



CHILDREN'S EDUCATION SOCIETY (Regd.)
THE OXFORD COLLEGE OF ENGINEERING

(Recognised by the Govt. of Karnataka, Affiliated to Visvesvaraya Technological University, Belagavi
Approved by A.I.C.T.E. New Delhi.

Recognised by UGC Under Section 2(f)
Bommanahalli, Hosur Road, Bangalore - 560 068.


Ph: 080-61754601/602, Fax: 080 - 25730551

E-mail: engprincipal@theoxford.edu Web: www.theoxfordengg.org

Details of research papers published

Index

| SL. No. | Particulars | Page No. |
|----------------|-----------------------------------|-----------------|
| 1. | Summary | 2 |
| 2. | Research papers published 2016-17 | 3 - 117 |
| 3. | Research papers published 2017-18 | 118 - 461 |
| 4. | Research papers published 2018-19 | 462 - 714 |
| 5. | Research papers published 2019-20 | 715 - 1059 |
| 6. | Research papers published 2020-21 | 1060 - 1221 |


PRINCIPAL
The Oxford College of Engineering
Bommanahalli, Hosur Road
Bengaluru-560 068



CHILDREN'S EDUCATION SOCIETY (Regd.)
THE OXFORD COLLEGE OF ENGINEERING
(Recognised by the Govt. of Karnataka, Affiliated to Visvesvaraya Technological University, Belagavi.
Approved by A.I.C.T.E. New Delhi.
Recognised by UGC Under Section 2(f)
Bommanahalli, Hosur Road, Bangalore - 560 068.
Ph: 080-61754601/602, Fax: 080 - 25730551
E-mail: engprincipal@theoxford.edu Web: www.theoxfordengg.org

Summary

In last 5 Academic Year, the faculty of The Oxford College of Engineering has published papers in various National & International Journals. There are total 2 National publications and 233 International publication in last 5 academic years.

| Sl. No | Academic Year | No. of Publication | |
|--------|---------------|--------------------|---------------|
| | | National | International |
| 1 | 2016-17 | 0 | 22 |
| 2 | 2017-18 | 2 | 48 |
| 3 | 2018-19 | 0 | 56 |
| 4 | 2019-20 | 0 | 59 |
| 5 | 2020-21 | 0 | 48 |
| Total | | 235 | |



CHILDREN'S EDUCATION SOCIETY (Regd.)
THE OXFORD COLLEGE OF ENGINEERING

(Recognised by the Govt. of Karnataka, Affiliated to Visvesvaraya Technological University, Belagavi.

Approved by A.I.C.T.E. New Delhi.

Recognised by UGC Under Section 2(f)

Bommanahalli, Hosur Road, Bangalore - 560 068.

Ph: 080-61754601/602, Fax: 080 - 25730551

E-mail: engprincipal@theoxford.edu Web: www.theoxfordengg.org

| Sl.No | Title of paper | Name of the author/s | Department of the teacher | Name of journal | Year of publication | ISSN number | Link to website of the Journal | Link to article/paper/abstract of the article | Is it listed in UGC Care list/Scopus/ Web of Science/other, mention |
|-------|---|------------------------|---------------------------|---|---------------------|----------------------|---|---|---|
| 1 | Tamper Detection using Watermarking Scheme and K-Mean Clustering for Bio Medical Images | Dr. R Kanagavalli | ISE | International Journal for Modern Trends in Science and Technology | 2016 | ISSN: 2455-3778 | https://www.ijmtst.com/ | http://www.ijmtst.com | UGC |
| 2 | A secured body sensor healthcare monitoring system for elderly couples | Jahnavi V | ISE | IJIRCCE | 2016 | 2320-9801, 2320-9798 | https://www.ijircce.com/ | http://ijircce.com/admin/main/storage/app/pdf/6q1lxIT6rpIMJWPCR IjYlJfGc7rycQfZqvj23xvY.pdf | Google Scholar |
| 3 | Congestion Control using Cross layer and Stochastic Approach in distributed networks networks | Selvarani R, Vinodha K | ISE | IJACSA | 2017 | - | http://www.ijacsa.thesai.org/ | https://thesai.org/Downloads/Volume8No3/Paper_28-Congestion_Control_using_Cross_layer_and_Stochastic.pdf | Google Scholar |



CHILDREN'S EDUCATION SOCIETY (Regd.)
THE OXFORD COLLEGE OF ENGINEERING

(Recognised by the Govt. of Karnataka, Affiliated to Visvesvaraya Technological University, Belagavi.

Approved by A.I.C.T.E. New Delhi.

Recognised by UGC Under Section 2(f)

Bommanahalli, Hosur Road, Bangalore - 560 068.

Ph: 080-61754601/602, Fax: 080 - 25730551

E-mail: engprincipal@theoxford.edu Web: www.theoxfordengg.org

| | | | | | | | | | |
|---|--|--|-----|---------|------|----------------------|---|---|----------------|
| 4 | Design and Development of Two Factor Authentication System for Eservices using DNA and Asymmetric Cryptography | Priyanka B J | ISE | IJRASET | 2017 | 2321-9653 | https://www.ijraset.com/ | https://www.ijraset.com/fileserve.php?FID=9023 | Google Scholar |
| 5 | Flow-Based Network Traffic Classification using Clustering Technique with MLA Approach | Tiveni Pujari | ISE | IJRASET | 2017 | 2321-9653 | https://www.ijraset.com/ | https://www.ijraset.com/fileserve.php?FID=9055 | Google Scholar |
| 6 | Robust and Secure Access Schema using Dual Factor Authentication and OTP using | Channappa Gowda D V | ISE | IJIRCCE | 2017 | 2320-9801, 2320-9798 | https://www.ijircce.com/ | http://ijircce.com/admin/main/storage/app/pdf/Qrhqhunc8EGLoZgj19KYVfjBUpj3Crrh1XeUuqJ.pdf | Google Scholar |
| 7 | Traffic Sign Recognition Using Convolution Neural Networks | S Visalini | ISE | IJIRCCE | 2017 | 2320-9801, 2320-9798 | https://www.ijircce.com/ | http://ijircce.com/admin/main/storage/app/pdf/aLQ8eDwVJJV0Vq3Dbkga6UecnNrGL6ArP2WO72uJ.pdf | Google Scholar |
| 8 | Lab-on-chip based optical biosensors for the application of dental fluorosis | D.L.Girijamba, Preeta Sharan, P.C.Srikanth | ECE | Optik | 2016 | 0030-4026 | https://www.journals.elsevier.com/optik | https://doi.org/10.1016/j.ijleo.2015.12.113 | SCI |



CHILDREN'S EDUCATION SOCIETY (Regd.)
THE OXFORD COLLEGE OF ENGINEERING

(Recognised by the Govt. of Karnataka, Affiliated to Visvesvaraya Technological University, Belagavi.

Approved by A.I.C.T.E. New Delhi.

Recognised by UGC Under Section 2(f)

Bommanahalli, Hosur Road, Bangalore - 560 068.

Ph: 080-61754601/602, Fax: 080 - 25730551

E-mail: engprincipal@theoxford.edu Web: www.theoxfordengg.org

| | | | | | | | | | |
|----|---|---|---------------|---|------|----------------------|---|---|----------------|
| 9 | Application of machine learning for real-time evaluation of salinity (or TDS) in drinking water using photonic sensors | Sandip Kumar Roy, Preeta Sharan | ECE | Drinking Water Engineering Science | 2016 | 19969 465, 19969 457 | https://www.drinking-water-engineering-and-science.net/ | https://doi.org/10.5194/dwes-9-37-2016 | Scopus |
| 10 | A novel quantum dot cellular automata for 4-bit code converters | Nandini G.Rao, P.C.Srikanth, Preeta Sharan | ECE | Optik, Elsevier | 2016 | 0030-4026 | https://www.journals.elsevier.com/optik | https://www.sciencedirect.com/science/article/abs/pii/S0030402615020379 | SCI |
| 11 | A Novel Image Compression Using Block Local Binary Pattern (LBP) with LZW | Ramya P Reddy | ECE | IJIREEICE | 2016 | 2321-2004, 2321-5526 | https://ijireeice.com/recent-issue-april-2016/ | https://www.ijireeice.com/upload/2016/april-16/IJIREEICE%2048.pdf | Google Scholar |
| 12 | Optimization of Crude Oil and PAHs Degradation by Stenotrophomonas rhizophila KX082814 Strain through Response Surface Methodology Using Box-Behnken Design | Praveen Kumar Siddalingappa, Virupakshappa, Manjunathi Bukkambudhi Krishnaswamy, Gaurav Mishra, and | Biotechnology | Hindawi Publishing Corporation Biotechnology Research International | 2016 | 2090-3146 | https://www.hindawi.com/journals/btri/2016/4769542/ | https://www.hindawi.com/journals/btri/ | Scopus |



CHILDREN'S EDUCATION SOCIETY (Regd.)
THE OXFORD COLLEGE OF ENGINEERING

(Recognised by the Govt. of Karnataka, Affiliated to Visvesvaraya Technological University, Belagavi.

Approved by A.I.C.T.E. New Delhi.

Recognised by UGC Under Section 2(f)

Bommanahalli, Hosur Road, Bangalore - 560 068.

Ph: 080-61754601/602, Fax: 080 - 25730551

E-mail: engprincipal@theoxford.edu Web: www.theoxfordengg.org

| | | | | | | | | | |
|----|--|---|---------------|---|------|-----------|---|---|----------------|
| | | Mohammed Ameenuddin Mehkri | | | | | | | |
| 13 | Bioremediation of Poly Aromatic Hydrocarbons (PAHs) and Crude Oil by Fungal Consortium from West Coast of Karnataka, India | S.V. Praveen Kumar, B.K. Manjunatha, Pavani Bhat, R. Veena, Swetha S. Pawate and M. Yogashree | Biotechnology | International Journal of Current Microbiology and Applied Sciences (IJCMAS) | 2016 | 2319-7692 | https://www.ijcmas.com/abstractview.php?ID=983&vol=5-10-2016&SN=44 | https://www.ijcmas.com/abstractview.php?ID=983&vol=5-10-2016&SN=44 | Scopus |
| 14 | Comparative Study of Symmetric and Asymmetric Structures using Response Spectrums | Mohammed Abdul Wasiq | Civil | IJSRD | 2016 | 2321-0613 | http://ijsrd.com/ | http://www.ijsrd.com/articles/IJSRDV4I40562.pdf | Google Scholar |
| 15 | Performance Study of High-Rise Buildings with Diagrid and Hexagrid Systems under Dynamic Loading | Deepika R | Civil | IJESC | 2016 | 2321-3361 | https://ijesc.org/ | https://doi.org/10.4010/2016.1084 | Google Scholar |
| 16 | Evaluation of Mechanical and Tribological | Pasanna M | Automobile | IJERAT | 2016 | 2454-6135 | https://ijagri.org/ijerati | https://ijagri.org/ijerati/index.php/ijerati/article/view/223 | Google Scholar |



CHILDREN'S EDUCATION SOCIETY (Regd.)
THE OXFORD COLLEGE OF ENGINEERING

(Recognised by the Govt. of Karnataka, Affiliated to Visvesvaraya Technological University, Belagavi.

Approved by A.I.C.T.E. New Delhi.

Recognised by UGC Under Section 2(f)

Bommanahalli, Hosur Road, Bangalore - 560 068.

Ph: 080-61754601/602, Fax: 080 - 25730551

E-mail: engprincipal@theoxford.edu Web: www.theoxfordengg.org

| | | | | | | | | | |
|----|---|--|--------------|-------------------------------------|------|----------------|---|---|----------------|
| | Characterization of Glass-Basalt Hybrid Composites | | | | | | rat/index.php/ijerat | | |
| 17 | Design of Rectenna for Energy harvesting from Ambient GSM and WLAN Frequency Bands | Vinay B E | Mechatronics | RUAS-SASTech Journal | 2016 | | https://research.msruas.ac.in/publications | http://www.sastechjournal.com/pdf/Journals/Oct2016/5.%20Design%20of%20Rectenna%20for%20Energy%20Harvesting%20from.pdf | Google Scholar |
| 18 | Enhanced Packet Dropping Algorithm and Neighbour Node Cluster Strategy for Intrusion Detection in MANET | Dr. M S Shashidhara | MCA | IJCAR Journals | 2016 | 2305-9184 | http://www.meacse.org/ijcar | www.meacse.org/ijcar/archives/97.pdf | UGC |
| 19 | Kinetic & Mechanistic study of Pd(II) catalysed oxidation deamination & decarboxylation of Glycine by Alkaline Permanganate | Dr Surekha M | Chemistry | IJAR, International | 2016 | ISSN-2820-5407 | https://www.journalijar.com/ | http://dx.doi.org/10.21474/IJAR01/3671 | UGC |
| 20 | Schur Convexity for Novel Ratio Of Difference of Means | Sreenivasa reddy Perla and S Padmanabhan | Mathematics | International Journal of Scientific | 2016 | 2347-3142 | https://www.arcjournals.org/international-journal- | https://www.arcjournals.org/pdfs/ijssimr/v4-i4/4.pdf | UGC |



CHILDREN'S EDUCATION SOCIETY (Regd.)
THE OXFORD COLLEGE OF ENGINEERING

(Recognised by the Govt. of Karnataka, Affiliated to Visvesvaraya Technological University, Belagavi.

Approved by A.I.C.T.E. New Delhi.

Recognised by UGC Under Section 2(f)

Bommanahalli, Hosur Road, Bangalore - 560 068.

Ph: 080-61754601/602, Fax: 080 - 25730551

E-mail: engprincipal@theoxford.edu Web: www.theoxfordengg.org

| | | | | | | | | | |
|----|---|--|-----------------|--|------|---------------|---|---|-------------------|
| | | | | c and Innovative Mathematical Research (IJSIMR) | | | of- scientific- and- innovative - mathematical- research | | |
| 21 | Roman Primary and Auxiliary Domination Number of a Graph | Mallikarjun B Kattimani and N C Hemalatha | Mathe matics | Internati onal Journal of Scientifi c and Research Publicati ons | 2016 | 2250- 3153 | https://www.ijsrp.org/research-paper-0516/ijsrp-p5306.pdf | https://www.ijsrp.org/research-paper-0516/ijsrp-p5306.pdf | Google Scholar |
| 22 | Roman Domination Number of a Graph | Mallikarjun B Kattimani and N C Hemalatha | Mathe matics | Internati onal Journal of Scientifi c and Research Publicati ons | 2016 | 2250- 3153 | https://www.ijsrp.org/research-paper-0616.php?rp=P545468 | https://www.ijsrp.org/aboutus.php | Google Scholar |



Advertisement

Main Menu

My Profile

Add Article

Searching By

Search more

PARTNERS

Advertise Your Business Here

Text Link AdBanner

Contact Us ?

Tamper Detection using Watermarking Scheme and K-Mean Clustering for Bio Medical Images

Journal: International Journal for Modern Trends in Science and Technology (IJMTST) (Vol.2, No. 11)

Publication Date: 2016-11-02

Authors : R. Suganya; R Kanagavalli;

Page : 180-185

Keywords : IJMTST;

Source : [Download](#) [Find It From : Google Scholar](#)

1. [Speed Estimation of Sensorless Induction Motor through Vector Control Using MRAS and Direct Synthesis Test](#)
2. [MRAS Observer for Sensorless Control of Induction Motor Using Fuzzy Pi Controller](#)
3. [THE ESTIMATION AND ADJUSTMENT OF ENERGETIC OPERATIONAL CONDITIONS OF SENSORLESS VECTOR-CONTROL SYSTEM WORKING UNDER INDUCTION MOTOR STATOR WINDING UNSYMMETRY](#)
4. [MODELLING ANALYSIS & DESIGN OF DSP BASED NOVEL SPEED SENSORLESS VECTOR CONTROLLER FOR INDUCTION MOTOR DRIVE](#)
5. [Speed Estimation of MRAS Based Induction Motor Drive Utilizing Machine's d- and q- Circuit Impedances Using PI and ANFIS Controller](#)

Abstract

In this paper, we focus image authentication and tamper detection using K-mean clustering based on fragile watermarking scheme. The two important aspects of the authentication watermarking scheme are Tamper detection and localization accuracy. In our scheme, clustering values of the watermarked image used as secret key. It can be detect any amendment is made to image and also point out the exact location that have been modified. Significant features of the schemes are reducing the time complexity and improving the PSNR value , with stand attacks. Original image is not required for verification

Other Latest Articles

1. [Power Quality Inverter on Photovoltaic SEPIC Converter](#)
2. [Graph Theory Matrix Approach in Selecting Optimal Combination of Operating Parameters](#)
3. [Circulating Current Fault-Tolerant Operation using MMC & PWM Compensation](#)
4. [Web Design Irrigation in Wireless Sensor Network Using Raspberry Pi](#)
5. [A STATCOM Control Scheme for Power Quality and THD Improvement](#)

Last modified: 2016-12-04 12:19:48

About ResearchBib Careers Contact us

Legal Terms of Service Privacy Policy Ad Choices Cookies



International Journal of Innovative Research in Computer and Communication Engineering

(An ISO 3297: 2007 Certified Organization)

Website: www.ijirccce.com

Vol. 5, Issue 6, June 2017

A Secured body Sensor healthcare Monitoring System for Elderly Peoples

Jahnavi V¹, P Kokila², Shruthi T S³, SamradhaRao⁴, Sujan Kumar⁵

UG Student, Department of ISE, The Oxford College of Engineering, Bommannahalli, Bengaluru, India¹

Assistant Professor, Department of ISE, The Oxford College of Engineering, Bommannahalli, Bengaluru, India²

UG Student, Department of ISE, The Oxford College of Engineering, Bommannahalli, Bengaluru, India³

UG Student, Department of ISE, The Oxford College of Engineering, Bommannahalli, Bengaluru, India⁴

UG Student, Department of ISE, The Oxford College of Engineering, Bommannahalli, Bengaluru, India⁵

ABSTRACT: The Internet of Things (IoT) has not been around for very long. Advances in information and communication technologies have led to the emergence of internet of things. The Internet of Things had evolved into a system using multiple technologies, ranging from the Internet to wireless communication. The usage of IoT technologies brings convenience of physicians and patients, since they are applied to various medical areas. The recent advances in wireless sensor networks and embedded computing technologies, miniaturized pervasive health monitoring devices have become practically feasible. The body sensor network (BSN) technology is one of the core technologies of IoT developments in healthcare system, where a patient can be monitored using a collection of tiny-powered and lightweight wireless sensor nodes. In addition to that of monitoring and analysis of physiological parameters, the recently proposed Body Sensor Networks (BSN) incorporates context aware sensing for increased sensitivity and specificity, but development of the body sensor network (BSN) technology in healthcare applications without considering security makes patient privacy vulnerable. At the specification, we mainly concentrate on the major security requirements in BSN-based modern healthcare system. Subsequently, the propose of a secure IoT-based healthcare system using BSN called BSN-Care, in which it can efficiently accomplish the security requirements.

KEYWORDS: BSN, data privacy, data integrity, authentication.

I. INTRODUCTION

The last few decades have witnessed a steady increase in life expectancy in many parts of the world leading to a sharp rise in the number of elderly people. A recent report from United Nations predicted that there will be 2 billion (22% of the world population) older people by 2050. In addition, research indicates that about 89% of the aged people are likely to live independently. However, medical research surveys found that about 80% of the aged people older than 65 suffers from at least one chronic disease causing many aged people to have difficulty in taking care of themselves. Accordingly, providing a decent quality of life for aged people has become a serious social challenge at that moment. The rapid proliferation of information and communication technologies is enabling innovative healthcare solutions and tools that show promise in addressing the aforesaid challenges. Now, Internet of Things (IoT) has become one of the most powerful communication paradigms of the 21st century. In the IoT environment, all objects in our daily life become part of the internet due to their communication and computing capabilities.

IoT extends the concept of the Internet and makes it more pervasive. IoT allows seamless interactions among different types of devices such as medical sensor, monitoring cameras, home appliances so on. Because of that reason IoT has become more productive in several areas such as healthcare system. In healthcare system, IoT involves many kinds of cheap sensors (wearable, implanted, and environment) that enable aged people to enjoy modern medical healthcare services anywhere, any time. Besides, it also greatly improves aged peoples quality of life. The body sensor network (BSN) technology is one of the most imperative technologies used in IoT-based modern healthcare system. It is basically a collection of low-power and lightweight wireless sensor nodes that are used to monitor the human body



International Journal of Innovative Research in Computer and Communication Engineering

(An ISO 3297: 2007 Certified Organization)

Website: www.ijircce.com

Vol. 5, Issue 6, June 2017

functions and surrounding environment. Since BSN nodes are used to collect sensitive (life-critical) information and may operate in hostile environments, accordingly, they require strict security mechanisms to prevent malicious interaction with the system. In this article, at first we address the several security requirements in in BSN based modern healthcare system. Propose of a secure IoT based healthcare system using BSN, called BSN-Care, which can guarantee to efficiently accomplish those requirement.

II. LITERATURE SURVEY

David Malan et al [1] propose the completion of an initial design of CodeBlue and prototypes of several of the components described herein. The pulse oximetry method has been completed and development of an ECG mote is currently underway. The use of an adaptive spanning-tree multi-hop routing algorithm, based on the Tiny OS Surge protocol, and the incorporation of a dynamic transmission power scaling to minimize interference. A lightweight public key infrastructure based on elliptic curve cryptography is currently being tested. A sophisticated programming model using abstract regions for routing, data sharing, and aggregation has also been developed. The disadvantages are i) Communication challenges: The first challenge is secure, reliable, ad hoc communication among groups of sensors and mobile, handheld devices. ii) Computational challenges: Sensor nodes have very limited computational power, and traditional security and encryption techniques are not well-suited to this domain.

Jason W.P.Ng et al [2] describes the ubiquitous monitoring system is presented for continuous monitoring of patients under their natural physiological states. The system provides the architecture for collecting, gathering and analyzing data from a number of biosensors. Particularly, the concept of BSN node is implemented which could form the basis for wireless intelligent modules for wearable and implantable sensors. In addition to the physiological parameters, the context awareness aspect is also included in the system to enhance the capturing of any clinical relevant episode. The demerit is the issues in the development of wearable/implantable sensors in BSN

Sideny Katz et al [3] propose the Index was originally derived from observations of old people with fracture of the hip, it was necessary to determine whether it could be applied to others as well. Observations of 1,001 individuals, to date, supported the original finding of an ordered relationship and demonstrated wide applicability. Of the 1,001 people, 96% could be classified by the Index (Table 3). Ninety per cent were 40 years old or older, and more than 60% were 60 or over. Most had more than one chronic disease. The primary clinical diagnoses associated with ADL disability were: fracture of the hip (250 persons), cerebral infarction (239), multiple sclerosis (138), arthritis (60), malignancy (30), cardiovascular disease exclusive of cerebral infarction (38), and amputation, paraplegia, or quadriplegia (67). In 38 other patients, the diagnoses were: cerebral palsy, Parkinson's disease, amyotrophic lateral sclerosis, peripheral neuropathy, or other neurological disease. Less commonly, primary diagnoses included such chronic diseases as asthma, emphysema, diabetes, blindness, cirrhosis, alcoholism, malnutrition, and obesity. The problem is they are not able to keep the track of chronic diseases.

Rajiv Chakravorty et al [4] describes the vast opportunity in the 'point-of-care' access and the capture and transmission of patient information will continue to drive the healthcare industry towards increased mobility. The importance is in the shifting awareness that mobility in healthcare settings increasingly refers to – the mobility of sensor/actuator devices, the healthcare providers (health 'outsourcing') and of the patient (users) themselves. MobiCare leverages the point-of-care patient access to offer important benefits like quality healthcare, a programmable service architecture, flexible service composition and a full-scale medical systems integration. MobiCare is an ongoing project and much work remains to be done. Besides a proof-of-concept prototype, there is a process of investigating other long-term, challenging research problems in MobiCare including the body sensor network security, reliable and secure sensor code updates and upgrades, the potential legal hurdles involved and the privacy issues that arise with dynamic remote code updates. The disadvantage is it is not reliable and secure.

Arun Kumar et al [5] elaborates the presentation of the first experimental evaluation of prominent device pairing methods. Results show that some simple methods (e.g., Visual Number and Image Comparison) are quite attractive overall, being fast and secure as well as acceptable by users. They naturally appeal to settings where devices have appropriate-quality displays. HAPADEP variant seems to be preferable for more constrained devices: it is fast, error-free and requires very little user intervention. LED Button or Vibrate-Button are best-suited for devices lacking screens, speakers and microphones. The demerit is user evaluation for each method is not yet done.

International Journal of Innovative Research in Computer and Communication Engineering

(An ISO 3297: 2007 Certified Organization)

Website: www.ijirccce.com

Vol. 5, Issue 6, June 2017

III. PROPOSED METHODOLOGY AND DISCUSSION

A. METHODOLOGY

Body Sensor Network (BSN) allows the integration of intelligent, miniaturized low-power sensor nodes in, on or around human body to monitor body functions and the surrounding environment. Generally, BSN consists of in-body and on-body sensor networks. An in-body sensor network allows communication between invasive/implanted devices and base station. On the other hand, an on-body sensor network allows communication between non-invasive/wearable devices and a coordinator. Each sensor node is integrated with bio-sensors such as blood pressure sensor, motion sensor, ECG etc.

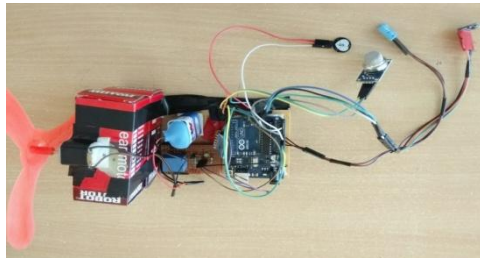


Fig.1: Hardware connections

i. Data Collection

Sensors collect the physiological parameters and forward them to a coordinator called Local Processing Unit (LPU), which can be a portable device such as PDA, smart-phone etc. The LPU works as a router between the BSN nodes and the central server called BSN-Care server, using the wireless communication. When the LPU detects any abnormalities then it provides immediate alert to the person that wearing the bio-sensors. When the BSN-Care server receives data of a person (who wearing several bio sensors) from LPU, then it feeds the BSN data into its database and analyzes those data. Subsequently, based on the degree of abnormalities, it may interact with the family members of the person, local physician, or even emergency unit of a nearby healthcare center.

ii. Lightweight Anonymous Authentication Protocol

The division of all security requirements (mentioned above) into two parts: network security, and data security. Network security comprises authentication, anonymity, and secure localization. On the other hand, data security includes data privacy, data integrity, and data freshness. Now, to the best of the knowledge there is no two-party authentication protocol which can achieve all the aforesaid properties of the network security. Hence, in order to achieve all the network security requirements a lightweight anonymous authentication protocol is used. Subsequently, to accomplish all the data security requirements we adopt OCB authenticated encryption mode.

In BSN-Care system, when a LPU wants to send the periodical updates to BSN-Care server, then the server needs to confirm the identity of LPU using a lightweight anonymous authentication protocol. In this section we describe our anonymous authentication protocol in details. The proposed authentication protocol consists of two phases: In Phase 1, the BSN-Care server issues security credentials to a LPU through secure channel, this phase is called registration phase. The Phase 2 of the proposed authentication protocol is the anonymous authentication phase, where before data transmission from the LPU to BSN-Care server, both the LPU and the server will authenticate each other. So, the objective of our proposed lightweight authentication scheme is as follows:

- To achieve mutual authentication property.
- To achieve anonymity property.
- To achieve secure localization property.
- To defeat forgery attacks.
- To reduce computation overhead.

International Journal of Innovative Research in Computer and Communication Engineering

(An ISO 3297: 2007 Certified Organization)

Website: www.ijirccce.com

Vol. 5, Issue 6, June 2017

IV. RESULT ANALYSIS

In the proposed work the Sensors are used to monitor elder people's body status and surrounding environment. The Elder people can be in touch with the family, doctor or care taker from remote place. During abnormal condition Automatic alert is sent to the family, doctor or care taker and automatic Control of the home appliances is achieved based on the body condition.

The data are collected using different sensors fig.1. The fig.2 describes the data stored in Android application, where P represent the Pulse, T represent Temperature, AS represent movement of object and CO represent the gas level of the environment. The predefined threshold level is fixed for pulse, temperature and toxic gas of the surrounding, if the values of any one of the mentioned point crosses the threshold value immediately message will be sent to the doctor, family members and to nearby hospital along the patient name, contact number and location as shown in fig.3



Fig.2: Data Stored In Android App



Fig.3: Message Intimation

V. CONCLUSION

The security and the privacy issues in healthcare applications using body sensor network (BSN). Subsequently, found that even though most of the popular BSN based research projects acknowledge the issue of the security, but they fail to embed strong security services that could be preserve patient privacy. Finally, the proposed system has a secured IoT based healthcare system using BSN, called BSN-Care, which can efficiently accomplish various security requirements of the BSN based healthcare system.

REFERENCES

- [1] David Malan, T. Fulford-Jones, M. Welsh, and S. Moulton, "CodeBlue: An ad hoc sensor network infrastructure for emergency medical care," in Proc. MobiSys Workshop Appl. Mobile Embedded Syst. (WAMES), Boston, MA, USA, Jun. 2004, pp. 1-8.
- [2] Jason W. P. Ng et al., "Ubiquitous monitoring environment for wearable and implantable sensors (UbiMon)," in Proc. 6th Int. Conf. Ubiquitous Comput. (UbiComp), Nottingham, U.K., Sep. 2004, pp. 1-2.



ISSN(Online): 2320-9801
ISSN (Print): 2320-9798

International Journal of Innovative Research in Computer and Communication Engineering

(An ISO 3297: 2007 Certified Organization)

Website: www.ijirccce.com

Vol. 5, Issue 6, June 2017

- [3] R. Weinstein, "RFID: A technical overview and its application to the enterprise," *IT Prof.*, vol. 7, no. 3, pp. 27–33, May/Jun. 2005.
- [4] R. Chakravorty, "A programmable service architecture for mobile medical care," in *Proc. 4th Annu. IEEE Int. Conf. Pervasive Comput. Commun. Workshop (PERSOMW)*, Pisa, Italy, Mar. 2006, pp. 531–536.
- [5] A.kumar, N.Saxena, G.Tusdik "Caveateptor: A comparative study of secure device pairing methods", in *Proc. IEEE Int. Conf. Pervasive Comput. Commun. (Per Com)*, Mar. 2009, pp. 1-10
- [6] P. Gope and T. Hwang, "Untraceable sensor movement in distributed IoT infrastructure," *IEEE Sensors J.*, vol. 15, no. 9, pp. 5340–5348, Sep. 2015.
- [7] P. Gope and T. Hwang, "A realistic lightweight authentication protocol preserving strong anonymity for securing RFID system," *Comput. Secur.*, vol. 55, pp. 271–280, Nov. 2015.
- [8] P. Kumar and H.-J. Lee, "Security issues in healthcare applications using wireless medical sensor networks: A survey," *Sensors*, vol. 12, no. 1, pp. 55–91, 2012.
- [9] K. Lorincz et al., "Sensor networks for emergency response: Challenges and opportunities," *IEEE Pervasive Comput.*, vol. 3, no. 4, pp. 16–23, Oct./Dec. 2004.
- [10] A. Wood et al., "ALARM-NET: Wireless sensor networks for assisted living and residential monitoring," *Dept. Comput. Sci., Univ. Virginia, Charlottesville, VA, USA, Tech. Rep. CS-2006-01*, 2006.
- [11] S. Pai et al., "Confidentiality in sensor networks: Transactional information," *IEEE Security Privacy Mag.*, vol. 6, no. 4, pp. 28–35, Jul./Aug. 2008.
- [12] Office for Civil Rights. United State Department of Health and Human Services Medical Privacy. National Standards of Protect the Privacy of Personal-Health-Information. [Online]. Available: <http://www.hhs.gov/ocr/privacy/hipaa/administrative/privacyrule/index.html>, accessed Jun. 15, 2011.
- [13] R. Chakravorty, "A programmable service architecture for mobile medical care," in *Proc. 4th Annu. IEEE Int. Conf. Pervasive Comput. Commun. Workshop (PERSOMW)*, Pisa, Italy, Mar. 2006, pp. 531–536.
- [14] J. Ko et al., "MEDiSN: Medical emergency detection in sensor networks," *ACM Trans. Embed. Comput. Syst.*, vol. 10, no. 1, pp. 1–29, Aug. 2010.

Congestion Control using Cross layer and Stochastic Approach in Distributed Networks

Selvarani R

Department of Computer science and Engineering
Alliance College of Engineering and Design
Bangalore, India

Vinodha K

Department of Information science and Engineering
The Oxford College of Engineering
Bangalore, India

Abstract—In recent past, the current Internet architecture has many challenges in supporting the magnificent network traffic. Among the various that affect the quality of communication in the massive architecture the challenge in maintaining congestion free flow of traffic is one of the major concerns. In this paper, we propose a novel technique to address this issue using cross layer paradigm based on stochastic approach with extended markovian model. The cross layer approach will bridge the physical layer, link layer, network layer and transport layer to control congestion. The resource provisioning operation will be carried out over link layer and the mechanism of exploring the congestion using stochastic approach will be implemented over the network layer. The Markov modeling is adopted to identify the best routes amidst of highly congested paths and it is carried out at the transport layer. An analytical research methodology will be adopted to prove that it is feasible to develop a technique that can identify the origination point of congestion and share the same with the entire network. It is found that this approach for congestion control is effective with respect to end to end delay, packet delivery ratio and processing time.

Keywords—Distributed Network System; cross layer; congestion; Traffic Flow; Rate Control Metric

I. INTRODUCTION

Internet plays a vital role in dissemination of knowledge and servicing seamless and ubiquitous communication in the present era. With the advancements in technologies like cloud computing and optical network, offering high speed data delivery, data storage and retrieval is not an impossible task [1] yet, there is still a problem with the existing internet architecture. A closer look into the existing internet architecture reveals that it is packed with various complexities Viz. incompatible in allowing connectivity with heterogeneous networks and its respective protocols, operating with various distributed networks [2][3]. The existing internet design principles can only permit networking with less complexity in its routing and communication process. These principles are not scalable for the requirement of the future internet architecture. The reason behind this is untrusted communication, more customer-oriented user environment, availability of many commercial network operators, data-centric utilities, and the worst part is intermittent connectivity [4]. Another challenging problem is its inclination towards Internet Protocol (IP) paradigm that makes it suitable for static internet users but not for mobile internet users. Therefore, whenever an application meets heterogeneity, it introduces a great deal of challenges for the network-based architecture and

at the same time, it also leads to significant problems of resource allocation that can potentially affect the quality of performance. The connection technique of this architecture is characterized by one-to-many and many-to-many connections and also supports smart virtualization process. The significance of user-based participation is quite high with compatibility of multi-hop transmission scheme [5]. Unfortunately, none of the above mentioned schemes are present even to a lesser extent in the existing internet architecture.

The present paper deals with the problems related to congestion control in future internet architecture. Although understanding the user-behavior over traffic and predicting it is an NP(nondeterministic polynomial time) hard problem, there are studies existing in past that has already focused on congestion control mechanism but less evidence of studies have focused towards congestion control in future internet architecture. Essentially, this is built over three components viz. service, architecture and infrastructure. The next problem is interoperability. Given a scenario of multiple and heterogeneous network, it is a challenging task to process the control messages. This phenomenon is definitely a big impediment towards congestion. The next issue is for a given congestion over the dynamic network, it is quite challenging to maintain a balance between identifying the point of congestion and processing heterogeneous control messages. Hence, it can be said that it is quite a difficult task to identify and mitigate the level of congestion in this architecture.

This paper presents a joint algorithm that incorporates cross layered mechanism with stochastic approach and Markov modeling to mitigate the potential issues of congestion in massive distributed system (future internet architecture). Section II reviews the existing literature for congestion control. The motivation and problem identification is discussed in section III. Section IV deal with the proposed study and its significant contribution. The algorithms that are implemented to attain the goals are presented in section V. The results of the proposed study are analyzed in Section VI. The concluding remarks are discussed in section VII.

II. RELATED WORK

The existing research in this area is revealed here.

Gholipour et al. [6] have carried out an investigation on congestion problems in sensor network. The working principal of the sensor network operate with distributed algorithm. Here the authors discussed a technique based on cost metric. The

results were compared with respect to energy and packet. Efthymiopoulos et al. [7] have presented a study on congestion minimization pertaining to real-time streaming. The authors have introduced a technique that can provide traffic management in different domains of the network based on the bandwidth. The system is purely made for the internet-based peer-to-peer traffic. Jose et al. [8] have presented a congestion minimization technique that evaluates the rate of communicating signals in highly distributed manner. The outcome of the study was evaluated with respect to transmission rate and found that it offers better rate control mechanism for minimizing the congestion. Zaki et al. [9] have presented a solution towards mitigating congestion that is witnessed over highly unpredictable mobile networks. The authors tested their finding over the continuous date occurred on 3G network. The outcome of the study was evaluated with respect to throughput and delay to find that proposed system offers better resiliency for internet-based congestion. Ichrak et al. [10] have also investigated the problems of congestion in TCP-IP(Transmission Control Protocol/Internet Protocol)based connection. Sonmez et al. [11] have presented a technique that focuses congestion identification and reduction owing to multimedia transmission. The study focuses on the congestion control and its effect on the quality of the transmitted multimedia files using fuzzy logic mechanism. The outcome of the study was evaluated with respect to Peak Signal-to-Noise Ratio (PSNR).

Reddy and Krishna [12] has presented cross layer approach in order to mitigate the congestion issues in mesh network using TCP New Reno protocol. They focused on efficient channel capacity optimizing during the massive multimedia transmission and the results were assessed using packet transmission rate and delay. A scheme for controlling the congestion over TCP-IP based network was presented by the authors Carofiglio et al. [13]. They has used the principle of active queue management to control the congestion and found that the technique possessed an effective window size, round trip time, and queue size. Further studies towards distributed system were carried out by Antoniadis et al. [14]. Although they worked on a small network, the principle applied was considered as a guiding factor for large scale distributed network as it focuses on addressing an effective traffic management technique using game theory. Cai et al. [15] have presented a model for controlling congestion in TCP-based communication system. The proposed methodology controls congestion over the wireless network based on node-to-node interactions. Using the case study of adhoc-based network, they have proved that their method offered better congestion control. Under the constraint of the fading channel, Ye et al [16] used probability theory to show that the congestion control model for vehicular network offered improvement in the energy efficiency and data packet transmission over adhoc-based networks. Similar kind of work was carried out by Bouassida and Shawky [17]. They presented dynamic scheduling algorithm based on the priority of the messages. The focused on improving data reliability of real-time vehicular network.

Kas et al. [18] have presented a technique for performing scheduling over dynamic channels. The aim of this is to

increase the throughput from application viewpoint. A specific level of weight is assigned to each node that is arbitrarily fine-tuned based on saturation level of the queue. The results were evaluated with respect to end-to-end delay and packet delivery ratio over Constant Bit Rate traffic. Li et al. [19] have investigated congestion control for delay-based network. The authors have compared their work with respect to voice and data traffic and showed that it can control congestion based on the available delay information. Misra et al. [20] has presented a unique technique based on automata theory for managing the congestion over wired network. The author have also applied stochastic-learning based mechanism and cellular automata for managing an effective queue size. The outcomes were assessed using sequence number, queue factor, etc. Uthra et al. [21] have proposed a rate control mechanism for governing the traffic so that efficient throughput can be managed to ensure transmission free from any sorts of collision. The outcome of the simulation-based study is recorded and compared with the existing predictive-based mechanism to control congestion and found that the presented system minimizes the traffic congestion and also enhances the traffic performance.

The following section presents the problem that is identified after reviewing the work that was carried out by researchers in the field of congestion control.

III. MOTIVATION AND PROBLEM IDENTIFICATION

The following are the areas to be considered for efficient performance of future Internet. The prevailing research in this area fail to address the following:-

- The network quality parameters like delay, latency and channel capacity are not considered efficiently for congestion control mechanism.
- The current cross layer design allows manipulation of various layer parameters which leads to complication of congestion control and error management. In addition to that it is observed that the complexity of identifying the source of congestion is difficult because of the inefficient handling of randomness of traffic in heterogeneous network.

IV. PROPOSED SYSTEM

The aim of the proposed system is to develop a novel algorithm that can identify the origin of congestion in distributed network system. Here, the emphasis on network resource allocation for dynamic data flow control is given. As future internet architecture will possess all the possible complexities of existing internet as well as other networking standards (owing to reconfigurable nature), it is essential to address the issues through empirical and analytical modeling. In addition to regular quality parameters our research addresses the issues related to air medium e.g interference and different levels of noise over wireless channel for modeling the traffic. This paper is a continuation of our work where we have offered a packet level congestion by introducing a parameter i.e., Rate Control Metric (RCM)[24]. This metric is designed to offer an efficient control over the highly distributed network. The system is designed with the principle of cross layer paradigm. The randomness in the heterogeneous network is studied

through stochastic based probability model. This system is viewed as a massive network through graph theory modeling for better analysis of traffic congestion. In order to study and mitigate the traffic congestion in heterogeneous network (Future internet architecture) the performance metric were analyzed through RCM.

In this research we have considered cross layer approach for effective communication between networks. The resource provisioning technique is enhanced through stochastic based approach where, the model based on markovian modeling provides an optimized search for favorable node for routing. This model supports in identifying the best possible node amidst of congested nodes for speedy transfer of data which enhances the throughput of the network.

A. Cross Layer network model

Identifying the origination point of congestion and determining the control messages for processing the routing process to mitigate congestion requires a robust mechanism. Cross-layered approach is used to overcome this problem by controlling physical layer, data link layer, network layer, and transport layer in the protocol stack of future internet architecture. The cross layer network model plays an important role in arbitrary provisioning of network resources for congestion control. The presented scheme uses a significant routing factor that supports dynamic communication through multiple hops. It also uses a scheme that controls and manages the rate of traffic flow to achieve the fairness in sharing of network resources. A cost efficient provisioning algorithm is designed that models a novel queuing technique for maintaining queue stability. One of the significant focuses of the presented technique is to include the scenarios of noise and interference. This approach helps in processing control messages of multiple layers to adjust the rate of traffic flow during peak hours and also select favorable nodes for communication between two different networks. Hence, the cross-layer scheme offers flexibility to process the control request with less delay and also ensures that it is applicable for distributed network with heterogeneity.

B. Stochastic Approach

The stochastic approach of the proposed system mainly involves an integrated implementation of resource provisioning, communication and controlling the traffic directions. This approach initializes the discrete networking states followed by selection of highly stabilized links, and apply provisioning. The system uses graph theory to design an algorithm that works over the distributed machines. The significant contribution of this approach is to develop a network model that uses noise and signal power to categorize the quality of the links. It also consider the constraints of first two layers (link, physical) where there is no assured link rate for assigned time instances in distributed networking system. There is also a possibility that the capacity of the route may vary over a period of time that will lead to a significant stochastic problem. In order to solve this issue, we have implemented Rate Control Metric (RCM) [24] that can extract the exact information about the traffic rate thereby giving more information about the capacity of the routes. In order to solve the problems related to computational complexity, we

also initialize a hypothetical matrix that stores and extracts the best provisioned values, which acts as alternative for the congestion states of traffic. Hence, there is no significant control overhead due to this. Moreover, the provisional matrix is regularly updated which makes the proposed system independent from any degree of congestion found in a specific transmission area.

C. Markov Modelling

The main aim of Markov Modeling is to optimize the stochastic approach used for congestion control. The goal of this module will be to minimize the end-to-end delay in distributed networking system. We apply probability theory along with Markov model to find out alternate routes by exploring non-congested paths for routing. Markov chain is used for mapping the network model that uses queuing theory over the layered design. (The study doesn't emphasize much on queuing mechanism explicitly as there is already robust mechanism specific to routing protocols in distributed network). The system maintains two types of traffics in a matrix i.e. local traffic and global traffic. Local traffic can be accessed at any instance of time and global traffic information can be accessed only when the node has better residual energy. The energy model based on first order radio model or Radio Frequency (RF) circuitry principle [26] will be implemented in the proposed system. The next section discusses the implementation of cross layer algorithm, stochastic approach algorithm and markov modeling.

V. ALGORITHM IMPLEMENTATION

A. Algorithm for Cross-Layer Approach

In this work, we address the mitigation of congestion in the distributed network system through cross layer approach. The algorithm and implementation are as depicted below.

Algorithm:

Input: n (nodes), ρ (queue)

Output: updation of Link

Start

1. init n, ρ , // n is the number of nodes & ρ is the queue size
2. Estimate generated packets pkt on condition

$$pkt = \left[\frac{\rho}{J} \right]_0^t$$

3. Define link cost

$$C_{s,d}(t) = \arg_{\max} [\Delta\rho]$$

4. $L[t] \rightarrow \{L_s, d[t]\}$

5. Define enhancement in cross-layer provisioning

$$L_c(t) = \int_0^L (\rho[x], (L_o - L_t)) dx$$

6. Select $\rightarrow \text{rand}[t] \in L \parallel \text{rand}[t] = L_c[t]$

7. update L[t]

End

The algorithm is formalized by considering the number of nodes n and initial queue size ρ . Fig.1 illustrates the complete process flow of the proposed cross layer based provisioning.

The queue stability of the distributed networking system is defined by the following equation which is used to filter out all the links that have their queue size tending to infinity.

$$\lim_{t_{cum} \rightarrow \infty} |\rho(t)| < \infty$$

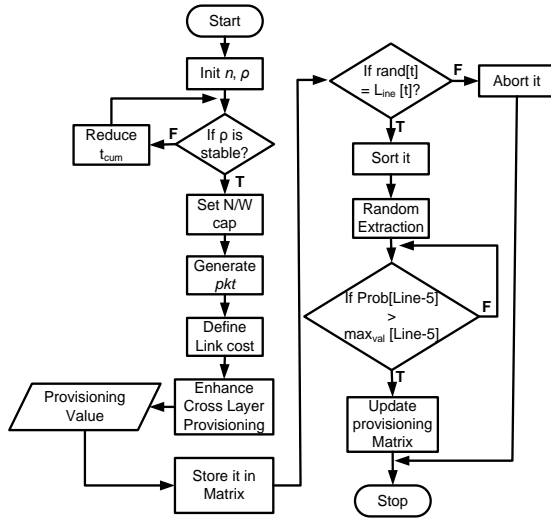


Fig. 1. Process flow for Cross Layer Provisioning

The link capacity of the network is expressed in terms of the pkt . Here, it is assumed that at time t the nodes in the network generate data packets equivalent to queue size ρ with controlled variables I and J (I and J are positive integers) are as shown in line2 of the algorithm. As the future internet architecture supports higher range of heterogeneity in device integration, there are possibilities of signal collision that leads to channel interference. In order to distinguish the quality of links (or routes) a new measurement link cost C is considered and is estimated based $\Delta \rho$, where the variable $\Delta \rho$ represents difference between the source queue ρ_s and destination queue ρ_d at the time t . The link provider metric $L[t]$ that is equivalent to $L_{s,d}[t]$, where L represents a matrix of provider that consist of non-colliding links between any source(s) and destination(d) is considered as the main parameter of the algorithm. It is assumed that initially the buffer is shared among each recipient node. The link provisioning matrix is updated considering the maximum value of the two arguments i.e. queue $\rho[x]$ and difference between outgoing capacity of link L_o and incoming capacity of link L_i .

The link provider will arbitrarily select an element from the matrix that satisfy the condition i.e. probability of selected element is equivalent to enhanced value (Line-6). It is updated as follows

$$L_c(t) = \int_0^L (\rho[x], (L_o - L_i)) dx$$

Here, the link metric $L[t]$ is estimated in terms of its queue size and the link capacity helps in the route selection process.

B. Algorithm for Stochastic Approach

In distributed networking system the traffic may undergo uncertainties like dynamic topology, random mobility etc. in high degree of randomness. The state of the network with uncertainty is analyzed through stochastic process in which the future node is identified with the theory of cross layer architecture. The nodes are initialized and their details are maintained on a data structure managed by graph theory. Owing to the distributed nature of the system, we assume that the control messages are free from errors or noise. After the implementation of cross-layer approach, we assume that there is no deviation or variance in the route capacity over the advancement of time.

Algorithm

Input: E_s (energy for transmitting), δ_s, d (gain factor of the power), β (capacity of the channel), ψ (noise density)

Output: Provisioning state

Start

1. Evaluate SNR

$$SNR_{s,d} = \frac{E_s \cdot \delta_{s,d}}{\beta \cdot \psi}$$

2. Evaluate capacity of link

$$L_{cap} = \beta \log_2(1 + SNR_{s,d})$$

3. Define duplicated groups

$$dp = \{dpS \mid s, d \in N, dpS \subseteq N_s \cap N_d\}$$

4. Function for duplicated groups

$$f(s, dp) = \{dpS \mid (s \in dpS) \wedge (dpS \subseteq dp) \wedge (|dpS| \geq 2)\}$$

5. If $s \subseteq S$ Than

6. for all $di \subseteq D$ do

7. $rcm(t) \leftarrow \text{argmin}(rcm_{max}, \text{scaler_mult}(t));$

8. Apply Algorithm-1

9. Transmit data from s to d

10. Update $\text{scaler_multi}(t) \rightarrow$ state of provisioning

End

The algorithm is implemented by defining a network model, Signal-to-Noise Ratio (SNR) and Link Capacity (Line-1 and 2 of the algorithm). The duplicate control messages for analysis purpose are generated using Line-3 of the algorithm. In the above algorithm the source node s is identified as s_{id} and matrix of duplicate control messages containing information

about s as $s.dp$. The duplicated groups are formulated using the equation as shown in Line-4. The cross layer architecture of the future internet is designed in such a way that each source node s can access its routing table N_s . For reliable routing during peak traffic the algorithm allows node s to construct multiple hops with other nodes for providing alternate routes. The one dimensional matrix is generated by scalar multiplication of s and dp and the same is stored at every node. However, for all the duplicate control messages dpS , only the node that has highest value of id is chosen and is used in the computation process. The algorithm looks for all the source nodes s (S is total source nodes) and attempts to control the flow of packets. It then checks all the respective destination nodes and uses rate control metric (RCM) [24] to further enhance the provisioning for the data transmission. Finally, with the help of cross layer provisioning algorithm the data is transmitted towards the destination d .

The significance of the stochastic based approach algorithm is that it further enhances the resource provisioning offered by cross-layer based provisioning technique at the link layer and also supports better communication in the network layer by favoring multiple hops routing in distributed networking system. Finally, the data transmission is improved by applying rate control metric [24] which assigns an appropriate rate at the transport layer for effective end to end communication. Hence, the algorithm completely supports the cross-layer paradigm for future internet architecture to ensure interoperability among heterogeneous networks and achieve efficient data transmission.

C. Algorithm for Markov Modeling

The Markov modeling is used to further strengthen the algorithm discussed in the above sections and to apply stochastic modeling to further enhance the congestion control algorithm and offer a better solution to control traffic congestion. In Markov modeling each node is represented as Mc that is composed of the total number of layers corresponding to $Lcap+1$ (numerically). The amount of data packets pkt processed on each layer should be equivalent to $Lcap$ such that $0 < pkt < Lcap$. We consider two different forms of layers Viz. passive layer PL and active layer AL . Passive layer represents the passive process when the nodes doesn't have any packet to forward ($pkt=0$) whereas in active layer, nodes always have packets for forwarding ($pkt>0$). As the future internet architecture possess different wireless nodes it is assumed that there are other feasible communication outages that will call for retransmission phenomenon. We denote ϕ as the amount of retransmission and Wn to be amount of unit trail of transmission. The algorithm for Markov modeling is given below.

Algorithm

Input: pkt (Packet), $Lcap$ (Link capacity w.r.t queue), PL (Passive Layer), AL (Active Layer), ϕ (Maximum amount of retransmission)

Output: Identification of free/busy routes

Start

1. init $pkt, Lcap, PL, AL, \phi$
2. Determine $TP, PP, \gamma P, IP$.
3. Define area of collision A
4. $\{s, d\} \in A_{s,d}, \forall A_{s,d} = A_s \cap A_d$
5. Obtain $|F_{s,d}| = A_s / A_{s,d}$
6. Evaluate size matrix $|A_{s,d}|, |F_{s,d}|$, and $|F_{d,s}|$
7. Estimate number of Nodes
 $size(|A_{s,d}|, |F_{s,d}|, \text{and } |F_{d,s}|) \cdot \text{network density}$
8. Estimate the probability of minimum transmission
 $p_{A_s} = 1 - \mathcal{G}$
9. Evaluate $b1, b2, b3$ & $Mc = \text{Algorithm-2}\{b1, b2, b3\}$
10. Find busy routes and free routes.

End

The problem of congestion in future internet architecture leads to network jamming that disrupt the process of identifying the best nodes for forwarding the data packets. This problem can be addressed by designing an algorithm that applies Markov modeling for evaluating the free and busy routes at the peak traffic situation. The algorithm takes the required inputs and computes maximum probability of passive state transition TP , preliminary state component PP , passive state probability component per states γP , and inter-arrival probability IP . Fig.2 shows the process flow for Markov modeling.

The Markov model is designed by considering three probability matrices viz. $b1, b2$ and $b3$. The matrix $b1$ and $b2$ represents the probability of a node identifying the busy channel in the first and second Markov process. The matrix $b3$ represents the feasibility that the packet forwarding process fails due to data packet collision or interference or noise. Line-3 shows the collision area A for the source node s . The area A is defined as a transmission zone where there is interference of the neighboring nodes resulting in traffic congestion in that particular transmission area. Hence, area A represents the possible congestion area. As shown in Line-4, it can be interpreted that both the sender node s and destination node d will lie within $A_{s,d}$. There can also be another possible transmission zone $F_{s,d}$ as per Line-5 which may be undetected in the area $A_{s,d}$. It means that there may be an area e.g. F , which goes undetected and the state of congestion is not determined owing to dynamic mobility of nodes in mobile networks. In this case a source node or any intermediate node in area $F_{s,d}$ cannot forward the message to destination node d .

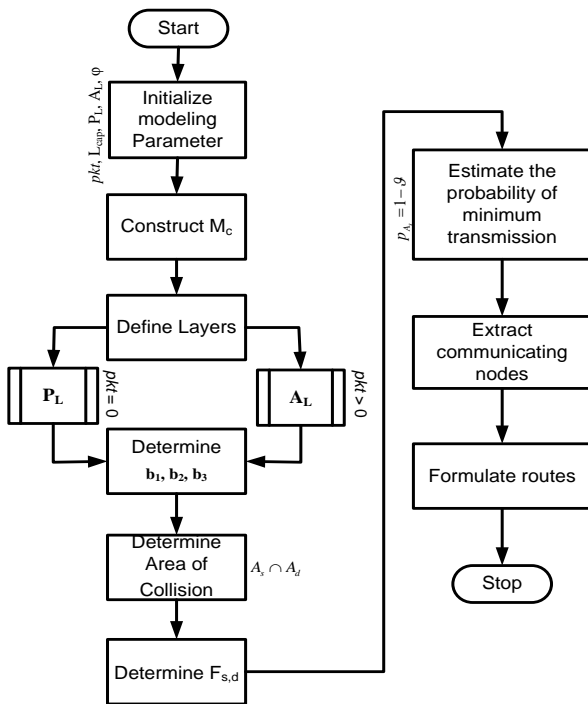


Fig. 2. Process Flow for Markov Modeling

The next phase of the algorithm is to compute the size of the transmission zones as per line-6. The algorithm computes the number of nodes in transmission zones by scalar multiplication of network size and network density as per line-7. The probability of minimum number of nodes required for forwarding data packets is computed as per Line-8. We use a simple variable ϑ that is equivalent to summation of the probability of all nodes carrying out data packet forwarding divided by total probability of the nodes forwarding data packets from the congested area. This phenomenon will mean that proposed Markov modeling attempts to find the existence of atleast one node which is in fair position to perform data transmission. The Markov modeling proceeds further to find similar kind of nodes and updates the matrix of data communication path that was previously managed by the algorithm of stochastic approach. The updated matrices helps to find the links between favorable nodes as the best possible alternate routes for packet forwarding during the peak traffic condition.

VI. RESULTS AND DISCUSSION

This section discusses about the results generated from the network simulation through NS2 simulator. The simulation parameters are as shown in Table 1.

TABLE. I. SIMULATION PARAMETERS

| Parameter | Value | Parameter | Value |
|--------------------------------|----------------|-------------------------------------|------------------|
| Network area(Simulation) area | 1000 x 1200 m2 | Control packet size | 32 bits |
| Simulation Time | 200 seconds | Data packet size | 2000 bytes |
| Routing Protocol | NetFlow | Antenna Model | Omni-directional |
| Pathloss exponent | 0.5 | Maximum Speed of node | 50 m/s |
| MAC Type | 802.11 | Minimum Speed node | 1m/s |
| Traffic Model | CBR/VBR | Transmission range | 10m |
| Mobility Model | Random | Transmission Energy consumption | 0.5 J |
| Channel Model | Urban | Receiving Energy consumption | 0.25J |
| Channel capacity | 300 Mbps | Ideal mode Energy consumption | 0.035 J |
| Channel sensing time | 0.2 sec | Sleep mode Power consumption | 0.02J |
| | | Initial battery Energy of each node | 10J |

The proposed work focuses in finding an effective solution for congestion control in distributed networking system. The performance parameters like packet delivery ratio, end-to-end delay and processing time are considered to analyze the effectiveness of the proposed system. It is benchmarked with similar studies of Otoshi et al. [25] and Sahuquillo et al. [27]. Otoshi et al. [25] who have presented a stochastic modeling with predictive analysis for identifying discrete states of traffic in distributed networking system. This technique has used a predictive control scheme to minimize the possibilities of predictive error considering network constraints e.g number of hops, length of the hops etc. The mean length of the hops was considered as cost function, which was subjected to optimization using CPLEX solver. The outcome of the work was quite convincing as it has offered better scalability for future internet architecture. Similarly, we consider the work carried out by Sahuquillo et al. [27] as it offers solution to the congestion control for a practical case study of distributed networking system eg. High Performance Computing. The authors have used a mechanism that integrates injection throttle and segregation of congested traffic. We perform a minor modification to techniques introduced in [25] [27] in order to make a suitable testbed for carrying out the comparative analysis. The parameters considered for analysis are end-to-end delay, packet delivery ratio and processing time.

A. Comparative Analysis of End-to-End Delay

The end to end analysis is carried out by transmitting the test data of 2000 bytes. The result is as shown in Fig.3.

The graph shows that proposed system is able to minimize the end-to-end delay to a larger extent as compared to existing studies of Otoshi et al. [25] and Sahuquillo et al. [27]. The reason behind this is the technique that is adopted for processing search request and control messages by the proposed system.

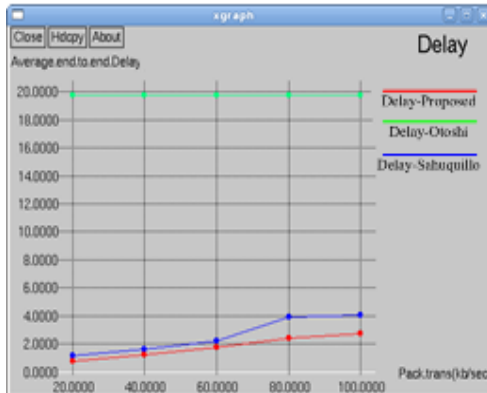


Fig. 3. Comparative Analysis of Delay (sec)

In the proposed system, owing to Markov modeling, it becomes essential for a node to obtain the significant address information of another communication node which could possibly reside in transmission zone of $F_{s,d}$ or $A_{s,d}$. As both $F_{s,d}$ and $A_{s,d}$ are different transmission zones, extraction of the node address will be a quite difficult. We simplify this problem by developing a cross layer paradigm that can carry out the task of processing control messages in transport layer thereby minimizing the complexity.

Here, the task of one layer is to aggregate the respective addresses of the nodes and keep on exchanging it with other layers. This operation of interoperability is managed by the network layer. It is the responsibility of the network layer for carrying out the processing of control message as it maintains the communication standards of each transmission zone. This process helps in identifying the point of congestion and makes it aware to the entire network. This process has two advantages viz. i) all nodes can quickly decide about alternate routes and decrease the impact of congestion during peak traffic and ii) degree of congestion at the origination point is reduced by implementing active queue management that directs the packets from highly congested area to less congested point. Hence, end-to-end delay of the proposed work is reduced in the presence of mobility of the nodes which varies at every simulation track points. The problem explored in Otoshi et al. [25] is a predictive scheme. Here, the stochastic processing is adapted to predict and identify the possible prediction error. Hence, the delay factor using this technique cannot be implemented for distributed system of dynamic nature like that of future internet architecture. Similarly, the work done by Sahuquillo et al. [27] have focused on identifying congestion by using control messages which is quite time consuming in its nature. Using Markov modeling, proposed system offers optimized solution for identifying the point of congested and

also offers best quality routes for packet forwarding thereby reducing the delay.

B. Comparative Analysis of Packet Delivery Ratio

Packet delivery ratio is computed by analyzing the amount of data packets received by the destination node to total amount of data transmitted by the source node. The result shown in Fig.4 exhibits that the proposed system offers better packet delivery ratio compared to Otoshi et al. [25] and Sahuquillo et al. [27]. This is because the proposed system provides a better processing of data generated by multiple networking domains in future internet architecture through cross layer paradigm. We start by analyzing the work done by Sahuquillo et al. [27]. The authors have implemented a technique where the incoming packets are organized at the input ports of the switches. The system emphasizes more on organization and less on queuing. This operation when implemented in our scenario reduces the packet delivery ratio. Moreover, the process of identification of the congestion and notify it to other nodes for updates are not discussed in that paper [27]. It is also not sure whether the updates were done over the highly congested area. This issue creates a negative impact on other neighboring nodes by consuming more time to take decision for routing. Hence, packet delivery ratio will be affected when this technique is used in future internet architecture.

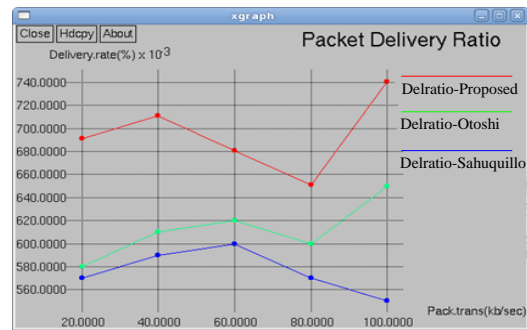


Fig. 4. Analysis of Packet Delivery Ratio

The technique proposed by Otoshi et al. [25] has used the concept of traffic engineering. This technique was implemented through stochastic modeling which is more predictive in nature. The predictive analytic model is assessed for its accuracy of traffic modeling using randomness by adopting traffic engineering with cost as a function on the stochastic model. This is much better than the technique discussed by Sahuquillo et al. [27] as it can accomplish better packet delivery ratio. The main drawback of this technique is that it uses control server to optimize the cost function which leads to less efficient distributed routing. Although, the authors have used relaxation mechanism to sort out this problem, but the probability factors assumed is less when compared to real-time traffic constraints. Hence, its packet delivery ratio is not better than the proposed system. The proposed system overcomes this problem by the algorithm-2 (stochastic) and algorithm-3 (Markov Modeling). These algorithms assist in identifying the best possible routes from non-congested area as well as congested area. The updating mechanism is quite instantaneous with a pause time of 0.0025 seconds in

simulation study that leads to better packet delivery ratio for a longer period of time.

C. Analysis of Processing Time

It is known that an effective congestion control mechanism must have a reduced processing time as far as possible. Lower the processing time means the network can ensure better instantaneous data delivery process. We analyze the processing time with increasing traffic load (packets per seconds). A closer look into the Fig 5 shows that processing time gets reduced linearly with increasing traffic load, which is one of the unique patterns of the proposed study. Usually with increased network traffic, the processing time should be increasing but due to cross layer approach the time complexity is reduced.

The cross layer approach bridges physical layer, link layer, network layer and transport layer. The provisioning operation is carried out over link layer, the mechanism of exploring the congestion using stochastic is implemented over network layer and Markov modeling for further optimizing the best routes (even from highly congested area) is carried out at the transport layer.

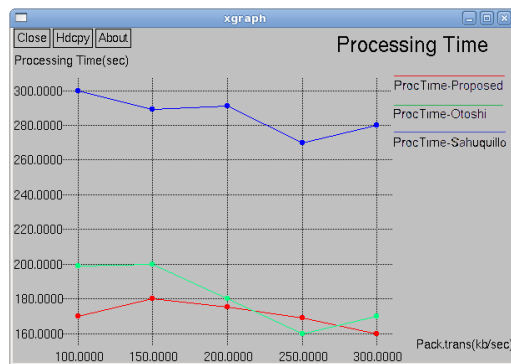


Fig. 5. Analysis of Processing Time

Hence, the system maintains different functionalities over different layers of protocol stack resulting in reduced processing time in the proposed system. For a given simulation environment, Otoshi et al. [25] and Sahuquillo et al. [27] work doesn't meet the demands of the distributed traffic scenario with dense congestion leading to higher processing time when compared to proposed system.

VII. CONCLUSION

Owing to the complexity in the design principle of distributed networking systems e.g. future internet architecture, the existing algorithms and techniques do not provide solution for mitigating congestion. The proposed system, therefore, presents a technique that uses conglomeration of cross layered approach, stochastic approach, and Markov modeling for addressing the problems of congestion in highly distributed networking system. We have adopted an analytical research methodology to prove that it is feasible to develop a technique that can identify the origination point of congestion and share the same with the entire network. The interesting point of implementation is that proposed technique attempts to use the existing network resources for harnessing the channel capacity in accordance with the state identified by the proposed system.

The outcome of the study were compared with existing system respect to end-to-end delay, packet delivery ratio, and processing time and found that proposed system offers better solution for congestion control.

REFERENCES

- [1] C. White, Data Communications and Computer Networks: A Business User's Approach, Cengage Learning, Computers, 2015
- [2] P. Verissimo, L. Rodrigues, Distributed Systems for System Architects, Springer Science & Business Media, Computers, 2012
- [3] N. Rajan, The Digitized Imagination: Encounters with the Virtual World, Taylor & Francis, Social Science, 2012
- [4] J. Holler, V. Tsiatsis, C. Mulligan, S. Avesand, S. Karnouskos, D. Boyle, "From Machine-to-Machine to the Internet of Things: Introduction to a New Age of Intelligence", Academic Press, Technology & Engineering, 2014
- [5] H-Y Wei, J. Rykowski, S. Dixit, WiFi, WiMAX and LTE Multi-hop Mesh Networks: Basic Communication Protocols and Application Areas, John Wiley & Sons, Technology & Engineering, 2013
- [6] M. Gholipour, A. T. Haghighat, M. R. Meybodi, "Hop-by-hop traffic-aware routing to congestion control in wireless sensor networks", *Springer- Eurasip Journal on Wireless Communications and Networking*, vol.15, 2015
- [7] N. Efthymiopoulos, A. Christakidis, M. Efthymiopoulou, "Congestion Control For P2P Live Streaming", *International Journal of Peer to Peer Networks*, Vol.6, No.2, August 2015
- [8] L. Jose, L. Yan, M. Alizadehy, G. Varghese, "High Speed Networks Need Proactive Congestion Control", *ACM-Proceedings of 14th ACM Workshop on Hot Topics in Network Article*, No.4, 2015
- [9] Y. Zaki, T. Potsch, J. Chen, "Adaptive Congestion Control for Unpredictable Cellular Networks", *ACM-SIGCOMM*, 2015
- [10] T. Ichrak, S. Nawal and A. Mustapha, "Systematic Mapping Study on the Congestion Control Problem in TCP/IP", *Contemporary Engineering Sciences*, Vol. 7, no. 27, pp.1509-1515, 2014
- [11] C. Sonmez, O. D. Incel, S. Isik, M. Y. Donmez, "Fuzzy-based congestion control for wireless multimedia sensor networks", *Springer-Eurasip Journal on Wireless Communications and Networkin*, vol. 63, 2014
- [12] C. P. Reddy, P. V. Krishna, "Cross Layer Based Congestion Control in Wireless Mesh Networks", *Cybernetics And Information Technologies*, Vol.14, No 2, 2014
- [13] G. Carofigli, M. Gallo, L. Muscariello and M. Papalini, "Multipath Congestion Control in Content-Centric Networks", *IEEE-Conference on Computer Communication Workshop*, pp.363-368, 2013
- [14] P. Antoniadis, S. Fdida, C. Griffin, Y. Jin, "Distributed medium access control with conditionally altruistic users", *Springer- Eurasip Journal on Wireless Communications and Networking*, vol.202, 2013
- [15] Y. Cai, S. Jiang, Q. Guan, and F R. Yu, "Decoupling congestion control from TCP (semi-TCP) for multi-hop wireless networks", *Springer-Eurasip Journal on Wireless Communications and Networking*, vol. 149, 2013
- [16] F. Ye, R. Yim, J. Zhang, S. Roy, "Congestion Control to Achieve Optimal Broadcast Efficiency in VANETs", *IEEE-International Conference on Communication*, pp.1-5, 2010
- [17] M. S. Bouassida and M. Shawky, "A Cooperative Congestion Control Approach within VANETs: Formal Verification and Performance Evaluation", *Hindawi Publishing Corporation, Eurasip Journal on Wireless Communications and Networking*, Article ID 712525, 2010
- [18] M. Kas, I. Korpeoglu, and E. Karasan, "Utilization-Based Dynamic Scheduling Algorithm for WirelessMesh Networks", *Hindawi Publishing Corporation, Eurasip Journal on Wireless Communications and Networking*, Article ID 312828, 2010
- [19] Y. Li, A. Papachristodoulou, M. Chiang, A. R. Calderbank, "Congestion control and its stability in networks with delay sensitive traffic", *Elsevier-Computer Networks*, vol.55, pp.20-32, 2011
- [20] S. Misra, B. J. Oommen, S. Yanamandra, "Random Early Detection for Congestion Avoidance in Wired Networks: A Discretized Pursuit

- Learning-Automata-Like Solution”, *IEEE Transactions On Systems, Man, And Cybernetics*, vol. 40, no. 1, February 2010
- [21] R. A. Uthra, S. V. K. Raja, A. Jeyasekar, A. J. Lattanze, “A probabilistic approach for predictive congestion control in wireless sensor networks”, *Journal of Zhejiang University-Science*, vol.15, Iss.3, pp.:187-199, 2014
- [22] K.Vinodha, R. Selvarani, “Congestion Control in Distributed Networks-a comparative study”, *Springer –Advances in Computer Science and Information Technology*, pp.115-123, 2012
- [23] K.Vinodha, R. Selvarani, “Congestion Control in Distributed Networking System-A Review”, *International Journal of Computer Applications*, Vol.83, No 6, December 2013
- [24] S. Rangaswamy and V. Krishnareddy, “An efficient traffic regulation mechanism for distributed networks”, *Springer- Eurasip Journal on Wireless Communications and Networking*, vol.154, 2015
- [25] T. Otoshiy, Y. Ohsitay, M. Muratay, “Traffic Engineering Based on Stochastic Model Predictive Control for Uncertain Traffic Change” *IEEE International Symposium on Integrated Network Management*, pp.1165-1170, 2015
- [26] A. Grebennikov, N. Kumar, B. S. Yarman, *Broadband RF and Microwave Amplifiers*, Taylor & Francis, Computers, 2015
- [27] J. E.Sahuquillo, E. G. Gran, P. J. Garcia, “Efficient and Cost-Effective Hybrid Congestion Control for HPC Interconnection Networks”, *IEEE Transactions On Parallel And Distributed Systems*, vol. 26, no. 1, January 2015



iJRASET

International Journal For Research in
Applied Science and Engineering Technology



INTERNATIONAL JOURNAL FOR RESEARCH

IN APPLIED SCIENCE & ENGINEERING TECHNOLOGY

Volume: 5 Issue: VII Month of publication: July 2017

DOI:

www.ijraset.com

Call:  08813907089

E-mail ID: ijraset@gmail.com

Design and Development of Two Factor Authentication System for E-Services Using DNA and Asymmetric Cryptography

Priyanka B J¹, Nalinakshi B. G², Dr. D Jayaramaih³

¹M.Tech, ²Associate professor, ³Prof and HOD, Dept. of ISE

The Oxford College of Engineering Karnataka, India.

Abstract: DNA cryptography is a new technology that uses biological concepts for encryption and decryption of data. There is a lot of growth in the field of mobile devices using for e-transaction using internet and wireless network. So To achieve secure communication and mutual authentication; two schemes are constructed from DNA hybridization and DNA digital coding techniques. Two factors authentication uses the OTP (One Time Password) and SAC (Server Authentication Code) for the better security. This paper presents a secure and efficient authentication mechanism for mobile e-banking services using RSA encryption and DNA cryptography. The comparative analysis between these schemes shows that DNA cryptography based authentication provides more security than the RSA based authentication in terms of computational complexity.

Keywords: DNA cryptography, DNA computing, Challenge-Response Authentication, Mobile security, Attacks.

I. INTRODUCTION

There are wide types of electronic services receiving smart phones have been growing rapidly. Using wireless technology the mobile phones started using e-service applications. The mobile phone users can access the internet through wireless communication in the field of wireless networks. All the mobile phone users are concerned about the security issues to use the e-services through the wireless internet. In order to achieve secured e-services, the four security functions such as integrity, confidentiality, non-repudiation and user authentication must be provided in wireless internet as in wired internet. By using any technology or applications to the wireless technology the security should be comparable with the wired technology.

Secure communication is nothing but a secure authentication is done to secure user and secret session key is established for confidentiality. As the methods and schemes grows for the cryptography, in parallel the same security schemes should be developed for the user authentication and key agreement. At the beginning of the cryptography the security is based on the passwords. The very first key agreement schema has been implemented by the Diffie and Helmen during the introduction of asymmetric key in the cryptography and since it does not provide secured authentication and vulnerable to attacks. Lamport has designed and proposed the very first authentication scheme based on the passwords. Most of these schemas depends public key cryptography. To overcome the drawbacks the hash function came into existence. By the Adleman's pioneering work DNA computing came into existing. By the design of his

DNA algorithm for solving the Hamiltonian problem, Adleman set the foundation for the research in the field of bio computing. Many researches thought after the results Adleman's experiments, because DNA's parallelism and large information storage capacity DNA computing can used in the field of cryptography to achieve the strong authentication. DNA cryptography increases the complexity of the problem by increasing its size so that an attacker requires huge number resources and efforts to break

This paper includes design and development of two protocol based on public key cryptography and DNA cryptography. By using the advantages of RSA algorithm and DNA techniques the problems in the web authentication scheme can be solved. Security analysis is done to prove that DNA based authentication scheme provides higher security than the public based scheme in terms of computational complexity and number attacks they overcome. Both the protocols two factors authentication schemes is done using OTP and SAC value, which are computed with different mathematical functions and DNA conversions.

II. LITERATURE SURVEY

Includes various types of authentication schemes, brief overview of the DNA cryptography and different techniques used in the DNA cryptography.

A. Authentication Scheme

There are many ways to provide the credentials for the authentication. The most commonly used method but not more secured is password authentication. Now a day the competitive e-commerce demands for methods that provides more protection when network resources includes highly sensitive data [9]. Smart cards and biometric authentication types provide this extra protection.

- 1) *Computer Recognition System*: it requires the installation of some small authentication software in the system. In the authentication process this can be verified as second authentication factor.
- 2) *Password Authentication*: is the most commonly used authentication form. Here user provides the username with password. The username are mostly a string of characters, numbers so it is vulnerable to guessing attack. Password may be easy to guess. By using digests for authentication the risk of eavesdropping can be minimised.
- 3) *Single Factor Authentication*: is a process where single credential is used to secure the critical data unauthorized access to system.
- 4) *Two factor authentication*: is a process where two credentials are used secure the unauthorized access to system and critical data.
- 5) *One Time Password (OTP)*: OTP authentication is a method to reduce the possibilities of compromised user credentials using login passwords that are only valid once. If an attacker is successful in sniffing the password that a user has used to enter in a site, it is of no use because the password is no longer valid. Moreover, it is highly difficult to predict the next password based on the previous one. Each time the OTP generated by the password-generating token are unique [3]. The function that generates such passwords must be non-invertible. There are three types of schemes to generate one-time passwords:

Based on time, such as Secure Id. Time-synchronization is required between the authentication server and the client providing the password. Based on a challenge (e.g. a random number chosen by the authentication server or transaction details) and a counter. Based on some internal data (e.g. the previous password) or counter (e.g. systems based on hash chains, such as S-Key [10])

Authentication is the very big issue now a day; the new protocol is designed for the purpose of achieving the high secured authentication using the public key encryption and DNA technology.

B. DNA Cryptography

With the lot of advances in the field of DNA computing the new technology has come into existence called as DNA cryptography which is far better than the traditional cryptography in point of providing authentication, security, integrity, storage capacity etc. In the DNA cryptography the encryption is done by converting the human readable form into bases of DNA strands, which creates a strong base for the authentication and digital signature. There are some techniques such a DNA digital coding and DNA indexing used for hiding the data. DNA indexing and DNA digital coding techniques are the most important for DNA Cryptography, a brief description about these two techniques are discussed in the previous chapter. The other few DNA Encryption Techniques are as described below:

C. DNA Digital Coding

DNA digital coding is the important technique used for encryption and decryption process which is based on the mapping of base pairs. DNA coding is done based on nucleotide bases A, C, T, G. such that A always makes pair with T and C always makes pair with G of two strands. In the mathematical point of view it is possible to produce 24 patterns but according to DNA complementary rules only 8 patterns are identified correctly such as 0123/CTAG, 0123/CATG, 0123/GTAC, 0123/GATC, 0123/TCGA, 0123/TGCA, 0123/ACGT, 0123/AGCT and among these 8 patterns, 0123/CTAG perfectly reflects the biological characteristics of four nucleotide bases.

Table1: DNA digital coding pattern [6]

| Digital coding | DNA code |
|----------------|----------|
| 00(0) | A |
| 01(1) | T |
| 10(2) | C |
| 11(3) | G |

III. CURRENT PRACTICES

There are many ways to provide the credentials for the authentication. The most commonly used method but not more secured is password authentication. Now a day the competitive e-commerce demands for methods that provides more protection when network resources includes highly sensitive data [9]. Smart cards and biometric authentication types provide this extra protection.

There are some OTP solutions based on a mobile phone. In [14, 15] a multichannel communication is used (Internet and GSM) in order to improve the security of the authentication scheme. In [13] a user logs in the web site using a username and a password. Then, a one-time password is sent via SMS to his mobile, and the user enters this data in the web authentication form. If it is correctly verified, the user is authenticated into the application. In this system the mobile is used as a mere point of reception, not as a hardware token that stores and computes keys.

On the other hand, In [14] what is sent though the GSM channel is a challenge. The mobile computes a one-time password using this challenge and sends it to his computer through a bluetooth connection. Finally, the password is forwarded to the server. The main trouble of these two schemes that rely on SMS messages to perform the authentication is that the session establishment between the user and the server is slow because SMS messages are not real-time. Thus, the system is not practical. On the other hand, users may want to connect to their Internet bank accounts from places in which there is no cellular connectivity (in some sensitive environments GSM signals are blocked), and these models do not allow it.

Other OTP solutions [15, 16] deal with a password generation in the mobile using as input a server challenge sent through the Internet connection. Once in the PC, the challenge is transferred to the mobile using a bluetooth channel. The problem is that bluetooth is usually not available from public access computers. Besides, it presents some relevant vulnerabilities and threats [17, 18] -most of which due to faulty implementations- that jeopardize the system.

Some other OTP mobile schemes focus on the speed of the process and base the generation of the one-time password on a time factor (no server challenge is needed). This is the case of the Free Auth Project [17]. The inconvenient of using this approach in a mobile context is the required time synchronization between the mobile and the server. Users roughly configure the clock of the mobile phone when they travel, and they are not very much concerned on setting the correct time zone. Hence, protocols based on absolute time are not feasible.

The MP-Auth scheme [18] uses the mobile as a secure device to store keys and encrypt passwords for web authentication. It is a one factor authentication mechanism that safeguards passwords from keyloggers, phishing attacks and pharming. Nevertheless, if an attacker learns a user password he can impersonate that user.

IV. PROPOSED SCHEME

The proposed scheme provides the secure authentication to the e-services. Both Asymmetric and DNA-OTP protocol follows same architecture for the communication.

A. DNA-OTP Scheme

The DNA-OTP scheme comprises of web server, a browser. Data transmission is very simple between mobile phone and client PC, so it does not require any communication channel like Bluetooth, it can entered by using keypad. The DNA-OTP scheme consists of three phases those are registration phase, authentication phase, transaction phase. In the registration phase the server sends the initialization key in DNA form to user who is interested in registration. These initialization keys are stored in the mobile phones for future authentication. After successful registration the user can access to the web services through the second phase that is authentication phase.

In the authentication phase the user sends his ID to the server, which computes the challenge in DNA sequence using DNA digital coding, replies with the challenge to user. The user computes the DOTP using challenge and other parameters and sends to the server. Server verifies the freshness of the submitted DOTP and determines whether the user is accepted or not. If the user is accepted the server will send the DSAC to the user. The user compares the received DSAC value with one he has computed using mobile phone. Once the DSAC values matches the transaction phase starts.

B. Asymmetric OTP Scheme

This scheme also includes three phases such as registration phase, authentication phase and transaction phase. In this scheme the public key encryption is used to generate the two factors required for the authentication. In the registration phase user provides the details to get register to the application service. Once the service is granted, server replies with the initialization key. Both user and server store their details in the DB. In authentication phase user provides username and password to gain access to the application.

Server replies with CH value if the login is successful. The client application computes OTP using RSA algorithm and enters the computed OTP value in the web site. Server verifies the received OTP if the value matches then first step of authentication is successful and displays SAC1 value. The user manually compares the both the values if matches then transaction phase starts. In the transaction phase the server sends the transaction ID to client and client generate the transaction authentication code and sends to the server and if the TAC is correct then actual transaction money takes place.

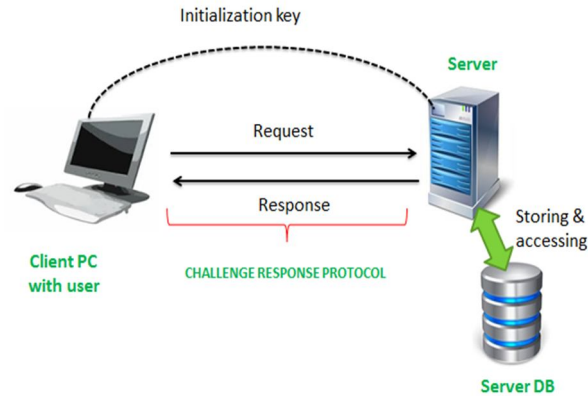


Figure2: System architecture.

V. SYSTEM DESIGN

The Figure3 shows the sequence diagram of the DNA-OTP deals with all three phases of the protocol, in registration phase the subscribed user sends his credential to register for the application. One the server receives the details of the user he generates and sends the DK0 that is initialisation key along with user id and server id. The user upon receiving the DK0 and other details, the user stores it in his mobile database by creating separate database for this server. At the same time the server creates database with user id. Server maintains the separate database for each individual user.

In the authentication phase comes after the registration phase, in this phase user sends the UID to server and server generates the DNA based DCH using random DNA sequence generator. User upon receiving the channel computes the temporary key by using the DCH and DK0. First he takes the hash of DCH using SHA 2 and resultant value is XOR with the DK0. Since DNA-OTP is two factors authentication schema so authentication is done in two steps using two generated secured values such as DOTP and DSAC.

The user and server both computes the values of the DOTP and DSAC values using the details stored in their data base. The user sends the DOTP to server and verifies whether the OTP computed by his is matches with this or not: if matches server will send the DSAC1 value to the user if not authentication fails at first step. After the success of first step authentication server sends the DSAC1 to user and user compares with his own generated DSAC value if matches then second step of authentication are successful if not authentication fails. Once the user authenticated successfully in both the steps the protocol enters to transaction phase. Here the server generates the DTID value and sends to user. The user upon receiving the DTID value he computes the DTA and sends to server, the server will verify the received DTA.

VI. COMPARATIVE SECURITY ANALYSES

In the asymmetric OTP there is a complexity in the key creation. RSA algorithm is limited to the prime numbers hence efficiency of generating primes are relatively low and difficult to generate secret one. The security of the RSA algorithm depends on the factoring the large prime numbers. The security can be threatened with the algorithm that decomposes a large number. The encryption and decryption needs a lot of calculation and speed of execution is slow and increases the time complexity. This scheme is vulnerable to the impersonation, even is users private keys are not available. The drawbacks of the asymmetric encryption scheme are overcome by DNA-OTP scheme.

The DNA-OTP scheme is developed using symmetric encryption, OTP, SAC and DNA hybridization to reduce the time complexity ($O(n)$). Time complexity of the encryption and decryption is increased in DNA algorithm because lot data conversions takes place while generating key value i.e. from normal text to ASCII then ASCII to binary and then binary to DNA sequence. To provide hybrid security in the authentication for e-banking DNA cryptography is combined with the traditional cryptography.

VII. EXPERIMENTS AND RESULTS

This chapter involves the average time taken by the RSA and DNA algorithm to encrypt and decrypt the file size of 2MB using different key size. In the following graph the decryption take taken by the DNA algorithm is more compare to RSA algorithm. From security point of view the algorithm which has higher decryption time lower transmission time is said to be highly secured. The DNA algorithm provides the higher complexity in generating the key values for the authentication and involves lot of data conversion for encrypting and decrypting the text file.

Table2: Values for the above graphs

| Key size(bits) | RSA algorithm | | DNA algorithm | |
|----------------|----------------------|----------------------|----------------------|----------------------|
| | Encryption time (ms) | Decryption time (ms) | Encryption time (ms) | Decryption time (ms) |
| 512 | 110 | 215 | 190 | 230 |
| 768 | 175 | 281 | 255 | 295 |
| 1024 | 251 | 348 | 300 | 375 |
| 1280 | 328 | 413 | 386 | 455 |
| 1536 | 404 | 479 | 425 | 570 |
| 1792 | 479 | 546 | 518 | 618 |
| 2048 | 552 | 611 | 585 | 699 |

Table3: Transmission time taken by the RSA and DNA-OTP schemes.

| Transmission time (ms) | | |
|------------------------|---------------|---------------|
| | RSA algorithm | DNA algorithm |
| 512 | 3315 | 3229.85 |
| 768 | 3320 | 3233.8 |
| 1024 | 3326 | 3239.85 |
| 1280 | 3308 | 3222.8 |
| 1536 | 3317 | 3235 |
| 1792 | 3322 | 3240.34 |
| 2048 | 3340 | 3250 |

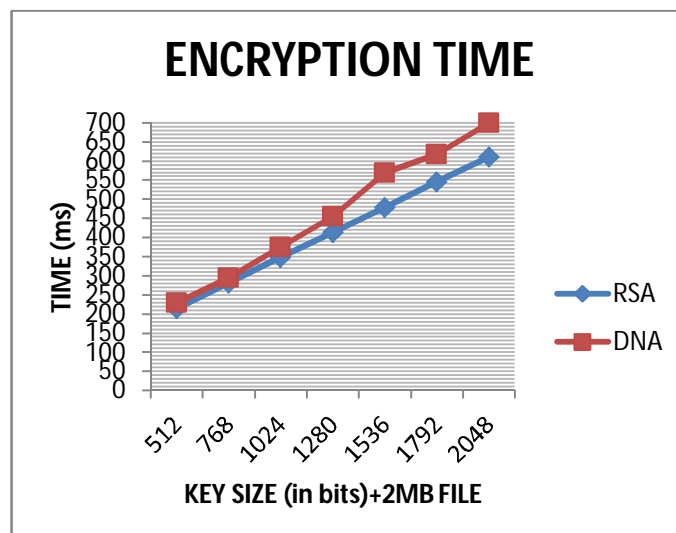


Figure4: Encryption time of DNA and RSA algorithm.

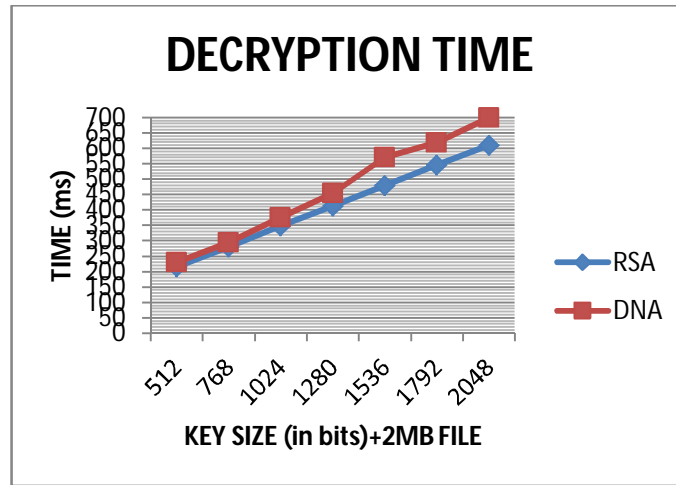


Figure5: Decryption time for DNA and RSA algorithm.

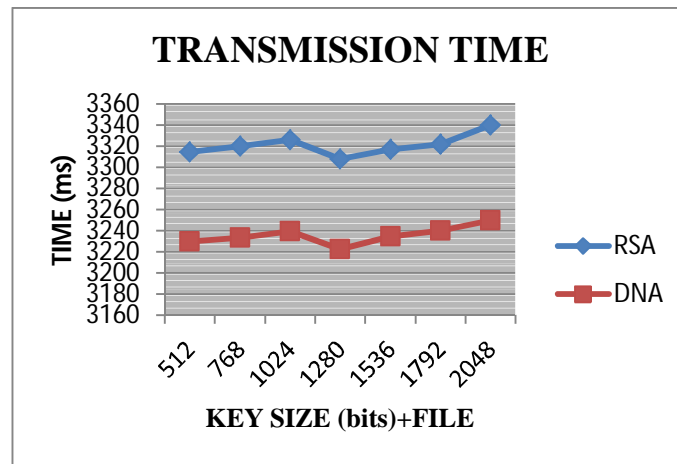


Figure6: Transmission taken by RSA and DNA algorithm.

$$\text{The average encryption time taken by the RSA algorithm} = \frac{(\text{Total taken to encrypt})}{(\text{Total number of keys})}$$

$$\frac{(100 + 175 + 251 + 328 + 404 + 479 + 552)ms}{7} = \frac{2289ms}{7} = 327ms$$

$$\text{The average encryption time taken by the DNA algorithm} = \frac{(\text{Total taken to encrypt})}{(\text{Total number of keys})}$$

$$\frac{(215 + 281 + 348 + 413 + 479 + 546 + 611)ms}{7} = \frac{2893ms}{7} = 413.28ms$$

$$\text{The average decryption time taken by the RSA algorithm} = \frac{(\text{Total taken to encrypt})}{(\text{Total number of keys})}$$

$$\frac{(190 + 255 + 300 + 386 + 425 + 518 + 585)ms}{7} = \frac{2659ms}{7} = 379.85ms$$

$$\text{The average encryption time taken by the DNA algorithm} = \frac{(\text{Total taken to encrypt})}{(\text{Total number of keys})}$$

$$\frac{(230 + 295 + 375 + 455 + 570 + 618 + 699)ms}{7} = \frac{3232ms}{7} = 461.71ms$$

From the above calculations the DNA algorithm takes 86.28 ms more than the RSA algorithm to encrypt the 2MB, 81.15ms more time than RSA algorithm to decrypt the and 0.08156 sec less transmission time than RSA algorithm when the different key size is used.

VIII. CONCLUSION

Current days e-services are very importance in many applications such as e-shopping, e- banking, e- ticket etc. but authentication is the main concern in all these applications. The aim of the protocol is to achieve the double layer authentication. One for authenticating the user with his ID and another is for authentication the server with his ID. The proposed protocol is providing the two step authentication with two different factors such as DNA-OTP and DSAC. The reason for the DNA technology for this protocol is because of its high computational power and unbreakable cipher text. An authentication done using RSA algorithm is less secured than the DNA based authentication in terms of complexity involved in logical computation, data conversions and matrix form involved in the DNA algorithm reduces time complexity of encryption and decryption.

IX. FUTURE WORK

In future, the designed protocol will be developed and implemented for real time application in any smart phone. This protocol will be implemented in the cloud for the purpose of storing the user details and focuses mainly on reducing possible attacks on it.

REFERENCES

- [1] He, Debiao, et al. "One-to-many authentication for access control in mobile pay-TV systems." *Science China Information Sciences* 59.5 (2016): 052108.
- [2] Misbahuddin, S. C. S, M. & Hashim, N. P. (2014). DNA for information security: A Survey on DNA computing and a pseudo DNA method based on central dogma of molecular biology. *International Conference on Computer and Communications Technologies*. 11 – 13 Dec, Hyderabad
- [3] R. R. Sinden, *International Journal of Innovative Research in Science, Engineering and Technology* (An ISO 3297: 2007 Certified Organization) Vol. 5, Issue 12, December 2016
- [4] William Stallings, *Cryptography and Network Security Principles and Practices*, Fourth Edition, 201
- [5] Al-Qayedi, A., Adi, W., Zahro, A., Mabrouk, A.: Combined web/mobile authentication for secure web access control. *IEEE Wireless Communications and Networking Conference (WCNC) 2* (March 2014) 677–68
- [6] Javheri, S. & Kulkarni, R. (2014). Secure Data communication and Cryptography based on DNA based Message Encoding. *International Journal of Computer Applications*, 98(16), 360-363.
- [7] C. Chou, K. Tsai, C. Lu. "Two ID-based authenticated schemes with key agreement for mobile environments". *J Super comput* 66:973-988, (2013)
- [8] Cheswick, W.R., Bellovin, S.M., Rubin, A.D.: *Firewalls and Internet Security: Repelling the Wily Hacker*. Addison-Wesley Longman Publishing Co., Inc., Boston, MA, USA (2013)
- [9] D. Wang, C. Ma. "Cryptanalysis of a remote user authentication scheme for mobile client C server environment based on ECC". *Information Fusion* 14, 498503, (2013)
- [10] Yunpeng Zhang and Liu He Bochen Fu. *Research on DNA Cryptography*, Applied Cryptography 2012
- [11] A. Atito , A. Khalifa , S. Z. Rida, *DNA-Based Data Encryption and Hiding Using Playfair and Insertion Techniques*(2011
- [12] Hakami, H. A., Chaczko, Z. & Kale, A. (2015). Review of Big Data Storage Based on DNA Computing, *Asia-Pacific Conference on. IEEE Computer Aided System Engineering (APCASE)*, 14-16 July, Educador, 113-117 [10] Hornweder, K. S. V. (2011)
- [13] *An Overview of Techniques and Applications of DNA Nanotechnology*, Technical Report UT-CS-11-682, (2011)
- [14] Iqbal, Z.: *Secure mobile one time passwords for web services* (master of science thesis). Technical report, Royal Institute of Technology (May 2011)
- [15] Hallsteinsen, S., Jorstad, I., Thanh, D.V.: Using the mobile phone as a security token for unified authentication. In: *Proc. of the International Conference on Systems and Networks Communications (ICSNC)*, Washington, DC, USA, IEEE Computer Society (2011).
- [16] Me, G., Pirro, D., Sarrecchia, R.: A mobile based approach to strong authentication on web. In: *Proc. of the International Multi-Conference on Computing in the Global Information Technology (ICCGI)*, Washington, DC, USA, IEEE Computer Society (2011) 67
- [17] Hager, C., Midkiff, S.: Demonstrating vulnerabilities in bluetooth security. *Global Telecommunications Conference. IEEE GLOBECOM 3* (Dec. 2003) 1420–1424 16. *Insight Consulting: How can bluetooth services and devices be effectively secured? Computer Fraud & Security* (1) (Jan. 2010) 4–7
- [18] FreeAuth Project: The freeauth. <http://www.freeauth.org> [Online; accessed on 10/2010].
- [19] Mannan, M., van Oorschot, P.C.: Using a personal device to strengthen password authentication from an untrusted computer. In: *Financial Cryptography (LNCS)*. Volume 4886. (2010) 88–103.



10.22214/IJRASET



45.98



IMPACT FACTOR:
7.129



IMPACT FACTOR:
7.429



INTERNATIONAL JOURNAL FOR RESEARCH

IN APPLIED SCIENCE & ENGINEERING TECHNOLOGY

Call : 08813907089  (24*7 Support on Whatsapp)



iJRASET

International Journal For Research in
Applied Science and Engineering Technology



INTERNATIONAL JOURNAL FOR RESEARCH

IN APPLIED SCIENCE & ENGINEERING TECHNOLOGY

Volume: 5 Issue: VII Month of publication: July 2017

DOI:

www.ijraset.com

Call:  08813907089

E-mail ID: ijraset@gmail.com

Flow-Based Network Traffic Classification Using Clustering Technique with MLA Approach

Triveni Pujari¹, Nalinakshi B. G², Dr.D Jayaramaiah³

^{1, 2, 3}Dept. Of ISE, The Oxford College of Engineering, Bengaluru-68, India.

Abstract: Network traffic classification is the process of categorizing network traffic according to various parameters into a number of traffic classes and it is necessary to maintain smooth operation of the network. There are so many methods to classify the network traffic. The proposed methods use machine learning algorithm i.e (MLA) approach. In MLA approach, a system learns from empirical data to automatically associate objects with corresponding classes. There are two types of MLAs one is supervised and the other is unsupervised. Supervised methods consist of labeled data to classify any flows into pre-defined traffic classes, but they cannot deal with unknown flows hence we use unsupervised clustering method along with supervised approach to cluster and classify both known and unknown flows. We applied hybridization of both supervised and unsupervised algorithm to achieve better accuracy. A number of real world traffic traces have been used to show the assessment of traffic classes and to test the proposed approach. The experimental results indicate that by incorporating special features of data packets in the course of clustering, enhances accuracy and cluster purity with significant improvement.

Keyword : Traffic classification, unsupervised machine learning, clustering, iterative approach, Wireshark, Tranalyzer

I. INTRODUCTION

Traffic classification (i.e., associating traffic flows with their source applications) has attracted increasing research efforts in the last decade. The explosion of this research area started when the traditional approach of relying on transport-level protocol ports became unreliable, mainly because of the increasing variety and complexity of modern Internet traffic and application-level protocols. The reason for the growth in Internet traffic data is due to the bandwidth-hungry applications like File Transfer applications, Video Streaming, Social Media Network (Facebook, Twitter etc.), Mobile applications, E-commerce websites, Stock Exchange data and much more. As the traffic data increases it is necessary to analyse, measure, and classify it as ISP and Network Administrators need it for various perspectives like network planning, traffic shaping, billing and to extract useful information. This task needs to be performed with various tools available in market (Ex: tcpdump, Wireshark etc.) These tools capture the network traffic and store it onto a local server for further processing.

Network traffic classification is the process of classifying traffic based on their applications. Nowadays due to the growth of internet users and bandwidth hungry applications the traffic generated in the network is very high. There are many methods for classification of network traffic, they all try to classify the network traffic accurately but classification accuracy is less. From the very beginning of the internet, since there were not so many users and therefore, not so many applications, traffic classification was done using the well-known ports defined by IANA [16]. Classification based on well-known TCP or UDP ports is becoming increasingly less effective, due to the numbers of networked applications are port-agile (allocating dynamic ports as needed), end users are deliberately using non-standard ports to hide their traffic, and use of Network Address Port Translation (NAPT) is widespread (for example a large amount of peer-to-peer file sharing traffic is using non-default ports).

Payload-based classification relies on some knowledge about the payload formats for every application of interest: protocol decoding requires knowing and decoding the payload format while signature matching relies on knowledge of at least some characteristic patterns in the payload. This approach is limited by the fact that classification rules must be updated whenever an application implements even a trivial protocol change, and privacy laws and encryption can effectively make the payload inaccessible.

To overcome the above issues we are using machine learning approach to classify the traffic. In our work we are implementing an unsupervised clustering approach to classify the network traffic because unsupervised is that of trying to find hidden structure in unlabelled dataset. Clustering analysis is one of the unsupervised approaches and it is the process of making set objects in such a

way that objects in the same group are more similar to each other than to those in other group. In our work we proposed automatic-learning algorithm using clustering techniques. Each flow indicates the packet size, packet length, inter-arrival time etc. So we can easily get the flow information for classification because these features are known to carry valuable information about the protocol and the applications that generated the flow.

II. LITERATURE SURVEY

The author in paper [1] proposes internet traffic classification using supervised learning algorithm and makes comparative analysis between machine learning algorithms. The main focus in this paper is the selection of feature sets. Hence it is concluded that the supervised decision tree based algorithms provide better performance and accuracy than the other supervised algorithms like KNN, naive Bayes etc. But accuracy of these decision tree based algorithms is poor while applying them for classifying P2P applications. According to author in paper [2] Self-learning classifier is an unsupervised clustering algorithm with an adaptive seeding approach. It helps to automatically identify the classes of traffic being checked and labelled. This algorithm automatically groups flows into pure clusters using statistical features. Hence this paper acts as a base to our project as it summarises the state of the art of cluster analysis and here the main target of the classification is flows. Each flow is characterised by simple metrics, like segment size and inter arrival times.

According to Zhang, jun, et al. in paper [3] the classification of network traffic was done by correlation information. The traditional methods suffer from a number of practical problems, such as dynamic ports and encrypted applications so machine learning techniques have been focused to classify the traffic. Machine learning can automatically search for and describe useful structural patterns in a supplied traffic dataset. The correlation analysis can improve the classification accuracy and system flexibility. The proposed approaches can be used for recognising unknown application from captured network traffic and semi supervised data mining for processing network packets.

We selected paper [4] to understand the self-adaptive approach for network traffic classification. The author presented a novel, fully automated Packet Payload Content (PPC) Based network traffic classification system. System learns new application in the network where classification is desired. Hence the proposed algorithms are for distilling the generated signatures, and showed that these signatures are practical for real time classification in the real world.

According to author in paper [5], this paper can facilitate collaboration, convergence on standard definitions and procedures. The described Traffic Identification Engine (TIE), an open source tool for network traffic classification, can be applied to both live traffic and previously captured traffic traces. It is also investigated that the performance of multi classification systems when applied to early classification. TIE has the ability to configure from which portion of traffic the features passed to the classifier can be extracted.

The author in paper [7] proposes an unsupervised learning, which is traffic clustering for classification, where labelled training data is difficult and new patterns keep emerging. In order to improve the accuracy of traffic clustering, they constrained clustering schemes, which make decisions by considering some background information are proposed. They use Gaussian mixture density and adapt an appropriate algorithm for estimating the parameters.

III. SYSTEM DESIGN AND METHODOLOGY

The proposed system overcomes the limitation of iterative classifiers. The semi supervised classifiers are using the internet traffic and also overcome the internet bots. The iterative filtering and multi batch seeding is applied to improve the performance. We propose an unsupervised traffic classification that uses both flow features and packet payload. Using a bag-of-words approach and latent semantic analysis, some clusters are identified. Auto-Learning achieves better results in terms of classification performance, provides fine grained visibility on traffic, and offers a simple self-seeding mechanism that naturally allows the system to increase its knowledge. The proposed homogeneous clustering algorithm achieves much better classification performance than existing traffic classification like k-means methods. Homogeneous algorithm improves the overall system performance and resource efficient since traffic reduction is used. The system architecture is as shown in figure.1.

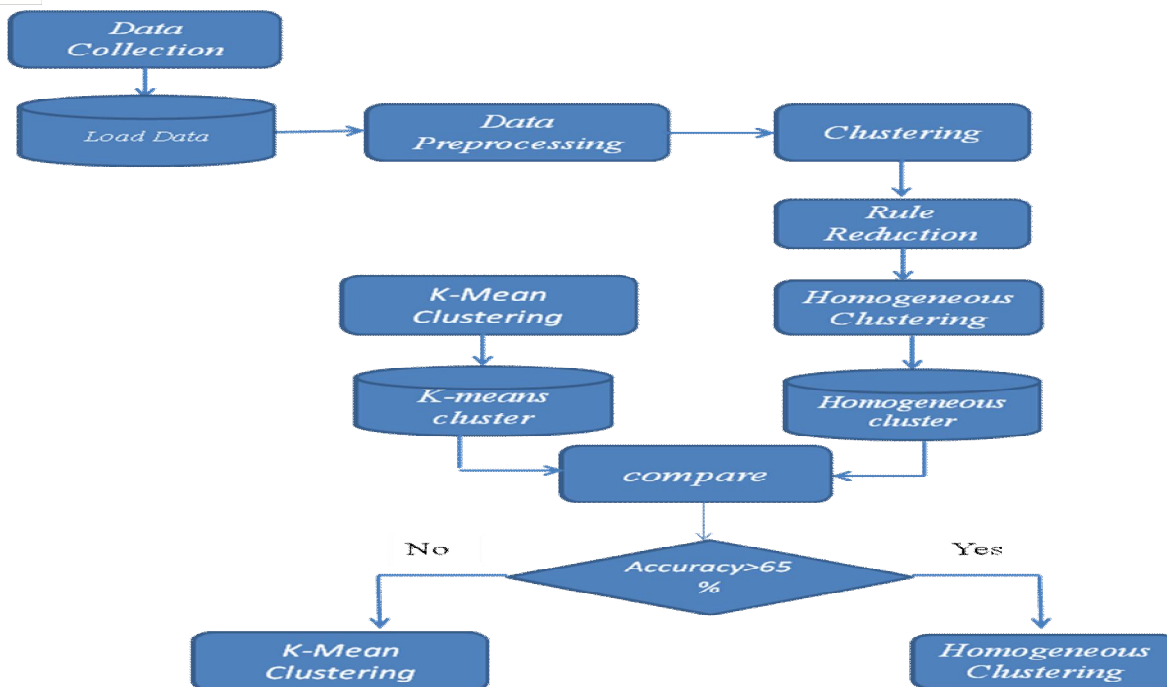


Fig.1 System Architecture

The functionalities of various software modules are explained below which includes four modules namely collection of dataset, data pre-processing, traffic reduction, and feature extraction.

A. Collect Dataset

Most commonly a data set corresponds to the contents of a single database table, or a single statistical data matrix, where every column of the table represents a particular variable, and each row corresponds to a given member of the data set. The data set lists values for each of the variables, such as height and weight of an object, for each member of the data set. Here the Wireshark tool is used to collect the dataset.

B. Data Pre-Processing

Data preparation and filtering steps can take considerable amount of processing time. It includes cleaning, normalization, transformation, feature extraction, and selection etc. Analysing data that has not been carefully screened for such problems can produce misleading results. Thus, the representation and quality of data is first and foremost before running an analysis.

C. Traffic Reduction

Traffic reduction method is one of the filtering method, it can reduce the data needed to be processed and hence increases the overall system performance. However, if a filter eliminates data improperly, bot detection rates could increase. Traffic Reduction can significantly improve the classification performance of many supervised classification algorithms.

D. Feature Extraction

Some of the behavior is distinguishable from normal behavior and hence features of the behavior can be extracted to detect bots. An ideal feature should be applicable to as many bots as possible. The features are collected in the feature extraction stage, like packet size, protocol, server port number, IP addresses etc and then the max membership principle is applied to the features to identify malicious ones. A packet is sent to the feature extraction stage if and only if its source or destination address is listed in the IP address list.

E. Clustering

Clustering is the process of grouping objects with similar features. In this paper the iterative clustering algorithm is used to classify the network traffic. In our work we are going to demonstrate how cluster analysis can be used to effectively identify groups of traffic. We are considering two unsupervised clustering algorithms, namely K-means and iterative homogeneous clustering for

network traffic classification. We evaluate these two algorithms and compare them with the previously used auto class algorithm, using empirical internet traces. Number of parameters used is six and based on these parameters there are three clusters formed with four classes namely FTP, HTTP, Telnet and SMTP. The comparison analysis made between existing K-means algorithm and proposed cluster algorithm. The graph (fig.7) shows the efficiency of proposed algorithm is better than that of existing algorithm. Clustering Algorithm analyses each batch of newly collected flows via the ProcessBatch(). It uses doiterative() function to make pure clusters the below algorithm shows the main loop of proposed algorithm.

This function takes in input

_B, the batch of new flows or dataset;

_U, the set of previous outliers that were not assigned to any class when processing the previous batch;

_S, the set of *seeding flows*, i.e., flows already analysed in past batches for which iterative clustering algorithm was able to provide a label;

As output, it produces

_C, the set of clusters;

_NS, the set of new seeds that are extracted from each cluster;

_U, which contains the set of new outliers;

Its main steps are

- 1) Clustering the dataset to get homogeneous subsets of flows,
- 2) Flow label assignment (function doLabeling()), and
- 3) Extraction of a new set of seeds (function extractSeeds()). Note that flows that are not assigned to any cluster are returned in the U set. Those flows are then aggregated in the next batch, so that they can eventually be aggregated to some cluster. In the following it details each step of the batch processing. Steps for malware detection or to detect the internet bots
- 4) Clustering the dataset to get homogeneous subsets of flows,
- 5) After homogeneous clustering rule reduction method is used
- 6) Extraction of a new set of rules (the source and destination address should be present in the IP address list)
- 7) Comparison between k-means and proposed homogeneous cluster method

IV. EXPERIMENTAL RESULTS

To carry out the experiment we have installed JDK 1.8 on our machine with net beans-IDE. It consists of packet sniffer program to capture and generate a Dataset. The implementation part consists of the following modules namely packet capturing, parameter selection, iterative clustering, labelling and classification.

A. Packet Capturing

This module is mainly used for capturing the packets to classify the traffic. It uses packet sniffer algorithm to capture the packet or packet capturing tools like Wireshark, netflow etc. Here Wireshark tool is used to capture the packet, it is one of the data capturing tools used to provide the structure of different networking protocols. It can also parse and display the fields, along with their meanings as specified by different networking protocols which are shown in the figure .2.

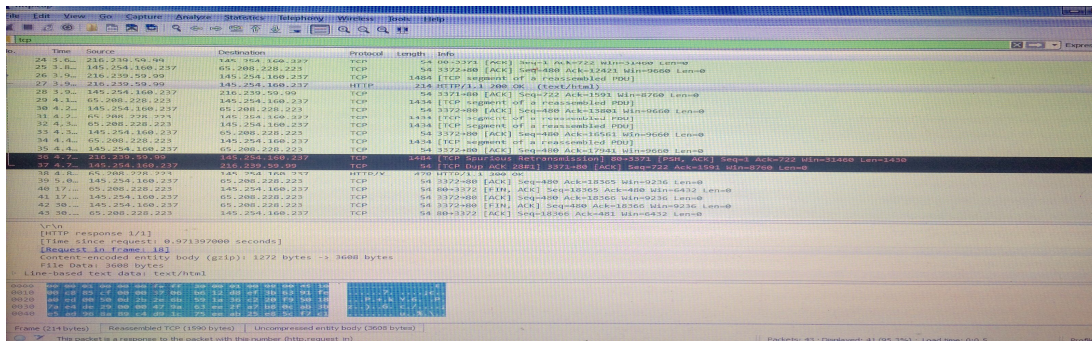


Fig.2. Wireshark Traffic Dump

- 1) *Tranalyzer2*: Tranalyzer2 is a lightweight flow generator and packet analyzer designed for simplicity, performance and scalability. The program is written in C and built upon the libpcap library. It provides functionality to pre- and post-process

IPv4/IPv6 data into flows and enables a trained user to see anomalies and network defects even in very large datasets, this is shown in figure.3.

```

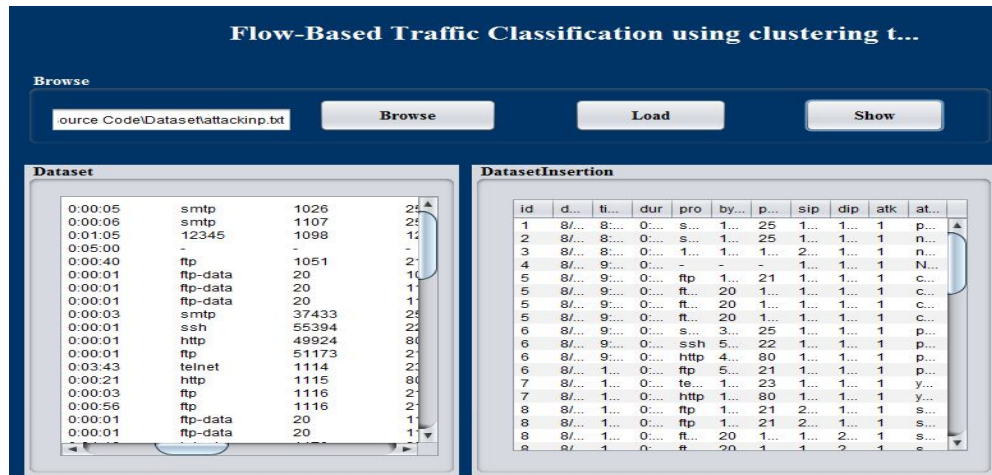
root@triveni-virtual-machine: /home/triveni/Downloads
Plugin directory does not exist.
Active plugins:
Start processing file: traffic.pcapng
BPF: (null)
Dump start: 1481209108.597831 sec : Thu 08 Dec 2016 20:28:28.597831
Finished processing, duration of file reading: 0.177565 seconds
Shutting down Tranalyzer 0.5.8...
Dump stop: 1481212696.130075 sec : Thu 08 Dec 2016 21:28:16.130075
Total dump duration: 3587.532244 sec
Number of processed packets: 14023
Number of processed traffic bytes: 8750300
Number of ARP packets: 0
Number of RARP packets: 0
Number of IPv4 fragmented packets: 0
Number of IPv6 fragmented packets: 0
Number of IPv4 packets: 14023
Number of IPv6 packets: 0
Number of processed IPv4 flows: 1251
A,B IPv4 flow asymmetry: 0.4644
max Number of IPv4 flows: 567
Average snapped Bandwidth: 19.513 KBit/s
Average full IP Bandwidth: 19.513 KBit/s
Average full raw Bandwidth: 19.513 KBit/s
root@triveni-virtual-machine: /home/triveni/Downloads#

```

Fig.3. parameter selection using tranlyzer2

- 2) *Iterative Clustering*: It uses doiterative () function to make pure clusters the below algorithm shows how the iterative clustering will work.
- 3) *Labelling*: Once flows have been clustered, the doLabeling (C0) procedure assigns a label to each cluster. For each cluster I in C0, flows are checked. If I contains some seeding flows, i.e., flows (extracted from S) that already have a label, a simple majority voting scheme is adopted: the seeding flow label with the largest frequency will be extended to all flows in I, possibly over-ruling a previous label for other seeding flows. More complicated voting schemes may be adopted. The below fig.2 shows the accuracy of the proposed iterative algorithm is more than that of the existing algorithms.

The below snapshots show the results obtained in our work which includes data loading, data pre-processing, clustering and the comparison between existing and proposed system in the form of accuracy.



| Dataset | | | |
|---------|----------|-------|----|
| 0:00:05 | smtp | 1026 | 24 |
| 0:00:06 | smtp | 1107 | 25 |
| 0:01:05 | 12345 | 1098 | 11 |
| 0:05:00 | - | - | - |
| 0:00:40 | ftp | 1051 | 21 |
| 0:00:01 | ftp-data | 20 | 11 |
| 0:00:01 | ftp-data | 20 | 11 |
| 0:00:01 | ftp-data | 20 | 11 |
| 0:00:03 | smtp | 37433 | 25 |
| 0:00:01 | ssh | 55394 | 22 |
| 0:00:01 | http | 49924 | 80 |
| 0:00:01 | ftp | 51173 | 21 |
| 0:03:43 | telnet | 1114 | 23 |
| 0:00:21 | http | 1115 | 80 |
| 0:00:03 | ftp | 1116 | 21 |
| 0:00:56 | ftp | 1116 | 21 |
| 0:00:01 | ftp-data | 20 | 11 |
| 0:00:01 | ftp-data | 20 | 11 |

| DatasetInsertion | | | | | | | | | | |
|------------------|-------|-------|------|-------|-------|------|------|------|-----|-------|
| id | d... | ti... | dur | pro | by... | p... | sip | dip | atk | at... |
| 1 | 8/... | 8... | 0... | s... | 1... | 25 | 1... | 1... | 1 | p... |
| 2 | 8/... | 8... | 0... | s... | 1... | 25 | 1... | 1... | 1 | n... |
| 3 | 8/... | 8... | 0... | 1... | 1... | 1... | 2... | 1... | 1 | n... |
| 4 | 8/... | 9... | 0... | - | - | - | 1... | 1... | 1 | N... |
| 5 | 8/... | 9... | 0... | ftp | 1... | 21 | 1... | 1... | 1 | c... |
| 5 | 8/... | 9... | 0... | ft... | 20 | 1... | 1... | 1... | 1 | c... |
| 5 | 8/... | 9... | 0... | ft... | 20 | 1... | 1... | 1... | 1 | c... |
| 5 | 8/... | 9... | 0... | ft... | 20 | 1... | 1... | 1... | 1 | c... |
| 6 | 8/... | 9... | 0... | s... | 3... | 25 | 1... | 1... | 1 | p... |
| 6 | 8/... | 9... | 0... | ssh | 5... | 22 | 1... | 1... | 1 | p... |
| 6 | 8/... | 9... | 0... | http | 4... | 80 | 1... | 1... | 1 | p... |
| 6 | 8/... | 1... | 0... | ftp | 5... | 21 | 1... | 1... | 1 | p... |
| 7 | 8/... | 1... | 0... | te... | 1... | 23 | 1... | 1... | 1 | y... |
| 7 | 8/... | 1... | 0... | http | 1... | 80 | 1... | 1... | 1 | y... |
| 8 | 8/... | 1... | 0... | ftp | 1... | 21 | 2... | 1... | 1 | s... |
| 8 | 8/... | 1... | 0... | ftp | 1... | 21 | 2... | 1... | 1 | s... |
| 8 | 8/... | 1... | 0... | ft... | 20 | 1... | 1... | 2... | 1 | s... |
| 8 | 8/... | 1... | 0... | ft... | 20 | 1... | 1... | 2... | 1 | s... |

Fig.4 load data

First we need to load the dataset for data pre-processing and for feature extraction which is shown in the fig.2. After loading the data, the data pre-processing phase takes place which is shown in fig.3. It includes cleaning, normalization, transformation, feature extraction, and selection etc

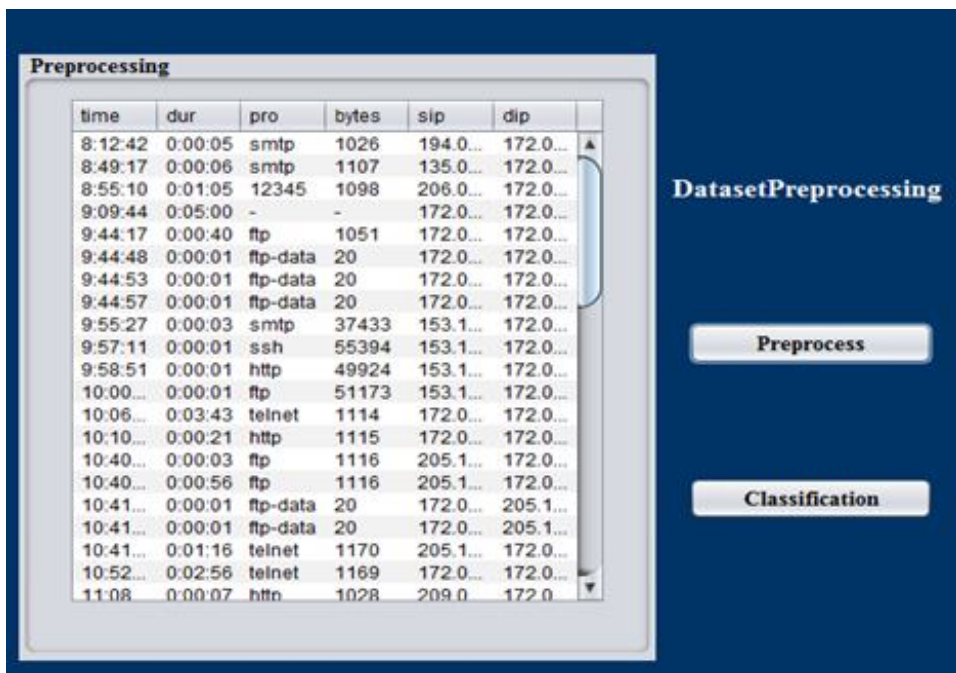


Fig.5 data pre-processing

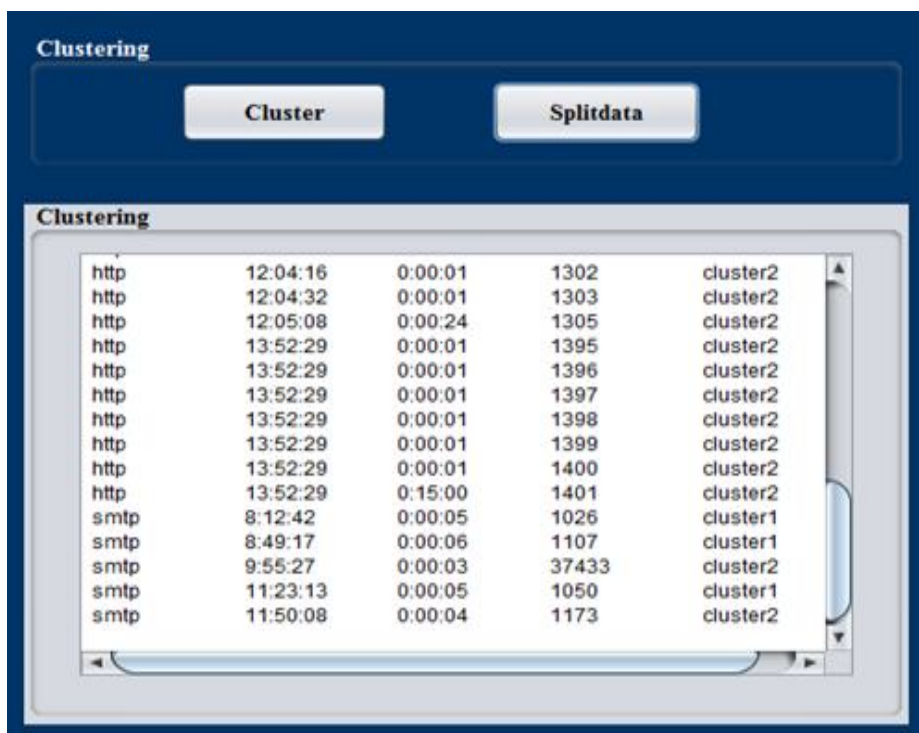


Fig.6 clustering

Cluster process group objects with similar characteristics. Objects are described by means of selected features which are shown in fig.4. In fig.5 shows the comparison between the proposed clustering algorithm and the existing K-means algorithm hence it is concluded that our proposed algorithm is more effective than existing algorithm.

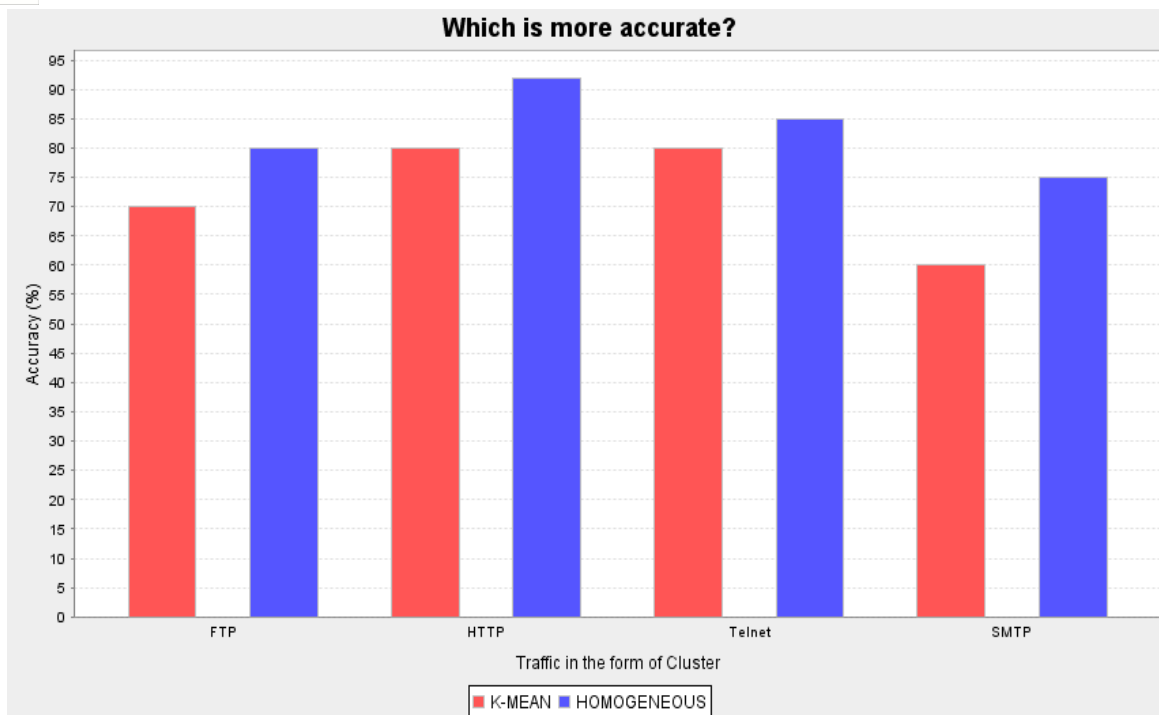


Fig.7 comparison between existing and proposed system

The accuracy graph shown in the figure .7 is the comparison between existing k-means algorithm and proposed clustering algorithm. Here X-axis indicates the generated clusters and Y-axis indicates the accuracy percentage. In this graph there are 4 clusters namely FTP, HTTP, Telnet and SMTP and it shows the percentage values.

V. CONCLUSION

The proposed homogeneous clustering MLA is used for distinguishing different kinds of traffic in a computer network. Here we are focusing on four different applications like FTP, HTTP, Telnet and SMTP. The homogeneous clustering method gives 90% accuracy than the existing k-means method in terms of purity or homogeneity of clusters and it also able to distinguish the traffic which appears to be similar, where an existing system cannot do.

VI. FUTURE SCOPE

The proposed algorithm which is considerably reduces the network traffic. Now the future work will be focusing on providing a good QOS, network security and minimize the network delay

REFERENCES

- [1] Kalaiselvi, T., and P. Shanmugaraja. "Internet Traffic Classification Using supervised Learning Algorithms–A Survey." (2016).
- [2] Grimaudo, Luigi, et al. "Select: Self-learning classifier for internet traffic." *IEEE Transactions on Network and Service Management* 11.2 (2014): 144-157.
- [3] Zhang, Jun, et al. "Network traffic classification using correlation information." *IEEE Transactions on Parallel and Distributed Systems* 24.1 (2013): 104-117.
- [4] Tongaonkar, Alok, et al. "Towards self adaptive network traffic classification." *Computer Communications* 56 (2015): 35-46.
- [5] De Donato, Walter, Antonio Pescapé, and Alberto Dainotti. "Traffic identification engine: an open platform for traffic classification." *IEEE Network* 28.2 (2014): 56-64.
- [6] Dainotti, Alberto, Antonio Pescapé, and Kimberly C. Claffy. "Issues and future directions in traffic classification." *IEEE network* 26.1 (2012).
- [7] Wang, Yu, et al. "Internet traffic classification using constrained clustering." *IEEE Transactions on Parallel and Distributed Systems* 25.11 (2014): 2932-2943.
- [8] Kim, Jeankyung, Jinsoo Hwang, and Kichang Kim. "High-Performance Internet Traffic Classification Using a Markov Model and Kullback-Leibler Divergence." *Mobile Information Systems* 2016 (2016).
- [9] Zhang, Jun, et al. "Network traffic classification using correlation information." *IEEE Transactions on Parallel and Distributed Systems* 24.1 (2013): 104-117.
- [10] Shafiq, Muhammad, et al. "Network Traffic Classification techniques and comparative analysis using Machine Learning algorithms." *Computer and Communications (ICCC), 2016 2nd IEEE International Conference on.* IEEE, 2016.
- [11] Alejandre, Francisco Villegas, Nareli Cruz Cortés, and Eleazar Aguirre Anaya. "Botnet Detection using Clustering Algorithms." *Research in Computing Science* 118 (2016): 65-75.
- [12] Hosseinpour, Farhoud, et al. "Artificial immune system based intrusion detection: Innate immunity using an unsupervised learning approach." *International Journal of Digital Content Technology and its Applications* 8.5 (2014): 1.



- [13] Katal, Supriya, and Asstt Prof Hardeep Singh. "A Survey of Machine Learning Algorithm in Network Traffic Classification." International Journal of Computer Trends and Technology (IJCTT).--Madurai, India: Seventh Sense Research Group 9.6 (2014): 301-304.
- [14] Finsterbusch, Michael, et al. "A survey of payload-based traffic classification approaches." IEEE Communications Surveys & Tutorials 16.2 (2014): 1135-1156.
- [15] Ranjan, Supranamaya, Joshua Robinson, and Feilong Chen. "Machine learning based botnet detection using real-time connectivity graph based traffic features." U.S. Patent No. 8,762,298. 24 Jun. 2014.
- [16] Narten, Thomas. "Guidelines for writing an IANA Considerations Section in RFCs." (2008).



10.22214/IJRASET



45.98



IMPACT FACTOR:
7.129



IMPACT FACTOR:
7.429



INTERNATIONAL JOURNAL FOR RESEARCH

IN APPLIED SCIENCE & ENGINEERING TECHNOLOGY

Call : 08813907089  (24*7 Support on Whatsapp)



Robust and Secure Access Schema using Dual Factor Authentication and OTP using Android Interface

Channappa Gowda D V

Assistant Professor, Dept. of ISE, The Oxford College of Engineering, Bangalore, Karnataka, India

ABSTRACT:The proposed system highlights one premium web services authentication system using dual factor in order to assure enhanced protection. As internet is flooded with illegal and malware application which are almost invisible to the generic user, hence there is a huge need to safe guard the clients who are actually paying for the services in order to maintain confidentiality and privacy. The proposed system provides a better score of authentication guarantee, which is very prominent for implementation purpose. A test bed is creating using windows OS and Android Mobile Interface (AMI), considering IMEI and IMSI information of a real time cellular phone. The proposed system highlights a novel dual-factor authentication scheme whereby a user's device produces multiples OTPs from an initial seed using the proposed production scheme.

KEYWORDS: One Time Password, Dual Factor Authentication, Android mobile interface

I. INTRODUCTION

Two-factor authentication is commonly found in electronic computer authentication, where basic authentication is the process of a requesting entity presenting some evidence of its identity to a second entity. Two-factor authentication seeks to decrease the probability that the requestor is presenting false evidence of its identity. The number of factors is important as it implies a higher probability that the bearer of the identity evidence indeed holds that identity in another realm (i.e.: computer system vs. real life). In reality there are more variables to consider when establishing the relative assurance of truthfulness in an identity assertion, than simply how many "factors" are used. Two-factor authentication is often confused with other forms of authentication. Two factor authentications require the use of two of the three regulatory-approved authentication factors. These factors are: Something the user knows (e.g., password, PIN); something the user has (e.g., ATM card, smart card); and something the user is (e.g., biometric characteristic, such as a fingerprint). According to proponents, TFA could drastically reduce the incidence of online identity theft, and other online fraud, because the victim's password would no longer be enough to give a thief permanent access to their information. However, many TFA approaches remain vulnerable to Trojan controlled websites and man in the middle attacks.[3] In addition to such direct attacks, three aspects must be considered for each of the 2 (or more) factors in order to fully realize the potential increase in confidence of authentication:

- The inherent strength of the mechanism, i.e. the entropy of a secret, the resistance of a token to cloning, or the uniqueness and reliability of a biometric.
- Quality of provision and management. This has many aspects, such as the confidence you can have that a token or password has been securely delivered to the correct user and not an imposter, or that the correct individual has presented himself for enrollment of his biometric, as well as secure storage and transmission of shared secrets, procedures for password reset, disabling a lost token, re-enrollment of a biometric, and prompt withdrawal of credentials when access is no longer required.
- Proactive fraud detection, e.g. monitoring of failed authentication attempts or unusual patterns of behavior which may indicate that an attack is under way, and suitable follow-up action.

Another solution suggests the utilization of signature chains to address the chain length restriction by involving public key techniques. This technique, however, also increases computation costs. Moreover, time-synchronized OTP



International Journal of Innovative Research in Computer and Communication Engineering

(An ISO 3297: 2007 Certified Organization)

Website: www.ijirccce.com

Vol. 5, Issue 6, June 2017

systems, which are typically based on an internal clock synchronized with a main server, are not applicable for mobile phones. In addition, due to the general nature of mobile phones (e.g., out of network, etc.); such synchronization cannot typically be guaranteed. To overcome the restrictions discussed above, this proposed system will discuss OTP production in the forward direction. This production will completely eliminate the mentioned limitations. Our idea is to produce multiple OTPs from an initial seed in a parallel process with the service provider itself, e.g., an online bank, by utilizing two different types of hash functions, which come with a nested chain. The resulting chain provides forwardness and infiniteness.

II. RELATED WORK

D.Parameswari and L.Jose [1] describes a method of implementing two factor authentication using SMS OTP - One Time Password to Secure an E-Transaction (SET). D.Parameswari and L.Jose provides the reader with an overview of the various parts of the system and the capabilities of the system. Generated One Time Password is valid for only a short user defined period of time and it is generated and verified using Secured Cryptographic Algorithm. FadiAloul, Syed Zahidi, Wassim El-Hajj [2] describes a method of implementing two factor authentication using mobile phones. They generated One Time Password is valid for only a short userdefined period of time and is generated by factors that are unique to both, the user and the mobile device itself. Additionally, an SMS-based mechanism is implemented as both a backup mechanism for retrieving the password and as a possible mean of synchronization. FadiAloul proposes and develops a complete two factor authentication system using mobile phones instead of tokens or cards.

Bogdan Groza, DorinaPetrica [3] Leslie Lamport in his paper Password Authentication with Insecure Communication proposed the use of one-way functions in order to obtain one time passwords. Because of their simplicity cryptographic hash functions are commonly used for such purpose. HavardRaddum, Lars Hopland Nest^oas, and KjellJ^orgen Hole [4] suggested two minor changes to Encap's protocol designs, one to bring the activation protocol's key generation in line with "best practice," and one to simplify the designs without reducing the security. The seriousness of the attacks shows how important a system-level analysis and testing can be to determine the level of security provided by protocols in a real system.

Stephen Chan, Stephen Lau, Jay Srinivasan, Adrian Wong [5] presented a prioritization of the work that needs to be done. OTP has very broad ranging effects and it is important that the most pressing issues be dealt with first. In addition, there is technology that needs to be developed and deployed-identified the work that we feel needs to be done, and prioritized it based on current observations. Chunhua Chen, Chris J. Mitchell, Shaohua Tang [6] show how Trusted Computing can be extended in a GAA-like framework to offer new security services. They then propose a general scheme that converts a simple static password authentication mechanism into a one-time password (OTP) system using the GAA key establishment service. Vipul Goyal, Ajith Abraham, SugataSanyal and Sang Yong Han [7] device a novel construction of hash chains. The basic idea here is to repeatedly require the insertion of user password after a fixed distance in the hash chain. The links at which the insertion of the password is required may be made public and stored at the host (server).

Kenneth G. Paterson and Douglas Stebila [8] consider the use of onetime passwords in the context of password-authenticated key exchange (PAKE), which allows for mutual authentication, session key agreement, and resistance to phishing attacks. Author describe a security model for the use of one-time passwords, explicitly considering the compromise of past (and future) one time passwords, and show a general technique for building a secure one-time-PAKE protocol from any secure PAKE protocol. Our techniques also allow for the secure use of pseudo randomly generated and time-dependent passwords.

Dinei Florencio and Cormac Herley [9] describe a service that allows users one-time password access to any web account, without any change to the server, without changing anything on the client, and without storing user credentials in-the-cloud. Employ a simple mapping of the arbitrary input password to restricted character set OTP's: thus every OTP is readable without ambiguity no matter what display or font is used, can be transmitted over SMS, and can be entered even on unfamiliar keyboards without the use of meta keys.

Anders Moen Hagalisletto and Arne Riiber [10] present a commercial protocol, developed by a Norwegian start-up copmany, for using a mobile terminal as a password calculator that could potentially be used towards any service provider on the internet. They report theirr experiences by specification, validation, and analysis of the protocol in particular the threat of phishing attacks is investigated.



International Journal of Innovative Research in Computer and Communication Engineering

(An ISO 3297: 2007 Certified Organization)

Website: www.ijirccce.com

Vol. 5, Issue 6, June 2017

Ryoichi Isawa and MasakatuMorii [11] propose a new one-time password scheme against the Hybrid Theft attack*1. The proposed scheme has three advantages: 1) secure against all the existing attacks, 2) based on only one-way hash function, and 3) a mutual authentication scheme. Compared with SAS-X (2), the proposed scheme is more secure because of the advantage 1, and can compute faster because of the advantage 2. SAS-X (2) is a one-way authentication scheme

Andrew Tillman [12] presents Many MLSs and associations are looking to implement improved security measures such as two factor authentication. Existing solutions are problematic in either cost and/or practicalityA solutions that use SMS would be a cost-effective and practical way in which to provide this functionality and as a result greatly increase the security of these important online resources. Alberto BenaventeMartínez, Spain [13] designs an authentication model that uses a onetime password (OTP) mechanism.

Password-authenticated key exchange was first introduced by Bellovin and Merritt in 1992 [14] as a protocol in which the client and server share a plaintext password and exchange encrypted information to allow them to derive a shared session key. A later variant [15], often called verifier-based, removed the requirement that the server have the plaintext password, instead having a one-way transformation of the password. The most extensively used model for the security of PAKE protocols is the Bellare-Pointcheval-Rogaway (BPR) model [16] and its extension [17] for verifier-based protocols. This model is the starting point of our model for the security of one-time-PAKE protocols. One particular such protocol is the PAK protocol [18, 19], which is the basis of our construction in the full version of this paper. Various authors have noted the value of using one-time passwords in authenticated key exchange protocols [20, 21, 22]. Abdalla et al. [23] (see also [24]) describe the OPKeyX protocol, a verifier-based one-time-PAKE protocol. It uses a hash chain to derive subsequent one-time passwords from a seed such that the server can verify but not compute the next password.

III. PROBLEM DESCRIPTION

This dual-factor authentication system suffers from the following shortcomings:

- SMS Cost: During every login request or transaction process, it is necessary to send an SMS-OTP from the bank to the user. This, in turn, will be costly to the bank with the consideration of statistics of bank's transactions
- SMS Lateness: The SMS transmission delay represents one of the major limitations of the traditional system.
- International Roaming: Travelling overseas creates restrictions on the SMS services. Turning off the roaming service will prevent the bank from sending the SMS-OTP, which in turn, stops the user from resuming any further processes.
- SMS Security: It can be said that while designing the GSM system, it had all security measures in mind, but as time passed and algorithms were cracked by the hackers, SMS-OTP based systems were not kept secure.

IV. PROPOSED SYSTEM

The main aim of the paper is to develop an architectural framework for dual factor authentication system, where the system will produce one time password (OTP) in the forward direction. The prime idea is to generate multiple OTPs from an initial seed in a parallel process with the service provider itself, e.g., an online bank, student file management, financial services etc. by utilizing two different types of hash functions, which come with a nested chain. The resulting chain provides forwardness and infiniteness and it should run on multiple systems of wired or wireless network. The cumulative architecture of the proposed system is as shown in Figure 1. The Lamport's idea has been extended with some modifications in order to generate infiniteness and forwardness, avoiding the use of public key cryptography. The shortcoming of those two parameters, infiniteness and forwardness, cause the several vulnerabilities shown with respect to the related work. A one-time password is valid for only one login session or transaction. OTP avoid a number of shortcomings which are associated with traditional (static) passwords. Dual-factor authentication is an approach to authenticate which requires the presentation of two different kinds of evidence that someone is who they say they are. It is a part of the broader family of multi-factor authentication, which is a defense in depth approach to security. Authentication is the act of confirming the truth of an attribute of a datum or entity. This might involve confirming the identity of a person, tracing the origins of an artifact, ensuring that a product is what it's packaging and labeling claims to

International Journal of Innovative Research in Computer and Communication Engineering

(An ISO 3297: 2007 Certified Organization)

Website: www.ijirccce.com

Vol. 5, Issue 6, June 2017

be, or assuring that a computer program is a trusted one. The proposed work mainly constitutes of two modules e.g. administrator (or service provider) and student. The administrator basically supervises the application by assisting in creation of account as well as relaying the services based on the digital content used by the student user. As the application will consist of a privilege access for the student, so an efficient and robust authentication as well as authorization is highly required.

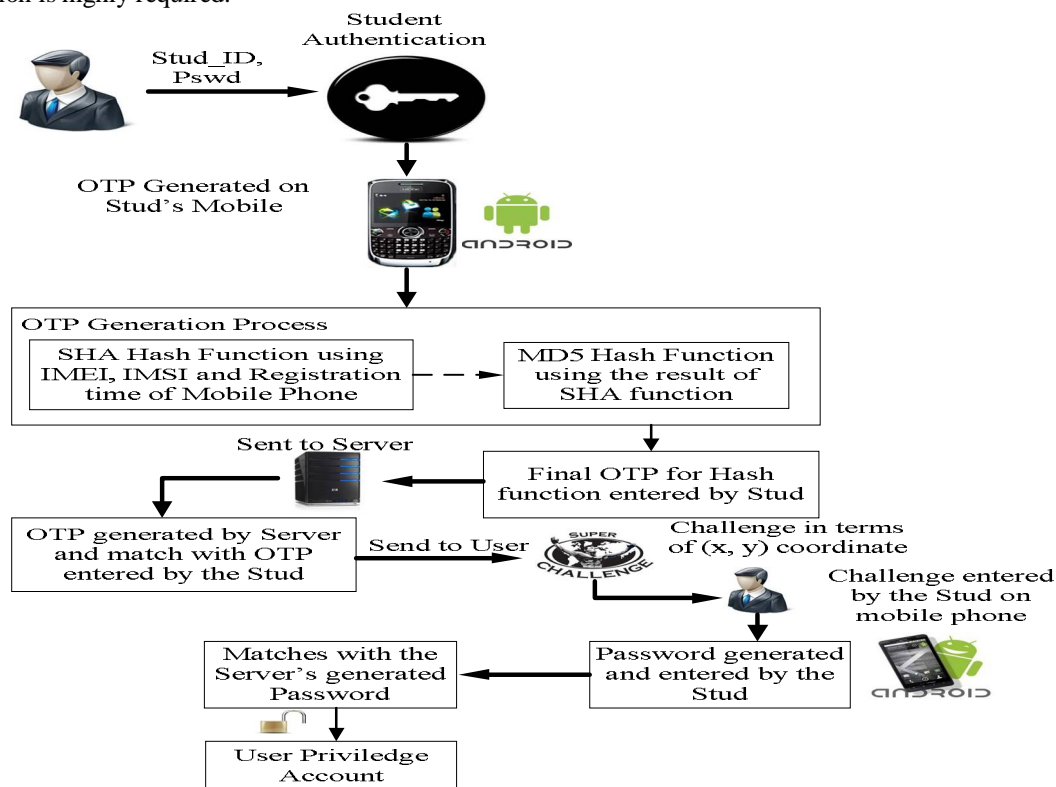


Figure 1: Proposed Architecture

The proposed system is mainly partitioned in three phases:

- **Enrollment Phase:** The student gets the two different hash functions, and an initial seed, established on their Android enabled mobile phone. To ensure that the information is completely shared with the service provider, the seed is produced by the shared and unique parameters of the host and user, e.g., the International Mobile Equipment Identity (IMEI), International Mobile Subscriber Identity (IMSI), and enrollment date.
- **Login and Authentication Phase:** The steps of the login and authentication process between the user and service provider are like this; the student logs in to the service provider's website, requesting access. As a response to this access request, a secure session is established, allowing the student to enter their authentication privileges, i.e., student's name and password, the first factor of authentication, what the student knows. Also the student provides the server with their OTP's current status. The current status allows the server to synchronize the generated seed with the student's current seed to get the same seed value on both sides before sending a challenge. The server randomly challenges the student with new indexes. The student enters those indexes, in their OTPgenerator to get the corresponding OTP. The student responds with this corresponding OTP. The server compares the received OTP with the calculated one. According to the server check, done in the previous step, the server will transfer an authorization execution or a communication termination.
- **Mathematical Illustration:** Through the enrollment process, the student gets two different hash functions, which could be SHA-1, and $h_B(.)$, which could be MD5, along with an initial seed, " S_{int} ," as the concatenation of the IMEI,



International Journal of Innovative Research in Computer and Communication Engineering

(An ISO 3297: 2007 Certified Organization)

Website: www.ijirccce.com

Vol. 5, Issue 6, June 2017

IMSI, and registration time, which could be “1234567891234561234567891234507012010200259” assuming IMEI is “123456789123456,” IMSI is “12345678912345,” and the registration time is “7/1/2012 20:02:59.” After logging into the service provider’s website using a different and static username and password, the first factor of authentication, the server asks the user for the OTP’s current status. If the student has generated numerous OTPs without using them, he might have reached an OTP status of, for example, “17.” The user will submit his current status to the server to allow the server to calculate the current seed $S_{\text{crt}}=H_A^{17}(S_{\text{int}})$ 1220848648030773785924867285680707842195071405780, which means that the server has calculated seventeen cascaded hashes of its initial seed “ S_{int} ,” using the SHA-1 algorithm, to be synchronized with the client. After that the server sends a random challenge value of new indexes, e.g., $x, y = 3, 4$, which means the user has to calculate his session OTP using this formula: $\text{OTP}=h_B^4(H_A^3(S_{\text{crt}}))= 68606061177919188523363813602016333158$. The server has to calculate the same value in a parallel process, and as soon as the client responds, the server will match the two values to give either a yes or no.

Static password has been long acknowledged as a big security and management headache to IT administrators of enterprises. Usually, a simple password was used repeatedly by a user or written down carelessly on a piece of paper. Unlike the traditional single-factor static password, one time password changes each time the user logs in. Thus, on one side, the users are forever freed from remembering static password by simply using a detached OTP generator or token; on the other side, sensitive personal information in the IT systems is better protected against unauthorized access since relay attacks are effectively prevented. To face the increasing security demands on IT systems nowadays, it is highly advised that enterprises introduce two-factor authentication methods into their IT infrastructure. The OTP solution, as the most adaptable and flexible scheme, is becoming the most popular information security solution in the field with cost-effective user OTP tokens and advanced security.

The proposed scheme can resist an off-line guessing attack because it uses strong passwords produced from strong hash functions. Moreover, replaying reusable passwords is restricted by encoding passwords to be used one time. However, it is necessary to prevent another token from becoming an OTP generator for the same user. A manual process should handle this situation.

V. SIMULATION RESULTS

The proposed system is designed on Windows 32-bit OS with 1.84 GHz processor with broadband connectivity of 100 Mbps. The programming is done on MyEclipse IDE. The experiment for the proposed system is done on real time Samsung Galaxy Smartphone with Android 2.2. Hence Android Development Tools (ADT) is used as it is a plug-in for the MyEclipse IDE that is designed to give a powerful, integrated environment in which to build Android applications. The proposed system will be experimented with active wireless connectivity between the system and Android enable device.

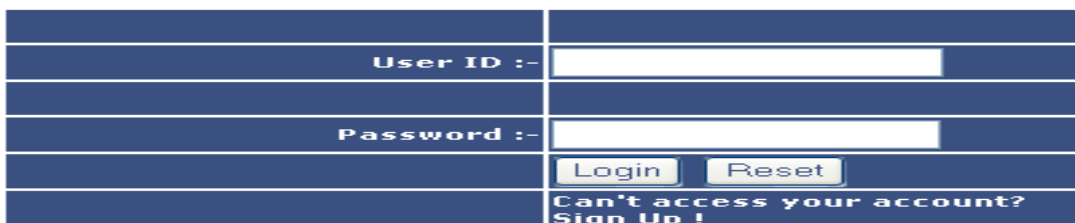


Figure 2: Student Login Options

THE ABOVE FIGURE 2 HIGHLIGHTS THE INITIAL AUTHENTICATION LOGIN FOR STUDENT. INITIALLY THE STUDENT HAS TO SIGN UP A NEW ACCOUNT WHERE THEY HAVE TO FURNISH ALL THE DETAILS AS SHOWN IN FIGURE 3.



International Journal of Innovative Research in Computer and Communication Engineering

(An ISO 3297: 2007 Certified Organization)

Website: www.ijirce.com

Vol. 5, Issue 6, June 2017

| | |
|---------------------|---|
| Name :- | <input type="text" value="Ravi"/> |
| College id :- | <input type="text" value="520923885"/> |
| Password :- | <input type="password" value="••••"/> |
| Confirm Password :- | <input type="password" value="••••"/> |
| Mobile No :- | <input type="text" value="7411666205"/> |
| Email :- | <input type="text" value="ravi.cbkinfotech@gmail.com"/> |
| Address :- | <input type="text" value="Mathikere Bangaluru Karnataka-560054"/> |
| IMEI No :- | <input type="text" value="0000000000000000"/> |
| IMSI No :- | <input type="text" value="3102600000000000"/> |
| Timestamps | <input type="text" value="1277931480000"/> |
| Your Question :- | <input type="text" value="How RU?"/> |
| Answer :- | <input type="text" value="I M GooD....."/> |
| | <input type="button" value="Submit"/> <input type="button" value="Reset"/> |

Figure 3: Sign-up Information feeding.

After the successful sign-up, the student can log in to their privilege account using the similar College ID as user ID and password, which was successfully fed at the time of sign up process

Are you human?
If yes.
Type the characters you see in the picture below




Figure 4: Captcha Authentication.

Once the student logs and their initial user ID and password is accepted, then they will be prompted to feed the random digital information displayed by Captcha application as shown in Figure 4. Now, after the successful sign up, the student can now perform initial login authentication for which they will be asked to feed OTP and Current status, both of which is generated at the Mobile interface as shown in Figure 5 and 6.

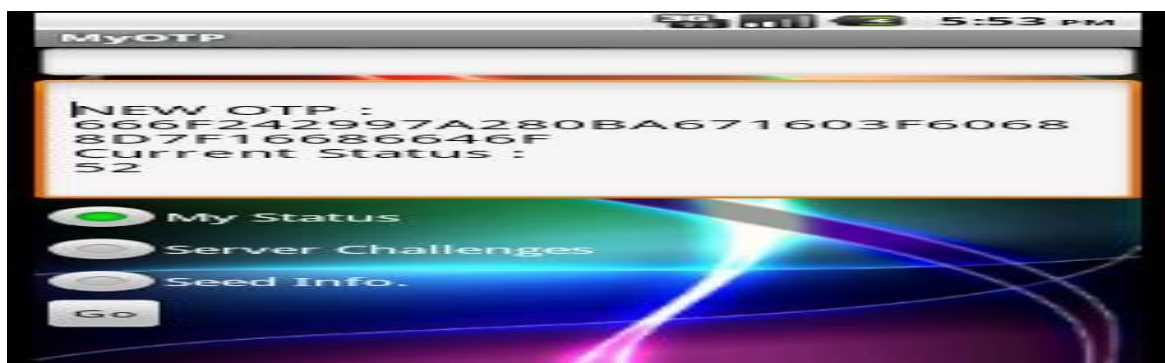


Figure 5: OTP & Current Status generation in Mobile interface

International Journal of Innovative Research in Computer and Communication Engineering

(An ISO 3297: 2007 Certified Organization)

Website: www.ijirce.com

Vol. 5, Issue 6, June 2017

| | |
|--------------------------------------|--------------------------------------|
| One Time Password :- | 13F60688D7F16686646F |
| Current Status :- | 52 |
| <input type="button" value="Login"/> | <input type="button" value="Reset"/> |

Figure 6: Feeding OTP and Current Status from mobile interface to web interface.

Once the OTP and current status is authenticated, the new index will be generated automatically in web interface as shown in Figure 7.

| | |
|-------------------------------------|----------|
| New Index :- | 108, 104 |
| <input type="button" value="Next"/> | |

Figure 7: Generation of new Index



Figure 8: Generation of OTP in Mobile Interface.

Once the new index value is authenticated in the mobile interface, the next sequence, it will generate a new OTP, in same mobile interface as shown in Figure 9. The student needs to take the newly generated OTP and feed in to their web-interface for final authentication as shown in Figure 10.

| | |
|-------------------------------------|---------------------|
| Enter Your New OTP :- | 3E38C29021E7CC54F93 |
| <input type="button" value="Next"/> | |

Figure 9: Feeding newly generated OTP in web interface.

VI. CONCLUSION AND FUTURE WORK

A new two-factor OTP-based authentication scheme has been proposed using Android mobile phones as they are becoming more and more powerful devices. This new authentication protocol provides forward and infinite OTP generation using two nested hash functions. The proposed approach has been illustrated to an online authentication process. This scheme achieves better characteristics than the other schemes discussed above. The proposed system is not limited to a certain number of authentications, unlike the previously-mentioned OTP hashing-based schemes and does not involve computationally expensive techniques to provide the infiniteness. The protocol doesn't require a token embedded server synchronized clock like. The approach eliminates the problems with utilizing OTPs with an SMS, consisting of the SMS cost and delay, along with international roaming restrictions. A detailed security analysis was also performed that covered many of the common types of attacks. The two factor authentication property has been achieved without restrictions.



International Journal of Innovative Research in Computer and Communication Engineering

(An ISO 3297: 2007 Certified Organization)

Website: www.ijirce.com

Vol. 5, Issue 6, June 2017

REFERENCES

- [1] D.Parneswari a*, L.Jose "SET with SMS OTP using Two Factor Authentication" Journal of Computer Applications (JCA) ISSN: 0974-1925, Volume IV, Issue 4, 2011.
- [2] Fadi Aloul, Syed Zahidi, Wassim El-Hajj "Two Factor Authentication Using Mobile Phones" Conference Location: Las Vegas, NV E-ISBN: 978-0-7695-4367-3 Print ISBN: 978-1-61284-427-5, 11 July 2011
- [3] Bogdan Groza, Dorina Petrica "ONE TIME PASSWORDS FOR UNCERTAIN NUMBER OF AUTHENTICATIONS" "Politehnica" University of Timisoara Department of Automation and Applied Informatics Bd. Vasile Parvan nr. 2, 302223 Timisoara, Romania
- [4] Håvard Raddum, Lars Hopland Nestås, and Kjell Jørgen Hole "Security Analysis of Mobile Phones Used as OTP Generators" P. Samarati et al. (Eds.): WISTP 2010, LNCS 6033, pp. 324–331, 2010. C. IFIP International Federation for Information Processing 2010.
- [5] Stephen Chan, Stephen Lau, Jay Srinivasan, Adrian Wong "One Time Password Authentication for Open High Performance Computing Environments" April 26, 2004
- [6] Chunhua Chen, Chris J. Mitchell, Shaohua Tang, "Ubiquitous One-Time Password Service using the Generic Authentication Architecture" China (No. 9351064101000003).
- [7] Vipul Goyal, Ajith Abraham, Sugata Sanyal and Sang Yong Han "The N/R One Time Password System" RFC 1321, April 1992.
- [8] Kenneth G. Paterson, Douglas Stebila "One-time-password-authenticated key exchange" September 4, 2009, p. 264-281 (Lecture Notes in Computer Science).
- [9] Dinei Florêncio and Cormac Herley "One-Time Password Access to any Server without Changing the Server" Proc. ISC '08, Taipei
- [10] Anders Moen Hagalisletto Arne Riiber "Using the mobile phone in two-factor authentication" The basic authentication mechanism is covered by the patent application document (PCT WO/2007/039806).
- [11] Alberto Benavente Martínez, Spain "One-Time Password Authentication Scheme to Solve Stolen Verifier Problem" L-022, back to the Intelligence Science and Technology.
- [12] Andrew Tillman "Two Factor Authentication Using SMS" Center for REALTOR® Technology Version 1.0
- [13] Alberto Benavente Martínez, Spain "Authentication model that uses One Time Passwords" Global Information Assurance Certification Paper 1 December 2003
- [14] Steven M. Bellovin and Michael Merritt. Encrypted key exchange: Password-based protocols secure against dictionary attacks. In Proceedings of the 1992 IEEE Computer Society Conference on Research in Security and Privacy. IEEE, May 1992. DOI:10.1109/RISP.1992.213269.
- [15] Steven M. Bellovin and Michael Merritt. Augmented encrypted key exchange: a password-based protocol secure against dictionary attacks and password file compromise. In Proc. 1st ACM Conference on Computer and Communications Security (CCS), pp. 244–250. ACM, 1993. DOI:10.1145/168588.168618.
- [16] Mihir Bellare, David Pointcheval, and Phillip Rogaway. Authenticated key exchange secure against dictionary attacks. In Preneel [Pre00], pp. 139–155. DOI:10.1007/3-540-45539-6_11.
- [17] Craig Gentry, Philip MacKenzie, and Zulfikar Ramzan. PAK-Z+, August 2005. URL <http://grouper.ieee.org/groups/1363/WorkingGroup/presentations/pakzplusv2.pdf>. Contribution to the IEEE P1363-2000 study group for Future PKC Standards.
- [18] Victor Boyko, Philip MacKenzie, and Sarvar Patel. Provably secure Password-Authenticated Key exchange using Diffie-Hellman. In Preneel [Pre00], pp. 156–171. DOI:10.1007/3-540-45539-6_12. Full version available as [BMP00b].
- [19] Philip MacKenzie. The PAK suite: Protocols for password-authenticated key exchange. Technical Report 2002- 46, DIMACS Center, Rutgers University, 2002. URL <http://dimacs.rutgers.edu/TechnicalReports/abstracts/2002/2002-46.html>.
- [20] Michel Abdalla, Olivier Chevassut, and David Pointcheval. One-time verifier-based encrypted key exchange, 2005. URL <http://www.di.ens.fr/~mabdalla/papers/ACP05-letter.pdf>. Extended abstract published as [ACP05a].
- [21] Liang Fang, Samuel Meder, Olivier Chevassut, and Frank Siebenlist. Secure password-based authenticated key exchange for web services. In Proc. 2004 Workshop on Secure Web Service (SWS), pp. 9–15. ACM, 2004. DOI:10.1145/1111348.1111350.
- [22] Douglas Stebila. Classical Authenticated Key Exchange and Quantum Cryptography. PhD thesis, University of Waterloo, 2009. EPRINT <http://hdl.handle.net/10012/4295>, URL <http://www.douglas.stebila.ca/research/papers/ste09/>.
- [23] Michel Abdalla, Olivier Chevassut, and David Pointcheval. One-time verifier-based encrypted key exchange. In Serge Vaudenay, editor, Public Key Cryptography (PKC) 2005, LNCS, volume 3386, pp. 47–64. Springer, 2005. DOI:10.1007/b105124. Full version available as [ACP05b].
- [24] Olivier Chevassut, Frank Siebenlist, and Mike Helm. Secure (one-time-) password authentication for the Globus toolkit. In GlobusWorld Conference, February 2005. URL <http://acs.lbl.gov/Projects/OPKeyX/Talks/GlobusWorld05/GlobusWorld05.html>.

Traffic Sign Recognition Using Convolution Neural Networks

S.Visalini

Assistant Professor, Dept. of ISE, The Oxford College of Engineering, Bangalore, Karnataka, India

ABSTRACT: Traffic signs have been designed to be easily readable for humans. For computer systems however, classifying traffic signs is still a challenging pattern recognition problem. Both image processing and machine learning algorithms are continuously refined to improve the recognition performance. A geo-coded traffic sign data set is constructed and used for training and testing the data for the recognition of the traffic signs. Instead of using handcrafted features such as HOG or SIFT which gives an accuracy around 75%, Convolutional Networks (ConvNets) use biologically-inspired multi-stage architectures that automatically learn hierarchies of invariant features. By applying ConvNets to the task, traffic sign classification becomes much easier and gives a better accuracy of about 85% - 95%. Using this recognition system, an application for the driver safety purpose is built. The application will keep the driver updated about the traffic signs which will lead in fewer to no mistakes while driving.

KEYWORDS: Traffic sign; Classification; Image detection, Convolutional Networks.

I. INTRODUCTION

Traffic signs or road signs are signs erected at the side of or above roads to give instructions or provide information to road users. The earliest signs were simple wooden or stone milestones. Later, signs with directional arms were introduced, for example, the fingerposts in the United Kingdom and their wooden counterparts in Saxony.

With traffic volumes increasing since the 1930s, many countries have adopted pictorial signs or otherwise simplified and standardized their signs to overcome language barriers, and enhance traffic safety. Such pictorial signs use symbols (often silhouettes) in place of words and are usually based on international protocols. Such signs were first developed in Europe, and have been adopted by most countries to varying degrees.

Road safety signs are primarily of three types:

1. **Mandatory Signs** - Mandatory signs are road signs which are used to set the obligations of all traffic which use a specific area of road. Unlike prohibitory or restrictive signs, mandatory signs tell traffic what it must do, rather than must not do. Most mandatory road signs are circular, may use white symbols on a blue background with white border or black symbols on a white background with a red border, although the latter is also associated with prohibitory signs.



Fig.1. Mandatory Signs

International Journal of Innovative Research in Computer and Communication Engineering

(An ISO 3297: 2007 Certified Organization)

Website: www.ijircce.com

Vol. 5, Issue 6, June 2017

2. **Cautionary Signs-** A warning sign is a type of traffic sign that indicates a hazard ahead on the road that may not be readily apparent to a driver. While designs vary, they usually take the shape of an equilateral triangle with a white background and thick red border.



Fig .2. Cautionary Signs

3. **Information Signs-** An information sign is a very legibly printed and very noticeable placard that informs people of the purpose of an object, or gives them instruction on the use of something. An example is a traffic sign such as a fuel pump.



Fig .3. Information Signs

The goals and objective of the project is to develop a method for traffic signs detection for vehicles that reduces the number of accidents while driving. This method will be developed as an automated software-hardware solution that will be supplied with the vehicle. To build a high performance traffic sign recognition system for Indian roads. Build dataset of Indian Traffic Road Signs. Build a classification system to recognize the road signs.

II. RELATED WORK

In [1]To design a good recognizer, many parameters should be taken into consideration. The recognizer should present a good discriminative power and low computational cost .It should be robust to the geometrical status of sign, such as the vertical or horizontal orientation, the size, and the position of the sign in the image. It should be robust to noise. The recognition should be carried out quickly if it is designed for real time applicationsIn [2]There are two main approaches in this field:Color-based approach allows reducing false positives results in the recognition process. These are based on segmentation by threshold in color space for image processing. andGreyscale methods concentrate on the geometry of the model to recognize it, color is used as a complementary technique to eliminate false positive results of classification. In [3]The images are pre-processed with several image processing techniques, such as, threshold techniques, Gaussian filter, Canny edge detection, Contour and Fit Ellipse. Then, the Neural Networks stages are performed to recognize the traffic for sign pattern. Objective is to reduce the search space and indicate only potential regions for increasing the efficiency and speed of the system. The traffic sign images are investigated to detect potential pixel regions which could be recognized.In [4]What makes CNNs such a good fit for working with image data?Their capacity can be controlled by varying their depth and breadth, and they also make strong and mostly correct assumptions about the nature of images (namely, stationary of statistics and locality of pixel dependencies). Thus, compared to standard feed forward neural networks with similarly-sized layers, CNNs have much fewer connections and parameters and so they are easier to train, while their theoretically-best performance is likely to be only slightly



International Journal of Innovative Research in Computer and Communication Engineering

(An ISO 3297: 2007 Certified Organization)

Website: www.ijircce.com

Vol. 5, Issue 6, June 2017

worse. This is a highly influential paper that kicked off a whole stream of work using deep convolutional neural networks for image processing. Two factors changed that made this possible: The availability of large enough datasets specifically, the introduction of ImageNet with millions of images, whereas the previous largest datasets had 'only' tens of thousands and The development of powerful enough GPUs to efficiently train large networks. In [5] For localization the classifier layers are replaced by a regression networks trained to predict bounding boxes at each spatial location and scale. The regression predictions are then combined, along with the classification results at each location. Training with multiple scales ensures predictions match correctly across scales, and exponentially increases the confidence of the merged predictions. Bounding boxes are combined based on the distance between their centres and the intersection of their areas, and the final prediction is made by taking the merged bounding boxes with maximum class scores. In [6] The use of ReLU activation "Deep convolutional neural networks with ReLUs train several times faster than their equivalents with tanh units Faster learning has a great influence on the performance of large models trained on large datasets" Using multiple GPUs (two!), and splitting the kernels between them with cross-GPU communication only in certain layers. The scheme reduces the top-1 and top-5 error rates by 1.7% and 1.2% respectively compared to a net with half as many kernels in each layer and trained on just one GPU. Using overlapping pooling. Let pooling layers be of size $z \times z$, and spaced s pixels apart. Traditionally pooling was used with $s = z$, so that there was no overlap between pools. Krizhevsky et al. used $s = 2$ and $z = 3$ to give overlapping pooling This reduced the top-1 and top-5 error rates by 0.4% and 0.3% respectively.

Traffic sign recognition has direct real-world applications such as driver assistance and safety, urban scene understanding, automated driving, or even sign monitoring for maintenance. It is a relatively constrained problem in the sense that signs are unique, rigid and intended to be clearly visible for drivers, and have little variability in appearance. Still, the dataset provided presents several difficult challenges due to real-world variability's such as viewpoint variations, lighting conditions (saturation, low-contrast), motion-blur, occlusions, sun glare, physical damage, colour fading, graffiti, stickers. Although signs are available in the training set, temporal information is not in the test set. The present project aims to build a robust recognizer without temporal evidence accumulation. Several existing approaches to road-sign recognition have used computationally-expensive sliding window approaches that solve the detection and classification problems simultaneously. But many recent systems in the literature separate these two steps. Detection is first handled with computationally-inexpensive, hand-crafted algorithms, such as colour thresholding. Classification is subsequently performed on detected candidates with more expensive, but more accurate, algorithms. Although the task at hand is solely classification, it is important to keep in mind the ultimate goal of detection while designing a classifier, in order to optimize for both accuracy and efficiency. Traffic Sign Recognition covers two problems: traffic sign detection (TSD) and traffic sign classification (TSC). The dataset is available only for Belgium and Germany. Mean accuracy built by A. de la Escalera, J. Ma Armingol, M. Mata "Traffic sign recognition and analysis for intelligent vehicles" using neural network system is 79.42%. This work does not use latest advances in the field of neural networks like convolutions.

Classification has been approached with a number of popular classification methods such as Neural Networks. Here we use the convolution neural network, The ConvNet. One advantage of ConvNets is that they can be run at very high speed on low-cost, small form-factor parallel hardware based on FPGAs or GPUs. Embedded systems based on FPGAs can run large ConvNets in real time, opening the possibility of performing multiple vision tasks simultaneously with a common infrastructure.

III. PROPOSED SYSTEM

Creating a dataset for Indian roads. The solution uses to propose recent advances in deep learning including convolution layers in addition to the feed forward neural network. Evaluate the performance of the system by considering additional signal like nearby detected signs. Building an application to demonstrate how this system can be used to improve driver safety.

- **User captured image:**

An image with traffic sign is captured by the user. The image must contain at least 1 traffic sign to be detected. The outcome of the image will also depend on the quality of the image. The better the resolution the better the accuracy.

International Journal of Innovative Research in Computer and Communication Engineering

(An ISO 3297: 2007 Certified Organization)

Website: www.ijircce.com

Vol. 5, Issue 6, June 2017

- **Traffic sign detection:**

The fed image is processed and searched for the traffic signs. The parameter checked are round, triangle, square, pentagonal, octagonal shapes with red, blue or yellow color surrounding it. A bounding box is put around the traffic sign.

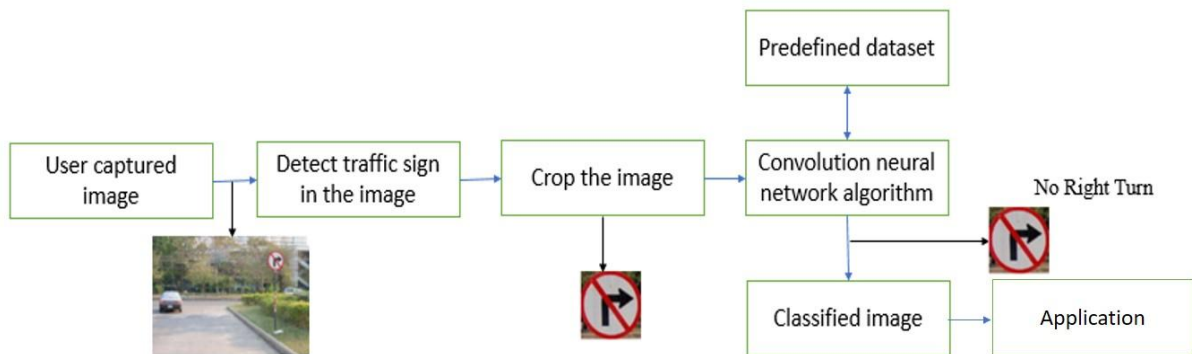


Fig .4. System Architecture Diagram

- **Crop image:**

Once the sign is detected then that image is cropped. The image within the bounding box is kept and the rest is discarded. That will help in the recognition process only to focus on the traffic sign.

- **Convolution neural network:**

A biologically-inspired, multilayer feed-forward architecture that can learn multiple stages of invariant features. Each stage is composed of a (convolutional) filter bank layer, a non-linear transform layer, and a spatial feature pooling layer. The spatial

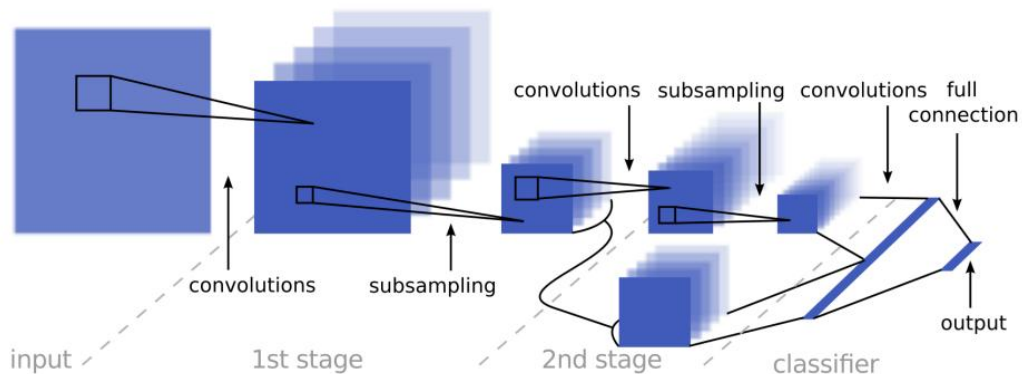


Fig . 5. Convolution Neural Network Architecture

pooling layers lower the spatial resolution of the representation, thereby making the representation robust to small shifts and geometric distortions, similarly to “complex cells” in standard models of the visual cortex. ConvNets are generally composed of one to three stages, capped by a classifier composed of one or two additional layers.

International Journal of Innovative Research in Computer and Communication Engineering

(An ISO 3297: 2007 Certified Organization)

Website: www.ijirccce.com

Vol. 5, Issue 6, June 2017

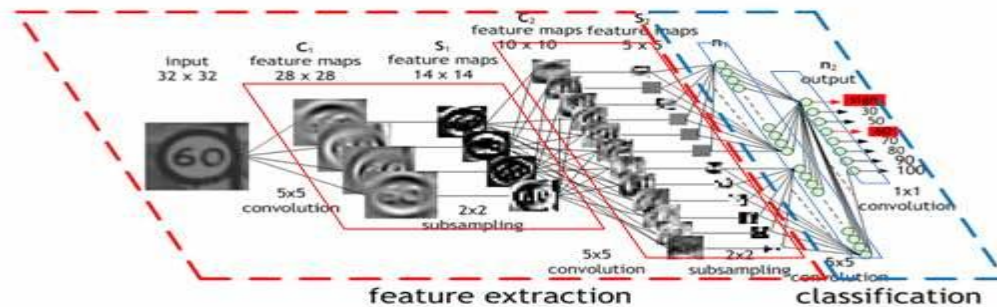


Fig .6. CNN feature extractor for Traffic Sign Classification

A gradient-based supervised training procedure updates every single filter in every filter bank in every layer so as to minimize a loss function.

- **Classified image:**

The image comes out of the classifier as a labelled traffic sign, the confidence score.

- **Predefined dataset:**

Traffic sign images are cropped and labelled which will be used for training the dataset.

- **Application:**

Using this traffic sign recognition system, an application is built to demonstrate improved driver safety. The application keeps the driver updated about the traffic signs and violations. This will reduce accidents due to human error.

IV. PSEUDO CODE

I) Dataset collection

Input: The recognition task requires a set of images with various traffic signs for classification.

Step 1: These images are obtained by taking pictures of traffic signs with geolocation using an android app developed for this purpose.

Step 2: The app monitors changes in geolocation and uses this information when a picture is taken. This information is written into a CSV file which is then downloaded to a common machine for aggregation and processing.

II) Image detection/processing:

Input: The captured and geocoded images are available in separate CSV files originating from separate instances of the app.

Step 1: A program merges all this data into a single dataset making it ready for processing.

Step 2: Before the images can be fed into a classifier, the following tasks must be carried out:

- The traffic signs in the image must be identified and a bounding box has to be marked around the signs
- The sign has to be extracted, labelled, for use as training data in the classifier

The size of the bounded area must be uniform across the dataset

Step 3: A web tool loads each image from the dataset onto a web page and the bounding box is marked. This information is added back into the dataset.

Step 4: The type of sign is also labelled.

Step 5: A script then crops all the bounding boxes and resizes them into a 30px * 30px image ready for the classification

International Journal of Innovative Research in Computer and Communication Engineering

(An ISO 3297: 2007 Certified Organization)

Website: www.ijirccce.com

Vol. 5, Issue 6, June 2017

V. SIMULATION RESULTS

The proposed Traffic sign recognition using Convolutional neural network and Screenshot for Driver Assistance Application are as shown in fig.7.

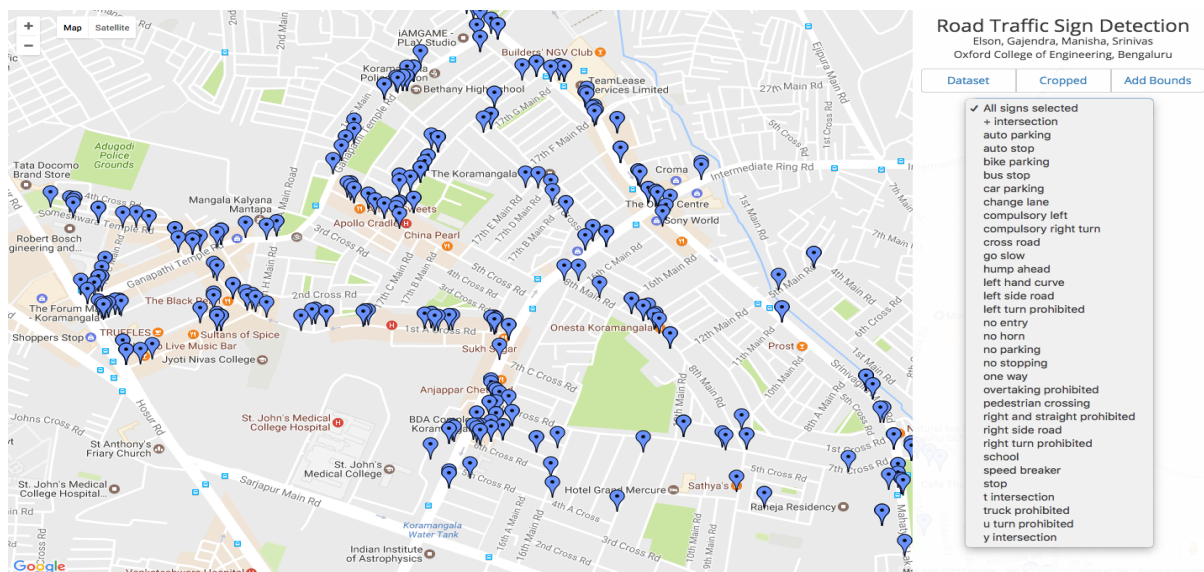


Fig.7.Screenshot for Driver Assistance Application

This web application will have a preloaded data set. Here we have collected traffic signs of 2 locations in Bangalore (HSR layout, Koramangala) and have loaded it in the map with its geo location. All the different signs are categorised into different groups (as shown on the right corner).

You can select a particular traffic sign. Here we have selected pedestrian crossing, only the pedestrian crossing tags in that area are shown and the rest are blurred.

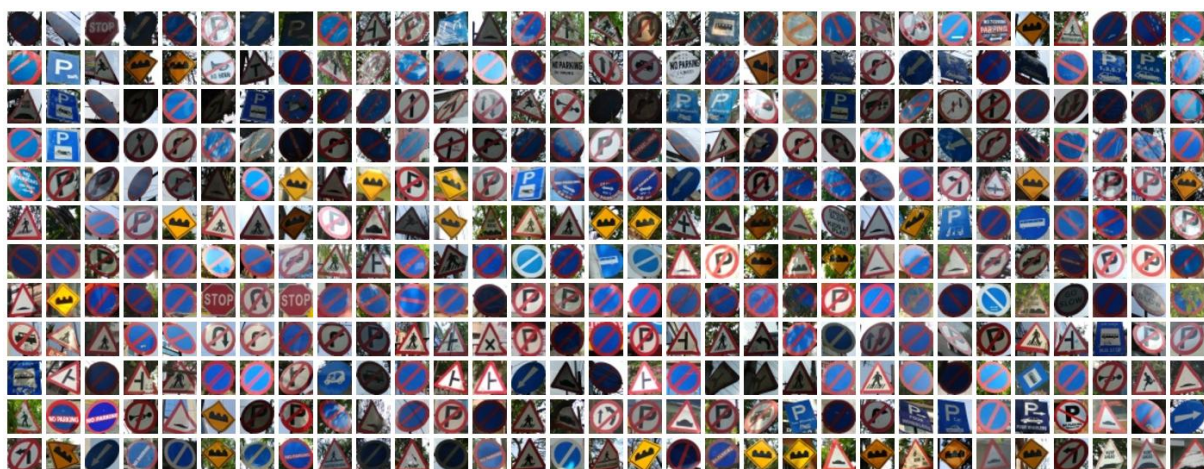


Fig.8.The dataset of the traffic sign

The dataset of the traffic sign is shown in fig.8., which was collected and cropped for the recognition purpose. Each of the image is cropped and resized to 32*32 p. We collected over 500 pictures in these 2 locations.

International Journal of Innovative Research in Computer and Communication Engineering

(An ISO 3297: 2007 Certified Organization)

Website: www.ijirccce.com

Vol. 5, Issue 6, June 2017

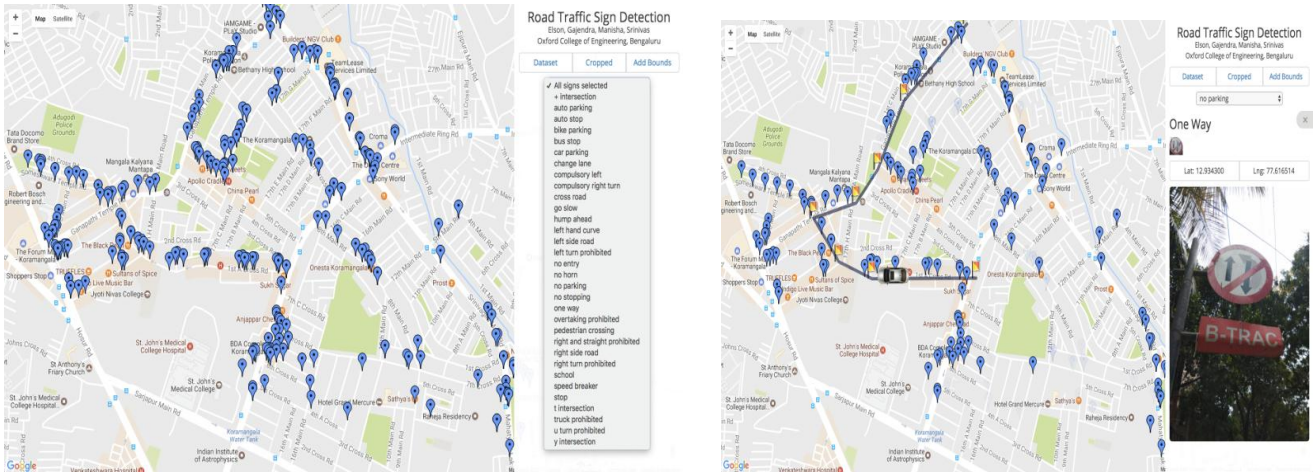


Fig .9. Screenshot for Driver Assistance Application for No parking

While conducting a simulation we need to give a start and a end location to a car, as the car moves in the given path the nearby traffic sign pops up. If there is any warning sign (hump ahead, school, pedestrian crossing etc,..) a pop up is shown on the right corner which gives a warning saying ‘go slow’ the pop up remains for 5 sec, every half a sec the color given to the pop up fades out and the end of the 5th sec it vanishes. when the car reaches the end location, if there is any no parking sign nearby it gives an alert saying ‘No parking here’ by which its understood for the driver not to park in that location. The Simulated graph for accuracy and Loss are shown in fig.10. and fig.11.

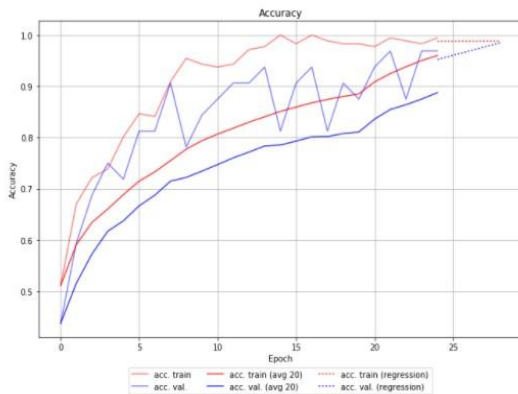


Fig .10. Accuracy for the Recognition

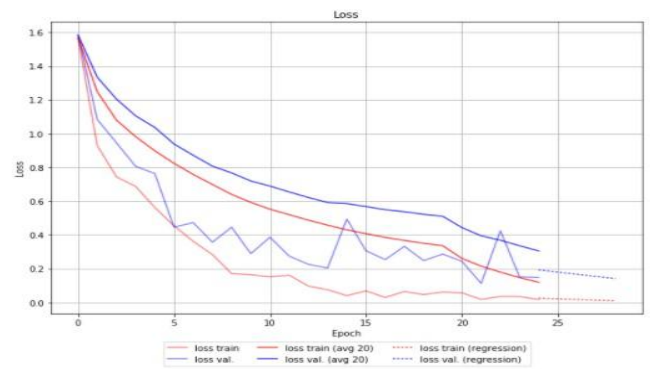


Fig .10. Loss/Error rate of the Recognition

VI. CONCLUSION AND FUTURE WORK

By applying ConvNets to the task, traffic sign classification becomes much easier and gives a better accuracy of about 85% - 95%. Using this recognition system, an application for the driver safety purpose is built. The application will keep the driver updated about the traffic signs for better driving assistance and safety. In future the driver assistance system can be used on cars to work according to the traffic signs and the recognition system can be used on self driving cars to learn and understand the traffic signs.



International Journal of Innovative Research in Computer and Communication Engineering

(An ISO 3297: 2007 Certified Organization)

Website: www.ijirccce.com

Vol. 5, Issue 6, June 2017

REFERENCES

1. Hasan FLEYEH1, Mark Dougherty, "Road And Traffic Sign Detection And Recognition", IEEE traffic sign recognition. Vol. 2 , pg:322-342, Aug 2016.
2. Auranuch Lorsakul, Jackrit Suthakorn, "Traffic Road Sign Detection And Recognition For Automotive Vehicles", IEEE NOMS 2014, vol. 13, Jun 2016.
3. Auranuch LorsakulTh, Jackrit Suthakorn "Traffic Sign Recognition for Intelligent Vehicle/Driver Assistance System Using Neural Network on OpenCV", IEEE URAI vol:12, pg:566-899, 2015
4. Lin et al., Krizhevsky et al., "ImageNet classification with deep convolutional neural networks", 2015.
5. Ralph D, Kim Bane, "Localization and detection in image processing", vol:5, pg:654-687, 2015
6. Goodfellow et al, "Maxout networks ", pg:345-356., 2014.
7. Sermanent et al, "overFeat: Integration using convolution networks", 2014
8. Christopher Rodrigues, "classification with Deep Convolution Neural Network", vol:10, 2011
9. L. Fletcher, N. Apostoloff, L. Petersson, and A. Zelinsky, "vision in and out of vehicles", IEEE Intell. Syst., Vol.18, no.3, pp.12-17, May/Jun. 2003
10. S. Lafuente-Arroyo, P. Gil-Jimenez, R. Maldonado-Bascon, F. Lopez-Ferreras and s. Maldonado-Bascon, "Traffic Sign shape classification evaluation I: SVM using distance to borders", in Proc, IEEE Intell. Veh. symp., Las Vegas, NV, , pp.557-562, June 2005
11. J. Miura, T. Kanda and Y. Shirai, "An active vision system for real-time traffic sign recognition", in proc. IEEE Intell. Transp. Sys., pp 52-57, Oct. 2000
12. A. de la Escalera, L. E. Moreno, M. A. Salichs and J. M. Armingol, "Road traffic sign detection and classification", IEEE trans. Ind. Electron., Vol.44, no.6, pp.848-859, Dec. 1997

BIOGRAPHY



S. Visalini has done her B.E in computer science from Adhiparasakthi Engineering college Affiliated to Anna University, M.E from RajaLakshmi Engineering College Affiliated to Anna University. She is currently working as the Assistant Professor in ISE Department of The Oxford College Of Engineering. She has presented a paper on Indoor location sensing using Bluetooth Technology in Journal of Engineering and IT Springer publications. She is guiding the M.Tech students in Network Engineering. She has around 9 years of teaching experience in leading educational Institutions in India. She has attended/conducted National and International level workshops, seminars and conferences.



Download PDF

[Download full issue](#)

Optik

Volume 127, Issue 6, March 2016, Pages 3480-3483

Lab-on-chip based optical biosensors for the application of dental fluorosis

D.L. Girijamba ^a, Preeta Sharan ^b, P.C. Srikanth ^c [Show more](#) [Outline](#) | [Share](#) [Cite](#) <https://doi.org/10.1016/j.ijleo.2015.12.113>[Get rights and content](#)

Abstract

Optical biosensors are powerful detection and analysis tool that has vast applications in biomedical research, healthcare, pharmaceuticals, environmental monitoring, and the battlefield. Biosensors consist of a biological entity that can be an enzyme, antibody, or nucleic acid that interacts with an analyte and produces the signal that is measured electronically. A variety of substances including nucleic acids, proteins (particularly antibodies and enzymes), lectins (plant proteins that bind sugar moieties) and complex materials (organelles, tissue slices, microorganism), can be used as the biological components. Fluoride content in drinkable groundwater directly affects the quality of drinking water. In this paper we have demonstrated a 2-dimensional photonic crystal based biosensor with line defect which can detect different fluorides in water. Simulation and analysis has been done for calcium fluoride, cesium fluoride, potassium fluoride, lithium fluoride and strontium fluoride and peak has been observed. One such major detection is to detect dental fluorosis caused by the fluorides present in water. Finite Difference Time Domain (FDTD) method has been used for the analysis. MEEP is Maxwell's Electromagnetic Equation Propagation simulation tool. The application of FDTD method is computation of transmission spectrum. MEEP is simulation package for the computation of transmission/reflection spectra, field patterns, resonant modes & frequencies in dielectric structures.

[< Previous](#)[Next >](#)

Keywords

PBG fluorosis

1. Introduction

Dental fluorosis is a alteration in the advent of the tooth's enamel. These variations can vary from hardlyperceptible white spots in mild forms to staining and pitting in the more severe forms. Dental fluorosis only occurs when younger children devour too much fluoride, from any source, over long periods when teeth are evolving under the gums. The advantageous effects of fluoride on dental caries are due predominantly to the topical effect of fluoride after the teeth have vented in the oral cavity. Biosensors function by coupling a biological sensing element with a detector system using a transducer [1] and biosensor for living cell [2]. Optical biosensors are powerful detection and analysis tool that has vast applications in biomedical research, healthcare, pharmaceuticals, environmental monitoring, and the battlefield [3]. Fluoride is a naturally occurring compound derived from fluorine, the 13th most abundant element on Earth. The basics of knowledge of Fluoride and Causes of fluoride in drinking water [4].

The organic bio molecules get excited from lower energy state to higher energy state, when optical beam is incident and lose their energy in the form of photons and relax to the ground state [5]. Maxwell's Curl equations are expanded in rectangular Coordinate

[Home](#) > [Methodology](#) > [TDS](#)Article [PDF Available](#)

Application of machine learning for real-time evaluation of salinity (or TDS) in drinking water using photonic sensors

September 2016 · [Drinking Water Engineering and Science](#) 9(2):37-45

DOI:10.5194/dwes-9-37-2016

Authors:

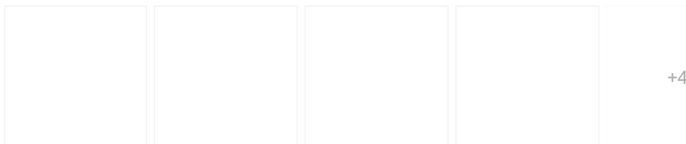
**Sandip Kumar Roy****Dr preeta Sharan**

The Oxford Educational Institutions

[Download full-text PDF](#)[Read full-text](#)[Download citation](#)[Copy link](#)[Citations \(4\)](#)[References \(27\)](#)[Figures \(9\)](#)

Abstract and Figures

The world is facing an unprecedented problem in safeguarding 0.4% of potable water, which is gradually depleting day-by-day. From a literature survey it has been observed that the refractive index (RI) of water changes with a change in salinity or total dissolved solids (TDS). In this paper we have proposed an automatic system that can be used for real-time evaluation of salinity or TDS in drinking water. A photonic crystal (PhC) based ring resonator sensor has been designed and simulated using the MEEP (MIT Electromagnetic Equation Propagation) tool and the finite difference time domain (FDTD) algorithm. The modelled and designed sensor is highly sensitive to the changes in the RI of a water sample. This work includes a real-time-based natural sequence follower, which is a machine learning algorithm of the naive Bayesian type, a sequence of statistical algorithms implemented in MATLAB with reference to training data to analyse the sample water. Further interfacing has been done using the Raspberry Pi device to provide an easy display to show the result of water analysis. The main advantage of the designed sensor with an interface is to check whether the salinity or TDS in drinking water is less than 1000?ppm or not. If it is greater than or equal to 2000?ppm, the display shows ?High Salinity/TDS Observed?, and if ppm are less than or equal to 1000?ppm, then the display shows ?Low salinity/TDS Observed?. The proposed sensor is highly sensitive and it can detect changes in TDS level because of the influence of any dissolved substance in water.



Evaluation of . Shows variation Design of the Salinity vs. RI of Transmitted salinity/TDS in... of RI with % of... two-dimensiona...water. The figur... spectrum for (a)...

Figures - available via license: [Creative Commons Attribution 3.0 Unported](#)

Content may be subject to copyright.

Discover the world's research

- 20+ million members
- 135+ million publications
- 700k+ research projects [Join for free](#)

[Public Full-text](#) (1)

Available via license: [CC BY 3.0](#)
Content may be subject to copyright.

Drink. Water Eng. Sci., 9, 37–45, 2016
www.drink-water-eng-sci.net/9/37/2016/
doi:10.5194/dwes-9-37-2016
© Author(s) 2016. CC Attribution 3.0 License.

Home > Mathematical Sciences > Dynamical Systems > Discrete Dynamical Systems > Cellular Automata

Article [PDF Available](#)

A novel quantum dot cellular automata for 4-bit code converters

January 2016 · *Optik - International Journal for Light and Electron Optics* 127(10)

DOI:10.1016/j.ijleo.2015.12.119

Project: [Currently Working on Surface Plasmonic Resonance based Optical Sensor](#)

Authors:



Nandini Rao
Dayananda Sagar Institutions



Srikanth P C
Malnad College of Engineering



Dr preeta Sharan
The Oxford Educational Institutions

[Download full-text PDF](#)

[Read full-text](#)

[Download citation](#)

[Copy link](#)



[Citations \(24\)](#) [References \(10\)](#) [Figures \(6\)](#)

Abstract and Figures

Quantum-dot cellular automata is a promising successor of CMOS technology. QCA proposed by Lent et al. is an emerging technology that offers an innovative approach for computing at nano-scale by monitoring the position of a single electron. This technology allows the implementation of logic devices using quantum dots instead of transistors, diodes. QCA technology has large potential in terms of high space density and power, possible to achieve miniaturization of circuits and high speed processing. The paper provides an efficient design and layout of code converters based on quantum-dot cellular automata using QCADesigner tool. In this paper a number of new results on binary to gray and gray to binary code converters and detailed simulation using QCAD designer tool is presented. We have performed a comparative study of proposed design with recent previous designs and proved that proposed design is efficient in terms of complexity, cell count, area usage and clocking.

Discover the world's research

- 20+ million members
- 135+ million publications
- 700k+ research projects [Join for free](#)



+1

QCA clock zones Layouts of AND XOR gate (a) QCA layout of (a) Layout of and QCA clock... gate and OR... graphical symb... XOR gate and (...binary to gray...

Figures - uploaded by [Dr preeta Sharan](#) Author content
Content may be subject to copyright.

[Public Full-text](#) (1)

Content uploaded by [Dr preeta Sharan](#) Author content
Content may be subject to copyright.

[Optik127 \(2016\) 4246–4249](#)

Contents lists available at [ScienceDirect](#)

Optik

journal homepage: www.elsevier.de/ijleo

A Novel Image Compression Using Block Local Binary Pattern (LBP) with LZW

Ramya.P.Reddy¹, Chrispin.Jiji²

Student, Department of ECE, TOCE, Bengaluru, India¹

Asst. Prof. Department of ECE, TOCE, Bengaluru, India²

Abstract: Image compression is aimed at reducing the data quantity, without degrading the image Quality beyond an acceptable threshold. The main advantage of LBP is it can give local texture pattern in an efficient manner. In this LBP values are used for the image compression. The description of image's local pattern results in an eight-bit binary description, but in order to restore the image from such a LBP description, the value of each central pixel is also needed. LZW coding which is simple and lossless technique is used for the LBP data compression. Finally result analysis is made based on performance parameters PSNR, MSE, SSIM.

Keywords: local binary pattern, local texture classification, Lempel-Ziv-Welch (LZW).

I. INTRODUCTION

In recent years, the development and demand of multimedia product grows increasingly fast, contributing to insufficient bandwidth of network and storage of memory device. Therefore, the theory of data compression becomes more and more significant for reducing the data redundancy to save more hardware space and transmission bandwidth. In computer science and information theory, data compression or source coding is the process of encoding information using fewer bits or other information bearing units than an unencoded representation. Compression is useful because it helps reduce the consumption of expensive resources such as hard disk space or transmission bandwidth. Nowadays, an amazing amount of data is generated every minute, e.g. (1) Google will receive 2 million search requests (2) facebook users upload and share more than 6,94,000 pieces of content (3) more than 184.8 billion e-mails are sent and received during a day. From above examples it is understood that image compression is important for many purposes. The Internet population globally has grown 6.59 percent from 2010 to 2011 and now it is all most 2.1 billion people, are using it to communicate, share, or store information. Mainly photos and videos occupy most of the space, with more than 8,000 photos shared each minute, e.g. Instagram share 3,600 new photos. Because of the explosively increasing information of image and video in various storage devices and Internet, the image and video compression technique becomes more and more important. Considering an average of 20MB/photo and a compression rate of 0.15, the predicted quantity of archived information is about 550 billion, 20MB i.e.73 bytes. In this project new method of image compression using LBP is proposed, this will saves more space when compared to the existing compression algorithms.

II. THEORETICAL ASPECTS

A. LOCAL BINARY PATTERN

The concept of Local Binary Pattern (LBP) was introduced by Ojala [1] as a fine texture scale descriptor, used to summarize the local structure of images. LBP

labels the image pixels and creates a binary number used for classification in computer vision This method takes each pixel and compares it with its neighbour's colour value. LBP is tolerant to monotonic illumination changes, an important advantage being its computational simplicity, therefore making possible real-time analysis. The LBP description is created by dividing the image into small 3x3 pixel matrices. The colour value of each central pixel is then compared with its eight neighbours whether these neighbour colour values are greater or less than the central point and a binary value is accordingly assigned to the corresponding bit. The algorithm is applied on a 3x3 neighbourhood, so for each central point there are eight neighbours, leading to an eight-bit value and a subsequent distinct label.

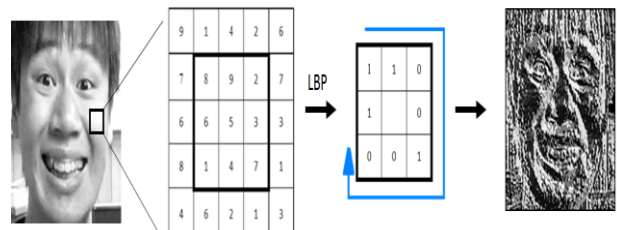


Fig.1 shows the local binary pattern for Small portion considering (3x3) block and its binary values.

B. Lempel-Ziv-Welch (LZW)

LZW is dictionary based algorithm, which is lossless in nature. This method was developed originally by Ziv and Lempel, and subsequently improved by Welch. As the message to be encoded is processed, the LZW algorithm builds a string table that maps symbol sequences to/from an N-bit index. The string table has 2N entries and the transmitted code can be used at the decoder as an index into the string table to retrieve the corresponding original symbol sequence. The sequences stored in the table can be arbitrarily long. A particular LZW compression algorithm takes each input sequence of bits of a given length (for example, 13 bits) and creates an entry in a table

(sometimes called a "dictionary" or "codebook") for that particular bit pattern, consisting of the pattern itself and a shorter code.

III. BLOCK DIAGRAM

1. The original image can be grey image or colour image if it is greyscale image then no operation is performed, if suppose it is colour a image is divided into R,G,B pixels separately and converts into bitmap image.

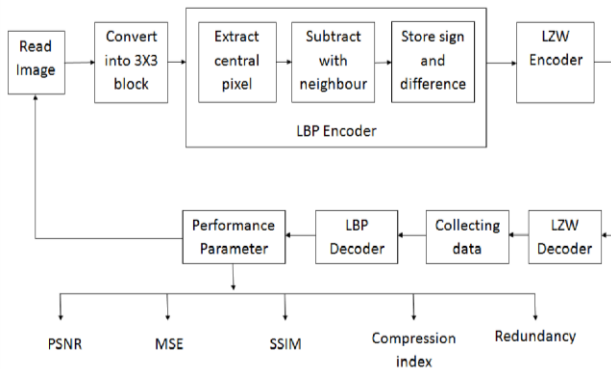


Fig. 2Block diagram of proposed system

2. From original image, two smaller images are created: one made of LBP codes and other containing the values for neighbourhood's centre pixels.
3. Pixels greyscale image is divided into 3*3 matrices. If it does not divide into image width or height, the borders matrices are filled in with random value 0's.
4. For every 3*3 matrix, the LBP code is calculated for every central grey value in each neighbourhood and results in eight-bit binary code.
5. Eight-bit pattern obtained based on conditions:
 - a) The value is "1" if pixel value is equal or greater than central pixel.
 - b) The value is "0" if pixel is less than central pixel.
6. Then its stores the value o central pixels, difference and the sign (i.e binary value).
7. Further LZW encoding algorithm is used to reduce the size of image.
8. Reconstruction can be done by decoding using LZW decoding algorithm. Further data regarding central pixel, sign and differences are collected and LBP decoder is used to retrieve the original information.
9. Finally the performance of original image with proposed model is examined.

IV. RELATED WORK ON IMAGE COMPRESSION

Image compression is a method of reducing the data quantity, without degrading the image quality beyond an acceptable threshold. This can be done by removing the redundancy present in the image. In information theory, data compression is the process of encoding information using fewer bits than the encoded representation, with the advantage of reducing the consumption of significant resources such as disk space or transmission bandwidth. Compression of an image requires storing the image in a bit flow/stream which is in binary 0's and 1's as compact as possible and decoding the image as accurately as

possible. The needed elements are an encoder and a decoder. The encoder receives the image and converts it into a series of binary data which are then transmitted or stored. The decoder re-creates the image as accurately as possible. The flow compression is described in Fig. 3.

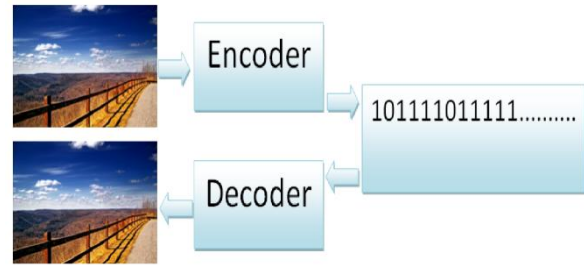


Fig.3 flow of image compression

Types of compression

- a. Lossy compression
- b. Lossless compression.

a. Lossy compression: It is a technique in which reconstructed image is not same as that of original image. It is irreversible process.
Eg. JPEG, MPEG.

b. Lossless compression: It is a technique in which reconstructed image is same as that of original image. It is reversible process.
Eg. LZW, Huffman coding

The important properties of a compression algorithm are the compression ratio and the reconstruction quality. The compression ratio is the report of bits numbers needed to represent the data before and after compression.

V. PROPOSED MODEL

The main aim of compression is not to degrade the image quality performance but can decrease the data quantity. In this paper the original image can be colour or grey scale image .If the image is colour then it is converted into grey scale image before applying it to LBP encoder.fig.4 shows the colour image and its grey scale.

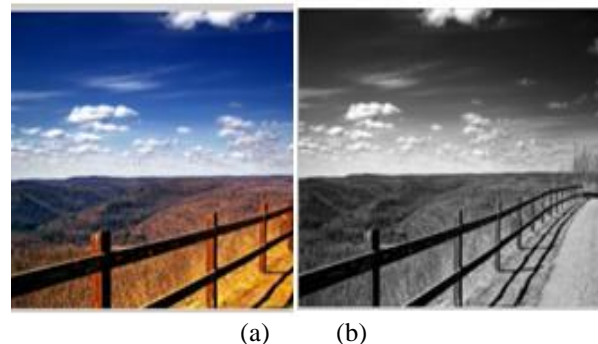


Fig 4 : image (a) shows colour image (174kb),image(b) shows grey scale image(174kb).

After converting the image to grey scale, the image is resized to 600*600 to make out blocks easily, then LBP encoding process is carried out where the image is divided into 3*3 blocks and for each block the central pixel value is obtained and their neighbouring pixel values and

difference is calculated and stored. The fig.5 shows the output of LBP encoder. As the LZW algorithm is dictionary based system it converts decimal value to ASCII values to encode the pixel values.

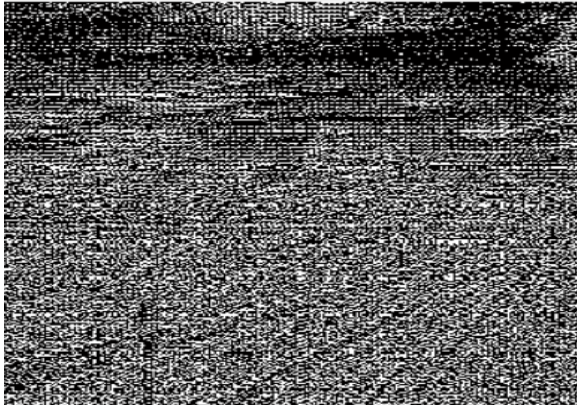


Fig 5 Output of LBP encoder

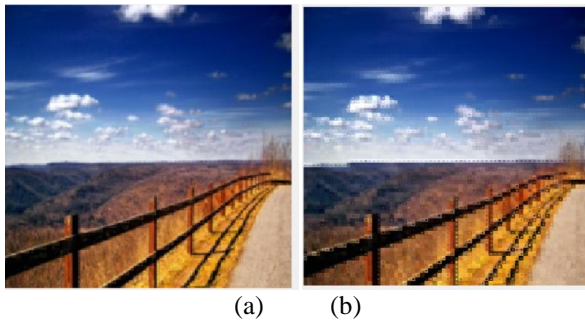


Fig.6 (a) reconstructed image based on 17% uniform distribution. (b) reconstructed image based on 17% of Gaussian distribution.

VI. EXPERIMENTAL RESULTS

The proposed method is implemented and analysis is done in MATLAB. The results are illustrated using different images shown in Fig 7. (a) Portrait image (b) ultrasound medical image

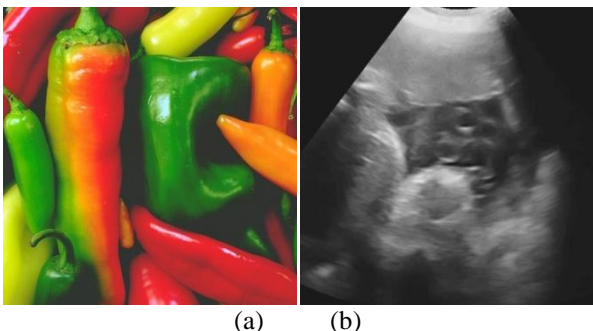


Fig 7 Shows test images taken to compare the performance

For testing purpose the reconstruction was performed on each image using four different percentage values for dispersion [8]. The uniform and Gaussian distribution are considered more the percentage of dispersion more is the pixel variation. Table I summarizes the results.

However, results proved that the lower the percentage, the

better the accuracy and similarity between images. An important advantage of the approach is the compression rate, especially when considered in the context of good SSIM values. Table II shows a comparison between the original image and compressed image. PSNR is the peak signal to noise ratio which should be more. MSE is the mean square error should be less. The compression ratio is original image to compressed image

TABLE I QUALITY OF RECONSTRUCTION OF IMAGES WITH STRUCTURAL SIMILARITY INDEX METRIC (SSIM)

| Fig 7 | Distribution | Limits of dispersion around central pixel | | | |
|-------|--------------|---|---------|---------|---------|
| | | 17% | 9% | 6% | 2% |
| (a) | Uniform | 0.92457 | 0.87229 | 0.81673 | 0.4834 |
| | Gaussian | 0.82878 | 0.77649 | 0.72094 | 0.3876 |
| (b) | Uniform | 0.92851 | 0.87622 | 0.82067 | 0.48733 |
| | Gaussian | 0.84814 | 0.79585 | 0.7403 | 0.40697 |

TABLE II COMPRESSION PERFORMANCE COMPARISON BETWEEN ORIGINAL IMAGE (Kb) AND COMPRESSED IMAGE (Kb)

| Test Image Fig 7 | Size of Original Image(Kb) | Size of Compressed Image(Kb) | Compression Ratio | Redundancy | SSIM | PSNR | MSE |
|------------------|----------------------------|------------------------------|-------------------|------------|---------|---------|---------|
| (a) | 139.477 | 32.411 | 4.3034 | 0.76762 | 0.92457 | 35.3852 | 18.9653 |
| (b) | 147.889 | 24.992 | 5.9175 | 0.83101 | 0.92851 | 39.1205 | 8.0248 |

VII. CONCLUSION

The public internet is a world-wide computer network through which images are sent, received and stored on hard disk or database. The main aim is to reduce the bandwidth and to maintain image quality. The multimedia technology is also developing rapidly. In the recent years, images has been widely used in day-to-day life such as, in financial records, military purpose, medical images, archaeological field. Hence the promising approach is image compression and also requires easy reliable restoration and retrieval. Therefore this paper presents the image compression using local binary pattern technique with LZW algorithm. The drawback can be information losses. SSIM is used to evaluate the quality of restoring i.e. upto 0.92. Apart from this in this proposed algorithm the performance of proposed system's PSNR, MSE, redundancy and compression index values are evaluated with original images it shows proposed method as better reliability and retrieval quality.

REFERENCES

- [1] T. Ojala, M. Pietikäinen, and D. Harwood, "A comparative study of texture measures with classification based on feature distributions", *Pattern Recognition*, vol. 19, no. 3, pp. 51-59, 1996.
- [2] D. Huang, C. Shan, M. Ardabilian, Y. Wang and L. M. Chen, "Local Binary Patterns and Its Application to Facial Image Analysis: A Survey", *IEEE Trans. on Systems*, vol. 41, pp. 765-781, 2011.
- [3] B. Da and N. Sang, "Local binary pattern based face recognition by estimation of facial distinctive information distribution", *Opt. Eng.*, vol. 48, no. 11, 2009.
- [4] T. Pajdla and J. Matas, "Face Recognition with local binary patterns", *ECCV 2004, LNCS 3021*, pp. 469-481, 2004.
- [5] L. Nanni, A. Lumini, and S. Brahmam, "Local binary patterns variants as texture descriptors for medical image analysis." *Artificial Intelligence in Medicine*, vol. 49, no. 2, pp. 117-125, 2010.
- [6] O. Ghita, D. Ilea, A. Fernandez and P. Whelan, "Local binary patterns versus signal processing texture analysis: a study from a performance evaluation perspective", *Sensor Review*, vol. 32, pp. 149 – 162, 2012.
- [7] Z. Wang and A. C. Bovik, "Mean squared error: love it or leave it? - A new look at signal fidelity measures", *IEEE Signal Processing Magazine*, vol. 26, no. 1, pp. 98-117, 2009.
- [8] Wang, E. P. Simoncelli, and A. C. Bovik, "Multi-scale structural similarity for image quality assessment", in *Proc. IEEE Asilomar Conf. Signals, Systems, Comput., Asilomar, CA*, vol. 2, pp. 1398-1402, Nov. 2003.
- [9] N. Khayati, W. Lejouad-Chaari and S. Sevestre-Ghalila, "A distributed image processing support system application to medical imaging", *Imaging Systems and Techniques, IST 2008*, pp. 261-264, 2008.

Research Article

Optimization of Crude Oil and PAHs Degradation by *Stenotrophomonas rhizophila* KX082814 Strain through Response Surface Methodology Using Box-Behnken Design

Praveen Kumar Siddalingappa Virupakshappa, Manjunatha Bukkambudhi Krishnaswamy, Gaurav Mishra, and Mohammed Ameenuddin Mehkri

Department of Biotechnology, The Oxford College of Engineering, Bengaluru 560068, India

Correspondence should be addressed to Manjunatha Bukkambudhi Krishnaswamy; professorbkm@gmail.com

Received 22 June 2016; Revised 27 September 2016; Accepted 13 October 2016

Academic Editor: Felipe Garcia-Rodriguez

Copyright © 2016 Praveen Kumar Siddalingappa Virupakshappa et al. This is an open access article distributed under the Creative Commons Attribution License, which permits unrestricted use, distribution, and reproduction in any medium, provided the original work is properly cited.

The present paper describes the process optimization study for crude oil degradation which is a continuation of our earlier work on hydrocarbon degradation study of the isolate *Stenotrophomonas rhizophila* (PM-1) with GenBank accession number KX082814. Response Surface Methodology with Box-Behnken Design was used to optimize the process wherein temperature, pH, salinity, and inoculum size (at three levels) were used as independent variables and Total Petroleum Hydrocarbon, Biological Oxygen Demand, and Chemical Oxygen Demand of crude oil and PAHs as dependent variables (response). The statistical analysis, via ANOVA, showed coefficient of determination R^2 as 0.7678 with statistically significant P value 0.0163 fitting in second-order quadratic regression model for crude oil removal. The predicted optimum parameters, namely, temperature, pH, salinity, and inoculum size, were found to be 32.5°C, 9, 12.5, and 12.5 mL, respectively. At this optimum condition, the observed and predicted PAHs and crude oil removal were found to be 71.82% and 79.53% in validation experiments, respectively. The % TPH results correlate with GC/MS studies, BOD, COD, and TPC. The validation of numerical optimization was done through GC/MS studies and % removal of crude oil.

1. Introduction

Bioremediation is an ecologically acceptable technology that employs the use of microorganisms to efficiently degrade pollutants [1]. The strain *Stenotrophomonas rhizophila* (PM-1) showed potential crude oil and PAHs degrading ability in our earlier report [2]. In the present study, an attempt has been made to optimize the process of bioremediation through Response Surface Methodology (RSM), which is a reliable and powerful tool for modelling and optimization of bioremediation processes [1].

In RSM, the Box-Behnken Design is having the maximum efficiency for an experiment involving three factors and three levels; further, the number of experiments conducted for this is much less compared to a central composite design. Box-Behnken Designs always have three levels for each factor and are purpose built to fit a quadratic model [3, 4]. The

Box-Behnken Design does not have runs at the extreme combinations of all the factors but compensates by having better prediction precision in the centre of the factor space. While a run or two can be botched in these designs the accuracy of the observations in the remaining runs is critical to the dependability of the model. Categorical factors can be added to these designs; however, the design is duplicated for every categorical treatment combination. It is well established that, in biological treatment processes, various operational parameters such as the level of temperature, salinity concentration, inoculum size, and pH directly influence the bacterial degradation performance of PAHs and crude oil [5]. Thus, to make the process more efficient, faster, and practically applicable, studies on the effect of each factor on the bacterial degradation of PAHs and crude oil appear essential [6]. Hence in this context, the present study was designed with an attempt to optimize cultural (pH, temperature, dose of

TABLE 1: Experimental range and the variables showing the limiting factors.

| Name | Unit | Type | Low | High |
|-----------------------------------|------|----------|-----|------|
| Temperature | °C | Factor | 25 | 40 |
| pH | | Factor | 5 | 11 |
| Salinity | | Factor | 5 | 20 |
| Inoculum size | ml | Factor | 5 | 20 |
| Total Petroleum Hydrocarbon (TPH) | % | Response | | |
| Biological Oxygen Demand (BOD) | mg/L | Response | | |
| Chemical Oxygen Demand (COD) | mg/L | Response | | |

inoculum, and salinity concentration) factors using conventional (one-factor-at-a-time) and statistical Response Surface Methodologies (RSMs) for degradation of crude oil and PAHs by the strain *Stenotrophomonas rhizophila* PM-1.

The present work discusses the use of Box-Behnken Design approach to plan the experiments for crude oil degradation with an overall objective of optimizing the process to degrade the crude oil.

2. Materials and Method

2.1. Soil Sampling and Isolation of Bacteria. The soil samples were collected from different localities of Western Ghats of Karnataka State, covering the oil spilled areas and the hydrocarbon degrading bacteria were isolated using R₂A media followed by serial dilution using standard protocols.

2.2. Preliminary Degradation Studies, PAHs, and Crude Oil Utilization Studies. The preliminary degradation was studied using redox indicator 2,6-dichlorophenolindophenol (DCPIP) [7]. The 2% PAHs and crude oil utilization by the bacterial isolate using Bacto Bushnell Hass broth was studied using decanol, hexadecane, toluene, dodecane, engine oil, benzene, octane, oleic acid, and naphthalene as sole carbon source and checked for utilization.

2.3. Experimental Design. The Box-Behnken factorial experimental design had employed four independent variables, namely, temperature (25, 30, 35, and 40°C), pH (5, 7, 9, and 11), salinity (5, 10, 15, and 20), and inoculum size (5, 10, 15, and 20 ml) as mentioned in Table 1. Each of the independent variables was studied at three levels (1, 0, and +1), with 29 experimental runs and one control. The levels were selected based on the results of experimental designs as shown in Table 2. The full strength media with 2% crude oil/PAHs act as a control. The statistical software Design-Expert® 10 (Stat-Ease, Inc., Minneapolis, MN, USA) was used to evaluate the analysis of variance ($P < 0.05$) to determine the significance of each term in the fitted equations and to estimate the goodness of fit in each case. In order to visualise the relationship between the experimental variables and responses, 3D plots are generated from the models. The optimum variables are obtained from the response surface.

2.4. Extraction of Residual Oil and Total Petroleum Hydrocarbon (TPH) Analysis. Based on the preliminary degradation

TABLE 2: Full-factorial Box-Behnken Design levels for the four independent variables showing total of 29 sets of experimentation work.

| Std | Run | Temp (°C) | pH | Salinity | Inoculum size (ml) |
|-----|-----|-----------|----|----------|--------------------|
| 8 | 1 | 32.5 | 8 | 20 | 20 |
| 16 | 2 | 32.5 | 11 | 20 | 12.5 |
| 12 | 3 | 40 | 8 | 12.5 | 20 |
| 18 | 4 | 40 | 8 | 5 | 12.5 |
| 23 | 5 | 32.5 | 5 | 12.5 | 20 |
| 6 | 6 | 32.5 | 8 | 20 | 5 |
| 11 | 7 | 25 | 8 | 12.5 | 20 |
| 20 | 8 | 40 | 8 | 20 | 12.5 |
| 14 | 9 | 32.5 | 11 | 5 | 12.5 |
| 29 | 10 | 32.5 | 8 | 12.5 | 12.5 |
| 25 | 11 | 32.5 | 8 | 12.5 | 12.5 |
| 22 | 12 | 32.5 | 11 | 12.5 | 5 |
| 21 | 13 | 32.5 | 5 | 12.5 | 5 |
| 19 | 14 | 25 | 8 | 20 | 12.5 |
| 1 | 15 | 25 | 5 | 12.5 | 12.5 |
| 28 | 16 | 32.5 | 8 | 12.5 | 12.5 |
| 13 | 17 | 32.5 | 5 | 5 | 12.5 |
| 5 | 18 | 32.5 | 8 | 5 | 5 |
| 10 | 19 | 40 | 8 | 12.5 | 5 |
| 7 | 20 | 32.5 | 8 | 5 | 20 |
| 4 | 21 | 40 | 11 | 12.5 | 12.5 |
| 9 | 22 | 25 | 8 | 12.5 | 5 |
| 27 | 23 | 32.5 | 8 | 12.5 | 12.5 |
| 15 | 24 | 32.5 | 5 | 20 | 12.5 |
| 3 | 25 | 25 | 11 | 12.5 | 12.5 |
| 24 | 26 | 32.5 | 11 | 12.5 | 20 |
| 2 | 27 | 40 | 5 | 12.5 | 12.5 |
| 17 | 28 | 25 | 8 | 5 | 12.5 |
| 26 | 29 | 32.5 | 8 | 12.5 | 12.5 |

results, the potential bacterial strains were selected and checked for the utilization capability of the crude oil. The isolates were inoculated into the conical flask containing Bacto Bushnell Hass broth in artificial sea water along with 2% crude oil and dextrose as additional carbon source [2]. The flask was monitored at regular intervals of time up to 15 days. The flasks were observed for any changes in the physical nature of the oil.

2.5. Biological Oxygen Demand (BOD) and Chemical Oxygen Demand (COD) Analysis. In order to assess the rate of degradation and PAHs utilization by the isolate *S. rhizophila* KX082814, the BOD and COD analysis were performed by following standard methods (APHA, 2001, and IS-3025).

2.6. GC/MS Analysis to Validate the RSM Design. The GC/MS analysis was performed using a MS-5973 spectrometer coupled to a Hewlett-Packard Model 6890 and GC equipped with a cool-on-column inlet and capillary direct interface. The instrument conditions were the following: capillary column HP-1MS, 60 m × 0.2 mm; helium column flow 1 ml/min;

TABLE 3: Showing the % TPH, BOD, and COD results of 29 experimental designs using *S. rhizophila* KX082814 when crude oil was used as sole carbon source on 15th day of incubation period.

| Std | Run | Temp (°C) | pH | Salinity | Inoculum size (ml) | % TPH | BOD (mg/l) | COD (mg/l) |
|-----|-----|-----------|----|----------|--------------------|-------|------------|------------|
| 8 | 1 | 32.5 | 8 | 20 | 20 | 53 | 153 | 226.8 |
| 16 | 2 | 32.5 | 11 | 20 | 12.5 | 56 | 189 | 245.6 |
| 12 | 3 | 40 | 8 | 12.5 | 20 | 52 | 178 | 286.5 |
| 18 | 4 | 40 | 8 | 5 | 12.5 | 51.89 | 196.5 | 258 |
| 23 | 5 | 32.5 | 5 | 12.5 | 20 | 68.5 | 221 | 356 |
| 6 | 6 | 32.5 | 8 | 20 | 5 | 61.53 | 216 | 341 |
| 11 | 7 | 25 | 8 | 12.5 | 20 | 67.84 | 256 | 382 |
| 20 | 8 | 40 | 8 | 20 | 12.5 | 53.52 | 188 | 256 |
| 14 | 9 | 32.5 | 11 | 5 | 12.5 | 65.23 | 225 | 358 |
| 29 | 10 | 32.5 | 8 | 12.5 | 12.5 | 70.25 | 241 | 442 |
| 25 | 11 | 32.5 | 8 | 12.5 | 12.5 | 69.05 | 221 | 395 |
| 22 | 12 | 32.5 | 11 | 12.5 | 5 | 65.2 | 198 | 305 |
| 21 | 13 | 32.5 | 5 | 12.5 | 5 | 62.59 | 225.6 | 298.5 |
| 19 | 14 | 25 | 8 | 20 | 12.5 | 53 | 184.2 | 219.9 |
| 1 | 15 | 25 | 5 | 12.5 | 12.5 | 61.52 | 205 | 298.5 |
| 28 | 16 | 32.5 | 8 | 12.5 | 12.5 | 64.25 | 236.5 | 336.8 |
| 13 | 17 | 32.5 | 5 | 5 | 12.5 | 68.54 | 295.6 | 358 |
| 5 | 18 | 32.5 | 8 | 5 | 5 | 60.21 | 258 | 356.5 |
| 10 | 19 | 40 | 8 | 12.5 | 5 | 58.5 | 187.5 | 265 |
| 7 | 20 | 32.5 | 8 | 5 | 20 | 63.25 | 225 | 398.5 |
| 4 | 21 | 40 | 11 | 12.5 | 12.5 | 55.26 | 198 | 268 |
| 9 | 22 | 25 | 8 | 12.5 | 5 | 59.25 | 189.65 | 258 |
| 27 | 23 | 32.5 | 8 | 12.5 | 12.5 | 64.58 | 242.6 | 421.2 |
| 15 | 24 | 32.5 | 5 | 20 | 12.5 | 61.22 | 215.8 | 395.8 |
| 3 | 25 | 25 | 11 | 12.5 | 12.5 | 60.25 | 210.5 | 298.5 |
| 24 | 26 | 32.5 | 11 | 12.5 | 20 | 62.54 | 235.6 | 329.5 |
| 2 | 27 | 40 | 5 | 12.5 | 12.5 | 58.21 | 189.58 | 298.5 |
| 17 | 28 | 25 | 8 | 5 | 12.5 | 59.52 | 178.5 | 258.5 |
| 26 | 29 | 32.5 | 8 | 12.5 | 12.5 | 55.68 | 153.8 | 221.35 |

pressure 18.5 psi; and split ratio 20 : 1. The initial temperature was 70°C and kept for 5 minutes with a temperature ramp of 14°C per minute and final temperature of 280°C was kept for 10 minutes with total run time 3024 minutes. A solvent delay was employed in order to prolong detector lifetime from 0 to 4.5 minutes. The solvent front reached the detector in 4.0 minutes and initial analyte retention time was approximately 7 minutes, so there was no loss of resolution due to initial solvent delay. The solvent used in all analyses was mixture of hexanes.

2.7. 16s rRNA Sequencing and NCBI Gene Bank Deposition. Bacterial identification was carried through 16s rRNA sequencing. Bacterial genomic DNA was isolated using the Insta Gene™ Matrix genomic DNA isolation kit Catalog # 732-6030. Using 16s rRNA universal primers gene fragment was amplified using MJ Research PTC-225 Peltier Thermal Cycler. The sequence obtained is deposited in the NCBI gene bank using the tool Sequin.

3. Results and Discussions

The present study was undertaken to examine the cumulative effect of four different parameters on degradation of crude oil and PAHs. The second-order polynomial coefficient for each term of the equation was determined through multiple regression analysis using the Design-Expert v.10. The experimental design and response for each trail were mentioned in Table 3. Maximum degradation was observed in case of run number 10 followed by 11, 17, and 7, where % degradation was found to be 70.25, 69.05, 68.54, and 67.84, respectively. It was noticed that the similar results were observed in case of runs number 10 and 11; this may be due to the identical experimental conditions, whereas in case of runs number 7 and 17, although the experimental conditions are different, the results show the highest rate of degradation was almost equal to the runs number 10 and 11. Hence according to the model, the runs number 10 and 11 as standard optimized conditions were selected as the optimum

TABLE 4: Diagnostics case statistics, experimental design, and results of Box-Behnken Design for crude oil and PAHs degradation.

| Run order | Actual value | Predicted value | Residual | Leverage | Internally studentized residual | Externally studentized residual | Cook's distance | Influence on fitted value DFFITS | Standard order |
|-----------|--------------|-----------------|----------|----------|---------------------------------|---------------------------------|-----------------|----------------------------------|----------------|
| 15 | 61.52 | 63.19 | -1.67 | 0.583 | -0.694 | -0.681 | 0.045 | -0.805 | 1 |
| 27 | 58.21 | 58.69 | -0.48 | 0.583 | -0.201 | -0.194 | 0.004 | -0.229 | 2 |
| 25 | 60.25 | 61.34 | -1.09 | 0.583 | -0.455 | -0.442 | 0.019 | -0.523 | 3 |
| 21 | 55.26 | 55.17 | 0.092 | 0.583 | 0.038 | 0.037 | 0.000 | 0.044 | 4 |
| 18 | 60.21 | 59.94 | 0.27 | 0.583 | 0.115 | 0.111 | 0.001 | 0.131 | 5 |
| 6 | 61.53 | 60.66 | 0.87 | 0.583 | 0.363 | 0.352 | 0.012 | 0.416 | 6 |
| 20 | 63.25 | 65.70 | -2.45 | 0.583 | -1.019 | -1.021 | 0.097 | -1.208 | 7 |
| 1 | 53.00 | 54.85 | -1.85 | 0.583 | -0.770 | -0.759 | 0.055 | -0.898 | 8 |
| 22 | 59.25 | 57.17 | 2.08 | 0.583 | 0.866 | 0.858 | 0.070 | 1.015 | 9 |
| 19 | 58.50 | 59.38 | -0.88 | 0.583 | -0.368 | -0.357 | 0.013 | -0.422 | 10 |
| 7 | 67.84 | 64.69 | 3.15 | 0.583 | 1.312 | 1.350 | 0.161 | 1.597 | 11 |
| 3 | 52.00 | 51.81 | 0.19 | 0.583 | 0.078 | 0.075 | 0.001 | 0.089 | 12 |
| 17 | 68.54 | 65.01 | 3.53 | 0.583 | 1.471 | 1.542 | 0.202 | 1.824 | 13 |
| 9 | 65.23 | 63.28 | 1.95 | 0.583 | 0.812 | 0.801 | 0.062 | 0.948 | 14 |
| 24 | 61.22 | 60.90 | 0.32 | 0.583 | 0.132 | 0.127 | 0.002 | 0.150 | 15 |
| 2 | 56.00 | 57.27 | -1.27 | 0.583 | -0.527 | -0.513 | 0.026 | -0.607 | 16 |
| 28 | 59.52 | 62.06 | -2.54 | 0.583 | -1.060 | -1.065 | 0.105 | -1.260 | 17 |
| 4 | 51.89 | 52.65 | -0.76 | 0.583 | -0.319 | -0.308 | 0.009 | -0.365 | 18 |
| 14 | 53.00 | 52.93 | 0.074 | 0.583 | 0.031 | 0.030 | 0.000 | 0.035 | 19 |
| 8 | 53.52 | 51.67 | 1.85 | 0.583 | 0.772 | 0.760 | 0.056 | 0.899 | 20 |
| 13 | 62.59 | 64.26 | -1.67 | 0.583 | -0.698 | -0.685 | 0.045 | -0.810 | 21 |
| 12 | 65.20 | 65.87 | -0.67 | 0.583 | -0.278 | -0.268 | 0.007 | -0.317 | 22 |
| 5 | 68.50 | 68.52 | -0.025 | 0.583 | -0.010 | -0.010 | 0.000 | -0.012 | 23 |
| 26 | 62.54 | 61.56 | 0.98 | 0.583 | 0.410 | 0.398 | 0.016 | 0.470 | 24 |
| 11 | 69.05 | 64.76 | 4.29 | 0.200 | 1.290 | 1.324 | 0.028 | 0.662 | 25 |
| 29 | 55.68 | 64.76 | -9.08 | 0.200 | -2.732 | -3.852 | 0.124 | -1.926 | 26 |
| 23 | 64.58 | 64.76 | -0.18 | 0.200 | -0.055 | -0.053 | 0.000 | -0.026 | 27 |
| 16 | 64.25 | 64.76 | -0.51 | 0.200 | -0.154 | -0.149 | 0.000 | -0.074 | 28 |
| 10 | 70.25 | 64.76 | 5.49 | 0.200 | 1.651 | 1.773 | 0.045 | 0.886 | 29 |

conditions to enhance the degradation. Further, the obtained optimized conditions from the RSM-BBD were confirmed and validated by experimental studies at standard conditions.

The obtained results were checked for their fitness to the model and obtained data was illustrated. The predicted and actual values for the model, Cook's distance, and studentized residuals illustrate the normal distribution and constant variance of the residuals; according to Table 4 and Figure 4, there were no points that were potentially powerful due to their location in the factor indicating the goodness of fit.

By the model, F -value of 3.31 implies that the model is significant (Table 5). Values of "Prob > F " less than 0.0500 indicate model terms are significant. In this case A , C , A^2 , and

C^2 are significant model terms as values greater than 0.1000 indicate the model terms are not significant. The lack of fit F -value of 0.19 implies the lack of fit is not significantly relative to the pure error. There is a 98.50% chance that a lack of fit F -value this large could occur due to noise. Nonsignificant lack of fit is good and we want the model to fit. The "Pred R^2 " of 0.3240 is not as close to the "Adj R^2 " of 0.5355 as one might normally expect; that is, the difference is more than 0.2. This may indicate a large block effect or a possible problem with our model and/or data. Things to consider are model reduction, response transformation, outliers, and so forth. All empirical models should be tested by confirmation runs. "Adeq Precision" measures the signal to noise ratio.

TABLE 5: Analysis of variances using ANOVA for response surface by quadratic model.

| Source | Sum of squares | df | Mean square | F-value | P value, Prob > F | |
|-----------------|----------------|----|--------------|--------------|-------------------|-----------------|
| Model | 639.46 | 14 | 45.68 | 3.31 | 0.0163 | Significant |
| A-temperature | 85.33 | 1 | 85.33 | 6.18 | 0.0262 | |
| B-pH | 21.60 | 1 | 21.60 | 1.56 | 0.2316 | |
| C-salinity | 76.86 | 1 | 76.86 | 5.56 | 0.0334 | |
| D-inoculum Size | 1.875E – 003 | 1 | 1.875E – 003 | 1.357E – 004 | 0.9909 | |
| AB | 0.71 | 1 | 0.71 | 0.051 | 0.8245 | |
| AC | 16.61 | 1 | 16.61 | 1.20 | 0.2914 | |
| AD | 56.93 | 1 | 56.93 | 4.12 | 0.0618 | |
| BC | 0.91 | 1 | 0.91 | 0.066 | 0.8010 | |
| BD | 18.36 | 1 | 18.36 | 1.33 | 0.2683 | |
| CD | 33.47 | 1 | 33.47 | 2.42 | 0.1419 | |
| A ² | 231.68 | 1 | 231.68 | 16.77 | 0.0011 | |
| B ² | 4.27 | 1 | 4.27 | 0.31 | 0.5871 | |
| C ² | 101.60 | 1 | 101.60 | 7.35 | 0.0169 | |
| D ² | 1.76 | 1 | 1.76 | 0.13 | 0.7268 | |
| Residual | 193.42 | 14 | 13.82 | | | |
| Lack of fit | 62.13 | 10 | 6.21 | 0.19 | 0.9850 | Not significant |
| Pure error | 131.28 | 4 | 32.82 | | | |
| Cor total | 832.88 | 28 | | | | |

Final Equation in Terms of Coded Factors

Total Petroleum Hydrocarbon (%TPH)

$$\begin{aligned}
 &= +64.76 - 2.67 * A - 1.34 * B - 2.53 * C - 0.013 \\
 &* D - 0.42 * AB + 2.04 * AC - 3.77 * AD \quad (1) \\
 &- 0.48 * BC - 2.14 * BD - 2.89 * CD - 5.98 \\
 &* A^2 + 0.81 * B^2 - 3.96 * C^2 - 0.52 * D^2,
 \end{aligned}$$

where A, B, C, and D are the coded values of the test variables (Table 6), temperature (°C), pH, salinity, and inoculum size (ml), respectively. The equation in terms of coded factors can be used to make predictions about the response for given levels of each factor. By default, the high levels of the factors are coded as +1 and the low levels of the factors are coded as -1. The coded equation is useful for identifying the relative impact of the factors by comparing the factor coefficients.

Final Equation in Terms of Actual Factors

Total Petroleum Hydrocarbon (TPH)

$$\begin{aligned}
 &= -71.82338 + 7.08541 * \text{Temperature} + 0.17307 \\
 &* \text{pH} + 1.05685 * \text{Salinity} + 3.81374 \\
 &* \text{Inoculum Size} - 0.018667 * \text{Temperature} \\
 &* \text{pH} + 0.036222 * \text{Temperature} * \text{Salinity} \\
 &- 0.067067 * \text{Temperature} * \text{Inoculum Size}
 \end{aligned}$$

$$\begin{aligned}
 &- 0.021222 * \text{pH} * \text{Salinity} - 0.095222 * \text{pH} \\
 &* \text{Inoculum Size} - 0.051422 * \text{Salinity} \\
 &* \text{Inoculum Size} - 0.10625 * \text{Temperature}^2 \\
 &+ 0.090120 * \text{pH}^2 - 0.070359 * \text{Salinity}^2 \\
 &- 9.24741E - 003 * \text{Inoculum size}^2 \quad (2)
 \end{aligned}$$

The equation in terms of actual factors can be used to make predictions about the response for given levels of each factor. Here, the levels should be specified in the original units for each factor. This equation should not be used to determine the relative impact of each factor because the coefficients are scaled to accommodate the units of each factor and the intercept is not at the centre of the design space. The Diagnostic Plots are as shown in Figures 1-5. Figure 1 shows the normal probability plot of the studentized residuals to check for normality of residuals. Figure 2 shows studentized residuals versus predicted values to check for constant error in the design. Figure 3 shows externally studentized residuals to look for outliers, that is, influential values of the design. Figure 4 shows Box-Cox plot for power transformations, where Cook's distance and studentized residual illustrate the normal distribution and constant variance of the residuals and Figure 5 shows the interactions among factors that influence crude oil and PAHs degradation by the isolate *S. rhizophila* (PM-1) KX082814.

The response surface curves show the relative effects of two variables, by keeping the other variable at fixed level,

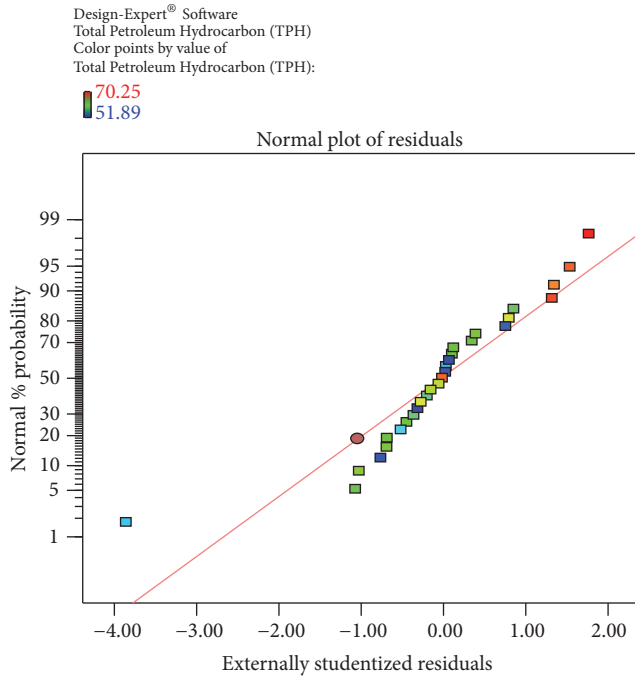


FIGURE 1: The Diagnostic Plots obtained by the Box-Behnken Design to evaluate the normal plot residuals using the normal % probability versus externally studentized residuals by the bacterial isolate *S. rhizophila* KX082814 for its crude oil degradation ability.

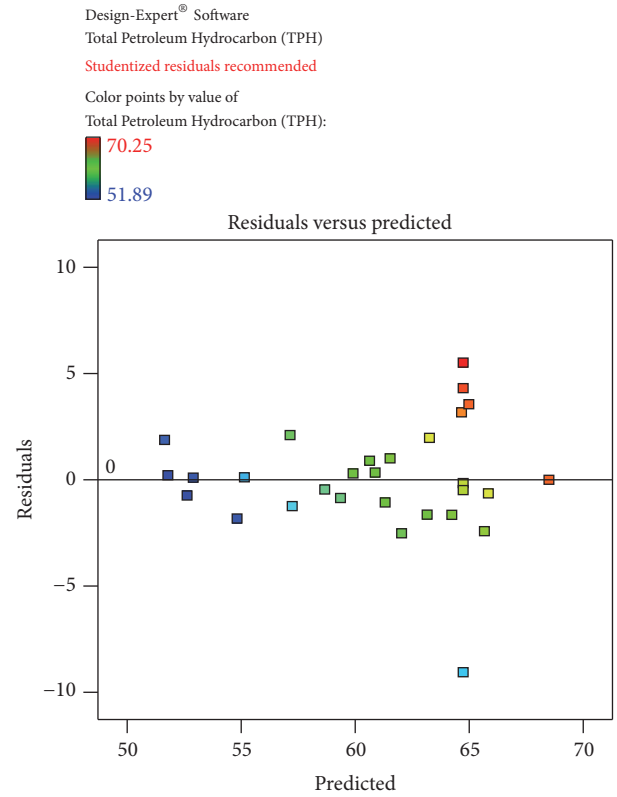


FIGURE 3: The Diagnostic Plots showing the recommended studentized residuals obtained by the Box-Behnken Design using the residual versus predicted by the bacterial isolate *S. rhizophila* KX082814 for its crude oil degradation ability.

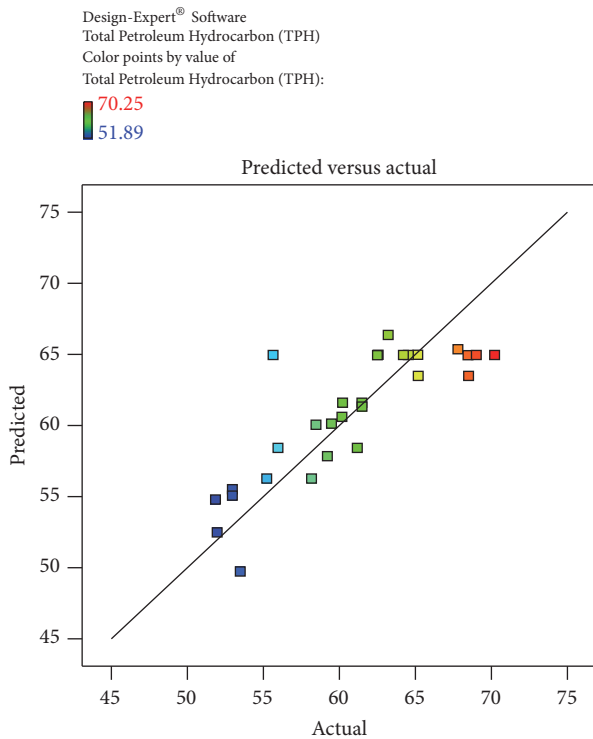


FIGURE 2: Predicted versus actual plot obtained by the Box-Behnken Design based on the % TPH of crude oil and PAHs degradation using the bacterial isolate *S. rhizophila* KX082814.

TABLE 6: Coded values of the test variables.

| Factor | Coefficient estimate | df | Standard error | 95% CI Low | 95% CI High | VIF |
|-----------------|----------------------|----|----------------|------------|-------------|------|
| Intercept | 64.76 | 1 | 1.66 | 61.20 | 68.33 | |
| A-temperature | -2.67 | 1 | 1.07 | -4.97 | -0.37 | 1.00 |
| B-pH | -1.34 | 1 | 1.07 | -3.64 | 0.96 | 1.00 |
| C-salinity | -2.53 | 1 | 1.07 | -4.83 | -0.23 | 1.00 |
| D-inoculum Size | -0.013 | 1 | 1.07 | -2.31 | 2.29 | 1.00 |
| AB | -0.42 | 1 | 1.86 | -4.41 | 3.57 | 1.00 |
| AC | 2.04 | 1 | 1.86 | -1.95 | 6.02 | 1.00 |
| AD | -3.77 | 1 | 1.86 | -7.76 | 0.21 | 1.00 |
| BC | -0.48 | 1 | 1.86 | -4.46 | 3.51 | 1.00 |
| BD | -2.14 | 1 | 1.86 | -6.13 | 1.84 | 1.00 |
| CD | -2.89 | 1 | 1.86 | -6.88 | 1.09 | 1.00 |
| A ² | -5.98 | 1 | 1.46 | -9.11 | -2.85 | 1.08 |
| B ² | 0.81 | 1 | 1.46 | -2.32 | 3.94 | 1.08 |
| C ² | -3.96 | 1 | 1.46 | -7.09 | -0.83 | 1.08 |
| D ² | -0.52 | 1 | 1.46 | -3.65 | 2.61 | 1.08 |

on crude oil degradation. The 3D plots and cubic designs are shown in Figures 6–9. The result obtained shows that pH of 8, temperature of 32.5°C, inoculum size of 12.5 ml, and salinity concentration of 12.5 were the best conditions to

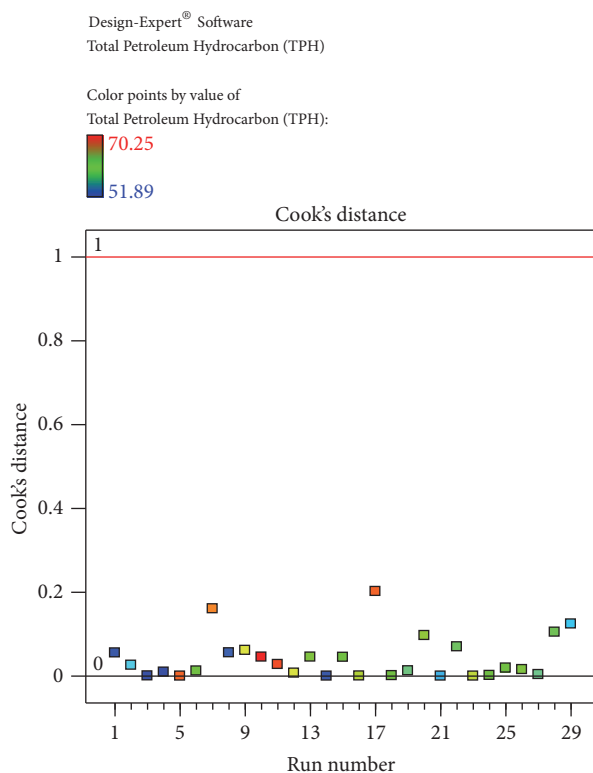


FIGURE 4: The Diagnostic Plots showing Cook's distance plot obtained by the Box-Behnken Design using Cook's distance versus run number by the bacterial isolate *S. rhizophila* KX082814 for its crude oil degradation ability.

TABLE 7: Assessment of rate of degradation by measuring BOD, COD, % TPH, and TPC for the bacterial isolate *S. rhizophila* (MP-1) KX082814 for observed and predicted optimum conditions through RSM-BBD.

| Test parameter | Observed optimum parameters through RSM-BBD | Validation of predicted optimum condition through RSM-BBD |
|----------------|---|---|
| TPC (cfu/ml) | 4.8×10^{-8} | 6.7×10^{-9} |
| TPH (%) | 71.82% | 79.53% |
| BOD (mg/L) | 253.5 | 325.2 |
| COD (mg/L) | 816 | 835.4 |

obtain maximum degradation of crude oil and PAHs using the bacterial isolate *S. rhizophila* KX082814. The optimal values for the variables as predicted by the RSM were found within the Box-Behnken Design region.

Validation of Optimization Process. Validation experiments were conducted in triplicate to determine the performance of *S. rhizophila* KX082814 and reproducibility of the results by evaluating the level of BOD, COD, TPC, % TPH, and GC/MS studies at the optimum favourable conditions through Box-Behnken Design and RSM (Table 7; Figure 10). The results showed $79.53 \pm 2.5\%$ of crude oil removal efficiency. The percentage error between the predicted and actual values was found to be 0.75%. The GC/MS study clearly indicates the

removal of majority of both aromatic and aliphatic hydrocarbons present in the crude oil (Figures 11 and 12; Table 8). A total of 42 different hydrocarbon components were observed in control sample, where after the bioremediation treatment with the isolate *S. rhizophila* (KX082814), it was noticed that only 20 hydrocarbon components remained in the test sample after 15th day. It was observed that majority of the components in the control samples are completely degraded and some peaks are converted to simpler hydrocarbon moieties. From the results the noticeable difference in the degradation process was clearly observed.

4. Conclusion

This study reveals the bioremediation of crude oil and PAHs utilization by the isolate *Stenotrophomonas rhizophila* (PM-1) with gene bank accession number KX082814 could be achieved up to $79.53 \pm 2.5\%$ by maintaining the optimum parameters, namely, temperature, pH, salinity, and inoculum size. The GC/MS studies also indicate that the degradation of majority of the hydrocarbon components, the statistical analyses, and the closeness of the experimental results and model predictions show the reliability of the regression model.

Competing Interests

The authors declare that there is no conflict of interests.

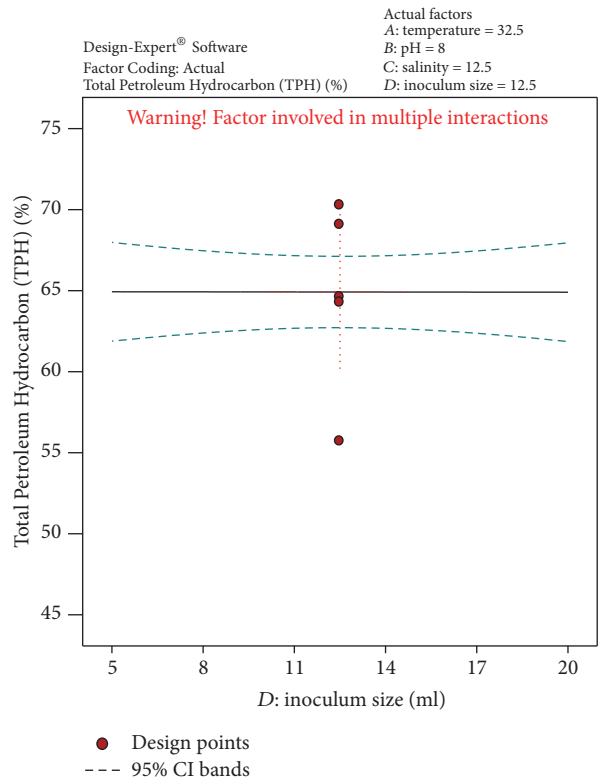
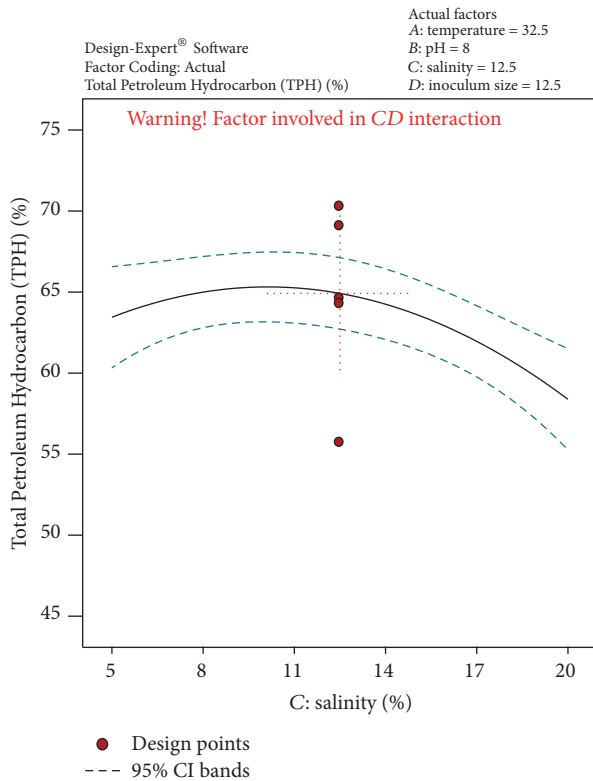
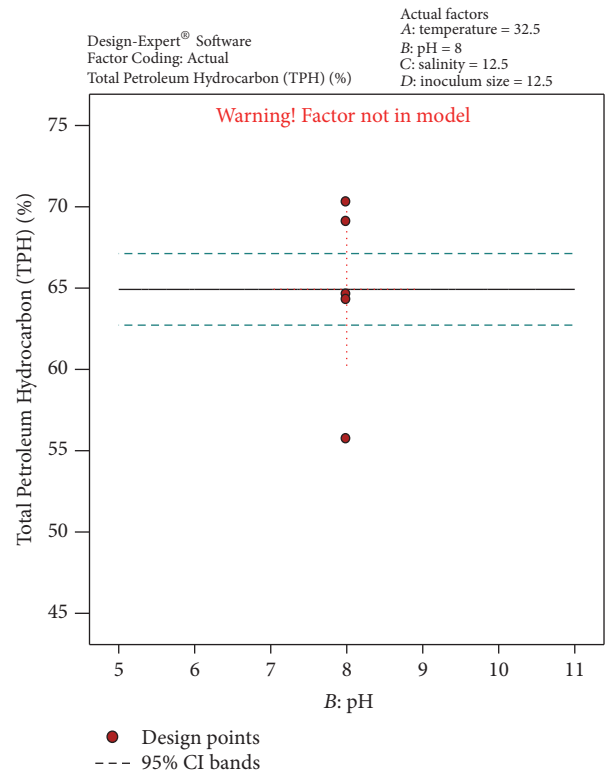
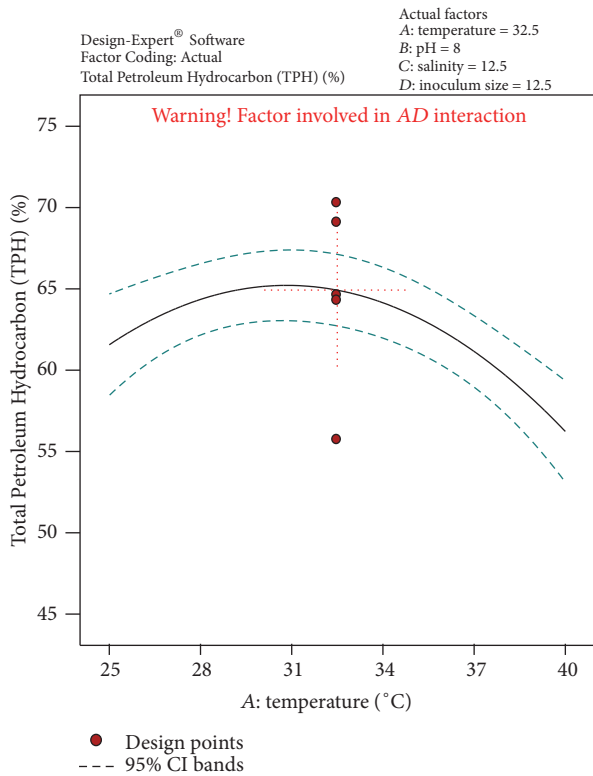


FIGURE 5: The Diagnostic Plots obtained by the Box-Behnken Design showing the interactions among factors that influence crude oil and PAHs degradation by the bacterial isolate *S. rhizophila* KX082814 for its crude oil degradation ability.

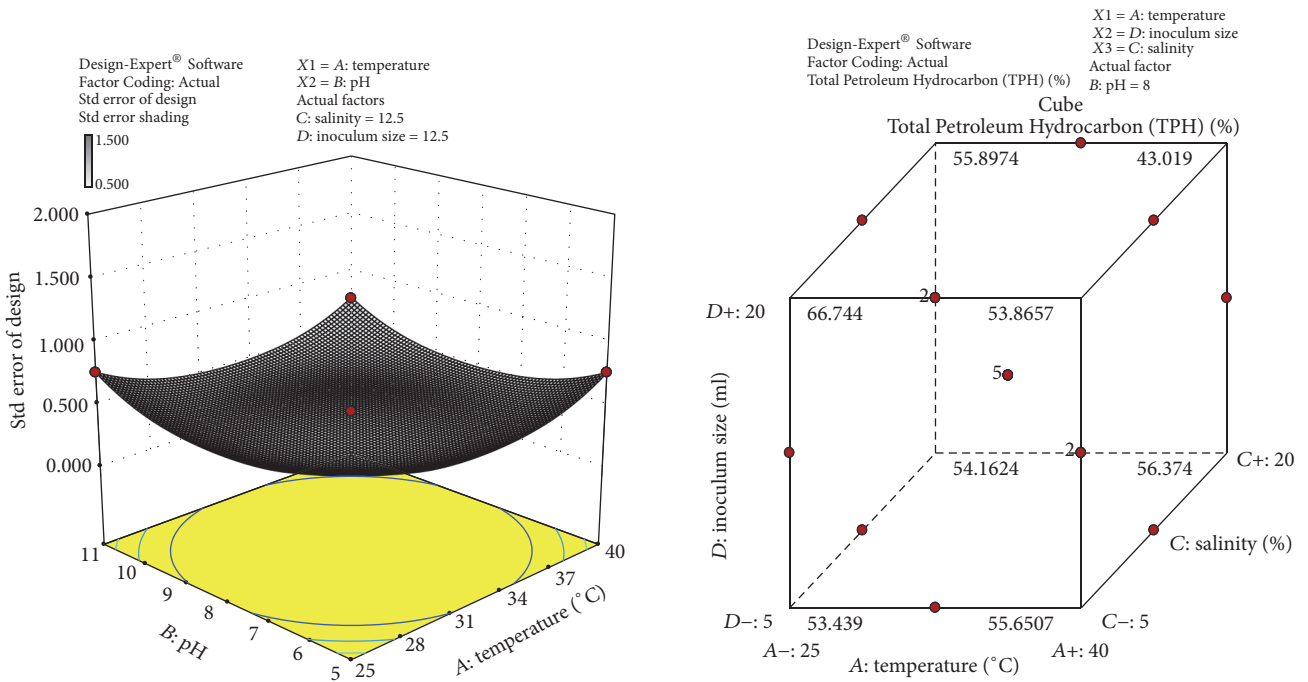


FIGURE 6: 3D response surface plot and Cube representation showing the standard error of design and interaction effect of factors that influence crude oil and PAHs degradation by the bacterial isolate *S. rhizophila* KX082814.

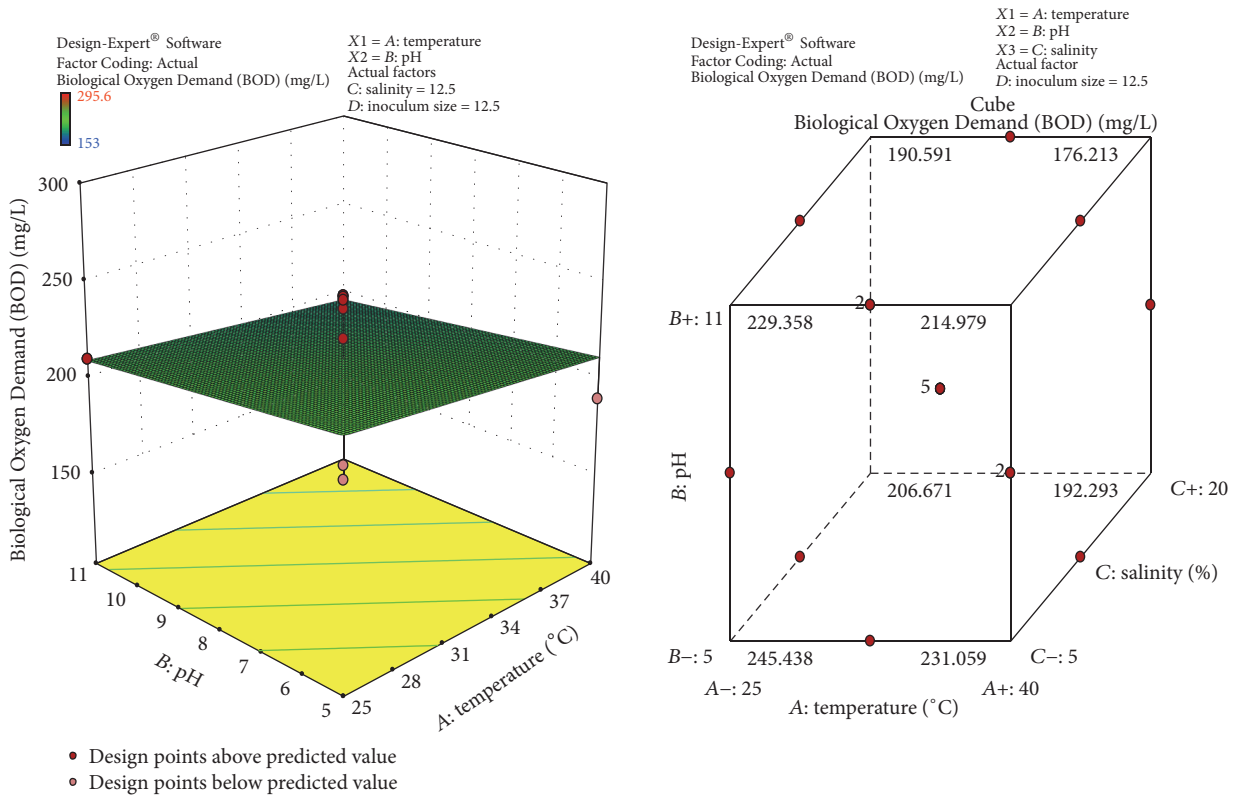


FIGURE 7: 3D response surface plot and Cube representation showing the interaction effect of factors that influence BOD of crude oil and PAHs degradation by the bacterial isolate *S. rhizophila* KX082814.

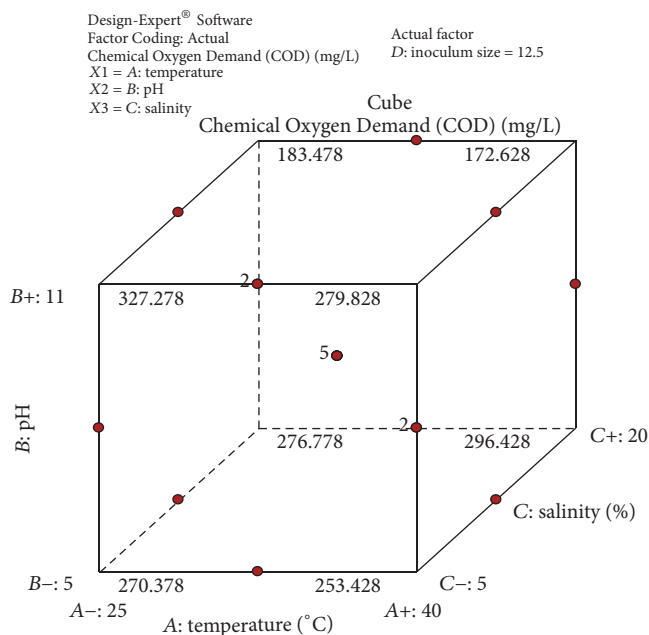
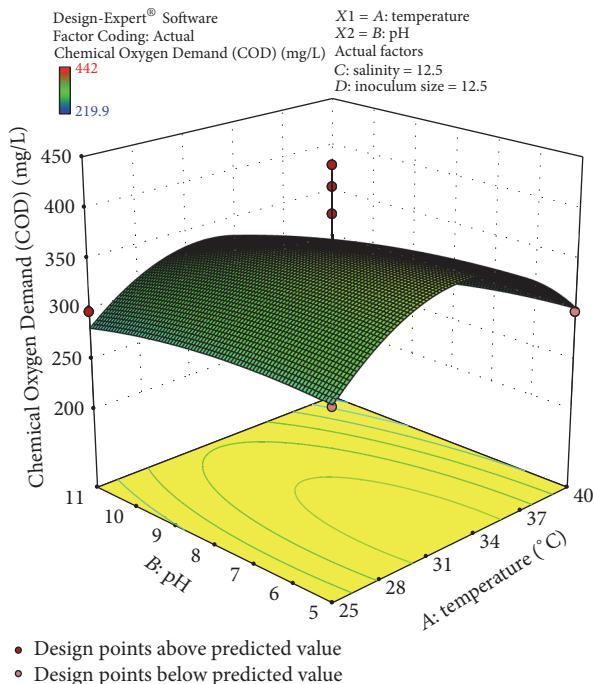


FIGURE 8: 3D response surface plot and Cube representation showing the interaction effect of factors that influence COD of crude oil and PAHs degradation by the bacterial isolate *S. rhizophila* KX082814.

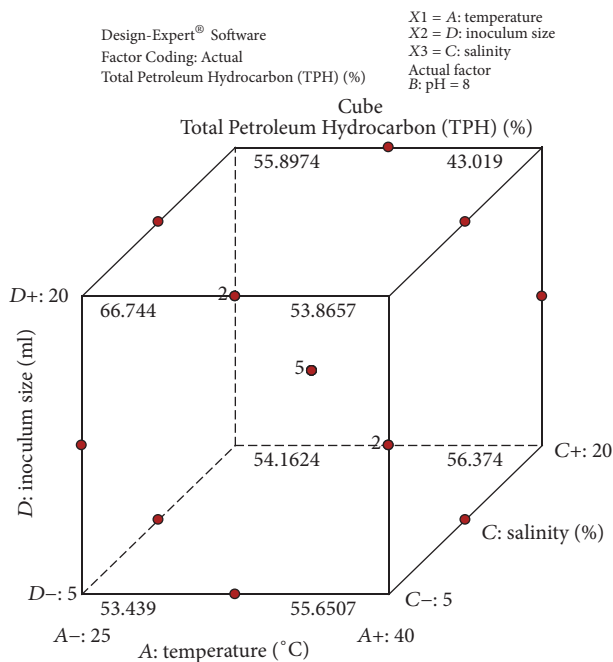
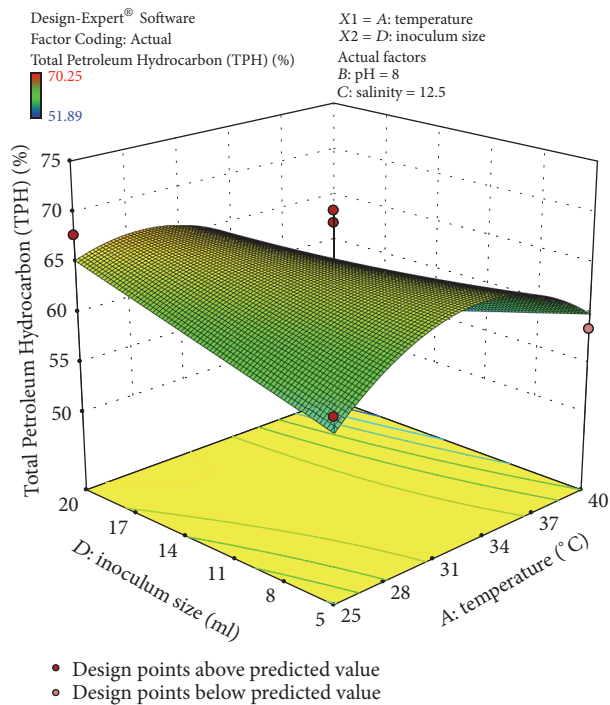


FIGURE 9: 3D response surface plot and Cube representation showing the interaction effect of factors that influence % TPH of crude oil and PAHs degradation by the bacterial isolate *S. rhizophila* KX082814.

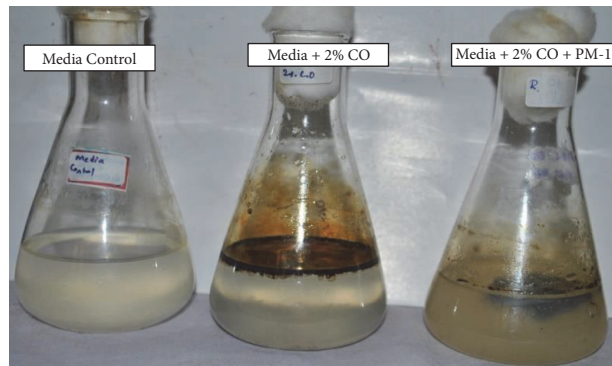


FIGURE 10: Validation of degradation using predicted optimum conditions (at temperature of 32.5°C, pH of 9, 12.5 of salinity, and 12.5 ml of inoculum size). From left the Media Control (FSM-ASW), Positive Control (FSM-ASW + 2% CO), and Test (FSM-ASW + 2%CO + PM-1 bacterial isolate) on 15th day of incubation time.

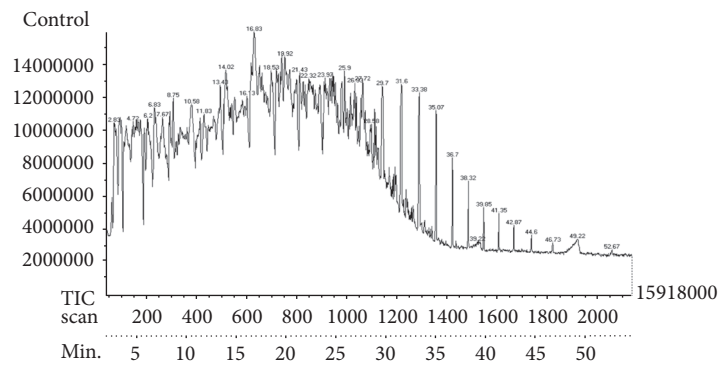


FIGURE 11: GC/MS chromatogram for 2% crude oil at 15th day of incubation shows persistence of total 40 different hydrocarbon components.

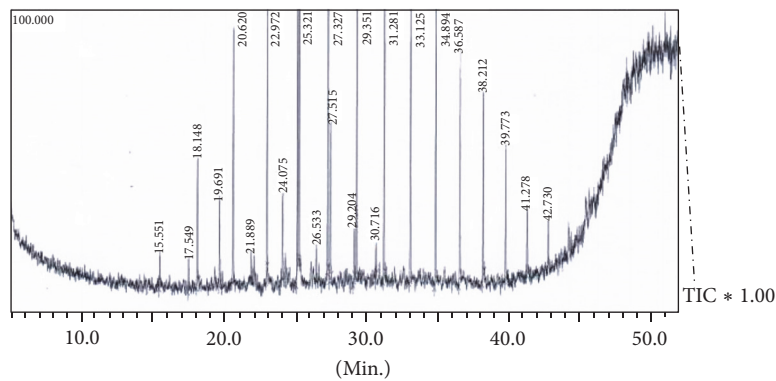


FIGURE 12: GC/MS chromatogram for 2% crude oil at 15th day of incubation shows persistence of total 23 different hydrocarbon components after being treated with the bacterial isolate *S. rhizophila* KX082814 on 15th day.

TABLE 8: Validation of crude oil degradation by GC/MS analysis after treatment with *S. rhizophila* (PM-1) KX082814 on 15th day.

| Major components of crude oil GC/MS | | | | Major residual components of crude oil after treatment | | | |
|-------------------------------------|---------|-------------------|--------|--|---------|-------------------|--------|
| Peak | R. time | Linear & branched | % area | Peak | R. time | Linear & branched | % area |
| 1 | 7.447 | C10H22 | 2.19 | 1 | 22.97 | C14H30 | 6.4 |
| 2 | 10.113 | C11H24 | 3.18 | 2 | 25.20 | C16H34 | 7.7 |
| 3 | 11.625 | C16H33Cl | 0.63 | 3 | 29.35 | C16H34 | 8.29 |
| 4 | 12.877 | C12H26 | 4.96 | 4 | 33.13 | C16H34 | 7.53 |
| 5 | 15.592 | C13H28 | 7.4 | 5 | 36.59 | C16H34 | 5.85 |
| 6 | 19.728 | C16H34 | 2.41 | 6 | 38.21 | C16H34 | 4.2 |
| 7 | 20.682 | C15H32 | 8.66 | 7 | 31.28 | C21H44 | 8.02 |
| 8 | 23.035 | C16H34 | 8.56 | 8 | 17.55 | C8H17I | 0.69 |
| 9 | 25.273 | C20H42 | 8.41 | 9 | 41.28 | C9H19I | 1.77 |
| 10 | 27.392 | C18H38 | 7.6 | 10 | 29.20 | C11H24 | 1.43 |
| 11 | 29.413 | C18H38 | 7.03 | 11 | 18.15 | C12H26 | 2.66 |
| 12 | 34.932 | C24H50 | 3.68 | 12 | 27.52 | C12H26 | 4.61 |
| 13 | 36.617 | C24H50 | 2.61 | 13 | 39.77 | C13H28 | 3.23 |
| 14 | 38.234 | C24H50 | 1.74 | 14 | 25.32 | C20H42 | 10.23 |
| 15 | 39.790 | C27H56 | 1.17 | 15 | 27.33 | C20H42 | 7.13 |
| 16 | 41.291 | C27H56 | 0.67 | 16 | 34.89 | C20H42 | 6.89 |
| 17 | 42.739 | C27H56 | 0.55 | 17 | 42.73 | C6H14 | 1.01 |
| 18 | 44.137 | C27H56 | 0.34 | 18 | 26.53 | C11H24 | 0.64 |
| 19 | 45.485 | C27H56 | 0.25 | 19 | 21.89 | C12H26 | 0.63 |
| 20 | 46.792 | C28H58 | 0.15 | 20 | 30.72 | C12H26 | 0.71 |
| 21 | 48.057 | C34H70 | 0.14 | | | | |
| 22 | 8.046 | C11H24 | 0.86 | | | | |
| 23 | 11.743 | C12H26 | 0.18 | | | | |
| 24 | 11.859 | C12H26 | 0.4 | | | | |
| 25 | 13.242 | C13H28 | 0.87 | | | | |
| 26 | 14.287 | C13H28 | 0.09 | | | | |
| 27 | 14.336 | C13H28 | 0.02 | | | | |
| 28 | 24.106 | C18H38 | 2.83 | | | | |
| 29 | 25.390 | C19H40 | 6.38 | | | | |
| 30 | 27.561 | C20H42 | 2.91 | | | | |

Acknowledgments

The authors thank Naval Research Board (Material Panel), DRDO, (DNRD/05/4003/NRB/291), the government of India for the financial support of this work. The authors are thankful to SAIF Centre, IIT Madras for GCMS facility, and management, principal, and head of department of Biotechnology, The Oxford College of Engineering, Bengaluru, for their constant support and facility.

References

- [1] S. E. Agarry and O. O. Ogunleye, "Box-Behnken design application to study enhanced bioremediation of soil artificially contaminated with spent engine oil using biostimulation strategy," *International Journal of Energy and Environmental Engineering*, vol. 3, article 31, 2012.
- [2] P. S. V. Kumar and B. K. Manjunatha, "Studies on hydrocarbon degradation by the bacterial isolate *Stenotrophomonas rhizophila* (PM-1) from the oil spilled regions of Western Ghats of Karnataka," *Science, Technology and Arts Research Journal*, vol. 4, no. 3, pp. 139–144, 2016.
- [3] S. E. Agarry, C. N. Owabor, R. O. Yusuf et al., "Enhanced bioremediation of soil artificially contaminated with kerosene: optimization of biostimulation agents through statistical experimental design," *Journal of Petroleum & Environmental Biotechnology*, vol. 3, article 120, 2012.
- [4] N. Debasmita and M. Rajasimman, "Optimization and kinetics studies on biodegradation of atrazine using mixed microorganisms," *Alexandria Engineering Journal*, vol. 52, no. 3, pp. 499–505, 2013.
- [5] O. Olawale, F. A. Oyawale, T. F. Adepoju, and S. Aikulolu, "Optimisation of diesel polluted soil using response surface methodology," *International Journal of Environmental Protection and Policy*, vol. 3, no. 6, pp. 194–202, 2015.
- [6] S. K. Garg, M. Tripathi, and N. Lal, "Response surface methodology for optimization of process variable for reactive orange 4 dye discoloration by *Pseudomonas putida* SKG-1 strain and

bioreactor trial for its possible use in large-scale bioremediation,” *Desalination and Water Treatment*, vol. 54, no. 11, pp. 3122–3133, 2015.

- [7] M. Youssef, G. E. El-Taweel, A. Y. El-Naggar, S. E. El-Hawary, M. A. El-Meleigy, and S. A. Ahmed, “Hydrocarbon degrading bacteria as indicator of petroleum pollution in Suez Canal, Egypt,” *World Applied Sciences Journal*, vol. 8, no. 10, pp. 1226–1233, 2010.



Hindawi

Submit your manuscripts at
<http://www.hindawi.com>



International Journal of Current Microbiology and Applied Sciences (IJCMAS)

[Join as a Reviewer](#)

[Login as a Reviewer](#)

Search

[Print this Article](#)

[PDF Full Text](#)

[How to Cite this Article](#)

[on Google](#)

[Google Scholar](#)

Indexed in



National Academy of
Agricultural Sciences (NAAS)

NAAS Score:
***5.38 (2020)**

[Effective from January 1, 2020]

[For more details click here](#)

ICV 2019: 96.39

Index Copernicus ICI Journals Master
List 2019 - IJCMAS--ICV 2019: 96.39

[For more details click here](#)

Announcement

[Volume-11, Issue-5 Published](#)

[Call for paper-Vol-11, Issue 6- June 2022.](#)

[Abstracting and Indexing](#)

[Aims and Scope](#)

[Article Processing Charges](#)

[Editorial Review and Acceptance](#)

[Plagiarism Prevention Policy](#)

[Author Guidelines](#)

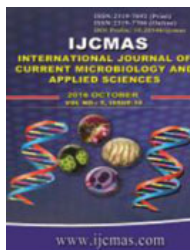
[Editorial Board](#)

[Subscription Information](#)

[See Guidelines to Authors](#)
[Current Issues](#)

[Download Publication Certificate](#)

Original Research Articles



PRINT ISSN : 2319-7692

Online ISSN : 2319-7706

Issues : 12 per year

Publisher : [Excellent Publishers](#)

Email : editorijcmas@gmail.com / submit@ijcmas.com

Editor-in-chief: Dr.M.Prakash

Index Copernicus ICV 2018: 95.39

NAAS RATING 2020: 5.38

[Int.J.Curr.Microbiol.App.Sci.2016.5\(10\): 386-396](#)

DOI: <http://dx.doi.org/10.20546/ijcmas.2016.510.044>

Bioremediation of Poly Aromatic Hydrocarbons (PAHs) and Crude Oil by Fungal Consortium from West Coast of Karnataka, India

S.V. Praveen Kumar, B.K. Manjunatha*, Pavani Bhat, R. Veena, Swetha S. Pawate and M. Yogashree

Department of Biotechnology, The Oxford College of Engineering, Bengaluru-560068 Karnataka, India

*Corresponding author

Abstract:

The present study primarily aims at developing an effective fungal consortium for the bioremediation of Poly Aromatic Hydrocarbons (PAHs) and crude oil. The hydrocarbon utilization capabilities of the potent isolated strains were studied for test hydrocarbons like benzene, toluene, naphthalene, paraffin and crude oil as model hydrocarbons for a period of 10 days. Degradation process was assessed by measuring percentage of TPH in residual oil, biological oxygen demand (BOD), chemical oxygen demand (COD), total plate count, UV spectrophotometric analysis and GC-MS studies. The study revealed that, among 45 isolated strains from PAHs/crude oil contaminated soil; four strains showed maximum degradation of crude oil & PAHs. 18s rRNA sequencing was used to identify the strains and, was identified as *Aspergillus terreus*, *Aspergillus aculeatus*, *Scedosporium boydii* and *Aspergillus sp.* The degradation process for this consortium was further optimized using Response Surface Method (RSM). The fungal isolates were also screened for biosurfactant production, Immobilization of the isolates on sodium alginate beads will be used as model of bioremediation studies.

Keywords: Bioremediation, Fungi, West Coast, PAHs, Crude oil, GC-MS.

[Download this article as](#)

How to cite this article:

Praveen Kumar, S.V., B.K. Manjunatha, Pavani Bhat, R. Veena, Swetha S. Pawate and Yogashree, M. 2016. Bioremediation of Poly Aromatic Hydrocarbons (PAHs) and Crude Oil by Fungal Consortium from West Coast of Karnataka. *Int.J.Curr.Microbiol.App.Sci.* 5(10): 386-396. doi: <http://dx.doi.org/10.20546/ijcmas.2016.510.044>



Comparative Study of Response of Symmetric and Asymmetric Structures using Response Spectrums

Mohammed Abdul Wasil¹ Varnitha M S²

¹ Student ²Associate Professor

^{1,2}The Oxford College of Engineering

Abstract— This article presents the comparative study of response of a symmetric and asymmetric structure when they are subjected to response spectrum analysis using the response spectrum developed using the equations provided in the Indian code book IS:1893:2002 and the response spectrum developed using the attenuation equation. The final results are studied to ascertain if there is any variation in the response of the structures subjected to both the response spectrums.

Key words: Response Spectrums, Asymmetric Structures

I. INTRODUCTION

Seismic hazards are one of the most devastating natural hazards among the various hazards due to their high degree of unpredictability and possibility of large scale damage to life and property in a matter of few seconds. With the advancement in various fields such as construction methods, designing of structures and methods of execution of the various typical projects, a need has been felt for the further revision of the Indian code book IS:1893:2002 which was last revised in the year 2002. Many changes were made in the code book such as updating various cities from zone 2 to zone 3 but the cause of which are still obsolete. The response spectrum provided in the Indian code has been used for a long time and has not been revised as per the needs. This response spectrum provided in the code book is used for every region of the country which appears to be inadequate. Different parts of the country has different seismic conditions and for every region using the same response spectrum is inappropriate as the results obtained may not properly ascertain the seismicity level of the region completely. Hence in order to take into consideration various factors such as the distance of the source from the site i.e., hypocentral distance, a site specific response spectrum is needed. In this article we have developed one such response spectrum using the attenuation equation. The attenuation equation used here is developed by S T G Raghukanth. This attenuation equation has been used for many other research work such as preparation of microzonation map for new Delhi city, preparation of seismic zonation map for Mumbai city and has also been used in the NDMA in the development of probabilistic seismic hazard map of India. The equation has also been used to study the seismicity of Bangalore city. Both the response spectrums acceleration values i.e., one from the code book developed for a certain time period and the other response spectrum developed using attenuation equation for the same time period are entered into the software ETABS 2013 for the symmetric and asymmetric structures. Analysis is carried out for the structures and the results are studied to ascertain whether there are any variations in the results of the structures for both the response spectrums. From the results we try to conclude the importance of updating the

response spectrum of the Indian code such that it can be applied to every region effectively.

II. METHODOLOGY

In order to carry out the comparative studies, firstly we have to develop the symmetric and asymmetric models respectively. The dimensions of the various components of the structures are determined by trial and error method. After the determination of the dimensions the symmetric and asymmetric models are prepared in the software ETABS 2013. The models developed are also checked using equivalent static method by comparing the base shear values obtained in the software with the base shear values calculated manually. Now the response spectrum is developed for a specific period using the equations from the code book IS:1893:2002 and the attenuation relation. It is to be noted that the response spectrum provided in the code book is not considered and the response spectrum is developed for different time period. The acceleration values obtained was using the formula from the IS:1893:2002 which is as follows

| Periods | Acceleration mm/s ² ,CRS | Acceleration mm/s ² ,NFR S | Accelerat ion mm/s ² ,FF RS |
|---------|-------------------------------------|---------------------------------------|--|
| 0 | 1 | 0.315 | 0.0877 |
| 0.01 | 1.015 | 0.314 | 0.0873 |
| 0.015 | 1.0225 | 0.592 | 0.1635 |
| 0.02 | 1.03 | 0.679 | 0.1873 |
| 0.03 | 1.045 | 0.723 | 0.2008 |
| 0.04 | 1.06 | 0.713 | 0.1985 |
| 0.05 | 1.075 | 0.687 | 0.1918 |
| 0.06 | 1.09 | 0.646 | 0.1828 |
| 0.075 | 1.1102 | 0.607 | 0.1705 |
| 0.09 | 1.135 | 0.578 | 0.1627 |
| 0.1 | 2.5 | 0.542 | 0.1537 |
| 0.15 | 2.5 | 0.433 | 0.1257 |
| 0.2 | 2.5 | 0.374 | 0.1096 |
| 0.3 | 2.5 | 0.287 | 0.0855 |
| 0.4 | 2.5 | 0.238 | 0.0724 |
| 0.5 | 2 | 0.206 | 0.0633 |
| 0.6 | 1.666 | 0.177 | 0.0542 |
| 0.7 | 1.4286 | 0.157 | 0.0489 |
| 0.8 | 1.25 | 0.14 | 0.0438 |
| 0.9 | 1.1111 | 0.124 | 0.0387 |
| 1 | 1 | 0.116 | 0.0364 |
| 1.2 | 0.8333 | 0.093 | 0.0295 |
| 1.5 | 0.6667 | 0.072 | 0.0232 |
| 2 | 0.5 | 0.051 | 0.0167 |
| 2.5 | 0.4 | 0.04 | 0.0132 |
| 3 | 0.333 | 0.03 | 0.01 |
| 4 | 0.25 | 0.02 | 0.0068 |

Table 1:

$Sa/g = 1+1.5T$ ($0.00 \leq T \leq 0.10$)
 $Sa/g = 2.50$ ($0.10 \leq T \leq 0.40$)
 $Sa/g = 1.00/T$ ($0.40 \leq T \leq 4.00$)
 Where, T - Time period
 Sa/g – Acceleration values

The acceleration values for the other response spectrum were obtained using the following attenuation equation as given below $\ln(Sa/g) = C1+C2+C3*M^2+C4*r+C5*\ln(r+C6e^{(C7*M)})+C8*\log(r)+\ln(\epsilon)$ Where C1, C2, C3, C4, C5, C6, C7, C8, $\sigma(\epsilon)$ are constants obtained from NDMA report(Development of Probabilistic seismic hazard map of India)
 Where
 r – Hypocentral distance in meters,
 M – Earthquake magnitude.

The hypocentral distance is taken as 12km(r) to obtain near field acceleration values and for far field it is taken as 52km(r). The magnitude M is taken as 7 for both the cases. Using the above two equations the values of accelerations are obtained. The values of acceleration are obtained for a specific time period. The time period and the acceleration values using the code book equations and the acceleration values obtained using attenuation equation for near and far field are shown in the table 1a. These values obtained using the equations are entered in the software ETABS 2013 along with the respective periods for individual symmetric and asymmetric structures. These values are entered in the software in the sub command 'Response spectrum' in the command 'Function'. After defining the response spectrum command we have to define the case RSX and RSY i.e., response spectrum in x – direction and y – direction in the load cases. After defining the load cases analysis is carried out and the required results are extracted for the purpose of comparison.

III. RESULTS

After the analysis of all the models is carried out the results are to be extracted for the purpose of comparison of the response of the structures. Here we developed and used three symmetric models and three asymmetric models for the purpose of analysis. One of the symmetric and asymmetric model is analysed using the response spectrum developed using the acceleration values obtained using the equation from the IS:1893:2002. Similarly one of the symmetric and asymmetric model is analysed using the response spectrum developed using the acceleration values obtained using attenuation equation for near field and one symmetric and asymmetric is analysed using the response spectrum for far field. In order to carry out the comparison the results are obtained for the following parameters

- 1) Story displacements
- 2) Story drifts
- 3) Story Shears

A. Story Displacements

A Story displacement is the amount of displacement that a structure can undergo when it is subjected to response spectrum analysis. Table 1 shows the amount by which each symmetric model subjected to various response spectrums has displaced and the graphs are shown in Fig 1. Similarly the displacements of asymmetric structures are shown in Table 2 and the graphs are shown in Fig 2.

| S | E | CRS | NFRS | FFRS |
|----|------|---------|---------|---------|
| | m | mm | mm | mm |
| 15 | 49 | 0.06223 | 0.00649 | 0.00213 |
| 14 | 45.8 | 0.0607 | 0.00633 | 0.00208 |
| 13 | 42.6 | 0.05865 | 0.00612 | 0.00201 |
| 12 | 39.4 | 0.0561 | 0.00585 | 0.00192 |
| 11 | 36.2 | 0.05313 | 0.00554 | 0.00182 |
| 10 | 33 | 0.04977 | 0.00519 | 0.00171 |
| 9 | 29.8 | 0.04606 | 0.0048 | 0.00158 |
| 8 | 26.6 | 0.04205 | 0.00439 | 0.00144 |
| 7 | 23.4 | 0.03776 | 0.00394 | 0.00129 |
| 6 | 20.2 | 0.0332 | 0.00347 | 0.00114 |
| 5 | 17 | 0.0284 | 0.00296 | 0.00097 |
| 4 | 13.8 | 0.02337 | 0.00244 | 0.0008 |
| 3 | 10.6 | 0.01812 | 0.00189 | 0.00062 |
| 2 | 7.4 | 0.01266 | 0.00132 | 0.00043 |
| 1 | 4.2 | 0.00698 | 0.00073 | 0.00024 |
| 0 | 0 | 0 | 0 | 0 |

Table 2:

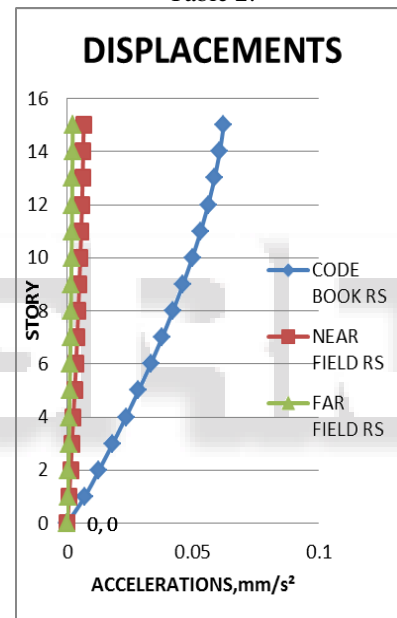


Fig. 1: Displacements

| S | E | CRS | NFRS | FFRS |
|----|------|---------|---------|---------|
| | m | mm | mm | mm |
| 15 | 49 | 0.06602 | 0.00678 | 0.00223 |
| 14 | 45.8 | 0.06425 | 0.0066 | 0.00217 |
| 13 | 42.6 | 0.06195 | 0.00636 | 0.00209 |
| 12 | 39.4 | 0.05914 | 0.00607 | 0.002 |
| 11 | 36.2 | 0.05589 | 0.00574 | 0.00189 |
| 10 | 33 | 0.05225 | 0.00537 | 0.00176 |
| 9 | 29.8 | 0.04826 | 0.00496 | 0.00163 |
| 8 | 26.6 | 0.04396 | 0.00452 | 0.00148 |
| 7 | 23.4 | 0.03938 | 0.00405 | 0.00133 |
| 6 | 20.2 | 0.03454 | 0.00356 | 0.00117 |
| 5 | 17 | 0.02946 | 0.00304 | 0.00099 |
| 4 | 13.8 | 0.02415 | 0.00249 | 0.00081 |
| 3 | 10.6 | 0.01862 | 0.00192 | 0.00063 |
| 2 | 7.4 | 0.01288 | 0.00133 | 0.00043 |
| 1 | 4.2 | 0.00694 | 0.00072 | 0.00023 |
| 0 | 0 | 0 | 0 | 0 |

Table 2: Story Displacements Asymm STR

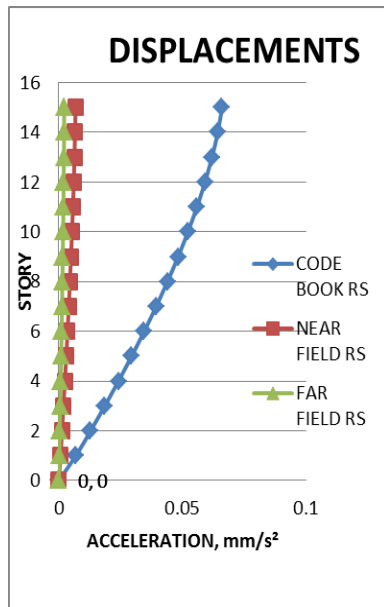


Fig. 2:

B. Story Drifts

The story drifts represent the amount by which each story of a structure subjected to seismic forces has drifted. The story drifts for the symmetric and the asymmetric structures analysed using the various developed response spectrums are shown in Table 3 and Table 4.

C. Story Shears

Story shear is the amount of shear developed or experienced at each story of a structure when the structure is subjected to seismic forces. The story shear for the symmetric and the asymmetric structures analysed using the various developed response spectrums are shown in Table 5 and Table 6.

| S | E | CRS | NFRS | FFRS |
|----|------|----------|----------|-----------|
| | m | | | |
| 15 | 49 | 1.30E-06 | 5.85E-08 | 1.877E-08 |
| 14 | 45.8 | 1.33E-06 | 8.23E-08 | 2.637E-08 |
| 13 | 42.6 | 1.38E-06 | 1.03E-07 | 3.284E-08 |
| 12 | 39.4 | 1.42E-06 | 1.18E-07 | 3.783E-08 |
| 11 | 36.2 | 1.47E-06 | 1.30E-07 | 4.193E-08 |
| 10 | 33 | 1.51E-06 | 1.40E-07 | 4.543E-08 |
| 9 | 29.8 | 1.55E-06 | 1.48E-07 | 4.826E-08 |
| 8 | 26.6 | 1.58E-06 | 1.55E-07 | 5.049E-08 |
| 7 | 23.4 | 1.61E-06 | 1.61E-07 | 5.247E-08 |
| 6 | 20.2 | 1.64E-06 | 1.66E-07 | 5.438E-08 |
| 5 | 17 | 1.67E-06 | 1.71E-07 | 5.607E-08 |
| 4 | 13.8 | 1.69E-06 | 1.75E-07 | 5.747E-08 |
| 3 | 10.6 | 1.71E-06 | 1.80E-07 | 5.876E-08 |
| 2 | 7.4 | 1.71E-06 | 1.90E-07 | 6.064E-08 |
| 1 | 4.2 | 1.66E-06 | 1.70E-07 | 5.674E-08 |
| 0 | 0 | 0 | 0 | 0 |

Table 3: Story Drifts Symm Str

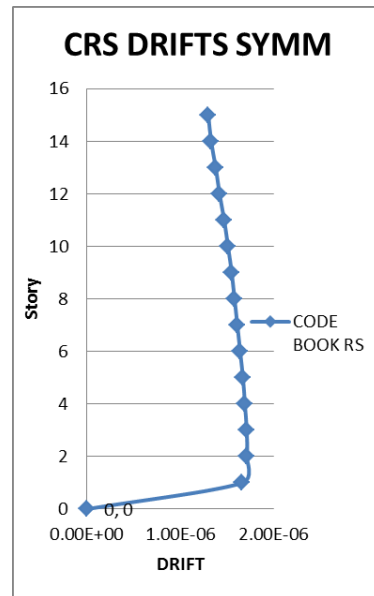


Fig. 3: Crs Drifts Symm

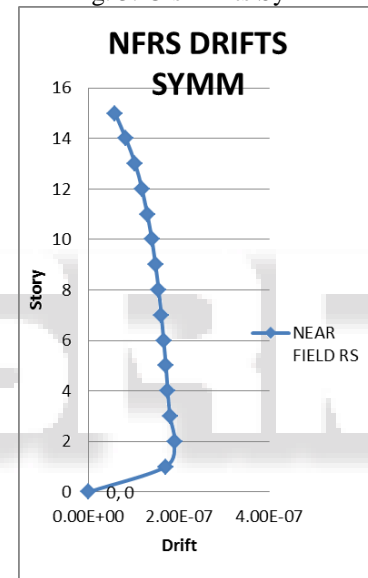


Fig. 4: Nfrs Drifts Symm

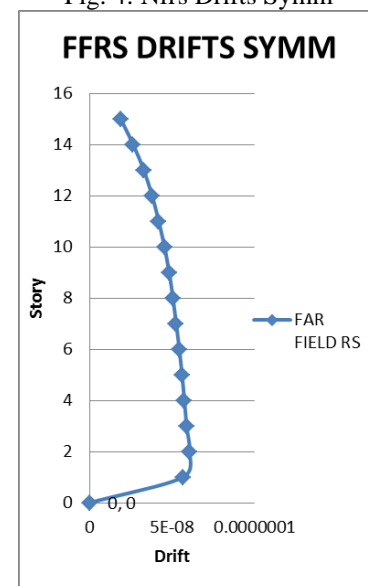


Fig. 5: Ffrs Drifts Symm

| S | E | CRS | NFRS | FFRS |
|----|------|---------|----------|----------|
| | m | | | |
| 15 | 49 | 1.3E-06 | 6.66E-08 | 2.13E-08 |
| 14 | 45.8 | 1.4E-06 | 9.14E-08 | 2.92E-08 |
| 13 | 42.6 | 1.5E-06 | 1.12E-07 | 3.60E-08 |
| 12 | 39.4 | 1.5E-06 | 1.3E-07 | 4.11E-08 |
| 11 | 36.2 | 1.5E-06 | 1.40E-07 | 4.52E-08 |
| 10 | 33 | 1.6E-06 | 1.50E-07 | 4.86E-08 |
| 9 | 29.8 | 1.6E-06 | 1.58E-07 | 5.12E-08 |
| 8 | 26.6 | 1.7E-06 | 1.63E-07 | 5.33E-08 |
| 7 | 23.4 | 1.7E-06 | 1.69E-07 | 5.52E-08 |
| 6 | 20.2 | 1.7E-06 | 1.74E-07 | 5.69E-08 |
| 5 | 17 | 1.7E-06 | 1.78E-07 | 5.84E-08 |
| 4 | 13.8 | 1.8E-06 | 1.82E-07 | 5.97E-08 |
| 3 | 10.6 | 1.8E-06 | 1.86E-07 | 6.1E-08 |
| 2 | 7.4 | 1.7E-06 | 1.92E-07 | 6.27E-08 |
| 1 | 4.2 | 1.7E-06 | 1.71E-07 | 5.56E-08 |
| 0 | 0 | 0 | 0 | 0 |

Table 4: Story Drifts Asymm Str

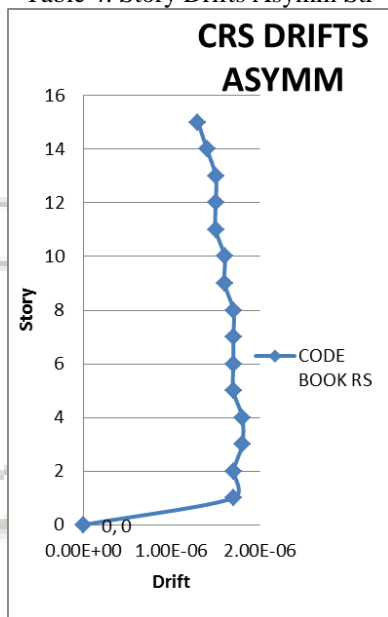


Fig. 6: Crs Drifts Asymm

| S | E | L | CRS | NFRS | FFRS |
|----|------|--------|--------|--------|--------|
| | m | | kN | kN | kN |
| 15 | 49 | Top | 0.2332 | 0.0254 | 0.0076 |
| | | Bottom | 0.2332 | 0.0254 | 0.0076 |
| 14 | 45.8 | Top | 0.4481 | 0.0482 | 0.0147 |
| | | Bottom | 0.4481 | 0.0482 | 0.0147 |
| 13 | 42.6 | Top | 0.6136 | 0.0651 | 0.0203 |
| | | Bottom | 0.6136 | 0.0651 | 0.0203 |
| 12 | 39.4 | Top | 0.7366 | 0.0775 | 0.0245 |
| | | Bottom | 0.7366 | 0.0775 | 0.0245 |
| 11 | 36.2 | Top | 0.834 | 0.0876 | 0.0279 |
| | | Bottom | 0.834 | 0.0876 | 0.0279 |
| 10 | 33 | Top | 0.9177 | 0.0965 | 0.0308 |
| | | Bottom | 0.9177 | 0.0965 | 0.0308 |
| 9 | 29.8 | Top | 0.9918 | 0.1042 | 0.0334 |
| | | Bottom | 0.9918 | 0.1042 | 0.0334 |
| 8 | 26.6 | Top | 1.0593 | 0.1109 | 0.0358 |
| | | Bottom | 1.0593 | 0.1109 | 0.0358 |
| 7 | 23.4 | Top | 1.1243 | 0.1174 | 0.0381 |
| | | Bottom | 1.1243 | 0.1174 | 0.0381 |

| | | | | | |
|---|------|--------|--------|--------|--------|
| 6 | 20.2 | Top | 1.1884 | 0.1243 | 0.0403 |
| | | Bottom | 1.1884 | 0.1243 | 0.0403 |
| 5 | 17 | Top | 1.2509 | 0.131 | 0.0424 |
| | | Bottom | 1.2509 | 0.131 | 0.0424 |
| 4 | 13.8 | Top | 1.3137 | 0.1374 | 0.0445 |
| | | Bottom | 1.3137 | 0.1374 | 0.0445 |
| 3 | 10.6 | Top | 1.3809 | 0.1442 | 0.0468 |
| | | Bottom | 1.3809 | 0.1442 | 0.0468 |
| 2 | 7.4 | Top | 1.4476 | 0.1513 | 0.0489 |
| | | Bottom | 1.4476 | 0.1513 | 0.0489 |
| 1 | 4.2 | Top | 1.4966 | 0.1569 | 0.0505 |
| | | Bottom | 1.4966 | 0.1569 | 0.0505 |
| 0 | 0 | Top | 0 | 0 | 0 |
| | | Bottom | 0 | 0 | 0 |

Table 5: Story Shears Symm Str

| S | E | L | CRS | NFRS | FFRS |
|----|------|--------|--------|--------|--------|
| | m | | kN | kN | kN |
| 15 | 49 | Top | 0.2284 | 0.0247 | 0.0076 |
| | | Bottom | 0.2284 | 0.0247 | 0.0076 |
| 14 | 45.8 | Top | 0.4348 | 0.0464 | 0.0145 |
| | | Bottom | 0.4348 | 0.0464 | 0.0145 |
| 13 | 42.6 | Top | 0.589 | 0.0621 | 0.0195 |
| | | Bottom | 0.589 | 0.0621 | 0.0195 |
| 12 | 39.4 | Top | 0.6999 | 0.0732 | 0.0232 |
| | | Bottom | 0.6999 | 0.0732 | 0.0232 |
| 11 | 36.2 | Top | 0.7864 | 0.0821 | 0.0262 |
| | | Bottom | 0.7864 | 0.0821 | 0.0262 |
| 10 | 33 | Top | 0.8616 | 0.09 | 0.0289 |
| | | Bottom | 0.8616 | 0.09 | 0.0289 |
| 9 | 29.8 | Top | 0.9291 | 0.0966 | 0.0312 |
| | | Bottom | 0.9291 | 0.0966 | 0.0312 |
| 8 | 26.6 | Top | 0.9909 | 0.1023 | 0.0331 |
| | | Bottom | 0.9909 | 0.1023 | 0.0331 |
| 7 | 23.4 | Top | 1.0509 | 0.108 | 0.0351 |
| | | Bottom | 1.0509 | 0.108 | 0.0351 |
| 6 | 20.2 | Top | 1.1099 | 0.1142 | 0.0372 |
| | | Bottom | 1.1099 | 0.1142 | 0.0372 |
| 5 | 17 | Top | 1.1669 | 0.1203 | 0.0392 |
| | | Bottom | 1.1669 | 0.1203 | 0.0392 |
| 4 | 13.8 | Top | 1.2247 | 0.1263 | 0.0411 |
| | | Bottom | 1.2247 | 0.1263 | 0.0411 |
| 3 | 10.6 | Top | 1.2889 | 0.1329 | 0.0432 |
| | | Bottom | 1.2889 | 0.1329 | 0.0432 |
| 2 | 7.4 | Top | 1.3544 | 0.1399 | 0.0453 |
| | | Bottom | 1.3544 | 0.1399 | 0.0453 |
| 1 | 4.2 | Top | 1.4023 | 0.1453 | 0.0469 |
| | | Bottom | 1.4023 | 0.1453 | 0.0469 |
| 0 | 0 | Top | 0 | 0 | 0 |
| | | Bottom | 0 | 0 | 0 |

Table 6: Story Shears Symm Str



Fig. 7: Nfrs Drifts Asymm

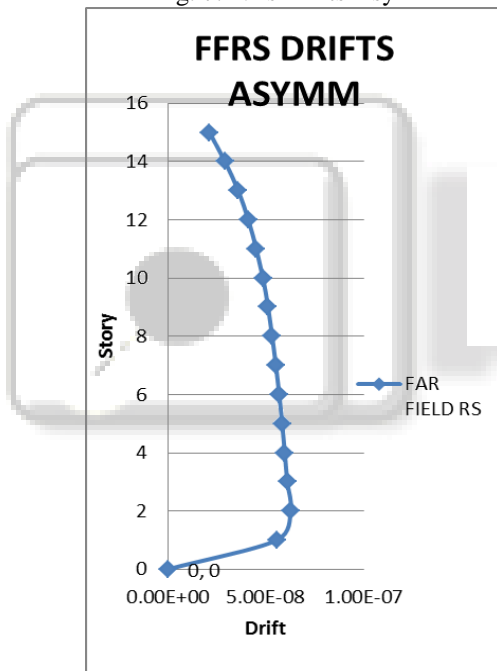


Fig. 8: Ffrs Drifts Asymm

IV. TERMS USED AND THEIR FULL FORMS

S – Story, E – Elevation, L – Location, CRS – Code book response spectrum (developed using IS:1893:2002 equations), NFRS – Near field response spectrum (developed using attenuation equation for a lower value of hypocentrals distance), FFRS – Far field response spectrum(developed using attenuation equation for a higher value of hypocentral distance)

The results have been obtained and the comparative study is carried out. It can be seen that the values of displacements for the structures analysed using the attenuation equation has lesser amount of displacement for both the near and far field response spectrum analysis as compared to the displacement values obtained for the structure analysed using the equation provided in the

IS:1893:2002. Similarly the values of story drifts and the story shears are comparatively higher for the structure analysed using the acceleration values obtained using the equations from IS:1893:2002 as compared to the values obtained for structure analysed using the acceleration values obtained using the attenuation equation. As the response values are higher for the structure analysed using the IS:1893:2002 equation the reinforcement to be provided in the structure are comparatively higher than the minimal amount required which results in higher dead load stresses in the structure and also leads to an uneconomical design. The main advantage of the attenuation equation is that it takes into consideration the hypocentral distance as well as the magnitude of the earthquake event consider, as a result of which we get the values with respect to the amount of seismicity felt in a specific region due to a certain magnitude of earthquake from the earthquake source. Depending upon these values the structural steel can be designed properly to incorporate the amount of seismicity felt in that specific region which also results in economical design. Hence it is very important that the Response spectrum provided in the IS:1893:2002 be revised appropriately so that it can accommodate each and every region of the country effectively.

V. SUMMARY & CONCLUSIONS

In this article response spectrum analysis has been carried by separately developing the response spectrums using the equations provided in the IS:1893:2002 and the attenuation equation. First the dimensions of the models to be developed are ascertained by trial and error method. The models developed are checked by using equivalent static method by comparing the base shear values obtained for the models developed in the software ETABS 2013 and the base shear values obtained manually. Now the acceleration values obtained using code book equations and the far field and near field acceleration values obtained from the attenuation equation are entered in 3 separate symmetric and asymmetric models and analysis is carried out. After the completion of analysis the results for the parameters displacements, drifts and shears are obtained. From the comparative study of the these parameters for various structures we obtain that the values obtained using IS:1893:2002 equations are comparatively higher as compared to the values for the far and near field equations. The values will lead to an uneconomical design of the structure and also develop extra stresses for the acceleration values of IS:1893:2002 equation, whereas the attenuation equation values gives results as per the seismic condition of the site and the distance from the source of seismic action which helps in providing economical design of structures and no extra stresses would be bared by the structure.

REFERENCES

- [1] Development Of Probabilistic Seismic Hazard Map Of India Final Report Technical Report
- [2] Of The Working Committee of Experts (Wce) Constituted By Natural Disaster Management Authority Govt Of India, New Delhi.
- [3] Seismic Hazard Estimation For Mumbai City. S. T. G. Raghu Kanth And R. N. Iyengar.

- [4] Seismic Hazard Mapping Of Delhi City. R.N.Iyengar1 And S.Ghosh, 13th World Conference On Earthquake Engineering, Vancouver, B.C., Canada, August 1-6, 2004, Paper No. 180.
- [5] Seismic Hazard Analysis For Bangalore Region, T.G.Sitharam And P.Anbazhagan, Natural Hazards (2007) 40:261 – 278, Doi 10.1007/S11069 – 006 – 0012 – Z.
- [6] Estimating Seismic Hazard For Central And Southern India, K.S. Jaiswal And R. Sinha., The 14th, World Conference On Earthquake Engineering, October 12-17, 2008, Beijing, China.
- [7] Probabilistic Seismic Hazard Studies Of East Coast Region Of India., L. Kanagarathinam
- [8] , G. R. Dodagoudar And A. Boominathan, The 14th, World Conference On Earthquake Engineering, October 12-17, 2008, Beijing, China.
- [9] Site Specific Seismic Hazard Assessment For Hyderabad City. K. Tirumala Reddy, P. Sreenivas Sarma And S. Jayaprakash Narayana, International Journal Of Earth Sciences And Engineering, Issn 0974 – 5904, Vol.03,No.05, October 2010, Pp.696 – 707.



Performance Study of High Rise Buildings with Diagrid and Hexagrid Systems under Dynamic Loading

Deepika R¹, Shivanand C.G², Dr. Amarnath K³
P G Student¹, Assistant Professor², Professor and HOD³

Department of Civil Engineering
The Oxford College of Engineering, Bangalore, Karnataka, India

Abstract:

Advances in technology, change in life style of people, requirements of present population has increased the growth of tall buildings. Load action on tall building are very much different than the low rise building, lateral loads due to wind and earthquake would produce more effect on high rise buildings. There are many lateral load resisting systems mainly classified into interior structures and exterior structures since diagrid and hexagrid systems are provided at outer periphery of buildings it comes under exterior structures. Normal bracing systems will be uneconomical, if number of stories are more than 25 hence, a new grid system has been developed i.e. diagrid system. As compared to other systems diagrid are aesthetically more pleasing and gives better stiffness to structures. Here, analysis of normal framing system without any load resisting system, diagrid with varied diagonal angles and hexagrid system will be conducted by using analysis and design software extended three dimensional analyses of building systems (ETABS V15.2). A regular floor plan of square shape of 30mx30m is considered, all structural members are designed as per IS 456-2000. Wind and earthquake parameters are considered from IS875- 1987 (part III) and IS1893-2002 respectively. Analysis results are compared in terms of storey drift, storey displacement, time period and overturning moment.

Keywords: diagrid, hexagrid, drift, displacement, overturning moment

I. INTRODUCTION

Tall building or high rise structures construction are more in this era; due to increase in population, economic prosperity and also due to the scarcity of lands high-rise structures are preferred. Height is main criteria in this kind of buildings, demand for tall buildings has increased because of increase in demand for business and residential space, advances in constructions, high strength structural elements, materials and also various software like Etabs, Staadpro etc these are analysis and design software's have provided growth of high rise structures.

In 19th century tall buildings were built in U.S.A but now a days due to people needs tall buildings are constructing every where this leads to sustainable development of society that is "development that meets the expectations and needs of present generation without compromising the ability of future generations to meet their requirements". According to studies and published articles in 1980, most of tall buildings were located in America and now recent studies shows that number of tall buildings and construction process is more in Asian countries, it is of about 32% and 24% in north America and Europe. Generally tall buildings are constructed and used for commercial office buildings, apartments etc.

Construction of tall buildings are not easy as that of normal conventional buildings due to the action of lateral loads, lateral displacement will induces bending and shear lag effects will be more so that in order to resist lateral loads new systems were invented known as lateral load resisting systems some of them are

- a) Interior structures
 - ❖ Rigid frame
 - ❖ Shear wall structure
 - ❖ Outrigger structure

- b) Exterior structures
 - ❖ Tube system
 - ❖ Diagrid system
 - ❖ Space truss
 - ❖ Exoskeleton structure
 - ❖ Super frame structure

Braced frames are structural elements those are mainly designed to resist earthquake loads and wind loads. Bracing system is highly efficient; they provide more strength and stiffness against horizontal shear because the diagonal member elements work in axial stress.

For tall steel buildings braces are used as lateral resisting systems in that mainly there are four types

- ❖ Single braces
- ❖ Double braces
- ❖ Triangular braces and
- ❖ Eccentric braces.

Usages of braces are not aesthetically good so those braces are usually provided in the interior of buildings. After braces tube structures, outrigger structures are introduced in 1960s. Architectures always wanted some new look for each and in order to meet their requirements a new load resisting system is recently introduced that is diagrid system.

Diagrid systems are better than conventional bracing systems because of following reasons

- ❖ Almost all conventional (vertical) columns were eliminated in case diagrid systems
- ❖ Diagrid are used in case skyscrapers (above 150m or 40 stories) and it is more economical but typical bracings are limited up to 25 storey building.

Diagrid are made up diagonal elements they are triangular structures with supporting beams, this system would provide more flexibility to interior planning and façade appearance is also improved because numbers of elements required are reduced. The diagrid structures are more efficient than conventional exterior braces systems this is only because almost all the vertical columns are eliminated, diagonal grid element alone itself carry all lateral and vertical loads, but conventional exterior braces carry only vertical loads. One of main advantage of this system is that up to 20% to 30% of steel can be saved at outer periphery compared normal conventional building. By using this system the high rise structures can be built to any shape like square, rectangle and curved structures etc.

II. METHODOLOGY

In this work comparison of hexagrid and diagrid with varied diagonal angles under dynamic loading are carried out. For the analysis a suitable plan of square shape is considered (G+29 building) dead loads and live loads are considered as per Indian standards.

In order to evaluate performance of all the models under dynamic loading seismic analysis is essential, columns are not provided at outer periphery for both diagrid and hexagrid and same dimensions are maintained.

III. COMMON BUILDING PARAMETERS

Table I: Building parameters

| Description | Value |
|-------------------------------------|----------------------|
| Plan dimension | 30mx30m |
| Height of building | 90m |
| Floor to floor height | 3m |
| Depth of slab | 120mm |
| Number of stories | 30 |
| Characteristic strength of concrete | 30N/mm ² |
| Characteristic strength of steel | 415N/mm ² |

A) Plan and elevation view:

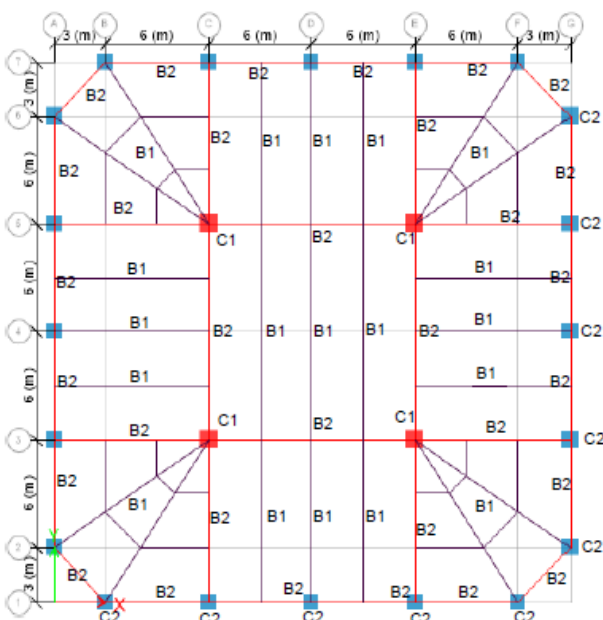


Figure 1: conventional building

Beam and column dimensions

B1 – 250mm*450mm

B2 – 300mm*600mm

C1 - 1000mm*1000mm

C2 – 900mm*900mm

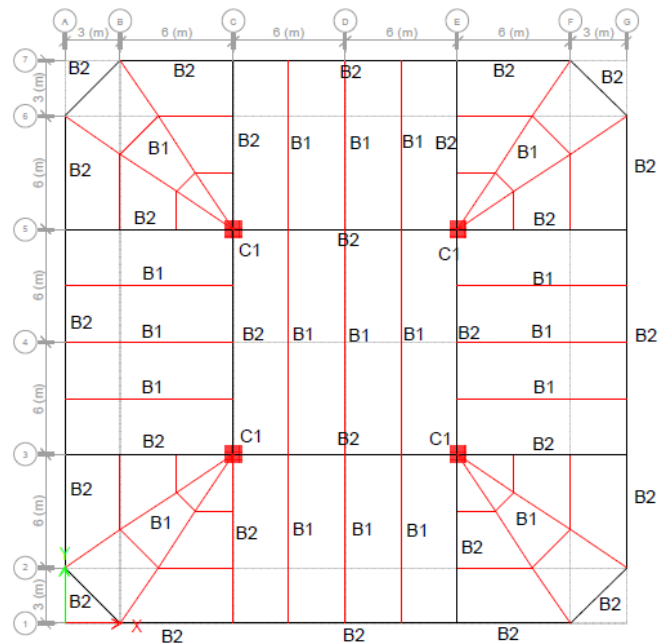


Figure 2: plan view for diagrid and hexagrid systems

Beam and column dimensions

B1 – 250mm*450mm

B2 – 300mm*600mm

C1 – 900mm*900mm

D1 – 450mm*450mm

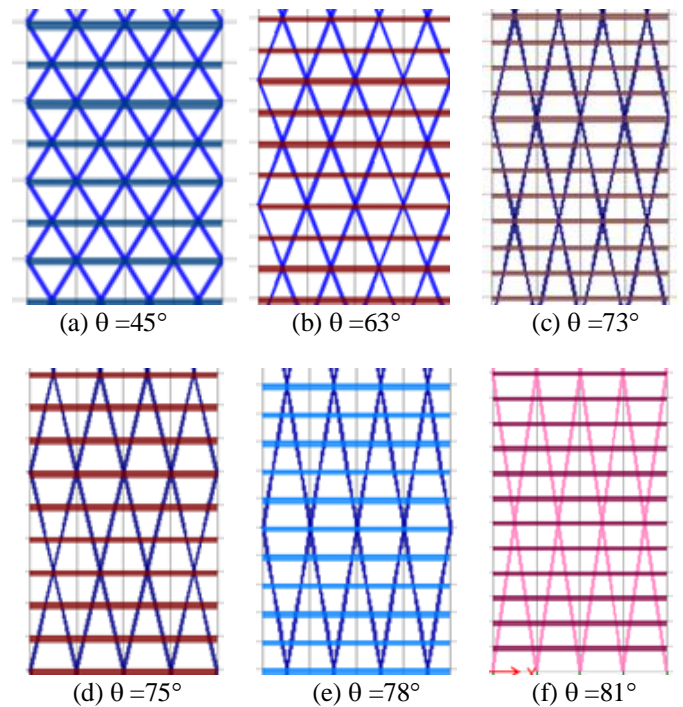


Figure 3: Elevation view of diagrid systems

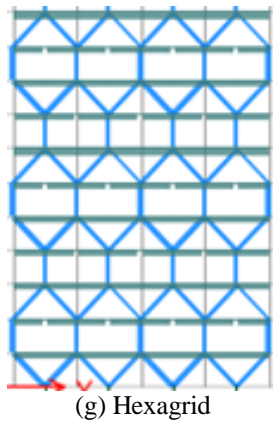


Figure 4: Elevation view of hexagrid system

B) Wind and seismic parameters

Table II: wind and seismic parameters

| PARAMETERS | |
|------------------------------|---------------------------|
| Seismic parameters | Wind parameters |
| Location: Amritsar | Wind speed, V_b : 47m/s |
| Zone: IV | Terrain category: 3 |
| Importance factor: 1.0 | Class C |
| Response reduction factor: 5 | $\theta < 3^\circ$ |
| Soil type: medium soil | $k_1, k_3 = 1$ |

IV. MODELING AND ANALYSIS

A) Diagrid and hexagrid structures:

In order to study the performance of diagrid and hexagrid buildings, analysis is done by using ETABS V15.2; this is one of sophisticated commercially used software for analysis of tall/high rise structures. This software is also used in the analysis and design of complex shaped building models including non-linear behaviors.

The dimensions and structural properties are maintained same for all models only diagonal angles are changed diagrid systems

- ❖ Normal conventional building without any load resisting system [R1]
- ❖ Diagrid building with diagonal angle of 45° [M1]
- ❖ Diagrid building with diagonal angle of 63° [M2]
- ❖ Diagrid building with diagonal angle of 73° [M3]
- ❖ Diagrid building with diagonal angle of 75° [M4]
- ❖ Diagrid building with diagonal angle of 78° [M5]
- ❖ Diagrid building with diagonal angle of 81° [M6]
- ❖ Hexagrid building [M7]

V. ANALYSIS RESULTS

Here, linear static, linear dynamic and non-linear dynamic analysis are performed and analysis results are represented in terms

- ❖ Storey drift
- ❖ Storey displacement
- ❖ Time period
- ❖ Overturning moment

A) Storey drifts:

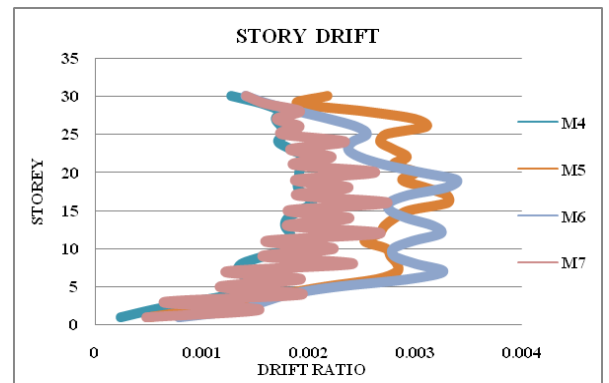
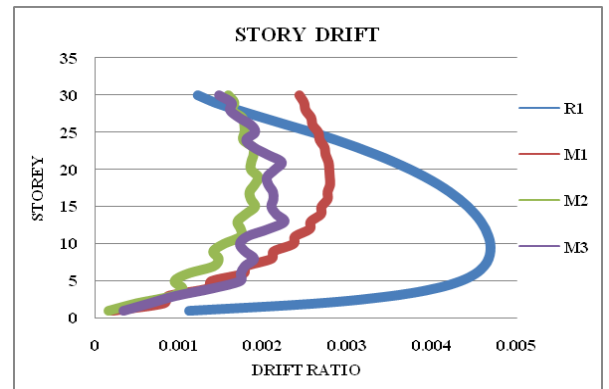


Figure 5: Storey drift ratio for different grid systems under earthquake load case

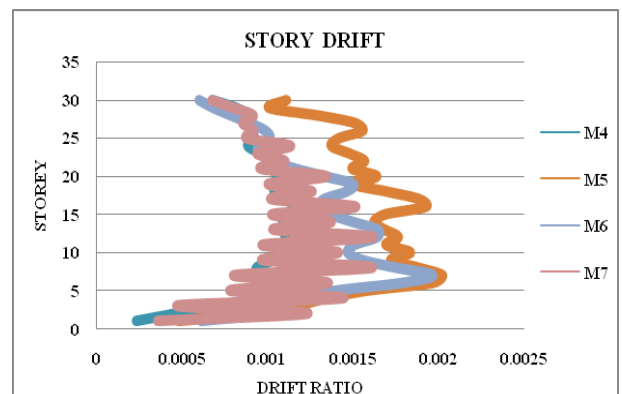
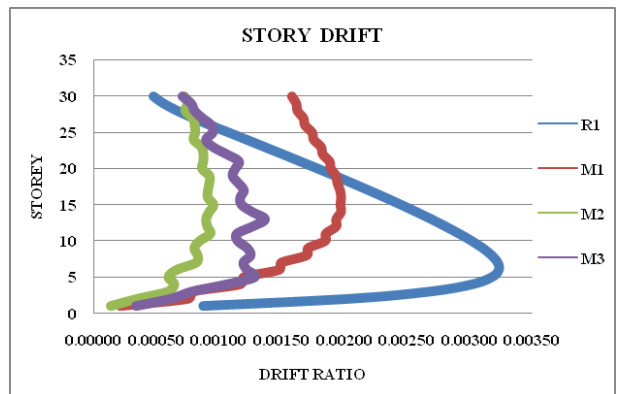


Figure 6: Storey drift ratio for different grid systems under wind load case

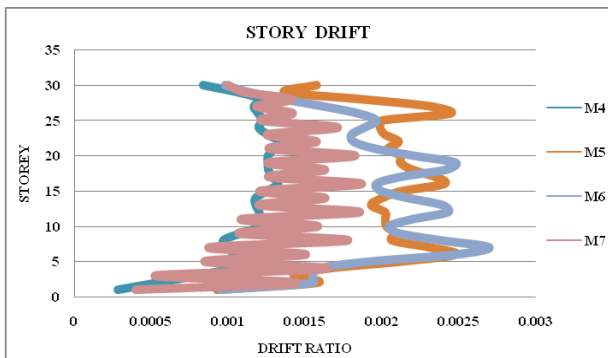
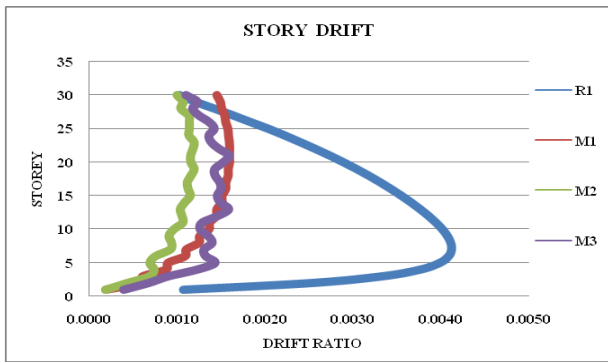


Figure 7: Storey drift ratio for different grid systems under response spectrum case

B) Storey displacement:

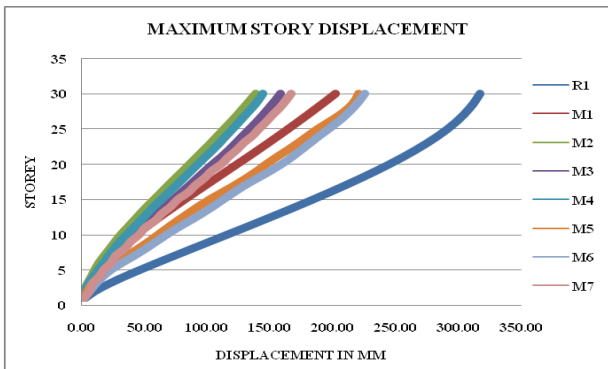


Figure 8: Storey displacement for different grid systems under earthquake load case

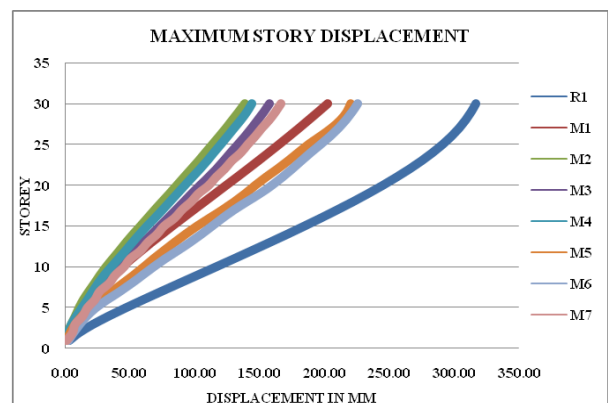


Figure 9: Storey displacement for different grid systems under wind load case

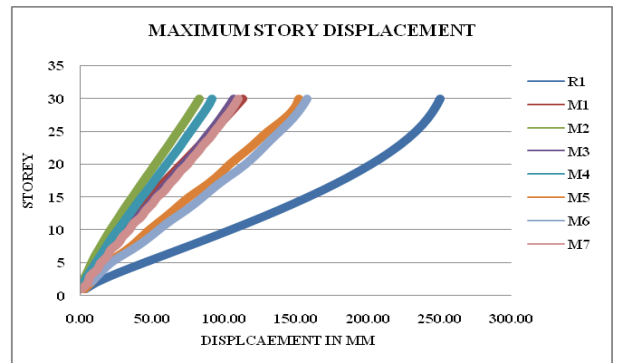


Figure 10: Storey displacement for different grid systems under response spectrum case

C) Overturning moment:

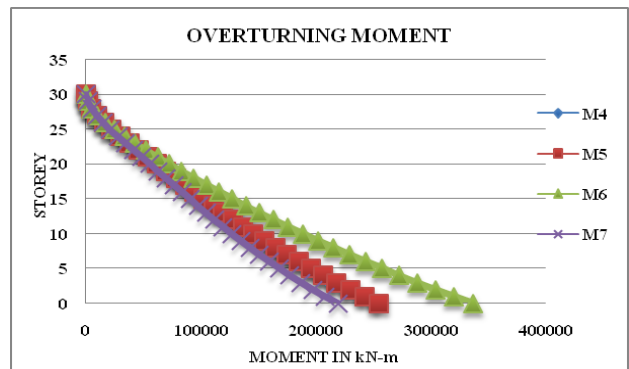
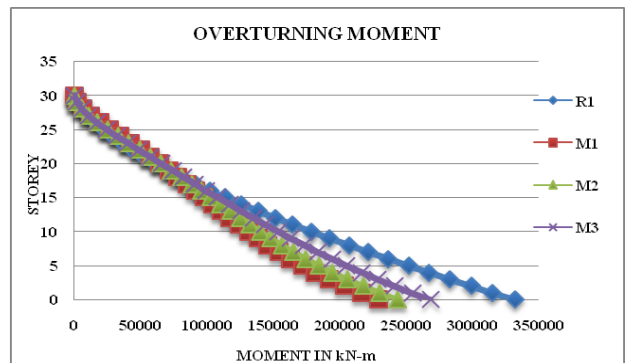


Figure 11: overturning moment for different grid systems under response spectrum case

D) Time period

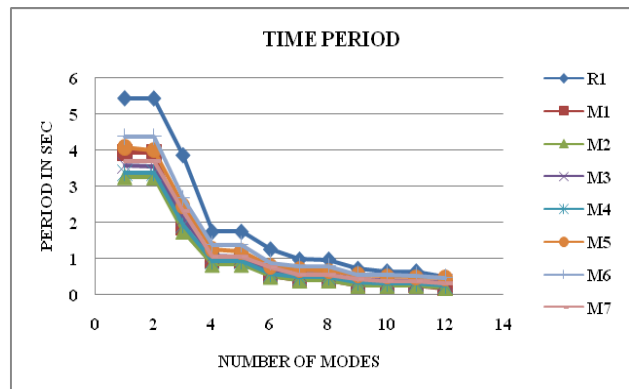


Figure 12: Time period for all models

Table III: Time period

| Models | Modes | |
|--------|-------|-------|
| | 1 | 12 |
| R1 | 5.433 | 0.488 |
| M1 | 3.926 | 0.198 |
| M2 | 3.268 | 0.199 |
| M3 | 3.577 | 0.335 |
| M4 | 3.381 | 0.26 |
| M5 | 4.082 | 0.466 |
| M6 | 4.382 | 0.477 |
| M7 | 3.69 | 0.319 |

VI. CONCLUSION

The present work is consists of analysis of diagrid systems with different diagonal angles i.e. 45°, 63°, 73°, 75°, 78°, 81° and analysis of hexagrid system. As we can see the results from above plots and we may conclude that

- Top storey displacement is less for diagrid system with diagonal angle of 63°
- Between the region 63° to 75° (diagonal angle) diagrid systems posses better stiffness, storey drift and storey displacement are less in this regions
- For hexagrid system also same section properties are maintained in order to study the performances but this system shows slightly higher storey displacement and drift compared to diagrid system (63° to 75°)
- Here we can notice that difference in storey displacement and storey drift of hexagrid and diagrid systems are not so high it is about 20mm to 30mm
- We know that as time period increases stiffness of member decreases, 63° diagrid system has less time period compared to other systems.

VII. REFERENCES

[1] Ali kheyroddin and Niloufar mashhadiali - Proposing the hexagrid system as a new structural system for tall buildings (Feb 2012)

[2] Barry Charnish and Terry Mc Donnell- the bow: unique diagrid structural system for sustainable tall buildings (2009)

[3] Giulia milana, franco Bontempi, pierluigi Olmati, konstantinos Gkoumas- Ultimate Capacity of Diagrid Systems for Tall Buildings in Nominal Configuration and Damaged State (Feb 2015)

[4] J. Kim, Y. Jun and Y.-Ho Lee- Seismic Performance Evaluation of Diagrid System Buildings (June 2010)

[5] Investigation of shear-lag effect in high-rise buildings with diagrid system- Johan Leonard (2005)

[6] Kavya A.J. B.K. Raghu Prasad- Comparative performance of octagrid and hexagrid lateral load resisting systems for tall building structure (Nov 2014)

[7] Khushbu Jania, Paresh V. Patelb- Analysis and design of diagrid structural system for high rise steel buildings (Jan 2013)

[8] Kyoung sun moon- Structural Design and Construction of Complex-Shaped Tall Buildings (2008)

[9] Kyoung-Sun Moon, John E. Fernandez and Jerome J. Connor- Diagrid structural systems for tall buildings: characteristics and methodology for preliminary design (2007)

[10] Lekshmi Mohan, C.K. Prasad Varma Thampan- Numerical Modelling and Evaluation of Hybrid Diagrid Structures (june-2015)

[11] Mr. Devaraja R, Rajalaxmi M Megadi- Analysis of curved perimeter diagrid lateral system (june-2014)

[12] Nishith B. Panchal, Dr. V. R. Patel, Dr. I. I. Pandya- Optimum angle of diagrid structural system (june-2014)

[13] Nishith B. Panchal, Dr. V. R. Patel- Diagrid structural system: strategies to reduce lateral forces on high rise building (April 2014)

[14] Rohit kumar singh, Dr. Vivek grag, Dr. Abhay Sharma- Analysis and design of concrete diagrid building and its comparison with conventional frame building (Sept 2014)

[15] Raghunath .D. Deshpandhe, Sadanand M. Patil, Subramanya Ratan- Analysis and comparison of diagrid and conventional structural system (2015)

[16] Ravi K Revankar, Talasadar R.G- Pushover Analysis of Diagrid Structure (Sept 2014)

[17] T M Boake- Diagrid structures: innovation and detailing

[18] Comparative Study of Pentagrid and Hexagrid Structural System for Tall Building- Taranath S.D, Mahantesh N.B (Aug 2014)

[19] Sree harsha J, K Raghu- Analysis of tall buildings for desired angle of diagrids (April 2015)

[20] Matin Alaghmandan, Payam Bahrami, Mahjoub Elnimeiri- The Future Trend of Architectural Form and Structural System in High-Rise Buildings

[21] IS-1893 (Part-2)-2002 Indian standard- criteria for earthquake resistant design of structures

[22] IS-875 (Part-1)-1987 code of practice for design loads (other than earthquake loads) for buildings and structures: part-1 for dead loads

[23] IS-875 (Part-2)-1987 code of practice for design loads (other than earthquake loads) for buildings and structures: part-2 for imposed loads

[24] IS-875 (Part-3)-1987 code of practice for design loads (other than earthquake loads) for buildings and structures: part-2 for wind loads

HOME / ARCHIVES / VOL. 2 NO. 1 (2016): VOLUME 2 SPECIAL ISSUE 1(MAY - 2016) / Articles

EVALUATION OF MECHANICAL AND TRIBOLOGICAL CHARACTERIZATION OF GLASS-BASALT HYBRID COMPOSITES

Keywords: Composite materials, Hybrid composite, silicon carbide, Basalt fibers, Glass fibers

ABSTRACT

Fiber reinforced polymer composites (FRPCs) are used in almost all type of advanced engineering structures like aircraft, boats, ships and, helicopters, automobiles, sporting goods, chemical processing equipment etc. In the field of composite materials the fiber reinforced composite consisting of one fiber is used for long time. The results would have appeared for certain area. This is because use of single fiber consisting of limited property. To overcome this problem the use of another fiber is made. This results in the form of hybrid composite. In this paper glass and basalt fibers are used in the form of hybrid composite. The characteristics of both the materials are discussed here. Epoxy binders are widely used as matrix in many FRPCs. They are a class of thermoset materials provide a unique balance of chemical and mechanical properties. For epoxy based fiber laminates, the typical reinforcements are glass, carbon, aramid and basalt fibers have been used to improve the overall properties of the composite laminate. By adding the filler to the composite material we can further improve the performance of composites. The filler use in this paper is the silicon carbide. The silicon carbide is known for its high hardness. Now a days hybrid composites used in the high level applications.

 PDF

PUBLISHED

2016-05-15

HOW TO CITE



Sign in to semanticscholar.org with Google

- A** Anup upadhyaya
anupmupadhyaya5@gmail.com
- n** ncsem mechanical
ncsemmechanical@gmail.com

4 more accounts

Corpus ID: 42535103

Design of Rectenna Energy Harvesting From Ambient GSM and WLAN Frequency Bands

E. VinayB., Pallaviram Sure, Rohini Deshpande · Published 2016

Ambient wireless energy harvesting is a process of collecting unused wireless energy, which is abundantly available around us. Most of today's wireless communication services use GSM 900, GSM 1800 and WLAN frequency bands. The energy in these three frequency bands are available at most of the places at all the times. For harvesting this energy, this paper targets the design of a multiband antenna that encompasses the above said three frequency bands completely. For this purpose, a planar... [Expand](#)

[\[PDF\] sastechjournal.com](#)

Save

Alert

Feed

[Abstract](#)

[Figures and Tables](#)

[11 References](#)

[Related Papers](#)

Figures and Tables from this paper



By clicking accept or continuing to use the site, you agree to the terms outlined in our Privacy Policy, Terms of Service, and Dataset License

ACCEPT & CONTINUE

Enhanced Packet Dropping Algorithm and Neighbour Node Cluster Strategy for Intrusion Detection in MANET

E.Selvi¹ and M.S. Shashidara²

¹Department of Computer Science, Asan Memorial College of Arts and Science, Chennai, India

²Department of MCA, The Oxford College of Engineering, Bangalore, India

Abstract

In MANET, every mobile node acts as both a transmitter and a receiver via bidirectional wireless links without requirements of any fixed network infrastructure. Intrusion-detection mechanisms effectively protect MANET from attacks using pre-distributed keys. Many intrusion detection systems were developed for MANET to improve the security level and to detect the malicious attackers in the network. However malicious node identification and their subsequent isolation from network and problems posed due to pre-distributed keys remained unsolved, compromising securing and therefore increasing the routing overhead. In this research work an Intrusion Detection technique to detect the malicious node by providing better security and reducing the routing overhead called Integrated Cluster and Highest Connectivity-based Packet Dropping (IC-HCPD) for mobile ad hoc network is presented. Neighbor Node-based Cluster Formation is designed in the proposed IC-HCPD technique aiming at reducing the routing overhead by obtaining the route using minimal distance. Consequently, the neighbor node possessing highest connectivity is selected as the Detection Manager using Cluster algorithm based on Highest Connectivity. Finally, the Detection Manager monitors the nodes entering into and leaving the network and identifies the faulty node and isolates the node from the network through Packet Dropping mechanism. The simulation results show that IC-HCPD technique can effectively improve average packet delivery ratio, reduces routing overhead for data delivery, and improves security as compared with those of the tested algorithms.

Keywords: Mobile ad hoc network, malicious node, pre-distributed keys, Highest Connectivity, Packet Dropping

1. Introduction

Due to the inherent vulnerabilities of mobile ad hoc networks, new intrusion detection measures need to be developed to efficiently safeguard the route from further being deteriorated. This work focuses on the detection of intruder nodes and isolating them from the network. Identity of polluters in MANET was identified [1] by applying a fully distributed technique with low computational overhead. In [2] enhanced adaptive acknowledgement model was introduced to improve the malicious node detection behavior rate. A virtual clustering [3] model was applied in heterogeneous network to improve the packet forwarding rate in the presence of malicious nodes. Another distributed technique [4], called as encounter-based distribution algorithm to detect the malwares with the aid of content-based signature was presented. Link state routing [5] is an efficient method to detect malicious node and isolate them from the network, so that the network does not get further disrupted. Surveying adjacent nodes was another mechanism used in [6] that resulted in minimizing the false alarm and also sending and checking packet for neighbor nodes being transmission.

Adaptive distribution mechanism for intrusion detection has been used for a long time [7]. This technique introduced a flexible responsive scheme in various attack scenarios with low network overhead. Evaluation of classification algorithms to detect malicious activities in MANET and their comparison results was presented in [8].

Intrusion detection systems were used in the past by several researchers using different methods to detect intrusions in networks in an efficient manner. However, most of these methods only detected the intruders only with high false alarm rate. Intelligent Agent intrusion detection model [9] was presented by integrating attribute selection, outlier detection, and enhanced multiclass SVM classification methods to detect anomalies with low false alarm rate. But, with the increase in the congestion rate, intrusion model did not work efficiently.

In this paper we propose a new intrusion detection method which is called Integrated Cluster and Highest Connectivity-based Packet Dropping (IC-HCPD). This method detects the malicious node with the help of the detection manager. The detection manager on the other hand based on the neighbor information performs clustering and detects the intruder or malicious node through packet dropping mechanism and isolates the node from the network. Consequently, routing overhead is decreased whereas the packet delivery ratio malicious node detection behavior rate is increased considerably in this method.

The rest of this paper is organized as follows: Section 2 presents a brief introduction of related works. Section 3 proposes our Integrated Cluster and Highest Connectivity-based Packet Dropping (IC-HCPD) method. In Section 4 the simulation results will be described. Finally Section 5 concludes our discussion.

2. Background and related work

Some recent studies have examined and discussed the problem of intrusion detection methods in mobile ad hoc network. Some of them will be surveyed in this section. An integrated cultural algorithm and artificial fish swarm algorithm [13] for anomaly detection of nodes was presented using optimized back propagation model. In [14], KNN classification algorithm was applied which detected the intrusion with high detection rate that separated normal nodes from abnormal nodes in purview of identifying the intruder nodes.

In [15], a new algorithm for preventing the network against jamming attack strategies using heuristic algorithm was designed. In [16], intrusion rate was reduced by protecting the location privacy using steiner tree aiming at improving the privacy and reducing the communication cost substantially. In [17], a framework for wireless mesh networks was designed using cooperative cross layer framework.

In [18], non parametric cumulative sum was used to detect the rate of intrusion against cognitive radio networks. By learning the normal operational model, the proposed intrusion detection system was able to detect anomalous or abnormal behavior arising from an attack. Attacks may also arise due to resource depletion. In [19], routing protocol layer was investigated to measure the VAMPIRE attacks through network wide energy usage

All of the above said methods perform intrusion detection by either compromising the security when providing routing overhead and vice versa. In this paper we propose a new algorithm that performs intrusion detection by identifying the malicious node and isolating the node from the network.

3. Proposed Intrusion Detection technique

In this section, first the problem statement is described, then the novel strategy for intrusion detection in MANET is proposed and finally the Neighbor Node-based Cluster Formation and Highest Connectivity-based Detection Manager strategies are presented.

3.1 Problem statement

The nodes in MANETs assume that other nodes seldom cooperate with each other to relay data, which is exploited by malicious nodes and propagate intrusive attacks across the network. The mobile nodes in MANET change the topology at a faster rate resulting in the increase in routing overhead.

With autonomous collection of mobile nodes, intrusion detection is one of the major topics being analyzed in Mobile Ad hoc Network. Distributed techniques were employed to infer the identity of malicious nodes and digital signature were applied to demonstrate higher malicious behavior detection rates.

However, conventional distributed techniques cannot isolate the malicious node and with the random nature of the network application of pre-distributed key pattern, increases the routing overhead substantially.

In our technique, we consider MANET as an undirected graph ‘ $G = (V, E)$ ’, with transmission range ‘ R ’ where ‘ V ’ represents the set of nodes and ‘ E ’ represents the set of bidirectional links. However, due to the presence of intruders that utilize the loophole to carry out the malicious behavior and therefore nodes gets compromised and more data packets cannot be successfully delivered to destinations.

The cluster head or detection manager selection is invoked on-demand in the proposed technique, and is aimed to reduce the routing overhead and therefore the communication costs. By classifying the mobile nodes in the network into clusters, the proposed technique allows the Detection Manager (DM) to identify the faulty node and isolate the node from the network. To achieve the goal of intrusion detection of malicious nodes in MANET, in the presence of malicious node, this paper design an intrusion detection technique where detection manager detect the malicious node and improve the packet delivery ratio and reduces the routing overhead using clustering technology.

3.2 Neighbor Node-based Cluster Formation

In this section, a Neighbor Node-based Cluster Formation is designed aiming at reducing the routing overhead and transmitting data packets in an intrusion free model. Fig 1 shows an example of Neighbor Node-based Cluster Formation for the selection of intermediate nodes.

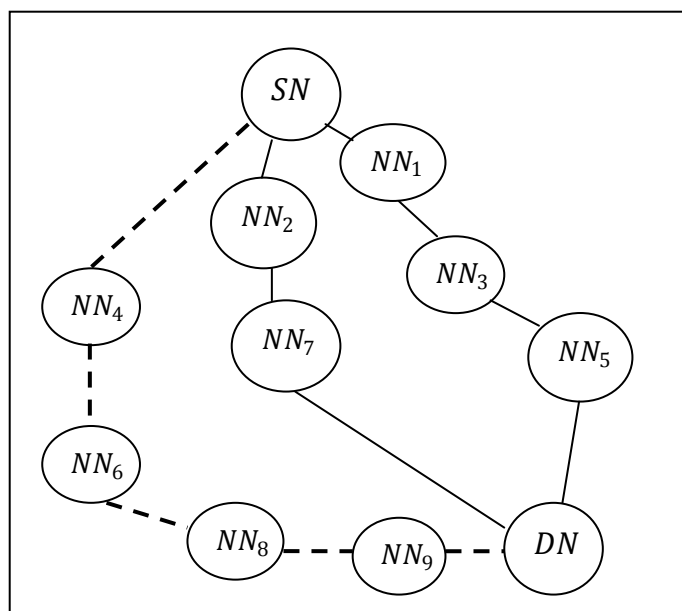


Fig.1 An example selection of intermediate nodes

As shown in fig 1, the source node is denoted as ‘ SN ’ and destination node by ‘ DN ’. Nine Neighbor Nodes ‘ $NN_1 - NN_7$ ’ exists between the source destination pair. Normal lines indicate the possible neighbor nodes through which routing can be proceeded whereas the dashed bold line denotes the final neighbor nodes selected through which transmission is forwarded.

In the proposed technique, the intermediate nodes from the source node ‘ SN ’ within the transmission range ‘ R ’ is measured to ensure secure routing through which data packets are transmitted and is formulated as given below.

$$IN = \sum_{i=1}^n \text{Min} (\text{Dis} (SN - NN_i)) \quad (1)$$

From (Eq.1), the distances between the source node and the neighbor nodes is first evaluated. Then, based on the result obtained, the minimum distance nodes are then selected as the intermediate nodes. If

more than one mobile node possesses similar minimal distance, then the residual distance is used as a basis to obtain the intermediate nodes and is formulated as given below.

$$IN = \sum_{i=1, j=2}^n \text{Min ResidualDis}(NN_i - NN_j) \tag{2}$$

In this way, by measuring the intermediate nodes, Neighbor Node-based Cluster Formation reduces the routing overhead and therefore minimizes the communication cost.

3.3 Highest Connectivity-based Detection Manager Selection

To achieve better packet delivery ratio, we need to keep track of the normal and malicious nodes to accordingly predict which route can be accessed through for packet or file transmission in the near future. With the intermediate nodes obtained using Neighbor Node-based Cluster Formation, the next step in the proposed technique is the identification of Detection Manager (DM). Every mobile node in MANET transmits or receives the data. The task of detection manager in the proposed work is to monitor the nodes which is entering and leaving the network and also identify the malicious node and isolate the node from the network.

In this work, a clustering algorithm based on highest connectivity or with maximum number of neighbors is selected as the cluster head or the Detection Manager (DM). In order to construct highest connectivity clustering, the node degree is measured on the basis of its' (i.e. source mobile node) distance from other mobile nodes in the network. Each mobile node broadcasts its id (i.e. Mobile ID) to the nodes that are within its transmission range 'R'. The structure of the broadcast information is as given below.

| | | | | |
|------------------|-----------|-----------|----------------------------|----------------------------|
| <i>Mobile ID</i> | <i>NN</i> | <i>NM</i> | <i>Weight_{NN}</i> | <i>Weight_{NM}</i> |
|------------------|-----------|-----------|----------------------------|----------------------------|

Fig 2 Broadcast Information

In order to measure the highest connectivity, the proposed technique obtains two parameters for selecting cluster head or detection manager along with the mobile node ID '*Mobile ID*' namely, neighbour node information '*NN*' and node mobility '*NM*' (as listed in fig 2). The neighbour node information comprises of the weight of neighbouring node '*Weight_{NN}*' present in its vicinity or transmission range 'R'.

On the other hand, the weight of the node mobility '*Weight_{NM}*' symbolizes the mobility of the nodes in network that depends upon the mobility pattern. Initially, the values of '*Weight_{NN}*' and '*Weight_{NM}*' are set to 0. With changes in the updates, the two values are incremented. These two parameters (values) along with the mobile node ID are used to measure the node capability. With this node capability, the mobile node that possesses high capability is selected as the cluster head or the detection manager '*DM_i*'.

$$DM_i = \text{Max} \sum_{i=1}^n (\text{Weight}_{NN}[IN] + \text{Weight}_{NM}[IN]) \tag{3}$$

From (Eq.3), the mobile node with maximum number of neighbors (i.e., maximum degree) is selected as the cluster head or detection manager. Mobile node possessing highest connectivity is considered as the detection manager. If two or more intermediate nodes possess the same capability, then the residual distance is used as given below.

$$DM_i = \text{Min ResidualDis} (\text{Max} \sum_{i=1}^n (\text{Weight}_{NN}[IN] + \text{Weight}_{NM}[IN])) \tag{4}$$

From (Eq.4), based on the minimum residual distance, detection manager is identified in the presence of more than one DM. By effective detection of DM, packet delivery ratio is improved significantly.

| |
|---|
| Input: Mobile ID ' <i>Mobile ID</i> ', Neighbor Node ' <i>NN</i> ', Node Mobility ' <i>NM</i> ', weight neighbouring node ' <i>Weight_{NN}</i> ', weight node mobility ' <i>Weight_{NM}</i> ', Source Node ' <i>SN</i> ', Destination Node ' <i>DN</i> ', Intermediate Node ' <i>IN₁ – IN₇</i> ', |
| Output: optimizes packet delivery ratio and reduces routing overhead |
| 1: Begin 2: Set ' <i>Weight_{NM}</i> ', ' <i>Weight_{NN}</i> ' to be 0 3: For each Source Node ' <i>SN</i> ' and Destination Node ' <i>DN</i> ' 4: Repeat 5: Measure Intermediate Nodes using (1) 6:if (more than one intermediate nodes obtained) 7:Measure Intermediate Nodes based on residual distance using (2) 8:End if 9: Until (Intermediate Nodes are obtained) 10: Obtain Detection Manager using (3) 11: If (more than one Detection Manager is obtained) 12:Measure Detection Manager based on residual distance using (4) 13: End if 14:End for 15: End |

Fig 3 Clustering algorithm based on Highest Connectivity

As shown in the fig 3, for each source destination pair, whenever a source node has to identify the best route to forward packets in MANET, intermediate nodes are measured. In the presence of more than one intermediate node minimum residual energy is used. Followed by this, the identification of detection manager is performed based on the highest connectivity. The highest connectivity or the maximum number of neighbors possessed by the intermediate nodes is then identified as the detection manager.

3.4 Packet Dropping-based Malicious Node Isolation model

Finally, Packet Dropping-based Malicious Node Isolation strategy aiming at improving the security is presented. As implied by the name, the detection manager in the network isolates the malicious node from communicating with other nodes in the network. In turn, this prevents the victim node from receiving data packets from other mobile nodes in the network.

The idea behind Packet Dropping-based Malicious Node Isolation strategy is that the link information is prevented from being spread to the entire network. As a result, these nodes will not be able to build a route to these target nodes. This attack is achieved by exploiting the Detection Manager Neighbor Node Relay Selection (DMNNRS) algorithm.

Each mobile node selects a set of its neighbor nodes ‘ NN ’. Only nodes, selected as ‘ NN ’ by the Detection Manager ‘ DM ’, are responsible for identifying the faulty node and isolate the node from the network. Fig 4 shows the DMNNRS algorithm.

| |
|--|
| Input: Mobile Node ‘ $MN_i = MN_1, MN_2, \dots, MN_n$ ’, Neighbor Node ‘ $NN_i = NN_1, NN_2, \dots, NN_n$ ’, Packet ‘ $P_i = P_1, P_2, \dots, P_n$ ’ |
| Output: Improves security and malicious node behavior detection rate |
| 1: Begin 2: For each Mobile Node ‘ MN_i ’ 3: Measure set of its neighbor nodes ‘ NN ’ 4: Obtains packets ‘ P_i ’ from its Neighbor Node ‘ NN_i ’ 5: If (‘ NN_i ’ forward ‘ P_i ’ with contents unchanged) or (‘ NN_i ’ do not drop) then 6: Forward ‘ P_i ’ to its ‘ NN_{i+1} ’ nodes 7: Else 8: Do not Forward ‘ P_i ’ to its ‘ NN_{i+1} ’ nodes 9: Remove ‘ NN_i ’ node from the network 10: End if 11: End for 12: End |

Fig 4 Detection Manager Neighbor Node Relay Selection algorithm

As shown in the fig 4, the Detection Manager randomly obtains the incoming packets of its neighbors. It passively listens to the communication to and from each of its neighbor nodes by auditing the contents of the HELLO message. If the contents of the HELLO message include the existence of all neighboring nodes along with the broadcast information (as provided in Fig 2), then the packets are sent to all the neighboring nodes.

On the other hand, if the contents of the HELLO message include a node not present in the network, then the packet cannot be forwarded due to the non-existence of the node and therefore packet drop occurs. Therefore, the mobile node is presumed as the malicious node by the Detection Manager and therefore isolated from the network. Here, in the proposed technique, intrusion detection is performed by means of detecting packet drops and modifications by the neighboring nodes. The deviation from normal behavior of a neighbor node is used as an indicator to identify the presence of the malicious node and isolate it from the network.

Fig 5 shows the Packet Dropping-based Malicious Node Isolation strategy to identify the malicious node and isolate it from the network. In the figure, Node 'A' is the attacking node and Node 'P' is the target node. The attacker node 'A' instead of sending HELLO messages including '{P, Q, R, S}', it sends a fake HELLO message that contains '{P, Q, R, S, T}' that include three neighbor nodes '{Q, R, S}' and one non-existent node '{T}'. According to the protocol, the target node 'P' will select the attacking node 'A'. So the node 'A' is the malicious node which drops the packet as identified by the DM and is isolated from the network.

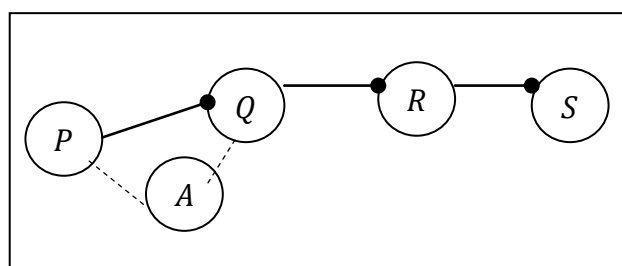


Fig 5 Packet Dropping-based Malicious Node Isolation strategy

In this way, a mechanism for detection of intrusion through packet dropping is presented based on cooperative nature of nodes in mobile ad hoc network. As a result, the faulty node that performs packet drop is identified as the malicious node and isolated from the network. This in turn ensures the security to a greater extent.

4. Simulation and performance comparison

To evaluate the proposed technique a real grid test bed simulator is required. However, to establish and maintain a real test bed is expensive. Instead, we choose a network simulator as the simulation tool. Many network simulators have been introduced, such as OPNET, NETSIM and NS2, among which NS2 is chosen since it provides a flexible and extensible simulation environment. In the following simulation, the existing intrusion detection techniques including Rateless Codes and Belief Propagation to Infer Identity of Polluters (RC-BP) [1], Enhanced Adaptive ACKnowledge (EAACK) [2] are implemented and compared with the IC-HCPD on a Mobile ad hoc network.

A random topology with a maximum of 70 nodes over a rectangle field was selected to test the proposed IC-HCPD and existing techniques RC-BP and EAACK respectively. The total dimension is fixed as 1500*1500m with the maximum transmission range of each mobile node being 250m and the duration of the simulation is 600s. Random way point model is used as the mobility model for each node.

The node speed is varied between 2m/s and 25m/s with the mobile node pause time is varied from 0 seconds to 300 seconds. In the result, for each metric, simulation is done for seven different seed values with taken for the result. Table 1 shows the parameters obtained that finally were used in the experiments.

Table 1 Parameters and values used in the experiment

| | |
|--------------------|----------------------------|
| Node density | 10, 20, 30, 40, 50, 60, 70 |
| Network area | 1500*1500m |
| Transmission range | 250m |
| Packets | 9, 18, 27, 36, 45, 54, 63 |
| Simulation period | 600s |
| Minimum node speed | 2m/s |
| Maximum node speed | 25m/s |
| Node pause time | 0 – 300 seconds |

4.1 Simulation results

The tested algorithms were run on the same experimental environment as listed in table 1 so their performance can be fairly compared. Several test metrics were used. Routing overhead is obtained on the basis of the neighboring nodes in network. The mobile nodes in MANET often change their location within network due to the random changes in topology. As a result, some stale routes are generated in the routing table resulting in unnecessary routing overhead. A good algorithm is one which reduces the routing overhead. The routing overhead is formulated as given below.

$$RO = \sum_{i=1}^n NN_i * Time (NN_i) \quad (5)$$

From (Eq.5), the routing overhead 'RO' is obtained on the basis of the neighbor nodes 'NN_i' and the time taken to obtain the neighboring nodes 'Time (NN_i)' in the network. Next, packet delivery ratio is used as the performance metric to measure the effectiveness of the proposed technique.

Packet delivery ratio is the ratio of number of packet actually delivered without duplication to destination verses the number of packet supposed to be received. This number or the packet delivery ratio represents the effectiveness and throughput of a protocol in delivering data to the intended receiver within the network.

$$PDR = \frac{P_d}{P_s} \quad (6)$$

From (Eq.6), the packet delivery ratio 'PDR' is measured using the packets delivered 'P_d' and the packets sent 'P_s' respectively. Finally, to evaluate the efficiency of the proposed technique, the rate of malicious behavior detection is measured.

Malicious behavior detection rate measures the rate of malicious nodes identified in the network. Due to different factors such as congestion, collision, packet drop, malicious behavior of a node is said to be observed. In the proposed technique, packet drop is used as a measure to detect intrusion in the network and is mathematically formulated as given below.

$$MBDR = \frac{\text{Packet drops detected}}{MN_i} \quad (7)$$

From (Eq.7), the malicious behavior detection rate 'MBDR' is observed on the basis of the number of nodes or node density 'MN_i'. In the following, each simulation was performed seven times to obtain the values of the three performance metrics.

4.2 Routing overhead

A node density of 70 listed in table were employed to simulate the routing overhead using the three methods Integrated Cluster and Highest Connectivity-based Packet Dropping (IC-HCPD) Rateless Codes and Belief Propagation to Infer Identity of Polluters (RC-BP) [1], Enhanced Adaptive ACKnowledge (EAACK) [2] on mobile ad hoc network.

Table 2 Average node density and routing overhead

| Node Density | Routing overhead (ms) | | |
|--------------|-----------------------|-------|-------|
| | IC-HCPD | RC-BP | EAACK |
| 10 | 0.38 | 0.45 | 0.60 |
| 20 | 0.52 | 0.59 | 0.64 |
| 30 | 0.78 | 0.85 | 1.09 |
| 40 | 0.95 | 1.03 | 1.18 |
| 50 | 1.05 | 1.12 | 1.26 |
| 60 | 1.15 | 1.22 | 1.35 |
| 70 | 1.28 | 1.35 | 1.50 |

A comparative analysis for routing overhead with respect to different mobile nodes was performed with the existing RC-BP [1] and EAACK [2] is listed in table. The increasing mobile nodes in the range of 10 to 70 are considered for experimental purpose in MANET.

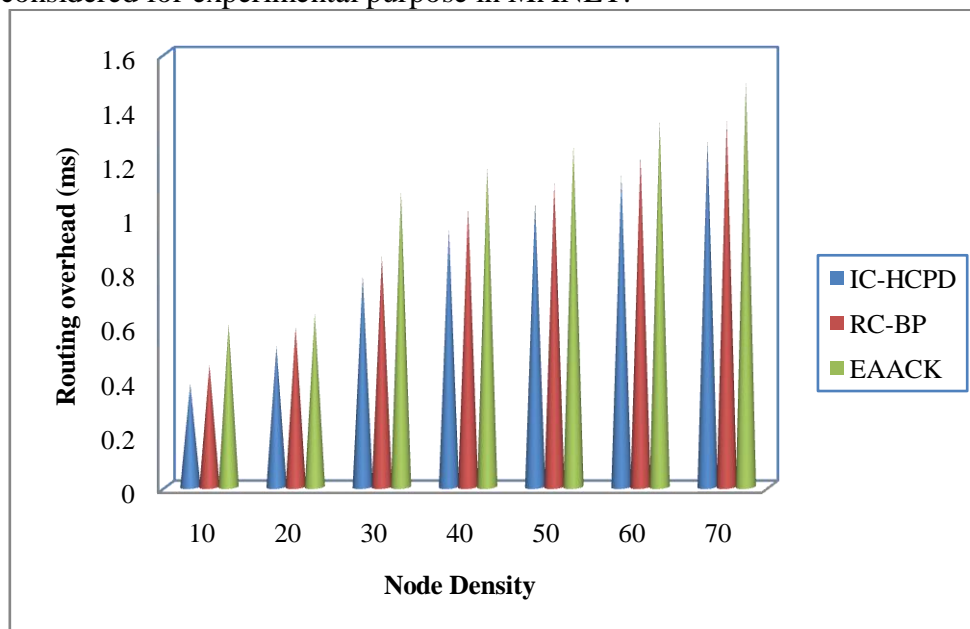


Fig 6 Routing overhead by varying the node density

Fig 6 shows the routing overhead for 70 nodes using the above mentioned intrusion detection techniques. As illustrated in fig, comparatively while considering more number of mobile nodes. In this simulation though three techniques have similar routing overhead, but were observed to be comparatively lesser when IC-HCPD was applied. The IC-HCPD method improves the routing overhead by considering neighbor node-based cluster formation that uses the minimum distance nodes for routing with respect to

different mobile nodes. The residual distance using the neighbor node information in IC-HCPD helps for any number of mobile nodes to obtain their neighbor information in a dynamic manner reducing the routing overhead by 9.64% compared to RC-BP and 28.50% compared to EAACK.

4.2 Packet Delivery Ratio

The experimental results in previous section have indicated that IC-HCPD method is more efficient than RC-BP and EAACK CR-DCST framework is more efficient than JSTM-EM and DIDS-WSN respectively in terms of routing overhead. In this section we compared IC-HCPD method with, RC-BP [1] and EAACK [2] to illustrate the effectiveness of applying clustering algorithm based on highest connectivity in terms of packet delivery ratio.

Table shows the performance of IC-HCPD, RC-BP and EAACK over different number of packets in terms of packet delivery ratio. From the table it is evident that the packet delivery ratio is observed to be high by applying the IC-HCPD method.

Table 3 Average packet delivery ratio and packets sent

| Packets | Packet Delivery Ratio (%) | | |
|---------|---------------------------|-------|-------|
| | IC-HCPD | RC-BP | EAACK |
| 9 | 92.35 | 82.45 | 80.32 |
| 18 | 94.19 | 84.24 | 81.12 |
| 27 | 95.23 | 85.28 | 82.16 |
| 36 | 89.21 | 79.26 | 76.14 |
| 45 | 91.35 | 81.40 | 78.28 |
| 54 | 93.28 | 83.33 | 80.21 |
| 63 | 95.89 | 85.94 | 82.82 |

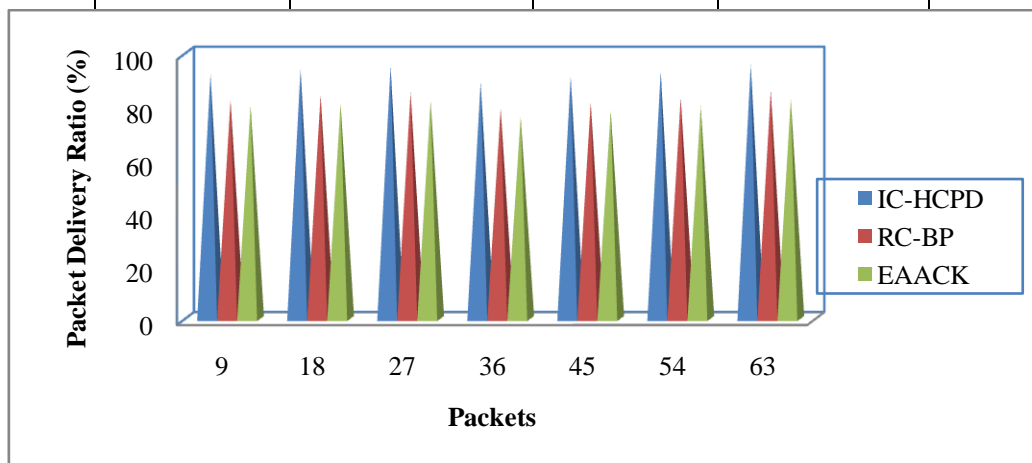


Fig 7 Packet delivery ratio by varying the packet density

Fig 7 displays the packet delivery ratio based on the changing number of packets. The mean packet delivery ratio of IC-HCPD method is improved by 11.15% and 1.46% compared to RC-BP and EAACK respectively. According to the highest connectivity as detected by the detection manager, the neighbor node that possesses maximum connectivity is selected as the route node through which the data or packets are forwarded. Therefore, with the highest connectivity, though existence of malicious nodes cannot be avoided, with the large number of neighbor nodes, the possibility of packet delivery ratio gets increased using the IC-

HCPD method when compared to RC-BP and EAACK. In case of the two existing methods, acknowledge information is used as a measure for data forwarding that ensures packet delivery. But the packet delivery ratio using IC-HCPD method was observed to be 10.68% improved and 1.39% improved when compared to the existing methods.

4.3 Malicious behavior detection rate

The malicious behavior detection rate using IC-HCPD method is provided in an elaborate manner in table with different number of mobile nodes and simulated using NS2 (as listed in table 4).

Table 4 Average malicious behavior detection rate

| Node density | Malicious behavior detection rate (%) | | |
|--------------|---------------------------------------|-------|-------|
| | IC-HCPD | RC-BP | EAACK |
| 10 | 51.35 | 42.85 | 34.16 |
| 20 | 62.14 | 53.09 | 45.09 |
| 30 | 75.83 | 66.67 | 58.67 |
| 40 | 78.14 | 69.05 | 63.05 |
| 50 | 80.35 | 71.28 | 67.28 |
| 60 | 84.16 | 75.13 | 69.13 |
| 70 | 89.23 | 80.18 | 73.18 |

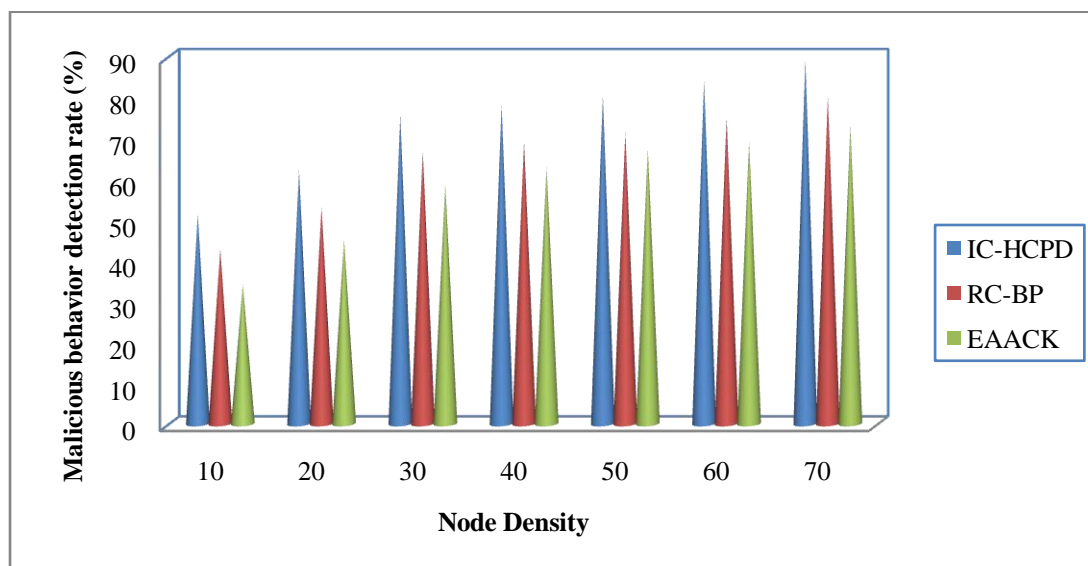


Fig 8 Measure of malicious behavior detection rate

Fig 8 shows the effect of malicious behavior detection rate for 70 mobile nodes. As node density increases, malicious behavior detection rate gets reduced. Here IC-HCPD outperforms the other methods as node density increases. The main reason is that the malicious behavior detection rate in the IC-HCPD method is made by isolating the malicious node based on the packet dropping rate. So the performance of the proposed Detection Manager Neighbor Node Relay Selection (DMNNRS) algorithm is improved by increasing the malicious behavior detection rate by 12.42% and 22.13% compared to RC-BP and EAACK.

5. Conclusion

Detecting intrusion in mobile ad hoc network is a complex task due to the intrinsic features of these networks, such as the higher node mobility, the lack of a fixed network infrastructure as well as the severe resource constraints. Therefore, there arises an urgent need to safeguard these communication networks and to propose efficient method in order to detect the intrusion at an early stage. In this article we provide an Integrated Cluster and Highest Connectivity-based Packet Dropping (IC-HCPD) that can be employed as intrusion detection method in MANETs. Results show that neighbor node selected based on the cluster formation may be a good paradigm to use when the goal is just to detect an intruder and isolate the intruding node from the network. The evaluation of the detection manager is performed considering highest connectivity that the intrusion detection process is completely distributed and maximum number of neighbor node exists in the network. Through the experiments using real traces, we observed that our intrusion detection method provided more accurate malicious behavior detection rate compared to the existing intrusion detection methods. In addition, our clustering algorithm based on highest connectivity effectively improved the packet delivery ratio and even reduced the routing overhead.

References

- [1] Rossano Gaeta, Marco Grangetto and Riccardo Loti, "Exploiting Rateless Codes and Belief Propagation to Infer Identity of Polluters in MANET", *IEEE Transactions on Mobile Computing*, Volume 13, Issue 7, July 2014, pp. 1482 – 1494.
- [2] Elhadi M. Shakshuki, Nan Kang and Tarek R. Sheltami, "EAACK—A Secure Intrusion-Detection System for MANETs", *IEEE Transactions on Industrial Electronics*, Volume 60, Issue 3, March 2013, pp. 1089 – 1098.
- [3] Peng Zhao, Xinyu Yang, Wei Yu and Xinwen Fu, "A Loose-Virtual-Clustering-Based Routing for Power Heterogeneous MANETs", *IEEE Transactions on Vehicular Technology*, Volume 62, Issue 5, June 2013, pp. 2290 – 2302.
- [4] Yong Li, Pan Hui, Depeng Jin, Li Su and Lieguang Zeng, "Optimal Distributed Malware Defense in Mobile Networks with Heterogeneous Devices", *IEEE Transactions on Mobile Computing*, Volume 13, Issue 2, February 2014, pp. 377 – 391.
- [5] Ahmed M. Abdalla, Imane A. Saroit, Amira Kotb and Ali H. Afsaria, "Misbehavior Nodes Detection and Isolation for MANETs OLSR Protocol", *Elsevier, Procedia Computer Science*, Volume 3, 2011, pp. 115 – 121.
- [6] Dina Sadat Jalali and Alireza Shahrbanooonezhad, "A Novel Method Intrusion Detection Based on Sending and Checking Packet for Neighbored Nodes in MANET", *Universal Journal of Communications and Network*, Volume 2, Issue 1, 2014, pp. 10 – 13.
- [7] Adnan Nadeem and Michael P. Howarth, "An Intrusion Detection & Adaptive Response Mechanism for MANETs", *Elsevier, Ad Hoc Networks*, Volume 13, 17 September 2013, pp. 1 – 28.
- [8] Sergio Pastrana, Aikaterini Mitrokotsa, Agustin Orfila and Pedro Peris-Lopez, "Evaluation of classification algorithms for intrusion detection in MANETs", *Elsevier, Knowledge-Based Systems*, Volume 36, December 2012, pp. 1 – 9.
- [9] S. Ganapathy, P. Yogesh and A. Kannan, "Intelligent Agent-Based Intrusion Detection System Using Enhanced Multiclass SVM", *Hindawi Publishing Corporation, Computational Intelligence and Neuroscience*, July 2012, pp. 10.
- [10] Jaeun Choi, Gisung Kim and Seun Kim, "A Congestion-Aware IDS Node Selection Method for Wireless Sensor Networks", *Hindawi Publishing Corporation, International Journal of Distributed Sensor Networks*, June 2012, pp. 6.
- [11] Nabil Ali Alrajeh and J. Lloret, "Intrusion Detection Systems Based on Artificial Intelligence Techniques in Wireless Sensor Networks", *Hindawi Publishing Corporation, International Journal of Distributed Sensor Networks*, September 2013, pp. 6.
- [12] Maha Abdelhaq, Raed Alsaqour and Shawkat Abdelhaq, "Securing Mobile Ad Hoc Networks Using Danger Theory-Based Artificial Immune Algorithm", *PLOS One*, 6 May 2015, pp. 1 – 16.

- [13] Xuemei Sun, Bo Yan, Xinzhong Zhang and Chuitian Rong, “An Integrated Intrusion Detection Model of Cluster-Based Wireless Sensor Network”, PLOS One, 8 October 2015, pp. 1 – 16.
- [14] Wenchao Li, Ping Yi, Yue Wu, Li Pan and Jianhua Li, “A New Intrusion Detection System Based on KNN Classification Algorithm in Wireless Sensor Network”, Hindawi Publishing Corporation, Journal of Electrical and Computer Engineering, June 2014, pp. 8.
- [15] Mingyan Li, Iordanis Koutsopoulos, and Radha Poovendran, “Optimal Jamming Attack Strategies and Network Defense Policies in Wireless Sensor Networks”, IEEE Transactions on Mobile Computing, Volume 9, Issue 8, August 2010, pp. 1119 – 1133.
- [16] Kiran Mehta, Donggang Liu and Matthew Wright, “Protecting Location Privacy in Sensor Networks against a Global Eavesdropper”, IEEE Transactions on Mobile Computing, Volume 11, Issue 2, February 2012, pp. 320 – 336.
- [17] Shafiullah Khan, Kok-Keong Loo, and Zia Ud Din, “Framework for Intrusion Detection in IEEE 802.11 Wireless Mesh Networks”, The International Arab Journal of Information Technology, Volume 7, Issue 4, October 2010, pp. 435 – 440.
- [18] Zubair Md. Fadlullah, Hiroki Nishiyama, Nei Kato and Mostafa M. Fouda, “An Intrusion Detection System (IDS) for Combating Attacks Against Cognitive Radio Networks”, IEEE Network, Volume 27, Issue 3, June 2013, pp. 1 – 8.
- [19] Eugene Y. Vasserman and Nicholas Hopper, “Vampire attacks: Draining life from wireless ad-hoc sensor networks”, IEEE Transactions on Mobile Computing, Volume 12, Issue 2, February 2013, pp. 1 – 15.
- [20] Wei Gao, Guohong Cao, Tom La Porta and Jiawei Han, “On Exploiting Transient Social Contact Patterns for Data Forwarding in Delay-Tolerant Networks”, IEEE Transactions on Mobile Computing, Volume 12, Issue 1, January 2013, pp. 151 – 165.



ISSN NO. 2320-5407

(/)

International Journal of Advanced Research (IJAR)

ISSN 2320-5407

A Peer Reviewed, Open Access, CrossRef In TRANSLATE

(<https://www.facebook.com/journalijar>) (<http://uk.linkedin.com/pub/international-journal-of-advanced-research/8a/b31/9/>) (<https://twitter.com/JOURNALIJAR>) (<https://plus.google.com/u/0/114567192354572386754>) (<https://journalijar-com.blogspot.in/>)

30
Mar 2017

KINETIC AND MECHANISTIC STUDY OF PALLADIUM (II) CATALYZED OXIDATION, DEAMINATION AND DECARBOXYLATION OF GLYCINE BY ALKALINE PERMANGANATE.

[Adarsha J. R. Sailasree S](#) (</search-result/?author=Adarsha J. R. Sailasree S>) , [SurekhaM](#) (</search-result/?author=SurekhaM>) and [Nandibewoor S. T.](#) (</search-result/?author=Nandibewoor S. T.>)

- 1 Department of Chemistry, Global Academy of Technology, Bangalore-560098.
- 2 Department of Chemistry, SriSairam College of Engineering, Bangalore-560078.
- 3 Department of Chemistry, The Oxford College of Engineering, Bommanahalli, Bangalore – 580068, India.
- 4 Department of Chemistry, Karnatak University, Dharwad, Karnataka, India.



Crossref (<http://search.crossref.org/?q=10.21474/IJAR01/3671>)

Cited-by

Abstract

Keywords

References

Cite This Article as

Corresponding Author

Kinetics of oxidation of glycine by permanganate in presence of Palladium(II) catalyst was studied spectrophotometrically. It was found that the reaction exhibits first order dependence on [catalyst] & [oxidant] and less than unit order in [glycine] and [alkali]. The data suggests that oxidation proceeds via formation of a complex between the substrate and the catalyst, which then reacts with one mole of permanganate in a slow step to form a

Schur Convexity Condition for Novel Ratio of Difference of Means

Sreenivasa Reddy Perla

The Oxford College of Engg
 Dept of Mathematics, VTU
 Bangalore, Karnataka. India.
srireddy_sri@yahoo.co.in

Padmanabhan S

RNSIT
 Dept of Mathematics, VTU
 Bangalore, Karnataka. India.
padmanabhanrnsit@gmail.com

K M Nagaraja

JSSATE
 Dept of Mathematics, VTU
 Bangalore, Karnataka. India.
nagkmn@gmail.com

Padmanava Samanta

Dept of Mathematics
 Berhampur University,
 Odissa.India.
dr.pns.math@gmail.com

Abstract: *In this paper, we study the different kind of convexities like Schur, Schur Geometric and Schur Harmonic convexities for novel ratio of difference of means.*

Keywords: *Schur convexity, Schur harmonic convexity, Schur Geometric convexity, ratio of difference of means and inequality.*

1. INTRODUCTION

The well-known means in literature such as arithmetic mean, geometric mean harmonic mean and contra harmonic mean are presented by pappus of Alexandria. In Pythagorean School on the basis of proportion and also some of the other means like Heron mean and Centriodal Mean are defined as follows [1,2] and some interesting results on above said means are discussed in [3-8].

For two positive real numbers a & b ;

$$\text{Arithmetic Mean} = A(a, b) = \frac{a+b}{2}$$

$$\text{Geometric Mean} = G(a, b) = \sqrt{ab}$$

$$\text{Harmonic Mean} = H(a, b) = \frac{2ab}{a+b}$$

$$\text{Contra Harmonic Mean} = C(a, b) = \frac{a^2 + b^2}{a+b}$$

$$\text{Heron mean} = H_e(a, b) = \frac{a + \sqrt{ab} + b}{3} \quad \text{and} \quad \text{Centriodal Mean } C_d(a, b) = \frac{2(a^2 + ab + b^2)}{3(a+b)}$$

Jamal Rooin and Mehdi Hassni [9], introduced the homogeneous functions $f(x)$ and $g(x)$, also established some convexity results and refinements to Ky-Fan-type inequalities. where

$$f(x) = \frac{a^x - b^x}{c^x - d^x} \quad \text{and} \quad g(x) = \ln \frac{a^x - b^x}{c^x - d^x} \quad \text{for } x \in (-\infty, \infty) \quad \text{and} \quad a > b \geq c > d.$$

In [10], authors studied the convexity(concavity) of the following ratio of difference of means.

$$M_{CAGH}(a, b) = \frac{C(a, b) - A(a, b)}{G(a, b) - H(a, b)}$$

$$M_{AH_eGH}(a, b) = \frac{A(a, b) - H_e(a, b)}{G(a, b) - H(a, b)}$$

$$M_{CH_eGH}(a,b) = \frac{C(a,b) - H_e(a,b)}{G(a,b) - H(a,b)} \qquad M_{C_dAGH}(a,b) = \frac{C_d(a,b) - A(a,b)}{G(a,b) - H(a,b)}$$

$$M_{CAH_eG}(a,b) = \frac{C(a,b) - A(a,b)}{H_e(a,b) - G(a,b)} \quad \text{and} \quad M_{CC_dGH}(a,b) = \frac{C(a,b) - C_d(a,b)}{G(a,b) - H(a,b)}$$

Some fruitful results related to Schur convexities were also found in [11-22].

In this paper, we study the Schur, Schur harmonic and Schur geometric convexity of ratio of means $M_{CAGH}(a,b)$, $M_{AH_eGH}(a,b)$, $M_{CH_eGH}(a,b)$ & $M_{CAH_eG}(a,b)$ and some applications of these ratio of difference of means.

2. PRELIMINARY RESULTS AND DEFINITIONS

In 1923, the Schur Convex function was introduced by I Schur, and proved many important applications to analytic inequalities. In 2003, X. M. Zhang propose the concept of Schur-geometrically convex function which is an extension of Schur-convexity function. In recent years, the Schur convexity, Schur geometrically convexity and Schur harmonic convexity have attracted the attention of a considerable number of mathematicians ([11],- [21]). For convenience of readers, we recall some definitions as follows:

Definition 2.1.[3,7] Let $x = (x_1, x_2, x_3, \dots, x_n)$ and $y = (y_1, y_2, y_3, \dots, y_n) \in R^n$

1. Let x is said to be majorized by y (in symbol $x < y$) $\sum_{i=1}^k x_i \leq \sum_{i=1}^k y_i$ for $k=1,2,3,\dots,n$ and

$$\sum_{i=1}^k x_i = \sum_{i=1}^k y_i \quad \text{where } x_1 \geq \dots \geq x_n \text{ and } y_1 \geq \dots \geq y_n \text{ are rearrangement of } x$$

and y in descending order.

2. $\Omega \subseteq R^n$ The function $\varphi : \Omega \rightarrow R^n$ is said to be schur convex function on Ω if $x < y$ on Ω implies $\varphi(x) \leq \varphi(y)$. φ is said to be a Schur concave function on Ω if and only if $-\varphi$ is Schur convex.

Definition 2.2.[22] Let $x = (x_1, x_2, x_3, \dots, x_n)$ and $y = (y_1, y_2, y_3, \dots, y_n) \in R^n_+$. $\Omega \subseteq R^n$ is called geometrically convex set if $x_1^\alpha y_1^\beta \dots x_n^\alpha y_n^\beta \in R^n$ for all x and y where $\alpha, \beta \in [0,1]$ with $\alpha + \beta = 1$. Let $\Omega \subseteq R^n_+$ The function $\varphi : \Omega \rightarrow R^n_+$ is said to be schur geometrically convex function on Ω if $(\ln x \dots \ln x_n) < (\ln y \dots \ln y_n)$ on Ω implies $\varphi(x) \leq \varphi(y)$. Let φ is said to be a Schur geometrically concave function on φ if and only if $-\varphi$ is Schur geometrically convex.

Definition 2.3.[3,7] The set $\Omega \subseteq R^n$ is called symmetric set if $x \in \Omega$ implies $px \in \Omega$ for every $n \times n$ permutation matrix p . The function $\varphi : \Omega \rightarrow R^n$ is said to be symmetric if every permutation matrix p ; $\varphi(px) = \varphi(x)$. for all $x \in \Omega$.

we introduce the ratio of difference of means as follows:

$$\frac{M_{CAGH}}{M_{AH_eGH}}(a,b) = \frac{C(a,b) - A(a,b)}{A(a,b) - H_e(a,b)} \qquad \frac{M_{CC_dGH}}{M_{C_dAGH}}(a,b) = \frac{C(a,b) - C_d(a,b)}{C_d(a,b) - A(a,b)}$$

$$\frac{M_{C_dAGH}}{M_{AH_eGH}}(a,b) = \frac{C_d(a,b) - A(a,b)}{A(a,b) - H_e(a,b)} \qquad \frac{M_{CC_dGH}}{M_{AH_eGH}}(a,b) = \frac{C(a,b) - C_d(a,b)}{A(a,b) - H_e(a,b)}$$

$$\frac{M_{C_dAGH}}{M_{AH_eGH}}(a,b) = \frac{C_d(a,b) - A(a,b)}{A(a,b) - H_e(a,b)} \qquad \frac{M_{CC_dGH}}{M_{AH_eGH}}(a,b) = \frac{C(a,b) - C_d(a,b)}{A(a,b) - H_e(a,b)}$$

Lemma 2.1.[3,7] Let $\Omega \subseteq R^n$ $\varphi : \Omega \rightarrow R$ is symmetric and convex function. Then φ is Schur convex on Ω .

Lemma 2.2.[9] For $a > b \geq c > d$. the function $f(x) = \frac{a^x - b^x}{c^x - d^x}$ where $x \in (-\infty, \infty)$ is

- i) Convex, if $ad - bc > 0$
- ii) Concave if $ad - bc < 0$
- iii) Equality holds if $ad - bc = 0$.

Lemma 2.3.[22] Let $\Omega \subseteq R^n$ be symmetric with non empty interior convex set and let $\varphi : \Omega \rightarrow R_+$ be continuous on Ω and differentiable on Ω^0 If φ is symmetric on Ω and for any on $x = (x_1, x_2, x_3, \dots, x_n) \in \Omega^0$. Then φ is

- (i) Schur convex (concave) if $s = (x_1 - x_2) \left(\frac{\partial \varphi}{\partial x_1} - \frac{\partial \varphi}{\partial x_2} \right) \geq 0 (\leq 0)$.
- (ii) Schur geometrically convex (concave) if $s = (\ln x_1 - \ln x_2) \left(x_1 \frac{\partial \varphi}{\partial x_1} - x_2 \frac{\partial \varphi}{\partial x_2} \right) \geq 0 (\leq 0)$.
- (iii) Schur harmonically convex (concave) if $s = (a - b) \left(x_1^2 \frac{\partial \varphi}{\partial x_1} - x_2^2 \frac{\partial \varphi}{\partial x_2} \right) \geq 0 (\leq 0)$.

3. SCHUR PROPERTIES ON RATIO OF DIFFERENCE OF MEAN

In this section, the Schur, Schur geometric and Schur harmonically convexities on ratio of difference of mean are established by finding the partial derivatives.

Theorem 3.1. The ratio of difference of means $\frac{M_{CC_dGH}}{M_{C_dAGH}}$ is

- (i) Schur convex.
- (ii) Schur geometrically convex.
- (iii) Schur harmonically convex is for all $a \geq b$.

Proof. Let $\frac{M_{CC_dGH}}{M_{C_dAGH}}(a,b) = \frac{C(a,b) - C_d(a,b)}{C_d(a,b) - A(a,b)}$

From lemma 2, Consider, $f(a,b) = CA - C_d^2 = \left(\frac{a^2 + b^2}{a+b} \right) \left(\frac{a+b}{2} \right) - \frac{4}{9} \left(\frac{a^2 + ab + b^2}{a+b} \right)^2$

By finding the partial derivatives of $f(a, b)$ and with simple manipulation gives

$$\frac{\partial f}{\partial a} = a - \frac{8}{9} \left(\frac{(a^2 + ab + b^2)a(a + 2b)}{(a + b)^3} \right) \text{ and } \frac{\partial f}{\partial b} = b - \frac{8}{9} \left(\frac{(a^2 + ab + b^2)b(2a + b)}{(a + b)^3} \right) \quad (1)$$

Proof of (i), from eqn (1), we have

$$\frac{\partial f}{\partial a} - \frac{\partial f}{\partial b} = (a - b) \left(1 - \frac{8(a^2 + ab + b^2)}{9(a + b)^2} \right) = (a - b) \left(\frac{a^2 + 10ab + b^2}{9(a + b)^2} \right)$$

$$\text{Then } s = (a - b) \left(\frac{\partial f}{\partial a} - \frac{\partial f}{\partial b} \right) = (a - b)^2 \left(\frac{a^2 + 10ab + b^2}{9(a + b)^2} \right) \geq 0 \text{ for all } a \& b$$

This verifies the condition for Schur convexity.

Proof of (ii), from eqn (1), we have

$$a \frac{\partial f}{\partial a} - b \frac{\partial f}{\partial b} = (a^2 - b^2) - \frac{8}{9} \left(\frac{(a^2 + ab + b^2)(a^3 - b^3 + 2ab(a - b))}{(a + b)^3} \right) \geq 0 \text{ for all } a \& b$$

$$\text{Then } s = (\ln a - \ln b) \left(a \frac{\partial f}{\partial a} - b \frac{\partial f}{\partial b} \right) = (\ln a - \ln b) \frac{a - b}{9(a + b)^3} (a^4 + b^4 + 14a^2b^2 + 2a^3b + 2ab^3) \geq 0$$

This verifies the condition for Schur geometrically convexity.

Proof of (iii), As above we have

$$\text{Then } s = (a - b) \left(a^2 \frac{\partial f}{\partial a} - b^2 \frac{\partial f}{\partial b} \right) = (a - b) \frac{(a^2 + 10ab + b^2)}{9(a + b)^2} \geq 0 \text{ for } a \& b$$

This verifies the condition for Schur Harmonically convex.

Thus the proof of theorem 3.1 is completed.

Theorem 3.2. The ratio of difference of means $\frac{M_{CC_dGH}}{M_{AH_eGH}}$ is

(i) Schur convex.

(ii) Schur geometrically convex.

(iii) Schur harmonically convex is for all $a \geq b$.

$$\text{Proof: Let } \frac{M_{CC_dGH}}{M_{AH_eGH}}(a, b) = \frac{C(a, b) - C_d(a, b)}{A(a, b) - H_e(a, b)}$$

From lemma 2, Consider, $f(a, b) = CH_e - AC_d$

$$= \left(\frac{a^2 + b^2}{a + b} \right) \left(\frac{a + b + \sqrt{ab}}{3} \right) - \left(\frac{a + b}{2} \right) \frac{2}{3} \left(\frac{a^2 + ab + b^2}{a + b} \right) = \frac{\sqrt{ab}}{3} \left(a + b - \frac{2ab}{a + b} - \sqrt{ab} \right)$$

By finding the partial derivatives of $f(a, b)$ and with simple manipulation gives

$$\frac{\partial f}{\partial a} = \frac{\sqrt{ab}}{3} \left(1 - \frac{2b^2}{(a+b)^2} - \frac{\sqrt{b}}{2\sqrt{a}} \right) + \left(a + b - \frac{2ab}{a+b} - \sqrt{ab} \right) \frac{\sqrt{b}}{6\sqrt{a}}$$

$$a \frac{\partial f}{\partial a} = \frac{\sqrt{ab}}{6} \left(\left(2a - \frac{4ab^2}{(a+b)^2} - \sqrt{ab} \right) + \left(a + b - \frac{2ab}{a+b} - \sqrt{ab} \right) \right) \quad (2)$$

similarly $b \frac{\partial f}{\partial b} = \frac{\sqrt{ab}}{6} \left(\left(2b - \frac{4a^2b}{(a+b)^2} - \sqrt{ab} \right) + \left(a + b - \frac{2ab}{a+b} - \sqrt{ab} \right) \right) \quad (3)$

Proof of (i), from eqs (2) & (3) we have

$$\text{Then } s = (a-b) \left(\frac{\partial f}{\partial a} - \frac{\partial f}{\partial b} \right) = \frac{(a-b)^2}{6(a+b)(\sqrt{ab})} (4ab + 2\sqrt{ab}(a+b) - a^2 - b^2) \geq 0 \text{ for } a \& b.$$

This verifies the condition for Schur convex.

Proof (ii), from eqs (2) & (3) we have

$$a \frac{\partial f}{\partial a} - b \frac{\partial f}{\partial b} = \frac{\sqrt{ab}}{6} \left(2a - 2b - \frac{4ab(b-a)}{(a+b)^2} \right)$$

$$\text{Consider, } s = (\ln a - \ln b) \left(a \frac{\partial f}{\partial a} - b \frac{\partial f}{\partial b} \right) = (\ln a - \ln b) \frac{\sqrt{ab}(a-b)}{3} \left(1 + \frac{2ab}{(a+b)^2} \right) \geq 0 \text{ for } a \& b$$

This verifies the condition for Schur geometrically convex.

Proof of (iii), from eqs (2) & (3) we have

$$a^2 \frac{\partial f}{\partial a} - b^2 \frac{\partial f}{\partial b} = \frac{\sqrt{ab}}{6} (a-b) \left(3a + 3b - 2\sqrt{ab} - \frac{2ab}{(a+b)} \right)$$

$$\text{Then } s = (a-b) \left(a^2 \frac{\partial f}{\partial a} - b^2 \frac{\partial f}{\partial b} \right) = \frac{\sqrt{ab}}{6} \frac{(a-b)}{(a+b)} (3(a^2 + b^2) + 4ab - 2\sqrt{ab}(a+b)) \geq 0 \text{ for } a \& b$$

This verifies the condition for Schur harmonically convex.

Thus the proof of theorem 3.2 is completed.

Theorem 3.3. The ratio of difference of means $\frac{M_{CAGH}}{M_{AH, GH}}$ is

- (i) Schur convex.
- (ii) Schur geometrically convex.
- (iii) Schur harmonically convex is for all $a \geq b$.

Proof: Similar argument as discussed in theorem 3.1 and 3.2 gives the proof of theorem 3.3.

REFERENCES

- [1] P. S. Bullen, Handbook of means and their inequalities, Kluwer Acad. Publ., Dordrecht, 2003.
- [2] G. H. Hardy, J. E. Littlewood and G. Polya, Inequalities, 2nd edition, Cambridge University Press, Cambridge, 1959.
- [3] A. M. Marshall and I. Olkin, Inequalities: Theory of Majorization and Its Application, New York : Academies Press, 1979.
- [4] K. M. Nagaraja, V. Lokesha and S. Padmanabhan, A simple proof on strengthening and extension of inequalities Adv. Stud. Contemp. Math., 17(1)(2008), 97-103.
- [5] I. J. Taneja, On a difference of Jensen inequality and its applications to mean divergence measures, RGMIA Research Report Collection, <http://rgmia.vu.edu.au>, 7(4)(2004), Art. 16. in:arXiv:math.PR/0501302
- [6] I. J. Taneja, Refinement of inequalities among means, Journal of Combinatorics, Information and System Sciences, 31(1-4)(2006), 343-364.
- [7] B. Y. Wang, Foundations of majorization inequalities, Beijing Normal Univ. Press, Beijing, China, 1990(in Chinese).
- [8] S. Wang and Y. Chu, The best bounds of combination of arithmetic and harmonic means for the Seiffert's mean, Int. J. Math. Analysis, 22(4) (2010), 1079-1084.
- [9] J. Roojin and M. Hassni, Some new inequalities between important means and applications to Ky-Fan types inequalities, Math. Ineq. and Appl., 10(3)(2007), 78-81
- [10] Naveenkumar. B, Sandeepkumar, V. Lokesha, and K. M. Nagaraja, Ratio of difference of means, International e Journal Mathematics and Engineering, 2(2),(2011)932-936.
- [11] Y. M. Chu and X. M. Zhang, The Schur geometrical convexity of the extended mean values, J. Convex Anal., 15(4)2008, 869-890.
- [12] N. Elezovic and J. Pecaric, Note on Schur-convex functions, Rocky Mountain Math., 29(1998), 853-856.
- [13] Huan Nan Shi, Jain Zang and Da-mao Li, Schur-geometric convexity for difference of means, Applied Mathematics E- Notes, 10(2010), 274-284.
- [14] V. Lokesha, K. M. Nagaraja, Naveen Kumar. B and Y.-D. Wu, Schur convexity of Gnan mean for two variables, Notes on Number theory and discrete mathematics, 17(4)(2011), 37-41.
- [15] K. M. Nagaraja and P. S. K. Reddy, Logarithmic convexity of double sequence, Scientia Magna, 7(2)(2011), 78-81
- [16] J. Sandor, The Schur-convexity of Stolarsky and Gini means, Banach J. Math. Anal., 1(2)(2007), 212-215.
- [17] H. N. Shi, Y. M. Jiang and W. D. Jiang, Schur-geometrically concavity of Gini mean, Comp. Math. Appl., 57(2009), 266-274.
- [18] H. N. Shi, Schur-convex functions relate to Hadamard-type inequalities, J. Math. Inequal., 1(1)(2007), 127-136.
- [19] H. N. Shi, S. H. Wu and F. Qi, An alternative note on the Schur-convexity of the extended mean values, Math. Inequal. Appl., 9(2)(2006), 219-224.
- [20] H. N. Shi, M. Bencze, S. H. Wu and D. M. Li, Schur convexity of generalized Heronian means involving two parameters, J. Inequal. Appl., V 2008, Art. ID. 879273, 9 pages doi:10.1155/2008/879273.
- [21] X. M. Zang, The Schur geometrical convexity of integral arithmetic mean, Inte. J. Pure Appl. Math., 41(7)(2007), 919- 925.

Roman Primary and Auxiliary Domination Number of a Graph

Mallikarjun B Kattimani and N C Hemalatha

The Oxford College of Engineering, Bangalore-560 068-India

Abstract- Let $G = (V, E)$ be a graph. The two disjoint proper subsets D_1 & D_2 of $V(G)$ are said to be roman primary dominating set and auxiliary dominating set of G respectively, if every vertex not in D_1 & D_2 is adjacent to at least one vertex in D_1 & D_2 . The domination number $\gamma_{pri}(G)$ is the minimum cardinality of a primary dominating set and the domination number $\gamma_{aux}(G)$ is the minimum cardinality of an auxiliary dominating set. Note that $\gamma_{pri}(G) \leq \gamma_{aux}(G)$. In this paper, we initiate a study of this new parameter.

Index Terms- domination number, primary domination number, and auxiliary domination number.

I. INTRODUCTION

The graphs considered here are simple, finite, nontrivial, undirected, connected, without loops or multiple edges or isolated vertices. For undefined terms or notations in this paper may be found in Harary [1].

Let $G = (V, E)$ be a graph. A set $D \subseteq V(G)$ is a dominating set of G if every vertex not in D is adjacent to at least one vertex in D . The domination number $\gamma(G)$ is the minimum cardinality of a dominating set.

While various parameters related to domination in graphs have been studied extensively. Let $G = (V, E)$ be a graph. The two disjoint proper subsets D_1 & D_2 of $V(G)$ are said to be roman primary dominating set and auxiliary dominating set of G respectively, if every vertex not in D_1 & D_2 is adjacent to at least one vertex in D_1 & D_2 . The domination number $\gamma_{pri}(G)$ is the minimum cardinality of a roman primary dominating set and the domination number $\gamma_{aux}(G)$ is the minimum cardinality

of an auxiliary dominating set. Note that $\gamma_{pri}(G) \leq \gamma_{aux}(G)$. In this paper, we initiate a study of this new parameter.

For example, Airspace control increases operational effectiveness by promoting the safe, efficient, and flexible use of airspace while minimizing restraints on airspace users (pilot and co-pilot). Airspace control (dominate) includes coordinating, integrating, and regulating airspace to increase operational effectiveness. Effective airspace control reduces the risk of unintended engagements against friendly, civil, and neutral aircraft, enhances air defense operations, and permits greater flexibility of joint operations. This motivates to our primary and

auxiliary dominating sets. And another example, parallel processing is the simultaneous use of more than one processor core to execute a program or multiple computational threads. Ideally, parallel processing makes programs run faster because there are more engines (cores) running it. In practice, it is often difficult to divide a program in such a way that separate cores can execute different portions without interfering with each other. Most computers have just one Processing unit, but some models have several, and multi-core processor chips are becoming the norm. Thus, we initiate a study of this new parameter.

II. RESULTS

We use the notation P_p , W_p , K_p , and C_p to denote, respectively, the path graph, wheel, complete graph, cycle graph with p vertices; the star graph with $p+1$ vertices, and $K_{m,n}$ the complete bipartite graph with $m+n$ vertices (see [1]).

We obtain the exact value of $\gamma_{pri}(G)$, $\gamma_{aux}(G)$ and $|V - (D_1 + D_2)|$ for some standard graphs, which are simple, to observe, hence we omit the proof. As usual, for a real number s , let $\lfloor s \rfloor$ be the greatest integer less than or equal to s , and $\lceil s \rceil$ be the least integer greater than or equal to s .

Proposition1. For any complete graph K_p with $p \geq 3$ vertices,

$$\gamma_{pri}(K_p) = \gamma_{aux}(K_p) = \gamma(G) = 1.$$

Proof. Suppose G is a complete graph with $p \geq 3$ vertices, since every pair of its vertices is adjacent. Clearly, by definition it proves that $\gamma_{pri}(K_p) = \gamma_{aux}(K_p) = \gamma(G) = 1$.

Proposition 2. For any cycle C_p , with

$$p \geq 4 \text{ vertices, } \gamma_{pri}(C_p) = \left\lceil \frac{p}{4} \right\rceil.$$

$$\text{and } \gamma_{aux}(C_p) = p - 3 \left\lfloor \frac{p}{4} \right\rfloor.$$

Proof. Let $G = (V, E)$ be a graph. The two disjoint proper subsets D_1 & D_2 of $V(G)$ are said to be primary dominating set and auxiliary dominating set of G respectively, Suppose Every vertex of D_1 set is contributing twice the number of vertices in $V - (D_1 \cup D_2)$

Proposition 3. For any wheel W_p , with $p \geq 5$ vertices, $\gamma_{pri}(P_p) = 1$, and $\gamma_{aux}(G) = P - 4$.

Prof. Suppose the graph is a wheel then we know that a wheel W_p having one vertex say v of maximum degree Δ , and remaining all other vertices are having degree three. Now, a vertex v and another two non adjacent vertices of W_p are also belongs to $V - (D_1 \cup D_2)$. Since primary domination number having exactly one vertex and $V - (D_1 \cup D_2)$ contains three vertices. Therefore auxillary domination number is $P - 4$.

Proposition 4. If G is a star, then $\gamma_{pri}(G) = 1$ and $\gamma_{aux}(G) = \Delta(G) - 1$.

Proof. Suppose G is a star and v being a vertex of maximum degree, then $\Delta(G) =$ number of pendent vertices. By the definition every vertex not in D_1 & D_2 is adjacent to at least one vertex in D_1 & D_2 , such that every pendant vertex of G must be belongs to D_1 or D_2 . Hence $\gamma_{pri}(G) = 1$ and $\gamma_{aux}(G) = \Delta(G) - 1$.

Proposition 5. If G is a complete bipartite graph with $m \leq n$ vertices, where, $m \geq 2$, then $\gamma_{pri}(K_{m,n}) = 1$, $\gamma_{aux}(K_{m,n}) = m - 1$.

Prof. Obviously follows from the definition; Hence we omit its proof.

Proposition 6. If G is a complete bipartite graph with $m \leq n$ vertices, then $\gamma_{pri}(G) + \gamma_{aux}(G) = \gamma(G) = m$.

Proof. Obviously, $\gamma(G) = m$. It is easy to notice that $\gamma_{pri}(G) + \gamma_{aux}(G) = n = m$. Hence the theorem is proved.

Proposition 7. Let G be a complete bipartite graph with $m \leq n$ vertices, where, $m \geq 2$, then $\gamma_{pri}(K_{m,n}) < \gamma(K_{m,n})$.

Proof. Obviously follows from the Proposition 4.

Proposition 8. If x be a pendent vertex of a graph G , then $x \in D_1$ or D_2 .

Proof. Clearly, every vertex not in D_1 & D_2 is adjacent to at least one vertex in D_1 & D_2 . Hence every pendant vertex of G must be belongs to D_1 or D_2 .

Next, we obtain a relationship between primary domination numbers with the domination number, since their proof are trivial, we omit the same.

Theorem 9. If G is a star or complete graph, then $\gamma_{pri}(G) = \gamma(G)$.

Theorem 10. If G be a complete bipartite graph with $m \leq n$ vertices, where, $m \geq 2$, then $\gamma_{pri}(G) < \gamma(G)$.

Proposition 11. If G is a complete bipartite graph with $m \leq n$ vertices, then $\gamma_{pri}(G) + \gamma_{aux}(G) = \gamma(G) = m$.

REFERENCES

- [1] F. Harary. Graph Theory, Addison-Wesley, Reading Mass.(1969).
- [2] Haynes, T. W., Hedetniemi, S.T. and Slater, P.J. (1998) - Domination in Graphs: Advanced Topics, Marcel Dekker, Inc., New York.
- [3] Haynes, T. W., Hedetniemi, S.T. and Slater, P.J.(1998) - Fundamentals of domination in graphs, Marcel Dekker, Inc., New York.
- [4] Allan, R.B. and Laskar, R.C. (1978) – On domination, independent domination numbers of a graph, Discrete Math., 23, pp.73 – 76.
- [5] Cockayne, E.J. and Hedetniemi, S.T. (1977) - Towards a theory of domination in graphs, Networks, 7, pp.247 – 261.
- [6] Cockayne, E. J., Dreyer, P.A., Hedetniemi, S.M. and Hedetniemi, S.T. (2004) - Roman domination in graphs, Discrete Math., 278, 11 – 22.
- [7] Ian Stewart (1999)-Defend the Roman Empire!, Scientific American, 281(6),136–139.

AUTHORS

First Author – Mallikarjun B Kattimani, The Oxford College of Engineering, Bangalore-560 068-India

Second Author – N C Hemalatha, The Oxford College of Engineering, Bangalore-560 068-India

Roman Domination Number of a Graph

Mallikarjun B Kattimani and N C Hemalatha

The Oxford College of Engineering, Bangalore-560 068-India

Abstract- A dominating set D of a graph $G = (V, E)$ is *roman dominating set*, if S and T are two subsets of D and satisfying the condition that every vertex u in S is adjacent to exactly one to one a vertex v in $V - D$ as well as adjacent to some vertex in T . The roman domination number of $\gamma_{rds}(G)$ of G is the minimum cardinality of a roman dominating set of G . In this paper many bounds on $\gamma_{rds}(G)$ are obtained and its exact values for some standard graphs are found. Also relationship with other parameter is investigated. We introduce Roman dominating set in which the interest is in dominating contains two types of subset.

Index Terms- Domination, Roman domination.

I. INTRODUCTION

The graphs considered here are simple, finite, nontrivial, undirected, connected, without loops or multiple edges or isolated vertices. For undefined terms or notations in this paper may be found in Harary [1].

Let $G = (V, E)$ be a graph. A set $D \subseteq V(G)$ is a dominating set of G if every vertex not in D is adjacent to at least one vertex in D . The domination number $\gamma(G)$ is the minimum cardinality of a dominating set.

Roman Emperor Constantine had the requirement that an army or legion could be sent from its home to defend a neighboring location only if there was a second army, which would stay and protect the home. Thus, there are two types of armies, stationary and traveling. Each vertex with no army must have a neighboring vertex with a traveling army. Stationary armies then dominate their own vertices, and its stationary army dominates a vertex with two armies, and the traveling army dominates its open neighborhood, which motivates to our roman domination number of a graph.

A dominating set D of a graph $G = (V, E)$ is *roman dominating set* if S, T are two subsets of D and satisfying the condition that every vertex u in S is adjacent to exactly one to one a vertex v in $V - D$ as well as adjacent to some vertex in T . The roman domination number of $\gamma_{rds}(G)$ of G is the minimum cardinality of a roman dominating set of G .

II. RESULTS

We use the notation $P_p, W_p, K_p,$ and C_p to denote, respectively, the *path, wheel, complete graph,* and *cycle* with p

vertices; $K_{1,p}$ star with $p + 1$ vertices, and $K_{m,n}$ complete bipartite graph with $(m + n)$ vertices (see [4]).

Theorem 1.

$$(1). \gamma_{rds}(C_p) = \left\lfloor \frac{p}{2} \right\rfloor + 1, \quad p \geq 3$$

$$(2). \gamma_{rds}(K_p) = p - 1, \quad p \geq 3$$

$$(3). \gamma_{rds}(W_p) = 3, \quad p \geq 4$$

$$(4). \gamma_{rds}(P_p) = \left\lceil \frac{p}{2} \right\rceil, \quad p \geq 3$$

$$(5). \gamma_{rds}(K_{m,n}) = m, \text{ where } m < n,$$

$$(6). \gamma_{rds}(K_{1,p}) = p = q = \Delta(K_{1,p})$$

Proof. Since, follows directly from the definition.

Theorem 2. For any graph $G, \gamma_{rds}(G) \leq p - 1$. equality holds when G a complete graph or a star.

Proof. Let D be a roman dominating set of G , such that S and T are two subsets of D , clearly, by the definition of roman dominating set the number of vertices in S are adjacent to a number of vertices in $(V - D)$ are equal. Then the number of vertices are in T are adjacent to a number of vertices in $(V - D)$ are greater than or equal to zero. Hence $\gamma_{rds}(G) \leq p - 1$.

Further, the complete graph or star achieves this bound.

Theorem 3. For any graph $G, p \geq 3$ vertices, a set S of independent $|m|$ cut vertices and each cut vertex is adjacent to a

$$\gamma_{rds}(T) = \sum_{i=1}^m \deg m_i$$

pendent vertex. Then

Proof. We know that, a dominating set D of a graph $G = (V, E)$ is *roman dominating set* if S, T are two subsets of D . Obviously, every cut vertex of S is adjacent to a pendent vertex u in $V - D$ as well as adjacent in T .

Thus,

$$\begin{aligned} &|N[S]| - |u| \\ \Rightarrow &|N(S)| \end{aligned}$$

$$\Rightarrow \gamma_{rds}(T) = \sum_{i=1}^{p-2} \deg_{ree} U_i \in S.$$

Theorem 4. For any graph G , $\gamma_{rds}(G) \geq \gamma(G)$.

Proof. Clearly, by the definition, roman dominating set is also a dominating set.

Theorem 5. For any graph G , $\frac{P}{\Delta + 1} \leq \gamma_{rds}(G)$.

Proof. It is known that $\frac{P}{\Delta + 1} \leq \gamma(G)$ and since $\frac{P}{\Delta + 1} \leq \gamma_{rds}(G)$, result holds

Theorem 6. For any graph G , $\gamma_{rds}(G) \leq p - 1$. And this bound is sharp.

Proof. Let D be a minimum dominating set of G . Then every vertex of $V - D$ except one vertex $v \in (V - D)$, then $D \cup (V - D) - 1$ is a roman dominating set. Thus $\gamma + P - \gamma - 1 = P - 1$.

The Complete graph K_p achieves this bound.

Theorem 7. If T is a tree with m cut vertices and if each cut vertex is adjacent to at least one end vertex except one is adjacent to exactly one end vertex, then $\gamma_{rds}(G) = m$.

Proof. Let C be the set of all cut vertices of tree T with $|C| = m$. Then $V - C$ is a dominating set of all end vertices with $|V - C| > m$. We know that S and T be the subset Stationary and travelling respectively of a roman dominating set. Here a cut vertex u which is adjacent to one end vertex is belongs to stationary set and $|C - u|$ cut vertices are belongs to travelling set, therefore C is a roman dominating set. Hence, the roman domination number of G $\gamma_{rds}(G) = m$.

Corollary 8. For any tree T , with $m \geq 2$ cut vertices, then $\gamma_{rds}(T) \leq m$.

Proof. Suppose, the tree T contain m number of cut vertices. Follows form the theorem 6. If some cut vertices is belongs $V - D$, by the definition $\gamma_{rds}(T) < m$.

The following propositions, corollary are straight forward and the proofs are omitted.

Propositions 9. If a graph G has cut vertex v and is adjacent to an end vertex, then $2 \leq \gamma_{rds}(G) \leq P - 1$.

Corollary 10. If a graph G has cut vertex, $P \geq 4$ vertices and every cut vertex has adjacent to at most two end vertices, then $\gamma_{rds}(G) = P - e$, where e be the end vertex.

REFERENCES

- [1] Allan, R.B. and Laskar, R.C. (1978) – On domination, independent domination numbers of a graph, Discrete Math., 23, pp.73 – 76.
- [2] Cockayne, E.J. and Hedetniemi, S.T. (1977) - Towards a theory of domination in graphs. Networks, 7, pp.247 – 261.
- [3] Cockayne, E. J., Dreyer, P.A., Hedetniemi, S.M. and Hedetniemi, S.T. (2004) - Roman domination in graphs, Discrete Math., 278, 11 – 22.
- [4] F. Harary, Graph Theory, Addison Wesley, Reading Mass., 1972.
- [5] Ian Stewart (1999)-Defend the Roman Empire!, Scientific American, 281(6),136–139.
- [6] Haynes, T. W., Hedetniemi, S.T. and Slater, P.J. (1998) - Domination in Graphs: Advanced Topics, Marcel Dekker, Inc., New York.
- [7] Haynes, T. W., Hedetniemi, S.T. and Slater, P.J.(1998) - Fundamentals of domination in graphs, Marcel Dekker, Inc., New York.
- [8] V R Kulli and M B Kattimani, Global Accurate Domination in Graphs, International Journal of Scientific and Research Publications, Volume 3, Issue 10, October 2013, ISSN 2250-3153.

AUTHORS

First Author – Dr. Mallikarjun Basanna Kattimani, M.Sc.,M.Phil.,PGDCA,Ph.D., Professor and HOD, Department of Engineering Mathematics, THE OXFORD COLLEGE OF ENGINEERING, Bommanahalli, Hosur Road, Bangalore-68 mallikarjun_8@yahoo.co.in, mathshodoxford@gmail.com 9740254828

Second Author – Mrs. N C Hemalatha, Asso. Prof. Department of Engineering Mathematics, THE OXFORD COLLEGE OF ENGINEERING, Bommanahalli, Hosur Road, Bangalore-68, Sharumunna7@gmail.com



CHILDREN'S EDUCATION SOCIETY (Regd.)
THE OXFORD COLLEGE OF ENGINEERING

(Recognised by the Govt. of Karnataka, Affiliated to Visvesvaraya Technological University, Belagavi.

Approved by A.I.C.T.E. New Delhi.

Recognised by UGC Under Section 2(f)

Bommanahalli, Hosur Road, Bangalore - 560 068.

Ph: 080-61754601/602, Fax: 080 - 25730551

E-mail: engprincipal@theoxford.edu Web: www.theoxfordengg.org

| Sl. No | Title of paper | Name of the author/s | Department of the teacher | Name of journal | Year of publication | ISSN number | Link to website of the Journal | Link to article/paper/abstract of the article | Is it listed in UGC Care list/Scopus/ Web of Science/other, mention |
|--------|---|--|---------------------------|-----------------|---------------------|-------------|---|---|---|
| 1 | MQTT-based Home Automation System Using Raspberry PI 3 Model B | Chandana P M, Clint Ulahannan Thomas,Harshith Ramesh Rai,Namita Y | ISE | IJCRT | 2017 | 2320-2882 | https://www.ijert.org | https://ijert.org/archive.php?vol=6&issue=2&page=1 | Google Scholar |
| 2 | MABIDaaS: Mutual Authentication and Financial Transaction Between Mobile Users using Blockchain based ID as a Service | Akshatha B M, Manasa J, Meghana K S, Sonal Salian, Dr. D. Jayaramaiah | ISE | IJCRT | 2017 | 2320-2882 | https://www.ijert.org | https://ijert.org/archive.php?vol=6&issue=2&page=1 | Google Scholar |



CHILDREN'S EDUCATION SOCIETY (Regd.)
THE OXFORD COLLEGE OF ENGINEERING

(Recognised by the Govt. of Karnataka, Affiliated to Visvesvaraya Technological University, Belagavi.

Approved by A.I.C.T.E. New Delhi.

Recognised by UGC Under Section 2(f)

Bommanahalli, Hosur Road, Bangalore - 560 068.

Ph: 080-61754601/602, Fax: 080 - 25730551

E-mail: engprincipal@theoxford.edu Web: www.theoxfordengg.org

| | | | | | | | | | |
|---|--|--|-----|-------|------|-----------|---|---|----------------|
| 3 | Study and Analysis of Most Sought after Big data Platforms and their Application for Network Analytics | Thendral N | ISE | IJCRT | 2017 | 2320-2882 | https://www.ijert.org | https://ijert.org/archive.php?vol=6&issue=2&page=1 | Google Scholar |
| 4 | Design and Implementation of an IoT System for Enhancing Proprioception Training | Archana D R, Ayesha Rahmath, Chandrashekar M, M Tuba Farheen, Dr D Jayaramaiah | ISE | IJCRT | 2017 | 2320-2882 | https://www.ijert.org | https://ijert.org/archive.php?vol=6&issue=2&page=1 | Google Scholar |
| 5 | An intelligent smartphone based approach using cloud computing and iot for risk-free driving | S.Kalaiselvi , Lakshmi L Menda , Navya V , Fiona Jothi Sylvester , Latha Shree N | ISE | IJCRT | 2017 | 2320-2882 | https://www.ijert.org | https://ijert.org/archive.php?vol=6&issue=2&page=1 | Google Scholar |



CHILDREN'S EDUCATION SOCIETY (Regd.)
THE OXFORD COLLEGE OF ENGINEERING

(Recognised by the Govt. of Karnataka, Affiliated to Visvesvaraya Technological University, Belagavi.

Approved by A.I.C.T.E. New Delhi.

Recognised by UGC Under Section 2(f)

Bommanahalli, Hosur Road, Bangalore - 560 068.

Ph: 080-61754601/602, Fax: 080 - 25730551

E-mail: engprincipal@theoxford.edu Web: www.theoxfordengg.org

| | | | | | | | | | |
|---|---|--|-----|-------|------|-----------|---|---|----------------|
| 6 | Detecting spam reviews on social media using network-based framework: netspam | P Kokila | ISE | IJCRT | 2017 | 2320-2882 | https://www.ijcrt.org | https://ijcrt.org/archive.php?vol=6&issue=2&page=1 | Google Scholar |
| 7 | Vehicle Detection in Fog and Night Condition using Block Matching and Color Enhancement Algorithm | Nivedha M,Pallavi R,Supriya S,Sushma R | ISE | IJCRT | 2017 | 2320-2882 | https://www.ijcrt.org | https://ijcrt.org/archive.php?vol=6&issue=2&page=1 | Google Scholar |
| 8 | Generating music from literature using topic extraction and sentiment analysis | Aafia Nausheen | ISE | IJCRT | 2017 | 2320-2882 | https://www.ijcrt.org | https://ijcrt.org/archive.php?vol=6&issue=2&page=1 | Google Scholar |
| 9 | A reliability system for filtering malicious information on social | Asma Nooren P, Chandana L V, Divya G A, Saniya Sadaf M | ISE | IJCRT | 2017 | 2320-2882 | https://www.ijcrt.org | https://ijcrt.org/archive.php?vol=6&issue=2&page=1 | Google Scholar |



CHILDREN'S EDUCATION SOCIETY (Regd.)
THE OXFORD COLLEGE OF ENGINEERING

(Recognised by the Govt. of Karnataka, Affiliated to Visvesvaraya Technological University, Belagavi.

Approved by A.I.C.T.E. New Delhi.

Recognised by UGC Under Section 2(f)

Bommanahalli, Hosur Road, Bangalore - 560 068.

Ph: 080-61754601/602, Fax: 080 - 25730551

E-mail: engprincipal@theoxford.edu Web: www.theoxfordengg.org

| | | | | | | | | | |
|----|--|--|-----|-------|------|---------------|---|---|-------------------|
| | network | | | | | | | | |
| 10 | MRCP-RMD: Resource allocation and Scheduling of jobs with Deadlines | Shashank G Hegde, Vinayak Suresh Pai, Vinitha S Bhat,Srinidhi L N | ISE | IJCRT | 2017 | 2320- 2882 | https://www.ijert.org | https://ijert.org/archive.php?vol=6&issue=2&page=1 | Google Scholar |
| 11 | Structure Design of Photonic Crystal Based MOEMS Accelerometer Sensor for Supplemental Restraint System in Automobile Passenger Safety | Sundar Subramanian , Anup M. Upadhyaya and Preeti Sharan | ECE | IJST | 201 | 0974- 5645 | https://dx.doi.org/10.17485/ijst/2017/v10i29/117327 | https://indjst.org/articles/structure-design-of-photonic-crystal-based-moems-accelerometer-sensor-for-supplemental-restraint-system-in-automobile-passenger-safety | UGC |



CHILDREN'S EDUCATION SOCIETY (Regd.)
THE OXFORD COLLEGE OF ENGINEERING

(Recognised by the Govt. of Karnataka, Affiliated to Visvesvaraya Technological University, Belagavi.

Approved by A.I.C.T.E. New Delhi.

Recognised by UGC Under Section 2(f)

Bommanahalli, Hosur Road, Bangalore - 560 068.

Ph: 080-61754601/602, Fax: 080 - 25730551

E-mail: engprincipal@theoxford.edu Web: www.theoxfordengg.org

| | | | | | | | | | |
|----|--|---|-----|---------------|------|-------------------|---|---|----------------|
| 12 | Performance Analysis of Reversible ALU in QCA | Rajinder Tiwari, Preeta Sharan | ECE | IJST | 2017 | 0974-5645 | https://dx.doi.org/10.17485/ijst/2017/v10i29/117324 | https://indjst.org/articles/performance-analysis-of-reversible-alu-in-qca | UGC |
| 13 | A Novel Imaging System for Removal of Underwater Distortion using Code V | Maik, Vivek Daniel, Stella Chrispin Jiji, A | ECE | IEIE | 2017 | 2287-5255 | http://koreascience.or.kr/journal/E1STIF.page | https://doi.org/10.5573/IEIESPC.2017.6.3.141 | Google Scholar |
| 14 | Deblurring Underwater Image Degradations Based on Adaptive Regularization | Chrispin A J, Nagaraj | ECE | IEEE Explorer | 2017 | 2471-7851 | https://doi.org/10.1109/ICCIC.2017.8524166 | https://ieeexplore.ieee.org/document/8524166 | Google Scholar |
| 15 | Underwater turbidity removal through ill-posed optimization with sparse modeling | Chrispin A J, Vivek | ECE | IEEE Explorer | 2017 | 978-1-5386-0813-5 | https://doi.org/10.1109/ICPSCI.2017.8392039 | https://ieeexplore.ieee.org/document/8392039 | Google Scholar |



CHILDREN'S EDUCATION SOCIETY (Regd.)
THE OXFORD COLLEGE OF ENGINEERING

(Recognised by the Govt. of Karnataka, Affiliated to Visvesvaraya Technological University, Belagavi.

Approved by A.I.C.T.E. New Delhi.

Recognised by UGC Under Section 2(f)

Bommanahalli, Hosur Road, Bangalore - 560 068.

Ph: 080-61754601/602, Fax: 080 - 25730551

E-mail: engprincipal@theoxford.edu Web: www.theoxfordengg.org

| | | | | | | | | | |
|----|--|---|---------|---------------|------|-----------------------|---|---|----------------|
| 16 | Variability Studies in Advanced Genotypes of Rice (Oryza sativa L) | .B Manjunatha, C. Malleshappa, Dr. Niranjana Kumara | ECE | IJCMA S | 2018 | 2319-7706 | http://www.ijcmas.com/ | https://doi.org/10.20546/ijcmas.2018.706.194 | Google Scholar |
| 17 | A Novel Technique for Enhancing Color of Undersea Deblurred Imagery | Chrispin Jiji · Nagaraj Ramrao | ECE | ASTES Journal | 2018 | | https://astesjournal.com/ | http://dx.doi.org/10.25046/aj030610 | Google Scholar |
| 18 | Enhancement of Underwater Deblurred Images using Gradient Guided Filter | Chrispin Jiji · Nagaraj Ramrao | ECE | IEEE Xplore | 2018 | | https://ieeexplore.ieee.org/Xplore/home.jsp | https://ieeexplore.ieee.org/document/9012305 | IEEE Xplore |
| 19 | Genetic variability studies and screening for blast resistance in advanced genotypes of rice (Oryza sativa L). | B Manjunatha, Kumara B N | BioTech | IJASR | 2017 | 2250-0057, 2321-00087 | http://www.tjprc.org/ | http://www.tjprc.org/publicshpapers/2-50-1513311888-57.IJASRDEC201757.pdf | Google Scholar |



CHILDREN'S EDUCATION SOCIETY (Regd.)
THE OXFORD COLLEGE OF ENGINEERING
 (Recognised by the Govt. of Karnataka, Affiliated to Visvesvaraya Technological University, Belagavi.

Approved by A.I.C.T.E. New Delhi.

Recognised by UGC Under Section 2(f)

Bommanahalli, Hosur Road, Bangalore - 560 068.

Ph: 080-61754601/602, Fax: 080 - 25730551

E-mail: engprincipal@theoxford.edu Web: www.theoxfordengg.org

| | | | | | | | | | |
|----|---|--------------|----|---|------|-----------------|---|---|----------------|
| 20 | Relationship of Nutrient molar ratio of microbial attached communities in organic matter utilization of Pachamalai forested stream. | K.Valarmathy | BT | International Journal of Advanced Multidisciplinary Research, | 2017 | ISSN: 2393-8870 | https://ijarm.com/pdfcopy/oct2017/ijarm4.pdf | https://ijarm.com/pdfcopy/oct2017/ijarm4.pdf | Google Scholar |
| 21 | Organic matter availability structures of microbial biomass and their activity in Pachamalai Forested stream in Tamilnadu. | K.Valarmathy | BT | International Journal of Advanced Research in Biological Sciences | 2017 | ISSN: 2348-8069 | https://ijarbs.com/pdfcopy/july2017/ijarbs26.pdf | https://ijarbs.com/pdfcopy/july2017/ijarbs26.pdf | Google Scholar |
| 22 | Organic matter decomposition by Aquatic fungi in the Pachamalai | K.Valarmathy | BT | International Journal of Advanced | 2017 | ISSN: 2393-8870 | https://ijarm.com/pdfcopy/june2017/ijarm13.pdf | https://ijarm.com/pdfcopy/june2017/ijarm13.pdf | Google Scholar |



CHILDREN'S EDUCATION SOCIETY (Regd.)
THE OXFORD COLLEGE OF ENGINEERING

(Recognised by the Govt. of Karnataka, Affiliated to Visvesvaraya Technological University, Belagavi.

Approved by A.I.C.T.E. New Delhi.

Recognised by UGC Under Section 2(f)

Bommanahalli, Hosur Road, Bangalore - 560 068.

Ph: 080-61754601/602, Fax: 080 - 25730551

E-mail: engprincipal@theoxford.edu Web: www.theoxfordengg.org

| | | | | | | | | | |
|----|--|---------------------------------|----|--|------|------------------------|--|--|-------------------|
| | forested stream contributed by streambed substrata. | | | ed Multidi sciplina ry Researc h | | | | | |
| 23 | 16s rDNA Based identification of bacteria in the organic matter of Pachamalai forested streams. | K.Valarmathy | BT | Internat ional Journal of Compre hensive Researc h in Biologi cal science s | 2017 | ISSN: 2393- 8560 | https://darshanpublishers.com/ijcrbs/cissuedec2017.html http://dx.doi.org/10.22192/ijcrbs.2017.04.12.001 | https://darshanpublishers.com/ijcrbs/cissuedec2017.html http://dx.doi.org/10.22192/ijcrbs.2017.04.12.001 | Google Scholar |
| 24 | Screening of antibacterial and antioxidant activities of Streptomyces species isolated from western Ghats from Karnataka | Dr.B.K.Manjunatha,Mr.Divakara R | BT | Internat ional Journal Of Creativ e Researc h Though ts | 2018 | ISSN: 2320- 2882 | https://www.ijcrt.org/papers/IJCRTOXFO015.pdf | https://www.ijcrt.org/papers/IJCRTOXFO015.pdf | UGC |



CHILDREN'S EDUCATION SOCIETY (Regd.)
THE OXFORD COLLEGE OF ENGINEERING
 (Recognised by the Govt. of Karnataka, Affiliated to Visvesvaraya Technological University, Belagavi.

Approved by A.I.C.T.E. New Delhi.

Recognised by UGC Under Section 2(f)

Bommanahalli, Hosur Road, Bangalore - 560 068.

Ph: 080-61754601/602, Fax: 080 - 25730551

E-mail: engprincipal@theoxford.edu Web: www.theoxfordengg.org

| | | | | | | | | | |
|----|--|--------------------------------|----|---|------|-----------------|---|---|-----|
| | | | | 25(IJC) | | | | | |
| 25 | Heavy metal ion detection using immobilized ALP enzyme | K.Valarmathy | BT | International Journal Of Creative Research Thoughts (IJCRT) | 2018 | ISSN: 2320-2882 | https://www.ijert.org/papers/IJCRTOXFO017.pdf | https://www.ijert.org/papers/IJCRTOXFO017.pdf | UGC |
| 26 | Isolation, characterization and biological activity of flax lectin | Dr.B.K.Manjunatha, Dr Suma T K | BT | International Journal Of Creative Research Thoughts | 2018 | ISSN: 2320-2882 | https://ijert.org/download.php?file=IJCRTOXFO020.pdf | https://ijert.org/download.php?file=IJCRTOXFO020.pdf | UGC |



CHILDREN'S EDUCATION SOCIETY (Regd.)
THE OXFORD COLLEGE OF ENGINEERING

(Recognised by the Govt. of Karnataka, Affiliated to Visvesvaraya Technological University, Belagavi.

Approved by A.I.C.T.E. New Delhi.

Recognised by UGC Under Section 2(f)

Bommanahalli, Hosur Road, Bangalore - 560 068.

Ph: 080-61754601/602, Fax: 080 - 25730551

E-mail: engprincipal@theoxford.edu Web: www.theoxfordengg.org

| | | | | | | | | |
|----|---|---------------------------------|----|--|------|-----------------|---|-----|
| | | | | (IJCRT) | | | | |
| 27 | Significance analysis of target profile in tuberculosis using gene interactions and insilico docking approach to find potential ligands | Dr.B.K.Manjunatha, Shambu M G | BT | International Journal Of Creative Research Thoughts (IJCRT) | 2018 | ISSN: 2320-2882 | https://www.ijcrt.org/papers/IJCRTOXFO025.pdf | UGC |
| 28 | Evaluation of bioremediation efficacy of A.flavusHQ010 119and Pencillium sp. KJ415574.1 strainsin used engine oil degradation | Dr.B.K.Manjunatha, Valarmathy K | BT | International Journal Of Creative Research Thoughts | 2018 | ISSN: 2320-2882 | https://www.ijcrt.org/papers/IJCRTOXFO032.pdf | UGC |



CHILDREN'S EDUCATION SOCIETY (Regd.)
THE OXFORD COLLEGE OF ENGINEERING

(Recognised by the Govt. of Karnataka, Affiliated to Visvesvaraya Technological University, Belagavi.

Approved by A.I.C.T.E. New Delhi.

Recognised by UGC Under Section 2(f)

Bommanahalli, Hosur Road, Bangalore - 560 068.

Ph: 080-61754601/602, Fax: 080 - 25730551

E-mail: engprincipal@theoxford.edu Web: www.theoxfordengg.org

| | | | | | | | | | |
|----|---|-------------------------------|----|--|------|-----------------|---|---|-----|
| | | | | (IJCRT) | | | | | |
| 29 | Screening of potential phytochemicals for wound healing. | Dr.B.K.Manjunatha, Tanusree C | BT | International Journal Of Creative Research Thoughts (IJCRT) | 2018 | ISSN: 2320-2882 | https://ijert.org/papers/IJCRTOXFO039.pdf | https://ijert.org/papers/IJCRTOXFO039.pdf | UGC |
| 30 | Isolation & Characterization Of Methanogenic Bacteria From Local Environment And Comparative Study Of Kinetics With | Salma Kausar M | BT | International Journal of Creative Research Thoughts | 2018 | ISSN: 2320-2882 | https://www.ijert.org/papers/IJCRTOXFO044.pdf | https://www.ijert.org/papers/IJCRTOXFO044.pdf | UGC |



CHILDREN'S EDUCATION SOCIETY (Regd.)
THE OXFORD COLLEGE OF ENGINEERING

(Recognised by the Govt. of Karnataka, Affiliated to Visvesvaraya Technological University, Belagavi.

Approved by A.I.C.T.E. New Delhi.

Recognised by UGC Under Section 2(f)

Bommanahalli, Hosur Road, Bangalore - 560 068.

Ph: 080-61754601/602, Fax: 080 - 25730551

E-mail: engprincipal@theoxford.edu Web: www.theoxfordengg.org

| | | | | | | | | | |
|----|---|-------------------------------|----|--|--------|-----------------|---|---|-----|
| | Traditional Biogas Producers. | | | (IJCRT) | | | | | |
| 31 | Construction of cancer diseasome through graph theoretical approach | Dr.B.K.Manjunatha, Tanusree C | BT | International Journal Of Creative Research Thoughts (IJCRT) | 2018 | ISSN: 2320-2882 | https://ijcrt.org/download.php?file=IJCRTOXFO057.pdf | https://ijcrt.org/download.php?file=IJCRTOXFO057.pdf | UGC |
| 32 | Radioprotective and immunomodulatory effects of Mesua Ferrea(Linn) from western ghats of India., in irradiated swiss albino | Dr.B.K.Manjunatha | BT | Journal of radiation research and applied sciences (Elsevier), | Jul-05 | 2314-7164 | https://www.sciencedirect.com/science/article/pii/S2314853518302646 | https://www.sciencedirect.com/science/article/pii/S2314853518302646 | SCI |



CHILDREN'S EDUCATION SOCIETY (Regd.)
THE OXFORD COLLEGE OF ENGINEERING

(Recognised by the Govt. of Karnataka, Affiliated to Visvesvaraya Technological University, Belagavi.

Approved by A.I.C.T.E. New Delhi.

Recognised by UGC Under Section 2(f)

Bommanahalli, Hosur Road, Bangalore - 560 068.

Ph: 080-61754601/602, Fax: 080 - 25730551

E-mail: engprincipal@theoxford.edu Web: www.theoxfordengg.org

| | | | | | | | | | |
|----|---|---------------|-------|-----------------|------|----------------------|---|---|----------------|
| | mice and splenic lymphocytes, | | | September 2017, | | | | | |
| 33 | Comparative study on regular and irregular rc structures under far and near field ground motion with base isolation | Sachin Mankal | Civil | IRJET | 2017 | 2395-0056, 2395-0072 | https://www.irjet.net/ | https://www.irjet.net/archives/V4/i8/IRJET-V4I8277.pdf | Google Scholar |
| 34 | Design of reinforced concrete structures using neural networks | Chandan.M.K | Civil | IRJET | 2017 | 2395-0056, 2395-0072 | https://www.irjet.net/ | https://www.irjet.net/archives/V4/i7/IRJET-V4I7420.pdf | Google Scholar |
| 35 | Ductility Of fly ash - slag based reinforced geopolymer concrete elements | Mahantesh N.B | Civil | EACEF | 2017 | - | https://www.matec-conferences.org/ | https://doi.org/10.1051/mateconf/201713801003 | Google Scholar |



CHILDREN'S EDUCATION SOCIETY (Regd.)
THE OXFORD COLLEGE OF ENGINEERING

(Recognised by the Govt. of Karnataka, Affiliated to Visvesvaraya Technological University, Belagavi.

Approved by A.I.C.T.E. New Delhi.

Recognised by UGC Under Section 2(f)

Bommanahalli, Hosur Road, Bangalore - 560 068.

Ph: 080-61754601/602, Fax: 080 - 25730551

E-mail: engprincipal@theoxford.edu Web: www.theoxfordengg.org

| | | | | | | | | | |
|----|--|----------------------|-------|-------|------|----------------------|---|---|----------------|
| | cured at room temperature. | | | | | | | | |
| 36 | Dynamic Analysis of Machine Foundation | Manohar D | Civil | IRJET | 2017 | 2395-0056, 2395-0072 | https://www.irjet.net/ | https://www.irjet.net/archives/V4/i8/IRJET-V4I899.pdf | Google Scholar |
| 37 | Performance Study of Elevated Water Tanks under Seismic Forces | Furquan Elahi Shaikh | Civil | IRJET | 2017 | 2395-0056, 2395-0072 | https://www.irjet.net/ | https://www.irjet.net/archives/V4/i7/IRJET-V4I7325.pdf | Google Scholar |
| 38 | Sesimic isolation by introducing large scale aggregates | Suhas Jain C B | Civil | IRJET | 2017 | 2395-0056, 2395-0072 | https://www.irjet.net/ | https://www.irjet.net/archives/V4/i8/IRJET-V4I8324.pdf | Google Scholar |
| 39 | Structural Analysis of Blast Resistant Buildings | Qureshi Rizwan | Civil | IRJET | 2017 | 2395-0056, 2395-0072 | https://www.irjet.net/ | https://www.irjet.net/archives/V4/i8/IRJET-V4I8233.pdf | Google Scholar |



CHILDREN'S EDUCATION SOCIETY (Regd.)
THE OXFORD COLLEGE OF ENGINEERING
 (Recognised by the Govt. of Karnataka, Affiliated to Visvesvaraya Technological University, Belagavi.

Approved by A.I.C.T.E. New Delhi.

Recognised by UGC Under Section 2(f)

Bommanahalli, Hosur Road, Bangalore - 560 068.

Ph: 080-61754601/602, Fax: 080 - 25730551

E-mail: engprincipal@theoxford.edu Web: www.theoxfordengg.org

| | | | | | | | | | |
|----|---|--|--------------|----------------------|------|----------------------|---|---|----------------|
| 40 | Study of vertical irregularity of tall rc structure under lateral load | Rahul | Civil | IRJET | 2017 | 2395-0056, 2395-0072 | https://www.irjet.net/ | https://www.irjet.net/archives/V4/i8/IRJET-V4I8275.pdf | Google Scholar |
| 41 | Dry sliding wear properties of za-alloy containing traces of impurities with and without heat treatment | Gurunagendra G R 1, Ravikeerthi C1, Dr. B R Raju | Auto mobile | IJRAM E | 2017 | 2321-3051 | http://www.ijrame.com/ | http://www.ijrame.com/ | Google Scholar |
| 42 | FIR Notch Filter with Rejection Bandwidth Tuning and Sharpening | Rohini Deshpande, Deepak Deshpande | Mechatronics | RUASS ASTech Journal | 2017 | - | https://research.msruas.ac.in/publications | https://research.msruas.ac.in/publications/fir-notch-filter-with-rejection-bandwidth-tuning-and-sharpening | Google Scholar |
| 43 | Dry sliding wear properties of za-alloy containing traces of impurities with and without heat treatment | Gurunagendra G R 1, Ravikeerthi C1, Dr. B R Raju | Auto mobile | IJRAM E | 2017 | 2321-3051 | http://www.ijrame.com/ | http://www.ijrame.com/ | Google Scholar |



CHILDREN'S EDUCATION SOCIETY (Regd.)
THE OXFORD COLLEGE OF ENGINEERING

(Recognised by the Govt. of Karnataka, Affiliated to Visvesvaraya Technological University, Belagavi.

Approved by A.I.C.T.E. New Delhi.

Recognised by UGC Under Section 2(f)

Bommanahalli, Hosur Road, Bangalore - 560 068.

Ph: 080-61754601/602, Fax: 080 - 25730551

E-mail: engprincipal@theoxford.edu Web: www.theoxfordengg.org

| | | | | | | | | | |
|----|--|---------------------|-----------|--|------|-----------|---|---|----------------|
| 44 | Quantum Based Adaptive Topology control for intrusion detection and isolation in MANET | Dr. M S Shashidhara | MCA | IRJET Journals | 2017 | 2395-0072 | https://www.irjet.net/ | https://www.irjet.net/archives/V4/i5/IRJET-V4I5334.pdf | UGC |
| 45 | Quantum Phase Shift for Energy Conserved Secured Data Communication in MANET | Dr. M S Shashidhara | MCA | International Journal of Communication Networks and Information Security | 2017 | 2073-607X | https://www.ijcnis.org/index.php/ijcnis | https://www.ijcnis.org/index.php/ijcnis/article/view/2365 | Google Scholar |
| 46 | Synthesis of bis(indolyl) methanes over mesoporous solid base ZrO ₂ /MgO catalysts under solvent free mild conditions | M.Shyamsundar | Chemistry | International Journal of porous materials Springer | 2017 | 1573-4854 | https://www.springer.com/journal/10934 | https://www.springer.com/journal/10934 | UGC/Scopus |



CHILDREN'S EDUCATION SOCIETY (Regd.)
THE OXFORD COLLEGE OF ENGINEERING

(Recognised by the Govt. of Karnataka, Affiliated to Visvesvaraya Technological University, Belagavi.

Approved by A.I.C.T.E. New Delhi.

Recognised by UGC Under Section 2(f)

Bommanahalli, Hosur Road, Bangalore - 560 068.

Ph: 080-61754601/602, Fax: 080 - 25730551

E-mail: engprincipal@theoxford.edu Web: www.theoxfordengg.org

| | | | | | | | | | |
|----|---|--------------------------------------|-----------|--------------------------------------|------|-----------|---|---|------------|
| | | | | r publicat ions | | | | | |
| 47 | Simple but efficient synthesis of bis (indolyl) methane's by the condensation of substituted benzaldehydes with indole over mesoporous ZrO ₂ -MgO green catalyst under solvent free conditions | M Shyamsundar/SZ Mohamed Shamshuddin | Chemistry | Journal of Porous Materials Springer | 2017 | 1573-4854 | https://www.springer.com/journal/10934 | https://www.springer.com/journal/10934 | UGC/Scopus |
| 48 | Mesoporous ZrO ₂ -Al ₂ O ₃ (ZA) mixed metal oxide is an efficient and reusable catalyst for the liquid phase O-methoxymethylat | M Shyamsundar, Prtahap S R | Chemistry | Journal of Porous Materials Springer | 2017 | 1573-4854 | https://www.springer.com/journal/10934 | https://www.springer.com/journal/10934 | UGC/Scopus |



CHILDREN'S EDUCATION SOCIETY (Regd.)
THE OXFORD COLLEGE OF ENGINEERING

(Recognised by the Govt. of Karnataka, Affiliated to Visvesvaraya Technological University, Belagavi.

Approved by A.I.C.T.E. New Delhi.

Recognised by UGC Under Section 2(f)

Bommanahalli, Hosur Road, Bangalore - 560 068.

Ph: 080-61754601/602, Fax: 080 - 25730551

E-mail: engprincipal@theoxford.edu Web: www.theoxfordengg.org

| | | | | | | | | | |
|----|---|--|-------------|--|------|-----------|---|---|----------------|
| | ion reaction under solvent free conditions | | | | | | | | |
| 49 | Convexity For Ratio of Difference of Some Special Means In Two Variables. | Sreenivasa reddy Perla and S Padmanabhan . | Mathematics | Advances in inequalities and application | 2017 | 2050-7461 | http://scik.org/ | http://scik.org/index.php/ai/article/view/2871 | Web of Science |
| 50 | Schur convexity of Bonferroni harmonic mean | Sreenivasa Reddy Perla & S. Padmanabhan | Mathematics | The Journal Analysis | 2018 | 2367-2501 | https://link.springer.com/article/10.1007/s41478-018-0110-9 | https://link.springer.com/article/10.1007/s41478-018-0110-9 | Scopus/UGC |

MQTT based Home Automation System Using Raspberry PI 3 model B

Chandana P M, Clint Ulahannan Thomas, Harshith Ramesh Rai, Namita Y
Final year B.E Students(UG)

Guided by: Mr. Chenappa Gowda, Assistant Professor, Department of ISE, TOCE
The Oxford College of Engineering, Bengaluru, India

Abstract : By the virtue of blooming automation industry and wireless connectivity, all the devices within the home can be connected. This improves the comfort, energy efficiency, indoor security, cost savings of the home. Small and constrained embedded devices are used to remotely monitor the conditions within home and control the home appliances. In such case, power consumption and network bandwidth become a major concern. A low power device that transmits messages through a less verbose protocol is needed. Owing to the ubiquitous availability of WiFi, all the appliances within home can be connected through a common gateway. An overview of a light weight Message Queuing Telemetry Transport (MQTT) protocol is presented here. In the prototype, we attempt to implement MQTT on Raspberry PI, a WiFi based development board. Sensors and actuators are connected to Raspberry PI and a Mosquitto based MQTT broker is established for remote monitoring and control. The use of MQTT hence achieves the desired result with a lower overhead and at about a 93% faster speed. The intruder detection is an added useful functionality to the system.

Index Terms- MQTT, Raspberry PI, Mosquitto, Home Automation, Intrusion Detection, Remote Appliance Control, Light-weight Protocol, WiFi, Remote Security Control, Embedded Devices.

1. INTRODUCTION

Home automation refers to remotely monitoring the conditions of home and performing the required actuation. Through home automation, household devices such as TV, light bulb, fan, etc. are assigned a unique address and are connected through a common home gateway. These can be remotely accessed and controlled from any PC, mobile or laptop. This can drastically reduce energy wastage and improve the living conditions besides enhancing the indoor security. Owing to the rapid growth in technology, the devices in the recent past are becoming smart. The real world devices are being equipped with intelligence and computing ability so that they can configure themselves accordingly. Sensors connected to embedded devices along with the low power wireless connectivity is facilitates to remotely monitor and control the devices. This forms an integral component of Internet of Things (IoT) network. can be correctly identified using Graphology. Internet of Things can be considered as a network of devices that are wirelessly connected so that they communicate and organize themselves based on the predefined rules. However these devices are constrained in terms of their resources. Hence light weight protocols such as MQTT, CoAP etc. are used for the data transmission over wireless connectivity. There are so many kinds of radio modules out of which GSM, 3G, WiFi, Bluetooth, Zigbee, etc. are common. However, owing to the surging number of WiFi hotspots and range sufficient to perform the required control and monitoring, WiFi is chosen as the mode of communication in the prototype and the devices are controlled through MQTT protocol implemented using Raspberry PI. MQTT is thus a light weight protocol that occupies low bandwidth and consumes less power. Considering the ease of wireless internet access through WiFi, MQTT client application is built on Raspberry PI. A prototype of MQTT based home automation system is implemented on Raspberry PI. The sensors and actuators connected to Raspberry PI are remotely monitored and controlled through a common home gateway. Thus the existing infrastructure can be used to enhance the home appliances and make them smart. This implementation provides an intelligent, comfortable and energy efficient home automation system. It also assists the old and differently abled persons to control the appliances in their home in a better and easier way.

2. LITERATURE REVIEW

Bluetooth based home automation system using cell phones

In Bluetooth based home automation system, the home appliances are connected to the Arduino BT board at input output ports using relay. The Bluetooth connection is established between Arduino BT board and phone for wireless communication. One circuit is designed and implemented for receiving the feedback from the phone, which indicate the status of the device.

Zigbee based home automation system using cell phones

To monitor and control the home appliances the system is designed and implemented using Zigbee. The device performance is record and store by network coordinators. For this the Wi-Fi network is used, which uses the four switch port standard wireless ADSL modern router. The message for security purpose first process by the virtual home algorithm and when it is declared safe it is re-encrypted and forward to the real network device of the home over Zigbee network, Zigbee controller sent messages to the end. To reduce the expense of the system and the intrusiveness of respective installation of the system Zigbee communication is helpful.

GSM based home automation system using cell phones

The home sensors and devices interact with the home network and communicates through GSM and SIM (subscriber identity module). The system use transducer which convert machine function into electrical signals which goes into microcontroller. The sensors of

system convert the physical qualities like sound, temperature and humidity into some other quantity like voltage. The microcontroller analysis all signal and convert them into command to understand by GSM module.

Home automation using RF module

The important goal of Home Automation System is to build a home automation system using a RF controlled remote. RF remote is combined to the microcontroller on transmitter side that sends ON/OFF signals to the receiver where devices are connected. By operating the stated remote switch on the transmitter, the loads can be turned ON/OFF globally using wireless technology.

MQTT Protocol

The basic concepts of it is publish/ subscribe and client/broker and its basic functionality is connect, publish, and subscribe. Also it has several good features like quality of service, retained messages, persistent session, last will and testament and SYS topics. MQTT decouples the space of publisher and subscriber. So they just have to know hostname/ IP and port of the broker in order to publish/subscribe to messages.

3. ARCHITECTURE AND FLOWCHART OF SYSTEM

In the prototype, we attempt to implement MQTT on Raspberry PI, a Wi-Fi based development board. Sensors and actuators are connected to Raspberry PI and a Mosquitto based MQTT broker is established for remote monitoring and control. The Architecture is shown in Figure 1 followed by the flowchart which is shown in Figure 2.

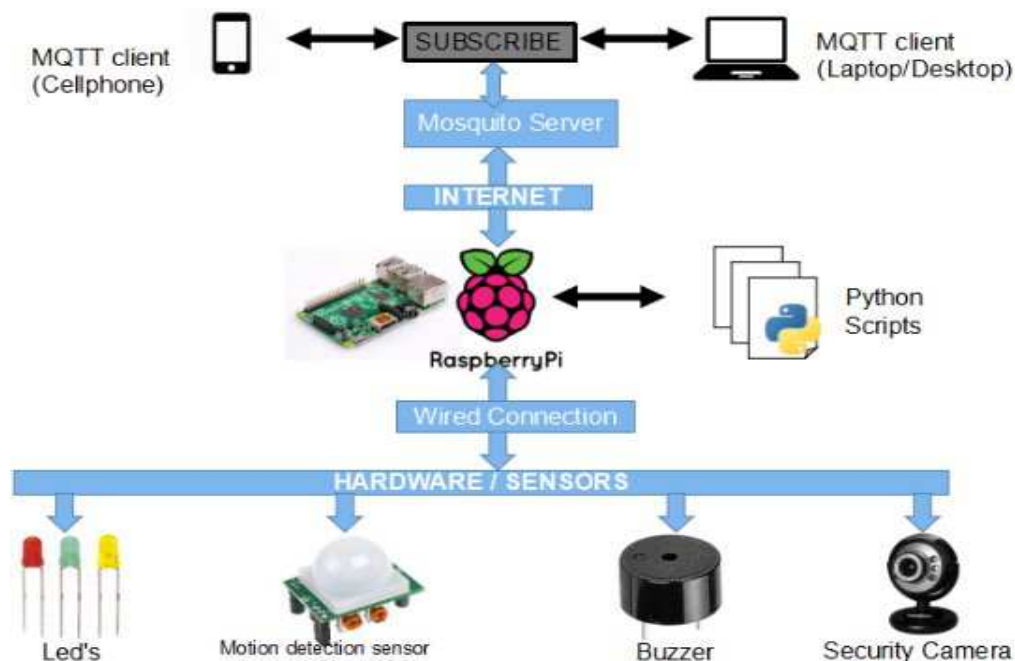


Figure 1: Architecture of MQTT-based Home Automation System

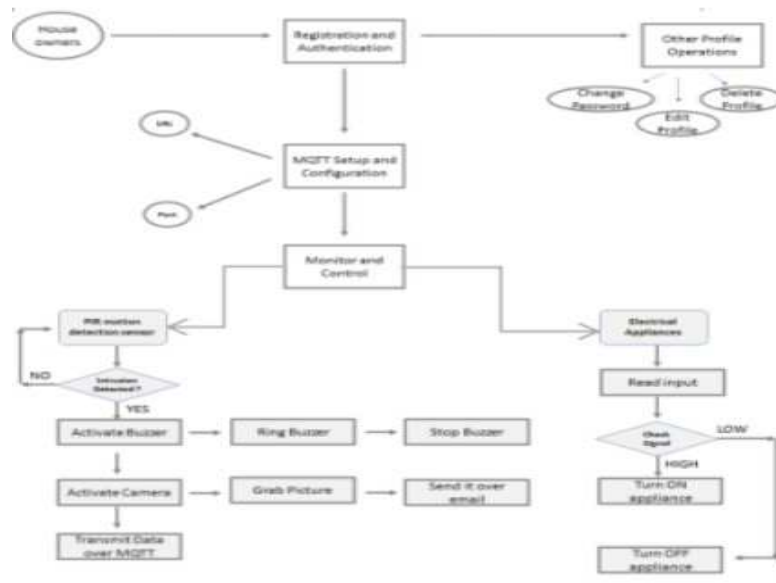


Figure 2: Flowchart of home automation system

The house owner initially performs Registration and Authentication, after which they can perform profile operations such as changing password, editing profile. Then MQTT Setup and Configuration is performed using URL and Port number, after which owner will be able to monitor and control the appliances. PIR motion detection sensor checks if the intruder is detected, if yes, it activates the Buzzer and Camera module. Buzzer rings for certain duration of time and then stops, Camera grabs the picture and sends it through mail to the end user. Electrical appliance module reads the input from user and checks the signal, if HIGH it turns ON the appliance, else turns OFF the appliance.

4. SET OF MODULES

The current work focuses on achieving an automated home control system which can be made a reality by breaking the entire set of operations into six modules as given below.

Module 1: User registration and headless Raspberry PI set up and configuration:

End user first creates account and logs in, after this end user can perform profile operations, then he should perform MQTT setup and configuration using URL and port number to indicate where MQTT server is present.

Algorithm:

Step 1: register the user by providing necessary credentials

Step 2: Setting up the raspberry pi:

-Write the Raspbian OS onto the SD card connected to the raspberry pi.

-Burn the OS into SD card after formatting it

-Configuring the raspberry pi:

-Install WinSCP software which helps in transferring files between the system and raspberry pi over a network using SSH.

-Install putty which helps to execute the programs as the Raspbian OS is built on Linux platform.

Module 2: Implementation of PIR motion detection module:

When unusual motion or movement is detected by PIR motion detection sensor, it transmits this data to the end user via Raspberry pi, which makes use of MQTT protocol for communication. Whenever intruder is detected it will automatically activate the buzzer and camera module.

Algorithm:

Step 1: align the motion sensor such that it is in the range of the camera view.

Step 2: do the necessary connections on the breadboard with the motion sensor.

Step 3: use M2F jumper cables to connect the corresponding breadboard pins to the Raspberry PI.

Module 3: Implement the Buzzer module:

Whenever the intruder is detected PIR motion detection sensor activates this buzzer, which rings for certain duration of time and stops. In this buzzer module we are making use of Piezo buzzer or passive buzzer.

Algorithm:

Step 1: do the necessary connections on the breadboard with the Piezo buzzer, as given below.

Step 2: use M2F jumper cables to connect the corresponding breadboard pins to the Raspberry pi. Connect one pin to ground (either one) and the other pin to a square wave out from a timer or microcontroller. For the loudest tones, stay around 4 KHz, but works quite well from 2KHz to 10KHz. For extra loudness, you can connect both pins to a microcontroller and swap which pin is high or low ('differential drive') for double the volume.

Module 4: Implementation of the Camera section:

Whenever the intruder is detected PIR motion detection sensor activates this camera section, which grabs the picture or image of the intruder and sends it to the user through email.

Algorithm:

Step 1: align the motion sensor such that it is in the range of the camera view.

Step 2: connect the web camera to the raspberry pi board via the USB connecting cable

Module 5: Implementation of the electrical appliances module:

This module enables the owners of the home to control the smart electrical appliances of their home from a remote Location (ideally a different geographical area). The end user will be provided with a couple of MQTT client applications to do this. The first one being the web application which will be developed from the scratch as part of this project research, and the second one will be the mobile application named 'MyMQTT'. There are several other readily available MQTT client applications for both android and IOS, which can be readily incorporated by the owners of the home to control the electrical appliances. As part of this project research is considered, we will enable the owners to perform the turn ON and turn OFF functionalities of the electrical appliances which can further be extended to various other features in the future work.

Module 6: Implement the MQTT module:

Initially configuration of Mosquitto server is done. when end users subscribe to this server, the server reads the input from user and forwards this data to raspberry pi which implements the operation, and when intrusion is detected it forwards the data to Mosquitto server, which will forward it to the cell phone or laptop which is subscribed to server.

Algorithm:

Step 1: execute SQL commands on MySQL to connect and import all packages.

Step 2: through putty, verify connections

Step 3: execute each of the previous modules.

Module 7: Implement the web server module:

This module is an end user interface through which the owner can control and access the home appliances.

Algorithm:

Step 1: Design the web page which accepts user credentials.

Step 2: using bootstrap to improve the look and feel of the web page.

Step 3: get the input from the user

Step 4: check if the input data is valid or not, if yes, go to step 5, else go to step 3

Step 5: enter the user's account and provide various available service options.

5. IMPLEMENTATION

This project is implemented considering the following aspects:

1. Usability Aspect:

The usability aspect of implementation of the project is realized using two principles:

- a: The project is implemented as a Java application.
- b: The user-friendly interface using Java's view architecture.

2. Technical Aspect:

The technical aspect of implementation of the project is realized as explained below:

STEP 1: INSTALL THE FOLLOWING SOFTWARES:

Servers: Apache Tomcat is to develop the product.

Database: MySQL is used as the database utility here, which is the world's most widely used open source relational database management system (RDBMS) that runs as a server providing multi-user access to a number of databases.

IDE: Eclipse is used as the Development environment on which the JAVA programs would be run.

The following steps should be followed to install eclipse:

-Installation of JVM: Regardless of the operating system, some Java virtual machine (JVM) has to be installed.

-Download Eclipse from the Eclipse Downloads page

STEP 2: WRITE IMAGE TO SD CARD:

Write the image to SD card. an image writing tool is to be used to install the image you have downloaded on your SD card.

Etcher is a graphical SD card writing tool that works on Mac OS, Linux and Windows, and is the easiest option for most users. Etcher also supports writing images directly from the zip file, without any unzipping required.

STEP 3: ADD "SSH" FILE TO THE SD CARD ROOT:

Enable SSH by placing a file named "ssh" (without any extension) onto the boot partition of the SD card

STEP 4: BOOT THE RASPBERRY PI:

The steps needed to be followed for this are:

1. Install mosquitto (MQTT) components.
2. Configure mosquitto and restart the service.
3. Run/ Test mosquitto

. STEP 5: DEVELOP THE WEB INTERFACE AND OTHER REQUIRED FILES AND EXECUTE:

On the Eclipse IDE, use javascript and java to develop required components for the communication and remote control of the appliances. Also use HTML, Bootstrap and related web development tools and languages to develop the user interface. Using these, give the necessary commands and execute the desired operations.

6. RESULTS

The Home Automation System was tested with respect to unit testing, integration testing and system testing with each providing 100% accurate results here is the report of the System testing which was carried out.

| Name of the Test | System Testing |
|-------------------|---|
| Item being tested | Over all functioning of GUI with all functions properly linked. |
| Sample Input | Sample intruder and the electrical appliances signal |
| Expected Output | All the modules working as expected |
| Actual Output | Each appliance reacts as per the signal given and intrusion aptly detected and image of intruder is sent immediately as E-mail. |
| Remarks | Successful |

The implementation of the system is carried out and the execution results are shown in the below images.



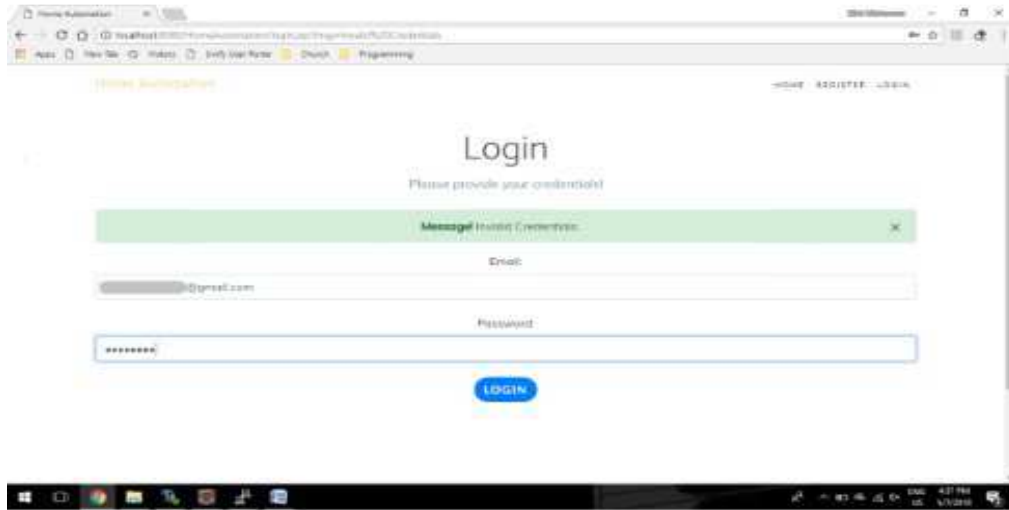


Figure.3. GUI of the MQTT-based Home Automation System

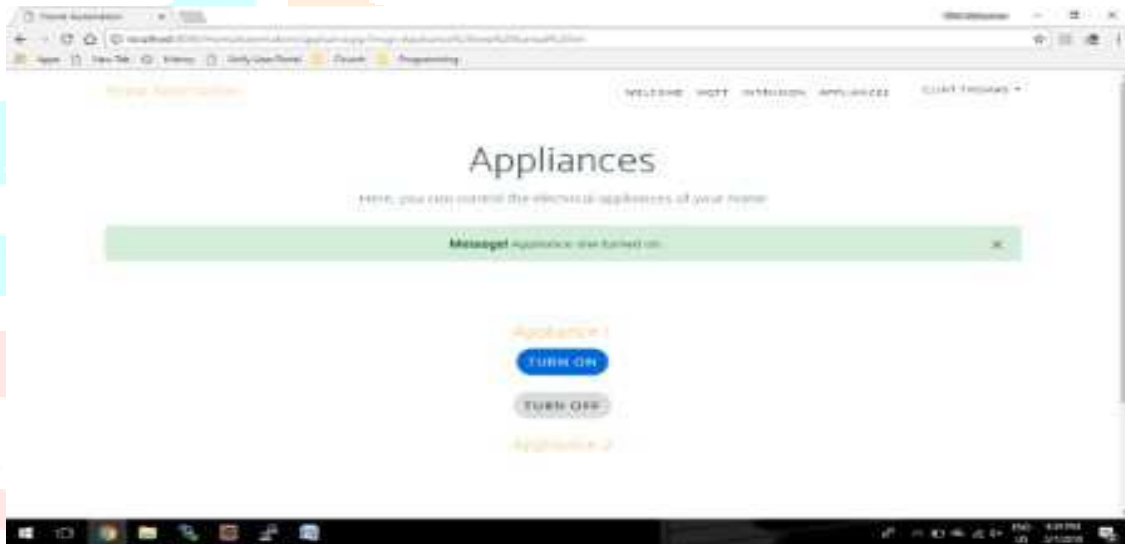


Figure 4: Appliance Control

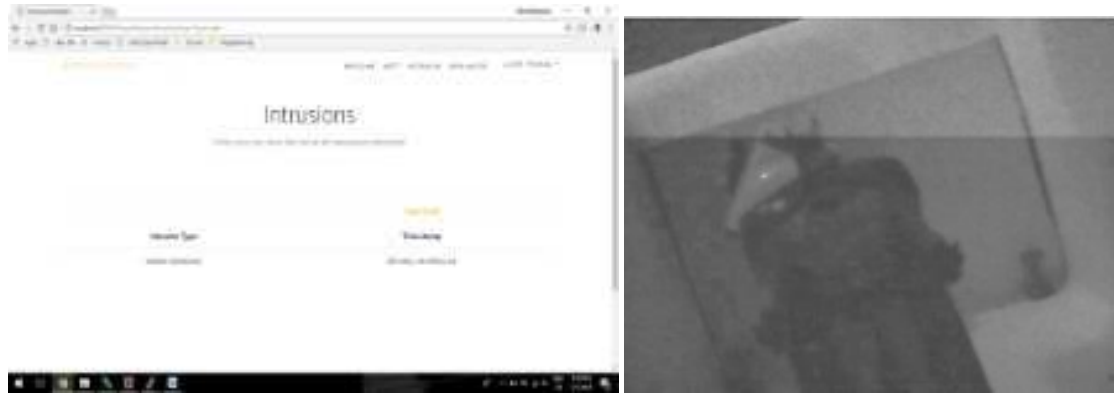


Figure 5: Intrusion detection notification and captured Intruder Image

CONCLUSION AND FUTURE SCOPE

MQTT is thus a light weight protocol that occupies low bandwidth and consumes less power. Considering the ease of wireless internet access through Wi-Fi, MQTT client application is built on Raspberry PI. A prototype of MQTT based home automation system is implemented on Raspberry PI. The sensors and actuators connected to Raspberry PI are remotely monitored and controlled through a common home gateway. Thus the existing infrastructure can be used to enhance the home appliances and make them smart. This implementation provides an intelligent, comfortable and energy efficient home automation system. It also assists the old and differently abled persons to control the appliances in their home in a better and easier way. A further scope in this work can be viewed in taking this further ahead. A cloud platform can be used to aggregate, analyze and visualize data. Customized GUI can be developed to remotely access the devices to monitor and control them. A household security system integrated with a home automation system can be developed which can provide additional services such as remote surveillance of security cameras over the Internet, or central locking of all perimeter doors and windows. Further research can help in development of Occupancy-aware control system, where it is possible to sense the occupancy of the home using smart meter-sand environmental sensors like CO₂ sensors, which can be integrated into the building automation system to trigger automatic responses for energy efficiency and building comfort applications.

Appliance control and integration with the smart grid and smart meter can be made a reality, taking advantage, instance, of high solar panel output in the middle of the dayrun washing machines. Leak detection, smoke and CO detectors can be made more efficient and reliable using this technology. Indoor positioning systems can be improved by home automation for the elderly and disabled. All of the above can be combined and a pet monitoring system can be realized which helps the people monitor activities in their absence.

REFERENCES

- [1] S. Nasrin and P.J. Radcliffe, "Novel protocol enables DIY home automation," in Telecommunication Networks and Applications Conference (ATNAC), 2014 Australasian, November 2014, pp.212-216.
- [2] H. ElKamchouchi and A. ElShafee, "Design and prototype implementation of SMS based home automation system," in Electronics Design, Systems and Applications (ICEDSA), 2012 IEEE International Conference on November 2012, pp.162-167.
- [3] Internet of Things: A Survey on Enabling Technologies, Protocols, and Applications, Ala Al-Fuqaha, Senior Member, IEEE, Mohsen Guizani, Fellow, IEEE, Mehdi Mohammadi, Student Member, IEEE, Mohammed Aledhari, Student Member, IEEE, and Moussa Ayyash, Senior Member, IEEE. IEEE COMMUNICATION SURVEYS & TUTORIALS, VOL. 17, NO. 4, FOURTH QUARTER 2015
- [4] A Smart Home Energy Management System Using IoT and Big Data Analytics Approach, IEEE Transactions on Consumer Electronics, Vol. 63, No. 4, November 2017.
- [5] Wireless Home Automation System and Security System using MQTT Protocol 2017 2nd IEEE International Conference On Recent Trends In ElectroInformation & Communication Technology, May 19-20, 2017, India
- [6] MQTT based Home Automation System Using ESP8266/ Raspberry Pi, Ravi Kishore Kodali and SreeRamya Soratkal, Department of Electronics and Communication Engineering, National Institute Of Technology, Warangal 506004 INDIA.
- [7] Mqttv3. 1protocol specification. [Online]. Available: <http://public.dhe.ibm.com/software/dw/webservices/wsmqtt/mqtt-v3r1.html>
- [8] Hivemq. [Online]. Available: <http://www.hivemq.com/blog/mqtt-essentials-part-1-introducing-mqtt>
- [9] Mqtt version 3.1.1 becomes an oasis standard. [Online]. Available: <https://www.oasisopen.org/news/announcements/mqtt-version-3-1-1-becomes-an-oasis-standard>
- [10] Oasis mqtt version 3.1.1. [Online]. Available: <http://docs.oasis-open.org/mqtt/mqtt/v3.1.1/os/mqtt-v3.1.1-os.html>



MABIDaaS: Mutual Authentication and Financial Transaction Between Mobile Users using Blockchain based ID as a Service

Akshatha B M, Manasa J, Meghana K S, Sonal Salian, Dr. D. Jayaramaiah
Department of Information Science and Engineering
The Oxford College of Engineering, Bengaluru-560068,India

Abstract:In recent times, most of the financial transactions are done through smartphones. Financial transactions contain data of high confidentiality; therefore, security is a main concern in these transactions. Every transaction should be recorded, and this information must be made non-tamperable. Authentication and Authorization of users must be done to check the authenticity of the users to avoid misuse of the data from an intruder. The proposed Mutual Authentication Blockchain based ID as a Service [MABIDaaS] [10] helps to achieve this. Our system uses blockchain technology for storing the transaction details of the user, cloud storage services for access rights, and Trusted Execution Environment [TEE] [11] for a secure execution of the transaction through mobile phones. This paper shows how the proposed system can be used for mutual authentication between two mobile users by using digital signature [3], key set and records the transacted data in the blocks as the data inserted into the blocks cannot be manipulated.

Index Terms–Blockchain, MABIDaaS, Digital Signature, Authentication, Key Generation, Access Rights.

I. INTRODUCTION

Mobile financial transactions [11] have become a popular mode of transaction. A common man can easily transfer money of any amount to another using merely his phone with a network connection. These kinds of applications require a degree of security, privacy protection and authenticity. The Blockchain based ID as a Service system aims to provide the necessary features.

Blockchain [1] is an open distributed ledger [5] that can record transactions between two parties efficiently. It can also be defined as a continuously growing list of records, known as blocks, which are linked to one another and also secured using cryptography. Transparency and incorruptible nature are the two important properties of Blockchain. Transparency data can be thought as public which is embedded in the network. Any unit of information on Blockchain cannot be manipulated or altered. The Blockchain needs no middleman for digital transactions. The Blockchain eliminates the risks that come with centralized [6] data. Nowadays security problems with the internet is familiar to everyone. Everyone relies on username/password system to protect the identity online. But the Blockchain security methods use encryption technology. The Public and Private keys are the basis for this technology. The public key acts as the users address on the Blockchain.

Trusted Execution Environment [TEE] [14] is introduced to provide a secure environment for exchange of information and financial transactions using private key and with the help of cloud storage. Cloud storage has brought a massive change in the storage industry. Software, platform, and infrastructure can be provided to users as a service from a cloud nowadays. Identity management could be also provided from the cloud to a user. In other words, the user could use an identity and authentication management infrastructure provided from the cloud as a form of IDaaS. [10] It would offer various benefits such as a reduced on-site infrastructure, integrated management with cloud services, and ease use. However, the use of IDaaS means outsourcing critical functions to a third party. All data related to identity and authentication (e.g., user account information, security credentials, etc.) is managed and controlled by the third party without knowing how the data is protected and processed on the cloud. The proposed system MABIDaaS uses cloud to allow the partner to evaluate the access permission rights of each of its registered users. The TEE implemented allows safe and secure transactions between the users without compromising the security using key generation and verification algorithm and transaction between user and partner using private key encryption. In the proposed system the cloud is made more secure and is accessible only by the partner using Secure Hash Algorithm(SHA).

II. EXISTING SYSTEM

Blockchain based ID as a Service is a system which helps in transaction between an individual user and the partner of the BIDaaS provider. The user can transact with the partner without registering himself with the partner if registration with the BIDaaS provider is done. The

BIDaaS provider stores the virtual ID and the public key of the user in the block. A user when requests the partner to its services, the partner checks the integrity of the user by checking if the ID sent by the user matches with the registered ID in the blockchain.

Once the confirmation is done, the partner takes the public key of the user to encrypt any data to be sent to the user using this key. Once the data is received by the user, he uses his private key to decrypt the data to get the original message.

The existing BIDaaS uses the blockchain to store the transaction details and works as an identity and authentication management but lacks in terms of security. Also, there is no constraint on the services permitted to each user which can result in posing as a threat to the financial transaction. This was a matter of concern in the field of finance, therefore there was a demand for a new type of BIDaaS.

Demand for BIDaaS with added security for Authentication

In any transaction, it is very important to validate both the peers identity before making a transaction. Thus, using Blockchain Technology, users can use an Identity and Authentication management infrastructure. This new feature also requires the functionalities of cloud computing. These days we observe that using cloud we can implement different softwares, Platforms, Infrastructures etc. This feature helps to reduce the on-site infrastructure that would be used otherwise. Every single transaction between the same or different users must be validated every time. This decreases the chances of deceit. Thus, it is important to implement BIDaaS so that crucial transactions in Blockchain are verified and protected from a third-party intrusion or viewing the transaction details. The use of Fingerprint Technology and encryption of the transaction details adds that extra edge to this new system and helps in providing extra security.

III. PROPOSED BLOCKCHAIN BASED ID AS A SERVICE- MABIDaaS

In this paper, we provide another version of BIDaaS which provides more security, authenticity and secrecy for more secure financial transactions. We have used the implementation of the Trusted Execution environment, Cloud for Storage and Key Generation for improving the existing system. Figure 1 shows the system architecture of the Proposed System.

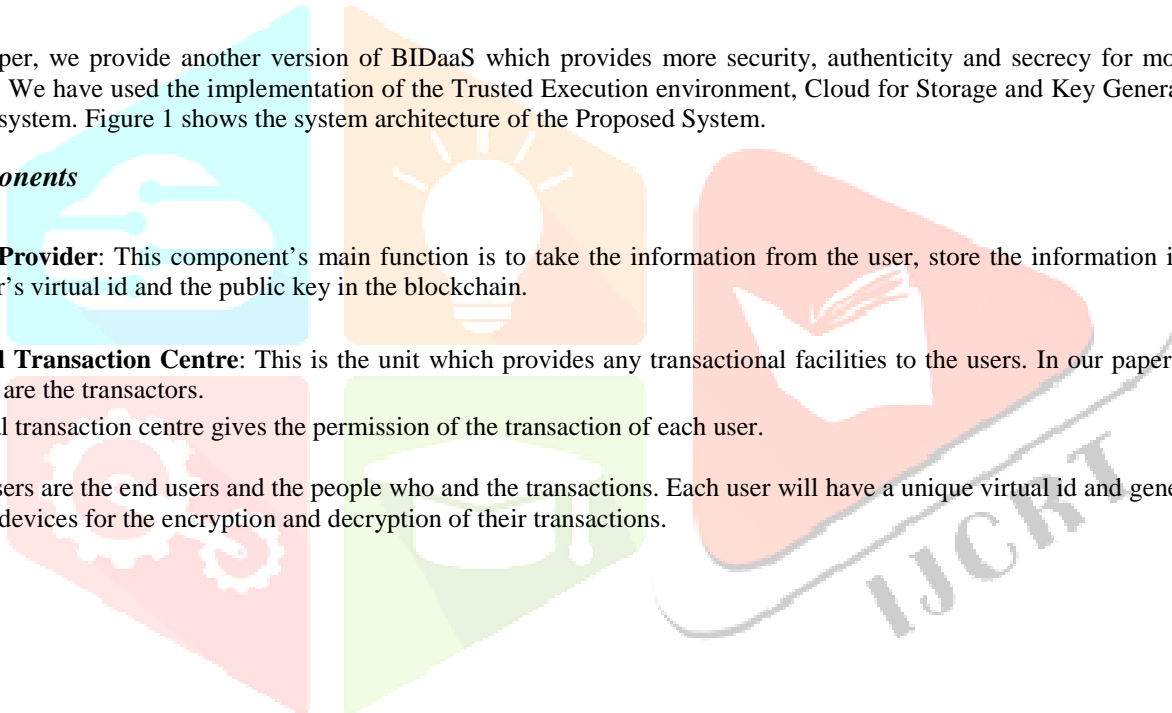
A. Components

1) **BIDaaS Provider:** This component's main function is to take the information from the user, store the information in the database and save the user's virtual id and the public key in the blockchain.

2) **Financial Transaction Centre:** This is the unit which provides any transactional facilities to the users. In our paper the FTC is a bank whose users are the transactors.

The financial transaction centre gives the permission of the transaction of each user.

3) **Users:** Users are the end users and the people who and the transactions. Each user will have a unique virtual id and generates a public key pair in their devices for the encryption and decryption of their transactions.



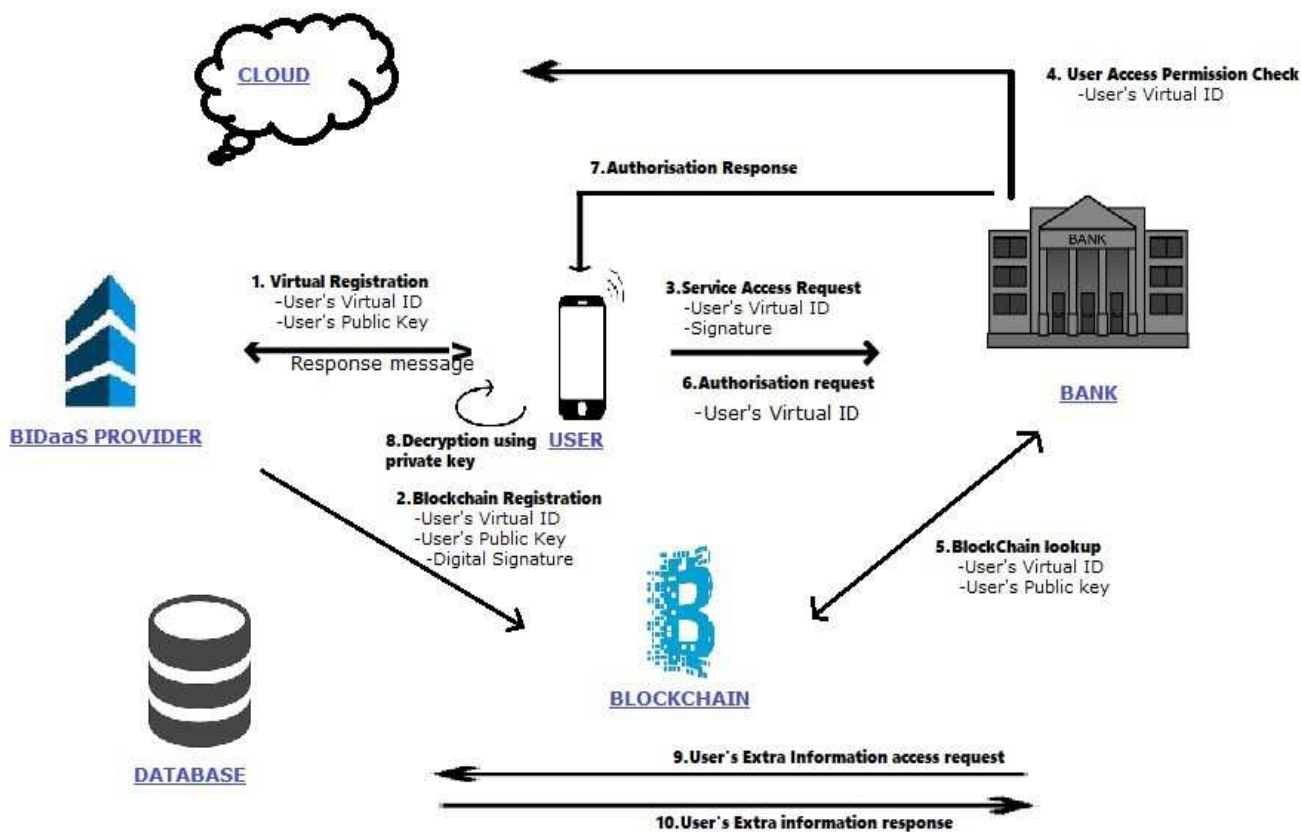


Fig 1: System Architecture of MABIDaaS

B. Procedures

- 1) Registration:** The process starts with the user registering with the BIDaaS provider which acts as a third-party verifier in the later stages. The user gives in the his/her account number, name, email id, phone number and the password. The user generates a public key pair in his/her device and stores the private key in his device and sends the public key to the provider. The BIDaaS provider inserts the user's virtual ID and the user generated public key into the block. The fingerprint of the user is taken during the registration process.
- 2) Login:** The user signs into his/her account by using the virtual id and password. The user has to authenticate by giving his/her fingerprint which is compared with the fingerprint taken during the registration process. The user sends an access request to the BIDaaS provider which generates an OTP and send it to the registered mobile number. This acts like another layer of authentication.
- 3) Add amount:** A user can transfer some amount from his bank account to the secret account which is used for the transaction, this amount detail is added into the block and the new variations on the amount is reflected in the block.
- 4) Transaction:** Once the user is successfully logged into their account, they get a list of activities that they can do. The user has to select another registered user with whom he/she wants to do any transaction. The Financial Transaction Centre [FTC] authorizes the transaction by checking with the cloud if the two users can proceed with the transactions.

For the transaction:

Key-Generation: One of the user generates a set of keys and encrypts it using the public key of the other user and sends it to them. The other user decrypts it using their private key

Single transaction: The user can transfer the amount details to the other user using the first key from the key set as a mode to encrypt the data. The receiver user can use the first key of the key set to decrypt the details and store it in the block.

The two communicating users can prove their authenticity by their digital signatures[3]. After the authenticity check, the users can generate a set of key and pass it to the other. Each key is used and discarded after respective transaction.

A user can login only through the given handset which holds his/her fingerprint and the transaction is run in the secure part of the OS called the Trusted Execution Environment.

DFD LEVEL 0

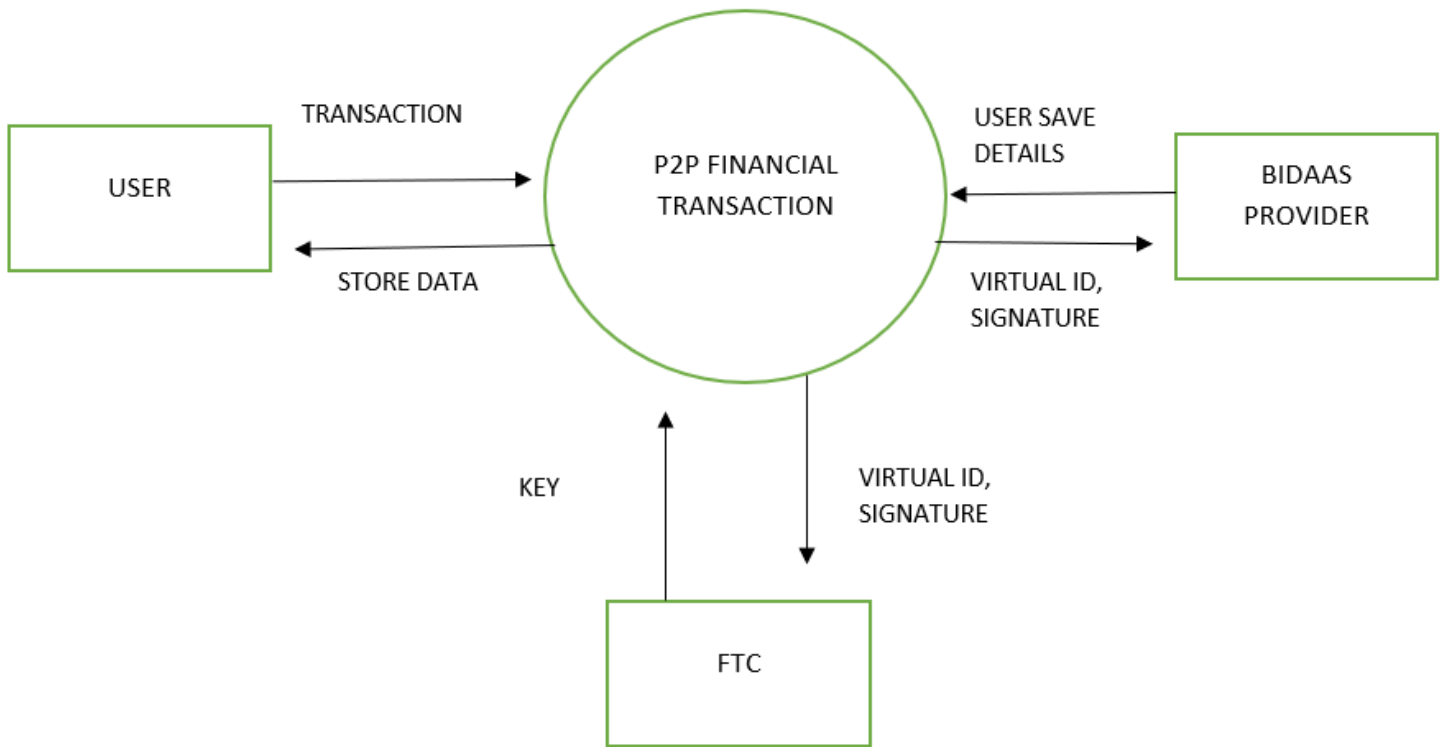


Figure 2: Data Flow Diagram of Level 0

DFD LEVEL 1

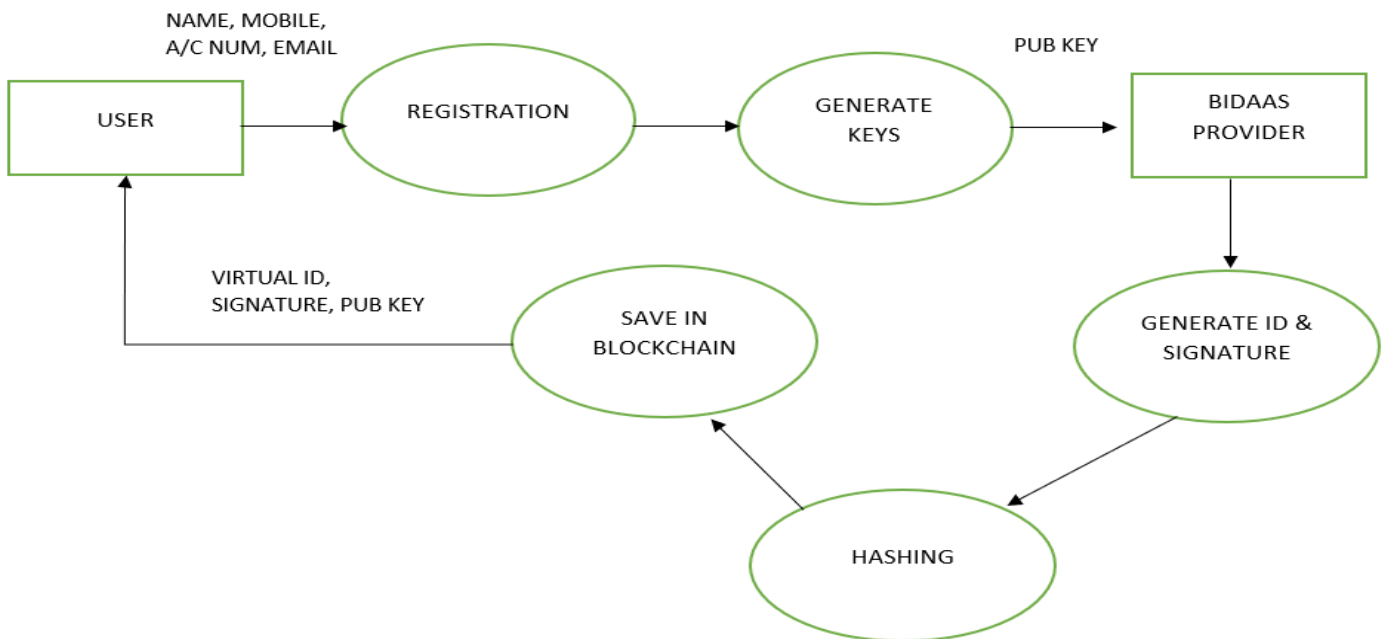


Figure 3: Data Flow Diagram of Level 1

DFD LEVEL 2

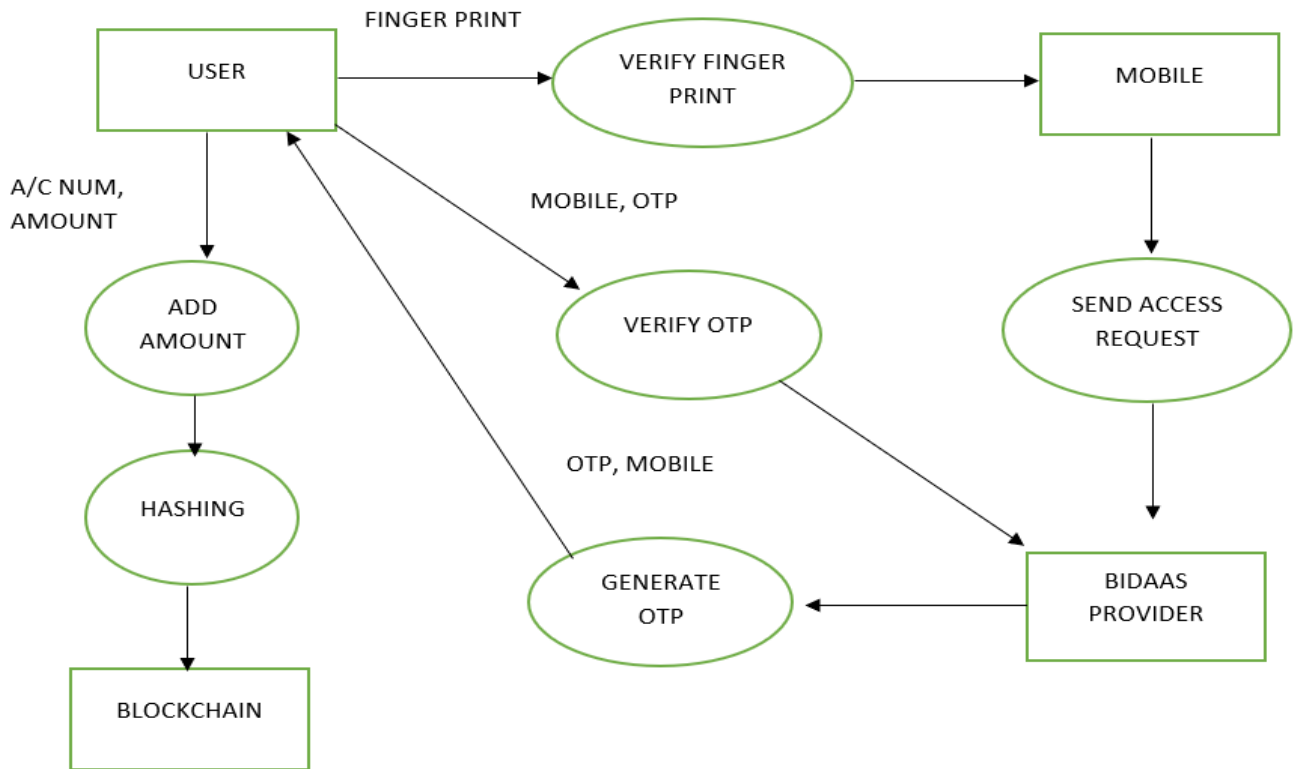
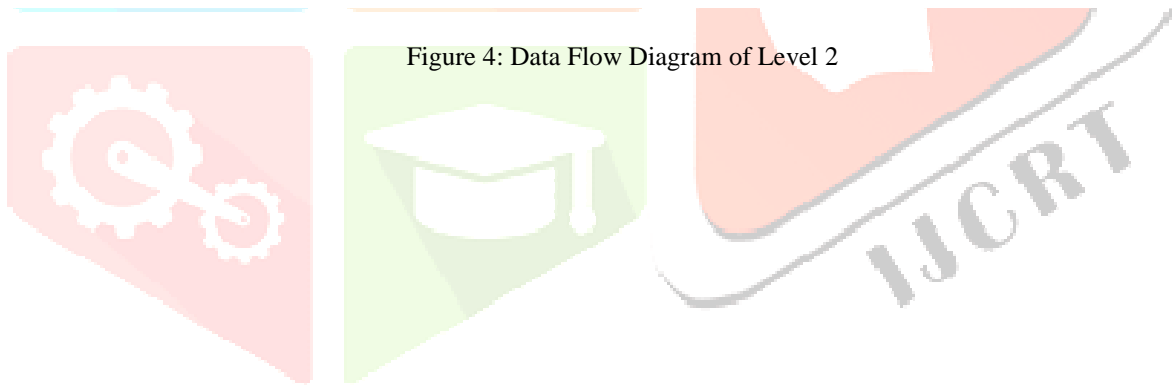


Figure 4: Data Flow Diagram of Level 2



DFD LEVEL 3

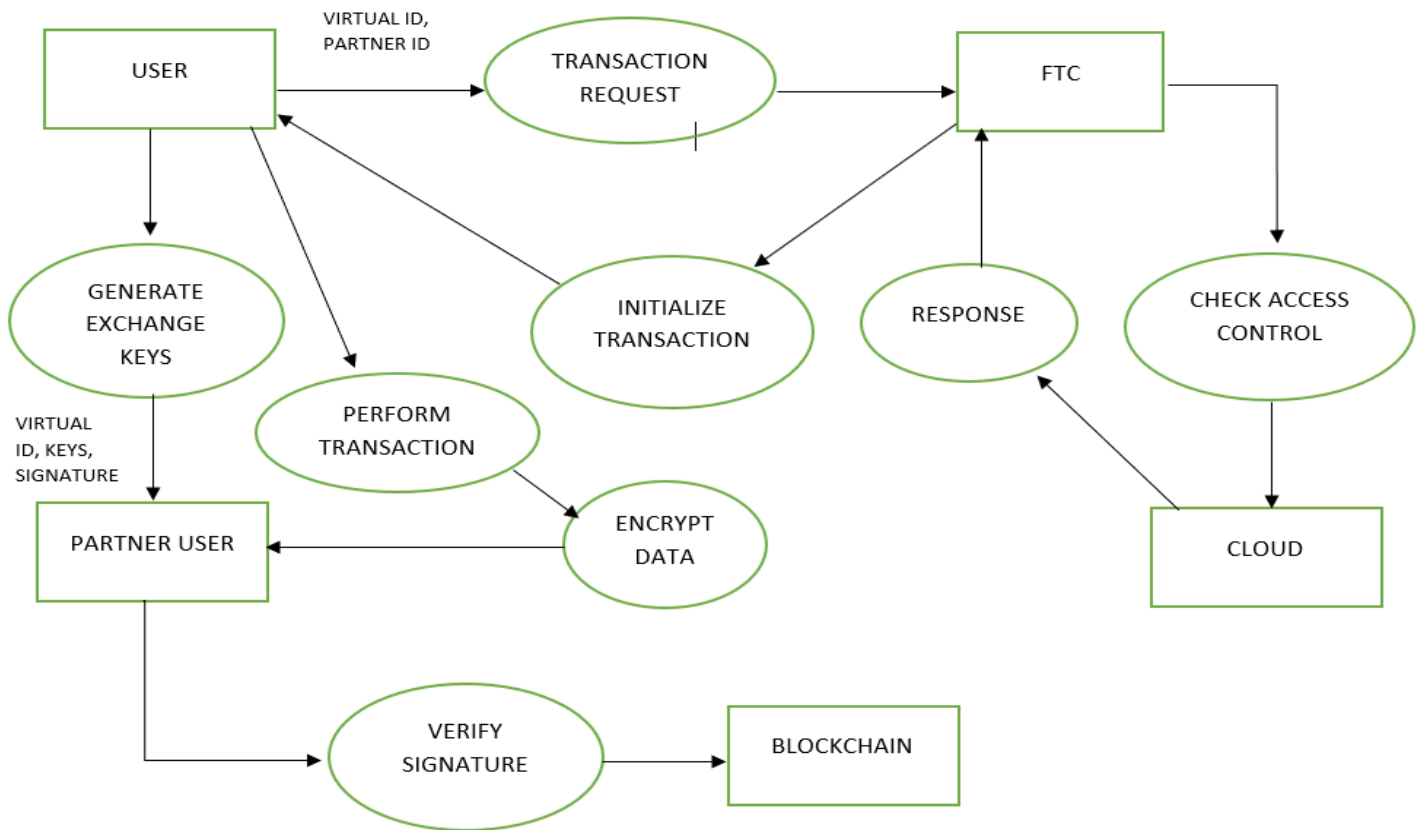


Figure 5: Data Flow Diagram of Level 3

DFD LEVEL 4

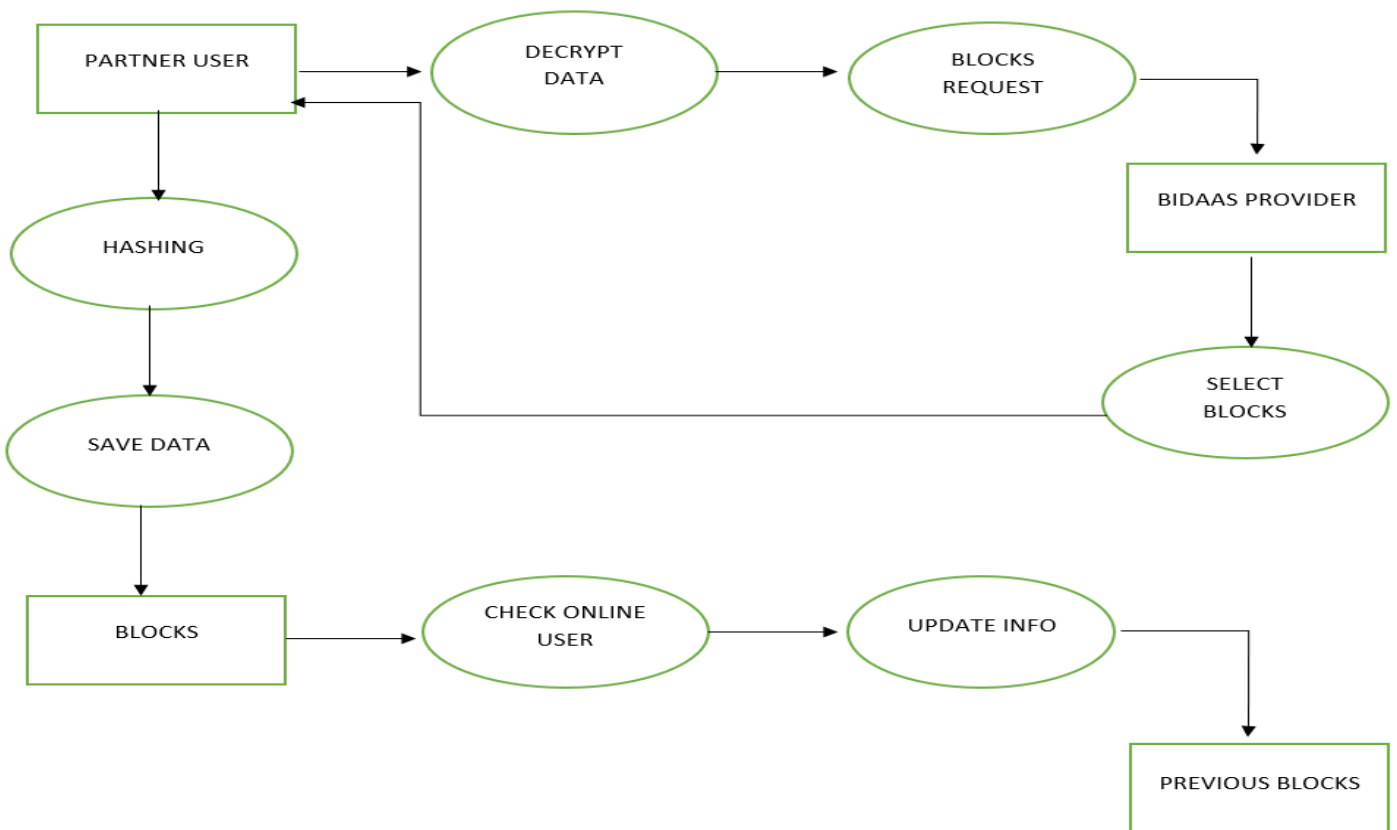


Figure 6: Data Flow Diagram of Level 4

C. Example

Let there be 2 users named X and Y respectively. Both of them register with the BIDaaS and their virtual ID and Public key is stored in the Blockchain. Now X wants to send Rs 500 to Y. X transfers Rs 1000 from his bank account to the account which handles the transaction. This amount is stored in the BIDaaS. X requests communication with Y from the Financial Transaction Centre [FTC]. The FTC checks for the access right permissions of both users. If permission is granted, the two users prove their authenticity with digital signature and X generates 10 keys and encrypts it using Y's public key and sends it to Y. Y decrypts the key set using his private key. A then encrypts Rs 500 using the first key of the key sets and sends it to Y. This transaction is stored in the blockchain. Y uses the same key from the key set and decrypts the message and updates its wallet amount which is appending this transaction into its device's block. Both X and Y then delete the key used for this transaction from the key set. 9 more transactions can be done after which one of the user has to generate another set of keys and send to the other.



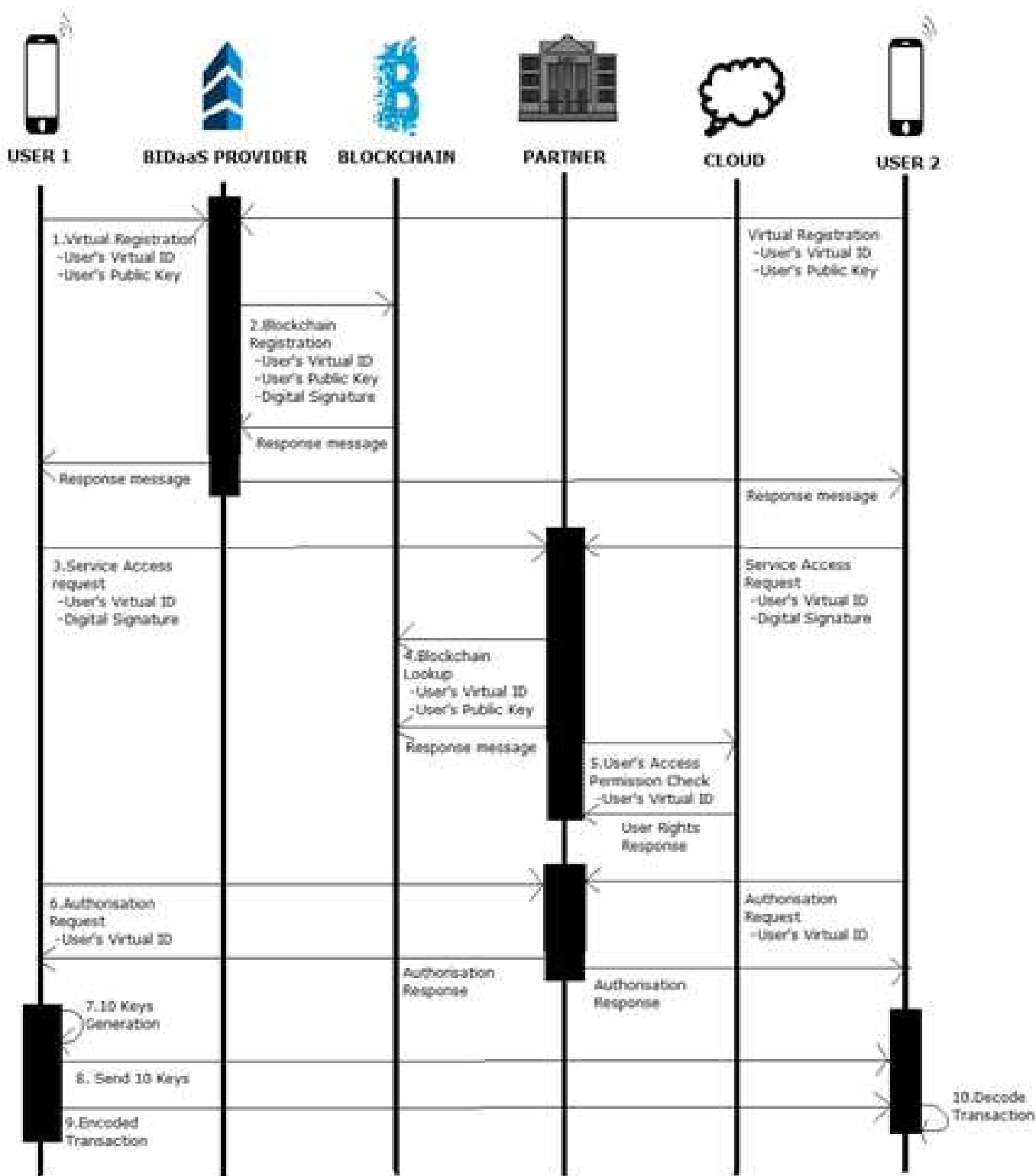


fig 2: Sequence diagram for a single transaction between two user

IV. FEATURES OF THE SYSTEM

A. Consensus Algorithm

The blockchain used here is a private blockchain. The miners are selected based on the computational power i.e., based on the timing, beginning time and end time is noted and the miners are selected. Each miner selected gets an amount as a reward.

B. Consortium Blockchain

The blockchain used here is a private blockchain which is not owned by the BIDaaS provider. The blockchain is a distributed ledger and is operated by consortium members. The user account information is accessed from the BIDaaS provider when needed, the user information is not shared among all consortium members present in the blockchain.

C. Provided User Information

Extra user information is provided to the BIDaaS provider and Financial Transaction Center (FTC). This is not only for storage purpose but also provide better privacy, avoiding the misuse of the information provided.

D. Use of virtual IDs

Every user is assigned by a virtual ID. This virtual ID assigned to the user is unique. The user can use the virtual ID if it is already registered in the blockchain.

E. Private Key of a User

Private key is a secret key which is stored in the user mobile. Each user has a different private key stored in an electronic device. Key generation material and other sensitive information is stored in the trusted execution environment.

F. Benefits to the BIDaaS Provider

The BIDaaS provider creates new sources of revenue by providing an identity and authentication management solution as well as providing existing user information to its partners.

G. Benefits to the User

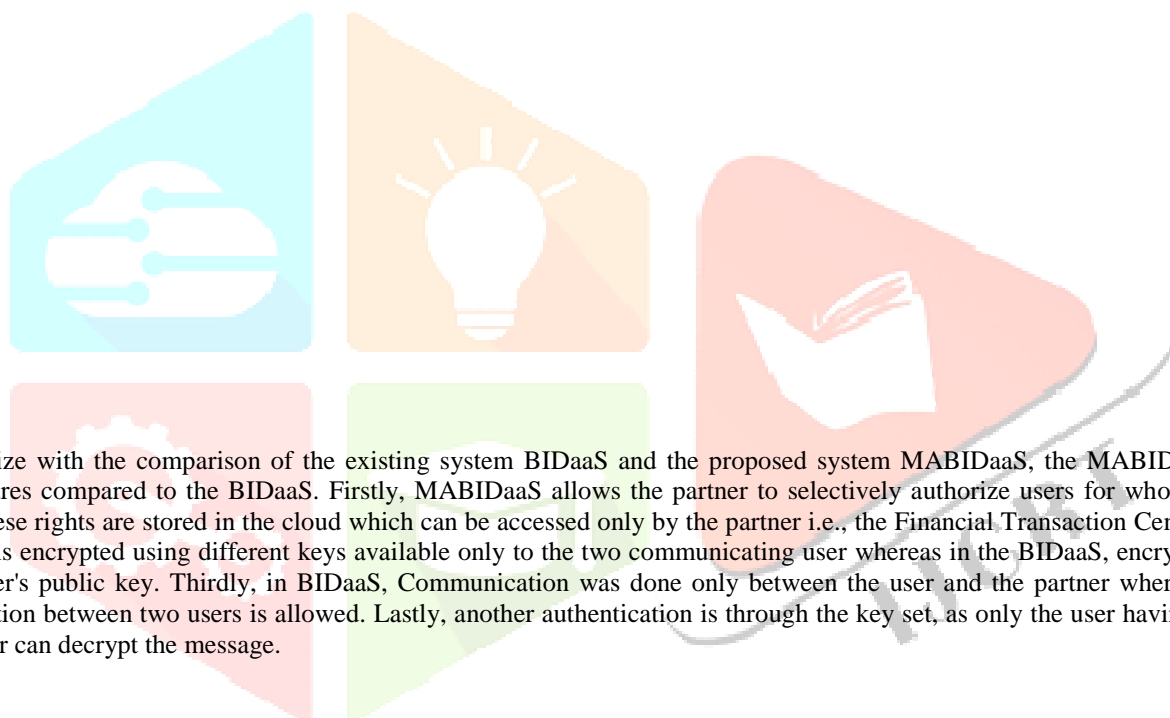
A better security is provided to the user by various levels of verification. Digital signature is included as well as key set exchange during transaction provides better security. The user details are registered in blockchain and it can be accessed when necessary and the details in the blockchain cannot be tampered hence provides a better security for transactions.

H. Benefits to the Financial Transaction Centre

Financial transaction center (FTC) which is the partner gets service request from the user. FTC looks up the blockchain for details and checks the permission rights for accessing the services, of the user from the cloud. The presence of the FTC extends its level in authorization by providing the access permission rights of the user.

Table 1: Comparison between BIDaaS and MABIDaaS

| Properties | BIDaaS | MABIDaaS |
|---------------------------------|--|---|
| Access rights | The BIDaaS system does not facilitate the use of cloud to store the access permission rights of its users. | The MABIDaaS system facilitates the use of cloud to store the user access rights. |
| Security | The security level in existing system is compromised due to the lack of sufficient authentication and verification protocols applied between partner-user and user-user communication. | More Security is achieved in MABIDaaS system using private key encryption algorithm. |
| Communication | Communication here takes place only between the partner and the user using wireless communication medium. | In MABIDaaS system, Communication occurs between partner-user and between user-user using wireless communication medium. This added feature helps to broaden the horizon of transactions that can occur in the environment. |
| Authentication Protocols | One layer of Authentication Protocol exists between the BIDaaS provider, Partner and the registered users. | Multiple Layers of Authentication protocol exists between the different components of the system, paving way for a more secure system than the existing system. |



To summarize with the comparison of the existing system BIDaaS and the proposed system MABIDaaS, the MABIDaaS provides more secure features compared to the BIDaaS. Firstly, MABIDaaS allows the partner to selectively authorize users for whom access rights are granted. These rights are stored in the cloud which can be accessed only by the partner i.e., the Financial Transaction Centre. Secondly, each transaction is encrypted using different keys available only to the two communicating user whereas in the BIDaaS, encryption is done using only the user's public key. Thirdly, in BIDaaS, Communication was done only between the user and the partner whereas in MABIDaaS, communication between two users is allowed. Lastly, another authentication is through the key set, as only the user having the key set same as the sender can decrypt the message.

V. CONCLUSION

MA-Blockchain based ID as a service focuses on the authentication and authorization. In this paper we have discussed an example which shows financial transactions between the mobile users using MABIDaaS. Security is provided by adding authentication in the form of key generation set and authorization through permission rights given to the user. Financial transaction centre checks the access rights of the user in the cloud. The act of providing the access rights to the user by storing it in the cloud has further improved the authorization measures of the system. Keys are generated and exchanged, and each key is used as a mode for encryption and decryption for each transaction respectively. The proposed system provides a secure transaction between the users without the partner having any knowledge of the financial transactions. Trusted Execution Environment is used in MABIDaaS which provides a secure area for the mobile application and the data loaded inside in terms to integrity and confidentiality. The proposed MABIDaaS has some room for improvement. The expansion of the area of network in which the transaction can take place between the user can smoothen the usage of the system.

REFERENCES

- [1] How the Blockchain Revolution Will Reshape the Consumer Electronics Industry. Jong-Hyouk Lee and Marc Pilkington, IEEE Consumer Electronics Magazine, Volume 6, Issue 3, July 2017.

- [2] Ethereum: A Secure Decentralized Generalized Transaction Ledger. DR.GavinWood,CTO Ethereum Project.
- [3] A Digital Signature Based On A Conventional Encryption Function. Ralph C. Merkle, 1987.
- [4] Making Byzantine Fault Tolerant Systems Tolerate Byzantine Faults. Allen Clement and Edmund Wong, Published in:Proceeding NSDI'09 Proceedings of the 6th USENIX symposium on Networked systems design and implementation, Boston, Massachusetts April 22 - 24, 2009.
- [5] Architecture of the Hyperledger Blockchain Fabric. Christian Cachin, IBM Research-Zurich, 2009.
- [6]Is Bitcoin a Decentralized Currency? Arthur Gervais, Ghassan O. Karame, SrdjanCapkun and VedranCapkun, IEEE Publication,Issue No. 03 - May-June (2014 vol. 12).
- [7]Two Bitcoins at the Price of One? Double-Spending Attacks on Fast Payments in Bitcoin. Ghassan O. Karame, Elli Androulaki and SrdjanCapkun, Published in: Proceeding CCS '12 Proceedings of the 2012 ACM conference on Computer and communications security, Raleigh, North Carolina, USA October 16 - 18, 2012.
- [8]Information Propagation in the Bitcoin Network. Christian Decker and Roger Wattenhofer, Published in: Peer-to-Peer Computing (P2P), 2013 IEEE Thirteenth International Conference on 9-11 Sept. 2013.
- [9]An Analysis of Anonymity in the Bitcoin System. Fergal Reid and Martin Harrigan, Volume 2, 7 May 2012.
- [10]BIDaaS: Blockchain Based ID as a Service. Jong-Hyouk Lee, published in IEEE,volume 20, 2017.
- [11]An Ecosystem of Trusted Execution environment of Smartphones- A potentially bumpy road, IEEE 2017.
- [12] Provably secure and lightweight identity-based authenticated data sharing protocol for cyber-physical cloud environment. ArijitKarati, Ruhul Amin, S.K HafizulIslam , Kim-Kwang Raymond Choo, Published in: IEEE, 08 May 2018
- [13]Secure cloud storage and Quick Keyword based Retrieval system.Songfeng Lu, Abdulruhman I Ahmed Abomakhelb, Published in :IEEE 2017
- [14] Open-TEE—An Open virtual trusted execution environment. Brian McGillion, TanelDettenborn, Thomas Nyman, N Asokan, IEEE 2015
- [15]Automated Partioning of Android applications for Trusted execution environment, Konstantin Rubinov,LuciaRosculete,Tulika Mitra, AbhikRoychoudhury, IEEE 2016

“Study and Analysis of Most Sought after Big data Platforms and their Application for Network Analytics”

Thendral N¹, Dr. Jayaramaiah²,

^{1,2}Dept of Information Science and Engineering, The Oxford College of Engineering, Bengaluru-68
natarajan.thendral@gmail.com¹, [dj-r-hodise@theoxford.edu](mailto:djr-hodise@theoxford.edu)²

Abstract: In Today’s world, we are getting technologically “connected”, all over with more and more data devices which collect lots information. This has resulted in large quantities of data in the form of images, text, videos and multimedia content, log files, etc. Small and Medium Enterprises (SME) are facing number of problems in collecting, storing, analyzing and exploring these large volumes of data. A number of Big Data Platforms have taken advantage of Hadoop open-source framework and are providing some support to handle the so called Big data of the organizations, Cloudera, HortonWorks, MapR, IBM InfoSphere Big Insight, Pivotal HD are a few Big data platforms currently available in the market. In this paper we carry out a comparative analysis of most sought after Big data platforms based on the operational, functional and performance characteristics of those platforms in general. We suggest that cloudera platform as the one which provides competitive advantage over the other platforms in terms of diagnostics, maintenance and performance analysis to be used as an acceptable tools for network Analytics.

Keywords: *Big Data, Distribution Hadoop, Diagnostics, Network Analytics.*

I. INTRODUCTION

Day after day, new innovations have delivered a lot of information that should be gathered, arranged, classified, moved, investigated, put away, etc. Currently, we are in the Big Data time in which a couple of distributors offer, arranged to-use spreads to manage a Big Data structure, To be particular Cloudera[2], Horton Works[1], MapR[3], IBM Infosphere Big Insights[4], and Pivotal HD[5] are the popular ones. The decision will be made on one or on the other arrangements as indicated by a few necessities. For instance, if the arrangement is open source, Maturity of the arrangement, and so on. A few releases have been supplemented with extra blocks, which make it conceivable to disentangle the task of the stages that retain parts complex due to the quantity of segments required. Accordingly, our work is to make a relative report on the fundamental Hadoop conveyance suppliers to characterize the qualities and shortcomings of every appropriation.

II. BIG DATA ARCHITECTURE

Before beginning with Big Data, one needs to ensure that all the fundamental segments of the design for breaking down all parts of a lot of information are set up. Engineering of a Big Data framework ought to have the capacity to explore the information sources in a quick and economical way. It ought to likewise have the accompanying layers: Data sources, Ingestion Layer, Visualization Layer, Hadoop Platform administration Layer, Hadoop Storage Layer, Hadoop Infrastructure Layer, Security Layer, and Monitoring Layer [11].



Figure 1: The Big Data architecture

This figure portrays the important segments of the engineering that ought to be a piece of a Big Data framework. It is important to pick open source or authorized structures to take full favorable position of the considerable number of highlights of the diverse segments of a Big Data framework [11].

III. UNDERSTANDING OF BIG DATA DISTRIBUTION ARCHITECTURES

In the midst of our investigation, we high light the structures of the particular spread Hadoop. Here there is the case of the five structures: Cloudera appropriation for Hadoop Platform, HortonWorks information platform, MapR Converged Data Platform, IBM Big information Platform, and pivotal HD business. The details are given in the succeeding paragraphs.

1. Cloudera Enterprise

Cloudera Enterprise is a superior minimal effort stage for directing investigation on information [1]. Cloudera Enterprise has the main local Hadoop Search motor and this stage furnishes its clients with dynamic information improvement highlight. Cloudera director incorporates propelled highlights like astute design defaults, modified observing, and powerful investigating which permit simple organization of Hadoop in any condition. Cloudera was right off the bat established by Hadoop specialists from Face book, Google, Oracle and Yahoo. This circulation is to a great extent in view of the segments of Apache Hadoop and it is supplemented by basically house segments for group administration. The point of Cloudera's plan of action isn't just to offer Licenses yet to offer help and preparing also. Cloudera offers a completely open source form of their stage (Apache 2.0 permit) [15].

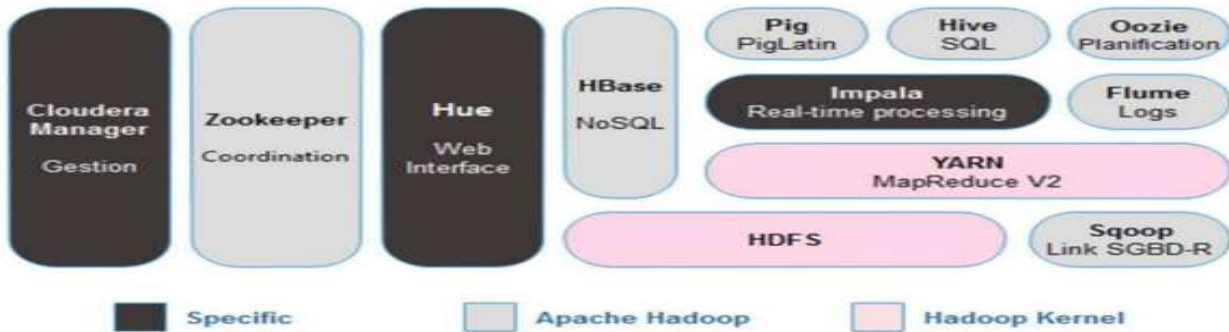


Figure2: Cloudera Distribution for Hadoop Platform (CDH)

2. HortonWorks Distribution

HortonWorks Distribution platforms(HDP) is the business' simply clear secure, undertaking arranged open source Apache™ Hadoop® scattering in light of a united plan (YARN). HDP watches out for the aggregate needs of data still, controls ceaseless customer applications and passes on capable enormous data examination that revive fundamental initiative and improvement [2].

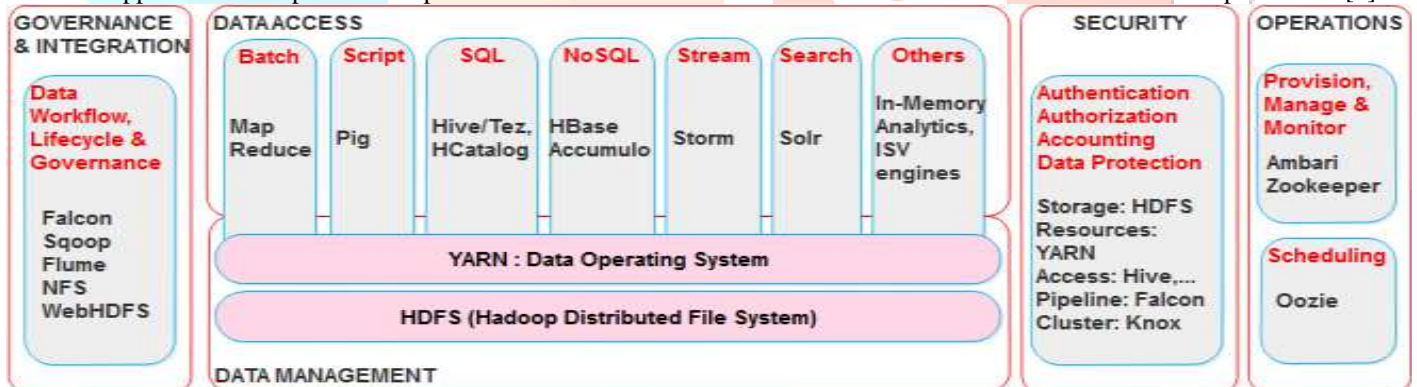


Figure 3: Horton Works Hadoop Platform (HDP)

Hortonworks Data Platform consolidates a versatile extent of taking care of engines that draw in one need to speak with comparable data in various courses, meanwhile. This infers applications for huge data examination can speak with the data in the best way: from gathering to insightful SQL[15] or low dormancy access with NoSQL. Creating use cases for data science, interest and spouting are also supported with Apache Spark, Storm and Kafka.

3. MapR Converged Data Platform

MapR Converged Data Platform is one single stage for enormous information applications. MapR's Platform depends on the idea of Polyglot Persistence which permits to use numerous information composes and organizes straightforwardly [2]. MapR, a merged information stage coordinates the energy of Hadoop and Spark with worldwide occasion gushing, continuous database capacities, and endeavor stockpiling, in this way empowering its clients to encounter the colossal energy of information [11].



Figure 5:MapR Architecture

The MapR Converged Data Platform tackles the emergency of multifaceted nature that outcomes from persistently sending workload-particular information storehouses. Inside a solitary stage on a solitary codebase, it unites the key advancements that make up a cutting edge information design, including an appropriated record framework, a multi-display NoSQL database, a distribute/buy in occasion spilling motor, ANSI SQL, and an expansive arrangement of open source information administration and examination innovations [16]. The MapR Converged Data Platform conveys speed, scale, and unwavering quality, driving both operational and systematic workloads in a solitary stage.

4. IBM InfoSphere

Enormous Insights Distribution Info Sphere Big Insights for Hadoop was right off the bat presented in 2011 of every two forms: the Enterprise Edition and the fundamental adaptation, which was a free download of Apache Hadoop packaged with a web administration support. In June 2013, IBM propelled the Infosphere BigInsights Quick Start Edition [4]. This new version gave enormous information volume investigation abilities on a business-driven stage. It the two joins Apache Hardtop’s Open Source arrangement with big business usefulness and henceforth, gives a huge scale investigation, portrayed by its versatility and adaptation to non-critical failure. In short, this distribution supports structured, unstructured and semi-structured data and offers maximum flexibility.

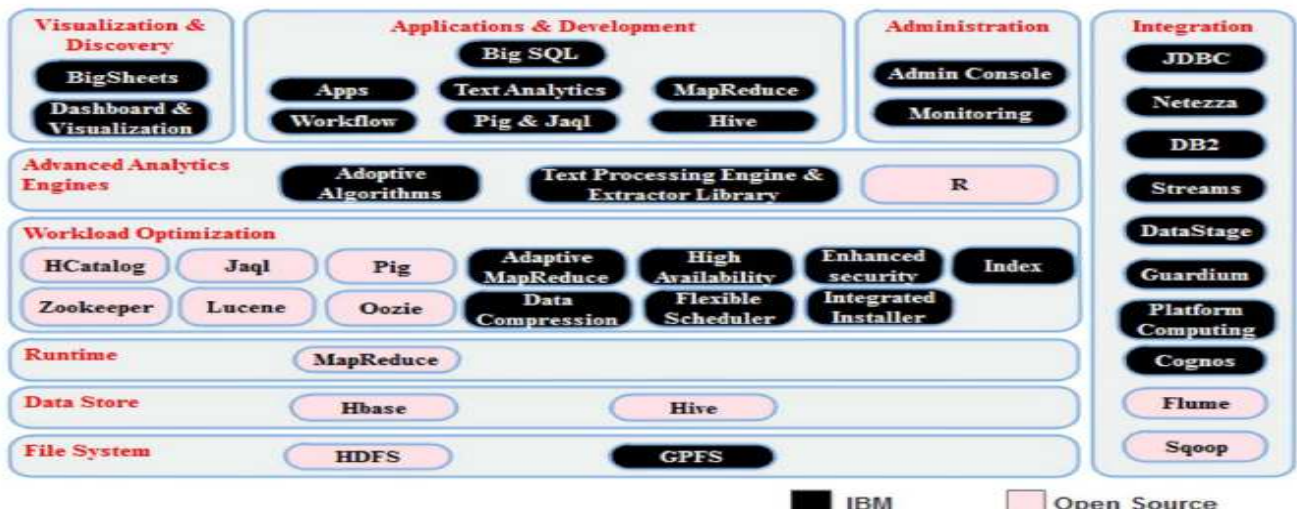


Figure6: IBM InfoSphere BigInsights Enterprise Edition

In spite of the fact that this condition incorporates a full Apache Hadoop stack, it is separated by various IBM segments that address the issues plot above [11]. In Big Insights Version 2.1, which ended up accessible in June 2013, these might be outlined as takes after:

5. Pivotal HD Distribution Pivotal Software, Inc.

(Pivotal) is a product and administrations organization situated in San Francisco and Palo Alto, California, with separate all together workplaces. The divisions incorporate Pivotal Labs for counseling administrations, the Pivotal Cloud Foundry improvement gathering, and item advancement assemble for the Big Data advertise. Urgent HD Enterprise is an economically upheld dissemination of Apache Hadoop [5]. The figure underneath indicates how every Apache and Pivotal part incorporates into the general engineering of Pivotal HD Enterprise.

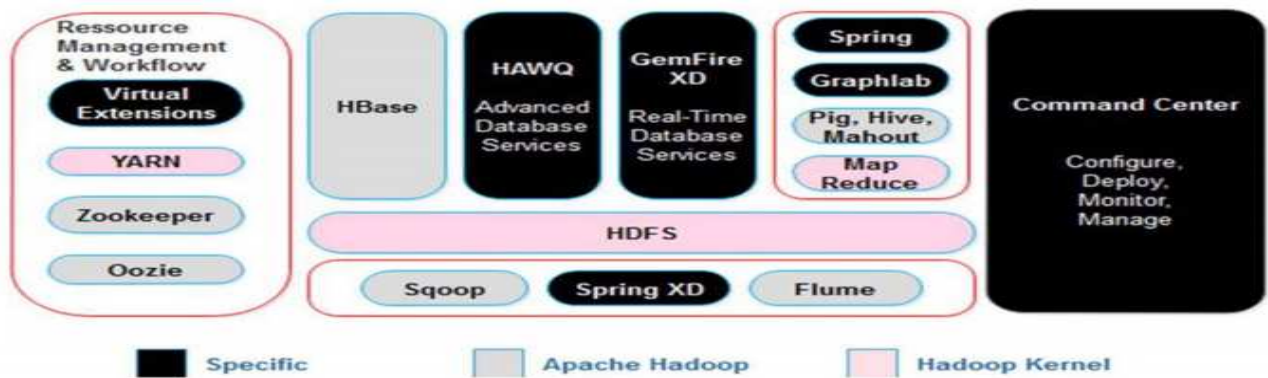


Figure 7: Pivotal HD Enterprise

Cloud Foundry does out two sorts of VMs: the part VMs that constitute the stage's structure, and the host VMs that host applications for the outside world. Inside CF, the Diego structure passes on the encouraged application stack over the entire host VMs, and keeps it running and balanced through demand surges, power outages, or distinctive changes. To deal with request, various host VMs run duplicate events of a similar application [6]. Cloud Foundry passes on application source code to VMs with everything the VMs need to assemble and run the applications locally.

IV. COMPARATIVE ANALYSIS OF MOST SOUGHT AFTER BIG DATA PLATFORMS BASED ON THE OPERATIONAL, FUNCTIONAL AND PERFORMANCE CHARACTERISTICS

With a specific end goal to assess appropriations, we attempted to recognize the qualities and shortcomings of the five major Hadoop distribution providers: Cloudera, HortonWorks, IBM InfoSphereBigInsights, MapR, and Pivotal.

A. *comparison based on Functional characteristics:*

| Platforms | Cloudera | Horton Works | MapR | IBM | Pivotal |
|-------------------------------------|--|--|--|--|---|
| Operational Characteristics | | | | | |
| Editor and Available Edition | <ul style="list-style-type: none"> Express Enterprise | Hortonworks Data Platform 2.5 | <ul style="list-style-type: none"> M3(free) M5 M7 | <ul style="list-style-type: none"> Quick Start Standard Enterprise | Pivotal Enterprise Edition |
| Administration Console | Cloudera manger | Ambari | MapR Control System | Web Console | Command center |
| Software Components | <ul style="list-style-type: none"> Cloudera Express Cloudera Impala Cloudera Search | <ul style="list-style-type: none"> Zeppelin Ambari User Views DSX | MapR software. | <ul style="list-style-type: none"> Big SQL Big R Adaptive MapReduce IBM GPFSTTM FPO | <ul style="list-style-type: none"> Command Center, Virtualization extensions and Isilon support |
| Ease of use | Powerful deployment, management and monitoring tools which are very much useful. | Very simple and easy-to-use sandbox which helps to getting started rapidly. | The most significant is the support for a native UNIX file system.. | Anyone can download the IOP platform for free of charge or select a supported offering and use it on premises | By using Spring Hadoop tool male easy deployment |

| | | | | | |
|----------------------------------|---------------------------|---------------------------------|--|--|-----------------------|
| Product version Evaluated | Cloudera Enterprise: 5.50 | Hortonworks Data platform: 2.30 | The MapR Distribution including Apache: 4.10 | IBM BigInsights for Apache Hadoop: 5.0 | HadoopPivotal HD: 3.X |
|----------------------------------|---------------------------|---------------------------------|--|--|-----------------------|

Table 1: Comparison based functional characteristics

The above table explains functional parameters of Available edition, Administration console, software components, ease of use and better manipulating facilities. The Cloudera platform provides better functional characteristics based on Apache Hadoop and projects effective use of open sources associated.

B. Comparison Based On Operational Characteristics:

| Platforms ↓ Operational Characteristics | Cloudera | Horton Works | MapffR | IBM | Pivotal |
|---|--|--|---|---|---|
| Open Source | Multiple version : Open source & Licensed | Open source | Licensed | Licensed | Multiple version : Open source & Licensed |
| Management Tools | Cloudera Manager | Ambari | MapR Control System | IBM Maxico Web console | Cloud Foundry |
| SQL Support | Impala | Stringer | Drill | IBMBig SQL | SQL |
| Market Presence | Highest score in market place Based on an evaluation compared to vendors | Next largest competitor with cloudera | Second highest current offering | This is also Strong competitor | Lowest score in market presence |
| Deployment | Deployment with Whirr toolkit. | Deployment with Ambari. Simple Deployment. | Through AWS Management Console. | IBM PureData System for Analytics. | BOSH and Ops Manager |
| Integration | Ease of integration using standard APIs and tools. | To ingest new data streams and additional volume as needed | Nagios integration and Ganglia integration. | Transforms data in any style and delivers it to any system. | Some tools available for integration. |

Table 2: Comparison based on operational characteristics

In the above table contains the comparative aspects of the five chosen platforms of Big data based on operational characteristics. The main objective of this comparison is to criticize which is the one for quick and easy deployment and Integrations of various API's.

C. Comparison based on Performance Characteristics:

| Platforms ↓ Functional Characteristics → | Cloudera | Horton Works | MapR | IBM | Pivotal |
|---|---|--|---|--|---|
| Flexibility | Offer great flexibility and capability with their services | Apache Tez for interactive access and Apache Slider for long-running applications. | Offer flexibility to Works out of the box with no special configuration required. | flexible data analysis features apply to data in a variety of formats | Pivotal Cloud Foundry uses a flexible approach called buildpacks |
| Security | provide data encryption | provide data encryption | provides encryption of data transmitted to, from and within a cluster | Provides encryption and masking of confidential data. | Secret-key cryptography. |
| Scalability | They offer great flexibility and capability with their services in such a way that it makes managing our various applications | Needed more support from Hortonworks during implementation and running of platform | Scalable architecture without single points of failure | Highly scalable storage platform to store and distribute very large data sets. | Greenplum running on DCA delivers scalability |
| High Availability | High Availability With a Load Balancer | Apache Hadoop 0.23.1 and HDFS NameNode high availability | High availability (HA) options for the NameNode and JobTracker. | For using HDFS replicated system based availability only. | Greenplum running on DCA delivers to assure availability and minimize downtime. |
| Data processing speed | With spark support Data processing, up to 100x in some cases. | Also working on improving computing speed. By using initiated Stinger | Apache Drill, a project backed by MapR to improve data processing speed | IBM InfoSphere Information Analyzer V8.1.1 provides efficient data processing speed. | HAWQ, a proprietary component able to process SQL-like queries 318x faster than Hive. |

Table 3: Comparison based on performance characteristics

The above Table describes a few parameters of performance like Flexibility, Data Processing speed, Scalability, High Availability, and Security. After analysing above performance characteristics, we conclude that Cloudera platform will provide reasonably good results for network analytics in terms of availability and processing speed.

V. ANALYZING CLOUDERA DISTRIBUTION FOR NETWORK ANALYTICS:

Cloudera platform provides an investigation stage and the most recent open source innovations to store, process, find, model and serve a lot of information. CDH, the Cloudera Hadoop dissemination, incorporates a few related open source ventures, for example, Hive and Impala. It likewise gives security and coordination a few equipment and programming items [15]. The Hive structure in Cloudera platform including Apache Hadoop enables clients to execute intuitive SQL questions straightforwardly against information put away in Hadoop Distributed File System (HDFS), Apache HBase or the Amazon Simple Storage Service.

A. General Architecture for Cloudera for Analytics:

Cloudera is a cutting edge programming arrangement composed particularly for information administration and investigation. The application offers what numerous specialists have marked as the world's speediest, least demanding, and most secure Apache Hadoop stage.

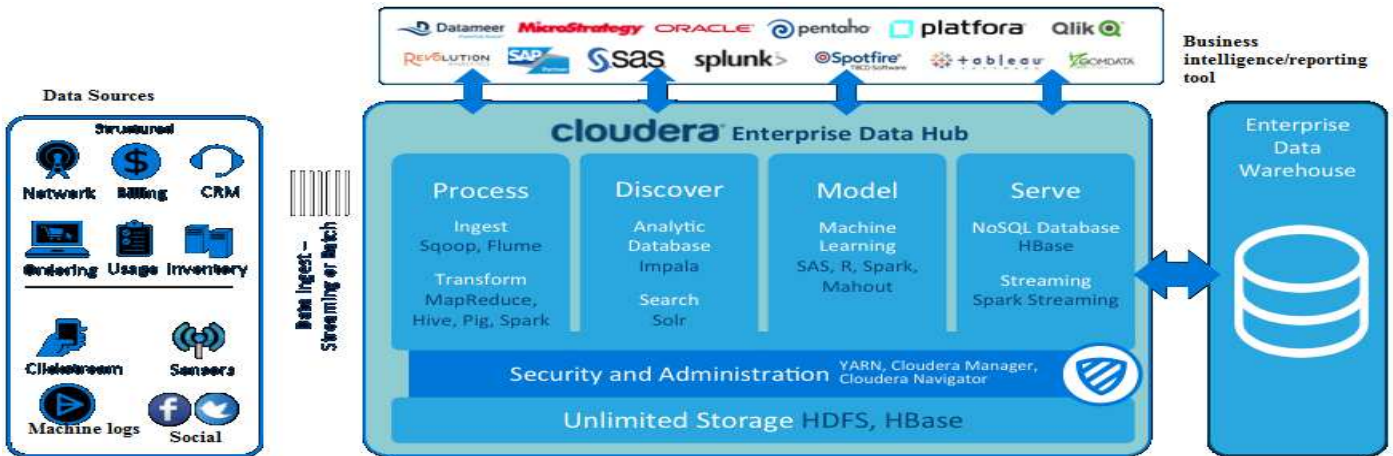


Figure 8: General Architecture for cloudera in analytics

With Cloudera Enterprise Data Hub (EDH), the framework changes the undertaking information administration scene by conveying the primary bound together stage for huge information [1]. The application gives ventures a solitary, bound together place to store, process, and break down every one of their information, engaging them to enhance the estimation of current speculations while empowering principal better approaches to get more an incentive from their information [8].

VI. IMPLEMENTING NETWORK ANALYTICS USING CLOUDERA DISTRIBUTION

CDH is the most total, tried, and mainstream dispersion of Apache Hadoop and related activities. CDH conveys the center components of Hadoop – versatile capacity and disseminated registering – alongside a Web-based UI and imperative venture abilities. CDH is Apache-authorized open source and is the main Hadoop answer for offer brought together group handling, intuitive SQL and intelligent inquiry, and part based access controls. Implementing network analytic by using following two tools, which is available in clouderaquickstart virtual machine [9].

- Apache Hive
- Hue

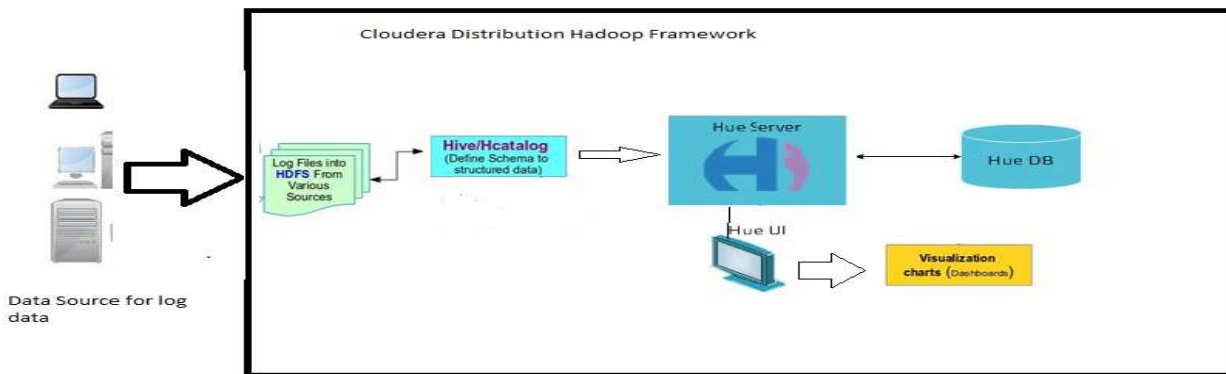


Figure9: Architecture of Network Analytics using cloudera

Logs are computer produced records that catch system and server activities data. They are helpful amid different phases of programming improvement, principally to debug and maintenance purposes and furthermore to manage arrange tasks. Here collecting log files from firewall system in terms of CSV file format. The sample log data for firewall system.

Sample log data for System alert event:

| Time | ID | Category | Group | Event | Msg. Type | Priority | Ether Type | Src. MAC | Src. Vendor | Src. Int. |
|------------------|------|-------------------|-------------------|------------------------------|----------------------------|-------------|------------|-------------------------|---------------|-----------|
| 05-10-2018 14:29 | 1226 | Network | Network Access | HTTPS Handshake | Simple Message String | Information | | 34525 2C:27:D7:2A:44:A5 | HEWLETT PACK | X0 |
| 05-10-2018 14:29 | 1233 | Firewall Settings | Multicast | Link-Local/Multicast IPv6 Pa | Standard Note Protocol | Notice | | 2048 BC:30:5B:E3:E7:1B | DELL | X0 |
| 05-10-2018 14:30 | 1431 | Network | Attacks | IP Spoof Detected | Standard Note Ethernet Net | Alert | | 34525 14:07:08:16:9B:C4 | PRIVATE | X3 |
| 05-10-2018 14:30 | 1226 | Network | Network Access | HTTPS Handshake | Simple Message String | Information | | 34525 14:07:08:16:9B:C4 | PRIVATE | X0 |
| 05-10-2018 14:30 | 1431 | Network | Attacks | ICMPv6 Packets Received | Standard Note Protocol | Information | | 2048 00:27:22:E8:74:0E | UBIQUITI NETW | X0 |
| 05-10-2018 14:31 | 1431 | Network | Attacks | IP Spoof Detected | Standard Note Ethernet Net | Alert | | 34525 14:07:08:16:9B:C4 | PRIVATE | X3 |
| 05-10-2018 14:31 | 1226 | Network | Network Access | HTTPS Handshake | Simple Message String | Information | | 34525 14:07:08:16:9B:C4 | PRIVATE | X0 |
| 05-10-2018 14:31 | 1233 | Firewall Settings | Multicast | Link-Local/Multicast IPv6 Pa | Standard Note Protocol | Notice | | 34525 2C:27:D7:27:96:60 | HEWLETT PACK | X2 |
| 05-10-2018 14:32 | 1233 | Firewall Settings | Multicast | Link-Local/Multicast IPv6 Pa | Standard Note Protocol | Notice | | 34525 2C:27:D7:27:96:60 | HEWLETT PACK | X3 |
| 05-10-2018 14:33 | 1431 | Network | Attacks | IP Spoof Detected | Standard Note Ethernet Net | Alert | | 2048 BC:30:5B:E3:E7:1B | DELL | X0 |
| 05-10-2018 14:33 | 1431 | Network | Attacks | IP Spoof Detected | Standard Note Ethernet Net | Alert | | 2048 BC:30:5B:E3:E7:1B | DELL | X0 |
| 05-10-2018 14:33 | 1226 | Network | Network Access | HTTPS Handshake | Simple Message String | Information | | 34525 14:07:08:16:9B:C4 | PRIVATE | X0 |
| 05-10-2018 14:33 | 1233 | Firewall Settings | Multicast | Link-Local/Multicast IPv6 Pa | Standard Note Protocol | Notice | | 34525 2C:27:D7:27:96:60 | HEWLETT PACK | X2 |
| 05-10-2018 14:33 | 1431 | Network | Attacks | IP Spoof Detected | Standard Note Ethernet Net | Alert | | 2048 BC:30:5B:E3:E7:1B | DELL | X0 |
| 05-10-2018 14:33 | 23 | Security Services | Attacks | IP Spoof Detected | Standard Note Ethernet Net | Alert | | 2048 BC:30:5B:E3:E7:1B | DELL | X0 |
| 05-10-2018 14:33 | 1226 | Network | Network Access | HTTPS Handshake | Simple Message String | Information | | 34525 14:07:08:16:9B:C4 | PRIVATE | X0 |
| 05-10-2018 14:34 | 1431 | Network | Attacks | ICMPv6 Packets Received | Standard Note Protocol | Information | | 34525 14:07:08:16:9B:C4 | PRIVATE | X3 |
| 05-10-2018 14:34 | 1431 | Network | Attacks | ICMPv6 Packets Received | Standard Note Protocol | Information | | 34525 14:07:08:16:9B:C4 | PRIVATE | X2 |
| 05-10-2018 14:34 | 1431 | Network | Attacks | ICMPv6 Packets Received | Standard Note Protocol | Information | | 34525 14:07:08:16:9B:C4 | PRIVATE | X3 |
| 05-10-2018 14:34 | 200 | Users | Authentication Ac | Admin Password Error From | Standard Note String | Warning | | | | X0 |
| 05-10-2018 14:34 | 1226 | Network | Network Access | HTTPS Handshake | Simple Message String | Information | | 34525 14:07:08:16:9B:C4 | PRIVATE | X3 |
| 05-10-2018 14:35 | 1233 | Firewall Settings | Multicast | Link-Local/Multicast IPv6 Pa | Standard Note Protocol | Notice | | 34525 2C:27:D7:27:96:61 | HEWLETT PACK | X4 |

Figure10: server status logs for firewall

Above log data are given as the input for our application in cloudera. The log data are having more than 1000 records for analysis. The records are store in the format of CSV file, and then it will be transferred to HDFS file location in /home/cloudera.

Hive Tool:

Hive tool used to create databases for analytical purpose. In analytical application server status logs data's are taking as the dataset to create tables. The following example use to create table for firewall data [15].

Example:

create table eventlog (eventstring,Src_ipstring,IP_PROTOCOLstring,Msg string.....) row format delimited fields terminated by',';

After creating table need to transfer data into table by using hive query.

load data localinpath '/home/cloudera/eventlog.csv' into table eventlog;

In hive tool we can query the database table for our network analysis basis. It will produce the data according to time taken for analysis the data. By using hive connectivity tools, visualize analytical data in graphs and charts.

Hue tool:

Hue is a web-based interactive query editor in the Hadoop stack that will helpful visualize and share data [15].

- Editor

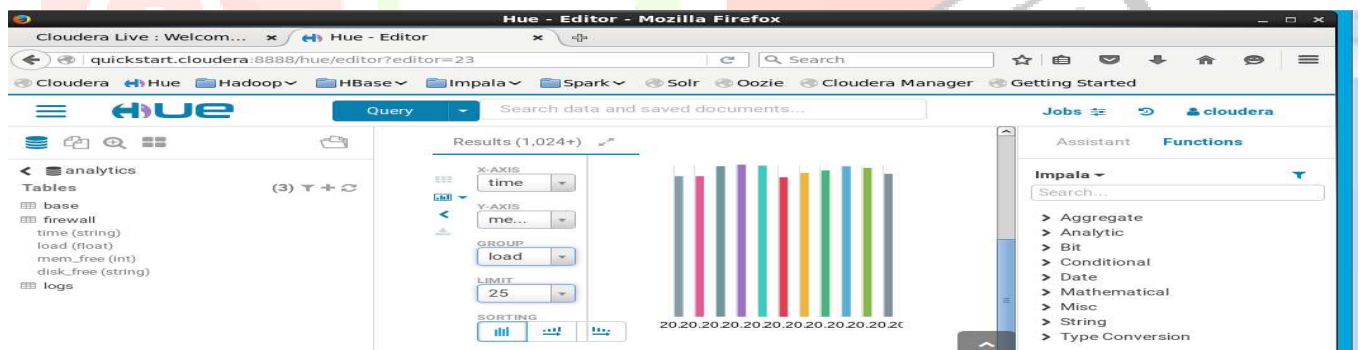


Figure 12: Graphs for System error status

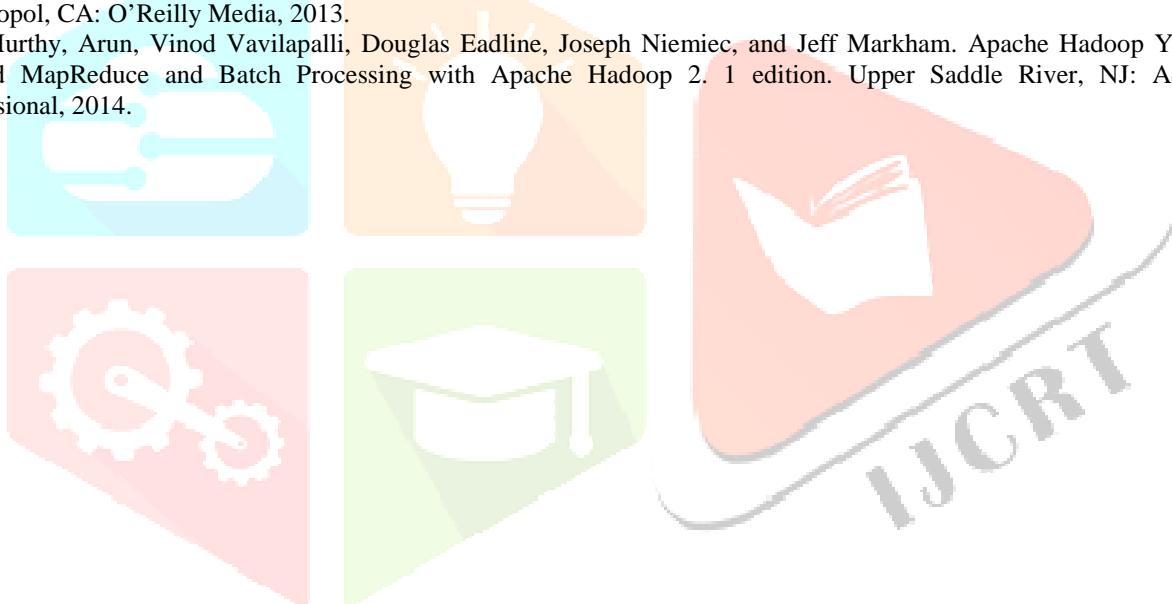
Therefore overview of cloudera Distribution for Network Analytics efficiently analyzed huge record with graphical manner. The objective of Hue's Editor is to make information questioning simple and gainful. It centers around SQL yet additionally bolsters work entries. It accompanies a shrewd auto finish, seek and labeling of information and question help.

VII. CONCLUSION AND FUTURE WORK

Many of the Big data platforms, and architecture frameworks differ in terms of their approach and level of details. Some are just proposed guidelines, whereas others have specific methodologies and critical aspects to follow. The majority of the platforms are abstract and generic in nature and hence the ability to work accurately is questionable. In this paper we analyzed a few open source Big data platforms like Cloudera, Horton Works, MapR, IBM and Pivotal. Our evaluation is based on both subjective measures like the ease of use and objective measures like the performance of each distribution, enabling users to make more informed decisions. According to our evaluation Cloudera offers additional management software as part of the commercial distribution so that Hadoop Administrators can configure, monitor and tune their hadoop clusters. Integrating the tools with Cloudera platform, will give best form of diagnostics and performance analysis. This is important to identify network failure and maintenance issues on prediction basis. Our future work is to expand this research to include more complex network analysis as well as multidimensional data to assist faster, diagnostics and improved performance.

References

- [1] HortonWorks Data Platform HortonWorks Data Platform: New Book. (2015).
- [2] Menon, R. (2014). Cloudera Administration Handbook
- [3] Dunning, T., & Friedman, E. (2015). Real-World Hadoop
- [4] Quintero, D. (n.d.). Front cover implementing an IBM InfoSphereBigInsights Cluster using Linux on Power.
- [5] Pivotal Software, I. (2014). Pivotal HD Enterprise Installation and Administrator Guide.
- [6] Sarkar, D. (2014). Pro Microsoft HDInsight. Berkeley, CA: Apress.
- [7] ThibaudChardonnens, “Big Data analytics on high velocity streams: specific use cases with Storm”, Software Engineering Group, Department of Informatics, University of Fribourg, Switzerland, 2013.
- [8] McKinsey Global Institute. Big data: The next frontier for innovation, competition, and productivity. Paper, June 2011. 7, 9, 10, 11
- [9] Nauman Sheikh, “Big Data, Hadoop, and Cloud Computing, Implementing Analytics”, Morgan Kaufmann, 2013.
- [10] C. Dobrea, and F. Xhafa b, “Intelligent services for Big Data science”, Future Generation Computer Systems, Volume 37, 2014, pp. 267-281.
- [11] Sawant, N., & Shah, H. (Software engineer). (2013). Big data application architecture & a problem-solution approach. Apress.
- [12] Lenovo, I. (2015). Lenovo Big Data Reference Architecture for Cloudera Distribution for Hadoop, (August).
- [13] Read, W., Report, T., & Takeaways, K. (2016). The Forrester Wave™: Big Data Hadoop Distributions, Q1 2016.
- [14] Gates, Alan, and Daniel Dai. Programming Pig: Dataflow Scripting with Hadoop. 2 edition. O'Reilly Media, 2016.
- [15] Capriolo, Edward, Dean Wampler, and Jason Rutherglen. Programming Hive: Data Warehouse and Query Language for Hadoop.1 edition. Sebastopol, CA: O'Reilly Media, 2012.
- [16] Ting, Kathleen, and JarekJarcecCecho. Apache Sqoop Cookbook: Unlocking Hadoop for Your Relational Database. 1 edition. Sebastopol, CA: O'Reilly Media, 2013.
- [17] Murthy, Arun, Vinod Vavilapalli, Douglas Eadline, Joseph Niemiec, and Jeff Markham. Apache Hadoop YARN: Moving beyond MapReduce and Batch Processing with Apache Hadoop 2. 1 edition. Upper Saddle River, NJ: Addison-Wesley Professional, 2014.



Design and Implementation of an IoT System for Enhancing Proprioception Training

Archana D R, Ayesha Rahmath, Chandrashekar M, M Tuba Farheen, Dr D Jayaramaiah
Department of Information Science and Engineering
The Oxford College of Engineering, Bengaluru-560068, India

ABSTRACT

One of the major issues relating to medical concern is, 'weakness and injuries in joints'. To facilitate proper correction for speedy recovery from damage caused at joints, specially the knee, we propose a system which uses wearable sensors. Whenever the bends around the joints is more and when the pressure at ankle exceeds the prescribed limit a feedback is sent to the patient and hence he/she can make the necessary correction. Also a graphical representation of the patient position and pressure will be maintained on a web page. This graph can provide an insight to physician or doctor regarding the exercises/movements occurred around the joints. The generic requirements like physical exercises for curing of injured, low strain practices of games and sports and also for the elderly people, movement can be effectively tracked and remotely controlled for better service and support by healthcare assistant. The primary function of this system is to enable high risk patients to be timely monitored and medicated to enhance the quality of their lifestyle.

Keywords— proprioception, wearable sensors, feedback

I. INTRODUCTION

Among the panoply of applications enabled by the IoT, smart and connected health care is a particularly important one. Networked sensors, either worn on the body or embedded in our living environments, make possible the gathering of information indicative of our physical and mental health. Captured on a continual basis effectively mined, such information can bring about a positive transformative change in the health care.

Proprioception is one of the most important sense also known as position sense. Proprioception allows us to accomplish complex tasks such as controlling our limbs without having to look at them for example, while driving. It can be impaired by diseases or injuries, and the patients will have difficulty with balance and coordination. This mostly affects elderly people and athletes.

Proprioceptive training involves exercises and the patients can record their improvement using wearable devices. In exercise therapy, the early rehabilitation stages, during which the patient works with the physical therapist several times each week. The patient is afterwards given instructions for continuing rehabilitation exercise by him/herself at home. This study develops a rehabilitation exercise assessment mechanism using wearable sensors in order to enable the patients with knee osteoarthritis to manage their own rehabilitation progress.

Using the available data, that has access to a large corpus of observation data for other individuals, the doctor can make a much better prognosis for your health and recommend treatment, early intervention, and life-style choices that are particularly effective in improving the quality of your health

II. CURRENT PRACTICES

The health parameters of the patient were measured and sent through Zigbee Communication protocol. The ZigBee technology provides a resolution for transmitting sensors data by wireless communication. Wearable sensor unit, attached to the patient's body, reads and transmits the patient's data to a portable ZigBee-based receiver carried around by a nurse or doctor or to a hospital server. The system is designed and built using the ZigBee modules (Nodes), sensors attached to the patient's body are interfaced to these Nodes. The complete Node is packaged in a light form and carried by the patient. Sensed data is transmitted to a ZigBee coordinator (Z-Coor) with a wide LCD display that is carried by the supervisor nurse or doctor on the hospital floor.

The XBee gateway shown in Figure1 is used to provide gateway functionality between the ZigBee network and the Ethernet. This gateway device collect data from the coordinator packetize it and via the TCP/IP layer, data is sent and stored in the main server where a database is used to keep records of the patient's history.

A Database is created that stores data such as threshold values for sensed data, these values are determined by the patient's physician and if the patient's readings exceed these values the system will automatically send an alarm SMS

using the GSM network to the doctor. The patient's records or history of readings of the various signs are maintained and an Apache webserver was used in the experimental set up.

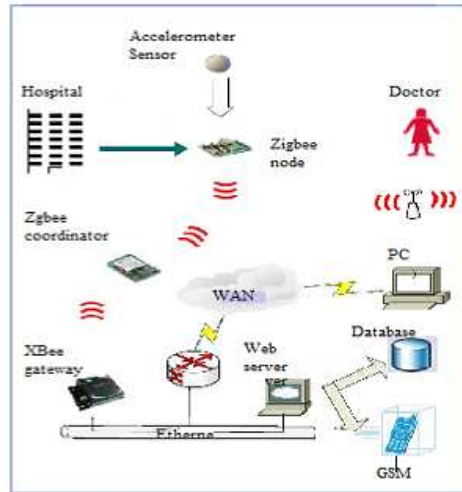


Figure 2.1: Patient health monitoring using Zigbee technology

III. BASIC ARCHITECTURE OF THE PROPOSED SYSTEM

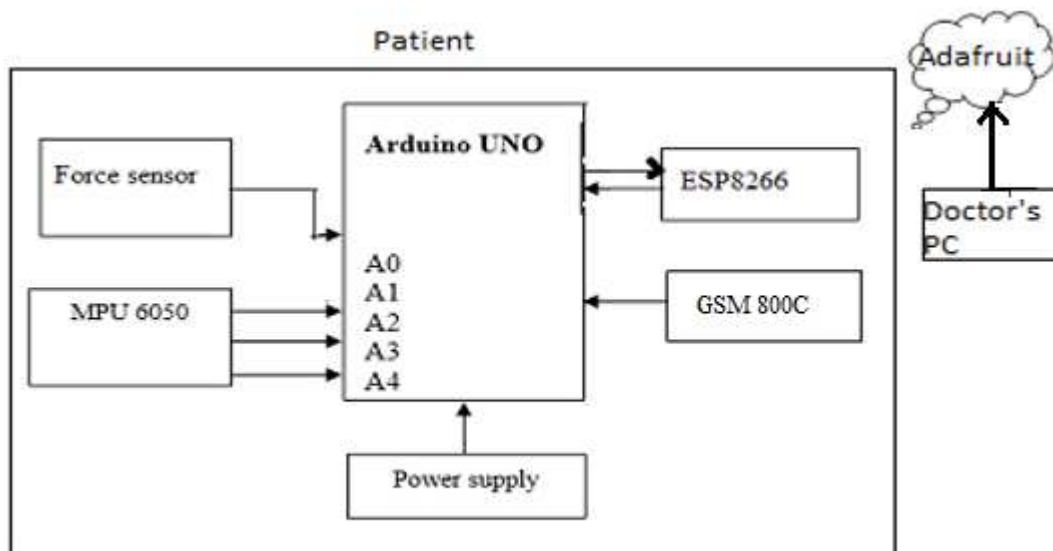


Figure 3.1: Block diagram for proposed system

We develop a healthcare monitoring system for both inpatients and outpatients for enhancing **proprioception training**, considering the cost, ease of application, accuracy and data security. The main idea of the designed system is continuous monitoring of the patients, over mobile phone and internet using wireless technologies. There are a number of exercises that can be performed to help train the proprioception such as balancing exercises, exercises while closing the eyes, strengthening exercises, squats, vertical jumps, are examples of ways that can help establish the connection between muscle fibers by building strength. The real-time monitoring system incorporates wearable sensors to extract medical information which helps finding out multiple parameters such as pressure, movement of the knee at the same time. The system has two interfaces, one for the patient and one for the doctor.

The patient interface is compromised of wearable sensors which extract medical information of the patient and transmit to the IoT server (Adafruit IO) via Wi-Fi. The doctor is provided with a unique user name and password to access the data obtained from the patient. The necessary feedback is sent via a SMS to the patient using GSM 800C module involving doctor’s advice for fast recovery.

The model consists of Arduino UNO board with microcontroller ATMEGA 328, accelerometer sensor with gyroscope features (MPU 6050), force sensors and Wi-Fi module. In this system for outpatients monitoring, ESP8266 wi-fi module collects the data from the sensors and sends the data to IoT server(Adafruit IO) for storage and further analysis through the website. The Protected data stored can be accessed anytime by the doctors.

IV. FEATURES OF THE PROPOSED SYSTEM

The proposed idea is a remote health monitoring system over mobile phone and internet using wireless technologies. The real-time monitoring system incorporates wearable sensors to extract medical information which helps finding out multiple parameters such as pressure, movement of the knee at the same time.

The system architecture is two tier 1) a patient interface that is wearable sensors 2) a web portal.

The patient interface is compromised of wearable sensors which extract medical information of the patient and transmit to the IoT server (Adafruit IO) via Wi-Fi. The doctor is provided with a unique user name and password to access the data obtained from the patient. The necessary feedback is sent via a SMS to the patient using GSM 800C module involving doctor’s advice for fast recovery. The proposed system has the ability to use multiple sensors which enables simultaneous monitoring of several parameters.

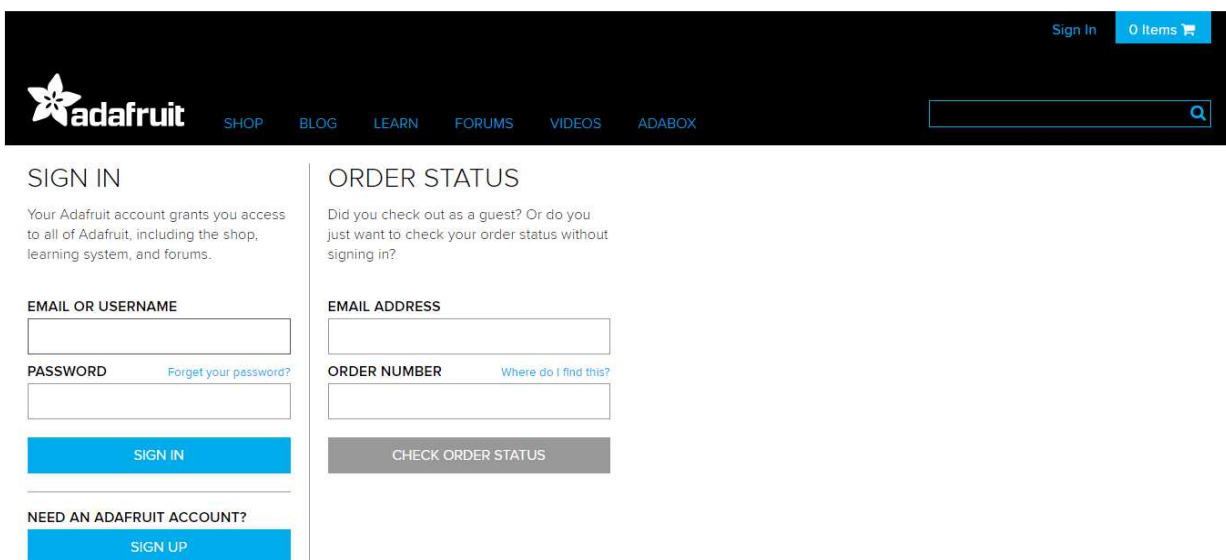


Figure 4.1: Adafruit login page

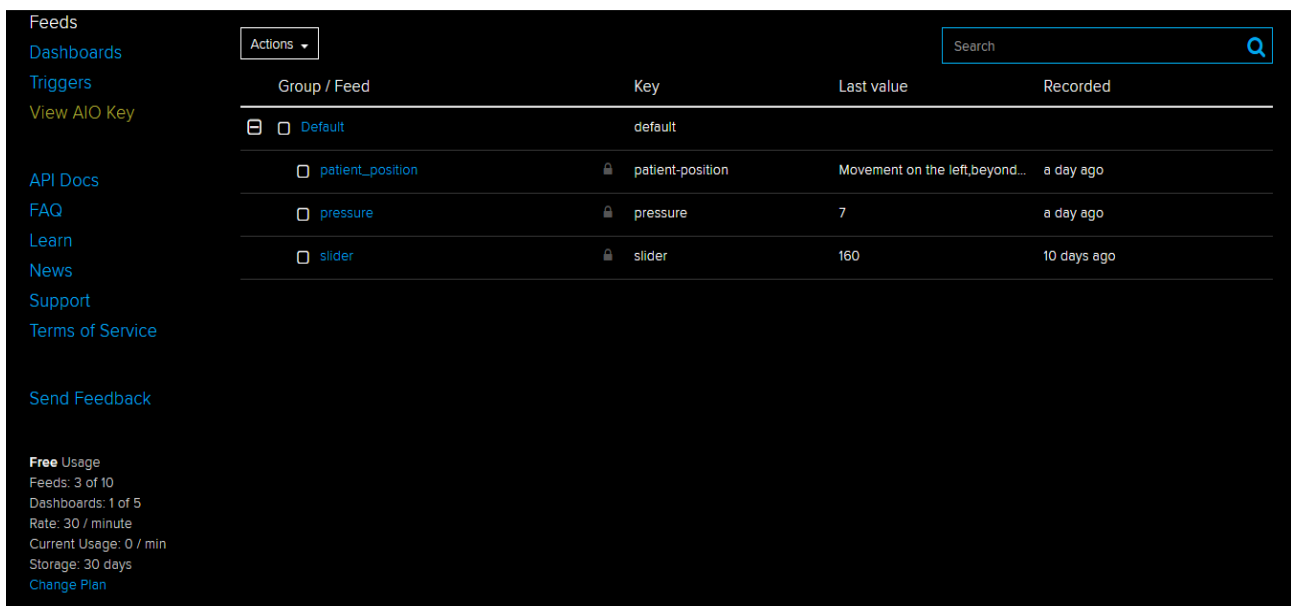


Figure 4.2: Adafruit Feeds with the sensed data

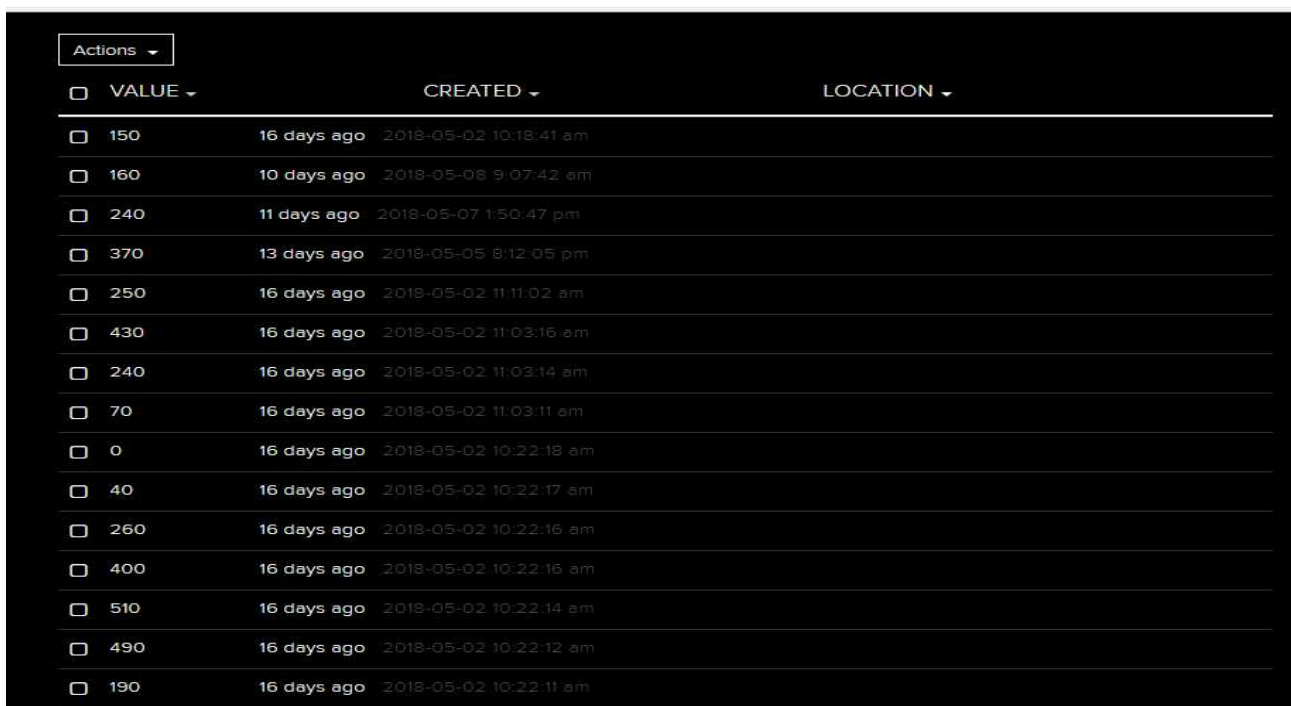


Figure 4.3: Adafruit feeds with sensed Pressure data

| Actions | VALUE | CREATED | LOCATION |
|---------|---|-------------|------------------------|
| | Movement on the left,beyond prescribed l... | 2 days ago | 2018-05-16 1:40:37 pm |
| | Movement on the left,beyond prescribed l... | 2 days ago | 2018-05-16 1:40:34 pm |
| | Movement on the left,beyond prescribed l... | 2 days ago | 2018-05-16 1:40:27 pm |
| | Movement on the left,beyond prescribed l... | 2 days ago | 2018-05-16 1:40:22 pm |
| | Movement on the left,beyond prescribed l... | 2 days ago | 2018-05-16 1:40:17 pm |
| | Movement on the left,beyond prescribed l... | 2 days ago | 2018-05-16 1:40:17 pm |
| | movement frontwards,beyond prescribed li... | 8 days ago | 2018-05-10 12:58:40 pm |
| | movement frontwards,beyond prescribed li... | 8 days ago | 2018-05-10 12:50:19 pm |
| | Movement on the right,beyond prescribed ... | 10 days ago | 2018-05-08 11:21:28 am |
| | Movement on the right,beyond prescribed ... | 10 days ago | 2018-05-08 11:21:22 am |
| | movement frontwards,beyond prescribed li... | 10 days ago | 2018-05-08 9:42:23 am |
| | Movement on the right,beyond prescribed ... | 10 days ago | 2018-05-08 9:35:26 am |
| | Movement on the left,beyond prescribed l... | 10 days ago | 2018-05-08 9:29:42 am |
| | Movement on the left,beyond prescribed l... | 10 days ago | 2018-05-08 9:29:41 am |
| | Movement on the left,beyond prescribed l... | 10 days ago | 2018-05-08 9:29:34 am |

Figure 4.4: Adafruit feeds with patient position details

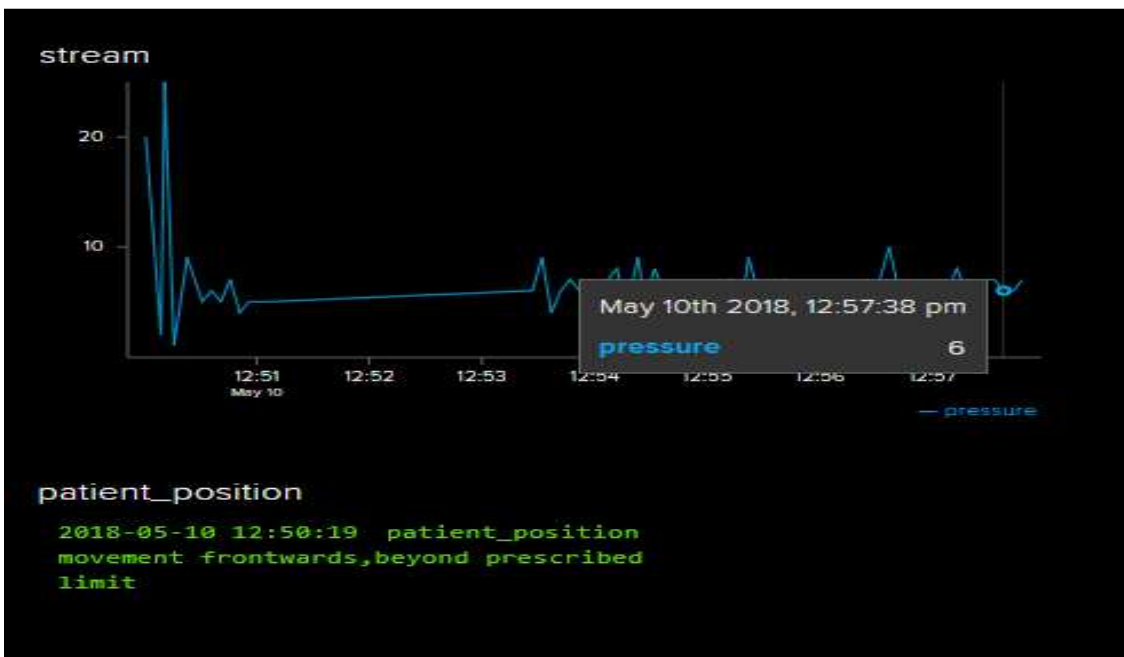


Figure 4.5: Adafruit Dashboard

The model consists of Arduino UNO board with microcontroller ATMEGA 328, accelerometer sensor with gyroscope features (MPU 6050), force sensors and Wi-Fi module. In this system for outpatients monitoring, ESP8266 wi-fi module collects the data from the sensors and sends the data to IoT server (Adafruit IO) for storage and further analysis through the website. The Protected data stored can be accessed anytime by the doctors.

MPU-6050: It has the ability to precisely and accurately track user motions, Motion Tracking technology can be used in applications ranging from health and fitness monitoring to location-based services.

Key features for this technology are small package size, low power consumption, high accuracy and repeatability, high shock tolerance, and application specific performance programmability – all at a low consumer price point. The MPU-6050 collects gyroscope and accelerometer data while synchronizing data sampling at a user defined rate.

FSR- Its key features are small size. It is capable of micro-force detection and high sensitivity, high sensitivity, high precision and high durability.

Data transmission from wearable sensors to IoT server

Data transmission process from sensors to IoT server via ESP-8266 Wi-Fi networks.

The sensors collect the data and transfer it to the IoT server (Adafruit IO) through ESP8266 Wi-Fi module.

The doctor is provided with a unique user id and password, where they can monitor multiple patients' health simultaneously by creating different dashboards and also observe the improvement of each patient from the stored data.

Feedback: The feedback is not only from the doctor after analysing the data in the IoT server, but also the patient is provided with immediate alert messages when there is any anomaly with reference to the predefined threshold values or the sensed parameters which vary based on the patients' age and condition using GSM 800C.

GSM 800C can transmit voice, SMS and data information with low power consumption. With the tiny size of 17.6*15.7*2.3mm, it can smoothly fit into slim and compact demands of customer design.

The alarming mechanism basically consists of data visualization, statistical pre-processing, and notifications.

The proposed alarming system is a generalized monitoring model that works on the principle of threshold values. It can be customized for individual monitoring due to the fact that the threshold values aren't the same for different age groups. The customized monitoring helps in setting adaptive boundary limits which keeps changing throughout the monitoring phase.

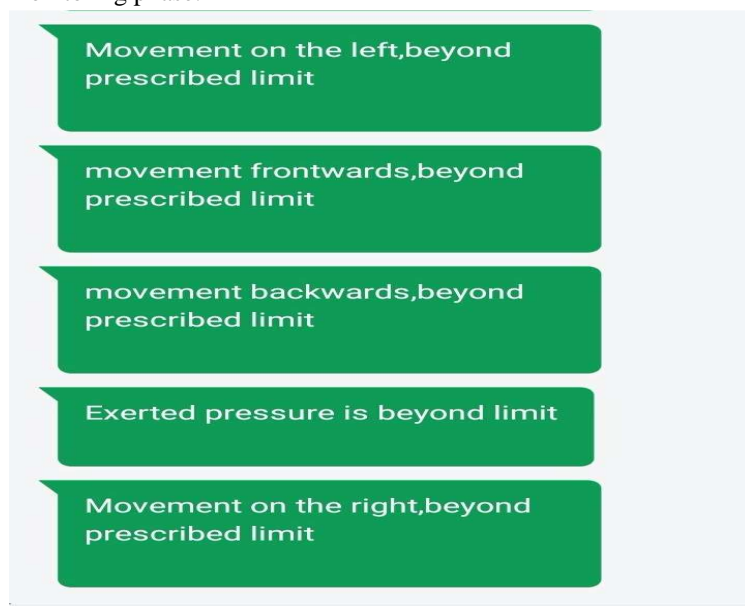


Figure 4.6: Feedback to patient via SMS

V. SPECIFIC HEALTHCARE APPLICATIONS

For people living with osteoarthritis (age range 45-65 years) rehabilitation based on exercise therapy is recommended, this model is useful to keep track of their movements which can enhance their joint function.

This model also helps the injured people specially the athletes who undergo a lot of physical and fitness training to ensure that they recover soon or have an easy going post-operative assessment by wearing the device and monitor their position so as to help him/her to do the exercises as prescribed.

For the physically disabled people if there are chances of improvement, this can help them to take the process slowly and gradually by monitoring movement and pressure exerted at ankle continuously.

VI. RESULTS AND CONCLUSION

The health care services are important part of our society and automating these services lessen the burden on humans and eases the measuring process. Also the transparency of this system helps patients to trust it. The sensors measure the required parameters and provide the data to the web server. When threshold value is reached, an alert message is sent to the user via SMS using GSM 800C and he/she can act more quickly. The ESP-8266 Wi-Fi module helps the server to update the patient data on website.

The development of low-cost, low-power, multifunctional wireless sensor nodes that are small in size and communicate untethered in short distances are used in our project. These tiny wireless sensor nodes, which consist of sensing, data processing, and communicating components, leverage the idea of sensor networks based on the collaborative effort of a large number of *nodes*. *Issues* such as long-term patient care in hospitals, support for elderly people at home can be resolved using this. The implemented real-time patient monitoring system, enables doctors to monitor the patients' health on a remote site, and provide timely advice according to their improvement. The system prevents the patients from re-hospitalization and monitoring multiple patients' health status simultaneously. The data are available for review on the central server, and can be accessed remotely by means of Adafruit Feeds. The system developed automatically alerts the patient when an anomaly is detected through SMS services. Besides bringing comfort to patients, there are commercial benefits in the area of reducing costs, rehospitalisation, and improving equipment and patient management.

VII. REFERENCES

- [1] Mangine, R.E.; Price, S. Innovative Approaches to Surgery and Rehabilitation. In Physical Therapy of the Knee; Mangine, R.E., Ed.; Churchill Livingstone: New York, NY, USA, 1988; pp. 191–220.
- [2] Taylor, P.E.; Almeida, G.J.M.; Kanade, T.; Hodgins, J.K. Classifying Human Motion Quality for Knee Osteoarthritis Using Accelerometers. In Proceeding of the 32nd Annual International Conference of the IEEE EMBS, Buenos Aires, Argentina, 31 August 2010; pp. 339–343.
- [3] Karantonis, D.M.; Narayanan, M.R.; Lovell, N.H.; Celler, B.G. Implementation of a Real-Time Human Movement Classifier Using a Triaxial Accelerometer for Ambulatory Monitoring. *IEEE Trans. Inf. Technol. Biomed.* 2006, 1, 156–167.
- [4] Ermes, M.; Pärkka, J.; Mantyjarvi, J.; Korhonen, I. Detection of Daily Activities and Sports with Wearable Sensors in Controlled and Uncontrolled Conditions. *IEEE Trans. Inf. Technol. Biomed.* 2008, 1, 20–26.
- [5] Luinge, H.J.; Veltink, P.H. Measuring orientation of human body segments using miniature gyroscopes and accelerometers. *Med. Biol. Eng. Comput.* 2005, 43, 273–282. 13.

- [6] Fahrenberg, J.; Foerster, F.; Smeja, M.; Muller, W. Assessment of posture and motion by multichannel piezoresistive accelerometer recordings. *Psychophysiology* 1997, 5, 607–612.
- [7] Ravi, N.; Dikhil, N.; Mysore, P.; Littman, M.L. Activity recognition from accelerometer data. In *Proceedings of the 7th Innovative Applications of Artificial Intelligence Conference*, Pittsburgh, PA, USA, 9 July 2005; pp. 1541–1546. 19.
- [8] Foerster, F.; Smeja, M.; Fahrenberg, J. Detection of posture and motion by accelerometry: A validation study in ambulatory monitoring. *Comp. Hum. Behav.* 1999, 15, 571–583. 20.
- [9] Foerster, F.; Fahrenberg, F. Motion pattern and posture: correctly assessed by calibrated accelerometers. *Behav. Res. Methods Instrum. Comput.* 2000, 3, 450–457. 21.
- [10] Godfrey, A.; Conway, R.; Meagher, D.; O'laighin, G. Direct measurement of human movement by accelerometry. *Med. Eng. Phys.* 2008, 10, 1364–1386.
- [11] Shull, P.B.; Jirattigalachote, W.; Hunt, M.A.; Cutkosky, M.R.; Scott, L. Delp. Quantified self and human movement: A review on the clinical impact of wearable sensing and feedback for gait analysis and intervention. *Gait Posture* 2014, 40, 11–19.
- [12] Brutovsky, J.; Novak, D. Low-cost motivated rehabilitation system for post-operation exercises. In *Proceeding of the 28th Annual International Conference of the IEEE Engineering in Medicine and Biology*, New York, NY, USA, 30 August–3 September 2006; pp. 6663–6666.
- [13] Tseng, Y.C.; Wu, C.H.; Wu, F.J.; Huang, C.F.; King, C.T.; Lin, C.Y.; Sheu, J.P.; Chen, C.Y.; Lo, C.Y.; Yang, C.W.; et al. A wireless human motion capturing system for home rehabilitation. In *Proceeding of the International Conference of Mobile Data Management*, Taipei, Taiwan, 18–20 May 2009; pp. 359–360.
- [14] Yeh, S.C.; Hwang, W.Y.; Huang, T.C.; Liu, W.K.; Chen, Y.T.; Hung, Y.P. A study for the application of body sensing in assisted rehabilitation training. In *Proceeding of the IEEE International Symposium on Computer, Consumer and Control*, Taichung, Taiwan, 4–6 June 2012; pp. 922–925. 29.
- [15] Zhou, H.; Hu, H. Human motion tracking for rehabilitation—A survey. *Biomed. Signal Process. Control* 2008, 1, 1–18.
- [16] Takeda, R.; Tadano, S.; Natorigawa, A.; Todoh, M.; Yoshinari, S. Gait posture estimation using wearable acceleration and gyro sensors. *J. Biomech.* 2009, 42, 2486–2494.

- [17] B. J. Miriviosky, L. N. Shulman, and A. P. Abernethy, "Importance of Health Information Technology, Electronic Health Records, and Continuously Aggregating Data to Comparative Effectiveness Research and Learning Health Care," *Journal of Clinical Oncology*, vol. 30, no. 34, 2012.
- [18] A. Avci, S. Bosch, M. Marin-Perianu, R. Marin-Perianu, P. Havinga, "Activity Recognition Using Inertial Sensing for Healthcare, Wellbeing and Sports Applications: A Survey," *23rd International Conference on Architecture of Computing Systems (ARCS)*, 2010.
- [19] V. I. Rejuso and C. Druzgalski, "Design of a Motorized Wobble Board for Load Sustainable Rehabilitative Training of Patients with Severe Ankle Injuries," *2016 Global Medical Engineering Physics Exchanges/ PAN American Health Care Exchanges (GMEPE / PAHCE)*.



AN INTELLIGENT SMARTPHONE BASED APPROACH USING CLOUD COMPUTING AND IOT FOR RISK-FREE DRIVING

S.Kalaiselvi , Lakshmi L Menda , Navya V , Fiona Jothi Sylvester , Latha Shree N

Asst. Prof , Student , Student , Student , Student

Department of Information Science and Engineering
The Oxford College of Engineering, Bangalore, Karnataka, India

Abstract : An intelligent Smartphone based approach using cloud computing and IoT for risk-free driving that will collect data using smart phone's GPS sensor, Accelerometer sensor and inform the driver about the condition of the road. The Android based application which will collect model inputs (longitude, latitude, and speed, acceleration data of vehicles) from a vehicle and send it to its nearest IoT-Fog server for processing the data quickly. It uses affinity propagation clustering approach which finds the location of road anomalies and accident prone area. It also provides a mechanism where the smart phone camera detects the driver's eyes using OpenCV to diagnose where he's in a dizzy state or not. This information will be stored in cloud for further use. With real-time analysis and auditory alerts of these factors, we can increase a driver's overall awareness to maximize safety.

IndexTerms : Smartphone, IoT, Fog, Cloud, Affinity Propagation clustering, Bumps/speed-breaker, OpenCV, Dizzy state detection

I. INTRODUCTION

In the present era vehicles have become an essential part of our life. But because of poor handling they have become a death angel for human life. Therefore safe driving becomes an important urge in life. Safe driving not only assures less time for driving but also it secures an accident-free drive. Though the risk in driving cannot be eradicated completely but it can be reduced. This is possible when the driver knows the road condition in advance. There are various road conditions due to which the Vehicle may fall unexpectedly leading to accidents with huge loss. The various road conditions include potholes, speed-breaker, etc. this system mainly focuses on detecting road accident using different machine learning algorithm and big data processing. After detecting the road conditions it plots them on the Google map to indicate the driver. It uses Affinity propagation clustering approach for training data and Random forest classifiers for validation of testing data. it mainly focuses on safe driving that is established on an IoT-based system. The IoT (Internet of things) based system refers to a system of internetworking connected devices embedded with actuators, sensors and network connectivity that enable these devices to collect and exchange data. An IoT system has been developed to detect road anomalies, accident-prone location and the driver's dizzy state. This is used for warning the drivers if there are any pothole, Bumps, speed-breaker and the accident prone area in their route. This IoT system also includes a fog based decision-making system. The fog refers to an architecture that provides services for computing, storing, and networking between the edge of the devices rather than routing everything through a central data center in the cloud. For calculating process clustering is need. Clustering is an Algorithm that is used to separate similar data points into intuitive groups. To arrange the regular data and irregular data it uses clustering .Fog has limited memory to store data. That's why it uses the cloud to store data for further use. Cloud refers to Internet-based computing which provides shared Computer processing resources and data, to the computer and other devices on demand .Here, the cloud is necessary to sync fog information with the cloud. The camera in the smart phone constantly focuses on the eyes of the driver and detects them using OpenCV. If the eyes are found close for more than 5 seconds, then an alarm will be raised so that the driver gets alerted. The presented work takes into account various factors leading to unsafe driving and presents a technique for evaluating the driving condition in advance.

II. LITERATURE SURVEY

In [1], it discusses the various data processing algorithms that are used to detect irregularity on the road using a mobile system. It also gives the optimal parameters and recommendations for the algorithm.(mednis 2011).In [2] ,the GPS sensor and accelerometer is used to gather the data about driving behavior and road anomalies and this data is analyzed based on a fuzzy system. In [3], the authors propose a Wi-Fi based architecture for pothole detection which gives prior warnings to the driver in case of detection of a pothole. The system consists of access points which are placed on the roadsides which broadcast the data

which is then received by the Wi-Fi enabled vehicles as they enter the area covered by the influence of the access points. The mobile nodes can also broadcast their response as feedback which when received by access point can be utilized for backend server processing. In [4], the authors develop a pothole detection system using 2D LiDAR and Camera. 2D LiDAR is used to find the distance and angle information of the road. The pothole detection algorithm and image-based pothole detection method is used to improve the accuracy of pothole detection and to obtain pothole shape. In [5], it uses an efficient unsupervised vision-based method for pothole detection without the need for training and filtering. It firsts detect asphalt pavements by analyzing RGB color space and performing image segmentation. A data set consisting of selected images from Google search engine is used which contains highly unstructured images taken from different cameras and shooting angles. The method uses manipulation of B component in RGB space and image segmentation it can be easily and widely adopted for hardware implementation. In [6] image pre-processing based on difference of Gaussian-Filtering and clustering based image segmentation methods are implemented for better results. The K-Means clustering based segmentation was preferred for its fastest computing time and edge detection based segmentation is preferred for its specificity. In [7], it develops a crowd sourced system to detect and localize potholes in multi-lane environments using accelerometer data from embedded vehicle sensors. This crowd sourced system reduces the required network bandwidth by determining road incline and bank angle information in each vehicle to filter acceleration components that do not correspond to pothole conditions. In [8] it proposes a smartphone-based driver assistance system which uses front and rear camera image recognition to help maintain the safety of the driver. The system uses a front camera image to detect the drowsiness of the driver, and a rear camera image to detect the vehicle in front. In [9] it describes an application called “Driver drowsiness detection” and the purpose of this application is to alert drivers so that they can be cautioned to pull over and stop driving in a drowsy state. It utilizes Haar-cascade Detection as well as template matching in OpenCV to detect and track the eyes using the front camera of an Android device. In [10], it proposes an eye blink monitoring algorithm that uses eye feature points to determine the open or closed state of the eye and activate an alarm if the driver is drowsy. By applying the Viola Jones algorithm we successfully detected the face region, Once the face is identified, the Region of Interest (ROI) is set to the face rectangle, detected by the Viola Jones algorithm. On this region again the Viola Jones Cascade classifier is applied to detect eyes. An accuracy of 94% has been recorded for the proposed methodology. Figure 1 shows the survey of the accidents that caused due to bad road conditions such as potholes, speed-breakers and the drowsiness of the driver.[12-15]

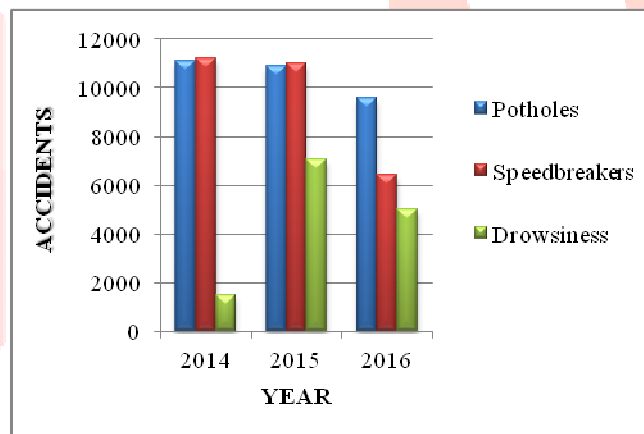


FIGURE 1: Survey of accidents caused due to bad road conditions and drowsiness

III. PROPOSED SYSTEM

The essential focal point of this framework is to identify the different street abnormalities well ahead of time and caution the client to guarantee chance risk-free driving. It requires an advanced mobile phone which keeps running on the Android working framework with inbuilt GPS sensor, Accelerometer sensor, and internet. The smart phone is placed in the car. Figure 2 represents the design of the model. The GPS of the advanced mobile phone gathers the constant area of the gadget. The speed of the car is ascertained by GPS and moving time. The accelerometer sensor has 3 axes. The estimation of x-pivot changes when the device is moved left or right. The estimation of y-pivot changes when the device is moved forward and backward. The estimation of z-hub changes when the device is moved up and down. It needs the z-hub esteem for separate potholes, speed breaker. The device is set in the car on a level plane for getting the exact information for z-pivot. Each gadget is associated with the haze. Here we are utilizing fog since it tackles the issue by keeping information nearer to the nearby PCs and gadgets, instead of directing everything through a central server in the cloud. Thus, the information exchange is speedier than the cloud and we will get the outcome rapidly. These gadgets are sending Latitude, Longitude, speed, and accelerometer

information to the fog constantly. The fog forms the information and sends the outcome to each cell phone and each fog. Fog has memory impediment that is the reason it likewise sends the outcome to the cloud to store data for additionally utilize.

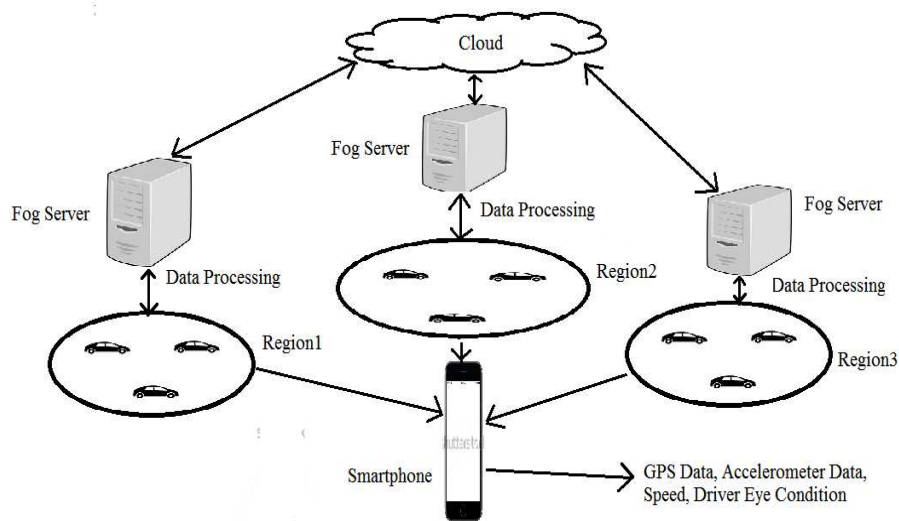


FIGURE 2: Design of the Model

A. Detecting different road anomalies

The information is sent to the closest fog from the advanced mobile phone each λ times. Here, λ is diverse time interim as indicated by various types of vehicle. At that point the information is computed to discover street oddities. If there is a pothole or speed-breaker, at that point each vehicle will back off on that area, and subsequent to passing it, the car will accelerate once more. Thus, for a specific zone if every one of the vehicles stoppages and speed ups again then haze will choose that there is a pothole or speed-breaker. For isolating speed-breaker and potholes, it will assess its z-pivot information. On the off chance that the z-pivot esteem is not as much as lower z-hub limit esteem then it is a pothole, if the z-hub esteem is higher than upper z-hub edge esteem, at that point it is speed breaker.

Algorithm 1: Detecting pothole and speed breaker

INPUT:

Sc: speed of current row

Sp: speed of pervious row

Sn: speed of next row

St: threshold speed

Sw: speed of the line after next row

Z : accelerometer z-hub estimation of current row

Zmax: most extreme edge for accelerometer z-hub

Zmin: least limit for accelerometer z-pivot

OUTPUT: Location of the pothole and speedbreaker

1. Fog database is read
2. while end of row do
3. if (Sc < Sth AND Sc > 0) AND (Z <= Zmin) And (Sp > Sc) AND (Sn > Sc) then
4. Save location of current row as pothole
5. end if
6. if (Sc < Sth AND Sc > 0) AND (Z >= Zmax) And (Sp > Sc) AND (Sn > Sc) then
7. Save location of current row as speed-breaker
8. end if
9. end while

B. Detecting accident prone areas

For finding accident prone area, it uses the previous data of accident. The data is collected from Accident Research Institute (ARI), BUET. This data holds some total accident in each area. For clustering these data, we again use Affinity propagation clustering algorithm.

Algorithm 2: Detecting accident prone areas

INPUT:

Thm: Threshold for moderate accident area

Thh: Threshold for highly accident area

An: Number of total accident in individual area

OUTPUT: Location of accident prone area

1. Read all row from cloud database
2. while End of row do
3. if ($An \geq Thm$) AND ($An < Thh$) then
4. Saving location of current row as moderate accident area
5. end if
6. if $An \geq Thh$ then
7. Saving location of current row as highly accident area
8. end if
9. end while

Algorithm 3 : Affinity propagation

$$r(i, k) \leftarrow s(y_i, y_k) - \max_{k \neq i} \{a(i, k) + s(y_i, y_k)\} \rightarrow (1)$$

$$a(i, k) \leftarrow \min \{0, r(k, k) + |i| \in \{i, k\} \max\{0, r(i, k)\}\} \rightarrow (2)$$

1. Initialize availabilities $a(i, k)$ to zero $\forall i, k$
2. do {
3. Update, using Equation (1), all the responsibilities given the availabilities
4. Update, using Equation (2), all the availabilities given the responsibilities
5. Combine availabilities and responsibilities to obtain the exemplar decisions
6. } until Termination criterion is met.

C. Detecting dizzy state of driver

The camera in the smart phone constantly focuses on the eyes of the driver and detects them using OpenCV. If the eyes are found close for more than 5 seconds, then an alarm will be raised so that the driver gets alerted. This system uses a front camera image to maintain driver safety. This system detects the driver's drowsiness by processing a front camera image, and alarms the driver. First, the face and eyes need to be detected from the front camera image in order to detect the drowsiness. The face and eyes can be detected by using Haar-like features. Face detection should come first to decrease the eye detection time by setting the region of interest (ROI). Second, drowsiness should be judged from the detected eye image it separates the eye image into white pixels that indicate the skin area and black pixels that indicate the eyeball area. It can be considered that the eye is closed if the number of black pixels decreases to less than 80% of the number of whole pixels according to PERCLOS (percentage of eye closure), and that the drowsiness is detected if the eye is closed for longer than 400ms. It can judge whether or not the driver is currently drowsy by checking these conditions in the front camera image.

IV. RESULTS

This section illustrates the output of the system. FIGURE 3 shows the screenshot that appears on the user interface on the Smartphone, where the driver can enter the source and destination of their journey. Here the current location of the driver can be selected as a source by clicking at the check box. The red flag indicates the source, green flag indicates the destination and the blue line indicate the path. The blue dot shows the current location of the user.

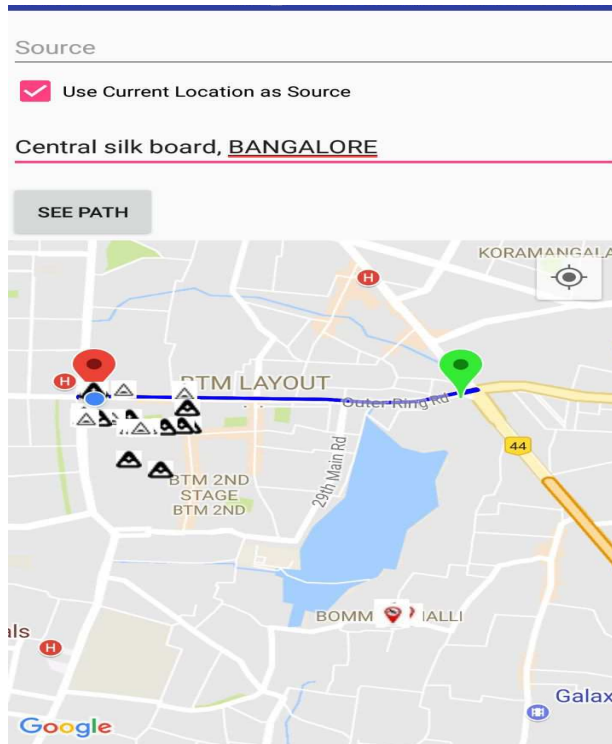


FIGURE 3 : User interface with entered source and destination

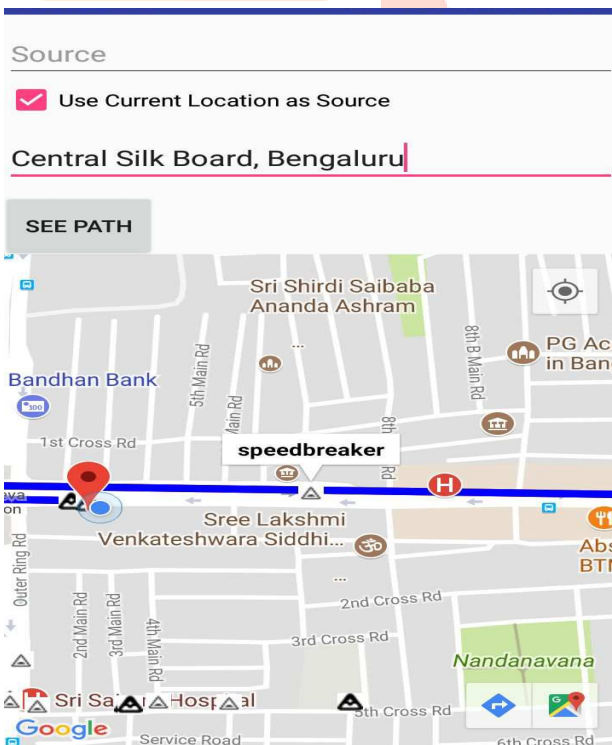


FIGURE 4: Spotting speed-breaker

The grey triangle in the FIGURE 4 indicate the speed breaker in the path, whenever the driver approaches the speed breaker, the application will give an indication of the approaching speed breaker with the help of voice alerts stating the distance of the speedbreaker from the drivers location.

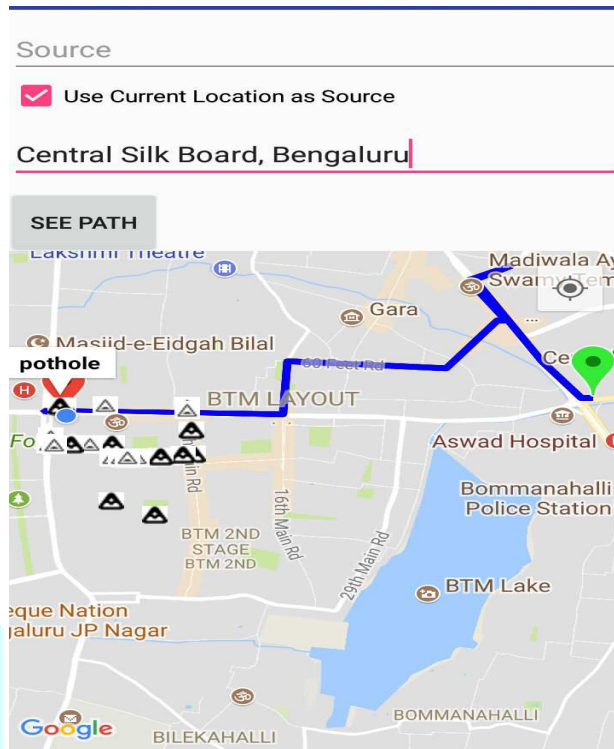


FIGURE 5: Spotting pothole

The black triangle in FIGURE 5 indicate the pothole in the path, whenever the driver approaches the pothole, the application will give an indication of the approaching pothole with the help of voice alerts stating the distance of the pothole from the drivers location.

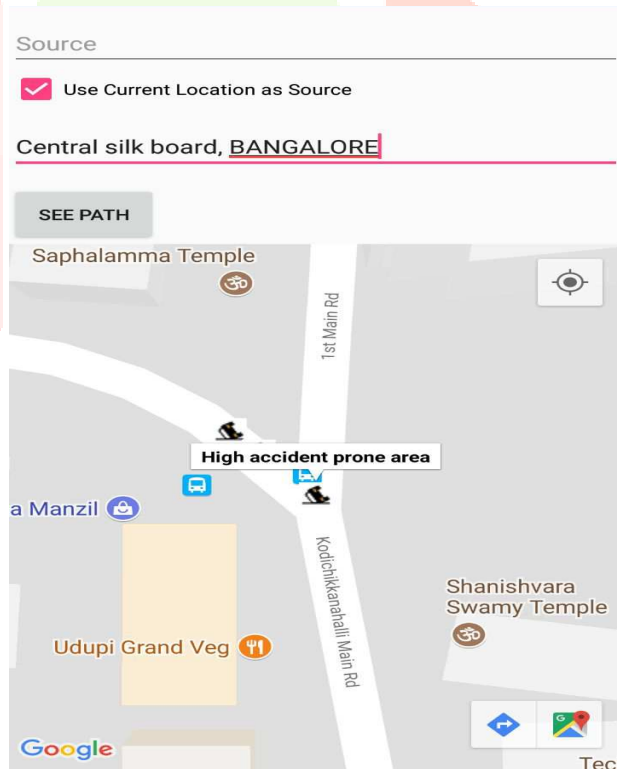


FIGURE 6: Detection of high accident prone area

The FIGURE 6 indicates the highly accidental prone areas .so when the user approaches these areas the user gets an alert so that the driver reduces their speed in order to avoid accidents. The notification to user will be in the form of voice alerts.

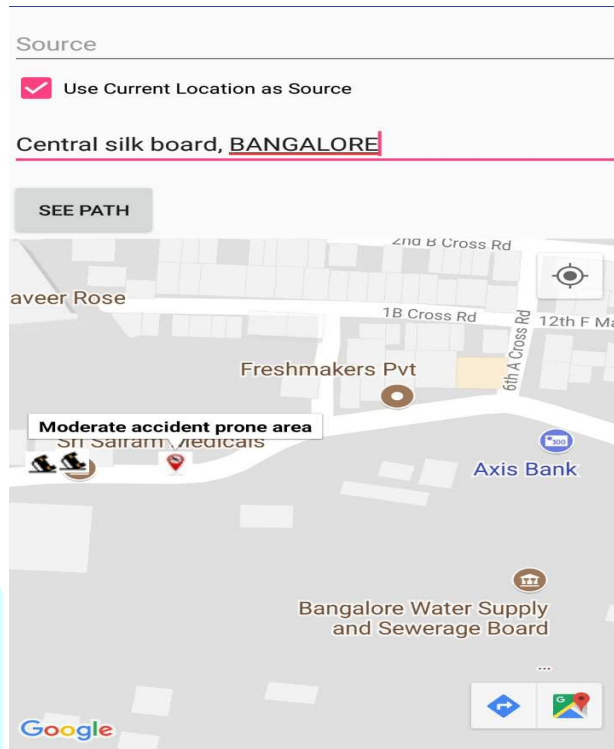


FIGURE 7: Detection of Moderate accident prone area

The FIGURE 7 indicates the moderate accident prone area. When the user approaches these areas the user gets an alert so that he reduces his speed in order to avoid accidents. The notification to user will be in the form of voice alerts.

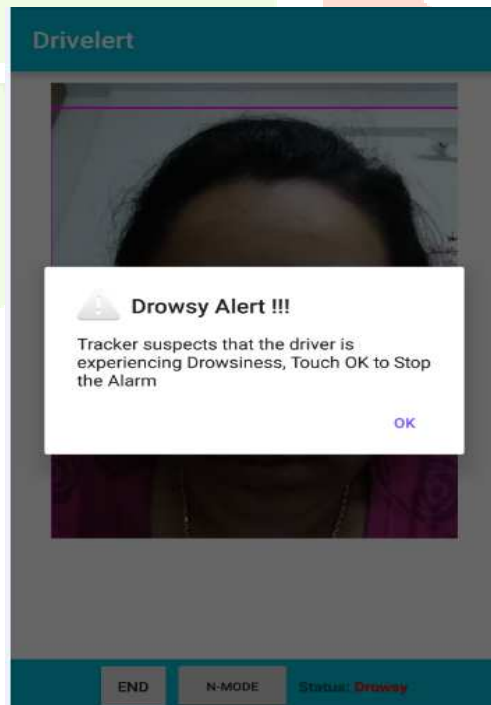


FIGURE 8: Drowsiness detection

Figure 8 detects the eyes of the user to indicate whether the driver is in dizzy state or not. In the above picture the Closed eyes is detected hence it produces an alarm to awaken the driver.

V. CONCLUSION

Road accidents can't be eradicated totally, however it can be controlled by demonstrating the state of the street to the vehicle driver. Consequently safe driving ends up a standout amongst the most regular desires in urban and in addition country life. Safe driving not just secures a mishap free drive it likewise guarantees less time for driving. In spite of the fact that driving can't be without hazard, one ought to know about the street conditions. The model sources of data (longitude, latitude, and speed, acceleration of vehicles) are obtained using Android application to have real-time implementation. Additionally, the model incorporates two computational insight strategies that are cloud and fog based framework. It utilizes Affinity propagation clustering algorithm on training data. It likewise gives a component where the advanced mobile phone camera identifies the driver's eyes utilizing OpenCV to analyze whether they are in dizzy state or not. The advanced cell is utilized expecting to evacuate the requirement for deploying particular sensors in a vehicle or at any street intersections. However, the essential goal of this approach is to have the capacity to give a continuous observing framework that can guarantee safe, accident-free and fast driving.

VI. REFERENCES

- [1] A. Mednis, G. Strazdins, R. Zviedris, G. Kanonirs, L. Selavo, dcoss, "Real time pothole detection using Android smartphones with accelerometers", in *Proc. International Conference on Distributed Computing in Sensor Systems and Workshops*, pp. 1-6, 2011.
- [2]R. K. Goregaonkar,S. Bhosale, "Assistance to Driver and Monitoring the Accidents on Road by using Three Axis Accelerometer and GPS System", *Proc. 1st International Conference*, vol.10, pp. 1-8, April 2014
- [3]Sudarshan S Rode, Shonil Vijay, Prakhar Goyal, Purushottam Kulkarni, Kavi Arya "Pothole Detection and Warning System: Infrastructure Support and System Design", in 2009 International Conference on Electronic Computer Technology
- [4]Byeong-ho Kang and Su-il Choi "Pothole Detection System using 2D LiDAR and Camera" in 2009 International Conference on Electronic Computer Technology
- [5]Amila Akagic, Emir Buza, Samir Omanovic "Pothole Detection: An Efficient Vision Based Method Using RGB Color Space Image Segmentation" in *MIPRO 2017*, May 22-26, 2017, Opatija, Croatia
- [6]K. Vigneshwar; B. Hema Kumar "Detection and counting of pothole using image processing techniques " in 2016 IEEE International Conference on Computational Intelligence and Computing Research (ICCIC)
- [7]Andrew Fox; B. V. K. Vijaya Kumar; Jinzhu Chen; Fan Bai "Multi-Lane Pothole Detection from Crowdsourced Undersampled Vehicle Sensor Data" in *IEEE Transactions on Mobile Computing*
- [8]Kyungwon Chang; Byung-Hun Oh; Kwang-Seok Hong "An implementation of smartphone-based driver assistance system using front and rear camera" in 2014 IEEE International Conference on Consumer Electronics (ICCE)
- [9]Aldila Riztiane; David Habsara Hareva; Dina Stefani; Samuel Lukas "Driver Drowsiness Detection Using Visual Information On Android Device " in 2017 International Conference on Soft Computing, Intelligent System and Information Technology (ICSIT)
- [10]Amna Rahman; Mehreen Sirshar; Aliya Khan "Real time drowsiness detection using eye blink monitoring " in 2015 National Software Engineering Conference (NSEC)
- [11] Mohd Abdullah Al Mamun,Amit Kumar Das "An Intelligent Smartphone Based Approach Using IoT for Ensuring Safe Driving" in 2017 International Conference on Electrical Engineering and Computer Science (ICECOS)
- [12]<https://qz.com/908870/speed-breakers-on-indian-roads-kill-more-than-10000-people-every-year/>
- [13]<https://www.hindustantimes.com/india-news/road-accidents-claimed-nearly-400-lives-every-day-in-india-in-2016/story-7DlmtDnvMYLLZVGxXKOaJN.html>
- [14]<https://www.pothole.info/the-facts/>
- [15]<http://internetofthingsagenda.techtarget.com/definition/fog-computing-fogging>

DETECTING SPAM REVIEWS ON SOCIAL MEDIA USING NETWORK-BASED FRAMEWORK: NETSPAM

¹P Kokila, ²Mir Mustafa Ali, ³Nikhil H M, ⁴Pooja Deshpande, ⁵Pratima Kulkarni

¹Assistant Professor, ²UG Student, ³UG Student, ⁴UG Student, ⁵UG Student,

¹Department of Information Science & Engineering,

¹The Oxford College of Engineering, Bangalore, India

Abstract : A lot of people rely on content available on social media for making decisions. The possibility that anyone can post a review provides a golden opportunity for spammers to write spam reviews about products and services. Identifying these spammers and the spam content is a very important topic in field of research and although a considerable number of studies have been done recently, but so far, the methodologies put forth still barely detect spam reviews, and none of them show the importance of each extracted feature type. This propose a novel framework, named *NetSpam*, which utilizes spam features for modeling review datasets as heterogeneous information networks to map spam detection procedure into a classification problem in such networks. Using the importance of spam features help us to obtain better results in terms of different metrics experimented on real-world review datasets from Yelp and Amazon websites. The results show that *NetSpam* is better than the existing methods using the features like review-behavioral, user-behavioral, review-linguistic, user-linguistic.

Keywords: *NetSpam, Social Network, Spammer, Spam Review, Fake Review, Heterogeneous Information Network*

I. INTRODUCTION

Information propagation is considered as an important source for producers in their advertising campaigns as well as for customers in selecting products and services. In the past years, people rely a lot on the written reviews in their decision-making processes, and positive/negative reviews encouraging/discouraging them in their selection of products and services. In addition, written reviews also help service providers to enhance the quality of their products and services. These reviews thus have become an important factor in success of a business while positive reviews can bring benefits for a company, negative reviews can potentially impact credibility and cause economic losses. The fact that anyone with any identity can leave comments as review provides a tempting opportunity for spammers to write fake reviews designed to mislead users' opinion. These misleading reviews are then multiplied by the sharing function of social media and propagation over the web. The reviews written to change users' perception of how good a product or a service are considered as spam and are often written in exchange for money Despite this great deal of efforts, many aspects have been missed or remained unsolved. One of them is a classifier that can calculate feature weights that show each feature's level of importance in determining spam reviews.

Spam minded informal conversations on social media (e.g. Twitter) shed light into their educational experiences, opinions, feelings, and concerns about the learning process. Data from such un-instrumented environments can provide valuable knowledge to inform student learning. Analyzing such data, however, can be challenging. The complexity of spam minded' experiences reflected from social media content requires human interpretation. However, the growing scale of data demands automatic data analysis techniques. Here data mining algorithm based on Spam filter is implemented which contains several steps like Data Collection from twitter, Cleaning the data by removing stop words, removal of non-letter and punctuation marks, probability of the words for various categories is estimated. For all the tweets Accuracy, Precision, Recall, F1 measure, Micro Averaged & Macro Averaged values are computed for each category and also for the various users. Therefore, its concluded based on average how many spam's minded have various categories of problems as well as extend this to the problems faced by which user.

Social media sites such as Twitter provide great venues for spam minded to share joy and struggle, vent emotion and stress, and seek social support. On various social media sites, spam minded discuss and share their everyday encounters in an informal and casual manner. Spam minded' digital footprints provide vast amount of implicit knowledge and a whole new perspective for educational researchers and practitioners to understand spam minded' experiences outside the controlled classroom environment. This understanding can inform institutional decision-making on interventions for at-risk spam minded, improvement of education quality, and thus enhance student recruitment, retention, and success. The abundance of social media data provides opportunities to understand spam minded' experiences, but also raises methodological difficulties in making sense of social media data for educational purposes. Just imagine the sheer data volumes, the diversity of Internet slangs, the unpredictability of locations, and timing of spam minded posting on the web, as well as the complexity of spam minded'

experiences. Pure manual analysis cannot deal with the ever-growing scale of data, while pure automatic algorithms usually cannot capture in-depth meaning within the data.

There is huge amount of data available in Information Industry. This data is of no use until converted into useful information. Analyzing this huge amount of data and extracting useful information from it is necessary. The extraction of information is not the only process that need to perform; it also involves other processes such as Data Cleaning, Data Integration, Data Transformation, Data Mining, Pattern Evaluation and Data Presentation. Once all these processes are over, we are now position to use this information in many applications such as Fraud Detection, Market Analysis, Production Control, Science Exploration etc.

Data Mining is defined as extracting the information from the huge set of data. In other words we can say that data mining is mining the knowledge from data. This information can be used for any of the following applications:

- Market Analysis
- Fraud Detection
- Customer Retention
- Production Control
- Science Exploration

II. METHODOLOGY

2.1 Hash tag Submission

This module is responsible for taking input the hash tags and then save the hash tags in the format of (HashTagID, HashTag and ProductID)

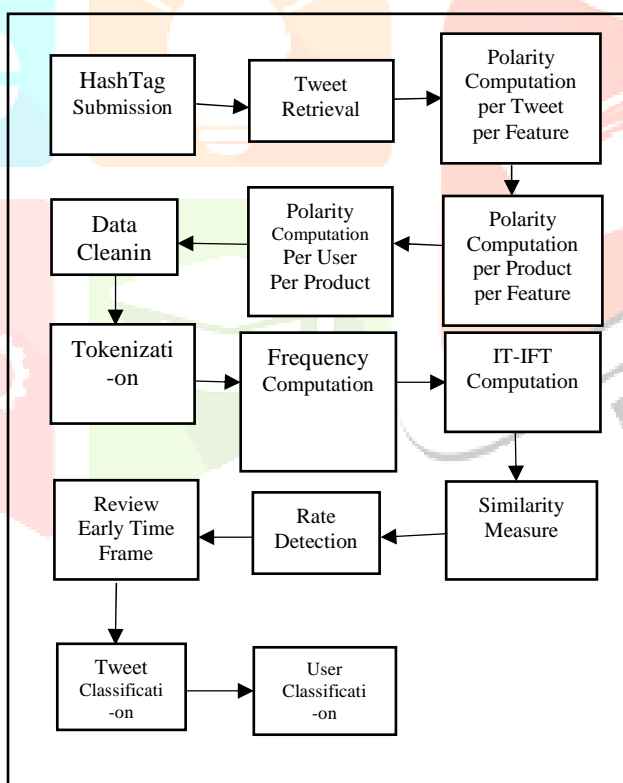


Fig.1: NetSpam Framework

2.1 Data Collection using Twitter

Twitter stores the reviews of the Products in the form of tweets which are associated with Hash Tags. This Module is responsible for Collecting tweets from Twitter by Passing the Hash Tag, APPID and Secret Key. APPID and Secret Key are unique generated IDs by twitter when application is created. Hash tag is a concept under which the users will be able to Tweet.

2.3 Polarity Computation per Tweet per Feature

This module is responsible for computing the sentiments of each tweet per feature. The positive sentiments, negative sentiments and neutral sentiments are found out per feature type. The feature types can be battery, memory, screen, touch and finally for each of the tweet the following matrix is computed.

Table.1: Tweet per feature

| Tweet ID | Product ID | Feature Type | Positive Sentiment | Negative Sentiment | User ID |
|---------------------|---|---|-------------------------------|-------------------------------|------------------------|
| Unique ID for Tweet | Product ID for which tweet has been performed | It can be any feature type like- Battery, Memory, | Positive Sentiments for Tweet | Negative Sentiments for Tweet | Unique ID for the User |

2.4 Polarity Computation per Tweet per Product

Polarity Computation per Tweet per Product is responsible for computation of polarity by computing the summation of polarities across tweets for the given product. Finally, the sentiment matrix can be defined as below

Table.2: Tweet per Product

| Product ID | Feature Type | Positive Sentiment | Negative Sentiment | User ID |
|---|---|-------------------------------|-------------------------------|------------------------|
| Product ID for which tweet has been performed | It can be any feature type like- Battery, Memory, | Positive Sentiments for Tweet | Negative Sentiments for Tweet | Unique ID for the User |

2.5 User Based Sentiments

The set of unique users are found out and then for each of the user the sentiments are added upper product

Table.3: User Based Sentiments

| Product ID | Positive Sentiment | Negative Sentiment | User ID |
|---|-------------------------------|-------------------------------|------------------------|
| Product ID for which tweet has been performed | Positive Sentiments for Tweet | Negative Sentiments for Tweet | Unique ID for the User |

2.6 Data Cleaning

Data Cleaning is used for removing the stop words from each of the tweets and clean them. After the data cleaning process is completed the clean data can be represented as a set CleanId ,CleanData ,UserId. CleanId is the unique Id associated with the Tweet, CleanData is the clean data after removal of clean data and UserId is the unique Id associated with the user.

2.7 Tokenization

The process of converting the statements into a sequence of words is called as tokenization

2.8 Frequency Computation

Frequency computation is a process of removing the repetition of tokens and hence removing the redundancy in the application. It is defined as number of times a token appears in the tweet

2.9 TF-IDF Computation

This is used to compute the inverse document frequency of each of the token and then multiply it by the text frequency.

$$IDF = \log (N/f)$$

Where,

N = number of tweets in which tweet exist

f = frequency of word

The TF-IDF is computed using the following equation

$$TF - IDF = f * IDF$$

2.10 Similarity Measure

Similarity Measure is responsible for finding the unique tokens between the tweets and then finding whether the tweets are similar based on the number of intersections and number of unions. Ratio of intersection sum and union sum will give the similarity measure.

2.11 Rate Deviation

Difference between the reviews of each of the users if certain users have more of such difference those are regarded as spam.

2.12 Early Time Frame Measure

This module takes the tweets and measures the duration in which tweets are performed by the users and if there are any tweets which have been given within certain duration repeatedly negative for a product.

2.13 Classification of Tweet

It measures the weight by computing the similarity between the tweets and then finding the sentiments score and then find the weight. If the weight exceeds the certain threshold the tweet is classified as spam otherwise it is not classified as spam.

2.14 Classification of Spam User

This is responsible for finding whether the user is spam users or not based on user's-based sentiments and the similarity measure of user's-based tweets.

2.15 Metapath Definition and Creation

A metapath is defined by a sequence of relations in the network schema. Table.2 shows all the metapath used in the proposed framework. As shown, the length of user-based metapath is 4 and the length of review based metapath is 2.

For metapath creation, we define an extended version of the metapath concept considering different levels of spam certainty. In particular, two reviews are connected to each other if they share same value. Hassanzadehet *al.* propose a fuzzy-based framework and indicate for spam detection, it is better to use fuzzy logic for determining a review's label as a spam or non-spam. Indeed, there are different levels of spam certainty. We use a step function to determine these levels. In particular, given a review u , the levels of spam certainty for metapath p_l (i.e., feature l) is calculated as $m_u^{p_l} = \frac{\lfloor s \times f(x_{lu}) \rfloor}{s}$, where s denotes the number of levels. After computing $m_u^{p_l}$ for all reviews and metapaths, two reviews u and v with the same metapath values (i.e., $m_u^{p_l} = m_v^{p_l}$) for metapath p_l are connected to each other through that metapath and create one link of review network. The metapath value between them denoted as $mp_{u,v} = mp_{u,l}$.

Using s with a higher value will increase the number of each feature's metapaths and hence fewer reviews would be connected to each other through these features. Conversely, using lower value for s leads us to have bipolar values (which mean reviews take value 0 or 1). Since we need enough spam and non-spam reviews for each step, with fewer numbers of reviews connected to each other for every step, the spam probability of reviews take uniform distribution, but with lower value of s we have enough reviews to calculate final spamicity for each review. Therefore, accuracy for lower levels of s decreases because of the bipolar problem and it decades for higher values of s , because they take uniform distribution. In the proposed framework, we considered $s = 20$, i.e. $m_u^{p_l} \in \{0, 0.05, 0.10, \dots, 0.85, 0.90, 0.95\}$.

Table.4: Features for users and reviews in four defined categories

| Spam Feature | User Based | Review Based |
|---------------------------|--|--|
| Behavioral Based Features | <p><i>Burstiness</i> [20]: Spammers, usually write their spam reviews in short period of time for two reasons: first, because they want to impact readers and other users, and second because they are temporal users, they have to write as much as reviews they can in short time.</p> $x_{BST}(i) = \begin{cases} 0 & (L_i - F_i) \notin (0, \tau) \\ 1 - \frac{L_i - F_i}{\tau} & (L_i - F_i) \in (0, \tau) \end{cases} \quad (1)$ <p>where $L_i - F_i$ describes days between last and first review for $\tau = 28$. Users with calculated value greater than 0.5 take value 1 and others take 0.</p> <p><i>Negative Ratio</i> [20]: Spammers tend to write reviews which defame businesses which are competitor with the ones they have contract with, this can be done with destructive reviews, or with rating those businesses with low scores. Hence, ratio of their scores tends to be low. Users with average rate equal to 2 or 1 take 1 and others take 0.</p> | <p><i>Early Time Frame</i> [16]: Spammers try to write their reviews asap, in order to keep their review in the top reviews which other users visit them sooner.</p> $x_{ETF}(i) = \begin{cases} 0 & (T_i - F_i) \notin (0, \delta) \\ 1 - \frac{T_i - F_i}{\delta} & (T_i - F_i) \in (0, \delta) \end{cases} \quad (2)$ <p>where $L_i - F_i$ denotes days specified written review and first written review for a specific business. We have also $\delta = 7$. Users with calculated value greater than 0.5 takes value 1 and others take 0.</p> <p><i>Rate Deviation using threshold</i> [16]: Spammers, also tend to promote businesses they have contract with, so they rate these businesses with high scores. In result, there is high diversity in their given scores to different businesses which is the reason they have high variance and deviation.</p> $x_{DEV}(i) = \begin{cases} 0 & otherwise \\ 1 - \frac{r_{ij} - avg_{e \in E_{ej}} r(e)}{4} & > \beta_1 \end{cases} \quad (3)$ <p>where β_1 is some threshold determined by recursive minimal entropy partitioning. Reviews are close to each other based on their calculated value, take same values (in $[0,1)$).</p> |
| Linguistic Based Features | <p><i>Average Content Similarity</i> [7], <i>Maximum Content Similarity</i> [16]: Spammers, often write their reviews with same template and they prefer not to waste their time to write an original review. In result, they have similar reviews. Users have close calculated values take same values (in $[0,1)$).</p> | <p><i>Number of first Person Pronouns, Ratio of Exclamation Sentences containing '!'</i> [6]: First, studies show that spammers use second personal pronouns much more than first personal pronouns. In addition, spammers put '!' in their sentences as much as they can to increase impression on users and highlight their reviews among other ones. Reviews are close to each other based on their calculated value, take same values (in $[0,1)$).</p> |

2.16 Classification

The classification part of *NetSpam* includes two steps; (i) *weight calculation* which determines the importance of each spam feature in spotting spam reviews, (ii) *Labeling* which calculates the final probability of each review being spam. Next we describe them in detail.

1) Weight Calculation: This step computes the weight of each metapath. We assume that nodes' classification is done based on their relations to other nodes in the review network; linked nodes may have a high probability of taking the same labels. The relations in a heterogeneous information network not only include the direct link but also the path that can be measured by using the metapath concept. Therefore, we need to utilize the metapaths defined in the previous step, which represent heterogeneous relations among nodes. Moreover, this step will be able to compute the weight of each relation path (i.e., the importance of the metapath), which will be used in the next step (Labeling) to estimate the label of each unlabeled review.

The weights of the metapaths will answer an important question; which metapath (i.e., spam feature) is better at ranking spam reviews? Moreover, the weights help us to understand the formation mechanism of a spam review. In addition, since some of these spam features may incur considerable computational costs (for example, computing linguistic-based features through *NLP* methods in a large review dataset), choosing the more valuable features in the spam detection procedure leads to better performance whenever the computation cost is an issue.

To compute the weight of metapath p_i , for $i = 1, \dots, L$ where L is the number of metapaths, we propose following equation:

$$W_{p_i} = \frac{\sum_{r=1}^n \sum_{s=1}^n mp_{r,s}^{p_i} \times y_r \times y_s}{\sum_{r=1}^n \sum_{s=1}^n mp_{r,s}^{p_i}}$$

where n denotes the number of reviews and $mp_{r,s}^p$ is a metapath value between reviews r and s if there is a path between them through metapath p_i , otherwise $mp_{r,s}^p = 0$. Moreover, $y_r(y_s)$ is 1 if review $r(s)$ is labeled as spam in the pre-labeled reviews, otherwise 0.

2) **Labeling:** Let $Pr_{u,v}$ be the probability of unlabeled review u being spam by considering its relationship with spam review v . To estimate Pr_u , the probability of unlabeled review u being spam, we propose the following equations:

$$Pr_u = \text{avg}(Pr_{u,1}, Pr_{u,2}, \dots, Pr_{u,n})$$

where n denotes number of reviews connected to review u .

It is worth to note that in creating the HIN, as much as the number of links between a review and other reviews increase, its probability to have a label similar to them increase too, because it assumes that a node relation to other nodes show their similarity. In particular, more links between a node and other non-spam reviews, more probability for a review to be non-spam and vice versa. In other words, if a review has lots of links with non-spam reviews, it means that it shares features with other reviews with low spamicity and hence its probability to be a non-spam review increases.

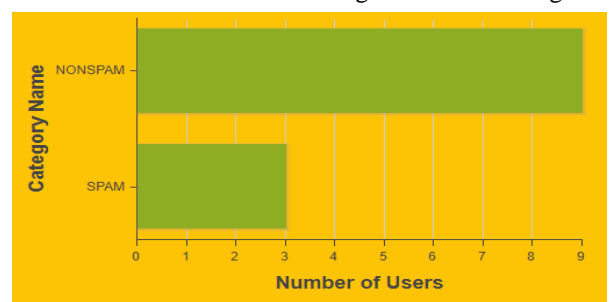
Table.5: Metapaths used in the NetSpam framework

| Row | Notation | Type | MetaPath | Semantic |
|-----|-------------|------|---|---|
| 1 | R-DEV-R | RB | Review-Threshold Rate Deviation-Review | Reviews with same Rate Deviation from average Item rate (based on recursive minimal entropy partitioning) |
| 2 | R-U-NR-U-R | UB | Review-User-Negative Ratio-User-Review | Reviews written by different Users with same Negative Ratio |
| 3 | R-ETF-R | RB | Review-Early Time Frame-Review | Reviews with same released date related to Item |
| 4 | R-U-BST-U-R | UB | Review-User-Burstiness User-Review | Reviews written by different users in same Burst |
| 5 | R-RES-R | RL | Review-Ratio of Exclamation Sentences containing '!'-Review | Reviews with same number of Exclamation Sentences containing '!' |
| 6 | R-PP1-R | RL | Review-first Person Pronouns-Review | Reviews with same number of first Person Pronouns |
| 7 | R-U-ACS-U-R | UL | Review-User-Average Content Similarity-User-Review | Reviews written by different Users with same Average Content Similarity using cosine similarity score |
| 8 | R-U-MCS-U-R | UL | Review-User-Maximum Content Similarity-User-Review | Reviews written by different Users with same Maximum Content Similarity using cosine similarity score |

III. CONCLUSION

This paper introduces a spam detection framework namely *NetSpam* based on a metapath concept as well as a new graph-based method to label reviews relying on a rank-based labeling approach. The performance of the proposed framework is evaluated by using two real-world labeled datasets of Yelp and Amazon websites. The observations shows that calculated weights by using this metapath concept can be very effective in identifying spam reviews and leads to a better performance. In addition, it is found that even without a train set, *NetSpam* can calculate the importance of each feature and it yields better performance in the features' addition process, and performs better than previous works, with only a small number of features. Moreover, after defining four main categories for features our observations show that the reviews behavioral category performs better than other categories, in terms of AP, AUC as well as in the calculated weights. The results also confirm that using different supervisions, similar to the semi-supervised method, have no noticeable effect on determining most of the weighted features, just as in different datasets.

| Tweet ID | Followers Probability | Tweet Probability | Friends Probability | Retweet Probability | Spam Probability | Similarity Probability | Rate Deviation Positive | Rate Deviation Negati | Rate Deviation Neutral |
|----------|-----------------------|-------------------|---------------------|---------------------|------------------|------------------------|-------------------------|-----------------------|------------------------|
| 316 | 0.045976596359 | 0.059426763652 | 0.061077843111 | 0.000429243854 | 0.051257761077 | 0.0982331257824843 | 0.0555555555555558 | 0.0699708454810504 | 0.0833333333333333 |
| 317 | 0.002203120485 | 0.005064485069 | 0.002072775221 | 0 | 0.16988286285 | 0.069636049578272 | 0.1388888888888892 | 0.0699708454810504 | 0.0833333333333333 |
| 318 | 0.052038774920 | 0.184224944472 | 0.032310202072 | 0 | 0.06254283551 | 0.08603406114221 | 0.0555555555555558 | 0.0616256450612243 | 0.0833333333333333 |
| 319 | 0.141798162380 | 0.207806946106 | 0.02379489917 | 0 | 0.09747775163 | 0.08751832384903 | 0.046875 | 0.0634110787172019 | 0.0895833333333333 |
| 320 | 0.007548396417 | 0.005706591245 | 0.063104560110 | 0 | 0.067567048693 | 0.0187688076237814 | 0.1510416666666667 | 0.0634110787172019 | 0.078125 |
| 321 | 0.015963594236 | 0.026589598774 | 0.027959971902 | 0 | 0.058293140048 | 0.1142408632914 | 0.046875 | 0.0634110787172019 | 0.0895833333333333 |
| 322 | 0.00191882065 | 0.000276362461 | 0.004283740211 | 0 | 0.078235530065 | 0.0761377329294819 | 0.0885416666666667 | 0.072157403262332 | 0.0579166666666667 |
| 323 | 0.16487289512 | 0.021635654288 | 0.129295255642 | 0.00008820079 | 0.09747775163 | 0.10987726169883 | 0.09375 | 0.048104952462321 | 0.0579166666666667 |
| 324 | 0.462002020809 | 0.261211643680 | 0.629600146061 | 0 | 0.06672451887 | 0.07559229680349 | 0.1149833333333333 | 0.07404402322616 | 0.0833333333333333 |
| 325 | 0.005092488826 | 0.02719103394 | 0.004291892355 | 0.012886135717 | 0.042470718221 | 0.11120473120075 | 0.0729166666666667 | 0.07404402322616 | 0.0833333333333333 |
| 326 | 0.02020538861 | 0.077318742378 | 0.017887015200 | 0 | 0.162160916883 | 0.0817664978162157 | 0.0520803333333333 | 0.07404402322616 | 0.0833333333333333 |
| 327 | 0.068519459423 | 0.026124262556 | 0.002579496471 | 0 | 0.051257761077 | 0.071903583018975 | 0.0833333333333333 | 0.244897995183676 | 0.0833333333333333 |



REFERENCES

1. S. Mukherjee, S. Dutta, and G. Weikum. Credible Review Detection with Limited Information using Consistency Features, In book: Machine Learning and Knowledge Discovery in Databases, 2016.
2. M. Luca and G. Zervas. Fake It Till You Make It: Reputation, Competition, and Yelp Review Fraud., SSRN Electronic Journal, 2016.
3. A. j. Minnich, N. Chavoshi, A. Mueen, S. Luan, and M. Faloutsos. Trueview: Harnessing the power of multiple review sites. In ACM WWW, 2015.
4. R. Shebuti and L. Akoglu. Collective opinion spam detection: bridging review networks and metadata. In ACM KDD, 2015.
5. Ch. Xu and J. Zhang. Combating product review spam campaigns via multiple heterogeneous pairwise features. In SIAM International Conference on Data Mining, 2014.
6. H. Li, Z. Chen, B. Liu, X. Wei, and J. Shao. Spotting fake reviews via collective PU learning. In ICDM, 2014.
7. B. Viswanath, M. Ahmad Bashir, M. Crovella, S. Guah, K. P. Gummadi, B. Krishnamurthy, and A. Mislove. Towards detecting anomalous user behavior in online social networks. In USENIX, 2014. G. Fei, A. Mukherjee, B. Liu, M. Hsu, M. Castellanos, and R. Ghosh. Exploiting burstiness in reviews for review spammer detection. In ICWSM, 2013.
8. L. Akoglu, R. Chandy, and C. Faloutsos. Opinion fraud detection in online reviews by network effects. In ICWSM, 2013.
9. A. Mukerjee, V. Venkataraman, B. Liu, and N. Glance. What Yelp Fake Review Filter Might Be Doing?, In ICWSM, 2013.
10. A. Mukherjee, A. Kumar, B. Liu, J. Wang, M. Hsu, M. Castellanos, and R. Ghosh. Spotting opinion spammers using behavioral footprints. In ACM KDD, 2013.
11. M. Ott, C. Cardie, and J. T. Hancock. Estimating the prevalence of deception in online review communities. In ACM WWW, 2012.
12. S. Feng, R. Banerjee and Y. Choi. Syntactic stylometry for deception detection. Proceedings of the 50th Annual Meeting of the Association for Computational Linguistics: Short Papers; ACL, 2012.
13. N. Jindal, B. Liu, and E.-P. Lim. Finding unusual review patterns using unexpected rules. In ACM CIKM, 2012.
14. S. Xie, G. Wang, S. Lin, and P. S. Yu. Review spam detection via temporal pattern discovery. In ACM KDD, 2012.
15. Y. Sun and J. Han. Mining Heterogeneous Information Networks; Principles and Methodologies, In ICCCE, 2012.
16. S. Feng, L. Xing, A. Gogar, and Y. Choi. Distributional footprints of deceptive product reviews. In ICWSM, 2012.
17. M. Ott, Y. Choi, C. Cardie, and J. T. Hancock. Finding deceptive opinion spam by any stretch of the imagination. In ACL, 2011.
18. G. Wang, S. Xie, B. Liu, and P. S. Yu. Review graph based online store review spammer detection, IEEE ICDM, 2011.
19. F. Li, M. Huang, Y. Yang, and X. Zhu. Learning to identify review spam. Proceedings of the 22nd International Joint Conference on Artificial Intelligence; IJCAI, 2011.
20. Y. Sun, J. Han, X. Yan, P. S. Yu, and T. Wu. Pathsim: Meta path-based top-k similarity search in heterogeneous information networks. In VLDB, 2011.
21. E.-P. Lim, V.-A. Nguyen, N. Jindal, B. Liu, and H. W. Lauw. Detecting product review spammers using rating behaviors. In ACM CIKM, 2010.

Vehicle Detection in Fog and Night Condition using Block Matching and Color Enhancement Algorithm

Nivedha M, Pallavi R, Supriya S, Sushma R
Final year B.E Students(UG)

Guided by: Mrs. R Suganya, Assistant Professor Department of ISE, TOCE
The Oxford College of Engineering, Bengaluru, India

Abstract: Fog is a big reason for road accidents. Images which are captured under bad weather conditions suffer low contrast so as their quality also degrade with the changes in atmosphere. The main reason behind this problem is that, the light capture by the lens is spread by the atmosphere. Fog reduces visibility to less than 1 kilometre. This paper aims to resolve the sight problem faced by car/other automobile drivers when driving in foggy weather condition and at night. For improving the visibility level of an image and reducing fog, various image enhancement methods are used. For improving the visibility level five major steps are used. First step is acquisition process of foggy / dark images. Second is estimation process. Third is enhancement process (improve visibility level, reduce fog). Next process is restoration process (restore enhanced image) while the final is the vehicle detection. The main aim of the paper is to review image enhancement and restoration methods for improving the quality and visibility level of an image which provide clear image in bad weather condition.

Index Terms—restoration process, foggy, estimation process, image enhancement, automatic braking.

1. INTRODUCTION

The images of outdoor scenes are usually degraded by the turbid medium (e.g., particles and water droplets) in the atmosphere. Haze, fog and smoke are such phenomena due to atmospheric absorption and scattering. Light from the atmosphere and light reflected from an object are scattered by the water droplets, resulting the visibility of the scene to be degraded. The two fundamental phenomena that are consequence of scattering are 'attenuation' and 'airlight'. Fog removal is a difficult task because fog depends on the unknown scene depth map information. Fog effect is the result of distance between camera and object. Hence removal of fog requires the estimation of airlight map or depth map.

The current fog removal method can be divided into two categories:

- (a) Image enhancement and
- (b) Image restoration.

Image processing is a method to perform some operations on an image, in order to get an enhanced image or to extract some useful information from it. It is a type of signal processing in which input is an image and output may be image or characteristics/features associated with that image. Nowadays, image processing is among rapidly growing technologies. It forms core research area within engineering and computer science disciplines too.

Image processing basically includes the following three steps:

- Importing the image via image acquisition tools.
- Analysing and manipulating the image.
- Output in which result can be altered image or report that is based on image analysis.

There are two types of methods used for image processing namely, analogue and digital image processing. Analogue image processing can be used for the hard copies like printouts and photographs. Image analysts use various fundamentals of interpretation while using these visual techniques. Digital image processing techniques help in manipulation of the digital images by using computers. The three general phases that all types of data have to undergo while using digital technique are pre-processing, enhancement, and display, information extraction. Improving the performance of vehicle-detection in different weather conditions becomes an important issue in vehicle-detection system because in the case of fine weather, the system would achieve good performance but however when it comes to bad weather like foggy environment and night condition the performance of many systems are not appreciable. The proposed method provides image enhancement and fog removal. Because of scarceness of data that are available in the foggy image, quality of image lower. Hence it is very much essential to make the image appropriate to human sight distinctive. Firstly we have to retain true color and striking differences of foggy image and retain the original image to obtain a clear image. Due to the lack of illumination at night, light will be from either other vehicles or from any light providing sources. So the brightness of image will be indistinct and contrast will be

literally less, most of the information are not perceivable by human eye. Images color will be the color of the light providing or light causing devices. Image's original color will be misrepresented. So it is very much necessary to enhance the image's characteristics to make better the execution of vehicle detection. In proposed system we make use of kalman filter for vehicle detection. Block matching algorithm is used for breaking images into fine blocks according to the type of image.

2. LITERATURE REVIEW

As Sensors are sensitive to weather conditions; video cameras could be used to record the traffic information at different weather conditions. We have sophisticated algorithms to analyze the traffic videos in real time and discover information of interest. Although some sensors could be more accurate, they could also be Intrusive and need a higher maintenance cost. We may need to embed weighing sensors in road to measure vehicle feature and classify vehicle size. In video surveillance systems, it is very complicated to extract more number of features from a video. It has been also inferred that more computations are required to calculate background model and to extract the key frames. In this paper, a novel algorithm is implemented which counts and classifies highway vehicles using regression. The algorithm proposed in this paper, starts with preprocessing the Low Quality videos by Removal of Noise using Bi-lateral filtering, followed by color image based Background mask generation using Multi-layer Background subtraction technique[1]. A fast performing kernel is designed which then used to extract the Foreground mask using Mixture of Gaussians. Finally Contour extraction and Cascaded Regression will results the foreground moving objects in the Low quality video.

A vehicle detection and counting system plays an important role in an intelligent transportation system, especially for traffic management. This paper proposes a video-based method for vehicle detection and counting system based on computer vision technology. The proposed method uses background subtraction technique[2] to find foreground objects in a video sequence. In order to detect moving vehicles more accurately, several computer vision techniques, including thresholding, hole filling and adaptive morphology operations, are then applied. Finally, vehicle counting is done by using a virtual detection zone. Experimental results show that the accuracy of the proposed vehicle counting system is around 96%.

Intelligent transportation systems have received a lot of attention in the last decades. Vehicle detection is the key task in this area and vehicle counting and classification are two important applications. In this study, the authors proposed a vehicle detection method which selects vehicles using an active basis model and verifies them according to their reflection symmetry. Then, they count and classify them by extracting two features: vehicle length in the corresponding time-spatial image and the correlation computed from the grey-level co-occurrence matrix of the vehicle image within its bounding box. A random forest is trained to classify vehicles into three categories: small (e.g. car), medium (e.g. van) and large (e.g. bus and truck). The proposed method is evaluated using a dataset including seven video streams which contain common highway challenges such as different lighting conditions, various weather conditions, camera vibration and image blurring[3]. Experimental results show the good performance of the proposed method and its efficiency for use in traffic monitoring systems during the day (in the presence of shadows), night and all seasons of the year.

Estimating the number of vehicles present in traffic video sequences is a common task in applications such as active traffic management and automated route planning. There exist several vehicle counting methods such as Particle Filtering or Headlight Detection, among others. Although Principal Component Pursuit (PCP) is considered to be the state-of-the-art for video background modeling, it has not been previously exploited for this task. This is mainly because most of the existing PCP algorithms are batch methods and have a high computational cost that makes them unsuitable for real-time vehicle counting. In this paper, we propose to use a novel incremental PCP-based algorithm[4] to estimate the number of vehicles present in top-view traffic video sequences in real-time. We test our method against several challenging datasets, achieving results that compare favorably with state-of-the-art methods in performance and speed: an average accuracy of 98% when counting vehicles passing through a virtual door, 91% when estimating the total number of vehicles present in the scene, and up to 26 fps in processing time.

Vehicle detection has been applied in many fields, such as intelligent transportation, video surveillance, driving assistance system and so on. In the case of fine weather, the state-of-the-art vehicle-detection systems may achieve good performance. However, the performance has a substantial decline in bad weathers, such as fog, night and so on. Therefore, improving the performance of vehicle-detection systems in different weather conditions becomes an important issue in vehicle-detection system[5]. In the fog or night, the quality of the images is reduced. In this paper, we propose some algorithms of image defogging and color enhancement in order to improve the performance of vehicle detection. The result of vehicle detection get much better after image processing in bad weathers.

3. METHODOLOGY

A. IMAGE ACQUISITION MODULE:

The program performs pre-processing of the image.

Step 1: Loading Image

Internal storage consists of number of images such as night, fog and normal images loaded from different sources. Few of these images from the internal storage are sent to the database.

Step 2: Extract RGB Component

Here the extraction of red, green, blue channels of a color image is been done.

1. Obtain the Red color plane of the image and display the red index of the image.
2. Obtain the Green color plane of the image and display the green index of the image.
3. Obtain the Blue color plane of the image and display the blue index of the image.

B. FEATURE EXTRACTION MODULE:

Features like mean and amount of white pixels in the image is extracted which helps in classification of images.

The program performs feature extraction of the image to identify if image is too foggy or less.

If the input image is colored, it should be converted to grey scale to perform computation on the grey scale image. The original version of the operator labels the image pixels by thresholding the 3×3 neighborhood of each pixel with the center value and summing the thresholded values. For this module input is gray scale image and output is features of the image.

• BLOCK MATCHING ALGORITHM

Step1: A block matching algorithm involves dividing the current frame of a video into macroblocks and comparing each of the macroblocks with a corresponding block and its adjacent neighbors in a nearby frame of the video (sometimes just the previous one).

Step2: A vector is created that models the movement of a macroblock from one location to another. This movement, calculated for all the macroblocks comprising a frame, constitutes the motion estimated in a frame.

Step3: The search area for a good macroblock match is decided by the 'search parameter', p , where p is the number of pixels on all four sides of the corresponding macro-block in the previous frame. The search parameter is a measure of motion. The larger the value of p , larger is the potential motion and the possibility for finding a good match. A full search of all potential blocks however is a computationally expensive task. Typical inputs are a macroblock of size 16 pixels and a search area of $p = 7$ pixels.

C. MACHINE LEARNING:

This module accepts the test image as input and matches it to one of the classes present in the training dataset, based on the feature values extracted from the input image. It classifies each row in test and returns the predicted class level group. Test must have the same number of columns as the data used to train the classifier in neural network, label sec indicates the group to which each row of test is assigned. Based on that the result is assigned to test variable. For this module, input the test image and trained dataset features and output is category of input image.

D. DENOISING MODULE:

Input will be gray scale or color image. The program performs feature denoising of the image so as to convert foggy image into better visibility. Output will be defogged image.

E. IMAGE ENHANCEMENT MODULE:

The image qualities of captured outdoor scenes are usually degraded due to bad weather such as fog, haze, smog, cloud and rain. Bad weather reduces visibility and contrast of the scene. The program performs image enhancement for better visibility. Input is gray scale or color image and output is enhanced image.

IMAGE ENHANCEMENT ALGORITHM

Algorithm 1 Adaptive Low-light Image Enhancement

Input: A low-light image I .

Output: An enhanced image E .

- 1: Apply superpixel segmentation on I , calculate α_{p_i} by Eq (1);
 - 2: Reverse the image I to get the image R ;
 - 3: Apply BM3D filter on R in two scales to get $b^{fine}(R)$ and $b^{coarse}(R)$, then combine them as Eq (3) to get the base layer $b(R)$;
 - 4: Apply first order differential on R to generate the noised detail layer $d_0(R)$;
 - 5: Using the structural filter to smooth $d_0(R)$ to generate the noise-free detail layer $d(R)$;
 - 6: Adaptively combine the noise-free detail layer $d(R)$ and the base layer $b(R)$ to obtain R' according the parameter α by Eq (2);
 - 7: Estimate the global atmosphere light A using R' ;
 - 8: Calculate the enhancement parameter $\omega(x)$ for each pixel as Eq (6);
 - 9: Estimate the transmission parameter $t(x)$ as Eq (5);
 - 10: Update $t(x)$ by using $P(x)t(x)$;
 - 11: Generate the dehazed image J by Eq (9) using R' ;
 - 12: Generate the final output E by reverse image J .
 - 13: **return** E ;
-

We firstly utilize the superpixel method to split the low-light image I into patches. For each patch we use the following method to determine the smoothing degree, assuming the noise is additive white Gaussian noise (AWGN). We use σ_{p_i} to denote the standard deviation and g_{p_i} to denote the local gradients of a superpixel p_i . Experimental observations show that the g_{p_i} in the flat patch increases greatly when AWGN is added into a clear image. Whereas, the g_{p_i} does not change a lot in the textural patch. On the other

hand, for the normalized image in the range [0, 1], the patch standard deviation σ_{p_i} varies in an order of magnitude. So we consider the normalized ratio α_{p_i} between σ_{p_i} and g_{p_i} to measure the patch noise-texture level as follows,

$$\alpha_{p_i} = \frac{\sigma_{p_i}}{g_{p_i}} \quad (1)$$

Based on the measurement of noise-texture level of each patch, we can adaptively apply our denoising algorithm. To facilitate denoising and utilize the dark channel prior dehazing algorithm for contrast enhancement, we invert the input image I using $R = 255 - I$. Enlightened by the unsharp masking filter, we define the denoised R as R_0 , and R_0 is obtained by the weighted combination of the base layer and the denoised detail layer of R .

$$R' = \alpha \cdot d(R) + b(R), \quad (2)$$

where $d(R)$ and $b(R)$ denote the noise-free detail layer and the base layer of R respectively. For a patch with small α , we add few details to constrain the noise degree. While, for a patch with large α , we add more details to the base layer. One good technique to get the base layer of an image is to smooth it using the BM3D filter, which can effectively attenuate AWGN. We utilize the noise-texture level coefficient α as a weight in generating the base layer.

$$b(R) = \alpha \cdot b^{fine}(R) + (1 - \alpha) \cdot b^{coarse}(R), \quad (3)$$

where $b^{fine}(R)$ and $b^{coarse}(R)$ respectively denote the smoothed result of the BM3D filter using a parameter half smaller and twice greater than the mean of the local standard deviation σ_{p_i} of the observed image I . To obtain the detail layer $d_0(R)$, we simply calculate the first order differential of the inverted image R . We find that the random noise tends to fuse with texture in the detail layer $d_0(R)$. So it is necessary to choose an appropriate algorithm to smooth the detail layer, while retaining useful texture we apply the structure smooth to the detail layer $d_0(R)$ to obtain a smooth and texture preserved result $d(R)$. Finally, we adaptively add the smoothed detail layer $d(R)$ back to the base layer $b(R)$ to get a noise-free and texture preserved image R_0 , as Equation (2).

Since the noise-free image R_0 is similar to the hazy image, we utilize efficient haze removal method to enhance its contrast. The algorithm is based on,

$$R' = t \cdot J + (1 - t) \cdot A, \quad (4)$$

where A is the global atmospheric light. J is the intensity of the original objects or scene without hazy depravation. t describes the percent of the light emitted from the objects or scene that reaches the camera. t is estimated using,

$$t(x) = 1 - \omega \cdot \min_{c \in \{r, g, b\}} \left(\min_{y \in \Omega(x)} \left(\frac{R'^c(y)}{A^c} \right) \right), \quad (5)$$

where $\Omega(x)$ is a local block centered at pixel x and the block size is 3×3 . ω is a weight coefficient, which is 0.8, to control the enhance degree.

$$\omega(x) = (1 - 10^{-\sqrt{\frac{\sum_{c \in \{r, g, b\}} (255 - I(x))^c}{3}}})^2, \quad (6)$$

where I is the intensity of the input low-light image, and c denotes the color channels. By applying the Equation (6), the weight coefficient ω is reduced when the pixel x is bright, and increased when the pixel x is dark. This adaptive adjustment can efficiently alleviate over-enhancement and under enhancement. We utilize the following process to estimate global atmosphere light A . To avoid the negative influence of random texture, we first smooth the R_0 with a 5×5 average filter, then we select the pixels whose minimum intensities in all color (RGB) channels are the 2% highest of all the pixels in the image. Among these pixels, we choose the pixel whose sum of RGB values is the highest. The RGB values of this selected pixel are used to represent the RGB values of the atmosphere A . Thus, according to Equation (4), we can recover the J by,

$$J = \frac{R' - A}{t} + A. \quad (7)$$

However, direct using of Equation (7) might lead to underenhancement for dark areas. To further optimize t , we introduce a multiplier P into Equation (7), and through extensive experiments, we find that P can be set as,

$$P = \begin{cases} 2t, & 0 < t < 0.5 \\ 1, & 0.5 < t < 1 \end{cases} \quad (8)$$

then the recovery equation becomes,

$$J = \frac{R' - A}{t \cdot P} + A. \quad (9)$$

F. VEHICLE DETECTION MODULE:

The program performs vehicle detection . For this module, we input a video and image is detected as output.

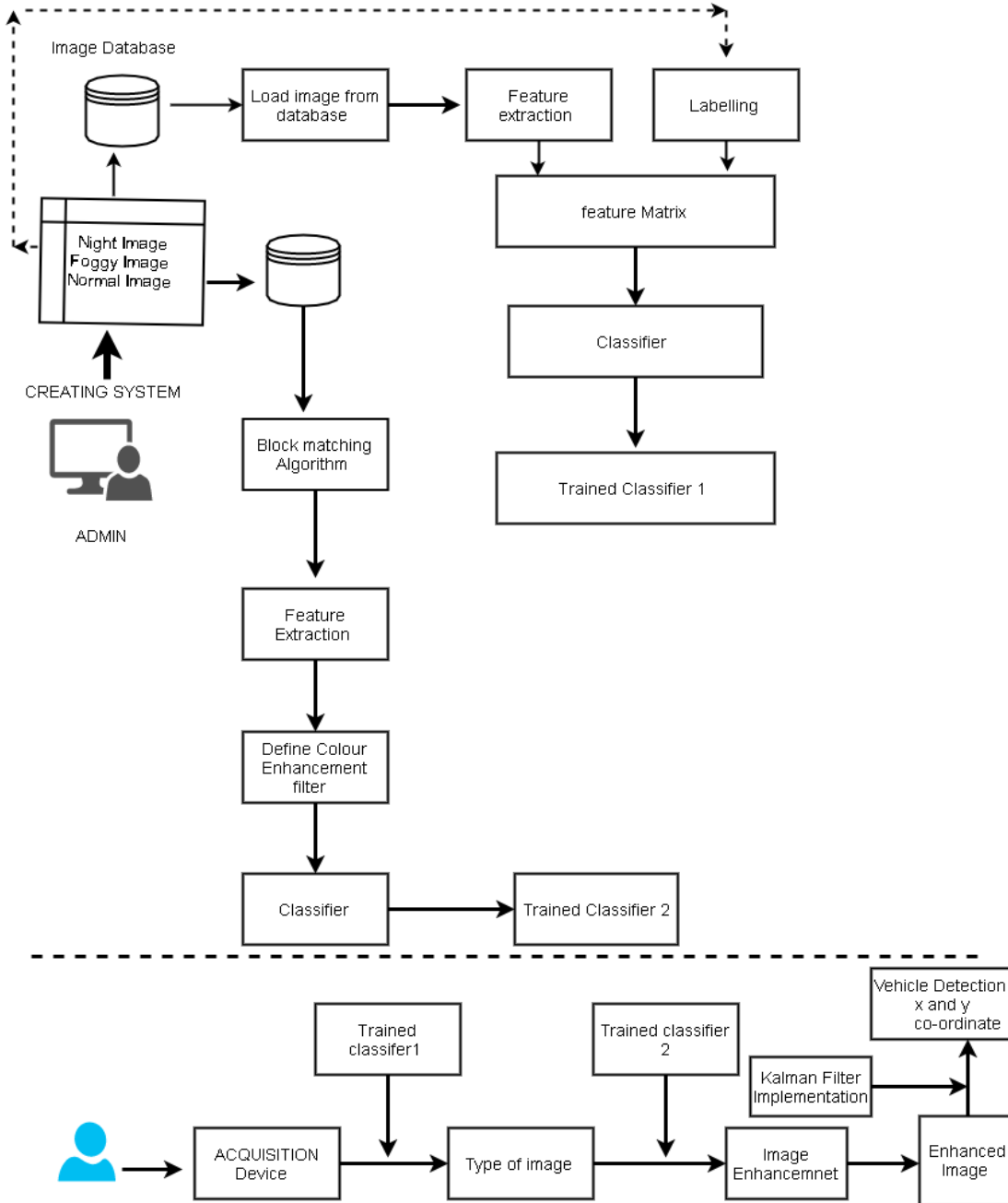


Figure 1: Architecture diagram of vehicle detection

EXPERIMENTAL RESULTS

The figure shown below gives the step by step operational output for our proposed system.

Defogging: The figure 2(a) and 2(b) demonstrates fog removal using the defog function. the picture on the left is taken on a foggy day with the defog function off. the picture on the right is the same scene taken with the defog function on. both pictures were captured with a camera. the defog feature adjusts contrast, color, and sharpness.



Figure 2(a): defogged image1



Figure 2(b): defogged image2

Color Enhancement: The purpose of color enhancement is to get finer details of an image and highlight the useful information. During the poor illumination condition the image appear darker or with lower contrast such image needs to be enhanced. Examples are shown below in figure 3(a) and 3(b).



Figure 3(a): color enhancement image1



Figure 3(b): color enhancement image2

Vehicle Detection: The detection of moving objects regions of change in the same image sequence which captured at different intervals, which also includes moving or motion vehicle detection and segmentation approach.

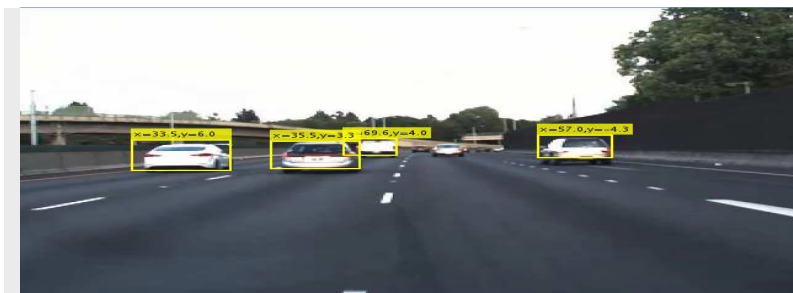


Figure 4: Vehicle detection

CONCLUSION

In the proposed system we choose algorithms for defogging the image, color enhancement prior to vehicle detection. The algorithm used for defogging will make the image's quality better. Color enhancement algorithm allows to increase visibility nature of scene.. This makes the image more appropriate to human sight. The proposed system can enhance the performance of vehicle detection and vehicle visibility in bad weathers.

FUTURE WORK

The system proposes a method which is able to detect vehicle but in future scope the vehicle braking system could be employed so as to provide a better ADAS (advanced driver-assistance system) system which is capable of not only detecting the vehicle but also providing braking assistance. The system can also be integrated with hardware model such that a real time model can be demonstrated with the existing algorithm.

REFERENCES

- [1] B. G. Rajagopal, N. Vishakraj, N. U. Kumar and P. Jothivenkatesh, " Vision-based system for counting of moving vehicles in different weather conditions," 2017 International conference of Electronics, Communication and Aerospace Technology (ICECA), Coimbatore, 2017,pp.86-91.doi: 10.1109/ICECA.2017.8203649.
- [2] Ohnishi, "A computer vision based vehicle detection and counting system," 2016 8th International Conference on Knowledge and Smart Technology (KST), Chiangmai, 2016, pp.224-227.doi: 10.1109/KST.2016.7440510.
- [3] S. Kamkar and R. Safabakhsh, "Vehicle detection, counting and classification in various conditions," in IET Intelligent Transport Systems, vol. 10, no. 6, pp. 406-413,82016. doi: 10.1049/iet-its.2015.0157.
- [4] J. Quesada and P. Rodriguez, "Automatic vehicle counting method based on principal component pursuit background modeling," 2016 IEEE International Conference on Image Processing(ICIP),Phoenix,AZ,2016,pp.3822-3826.doi: 10.1109/ICIP.2016.7533075.
- [5] Xuerui Dai, Xue Yuan, Jing Zhang, Liping Zhang, "Improving the performance of vehicle detection system in bad weathers," 2016 IEEE.
- [6] Kamkar, S., Safabakhsh, R.: 'Vehicle detection, counting and classification in various conditions', IET Intell. Transp. Syst., 2016, 10, (6), pp. 406–413.
- [7] G. N. Swamy and S. Srilekha, "Vehicle detection and counting based on color space model," 2015 International Conference on Communication.
- [8] P. Valiere, L. Khoudour, A. Crouzil and D. N. T. Cong, "Robust vehicle counting with severe shadows and occlusions," 2015 International Conference on Image Processing Theory, Tools and Applications (IPTA), Orleans, 2015, pp. 99-104.unications and Signal Processing(ICCSP),Melmaruvathur,2015,pp.0447-0450.doi: 10.1109/ICCSP.2015.7322928.
- [9] Liu, Y., Tian, B., Chen, S., et al.: 'A survey of vision-based vehicle detection and tracking techniques in ITS'. IEEE Int. Conf. Vehicular Electronics and Safety (ICVES), Dongguan, China, July 2013, pp. 72–77.
- [10] Li, Y., Wang, F.Y., Li, B., et al.: 'A multi-scale model integrating multiple features for vehicle detection'. Int. IEEE Conf. Intelligent Transportation Systems (ITSC), The Hague, The Netherlands, May 2013, pp. 399–403.
- [11] Held, D., Levinson, J., Thrun, S.: 'A probabilistic framework for car detection in images using context and scale'. IEEE Int. Conf. Robotics and Automation (ICRA), Saint Paul, USA, June 2012, pp. 1628–1634.
- [12]Wu, K., Xu, T., Zhang, H.: 'Overview of video-based vehicle detection technologies'. 6th Int. Conf. Computer Science & Education (ICCSE), Singapore, Singapore, August 2011, pp. 821–825.
- [13] Atiq, H.M., Farooq, U., Ibrahim, R., et al.: 'Vehicle detection and shape recognition using optical sensors: a review'. Second Int. Conf. Machine Learning and Computing (ICMLC), Bangalore, India, February 2010, pp. 223–227.
- [14] Tsai, L.W., Hsieh, J.W., Fan, K.C.: 'Vehicle detection using normalized color and edge map', IEEE Trans. Image Process., 2007, 16, (3), pp. 850–864.
- [15] Jia, Y., Zhang, C.: 'Front-view vehicle detection by Markov chain Monte Carlo method', Pattern Recognit., 2009, 42, (3), pp. 313–321.

GENERATING MUSIC FROM LITERATURE USING TOPIC EXTRACTION AND SENTIMENT ANALYSIS

¹ Aafia Nausheen, ² Abhilasha Yadav, ³ Ashley Thomas, ⁴ Gayathri M

Under the guidance of Mrs. Varsha Nilugal, Assistant professor,
Department of Information Science and Engineering, The Oxford College of Engineering,
Bangalore, Karnataka, India.

Abstract: This study presents Tambr, a new software for translating literature into audio using Topic Extraction and Sentiment Analysis for the way in which their timbre relates to the meaning and sentiment of the topics conveyed in the story. The durations, intervals and pitches of the output audio are generated using sentiment analysis which corresponds to sentiment of the text. Natural language processing algorithms are used for topic extraction in the text. Sentiment analysis is used to vary the intensity of the audio. The sounds generated by the system are very characteristics of ambiance music, as the emphasis was placed on selecting musical timbres that match with the themes of the text.

Index Terms - Topic Extraction, Sentiment Analysis, Natural Language Processing, Text Summary, Tambr.

I. INTRODUCTION

Musical timbre is one of the most defining characteristics of how a piece of music sounds. Timbre refers to the character and quality of a sound, as opposed to the pitch or loudness. A saxophone and an electric guitar, for example, could play the same notes, but would still be distinguishable as different instruments; that difference is in their timbre. Because of the large number of features that define the timbre of a sound, be it from an acoustic musical instrument or a computer generated synthesizer, academic discussion of timbre is often limited.

TransProse is an existing software that automatically generates musical pieces from text. TransProse uses known relations between elements of music such as tempo and scale, and the emotions they evoke.

Further, it uses a novel mechanism to determine sequences of notes that capture the emotional activity in text. Transpose focuses on novels and generate music that captures the change in the distribution of emotion words.

Although, TransProse has several advantages, there are certain challenges that it faces such as generating sequences of notes, given the infinite possibilities of pitch, duration, and order of the notes. Computational approaches to analyzing timbre are still in their early stages and are often limited. It also lacks intentional harmony and discord between the melodies. It is unable to evaluate the impact of textual features such as the length of the novel and the style of writing on the generated music.

Tambr is a new software that we are proposing for translating literature into sound using multiple synthesized voices selected for the way in which their timbre relates to the meaning and sentiment of the topics conveyed in the story. It uses sentiment analysis to generate the pitches, durations, and intervals of the output audio in a way corresponding to the sentiment of the novel. It also uses natural language processing algorithms to extract the topics in the novel. It varies the intensity of notes based on sentiment analysis. It takes musical timbre into account when selecting voices.

There are several applications of the proposed software which include helping People with learning disabilities. Some people have difficulty reading large amounts of text due to dyslexia and other learning disabilities. Translating text into audio on the basis of sentiment helps. Supporting people who have literacy difficulties. Some people have basic literary levels. By offering them an option to hear the text instead of reading it, they can get valuable information in a way that is more comfortable for them. Aiding people who speak the language but do not read it - Many people who come to a new country learn to speak and understand the native language effectively, but may still have difficulty reading in a second language. This allows them to take in the information in a way they are more comfortable with, making your content easier to comprehend and retain. Assisting people who multitask. A busy life often means that people do not have time to do all the reading they would like to do online. Having a chance to listen to the content instead of reading it allows them to do something else at the same time. It benefits people with visual impairment. Text to speech can be a very useful tool for the mild or moderately visually impaired. Even for people with the visual capability to read, the process can often cause too much strain to be of any use or enjoyment. With text to speech, people with visual impairment can take in all manner of content in comfort instead of strain. Guiding people with different learning styles. Some people are auditory learners, some are visual learners, and some are kinesthetic learners – most learn best through a combination of the three. This system helps people to read with better understanding of the pronunciation of words. These are some of the main applications of the proposed system. It is very helpful for millions of people in their day-to-day lives. This system is useful for children as well as adults. There are several other applications but only a few have been listed in this article.

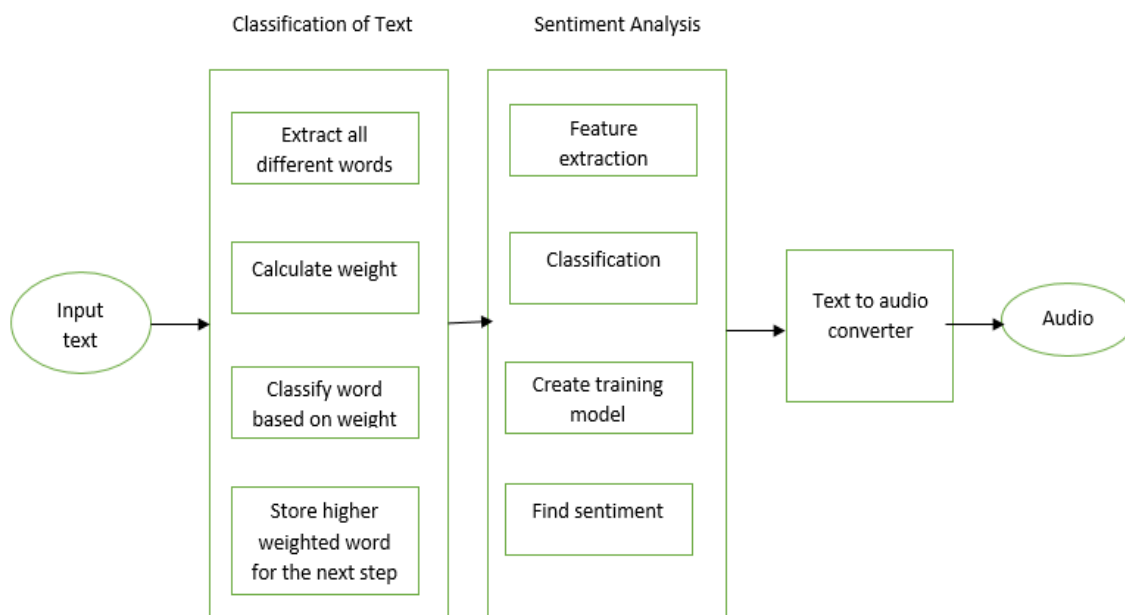


Figure 1: Proposed System Architecture

1.1 Text Summarization

Text summarization is the problem of creating a short, accurate, and fluent summary of a longer text document. Automatic text summarization methods are greatly needed to address the ever-growing amount of text data available online to both better help discover relevant information and to consume relevant information faster. There is an enormous amount of textual material, and it is only growing every single day. Think of the internet, comprised of web pages, news articles, status updates, blogs and so much more. The data is unstructured and the best that we can do to navigate it is to use search and skim the results. There is a great need to reduce much of this text data to shorter, focused summaries that capture the salient details, both so we can navigate it more effectively as well as check whether the larger documents contain the information that we are looking for. Automatic text summarization, or just text summarization, is the process of creating a short and coherent version of a longer document. There are two main approaches to summarizing text documents. They are extractive methods and abstractive methods. They are explained further in detail.

1.1.1 Extractive Methods

Extractive text summarization involves the selection of phrases and sentences from the source document to make up the new summary. Techniques involve ranking the relevance of phrases in order to choose only those most relevant to the meaning of the source.

1.1.2 Abstractive Methods

Abstractive text summarization involves generating entirely new phrases and sentences to capture the meaning of the source document. This is a more challenging approach but is also the approach ultimately used by humans. Classical methods operate by selecting and compressing content from the source document.

1.2 Sentiment Analysis

Natural language processing is only half the battle though. Human communication isn't just words and their explicit meanings. Human communication is nuanced and complex. You can tell based on the way a friend asks you a question whether they're bored, angry, or curious. Sentiment is like a combination of tone of voice, word choice, and writing style all rolled into one. As shown in Fig.2, the input to natural language processing will be a simple stream of Unicode characters (typically UTF-8). Basic processing will be required to convert this character stream into a sequence of lexical items (words, phrases, and syntactic markers) which can then be used to better understand the content. The basics include: Structure extraction – identifying fields and blocks of content processing and understanding. Tokens can be words, numbers, identifiers or punctuation (depending on the use case). Lemmatization / Stemming which reduces word variations to simpler forms that may help increase the coverage of NLP utilities. Lemmatization is strongly preferred to stemming if available. Search Technologies has lemmatization for English and our partner, Basis Technologies, has lemmatization for 60 languages. Decompounding for some languages (typically Germanic, Scandinavian, and Cyrillic languages), compound words will need to be split into smaller parts to allow for accurate NLP. Entity extraction for identifying and extracting entities (people, places, companies, etc.) is a necessary step to simplify downstream processing. There are several different methods: regex extraction, dictionary extraction, complex pattern-based extraction and

statistical extraction. Phrase extraction which extracts sequences of tokens (phrases) that have a strong meaning which is independent of the words when treated separately. These sequences should be treated as a single unit when doing NLP. For example, “Big Data” has a strong meaning which is independent of the words “big” and “data” when used separately. All companies have these sorts of phrases which are in common usage throughout the organization and are better treated as a unit rather than separately. Techniques to extract phrases include: part of speech tagging, statistical phrase extraction and hybrid. Based on tagging, Identify and mark sentence, phrase, and paragraph boundaries. These markers are important when doing entity extraction and NLP since they serve as useful breaks within which analysis occurs. Language identification will detect the human language for the entire document and for each paragraph or sentence. Language detectors are critical to determine what linguistic algorithms and dictionaries to apply to the text. Tokenization in order to divide up character streams into tokens which can be used further.

1.3 Decide on Macro versus Micro Understanding

Before you begin, you should decide what level of content understanding is required:

1.3.1 Macro Understanding provides a general understanding of the document as a whole. It is typically performed with statistical techniques which are used for: clustering, categorization, similarity, topic analysis, word clouds, and summarization.

1.3.2 Micro Understanding extracts understanding from individual phrases or sentences. It is typically performed with NLP a technique which are used for: extracting facts, entities (see above), entity relationships, actions, and metadata fields.

1.4 Macro Understanding

Once you have decided to embark on your NLP project, if you need a more holistic understanding of the document this is a “macro understanding.” This is useful for: classifying / categorizing / organizing records, clustering records, extracting topics, general sentiment analysis, record similarity, including finding similarities between different types of records (for example, job descriptions to résumés / CVs), keyword / key phrase extraction, duplicate and near-duplicate detection, summarization / key sentence extraction and semantic search.

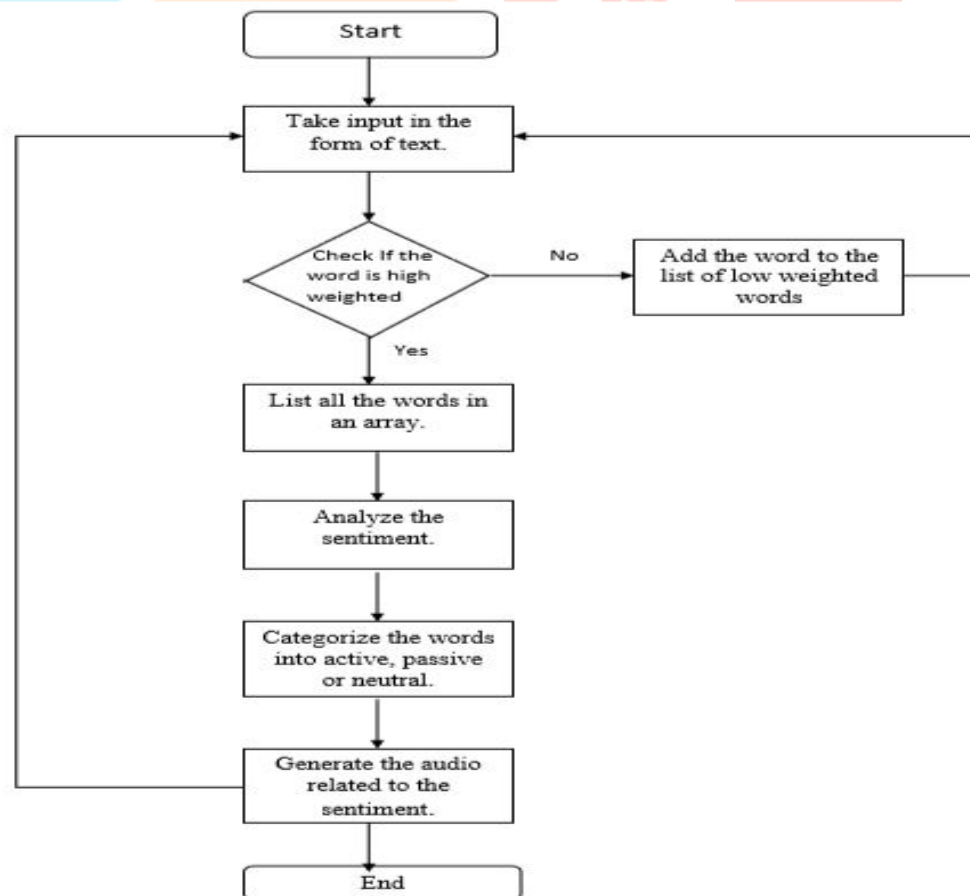


Figure 2: Flow Chart

II. ALGORITHM

1. Take the full CONTENT and split it into PARAGRAPHS.
2. Split each paragraph into SENTENCES.
3. Compare every sentence with every other. This is done by Counting the number of common words and then Normalize this by dividing by average number of words per sentence
4. These intermediate scores/values are stored in an INTERSECTION matrix
5. Create the key-value dictionary
 - Key: Sentence
 - Value: Sum of intersection values with this sentence
6. From every paragraph, extract the sentences with the highest score.
7. Sort the selected sentences in order of appearance in the original text to preserve content and meaning.

III. CONCLUSION

The software will transform each paragraph of the text providing a weight of how relevant each word is to a given paragraph based on the number of other paragraphs in which it appears. It generates a list of topics, where each topic is a set of, at most, ten terms that define the topic. It interprets the sequence of sentiment scores for each sentence as a series of signals generated by the sentiment analysis module corresponding a sensible way with the plot structure that a reader can verify in the text. This system will generate audio that is related to the characteristic ambiance of the text. It provides intentional harmony and discord between the audio.

IV. ACKNOWLEDGEMENT

We would like to specially thank Mrs.VarshaNilugal, Assistant Professor, Department of Information Science, The Oxford College of Engineering, for her advice, contribution and encouragement throughout this project. We would also like to thank Dr. D Jayaramiah, Professor and Head of Information Science Department, The Oxford College of Engineering, for his constant support and encouragement.

REFERENCES

- [1] K. Siedenbug, I. Fujinaga, and S. McAdams, "A comparison of approaches to Timbre descriptors in music information retrieval and music psychology," J. New Music Research, vol. 45, no. 1, 2016.
- [2] H. Davis and Saif M. Mohammad, "Generating music from literature," in Proc. EACL Workshop on Computational Linguistics for Literature, 2014.
- [3] P.N. Vassilakis, "Representing sound energy, phase, and interference using three-dimensional signals" presented at the 153rd meeting of the Acoustical Society of America, Salt Lake City, UT, 2007
- [4] Eck, D., and Lapalme, J. 2008. "Learning musical structure directly from sequences of music", UniversityofMontreal, Department of Computer Science, CP 6128.
- [5] H. L. F. Helmholtz, "On the Sensations of Tone as a Physiological Basis for the Theory of Music", 2nd ed., A.J. Ellis, Trans. New York: Dover Publications, Inc., 1885 (1954).
- [6] G. von Békésy, "Experiments in Hearing. New York: Acoustical Society of America Press", 1960 (1989).
- [7] E. Terhardt, "On the perception of periodic sound fluctuations (roughness)", Acustica, vol. 30(4), pp. 201-213, 1974.
- [8] R. Plomp, "The ear as a frequency analyzer", J. Acoust. Soc. Am., vol. 36(9), pp. 1628-1636, 1964.
- [9] E. Zwicker, "Subdivision of the audible frequency into critical bands," J. Acoust. Soc. Am., vol. 33(2), pp. 248-249, 1961.
- [10] M. Campbell and C. Greated, "The Musician's Guide to Acoustics", 2nd ed. New York: Oxford University Press, 1994.

A RELIABILITY SYSTEM FOR FILTERING MALICIOUS INFORMATION ON SOCIAL NETWORK

Asma Nooren P, Chandana L V, Divya G A, Saniya Sadaf M
Final year B.E Students(UG)

Guided by: Mrs.Vinodha k, Assistant Professor Department of ISE, TOCE
The Oxford College of Engineering, Bengaluru ,India

Abstract : The role of social network is to enable individuals to simultaneously share information with their peers. The communities meet in person or share ideas and experiences over internet. Unfortunately the social network is misused to spread malicious information which adversely effects the society.This malicious information affects the sentiments of people and also the reputation of social network. For example during 2016 election, voting polls were falsely predicted and spread all over social media but later due to false predictions it deeply affected the sentiments of the political parties. In this work, we are focusing on fastest growing social media profoundly known as twitter. To overcome the impact of the malicious information, in our work we propose a technique which is modelled analytically by considering reputation of social network and user experience to access, analyse and validate the information .The proposed system will be validated with respect to reliable tweets obtained which will prove that the impact of malicious information will be reduced by 24% compared to existing system.

Keywords— Reliability, Reputation, Classification, User experience, Feature-Ranking, Twitter.

1. INTRODUCTION

Information reliability on Twitter has been a trending topic among researchers in the fields of both computer and social sciences, due to the recent evolution of this platform as a tool for information dissemination. Twitter enables to transfer the information in a cost-effective manner. It has now become the source of news among variety of users around the globe.

The main characteristics feature of this platform is to deliver the content in a tailored manner which allows the users to obtain news regarding their topics of choice. The development of various techniques to verify the information obtained from Twitter has been a challenging task. In this paper, we propose a reliability analysis system for assessing information on Twitter to prevent the rapid growth of fake or malicious information.

2. LITERATURE REVIEW

A new model for classifying social media users according to their behaviours.

M. Al-Qurishi et.al[1] has proposed a new model for classifying social media users according to their behaviors. Facebook and Twitter are the most popular social media that are being used as a means of social communication and sharing thoughts, knowledge and even news. Classifying huge information from these social medias using traditional data mining classification algorithms is time consuming task which needs huge processing and memory space. The authors have proposed a new approach for classifying information in social network that can give accurate result similar to support vector machine (SVM) with less processing time and consuming less memory space compare to SVM.

A Multi-stage Credibility Analysis Model for Microblogs.

M. AlRubaian et.al[2] proposed a multistage credibility analysis model for microblogs Currently, microblogs are well-known social network, which are one of the most important sources of information. In this paper, a multi-stage credibility analysis framework is proposed to prevent the proliferation of fake or malicious information on twitter. They used Naive Bayes classifier and it is enhanced by considering the relative importance of the used features to improve the classification.

A model for recalibrating credibility in different contexts and languages - A twitter case study.

A. A. AlMansour et.al[3] intended a model for recalibrating credibility in different contexts and languages. Due to the growing dependence on the WWW User- Generated Content (UGC) as a primary source for information and news, the research on web

credibility is becoming more important and more prone to threat. So this work proposes a general model to assess information credibility on UGC different platforms, including Twitter.

A Novel Prevention Mechanism for Sybil Attack in Online Social Network.

Maged AlRubaian et al.[4] suggested Sybil Defense Techniques in Online Social Networks which is a Survey regarding the problem of malicious activities in online social networks, such as Sybil attacks and use of fake identities. In this paper, they provide a comprehensive survey of literature from 2006 to 2016 on Sybil attacks in online social networks and they have reviewed existing Sybil attacks, in the context of online social networks. then they have provided a new taxonomy of Sybil attack defense.

Interactive interfaces for complex network analysis: An information credibility perspective.

J. Schaffer et al.[5] Interactive interfaces for complex network analysis: An information credibility perspective This study reveals about the impact of visualization and interaction strategies for extracting quality information from complex networks such as microblogs. Interactive node-link graph and a novel approach are the two approaches, where content is separated into interactive lists based on data properties. These two approaches are applied to overcome the problem of extracting quality information from complex networks.

3. DESIGN OF RELIABLE SYSTEM FOR FILTERING MALICIOUS CONTENT

A reliable system for filtering malicious information on twitter incorporates four components which is as depicted in the fig 3.1 and the incorporated components are: 1)Reputation of social network 2)User acceptance level 3)Feature ranking algorithm 4)Reliable classifier engine.

These components work in an algorithmic form to access, analyse and validate information and this is passed as input to decision based threshold (Dth).If $Dth > 80$ the information is rejected being malicious otherwise the information is accepted which are the reliable tweets. These results are stored in database which can be accessed for future use.

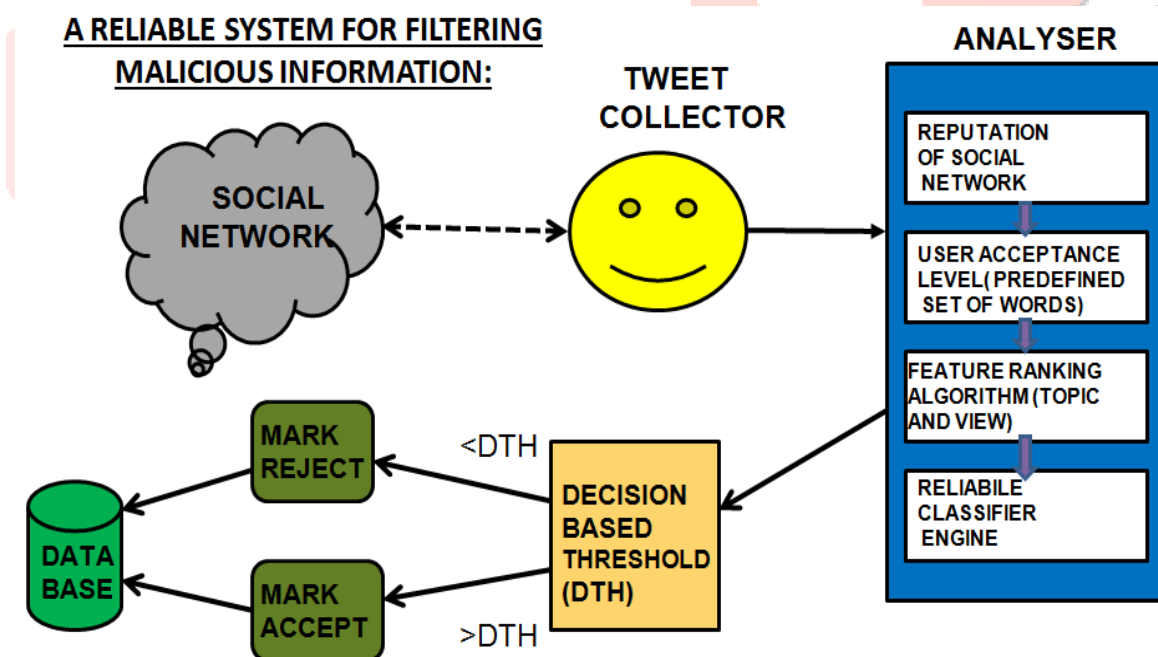


Figure 3.1: A Reliable system for filtering malicious information on twitter.

The working of reliable system involves the following units:-

Social Network:- It's a dedicated website which enables individuals to communicate with each other by posting information, comments, images, messages etc.

For example:-twitter,facebook,whatsapp,instagram

Tweet Collector:- It is a component responsible to collect the recent tweets from twitter using search and stream APIs.

Analyser :- comprises of four components which are user reputation, feature ranking, reliable classifier and user acceptance .These components work in an algorithmic form to access ,analyse and validate information collected from twitter .

Decision Based Threshold(Dth):- The results of analyser are fed to decision based component,where the threshold value is set to 80(which represents the total number of tweets collected from twitter). If $Dth > 80$ the information is rejected being malicious otherwise when $Dth < 80$ the information is accepted.

Database:- The validated results are stored in a database which can be accessed for future use.

4. ALGORITHM DESIGN AND IMPLEMENTATION

ANALYSIS OF USER RELIABILITY AND REPUTATION.

User reputation component verifies the reliability of the users and how far the information tweeted by these reputed users is trustworthy. Consequently, in this process we calculate reputation score (R) and the steps for calculating R is as followed;

Algorithm:-

Step 1: procedure CalcUserReputation (User, Tweets)

Step 2: If Tweets is empty then return 0

If User is verified then return 1

Step 3: For each $u \in \text{User}$, Calculate Users Activity Influence and Sentiment History

* UserActivity $I^p(u_i) = \sum_{u \in U, p \in T} u_i / |T|$

Where I is initial activity, p is particular topic, ui is ith user, T is tweets.

* UserInfluence $UI^{pEP} = SP^p(u_i) + I^p(u_i)$

Where SP is social popularity.

* UserSentimentHistory $\Delta_{ui} = \sum T_{ui}^+ / \sum T_{ui}^+ + \sum |T_{ui}^-|$

Where T_{ui}^+ is positive tweet of i^{th} user, T_{ui}^- is negative tweet of i^{th} user

Step 4: The reputation R is given by,

$R = \text{sentiment history (SH)} * \text{user influence (UI)}$

Step 5: End process

PRIORITIZING FEATURES BASED ON RE-TWEET COUNT.

Feature ranking component returns the reliability of tweets, i.e, it tells us how far a tweet can be trusted based on re-tweet counts. Higher the re-tweet count for a tweet more the particular tweet can be trusted. Judgement matrix for feature ranking (FR) consisting features (F) are given as follows

$$F(R) = \begin{pmatrix} 1 & f_{12} & \dots & f_{1n} \\ f_{21} & 1 & \dots & f_{2n} \\ \vdots & \vdots & \ddots & \vdots \\ f_{n1} & f_{n2} & \dots & 1 \end{pmatrix}$$

Algorithm

Step 1:Procedure FEATURERANK(FR)

Step 2:For each column $C \in FR$

Step 3:Normalizing features is given by (S) where , $S \leftarrow \sum_{i \in c} (F_i)$ with respect to the row.

Step 4:End for.

Step 5:for each feature $F_i \in FR$

Step 6: $FR^{\wedge} \leftarrow$ normalizing FR by dividing each entry on S

Step 7:calculate a list of all the ranked features with respect to

$$RC = \left[\frac{\prod_{j=1}^n f_{ij}^{1/n}}{\left(\sum_{i=1}^n \left[\prod_{j=1}^n f_{ij} \right]^{1/n} \right)} \right]$$

Step 8:End for

Step 9:RF \leftarrow create a list of all the ranked features with respect to RC

Step 10:return RF

Step 11:end procedure.

CLASSIFICATION OF TWEETS.

The main aim of reliable classifier engine is to classify positive, negative and neutral tweets and eliminates the negative tweets. The classification is based on naïve baye's concept.

$$P(A/C) = \frac{P(C/A) P(A)}{P(C)}$$

Where,

A is feature or attribute of training data,

C is conditions applied on training data,

P(A/C) is probability of attribute based on condition.

P(C/A) is probability of condition based on attribute.

P(A) is probability of attribute.

P(C) is probability of condition.

The following function shows the classification of positive and negative tweets.

```
<p class="postweet">//for positive tweets
<%
out.print("@ " + tweet.getUser().getScreenName() + " - " + tweet.getText());
set--;
}
} else if (score <= -1) {
neg++;
if (set > 0) {
%>
</p>
<p class="negtweet">//for negative tweets
<%
out.print("@ " + tweet.getUser().getScreenName() + " - " + tweet.getText());
set--;
}
} else if ((score < 1) && (score > -1))
{
neu++;
if (set > 0) {
%>
</p>
```

USER SEARCH HISTORY ANALYSIS.

In user search history analysis we determine the topic of interest of a particular user based on their respective search history. The frequently searched topic in the user's search history will be the most reliable topic for the user by this we can obtain the set of tweets which are more trustworthy from the user point of view.

The following function is used to access user's sentiment history

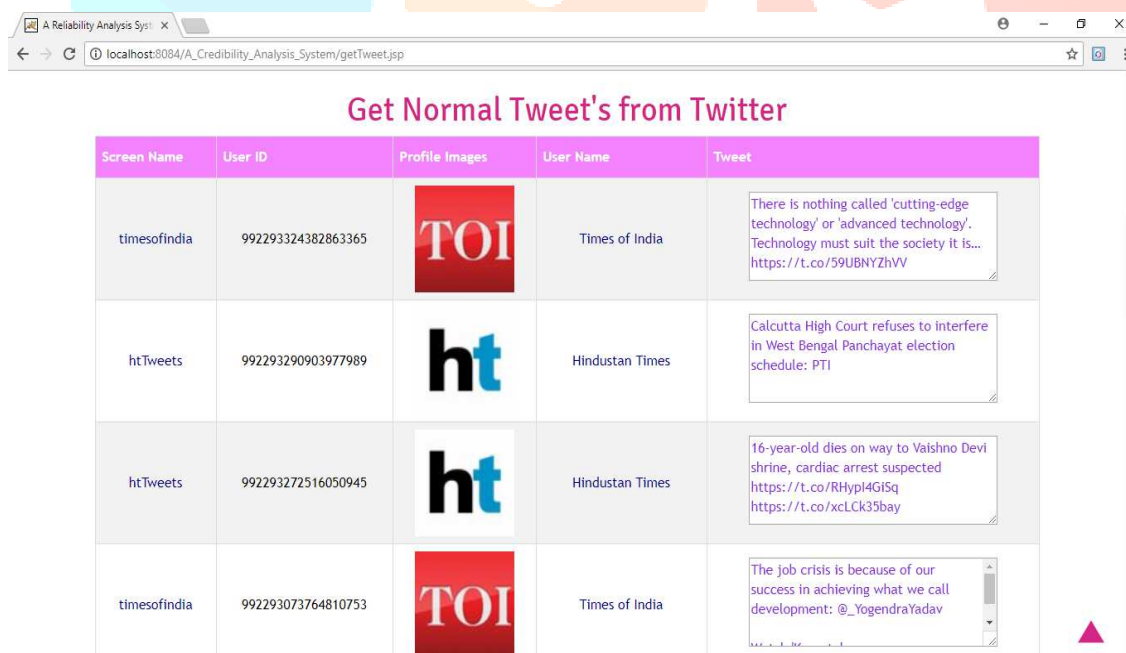
```
<center><h4>Get User Sentiment Search History </h4></center>
<div class="center btmspace-80">
<%
ConfigurationBuilder cf = new ConfigurationBuilder();
cf.setDebugEnabled(true)
.setOAuthConsumerKey("aV8lanFby7bTEMI2JXfJPiuB7")
.setOAuthConsumerSecret("3Di9ULBEzWt1PJUtCgvUnU7vXvvVE74cdxrNA7pfVeF1sTSSsty")
.setOAuthAccessToken("759307560369303553-X1kMf7u6BapUEMqQIQRMaR9fCuXgoyd")
.setOAuthAccessTokenSecret("awCfmbazBXRyk1ddMF7sUaCSD1Xkr4cYc6T7QsAncpC2g");
TwitterFactory tf = new TwitterFactory(cf.build());
twitter4j.Twitter twitter = tf.getInstance();
java.util.List<Status> status = twitter.getHomeTimeline(); %
```

5. RESULT'S DISCUSSION

We validate our system on different datasets of Twitter content, Our results show that the system which involved a reputation-based component, reliable classifier engine, user acceptance component and feature ranking algorithm provides a significant and accurate reliability assessment. The major outcomes of our proposed system is that on validating information with respect to error rate the impact of malicious information will be reduced by 24% when compared to existing system.

We are assessing the recent tweets from twitter using stream and search API.

The figure 5.1 illustrates the example of assessing the recent tweets from the twitter.







| Screen Name | User ID | Profile Images | User Name | Tweet |
|--------------|--------------------|---|-----------------|--|
| timesofindia | 992293324382863365 |  | Times of India | There is nothing called 'cutting-edge technology' or 'advanced technology'. Technology must suit the society it is... https://t.co/59UBNYZhVv |
| htTweets | 992293290903977989 |  | Hindustan Times | Calcutta High Court refuses to interfere in West Bengal Panchayat election schedule: PTI |
| htTweets | 992293272516050945 |  | Hindustan Times | 16-year-old dies on way to Vaishno Devi shrine, cardiac arrest suspected https://t.co/RHypl4GiSg https://t.co/xcLck35bay |
| timesofindia | 992293073764810753 |  | Times of India | The job crisis is because of our success in achieving what we call development: @_YogendraYadav |

Fig 5.1 : Example for extracting recent tweets from twitter.

Here we rank the tweets based on retweet count. Higher the retweet count more the trustworthy of the tweet.

In the fig 5.2, the topic NDTV has the highest retweet count of 6. Therefore it is more reliable when compared to other tweets.

| User ID | ScreenName | Profile Images | User Name | Tweet | Re Tweet Count |
|--------------------|--------------|----------------|-----------------|--|----------------|
| 992292385584435202 | ndtv | | NDTV | #Blog: Ravish Kumar on his photo with earphones going viral | 6 |
| 992292451854442496 | timesofindia | | Times of India | . Saugata Bhattacharya and are discussing Digital disruption: Is India ready for im... | 4 |
| 992292273403527168 | ndtv | | NDTV | "Sidaramaiah Supported Jihadi Elements": Yogi Adityanath In Karnataka #NDTVNewsBeps | 4 |
| 992292026958794753 | htTweets | | Hindustan Times | RT #Deadpol a Titanic, gets #CelineDion to sing theme song. Watch | 3 |

Fig 5.2 : Features ranked based on re-tweet count.

Fig 5.3 gives the sample output of user reputation where the reliability of user is verified based on reputation score. So here the reliable user is *ht* with the highest reputation score of 795858.

| User ID | ScreenName | Profile Images | User Name | Tweet | User Reputation Score |
|--------------------|------------|----------------|-----------------|---|-----------------------|
| 992293290903977989 | htTweets | | Hindustan Times | Calcuta High Court refuses to interfere in West Bengal Panchayat election schedule: PTI | 7.95858 |
| 992293272516050945 | htTweets | | Hindustan Times | -year-old dies on way to Vaishno Devi shrine, cardiac arest suspected | 7.95858 |
| 992292924237860870 | htTweets | | Hindustan Times | President Xi Jinping says Marxism stil 'totally corect' for China | 7.95858 |
| 992292762362900480 | htTweets | | Hindustan Times | PC Jewelers wipes out \$2. market cap after founder gifted shares to family | 7.95858 |

Fig 5.3: Tweets based on user reputation score.

This component classifies the positive, negative and neutral tweets and eliminates the negative tweets.

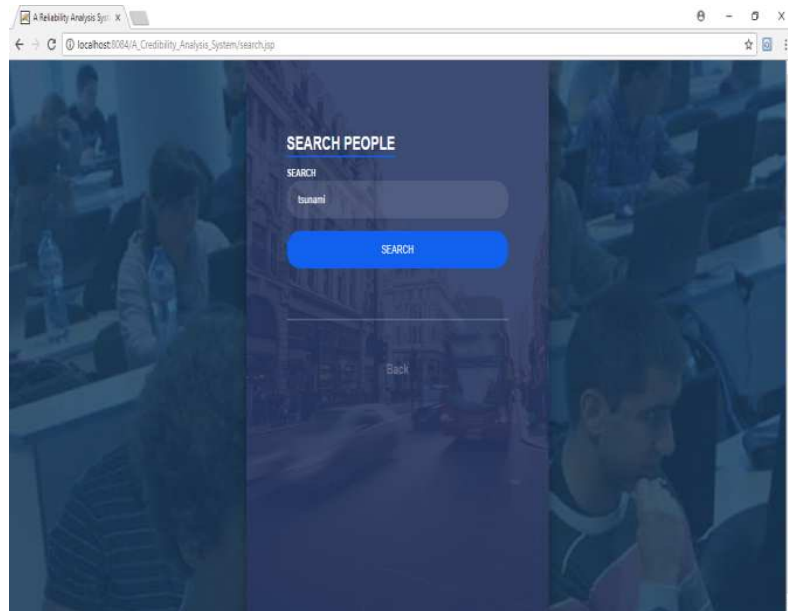


Fig 5.4: This snapshot illustrates searching of tweets

The result of the topic tsunami has 33.33% of positive and 33.33% of negative tweets as shown in the fig 5.5.

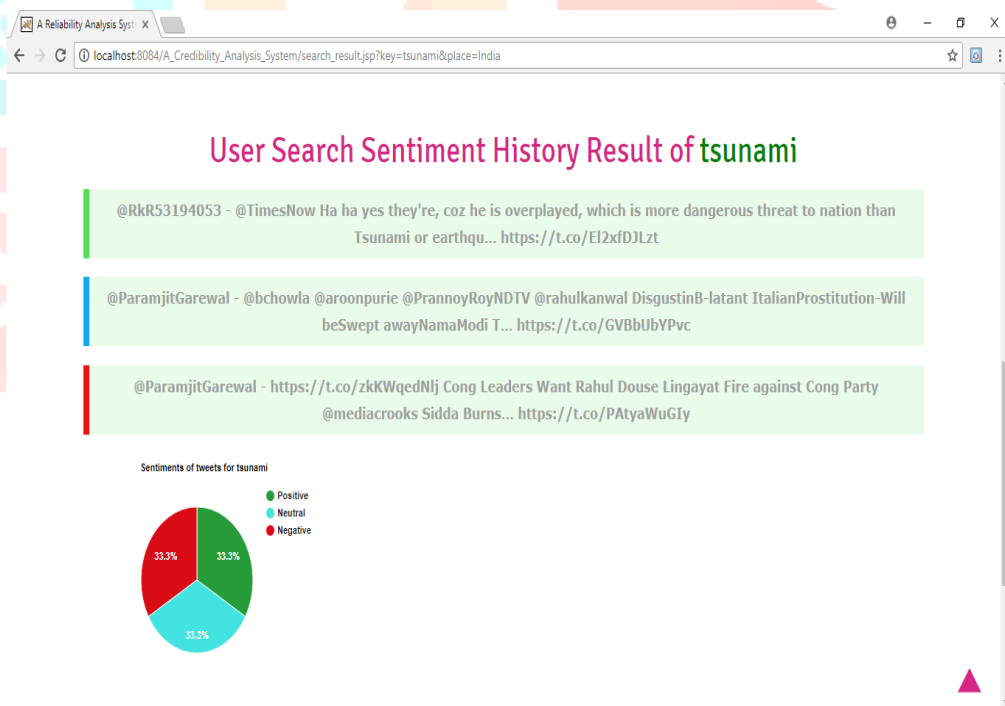


Fig 5.5: Classification of positive and negative tweets for the topic tsunami.

In fig 5.6 we notice that the negative tweets are eliminated for the tsunami

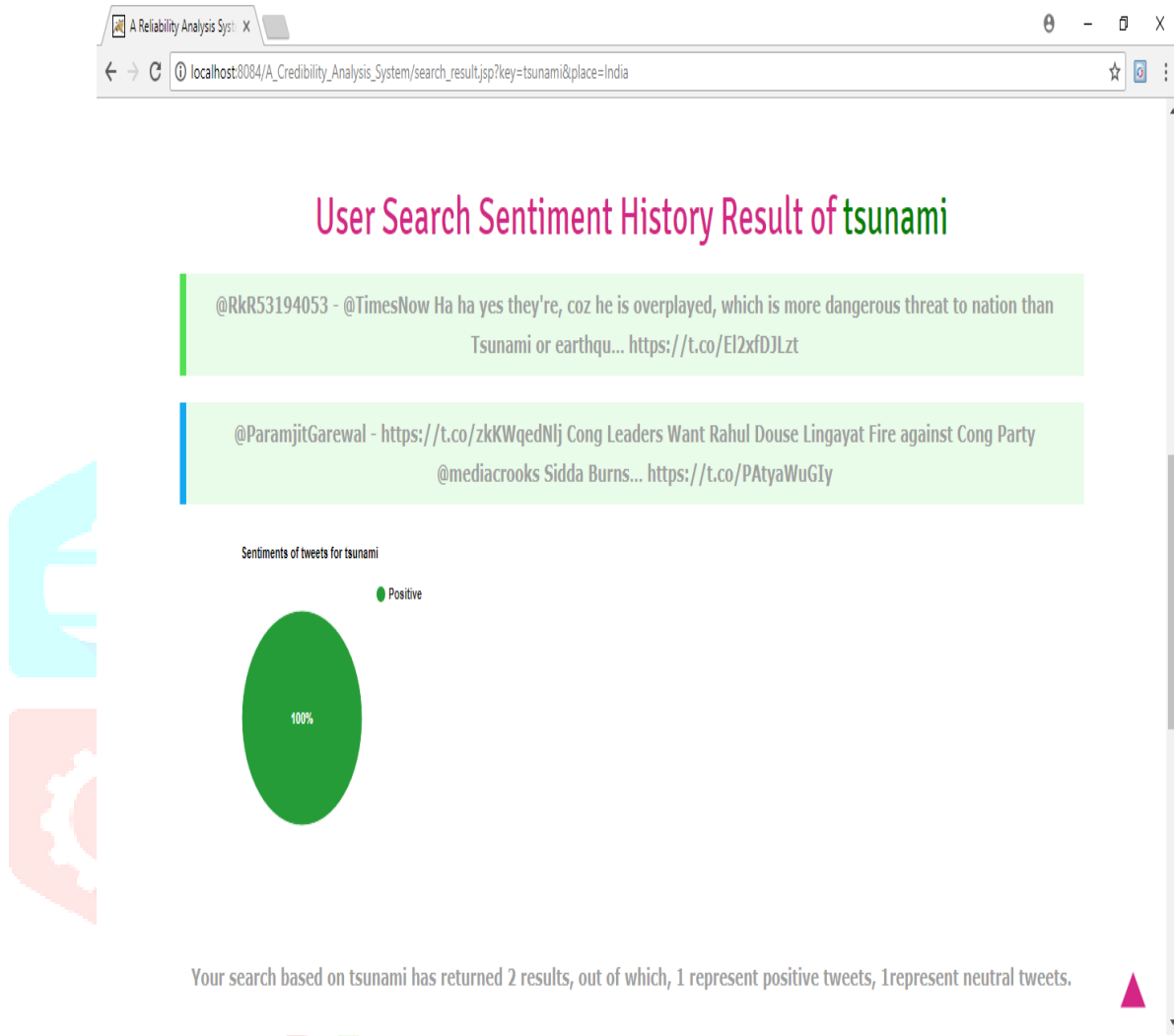


Fig 5.6: Elimination of negative tweets for the topic tsunami

Fig 5.7 gives idea about the user’s preferences based on their search history. In this example the users most search topic is csk.



Fig 5.7: User’s search history.

Fig 5.8 gives the performance of reliable system for filtering malicious content which is in the form of a pie chart. This pie chart gives the comparison of proposed system with the existing system. Here we notice that the proposed system shows the greater efficiency compared to existing system.

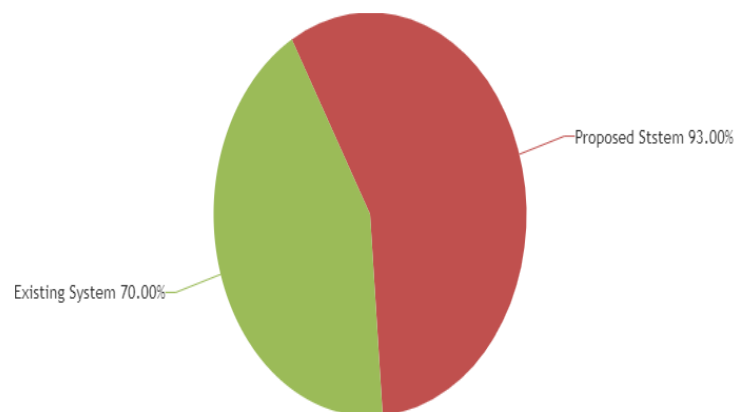


Fig 5.8: Performance of reliable system for filtering malicious content

6. CONCLUSIONS AND FUTURE WORK

Conclusions:

Social networks like twitter, facebook etc play a vital role in exchanging information among people. The information exchanged through these social networks maybe malicious and it may have an adverse affect on the sentiments of people.

To overcome the dissemination of malicious information which affects the sentiment of the people we proposed a reliable system which includes four components integrate together and work in an algorithmic form as a result of which we can observe that the error rate is reduced by 24%.

Future work:

The system can be improved and extended with the following aspects in future:

- The system which is getting implemented with four major components to reduce malicious information is best suited and possibly the most essential design which could have happened now.
- In future by the technology being changed or there are things invented everyday, there are expectations that the malicious information could be further reduced by more than 24%.
- Also in future our system can be programmed as a weapon to identify the inconsistent users who are frequently tweeting malicious information.
- The system can be implemented with different features, one of them is elimination of negative tweets prior it is being posted.

7. REFERENCES

- [1] M. Al-Qurishi, R. Aldrees, M. AlRubaian, M. Al-Rakhami, S. M. M. Rahman, and A. Alamri, "A new model for classifying social media users according to their behaviors," in Web Applications and Networking (WSWAN), 2015 2nd World Symposium on, 2015, pp.15
- [2] M. AlRubaian, M. Al-Qurishi, M. Al-Rakhami, S. M. M. Rahman, and A. Alamri, "A Multi-stage Credibility Analysis Model for Microblogs," presented at the Proceedings of the 2015 IEEE/ACM International Conference on Advances in Social Networks Analysis and Mining 2015, Paris, France, 2015 .
- [3] A. A. ALMANSOUR, L. BRANKOVIC, AND C. S. ILIOPOULOS, A MODEL FOR RECALIBRATING CREDIBILITY IN DIFFERENT CONTEXTS AND LANGUAGES - A TWITTER CASE STUDY.
- [4] Majed AlRubaian, Muhammad Al-Qurishi, Sk Md Mizanur Rahman, and A. Alamri, "A Novel Prevention Mechanism for Sybil Attack in Online Social Network," presented at the WSWAN'2015, 2015.
- [5] J. Schaffer, B. Kang, T. Hollerer, H. Liu, C. Pan, S. Giyu, and J. O'Donovan, "Interactive interfaces for complex network analysis: An information credibility perspective," in Pervasive Computing and Communications Workshops (PERCOM Workshops), 2013 IEEE International Conference on, 2013, pp. 464-469.
- [6] A. A. AlMansour, L. Brankovic, and C. S. Iliopoulos, "Evaluation of credibility assessment for microblogging: models and future directions," in Proceedings of the 14th International Conference on Knowledge Technologies and Data-driven Business, 2014, p. 32.
- [7] Majed AlRubaian, Muhammad Al-Qurishi, Sk Md Mizanur Rahman, and A. Alamri, "A Novel Prevention Mechanism for Sybil Attack in Online Social Network," presented at the WSWAN'2015, 2015
- [8] C. Castillo, M. Mendoza, and B. Poblete, "Information credibility on twitter," presented at the Proceedings of the 20th international conference on World wide web, Hyderabad, India, 2011.
- [9] S. Y. Rieh, M. R. Morris, M. J. Metzger, H. Francke, and G. Y. Jeon, "Credibility Perceptions of Content Contributors and Consumers in Social Media," 2014.
- [10] M. R. Morris, S. Counts, A. Roseway, A. Hoff, and J. Schwarz, "Tweeting is believing?: understanding microblog credibility perceptions," in Proceedings of the ACM 2012 conference on Computer Supported Cooperative Work, 2012, pp. 441-450.
- [11] Pal, A. and Counts, S. What's in a @name? How Name Value Biases Judgment of Microblog Authors. in Proc. ICWSM, AAAI (2011)

- [12] A. Gupta, P. Kumaraguru, C. Castillo, and P. Meier, "Tweetcred: Real-time credibility assessment of content on twitter," in Social Informatics, ed: Springer, 2014, pp. 228-243
- [13] Metaxas, Panagiotis Takas, Samantha Finn, and Eni Mustafaraj. "Using TwitterTrails. com to Investigate Rumor Propagation." Proceedings of the 18th ACM Conference Companion on Computer Supported Cooperative Work & Social Computing. ACM, 2015
- [14] A. Gupta and P. Kumaraguru, "Credibility ranking of tweets during high impact events," in Proceedings of the 1st Workshop on Privacy and Security in Online Social Media, 2012, p. 2
- [15] M. Mendoza, B. Poblete, and C. Castillo, "Twitter Under Crisis: Can we trust what we RT?," in Proceedings of the first workshop on social media analytics, 2010, pp. 71-79
- [16] Westerman, D., Spence, P.R., and Van Der Heide, B.: 'A social network as information: The effect of system generated reports of connectedness on credibility on Twitter', Computers in Human Behavior, 2012, 28, (1), pp. 199-206
- [17] B. Kang, J. O'Donovan, and T. Höllerer, "Modeling topic specific credibility on twitter," in Proceedings of the 2012 ACM international conference on Intelligent User Interfaces, 2012, pp. 179-188
- [18] Y. Ikegami, K. Kawai, Y. Namihira, and S. Tsuruta, "Topic and Opinion Classification Based Information Credibility Analysis on Twitter," in Systems, Man, and Cybernetics (SMC), 2013 IEEE International Conference on, 2013, pp. 4676-4681



MRCP-RMD: Resource allocation and Scheduling of jobs with Deadlines

Shashank G Hegde, Vinayak Suresh Pai, Vinitha S Bhat, Srinidhi L N

Final year B.E Students(UG)

Guided by: Mrs. Visalini S, Assistant Professor Department of ISE, TOCE
The Oxford College of Engineering, Bengaluru, India

Abstract : MRCP-RM: Big Data is the problem raised due to large storage of dataset and traditional data processing. Data processing from large set of data holds great disadvantages over time constraint, in order to overcome this constraint Deadline(priority scheduling) is introduced in this research. The method for Resource Allocation and Scheduling of Map Reduce Jobs with Deadlines, which focuses on resource allocation and scheduling of MapReduce jobs according to client's requirements. Big data is the domain used for resource allocation and scheduling of jobs. Parallel processing on distributed data of commodity hardware in a reliable, fault-tolerant manner. An open stream of MapReduce jobs with SLA (Service Level Agreement) on a distributed computing environment i.e. HDFS (Hadoop Distributed File System). Hadoop distributed file system allows storing and effective retrieval of data. Existing Hadoop scheduler do not support completion time guarantee and performance of completion of jobs is less. Algorithm used is MRCP-RM (MapReduce Constraint Programming based on resource allocation). MRCP-RM not only maps all the newly submitted jobs but also remaps the tasks of jobs that have previously been executed but have not started executing. Scheduler consists of MRCP-RM code in which the data are sorted and shuffled and deadline control is achieved by setting job priorities at scheduling phase. The goal of this project is to enhance the performance, scalability and throughput over deadline control by 15% to 18%.

Index Terms—Resource allocation, constraint programming and scheduling of jobs.

1. INTRODUCTION

Big Data is the term that refers not only to the large volumes of data but it is also concerned about the complexity of the data and the speed at which it is getting generated. It is generally described by using three characteristics, widely known as 3 V's:

- **VOLUME**

The size is one of the characteristics that define big data. Big data consists of very large data sets. However, it should be noted that it is not the only one parameter and for data to be considered as big data, other characteristics must also be evaluated.

- **VELOCITY**

The speed at which the data is being generated is an important factor. For example, in every one second thousands of tweets are tweeted on microblogging platform, Twitter. Even if the size of each individual tweet is 140 characters, the speed at which it is getting generated makes it an eligible data set that can be considered as big data.

- **VARIETY**

Big data comprises data in all formats: structured, unstructured or combination of both. Generally, it consists of data sets, so complex that traditional data processing applications are not sufficient to deal with them. All these characteristics make it difficult for storing and processing big data using traditional data processing application software's. Two papers published by Google, build the genesis for Hadoop. Hadoop is an open source frame-work used for distributed storage and parallel processing on big data sets. Two core components of Hadoop are:

- **HADOOP DISTRIBUTED FILE SYSTEM (HDFS)**

Used for distributed storage of data. The input file is first split into blocks of equal size except the last block which are then replicated across Data Nodes. Currently, default block size is 128 MB which was previously 64 MB and default replication factor is 3. Block size and replication factors are configurable parameters.

- **MAPREDUCE**

For parallel processing on distributed data on cluster of commodity hardware in a reliable, fault-tolerant manner.

A MapReduce job usually splits the input data-set into independent chunks which are processed by the map tasks in a completely parallel manner. The framework sorts the outputs of the maps, which are then input to the reduce tasks.

There are plenty of resources available that describe the detailed architecture of Hadoop and about how it works. Anyone who is not aware about what Hadoop is at all and how it can help manage big data is suggested to get a basic understanding of it before continuing here since basic understanding of Hadoop is required to understand the concepts discussed in following sections.

2. LITERATURE REVIEW

Deadline-based Workload Management for MapReduce Environments: Pieces of the Performance Puzzle.

Author: Abhishek Verma, Ludmila Cherkasova, Vijay S. Kumar, Roy H. Campbell.

Design of new schedulers for Mapreduce environment to enhance the workload management for processing Mapreduce jobs with deadlines. A policy for job ordering in the processing queue. Allocation and de-allocation spare resources in the system among the active jobs.

Engineering Resource Management Middleware for Optimizing the Performance of Clouds Processing MapReduce Jobs with Deadlines

Norman Lim, Shikharesh Majumdar, & Peter Ashwood-Smith

Software packages to formulate and solve the matchmaking and scheduling problems. High resource utilization and adequate revenue. Achieve high system performance.

A Constraint Programming-Based Resource Management Technique for Processing MapReduce Jobs with SLAs on Clouds

Peter Ashwood-Smith Norman Lim and Shikharesh Majumdar.

Effective technique for resource management on clouds for jobs characterized by an end-to-end SLA comprising an earliest start time, execution time, and deadline.

Scheduling in MapReduce-like Systems for Fast Completion Time

Hyunseok Chang, Murali Kodialam, Ramana Rao Kompella, T. V. Lakshman, Myungjin Lee, Sarit Mukherjee

A linear program that minimizes the job completion times to solve the problem. Achieve feasible schedules within a small constant factor of the optimal value of the objective function.

MARLA: MapReduce for Heterogeneous Clusters

Zacharia Fadika 1, Elif Dede 2, Jessica Hartog 3, Madhusudhan Govindaraju

Efficient and swift processing of large scale data with a cluster of compute nodes. Performing well not only in homogeneous settings, but also when the cluster exhibits heterogeneous properties.

The performance gains exhibited by our approach against Apache Hadoop and MARIANE in data intensive and compute intensive applications.

3. SYSTEM ARCHITECTURE

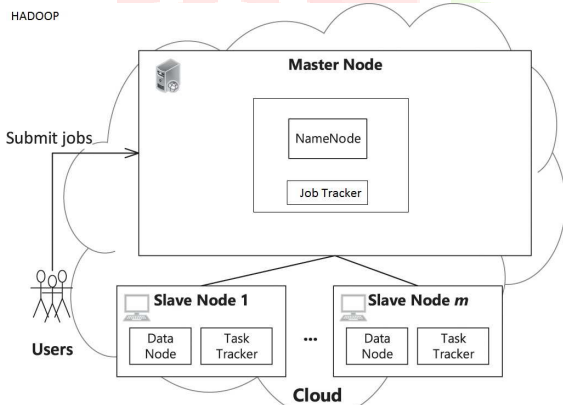


Figure:3.1

HDFS(STORAGE):

HDFS is designed for storing very large files with streaming data access and running on clusters of commodity hardware.

A dataset is typically generated or copied from source and then various analysis is performed on that data set over time.

MAPREDUCE(COMPUTATION):

Map –Reducing is a processing technique that allows scalability across hundreds or thousands of servers in a Hadoop clusters.

Map-Reduce algorithms contain two important tasks map and reduce. The shuffle and sort process is dependent mainly on value of data sets, At last we are scheduled and Map-Reducing jobs

JOB TRACKER:

This resides in master node and is responsible for accepting job compliances from clients scheduling task to run on nodes, and providing executive functions such as condition and task progress watching to the bunch.

TASK TRACKER:

This accepts task from the JobTracker, initiate to the user program to execute these jobs locally and reports are sent to the JobT immediately.

NAMENODE (MASTER NODE):

The name node is a master of all daemons and is use to map the block and store file in HDFS format.

SECONDARY NAME NODE:

Performs name node operation log check point. Acts as a backup for Name node

DATA NODE (SLAVE NODE):

The Data Node is used in creation, insertion and deletion of data or files based on the order of name node.

Data flow diagrams:

DFD-L0:



Figure:3.2

DFD-L1:

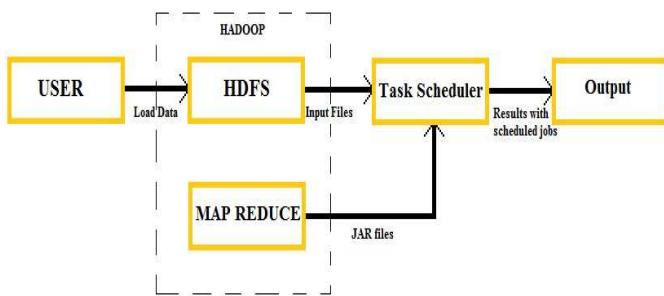


Figure:3.3

DFD-L2:

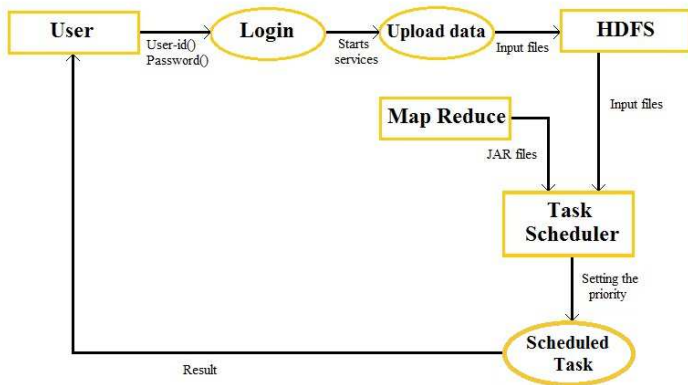


Figure:3.4

Data Flow:

The data flow diagram shows the flow of data from end user to appliances. The user has to register using user id and password in order to submit the query in the cloud server. The query will be processed using process user query event. The HDFS redirects the query to the task scheduler which resides in the Name Node.

The task will be scheduled and directed to the data node. The jobs are scheduled and submitted back to task scheduler. The chunks of data are merged and the results are produced to user

4. MODULE SETS

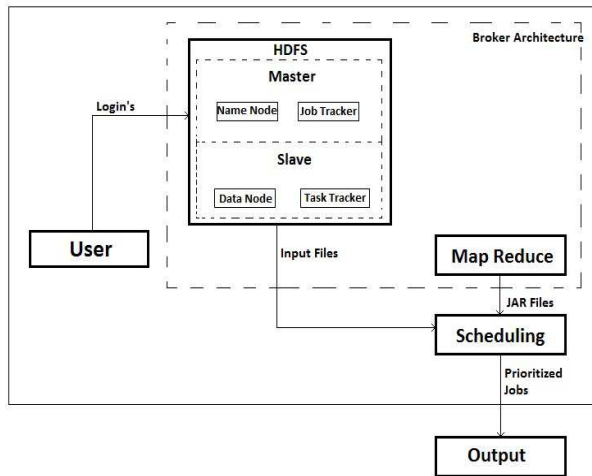


Figure:4.1

Admin/User: User logs into system using user-id and password. Authorization is needed to identify the user. Only authenticated users can access the system. Admin/User has to start all Hadoop services.

HDFS: It is used to store files in distributed manner. Namenode has meta data where as Datanode will be having actual data. All the input files are stored from local to hdfs using commands. Files are stored in form of chunks, default size is 64MB and can vary up to 1024MB. Replication Factor is 3. Parallel processing is done, to extract data from HDFS.

Map Reduce: It produces key; value pairs. It consists of 3 classes Mapper, Reducer and Driver class. Driver class is a main class used during compilation. It provides key and value pairs for given input files and also removes duplication. All programs are compiled here using JAR files, Driver class name, Input file and Output directory.

Scheduling: Each JAR file generates unique job-id. Priorities to each job-id is assigned according to client's/user requirement. It prioritizes each jobs and executes it as early as possible by increasing scalability and throughput.

5. IMPLEMENTATION

STEP: 1

- User login's to system.
- Opens terminal and starts all hadoop services using "start-all.sh" command.
- 3 times password should be entered to start all the services.
- Using "jps" command, we can check all the hadoop daemons running and also to check the activities of all the nodes.

```

tags.csv (~/Desktop/mov) - gedit
File Edit View Search Documents Help
tags.csv X
userId,timestamp,movieId,tag
18,1240597180,4141,Mark Waters
65,1368150878,208,dark hero
65,1368150879,353,dark hero
65,1368149983,521,noir thriller
65,1368150878,592,dark hero
65,1368149876,660,bollywood
65,1368150160,898,screwball comedy
65,1368149983,1248,noir thriller
65,1368150855,1391,mars
65,1368150217,1617,neo-noir
65,1368149925,1694,jesus
65,1368149983,1783,noir thriller
65,1368149925,2022,jesus
65,1368151314,2193,dragon
65,1368151266,2353,conspiracy theory
65,1368150855,2662,mars
65,1368149983,2726,noir thriller
65,1368149925,2840,jesus
65,1368149926,3052,jesus
65,1368149876,5135,bollywood
65,1368149949,6539,treasure
65,1368150879,6874,dark hero
65,1368149983,7013,noir thriller
65,1368149925,7318,jesus
65,1368150812,8529,stranded
65,1368151266,8622,conspiracy theory
65,1305008715,27803,Oscar (Best Foreign Language Film)
65,1304957153,27866,New Zealand
65,1304958354,46882,surreal
65,1304958359,46882,unusual
65,1368149876,51884,bollywood
65,1304957612,56652,cute
  
```

Figure:5.1

STEP: 2

- Hadoop uses HDFS to store files in form of chunks.
- Create a directory under root, where all the input data is to be stored.
- Using “cd” change the directory, where input data is stored.
- Using “hadoop fs -put filename.extension /(enter)” command, load all the required input data files from local to hadoop (HDFS).
- Open browser and type <http://localhost:50070>.
- Click on [Browse File System](#) to see whether the files are load into hadoop(HDFS).

STEP: 3

- In this, we have totally 4 programs i.e.
 1. Map Reduce.
 2. Partitioner.
 3. Frequency.
 4. Distinct.
- Create jar files of these programs using Eclipse.
- In terminal, using “hadoop jar /root/name_of_jar.jar driver_class_name / input_file /output_directory” to execute the input files using jar files.
- For each program single job-id will be created.
- Change the configuration of fair scheduler and mapred xml files in filesystem/usr/local/Hadoop/conf folder.
- Reboot the system once configuration are changed.
- Run the jar files once again
- Using “hadoop job -list” command check currently running jobs.
- Once the job-id is created.
- Set priority to jobs using “hadoop job -set-priority”.
- Valid values for priority are : VERY_HIGH, HIGH, NORMAL, LOW, VERY_LOW.
- Syntax is “hadoop job -set-priority values job-id”.

```

root@localhost:~# hadoop job -list
Warning: $HADOOP_HOME is deprecated.
0 jobs currently running
JobId State StartTime Username
[root@localhost ~]# hadoop job -list
Warning: $HADOOP_HOME is deprecated.
1 jobs currently running
JobId State StartTime Username
job_201805070300_0001 4 1525687388746 root

root@localhost:~# hadoop jar /root/d1.jar Distinct /tags.csv /d3
Warning: $HADOOP_HOME is deprecated.
18/05/07 03:03:06 INFO input.FileInputFormat: Total input paths to process : 1
18/05/07 03:03:06 INFO util.NativeCodeLoader: Loaded the native-hadoop library
18/05/07 03:03:06 WARN snappy.LoadSnappy: Snappy native library not loaded
18/05/07 03:03:09 INFO mapred.JobClient: Running job: job_201805070300_0001
18/05/07 03:03:10 INFO mapred.JobClient: map 0% reduce 0%
18/05/07 03:03:45 INFO mapred.JobClient: map 70% reduce 0%
18/05/07 03:03:48 INFO mapred.JobClient: map 100% reduce 0%
18/05/07 03:04:00 INFO mapred.JobClient: map 100% reduce 73%
18/05/07 03:04:12 INFO mapred.JobClient: map 100% reduce 100%
18/05/07 03:04:21 INFO mapred.JobClient: Job complete: job_201805070300_0001
18/05/07 03:04:21 INFO mapred.JobClient: Counters: 29
18/05/07 03:04:21 INFO mapred.JobClient: Job Counters
18/05/07 03:04:21 INFO mapred.JobClient: Launched reduce tasks=1
18/05/07 03:04:21 INFO mapred.JobClient: SLOTS_MILLIS_MAPS=39117
18/05/07 03:04:21 INFO mapred.JobClient: Total time spent by all reduces waiting after reserving slots (ms)=0

root@localhost:~# hadoop -set-priority job_201805070300_0001
Warning: $HADOOP_HOME is deprecated.
Unrecognized option: -set-priority
Error: Could not create the Java Virtual Machine.
Error: A fatal exception has occurred. Program will exit.
[root@localhost ~]# hadoop -set-priority job_201805070300_0001 HIGH
Warning: $HADOOP_HOME is deprecated.
Unrecognized option: -set-priority
Error: Could not create the Java Virtual Machine.
Error: A fatal exception has occurred. Program will exit.
[root@localhost ~]# hadoop -set-priority job_201805070300_0001 HIGH
Warning: $HADOOP_HOME is deprecated.
Changed job priority.
[root@localhost ~]#

```

Figure:5.2

STEP: 4

- Open browser and type <http://localhost:50030>.
- Click on completed jobs to view the output.

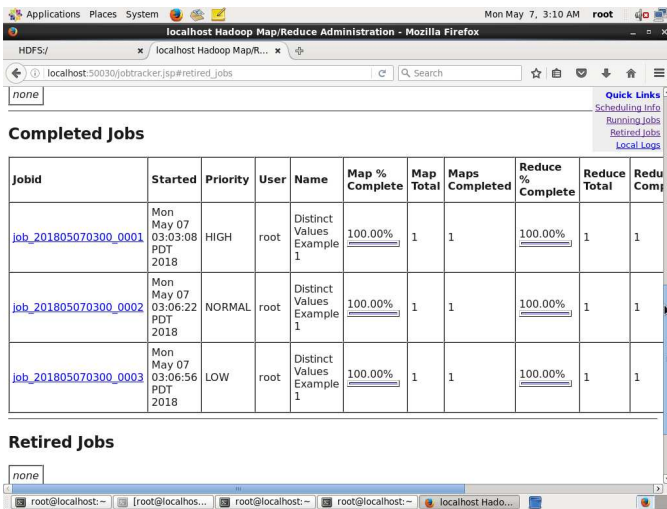


Figure:5.3

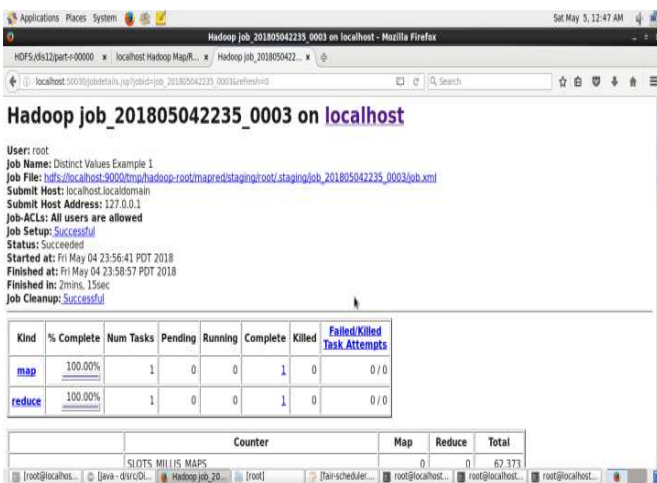


Figure:5.4

6. EXPERIMENTAL RESULTS

In this research there are three jobs given as input logs i.e., tags.csv,movies.csv,ratings.csv. These file consist details like movie id,timestamp,ratings,year,type of movies .

The final browser screen would appear with columns as JOBID,STARTED,PRIORITY,USER,NANE,MAP AND COMPLETED REDUCE TOTAL,REDUCE COMPLETE. The job id is unique for every job. This id will display the starting and ending time of the job.The priorities are like HIGH,VERY HIGH,NORMAL,LOW,and VERY LOW.

The priority is set during scheduling.

SCALABILITY:

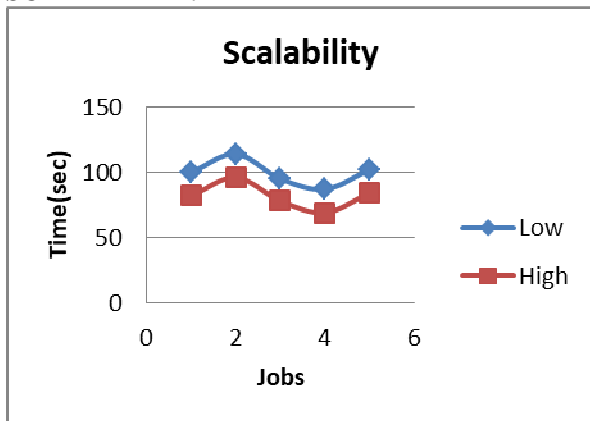


Figure:6.1

Existing system takes more time to complete 5 jobs because of low priority, whereas in proposed system it takes less time to complete 5 jobs because we are setting priority to high. Thus we are able to complete more number of jobs compared to existing one. With extra 15% to 18% efficiency than existing one.

THROUGHPUT:

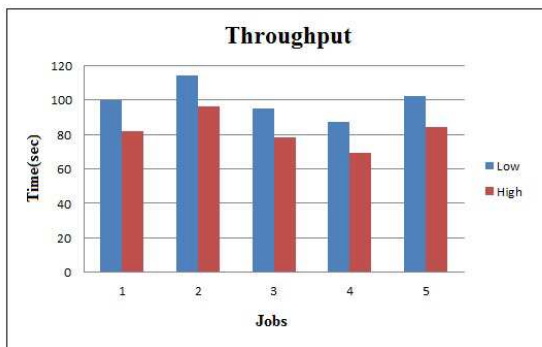


Figure:6.2

It takes less time to complete jobs. Thus we can complete extra 15% to 18% of the jobs early compared to existing system.

7. CONCLUSION AND FUTURE WORK

The goal of this research is devising effective matchmaking and scheduling techniques for efficiently processing an open stream of MapReduce jobs with SLAs on a distributed computing environment with m resources, such as a private cluster or a set of resources acquired a priori from a public cloud. A key research objective is to achieve high system performance while ensuring matchmaking and scheduling overhead is low. A constraint programming based resource management technique called MRCP-RM that can efficiently perform matchmaking and scheduling of an open stream of MapReduce jobs with SLAs. A constraint programming based resource management technique called MRCP-RMD that can efficiently perform matchmaking and scheduling of an open stream of MapReduce jobs has been implemented. The implementation was successful with effective prioritization of jobs; hence one can infer that hadoop is apt when it comes to resource allocation and management.

Demonstration of effectiveness as reflected in the ability to achieve high system performance while incurring a small overhead was possible

Following achievements were made:

- 1) Throughput control.
- 2) Improved Scalability.
- 3) Effective usage of resources.

All the factors mentioned above leads to customer satisfaction and also helps cut costs for the company by effective resource management.

REFERENCES

1. N. Lim, S. Majumdar, and P. Ashwood-Smith, "Engineering resource management middleware for optimizing the performance of clouds processing MapReduce jobs with deadlines," in Proc. Int. Conf. Perform. Eng., Mar. 24-26, 2014, pp. 161–172.
2. N. Lim, S. Majumdar, and P. Ashwood-Smith, "A constraint programming-based resource management technique for processing. MapReduce jobs with SLAs on clouds," in Proc. Int. Conf. Parallel Process, Sep. 9-12, 2014, pp. 411–421
3. Verma, L. Cherkasova, V. S. Kumar, and R. H. Campbell, "Deadline-based workload management for MapReduce environments: Pieces of the performance puzzle," in Proc. Netw. Operations Manage. Symp, Apr.16-20, 2012, pp. 900–905.
4. Z. Fadika, E. Dede, J. Hartog, and M. Govindaraju, "MARLA: MapReduce for heterogeneous clusters," in Proc. IEEE/ACM Int. Symp. Cluster Cloud Grid Comput, May 13-16, 2012, pp. 49–56
5. H. Chang, M. Kodialam, R. R. Kompella, T. V. Lakshman, M. Lee, and S. Mukherjee, "Scheduling in mapreduce-like systems for fast completion time," in Proc. IEEE INFOCOM, Apr. 10-15, 2011, pp. 3074–3082.



Indian Journal of Science and Technology

[HOME](#) / [ARTICLES](#)

/ Structure Design of Photonic Crystal Based MOEMS Accelerometer Sensor for Supplemental Restraint System in Automobile Passenger Safety

ARTICLE

VIEWES 141

PDF 53

Abstract

Full-Text PDF



Indian Journal of Science and Technology

DOI: [10.17485/ijst/2017/v10i29/117327](https://doi.org/10.17485/ijst/2017/v10i29/117327)

Year: 2017, Volume: 10, Issue: 29, Pages: 1-6

Original Article

Structure Design of Photonic Crystal Based MOEMS Accelerometer Sensor for Supplemental Restraint System in Automobile Passenger Safety

Sundar Subramanian^{1*}, Anup M. Upadhyaya² and Preeta Sharan²

¹Centre for Emerging Technologies, Jain University, Bangalore – 560069, Karnataka, India;

sundar3172@gmail.com

²Department of

Mechanical Engineering, Department of Electronics and Communication Engineering, The Oxford

College of Engineering, Bangalore – 560068, Karnataka, India; upadhyayaanup74@gmail.com,

sharanpreeta@gmail.com

*Author For Correspondence

Sundar Subramanian

Centre for

Emerging Technologies, Jain University, Bangalore – 560069, Karnataka, India;

sundar3172@gmail.com



This work is licensed under a [Creative Commons Attribution 4.0 International License](https://creativecommons.org/licenses/by/4.0/).

ABSTRACT

Leading cause of human death in most of country is roadway crashes. Supplemental restraint system playing vital role in preventing and protecting the passengers and drivers in case of accidents thereby providing chance of last line of defence against serious injuries. So there is



Year: 2017, Volume: 10, Issue:

29



Citations

Citation Indexes: 1

[see details](#)



Indian Journal of Science and Technology

[HOME](#) / [ARTICLES](#) / Performance Analysis of Reversible ALU in QCA

ARTICLE

VIEWES 200

PDF 540

Abstract

Full-Text PDF



Indian Journal of Science and Technology

DOI: [10.17485/ijst/2017/v10i29/117324](https://doi.org/10.17485/ijst/2017/v10i29/117324)

Year: 2017, Volume: 10, Issue: 29, Pages: 1-5

Original Article

Performance Analysis of Reversible ALU in QCA

Rajinder Tiwari^{1*}, Deepika Bastawade², Preeta Sharan² and Anil Kumar¹

¹Department of ECE, ASET, Amity University, Lucknow – 226028, Uttar Pradesh, India; rtiwari@amity.edu, akumar3@lko.amity.edu

²Department of ECE, The Oxford College of Engineering, Bengaluru – 560068, Karnataka, India; Deepikabastawade14@gmail.com, sharanpreeta@gmail.com

*Author For Correspondence

Rajinder Tiwari

Department of ECE, ASET, Amity University, Lucknow – 226028, Uttar Pradesh, India; rtiwari@amity.edu



This work is licensed under a [Creative Commons Attribution 4.0 International License](https://creativecommons.org/licenses/by/4.0/).

ABSTRACT

Quantum spot Cell Automata (QCA) based reversible method of reasoning is the foundations of creating nanotechnological figuring structures. It ensures enormously low power usage with high thickness and working repeat. Programmable reversible method of reasoning is ascending as an approaching basis arrangement style for execution in present day nanotechnology and quantum preparing with unimportant impact on circuit warm period. Late advances in reversible method of reasoning using and quantum PC figuring mull over improved PC building and math basis unit designs. This work focuses on plan of a powerful reversible ALU (Arithmetic Logic Unit) and its affirmation in QCA. We have considered existing 3×3 M-R Gate as the essential building block, a 4×4 reversible method of reasoning entryways (M-R Gate with



Year: 2017, Volume: 10, Issue:

29



Citations

Citation Indexes: 4

Captures

Readers: 1

[see details](#)

IEIE Transactions on Smart Processing and Computing

Volume 6 Issue 3 / Pages.141-150 / 2017 / 2287-5255(eISSN)

The Institute of Electronics and Information Engineers (대한전자공학회)



A Novel Imaging System for Removal of Underwater Distortion using Code V



DOI QR Code

Maik, Vivek (Department of Electronics and Communication, The Oxford College of Engineering) ;

Daniel, Stella (Department of Electronics and Communication, The Oxford College of Engineering) ;

Chrispin Jiji, A. (Department of Electronics and Communication, The Oxford College of Engineering)

Received : 2017.01.03 Accepted : 2017.03.24 Published : 2017.06.30

<https://doi.org/10.5573/IEIESPC.2017.6.3.141>

Copy

Citation

PDF

KSCI

Abstract

Images obtained from underwater are usually degraded due to the environmental conditions. Some of the typical degradation factors include turbidity and color degradation. These degradations can be attributed to the absorptive and scattering properties of underwater degradation in terms of optical parameters, such as modulation transfer function (MTF), optical transfer function (OTF), point spread function (PSF), and color constancy. In this paper, we use the CODE V optical simulation software to mimic underwater conditions and model the imaging platform, thereby studying various parameters, such as PSF and MTF, and we use the PSF to remove the underwater turbidity. Experimental results show increased performance with the algorithm, compared to other existing methods.

Keywords

CODEV; PSE; Turbidity

File



Download PDF

References

1. B. McGlamery, "A computer model for underwater camera system," in Ocean Optics VI, S. Q. Duntley, Ed., vol. 208 of Proceedings of SPIE, pp. 221-231, 1979.
2. J. S. Jaffe, "Computer modeling and the design of optimal underwater imaging systems," IEEE Journal of Oceanic Engineering, vol. 15, no. 2, pp. 101-111, 1990. <https://doi.org/10.1109/48.50695>
3. C. Funk, S. Bryant, and P. Heckman, "Handbook of underwater imaging system design," Tech. Rep. TP303, Naval Undersea Center, San Diego, Calif, USA, 1972.
4. T. H. Dixon, T. J. Pivrotto, R. F. Chapman, and R. C. Tyce, "A range-gated laser system for ocean floor imaging," Marine Technology Society Journal, vol. 17, 1983.
5. J. McLean and K. Voss, "Point spread functions in ocean water: comparison between theory and experiment," Applied Optics, vol. 30, pp. 2027-2030, 1991. <https://doi.org/10.1364/AO.30.002027>
6. K. Voss, "Simple empirical model of the oceanic point spread function," Applied Optics, vol. 30, pp. 2647-2651, 1991.



IEEE Xplore

Browse My Settings Help

Institutional Sign In

Institutional Sign In

All



ADVANCED SEARCH

Conferences > 2017 IEEE International Confe...

Deblurring Underwater Image Degradations Based on Adaptive Regularization

Publisher: IEEE

Cite This

PDF

A.J Chrispin ; R Nagaraj All Authors

1 Paper Citation

71 Full Text Views



Alerts

Manage Content Alerts

Add to Citation Alerts

More Like This

Fast and Accurate Solution of the Inverse Problem for Image Reconstruction Using Electrical Impedance Tomography
IEEE Transactions on Magnetics
Published: 2019

Comparison of Dictionary-Based Image Reconstruction Algorithms for Inverse Problems
2020 28th Signal Processing and Communications Applications Conference (SIU)
Published: 2020

Show More

Abstract



Document Sections

- I. Introduction
- II. Related Works
- III. Sparse Domain for Deblurring Underwater Images
- IV. Adaptive Regularization
- v. Results and Analysis

Show Full Outline

Authors

Figures

References

Citations

Keywords

Metrics

More Like This

Abstract: Images attained from underwater are typically corrupted by features such as poor perceptibility, bright object, color reduced, blurred and noise. Rebuilding of appearance... [View more](#)

Metadata

Abstract: Images attained from underwater are typically corrupted by features such as poor perceptibility, bright object, color reduced, blurred and noise. Rebuilding of appearance after its distorted and blaring complement remains a challenging problem. The ill-posed nature of the problematic means on no account of specific solution so any solution is an estimated of the actual solution and this often leads to inconsistency in the form of degradation as complete smoothing of the reconstructed image. The sparse dominion systems provide unusual solutions to this inverse problem by giving the l_1 -norm sparsity prior to eliminate underwater image degradations. In this paper, we present adaptive regularization to confine the image patches residence on the inherent smoothing and include the image nonlocal self-similarity into sparse dominion to recover the exactness to reconstruct the expected image. The tentative consequences by means of the proposed technique contribute enhanced performance than former state-of-the-art techniques.

Published in: 2017 IEEE International Conference on Computational Intelligence and Computing Research (ICIC)

Date of Conference: 14-16 Dec. 2017 **INSPEC Accession Number:** 18248590

Date Added to IEEE Xplore: 08 November 2018 **DOI:** 10.1109/ICIC.2017.8524166

Publisher: IEEE

ISBN Information:

Conference Location: Coimbatore, India


ISSN Information:


 Contents


I. Introduction


Images are the key causes of information. Catching an image accurately as it seems in the actual world remains very challenging and unbearable. The excellence, however, of underwater imageries stays still poorer than that report in the airborne meanwhile restrictions enforced by physical possessions [1] of the water medium. In case of taking photographs or imaging schemes these are formed by distorting act began due to unsuitable converging of camera lens and huge quantity of separable elements in water, noise, the discrepancy in the illumination of image, poor perceptibility due to light reduction, bluish presence etc. To progress the excellence of the underwater image we go for image restoration or image de-blurring or image deconvolution to assessment or improve an original imageries from a distorted or degraded appearance. Undertaking this usually entails constructing scientific representations of the degradation and using several signal processing systems. We propose an effective and active means termed image restoration whose ultimate objective is to develop the accurate picture from the retrieval of a deteriorated image and the actual target from the inversion of attained evidence to evaluate the novel imageries commencing the distortions or degradations. To contract through underwater imageries, former we entail towards learning the physical properties of water as intermediate which mostly reasons the distortion possessions normally existent in typical imageries like air. The perceptibility of underwater imageries stays unfortunate owing to bright reduction by way of consequence aiming cloudy. Huge quantity of specific elements in underwater normally that is imperceptible to unprotected eye by means of floating elements roots the muddiness or dimness named as Turbidity to outcomes in distorting or mixed with noise, causing in decreased image eminent structures. The distortion in underwater imageries similarly happens owing to defocusing and inappropriate principal point. The perceptibility range can be enlarged with non-natural lighting incline to illumine the act popularly not same, creating a luminous spot in the midpoint of appearance by way of unwell illumined part adjoining it. In underwater, for instance the quantity of light diminishes while we drive shallower and shallower the color lessens which rest continuously their wavelengths and only blue hue journeys extended submerged owing towards little wavelength and this creates the underwater imageries intensely controlled through blue hue. The key problems arise in submerged imageries are muddling, blaring, reduced perceptibility, little divergence, hue lessened. However we stay typically on distortion and blaring imageries. Underwater images are intensely degraded by causes which reasons blur and noisy in images are optical properties in water medium, turbidity (haziness or cloudiness) defocusing (out of focus) and these are united into unique function called Point Spread Function (PSF). The problem statement is specified through


$$y = Hx + n \tag{1}$$


- [Authors](#) 

- [Figures](#) 

- [References](#) 

- [Citations](#) 

- [Keywords](#) 

- [Metrics](#) 

Loading [MathJax]/extensions/MathMenu.js

IEEE Personal Account

Purchase Details

Profile Information

Need Help?

Follow

CHANGE USERNAME/PASSWORD

PAYMENT OPTIONS

COMMUNICATIONS PREFERENCES

US & CANADA: +1 800 678 4333



VIEW PURCHASED DOCUMENTS

PROFESSION AND EDUCATION

WORLDWIDE: +1 732 981 0060

TECHNICAL INTERESTS

CONTACT & SUPPORT

[About IEEE Xplore](#) | [Contact Us](#) | [Help](#) | [Accessibility](#) | [Terms of Use](#) | [Nondiscrimination Policy](#) | [IEEE Ethics Reporting](#) | [Sitemap](#) | [Privacy & Opting Out of Cookies](#)
A not-for-profit organization, IEEE is the world's largest technical professional organization dedicated to advancing technology for the benefit of humanity.

© Copyright 2021 IEEE - All rights reserved. Use of this web site signifies your agreement to the terms and conditions.

IEEE Account

Purchase Details

Profile Information

Need Help?

» Change Username/Password

» Payment Options

» Communications Preferences

» **US & Canada:** +1 800 678 4333

» Update Address

» Order History

» Profession and Education

» **Worldwide:** +1 732 981 0060

» View Purchased Documents

» Technical Interests

» Contact & Support

[About IEEE Xplore](#) | [Contact Us](#) | [Help](#) | [Accessibility](#) | [Terms of Use](#) | [Nondiscrimination Policy](#) | [Sitemap](#) | [Privacy & Opting Out of Cookies](#)

A not-for-profit organization, IEEE is the world's largest technical professional organization dedicated to advancing technology for the benefit of humanity.

© Copyright 2021 IEEE - All rights reserved. Use of this web site signifies your agreement to the terms and conditions.



Institutional Sign In

All



ADVANCED SEARCH

Conferences > 2017 IEEE International Confe...

Underwater turbidity removal through ill-posed optimization with sparse modeling

Publisher: IEEE

Cite This

PDF

A. Chrispin Jiji ; M Vivek All Authors

1 Paper Citation

39 Full Text Views



Alerts

Manage Content Alerts

Add to Citation Alerts

More Like This

Echo State Networks With Orthogonal Pigeon-Inspired Optimization for Image Restoration IEEE Transactions on Neural Networks and Learning Systems Published: 2016

A Majorize–Minimize Strategy for Subspace Optimization Applied to Image Restoration IEEE Transactions on Image Processing Published: 2011

Show More

Abstract



Document Sections

- I. Introduction
- II. Supervised Sparse Modelling with Dictionary Update
- III. Learning Compact Dictionary Adaptive Sparse Domain Selection
- IV. Local Auto Regressive Sparsity Adaptation
- V. Non-Local Self-Similarity Sparsity Adaptation

Abstract:In this paper, we incorporate an underwater deblurring method for the minimization of an energy function. The incorporated method uses ill-posed and sparse modeling for d... **View more**

Metadata

Abstract: In this paper, we incorporate an underwater deblurring method for the minimization of an energy function. The incorporated method uses ill-posed and sparse modeling for deblurring. The blur modeling is done for typical underwater turbidity which can be restored through the proposed algorithm. The incorporated algorithm uses intelligent adaptivity through the uses of trained dictionaries from local as well as global features. The result analysis showed that by achieving better image quality so far as for the performance metrics and also the performance of visual quality of the estimated image.

Published in: 2017 IEEE International Conference on Power, Control, Signals and Instrumentation Engineering (ICPCSI)

Date of Conference: 21-22 Sept. 2017 **INSPEC Accession Number:** 17860847

Date Added to IEEE Xplore: 21 June 2018 **DOI:** 10.1109/ICPCSI.2017.8392039

ISBN Information:

Publisher: IEEE

Conference Location: Chennai, India

Show Full Outline

Authors

Figures

References

Citations

Keywords

Metrics

Contents

I. Introduction

Underwater image deblurring is a challenging and vital part of image capture since most of the underwater image suffer from turbidity. The

Home 4 More ▾



Article Full-text available

Variability Studies in Advanced Genotypes of Rice (Oryza sativa L.)

October 2018 · Bioscience Trends 10(41):8707-8708

B. Manjunatha · Dr Niranjana Kumara

Research Interest ⓘ

Citations

Recommendations

Reads ⓘ

[See details](#)

1.6

2

0 new 0

1 new 23

Download

Share ▾ More ▾

Overview

Stats

Comments

Citations (2)

References (6)



Abstract and figures

The experiment was composed of 25 advanced rice genotypes with three replications in RCBD conducted in Agricultural and Horticultural Research Station, Ponnampet, University of Agricultural and Horticultural Sciences, Shivamogga. The traits panicles per square metre and yield kg/ha had higher GCV and PCV as well as high genetic variability and phenotypic variability. Yield kg/ha had high heritability coupled with GCV and PCV.



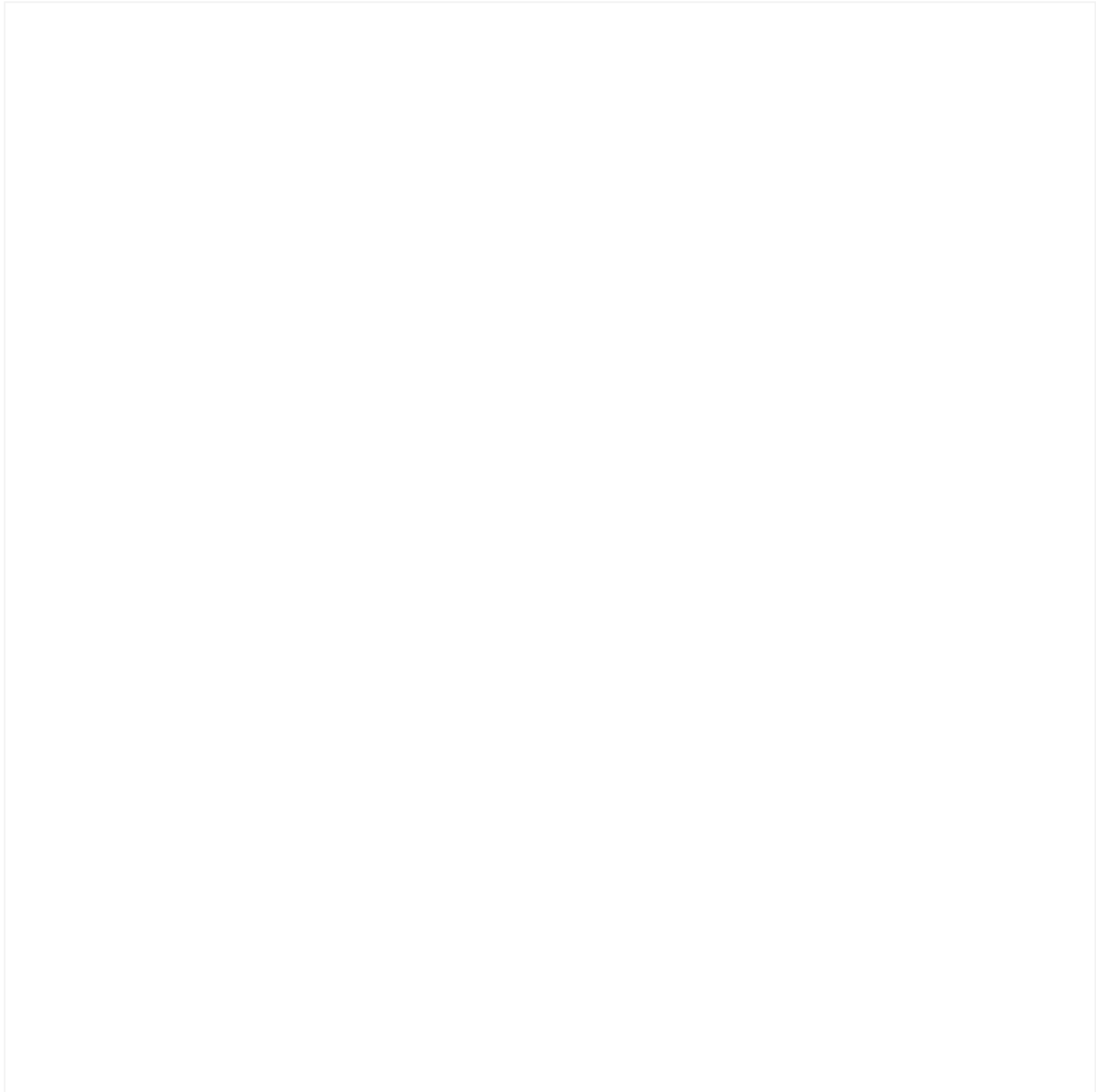


Figure content uploaded by [B. Manjunatha](#) Author content
Content may be subject to copyright.

 Public Full-text 1

Content uploaded by [B. Manjunatha](#) Author content
Content may be subject to copyright.

TRENDS IN BIOSCIENCES VOL 10-





Similar research

Genetic variability for quantitative and qualitative traits of radish (*Raphanus sativus* L.)

Article

Full-text available

February 2021

Vinay Kumar Mashkey · Balaji Vikram · K R Maurya

The present investigation entitled Genetic Variability for Quantitative and Qualitative traits of Radish which was carried out during 2019-2020 at the Horticultural Research Farm, of Department of Horticulture, AKS University, Sherganj, Satna (M.P.). Seeds were sown directly in the field on of 15 t...

2 Reads · 1 Citation

Download

Recommend Follow Share

Studies on Variability, Heritability and Genetic Advance for Quantitative Traits in Rice (*Oryza sativa* L)

Article

Full-text available

January 2018

Malleshappa C And · Dr Niranjana Kumara · B. Manjunatha

21 Reads

Download

Recommend Follow Share

Qualitative Characterization of Gum Guar (*Cymopsis tetragonoloba* L.) Genotypes

Conference Paper

Full-text available

February 2017 · International conference on chemical, agricultural and biological sciences

Dr Niranjana Kumara

—Eighty five guar (*Cymopsis tetragonoloba* L.) genotypes were collected from NBPGR, RRS, Jodhpur, Rajasthan and conducted field experiment in University of Agricultural and Horticultural Sciences, Shivamogga, Karnataka, India in the year 2014 (Kharif). The experiment was laid in RCBD and its...

171 Reads

Download


Recommend Follow Share



Genetic Variability Studies and Screening for Blast Resistance in Elite Genotypes of Rice (Oryzasativa L.)

Article [Full-text available](#)

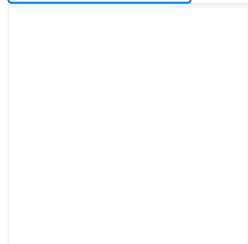
January 2017 · International Journal of Agricultural Science and Research

 Dr Niranjana Kumara

37 Reads

[Download](#)

[Recommend](#) [Follow](#) [Share](#)



Generation Mean Analysis for Yield and Quality Traits in Aromatic Genotypes of Rice (Oryza sativa L.)

Article [Full-text available](#)

December 2017

 Dilruba A. Bano ·  Sheo P Singh ·  Showkat A Waza

The present investigation in aromatic rice (*Oryza sativa* L.) was undertaken for studying the magnitude of gene action in three cross combination for eight yield and nine quality traits deploying generation mean analysis following six parameter model for parents (P1 and P2), F1, F2, BC1 and...

408 Reads · 2 Citations

[Download](#)

[Recommend](#) [Follow](#) [Share](#)

[View more related research](#)



Home 4 More ▾



Article Full-text available

A Novel Technique for Enhancing Color of Undersea Deblurred Imagery

January 2018

DOI: [10.25046/aj030610](https://doi.org/10.25046/aj030610)

Chrispin Jiji · Nagaraj Ramrao

Research Interest ⓘ

Citations

Recommendations

Reads ⓘ

[See details](#)

0.7

1

0 new 0

1 new 21

Download

Share ▾

More ▾

Overview

Stats

Comments

Citations (1)

References (30)



Abstract and figures

Exploring the ocean underneath has always been an area of great scientific and environmental concern. However, the study of underwater environment was very difficult due to the extreme conditions. Undersea descriptions undergo severe distortion attributed to absorptive as well as scattering properties. Absorption substantially removes illumination, whereas a ray of light redirected in several path when it interacts by substance. Because of these, undersea descriptions encompass blur as well as color loss. In this paper we suggested an effective technique namely, a turbidity removal method for deblurring the image. If the deblurred image has a lighting problem, we make use of a color-correction method to find the clear image. Our substantial qualitative and quantitative assessment expose that the proposed algorithm progress the excellence as well as lessen color distortion loyally, also improves the state-of-the-art undersea technique. © 2018 Advances in Science, Technology and Engineering Systems. All rights reserved.



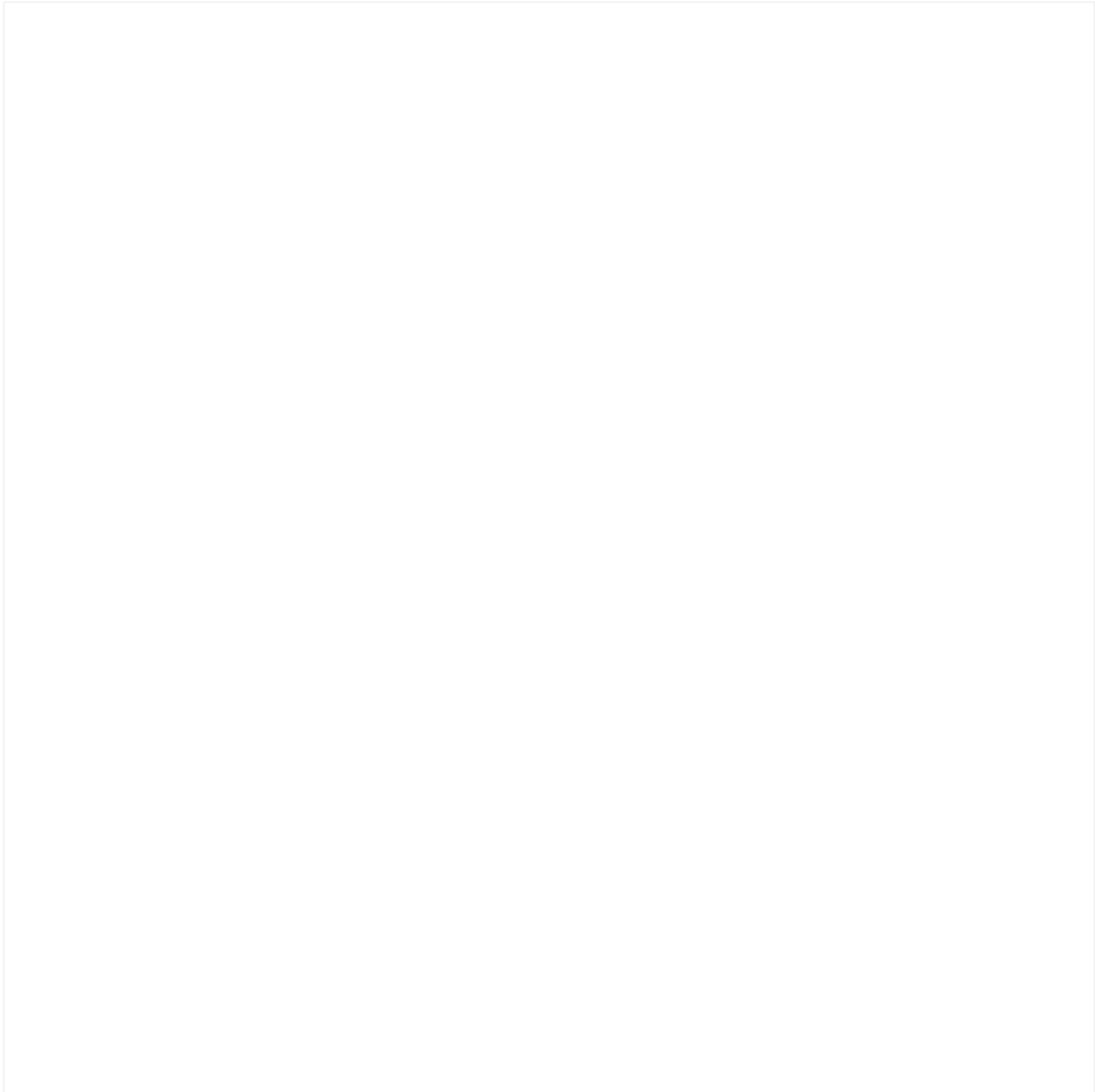

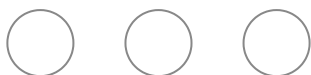


Figure content uploaded by [Chrispin Jiji](#) Author content
Content may be subject to copyright.

 Public Full-text 1

Content uploaded by [Chrispin Jiji](#) Author content
Content may be subject to copyright.





A Novel Technique for Enhancing Color of Undersea Deblurred Imagery

Chrispin Jiji*, Nagaraj Ramrao

Department of Electronics and Communication, The Oxford College of Engineering, Oxford Insti

ARTICLE INFO

Article history:

Received: 18 September, 2018

Accepted: 23 October, 2018

Online: 01 November, 2018

Keywords:

Underwater

Image Deblurring

Image Enhancement

ABSTRACT

Exploring the ocean underneath has always been environmental concern. However, the study of undersea due to the extreme conditions. Undersea descriptions are absorptive as well as scattering properties. illumination, whereas a ray of light redirected in substance. Because of these, undersea descriptions are In this paper we suggested an effective technique named deblurring the image. If the deblurred image has a color-correction method to find the clear image. quantitative assessment expose that the proposed algorithm as lessen color distortion loyally, also improves the sta

1. Introduction

Images captured in undersea has plays a vital basis of interest within various branches of technical and systematic explores [1], such as examining underneath infrastructures [2] as well as cables [3], detecting manmade objects [4], managing undersea vehicle [5], marine biology investigate [6], and archaeology [7]. Apart of normal descriptions, undersea descriptions undergo reduced visibility ensuing attenuation of the propagated illumination, mainly owing to absorption along with scattering effect. In this paper, we use image processing acting extensive interest over earlier years due to its challenging nature and its importance for the surroundings. Improving undersea scene excellence separates the problem into image restoration and image Enhancement

Visibility in undersea imagery is usually blurry, but having large number of particles underneath cause's cloudiness or more haziness, called turbidity, which causes blur in undersea imagery. To remove any blur, we usually use restoration problem with estimated or known PSF matrix.

$$b = h * d + n \quad (1)$$

If the deblurred image is use image enhancement to difficulty during lighting or reduces illumination, practical Figure 1. The objects by are imperceptible, and colors go

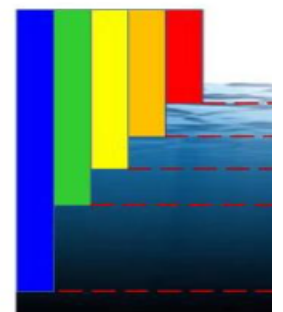


Figure 1: Dissimilar illum

Define abbreviations and ac the text, even after they have use abbreviations in the title



estimated directly as it varies depending on blur itself. Existing system uses some prior to estimate point spread function (PSF) for restoration of undersea blurred imagery.

undersea imagery is subject to picture excellence. As a result to compensate light conditions for restoration as well as e

*A. Chrispin Jiji, 8951627124 & chrispinjij@gmail.com

<https://dx.doi.org/10.25046/aj030610>



Home 4 More ▾



Article Full-text available

An Underwater Image Enhancement via Wavelet domain Gradient Guided Filter

December 2018 · International Journal of Engineering & Technology 7(4.38):944

DOI: [10.14419/ijet.v7i4.38.27614](https://doi.org/10.14419/ijet.v7i4.38.27614)

Chrispin Jiji · Nagaraj Ramrao

Research Interest ⓘ

Citations

Recommendations

Reads ⓘ

[See details](#)



--

0

0 new 0

1 new 9

Download

Share ▾

More ▾

Overview

Stats

Comments

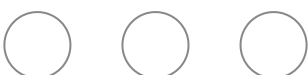
Citations

References (22)



Abstract and figures

Pictures confined in underneath are often yield limited visibility and low dissimilarity due to haze in undersea. Existing approaches enhance pictures but frequently undergo noise issue; this paper presents a hybrid method for solving mage enhancing difficulty in frequency domain. Firstly, we propose locally adaptive Non locally robust regularization to deblur the image. The deblurred image has small gray-level rate in any color channel. Secondly we used an open dim channel scheme to increase visibility in low-intensity rate. Thirdly, gradient guided filter to enhance the details. Later, we use the soft-thresholding process to decrease noise in high-intensity rate to advance texture information. Finally, image is well enhanced via wavelet domain gradient guided filter. The projected technique intends to raise perceptual visibility, keep extra texture information as well lower noise effect. The performance evaluations prove that projected scheme give up better results by existing methods.



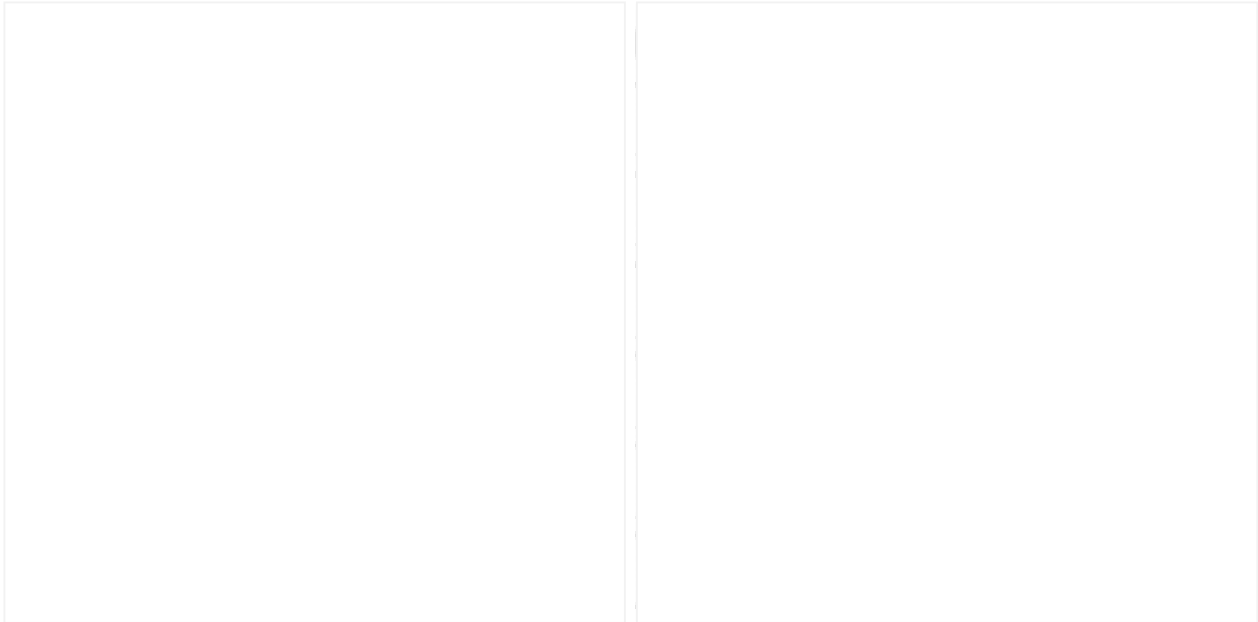

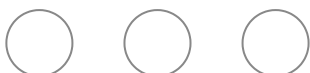


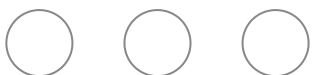
Figure content uploaded by [Chrispin Jiji](#) Author content
Content may be subject to copyright.

 Public Full-text 1

Content uploaded by [Chrispin Jiji](#) Author content
Content may be subject to copyright.

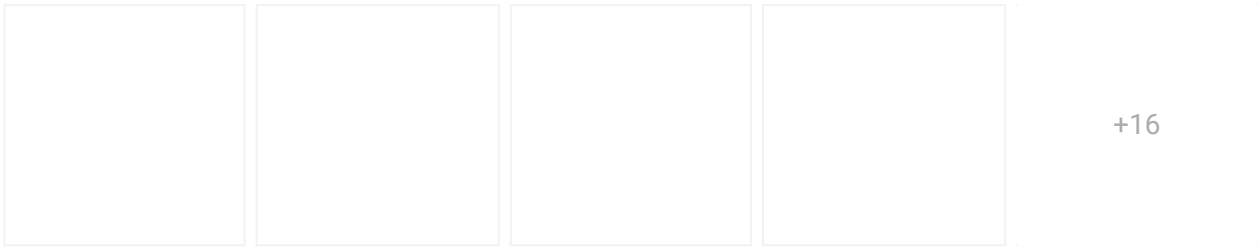
Page 1





Copyright © 201

Similar research



Underwater Image Enhancement by Wavelength Compensation and Dehazing

Article [Full-text available](#)

December 2011 · IEEE Transactions on Image Processing

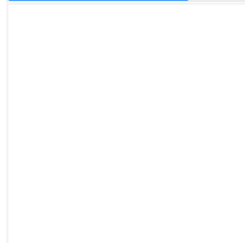
 John Y. Chiang ·  Ying-Ching Chen

Light scattering and color change are two major sources of distortion for underwater photography. Light scattering is caused by light incident on objects reflected and deflected multiple times by particles present in the water before reaching the camera. This in turn lowers the visibility and...

5,335 Reads · 543 Citations

[Download](#)

[Recommend](#) [Follow](#) [Share](#)



A Novel Technique for Enhancing Color of Undersea Deblurred Imagery

Article [Full-text available](#)

January 2018

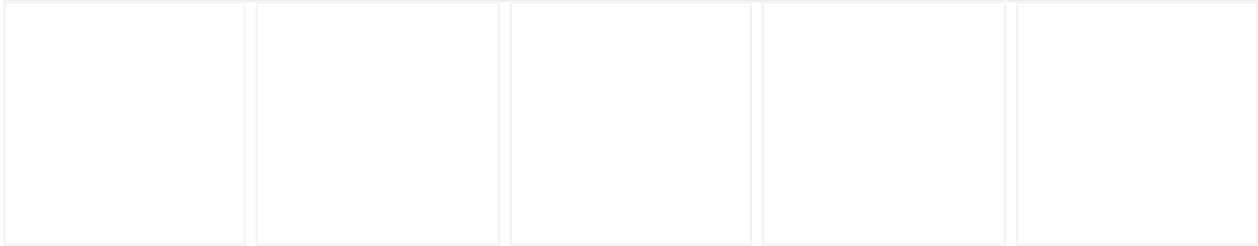
 Chrispin Jiji ·  Nagaraj Ramrao



21 Reads · 1 Citation

[Download](#)

[Recommend](#) [Follow](#) [Share](#)



Texture filtering based physically plausible image dehazing

Article [Full-text available](#)

June 2016 · The Visual Computer

Chunxiao Liu · Jinwei Zhao · Yiyun Shen · [...] · Yi Ouyang

To address the issues of false candidate atmospheric light, halo effects and color distortion in sky regions, a physically plausible single image dehazing algorithm is proposed based on texture filtering. First, gamma correction based preprocessing is applied to the luminance channel of the...

50 Reads · 13 Citations

[Download](#)

[Recommend](#) [Follow](#) [Share](#)

Single underwater image enhancement using depth estimation based on blurriness

Conference Paper [Full-text available](#)

September 2015 · 2015 IEEE International Conference on Image Processing (ICIP)

Yan-Tsung Peng · Xiangyun Zhao · Pamela Cosman

208 Reads · 74 Citations

[Download](#)

[Recommend](#) [Follow](#) [Share](#)

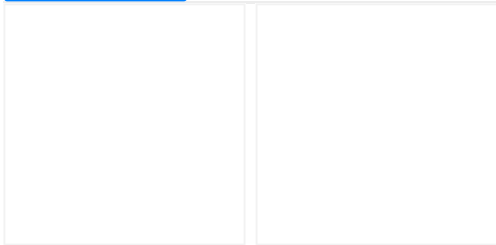


Image Haze Removal Using Dark Channel Prior and Inverse Image

Article [Full-text available](#)

January 2016 · MATEC Web of Conferences

Lei Shi · Xiao Cui · Li Yang · [...] · Jing Shi

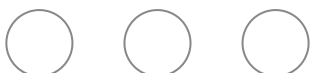
Image haze removal using dark channel prior is prone to encountering color distortion in sky and brightness region. To solve the problem, we proposed an improved method based on inverse image and dark channel prior. Firstly, we applied inverse image to estimating a new transmission map. Th...

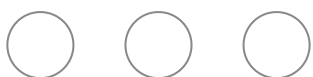
81 Reads · 6 Citations

[Download](#)

[Recommend](#) [Follow](#) [Share](#)

[View more related research](#)





See discussions, stats, and author profiles for this publication at: <https://www.researchgate.net/publication/328333705>

Variability Studies in Advanced Genotypes of Rice (*Oryza sativa* L.)

Article in *Bioscience Trends* · October 2018

CITATIONS

2

READS

19

2 authors:



B. Manjunatha

University of Agricultural & Horticultural

9 PUBLICATIONS 8 CITATIONS

[SEE PROFILE](#)



Dr Niranjana Kumara

The Trans-disciplinary University

23 PUBLICATIONS 27 CITATIONS

[SEE PROFILE](#)

Some of the authors of this publication are also working on these related projects:



AICRP on Rice [View project](#)

Variability Studies in Advanced Genotypes of Rice (*Oryza sativa* L.)

B. MANJUNATHA AND B. NIRANJANJA KUMARA

All India Coordinated Research Project, Agricultural and Horticultural Research Station, Ponnampet,
University of Agricultural and Horticultural Sciences, Shivamogga, Karnataka
email : manjugpb@gmail.com

ABSTRACT

The experiment was composed of 25 advanced rice genotypes with three replications in RCBD conducted in Agricultural and Horticultural Research Station, Ponnampet, University of Agricultural and Horticultural Sciences, Shivamogga. The traits panicles per square metre and yield kg/ha had higher GCV and PCV as well as high genetic variability and phenotypic variability. Yield kg/ha had high heritability coupled with GCV and PCV.

Key words Heritability, Rice, Variability,

Rice (*Oryza sativa* L.) is regarded as one of the major cereal crops with high agronomic and nutritional importance. It is a major source of human food for more than half of the world's population [1]. Rice is a self-pollinated cereal crop belonging to the family Gramineae (Synonym-*Poaceae*) under the order *Cyperales* and class *Monocotyledon* having chromosome number $2n=24$ [1]. The genus *Oryza* includes a total of 25 recognized species out of which 23 are wild species and two, *Oryza sativa* and *Oryza glaberrima* are cultivated [2]. It can survive as a perennial crop and can produce a ratoon crop for up to 30 years but cultivated as annual crop and grown in tropical and temperate countries over a wide range of soil and climatic condition. Rice and agriculture are still fundamental to the economic development of most of the Asian countries. Rice plays a central role in politics, society and culture, directly or indirectly employs more people than any other sector. Farmers need to achieve good yields without harming the environment so that they can make a good living while providing the rice-eating people with a high-quality, affordable staple. Underpinning this, a strong rice research sector can help to reduce costs, improve production and ensure environmental sustainability. Indeed, rice research has been a key to productivity and livelihood.

Yield enhancement is the major breeding objective in rice breeding programmes and knowledge on the nature and magnitude of the genetic variation governing the inheritance of quantitative characters like yield and its components is essential for effective genetic improvement. A critical analysis of the genetic variability parameters, namely, Genotypic Coefficient of Variability (GCV), Phenotypic Coefficient of Variability (PCV), heritability and genetic advance for different traits of economic importance is a major pre-requisite for any plant breeder to work with crop improvement programs. The present investigation was undertaken in this context to elucidate information on variability, heritability, genetic advance, character associations and path of effect in promising rice genotypes. A good knowledge of genetic resources might also help in

identifying desirable genotypes for future hybridization program.

MATERIAL AND METHODS

The experiment was carried out during *kharif*, 2012 at Agricultural and Horticultural Research station, Ponnampet under University of Agricultural and Horticultural Sciences, Shivamogga, Karnataka. The material comprised of 25 advanced rice genotypes (Table 1) sown in a Randomized Complete Block Design with three replications with spacing of 20 x 15 cm. Data were recorded on five randomly selected plants in each entry in each replication for the traits days to 50% flowering, Plant height (cm), Productive tillers/m² and Yield kg/ha. The data subjected to INDOSTAT software to estimate Genetic coefficient of variation (%), phenotypic coefficient of variation (%), Heritability (%) (Broad sense), Genetic Advance and Genetic Advance as percent of mean. The estimates for variability treated as per the categorization proposed by Siva Subramanian and Madhavamenon [4], heritability and genetic advance as percent of mean estimates according to criteria proposed by Johnson *et al.* [2].

RESULTS AND DISCUSSION

In the present experiment, analysis of variance revealed the existence of significant differences among genotypes for all traits studied. The mean, variability estimates *i.e.*, Genetic coefficient of variation (%), phenotypic coefficient of variation (%), Heritability (%) (Broad sense), Genetic Advance as percent of mean are presented in Table 2. All traits under studied have higher phenotypic coefficient of variation than genotypic coefficient of variation. The magnitude of phenotypic coefficient of variation and genotypic coefficient of variation was moderate to high for the traits panicles per square metre and yield [3, 5]. The high PCV observed for yield per hectare [5]. The high GCV obtained for number of panicles per square metre indicating the improvement is possible through selection. Genotypic coefficient of variation measures the extent of genetic variability percent for a trait but does not assess the amount of genetic variation which is heritable. Heritability estimates were high for all the characters. The heritability estimates along with genetic advance can be useful to predict effect of selection in selection programmes. The traits like days to fifty percent flowering, yield kg/ha [7] and Plant height (cm) exhibited higher magnitude of genetic advance as percent of mean. The traits plant height (cm), days to fifty percent flowering, panicles per square metre and yield kg/ha have high heritability along with genetic advance as percent of mean indicate that these characters attributable to additive gene effects which are fixable revealing that improvement in these characters would be possible through direct selection.

Table 1. List of advanced rice genotypes used in Experiment.

| Serial number | Genotypes | Serial number | Genotypes |
|---------------|-----------|---------------|---------------|
| 1 | IET 22164 | 14 | IET 22486 |
| 2 | IET 22155 | 15 | IET 22489 |
| 3 | IET 22199 | 16 | Samba Mahsuri |
| 4 | Tunga | 17 | Swarna |
| 5 | IET 22461 | 18 | IET 22862 |
| 6 | IET 22462 | 19 | IET 22260 |
| 7 | IET 22223 | 20 | IET 22264 |
| 8 | IET 22439 | 21 | IET 22458 |
| 9 | IET 22477 | 22 | IET 22859 |
| 10 | IET 22490 | 23 | CRHR-32 |
| 11 | IET 22488 | 24 | IET 23486 |
| 12 | IET 22493 | 25 | BPT 5204 |
| 13 | IET 22449 | | |

Table 2. Variability, Heritability and Genetic Advance for quantitative traits in rice.

| Character | Mean | Range | Genetic coefficient of variation (%) | Phenotypic coefficient of variation (%) | Heritability (%) | Genetic advance (%) | Genetic advance as percent mean |
|---------------------------------|------|-----------|--------------------------------------|---|------------------|---------------------|---------------------------------|
| Days to fifty percent flowering | 115 | 91-140 | 10.90 | 11.04 | 0.98 | 25.88 | 22.46 |
| Plant height(cm) | 72 | 52-102 | 17.78 | 18.40 | 0.93 | 25.18 | 35.44 |
| Panicles per m ² | 398 | 185-581 | 21.05 | 23.65 | 0.80 | 154.00 | 38.66 |
| Yield kg/ha | 3538 | 1936-6773 | 31.6 | 32.36 | 0.95 | 2248.00 | 63.54 |

LITERATURE CITED

- Shajedur Hossain., Maksudulhaque M. D and JamilurRahaman., 2015, Genetic variability and association analysis in rice. *International Journal of Applied Biology and Pharmaceutical Technology*. **5(2)**: 63-65.
- Johnson, H.W. Robinson, H.F. and Costock, R.E. 1955. Estimates of genetic and environmental variability in Soyabean. *Agronomy Journal*, **47(7)**: 314-318.
- Roy, B. Hossain, M. and Hossain, F. 2001., Genetic variability in yield components of rice (*Oryza sativa* L.). *Environment and Ecology*. **19(1)**: 186-189
- Siva Subramanian, S. and Madhavamenon, P. 1973. Combining ability in rice. *Madras Agricultural Journal*. **60**: 419-421
- Thirumala Rao, V. Chandra Mohan, Y. Bhadr, D. Bharathi, D. and Venkanna,. V. 2014.
- Venkanna, V., Lingaiah, N., RajuCh and Rao, V.T. 2014. Genetic studies for quality traits of F₁ population of rice (*Oryzasativa* L.). *International Journal of Applied Biology and PharmaceuticalTechnology*. **5(2)**: 125-127.
- Vaithiyalingan, M. and Nadarajan, N. 2006. Genetic variability, heritability and genetic advance in F₁ population of inter sub-specific crosses of rice. *Crop Research*. **31(3)**: 476-477.

Received on 03-11-2017

Accepted on 05-11-2017

Relationship between microbial biomass and extracellular enzymes: a study of Pachamalai forested streams

K. Valarmathy^{1*}, R. Stephan², B.K.Manjunath¹

^{1*}Department of Biotechnology, The Oxford Engineering College of Engineering, Bangalore, Karnataka, India.
(mathy.valar@gmail.com)

²Department of Plant Biotechnology Unit, PG & Research Department of Botany, Government Arts College, Ariyalur, Tamil Nadu, India.

Abstract

In forest environments, aquatic micro fungi play a critical role in organic matter breakdown. These microorganisms break down refractory substances like lignin, allowing the microbial population to effectively use organic material. In Pachamalai rainforest streams, the primary inflow of allochthonous organic materials occurs in the autumn and is enriched with luxurious microbiota. Our study aimed to determine the relationship between microbial biomass and extracellular enzymes from the streams of Pachamalai forests. The physicochemical properties of leaves and the activity of the microbial flora on the organic matter degradation were also determined. The C: N, C: P, and N: P biofilm molar ratios were calculated based on the total N, P, and C contents of two leaves species viz. *Morinda tinctoria* and *Pongamia pinnata* leaves. The hydrolytic and oxidative enzyme activity of the leaf substrata was analysed by earlier known methods. *Morinda tinctoria* leaves had a faster breakdown with a decrease in leaf toughness relative to *P. pinnata*. Extracellular enzyme assays revealed that *M. tinctoria* had higher hydrolytic enzyme activity when compared to *P. pinnata*. From our study, it is conclusive that the microbiota associated with both the leaf species have significant extracellular enzymatic activity in degrading the polysaccharides and lignin. This plays a significant role in the stream biota and influences the ecosystem.

Keywords: Extracellular enzymes, forested stream, sporulation, microbial biomass, *Morinda tinctoria*, *Pongamia pinnata*

1. Introduction

Small streams to huge rivers, running waters usually occur in a wide range of climate, vegetation, terrain, and geological conditions (Allan J et al., 1995). Several studies have found persistent variations in biogeochemical features, hydrological parameters (Gasith et al., 1999) and biological structure and function across streams from different biomes and ecoregions. One of the most intriguing topics in earth sciences is the close interaction between abiotic conditions and the soil biosphere, which has enormous consequences for both environmental and human health (Van Elsas et al., 2008). It is not astonishing that the soil formation with a high degree of fertility is the consequence of hundreds of

years evolution of the soil due to the complex interactions between various factors (Harrison et al.,2008). The soil matrix, as well as chemical and physical characteristics of soils, such as the quality and amount of soil organic matter, pH, and redox conditions, have a significant impact on the form and function of microbial communities in soils (Lombard et al.,2011) . The size of the channel, the flow of water, and the form of the banks influence the development of biological communities(Allan J et al., 1995). Microbial communities may form in both organic (wood and leaves) and inorganic (cobles, gravel, rocks and sand) stream benthic substrata, and are comprised of algae, bacteria, fungi, and protozoa embedded in an extra polymeric material matrix(Locket al.,1984). The community structure and function may change depending on the presence of various microbial species in the substratum (Romani et al., 2000). One of the primary factors of stream water chemistry may be the chemical composition of particles in the watershed(Berner et al.,1987) . Microbial diversity in lotic settings is less often researched than in marine and lake ecosystems, according to a recent report of microbial diversity studies in aquatic habitats(Zinger et al.,2011) . With landscapes, streams and rivers are the foci of microbially mediated carbon (C) and nutrient metabolism(Valarmathy et al.,2017). Before the advent of molecular techniques, bacterial diversity was particularly difficult to characterize, beyond distinguishing gram-negative from gram-positive organisms or doing plate counts on selective medium(Milner et al.,1984) . In the stream ecosystem, fungi and bacteria are the primary producers of extracellular enzymes responsible for polysaccharides hydrolysis, lignin oxidation, breakdown of peptides, and organic phosphorus compounds peptides(Romani et al., 2014) . Physical forces, as well as the activities of microbes such as aquatic hyphomycetes, promote leaf degradation in streams(Barlocher,1992) . The activities of these organisms accompanied by chemical reactions, cause changes in litter quality (e.g., increases in N and P concentrations) and loss of litter mass. To evaluate microbe colonization patterns (Gessner et al.1993) , to assess the ecological state of the stream ecosystem(Panet al., 1996) , and to study the interactions between microbial groups and species in the group, a community composition investigation is essential(Rieret al., 2001 ; Gulis et al., 2003) . It seems easier to identify algal and fungal species up against the bacterial diversity in the streams.

Our study aimed to determine the relationship between microbial biomass and extracellular enzymes from the streams of Pachamalai forests. It will also give an insight into the physicochemical properties of leaves and the activity of the microbial flora on organic matter degradation.

2. Material and Methods

2.1 Estimation of physicochemical properties of leaves

The microbial communities like fungi are usually found in leaf substrate and leaf tissues. Therefore, the physical and chemical properties of the leaves are largely responsible for the development of the

microbial community on organic substrata. In our study, chemical properties such as Carbon (C), Nitrogen (N) and Phosphorus (P), and Lignin content were determined.

2.1.1 Determination of Carbon, Nitrogen and phosphorus content

Leaf circles were dried and the weights of subsamples were recorded. These leaf circles were placed in the tin foil crucibles and then inside the CN Elemental Analyzer. The phosphorus content of the leaf subsamples was determined by basic digestion using NaOH by autoclaving(Grasshoff et al., 1980) at 110°C for 90 min. Further the C: N, C: P, and N: P biofilm molar ratios were calculated based on the total N, P, and C contents of the leaves.

2.1.2 Estimation of Lignin Content

Pongamia pinnata and Morinda tinctoria species were considered for the estimation of Lignin content. According to the method of Iiyama & Wallis (1990), the leaf circles were first digested with a mixture of 4% perchloric acid and 25% acetyl bromide (in acetic acid medium) at 70°C for 30 min. The equation of Morrison(Morrison et al., 1972) was used to determine the lignin content of the samples.

2.2 Enzyme activity

The enzyme activity of the microbial flora associated with leaves was tested to determine the activity of hydrolytic and oxidative enzymes.

2.2.1 Estimation of Hydrolytic enzyme assays

The extracellular enzyme activity was measured using the methodology described by Romani & Sabater(Romani et al.,2001) . Six diverse hydrolytic enzyme assays were performed in this study namely -glucosidase, β -xylosidase, cellobiohydrolase, phosphatase, leucine-aminopeptidase, and β -glycosaminidase activity. These assays determined the decomposition rate of compounds viz. polysaccharides, organic phosphorus, peptides, and chitin respectively. All these assays were performed at the Indian Institute of Food Processing Technology (IIFPT), Tanjore, Tamilnadu and the obtained results were utilized for further studies.

2.2.2 Estimation of Oxidative enzymes assay

The microbiological colonies on stream substrata were also analyzed for the phenoloxidase and peroxidase enzyme activities. Fungi produce ligninolytic peroxidases and phenol oxidase which oxidize lignin polymer to generate aromatic radicals(Hammel et al.,1997) . In this study, L-3,4-dihydroxyphenylalanine (L-DOPA) is an electron-donor substrate used for the detection of phenoloxidase activity. The oxidative enzyme activity assay was carried out at IIFPT, Tanjore, Tamilnadu and the results were further utilized for the study.

2.3 Estimation of Fungal Sporulation Rates

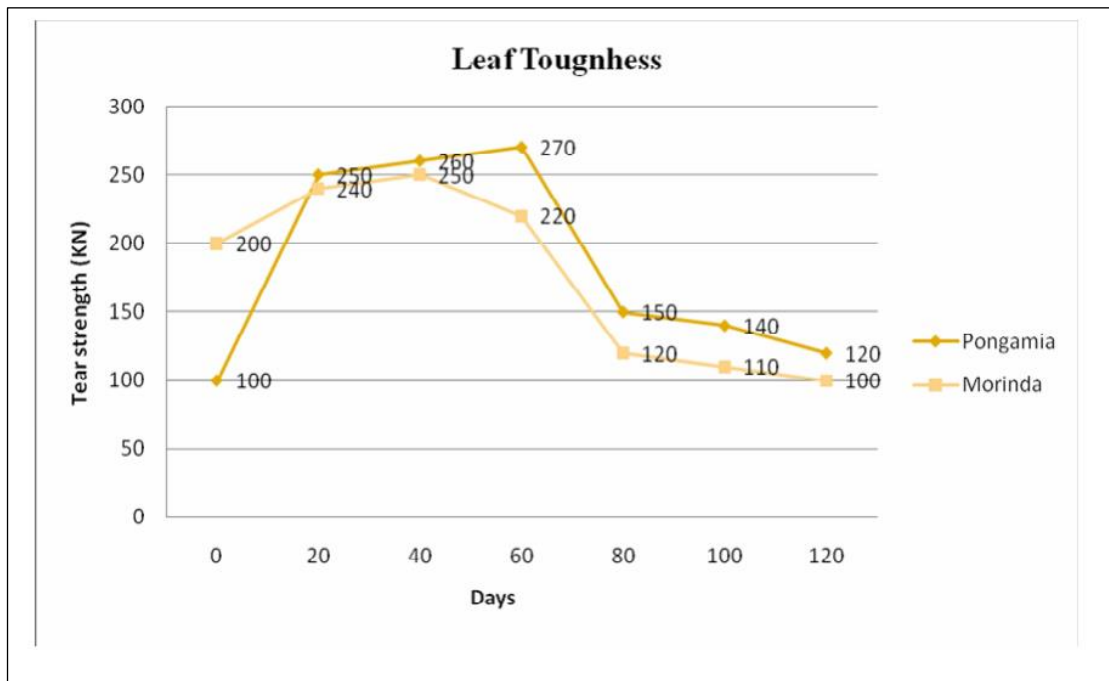
Leaf discs of *P. pinnata* and *M. tinctoria* were used to measure the sporulation rates of aquatic hyphomycetes. Sand samples, tiles, and leaves were washed with sterile water before incubation to remove the surface deposits of biofilms. Pyrex flasks of 250ml containing 100ml sterilized steam water were used to incubate the substratum samples. The samples were all incubated in a shaking bath at 80rpm, 10°C for 48 h to induce sporulation. Later, 25µL of 0.5% (w/v) Triton X-100 solution was added and 20ml of the conidial suspension was passed through Nitrocellulose membranes (5µm pore size, Whatman). The membranes retained the conidial spores which were later stained with 0.1% Trypan Blue (Baldy et al., 2002). The retained conidial spores were stained with 0.1% Trypan blue (dissolved in 60% lactic acid). Leaf samples were counted at 400× magnification, whereas the fine and coarse samples of substrata were counted using the whole filter. Sporulation rates were expressed as below:

$$\text{Sporulation rate} = \frac{\text{number of conidia produced}}{\text{unit surface area and time}} \text{ cm}^2 \cdot \text{day}$$

3. Results and Discussion

Field observations suggest that *M. tinctoria* leaves had a faster decomposition rate when compared to *P. pinnata*. It was also found that *P. pinnata* only remained in the litter bags after 58 days. The faster breakdown was seen in *M. tinctoria* accompanied by a decrease in leaf toughness on Day 7 while compared to *P. pinnata* (Figure 1).

Figure 1. Leaf tear strength of the two-leaf species, *M. tinctoria* and *P. pinnata* in the litter bag experiment.



Values are represented as mean (n=3) and standard errors of each sampling date.

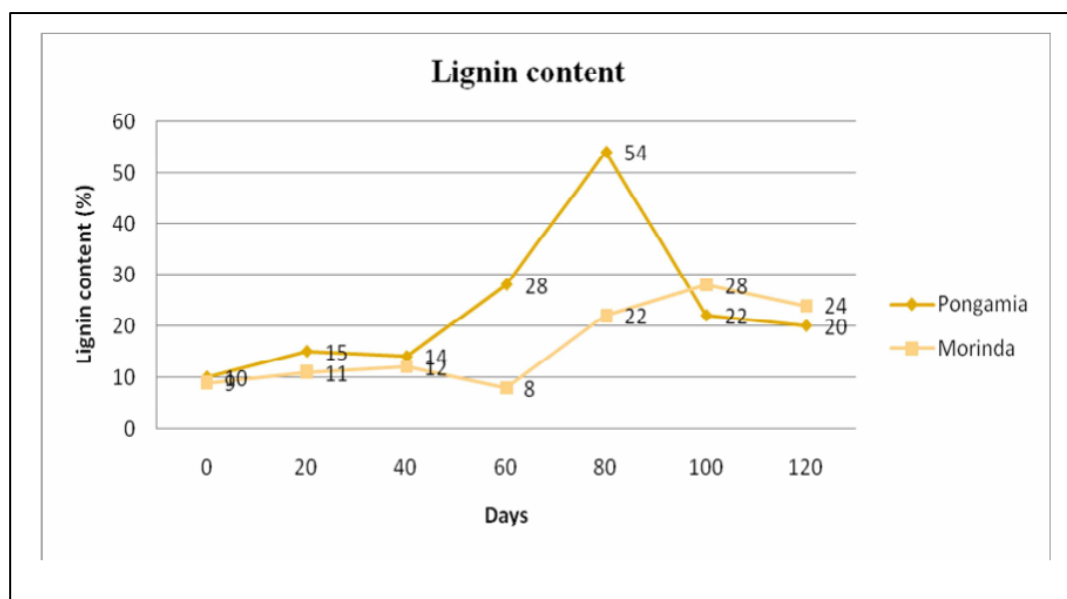
Experimentally, it was observed that the nutrient molar ratios C:N and C:P in leaves showed a drastic decrease on Day 7 and Day 17. Statistical significance was observed only in the decreasing trend of C:N ratio. Meanwhile, no drastic changes were observed in the N:P ratio during the experiment. Table 1 explains the difference in the nutrient molar ratios between *M. tinctoria* and *P. pinnata*.

Table 1. The molar ratios C: N, C: P and N: P of the two-leaf species as obtained in the litter bag experiment.

| Days | C: N | | C: P | | N: P | |
|------|-------------------------------|---------------------------------|-------------------------------|---------------------------------|-------------------------------|----------------------------------|
| | <i>P. pinnata</i> Mean(SE) | <i>M. tinctoria</i> Mean(SE) | <i>P. pinnata</i> Mean(SE) | <i>M. tinctoria</i> Mean(SE) | <i>P. pinnata</i> Mean(SE) | <i>M. tinctoria</i> Mean (SE) |
| 0 | 75.5 (0.5) | 90.4 (2.4) | 838.7(120.4) | 710.4 (68.2) | 70.5 (11.5) | 50.0 (2.5) |
| 1 | 64.5 (0.8) | 95.5 (12.2) | 864.2 (116.1) | 2245.5 (490.6) | 94.2(26.2) | 148.6(12.0) |
| 2 | 92.1 (10.9) | 96.6 (16.4) | 838.5 (260.4) | 1875.2(782.2) | 65.1 (24.1) | 128.1 (41.0) |
| 4 | 81.5 (1.0) | 91.1 (4.4) | 1344.4 (92.8) | 1306 (198.4) | 106.7 (7.5) | 95.4 (15.0) |
| 7 | 92.3(0.4) | 68.2(5.7) | 986.0(102.6) | 1072.1 (95) | 71.1(9.6) | 100.6 (4.8) |
| 17 | 56.9 (0.5) | 45.7 (0.8) | 564.2 (58.2) | 390 (30.3) | 62.1 (2.2) | 52.4 (1.4) |
| 28 | 38.4 (1.4) | 36.1 (1.0) | 451.4(26.5) | 386.2 (34.0) | 74.5(4.2) | 64.2 (5.4) |
| 44 | 52.4 (0.2) | 45.7(0.9) | 506.1 (61.3) | 403.2 (62.4) | 62.2(7.8) | 56.4 (8.6) |
| 58 | 44.6 (5.5) | 42.4 (2.6) | 492.2 (124.2) | 621.1 (136) | 65.6 (10.6) | 92.1 (12.4) |
| 73 | 49.5 (2.1) | 656.1 (24.3) | 85.1(2.2) | | | |
| 93 | 35.1 (2.6) | 322.5(34.2) | 60.2 (10) | | | |
| 112 | 54.2 (1.0) | 476.2(28.4) | 56.1(4.3) | | | |

Our study showed that the content of lignin was in a similar range between different leaf species, however, during breakdown the changes in the percentage of lignin were noticed (Figure 2).

Figure 2. Percentage of lignin content in the leaves of *M. tinctori* and *P. pinnata* during the degradation procedure.



Values are represented as mean (n=3) and standard errors of each sampling date.

Hydrolytic and oxidative enzyme assays revealed that the polysaccharide and lignin degradation increased during the breakdown experiment (Table 2). The polysaccharide degrading activities in *M. tinctoria* showed an increasing trend during week 2 (Day 7- Day 17), a sharp peak was noted on Day 44 and then decreased on day 56 (Figure 3.2a). A similar trend was observed in the activities of *P. pinnata* leaves. The evaluation of phenol-oxidase assay exposed that a common pattern was noticed among the two leaf species i.e., an increase after Day 7, a plateau on Day 17, and further extended until the end of the experiment (Figure 3.2b). It is evident from hydrolytic enzyme activity that *M. tinctoria* had higher activity when compared to *P. pinnata*, however, the other activities had many similarities between the two species. Biomass-specific enzyme assays showed higher activity in *P. pinnata* leaves than in *M. tinctoria* (Figure 3.2c). This suggests that the microbial biomass on *P. pinnata* had better decomposing activity than that of *M. tinctoria*. Moreover, a sharp peak was observed in the enzyme activity per unit of microbial carbon at the onset of the experiment that gradually decreased later (Figure 4).

Table 2. Extracellular enzyme activities in *P. pinnata* and *M. tinctoria* leaves, and leaf physical and chemical properties during the breakdown experiment.

| | C: N | C: P | Toughness |
|------------------------|----------|----------|-----------|
| Pongamia (n=12) | | | |
| β-glucosidase | -0.825** | -0.786** | -0.821** |
| β-xylosidase | -0.75** | -0.742** | -0.810** |
| cellobiohydrolase | -0.650** | -0.756** | -0.614** |
| phenol oxidase | -0.784** | -0.736** | -0.768** |

| | | | |
|-----------------------|----------|----------|----------|
| bacterial biomass | -0.690** | -0.712** | -0.784** |
| fungal biomass | -0.612* | -0.625** | -0.822** |
| Morinda (n=12) | | | |
| β-glucosidase | -0.910** | -0.748* | -0.878** |
| β-xylosidase | -0.754* | ns | -0.836** |
| cellobiohydrolase | -0.716* | ns | -0.824** |
| phenol oxidase | -0.798** | -0.677* | -0.796* |
| bacterial biomass | -0.886** | -0.693* | -0.948** |
| fungal biomass | ns | ns | Ns |

Note: Significant correlations are indicated by asterisks [(*) for P<0.05 and (**) for P< 0.005] while the not significant are indicated by (ns).

Figure 3. Graphical representation of enzyme activities during the breakdown of the two leaf species (a) β-glucosidase, (b) β-xylosidase, (c) cellobiohydrolase and (d) Phenol oxidase.

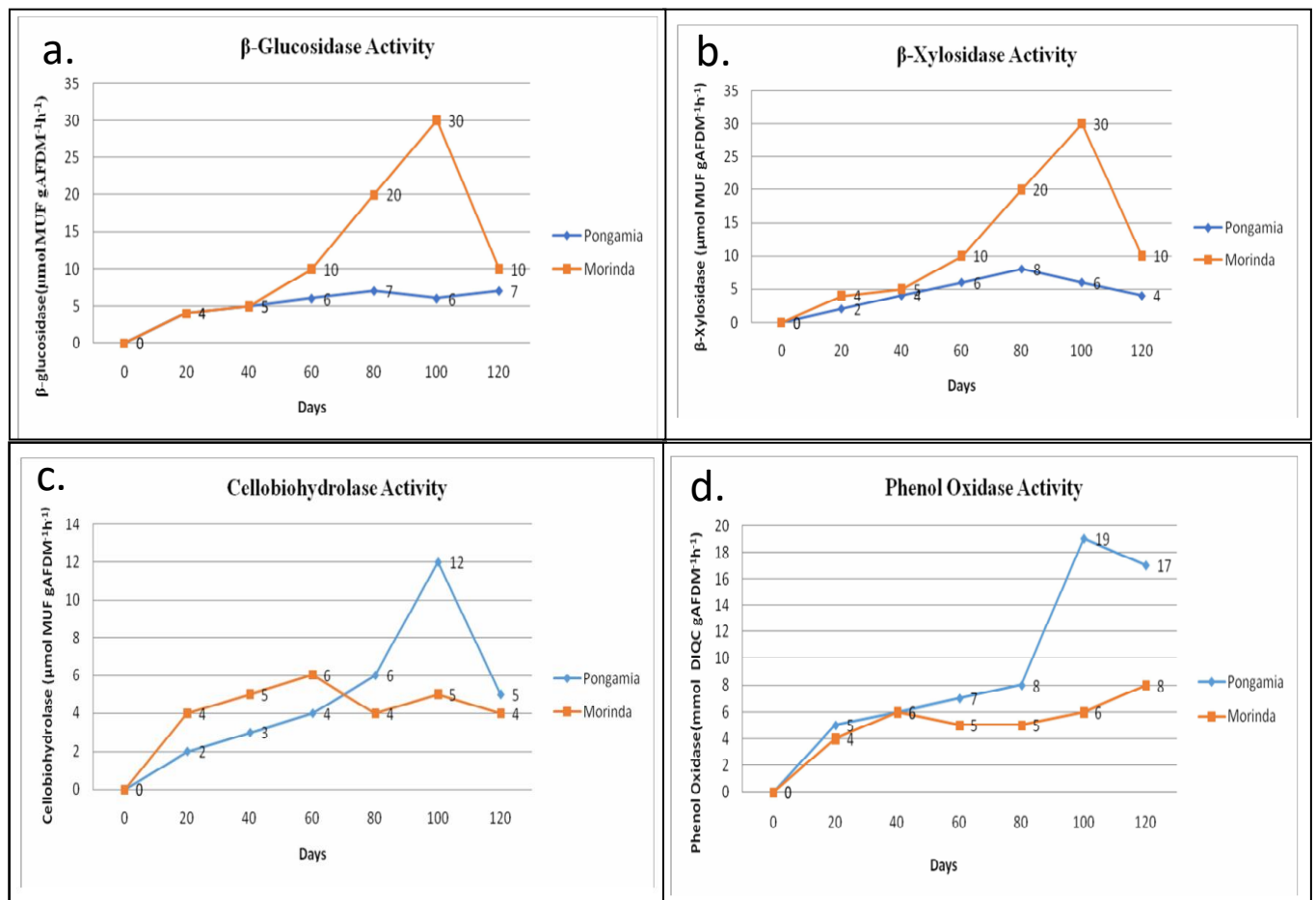
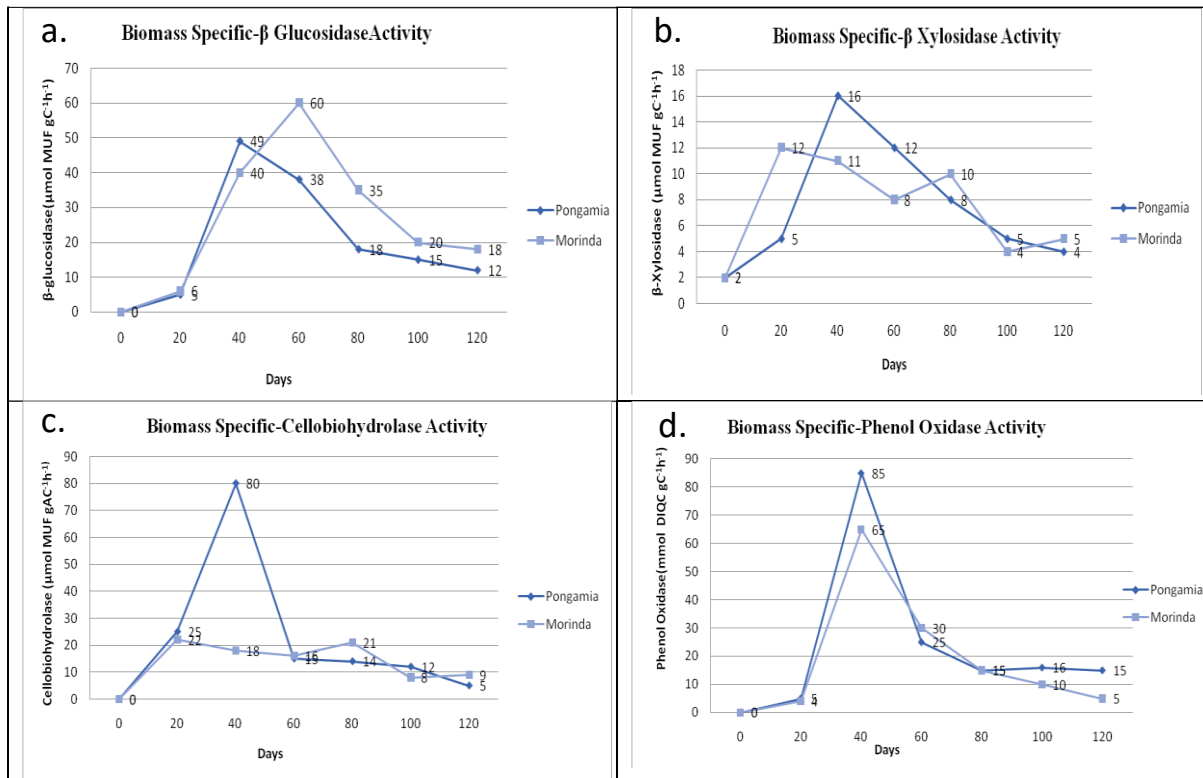


Figure 4. Biomass specific enzyme activities of (a) β -glucosidase, (b) β -xylosidase, (c) cellobiohydrolase and (d) Phenol oxidase on the two-leaf species during the experiment.



Sporulation rates greatly varied among the two-leaf species as shown in Table 3. It was studied that the fungal sporulation rates were higher in organic substrata than those of the inorganic substrata. *P. pinnata* leaves recorded the highest fungal sporulation rates. Finally, we could conclude that a prolonged enrichment experiment affected the inorganic substrata sporulation meanwhile addition of nutrients could not generate any effect of significance (Table 3).

Table 3. Analysis of variance considering the effect of different factors on sporulation rates.

| Sources | Sporulation rates |
|----------------------------------|-------------------|
| Substrate (S) | F3.32 = 162.50 |
| | P < 0.001 |
| Long - term Enrichment (E) | F1.32 = 8.04 |
| | P < 0.01 |
| Short-term Nutrient Addition (N) | F1.32 = 0.18 |
| | P = 0.626 |
| S x E | F3.32 = 7.06 |
| | P < 0.0001 |

| | |
|------------------|--------------|
| S x N | F3.32 = 1.20 |
| | P=0.302 |
| E x N | F1.32 = 0.64 |
| | P=0.410 |
| S x E x N | F3.32 = 6.08 |
| | P < 0.005 |

Berg (1986) proposed that the decomposition of fresh leaves begins with the easily mineralized fractions of non-lignified carbohydrates, followed by the mineralization of more refractory fractions of lignified carbohydrates in later stages. CBH activity was high for the entire period in the Koraiyaru stream after leaf fall peak (October), but P and PO activity increased only after several weeks. This finding suggests that OM decomposition began with cellulose degradation and progressed to the degradation of lignin-related chemicals. In our earlier study, rDNA methods revealed a higher bacterial species richness. The degradation of organic materials followed a distinct temporal pattern, with notable changes in enzyme activity and ergosterol levels between substrata. Berg(1986) proposed that the decomposition of fresh leaves begins with the easily mineralized fractions of non-lignified carbohydrates, followed by the mineralization of more refractory fractions of lignified carbohydrates in later stages. CBH activity was high for the entire period in the Koraiyaru stream after the leaf fall peak (October), but P and PO activity increased only after several weeks.

Physico-chemical factors, such as discharge and dissolved inorganic nitrogen DIN, might, nevertheless, influence the enzymatic activity time-pattern. Several studies in forested streams in the autumn or early winter suggest that the majority of the nitrate in the catchment of the streams is mobilized(Gasith et al.,1997; Bernal et al., 2002) . The weathering of dissolved and particulate organic matter deposited on the soil after the dry period (summer) caused N content in stream water to be positively connected with lignocellulosic activities (P and PO). As a result, in a system where N may be a scarce resource, nitrate availability boosted fungal activity (Romani et al., 2004). The enzymatic activity of biofilms varied between species' leaves, which could be due to changes in leaf composition (C:N ratio, lignin content, polyphenol content, leaf durability)(Griffin, 1994). Lower enzymatic activity for the biofilm on *P. pinnata* was identified in previous research on leaf decomposition in soil and other aquatic habitats, and similar results were observed in *P. pinnata* species of our study. The high C:N ratio recorded in this substratum could be the reason for the material's low mineralization(Bernal et al.,2003).

Baldy et al.,(1995) supported our current work by demonstrating the role of bacteria in the late phases of the leaf breakdown process. Throughout the study period, estimates of ergosterol

concentration per stream reach demonstrated a progression of fungal biomass, which dropped only after the majority of the material had been treated. In the forested stream of Pachamalai, rDNA methods confirmed a higher bacterial species richness (Valarmathy et al., 2017). In terms of selection and colonization of streambed substrata during the fall, the fungi may be called facultative microorganisms. They take advantage of a new allochthonous CPOM that was introduced to the system in the fall. Our work is a clear evidence of the influence of microbiota on the stream in aquatic environment.

Conclusion

In conclusion, our study have given an insight into the microbiota associated with both the leaf species and their role in extracellular enzymatic activity in degrading. Also, out of the two species *P. pinnata* showed significant content of polysaccharides and lignin degradation activity than that of *M. tinctoria*. This plays a significant role in the stream biota and influences the ecosystem.

Acknowledgments

The authors would like to thank the Plant Biotechnology Unit, PG and Research Department of Botany, Government Arts College Ariyalur for providing all the facilities for conducting this research.

References

- [1] Allan, J., Stream ecology: Structure and function of running waters. Chapman & hall, London 255, **(1995)**.
- [2] Gasith, A., and Resh, V.H., Stream in Mediterranean climate regions: abiotic influence and biotic responses to predictable seasonal events, *Annu. Rev. Ecol. Syst.*, 30, 51-81 **(1999)**.
- [3] Van Elsas, J.D., Costa, R., Jansson, J., Sjoling, S., Bailey, M., Nalin, R., Vogel, T.M. and Van Overbeek. L., The metagenomics of disease-suppressive soils – experiences from the METACONTROL project, *Trends Biotechnol.*, 26:591–601 **(2008)**.
- [4] Harrison, R. B., and Strahm, B., Soil formation, *Encycl. Ecol.*, 2008; 3291–3295, **(2008)**.
- [5] Lombard, N., Prestat, E., van Elsas, J. D., and Simonet, P., Soil specific limitations for access and analysis of soil microbial communities by metagenomics, *FEMS Microbiol. Ecol.*, 78, 31–49 **(2011)**.
- [6] Lock, M.A., Wallace, R.R., Costerton, J.W., Ventullo, R.M. and Charlton, S.E., River epilithon: Toward a structural – functional model, *Oikos*, 42, 10-22 **(1984)**.
- [7] Romani, A.M. and Sabater, S., Influence of algal biomass on extracellular enzymes activity in river biofilms. *Microbial Ecol.* 40, 16-24 **(2000)**.
- [8] Berner, E.K., and Berner, R.A. The global water cycle: Geochemistry and environment. Prentice-Hall, Englewood Cliff **(1987)**.

- [9] Zinger, L., Amaral-Zettler, L. A., Fuhrman, J. A., Horner-Devine, M. C. and Huse, S.M., Global patterns of bacterial beta-diversity in seafloor and seawater ecosystems, *PLoS One* 6, 24570 (2011).
- [10] Valarmathy, K., and Stephan, R., Relationship of Nutrient molar ratio of microbial attached communities in organic matter utilization of Pachamalai forested stream, *Int. J. Adv. Multidiscip. Res.* 4(10), 18-28 (2017).
- [11] Milner, C.R. and Goulder, R., Bacterioplankton in an urban river : The effects of a metal-bearing tributary. *Water Res.* 18, 1395–1399 (1984).
- [12] Romani, A.M., Giorgi, A., Acuna, V. and Sabater, S., The influence of substratum type and nutrient supply on biofilm organic matter utilization in streams. *Limnol. Oceanogr.*, 49, 1713-1721 (2004).
- [13] Barlocher, F., *The ecology of aquatic hyphomycetes*. Springer-Verlag, Berlin (1992).
- [14] Gessner, M.O. and Chauvet, E., Ergosterol-to-biomass conversion factors for aquatic hyphomycetes. *App. Environ. Microbiol.*, 59, 502-507 (1993).
- [15] Pan, Y., Stevenson, R.J., Hill, B.H., Herlihy, A.T., and Collins, G.B., Using diatoms as indicators of ecological conditions in lotic systems: A regional assessment. *J. North Am. Benthol. Soc.*, 15, 481-495 (1996).
- [16] Rier, S.T. and Stevenson, R.J. Relation of environmental factors to density of epilithic lotic bacteria in 2 ecoregions. *J. North Am. Benthol. Soc.*, 20(4), 520-532 (2001).
- [17] Gulis, V., and Suberkropp, K., Effect of inorganic nutrients on relative contributions of fungi and bacteria to carbon flow from submerged decomposing leaf litter. *Microbial Ecol.* 2003; 45:11–19 (2003).
- [18] Grasshoff, K., Ehrhardt, M., and Kremling, K., *Methods of seawater analysis*. Second, Revised and extended Edition. Verlag Chemie, Weinheim, (1983).
- [19] Iiyama, K., and Wallis, A.F.A., Determination of lignin in herbaceous plants by an improved acetyl bromide procedure. *J. Sci. Food Agric.* 51, 145-151 (1990).
- [20] Morrison, I.M., A Semi micro method for the determination of lignin and its use in predicting the digestibility of forage crops. *J. Sci. Food Agric.* 23, 455-463 (1972).
- [21] Romani, A.M., and Sabater S., Structure and activity of rock and sand biofilms in a Mediterranean stream. *Ecology* 82, 3232-3245 (2001).
- [22] Hammel, K.E., Fungal degradation of lignin. In: *Driven by nature: Plant litter quality and decomposition*, pp. 35-45. CAB, International, Willingford, (1997).

[23] Baldy, V., Chauvet, E., Charcosset, J.Y., and Gessner, M.O., Microbial dynamics associated with leaves decomposing in the mainstem and floodplain of a large river. *Aquat. Microb. Ecol.* 28, 25–36 **(2002)**.

[24] Berg. Nutrient release from litter and human in coniferous forest soils: A mini-review. *Scand. J. For. Res.* 1, 359-369 **(1986)**.

[25] Gasith, A., and Resh, V.H., Streams in Mediterranean climate regions: abiotic influences and biotic response to predictable seasonal events. *Annu. Rev. Ecol. Evol. Syst.* 30, 51-81 **(1999)**.

[26] Bernal, S., Butturini, A., Nin, E.F., and Sabater, S., Variability of DOC and nitrate responses to storms in a small Mediterranean forested catchment. *Hydrol. Earth Syst. Sci.* 6,1031-1041 **(2002)**.

[27] Griffin, D.H., *Fungal physiology*, 2 edn. Wiley-Liss, New York **(1994)**.

[28] Bernal, S., Butturini, A., Nin, E.F., and Sabater, S. Leaf litter dynamics and nitrous oxide emission in a Mediterranean riparian forest implications for soil nitrogen dynamics. *J. Environ. Qual.* 32, 191-197 **(2003)**.

[29] Baldy, V., Gessner, M.O., and Chauvet, E. Bacteria, fungi and the breakdown of leaf litter in a large river. *Oikos* 74, 93-102 **(1995)**.

[30] Valarmathy, K., and Stephan, R., 16s rDNA based identification of bacteria in the organic matter of Pachamalai forested streams. *Int. J. Comp. Res. Biol. Sci.* 4(12), 1-10 **(2017)**.



Organic matter availability structures of microbial biomass and their activity in Pachamalai Forested stream in Tamilnadu.

K.Valarmathy and R. Stephan*

Department of Biotechnology, The Oxford College of Engineering, Bangalore- 68.

* Plant Biotechnology Unit, PG & Research Department of Botany, Government Arts College, Ariyalur- 621 718.

*Corresponding author: stephan.biotech@gmail.com

Abstract

Microbial biomass (bacteria, fungi, algae) and the activity of extracellular enzymes used in the decomposition of organic matter among different benthic substrata over one hydrological year in a Pachamalai stream. Microbial heterotrophic biomass (bacteria plus fungi) except during short periods of high light availability in the spring and winter. Bacterial and fungal biomass increased with the decomposition of cellulose and hemicellulose compounds from leaf material. Later, lignin decomposition was stimulated in fine (sand, gravel) and coarse (rocks, boulders and cobbles) substrata by the accumulation of fine detritus. In the drought provoked an earlier leaf fall. The resumption of the water flow caused the weathering of riparian soils and subsequently a large increase in dissolved organic carbon and nitrate, which led to growth of bacteria and fungi.

Keywords: Microbial diversity; microbial population; bacterial community; organic matter.

Introduction

Microbial heterotrophs (bacteria and fungi) can produce a broad range of substrate – specific enzymes that enable allochthonous and autochthonous organic matter (OM) mineralization (Arnosti, 2003). This substratum is decomposed by physical, chemical, and biological factors. Lignocelluloses the major components of biomass are degraded by that enzyme itself. Natural disturbance, from seasonal changes rainfall and tree fall, to hurricane damage, cause population shifts and changes to communities of bacteria (Lyautey, *et al.*, 2005). To understand the ecology of these microorganisms, their interactions, and the functions they perform, it is important to study them in their natural habitats (Sterflinger, *et al.*, 1998).

Leaf breakdown in streams is caused by the joint action of physical factors, the activity of microorganisms, such as aquatic hypomyces (Barlocher, 1992).

Microorganisms like bacteria and fungi are among the few organisms that secrete enzymes that can break down large molecules, such as cellulose, chitin, and lignin, into smaller compounds that can be taken up by the biota (Sinsabaugh, and Linkins. 1990.). The untapped diversity of microorganisms is a resource for new genes and organisms of value to biotechnology. The diversity patterns of microorganisms can be used for monitoring and predicting environmental change.

In present study water sediments and leaf litter samples were collected from streams of Mayiluthu and Koraiyar streams in Pachamalai hills situated in Trichy Dt. Tamil Nadu. To study the role of different microbial groups as decomposers in the littoral area and their metabolic and structural responses of sediment in microbial communities to the addition of different carbon substances have been assessed.

Materials and Methods

Study area

In the study area are Pachamalai hills, located in Trichy District. Tamilnadu, india. situated 3000 feet above sea level lying between 78° 31' East and 11° 28' North and 11° 10' South and 78° 20' West Latitude. In the Pachamalai forested streams several streams are present. In present work all samples were collected in Koraiyar and Mayiluthu streams.

Sampling

Monthly samples were taken (from March 2015 until February 2016) at different scales of coarse particulate organic matter (CPOM), POM transported by the water, and water nutrient concentration. The visually estimated the relative cover (%) of coarse substrata (cobbles, boulders and rocks), fine substrata (gravel and sand), leaves (distinguishing the relative cover of *Pongamia pinnata*, *Morinda tinctoria* and *Acacia nilotica*), branches and fine detritus.

At the habitat scale, collected distinct benthic substrata (leaves, sand and tiles) Analysed them for microbial biomass (algae bacteria and fungi) and extracellular enzyme activity (α-glucosidase, α-xylosidase, leucine-aminopeptidase, phosphatase, cellobiohydrolase and phenoloxidase activity). Benthic substrata were classified as coarse (rocks, boulders and cobbles), fine (sand) or leaves (the three dominant species in the reach; *Pongamia pinnata*, *Morinda tinctoria* and *Acacia nilotica*).

In this sample the following parameter was analyzed

I. Physical and chemical parameters

In this water sample dissolved oxygen, PH, conductivity, were measured temperature, dissolved organic carbon (DOC), dissolved inorganic carbon (DIC), dissolved N and P concentration and then total nitrate and phosphate concentrations were determined by the standard methods (APHA, 1998).

II. Coarse particulate organic matter (CPOM)

During the period March 2015- February 2016, total CPOM input in the two streams was analysed by a monthly collection of leaf and plant materials accumulated in five traps distributed along the reach and suspended 1 cm above the water surface. The traps consisted of a square wooden frame (1X1 m) and a nylon net the CPOM materials collected were dried at 80° C for 48h and then weighed.

III. Extra cellular enzymes activity

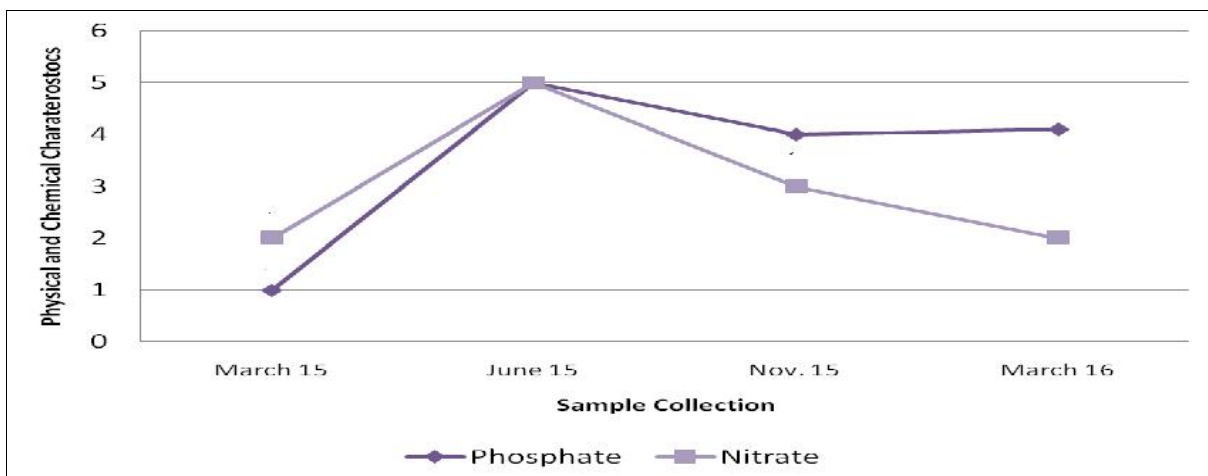
In the study, several hydrolytic and oxidative extracellular enzymes activities were analyzed the samples consisted of 1 leaf disk, 1 piece of branch 1ml of sand volume, 1 gravel grain and 1 liter placed in glass vials filled with stream water (5 ml) and kept cold (4° C) until arrival at the laboratory. A total of six different hydrolytic enzymes assays were performed by polysaccharide compounds degradation by means of the β- glucosidase, β- Xylosidase, Cellobiohydrolase, Phosphatase. Peptidase and Phenol oxidase using the methodology described by (Romani et al., 2001). In the all three parameters sample was collected by triplicate and the data was carried out in statistical analysis.

Results

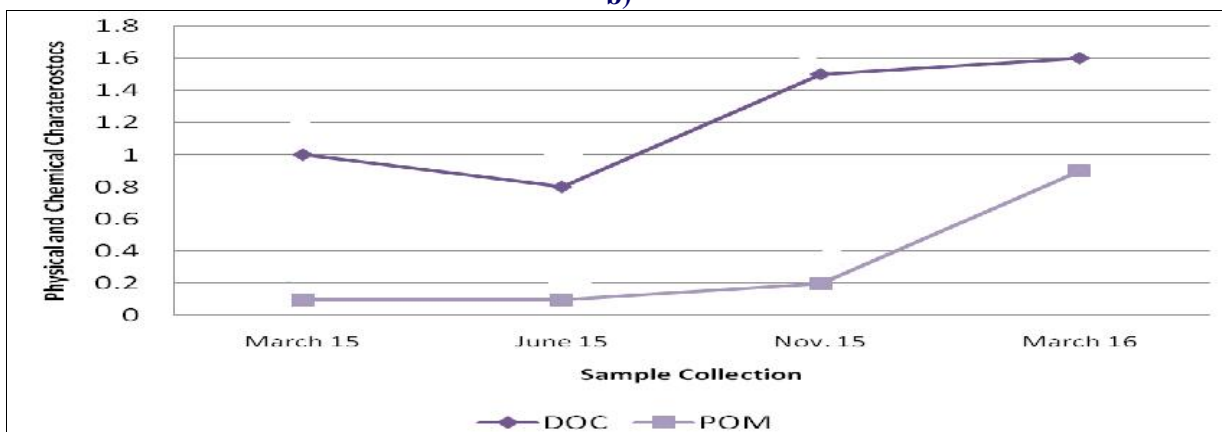
Environmental variables and stream characteristics

Rainfall is generally highest in spring and autumn, however total rainfall can vary from year to year. During the study period temperature varied between 16° C and 26° C. Stream discharge was highest in the autumn (in October) and dramatically decreased in early summer (in June) to zero flow in July and August. The first rainfall in September restored the stream's water flow and increased its dissolved nutrient content (nitrate, phosphate and DOC) (Figures .1 a,b,c). Stream water was low in P and high in N most of the year, the majority of CPOM input occurred during autumn (especially in October), but there was a secondary peak in spring (March). In both cases, the largest input of CPOM came from *Pongamia pinnata* (L). CPOM standing stock and POM transport were particularly high in September, shortly after water flow resumed. However spates in October rapidly washed the accumulated CPOM downstream (Fig- 1c).

a)



b)



c)

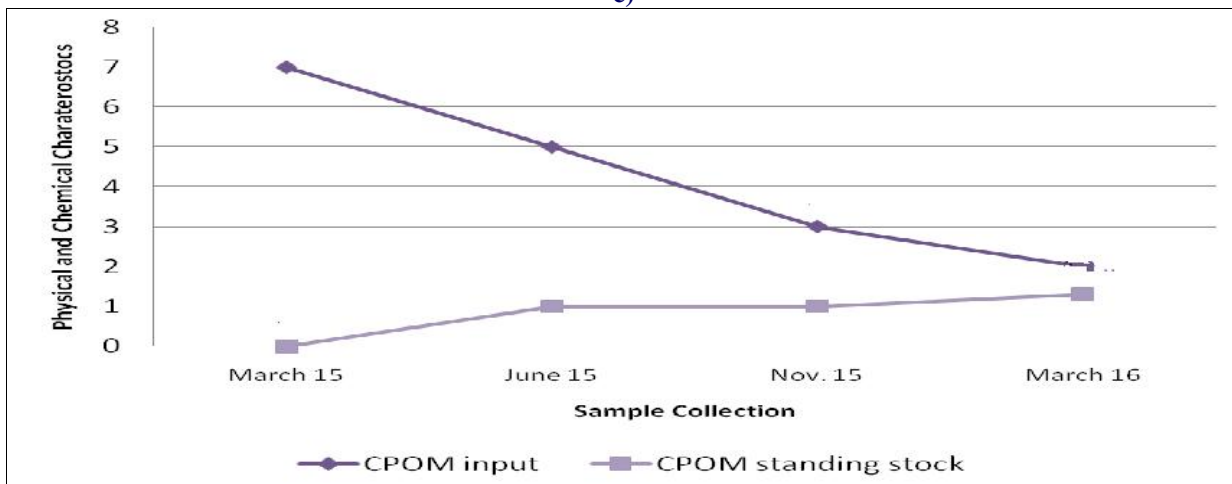
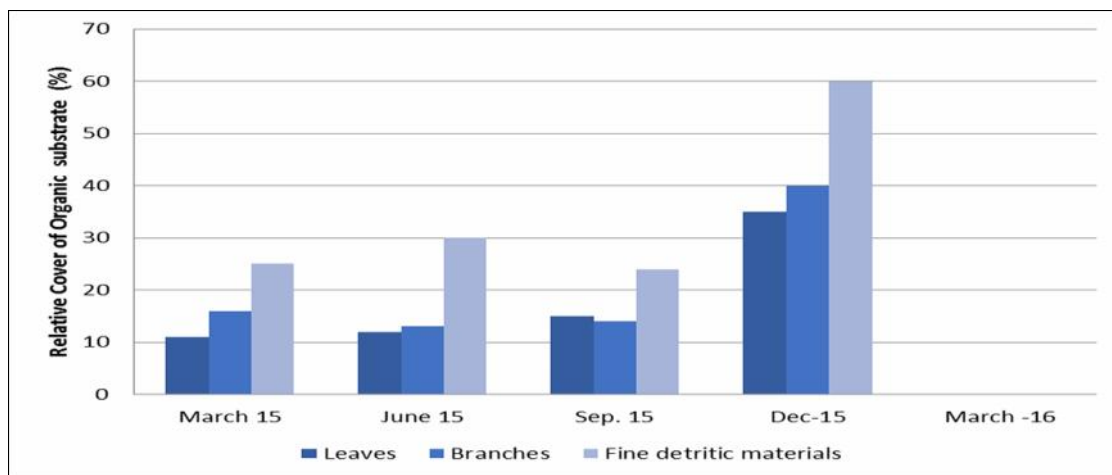


Figure – 1 Physical and chemical characteristics of the Pachamalai stream water during the study period. Values of phosphate (g) and nitrate (mg) (a), dissolved organic carbon (mg) and particulate organic matter (POM) in transport (b), and CPOM input and standing stock (c) are shown. Low or Zero flow occurred from the end of June to early September- 2015.

Mean wetted surface area was 71.6 ± 4.2 . Coarse substrata covered 70% of this area, while 30% was covered by fine substrata (Figure .2 a, b). Coarse substrata dominated in the centre of the channel, while gravel and sand accumulated in pools and in the depositional zones near the banks. October rainfall increased the fine substrata cover to 52% of the total surface area of the reach. The decrease in water level from June onwards narrowed the wetted channel and

resulted in the loss of depositional zones and in the subsequent predominance of coarse substrata (up to 75% of reach surface). Leaf accumulation in the autumn covered as much as 80% of the total wetted surface area, while fine detritus were more abundant in spring and winter (up to 28% of reach area). The highest accumulation of branches occurred in autumn.

a)



b)

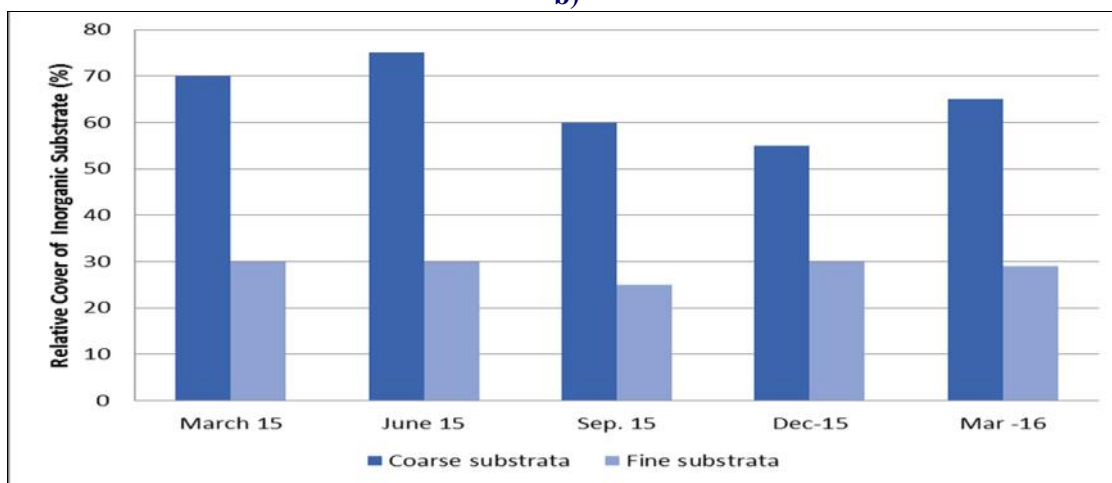


Figure : 2 Relative coverage (%) at each sampling time of the inorganic (coarse and fine substrata) and organic (leaves, branches, fine detritic materials) benthic substrata in the studied

Comparison of microbial biomass among substrata

Reach-scale values of bacterial, fungal and algal biomass in the different benthic substrata varied seasonally (ANOVA, T effect, $P < 0.005$; Figure. 3). Bacterial and fungal biomass peaked in September, although their temporal variations also depended on the substratum type. Bacterial standing stock on fine substrata and tiles was highest during spring, which

coincides with the higher algal biomass episode (Figures. 3 a&c). Each microbial group showed certain preferences in substratum colonization (Figure .3). In general, bacteria mainly accumulated on tiles, except in September when submerged leaves were preferred, fungi colonised leaves while algae accumulated on tiles. Fungi dominated in the biomass of the microbial

community (up to 9 gC m^{-2} , in autumn), followed by algae (up to 6.9 gC m^{-2} in spring) and bacteria (up to 0.21 gC m^{-2} , in autumn; Figure.3).

The microbial autotrophic heterotrophic C ratio shifted from being highly autotrophic in spring and winter (ratio of 3 and 2.1, respectively) to highly heterotrophic in autumn (ratio of 0.1).

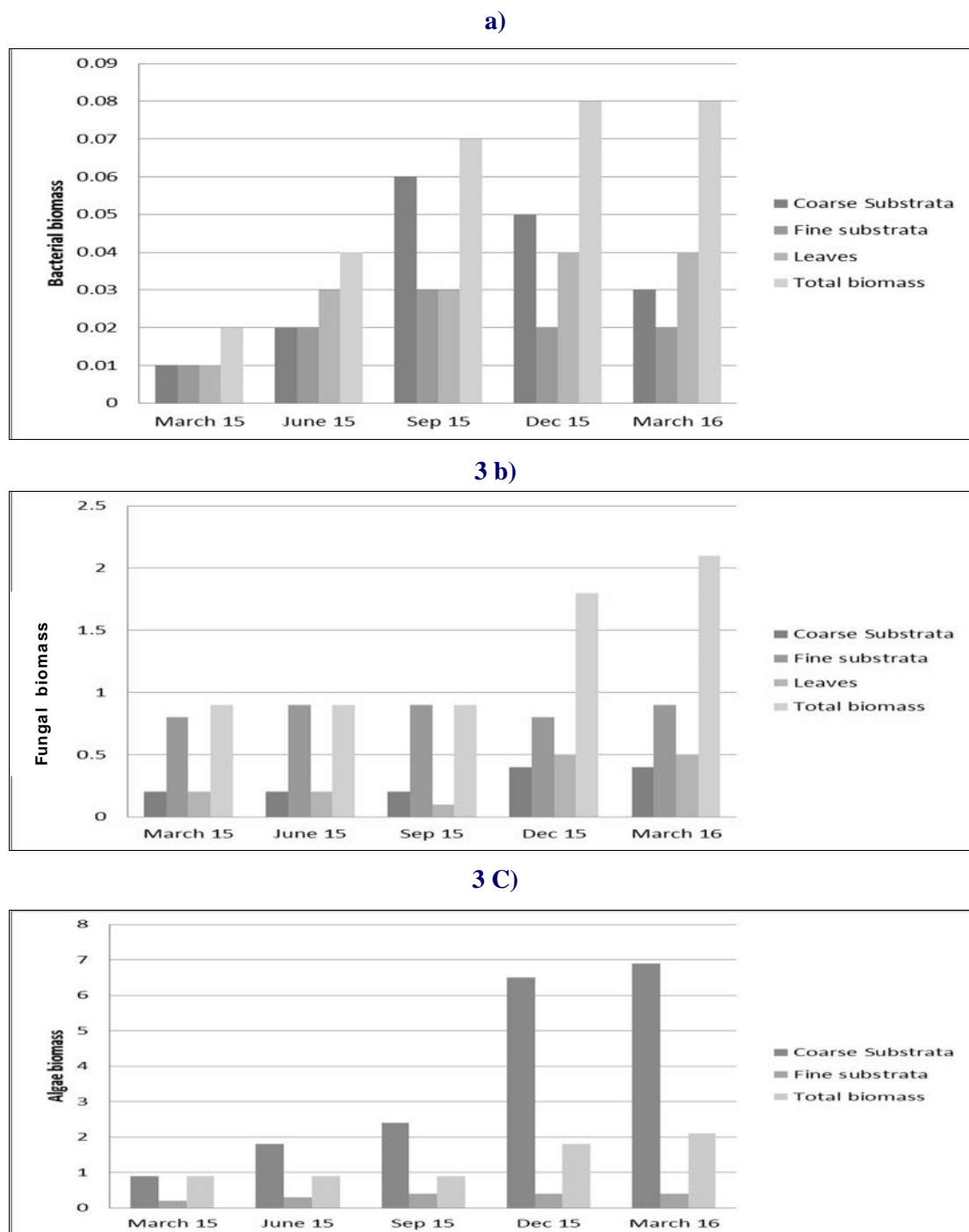


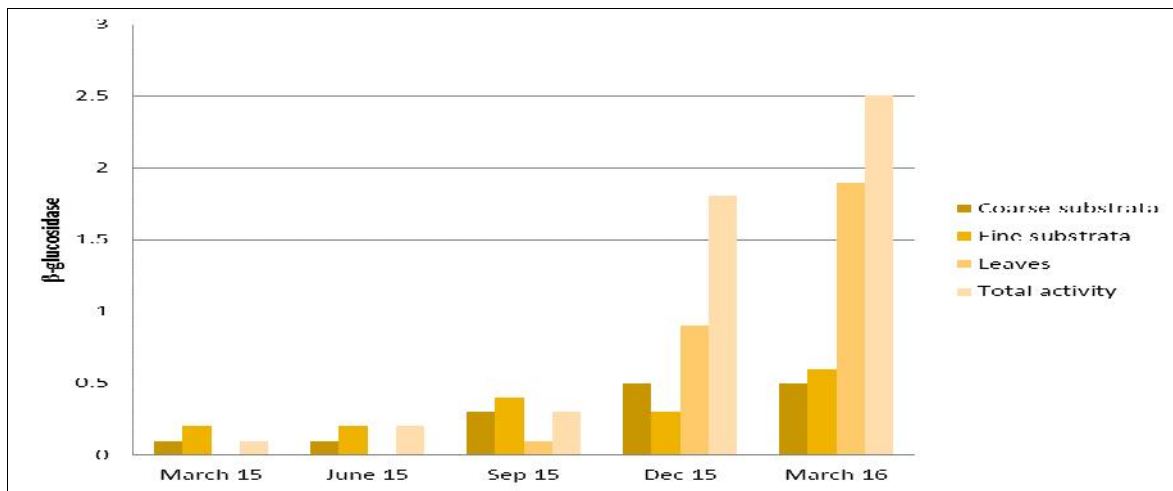
Figure – 3 Biomass of bacteria (a), Fungi (b) and algae (c) expressed in terms of carbon per unit of reach surface area on different benthic substrata (leaves, coarse and fine substrata) in the study reach. Total values of benthic microbial biomass accumulated in the reach (biomass in coarse and fine substrata and leaves) are also shown.

Extracellular enzyme activity

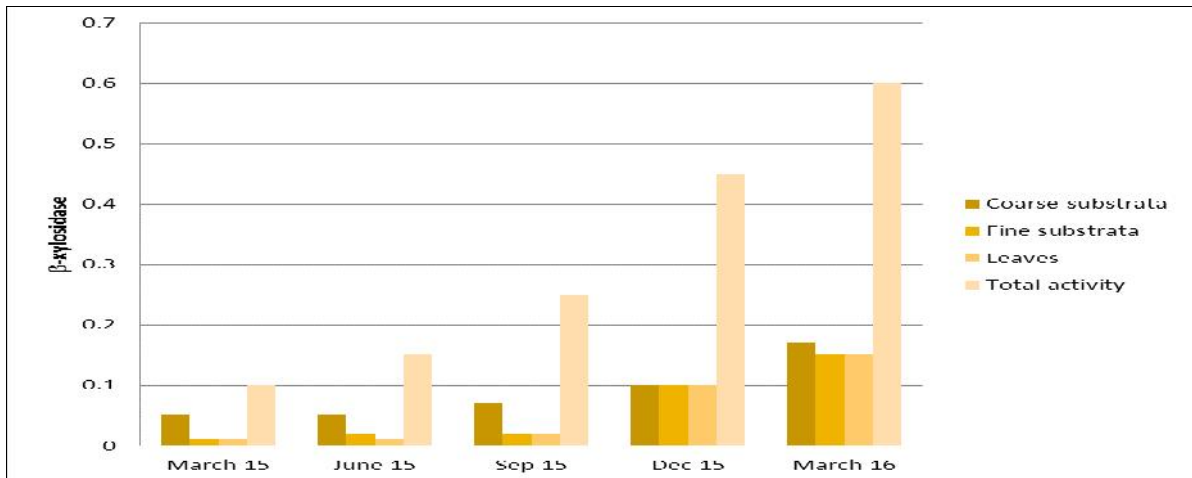
Enzyme activity in different substrata demonstrated a marked seasonally (Figure. 4). The activity of three enzymes involved in polysaccharide degradation (β -glucosidase, β -xylosidase and cellobiohydrolase) peaked in early autumn (September), coinciding with the rise in benthic heterotrophic biomass (Figures 4 a, b & c). However, β -glucosidase activity was highest between June and October, while β -xylosidase activity peaked between May and November. There was a sharp increase in cellobiohydrolase activity between June and September and again in February the following year. Phosphatase and phenol oxidase activity steadily increased in spring and peaked in September (Figures. 4 d & e), activity then decreased during the autumn and recovered in winter. Trends in peptidase activity contrasted with that of other enzymes (Figure.4 f).

The temporal dynamics of each enzyme activity varied with benthic substratum type, except in the case of the phenol oxidase activity ($P = 0.33$). In general, polysaccharide-degrading enzymes were most active (β -glucosidase and β -xylosidase) in leaf material, while phosphatase and peptidase prevailed on tiles. However, cellobiohydrolase activity did not differ between substrata. The decomposition of lignocellulosic compounds was most common on fine substrata. In general, the capacity of benthic communities in the decomposition of simple C molecules (β -glucosidase, Figure. 4 a) was 100 times greater than their capacity to decompose hemicelluloses and celluloses (β -xylosidase and cellobiohydrolase, Figure .4 b & c). The greatest capacity was that measured for organic phosphorus compounds and peptide decomposition (Figures.4 d & f).

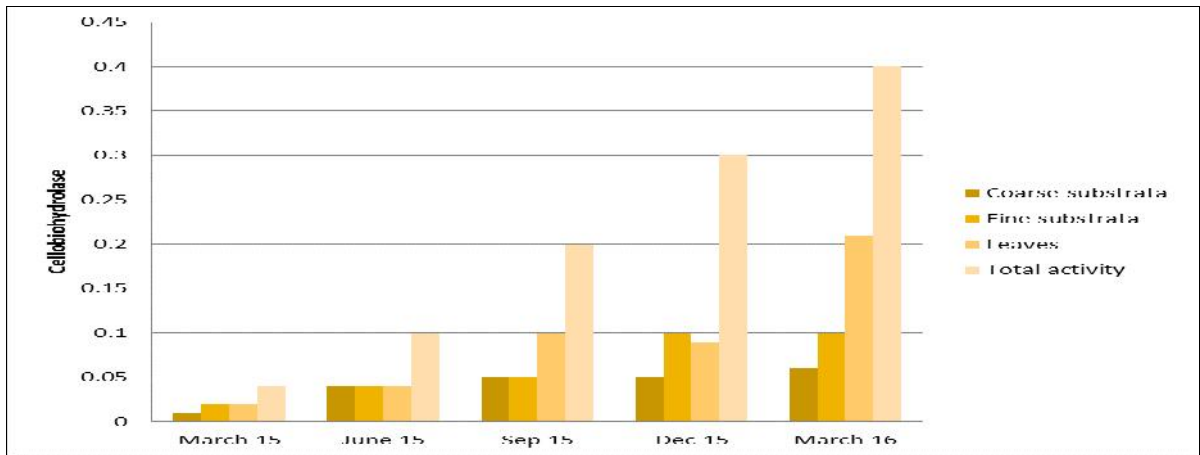
a)



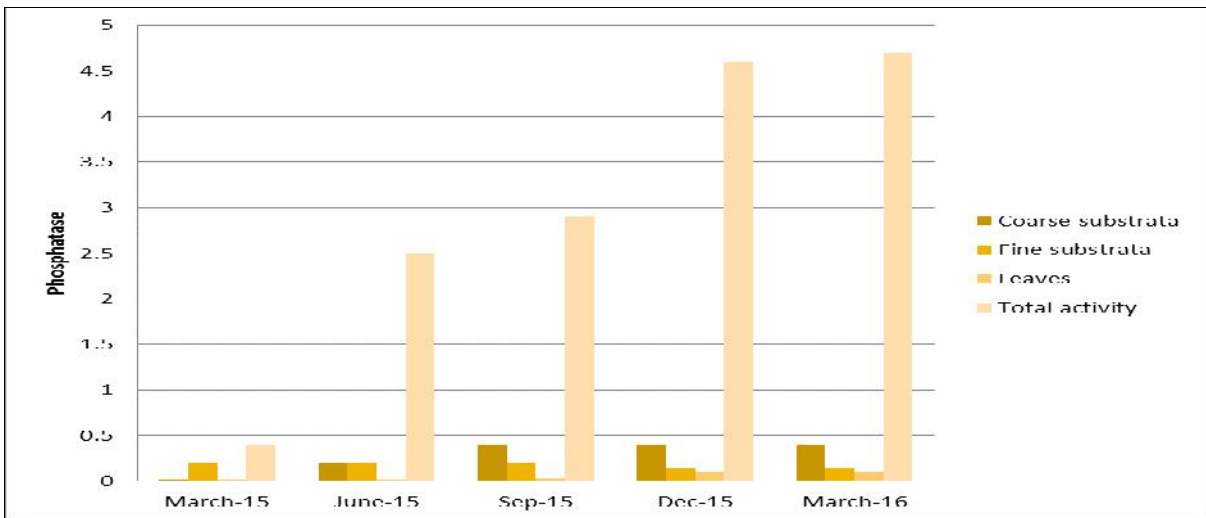
b)



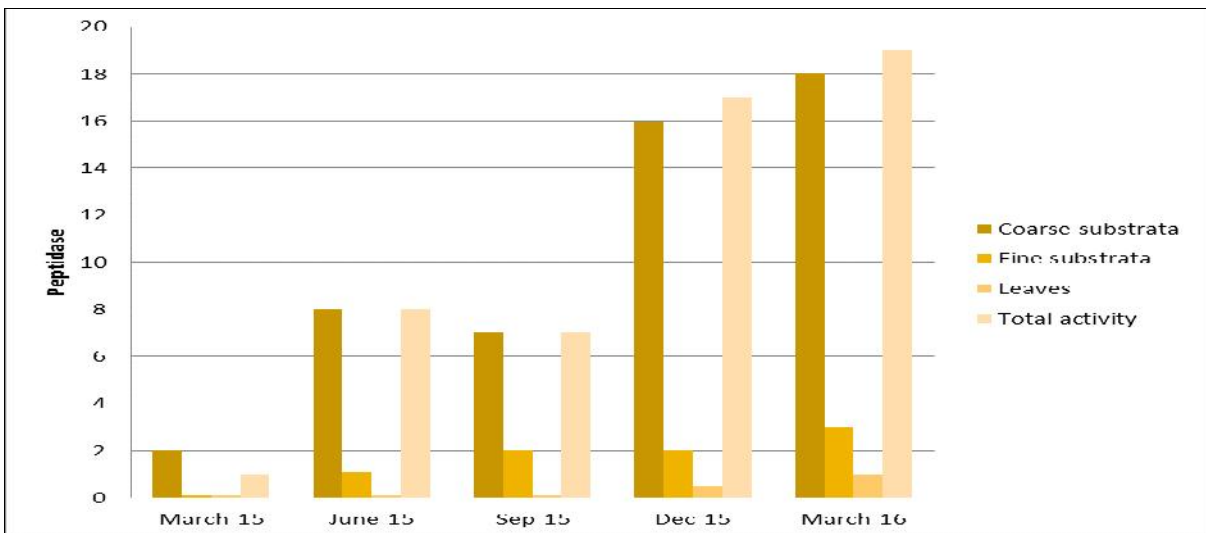
c)



d)



e)



f)

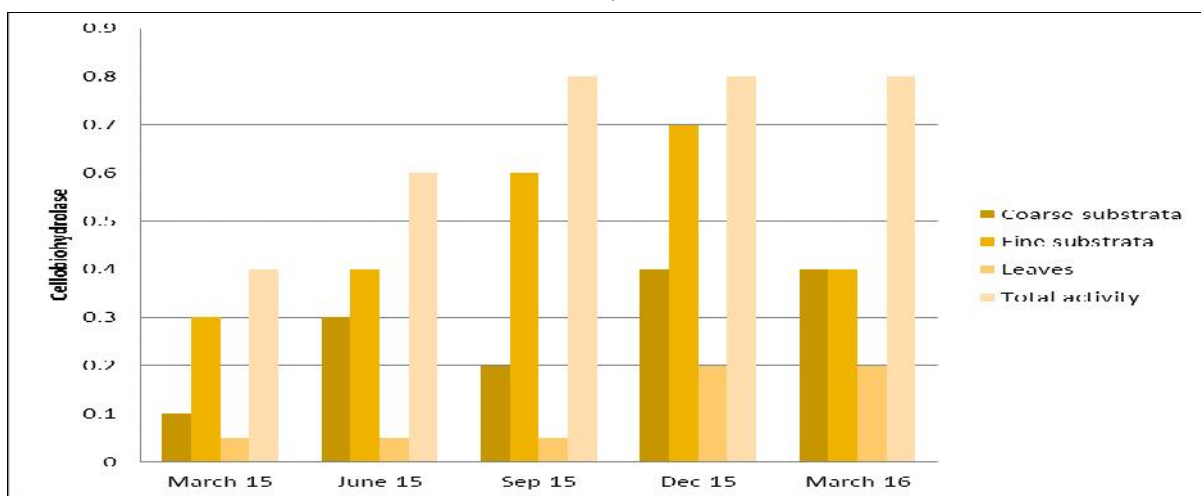


Figure – 4 : Extra cellular enzymes activity [(a) β - glucosidase, (b) β -xylosidase, (c) cellobiohydrolase, (d) phosphatase, (e) peptidase, and (f) phenol oxidase. Total values of different enzyme activity (- activity in coarse and fine substrata and leaves) in the reach are also shown.

Discussion

Our observations on enzyme activity and microbial biomass reveal two distinct periods of high microbial enzyme activity: the first is in late winter-early spring, and the second in late summer-autumn. In late winter-spring, light reaching the stream bed was not restricted by canopy cover, which caused an increase in water temperature. For a short period, there was a sharp increase in autotrophic biomass, particularly on coarse substrata, resulting in a dense autotrophic population (high autotrophic: heterotrophic C ratio). The highest algal peak occurred in periods of relatively low dissolved inorganic nutrient concentration (June 2015), which is consistent with theories of light-dependant algal development in forested streams (Mallory & Richardson, 2005; Taulbee et al., 2005; Ylla et al., 2007). During this period, it is likely that algae outcompeted bacteria for dissolved inorganic nutrients (Rier & Stevenson, 2002). Peptidase activity was highest during periods of greatest algal biomass development in coarse substrata. This relationship may indicate the use of algal exudates (mainly peptidic molecules) by bacteria (Romaní et al., 2004), since bacterial enzyme production (especially peptidases) can be stimulated by active algal photosynthesis (Espeland et al., 2001). During this period, heterotrophic microbial activity may depend largely on the use of autochthonous sources.

The second episode of high microbial enzyme activity is based on allochthonous OM sources, especially leaf litter from the riparian forest. The activity of polysaccharide-degrading enzymes (involved in the degradation of cellulose and hemicellulose compounds) was associated mainly with the CPOM

standing stock in the reach. The magnitude and duration of high enzyme activity can be explained by temporal shifts in organic matter supply, as well as by changes in the storage capacity of sediments (Wilczek et al., 2005). Although this heterotrophic episode is correlated with leaf litter input and accumulation in the stream, microbial benthic communities also showed active decomposition activity during the winter. At this time, the decomposition of lignocellulose (phenol oxidase activity) and organic phosphorus compounds (phosphatase) was greatest in coarse substrata where fine detritus accumulated.

Conclusion

Microbial heterotrophic biomass (bacteria plus fungi) was generally higher than autotrophic biomass (algae), except during short periods of high light availability in the spring and winter. During these periods, sources of organic matter (OM) shifted towards autochthonous sources derived mainly algae, which was demonstrated by high algal biomass and peptidase activity in benthic communities. Heterotrophic activity peaked in the autumn. Bacterial and fungal biomass increased with the decomposition of cellulose and hemicellulose compound from the leaf material. Later, lignin decomposition was stimulated in fine (sand, gravel) and Coarse (Rocks, boulders and cobbles) substrata by the accumulation of fine detritus. The Koraiyaru falls and Mayiluthu summer drought provoked an earlier leaf fall. The resumption of the water flow caused the weathering of riparian soils and subsequently a large increase in dissolved organic carbon and nitrate, which led to growth of bacteria and fungi.

Acknowledgments

Authors thank to Plant biotechnology unit, PG and Research Department of Botany, Government Arts College, Ariyalur for providing all facilities.

References

1. Apha, (1998). Standard methods for the examination of water and waste water. 20th editions American Public Health Association, Washington DC.
2. Arnosti., C. (2003). Microbial extracellular enzymes and their role in dissolved organic matter cycling. In aquatic ecosystem: interactivity of dissolved organic matter, PP 315-342. Academic press, California.
3. Barlocher, F., (1992). The ecology of Aquatic hyphomycetes. Springer-Verlag, Berlin.
4. Espeland, E.M., Francoeur, S.N. and Wetzel, R.G. (2001). Influence of algal photosynthesis on biofilm bacterial production and associated glucosidase and xylosidase activities. Microbial ecology, 42,524-530.
5. Lyautey, E., Jackson, C.R., Cayrou, J., Rols, J.L., and Garaetian, F. (2005). Bacterial community succession in natural river biofilm assemblages, Microbial Ecology, 50, 589-601.
6. Mallory, M.A and Richardson, J. S. (2005). Complex interaction of light, nutrients and consumer density in a stream periphyton-grazer (tailed frog tadpoles) system. Journal of Animal Ecology, 74. 1020-1028.
7. Rier, S. T. and Stevenson, R.J. (2002). Effects of light, dissolved organic carbon, and inorganic nutrients on the relationship between algae and heterotrophic bacteria in stream periphyton, Hydrobiologia, 489, 179-184.
8. Romani, A.M., and Sabater, S. (2001). Structure and activity of rock and sand biofilms in a Mediterranean stream, Ecology 82, 3232-3245.
9. Romani, A.M., Giorgi, A., Acuna. V. and Sabater, S. (2004). The influence of substratum type and nutrient supply on biofilm organic matter utilization in streams Limnology and Oceanography, 49, 1713-1721.
10. Sinsabaugh, R. L., and A. E. Linkins. (1990). Enzymatic and chemical analysis of particulate organic matter from a boreal river. Freshwater Biol. 23:301-309
11. Sterflinger, K., W. E. Krumbein, and A. Schwiertz. (1998). A protocol for PCR *in situ* hybridization of hyphomycetes. Int. Microbiol. 1:217-220.
12. Taulbee, W.K., Cooper, S.D. and Melack, J.M. (2005). Effect of nutrient enrichment on algal biomass across a natural light gradient. Archiv fur Hydrobiologie, 164, 449-464.
13. Wilczek, S., Fischer, H. and Pusch. M.T. (2005). Regulation and seasonal dynamics of extracellular enzyme activities in the sediments of a large lowland river Microbial Ecology, 50, 253-267.
14. Ylla, I., Romani, A.M. and Saater, S. (2007). Differential effects of nutrients and light on the primary production of stream algae and mosses. Fundamental and Applied Liminology, 170, 1-10.

| Access this Article in Online | |
|--|--|
|  | Website: www.ijarbs.com |
| | Subject: Biodiversity |
| Quick Response Code | |
| DOI: 10.22192/ijarbs.2017.04.07.026 | |

How to cite this article:

K.Valarmathy and R. Stephan. (2017). Organic matter availability structures of microbial biomass and their activity in Pachamalai Forested stream in Tamilnadu. Int. J. Adv. Res. Biol. Sci. 4(7): 209-217.

DOI: <http://dx.doi.org/10.22192/ijarbs.2017.04.07.026>

Research Article

DOI: <http://dx.doi.org/10.22192/ijamr.2017.04.06.013>

Organic matter decomposition by Aquatic fungi in the Pachamalai forested stream contributed by streambed substrata

K. Valarmathy and R. Stephan*

Department of Biotechnology, The Oxford College of Engineering, Bangalore- 68.

* Plant Biotechnology Unit, PG & Research Department of Botany, Government Arts College, Ariyalur- 621 718. Tamil Nadu - India.

*Corresponding Author: stephan.biotech@gmail.com

Abstract

Aquatic micro fungi play the fundamental role in organic matter decomposition in all the forested ecosystems. These micro-organisms degrade recalcitrant compounds like lignin, thereby enhancing the utilization of organic material by the microbial community. The main input of allochthonous organic matter in Pachamalai forested streams occurs during the autumn. In-stream breakdown processes can be affected by high physical erosion during floods but changes in stream water chemistry may also affect the decomposition enzymatic activities of stream microorganisms. Two ligninolytic activities (Phenol oxidase and Peroxidase) and a cellulolytic activity (cellobiohydrolase) were measured in leaves, branches, sand and gravel substrata in a reach of a Pachamalai forested stream. Highest ligninolytic activities were measured in biofilm developed on inorganic substrata (sand and gravel) were also accumulated the highest fungal biomass. Similarly, cellulolytic activities were significantly higher in biofilm on organic substrata (leaves and branches). Physical and chemical factors, such as discharge and stream water nutrient concentration DIN (Dissolved Inorganic Nitrogen) were affecting the enzymatic activities, particularly enhancing phenol oxidase. Moreover, the chemical composition of the available organic matter OM (high cellulose in leaves, high lignin in fine detritic materials) strongly influenced the decomposition activity in each biofilm. A precise description and quantification of the benthic substrata was used to obtain enzymatic activity values in terms of stream reach. These results showed a temporal pattern in the decomposition activities in the reach, beginning with the decomposition of cellulose (October) followed by lignin compounds (November and December).

Keywords

Forrested stream,
Fungi,
Pachamalai,
Pongamia pinnata, and
Morinda tinctoria.

Introduction

Running waters are enormously diverse, they range from small streams to large rivers and occurs under widely differing conditions of climate, vegetation, topography and geology. In forested streams where light is a limiting factor for primary production, energy sources are mainly allochthonous (leaf litter), the metabolic

processes being typically heterotrophic (Minshall et al., 1983). In Pachamalai forested streams, the greatest input of plant material occurs in autumn, thereby providing the potential for decomposition processes. The initial breakdown of leaves in the stream is mainly carried out by aquatic hyphomycetes (Suberkropp &

Klug, 1976; Findlay & Arsuffi, 1989; Gessner & Chauvet, 1994; Mathuriau & Chauvet, 2002), while the contribution of bacteria is lower (Hieber & Gessner, 2002). This group of fungi is crucial in decomposition process as it breaks down lignified carbohydrates, which constitute a natural protection of polysaccharide components against enzymatic attack (Griffin, 1994). After cellulose, lignin is the most abundant form of aromatic carbon in the world. Lignin degradation does not provide a primary source of carbon and energy for fungal growth, but decay processes and utilization of carbohydrates for fungal growth can occur only with the coordinate degradation of this carbon (Griffin, 1994). Studies on the decomposition of organic matter (OM) have mainly focused on organic substrata (leaves and wood; e. g. Gessner & Chauvet 1994; Pozo et al., 1998; Diez et al., 2002). The accumulation of decomposing material occurs in streams. Specifically, sand sediments accumulate large amounts of fine detritic materials in a forested Pachamalai stream was evaluated, and studied the way in which their role was shared between the distinct streambed substrata (leaves, sand, gravel and branches) where substantial OM decomposition may occur. Decomposition process may be related to variations in inorganic nutrient availability. It has been observed that the addition of nitrogen increases cellulolytic activity and decreases lignin-degrading phenol oxidase activity (Carreiro et al., 2000). Moreover, the chemical nature of streambed substrata, such as the tannin content or the physical properties of leaves (high waxy cuticles), has been proposed as a major determinant of breakdown rate (Barlöcher et al., 1995). Sinsabaugh et al. (1992) determined that phenol oxidase activity was substrate-related but not site-related.

In the present study ligninolytic and cellulolytic enzyme activities were measured on gravel and sand, on the leaves of several species (*Acacia nilotica*, *Pongamia pinnata*, and *Morinda tinctoria*) and on branches, to determine the most active site of organic matter decomposition (OM) among the substrata types. The relationships between enzymatic activities and fungal biomass (ergosterol content) of biofilms were studied in each substratum, and also, with the physical-chemical parameters of stream water to establish which variables were controlling the decomposition process in the pachamalai forested streambed substrata.

Materials and Methods

Study area

In the study area are Pachamalai hills, located in Trichy District, Tamilnadu, India. situated 3000 feet above sea level lying between 78° 31' East and 11° 28' North and 11° 10' South and 78° 20' West Latitude. In the Pachamalai forested streams several streams are present. The study samples were collected in Koraiyar and Mayiluthu streams.

Sampling

Sampling of leaves, branches, sand and gravel was performed in the Pachamalai stream reach at fortnight intervals from October 2014 to January 2015 (for a total of seven sampling dates). In total, 9 substrata types (defined as follows) were sampled. Leaves of three species were collected: *Acacia nilotica*, *Pongamia pinnata*, and *Morinda tinctoria*, considering separately the leaves just fallen into the stream (as fresh leaves) and those being already immersed (as decaying leaves). Branches, sand and gravel samples were collected as well.

The stream bed is made up of different substrata of both inorganic rocks, cobbles, sand and organic leaves, wood. The organic matter rocks, cobbles and boulders was collected using ceramic tiles placed in the substrata of surface area were glued on to stream cobbles and immersed in the stream for colonization 5-6 weeks before sampling. The gravel samples were taken directly from the stream bed and the sand substratum was sampled with plastic container. The organic matter of leaves was used to cut leaf discs from the entire leaf and branches 0.5 to 1.5 cm were cut in pieces of 1.5 cm in length. In all cases, the surface area of the whole substratum was considered as potential surface area colonized by microbes.

At each sampling time, the different substrata were analyzed for ergosterol concentration and extracellular enzyme activity Cellobiohydrolase (CBH), Phenol oxidase (PO) and Peroxidase (P) activity. In the fungal biomass ergosterol concentration analysis was investigated in leaves of different species (*Acacia nilotica*, *Pongamia pinnata*, and *Morinda tinctoria* fine substrata (sand, gravel) and coarse substrata (Cobbles, boulders and rocks). The above sample ergosterol were isolated and analyzed HPLC by the method of (Gessner & Schmitt, 1996)

In the different substrata extracellular enzymes activity cellobiohydrolase (CBH), Phenol oxidase (PO) and Peroxidase (P) activity was analyzed using the samples consisted of 1 leaf disc, 1 piece of branch, 1ml of sand volume, 1 gravel grain and 1 tile placed in glass vials filled with stream water (5ml). The hydrolytic cellobiohydrolase enzymes activity was investigated by (Romani et al., 2001) and the samples was measured at 365-455 nm wave length at UV-Spectrum photometer. The oxidase enzymes phenol oxidase and peroxidase was investigated by Mason, 1984 and Singabangh & Linkins, 1994) the sample measured at 460nm for the stream substrata and the data were performed for both enzymes and taken in to account for final activity calculations. Moreover, temperature, conductivity, pH, dissolved oxygen and light were measured in the field with portable meters and water samples for Ammonia, Nitrate, Phosphate and dissolved organic and inorganic carbon (DOC and DIC) determination were using the standard protocol (APHA, 1998).

Statistical analyses

In all the sample parameters the data was collected by triplicate. Differences between enzymatic activities and ergosterol concentration (fungal biomass) of the distinct streambed substrata and over time were analysed using a mean and standard deviation (SD).

Results

Water physico-chemistry

The physico-chemical parameters varied considerably during the study period. There was a progressive decrease in stream water temperature, which reached the lowest values in January 2015 (Table -1). Discharge increased up to 10 times the basal flow throughout the study period, producing drastic increases in inorganic nutrients (especially nitrate) and to a lesser extent in DOC. Discharge variations also caused changes in the proportions of substrata during autumn (Table -2). The leaf litter material tall peak during October and November covered nearly 50% of the streambed surface area and accumulation of fine detritic materials respectively.

Table -1 Physical and chemical characteristics of the Pachamalai forested stream water during the study period. Values for water nutrient concentrations are means (n=3) and those for temperature and discharge are individual values of each of the seven sampling dates. Mean for all period are also shown.

| Date | 02-10-2014 | 16-10-2014 | 30-10-2014 | 13-11-2014 | 27-11-2014 | 17-12-2014 | 13-01-2015 | Mean |
|--------------|------------|------------|------------|------------|------------|------------|------------|-------|
| Temp (°C) | 12.4 | 15 | 13.1 | 12.0 | 8.4 | 8.1 | 3.8 | 10.4 |
| Disch (L/s) | 6.5 | 28.4 | 19.4 | 18.5 | 84.6 | 45.2 | 26.4 | 32.7 |
| NO3-N (µg/L) | 10.2 | 510.2 | 102.2 | 28.2 | 72.1 | 830.1 | 560.2 | 399.0 |
| P (µg/L) | 2.2 | 11.1 | 4.3 | 3.4 | 12.2 | 14.4 | 3.6 | 7.3 |
| DOC (mg/L) | 2.4 | 4.5 | 4.0 | 3.2 | 4.2 | 1.2 | 3.2 | 3.2 |

Table -2 Benthic substrata description of the Pachamalai forested stream reach during autumn-winter 2014/15. Values are the percent of each substratum occupying the streambed.

| Sampling date | Rock | Sand-gravel | Branches | Decaying leaves | Fresh leaves | Detritic material |
|---------------|------|-------------|----------|-----------------|--------------|-------------------|
| 02-10-2014 | 62.2 | 34.2 | 1.12 | 4.40 | 28.10 | 41.52 |
| 16-10-2014 | 62.2 | 34.2 | 0.82 | 2.60 | 21.12 | 11.80 |
| 30-10-2014 | 62.2 | 34.2 | 0.85 | 4.24 | 45.72 | 11.24 |
| 13-11-2014 | 62.2 | 34.2 | 1.54 | 14.22 | 42.03 | 11.10 |
| 27-11-2014 | 64.0 | 32.0 | 2.18 | 18.40 | 12.14 | 2.16 |
| 17-12-2014 | 58.0 | 40.0 | 1.80 | 25.72 | 0.35 | 5.08 |
| 13-01-2015 | 64.0 | 34.0 | 2.06 | 9.14 | Absent | 6.50 |

Extracellular enzyme activities

streambed substrata and throughout the study period (Figure -1).

There were significant differences in CBH and PO activities between biofilms developed on different

Figure – 1 Enzymatic activities (CBH, PO and P)in (A- 1,2,3,) sand and gravel , (B- 1,2,3) fresh leaves, (C- 1,2,3) decaying leaves and branch during 2014-2015 in Pachamalai forested stream. Values are means and SE of activity in each substratum (4 replicates) during the 7 sampling dates. (CBH-PO-P)

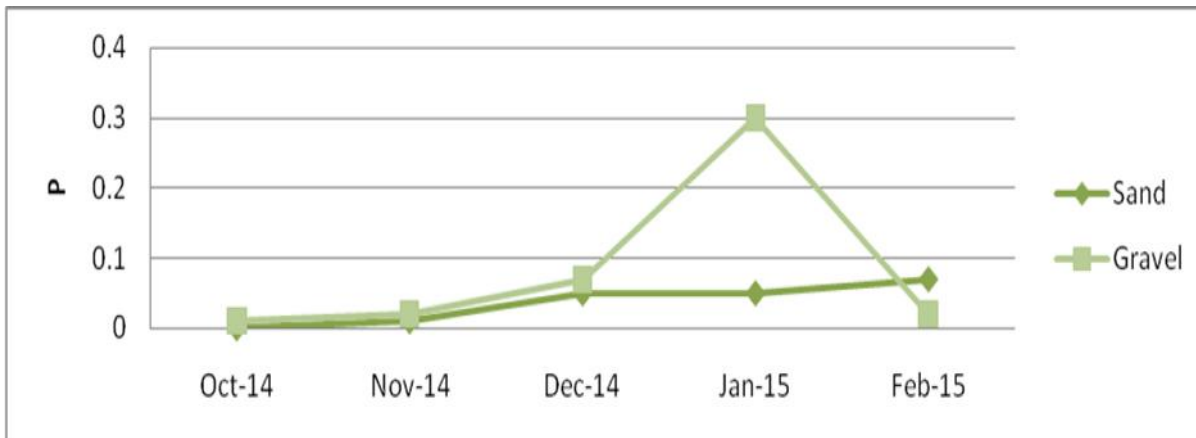
1. A



1



2

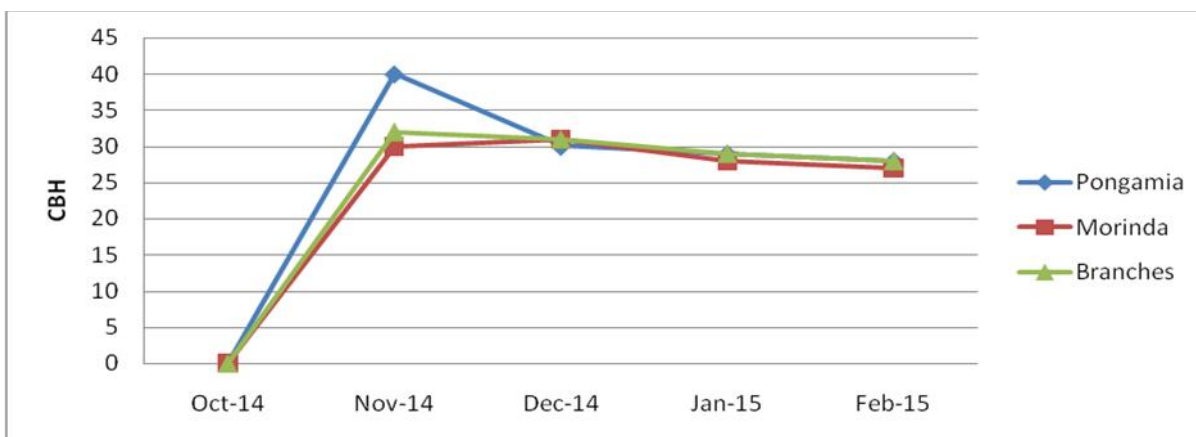


3

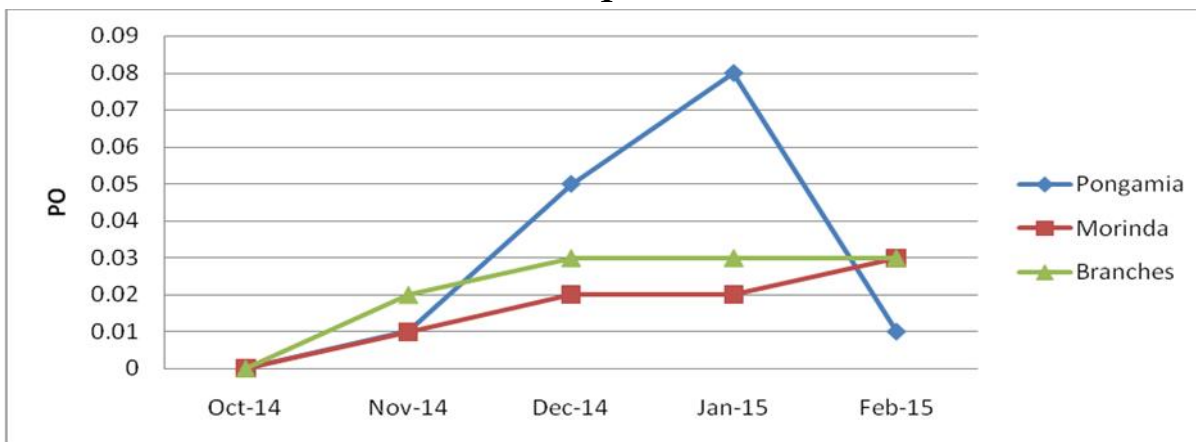
P activity showed significant differences among substrata but not over time . CBH activity was significantly higher biofilms developed on organic substrata, while PO and P were significantly higher in those growing on inorganic substrata. The highest CBH activities were detected in biofilms of decaying *Morinda tinctoria* Roxb leaves (Figure-1), followed by *Acacia nilotica* Wild, *Morinda tinctoria* Roxb and branches. The lowest CBH activity values were observed in biofilms of fresh leaves, sand and gravel substrata. Biofilm on sand and gravel showed

the highest PO activity compared with that in organic substrata communities (Figure -1). Among leaf species, the highest PO activity was measured in the biofilm on fresh and decaying leaves of *Acacia nilotica* Wild while the lowest was on fresh *Morinda tinctoria* Roxbleaves. The highest P activity was registered in sand and gravel biofilm, Among leaves, the highest P activity was detected in biofilm on fresh and decaying *Morinda tinctoria* Roxb leaves while the lowest was on fresh *Morinda tinctoria*, *Roxb* leaves.

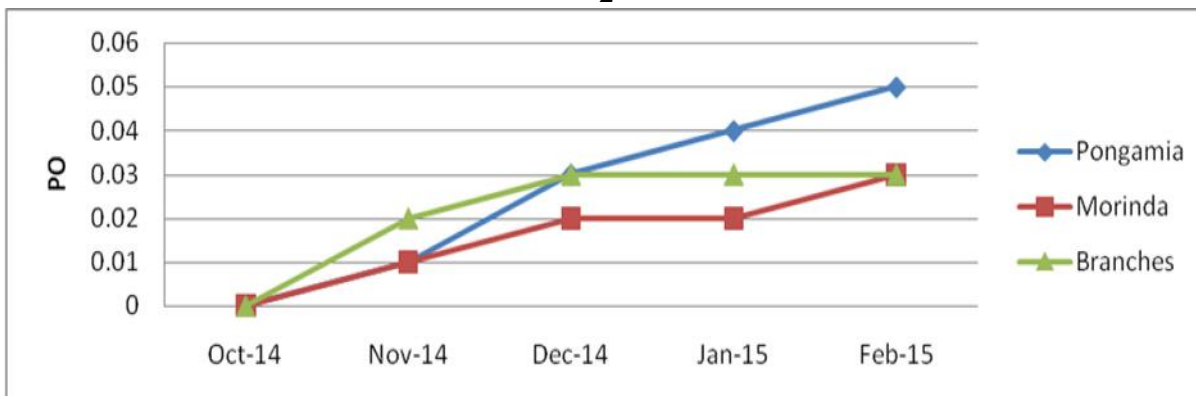
1. B



1

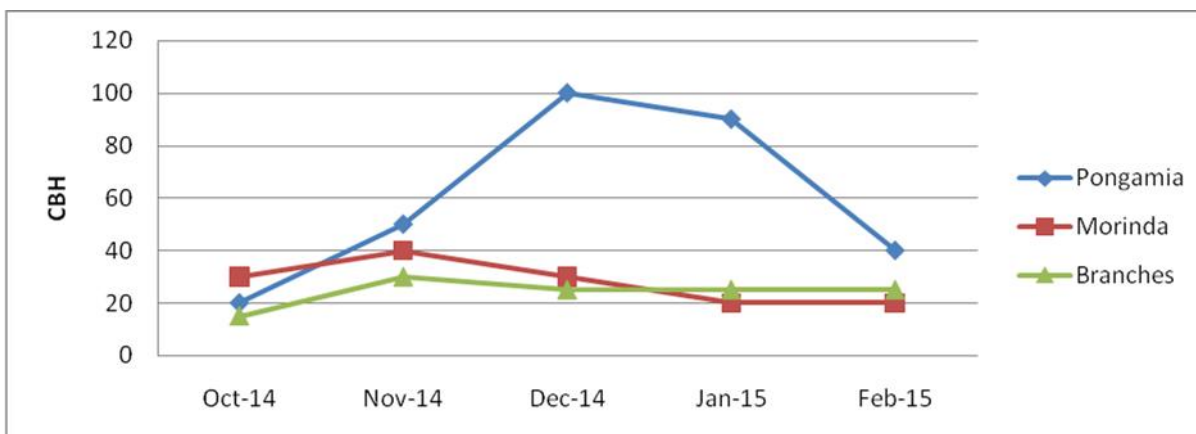


2

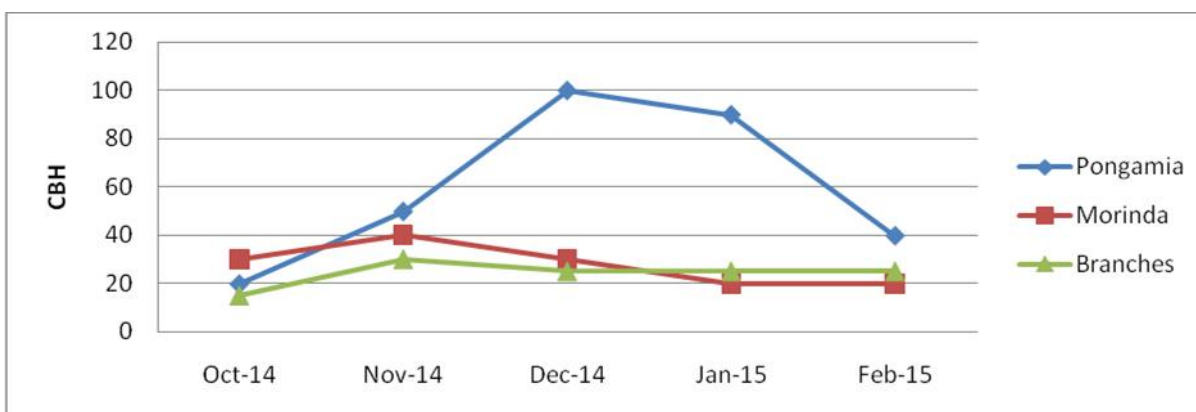


3

1. C



1



2



3

Ergosterol content

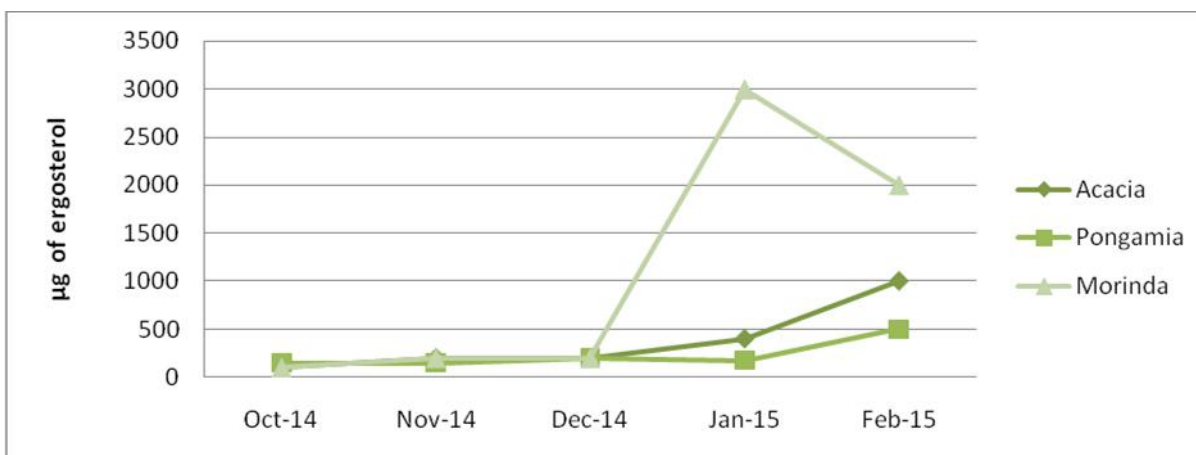
A general increase in fungal biomass occurred at the end of autumn in all the substrata (Figure -2). Ergosterol content showed differences over time and among substrata. Fungal biomass was higher on

inorganic substrata, particularly on sand, than on leaves and branches. Ergosterol on sand was 10-fold higher than that on gravel among leaf species *Acacia nilotica* Wild accounted for the highest fungal biomass.

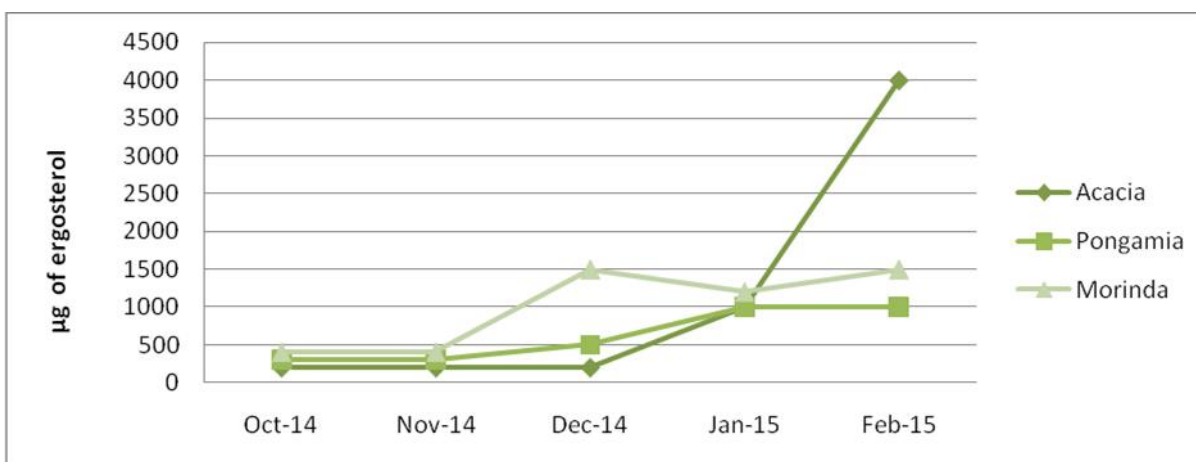
Figure – 2 Ergo sterol content on the streambed substrata during autumn-winter 2014/15 in the Pachamalai forested streams (a) sand and gravel, (b) Fresh leaves, (c) decaying leaves and branches. Values are mean and SE of ergosterol in each substratum (3 replicates) during the 7 sampling dates.



A



B



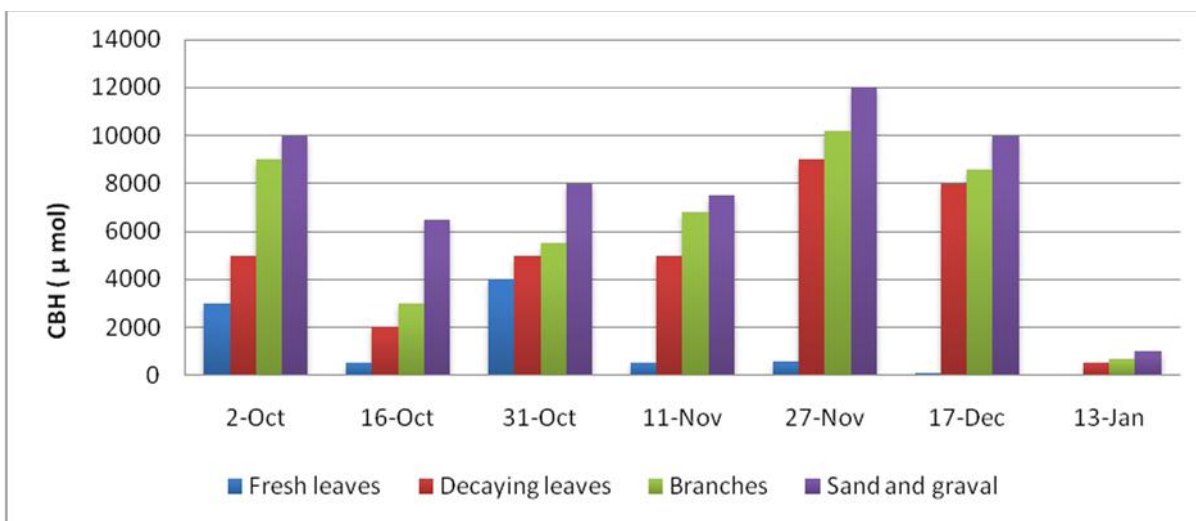
C

Stream reach capacity on OM decomposition

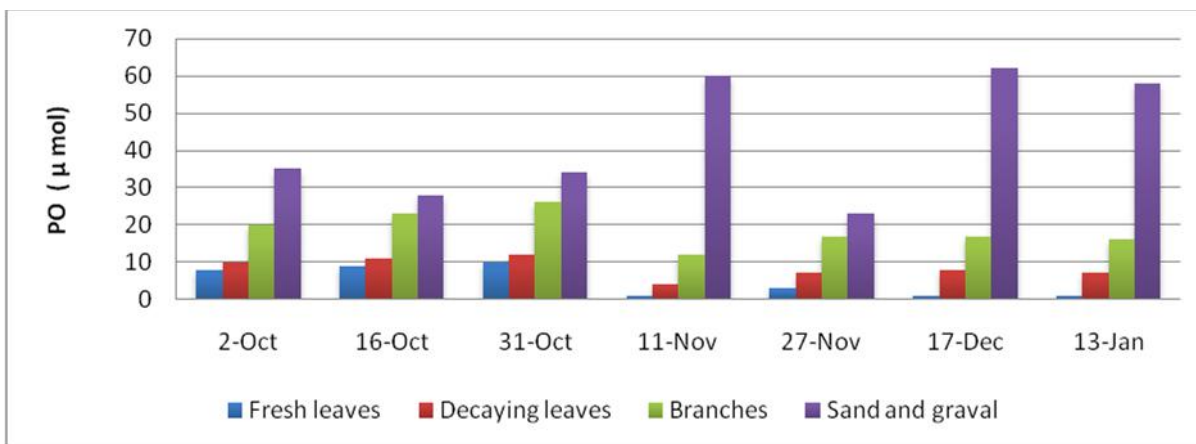
The stream reach capacity for the different enzyme activities was calculated after considering the activities by the corresponding percent of substrata occupying the streambed. High values of CBH were characteristic of the whole study period. Both PO and P increased after several weeks (Figure-3). Biofilm in sand and gravel were responsible for the high values of PO and P activities. CBH showed higher values in

biofilms on organic substrata, being initially higher on fresh leaves and later increasing on decaying leaves. Maximum fungal biomass was reached in November and December. Ergosterol was first accumulated on fresh and decaying leaves (November) but was later more abundant on sand-gravel (Figure -4). Lignocellulosic activities were correlated with the ergosterol content of decaying leaves and branches (PO activity) and sand-gravel substrata (P activity).

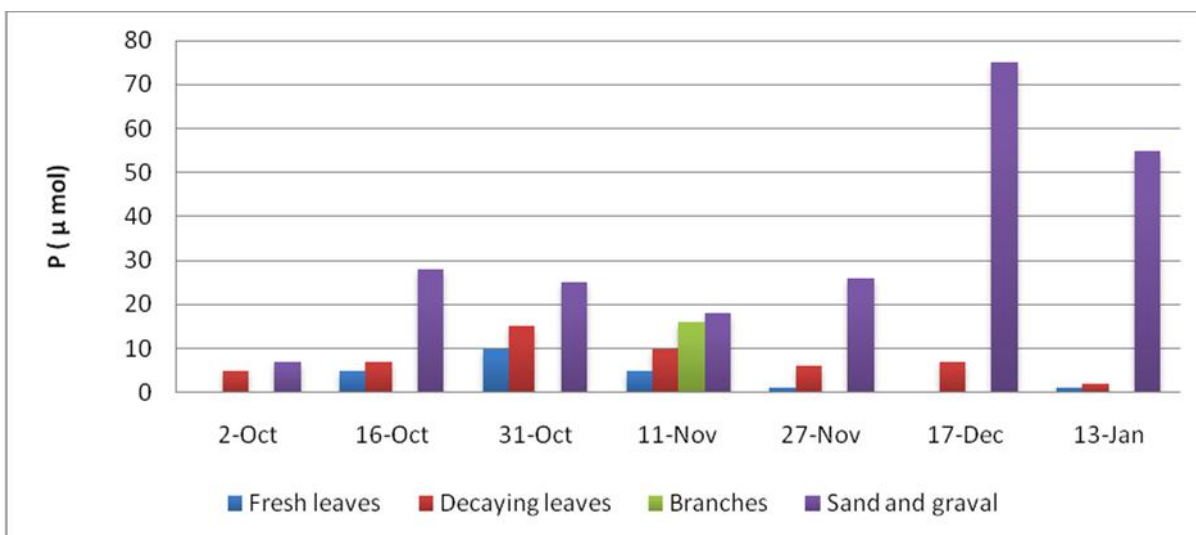
Figure – 3 Enzymatic activity of a-CBH, b-PO and c- P values corrected by real surface area occupied by each substratum in the Pachamalai forested stream (2014-15).



A

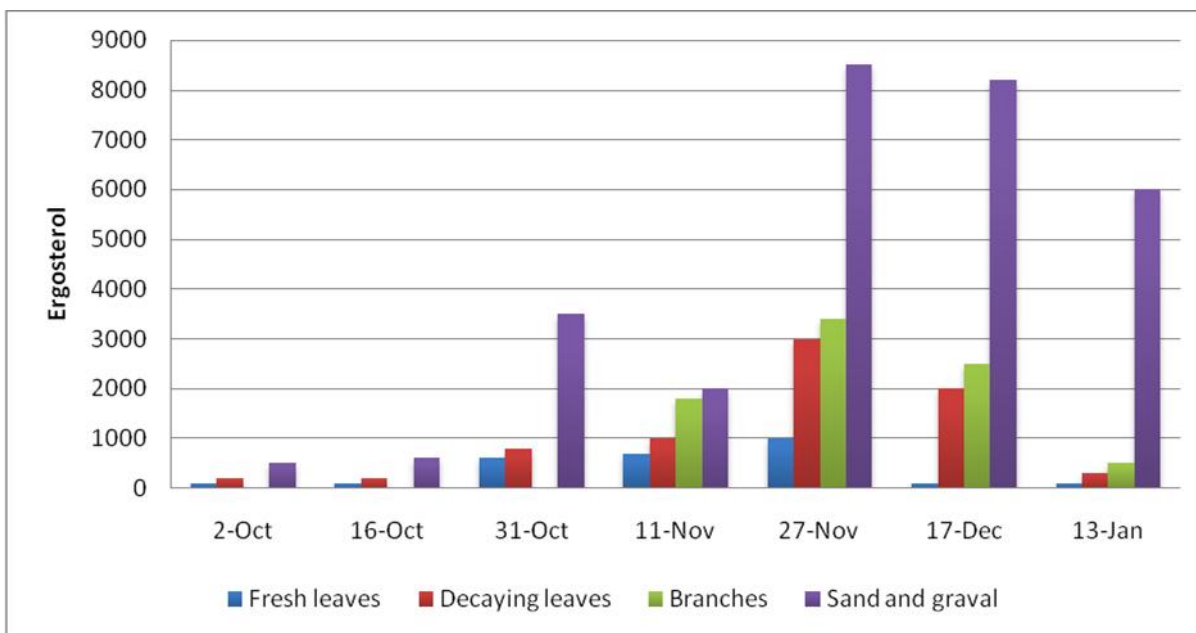


B



C

Figure – 4 Ergosterol content corrected by real surface area occupied by each substratum in the Pachamalai forested streams (2014-15)



Discussion

Organic matter decomposition showed a clear temporal pattern and remarkable differences in the enzymatic activities and ergosterol content between substrata. According to the model of Berg (1986), the decomposition of fresh leaves begins with the easily mineralised fractions of non-lignified carbohydrates, whereas later stages are characterized by mineralization of more recalcitrant fractions of lignified carbohydrates. In the Koraiyaru stream, after leaf fall peak (October), CBH activity was high for the

whole period, while P and PO activities increased only after several weeks. This observation indicates that OM decomposition began with cellulose decomposition followed by degradation of lignin related compounds. However, physico-chemical parameters, such as discharge and dissolved inorganic nitrogen DIN, may also determine the time-pattern of the enzymatic activity. Several studies in autumn or early winter in forested streams (Gasith & Resh, 1999) may mobilise most of the nitrate in the catchment of the streams (Bernal *et al.*, 2002).

After the dry period (summer), caused the weathering of dissolved and particulate organic matter accumulated on soil, and N concentration in streamwater was positively correlated with lignocellulosic activities (P and PO). Therefore, fungal activities were enhanced by nitrate availability in a system where N may be a limiting resource (Romaní *et al.*, 2004). An enhancement of lignocellulosic activities by the water N content has been observed in other systems (Alvarez & Guerrero, 2000). However, Carreiro *et al.* (2000) described the inhibition of these activities by high N concentrations.

Differences between biofilms colonising organic or inorganic substrata were evident in Pachamalai forested stream. Lignocellulosic activities were higher on inorganic substrata biofilm (developed on sand and gravel) while CBH was higher in biofilm developed on organic substrata (leaves and branches). High ligninolytic activities in sand and gravel biofilm were caused by the large accumulation of fine detritic material derived from decomposition of coarse particulate organic matter (CPOM). The largest accumulation of this material occurred in the slow-moving habitats, coinciding with stream pools or littoral zones where sand and gravel were the main substrata. The fine detritus accumulated in these substrata might be composed by a higher proportion of lignin (Yeager & Sinsabaugh, 1998; Sinsabaugh & Findlay, 1994). The lower CBH activity of biofilm growing on sand and gravel indicates the low availability of cellulose compounds in fine detritic particles. In contrast, high CBH activity in biofilms developed on organic substrata could reflect the availability of cellulolytic compounds on leaves and branches.

The enzymatic activities of biofilms differed on the leaves of different species, which might be attributable to differences in leaf composition (C: N ratio, lignin content, polyphenol content, leaf durability; Griffin, 1994). Similar results observed in *Pongamia pinnata* species of our study the lower enzymatic activities for the biofilm on *Pongamia pinnata* was already observed in previous studies developed on leaf decomposition in soil and in other aquatic habitats. The high C:N ratio measured in this substratum (Bernal *et al.*, 2003; Ostrofsky, 1997) may be pointed out as the cause of low mineralization observed for this material. Similarly slower breakdown of *Platanus* leaves than other indigenous Mediterranean leaf species (e. g. *Populus nigra*; Casas & Gesner, 1999) is probably caused by the higher lignin and other

recalcitrant compounds content in the former or observed (Ostrofsky, 1997). In contrast, high CBH and P activities were recorded in biofilms on *Acacia nilotica* leaves, highest PO was measured differences in PO activities between biofilms of leaf material of plant species are probably related to the inhibition effect of phenolic compounds (Pind *et al.*, 1994). Likewise the lower polyphenol content of *Alnus glutinosath* than *Populus nigra* leaves (Pereira *et al.*, 1998) may imply a higher PO activity. This distinct enzymatic behaviour determines a faster decomposition of *Acacia nilotica* leaves in the stream reach, followed by those of *Morinda tinctoria* and finally by *Pongamia pinnata*.

Similarly fungal biomass was generally related with the enzymatic activities measured in the different substrata, indicating that fungi were responsible for most of decomposition processes that occurred in the stream in autumn (Griffin, 1994). The similar PO activity values measured in biofilm in sand and gravel substrata, but the lower fungal biomass in gravel, may be related to a higher proportion of fungi with PO ability (white rot fungi, Dix & Webster, 1995) on gravel than on sand. However, this activity in gravel could also be produced by some microorganisms (e. g. bacteria) using at least part of the degradation intermediates of lignin generated by fungi (Rüttimann *et al.*, 1991). The present study was supported by Baldy *et al.* (1995) where demonstrated the importance of bacteria in the late stages of the breakdown process of leaves.

The estimates of ergosterol concentration per stream reach showed a progression of fungal biomass throughout the study period, which decreased only after most of the material had been processed. The fungi could be considered as facultative microorganisms in the sense of selection and colonization of streambed substrata during the fall. They use the new allochthonous CPOM that entered the system during autumn. When leaf material was carried downstream, the fungi remained active on the fine detritic materials derived from the breakdown of leaves and branch materials, therefore achieving a complete decomposition of all the material that entered the reach during this season.


Acknowledgments

Authors thank to Plant biotechnology unit, PG and Research Department of Botany, Government Arts College Ariyalur for providing the all facilities.

References

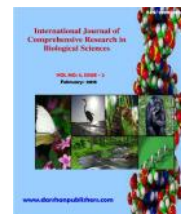
1. Alvarez, S. & Guerrero, M.C (2000) . Enzymatic activities with decomposition of particulate organic matter in two shallow ponds. *Soil biology and biochemistry*, 32, 1941-1951.
2. Apha, 1998. Standard methods for the examination of water and waste water. 20th editions American Public Health Association, Washington DC.
3. Baldy, V., Gessner, M.O & Chauvet, E. (1995). Bacteria, Fungi and the breakdown of leaf litter in a large river. *Oikos*, 74, 93-102.
4. Barlocher, F., Canhoto, C. & Graca, M.A.S. (1995) Fungal colonization of alder and eucalypt leaves in two streams in central Portugal. *Archiv fur Hydrobiologie*, 133, 57-68.
5. Berg, B. 1986. Nutrient release from litter and human in coniferous forest soils: a mini review. *Scandinavian journal of forest research*, 1, 359-369.
6. Bernal, S., Butturini, A., Nin, E., F & Sabater, S. (2002). Variability of DOC and nitrate responses to storms in a small Mediterranean forested catchment. *Hydrology and earth system sciences*, 6. 1031-1041.
7. Bernal, S., Butturini, A., Nin, E., F & Sabater, S. (2003). Leaf litter dynamics and nitrous oxide emission in a Mediterranean riparian forest implications for soil nitrogen dynamics. *Journal of environmental quality*, 32, 191-197.
8. Carreiro, M.M., Sinsaaugh, R.L., Repert, D.A & Parkhurst, D.F. (2000). Microbial enzyme shifts explain litter decay response to simulated nitrogen deposition *Ecology*, 81, 2359-2365.
9. Casas, J. & Gessner, M.O. 1999. Leaf litter breakdown in a Mediterranean stream characterized travertine precipitation. *Freshwater Biology*, 41, 781-793.
10. Diez, J., Elozegi, A., Chauvel, E. & Pozo, J. 2002. Breakdown of wood in the Aguera stream. *Freshwater Biology*, 47, 2205- 2215.
11. Dix, N. & Webster, J. (1995) *Fungal Ecology* Chapman and Hall, New York.
12. Findlay, S.G. & Arsuffi, T.i. 1989. Microbial growth and detritus transformation during decomposition of leaf litter in a stream. *Freshwater Biology*, 21, 261-269.
13. Gasith, A. & Resh, V.H. 1999. Streams in Mediterranean climate regions: abiotic influences and biotic response to predictable seasonal events. *Annual Review of Ecology and systematics*, 30, 51-81.
14. Gessner, M.O. & Chauvel, E. 1994. Importance of stream microfungi in controlling breakdown rates of leaf litter. *Ecology*, 75, 1807-1817.
15. Griffin, D.H. 1994. *Fungal physiology*, 2 edn. Wiley-Liss, New York.
16. Hieber, M. & Gessner, M.O. 2002. Contribution of stream detritivores, fungi, and bacteria to leaf breakdown based on biomass estimates, *Ecology*, 83, 1026-1038.
17. Mathunau, C. & Chauvel. E. 2002. Breakdown of leaf litter in a neotropical stream. *Journal of the north American Benthological Society*, 21 384-396.
18. Minshall, G.W., Petersen, R.C. Cummins, K. W., Bott, T.L., Sedell, J. R., Cushing, C.C & Vanotte, R.L. 1983. Interbiome comparison of stream ecosystem dynamics *Ecological Monographs*, 53, 1-25.
19. Ostrofsky, M.L. 1997. Relationship between chemical characteristics of autumn-shed leaves and aquatic biofilms in a northeastern Ohio stream. *Journal of the North American Benthological Society*, 16, 750-759.
20. Pereira, A. P., Graca, M.A.S. & Molles, M. 1998. Leaf litter decomposition in relation to litter physico-chemical properties, fungal biomass, arthropod colonization, and geographical origin of plant species, *Pedobiologia*, 42, 316-327.
21. Pind, A., Freeman, C & Lock, M.A. 1994. Enzymic degradation of phenolic materials in peatlands measurement of phenol oxidase activity. *Plant and Soil*, 159, 227-231.
22. Romani, A.M., Giorgi, A., Acuna. V. and Sabater, S. 2004. The influence of substratum type and nutrient supply on biofilm organic matter utilization in streams *Limnology and Oceanography*, 49, 1713-1721.
23. Ruttimann, C., Vicuna, R., Mozuch, M.D. & Kirk, T.K 1991. Limited bacterial mineralization of fungal degradation intermediates from synthetic lignin. *Applied and Environmental Microbiology*, 57, 3652-3655.

24. Sinsabaugh, R.L., & Findlay, S. 1994. Enzymatic models for estimating decomposition rates of particulate detritus. *Journal of the North American Benthological Society*, 13, 160-169.
25. Sinsabaugh, R.L., Antibus, R.K., Linkins, A.E., McClaugherty, C.A. Rayburn, L., Repert, D. & Weiland, T. 1992. Wood decomposition over a first-order watershed. Mass loss as a function of lignocellulose activity. *Soil biology and Biochemistry*, 24, 743-749.
26. Yeager, P.E. & Sinsabaugh, R.L. 1998. Microbial diversity along a sediment detrital particle size gradient. *Aquatic ecology*, 32, 281- 289.

| Access this Article in Online | |
|--|--|
|  | Website: www.ijarm.com |
| | Subject: Biodegradation |
| Quick Response Code | |
| DOI: 10.22192/ijamr.2017.04.06.013 | |

How to cite this article:

K Valarmathy and R. Stephan. (2017). Organic matter decomposition by Aquatic fungi in the Pachamalai forested stream contributed by streambed substrata. *Int. J. Adv. Multidiscip. Res.* 4(6): 105-116.
DOI: <http://dx.doi.org/10.22192/ijamr.2017.04.06.013>



Research Article

16s rDNA BASED IDENTIFICATION OF BACTERIA IN THE ORGANIC MATTER OF PACHAMALAI FORESTED STREAMS

K. Valarmathy¹ and R. Stephan*

¹ Department of Biotechnology, The Oxford Engineering College of Engineering, Bangalore- 68.

* Plant Biotechnology Unit, PG & Research Department of Botany, Government Arts College, Ariyalur- 621 718.

*Corresponding Author: stephan.biotech@gmail.com

Abstract

Molecular tools to monitor bacterial diversity in complex microbial assemblages have developed during the last decade using 16S ribosomal DNA based polymerase chain reaction (PCR). The organic matter samples from Koraiyar and Mayiluthu forested streams of Pachamalai hills were subjected to DNA extraction and the resultant amplicons of the genomic DNA were amplified by PCR using universal primers. The resultant amplicons of PCR assays were subjected to electrophoresis and PCR fitness was identified. The molecular detection of 16S rDNA sequence of samples from both stream was done. This showed the availability of a simple method to confirm the bacterial colonization on a broad range of species and this would be useful in the evaluation of organic matter degradation in streams.

Keywords: PCR, 16S rDNA, primers, Koraiyar, Mayiluthu.

Introduction

Identification of bacteria is traditionally performed by isolation of the organisms and the study of their phenotypic characteristics, including Gram staining, morphology, culture requirements and biochemical reactions. However, these methods of bacterial identification have major drawback. Firstly, they cannot be used for noncultivable organisms. Second, we are occasionally faced with organisms exhibiting biochemical characteristics that do not fit into patterns of any known genus and species. Third, identification of slow growing organisms

would be extremely slow and difficult (Woo et al., 2003). Since the discovery of PCR and DNA sequencing, comparison of the gene sequences of bacterial species showed that the 16S rDNA gene is highly conserved within a species and among species of the same genus, and hence, can be used as the new technique for identification of bacteria to the species level (Oleson and Woese, 1993).

Aquatic microbial diversity is well understood to be a key component of aquatic ecosystem functioning (Conter and Biddanda, 2002; Gessner

et al., 2010), and major advances toward linking microbial diversity with ecosystem function have been made in aquatic system (Horner- Devine *et al.*, 2013). A recent survey of microbial diversity studies in aquatic habitats showed that microbial diversity in lotic environments is less commonly studied than in marine and lake ecosystems (Zinger *et al.*, 2012). Stream and rivers are hotspots of microbially mediated carbon (C) and nutrient processing with landscapes (Hynes, 1975; Fisher *et al.*, 1998; McClain *et al.*, 2003). Bacterial diversity was particularly difficult to define, beyond differentiating gram-negative from gram-positive cells (Geesey *et al.*, 1977) or conducting plate counts on selective media (Millner and Goulder, 1984), before the availability of molecular tools. The application of molecular techniques to measure stream microbial diversity produced new insights. Following the establishments of the ribosomal rRNA gene as a conserved marker of taxonomic lineage (Pace, 1997), studies on water column biota began to resolve longitudinal patterns in microbial diversity (Crump *et al.*, 1999; Crump and Baross, 2000), and efforts to integrate molecular and traditional tools in studies of fungal diversity were mounted (Nikoicheva *et al.*, 2003; Nikolcheva and Barlocher, 2005).

Materials and Methods

Sampling procedure

Sampling of epilithic biofilms was performed using sand blasted glass tiles of 9.6 cm² of surface area. Two tiles were scraped per replicate using a sterile cell scraper and suspended in 1 ml sterile stream water.

Isolation of Bacteria

The samples were collected in a sterile plastic container and transported to laboratory for bacteriological analysis. Bacterial isolates were screened on Nutrient Agar (NA) plates by the standard pour plate method. Plates were incubated at 37°C for 24h. A total of one hundred and forty-four isolates were obtained, after incubation.

Two isolate was selected from the group of isolates and used for further studies. The isolated bacteria were identified based on colony characteristics, gram staining methods and by various biochemical tests as given by Bergey's (1984) Manual of Determinative bacteriology.

Biochemical Characterization of the bacteria

The selected bacterial strain was grown in nutrient broth culture medium containing 2.5% peptone, 1.0% yeast extract, and 0.5% beef extract. Cultures (50 ml in 250-ml conical flasks) were inoculated with 5% (v/v) inoculums and incubated at 37 °C with vigorous orbital shaking at 120-150 rpm. To make a solid medium, 1.5% agar was added to the broth (Himedia, India). The shape and color of the colonies were examined under the microscope after Gram staining. Isolates were biochemically analyzed for the activities of Oxidase, Catalase and MR-VP test, Urease test, Motility, Indole production (Table- 1) and Citrate utilization (Table- 2) tests were also conducted. These tests were used to identify the isolates according to Bergey's Manual of Determinative bacteriology.

Bacterial DNA isolation

Bacterial genomic DNA was isolated as per the standard protocol (Hoffman and Winston, 1987). Nutrient broth was inoculated with single colony and cultured for overnight at 37°C. Cells were harvested from 5 mL of the culture and to this 100µL of lysozyme was added and incubated at Room temperature for 30 min, followed by the addition of 700µL of cell lysis buffer (Guanidiniumisothiocyanate, SDS, Tris- EDTA). The contents were mixed by inverting the vial for 5 min with gentle mixing till the suspension looked transparent. 700µL of isopropanol was added on to the top of the solution and were mixed gently till white strands of DNA were seen. The DNA was extracted from the aqueous layer was precipitated with ethanol. The DNA pellet was dried and dissolved in 50µL of 1X TE buffer. The purity of the DNA was analyzed by running on 0.8% agarose gel stained with ethidium

bromide (0.5 µg/µL). A single intense band with slight smearing was noted.

The extracted genomic DNA was used as template DNA for the universal bacterial primers (Forward primer 5'-AGAGTTTGATCCTGGCTCAG-3' and reverse primer (5' GGTTACCTTGTTACGACTT 3') were used for the amplification of the 16S rRNA gene fragment. The reaction mixture of 50µl consisted of 10 ng of genomic DNA, 2.5 Units of Taq DNA polymerase, 5µl of 10X PCR amplification buffer (100 mMTris- HCl, 500 mMKCl pH-8.3), 200µM dNTP, 10 p moles each of the two universal primers and 1.5mM MgCl₂. Amplification was done by initial denaturation at 94°C for 3min, followed by 40 cycles of denaturation at 94°C for 30 seconds, annealing temperature of primers was 55°C for 30 second and extension at 72°C for 1 minute. The final extension was conducted at 72°C for 10 minutes.

Agarose Gel Electrophoresis

10 µL of the reaction mixture was then analyzed by submarine gel electrophoresis using 1.0 % agarose with ethidium bromide (0.5 µg/µL) as per the standard protocols (Sambrook *et al.*, 2001) at 80V/cm and the reaction product was visualized under Gel Documentation System (Alpha Innotech).

Purification of PCR Product by Exosap-IT

The PCR product was subjected to purification by using Exosap-IT. It is a mixture of Exonuclease I and Shrimp Alkaline Phosphatase that removes left over primers and free nucleotides from the PCR reaction. To 5 µL of PCR product add 2 µL of Exosap. Further the samples were incubated at 37°C for 15 minutes for the degradation of primers and free nucleotides. Then the Tube was transferred to water bath at 80°C and incubated for 15 minutes to inactivate the Exosap-IT enzyme. The sample was then ready for sequencing reaction.

DNA sequencing of 16S rRNA gene fragment

The 16S rRNA purified PCR product (100ng concentration) was subjected for the amplification of the 16S rRNA gene.

PCR amplification of 16S rRNA gene:

PCR reaction was performed in a gradient thermal cyclor (Eppendorf, Germany). The sequencing using ABI DNA 3730 XL sequencer (Applied BiosystemInc). Sequencing of the 16S rRNA gene of the bacterial isolate was done from both the directions, the sequence obtained was subjected to BLAST search and the bacterial species were determined. The percentages of sequence matching were also analyzed.

Computational analysis (BLAST) and Identification of Bacterial species

BLAST (Basic Local Alignment Search Tool) is a web-based program that is able to align the search sequence to thousands of different sequences in a database and show the list of top matches. This program can search through a database of thousands of entries in a minute. BLAST (Altschule *et al.*, 1990) performs its alignment by matching up each position of search sequence to each position of the sequences in the database. For each position BLAST gives a positive score if the nucleotides match, it can also insert gaps when performing the alignment. Each gap inserted has a negative effect on the alignment score, but if enough nucleotides align as a result of the gap, this negative effect is overcome and the gap is accepted in the alignment. These scores are then used to calculate the alignment score, in "bits" which is converted to the statistical E-value. The lower the E-value, the more similar the sequence found in the database is to query sequence. The most similar sequence is the first result listed.

Results and Discussion

Bacterial population analysis in biofilms

PCR amplification of DNA extracted from epilithic biofilm was performed on samples of Pachamalai forested stream. The traditional identification of bacteria on the basis of phenotypic characteristics is generally not as accurate as identification based on genotypic methods. Comparison of the bacterial 16S rRNA gene sequence has emerged as a preferred genetic technique. The sequence of the 16S rRNA gene has been widely used as a molecular clock to estimate relationships among bacteria (phylogeny), but more recently it has also become important as a means to identify an unknown bacterium to the genus or species level. The use of 16S rRNA gene sequences to study bacterial phylogeny and taxonomy has been by far the most common housekeeping genetic marker used for a number of reasons. These reasons include (i) its presence in almost all bacteria, often existing as a multigene family, or operons (ii) the function of the 16S rRNA gene over time has not changed, suggesting that random sequence changes are a more accurate measure of time (evolution); and (iii) the 16S rRNA gene (1,500 bp) is large enough for informatics purposes (Patel, J. B. 2001). The rRNA based analysis is a central method in microbiology used not only to explore microbial diversity but also to identify new strains.

Total of one hundred and forty-four isolates obtained, from the Pachamalai forested stream two isolate were used for further analysis. Isolated colony from mixed populations, on nutrient agar plates were characterized and sub cultured to obtain pure cultures, and the isolated bacteria were identified based on colony characteristics, and were biochemically analyzed for the activities of Oxidase, Catalase, MR-VP test, Urease test, Motility, Indole production (Table- 1), Sugar utilization test (Table -2) and Gram staining (Figure: 1) tests. From the tests the isolate was found to be *Bacillus spp.*, further confirmation was done using molecular approach. Bacterial

genomic DNA was isolated as per the standard protocol (Hoffman and Winston, 1987). The presence of bacterial genomic DNA isolated was confirmed on 0.8% agarose gel stained with ethidium bromide. An intense single band was seen along with the DNA marker. (Fig-2) The extracted DNA was used as template for amplification of 16S rRNA gene. The universal primers 27F and 1429R were used for the amplification and sequencing of the 16S rRNA gene fragment. The optimum annealing temperature was found to be 55°C. An intense single band was visible on 1% agarose gel stained with ethidium bromide (Figure: 2). The PCR product was subjected to sequencing using BDT V3.1 cycle sequencing kit on ABI 3730 XL genetic analyzer from both forward and reverse directions. The two sequences (Figure: 3) obtained were compared with the NCBI gene bank database using BLAST search program (<http://www.ncbi.nlm.nih.gov>) (Marchler– Bauer *et al.*, 2000; Pruitt *et al.*, 2005). The percentages of sequence matching were also analyzed. The homology search made using BLAST sequence 1 showed 99 – 100% maximum identity with that of *Bacillus subtilis strain B5501A*, NCBI Gene Bank Accession No: FJ 55787.1 and E-value equal to 0 for all closely related taxa. Other close homologs of the isolate showing 99% similarity with, *Bacillus tequilensis* BK206 99%, 99% similarity with *Bacillus vallismortis*, and 95% *Paeni Bacillus polymaxa*, *Bacillus velezensis* P42, *Bacillus amyloquelaciens - L51*, *Bacillus sigmensis* IHBB16121, *Bacillus licheniform*, and the sequence 2 showed maximum identity with that of *Leptotrichia species* EB007, *Leptolyngbya Species –L21- BG2* and with *Cyanobacterium phormidium*. Sequences of the bacterial isolates were used for the construction of the phylogenetic dendrogram to know the genetic relatedness between the bacterial isolates. All the closely related homologs of identified bacteria were used for the construction of the phylogenetic dendrogram to know their evolutionary origin. The dendrogram showing the relation between *Bacillus subtilis* strain B5501A and *Leptolyngbya 12077* and their close homologs is shown in (Figure:4a, b).

Table -1: Physio–biochemical characteristics of the isolate *Bacillus subtilis* B5501A

| Test | Observation |
|-------------------------|--|
| Gram's stain | Gram Positive |
| Spore staining | Central, oval, bulging |
| Cell shape | Rods |
| Cell size | >3µm |
| Colony character | White, raised irregular |
| Motility | + |
| Catalase | + |
| Oxidase | - |
| Indole | - |
| Methyl red | - |
| Voges-Proskauer | - |
| Citrate utilization | + |
| Casein utilization | + |
| Starch hydrolysis | + |
| Urea hydrolysis | - |
| Growth at 50°C | + |
| Growth in 10% NaCl | - |
| Anaerobic growth | + |
| TSI (Triple Sugar Iron) | Acid slant/ alkaline butt, gas, no H ₂ S produced |

+,Positive , -Negative

Table-2: Sugar utilization test

| Sugar utilization | Result (acid/ gas) |
|-------------------|--------------------|
| Glucose | +/- |
| Galactose | +/- |
| Arabinose | +/- |
| Mannitol | -/- |
| Maltose | +/- |
| Mannose | +/- |
| Raffinose | -/- |
| Rhamnose | -/- |
| Sucrose | +/- |
| Lactose | +/- |
| Fructose | +/- |
| Xylose | +/- |

+ /Positive - / Negative

Figure –1 – Bacillus strain (Gram Staining)

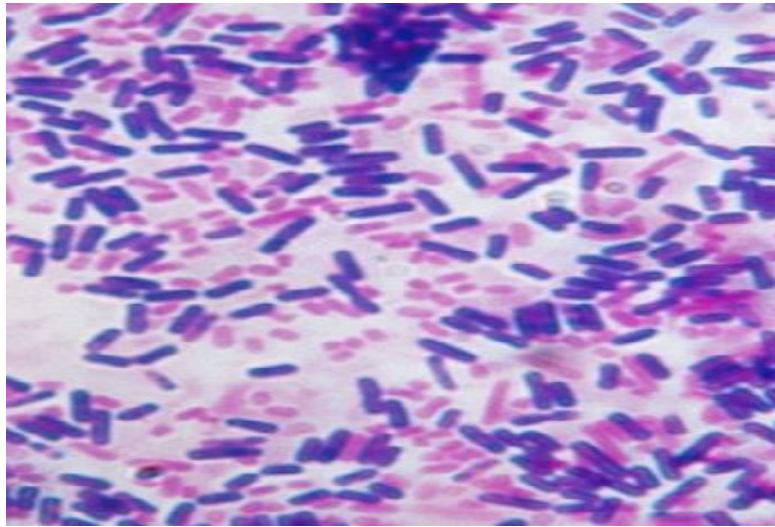
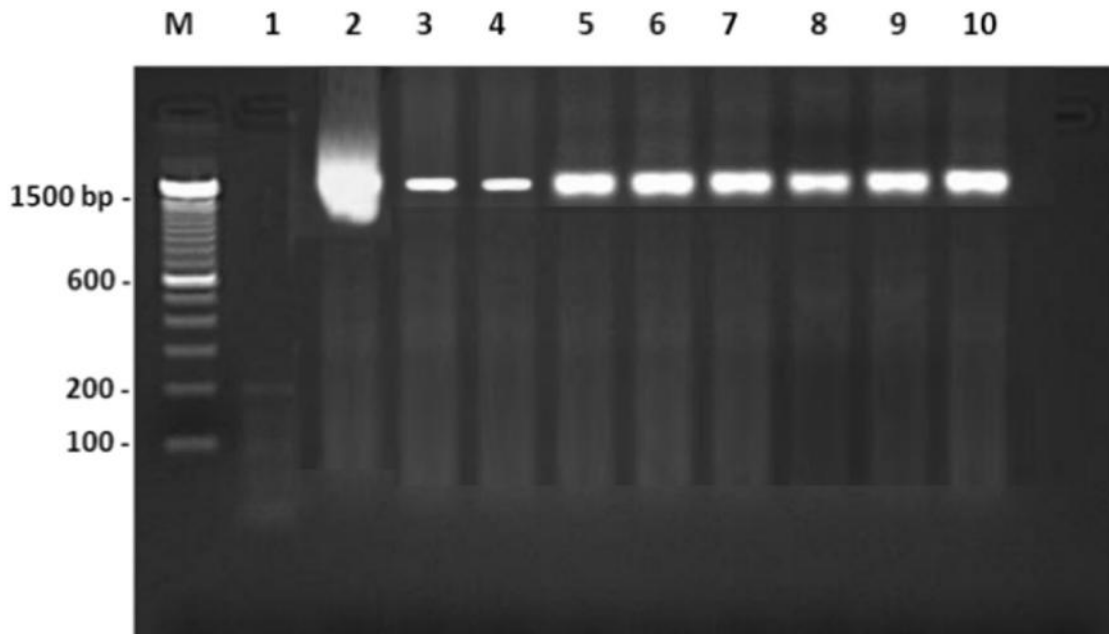


Figure- 2- Gel image of 16S rRNA amplicon



Lane – M - DNA marker,
Lane- 1 -Negative control
Lane – 2 -Positive control (genomic DNA)
Lane-3 to 10 -16S rRNA amplicon band

Figure- 3 - Partial sequence of PCR product of 16S rRNA gene

a. sequence-1 b. sequence-2

(a)

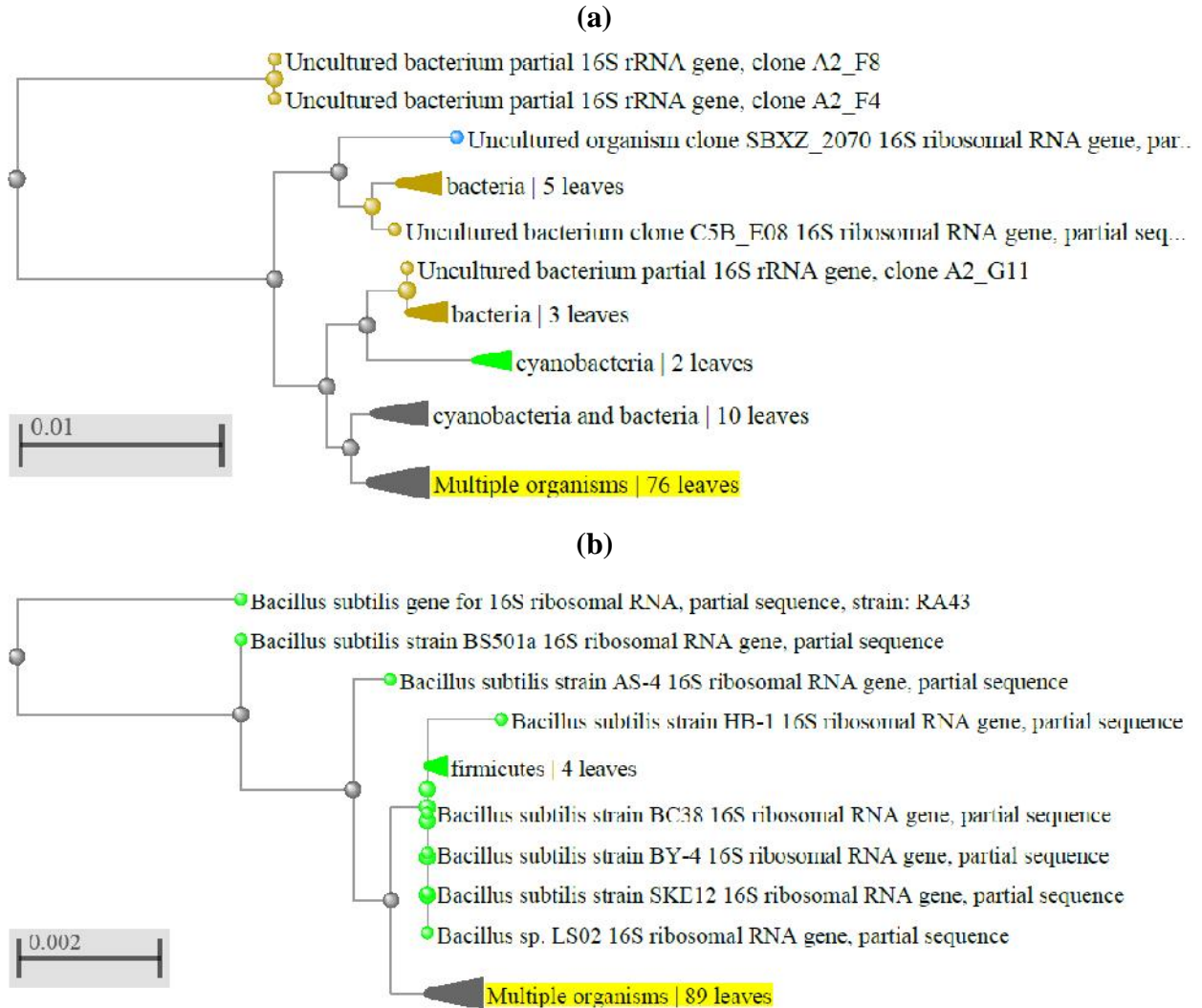
ACGCGATAAGTATCCCGCCTGGGGAGTACGCACGCAAGTGTGAAACTCAAAGGAATTGACGGGGGCCCGACA
AGCGGTGGAGTATGTGGTTTAATTCGATGCAACGCGAAGAACCCTTACCAGGGCTTGACATCCCTCGAATCCT
CTTGAAAGAGAGGAGTGCCTTCGGGAGCGAGGAGACAGGTGGTGCATGGCTGTCTGTCAGCTCGTGTCTGTGAG
ATGTTGGGTTAAGTCCCGCAACGAGCGCAACCCACGTCTTATGTTGCCAGCATTGAGTTGGGCACTCTGGGG
AGACTGCCGGGGACAACCTCGGAGGAAGGTGTGGATGACGTCAAGTCATCATGCCCTTACGTTCTGGGCTAC
ACACGTACTACAATGCTTCGGACAAAGGGCAGCCAAGTACGATAGTGTAGCTAATCCATAAAACCGAGGCAC
AGTTCAGATTGCAGGCTGCAACTCGCCTGCATGAAGGAGGAATCGCTAGTAATCGCCGGTCAGCATAACGGCG
GTGAATACGTTCCCGGGCCTTGTACACACCCGCCGTACACCCATGGGAGCATAACGTCCTACGGGAGAAAGCA
GGGGACCTTCGGGCCTTTCGCTATCAGATGAGCCTAGGTTCGGATTAGCTAGTTGGTGAGGTAATGGCTCACC
AAGGCGACGATCCGTAACCTGGTCTGAGAGGATGATCAGTCACACTGGAACCTGAGACACGGTCCAGACTCCTA
CGGGAGGCAGCAGTGGGGAATATTGGACAATGGGCGAAAGCCTGATCCA
GCCATGCCGCGTGTGTGAAGAAGGTCTTCGGATTGTAAAGCACTTTAAGTTGGGAGGAAGGGCAGTTGCCTA
ATACGTAACTGTTTTGACGTTACCGACAGAATAAGCACCGGCTAACTCTAACGCTGGCGGCAGGCCTACGGA
CGGGTGAGTAATGCC TAGGAATCTGCCTGGTAGTGGGGGATAACGCTCGGAAACGGACGCTAATACCGCATA
CGTCTACGGGAGAAAGCAGGGGACCTTCGGGCCTTTCGCTATCAGATGAGCCTAGGTTCGGATTAGCTAGTT
GGTGAGGTAATGGCTCACCAAGGCGACGATCCGTAACCTGGTCTGAGAGGGATGATCAGTCACACTGGAACCTG
AGACACGGTCCAGACTCCTACGGGAGGCAGCAGTGGGGAATATTGGACAATGGGCGAAAGCCTGATCCAGCC
ATGCCGCGTGTGTGAAGAAGGTCTTCGGATTGTAAAGCACTTTAAGTTGGGAGGAAGGTTAAGCACTCCGCC
TGGGGAGTACGGCCGCAAGGCTGAAACTCAAAGGAATTGACGGGGGCCCGCACAAAGCGGTGGAGCATGTGGT
TTAATTCGAAGCAACGCGAAGAACCCTTACCAGGTCTTGACATCCTCTGACAACCCTAGAGATAGGGCTTTCC
CCTTTCGGGGGACAGAGTGACAGGTGGTGCATGGTTGTCTGTCAGCTCGTGTCTGTGAGATGTTGGGTTAAGTC
CCGCACGAGCGCAACCCTTTGATCTTAGTGACGATCAGTGGCACCTCTA
AGGTGACTGCGTGACAACGAGAGGTGGGGATGACGTCAATCATCATGCCCTTATGACCTGGGCTACAAGAG
AGTTGATCCTGGCTCAGGACGAACGCTGGCGGCGTGCCTAATACATGCAAGTCGAGCGGACAGATGGGAGCT
TGCTCCCTGATGTTAGCGGCGGACGGGTGAGTAACACGTGGGTAACCTGCCTGTAAGACTGGGATAACTCCG
GGAAACCGGGGCTAATACCGGATGGTTGTTTGAACCGCATGGTTCAAACATAAAAGGTGGCTTCAGCAGTAG
GGAATCTTCCGCAATGGACGAAAGTCTGACGGAGCAACGCCGCGTGAGTGATGAAGGTTTTTCGGATCGTAAA
GCTCTGTTGTTAGGGAAGAACAAGTACCGTTCGAATAGGGCGGTACCTTGACGGTACCTAACACATGCAAGT
CGAGCGGCAGCACGGTACTTGTACCTGGTGGCGAGCGG

(B)

AACGCTGGCGGCAGGCCTAACACATGCAAGTCGAGCGGCAGCACGGGTACTTGTACCTGGTGGCGAGCGGCG
GACGGGTGAGTAATGCCTAGGAATCTGCCTGGTAGTGGGGGATAACGCTCGGAAACGGACGCTAATACCGCA
TACGTCCTACGGGAGAAAGCAGGGGACCTTCGGGCCTTTCGCTATCAGATGAGCCTAGGTTCGGATTAGCTAG
TTGGTGAGGTAATGGCTCACCAAGGCGACGATCCGTAACCTGGTCTGAGAGGGATGATCAGTCACACTGGAAC
TGAGACACGGTCCAGACTCCTACGGGAGGCAGCAGTGGGGAATATTGGACAATGGGCGAAAGGGCGGTGGCG
GGTGCTATAATGCAGTCGAGCGAATCGATGGGAGCTTTCCTGAGATTAGCGGCGGACGGGTGAGTAACA
CGTGGGCAACCTGCCTATAAGACTGGGATAACTTCGGGAAACCGGAGCTAATACCGGATACGTTCTTTTCTC
GCATGAGAGAAGATGGAAAGACGGTTTACGCTGTCACTTATAGATGGGCCCGCGGCGCATTAGCTAGTTGGT
GAGGTAATGGCTCACCAAGGCGACGATGCGTAGCCGACCTGAGAGGGTGTATCGGCCACACTGGGACTGAGAC
ACGGCCCAGACTCCTACGGGAGGCAGCAGTAGGGAATCTTCCGCAATGGACGAAAGTCTGACGGAGCAACGC
CGCGTGAACGAAGAAGGCCTTCGGGTCGTAAAGTTCTGTTGTTAGGGAAGTTACCAGGTCTTGACATCCTCT
GACAATCCTAGAGATAGGACGTCCCCTTCGGGGGACAGAGTGACAGGTGGTGCATGGTTGTCTGTCAGCTCGTG
TCGTGAGATGTTGGGTTAAGTCCCGCAACGAGCGCAACCCTTTCGATCTTAGTTGCCAGCATTAGTTGGGCAC
TCTAAGGTGACTGCCGGTGACAAACCGGAGGAAGGTGGGGATGACGTCAAATCATCATGCCCTTATGACCT

GGGCTACACACGTGCTACAATGGACAGAACAAGGCAGCGAAACCGCGAGGTTAAGCCAATCCCACAAATCT
 GTTCTCAGTTCGGATCGCAGTCTGCAACTCGACTGCGTGAAGCTGGAATCGCTAGTAATCGCGGATCAGCAT
 GCCGCGGTGAATACGTTCCCGGGCCTTGTACACACCGCCCGTACACCACGAGAGTTTCGTAACACCCGAAGC
 CGGTGAGGTAACCTTTTAGGAGCCAGCCGCGAAGG
 TGGGACAGATGATTGGGGTGAAGTCGTAACAAGGTAACC

**Figure- 4- Phylogenetic tree representing close homologs of
 a. uncultured bacterial clone. b. *Bacillus subtilis***



Nikolcheva, L. G and F. Barlocher, 2004. Using taxon-specific primers study on demonstrated the presence of these major fungal taxa and found ascomycetes to be the main group of fungi colonizing decaying leaves in streams. In contrast rDNA approaches confirmed higher bacterial species richness in the Pachamalai forested stream.

Conclusion

Patterns of biofilm formation were investigated in Mayiluthu and Koraiyar streams of Pachamalai forest. From the results it was understood that a higher amount of particulate organic matter standing stock was found in the Mayiluthu stream channel. From the tests conducted the isolate was found to be *Bacillus species* and the obtained dendrogram showed that there is a relation between *Bacillus subtilis* strain B5501A.

Acknowledgments

The authors would like to thank the Department of Botany, Government Arts College, Ariyalur, Tamil Nadu, India for provided the required facility for this study.

References

1. Altschul, S. F., Gish, W., Miller, W., Myers, E. W., and Lipman, D. J. (1990). Information about the BLAST. *Journal of Molecular Biology*, 401-403.
2. Araya, M., Peña C., Pizarro, F., and Olivares, M. (2003). Gastric response to acute copper exposure. *Science of the Total environment*, 303(3), 253-7.
3. Battin, T. J., Kaplan, L. A., Newbold, J. D., Cheng, X.H., and Hansen, C. (2003). Effects of current velocity on the nascent architecture of stream microbial biofilms. *Applied and Environmental Microbiology*, 69, 5443-5452.
4. Cotner, J. B., and Biddanda, B. A. (2002). Small players, large role: microbial influence on biogeochemical processes in pelagic aquatic ecosystems. *Ecosystems* 5, 105–121. doi: 10.1007/s10021-001-0059-3.
5. Crump, B. C., and Baross, J. A. (2000). Archaea plankton in the Columbia river, its estuary and the adjacent coastal ocean, USA. *FEMS Microbiol. Ecol.* 31, 231–239. doi: 10.1111/j.1574-6941.2000.tb00688.x
6. Crump, B. C., Armbrust, E. V., and Baross, J. A. (1999). Phylogenetic analysis of particle-attached and free-living bacterial communities in the Columbia river, its estuary, and the adjacent coastal ocean. *Applied and Environmental Microbiology*. 65, 3192–3204.
7. Emtiazi, F., Schwartz, T., Marten, S.M., Krolla- Sidenstein, P., and Ost, U. (2004). Investigation of natural biofilms formed during the production of drinking water from surface water embankment filtration. *Water Research*, 38, 1197-1206.
8. Fisher, S. G., Grimm, N. B., Martí, E., Holmes, R. M., and Jones, J. B. (1998). Material spiraling in stream corridors: a telescoping ecosystem model. *Ecosystems* 1, 19–34. doi: 10.1007/s100219900003
9. Gasith, A., and Resh, V.H. (1999). Stream in Mediterranean climate regions: abiotic influence and biotic responses to predictable seasonal events. *Annual Review of ecology and Systematics*, 30, 51-81.
10. Geesey, G. G., Richardson, W. T., Yeomans, H. G., Irvin, R. T., and Costerton, J. W. (1977). Microscopic examination of natural sessile bacterial populations from an alpine stream. *Canadian Journal of Microbiology*, 23, 1733–1736. doi: 10.1139/m77-249.
11. Gessner, M. O., Swan, C. M., Dang, C. K., Mckie, B. G., Bardgett, R. D., and Wall, D. H. (2010). Diversity meets decomposition. *Trends in Ecology and evolution*, 25, 372–380. doi: 10.1016/j.tree.2010.01.010.
12. Horner-Devine, M. C., Leibold, M. A., Smith, V. H., and Bohannan, B. J. M. (2003). Bacterial diversity patterns along a gradient of primary productivity. *Ecology Letters*. 6, 613–622. doi: 10.1046/j.1461-0248.2003.00472. x.
13. Hynes, H. B. N. (1975). The stream and its valley. *Verh. Int. Ver. Theor. Angew. Limnol.* 19, 1–15.
14. Jackson, C. R., Churchill, P. F., and Roden, E.E. (2001). Successional changes in bacterial assemblage structure during epilithic biofilm development. *Ecology*, 82, 555-566.
15. Lyautey, E., Jackson, C.R., Cayrou, J., Rols, J.L., and Garaetian, F. (2005). Bacterial community succession in natural river biofilm assemblages, *Microbial Ecology*, 50, 589-601.
16. Lyautey, E., Teissier, S., Charcosset, J. Y., Rols, J.L., and Garaetian, F. (2003). Bacterial diversity of epilithic biofilm assemblages of an anthropized river section, assessed by DGGE analysis of a 16S r DNA fragment. *Aquatic Microbial Ecology*, 33, 217-224.
17. Marchler-Bauer, A., Panchenko, A. R., Shoemaker, B. A., Thiessen, P. A., Geer, L. Y., and Bryant, S. H. (2000). CDD: a database of conserved domain alignments with links to domain three - dimensional structure. *Journal of Nucleic acid research*, 30, 281-283.

18. McClain, M. E., Boyer, E. W., Dent, C. L., Gergel, S. E., Grimm, N. B., Groffman, P. M., et al. (2003). Biogeochemical hot spots and hot moments at the interface of terrestrial and aquatic ecosystems. *Ecosystems* 6, 301–312. doi: 10.1007/s10021-003-0161-9.
19. Milner, C. R., and Goulder, R. (1984). Bacterioplankton in an urban river - the effects of a metal-bearing tributary. *Water Research*, 18, 1395–1399. doi: 10.1016/0043-1354(84)90009-5.
20. Nagpal, M. I., Fox, K.F., and Fox, A. (1998). Utility of 16S-23S rRNA spacer region methodology: how similar are interspace regions within genome and between strains for closely related organisms? *Journal of Microbiological methods*, 33, 211-219.
21. Nikolcheva, L. G., and Barlocher, F. (2005). Seasonal and substrate preferences of fungi colonizing leaves in streams: traditional versus molecular evidence. *Environmental Microbiology*, 7, 270–280. doi: 10.1111/j.1462-2920.2004.00709. x.
22. Nikolcheva, L. G., Cockshutt, A. M., and Barlocher, F. (2003). Determining diversity of freshwater fungi on decaying leaves: comparison of traditional and molecular approaches. *Applied and Environmental Microbiology*, 69, 2548–2554. doi: 10.1128/AEM.69.5.2548-2554.2003.
23. Olsen, G. J. and Woese, C. R. (1993). Ribosomal RNA: a key to phylogeny. *FASEB*, J;7:113-123.
24. Pace, N. R. (1997). A molecular view of microbial diversity and the
- Int. J. Compr. Res. Biol. Sci.*(2017).4(12):1-10 biosphere. *Science* 276, 734–740. doi: 10.1126/science.276.5313.734.
25. Patel, J. B. 2001, 16S rRNA gene sequencing for bacterial pathogen identification in the clinical laboratory. *Mol. Diagn.* 6,313-321.
26. Pruitt, K. D., Tatusova, T., and Maglott, D. R. (2005). NCBI reference sequence: a cultured non-redundant sequence database of genomes, transcripts, and proteins. *Journal of Nucleic Acids Research*, 33, D501–D504.
27. Sambrook, J; Fritsch, E. F. and Maniatis, T.(1989), *Molecular Cloning, A laboratory manual*, 2nd Edn (ColdSpring Harbor Laboratory, ColdSpring Harbor, NY).
28. Woo, P. C. Y., Ng, K. H. L., Lau, S. K. P., Yip, K., Fung, A. M. Y., Leung, K., Tam, D. M. W., Que, T. and Yuen, K. (2003). Usefulness of the MicroSeq 500 16S Ribosomal DNA-Based Bacterial Identification System for Identification of Clinically Signification Bacterial Isolates with Ambiguous Biochemical Profiles. *Journal of Clinical Microbiology*, 1996-2001.
29. Zinger, L., Gobet, A., and Pommier, T. (2012). Two decades of describing the unseen majority of aquatic microbial diversity. *Mol. Ecol.* 21, 1878–1896. doi: 10.1111/j.1365-294X.2011.05362. x.

| Access this Article in Online | |
|--|---|
|  | Website: www.darshanpublishers.com |
| | Subject: Biodiversity |
| Quick Response Code | |
| DOI:10.22192/ijcrbs.2017.04.12.001 | |

How to cite this article:

K. Valarmathy and R. Stephan. (2017). 16s rDNA Based identification of bacteria in the organic matter of Pachamalai forested streams. *Int. J. Compr. Res. Biol. Sci.* 4(12): 1-10.
 DOI: <http://dx.doi.org/10.22192/ijcrbs.2017.04.12.001>

Screening Of Antibacterial And Antioxidant Activities Of *Streptomyces* Species Isolated From Western Ghats Region Of Karnataka

Almas Fathima, Daaniyah Belgami, S S Naziya Saba, Smriti Aurora, B K Manjunatha and Divakara R
Department of Biotechnology, The Oxford College of Engineering, Bommanahalli, Bengaluru-560068

ABSTRACT

Soil *Actinomycetes*' secondary metabolites possess wide range of biologically active compounds and are the potential source of novel bioactive metabolites. Currently *Actinomycetes* emerged as an important source for bioactive natural products with chemical diversity. In this study, *Actinomycetes* strain was isolated from the Western Ghats region of Karnataka and characterized by the 16S rRNA gene sequence. The strain was identified as *Streptomyces* species. The strain was characterized for antioxidant and antibacterial activity. The isolated strain exhibited broad spectrum of antibacterial activity against Gram positive bacteria (*S. aureus* and *B. subtilis*) and Gram negative bacteria (*P. aeruginosa* and *E. coli*). The ethyl acetate extract showed 86.6 % and 98 % of 2, 2-diphenyl-1-picrylhydrazyl (DPPH) and 2, 2'-azinobis-(3-ethylbenzothiazoline-6-sulfonic acid) radical scavenging assay at 11 mg/ml and 8.25 mg/ml respectively. However, purification and further characterization of bioactive metabolites from *Streptomyces* species is required for their optimum utilization towards antibacterial and antioxidant purposes.

INTRODUCTION

Actinomycetes are a group of prokaryotic organisms belonging to subdivision of the Gram-positive bacteria phylum. Most of them are grouped under subclass Actinobacteridae, order Actinomycetales. The members of this order are characterized by the high G+C content which accounts about >55 mol% in their DNA (Stackebrandt *et al*, 1997). These are one of the richest source of important natural products especially antibiotics. So far, approximately 10,000 antibiotics were reported, and almost half of them are produced by soil actinomycetes *Streptomyces* (Lazzarini *et al*, 2000). Bioactive metabolites produced from *Streptomyces* have high commercial value and important applications in human as well as livestock medicine and in agriculture (Wathe *et al*, 2001). The biological active compounds produced by actinomycetes are being used as antibiotics, immunosuppressant, extracellular hydrolytic enzymes, plant growth promoters, lytic enzymes, herbicides, insecticides, antitumor agents and siderophores. Approximately World's 80% antibiotics are obtained by actinomycetes, majorly from genus *Streptomyces* and *Micromonospora* (Pandey *et al*, 2004).

Chemotherapy using antimicrobial agents has been a leading cause for the rise of average life expectancy in the past Century. However, infectious agents that have become resistant to antibiotic drug therapy are an increasing public health problem. Currently, about 70% of the bacteria which cause infections to humans in hospitals are resistant to at least one of the drugs most commonly used for treatment of infection caused by them. Certain organisms are resistant to all approved antibiotics and infections caused by these organisms can only be treated with experimental and potentially toxic drugs. The increase in antibiotic resistance of bacterial will cause community acquired infections and also causes morbidity (Bisht *et al*, 2009). Development of antibiotic resistance in bacteria, as well as economic incentives has resulted in identification new antibiotic strains of actinomycetes in order to maintain a pool of effective drugs at all times (Stephen & Kennedy, 2011).

Free radicals and oxidants play a dual role as both toxic and beneficial compounds, since they can be either harmful or helpful to the body. It has been implicated in the development of many human diseases. A few of them include arthritis, inflammatory diseases, kidney diseases, cataracts, inflammatory bowel disease, colitis, lung dysfunction, pancreatitis, drug reactions, skin lesions and aging (Lakhtakia *et al*, 2011). They are produced either from normal cell metabolism *in situ* or from external sources (like pollution, cigarette smoke, radiation and medication). When an overload of free radicals cannot gradually be destroyed, their accumulation in the body generates a phenomenon called oxidative stress. This process plays a major part in the development of several chronic and degenerative illnesses (Pham-Huy *et al*, 2008).

Moreover, it has been shown that antioxidants and free radical scavengers are crucial in the prevention of pathologies, in which reactive oxygen species (ROS) or free radicals are implicated (Rathna Kala and Chandrika, 1993). Synthetic antioxidants have been used in stabilization of foods (Hajji *et al*, 2010). But their use is being restricted nowadays because of their toxic and carcinogenic effects (Kekuda *et al*, 2010). Thus, interest in finding natural antioxidants, without any undesirable effects has increased greatly (Rechner *et al*, 2002). Oxidative stress is ultimately involved in endothelial dysfunction, a condition which is evident in adults suffering from various cardiovascular diseases including thalassemia (Shinar and Rachmilewitz, 1990; Hebbel, 1990; Grinberg *et al*, 1995). Antioxidant and other supportive therapies protect red blood cells against oxidant damage (Filburn, 2007; Kukongviriyapan *et al*, 2008). It is well known that the generation of free radicals happens because of microbial infection which leads to DNA damage (Maeda and Akaike, 1998). In the present study, we point out biological activities of secondary metabolites produced by actinomycetes in effort to combat infectious diseases.

MATERIALS AND METHODS

Soil sampling and pretreatment: Soil samples were collected from forest areas of Western Ghat region of Karnataka and Kerala. Each collection will be made from 10-15 cm depth of the soil. These were air-dried for 1 week, crushed and sieved. The sieved soils were then used for actinomycetes isolation.

Isolation of Actinomycetes: Each sample were air-dried at room temperature (about 25 ± 2 °C) for 5 to 7 days and then ground in a mortar and used for further study. Dilution technique was used to isolate actinomycetes from the soil samples. Soil samples were serially diluted with sterile 0.9% (w/v) saline solution to give final concentrations of 10^{-2} and 10^{-3} . Using a sterile glass rod, the soil suspensions were spread onto sterile Glycerol Asparagine Agar (GAA). All plates were incubated at 28 °C for 7 days.

Characterization of actinomycetes: The isolated actinomycetes were characterized by morphological and biochemical methods. Morphological characterization was done by macroscopic and microscopic methods. Microscopic characterization was carried out by cover slip culture method (Kawato and Sinobu, 1979) by observing mycelium structure, color and arrangement of conidiospore and arthospore on the mycelium through the oil immersion (100X). The observed morphological characters were compared with Bergey's manual of determinative bacteriology and the isolate was characterized.

Screening for antimicrobial activity: Antimicrobial activities of isolates were tested preliminarily by cross streak method on Nutrient Agar plates (Egorov, 1985). Actinomycetes isolates were streaked across diameter on nutrient agar plates. After incubation at 28 °C for 6 days, 24 hrs cultures of test organisms were streaked perpendicular to the central strip of actinomycetes culture. All plates were again incubated at 37 °C for 24 hrs and zone of inhibition was measured.

Extraction of antimicrobial compounds: The antibacterial compounds were isolated from the actinomycetes isolates by following Westley *et al*, 1979 and Liu *et al*, 1986 method with slight modifications. The selected antagonistic actinomycete isolates were inoculated into Yeast Extract Malt Extract (YEME) broth, and incubated at 28 °C in a shaker (200-250 rpm) for seven days. After incubation the broths were filtered through Whatman No.1 filter paper. To the culture filtrate, equal volume ethyl acetate was added and shaken vigorously for 1 hr for the extraction of antimicrobial compound. The ethyl acetate extract was evaporated to dryness in rotary flash evaporator. The extracts were tested for their antimicrobial activity by well diffusion method (Sen *et al*, 1995) against the test pathogens. The antimicrobial efficacy was assessed by measuring the zone of inhibition after 24 hrs of incubation.

DETERMINATION OF ANTIOXIDANT ACTIVITY:

DPPH scavenging activity: DPPH scavenging activity of the EA extract was determined by the method of Manjunatha *et al*, 2013 with slight modifications. 100 µM methanol DPPH solutions were mixed with different concentrations of EA extract. Ascorbic acid (standard) was used as positive control. The tubes were incubated at room temperature in dark for 30 min and the optical density was measured at 517 nm. The absorbance of the control, DPPH• alone (containing no sample), was also noted (Khalaf NA, 2008). The percentage of radical scavenging activity of the extract against the stable DPPH• was calculated using following equation:

$$\% \text{ DPPH}\cdot \text{ Scavenging activity} = [A_{\text{control}} - A_{\text{sample}}] / A_{\text{control}} \times 100$$

ABTS scavenging activity: To generate ABTS radical cation, 50ml of 2mM ABTS and 0.3mL of 17mM Potassium persulfate were mixed together and incubated in the dark for 12-16 h to develop Prussian blue colored ABTS^{•+} solution which has an absorption maxima at 734nm [Re *et al.*, 1999]. To determine scavenging activity of extracts of different concentrations was added to 1.6ml of ABTS^{•+} solution. The absorbance was measured at 734nm after 20 minutes at room temperature. All readings were performed in triplicates and the free radical scavenging activity was calculated from equation:

$$\% \text{ ABTS Scavenging activity} = [A_{\text{control}} - A_{\text{sample}}] / A_{\text{control}} \times 100$$

Molecular characterization of actinomycetes strain by 16S rDNA sequence: The actinomycetes strain was grown at 30 °C for 5 days in shake flasks, containing 100 ml of ISP 2 medium (4 g/l yeast extract, 10 g/l malt extract and 4 g/l glucose). Mycelium was obtained by centrifugation and washed twice with bi-distilled water. Approximately, 200 mg of mycelium were used for genomic DNA extraction as follows: the sample was dispersed in 800 µl of the lysis solution (100mM Tris-HCl, pH 7.4, 20mM EDTA; 250mM NaCl; 2% SDS; 1 mg/ml; lysozyme; 100 µl H₂O), added with 5 µl of RNase (50 mg/ml) and incubated at 37 °C for 60 min. Then 10 µl of proteinase K solution (20 mg/ml) were added, and the lysis solution was reincubated at 65 °C for 30 min. The lysate was extracted two times with an equal volume of phenol, centrifuged and then re-extracted with chloroform (v/v) to remove residual phenol. DNA was precipitated by adding NaCl (at a final concentration of 150 mM) and 2 volumes of 95% cool ethanol. After centrifugation, the DNA was cleaned with 50 µl of ethanol 70%, centrifuged, and then re-suspended in 50 µl of TE buffer (10mM Tris-HCl, pH 7.4; 1mM EDTA, pH 8.0). The DNA purity and quantity were checked by spectrophotometer at 260 and 280 nm.

PCR amplification of the 16S rDNA of actinomycetes strain was performed using two primers: 27f (50-AGAGTTTGATCCTGGCTCAG-30) and 1492r (50-GGTTACCTTGTTACGACTT-30). The 16S rDNA was amplified by PCR using Promega kit. The final volume of reaction mixture of 50 µl contained 1X PCR buffer (10mM Tris-HCl, 50mM KCl, pH 9.0 at 25 °C), 1.5mM MgCl₂, 200 mM of each dNTP, 1mM of each primer, 1.25 U of Taq DNA polymerase and 500ng of template DNA. The amplification was performed according to the following profile: an initial denaturation step at 98 °C for 3 min, after which Taq DNA polymerase was added, followed by 30 amplification cycles of 94 °C for 1 min, 52 °C for 1 min and 72 °C for 2 min, and a final extension step of 72 °C for 10 min. The PCR product was detected by agarose gel electrophoresis and was visualized by UV fluorescence after ethidium bromide staining.

The PCR products obtained were submitted to Genome Express for sequence determination. The same primers as above and an automated sequencer were used for this purpose. The sequence determined was compared for similarity level with the reference species of bacteria contained in genomic database banks, using the NCBI Blast available at the ncbi.nlm.nih.gov Web site.

RESULTS

Cultural characteristics and Microscopic study:

The actinomycetes isolate was named as SBR1 (1). The colony characteristics of the isolate were studied on the GAA, Inorganic salt-starch agar (ISSA) and Oat Meal Agar (OMA) media. The growth was good on GAA and ISSA whereas moderate growth was observed on OMA. The color of substrate and aerial mycelium varied in different media. The organism produced colonies of 3 mm diameter, white colony with secondary black metabolites, blue pigmentation, greys at centre and hard on GAA with inhibition of neighbored colony, on oat meal agar it produced colony with poor growth, 3 mm diameter, cream colored spores with entire and umbonate margin, on ISSA colonies were light cream colored entire, elevated margin, good growth, outer periphery shows ring of spores. The organism was gram positive and positive for starch hydrolysis, casein hydrolysis and lecithinase and lipase production, negative for gelatine hydrolysis, citrate utilization. Based on morphological biochemical and on characterization of the organism it was shown to be *Streptomyces* sp.

Table 1: Cultural characteristics of SBR 1(1)

| Media | Growth | Substrate mycelium | Aerial mycelium | Diffusible pigment |
|-------|----------|--------------------|-----------------|--------------------|
| GAA | Good | Grey | White | Blue |
| OMA | Moderate | Grey | Cream | --- |
| ISSA | Good | Grey | White | --- |

Preliminary antibacterial activity and MIC: A total of 7 isolates were recovered from the soil samples. All the isolates were subjected for cross streak method in order to assess antagonistic property against gram negative and gram positive bacteria. Presence of clear zone or reduced growth of test bacteria near the growth of actinomycetes was considered as positive for antagonistic activity. All the isolates were potent enough to inhibit at least one of the test bacteria. SBR 1(1) showed prominent inhibition of test bacteria in cross streak technique, so it was selected for further study.

The antibacterial efficacy of the ethyl acetate extract of SBR 1(1) is studied using 3 Gram positive and 2 Gram negative bacteria. It was observed that extract was having broad spectrum antibacterial activity inhibiting both Gram positive and Gram negative bacteria. The study of MIC has shown that MIC of ethyl acetate extract was <25 µg for Gram positive bacteria (*B. subtilis* and *S. aureus*) and 75 µg for Gram negative bacteria (*E. coli*) (Table 2 & 3; Figure 1).

Table 2: Antibacterial activity of ethyl acetate extract of isolate SBR 1(1)

| Test Bacteria | Zone of inhibition in cm | | |
|--------------------|--------------------------|-------------------------------|------|
| | SBR 1(1) | Standard (Streptomycin 10 µg) | DMSO |
| <i>B. cereus</i> | 2.6 | 2.0 | 0.0 |
| <i>E. coli</i> | 2.0 | 1.1 | 0.0 |
| <i>B. subtilis</i> | 2.7 | 1.9 | 0.0 |
| <i>S. aureus</i> | 2.5 | 2.4 | 0.0 |
| <i>P. putida</i> | 1.0 | 1.3 | 0.0 |

Table 3: Minimum Inhibitory Concentration (MIC) of ethyl acetate extract of isolate RHC-1

| Test bacteria | MIC for ethyl acetate extract of isolate SBR 1(1) Zone of Inhibition in cm | | | | |
|--------------------|--|-------|-------|-------|--------|
| | Standard 10 µg | 25 µg | 50 µg | 75 µg | 100 µg |
| <i>E. coli</i> | 2.5 | - | - | 1.1 | 1.3 |
| <i>B. subtilis</i> | 1.2 | 1.5 | 1.7 | 1.8 | 1.9 |
| <i>S. aureus</i> | 1.8 | 1.2 | 1.4 | 1.5 | 1.7 |



Figure 1: MIC for ethyl acetate extract of RHC-1

Screening of antioxidant activity:

DPPH Radical Scavenging Assay: Study of DPPH scavenging ability of the extract showed that ethyl acetate extract has free radical scavenging ability but the activity of extract is less when compared with the ascorbic acid standard. DPPH scavenging studies have revealed that the extract possesses 86.6% scavenging ability at a concentration of 11 mg/ml and the DPPH free radical scavenging ability of the extract was dose dependent (Figure. 2).

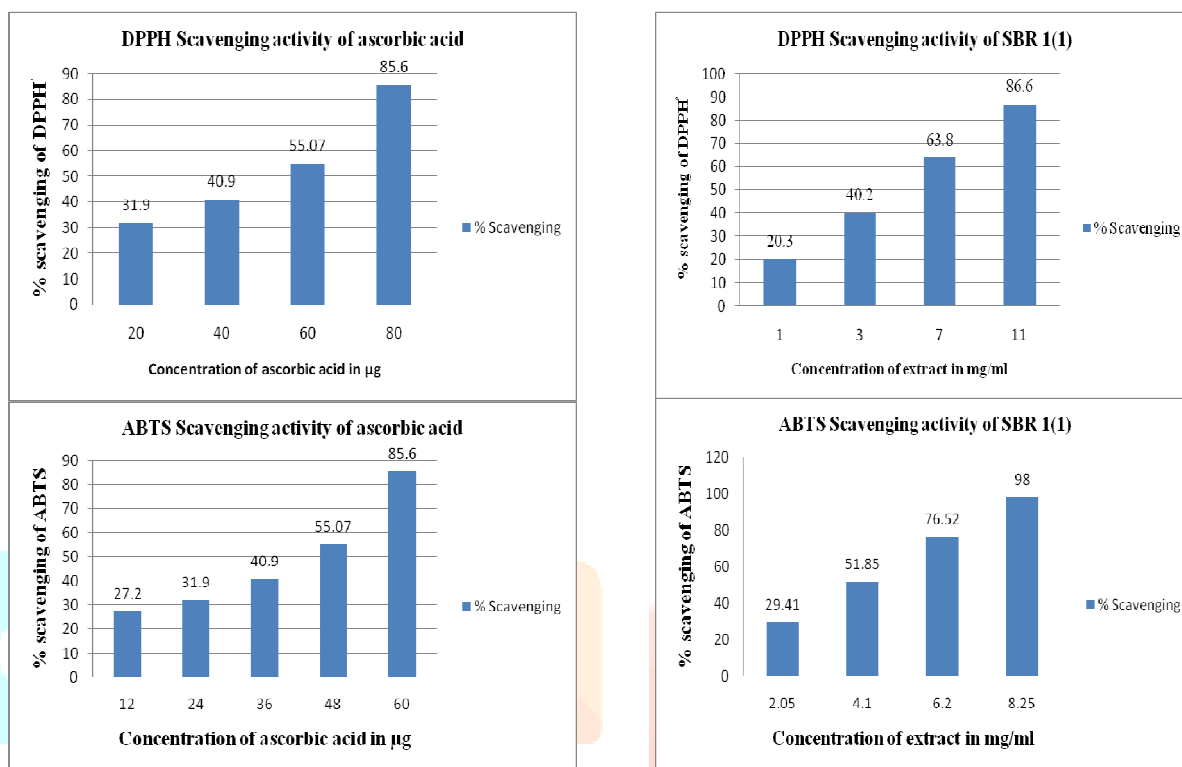


Figure 2: Antioxidant activity of ethyl acetate extract of SBR 1(1)

Assay of ABTS scavenging activity: ABTS scavenging studies have revealed that the ethyl acetate extract of SBR 1(1) is capable of scavenging the ABTS radical efficiently. But ability of the extract is less when compared with ascorbic acid standard. The ethyl acetate extract had 98% scavenging activity at a concentration of 8.25 mg/ml. Even ABTS free radical scavenging ability of the extract is also dose dependent (Figure 2).

Molecular characterization by 16S rDNA sequencing: Through 16S rDNA sequence analysis, an amplified fragment of 747 bp was obtained and compared with sequences of the reference species of bacteria contained in genomic database banks. The similarity level ranged from 96.3% to 97.8% with *Streptomyces* species 13636G having the closest match. The phylogenetic tree obtained by applying the neighbor joining method is illustrated in Fig. 8. The sequence results for SBR 1(1) as follows:

```
GGCGTTTTTTCGCTCTCAGCGTCAGTAATGGCCCAGAGATCCGCCTTCGC
CACCGGTGTTCTCCTGATATCTGCGCATTTACCGCTACACCAGGAATT
CCGATCTCCCTACCACACTCTAGCTAGCCCGTATCGAATGCAGACCCGG
GGTTAAGCCCCGGGCTTTCACATCCGACGTGACAAGCCGCCTACGAGCTC
TTTACGCCAATAAATTCCGGACAACGCTTGCGCCCTACGTATTACCGCGG
CTGCTGGCACGTAGTTAGCCGGCGCTTCTTCTGCAGGTACCGTCACTTGC
GCTTCTCCCTGCTGAAAGAGGTTTACAACCCGAAGGCCGTCATCCCTCA
CGCGCGTCGTCATCAGGCTTTCGCCCATTTGTGCAATATTCCCACTG
CTGCCCTCCGTAGGATGCTGGGCCGTGTCTCAGTCCCAGTGTGGCCGGTC
GCCCTCTCAGGCCGGCTACCCGTCGCTCGCCTTGGTAGGCCATTACCCAC
CAACAAGCTGATAGGCCGCGGGCTCATCCTTACCCGCCGAGCTTTCAAC
CCCGTCCCATGCGGAACAGAGTATTATCCGGTATTAGACCCCGTTTCCAG
GGCTTGTTCCAGAGTGAAGGGCAGATTGCCACGTGTTACTACCCGTTT
GCCACTAATCCACCACCGAAGCGGCTTCATCGTTTCCGACTTGCATGTGTTA
AGCACGCCGCCAGCGTTCGTCTGAGCTGTTTTAAAACTTAAAAAC.FASTA
```

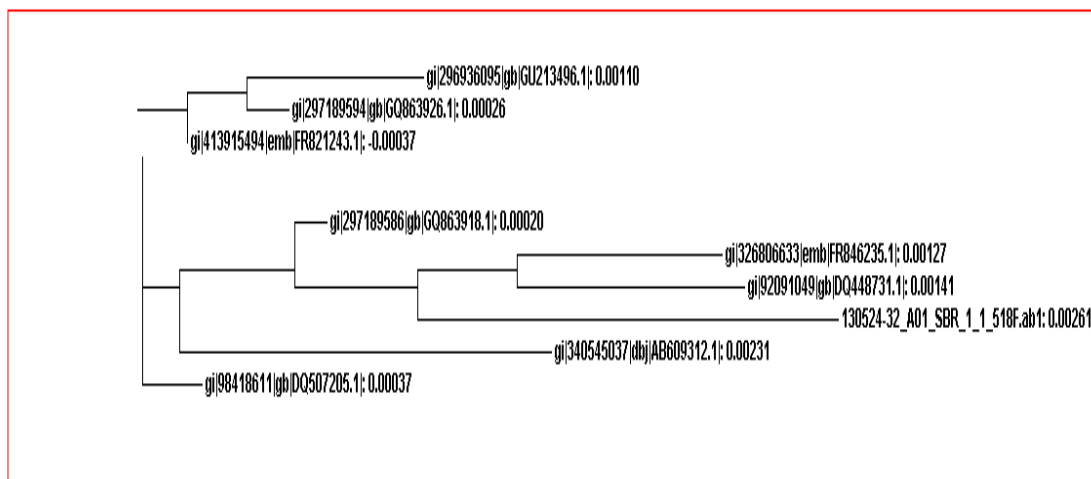



Figure 3:

Phylogram based on 16S rDNA sequences showing the relations between strain SBR 1(1) and type species of the genus *Streptomyces*

DISCUSSION

Western Ghats of India are the less explored regions for actinomycetes diversity and this study has shown that Western Ghats contain diverse species producing the antibiotic. The plant root primarily determines the nature and abundance of the rhizosphere soil microflora, when conditions affect root growth or metabolism, it will be reflected in quantitative and qualitative changes in microbial populations of rhizosphere. Conversely, microbial communities can affect rooting patterns, stimulate and promote plant root growth (e.g., release of hormones, neutralizing toxic substances, etc.), and influence the supply of available nutrients for plant uptake. Microbial turnover of rhizo-deposits plays an important role in carbon flow through soils [Rathna Kala and Chandrika, 1993; Rechner et al, 2002; Behal, 2003; Kekuda et al., 2010]. Actinomycetes are an important class of bacteria and constitute one of the important groups of the rhizosphere microflora. Members of *Streptomyces* are most abundant in soil and accounts for about 90% of actinomycetes isolated from soil [Shinar and Rachmilewitz, 1990; Rathna Kala and Chandrika, 1993; Khamna et al., 2009;]. In the present study, we have recovered 07 actinomycetes isolates from a rhizosphere soil collected at Western Ghats of Karnataka. All the isolates were subjected to primary screening for antibacterial activity by cross streak method. This dual culture method is widely used to screen the ability of actinomycetes strains to produce antimicrobial metabolites [Shinar and Rachmilewitz, 1990, Hebbel et al., 1990; Kekuda et al., 2012]. Out of 07 isolates, all the 7 isolates have shown inhibition of all test bacteria. We have selected a potent isolate SBR 1(1) which inhibited both gram positive and Gram negative bacteria. The characterization of SBR 1(1) revealed that the isolate is a *Streptomyces* species. The life cycle of *Streptomyces* provides 3 distinct features for microscopic characterization namely vegetative mycelium, aerial mycelium bearing chains of spores and the characteristic arrangement of spores and the spore ornamentation. The latter two features produce most diagnostic information [Kukongviriyapan et al., 2008, Filburn et al., 2007]. Details on cultural and microscopic characteristics together with biochemical properties assisted the researchers to classify actinomycetes as members of the genus *Streptomyces*. Many studies have been carried out where the actinomycetes isolates were identified as species of *Streptomyces* based these properties or characteristics (Ceylan et al, 2008; Pham-Huy et al, 2008; Grinberg, 1995; Maeda and Akaike, 1998; Jeffrey et al, 2007; Sahin and Ugur, 2003). In the present study, the cultural and microscopic characteristics of the isolate SBR1(1) were consistent with its classification as a member of the genus *Streptomyces*.

The members of *Streptomyces* can be distinguished from other sporing actinomycetes based on morphology and hence morphology plays an important role in the Antimicrobial agents play an indispensable role in decreasing morbidity and mortality associated with infectious diseases caused by bacteria, fungi, viruses and parasites. However, selective pressure exerted by the use of antimicrobial drug became the major driving force behind the emergence and spread of drug-resistance pathogens. In addition, resistance has been developed in pathogens after discovery of major class of antimicrobial drugs, varying in time from as short as 1 year in case of penicillin to >10 years in case of Vancomycin (Jeffrey et al, 2007). This alarming situation necessitated search of new bioactive compounds capable of acting against pathogens in particular drug resistant pathogens. It is well known that microorganisms, in particular bacteria and fungi are an unexhaustible source of natural compounds having several therapeutic applications. In the present study, it was found that both Gram positive bacteria and Gram negative bacteria were susceptible to high extent (Singh et al, 2006; Pandey et al, 2004).

Free radicals are chemical species containing one or more unpaired electrons that make them highly unstable and cause damage to other molecules by extracting electrons from them in order to attain stability. In recent years much attention has been devoted to natural antioxidant and their association with health benefits (Ali et al, 2008).

DPPH is a stable, organic and nitrogen centered free radical, it has absorption maximum band around 515-528 nm (517 nm) in alcoholic solution. It accepts an electron or hydrogen atom and becomes a stable diamagnetic molecule. Though a number of *in vitro* assays have been developed to evaluate radical scavenging activity of compounds, the model of scavenging of the stable DPPH radical is one of the widely used protocols. The effect of antioxidants on scavenging DPPH radical is due to their hydrogen donating ability. In this assay, the antioxidants reduce the purple colored DPPH radical to a yellow colored compound diphenylpicrylhydrazine, and the extent of reaction will depend on the hydrogen donating ability of the antioxidants. In the

present study, a decrease in the absorption of DPPH solution in the presence of various concentrations of ethyl acetate extract was measured at 517 nm. It was observed that the radical scavenging activities of extract and ascorbic acid increased on increasing concentration. The scavenging effect of ethyl acetate extract was much lesser when compared with ascorbic acid. Although the scavenging abilities of extract was lesser, it was evident that the extracts showed hydrogen donating ability and therefore the extract could serve as free radical scavengers, acting possibly as primary antioxidants (Ali *et al*, 2008).

The ABTS radical cation decolorization assay is one of the methods for the screening of the antioxidant activity (Re *et al*, 1999). Therefore, the ABTS radical scavenging activity of the ethyl acetate extract was determined. The results indicated that the ethyl acetate extract showed a lesser tendency to decay ABTS radicals at low concentrations of reaction than at high concentrations (Fig. 6). The extract scavenged ABTS radicals in a concentration-dependent manner. The ABTS antioxidant assay, also known as the Trolox equivalent anti-oxidant capacity (TEAC) assay, assesses the total radical scavenging capacity of the plant extracts. This is determined through the ability of these extracts to scavenge the long-lived specific ABTS radical cation chromophore in relation to that of Trolox, the water-soluble analogue of vitamin E [Zhong *et al.*, 2011].

The antioxidant activities of recognized antioxidants have been attributed to various mechanisms, including the prevention of chain initiation, binding of transition metal ion catalysts, decomposition of peroxides, prevention of hydrogen abstraction, and radical scavenging [Diplock, 1997].

According to the results of the DPPH radical-scavenging assay and ABTS radical-scavenging assay, it was found that the isolate SBR 1(1) had antioxidant abilities.

CONCLUSION:

In this study, the results have suggested that actinomycetes isolate RHC-1 has closely related with *Streptomyces* spp. 13636G, having the capability to show antimicrobial and antioxidant activity and the present study highlights the necessity of further researches towards the goal of searching for novel bioactive compounds from less explored regions like Western Ghats.

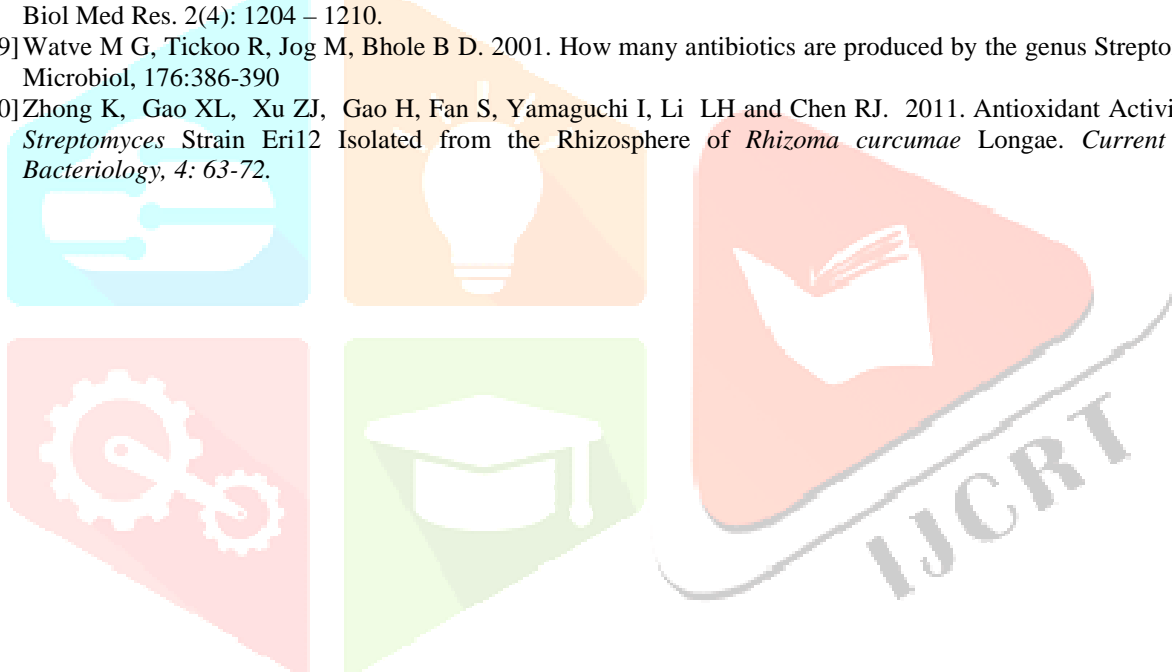
Acknowledgement:

We express our deep gratitude to Founder Chairman Sri. NarasaRaju, President Sri. Ramesh Raju, Principal Dr. R. V. Praveen Gowda and Head, Dept. of Biotechnology Dr. Manjunath B K, The Oxford College of Engineering, Bangalore, for providing facilities to conduct work and kind support and encouragement.

REFERENCES:

- [1] Amit Pandey, Imran Ali, Kailash Singh Butola, TanushriChatterji, Vidyottma Singh. 2004. Isolation and characterisation of actinomycetes from soil and evaluation of antibacterial activities of actinomycetes against pathogens. *ActaBiol Med Exper*, 15:113-115
- [2] Behal V. 2003. Alternative sources of biologically active substances. *Folia Microbiol (Praha)*; 48:563-71.
- [3] Bisht R, Katiy ARA, Singh R, Mittal P. 2009. Antibiotic Resistance –A Global Issue of Concern. *Asian Journal of Pharmaceutical and Clinical Research*. 2 (2); 34-39.
- [4] Ceylan O, Okmen G and Ugur A.2008.Isolation of soil *Streptomyces* as source antibiotics active against antibiotic-resistant bacteria.*EurAsian Journal of BioSciences*.2, 73-82.
- [5] Diplock, AT. 1997. Will the 'good fairies' please prove to us that vitamin E lessens human degenerative disease. *Free Rad.Res*.27 (5),511-532.
- [6] Filburn CR, Kettenacker R, Griffin DW. 2007. Bioavailability of a silybin-phosphatidylcholine complex in dogs. *J Vet PharmacolTher*; 30:132-8.
- [7] Grinberg LN, Rachmilewitz EA, Kitrossky N, Chevion M. 1995. Hydroxyl radical generation in β -thalassemia red blood cells. *Free Rad Biol Med*; 18:611-5.
- [8] Hajji M, Jarraya R, Lassoued I, Masmoudi O, Damak M, Nasri M. 2010. GC/MS and LC/MS analysis, and antioxidant and antimicrobial activities of various solvent extracts from *Mirabilis jalapa* tubers. *Process Biochem*; 45:1486-93.
- [9] Hebbel RP, Leung A, Mohandas N.1990. Oxidation-induced changes in microheologic properties of the red cell membrane. *Blood*; 76:1015-20.
- [10] Jeffrey L.S.H., A.M. Sahilah, R. Son and S. Tosiah. 2007. Isolation and screening of actinomycetes from Malaysian soil for their enzymatic and antimicrobial activities. *J. Trop. Agric. and Fd. Sc*. 35(1): 159– 164.
- [11]Kekuda PTR, Shobha KS, Onkarappa R, Gautham SA, Raghavendra HL. 2012. Screening biological activities of a *Streptomyces* species isolated from soil of Agumbe, Karnataka, India, *International Journal of Drug Development and Research*, 4(3), 104-114.
- [12]Kekuda PTR, Shobha KS, Onkarappa R. 2010. Studies on antioxidant and anthelmintic activity of two *Streptomyces* species isolated from Western Ghat soil of Agumbe, Karnataka, *Journal of Pharmacy Research*, 3(1), 26-29.
- [13]Khamna S, Yokota A, Lumyong S. 2009. Actinomycetes isolated from medicinal plant rhizosphere soils: diversity and screening of antifungal compounds, indole-3-acetic acid and siderophore production, *World Journal of Microbiology and Biotechnology*, 25(4), 649-655.
- [14]Kukongviriyapan V, Somparn N, Senggunprai L, Prawan A, Kukongviriyapan U, Jetsrisuparb A. 2008. Endothelial Dysfunction and Oxidant Status in Pediatric Patients with Hemoglobin E-beta Thalassemia. *PediatrCardiol*; 29:130-5.
- [15]Lakhtakia R, Ramji MT, Lavanya K, Rajesh K, Jayakumar K, Sneha C, Narayan A, Ramya B, Ramana G, Chari PVB, Chaitanya KV.2011. The role of antioxidants in human health maintenance: Small molecules with infinite functions. *IJPSR*; 2:1395-402.
- [16]Lazzarini A, Cavaletti L, Toppo G and Marinelli F. 2000. Rare genera of actinomycetes as potential producers of new antibiotics.*Antonie van Leeuwenhoek* 78:399–405

- [17] Maeda H, Akaike T. 1998. Nitric oxide and oxygen radicals in infection, inflammation, and cancer. *Biochemistry (Moscow)*; 63:854-65.
- [18] Manjunatha BK, Syed Murthuza, Divakara R, Archana M, Sarvani RJ, Verghees S, Paul K. 2013. Antioxidant and anti-inflammatory potency of *Mesua ferrea* L. *Indian Journal of Applied Research*. 3(8); 55-59.
- [19] Pandey, B. Ghimire, P. Agrawal, V.P. 2004. Studies on antibacterial activity of Actinomycetes isolated from the Khumbu region of Nepal. *J Biol.Sci.*, 23:44-53.
- [20] Pham-Huy LA, He H, Pham-Huyc C. 2008. Free radicals, antioxidants in disease and health. *Int J Biomed Sci*; 4:89-96.
- [21] Rathna Kala R, Chandrika V. 1993. Effect of different media for isolation, growth and maintenance of actinomycetes from mangrove sediments. *Indian J Mar Sci*; 22:297-9.
- [22] Re R, Pellegrini N, Proteggente A, Pannala A, Yang M, Rice-Evans C. 1999. Antioxidant activity applying an improved ABTS radical cation decolorization assay. *Free Radical Biol. Medicine*. 26(9):1231-1237.
- [23] Rechner AR, Kuhnle G, Bremmer P, Hubbard GP, Moore KP, Rice-Evans CA. 2002. The metabolic fate of dietary polyphenols in humans. *Free Radic Biol Med*; 33:220-35.
- [24] Sahin N, Ugur A. 2003. Investigation of the antimicrobial activity of some *Streptomyces* isolates, *Turkish Journal of Biology*, 27, 79-84.
- [25] Shinar E, Rachmilewitz EA. 1990. Oxidative denaturation of red blood cells in thalassemia. *Semin Hematol*; 27:70-82.
- [26] Singh, S.L., Baruha, I and Bora, T.C. 2006. Actinomycetes of loktak habitat isolation and screening of antimicrobial activity. *Biotech*. 5 (2): 217-221.
- [27] Stackebrandt E, Rainey F A and Ward-Rainey N L. 1997 Proposal for a new hierarchic classification system, Actinobacteria classis Nov. *Int. J. Syst. Bacteriol*, 47:479-491.
- [28] Stephen T Odonkor & Kennedy K Addo. 2011. Bacteria Resistance to Antibiotics: Recent Trends and Challenges. *Int J Biol Med Res*. 2(4): 1204 – 1210.
- [29] Watve M G, Tickoo R, Jog M, Bhole B D. 2001. How many antibiotics are produced by the genus *Streptomyces*? *Arch. Microbiol*, 176:386-390
- [30] Zhong K, Gao XL, Xu ZJ, Gao H, Fan S, Yamaguchi I, Li LH and Chen RJ. 2011. Antioxidant Activity of a Novel *Streptomyces* Strain Eri12 Isolated from the Rhizosphere of *Rhizoma curcumae* Longae. *Current Research in Bacteriology*, 4: 63-72.



Heavy metal ion detection using Immobilized ALP enzyme

K.Valarmathy*, Kala Sai Sarwani, H. Geethabhai, Eric Joseph

Department of Biotechnology, The Oxford College of Engineering, Bommanhalli, Bangalore-560068
mathy.valar@gmail.com

Abstract: Environment pollution by toxic heavy metals (HM) presents a real life threat for human health. Accumulation of heavy metals like Cadmium, Mercury, Cobalt and Copper in water causes toxic actions if the tolerance level is exceeded. Alkaline Phosphatase (ALP) activity was used for estimation of heavy metal ions in drinking water. It was based on inhibition of Alkaline Phosphatase enzyme activity exerted by metal ions. Kinetics of ALP was performed and maximum activity was found to be at using 2U/ml concentration of enzyme and hence was chosen for further studies. ALP immobilization was carried out by sol-gel method and sodium alginate method on two different surfaces: glass and stainless steel. Inhibition characteristics of ALP were tested using different concentrations of individual heavy metals ranging from 10mM to 10⁻⁵mM and also using combination of heavy metals of concentration 10⁻⁴mM. The reaction showed uncompetitive inhibition. Amongst the four heavy metals used, the amount of inhibition was found to be more in mercury compared to other metals.

Index Terms— Alkaline Phosphatase, Sol-Gel, Inhibition, metal ions

1. INTRODUCTION

The accumulation of toxic substances in the environment continuously increases due to diverse pollutants from the industries. Heavy metals in drinking water pose a serious threat to human health if the respective tolerance level is exceeded. Populations are exposed to heavy metals primarily through water consumption, but few heavy metals can accumulate in the human body (e.g., in lipids and gastrointestinal system) and may induce cancer and other risks. Hence, fast and accurate detection of metal ions has become a critical issue. Due to the high toxicity caused by the heavy metal ions there is an obvious need to determine them rapidly at trace levels. The present investigation aims determining heavy metal ions based on the inhibition studies of ALP on different metals.

2. MATERIALS AND METHODS

2.1 ENZYME KINETIC STUDIES

2.1.1 PNP STANDARD CURVE:

Enzyme kinetics was studied by plotting the pNP Standard Curve and carrying out the Enzyme Activity Assay by using 0.05M p-nitro phenyl phosphate (pNPP) as the substrate. The release of p-nitrophenol (pNP) in the reaction mixture (2.5ml) was continuously measured at 405nm spectrophotometrically (Thermo-Fischer), over the linear period. Different concentrations of standard pNP ranging from 0µg to 50µg were taken in a series volume of different test tubes. 1ml of distilled water is added to the test tubes. 2ml of 0.1M Sodium Hydroxide was added to make up the final reaction mixture to 4ml. Absorbance readings were taken at 405nm.

2.1.2 INHIBITION STUDIES OF FREE ALP WITH DIFFERENT HEAVY METAL IONS:

The effect of Hg²⁺, Cu²⁺, Co²⁺ and Mn²⁺ on ALP activity was studied. Various concentrations of the chosen heavy metals were added to the 0.1M Sodium Carbonate-Bicarbonate buffer followed by the addition of 0.1ml

enzyme. 1ml of 0.05M p-NPP substrate was then added to study the inhibition of the enzyme activity. 1ml of 0.2M NaOH was added to the final reaction mixture and the absorbance was measured at 405 nm spectrophotometrically.

2.2 IMMOBILIZATION OF ENZYME

2.2.1 SOL GEL METHOD

The stock gel solution for immobilization was prepared by adding 570 μ l of methanol 50 μ l of TEOS and 10 μ l of 3.8% CTAB (Cetyl Tri methyl Ammonium Bromide) solution in a small test tube at room temperature The solution was vigorously mixed. It was then cooled to 4 $^{\circ}$ C immediately after mixing. The enzyme stock solution was prepared by dissolving a known quantity of ALP in 50ml 0.02M phosphate buffer (pH- 7.0).The enzyme solution was cooled at 4 $^{\circ}$ C.

2.2.2 SODIUM ALGINATE METHOD (SA):

The sodium alginate method was performed by adding 0.6gms of Sodium alginate to 20ml of distilled water(solution 1) and 50 μ l of ALP (2U/ml) (solution 2). The Solution 1 and 2 were mixed and stirred for 30 minutes covering the electrode.

2.3 ACTIVITY OF IMMOBILIZED ENZYME ON DIFFERENT SURFACES

Immobilization was performed on two different types of surfaces (Glass and Stainless Steel) and by two different methods (Sol Gel and Sodium Alginate). 1ml of pNPP substrate was added to 0.4ml sodium carbonate-bicarbonate buffer .The enzyme immobilized glass beads, stainless steel fork prangs and stainless steel plates were added and incubated at 37 $^{\circ}$ C for 15minutes. glass beads, stainless steel fork prangs and stainless steel plates were removed. 1ml NaOH was then added and absorbance was measured at 405nm. Enzyme was not immobilized on the glass surface using the Sol Gel method as it specifically requires a conducting medium

2.4 pNPP SUBSTRATE KINETICS

The primary function of the inhibitor is to reduce the rate of reaction. Hence the need to study the rate of the reaction is highly necessary to study the properties of inhibition.

2.4.1 pNP ASSAY

Various volumes of standard pNP (0, 0.2, 0.4, 0.6, 0.8, 1.0 ml) were taken in a series of test tubes. The Volume was made upto 1ml using distilled water. 2ml of 0.1M NaOH was then added to all the test tubes and absorbance was measured at 405nm

2.4.2 pNPP ASSAY

1ml of different concentrations of pNPP was added to 0.4ml buffer followed by the addition of 0.1ml enzyme. It was then incubated at 37 $^{\circ}$ C for 5minutes. 1ml of 0.2M NaOH was then added to the test tubes and the absorbance was measured at 405nm.

2.4.3 MM PLOT FOR pNPP SUBSTRATE

The Michaelis-Menton plot was plotted for the substrate to find the rate of the reaction. It is a plot with concentration on x-axis and activity on y-axis. The formula used to calculate the activity is:-

Activity = (concentration of pNP x dilution factor) in μ mol/min
(mol. wt of pNP x Vol. of enzyme x Incubation time)

2.4.3 LB PLOT OF pNPP

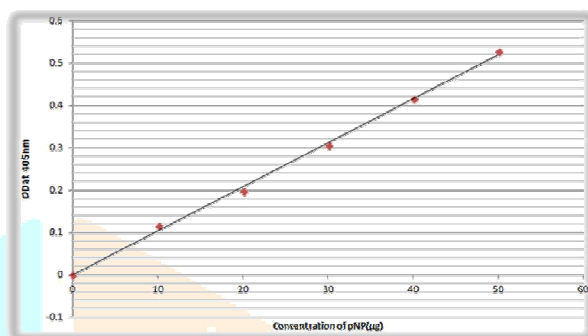
The Lineweaver-Burk plot is widely used to determine important terms in enzyme kinetics, such as K_m and V_{max} . The y-intercept of such a graph is equivalent to the inverse of V_{max} . The x-intercept of the graph represents $-1/K_m$. It also gives a quick, visual impression of the different forms of enzyme inhibition. The LB plot was plotted for the substrate to use as a reference to fine the type of inhibition exhibited by the heavy

metals.

3. RESULTS AND DISCUSSION

3.1 STANDARDIZATION OF pNP

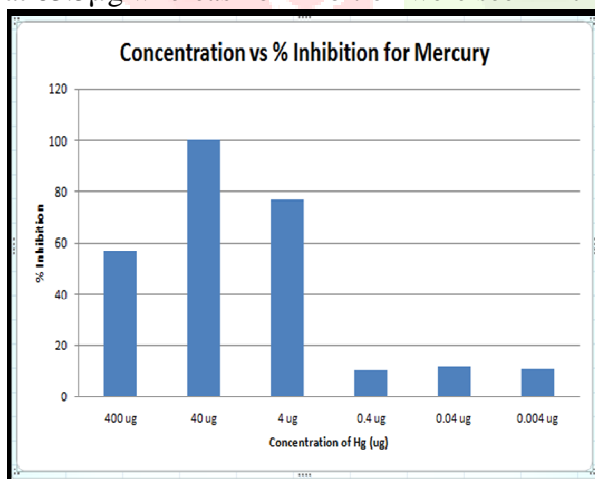
A graph was plotted with concentration of pNP taken on the x-axis and absorbance on y-axis. From the results it was observed that there was a linear increase in the absorbance level against increasing concentrations of pNP



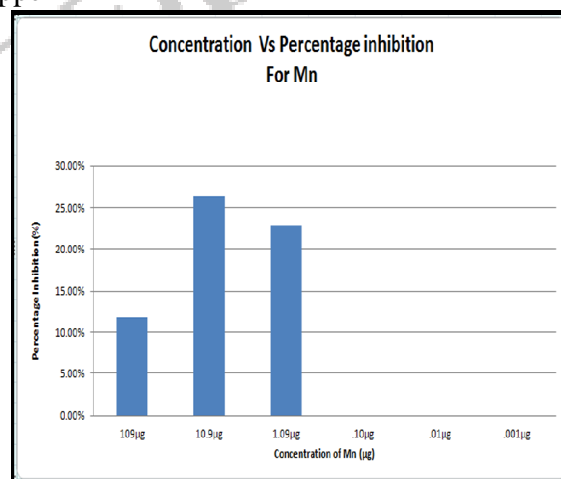
Graph 1: Standard Curve for pNP

3.2 INHIBITION STUDIES OF THE FREE ENZYME ALP

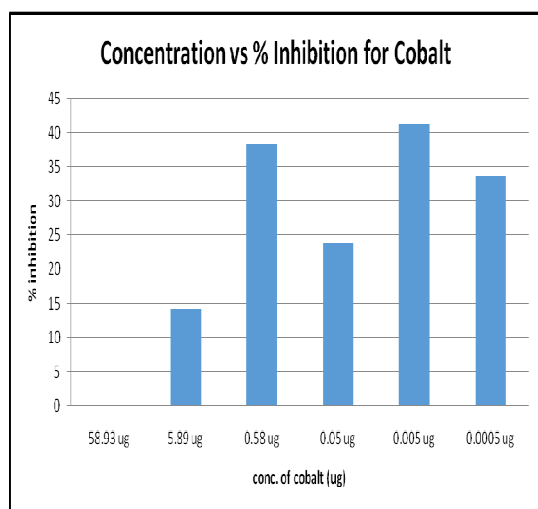
The compounds HgCl_2 , MnSO_4 , CoSO_4 and CuSO_4 were used as inhibitors and the percentage inhibition exerted by the respective individual heavy metals i.e. Hg^{2+} , Mn^{2+} , Co^{2+} and Cu^{2+} is given below. The percentage inhibition was calculated for different concentrations of Mercury, Manganese, cobalt and copper.. It was found that maximum inhibition was exhibited by $40\mu\text{g}$ of Mercury whereas minimum inhibition was shown by $0.4\mu\text{g}$ of Mercury and maximum inhibition was exhibited by $10.9\mu\text{g}$ of Manganese whereas no inhibition was seen after concentrations of $0.10\mu\text{g}$. It was found that maximum inhibition was exhibited by $0.005\mu\text{g}$ of Cobalt whereas no inhibition was seen in $58.93\mu\text{g}$ of Cobalt and it was found that high inhibitions were seen in $6.35\mu\text{g}$ and $0.06\mu\text{g}$ concentrations of Copper, lesser inhibition at $63.5\mu\text{g}$ whereas no inhibition were seen in the by $0.4\mu\text{g}$ of Copper



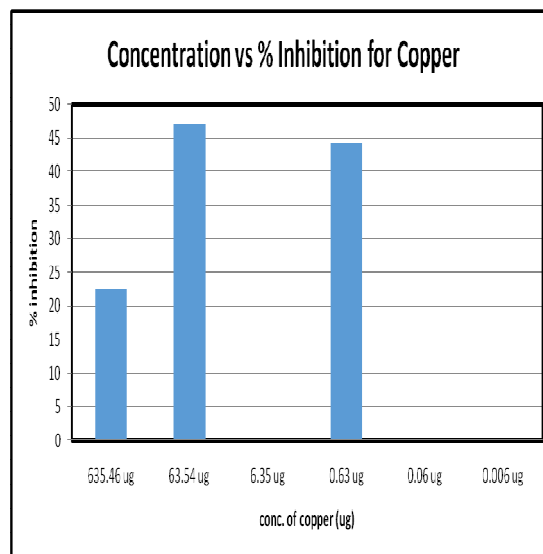
Graph 2: Concentration of Mercury vs. Percentage Inhibition



Graph 3: Concentration of Manganese vs. Percentage Inhibition



Graph 4: Concentration of Cobalt vs. Percentage Inhibition



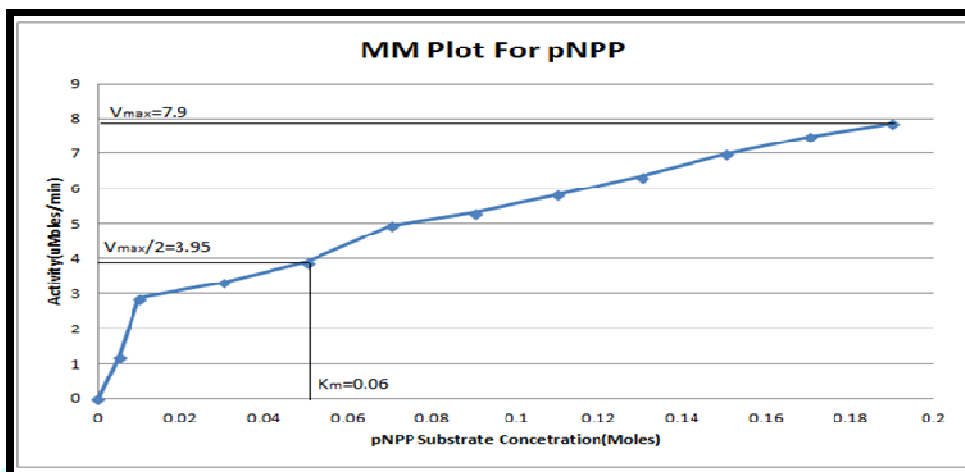
Graph 5: Concentration of Copper vs. Percentage Inhibition

3.3 RESULTS OF ACTIVITY OF IMMOBILIZED ENZYME ON DIFFERENT SURFACES

Immobilization was performed on two different types of surfaces (Glass and Stainless Steel) and by two different methods (Sol Gel and Sodium Alginate). The test was performed to find the activity of the immobilized enzyme on the glass beads. The sample (S) which had the enzyme immobilized glass beads showed negligible activity while the left over Sodium Alginate Extract (E) of the glass beads comparatively showed some activity. This showed that the enzyme had not been immobilized on to the glass surface using this method. The ALP immobilized prongs were tested for enzyme activity for a period of one week. The Immobilized enzyme showed high activity on the 1st day, which steadily decreased on the 2nd day and was almost negligible on the 7th day. This concluded that the enzyme showed stability for 1 week when it was immobilized with Sodium Alginate. For the Sol Gel Immobilized Surface, activity was found to be maximum on the 1st day which decreased over the 2nd and the 7th day. Moreover the activity for Stainless Steel Fork Prongs using Sodium Alginate Method had considerable good activity on day 2 whereas for the Sol Gel Immobilized prongs lost a greater amount of activity on the day 2 itself. Here the Sodium Alginate Immobilized Surface was tested for enzyme activity. This experiment showed considerably good activity on the 1st day which was rapidly lost on the 2nd. The results did not require us to proceed with testing the activity further ahead. The sol gel immobilized enzyme surface was then tested for enzyme activity. For this type of immobilization, the activity had reduced drastically from the 1st day to the 2nd. Moreover the activity for Stainless Steel Plates using Sol Gel method seemed to exhibit higher activity than that of the Sodium Alginate Method. The inhibition characteristics for four different metals i.e. Mercury, manganese, cobalt, copper were tested. All the metals were found to produce 100% inhibition.

3.4 MM PLOT FOR pNPP SUBSTRATE

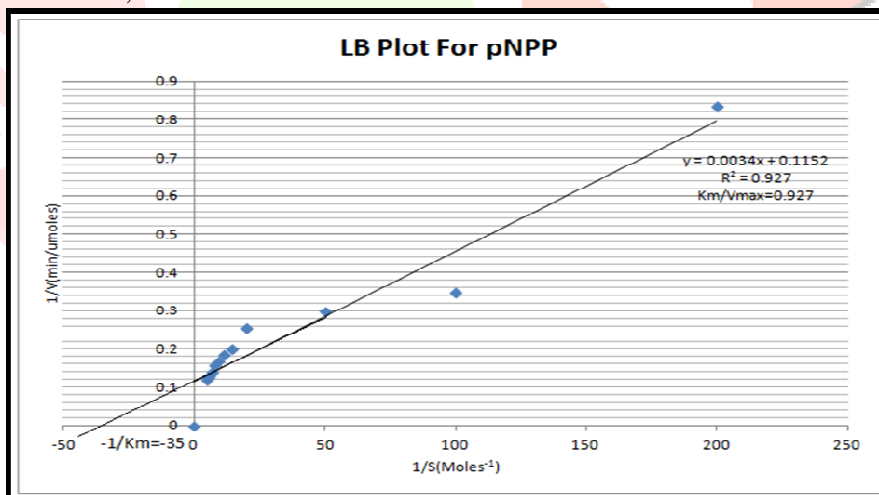
In the Michaelis-Menton curve obtained, it was seen that the rate of the reaction was found to increase with increasing concentrations of the substrate. This would tell us about the amount of the product pNP formed from the substrate pNPP. From the graph the V_{max} was found to be 7.9 and the K_m value was found to be 0.06



Graph 7: MM plot for substrate

3.5 LB PLOT OF PNPP

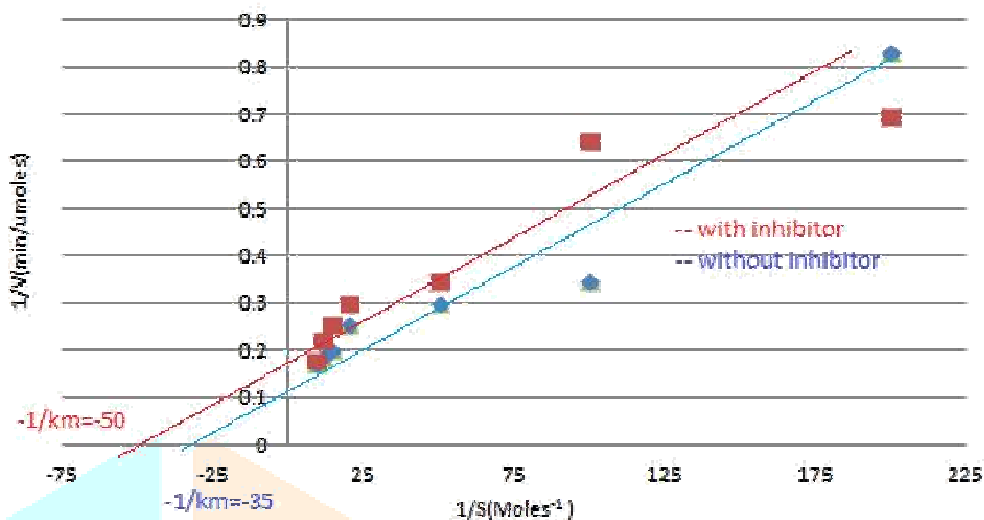
From the resulting LB plot, the substrate was used as a reference to find the type of inhibition exhibited by the heavy metals. From this, the K_m was found to be 0.028 and V_{max} was found to be 0.0302.



Graph 8: LB plot of pNPP

3.6 TYPE OF INHIBITION

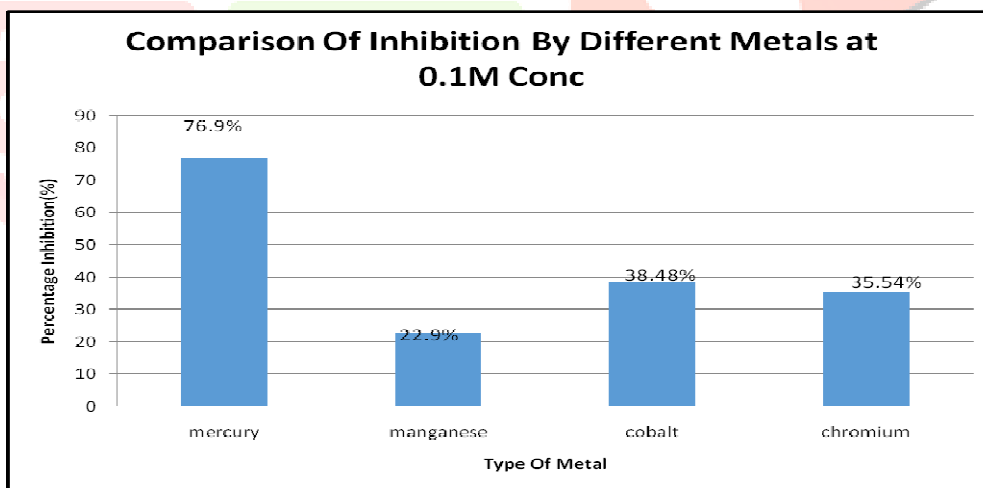
The Lineweaver-burk plot was plotted for the substrate with and without the inhibitor and the inhibition was found to be of uncompetitive type. Uncompetitive inhibition implies that the inhibitor can bind only to the substrate-enzyme complex. This was concluded due to the parallel slopes obtained for the respective curves.



Graph 9: LB plot with inhibitor

3.7 COMPARISON OF INHIBITION BY DIFFERENT METALS AT 0.1 M CONCENTRATIONS

The results obtained were plotted on a graph. It was found that Mercury exhibited maximum inhibition of 76.9% while Manganese seemed to show the least inhibition of 22.9%.



Graph 10: Comparison of Inhibition by Different Metals

4. CONCLUSION

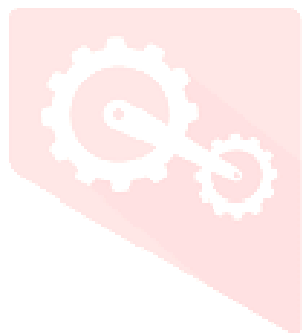
The present study concluded that maximum activity for Alkaline Phosphatase enzyme was exhibited at 2U/ml concentration. Hence, this concentration was chosen for further work. On comparing the immobilization by the two techniques used, we observed that Sodium Alginate immobilized surface retained higher activity compared to Sol gel immobilized surface. By studying the effect of various

heavy metals on the free and immobilized enzyme, it was found that Mercury exhibited maximum inhibition on the activity of the enzyme Alkaline Phosphatase and Manganese was found to have the least inhibition. The heavy metals Copper and Cobalt showed unstable inhibition readings due to the inherent color exhibited by them which caused hindrance in Absorbance readings. The concentration range of heavy metals that can be detected by using this sensor is 10-4mM to 10mM .A Line weaver – Burk plot was plotted for the pNPP substrate with and without the inhibitor. The graph obtained showed that the inhibition was of uncompetitive type. This implies that the enzyme inhibitor can bind only to the complex formed between the enzyme and the substrate. This could imply that the binding site for the inhibitor is accessible only after the enzyme has bound to its substrate.

5. REFERENCES

1. R. Ilangoan, D. Daniel, A. Krastanov, C. Zachariah & R. Elizabeth (2006) Enzyme based Biosensor for Heavy Metal Ions Determination, *Biotechnology & Biotechnological Equipment*, 20:1, 184-189.
2. Maitha M. Alnuaimi, Ibtesam A Saeed and S. Salman Ashraf (2012) Effect of various heavy metals on the enzymatic activity of E.coli ALP, *International Journal of Biotechnology and Biochemistry*, Vol 8, 47-59.
3. Lata Sheo Bachan Upadhyay and Nishant Verma (2015) ALP inhibition based conductometric biosensor for phosphate estimation in biological fluids., *Elsevier*, Vol 68, 611-616.
4. Abollino, O., Aceto, M., Malandrino, M., Mentasti, E., Sarzanini, C., Barberis, R., (2002). Distribution and mobility of metals in contaminated sites. Chemometric investigation of pollutant profiles. *Environ. Pollut.* 119: 177-193.
5. Alpat, S., Alpat, S.K., Adirci, B.H.C., Yas, a, I. and Telefoncu, A. (2008) A novel microbial biosensor based on *Circinella* sp. modified carbon paste electrode and its voltammetric application. *Sens. Actuators B* 134(1): 175–181.
6. Alpat, S.K., Alpat, S., Kutlu, B., Zbayrak, O.O. and B'uy'ukis, ik, H.B. (2007) Development of biosorption-based algal biosensor for Cu(II) using *Tetraselmis chuii*. *Sens. Actuators B* 128(1): 273–278.
7. Amine A., Mohammadi H., Bourais I. and Palleschi G. (2006) Enzyme inhibition-based biosensors for food safety and environmental monitoring. *Biosens. Bioelectron.* 21: 1405–1423.
8. Amine A., Mohammadi H., Bourais I. and Palleschi G. (2006) Enzyme inhibition-based biosensors for food safety and environmental monitoring. *Biosens. Bioelectron.* 21: 1405–1423.
9. Anh, T.M., Dzyadevych, S.V., Prieur, N. (2006) Detection of toxic compounds in real water samples using a conductometric tyrosinase biosensor. *Materials Science and Engineering C* 26(2-3): 453–456
10. Appenroth, K.J. (2010) Definition of “Heavy Metals” and their role in biological systems, Sherameti, I. and Varma, A. (eds.), *Soil Heavy Metals*, Soil Biology. 19: 19-29. DOI 10.1007/978-3-642-02436-8_2, © Springer-Verlag Berlin Heidelberg 2010
11. Babkina, S.S. and Ulakhovich, N.A. (2004) Amperometric biosensor based on denature DNA for the study of heavy metals complexing with DNA and their determination in biological, water and food samples. *Bioelectrochem.* 63(1-2): 261–265.
12. Bagal-Kestwal, D., Karve, M. S., Kakade, B. and Pillai, V. K. (2008) Invertase inhibition based electrochemical sensor for the detection of heavy metal ions in aqueous system: application of ultra-microelectrode to enhance sucrose biosensor's sensitivity. *Biosens. Bioelectron.* 24(4): 657– 664.

13. Barcelo, J., Poschenrieder, C. (2004) Structural and ultrastructural changes in heavy metal exposed plants. In: Prasad MNV (ed) Heavy metal stress in plants, 3rd edn. Springer, Berlin, 223–248
14. Barrocas, P.R.G., Landing, W.M. and Hudson, J.M. (2010) Assessment of mercury(II) bioavailability using a bioluminescent bacterial biosensor: practical and theoretical challenges. *J. Environ. Sc.* 22(8): 1137– 1143.
15. Belkin, S., (2003) Microbial whole-cell sensing systems of environmental pollutants. *Curr. Opin. Microbiol.* 6: 206-212
16. Bentley A., Atkinson A., Jezek J. and Rawson D. M. (2001) Whole cell biosensor electrochemical and optical approaches to ecotoxicity testing. *Toxicol. Vitro* 15: 469-475.
17. Berezhtskyy, A.L., Sosovska, O.F., Durrieu, C., Chovelon, J., Dzyadevych, S.V., Tran- Minh, C. (2008) Alkaline phosphatase conductometric biosensor for heavy-metal ions determination. *ITBM-RBM* 29(2–3): 136–140.
18. Biran, R., Babai, L., Klimentiy, J., Rishpon and Ron, E.Z. (2000) Online and in situ monitoring of environmental pollutants: electrochemical biosensing of cadmium. *Environ Microbiol.* 2: 285-290
19. Blake, D.A., Jones, R.M., Blake, R.C. 2nd, Pavlov, A.R., Darwish, I.A., Yu, H. (2001)
20. Antibody-based sensors for heavy metal ions. *Biosens. Bioelectron.* 16(9–12): 799–809.
21. Bontidean, A., Mortari, S. and Leth N.L. (2004) Biosensors for detection of mercury in contaminated soils, *Environ. Poll.* 131(2): 255–262.
22. Bontidean, C., Berggren, G., Johansson, E., Csoregi, B., Mattiasson, J.R., Lloyd, K.J., Jakeman and Brown, N.L. (1998) Detection of Heavy Metal Ions at Femtomolar Levels
23. Using Protein-Based Biosensors. *Anal. Chem.* 70: 4162-4169.
24. Bontidean, I. (2002) Design, development and applications of highly sensitive protein based capacitive biosensors. Lund University Dissertation Abstracts.
25. Bontidean, I., Ahlqvist, J. and Mulchandani, A. (2003) Novel synthetic phytochelatin based capacitive biosensor for heavy metal ion detection. *Biosens. Bioelectron.* 18(5-6): 547– 553



ISOLATION, CHARACTERIZATION AND BIOLOGICAL ACTIVITY OF FLAX LECTIN

¹Dr Suma TK, ²Vasudha TK, ²Raghavi G, ²Rajalakshmi V, ²Nisha S, ²Priyadarshini M, ²B Preethi, ²M Vaishali Krishna and ³Dr BK Manjunath

¹Asst Professor, ²Student, ³Professor and Head
Department of Biotechnology
The Oxford College of Engineering, Bangalore, India
For correspondence – tksuma@gmail.com

Abstract: Lectins are a class of non-covalent carbohydrate-binding proteins of non-immune origins; possessing at least one non-catalytic domain, they can reversibly recognize and bind to monosaccharides or oligosaccharides. Legume lectins have been demonstrated to possess antifungal and antiproliferative potency on tumor cells. Seed lectin from *Linum usitatissimum* (flax) was extracted and partially purified by acetone precipitation followed by DEAE-cellulose ion exchange chromatography and Sephadex G-100 gel filtration chromatography. Carbohydrate binding specificity of lectin was determined by the hemagglutination method and found to be specifically binding to N-acetyl galactosamine. Purified lectin was characterized for their biological activity like antiproliferative, antioxidant, anti-inflammatory and antimicrobial activity using *in vitro* assays and found to possess significant biological activities.

(Index terms : flax, lectin, hemagglutination, carbohydrate binding, anti-oxidant)

I. INTRODUCTION

Lectins are proteins/glycoproteins which bind reversibly to carbohydrates. Lectins with specific carbohydrate specificity have been isolated from distinct sources such as viruses, bacteria, fungi, algae, animals, and plants [Sharon and Lis 2004]; they show specificity to distinct carbohydrates, such as mannose, sialic acid, fucose, N-acetylglucosamine, galactose/N-acetylgalactosamine, complex glycans, and glycoproteins [Wu A. M *et al* 2009].

Recent studies have demonstrated the potential of lectins from different origin and carbohydrate specificities as antifungal and antiparasitic agents [Hamed *et al* 2017]. Plant lectins investigated for antifungal potential, mainly against phytopathogenic species, have most reported antifungal effects binding to hyphae, causing inhibition of growth and prevention of spore germination.

Lectins from several origins exert cytotoxic effects such as inhibition of proliferation and activation of cell death pathways, on different types of cancer cells. In addition, many anticancer lectins usually possess low cytotoxicity to nontransformed cells. This fact is probably associated with the distinct expression of glycans on surface of cancer and normal cells, allowing lectins specifically to recognize malignant cells [Przybyło *et al* 2002, Varki *et al* 2009]. Since lectins have the property to bind carbohydrates their ability to antagonize, *in vivo*, neutrophil migration induced by inflammatory stimuli is well established (Alencar NM *et al* 2004). There is also data to suggest that some lectins down-regulate telomerase activity and hence inhibit angiogenesis (Sharon and Lis, 2004). A natural outcome of these studies has been the application of several lectins as therapeutic agents which favorably bind to cancer cell membranes or their receptors, thereby triggering cancer cell agglutination which translates into cytotoxicity, apoptosis, and inhibition of tumour growth (Sharon and Lis, 2004).

With the background of a wide variety of lectins isolated from diverse sources and studied for multiple biological activities, the current project was formulated to identify potential novel sources of lectins with useful properties. Flax seed or *Linum usitatissimum* is important in the nutraceutical market, as an alternate source of fish oil being naturally high in polyunsaturated fatty acids (PUFA). Intake of flaxseed in daily diet may reduce the risk of cardiovascular diseases such as coronary heart disease and stroke. There is also evidence that flax has anticancer effects in breast, prostate and colon cancers. Information on lectins isolated from flax seeds and their properties is very little. The focus of the present study was to isolate, purify and characterize lectin from the seeds of *Linum usitatissimum* (flax) and analyze *in vitro* antioxidant, anti-inflammatory and antiproliferative activities.

II. MATERIALS AND METHODS

a) Materials

Human blood of groups A, B and O were collected from healthy persons. Animal blood was collected from nearby veterinary hospitals. Flax (*Linum usitatissimum*) seeds were obtained from local markets.

b) Extraction of lectin

Dry seeds were first powdered in a blender. Seed powders were then weighed and extracted using cold extraction buffer, 1X PBS overnight at 4°C. The extract was then centrifuged for 15 minutes at 10,000 rpm at 4°C and clear supernatant was collected. Protein was estimated by Bradford method using BSA as a standard protein (Bradford 1976).

c) Hemagglutination activity of lectins

Seed extracts were assayed for the presence of lectin with whole blood of different blood types (Jawade AA et al 2016). 10µl of whole blood was used as negative control. 10µl of human blood types A, B, AB and O are taken on a clean and dry slide. The whole blood was mixed with 20µl of seed extract and hemagglutination observed.

In order to confirm that hemagglutination is due to lectin interacting with RBC cell surface carbohydrates, agglutination test of lectin was done by using 2% suspension of erythrocytes (Deshpande&Patil 2003). 50µl of 2% RBC suspension was mixed with 20µl of seed extract and hemagglutination observed.

Hemagglutination assay was also performed in 96 well plates (John Shi et al., 2007). 50µl of PBS and 10µl each of whole blood of human blood types A, B, AB and O was added to wells. 20µl of sample was then added to the wells. 50µl of PBS and 10µl of whole blood of any blood type served as negative control. Hemagglutination was observed after one hour.

d) Carbohydrate inhibition assay

Agglutination inhibition assay was done by testing the ability of different carbohydrates like disaccharides, pentoses, hexoses, oligosaccharides to inhibit the agglutination (Kurokawa et al. 1976). To confirm sugar specificity of extracted lectins, 100 µl of 500 mM sugar solutions were incubated with 100 µl lectin for 30 minutes at room temperature. 20µl of incubated mixture was mixed with 50µl of 2% RBC suspension. Hemagglutination or its absence was observed under a transilluminator.

e) Purification of lectin

Crude lectin extract was fractionated using ammonium sulfate salt (0 - 75%) (Devi et al., 2014). The salt precipitate was allowed to stand overnight in the cold for complete precipitation. After centrifugation, pellets were suspended in minimal volume of 1X PBS buffer and extensively dialysed against the extraction buffer for 24 hr in the cold for complete salt removal. Alternatively, crude extracts were treated with ice-cold acetone at 4°C and allowed for complete precipitation overnight. The precipitate was then centrifuged, air dried and dissolved in PBS. Protein concentration and hemagglutination activity were determined for the precipitates.

f) Chromatographic separation of lectin (Devi et al., 2014)

Acetone-precipitated flax seed extract was fractionated on a Sephadex G-100 gel filtration column equilibrated with 1X PBS, pH 7.4. Fractions were collected at a flow rate of 0.5ml/min and the protein was monitored by measuring absorbance at 280nm. Hemagglutination activities of the fractions were then assayed. The fractions containing hemagglutinating activities were pooled and again loaded on to a DEAE-cellulose ion exchange column pre-equilibrated with 1X PBS, pH 7.4. Fractions of 1 ml volume each were collected at a flow rate of 1 ml/min. The bound proteins were eluted with 1M KCl in 1X PBS, pH 7.4. All fractions were measured for absorbance at 280nm as well as for hemagglutination activity.

g) SDS-PAGE

Polyacrylamide gel electrophoresis of lectin samples was performed by the method of Laemmli (1970) with 15% polyacrylamide gel in the presence of sodium dodecyl sulfate (SDS) and 2-mercaptoethanol (SDS-PAGE). After electrophoresis the gel was stained with 0.2% Coomassie brilliant blue (R250) (Bluh et al 1987) and then destained.

h) pH and temperature stability studies

The effect of pH on activity of lectin was studied using different buffers in the pH range of 4-9 by the method described earlier (Devi et al., 2014). The thermal behavior of the partially purified lectin was also evaluated by incubating the lectin sample at temperatures of 17°C–77°C for 15min.

i) Antioxidant activity of lectin

Antioxidant activity of lectin was assessed by DPPH (1,1-diphenyl-2-picrylhydrazyl) radical scavenging assay (Janardhan et al 2014) and ABTS (2, 2'-azinobis, 3-ethylbenzothiazoline-6-sulfonic acid di-ammonium salt) radical scavenging assay (Lee et al 2014). Standard used in assay was ascorbic acid.

j) Anti-inflammatory activity of lectin

To assess the anti-inflammatory activity of flax lectin, proteinase inhibition assay was performed according to the modified method of Oyedepo et al 1995 and Sakat et al 2010 and inhibition of albumin denaturation technique according to Mizushima et al 1968 and Sakat et al 2010 with minor modifications. The percentage inhibition of proteinase inhibitory and protein denaturation activity was calculated.

k) Anti-proliferative activity of lectins

MCF-7 and HEPG2 cell line were cultured in DMEM and EMEM medium respectively supplemented with 10% inactivated Fetal Bovine Serum (FBS), penicillin (100 IU/ml), streptomycin (100 µg/ml) in a humidified atmosphere of 5% CO₂ at 37°C until confluent. The cells were dissociated with TPVG solution (0.2 % trypsin, 0.02 % EDTA, 0.05 % glucose in PBS). The viability of the cells is checked and centrifuged. Further, 50,000 cells / well of MCF-7 and HEPG2 were seeded in a 96 well plate and incubated for 24 hrs at 37°C, 5 % CO₂ incubator. The monolayer cell

culture was trypsinized and the cell count was adjusted to 1.0×10^5 cells/ml using respective media containing 10% FBS. To each well of the 96 well microtiter plate, 100 μ l of the diluted cell suspension (50,000cells/well) was added. After 24 h, when a partial monolayer was formed, 100 μ l of different concentrations of test samples were added and plates incubated at 37°C for 24hrs in 5% CO₂ atmosphere. Later, test solutions in the wells were discarded and 100 μ l of MTT (5 mg/10 ml of MTT in PBS) was added to each well and incubated for 4 h at 37°C. The supernatant was removed and 100 μ l of DMSO was added and the plates were gently shaken to solubilize the formed formazan. The absorbance was measured using a microplate reader at a wavelength of 590 nm. The percentage growth inhibition was calculated using the following formula and concentration of test drug needed to inhibit cell growth by 50% (IC₅₀) values is generated from the dose-response curves for each cell line. % Inhibition = $100 - (\text{OD of sample}/\text{OD of Control}) \times 100$.

III. RESULTS AND DISCUSSION

Lectins were extracted from flax seeds into PBS and precipitated using salt or acetone. All extracts were tested for hemagglutination with human and animal blood. Table 1 shows hemagglutination of human blood types and animal blood by flax seed extracts. It showed hemagglutination reaction with only human blood group A (and AB) indicating its specificity to N-Acetylgalactosamine (Fig. 1).

Table 1 : Agglutination study of *Linum usitatissimum* seed lectin with human and animal erythrocytes

| Erythrocytes | Agglutination |
|--------------|---------------|
| Human 'O' | - |
| Human 'A' | +++ |
| Human 'AB' | +++ |
| Human 'B' | - |
| Rabbit | - |
| Sheep | - |
| Hen | - |

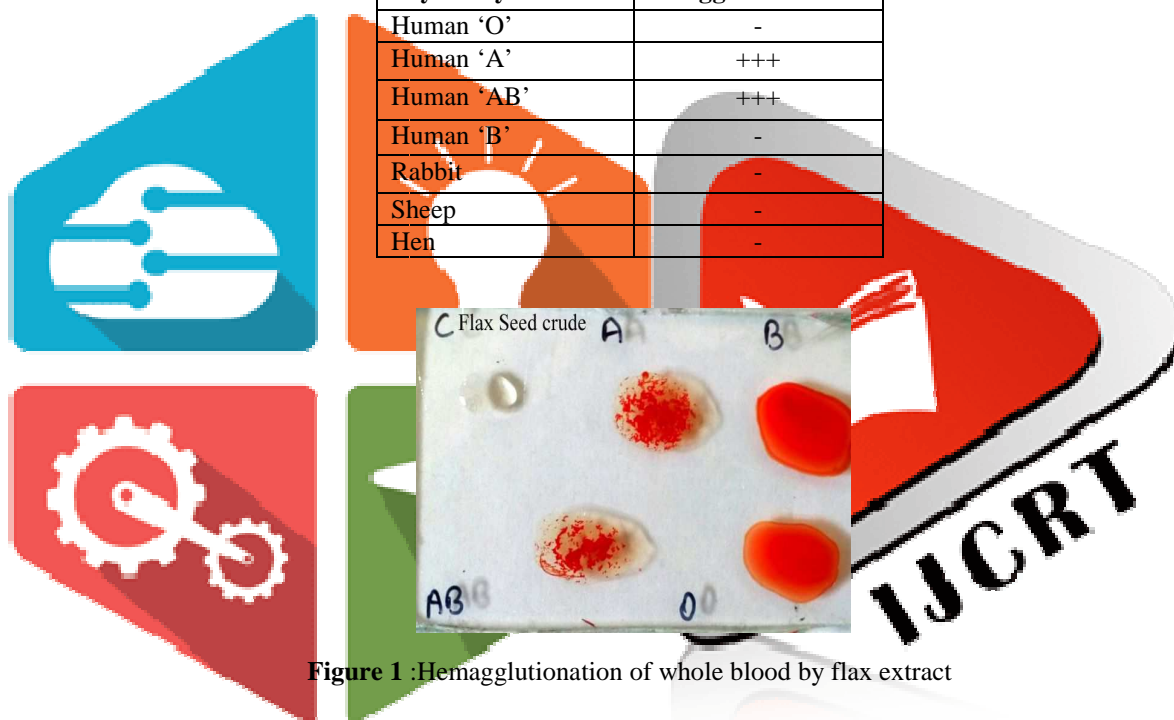


Figure 1 : Hemagglutination of whole blood by flax extract

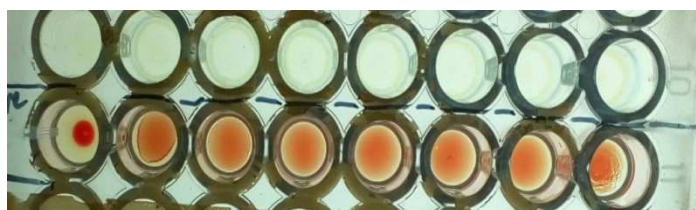


Figure 2: Hemagglutination assay in 96 well plate

Hemagglutination assay was also performed by using human erythrocyte suspension in microtitre plates. Formation of red button of RBCs at the bottom of the well indicated absence of hemagglutination. (Fig. 2).

In order to determine the absolute specificity of flax lectins towards various carbohydrates, carbohydrate inhibition assay was carried out. Table 2 shows the inhibition of lectin by different carbohydrates. Flax lectin was inhibited by N- Acetyl galactosamine (GalNac) alone and no other carbohydrate indicating the absolute specificity of this lectin for GalNac.

Table 2: Inhibition of lectin by different carbohydrates

| Carbohydrates | Agglutination |
|---------------|---------------|
|---------------|---------------|

| | | |
|------------------------|-----|--|
| Glucose | +++ | - = inhibits lectin + = does not inhibit lectin |
| Galactose | +++ | |
| Mannose | +++ | |
| Lactose | +++ | |
| Fucose | +++ | |
| N-acetyl galactosamine | - | |

Flax lectin was purified from the acetone precipitated extract using Sephadex G-100 gel filtration column equilibrated with 1X PBS buffer, pH 7.4. Fig. 3 gives the purification profile of flax lectin by gel filtration chromatography. Hemagglutination activity was detected in the initial fractions (maximum in fraction 3) denoting the high molecular weight of the purified lectin. None of the later eluting protein peaks showed any trace of hemagglutination activity. Although gel filtration chromatography is commonly employed for lectin separations (Zhang et al 2014), such purification of *Linum usitatissimum* lectin using Sephadex G-100 has not been reported earlier.

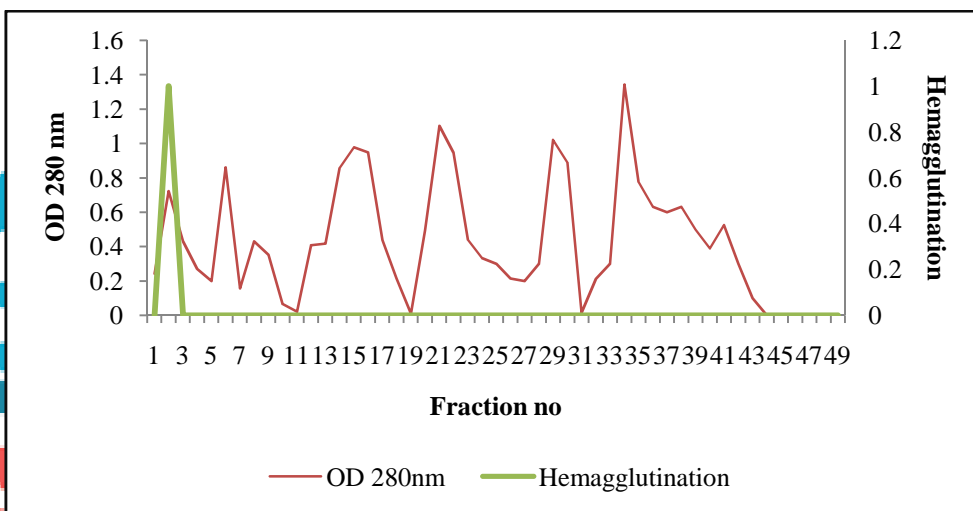


Figure 3: Sephadex G-100 gel filtration purification profile of flax lectin

Flax lectins were further purified on DEAE cellulose ion exchange column. The fractions were assayed for protein by measuring their absorbance at 280nm as well as for the hemagglutination activity. Among the fractions collected, activity was recovered in the unbound fractions and no activity was seen in bound (Fig. 4), indicating its anionic nature.

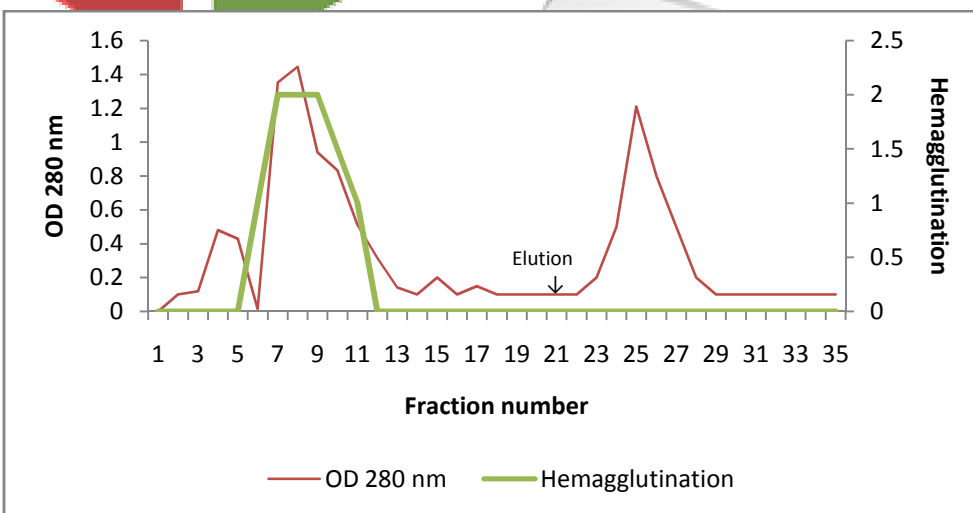


Figure 4: DEAE-cellulose ion exchange purification profile of flax lectin

SDS-PAGE analysis of lectin at each stage of purification was done to determine purity as well as molecular weight. Fig. 5 shows the gel profile of crude and partially purified flax lectin preparation on a 15% SDS-PAGE gel. In comparison with crude extract

and salt and acetone precipitates, different types of protein bands were seen in unbound and gel filtration fraction signifying a level of purification. The presence of protein bands in between that of BSA and lysozyme molecular markers shows that the molecular weight of the lectin or its subunits is between 14.3 kDa (lysozyme) and 66.5 kDa (Bovine serum albumin). This profile of unbound and gel filtration fractions was associated with hemagglutination activity while bound had no hemagglutination activity.

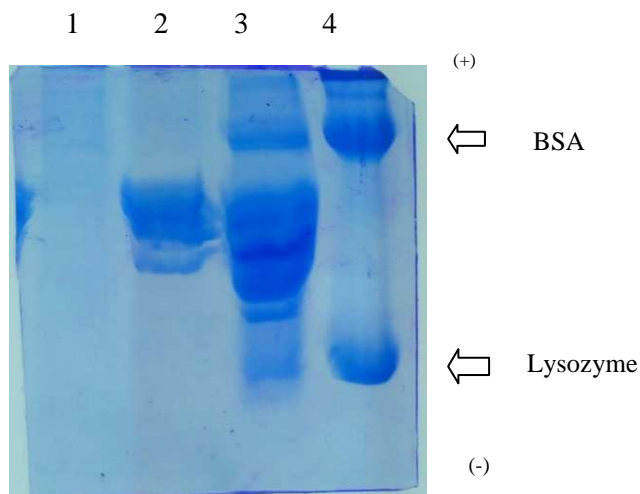


Figure 5: SDS-PAGE profile of flax crude and partially purified samples. 15% polyacrylamide gel was run with following samples and stained with Coomassie Brilliant Blue for visualization. From left to right: Lane 1: Gel-filtration pooled fraction, Lane 2: Flax ion-exchange unbound fraction, Lane 3: acetone precipitate, Lane 4: BSA + Lysozyme molecular marker.

The antioxidant activity of lectins has been well-established (Sadananda *et al.*, 2014). Anti-oxidant assays of DPPH and ABTS were performed for lectin extracts. The percentage scavenging activity of flax lectin was tested against that of ascorbic acid which is known to have potent antioxidant activity (Fig. 6 and 7). The IC₅₀ value for flax lectin was found to be 3.008 mg/ml. The IC₅₀ value for ascorbic acid at same concentration as lectin was found to be 3.018mg/ml.

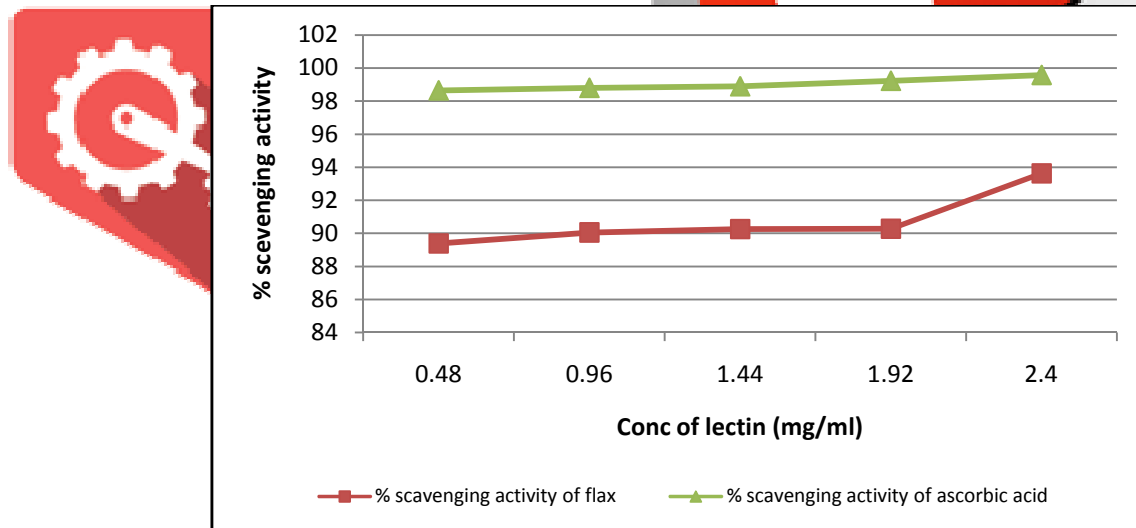


Figure 6: Antioxidant activity of flax lectin by DPPH assay. The reduction capability of DPPH radical was determined by the decrease in its absorbance at 517nm which is induced by different antioxidants.

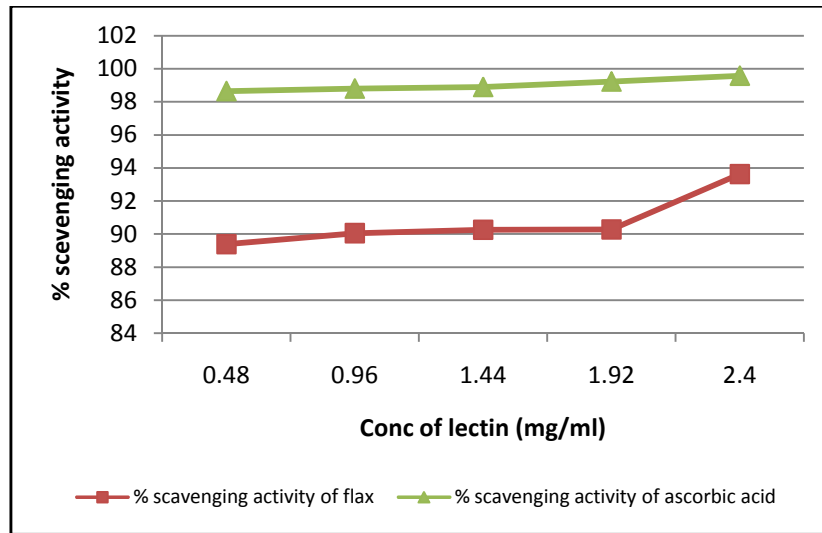


Figure 7: Antioxidant activity of flax lectin by ABTS assay. The decrease in absorbance due to scavenging of the proton radicals is monitored spectrophotometrically at 734nm

Lectins have been shown to have anti-inflammatory activity (Janaina K.L. Campos *et al.*, 2016). Proteinase inhibition assay and albumin denaturation assays were performed to demonstrate anti-inflammatory activity. Fig. 8 shows the anti-inflammatory activity of flax lectin. Flax lectin exhibited significant antiproteinase activity at different concentrations and showed 100% inhibition at 3.2mg/ml of lectin.

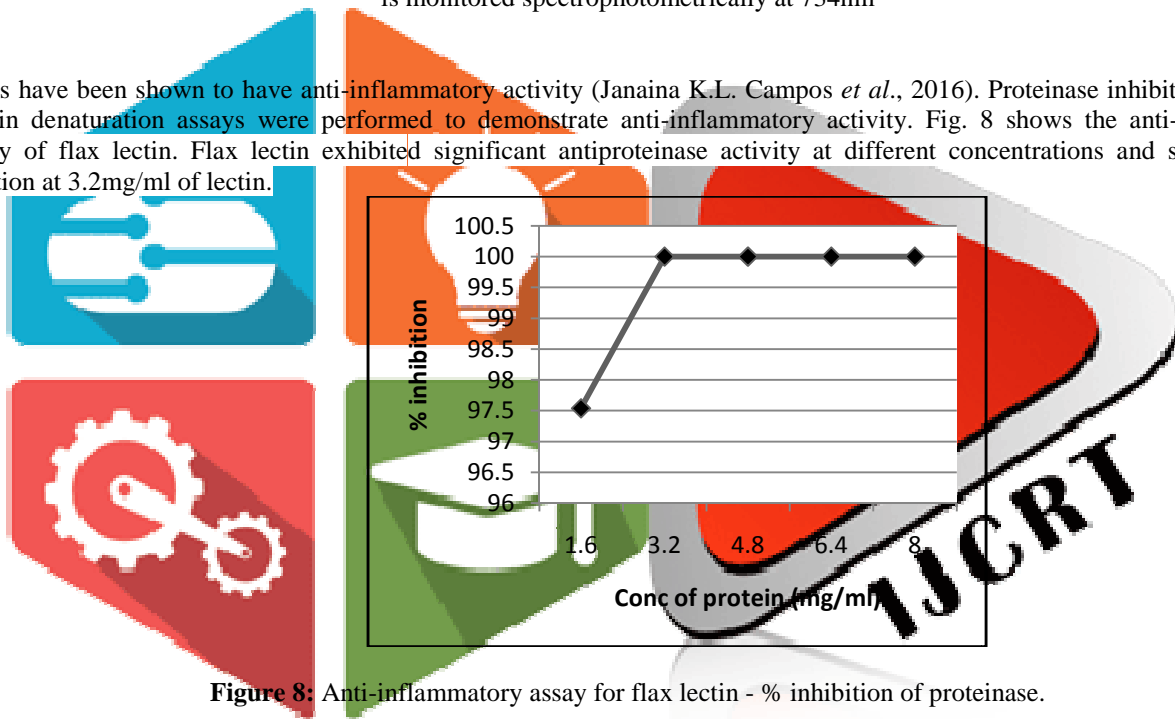


Figure 8: Anti-inflammatory assay for flax lectin - % inhibition of proteinase.

As part of the investigation on the mechanism of the anti-inflammation activity, ability of lectin to inhibit protein denaturation was studied (Fig. 9). It was effective in inhibiting heat induced albumin denaturation. Inhibition of 100% was observed at 8 mg/ml for flax lectin.

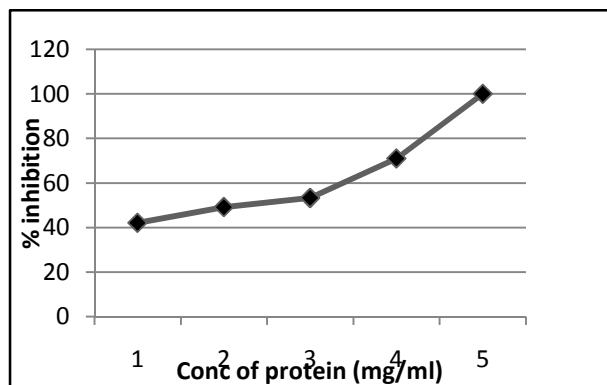


Figure 9: Anti-inflammatory assay for flax lectin - % inhibition of protein denaturation.

Flax lectins were tested for their pH stability by incubating the lectins in buffers of different pH. The lectins showed remarkable pH stability in the range 4-9 which was confirmed by hemagglutination of the lectins after incubation. When tested at a range of temperatures between 17-100°C, flax and lectins showed decreased activity beyond 57°C.

To evaluate the cytotoxic effect of flax lectin against cancer cells, human breast carcinoma cells (MCF-7) were incubated with different dosages of flax lectin samples. After 24 hours of incubation, cell viability was determined by MTT assay. Flax lectin extract was found to induce cell toxicity in a concentration dependant manner (Table 4). Dose response curves between the range 10µg/ml to 320µg/ml express decreased number of viable cells with increase in the concentration of compound. Results indicate that the cytotoxic effect steadily strengthens with increase in concentration.

Table 4: Cytotoxicity assays using flax lectin

| MCF-7 | | | |
|----------------------------|-------------|-------------|--------------|
| Sample | Conc. µg/ml | OD at 590nm | % inhibition |
| <i>Linum usitatissimum</i> | 10 | 0.911 | 4.27 |
| | 20 | 0.875 | 7.95 |
| | 40 | 0.833 | 12.47 |
| | 80 | 0.811 | 14.78 |
| | 160 | 0.766 | 19.50 |
| | 320 | 0.721 | 24.19 |

IV. CONCLUSION

Very little information is currently available on flax seed lectins. In one study, hemagglutination activity and carbohydrate specificity of lectin seedlings revealed their role in plant adaptation to abiotic stresses (Levchuket *et al* 2013). A similar study on amaranth-like lectin genes in flax induced by defence hormones has also been reported (Kashfia Faruque *et al* 2015).

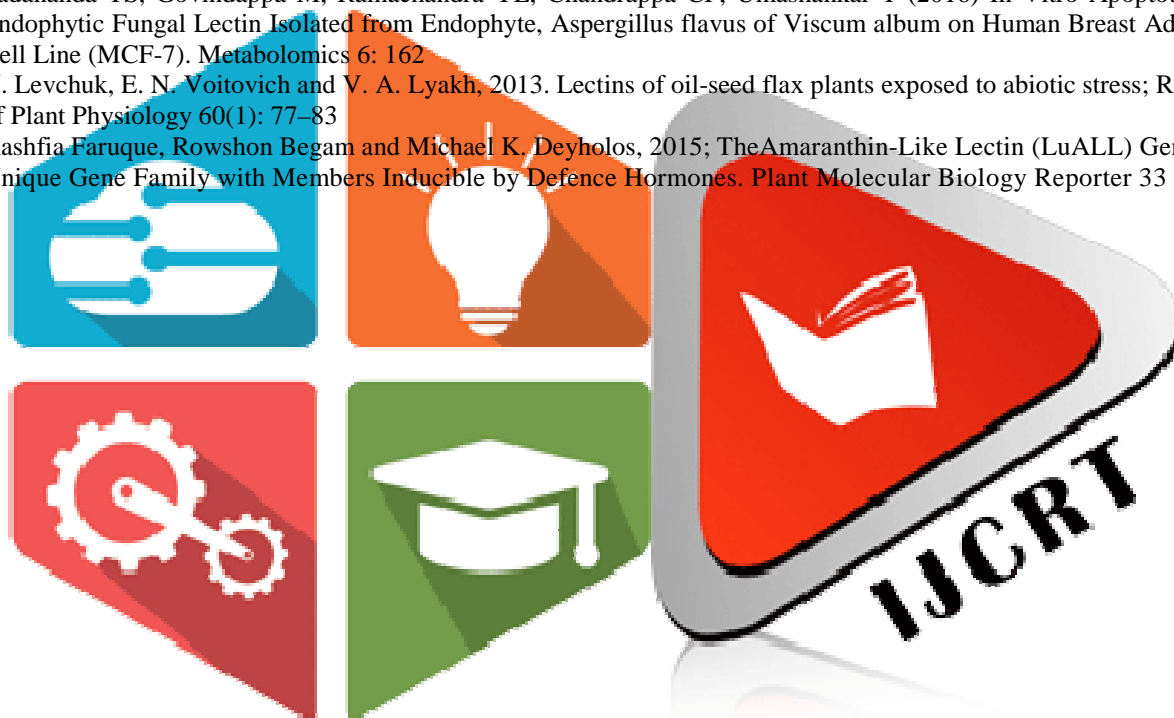
The current report sheds light on the hemagglutination activity, carbohydrate specificity, purification strategies and biological activity of flax seed lectins. *Linum usitatissimum* (Flax) lectin extracts were found to be specific to N-Acetylgalactosamine. Purification was achieved by concurrent use of gel filtration and ion exchange chromatography and it was found to be a high molecular weight cationic protein. Purified lectin was shown to possess anti-oxidant, anti-inflammatory and anti-proliferative properties and remarkable pH and temperature stability. These results support the general finding of lectins to be biologically active in different ways. Further work is warranted to establish possible utilization of flax lectin for specific applications.

Acknowledgment

V. References

- Nathan, Sharon and Halina Lis, 2004; History of lectins: from hemagglutinins to biological recognition molecules; *Glycobiology* 14 (11): 53R-62R
- Wu AM, Lisowska E, Duk M and Yang Z, 2009; Lectins as tools in glycoconjugate research; *Glycoconj* 26(8):899-913.
- Hamed El-SE, Ibrahim El-AMM, Mounir SM (2017) Antimicrobial Activities of Lectins Extracted from Some Cultivars of *Phaseolus vulgaris* Seeds. *J MicrobBiochemTechnol* 9:109-116
- Przybylo M, Hoja-Lukowicz D, Litynska A and Laidler P. 2002; Different glycosylation of cadherins from human bladder non-malignant and cancer cell lines. *Cancer Cell Int.* 18;2:6.
- Varki A, Varki NM and Borsig L, 2009; Molecular basis of metastasis (correspondence). *N. Engl. J. Med.* 360: 1678-1680
- Nylane M.N. Alencar, Ana M.S. Assreuy, David N. Criddle, Emmanuel P. Souza, Pedro M.G. Soares, AlexandreHavt, Karoline S. Aragao, Daniel P. Bezerra, Ronaldo A. Ribeiro, Benildo S. Cavada, 2004. VataireaMacrocarpaLectin Induces Paw Edema With Leukocyte Infiltration. *Protein & Peptide Letters* 11(2), 195-200
- Bradford, Marion (1976). "A Rapid and Sensitive Method for the Quantification of Microgram Quantities of Protein Utilizing the Principle of Protein-Dye Binding" (PDF). *Analytical Biochemistry*. 72: 248–254.
- Jawade AA, Pingle SK, Tumane RG, Sharma AS, Ramteke AS & Jain RK (2016) Isolation and characterization of lectin from the leaves of *Euphorbia tithymaloides* (L.). *Tropical Plant Research* 3(3): 634– 641)
- Deshpande&Patil 2003
- John Shi, Sophia Jun Xue, Yukio Kakuda, Sanjallic, and Daniel Kim; 2007; Isolation and characterization of lectins from kidney beans (*Phaseolus vulgaris*); *Process Biochemistry* 42: 1436–1442.
- Kurokawa T, Tsuda M and Sugino Y, 1976. Purification and characterization of a lectin from *Wistaria floribunda* seeds. *J Biol Chem.* 251(18):5686-93
- B. Gayatri Devi and K.P.J HemaLatha. 2014; Isolation, Partial Purification and Characterization of Alkaline Serine Protease from seeds of *CucumisMelo* Var. *International Journal of Research in Engineering and Technology.* 3:6

13. Helmut Blum, HildburgBeier and Hans J. Gross; 1987; Improved silver staining of plant proteins, RNA and DNA in polyacrylamide gels; *Electrophoresis* 8(2): 93-99
14. Janardhan A, Kumar AP, Viswanath B, Saigopal DV and Narasimha G. 2014. Production of bioactive compounds by actinomycetes and their antioxidant properties. *Biotechnol Res Int.* 2014:217030.
15. Lee DR, Lee SK, Choi BK, Cheng J, Lee YS, Yang SH and Suh JW, 2014. Antioxidant activity and free radical scavenging activities of *Streptomyces* sp. strain MJM 10778. *Asian Pac J Trop Med.* 7(12):962-7
16. O.O. Oyedapo & A. J. Famurewa, 1995. Antiprotease and Membrane Stabilizing Activities of Extracts of *FagaraZanthoxyloides*, *OlaxSubscorpioides* and *TetrapleuraTetraptera*. *International Journal of Pharmacognosy* 33(1), 65-69
17. Sakat S, Juvekar AR, Gambhire MN. 2010 In vitro antioxidant and anti-inflammatory activity of methanol extract of *Oxalis corniculata* Linn. *International Journal of Pharma and Pharmacological Sciences*; 2(1):146-155
18. Mizushima Y and Kobayashi M. 1968 Interaction of anti-inflammatory drugs with serum proteins, especially with some biologically active proteins. *J of Pharma Pharmacol*; 20:169- 173.
19. T. S. Sadananda, M. Govindappa and Y. L. Ramachandra, 2014; In vitro Antioxidant Activity Of Lectin from Different Endophytic Fungi of *Viscum album* L; *British Journal of Pharmaceutical e research* 4(5): 01-15.
20. Janaína K.L. Campos, Chrisjacele S.F. Araújo, Tiago F.S. Araújo, Andréa F.S. Santos, José A. Teixeira, Vera L.M. Lima, Luana C.B.B. Coelho, 2016; Antiinflammatory and antinociceptive activities of *Bauhinia monandra* leaf lectin. *Biochimie* 01: 62–68.
21. Weiwei Zhang, Guoting Tian, Xueran Geng, Yongchang Zhao, Tzi Bun Ng, Liyan Zhao and Hexiang Wang. 2014. Isolation and Characterization of a Novel Lectin from the Edible Mushroom *Stropharia rugosoannulata*. *Molecules* 19, 19880-19891
22. Sadananda TS, Govindappa M, Ramachandra YL, Chandrappa CP, Umashankar T (2016) In Vitro Apoptotic Activity of Endophytic Fungal Lectin Isolated from Endophyte, *Aspergillus flavus* of *Viscum album* on Human Breast Adenocarcinoma Cell Line (MCF-7). *Metabolomics* 6: 162
23. N. Levchuk, E. N. Voitovich and V. A. Lyakh, 2013. Lectins of oil-seed flax plants exposed to abiotic stress; *Russian Journal of Plant Physiology* 60(1): 77–83
24. Kashfia Faruque, Rowshon Begam and Michael K. Deyholos, 2015; TheAmaranthin-Like Lectin (LuALL) Genes of Flax: a Unique Gene Family with Members Inducible by Defence Hormones. *Plant Molecular Biology Reporter* 33 (3), 731–741.



SIGNIFICANCE ANALYSIS OF TARGET PROFILE IN TUBERCULOSIS USING GENE INTERACTIONS AND INSILICO DOCKING APPROACH TO FIND POTENTIAL LIGANDS

Dr. Manjunath, Shambhu M.G Apeksha, Chandana N, Lakshmi S, Mounika S.

Department of Biotechnology, The Oxford College of Engineering, Bengaluru-560068

*correspondence should be addressed to Mr Shambhu M G : shambhumg13@gmail.com

Abstract: Tuberculosis is a common and deadly infectious disease caused by *Mycobacteria*. WHO estimates that one third of global population is infected with *Mycobacterium tuberculosis*. Tuberculosis is a Multidrug resistant since there are a lot of mutations occur in genes. Our study focused on uncharacterized mutated tuberculosis target identification by using Systems Biology Approach, which is used to find the better drug targets. From the advance search by using UniProt we observed seven receptors are the significant targets 2CCA, 1P44, 3VZ1, 3IFZ, 1KOR, 2EYQ. Tuberculosis target candidates are screened and validated by docking studies using Auto dock Software. Analysis has revealed that among 14 ligands it has been observed that Josamycine and Rifapentine showed a better interaction score (-10.3 kcal/mol and -12.7 kcal/mol) and could be potential ligands. These potential ligands have also shown better ADMET properties in *Insilico* studies by using ADMET SAR software.

1. INTRODUCTION

Tuberculosis (TB) is caused by *Mycobacterium tuberculosis*. TB is an infectious disease that usually affects the lungs. Some strains of the TB bacteria developed resistance to the standard drugs through genetic changes [2]. TB affects 24% of world's total population. According to WHO its world's top infectious disease, about 5000 people deaths occurs everyday. *Mycobacterium tuberculosis* (MTB) is a rod shaped bacteria that can thrive only human beings [3]. TB is often called Multidrug resistance (MDR). The TB bacteria has natural defences against some drugs, and can acquire drug resistance through genetic mutations. The bacteria does not have the ability to transfer genes for resistance between organisms through plasmids some mechanisms of drug resistance include: **Cell wall:** The cell wall of *M. tuberculosis* (TB) contains complex lipid molecules which act as a barrier to stop drugs from entering the cell [9]. **Drug modifying & inactivating enzymes:** The TB genome codes for enzymes (proteins) that inactivate drug molecules. These enzymes usually phosphorylate, acetylate, or adenylate drug compounds. **Drug efflux systems:** The TB cell contains molecular systems that actively pump drug molecules out of the cell. **Mutations:** Spontaneous mutations in the TB genome can alter proteins which are the target of drugs [6], making the bacteria drug resistant. In the present study, Initially the receptors are obtained from the target pathogen database 30 receptors were obtained from the literature survey. Among the 30 receptors, 7 potential genes were obtained by string software. Validation was performed using Rampage software. Homology model was performed for all seven receptors. Among the seven receptors, only two receptors model was not found. These two receptors model was built using Swiss model and validated using Rampage and ERATT tool. Fourteen potential ligands were obtained from drug bank. These ligands satisfied and passed Lipinski's rule which were performed to obtain better drug candidates. Interaction studies between the receptors and ligands were observed by docking studies by using Autodockvina software. It was observed that among the 14 ligands, two ligands showed good interaction studies they are Rifapentine and Josamycin. *Insilico* ADMET properties predictions was performed using ADMET SAR SOFTWARE.

2. MATERIALS AND METHODS

2.1 IDENTIFICATION AND PREPARATION OF TARGET PROTEIN

Target identification is the process of identifying the direct molecular target for example protein or nucleic acid of a small molecule. In clinical pharmacology, target identification is aimed at finding the efficacy target of a drug/pharmaceutical. Target proteins are functional biomolecules that are addressed and controlled by biologically active compounds [1]. Target proteins control the action and the kinetic behaviour of drugs within the organism. Initially by using database Target pathogen and literature review 4000 genes was obtained which occurred in Tuberculosis [1]. These 4000 genes was further analyzed and screened by using the string software. By using string software on the basis of protein-protein interaction 30 potential genes were screened based on their functions and characteristics using UniProt advance filters.

2.2 GENES NETWORK STUDIES

Using string database these 30 genes were screened based on their functions and characteristics using UniProt advance filters .Seven significant genes involved in tuberculosis were shortlisted among 30 targets. All the 7 targets were further studied based on structural information[15]. Among these seven targets we observed that 2 targets did not have the structure which was further modelled using Swiss model.

2.3 HOMOLOGY MODELLING

The Homology Modelling server template library ExpDB is extracted from the PDB. To select templates for a given protein, the sequences of the template structure library are searched. If these templates cover distinct regions of the target sequence, the modeling process will be split into separate independent batches. Homology modelling was used for the construction of atomic resolution model of the target protein. Swiss model was used to obtain 3d protein structure models for the genes which we have selected for finding the better drug candidate. The template protein of gabD1 is 3VZL and of mfd is 2EYQ. For two protein the model was built based on template as the structure was not available and this was done using Swiss model.

2.4 VALIDATION

The Ramachandran plot has been the mainstay of protein structure validation for many years. Its detailed structure has been continually analysed and refined as more and more experimentally determined models of protein 3D structures have become available, particularly at high and ultra-high resolution. These plots are typically split in forbidden and allowed regions. Around 40% of all the amino acids in a structure are contained in just the 2% of the Ramachandran plot the so called "allowed areas". Rampage revealed the information of the dihedral angles of residues with respect to protein structures. Ramachandran plot was analysed for the 2 protein models by giving the pdb format. Validation was done using the ERRAT tool and this tool analyzes the statistics of non-bonded interactions between different atom types and plots the value of the error function versus position of a 9-residue sliding window, calculated by a comparison with statistics from highly refined structures. We uploaded the pdb file of modeled protein and we obtained a graph which specifies the error % and the warning %. These graphs were used for the validation process.

2.5 SCREENING OF LIGANDS

The ligands were collected from the DRUGBANK and advance search. The ligands were screened based on the Lipinski's rule which states that poor adsorption is anticipated, if the molecular weight is greater than 500 LogP is greater than 5 and hydrogen bond acceptors is greater the all the ligands should satisfies Lipinski's rule and also indicates good drug candidates. In our study 14 potential ligands were screened[17].

2.6 DOCKING

AutoDockVina, a new program for molecular docking and virtual screening, is presented. AutoDockVina significantly improves the accuracy of the binding mode predictions, than the Autodock 4. Six targets were docked with the selected 14 ligands. The best interaction is taken based on the score given by autodockvina. The general functional form of the conformation-dependent part of the scoring function AutoDockVina (referred to as Vina here) is designed to work with is [7],

$$c = \sum_{i < j} f_{t_i t_j}(r_{ij}),$$

Where the summation is over all of the pairs of atoms that can move relative to each other, normally excluding 1–4 interactions, *i.e.* atoms separated by 3 consecutive covalent bonds. Here, each atom i is assigned a type t_i , and a symmetric set of interaction functions $f_{t_i t_j}$ of the interatomic distance r_{ij} should be defined.

$$c = c_{\text{inter}} + c_{\text{intra}}$$

This value can be seen as a sum of intermolecular and intramolecular contributions [7]. The optimization algorithm, described in the following section, attempts to find the global minimum of c and other low-scoring conformations, which it then ranks.

2.7 ADMET (Absorption, Distribution, Metabolism, Excretion, and toxicity) Test

ADMET stands for Adsorption, Distribution, Metabolism, Excretion, Toxicity. To select drug-like molecule, ADMET SAR software was used to screen the selected five molecules based on filters namely Lipinski's rule [16], Quantitative Estimate of Drug likeness. The selected compounds in SDF format was given to the ADMET software interface and proceeded to calculate the properties.

3. RESULTS AND DISCUSSIONS

3.1 IDENTIFICATION OF TARGET PROTEIN

After the characterization of genes we obtained 1373 unknown genes. Analysis of genes was carried out based on their functional characteristics. Among the 30 targets, 7 targets have to be further analyzed through network analysis. The mapping of genes was carried out using UniProt ID mapping. The several specific genes were obtained as such when provided with identifiers from UniProtKB AC/ID to PDB.

3.2 Gene interaction network analysis

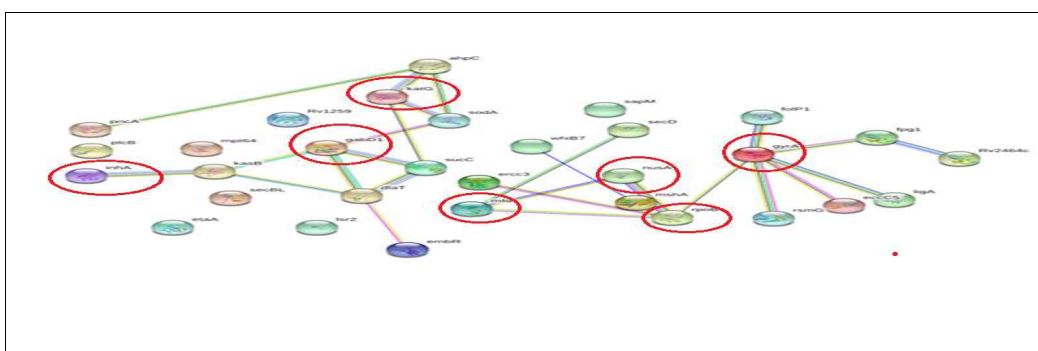
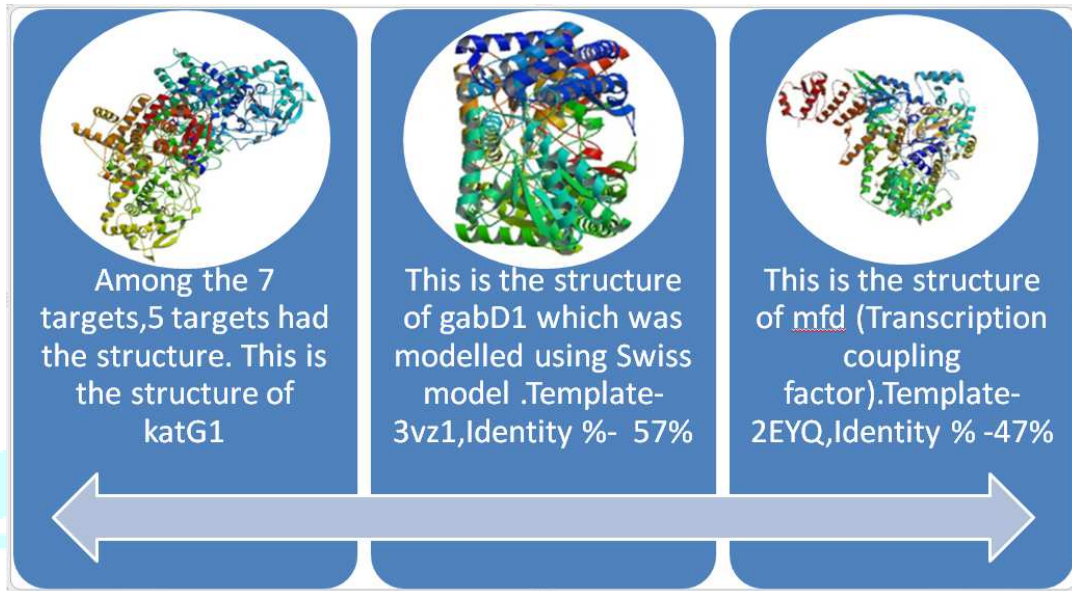


Fig 2: protein-protein interactions where done using the string database and 7 targets were found to have better interactions and those genes were inhA, katG, r

The 30 Target protein which were obtained from the advance search n the characterized genes, these were given to string software and using the string software we found out the gene-gene interactions and among the 30 genes we found that 7 genes had the better drug interactions and based on these interactions the 7 genes were shortlisted and those are the inhA,katG,rpoB,gabD1,mfd,gyrA,nusA. Among these 7 genes 5[22] had the structures and 2 did not have the structures which were modelled using the homology modeling.

3.2 HOMOMOLOGY MODELLING



In the homology modelling we used the swiss model software and the 2 genes which did not have the structure was built a model and the template was found for the these genes and we obtained the structure.

3.3 VALIDATION

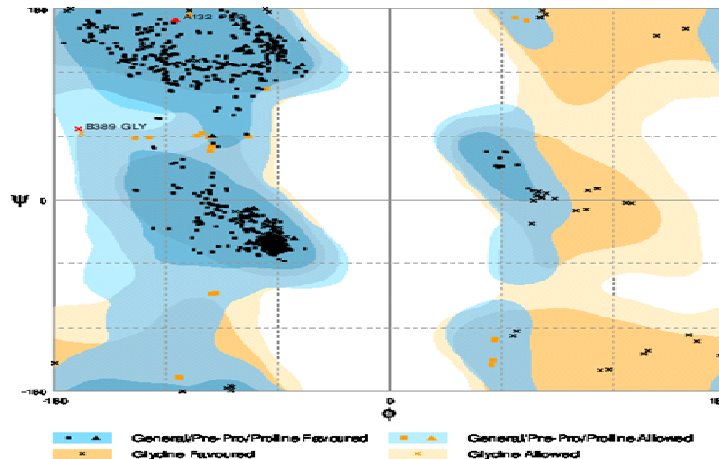


FIGURE 8:
 Number of residues in favoured region (~98.0% expected) : 881 (97.5%)
 Number of residues in allowed region (~2.0% expected) : 21 (2.3%)

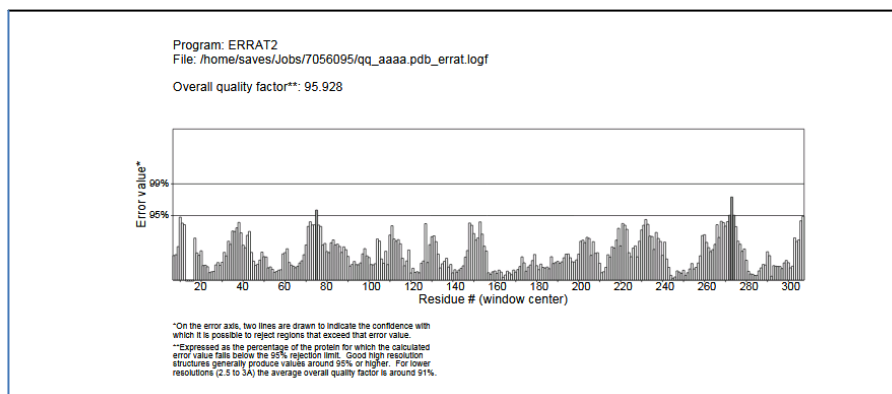


Fig 7 : Validation of molecules using ERRAT tool

3. 4 DOCKING

Autodockvina was performed to predict the bound conformation the binding affinity[23].The grid maps will be automatically formed by the software.The configuration values will be saved in a text file called conf.The PDBQT file of target and the ligand was obtained.

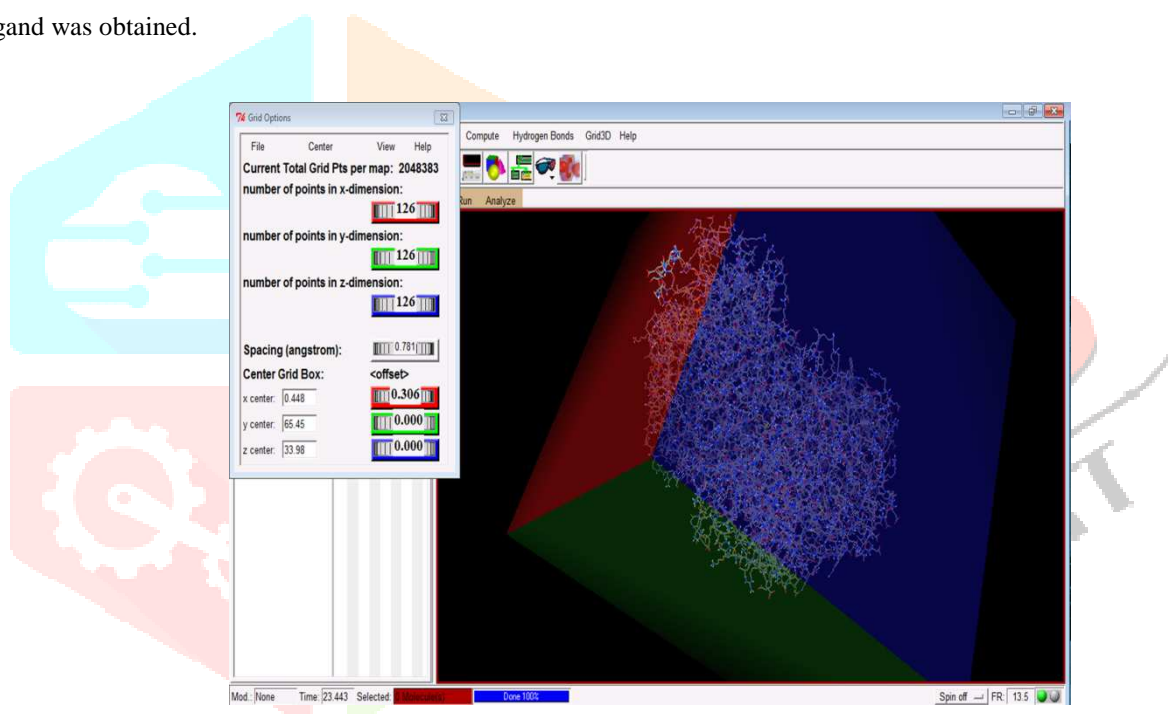


Fig8:Grid box formed by the Autodock for 1KOR.

Similarly the grid box and the configuration was done for other genes.14 ligands were taken for docking purpose, where Josamycine and Rifapentine showed the better result compared to other ligands.

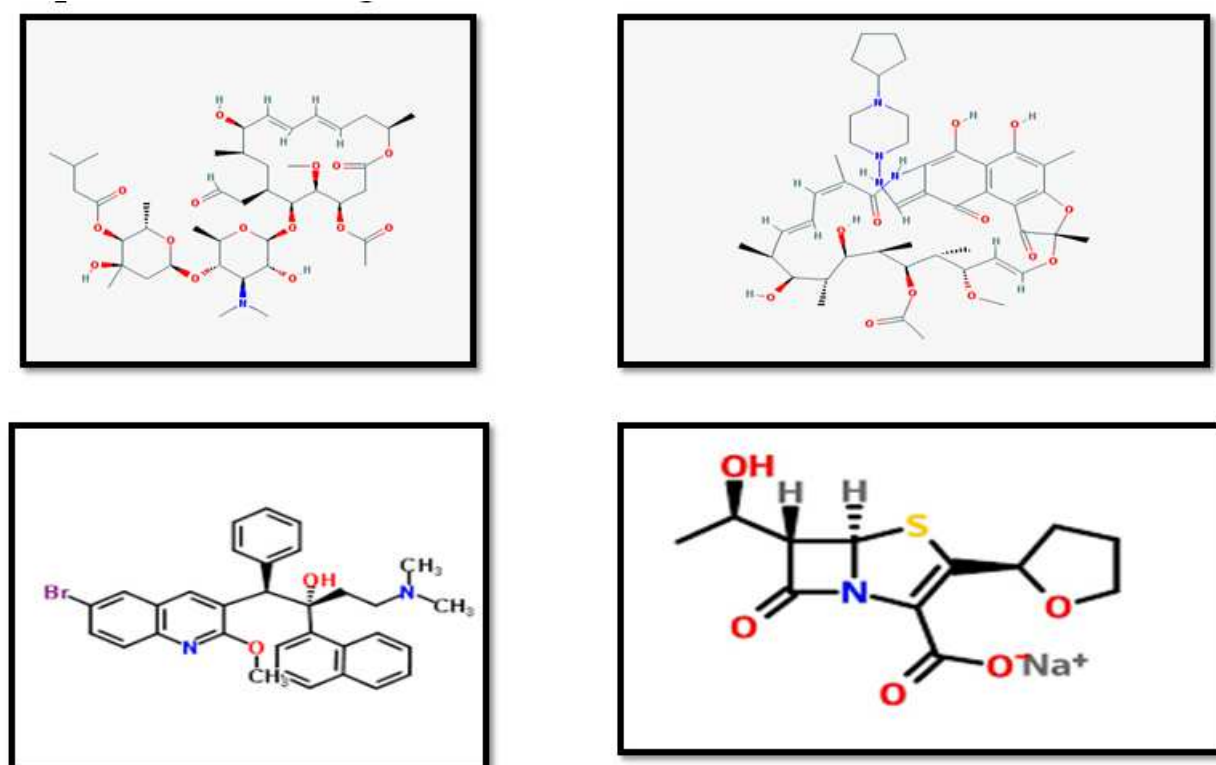


Fig9 : Ligands structure a.Josamycin, b.Rifampentine, c.Bedaquiline, d.Faropenem

Further the command prompt was used to run the program, where the conffile ,gene and ligand pdbqt file was saved in one folder.Further the docking analysis is performed based on the binding energy value and the interaction was analysed using pymol software.

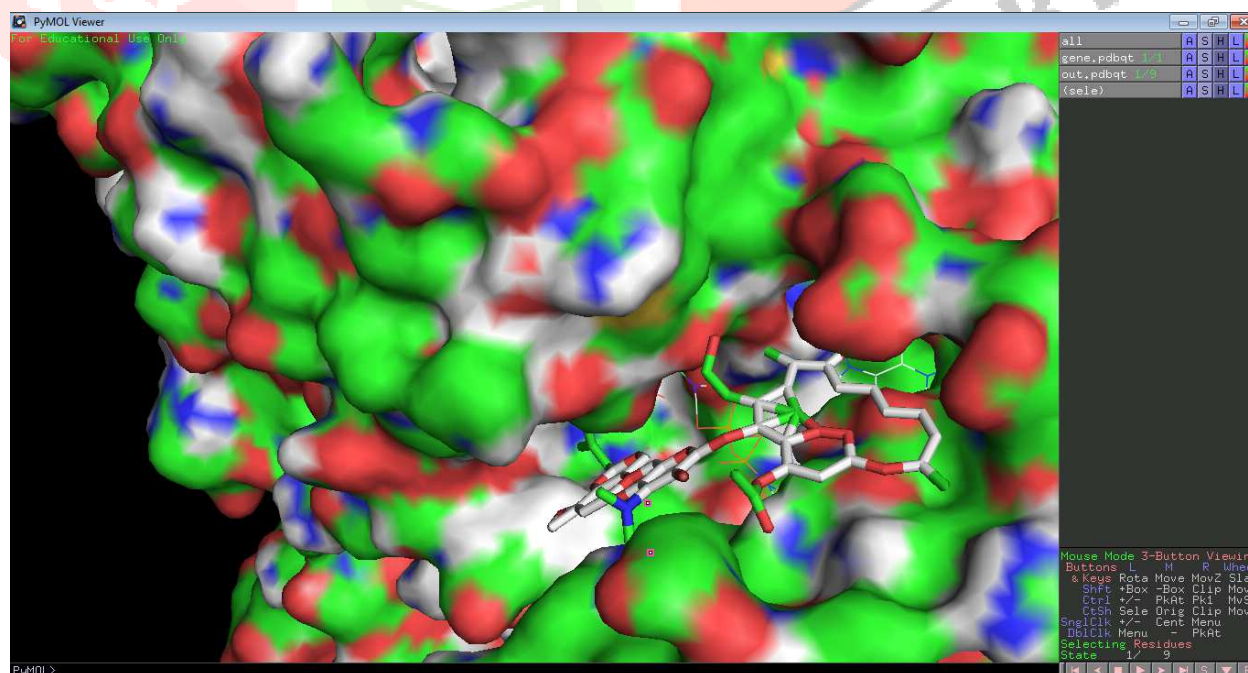


Fig10: Docking result of Josamycin which is docked with the 1KOR

Rifapentine was shown the better result for the gene 2CCA.

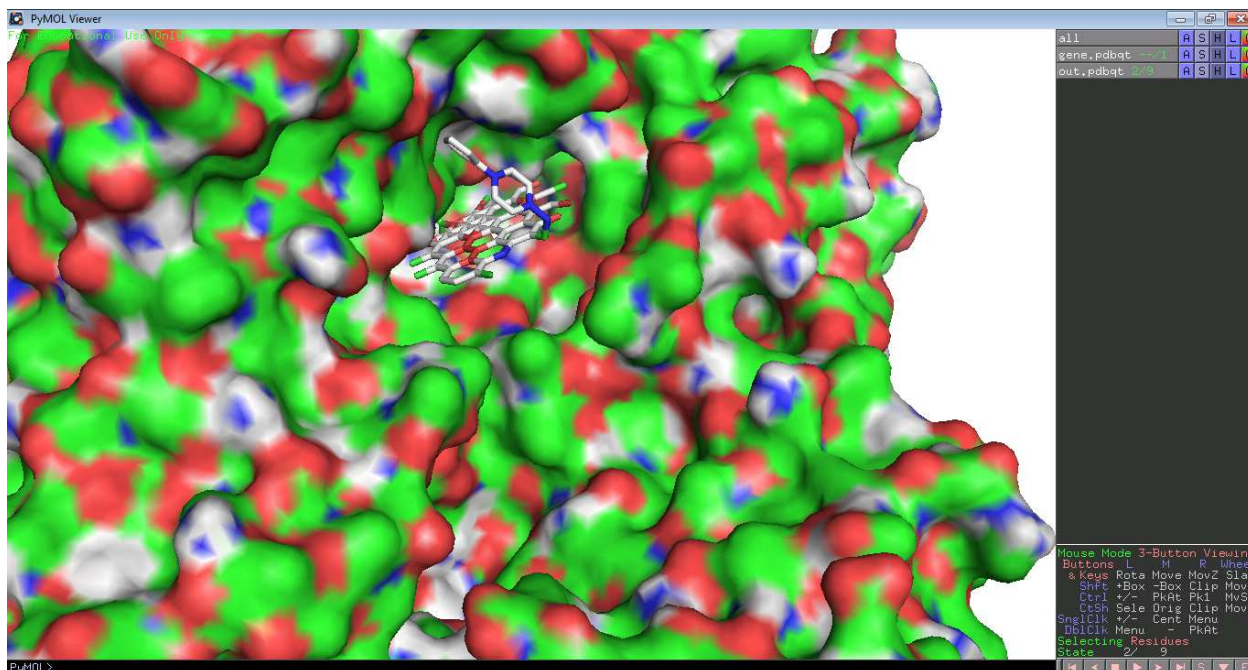


Fig15: 2CCA was docked with the ligand Rifapentine.

Docking was performed between the 6 genes and the listed ligands using the autodockvina. The software will predict the proper binding site. Further the analysis of the result was done based on the values.

| 1 | LIGANDS | 2CCA | 1P44 | 3VZ1 | 3IFZ | 1KOR | 2EYQ |
|----|------------------------------------|-------|-------|-------|-------|-------|-------|
| 2 | 5 Amino-1,3,4,thiadiazole -2 thiol | -4.6 | -3.7 | -4.4 | -3.7 | -4 | -4.1 |
| 3 | Bedaquiline | -9.8 | -8.2 | -8.2 | -9.9 | -9.3 | -8.7 |
| 4 | Delamanid | -8 | -9 | -9.7 | -9.5 | -8 | -9.2 |
| 5 | Faropenem | -8.1 | -6.6 | -6.1 | -6.3 | -7.1 | -7 |
| 6 | Isoniazid | -5.8 | -4.7 | -4.9 | -4.3 | -4.7 | -4.7 |
| 7 | Josamycin | -9.2 | -9 | -9.1 | -9.3 | -10.3 | -10.1 |
| 8 | KanamycinA | -8.1 | -9.2 | -7.4 | -7.5 | -8.2 | -9.1 |
| 9 | Levofloxacin | -7.4 | -8.9 | -6.8 | -7.1 | -7.3 | -7.7 |
| 10 | Pretomanid | -7.2 | -7.8 | -7.4 | -7.3 | -7.9 | -8.2 |
| 11 | Protionamide | -5.2 | -7 | -5.2 | -5 | -5.3 | -5.2 |
| 12 | Pyrazinamide | -5.1 | -4.8 | -5.3 | -4.2 | -4.8 | -4.6 |
| 13 | Rifapentine | -12.7 | -10.9 | -11.8 | -12.4 | -11.8 | -13.1 |
| 14 | SQ-109 | -5 | -5.1 | -6.2 | -5.1 | -6.7 | -6.8 |
| 15 | Terizidone | -7.2 | -7 | -6.6 | -6.4 | -8 | -6.7 |



3.5 ADMET PROPERTIES

| SL.NO | LIGAND NAME | PROPERTY | MODEL | RESULT | PROBABLIITY |
|-------|-------------|--------------|-----------------------------|-----------------|-------------|
| 1 | REFAPENTINE | ABSORPTION | Blood-Brain Barrier | BBB- | 0.9659 |
| | | | Human Intestinal Absorption | HIA+ | 0.66848 |
| | | DISTRIBUTION | Subcellular localisation | Mitochondria | 0.5477 |
| | | METABOLISM | CYP450IA2 Inhibitor | Non-Inhibitor | 0.8865 |
| | | TOXICITY | Carcinogens | Non-carcinogens | 0.8147 |
| 2 | JOSAMYCINE | ABSORPTION | Blood-Brain Barrier | BBB- | 0.9659 |
| | | | Human Intestinal Absorption | HIA+ | 0.5235 |
| | | DISTRIBUTION | Subcellular localisation | Mitochondria | 0.5110 |
| | | METABOLISM | CYP450IA2 Inhibitor | Non-Inhibitor | 0.9070 |
| | | TOXICITY | Carcinogens | Non-carcinogens | 0.9287 |

ADMET properties of Rifapentine and Josamycine.

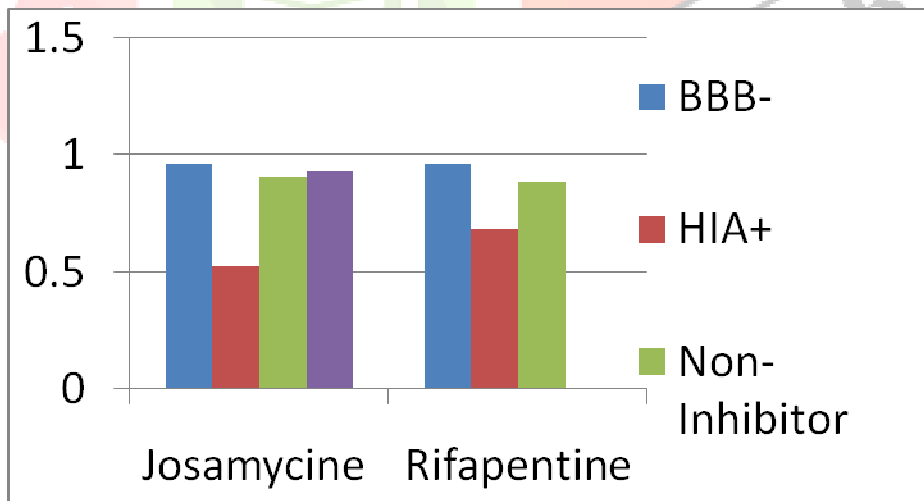


Fig16 : Result of ADMET properties.

4. CONCLUSION

Tuberculosis (TB) is caused by *Mycobacterium tuberculosis*. TB is an infectious disease that usually affects the lungs. Some strains of the TB bacteria developed resistance to the standard drugs through genetic changes and *Mycobacterium tuberculosis* (MTB) is a rod shaped bacteria that can thrive only human beings .TB is often called Multidrug resistance(MDR) or Multi drug resistance is antimicrobial resistance shown by a species of microorganisms to multiple anti-microbial drugs .MDR is most threatening to public health. MDR bacteria that is resist multiple antibiotics

A dataset of genes was reviewed using the TARGET PATHOGEN database where the characterization of the genes were carried out such that separate the characterized genes and uncharacterized genes and we concentrated on the un characterized genes for our project and among the 4000 genes we obtained 1373 characterized gens and 2627 of characterized genes.

These genes were further shortlisted to 30 genes based on their functional characteristics which were suitable for the *Mycobacterium tuberculosis*. Further to know the gene-gene interactions of these 30 genes, these genes were submitted to gene interaction analysis.

In the gene network analysis we used the STRING software to find out the gene-gene interaction where we submitted 30 genes to STRING and gene network was formed from which 6 genes were shortlisted because they had better drug interactions.

Modelling of the protein was carried out using SWISS MODEL .Among the seven genes which had better interactions, two genes did not have the structure so they were modelled using the SWISS MODEL and the template was obtained for these 2 targets.

Validation of these structures obtained from SWISS MODEL was carried out using RAMPAGE and ERRAT tool was also used for the validation of the structures.RAMPAGE showed the allowed regions and favourable regions based on which the modelled structures were validated and in ERAT tool the percentage of error and the warning percentage were given and 99% of the residues were below the threshold and 1% of which were above the threshold. Thus the modelled structures were validated.

Further the docking studies were carried out using AUTODOCK VINA software and the docking results showed that two ligands had better interaction score and those were REFAPENTINE (-13.1 kcal/mol) and JOSAMYCINE (- 10.1 kcal/mol). ADMET properties were studied using ADMET SAR software and these two ligands also showed better properties compared to other ligands and these ligands are non-carcinogenic and non-toxic.

Hence we conclude that based on the docking studies and ADMET properties ,two ligands REFAPENTINE (-13.1 kcal/mol) and JOSAMYCINE (- 10.1 kcal/mol) have shown better interactions and these can be the potential drug molecules for Tuberculosis.

ACKNOWLEDGEMENT

The Authors would like to thank CCMC-VGST (under KFIST Level 1) Govt of Karnataka , Department of Biotechnology and the management TOCE Bengaluru for the support and Infrastructure provided and for their undiminished encouragement and valuable inputs for the project.

5.REFERENCE

1. Sosa EJ, Burguener G, Lanzarotti E Target-Pathogen: a structural bioinformatic approach to prioritize drug targets in pathogens , journal nucleic acids research. published in 2018.
2. Nisha T,nair,Shefin Nisthar identification of novel drug candidate against Mycobacterium Tuberculosis Inh A protein through computer aided drug discovery, journal, Indian journal of pharmaceutical education and research. published in 2016.
3. V.R.Bollela, E.I.Nambuurete, Detection of kat G and inh A mutations to guide isoniazid and ethionamid use of drug resistant tuberculosis and journal is HHS PUBLIC ACCESS published in 2016.
4. Marva Seifert, Donald Catanzaro, Genetic mutations associated with isoniazid resistance in mycobacterium tuberculosis and the journal is PLOS ONE published in 2015.
5. Danil V Zimenkov, Olga V Antonova, Detection of second line drug resistance in mycobacterium tuberculosis using oligonucleotides microarrays and journal is BMC INFECTIOUS DISEASES and it is published in 2013.
6. Wanil Kang, Yu Pang, Current status of new tuberculosis vaccine in children and the journal is HUMAN VACCINE IMMUNOTHERAPEUTICS and it is published in 2016.
7. Marva V.J, Autodock Vina:Improving the speed and accuracy of docking with scoring function and journal is HHS PUBLIC ACCESS published in 2011.
8. Charles C Wang, System approach to tuberculosis vaccine development and journal is RESPIROLOGY published in 2013.
9. Asad Amir, Khyti Rana, M TB H37 RV , In silico drug targets, Identification by metabolic pathway analysis and the journal is INTERNATIONAL JOURNAL OF EVOLUTIONARY BIOLOGY published in 2014.
10. Mustafa AS, In silico analysis and experimental variation of M TB specific protein and peptides M TB for immunological diagnosis and vaccine development, journal MEDICAL PRINCIPLE AND PRACTICE published in 2013.
11. Beban Kai Sheng Chung, Thomas dick, In silico analysis for discovery of tuberculosis drug targets, journal ANTIMICROBIAL CHEMOTHERAPY published in 2013.
12. Edivi W Tiwemera, Natural history of tuberculosis duration and fatality of untreated pulmonary TB in HIV negative patients, journal PLOS ONE published in 2011.
13. Molebogeng X Rangaka, Controlling the seed beads of TB, Diagnosis and tereatment of TB infection, journal HSS PUBLIC ACCESS published in 2015.
14. Ragini Singh, Basanhi Ramachandran, In silico based high throughput screening for discovery of novel combinations of TB treatment, journal ANTIMICROBIAL AGENTS AND CHEMOTHERAPY published in 2015.

15. Dipendra Gurnung, String software,intelligent predictive string search algorithm, journal SCIENCE DIRECT published in 2016.
16. V.C Sheng, Comprehensive source and free tool for assessment of chemical ADMET properties, journal CHEMICAL INFORMATION AND MODELLING published in 2012.
17. David S Wishart, Comprehensive resource for in silico drug discovery and exploration, journal NUCLEIC ACID RESEARCH published in 2006.



Evaluation of bioremediation efficacy of *A.flavus* HQ010119 and *Pencillium sp.* KJ415574.1 strains in used engine oil degradation

Sriraksha H G, Drishya T D, Durgashree C, Sisira Anil, Manjunatha B K*, Praveen Kumar S V and Valarmathy K

Department of Biotechnology, The Oxford College of Engineering, Hosur Main Road, Bommanahalli, Bengaluru, 560068, Karnataka, India

Abstract: In the present paper, we report the hydrocarbon degrading ability of *A.flavus* HQ010119 and *Pencillium sp.* KJ415574.1 fungal strains in used engine oil. Parameters viz., %Total petroleum hydrocarbon (TPH) analysis, BOD,COD analysis and ability to produce biosurfactant were assessed. Among the strain tested, *A.flavus* was able to degrade 50% of hydrocarbons followed by *Pencillium sp.* 46.42% degradation after 20 days of incubation.

Keywords: Used engine oil, TPH, fungal isolates, biosurfactant

INTRODUCTION

The increase in the consumption of petroleum fractions has led to the rapid increase in the pollution of soil by used motor oil (UMO). The environment (soil and water) is highly contaminated with hydrocarbons by the disposal of used oils (engine oil, diesel or jet fuels). In today's world, oil spills at auto-mechanic workshops have been left uncared for over the years in many countries, and continuous accumulation of the oil is of high environmental concern as a result of hazard associated with it [Abdulsalam *et al.*, 2012]. The attention of researchers have shifted towards the remediation of the environment (soil and water) polluted with hydrocarbons especially the polycyclic aromatic hydrocarbons (PAHs) due to the fact that most of the PAHs causes cancer, gene mutation and are very toxic [Clemente *et al.*, 2001]. PAHs are toxic, carcinogenic and mutagenic so their presence in environment is of great concern and has deleterious effect on human health. The Release of persistent, bioaccumulative and toxic chemicals (benzene, toluene, ethylbenzene, xylene and polycyclic aromatic hydrocarbon) cause health and environmental hazards. These pollutants find their way into plant tissues, animals and human beings by the movement of hazardous constituents in the environment [Ebenezer, 2013]. Soil polluted with spent and fresh motor oil also create a serious effect on plant tissues, soil components, and its microorganisms, human and other animal health [Stephen, E. *et al.*, 2011]. Excess spillage of the oil causes fire hazards which lead to loss of lives and properties

Bioremediation is the naturally occurring process by which microorganisms transform environmental contaminants into harmless endproducts, in order to obtain the sources of carbon and energy. During the process of bioremediation, which involves the activity of microorganisms to remove pollutants, environmental parameters such as temperature, pH, oxygen and moisture content, are optimized to achieve accelerated biodegradation. Basically, there are two different approaches to bioremediation technologies, depending on the pollution situation and type of micro-organisms being used. The first is the one which involves the activation of the indigenous microflora in the polluted area by addition of nutrients and forming the best conditions of other chemical, physical and biological factor, or known as biostimulation. The second (bioaugmentation) is the one which involves the addition of oiloxidizing micro-organisms isolated from other sites, or addition of genetically engineered micro-organisms [Amund O *et al.*, 1987]

Although many species of bacteria and algae have been found to be efficient in degradation of low molecular weight hydrocarbons, for degradation of high molecular weight hydrocarbons, fungal species are preferred (Potin *et al.*, 2004). This is because use of fungi is economical since they grow on inexpensive substrates like forest and agricultural wastes. Also, fungi have the ability to produce many extracellular enzymes that can degrade a range of hydrocarbons (Vanishree *et al.*, 2014) and they can produce sufficiently large quantities of biosurfactant, which help in increasing the rate of biodegradation.

MATERIALS AND METHODS

3.1 Sample collection and Isolation of fungi:

The soil samples were collected from different localities of Western Ghats of Karnataka State, covering the oil spilled areas and the hydrocarbon degrading fungi were isolated using R2A media followed by serial dilution against protocols.

3.2 Hydrocarbon utilization studies:

Equal numbers of Erlenmeyer flasks (50/150ml) were taken, to which artificial seawater and Full strength media were added (Austin, 1993). All the flasks were autoclaved and cooled to room temperature. To each of the flasks, 2% test hydrocarbon was added. The test hydrocarbon was used Engine oil. Finally, a loop full of the pure fungal colony was inoculated into the media in aseptic conditions.

3.2.1 Biomass estimation:

After the incubation period, the biomass of inoculated strain is expected to increase significantly, which would indicate that the strain has the potential to use the test hydrocarbon as energy source, and thus multiply in number. To determine the increase in biomass, the flask weight was taken before and after incubation period.

3.2.4 Gravimetric method of % TPH analysis:

After incubation period, the concentration of residual hydrocarbons in the flasks was evaluated using gravimetric method (Al-Nasrawi, 2012; Ijah *et al.*, 1992; Bartha *et al.*, 1984). Each sample was added to separating funnel along with 10ml of petroleum ether, and shaken thoroughly. It was then allowed to settle and the organic phase containing solvent and residual hydrocarbons was collected into a pre-weighed petriplate. The petriplates were allowed to air dry for 24-48hrs, and the final weight was measured. The difference in final and initial weights was calculated, and this value was considered as weight of test. The same process was repeated for control flask, and the subtracted value was considered as weight of control. Percentage degradation of TPH was calculated as:

$$\% \text{ degradation} = \frac{\text{Weight of control} - \text{Weight of test}}{\text{Weight of control}} \times 100$$

3.2.2 Biological Oxygen Demand:

Tests for Biological Oxygen Demand in the incubated flasks were performed according to the method described by IS: 3025 (Part 44). Finally BOD level was calculated as:

$$BOD \left(\frac{mg}{L} \right) = \frac{(D_0 - D_5 - BC) \text{Volume of the diluted sample}}{\text{Volume of sample taken}}$$

Where D_0 is the initial dissolved oxygen (DO) for the diluted sample (in mL), D_5 is the dissolved oxygen (DO) at the end of 5 days for the diluted sample, BC is Blank Correction ($C_0 - C_5$ i.e. initial DO of blank – DO of blank after 5 days).

3.2.3 Chemical Oxygen Demand:

Tests for Chemical Oxygen Demand in the incubated flasks were done according to the method described by IS: 3025 (Part 58). COD was calculated as:

$$COD \left(\frac{mg}{L} \right) = \frac{(A - B \times N \times 8 \times 1000)}{\text{Volume of sample taken}}$$

Where A= Volume of Ferrous Ammonium Sulphate for blank, B= Volume of Ferrous Ammonium Sulphate for sample, N= Normality of Ferrous Ammonium Sulphate

3.2.5 UV-Visible Spectrophotometer analysis:

After gravimetric estimation, the residues from the petri plates were re-extracted using petroleum ether (2ml), and added into tubes, and analysed using UV-visible spectrophotometer. The spectra were recorded in (Thermo Evolution 201) UV/VIS spectrophotometer ranging 200-800 nm. Since the wavelength is unknown, the whole range of UV and visible wavelength (200-800nm) was analysed. For blank, the solvent (petroleum ether) was used.

3.3 Screening for biosurfactant production:

A loop full of pure culture was inoculated in a series of test tubes containing 10ml of Sabouraud Dextrose Broth (SDB) each. After incubation for 24hrs, the cultures were centrifuged at 10000 rpm for 20 minutes and the supernatant (cell free broth) was retained for further tests.

3.3.1 Emulsifying index test (E_{24}):

2mL of the used engine oil was mixed with 2mL supernatant in a test tube, and vortexed at high speed for 2 minutes. The test tubes were allowed to stand for 24 hours following which the height of the emulsion formed and the total height of the solution was measured (Suganya, 2013; Sarubbo, 2006). Emulsifying index was calculated as:

$$E_{24} = \frac{\text{Height of emulsion formed (cm)}}{\text{Total height of the solution (cm)}} \times 100$$

3.3.2 Oil dispersion test:

About 20mL of distilled water was taken in a petri plate. 2mL of the used engine oil was added, followed by the addition of 1mL of supernatant to the center. Formation of clear zones was considered as positive result (Nalini *et al.*, 2013).

3.3.3 Drop collapse test:

Single drops of used engine oil, when added to the wells of a microtitre plate develop into a dome shaped droplets. To each of the wells, 10 μ L of the supernatant was added on top of the drop of hydrocarbon. If the shape of the drop of hydrocarbon flattens, it was considered positive result (Chandran *et al.*, 2010).

3.4 Detection of Enzyme activity:

Microorganisms produce certain enzymes that catalyse the degradation process, thereby reducing the time. The activity of such enzymes is to be identified. One of such enzymes of importance for degradation studies is dehydrogenase enzyme. For the detection of dehydrogenase activity, 5g of soil sample was mixed with 5mL of 2, 3, 5-triphenyl tetrazolium chloride (TTC) and incubated for 24hrs at 37 $^{\circ}$ C. TTC solution was prepared by mixing 5 g/L of TTC with 0.2 M Tris-HCl buffer, pH 7.4. After incubation, two or three drops of concentrated H₂SO₄ were added in order to stop the reaction. It was then mixed with 5mL of hydrocarbon, mixed thoroughly, and allowed to stand for 30mins at room temperature. Later, the contents were centrifuged at 1000 RPM for 20mins. Absorbance of the extract was measured at 492 nm. Finally, the presence of dehydrogenase is said to be confirmed if the OD value is above 0.5 (Soleimani *et al.*, 2010; Cheema *et al.*, 2009).

RESULTS AND DISCUSSION

1. Gravimetric method of % TPH analysis:

Bioremediation study of used engine oil using *A.flavus* HQ010119 and *Pencillium sp.* KJ415574.1 with incubation of 20 days is presented here. Gravimetric method of % TPH analysis study revealed that *A.flavus* (BNG-05) showed 50% degradation and *Pencillium sp.* (T-2) showed 46.42% degradation (table 2), (fig 2)

2. BOD:

Measurement of consumed oxygen by aquatic microorganisms to decompose or to oxidize organic matter is analyzed. High BOD has high pollution potential if discharged untreated into a water course because it can result in severe depletion of oxygen content of the water and thus kill aquatic animals. The analysis revealed that the BOD level decreased after every five days of incubation (fig 3).

3. COD:

The requirement of dissolved oxygen for the oxidation of organic and inorganic constituents is measured. Usually cod results are typically higher than BOD values and it decreased after the bioremediation process. The chemical oxygen demand (COD) for fungal isolates inoculated with used engine oil, after every 5 days of incubation, was assessed by APHA method 5210 B. (fig 4).

4. UV analysis:

After gravimetric analysis of the residual hydrocarbons, the residues are re-extracted and the absorbance is measured using a UV-visible spectrophotometer. The maximum wavelength (λ_{max}) is given in the bracket for each sample. The change in λ_{max} value indicates the loss of conjugation and breakdown of molecular structure of oil thereby proving the degradation of used engine oil by the isolates

5. Biosurfactant analysis:

Biosurfactant can increase the surface area of hydrophobic materials, such as pesticides and other hydrocarbons in soil and water environment, thereby increasing their water solubility. Hence, the presence of surfactant may increase microbial degradation of pollutants. In emulsification test (E_{24}) it is observed that *A.flavus* and *Pencillium sp.* showed emulsification index nearby to 50%.

Drop collapse test, when an oil drop was added to the wells of a microtitre plate, it formed a dome shaped convex droplet. The ability of the biosurfactant to disturb this structure and cause it to collapse was considered as positive result. The collapsed structure appeared flat in shape, compared to the non-collapsed structure after the addition of biosurfactant produced *A.flavus* and *Pencillium sp.* (table 3). Oil dispersion test depicts the capacity of biosurfactant produced by the potent organism to disturb the surface of oil, by altering the surface tension. This is important because it can help in dispersing large droplets of oil, making them smaller and more available to the microorganisms for degradation. The ability of the biosurfactant to disturb the oil surface

is considered positive result. (Nalini *et al.*, 2013), (table 4).The results for oil dispersion test reveals the biosurfactant produced by *A.flavus* and *Pencillium sp.* which were capable of dispersing oil surface.

6. Enzyme screening

The activity of dehydrogenase enzyme was assessed by measuring the reduction of 2, 3, 5 - triphenyl tetrazolium chloride (TTC) to 1, 3, 5 - triphenyl formazan (TPF). The OD₄₉₂ values for the fungal strains were used to determine the presence or absence of the enzyme. OD values above 0.5 were considered to be positive result.Both *A.flavus* and *Pencillium sp* showed positive for the test.

Table 1: List of potent isolates used for degradation studies along their percentage of biodegradation.

| Fungal strain | 5 th day | 10 th day | 15 th day | 20 th day |
|---------------|---------------------|----------------------|----------------------|----------------------|
| BNG-05 | 18.51 | 27.7 | 41.66 | 50 |
| T-2 | 13.70 | 18.94 | 33.33 | 46.42 |

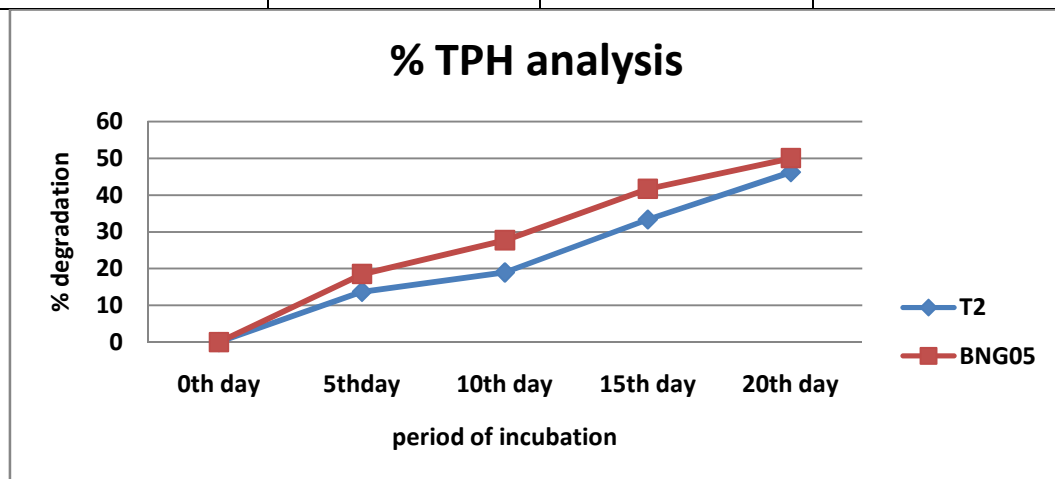


Fig 1: Day wise degradation of used engine oil by potent fungi, where graph show %TPH of all the isolates up to 20 days of incubation

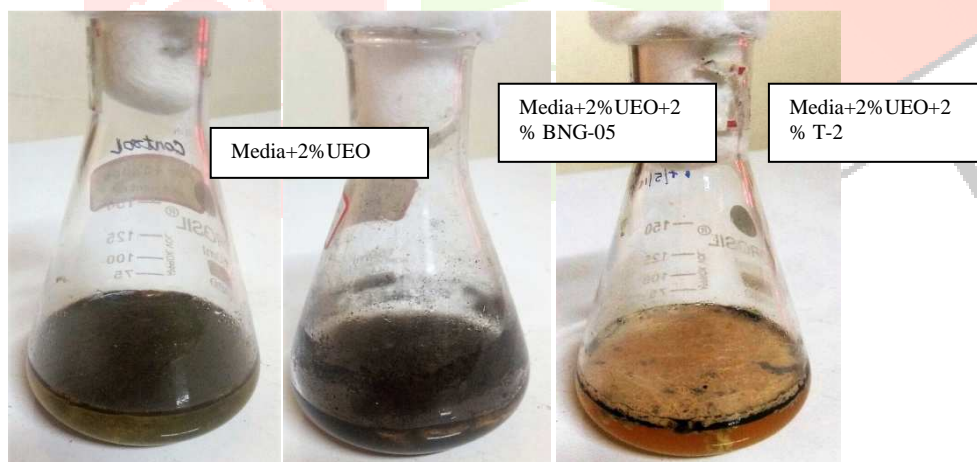


Fig 2: Degradation of used engine oil by fungal isolates BNG O5 andT-2 after 20 days of incubation

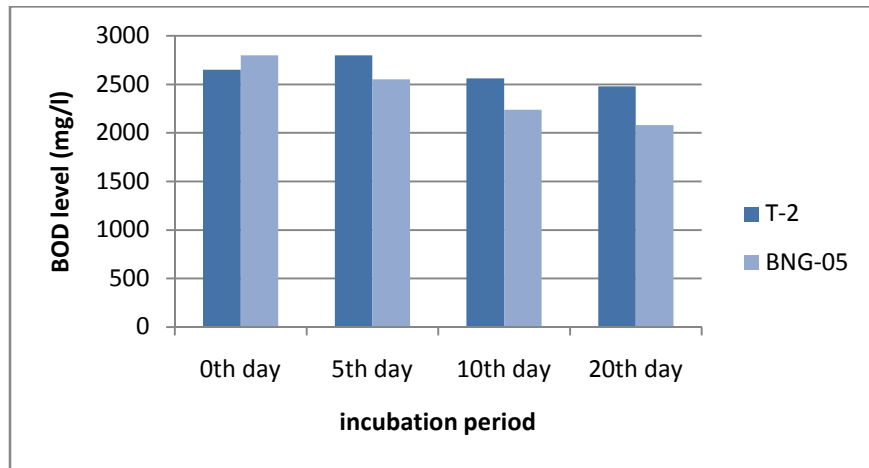


Fig 3: BOD level of fungal isolates inoculated with used engine oil after 20days of incubation

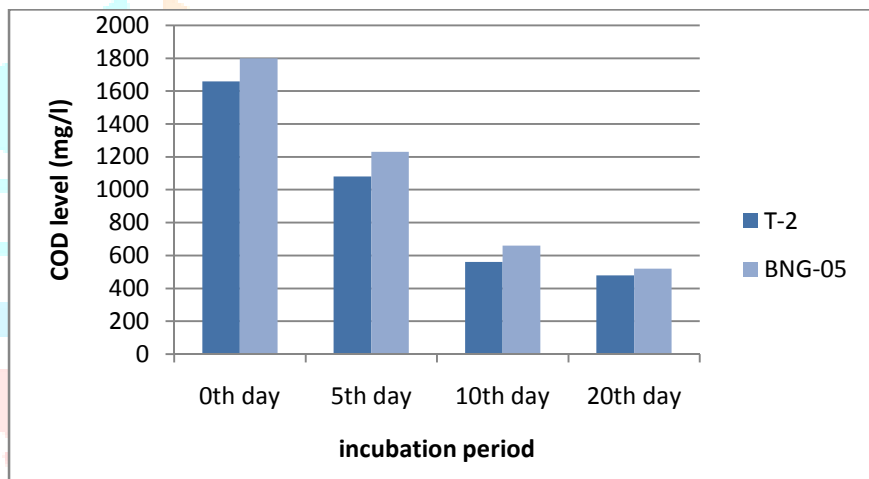
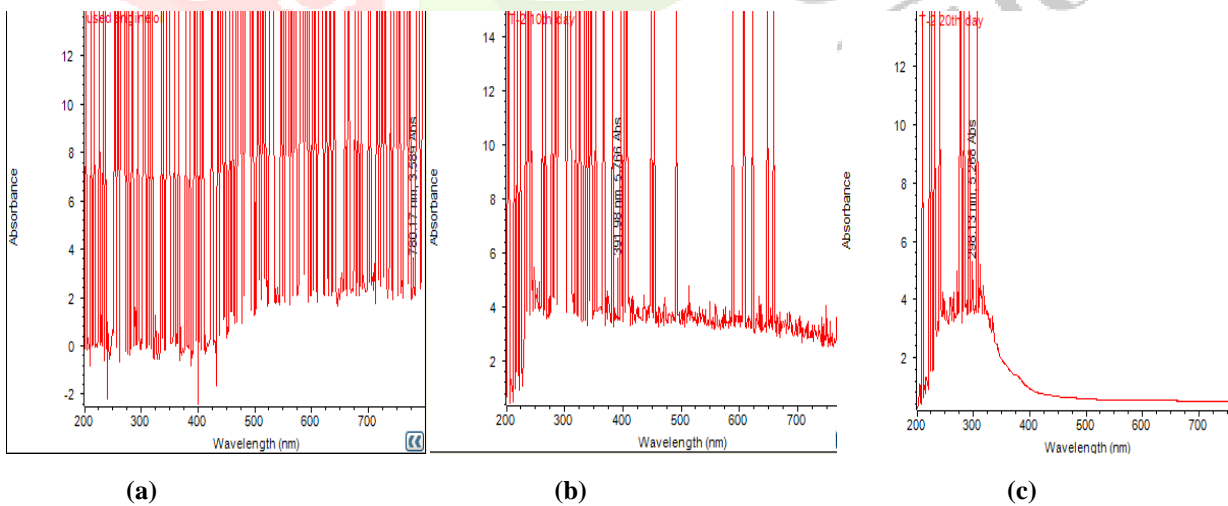
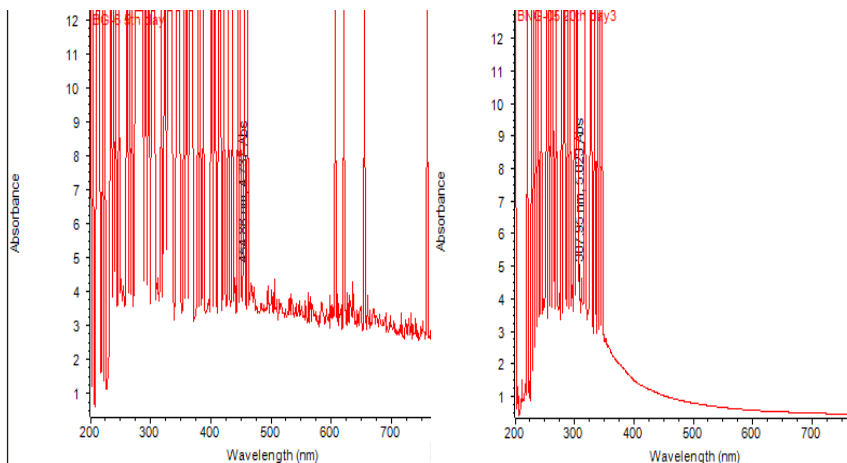


Fig 4: COD level of fungal isolates inoculated with used engine oil after 20days of incubation





(d) (e)

Fig 5 :Uv analysis for (a) used engine oil $\lambda_{max}=780nm$, test incubated with *A.flavus* (b) 5th day $\lambda_{max}=391.98nm$, (c) 20th day $\lambda_{max}=298.13nm$, test incubated with *Pencillium sp* (d) 5th day $\lambda_{max}=454.88nm$,(e) 20th day $\lambda_{max}=307.95nm$

Table 2:Emulsification test

| Sl. No. | Sample name | Emulsification layer length (cm) | Height of the solution (cm) | Emulsification index (E ₂₄ in %) |
|---------|-------------|----------------------------------|-----------------------------|---|
| 1 | T2 | 1.1 | 2.6 | 42.31 |
| 2 | BNG05 | 1.3 | 2.8 | 46.43 |

Table 3: Results for drop collapse test

| Sl. No | Sample name | Shape of drop for Engine oil |
|--------|-------------|------------------------------|
| 1 | T2 | Flat |
| 2 | BNG05 | Flat |

CONCLUSION

The present study reveals the potency of *A.flavus* HQ10119 and *Pencillium sp.* KJ415574.1 isolated from different localities of West Coast of Karnataka, to degrade used engine oil components and convert into less toxic components. Further optimization of process parameters and immobilization studies need to be undertaken to enhance the degradation in both ex-situ and in-situ environment.

ACKNOWLEDGEMENT

We would like to thank, Head of the Department. Department of Biotechnology, The Oxford College of Engineering for the infrastructure and encouragement.

REFERENCES

[1] Abdulsalam, S. Adefia, S. S. Bugaje, I. M. and Ibrahim, S, “Bioremediation of Soil Contaminated With Used Motor Oil in a Closed System,” J. Bioremediation Biodegrad., vol. 3, no. 12, pp. 3–9, 2012.
 [2] Al-Nasrawi, Hussain. 2013. “Biodegradation of Crude oil by fungi isolated from Gulf of Mexico”. J. Bioremed. Biodegrad. 3(4):1-6.
 [3] Amund OO, Adebawale AA, Ugoji EO (1987) Occurrence and characteristics of hydrocarbon utilizing bacteria in nigerian soils contaminated with spent motor oil. Indian J Microbiol 27: 63-67.
 [4] Bartha, Richard., Lanzilotta, R. P., and Pramer, David. 1966. “Stability and Effects of Some Pesticides in Soil”. Applied Microbio. 15(1):67-75.

- [5]Chandran, P., Das, N. 2011. "Characterization of sophorolipid biosurfactant produced by Yeast species grown on diesel oil". Int. J. of Science and Nature. 2:63-71.
- [6]Clemente, A. R. Anazawa, T. A. and Durrant, L. R, "Biodegradation of Polycyclic Aromatic Hydrocarbons by Soil Fungi," Brazilian J. Microbiol., vol. 32, pp. 255–261, 2001.
- [7]Ebenezer, L. A, "Bioremediation of Hydrocarbon Contaminated Soil Using Compost, NPK Fertilizer and Cattle Bile as Amendment Materials," Kwame Nkrumah University of Science and Technology, 2013.
- [8]. Ijah,U.J.J.: The potential use of chickendrop microorganisms for oil spillremediation. *The Environmentalist.*,**23**, 8995 (2003).
- [9]Nalini, S., Parthasarathi, R., Thandapani, C.M. 2013. "Isolation, Screening and characterization of biosurfactant produced by *Bacillus sp.* from automobile oil contaminated soil". Int. J. of Pharmaceutical & Biological Archives 4(1):130-135.
- [10]Potin, Olivier., Catherine Rafin, Etienne Veignie. 2004. "Bioremediation of an aged polycyclic aromatic hydrocarbons (PAHs)-contaminated soil by filamentous fungi isolated from the soil". Int. Biodeterioration & Biodegrad. 54:45 – 52.
- [11]Soleimani, Mohsen., Majid Afyuni, Mohammad Hajabbasi, A., Farshid Nourbakhsh, Mohammad Sabzalian, R., Jan Christensen, H. 2010. "Phytoremediation of an aged petroleum contaminated soil using endophyte infected and non-infected grasses". Chemosphere. 81:1084–1090.
- [12]Stephen, E. and Ijah, U. J. J, "Comparison Of Glycine Max and Sida Acuta in the Phytoremediation Of Waste Lubricating Oil Polluted Soil," Nat. Sci., vol. 9, no. 8, pp. 190–193, 2011
- [13]Suganya, R.S. 2013. "Screening Optimization and Production of Biosurfactants from *Bacillus* and *Pseudomonas* Species". Int. J. Curr Pharm Res. 5(1):19-23
- [14].Uzoamaka, G.O., T. Floretta and M.O. Florence: Hydrocarbon degradation potentials of indigenous fungal isolates from petroleum contaminated soils. *J. Phy. Nat. Sci.*, 3, 1-6 (2009).
- [15]Vanishree, M., Thatheyus, A.J., Ramya, D. 2014. "Biodegradation of petrol using fungus *Penicillium sp.*" Science Int. 2(1): 26-31.



SCREENING OF POTENTIAL PHYTOCHEMICALS FOR WOUND HEALING

¹Dr. B.K. Manjunatha*, ²Tanusree Chaudhuri, ³B.S. Rithu, ⁴K Soundarya Vadhulas, ⁵Harish.M

¹ Professor and Head of Department, ² Assistant professor, ^{3,4,5} Student
Department of Biotechnology,
The Oxford College of Engineering, Bengaluru, Karnataka-
560068, India.

Abstract: Traditional therapies, including the use of dietary components for wound healing and skin regeneration, are very common in Asian countries such as China and India. The increasing evidence of health-protective benefits of phytochemicals, components derived from plants is generating a lot of interest, warranting further scientific evaluation and mechanistic studies. Among different plants showing positive activity towards wound healing, *Capparis spinosa*-*C. spinosa* has many active constituents such as flavonoids such kaempferol and quercetin. Nature fruits of *C. spinosa* have glucose as 1-H Indole-3-acetonitrile etc, whereas *C. zeylanica* has reported to have fatty acids such as E-octodec-7enynoic acid isolated from chloroform extract of the roots. Extracts of *C. decidua* stems and flowers showed insecticidal and oviposition inhibitory activities against *Bruchus chinensis*. The phytochemical from these plant extracts were found to possess significant wound healing promoting activity. In the present study, we have identified 12 potent active constituents viz., Capparis spine, Glucocapparin, kaempferol, kaempferol-7-rhamnoside, Polyprenols, Proline betaine, Quercetin, Quercetin-3-rutinoside, Rhamnetin, Rutin, Saccharose, Sinigrin for wound healing promoting ability. These active constituents were subjected for docking study using a well established target GSK 3 Beta responsible for wound healing process in human. Our results, indicated that Capparis spine, Glucocapparin, kaempferol, Polyprenols, Quercetin, Quercetin-3-rutinoside, Rhamnetin have a potent wound healing property among other compounds. In vivo/ in vitro studies to validate the present finding and to understand the exact mechanism and potential targets of these phytochemicals are under process.

Keywords: Wound healing, Ethanol leaf extract, *C. decidua*, *C. spinosa* and *C. Zeylanica*, Antimicrobial activity, Docking.

I. INTRODUCTION

Wound infection has become a major medical distress in recent years. Wound is defined simply as the disruption of the cellular and anatomic continuity of a tissue. Wound may be originated by physical, chemical, thermal, microbial or immunological insult to the tissue. Wound healing is a structured biological process that restores tissue continuity after injury and is a combination of physical, chemical and cellular events that recreate the wounded tissue or replace it with collagen. Wound healing can be divided into three stages, including inflammation, proliferation and re-modelling and maturation phases which includes the interaction of various cells, cytokines and growth factors. The normal healing starts immediately after the injury. When blood spills at the site of injury, the blood platelets interact with collagen and other components of the extracellular matrix. This stimulates the release of clotting factors as well as essential growth factors and cytokines such as platelet-derived growth factor (PDGF) and transforming growth factor beta (TGF- β). The inflammatory phase begins after the migration of neutrophils to the wound site to clean the tissue. The fibroblasts migrate into the tissue to unfold into the proliferative phase and deposit new extracellular matrix. This new collagen matrix gets cross linked and organized.

Capparis is one of the important genus of the family Capparidaceae. Leaves of *Capparis decidua* are used as plaster for boils and swellings, to relieve tooth ache, as antidote to poison, stem bark as laxative, anthelmintic, in treating cough, asthma and inflammation, fruits in cardiac troubles, root and root bark in fever and rheumatism (Chopra, et al., 1956), fruits are known as appetizer, stem bark is used in the treatment of cardiac diseases, whole plant is used in debility, joint pains, pyorrhoea, rheumatism, skin disorders (Keshava Murthy, 1994), fruits and shoots are reported for hypolipidaemic (Purohit and Vyas, 2005), antistress and antidiabetic (Yadav, et al., 1997), anti-inflammatory activity. Leaves of *C. spinosa* are used as poultice in gout, in nervous disorders, stem bark is used in treating paralysis, rheumatism, tooth ache and tuberculosis (Keshava Murthy, 1994), root bark as tonic, diuretic, expectorant, anthelmintic, analgesic, in rheumatism, paralysis, enlarged spleen and tubercular glands (Chopra, et al., 1956), antihepatitis, anti-inflammatory, antifungal, antidiabetic, in treating chondrocytes (Panico, et al., 2005), as hypolipidaemic (Eddouks, et al., 2005), as anti-allergic and antihistaminic (Trombetta, et al., 2005), as antioxidant (Bonina, et al., 2002; Germano, et al.,

2002). The plant contains glucoside, triglucoside, rutin, pentosans, ronic acid, pectic acid and saponin (Chopra, et al., 1956), glucosinolates, fatty acid, sterol and tocopherol (Matthaus and Ozcan, 2005). Leaves of *C. zeylanica* is used in treating cholera, fruits in treating blisters and boils, roots in treating coryza, elephantiasis, hemiplegia, neuralgia, oedema, piles, pneumonia, rheumatism, snakebite, ulcer and vomiting (Keshava Murthy, 1994), as sedative, in treating cholera and stomachic, the plant contains an alkaloid, phytosterols, water soluble acids (Chopra, et al., 1956) and E-octadec-7-en-5-ynoic acid. The tribal groups of Davanagere district, Karnataka state, India use leaves of above mentioned plants in healing septic wound (Fresh leaves were ground with lime juice and mixed with one teaspoon full of honey, a thick paste so obtained is applied to septic wounds) (Manjunatha, 2002).

Critical review of the literature revealed that the wound healing potency of these plants has not been subjected to clinical evaluation. In the present study, we have identified 12 potent active constituents viz., Capparispinine, Glucocapparin, kaempferol, kaempferol-7-rhamnoside, Polyphenols, Proline betaine, Quercetin, Quercetin-3-rutinoside, Rhamnetin, Rutin, Saccharose, Sinigrin for wound healing promoting ability. These active constituents were subjected for docking study using a well established target GSK 3 Beta responsible for wound healing process in human. Our results, indicated that Capparispinine, Glucocapparin, kaempferol, Polyphenols, Quercetin, Quercetin-3-rutinoside, Rhamnetin have a potent wound healing property among other compounds. In vivo/ in vitro studies to validate the present finding and to understand the exact mechanism and potential targets of these phytochemicals are under process.

II. MATERIALS AND METHODS

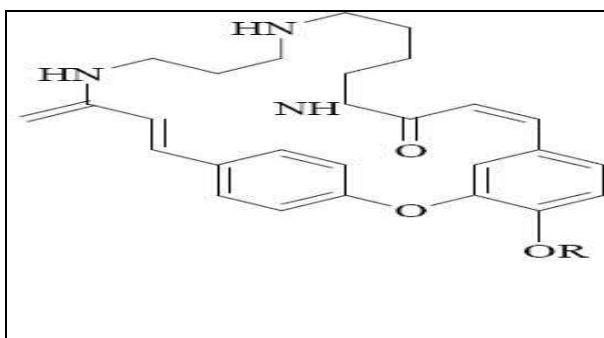
1. **Target Identification:** Glycogen synthase kinase-3 (GSK-3) is a widely expressed and highly conserved serine/threonine protein kinase encoded by 2 genes, GSK3A and GSK3B. Both Gsk3b-CKO mice and fibroblasts showed elevated expression and production of endothelin-1 (ET-1) compared with control mice and cells. Antagonizing ET-1 reversed the phenotype of Gsk3b-CKO fibroblasts and mice. Thus, GSK-3beta appears to control the progression of wound healing and fibrosis by modulating ET-1 levels. These results suggest that targeting the GSK-3beta pathway or ET-1 may be of benefit in controlling tissue repair and fibrogenic responses in vivo. So, we performed Automated docking was used to determine the orientation of inhibitors bound in the active site of GSK3-b. The protein structure file 1Q5K was taken from PDB (www.rcsb.org/pdb) was edited by removing the hetero atoms, adding C terminal oxygen (Binkowski et al., 2003).
2. **Ligand Identification:** 12 ligands namely Capparispinine, Glucocapparin, kaempferol, kaempferol-7-rhamnoside, Polyphenols, Proline betaine, Quercetin, Quercetin-3-rutinoside, Rhamnetin, Rutin, Saccharose, Sinigrin was identified through literature, which have potential wound healing activity belonging to *Capparis spp.* All ligands were searched for the three dimensional structure in the pubchem database, and nonpolar hydrogen atoms were merged in the corresponding three dimensional structure.
3. **Docking:**
 1. **Target preparation:** The following steps were followed to prepare the protein file: First the water molecules were removed from protein. Next, we need to add hydrogen because X-ray crystallography usually does not locate hydrogen; hence most PDB files do not include them. Later pdbqt file of protein was generated.
 2. **Ligand preparation:** to generate the ligand pdbqt file, the following steps were followed. In Autodock Tools, torsion tree and no of torsions were selected. And finally it was saved Save as .pdbqt
 3. **Autodock vina working protocol:** Docking studies were carried out using AUTODOCK software. AUTODOCK Vina is a suite of automated docking tools. Autodock Vina was performed in the cmd command terminal using the following command.

```
"C:\Program Files (x86)\The Scripps Research Institute\Vina\vina.exe" -- config conf.txt -- log log.txt.
```
4. **Visualization of docking results:** PyMOL and DISCOVERY STUDIO are the software used for visualization of interactions between targets and ligands. These help in finding in different types of interactions between our ligand and the target molecule.

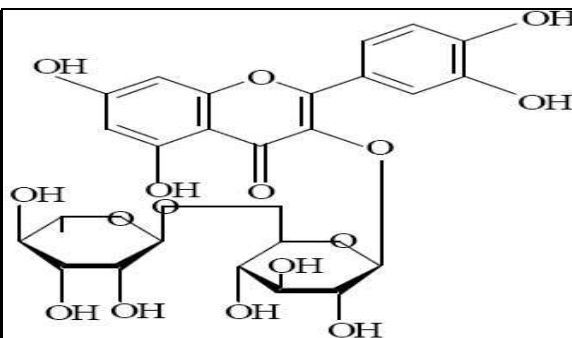
III. RESULTS AND DISCUSSION:

1. 12 ligands namely Capparispinine, Glucocapparin, kaempferol, kaempferol-7-rhamnoside, Polyphenols, Proline betaine, Quercetin, Quercetin-3-rutinoside, Rhamnetin, Rutin, Saccharose, and Sinigrin was identified through

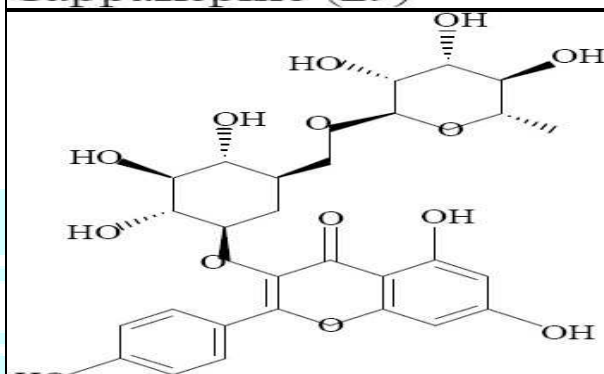
literature, which have potential wound healing activity belonging to *Capparis spp.* The structure of all the 12 ligands are as follows:



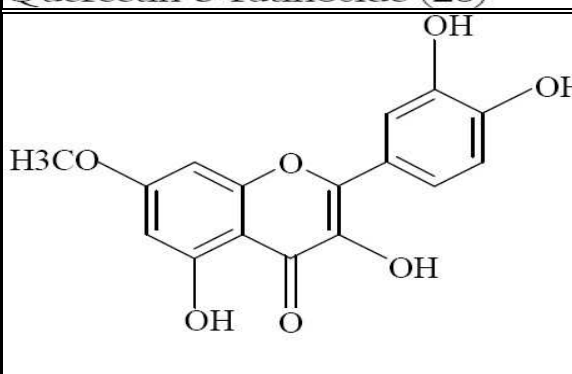
Capparispine (29)



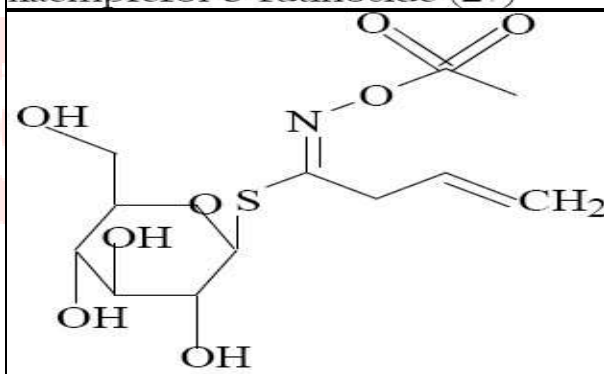
Quercetin-3-rutinoside (28)



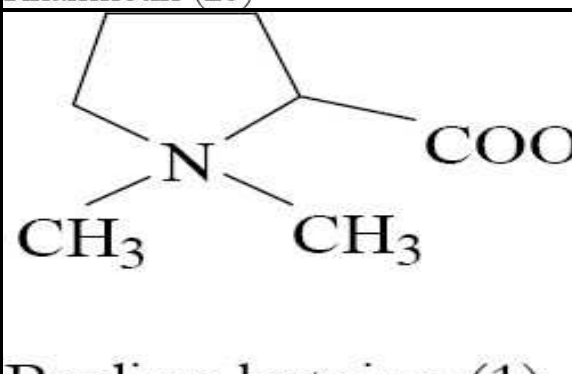
kaempferol-3-rutinoside (27)



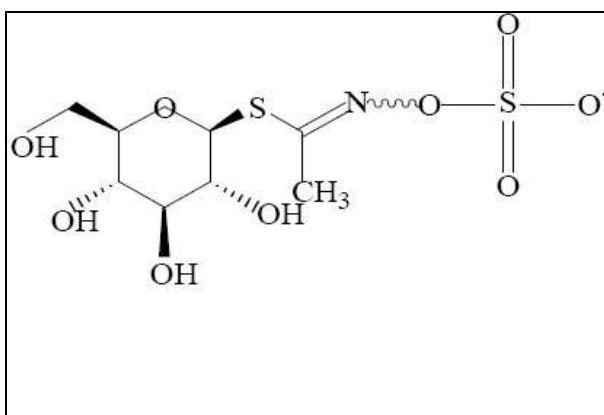
Rhamnetin (25)



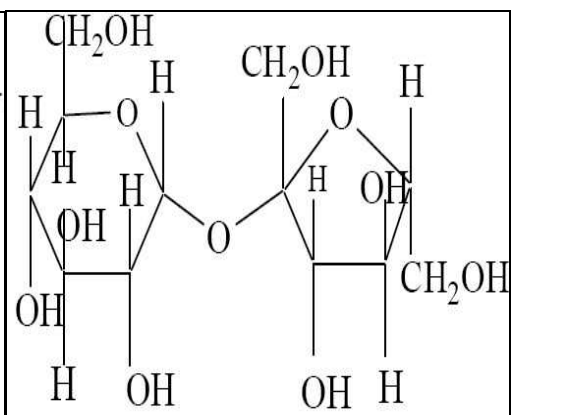
Sinigrin (44)



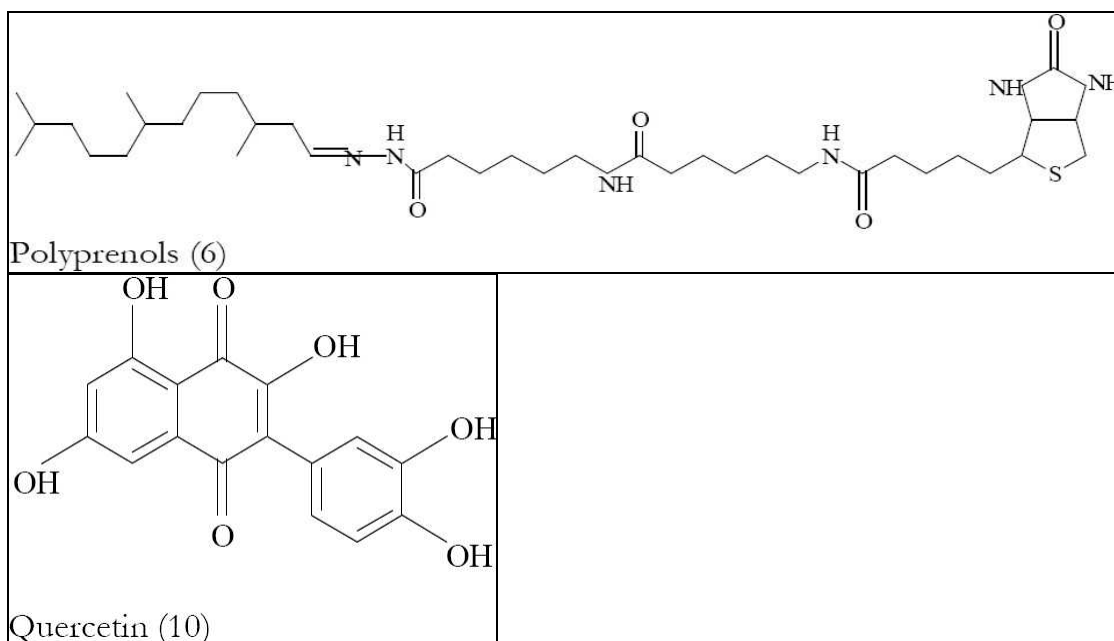
Proline betaine (1)



Glucocapparin (43)



Saccharose (7)



The protein structure file 1Q5K was taken from PDB (www.rcsb.org/pdb) was edited by removing the hetero atoms, adding C terminal oxygen is being given as follows:

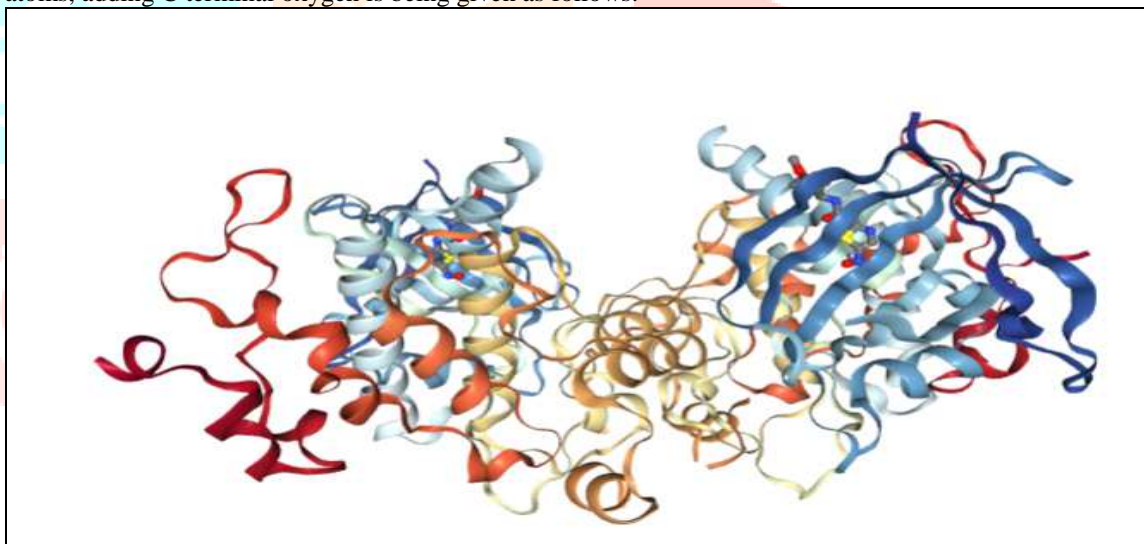


Figure1: Structure of 1Q5K protein

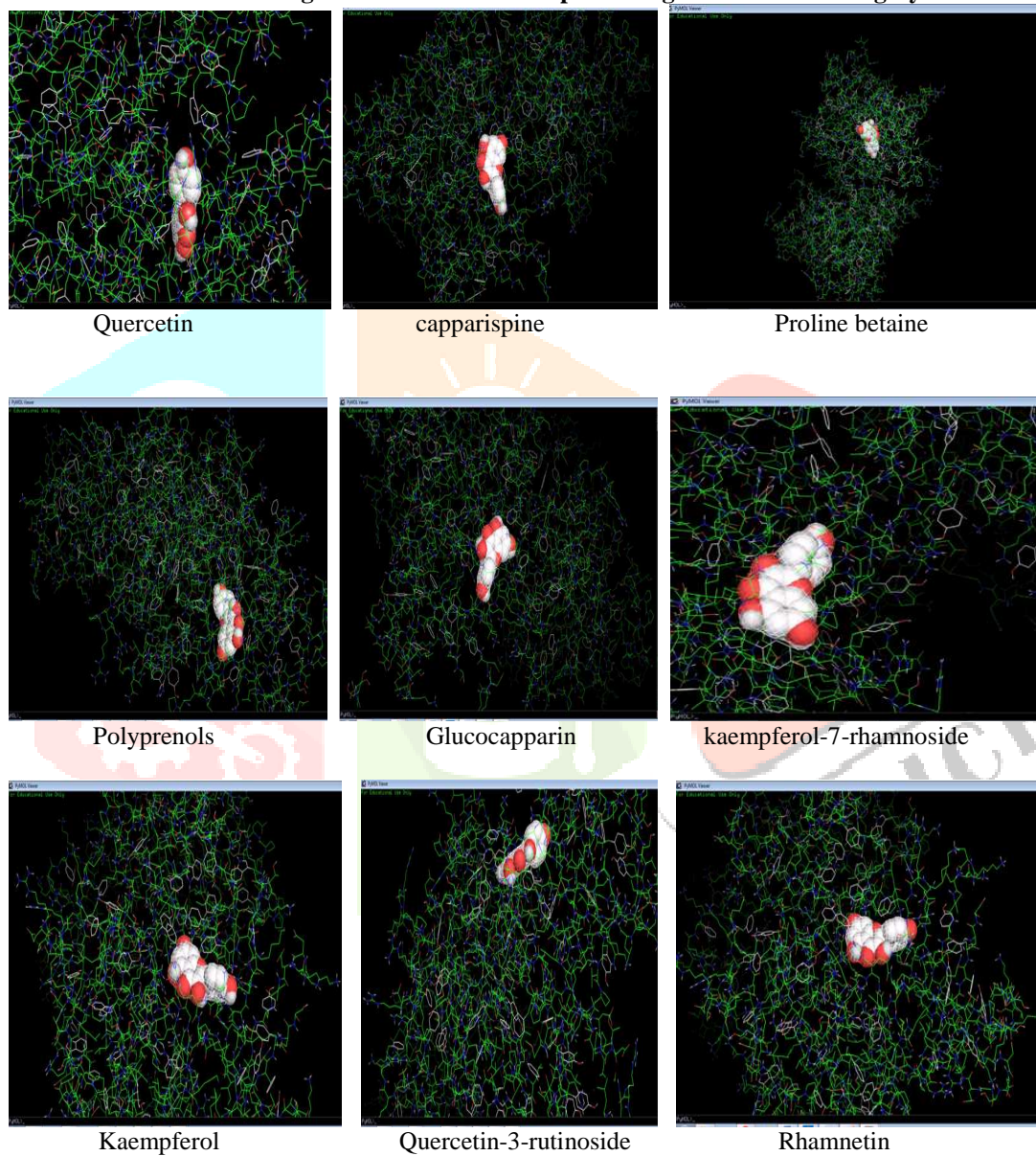
Using Autodock Vina software, docking is done and the results are obtained in the form of dlq files. These files are converted to PDBQT files and then into PDB file. Binding energy score and corresponding PDB structure is obtained for the runs. The run giving the highest negative score for estimated binding energy in kcal/mol is considered for complex file formation.

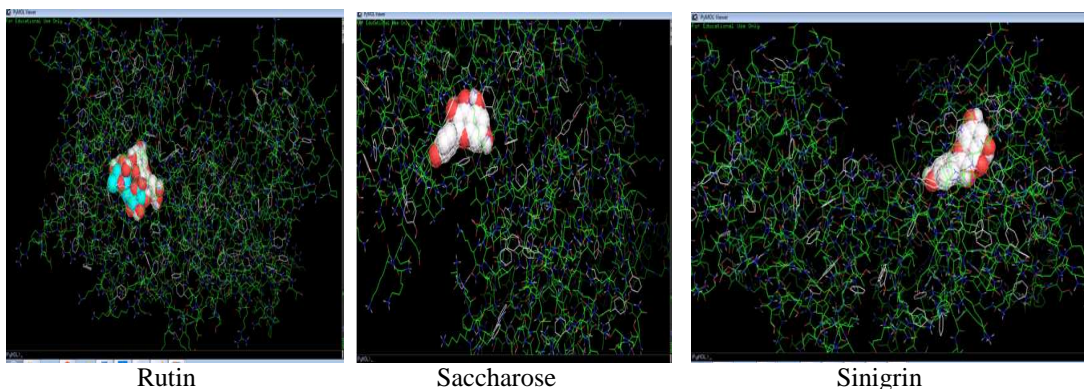
Table-1
Affinity values after Docking studies.

| Sl no. | Ligand Compounds | Affinity values |
|--------|-------------------------|-----------------|
| 1 | Capparispine | -8.4 |
| 2 | Glucocapparin | -8.4 |
| 3 | kaempferol | -8.4 |
| 4 | kaempferol-7-rhamnoside | -7.4 |
| 5 | Polyrenols | -8.4 |

| | | |
|----|------------------------|------|
| 6 | Proline betaine | -8.1 |
| 7 | Quercetin | -8.4 |
| 8 | Quercetin-3-rutinoside | -8.4 |
| 9 | Rhamnetin | -8.4 |
| 10 | Rutin | -9.1 |
| 11 | Saccharose | -8.4 |
| 12 | Sinigrin | -8.5 |

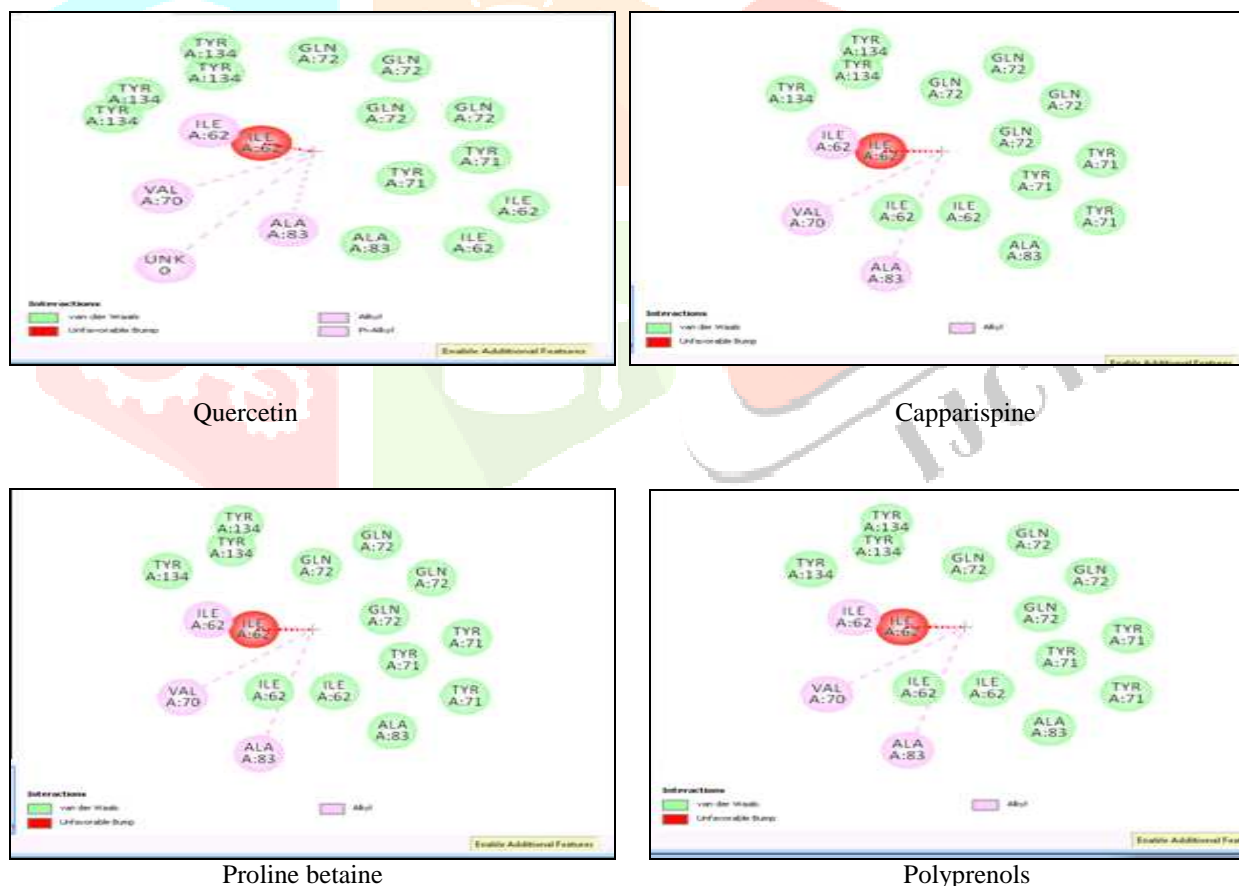
Figure 2: Visualization of protein-ligand structure using Pymol.

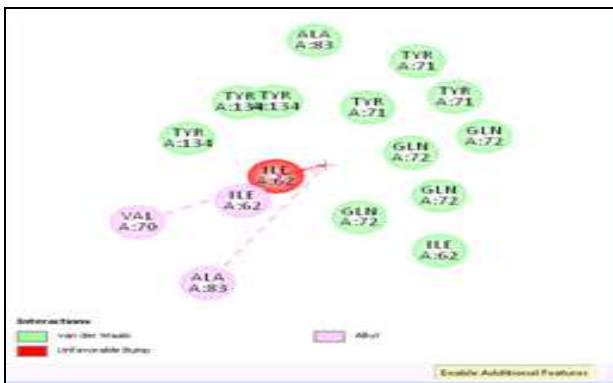




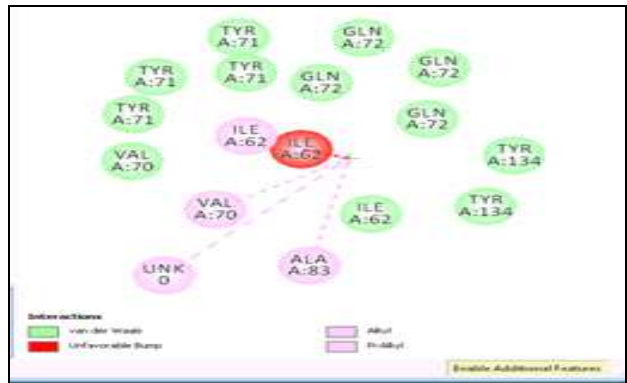
From the docked complex, pharmacophore is being identified and analyzed through protein ligand 2-D interaction. It is being observed that the Tyr and Gln are the most two important amino acids present in the active site of the target protein, making the favourable interaction with the ligand molecule.

Figure3: Protein ligand 2-D interaction of Pharmacophore

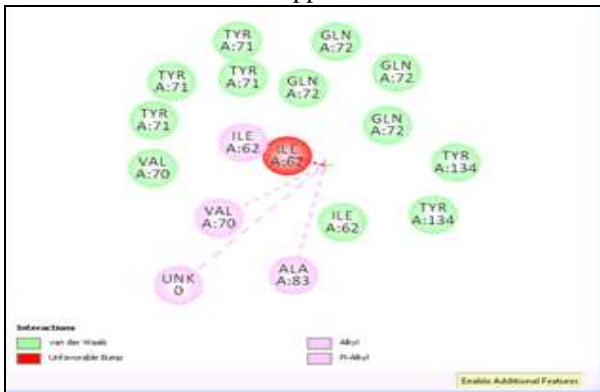




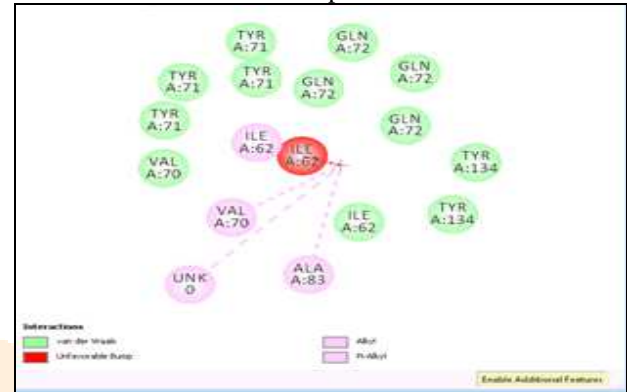
Glucocapparin



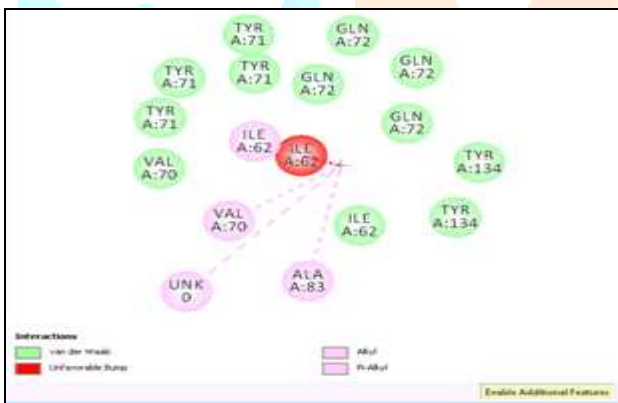
kaempferol-7-rhamnoside



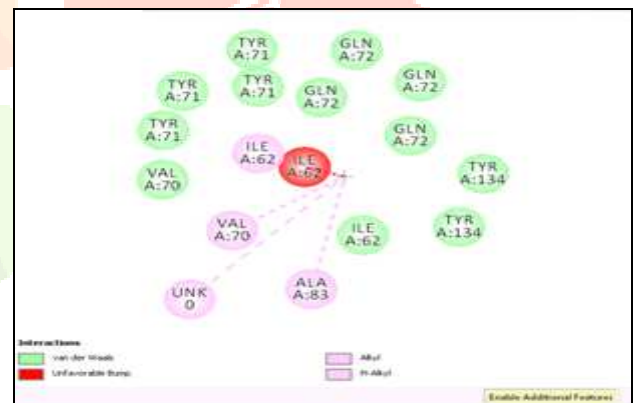
Kaempferol



Quercetin-3-rutinoside



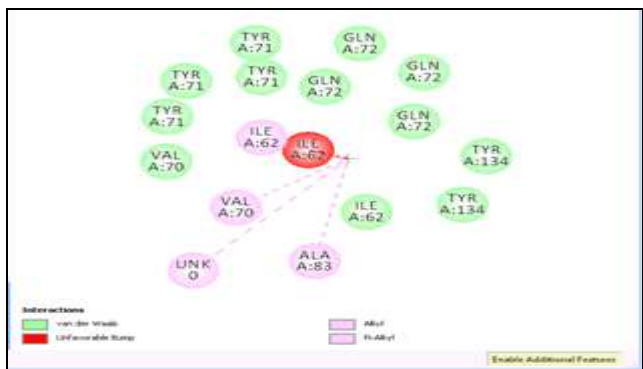
Rhamnetin



Rutin



Saccharose



Sinigrin

Table 2: Analysis of Pharmacophore

| Name | environmental definition |
|------|--------------------------|
|------|--------------------------|

| | |
|---------------------------|--------------------|
| Van der walls interaction | Val, Tyr, Gln, Ile |
| Alkyl, pi-alkyl | Val, Ile and ala |

IV. DISCUSSION

In the present investigation preliminary phytochemical analysis revealed the presence of glycosides, triterpenoids, flavonoids, alkaloids, saponins, sterols and tannins. These phytoconstituents are known to inhibit lipid peroxidation and increases the viability of collagen fibrils by increasing the strength of collagen fibers, by increasing the circulation, by preventing the cell damage and by promoting the DNA synthesis (Geite, et al., 2002). Thus wound healing potency of *C. decidua*, *C. spinosa* and *C. zeylanica* may be attributed to the antibacterial and antioxidant property of the phytoconstituents present in them which may be either due to their individual or additive effect which help the process of wound healing. Among the ligands studied for wound healing Capparispine, Glucocapparin, kaempferol, Polyphenols, Quercetin, Quercetin-3-rutinoside, Rhamnetin showed very high potential towards wound healing.

V. ACKNOWLEDGEMENTS

The authors is very grateful to Girimaji N. Raj Gopal, S.V.Thimmaiah and Prof. Darmanada Rao National Educational Society, Shimoga.

VI. REFERENCES

- Ageel, A.M., Parmar, N.S., Mossa, J.S., Al-Yahya, M.A., Al-Said, M.S. and Tariq, M., *Agents Actions*, 1986, 17(3-4), 383.
- Azad, S. 2002. Essentials of surgery. PARAS Medical Publishers, Hyderabad, India.
- Bonina, F., Puglia, C., Ventura, D., Aquino, R., Tortora, S., Sacchi, A., Saija, A., Tomaino, A., Pellegrino, M.L. and de Caprariis, P. 2002. *In vitro* antioxidant and *in vivo* photoprotective effects of a lyophilized extract of *Capparis spinosa* L. buds. *J. Cosmet. Sci.* 53(6), 321-335.
- Calis, I., Kuruuzum-Uz, A., Lorenzetto, P.A. and Ruedi, P., *Phytochem.*, 2002, 59(4), 451.
- Chopra, R.N., Nayar, S.L. and Chopra, I.C. 1956. Glossary of Indian Medicinal Plants. C.S.I.R. Publications, New Delhi.
- Ehrlich, H.P. and Hunt, T.K. 1968. Effect of cortisone and vitamin A on wound healing. *Ann. Surg.* 167, 324.
- Germano, M.P., De Pasquale, R., De Angelo, V., Catania, S., Silvari, V. and Costa, C. 2002. Evaluation of extracts and isolated fraction from *Capparis spinosa* L. buds as an antioxidant source. *J. Agric. Food Chem.* 50(5), 1168-1171.
- Getie, M., Gebre Mariam, T., Reitz, R. and Neubert, R.H. 2002. Evaluation of the release profiles of flavonoids from topical formulations of the crude extract of the leaves of *Dodonea viscosa* (Sapindaceae). *Pharmazie.* 57, 320-322.
- Haque, M.E., Haque, M., Rahman, M.M., Rahman, M.M., Khondkar, P., Wahed, M.I., Mossadik, M.A., Gray, A.I. and Sarker, S.D., *Fitoter.*, 2004, 75(2), 130.
- Keshavamurthy, K.R. 1994. Medicinal plants of Karnataka. Karnataka Forest Department (ed.), Bangalore, India.
- Kokate, C.K., Purohith, A.P. and Gokhale, S.B. 1990. Pharmacognosy. Nirali Prakashan, Pune.
- Lee, K.H. 1968. Studies on mechanism of action of salicylates, retardation of wound healing by aspirin. *J. Pharm. Sci.* 57(6), 1042-1043.
- Manjunatha, B.K. 2002. Floristic composition of davanagere district, Karnataka, India. Ph. D. Thesis, Kuvempu University, Shankaraghatta, Karnataka, India.
- Matthaus, B. and Ozcan, M. 2005. Glucosinolates and fatty acid, sterol and tocopherol composition of seed oils from *Capparis spinosa* Var. *spinosa* and *Capparis ovata* Desf. Var. *canescens* (Coss.) Heywood. *J. Agric. Food Chem.* 53 (18) 7136-7141.
- Morton, J.P. and Malone, M.H. 1972. Evaluation of vulnerary activity by an open wound procedure in rats. *Arch. Int. Pharmacodyn.* 196(6), 117-136.
- Panico, A.M., Cardile, V., Garufi, F., Puglia, C., Bonina, F. and Ronsisvalle, G. 2005. Protective effect of *Capparis spinosa* on chondrocytes. *Life Sci.* 77 (20) 2479-2488.
- Patil, M.B., Jalalpure, S.S. and Nagoor, V.S. 2004. Wound healing activity of the roots of *Eclipta alba* Linn. *Indian Drugs.* 41(1), 40-45.
- Purohit, A. and Vyas, K.B. 2005. Hypolipidaemic efficacy of *Capparis decidua* fruit and shoot extracts in cholesterol fed rabbits. *Indian J. Exp. Biol.* 43 (10) 863-866.
- Trombetta, D., Occhiuto, F., Perri, D., Puglia, C., Santagati, N.A., De Pasquale, A., Saija, A. and Bonina, F. 2005. Antiallergic and antihistaminic effect of two extracts of *Capparis spinosa* L. flowering buds. *Phytother Res.* 19 (1): 29-33.

20. Woessner, J.F. 1963. The determination of hydroxyproline in tissue and protein samples containing small proportions of the iminoacid. *Archiv. Biochem.* 93, 440-447.
21. Yadav, P., Sarkar, S. and Bhatnagar, D., *Pharmacol. Research*, 1997, 36(3), 221.



ISOLATION & CHARACTERIZATION OF METHANOGENIC BACTERIA FROM LOCAL ENVIRONMENT AND COMPARATIVE STUDY OF KINETICS WITH TRADITIONAL BIOGAS PRODUCERS.

*¹Salma Kausar.M, ²Jhansi v, ³S.Niveditha, ⁴Harshitha Ananthrama

¹Assistant Professor, ^{2,3,4}Student

Department of Biotechnology

The Oxford College of Engineering, Bangalore -560068, India

Author for correspondence

Salma Kausar.M

msalmakausar@gmail.com

Abstract: In the present study the soil samples from paddy field (kalikiri Andhra Pradesh), Karnataka compost development corporation limited (KCDC, kudlu village, Bangalore) & spent waste from floating type biogas plant were collected and methanogens were isolated, characterized & subjected to growth under anaerobic conditions by providing the kitchen and vegetable market waste as the substrate the kinetic study was carried out. A total of 16 isolates were obtained from the sample. The morphology and phenotypic characteristics were studied by performing various biochemical tests which revealed that the organism were anaerobes. Biogas production was carried out by using anaerobic digester. Paddy field and Biogas sample showed maximum production of biogas than KCDC. But mixed consortia had a very high degrading ability in very short period of time up to 92.95%.

(keywords- municipal solid waste, methanogens, anaerobic digestion, Modified Gompertz equation, biogas production)

I. INTRODUCTION

Municipal Solid Waste (MSW), commonly known as trash or garbage and as refuse or rubbish, is a waste type consisting of everyday items that are discarded by the public. "Garbage" can also refer specifically to food waste, as in a garbage disposal. The composition of municipal solid waste varies greatly from municipality to municipality,^[1] and it changes significantly with time. Biodegradable waste can be commonly found in municipal solid waste (sometimes called biodegradable municipal waste). Biodegradable waste: food and kitchen waste, green waste, paper (most can be recycled although some difficult to compost plant material may be excluded ^[2]). In the absence of oxygen, much of this waste will decay to methane by anaerobic digestion.^[3] Biodegradable waste includes any organic matter in waste which can be broken down into carbon dioxide, water, methane or simple organic molecules by micro-organisms and other living things using composting, aerobic digestion, anaerobic digestion or similar processes. Anaerobic digestion is a collection of processes by which microorganisms break down biodegradable material in the absence of oxygen.^[4] The process is used for industrial or domestic purposes to manage waste or to produce fuels. Much of the fermentation used industrially to produce food and drink products, as well as home fermentation, uses anaerobic digestion. Anaerobic digestion (AD) occurs naturally in some soils and in lake and oceanic basin sediments, where it is usually referred to as "anaerobic activity".^{[5][6]} This is the source of marsh gas methane as discovered by Alessandro Volta in 1776.^{[7][8]} The digestion process begins with bacterial hydrolysis of the input materials. Insoluble organic polymers, such as carbohydrates, are broken down to soluble derivatives that become available for other bacteria. Acidogenic bacteria then convert the sugars and amino acids into carbon dioxide, hydrogen, ammonia, and organic acids. These bacteria convert these resulting organic acids into acetic acid, along with additional ammonia, hydrogen, and carbon dioxide. Finally, methanogens convert these products to methane and carbon dioxide.^[9] The methanogenic archaea populations play an indispensable role in anaerobic wastewater treatments.^[10] Anaerobic digestion (AD) is used as part of the process to treat biodegradable waste and sewage sludge. As part of an integrated waste management system, anaerobic digestion reduces the emission of landfill gas into the atmosphere. The nutrient-rich digestate produced can be used as fertilizer. Methanogens are microorganisms that produce methane as a metabolic byproduct in anoxic {low level oxygen} conditions. They belong to the domain of archaea most of them have cell wall. They occur in 2 forms cocci, bacilli, consume H₂ & CO₂. Methanogens are responsible for marsh gas {bio gas} production. They are obligate anaerobes, extremophiles, living in the guts of cows, deep in swamps and even in the muck from sewage treatment plants. Methanogenesis or bio methanation is the formation of methane by microbes known as methanogens. Methanogenesis is sensitive to both high and low pH's and occurs between pH 6.5 and pH 8.^[11] The remaining, indigestible material the microbes cannot use and any dead bacterial remains constitute the digestate.^[12]

II. MATERIALS AND METHODS

A. Collection of samples

The samples from three different places, soil sample from paddy field(PD) of kalikiri Andhara Pradesh, fine manure sample from Karnataka compost development corporation limited(KCDC) and spent from floating type biogas plant(BG)of chikballapura were collected in sterile zip-lock plastic maintaining aseptic conditions. The collected samples were brought to the laboratory for isolation and characterization.

B. Construction of anaerobic chamber

The chamber was constructed by using polycarbonate material & anaerobic condition was maintained by complete removal of oxygen.

C. Isolation of methanogens

Methanogenic organisms were grown in Thioglycollate media^[13] by serial dilution of sample and by using pour plate & spread plate method. (Basic Practical Microbiology A Manual by Society for General Microbiology (SGM)). Identification of bacterial isolates was done on the basis of their colony characteristics on the basal media & Gram staining^[13].

D. Fluorescence test

Fluorescence is presumptive evidence for methanogenic bacteria, but definitive proof requires further characterization.^[13] To observe the presence of fluorescence, the isolated colony plates were directly placed in UV Trans-illuminator & checked for blue green fluorescence.

E. Agar deep culture

An agar deep culture produced by a deep inoculation into a solid medium (thioglycollate agar media) that is used especially for the growth of anaerobic bacteria (Harley J.P. And Prescott Lansing L.M. 2002. Laboratory Exercises in Microbiology, 5th Ed. McGraw-Hill Higher Education, New York, NY, USA). The inoculation was carried out using a sterile needle loop. The obtained isolates were subculture in liquid BM3 media.^[14]

F. Cell count and motility test

The cell count was performed by using hemocytometer and the results were recorded. Motility test was carried out using hanging drop technique to identify motile & non-motile isolates.^[13] Gram's staining was carried out for the obtained isolates in order to study their morphology (Pioneers in Medical Laboratory Science: Christian Gram 1884)^[15].

G. Biochemical tests

Biochemicals tests such as IMViC, urease, TSI, catalase, carbohydrate fermentation tests, starch test were performed in order to identify bacterial species based on the differences in the biochemical activities of bacteria.

H. Antibiotic sensitivity test

Antibiotic sensitivity test was carried out by disc diffusion technique using streptomycin (10mcg) and the results were recorded.

I. Waste collection and processing

Kitchen Waste (KW) was collected from houses of residential area (H S R layout) & vegetable market waste were collected from Madiwala vegetable market. The waste along with inoculum (3:1 ratio) was fed to screw capped pet bottles and the setup was left at room temperature for the production of biogas through AD. Cow Manure (CM) was collected from Mallela (Pileru, Andhra Pradesh). The wastes were cut into small size & blended in order to reduce size to ease the process of digestion.

J. Liquid displacement setup

A simple lab-scale experiment was fabricated using digesters. Each digester was made of plastic pet bottles. In this study the volume of produced gas was measured by water displacement method considering the volume of the generated gas equal to that of expelled water in the water collector. Each digester was connected to water chamber (plastic bottles) by a plastic pipe (gas pipe) which was used to pass the produced gas into water chamber. Another glass pipe (water pipe) was used to take the displaced water from the water chamber to the water collector which was fitted & air sealed. Both the ends of the gas pipe were inserted just at the top of the digester and the water chamber. The water pipe was inserted just bottom of the water chamber and top of water collector. The set up is illustrated in figure 1.

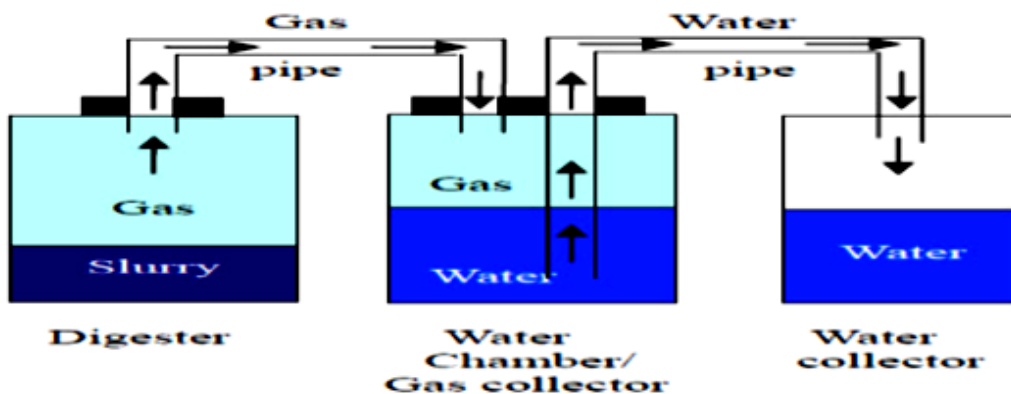


Fig 1: schematic diagram of the lab-scale experimental set-up [16]

K. Solid Analysis

- **Moisture content(MC):** The MC is the water content that is present in the reaction mixture. The water present in the reaction mixture was measured by the direct method of determination.

$$\text{Moisture Content (\%)} = \frac{W2 - W3}{W2 - W1} * 100$$

Where

W1= weight of the container; W2= weight of the container and sample before drying; W3= weight of the container and sample after drying.

- **Total solids(TS):** Total solids include both the suspended solids and the dissolved solids which are obtained by separating the solid and liquid phase by evaporation. These solids are the substrate components that will be utilized for the production of the biogas.

$$\text{Total Solids (\%)} = 100 - \text{Moisture (\%)}$$

- **Volatile Solids(VS):** the solids that remain after drying, evaporating or filtration were then ignition at 600° C. the sample turn to ash.

$$\text{Volatile solids (\%)} = \frac{W2 - W3}{W2 - W1} * 100$$

Where

W1= weight of the dish; W2= weight of the dried residue and dish; W3= weight of the residue and dish after ignition.

III. Result and Discussion

The samples were successfully collected in sterile zip-lock plastic maintaining aseptic conditions. The anaerobic chamber was constructed and anaerobic condition was maintained. The isolation of methanogens was carried out by using different dilutions of sample (10⁻², 10⁻³, 10⁻⁴). Pure cultures were selected by streaking the individual colony on TG agar plates. Pentagon streak was carried out in order to check whether the culture consists of only one organism. A total of 16 bacterial strains were identified by standard bacteriological identification procedure from the three samples. They were named as KC1-KC5 (obtained from KCDC), BG1-BG5(biogas plant) and PF1-PF6(paddy field) respectively. Microscopic examinations were carried out by gram staining and motility test. The results obtained are given in table 1.

Table1: result for cell count, gram's staining, motility test

| Sl. No. | Strain No. | Cell Count(Cells/ml) | Gram's Staining | Shape | Motility |
|---------|------------|----------------------|-----------------|---------|-------------|
| 1. | KC1 | 35*10 ⁴ | Gram Negative | Cocci | Motile |
| 2. | KC2 | 27*10 ⁴ | Gram Negative | Cocci | Motile |
| 3. | KC3 | 49*10 ⁴ | Gram Negative | Cocci | Non -Motile |
| 4. | KC4 | 50*10 ⁴ | Gram Negative | Cocci | Motile |
| 5. | KC5 | 50*10 ⁴ | Gram Negative | Cocci | Non -Motile |
| 6. | BG1 | 19*10 ⁴ | Gram Negative | Bacilli | Non- Motile |
| 7. | BG2 | 27*10 ⁴ | Gram Negative | Bacilli | Motile |
| 8. | BG3 | 24*10 ⁴ | Gram Negative | Bacilli | Motile |
| 9. | BG4 | 48*10 ⁴ | Gram Negative | Bacilli | Motile |
| 10. | BG5 | 26*10 ⁴ | Gram Negative | Bacilli | Motile |

| | | | | | |
|-----|-----|--------------------|---------------|---------|------------|
| 11. | PF1 | 21*10 ⁴ | Gram Negative | Cocci | Non-Motile |
| 12. | PF2 | 48*10 ⁴ | Gram Negative | Bacilli | Non-Motile |
| 13. | PF3 | 31*10 ⁴ | Gram Negative | Bacilli | Non-Motile |
| 14. | PF4 | 28*10 ⁴ | Gram Negative | Bacilli | Motile |
| 15. | PF5 | 48*10 ⁴ | Gram Negative | Bacilli | Non-Motile |
| 16. | PF6 | 23*10 ⁴ | Gram Negative | Cocci | Non-Motile |

a. Fluorescence test

Fluorescence test was carried out for the identification of methanogenic bacteria containing the F420 coenzyme which shows blue-green fluorescence by methanogenic bacteria and is readily distinguishable from the white-yellow fluorescence occasionally observed in non-methanogenic colonies. The strains showed no fluorescence indicating the absence of F240 co-enzyme production

b. Butt Culturing

The isolates were found to be anaerobic & few isolates developed cracks in agar indicating the gas production.

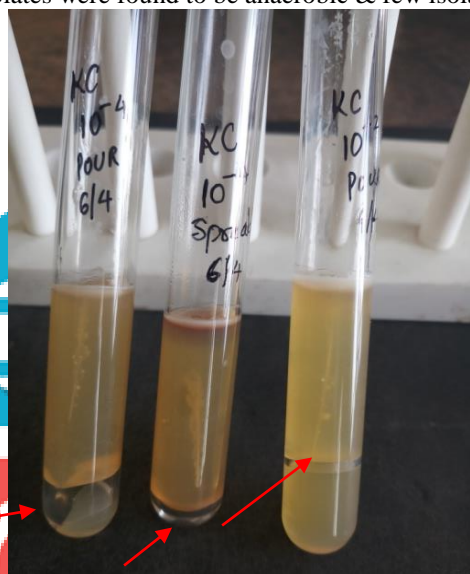


Fig2a: results for butt culture technique with gas production

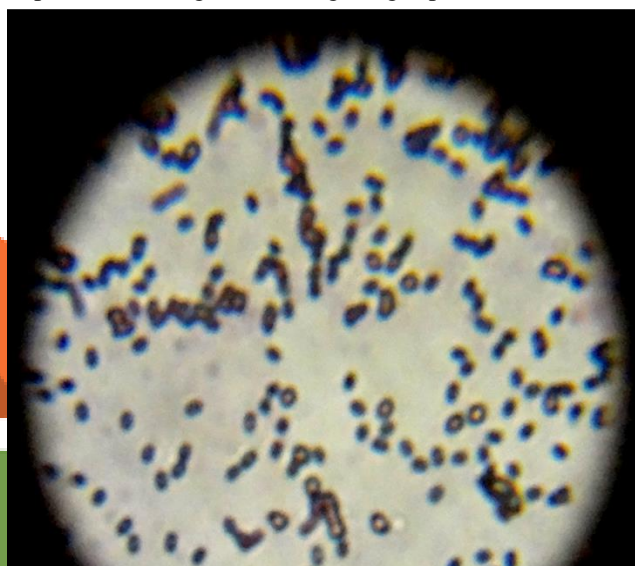


Fig 2b: results for grams staining indicating gram negative cocci shaped microbe.

c. Biochemical tests

Table 2: result for biochemical tests

| SL.NO | STRAIN NO | I | M | V | CI | C | TSI | U | CHF | SHT |
|-------|-----------|-----|-----|-----|-----|-----|-----|-----|-----|-----|
| 1 | KC1 | -ve | +ve | -ve | +ve | +ve | +ve | +ve | +ve | +ve |
| 2 | KC2 | -ve | +ve | -ve | +ve | +ve | +ve | +ve | +ve | +ve |
| 3 | KC3 | -ve | +ve | -ve | +ve | +ve | +ve | +ve | +ve | +ve |
| 4 | KC4 | -ve | -ve | -ve | +ve | -ve | +ve | +ve | +ve | +ve |
| 5 | KC5 | -ve | +ve | -ve | +ve | -ve | +ve | +ve | +ve | +ve |
| 6 | BG1 | -ve | -ve | -ve | +ve | -ve | +ve | +ve | +ve | +ve |
| 7 | BG2 | -ve | +ve | -ve | -ve | +ve | +ve | -ve | +ve | +ve |
| 8 | BG3 | -ve | +ve | -ve | +ve | +ve | +ve | -ve | +ve | +ve |
| 9 | BG4 | -ve | -ve | -ve | +ve | +ve | +ve | +ve | +ve | +ve |
| 10 | BG5 | -ve | +ve | -ve | +ve | +ve | +ve | -ve | +ve | +ve |
| 11 | PF1 | -ve | +ve | -ve | +ve | +ve | +ve | +ve | +ve | +ve |
| 12 | PF2 | -ve | +ve | -ve | +ve | -ve | +ve | -ve | +ve | +ve |

| | | | | | | | | | | |
|----|-----|-----|-----|-----|-----|-----|-----|-----|-----|-----|
| 13 | PF3 | -ve | +ve | -ve | +ve | -ve | +ve | +ve | +ve | +ve |
| 14 | PF4 | -ve | +ve | -ve | +ve | +ve | +ve | +ve | +ve | +ve |
| 15 | PF5 | -ve | +ve | -ve | +ve | +ve | +ve | +ve | +ve | +ve |
| 16 | PF6 | -ve | -ve | -ve | +ve | -ve | +ve | -ve | +ve | +ve |

I-Indole test

M-Methyl red test

V-Voges Proskauer test

CI-Citrate test

C-Catalase test

TSI-Triple Sugar Iron test

U-Urease test

CHF-Carbohydrate Fermentation Test

SHT-Starch Hydrolysis test

d. Antibiotic sensitivity test

The results of antibiotic sensitivity test are given in table3.

Table3: results of antibiotic sensitivity test

| Sl.no | Strain no | Antibiotic sensitivity | MIC(cm) |
|-------|-----------|------------------------|---------|
| 1 | KC1 | +ve | 1.8 |
| 2 | KC2 | +ve | 1.0 |
| 3 | KC3 | +ve | 2.0 |
| 4 | KC4 | -ve | 1.7 |
| 5 | KC5 | +ve | 2.05 |
| 6 | BG1 | +ve | 1.1 |
| 7 | BG2 | +ve | 1.2 |
| 8 | BG3 | +ve | 2.0 |
| 9 | BG4 | +ve | 0.9 |
| 10 | BG5 | +ve | 1.1 |
| 11 | PF1 | +ve | 1.7 |
| 12 | PF2 | +ve | 1.5 |
| 13 | PF3 | +ve | 1.8 |
| 14 | PF4 | +ve | 1.5 |
| 15 | PF5 | +ve | 1.5 |
| 16 | PF6 | +ve | 0.8 |

e. Liquid displacement

The biodegradable waste was fed into the screw capped PET bottles along with crude sample in 3:1 ratio (vegetable waste: inoculums), 4%NH₄OH, 1.5%NaOH, 4g of cow manure(CM) was added to enhance the process of gas production.1.5%NaOH is used to maintain the alkaline (6.8 to 7.2) condition. The setup was left at room temperature for 20 days. The results are tabulated as follows

Amount of liquid displaced is tabulated as

Table4: Amount of liquid displaced in ml (crude sample)

| Duration(days) | Sample 1 (PF) | Sample2(KC)* | Sample3(BG) |
|----------------|---------------|--------------|-------------|
| 0 | 860 | 0 | 30 |
| 5-10 | 35.6 | 0 | 0 |
| 10-15 | 62.95 | 0 | 542 |
| 15-20 | 10 | 57 | 90 |

*- after 20th day KCDC produced gas but other samples were already converted into organic matter.

Table 5: Amount of liquid displaced in ml (result for isolated strains)

| Sl | Strain no | Duration(days) | Liquid displaced(ml) |
|----|-----------|----------------|----------------------|
|----|-----------|----------------|----------------------|

| | | | |
|----|-----|-------|-----|
| no | | | |
| 1 | BG1 | 0-5 | - |
| | | 5-10 | - |
| | | 10-15 | - |
| | | 15-20 | - |
| 2 | BG2 | 0-5 | - |
| | | 5-10 | - |
| | | 10-15 | - |
| | | 15-20 | 6.2 |
| 3 | BG3 | 0-5 | - |
| | | 5-10 | - |
| | | 10-15 | - |
| | | 15-20 | - |
| 4 | BG4 | 0-5 | - |
| | | 5-10 | - |
| | | 10-15 | 100 |
| | | 15-20 | 250 |
| 5 | BG5 | 0-5 | - |
| | | 5-10 | - |
| | | 10-15 | - |
| | | 15-20 | 45 |
| 6 | PF1 | 0-5 | - |
| | | 5-10 | - |
| | | 10-15 | - |
| | | 15-20 | - |
| 7 | PF2 | 0-5 | - |
| | | 5-10 | - |
| | | 10-15 | - |
| | | 15-20 | - |
| 8 | PF3 | 0-5 | - |
| | | 5-10 | - |
| | | 10-15 | - |
| | | 15-20 | - |
| 9 | PF4 | 0-5 | - |
| | | 5-10 | - |
| | | 10-15 | - |
| | | 15-20 | - |
| 10 | PF5 | 0-5 | 67 |
| | | 5-10 | - |
| | | 10-15 | - |
| | | 15-20 | - |
| 11 | PF6 | 0-5 | - |
| | | 5-10 | - |
| | | 10-15 | - |
| | | 15-20 | - |

f. Solid analysis

Moisture content and Total solids(TS) were determined gravimetrically after drying in oven at 105 °C. Volatile solids (VC) content was analysed by ignition dried sample at 600 °C for 2 hours and determining the ash free dry weight.

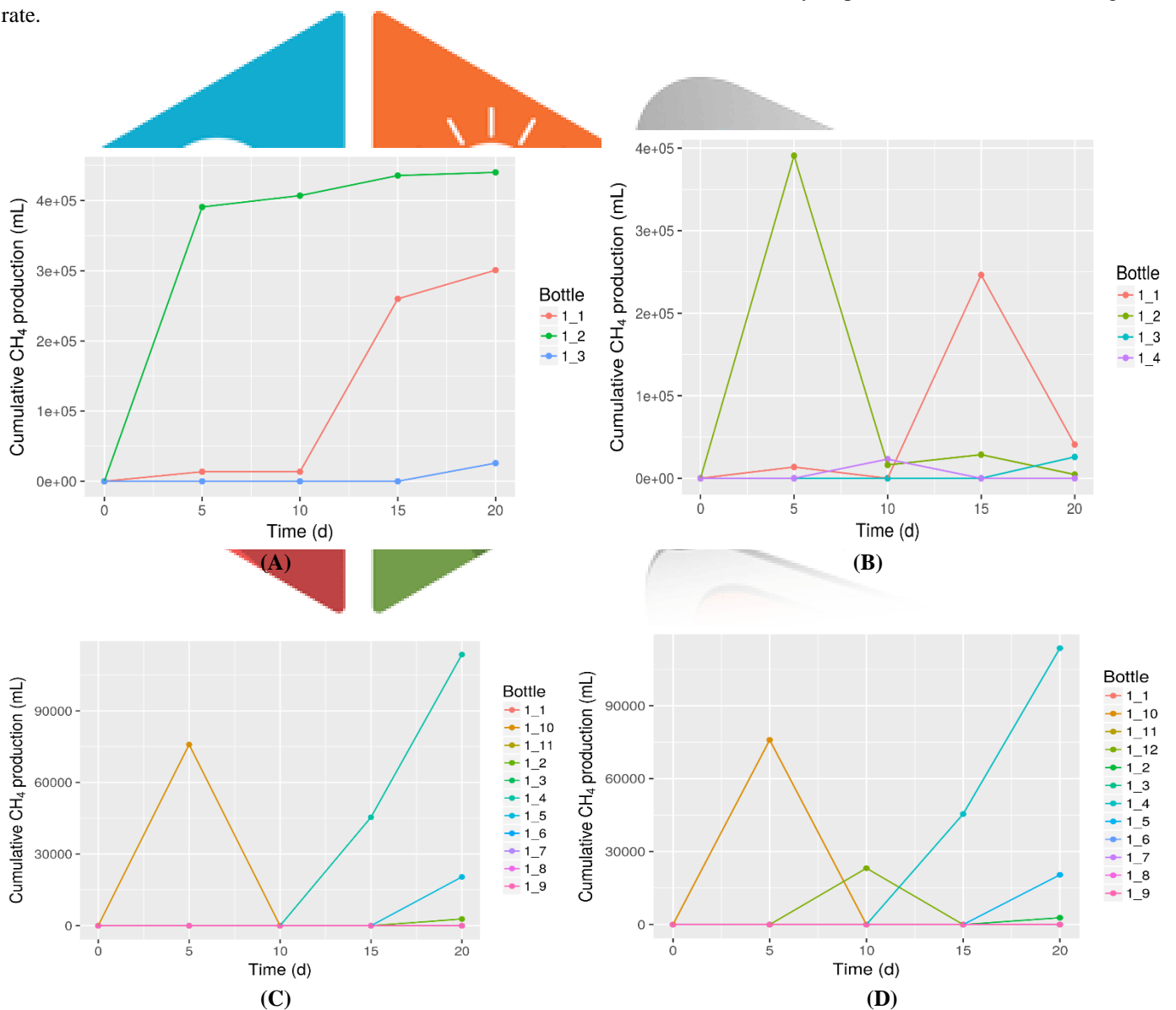
Table 6: Solid analysis of the crude sample

| SAMPLE | MC (%) | TC (%) | VC (%) |
|--------|--------|--------|--------|
| B1 | 94.4 | 5.6 | 88.14 |
| B2 | 92.03 | 7.97 | 89.71 |
| P1 | 92.7 | 7.3 | 77.05 |
| P2 | 95.60 | 4.4 | 74.29 |
| F2 | 94.9 | 5.1 | 75.55 |
| F3 | 94.7 | 5.3 | 68.42 |

Table7: Solid analysis of the isolated sample

| STRAIN | MC (%) | TC (%) | VC (%) |
|--------|--------|--------|--------|
| BG2 | 92.54 | 7.46 | 82.78 |
| BG4 | 78.93 | 6.16 | 80.59 |
| PF5 | 88.2 | 11.8 | 88.35 |
| MIX | 92.95 | 7.05 | 78.93 |

It was seen that after isolation the strain BG2 and mixed consortia (mix) had the ability to produce more amount of biogas at faster rate.



Graphs: Cumulative biogas production of (A) crude sample(1_1-BG,1_2-PF,1_3-KC) ;(B) crude sample with mix consortia(1_1-BG,1_2-PF,1_3-KC,1_4-Mix) ;(C) isolated sample (1_1to 1_5-BG,1_6 to 1_11-PF) ;(D) isolated sample with mix consortia (1_1to 1_5-BG,1_6 to 1_11-PF, 1_12-mix).

IV. Discussion

The study of biogas production from different substrate were conducted in anaerobic digester. The organisms were grown anaerobically using thioglycolate media. The morphology and phenotypic characteristics were studied by performing various biochemical tests which revealed that the organism were anaerobes. The biogas production was monitored and measured by liquid displacement study at regular intervals. A good substrate characterization is important in prediction of biogas potential from different substrates. The above graph indicates that mixed consortia had high degrading ability when compared to crude samples and isolated strains. Thus, speeding up the process of conversion of waste into organic matter. The moisture content of substrates ranged from 88% to 94%, this indicated that the substrate had enough moisture content for anaerobic digestion. The volatile solid of substrates ranged from 76% to 88%, this indicated that the substrate was rich in organic solid content that was to be converted to biogas.

V. Conclusion

It is concluded that individual strains had a potential to degrade the waste to organic matter in short period of time indicating a faster degradation rate compared to crude samples. The crude sample showed high amount of water displacement with increasing time, indicating the slow rate of degradation of waste into organic matter but higher rates of biogas production. From the graph, it was found that the mixed consortia have a high degrading ability in a short period of time. So, it can be concluded that mixed consortia gave a better result than the individual strains and can be used for speeding up the process.

VI. Acknowledgment

The satisfaction and euphoria that accompany the successful completion of any task would be incomplete without mention of the people who made it possible, whose constant guidance and encouragement crowded our efforts with success.

We would start by thanking the Chairman **Shri. S Narasimha Raju** of The Oxford College of Engineering for the opportunity, infrastructure and facilities provided for executing the work.

We thank our principal **Dr. R V Praveena Gowda** for providing necessary resources.

We thank **Dr.B.K. Manjunatha**, Professor and Head, Department of Biotechnology, The Oxford College of Engineering.

we would like to sincerely thank our guide **Ms. Salma Kausar.M**, Assistant Professor, Department of Biotechnology for her valuable suggestions without her help the completion of the project would not be possible.

We thank all faculty members of Department of Biotechnology for their necessary guidance and support. We also thank all non-teaching staff members for providing the support, help and cooperation without which the project would have been incomplete.

Our sincere thanks to all those who have directly or indirectly supported us in all aspects in bringing out this project efficiently and successfully.

We would like to thank our parents for their moral support.

Above all we thank the supreme lord for constantly helping us to overcome the hurdles and giving us the strengths to execute this project.

We would like to thank **Dr. Padma** principal The Oxford College of Pharmacy and **Ms. Sona** the faculty for their guidance.

The Authors would like to thank **Mrs.Vasantha & Mr. Obul Reddy** (owners of paddy field), the head and the staff of Karnataka compost development corporation ltd., kudlu village, **Mr. Awala Murthy** for helping us to collect the biogas plant samples.

We gratefully thank **Mr. Challa Bhaskar Reddy & Mrs. Ramadevi** for permitting us to collect the cow manure sample.

VII. References

- 1) **Kumar, Sunil; Dhar, Hiya; Nair, Vijay V.; Bhattacharyya, J. K.; Vaidya, A. N.; Akolkar, A. B. (2016).** "Characterization of municipal solid waste in high-altitude sub-tropical regions". *Environmental Technology*. 37: 2627–2637
- 2) "Organics -Green Bin". Christchurch City Council. Retrieved 19 March 2016
- 3) **CSL London Olympics Waste Review.** cslondon.org
- 4) National Non-Food Crops Centre. "NNFCC Renewable Fuels and Energy Factsheet: Anaerobic Digestion", Retrieved on 2011-11-22
- 5) **Koyama, Tadashi (1963).** "Gaseous metabolism in lake sediments and paddy soils and the production of atmospheric methane and hydrogen". *Journal of Geophysical Research*. **68** (13): 3971–3973. Bibcode:1963JGR...68.3971K.
- 6) **Pamatmat, Mario Macalalag; Bhagwat, Ashok M. (1973).** "Anaerobic metabolism in Lake Washington sediments" (PDF). *Limnology and Oceanography*. pp. 611–627. Bibcode:1973LimOc. 18..611P.
- 7) **Zehnder, Alexander J. B. (1978).** "Ecology of methane formation". In Mitchell, Ralph. *Water pollution microbiology 2*. New York: Wiley. pp. 349–376. ISBN 978-0-471-01902-2.
- 8) **MacGregor, A. N.; Keeney, D. R. (1973).** "Methane formation by lake sediments during in vitro incubations". *Journal of the American Water Resources Association (JAWRA)*. **9** (6): 1153–1158. Bibcode:1973JAWRA.
- 9) Anaerobic digestion reference sheet, waste.nl
- 10) **Tabatabaei, Meisam (2010).** "Importance of the methanogenic archaea populations in anaerobic wastewater treatments". *Process Biochemistry*. **45**: 1214–1225.
- 11) "Anaerobic Digester: How It Works [Process] | GreenTheFuture.com".
- 12) "Landfill Gas & Biogas Analyzers | Nova Gas". Nova Gas.
- 13) **S. Dash* and P. Ray (2016)** Comparative Analysis of Different Biodegradable Wastes for Better Biogas Production *International Journal of Current Microbiology and Applied Sciences* ISSN: 2319-7706 Volume 5 Number 7 (2016) pp. 576-585
- 14) **Elizabeth R. Fielding, David B. Archer, Everly Conway de Macario and Alberto J. L. Macario (1988)** Isolation and Characterization of Methanogenic Bacteria from Landfills) vol-54 pg. no 835-836
- 15) **Amrita Saha* and Subhas Chandra Santra (2014)** Isolation and Characterization of Bacteria Isolated from Municipal Solid Waste for Production of Industrial Enzymes and Waste Degradation. *J Microbiol Exp* 1(1): 00003. Volume 1 Issue 1 - 2014 Department of Environmental Science, University of Kalyani, India
- 16) **Dhadse, S., Kankal, N.C. and Kumari, B. (2012).** Study of diverse methanogenic and non-methanogenic bacteria used for the enhancement of biogas production. *Int. J. Life Sci. Biotechnol. Pharma Res*, 1.
- 17) **Aisha Khalid and Shagufta Naz, (2013)** Isolation and Characterization of Microbial Community in Biogas Production from Different Commercially Active Fermentors in Different Regions of Gujranwala Department of Biotechnology and Microbiology, Lahore College for Women University, Pakistan-*International Journal of Water Resources and Environmental Sciences* 2(2): 28-33, 2013
- 18) **Srinidhi Adiga, Ramya R., Shankar B. B., Jagadish H. Patil and Geetha C. R. (2012)** Kinetics of Anaerobic Digestion of Water Hyacinth, Poultry Litter, Cow Manure and Primary Sludge: A Comparative Study 2012 2nd International Conference on Biotechnology and Environment Management IPCBEE vol.42
- 19) **T. Edwards and B.C. McBride (1975),** New method for isolation and identification of methanogenic bacteria, *applied microbiology* vol.29, no4, p.540-545.
- 20) **Michaela Stieglmeier, Reinhard Wirth, Gerhard Kminek and Christine Moissl-Eichinger. (2009),** Cultivation of Anaerobic and Facultatively Anaerobic Bacteria from Spacecraft-Associated Clean Rooms, *applied and environmental microbiology*, p. 3484–3491 Vol. 75, No. 11
- 21) **Amrita saha and Subhas chandra Santra (2014)** Isolation and Characterization of Bacteria Isolated from Municipal Solid Waste for Production of Industrial Enzymes and Waste Degradation, Department of Environmental Science Volume 1 Issue 1, University of Kalyani, India.
- 22) **J. A Ladapo and M.A. Barlaz, (1997),** Isolation and Characterization of refuse methanogens, *Journal of applied microbiology*, **82**,751-758
- 23) **Salma A. Iqbal, Shahinur Rahaman, Mizanur Rahman, Abu Yousuf, (2014)** Anaerobic digestion of kitchen waste to produce biogas, Elsevier, *Procedia Engineering*, vol 90, 2014, pp 657-662
- 24) **Mythili Ravichandran, Prathaban Munisamy, Sharmila Devi Natarajan and Chandrasekar Varadharaju (2016)** Rare detection and identification of methanogenic bacteria from diverse ecological niches in India for carbon balance and management in our environment. Department of microbiology, K.S. Ramasamy college of arts and science, Tiruchengode, Tamilnadu.
- 25) **Bouallagui H, BenCheikh R, Marouani L, Hamdi M. Mesophilic (1992)** biogas production from fruit and vegetable waste in tubular digester, *Bioresour Technol*, pp 39-48
- 26) **Emma Kreuger, Ivo Achu and Lovisa Björnsson, (2011)** Ensiling of crops for biogas production: effects on methane yield and total solids determination, *Biotechnology for Biofuels*, 2011.

- 27) **Anthony Njuguna Matheri, Iaeng, Mohamed Belaid, Tumisang Seodigeng, and Catherine Jane Ngila. (2016)**
Modelling the kinetic of biogas production from co-digestion of pig waste and grass clippings. Proceedings of world congress on Engineering 2016 vol 2 wce, London, U.K



Construction of Cancer Diseasome through Graph Theoretical Approach

Chetan H, Shujaat Afzal, Tanusree Chaudhuri, B. K. Manjunath

Student, Student, Asst. Professor, Head of the Department

Department of Biotechnology, The Oxford College Of Engineering, Bangalore, India

Abstract

Diseasome is a collection of networks that relates human diseases with the disease causing human genes. A network of disorders and disease genes linked by known disorder–gene associations offers a platform to explore in a single graph-theoretic framework all known phenotype and disease gene associations, indicating the common genetic origin of many diseases. The Online Mendelian Inheritance in Man (OMIM) is used as the data source for disease-gene relations in Diseasome. Mouse is the primary model organism to study mammalian genetics. The genome of mouse is incisively and specifically modified and controlled to study the mutations in the human genome, to discover the molecular mechanisms of various complex human diseases such as cancers, diabetes, hereditary and neurological disorders. Researchers have already identified that, essential human genes are likely to encode hub proteins and are expressed widely in most tissues, suggesting that disease genes also would play a central role in the human interactome. In our present study we have constructed and classified the human diseasome network for cancer for the better understanding of disease gene association in different types of cancer. This project aims to map the human cancer disease network onto the mouse genotype/phenotype data pertaining to different types of cancer, by generating multi-partite networks of human cancer vs – human/mouse genes – phenotypic abnormalities observed in targeted knock-out-mouse models in cancer. The resulting networks will enrich the effort to curate specific symptoms and effects of different types of cancer to improve medical diagnosis.

Key words: Cancer, Human, Mouse, OMIM, Disease, Diseasome

I. Introduction:

Diseasome is a compilation of networks between human diseases with the genes causing disease (Goh et al., 2007). It is a network based study that relates human genetic disorders with the corresponding genes (Martisoni M et al., 2006). Genes associated with similar disorders show both higher likelihood of physical interactions between their products and higher expression profiling similarity for their transcripts, supporting the existence of distinct disease-specific functional modules (Hulbert AJ 2008). The Online Mendelian Inheritance in Man (OMIM) is used as the data source for disease-gene relations in Diseasome (Joanna S. Amberger et al., 2004). Mouse is the primary model organism to study mammalian genetics. The Genetic resemblance between mouse and human organisms is the reason behind using mouse as a model organism to study human diseases (McKusick, V.A., 1998). More than 90% of the mouse and human genomes can be divided into related conserved syntenic regions, which show the gene order in the genomes (Robert L. Perlman., 2016). The Diseasome mapping consists of multiple networks namely: the human disease network (HDN), the disease genes network (DGN) and the bi-partite human disease and gene network. In the study of, Goh et al. It was proposed that the disorders can be associated with each other using the shared disease-causing genes. The main list of Diseasome contained 1,284 disorders and 1,777 disease genes and all diseases are categorized based on 22 distinct disease classes (Olson H et al., 2000). Diseasome particularly focuses on the molecular relationships between genetic variation and phenotypic information, and it is a seminal work in terms of discovering the mechanisms of complex diseases. It is important here to note that, revealing complex disease mechanisms is one of the most crucial problems in biomedical research, currently (Botstein and Risch, 2003, Kann, 2009). It had already been stated in the literature that many human diseases occur due to the factors related to genetic variations (Hirschhorn and Daly, 2005). Up to date, various databases are constructed for annotating the relations between genes and diseases of human such as OMIM (Hamosh et al., 2005), CTDTM (Davis et al., 2010) and NHGRI-EBI GWAS catalog (Welter et al., 2013). Due to the nature of database curation process the associations are not complete, so the integration of multiple existing resources usually leads to more comprehensive view of the current biomedical knowledge.

Cancer, is one of leading cause of death worldwide. There are several analysis that have been performed, which enables the better understanding towards cancer proteomics by deciphering genetic and epigenetic data for gene regulatory networks analysis. These data has uncovered very important protein-protein interaction (PPI) pairs which are integrative part of the cancer network.

In our present study we have created a diseasome network for different types of cancer, which will eventually help us to better understand the cancer processes to identify biomarkers and therapeutic targets, and predict the prognosis of cancer in acute cancer patients.

II. Materials and methods:

2.1 DATA DOWNLOAD AND PROCESSING :

Curated morbid map file was being downloaded from Online Mendelian Inheritance in man (OMIM). Morbid Map (MM) of the OMIM is one of the most comprehensive and highly curated disorder gene association database. The OMIM MM shows the cytogenetic map location of disease genes in OMIM. The link www.omim.org is being opened up, wherein download tab in menu is selected and registration for download is done.

Two different datasets about human and mouse organisms were extracted. Dataset 1 contains the Human disease – human gene relation information and downloaded from Disasome resource and the Dataset 2 contains Mouse affected system (phenotype) – mouse gene information derived from MGI and Human data were downloaded from OMIM. Mouse genes attribute was chosen as a foreign key, to relate these two sets.

2.2 DATASET DOWNLOAD FROM DISEASOME & DATA PROCESSING:

Disasome dataset was created from curated OMIM data, that has been used as the source to constitute Dataset 1. It includes disease ID, disease name, disorder class, size (s) that show the number of associated genes, degree (k) shows number of disorder classes it connects to, class degree (K) is the number of distinct disorder classes it connects to and genes written as comma delimited at the last column.

The curated table contains the Disease ID, Disorder name, Human Gene Symbols, OMIM ID, Chromosome Position of the related gene and Disorder Class information. Disorder names were aligned in an alphabetical order and distinct consecutive numbers are given in ascending order starting from 1. These numbers are called as Disease ID and assigned for analysis in Gephi. Disorder names are distinctly ordered with their related human genes and in accordance OMIM IDs are retrieved. If a disorder has more than one genes related to it, these genes are separated with comma.

Mouse orthologues of human genes were converted and extracted with the online converter tool called as HCOP: Orthologue Predictions Search.

2.3 DATASET DOWNLOAD FROM MGI & DATA PROCESSING:

Mouse affected systems information (i.e. phenotypes) was collected from the MGI database. Collected mouse orthologue genes with HCOP were imported to the MGI batch summary tool for creating Dataset 2.

Only the targeted null/knock-out mouse genes were taken into consideration during the generation of Dataset 2.

The dataset 2 includes affected system information with unique “Mammalian phenotype ID” of all recorded mouse genes with marker symbols in that database. It also provides unique MGI IDs for these genes, allele type and allele attribute information.

2.4 Collection of Cancer data: Curated Morbid map from dataset 1 was searched rigorously for different types of cancer information. A total set of 74 different types of cancer with the involvement of 202 gene was identified. Dataset 2 was constructed for this set following the process in 2.3.

2.5 INTEGRATION OF DATA & GENERATING THE NETWORKS.

The data integration was based on connecting human diseases and mouse affected systems (i.e. phenotypes) by using mouse/human orthologous genes. We have followed the genes as nodes strategy to generate the networks.

Human diseases are indirectly connected to the mouse phenotypes (i.e. affected systems) while using mouse/human orthologous genes as the mediator. Relations in-between genes-diseases-phenotypes. Human diseases are indirectly connected to the mouse phenotypes (i.e. affected systems) while using mouse/human orthologous genes as the mediator.

III Result and Discussion:

3.1 Creation of Dataset 1:

Dataset 1 was created with required disease name corresponding disease ID, human genes, OMIM ID, Chromosome Position of the related gene and Disorder Class information. Disorder names were aligned in an alphabetical order and distinct consecutive numbers are given in ascending order starting from 1. These numbers are called as Disease ID and assigned for analysis in Gephi. The Figure 3.1 shows a screenshot the curated dataset1

| Disease ID | Disorder name | Gene symbols | OMIM ID | Chromosome | Class | |
|------------|---------------|--|---|------------|---------------|-------------------|
| 2 | 427 | Diabetes mellitus, type 1, 125853 (3) | AKT2 | 164731 | 19q13.1-q13.2 | Endocrine |
| 3 | 427 | Diabetes mellitus, type 1, susceptibility to, 125853 (3) | IFF1 | 600733 | 13q12.1 | Endocrine |
| 4 | 918 | Lung cancer, 211980 (3) | KRAS2, RASK2 | 190070 | 12p12.1 | Cancer |
| 5 | 918 | Lung cancer, 211980 (3) | PPP2R1B | 603113 | 11q22-q24 | Cancer |
| 6 | 918 | Lung cancer, 211980 (3) | SLC22A1L, BWSCR1A, IMPT1 | 602631 | 11p15.5 | Cancer |
| 7 | 918 | Lung cancer, somatic, 211980 (3) | MAP3K8, COT, EST, TPL2 | 191195 | 10p11.2 | Cancer |
| 8 | 1324 | Rheumatoid arthritis, progression of, 180300 (3) | IL10, CSF | 124092 | 1q31-q32 | Connective tissue |
| 9 | 1324 | Rheumatoid arthritis, susceptibility to, 180300 (3) | MHC2TA, C2TA | 600005 | 16p13 | Connective tissue |
| 10 | 1324 | Rheumatoid arthritis, susceptibility to, 180300 (3) | NFKB1L1 | 601022 | 6p21.3 | Connective tissue |
| 11 | 1324 | Rheumatoid arthritis, susceptibility to, 180300 (3) | PADI4, PADI5, PAD | 605347 | 1p36 | Connective tissue |
| 12 | 1324 | Rheumatoid arthritis, susceptibility to, 180300 (3) | PTPN8, PEP, PTPN22, LYP | 600716 | 1p13 | Connective tissue |
| 13 | 1324 | Rheumatoid arthritis, susceptibility to, 180300 (3) | RUNX1, CBF4A, ANK1 | 151385 | 21q22.3 | Connective tissue |
| 14 | 1324 | Rheumatoid arthritis, susceptibility to, 180300 (3) | SLC22A4, OCTN1 | 604190 | 5q31 | Connective tissue |
| 15 | 1324 | Rheumatoid arthritis, systemic juvenile, susceptibility to, MF | MF | 153620 | 22q11.2 | Connective tissue |
| 16 | 1304 | Rapid progression to AIDS from HIV1 infection (3) | CX3CR1, GFR13, V28 | 601470 | 3pter-q21 | Immunological |
| 17 | 1305 | Rapp-Hodgkin syndrome, 129400 (3) | TP73L, TP63, KET, EEC3, SHFM4, LMS, RHS | 603273 | 3q27 | multiple |
| 18 | 70 | AIDS, delayed/rapid progression to (3) | KIR3DL1, NKAT3, NKB1, AMB11, KIR3DS1 | 604946 | 19q13.4 | Immunological |
| 19 | 70 | AIDS, rapid progression to, 609423 (3) | IFNG | 147570 | 12q14 | Immunological |
| 20 | 70 | AIDS, resistance to (3) | CXCL12, SDF1 | 600835 | 10q11.1 | Immunological |
| 21 | 1043 | Mycobacterium tuberculosis, susceptibility to infection by | NRAMP1, NRAMP | 600266 | 2q35 | Immunological |
| 22 | 1400 | Sjogren-Larsson syndrome, 270200 (3) | ALDH3A2, ALDH10, SLS, FALDH | 609523 | 17p11.2 | Metabolic |
| 23 | 1454 | Stroke, susceptibility to, 1, 606799 (3) | PDE4D, DPDE3, STRK1 | 600129 | 5q12 | Cardiovascular |
| 24 | 1454 | Stroke, susceptibility to, 601367 (3) | ALOX5AP, FLAP | 603700 | 13q12 | Cardiovascular |
| 25 | 1533 | Tuberculosis, susceptibility to (3) | IFNGR1 | 107470 | 6q23-q24 | Respiratory |

FIGURE 3.1: Sample Dataset 1

For our present study, we have identified 74 different types of cancer, with 202 human genes with their OMIM Id, chromosome location.

| | A | B | C | D | E | F |
|----|------------|---|--------------------------------|---------|---------------|--------|
| | DISEASE ID | DISEASE NAME | HUMAN GENE | OMIM ID | CHROMOSOME | CLASS |
| 2 | 207 | Bladder cancer, 109800 (3) | FGFR3, ACH | 134934 | 4p16.3 | Cancer |
| 3 | 207 | Bladder cancer, 109800 (3) | KRAS2, RASK2 | 190070 | 12p12.1 | Cancer |
| 4 | 207 | Bladder cancer, 109800 (3) | RB1 | 180200 | 13q14.1-q14.2 | Cancer |
| 5 | 207 | Bladder cancer, somatic, 109800 (3) | HRAS | 190020 | 11p15.5 | Cancer |
| 6 | 228 | Breast and colorectal cancer, susceptibility to (3) | CHEK2, RAD53, CHK2, CDS1, LFS2 | 604373 | 22q12.1 | Cancer |
| 7 | 228 | Breast cancer, 114480 (3) | PK3CA | 171834 | 3q26.3 | Cancer |
| 8 | 228 | Breast cancer, 114480 (3) | PPM1D, WIP1 | 605100 | 17q22-q23 | Cancer |
| 9 | 228 | Breast cancer, 114480 (3) | SLC22A1L, BWSCR1A, IMPT1 | 602631 | 11p15.5 | Cancer |
| 10 | 228 | Breast cancer, 114480 (3) | TP53, P53, LFS1 | 191170 | 17p13.1 | Cancer |
| 11 | 228 | Breast cancer-1 (3) | BRCA1, PSCP | 113705 | 17q21 | Cancer |
| 12 | 228 | Breast cancer 2, early onset (3) | BRCA2, FANCD1 | 600185 | 13q12.3 | Cancer |
| 13 | 228 | Breast cancer (3) | TSG101 | 601387 | 11p15.2-p15.1 | Cancer |
| 14 | 228 | Breast cancer, early-onset, 114480 (3) | BRIP1, BACH1, FANCI | 605882 | 17q22 | Cancer |
| 15 | 228 | Breast cancer, invasive intraductal (3) | RAD54L, HR54, HRAD54 | 603615 | 1p32 | Cancer |

Figure 3.2: Dataset 1 for cancer diseases

3.2 Creation of Dataset 2:

Dataset 2 consists of phenotype terms with their MP ID's and targeted knock-out mouse orthologues of human genes. Human gene column again was added for the ease of understanding. This dataset is based on mouse data. Mouse affected systems information (i.e. phenotypes) was collected from the MGI database. An example dataset 2 is described in figure 3.3

| 1 MP ID | AFFECTED SYSTEM (PHENOTYPE) | MOUSE GENE | HUMAN GENE | DISEASE ID | HUMAN DISEASE | DISORDER CLASS |
|---------------|--|------------|------------|------------|----------------------------|-------------------|
| 2 MP:0002078 | abnormal glucose homeostasis | Akt2 | AKT2 | 427 | Diabetes mellitus, type II | Endocrine |
| 3 MP:0014169 | decreased brown adipose tissue mass | Akt2 | AKT2 | 427 | Diabetes mellitus, type II | Endocrine |
| 4 MP:0009356 | decreased liver triglyceride level | Akt2 | AKT2 | 427 | Diabetes mellitus, type II | Endocrine |
| 5 MP:0030022 | decreased muscle cell glucose uptake | Akt2 | AKT2 | 427 | Diabetes mellitus, type II | Endocrine |
| 6 MP:0014146 | decreased white adipose tissue mass | Akt2 | AKT2 | 427 | Diabetes mellitus, type II | Endocrine |
| 7 MP:0005378 | growth/size/body region phenotype | Akt2 | AKT2 | 427 | Diabetes mellitus, type II | Endocrine |
| 8 MP:0000316 | cellular necrosis | Kras2 | KRAS2 | 918 | Lung cancer | Cancer |
| 9 MP:0010856 | dilated respiratory conducting tubes | Kras2 | KRAS2 | 918 | Lung cancer | Cancer |
| 10 MP:0005379 | endocrine/exocrine gland phenotype | Kras2 | KRAS2 | 918 | Lung cancer | Cancer |
| 11 MP:0010771 | integument phenotype | Kras2 | KRAS2 | 918 | Lung cancer | Cancer |
| 12 MP:0010768 | mortality/aging | Kras2 | KRAS2 | 918 | Lung cancer | Cancer |
| 13 MP:0002006 | neoplasm | Kras2 | KRAS2 | 918 | Lung cancer | Cancer |
| 14 MP:0001954 | respiratory distress | Kras2 | KRAS2 | 918 | Lung cancer | Cancer |
| 15 MP:0010768 | mortality/aging | Kras2 | KRAS2 | 918 | Lung cancer | Cancer |
| 16 MP:0005387 | immune system phenotype | Pad | PAD | 1324 | Rheumatoid arthritis | Connective tissue |
| 17 MP:0004924 | abnormal behavior | Pad | PAD | 1324 | Rheumatoid arthritis | Connective tissue |
| 18 MP:0003935 | abnormal craniofacial development | Tp73l | TP73L | 1305 | Rapp-Hodgkin syndrome | multiple |
| 19 MP:0000428 | abnormal craniofacial morphology | Tp73l | TP73L | 1305 | Rapp-Hodgkin syndrome | multiple |
| 20 MP:0001672 | abnormal embryo development | Tp73l | TP73L | 1305 | Rapp-Hodgkin syndrome | multiple |
| 21 MP:0010942 | abnormal respiratory epithelium morphology | Tp73l | TP73L | 1305 | Rapp-Hodgkin syndrome | multiple |
| 22 MP:0000549 | absent limbs | Tp73l | TP73L | 1305 | Rapp-Hodgkin syndrome | multiple |
| 23 MP:0005380 | embryo phenotype | Tp73l | TP73L | 1305 | Rapp-Hodgkin syndrome | multiple |
| 24 MP:0010771 | integument phenotype | Tp73l | TP73L | 1305 | Rapp-Hodgkin syndrome | multiple |
| 25 MP:0010768 | mortality/aging | Tp73l | TP73L | 1305 | Rapp-Hodgkin syndrome | multiple |

Figure 3.3: Sample dataset for dataset 2

For this project 1567 mouse affected systems information (i.e. phenotypes) was collected from MGI report along with their MP ID's. These mouse affected systems were aligned to their corresponding human orthologs and dataset 3 was created for the construction of cancer Diseases. Figure 3.4 shows the glimpse of cancer diseases.

| MOUSE GENE | HUMAN GENE | MP ID | phenotype |
|------------|------------|------------|--|
| Mdm2 | MDM2 | MP:0005384 | cellular phenotype |
| Mdm2 | MDM2 | MP:0006043 | decreased apoptosis |
| Mdm2 | MDM2 | MP:0001262 | decreased body weight |
| Mdm2 | MDM2 | MP:0000333 | decreased bone marrow cell number |
| Mdm2 | MDM2 | MP:0001698 | decreased embryo size |
| Mdm2 | MDM2 | MP:0002875 | decreased erythrocyte cell number |
| Mdm2 | MDM2 | MP:0005378 | growth/size/body region phenotype |
| Egfr | EGFR | MP:0002161 | abnormal fertility/fecundity |
| Egfr | EGFR | MP:0000763 | abnormal filiform papillae morphology |
| Egfr | EGFR | MP:0006257 | abnormal fungiform papillae morphology |
| Egfr | EGFR | MP:0008325 | abnormal gonadotroph morphology |
| Braf | BRAF | MP:0002182 | abnormal astrocyte morphology |
| Braf | BRAF | MP:0000297 | abnormal atrioventricular cushion morphology |
| Braf | BRAF | MP:0010029 | abnormal basicranium morphology |
| Braf | BRAF | MP:0001614 | abnormal blood vessel morphology |
| Braf | BRAF | MP:0001777 | abnormal body temperature homeostasis |
| Braf | BRAF | MP:0004259 | small placenta |
| Braf | BRAF | MP:0001209 | spontaneous skin ulceration |
| Braf | BRAF | MP:0005426 | tachypnea |
| ErbB2 | ERBB2 | MP:0000920 | abnormal myelination |
| ErbB2 | ERBB2 | MP:0003871 | abnormal myelin sheath morphology |

Figure 3.4 : dataset 2 for Cancer

3.4 Construction of Dataset 3:

Dataset 1 and Dataset 2 were merged by integrating the human and mouse data tables to create Dataset 3. A link was established between human and mouse data using the targeted knock-out mouse orthologues of human genes. A sample dataset 3 is shown in figure 3.5.

| MP ID | AFFECTED SYSTEM (PHENOTYPE) | MOUSE GENE | HUMAN GENE | DISEASE ID | HUMAN DISEASE | DISORDER CLASS |
|------------|--|------------|------------|------------|----------------------------|-------------------|
| MP:0002078 | abnormal glucose homeostasis | Akt2 | AKT2 | 427 | Diabetes mellitus, type II | Endocrine |
| MP:0014169 | decreased brown adipose tissue mass | Akt2 | AKT2 | 427 | Diabetes mellitus, type II | Endocrine |
| MP:0009356 | decreased liver triglyceride level | Akt2 | AKT2 | 427 | Diabetes mellitus, type II | Endocrine |
| MP:0030022 | decreased muscle cell glucose uptake | Akt2 | AKT2 | 427 | Diabetes mellitus, type II | Endocrine |
| MP:0014146 | decreased white adipose tissue mass | Akt2 | AKT2 | 427 | Diabetes mellitus, type II | Endocrine |
| MP:0005378 | growth/size/body region phenotype | Akt2 | AKT2 | 427 | Diabetes mellitus, type II | Endocrine |
| MP:0000316 | cellular necrosis | Kras2 | KRAS2 | 918 | Lung cancer | Cancer |
| MP:0010856 | dilated respiratory conducting tubes | Kras2 | KRAS2 | 918 | Lung cancer | Cancer |
| MP:0005379 | endocrine/exocrine gland phenotype | Kras2 | KRAS2 | 918 | Lung cancer | Cancer |
| MP:0010771 | integument phenotype | Kras2 | KRAS2 | 918 | Lung cancer | Cancer |
| MP:0010768 | mortality/aging | Kras2 | KRAS2 | 918 | Lung cancer | Cancer |
| MP:0002006 | neoplasm | Kras2 | KRAS2 | 918 | Lung cancer | Cancer |
| MP:0001954 | respiratory distress | Kras2 | KRAS2 | 918 | Lung cancer | Cancer |
| MP:0010768 | mortality/aging | Kras2 | KRAS2 | 918 | Lung cancer | Cancer |
| MP:0005387 | immune system phenotype | Pad | PAD | 1324 | Rheumatoid arthritis | Connective tissue |
| MP:0004924 | abnormal behavior | Pad | PAD | 1324 | Rheumatoid arthritis | Connective tissue |
| MP:0003935 | abnormal craniofacial development | Tp73l | TP73L | 1305 | Rapp-Hodgkin syndrome | multiple |
| MP:0000428 | abnormal craniofacial morphology | Tp73l | TP73L | 1305 | Rapp-Hodgkin syndrome | multiple |
| MP:0001672 | abnormal embryo development | Tp73l | TP73L | 1305 | Rapp-Hodgkin syndrome | multiple |
| MP:0010942 | abnormal respiratory epithelium morphology | Tp73l | TP73L | 1305 | Rapp-Hodgkin syndrome | multiple |
| MP:0000549 | absent limbs | Tp73l | TP73L | 1305 | Rapp-Hodgkin syndrome | multiple |
| MP:0005380 | embryo phenotype | Tp73l | TP73L | 1305 | Rapp-Hodgkin syndrome | multiple |
| MP:0010771 | integument phenotype | Tp73l | TP73L | 1305 | Rapp-Hodgkin syndrome | multiple |
| MP:0010768 | mortality/aging | Tp73l | TP73L | 1305 | Rapp-Hodgkin syndrome | multiple |

Figure 3.5: Sample Dataset 3

Again, we have created a dataset 3 for the construction of cancer diseaseome with name of different types of cancer, disease ID(3 is specified for cancer), phenotype, mouse and human gene, MP ID's . Figure 3.6 shows the cancer diseaseome

| MP ID | MOUSE GENE | HUMAN GENE | HUMAN DISEASE | phenotype | CLASS |
|------------|------------|------------|---|---|--------|
| MP:0005384 | Mdm2 | MDM2 | Accelerated tumor formation, susceptibility to (3) | cellular phenotype | CANCER |
| MP:0006043 | Mdm2 | MDM2 | Accelerated tumor formation, susceptibility to (3) | decreased apoptosis | CANCER |
| MP:0001262 | Mdm2 | MDM2 | Accelerated tumor formation, susceptibility to (3) | decreased body weight | CANCER |
| MP:0000333 | Mdm2 | MDM2 | Accelerated tumor formation, susceptibility to (3) | decreased bone marrow cell number | CANCER |
| MP:0001698 | Mdm2 | MDM2 | Accelerated tumor formation, susceptibility to (3) | decreased embryo size | CANCER |
| MP:0002875 | Mdm2 | MDM2 | Accelerated tumor formation, susceptibility to (3) | decreased erythrocyte cell number | CANCER |
| MP:0005378 | Mdm2 | MDM2 | Accelerated tumor formation, susceptibility to (3) | growth/size/body region phenotype | CANCER |
| MP:0002161 | Egfr | EGFR | Adenocarcinoma of lung, response to tyrosine kinase inhib | abnormal fertility/fecundity | CANCER |
| MP:0000763 | Egfr | EGFR | Adenocarcinoma of lung, response to tyrosine kinase inhib | abnormal filiform papillae morphology | CANCER |
| MP:0006257 | Egfr | EGFR | Adenocarcinoma of lung, response to tyrosine kinase inhib | abnormal fungiform papillae morphology | CANCER |
| MP:0008325 | Egfr | EGFR | Adenocarcinoma of lung, response to tyrosine kinase inhib | abnormal gonadotroph morphology | CANCER |
| MP:0002182 | Braf | BRAF | Adenocarcinoma of lung, somatic, 211980 (3) | abnormal astrocyte morphology | CANCER |
| MP:0000297 | Braf | BRAF | Adenocarcinoma of lung, somatic, 211980 (3) | abnormal atrioventricular cushion morphol | CANCER |
| MP:0010029 | Braf | BRAF | Adenocarcinoma of lung, somatic, 211980 (3) | abnormal basicranium morphology | CANCER |
| MP:0001614 | Braf | BRAF | Adenocarcinoma of lung, somatic, 211980 (3) | abnormal blood vessel morphology | CANCER |
| MP:0001777 | Braf | BRAF | Adenocarcinoma of lung, somatic, 211980 (3) | abnormal body temperature homeostasis | CANCER |
| MP:0004259 | Braf | BRAF | Adenocarcinoma of lung, somatic, 211980 (3) | small placenta | CANCER |
| MP:0001209 | Braf | BRAF | Adenocarcinoma of lung, somatic, 211980 (3) | spontaneous skin ulceration | CANCER |
| MP:0005426 | Braf | BRAF | Adenocarcinoma of lung, somatic, 211980 (3) | tachypnea | CANCER |
| MP:0000920 | ErbB2 | ERBB2 | Adenocarcinoma of lung, somatic, 211980 (3) | abnormal myelination | CANCER |
| MP:0003871 | ErbB2 | ERBB2 | Adenocarcinoma of lung, somatic, 211980 (3) | abnormal myelin sheath morphology | CANCER |

Figure 3.6: Cancer Dataset 3

3.5 Clustering and analysis of the network:

The network visualisation was done in gephi tool. The disease names were taken as nodes and the edges was for assigned for the phenotypes. The network for different types of cancer was created, which has been shown in figure 3.7. In this figure the genes partening to different types of cancer is used as the nodes, and phenotypes for cancer is being used as the edges. After analysis of the network it is being observed a very high modularity in cancer phenotypes. Specially the genes, that are present at the core of the network shows similar kind of phenotypes rather than the nodes present on the surface of the network.

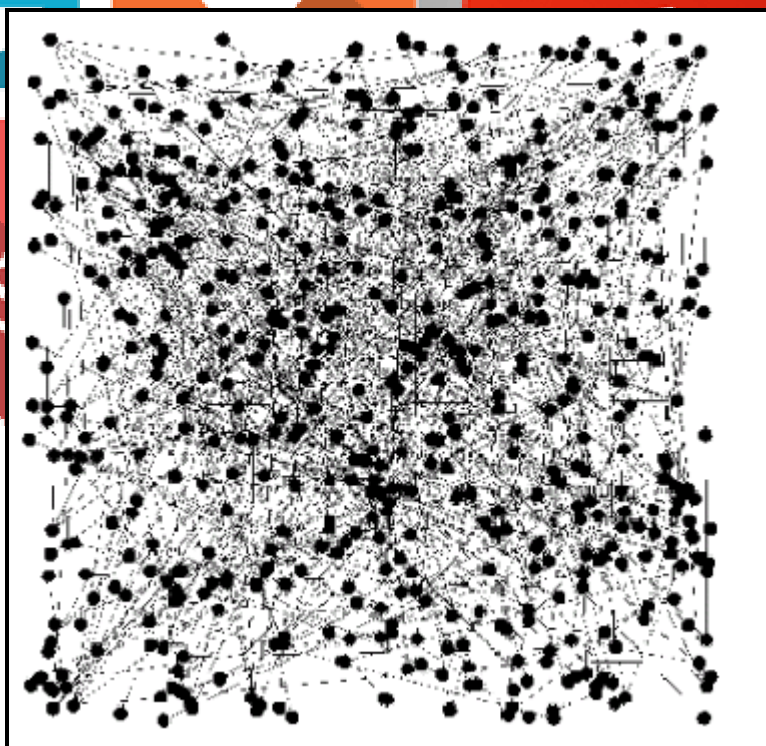


Figure 3.7 Cancer Diseaseome.

So, to analyze the genes present in the network, we have reconstructed the network only with the genes as nodes without edges. This time we have used a unique color code for the genes. The color code is shown in figure 3.8(a). The network is reconstructed using the color code in 3.8(b). In this new network it is being observed that KRAS2 is the gene that shows majority of the phenotypes in cancer (Fig 3.8 a)

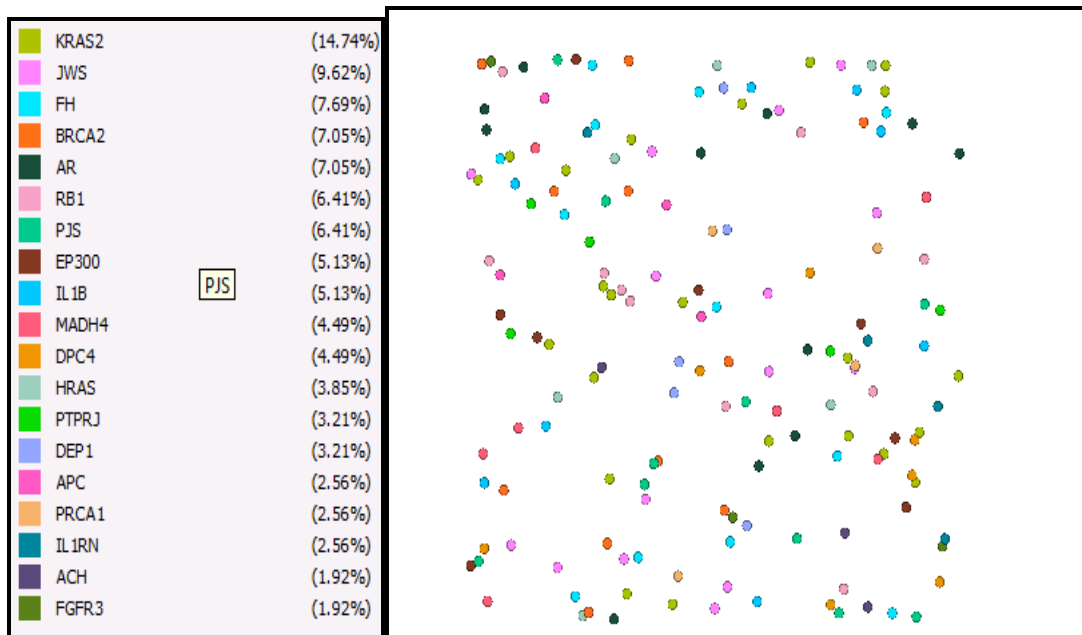


Figure 3.8: a) colour codes of genes. b) network constructed according to the colour code.

So, to analyze, the core part of the network more intensely as well as the phenotypes associated with it, we decided to break the main network into different modules. Figure 3.9 shows the modularity in the cancer network. After analysis of the modularity in the cancer network, it has been found that there are 813 different modules that are present and the most dominant phenotypes in cancer are nervous system phenotype modularity 34, abnormal dermis papillary layer morphology modularity 27, abnormal embryo development modularity 21 etc.

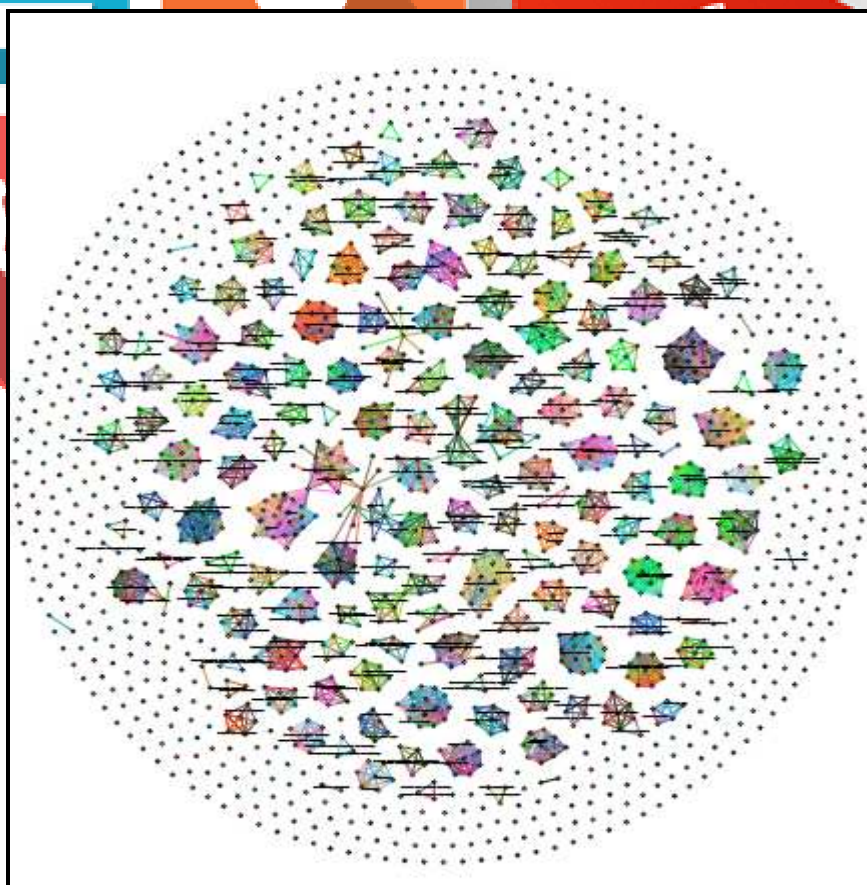


Fig 3.9: Modularity in cancer network.

so, to make our conclusion more apprehensive, we have given detailed diagram of some of the modularity in the following figure 3.10.

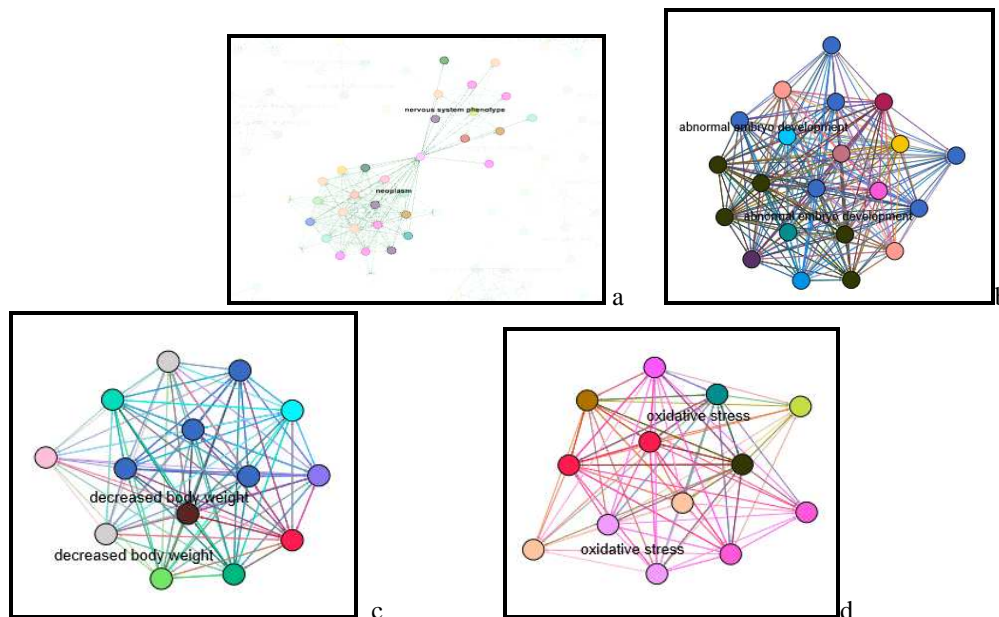


Figure 3.10: a) Cluster of neoplasm and nervous system phenotype b) Cluster of abnormal embryo development c) Cluster of decreased body weight d) Cluster of oxidative stress.

In our present study , we have even listed out the major phenotypes that occur during different types across different stages of cancer. Table 3.1 shows a detailed list of mostly occur phenotypes in cancer.

| phenotype | modularity_class | No of Occurance |
|---|------------------|-----------------|
| nervous system phenotype | 119 | 34 |
| abnormal dermis papillary layer morphology | 298 | 27 |
| abnormal embryo development | 771 | 21 |
| ventricular septal defect | 328 | 16 |
| decreased incidence of tumors by chemical induction | 108 | 16 |
| enlarged thymus | 62 | 16 |
| increased tumor incidence | 565 | 15 |
| decreased embryo size | 291 | 15 |
| premature death | 302 | 14 |
| decreased body weight | 35 | 14 |
| prenatal lethality, incomplete penetrance | 741 | 13 |
| no abnormal phenotype detected | 562 | 13 |
| abnormal thyroid-stimulating hormone level | 307 | 13 |
| abnormal bone marrow cell morphology/development | 339 | 12 |
| increased apoptosis | 146 | 12 |
| increased thyrotroph cell number | 83 | 12 |
| respiratory distress | 512 | 11 |
| abnormal cell physiology | 340 | 11 |
| cardiovascular system phenotype | 332 | 11 |
| abnormal hematopoietic system morphology/development | 299 | 11 |
| increased or absent threshold for auditory brainstem response | 281 | 11 |
| abnormal long bone diaphysis morphology | 173 | 10 |
| decreased cardiac muscle contractility | 153 | 10 |
| abnormal coat appearance | 121 | 10 |
| abnormal myocardium layer morphology | 9 | 10 |

Table 3.1: The common phenotypes of all cancer.

In our present study, we have created diseaseome for all types of cancer in human. From the diseaseome, we have identified the major phenotypes that occur from different types to different stages of cancer. This analysis of diseaseome has been carried out using knockout mouse model will help in characterization of different types of cancer. This study will have a significant impact on the development of methodological approaches toward precise identification of pathological cells and would allow for more effective detection of cancer-related changes.

IV Reference:

1. KWANG-IL GOH, MICHAEL E. CUSICK, DAVID VALLE, BARTON CHILDS, MARC VIDAL, AND ALBERT-LÁSZLÓ BARABÁSI, 2007. **THE HUMAN DISEASE NETWORK**
2. McKusick, V.A. (1998) Mendelian Inheritance in Man. A Catalog of Human Genes and Genetic Disorders, 12th edn. Johns Hopkins University Press, Baltimore, MD.
3. Ada Hamosh*, Alan F. Scott, Joanna S. Amberger, Carol A. Bocchini and Victor A. McKusick, 2004 Online Mendelian Inheritance in Man (OMIM), a knowledgebase of human genes and genetic disorders.
4. Olson H, Betton G, Robinson D et al., 2000 Concordance of the toxicity of pharmaceuticals in humans and in animals.; 32:56–67.
5. Martignoni M, Groothuis GM, de Kanter R. 2006 Species differences between mouse, rat, dog, monkey and human CYP-mediated drug metabolism, inhibition and induction. *Expert Opin Drug Metab Toxicol* ;2:875–94.
6. Suarez RK, Darveau CA. 2005 Multi-level regulation and metabolic scaling. *J Exp Biol*;208:1627–34.
7. Hulbert AJ 2008. The links between membrane composition, metabolic rate and lifespan. *Comp Biochem Physiol A Mol Integr Physiol* ;150:196–203.
8. Berry RJ, Bronson FH 1992. Life history and bioeconomy of the house mouse. *Biol Rev Camb Philos Soc* ;67:519–50.
9. Phelan JP, Rose MR. 2005 Why dietary restriction substantially increases longevity in animal models but won't in humans. *Age Res Rev* ;4:339–50.
10. Nguyen TL, Vieira-Silva S, Liston A et al. 2015 How informative is the mouse for human gut microbiota research? *Dis Model Mech* ;8:1–16.
11. Mestas J, Hughes CC. 2004 Of mice and not men: differences between mouse and human immunology. *J Immunol* ;172:2731–8.
12. Nachman MW, Searle JB. 1995 Why is the house mouse karyotype so variable? *Trends Ecol Evol* ;10:397–402.
13. Austad SN. 2002 A mouse's tale. *Nat Hist* ;111:64–70.
14. Paigen K. 2003 One hundred years of mouse genetics: an intellectual history the classical period (1902–1980). *Genetics* 2003;163:1–7.

Acknowledgement:

We sincerely thank the management of The Oxford College of Engineering and VGST for providing this opportunity to work.



Radioprotective and immunomodulatory effects of *Mesua ferrea* (Linn.) from Western Ghats of India., in irradiated Swiss albino mice and splenic lymphocytes

Syed Murthuza , Bukkambudhi Krishnaswamy Manjunatha  

Show more 

 Outline |  Share  Cite

<https://doi.org/10.1016/j.jrras.2017.09.001>

[Get rights and content](#)

Under a Creative Commons [license](#)

[Open access](#)

Abstract

The present study reports the efficacy of *Mesua ferrea* (Linn.) extract in mitigating radiation induced toxicity along with immunomodulatory property. Swiss albino mice, splenic lymphocytes and plasmid pBR322 DNA were used to evaluate the radioprotective effect by exposing them to 6Gy EBR or 4 Gy gamma radiation. In this study, *Mesua ferrea* methanolic (MfM) or aqueous extracts (MfA) significantly protected pBR322 DNA against radiation induced strand breaks. Both the extracts significantly offered protection against radiation-induced apoptosis as indicated by propidium iodide staining and DNA ladder assay. MfM or MfA significantly scavenged radiation derived free radicals indicating their antioxidant potential. MfM or MfA were orally administered to Swiss albino mice at 250 or 200 mg/kg body weight respectively for 7 days. The study showed significant increase in the levels of glutathione, and activities of endogenous antioxidant enzymes superoxide dismutase & catalase. Administration of MfA or MfM to mice significantly reduced electron beam radiation (EBR; 6Gy) induced increase in MDA levels. Immunomodulatory efficacy of MfM and MfA was evaluated using concanavalin-A (Con-A) induced proliferation of CFSE labelled splenic lymphocytes. Both the extracts significantly reduced proliferation in a dose-dependent manner. Further, MfM or MfA treatment prevented EBR induced histopathological changes in jejunum, spleen, liver and kidney. This demonstrates that the plant *Mesua ferrea* has promising antioxidant, radioprotective and immunomodulatory activity which may be attributed to the active constituents present in it.

Keywords

Radioprotection; DNA damage; Antioxidant enzymes; Proliferation; Reactive oxygen species; *Mesua ferrea*

1. Introduction

Radiotherapy is a dominant mainstay treatment modality of various solid cancers ([Baskar, Dai, Wenlong, Yeo, & Yeoh, 2014](#)), but is reported to induce secondary cancers by causing damage to rapidly multiplying normal cells ([Robbins and Zhao, 2004](#)). Though the treatment regime helps in extending the life-span of cancer patients depending on the type and stage of cancers, it has led to the development of secondary cancers, some of which are more severe than the primary cancer ([Little, 2001](#)), indicating the need for identifying drugs which can control the growth of malignant tissue leaving the normal cells with little or no side effect.

Exposure of cells to ionizing radiation generates reactive oxygen species (ROS) and reactive nitrogen species (RNS) which in turn cause cellular damage via lipid peroxidation, protein oxidation and DNA alterations. DNA damage can result in cell death or cancer. Lipid peroxidation products are reported to bind to DNA and induce mutagenesis. Free radical mediated damage to the protein can result in loss of function of DNA repair enzymes leading to mutagenesis and carcinogenesis ([Devasagayam et al., 2004](#), [Gracy et al., 1999](#); & [Cheeseman & Slater, 1993](#)). Plant derived molecules with potent antioxidant activity could mitigate radiation induced damage to normal cells/tissues.

M. ferrea (Linn.) is a well-known evergreen tropical tree (Clusiaceae) commonly known as Naga sampige (Kannada), Naga kesara (Sanskrit), and Cobra saffron (English) widely grow in Southern Asia, used in the Indian traditional medicinal system for the treatment of fever, dyspepsia, microbial infections ([Sumitra, Kalpana, & Jigna, 2013](#)), renal diseases ([Dennis & Akshaya, 1998](#)), liver disorders ([Garg, Sharm, Ranjan, Atrri, & Mishra, 2009](#)). In Malaysia and India, a mixture of pounded kernels and seed oil is used for poulticing wounds. The seed-oil of *M. ferrea* is used for treating itch, other skin eruptions and rheumatism ([Orwa, Mutua, Kindt, Jamnadass, & Simons, 2009](#)). The plant is reported for its wound healing ([Choudhary, 2012](#)) anti-inflammatory, antioxidant, anticancer ([Abhilash & Ramesh, 2012](#)), analgesic ([Hassan, Ali, Alimuzzaman, & Rihan, 2006](#)), antiarthritic ([Rastogi and Mehrotra, 1990-94](#)) and immunomodulatory activity ([Manoj, Sanjay-Kumar, Lokesh, & Manohara, 2012](#)). The stem bark contains 4-alkyl and 4-phenylcoumarin ([Luisella-Verotta et al., 2004](#)), pyranoxanthones, mesuaferrin-A, mesuaferrin-B, caloxanthone-C, 1-8-dihydro-3-methoxy-6-methylanthraquinone, β -sitosterol, friedelin and betulinic acid ([Soek Sin The et al., 2011](#)) which are promising therapeutic compounds. Seed oil contains phenyl coumarin, mesuol (5,7-dihydroxy-8-isopentenyl-6-isobutyryl-4-

phenylcoumarin), mesuone, mammeigin, mesaugin and coumarin. The stamen extract contains α -amyrin, β -amyrin, β -sistosterol mesuaxanthone-B and mesuanic acid (Raju, Srimannarayana, & Subbarao, 1976).

Development of radioprotective agents has been the subject of intense research in recent years, in view of their potential to improve the therapeutic index in radiotherapy. Hence the search for alternative sources, including bioactive principles of plant origin, has been an ongoing task worldwide. Since radiation-induced genotoxicity is predominantly a free radical mediated effect on DNA, plant-derived bioactive compounds with their antioxidant potential may render radioprotection to normal tissues. In this context, the present work was carried out to screen the plant *M. ferrea* for its radioprotective and anti-proliferative activity.

2. Materials and methods

2.1. Reagents and chemicals

m-phosphoric acid, sodium chloride, EDTA, disodium hydrogen phosphate, 5, 5'-dithiobis (2 nitro-benzoic acid), trichloroacetic acid, 2-thiobarbituric acid, HCl, malonaldehyde bis (dimethyl acetal), dimethyl sulfoxide (DMSO), 5-(and-6)-carboxy-2,7-dihydrodichlorofluorescein diacetate ($H_2DCF-DA$), RPMI 1640, fetal bovine serum (FBS), agarose, propidium iodide (PI), trizma base, triton X-100, sodium citrate, Tween 20 and ethidium bromide were procured from Sigma-Aldrich USA. Hydrogen peroxide, potassium dihydrogen phosphate, nitroblue tetrazolium chloride, riboflavin, and methionine were purchased from HiMedia, Mumbai. Concanavalin-A was obtained from Calbiochem, USA. Carboxyfluorescein diacetate succinimidyl ester (CFSE) was procured from Molecular Probes, USA. Plasmid pBR322 DNA was obtained from Aristogene, Bangalore.

2.2. Collection and extraction

The stem bark of *Mesua ferrea* (Linn.) was collected from the Shettyhalli reserve forest, Western Ghats of Karnataka. Identified and authenticated sample was deposited for further reference in the Department of Biotechnology, TOCE Bangalore. The plant material was shade dried and powdered mechanically using a domestic electric blender, powdered samples were stored in airtight glass containers for further study. About 250 g of plant material was subjected to soxhlation using methanol for approximately 48 h. An aqueous extract was also prepared using double distilled water. Extracts were filtered, concentrated to dryness in vacuum under reduced pressure using rotary flash evaporator (IKA-German) (Shobowale, Ogbulie, Itoandon, Oresgun, & Olatope, 2013;; Akinmoladun, Ibukun, Afor, Obuotor, & Farombi, 2007).

2.3. Irradiation

The electron beam irradiation (EBR) work was carried out at Microtron center, Mangalore University, Mangalore, Karnataka, India. The un-anaesthetised animals were restrained in well-ventilated perspex boxes and exposed to whole-body EBR at a distance of 30 cm from the beam exit point of the microtron accelerator at a dose rate of ~ 100 cGy/min. pBR322 plasmid DNA

and murine splenic lymphocytes suspended in RPMI medium were exposed to α -radiation using a ^{60}Co source at a dose rate of 0.89 Gy/min in Blood Irradiator, BRIT, Mumbai, India.

2.4. Plasmid pBR322 DNA damage studies

Plasmid pBR322 DNA was used to study the radioprotective efficacy of MfM or MfA in cell free system (Umang, Kunwar, Srinivasan, Nanjan, & Priyadarsini, 2009). Agarose gel (1%) was prepared in 130 mM tris-borate/2.5 mM EDTA (TBE) buffer. Ethidium bromide (0.5 $\mu\text{g}/\text{ml}$) was added in the gel preparation to enable the visualization of the DNA bands in a UV transilluminator. The gel was submerged in an electrophoresis tank filled with TBE buffer. About 200 ng of pBR322 DNA was suspended in 20 μl of 10 mM sodium phosphate buffer, pH 7.4 and exposed to an absorbed dose of 50 Gy γ -radiation dose both in the absence or presence of varying concentration of MfM and MfA. The samples were mixed with loading dye (0.25% bromophenol blue and 30% glycerol) and loaded into the wells. Electrophoresis was carried out at 60V to separate the open circular (OC) and the super coiled (SC) form of DNA. The movement of the DNA bands was visualized on a UV transilluminator.

2.5. Isolation of lymphocytes

Lymphocytes were isolated from the spleen of Swiss albino mice following the method of Sharma et al., 2007a, Sharma et al., 2007b. The whole spleen was put in a 15 ml tube containing RPMI medium, squeezed gently against a sterile mesh using the piston. Then erythrocytes were lysed by brief hypotonic shock and cells were counted in a hemocytometer. Cells were cultured in a 24-well tissue culture plate containing RPMI media with 1 \times antibiotics (penicillin & streptomycin), 10% FBS, at cell density of 1×10^6 cells/ml. Cells were cultured for indicated time points at 37 $^\circ\text{C}$ in a 95% relative humidity and at 5% CO_2 atmosphere.

2.6. Estimation of apoptosis

Apoptosis of irradiated splenic lymphocytes was studied following the method of Sharma et al., 2007a, Sharma et al., 2007b. Lymphocytes were pre-incubated with various concentration of *Mesua ferrea* methanol extract (100, 50 25 and 10 $\mu\text{g}/\text{ml}$) for 2 h and then exposed to 4 Gy γ -radiation dose. The cultured cells were harvested by centrifugation for 2 min at 13500 rpm and the pellet was resuspended in 1 ml propidium solution and stored at 4 $^\circ\text{C}$ in dark. After 24 h, cells were acquired using a flow cytometer and percent apoptotic cells was determined by analyzing pre-G1 population (less than 2n DNA content) using FlowJo[®] software.

2.7. DNA ladder assay

DNA ladder assay was performed according to the Checker et al., 2008. The cultured lymphocytes were pre-incubated with various concentrations of *Mesua ferrea* methanol (50, 25 and 10 $\mu\text{g}/\text{ml}$) and aqueous extracts (50, 25 and 10 $\mu\text{g}/\text{ml}$) for 2 h and then exposed to 4 Gy γ -radiation dose and cultured for 24 h at 37 $^\circ\text{C}$ in 5% CO_2 incubator, washed with 1X PBS and resuspended in 50 μl DNA lysis buffer and incubated at 55 $^\circ\text{C}$ for 1 h. Then 10 μl RNase (1 mg/ml) was added to degrade RNA and incubated for 1 h at 55 $^\circ\text{C}$, RNase was inactivated by incubating at

65 °C for 5 min followed by addition of 10 µl 6X loading dye. 20 µl sample was loaded into the each well in 1.8% Agarose gel. Electrophoresis was carried out at 65V for one hour and DNA was visualized by ethidium bromide staining under UV illumination using Gel Doc system.

2.8. Measurement of reactive oxygen species

The levels of ROS were measured according to [Wang et al., 2008](#), by staining the cells with H₂DCFDA. Lymphocytes were pre-incubated with *Mesua ferrea* methanol and aqueous extracts (100, 50, 25 & 10 µg) for 2 h in RPMI medium, stained with H₂DCFDA (20 µM, 30 min 37 °C) and were exposed to 4 Gy γ-radiation dose. Change in fluorescence was monitored at excitation/emission 485/535 nm using microplate based spectrofluorimeter (Synergy Hybrid, Biotek).

2.9. Estimation of reduced glutathione

Glutathione was estimated following the method of [Sedlak & Lindsay, 1968](#). Proteins were precipitated using 10% TCA, centrifuged and 0.5 ml of the supernatant was mixed with 0.3 M phosphate buffer and 0.006 mM DTNB. The mixture was incubated for 1min and the absorbance was measured at 412 nm against appropriate blank. The glutathione content was calculated by using standard plot under the same experimental condition.

2.10. Estimation of membrane lipid peroxidation

Lipid peroxidation was studied following the method described by [Braugher et al., 1987](#). In brief, the liver homogenate was incubated with 15% TCA, 0.375%TBA and 5N HCl at 95 °C for 15 min, the mixture was cooled, centrifuged and the absorbance of the supernatant was measured at 532 nm against appropriate blank. The amount of Malondialdehyde (MDA) was determined by using $\epsilon = 1.56 \times 10^5 \text{ M}^{-1} \text{ cm}^{-1}$.

2.11. Estimation of superoxide dismutase activity

The estimation of superoxide dismutase enzyme was carried out by [Misra and Fridovich, 1972](#) method. The substrate used for the assay consists of nitro blue tetrazolium chloride which reacts with superoxide anions to produce formazan which is a blue colored complex. Superoxide anions were produced upon illumination of riboflavin in the presence of methionine as an electron donor. The SOD present in the sample will act on the superoxide anions produced by riboflavin and they reduce the net superoxide anions in the substrate leading to decreased production of formazan manifested by decreased intensity of the blue color formed. The decrease in the formation of formazan is directly proportional to SOD activity in the sample, 50% decrease in the formation of formazan is taken as one unit of SOD ([Geller & Winge, 1983](#)).

2.12. Estimation of catalase activity

Catalase activity was carried by the method of [Luck, 1974](#), p.885. Take 3 ml of Hydrogen peroxide phosphate buffer and mix in 0.01–0.04 ml sample with a glass stirrer flattened at one end. Note

the time Δt required for a decrease in absorbance (240 nm) from 0.45 to 0.4. This value is used for calculations if it is greater than 60 s repeat the measurements with a more concentrated solution of the sample.

2.13. Mitogen-induced proliferation assay

The anti-proliferative assay was carried out following the method of [Wilankar et al., 2011](#). Lymphocytes were stained with cell tracker dye (CFSE), cells (2×10^6 cells/well) were cultured in RPMI medium containing 10% FBS. Extracts were added in different concentrations and stimulated with Concanavalin A (2.5 $\mu\text{g}/\text{ml}$) in respective wells and incubated for 72 h at 37°C in a 95% relative humidity, 5% CO₂ atmosphere. The cells were harvested and fixed with 1% paraformaldehyde at 4°C for 20–25 min. After fixing, Hoechst-33342 (10 $\mu\text{g}/\text{ml}$) was added and samples were acquired on a flow cytometer and analyzed using FlowJo software.

2.14. Histopathological studies

Animals were divided into five groups of six animals each. Group I–normal control, group II–whole body electron beam irradiated (6 Gy) (treated with vehicle only), Group III– treated orally with MfM before (6 Gy), Group IV received MfM post-irradiation (6 Gy), Group-V received *M. ferrea* aqueous stem bark extract before irradiation, Group VI received MfA once daily for 7 consecutive days. Animals of Group IV & VI were exposed to EBR on day 7 and all animals were sacrificed on 8th day. Slice of jejunum, spleen, liver & kidney were fixed in 4% formaldehyde, embedded in paraffin wax, sectioned at 5 μm thickness and stained with haematoxylin and eosin stains. Detailed microscopic examination of these organs was carried out.

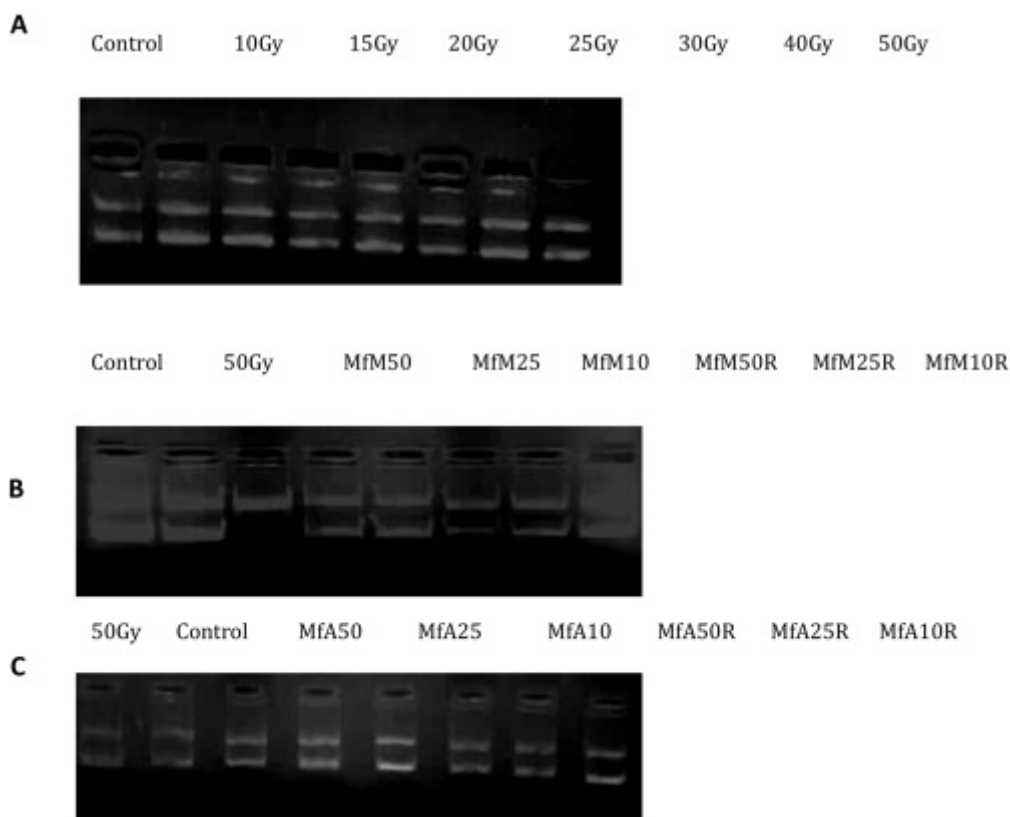
2.15. Statistical analysis

The statistical analysis was performed using one-way ANOVA analysis.

3. Results

3.1. Effect of *Mesua ferrea* extracts on pBR322 DNA damage study

The efficacy of *Mesua ferrea* extract in protecting DNA damage due to radiation was studied using pBR-322 plasmid DNA model. It was found that Plasmid DNA on exposure to 50 Gy γ -radiation underwent complete conversion into open circular form from super coiled form as indicated in [Fig. 1 A–C](#). In plasmid DNA treated with varying concentrations of MfM or MfA (10, 25 & 50 μg), significant protection was observed against radiation induced strand breaks.



Download : [Download high-res image \(248KB\)](#)

Download : [Download full-size image](#)

Fig. 1. Effect of *Mesua ferrea* extracts on pBR322 DNA damage by 4 Gy γ -irradiation: Agarose gel electrophoresis image, depicting super coiled (SC) and nicked open circular (OC) forms of plasmid DNA exposed to 10, 15, 20, 25, 30, 40, 50 Gy radiation dose for dose fixation (A). pBR322 plasmid DNA exposed to 50 Gy γ -radiation induced strand breaks. Treatment with (B) *Mesua ferrea* methanol and (C) aqueous extracts at (50, 25 and 10 μ g) concentrations before 1 h of radiation exposure gives a dose dependent.

3.2. Effect of *Mesua ferrea* extract on γ -radiation induced apoptosis in lymphocytes

Exposure of murine splenic lymphocytes to 4 Gy dose of γ -radiation resulted in significantly higher induction of apoptosis as compared to control group indicating severe damage to the lymphocytes. Lymphocytes pre-treated with MfM extract prior to radiation exposure exhibited dose dependent protection against cell death. MfM (100 μ g) per se did not induce apoptosis in lymphocytes as shown in overlaid flow cytometric histograms (Fig. 2A). The cells showing hypodiploid DNA content were gated and percent cell death is shown as bar graph (Fig. 2B).

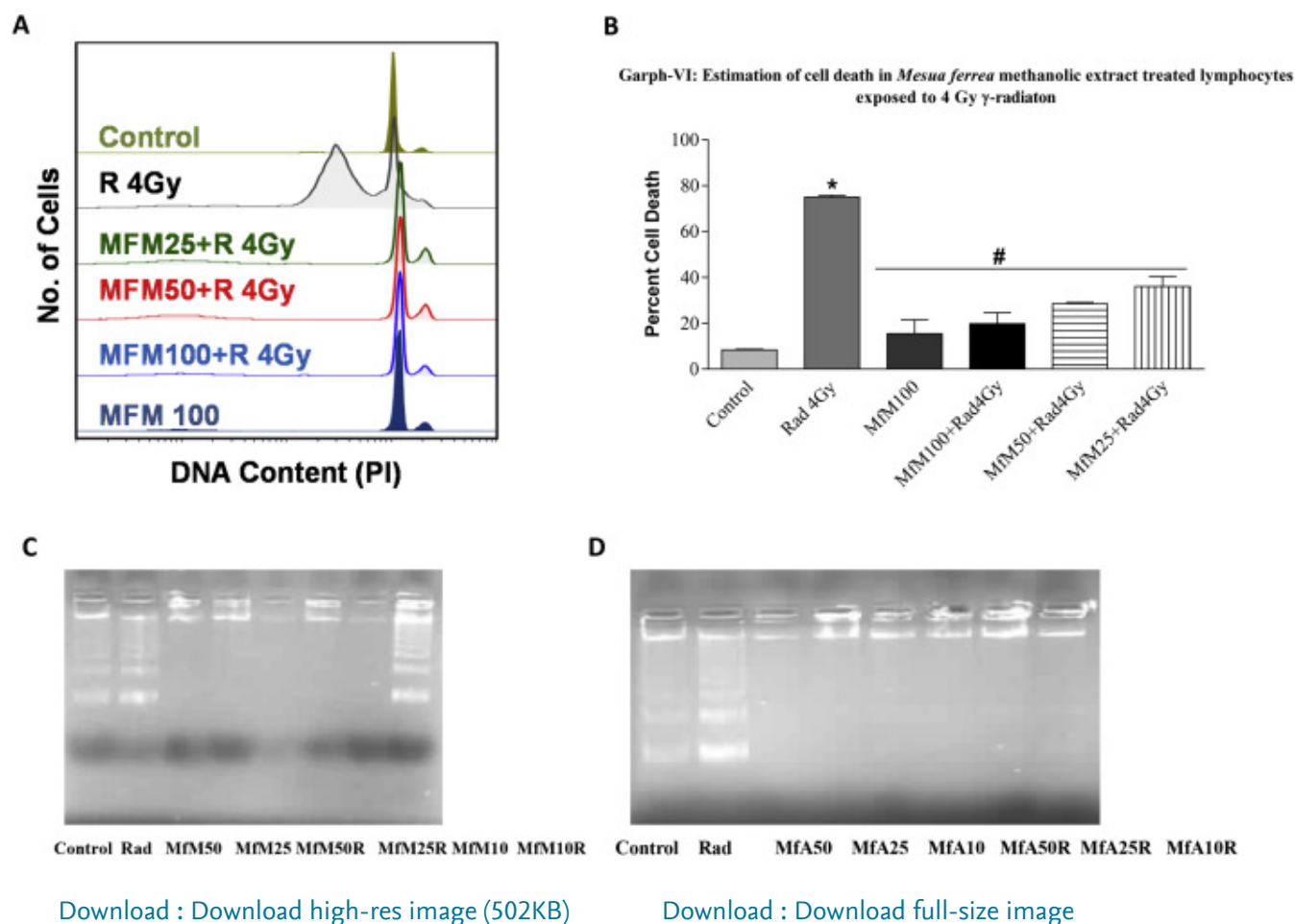


Fig. 2. Lymphocytes were pre-incubated with indicated concentrations of *Mesua ferrea* methanol extract for 2 h and then exposed to 4 Gy radiation dose. Representative overlaid flow cytometric histograms are shown (A). Bar graph represents percent cell death (B). * $p < .05$ as compared to control, # $p < .05$ as compared to radiation. Lymphocytes were preincubated with various concentration of (C)*Mesua ferrea* methanol (50, 25 and 10 μ g) and (D) aqueous extracts (50, 25 and 10 μ g) for 2 h and then exposed to 4 Gy radiation dose radiation dose and cultured for 24 h at 37°C in 5% CO₂ incubator. DNA ladder indicates the cells undergoing apoptosis.

3.3. Effect of *Mesua ferrea* extracts on radiation induced apoptosis (DNA ladder)

DNA fragmentation is a hallmark of apoptosis. This assay was used to confirm the radioprotective efficacy of MfM and MfA. Exposure of lymphocytes to 4Gy radiation induced DNA ladder pattern indicating cells undergoing apoptosis (Fig. 2C and D). However, pretreatment of lymphocytes with MfM or MfA of different concentrations prevented radiation induced DNA fragmentation. Neither MfM nor MfA induced DNA fragmentation but inhibited basal apoptosis.

3.4. Effects of *Mesua ferrea* on radiation-induced ROS generation

Since, radiation mediated cellular damage is mediated through generation of reactive oxygen species, intracellular ROS levels were measured using redox-sensitive fluorescent probe DCF-

DA. Interestingly, both MfM and MfA scavenged basal ROS levels in lymphocytes. Radiation induced significant increase in ROS levels in lymphocytes but pre-treatment with MfM or MfA resulted significant decrease in DCF fluorescence suggesting radical scavenging activity (Fig. 3A and B).

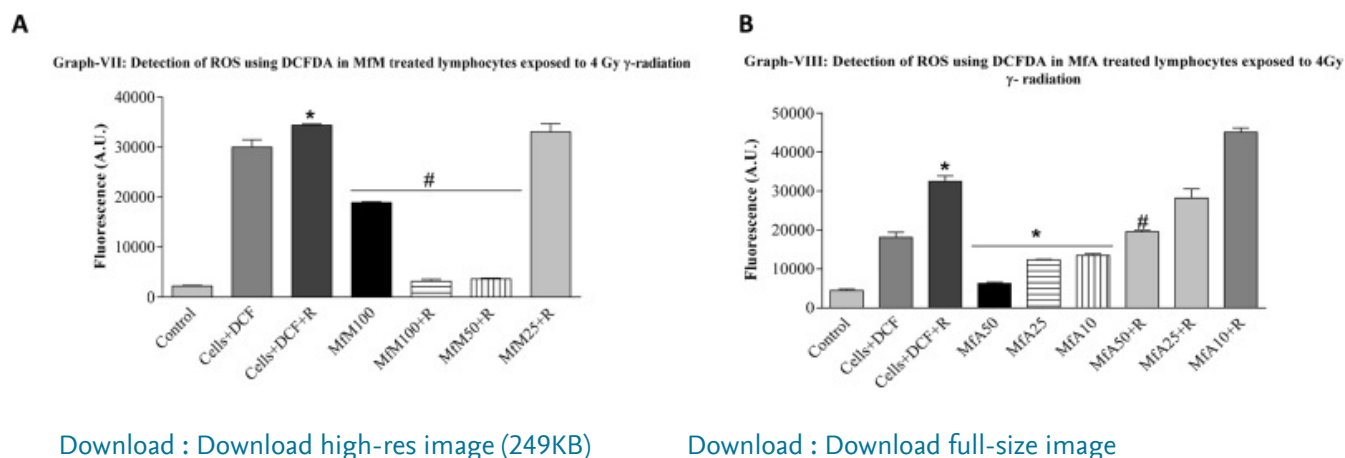
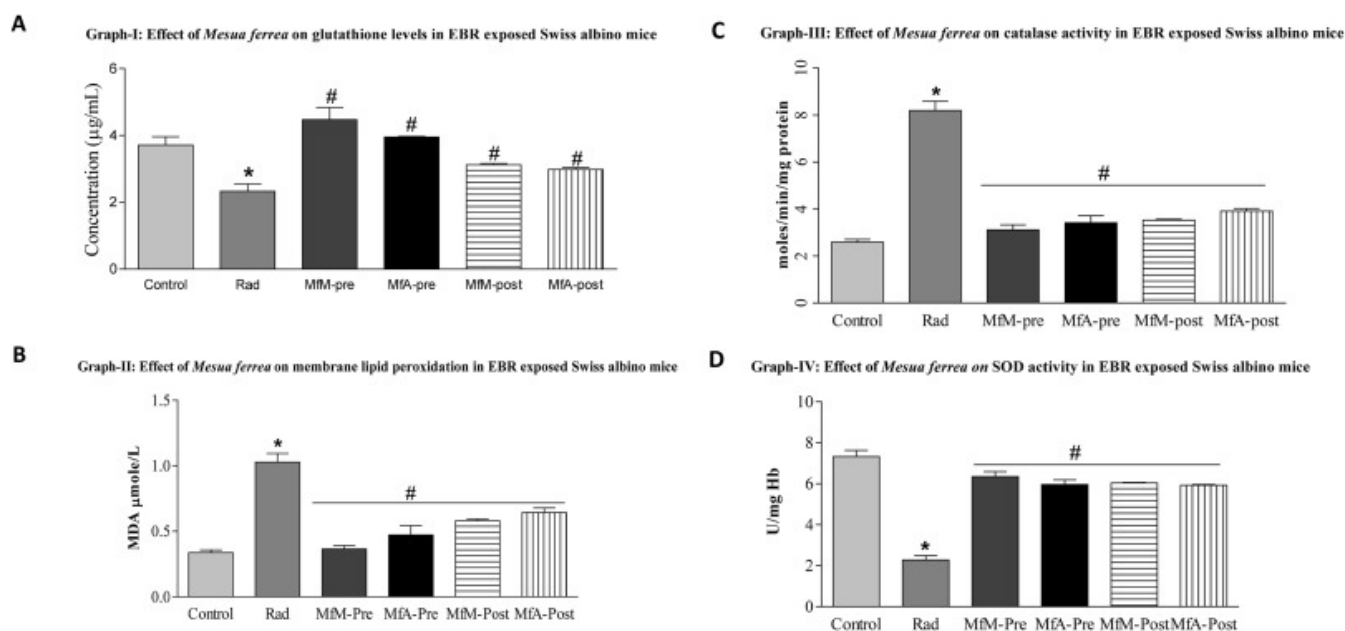


Fig. 3. Lymphocytes were pre-incubated with indicated concentrations of *Mesua ferrea* methanol (A) or aqueous extracts (B) for 2hrs in RPMI medium, stained with H₂DCF-DA (20 μ M, 30 min at 37 $^{\circ}$ C). Levels of intracellular ROS were estimated by monitoring the fluorescence of DCF (Ex. 485 nm/Em. 535 nm). * p < .05, as compared to control, # p < .05, as compared to radiation.

3.5. Effect of *Mesua ferrea* on serum GSH levels

Fig. 4A shows the effect of pre and post administration of MfM or MfA on EBR induced changes in plasma GSH levels in vivo. Exposure of mice to 6 Gy EBR resulted in significant reduction in plasma levels of reduced GSH. Oral administration of MfM or MfA to mice before as well as after exposure to EBR significantly abrogated EBR induced decrease in plasma GSH levels.



[Download : Download high-res image \(411KB\)](#)[Download : Download full-size image](#)

Fig. 4. The effect of *Mesua ferrea* methanol or aqueous on glutathione levels in the serum of mice prior to or post 6Gy EBR exposure (A). * $p < .05$ as compared to control, # $p < .05$ as compared to radiation. The effect of *Mesua ferrea* methanol or aqueous on membrane lipid peroxidation prior to or post 6 Gy EBR exposure (B), * $p < .05$ as compared to control, # $p < .05$ as compared to radiation. The effect of *Mesua ferrea* methanol or aqueous on catalase activity prior to or post 6 Gy EBR exposure (C) * $p < .05$, as compared to control, # $p < .05$, as compared to radiation. The effect of *Mesua ferrea* methanol or aqueous on SOD activity prior to or post 6 Gy EBR exposure (D) * $p < .05$, as compared with control, # $p < .05$, as compared to radiation.

3.6. Effect of *Mesua ferrea* on EBR induced malondialdehyde levels in serum

Fig. 4B shows the effect of pre and post administration of MfM or MfA on EBR induced changes in membrane lipid peroxidation in vivo. Exposure of mice to 6Gy EBR resulted in significant increase in membrane lipid peroxidation as compared to control. Oral administration of MfM or MfA before as well as after exposure significantly reduced EBR induced increase in membrane lipid peroxidation as measured by changes in MDA levels.

3.7. Effect of *Mesua ferrea* on EBR induced catalase activity

Fig. 4C shows the effect of pre and post administration of MfM or MfA on EBR induced changes in catalase enzyme activity in vivo. Exposure of mice to 6 Gy EBR resulted in more than two-fold increase in catalase activity as compared to control. Oral administration of MfM or MfA pre or post exposure significantly reduced EBR induced increase in catalase activity.

3.8. Effect of *Mesua ferrea* on EBR induced SOD activity

Fig. 4D shows the effect of pre and post administration of MfM or MfA on EBR induced changes in SOD enzyme activity in vivo. Exposure of mice to 6Gy EBR resulted in significant decrease in SOD activity as compared to that in control. Oral administration of MfM or MfA to mice pre or post exposure to EBR significantly abrogated the EBR induced reduction in SOD activity.

3.9. Effect of MfM and MfA on mitogen-induced proliferation of lymphocytes

The effect of MfA or MfM extracts on Con-A induced proliferation of murine T-cells was measured by CFSE dye dilution. Con-A treatment induced proliferation of T cells as evinced from increase in daughter cells as shown in the overlaid flow cytometric histograms in Fig. 5A and C. Both MfM as well as MfA inhibited mitogen induced proliferation of T cells in a dose dependent manner as shown by decrease in daughter cells (Fig. 5B and D).

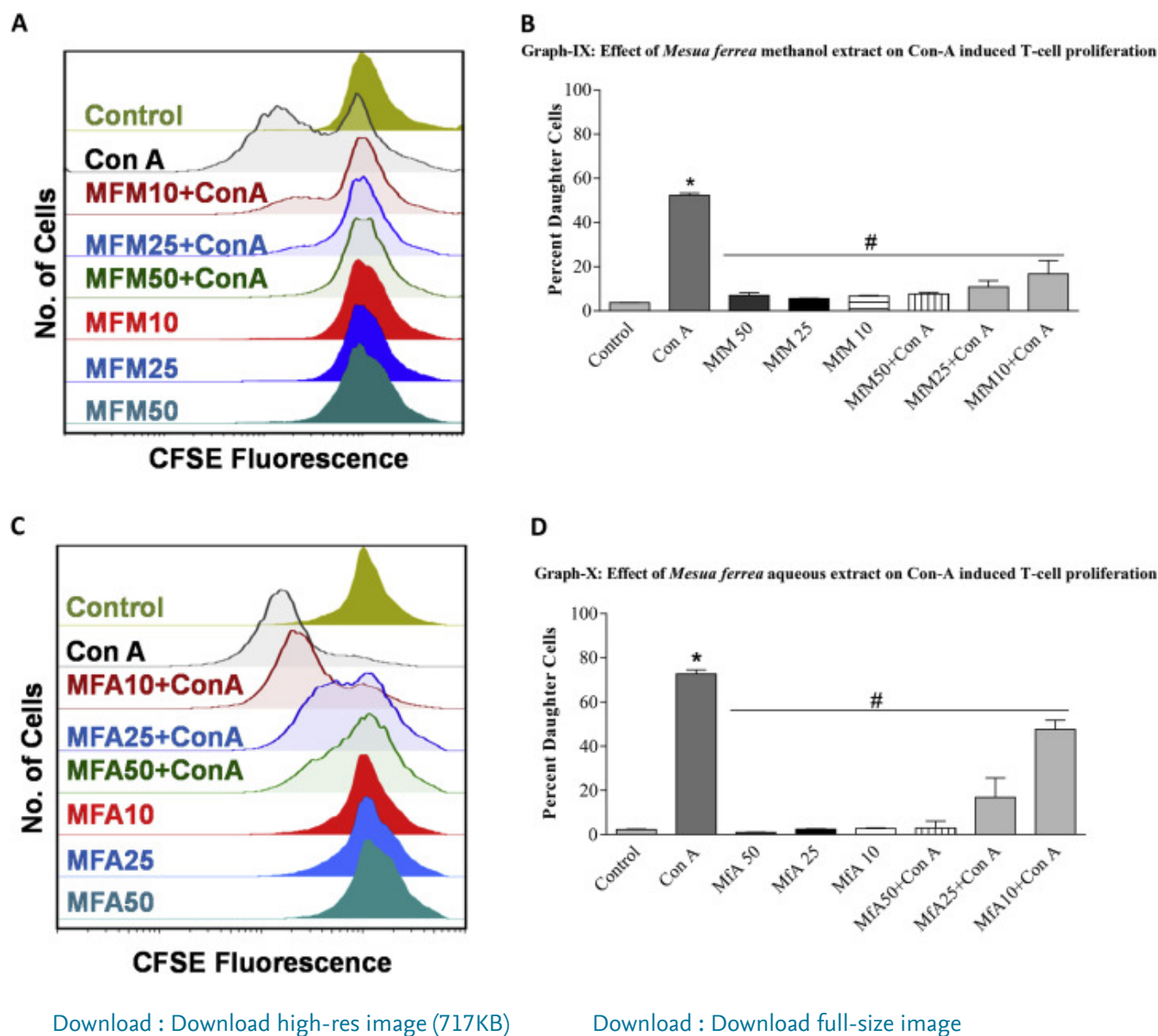
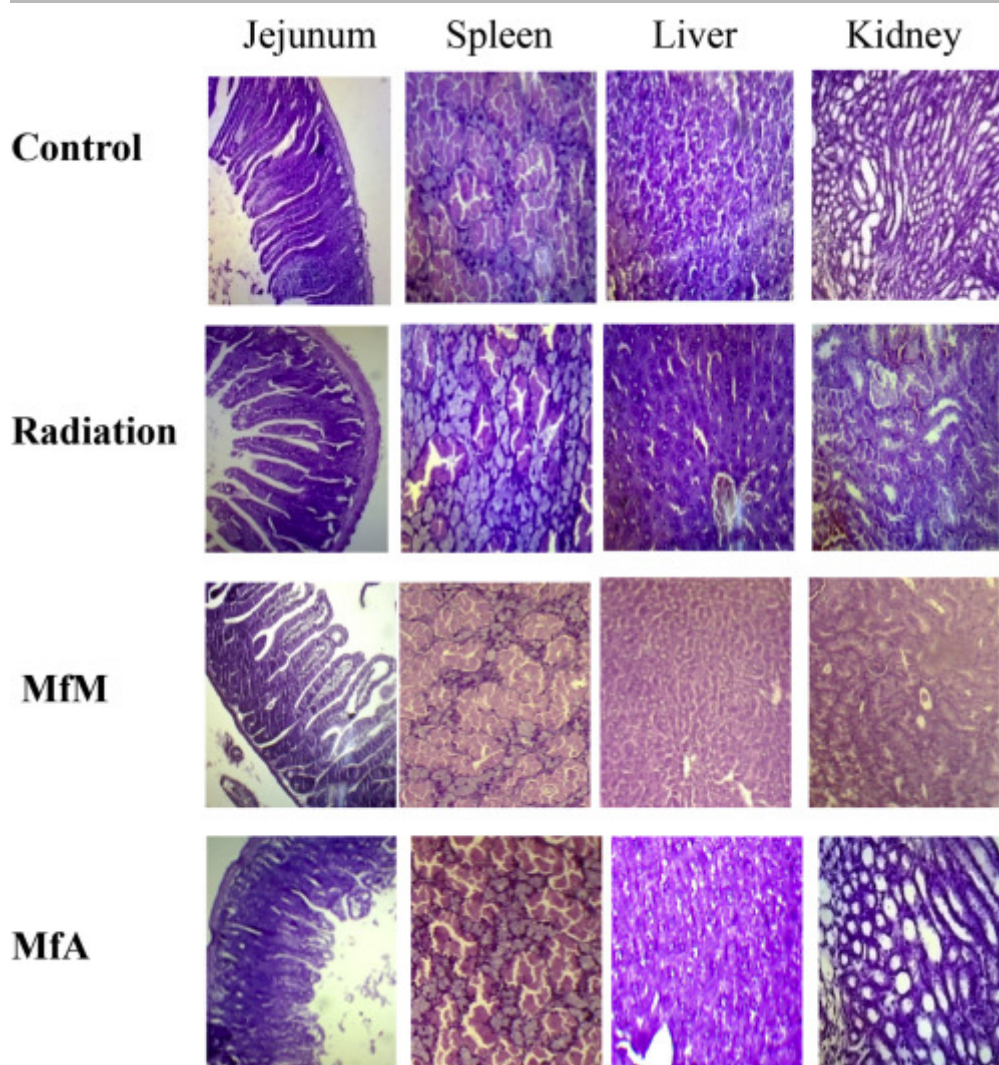


Fig. 5. Effect of *Mesua ferrea* methanol or aqueous extracts on Con-A induced T-cell proliferation was monitored by CFSE dye dilution method. Representative flow-cytometric histograms are shown (A & C). Bar graph represents percent daughter cells (B & D). * $p < .05$, as compared to control, # $p < .05$, as compared to Con A treated group.

3.10. Effect of administration of MfM or MfA on histopathological changes induced by EBR

The effect of MfM or MfA administration on 6 Gy EBR induced damage to organs of mice was studied by necropsy followed by histopathology. The representative tissue sections of mice from different treatment groups are shown in Fig. 6. The architecture of jejunum, spleen, liver and kidney was altered in EBR exposed mice indicating severe injury to these organs. In radiation group, the damage to the inner and outer muscularis, lamina propria of villi shows the damage to jejunum, scattered histiocytes shows the damage to spleen, appearance of fatty lobules indicates damage to hepatocytes and appearing of lesions, glomerular collapse shows the

damage to nephrocytes (Fig. 6). Oral administration of MfM or MfA significantly reduced the radiation induced damage to jejunum, spleen, liver and kidney as shown by normal architecture of cells in the histological sections of these organs.



[Download : Download high-res image \(1MB\)](#)

[Download : Download full-size image](#)

Fig. 6. Effect of *Mesua ferrea* methanol & aqueous on organs of mice exposed to 6 Gy EBR, compared with control exhibits normal architecture of jejunum, spleen, liver and kidney. In radiation group damage to the inner and outer muscularis, lamina propria of villi shows the damage to jejunum Scattered histiocytes shows the damage to spleen Appearance of fatty lobules indicates damage to hepatocytes and Appearing of lesions, Glomerular collapse shows the damage to nephrocytes.

4. Discussion

The development of effective radioprotectors and therapeutic drugs is of great importance in view of their potential application in cancer treatment and diagnosis. It is well established that phyto-constituents have potential application in mitigating the toxic effects of free radicals

generated in the body (Manjunatha et al., 2013). Many synthetic as well as natural compounds have been investigated for their efficacy to protect against radiation-induced cellular damage. Radiation generates free radicals which lead to a cascade of events leading to cellular damage. Hence scavenging of these intra-cellular free radicals can minimize the radiation-induced damage.

We have evaluated the efficacy of MfM and MfA on γ -radiation induced damage in pBR322 DNA. On exposure to 50Gy γ -radiation, the super coiled (SC) form of DNA got converted to the open coiled (OC) form and in presence of extracts, there is a diminution in the damage to the SC form on treatment with different concentrations of MfM or MfA (Vinutha et al., 2015, Sandur et al., 1999). Radiation-induced apoptosis in lymphocytes was assessed by DNA fragmentation as well as PI staining followed by flow cytometry. MfM and MfA significantly reduced the extent of radiation-induced apoptosis as indicated by a decrease in the percentage of fragmented DNA and decrease in pre-G1 population (Nazir et al., 2011, Sminaa et al., 2011). Both the extracts scavenged radiation derived free radicals in lymphocytes suggesting that these extracts not only act as antioxidants in cell free system but also in cellular models.

GSH is the most abundant thiol containing antioxidant inside cells and is known to participate in many metabolic processes. GSH is typically found in a highly reduced state and maintains the appropriate redox status of the sulfhydryl groups in proteins involved in nucleic acid biosynthesis and DNA repair in addition to standard antioxidant functions. Oxidative damage to organisms is connected with the progressive accumulation of oxidized products of ROS (Saghi Ghaffari, 2008). It is also involved as an antioxidant in the detoxification of products from the ROS-promoted oxidation of lipids such as malonic dialdehyde and 4-hydroxy-2-nonenal. In the present study, we found that MfM and MfA significantly restored the EBR induced depletion of reduced serum GSH levels in mice. The restoration in reduced GSH levels in MfM and MfA treated groups could be responsible for the radioprotective efficacy of these herbal extracts.

Changes in activity of antioxidant enzymes such as SOD and Catalase can result in accumulation of H_2O_2 and superoxide radicals which can perturb cellular redox balance (Volodymyr I. Lushchak, 2012 & Svetlana, Borislav, & Georgi, 2013). Oxidative stress leads to tissue damage, and antioxidant supplementation may delay or prevent such damage (Naveen, Suchetha, Ganesh, Damodar, & Madhu, 2011). In the present study, oral pre-administration of MfA or MfM exhibited a significant increase in antioxidant enzyme activity in the animals exposed to EBR. This clearly indicates that the active constituents in the extract could offer radioprotection by up-regulating the antioxidant enzymes SOD but not catalase.

MDA is a reliable biomarker for oxidative stress generated by free radical attack on phospholipids and circulating lipids of cell membrane (Savita et al., 2010; & Ohkawa et al., 1979). Lipid peroxidation is a highly destructive process that alters the structure and function of cellular membrane and physico-chemical properties of membrane-bound enzymes and proteins receptors (Agarwal & Kaler, 2001). In the present study MfA and MfM significantly reduced EBR

induced increase in MDA levels indicating their potency in controlling deleterious effects of radiation on cell membrane.

Peripheral T-lymphocytes have been reported to proliferate in vivo in response to infection (Rocha, Dautigny, & Pereira, 1989;; Modigliani, Coutinho, Defranoux, Coutinho, & Bandeira, 1994). T cell activation and proliferation is also associated with inflammation. In the present report, the anti-proliferative effect of *Mesua ferrea* methanolic and aqueous extracts was investigated in terms of suppression of T-cell proliferation induced by Con A. Both MfM and MfA inhibited Con-A induced proliferation of T-cells in a dose-dependent manner. These results show anti-inflammatory and immuno-suppressive potential of MfM and MfA. Histopathological studies revealed that administration of MfM and MfA protected jejunum, spleen, liver and kidney against EBR induced tissue damage.

5. Conclusion

From our investigation, it is evident that the plant *Mesua ferrea* contains potent phyto-constituents which can scavenge free radicals through its antioxidative ability and regulate the activity of antioxidant enzymes. It can be concluded that the radioprotective and Immunomodulatory effects of the plant can be attributed to its antioxidant potency. However, further work is required to reveal the molecular mechanism of the protecting the radiation-induced damage by MfM and MfA.

Conflict of interest

The authors do not have any potential conflicts of interest.

Acknowledgements

The authors are greatly thankful to Dr. Rahul Checker, Dr. Deepak Sharma and Dr. Santosh K. Sandur for providing help in carrying out experiments at Bhabha Atomic Research Center, Mumbai. We are also thankful to Board of Research in Nuclear Science, Government of India for the financial support (SanctionNo.2012/34/21/BRNS). We greatly acknowledge the support of Department of Biotechnology, The Oxford College of Engineering Bangalore.

LIST OF ABBREVIATIONS

EBR

Electron beam radiation

Gy

Gray

SOD

Superoxide dismutase

GSH

Glutathione

MDA

Malondialdehyde

DTNB

5,5-dithio-bis-(2-nitrobenzoic acid)

BSA

Bovine serum albumin

TCA

Trichloroacetic acid

DMSO

Dimethyl Sulfoxide

DCF-DA

2',7'-dichlorodihydrofluorescein diacetate

FBS

Fetal bovine serum

RPMI medium

Roswell Park Memorial Institute Medium

PI

Propidium Iodide

TBE

Tris/Borate/EDTA

Con-A

Concanavalin A

CFSE

Carboxy fluorescein diacetate succinimidyl ester

ROS

Reactive oxygen species

SC

Super coiled

OP

Open circular

MfM

Mesua ferrea Methanol extract

MfA

Mesua ferrea Aqueous extract[Recommended articles](#)

References

[Abhilash and Ramesh, 2012](#) N. Abhilash, K.V. Ramesh**In vitro Antioxidant, in silico Anti-inflammatory and Anti-cancer activity of *Mesua ferrea***

Research & Reviews: Journal Herbal Science, 3 (1) (2012), pp. 27-34

[Google Scholar](#)[Agarwal and Kaler, 2001](#) A. Agarwal, R.K. Kaler**Radiation-induced peroxidative damage: Mechanism and significance**

Indian Journal of Experimental Biology, 39 (2001), pp. 291-309

[View Record in Scopus](#) [Google Scholar](#)[Akinmoladun et al., 2007](#) A.C. Akinmoladun, E.O. Ibukun, E. Afor, E.M. Obuotor, E.O. Farombi**Phytochemical constituent and antioxidant activity of extract from the leaves of *Ocimum gratissimum***

Scientific Research and Essays, 2 (5) (2007), pp. 163-166

[View Record in Scopus](#) [Google Scholar](#)[Baskar et al., 2014](#) R. Baskar, J. Dai, N. Wenlong, R. Yeo, K.W. Yeoh**Biological response of cancer cells to radiation treatment**

Frontiers in Molecular Biosciences, 1 (24) (2014), pp. 1-9

[Google Scholar](#)[Braughler et al., 1987](#) J.M. Braughler, J.F. Pregoner, R.L. Chase, L.A. Duncan, E.J. Jacobsen, J.M.

McCall

Novel 21-amino steroid as potent inhibitors or iron-dependent lipid peroxidation

Journal of Biological Chemistry, 262 (1987), pp. 10438-10440

[Article](#)  [Download PDF](#) [View Record in Scopus](#) [Google Scholar](#)[Checker et al., 2008](#) R. Checker, C. Suchandra, D. Sharma, G. Sumit, V. Prasad, A. Sharma, *et al.***Immunomodulatory and radioprotective effects of lignans derived from fresh nutmeg mace (*Myristica fragrans*) in mammalian splenocytes**

International Immunopharmacology, 8 (2008), pp. 661-669

[Article](#)  [Download PDF](#) [View Record in Scopus](#) [Google Scholar](#)[Cheeseman and Slater, 1993](#) K.H. Cheeseman, T.F. Slater**An introduction to free radical biochemistry**

British Medical Bulletin, 49 (3) (1993), pp. 481-493

[CrossRef](#) [Google Scholar](#)

[Choudhary, 2012](#) G.P. Choudhary

Wound healing activity of the ethanolic extract of *Mesua ferrea* Linn

International Journal of Advances in pharmacological Biology and chemistry, 1 (3) (2012), pp. 369-371

[View Record in Scopus](#) [Google Scholar](#)

[Dennis and Akshaya, 1998](#) T.J. Dennis, K.K. Akshaya

Constituents of *Mesua ferrea*

Fitoterapia, 69 (1998), pp. 291-304

[View Record in Scopus](#) [Google Scholar](#)

[Devasagayam et al., 2004](#) T.P.A. Devasagayam, J.C. Tilak, K.K. Boloor, S.S. Ketaki, S.G. Saroj, R.D. Lele

Free radicals and antioxidants in human Health: Current status and future prospects

Journal of the Association of Physicians of India, 54 (2004), pp. 794-804

[Google Scholar](#)

[Garg et al., 2009](#) S. Garg, a K. Sharm, R. Ranjan, P. Atrri, P. Mishra

In-vivo antioxidant activity and hepatoprotective effect of methanolic extracts of *Mesua ferrea* L

International Journal of Pharmacy and Technical Research, 1 (2009), pp. 1692-1696

[View Record in Scopus](#) [Google Scholar](#)

[Geller and Winge, 1983](#) B.L. Geller, D.R. Winge

A method for distinguishing Cu, Zn-and Mn-containing superoxide dismutases

Analytical Biochemistry, 128 (1) (1983), pp. 86-92

[Article](#)  [Download PDF](#) [View Record in Scopus](#) [Google Scholar](#)

[Ghaffari, 2008](#) Saghi Ghaffari

Forum review- oxidative stress in the regulation of normal and neoplastic hematopoiesis

Antioxidants and Redox Signaling, 10 (11) (2008), pp. 1923-1940

[CrossRef](#) [View Record in Scopus](#) [Google Scholar](#)

[Gracy et al., 1999](#) R.W. Gracy, J.M. Talent, Y. Kong, C.C. Conard

Reactive oxygen species: The unavoidable environmental insults

Mutation Research, 428 (1999), pp. 17-22

[Article](#)  [Download PDF](#) [View Record in Scopus](#) [Google Scholar](#)

[Hassan et al., 2006](#) M.T. Hassan, M.S. Ali, M. Alimuzzaman, S.Z. Rihan

Analgesic activity of *Mesua ferrea* linn

Dhaka University Journal of Pharmaceutical Sciences, 5 (1-2) (2006), pp. 73-75

[View Record in Scopus](#) [Google Scholar](#)

[Little, 2001](#) M.P. Little

Cancer after exposing to radiation in the course of treatment for the benign and malignant disease

The Lancet Oncology, 2 (2001), pp. 212-220

[Article](#)  [Download PDF](#) [View Record in Scopus](#) [Google Scholar](#)

[Luck, 1974](#) H. Luck

2 (ED. bergmeyer)

Methods in enzymatic analysis, Academic Press, New York (1974)

p.885

[Google Scholar](#)

[Luisella-Verotta et al., 2004](#) Luisella-Verotta, L. Erminio, V. Giovanni, V.F. Paola, G.N. Maria, R. Alessandro, *et al.*

4-Alkyl- and 4-phenylcoumarins from *Mesua ferrea* as promising multidrug resistant antibacterials

Phytochemistry, 65 (2004), pp. 2867-2879

[Google Scholar](#)

[Manjunatha et al., 2013](#) B.K. Manjunatha, Syed-Murthuza, R. Divakara, M. Archana, R.J. Sarvani, V. Steffina, *et al.*

Antioxidant and antiinflammatory activity potency of *Mesua ferrea* linn

Paripex-Indian Journal of the Applied Research, 3 (8) (2013), pp. 55-59

[View Record in Scopus](#) [Google Scholar](#)

[Manoj et al., 2012](#) K.C. Manoj, D.S. Sanjay-Kumar, T. Lokesh, K.P. Manohara

In-vivo antioxidant and immunomodulatory activity of mesuol isolated from *Mesua ferrea* L. seed oil

International Immunopharmacology, 13 (2012), pp. 386-391

[Google Scholar](#)

[Misra and Fridovich, 1972](#) Misra, Fridovich

The role of superoxide anion in the autoxidation of epinephrine and a simple assay for superoxide dismutase

Journal of Biological Chemistry, 247 (1972), pp. 3170-3175

[Article](#)  [Download PDF](#) [Google Scholar](#)

[Modigliani et al., 1994](#) Y. Modigliani, G. Coutinho, O.B. Defranoux, A. Coutinho, A. Bandeira
Differential contribution of thymic outputs and peripheral expansion in the development of peripheral T cell pools

European Journal of Immunology, 24 (5) (1994), pp. 1223-1227

[CrossRef](#) [View Record in Scopus](#) [Google Scholar](#)

[Naveen et al., 2011](#) P. Naveen, K.N. Suchetha, S. Ganesh, G.K.M. Damodar, L.N. Madhu

Radioprotective effect of *Nardostachys jatamansi* against whole body electron beam induced oxidative stress and tissue injury in rats

Journal of Pharmacy Research, 4 (7) (2011), pp. 2197-2200

[View Record in Scopus](#) [Google Scholar](#)

[Nazir et al., 2011](#) M.K. Nazir, S.K. Sandur, R. Checker, D. Sharma, T.B. Poduval, K.B. Sainis
Pro-oxidants ameliorate radiation-induced apoptosis through activation of the calcium–ERK1/2–Nrf2 pathway

Free Radical Biology and Medicine, 51 (2011), pp. 115-128

[Google Scholar](#)

[Ohkawa et al., 1979](#) H. Ohkawa, N. Ohishi, K. Yagi
Assay for lipid peroxide in animal tissue by thiobarbituric acid reaction

Analytical Biochemistry, 95 (1979), pp. 351-358

[Article](#)  [Download PDF](#) [Google Scholar](#)

[Orwa et al., 2009](#) C. Orwa, A. Mutua, R. Kindt, R. Jamnadass, A. Simons
Agroforestry database: A tree reference & selection guide version 4.0

World Agroforestry Kenya (2009)

[Google Scholar](#)

[Raju et al., 1976](#) M.S. Raju, G. Srimannarayana, N.V. Subbarao
Structure of Mesuaferrone-B a new biflavane from the stamens of *Mesua ferrea* linn

Tetrahedron Letters, 49 (1976), pp. 4509-4512

[Article](#)  [Download PDF](#) [View Record in Scopus](#) [Google Scholar](#)

[Rastogi and Mehrotra, 1990-94](#) R.P. Rastogi, B.N. Mehrotra
Compendium of Indian medicinal plants, Vol. 4, Central Drug Research Institute
Lucknow (1990-94), p. 472

[Robbins and Zhao, 2004](#) M.E.C. Robbins, W. Zhao
Chronic and radiation-induced late normal tissue injury: A review
International Journal of Radiation Biology, 80 (4) (2004), pp. 251-256

[View Record in Scopus](#) [Google Scholar](#)

[Rocha et al., 1989](#) B. Rocha, N. Dautigny, P. Pereira
Peripheral T lymphocytes: Expansion potential and homeostatic regulation of pool sizes and CD4/CD8 ratios in vivo

European Journal of Immunology, 19 (1989), pp. 905-911


[CrossRef](#) [View Record in Scopus](#) [Google Scholar](#)


[Sandur et al., 1999](#) S.K. Sandur, R.C. Chaubey, T.P. Devasagayam, K.I. Priyadarsini, P.S. Chauhan
Inhibition of radiation-induced DNA damage in plasmid pBR322 by chlorophyllin and possible mechanism(s) of action


Mutation Research, 425 (1999), pp. 71-79


[Google Scholar](#)

[Savita et al., 2010](#) V. Savita, L.G. Manju, D. Ajaswara, S. Sanghmitra, K.S. Sandeep, J.S.F. Swaran
Modulation of ionizing radiation-induced oxidative imbalance by semi-fractionated extract of Piper betel an in vitro and in vivo assessment
Oxidative Medicine and Cellular Longevity, 3 (1) (2010), pp. 44-52
[Google Scholar](#)

[Sedlak and Lindsay, 1968](#) J. Sedlak, R. Lindsay
Estimation of total, protein-bound, and nonprotein sulfhydryl groups in tissue with Ellman's reagent
Analytical Biochemistry, 25 (1968), pp. 192-205
[Article](#)  [Download PDF](#) [Google Scholar](#)

[Sharma et al., 2007a](#) D. Sharma, S.K. Sandur, R. Rashmi, S. Khanam, K.B. Sainis
Differential modulation of mitogen-driven proliferation and homeostasis-driven proliferation of T cells by rapamycin, Ly294002 and chlorophyllin
Molecular Immunology, 44 (2007), pp. 2831-2840
[Article](#)  [Download PDF](#) [View Record in Scopus](#) [Google Scholar](#)

[Sharma et al., 2007b](#) D. Sharma, S.K. Sandur, K.B. Sainis
Antiapoptotic and immunomodulatory effects of chlorophyllin
Molecular Immunology, 44 (2007), pp. 347-359
[Article](#)  [Download PDF](#) [View Record in Scopus](#) [Google Scholar](#)

[Shobowale et al., 2013](#) O. Shobowale, N.J. Ogbulie, E.E. Itoandon, M.O. Oresegun, S.O.A. Olatope
.Phytochemical and antimicrobial evaluation of aqueous and organic extracts of calotropis procera ait leaf and latex
Nigerian Food Journal, 1 (2013), pp. 77-82
[Article](#)  [Download PDF](#) [View Record in Scopus](#) [Google Scholar](#)

[Sminaa et al., 2011](#) T.P. Sminaa, S. Deb, T.P.A. Devasagayam, S. Adhikarib, K.K. Janardhanan
Ganoderma lucidum total triterpenes prevent radiation-induced DNA damage and apoptosis in splenic lymphocytes in vitro
Mutation Research, 726 (2011), pp. 188-194
[Google Scholar](#)

[Soek Sin The et al., 2011](#) Soek Sin The, G. Cheng Lian Ee, M. Rahmani, Yun Hin Taufiq Yap, Rusea Go, Siau Hui Mah
Pyranoxanthenes from Mesua ferrea
Molecules, 16 (2011), pp. 5647-5654
[Google Scholar](#)

[Sumitra et al., 2013](#) C. Sumitra, R. Kalpana, P. Jigna
Indian medicinal herb: Antimicrobial efficacy of Mesua ferreaL. seed extracted in different solvents against infection causing pathogenic strains

Journal of Acute Disease (2013), pp. 277-281

[Google Scholar](#)

[Svetlana et al., 2013](#) G. Svetlana, P. Borislav, B. Georgi

Radioprotective effect of *Haberlea rhodopensis* (Firr.) leaf extract on γ -radiation induced DNA damage, lipid peroxidation and antioxidant levels in rabbit blood

Indian Journal of Experimental Biology, 51 (2013), pp. 29-36

[Google Scholar](#)

[Umang et al., 2009](#) S. Umang, A. Kunwar, R. Srinivasan, M.J. Nanjan, K.I. Priyadarsini

Differential free radical scavenging activity and radioprotection of *Caesalpinia digyna* extracts and its active constituent

Journal of Radiation Research, 50 (2009), pp. 425-433

[Google Scholar](#)

[Vinutha et al., 2015](#) K. Vinutha, S.M. Vidya, K.N. Suchetha, S. Ganesh, H.G. Nagendra, Pradeepa, *et al.*

Radioprotective activity of *Ficus racemosa* ethanol extract against electron beam induced DNA damage in vitro, in vivo and in silico

International Journal of Pharmacy and Pharmaceutical Sciences, 7 (6) (2015), pp. 110-119

[View Record in Scopus](#) [Google Scholar](#)

[Lushchak, 2012](#) Volodymyr-I. Lushchak

Glutathione homeostasis and Functions: Potential targets for medical interventions

Journal of Amino Acids, 2012 (2012), pp. 1-26

[CrossRef](#) [Google Scholar](#)

[Wang et al., 2008](#) C.C.C. Wang, Y.M. Chiang, S.C. Sung, Y.L. Hsu, J.K. Chang, P.L. Kuo

Plumbagin induces cell cycle arrest and apoptosis through reactive oxygen species/c-Jun N-terminal kinase pathways in human melanoma A375.S2 cells

Cancer Letters, 259 (1) (2008), pp. 82-98

[Article](#)  [Download PDF](#) [View Record in Scopus](#) [Google Scholar](#)

[Wilankar et al., 2011](#) C. Wilankar, D. Sharma, R. Checker, M.K. Nazir, R.S. Patwardhan, A. Patil, *et al.*

Role of immunoregulatory transcription factors in differential immunomodulatory effects of tocotrienols

Free Radical Biology and Medicine, 51 (1) (2011), pp. 129-143

[Article](#)  [Download PDF](#) [View Record in Scopus](#) [Google Scholar](#)

Cited by (0)

Peer review under responsibility of The Egyptian Society of Radiation Sciences and Applications.



Copyright © 2022 Elsevier B.V. or its licensors or contributors.
ScienceDirect® is a registered trademark of Elsevier B.V.



COMPARATIVE STUDY ON REGULAR AND IRREGULAR RC STRUCTURES UNDER FAR AND NEAR FIELD GROUND MOTION WITH BASE ISOLATION

SACHIN MANKAL¹, KARUNA S²

¹M.TECH student, Dept. of Civil Engineering, The oxford college of engineering, Bangalore, Karnataka, India

²Assistant Professor, Dept. of Civil Engineering, The oxford college of engineering, Bangalore, Karnataka, India

Abstract - An Earthquake is characterized as the sudden movement of Earth's crust. Earthquakes are caused by the release of build-up stress within rocks along geological faults or by the movement of magma in volcanic territories. From previous Earthquakes it is seen that earthquakes results in mass destruction which further leads in loss of life. In order to overcome this and to build the Earthquake resistant structures base isolation technique can be used. In this thesis the comparative study on 20 storey regular and irregular RC frame structure under far and near field ground motion with and without base isolation is carried out. Nonlinear time history analysis is done using Kobe (HIK) and Bhuj earthquake data as far and near field ground motions respectively using ETABS 2013 FEM package. Lead rubber bearing (LRB) isolator is considered as isolation system where LRB is designed manually. The parameters considered for this study are base shear, storey displacement, acceleration, velocity, storey drift and time period. In this thesis the variation of parameters, for regular and irregular structure under far and near field ground motion with and without base isolation is studied.

Key Words: Lead rubber bearing (LRB), Near field ground motion, Far field ground motion, Base isolation.

1. INTRODUCTION

An Earthquake is characterized as the sudden movement of Earth's crust. Earthquakes are caused by the release of build-up stress within rocks along geological faults or by the movement of magma in volcanic territories. Major Earthquakes doesn't happen much of the time, yet are generally damaging. Major earthquakes usually do not occur alone when one such earthquake happens there is usually another one at the nearby location. There are smaller earthquakes that occur in the same place before the larger earthquake follows. It causes various damaging effect at places they act. It causes severe damage to the buildings and great loss of life. Hence buildings under seismic prone regions should be designed such that it resists the earthquake without any failure. The sites which are nearer to the fault line are highly affected than the sites which are located far from the fault line.

1.1 Some important definitions

Fault: A fracture having significant movement in parallel with its plane is known as fault. The energy released during the quick slippage of faults results in earthquakes.

Near Field: The field or site which is in the range of 10km to 15km from the fault line is called as near field.

Far Field: When the distance of site or field is more than 20km from the fault line then it is called as Far Field.

The near field earthquake contains high frequency, long period, large amplitude pulses and higher accelerations when compared to far field ground motions. From the fluctuating nature of near field, evaluation of structural response is difficult. They are denoted by simple analogous pulse models of simplified motions composed of important near field aspects for their simplification.

1.2 Base isolation system

A conventional method for making earthquake safe structures is to plan a firm and sufficiently solid structure with the goal that it could oblige expected lateral forces. This may not be the most cost effective technique. The issue with this method is that the building needs to assimilate all the horizontal forces prompted by the seismic ground motion.

The system of base isolation permits to avoid the already mentioned issue. Loss of life in previous earthquakes has constrained the engineers and researchers to consider new and new strategies and techniques to protect the structures from powerful forces of earthquake. The technique of base isolation was developed trying to moderate the impacts of earthquakes on structures during earthquake attacks and has been ended up being one of the exceptionally powerful methods in the previous few years.

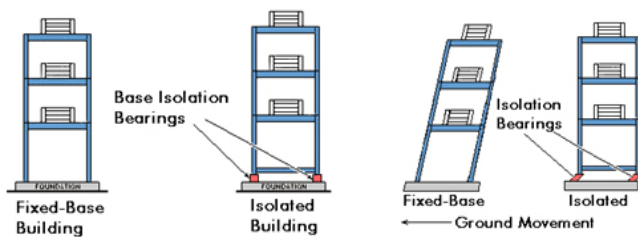


Fig -1: Performance of Fixed Base and Isolated Base structure

1.3 Classification of Base Isolation system

The devices are classified as

1. Elastomeric system.
2. Sliding system.

Elastomeric system is further classified as

1. Natural Rubber Bearings.
2. Lead Rubber Bearings.
3. High Damping Rubber Bearings.

Among these Elastomeric system Lead Rubber Bearing is used in this project

Lead Rubber Bearings

In contrast with natural rubber bearings, lead rubber bearings have a greatly improved ability to give sufficient stiffness to wind loads and better damping qualities.

The lead rubber bearing arrangement is the same as that of natural rubber bearings, apart from there is one cylindrical lead plugs in the center this along with rubber makes the device exhibit bilinear behavior. Under low service wind loads, high stiffness of the lead plug draws in the greater part of the load and the arrangement demonstrates high stiffness.

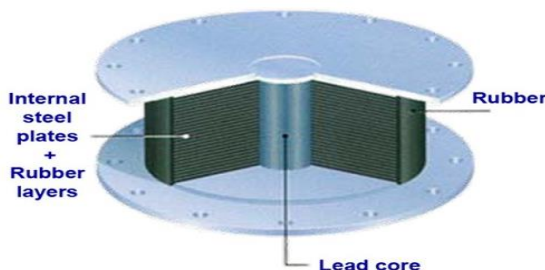


Fig -2: Lead Rubber Bearing

2. SCOPE OF THE STUDY

- From previous Earthquakes it is seen that earthquakes results in mass destruction which further leads in loss of life. In order to overcome

this and to build the Earthquake resistant structures base isolation technique can be used.

- Symmetrical structures impact in a similarly uniform distribution of seismic forces over its segments. Unsymmetrical structures result in uncertain distribution of forces. So the behaviour of regular structures over regular structure is studied.
- The sites which are nearer to the fault line are highly affected than the sites which are located far from the fault line. so the behaviour of structures under near field and far field ground motions are studied.

3. METHODOLOGY AND ANALYSIS

3.1 DETAILS OF PLAN

The plan has 5 x 4 bays, length of each bay is considered as 4m. SMRF (Frame) of 20 storey with regular and irregular in plan is considered. The storey height is same for all the building models considered for analysis.

3.2 PARAMETERS CONSIDERED FOR ANALYSIS

1. Type of structure: Special Moment resisting frame
2. Number of stories: 20
3. Earthquake Zone: V (as per IS 1893:2000)
4. Floor to floor height: 3m
5. Concrete grade: M30
6. Grade of steel: Fe 500
7. Column: 400mm x 700mm
8. Beam: 200mm x 500mm
9. Slab depth: 175mm
10. Super dead load (floor load): 1.5 kN/m²(as per IS 875 (Part 1))
11. Live load: 3 kN/m²(as per IS 875 (Part 2))
12. Live load on top floor: 1.5 kN/m²(as per IS 875 (Part 2))
13. Super dead load (floor load) on top floor: 0.75 kN/m²(as per IS 875 (Part 1))
14. External wall Load: 10kN/m
15. Parapet wall load (1m): 4kN/m
16. Importance factor: 1(as per IS 1893:2000)
17. Response reduction factor: 5 (as per IS 1893:2000)

3.4 MODEL DESCRIPTION

The plan and Elevation of models considered are as follows:

- Model R1: Regular structure with Fixed Base.
- Model R2: Regular structure with Isolated Base.
- Model IR1: Irregular structure in which projection provided are 40% and 50% in X and Y directions respectively with Fixed Base.
- Model IR2: Irregular structure in which projection provided are 60% and 50% in X and Y directions respectively with Fixed Base.

- Model IR3: Irregular structure in which projection provided are 40% and 50% in X and Y directions respectively with Isolated Base.
- Model IR4: Irregular structure in which projection provided are 60% and 50% in X and Y directions respectively with Isolated Base.
- Model R3: Regular structure with Fixed Base. (Far Field)
- Model IR5: Irregular structure in which projection provided are 40% and 50% in X and Y directions respectively with Fixed Base. (Far Field)
- Model IR6: Irregular structure in which projection provided are 60% and 50% in X and Y direction respectively with Fixed Base. (Far Field)

3.5 ETABS MODEL

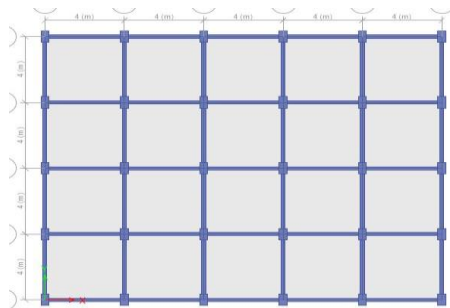


Fig -5 Plan view of Model

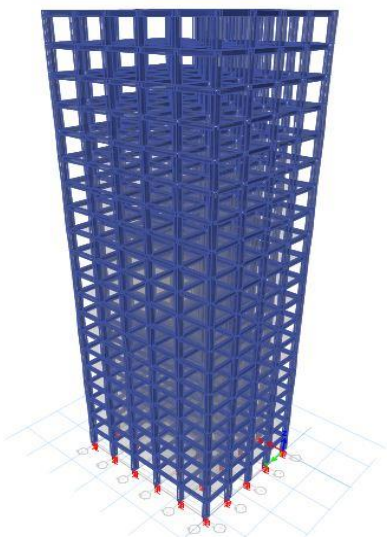


Fig -6 Isometric view of Model

The dynamic (Time history) analysis of G+20 storey RC framed structure is carried out using “ETABS 2013” software, Loading is applied as per IS1893-2000 and IS:875 (part 2). Bhuj earthquake data is used for analysis of structure as near field and Kobe HIK earthquake record is used for analysis under far field.

After the analysis of the structure the LRB Base isolator is designed by considering the maximum Base reaction obtained from the analysis of fixed base structure using ETABS 2013 software.

3.6 Design of Base Isolator (As per UBC 1997 & IS 1893-2000)

Lead rubber bearing type of isolator is used for analysis of the structure and to find the properties of LRB the design is carried out.

3.7 Codal Provisions for Design of Base Isolator

The LRB Base Isolator is designed as per UBC-1997 and IS 1893-2000. Some of the important data required for the Design of LRB are:

1. Seismic zone Factor (Z) = Zone V (Table 16I UBC 1997)
2. Soil profile type = Sc (Table 16J UBC 1997)
3. Seismic coefficient (Ca) = 0.36 (Table 16Q UBC 1997)
4. Seismic coefficient (Cv) = 0.54 (Table 16R UBC 1997)
5. Importance Factor (I) = 1 (Table 16K UBC 1997)
6. Response reduction factor (R) = 5 (Table 16N UBC 1997)
7. Seismic Source type = B (Table 16U UBC 1997)
8. Damping Coefficient (Bd) = 1 (Table 16C UBC 1997)
9. Damping Coefficient (Bm) = 1 (Table 16C UBC 1997)
10. Near source factor (Na) = 1 (Table 16S UBC 1997)
11. Near Source factor (Nv) = 1 (Table 16T UBC 1997)
12. Damping Beff = 5% (From IS 1893-2000 for RC structures)
13. Weight of the structure (W) = 7036 KN (From Analysis)

The Design procedure of LRB base isolator is referred from DESIGN OF SEISMIC ISOLATED STRUCTURE by James M.Kelly and Farzad Naeim.

STEP 1: Calculation of Design displacement (Dd)

Assume design time period as Td = 2.5 seconds. g = 9.81

$$Dd = \frac{g}{4\pi^2} * \frac{CvTd}{Bd}$$

STEP 2: Calculation of Effective Stiffness (Keff)

$$Keff = \frac{W}{g} * \left[\frac{2\pi}{Td} \right]^2$$

STEP 3: Calculation of Energy dissipated per cycle (Wd)

$$Wd = [2\pi * Keff * Dd^2 * Beff]$$

STEP 4: Calculation of characteristics strength (Q)

$$Q = \left[\frac{W}{4Dd} \right]$$

STEP 5: Calculation of Stiffness in rubber (K2)

$$K2 = \left[K_{eff} - \frac{Q}{Dd} \right]$$

STEP 6: Calculation of Yield Displacement (Dy)

$$Dy = \left[\frac{Q}{K1 - K2} \right] \text{ We know that } K1 = 10K2$$

STEP 7: Recalculation of Q to Qr $Qr = \frac{Wd}{4[Dd - Dy]}$

STEP 8: Calculation of area & Diameter of Lead Plug
(Assume Yield strength of lead core in between 7 to 8.5 Mpa)
Area of lead plug needed is

$$A_{pb} = \frac{Qr}{\sigma_{ypb}} \text{ where } (\sigma_{ypb} = 8.5 \text{ Mpa})$$

Diameter of lead plug is

$$A = \frac{\pi d^2}{4}$$

STEP 9: Revising rubber stiffness Keff to Keff(R)

$$K_{eff}(R) = \left[K_{eff} - \frac{Qr}{Dd} \right]$$

STEP 10: Total thickness of rubber layer (tr)

$$tr = \frac{Dd}{\gamma} \text{ Where } \gamma = 100\% \text{ (Max shear strain of rubber)}$$

STEP 11: Area of Bearing (Alrb)

$$Alrb = \left[\frac{K_{eff}(R) * tr}{G} \right] G = \text{Shear modulus of rubber}$$

(Ranging between 0.4 to 1.1 Mpa) Adopt G = 0.8 Mpa

STEP 12: Diameter of Bearing (ϕ_{lrb})

$$\phi_{lrb} = \sqrt{\frac{4A}{\pi}}$$

STEP 13: Shape Factor (S)

$$S = \left[\frac{1}{2.4} * \frac{fv}{fh} \right]$$

Take horizontal Period to be 2.5 seconds

$$fh = \frac{1}{2.5} \quad fh = 0.4 \text{ HZ} \quad fv = 10 \text{ HZ}$$

W.K.T $S = \left[\frac{\phi_{lrb}}{4t} \right]$ Where t is thickness of single rubber layer

Number of rubber layers = $\frac{tr}{t}$

STEP 14: Dimensions of lead rubber Bearing (LRB)

- Let the thickness of shim plates be 3mm
- Number of shim plates = (No of rubber layers - 1)

End plate thickness is between 19.05mm to 38.1mm

Therefore adopt 35mm as thickness of End plate.

STEP 15: Compression Modulus Ec

$$Ec = \left[6GS^2 \left[1 - \frac{6GS^2}{K} \right] \right] \text{ Where } K = 2000 \text{ Mpa}$$

STEP 16: Horizontal stiffness (Kh)

$$Kh = \frac{GAlrb}{tr}$$

STEP 17: Vertical stiffness (Kv)

$$Kv = \frac{Ec * Alrb}{tr}$$

| Property | Value |
|-----------------------------|------------------|
| Effective stiffness (Keff)R | 4172.405 KN/m |
| Horizontal stiffness (Kh) | 4171.940 KN/m |
| Vertical stiffness (Kv) | 2008870.737 KN/m |
| Characteristic strength(Qr) | 120.322 KN |
| Post yield stiffness ratio | 0.1 |
| Damping | 5% |

Table-1 Properties of LRB required in Etabs 2013

4. RESULTS AND DISCUSSIONS

This section presents the results and discussions of seismic analysis of regular and irregular RC structure under near field and far field ground motion with base isolation considering very extreme seismic zone (Zone V), The results of Nonlinear dynamic analysis of regular and irregular RC structure under near field and far field ground motion with base isolation has been discussed below.

1. Base Shear
2. Maximum storey displacement
3. Storey drift

4.1 Base Shear

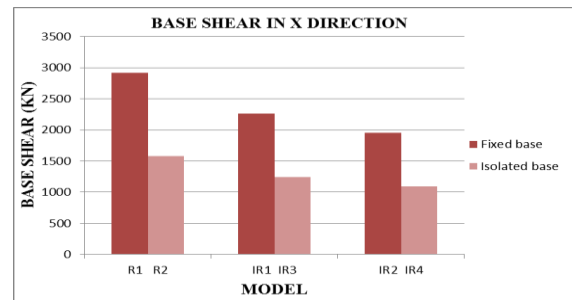


Fig-8 Base shear for R1, R2, IR1, IR3, IR2 and IR4 in X direction

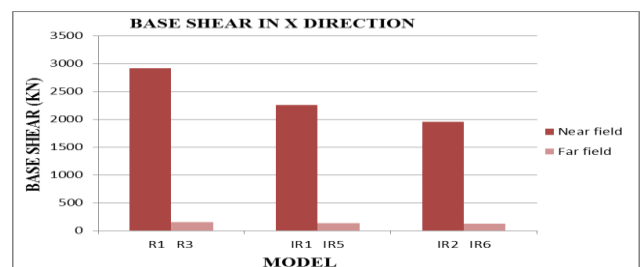


Fig-10 Base shear for R1, R3, IR1, IR5, IR2 and IR6 in X direction

COMPARISON AND DISCUSSION

- From the figures it is observed that the base shear for regular model (R1) is maximum and the base shear is reduced in irregular models IR1 and IR2 (re-entrant corners offset is increased).
- When the Fixed base models(R1,IR1,IR2) and Isolated base models(R2,IR3,IR4) are compared, base shear in isolated base is reduced by 45% in both X and Y directions.
- When the the structure under near field ground motion is compared with strucutre under far field ground motion base shear is very negligible under far field ground motion in both X and Y directions.

| MODEL | BASE SHEAR (KN) | |
|-------|-----------------|-------------|
| | X Direction | Y Direction |
| R1 | 2918.817 | 2561.228 |
| R2 | 1576.16 | 1383.16 |
| R3 | 148.833 | 269.981 |
| IR1 | 2260.464 | 2117.245 |
| IR2 | 1953.576 | 1807.932 |
| IR3 | 1243.255 | 1164.48 |
| IR4 | 1094.002 | 1012.85 |
| IR5 | 132.7903 | 229.2232 |
| IR6 | 120.7655 | 199.3618 |

Table-2 Base shear for all the models

4.2 MAXIMUM STOREY DISPLACEMENT

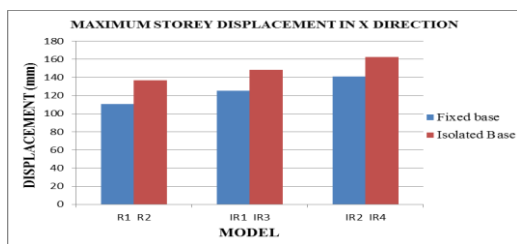


Fig-11 Maximum storey displacement for R1, R2, IR1, IR3, IR2 and IR4 in X direction

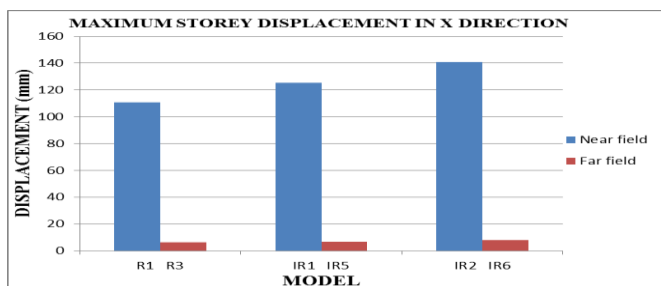


Fig-12 Maximum storey displacement for R1, R3, IR1, IR5, IR2 and IR6 in X direction

COMPARISON AND DISCUSSION

- From figures it is witnessed that the storey displacement increases as the elevation of the structure increases and when comparing the irregular model with the regular one the displacement increases with increase in irregularity in both X and Y directions.
- The displacement in isolated base structure is more than the fixed base structure in both X and Y direction due to isolator.
- When the structure under near field ground motion is compared with strucutre under far field ground motion storey displacement is very negligible under far field ground motion in both X and Y directions.

| MODEL | DISPLACEMENT (MM) | |
|-------|-------------------|-------------|
| | X Direction | Y Direction |
| R1 | 110.8 | 89.4 |
| R2 | 137 | 120.5 |
| R3 | 6.1 | 4.8 |
| IR1 | 125.4 | 111.7 |
| IR2 | 140.9 | 128.2 |
| IR3 | 148.3 | 136.1 |
| IR4 | 162.6 | 152.1 |
| IR5 | 6.8 | 6.1 |
| IR6 | 8 | 7.4 |

Table-3 Maximum storey displacement values for all the models

4.2 STOREY DRIFT

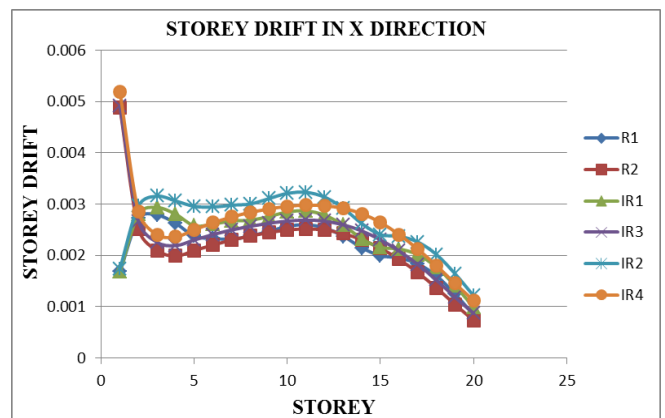


Fig-13 Storey Drift for R1, R2, IR1, IR3, IR2 and IR4 in X direction

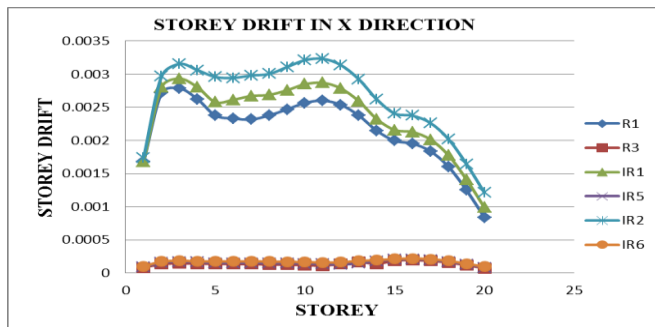


Fig-14 Maximum storey displacement for R1, R3, IR1, IR5, IR2 and IR6 in X direction

6. REFERENCES

1. C.P. Providakis (2007), Effect of LRB isolators and supplemental viscous dampers on seismic isolated buildings under near-fault excitations.
2. Ms. Minal Ashok Somwanshi and Rina N Pantawane (2015), Seismic Analysis of Fixed Based and Base Isolated Building Structures.
3. Vinodkumar Parma, G.S.Hiremath (2014), Effect of base isolation in multistoried RC irregular building using time history analysis.
4. Syed Ahmed Kabeer KI, Sanjeev Kumar K.S (2014), Comparison of Two Similar Buildings with and without Base Isolation.
5. H. R. Tavakoli, H. Gilani & G. R. Abdollahzadeh (2012), Comparative Evaluation of Seismic Parameters for Near-Fault and Far- Fault Earthquakes.
6. A. GHOBARAH (2004), Response of structures to near-fault ground motion.
7. VENKATESH, Mr.ARUNKUMAR.H.R (2016), Dynamic analysis of 11 storey rc structure by providing lead rubber bearing as base isolation system.
8. M. Davoodi, M. Sadjadi & P. Goljahani, M. Kamalian (2012), Effects of Near-Field and Far-Field Earthquakes on Seismic Response of SDOF System Considering Soil Structure Interaction.
9. Reza S. Jalali, Mohammad Nouripour Azgomi, Mihailo D.Trifunac (2013), In-plane response of two-story structures to near-fault ground motion.
10. James M.Kelly and Farzad Naeim, Design of Seismic Isolated Structure from theory of practice, John Wiley and sons, 1999.
11. IS: 456-2000, "Code of Practice for Plain and Reinforced Concrete", Bureau of Indian Standard, New Delhi, India.
12. James M Kelly, Earthquake resistant Design with Rubber, Springer-Verlag, 1st edition, 1993.
13. IS 1893 (Part 1): 2002, "Criteria for Earthquake Resistance Design of Structures", part 1 General Provisions and Buildings, fifth revision, Bureau of Indian Standards, New Delhi, India.
14. Uniform Building Code. International Conference of Building Officials. Whittier, CA. 1997.
15. IS 875-2: Code of Practice for Design Loads (Other Than Earthquake) For Buildings And Structures.

7. BIOGRAPHIES



Sachin Mankal, pursuing post-graduation in Structural Engineering Department at The oxford college of Engineering, Bengaluru, Karnataka, India

COMPARISION AND DISCUSSION

- From the storey drift plot it is observed that in all the models with fixed base and isolated base under near field ground motion, the drift is maximum at storey 11 in X direction.
- From Fig13 it is observed that the drift is maximum in model IR2 along X direction
- When the structure under near field ground motion is compared with strucutre under far field ground motion storey drift is very negligible under far field ground motion in both X and Y directions.

5. CONCLUSION

- The base shear of regular model is maximum and the base shear is reduced in irregular models.
- When the Fixed base models and Isolated base models are compared, base shear in isolated base is reduced by 45% which increases the stability of the structure.
- Base shear of structures under far field ground motion is very less when compared to structures under near field ground motions.
- The storey displacement increases with increase in storey, and the displacement insreases with increase in irregularity in both X and Y directions.
- The displacement of structure with base isolation is greater than the structure with fixed base.
- The displacement of structure under far field ground motion is very negligible when compared with near field ground motion.
- The acceleration and velocity of regular structure is greater than the irregular structure, whereas the displacement is maximum in irregular structure.
- Due to base isolation the acceleration and velocity is reduced in isolated structures when compared to fixed base structure.
- Acceleration and velocity of structure under near field ground motion is greater than the structures under far field ground motion.



Karuna S working as an assistant professor in department of Civil engineering at The oxford college of Engineering, Bengaluru, Karnataka, India.

Design of reinforced concrete structures using neural networks

Chandan.M.K¹, Raghu Prasad.B.K², Amarnath.K³

¹Student, The Oxford College of Engineering, Bangalore

²Retd.IISc Professor, Bangalore

³ Professor and Head, Dept. of Civil Engineering, The Oxford college Of Engineering, Karnataka, India

Abstract - Optimization techniques play an important role in structural design. The purpose is to find the best ways so that a designer or a decision maker can derive maximum benefit from the available resources. In the present study a column, a beam and a G+4 storey model are modelled using STAAD PRO v8i software. Static analysis of the structure is carried out and the results like axial forces (P), bending moments (M), support reactions(R) are recorded. The results are tabulated along with other parameters like Area of steel(Ast), Breadth of beam (B), Depth of beam or slab (D), Characteristic compressive strength of concrete (fck), Characteristic strength of steel (fy), Design bending moment (Mu) and percentage of steel (pt). The design of Reinforced concrete members under uni axial bending is done manually as per IS-456:2000 and SP 16 and percentage of steel is calculated and noted down. The results from the static analysis of the structure which are in tabulated form are tested and trained in MATLAB neural network toolbox. The predicted values for the percentage of steel by neural network toolbox are noted down. The percentages of error for the predicted values are almost negligible when compared to those obtained by conventional method for most of the cases and are in good agreement with one another.

Key Words: Optimization, Artificial Neural Network, STAAD PRO, MATLAB, IS-456 : 2000 etc...

1. INTRODUCTION

The artificial neural network (ANN) was developed 50 years ago. ANNs are the simplifications of biological neural networks. The neural networks are very important tool for studying the structure of human brain. Due to the complexity and for complete understanding of biological neurons, many architectures of ANN have been reported in the present study.

1.1 Aim of neural networks

The aim of neural networks is to replicate the human ability to adapt to changes taking place in the current environment. This depends on the capability to learn from the events that have happened in the past and to be able to apply that to future situations.

For example: The decisions made by trainee doctors are rarely based on a single symptom due to complexity of human body. But an experienced doctor is far more likely to make a good and effective decision than a trainee, because

from his past experiences he knows what to look out for and what not to worry about. Similarly it would be beneficial if machines too, could utilize past events as part of the criteria on which their decisions are based, and this is the role that neural networks seek to fill.

1.2 Artificial neural networks

ANNs consist of a number of processing units analogous to neurons in the brain called nodes. Each node has a function called node function which are associated with a set of local parameters. The local parameters determine the output of the node when input is given. If the local parameters are modified, the node functions may get altered. Hence, the artificial neural networks can be defined as the information-processing system in which the elements called neurons, process the information.

1.3. Structure of neural network

The neural networks can be single layered or multi-layered. A single layered neural network is composed of two input neurons and one output neuron. A multi-layered artificial neural network(MNN) consists of input layer, output layer and a hidden layer of neurons. The hidden layer of neurons is also called as intermediate layer of neurons. A three layered neural network is shown in the figure below.

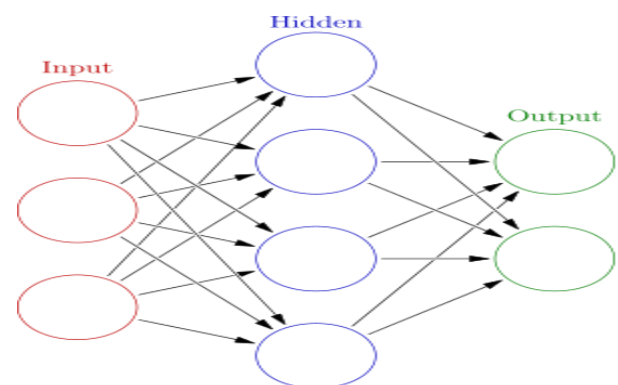


Fig -1:

The above figure shows densely interconnected three layered static neural network in which each circle represents an artificial neuron.

In a MNN, the input layer is connected to hidden layer and the hidden layers are inter-connected to layer of outputs. The neurons in the input layer represent the information that is fed into the network. The activity of neurons in the intermediate layer depends on the activity of neurons in input layer. Likewise, the activity of neurons in the output layer depends on the activity of neurons in the intermediate layer.

2. PARAMETERS IN THE STUDY

- Pu Axial load
- B Breadth of member
- D Overall depth of member
- Ast Area of steel
- fck Characteristic compressive strength of concrete or grade of concrete
- fy Characteristic strength of steel or grade of steel
- Mu Design bending moment
- Pt Percentage of steel

3. ANALYTICAL STUDY

From the analysis of G+4 storey structure carried out in STAAD PRO software results are taken. The design of columns loaded axially under uni-axial bending and the design of simply supported singly reinforced beams are done as per IS:456-2000 and SP-16 code books. The same design of columns and beams of the G+4 storey structure is carried out in neural network toolbox of MATLAB in the form of trained computer programme. Both the cases are compared with one another.

Table 1: Input values calculated for short columns using excel spread sheets for 10 sets

| | | | | | | | | | | |
|-------------------------------------|---------|---------|---------|---------|----------|----------|----------|----------|----------|----------|
| No. of sets | 1 | 2 | 3 | 4 | 5 | 6 | 7 | 8 | 9 | 10 |
| Pu (N) | 761967 | 578928 | 512476 | 135530 | 724123 | 379050 | 871473 | 847200 | 912968 | 642114 |
| Breadth (mm) | 230 | 230 | 230 | 230 | 230 | 230 | 230 | 230 | 230 | 230 |
| Depth (mm) | 600 | 600 | 600 | 380 | 600 | 600 | 600 | 600 | 600 | 600 |
| Moment (N-mm) | 5895000 | 8726000 | 8716000 | 1397000 | 87331000 | 75315000 | 74193000 | 82397000 | 64645000 | 25650000 |
| Cover (mm) | 40 | 40 | 40 | 40 | 40 | 40 | 40 | 40 | 40 | 40 |
| Factored load (N) | 761967 | 578928 | 512476 | 135530 | 724123 | 379050 | 871473 | 847200 | 912968 | 642114 |
| Grade of concrete | 25 | 25 | 25 | 25 | 25 | 25 | 25 | 25 | 25 | 25 |
| Grade of steel (N/mm ²) | 500 | 500 | 500 | 500 | 500 | 500 | 500 | 500 | 500 | 500 |
| % of steel | 2 | 0.8 | 0.8 | 0.8 | 1.3 | 1.2 | 2.3 | 2 | 2.2 | 1.4 |

Table 2 : Training data for short column for 10 sets

| | | | | | | | | | | |
|--|---------|---------|---------|---------|----------|----------|----------|----------|----------|----------|
| No. of sets | 1 | 2 | 3 | 4 | 5 | 6 | 7 | 8 | 9 | 10 |
| Pu (N) | 761967 | 578928 | 512476 | 135530 | 724123 | 379050 | 871473 | 847200 | 912968 | 642114 |
| Breadth (mm) | 230 | 230 | 230 | 230 | 230 | 230 | 230 | 230 | 230 | 230 |
| Depth (mm) | 600 | 600 | 600 | 380 | 600 | 600 | 600 | 600 | 600 | 600 |
| Moment (N-mm) | 5895000 | 8726000 | 8716000 | 1397000 | 87331000 | 75315000 | 74193000 | 82397000 | 64645000 | 25650000 |
| Cover (mm) | 40 | 40 | 40 | 40 | 40 | 40 | 40 | 40 | 40 | 40 |
| Factored load (N) | 761967 | 578928 | 512476 | 135530 | 724123 | 379050 | 871473 | 847200 | 912968 | 642114 |
| Grade of concrete (N/mm ²) | 25 | 25 | 25 | 25 | 25 | 25 | 25 | 25 | 25 | 25 |
| Grade of steel (N/mm ²) | 500 | 500 | 500 | 500 | 500 | 500 | 500 | 500 | 500 | 500 |

Table 3 : Input values calculated for simply supported beams using excel sheets for 10 sets.

| | | | | | | | | | | |
|---|-----------|-----------|----------|----------|-----------|-----------|-----------|-----------|-----------|-----------|
| Beam No. | 252 | 245 | 247 | 246 | 244 | 251 | 253 | 272 | 273 | 255 |
| Cover | 25 | 25 | 25 | 25 | 25 | 25 | 25 | 25 | 25 | 25 |
| Depth (mm) | 600 | 600 | 600 | 600 | 600 | 600 | 380 | 600 | 600 | 600 |
| Span Moment (N-mm) | 75400000 | 103000000 | 43500000 | 43000000 | 101000000 | 74800000 | 62600000 | 54500000 | 186000000 | 55400000 |
| Left hand support moment (N-mm) | 102000000 | 156000000 | 63200000 | 77200000 | 175000000 | 111000000 | 93300000 | 174000000 | 308000000 | 98400000 |
| Right hand support moment | 112000000 | 157000000 | 71400000 | 58300000 | 152000000 | 104000000 | 146000000 | 103000000 | 310000000 | 179000000 |
| f _{ck} (N/mm ²) | 25 | 25 | 25 | 25 | 25 | 25 | 25 | 25 | 25 | 25 |
| F _y | 500 | 500 | 500 | 500 | 500 | 500 | 500 | 500 | 500 | 500 |
| Percentage of steel at mid span | 0.30 | 0.37 | 0.20 | 0.19 | 0.36 | 0.32 | 0.27 | 0.19 | 0.71 | 0.19 |
| Percentage of steel at left hand support | 0.36 | 0.58 | 0.22 | 0.27 | 0.66 | 0.39 | 0.38 | 0.65 | 1.22 | 0.35 |
| Percentage of steel at right hand support | 0.4 | 0.63 | 0.25 | 0.2 | 0.56 | 0.37 | 0.37 | 0.37 | 1.23 | 0.68 |

Table 4: Training data for simply supported beam for 10 sets

| | | | | | | | |
|-------------|----------|--------------|------------|----------------------------------|------------|--|-------------------------------------|
| 10 | 252 | 230 | 600 | 75.4 | 40 | 25 | 500 |
| 9 | 245 | 230 | 600 | 103 | 40 | 25 | 500 |
| 8 | 247 | 230 | 600 | 43.5 | 40 | 25 | 500 |
| 7 | 246 | 230 | 600 | 43 | 40 | 25 | 500 |
| 6 | 244 | 230 | 600 | 101 | 40 | 25 | 500 |
| 5 | 251 | 230 | 600 | 74.8 | 40 | 25 | 500 |
| 4 | 253 | 230 | 380 | 62.6 | 40 | 25 | 500 |
| 3 | 272 | 230 | 600 | 54.5 | 40 | 25 | 500 |
| 2 | 273 | 230 | 600 | 186 | 40 | 25 | 500 |
| 1 | 255 | 230 | 600 | 55.4 | 40 | 25 | 500 |
| No. of sets | Beam no. | Breadth (mm) | Depth (mm) | Span Moment $\times 10^6$ (N-mm) | Cover (mm) | Grade of concrete (N/mm ²) | Grade of steel (N/mm ²) |

3.1 Optimized response spectrum results in MATLAB

The response spectrum analysis of the above mentioned G+4 storey structure is carried out in STAAD PRO software and the maximum results of nodal displacement, moments and base shear are taken.

Table 5 : Input data

| | |
|--------------------------------|---------|
| Total height of the structure | 21 m |
| Maximum width of the structure | 21.03 m |
| Zone | 0.1 |
| Number of storeys | 7 |
| Number of bays | 5 |

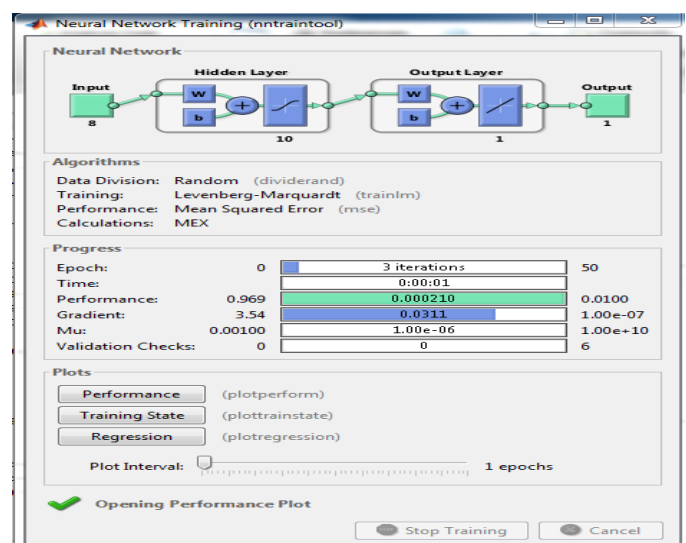
Table 6 : Target data obtained from Response spectrum analysis using STAAD PRO

| | |
|---|-------------|
| Maximum base shear | 996.42 kN |
| Maximum nodal displacement in X direction | 48.84 mm |
| Maximum nodal displacement in Y direction | 3.733 mm |
| Maximum nodal displacement in Z direction | 70.214 mm |
| Maximum moments in X direction | 104.14 kNm |
| Maximum moments in Y direction | 2.009 kNm |
| Maximum moments in Z direction | 107.657 kNm |

4. Results and discussions

4.1 Results for 10 sets of input of short columns

$y_1 =$
2.2125 2.0804 1.9994 1.8955 2.5822 2.5717 2.4263 2.5640 2.6012 2.5350



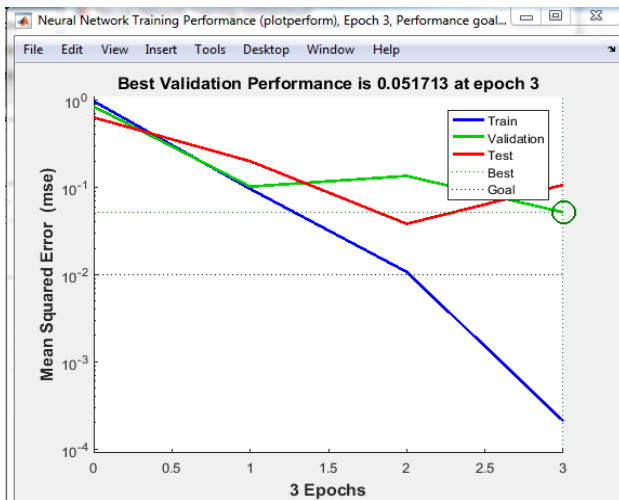
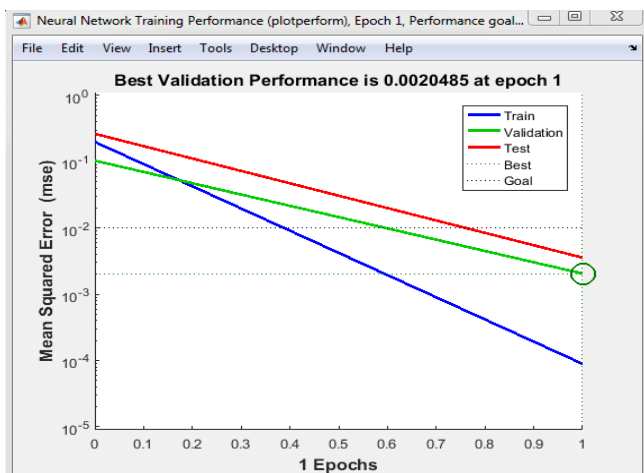
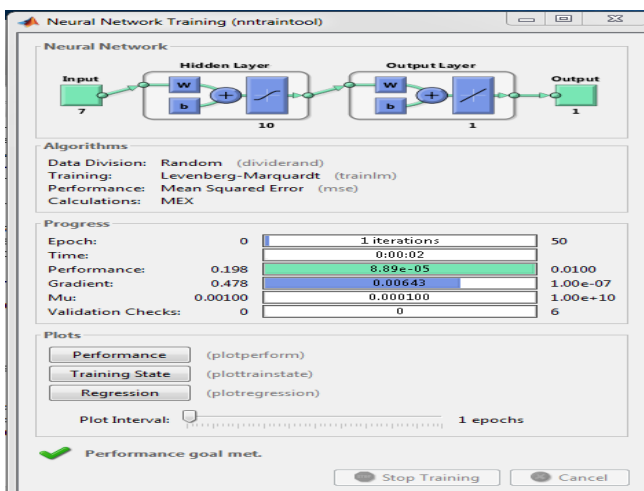


Table 7 : Percentage of errors in the design of short column

4.2 Results for 10 sets of input of simply supported beams

y1 =
0.5962 0.3129 0.3792 0.6414 0.6526 0.6183 0.9586 0.7797 0.6357 0.6342



| | | | | | | | | | | | | |
|--|--------|-----|-----|----------|----|--------|----|-----|--|-----|--------|--------|
| | 761967 | 230 | 600 | 5895000 | 40 | 761967 | 25 | 500 | | 2 | 1.93 | -0.035 |
| | 578928 | 230 | 600 | 8726000 | 40 | 578928 | 25 | 500 | | 0.8 | 0.9755 | 0.219 |
| | 512476 | 230 | 600 | 8716000 | 40 | 512476 | 25 | 500 | | 0.8 | 0.7960 | -0.005 |
| | 135530 | 230 | 380 | 1397000 | 40 | 135530 | 25 | 500 | | 0.8 | 0.7791 | -0.026 |
| | 724123 | 230 | 600 | 87331000 | 40 | 724123 | 25 | 500 | | 1.3 | 1.2893 | -0.008 |
| | 379050 | 230 | 600 | 75315000 | 40 | 379050 | 25 | 500 | | 1.2 | 1.1705 | -0.025 |
| | 871473 | 230 | 600 | 74193000 | 40 | 871473 | 25 | 500 | | 2.3 | 2.305 | 0.002 |
| | 847200 | 230 | 600 | 82397000 | 40 | 847200 | 25 | 500 | | 2 | 2.003 | 0.002 |
| | 912968 | 230 | 600 | 64645000 | 40 | 912968 | 25 | 500 | | 2.2 | 2.588 | 0.176 |
| | 642114 | 230 | 600 | 25650000 | 40 | 642114 | 25 | 500 | | 1.4 | 1.4030 | 0.002 |
| Pu (N) | | | | | | | | | | | | |
| B (mm) | | 230 | 600 | | | | | | | | | |
| D (mm) | | 230 | 600 | | | | | | | | | |
| Mu | | | | 25650000 | 40 | | | | | | | |
| Cover (mm) | | | | | 40 | | | | | | | |
| Factored load (N) | | | | | | 642114 | | | | | | |
| Fek (N/mm ²) | | | | | | | 25 | | | | | |
| Fy (N/mm ²) | | | | | | | | 500 | | | | |
| Desired value of percentage of steel | | | | | | | | | | 1.4 | | |
| Predicted value of percentage of steel | | | | | | | | | | | 1.4030 | |
| % error | | | | | | | | | | | | 0.002 |

Table 8 : Percentage of errors in the design of simply supported beam

| | | | | | | | | | | |
|--|-----------|-----------|----------|----------|-----------|-----------|-----------|-----------|-----------|-----------|
| Beam No. | 252 | 245 | 247 | 246 | 244 | 251 | 253 | 272 | 273 | 255 |
| Cover | 25 | 25 | 25 | 25 | 25 | 25 | 25 | 25 | 25 | 25 |
| Depth (mm) | 600 | 600 | 600 | 600 | 600 | 600 | 380 | 600 | 600 | 600 |
| Span Moment | 75400000 | 103000000 | 43500000 | 43000000 | 101000000 | 74800000 | 62600000 | 54500000 | 186000000 | 55400000 |
| Left hand support | 102000000 | 156000000 | 63200000 | 77200000 | 175000000 | 111000000 | 93300000 | 174000000 | 308000000 | 98400000 |
| Right hand support | 112000000 | 157000000 | 71400000 | 58300000 | 152000000 | 104000000 | 146000000 | 103000000 | 310000000 | 179000000 |
| fek (N/mm ²) | 25 | 25 | 25 | 25 | 25 | 25 | 25 | 25 | 25 | 25 |
| Fy | 500 | 500 | 500 | 500 | 500 | 500 | 500 | 500 | 500 | 500 |
| Percentage of steel at mid span | 0.30 | 0.37 | 0.20 | 0.19 | 0.36 | 0.32 | 0.27 | 0.19 | 0.71 | 0.19 |
| Percentage of steel at left hand support | 0.36 | 0.58 | 0.22 | 0.27 | 0.66 | 0.39 | 0.38 | 0.65 | 1.22 | 0.35 |
| Percentage of steel at right | 0.4 | 0.63 | 0.25 | 0.2 | 0.56 | 0.37 | 0.37 | 0.37 | 1.23 | 0.68 |

5. Conclusion

Predicted values from the Artificial neural network (ANN) for the design of Reinforced concrete columns, beams are very close to those obtained from conventional design using IS:456-2000. The errors are quite low in the predicted values. Similarly, the maximum values of base shear, nodal displacements and moments from the analysis are compared with those from the predicted values using artificial neural network. The two are very close to one another. Therefore, it can be said such a well trained artificial neural network can be used to perform design.

References

1. K.Karthikeyan, Dr.R.Mercy Shanthi, "Optimization of RC columns using artificial neural network", International journal of scientific & engineering research volume 7, issue 4, April 2016.
2. Abu-bakr A. A. Aga, Fathelrahman M. Adam, "Design optimization of reinforced concrete frames", open journal of civil engineering, published in March 2015.
3. Sara .A. Babiker, Fathelrahman.M . Adam, Abdelrahman E. Mohamed, "Design optimization of reinforced concrete beams using artificial neural network", International journal of engineering inventions volume 1, issue 8, October 2012.
4. S.A.Bhalchandra, P.K.Adsul, "Cost optimization of doubly reinforced rectangular beam section", International journal of modern engineering research (IJMER) volume 2, issue 5 Sept- Oct 2012.
5. Jagbir Singh, Sonia Chutani, "A survey of modern optimization techniques for reinforced concrete structural design", International journal of engineering science invention research & development volume 2, issue 1, July 2015.
6. S.Ramamrutham, "Design of reinforced concrete structures", Dhanpat rai publishing company.
7. H.Sudarsana Rao, B.Ramesh Babu, " Optimized column design using genetic algorithm based neural networks" Indian journal of Engineering and Material science, 2006.
8. N.Jayaramappa, A.Krishna, B.P.Annpurna and T.Kiran, "Prediction of Base shear for three dimensional RC frame subjected to Lateral load using Artificial Neural Network" Indian Journal of science and technology, 2014.

9. Zulkifli Muhammad, "Frame Optimization using Neural Network" International journals on science and technology.
10. "Application of Neural network in civil engineering problems" by D.S.Jeng , D.H.Cha and M.Blumenstein, 2003.
11. Applications of Artificial Neural Network in Construction Engineering and Management by Megha Jain K.K.Pathab, 2014.
12. "Counterpropagation Neural Networks in Structural Engineering" by Hojjat Adeli, 2006.
13. Analysis of infilled frames- A study using Neural Network, by N.Muralikrishna and Dr.Gangadharan, 1999.
14. "Predicting the life of concrete structures using neural networks" by N.R.Buenfeld, 1998.
15. Neural Networks approaches to weight simple truss design problem by Hyeong - taek & C.Johnyoon, 1994.
16. Rafiq.M.Y, Genetic algorithms in optimum design, capacity check and final detailing of reinforced concrete columns, School of civil and engineering University of Plymouth, Plymouth, 1995.
17. Senoui.A.B and Abdul-Salam.M.A, Prediction of reinforced concrete beam depth Using Neural Networks, Engineering Journal of the University of Qatar, 1998.
18. ACI committee 318, Building code requirements for structural concrete, ACI 318-08, American Concrete Institute, 2008.
19. Bureau of Indian standards, IS 456:2000, Code of Practice for Plain and reinforced Concrete, 2000.
20. AL-Salloum.Y.A and Siddqi .G.H, Cost optimum design of concrete beams, ACI structural journal, Vol.91, No.6,1994.
21. Lee.C. and Ahn.J, "Flexural Design of Reinforced Concrete frames by Genetic Algorithm, Journal for Structural Engineering, 2003.
22. Guerra.A. and Kiouisis.P.D," Design Optimization of Reinforced Concrete Structures", Computers and Concrete, 2006.
23. Yousuf.S.T, Alsaffar. I.S and Ahmed.S.M. , "Optimum design of Singly and Doubly Reinforced Concrete Rectangular Beam Sections : Artificial Neural Networks Application, Iraqi Journal of civil Engineering, 2010.

Ductility Of fly ash - slag based reinforced geopolymer concrete elements cured at room temperature.

Mahantesh N.B. ^{1*}, Amarnath. K. ², and Raghuprasad B. K. ³

¹ Alliance University, Bangalore, India

^{2,3} The Oxford College of Engineering, Bangalore, India

Abstract. Ductility of the flexural element is the main governing property for healthy performance of structural element. Although numerous factors contribute towards the ductility of Reinforced Geopolymer Concrete (RGPC) elements, low calcium based fly ash and GGBS have chemical proportions which make RGPC develop significant ductility along with steel reinforcement – when mixed in an intelligent way satisfying structural and economic conditions. In the present research work influence of low calcium fly ash, GGBS, River sand, M-sand, Steel Grade, manufactured fibres and natural fibres are used to study the ductile behaviour of RGPC sections by load testing 51 under reinforced flexural elements. The study reveals that fly ash - slag based reinforced flexural elements behave in line with OPC based RCC elements. The provisions mentioned in Indian RC designer IS:456-2000 can be used to predict the flexural behaviour of reinforced geopolymer concrete elements. The average flexural ductility of these test specimens observed to lie in between 2 & 3.

Keywords: Ductility, Geopolymer concrete, fly ash, slag, large deflections, flexural behaviour, River sand, Manufactured Sand.

1) INTRODUCTION

Geopolymer Concrete an environmentally friendly concrete having good structural skills is known structural concrete for the last 50 years, but still ordinary Portland Cement Concrete holds the first place in all construction activities. The manufacturing process of geopolymer concrete needs urgent attention to develop a process which suits the requirement of a most consumed private sector of concrete industry like fast moving consumer product (**FMCG**). Low calcium based fly ash geopolymer concrete essentially need heat or steam curing which make them unsuitable for cast in situ applications. The cost of curing is the additional factor which has made geopolymer concrete unpopular in most of the construction activities, especially in reinforced concrete structural elements.

*corresponding author: mahanteshb@rediffmail.com

Ambient curing is the most effective remedy to solve this issue. Industrial waste like slag (ground granulated blast furnace slag), when mixed with fly ash, develops strength at ambient temperature without heat or steam curing keeping the final strength same. During the past 10 - 15 years partial replacement of cement by fly ash & GGBS is becoming popular because of economic reasons in these sectors of concrete industry, giving ample evidence and data for a complete replacement.

2) MATERIALS USED AND PROPERTIES.

Fly ash used in this work was collected from Raichur thermal power plant in Karnataka, having sp.gr 2.15, Silicon dioxide (SiO₂) 61.98%, Aluminium oxide (Al₂O₃) 26.06%, calcium oxide(Cao) 3.05% confirming to grade 1 of IS 3812. *Slag – ground granulated blast furnace slag*, was procured from Jindal Steel Plant Bellary-Karnataka, having sp.gr 2.62, Silicon dioxide (SiO₂) 33.88%, Aluminum oxide (Al₂O₃) 18.02%, calcium oxide(Cao) 34.98% confirming to IS 12089.

Manufactured-Sand (M-sand), crushed from granite stone, having Sp.gr 2.45, Fineness Modulus (F.M) 2.70 and *River Sand* of sandstone origin having F.M 2.62 confirming to Zone III of IS 383-1970 are used as fine aggregates and tested as per IS 2386. *Coarse aggregates* of granite origin of sizes 20mm, 12.5mm & 4.75mm tested as Per IS2386. These coarse aggregates have water absorption capacity 0.5% by weight at room temperature 16 to 28 degrees Celsius.

Sodium hydroxide of 97% purity and *sodium silicates* with Na₂O=14.7%, SiO₂=29.41%, water = 59.9% by mass are used as Alkaline Activator Solution using ratio of Na₂SiO₃/ NaOH = 2.5. *Sulphonated naphthalene* based superplasticiser, i.e. Conplast SP430 DIS distributed by FOSROC chemicals Bangalore used. Reinforcement is of Fe415 and Fe500 grades.

Four types of fibres used. They are (1) waste fibres produced from workshop lathe machine labelled as **LMF** (Lathe machine waste fibre) (2) factory made hook ended steel fibres marked as **SF2** of aspect ratio 71 from Bekeart Pvt. Ltd, (3) plane steel fibres without hook end labelled as **SF1** from Nevatia Steel & Alloys Pvt Ltd (4) Polyester fibres marked as **PF** from Recron 3s Pvt Ltd placed sourced from South Indian Private Companies.

Table 1: Constituents for 1m³ of Geopolymer Concrete

| S.No. | Materials | Weight (kg) | Specifications |
|-------|--|-------------|--|
| 1 | Fly ash | 276 | 70% of total fly ash |
| 2 | GGBS (30%) | 120 | 30% of total fly ash |
| 3 | 20mm to 12mm size CA | 451 | 35% of total CA |
| 4 | 12mm to 4.75mm CA | 451 | 35% of total CA |
| 5 | 4.75mm & down sizes | 389 | 30% of total CA |
| 6 | River sand | 111 | 20% of total FA |
| 7 | M-sand | 444 | 80% of total FA |
| 8 | Sodium hydroxide of 8M | 45 | 97% purity |
| 9 | Sodium Silicate(Na ₂ SiO ₃) | 113 | Na ₂ O14.7%, SiO ₂ 29.4% |
| 10 | Super plasticizer | 3.6 | SP430DIS (1.5%) |
| | NOTATION: FA: Fine aggregate, CA: Coarse aggregate | | |

Table 1 shows the mix proportions used for all reinforced geopolymer concrete specimens listed in Table 2.

3) SPECIMEN PREPARATION

Alkaline Activator Solution (AAS) is prepared 24 hours before mixing of concrete. Molarity of the NaOH solution (SHS) determined by the relation $M = 0.25PD$. M is the molarity of NaOH solution, P is concentration of sodium, D is the density of SHS for P. Therefore to get 1 liter of SHS of 8, 10 and 12 Molarity (255+745), (306+694) and (354+646) of (Sodium Hydroxide pallets in gms + water in gms) added respectively [4]. Cover blocks of 10mm thick are used for all specimen to provide clear uniform cover to reinforcements. Compaction of geopolymer concrete while filling in formwork containing reinforcement is done by using vibrators. The side from work removed after 24 hours of casting and specimen are left to room temperature curing which varied from 16 degrees Celsius at night & 28 degrees Celsius during peak daytime.

4) SPECIMEN DETAILS

To know the ductile capacity of reinforced flexural elements, different parameters which affect the ductility of components taken into considerations and a careful grouping of different specimens to be tested are listed. In all 41 slabs were tested having four different sizes $1.3m \times 0.65m$, $1m \times 1m$, $0.8m \times 0.8m$, $0.975m \times 0.65m$ with aspect ratios 1, 1.5 and 2.0. Two types of loads were applied, i.e. CPL Central Point Load and UDL – Uniformly Distributed Load using monotonically increasing load in 50Mton Loading frame.

Table 2: Specimen Groups

| Group Name Fine Agg. - Molarity | No & Element | Size mm L x B x D | Ast- N_x-N_L | fy- fck- & curing days |
|--|-----------------|--|--------------------|---------------------------|
| A1:MS-8M | 8-Slabs | 1300 x 650 x 75 | 8mm – 4# & 7# | Fe500-57.87-36 |
| A2:MS-10M | 8-Slabs | 975 x 650 x 75 | 8mm – 4#& 6# | Fe500-45.96-26 |
| A3: MS-12M | 8-Slabs | 800 x 800 x 75 | 8mm – 5#& 5# | Fe500-41.70-22 |
| B1, B2, B3: MS-8M | 12-Slabs | 1000 x 1000 x 60 | 8mm –7# &7# | Fe415-44.20-14 |
| C1: RS-8M | 05-Slabs | 1000 x 1000 x 60 | 8mm –11#&11# | Fe415-35-14 |
| D: BM1to BM10 RS-8M | 10-Beams | Top :02#-8mm Bot: 03#-12mm 2L-8mm-100c/c | B=150mm D=210mm | Fe415-35-14 |
| Notation: MS- Manufactured sand , RS- River sand : N_x & N_L rebars parallel to Shorter & Longer Sides, Fe500- yield stress 533Mpa & Ultimate stress 587Mpa, Fe415- yield stress 423 Mpa and Ultimate stress 502Mpa, SS- Short sides simply supported & remaining sides free, fck – cube compressive strength Mpa, PF – polyester fibers. PL-plain GPC | | | | |

5) LOAD TESTING OF SPECIMENS

Testing of slabs is done by applying crucial point loads and uniformly distributed loads by using 50Mton self-straining loading frame with electrically operated hydraulic jack. The

two-point load system at a $L/3$ distance from both support ends of the beams applied for all the beams. Then the deflections are measured under load points and at the centre of the beam. On the day of testing flexural members - cubes and cylinders were tested.

6) NUMERICAL COMPUTATIONS

Among the most widely used and easily available aggregates, Granite holds the first place having Young's Modulus varying from 10 – 70 GPa - far above the values of sandstone rocks, i.e. 1- 20 GPa. When Manufactured sand of granite origin as fine aggregate mixed with coarse aggregates of granite origin, with fly ash: slag at 70:30 the resulting composite of granite based geopolymer concrete develops better structural properties. The IS:456-2000 describes the relations between compressive strength and flexural strength, modulus of elasticity as $f_{cr}=0.7\sqrt{f_{ck}}$ [2] and $E_c= 5000\sqrt{f_{ck}}$ after 28 days of curing [9]. These expressions are very closely following for fly ash: GGBS ratio at 70:30. [3]

All slabs and beams are analysed using conventional elastic theory for the applied loads and provided boundary condition using geometrical & material properties like compressive strength, steel strength as listed in Table 1. The failure mechanism of reinforced geopolymer concrete flexural elements follows the conventional OPC based RCC behaviour. The numerical computations are done using IS 456-2000. Until the appearance of the first crack at centre bottom of slab and beam, the composite is linearly elastic. Assessing the strength at this stage, using a full section of concrete results into more moment of inertia gives fewer deflections than measured ones. The composite continues to behave linearly elastic till tensile steel yields. Deflection calculations based on the effective moment of inertia using local code give noticeably matching with actual deflections.

Using $0.67f_{ck}$ as peak stress in compression concrete with parabolic stress blocks gives maximum strain 0.0020 to 0.0025, whereas using $0.85f_{ck}$ with rectangular stress block gives strains around 0.003 to 0.0035. Failure loads from both peak stresses are acceptably same. The tensile stress of concrete at all stages are neglected. Calculated flexural cracks widths and measured ones are closely matching and are within acceptable limits at service loads. Beyond this stage, the specimen is said to have failed structurally. Further loading on the specimen is treated as post failure stage where significant deflections are observed.

7) FLEXURAL DUCTILITY OF GEOPOLYMER CONCRETE

If the constituent materials of concrete are ductile, then the concrete can be made more ductile by adding tension steel to develop the desired ductility so that the structures respond elastically at low cost. The plain geopolymer concrete under increasing flexure stress develops compression strains from 0.0010 to 0.0045 [5]. While reinforcement steel (Fe415) 0.0045 to 0.015 (yielding to failure). This reflects on strain ductility of 4.5 for GPC and steel 3.33. These values indicate the possible ductility of resulting composite, i.e. RGPC when subjected to pure flexural stresses.

For the known geometrical & material properties - analytically yield load F_y & ultimate load F_u is determined. Corresponding deflections Δ_y & Δ_u are read from load Vs deflection curves are drawn by using laboratory measurements. Then Ductility (*calculated*) = Δ_u / Δ_y , and Ductile Load $D.L = F_u/F_y$. Similarly, Strain Hardening Slope for calculated one = $SHS_{cal} = \text{Ductile Load (calculated)}/\text{Ductility (cal)}$

Similarly, Ductility(*measured*) = Δ_{um}/Δ_y , Δ_{um} is the maximum deflection the component undergone under maximum applied load F_{um} and Δ_y is the measured deflection at yielding

of steel. Then Ductile Load $D.L_m = F_{um}/F_y$. Similarly, Strain Hardening Slope for measured one = SHS mea = Ductile Load (measured)/Ductility (mea)

Ductility (calculated) & Ductility (measured) represent the minimum and maximum ductility developed by GPC. The Average Displacement Ductility is the average ductility between these two values, having more probability develops under Normal Quality Control.

8) RESULTS AND DISCUSSION

The mix design used is based on 77% of total aggregates to produce 40Mpa after ambient curing at 16 to 28 degrees Celsius for seven days which includes 24 hours of the rest period. Although M-sand and R-sand have nearly same fineness modulus, using Manufactured sand, the mix provided more than 40 Mpa, while using River-sand produced less than 40 Mpa compressive strength. The main reason for the difference in strength may be due to the difference in rock origins of fine aggregates & coarse aggregate, i.e. M- sand being granite origin mixing with coarse granite aggregates produces excellent bonding, whereas River sand being Sandstone origin produced less bonding with coarse granite aggregates. Moreover, the basic compressive strength of granite (100 to 250Mpa) is more than sandstone (20 to 170 Mpa) making granite based concrete stronger.

With steel fibres, the composites develop improved strengths while PF produced a marginal increase in strength. This indicates that all four types of fibres used were able to develop a good bond with GPC mixture of both types of fine aggregate. The increased compressive strengths are attributed to the property of fibres in delaying the failure by increased deflections.

Fig.1 to Fig.3 represent the developed deflections of the first set of slabs **Group A**. Compared to UDL; Central point loads develop steep & sudden deflections at all the three stages of loading. The first appearance of a crack in tension concrete, yielding of tension steel and development of peak compressive stresses - passed within a short difference of loads because of stress concentration under the load.

Group B slabs: Compared to Fe500 steel, Fe415 steel is more ductile. As seen from Fig 4, Fig 5 & Table 2- it has produced ductility of slabs around 2.81 without fibres. Manufactured steel fibres increased the average ductility to 3.15, while the lathe machine fibres could develop around 2.79 and did not influence much on ductility. The lathe machine fibres are of random sizes in a loop form and thus could not align themselves along the major bending axis. However, it is expected that increased percentage and reducing the sizes by cutting them down to aspect ratio 30 could produce more ductility which is cost effective also.

In Group C: As seen from Fig. 6 & table 2 the average ductility of slabs was limited to 1.64. Using steel fibres slight increase in ductility observed while marginal improvement in ductility was observed using polyester fibres.

In Group D all beams are subjected to two-point load system & beams with steel fibres developed slightly better ductility compared to 4 beams with polyester fibres. As seen from strength tests on cubes and cylinders, river sand of the type used has the less basic compressive strength right from its parent rock, i.e. Sand Stone has less compressive strength than Granite stone. In addition to this - river and does not develop enough bond with fibres and thus develops less ductility compared to M-sand.

As seen from strength tests on cubes and cylinders, river sand of the type used has less basic compressive strength right from its parent rock. That is, Sand Stone has less compressive strength than Granite stone. In addition to this, the river sand does not develop enough bond with fibres and thus develops less ductility compared to M-sand.

The applied load Vs measured deflections of all specimens listed from Fig. 1 to 7. Table 3 shows the list of observed ductilities of all 51 test specimens. These results indicate that M sand based RGPC specimens are more ductile than R-Sand based specimens. With steel fibre, these specimens may further enhance the composite ductility.

Table 4 broadly summarises the ductilities interms of two fine aggregates used. Addition of steel fibres at 1 to 1.5% could increase the ductility of M-Sand and R-Sand based RGPC. The combination M-Sand with Fe415 reinforcement & steel fibres produce maximum ductility of **2.97**. However, R-Sand with Fe415 reinforcement without any fibres produces the lowest ductility of **1.91**.

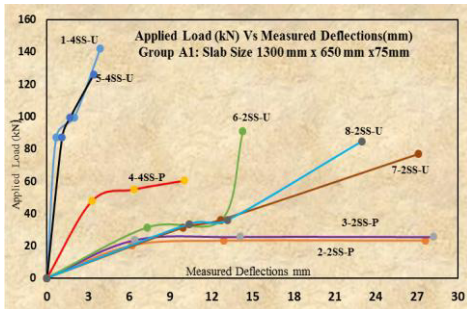


Fig. 1: Applied Load (kN) Vs Measured Deflection (mm) for Group A1- specimens

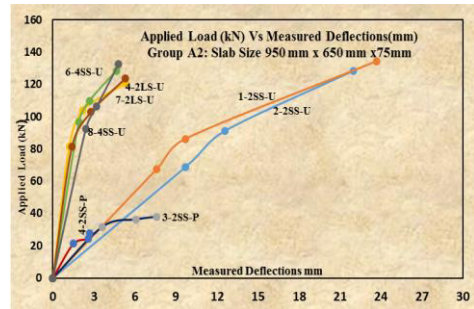


Fig. 2: Load (kN) Vs Measured Deflection (mm) for Group A2- specimens

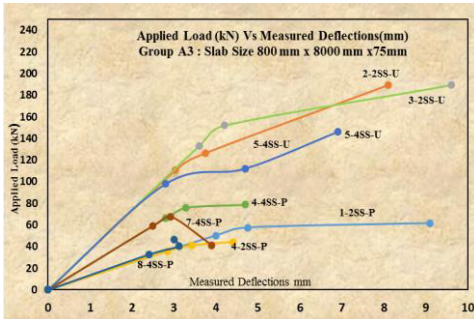


Fig. 3: Load (kN) Vs Measured Deflection (mm) for Group A3- specimens

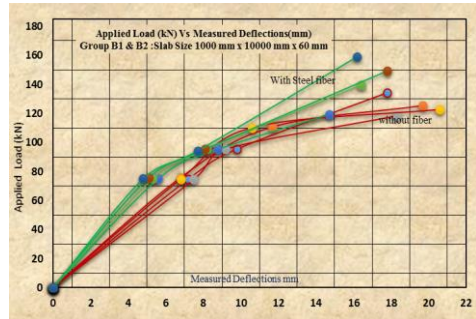


Fig. 4: Load (kN) Vs Measured Deflection (mm) for Group B1 & B2- specimens

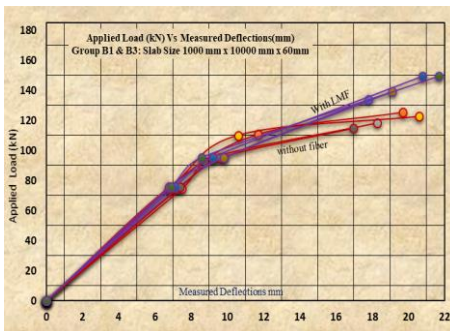


Fig. 5: Load (kN) Vs Measured Deflection (mm) for Group B1-& B3 specimens

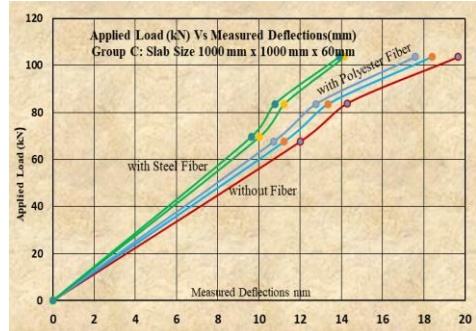


Fig. 6: Load (kN) Vs Measured Deflection (mm) for Group C specimens

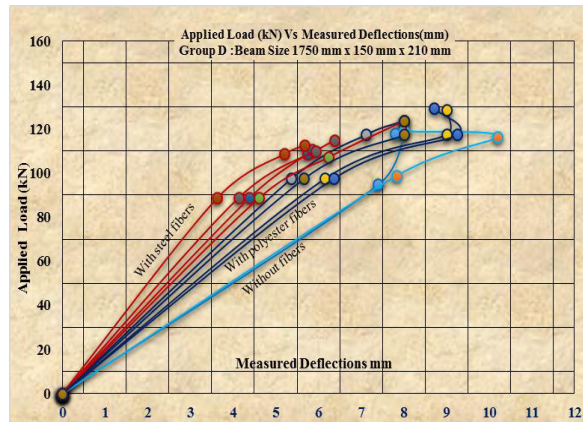


Fig. 7: Load (kN) Vs Measured Deflection (mm) for Group D specimens

Table 3 : Ductility Index of Reinforced Geopolymer Beams & Slab

| Sl.No | Component | Fine Agg | Fibers | f_y | f_{ck} | Molarity | D.I (Cal) | D.L (Cal) | D.I (Mea) | D.L (Mea) | SHS | No of Specime | Remarks | |
|-------|--------------------------|----------|--------|-------|----------|----------|-----------|-----------|-----------|-----------|------|---------------|----------|--|
| 1 | Reinforced Two Way Slabs | M-Sand | Nil | Fe500 | 57.87 | 8M | 1.87 | 1.15 | 3.46 | 1.81 | 0.65 | 8 | | |
| 2 | | M-Sand | " | " | 45.9 | 10M | 1.56 | 1.22 | 2.74 | 1.51 | 0.59 | 8 | | |
| 3 | | M-Sand | " | " | 41.7 | 12M | 1.26 | 1.14 | 2.02 | 1.30 | 0.67 | 8 | | |
| 4 | | M-Sand | Nil | Fe415 | 44.7 | 8M | 1.47 | 1.37 | 2.81 | 1.67 | 0.94 | 4 | | |
| 5 | | M-Sand | Steel | " | 49.6 | 8M | 1.58 | 1.26 | 3.15 | 1.89 | 0.80 | 4 | 1%, 1.5% | |
| 6 | | M-Sand | LMF | " | 58.7 | 8M | 1.32 | 1.26 | 2.79 | 1.83 | 0.96 | 4 | 1%, 1.5% | |
| 7 | | R-Sand | Nil | " | 35.0 | 8M | 1.19 | 1.22 | 1.64 | 1.54 | 1.02 | 1 | | |
| 8 | | R-Sand | PF | " | 37.6 | 8M | 1.19 | 1.22 | 1.64 | 1.54 | 1.02 | 2 | 0.50% | |
| 9 | | R-Sand | Steel | " | 38.1 | 8M | 1.12 | 1.20 | 1.68 | 1.56 | 1.07 | 2 | 1.50% | |
| 10 | Singly Reinforced Beams | R-Sand | Nil | Fe415 | 35.00 | 8M | 1.50 | 1.21 | 2.17 | 1.50 | 0.80 | 2 | | |
| 11 | | R-Sand | Steel | Fe415 | 38.08 | 8M | 1.46 | 1.21 | 2.25 | 1.58 | 0.83 | 4 | 1.50% | |
| 12 | | R-Sand | PF | Fe415 | 37.6 | 8M | 1.35 | 1.22 | 2.19 | 1.50 | 0.92 | 4 | 0.50% | |
| 13 | Average Value : | | | | | | | 1.41 | 1.22 | 2.38 | 1.60 | 0.86 | 51 | |

Notations used : D.I- Ductility Index, D.L- Ductile load, SHS - Strain Hardneing Slope ,cal-calculated, mea-measured

Table 4 : Ductility Ranking of RGPC specimens

| S.No | F. A | F_y | Fiber | DI_{cal} | DI_{mea} | SHS | D.R |
|-------------------------|--------|-------|-------|-------------|-------------|-------------|------------|
| 1 | M-sand | Fe415 | Steel | 1.45 | 2.97 | 0.88 | I |
| 2 | M-sand | Fe415 | Nil | 1.47 | 2.81 | 0.94 | II |
| 3 | M-sand | Fe500 | Nil | 1.56 | 2.74 | 0.64 | II |
| M-Sand (Average) | | | | 1.49 | 2.84 | 0.82 | |
| 1 | R-sand | Fe415 | Steel | 1.29 | 1.97 | 0.95 | |
| 2 | R-sand | Fe415 | PF | 1.27 | 1.92 | 0.97 | III |
| 3 | R-sand | Fe415 | Nil | 1.35 | 1.91 | 0.91 | |
| R-Sand (Average) | | | | 1.30 | 1.93 | 0.94 | |

9) CONCLUSIONS

Following conclusions are drawn based on room temperature cured fly ash- slag based reinforced geopolymer concrete flexural elements.

- The flexural behaviour of Reinforced Geopolymer Concrete is similar to Conventional OPC based RCC elements. IS: 456-2000 of Indian RC Design Code can be used to estimate all structural design related output.
- Using M-sand ductility of GPC could be in the range **1.50 to 2.85** and Using River sand it could be in the range **1.30 to 1.95**. The average of these two ductilities of RGPC lies between **1.4 and 2.40**.
- If fine aggregates and coarse aggregates are of the same rock origin, then the ductility of GPC is more with appreciable bond strength.
- Using proper steel grade & fibres at 10 to 15% could increase the strength and ductility of GPC.

REFERENCES

- [1] Prakash Desai, K. U. Muthu, A brief review on strength, deflection and cracking of rectangular, skew and circular reinforced concrete slabs, *Indian Institute of Science*, 91-108,(Mar-Apr. 1988).
- [2] Djwantoro Hardjito, Studies on Fly Ash-based Geopolymer Concrete, *Thesis Report, Curtin University of Technology*, (Nov.2005).
- [3] Radhakrishna et al., Strength Characteristics of Open Air Cured Geopolymer Concrete, *Transactions of the Indian Ceramic Society*, (Feb.2014).
- [4] Rajamane et al., Quantities of Sodium hydroxide solids and water to prepare sodium hydroxide solution of given molarity for geopolymer concrete mixes, *ICI technical paper*, (Sept. 2014).
- [5] N. Ganesan et al., Development of stress block parameters for geopolymer concrete, *The Indian Concrete Journal*, vol **89**, Issue 9, pp 47-56, (Sept. 2015).
- [6] Mahantesh et al., Flexural behaviour of fly ash-slag based reinforced geopolymer concrete flexural elements cured at room temperature, *IJTAM*, ISSN 0973-6085, Volume **12**, Number 4, PP 845-856, (2017).
- [7] Mahantesh et al. , Strength and Deformation Behavior of Reinforced Geopolymer Concrete Flexural Elements, *IJCET*, ISSN 0976-6316, Volume **8**, Issue 5, PP 1108 – 1121, (May 2017).
- [8] Robert Park & Thomas Paulay, *Reinforced Concrete Structures*, John Wiley & Sons, INC.UK, (2013).
- [9] IS 456-2000, Indian standard code of practice for plain and reinforced concrete for general building construction, *Bureau of Indian Standards - New Delhi*, (2000)
- [10] Sumajouw and Rangan, Low Calcium Fly Ash-based Geopolymer Concrete: Reinforced Beams and Columns, *Research Report GC3, Curtin University of Technology*, (2006).

ACKNOWLEDGEMENTS

- The Authors wish to express their grateful feelings and thank the management of **Alliance University** and **The Oxford College of Engineering – Bangalore**, for their kind support while investigating this research work during 2013 - 2016.
- The Authors also wish to thank **EACEF 2017** for their excellent support during the conference at Seoul- South Korea.

Dynamic Analysis of Machine Foundation

Manohar.D¹, B.K. Raghu Prasad², Dr.K. Amarnath³

¹Student, The oxford College of Engineering, Bangalore, Karnataka, India

²Former Professor, The Oxford College of Engineering, Bangalore, Karnataka, India

³HOD, Civil Department, The Oxford College of Engineering, Bangalore, Karnataka, India

Abstract – The analysis of Machine Foundation involves not only static loads but also the dynamic loads which are caused due to the working of the machine. Therefore, the machine foundation should survive these loads. Therefore, it becomes vital to reduce the natural frequency of soil beneath the foundation. One such treatment is to prepare a layered soil beneath the foundation by trenching the soil and placing different types of isolation materials.

Key Words: Frame foundation, Sinusoidal load, Rubber, Rock basalt, Springs, etc

1. INTRODUCTION

The dynamic loads that act on the machine foundations may be caused due to various reasons such as vibrations of machines while in running conditions, due to the vehicles moving on top of the foundations, in case of impact machines due to the impact of hammers, nuclear blasts in the vicinity, shock waves etc.

Therefore, as a designer one should be thorough with the ways with which these dynamic loads can be transmitted from machines to the soil beneath the foundation which can either be done by providing an elastic support such as rubber or a spring underneath the foundation in order to reduce the vibrations.

2.0 RECENT STUDIES AND OBJECTIVE

Shamsher Prakash (2006) discusses the method for determining the responses of foundations subjected to vibrating loads. Here the soil-foundation system is assumed as spring mass – dashpot model. Here the block foundation is considered. Mulugeta (2003) aims at incorporating impedance function by using expressions and dimensionless graphs for determining the dynamic stiffness and dashpot coefficients. In the paper by Piyush K (2014) reciprocating machines are installed on a block foundation on the ground surface as well as placed at different depths. Here the values of frequency and amplitude in different modes of vibration are compared.

Karlik (2013) has presented on the sensitivity and reliability analysis of machine foundation depending on the soil stiffness. Silipus (2015) has discussed the analytical and numerical models as how complex have to be in order to model the vertical dynamic response of machine foundation system. S. Patel has studied the foundation supporting rotary

type of machines. There two types of rotary machines under consideration in his paper Attar (2016) has presented methods to reduce vibrations by different isolation materials which are placed between the block foundation and the machinery. Nikhil (2016) presents the test sample for a roto dynamic model at various speed. It also discusses the various types of foundation which produces min vibration for a particular type of machine.

2.1 Objective

In design of machine foundation, it is vital to reduce the natural frequency of the soil beneath the foundation, which by doing so the vibrations produced can be easily dealt with.

One such treatment is to prepare a layered soil beneath by trenching the soil and prepare a layered soil by proper combination of different types. In this thesis, an attempt is made to reduce the vibrations transferred from machines to the foundations (frame type) by using layered soil medium underneath the foundation.

3.VIBRATION ISOLATION FOR MACHINE FOUNDATION

Even if the machines are rigidly connected to the floor ,the vibrations created by these machines get transmitted through the floor and to the soil below the foundation which will be large,even at long distances the transmitted vibrations create harmful effects. Also when these machine foundations are provided with elastic material there is a danger of creating resonance condition due to elasticity of the material

3.1 Following steps will help to reduce the vibrations upto a certain extent

- (i) **Selection of sites for the foundations** : The machinery and the foundation should be located as far as possible from the foundations of adjacent structures in order to reduce the vibrations felt by the adjacent structures.
- (ii) **Dynamic loads should be well balanced:** The machine should be so balanced that even after the dynamic loads are applied it should be nullified without causing any harmful effects.

(iii) **Providing Suitable foundations** :Depending on the type of machine ,the load coming on the foundation ,its operating freequency ,the designer should design the foundation in such a manner so as to reduce the vibrations being transmitted from machine to the soil below the foundation

(iv) **Providing proper isolation:** When machine foundations are unavoidably very close to the adjoining structures, the care should be taken to properly isolate the other structures from machine foundation by proving isolation material such as rubber or wood below the machine foundation.

4. ANALYTICAL STUDY

Frame Foundation

Frame type machine foundations usually consists of structural members such as beams, columns and slabs. The slabs are placed at the top in order to support the machinery. These structural members are constructed either in RCC or composite materials.

Section properties

Column section- 200mmX450mm

Beam section -200mmx300mm

Slab 200mm

Loading

Dead load of machine -2000 kg

Operating frequency - 1500 rpm – 25 cycles/sec

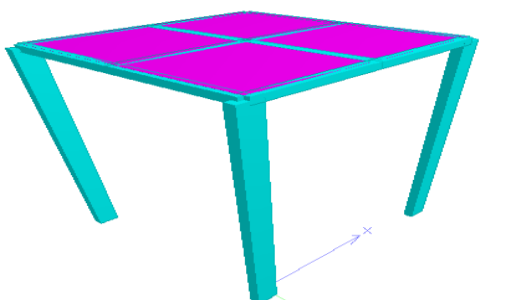
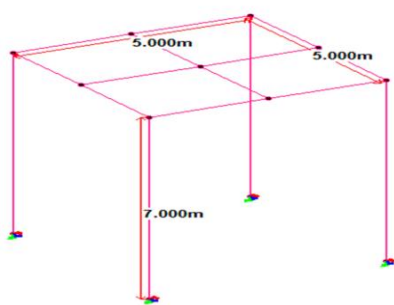


Fig -1: STAAD model

4.1 Determining the natural frequency of the system and plotting frequency response curves

Considering that the columns are infinitely rigid, the slab stiffness can be determined using the slab deflection formula:

$$Y_{max} = 0.0454x(q_0 \times a^4) / (Eh^3)$$

Here q = Load

a = slab dimensions = 5m

E = Young's modulus of concrete = 40Gpa

h = thickness of the slab = 0.2m

considering Ymax as unity we get load as 11.27 kN/ m, this is also the stiffness of the slab. On comparing the slab stiffness with the stiffness of the spring we can neglect the slab stiffness since it is very small.

$$1/K_{eff} = (1/11.27) + (1/15000)$$

Therefore $K_{eff} = 11.26 \text{ kN/ m}$

$$\text{Frequency} = 1/2\pi (\text{sqrt} (k/m))$$

$$= 0.37 \text{ Hz}$$

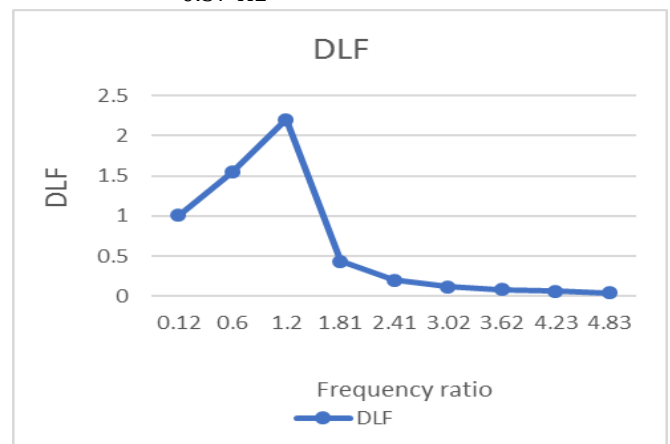


Chart -1: For K = 15000 kN/ m

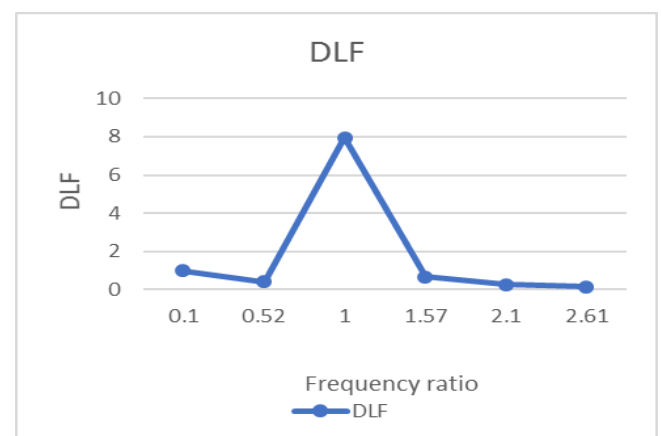


Chart -2: For K = 20000 kN/ m

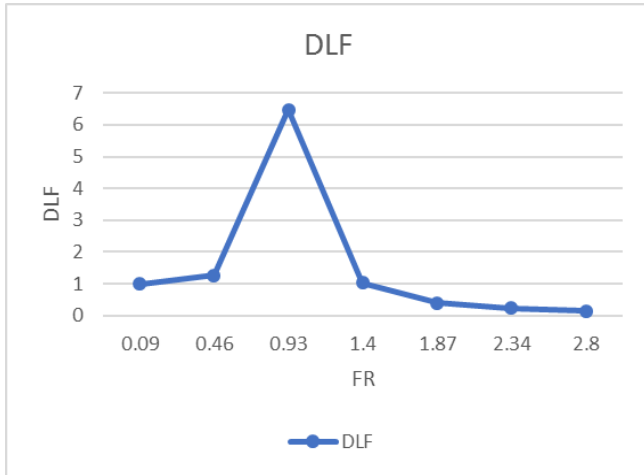


Chart -3: For K = 25000 kN/ m

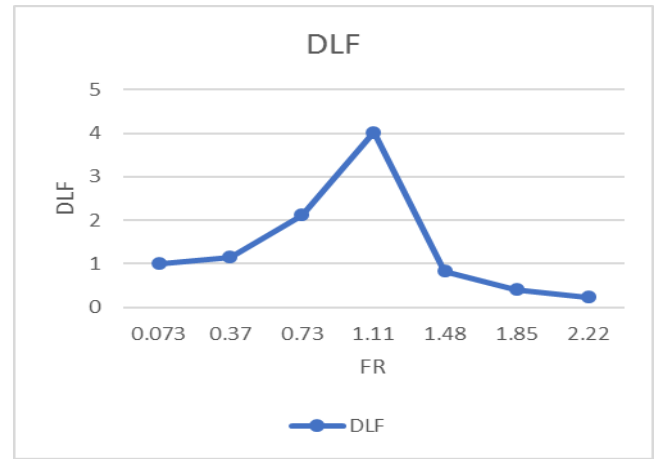


Chart -6: For K = 40000 kN/ m

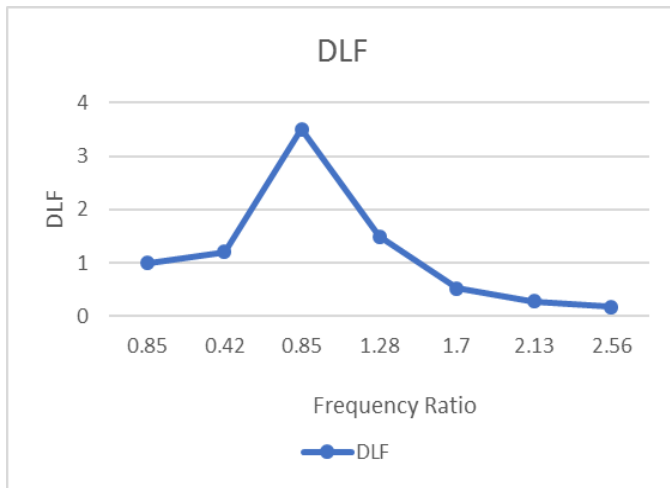


Chart -4: For K = 30000 kN/ m

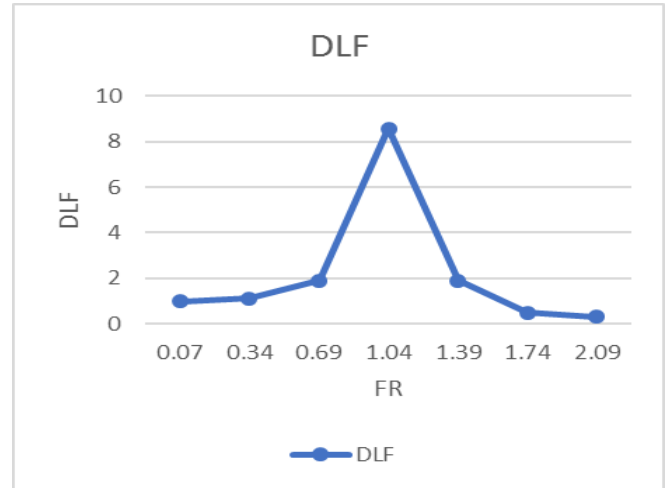


Chart -7: For K = 45000 kN/ m

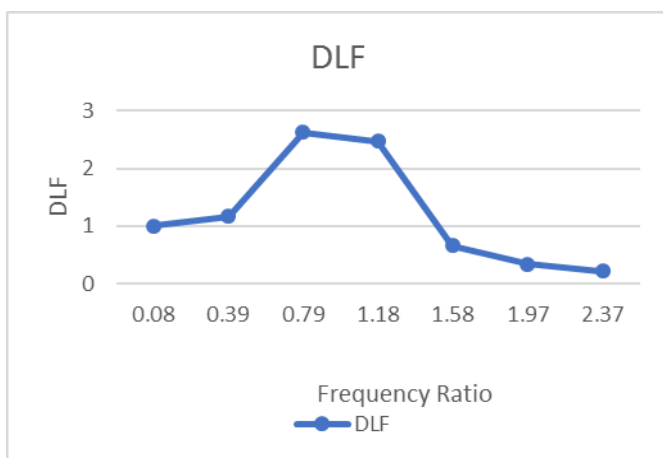


Chart -5: For K = 35000 kN/ m

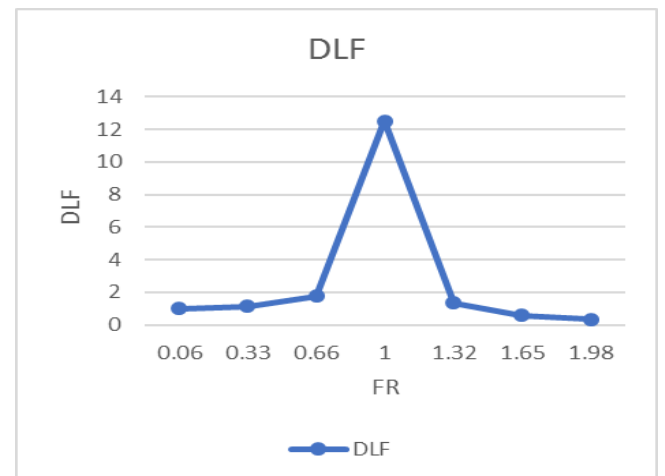


Chart -8: For K = 50000 kN/ m

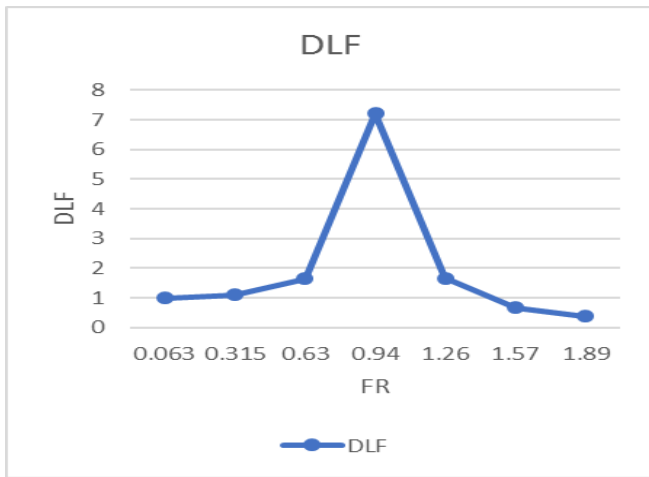


Chart -9: For K = 55000 kN/ m

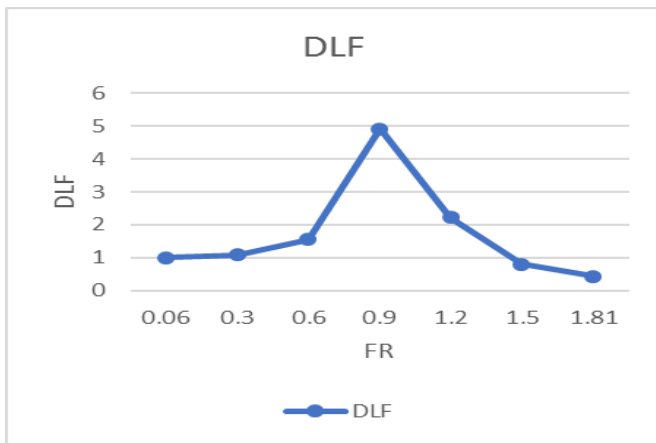


Chart -10: For K = 60000 kN/ m

4.2 Plotting transmissibility curves

It is the ratio of maximum amplitude i.e., the force transmitted to the foundation to the amplitude of applied force is known as transmissibility of the support system.

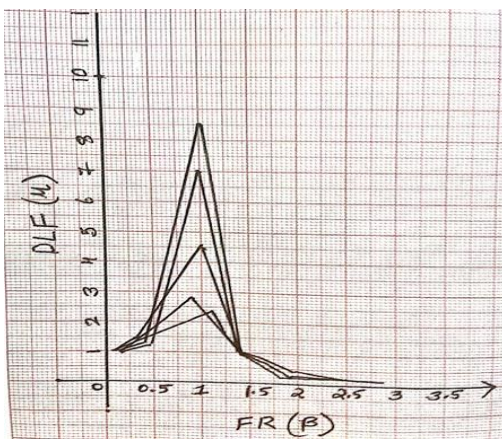


Fig -1: Transmissibility curve

5.1 Machine foundation with spring supports

In this model the frame foundation is supported by a spring support as shown below. Some of the practical examples of machine foundations supported by spring supports

Here an attempt is made to try and reduce the vibration transmitted from machine to the soil beneath the foundation by providing spring supports

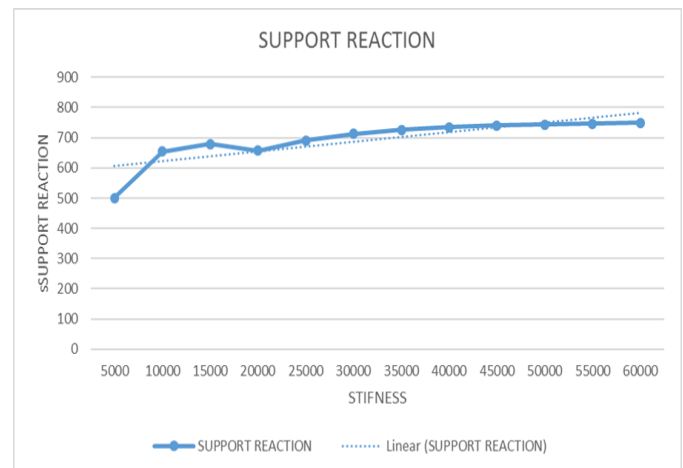


Chart -11: stiffness v/s support reaction

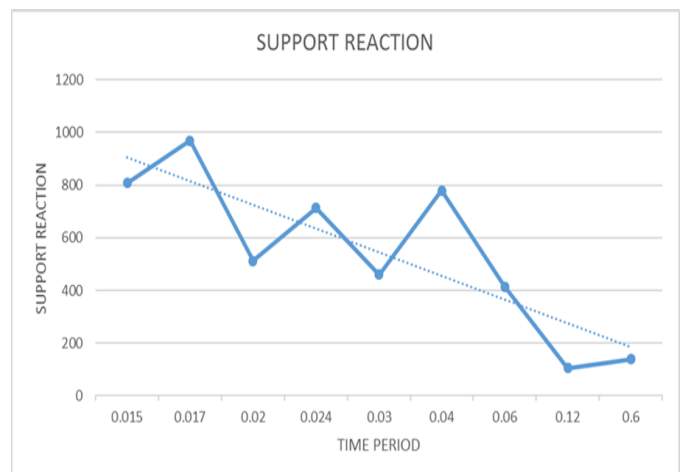


Chart -12: Time period v/s support reaction

| STIFNESS (kN/m) | SUPPORT REACTION (KN) |
|-----------------|-----------------------|
| 5000 | 515.5 |
| 10000 | 683.3 |
| 15000 | 676.7 |
| 20000 | 746.2 |
| 25000 | 780 |
| 30000 | 794 |
| 35000 | 799 |
| 40000 | 799.5 |
| 45000 | 798.5 |
| 50000 | 796.5 |
| 55000 | 794.4 |
| 60000 | 792 |

Table -1: Data for support reaction v/s stiffness

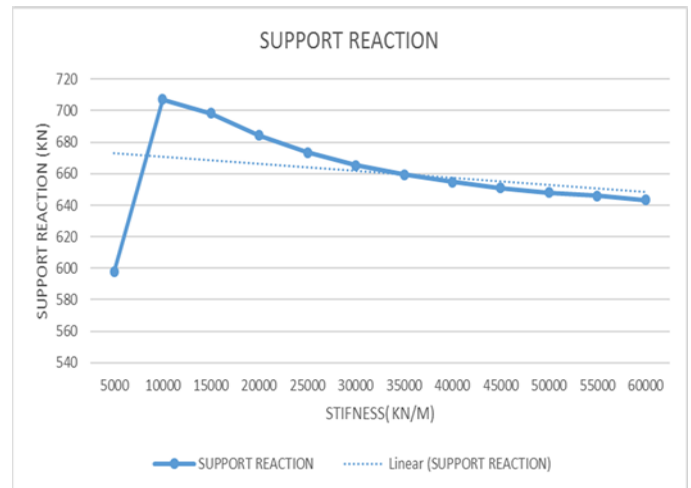


Chart -14: stiffness v/s support reaction

| STIFNESS (kN/m) | SUPPORT REACTION (KN) |
|-----------------|-----------------------|
| 5000 | 597.7 |
| 10000 | 707 |
| 15000 | 698.4 |
| 20000 | 684.2 |
| 25000 | 673.4 |
| 30000 | 665.4 |
| 35000 | 659.3 |
| 40000 | 654.7 |
| 45000 | 651 |
| 50000 | 648 |
| 55000 | 646 |
| 60000 | 643.4 |

Table -2: Data for support reaction v/s stiffness

5.2 Machine foundation provided with a hard material (Rock basalt) below the frame foundation

Material properties assigned in stadd model

Young's modulus – 1.96×10^7

Poisson's ratio – 0.15

Frequency – 25 Cycles/sec

In this model the frame foundation is supported by layers of hard material such as rock basalt with the following material properties as listed above.

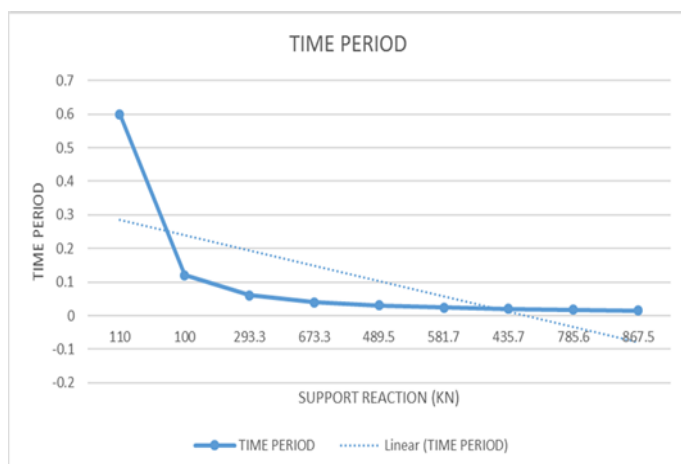


Chart -13: Time period v/s support reaction

5.3 Machine foundation provided with a soft material (Rubber) under the foundation

Material properties assigned in stadd model

Young's modulus -50000 kN/m²

Poissons ratio -0.48

Shear modulus-20000 kN/m²

Stiffness – 25000 kN/m

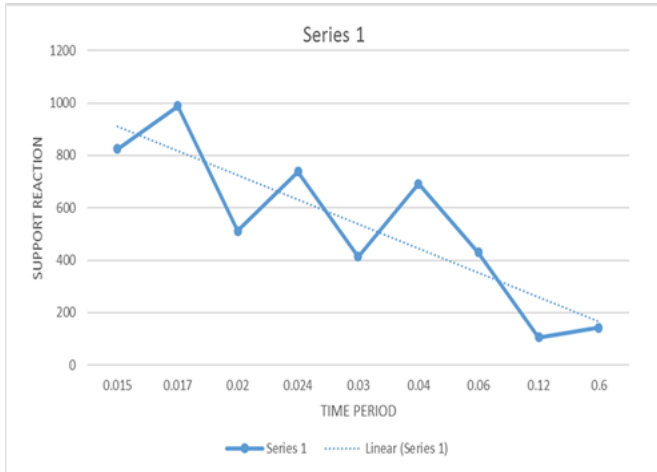


Chart -15: Time period v/s support reaction

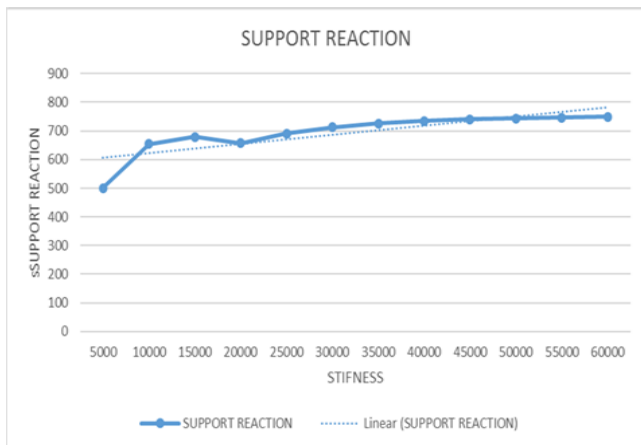


Chart -16: stiffness v/s support reaction

| Stiffness (kN/m) | Support reaction (KN) |
|------------------|-----------------------|
| 5000 | 301.1 |
| 10000 | 654.7 |
| 15000 | 678.5 |
| 20000 | 656.7 |
| 25000 | 691.5 |
| 30000 | 712.3 |
| 35000 | 725.6 |
| 40000 | 734.3 |
| 45000 | 740.2 |
| 50000 | 744.2 |
| 55000 | 747.1 |
| 60000 | 749.1 |

Table -3: Data for support reaction v/s stiffness

6. FINAL COMPARISON AND CONCLUSION

(1) From the above list of tables, we can conclude that the support reactions are considerably reduced when the Rock-Basalt material is laid as a bed in number of layers below the frame foundation

(2) Support reaction by using rock basalt is reduced by 106 kN when compared to the reactions by using a rubber material and also by 148 kN when springs are used

(3) Therefore, a hard material such as rock prevents the vibrations better from being transmitted from machine to the soil below the foundation when compared with rubber and springs as a isolation material.

7. REFERENCES

[1] Bhatia, K. G., Foundation for Industrial Machines, Handbook for Practical Engineers, D-CAD Publisher, New Delhi, 2009, ISBN: 978-81-906032-2-5

[2] Gazetas, G., Foundation vibrations, Foundation Engineering Handbook, (H.Y. Fang, editor), Van Nostrand Reinhold, New York, 1991

[3] Králik, J. Králik, J. jr., Probability and Sensitivity Analysis of Machine Foundation and Soil Interaction. Applied and Computational Mechanics

[4] Gazetas, G., Analysis of Machine Foundations, State of the Art of Soil Dynamics and Earthquake Engineering, Volume 2, 1983

[5] Arora, K.R., Soil Mechanics and Foundation Engineering, 4th ed. Delhi Standard

[6] Rirchart, F.E., Foundation Vibration, in Foundation Engineering Hand Book

[7] Foundations for vibrating machines' by Shamsher Prakash (USA):

[8] Vibration analysis and design of block type machine foundation interacting with the soil' by Mulugeta 2003

[9] Dynamic analysis of machine foundation - National conference 2014

[10] Sensitivity analysis of soil-foundation-machine interaction on layered soil' by Karlik 2013

[11] Behavior of machine foundation subjected to vertical dynamic loading' by Silipus 2015

[12] Dynamic analysis of machine foundation supporting rotary machine' by S. Patel 2015

[13] Economical methods of reducing vibrations of machine foundation' by Attar 2014

[14] Vibration analysis of roto dynamic madel'Nikhil 2016

Performance Study of Elevated Water Tanks under Seismic Forces

Furquan Elahi Shaikh¹, B K Raghuprasad², Amarnath K³

¹M.Tech, Department of Civil Engineering, The Oxford College of Engineering & Technology, Bengaluru, Karnataka, India

^{2,3}Professor, Department of Civil Engineering, The Oxford College of Engineering & Technology, Bengaluru, Karnataka, India

Abstract – Elevated water tanks are frequently used in seismic active regions and because of that the seismic behavior of them needs to be carefully analyzed and dealt with. Due to lack of understanding most of the elevated tanks were damaged in the past earthquakes and hence there is a need to properly understand the different factors governing the design. At present, IS 1893:1984 describes the seismic force criteria for elevated water tanks. The code does not take into account for the convective and impulsive pressure in the analysis of the tank and also assumes the tank to be a single degree of freedom system. The objective of this work is to assess the impact of earthquake forces on two types of tank systems based on their support mainly classified as Framed Staging and Shaft Staging. Response Spectrum Analysis is carried out and behavior of these staging systems is studied as per draft code Part II of IS 1893:2006 and IITk's GSDMA guidelines. Parameters such as Base Shear, Nodal Displacement, Overturning Moment, and Vibration Analysis are obtained from an FEM software STAAD-Pro.

Key Words: Frame Type Staging, Shaft Type Staging, Single degree of freedom, Impulsive pressure, Convective pressure.

1. INTRODUCTION

The progress in the scientific research into the dynamic behavior of liquid storage tanks reflects the increasing significance of these structures. Early uses for liquid containers were found in the petroleum industry and in municipal water supply systems. As time progressed the use of these types of storage is not just limited to storage of flammable liquids or water but also extended to nuclear reactor installation and thus making the study of their vibration properties a matter of prime importance. Safety of elevated tanks is of significant importance as tanks carrying large volume of different types of liquids within them. Water tanks are circular, rectangular, square, conical or intze type. Based on their supporting system elevated tanks can be classified as framed staging and shaft staging tanks. Due to the importance of water in dire circumstances such as an earthquake this study is primarily focused on the seismic performance of an elevated water tank. The objective of this study is to analyze the two types of elevated water tanks namely

Frame type and Shaft type using FEM software STAAD-Pro and compare their results and establish which one is better performing under seismic loads. The seismic design criteria in India is given by IS 1893-2002 (Part I) which illustrates minimum loading standards and IS 4326-1993 which gives the design and detailing requirements for constructions of building structures.

2. LITERATURE REVIEW

Significant research was carried out on seismic design of liquid storage tanks and a few published works on seismic response characteristics of reinforced concrete water tanks. G.W. Housner [1] investigated the response of the tanks which were supported on ground and elevated tanks during the Chilean earthquake of May 1960. He studied that when an elevated water tank is completely filled or completely empty it may be treated as a single degree of freedom system. Whereas when the tank is partially filled with water the same idealization does not hold good and hence stated the convective effect in the tank which was primarily due to the sloshing of water to the tank wall. Jain Sudhir k [2] investigated that the IS code provisions and observed there was absence of a proper value which should take into consideration the performance factor of the tank. Analysis of few tanks suggested that the idealization based on the code is not adequate enough to counter the lateral forces differences and the final result depends heavily on the dimensions of the tank and the stiffness of support system. Durgesh C Rai [3] investigated that the current design of the circular shaft type staging was very poor and the tanks designed using those parameters were extremely vulnerable under lateral loads. He also studied the tanks which were damaged in 2001 Bhuj earthquake and that was taken as a benchmark in his study. Pavan S Ekbote [4] studied the response of the elevated tank and considered certain parameters and theories which were recommended by G.W Housner [1] which are more acceptable and are being adopted in many of the international codes. Their aim was to study the performance of the elevated water tanks under different kinds of staging patterns. Rupachandra J Aware [5] investigated and studied the seismic performance of circular elevated water tank as per the draft code of IS 1893:2002 (part 2). It was mentioned that complex pattern of stresses are developed in the staging and

circular walls of the tank. Their objective was to analyze the tank at different staging height corresponding to different seismic zones of India. Dona Rose K J [6] studied the response of an elevated circular type water tanks to dynamic forces. Tanks of various capacities with different staging height are modeled using ANSYS software. The analysis is carried out for two cases namely, tank full and half level condition considering the sloshing effect along with hydrostatic effect. Time history analysis using draft code of IS 1893-2002 (part2) and the acceleration data from El Centro earthquake was taken. The peak displacements and base shear obtained from the analysis were also compared along with displacements. Jay Lakahnakiya [7] analyzed the hydrodynamic pressure of intze tank and comparison of the cost of water tank for different staging conditions like shaft and frame type. Staging part was analyzed in Staad Pro. V8i and the design was done in excel worksheet. After the complete design the quantity of material has been found and then costing of water tank is done using supply and sewage board. Mor Vytankatesh K. et al [8] studied the impact of seismic forces on RC shaft and framed type with different capacities which were placed in different seismic zones. Comparison of elevated tanks with different system capacities and seismic zones states that these parameters may considerably change the seismic behavior of tanks.

3. OBJECTIVE

- To determine the hydrodynamic effects on elevated water tank, with different supporting systems i.e., framed staging and concrete shaft placed in different seismic zones, using the Housner’s model.
- To determine maximum nodal displacement at the top.
- Free vibration analysis for both frame type and shaft type staging in Zone II and Zone IV.
- To determine overturning moment over the height for frame type and shaft type staging.
- To determine base shear for frame type and shaft type staging.

4. DESCRIPTION OF HOUSNER’S (1963) (1) MODEL

Elevated water tanks usually are never completely filled, due to which considering it as single degree of freedom system is not satisfactory. Therefore a partially filled tank cannot be idealized as a single degree of freedom system without taking into account the sloshing effect. The lateral stiffness for the frame type staging can be calculated by any FEM based software or manually, whereas the stiffness calculation for the shaft type staging is calculated by applying a horizontal force at the center of gravity of the tank and the unit nodal displacements are noted.

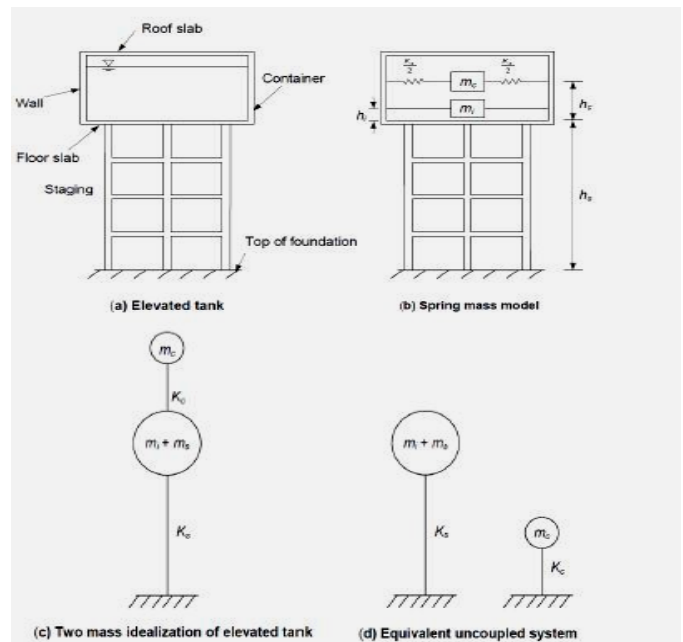


Fig 1 Two mass idealization as proposed by Housner

When the liquid mass in the tank is divided into two parts as shown in the above figure 1, the mass which vibrates along with the tank wall is called the impulsive mass. The mass which vibrates relative to the tank wall is called the convective mass. Housner (1963) [1] explained about the two mass model of elevated tank. In figure 1 we can see the masses “ m_c ” and “ m_i ” which represent the convective and impulsive masses respectively and “ K_c ” is corresponding stiffness. Figure 2 shows the pattern in which the impulsive and convective pressures are to be applied with “ h_i ” and “ h_c ” being the heights of the impulsive pressure (including base pressure) and convective pressure (including base pressure) respectively.

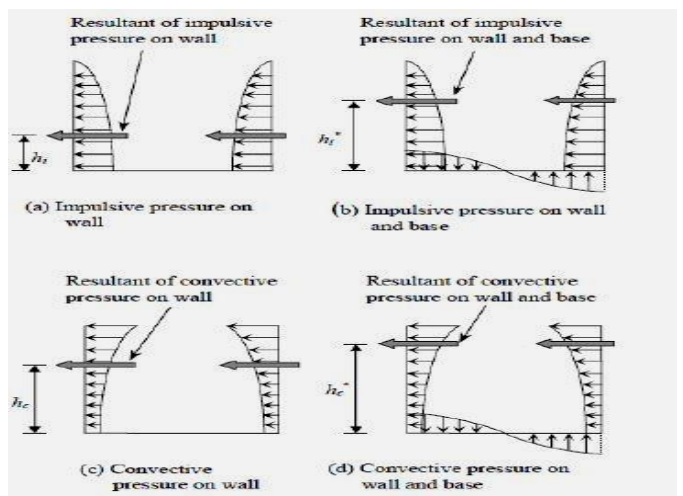


Fig 2 Hydrodynamic Pressure Distribution on Tank Walls

Parameters of elevated water tank

| Sl. No | Parameters | Values |
|--------|-------------------------------|------------------------------------|
| 1 | Diameter of the tank | 10 m |
| 2 | Height of Cylindrical Wall | 3 m |
| 3 | Thickness of Cylindrical Wall | 200 mm |
| 4 | Height of Staging | 20 m |
| 5 | Number of Columns | 8 |
| 6 | Size of Column | 600 x 600 mm |
| 7 | Size of Top Ring Beam | 200 x 600 mm |
| 8 | Size of Bottom Ring Beam | 200 x 600 mm |
| 9 | Size of Bracing | 200 x 400 mm |
| 10 | Thickness of Top Dome | 120 mm |
| 11 | Thickness of Bottom Dome | 200 mm |
| 12 | Density of Concrete | 25 kN/m ³ |
| 13 | Zone | II & IV |
| 14 | Response Reduction Factor | 2.5 |
| 15 | Importance Factor | 1.5 |
| 16 | Type of Soil | Hard (zone II), Soft (Zone IV) |

Table 1 Parameters of the Elevated Tank

| Values of Partial Safety Factor γ_f for Loads (Clauses 18.2.3.1, 36.4.1 and B- 4.3) | | | | | | |
|---|-------------------------|-----|-----|-------------------------------|-----|-----|
| Load Combination | Limit State of Collapse | | | Limit State of Serviceability | | |
| | DL | IL | WL | DL | IL | WL |
| (1) | (2) | (3) | (4) | (5) | (6) | (7) |
| DL + IL | 1.5 | | 1.0 | 1.0 | 1.0 | - |
| DL + WL | 1.5 | - | 1.5 | 1.0 | - | 1.0 |
| | or 0.9 ⁽¹⁾ | | | | | |
| DL + IL + WL | 1.2 | | | 1.0 | 0.8 | 0.8 |

Table 2 Applied Load Combinations

NOTES

1. While considering earthquake effects substitute EL for WL.
2. For the limit state of serviceability, the values of γ_f given in this table for short term effects. While assessing the long term effects due to creep the dead load and hat part of the live load likely to be permanent may only be considered.
3. (1) This value is to be considered when stability against overturning or stress reversal is critical.

5. ELEVATED TANK WITH FRAME TYPE STAGING

Frame type stagings are used widely as compared to shaft type staging primarily because they are much better in performance. Earthquakes in the recent past have proved that the frame type staging performs much better than the shaft type staging. It primarily performs better because of the higher redundancy and due to the fact that it more ductile. The frame type staging consists of combination of beams and columns which makes it much more ductile and performs better in the event of an earthquake. The geometric properties of the tank primarily depend on the capacity and the height of the staging may vary from 10 to 20m. Generally for circular type of tank the diameter usually depends on the capacity.



Fig 3 Framed Type model prepared in Staad-Pro

6. ELEVATED TANK WITH SHAFT TYPE STAGING

Due to their ease of construction and more solid form the shaft type staging is adopted for larger capacities. Earthquakes in the recent past have proved that the shaft type staging is much more vulnerable as compared to the frame type staging. The lack of ductility and also lower redundancy of the shaft adds to the vulnerability of it.

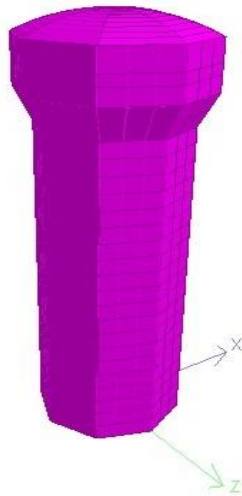


Fig 4 Shaft Type model prepared in Staad-Pro

However for STAAD Pro analysis the pressures applied on the base of the wall of the tank and on the base slab are taken to be

- i. $\rho g h_i^*$ (impulsive mode) = $1 \times 9.81 \times 4.44 = 43.55 \text{ kN/m}^2$
- ii. $\rho g h_c^*$ (convective mode) = $1 \times 9.81 \times 3.67 = 36.00 \text{ kN/m}^2$

Where

ρ = Density of Water (kN/m^3).
 g = Acceleration due to gravity (m/sec^2).
 h_i^* = Height of Impulsive mass above the bottom of the tank (including base pressure).
 h_c^* = Height of Convective mass above the bottom of the tank (including base pressure).
 The shaft type staging can also be imagined as an inverted pendulum and hence it can be assumed that maximum resistance is going to be offered by the hollow shaft section. The load carrying capacity can be seriously hampered if there is any damage to the staging at the critical section. The dimensions of the tank primarily depend on the capacity and the height of the staging may vary from 10 to 20m. Generally for circular type of tank the diameter usually depends on the capacity it is supposed to carry but the thickness of the shaft usually varies between 120 mm to 200mm.

7. RESULTS AND DISCUSSION

1. Results for Convective Pressure

i. Time Period

| Convective Mode | | |
|-----------------|------------|------------|
| Mode | Frame Type | Shaft Type |
| 1.00 | 2.09340 | 0.31858 |

| | | |
|------|---------|---------|
| 2.00 | 2.09340 | 0.31858 |
| 3.00 | 1.43227 | 0.12214 |
| 4.00 | 0.21799 | 0.07298 |
| 5.00 | 0.21788 | 0.07298 |
| 6.00 | 0.19351 | 0.06481 |

Table 3 Time Period for Frame & Shaft type Staging

- Time periods in various modes for the frame type staging are much higher compared to those of shaft type staging.

ii. Comparison of Base Shear

| Base Shear (kN) | | |
|-----------------|---------|---------|
| Type of Staging | Zone II | Zone IV |
| Shaft | 567.81 | 1848.52 |
| Frame | 369.77 | 981.46 |

Table 4 Base Shear Results for frame & Shaft type Staging

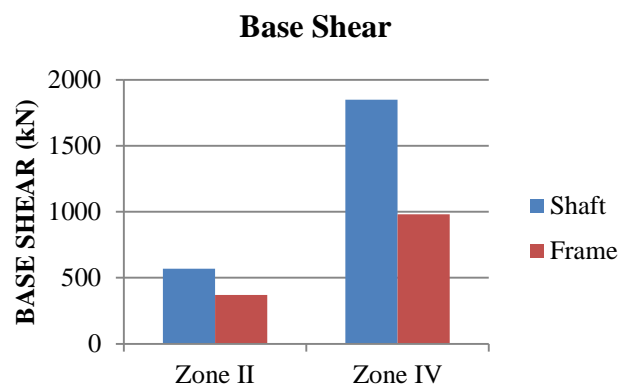


Chart-1 Base Shears in Convective Mode

- Figure 5 shows that the base shears for the frame type staging in Zone II and Zone IV are comparatively lower compared to those of shaft type staging.

iii. Nodal Displacements in Convective Mode

| Nodal Displacements (mm) | | |
|--------------------------|---------|---------|
| Type of Staging | Zone II | Zone IV |
| Shaft | 3.509 | 11.331 |
| Frame | 70.069 | 231.98 |

Table 5 Nodal Displacements for frame & Shaft type Staging

Nodal Displacement

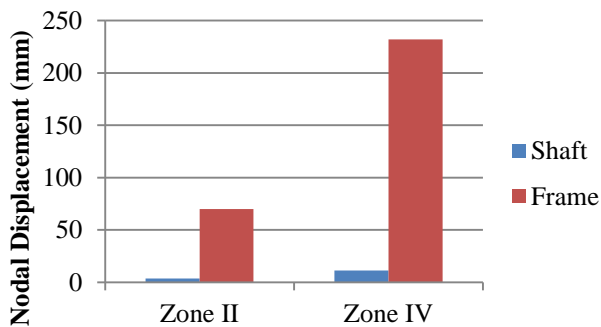


Chart-2 Nodal Displacements in Convective Mode

- From the above figure it is clear that the nodal displacements are higher for the frame type staging as compared to those of shaft type staging.
- It also proves that the frame type staging is more flexible as compared to shaft type staging.

iv. Overturning Moments in Convective Mode

| Overturning Moments (kN-m) | | |
|----------------------------|---------|---------|
| Type of Staging | Zone II | Zone IV |
| Shaft | 323.61 | 1424.66 |
| Frame | 232.631 | 732.113 |

Table 6 Overturning Moment for Frame & Shaft type Staging

Overturning Moment

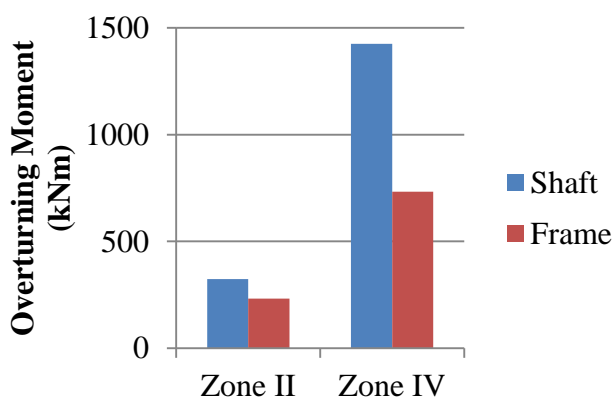


Chart-3 Overturning Moment

- Since overturning moment is a governing factor in the design of an elevated water tank, it is observed that the overturning moment is higher for the shaft type staging as compared to frame type staging.

2. Result for Impulsive Pressure

i. Time Period

| Impulsive Mode | | |
|----------------|------------|------------|
| Mode | Frame Type | Shaft Type |
| 1.00 | 2.214770 | 0.341130 |
| 2.00 | 2.214770 | 0.341130 |
| 3.00 | 1.521870 | 0.129660 |
| 4.00 | 0.218130 | 0.073630 |
| 5.00 | 0.218140 | 0.073630 |
| 6.00 | 0.193500 | 0.067270 |

Table 7 Time Period Results for Frame & Shaft type Staging

- Time periods for the frame type staging are much higher as compared to those of shaft type staging.
- Also as seen in the above table the time periods in impulsive mode values are much higher as compared to those in convective mode.

ii. Base Shear

| Base Shear (kN) | | |
|-----------------|---------|---------|
| Type of Staging | Zone II | Zone IV |
| Shaft | 710.46 | 2855.44 |
| Frame | 629.03 | 2507.02 |

Table 8 Base Shears for frame & Shaft type Staging

Base Shear

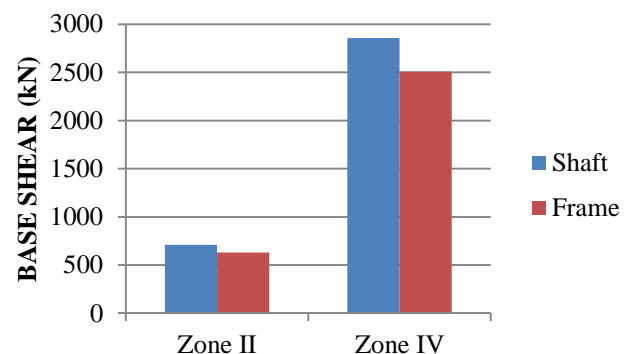


Chart-4 Base Shears in Impulsive Mode

- Figure 8 shows that the Base shears for the frame type staging in Zone II and Zone IV are comparatively lower compared to those in shaft type staging.
- It can also be seen that the base shear values of the impulsive mode are higher as compared convective mode.

iii. Nodal Displacements

| Nodal Displacements (mm) | | |
|--------------------------|---------|---------|
| Type of Staging | Zone II | Zone IV |
| Shaft | 38.66 | 154.22 |
| Frame | 148.53 | 600.707 |

Table 9 Nodal Displacements in Impulsive Mode

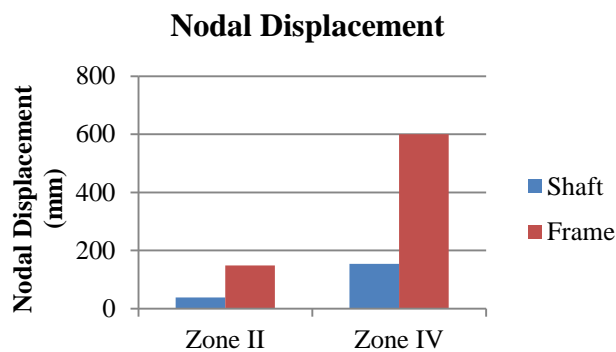


Chart-5 Nodal Displacements in Impulsive Mode

- From the above figure it is clear that the nodal displacements are higher for the frame type staging compared to those in shaft type staging.
- It may also be seen in the impulsive mode that the displacement values are much higher compared to those in convective mode.

iv. Overturning Moments

Table 10 Overturning Moments for Frame & Shaft type Staging

| Overturning Moments (kN-m) | | |
|----------------------------|---------|---------|
| Type of Staging | Zone II | Zone IV |
| Shaft | 829.52 | 2420.14 |
| Frame | 466.026 | 1871.95 |

Overturning Moment

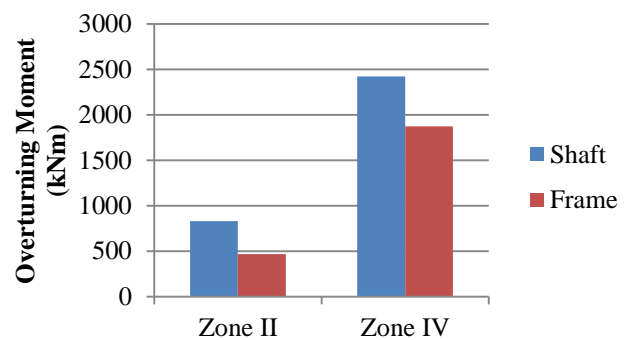


Chart-6 Overturning Moment

- Since overturning moment is a governing factor in the design of an elevated water tank, it is observed that the overturning moment is higher for the shaft type staging as compared to that in frame type staging.
- Also the overturning moment values in impulsive mode are much higher as compared to the convective mode.

8. CONCLUSIONS

- Base shear is higher in the shaft type staging as compared to the frame type staging for convective and impulsive mode.
- The increment in base shear is much higher as compared to hard soil to soft soil.
- The nodal displacement values in shaft type are very low as compared to the frame type staging which suggests that the frame type staging is much more flexible and can return to its original position after a large deflection from its mean position.
- The nodal displacement values are much higher in impulsive mode as compared to convective mode.
- The shaft type staging has higher base shear values but lower nodal displacements values suggesting that the shaft type staging is brittle compared to frame type staging.
- During designing an elevated water tank primary importance is given to the overturning moment, since large mass accumulates at the top of slender supporting system it is observed that the overturning moment for frame staging is less than that of tanks supported on shaft type staging.
- Time period in convective and impulsive are similar for both frame type and shaft type staging.
- Sloshing wave height is approximately same for the tanks, as it majorly depends on the capacity of the tank.

REFERENCES

- [1] Geroge W. Housner, "The Dynamic Behavior of Water Tanks", Bulletin of the Seismological Society of America.
- [2] Jain Sudhir K , Sameer U , "Seismic Design of Frame Staging for Elevated Water Tanks"
- [3] Durgesh C. Rai, "Review of Code Design Forces For Shaft Supports of Elevated Water Tanks"
- [4] Pavan S Ekbote, Dr Jagadish G Kori, "Seismic Behavior of RC Elevated Water Tank Under Different Types Of Staging Patterns", Journal of Engineering, Computers & Applied Sciences
- [5] Dona Rose K J, Sreekumar M, Anumod A S, "A Study of Overhead Water Tanks Subjected to Dynamic Loads", International Journal of Engineering Trends & Technology
- [6] Jay Lakhanakiya, Prof. Hema J. Shah, "A Parametric Study of an Intze Tank Supported on Different Stagings" International Journal for Scientific Research & Development
- [7] Mor Vyankatesh K, More Varsha T, "Comparative Study on Dynamic Analysis of Elevated Water Tank Frame Staging & Concrete Shaft Supported, IOSR Journal of Mechanical & Civil Engineering.
- [8] Rupachandra J. Aware, Dr. Vageesha S. Mathada, "Seismic Performance of Circular Elevated Water", International Journal of Science and Research.
- [9] IITK-GSDMA Guidelines for Seismic Design of Liquid Storage Tanks.

SEISMIC ISOLATION BY INTRODUCING LARGE SIZED AGGREGATES

Suhas Jain C B¹, Dr. B K Raghu Prasad², Dr. Amarnath K³

¹Student, M-Tech Structural Engineering, The Oxford College Of Engineering, Karnataka, India

²Professor, Dept. of Civil Engineering, IIS-c, Karnataka, India

³HOD & Professor, The Oxford College Of Engineering, Karnataka, India

Abstract - The system comprising of the use of large sized aggregates as isolating material is discussed in this paper. The attempt is made to understand the mechanism of the system which is pivoted on the phenomenon of stiffness and collision between the accommodated aggregates in system. It is a passive way of Seismic Isolation and exerted seismic force is conveyed through the system via collision between accommodated aggregates leading in dissipation of seismic energy. The arrangement of system encouraging lesser value of work done is more suitable for Isolation. The above discussed work is done using Staad-pro v8i software

proceeded by dumping preconceived mass of stone aggregates in excavated foundation pit. If scenario demands, covering may be provided along the periphery of the mass to prevent against penetration of mass in to surrounding earth. The provided mass is compacted to a known density. Subsequently raft is placed on the arrangement. The typical layout of the raft coupled with aggregate Isolating system is shown in the following figure.

Key Words: Seismic Isolation, Time history analysis

1. INTRODUCTION

Seismic Isolation concept was first reported by John Milne during 1890s and later on widely implemented as seismic protection system in seismic prone areas. The term Base refers to Foundation of the Structure and Isolation refers to reducing the interaction between the Ground and structure resting over it. Base Isolation is a Passive way to reduce demand and it is simple design approach to reduce the earthquake damage potential. Three major things a Base Isolation system should accomplish are,

- Horizontal Flexibility
- Energy Dissipation
- Vertical Flexibility

1.1 Seismic Isolation Devices

- Laminated Rubber bearing (Elastomeric bearing)
- Viscous Fluid Damper
- Lead Rubber Bearing
- Spherical Sliding Bearing (Friction Pendulum)

Although the installation of the above mentioned damping devices reduce the seismic response in structures, they are limited in practice due to their high cost. As a result application of this system is restricted to projects where its benefit exceeds cost requirement. This major drawback can be fulfilled by replacing the above mentioned devices with naturally available stone aggregates crushed to required proportions. The Isolating system discussed here is assumed to be well suited for Raft foundation. Initially penetration test is conducted to make sure that the available earth after excavation is hard enough to bear the aggregates against penetration of the same in to the surrounding earth. It is

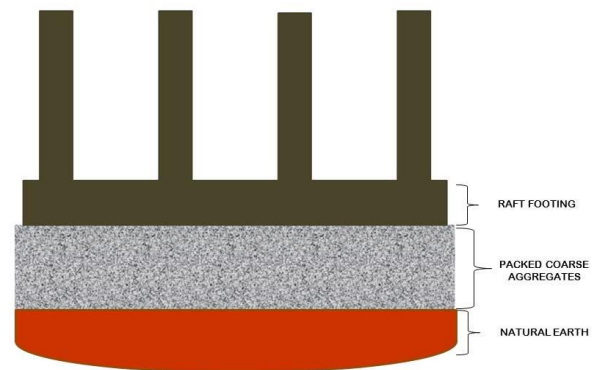


Fig 1.1 RAFT COUPLED WITH LARGE SIZED AGGREGATE

(The figure represents the position of aggregates in discussing Isolating system)

As mentioned above, typical section across the raft representing the position of stone aggregates without any covering provided along the periphery of the arrangement is shown in above figure. In case of any existence of adverse ground condition (silty sand, moist earth) is noticed near foundation, Tar sheet as covering material may be provided along the periphery of the stone aggregates to make the Isolating system water proofing and also to held the stone aggregates in position to withstand against dispersion of aggregates in to surrounding Earth.

2. METHODOLOGY

The system comprises the use of large sized aggregates as isolating material. The mechanism of the system is pivoted on the phenomenon of stiffness and collision between the accommodated aggregates in system. It is a passive way of

Seismic Isolation, Seismic force is conveyed through the system via collision between accommodated aggregates.

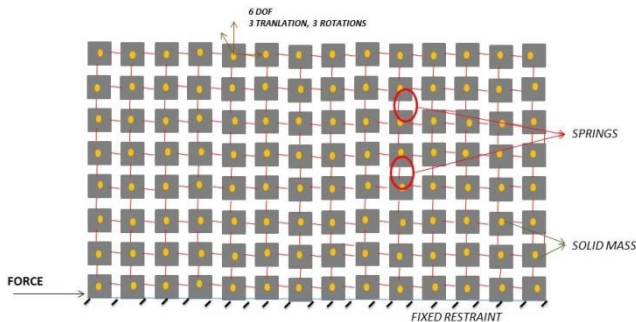


Fig 1.2 Typical section of system

(Figure represents the typical section of Isolating system where the stone aggregates are connected by links/springs)

During the process, the gained collision intensity by aggregates is directly proportional to dissipated seismic energy unless the boundary conditions are considered. The vital boundary conditions to be considered are,

- Density of surrounding earth (naturally of Lithosphere)
- Surface hardness and moisture content of bounding earth
- Weight of Structure

The layers of solid masses are modeled and the bottom most layer of solid masses are assigned fixed restraint. All solid masses are connected to each other by springs assigning the stiffness values varying from zero for very loose condition to infinity for very stiff/rigid condition. Thus the bottom layer is made fixed to ground and the subsequent upper layers are subjected to experience all 6 Degrees of Freedom and its magnitude will vary with respect to varying stiffness of connecting springs and applied lateral force. The stiffness values assigned are according to the compaction of aggregates mass in actual practice. The analysis is done by assigning uniform stiffness for springs. With reference to compaction of whole mass of aggregate in actual, the exact stiffness between any two solid masses is unpredictable and thus the stiffness values of spring shall be randomly varied for analysis purpose. The behavior of system is analyzed for free vibration state and subsequently the structure is made to rest on the system and responses are compared with conventional structure.

It is known that largely arranged particles when hit each other, they dissipates energy through heat. In fact loose and non-uniformly packed particles are much more effective. While packing certain sensitive electronic instruments, they are surrounded by loosely and randomly arranged thermocole particles filled with air, the idea being that under impact to the bag containing the instrument, the thermocole particles collide each other smoothly as suspension is

provided in the form of air filling in them, leading to less impact on instrument. This phenomenon is been carried here by replacing individual thermocole units by stone aggregates, air filling is replaced by soil mass and link elements, impact on bag is here considered as adverse seismic activity and finally instrument inside the bag is replaced by the structure.

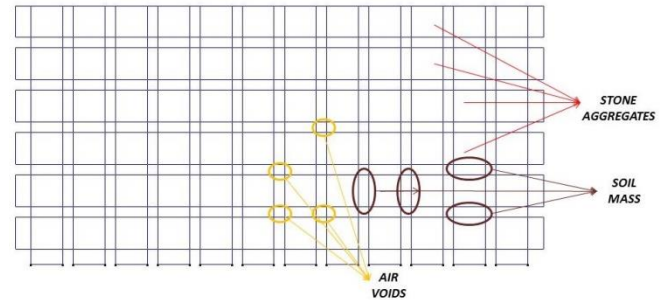


Fig 1.3 TYPICAL SECTION OF ISOLATING SYSTEM MODELED IN STAAD-PRO

(Arrangement of aggregates in typical section modeled in Staad-pro software is shown in the figure. Here the soil mass is provided as link element between stone aggregates)

As shown in the above figure the stone aggregates are packed by providing soil mass and air gap in between them. The modeling of isolating system is done in *Staad pro V8i* software. Initially the material properties of stone aggregate, soil mass and link elements are defined. The provision is provided in *Staad pro* software to model solid elements and thus each stone aggregate is modeled as solid element by assigning their respective property. The connection between the stone aggregates is done in two ways i.e. by providing,

- a) line element at corners of solid stone mass assigning preconceived stiffness/Young's Modulus value.
- b) Solid element of soil mass at all edges of stone aggregate.

The study is carried out by considering the Time History analysis data of El Centro Earthquake. The deformed shape of typical section under the application of seismic force is shown in the following figure,

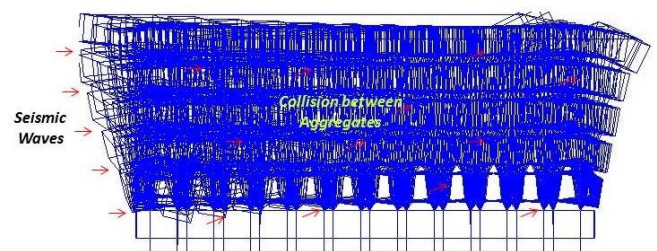


Fig 1.4 BEHAVIOUR OF AGGREGATES

The above mentioned typical section is made to experience the seismic activity and as expected earlier we noticed the deformed pattern of arrangement represents significantly the existence of collision between the stone aggregates. Analyzing the behavior of system, conclusion can be drawn that propagation of seismic waves through the arrangement occurs via collision between the accommodated aggregates and leading to dissipation of seismic energy. However impact being contact mechanics, is not modeled in the present work. The springs representing the resistance between the aggregates deform to absorb the energy. The problem is considered as linear, if non-linearity and hysteresis curve are considered, even the dissipated energy can be obtained. Thus the Raft is suspended from impact of adverse seismic waves. The soil mass provided between stones offers suspension for inter-particle collision and in turn the whole arrangement of Isolation system offers suspension against direct impact of adverse seismic waves on structure.

The System is assumed to be well suited for Raft footing. Initially penetration test is conducted to make sure that the available Earth after excavation is hard enough to bear the aggregates against penetration of the same in to earth. It is proceeded by dumping calculated mass of aggregates in excavated pit. If scenario demands , the covering may be provided along the periphery of the mass to persist against penetration of mass in to the surrounding earth. The provided mass is compacted to preconceived density. All sectional properties, physical properties must achieve preconceived data. Subsequently Raft is made to settle above the arrangement as shown in typical section.

3. MODELLING OF ISOLATING SYSTEM

The heart of the Isolating system is being the nature of aggregates, each aggregate is modeled as solid element and assigned with respective properties of naturally available stone aggregate. Provision to model solid element and assigning required properties to same is been provided in *Staad Pro* software.

The system is assemblage of a large number of aggregates. In order to analyze its behavior, initially modeling of single unit composed of 2 stone masses fastened by links and soil mass is done. Subsequently number of units are increased to achieve required size.

A typical model including two solid elements connected to each other by line elements provided as link at all four corners of solid is shown in the following Figure.

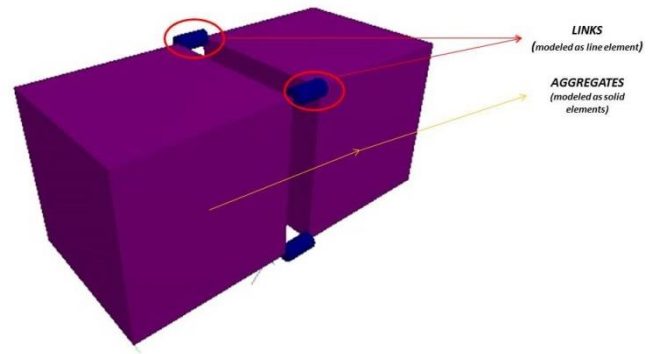


Fig 1.5: MODEL OF TWO STONE MASS

(Single unit of the Isolating system is shown in figure which is composed of 2 stone masses connected to each other by line elements to act as link of desired stiffness)

As mentioned above, all modeling and analysis work is done in *Staad Pro V8i* software. Modeling of stone aggregate of required size is done using Draw Solid command. Keeping the size of aggregate as reference eight nodes are created and is proceeded by drawing solid element using **Add 8 Noded Solids** command. Subsequently Line element of preconceived thickness & stiffness properties is drawn between the stone aggregates.

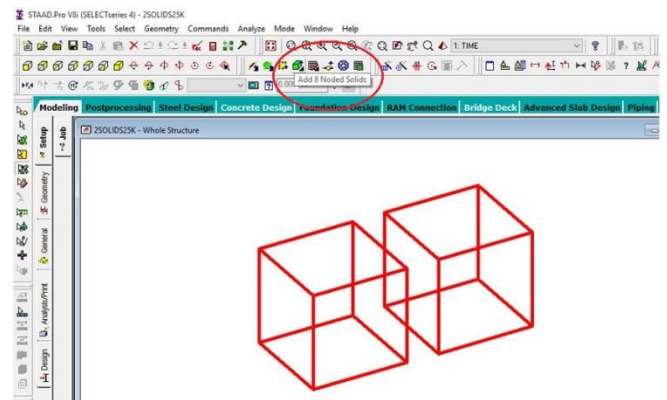


Fig 1.6: STAAD PRO- 2 SOLID MODEL

(Typical modeling of two solid masses in Staad-Pro software is shown in above figure)

The project is carried out by considering 60mm size of stone aggregate and 20mm diameter of circular line element which is provided as link element as standard size. Stiffness of link elements is varied from 0.001 to 10^7 KN/m. All corners of adjacent solids are connected with link elements. The stiffness values assigned for beam elements & corresponding Young's & Shear Modulus are as follows,

Table -1: Properties of Line elements

| STIFFNESS (K KN/m) | YOUNG'S MODULUS (E KN/m ²) | SHEAR MODULUS (G KN/m ²) |
|-----------------------|---|---|
| 0.01 | 0.32 | 0.1455 |
| 0.1 | 3.2 | 1.4545 |
| 1.0 | 32 | 14.5455 |
| 100 | 3200 | 1454.5455 |
| 10000 | 3.2x10 ⁵ | 145454.54 55 |
| 25x10 ⁵ | 8x10 ⁷ | 3.6x10 ⁷ |
| 50x10 ⁵ | 2x10 ⁸ | 9x10 ⁷ |
| 1x10 ⁷ | 3.2x10 ⁸ | 1.45x10 ⁸ |

Similarly, a typical model including two stone aggregates connected to each other by soil mass modeled as solid element is provided as link member at edges of solid is shown in the following Figure.

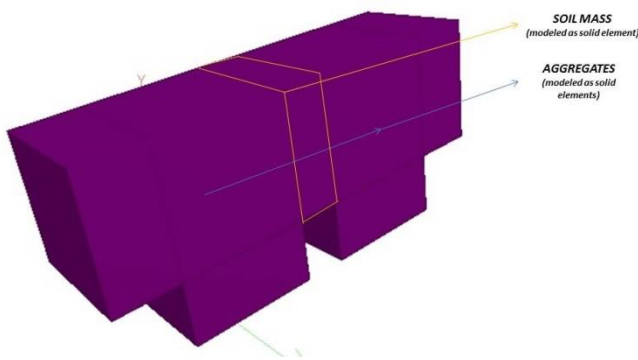


Fig 1.7: Two stones plugged with soil mass

(Single unit representing the Soil mass as connecting element between two stones is shown in above figure)

As shown in above Figure, soil mass is sandwiched between stone aggregates. The highlighted part in figure represents soil mass. Young's Modulus of soil mass is varied from 15000 KN/m² for loose soil mass to 30000 KN/m² for fully compacted soil mass & is directly proportional to stiffness between aggregates. The values of E and G of soil mass are,

Table 1.2: Properties of Soil mass

| Young's Modulus, E (KN/m ²) | Shear Modulus, G (KN/M ²) | Stiffness, K (KN/m) |
|---|---|---------------------------|
| 15000 (loose) | 5358 | 2700 |
| 20000 (medium) | 7145 | 3600 |
| 25000 (stiff) | 8929 | 4500 |
| 30000 (fully compacted) | 10715 | 5400 |

The solid masses modeled along the periphery of the system are assigned with the properties of Earth crust. The material properties of Stone, Crust, Sand, Horizontal and Vertical line elements of a typical example model is shown in the Figure below. By keeping the material property of stone and Crust as constant, the properties of sand and horizontal links are varied by assigning the properties listed out in Table 1.3

Table 1.3: Material Properties

| Name | E kN/m ² | Poisson's Ratio | Density kN/m ³ | Alpha E-6/K | Fy kN/m ² | Fu kN/m ² | Ry | Rt | Fcu kN/m ² |
|----------|------------------------|-----------------|------------------------------|----------------|-------------------------|-------------------------|-------|-------|--------------------------|
| STONE | 55E6 | 100E-3 | 27.001 | 0.000 | 0.000 | 0.000 | 1.000 | 1.000 | 0.000 |
| CRUST | 76.8E6 | 200E-3 | 23.001 | 0.000 | 0.000 | 0.000 | 1.000 | 1.000 | 0.000 |
| SAND | 25000.107 | 400E-3 | 22.001 | 0.000 | 0.000 | 0.000 | 1.000 | 1.000 | 0.000 |
| STEEL | 199.9E6 | 300E-3 | 76.822 | 3.333 | 248.2E3 | 399.9E3 | 1.200 | 1.500 | 0.000 |
| CONCRETE | 21.72E6 | 170E-3 | 23.617 | 2.778 | 0.000 | 0.000 | 0.000 | 0.000 | 27579.029 |
| HZELINK | 3.200 | 100E-3 | 15.001 | 0.000 | 0.000 | 0.000 | 1.000 | 1.000 | 0.000 |
| VLELINK | 320E6 | 100E-3 | 15.001 | 0.000 | 0.000 | 0.000 | 1.000 | 1.000 | 0.000 |

The properties of connecting elements listed out in Table 1.3 is kept as standard and number of models with different sizes, cross sections, loadings were created and link elements in each model is assigned with each material property. Thus the behavior of each different model is studied by assigning all stiffness properties mentioned in Tables 1.3 above. The gap between the stones aggregates in actual site varies, but for modeling purpose uniform gap of thickness 20mm filled with soil mass is considered.

The different sizes of system are modeled for the analysis purpose and is varied from 0.0005 m³ to 4 m³.

The following list of sizes of arrangement are considered for analysis purpose,

1. (0.06 x 0.18 x 0.08) m
2. (0.14 x 0.18 x 0.08) m
3. (0.14 x 0.18 x 0.16) m
4. (0.06 x 1.00 x 0.50) m
5. (0.06 x 1.62 x 0.82) m
6. (1.00 x 1.00 x 0.25) m
7. (1.00 x 1.00 x 0.50) m
8. (1.40 x 1.40 x 0.25) m
9. (1.40 x 1.40 x 0.50) m
10. (4.00 x 4.00 x 0.25) m

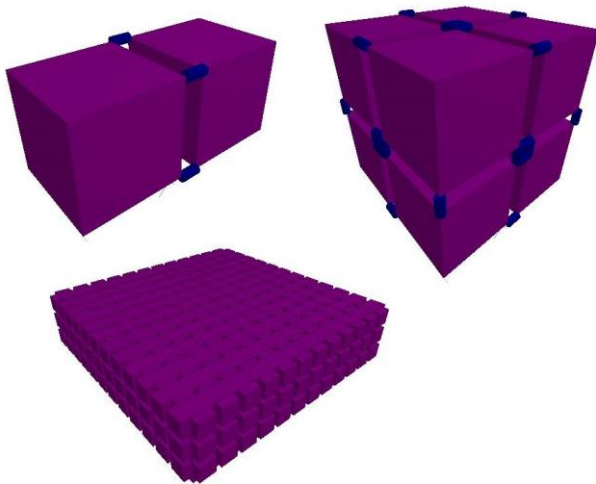


Fig 1.8 : Different sizes of system

(Figure shows the different sizes and arrangement of stone masses, soil masses and line elements)

All the modeled sections are analyzed by applying vertical load where the load denotes weight of structure in actual. The application of vertical load is carried out by placing Plate element of concrete material of suitable sections satisfying desired load quantity above the arrangement of aggregates. The Plate element resembles the raft footing in actual which made it to use as loading element here & all models are assigned with constant seismic parameters of El Centro Earthquake. The typical section of loading on Isolating system and loads applied for analysis purpose corresponding to cross section of plate element are as follows,

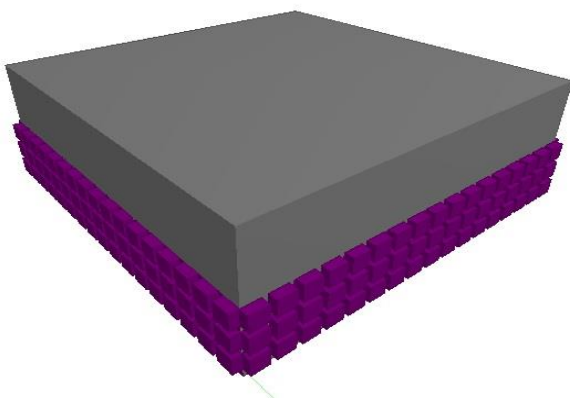


Fig 1.9: Loading on system

(Plate element as loading material is placed above the arrangement is shown here)

Table 1.4 (a) & (b) : Sizes of Plate element corresponding to loading

| PLATE DIMENSION (L x B x D) m | LOAD in KN |
|-------------------------------|------------|
| (0 x 0 x 0) | 0 |
| (0.94 x 0.94 x 0.05) | 1.00 |
| (0.94 x 0.94 x 0.1) | 2.00 |
| (0.94 x 0.94 x 0.2) | 4.24 |
| (0.94 x 0.94 x 0.4) | 8.50 |
| (0.94 x 0.94 x 1.6) | 12.72 |
| (0.94 x 0.94 x 0.8) | 17.00 |
| (0.94 x 0.94 x 1.0) | 21.20 |
| PLATE DIMENSION (L x B x D) m | LOAD in KN |
| (0 x 0 x 0) | 0 |
| (1.34 x 1.34 x 0.023) | 1.00 |
| (1.34 x 1.34 x 0.046) | 2.00 |
| (1.34 x 1.34 x 0.100) | 4.30 |
| (1.34 x 1.34 x 0.197) | 8.50 |
| (1.34 x 1.34 x 0.300) | 13.00 |
| (1.34 x 1.34 x 0.394) | 17.00 |
| (1.34 x 1.34 x 0.500) | 21.55 |

The above mentioned loadings in Table (a) & (b) are done for sections (1.00 x 1.00 x 0.25)m, (1.00 x 1.00 x 0.50)m, (1.40 x 1.40 x 0.25)m, (1.40 x 1.40 x 0.50)m only.

The analysis is carried out for different compaction values. Predominantly Compaction value is used to fix/check the depth of system. The compaction value of system can be varied by two criteria, i.e. by keeping volume as constant,

1. Increasing stiffness/Young's Modulus of connecting element

The system is composed of large number of units containing 2 stone mass & a link each, values of stiffness & Young's modulus of links is directly proportional to compaction value of system. The various values of stiffness & Young's modulus is shown in Table (1) & (2) are assigned and analysis is carried out.

2. Increasing number of stone count by reducing thickness of soil element.

Parallel way of varying compaction value of system is by keeping volume as constant thickness of link element is varied which in turn leads to number of stone count. Unit density of stone mass is same, variation in its count with constant system's volume leads to variation in density of system. Density of any system is directly proportional to compaction value.

The bottom most layer of Stone aggregates existing in contact with Ground below are assigned Fixed restraint and the layers above are connected by providing links. The typical arrangement is shown in following Figure,

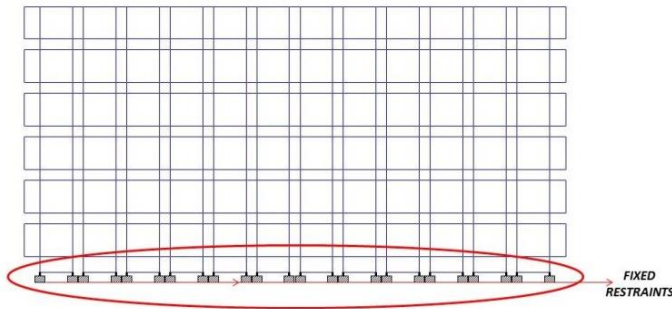


Fig 1.10 : Support restraint

(All the joints which are in direct contact with below ground are assigned with fixed restraint)

The periphery stone aggregates along the direction of seismic wave are assigned with load of El Centro earthquake data. The earthquake load is assigned to highlighted solid masses of the arrangement shown in below Figure,

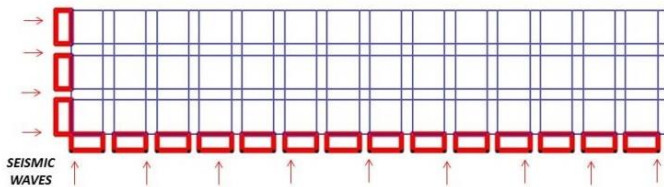


Fig 1.11 : Application of Earthquake load

(The highlighted masses along the periphery are assigned with earthquake load)

For Time-History analysis purpose El Centro earthquake data is assigned for all models and comparison is done assuming the system is free from other external disturbances. The acceleration values of El Centro Earthquake for a time period up to 2.24 seconds are considered for analysis purpose.

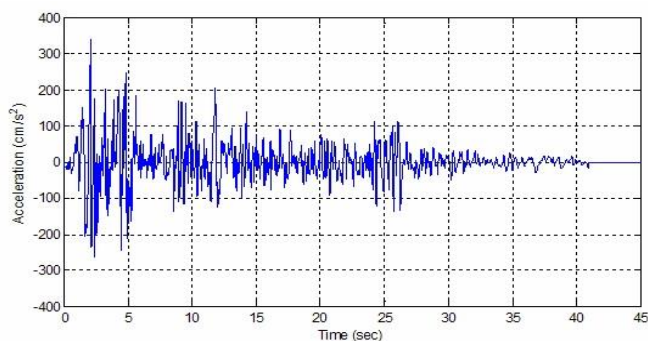


Fig 1.12 : Acceleration-Time History Plot

(Ground motion data recorded at a site in El Centro, California Imperial Valley earthquake of May 18, 1940 is shown in figure)

The number of modes are restricted to 10 in the study and the first mode shape of a typical arrangement is shown

below. The analysis of all models with different size, cross sections, loadings, stiffness of connecting members is carried out by assigning the time period and corresponding acceleration data of El Centro earthquake.

Initially the behavior of two stone aggregates linked with sand mass and surrounded by crust element is drawn and subsequently the number of all elements are increased and relative responses are drawn. The example models and their Natural Frequency, deflected shape along with size, corresponding Stiffness/Young's Modulus of connecting element, Mass participation factors, Time-Acceleration curve, Base reaction and Work done are listed below. The mentioned parameters are determined for all models categorized under different stiffness, sizes, varying imposed loads, but the most efficient models and their behavior are listed out below. The case in which the value of work done is less, that arrangement is highly encouraged for isolating system.

Ex 1- Size = (0.06 x 0.18 x 0.08) m
 Young's Modulus (E) = 30000 kN/m²
 Load = Selfweight

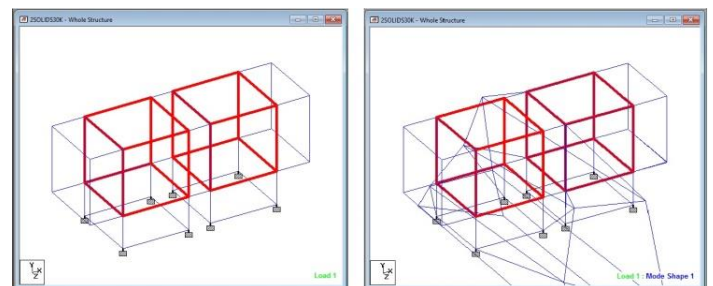


Fig 1.13 : Model & First Mode shape

Model of two stone masses of 60mm size each is highlighted in figure connected to one other by soil mass of thickness being 20mm is shown in figure. The material property of soil mass assigned with very less stiffness value whose Young's modulus being 15000 kN/m². All the supports are assigned Fixed restraint. The analysis is done considering El-Centro earthquake data the very first mode shape of arrangement is shown above.

Table 1.5 : Frequency, Period & corresponding Mode numbers

| MODE | FREQUENCY HZ | Period seconds |
|------|-----------------|-------------------|
| 1 | 5200.858 | 1.92 E-04 |
| 2 | 5452.817 | 1.83 E-04 |
| 3 | 8394.354 | 1.19 E-04 |
| 4 | 14505.285 | 6.89 E-05 |
| 5 | 14791.881 | 6.76 E-05 |
| 6 | 15753.601 | 6.35 E-05 |
| 7 | 16017.562 | 6.24 E-05 |
| 8 | 17724.048 | 5.64 E-05 |
| 9 | 17752.864 | 5.63 E-05 |
| 10 | 19593.991 | 5.1 E-05 |

The vales of frequencies, periods for corresponding modes are tabulated. The gradual decrease of time period and increase in frequency is observed in the analysis.

Table 1.6 : Mass Participation Factors

MASS PARTICIPATION FACTORS IN PERCENT

| MODE | X | Y | Z | SUMM-X | SUMM-Y | SUMM-Z |
|------|-------|-------|-------|--------|--------|--------|
| 1 | 0.00 | 0.00 | 37.93 | 0.000 | 0.000 | 37.930 |
| 2 | 22.48 | 17.49 | 0.00 | 22.482 | 17.485 | 37.930 |
| 3 | 0.00 | 0.00 | 0.17 | 22.482 | 17.485 | 38.104 |
| 4 | 44.52 | 7.95 | 0.00 | 67.001 | 25.433 | 38.104 |
| 5 | 0.00 | 0.00 | 5.13 | 67.001 | 25.433 | 43.233 |
| 6 | 0.00 | 0.00 | 16.85 | 67.001 | 25.433 | 60.080 |
| 7 | 0.00 | 0.00 | 0.01 | 67.001 | 25.433 | 60.091 |
| 8 | 0.74 | 2.03 | 0.00 | 67.740 | 27.459 | 60.091 |
| 9 | 0.00 | 0.00 | 0.41 | 67.740 | 27.459 | 60.497 |
| 10 | 0.00 | 16.26 | 0.00 | 67.742 | 43.720 | 60.497 |

The mass participation values and its cumulative weight of above model in all global directions is shown in above Table. The arrangement is experiencing maximum response/deformation in global X-direction.

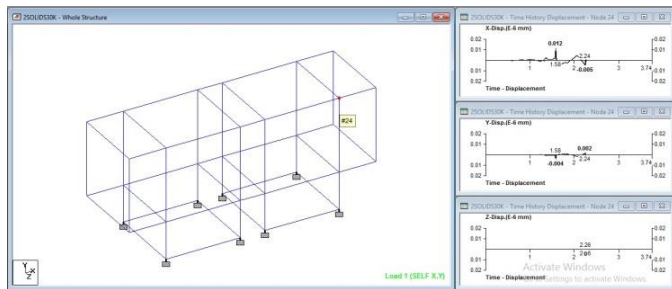


Fig 1.14 : Model & Time v/s Displacement spectra

The spectra relating Time and acceleration values in all three i.e. X, Y and Z direction is shown in above figure. The arrangement is experiencing maximum acceleration at time 1.58 s. The acceleration is very much less in Z- direction.

Table 1.7 : Base Reaction

| 2SOLIDS30K - Support Reactions: | | | | | | | |
|---------------------------------|--------|------------------|----------------|------------------|---------|---------|---------|
| All Summary Envelope | | | | | | | |
| Node | L/C | Horizontal Fx kN | Vertical Fy kN | Horizontal Fz kN | Moment | | |
| | | | | | Mx kN-m | My kN-m | Mz kN-m |
| 13 | 1 TIME | -0.000 | -0.000 | 0.000 | 0.000 | 0.000 | 0.000 |
| | 2 DL | 0.000 | 0.004 | -0.000 | 0.000 | 0.000 | 0.000 |
| 14 | 1 TIME | -0.000 | -0.000 | -0.000 | 0.000 | 0.000 | 0.000 |
| | 2 DL | 0.000 | 0.004 | 0.000 | 0.000 | 0.000 | 0.000 |
| 15 | 1 TIME | -0.000 | 0.000 | 0.000 | 0.000 | 0.000 | 0.000 |
| | 2 DL | -0.000 | 0.002 | 0.000 | 0.000 | 0.000 | 0.000 |
| 16 | 1 TIME | -0.000 | 0.000 | -0.000 | 0.000 | 0.000 | 0.000 |
| | 2 DL | -0.000 | 0.002 | -0.000 | 0.000 | 0.000 | 0.000 |
| 25 | 1 TIME | -0.000 | 0.000 | -0.000 | 0.000 | 0.000 | 0.000 |
| | 2 DL | -0.000 | 0.004 | -0.000 | 0.000 | 0.000 | 0.000 |

| 2SOLIDS30K - Statics Check Results | | | | | | | |
|------------------------------------|------------|-------|--------|--------|---------|---------|---------|
| L/C | | Fx kN | Fy kN | Fz kN | Mx kN-m | My kN-m | Mz kN-m |
| 2 | Loads | 0.000 | -0.023 | 0.000 | -0.001 | 0.000 | -0.002 |
| | Reactions | 0.000 | 0.023 | -0.000 | 0.001 | -0.000 | 0.002 |
| | Difference | 0.000 | 0.000 | -0.000 | 0.000 | -0.000 | -0.000 |

Under the action of ground motion on arrangement, the stone masses in the top layer experiencing maximum deformation is noticed. The base reaction and displacement experienced by the top most stone mass is highlighted in Table.

Table 1.8 : Work done

| Sl No. | Direction | Displacement M | Base reaction kN | Work done kN-m |
|--------|-----------------------------------|----------------|------------------|----------------|
| 1 | X | 0.012 | 0.004 | 2.5 E-05 |
| 2 | Y | 0.004 | | 1.6 E-05 |
| 3 | Z | 0.000 | | 0 |
| 4 | equilibrium $(x^2+y^2+z^2)^{0.5}$ | 0.012 | | 4.8 E-05 |

Work done = Base reaction x Lateral displacement

The model experiencing less values of work done is more suitable and efficient arrangement. The work done values in directions X, Y, Z and equilibrium state are tabulated above.

Ex 2- Size - (1.40 x 1.40 x 0.25) m
 Young's Modulus (E) = 30000 kN/m²
 Load = 21.55 kN

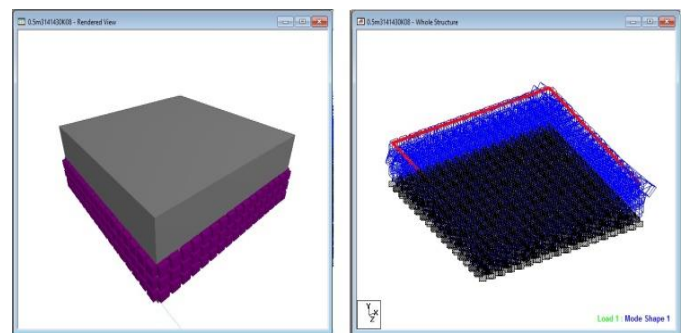


Fig 1.15 : Model & First Mode shape

Model of system of size being 0.50 m³ composed of stone masses of 60mm size each connected to one other by soil mass of thickness being 20mm is shown in figure. The material property of soil mass assigned with high stiffness value whose Young's modulus being 30000 kN/m². All the supports are assigned Fixed restraint. The loading on arrangement is done in the form of Plate element. The analysis is done considering El-Centro earthquake data and the very first mode shape of arrangement is shown above.

Table 1.9 : Frequency, Period & corresponding Mode numbers

| Mode | Frequency Hz | Period seconds |
|------|--------------|----------------|
| 1 | 274.099 | 0.004 |
| 2 | 330.077 | 0.003 |
| 3 | 366.409 | 0.003 |
| 4 | 369.628 | 0.003 |
| 5 | 384.286 | 0.003 |
| 6 | 388.686 | 0.003 |
| 7 | 396.625 | 0.003 |
| 8 | 406.651 | 0.002 |
| 9 | 426.512 | 0.002 |
| 10 | 427.613 | 0.002 |

The values of frequencies, periods for corresponding modes are tabulated. The gradual decrease of time period and increase in frequency is observed in the analysis.

Table 1.10 : Mass Participation Factors

MASS PARTICIPATION FACTORS IN PERCENT

| MODE | X | Y | Z | SUMM-X | SUMM-Y | SUMM-Z |
|------|------|------|-------|--------|--------|--------|
| 1 | 0.00 | 0.00 | 15.10 | 0.000 | 0.000 | 15.104 |
| 2 | 0.01 | 0.03 | 0.00 | 0.012 | 0.033 | 15.104 |
| 3 | 0.00 | 0.00 | 0.03 | 0.012 | 0.033 | 15.129 |
| 4 | 1.62 | 9.56 | 0.00 | 1.628 | 9.591 | 15.129 |
| 5 | 0.05 | 0.47 | 0.00 | 1.680 | 10.062 | 15.129 |
| 6 | 0.00 | 0.00 | 0.08 | 1.680 | 10.062 | 15.207 |
| 7 | 0.00 | 0.00 | 0.01 | 1.680 | 10.062 | 15.218 |
| 8 | 0.01 | 0.31 | 0.00 | 1.690 | 10.374 | 15.218 |
| 9 | 0.00 | 0.00 | 0.00 | 1.690 | 10.374 | 15.220 |
| 10 | 0.00 | 0.10 | 0.00 | 1.690 | 10.476 | 15.220 |

The mass participation values and its cumulative weight of above model in all global directions are shown in above Table. The arrangement is experiencing maximum response/deformation in global Z-direction.

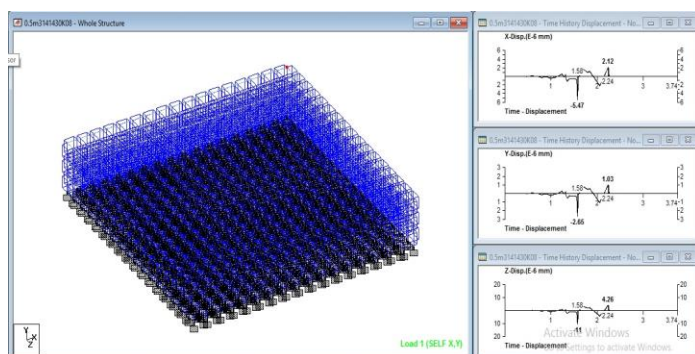


Fig 1.16 : Model & Time v/s Displacement spectra

The spectra relating Time and acceleration values in X, Y and Z directions is shown in above figure. The arrangement is experiencing maximum acceleration at time 1.58 s.

Table 1.10 : Base Reaction

| 0.5m3141430K08 - Support Reactions: | | | | | | | |
|-------------------------------------|--------|------------------|----------------|------------------|---------|---------|---------|
| All Summary Envelope | | | | | | | |
| Node | L/C | Horizontal Fx kN | Vertical Fy kN | Horizontal Fz kN | Moment | | |
| | | | | | Mx kN-m | My kN-m | Mz kN-m |
| 8570 | 1 TIME | 0.000 | -0.000 | 0.000 | 0.000 | 0.000 | 0.000 |
| | 2 DL | -0.006 | 0.297 | -0.072 | 0.000 | 0.000 | 0.000 |
| 8577 | 1 TIME | 0.000 | 0.000 | -0.000 | 0.000 | 0.000 | 0.000 |
| | 2 DL | 0.200 | 1.374 | -0.200 | 0.000 | 0.000 | 0.000 |
| 8578 | 1 TIME | 0.000 | 0.000 | 0.000 | 0.000 | 0.000 | 0.000 |
| | 2 DL | 0.127 | 0.945 | 0.036 | 0.000 | 0.000 | 0.000 |
| 8579 | 1 TIME | 0.000 | 0.000 | 0.000 | 0.000 | 0.000 | 0.000 |
| | 2 DL | -0.027 | 0.428 | 0.027 | 0.000 | 0.000 | 0.000 |
| 8580 | 1 TIME | 0.000 | -0.000 | 0.000 | 0.000 | 0.000 | 0.000 |
| | 2 DL | -0.036 | 0.945 | -0.127 | 0.000 | 0.000 | 0.000 |

| 0.5m3141430K08 - Statics Check Results | | | | | | | |
|--|------------|--------|---------|-------|---------|---------|---------|
| L/C | | Fx kN | Fy kN | Fz kN | Mx kN-m | My kN-m | Mz kN-m |
| 2 | Loads | 0.000 | -30.984 | 0.000 | -20.759 | 0.000 | -20.759 |
| | Reactions | -0.000 | 30.984 | 0.000 | 20.759 | 0.000 | 20.759 |
| | Difference | -0.000 | -0.000 | 0.000 | -0.000 | 0.000 | -0.000 |

Under the action of ground motion on arrangement, the stone masses in top layer experiencing maximum deformation is noticed. The base reaction and displacement experienced by the top most stone mass is highlighted in above Table.

Table 1.11 : Work done

| Sl No. | Direction | Displacement (mm) | Base reaction (kN) | Work done (kN-mm) |
|--------|---------------------------------------|-------------------|--------------------|-------------------|
| 1 | X | 5.47 | 0.428 | 2.34 |
| 2 | Y | 2.65 | | 1.13 |
| 3 | Z | 11.00 | | 4.70 |
| 4 | equilibrium $(x^2 + y^2 + z^2)^{0.5}$ | 12.56 | | 5.37 |

Work done = Base reaction x Lateral displacement

The model experiencing less values of work done is more suitable and efficient arrangement and the work done values in directions X, Y, Z and equilibrium state are tabulated above.

The response of system composed of stone masses connected to one another through springs/line elements greatly depends on assigned stiffness values for link elements ranging from very loose/ zero stiffness to very large stiffness value when the aggregates are in rigid contact.

However the arrangement in which the work done value is less, is more encouraged, here the arrangement of isolation system consisting soil mass of Young's modulus 30000 kN/m² is adopted for further work which includes the comparison between conventional fixed base structure and structure plugged with isolation system.

The typical twenty storied single bay framed structure is considered for the comparison purpose whose plan dimensions being (3x3) m and height of complete structure being 60 m. The size of Isolating system is (4x4x0.5) m, size of stone mass is 60mm and thickness of soil mass between stone aggregates is 20mm.

The analysis of framed model is done in two cases,
case i. Framed model with Isolated footings with fixed restraints at base

case ii. Framed model with Raft footing rested on Isolating system

The analysis is done using *Staad-Pro V8i* software and the deformed shape of both structures relative to case i and case ii is shown in figure below,

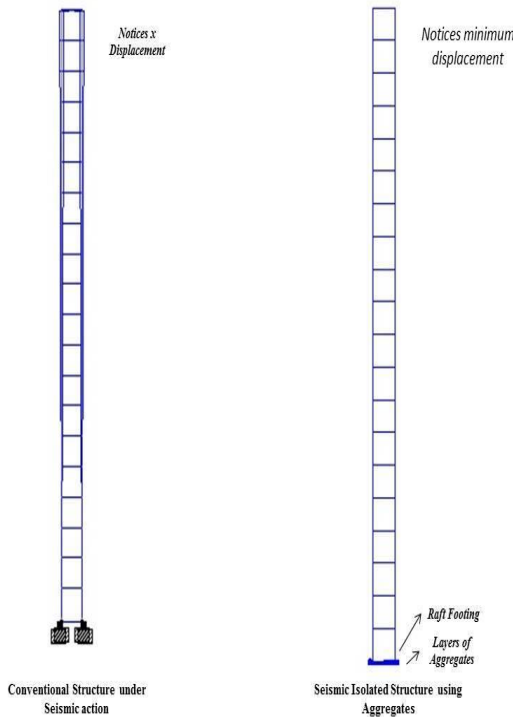


Fig 1.17 Deformed shape of Structure

(The deformed shape of structure with fixed restraint-left and base structure using large sized aggregates-right is shown in above figure)

| MODE | FREQUENCY HZ | Period seconds | MODE | FREQUENCY HZ | Period seconds |
|------|--------------|----------------|------|--------------|----------------|
| 1 | 0.361 | 2.770 | 1 | 0.313 | 3.200 |
| 2 | 0.410 | 2.437 | 2 | 0.328 | 3.050 |
| 3 | 0.712 | 1.405 | 3 | 0.353 | 2.830 |
| 4 | 1.259 | 0.794 | 4 | 0.397 | 2.520 |
| 5 | 1.626 | 0.615 | 5 | 0.513 | 1.950 |
| 6 | 2.145 | 0.466 | 6 | 0.689 | 1.450 |
| 7 | 2.462 | 0.406 | 7 | 0.950 | 1.052 |
| 8 | 3.348 | 0.299 | 8 | 1.351 | 0.740 |
| 9 | 3.563 | 0.281 | 9 | 1.695 | 0.590 |
| 10 | 3.607 | 0.277 | 10 | 1.815 | 0.551 |

Fig 1.18: Periods of Isolated and conventional structure

The periods of isolated structure is found to be more compared to that of conventional one. The structure provided with fixed restraint at base is experienced a displacement of around 17 mm at top node of structure. Whereas we noticed very less or zero displacement in the same node of Isolated structure. The story drift plot for conventional and isolated structure is shown in following figure.

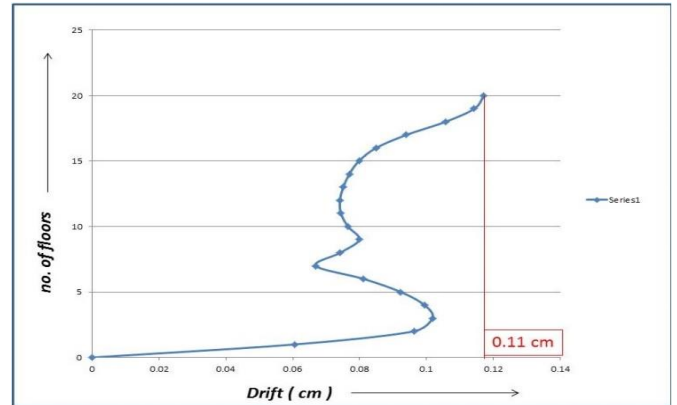


Fig 1.19: Story drift plot for conventional structure

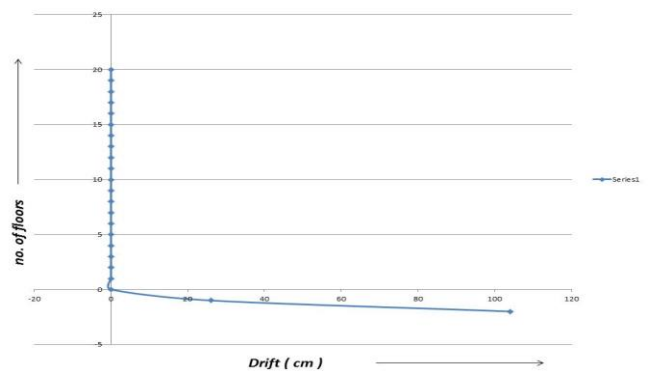


Fig 1.20: Story drift plot for base isolated structure

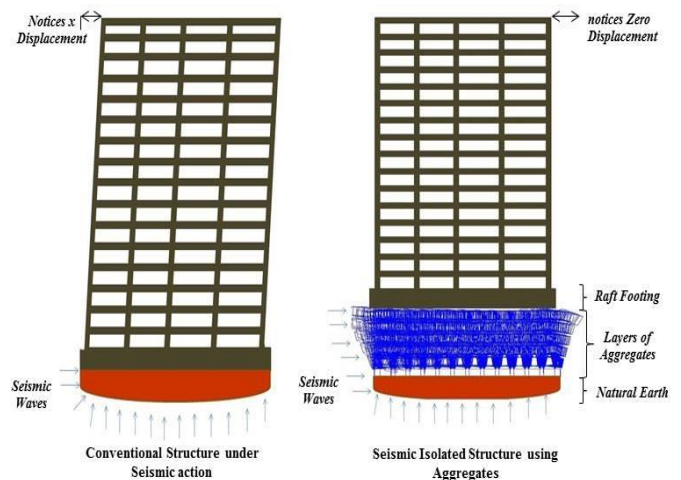


Fig 1.21: Comparison of conventional & Isolated structure

CONCLUSIONS:

- The periods of isolated structure are marginally more compared to those of conventional one.
- The technique presented in the paper involves filling up an excavated pit of certain known designed dimensions and just filling the pit with loose boulders/stones or in general coarse aggregates.
- The technique can be called as passive isolation. It is easy to construct. The materials locally available can be employed and therefore does not involve much transportation and energy. It can therefore be classified under sustainable technology.
- The system in which the Young's modulus of soil is assigned with 30000kN/m^2 (fully compacted soil mass) is concluded as efficient one in this study.
- The displacement at topmost node is very much less in Isolated structure compared to that of conventional one.
- The work done in the case of an isolated structure is least which is also an encouraging feature.
- Any structure built on such an isolated system shows much less displacement at the top compared to that of the conventional which proves that such passive isolation works well even when subjected to an earthquake ground motion.
- The drift of such a structure is almost nil which is very encouraging.

ACKNOWLEDGEMENT

It is with a feeling of great pleasure that I would like to express my most sincere heartfelt gratitude Sri. Dr. B K Raghu Prasad & Dr. Amarnath K for their valuable guidance.

REFERENCES

- [1] Anand S.Arya, "Concepts & techniques for seismic base-isolation of structures" ISBN 9054100605
- [2] Kubilay Kaptan, "Seismic Base Isolation & Energy absorbing devices", European Scientific Journal
- [3] Gabriel Danila, "Seismic response control of buildings using Base Isolation", IJMCS Vol 1
- [4] Saiful Islam, "Seismic isolation in buildings to be practical reality", JETR, Vol. 3(4)
- [5] Dynamics of Structures, Anil K Chopra, Etc.....

Structural Analysis of Blast Resistant Buildings

Qureshi Rizwan¹, Shivanand Ghule², Amarnath K³

¹M.Tech, Department of Civil Engineering, The Oxford College of Engineering, Bengaluru, Karnataka, India

^{2,3}Professor, Department of Civil Engineering, The Oxford College of Engineering, Bengaluru, Karnataka, India

Abstract: The objective of this study is to shed light on blast resistant building design theories. The general aspects of explosion process have been presented to clarify the effects of explosives on buildings. The main aim of this work is to compare the responses of the structure having shear wall and the structure having braces. Thus, analysing which structure is more blast resistant. Blast loads of explosives weighing 150kg and 250kg is subjected on both the models at distances 25m & 50m. Responses of both the models are observed.

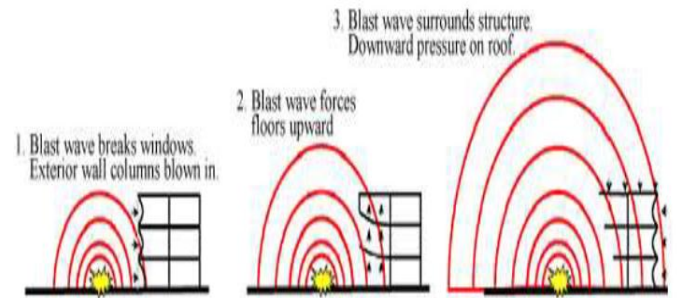


Fig 1: Blast effects

INTRODUCTION

An explosion can be defined as rapid liberation of potential energy followed by huge eruption of energy in the atmosphere. The energy released during explosion is converted into thermal energy radiation and some part of energy forms shock waves which expand radially.

Many incidents have taken place around the world where the structures are subjected to blast induced impulsive loads due to fanatic activities in the past few years. This has lead to threat to life and property. Blast resistant design is a specialized area to which structural engineers are not exposed meticulously as this design is comprehensively used only for military setups. Various types of finite element tools and software are available for blast resisting design of structures.

STRUCTURAL ASPECTS OF DESIGN FOR BLASTS LOADING

Whenever an explosion takes place the front face of the building experiences maximum over pressure due to reflection. The sides and terrace of the building experiences no reflected waves. The back side of the building experiences zero pressure unless the blast wave has travelled throughout the structure. There will be a lag of time in the formation of pressure and loads on the front and back sides.

LITERATURE REVIEW

R.D. Ambrosini & B M Luccioni (2003): They conducted study on reinforced concrete building and did the analysis of structural failure due to blast load. The whole process of explosion charge to the complete destruction of the structure is reproduced, including the proliferation of blast wave and its effects on the structure. Their journal includes comparison that the damage occurred by explosive charge with images along with the simulation procedure.

Mayor Baxani et al. (2015): He studied the dynamic response of Masonry wall subjected to blast load of charge 0.5kg at a distance of 0.5m from the wall. Langrangian and Eulerian methods are incorporated to implement the required parameters of blast load. Finite Element analysis tool Autodyne was used. The idea of this work was to investigate the local effect and global response of the masonry wall. The analysis results were obtained in terms of acceleration, velocity for charges on the ground and in air, it was found that the maximum acceleration for both air blast and ground blast 11.772 mm/s² and 8.14 mm/s² respectively.

METHODOLOGY

The calculations are based on **IS: 4991-1968** which is the criteria for blast resistant design of structures for explosions above ground.

Models used:

Model 1: Shear wall of thickness 150mm
 Model 2: Structure having Braces of Steel

Case Study:

- Case 1- Blast load of 150kg explosive at 25m standoff distance
- Case 2- Blast load of 150kg explosive at 50m standoff distance
- Case 3- Blast load of 250kg explosive at 25m standoff distance
- Case 4- Blast load of 250kg explosive at 50m standoff distance

STRUCTURAL DETAILS

Description of Model:

| Table 1: Description of Model | |
|--|----|
| No. of bays in x-direction | 4 |
| No. of bays in y-direction | 4 |
| Width of single bay in both directions | 4m |
| No. of Storeys | 20 |
| Height of each storey | 3m |

Structural elements:

| Table 2: Structural Elements | | |
|------------------------------|---------------|--------|
| Column | 600mm x 600mm | M40 |
| Beam | 350mm x 550mm | M30 |
| Slab | 140mm thick | M30 |
| Plinth | 900mm thick | M30 |
| Steel | | Fe 500 |

General loading:

| Table 3: Loadings | |
|-------------------|-----------------------|
| Live load | 3kN/m ² |
| Floor finish | 1.5 kN/m ² |
| Imposed loads | 2 kN/m ² |

Model 1: shear walls of 150mm thickness is used

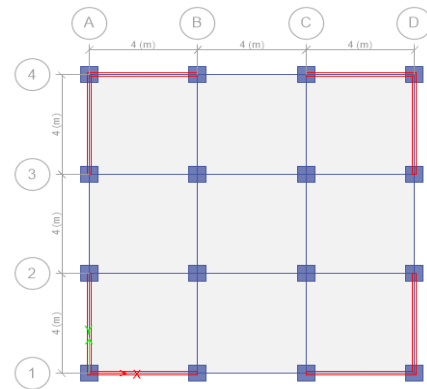


Fig 2: Plan view



Fig 3: Elevation

Model 2: Steel bracing of X-shape. ISWB550 steel has been used.

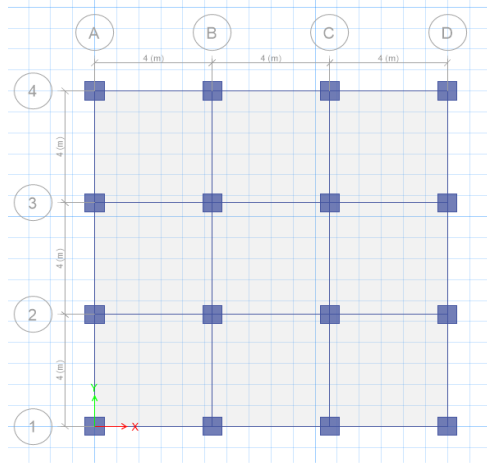


Fig 4: Plan view

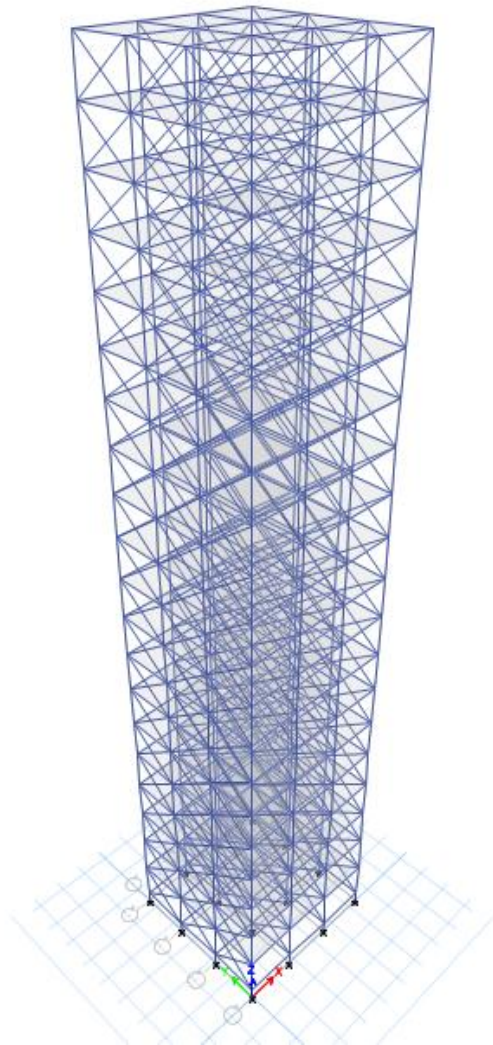


Fig 5: Elevation

RESULTS:

Case 1: when 150kg of explosive is used at 25m standoff distance

Storey displacement

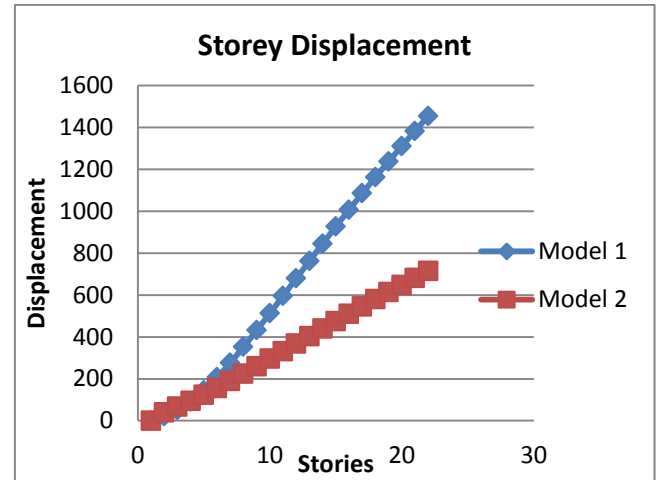


Fig 6: Comparison of Storey Displacement

| Table 4: Storey Displacement | | |
|------------------------------|---------|---------|
| | Model 1 | Model 2 |
| Storeys | mm | mm |
| Base | 0 | 0 |
| PLINTH | 21.4 | 40.3 |
| Story1 | 49.7 | 67.7 |
| story2 | 91.1 | 94.9 |
| Story3 | 144.5 | 124.1 |
| Story4 | 207.2 | 155.9 |
| Story5 | 277.1 | 189.4 |
| Story6 | 352.5 | 224.2 |
| Story7 | 431.6 | 259.8 |
| Story8 | 513.2 | 295.9 |
| Story9 | 596.1 | 332.2 |
| Story10 | 679.3 | 368.7 |
| Story11 | 762.7 | 403.5 |
| Story12 | 845.2 | 439.2 |
| Story13 | 926.8 | 474.9 |
| Story14 | 1006.9 | 510.4 |
| Story15 | 1085.5 | 545.6 |
| Story16 | 1162.3 | 580.4 |
| Story17 | 1237.5 | 614.7 |
| Story18 | 1311 | 648.4 |
| Story19 | 1383 | 681.6 |
| Story20 | 1453.9 | 714.2 |

Storey Drift

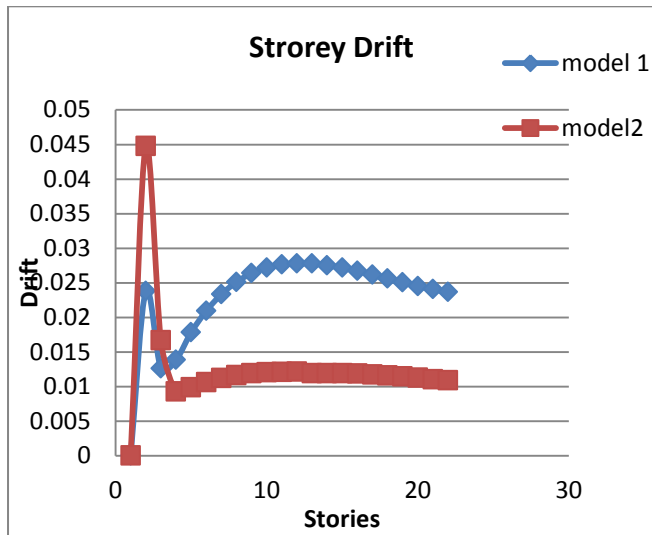


Fig 7: Comparison of Storey Drift

| Table 5 : Storey Drift | Model 1 | Model 2 |
|------------------------|----------|----------|
| Storeys | | |
| Base | 0 | 0 |
| Plinth | 0.02382 | 0.044747 |
| 1 | 0.012601 | 0.016684 |
| 2 | 0.013856 | 0.009288 |
| 3 | 0.01783 | 0.009887 |
| 4 | 0.020938 | 0.010624 |
| 5 | 0.023338 | 0.011205 |
| 6 | 0.025124 | 0.011619 |
| 7 | 0.026383 | 0.011896 |
| 8 | 0.027196 | 0.012053 |
| 9 | 0.027641 | 0.012108 |
| 10 | 0.027791 | 0.012155 |
| 11 | 0.02778 | 0.011921 |
| 12 | 0.027532 | 0.011922 |
| 13 | 0.027177 | 0.011909 |
| 14 | 0.026718 | 0.011846 |
| 15 | 0.026188 | 0.011743 |
| 16 | 0.025621 | 0.011605 |
| 17 | 0.025052 | 0.01144 |
| 18 | 0.024511 | 0.011255 |
| 19 | 0.024066 | 0.011057 |
| 20 | 0.023682 | 0.010878 |

Case 2: when 150kg explosive used at 50m standoff distance.

Storey Displacement

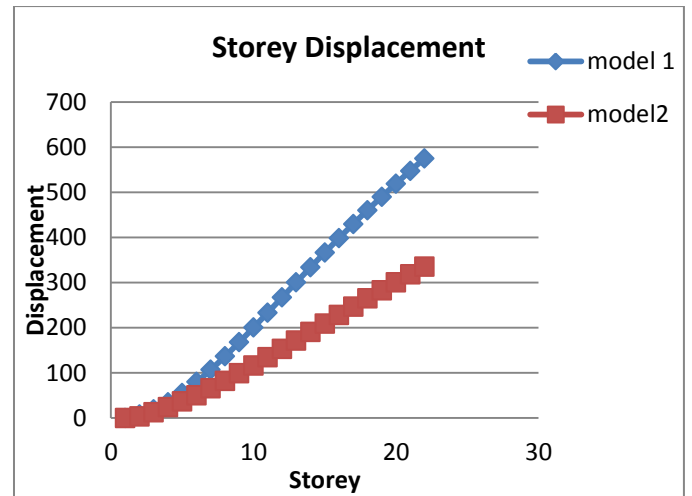


Fig 8: Comparison of lateral displacement

| Table 6: Storey Displacement | Model 1 | Model 2 |
|------------------------------|---------|---------|
| Storeys | mm | mm |
| Base | 0 | 0 |
| PLINTH | 7.9 | 3.3 |
| 1 | 18.7 | 12.5 |
| 2 | 34.8 | 23.7 |
| 3 | 55.3 | 36.3 |
| 4 | 79.7 | 50.3 |
| 5 | 107 | 65.6 |
| 6 | 136.6 | 81.8 |
| 7 | 167.8 | 98.8 |
| 8 | 200.3 | 116.4 |
| 9 | 233.4 | 134.6 |
| 10 | 266.9 | 153 |
| 11 | 300.4 | 171.7 |
| 12 | 333.6 | 190.5 |
| 13 | 366.3 | 209.3 |
| 14 | 398.4 | 228.1 |
| 15 | 429.8 | 246.6 |
| 16 | 460.4 | 265 |
| 17 | 490.2 | 283 |
| 18 | 519.2 | 300.8 |
| 19 | 547.5 | 318.2 |
| 20 | 575.1 | 335.3 |

Storey Drift

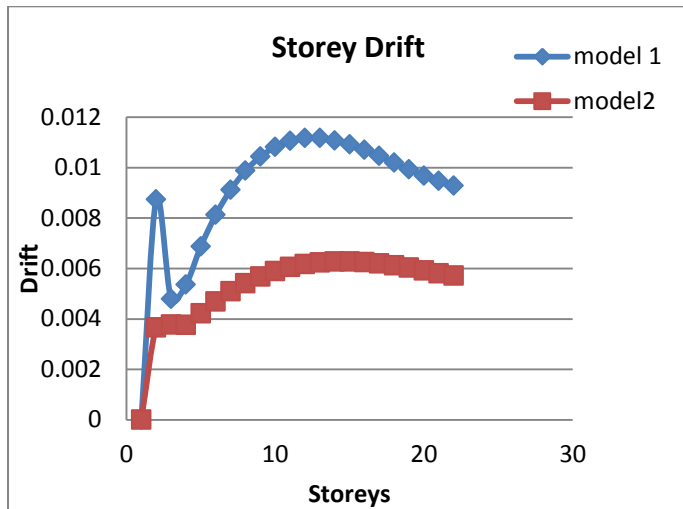


Fig 9: Comparison of Storey drift

| Table 7: Storey Drift | Model 1 | Model 2 |
|-----------------------|----------|----------|
| Storeys | | |
| Base | 0 | 0 |
| PLINTH | 0.008729 | 0.003665 |
| 1 | 0.004794 | 0.003771 |
| 2 | 0.005358 | 0.003764 |
| 3 | 0.006873 | 0.004221 |
| 4 | 0.008124 | 0.004692 |
| 5 | 0.009114 | 0.005088 |
| 6 | 0.009874 | 0.005416 |
| 7 | 0.010434 | 0.005683 |
| 8 | 0.010821 | 0.005894 |
| 9 | 0.011057 | 0.006054 |
| 10 | 0.011165 | 0.006168 |
| 11 | 0.011165 | 0.00624 |
| 12 | 0.011076 | 0.006275 |
| 13 | 0.010916 | 0.006276 |
| 14 | 0.010704 | 0.006247 |
| 15 | 0.010458 | 0.006193 |
| 16 | 0.010192 | 0.006118 |
| 17 | 0.009925 | 0.006026 |
| 18 | 0.009671 | 0.005921 |
| 19 | 0.009466 | 0.005808 |
| 20 | 0.009275 | 0.005711 |

Case 3: when 250kg of explosive is used at 25m standoff distance.

Storey Displacement



Fig 10: Comparison of lateral displacement

| Table 8: Storey Displacement | Model 1 | Model 2 |
|------------------------------|---------|---------|
| Storeys | mm | mm |
| Base | 0 | 0 |
| PLINTH | 11.1 | 48 |
| 1 | 46 | 97.5 |
| 2 | 99.9 | 151.1 |
| 3 | 166.8 | 211.6 |
| 4 | 244.7 | 279.3 |
| 5 | 331.1 | 352.7 |
| 6 | 423.5 | 430.8 |
| 7 | 520 | 512.8 |
| 8 | 619.1 | 597.9 |
| 9 | 719.4 | 685.4 |
| 10 | 819.6 | 774.4 |
| 11 | 918.7 | 864.6 |
| 12 | 1016.2 | 955.3 |
| 13 | 1111.3 | 1046 |
| 14 | 1203.6 | 1136.4 |
| 15 | 1293 | 1225.9 |
| 16 | 1379.2 | 1314.4 |
| 17 | 1462.5 | 1401.6 |
| 18 | 1542.8 | 1487.3 |
| 19 | 1620.8 | 1571.4 |
| 20 | 1695.9 | 1654.1 |

Storey Drift

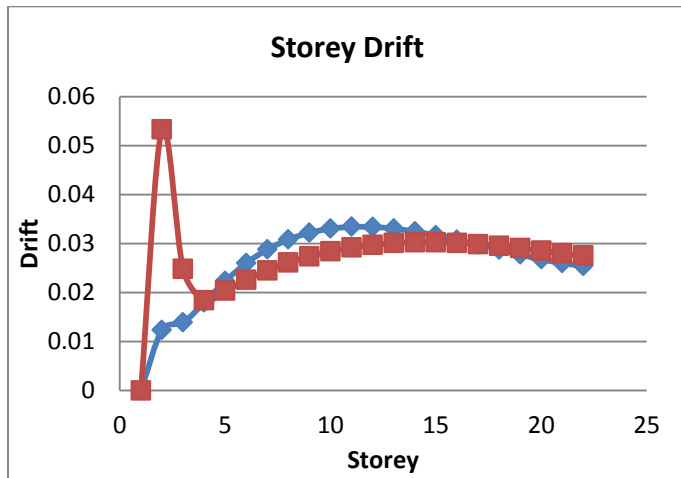


Fig 11: Comparison of Storey drift

| Table 9: Storey Drift | Model 1 | Model 2 |
|-----------------------|----------|----------|
| Storeys | | |
| Base | 0 | 0 |
| PLINTH | 0.012332 | 0.053297 |
| 1 | 0.013897 | 0.024798 |
| 2 | 0.017958 | 0.018405 |
| 3 | 0.022339 | 0.020365 |
| 4 | 0.02603 | 0.022616 |
| 5 | 0.028824 | 0.024531 |
| 6 | 0.030854 | 0.026112 |
| 7 | 0.032237 | 0.027399 |
| 8 | 0.033069 | 0.028419 |
| 9 | 0.033437 | 0.029194 |
| 10 | 0.033418 | 0.029747 |
| 11 | 0.033081 | 0.030099 |
| 12 | 0.032493 | 0.030269 |
| 13 | 0.031711 | 0.030277 |
| 14 | 0.030792 | 0.030143 |
| 15 | 0.029789 | 0.029886 |
| 16 | 0.028755 | 0.029526 |
| 17 | 0.027744 | 0.029083 |
| 18 | 0.0268 | 0.02858 |
| 19 | 0.026029 | 0.028042 |
| 20 | 0.025406 | 0.027566 |

Case 4: when 250kg explosive is used at 50m standoff distance.

Storey Displacement

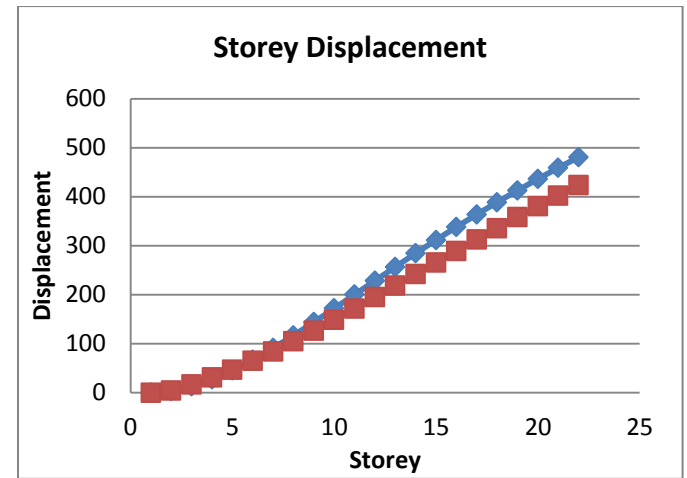


Fig 12: Comparison of lateral displacement

| Table 10: Storey Displacements | Model 1 | Model 2 |
|--------------------------------|---------|---------|
| Storeys | mm | mm |
| Base | 0 | 0 |
| PLINTH | 3.3 | 4.7 |
| 1 | 12.8 | 16.6 |
| 2 | 27.4 | 31 |
| 3 | 45.8 | 47 |
| 4 | 67.3 | 64.9 |
| 5 | 91.3 | 84.3 |
| 6 | 117.1 | 104.9 |
| 7 | 144.1 | 126.4 |
| 8 | 172 | 148.8 |
| 9 | 200.3 | 171.7 |
| 10 | 228.6 | 195 |
| 11 | 256.8 | 218.6 |
| 12 | 284.5 | 242.2 |
| 13 | 311.7 | 265.9 |
| 14 | 338.2 | 289.4 |
| 15 | 363.8 | 312.7 |
| 16 | 388.7 | 335.8 |
| 17 | 412.8 | 358.4 |
| 18 | 436.1 | 380.6 |
| 19 | 458.9 | 402.4 |
| 20 | 480.8 | 423.9 |

Storey Drift

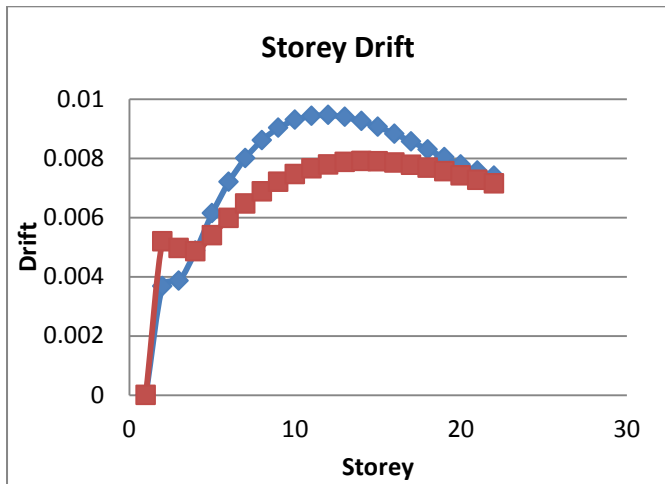


Fig 13: Comparison of Storey drift

| Table 11 : Storey Drift | Model 1 | Model 2 |
|-------------------------|----------|----------|
| Storeys | | |
| Base | 0 | 0 |
| PLINTH | 0.003681 | 0.005192 |
| 1 | 0.00386 | 0.004963 |
| 2 | 0.004874 | 0.004854 |
| 3 | 0.006141 | 0.005395 |
| 4 | 0.007196 | 0.00598 |
| 5 | 0.008006 | 0.00647 |
| 6 | 0.008607 | 0.006874 |
| 7 | 0.009028 | 0.0072 |
| 8 | 0.009295 | 0.007457 |
| 9 | 0.009431 | 0.00765 |
| 10 | 0.009457 | 0.007785 |
| 11 | 0.009391 | 0.007868 |
| 12 | 0.009253 | 0.007903 |
| 13 | 0.009059 | 0.007897 |
| 14 | 0.008824 | 0.007854 |
| 15 | 0.008564 | 0.007778 |
| 16 | 0.008294 | 0.007677 |
| 17 | 0.008028 | 0.007554 |
| 18 | 0.00778 | 0.007416 |
| 19 | 0.00758 | 0.007268 |
| 20 | 0.007407 | 0.007144 |

CONCLUSIONS

- 1) With the increase in Blast load and decrease in the Standoff distance, the Displacement and Storey Drift increases rapidly. So the response of the structure completely depends on the standoff distance and blast load.
- 2) The maximum displacements are 1695.9mm and 1654.1mm for 250kg explosive from 25m standoff distance. And 1453.9mm & 714.2mm was the maximum displacement for 150kg explosive at 25m standoff distance.
- 3) For model 2 having steel braces the storey displacement is reduced to 58% and storey drift are reduced to 52.2% for 150kg of explosive.
- 4) Here, while using 250kg of explosive the thickness of shear wall was increased to 250mm but the grade of concrete used is M40 only.
- 5) In case 3 and case 4, where the thickness of shear wall is increased (Model 1) the difference in the response of both the models was effectively reduced.
- 6) The responses of both Model 1 and Model 2 at their respective distances are obtained.

REFERENCES

- 1) Kocaz Z. (2004) Blast Resistant Building Design, MSc Thesis, Istanbul Technical University, Istanbul, Turkey.
- 2) Hill J.A., Courtney M.A. (1995). The structural Engineer's Response to Explosion Damage. The Institution of Structural Engineer's Report, SETO Ltd, London.
- 3) Mays G.C., Smith P.D. (1995). Blast Effects on Buildings, Thomas Telford Publications, Heron Quay, London.
- 4) Yandzio E., Gough M. (1999). Protection of Buildings against Explosions, SCI Publication, Berkshire, U.K
- 5) "Structures to Resist the Effects of Accidental Explosions," Dept. of the Army Tech. Manual, TM5-1300, Dept. of the Navy Pub. NAVFAC P-397, Dept. of the Air Force Manual, AFM 88- 22, June 1969.

STUDY OF VERTICAL IRREGULARITY OF TALL RC STRUCTURE UNDER LATERAL LOAD

RAHUL¹, SHIVANAND C G²

¹M Tech, Department of Civil Engineering, The Oxford College of Engineering & Technology, Bengaluru, Karnataka

²Assistant Professor, Department of Civil Engineering, The Oxford College of Engineering & Technology, Bengaluru, Karnataka, India

Abstract - To study the behaviour of the building when the structure is subjected to the lateral loads (earthquake load and the wind load). For the urbanization and for the aesthetic purpose many irregular structures have been designed. As we all know that for good behaviour of the structure it is essential that the structure should be regular. Understanding the behaviour of the Setback building and comparing them with the building without setback building (Regular building) under the lateral load, Similarly for the Mass irregularity. Modelling and analysis of the models is been carried out using the Etabs 2013 software. The present study is limited for analysis of RC structure for lateral loads (EL & WL). The behaviour of the G+30 storey Regular building, Setback building and Mass irregularity building was studied. These building are analysed using Response Spectrum Method. The effect of the setback irregularity and mass irregularity is been studied by considering the parameter such as Storey displacement, storey drift, storey stiffness, Base shear and Time period and they are compared with the regular building.

Key Words: Mass Irregularity, Setback, Storey displacement, base shear, Time period & Response spectrum Analysis

1. INTRODUCTION

Earthquake is the most devastating and destructive of all the natural calamities. Earthquake is distinctive shaking of the earth surface which results in damage of the structures and causes several hundreds of casualties or loss of life. The earthquake is caused due to the energy released at the movement of faulty rocks. There will be continuous movement of the rock. The earthquake occurred in past days proves that effect on the building Structures, loss of human lives, damage on the ancient structures, flyovers bridges etc. this will directly affect the growth of the country. Many researches are carried out to design an earthquake resistant structure, but still it is not been possible to design the earthquake resistant structure without causing damage. In order to overcome this problem we need to know the seismic performance of the structure or building with various aspects, which will help us to design the structure which will resist the frequent

minor earthquake and gives sufficient caution whenever it is exposed to major earthquakes. Hence in present study there an effort made to study the behaviour of vertical irregular RC structure with mass and set back irregularity.

1.1 Scope of Study

The seismic performance of the RC structures mainly depends on the shape of the building and the structural system of the building. While symmetrical buildings effect in an equally uniform distribution of seismic forces all over its components. Unsymmetrical buildings result in tremendous indeterminate distribution of forces making the analysis and prediction becomes complicated. A desire to create an aesthetic and functionally efficient structure drives architects to perceive wonderful as well as imaginative structures. Earthquake resistant engineering emphasis the inconvenience of using irregular plans, recommending as an alternative the use of simple shapes. The effects that cause seismic action in irregular structures were observed in many recent earthquakes.

Furthermore to design and analyse an irregular building a considerably high level of engineering and designer effort are required, whereas a poor designer can design and analyse a simple architectural features. In other words, damages in those with irregular features are more than those in regular one. Therefore, irregular structures need a more cautious structural analysis to reach an appropriate behavior during a devastating earthquake.

1.2 OBJECTIVE OF STUDY

In this present study, The study of vertical irregularity and Mass irregularity of tall RC structure under lateral loads is carried out using Response Spectrum Analysis. Modelling and Analysis is done using Etabs 2013.

2. DESCRIPTION OF MODEL

The plan area of (35X25m) and equal length of 5m are considered. The building considered is an ordinary moment resisting frame of 30 story's with two types of irregular configurations. The different irregularities are

mass irregularity and the setback. The stormy height is uniform throughout for all the building models considered for analysis. The software used for analysis of the frame models is ETABS 2013.

Modeling

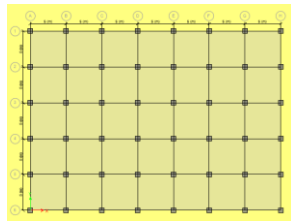


Fig-1 Regular Plan

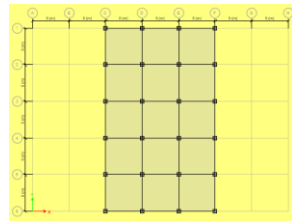


Fig-2 Setback Plan

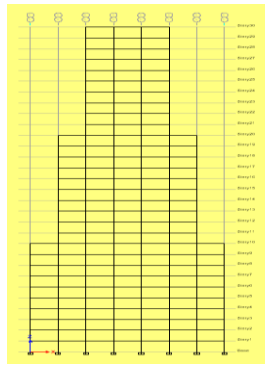


Fig-3 Model M1VZ5

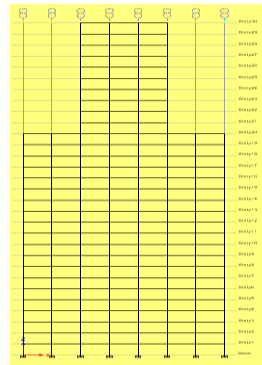


Fig-4 Model M2VZ5

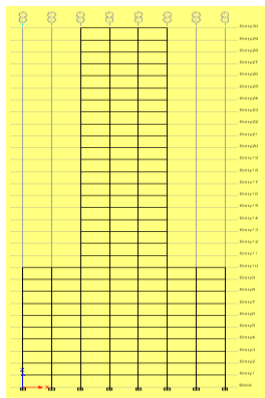


Fig-5 Model M3VZ5

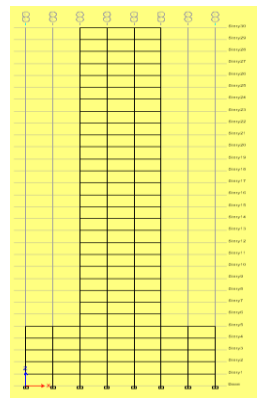


Fig-6 Model M3VZ5

The plan and elevations of models considered are as follows

MODEL RMZ5 - Building in rectangular shape with regular configuration for Zone 5.

MODEL RMZ2 - Building in rectangular shape with regular configuration for Zone 2.

MODEL M1VZ5 - Building with setback in 10th to 20th and 20th to 30th floors at 5m at regular 10 floors interval (ZONE 5).

MODEL M2VZ5 - Building with setback from 20th floor (ZONE 5).

MODEL M3VZ5 - Building with setback from 10th floor (ZONE 5).

MODEL M4VZ5 - Building with setback from 5th floor (ZONE 5).

MODEL MMZ5 - Building with mass irregularity at 10th, 20th and 30th floor for (Zone 5).

MODEL MMZ2 - Building with mass irregularity at 10th, 20th and 30th floor for (Zone 2).

The above mentioned models are considered for zone 5 and similarly same models are considered for zone 2 and they are named as RMZ2, model M1VZ2, model M2VZ2. Model M3VZ2 and model M4VZ2

Table-1 PARAMETERS CONSIDERED FOR ANALYSIS

| Particulars | Quantity |
|----------------------------|--------------------|
| Type of the structure | SMRF |
| Number of stories | 30 |
| Seismic zone | 5 & 2 |
| Floor height | 3m |
| Grade of concrete | M40 & M25 |
| Grade of steel | Fe550, Fe415 |
| Type of the soil | Soft Soil |
| Importance factor | 1 |
| Response reduction factor: | 5 |
| Live load | 3KN/m ² |
| Wind Speed | 50 km/s |
| Terrain category | 4 |
| Class of the structure | C |

Table-2 BEAM AND COLUMN SIZE DIMENSION

| Ticulars | Dimensions | Grade of concrete |
|-------------------------|------------|-------------------|
| Beam Size | | |
| 1- 10 floors | 300X550mm | M40 |
| 11-20 floors | 300X500mm | M40 |
| 21-30 floors | 300X400mm | M40 |
| Column Size | | |
| 1- 10 floors | 650X650mm | M40 |
| 11-20 floors | 550X550mm | M40 |
| 21-30 floors | 500X500mm | M40 |
| Thickness of slab | 150mm | M25 |
| Interior wall thickness | 150mm | |
| Exterior wall thickness | 200mm | |

Table-3 LOAD DETAILS

| Particulars | Quantity |
|--------------------------|-----------------------|
| Live load | 3 kN/m ² |
| Live load on top roof | 1.5 kN/m ² |
| Floor Finish | 1.8 kN/m ² |
| Floor Finish on top roof | 1.2 kN/m ² |
| Mass Irregularity load | 25 kN/m ² |

2. RESULTS AND DISCUSSIONS

This chapter represents the results and discussions of seismic analysis of vertical irregularities of RC tall Structures. Considering the different seismic zones that is Zone 5 and Zone 2, and the method of analysis is Response Spectrum Method. The results of both mass irregularity and the results of setback are discussed by considering the following parameters.

1. Storey Displacement
2. Storey Drift
3. Storey Stiffness
4. Base shear
5. Time Period

Comparison of Storey Displacement X-Direction

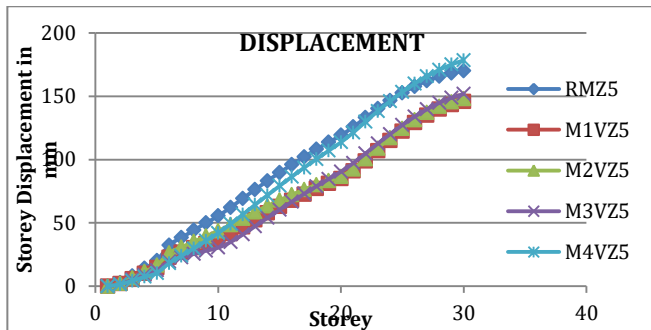


Chart-1 Setback results of storey displacement for Zone 5.

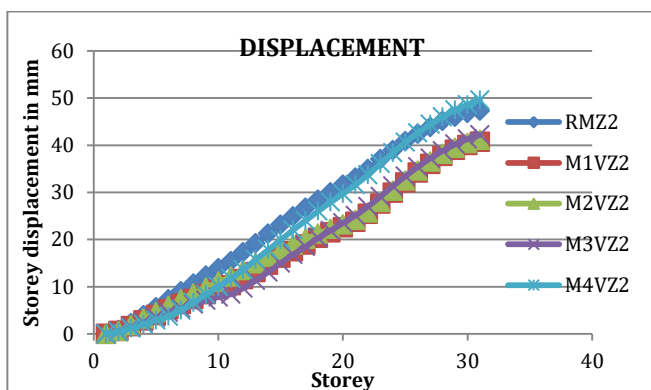


Chart-2 Setback results of storey displacement for Zone 2.

✓ It is observed from chart-1 and chart-2 that displacement increases with increase in storey in both the directions that is in X direction.

✓ Comparing all the models with regular model (RMZ5), it is seen that model M1VZ5 (Setback irregularity at 5th storey) has the higher displacement values.

✓ Comparing chart-1 and chart-2 it represents that the displacement of structure in zone 5 is maximum than displacement of the structure in zone 2.

Comparison of Storey Displacement X-Direction.

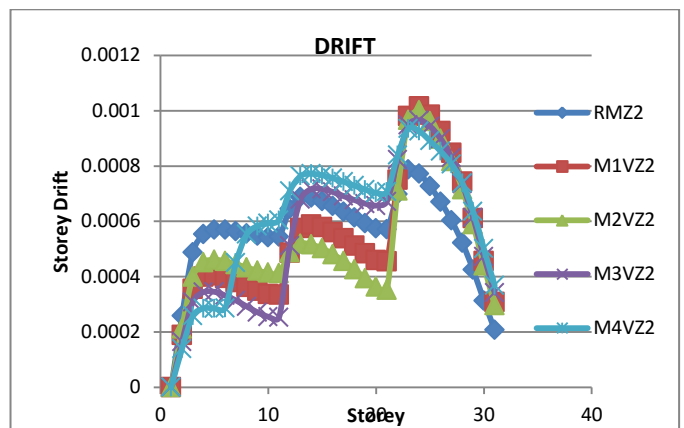


Chart-3 Setback results of storey drift for Zone 5.

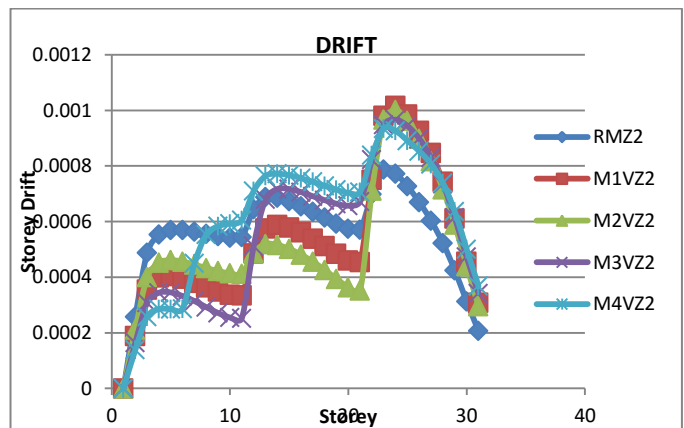


Chart-4 Setback results of storey drift for Zone 2.

✓ The storey drift is maximum in model M1VZ5 and increased by 22% when compared with regular model RMZ5.

✓ The storey drift is maximum in model M1VZ2 and increased by 24% when compared with regular model RMZ2.

✓ Comparing of all models in zone 5 (RMZ5, M1VZ5, M2VZ5, M3VZ5 and M4VZ5) with models in zone2 (RMZ2, M1VZ2, M2VZ2, M3VZ2 and M4VZ2) it is observed that models in zone 5 has the higher storey drift values.

Comparison of base shear results X-Direction

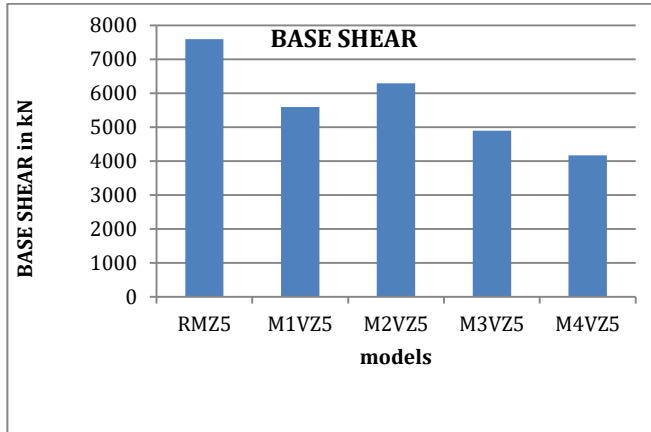


Chart-5 setback base shear results for zone 5

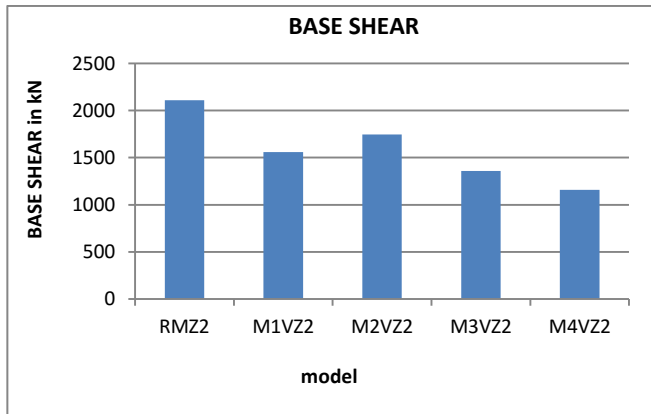


Chart-5 setback base shear results for zone 2

Table-4 Base shear

| BASE SHEAR in kN | | |
|------------------|-------------|-------------|
| MODEL | X direction | Y direction |
| RMZ5 | 7589.622 | 7538.308 |
| MMZ5 | 7836.24 | 7783.111 |
| RMZ2 | 2108.568 | 2094.312 |
| MMZ2 | 2176.787 | 2162.027 |

- ✓ Base shear of regular model (RMZ5) and Setback irregularity models along X is been presented in chart-5 & 6 for Zone 5 & zone2 respectively.
- ✓ It is observed that the base shear is maximum in regular model compared with model with setback irregularity.

- ✓ The base shear in models M1VZ5, M2VZ5, M3VZ5 and M4VZ5 reduced by 26%, 17%, 35 and 45% respectively when compared with regular model RMZ5.
- ✓ Comparing of all models in zone 5 (RMZ5, M1VZ5, M2VZ5, M3VZ5 and M4VZ5) with models in zone2 (RMZ2, M1VZ2, M2VZ2, M3VZ2 and M4VZ2) it is observed that base shear of models at zone5 has the higher values.

RESULTS OF MASS IRREGULARITY

BASE SHEAR RESULTS

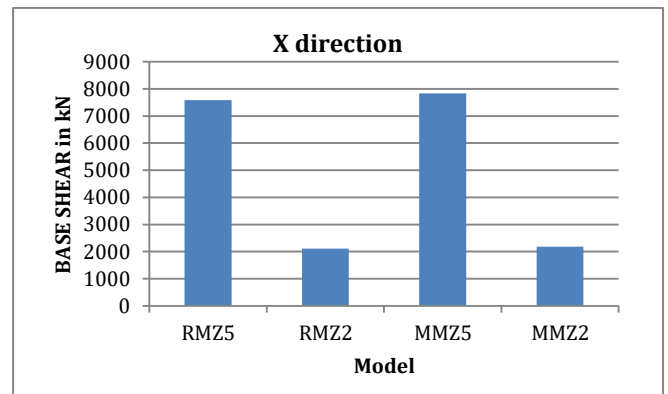


Chart-7 Base shear results for zone 5 & 2

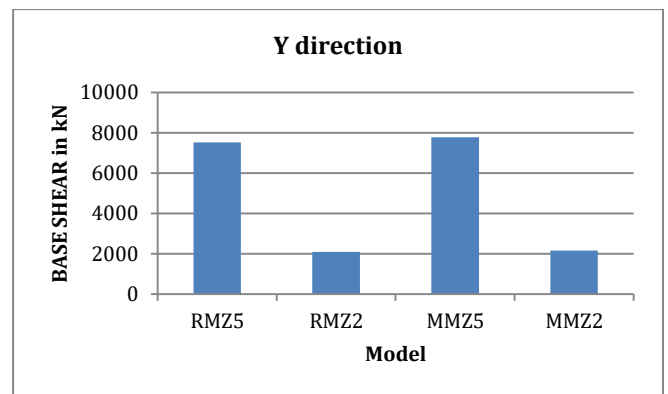


Chart-8 Base shear results for zone 5 & 2

- ✓ Base shear of regular model (RMZ5) and Mass irregularity model along X and Y-direction is been presented in figure 5.8.1 and figure 5.8.2 for Zone 5 respectively. Similarly Base shear of regular model (RMZ5) and Mass irregularity models along X and Y-direction is been presented in figure 5.8.3 and figure 5.8.4 for Zone 2 respectively.
- ✓ It is observed that the base shear is maximum in mass irregularity model compared with model with regular model.

✓ Comparing the model RMZ5 in zone 5 with model RMZ2 in zone2 it is observed that models in zone 5 has the higher base shear values.

Table-5 Base shear

| BASE SHEAR in kN | | |
|------------------|-------------|-------------|
| MODEL | X direction | Y direction |
| RMZ2 | 2108.5684 | 2094.312 |
| M1VZ2 | 1560.4699 | 1570.135 |
| M2VZ2 | 1745.9683 | 1705.54 |
| M3VZ2 | 1359.9852 | 1343.45 |
| M4VZ2 | 1157.0767 | 1175.759 |

STOREY DRIFT RESULTS

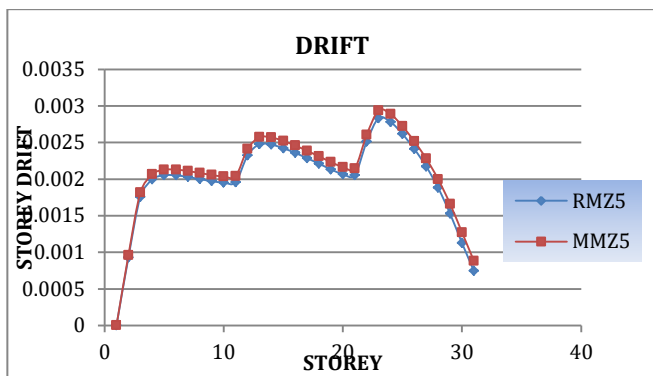


Chart-9 Storey Drift results for zone 5

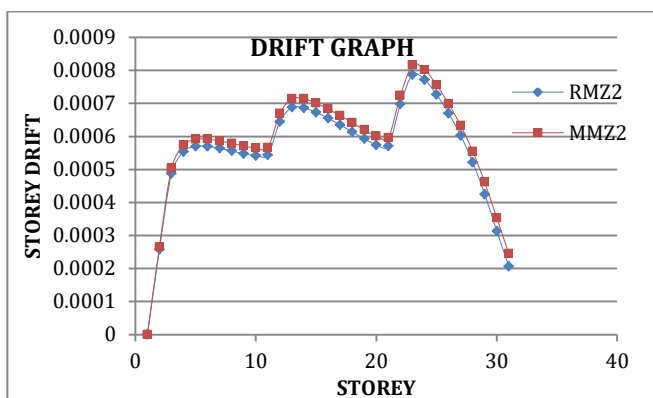


Chart-10 Storey Drift results for zone 2

- ✓ Storey drift of regular model (RMZ5) and Mass irregularity model along X and Y-direction is been presented in figure 5.7.1 and figure 5.7.2 for Zone 5 respectively.
- ✓ The storey drift is maximum in model MMZ5 and increased by 3.5% when compared with regular model RMZ5.

- ✓ The storey drift is maximum in model MMZ2 and increased by 3% when compared with regular model RMZ2.
- ✓ Comparing the model RMZ5 in zone 5 with model RMZ2 in zone2 it is observed that models in zone 5 has the higher storey drift values

3. CONCLUSIONS

- ✓ From the present study it is concluded that the building with irregular structural configuration are subjected to severe damage when compared to the regular structure.
- ✓ During earthquake structure located in zone 2 are less affected when compared to the structure located at zone 5.
- ✓ There is difference in the base shear in all models this is due to the seismic weight of the building.
- ✓ The storey lateral displacement of mass irregular frame will increase as the heavy mass floor level increases in the buildings. Regular frame has the least displacement.
- ✓ At last, we finish up from the outcomes unpredictable structures are to be treated with appropriate plan and ought to be trailed by all IS code procurements given the guidelines

REFERENCES

[1] Neha P. Modakwar¹, Sangita S. Meshram², Dinesh W. Gawatre³ "Seismic Analysis of Structures with Irregularities" IOSR Journal of Mechanical and Civil Engineering (IOSR-JMCE).

[2] N.Anvesh ¹, Dr. Shaik Yajdani², K. Pavan kumar³ "Effect of Mass Irregularity on Reinforced Concrete Structure Using Etabs" International Journal of Innovative Research in Science, Engineering and Technology Vol. 4, Issue 10, October 2015.

[3] C.M. Ravi Kumar¹, K.S. Babu Narayan², M.H. Prashanth³, H.B Manjunatha⁴ and D. Venkat Reddy⁵ "SEISMIC PERFORMANCE EVALUATION OF RC BUILDINGS WITH VERTICAL IRREGULARITY" ISET GOLDEN JUBILEE SYMPOSIUM, October 20-21, 2012.

[4] Rupesh R. Pawade¹, Dr.M.N.Mangulkar² "Influence of Combine Vertical Irregularities in the Response of Earthquake Resistance Rc Structure" IOSR Journal of Mechanical and Civil Engineering (IOSR-JMCE) Volume 14, Issue 1 Ver. IV (Jan. - Feb. 2017).

[5] J. Shaikh Sameer¹, S. B. Shinde² "SEISMIC RESPONSE OF VERTICALLY IRREGULAR RC FRAME WITH MASS IRREGULARITY" International Journal of Civil Engineering and Technology (IJCIET) Volume 7, Issue 5, September-October 2016.

[6] Ravindra N. Shelke¹, U. S. Ansari² "SEISMIC ANALYSIS OF VERTICALLY IRREGULAR RC BUILDING FRAMES"

International Journal of Civil Engineering and Technology (IJCIET) Volume 8, Issue 1, January 2017.

[7] Rahul Ghosh¹, Rama Debbarma² “Performance evaluation of setback buildings with open ground storey on plain and sloping ground under earthquake loadings and mitigation of failure” Int J Adv Struct Eng, 27 January 2017.

[8] Suchita Hirde^À and Romali Patil^{À*} “Seismic Performance of Setback Building Stiffened with Reinforced Concrete Shear Walls” International Journal of Current Engineering and Technology Vol.4, No.3 (June 2014).

[9] Oman Sayyed¹, Suresh Singh Kushwah², Aruna Rawat³ “Effect of Infill and Mass Irregularity on RC Building under Seismic Loading”, International Research Journal of Engineering and Technology (IRJET), Volume: 04 Issue: 02 | Feb -2017.

[10] Aashish Kumar, Aman Malik, Neeraj Mehta “Seismic Response of Set-Back Structure” International Journal of Engineering and Technical Research (IJETR) ISSN: 2321-0869, Volume-3, Issue-6, June 2015.

BIOGRAPHY:



RAHUL
BTECH IN CIVIL ENGINEERING FROM
ACHARYA COLLEGE OF ENGINEERING,
MTECH IN STRUCTURAL
ENGINEERING FROM THE OXFORD
COLLEGE OF ENGINEERING

DRY SLIDING WEAR PROPERTIES OF ZA-ALLOY CONTAINING TRACES OF IMPURITIES WITH AND WITHOUT HEAT TREATMENT

Gurunagendra G R¹, Ravikeerthi C¹, Dr. B R Raju²

¹Associate Professor, Department of Mechanical Engineering, Global Academy of Technology, Bangalore, India

Assistant Professor, Department of Mechanical Engineering, Academy of Technology, Bangalore, India

²Professor and Head Department of Automobile Engineering, TOCE Bangalore

ABSTRACT

ZA-8, ZA-12, ZA-27 are the family of ZA alloys widely used as Low cost Bearing materials in High load and Low speed applications. These alloys with low cost, low energy requirement for shaping, excellent cast ability, and high strength properties are better than some bronze bearing alloys, but they still have restricted application especially due to the deterioration of mechanical and wear resistance properties at temperatures exceeding 100°C. Aluminium is one of the major alloying elements in Zn alloy systems where it imparts fluidity to the alloys. In practice, the amount of Al added to Zn-based alloys in order to attain good engineering properties varies over a wide range. Against this background, the present research work has been undertaken with an objective to explore the potential of ZA alloys as a bearing material and to investigate the effect of alloying elements at room temperature on the Tribological behaviour of the ZA alloy. Zinc and aluminium are low cost bearing materials compared to conventional bearing material and this work is an attempt to find a possible use of such economical materials which might gainfully be employed as low cost, high strength and wear resistant alloys.

KEYWORDS: High load, Low speed, bearing materials

1. INTRODUCTION

The group of zinc-aluminium (ZA) alloys was developed in 1970s and became a substitute for brass and cast malleable iron to produce the wear-resistant parts. These alloys with low cost, low energy requirement for shaping, excellent cast ability, and high strength properties are equivalent or better than some standard bronze bearing alloys, but they still have limited application especially due to the deterioration of mechanical and wear resistance properties at temperatures exceeding 100°C. Aluminium is one of the major alloying elements in Zn alloy systems where it imparts fluidity to the alloys. In practice, the amount of Al added to Zn-based alloys in order to

attain good engineering properties varies over a wide range. The effect of different Al contents (namely 8, 12, 20 and 27) on the microstructure and tensile properties of Zn based alloy has increased strength and wear resistance. Zinc-Aluminium alloys are known to possess excellent bearing properties particularly at high load and low speed. They have found increasing use for many applications and have competed effectively against copper, aluminium and iron-base foundry alloys. However, the elevated temperature ($> 100^{\circ}\text{C}$) properties of zinc aluminium alloys are unsatisfactory and restrict their use in some applications. One promising approach to improve the elevated temperature properties was reinforcing the alloys with SiC fibers or particles, alumina particles and fibres, glass fibres etc.

All the zinc-aluminium alloys have excellent resistance to corrosion in a variety of environments. However, there has been a lack of specific corrosion data of zinc-aluminium based MMCs and their corrosion resistance to date, because of very limited use of zinc-aluminium alloys as matrix material for MMCs. Most of the commercial work on MMCs has focused on aluminium as the matrix metal. The combination of light weight, environmental resistance and favourable mechanical properties has made aluminium alloys very popular for use as a matrix metal. Aluminium and its alloys have been used as a matrix for a variety of reinforcements: continuous boron, Al_2O_3 , SiC and graphite fibers, various particles, short fibers and whiskers. As a result, advanced metal matrix composites with improved mechanical, physical and tribological characteristics, were obtained. The ZA alloys are suitable for casting by sand, permanent mould, shell mould and high-pressure die casting methods. These alloys exhibit mechanical properties equal to or exceeding those of conventional zinc die casting alloys and those of cast iron, aluminium and copper alloys. In addition, they have excellent bearing properties, wear resistance and machinability. Advantage of cast properties include low melting temperatures and hence low melting energy consumption, increased die life and mould stability. They can be readily cast in thin sections in sand moulds. It is also appreciated that the microstructure of ZA alloys, as it is true for any alloy, is associated with various factors such as compositions of alloy, production techniques adopted etc., and that even a very small change in one of these factors can seriously affect the quality, performance of the material. Hence, this leads to the argument that the field of microstructure, phase formation and wear properties of ZA alloys with different compositions still remains open for investigation for various purposes in industry.

2. EXPERIMENTAL PROCEDURE OF WEAR TEST:

The Alloy was prepared using Liquid Metallurgy route using Pure Zinc (99% pure) and Aluminium (99% pure) using Weight method. Composition as shown in the Table 1.

| Obtained by optical emission spectrum with traces of Impurities. | | | | | | | | | | | | |
|--|--------|-----|-------|-------|------|-------|-------|------|-------|-------|-------|-------|
| Composition | Zn | Al | Sn | Cd | Cu | Fe | Pb | Bi | Mg | Ag | Sb | Si |
| Percentage | 88.480 | 9.8 | 0.094 | 0.007 | 0.01 | 0.600 | 0.032 | 0.08 | 0.236 | 0.008 | 0.264 | 0.353 |

Dry sliding wear tests for different number of specimens was conducted by using a pin-on disc machine (Model: Wear & Friction Monitor TR-20) supplied by DUCOM is shown in Figure 1.

SPECIFICATIONS

| | |
|----------------------------|---------------------------------------|
| APPARATUS | : TRIBOMETER (DUCOM PVT LTDBANGALORE) |
| DISC ROTATION SPEED | : 200-2000 RPM |
| SLIDING SPEED | : 0.5-10 M/S |
| TRACK DIAMETER | : 50-100 MM |
| WEAR RANGE | : 1-2000 μ |
| LOAD | : 5-200 N |
| POWER | : 2KVA, 230V |
| SPECIMEN STANDARD | : ASTM G99 |



Figure 1: Pin on Disc Machine

The pin was held against the counter face of a rotating disc (EN31 steel disc) with wear track diameter 100 mm. The pin was loaded against the disc through a dead weight loading system. The wear test for all specimens was conducted under the normal loads of 1kg, 2kg and a sliding velocity of 2 and 4 m/s.

Wear tests were carried out for a total sliding distance of approximately 1250 m under similar conditions as discussed above. The pin samples were 30 mm in length and 6 mm in diameter. The surfaces of the pin samples were slides using emery paper (80 grit size) prior to test in order to ensure effective contact of fresh and flat surface with the steel disc. The samples and wear track were cleaned with acetone and weighed (up to an accuracy of 0.0001 gm using microbalance) prior to and after each test. The wear rate was calculated from the height loss technique and expressed in terms of wear volume loss per unit sliding distance.

In this experiment, the test was conducted with the following

Parameters:

- Load
- Speed
- Distance

In the present experiment the parameters such as speed, time and load are kept constant throughout for all the experiments. These parameters are given in Table.

Table 2: Parameter taken constant during sliding wear test

| | |
|----------------------|--|
| Pin material | ZA-alloy |
| Disc material | EN 31 steel |
| Pin dimension | Cylinder with diameter 6 mm height 30 mm |
| Sliding speed (rpm) | 400 |
| Normal load (kg) | 1, 2, 3 |
| Sliding distance (m) | 1250 |

3. PIN-ON-DISC TEST

In this study, Pin-on-Disc testing method was used for tribological characterization. The test procedure is as follows:

- Initially, pin surface was made flat such that it will support the load over its entire cross-section called first stage. This was achieved by the surfaces of the pin sample ground using emery paper (80 grit size) prior to testing
- Run-in-wear was performed in the next stage/ second stage. This stage avoids initial turbulent period associated with friction and wear curves
- Final stage/ third stage is the actual testing called constant/ steady state wear. This stage is the dynamic competition between material transfer processes (transfer of material from pin onto the disc and formation of wear debris and their subsequent removal). Before the test, both the pin and disc were cleaned with ethanol soaked cotton (Surappa et al 2007)

Before the start of each experiment, precautionary steps were taken to make sure that the load was applied in normal direction. Figure represents a schematic view of Pin-on-Disc setup.

Table 3: Process parameters and levels

| Sl no. | Load (N) | Sliding Speed, S (rpm) | Sliding Distance, D (m) |
|--------|----------|------------------------|-------------------------|
| 1 | 10 | 400 | 1250 |
| 2 | 20 | 400 | 1250 |
| 3 | 30 | 400 | 1250 |

WEAR TEST

Dry sliding wear tests for the ZA have been conducted using pin-on-disc Tribometer (m/s Ducom Bengaluru). The test have been conducted in air. Wear test have been conducted using cylindrical sample ($\phi 12\text{mm} \times 30\text{mm}$) that had flat surface in contact region and the rounded corner. The pin is held stationary against counterface of 100mm diameter rotating disc made of En-32 steel having HRC65.

The wear test have been conducted under three normal loads 1kg, 2kg, 3kg and at fixed sliding speed of 2.094m/s. Each wear test have been carried out for the sliding distance of 1.8km. Tangential force has been monitored continuously. Height was is measured from graph using slope and converted to volume loss data and wear rate is determined.

4. WEAR CALCULATION

1. Area, Cross sectional Area $A = \frac{\pi d^2}{4}$
2. Volume loss,
Volume loss = Cross sectional Area x Height loss
3. Wear rate
Wear rate = Volume loss / Sliding distance
4. Wear resistance,
Wear resistance = 1/ Wear rate
5. Specific wear rate,
Specific wear rate = Wear rate/load

Table 4: Wear rate Results at as Cast condition

| Sl No | Load | | Height Loss | | | Time Sec | Distance covered m | Wear Rate (mm ³ /m) ×10 ⁻³ | Friction Force N | Coefficient of Friction |
|-------|------|----|----------------------|----------------------|--|-------------|-----------------------|--|---------------------|-------------------------|
| | Kg | N | H ₁ μm | H ₂ μm | H ₁ - H ₂ μm | | | | | |
| 1 | 1 | 10 | 53.5 | 49.7 | 3.85 | 50 | 104.71 | 1.03 | 2.98 | 0.298 |
| 2 | 2 | 20 | 51.08 | 38.26 | 12.82 | 50 | 104.71 | 3.46 | 10.1 | 0.505 |
| 3 | 3 | 30 | 88.44 | 77.95 | 10.49 | 50 | 104.71 | 2.83 | 14.27 | 0.475 |

| Load(N) | Wear resistance (m /mm ³) |
|---------|--|
| 10 | 970.87 |
| 20 | 288.91 |
| 30 | 353.09 |

| Load(N) | Specific wear rate ×10 ⁻⁴ mm ³ / N m |
|---------|--|
| 10 | 1.03 |
| 20 | 1.73 |
| 30 | 0.943 |

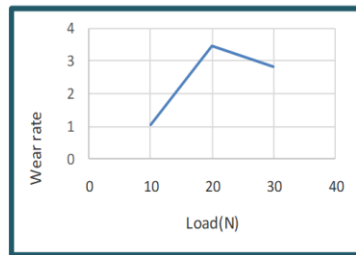


Figure 1: Load vs Wear Rate

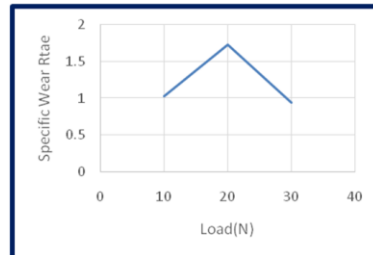


Figure 2: Load vs Specific Wear rate

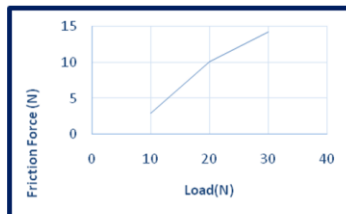


Figure 3: Load vs Friction Force

Table 5: Wear rate Results after Heat Treatment

| Sl No | Load | | Height Loss | | | Time Sec | Distance covered m | Wear Rate (mm ³ /m) ×10 ⁻³ | Friction Force N | Coefficient of Friction |
|-------|------|----|----------------------|----------------------|--------------------------------------|-------------|-----------------------|--|---------------------|-------------------------|
| | Kg | N | H ₁ μm | H ₂ μm | H ₁ -H ₂ μm | | | | | |
| 1 | 1 | 10 | 44.78 | 42.22 | 2.56 | 50 | 104.71 | 0.691 | 4.72 | 0.21 |
| 2 | 2 | 20 | 58.96 | 43.92 | 15.04 | 50 | 104.71 | 4.06 | 8.71 | 0.22 |
| 3 | 3 | 30 | 93.85 | 70.52 | 23.33 | 50 | 104.71 | 6.29 | 13.62 | 0.22 |

| Load | Wear resistance (m/mm ³) |
|------|--------------------------------------|
| 1 | 1447.17 |
| 2 | 246.3 |
| 3 | 158.98 |

| Load | Specific Wear rate ×10 ⁻⁴ (mm ³ /Kg-m) |
|------|---|
| 1 | 0.691 |
| 2 | 2.03 |
| 3 | 2.09 |

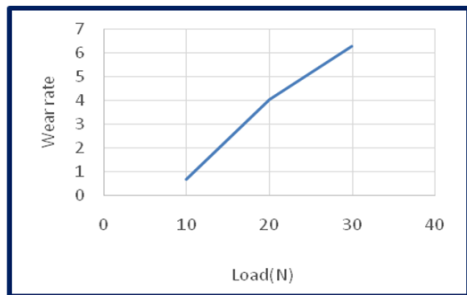


Figure 1: Load vs Wear Rate

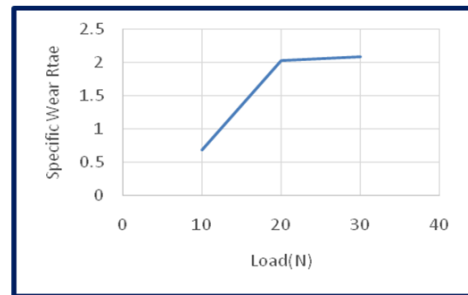


Figure 2: Load vs Specific Wear rate

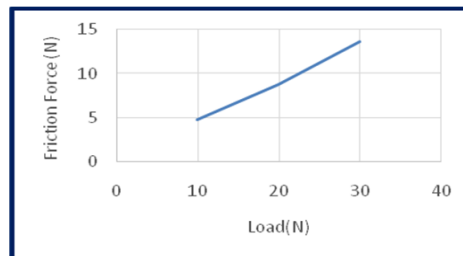
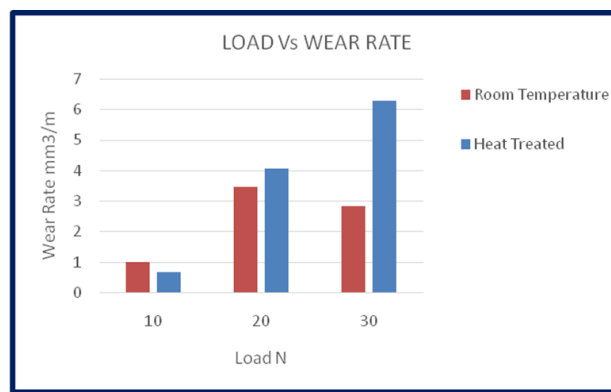


Figure 3: Load vs Friction Force

COMPARISON CHART:



5. CONCLUSION

ZA alloy is a competitive Bearing alloy that shows improvement in both Mechanical and Tribological properties compared with phosphor bronze, SAE 660 alloy and Cast Iron. As a First step towards developing a new material for the tribological applications for component used in various industrial applications.

Finally, at the end of completing the dry sliding wear test on the developed Low Aluminium and High Zinc alloy (ZA) there is a very low wear rate observed for heat treated alloy when compared to room temperature for Normal load of 10N, but wear rate increases at higher loaded for heat treated alloy.

There is more scope for further research by changing the process of fabrication of alloy and also Reinforcing with hard phase Reinforcements like Sic, Al₂O₃, graphite, MoS₂etc.

BIBLIOGRAPHY

1. S.Rajasekaran, N.K.Udayashankar, and Jagannath Nayak: T4 and T6 Treatment of 6061 Al-15 Vol.% SiCP Composite International Scholarly Research Network ISRN Materials Science Volume 2012, Article ID 374719, 5 pages doi:10.5402/2012.
2. Prasad, B. K. A.K. Patwardhan, A.H. Yegneswaran "Dry sliding wear characteristics of some Zinc-aluminium alloys: a comparative study with a conventional bearing bronze at a slow speed", Wear, Volume 199, 1996, 142-151
3. B.K. Prasad, A.K. Patwardhan, and A.H. Yegneswaran, "Characterization of the wear response of a modified Zinc-based alloy Vis-Avis a conventional Zinc-based alloy and a bearing bronze", Metall. Mater. Trans., Vol 27A, 1996, 3513-3523
4. Yuanyuan, Tungwai, Wei Xia, Wen Zhang "Effect of Mn content on the tribological behaviour of ZA27% Al-2% Cu alloy" Wear, Volume 198, 1996, 129-135.
5. B. Bobic, S. Mitrovic, M. Babic, I. Bobic: Corrosion of Aluminium and Zinc-Aluminium Alloys Based Metal-Matrix Composites, Tribology in Industry, Vol. 31, No. 3&4, pp. 44-52, 2009.
6. Kubel, E.J.: Expanding horizons for ZA alloys. Adv. Mater. Process. Inc. Met. Prog. 7, 51-57 (1987)
7. Goodwin, F., Ponikvar, A.: Engineering properties of zinc alloys, 3rd edn. ILZRO, Durham (1989)
8. Barnhurst, R.J.: Designing zinc alloy bearings. J. Mater. Des. 12, 279-285 (1990)
9. Pandey, J.P., Prasad, B.K.: Sliding wear response of a zinc-based alloy compared to a copper-based alloy. Metall. Mater. Trans. 29, 1245-1255 (1989)
10. Rac, A., Babic, M., Ninkovic, R.: Theory and practice of Zn-Al sliding bearings. J. Balkan Tribol. Assoc. 7, 234-240 (2001).
11. Babic, M., Ninkovic, R.: Zn-Al alloys as tribomaterials. Tribol. Ind. 26, 3-7 (2004)
12. Babic, M., Ninkovic, R., Rac, A.: Sliding wear behavior of Zn-Al alloys in conditions of boundary lubrication. The Annals of University "Dunãrea de Jos" of Galati Fascicle VIII. Tribology, 60-64 (2005)
13. Choudhury, P., Das, S., Datta, B.K.: Effect of Ni on the wear behavior of a zinc-aluminum alloy. J. Mater. Sci. 37, 2103-2107 (2002). doi:10.1023/A:1015297904125
14. Sharma, S.C., Girish, B.M., Kamath, R., Satish, B.M.: Graphite particles reinforced ZA-27 alloy composite materials for journal bearing application. Wear 219, 162-168 (1998). doi:10.1016/S0043-1648(98)00188-4
15. Gervais, E., Barnhurst, R.J., Loong, C.A.: An analysis of selected properties of ZA alloys. J. Met. 37, 43-47 (1985)
16. Zhu, Y.H., Biao, Y., Wei, H.: Bearing wear resistance of monotectoid Zn-Al based alloy (ZA-35). J. Mar. Sci. Technol. 11, 109-113 (1995)
17. Lyon, R.: High strength zinc alloys for reengineering applications in the motor car. Met. Mater. 1, 55-57 (1985)
18. Bobic, I., Ninkovic, R., Babic, M.: Structural and mechanical characteristics of composites with base matrix of RAR27 alloy reinforced with Al₂O₃ and SiC particles. Tribol. Ind. 26, 21-26 (2004)
19. Prasad, B.K., Patwardhan, A.K., Yegneswaran, A.H.: Microstructure-property characterization of some Zn-Al alloys: effects of heat treatment parameters. Z. Metallk. 87, 967-972 (1996)
20. Prasad, B.K.: Influence of heat treatment parameters on the lubricated sliding wear behavior of a zinc-based alloy. Wear 257, 1137-1144 (2004). doi:10.1016/j.wear.2004.07.006



Your cart is empty

IOS Press Ebooks

Guest Access ?

Register | Log in

[Home](#)
[Ebooks](#)
[Open Access](#)
[About IOS Press](#)
[Contact](#)
[FAQ](#)
Search**> SEARCH****Browse by subject**

Administrative Sciences
 Applied Physics
 Biochemistry, Medicine & Health
 Chemistry
 Computer & Communication Sciences
 Ehlers-Danlos syndrome
 Electronics & Mechanics
 Engineering
 Environmental Sciences
 Geographic Information Science
 Geosciences
 Health Information Technology
 Heritable connective tissue disorders
 Housing
 Hypermobility
 International Security
 Life & Behavioural Sciences
 Linked Data
 Management
 Manufacturing
 Marine Technology
 Mathematics
 Neurosciences
 Physics
 Physics & Instrumentation
 Public Health
 Rehabilitation & Assistive Technology
 Security & Terrorism
 Social Sciences:
 Economics/Policy/Management
 Sustainability
 Technology
 Townplanning & Architecture
 Transportation Sciences

**FIR Notch Filter with Rejection Bandwidth Tuning and Sharpening**

Authors Rohini Deshpande, Deepak Deshpande

Pages 364 - 371

DOI 10.3233/978-1-61499-828-0-364

Series [Frontiers in Artificial Intelligence and Applications](#)Ebook [Volume 299: Fuzzy Systems and Data Mining III](#)**Abstract**

Two novel design methodologies for the FIR notch filter (NF) are proposed: i) Design with rejection bandwidth (RBW) tuning, ii) Design with narrow RBW. In both methodologies, basic FIR notch filter is evolved from second order IIR notch filter. In the first design, a relationship between pole radius 'r' and RBW is developed for different values of notch frequencies and filter lengths. Such developed relation is used to design an FIR notch filter for the specified RBW, notch frequency and given length. In the second methodology, design of FIR notch filter with highly narrow RBW is suggested. Reduction in the RBW is achieved by choosing high value of 'r' for FIR NF designed from a second order infinite impulse response (IIR) prototype filter and then by using an amplitude change function (ACF): $H(z)(2 - H(z))$.

\$35.00 / €27.50 / £22.00**Add PDF to cart****Contact**

North America
 Europe
 Asia

IOS Press Copyright 2021

[Disclaimer](#)
[Terms of use](#)
[Privacy Policy](#)
[Contact](#)
[FAQ](#)

**FOLLOW US
ON TWITTER**

QUANTUM BASED ADAPTIVE TOPOLOGY CONTROL FOR INTRUSION DETECTION AND ISOLATION IN MANET

E.Selvi¹, M.S. Shashidhara²

¹Asst. Professor, Department of Computer Science, Asan Memorial College of Arts and Science, Chennai, India.

²Head of the Department, Department of MCA, The Oxford College of Engineering, Bangalore, India.

ABSTRACT: A mobile ad hoc network (MANET) is an infrastructure-less network where the number of mobile nodes is independently moved in a random direction within the transmission range of the network. Due to the movement of mobile nodes, the network topology is changed arbitrarily. Therefore, various intrusions are presented in MANET. For accurate and robust intrusion detection against several attack and deceiving actions, SIEVE technique was designed in MANET. However, node mobility of the ad hoc network restricts the BP algorithm efficiency and it's difficult to identify attack behavior. Therefore, security is a most important concern in decentralized structure of mobile network. In order to develop the intrusion detection and isolation in MANET, Quantum based Adaptive Topology Control (QATC) technique is developed. In QATC, an adaptive topology control is designed to adjust the transmission range of the mobile nodes to extend the lifetime of networks by retaining the network connectivity. This topology leaves maximum possible nodes connected in a cluster zone with minimum energy consumption and transmission interference. This helps to increase the packet delivery ratio. After this, the arriving and leaving nodes are monitored and the malicious node is identified from the network, through Quantum Mechanism. Quantum mechanism is typically used to detect the malicious node from the network using specific key distribution. Due to this, the malicious nodes are easily detected and isolated, aiming at improving the Malicious node detection rate with minimum time. A simulation result shows that the Quantum based Adaptive Topology Control (QATC) technique achieves higher packet delivery ratio, malicious node detection rate and reduces energy consumption, and time to identify the malicious node compared to state-of-the-works.

KEYWORDS: Mobile ad hoc network (MANET), malicious node, Adaptive Topological Control, Quantum Mechanism, intrusion detection, intrusion isolation

I.INTRODUCTION

A mobile ad hoc network is an infra-structure less network which can establish the route path through collection of intermediate mobile nodes. In MANET, the mobile nodes are randomly moved in any direction. Due to the mobility of node, the transmission range of the networks is varied accordingly. By varying the transmission range, several intrusions continuously attack the network's accessibility through common techniques such as flooding, black hole and denial of service (DoS). The mobile nodes perform packet transmission from one end to another end with the mobility of nodes and due to this wide range of intrusion occurs in MANET. Therefore, several review techniques are expensively developed.

MANET processed with two different types of modes such as single-hop and multi-hop. The nodes in MANETs assume that other nodes are always combined with each other to communicate data, which is exploited by malicious nodes and propagate intrusive attacks across the network. Intrusion detection system is developed for MANET to improve the security level and to detect the malicious attackers in the network.

To obtain accurate and robust intrusion detection against several attack and deceiving actions, SIEVE technique was designed in [1] to infer Identity of Polluters in MANET by exploiting Rate less Codes and Belief Propagation (BP). The BP algorithm evaluates the identity of malicious nodes residing upon the network with simple pollution detection mechanism. SIEVE technique ensures multi-party download or collaboration attack detection with minimal computational, memory and communication resources. However, node mobility of the ad hoc network restricts the BP algorithm efficiency, as it affects key Pre-distribution, identifying routing mechanisms and attack behavior.

To improve the routing performance in MANET, Energy-Aware Routing Algorithm was introduced in [2] along with RMECR and RMER. Reliable Minimum Energy Cost Routing (RMECR) addresses requirements of ad hoc

networks: energy-efficiency, reliability, and extending network lifetime. Reliable Minimum Energy Routing (RMER) is an energy-efficient routing algorithm which minimizes the route of total energy required for end-to-end packet traversal. However, the RMECR and RMER algorithm, for extending the network lifetime cannot be implemented for varying conditions.

The objective of the thesis is organized as follows. Quantum based Adaptive Topology Control (QATC) technique is introduced to develop the intrusion detection and effective isolation in MANET. Initially, an adaptive topology control technique is applied to adjust the transmission range of the mobile nodes to extend the lifetime of Adhoc networks by changing the network connectivity and improving the network lifetime. This topology also increases the packet delivery ratio and maximum possible nodes are connected in a cluster zone with minimum energy consumption and transmission interference. Then, the quantum mechanism is used to monitor and detect the malicious node from the network using key distribution followed by isolation of malicious nodes from the network for increasing the transmission.

The rest of the paper is organized as follows. In Section 2, a summary of different routing techniques to prevent intrusion in mobile ad-hoc network are explained. In Section 3, the proposed framework of Quantum based Adaptive Topology Control (QATC) technique with the help of diagram is described. In Section 4, simulation environment is provided with detailed analysis of results explained in Section 5. In Section 6, the concluding remarks are included.

II.RELATED WORK

Intrusion detection is a type of vulnerable attack in wireless mobile ad hoc networks that can occur during packet transmission between the mobile nodes. A new IDS scheme was introduced in [3] and selects novel cluster leader selection process and a hybrid IDS using Vickrey-Clarke-Groves which provides the intrusion detection service. However, it does not increase the intrusion detection rate. An approach based on a multivariate Hotelling's T2 statistical analysis technique was designed in [4] for intrusion detection in network environments. In [5], a lightweight system to discover the new characteristics of Sybil attackers with lack of centralized trusted third party. However, variable transmit powers and hidden attacks are the major issues in the network. A secure routing scheme was developed in [6] ID-based encryption for route discovery.

An integrated detection model was developed in [7] cluster-based wireless sensor network for increasing detection rate and reducing false rate. In [8], the classification methods are developed for intrusion detection for MANETs. The datasets cover various attack types, levels of network mobility and several data collection intervals for the intrusion detection system.

An intrusion detection and adaptive response mechanism was developed in [9] for identifying a range of attacks and provides an effective response in MANETs. An effective intrusion-detection system [10] named as EAACK particularly developed for MANETs obtains higher malicious-behavior-detection. However, the network overhead was not reduced to a required level.

An Adaptive Three Acknowledgements (A3ACKs) intrusion detection system was developed in [11] for reducing the receiver collision, restricted transmission power and attacks in MANET. A novel Intrusion Detection System was designed in [12] using the trust evaluation metrics for identifying the flooding DDOS attacks in MANET. In [13], Machine learning based intrusion detection systems for MANETs was described and it has the difficulties when constructing the topology of the network.

An intrusion detection system was designed in [14] based on K -nearest neighbor classification algorithm in wireless sensor network for improving the intrusion detection accuracy. Risk assessment in mobile applications have received greater attention never before with the increasing use of its applications worldwide. In [15], attacks related to mobile applications and measure for avoiding the risk assessment baseline on sensitive information and permission revocation is discussed. But, channel quality information with respect to mobile applications was not concentrated.

To analyze the performance of a base station (BS) coordination strategy, Stochastic Geometry Approach was developed in [16]. A neighbor coverage-based probabilistic rebroadcast protocol was proposed in [17], to consider the information about uncovered neighbors (UCN), connectivity metric and local node density to calculate the rebroadcast probability. Cooperation Scheme was implemented in [18] to carry out both selection combination and maximum ratio at destination in the network to improve the lifetime. The survey of several intrusion detection approaches was developed in MANET [19]. A danger theory-based artificial immune algorithm was designed in [20] using mobile dendritic cell algorithm for identifying the flooding-based attacks in MANETs.

Based on the above mentioned methods and techniques, an efficient Quantum based Adaptive Topology Control (QATC) Technique is developed to increase the network transmission range and intrusion detection in MANET. The brief explanation about the intrusion detection is explained in the forth coming section.

III. QUANTUM BASED ADAPTIVE TOPOLOGY CONTROL (QATC) TECHNIQUE IN MANET

In Quantum based Adaptive Topology Control (QATC) Technique, we consider MANET be the connected path link set of 'G' with sub graphs. The connected path link graph $G <V, E>$ where 'V' represents the set of nodes and 'E' represents the set of bidirectional edges. Due to the presence of intrusion, that utilize the ambiguity to carry out the malicious behavior and therefore nodes gets compromised and number of packets are not successfully received at the destinations within the transmission range. In order to overcome the above issues during transmission, the quantum based adaptive topological control technique is proposed aiming at detecting and isolating the intrusion effectively. Therefore, the packet delivery ratio is increased with minimum energy consumption.

Initially, the number of mobiles in network is grouped to form a cluster. Due to the variation in network transmission range, the number of intrusion can easily affect the network system performance. The proposed adaptive topology control technique is applied for adjusting the transmission range of the mobile nodes. This topology is also keeping the maximum number of nodes in cluster zone with minimum energy consumption. In order to achieve the intrusion detection and isolation in MANET, Quantum mechanism is applied on the cluster with minimum transmission interference.

A. Adaptive topology control technique

Adaptive topology control is used in MANET to alter the transmission range of the network. The topology control is also used to improve network wide connectivity, minimum energy and reduces interference between nodes. Initially, cluster is formed based on the intermediate nodes between the source nodes to destination. The source node is denoted as 'SN' and destination node 'DN'. The Neighbor Nodes exists between the source and destination pair. The entire possible neighbor nodes are grouped through which routing can be established from source to destination.

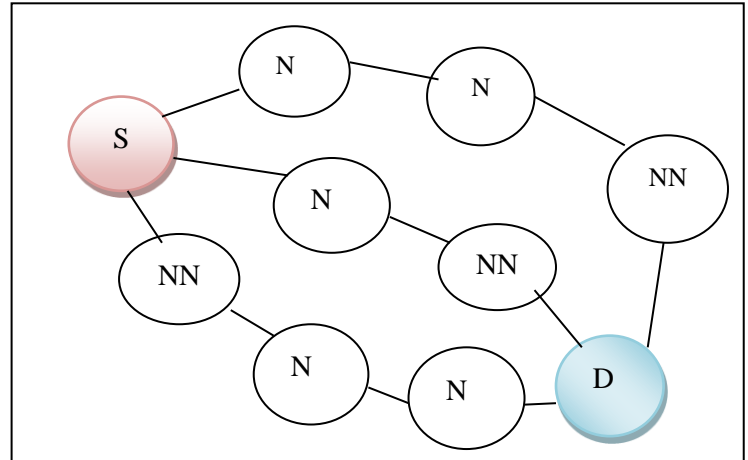


Fig-1: Formation of cluster in MANET

Fig 1 illustrates the cluster formation in MANET and complete clustering provides effective connection where the link between all the clusters contain all element pair of nodes which creates the route path. The node vertex 'V' and edges 'E' are combined together to cluster the movable nodes of similar connected path links. The initial step uses the node with maximum degree of cluster connected path links. The application of clustering increases the broadcasting performance.

Consider a number of mobile nodes are deployed randomly throughout the network. It is assumed that all the nodes are equipped and fully connected at maximum transmission range TR_{max} . The objective of the Adaptive topology control is to provide a controllable and, minimal energy cost. The proposed Adaptive topology control consists of three phases such as discovery phase, topology construction phase, topology maintenance phase. At first, each mobile node determines its one-hop neighbors for establishing the route path. Mobile base station node begins the topology construction (TC) phase by transmitting a control message in second phase. Between the other nodes, the control message has information on limited neighborhood connectivity. Finally, the topology maintenance is carried out to avoid separated networks because of few control message losses.

Initially, the source node 'SN' broadcasts the control message at the maximum transmission range TR_{max} . A reliable one-hop broadcast mechanism can be used to find the one hop neighbors. This helps to reduce the possibility of undiscovered node by its neighbors.

The intermediate nodes from the source node 'SN' within the transmission range ' TR_{max} ' is measured to ensure secure routing through which data packets are

transmitted, the intermediate nodes are calculated as follows,

$$IN = \sum_{i=1}^n \text{Min} (\text{Dis} (SN - NN_i)) \quad \text{eq. (1)}$$

From eq. (1), the distances between the source node and the neighbor nodes is first evaluated. Then, based on the result obtained, the minimum distance nodes are then selected as the intermediate nodes. Based on this distance measure, the route path is selected for efficient transmission.

Step 1: Discovery phase

In discovery phase, the route is established between source and destination. The main objective is to make all the nodes receive the discovery message and formulate an entire neighbor list. After the successful reception of the control message from source node SN, the neighboring node 'NN' estimates its distance and maintains the route. The entire neighboring list is maintained and it consists of different neighbor identity and distance between the nodes. The neighbor list is then stored in ascending order.

Step 2: Topology construction (TC) phase

In proposed adaptive topology control technique, each node chooses a set of neighbors by overhearing the continuous transmission between its neighboring nodes. The neighboring node is selected to distribute its control message. Nodes that are closer to the source node are given higher priority as compared to the farther ones. The control message is also used to maintain proper value of hop distance towards the source node. As the TC phase proceeds, the control message broadcast in a limited manner such that each node communicates the control message only once. Each node maintains the following features such as Identity, backbone, hop count and neighboring list.

Step 3: Topology maintenance phase

This section describes a where the control message is lost and not successfully received at the destination. The loss of control message is major issue, because it contains information about the neighboring node. Due to this, the asymmetric routes are established where the selected neighboring node not able to extend its transmission range. Therefore, the proposed topology control technique is developed for altering the transmission range. Each node received control message from all its one-hop neighbors. Then it transmits the

Request (RREQ) message at maximum transmission range TR_{max} . During the reception, only the neighboring node responds with the Reply (RREP) message. Finally, on receiving the RREP message, the source node alters its transmission range with minimum energy cost to include neighboring node by retaining the network connectivity.

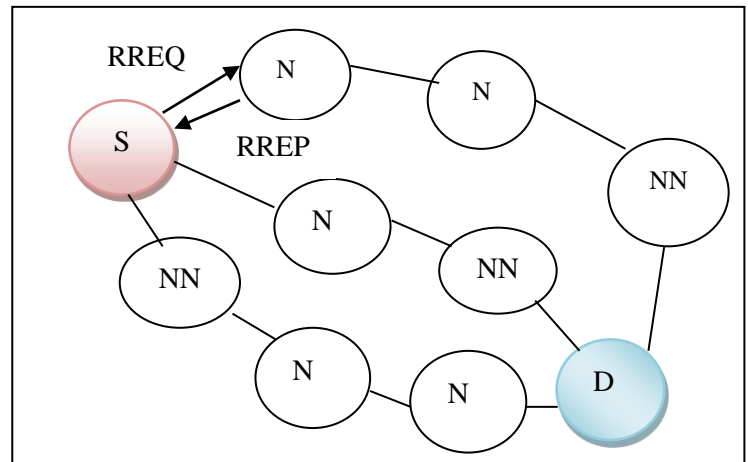


Fig-2: Network connectivity based on request and reply message

As shown in fig 2, Network connectivity based on request and reply message distribution is described in topology maintenance phase. The algorithmic description of the adaptive topology control technique is explained as below.

Input: Mobile Node $MN_i = MN_1, MN_2, \dots, MN_n$, Neighbor Node $NN_i = NN_1, NN_2, \dots, NN_n$,

RREP message, RREQ message

Output: Extend the transmission range of the mobile network

Begin

For each Source Node 'SN' and Destination Node 'DN'

Measure the intermediate node using minimum distance by (1)

Route Discovery phase

Step 1: obtain the information about the neighboring node

Step 2: Arrange the neighbor list in ascending order of distance

Topology construction phase

Step 3: Each node selects neighbor node to transmit a control message

Step 4: Broadcast the control message at TR_{max}

Step 5: Maintain the value of hop distance towards source node

Topology maintenance phase

Step 6: if (Each node received control message from all its one-hop neighbors)

Step 7: else

Step 8: Send RREQ message from SN to NN at TR_{max}

Step 9: Sends the Reply (RREP) message from NN to SN

Step 10: SN receives the RREP message

Step 12: SN extends its transmission range and improves connectivity with minimum energy cost

Step 13: end if

Step 14: end for

Step 15: end

Algorithm 1. Adaptive topology control algorithm

As shown in the above algorithm, it is adaptive to different transmission range of the mobile nodes. In discovery phase, the neighboring nodes are identified among the number of movable node in MANET for establishing the route path from source to destination. Then, the neighboring information is listed and sorted in ascending order. In second phase, topology is constructed. The topology construction control message is distributed for all the nodes at a transmission range TR_{max} . Due to this, the hop distance is maintained. In third phase, topology maintenance is performed for improving the network lifetime with minimum energy cost. This topology leaves maximum possible nodes connected in a one cluster zone with minimum energy consumption and transmission interference. As a result, it helps to increase the packet delivery ratio.

B. Quantum based secure transmission in MANET

The successful topology construction and maintenance is carried out to improve the network

connectivity. Due to increasing the network transmission range, several intrusions affects the network performance. In order to reduce the intrusion in MANET, the quantum mechanism is applied for secured transmission through quantum key distribution. The application of quantum mechanism provides the sharing of a secret encryption key between the mobile nodes within the transmission range. The Intrusion Detection and isolation approach to enhance high security mobile Adhoc networks effectively detect malicious node behavior. The flow diagram of the shared key distribution is organized as shown in fig 3

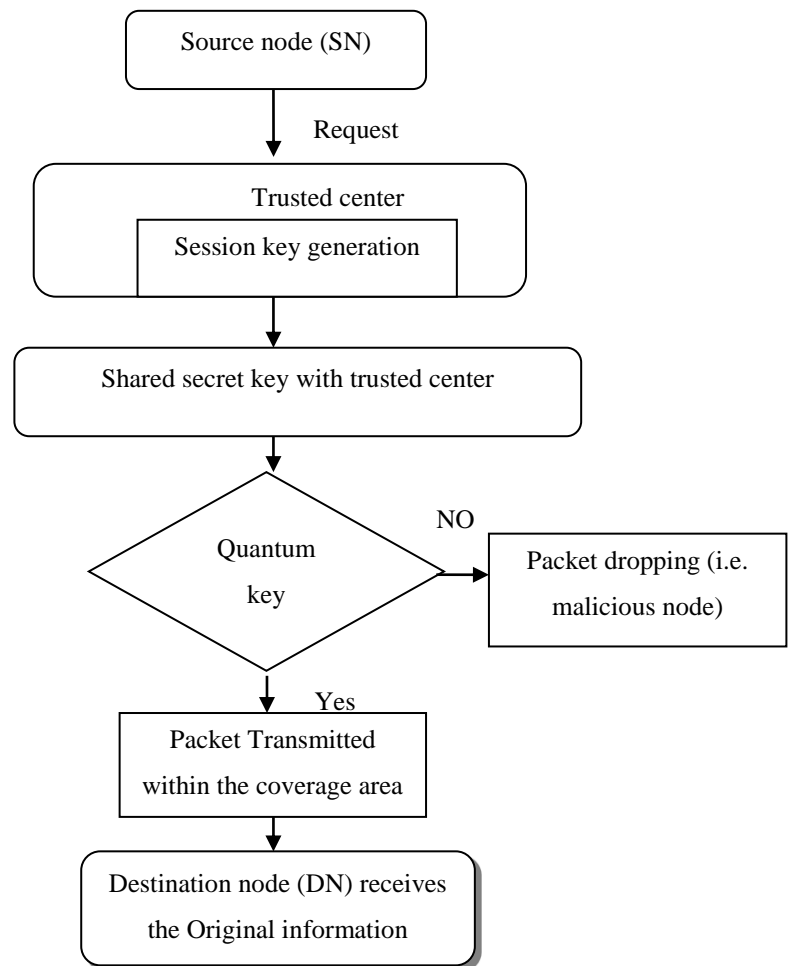


Fig 3. Flow process of quantum based key distribution

As shown in fig 3, Quantum cryptography uses quantum mechanics to enhance secure communication. It enables two parties' source node and destination to produce a shared random key to encrypt and decrypt information. An important cryptography is the ability of the nodes to detect the third party (i.e. intrusion) trying to obtain a knowledge of the key.

Quantum based key distribution depends on the principle of quantum for detecting the intrusion without disturbing the transmission. The quantum network facilitates the distribution of a secret encryption key between the nodes. The two nodes are exchanging a key with contact to achieve perfect secrecy for transmission. The ability of the source and destination to use the shared key helps to detect the intrusion. A trusted center generates a random number and a session key. It distributes the session key to the source node for encryption. Also, it distributes the same session key to the receiver side for decryption. Then the quantum key is generated using quantum information and session key. The four types of the input bit with the key value is obtained as follows,

- The input value is 0 and 0, the quantum key generate $0.707(|0\rangle + |1\rangle)$
- The input value is 1 and 0, then $0.707(|0\rangle - |1\rangle)$
- The value is 0 and 1, then $|0\rangle$
- The value is 1 and 1, then $|1\rangle$

If the shared secret key is matched with the quantum key, the transmission is performed effectively within the range. Otherwise, Packet Dropping occurs aiming at improving the security of the mobile network. This is used to detect the malicious node (i.e. intrusion) and prevents it from receiving data packets from other mobile nodes in the network.

Step 1: Malicious node isolation approach

Upon the successful detection of intrusion in MANET, the isolation is performed accordingly. The intrusion is established during the transmission packet form source to destination. A Malicious node isolation approach is used to detect the intrusion and make aware the nodes about malicious node. The source node monitors whether the data packets are transmitted or dropped by the suspected nodes. If there is packet drop then the node is isolated and distributes the attack isolation message to all normal behavior nodes thus preventing further intrusion attack.

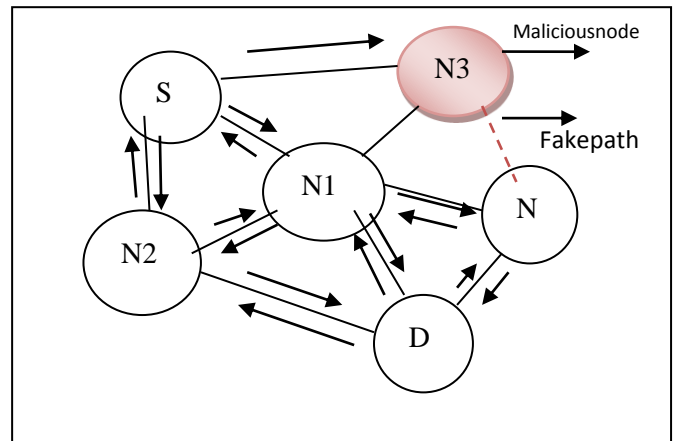


Fig 4 Malicious node behavior

In fig 4, the malicious node behavior process is described. When a node N3 is identified as the malicious node, the isolation of the node is carried out from the network. According to Malicious node isolation approach in QATC, the source node transmits an attack isolation message to inform other normal nodes in transmission range of the network. Simultaneously, the nearby nodes can receive this message. Due to this, the malicious node is isolated by removing it from the path and preventing the data packets from reaching it.

At first, the source node sends an attack isolation message to all the nodes in the network then the nodes verifies the presence of malicious node. If all nodes identify the malicious node then they detect the particular malicious path where malicious node is present. Thus the malicious node is isolated and it has fake link with other nodes in the network. After isolating the malicious node, the source node retransmits the data packets through other alternative path. For increasing the transmission, neighboring nodes do not have malicious node in routing process and also does not receive any request message from malicious node. Followed by this, the malicious nodes are isolated from the network graph and rest of the network remains connected and easily identifies the packet drop. This helps to improve the network security during the packet transmission in MANET.

IV EXPERIMENTAL SETTINGS

An efficient Quantum based Adaptive Topology Control (QATC) technique is implemented in NS-2 simulator with the network range of 1500*1500 m size. The mobile network consists of 70 nodes in the network structure and uses the Random Way Point (RWM) model. The RWM uses typical number of mobile nodes for locating

the movable nodes. The dynamic changing topology uses the Ad hoc On-demand Distance Vector (AODV) routing protocol to perform the experimental work.

The node speed is varied between 2m/s and 25m/s and the mobile node pause time is varied from 0 seconds to 300 seconds. As a result, for each metric, simulation is done for seven different seed values which are taken for the result. The simulations parameters are obtained that are used in the experiments are listed in table 1.

Table-1: Parameters value

| Parameter | Value |
|--------------------|----------------------------|
| Node density | 10, 20, 30, 40, 50, 60, 70 |
| Network area | 1500*1500m |
| Transmission range | 250m |
| Packets | 9, 18, 27, 36, 45, 54, 63 |
| Simulation period | 600s |
| Minimum node speed | 2m/s |
| Maximum node speed | 25m/s |
| Node pause time | 0 – 300 seconds |
| Mobility model | Random Way Point |
| Network simulator | NS 2.34 |

Experiment is conducted on the factors such as packet delivery ratio, malicious behavior detection rate, energy consumption, time to identify the intrusion. These parameters result percentage of the QATC technique is compared against the existing intrusion detection techniques including SIEVE technique [1] and Energy-Aware Routing Algorithm [2].

V SIMULATION RESULTS AND ANALYSIS

To validate the efficiency and theoretical advantages of the proposed Quantum based Adaptive Topology Control (QATC) technique with SIEVE technique

[1] and Energy-Aware Routing Algorithm [2] simulation results under NS2 are presented. The experiment is conducted on the factors such as packet delivery ratio, malicious behavior detection rate, energy consumption, and time to identify the intrusion. Performance is evaluated along with the following metrics with help of tables and graph values.

A. Impact of Packet delivery ratio

Packet delivery ratio using QATC technique is defined as the ratio of numbers of packets sent by source nodes to the number of packets successfully received at the destination nodes in MANET.

$$PDR = \frac{\text{No.of packet}_R}{\text{No.of packet}_S} * 100 \quad \text{eq. (2)}$$

From eq.(2), packet delivery ratio PDR is $\frac{\text{packet}_R}{\text{packet}_S}$ number of packet received, packet_S No. of packet sent. It is measured in terms of percentage (%). Higher the packet delivery ratio more efficient the method is said to be.

Table 2 Tabulation for packet delivery ratio

| No. of packet sent | Packet Delivery ratio (%) | | |
|--------------------|---------------------------|-----------------|---------------------------------|
| | QATC | SIEVE technique | Energy-Aware Routing Algorithms |
| 9 | 91.36 | 85.69 | 81.36 |
| 18 | 92.74 | 87.37 | 82.98 |
| 27 | 93.12 | 88.68 | 84.63 |
| 36 | 94.63 | 88.97 | 85.74 |
| 45 | 95.23 | 89.36 | 85.98 |
| 54 | 95.69 | 90.10 | 86.25 |
| 63 | 96.31 | 91.36 | 87.36 |

The simulation values of packet delivery ratio based on the number of packet sent is illustrated in table 2. The convergence plot of seven different values is shown in chart-1.

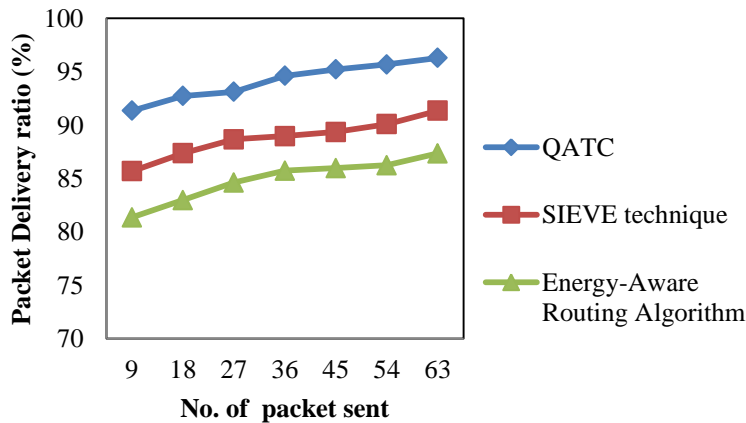


Chart-1: Measure of packet delivery ratio

Chart-1 illustrates the simulation results of packet delivery ratio with number of packet transmitted and it varies from 9 to 63. From the figure, it is clear that the proposed QATC technique achieves higher packet delivery ratio as compared to existing SIEVE technique [1] and Energy-Aware Routing Algorithm [2]. Due to this, the adaptive topology control technique is applied in proposed QATC. This topology uses the discovery phase to establish the route path by identifying the one hop neighbor. The path links are established where the selected neighboring node to extend its transmission range. This in turn improves the packet delivery ratio by 6% compared to existing SIEVE technique [1]. In addition, QATC efficiently identifies the malicious node for effective transmission. As a result, the packet delivery ratio is improved by 10% compared to Energy-Aware Routing Algorithm [2].

B. Impact of Malicious behavior detection rate

Malicious behavior detection rate in QATC technique measures the rate of malicious nodes identified in the mobile network. Due to the packet drop, malicious behavior of a node is observed. In the proposed technique, packet drop is used as a measure to detect intrusion in the network and is mathematically formulated as given below.

$$MBDR = \frac{\text{Detect dropped packet}}{\text{total no.of node}} \quad \text{eq. (3)}$$

From eq.(3), the malicious behavior detection rate 'MBDR' is observed which is ratio of detecting the number of dropped packet to the total number of nodes in MANET.

Table 3 Tabulation for Malicious behavior detection rate

| No. of mobile nodes | Malicious behavior detection rate (%) | | |
|---------------------|---------------------------------------|-----------------|--------------------------------|
| | QATC | SIEVE technique | Energy-Aware Routing Algorithm |
| 10 | 78.35 | 64.36 | 61.35 |
| 20 | 81.24 | 68.24 | 65.65 |
| 30 | 82.36 | 73.31 | 70.36 |
| 40 | 84.67 | 75.36 | 73.52 |
| 50 | 85.34 | 79.24 | 76.34 |
| 60 | 88.74 | 80.32 | 78.69 |
| 70 | 90.32 | 81.36 | 79.67 |

The malicious behavior detection rate using QATC technique is evaluated with two different methods SIEVE technique [1] and Energy-Aware Routing Algorithm [2] as shown in table 3. The simulation results of three different techniques are illustrated in Chart-2.

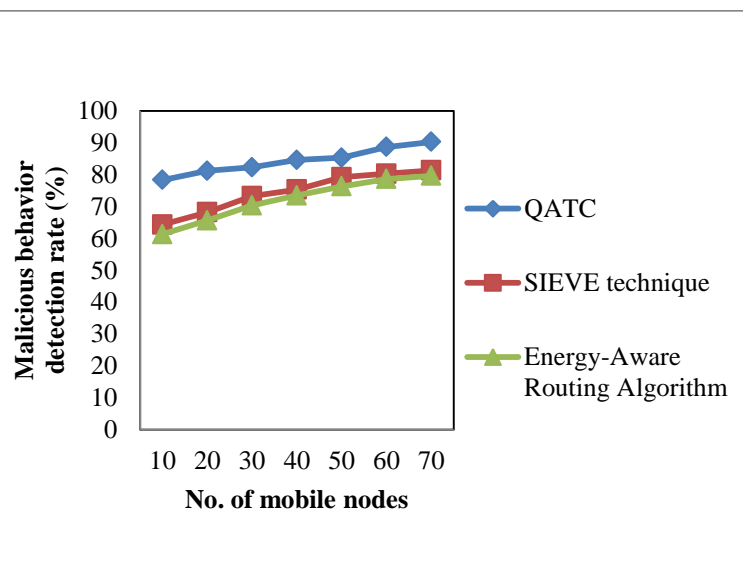


Chart-2: Measure of Malicious behavior detection rate

Chart 2 depicts the simulation of malicious behavior detection rate with respect to number of mobile nodes in MANET. The figure illustrates; our proposed QATC technique improved the performance of malicious behavior detection rate than the other state-of-art-methods [1] [2]. This is because, the malicious behavior detection rate in the QATC technique is made by detecting the malicious node using Quantum based key distribution, based on the principle of quantum. By using this key distribution mechanism, the intrusions are effectively detected without disturbing the transmission. So the performance of the proposed QATC technique is improved and increases the malicious behavior detection rate by 24% and 29% compared to SIEVE technique [1] and Energy-Aware Routing Algorithm [2] respectively.

C. Impact of energy consumption

Energy consumption using QATC technique method is the product of number of mobile nodes, power (in terms of watts) and time (in terms of seconds). The energy consumption is measured in terms of Joules (J). The mathematical formulation for energy consumption used is expressed as follows,

$$EC = No. of nodes * Power * Time \quad eq. (4)$$

'EC' is the energy consumption where the energy consumed by mobile nodes to reach destination.

Table 4 Tabulation for Energy consumption

| No. of nodes | Energy consumption (Joules) | | |
|--------------|-----------------------------|-----------------|--------------------------------|
| | QATC | SIEVE technique | Energy-Aware Routing Algorithm |
| 10 | 26.64 | 38.12 | 32.54 |
| 20 | 35.30 | 39.33 | 37.58 |
| 30 | 38.53 | 41.56 | 40.64 |
| 40 | 40.13 | 44.27 | 43.32 |
| 50 | 41.21 | 47.22 | 45.65 |
| 60 | 42.14 | 50.12 | 46.54 |
| 70 | 44.22 | 51.58 | 48.24 |

The energy consumption of proposed QATC technique and SIEVE technique [1] and Energy-Aware Routing Algorithm [2] are described in table 4. The comparison results of three different methods are illustrates the following chart 3.

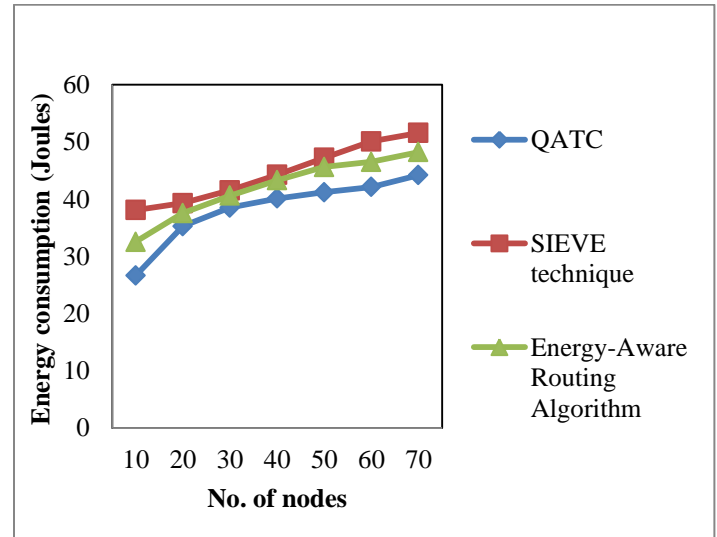


Chart-3: Measure of Energy consumptionThe energy consumption based on different mobile nodes with three different methods QATC technique, SIEVE technique [1] and Energy-Aware Routing Algorithm [2] performed is extensively shown in figure 7. As illustrated in figure 7, while increasing the number of mobile nodes in MANET, the energy consumption is increased in all the three methods but comparatively it is reduced in QATC technique. In QATC technique, the clustering is performed on the mobile node, then the routing path is selected for efficient transmission with minimum energy consumption. In addition, by applying topology control technique, the topology maintenance phase is carried out to improve the network connectivity. This topology will leave maximum possible nodes connected in a cluster zone with minimum possible energy consumption and transmission interference. Therefore the energy consumption is reduced by 18 % compared to SIEVE technique [1] and 10% compared to Energy-Aware Routing Algorithm [2] respectively.

D.Impact of time to identify the Malicious node

The time to identify the black hole node is measured using the number of node and the time taken to identify packet dropping during the packet transmission in MANET. The mathematical formulation for time is as given below.

$$T_{MN} = \text{No. of node} * \text{Time (Identifying malicious node)}$$

eq.(5)

From eq.5, where T_{MN} time to identify the malicious node, which is measured in terms of milliseconds (ms).

Table 5 Tabulation for Time to identify the malicious node

| No. of node | Time to identify the malicious node (ms) | | |
|-------------|--|-----------------|--------------------------------|
| | QATC | SIEVE technique | Energy-Aware Routing Algorithm |
| 10 | 1.17 | 1.56 | 1.24 |
| 20 | 1.25 | 1.63 | 1.55 |
| 30 | 1.79 | 2.14 | 1.97 |
| 40 | 1.95 | 2.63 | 2.45 |
| 50 | 2.74 | 3.12 | 2.99 |
| 60 | 3.31 | 4.25 | 3.87 |
| 70 | 4.22 | 4.68 | 4.55 |

As shown in table 5, the analysis of malicious node identification time based on the number of node ranges from 10 to 70. The results of malicious node identification time using QATC technique, SIEVE technique [1] and Energy-Aware Routing Algorithm [2] is shown in chart 4.

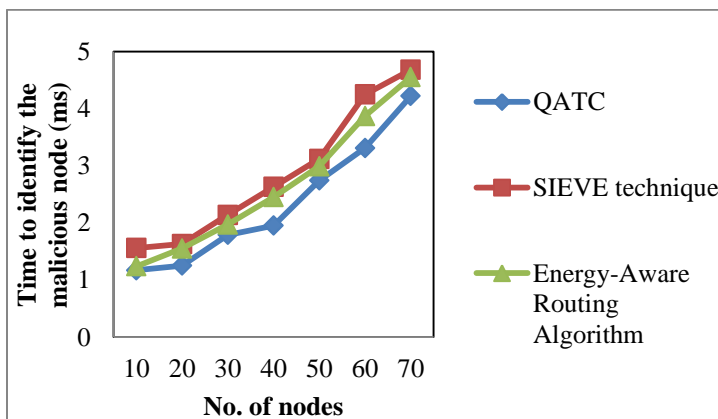


Chart-4: Measure of Time to identify the malicious node

Chart 4 reveals the simulation results of time to identify the malicious node with respect to number of mobile node in MANET. The figure illustrates, our proposed QATC technique improves the performance by reducing the time taken to identify the malicious node than the other state-of-art- methods [1] [2]. Due to this, the quantum based shared key distribution effectively identifies the malicious node to enhance secure communication. It enables two parties' source node and destination node to use shared random key to encrypt and decrypt information. Quantum based key distribution is used to detect the intrusion with minimum time. The intrusion detection time is reduced by 24% and 14% compared to SIEVE technique [1] and Energy-Aware Routing Algorithm [2].

VI CONCLUSION

In this paper, an efficient Quantum based Adaptive Topology Control (QATC) technique is developed for detecting the intrusion and isolation in MANET. Initially, an adaptive topology control is used in three phases for adjusting the transmission range of the mobile nodes to extend the network lifetime of Adhoc networks by maintaining the network connectivity. The adaptive topology establishes the effective route path with minimum energy consumption and transmission interference. After that, Quantum mechanism is applied by using the key distribution. The quantum network facilitates the distribution of a secret key between the nodes. The two nodes are exchanging a key with contact to achieve perfect secrecy for transmission. Finally, the detected malicious nodes are isolated by removing from the path and prevents the data packets from reaching them. The simulation results also reveal that the QATC technique improves the packet delivery ratio and minimizes the energy consumption. Therefore, the QATC technique also increases the malicious behavior detection rate with minimum time compared to state-of-art methods.

VII REFERENCES

[1] Rossano Gaeta, Marco Granetto, and Riccardo Loti, "Exploiting Rateless Codes and Belief Propagation to Infer Identity of Polluters in MANET", IEEE TRANSACTIONS ON MOBILE COMPUTING, VOL.13, NO.7, JULY 2014

[2] Javad Vazifehdan, R. Venkatesha Prasad, and Ignas Niemegeers, "Energy-Efficient Reliable Routing Considering Residual Energy in Wireless Ad Hoc Networks", IEEE TRANSACTIONS ON MOBILE COMPUTING, VOL. 13, NO. 2, FEBRUARY 2014

- [3] Basant Subba, Santosh Biswas, Sushanta Karmakar, "Intrusion detection in Mobile Ad-hoc Networks: Bayesian game formulation", *Engineering Science and Technology, an International Journal*, Elsevier, 2015
- [4] Aneetha Avalappampatty Sivasamy and Bose Sundan., "A Dynamic Intrusion Detection System Based on Multivariate Hotelling's T2 Statistics Approach for Network Environments", *The Scientific World Journal*, Hindawi Publishing Corporation, Volume 2015, Article ID 850153, 9 pages
- [5] Sohail Abbas, Madjid Merabti, David Llewellyn-Jones, and Kashif Kifayat, "Lightweight Sybil Attack Detection in MANETs", *IEEE Systems Journal*, Volume 7, Issue 2, 2013, Pages 236 – 248
- [6] Sayyed Musaddique, S.S.Hippargi, Attar Shuaib, "Advanced Secure Intrusion Detection System for MANET", *International journal of innovative research in electrical, electronics, instrumentation and control engineering*, vol. 3, issue 12, December 2015
- [7] Xuemei Sun, Bo Yan, Xinzhong Zhang, Chuitian Rong., "An Integrated Intrusion Detection Model of Cluster-Based Wireless Sensor Network", *Plos one journal*, 2015
- [8] Aikaterini Mitrokotsa, Christos Dimitrakakis, "Intrusion detection in MANET using classification algorithms: The effects of cost and model selection", *Ad Hoc Networks*, Elsevier, Volume 11, 2013, pages 226–237
- [9] Adnan Nadeem, Michael P. Howarth, "An intrusion detection & adaptive response mechanism for MANETs", *Ad Hoc Networks*, Elsevier, volume 13, 2014, Pages 368–380
- [10] Elhadi M. Shakshuki, Nan Kang, and Tarek R. Sheltami, "EAACK—A Secure Intrusion-Detection System for MANETs", *IEEE transactions on industrial electronics*, VOL. 60, NO. 3, MARCH 2013
- [11] Tarek Sheltami, Abdulsalam Basabaa, Elhadi Shakshuki, "A3ACKs: adaptive three acknowledgments intrusion detection system for MANETs", *Journal of Ambient Intelligence and Humanized Computing*, Springer, August 2014, Volume 5, Issue 4, pp 611-620
- [12] M. Poongodi and S. Bose, "A Novel Intrusion Detection System Based on Trust Evaluation to Defend Against DDoS Attack in MANET", *Arabian Journal for Science and Engineering*, Springer, December 2015, Volume 40, Issue 12, pp 3583-3594
- [13] Lediona Nishani and Marenglen Biba, "Machine learning for intrusion detection in MANET: a state-of-the-art survey", *Journal of Intelligent Information Systems*, Springer, April 2016, Volume 46, Issue 2, pp 391-407
- [14] Wenchao Li, Ping Yi, Yue Wu, Li Pan, and Jianhua Li., "A New Intrusion Detection System Based on KNN Classification Algorithm in Wireless Sensor Network", *Journal of Electrical and Computer Engineering*, Hindawi Publishing Corporation, Vol. 2014, Article ID 240217, pp.1-8,2014
- [15] Yiming Jing, Gail-Joon Ahn, Ziming Zhao and Hongxin Hu, "Towards Automated Risk Assessment and Mitigation of Mobile Applications", *IEEE Transactions on Dependable and Secure Computing*, Volume:PP, Issue: 99, Oct 2014
- [16] Namyoon Lee, David Morales-Jimenez, Angel Lozano, and Robert W. Heath, "Spectral Efficiency of Dynamic Coordinated Beam forming: A Stochastic Geometry Approach", *IEEE TRANSACTIONS ON WIRELESS COMMUNICATIONS*, VOL. 14, NO. 1, JANUARY 2015
- [17] Xin Ming Zhang, En Bo Wang, Jing Jing Xia, and Dan Keun Sung, "A Neighbor Coverage-Based Probabilistic Rebroadcast for Reducing Routing Overhead in Mobile Ad Hoc Networks", *IEEE TRANSACTIONS ON MOBILE COMPUTING*, VOL. 12, NO. 3, MARCH 2013
- [18] Yong Zhou, and Weihua Zhuang, "Throughput Analysis of Cooperative Communication in Wireless Ad Hoc Networks with Frequency Reuse", *IEEE TRANSACTIONS ON WIRELESS COMMUNICATIONS*, VOL. 14, NO. 1, JANUARY 2015
- [19] Ehsan Amiria, Hassan Keshavarz, Hossein Heidari, Esmail Mohamadi, Hossein Moradzadeh, "Intrusion Detection Systems in MANET: A Review", *Procedia - Social and Behavioral Sciences*, Elsevier, volume 129, 2014, 453 – 459
- [20] Maha Abdelhaq, Raed Alsaqour, Shawkat Abdelhaq, "Securing Mobile Ad Hoc Networks Using Danger Theory-Based Artificial Immune Algorithm", *plos one journal*, May 6, 2015

Quantum Phase Shift for Energy Conserved Secured Data Communication in MANET

E.Selvi¹, M. S. Shashidhara²

¹Department of Computer Science, Asan Memorial College of Arts and Science, Chennai, India

²Department of MCA, The Oxford College of Engineering, Bangalore, India

Abstract: A Mobile Ad-Hoc Network(MANET) is a structure-less network where the mobile nodes randomly moved in any direction within the transmission range of the network. Due to this mobility, wide range of intrusion occurs in MANET. Therefore, Intrusion Detection Systems (IDS) are significant in MANETs to identify the malicious behavior. In order to improve the secured data communication an efficient Quantum Phase Shift Energy Conserved Data Security (QPSEC-DS) technique is introduced. The Quantum Phase Shift (QPS) technique is used for ensuring the security during the data transmission from sender to receiver in MANET. Initially, the quantum based approach is used to encrypt the information using QPS at the sender through secret key distribution. The receiver side also performs the same QPS, and then the encrypted bit is received successfully. This in turns attains the secured packet transmission without any malicious node in the MANET. Based on the phase shifting, the energy conservation between the sender and receiver is measured for transmitting the data packet using QPSEC-DS technique. Also, the enhanced Dynamic Source Routing (DSR) protocol is applied in QPSEC-DS technique is implemented to improve the energy management and secured data communication between the source and destination in an efficient manner. The QPSEC-DS technique conducts the simulations work on parameters including packet delivery ratio, energy consumption, communication overhead and end to end delay.

Keywords: Mobile ad hoc network (MANET), Quantum phase shift (QPS), Energy conservation, Intrusion Detection Systems (IDS), Dynamic source routing (DSR) protocol.

1. Introduction

A MANET is arranged with a group of mobile nodes based on the multi-hop approach without any centralized administration. In MANET, every mobile node act as a sender and a receiver via bidirectional wireless and it does not contain any permanent network infrastructure. Intrusion-detection mechanisms effectively protect MANET from attacks. Most recently, intrusion attacks are created by forming the black hole attacks in MANET. Therefore, IDS is developed in MANET to improve the security level and to detect the malicious attackers in the network. Several secured data transmission and energy efficient techniques are explained with the help of literature.

An Enhanced Adaptive Acknowledgment (EAACK) intrusion-detection system was developed in [1] for detecting the malicious activities. However, EAACK does not reduce the network overhead and also energy efficient secured data transmission is the difficult issue. Energy-Aware and Error Resilient (EAER) routing protocol was designed in [2] for improving the packet delivery with minimum energy

consumption. However, the secured transmission remained unaddressed.

In [3], standard ad hoc on-demand multi-path distance vector protocol was introduced to improve packet delivery ratio with minimum delay, overhead and it also offered security against vulnerabilities and attacks. A Report-based payment scheme (RACE) was developed in [4] for securing the payment and accurately detecting malicious nodes without false declaration. However, intermediate nodes cannot make confirmation for packet transmission.

A MANET has been highly susceptible to several attacks because of random motion of mobile nodes in network. Due to this, a risk-aware response approach was introduced in [5] to systematically handle identified routing attacks. However, it included node reputation and attack frequency with adaptive decision model and energy management was considered to be a challenging issue. In [6], Reliable and Energy Efficient Protocol was developed for improving packet delivery ratio, energy consumption, and throughput. Danger-theory based artificial immune algorithm was designed in [7] to improve security through multipath routing by means of attack detection. However, the performance of this method was not proved to be efficient.

Residual Energy based Reliable Multicast Routing Protocol (RERMR) was designed in [8] to improve network lifetime and also increased packet delivery rate. However, security in optimized multicast routing was unaddressed. Hybrid method was developed in [9] for minimizing energy consumption and execution time through multipath routing in MANET. Different routing protocol was designed in [10] for identifying malicious activities during secured data transmission in MANET.

With the above considerations, main contribution of the research work is arranged as follows. An efficient Quantum Phase Shift Energy Conserved Data Security (QPSEC-DS) technique is proposed with the objective of improving the security during data packet transmission with minimum energy conservation in MANET. Then the Quantum phase shift is carried out to improve the security for transmitting the data packet from the sender to the receiver side. Initially, the Quantum based approach utilizes the shared random key to encrypt and decrypt the information using phase shift between the sender and the receiver in a secured manner. Next, the Quantum key distribution is efficiently detects the intrusion node and improves the security for packet transmission in MANET. With the aid of energy conserved data communication, the shifting position is evaluated for preserving the data transmission with lesser energy

Article [Publisher preview available](#)Simple but efficient synthesis of bis(indolyl)methanes by the condensation reaction of substituted benzaldehydes with indole over mesoporous ZrO₂-MgO green catalysts under solvent free conditions

Springer

August 2017 · *Journal of Porous Materials* 24(4)

DOI:10.1007/s10934-016-0340-7

Authors:

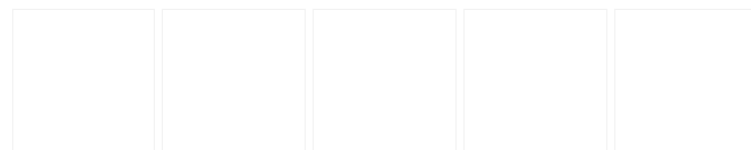
**Shyam Sundar**
The Oxford Educational Institutions**SZ Mohamed Shamsuddin****V. T. Vasanth****T. E. Mohankumar**[Read publisher preview](#)[Request full-text](#)[Download citation](#)[Copy link](#)

To read the full-text of this research, you can request a copy directly from the authors.

[Citations \(5\)](#)[References \(49\)](#)[Figures \(5\)](#)

Abstract and Figures

Solid base catalytic materials such as ZrO₂, MgO, ZrO₂-MgO were prepared by either precipitation or impregnation method and characterized by, BET, CO₂-TPD, PXRD, FT-IR, ICP-OES and TEM techniques. These catalysts were used for the synthesis of bis(indolyl)methanes by the condensation of different benzaldehydes with indole under solvent free conditions in shorter reaction times (20 min) at moderate temperature (70 °C). ZrO₂/MgO catalyst was found to be highly basic and also resulted in high yields of bis(indolyl)methanes up to ~99%. This methodology offers several advantages such as high quality yields, easy procedure, mild and environmentally benign conditions. TEM studies revealed that ZrO₂-MgO is mesoporous (25–45 nm) in nature. ZrO₂-MgO catalysts were found to be economical, efficient and were found to be highly active, recyclable and reusable up to six reaction cycles without much loss of their activity.



PXRD patterns of FTIR spectra of ZrO₂, MgO and... ZrO₂, MgO and... TEM images of ZrO₂-MgO at a... bis(indolyl)... Possible mechanism for...

Figures - available from: [Journal of Porous Materials](#)This content is subject to copyright. [Terms and conditions](#) apply.

Discover the world's research

- 20+ million members
- 135+ million publications
- 700k+ research projects [Join for free](#)

Publisher Preview (1)A preview of this full-text is provided by Springer Nature. · [Learn more](#)[Preview content only](#)Content available from [Journal of Porous Materials](#)
This content is subject to copyright. [Terms and conditions](#) apply.

J Porous Mater (2017) 24:1003–1011
DOI 10.1007/s10934-016-0340-7

Simple but efficient synthesis of bis(indolyl)methanes

Article [Publisher preview available](#)Simple but efficient synthesis of bis(indolyl)methanes by the condensation reaction of substituted benzaldehydes with indole over mesoporous ZrO₂-MgO green catalysts under solvent free conditions

Springer

August 2017 · *Journal of Porous Materials* 24(4)

DOI:10.1007/s10934-016-0340-7

Authors:

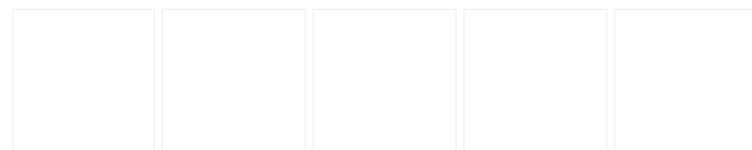
**Shyam Sundar**
The Oxford Educational Institutions**SZ Mohamed Shamsuddin****V. T. Vasanth****T. E. Mohankumar**[Read publisher preview](#)[Request full-text](#)[Download citation](#)[Copy link](#)

To read the full-text of this research, you can request a copy directly from the authors.

[Citations \(5\)](#)[References \(49\)](#)[Figures \(5\)](#)

Abstract and Figures

Solid base catalytic materials such as ZrO₂, MgO, ZrO₂-MgO were prepared by either precipitation or impregnation method and characterized by, BET, CO₂-TPD, PXRD, FT-IR, ICP-OES and TEM techniques. These catalysts were used for the synthesis of bis(indolyl)methanes by the condensation of different benzaldehydes with indole under solvent free conditions in shorter reaction times (20 min) at moderate temperature (70 °C). ZrO₂/MgO catalyst was found to be highly basic and also resulted in high yields of bis(indolyl)methanes up to ~99%. This methodology offers several advantages such as high quality yields, easy procedure, mild and environmentally benign conditions. TEM studies revealed that ZrO₂-MgO is mesoporous (25–45 nm) in nature. ZrO₂-MgO catalysts were found to be economical, efficient and were found to be highly active, recyclable and reusable up to six reaction cycles without much loss of their activity.



PXRD patterns of FTIR spectra of ZrO₂, MgO and... ZrO₂, MgO and... TEM images of ZrO₂-MgO at a... bis(indolyl)... Possible mechanism for...

Figures - available from: [Journal of Porous Materials](#)This content is subject to copyright. [Terms and conditions](#) apply.

Discover the world's research

- 20+ million members
- 135+ million publications
- 700k+ research projects [Join for free](#)

Publisher Preview (1)A preview of this full-text is provided by Springer Nature. · [Learn more](#)[Preview content only](#)Content available from [Journal of Porous Materials](#)
This content is subject to copyright. [Terms and conditions](#) apply.

J Porous Mater (2017) 24:1003–1011
DOI 10.1007/s10934-016-0340-7

Simple but efficient synthesis of bis(indolyl)methanes

Article [Publisher preview available](#)Mesoporous ZrO₂-Al₂O₃ (ZA) mixed metal oxide as an efficient and reusable catalyst for the liquid phase O-methoxymethylation reaction under solvent free conditions SpringerOctober 2018 · *Journal of Porous Materials* 25(5)DOI: [10.1007/s10934-017-0537-4](https://doi.org/10.1007/s10934-017-0537-4)Project: [PhD work](#)


Authors:



S. R. Pratap

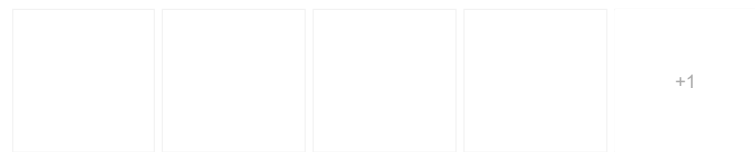
Shyam Sundar
The Oxford Educational Institutions

SZ Mohamed Shamsuddin

[Read publisher preview](#)[Request full-text](#)[Download citation](#)[Copy link](#) To read the full-text of this research, you can request a copy directly from the authors.[Citations \(5\)](#)[References \(61\)](#)[Figures \(6\)](#)

Abstract and Figures

Mixed metal oxide based solid acids like ZrO₂-Al₂O₃ (ZA) with Al₂O₃ different loadings (2, 4, 6, 8 and 10 mol%) were prepared by wet impregnation method and characterized by PXRD, NH₃-TPD, BET, ICP-OES, SEM, and TEM techniques. These solid acids were evaluated for their catalytic activity in the synthesis of a series of O-methoxymethylated products under solvent-free conditions at a moderate temperature in shorter reaction time (~20 min). This is achieved by various substituted alcohols and dimethoxy methane in good yields. Solid acids containing ZA used in this study exhibited good catalytic activity in the reaction. In case of 6 mol% ZA which has highest surface acidity, surface area and catalytically active tetragonal phase was found to be highest active in the O-methoxymethylation reaction up to ~99% yield. These catalysts were found to be reactivable and reusable.



PXRD patterns of SEM images a TEM images a Effect of O-
2% ZrO₂/Al₂O₃ 4% ZA, b 6% ZrO₂/Al₂O₃ 4% ZA, b 6% ZrO₂/Al₂O₃ reusability of 6% ZrO₂/Al₂O₃ methoxymethyl...

Figures - available from: [Journal of Porous Materials](#)

This content is subject to copyright. [Terms and conditions](#) apply.

Discover the world's research

- 20+ million members
- 135+ million publications
- 700k+ research projects [Join for free](#)

 Publisher Preview (1)

A preview of this full-text is provided by Springer Nature. [Learn more](#)
[Preview content only](#)

Content available from [Journal of Porous Materials](#)
This content is subject to copyright. [Terms and conditions](#) apply.

Journal of Porous Materials (2018) 25:1265–1273
<https://doi.org/10.1007/s10934-017-0537-4>



USER

Username Password Remember me

Reset Password

Email

INFORMATION

- [For Authors](#)

JOURNAL
CONTENT

Search

All

Browse

- [By Issue](#)
- [By Author](#)
- [By Title](#)

[HOME](#)[ABOUT](#)[TABLE OF CONTENTS](#)[EDITORIAL BOARD](#)[CONTACT](#)[Home](#) > [Vol 2017 \(2017\)](#) > [Perla](#)

Convexity for ratio of difference of some special means in two variables

Sreenivasa Reddy Perla, S. Padmanabhan, V. Lokesh, Sandeep Kumar

Abstract

In this paper, we study the Schur properties of convexities(concave) like Schur, Schur Geometric, Schur Harmonic convexities on the ratio of difference of means obtained by arithmetic mean, geometric mean, harmonic mean, contra harmonic mean, heron mean and root-square means. Also, established some inequalities related to these means.

Full Text: [PDF](#)**Published:** 2016-12-01**How to Cite this Article:**

Sreenivasa Reddy Perla, S. Padmanabhan, V. Lokesh, Sandeep Kumar, Convexity for ratio of difference of some special means in two variables, Adv. Inequal. Appl., 2017 (2017), Article ID 2

Copyright © 2017 Sreenivasa Reddy Perla, S. Padmanabhan, V. Lokesh, Sandeep Kumar. This is an open access article distributed under the [Creative Commons Attribution License](#), which permits unrestricted use, distribution, and reproduction in any medium, provided the original work is properly cited.

Advances in Inequalities and Applications

ISSN 2050-7461

Editorial Office: office@scik.org

Copyright ©2021 SCIK Publishing Corporation

[Download PDF](#)[Download PDF](#)

Original Research Paper | [Open Access](#) |
[Published: 16 July 2018](#)

Schur convexity of Bonferroni harmonic mean

[Sreenivasa Reddy Perla](#)  & [S. Padmanabhan](#)

[The Journal of Analysis](#) **27**, 137–150 (2019)

1071 Accesses | **1** Citations | [Metrics](#)

Abstract

In this paper, we research the Schur convexity, Schur geometric convexity and Schur harmonic convexity of the Bonferroni harmonic mean. Some inequalities identified with the Bonferroni harmonic mean are set up to represent the utilizations of the acquired outcomes.

Introduction

Arithmetic, Geometric and Harmonic means are three important means, which have been extensively used in the information aggregation [[5](#), [6](#), [7](#), [11](#), [12](#), [17](#), [18](#), [19](#), [35](#), [36](#)]. For a collection of real numbers a_i ($i = 1, 2, \dots, n$), the Arithmetic mean (AM), the Geometric mean (GM) and the Harmonic mean (HM) are defined by:



AUTHORS INSTRUCTIONS

- [Forthcoming articles](#)
- [Instructions to Authors](#)
- [Copyright Form](#)
- [Human and Animal Rights](#)
- [Article Tracking](#)
- [Certificate and Acceptance](#)
- [Cover page](#)
- [Anti-Plagiarism Policy](#)
- [Open Access and Licensing](#)
- [Publication Ethics and Malpractice Statement](#)
- [Proofs](#)
- [Submission](#)
- [Review Procedure](#)

SUBMIT YOUR ARTICLE

IMPACT FACTOR

INDEXED-IN

- [Impact Factor](#)
- [Indexed In](#)

SUBJECT AREA

Life Sciences

- [Agricultural](#)
- [Biological Sciences](#)
- [Biotechnology,](#)
- [Biochemistry](#)
- [Genetics](#)
- [Molecular Biology](#)
- [Environmental Science](#)

[More](#)

Schur-convexity for ginimean of n variables

NAAS SCORE

Author: Sreenivasa Reddy Perla., Padmanabhan S and V Lokesha

Schur-convexity, Schur-geometric convexity and Schur-harmonic convexity for Gini mean of n variables are investigated, and some mean value inequalities of n variables are established.

Download PDF: [4103--A--2017.pdf](#)

DOI: DOI: <http://dx.doi.org/10.24327/ijcar.2017.6698.0998>

Select Volume: Volume6



National Agricultural & Veterinary Extension
NAAS
***3.07 (C)**
[Effective from 2017-2018]
For more details visit [http://naas.aicr.org](#)

JOURNAL DOI



IMPACT FACTOR

Impact Factor
2017

ANNOUNCEMENT

Call for papers - Manuscript processing and public journal

MODEL CERTIFICATE

TRACK YOUR ARTICLE

COPYRIGHT F



CHILDREN'S EDUCATION SOCIETY (Regd.)
THE OXFORD COLLEGE OF ENGINEERING
 (Recognised by the Govt. of Karnataka, Affiliated to Visvesvaraya Technological University, Belagavi.

Approved by A.I.C.T.E. New Delhi.

Recognised by UGC Under Section 2(f)

Bommanahalli, Hosur Road, Bangalore - 560 068.

Ph: 080-61754601/602, Fax: 080 - 25730551

E-mail: engprincipal@theoxford.edu Web: www.theoxfordengg.org

| Sl.No | Title of paper | Name of the author/s | Department of the teacher | Name of journal | Year of publication | ISSN number | Link to website of the Journal | Link to article/paper/abstract of the article | Is it listed in UGC Care list/Scopus/Web of Science/other, mention |
|-------|--|---|---------------------------|---|---------------------|-----------------|---|---|--|
| 1 | Trust based resource selection with optimization technique | E. Saravana Kumar, K. Vengatesan | CSE | Cluster Computing | 2018 | 1573-7543 | https://www.springer.com/journal/10586 | https://doi.org/10.1007/s10586-018-2362- | UGC/Scopus |
| 2 | Biclustering of gene expression data using biclustering iterative signature algorithm and biclustering coherent column | E Saravanan Kumar, K Vengateshan, C Rajan | CSE | International Journal of Biomedical Engineering and Technology | 2018 | 1752-6426 | https://www.inderscience.com/ | https://dx.doi.org/10.1504/IJBET.2018.089968 | Scopus |
| 3 | Characterization Breast Cancer Histology Images using Deep Learning | R Gayathri, R Latha | CSE | Characterization Breast Cancer Histology Images using Deep Learning | 2018 | ISSN: 2248-9622 | https://www.frontiersin.org/articles/10.3389/fgene.2019.00080/full | https://www.frontiersin.org/journals/genetics | Scopus |



CHILDREN'S EDUCATION SOCIETY (Regd.)
THE OXFORD COLLEGE OF ENGINEERING

(Recognised by the Govt. of Karnataka, Affiliated to Visvesvaraya Technological University, Belagavi.

Approved by A.I.C.T.E. New Delhi.

Recognised by UGC Under Section 2(f)

Bommanahalli, Hosur Road, Bangalore - 560 068.

Ph: 080-61754601/602, Fax: 080 - 25730551

E-mail: engprincipal@theoxford.edu Web: www.theoxfordengg.org

| | | | | | | | | | |
|---|--|---------------------|-----|-------|------|-----------|---|---|----------------|
| 4 | AIR QUALITY ANALYSIS USING MACHINE LEARNING | Bitty Cleatus | ISE | JETIR | 2019 | 2349-5162 | https://www.jetir.org/psearch.php | https://www.jetir.org/papers/JETIRCD06024.pdf | Google Scholar |
| 5 | SMART ROBOTIC GARBAGE MANAGEMENT SYSTEM | Syed Mohamed Faizan | ISE | JETIR | 2019 | 2349-5162 | https://www.jetir.org/psearch.php | https://www.jetir.org/papers/JETIRCD06027.pdf | Google Scholar |
| 6 | VIRTUALA – The Smart Glass | Mayuri Munnolimath | ISE | JETIR | 2019 | 2349-5162 | https://www.jetir.org/psearch.php | https://www.jetir.org/papers/JETIRCD06023.pdf | Google Scholar |
| 7 | SOURCE CODE GENERATOR USING SPEECH | Akshata V Kulkarni | ISE | JETIR | 2019 | 2349-5162 | https://www.jetir.org/psearch.php | https://www.jetir.org/papers/JETIRCD06026.pdf | Google Scholar |
| 8 | A NOVEL TRAFFIC MANAGEMENT SYSTEM USING CANNY EDGE DETECTION | Ankit Kumar Mishra | ISE | JETIR | 2019 | 2349-5162 | https://www.jetir.org/psearch.php | https://www.jetir.org/papers/JETIRCD06025.pdf | Google Scholar |



CHILDREN'S EDUCATION SOCIETY (Regd.)
THE OXFORD COLLEGE OF ENGINEERING

(Recognised by the Govt. of Karnataka, Affiliated to Visvesvaraya Technological University, Belagavi.

Approved by A.I.C.T.E. New Delhi.

Recognised by UGC Under Section 2(f)

Bommanahalli, Hosur Road, Bangalore - 560 068.

Ph: 080-61754601/602, Fax: 080 - 25730551

E-mail: engprincipal@theoxford.edu Web: www.theoxfordengg.org

| | | | | | | | | |
|----|---|---|-----|----------------------------|------|-----------|---|----------------|
| 9 | Emotion Detector for Medical Application | Abhishek M.S | ISE | JETIR | 2019 | 2349-5162 | https://www.jetir.org/papers/JETIRCD06020.pdf | Google Scholar |
| 10 | ANALYSIS OF LOAD BALANCING ON DISTRIBUTED FILE SYSTEM FOR EFFECTIVE DATA RETRIVAL | Salini R S | ISE | JETIR | 2019 | 2349-5162 | https://www.jetir.org/papers/JETIRCD06022.pdf | Google Scholar |
| 11 | FACE RECOGNITION USING LOW QUALITY IMAGES | Mohamed Alkib Javed | ISE | JETIR | 2019 | 2349-5162 | https://www.jetir.org/papers/JETIRCD06021.pdf | Google Scholar |
| 12 | Design and implementation of crossbar scheduler for system-on-chip network in quantum dot | Gunjan Thakur, Mrinal Sarvagya, Preeta Sharan | ECE | Internet Technology letter | 2018 | 2476-1508 | https://onlinelibrary.wiley.com/journal/24761508 | Web of Science |



CHILDREN'S EDUCATION SOCIETY (Regd.)
THE OXFORD COLLEGE OF ENGINEERING
 (Recognised by the Govt. of Karnataka, Affiliated to Visvesvaraya Technological University, Belagavi.

Approved by A.I.C.T.E. New Delhi.

Recognised by UGC Under Section 2(f)

Bommanahalli, Hosur Road, Bangalore - 560 068.

Ph: 080-61754601/602, Fax: 080 - 25730551

E-mail: engprincipal@theoxford.edu Web: www.theoxfordengg.org

| | | | | | | | | | |
|----|---|--|-----|---|------|-------------|---|---|--------|
| | cellular automata technology | | | | | | | | |
| 13 | Wavelength selectivity using adaptive shortest path algorithm for optical network | P. Piruthivira jDr preeta Sharan Dr preeta Sharan N. Ramrao | ECE | Pertanika Journal of Science and Technology | 2018 | 1527-1538 | http://www.pertanika.upm.edu.my/ | https://www.researchgate.net/publication/326990281_Wavelength_selectivity_using_adaptive_shortest_path_algorithm_for_optical_network | Scopus |
| 14 | Photonic crystal based micro mechanical sensor in SOI platform | Indira Bahaddur, Srikanth P C, Dr preeta Sharan | ECE | Pertanika Journal of Science and Technology | 2018 | 1481 - 1488 | http://www.pertanika.upm.edu.my/ | https://www.researchgate.net/publication/326990336 | Scopus |
| 15 | A novel imaging system for underwater haze enhancement | A Chrispin Jiji, R Nagraj | ECE | Springer | 2018 | | https://link.springer.com/ | https://link.springer.com/article/10.1007/s41870-019-00312-y | Scopus |



CHILDREN'S EDUCATION SOCIETY (Regd.)
THE OXFORD COLLEGE OF ENGINEERING

(Recognised by the Govt. of Karnataka, Affiliated to Visvesvaraya Technological University, Belagavi.

Approved by A.I.C.T.E. New Delhi.

Recognised by UGC Under Section 2(f)

Bommanahalli, Hosur Road, Bangalore - 560 068.

Ph: 080-61754601/602, Fax: 080 - 25730551

E-mail: engprincipal@theoxford.edu Web: www.theoxfordengg.org

| | | | | | | | | | |
|----|---|--|-----|---------------|------|-----------|--|---|----------------|
| 16 | Hybrid Technique for Enhancing Underwater Image in blurry conditions | Chrispin Jiji, Nagraj Ramaro | ECE | ASTES | 2018 | 2415-6698 | https://astesjournal.com/ | https://astesjournal.com/v04/i02/p43/ | Google Scholar |
| 17 | Link Based Routing Algorithm for the Desired Quality of Service of a Network | R.Bhargava Rama Gowd, S.Thenappan, GiriPrasad M.N | ECE | IJEAT | 2018 | 2249-8958 | https://www.ijeat.org/ | https://www.ijeat.org/wp-content/uploads/papers/v8i4/C5922028319.pdf | Google Scholar |
| 18 | Highly sensitive lab-on-chip with deep learning AI for detection of bacteria in water | Shaikh Afzal Nehal, Debpriyo Roy, Manju Devi & T. Srinivas | ECE | IJIT Springer | 2018 | 2511-2104 | https://link.springer.com/ | https://link.springer.com/article/10.1007%2Fs41870-019-00363-1 | Scopus |
| 19 | Design and Implementation of Secure Cryptographic Algorithm | Snehapriya M, Manju Devi | ECE | PICES | 2018 | 2566-932X | http://pices-journal.com/ojs/index.php/pices | http://pices-journal.com/ojs/index.php/pices/article/view/185 | Google Scholar |



CHILDREN'S EDUCATION SOCIETY (Regd.)
THE OXFORD COLLEGE OF ENGINEERING
 (Recognised by the Govt. of Karnataka, Affiliated to Visvesvaraya Technological University, Belagavi.

Approved by A.I.C.T.E. New Delhi.

Recognised by UGC Under Section 2(f)

Bommanahalli, Hosur Road, Bangalore - 560 068.

Ph: 080-61754601/602, Fax: 080 - 25730551

E-mail: engprincipal@theoxford.edu Web: www.theoxfordengg.org

| | | | | | | | | | |
|----|--|--------------------------------|-----|---------------|------|-------------------|---|---|----------------|
| | Using Vedic-Mathematics | | | | | | | | |
| 20 | A Novel Low Power MUX based Dynamic Barrel Shifter using Footed Diode Domino Logic | Bharathesh Patel N, Manju Devi | ECE | IJITEE | 2018 | 2278-3075 | https://www.ijitee.org/ | https://www.ijitee.org/wp-content/uploads/papers/v8i6s3/F10630486S319.pdf | Scopus |
| 21 | Evolution of Wireless Communication along with Encoders | Rashmi R, Manju Devi | ECE | IJITEE | 2018 | 2278-3075 | https://www.ijitee.org/download/volume-9-issue-1/ | https://www.ijitee.org/wp-content/uploads/papers/v9i1/A5259119119.pdf | Scopus |
| 22 | Enhancement of Underwater Deblurred Images using Gradient Guided Filter | .Chrispin Jiji ; R Nagaraj | ECE | IEEE Explorer | 2018 | 978-1-5386-2440-1 | https://doi.org/10.1109/RTEICT42901.2018.9012305 | https://ieeexplore.ieee.org/document/9012305 | Google Scholar |



CHILDREN'S EDUCATION SOCIETY (Regd.)
THE OXFORD COLLEGE OF ENGINEERING
 (Recognised by the Govt. of Karnataka, Affiliated to Visvesvaraya Technological University, Belagavi.

Approved by A.I.C.T.E. New Delhi.

Recognised by UGC Under Section 2(f)

Bommanahalli, Hosur Road, Bangalore - 560 068.

Ph: 080-61754601/602, Fax: 080 - 25730551

E-mail: engprincipal@theoxford.edu Web: www.theoxfordengg.org

| | | | | | | | | | |
|----|--|-----------------------------|-----|---------------|------|-----------|---|---|----------------|
| 23 | An Underwater Image Enhancement via Wavelet domain Gradient Guided Filter | Chrispin JijiNagaraj Ramrao | ECE | IEEE Explorer | 2018 | 2227-524X | http://dx.doi.org/10.14419/ijet.v7i4.38.27614 | https://www.researchgate.net/publication/334452936_An_Underwater_Image_Enhancement_via_Wavelet_domain_Gradient_Guided_Filter | Google Scholar |
| 24 | A Novel Technique for Enhancing Color of Undersea Deblurred Imagery | Chrispin JijiNagaraj Ramrao | ECE | ASTES | 2018 | 2415-6698 | DOI: 10.25046/aj030610 | https://astesj.com/v03/i06/p10/ | Scopus |
| 25 | Design and Performance Analysis of Differential Amplifier for Various Applications | M R Jyoti | ECE | JCTN | 2018 | 1546-1955 | https://www.ingentaconnect.com/content/asp/jctn | https://doi.org/10.1166/jctn.2018.7652 | Google Scholar |



CHILDREN'S EDUCATION SOCIETY (Regd.)
THE OXFORD COLLEGE OF ENGINEERING
 (Recognised by the Govt. of Karnataka, Affiliated to Visvesvaraya Technological University, Belagavi.

Approved by A.I.C.T.E. New Delhi.

Recognised by UGC Under Section 2(f)

Bommanahalli, Hosur Road, Bangalore - 560 068.

Ph: 080-61754601/602, Fax: 080 - 25730551

E-mail: engprincipal@theoxford.edu Web: www.theoxfordengg.org

| | | | | | | | | | |
|----|--|-------------------------------------|-----|---|------|-----------|---|---|--------|
| 26 | Constructing PV Array and Power Calculation Using ANFIS Controller based MTPP | Madhavi Dasari and Dr. V.S. Bharath | EEE | Journal of Advanced Research in Dynamical and Control Systems | 2018 | 1943-023X | https://www.jardcs.org/abstract.php?id=1267 | https://www.jardcs.org/index.php | Scopus |
| 27 | FireFly ANN Based UPQC-S PV Array System for Power Enhancement | Madhavi Dasari and V.S. Bharath | EEE | Journal of Green Engineering (JGE) | 2019 | 1904-4720 | http://www.jgenng.com/wp-content/uploads/2019/12/volume9-issue4-012.pdf | http://www.jgenng.com/wp-content/uploads/2019/12/volume9-issue4-012.pdf | Scopus |
| 28 | In vitro and in vivo evaluation of anti-inflammatory potency of Mesua ferrea, Saraca asoca, Viscum album & Anthocephalus cadamba in murine | Dr. B.K.Manjunatha | BT | Beni-Suef University Journal of Basic and Applied Sciences (Elsevier),7 | 2018 | 2314-8543 | https://www.sciencedirect.com/science/article/pii/S2314853518302646 | Beni-Suef University Journal of Basic and Applied Sciences ScienceDirect.com by Elsevier | Scopus |



CHILDREN'S EDUCATION SOCIETY (Regd.)
THE OXFORD COLLEGE OF ENGINEERING

(Recognised by the Govt. of Karnataka, Affiliated to Visvesvaraya Technological University, Belagavi.

Approved by A.I.C.T.E. New Delhi.

Recognised by UGC Under Section 2(f)

Bommanahalli, Hosur Road, Bangalore - 560 068.

Ph: 080-61754601/602, Fax: 080 - 25730551

E-mail: engprincipal@theoxford.edu Web: www.theoxfordengg.org

| | | | | | | | | | |
|----|---|---|----|---|------|-----------|---|---|----------------|
| | macrophages raw 264.7 cell lines and Wistar albino rats | | | | | | | | |
| 29 | Grating based pressure monitoring system for subaquatic application | Regina Mathias, Ambresh P. Ambalgi, Anup M. Upadhyay a | ME | International Journal of Information Technology | 2018 | 2511-2112 | https://www.springer.com/journal/41870 | https://doi.org/10.1007/s41870-018-0128-x | UGC |
| 30 | Processing and Mechanical Characterization of 8 wt. % of Micro B4C Particulates Reinforced Al7020 Alloy Composites | Raviprakash M | ME | Journal of Emerging Technologies and Innovative Research | 2018 | 2349-5162 | https://www.jetir.org/ | https://www.jetir.org/papers/JETIR1804245.pdf | Google Scholar |
| 31 | Design and Analysis of Effect of Core Thickness in UAV Wing | Raviprakash M | ME | International Journal for Ignited Minds (IJIMIINDS) | 2018 | 2349-2082 | http://www.ijiminds.com/ | http://www.ijiminds.com/allarticles/article_138_0.pdf | Google Scholar |



CHILDREN'S EDUCATION SOCIETY (Regd.)
THE OXFORD COLLEGE OF ENGINEERING

(Recognised by the Govt. of Karnataka, Affiliated to Visvesvaraya Technological University, Belagavi.

Approved by A.I.C.T.E. New Delhi.

Recognised by UGC Under Section 2(f)

Bommanahalli, Hosur Road, Bangalore - 560 068.

Ph: 080-61754601/602, Fax: 080 - 25730551

E-mail: engprincipal@theoxford.edu Web: www.theoxfordengg.org

| | | | | | | | | | |
|----|---|----------------|---------------|--|------|---|---|---|----------------|
| 32 | Processing and Mechanical Characterization of Nano B4C Particulates Reinforced Al2218 alloy Composites | Raviprakash M | ME | International Journal of Advanced Mechanical Engineering | 2018 | http://www.ripublication.com/ | http://www.ripublication.com/ | https://www.ripublication.com/ijamev8n18/ijamev8n1_10.pdf | Google Scholar |
| 33 | Isolation & Characterization Of Methanogenic Bacteria From Local Environment And Comparative Study Of Kinetics With Traditional Biogas Producers. | Salma Kausar M | Biotechnology | International Journal Of Creative Research Thoughts | 2018 | ISSN: 2320-2882 | https://ijcrt.org/ | https://ijcrt.org/ | UGC |
| 34 | Heavy metal ion detection using immobilized ALP enzyme | K. Valarmathy | Biotechnology | International Journal Of Creative Research Thoughts | 2018 | ISSN: 2320-2882 | https://ijcrt.org/ | https://ijcrt.org/ | UGC |



CHILDREN'S EDUCATION SOCIETY (Regd.)
THE OXFORD COLLEGE OF ENGINEERING

(Recognised by the Govt. of Karnataka, Affiliated to Visvesvaraya Technological University, Belagavi.

Approved by A.I.C.T.E. New Delhi.

Recognised by UGC Under Section 2(f)

Bommanahalli, Hosur Road, Bangalore - 560 068.

Ph: 080-61754601/602, Fax: 080 - 25730551

E-mail: engprincipal@theoxford.edu Web: www.theoxfordengg.org

| | | | | | | | | | |
|----|--|---------------------------------|----------------|---|------|-----------------|--|---|-----|
| 35 | Screening of potential phytochemicals for wound healing. | Dr.B.K.M anjunatha, Tanusree C | Biotechnol ogy | International Journal Of Creative Research Thoughts | 2018 | ISSN: 2320-2882 | https://ijcrt.org / | https://ijcrt.org/ | UGC |
| 36 | Screening of antibacterial and antioxidant activities of Streptomyces species isolated from western Ghats from Karnataka | Dr. Kusum Paul, Shambu M G | Biotechnol ogy | International Journal Of Creative Research Thoughts | 2018 | ISSN: 2320-2882 | https://ijcrt.org / | https://ijcrt.org/ | UGC |
| 37 | Construction of cancer diseasome through graph theoretical approach | Dr.B.K.M anjunatha, Tanusree C | Biotechnol ogy | International Journal Of Creative Research Thoughts | 2018 | ISSN: 2320-2882 | https://ijcrt.org / | https://ijcrt.org/papers/IJCRTOXF0057.pdf | UGC |
| 38 | Isolation, characterization and biological activity of flax lectin | Dr.B.K.M anjunatha, Dr Suma T K | Biotechnol ogy | International Journal Of Creative Research Thoughts | 2018 | ISSN: 2320-2882 | https://ijcrt.org / | https://ijcrt.org/papers/IJCRTOXF0020.pdf | UGC |



CHILDREN'S EDUCATION SOCIETY (Regd.)
THE OXFORD COLLEGE OF ENGINEERING
 (Recognised by the Govt. of Karnataka, Affiliated to Visvesvaraya Technological University, Belagavi.

Approved by A.I.C.T.E. New Delhi.

Recognised by UGC Under Section 2(f)

Bommanahalli, Hosur Road, Bangalore - 560 068.

Ph: 080-61754601/602, Fax: 080 - 25730551

E-mail: engprincipal@theoxford.edu Web: www.theoxfordengg.org

| | | | | | | | | | |
|----|---|------------------------------------|----------------|---|------|----------------------|---|---|----------------|
| 39 | Significance analysis of target profile in tuberculosis using gene interactions and insilico docking approach to find potential ligands | Dr.B.K.M anjunatha, Shambu M G | Biotechnol ogy | International Journal Of Creative Research Thoughts | 2018 | ISSN: 2320-2882 | https://ijcrt.org / | https://ijcrt.org/papers/IJCRTOXF0025.pdf | UGC |
| 40 | Morphological characterization of Pyricularia oryzae causing blast disease in rice (Oryza sativa L.) from different zones of Karnataka | B Manjunatha and M Krishnappa | BioTech | Journal of Pharmacognosy and Phytochemistry | 2018 | 2278-4136, 2349-8234 | https://www.phytojournal.com/ | https://www.phytojournal.com/archives/2019/vol18issue3/PartBC/8-3-279-550.pdf | Google Scholar |
| 41 | Stability Analysis for Yield and Yield Attributing Traits in Rice (Oryza sativa L.) | B Manjunatha, Dr. Niranjana Kumara | BioTech | IJCMAS | 2018 | 2319-7962, 2319-7706 | https://www.ijcmas.com/ | https://www.ijcmas.com/abstractview.php?ID=8341&vol=7-6-2018&SNo=194 | Google Scholar |



CHILDREN'S EDUCATION SOCIETY (Regd.)
THE OXFORD COLLEGE OF ENGINEERING

(Recognised by the Govt. of Karnataka, Affiliated to Visvesvaraya Technological University, Belagavi.

Approved by A.I.C.T.E. New Delhi.

Recognised by UGC Under Section 2(f)

Bommanahalli, Hosur Road, Bangalore - 560 068.

Ph: 080-61754601/602, Fax: 080 - 25730551

E-mail: engprincipal@theoxford.edu Web: www.theoxfordengg.org

| | | | | | | | | | |
|----|---|---|---------|--|------|----------------------|---|---|----------------|
| 42 | Performance Evaluation of Maize Hybrids (Zea mays L.) | B Manjunatha, Dr. Niranjana Kumara | BioTech | IJCMAS | 2018 | 2319-7962, 2319-7706 | https://www.ijcmas.com/ | https://doi.org/10.20546/ijcmas.2018.711.139 | Google Scholar |
| 43 | Genetic variability, path analysis, character association for yield and its attributing traits in F population of cross BPT-5204 × IET-21214 in rice (Oryza sativa L.). | Pradeep,P, Malleshappa, C., Manjunatha, B., Kumara, B. N., Harish, D. | BioTech | Environment and Ecology | 2018 | 0970-0420 | https://www.environmentandecology/ | https://www.environmentandecology.com/publication-volume-362018/ | Google Scholar |
| 44 | In vitro and in vivo evaluation of anti-inflammatory potency of Mesua ferrea, Saraca asoca, | Syed Murthuza, B.K. Manjunatha | BioTech | Beni-Suef University Journal of Basic and Applied Sciences | 2018 | 2314-8535 | https://www.sciencedirect.com/science/journal/23148535 | https://www.sciencedirect.com/science/article/pii/S2314853518302646 | Scopus |



CHILDREN'S EDUCATION SOCIETY (Regd.)
THE OXFORD COLLEGE OF ENGINEERING

(Recognised by the Govt. of Karnataka, Affiliated to Visvesvaraya Technological University, Belagavi.

Approved by A.I.C.T.E. New Delhi.

Recognised by UGC Under Section 2(f)

Bommanahalli, Hosur Road, Bangalore - 560 068.

Ph: 080-61754601/602, Fax: 080 - 25730551

E-mail: engprincipal@theoxford.edu Web: www.theoxfordengg.org

| | | | | | | | | | |
|----|--|--|------------|----------------|------|-----------------|---|---|----------------|
| | Viscum album & Anthocephalus cadamba in murine macrophages raw 264.7 cell lines and Wistar albino rats | | | | | | | | |
| 45 | Analysis and Design of Blast Resistant Structures | Sharlin Sheeba B. K. Raghu Prasad | Civil | IJERT | | 2278-0181 | http://www.ijert.org/ | https://www.ijert.org/volume-08-issue-08-august-2019 | Google Scholar |
| 46 | Response of RCC Asymmetric Building Subjected to Earthquake Ground Motions | Davda Karan Kishorbha i Prof. B.K. Raghu Prasad Prof. Amarnath K | Civil | IJERT | 2018 | 2278-0181 | http://www.ijert.org/ | https://www.ijert.org/volume-08-issue-07-july-2019 | Google Scholar |
| 47 | Case hardening effects on mechanical | Raju B R | Automobile | IJCRT Journals | 2018 | ISSN: 2320-2882 | https://ijcrt.org/ | https://ijcrt.org/papers/I | UGC |



CHILDREN'S EDUCATION SOCIETY (Regd.)
THE OXFORD COLLEGE OF ENGINEERING

(Recognised by the Govt. of Karnataka, Affiliated to Visvesvaraya Technological University, Belagavi.

Approved by A.I.C.T.E. New Delhi.

Recognised by UGC Under Section 2(f)

Bommanahalli, Hosur Road, Bangalore - 560 068.

Ph: 080-61754601/602, Fax: 080 - 25730551

E-mail: engprincipal@theoxford.edu Web: www.theoxfordengg.org

| | | | | | | | | | |
|----|---|---------------------|------------|----------------|------|-----------------|---|---|----------------|
| | properties in graphite reinforced al6061 mmcs | | | | | | | JCRTOXF0021.pdf | |
| 48 | Investigation on Mechanical and Tribological Characterization of Nano Particulate Filled Fiber Reinforced Hybrid Composites for Automobile Applications | Raju B R | Automobile | IJCRT Journals | 2018 | ISSN: 2320-2882 | https://ijcrt.org/ | https://ijcrt.org/download.php?file=IJCRTOXF0048.pdf | Google Scholar |
| 49 | A simple Approach on Premises Deployment Model Techniques Provider with Encrypt Transfers Technology | Dr. M S Shashidhara | MCA | IJCRT Journals | 2018 | 2320-2882 | https://ijcrt.org/ | http://www.ijcnis.org/index.php/ijcnis/issue/view/26 | UGC |



CHILDREN'S EDUCATION SOCIETY (Regd.)
THE OXFORD COLLEGE OF ENGINEERING

(Recognised by the Govt. of Karnataka, Affiliated to Visvesvaraya Technological University, Belagavi.

Approved by A.I.C.T.E. New Delhi.

Recognised by UGC Under Section 2(f)

Bommanahalli, Hosur Road, Bangalore - 560 068.

Ph: 080-61754601/602, Fax: 080 - 25730551

E-mail: engprincipal@theoxford.edu Web: www.theoxfordengg.org

| | | | | | | | | | |
|----|--|----------------------------------|-----|----------------|------|-----------|---|---|-----|
| 50 | An Empirical study on Ticket Classification using Machine learning in Osticket System | Dr. M S Shashidhara | MCA | IJCRT Journals | 2018 | 2320-2883 | https://ijcrt.org/ | http://www.ijcrt.org/viewfull.php?&p_id=IJCRT1705154 | UGC |
| 51 | Study On Eye Troubles Using Palm Print And Image Processing Technique | Dr. M S Shashidhara | MCA | IJCRT Journals | 2018 | 2455-1457 | https://ijcrt.org/ | http://www.ijrter.com/papers/volume-2/issue-5/study-on-eye-troubles-using-palm-print-and-image-processing-technique.pdf | UGC |
| 52 | A Simple Approach on Web Based Classification of Face Recognition Based on Individual Data | Dharamvir, Dr. Poornima Nataraja | MCA | IJCRT Journals | 2018 | 2320-2882 | https://ijcrt.org/ | https://ijcrt.org/download.php?file=IJCRTOXFO065.pdf | UGC |



CHILDREN'S EDUCATION SOCIETY (Regd.)
THE OXFORD COLLEGE OF ENGINEERING
 (Recognised by the Govt. of Karnataka, Affiliated to Visvesvaraya Technological University, Belagavi.

Approved by A.I.C.T.E. New Delhi.

Recognised by UGC Under Section 2(f)

Bommanahalli, Hosur Road, Bangalore - 560 068.

Ph: 080-61754601/602, Fax: 080 - 25730551

E-mail: engprincipal@theoxford.edu Web: www.theoxfordengg.org

| | | | | | | | | | |
|----|---|--|-------------|---|------|--|---|---|----------------|
| | using Internet on Things and its Applications | | | | | | | | |
| 53 | In Silico Identification of Piperazine Linked Thiohydantoin Derivatives as Novel Androgen Antagonist in Prostate Cancer Treatment | Dr. Shipra Bhati | Chemistry | International journal of Peptide Research and Therapeutics-Springer | 2018 | ISSN: 1573-3149 (Print) 1573-3904 (Online), IF-1.219 | https://doi.org/10.1007/s10989-018-9734-5 | https://link.springer.com/article/10.1007/s10989-018-9734-5 | UGC |
| 54 | An extension of golden section algorithm for n-variable functions with MATLAB code | G Sandhya Rani , Sarada Jayan and K V Nagaraja | MATHEMATICS | IOP Science | 2018 | 1757-899X | https://iopscience.iop.org/article/10.1088/1757-899X/577/1/012175 | https://iopscience.iop.org/journal/1757-899X | Goolge Scholar |
| 55 | CONVEXITY FOR THE PROPORTION OF ONE MEAN WITH RESPECT | SREENIVASA REDDY PERLA ,S PADMANABHAN | MATHEMATICS | Journal of Emerging Technologies and Innovative Research | 2018 | 2349-5162 | http://www.imvibl.org/buletin/bulletin_imvi_6_2_2016/buletin_imvi_6_2 | http://www.imvibl.org/buletin/bulletin_imvi_6_2_2016/buletin_imvi_6 | Goolge Scholar |



CHILDREN'S EDUCATION SOCIETY (Regd.)
THE OXFORD COLLEGE OF ENGINEERING

(Recognised by the Govt. of Karnataka, Affiliated to Visvesvaraya Technological University, Belagavi.

Approved by A.I.C.T.E. New Delhi.

Recognised by UGC Under Section 2(f)

Bommanahalli, Hosur Road, Bangalore - 560 068.

Ph: 080-61754601/602, Fax: 080 - 25730551

E-mail: engprincipal@theoxford.edu Web: www.theoxfordengg.org

| | | | | | | | | | |
|----|--|--|-------------|--|------|-----------|---|---|----------------|
| | TO ANOTHER PROPORTION OF MEAN | | | | | | _2015_241_249.pdf | _2_2015_241_249.pdf | |
| 56 | ON SCHUR M- POWER CONVEXITY FOR PROPORTION OF DISTINCTION OF SOME SPECIAL MEANS IN TWO VARIABLES | SREENIVASA REDDY PERLA AND S PADMANABHAN | MATHEMATICS | Journal of Emerging Technologies and Innovative Research | 2018 | 2349-5162 | https://www.jetir.org/papers/JETIR1905G43.pdf | https://www.jetir.org/papers/JETIR1905G43.pdf | Google Scholar |

[Download PDF](#)

Published: 08 March 2018

Trust based resource selection with optimization technique

[E. Saravana Kumar](#)  & [K. Vengatesan](#)

Cluster Computing. **22**, 207–213 (2019)

105 Accesses | **4** Citations | [Metrics](#)

Abstract

Grid computing is distributed computing that coordinates and utilizes computing power, data storage, applications and network resources in dynamic and geographically dispersed organizations. Resource management and application scheduling are two major grid computing problems. Resources are heterogeneous regarding power, architecture, configuration and availability complicating task scheduling. The aim of grid scheduling is in reducing makespan. In grid applications, users should be ensured reliable transactions. Trust is multi-dimensional factor and depends on components like entity reputation, policies and opinions of the entity. A trust based scheduling approach is proposed in this study.

Introduction



[International Journal of Biomedical Engineering and Technology](#) > [2018 Vol.26 No.3/4](#)

Title: [Biclustering of gene expression data using biclustering iterative signature algorithm and biclustering coherent column](#)

Authors: E. Saravana Kumar; K. Vengatesan; R.P. Singh; C. Rajan

Addresses: Adhiyamaan College of Engineering, Hosur, Tamil Nadu, India ' Sri Satya Sai University of Technology and Medical Sciences, Sehore, Madhya Pradesh, India ' Sri Satya Sai University of Technology and Medical Sciences, Sehore, Madhya Pradesh, India ' KSR College of Technology, Tiruchengode, Tamil Nadu, India

Abstract: Clustering has various methods for solving the different research problems in biological domain. Analysis of gene expression data in biomedical filed is very critical task, in which various algorithms are proposed under different experimental conditions. In this proposed work the gene expression data are tested with Biclustering Bimax and Biclustering Iterative Signature Algorithm (ISA) and Biclustering Coherent Column; the experimental result show the Biclustering ISA has demonstrated a coherent manifestation contour only in the surfeit of subset of microarray experiments and produced momentous result.

Keywords: clustering; gene expression; biclustering; iterative signature algorithm formatting.

DOI: [10.1504/IJBET.2018.089968](#)

International Journal of Biomedical Engineering and Technology, 2018 Vol.26 No.3/4, pp.341 - 352

Received: 20 May 2017

Accepted: 17 Jul 2017

Published online: 15 Feb 2018 *

Full-text access for editors Access for subscribers Purchase this article

Comment on this article

Keep up-to-date

[Our Blog](#)

[Follow us on Twitter](#)

[Visit us on Facebook](#)

[Our Newsletter \(subscribe for free\)](#)

[RSS Feeds](#)

[New issue alerts](#)

[Return to top](#)

[Contact us](#) [About Inderscience](#) [OAI Repository](#) [Privacy and Cookies Statement](#) [Terms and Conditions](#) [Help](#) [Sitemap](#)

© 2021 Inderscience Enterprises Ltd.

Characterization Breast Cancer Histology Images using Deep Learning

R Gayathri, R Latha

IV Semester M.Tech., Department of Computer Science and Engineering, The Oxford College of Engineering, Bangalore-560068

Assistant Professor, Department of Computer Science and Engineering, The Oxford College of Engineering, Bangalore-560068,India.

ABSTRACT:

The paper employs deep learning to classify breast cancer histopathological image into normal, benign and malignant subclasses *in situ* carcinoma and invasive carcinoma categories. The classification is mainly based on cells' density, variability, and organization along with overall tissue structure and morphology. Smaller and larger patches of histological images are extracted that includes cell-level and tissue-level features. Here, Patches are screened by Clustering algorithm and CNN is used to select the discriminative patches. The proposed approach is applied to the multi-class classification of breast cancer histology images. It achieves initial test achieves of 95% accuracy and on the overall test, 88.89% accuracy.

Keywords: Breast cancer histology images, CNN, image classification.

Date of Submission: 06-07-2020

Date of Acceptance: 21-07-2020

I. INTRODUCTION:

Breast cancer is the most common cancer and the second main cause of cancer for death in women, after lung cancer. The chance of any woman dying from breast cancer is around 1 in 37, or 2.7 percent [1]. The diagnosis from a histology image is the gold standard in diagnosing considerable types of cancer. Pathologists analyse the regularities of cell shapes, density, and tissue structures by examining a thin slice of tissue under an optical microscope and determine cancerous regions and malignancy degree. Due to the complexity and diversity of histology images, the manual examination requires abundant knowledge and experience of the pathologists and is fairly time-consuming and error-prone [2]-[4].

II. RELATED WORK:

In the 2012 ImageNet image classification competition, the deep learning model AlexNet won the champion [5]. In study, Spanhol et al. [6], [7] constructed a dataset of 7909 breast cancer histology images named BreakHis acquired on 82 patients. Spanhol et al. used six different feature extractors to extract features from the image, and provided four classifiers for each feature extractor for final classification. The final correct rate was 80% to 85%. Bayramoglu et al. put together four different magnifications for uniform training and tested them separately at a single magnification [8]. They trained AlexNet based on the extraction of

patches obtained randomly or by a sliding window mechanism from breast cancer images with multiple magnifications and combined the patch probabilities with three fusion rules for final classification. Wang et al. [9] used sampling patches to train a CNN to make patch-level predictions, then aggregated the results to create tumour probability heatmaps and made slide-level predictions. The methodology was tested on the Camelyon16 dataset including 400 WSIs [10]. In [11], context-aware stacked convolutional neural networks for 3-class classification of breast WSIs were presented. Bejnordi et al. used a CNN trained by high pixel resolution patches to extract cell-level features primarily, followed by a second CNN. Then, large input patches were used to train the stacked CNNs to learn both cellular information and global tissue structures.

III. PROPOSED SOLUTION:

In this paper, deep learning is employed to construct a CAD model, and the pathological images of breast cancer are divided into benign and malignant. In the work herein described, histology image classification was performed by processing several patches with fixed size. Microscopically, cancer cells have distinguishing histological features. Therefore, referring to the pathologists' diagnostic process, features related to cells and global tissue structures extracted from two kinds of patches with

different sizes will improve the performance of the classification of breast cancer histology images into one of the 4 target classes. The labels of histology images for the classification task given by the pathologists are based on the whole images. Larger size patches sampled from a histology image contain sufficient information so that the image label can be used for the patches. However, cell-level patches extracted from high resolution histology images, especially ultra-high resolution WSIs, may not contain sufficient diagnostic information. There exist some patches with large areas of fat cells and stroma, sparse breast cells, and normal patches extracted from malignant histology images. CNNs trained by these patches can't extract discriminative features. Consequently, we present a methodology to automatically screen more discriminative patches based on clustering algorithm and convolutional neural network. Based on the above two aspects, the main objective of this paper is to

propose a comprehensive and effective scheme for the multi-classification of breast histology images in order to improve the diagnostic performance. To achieve this, the main contributions of our work can be summarized as follows: (i) We propose a patch sampling strategy to extract two kinds of patches with different sizes to preserve essential information and contain cell-level and tissue-level features respectively., (ii) We design a patch selecting method to select more discriminative patches based on CNN and K-means., (iii) We design a classification framework which extracts features from the patches using the feature extractors and compute the final feature of each whole image for classification through a classifier.

Stain inconsistency of histology images, due to differences in color responses of slide digital scanners, will affect the performance of image analysis. As can be seen from Fig. 1, the images in the dataset have large stain variation.

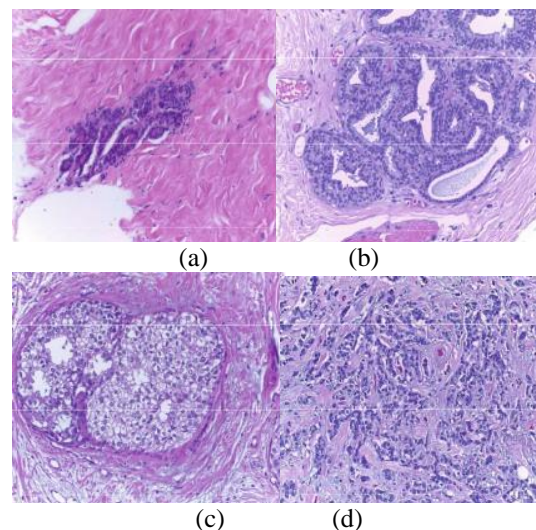


FIGURE 1. H&E stained images from each type, (a): normal tissue, (b): benign abnormality, (c): in situ carcinoma, and (d): invasive carcinoma.

To this end, stain normalization is essential prior to other processes. There are various researches for stain normalization in histology images [12], [13]. In this paper, we use a method proposed by Reinhardt *et al.* [14], which transforms the RGB images to the decorrelated $l\alpha\beta$ color space, followed by computing the means and standard deviations for each channel separately in $l\alpha\beta$ space and a set of linear transforms in order to match the color distribution of the source and target images, finally, converts the results back to RGB.

IV. DATASET:

This section is dedicated to introducing the dataset used in our work and pre-processing of

images. The dataset is from the bioimaging 2015 breast histology classification challenge [15], composed of high-resolution (2048×1536 pixels) and H&E stained breast cancer histology images. The images were digitized with a magnification of 200x and pixel size of $0.42\mu\text{m} \times 0.42\mu\text{m}$. Two pathologists labeled images as normal, benign, *in situ* carcinoma or *invasive* carcinoma according to the predominant cancer type in each image, without specifying the area of interest. Fig. 1 illustrates images from each class mentioned in the dataset.

This dataset composed of a training set of 249 images, an initial test set of 20 images and an extended test set of 16 images with increased

ambiguity is publicly available at <https://rdm.inesctec.pt/dataset/nis-2017-003>. The main goal of this paper is to propose an effective scheme for the multi-class breast histology images classification.

V. PROPOSED ARCHITECTURE:

The multi-classification scheme of breast histology images is presented in this section. We introduce the overall framework at first, and then describe each process in detail. Fig. 2 illustrates the framework of our approach used for multi-class classification of breast histology images.

A. Framework:

The main processes can be summarized as follows: (i) We extract two kinds of patches with different sizes by a sliding window mechanism from breast cancer histology images to preserve essential information and contain cell-level and tissue-level features, and then train two CNNs as feature extractors respectively. (ii) We split the small patches into multiple clusters using k-means clustering algorithm and select more discriminative patches based on the network trained by small patches to retrain the network. (iii) We extract features from the selected smaller patches and larger patches using the feature extractors and compute the final feature of each whole image to train a classifier for classification.

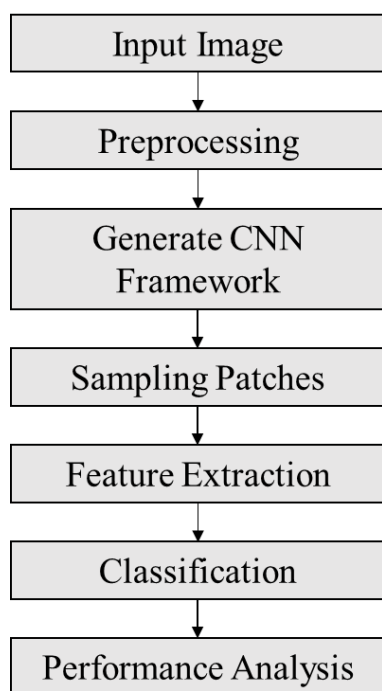


Figure 2. System Architecture

B. CNN Training:

Our goal is to classify the breast histology image into four classes: normal tissue, benign tissue, *in situ* carcinoma and *invasive* carcinoma. The performance of classification is highly dependent on the information extracted from the images. We use features related to breast cells and global tissue structures to represent each whole image. Firstly, because the arrangement of cancer cells is extremely disordered and the cancerous cells have atypia such as larger nuclei and inconsistent morphology, therefore, cell-level features including the nuclei information, such as shape and variability, as well as cells organization features like density and morphology, are used to diagnose whether cells are cancerous. The pixel size of the breast histology images in the dataset is $0.42\mu m \times 0.42\mu m$, and the radius of cells is between 3 and 11 pixels approximately. Consequently, we extract small patches of 128×128 pixels to contain cell-level features. Secondly, the structure of the diseased tissue may be atypical. *In situ* carcinoma is a carcinoma growth of minor grade precancerous, with no invasion of the surrounding tissue within a particular tissue compartment in the mammary duct. Interestingly, *invasive* carcinoma does not confine itself to the initial tissue compartment [16]. Therefore, tissue structure information is essential to differentiate between *in situ* and *invasive* carcinomas. It is unpractical for CNNs to extract features from a histology image with a large size directly. According to the size of images in the provided dataset, we extract patches of 128×128 pixels to contain the global tissue structure information. We extract patches by a sliding window mechanism from breast cancer histology images. The patches of 128×128 pixels are small and focus on cell-related characteristics, therefore, we extract contiguous non-overlapping patches from the breast histology images. In addition, we extract overlapping 128×128 pixels patches with a 50% overlap to contain continuous tissue morphology and structure information. All extracted patches are given the same label as the corresponding histology image.

C. FEATURE EXTRACTOR:

The histology images have different cell morphology, texture, tissue structures, and so on. The representation of complex features is significant for the classification task. The handcrafted feature extraction method needs abundant expert domain knowledge, and it is labour-intensive and difficult to extract discriminative features. CNNs can directly extract representative features from images, and have achieved remarkable results in various fields. ResNet50 [17] is used as a feature extractor in this

paper because it is a classical CNN and easy to train compared to other deeper models under the premise of ensuring the extraction of usability features. The deep residual learning framework (ResNet) is proposed by He and Sun [18] to address the degradation of deep networks. Formally, the desired underlying mapping is denoted as $H(x)$, then the stacked nonlinear layers are fitted to another mapping of $F(x) := H(x) - x$ and the original mapping is rewritten as $F(x) + x$. The formula of $F(x) + x$ is implemented by feed-forward neural networks with "shortcut connections" which perform the identity mapping. For deeper nets, a bottleneck design which uses a stack of 3 layers instead of 2 for each residual function is proposed. The ResNet50 consists of 16 "bottleneck" building blocks and takes as input a $\{3, 224, 224\}$ RGB image.

The training of ResNet50 from scratch requires a large number of training images to avoid overfitting. However, because of the paucity of histology images in our dataset, we adapt a transfer learning strategy [20], [21] and use ResNet50 pre-trained on the ImageNet dataset [22]. We remove the top layer of the network and add a softmax classifier with 4 neurons, then, we resize the patches of 128×128 pixels to 224×224 pixels for fine-tuning two modified networks as original feature extractors and the trained networks are denoted as ResNet50-512 and ResNet50-128 respectively. 2048-dimensional features of patches can be obtained from the global average pooling layer of ResNet50.

For the multi-class classification of breast cancer histology images, the sampling strategy of two kinds of patches, the screening method of 128×128 pixels patches and feature extractors based on ResNet50 have been introduced above.

Then, we rescale the extracted patches of 128×128 pixels and selected patches of 128×128 pixels corresponding to each image in the training set, and feed them into the fine-tuned ResNet50-512 and ResNet50-cluster respectively to obtain the 2048-dimensional features group, which can represent the cells and tissue structures information of the image. In order to obtain the final feature of an image, we employ the P-norm pooling fusion method [19] and the formulation is as follows:

$$f_p(v) = \left(\frac{1}{N} \sum_{i=1}^N v_i^p \right)^{\frac{1}{p}}$$

Here, N represents the number of patches, v_i denotes the 2048-dimensional feature of the i -th patch and $P \in \{3, 4, 5, 6, 7, 8, 9, 10, 11, 12, 13, 14, 15, 16, 17, 18, 19, 20\}$ is used in our paper. At last, the image-wise features of histology images in the training set are used to train the SVM classifier for multi-class breast cancer histology classification.

VI. PERFORMANCE EVALUATION: IMAGE-WISE CLASSIFICATION:

We use the normalized breast histology images in the test set to verify the approach proposed in this paper. The procedure of the experiment is as follows:

- The sampling strategy introduced in Section V.B is used to extract contiguous non-overlapping patches of 128×128 pixels and patches of 128×128 pixels with 50% overlap from the test images.
- The ResNet50-cluster fine-tuned by patches of 128×128 pixels in the selected clusters is sensitive to more discriminative patches, therefore, we use the network to predict the smaller patches and select patches with classification probability higher than a set threshold.
- We rescale the selected patches of 128×128 pixels corresponding to each test image to 224×224 pixels, and feed them into the fine-tuned ResNet50-512 and ResNet50-cluster respectively to obtain the 2048-dimensional features group.
- We employ the 3-norm pooling method to compute the final feature of each image and make final classification by using SVM.

The patches of 128×128 pixels are predicted using the ResNet50-cluster, and the patches with classifier probability higher than 90% are retained. Four test images are classified into wrong categories, three of which belong to the extended test set, and the remaining one labelled as normal is classified as benign.

The calculation formulas are as follows:

$$Accuracy = \frac{TP+TN}{TP+TN+FP+FN} \dots \dots (2)$$

$$Precision = \frac{TP}{TP+FP}, Recall = \frac{TP}{TP+FN} \dots \dots (3)$$

$$F = \frac{2 \times Precision \times Recall}{Precision + Recall} \dots \dots \dots (4)$$

$$Macro-F = \frac{1}{N} \sum_{i=1}^N F_i \dots \dots \dots (5)$$

Here, TP (true positive) is the number of positive cases that are classified as positive. Analogously, TN, FN and FP represent the numbers of true negatives, false negatives and false positives respectively. The recall represents the percentage of positive samples that are correctly classified, which is more clinically relevant. Macro-F, also known as macro-averaging, is used to evaluate the performance of multi-classification globally and is computed by first computing the F-scores for the n categories then averaging these per-category scores to compute the global means.

The image-wise accuracy of the initial test set and overall test set is 95% and 88.89% respectively. According to the confusion matrix, precision, recall and F-score of each class can be obtained respectively, as shown in Table 2. The value of

macro-F calculated according to formula (5) is 89.14%.

| Results | Normal | Benign | InSitu | Invasive |
|-----------|--------|--------|--------|----------|
| Precision | 0.875 | 0.75 | 1.0 | 1.0 |
| recall | 0.78 | 1.0 | 0.89 | 0.89 |
| F-Score | 0.825 | 0.857 | 0.942 | 0.942 |

Table 2: The Performance of the proposed model.

VII. RESULTS AND DISCUSSION:

In our work, we extract smaller patches of 128×128 pixels from the breast histology images to contain cell-level and tissue-level features, then, we screen discriminative 128×128 pixels patches based on clustering algorithm and CNN. Through comparative experiments, it is proved that the method proposed in this paper can effectively improve the performance of multi-classification of breast histology images. We contrast the aftereffects of our methodology and the benchmark strategy proposed in [23] (CNNCSVM) and the near result is appeared in Table 11. Araújo et al. utilized the equivalent dataset as us and extricated patches of 512×512 pixels. They utilized their very own CNN planned and accomplished a best exactness of 77.8% of multi-classification with enlarged dataset. It very well may be seen that our methodology has a considerable improvement in exactness and review contrasted and the benchmark conspire, particularly in the classification of benevolent what's more, in situ carcinoma pictures.

VIII. CONCLUSION:

In this paper, we propose an effective method to classify the H&E stained breast histology images into four classes: normal tissue, benign lesion, in-situ carcinoma and invasive carcinoma. Due to the atypia of cancerous cells and the difference in tissue morphology and structures between in situ carcinoma and invasive carcinoma, we extract patches of 128×128 pixels from the histology images to contain different levels features.

REFERENCES:

- [1]. N. Christian. (2018). *What You Need to Know About Breast Cancer*. [Online]. Available: <https://www.medicalnewstoday.com/articles/37136.php>
- [2]. M. N. Gurcan, L. E. Boucheron, A. Can, A. Madabhushi, N. Rajpoot, and B. Yener, "Histopathological image analysis: A review," *IEEE Rev. Biomed. Eng.*, vol. 2, pp. 147-171, 2009.
- [3]. L. He, L. R. Long, S. Antani, and G. Thoma, "Computer assisted diagnosis in histopathology," *Sequence Genome Anal., Methods Appl.*, vol. 3, pp. 271-287, 2010.
- [4]. L. He, L. R. Long, S. Antani, and G. R. Thoma, "Histology image analysis for carcinoma detection and grading," *Comput. Methods Programs Biomed.*, vol. 107, no. 3, pp. 538-556, 2012.
- [5]. A. Krizhevsky, I. Sutskever, and G. Hinton, "Imagenet classification with deep convolutional neural networks," *Advances in neural information processing systems*. 2012.
- [6]. F. A. Spanhol, L. S. Oliveira, L. Heutte, and C. Petitjean, "A dataset for breast cancer histopathological image classification," *IEEE Trans. Biomed. Eng.*, vol. 63, no. 7, pp. 1455-1462, Jul. 2016.
- [7]. F. A. Spanhol, L. S. Oliveira, L. Heutte, and C. Petitjean, "Breast cancer histopathological image classification using convolutional neural networks," in *Proc. IEEE Int. Joint Conf. Neural Netw. (IJCNN)*, Jul. 2016, pp. 2560-2567.
- [8]. N. Bayramoglu, J. Kannala, and J. Heikkilä, "Deep learning for magnification independent breast cancer histopathology image classification," 2016 23rd International conference on pattern recognition (ICPR). IEEE, 2016.
- [9]. D. Wang, A. Khosla, R. Gargeya, H. Irshad, and A. H. Beck. (2016). "Deep learning for identifying metastatic breast cancer." [Online]. Available: <https://arxiv.org/abs/1606.05718>
- [10]. B. E. Bejnordi et al., "Diagnostic assessment of deep learning algorithms for detection of lymph node metastases in women with breast cancer," *JAMA*, vol. 318, no. 22, pp. 2199-2210, Dec. 2017.
- [11]. B. E. Bejnordi et al., "Context-aware stacked convolutional neural networks for classification of breast carcinomas in whole-slide histopathology images," *J. Med. Imag.*, vol. 4, no. 4, p. 044504, 2017.

- [12]. A. Vahadane et al., "Structure-preserved color normalization for histological images," in Proc. IEEE 12th Int. Symp. Biomed. Imag. (ISBI), Apr. 2015, pp. 1012_1015.
- [13]. M. Macenko et al., "A method for normalizing histology slides for quantitative analysis," in Proc. IEEE Int. Symp. Biomed. Imag., Nano Macro (ISBI), Jun./Jul. 2009, pp. 1107_1110.
- [14]. E. Reinhard, M. Adhikhmin, P. Shirley, and B. Gooch, "Color transfer between images," IEEE Comput. Graph. Appl., vol. 21, no. 5, pp. 34_41, Sep./Oct. 2001.
- [15]. A. Pêgo and P. Aguiar. (2015). Bioimaging. [Online]. Available: <http://www.bioimaging2015.ineb.up.pt/datas/et.html>
- [16]. A. K. Mary. (2018). Breast Cancer. [Online]. Available: <https://www.merckmanuals.com/home/women-s-health-issues/breast-disorders/breast-cancer>
- [17]. K. He, X. Zhang, J. Sun, and S. Ren, "Deep residual learning for image recognition," in Proc. IEEE Conf. Comput. Vis. Pattern Recognit., 2016, pp. 770_778.
- [18]. K. He and J. Sun, "Convolutional neural networks at constrained time cost," in Proc. IEEE Conf. Comput. Vis. Pattern Recognit., Jun. 2015, pp. 5353_5360.
- [19]. Y. L. Boureau, J. Ponce, and Y. LeCun, "A theoretical analysis of feature pooling in visual recognition," in Proc. 27th Int. Conf. Mach. Learn.(ICML), 2010, pp. 111_118.
- [20]. J. Yosinski, J. Clune, H. Lipson, and Y. Bengio, "How transferable are features in deep neural networks?" in Proc. Adv. Neural Inf. Process. Syst., 2014, pp. 3320_3328.
- [21]. N. Tajbakhsh et al., "Convolutional neural networks for medical image analysis: Full training or _ne tuning?" IEEE Trans. Med. Imag., vol. 35, no. 5, pp. 1299_1312, May 2016.
- [22]. J. Deng, W. Dong, L.-J. Li, K. Li, L. Fei-Fei, and R. Socher, "ImageNet: A large-scale hierarchical image database," in Proc. IEEE Conf. Comput. Vis. Pattern Recognit., Jun. 2009, pp. 248_255.
- [23]. T. Araújo et al., "Classification of breast cancer histology images using convolutional neural networks," PLoS ONE, vol. 12, no. 6, p. e0177544, 2017.

AIR QUALITY ANALYSIS USING MACHINE LEARNING

¹Bitty Cleatus, ²Heeba Mouinuddin, ³Khushi Singh, ⁴Lakshmi Madhumitha P, ⁵Ms.Indu

¹Student, ²Student, ³ Student, ⁴ Student, ⁵Asst Professor

¹Information Science and Engineering

¹The Oxford College of Engineering, Bangalore,
India

Abstract: With the rapid development of urbanization and industrialization, many developing countries are suffering from heavy air pollution. Current air quality prediction methods mainly use shallow models; however, these methods produce unsatisfactory results. The three important topics involved in urban air computing are interpolation, prediction, and feature analysis of fine-gained air quality and the solutions to these topics can provide extremely useful information to support air pollution control, and consequently generate great societal and technical impacts. The related existing work solves the three problems separately by different models. The proposed approach utilizes the unlabelled spatio-temporal data to improve the performance of the interpolation and the prediction, and performs feature selection and association analysis, results reveals the variation in the air quality. This paper focuses on applicability of machine learning algorithms in operational conditions of air quality monitoring for predicting the daily peak concentration of a major photochemical pollutant from point measurements of a local monitoring station for the smaller places of the cities. The aim of the research reported here is the investigation of applicability of machine learning techniques for air quality forecasting in operational conditions.

Key Words: Interpolation, Prediction, Feature analysis, Air quality, Semi supervised learning, unlabelled spatio-temporal data.

I.INTRODUCTION

The interpolation, prediction, and feature analysis of fine-gained air quality are three important verticals of the area of urban air computing. Interpolation targets to solve the problem that there are limited air-quality-monitor-stations. A precise prediction provides valuable insight to protect humans from ill effect of the air pollution. A reasonable feature analysis provides details of the variation in the air quality.

There are several challenges for urban air computing as the related data have some special characteristics.

There are insufficient air-quality-monitor stations in a city due to the high cost of building and maintaining. Also, it is expensive to obtain labelled training samples for the fine-gained air quality.

There are lot of missing and incomplete data from the air-quality-monitor-stations. This could be because of the periodical maintenance, frequency of collection and other issues.

It's difficult to identify the kind of data that are relevant features for interpolation and prediction, and the key factors for environment departments to prevent and control air pollution. This is because there is not clearly accepted factor for the cause of air pollution. This paper addresses all these challenges by utilizing the information contained in the unlabelled data and the spatio-temporal data, and performing feature selection and association analysis for the urban air related data.

II.PROBLEM STATEMENT

The increase in the pollution, a smaller number of devices monitoring the air quality but forward various health hazards and poorly managed air pollution. The interpolation, prediction, and feature analysis of fine-gained air quality are three important verticals in the area of air pollution analysis. The solutions to these three verticals can provide extremely useful insight to support air pollution control, and consequently generate great societal and technical impacts. Most of the existing work solves the three problems separately by different models.

III. PROPOSED SYSTEM

The paper is motivated to address all these challenges by utilizing the information contained in the unlabelled data and the spatio-temporal data, and performing feature selection and association analysis for the urban air related data. Though labelled data are difficult or expensive to obtain, large amounts of unlabelled examples can often be gathered cheaply. In general, unlabelled data can help in providing information to better exploit the geometric structure of the data. Moreover, most of the urban air related data contain both space and time information.

The first step is determining a subset of the initial features is called feature selection. The selected features are expected to contain the relevant information from the input data, so that the desired task can be performed by using this reduced representation instead of the complete initial data.

The feature extraction starts from an initial set of measured data and builds derived values (features) intended to be informative and non-redundant, facilitating the subsequent learning and generalization steps.

When the input data to an algorithm is too large to be processed and it is suspected to be redundant, then it can be transformed into a reduced set of features.

The learning algorithm finds patterns in the training data that map the input data attributes to the target, and it outputs an ML model that captures these patterns. Once the build model is tested then we will pass real time data for the prediction. Once prediction is done then we will analyse the output to find out the crucial information.

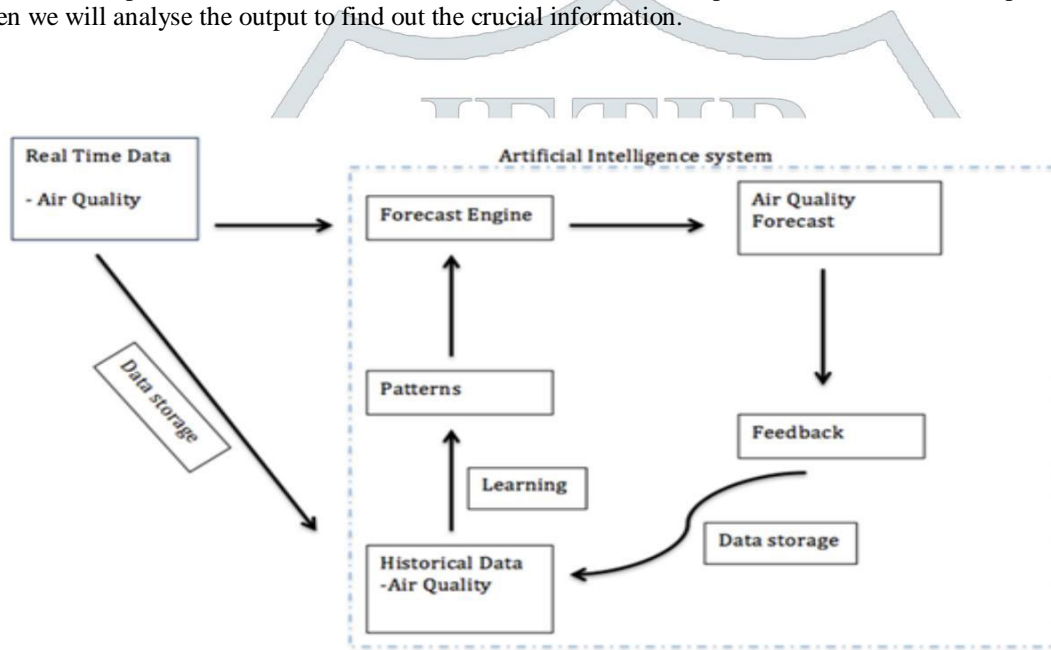


Fig: Design Consideration of the Proposed System

III. RESEARCH METHODOLOGY

3.1 Modules Description

Pre-processing of Captured Image

Real Time air quality data collection

The primary data collected from the online sources remains in the raw form of statements, digits and qualitative terms. The raw data contains error, omissions and inconsistencies. Various techniques have been incorporated for the pre-processing & cleaning of the raw data. Post the pre-processing of the raw data it is feed to forecast engine and persisted in Historical Data.

Forecast Engine

The forecast engine does the feature selection. The features extraction starts from an initial set of measured data and builds derived values (features) intended to be informative and non-redundant, facilitating the subsequent learning and generalization steps.

Air Quality Forecast

Based on the real time air quality data and model trained, this layer does the prediction. Once prediction is done then we will analyze the output to find out the crucial information.

Feedback

The prediction is further feedback and persisted to the historical data. This is later used by the Patterns module for the analysis and training of the Machine Learning model for the prediction.

Patterns

This module involves the training the model based on the historical data and feedback from the forecast engine. The learning algorithm finds patterns in the training data that map the input data attributes to the target, and it outputs an ML model that captures these patterns. The build model is further tested for the accuracy.

3.2 Result Analysis

In this section, the performance of the system is checked with respect to the real time air quality statistics collected.



Fig: Accuracy of a sample air quality data

The above pie chart depicts the accuracy of the proposed system in predicting the urban air quality.

3.3 Future Work

The current algorithm uses the Random forest algorithm for classification of the air quality. In future work, the artificial neural network can be implemented for the classification problem.

IV.CONCLUSION

In this project the three important topics in the area of urban air computing: the interpolation, prediction, and feature analysis of fine-grained air quality has been computed. The solutions to these topics can provide crucial information to support air pollution control, and consequently generate great societal and technical impacts. Most existing efforts focus on solving the three problems separately by establishing different models. In this paper, we develop a general and effective approach to unify the interpolation, prediction, feature selection and analysis of the fine-grained air quality into one model. In order to improve the performance of interpolation and prediction, we utilize the intrinsic characteristics of the spatio-temporal data and the information contained in the unlabeled data by embedding spatio-temporal semisupervised learning on the output layer of neural network.

V.ACKNOWLEDGMENT

The satisfaction and euphoria that accompany the successful completion of any task would be incomplete without the mention of people who made it possible whose constant guidance and encouragement crowned our effort with success. We would like to express our gratitude to Dr. Praveena Gowda, Principal, The Oxford College of Engineering for providing us a congenial environment and surrounding to work in. Our hearty thanks to Dr. R. Kanagavalli, Professor & Head, Department of Information Science and Engineering, The Oxford College of Engineering for her encouragement and support. Guidance and deadlines play a very important role in successful completion of the project report on time. We convey our gratitude to Ms. Indu K S, Assistant Professor, Department of Information Science and Engineering for having constantly monitored the completion of the Project Report and setting up precise deadlines. Finally a note of thanks to the Department of Information Science and Engineering, The Oxford College of Engineering, both teaching and non-teaching staff for their cooperation extended to us.

VI. REFERENCES

- [1] Zhongang Qi, Tianchun Wang, Guojie Song, Weisong Hu, Xi Li*, Zhongfei (Mark) Zhang “Deep Air Learning: Interpolation, Prediction, and Feature Analysis of Fine-grained Air Quality”, IEEE transactions on knowledge and data engineering 2018.
- [2] Hsun-Ping Hsieh, Shou-De Lin, Yu Zheng “Inferring Air Quality for Station Location Recommendation Based on Urban Big Data”, in Proceedings of the 21th ACM SIGKDD International Conference on Knowledge Discovery and Data Mining, ser. KDD '15, 2015, pp. 437– 446.
- [3] Dora Erdos, Vatche Ishakian, Andrei Lapets, Evimaria Terzi, Azer Bestavros “The Filter Placement Problem and its Application to Minimizing Information Multiplicity “, vol. 2, no. 1, pp. 1–127, 2009.
- [4] Lixin Li, Xingyou Zhang, James B.Holt, Jie Tian, Reinhard Piltner “Spatiotemporal Interpolation Methods for Air Pollution Exposure”, in Symposium on Abstraction, Reformulation, and Approximation, 2011.
- [5] David Hasenfratz, Olga Saukh, Silvan Sturzenegger, Lothar Thiele “Participatory Air Pollution Monitoring Using Smartphones”.
- [6] Dmytro Karamshuk, Anastasios Noulas, Salvatore Scellatu, Vincenzo Nicosia, Cecilia Mascolo “Geo-Spotting: Mining Online Location-based Services for Optimal Retail Store Placement”
- [7] Yu Zheng, Xiuwen Yi, Ming Li, Ruiyuan Li, Zhangqing Shan, Eric Chang, Tianrui Li “Forecasting fine grained air-quality based on big data”, in Proceedings of the 21th ACM SIGKDD International Conference on Knowledge Discovery and Data Mining, ser. KDD '15, 2015.
- [8] Salimol Thomas & Robert B. Jacko “Model for Forecasting Expressway Fine Particulate Matter and Carbon Monoxide Concentration: Application of Regression and Neural Network Models”
- [9] Yu Zheng, Furui Liu, Hsun-Ping Hsieh “U-Air- When Urban Air Quality Inference Meets Big Data”, in Proceedings of the 19th ACM SIGKDD International Conference on Knowledge Discovery and Data Mining, ser. KDD '13, 2013, pp. 1436–1444.



SMART ROBOTIC GARBAGE MANAGEMENT SYSTEM

¹Syed Mohomed Faizan, ²Aishwarya G Shenoy, ³Adiba Anjum, ⁴Ms. Kalaiselvi

¹Student, ²Student, ³Student, ⁴Assistant Professors

^{1,2,3,4} Information Science and Engineering

^{1,2,3,4} The Oxford College of Engineering, Bangalore, India

Abstract : “Swachh Bharat Abhiyaan” is a national campaign initiated by the Government of India, which covers 4,041 cities and towns, to clean the streets, roads and infrastructure of the country. The main motto of the mission is to cover all the rural and urban areas of the country. With increase in population, the scenario of cleanliness with respect to garbage management is degrading tremendously. The overflow of garbage in public areas creates the unhygienic condition in the nearby surrounding. It may provoke several serious diseases amongst the nearby people. It also degrades the valuation of the area. To avoid this and to enhance the cleaning, ‘**smart robotic garbage management system**’ is proposed. The proposed automated robotic dustbin can sense human being approaching towards it and opens the upper lid and alerts the user to use the dustbin. If the waste falls outside the dustbin it can sense and alert the user.

Index Terms -Image processing, Machine Learning, IOT, K Means Clustering Algorithm, Waste Management

I. INTRODUCTION

Waste management is a global issue but its consequences are more pronounced in developing countries. World is facing as well as enjoying Urbanization. In urban life waste is the major issue. How, where and when waste should be disposed is the burning issue. In India, solid waste management system has failed to keep pace with social and economic development in several regions. Solid waste management is one of the most challenging issues, which are facing a serious pollution problem due to the huge quantities of solid waste. The inefficiency in management of municipal solid waste can adversely affect public health, environment and our economy. Considering sustainability for the smart city concept, major issues faced by most of the smart cities will be enormous .

At various stage of Solid Waste Management process the problems which cities face today will be acute if not addressed in a smart manner due to the Urbanization pressure and its multifarious effects on the local as well as regional environment .The automated robotic smartbin can sense human being approaching towards it and opens the upper lid and alerts the user to use the smartbin. If the waste falls outside the smartbin it can sense and alert the user.

The automated robotic smartbin can segregate the wet and dry materials and put it in the respective chambers. Once a particular chamber is filled up the bottom lid opens up and dumps the waste in the lower part of the smartbin. The robotic smartbin comes with a HD camera that monitors the nearby area and processes the captured images and detects if any waste is there. If waste is detected the robotic smartbin moves towards it and picks it up.

Robotics is related to electronics, mechanics, and software technology. Today research on robotics is focused on developing systems which exhibit modularity, flexibility, redundancy, fault-tolerance. A general and extensible software environment and seamless connectivity to other machines are some of the characteristics some researchers focus on completely automating a manufacturing process or a task. Robots are normally designed by providing sensor based intelligence to the robot arm, while others try to solidify the analytical foundations on which many of the basic concepts in robotics are built.

II. PROBLEM STATEMENT

In our daily life we face many difficulties while moving on the streets, walking inside the park, walking on the roadside, market areas due to improper management of waste materials. Most of the time not only human beings even street dogs tend to scatter the waste because of which the diseases spread easily. Few reasons for this kind of situation are improper management of the waste material, improper adequate installation of the dustbin in various areas, as well as the untimely collection of waste which leads to unhygienic surroundings such as bad smell and spread of diseases. One more important cause is the inherent habit of the humans to dump the waste due to lack of dustbins in the neighborhood. This leads to decomposition of the waste for prolonged time leading to certain chemical reactions in the environment. Lack of knowledge about proper waste management.

While doing the research work and interviewing the common people and the government authorities associated with the garbage management (Municipal corporations) of various places, few very common things turned up : A nation always possess rules , regulations and technologies but the matter of grave concern is that the linking factor is missing, faithful following of duties by the officers and low grade workers is nowhere to be seen. Here arises a urgent need of developing a system which can handle the situation intelligently before it's too late. There is a tendency for accuracy to vary greatly as well as delay in readings. Those problems may be enlarged in real time applications.

An efficient waste management is a pre requisition for maintain a safe and green environment as there are increasing all kinds of waste disposal which is lacking in the environment. In most of the system, waste separation is done according to the type of the waste i.e. dry or wet. Similarly, the waste separation is done also on the basis of the type of garbage bin located at various locations. Over the last few decades, plenty of remedial ways were suggested dispensing with filled level detection of garbage vehicle, though it is still a tough challenge /arduous task. The detection of the fill-level for different garbage collection vehicle presents many difficulties due to the various irregularities of the bin-filling process, such as the irregular shape and the variety of the included materials .

PROPOSED SYSTEM

To solve the problems, IR, Ultrasonic Sensor, Camera and robotics technologies could be used to reduce cleaner's workload and assure a clean environment. The Camera can rotate and capture image. The captured image is processed and detect the waste product or material and put a laser light beam to it. The LDR follows the light and reach the waste material. The robotic smartbin can capture the waste and put it into the bin. The robotic smart bin can detect the dry and wet material put into it and dump it into the respective chamber.

III. RESEARCH METHODOLOGY

3.1 Modules Description

1. Controlling Lids

The robotic smartbin has two lids, one on the top and another in the bottom. When it detects that someone is approaching towards it, the upper lid of the smartbin opens up so that we can dump the waste inside the smartbin. When the upper chamber of the smartbin fills up with waste, the lower lid opens up and dumps all the waste into the lower chamber and sends a message to the care taker to clean the lower chamber. PIR sensor is used to detect the motion of the people coming to the garbage bin with trash while the bin is at full status and block adding of any more garbage to the bin through informing them by speaker. An individual PIR sensor detects changes in the amount of infrared radiation impinging upon it, which varies depending on the temperature and surface characteristics of the objects in front of the sensor. Objects of similar temperature but different surface characteristics may also have a different infrared emission pattern, and thus moving them with respect to the background may trigger the detector as well. When an object, such as a human, passes in front of the background, such as a wall, the temperature at that point in the sensor's field of view will rise from room temperature to body temperature, and then back again.

2. Segregate the wet and dry waste

There are two chambers (partitions) in the smartbin. One chamber is for wet waste and another one is for dry waste. When we dump waste into the smartbin, it can detect what type of the waste i.e. wet or dry. If wet waste is detected then the upper lid will rotate towards the wet chamber and dump the waste. If dry waste is detected then the upper lid will rotate towards the dry chamber and dump the waste. Moisture sensors measure the volumetric water content in the waste. The Moisture Sensor uses capacitance to measure dielectric permittivity of the surrounding medium. In waste, dielectric permittivity is a function of the water content. The sensor averages the water content over the entire length of the sensor. There is a 2 cm zone of influence with respect to the flat surface of the sensor, but it has little or no sensitivity at the extreme edges. Moisture sensors typically refer to sensors that estimate volumetric water content. The dielectric constant of a certain volume element around the sensor is obtained by measuring the speed of propagation along a buried transmission line. The moderator properties of water for neutrons are utilized to estimate waste moisture content between a source and detector probe. Measuring how strongly the waste resists the flow of electricity between two electrodes can be used to determine the waste moisture content. The amount of water present can be determined based on the voltage the waste produces because water acts as an electrolyte and produces electricity. The technology behind this concept is the galvanic cell.

3. Moving in a Path

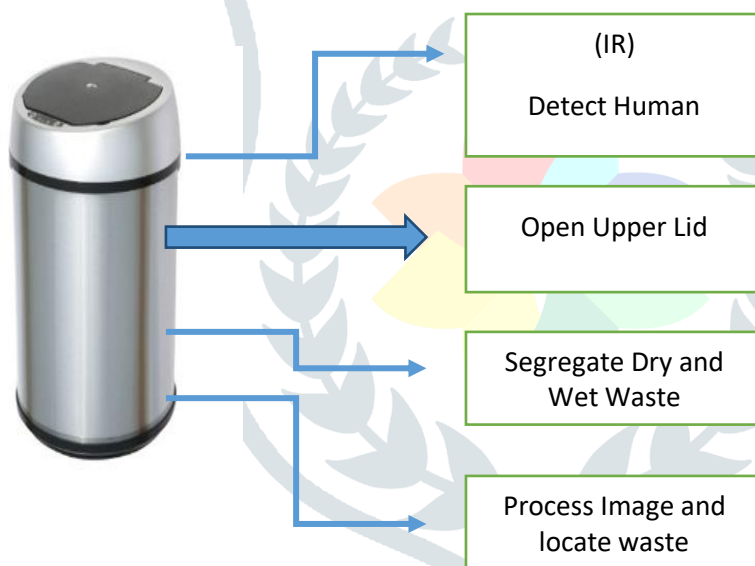
The robotic smartbin can move on the specified path in the park. On the move if it detects any obstacle then it stops, changes its direction and then continues moving. It helps us to get the smartbin near to us most of the time. A stepper motor or step motor or stepping motor is a brushless DC electric motor that divides a full rotation into a number of equal steps. The motor's position can then be commanded to move and hold at one of these steps without any position sensor for feedback (an open-loop controller), as long as the motor is carefully sized to the application in respect to torque and speed. Stepper motors effectively have multiple "toothed" electromagnets arranged around a central gear-shaped piece of iron. The main idea behind it is a programmable robotic vehicle with a dustbin having recyclable and non recyclable compartments on it. The bots can be placed on different designed locations in an area where they will behave as normal dustbin for collecting the waste, once the compartments of dustbin are full it will move to the dumping site by following a painted path and will return back to its location after dumping. The dumping of waste at the dumping sites can also be timed such that it matches with the time at which municipal waste collector vehicles will arrive at the dumping site to collect the waste (it can also have a default dumping time). The additional features such as proximity sensor that will open the dustbin lid automatically when someone try to put waste in the dustbin and some praising mechanism either a gesture or through some digital means will attract the public to use this dustbin. Moreover there are limitless additional features that can be added depending upon the place where the bot is being used.

4. Detect and collect waste

The smartbin is installed with a HD camera. While moving, it keeps on monitoring the surrounding and captures images. The captured image is processed and if any waste packets are detected, it targets the waste, moves towards it, picks up the waste packet and dumps inside it. Ultrasonic sensors measure distance by using ultrasonic waves. The sensor head emits an ultrasonic wave and receives the wave reflected back from the target. Ultrasonic Sensors measure the distance to the target by measuring the time between the emission and reception. An infrared sensor is an electronic device, that emits in order to sense some aspects of the surroundings. An IR sensor can measure the heat of an object as well as detects the motion. These types of sensors measures only infrared radiation, rather than emitting it that is called as a passive IR sensor.

5. Automatic alert

The smart bin has an additional functionality of updating the status of the bin. The smart bin is connected to an application through a Bluetooth device. The application has the capability of detecting the amount of waste filled in the smart bin. The ultrasonic sensor attached to the smart bin helps with this functionality. The application sends an alert to the user as well as the garbage collector as soon as the smartbin is filled. A notification prompt is sent to the registered mobile phone and the user can monitor the waste filled in the smart bin. Bluetooth is a wireless technology standard for exchanging data between fixed and mobile devices over short distances using short-wavelength UHF radio waves in the industrial, scientific and medical radio bands, from 2.400 to 2.485 GHz, and building personal area networks (PANs). Bluetooth is a packet-based protocol with a master/slave architecture. One master may communicate with up to seven slaves in a piconet. All devices share the master's clock. Packet exchange is based on the basic clock, defined by the master, which ticks at 312.5 μ s intervals. A master BR/EDR Bluetooth device can communicate with a maximum of seven devices in a piconet (an ad-hoc computer network using Bluetooth technology), though not all devices reach this maximum. The devices can switch roles, by agreement, and the slave can become the master. Android software development is the process by which new applications are created for devices running the Android operating system. Some languages/programming tools allow cross-platform app support, i.e. for both Android and iOS. Through the Bluetooth device, a notification prompt is sent to the mobile device and a message stating the smart bin is filled will be achieved. The garbage collector can hence come and pick up the waste.



IV. RESULT AND DISCUSSION

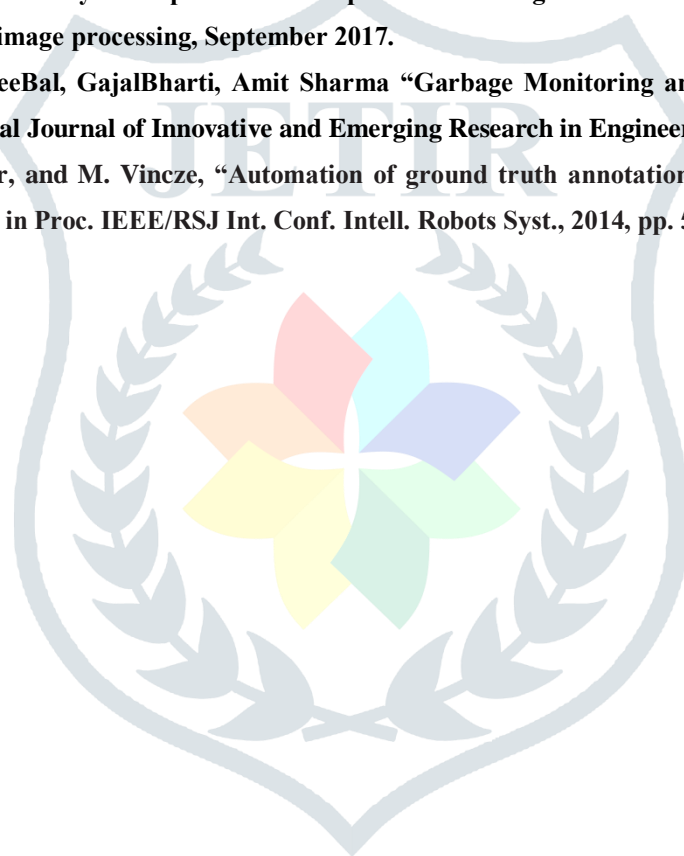
The system presents a parallel approach, based on robotics and image processing to construct a smart robotic garbage management system, with the aim of improving the cleanliness of the society. In this proposed system, IR, Ultrasonic Sensor, Camera and robotics technologies could be used to reduce cleaner's workload and assure a clean environment. The Camera installed to the smartbin can rotate and capture images. The captured image is processed and detect the waste product or material and put a laser light beam to it. The LDR follows the light and reach the waste material. The robotic smartbin can capture the waste and put it into the bin. The robotic smartbin can detect the dry and wet material put into it and dump it into the respective chamber. The accuracy is 90% and can enhanced in the future with more technology. This proposed model is a great step forward to clean the environment contributing towards the campaign "Swacch Bharat Abhiyan". It provides a smarter way of handling garbage by collecting and segregating the different types of wastes. There will be proper monitoring of workers and all the work is done in a systematic way. The automatic alert feature also avoids the unnecessary travel done by the workers to collect the waste. Thus, it is a good initiative towards #CleanIndia.

V.ACKNOWLEDGMENT

This proposed model is a great step forward to clean the environment contributing towards the campaign “Swacch Bharat Abhiyan”. It provides a smarter way of handling garbage by collecting and segregating the different types of wastes. There will be proper monitoring of workers and all the work is done in a systematic way. The automatic alert feature also avoids the unnecessary travel done by the workers to collect the waste. Thus, it is a good initiative towards #CleanIndia. Although there is a lot of up gradation in the way of handling the garbage, there are a few more improvements. The smartbin should be able to deviate its path when an obstacle comes in front of it which is a future work to be done. The smartbin should have a wider range of database in order to distinguish between various particles. Solar cells should be used for an even more efficient working.

REFERENCES

- [1] Hongliang Wang “Master Thesis RFID Guardian Back-end Security Protocol” IEEE Transactions on image processing, October 2018.
- [2] Suyog Gupta and Dr. Pradeep Kumar “Real Time Solid Waste Monitoring and Management System: A Case Study of Kanpur City”, International Journal of Science, Environment ISSN 2278-3687 (O) and Technology, Vol. 4, No 2, 2015.
- [3] Devang D Kapadia, Ashish Pandey “Prospects and Perspectives of Integrated Solid Waste Management in Smart Cities” IEEE Transactions on image processing, September 2017.
- [4] Nimmi Pandey, Shubhashree Bal, Gajal Bharti, Amit Sharma “Garbage Monitoring and Management using Sensors, RF- ID and GSM” International Journal of Innovative and Emerging Research in Engineering Volume 2, Issue 3, 2015.
- [5] A. Aldoma, T. Faulhammer, and M. Vincze, “Automation of ground truth annotation for multi-view RGB-D object instance recognition datasets,” in Proc. IEEE/RSJ Int. Conf. Intell. Robots Syst., 2014, pp. 5016–5023.



VIRTUALA – The Smart Glass

¹Mayuri Munnolimath, ²Saba Kausar, ³Shehza Hussain, ⁴Varsha Lokesh, ⁵Dr. R. Kanagavalli
^{1,2,3,4}Student, ⁵Head of department,
^{1,2,3,4,5}Department of Information Science and Engineering.
^{1,2,3,4,5}The Oxford College of Engineering, Bengaluru, India.

ABSTRACT: Virtuala is a new smart glass system for alzheimers patients. The glasses will be able to capture images through the HD camera already built-in on the glasses by using face recognition and the augmented reality information returns to the person wearing them. For instance, if any person is looking at an individual through these glasses then they could see their information on the display using led. There are two IR sensors on either sides of the device that help in gesture control. The Bluetooth and hotspot connectivity enables the device to display incoming calls and messages through the app installed in the users phone. This smart glass system can visualize the world for the blind, give voice instructions and hints through wireless bone conduction headphones This application can detect and recognize person's face and give corresponding voice hints to the blind. It also helps the user in receiving the call/ message and sends an alert to the user android application.

Key Words: Smart glass system, alzheimer, face recognition, voice hints.

I.INTRODUCTION

VR is in the business of creating a whole new world and transporting the user to them, AR is the phenomenon of supplementing the real world around us with computer-generated data. The main agenda of Project Glass augmented reality Head-Mounted Display (HMD) products would be the hands-free displaying of information that is vastly and currently available to most smart phone users Glasses will feature augmented reality and virtual reality. The glasses are basically wearable computers that will use the Android software that powers Android smart phones.



Fig.1 VR glasses

Augmented reality is the integration of digital information with the users environment in real time. It uses the existing environment and overlays the new information on top of it. The technology is used in many industries including healthcare, public safety, gas and oil, tourism and marketing.

PROBLEM STATEMENT

The problems identified in the already existing system are as that people with alzheimers disease suffer a lot every now and then as they cannot remember most of the things in their life. They cannot even remember their family members and friends. So because of that they need to put lots of pressure on their mind to recall their names and other details. They tend to forget events and people around them who play a very important role in their daily life. So there is a huge requirement of some standard technology to help them to remember their family members, friends or other things in their daily life.

PROPOSED SYSTEM

The glasses will help the Alzheimer patients in recognizing people around them, thus leading to the improvement of their health conduction. The glasses also reminds them about events related family, friends, doctors etc. The need for such a system was most required as it simplifies the patients needs and solves the problems on a daily basis.

II. RESEARCH METHODOLOGY

2.1 Module Description

MODULE 1: FACE DETECTION

VIOLA AND JONES' HAAR-LIKE FEATURES AND CASCADE CLASSIFIERS.

The typical cascade classifier is the very successful method of Viola and Jones for face detection [3-4]. Generally, many object detection tasks with rigid structure can be addressed by means of this method. The cascade classifier is a tree-based technology, in which Viola and Jones used Haar-like features for human face detection. The Haar-like features by default are shown in Figure 2, which can be used in the detection of the face once the image is captured.

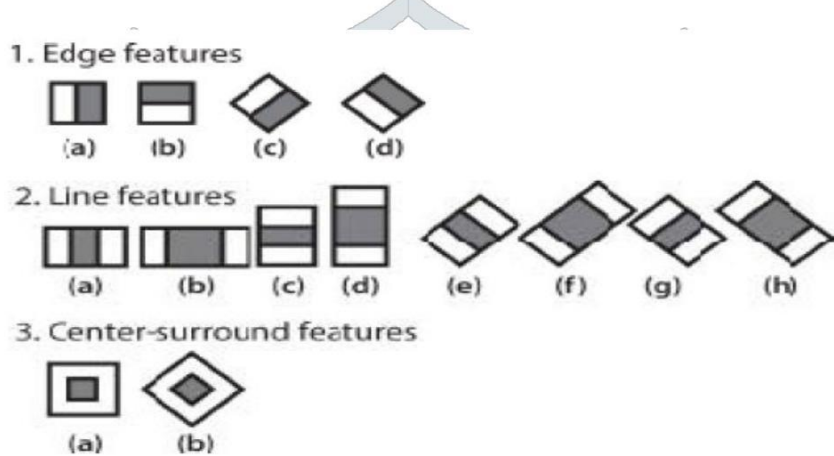


Fig.2 Haar-like features from the OpenCV source distribution

The Viola-Jones' detector uses AdaBoost, called a rejection cascade, which is a series of nodes, with each node being a definite multi-tree AdaBoosted classifier.

Fig 3 shows the Viola-Jones' rejection cascade, composed of many boosted classifier groups of decision trees trained on the features from faces and non-faces or other training objects to be detected.

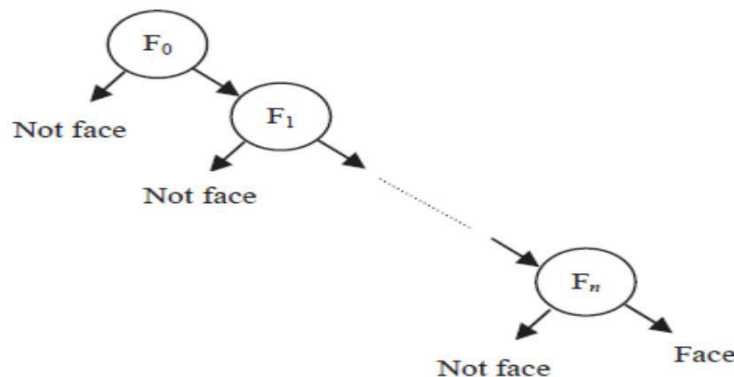


Fig.3 Rejection cascade by Viola-Jones

Each node being a multi-tree of boosted classifiers trained in such a way that almost all non-faces are rejected at the last node nearly without missing a real human face.

B. Color Model HSV and histogram matching

The HSV color model is an ideal tool for developing image processing algorithms based on color descriptions, which are natural and intuitive to human observers of images. The HSV model decouples the intensity (V) from color dimensions, hue (H) and saturation (S). After the RGB-HSV transform, hue is a color attribute that tells the observer what color is perceived (pure yellow, green, or red). For people of a specific race, for instance yellow race, the face skin color follows specific distribution, which does not change a lot under different light conditions according to principle of color constancy. Thus the hue is a relatively robust feature that carries skin tone information.

C. Eyes detection and mouth detection within a human face candidate

By means of Haar-like features and taking the advantage of conception of cascade classifiers, one can design and implement eyes and mouth detections. Similarly to rejection cascade for human face, the classifiers for eyes and mouth detections are used as weak classifiers, making the whole classification system stronger.

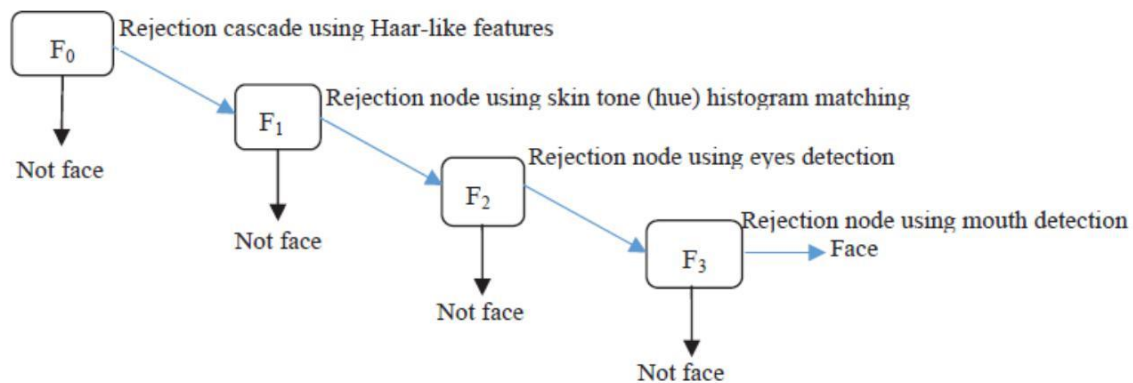


Fig.4 Proposed framework of human face detection cascade

Note 1: Training for obtaining prototype of skin hue histogram

The proposed human face detection is implemented with the help of OpenCV. However, at the stage of skin hue histogram matching, the prototype of histogram should be obtained before the test phase of human face detection.

Note 2: Implementation of initial face detection

The block F0 is itself a cascade of classifiers using Haar-like features. The cascade classifier supplied OpenCV will be used, so it needs not additional training in the work.

Note 3: Implementation of eyes and mouth detections

The eyes and mouth detections are also implemented by calling modules in OpenCV, so it needs not a training process before the stage of test either. The histogram matching means comparison of two histograms so as to measure the difference between a human face candidate's skin hue histogram and the prototype of hue histogram of training (real) human faces.

MODULE 2: FACE RECOGNITION

PRINCIPAL COMPONENT ANALYSIS

Principal Component Analysis, or PCA, is a statistical method used to reduce the number of variables in a dataset. It does so by lumping highly correlated variables together. Naturally, this comes at the expense of accuracy. However, if you have 50 variables and realize that 40 of them are highly correlated, you will gladly trade a little accuracy for simplicity. Suppose there are two variables:

1. Dow Jones Industrial Average, or DJIA, a stock market index that constitutes 30 of America's biggest companies, such as Hewlett Packard and Boeing.
2. S&P 500 index, a similar aggregate of 500 stocks of large American-listed companies. It contains many of the companies that the DJIA comprises.

Step 1 – Standardize: Standardize the scale of the data. I have already done this, by transforming the data into daily % change. Now, both DJIA and S&P data occur on a 0-100 scale.

Step 2 – Calculate covariance: Find the covariance matrix for the data. As a reminder, the covariance between DJIA and S&P – $\text{Cov}(\text{DJIA}, \text{S\&P})$ or equivalently, $\text{Cov}(\text{DJIA}, \text{S\&P})$ – is a measure of how the two variables move together.

Step 3 – Deduce eigens: The above points are represented in 2 axes: X and Y. In theory, PCA will allow us to represent the data along one axis. This axis will be called the principal component, and is represented by the black line.

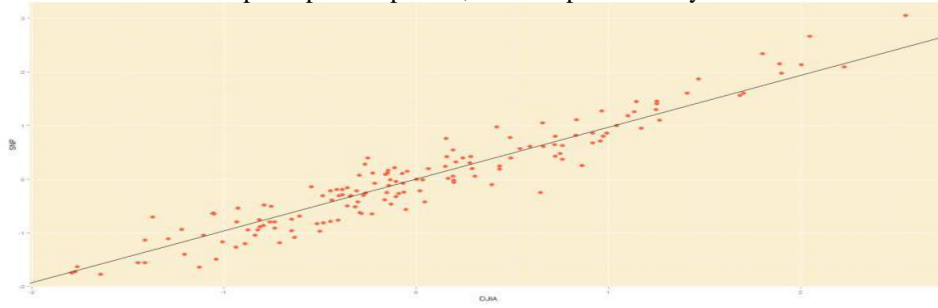


Fig.5 Deduce eigens

To convert the data into the new axes, multiply the original DJIA, S&P data by eigenvectors, which indicate the direction of the new axes (principal components).

Step 4 – Re-orient data: Since the eigenvectors indicates the direction of the principal components (new axes), we will multiply the original data by the eigenvectors to re-orient our data onto the new axes. This re-oriented data is called a score.

Step 5 – Plot re-oriented data:

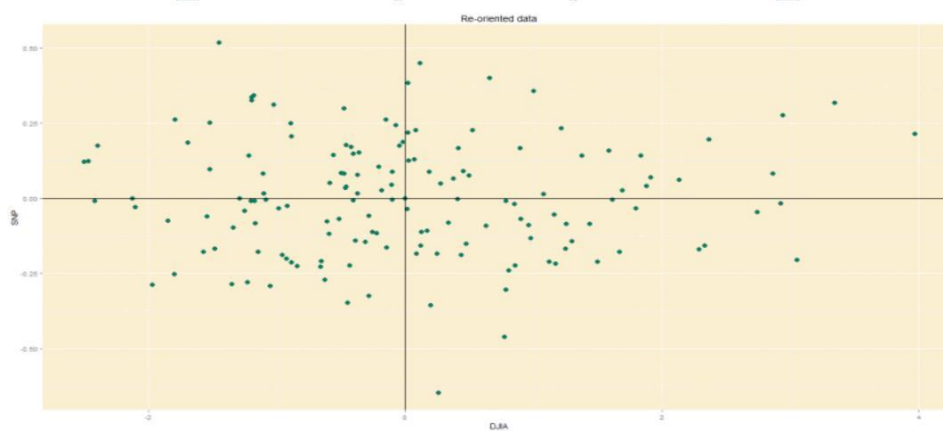


Fig.6 Plot re-oriented data

Step 6 – Bi-plot: A PCA would not be complete without a bi-plot. This is basically the plot above, except the axes are standardized on the same scale, and arrows are added to depict the original variables, lest we forget.

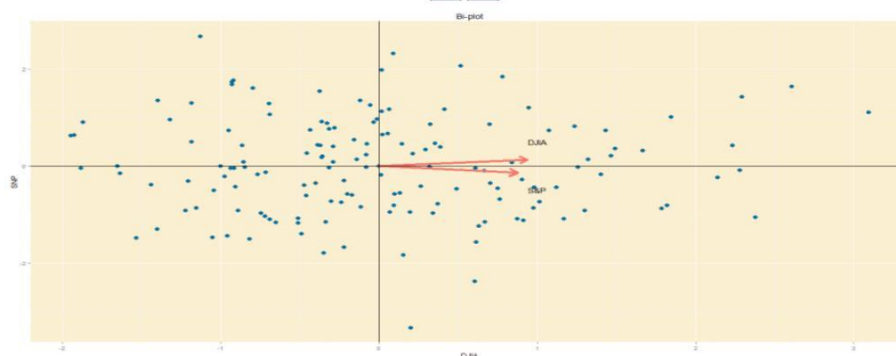


Fig.7 Bi plot

Axes: In this bi-plot, the X and Y axes are the principal components.

Points: These are the DJIA and S&P points, re-oriented to the new axes.

Arrows: The arrows point in the direction of increasing values for each original variable. For example, points in the top right quadrant will have higher DJIA readings than points in the bottom left quadrant. The closeness of the arrows means that the two variables are highly correlated.

2.2 Result Analysis

The server for the admin for adding the images is shown in Figure 8, where a persons image with name, mobile no and relationship is added. This image is later used for comparison.

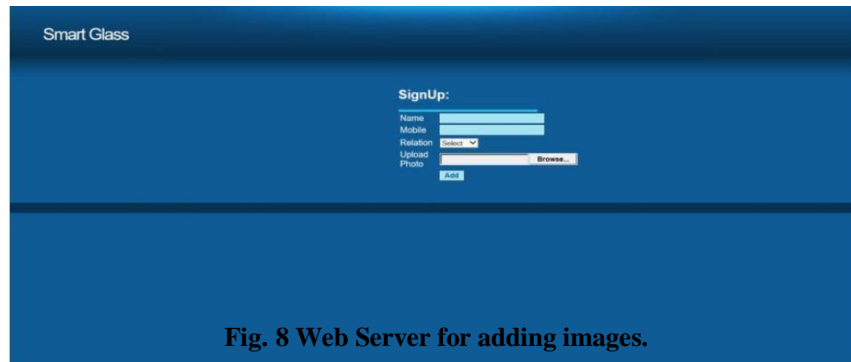


Fig. 8 Web Server for adding images.

The pi camera mounted the glasses captures the image of the person and with the help of haar cascade which is used for the face detection the system prompts that a face has been detected, the captured image is converted into grey scale as shown in the Figure 9, for the detection processed image to now be recognized.

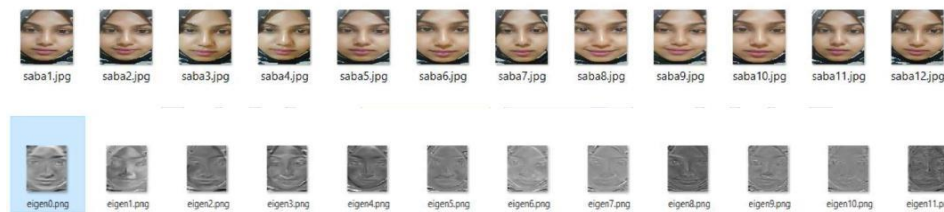


Fig.9 Conversion of captured images into eigens

Once the image has been detected it is now recognized with the help of PCA which is the method used for face recognition, the captured image is compared with the images stored in the server and the result is shown with the name of the person whose face matches the captured image. The glasses also features the incoming calls and messages on the display, this is achieved with the app installed in persons phone, the glasses are connected via hotspot to the phone, the app for call and messages is shown in the Figure 10.

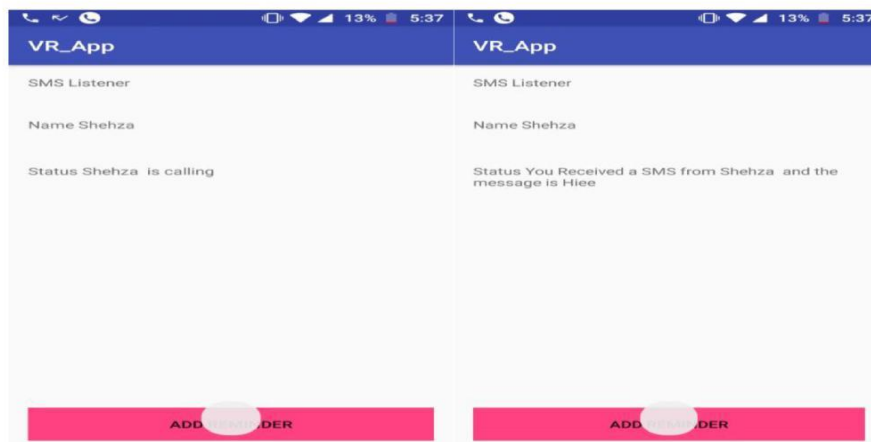


Fig.10 App for calls and messages

The incoming calls and messages are shown on the display of the glass successfully, which is shown in the figure 11. The glasses also display reminders of events thereby helping the alzheimers patients in remembering important events.

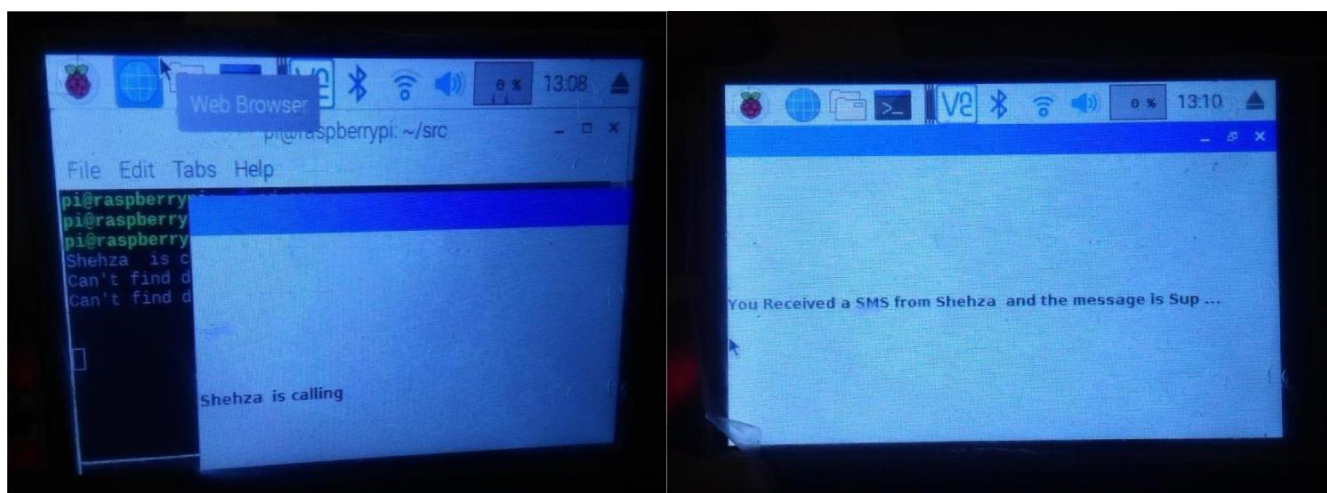


Fig 11 Display of incoming calls and messages

Thus the wearable glasses help the alzheimers patients in their day to day life making their lives simpler by reminding them of the events, being able to recognise the faces of the people around them like their family, friends , doctors etc. This makes the entire system a great help for patients.

2.3 Future Work

The device can be further optimized to fit the users needs, by improving the structure and the architecture of the system. The system could be more compact for it to be handled in a convenient manner. The glasses can be made according the eye sight of the person wearing it. Thus, improving the system features and capabilities.

III.CONCLUSION

The project aims at serving the Alzheimer patients who face a lot of issues in the everyday life. The disease is such that it gets inevitable for them to carry out their daily chores smoothly such as remembering their family and friends faces, time to meet their doctors and take medicines. These problems are made easy with the device designed. It helps them remember their family members and friends. It also reminds them about taking the medicines and appointment with the doctors. It displays the incoming calls and messages through the Bluetooth.

IV.ACKNOWLEDGMENT

The satisfaction and euphoria that accompany the successful completion of any task would be incomplete without the mention of people who made it possible whose constant guidance and encouragement crowned our effort with success. We would like to express our gratitude to Dr. Praveena Gowda, Principal, The Oxford College of Engineering for providing us a congenial environment and surrounding to work in. Our hearty thanks to Dr. R. Kanagavalli, Professor & Head, Department of Information Science and Engineering, The Oxford College of Engineering for her encouragement and support. Guidance and deadlines play a very important role in successful completion of the project report on time. We convey our gratitude to Dr. R. Kanagavalli, Professor & Head, Department of Information Science and Engineering for having constantly monitored the completion of the Project Report and setting up precise deadlines. Finally a note of thanks to the Department of Information Science and Engineering, The Oxford College of Engineering, both teaching and non-teaching staff for their cooperation extended to us.

REFERENCES

- [1] Feng Lan, Guangtao Zhai and Wei Lin “Lightweight Smart Glass System with Audio Aid for Visually Impaired People.”
- [2] Rajashree Tripathy, R N Daschoudhury “Real-time Face Detection and Tracking Using Haar Classifier on SoC.”
- [3] Nanoka Sumi and Vasily Moshnyaga, “A Novel Face Recognition for Smart Glasses,”
- [4] Rodney E. Peters, Richard Pak & Gregory D. Abowd , “Finding Lost Objects: Informing the Design of Ubiquitous Computing Services for the Home,”.
- [5] Hermann Schweizer, “ Smart glasses: technology and applications,”
- [6]Christian Frank, Philipp Bolliger , Christof Rounder and Wolfgang Keller, “Objects calling home locating objects using mobile phones”
- [7]Shervin EMAMI,Valentin Petrut SUCIU, “Facial Recognition using openCV,”.
- [8]P.Viola,M.Jones, Rapid Object Detection Using a Boosted Cascade of Simple Features,IEEE conf.comp.Vision & Pattern Recognition , 2001.
- [9]Andera Colaco et al.Mime: compact,low powder 3D gesture sensing for interaction with head mouted displays. In proceeding of the 26th annual ACM symposium on User interface software and technology (USIT’ 13)
- [10] P.Viola and M Jones , “Rapid object detection using a boosted classifier of simple features ”, In Proceedings of IEEE Conference on Computer Vision and Pattern Recognition, 2001,vol 1,pp.511-518



SOURCE CODE GENERATOR USING SPEECH

¹Akshata V Kulkarni, ²Deekshitha R, ³Fanoos Fathima, ⁴Dr. R.Kanagavalli

^{1,2,3,4}Department of Information Science and Engineering,

^{1,2,3,4}The Oxford College of Engineering, Bengaluru, India

ABSTRACT: Researchers have shown that most effort of today's software development is maintenance and evolution. Developers often use integrated development environments, debuggers and tools for code search, testing, and program understanding to reduce the tedious tasks. Interaction with software development environments can be frustrating for the growing numbers of developers who suffer from repetitive strain injuries (RSI) and other disabilities that make typing difficult or impossible. Speech interfaces can be used to help developers reduce their dependence on typing, reducing the onset of RSI among computer users, and increasing access for those who already have motor disabilities. We have proposed a system to generate code automatically based on speech. The speech input is processed and based on that the code will be automatically generated.

Key Words: Speech to text, code generation, mapping the text, Speech Interface

I.INTRODUCTION

Speech Recognition, it is the ability of the machine or program to evaluate word, idiom or a sentence in spoken expression and convert those words into a machine readable format. The more sophisticated software has the ability to obtain natural language as well. Speech recognition works using algorithms through acoustic and language modeling. In addition, acoustic modeling represents the link between linguistic units of speech and audio signals; whereas language modeling matches sound with string to help categorize between words that sound similar. Additionally, Hidden Markov Models are used as well to make materialistic patterns in a speech to enhance accuracy with the system. Furthermore, it is seen that a person working on a computer cannot work or type for longer duration because if they can then there will be an issue of back or wrist pain that will be pernicious for the human body, but it can be avoided easily by switching from typing to speaking whenever needed. Research has shown that more than 60% of software engineering resources are spent on maintenance. Software maintenance is the process of modifying a software system after delivery to fix bugs, improve performance, or adapt to a changing environment. Software maintenance requires code comprehension, as reading and understanding source code is the prerequisites of any modification. Program comprehension is time-consuming and cost most of developers' time.

II.PROBLEM STATEMENT

Code Generation techniques depends on textual documentation which are highly prone to syntactical errors. Manually defining every programming construct is tedious and time consuming. There is a lack of flexibility and efficiency of software developers.

PROPOSED SYSTEM

The proposed system helps in generating the source code and also compiling the code to check for various errors and bugs, which helps in reducing the time taken to code by the developers. The proposed system allows the user to be able to generate the syntax of various inputs that helps reduce the time taken for developing a project. Speech to text conversion is done using an android app. Process the text using NLP by using NLP server. The text generated is mapped with the corresponding instructions. Finally, generated code is added in the appropriate part of the program.

Advantages:

- Easy to code
- Less time for the development phase
- Cost efficient
- Bug-free code
- Programming-by-voice can enable motor-impaired software engineers to program, albeit at reduced efficiency compared to an unimpaired programmer.



Fig: System Architecture of the proposed system

III. RESEARCH METHODOLOGY

3.1 Modules Description

Speech Processing:

The speech input is processed using Google API and is converted into text. The generated text is then sent to the Tomcat server and further sent to the NLP server.

The communication between the Android app and the Tomcat server is done using HTTP protocol. The user can work on multiple projects from the same app. Based on the selected project, the app sends the request to the web server and the server on receiving the request starts the respective project.

NLP Server

The NLP server starts listening on a particular port number. Once the server receives a request from the user, it sends the instruction to the NLP server to process it. Once NLP server receives the input from the web server, it processes the input to find out the part of the speech. Based on the process input, it starts the next process that is mapping. If there is no pre-defined command, it invokes the machine learning algorithm like naïve based classification and finds the appropriate command.

A white point is a set of values or that serve to define the color "white" in image capture, encoding, or reproduction. It is used to calculate the traffic density by comparing the number of white pixels to the number of black pixels. This gives an estimation of the traffic density in the lane.

Mapping:

Once the mapping process is invoked, it tries to map the input with the predefined instructions. If it finds exactly the matched instruction, it adds the code segment into the project or to a respective class. As we are handling object oriented programming, user has simple and easy-to-use instructions and the details are found in the app itself.

For example:-

a) If the user wants to create a new class he/she can just say "create a class" then the mapper will send the instruction to the server to ask for the name of the class. User can tell the name of the class and based on that, the mapper will create a class with the given name. If a class with the same name is already present in the same package of the project, then server will not create any class for it and sends the notification to the user.

b) if the user gives the input like, “create a method with the name ‘xyz’ with no return type” then the app sends the instruction to the server to create a method with the name xyz which does not return any type and server adds it in the current class.

Like this, the user can create different types of methods with parameters or without parameters, with different return types. The mapper is capable of handling few features of object oriented programming like creating a class, handling inheritance and polymorphism, different logic like- if else, for loop, while loop, do-while loop and many more.

The structural setup methodology is wired with working up a fundamental essential framework for a system. It incorporates perceiving the genuine parts of the structure and exchanges between these fragments. The starting design technique of perceiving these subsystems and working up a structure for subsystem control and correspondence is called development demonstrating plot and the yield of this framework method is a depiction of the item basic arranging. The proposed design for this framework is given beneath. It demonstrates the way this framework is outlined and brief working of the framework.

3.2 Result Analysis

In this section, we discuss the time taken for the development time of source codes. The development time has been readily decreased with the use of speech as input. The dataset required for the code generation is mapped to a dictionary for speech recognition. The dataset contains readily available syntaxes that are required for the code generation and hence the time consumed is considerably decreased. The syntax is automatically generated and the corresponding packages that are needed for the java programming is also called. Bug free source codes can thus be generated by using this system.

3.3 Future Work

Since the system developed uses only one programming language and the generation of only that language’s code/syntax is done. In the future work, we can integrate multiple programming languages and their functionalities. Java may also contain ambiguity with respect to variables and the interfaces used in the programs which creates a limitation for automatically generate the code.

IV.CONCLUSION

Speech-based programming also may provide insight into better forms of high-level interaction. With more study, different user interface designs, and better analysis, software developers will one day be able to use speech-based programming to compete effectively in the workforce. The system will be able to add pre-defined logic automatically. The proposed application will be able to generate code based on speech as an input by recognizing the speech, converting to text and then map it to the pre-defined code and thus ad the corresponding code.

V.ACKNOWLEDGMENT

The satisfaction and euphoria that accompany the successful completion of any task would be incomplete without the mention of people who made it possible whose constant guidance and encouragement crowned our effort with success. We would like to express our gratitude to Dr. Praveena Gowda, Principal, The Oxford College of Engineering for providing us a congenial environment and surrounding to work in. Our hearty thanks to Dr. R. Kanagavalli, Professor & Head, Department of Information Science and Engineering, The Oxford College of Engineering for her encouragement and support. Guidance and deadlines play a very important role in successful completion of the project report on time. We convey our gratitude to Dr. R. Kanagavalli, Professor & Head, Department of Information Science and Engineering for having constantly monitored the completion of the Project Report and setting up precise deadlines. Finally a note of thanks to the Department of Information Science and Engineering, The Oxford College of Engineering, both teaching and non-teaching staff for their cooperation extended to us.

REFERENCES

- [1] Juan Zhai, Lin Tan, Feng Qin-Automatic Model Generation from Documentation for Java API Functions.978-1-4503-3900-1/16/05...\$15.00©2016 IEEE
- [2] Kaveendra Lunuwilage, Thelijjagoda ,Sameera Abeysekara -Web Based Programming Tool with Speech Recognition for Visually Impaired Users.978-1-5386-4602-1/17/\$31.00©2017 IEEE
- [3] Fagui Mao,Xuyang Cai,Beijun Shen,Yong Xia-Operational Pattern Based Code Generation for Management Information System: An Industrial Case Study.978-1-5090-2239-7/16/\$31.00 copyright 2016 IEEE
- [4] Lutfi Kerem Senel, Ihsan Utlu ,Veysel Yucesoy.-Semantic Structure and Interpretability of Word Embeddings.2329-9290©2018 IEEE
- [5] Takafumi Moriya, Tomohiro Tanaka-Evolution- Strategy-based Automation of System Development for High-Performance Speech Recognition. 2329-9290 © 2018 IEEE
- [6] Shahab Nadir, Prof. Detlef Streitferdt -Software code generator in automotive field 978-1-4673-9795-7/15 \$31.00 © 2015 IEEE
- [7] Victor Guana, Eleni Stroulia-ChainTracker: Towards a Comprehensive Tool for Building Code-Generation Environments. 1063-6773/14 \$31.00 © 2014 IEEE
- [8] GlotNet—A Raw Waveform Model for the Glottal Excitation in Statistical Parametric SpeechSynthesis
Lauri Juvela ; Bajibabu Bollepalli ; Vassilis Tsiaras ; Paavo Alku
- [9] An Efficient Framework for Sentence Similarity Modeling Zhe Quan ; Zhi-Jie Wang ; Yuquan Le ; Bin Yao ; Kenli Li ; Jian Yin
- [10] Semantic Speech Retrieval With a Visually Grounded Model of Untranscribed Speech Herman Kamper ; Gregory Shakhnarovich ; Karen Livescu IEEE/ACM Transactions on Audio, Speech, and Language Processing



A NOVEL TRAFFIC MANAGEMENT SYSTEM USING CANNY EDGE DETECTION

¹Ankit Kumar Mishra, ²Austin Emmanuel T, ³Jayashree S, ⁴Ms P Kokila

¹Student, ²Student, ³Student, ⁴Assistant Professors

^{1,2,3,4}Information Science and Engineering

^{1,2,3,4}The Oxford College of Engineering, Bangalore, India

Abstract: Currently the traffic control system in place in our country is non-flexible and non-adaptive to the ever-growing number of vehicles on the road. It does not take into account the changing traffic density during the different hours of the day. Consequently, the roads get congested frequently and intersections get blocked. Time and fuel, two highly important resources are wasted in this inefficient working of the present-day system. This system proposes a dynamic system that overcomes all these drawbacks. The Proposed system uses cameras installed at the red lights and intersections to monitor the traffic dynamically and then processes this information using image processing, computes the volume of the real time traffic, sets the timer of the signal accordingly. The system uses Canny Edge Detection algorithm to effectively calculate the traffic density and uses Arduino board and OpenCV to control traffic signals. The system also monitors if there is any scope of congestion at the intersection and adjusts the timer to prevent it. The entire system works autonomously and has a quick turnaround time, saving critical resources at every junction.

Keywords: Image Processing, Canny Edge Detection Algorithm, Traffic density, Traffic control system

I. INTRODUCTION

As the population of the modern cities is increasing day by day, vehicular travel is increasing which is leading to congestion problem. Traffic congestion has been causing many critical problems and challenges in the major and most populated cities. Due to this traffic congestion there is more wastage of time. The steady increase in the number of automobiles on the road has amplified the importance of managing traffic flow efficiently to optimize utilization of existing road capacity. High fuel cost and environmental concerns also provide important incentives for minimizing traffic delays. The system is intended to overcome the drawbacks, which are there in the existing systems implemented until now for the traffic management system. This system uses cameras installed at intersections to monitor traffic dynamically. It then processes the extracted information using an algorithm called Canny Edge Detection, computes the volume of traffic and sets the timer of the signal accordingly. Canny Edge Detection is the best algorithm to detect the vehicles because it uses multi-stage algorithm to detect the captured images. It also monitors the scope of congestion at the intersection and adjusts the timer to prevent it. The entire system works autonomously and has a quick turnaround time, saving critical resources at every junction.

Traffic congestion is a serious issue. In the existing system, signal times are fixed and it does not depend on the density of traffic. Large red light delays lead to traffic congestion. In this paper, a traffic control system is implemented in which signal timings are updated based on the traffic density. The system is using OpenCV and Arduino. Image processing of traffic video is done in OpenCV. The system uses Canny Edge Detection technique to compute the traffic density.

II. PROBLEM STATEMENT

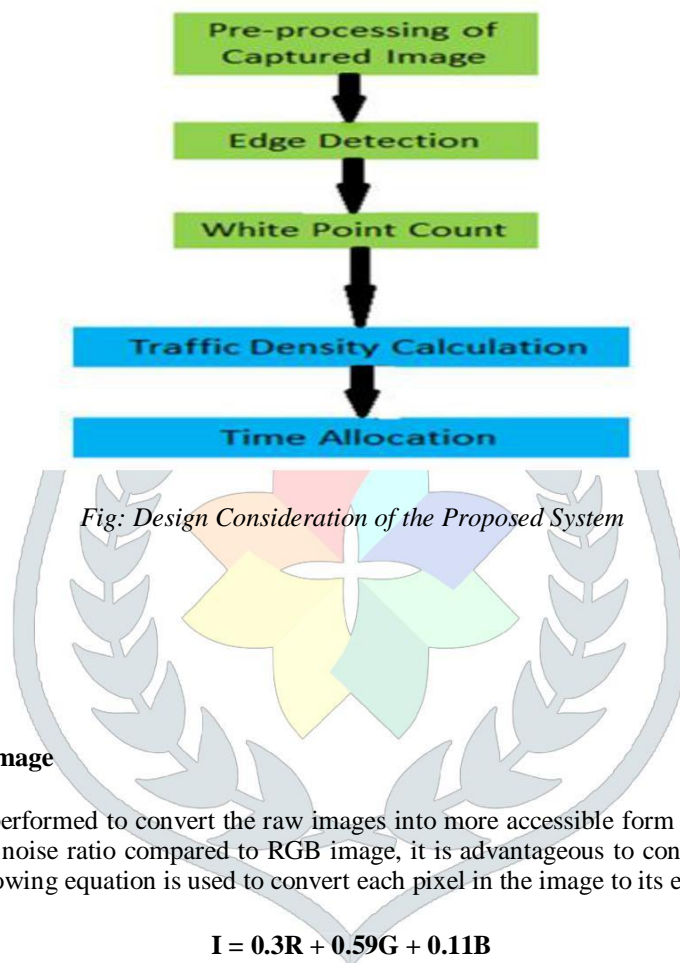
With increase in the number of vehicles on the road today causes traffic congestion near junctions. The main effect of this matter is lot of time of the people is wasted on the road itself. At certain times in junctions, sometimes even if there is no traffic, people have to wait, because the traffic light remains red for the present time period, the road users should wait until the light turns to green. The present traffic control is not dynamic and predefined which does not relay on present traffic.

PROPOSED SYSTEM

The proposed system helps in changing the traffic lights dynamically, which helps in reducing the congestion of the traffic and more importantly, allows smooth functioning of the traffic. The proposed system changes RGB images to Gray-Scale images for further processing. Canny Edge Detection Algorithm is used for the edge detection. Images are smoothed by applying Gaussian filter. At last, with the help of white point count, the density of the traffic is calculated for various lanes, which helps in varying the time of the traffic signals.

Advantages:

- It reduces the manpower required to operate the traffic signals.
- It reduces the need for additional hardware that might incur extra cost.
- Use faster algorithms that will not delay the system when used in real time.
- Dynamic traffic signal times to regulate traffic based on traffic density.



III. RESEARCH METHODOLOGY

3.1 Modules Description

Pre-processing of Captured Image

Image pre-processing is performed to convert the raw images into more accessible form for edge detection. As Gray scale images have superior signal to noise ratio compared to RGB image, it is advantageous to convert RGB images into Gray scale for further processing. The following equation is used to convert each pixel in the image to its equivalent Gray scale form:

$$I = 0.3R + 0.59G + 0.11B$$

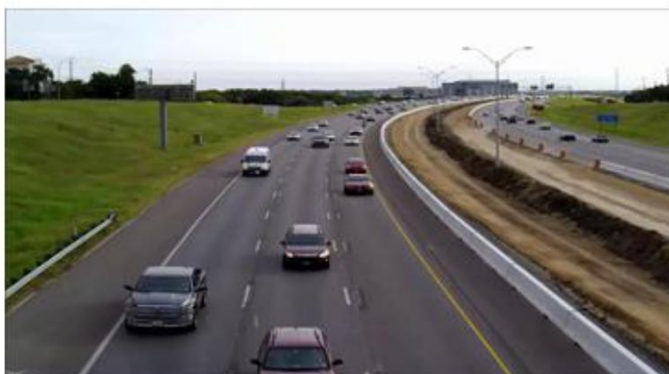


Fig: RGB to Gray Scale Image Conversion

Edge Detection

Edge detection is used to identify distinct shapes. It is used for isolating different shapes of the vehicles from rest of the image. After comparing different edge detectors, Canny Edge Detector is found to be most suitable for this application. Images are smoothed by applying Gaussian filter to reduce unwanted texture and details.

The Canny Edge Detection algorithm can be broken down into the five following steps:

- Apply Gaussian filter to smoothen the image in order to remove the noise
- Find the intensity gradients of the image
- Apply non-maximum suppression to get rid of spurious response to edge detection
- Apply double threshold to determine potential edges

- Track edge by hysteresis: Finalize the detection of edges by suppressing all the other edges that are weak and not connected to strong edges

The Canny algorithm contains a number of adjustable parameters, which can affect the computation time and effectiveness of the algorithm.

- The size of the Gaussian filter: the smoothing filter used in the first stage directly affects the results of the Canny algorithm. Smaller filters cause less blurring, and allow detection of small, sharp lines. A larger filter causes more blurring, smearing out the value of a given pixel over a larger area of the image. Larger blurring radii are more useful for detecting larger, smoother edges – for instance, the edge of a rainbow.
- Thresholds: the use of two thresholds with hysteresis allows more flexibility than in a single-threshold approach, but general problems of thresholding approaches still apply. A threshold set too high can miss important information. On the other hand, a threshold set too low will falsely identify irrelevant information (such as noise) as important. It is difficult to give a generic threshold that works well on all images. No tried and tested approach to this problem yet exists.

White Point Count

A white point is a set of values or that serve to define the color "white" in image capture, encoding, or reproduction. It is used to calculate the traffic density by comparing the number of white pixels to the number of black pixels. This gives an estimation of the traffic density in the lane.



White point count: 61659 pixels



White point count: 13302 pixels

Time allocation

Time allocation is done based upon the white point count of the traffic on the road at that particular time. The number of white pixels of the edge detected image and total number of pixels gives the density percentage.

$$\% \text{density} = \frac{\text{No. of white pixels}}{\text{Total no. of pixels}}$$

- If the density is between 0 to 10% - green light is on for 10 seconds.
- If the density is between 10 to 50% - green light is on for 30 seconds.
- If the density is between 50 to 70% - green light is on for 40 seconds.
- If the density is between 70 to 90% - green light is on for 60 seconds.
- If the density is between 90 to 100% - green light is on for 90 seconds.

Arduino-Python Interfacing

The system is based on OpenCV and Arduino. Camera captures the video. It is send to PC and opencv is used for image processing. It also consists of Arduino which controls the signal timings to which LED's are connected. The entire algorithm for image processing is implemented in OpenCV. The hardware interface of Arduino is interfaced to OpenCV is through pyserial Software. After interfacing, density calculated is used to allocate time for the lanes. LEDs of each lane connected to Arduino glow based on time allocated.

Configuring LED

LED's is used to represent the traffic signal of each traffic lane . Two arrays of LEDs with each array encompassing a red and a green LED for two lanes. Python programming language is used for image processing and Arduino development board is used to control the LEDs. The inputs of these LEDs are connected to the digital I/O pins of the Arduino. All of the pins have common ground connected to the ground of Arduino. LEDs are controlled by the output pins of the Arduino, which are controlled by the time, allocated to each consecutive lane.

3.2 Result Analysis

In this section, the performance of the system is checked with respect to White Point Count, calculation of the Traffic Density and glowing of LEDs with respect to Arduino-Python interfacing after the Time Allocation. The Time Allocation for various lanes is accurate and it helps in performing the traffic control smoothly suggests the proposed system to be an efficient solution. The proposed system helps in reducing manpower required to operate the traffic signals. It reduces the need for additional hardware that might incur extra cost. The following table suggests the calculation of white point count, calculation of traffic density related to the white point count and time allocation for the respective LEDs for two lanes.

| Lanes | White Point Count | Traffic Density | Time Allocation |
|--------|-------------------|-----------------|-----------------|
| Lane 1 | 30720 | 10% | 20 Seconds |
| Lane 2 | 156600 | 50.97% | 30 Seconds |
| Lane 1 | 195643 | 63.68% | 40 Seconds |
| Lane 2 | 222278 | 72.35% | 50 Seconds |
| Lane 1 | 276940 | 90.1% | 60 Seconds |

Table: Time Allocation for Signals based upon the calculated traffic density

So, the table shows the variation and an improvement which indicates an efficient processing of the proposed system.

3.3 Future Work

In future work Raspberry pi microcontroller can be used which will directly integrate the opencv software there is no need to install the opencv in the system. With the help of raspberry pi we can provide the view of the traffic to the traffic controller room so that the green signal will be provided for the longer time in the required area during the signal in order to avoid the unnecessary waiting time during the signal.

IV. CONCLUSION

The system presents a novel approach, based on Canny Edge Detection (CED) algorithm to construct a traffic management system, with the aim of improving the traffic conditions. In this proposed system, the images are captured at intersections, and then they are processed using CED algorithm. After that, the calculation of the density of the traffic is done using the white point count, and dynamically the signal times are changed depending on the intensity of traffic. Therefore, the system autonomously controls the traffic, involving lower human power with virtually no new installation cost. This model is an attempt to detect the density of vehicles on road in real time. The implementation of the proposed system will help in attaining great accuracy. The increase in accuracy for the tested dataset will help a lot by avoiding the traditional edge detection methodology, which are not so effective in achieving the proper traffic management. Moreover, this will also contribute in a much faster overall computing process.

V. ACKNOWLEDGMENT

The satisfaction and euphoria that accompany the successful completion of any task would be incomplete without the mention of people who made it possible whose constant guidance and encouragement crowned our effort with success. We would like to express our gratitude to Dr. Praveena Gowda, Principal, The Oxford College of Engineering for providing us a congenial environment and surrounding to work in. Our hearty thanks to Dr. R. Kanagavalli, Professor & Head, Department of Information Science and Engineering, The Oxford College of Engineering for her encouragement and support. Guidance and deadlines play a very important role in successful completion of the project report on time. We convey our gratitude to Ms. P Kokila, Assistant Professor, Department of Information Science and Engineering for having constantly monitored the completion of the Project Report and setting up precise deadlines. Finally a note of thanks to the Department of Information Science and Engineering, The Oxford College of Engineering, both teaching and non-teaching staff for their cooperation extended to us.

REFERENCES

- [1] Shahebgouda Halladamani, Radha R C “Development of Closed Loop Traffic Control System using Image Processing” International Conference on Energy, Communication, Data Analytics and Soft Computing (ICECDS-2017), 978-1-5386-1887-5/17/©2017 IEEE
- [2] Busarin Eamthanakul, Mahasak Ketcham, Narumol Chumuang “The Traffic Congestion Investigating System by Image Processing from CCTV Camera”, 978-1-5090-5210-3/17/©2017 IEEE
- [3] Aman Dubey, Aksdeep, Sagar Rane “Implementation of an Intelligent Traffic Control System and Real Time Traffic Statistics Broadcasting” International Conference on Electronics, Communication and Aerospace Technology (ICECA 2017), 978-1-5090-5686-6/17/ ©2017 IEEE
- [4] Elizabeth Basil, S D Sawant “IoT based Traffic Light Control System using Raspberry Pi” International Conference on Energy, Communication, Data Analytics and Soft Computing (ICECDS-2017), 978-1-5386-1887-5/17/ ©2017 IEEE
- [5] Pranav Maheshwari, Deepanshu Suneja, Praneet Singh, Yogeshwar Mutneja “Smart Traffic Optimization using Image Processing”, 978-1-4673-6747 -9/15/\$31.00 ©2015 IEEE
- [6] Anurag Kanungo, Ayush Sharma, Chetan Singla “Smart Traffic Lights Switching and Traffic Density Calculation using Video Processing”, 978-1-4799-2291-8/14/©2014 IEEE
- [7] Shubham Sahu, Dipanjan Paul, S Senthilmurugan “DENSITY BASED TRAFFIC SIGNAL CONTROL USING ARDUINO AND IR SENSORS”, SRM Institute of Science & Technology, Chennai – April 2018 (International Journal of Novel Research and Development - (IJNRD)
- [8] Partha Narayan Chowdhury, Tonmoy Chandra Ray, Jia Uddin “A Vehicle Detection Technique for Traffic Management using Image Processing” BRAC University Dhaka, Bangladesh - April 2018 [1] Matlab Image Processing and Video Processing Toolbox <http://www.mathworks.in/products/image/>
- [9] Image Subtraction Technique from Matlab <http://www.mathworks.in/help/images/ref/imshowsubtract.html>
- [10] Khekare, G.S.; Sakhare, A.V., "A smart city framework for intelligent traffic system using VANET," *Automation, Computing, Communication, Control and Compressed Sensing (iMac4s), 2013 International Multi-Conference on*, vol., no., pp.302,305, 22-23 March 2013
- [11] Badura, S.; Lieskovsky, A., "Intelligent Traffic System: Cooperation of MANET and Image Processing," *Integrated Intelligent Computing (ICIIC), 2010 First International Conference on*, vol., no., pp.119,123, 5-7 Aug. 2010
- [12] Yang Xiao; Yu-ming Xie; Lingyun Lu; Shuang Gao, "The traffic data compression and decompression for intelligent traffic systems based on two-dimensional wavelet
- [13] Naruemol Chumuang and Mahasak Ketcham “Handwriting Thai Signature Recognition System based on Multilayer Perceptron and Radial Basis Network” International Conference on Advanced Computational Technology and Creative Media (ICACTION 2014) 14- 15 August, 2014.
- [14] N. Hnoohom, N. Chumuang and M. Ketcham, "Thai Handwritten Verification System on Documents for the Investigation," 2015 11th International Conference on Signal-Image Technology & Internet-Based Systems (SITIS), Bangkok, 2015, pp. 617-622. doi: 10.1109/SITIS.2015.70
- [15] Mahasak Ketcham, Worawut Yimyam, Narumol Chumuang. “Segmentation of Overlapping Isan Dhamma Character on Palm Leaf Manuscript’s with Neural Network,” Recent Advances in Information and Communication Technology 2016, vol. 463 of the series Advances in Intelligent Systems and Computing, pp. 55-65, 2016. [10] P.G. Michalopoulos, "Vehicle Detection Video through Image Processing: The Autoscope System," IEEE Trans. Vehicular Technology”, vol. 40, no. 1, 1991, pp. 21–29.
- [16] Rafael C. Gonzalez, Richard E. Woods, “Digital Image Processing”, Addison-Wesley Publishing Company, September 1993.
- [17] Rita Cucchiara , Costantino Grana , Massimo Piccardi , Andrea Prati , Stefano Sirotti , Improving Shadow Suppression in Moving Object Detection with HSV Color Information
- [18] Shu-Ching Chen, Mei-Ling Shyu, Chengcui Zhang, and Jeff Strickrott, “Spatio-Temporal Vehicle Tracking and Indexing”, <http://www.cs.fiu.edu/~jstric01/>.
- [19] P. Khakham, N. Chumuang and M. Ketcham, "Isan Dhamma Handwritten Characters Recognition System by Using Functional Trees Classifier," 2015 11th International Conference on Signal-Image Technology & Internet-Based Systems (SITIS), Bangkok, 2015, pp. 606-612. doi: 10.1109/SITIS.2015.68
- [20] N. Chumuang and M. Ketcham, "Intelligent handwriting Thai Signature Recognition System based on artificial neuron network," TENCON 2014 - 2014 IEEE Region 10 Conference, Bangkok, 2014, pp. 1-6. doi: 10.1109/TENCON.2014.7022415

Emotion Detector for Medical Application

¹Abhishek M.S, ²Akshay P Shetty, ³Anshu Agarwal, ⁴Darel V Johny, ⁵Ms. Suganya R,
¹²³⁴Student, ⁵Asst Professor,
¹²³⁴⁵Department of Information Science and Engineering,
¹²³⁴⁵The Oxford College of Engineering, Bangalore, India.

Abstract: The purpose of this project is to detect the emotion of a user by using three parameters i.e., PPG sensor, temperature sensor and GSR sensor. The proposed system monitors and processes PhotoPlethysmoGraph (PPG), Galvanic Skin Response (GSR) and temperature sensor values. A PPG sensor is used to estimate a person's heart rate, a GSR sensor is used to detect the person's skin conductance and the temperature sensor is used to get the user's body temperature. An Arduino microcontroller is paired with an Android device via a Bluetooth Low Energy (BLE) wireless connection, to monitor the signals received from the Arduino microcontroller. All these signals are received in the android app where it detects and shows the emotion of the user. Such a system could be used in hospitals, for home-care, or by athletes, students, and people suffering from heart diseases. However, the primary audience is vulnerable people who need home-care.

Index Terms - PhotoPlethysmoGraph (PPG), Galvanic Skin Response (GSR), Temperature sensor, Emotion, Android App and Vulnerable People.

I. INTRODUCTION

The Emotion Detector project is divided into two parts, the Arduino circuitry and the Android application. Hence, the system consists of two subsystems; the first subsystem is composed of an Arduino microcontroller and three sensors (i.e. PPG, Temperature and GSR sensors), while the second subsystem is composed of an Android monitoring application. Generally speaking, all signal acquisition will be done within the Arduino microcontroller subsystem. Android (4.3+) is the platform used to develop the application, while the Android device is simply a receiver and a sender. It receives the PPG, GSR and Temperature sensor readings along with the heart rate as it sends the start/stop command for the acquisition of each signal to the Arduino microcontroller. The Android application then plots the corresponding waveforms, and processes them to extract related parameters. The inter-communication between the Arduino microcontroller and the Android device is established through a BLE connection. The GSR sensor that is used has Grove connectors, thus a Grove shield is needed for pairing it with the Arduino microcontroller. The Grove shield identifies the corresponding pins of the Arduino microcontroller, and allows the connection of additional sensors and/or other shields. The team was able to accomplish all of the proposed milestones. A working circuit consisting of an Arduino UNO microcontroller, a PPG sensor, a GSR sensor, a temperature sensor and a BLE module was developed. The GUI of the Android application was developed, and the application's functionalities were implemented. Also PPG, Temperature and GSR signals were successfully displayed on the developed application. Application users would now be able to register multiple patients' profiles, connect to the Arduino microcontroller, monitor the PPG and GSR signals, and share information with a selected emergency contact.

II. OBJECTIVES

Emotions represent the mood of a person. They are influenced by personality and temperament and determine the behaviour of a person, being closely linked to the nervous system. A definition according to Daniel Schechter says that emotions are positive or negative experiences that are associated with a particular pattern of psychological activity. In the current context, the trend in technology is tilted largely towards developing applications that increase the comfort of people and the interaction between humans and computers. Everything becomes more oriented to mobile applications. Our purpose was to develop a practical mobile application which determines the mood of users, based on several essential physical parameters collected from sensors. Moreover, the application acts as a recommender system, by suggesting the user musical items according to their mood. According to medicine and psychology, emotions are generated by the same central nervous system that controls the entire body, so if a person is experiencing different moods, the system increases or decreases the oxygen levels in the muscles, temperature or pulse. It works like an automatic system. A team of researchers from Aalto University, Finland has found that body temperature changes depending on the mood of the individual due to system response and nervous emotions, as set out in. Furthermore, their research is resumed in a diagram of the human body showing how temperature changes in different emotions.

III. METHODOLOGY

To ensure synchronous transmission and minimize transmission delays, the rate at which the points were transmitted was made equal to the sampling rate of the analog data from the sensor. This was done using the same interrupt timer for both the sampling and transmission processes. The timer was set as such that it interrupted every 2ms (sampling period) to sample a PPG point and then send right away through the serial UART port to the application.

When dealing with the serial transmission of the points, each waveform point was sent followed by a heart rate value corresponding to an approximated number of points between the first and the second peak of the PPG signal (the distance between the peaks represents an inter-beat interval). An Arduino loop function was used to facilitate continuous transmission of data to the real-time monitoring system.

Moreover, to make the monitoring more informative and efficient, heart rate variability was also investigated using 5 common (HRV) parameters for normal R-R heartbeat (NN) intervals [6]. They are as follows:

- Mean of the NN intervals
- Standard deviation (SD) of the NN intervals
- The Coefficient of Variation (CV) of the NN intervals (the ratio of the standard deviation to the mean)
 - The Standard Deviation of Successive Differences (SDSD) of NN intervals

$$SDSD = \sqrt{\frac{\sum_{i=1}^{n-1} (D_i - D_{mean})^2}{n-1}}$$

Where:

- i = interval index,
- n = number of total intervals,
- (n - 1) = number of interval differences,

- The Root Mean Square of Successive Differences (RMSSD) of NN intervals

$$RMSSD = \sqrt{\frac{\sum_{i=1}^{n-1} D_i^2}{n-1}}$$

Where:

- i = interval index,
- n = number of total intervals,
- (n - 1) = number of interval differences.

For analyzing the GSR signal, four parameters were used:

- Mean
- Standard deviation
- Kurtosis
- Skewness

The mean of the signal represented its baseline. The standard deviation indicated changes in the signal relative to its baseline. Kurtosis, was used to measure the flatness of the signal relative to the normal distribution. Generally, a positive value for kurtosis indicates that the signal is Leptokurtic (more flat than the normal distribution) while a negative value means the signal is less flat than the normal distribution, or platykurtic. The implemented formula for Kurtosis is the following

$$Kurtosis(x_1 \dots x_N) = \left\{ \frac{1}{N} \sum_{j=1}^N \left[\frac{x_j - \bar{x}}{\sigma} \right]^4 \right\} - 3,$$

Skewness was determined to indicate the symmetry of the GSR signal relative to its baseline. A positive skewness would indicate that the signal is skewed to the right while a negative.

$$Skewness(x_1 \dots x_N) = \frac{1}{N} \sum_{j=1}^N \left[\frac{x_j - \bar{x}}{\sigma} \right]^3$$

IV. SYSTEM DESIGN

4.1 Design Consideration

The design considerations are formulated to bring to the attention of the designers in applying the universal accessibility design principles and requirements to buildings and facilities. They can also be used to identify barriers in existing buildings. The design considerations are categorized into sub groups and presented as bullet points for ease of reference. The respective best practices section for key issues in each sub-group has been indicated. In addition to academic principles and theories, these considerations have also incorporated practical findings as discussed in Section 4 in the case studies, the analysis from the surveys, and the interviews with users and professionals. Several structural design considerations should be taken into account for economical and efficient welding. Many of these apply to other joining methods, and all apply to both subassemblies and the complete structure.

4.2 Block Diagram

A block diagram is a diagram of a system in which the principal parts or functions are represented by blocks connected by lines that show the relationships of the blocks. They are heavily used in engineering in hardware design, electronic design, software design, and process flow diagrams. Block diagrams are typically used for higher level, less detailed descriptions that are intended to clarify overall concepts without concern for the details of implementation. Contrast this with the schematic diagrams and layout diagrams used in electrical engineering, which show the implementation details of electrical components and physical construction.

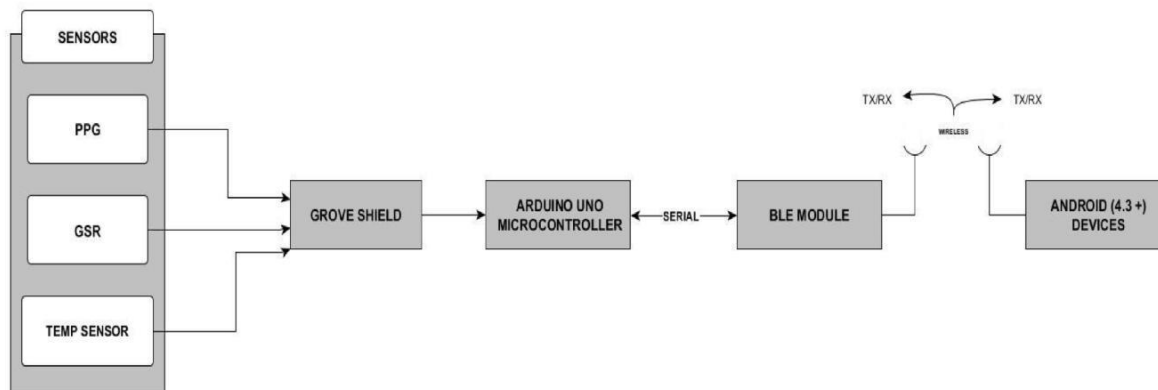


Fig 4.2 Block diagram of Emotion Detector

4.3 System Architecture

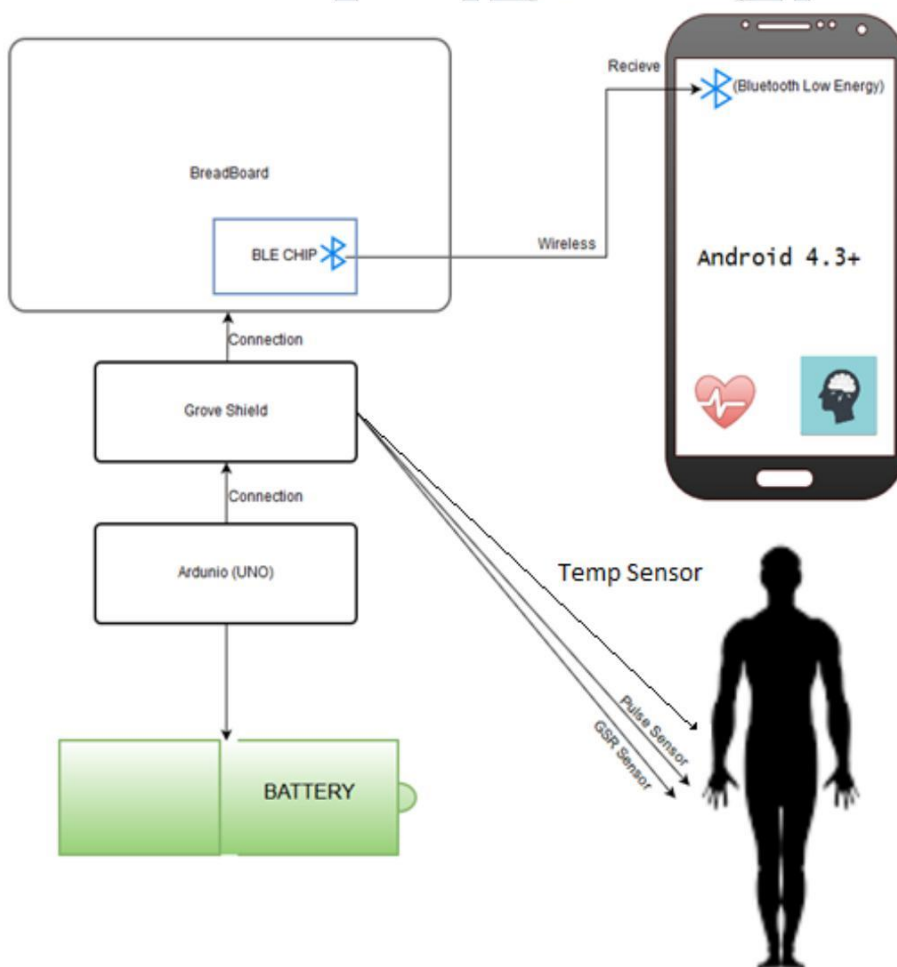


Fig 4.3 System Architecture of the Proposed System

A system architecture or systems architecture is the conceptual model that defines the structure, behavior, and more views of a system.[1] An architecture description is a formal description and representation of a system, organized in a way that supports reasoning about the structures and behaviors of the system.

A system architecture can consist of system components and the sub-systems developed, that will work together to implement the overall system. There have been efforts to formalize languages to describe system architecture, collectively these are called architecture description languages (ADLs).

V. TEST CASES AND ANALYSIS

5.1 Test Cases

| Test ID | Test Case Description | Expected output | Actual output | Status |
|---------|--|--|---|--------|
| 1 | The User enters their details and clicks register. | A message should show telling the user they are registered. | A message is shown telling the user they are registered | PASS |
| 2 | User Enters correct Login ID | The user should be directed to the Monitoring page | The user is directed to the monitoring page | PASS |
| 3 | User enters wrong login ID | The User is asked to register first | The user is asked to Register | PASS |
| 4 | The user is asked to grant permission to the app to use blue tooth | If the user clicks deny, user should direct back to login page | The user is directed back to login page | PASS |
| 5 | The user is asked to grant permission to the app to use blue tooth | If the user clicks Accept it moves to the monitoring page | The focus moves to monitoring page | PASS |
| 6 | The user tries to connect to a Bluetooth module | If the module is present it should connect | The Bluetooth module connects | PASS |
| 7 | Trying to get PPG sensor values | The values should be shown on the screen | The values are shown on the screen | PASS |
| 8 | Trying to get Temperature sensor values | The values should be shown on the screen | The values are shown on the screen | PASS |

VI. RESULTS AND DISCUSSION

6.1 Results of Descriptive Statics of Study Variables

The Mood Detector application is designed to detect the mood of the user by analyzing 3 physical parameters (pulse, skin electro conductivity and temperature) and by using a machine learning algorithm which is trained with data from the users. The application has been tested repetitively until the results generated by the learning algorithm have been validated 100%, thus confirming that the machine learning algorithms provides the correct output. The measuring device can be improved in order to obtain smaller dimensions, so it can be worn on the wrist, similar to fitness bracelets designed for athletes. The application can be extended on other platforms such as iOS or Web platform. Also, the music database can be extended to a richer playlist, and the application can be reconsidered so as to recommend things in varied fields such as books, movies, theater, events, or places.

6.2 Inference

The Mood Detector application is designed to detect the mood of the user by analyzing 3 physical parameters (pulse, skin electro conductivity and temperature) and by using a machine learning algorithm which is trained with data from the users. The application has been tested repetitively until the results generated by the learning algorithm have been validated 100%, thus confirming that the machine learning algorithms provides the correct output. The measuring device can be improved in order to obtain smaller dimensions, so it can be worn on the wrist, similar to fitness bracelets designed for athletes. The application can be extended on other platforms such as iOS or Web platform. Also, the music database can be extended to a richer playlist, and the application can be reconsidered so as to recommend things in varied fields such as books, movies, theater, events, or places.

6.3 Future Work

We can add better algorithm of machine learning or deep learning algorithm for larger amount of data with more accuracy. Later we can try to predict in how many days it will take to cure a person. This can be used in cooperate world for knowing different emotional behaviour of employee for providing them better ways of motivation.

6.4 Acknowledgement

The satisfaction and euphoria that accompany the successful completion of any task would be incomplete without the mention of people who made it possible whose constant guidance and encouragement crowned our effort with success. We would like to express our gratitude to Dr. Praveena Gowda, Principal, The Oxford College of Engineering for providing us a congenial environment and surrounding to work in. Our hearty thanks to Dr. R. Kanagavalli, Professor & Head, Department of Information Science and Engineering, The Oxford College of Engineering for her encouragement and support. Guidance and deadlines play a very important role in successful completion of the project report on time. We convey our gratitude to Ms. Suganya R, Asst. Professor, Department of Information Science and Engineering for having constantly monitored the completion of the Project Report and setting up precise deadlines. Finally, a note of thanks to the Department of Information Science and Engineering, The Oxford College of Engineering, both teaching and non-teaching staff for their cooperation extended to us.

References

- [1] "Self-Monitoring of Emotions and Mood Using a Tangible Approach". Federico Sarzotti Department of Computer Science, University of Torino, 10124 Turin, Italy; sarzotti@di.unito.it. This paper is an extended version of paper presented at the HCI International 2015 Parallel Session on Quantified Self and Personal Informatics entitled "Engaging Users in Self-Reporting Their Data: A Tangible Interface for Quantified Self". Received: 1 November 2017; Accepted: 19 December 2017; Published: 8 January 2018
- [2] Emotion Recognition Using Finger Tip Temperature: First Step towards an Automatic System "Smart image detection using Image Processing", 978-1-4673-6747 -9/15/\$31.00 ©2016 IEEE
- [3] Akshay Chamoli Ex. Student of Computer Science Computer Science & Engineering Department, Pondicherry University, Puducherry, India "Detection of Emotion in Analysis of Speech Using Linear Predictive Coding Techniques (L.P.C)" 978-1-4799-2291-8/14/©2015 IEEE
- [4] Henry Candra*, Mitchell Yuwono, Rifai Chai, Hung T. Nguyen, and Steven "Classification of Facial-Emotion Expression in the Application of Psychotherapy using Viola-Jones and Edge-Histogram of Oriented Gradient" 978-1-4799-2291-8/14/©2014 IEEE
- [5] Emotion Recognition Using Finger Tip Temperature: First Step towards an automatic System G. Shiva Kumar and P. A. Vijay
- [6] Galvanic Skin Response Data Classification for Emotion Detection Sri Kusrohmaniah, Sebastian Bagya Gunawan, Pranowo, Anton Satria Prabuwono, Departement of Informatics Engineering. Universitas Atma Jaya Yogyakarta, Yogyakarta 55281, Indonesia Psychology Department, Universitas Gajah Mada, Yogyakarta, Indonesia, 2014 IEEE
- [7] Jui-Le Chen, Jun-Ying Chen, Sheng-Ting Huang, Qi-Chen Ye, Qi-Wen Gung, and Shih-Pang Tseng, Department of Computer Science and Entertainment Technology, Tajen University, Pingtung 978-1-4799-2291-8/14/©2013 IEEE
- [8] Mood Detector – On Using Machine Learning to Identify moods and Emotions Alexandra Cernian, Adriana Olteanu, Dorin Carstoiu, Cristina Mares Faculty of Automatic Control and Computers University Politehnica of Bucharest Bucharest, Romania.
- [9] A Study on Real-Time Pulse Sensor Interface with System-on-Chip Architecture Lim Chun Keat¹, Asral Bahari Jambek² and Uda Hashim³ ^{1,2}School of Microelectronic Engineering, University Malaysia Perlis, Perlis, Malaysia ³Institute of Nano Electronic Engineering, Universiti Malaysia Perlis, Perlis, Malaysia.
- [10] EEG-based emotion recognition using self-organizing map for boundary detection Reza Khosrowabadi, Hiok Chai Quek and Abdul Wahab Center for Computational Intelligence, School of Computer Engineering, Nanyang Technological University,

ANALYSIS OF LOAD BALANCING ON DISTRIBUTED FILE SYSTEM FOR EFFECTIVE DATA RETRIVAL

¹Salini R S, ²Nadiya S, ³Ramya K M, ⁴Sreelakshmi V, ⁵Vinodha K

¹Student, ²Student, ³ Student, ⁴ Student, ⁵Assistant professor
Information Science and Engineering

The Oxford College of Engineering, Bangalore, India

Abstract– Load Balancing and Resource utilization are two important factors of DFS(Distribution File System). HDFS(Hadoop Distribution File System) plays a key role in Cloud computing environment and BigData analytics. In the present DFS, the file chunk distribution is dependent on central node which is susceptible for bottleneck and single point of failure. HDFS Uses 3 types of nodes Viz., namenode, secondary namenode and datanode to overcome single point failure. In this paper, the challenges faced in DFS are analyzed and a novel algorithm is proposed to address them. The imbalance in data access is due to the conventional parallel file system striping policies used for unevenly distribution of data among storage nodes. To overcome this HDFS stores each data unit, referred as chunk file, with several copies based on a relative random policy, which can result in an even data distribution among storage nodes. Based on the data retrieval policy in HDFS, if a storage node contains more requested data, the probability of accessing that node will be high resulting in bottleneck situation. To reduce the imbalanced access of data Opass method is used. Opass adopts new matching-based algorithms to match processes to data so as to compute the maximum degree of data locality and balanced data access. Furthermore, to retrieve the data fastly distribution algorithm and map reduce techniques are used.

IndexTerms – Parallel data access, Distributed file system, HDFS, MapReduce.

I.INTRODUCTION

A file system is a process that manages data storage and access on a hard disk drive(HDD). Distributed file systems such as GFS, HDFS, QFS or ceph, could be directly deployed on the disks of cluster nodes to reduce data movements. When storing a data set, distributed file systems will usually divide the data into small chunk files and randomly distribute them with several identical copies. Hadoop is an open source distributed processing framework that manages data processing and storage for big data applications running in clustered systems. The Hadoop Distributed File System (HDFS) is the primary data storage system used by Hadoop applications. It employs a NameNode and DataNode architecture to implement a distributed file system that provides high performance access to data across highly scalable Hadoop clusters. When retrieving data from HDFS, a client process will attempt to read the data from the disk that it is running on. If the required data is not on the local disk then the process will read from another node that contains the required data. The data requests from the parallel processes are referred to as parallel data requests. These data requests can be issued from Hadoop MapReduce applications, but also from MPI applications [2]. MapReduce is a

programming framework that allows the user to perform distributed and parallel processing on large data sets in a distributed environment. Map Reduce consists of two distinct tasks – Map and Reduce. The message passing interface is a standardized means of exchanging messages between multiple computers running a parallel program across distributed memory.

Unfortunately, the data requests from parallel processes or executors in big data processing will be served in an imbalanced fashion on the distributed storage servers and these parallel requests over the storage will compete for shared resources. Parallels Access is the simplest, fastest, and most reliable way to remotely access all your Windows/Mac applications and files on your iPhone, iPad, or Android phone or tablet. The Hadoop file system can allow parallel programs to access data by using its libHDFS library. The I/O interface, like hdfsread and hdfswrite, will be used to read/write data from/to HDFS. Another method is to use an I/O virtual translation layer to translate the parallel I/O operations. [1] Load balancing concept in a distributed system and a fully distributed load balancing algorithm mainly overcomes the load imbalance problem by using load balance Nearest Search algorithm but couldn't achieve Downtime, Limited control and

Vendor lockin.[2] DataMPI, which provided following MPI specifications: Dichotomic, Dynamic, Data-centric, and Diversified features .It provides advantages in performance and flexibility, but not able to reduce I/O response time, So SCALER is used. [3] SCALER, which allows MPI based applications to directly access HDFS without extra data movement and achieves the design goal efficiently such as Scalable parallel file write performance, Reducing I/O response time and Effective buffer for burst write workload. But this system is not suitable for small files. [4] A new methodology for managing read-write file sets across multiple file servers of a Distributed File System, thus balancing the load of file access requests across servers.It uses rule-based data mining technique and graph theory algorithms.

In section 2 represents an overview of HDFS andh MapReducing technique followed in document by section 3 that presents related work and followed by section4 presents existing models on HDFS. Various open research issues are presented in Section 5. Section 6 presents about opass technologies. A results explanation is given in Section 7 followed by concluding remarks in Section 8 .

II. HDFS AND MAPREDUCING TECHNIQUE

The Hadoop Distributed File System (HDFS) is a distributed file system designed to run on commodity hardware. It is highly fault-tolerant and provides high throughput access to application data. It is designed to be deployed on low-cost hardware and is suitable for applications that have large data sets. It is designed to reliably store very large files across machines in a large cluster. It stores each file as a sequence of blocks. The blocks of a file are replicated for fault tolerance. The block size and replication factor are configurable per file. An application can specify the number of replicas of a file. The replication factor can be specified at file creation time and can be changed later. Files in HDFS are write-once and have strictly one writer at any time.

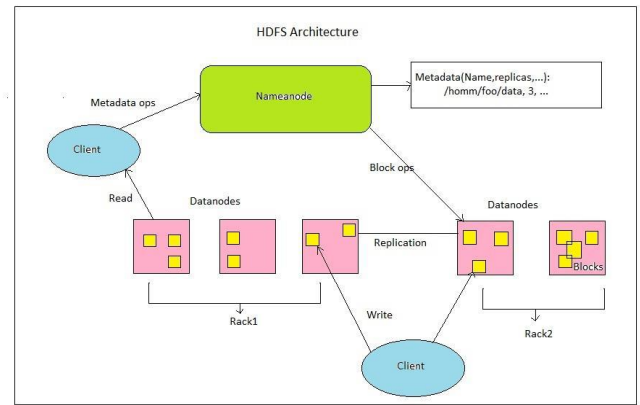


Fig 1. HDFS Architecture

HDFS has master/slave architecture.As shown in fig1, an HDFS cluster consists of a single NameNode which is a master server that manages the file system namespace and regulates access to files by clients and there are a number of DataNodes, usually one per node in the cluster, which manage storage attached to the nodes that they run on. The NameNode and DataNode are pieces of software designed to run on commodity machines.

These machines typically run a GNU/Linux operating system (OS). HDFS is built using the Java language; any machine that supports Java can run the NameNode or the DataNode software. Usage of the highly portable Java language means that HDFS can be deployed on a wide range of machines. A typical deployment has a dedicated machine that runs only the NameNode software. Each of the other machines in the cluster runs one instance of the DataNode software.

The architecture does not preclude running multiple DataNodes on the same machine but in a real deployment that is rarely the case. HDFS exposes a file system namespace and allows user data to be stored in files.Internally, a file is split into one or more blocks and these blocks are stored in a set of DataNodes. The DataNodes are responsible for serving read and write requests from the file system's clients. It also performs block creation, deletion, and replication upon instruction from the NameNode.The NameNode executes file system namespace operations like opening, closing, and renaming files and directories and makes all decisions regarding replication of blocks.It also determines the mapping of blocks to DataNodes. It periodically receives a Heartbeat and a Block report from each of the DataNodes in the cluster.Receipt of a Heartbeat implies that the datanode is functioning properly.

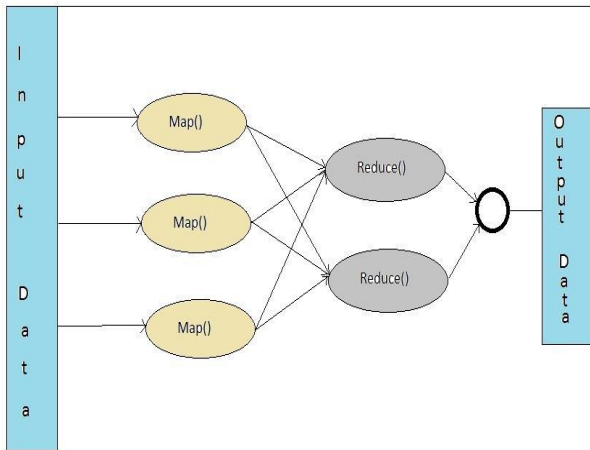


Fig2. Operation of MapReduce

Hadoop MapReduce is a software framework which is basically used for easy writing applications to process vast amounts of data in-parallel on large clusters of commodity hardware in a reliable and fault-tolerant manner. A MapReduce *job* usually splits the input data-set into independent chunks which are processed by the *map tasks* in a completely parallel manner as shown in fig2. The framework sorts the outputs of the maps, which are then input to the *reduce tasks*. Typically both the input and the output of the job are stored in a file-system. The framework takes care of scheduling tasks, monitors them and re-executes the failed tasks. Typically, the MapReduce framework and the Hadoop Distributed File System are running on the same set of nodes.

This configuration allows the framework to effectively schedule tasks on the nodes where data is already present, resulting in very aggregate bandwidth across the cluster. The MapReduce framework consists of a single master JobTracker and one slave TaskTracker per cluster-node. The master is responsible for scheduling the jobs' component tasks on the slaves, monitoring them and re-executing the failed tasks. The slaves execute the tasks as directed by the master.

The MapReduce framework operates on <key, value> pairs, that is, the framework views the input to the job as a set of <key, value> pairs and produces a set of <key, value> pairs as the output of the job, conceivably of different types. The key and value classes have to be serializable by the framework and hence need to implement the Writable interface and also need to implement the WritableComparable interface to facilitate sorting by the framework.

III. RELATED WORK

Radha G. Dobale[1] discussed the load balancing concept in a distributed manner and a fully distributed load balancing algorithm is proposed to cope with the load imbalance problem. The load balance Nearest Search algorithm is used to migrate one user's whole file into any other node instead of partitioning a file into a no. of chunks. Radha G. Dobale[1] achieved Load balancing, Scalability, Availability and Maintenance, but couldn't achieve Downtime, Limited control and Vendor lockin.

Xiaoyi Lu[2] proposed DataMPI, which provided following MPI specifications: Dichotomic, Dynamic, Data-centric, and Diversified features. Performance experiments showed that DataMPI has significant advantages in performance and flexibility, while maintaining high productivity, scalability, and fault tolerance of Hadoop.

Xiaoyi Lu[3] was not able to reduce I/O response time. Xi Yang[3] introduced a system solution, named SCALER, which allows MPI based applications to directly access HDFS without extra data movement. SCALER supports N-1 file write at both the inter-block level and intra-block level. Experimental results confirm that SCALER achieves the design goal efficiently such as Scalable parallel file write performance, reducing I/O response time and Effective buffer for burst write workload. Here, this system is not suitable for small files.

Valeria Cardellini[4] proposed system that reviewed the state of art in load balancing techniques on distributed web server systems and analyzed the efficiencies. Popular websites can neither rely on a single powerful server nor on independent mirrored servers to support the ever increasing request load. Scalability and availability can be provided by the distributed web server architecture that schedule client requests among the multiple server nodes in a user-transparent way. The proposed system was able to eliminate server overhead and bottleneck but had limited applicability, increased latency time and dispatcher bottleneck.

Amit Gajbhiye[5] discussed about Global Server Load Balancing with Networked Load Balancers for Geographically Distributed Cloud Data-Centres and critically analysed the state-of-the-art techniques used for Global Server Load Balancing and have proposed a novel model of

networked load balancers for load balancing across the datacenters in cloud computing environment. The proposed model overcomes the shortcomings of existing DNS based load balancing by considering current load status of datacenter, by making time to live of DNS server cache redundant and by finding the exact location by real IP of end user. The proposed system achieved Load balancing with networking among load balancers in datacenters in distributed environment, A novel load calculation was done and Response time was reduced to transfer the request across multiple datacenters. The system was unable to Deploy the model in real time environment.

Alexandra Glagoleva [6] presented a new methodology for managing read-write file sets across multiple file servers of a Distributed File System, thus balancing the load of file access requests across servers. The proposed methodology is based on a rule-based data mining technique and graph theory algorithms. The rule-based technique generates rules from access request data to identify present file access patterns in the system. The algorithm for fileset relocation is based on the graph coloring problem.

IV.EXISTING SYSTEM MODELS

1.MapReduce technique for parallel-automata analysis of large scale rainfall data:

MapReduce is a technique for executing exceedingly parallelizable and distributable algorithms across huge datasets utilizing countless PCs. Utilizing MapReduce with Hadoop, the large-scale rainfall could be determined without adaptability issues. Vast scale rainfall information assumes an imperative part in farming field thus early expectation of rainfall is important for the better financial development of a nation. information for accurate rainfall Big Data innovation like Hadoop have developed to fathom the difficulties and issues of huge information utilizing distributed computing.

In this model the huge scale rainfall information is anticipated by utilizing MapReduce system which plays out the capacities which are required and decrease the task to get proficient arrangements through taking the information and isolating into smaller tasks. The three Regression Automata (RA) algorithms such as Linear Regression automata, Support Vector Regression Automata and Logistic Regression Automata are utilized to forecast the future esteem of large scale rainfall data. This model also serves as a tool that takes in the rainfall information from diminished

information as input and predicts the future rainfall. The outcomes obviously demonstrate that the all the three RA models can anticipate the rainfall productively in different terms, such as, error rate, coefficients and mean square error.

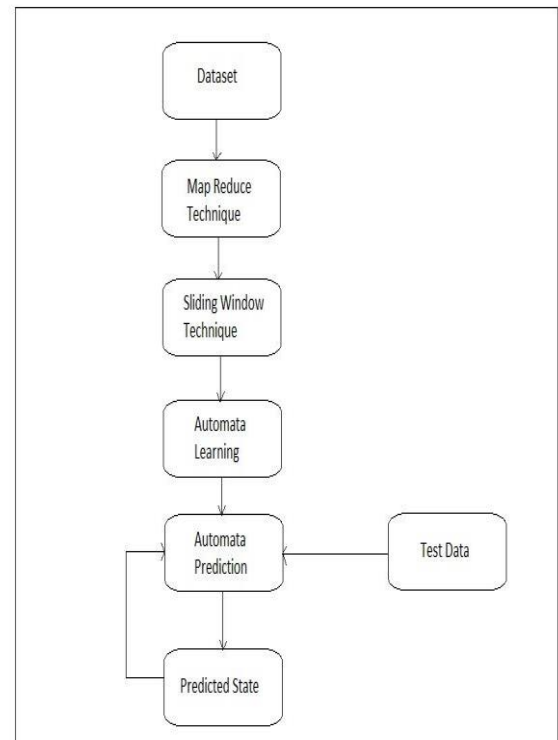


Fig 3. Map reduce technique for parallel-automata analysis.

2.Unstructured Data Analysis on Big Data using Map Reduce:

Large amount of unstructured data needs structural arrangement for processing the data. Hadoop is binary compatible with Map reduce. Map Reduce is a shuffling strategy to perform filtering and aggregation of data analysis tasks. Map is nothing but the filtering technique used for filtering the datasets and similarly Reduce is a technique used for aggregation of data sets. In the real time scenario, the volume of data used linearly increases with time.

Social networking sites like Facebook, Twitter discovered the growth of data which will be uncontrollable in the future. In order to manage the huge volume of data, the proposed method will process the data in parallel as small chunks in distributed clusters and aggregate all the data across clusters to obtain the final processed data. In Hadoop framework, MapReduce is used to perform the task of filtering, aggregation and to maintain the efficient storage structure. The data are preferably refined using collaborative filtering, under the prediction mechanism of particular data needed by the user. Collaborative Filtering Technique is used to generate recommendations based on user data. Sentiment Analysis is a technique which uses natural

language processing and Text analysis techniques for predicting the user sentiments based on polarity.

The proposed method is enhanced by using the techniques such as sentiment analysis through natural language processing for parsing the data into tokens and emoticon based clustering. The process of data clustering is based on user emotions to get the data needed by a specific user. The results show that the proposed approach significantly increases the performance of complexity analysis.

3. Mining on Big Data Using Hadoop MapReduce Model:

The proposed hadoop model consists of five tools namely data preprocessing, data migration with sqoop, data analytics with hive, data analytics with pig and data analytics with map reduce. Data preprocessing module is used to create data set for making item-set of product.

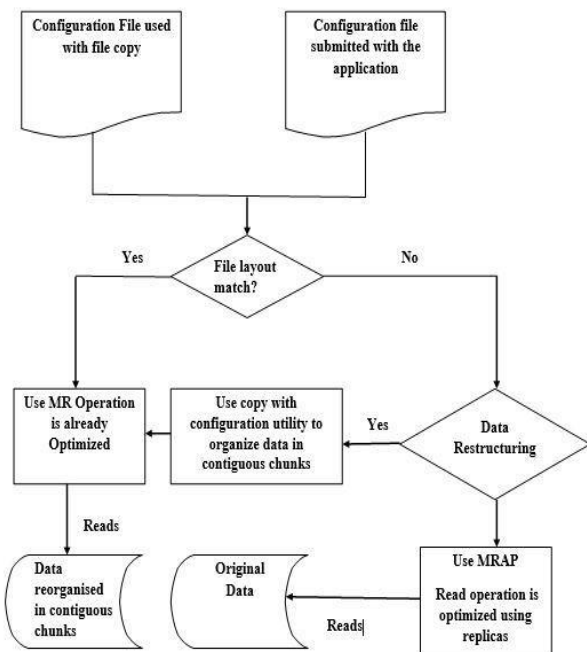


Fig 4. MRAP Technique for Date Restructuring

The data migration with sqoop module is used to transfer the dataset into Hadoop. Sqoop is a tool for transferring data between databases and Hadoop. With the help of this module the dataset is fetched into Hadoop using sqoop tool. Sqoop is used to perform many functions, such as to fetch the particular column or to fetch the dataset with specific condition that will be supported by sqoop tool and data will be stored in Hadoop. Data analytic with hive module is used to analyze structure language. Hive is a data ware house system for Hadoop.

It runs structured query language (SQL) like queries called hive query language (HQL). The HQL is converted internally to map reduce jobs.

Hive was introduced by Facebook. Hive supports functions like data definition language (DDL), Data manipulation language (DML) and user defined functions. In this module the dataset is analyzed using hive tool which will be stored in Hadoop. To analyze dataset hive is used with HQL. Using hive Partition, Bucketing can be performed. The module of data analytic with pig is also used to analyze data set.

Apache pig is a high level data flow platform to execute map reduce programs with Hadoop. Data analytic with map reduce module is also used analyze data set with map reduce. Map reduce is a processing technique using program model of java for distributed computing. The map reduce algorithm contains two important tasks such as map and reduce. The task map is used to map with chart, record, plot, drawing, plan and diagram etc. Whereas task reduce is used to minimize the dimension.

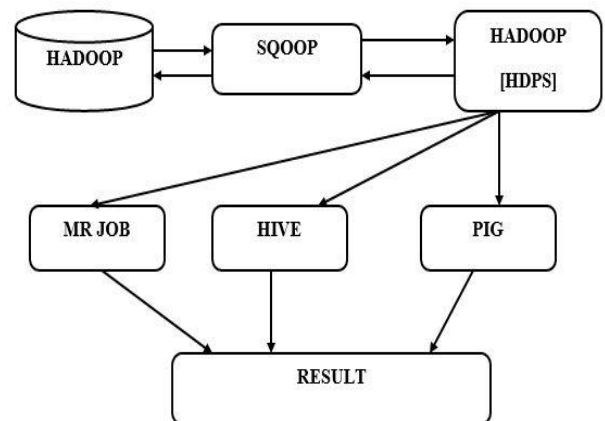


Fig 5. Hadoop MapReduce Technique on mining

V. ISSUES IN HADOOP MAPREDUCE

Challenge 1: lack of performance and scalability
The hadoop mapreduce programming model do not provide a fast, scalable distributed resource management solution. Organisations require a distributed Mapreduce solution that can deliver competitive advantage by solving wider range of data intensive analytic problems faster. The mapreduce implementation should help organizations run complex data simulation with submillisecond latency, high data throughput and Thousands of mapreduce tasks completed per seconds depending on complexity.

Challenge 2: Lack of flexible resource management. The hadoop MapReduce programming model are not able to react quickly to real time changes in application or user demands. Based on the volume of tasks, the priority of the job and time varying resource allocation policies, mapreduce jobs should be able to quickly grow or shrink the number of

concurrently executing tasks to maximize throughput, performance and cluster utilization while respecting resource ownership and sharing policies.

Challenge3: Lack of application deployment support. The hadoop MapReduce programming model do not make it easy to manage multiple application integrations on production-scale distributed system with automated application service deployment capability.

Challenge4: Lack of quality of service assurance. The hadoop Mapreduce programming model are not optimized to take full advantage of modern multicore servers. The implementation should allow for both multithreaded and single threaded tasks and be able to schedule them with a view to maximize cache effectiveness and data locality into consideration.

Challenge 5: Lack of multiple data source support. The hadoop Mapreduce programming model only support a single distributed file system, the most common being HDFS. A complete implementation of the MapReduce programming model should be flexible enough to provide data access across multiple distributed file systems. In this way, existing data does not need to be moved or translated before it can be processed. MapReduce services need visibility to data regardless of where it resides.

Challenge 6: Privacy and security challenges. There are issues in auditing, access control. Authentication and privacy when performing mapper and reducer jobs. To solve the mentioned challenges in this section, the following opass methodologies are used.

VI. METHODOLOGY

1. Encoding Process:

The parallel data read requests can be served in a balanced way through maximizing the degree of data locality read. To achieve this, we retrieve data distribution information from storage and build the locality relationship between processes and chunk files, where the chunk files will be associated with data processing operators/ tasks according to different parallel applications [16].

Map reduce background: MapReduce is a programming model suitable for processing of huge data. Hadoop is capable of running MapReduce programs written in various languages: Java, Ruby, Python, and C++.

MapReduce programs are parallel in nature, thus are very useful for performing large-scale data analysis using multiple machines in the cluster. MapReduce consists of several components, including:

- Job Tracker -- the master node that manages all jobs and resources in a cluster
- Task Trackers -- agents deployed to each machine in the cluster to run the map and reduce tasks.

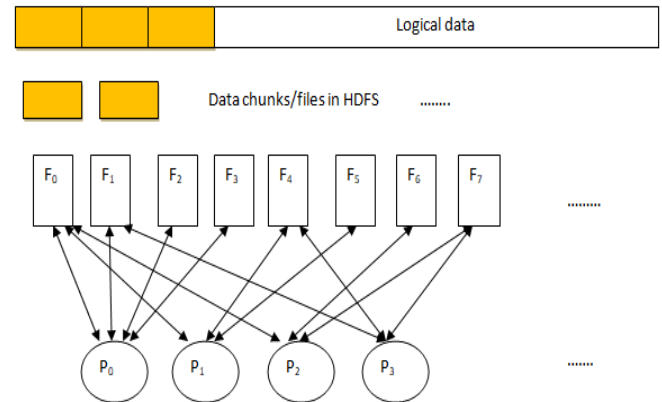


Fig 6. A bipartite matching example of processes and chunk files [16].

- JobHistoryServer -- a component that tracks completed jobs, and is typically deployed as a separate function or with Job Tracker.

The basic architecture of map reduce is as shown in fig 2. The term MapReduce actually refers to two distinct jobs that Hadoop programs perform. The first is the map job, which takes a set of data and converts it into another set of data, where individual elements are broken down into tuples (key/value pairs). The reduce job takes the output from a map as input and combines those data tuples into a smaller set of tuples. Both these functions can be prototyped as follows:

$\text{Map}(K1, V1) \rightarrow [(K2, V2)]$.

$\text{Reduce}(K2, \{V2\}) \rightarrow [(K3, V3)]$.

When a file is divided into equal sized blocks (64MB-128MB) and each block is assigned to a cluster, the job tracker starts a map task for each data block and typically assigns it to the task tracker on the machine. Each data block will have a mapper. Each mapper will have a corresponding reducer. The mapper performs map function and we get the intermediate results. This intermediate results enters the reduce phase. The reducer performs reduce function. The results of all task tracker are combined to get the output.

Matching-Based Algorithm for Tasks with Multi-Data Inputs is used for encoding process. This algorithm is accessed through port number 50070.

2. Optimizing Parallel Single Data Access in DFS:

The overall execution time for parallel data analysis will be decided by longest running process. For a single task with multiple data inputs as shown in fig 7, the required inputs may be placed on a multiple data nodes, which imply that some of the data associated with given task may be local to the process assigned to that task and some might be remote so, tasks with multiple inputs will complicate the matching of processes to data. we propose a novel matching based algorithm for this type of parallel data accesses. Our algorithm aims to associate each process with data processing tasks, such that a large amount of data can be read locally. We assign each process with the equal number of tasks for parallel execution. Our algorithm achieves the optimal matching value from the perspective of each process. To begin, we compute the amount of co-located data associated with each task and each process and encode these values as the matching values between them and we will find a task .

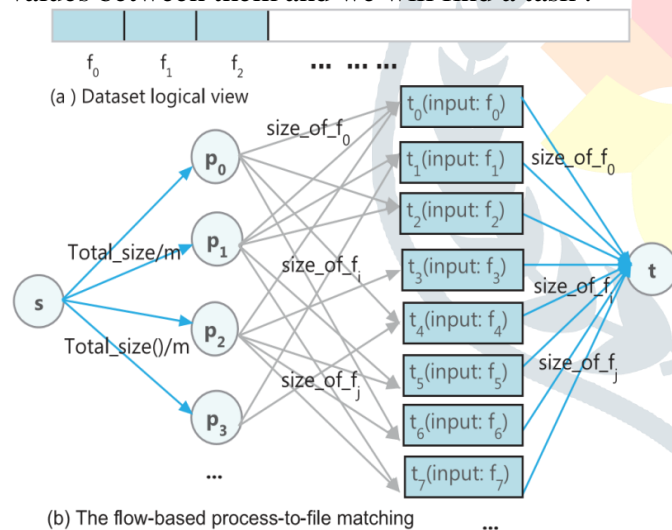


Fig 7. The matching-based process-to-file configuration for single-data access[16].

3. Optimizing Parallel Multi-Data Read Access in DFS:

In previous method we are accessing single data but here we are accessing multiple data. We propose a novel matching based algorithm for this type of parallel multi-data read access. Our algorithm aims to associate each process with data processing tasks such that a large amount of data can be read locally.

4. Opass for Parallel Data Read Access in DFS:

HDFS uses an r-way replication to provide high availability. Files in HDFS are referred as chunks

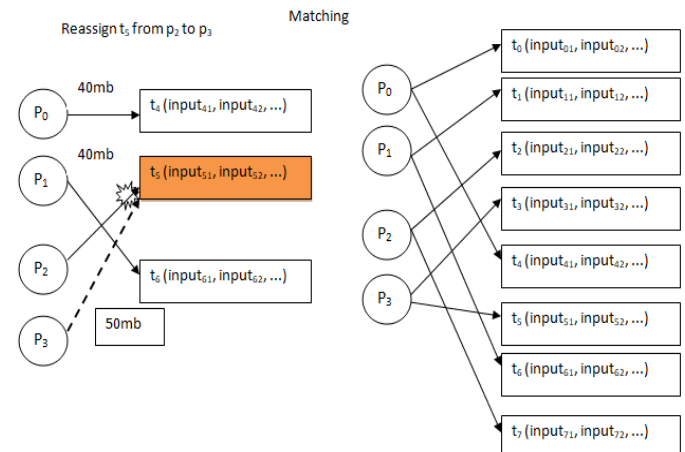


Fig 8 The process-to-data matching example for multiple data assignment[16].

and each chunk will be copied to r DataNodes. When a read request is initiated for a chunk, by default, the NameNode will return a sorted list of DataNodes that holds the requested chunk. The nearest Data Node will be picked to serve the read request. When the degree of imbalance crosses a pre-defined threshold, we will replace the default locality driven read strategy with our matching based method.

Distribution algorithm is used to evenly distribute the read requests for file's chunks. In fig 9, Capacity is determined by each Data Node's current number of chunks served and the number of chunks of newly requested file. Expected matching is denoted in red dotted line.

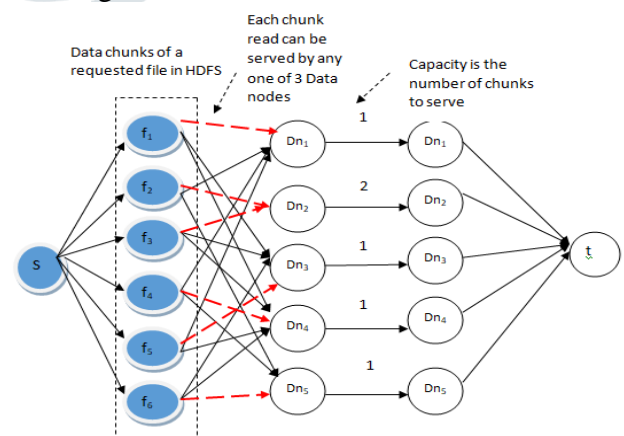


Fig 9. Balanced file read requests matching using network flow[16].

Algorithm 1. Algorithm to read chunks in distributed file system.

Let the file f consists of m chunks stored on n DataNodes.

Let the set $NP = \{np_0, np_1, \dots, np_{n-1}\}$ represent the current number of chunk data requests served by data nodes.

Let the set $P = \{p_0, p_1, \dots, p_{n-1}\}$ represent the number of chunk data requests for file F that the data nodes will serve.

Let the set $l = \{l_0, l_1, \dots, l_{n-1}\}$ represent the number of chunks of F that each Data nodes holds.

Input: m, n, P, NP ; **Output:** P

Steps:

Find the maximum number of read requests served by current data nodes: $np_j = \text{Max}(nP)$

* assign m chunks to n data nodes */

For np_i in NP and $np_i < np_j$ do

if $np_j - np_i > l_i$ then

$p_i = l_i$; $m = m - p_i$;

else

$p_i = np_j - np_i$; $m = m - p_i$;

end if

while $m > 0$ do

for np_i in PC and $m > 0$ do

if $p_i < l_i$ then

$p_i = p_i + 1$; $m = m - 1$

end if

end for

end while

Algorithm2.Dijkstra's algorithm

1. Mark all nodes unvisited. Create a set of all the unvisited nodes called the *unvisited set*.
2. Assign to every node a tentative distance value: set it to zero for our initial node and to infinity for all other nodes. Set the initial node as current.
3. For the current node, consider all of its unvisited neighbours and calculate their *tentative* distances through the current node. Compare the newly calculated *tentative* distance to the current assigned value and assign the smaller one. For example, if the current node A is marked with a distance of 6, and the edge connecting it with a neighbour B has length 2, then the distance to B through A will be $6 + 2 = 8$. If B was previously marked with a distance greater than 8 then change it to 8. Otherwise, keep the current value.
4. When we are done considering all of the unvisited neighbours of the current node, mark the current node as visited and remove it from the *unvisited set*. A visited node will never be checked again.

5. If the destination node has been marked visited (when planning a route between two specific nodes) or if the smallest tentative distance among the nodes in the *unvisited set* is infinity (when planning a complete traversal; occurs when there is no connection between the initial node and remaining unvisited nodes), then stop. The algorithm has finished.
6. Otherwise, select the unvisited node that is marked with the smallest tentative distance, set it as the new "current node", and go back to step 3.

VII. RESULT:

To test OPASS on parallel processing applications, we record the I/O time taken to read each chunk files by comparing with three metrics, the average sI/O time taken to read all chunk files, the maximum I/O time and the minimum I/O time as shown in fig 10,11. Fig 10. represents reading data from HDFS without implementing opass . This shows that the I/O time become more variant has the cluster size increases. the maximum I/O time increases drastically while the minimum I/O time remains constant. For instance, on the 16 node to 80 node cluster the maximum I/O time to read a chunk file reaches from 7 X to 18X. This is not suitable for parallel programs which has longest operation for execution.

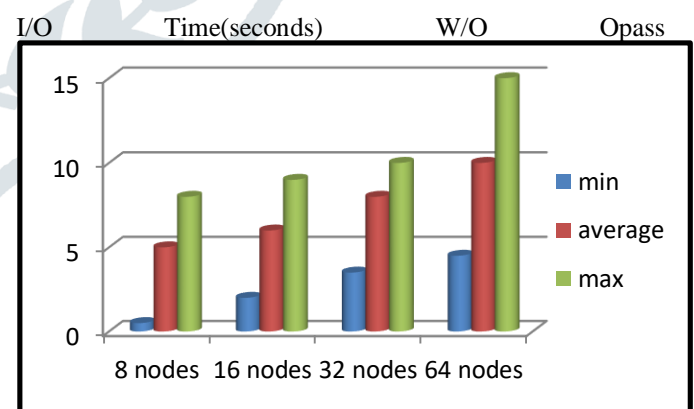


Fig 10. Read data from HDFS without Opass.

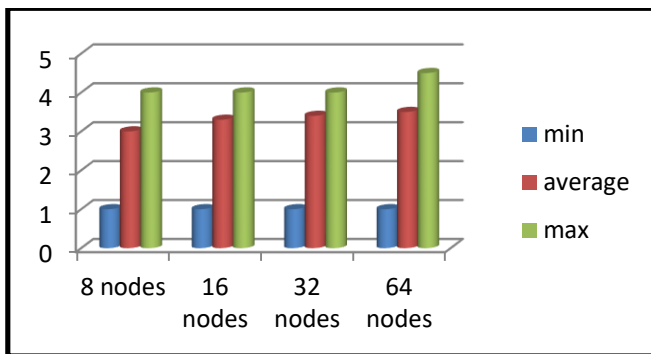


Fig. 11. Read data from HDFS with Opass.

With the use of Opass, as shown in Fig. 11, the I/O performance remains constant as the cluster size increases, with an average I/O time of around 0.9 seconds. With the use of Opass, the I/O time during the entire execution is approximately one to two seconds. In all, the average I/O operation time with the use of Opass is a quarter of that without opass.

VIII. CONCLUSION

In this paper the problems of parallel data reads/writes on distributed file systems is analysed due to the lack of consideration of data distribution, parallel data requests are often served in an imbalanced and remote fashion.

To overcome the imbalance fashion in distributed file system, opass methods are used. The data retrieve is improved by 10% compared to existing system.

In future, on hadoop for dynamic and iterative processing we are trying to identify the data changes whenever there is a dynamic updation using FP algorithm.

ACKNOWLEDGMENT

We would like to express our gratitude to Dr. Praveena Gowda, Principal, The Oxford College of Engineering for providing us a congenial environment and surrounding to work in. Our hearty thanks to Dr. R. Kanagavalli, Professor & Head, Department of Information Science and Engineering, The Oxford College of Engineering for her encouragement and support. We convey our gratitude to Dr. Vinodha K, Asst. Professor, Department of Information Science and Engineering for having constantly monitored the completion of the Project Report and setting up precise deadlines.

References:

- [1] Review of Load Balancing for Distributed Systems in Cloud
- [2] DataMPI: Extending MPI to Hadoop-like Big Data Computing
- [3] SCALER: Scalable Parallel File Write in HDFS

[4] Title Dynamic Load Balancing on Web-server Systems

[5] Amit Gajbhiye discussed about Global Server Load Balancing with Networked Load Balancers for Geographically Distributed Cloud Data-Centres and critically analysed the state-of-the art techniques used for Global Server L

[6] Alexander Glagoleva presented a new methodology for managing read-write file sets across multiple file servers of a distributed file system, thus balancing the load of file access requests.

[7] Apache Hadoop YARN: Yet Another Resource Negotiator

[8] G. King, "Big Data is Not About the Data!" Presentation (Harvard University USA, 19 November 2013).

[9] Samee U. Khan Enabling Big Data Complex Event Processing for Quantitative Finance through a Data- Driven Execution.

[10] T. H. Davenport and J. Dyché, "Big data in big companies," International Institute for Analytics.

[11] B. Fang, P. Zhang, in BigData in Finance. Big Data Concepts, Theories, and Applications, ed. by S. Yu, S. Guo (Springer International Publishing, Cham, 2016).

[12] T.-C. Dao and S. Chiba, "HPC-reuse: Efficient process creation for running MPI and Hadoop MapReduce on supercomputers," in Proc. 16th IEEE/ACM Int. Symp. Cluster Cloud Grid Comput., 2016, pp. 342–345.

[13] A. Darling, L. Carey, and W.-C. Feng, "The design, implementation, and evaluation of mpiblast," presented at the ClusterWorld, San Jose, CA, USA, 2003.

[14] J. Dean and S. Ghemawat, "MapReduce: Simplified data processing on large clusters," Commun. ACM, vol. 51, no. 1, pp. 107–113, 2008.

[15] L. R. Ford Jr and D. R. Fulkerson, "A suggested computation for maximal multi-commodity network flows," Manag. Sci., vol. 5, no. 1, pp. 97–101, 1958.

[16] "Achieving Load Balance for Parallel Data Access on Distributed File Systems", Dan Huang, Dezhi Han, Jun Wang, Jiangling Yin, Xunchao Chen, Xuhong Zhang, Jian Zhou, and Mao Ye, vol.67,no.3, 2018

FACE RECOGNITION USING LOW QUALITY IMAGES

¹Mohamed Alkib Javed, ²Prince Kumar, ³Syed Abdul Mannan, ⁴Yash Badia, ⁵Mr. Yadhukrishna MR
¹Student, ²Student, ³Student, ⁴Student, Assistant Professor Dept. of ISE
¹Information Science and Engineering
¹The Oxford College of Engineering, Bangalore, India

Abstract : Sparse-representation based classification (SRC) has been appearing great execution for face recognition as of late. Be that as it may, SRC isn't great at face recognition with low-quality pictures (e.g., camouflaged, undermined, impeded, etc.) which regularly show up in handy applications. To take care of the issue, In Face Recognition using low quality images(FRULQI), we propose a novel SRC based strategy for face recognition with low-quality images. In SLCR, we use low-position grid recuperation on the preparation dataset to acquire low-position segments and non-low-position segments, which are utilized to develop the word reference. The new dictionary is equipped for depicting facial element better, particularly for low- quality face tests. Besides, the base class-wise recreation remaining is utilized as the acknowledgment rule, prompting a generous enhancement for the proposed SLCR's execution. Broad trials on benchmark face databases exhibit that the proposed technique is reliably better than other sparse-representation based methodologies for face acknowledgment with low-quality pictures.

Index Terms - Face recognition, sparse-representation based classification , low quality images.

I. INTRODUCTION

The face recognition has been the most celebrated biometric methodology in view of its huge application potential in the earlier decades. Satisfactory and constructive getting ready tests guarantee a better than average component depiction for portraying the characteristics of an individual's face. In any case, truly, the image of each individual is much of the time covered, undermined or blocked. Henceforth, face recognition with low-quality pictures is more trying than the one with sufficient and extraordinary pictures. This paper bases on the endeavor of face recognition with low-quality pictures. The practicality of feature extraction is critical for face recognition. Principal component analysis (PCA) is a commonplace procedure for dimensionality decline.

In development, there are various procedures, for instance, straight discriminant investigation (LDA), probabilistic subspace learning and region conservation (Laplacian face, etc. In any case, it is a troublesome endeavor for these procedures to light up special cases or pitiful uproar. To help this issue, a couple of strategies for solid PCA have been proposed. Among them, low-position grid recuperation (LR) is a key technique, which can disconnect debased information from the planning face pictures better than PCA. As requirements be, low-position parts gotten by LR would better fill the gathering need.

The execution of the classifier is significant for face recognition. Closest neighbor (NN) classifier is broadly connected for its effortlessness. Expansions of NN classifier, closest component line (NFL), closest element plane (NFP), closest element space (NFS) and direct relapse classifier (LRC), consider the connection between the testing picture and the preparation pictures of each class independently. Not the same as the previously mentioned classifiers, sparse-representation based characterization (SRC) which considers the testing picture as a direct blend of the preparation dataset has been proposed for face recognition and accomplished fulfilling results.

Be that as it may, SRC is unequipped for performing admirably when the preparation dataset is under-examined or defiled. To beat this inadequacy, some all-encompassing SRC methods have been proposed. SRC with Markov arbitrary fields to address the mask face recognition issue with substantial adjacent occlusion. SRC to deal with the misalignment, posture and light invariant recognition issue. Another thought of strong relapse and proposed a regularized powerful coding (RSC). A strategy utilization of the correntropy prompted powerful blunder metric and displayed the correntropy based sparse-representation calculation (CESR). A strategy for class-wise sparse-representation (CSR) to handle the issues of the ordinary example savvy sparse-representation.

In this paper, we focus on the dictionary advancement of SRC to grasp face recognition with low-quality pictures and propose a sparse low-position part based representation (SLCR) which is amazing for under-examined, covered, demolished and obstructed face recognition. In the proposed strategy, the crucial responsibility is the utilization of the low-position part breaking down to build up the dictionaries. Low-position part and non-low-position portion procured by LR from the arrangement tests present the powerful features and the other related with an obstacle, oddity or sparse confusion, separately, which would add to correct recognition.

PROBLEM STATEMENT

With the substantial interest of Biometric based verification these days and innovation developing quickly, we never again can depend on unique finger impression based confirmation and a new technique for face recognition is coming into the picture. However, when the picture is caught by let say CCTV cameras the nature of the picture is to some degree twisted and is undermined. We are in a need of a framework that can identify faces not withstanding when the picture quality is low. We here are proposing the technique that can without much of a stretch improve the proficiency and help us in setting a benchmark.

PROPOSED SYSTEM

A sparse low-rank component based representation (SLCR) which is an expansion of sparse-representation based grouping (SRC). Consequently, we compare the outcomes between SLCR and other SRC based techniques. In this area, we initially pick three face databases (the all-inclusive Yale B[38], CMU Multi-PIE and AR face databases) to compare the execution of our technique with LR, SRC, LRSI, SSRC and SDR-SLR in various test conditions. Moreover, we check the execution of SLCR and other SRC based strategies on the LFW database in regular circumstances. Likewise, all analyses are rehashed multiple times and each time we pick an alternate preparing set and testing set. Preparing set and testing set are from a similar database. Both of them contain distinctive examples of a similar individual. Accordingly, the number of impostor tests in the preparation set and testing set is 0 with the goal that the false match rate (FMR) is 0% in all analyses. We utilize the false non-match rate (FNMR) at a 0% FMR to demonstrate the aftereffects of tests.

II. RESEARCH METHODOLOGY

Modules Description

Reading, Training and Testing: We are utilizing the informational index called Yale B database. Which contains the pictures in various quality and light source. Aggregate of 40 people picture and 65 pictures of a solitary individual. The element of each picture is 192 x 168. We will utilize 80% of information for training and rest 20% of information for the testing.

Mean Image: Mean picture is utilized to light up the present picture and after that further, it's utilized for face recognition. We are utilizing a mean picture in light of the fact that the current picture may be dull and features won't be properly extracted.

Salt and pepper noise: We have to include white and dark pixels randomly in the picture network for that we utilize salt-and-pepper noise. We utilize this noise just to check whether the calculation is sufficiently proficient to perceive the picture or not. We are utilizing 20% of salt-and-pepper noise.

Eigen Faces and Downsample: Here we are reconstructing the image using the Eigenvector values. Because in order to do the sparse matrix we need Eigenvalues and multiply with the Transpose to the actual matrix. Down sampling image reduces the number of samples that can represent the signal or feature. Only important features are allowed to scream out.

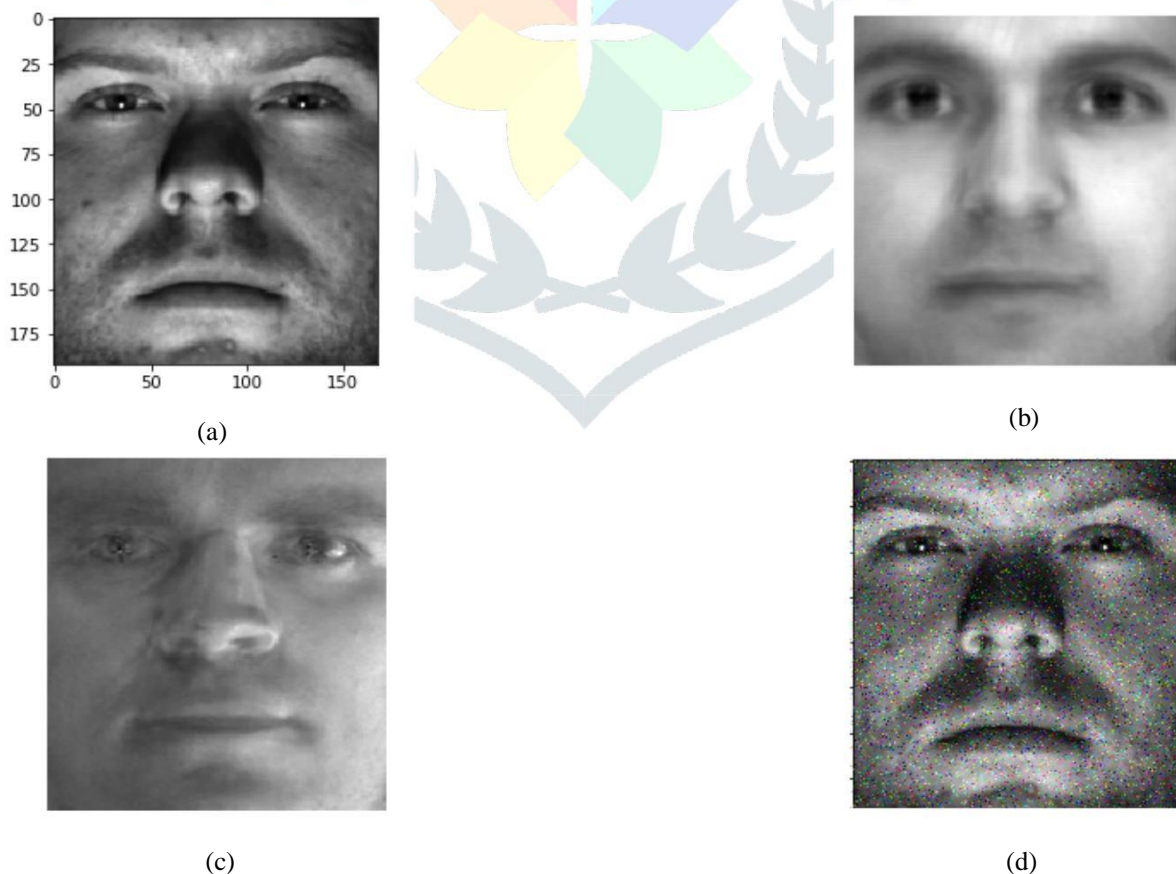


Fig. 1 (a) Sample image of Yale B (b) Mean image (c) Eigen Faces (d) Image with 20% salt and pepper noise.

Sparse Low-rank Component based Representation (SLCR): Inspired by individual qualities of SRC and low-rank matrix recovery, in this paper, we propose another sparse low-rank component-based representation (SLCR) for low-quality face recognition. We start with the inspirations of our work. For the past lexicon based SRC techniques, SSRC basically applies centroid pictures to catch the class-explicit data. SDR-SLR applies the reproduced pictures by the

particular vectors relating to the biggest solitary incentive to instate word reference. The trials report that SDR-SLR is better than SSRC for face recognition. SDR-SLR applies particular esteem disintegration (SVD) to get class-explicit data to instate the word reference. For the matrix disintegration, SVD is equivalent to PCA. By PCA, the preparation of dataset D can be disintegrated into

$$D = L + N$$

where L is the principal component (i.e., class-explicit data in SDR-SLR), N is the non-principal component (i.e., non-class-explicit data in SDR-SLR).

RESULT AND DISCUSSION

As already mentioned the extended Yale B database consists of 2740 frontal face images of 38 subjects while each picture is taken under different lab controlled lighting conditions. The CMU Multi-PIE database contains face pictures caught in four sessions with varieties in brightening, demeanor, and posture. Furthermore, we pick a subset of the dataset set comprising of 1360 frontal pictures for 68 people. The AR database contains more than 4000 frontal pictures for 126 people. We pick a subset of the dataset set comprising of 702 frontal pictures for 54 people on the AR database and these pictures incorporate increasingly facial varieties, including brightening change, articulations, and facial masks. The edited pictures of one individual from the all-encompassing Yale B, CMU Multi-PIE and AR databases are appeared in Fig.2 (a),(b),(c) separately.

The examination intends to test the adequacy of the proposed SLCR on the preparation dataset tainted by various dimensions of clamor. We select the all-encompassing Yale B, CMU Multi-PIE and AR databases to test and all preparation tests are undermined by various dimensions of clamor. The preparation pictures are from the all-encompassing Yale B, CMU Multi-PIE and AR databases separately, and from left to right, the preparation pictures are defiled by salt-and pepper clamor from 5% to 30%, individually. Considering various databases having an alternate example measure, we arbitrarily pick 20 and 30 pictures for every person from the all-inclusive Yale B database, 5 and 6 pictures for each person from PIE and AR databases as the preparation set and the rest as the testing set, individually.

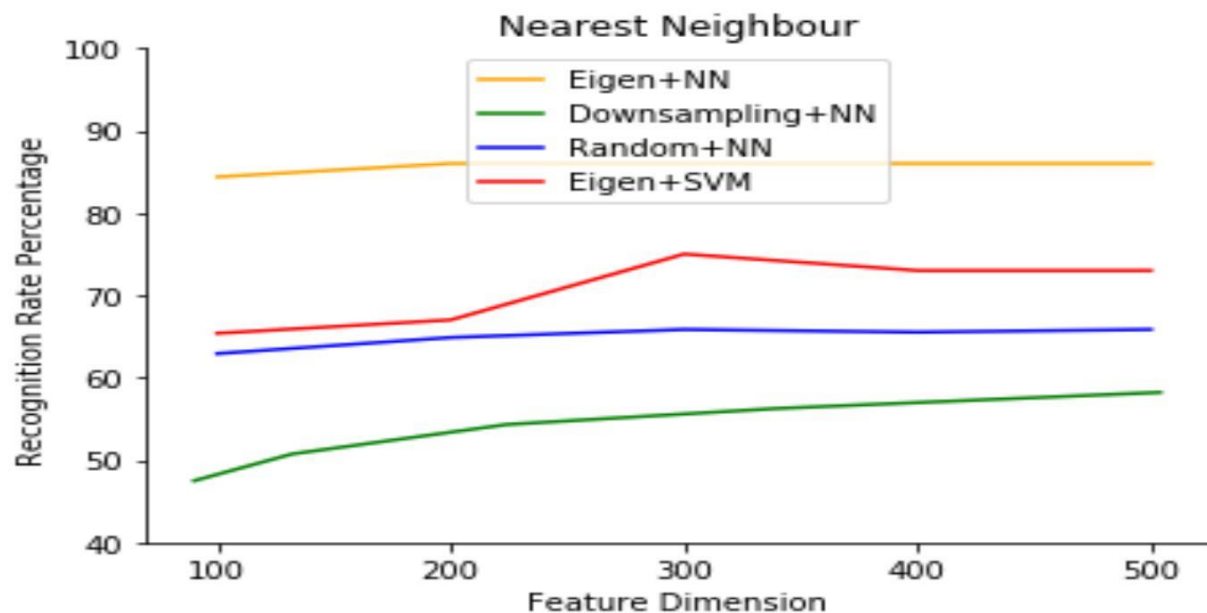


Fig. 2 Different accuracy with both the classifiers the SVM and KNN

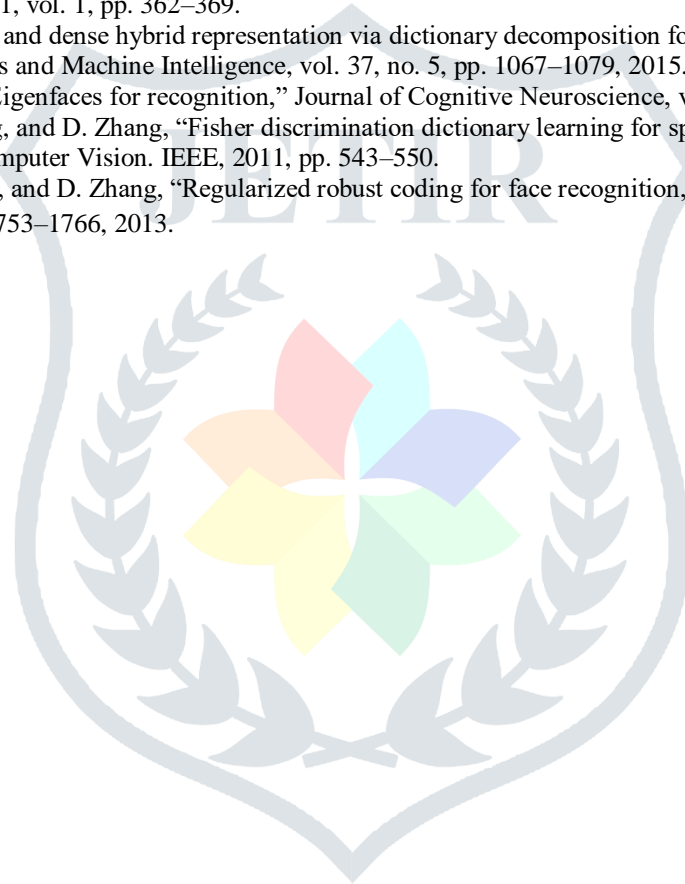
Here the Down sampled image, Random image (that includes salt and pepper noise), Eigen with both the classifier the K-nearest neighbor and SVM are included. The accuracy is better in both the case for Eigen values i.e. the algorithm we are proposing and is low for the existing methods. From here we can propose that SLCR is best fit for the low quality images.

III.ACKNOWLEDGMENT

Our proposed SLCR reliably beats other sparse representation based methods for face acknowledgment with low-quality pictures. Subsequently, we break down the motivation behind why the proposed SLCR can genuinely well take care of the acknowledgment issue of low quality face pictures. We pick a precedent in commotion examinations to delineate the strategy of the above analyses. Actually, SLCR utilizes low-position grid recuperation to get the low-position segment and non-low position part which have less commotion in all face pictures. As such, the dictionary in SLCR not exclusively can depict facial highlights well yet in addition can decrease the effect of commotions. The better commotion fitting capacity of SLCR along these lines prompts better face acknowledgment execution. The procedure of dictionary construction in SLCR can evacuate loads of data brought about by clamors. In the meantime, the dictionary in SLCR keeps up more assorted variety than the other methods. Accordingly, SLCR accomplishes hearty execution in these examinations. For different databases and other low quality pictures (i.e., disguised and occluded), the circumstance is comparative.

REFERENCES

- [1] T. Larrain, J. S. Bernhard, D. Mery, and K. W. Bowyer, "Face recognition using sparse fingerprint classification algorithm," *IEEE Transactions on Information Forensics and Security*, vol. 12, no. 7, pp. 1646–1657, 2017.
- [2] F. De la Torre and M. J. Black, "Robust principal component analysis for computer vision," in *IEEE International Conference on Computer Vision*. IEEE, 2001, vol. 1, pp. 362–369.
- [3] X. Jiang and J. Lai, "Sparse and dense hybrid representation via dictionary decomposition for face recognition," *IEEE Transactions on Pattern Analysis and Machine Intelligence*, vol. 37, no. 5, pp. 1067–1079, 2015.
- [4] M. Turk and A. Pentland, "Eigenfaces for recognition," *Journal of Cognitive Neuroscience*, vol. 3, no. 1, pp. 71–86, 1991.
- [5] M. Yang, L. Zhang, X. Feng, and D. Zhang, "Fisher discrimination dictionary learning for sparse representation," in *IEEE International Conference on Computer Vision*. IEEE, 2011, pp. 543–550.
- [6] M. Yang, L. Zhang, J. Yang, and D. Zhang, "Regularized robust coding for face recognition," *IEEE Transactions on Image Processing*, vol. 22, no. 5, pp. 1753–1766, 2013.



Home > Political Science > Qualitative and Multi-method Research > QCA

Article

Design and Implementation of Crossbar Scheduler for System-On-CHIP (SOC) Network in Quantum dot Cellular Automata (QCA) Technology

January 2018 · Internet Technology Letters 1(5):e26

DOI:10.1002/itl2.26

Authors:



Gunjan Thakur



Mrinal Sarvagya
Reva Group of Educational Institutions



Dr preeta Sharan
The Oxford Educational Institutions

Request full-text

Download citation

Copy link



To read the full-text of this research, you can request a copy directly from the authors.

Citations (3) References (16)

Abstract

SoC provides a comprehensive solution to the design challenges involved in the domain of telecommunication network, multimedia and consumer electronics. One of the crucial component of any SoC network is the crossbar based switching circuit which synchronize the network traffic and provides a congestion free path for communication. With the increase in number of on-chip components the power consumed by crossbar schedulers takes a significant amount of the entire power budget. This indicates the need for techniques to reduce the area and energy consumption of on-chip schedulers. In this paper we have proposed the design of on-chip schedulers for implementation in Quantum Dot Cellular (QCA) technology. QCA is the latest Nano computation technology and emerging as an alternative to replace the conventional CMOS devices. The salient features of QCA are highly dense structure, extremely low power consumption and very high processing speed. The proposed on-chip scheduler circuit has been simulated using QCA Designer tool. To perform a fair comparison, we also synthesized the proposed design in CMOS technology. The results obtained from comparison indicates that the QCA circuits occupy less area and power consumption than the traditional CMOS technology.

Discover the world's research

- 20+ million members
- 135+ million publications
- 700k+ projects [Join for free](#)

No full-text available

To read the full-text of this research, you can request a copy directly from the authors.

Request full-text PDF

Citations (3)

References (16)

... The fundamental unit of a QCA device is the QCA cell [10, 11], considered here to have the standard size of 18 nm × 18 nm. Each QCA cell contains four quantum dots with diameter of 5 nm, placed on the four corners of a square [11]. ...

Article

Wavelength selectivity using adaptive shortest path algorithm for optical network

July 2018 · *Pertanika Journal of Science and Technology*, 26(3):1527-1538

Authors:



P. Piruthiviraj
New Horizon College of Engineering



Dr preeta Sharan
The Oxford Educational Institutions



N. Ramrao

Request full-text

Download citation

Copy link



To read the full-text of this research, you can request a copy directly from the authors.

Abstract

The problem of routing and wavelength assignment is apparent in the dynamic all-optical network that plays an important role in the optical transport layer network. It is solved by minimising the connection blocking since the grooming adaptive shortest path algorithm shows comparably better results in terms of the calculation to find blocking probability. The shortest path algorithm used in this paper contains the present network state information, and each node creates a shortest path tree towards all the other nodes, which form node pairs by connecting each branch in the tree. The adaptive shortest path algorithm will find the shortest path throughout the network path and it chooses the best path from the available source-destination. Considering the number of nodes as 14 and comparing for different topology, it has been observed that the wavelength usage in each node varies with respect to different topology. Additionally, a comparative study of wavelength usage has been achieved for topologies like random, ring and tree.

Discover the world's research

- 20+ million members
- 135+ million publications
- 700k+ projects [Join for free](#)

No full-text available

To read the full-text of this research, you can request a copy directly from the authors.

Request full-text PDF

Citations (0)

References (0)

ResearchGate has not been able to resolve any citations for this publication.

Recommended publications [Discover more](#)

Article

A New Network Coding Structure and Its Application on GEMNET Backbone

[Home](#) > [Optical Devices](#) > [Physics](#) > [Optics](#) > [Photonic Crystals](#)

Article [PDF Available](#)

Photonic crystal based micro mechanical sensor in SOI platform

July 2018 · *Pertanika Journal of Science and Technology*, 26(3):1481-1488

Project: [Photonic based BioSensor](#)

Authors:



Indira Bahaddur
Malnad College of Engineering



Dr preeta Sharan
The Oxford Educational Institutions



Srikanth P C
Malnad College of Engineering

[Download full-text PDF](#)

[Read full-text](#)

[Download citation](#)

[Copy link](#)



[References \(10\)](#)

Abstract

Two-dimensional photonic crystals with nano-rod configuration integrated in a silicon-on insulator are analysed in this study. A photonic crystal waveguide suspended over a silicon substrate then weight can be applied on that substrate to change the displacement of substance and to measure sensitivity for pressure in terms of micro units. The overall objective of this work is to detect displacement, which indicates the force applied on the slab with photonic crystals that have line defects. Stress and displacement of the slab reveal the pressure applied. Stress is calculated by the power distribution/excitation in the slab. The displacement of the slab is due to the force, while pressure is determined by the photonic crystal sensor. The quality and sensitivity of the sensor are 1496 and 1200 RIU, respectively. The transmission spectrum is 0.1 micron to 0.5 microns shift, respectively, which are found to be distinct.

Discover the world's research

- 20+ million members
- 135+ million publications
- 700k+ research projects [Join for free](#)

[Public Full-text](#) (1)

Content uploaded by [Srikanth P.C.](#) Author content
Content may be subject to copyright.

Pertanika J. Sci. & Technol. 26 (3): 1481 - 1488 (2018)

SCIENCE & TECHNOLOGY

Journal homepage: <http://www.pertanika.upm.edu.my/>

Photonic Crystal Based Micro Mechanical Sensor in SOI Platform

Indira Bahaddur^{1*}, Preetha Sharan² and P. C. Srikanth¹


¹Department of ECE, Malnad College of Engineering, Hassan, India

²ECE, Oxford College of Engineering, Bangalore, India

ABSTRACT

- Original Research
- [Published: 24 April 2019](#)

A novel imaging system for underwater haze enhancement

- [A. Chrispin Jiji](#)  &
- [R. Nagaraj](#)

[International Journal of Information Technology](#)

12, 85–90 (2020)

- 84 Accesses
- [Metrics](#)

Abstract

Images captured underneath water is badly corrupted with spreading of element, which decrease the dissimilarity, alter color, as well as build point description hard on the way to recognize, by human visualization. For that reason deblurring will be a significant problem to control the underneath cause and to get better visual outcome of the picture. The projected scheme is primarily for improving deblurred imagery visibility. Dim channel preceding is mainly for removing mist, beside gradient guided strain headed for processing the picture owing towards

Hybrid Technique for Enhancing Underwater Image in blurry conditions

Chrispin Jiji^{*2}, Nagaraj Ramrao¹

¹Department of ECE, The Oxford College of Engineering, Bengaluru-560068, Karnataka, India

²Kalasalingam Academy of Research and Education, Krishnankoil-626126, Tamilnadu, India

ARTICLE INFO

Article history:

Received: 03 March, 2019

Accepted: 10 April, 2019

Online: 17 April, 2019

Keywords:

Image Restoration

Image Enhancement

Color Adjustment

Hybrid Technique

ABSTRACT

Enhancing underwater visualization using hybrid technique is generally employed into oceanic production. Through growing oceanic learning, undersea processing has drawn extra importance owing towards necessary task of picture towards attaining data. Although, suitable to reality of dust-like constituent and beam reduction, undersea descriptions continually experience small contrast and color alteration. In this paper, we estimate submerged beam transmission progression also intend an effectual means to defeat the backscatter trouble. Our scheme generally includes three steps; first, we reconstruct the picture using adaptive regularization. Second, we separate the reconstructed picture with weighted decomposition; third, we exploit color adjustment along with dehazed process via gradient guided filter towards holding dual mechanisms independently; at last, re-establish fine effect, we use hybrid technique for enhancing the picture. The tentative outcome illustrates that our proposed process extensively get better quality of unclear submerged descriptions. In common, our proposed method verified as well-performed and effectual than existing technique.

1. Introduction

In the modern years, scientists and researchers have exposed their main concern in capturing the aquatic life beneath the water. Although the statement that 70% of the globe encloses water includes enormous energy, abundant mineral assets and biological resources. The living beneath the water is still not as much look at. Conversely, challenges related by capturing descriptions beneath the water have been complex to defeat, owing to carry-over haze and color cast. The muddy nature of water suitable to process element such as mineral deposits, sand and plankton, showed a huge difficulty in undersea look at region. These elements set up lack of clarity in undersea descriptions which spoils the clearness and ocular analysis of the picture and in turn, inappropriate for any advance use. Researchers have finished that the spreading and absorption property of beam underneath are the chief basis for this deformation [1]. While water is roughly 800 times denser than air, so when beam penetrate from air to water, it come across reflection fact at the surface owing to which only unfair measure of beam go through water. Afterwards the beam undergoes spreading cause when it strikes and element and minerals suspend in water. Scattering diverges the beam in dissimilar directions which diminish the measure of beam falling on the object captured

underneath. The end effect of spreading outcome is that the undersea captured descriptions are dim in look [2]. A further problem is causal to lack of clarity of picture that the water molecules take up certain measure of beam when beam hit on them. Because the mass of water is larger than air, it employs dissimilar absorption possessions for diverse beam wavelengths, so the color of undersea descriptions is typically deformed. Generally, red part vanishes first as of its highest wavelength, where blue beam, by small wavelength, convey the greatest path beneath water. Therefore, undersea descriptions are often dominated via blue color. In common, color cast and beam scattering reason deviate color along with contrast degradation into descriptions attained undersea as shown in Figure 1.

In contrast, our system uses dual phases specifically Adaptive Regularization for restoration and Hybrid technique intended for improving its quality. In this work we suggested for merging the thought mainly dictionary knowledge by structural cluster along with picture restoring functions.

Our advance establishes novel regularization to beat a superior stability among local and non-local strength. Generally, our algorithm interprets learning through local and non-local similarity give inference of each picture elements. The restored picture decomposes into dissimilar elements for signifying their

*Chrispin Jiji, 8951627124 & chrispinjij@gmail.com

New Approaches in Engineering Research Vol. 3

(<https://stm.bookpi.org/NAER-V3/index>)

Home (<https://stm.bookpi.org/NAER-V3/index>) / Books
/ New Approaches in Engineering Research Vol. 3 (<https://stm.bookpi.org/NAER-V3/issue/view/176>)
/ Chapters



(<https://stm.bookpi.org/NAER-V3/issue/view/176>)

[Study on Link Based Routing Algorithm for the Desired Quality of Service of a Network](https://stm.bookpi.org/NAER-V3/issue/view/176)

R. Bhargava Rama Gowd ; T. Someshwari ; S. Thenappan ; M. N. Giri Prasad

New Approches in Engineering Research Vol. 3, 21 June 2021, Page 90-102

<https://doi.org/10.9734/bpi/naer/v3/10377D> (<https://doi.org/10.9734/bpi/naer/v3/10377D>)

Published: 2021-06-21

[View Article](#) 

[Cite](#) 

[Statistics](#) 

[Share](#) 

Abstract

Routing algorithms play an important role in the network performance calculation where Quality of service matters there are two types of routing algorithms: Local and Global Routing. Local routing allows for more effective decision-making than global routing [1]. This

Home 4 More ▾



Article

Highly sensitive lab-on-chip with deep learning AI for detection of bacteria in water

September 2019 · International Journal of Information Technology 12(13)

DOI: [10.1007/s41870-019-00363-1](https://doi.org/10.1007/s41870-019-00363-1)

Shaikh Afzal Nehal · Debpriyo Roy · Manju Devi · T. Srinivas

Research Interest

Citations

Recommendations

Reads

[See details](#)

4.5

6

0 new 0

0 new 106

Request full-text

Share ▾

More ▾

Overview

Stats

Comments

Citations (6)

References (16)



Abstract

Artificial Intelligence (AI) has provided a new insight on how to make better predictions in water quality. AI uses convolutional neural networks (CNN) modeled after the human brain. In this work we have started implementing deep learning techniques to predict level of bacterial contaminants in water. A look-up table is used to classify the level of sensing parameters based on signature of the bacteria. AI will be very helpful for accurate prediction based on signature as identified by the sensor. We have simulated an AI-based lab-on-chip application platform that can detect the contamination using the output from Photonic Crystal based optical biosensor. The presence of bacteria in water changes the output spectral behavior. By training with the different samples, design of input layer was optimized for bacteria in water. Optical biosensors are generally light weight, small and portable and less noisy system and works without electric power. The AI technique helped to distinctly predict the presence of Escherichia coli bacteria. Research concludes with the probability of accuracy of 95% detection based on output spectrum and identified training data.

Public Full-texts



[Home](#) / [Archives](#) / [Vol. 3 No. 2 \(2019\): Issue 2 - May 2019](#) / [Articles](#)

Design and Implementation of Secure Cryptographic Algorithm Using Vedic Mathematics

Snehapriya M

The Oxford College of Engineering, Bangalore, India

Manju Devi

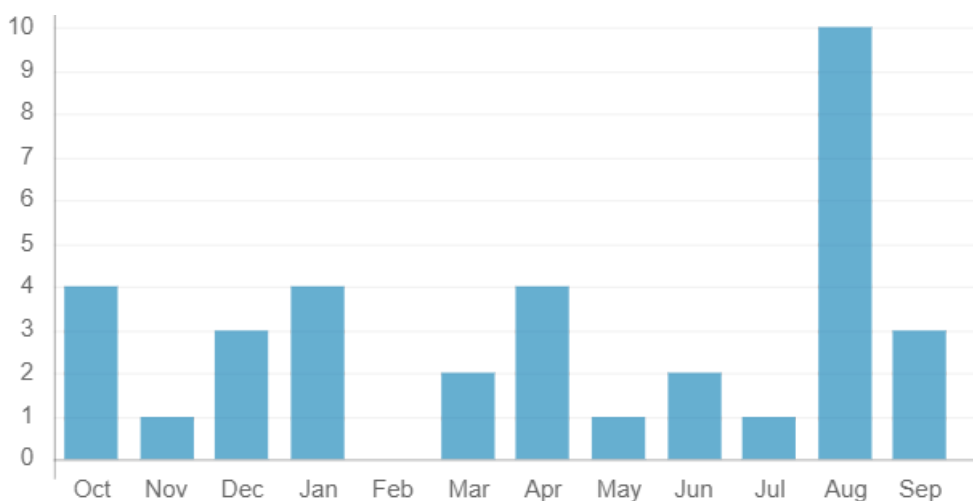
The Oxford College of Engineering, Bangalore, India

Keywords: Cryptography, AES, MATLAB, Modelsim, Vedic-Mathematics

Abstract

In the world of digitization, security is the main aspect and security of data plays an important role in communication and the field of electronics. One of the highly flexible security standard algorithm, AES provides a secure communication over the network. This paper explains the importance of the AES with the combination of Vedic-mathematics. There are mainly four steps in AES, which include add-round key, subbytes, shift-rows, mix-columns. This paper mainly concentrates on mix-columns. The analysis and simulation is done using MATLAB, Modelsim tools. This method of implementing AES using Vedicmathematics improves the performance in terms of speed, power and area.

Downloads





Home > Other

A Novel Low Power MUX based Dynamic Barrel Shifter using Footed Diode Domino Logic

5 10

International Journal of Innovative Technology and Exploring Engineering (IJITEE)
ISSN: 2278-3075, Volume-8, Issue-6S3, April 2019

1 / 5

A Novel Low Power MUX based Dynamic Barrel Shifter using Footed Diode Domino Logic

Bharathesh Patel N, Manju Devi

Abstract— The choice of the Complementary Metal Oxide Semiconductor logic to be used for implementation depend on the given specified optimization and the performance constraints that the finished chip is required to meet. Dynamic logic provides better performance for higher fan in and complex logic circuits and also with the increasing level of integration, high speed and low power dissipation have become the mandatory requirements for any logic design along with the performance.

Many design logics are available within Dynamic Logic stream. One of the popular logic is the Domino logic (DL) for low power dissipation and high- speed. This paper presents a comparative study and analysis of Barrel Shifter using Pseudo nMOS multiplexer and Footed Diode Domino (FDD) multiplexer.

Keywords— Domino CMOS circuits, Dynamic Logic, Pre-charge, Evaluation, Barrel Shifter, Pseudo nMOS, charge sharing, Power consumption.

1. INTRODUCTION

A Barrel shifter is a logic circuits extensively used in embedded digital signal processors as well as in general purpose processors to manipulate the data as rotating and shifting information is required in a few fields including bit-indexing, arithmetic tasks and variable-length coding. Several patents and copyrighted research articles efficient designed and implementation for barrel shifters [1-2].

A shifter is designed to shift and rotate the data by specified number of bits logically or arithmetically either left or right. With the increasing level of integration there is always a need to reduce the delay of operation and reduction in the power consumption. This paper presents 2 different designs of Barrel shifter using multiplexer and dynamic multiplexer and compares both in terms of power and delay [3-6]

Pseudo nMOS rationales are the most widely recognized type of CMOS ratioed rationale which Provides high speed for large fan in circuits but suffers from static power consumption [7]

Dynamic logic is widely used in high performance microprocessors and is attractive for high speed circuits as compared to static logic. Dynamic circuits use fifty percent of

clock flag. Footed Diode Domino rationale is one of the domino rationale which defeats the issue of debasement of execution because of proliferation of pre-charge beat.

A. Shift & Rotate Tasks

In this report, the input operand as denoted X and W defined as shift/rotate operation and Y denoted as shifted/rotated output result. X is defined as an m-bit esteem, m term is a number intensity of 2. Consequently, W is a logarithm of 2(m) bit number speaking to values from 0 to m-1. The bi-directional barrel shifters introduced here can perform six unique tasks: shift right arithmetic (SRA), shift right logical (SRL), rotate left (RL), shift left logical (SLL), shift left arithmetic (SLA), & rotate right (RR).

Table 1 gives a case of these tasks. In this input vector X is signified as x7x6x5x4x3x2x1x0 and the S/R sum W is a 3 bit vector indicated as b2b1b0 and the yield vector is meant as y7y6y5y4y3y2y1y0 and Table 2 demonstrates the task control bits.

Table I Shift And Pivot Models

| Operation | y7y6y5y4y3y2y1y0 |
|-----------|------------------|
| 3-bit SRL | 000a7a6a5a4a3 |
| 3-bit SRA | a7a7a7a7a6a5a4a3 |
| 3-bit RR | a2a1a0a7a6a5a4a3 |
| 3-bit SLL | a4a3a2a1a0000 |
| 3-bit SLA | a7a3a2a1a0000 |
| 3-bit RL | a4a3a2a1a0a7a6a5 |

Table II. Operation Control Bits

| 'Rotate' | 'Left' | 'Arithmetic' | Task |
|----------|--------|--------------|------|
| H | H | X' | RL |
| L | H | L | SLL |
| H | L | X' | RR |
| L | H | H | SLA |
| L | L | H | SRA |
| L | L | L | SRL |

- SRL task of a W-bit is RS & value 1's the higher W bits of the outcome to 0's.



Evolution of Wireless Communication along with Encoders

Rashmi R, Manju Devi

Abstract: Now a days technology drastically increasing, leads to increase in communication also. Internet of Things (IOT) is very basic fundamental necessary to the consumers in this decade, which requires a communication path mainly from end to end. By understanding this technology growth, took as motivation and started a survey for turbo decoder architecture in Long Term Evolution (LTE) and 3GPP-LTE communication. Different generation technologies adopt different kinds of encoder as well as decoder to encrypt the data which can be sent from source devices to destination devices, which consists parameters like data rate, frequency used to transmit and speed of transitioning i.e., encoding and decoding the data at the transmitter as well as receiver. This paper represents a survey on different architectures of turbo decoder in LTE communication which can give a brief idea about the communication and also the usage of turbo encoder in various applications. Initially we look back a history and development of a communication system till LTE. Later we discuss the different technologies and topologies on turbo decoder along with its architecture, advantage and disadvantage.

Keywords : IOT, LTE, Turbo Encoder, Communication, Encoding and Decoding

I. INTRODUCTION

Wireless communication is the communication between the two or more systems or points that are not connected through electrically. The radio waves are used in the most common wireless technologies. Cellular network communication is a kind of addicted technology and also widely accepted technology in a current generation, which is also be a very good research area for researchers. The LTE communication system is not the initial development of communication system and also turbo decoder is not the initial decoder. Lot of researchers are under research to increase the communication speed between the two different systems and also to optimize it. The main agenda of this paper is to understand the previous research work and to extract the problems or disadvantage intact to it.

II. HISTORY OF TELECOMMUNICATION

In Africa, America and some in some parts of Asia the telecommunication was begun by using the smoke signals and drums. Semaphore telegraphy is the early communication system using pivoting shutter and tower system to convey the information by Visual signals and information is encoded by the positioning of mechanical elements. The French scientist

named Claude chappe invented Semaphore telegraphy in 1792. This system was constructed using a wooden bean to show the symbols and communication was established between Lille and Paris.

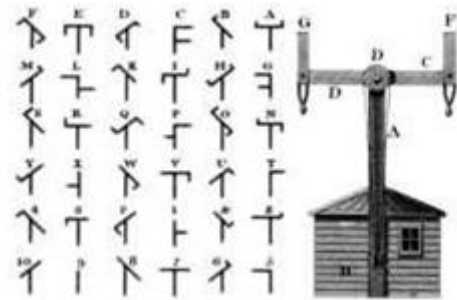


Fig1: Chappe telegraphy and code of letters and symbols associated with it.

Fig 1 represents the Chappe telegraphy model and code of letters and symbols associated with it. Later in 1726 electrical communication system initially unsuccessful where the great scientists like Laplace, Gauss and Ampere were involved in invention. In 1816 the scientist and inventor Sir Francis Ronalds invented first working telegraphy with the help of static electricity. Later in 1838 William Fothergill cooke and Charles wheat stone patented a six wire and five needle system and it is commercially available to customers to communicate around 21 kilometre (KM). This is the first electromagnetic telegraphy mounted on a device. Also in 1838, Samuel Morse and Alfred Vali combined electrical telegraphy and logging device (recording message on paper tape). This Morse telegraphy was simple and highly efficient by Morse coding and the same coding is précised by Hoffman code over 100 years later in digital communication. This technology was spread over 32000 KM in United States (US).

Fig 2 and Fig 3 represents the Morse code receiver along with recording on paper tape as well as the comparison of current standard with Morse code. Later in 1878-79 Alexander Graham Bell invented electrical telephone based on harmonic telegraphy. This technology was expanded between the two countries that is United States (US) and United Kingdom (UK). G. G. Hubbard and Alexander G. Bell were started the first company on telephone named Bell telephone company in US, now it is American Telephone and telegraph (AT&T), largest voice device communication company in world till now.

Revised Manuscript Received on November 05, 2019.

Rashmi R¹, Dept. of Electronics & Communication Engg, Vemana Institute of Technology, Bengaluru, India. Email: rashmiram@gmail.com

Manu Devi, Dept. of Electronics & Communication Engg, The Oxford college of Engineering, Bengaluru, India. Email: manju3devi@gmail.com

The first voice communication call which is transcontinental occurred on 25th January 1915,



Fig 2: Morse code receiver along with recording on paper tape



Fig 3: Comparison of current standard with Morse code
 it was commercially marketed across globe, transatlantic voice communication was impossible to customers until 1927. In 1880 Alexander G Bell and C. S. Tainter experimentally achieved the world’s first wireless telephone voice call by photophones with modulated lightbeams projected, which was implemented in military and optical fibre communication. Finally in 1956, the operational first transatlantic telephone cable which would has more than 100’s of electronic amplifiers came into exist (before the six years of Telstar launch). The static Public Switched Telephone Network (PSTN) relay for telephone calls by land line telephones to earth station which was communicated via geostationary satellite. In 20th century the technology was improvised and the communication was done through submarine communication cables by using optic fibre cables. Later in 1979 the satellite communication technology is drastically impacted with a host of commercial satellites for mobile phones, Radio’s, Television’s and internet access. Later in 1990’s, satellite communication price keeps on dropping significantly. In early 2004, Japan proposed the LTE for the first time internationally with data speed of 144Mbits/s. In 2007, Infineon found the first RF transceiver which supports LTE functionality on a chip with RF silicon processor in CMOS logic. In 2011, the researchers under gone lot of research and found a 4G LTE in south Asia (Srilanka) with a data speed of 96Mbits/s. The above section can insist the brief survey of wired and wireless telephone communication and also incorporates the drastic development in the technology along with significant decrease in the price of communication. Further we explain the specific functionality of decoders which are main part of communications and also their application along with demerits of it. The agenda of this survey is to get the at most

solution for the various demerits of Turbo encoder in the present LTE technology. In 2019 there were in and around 717 operators who have launched LTE networks across globe as per Global Mobile Suppliers Association (GMPS) survey.

III. IMPLIMENTATION OF TURBO CODER AND DECODER ARCHITECTURE FOR VARIOUS REAL TIME APPLICATIONS

The various applications like finding the maximum or minimum number a large number set, MAP decoder, mobile WiMAX and 3GPP-LTE, LTE communication and so many. In this paper we try to interpret some real time applications and usage of Turbo coder as well as decoder.

A.Field Programming Gate Array (FPGA) implementation by using parallel high speed Maximum A Posterior (MAP) decoders, in this work, the aim is to implement the designed FPGA for High speed parallel architecture for MAP probabilities decoder. Turbo principle is used by turbo equaliser to perform the digital communication. The turbo decoding can achieve a close performance of Shannon’s theoretical limit and also improves the performance of the digital communication receiver. The very high throughput can be achieved by building a sliding window approach by parallel systolic scheme. Maximum of 1.6 Gb/s is achieved by implementing a 8-state MAP decoder which need to place at the receiver end. MAP decoder is the optimised technique to minimise the bit error rate (BER). Due to this reason and results, it can be used in the mitigate channel impairments which can be found in the high speed optical fibre. To conclude the overall architecture is to achieve a throughput of 1.6Gbps with the help of 8 state max-log-Map equalizer for commercial GPP 4 channel, also provides the increase in the speed of communication as its future scope. Table 1 refers the comparison of different soft in/soft out (SISO) decoders throughput. Fig 4 represents the systolic architecture that is been implemented with 8-state max-log-MAP [1].

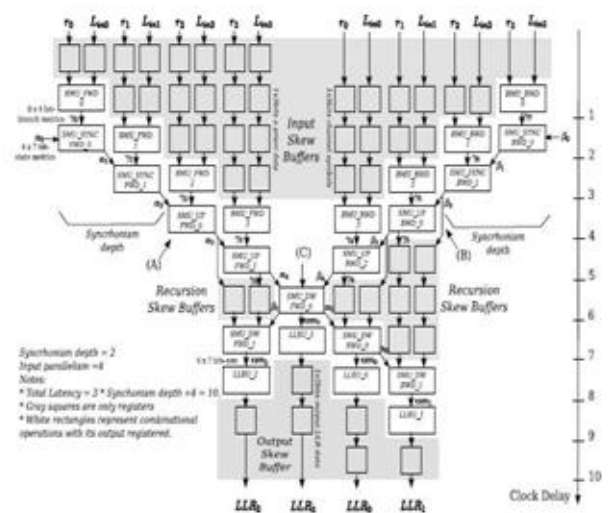


Fig 4: Implemented Systolic 8-state max-log-MAP architecture



B.Parallel Radix-4 Uniform turbo decoder for 3GPP-LTE technology as well as mobile WiMAX technology are been implemented to give support the current 4G wireless communication. In this approach the new hard-core sharing hardware architecture which consists of 8 retimed radix-4 SISO decoder. This architecture enables good throughput and two modes of parallel hardware interweavers to support the regular permutation (ARP) and quadratic polynomial permutation (QPP) interleaver. Fig 5 represents the Overall architecture of Radix-4 Uniform turbo decoder with multiplexing in time. In parallel turbo decoding system is the single chip and it has a collusion free access for the ARP or QRP interleaver which is been defined in WiMAX/3GPP-LTE standards for mobiles. Here each SISO decoder in parallel turbo decoder accesses particular memory by finding a specific address computed in the interleavers. In conventional add-compare-select (ACS) block the cascade the two-input ACS has a drawback of more time consumption as well as limiting operating frequency. For this, applying a retiming as well as migrating of common operator can reduce the time consumption by enabling the turbo decoder to perform operations in high frequency and also provides higher throughput. The memory sharing was achieved with by radix 4 Uniform single binary turbo decoding which interchanges the two extrinsic data values. Finally the two hardwares are combined by using dual mode hardware

interleaver, which consists of WiMAX as well as 3GPP-LTE on a single chip. By using two accumulator based circuit, the exact value of flip flop will disables the mobile WiMAX mode. The results of those decoders exhibits 100Mb/s in case of 8 iterations and also throughput can also made more in case of future work [2].

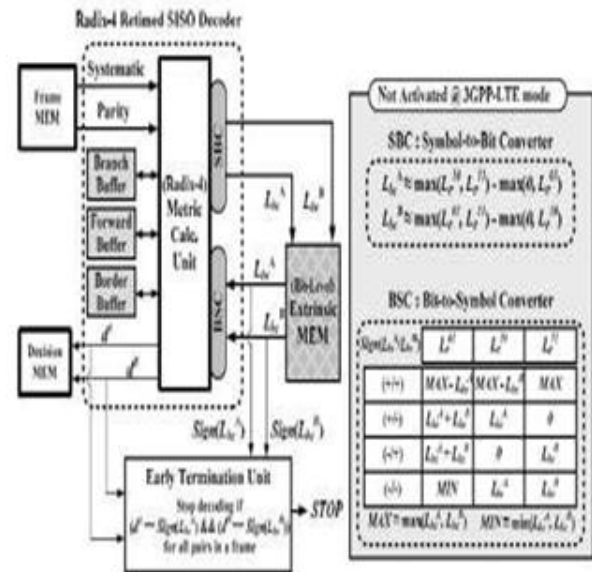


Fig 5: Overall architecture of Uniform turbo decoder with time multiplexing

Table 1: Throughput comparison between different SISO detectors

| Sl No. | Tech | Clock | Throughput iteration | Algorithm |
|--------|--------|--------|----------------------|-------------|
| 1 | 180n | 145MHz | 144Mbps | log-MAP |
| 2 | Virtex | 310MHz | 139Mbps | MAX scale |
| 3 | Virtex | 56MHz | 79.2Mbps | MAP |
| 4 | 180n | 500MHz | 500Mbps | SOVA |
| 5 | 130n | 750MHz | 750Mbps | log-MAP |
| 6 | Virtex | 100MHz | 1.6Gbps | max-log MAP |

C.As turbo code reduces the received error signals in LTE channel and optimization of this turbo code takes good field of research. In the year 2011, the new innovative and optimize 8-level turbo encoder algorithm is designed along with VLSI architecture for LTE. Also this architecture is based upon 3GPP standards and employs dual RAM turbo code interleaver, optimize 8-level parallel architecture, efficient 8-level index generator and recursive pair matching. The recursive pairwise matching technique used here to minimize the quantity of additions. The dual RAM in turbo code interleaver reduces the clock latency.

D.An 3rd order reconfigurable energy efficient continuous time $\Sigma\Delta$ modulator is presented which can be applicable for 4G-LTE system. By switching between feed forward (FF) and feed backward (FB) in the flexibility architecture, the power consumption is reduced hence it is introduced in all the core blocks (amplifier, feedback DAC and multi-bit quantizer). The FF has a drawback of high speed indispensable summing block in spite of that it has a less output swing with power efficient integrator in it. FB architecture has a capacity of enabling robust NTF design

which required for 3rd order reconfigurable $\Sigma\Delta$ modulator in FF architecture.

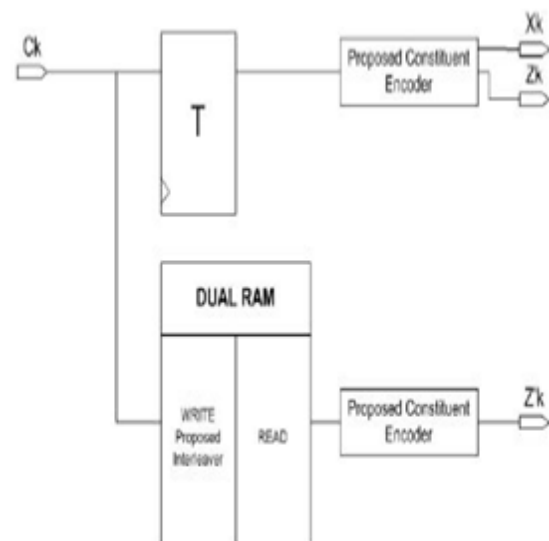


Fig 6: Block diagram of Turbo encode architecture

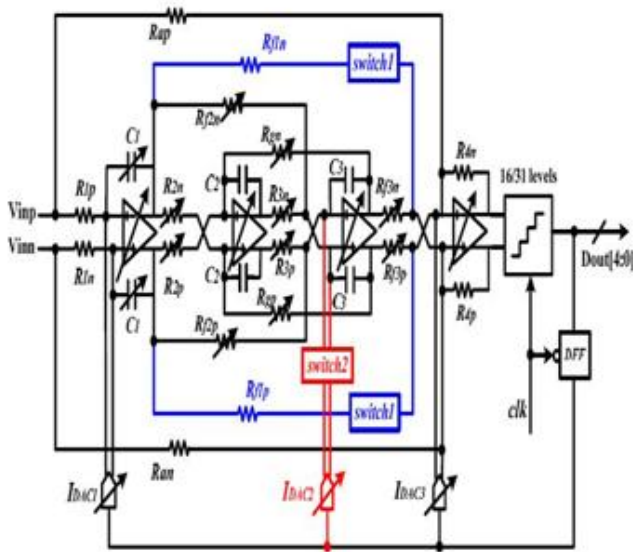


Fig7: 3rd- order reconfigurable $\Sigma\Delta$ modulator architecture

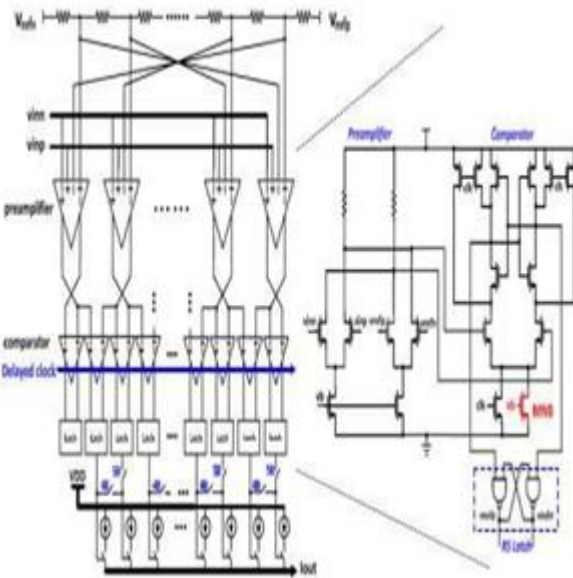


Fig 8: Flexible architecture of multi bit quantiser and FB DAC

Fig 7 represents the architecture of 3rd-order reconfigurable $\Sigma\Delta$ continuous time modulator. Fig 8 represents the Flexible architecture with multi bit interpolating quantiser along with FB DAC. Finally, the architecture is implemented by using 130nm CMOS Technology, the modulator results are 5/10/15/20 MHz over SNR of 72.7/ 66.7 /60 /59 dB for 1.2V and the Power consumed is 8/14.7/16/21 mW. The future scope is to extend the reconfigurable signal bandwidth range [4].

E. High speed architecture to find a generic min/max values, which address is presented. The proposed method is extended from earlier work on LZC architecture. Also this

method explains about quantum cellular architecture (QCA), which provides considerable advantage in terms of frequency of clock and power consumption. In this proposed architecture, to obtain the g th best value in the random list of „ k “ elements, and g value will be any value between 1 to k . This search of the value is important part in iterative channel decoder. It is an efficient hardware with less complexity as well as less latency, when the co-ordinates of the unsigned set of „ k “ larger values. The results are obtained after synthesis with a 90nm CMOS standard Cell Technology which provides the best specific values for g and k . The QCA is also used for regulation and scalable properties, which reduces lower power and high speed. To achieve all these certain topologies were taken into consideration, on a first stage each of the k element has 2^n bits with one hot code, this hot code determines the maximum value and in 2nd stage add of maximum value is determined. These two stages describes the leading zero counter (LCZ). A pipeline version of this architecture also achieved by increasing the throughput and also longer latency at the same cost with clock period of 0.32nsec. Fig 9 represents the internal architecture of decoder [5].

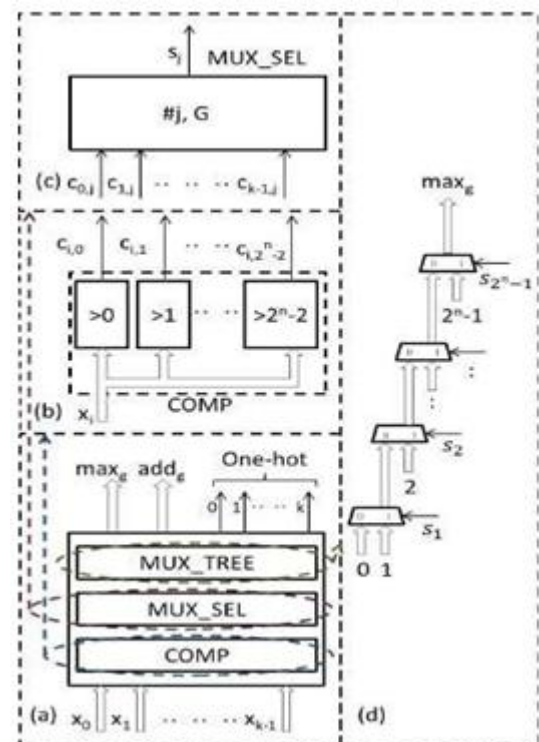


Fig 9: (a) Overall Architecture and main units, (b) Parallel Comparators, (c) Signal select on Generation and (d) Multiplexer

IV. CONCLUSION

The overall aim of this paper is to brief out the evolution of the wireless communication system along with encoder. Here initially we have approached to explain the stage by stage growth in wired communication system to wireless communication system along with associated data coders and decoders. In further section, discussion of some important real time implemented architectures and algorithms for Turbo coder and decoder which needed for current generation (4G), 3GPP, WiMAX technologies. The main drawback of turbo coder is high decoding latency.



The main challenges present in turbo coding architecture are:

- i. More time consumption due to iterative nature of the decoding algorithm.
- ii. MAP decoders recursion in forward or backward flow.
- iii. The interleavers/deinterleavers units between MAP decoder.

Finally tracking these problem statements and to provide the optimised solution to them will be future scope, it enables the less time and more latency to LTE communication system with better data rates.

REFERENCES

1. Martin I. del Barco, Gabriel N. Maggio, Damian A. Morero, et. al., "FPGA Implementation of High-Speed Parallel Maximum A Posteriori (MAP) Decoders", pp no., 98-102, ISBN 978-9-8725-1029-9, IEEE Catalog number CFP0954E.
2. Ji-Hoon Kim, In-Cheol Park," A Unified Parallel Radix-4 Turbo Decoder for Mobile WiMAX and 3GPP-LTE", pp no., 487-490 , 978-1-4244-4072-6/09/\$25.00 ©2009 IEEE
3. Ardimas Andi Purwita, Arnaud Setio, Trio Adiono, "Optimized 8-Level Turbo Encoder Algorithm and VLSI Architecture for LTE", International Conference on Electrical Engineering and Informatics, Bandung, Indonesia, 17-19 July 2011, 978-1-4577-0752-0/11/\$26.00 ©2011 IEEE
4. Jing Li, Ruiyuan Zhu1, Ting Yi, Bill Liu, Zhiliang Hong," An Energy-Efficient 5-MHz to 20-MHz, 12-bit Reconfigurable Continuous-Time $\Sigma\Delta$ Modulator for 4G-LTE Application", 978-1-4799-1235-3/13/\$31.00 ©2013 IEEE
5. *Andrea Dario Giancarlo Brololi, Juan Chi Wang,* " A FAST ARCHITECTURE FOR FINDING MAXIMUM (OR MINIMUM) VALUES IN A SET", IEEE International Conference on Acoustic, Speech and Signal Processing (ICASSP), 2014
6. Berrou, A. Glavieux and P. Thitimajshima, "Near Shannon Limit ErrorCorrecting Coding and Decoding: Turbo-Codes," Proceedings of International Conference on Communication, pp. 1064-1070, 1993.
7. 3rd Generation Partnership Project; Technical Specification Group Radio Access Network; Evolved Universal Terrestrial Radio Access (E-UTRA)," Multiplexing and Channel Coding (Release 9) 3GPP Organizational Partners TS 36.212, Rev. 8.3.0, May 2008.
8. 3rd Generation Partnership Project; Technical Specification Group Radio Access Network; Evolved Universal Terrestrial Radio Access (E-UTRA)," Multiplexing and Channel Coding (Release 10) 3GPP Organizational Partners TS 36.212, Rev. 10.0.0, 2011.
9. C-C. Wong and H-C. Chang, High-Efficiency Processing Schedule for Parallel Turbo Decoders Using QPP Interleaver," IEEE Transactions on Circuits and Systems I: Regular Papers, vol. 58, no. 6, pp. 1412-1420, June-2011.
10. C. Lin, C. Chen, E. Chang and A. Wu, "Reconfigurable Parallel Turbo Decoder Design for Multiple High-Mobility 4G Systems," Journals of Signal Processing Systems (Springer US), pp. 1-14, 2013.
11. Y. Sun and J. R. Cavallaro, "Efficient Hardware Implementation of a Highly-Parallel 3GPP LTE/LTE-Advanced Turbo Decoder," INTEGRATION, the VLSI Journal, vol. 44, pp. 305-315, 2011.
12. S. Belfanti, C. Roth, M. Gautschi, C. Benkeser and Q. Huang, "A 1Gbps LTEAdvanced Turbo-Decoder ASIC in 65nm CMOS," IEEE Symposium on VLSI Circuits (VLSIC), pp. C284-C285, 2013.
13. T. Inseher, F. Kienle, C. Weis and N. Wehn, "A 2.15 GBit/s Turbo Code Decoder for LTE Advanced Base Station Applications," International Symposium on Turbo Codes and Iterative Information Processing (ISTC), pp. 21-25, 2012.
14. D. Talbot, A Banner Year for Mobile Devices," MIT Technology Review, COMMUNICATION NEWS, December-2012.
15. Anghel, Cristian, Cristian Stanciu, and Constantin Paleologu. "Sorting methods used in parallel turbo decoding for LTE systems." In Signals, Circuits and Systems (ISSCS), 2015 International Symposium on, pp. 1-4. IEEE, 2015.
16. Mishra, Shivshankar, Harshit Shukla, and Suneel Madhekar. "Implementation of Turbo decoder using MAX-LOGMAP algorithm

in VHDL." In 2015 Annual IEEE India Conference (INDICON), pp. 1-6. IEEE, 2015.

17. Bahirgonde, Prabhavati D., and Shantanu K. Dixit. "Low complexity modified constant Log-Map algorithm for radix-4 turbo decoder." In Pervasive Computing (ICPC), 2015 International Conference on, pp. 1-4. IEEE, 2015.
18. Shrestha, Rahul, and Roy Paily. "Hardware Implementation and Testing of Log-MAPP Decoder Based on Novel Un-Grouped Sliding-Window Technique." In Electronic System Design (ISED), 2014 Fifth International Symposium on, pp. 171-175. IEEE, 2014.

AUTHORS PROFILE



Rashmi R currently working as Assistant Professor in the Department of Electronics & communication Engineering at Vemana Institute of Technology, Bengaluru. She has BE and M. Tech Degrees in Digital Communication and Networking. She has 8 years of experience in Teaching and Administration. Her area of Research includes Digital Communication. She has published more than 7 papers both in National and International Journals. She is a member of many professional bodies like ISTE, IACSIT, IAENG, IFERP. **Email: rashmiramreddy@gmail.com**



Dr Manju Devi is working as Professor and head in the department of ECE at The Oxford College of Engineering Bangalore. She has worked as Vice-Principal and professor at BTLIT, Bangalore. She obtained her B.E (ECE) degree in 1996 from Anna University, M.Tech degree in Applied Electronics from BMSCE, and Ph,D from Visvesvaraya Technological University (VTU), Karnataka. She has almost twenty two years of academic teaching experience and worked for both NBA and NAAC. She has almost 75 publications in international conference and journals. She is guiding eight students from Visvesvaraya Technological University (VTU), Karnataka. Her areas of interest are VLSI design, Analog and Mixed mode VLSI design and Digital Electronics. **Email:manju3devi@gmail.com**



Institutional Sign In

All



ADVANCED SEARCH

Conferences > 2018 3rd IEEE International C...

Enhancement of Underwater Deblurred Images using Gradient Guided Filter

Publisher: IEEE

Cite This

PDF

A.Chrispin Jiji ; R Nagaraj All Authors

50 Full Text Views



Alerts

Manage Content Alerts

Add to Citation Alerts

More Like This

A Fast Sand-Dust Image Enhancement Algorithm by Blue Channel Compensation and Guided Image Filtering
IEEE Access
Published: 2020

An Experimental-Based Review of Image Enhancement and Image Restoration Methods for Underwater Imaging
IEEE Access
Published: 2019

Show More

Abstract



Downl

PDF

Document Sections

- I. Introduction
- II. Related Work
- III. Enhancing Underwater Deblurred Imagery
- IV. Proposed Filter
- V. Experimental Results

Show Full Outline

Authors

Figures

References

Keywords

Metrics

More Like This

Abstract:Underwater imagery is extremely essential owing to the eminence of imagery which captures underwater. While capturing such imagery, excellence of descriptions corrupt owi... **View more**

Metadata

Abstract:

Underwater imagery is extremely essential owing to the eminence of imagery which captures underwater. While capturing such imagery, excellence of descriptions corrupt owing to various factor similar to wrinkle within water, lack of accessibility of radiance, organic material dissolve in water as well as images capture as of a very little distance. Hence it should be process before applying it on this imagery. Existing weighted guided filter be able to lessen halo artifacts but it fail to maintain boundaries. In our paper, we propose to overcome this drawback by using gradient domain guided image filter which will improve the excellence, restrain the blare, and conserve the boundaries into imagery. Tentative effect shows improved performance, evaluated to former schemes, mainly close to the boundaries.

Published in: 2018 3rd IEEE International Conference on Recent Trends in Electronics, Information & Communication Technology (RTEICT)

Date of Conference: 18-19 May 2018 **INSPEC Accession Number:** 19410910

Date Added to IEEE Xplore: 27 February 2020 **DOI:** 10.1109/RTEICT42901.2018.9012305

Publisher: IEEE

ISBN Information:

Conference Location: Bangalore, India

I. Introduction

Underwater bad imaging situation, like blur, the excellence of images corrupt brutally owing to the influence of element in the underwater. Imperfect element will disperse radiance and consequence in reduction of reflected radiance commencing the scene along with the scattered radiance resolve the radiance received by means of the camera and change the image dissimilarity and colour [1]. Consequently, it is essential for computer vision system to get better visual possessions. Image deblurring technique, is to reduce interference due to haze by particular approach, in order to acquire acceptable visual effect and attain more useful information [2]. Also removes useless possessions and is often considered as an image enhancement system. conversely, it differ from conventional noise deduction and dissimilarity improvement method as the degradation to representation pixels that is induce by the existence of haze depends on the distance among the object and the attainment device and the local density of the blur [3]. These methods not take the effect of the degradation interested in description, but mostly employ targeted method to get better contrast and detail of the representation. Image enhancement based method is not necessary to resolve the substantial form of image degradation, but somewhat directly improve the image contrast and excellence from the perception.

Underwater image enhancement method presents a means towards getting better the item detection within undersea situation. At hand bunch of explore happening intended for the development of picture excellence, however inadequate effort have made in to the part of underneath imagery, since underneath location picture obtain distorted owing near reduced visibility situation along with property resembling "assimilation", "evidence", "flexible of brightness, "denser intermediate", as well as "dissemination" etc. These are the significant part which sources the deprivation of underneath descriptions. Next difficulty regarding the density is well thought-out 800 times denser than atmosphere. Consequently, once illumination emission progress from e atmosphere into water, it is partially reproduce furthermore partially go through it. The entire illumination quantity too begins dropping. Likewise, particle underneath besides take in quantity of illumination. Because of these underneath imagery are reaching dim and dim since the depth raises. But also colors fall off based on the wavelength. Which build the descriptions subject merely with blue color of any object under the water is affected. In addition, the haze descriptions include slight intensity, slight dissimilarity and so on. When an underwater image [4] is captured, it is necessarily to right and regulate the image. The filter use normally improves the image excellence, suppress the noise, and conserve the boundaries in an image. Consequently boundary preserving filters are used for underwater dispensation. The projected scheme is to incorporate a precise initial categorize boundary sensitive restraint which conserved to a large extent. Tentative consequences of application illustrate that the resulting algorithms generate imagery by means of enhanced visual excellence.

Sign in to Continue Reading

- [Authors](#) ▼
- [Figures](#) ▼
- [References](#) ▼
- [Keywords](#) ▼
- [Metrics](#) ▼

IEEE Personal Account

Purchase Details

Profile Information

Need Help?

Follow

CHANGE USERNAME/PASSWORD

PAYMENT OPTIONS

COMMUNICATIONS PREFERENCES

US & CANADA: +1 800 678 4333



VIEW PURCHASED DOCUMENTS


PROFESSION AND EDUCATION

WORLDWIDE: +1 732 981 0060

Loading [MathJax]/extensions/MathZoom.js

TECHNICAL INTERESTS

CONTACT & SUPPORT

[About IEEE Xplore](#) | [Contact Us](#) | [Help](#) | [Accessibility](#) | [Terms of Use](#) | [Nondiscrimination Policy](#) | [IEEE Ethics Reporting](#)  | [Sitemap](#) | [Privacy & Opting Out of Cookies](#)
A not-for-profit organization, IEEE is the world's largest technical professional organization dedicated to advancing technology for the benefit of humanity.

© Copyright 2021 IEEE - All rights reserved. Use of this web site signifies your agreement to the terms and conditions.

IEEE Account

- » [Change Username/Password](#)
- » [Update Address](#)

Purchase Details

- » [Payment Options](#)
- » [Order History](#)
- » [View Purchased Documents](#)

Profile Information

- » [Communications Preferences](#)
- » [Profession and Education](#)
- » [Technical Interests](#)

Need Help?

- » **US & Canada:** +1 800 678 4333
- » **Worldwide:** +1 732 981 0060
- » [Contact & Support](#)

[About IEEE Xplore](#) | [Contact Us](#) | [Help](#) | [Accessibility](#) | [Terms of Use](#) | [Nondiscrimination Policy](#) | [Sitemap](#) | [Privacy & Opting Out of Cookies](#)

A not-for-profit organization, IEEE is the world's largest technical professional organization dedicated to advancing technology for the benefit of humanity.

© Copyright 2021 IEEE - All rights reserved. Use of this web site signifies your agreement to the terms and conditions.

An Underwater Image Enhancement via Wavelet domain Gradient Guided Filter

Chrispin Jiji, Nagaraj Ramrao

Department of ECE, The Oxford College of Engineering, Bangalore, India
chrispinjij@gmail.com, nagarajramrao@gmail.com

Abstract

Pictures confined in underneath are often yield limited visibility and low dissimilarity due to haze in undersea. Existing approaches enhance pictures but frequently undergo noise issue; this paper presents a hybrid method for solving mage enhancing difficulty in frequency domain. Firstly, we propose locally adaptive Non locally robust regularization to deblur the image. The deblurred image has small gray-level rate in any color channel. Secondly we used an open dim channel scheme to increase visibility in low-intensity rate. Thirdly, gradient guided filter to enhance the details. Later, we use the soft-thresholding process to decrease noise in high-intensity rate to advance texture information. Finally, image is well enhanced via wavelet domain gradient guided filter. The projected technique intends to raise perceptual visibility, keep extra texture information as well lower noise effect. The performance evaluations prove that projected scheme give up better results by existing methods.

Keywords: Underwater image enhancement, Dehazing, Wavelet domain Gradient guided filter.

1. Introduction

Acquiring clear descriptions in ocean environment is a significant problem in oceanography engineering [1]. The key challenges that ocean imaging suffer from severe degradation due to scattering by impurity and organisms in water. The underwater image quality plays an essential task for examining survey of undersea populations, ocean mines, shipwrecks, coral reefs, telecommunication cables and evaluating biological surroundings. Acquiring ocean descriptions is tough typically owing to haze causes light reflections, scatterers by element underneath and color alteration owing towards wavelength reduction [2] results blur, partial visibility and color variation. The element such as sand, minerals and plankton also results haze. The reflected beam from substance propagates to camera absorb and scatterers the ray. The multi-scattering process in [3] dissolves the ray keen on homogeneous surroundings of illumination. Usually processing underneath descriptions focuses to balance both scatterers or color deformation. The elimination of scatterers deformation contain polarization property balance visibility [4] to enhance undersea descriptions [5] and joining point spread and modulation transfer function decreases causes of blur [6]. Image enhancement based scheme do not acquire causes of degradation but mainly improve dissimilarity details as well as visual property. Recently lots of researchers have widened pre-processing schemes for enhancing undersea descriptions. Traditional schemes increase perceptual eminence but failed to balance adaptive degradation. To undertake these issue a few researchers added more information for haze reduction. As scatters were indefinite task of depth was frequently under constrained. Although this method is mainly for improving haze visibility and generate exciting outcome but fail to support color because enhanced imagery does not always enclose maximum dissimilarity. In modern day's major development of haze elimination employ reasonable

priors or assumptions to exploit local dissimilarity for enhancement.

In this paper, we use hybrid undersea image enhancement method to enhance image via wavelet domain gradient guided filter. Our contributions are five-fold: (1) locally adaptive non locally robust regularization for deblurring the image; (2) use open dim channel model to improve visibility efficiently; (3) gradient guided filter to enhance details; (4) exploit soft thresholding for noise removal; and (5) projected approach boost perceptual visibility as well as details, but decrease noise effect. Tentative outcome prove that the projected scheme removes blur, advance visibility, enhance details and remove noise more faithfully with state-of-the-art process.

The paper is organized as follows. Section 2 provide a review of prior art. Section 3 includes details of projected method. Section 4 presents tentative outcome and analysis. The last section concludes our paper.

2. Previous Art

In this section conventional dehazing methods are summarized with wavelet domain gradient guided filter. Image enhancement methods not necessary for solving substantial type of degradation, but relatively enhance the picture from human visual perception. Histogram equalization [6] represents a basic algorithm to solve small dissimilarity imagery. It compresses brightness to get more uniform exposure characteristics but causes "halo" and brilliance distortion. The contrast limited adaptive histogram equalization [7] scheme remove fog effects, but lead to noise amplification in some hazy imagery. Multi-scale Retinex [8] is to boost dissimilarity and brilliance, but lead to halo phenomena in some sharp boundary or cause whole picture too bright. Homomorphic filtering [9] based light model practiced foggy color imagery and

Home 14 More ▾



Article Full-text available

A Novel Technique for Enhancing Color of Undersea Deblurred Imagery

January 2018

DOI: [10.25046/aj030610](https://doi.org/10.25046/aj030610)

 Chrispin Jiji · Nagaraj Ramrao

Research Interest ⓘ

Citations

Recommendations

Reads ⓘ

[See details](#)

 0.7

1

0 new 0

0 new 19

Download

Share ▾

More ▾

Overview

Stats

Comments

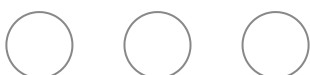
Citations (1)

References (30)



Abstract and figures

Exploring the ocean underneath has always been an area of great scientific and environmental concern. However, the study of underwater environment was very difficult due to the extreme conditions. Undersea descriptions undergo severe distortion attributed to absorptive as well as scattering properties. Absorption substantially removes illumination, whereas a ray of light redirected in several path when it interacts by substance. Because of these, undersea descriptions encompass blur as well as color loss. In this paper we suggested an effective technique namely, a turbidity removal method for deblurring the image. If the deblurred image has a lighting problem, we make use of a color-correction method to find the clear image. Our substantial qualitative and quantitative assessment expose that the proposed algorithm progress the excellence as well as lessen color distortion loyally, also improves the state-of-the-art undersea technique. © 2018 Advances in Science, Technology and Engineering Systems. All rights reserved.



Home More ▾



Article

Design and Performance Analysis of Differential Amplifier for Various Applications

November 2018 · Journal of Computational and Theoretical Nanoscience 15(11):3501-3508

DOI: [10.1166/jctn.2018.7652](https://doi.org/10.1166/jctn.2018.7652)

Jyoti M R · H Chetan · Manjudevi

Research Interest

Citations

Recommendations

Reads

[See details](#)

0.4

0

0 new 0

4 new 544

Request full-text

Share ▾

More ▾

Overview

Stats

Comments

Citations

References



Abstract

With continuous growing trends in the semiconductor industry towards the reduced power dissipation, high gain and decrease in the transistor channel length, designing of high performance circuits becomes more critical. For various application the input stage is differential amplifier because of its best advantages. In this work, we have worked on Differential amplifier which is designed and implemented with gain higher than 40 dB. The design uses a current mirror with miller compensation. This work also includes design and analysis of two stage op-amp and folded cascade op-amp to give gain higher than 70 dB and tradeoffs among the parameters such as gain, gain-bandwidth, power dissipation, current, area, trans conductance is explained. The simulations have been performed for differential amplifier, two-stage amplifier with Wilson mirror and folded cascade operational amplifier (FCOA) using VLSI CAD tool. The proposed designs have low power dissipation, high gain and high gain bandwidth. Therefore the postulation incorporates outline and recreation of two-stage operational amplifier and a folded cascade amplifier for better performance and good stability. With this differential amplifier simulation we could achieve better gain of 42 dB and 72 dB using two stage amplifier and cascade amplifier respectively.



ARCHIVES

Constructing PV Array and Power Calculation Using ANFIS Controller based MTPP

👤 Madhavi Dasari and Dr.V.S. Bharath

Abstract

At the present time, it has been emerging thought in the direction of use photovoltaic (PV) system. The paper which presents the new creative method for improve the efficiency and optimization of the PV scheme. Topology of PV scheme which includes maximized tracking of power point (MTPP) controller has discussed. The main goal to perform a special concern with ANFIS algorithm where the algorithm is combined with fuzzy inference system (FIS) and neural network which improves the PV array performance. This paper shows a deep survey and MTPP controller design to protect a high performance of PV system which can be carefully chosen for practical implementation issue. Based on fast changing radiation, the method is compared with conductance of incremental in Conventional (CI). The ANFIS on basis of MTPP scheme performs fast which provides better outcomes less than the alteration of solar irradiation. The execution is performed using MATLAB/SIMULINK software.

📖 Volume 11 | 06-Special Issue

📄 Pages: 271-280

📄 Download PDF

← Back to Archives (archives.php)

Login (login.php)

JARDCS

Journal of Advanced Research in Dynamical and Control Systems presents peer-reviewed survey and original research articles.

Quick Links

Scope of JARDCS (scope.php)

For Contributors (contributors.php)

Online Submission (submission.php)

Article Tracking (article-tracking.php)

Contact (contact.php)

Publication Ethics & Malpractice Statement (publication-ethics-malpractice-statement.php)

Archives

Current Issue (current-issue.php)

All Archives (archives.php)

Special Issues (special-issue.php)



FireFly ANN Based UPQC-S PV Array System for Power Enhancement

¹Madhavi Dasari and ²V.S. Bharath

¹Research Scholar, Department of EEE, Oxford College of Engineering, VTU, Karnataka, India. E-mail: madhavi.81d@gmail.com

²Professor, Department of EEE, Oxford College of Engineering, VTU, Karnataka, India.

Abstract

In this research work, the action of power outcome from the PV array is controlled and enhanced. This work is proposed to control the scheme applied on variable irradiance with altering the power connections by two-level inverter controlling strategy. Firefly ANN approach is applied to analyse the PQ theory and fundamental harmonics in voltages. It is done using (Firefly Based Neural Networks-Anfis Controller)-FANN-AC scheme. This contribution is used to develop the two stages controlling approach that adjust the DC voltages. 3 phase non-linear load conditions and its effects on source voltages and currents are considered. This work is implemented in MATLAB -15b, Simulink design is implemented to observe the variable irradiance changes and non-linear load conditions, limit harmonic distortion in the current.

Keywords: Controllers, Neural Networks, Power Quality analysis, PV array, UPQC.

1 Introduction

As day by day, growth in electricity utilisation leads to the identification of the alternate energy sources such as renewable resource energy systems along with existing solar and advanced solar power source units. UPQC assisted to minimising the hysteresis losses by accessing both

Journal of Green Engineering, Vol. 9_4, 638–657. Alpha Publishers

This is an Open Access publication. © 2019 the Author(s). All rights reserved

shunt and series controlling circuits. This controlling strategy is accessed by many researchers, and we followed the same in our approach with a limitation and to compensate the voltage sag and swell. Firefly based ANN approach is applied to PO method and this enhanced the voltage levels and minimised the harmonics at different sections. However, in our approach, we followed our principle to work on a series active filter rather than the shunt, which helps to regulate the voltages and minimises the sag levels occurred in the PV array system. In power electronics systems, power quality (PQ) is considered as an essential concern in the present era. It is fundamental, especially with the presentation of best in class gadgets, whose general execution is defenceless to the top-notch of intensity provided. Power quality issue is an event concerning shifting voltages, current or recurrence those results in a disappointment of end-use gadget [1]. The fundamental objective of conceiving UPQC is the consolidated utilisation of gathering vivacious and shunt-enthusiastic channels mainly to repay poor-arrangement current and sounds because the SCR oversaw capacitor banks make up for responsive power in power recurrence terms [2]. Displaying and recreation of custom power conditioners appear at be inescapable as vitality hardware-based absolutely framework used for expanding the quality top of the line in circulation systems [3].

2 Literature Review

In [3] authors proposed a control methodology of vector control for the lattice associated single-stage VSI in the photovoltaic framework the goal of the matrix associated inverter control is to keep up the DC-interface voltage and autonomous dynamic and responsive power stream.

In [4] suggested that the principle framework benefits that microgrids can offer to the central system, just as the future patterns in the advancement of their task and control for the following future, are displayed and discussed. Using the savvy fuzzy rationale control for DC connect adjustment dependent on the evenness property, we proposed a straightforward answer for the quick reaction and adjustment issues in the nonlinear power electronic framework.

Some authors proposed MPPT calculations (P&O and INC) make the yield intensity of the PV framework to be preserved at the most extreme while the illumination also temperature differed also changes the PV producer to the heap.

The all-inclusive advantage of the UPQC incorporated the result: it has an equivalent trademark to SCR controlled capacitor banks of achieving load pay following in illustration the consistent sinusoidal flows inside the current control mode [4, 5]. Additionally the most extreme power quality improvement apparatus for vulnerable nonlinear burdens, which need genuine sinusoidal information supply [6].

UPQC worked in unmistakable potential setups for unmarried-stage (2-wire). Also, three-stage (three-twine and four-wire) systems, different repayment methods, and current patterns additionally situated in the field [7]. Along these lines, this conditioner can procure sensible quality top-notch advancement, diminishing the vitality aggravations which are given to the clients through the mains the utilisation of the arrangement unit. Other places for PQ (i.e., mains vitality interferences) can be presented to the clients (custom quality) commencing the shunt units [8]. To repeat the essential guideline of UPQC is to make specific magnificent supply voltage and payload present-day unsettling influences, explicitly, droops, swell, irregularity, music, responsive flows, and forefront unbalance delivered by utilising the nonlinear burdens [9, 10].

The control sign given to the UPQC plays a massive job in sorting out a superior task of the apparatus. Regular control plans comprehensively utilised withstanding the control plans got from engineered knowledge which additionally recorded inside the writing. Utilizations of a couple of cutting edge numerical riggings in like and wavelet revamp particularly, in power astounding additionally are completed. A vast arrangement of writing ensuring uses of fuzzy good judgment, proficient structures, neural systems, and hereditary calculations in vitality quality is in like manner developing [11]. The ANN-based controller intends for the advanced administrator of the shunt-lively power channel and talented disconnected the utilisation of certainties from the conventional corresponding crucial controller [12]. Accordingly, a virtual controller-based at the TMS320F2812 DSP stage that did for the reference period for not holding control schemes proposed [13].

3 Problem Identification

Overall writing clarifies about sun-powered related information. Likewise, PV frameworks are planned yet need to demonstrate and tried with the proposed controller, to give the most extreme power yield. The control plan of Grid-associated PV framework investigated for giving the ideal PV power also in elevation calibre of present infused hooked on the lattice and, hence, elevated power quality; this was neglected to clarify in above literature [1-26]. The second thing is the essential factors to be considered in PQ measurement and tested the PV system with variable solar irradiance. Power quality control is possible with the proposed method not there in existed methods. Along with the enhancement of PQ, the transient response and stability of the grid associated PV scheme examined with proposed research work. Using the above identifications to analyse the characteristics of PV systems and mitigate the PQ issues and behaviour of voltage and current loops for regulating the dc connection voltage also the output inverter current [15]. At last to infuse vitality hooked on the lattice at solidarity power factor also current through short consonant twisting.

4 Methodology

In this selection, PV array collects the voltage from solar panels depending on the radiance intensity from the sun, this may vary for different seasons and time. Below figure.1 and 2.explained that ANFIS controller-based work with the help of firefly algorithm using neural networks phenomenon. With this above diagram, we are reducing the power alterations and irradiance problem. The proposed approach will help the system to get better efficiency and unity power factor.

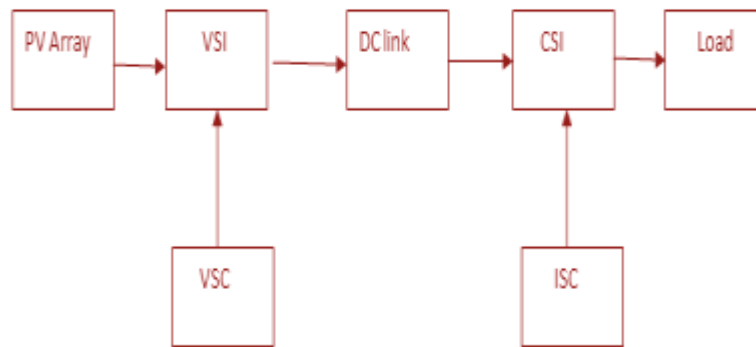


Figure 1 Existing Methodology

In another research paper[14] prescribed the use of fuzzy decision-making ability (FL) approach inside microgrid power framework based absolutely at the most extreme current vitality moulding framework contraptions which incorporate Unified/Power/Quality Conditioner (UPQC). Thus [15, 16], a straight quadratic controller (LQR) oversee method implanted through the ANN is utilised to organise the activity of the arrangement also shunt VSIs of the UPQC. In some other advancement, a regulator set of standards dependent on wavelet revise for UPQC to stifle present-day music and voltage hangs is proposed [17]. Along these lines, in [18], the developers stress the upgrade of vitality palatable with the guide of the use of UPQC with fuzzy appropriate judgment controller (FLC) as well as counterfeit neural network organiser on the customary relative principal (PI) regulator. In [19], the assurance of voltage references for arrangement fiery power get out is cultivated dependent on a stable III-section advanced fragment bolted circle (DSLL) device utilising a fuzzy controller.

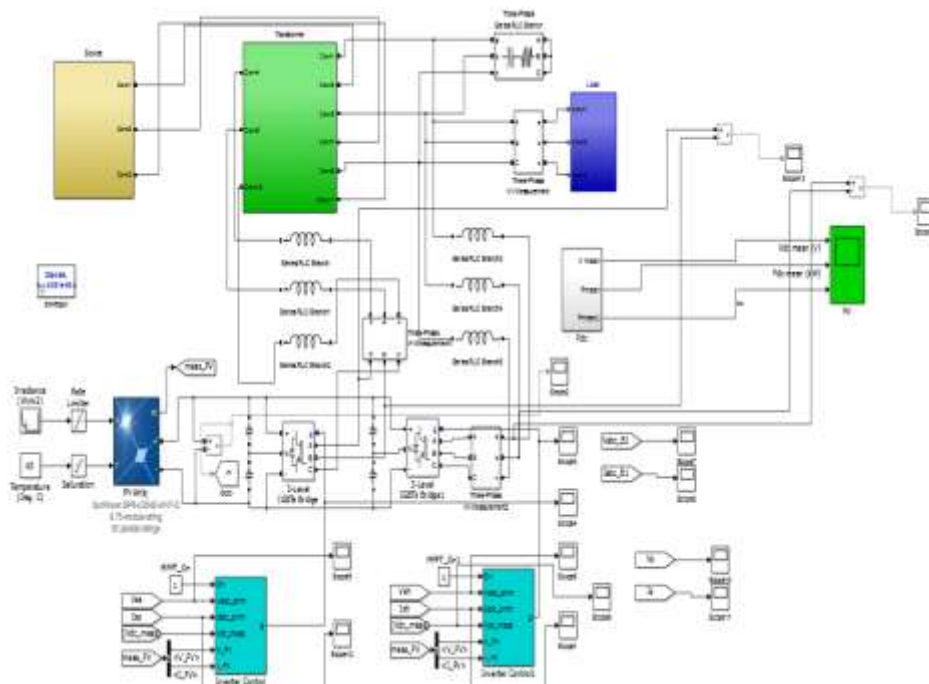


Figure 2 Existing Work -Without Neural Networks and FireFly Optimization

4.1 Proposed Work

It discovered that the dynamic steadiness of the power framework can upgrade by enhancing a transient balancing out sign got from deviation in speed, terminal recurrence, quickening power, rotor point and so forth., on the ordinary voltage blunder sign of AVR. Thus, Power System Stabilizer (PSS) is created to deliver these transient balancing out the sign to help in damping the annoyance motions utilising the balance of generator excitation signal by applying PSS yield as a strengthening control sign to the AVR this work is conceivable with FFNN-AC.

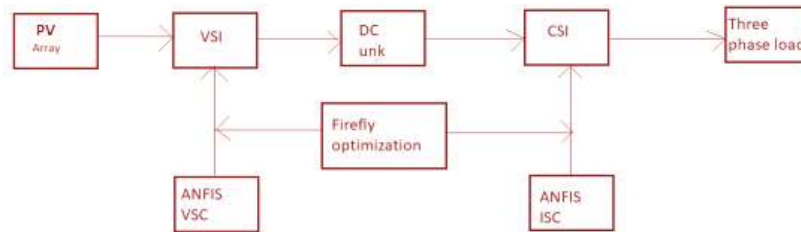


Figure 3 proposed FFNN-AC method

In this section, proposed work PV array is collected the voltage from solar panels depending on the radiance intensity from the sun, this does not vary for different seasons and time. Above fig.3 and 4a explained that ANFIS controller-based work with the help of firefly algorithm using neural networks phenomenon. With this above diagram, we are reduced the power alterations and irradiance problem. Current and voltage controller assisted the system to get better efficiency and unity power factor.

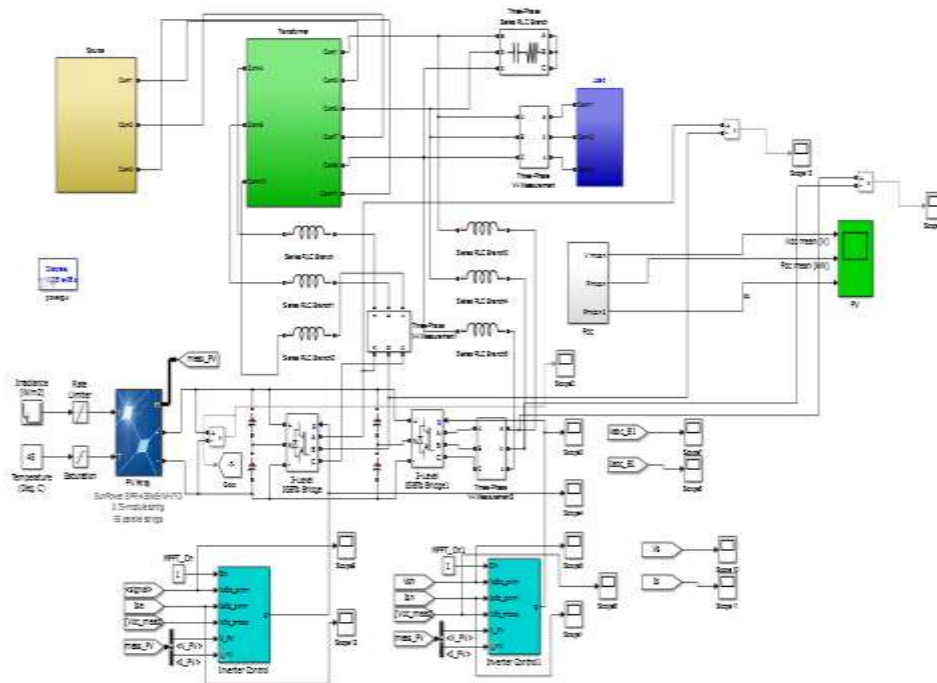


Figure 4a ANFIS-NN-FireFly Model

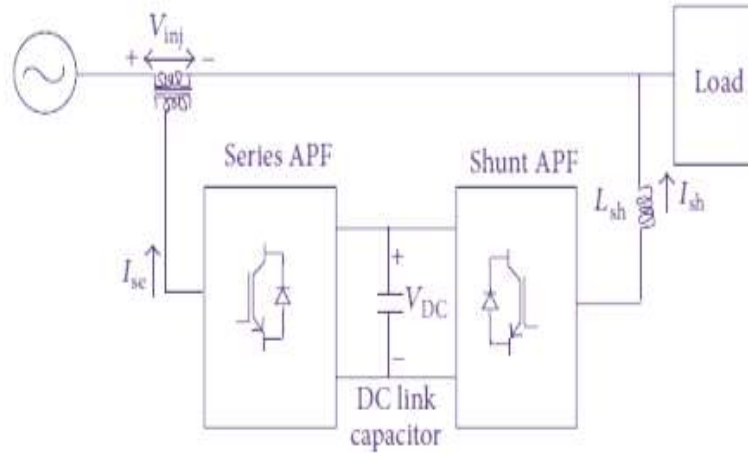


Figure 5 Block diagram

UPQC controlling strategy: Our approach is dependent on the phasor diagram for PV-array based UPQC shown in figure 5.

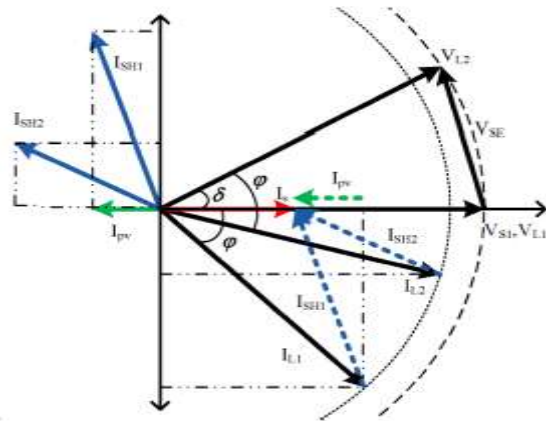


Figure 6 PV-UPQC phasor diagram

Here Inverter shunt currents given by I_{sh} , current from PV array denoted by I_{pv} , load current represented by I_L . V_s , V_L , V_{se} given as Source voltage, Load voltage, Series voltage respectively shown in fig.6 From fig. 7 source voltage of the circuit is given by

$$V_{inj} = V_0 \sqrt{x^2 + 2(1-x)(1-\cos\alpha)} \quad (1)$$

UPQC approach used in this approach helps in injecting the voltages to load and gets out from voltage sag condition. The derivation is carried out from [14]. Then this is followed by using Firefly based Neural network optimisation for controlling the sag voltages in the series compensator.

4.1.2 Firefly Based NN

The idealised behaviour of these fireflies could summarise as follows: fireflies are unisex, so they attract others regardless of their sex. In this algorithm, it assumed that the brightness of a firefly defines its attractiveness. This brightness is then encoded to objective functions $f(x)$ for $x \in S \subset \mathbb{R}^n$, considering as a continuous constrained optimisation problem.

Firefly will train by controlling the weights parameter at each step and also compares with the positions this relatively reduces the PLL utility and minimises the sag voltages due to the position acquisition. Our approach limits the values-based maximum light penetration by each firefly and its position with respective error weight option. The following steps help us for training ANN using Firefly algorithm and make us learn how optimisation carried.

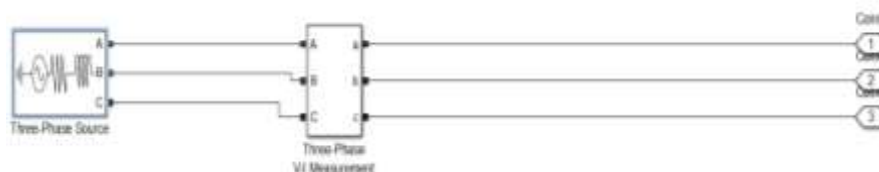


Figure 7 Source circuit

Fig.7 represents the three-phase source and measurement system which helps the microgrid system developed in this paper as an external compensator.

ANN OPTIMIZED BY FIREFLY represented in figure 9

Input: Object related to the source

STEP 1: Assign neural network with input, hidden and output layers.

STEP 2: Based Light maximisation principle update weights of neurons.

Step 3: Repeat step 2 until the best light penetrating limit acquired.

Step 4: Verify the best firefly was selected or not

Step 5: If not selected repeat Step 2

Step 6: If best obtained

Step 6.1: Update the weights and generate the best-minimised error value.

Step 7: Repeat step 2 to Step 6 until the best samples obtained.

Step 8: Compare originals limits with this Firefly neural network.

Output: The output of FIREFLY optimiser compensates the sag voltages in the series compensator.

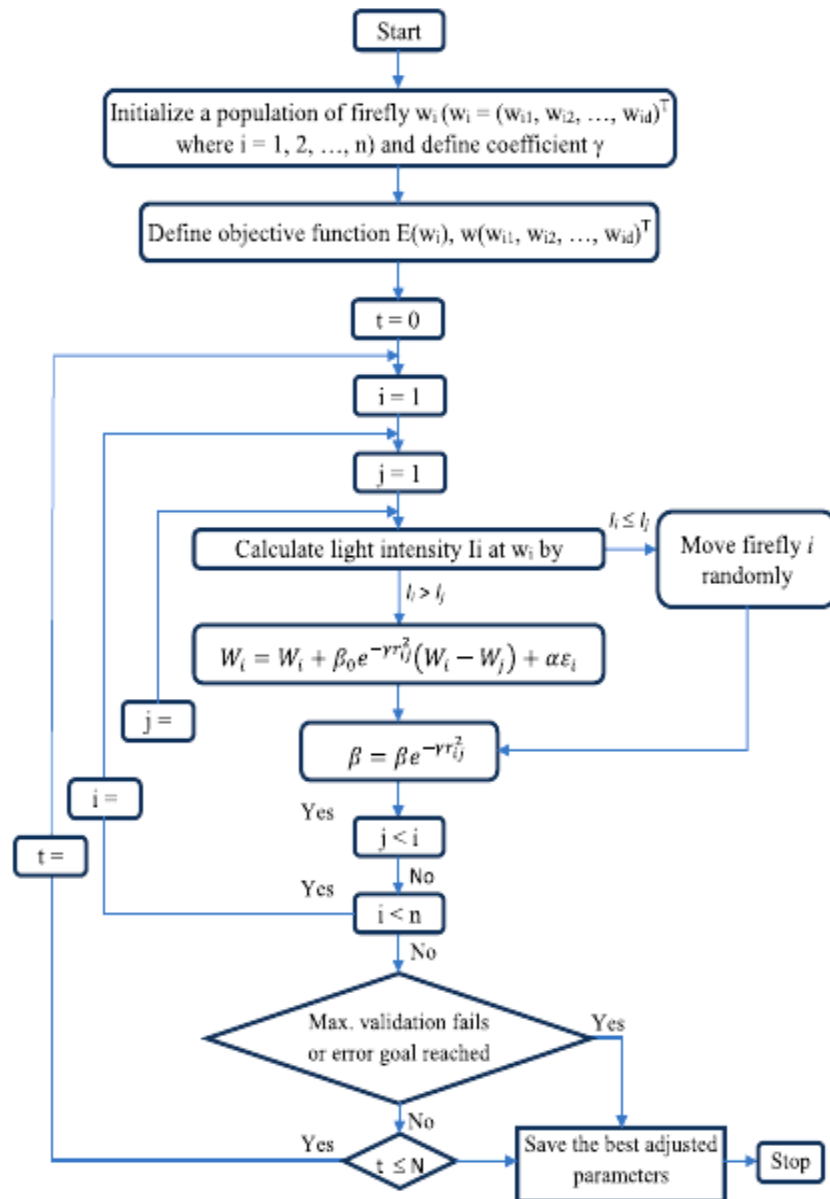


Figure 9 Flow chart for ANN with Firefly optimisation.

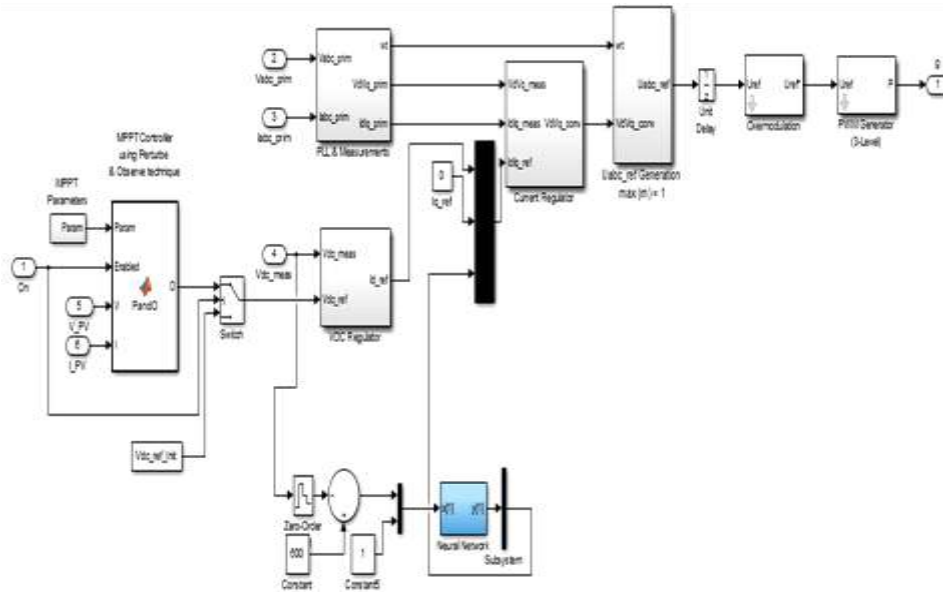


Figure 10 Series controller circuit

Figure 9 shows that Flow chart for ANN with Firefly optimisation. Fig.10 explains that series controller of circuit here system power quality is more compared to the shunt system, but the time factor is a concern.

4.1.3 Neural Networks Role

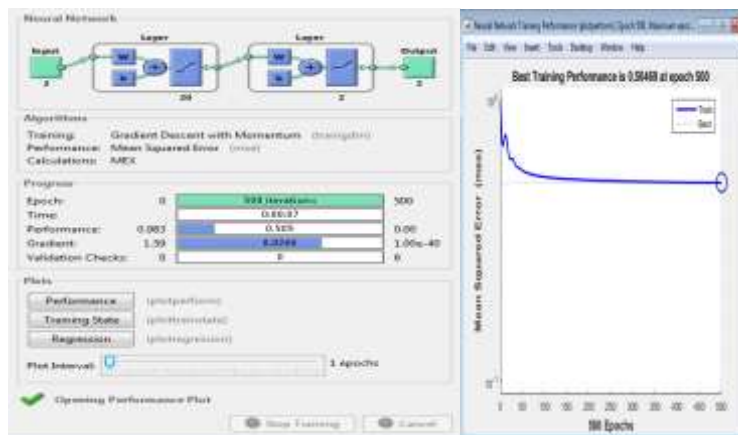


Figure 11 a) Neural Networks Role b) input voltage

5 Results and Discussions

Fig.11a. explained that neural networks data processing from controller here using layers phenomena analysing the performance, training state, regression.

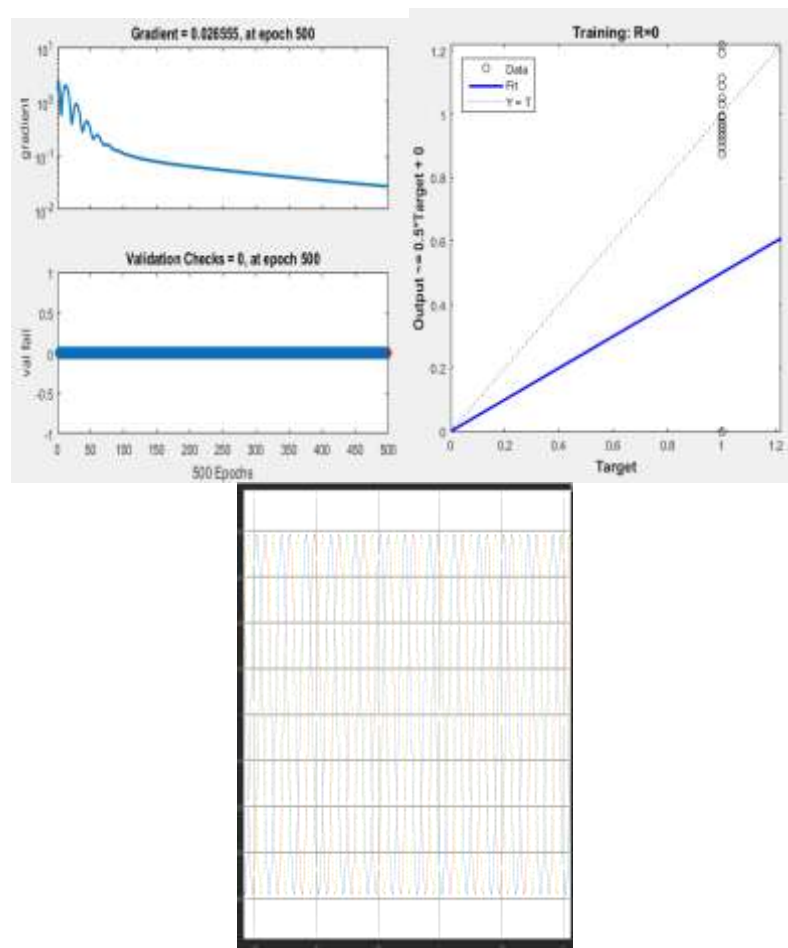


Figure 12 Input voltage from grid source and analysis 13 b) validation of echo's 13 c) target Vs output variation

Fig.12 gives the training performance limits and validating the data error minimisation using gradient the best-minimised outcome from neural networks will help in compensating the deflections in source voltages in both sag and swell modes.

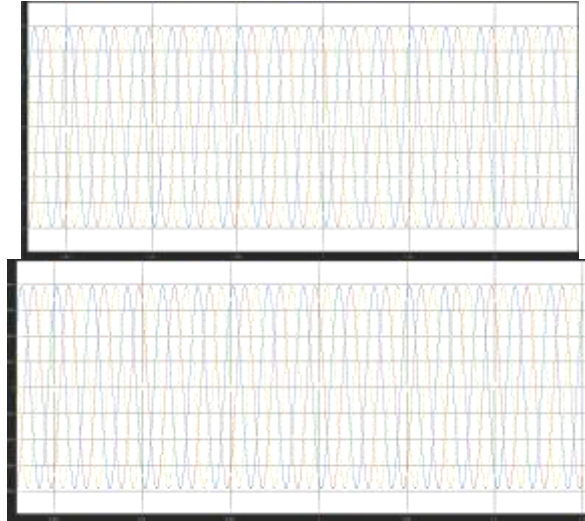


Figure 13 d) Source currents e)Load Voltages at non-linear conditions

Fig.13d) shows that source current from grid this current have so many disturbances depending on sun intensity. Fig.13e)explains that load voltage at conditions of nonlinearity here we apply FFNN-AC method. Such that reducing the sag and swings.

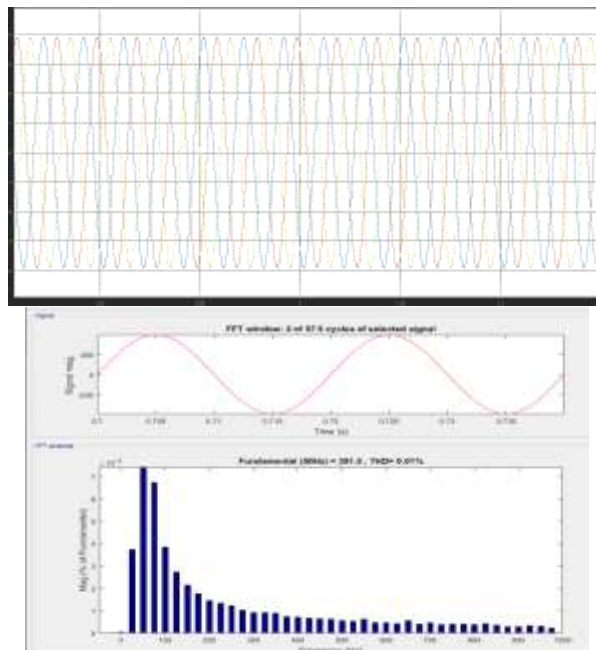


Figure 14 a) Load Currents at non-linear conditions b)THD (threshold) for source voltages

Fig.14 a) explains that load current at conditions of non-linearity here we apply FFNN-AC method. Such that reducing the sag and swings. Fig.14 b) source voltage from different sources here fundamental frequency is 50Hz THD=0.01%

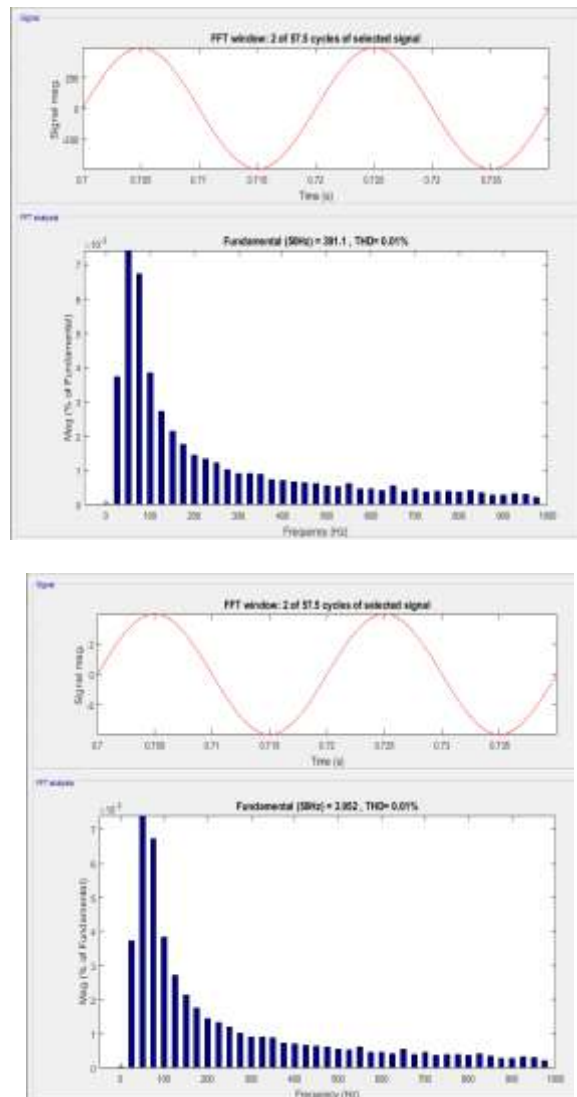


Figure15a) THD for load voltages 15b) THD at a source current

Fig.15a) source voltage from different loads and the fundamental frequency is 50Hz THD=0.01% . Fig. 15b) source voltage from different source current and fundamental frequency is 50Hz THD=0.01%

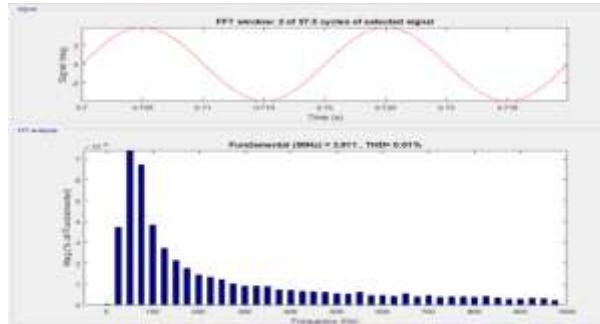


Figure 16 Harmonic distortion for load current

Fig.16 source voltage from different load current and the fundamental frequency is 50Hz THD=0.01%

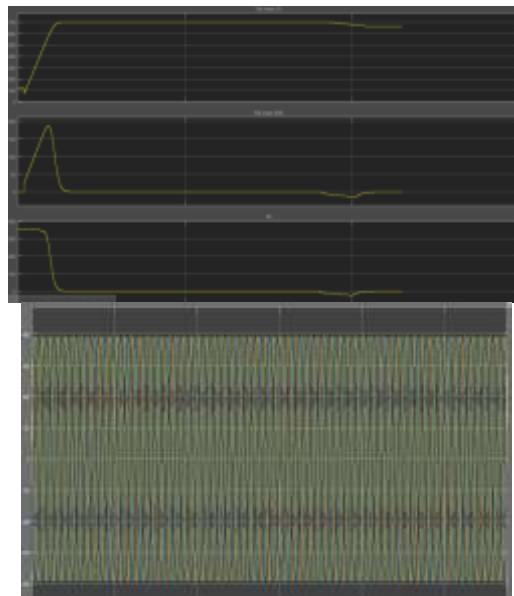


Figure 17. p_{dc} , v_{dc} , i_{dc} model

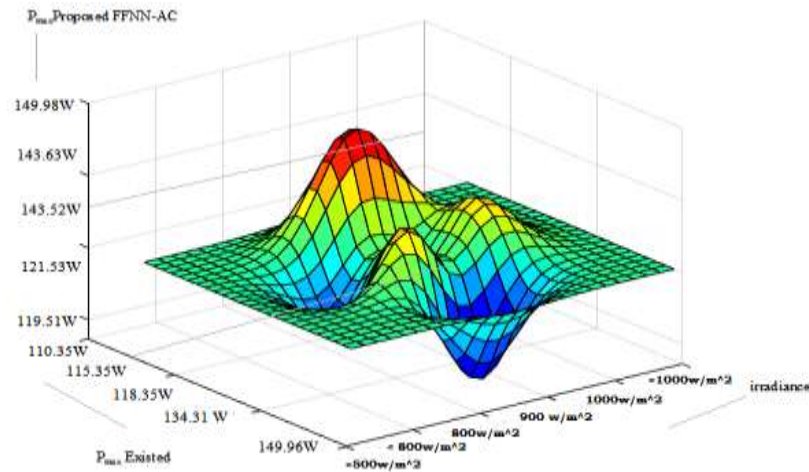


Figure 18 final comparison surface graphs

Here, p_{dc} , v_{dc} , i_{dc} model is depicted in Fig 17 and Fig.18 explained that final comparison graph between irradiance, Pmax Existed work, Pmax proposed work we achieved good improvement in power quality, stability and efficiency.

5.CONCLUSION

In this Research, the displaying and the “Simulink_models” of the entire made out of PV “generator”, support conversation and M_PPT calculations (FFNN-AC) exhibited. As per the consequences of the recreation, we reason that The PV generator execution breaks down with expanding HEAT, diminishing of sunlight based illumination and variety of the electrical burden. The MPPT calculation FFNN-AC make the yield intensity of the PV framework to reserved at the most extreme when the illumination and “temperature” changed and modifies the PV generator to the heap.

6 References

[1] Tahiri, F. E., Chikh, K., Khafallah, M., &Saad, “Comparative study between two Maximum Power Point Tracking techniques for photovoltaic system” International Conference on Electrical and Information Technologies (ICEIT) 978-1-4673-8469-8/16.

[2] Joan Rocabert, Alvaro Luna, FredeBlaabjerg and Pedro Rodriguez, "Control of Power Converters in AC Microgrids," IEEE Transactions on Power electronics, vol. 27, no. 11, pp.4734-49, 2012.

- [3] Thounthong, Phatiphat, ArkhomLuksanasakul, PoolsakKoseeyaporn, and Bernard Davat, "Intelligent model-based control of a standalone photovoltaic/fuel cell power plant with supercapacitor energy storage," *IEEE Transactions on Sustainable Energy*, vol.4, no. 1, pp.240-249, 2013.
- [4] S.Samerchur, S. Premrudeepreechacharn, Y.Kumsuwun and K.Higuchi. "Power control of single-phase voltage source inverter for grid-connected photovoltaic systems" in *Power Systems Conference and Exposition (PSCE)*, pp. 1-6, 2011.
- [5] Dong Cao, Shuai Jiang, Xianhao Yu, and Fang ZhengPeng, "Low-cost semi-Z-source inverter for single-phase photovoltaic systems," *IEEE Transactions on Power Electronics*, vol.26, no. 12, pp.3514-3523, 2011.
- [6] Soumyadeep Ray, MadichettySreedhar and AbhijitDasgupta, "ZVCS based high-frequency link grid-connected SVPWM applied three phases three-level diode clamped inverter for photovoltaic applications," in *Power and Energy Systems Conference: Towards Sustainable Energy*, pp. 1-6, 2014.
- [7] Matthias Klatt, Alicia Dorado, Jan Meyer, Peter Scheiner, Jürgen Backes, Ran Li, and Dresden–Germany Dresden–Germany Stuttgart–Germany, "Power quality aspects of rural grids with high penetration of microgeneration, mainly PV-installations," *Proceedings of the 21st International Conference on Electricity Distribution*, pp.1-4, 2011.
- [8] Chandani.Chovatia, Narayan P. Gupta, and Preeti N. Gupta, "Power Quality Improvement in a PV Panel connected Grid System using Shunt Active Filter," *International Journal of Computer Technology and Electronics Engineering (IJCTEE)*, vol.2, no. 4, pp.41-45, 2012.
- [9] A.Hari Prasad, Y.Rajasekhar Reddy and P.V. Kishore, "Photovoltaic Cell as Power Quality conditioner for Grid-connected system." *International Journal of Scientific and Engineering Research*, vol.2, no.10, pp.1-8, 2011
- [10]RiadKadri, Jean-Paul Gaubert, and Gerard Champenois. "An improved maximum power point tracking for photovoltaic grid-connected inverter based on voltage-oriented control," *IEEE Transactions on Industrial Electronics*, vol. 58, no.1, pp. 66-75, 2011.
- [11]S.A.Lakshmanan, B. S. Rajpour hit, and Amit Jain, "A novel current-controlled SVPWM technique for the grid-connected solar PV system." In *PES General Meeting Conference & Exposition*, pp.1-5, 2014.
- [12]Yongheng Yang and Frede Blaabjerg, "Low-Voltage Ride-Through Capability of a Single-Stage Single-Phase Photovoltaic System Connected to the Low-Voltage Grid", *International Journal of Photo energy*, pp.1-9, 2013.
- [13]A.Mahmud, H.R Pota and M.J. Hossain, "Nonlinear Current Control Scheme for a Single-Phase Grid-Connected Photovoltaic System." *IEEE Transactions on Sustainable Energy*, vol.5, no.1, pp.218-27, 2014.

- [14] Masoud Farhoodnea, Azah Mohamed, Hussain Shareef, and HadiZayandehroodi, "Power Quality Analysis of Grid-Connected Photovoltaic Systems in Distribution Networks," *Przeglad Elektro techniczny*, pp.208-13, 2013.
- [15] N. Kumarasabapathy and P. S. Manoharan, "MATLAB Simulation of UPQC for Power Quality Mitigation Using an Ant Colony Based Fuzzy Control Technique," *The Scientific World Journal*, vol. 2015, Article ID 304165, 9 pages, 2015.
- [16] J. Bratt, "Grid connected PV inverters: Modeling and simulation", Thesis Presented to the Faculty of San Diego State University, 2011.
- [17] A. Nordin and A. Omar "Modeling and Simulation of Photovoltaic (PV) Array and Maximum Power Point Tracker (MPPT) for Grid-Connected PV System", 3rd International Symposium & Exhibition in Sustainable Energy & Environment, 2011.
- [18] Q. Chunqing, Y. Yong and S. Ji, "Deadbeat Decoupling Control of Three-phase Photovoltaic Grid-connected Inverters", *IEEE International Conference on Mechatronics and Automation*. 2009.
- [19] R. Benadli, B. Khiari and A. Sellami, "Three-Phase Grid-Connected Photovoltaic System with Maximum Power Point Tracking Technique Based On Voltage-Oriented Control and Using Sliding Mode Controller", 6th International Renewable Energy Congress, 2015.
- [20] F. Ding, P. Li, B. Huang, F. Gao, C. Ding and C. Wang, "Modeling and Simulation of Grid-connected Hybrid Photovoltaic/Battery Distributed Generation System", *International Conference on Electricity Distribution*, 2010.
- [21] M. Makhlof, F. Messai, H. Benalla, "Modeling and simulation of gridconnected photovoltaic distributed generation system", *Journal of Theoretical and Applied Information Technology*, vol. 45 no.2, 2012.
- [22] F.E. Tahiri, K. Chikh, M. Khafallah and A. Saad, "Comparative study between two Maximum Power Point Tracking techniques for Photovoltaic System", 2nd International Conference on Electrical and Information Technologies ICEIT, 2016.
- [23] J. Jiang, T. Huang, Y. Hsiao and C. Chen, "Maximum Power Tracking for Photovoltaic Power Systems", *Tamkang Journal of Science and Engineering*, vol. 8, no 2, pp. 147-153, 2005.
- [24] L. Abderezak, B. Aissa and S. Hamza, "Comparative study of three MPPT algorithms for a photovoltaic system control", *World Congress on Information Technology and Computer Applications (WCITCA)*, 2015.
- [25] D. Dera, T. Kerekes, R. Teodorescu and F. Bladbjerg, "Improved MPPT algorithms for rapidly changing environmental conditions", *Power Electronics and Motion Control Conference*, 2006.
- [26] S. Mohammed, D. Devaraj, T. P. Ahamed, "Maximum Power Point Tracking System for Stand-Alone Solar PV Power System Using Adaptive Neuro-Fuzzy Inference System", *Biennial International*

Conference on Power and Energy Systems: Towards Sustainable Energy (PESTSE), 2016.

Biographies




Ms. Madhavi Dasari has obtained her B.E degree from Visvesvaraya Technological University, Belagavi in the year 2004. She obtained her M.Tech degree from JNTU, Kakinada in the year 2011. Her research include power quality, photovoltaic systems, artificial intelligence and renewable energy.



Mr. V. S. Bharath, has obtained his B.E degree from Madras University, Chennai in the year 1998. He obtained his M.E degree from Annamallai University, Chidambaram in the year 2002. He completed his Ph.D at Bharath University, Chennai in the year 2015. He has published over 20 Technical papers in National and International Conference proceeding/Journals. His area of interest is Inverter fed AC drives.

Original Research | Published: 18 May 2018

Grating based pressure monitoring system for subaquatic application

[Regina Mathias](#) , [Ambresh P. Ambalgi](#) & [Anup M. Upadhyaya](#)

International Journal of Information Technology **10**, 551–557 (2018)

105 Accesses | **3** Citations | [Metrics](#)

Abstract

In this work we proposed fibre Bragg grating (FBG) based pressure sensor, to detect the pressure in subaquatic application. For specific underwater pressure intervals, change in wavelength of FBG sensor is simulated with photonic design software. Obtained results exhibited distinct shift in peak resonant wavelength with wavelength ranging from 1550 to 1556 nm with Q factor of 1,32,280. FBG encapsulated mechanical model designed and analyzed to investigate strain behavior due to pressure application. **Pressure and strain change values are overlapping for the operable wavelength of 1.5625 during mechanical and optical analysis. Absolute sensitivity of sensor found to be 0.04644/RIU.** This proposed sensor can play significant roles in studying underwater diving conditions.



Journal of Emerging Technologies and Innovative Research

(An International Scholarly Open Access Journal, Peer-reviewed, Refereed Journal)
Impact factor 7.95 Calculate by Google Scholar and Semantic Scholar | AI-Powered Research Tool, Multidisciplinary, Monthly, Multilanguage Journal

UGC Approved Journal no 63975

ISSN: 2349-5162 | ESTD Year : 2014
Call for Paper
Volume 8 | Issue 9 | September 2021

JETIR **E**XPLORE- Search Thousands of research papers

Send message...

- Home
- Editorial / RMS ▼
- Call For Paper
- Research Areas
- For Author ▼
- Current Issue
- Archives ▼
- NEW
- FAQs
- Contact Us

Indexed in:

Volume 5 Issue 4
April-2018
eISSN: 2349-5162

UGC and ISSN approved
7.95 impact factor UGC
Approved Journal no
63975

7.95 impact factor calculated
by Google scholar

Unique Identifier

Published Paper ID:
JETIR1804245

Registration ID:
181313

Page Number

123-128

Post-Publication

- Download eCertificate,
- Confirmation Letter
- editor board member
- JETIR front page
- Journal Back Page
- UGC Approval 14 June W.e.f of CARE List UGC Approved Journal no 63975

Share This Article

Important Links:

- [Current Issue](#)
- [Archive](#)
- [Call for Paper](#)
- [Submit Manuscript online](#)

Jetir RMS

Title

Processing and Mechanical Characterization of 8 wt. % of Micro B4C Particulates Reinforced Al7020 Alloy Composites

Authors

Raviprakash M
 R Saravanan
 Madeva Nagaral
 V Auradi

Abstract

In the current study, an investigation made on fabrication of B4C reinforced Al7020 alloy composites and evaluation of properties. Al7020-8 wt. % of B4C composites were synthesized by liquid stir casting process. Microstructural characterization was carried out by using scanning electron microscope and energy dispersive spectroscopy. Prepared composites were evaluated for density, hardness and tensile strength as per ASTM standards. Scanning electron micro photographs revealed the distribution of B4C particulates in the Al matrix and were confirmed by EDX analysis. Further, density of Al7020-8 wt. % of B4C composites exhibited lesser density as compared to base alloy. B4C particulates reinforced composites were shown more enhanced properties as compared to A7020 alloy.

Key Words

Al7020 Alloy, B4C particulates, Microstructure, Hardness, Tensile Strength

Cite This Article

"Processing and Mechanical Characterization of 8 wt. % of Micro B4C Particulates Reinforced Al7020 Alloy Composites", International Journal of Emerging Technologies and Innovative Research (www.jetir.org), ISSN:2349-5162, Vol.5, Issue 4, page no.123-128, April-2018, Available : <http://www.jetir.org/papers/JETIR1804245.pdf>

ISSN

2349-5162 | Impact Factor 7.95 Calculate by Google Scholar

An International Scholarly Open Access Journal, Peer-Reviewed, Refereed Journal Impact Factor 7.95 Calculate by Google Scholar and Semantic Scholar | AI-Powered Research Tool, Multidisciplinary, Monthly, Multilanguage Journal Indexing in All Major Database & Metadata, Citation Generator

Cite This Article

"Processing and Mechanical Characterization of 8 wt. % of Micro B4C Particulates Reinforced Al7020 Alloy Composites", International Journal of Emerging Technologies and Innovative Research (www.jetir.org | UGC and issn Approved), ISSN:2349-5162, Vol.5, Issue 4, page no. pp123-128, April-2018, Available at : <http://www.jetir.org/papers/JETIR1804245.pdf>

Publication Details

Published Paper ID: JETIR1804245

Registration ID: 181313

Download PDF



Downloads

0002615

Print This Page



Impact Factor:

7.95 WhatsApp Contact
 Click Here
Impact Factor Calculation click here

Current Call For Paper

Volume 8 | Issue 9
September 2021

Call for Paper
Click Here For More Info

Contact Us
 Click Here

Important Links

- [Current Issue](#)
- [Archive](#)
- [Call for Paper](#)
- [Submit Manuscript online](#)

Jetir RMS



Design and Analysis of Effect of Core Thickness in UAV Wing

Puttappa H R¹, Ravi Prakash M² & Madhusudhan Reddy³

¹P G Scholar, Dept of Mechanical Engineering, The Oxford College of Engineering, Bengaluru.

^{2,3}Asst. Prof, Dept of Mechanical Engineering, The Oxford College of Engineering, Bengaluru.

ABSTRACT: Sandwich construction is enormously used in airliner, rocket and satellite structures because of high strength to weight ratio. Sandwich constructed with thin, high strength and high stiffness sheets of fiber or metallic composite material divided by a thick layer of less density substance as shown in Figure 1. The thicker sheet of less density substance commonly known as core material having light foam type (e.g. Rohacell or Nomex core as shown in Figure 2 or metallic honeycomb as shown in Figure 3 or corrugated core as shown in Figure 4). The core material adhesively bonded to the face sheets.

A sandwich-prepared composite is an exceptional class of composite materials which is fabricated by combining two thin substances but having rigid films with lightweight but having wide core. The core substance is typically prepared which is having less strength substance; however it is having high thickness present the sandwich composite which is having larger bending stiffness and when we take it as whole material will be having less density.

The open and closed compartment prepared foams made up of with the following materials.

- Balsa wood
- Polyvinylchloride
- Honeycombs and
- Syntactic foams are frequently used core materials.

This open and closed compartment metal foam can be called as core materials.

KEYWORDS: Core Thickness, Composite, UAV, Rustom, Wing, Honeycomb, Stress, Strain, Bending Moment, Nestron.

1. INTRODUCTION

Laminates which is made up of glass or carbon fiber-reinforced thermoplastics or largely used thermo set polymers (polyesters, epoxies...) are extensively formed as skin substance. In some of the cases Sheet metal is acts as a skin material.

Main factors depend of the composite material strength is as follows:

The external skins: If the sandwich covered by face sheets on both sides and the whole sandwich is stressed by applying

forces on the core of the beam, and then the bending moment will happens by means of shear forces in the sandwich. The outcome of the shear forces are tension in bottom skin face sheet and compression on the top skin face sheet. The core material separated between top and bottom face sheet. If I increase the thickness of the core the composite material will be stronger as stronger. This working principle is same as I beam concept.

Between the core and the skin the adhesive acts as resin: after applying a load on the composite the shear stress on the core and the face material will going to change rapidly. There will be a small amount of shear stress due to applied load and due to bending on the adhesive cannot be neglected. If the adhesive bond between the top face sheet and core material and also core material and bottom face should not be weak because of this there may be leads to a de-lamination.

1.1 Advantage of Sandwich Constructed Composites:

- There is improved bending stiffness to weight ratio when I compared with monolithic construction.
- There is a high resistance to mechanical properties and this leads to a more sonic fatigue.
- There is better damping feature when compared to other materials.
- There is better improvement in the thermal insulation.

But for this project I am going to use specific set of material for the sandwich construction which is already pre determined. I am going to use foam as the core and carbon fiber in the face.

1.2 RUSTOM II

The Aeronautical Development Establishment, a laboratory under the DRDO, in collaboration with HAL and Bharath Electronics Limited, is developing a largely indigenous RUSTOM II which will be in the same class as the predator of the US. It will field advanced capabilities, additional payloads and an endurance of 24 hours. Maiden flight is scheduled for February 2014 and the \$342.25 million RUSTOM II project for 10 RUSTOM II UAV's, spare vehicles and support equipments is planned to be completed by august 2017. Unmanned Aerial Vehicle having medium altitude long endurance. Properties which elaborates the RUSTOM are given below in the table.

| | |
|--------------------|--------------|
| Speed | 125-175 Kmph |
| Maximum Altitude | 32000 Feet |
| Operating Altitude | 20000 Feet |
| Maximum Speed | 225 Kmph |
| Stall Speed | 110 Kmph |

Table 1: Important Parameters of RUSTOM 2.

1.3 Wing of the Unmanned UAV

Wing of the RUSTOM UAV is designed on the concept of two spar wing configuration and it's a high wing.

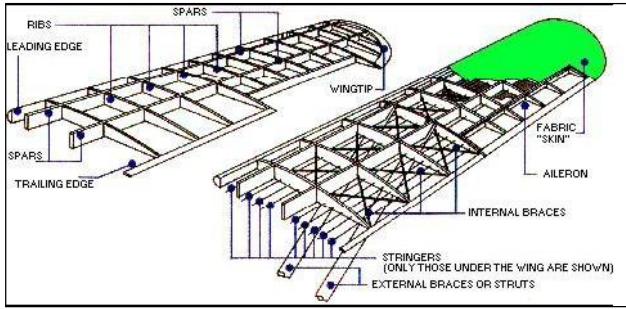


Fig 1: Two Spar Wing Configurations

2. ANALYSIS PROCEDURE

The procedure there were adopted has been described in detailed in this chapter. It includes design of the sandwich constructed composite in CATIA V5 and analyzing it in MSC Nastran. It also includes analysis of sandwich constructed composite by two methods.

1. Three point bending method
2. Linear static analysis

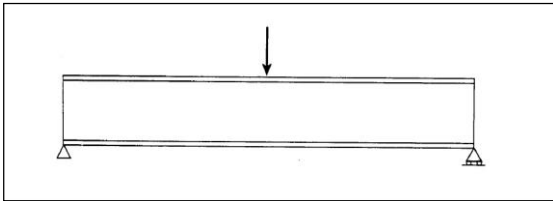


Fig 2: Sandwich Beam is analyzed using Three Point Bending.

To demonstrate the potentials and drawbacks of obtainable sandwich theories, here I am explaining the sandwich beam using three point bending load. The overall behavior and local behavior nearest to the load applied and also considered the support in the beam. And I have to find overall behavior

and local behavior for two various sandwich core thicknesses.

2.1 Core Thickness: 5mm, 10mm

The core thickness with 5mm and 10mm is analyzed and compared with the classical theory and superposition approach theory.

As per classical theory is considered in this example, the faces thickness is less compared to sandwich thickness and the core is weaker than that of the faces. The deformations are considered are the combination of two quite individual parts. The initial deformation happens because of the deformation as per the ordinary beam theory. The next deformation is happens because of deformation as per the shear deformation in the core. By considering these above points the differential equations are derived as follows.

$$D_s \cdot \frac{d^4 w_b}{dx^4} = 0 \text{ (ordinary beam theory)}$$

$$\frac{dw_s}{dx} = \frac{-F/2}{A_s G_c} \text{ (shear deformation)}$$

Where,

$$D_s = \frac{b_s E_f d_f E_f d_b d^2}{E_f d_t + E_f d_b}$$

$$A_s = b_s d$$

$$d = \frac{d_t}{2} + 2 + \frac{d_b}{2}$$

$$c = h_s - (d_t + d_b)$$

In these equations w_b and w_s are the perpendicular displacements because of bending respectively shear deformations. D_s can be referred as flexural rigidity and $A_s G_c$ is referred as sandwich beam shear stiffness. No apply boundary conditions as $x=0$ and $x=l/2$ is:

$$\phi_b(x=0) = 0$$

$$w_b(x=l_s/2) = 0$$

$$D(x=l_s/2) = -F/2$$

$$M(x=l_s/2) = 0$$

$$w_s(x=l_s/2) = 0$$

After applying boundary condition rotation of the beam is referred as ϕ_b , shear force is referred as D and the bending moment is referred as M . Deflection due to bending and shear can be solved by using analytical method by applying boundary conditions, the equation can be written as follows;

$$w_b(x) = \frac{F}{12D_s} x^3 - \frac{Fl_s}{8D_s} x^2 + \frac{Fl_s^3}{48D_s}$$

$$w_s(x) = \frac{-F}{2A_s G_c} x + \frac{Fl_s}{4A_s G_c}$$

By using derived constitutive relations we can easily calculate the shear force, bending moment, shear stress and membrane stress in the core and faces.

Sandwich beam stresses strains are found out by

Axial Strain:

$$\epsilon_{xx}(x, z) = -z \frac{d^2 w}{dx^2}$$

Axial Stress:

$$\sigma_{xx}(x, z) = -zE(z) \frac{d^2 w}{dx^2}$$

2.2 Bending Moment of the Beam

$$M_x(x) = \int z \sigma_{xx} dz = - \left(\int z^2 E(z) dz \right) \frac{d^2 w}{dx^2} = -D \frac{d^2 w}{dx^2}$$

The quantity D is called the flexural stiffness

By considering the above equations and I can say the stress in the sandwich beam which is having core thickness $2h$, the modulus elasticity of core E^c , face sheet thickness of two numbers f the modulus elasticity of fiber E^f can be written as below equation.

$$\sigma_{xx}^f = \frac{zE^f M_x}{D}$$

$$\sigma_{xx}^c = \frac{zE^c M_x}{D}$$

$$\tau_{xz}^f = \frac{Q_x E^f}{2D} [(h+f)^2 - z^2]$$

$$\tau_{xz}^c = \frac{Q_x}{2D} [E^c(h^2 - z^2) + E^f f(f+2h)]$$

3. LINEAR STATIC ANALYSIS

When loads apply on a body, the body get deforms and the loads will be transmitting all the way through the body. The state of equilibrium induces when the external loads induce internal forces and reactions to render the body.

Linear Static analysis calculates the following;

1. Displacements
2. Strains
3. Stresses and
4. Reaction forces under the effect of applied loads.

3.1 Assumption of Linear Static Analysis

Static Assumption: To get full magnitude the loads should apply slowly and gradually. The loads remain constant (time-invariant) once after reaching their full magnitudes. Due to

negligibly small accelerations and velocities the above assumption I can conclude inertial and damping forces are neglected. In many cases induces considerable inertial and damping forces that cannot be neglected due to dynamic loads change with time.

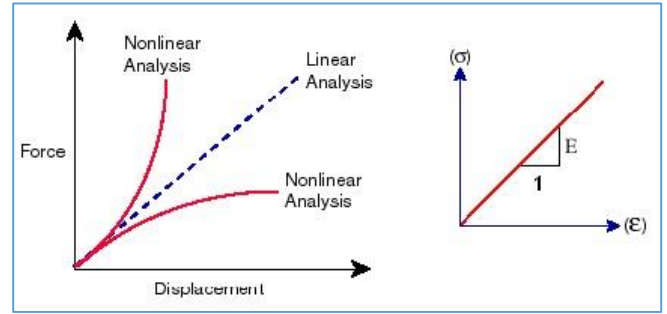


Fig 3: Assumption of Linear static analyses

Linear static analysis for this sandwich panel is done with the help of software package MSC nastran.

With the help of linear static method, ply stress in each ply is found. And ply stress for the various.

In this example a classical theory, a superposition approach theory is compared for the above two core thickness.

Deflection of sandwich panel along the x axis with separate deflection value accounting shear and bending with total deflection

3.2 Deflection of Sandwich Panel along the X Axis Core Thickness 5mm

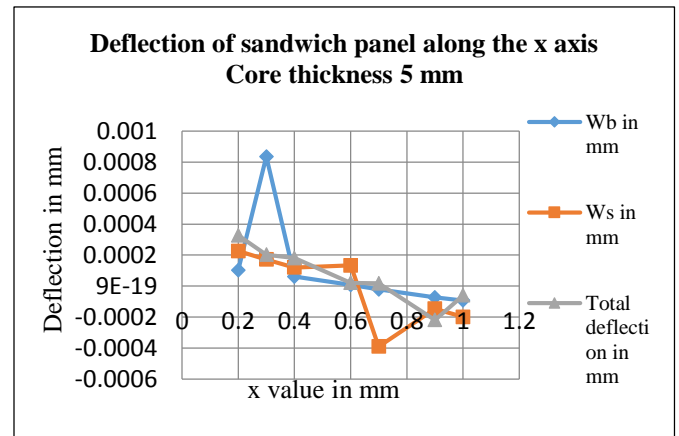


Fig 4: Deflection of Sandwich Panel along the X Axis Core Thickness 5mm.

3.3 Comparison of Theories for Stress Due to Bending for 5 mm

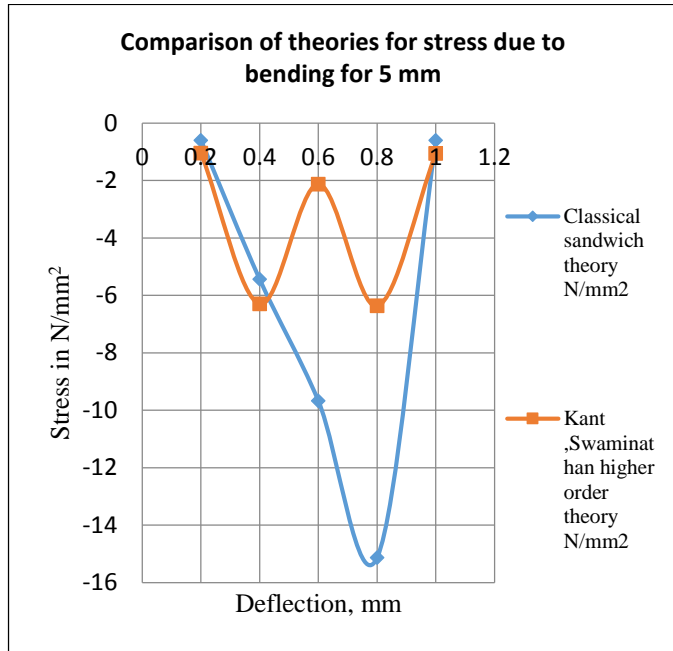


Fig 5: Comparison of Theories for Stress due to Bending For 5mm.

3.4 Comparison of Theories for Axial Strain for 5mm

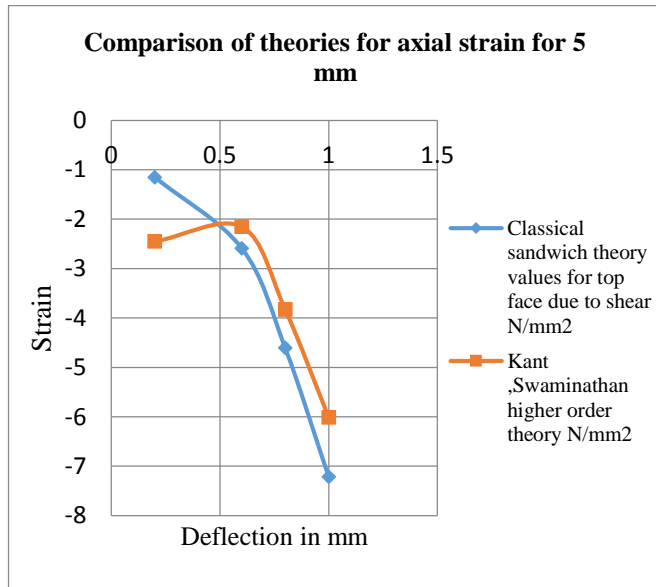


Fig 6: Comparison of Theories for Axial Strain for 5 mm.

3.5 Comparison of Theories for Displacement Due To Shear 5mm (Top)

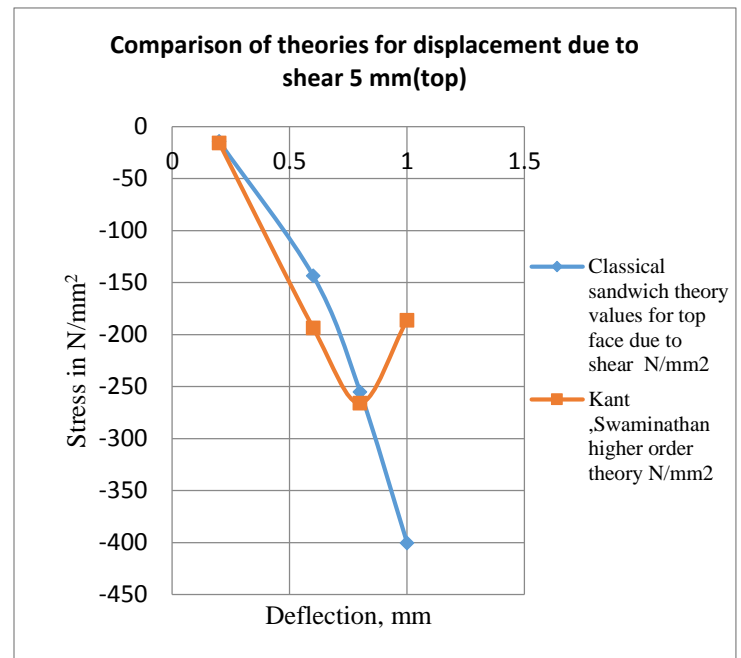


Fig 7: Comparison of Theories for Displacement due to Shear 5mm (top).

3.6 Deflection along Y Direction for 10mm Core Thickness

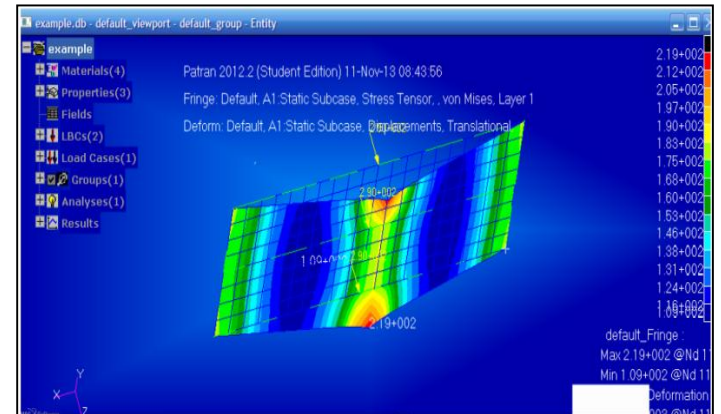


Fig 8: Deflection along Y Direction for 10mm Core Thickness.

3.7 Comparison of Theories with MSC Nastran for 5mm Displacement due to Bending

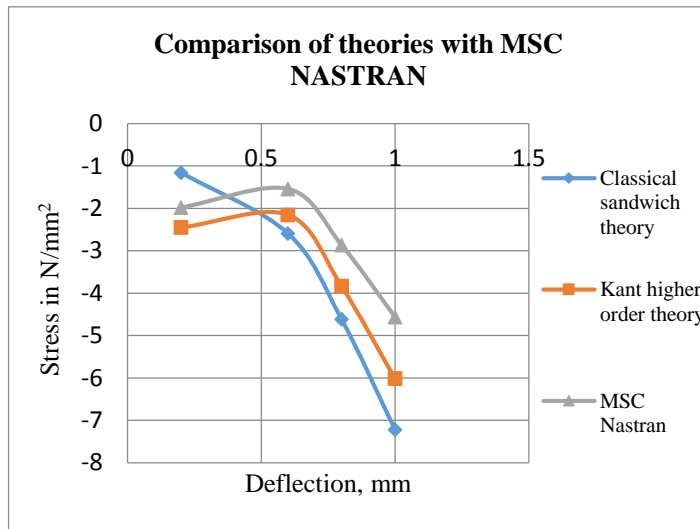


Fig 9: Comparison of Theories with MSC Nastran for 5mm Displacement due to Bending.

3.8 Stress Variation along Y Direction for 10mm Core Thickness

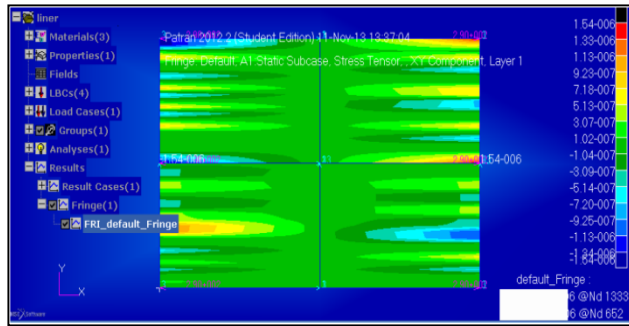


Fig 10 - Stress Variation along Y Direction for 10mm Core Thickness.

4. CONCLUSION

So, based on the classical theories to the highly advanced theories, we come to conclusion that sandwich panel with high core thickness has high stiffness and flexural rigidity. Moreover this is confirmed with the help of overall stiffness value from the theories.

This is further more that this phase of project work is concerned with the study of sandwich theories and a software package relates to sandwich constructed composites.

Since software package we concerned in this project gives exact results.

So, it is worth to continue our project with the help of this software packages.

Moreover, from this observation sandwich panel with foam proves better than honey comb core.

Then the given two material ROAHCELL r51 and carbon t300 are highly efficient when compare with other combination.

REFERENCE

1. Torayca t300 data sheet “fiber, composite properties of carbon t300”.
2. Msc/patran laminate modeler course pat 325
3. Paulkuhn, “Analysis Of &Par Cantilever Wings with Special Reference to Torsion and Load Transference”.
4. Deshpande, “The Design of Sandwich Panels with Foam Core”.
5. Ijsbrand j. Van straalen “Comprehensive Overview Of Theories For Sandwich Panels”
6. B. Woodward, M. Kashtalyan. “Bending response of sandwich panels with graded core: 3d elasticity analysis”.
7. Salih n. Akour et al., “Effect of core material stiffness on sandwich Panel behavior beyond the yield limit”.
8. T. Kant et al., “Analytical Solutions For The Static Analysis Of Laminated Composite And Sandwich Plates Based On A Higher Order Refined Theory”
9. Aditya kotikalpudi “aerodynamic analysis using xflr-5”.
10. S.Rajagopal and Ranjan ganguli “Multidisciplinary Design Optimization of Long Endurance Unmanned Aerial Vehicle Wing”.

Processing and Mechanical Characterization of Nano B₄C Particulates Reinforced Al2218 alloy Composites

¹Vidyadhar Pujar, ²Srinivas H K, ³Madeva Nagaral

¹Research Scholar, Department of Mechanical Engineering, Don Bosco Institute of Technology, Bangalore, Karnataka, India & Assistant Professor, Department of Mechanical Engineering, Oxford College of Engineering, Bangalore, Karnataka, India.

²Professor, Department of Mechanical Engineering, SJBIT, Bangalore, Karnataka, India.

³Design Engineer, Aircraft research and Design Centre, HAL, Bangalore, Karnataka, India.

**Corresponding Author E-mail: v8123340411@gmail.com*

Abstract

In the current era of aerospace, automobile and other various industries, light weighed aluminium metal matrix nano composites plays a very major role. Nano metal matrix composites are composed of base material as metallic which is reinforced with ceramic particulate as reinforcement material. This paper consists of the preparation of nano composites by stir casting process by the addition of nano B₄C particulates into the Al2218 matrix by varying different weight percentages of 2% and 4% at a temperature of 730°C-750°C. Further once the nano composites are prepared, these are subjected to characterization, the SEM revealed that there was good uniform distribution of nano particles in the aluminum by exhibiting a good bonding with matrix and EDS confirmed the presence of B and C elements. Different mechanical properties were conducted like hardness, ultimate tensile strength and yield strength, which revealed that there was an increase the mechanical properties than compared to the base metal.

Key Words: Al2218 Alloy, nano B₄C, Stir casting, Nano composites, mechanical properties

1. Introduction

Nano metal matrix composites play a vital role in the current and modern technology. Usually micro ceramic particles are picked up for better yield and ultimate strength of the metal. But however the ductility of MMCs deteriorates with high ceramic particles absorption. So the nano particles reinforcement can significantly replaced in the place

of micro particles which enhance the mechanical strength of the matrix more effectively and there by promoting the particle hardening mechanism than micron particles [1, 2].

Aluminum alloys as a matrix phase are widely used in aerospace, automobile and marine industries due to their various properties like low density, good mechanical properties, better corrosion resistance, and low thermal coefficient of expansion as compared to other conventional metals and alloys and also the cost of production is relatively low [3, 4]. Because of these characters they form a very strong and good contender in many of the applications [5]. However, the mechanical properties such as strength, elastic modulus and wear resistance are not enough for industrial applications; therefore, they are reinforced by various ceramic reinforcements such as Al_2O_3 , SiC, graphite etc., [6, 7]. But nano B_4C ceramic particles as reinforcement made a remarkable trend and have recently been used for the better improvement of the mechanical and wear properties in Aluminum matrix composites by offering extremely high hardness, better strength, chemical stability and increase in thermal stability [8]. In addition, a limited work has been done on aluminum matrix composites by reinforcing with nano B_4C because of its high cost of raw material and poor wetting. B_4C is the third hardest material and it possesses an excellent hardness, low specific gravity, and high melting point therefore, which is a best suitable reinforcement material for nano metal matrix composites having density less than aluminum [9]. The Al- B_4C nano composites are used in different applications like bicycle frame, armor tanks, containment of nuclear waste, bullet proof vests, neutron absorber in nuclear power plant, Because the absorption of thermal neutrons produces heat and therefore the temperature of the material increases such that the Al-nano B_4C composites may experience long-term exposure for estimated temperatures [10].

Many different fabrication techniques are generally available for the fabrication of nano metal matrix composites, such as powder metallurgy, mechanical alloying, high-energy ball milling, nano-sintering, spray deposition, and variety of casting techniques [11]. Nevertheless mechanical stir casting process by the formation of vortex method is one of the best technique because, it is relatively inexpensive and it can be used to disperse nano sized B_4C particles in molten aluminium without forming agglomeration and clustering by the addition of nano ceramic particles in steps of two stages into the molten matrix and obtaining a good wetting by the proper selection of parameters like stirring speed, time, temperature of molten metal, preheating temperature of the mould and ceramic particle along with uniform feed rate of the reinforcement [4]. Even though stir casting allows producing components in bulk at a low cost of production with different complex geometries, but there are some disadvantages with it such as porosity, blowholes and proper distribution of the nano ceramic reinforcing particles between the metal matrixes. Due to this the mechanical properties often leads to degradation. However this problem occurs when the volume fraction of the reinforcement is high in the ratio of composites.

The present research work is done by the preparation of nano metal matrix composites by the addition of nano B_4C in Al2218 melt at a temperature of 730°C - 750°C by stir casting process. During the composite preparation the pre-heated mix containing of

nano B₄C particles and K₂TiF₆ flux was added into the melt to enhance wetting and incorporation of nano B₄C particles into molten melt of Al2218. Further the prepared nano composites were subjected to evaluation of mechanical properties for the better enhancement compared to base metal.

2. Experimental Details

2.1 Process parameters – Matrix and Reinforcement

Al2218 is a 2000 series aluminum alloy which as major content of copper along with magnesium and it is formulated as wrought product and used a primary matrix material. Among aluminium alloys, Al2218 is chosen because it as a low density of 2.8 g/cm³ and used in various applications like jet engines, structural and tubing due to its excellent machinability characteristics. Because of high content of copper and magnesium the materials becomes age hardenable with good strength, corrosion resistance and has good weldability. Table 1 illustrates the chemical composition of Al2218 alloy.

Table 1: Shows the chemical composition of the Al2218 alloy used in the present study

| Elements | Si | Fe | Cu | Mg | Ni | Zn | Ti | Mn | Al |
|------------|------|-----|-----|-----|-----|------|------|------|-----|
| Weight (%) | 0.90 | 1.0 | 4.5 | 1.8 | 1.7 | 0.25 | 0.10 | 0.20 | Bal |

For the present work the nano B₄C is used as secondary reinforcement particle which was procured from Reinste Nano Venture, Delhi, having a particle dia size of 500nm. The different physical characteristics like hard strength, catalyst support and as neutron absorber makes nano B₄C as a researchers and engineers choice for various applications by increasing mechanical and tribological properties. Aluminum is reinforced with nano B₄C because it a low density which is less than the matrix material which contributes to weigh saving and as high melting point up to 2350⁰C along with excellent chemical and thermal stability. Hence, nano B₄C reinforced aluminum matrix composite has expanded more attraction towards stir casting method with low coast.

2.2 Preparation of Nano Metal Matrix Composites

For the preparation of metal matrix nano composites stir casting technique is chosen because of less expensive and suitable for bulk production of components. The nano composites containing 2 and 4 wt. % of nano B₄C particulates were prepared from stir casting process technique. Initially the required amount of nano B₄C and the cast iron die are preheated to a temperature of 400 C. On the other part, the calculated amount of Al2218 was weighed and placed in a graphite crucible inside a electric furnace and heated to temperature of 750 C, so that the entire raw materials coverts into an molten

phase at a melting temperature of 660°C. After the complete melting of Al2218, the degassing powder known as Solid Hexa Chloro Ethane (C₂Cl₆) is introduced into the molten melt so that the unwanted adsorbed gases are forced out from the melt. The molten melt is disturbed by dipping a zirconium coated mechanical stirrer to form a clear vortex by stirring mechanism at a speed of 300rpm. Once the vortex is formed then the preheated nano ceramic particles along with the proper proportion ratio of K₂TiF₆ is introduced into the molten melt by a constant feed rate. At every each stage the continues stirring process is carried out before and after the pouring of mixture of nano B₄C and K₂TiF₆ to avoid clustering of particulates and to have uniform homogenous distribution of nano particulates in the melt. After continues stirring, the entire molten metal was poured into preheated cast iron die.

The prepared nano composites were machined as per the standards for characterization purpose. After confirming the uniform homogenous distribution of nano particles in the matrix by SEM and the presence of B and C elements by EDS, the mechanical behaviour of as cast Al2218 alloy and its nano composites were further evaluated as per ASTM standards.

3. Results and Discussions

3.1 Characterization by SEM and EDS

The Scanning Electron Microscope is used to examine the reinforcement pattern and the proper distribution of nano particles from the prepared nano composite. A piece of cut section was taken from the casted specimen and grinded using 220 grit SiC paper followed by 400, 600, 800 and 1000 grades of emery paper. Then the samples were mechanically polished and etched by Keller's reagent (HCL+ HNO₃+HF+Water) to obtain the better contrast of the microstructure.

Figure 1a shows the scanning electron photographs of as cast Al2218 alloy. Similarly figure 1b showing 2 wt. % nano B₄C reinforced composites and figure 1c showing scanning electron photographs of 4 wt. % of nano B₄C particulates reinforced composites respectively. From the scanning electron photographs, it is revealed that there is uniform homogenous distribution of secondary phase of nano particulates in the Al2218 alloy matrix without any agglomeration. It is also observed that there is an excellent interfacial bonding between the nano B₄C and Al2218 alloy matrix, which further enhances the properties of Al2218 alloy. In the case of Al2218-4 wt. % nano B₄C composites, there are more particulates in the Al2218 matrix, which shows good castability and wettability of Al2218 alloy with ceramic reinforcements.

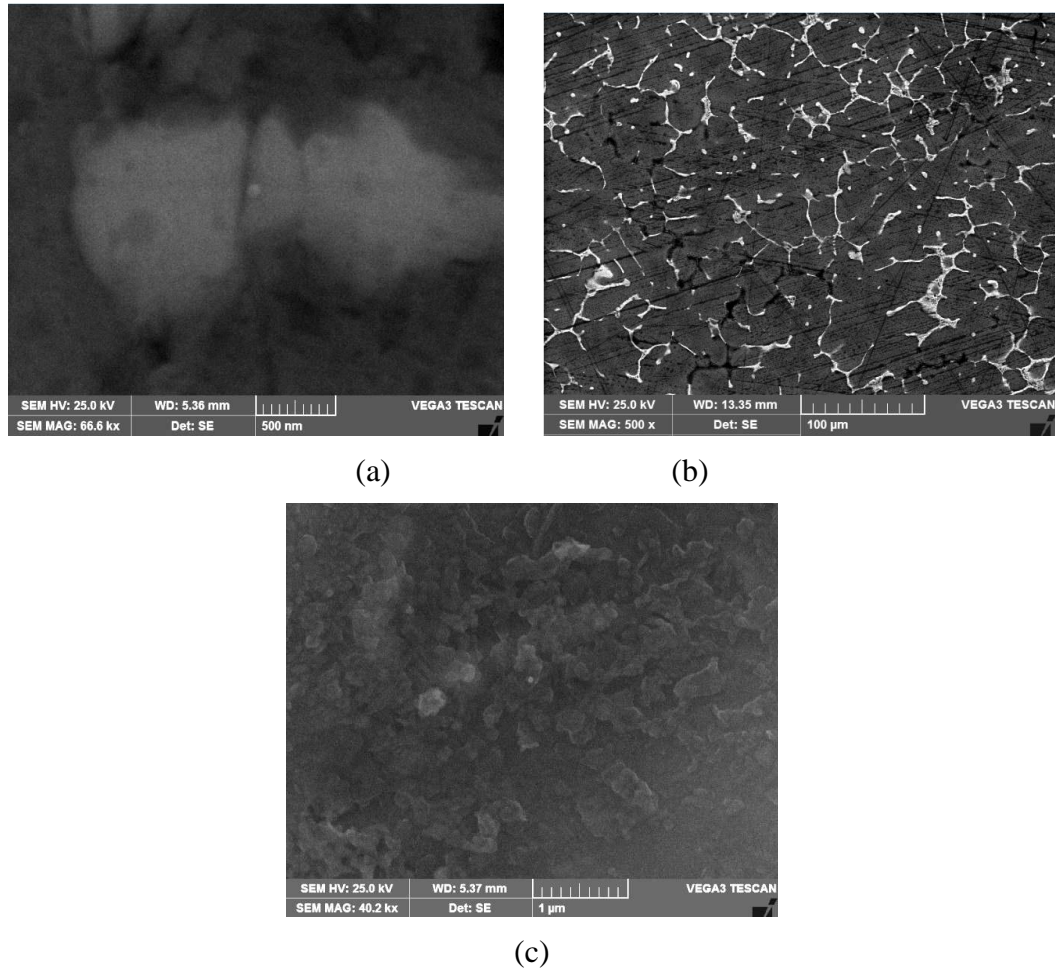


Figure 1: Scanning electron micrographs of (a) as cast Al2218 alloy (b) Al2218-2% B₄C and (c) Al2218-4% B₄C composites

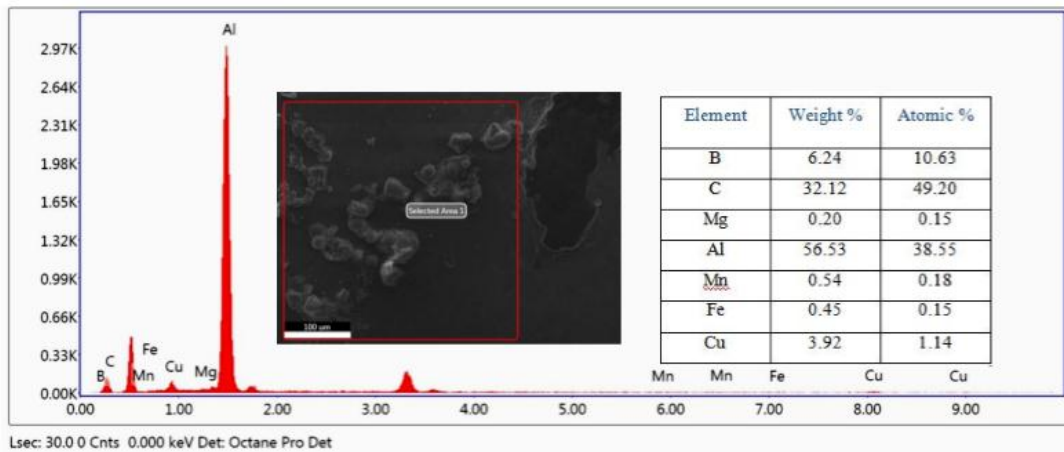


Figure 2: Scanning electron micrographs of (a) as cast Al2218 alloy (b) Al2218-2% B₄C and (c) Al2218-4% B₄C composites

EDS analysis confirms the presence of Boron Carbide particulates in Al2218 alloy matrix in the form of B and C elements along with Al and Cu elements (figure 2).

3.2 Hardness Measurements

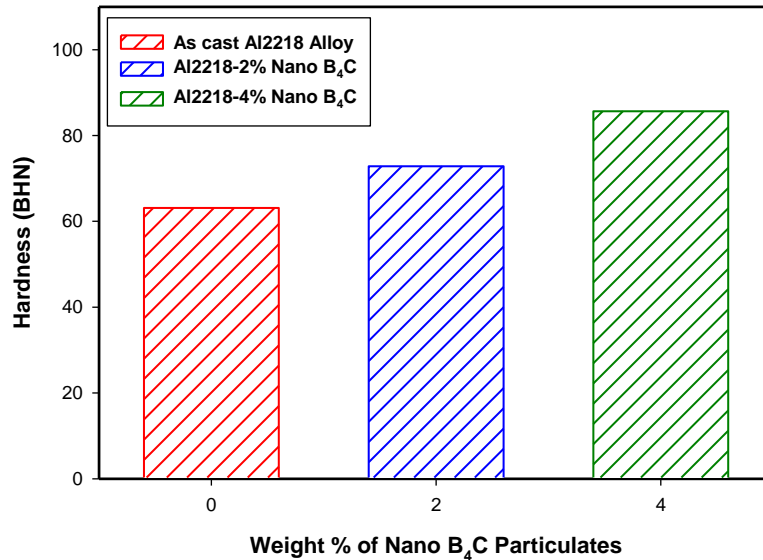


Figure 3: Hardness of Al2218 alloy and its nano B₄C composites

Figure 3 shows the effect of nano B₄C particulates on the hardness of Al2218 alloy. From the graphs, it is noted that nano particles reinforced composites showed more hardness strength as compared to the Al base matrix. Further, as weight percentage of nano B₄C increases from 0 to 4 %, in Al2218 composites, it is observed that hardness increased from 63.13 BHN to 85.66 BHN. This increase in hardness is mainly due to the presence of nano ceramic particulates in the matrix. These particulates act as the barrier for dislocations [12, 13].

The higher hardness values for composites containing finer nano B₄C particles can be attributed to the larger surface area of these particles in contact with the matrix alloy. Therefore, due to the co-efficient of thermal expansion mismatch between Al2218 and B₄C phases, higher dislocations densities are generated during processing [14].

3.3 Ultimate and Yield Strength

Figure 4 showing the effect of nano B₄C particulates on the tensile behavior of Al2218 alloy. From the graphs, it is noted that nano composites showed more ultimate and yield strength as compared to the Al2218 base matrix. Further, as weight percentage of nano B₄C increases from 2 to 4 %, in Al2218 composites, it is observed

that UTS increased from 208 MPa to 229 MPa, for base alloy it is found that 195 MPa. This increase in UTS and YS is mainly due to the presence of ceramic particulates in the matrix. These particulates act as the barrier for dislocations [15].

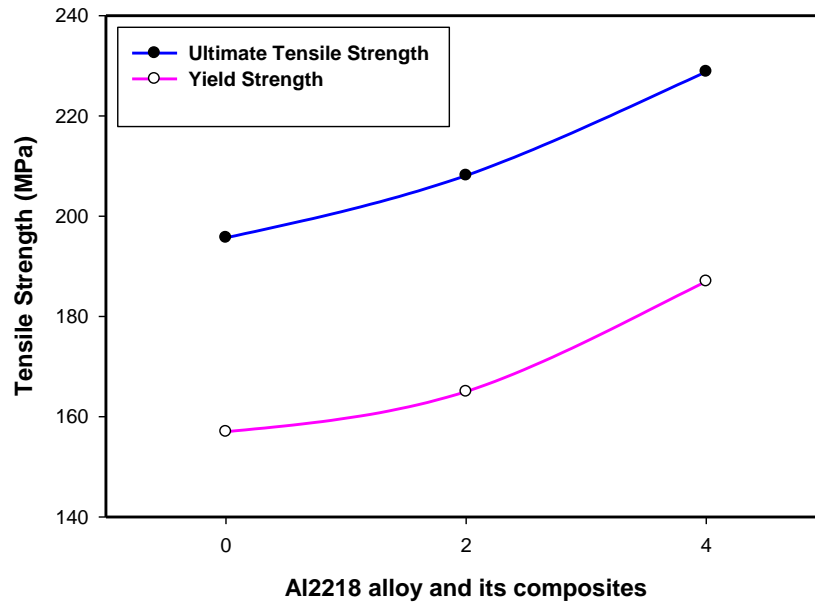


Figure 4: Ultimate and yield strength of Al2218 alloy and its nano B₄C composites

Further, the yield strength of Al2218-nano composites enhanced due to the presence of B₄C particulates. The mechanical properties of nano particulate reinforced MMCs are controlled by a complex interaction between the Al matrices and reinforcements. The addition of a reinforcing phase of different elastic properties induces strain concentration. In order to maintain the displacement compatibility across the interface when a far-field strain is applied, dislocations are generated at the composite interface [16]. Also, the difference in thermal expansion coefficients between the two phases necessitates the generation of dislocations to accommodate thermal strain on changing temperature.

3.4 Percentage Elongation

The improvement in UTS is, be that as it may, associated with a lessening in flexibility, which decreases as evidently appeared in figure 5. Expanding the wt. % of nano B₄C in the composite opposes the flowability of aluminum framework and diminishes the bendable aluminum compound network content which brings about the lessening of % prolongation of the composite [17].

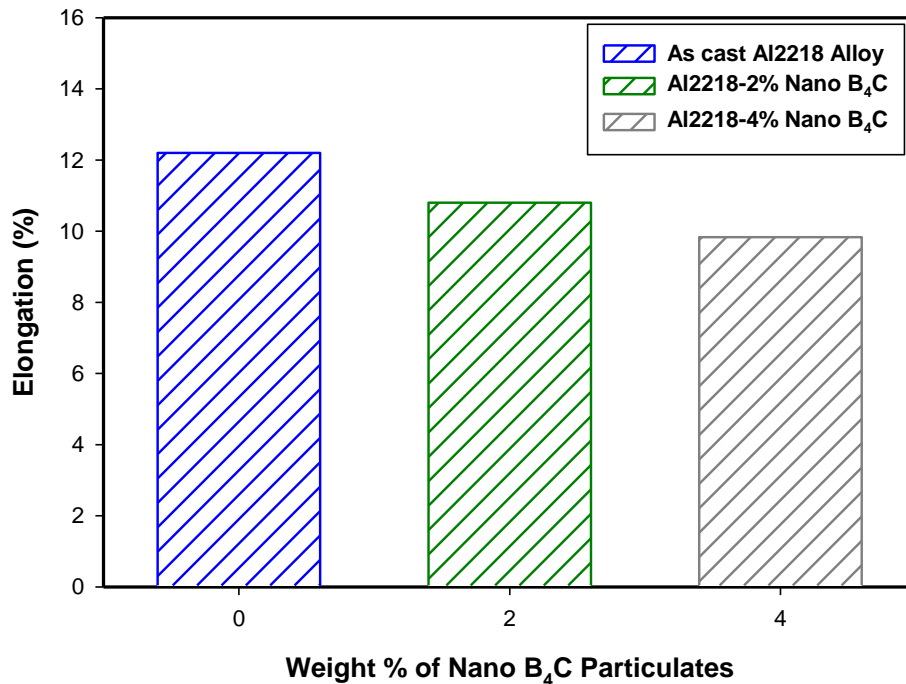


Figure 5: Percentage elongation of Al2218 alloy and its nano B₄C composites

4. Conclusion

In this research, nano B₄C-Al2218 composites have been fabricated by stir casting method by taking 2 and 4 wt. % of reinforcement. The microstructure, ultimate tensile strength, yield strength, percentage elongation of prepared samples is studied. The matrix is almost pore free and uniform distribution of nano particles, which is evident from SEM microphotographs. The EDS analysis confirms the presence of nano B₄C particles in the Al alloy matrix. The mechanical properties of Al2218-2 and 4wt. % nano B₄C composites are superior to those of unreinforced material. The ultimate tensile strength of Al2218 alloy is increased from 195 MPa to 229 MPa for 4 wt. % nano composites. Percentage elongation of nano B₄C composites decreased as compared to the unreinforced Al2218 alloy.

REFERENCES

- [1] Xiao-Hui Chen, Hong Yan, Solid-liquid interface dynamics during solidification of Al 7075-Al₂O₃ based metal matrix composites, *Materials and Design*, 94, 2016, pp. 148-158.
- [2] J. Hashim, L. Looney, M. S. J. Hashim, The wettability of SiC particles by molten aluminium alloy, *Journal material processing Technology*, Vol. 119, 2001.

- [3] Jayasheel I Harti, T. B. Prasad, Madeva Nagaral, Pankaj Jadhav and V. Auradi, Microstructure and dry sliding wear behavior of Al2219-TiC composites, *Materials Today Proceedings*, 4, 10, 2017, pp. 11004-11009.
- [4] H. H. Kim, J. S. S. Babu and C. G. Kang, Fabrication of A356 aluminium alloy matrix composite with CNTs-Al₂O₃ hybrid reinforcements, *Materials Science and Engineering A*, 573, 2013, pp. 92-99.
- [5] G. Rama Rao and Padmanabhan, Fabrication and mechanical properties of aluminium-boron carbide composites, *International Journal of Materials and Biomaterials Applications*, Vol. 2, No. 3, 2012, pp. 15-18.
- [6] Krishna Dama, Prashanth L, Madeva Nagaral, Rakesh Mathapati, Hanumanthrayagouda M B, "Microstructure and mechanical behavior of B₄C particulates reinforced ZA27 alloy composites," *Materials Today Proceedings*, 4, 8, pp. 7546-7553, 2017.
- [7] Madeva Nagaral, V Auradi, S A Kori, Reddappa H N, Jayachandran and Veena Shivaprasad, "Studies on 3 and 9 wt.% B₄C particulates reinforced Al7025 alloy composites", *American Institute of Physics Proceedings*, Vol. 1859, 020019, 2017.
- [8] C. S. Ramesh, R. Keshavamurthy, B. H. Channabasappa, S. Promod, Friction and wear behaviour of Ni-P coated Si₃N₄ reinforced 6061-Al composites, *Tribology Int.*, 43, 2010, 623-624.
- [9] Madeva Nagaral, R. Pavan, P. S. Shilpa and V. Auradi, Tensile behavior of B₄C particulate reinforced Al2024 alloy metal matrix composites, *FME Transactions*, 45, 2017, 93-96.
- [10] R.Vijay, C. Elanchezhian, M. Jaivignesh, S. Rajesh and C. Parswajinan, Evaluation of mechanical properties of aluminium alloy alumina boron carbide metal matrix composites, *Materials and Design*, Vol. 58, 2014, pp. 332-338.
- [11] P. Dora Siva and S. Chintada, Hybrid composites a better choice for high wear resistant materials, *Journal of Materials Research and Technology*, Vol. 3, No. 2, 2014, pp. 172-178.
- [12] Jaswinder Singh and Amit Chauhan, Overview of wear performance of aluminium matrix composites reinforced with ceramic materials under the influence of controllable variable, *Ceramics International*, 42, 2016, pp. 56-81.
- [13] S. Ghanaraja, Subrata Ray and S. K. Nath, Synthesis and mechanical properties of cast alumina nano particle reinforced metal matrix composites, *Materials Today Proceedings*, 2, 2015, pp. 3656-3665.
- [14] Dinesh Patidar and R S Rans, Effect of B₄C particle reinforcement on the various properties of aluminium matrix composites: a survey paper, *Materials Today Proceedings*, 4, 2017, pp. 2981-2988.
- [15] Madeva Nagaral, B. K. Shivananda, V. Auradi, K. I. Parashivamurthy and S. A. Kori,

- Mechanical behavior of Al6061-Al₂O₃ and Al6061-Graphite composites, *Materials Today Proceedings*, 4, 10, 2017, pp. 10978-10986.
- [16] M. Nagaral, S. Attar, H. N. Reddappa and V. Auradi, Suresh Kumar and Raghu, S.: Mechanical behavior of Al7025-B₄C particulate reinforced composites, *Journal of Applied Mechanical Engineering*, 4:6, 2015.
- [17] Pankaj R Jadhav, B R Sridhar, Madeva Nagaral, Jayasheel Harti, "Evaluation of mechanical properties of B₄C and graphite particulates reinforced A356 alloy hybrid composites," *Materials Today Proceedings*, 4, 9, pp. 9972-9976, 2017.

ISOLATION & CHARACTERIZATION OF METHANOGENIC BACTERIA FROM LOCAL ENVIRONMENT AND COMPARATIVE STUDY OF KINETICS WITH TRADITIONAL BIOGAS PRODUCERS.

*¹Salma Kausar.M, ²Jhansi v, ³S.Niveditha, ⁴Harshitha Ananthrama

¹Assistant Professor, ^{2,3,4}Student

Department of Biotechnology

The Oxford College of Engineering, Bangalore -560068, India

Author for correspondence

Salma Kausar.M

msalmakausar@gmail.com

Abstract: In the present study the soil samples from paddy field (kalikiri Andhra Pradesh), Karnataka compost development corporation limited (KCDC, kudlu village, Bangalore) & spent waste from floating type biogas plant were collected and methanogens were isolated, characterized & subjected to growth under anaerobic conditions by providing the kitchen and vegetable market waste as the substrate the kinetic study was carried out. A total of 16 isolates were obtained from the sample. The morphology and phenotypic characteristics were studied by performing various biochemical tests which revealed that the organism were anaerobes. Biogas production was carried out by using anaerobic digester. Paddy field and Biogas sample showed maximum production of biogas than KCDC. But mixed consortia had a very high degrading ability in very short period of time up to 92.95%.

(**keywords-** municipal solid waste, methanogens, anaerobic digestion, Modified Gompertz equation, biogas production)

I. INTRODUCTION

Municipal Solid Waste (MSW), commonly known as trash or garbage and as refuse or rubbish, is a waste type consisting of everyday items that are discarded by the public. "Garbage" can also refer specifically to food waste, as in a garbage disposal. The composition of municipal solid waste varies greatly from municipality to municipality,^[1] and it changes significantly with time. Biodegradable waste can be commonly found in municipal solid waste (sometimes called biodegradable municipal waste). Biodegradable waste: food and kitchen waste, green waste, paper (most can be recycled although some difficult to compost plant material may be excluded ^[2]). In the absence of oxygen, much of this waste will decay to methane by anaerobic digestion.^[3] Biodegradable waste includes any organic matter in waste which can be broken down into carbon dioxide, water, methane or simple organic molecules by micro-organisms and other living things using composting, aerobic digestion, anaerobic digestion or similar processes. Anaerobic digestion is a collection of processes by which microorganisms break down biodegradable material in the absence of oxygen.^[4] The process is used for industrial or domestic purposes to manage waste or to produce fuels. Much of the fermentation used industrially to produce food and drink products, as well as home fermentation, uses anaerobic digestion. Anaerobic digestion (AD) occurs naturally in some soils and in lake and oceanic basin sediments, where it is usually referred to as "anaerobic activity".^{[5][6]} This is the source of marsh gas methane as discovered by Alessandro Volta in 1776.^{[7][8]} The digestion process begins with bacterial hydrolysis of the input materials. Insoluble organic polymers, such as carbohydrates, are broken down to soluble derivatives that become available for other bacteria. Acidogenic bacteria then convert the sugars and amino acids into carbon dioxide, hydrogen, ammonia, and organic acids. These bacteria convert these resulting organic acids into acetic acid, along with additional ammonia, hydrogen, and carbon dioxide. Finally, methanogens convert these products to methane and carbon dioxide.^[9] The methanogenic archaea populations play an indispensable role in anaerobic wastewater treatments.^[10] Anaerobic digestion (AD) is used as part of the process to treat biodegradable waste and sewage sludge. As part of an integrated waste management system, anaerobic digestion reduces the emission of landfill gas into the atmosphere. The nutrient-rich digestate produced can be used as fertilizer. Methanogens are microorganisms that produce methane as a metabolic byproduct in anoxic {low level oxygen} conditions. They belong to the domain of archaea most of them have cell wall. They occur in 2 forms cocci, bacilli, consume H₂ & CO₂. Methanogens are responsible for marsh gas {bio gas} production. They are obligate anaerobes, extremophiles, living in the guts of cows, deep in swamps and even in the muck from sewage treatment plants. Methanogenesis or bio methanation is the formation of methane by microbes known as methanogens. Methanogenesis is sensitive to both high and low pH's and occurs between pH 6.5 and pH 8.^[11] The remaining, indigestible material the microbes cannot use and any dead bacterial remains constitute the digestate.^[12]

II. MATERIALS AND METHODS

A. Collection of samples

The samples from three different places, soil sample from paddy field(PD) of kalikiri Andhara Pradesh, fine manure sample from Karnataka compost development corporation limited(KCDC) and spent from floating type biogas plant(BG)of chikballapura were collected in sterile zip-lock plastic maintaining aseptic conditions. The collected samples were brought to the laboratory for isolation and characterization.

B. Construction of anaerobic chamber

The chamber was constructed by using polycarbonate material & anaerobic condition was maintained by complete removal of oxygen.

C. Isolation of methanogens

Methanogenic organisms were grown in Thioglycollate media^[13] by serial dilution of sample and by using pour plate & spread plate method. (Basic Practical Microbiology A Manual by Society for General Microbiology (SGM)). Identification of bacterial isolates was done on the basis of their colony characteristics on the basal media & Gram staining^[13].

D. Fluorescence test

Fluorescence is presumptive evidence for methanogenic bacteria, but definitive proof requires further characterization.^[13] To observe the presence of fluorescence, the isolated colony plates were directly placed in UV Trans-illuminator & checked for blue green fluorescence.

E. Agar deep culture

An agar deep culture produced by a deep inoculation into a solid medium (thioglycollate agar media) that is used especially for the growth of anaerobic bacteria (Harley J.P. And Prescott Lansing L.M. 2002. Laboratory Exercises in Microbiology, 5th Ed. McGraw-Hill Higher Education, New York, NY, USA). The inoculation was carried out using a sterile needle loop. The obtained isolates were subculture in liquid BM3 media.^[14]

F. Cell count and motility test

The cell count was performed by using hemocytometer and the results were recorded. Motility test was carried out using hanging drop technique to identify motile & non-motile isolates.^[13] Gram's staining was carried out for the obtained isolates in order to study their morphology (Pioneers in Medical Laboratory Science: Christian Gram 1884)^[15].

G. Biochemical tests

Biochemicals tests such as IMViC, urease, TSI, catalase, carbohydrate fermentation tests, starch test were performed in order to identify bacterial species based on the differences in the biochemical activities of bacteria.

H. Antibiotic sensitivity test

Antibiotic sensitivity test was carried out by disc diffusion technique using streptomycin (10mcg) and the results were recorded.

I. Waste collection and processing

Kitchen Waste (KW) was collected from houses of residential area (H S R layout) & vegetable market waste were collected from Madiwala vegetable market. The waste along with inoculum (3:1 ratio) was fed to screw capped pet bottles and the setup was left at room temperature for the production of biogas through AD. Cow Manure (CM) was collected from Mallela (Pileru, Andhra Pradesh). The wastes were cut into small size & blended in order to reduce size to ease the process of digestion.

J. Liquid displacement setup

A simple lab-scale experiment was fabricated using digesters. Each digester was made of plastic pet bottles. In this study the volume of produced gas was measured by water displacement method considering the volume of the generated gas equal to that of expelled water in the water collector. Each digester was connected to water chamber (plastic bottles) by a plastic pipe (gas pipe) which was used to pass the produced gas into water chamber. Another glass pipe (water pipe) was used to take the displaced water from the water chamber to the water collector which was fitted & air sealed. Both the ends of the gas pipe were inserted just at the top of the digester and the water chamber. The water pipe was inserted just bottom of the water chamber and top of water collector. The set up is illustrated in figure 1.

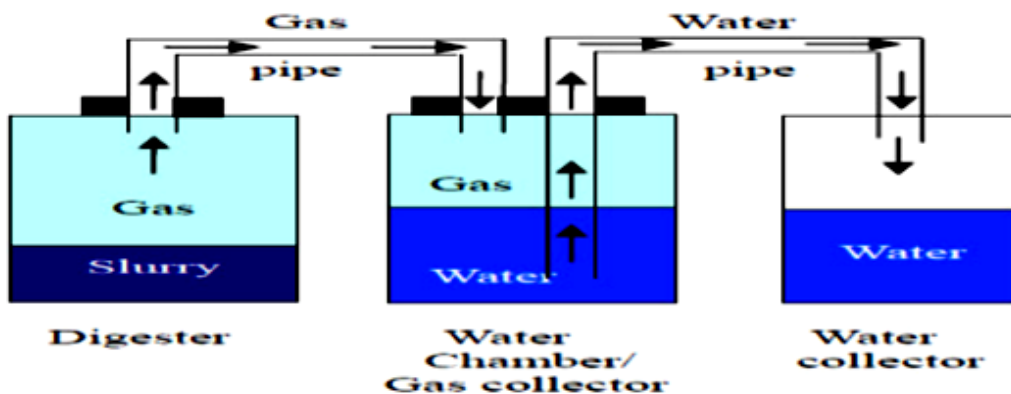


Fig 1: schematic diagram of the lab-scale experimental set-up [16]

K. Solid Analysis

- **Moisture content(MC):** The MC is the water content that is present in the reaction mixture. The water present in the reaction mixture was measured by the direct method of determination.

$$\text{Moisture Content (\%)} = \frac{W2 - W3}{W2 - W1} * 100$$

Where

W1= weight of the container; W2= weight of the container and sample before drying; W3= weight of the container and sample after drying.

- **Total solids(TS):** Total solids include both the suspended solids and the dissolved solids which are obtained by separating the solid and liquid phase by evaporation. These solids are the substrate components that will be utilized for the production of the biogas.

$$\text{Total Solids (\%)} = 100 - \text{Moisture (\%)}$$

- **Volatile Solids(VS):** the solids that remain after drying, evaporating or filtration were then ignition at 600° C. the sample turn to ash.

$$\text{Volatile solids (\%)} = \frac{W2 - W3}{W2 - W1} * 100$$

Where

W1= weight of the dish; W2= weight of the dried residue and dish; W3= weight of the residue and dish after ignition.

III. Result and Discussion

The samples were successfully collected in sterile zip-lock plastic maintaining aseptic conditions. The anaerobic chamber was constructed and anaerobic condition was maintained. The isolation of methanogens was carried out by using different dilutions of sample (10⁻², 10⁻³, 10⁻⁴). Pure cultures were selected by streaking the individual colony on TG agar plates. Pentagon streak was carried out in order to check whether the culture consists of only one organism. A total of 16 bacterial strains were identified by standard bacteriological identification procedure from the three samples. They were named as KC1-KC5 (obtained from KCDC), BG1-BG5(biogas plant) and PF1-PF6(paddy field) respectively. Microscopic examinations were carried out by gram staining and motility test. The results obtained are given in table 1.

Table1: result for cell count, gram's staining, motility test

| Sl. No. | Strain No. | Cell Count(Cells/ml) | Gram's Staining | Shape | Motility |
|---------|------------|----------------------|-----------------|---------|-------------|
| 1. | KC1 | 35*10 ⁴ | Gram Negative | Cocci | Motile |
| 2. | KC2 | 27*10 ⁴ | Gram Negative | Cocci | Motile |
| 3. | KC3 | 49*10 ⁴ | Gram Negative | Cocci | Non -Motile |
| 4. | KC4 | 50*10 ⁴ | Gram Negative | Cocci | Motile |
| 5. | KC5 | 50*10 ⁴ | Gram Negative | Cocci | Non -Motile |
| 6. | BG1 | 19*10 ⁴ | Gram Negative | Bacilli | Non- Motile |
| 7. | BG2 | 27*10 ⁴ | Gram Negative | Bacilli | Motile |
| 8. | BG3 | 24*10 ⁴ | Gram Negative | Bacilli | Motile |
| 9. | BG4 | 48*10 ⁴ | Gram Negative | Bacilli | Motile |
| 10. | BG5 | 26*10 ⁴ | Gram Negative | Bacilli | Motile |

| | | | | | |
|-----|-----|--------------------|---------------|---------|------------|
| 11. | PF1 | 21*10 ⁴ | Gram Negative | Cocci | Non-Motile |
| 12. | PF2 | 48*10 ⁴ | Gram Negative | Bacilli | Non-Motile |
| 13. | PF3 | 31*10 ⁴ | Gram Negative | Bacilli | Non-Motile |
| 14. | PF4 | 28*10 ⁴ | Gram Negative | Bacilli | Motile |
| 15. | PF5 | 48*10 ⁴ | Gram Negative | Bacilli | Non-Motile |
| 16. | PF6 | 23*10 ⁴ | Gram Negative | Cocci | Non-Motile |

a. Fluorescence test

Fluorescence test was carried out for the identification of methanogenic bacteria containing the F420 coenzyme which shows blue-green fluorescence by methanogenic bacteria and is readily distinguishable from the white-yellow fluorescence occasionally observed in non-methanogenic colonies. The strains showed no fluorescence indicating the absence of F240 co-enzyme production

b. Butt Culturing

The isolates were found to be anaerobic & few isolates developed cracks in agar indicating the gas production.

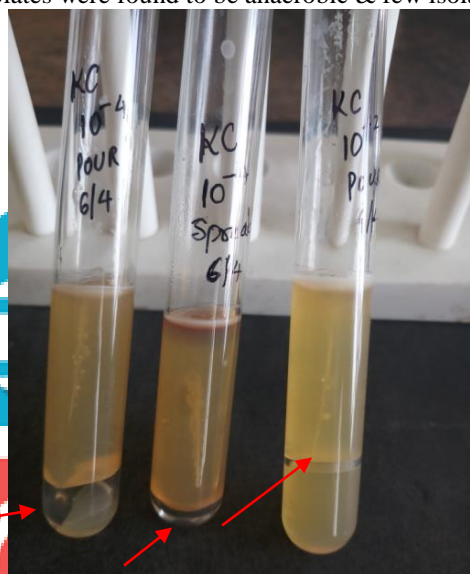


Fig2a: results for butt culture technique with gas production

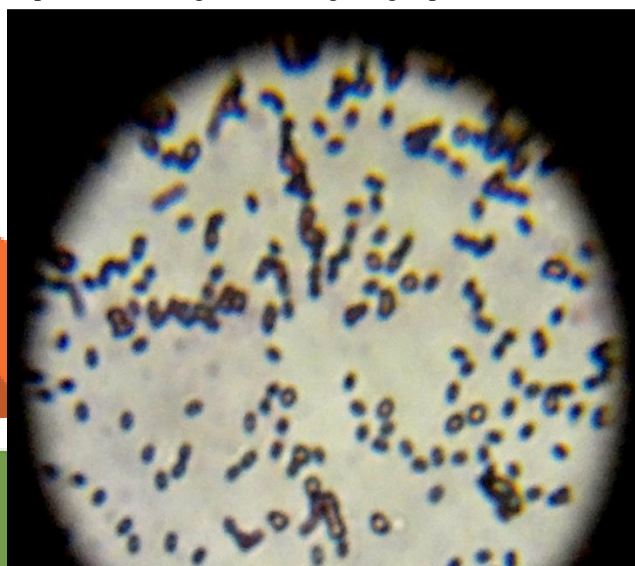


Fig 2b: results for grams staining indicating gram negative cocci shaped microbe.

c. Biochemical tests

Table 2: result for biochemical tests

| SL.NO | STRAIN NO | I | M | V | CI | C | TSI | U | CHF | SHT |
|-------|-----------|-----|-----|-----|-----|-----|-----|-----|-----|-----|
| 1 | KC1 | -ve | +ve | -ve | +ve | +ve | +ve | +ve | +ve | +ve |
| 2 | KC2 | -ve | +ve | -ve | +ve | +ve | +ve | +ve | +ve | +ve |
| 3 | KC3 | -ve | +ve | -ve | +ve | +ve | +ve | +ve | +ve | +ve |
| 4 | KC4 | -ve | -ve | -ve | +ve | -ve | +ve | +ve | +ve | +ve |
| 5 | KC5 | -ve | +ve | -ve | +ve | -ve | +ve | +ve | +ve | +ve |
| 6 | BG1 | -ve | -ve | -ve | +ve | -ve | +ve | +ve | +ve | +ve |
| 7 | BG2 | -ve | +ve | -ve | -ve | +ve | +ve | -ve | +ve | +ve |
| 8 | BG3 | -ve | +ve | -ve | +ve | +ve | +ve | -ve | +ve | +ve |
| 9 | BG4 | -ve | -ve | -ve | +ve | +ve | +ve | +ve | +ve | +ve |
| 10 | BG5 | -ve | +ve | -ve | +ve | +ve | +ve | -ve | +ve | +ve |
| 11 | PF1 | -ve | +ve | -ve | +ve | +ve | +ve | +ve | +ve | +ve |
| 12 | PF2 | -ve | +ve | -ve | +ve | -ve | +ve | -ve | +ve | +ve |

| | | | | | | | | | | |
|----|-----|-----|-----|-----|-----|-----|-----|-----|-----|-----|
| 13 | PF3 | -ve | +ve | -ve | +ve | -ve | +ve | +ve | +ve | +ve |
| 14 | PF4 | -ve | +ve | -ve | +ve | +ve | +ve | +ve | +ve | +ve |
| 15 | PF5 | -ve | +ve | -ve | +ve | +ve | +ve | +ve | +ve | +ve |
| 16 | PF6 | -ve | -ve | -ve | +ve | -ve | +ve | -ve | +ve | +ve |

I-Indole test

M-Methyl red test

V-Voges Proskauer test

CI-Citrate test

C-Catalase test

TSI-Triple Sugar Iron test

U-Urease test

CHF-Carbohydrate Fermentation Test

SHT-Starch Hydrolysis test

d. Antibiotic sensitivity test

The results of antibiotic sensitivity test are given in table3.

Table3: results of antibiotic sensitivity test

| Sl.no | Strain no | Antibiotic sensitivity | MIC(cm) |
|-------|-----------|------------------------|---------|
| 1 | KC1 | +ve | 1.8 |
| 2 | KC2 | +ve | 1.0 |
| 3 | KC3 | +ve | 2.0 |
| 4 | KC4 | -ve | 1.7 |
| 5 | KC5 | +ve | 2.05 |
| 6 | BG1 | +ve | 1.1 |
| 7 | BG2 | +ve | 1.2 |
| 8 | BG3 | +ve | 2.0 |
| 9 | BG4 | +ve | 0.9 |
| 10 | BG5 | +ve | 1.1 |
| 11 | PF1 | +ve | 1.7 |
| 12 | PF2 | +ve | 1.5 |
| 13 | PF3 | +ve | 1.8 |
| 14 | PF4 | +ve | 1.5 |
| 15 | PF5 | +ve | 1.5 |
| 16 | PF6 | +ve | 0.8 |

e. Liquid displacement

The biodegradable waste was fed into the screw capped PET bottles along with crude sample in 3:1 ratio (vegetable waste: inoculums), 4%NH₄OH, 1.5%NaOH, 4g of cow manure(CM) was added to enhance the process of gas production.1.5%NaOH is used to maintain the alkaline (6.8 to 7.2) condition. The setup was left at room temperature for 20 days. The results are tabulated as follows

Amount of liquid displaced is tabulated as

Table4: Amount of liquid displaced in ml (crude sample)

| Duration(days) | Sample 1 (PF) | Sample2(KC)* | Sample3(BG) |
|----------------|---------------|--------------|-------------|
| 0 | 860 | 0 | 30 |
| 5-10 | 35.6 | 0 | 0 |
| 10-15 | 62.95 | 0 | 542 |
| 15-20 | 10 | 57 | 90 |

*- after 20th day KCDC produced gas but other samples were already converted into organic matter.

Table 5: Amount of liquid displaced in ml (result for isolated strains)

| Sl | Strain no | Duration(days) | Liquid displaced(ml) |
|----|-----------|----------------|----------------------|
|----|-----------|----------------|----------------------|

| | | | |
|----|-----|-------|-----|
| no | | | |
| 1 | BG1 | 0-5 | - |
| | | 5-10 | - |
| | | 10-15 | - |
| | | 15-20 | - |
| 2 | BG2 | 0-5 | - |
| | | 5-10 | - |
| | | 10-15 | - |
| | | 15-20 | 6.2 |
| 3 | BG3 | 0-5 | - |
| | | 5-10 | - |
| | | 10-15 | - |
| | | 15-20 | - |
| 4 | BG4 | 0-5 | - |
| | | 5-10 | - |
| | | 10-15 | 100 |
| | | 15-20 | 250 |
| 5 | BG5 | 0-5 | - |
| | | 5-10 | - |
| | | 10-15 | - |
| | | 15-20 | 45 |
| 6 | PF1 | 0-5 | - |
| | | 5-10 | - |
| | | 10-15 | - |
| | | 15-20 | - |
| 7 | PF2 | 0-5 | - |
| | | 5-10 | - |
| | | 10-15 | - |
| | | 15-20 | - |
| 8 | PF3 | 0-5 | - |
| | | 5-10 | - |
| | | 10-15 | - |
| | | 15-20 | - |
| 9 | PF4 | 0-5 | - |
| | | 5-10 | - |
| | | 10-15 | - |
| | | 15-20 | - |
| 10 | PF5 | 0-5 | 67 |
| | | 5-10 | - |
| | | 10-15 | - |
| | | 15-20 | - |
| 11 | PF6 | 0-5 | - |
| | | 5-10 | - |
| | | 10-15 | - |
| | | 15-20 | - |

f. Solid analysis

Moisture content and Total solids(TS) were determined gravimetrically after drying in oven at 105 °C. Volatile solids (VC) content was analysed by ignition dried sample at 600 °C for 2 hours and determining the ash free dry weight.

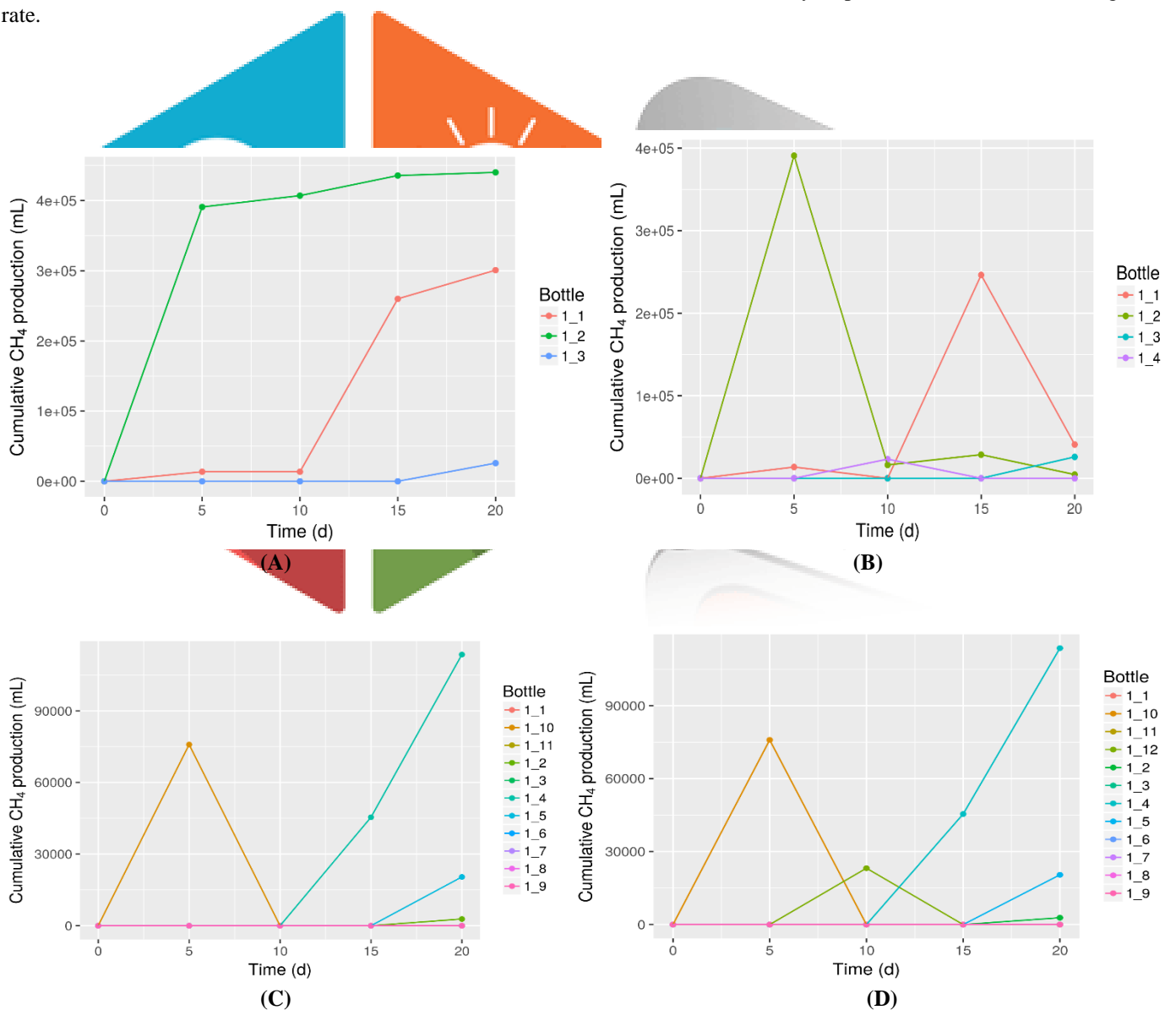
Table 6: Solid analysis of the crude sample

| SAMPLE | MC (%) | TC (%) | VC (%) |
|--------|--------|--------|--------|
| B1 | 94.4 | 5.6 | 88.14 |
| B2 | 92.03 | 7.97 | 89.71 |
| P1 | 92.7 | 7.3 | 77.05 |
| P2 | 95.60 | 4.4 | 74.29 |
| F2 | 94.9 | 5.1 | 75.55 |
| F3 | 94.7 | 5.3 | 68.42 |

Table7: Solid analysis of the isolated sample

| STRAIN | MC (%) | TC (%) | VC (%) |
|--------|--------|--------|--------|
| BG2 | 92.54 | 7.46 | 82.78 |
| BG4 | 78.93 | 6.16 | 80.59 |
| PF5 | 88.2 | 11.8 | 88.35 |
| MIX | 92.95 | 7.05 | 78.93 |

It was seen that after isolation the strain BG2 and mixed consortia (mix) had the ability to produce more amount of biogas at faster rate.



Graphs: Cumulative biogas production of (A) crude sample(1_1-BG,1_2-PF,1_3-KC) ;(B) crude sample with mix consortia(1_1-BG,1_2-PF,1_3-KC,1_4-Mix) ;(C) isolated sample (1_1to 1_5-BG,1_6 to 1_11-PF) ;(D) isolated sample with mix consortia (1_1to 1_5-BG,1_6 to 1_11-PF, 1_12-mix).

IV. Discussion

The study of biogas production from different substrate were conducted in anaerobic digester. The organisms were grown anaerobically using thioglycolate media. The morphology and phenotypic characteristics were studied by performing various biochemical tests which revealed that the organism were anaerobes. The biogas production was monitored and measured by liquid displacement study at regular intervals. A good substrate characterization is important in prediction of biogas potential from different substrates. The above graph indicates that mixed consortia had high degrading ability when compared to crude samples and isolated strains. Thus, speeding up the process of conversion of waste into organic matter. The moisture content of substrates ranged from 88% to 94%, this indicated that the substrate had enough moisture content for anaerobic digestion. The volatile solid of substrates ranged from 76% to 88%, this indicated that the substrate was rich in organic solid content that was to be converted to biogas.

V. Conclusion

It is concluded that individual strains had a potential to degrade the waste to organic matter in short period of time indicating a faster degradation rate compared to crude samples. The crude sample showed high amount of water displacement with increasing time, indicating the slow rate of degradation of waste into organic matter but higher rates of biogas production. From the graph, it was found that the mixed consortia have a high degrading ability in a short period of time. So, it can be concluded that mixed consortia gave a better result than the individual strains and can be used for speeding up the process.

VI. Acknowledgment

The satisfaction and euphoria that accompany the successful completion of any task would be incomplete without mention of the people who made it possible, whose constant guidance and encouragement crowded our efforts with success.

We would start by thanking the Chairman **Shri. S Narasimha Raju** of The Oxford College of Engineering for the opportunity, infrastructure and facilities provided for executing the work.

We thank our principal **Dr. R V Praveena Gowda** for providing necessary resources.

We thank **Dr.B.K. Manjunatha**, Professor and Head, Department of Biotechnology, The Oxford College of Engineering.

we would like to sincerely thank our guide **Ms. Salma Kausar.M**, Assistant Professor, Department of Biotechnology for her valuable suggestions without her help the completion of the project would not be possible.

We thank all faculty members of Department of Biotechnology for their necessary guidance and support. We also thank all non-teaching staff members for providing the support, help and cooperation without which the project would have been incomplete.

Our sincere thanks to all those who have directly or indirectly supported us in all aspects in bringing out this project efficiently and successfully.

We would like to thank our parents for their moral support.

Above all we thank the supreme lord for constantly helping us to overcome the hurdles and giving us the strengths to execute this project.

We would like to thank **Dr. Padma** principal The Oxford College of Pharmacy and **Ms. Sonu** the faculty for their guidance.

The Authors would like to thank **Mrs.Vasanth & Mr. Obul Reddy** (owners of paddy field), the head and the staff of Karnataka compost development corporation ltd., kudlu village, **Mr. Awala Murthy** for helping us to collect the biogas plant samples.

We gratefully thank **Mr. Challa Bhaskar Reddy & Mrs. Ramadevi** for permitting us to collect the cow manure sample.

VII. References

- 1) **Kumar, Sunil; Dhar, Hiya; Nair, Vijay V.; Bhattacharyya, J. K.; Vaidya, A. N.; Akolkar, A. B. (2016).** "Characterization of municipal solid waste in high-altitude sub-tropical regions". *Environmental Technology*. 37: 2627–2637
- 2) "Organics -Green Bin". Christchurch City Council. Retrieved 19 March 2016
- 3) **CSL London Olympics Waste Review.** cslondon.org
- 4) National Non-Food Crops Centre. "NNFCC Renewable Fuels and Energy Factsheet: Anaerobic Digestion", Retrieved on 2011-11-22
- 5) **Koyama, Tadashi (1963).** "Gaseous metabolism in lake sediments and paddy soils and the production of atmospheric methane and hydrogen". *Journal of Geophysical Research*. **68** (13): 3971–3973. Bibcode:1963JGR...68.3971K.
- 6) **Pamatmat, Mario Macalalag; Bhagwat, Ashok M. (1973).** "Anaerobic metabolism in Lake Washington sediments" (PDF). *Limnology and Oceanography*. pp. 611–627. Bibcode:1973LimOc. 18..611P.
- 7) **Zehnder, Alexander J. B. (1978).** "Ecology of methane formation". In Mitchell, Ralph. *Water pollution microbiology 2*. New York: Wiley. pp. 349–376. ISBN 978-0-471-01902-2.
- 8) **MacGregor, A. N.; Keeney, D. R. (1973).** "Methane formation by lake sediments during in vitro incubations". *Journal of the American Water Resources Association (JAWRA)*. **9** (6): 1153–1158. Bibcode:1973JAWRA.
- 9) Anaerobic digestion reference sheet, waste.nl
- 10) **Tabatabaei, Meisam (2010).** "Importance of the methanogenic archaea populations in anaerobic wastewater treatments". *Process Biochemistry*. **45**: 1214–1225.
- 11) "Anaerobic Digester: How It Works [Process] | GreenTheFuture.com".
- 12) "Landfill Gas & Biogas Analyzers | Nova Gas". Nova Gas.
- 13) **S. Dash* and P. Ray (2016)** Comparative Analysis of Different Biodegradable Wastes for Better Biogas Production *International Journal of Current Microbiology and Applied Sciences* ISSN: 2319-7706 Volume 5 Number 7 (2016) pp. 576-585
- 14) **Elizabeth R. Fielding, David B. Archer, Everly Conway de Macario and Alberto J. L. Macario (1988)** Isolation and Characterization of Methanogenic Bacteria from Landfills) vol-54 pg. no 835-836
- 15) **Amrita Saha* and Subhas Chandra Santra (2014)** Isolation and Characterization of Bacteria Isolated from Municipal Solid Waste for Production of Industrial Enzymes and Waste Degradation. *J Microbiol Exp* 1(1): 00003. Volume 1 Issue 1 - 2014 Department of Environmental Science, University of Kalyani, India
- 16) **Dhadse, S., Kankal, N.C. and Kumari, B. (2012).** Study of diverse methanogenic and non-methanogenic bacteria used for the enhancement of biogas production. *Int. J. Life Sci. Biotechnol. Pharma Res*, 1.
- 17) **Aisha Khalid and Shagufta Naz, (2013)** Isolation and Characterization of Microbial Community in Biogas Production from Different Commercially Active Fermentors in Different Regions of Gujranwala Department of Biotechnology and Microbiology, Lahore College for Women University, Pakistan-*International Journal of Water Resources and Environmental Sciences* 2(2): 28-33, 2013
- 18) **Srinidhi Adiga, Ramya R., Shankar B. B., Jagadish H. Patil and Geetha C. R. (2012)** Kinetics of Anaerobic Digestion of Water Hyacinth, Poultry Litter, Cow Manure and Primary Sludge: A Comparative Study 2012 2nd International Conference on Biotechnology and Environment Management IPCBEE vol.42
- 19) **T. Edwards and B.C. McBride (1975),** New method for isolation and identification of methanogenic bacteria, *applied microbiology* vol.29, no4, p.540-545.
- 20) **Michaela Stieglmeier, Reinhard Wirth, Gerhard Kminek and Christine Moissl-Eichinger. (2009),** Cultivation of Anaerobic and Facultatively Anaerobic Bacteria from Spacecraft-Associated Clean Rooms, *applied and environmental microbiology*, p. 3484–3491 Vol. 75, No. 11
- 21) **Amrita saha and Subhas chandra Santra (2014)** Isolation and Characterization of Bacteria Isolated from Municipal Solid Waste for Production of Industrial Enzymes and Waste Degradation, Department of Environmental Science Volume 1 Issue 1, University of Kalyani, India.
- 22) **J. A Ladapo and M.A. Barlaz, (1997),** Isolation and Characterization of refuse methanogens, *Journal of applied microbiology*, **82**,751-758
- 23) **Salma A. Iqbal, Shahinur Rahaman, Mizanur Rahman, Abu Yousuf, (2014)** Anaerobic digestion of kitchen waste to produce biogas, Elsevier, *Procedia Engineering*, vol 90, 2014, pp 657-662
- 24) **Mythili Ravichandran, Prathaban Munisamy, Sharmila Devi Natarajan and Chandrasekar Varadharaju (2016)** Rare detection and identification of methanogenic bacteria from diverse ecological niches in India for carbon balance and management in our environment. Department of microbiology, K.S. Ramasamy college of arts and science, Tiruchengode, Tamilnadu.
- 25) **Bouallagui H, BenCheikh R, Marouani L, Hamdi M. Mesophilic (1992)** biogas production from fruit and vegetable waste in tubular digester, *Bioresour Technol*, pp 39-48
- 26) **Emma Kreuger, Ivo Achu and Lovisa Björnsson, (2011)** Ensiling of crops for biogas production: effects on methane yield and total solids determination, *Biotechnology for Biofuels*, 2011.

- 27) **Anthony Njuguna Matheri, Iaeng, Mohamed Belaid, Tumisang Seodigeng, and Catherine Jane Ngila. (2016)**
Modelling the kinetic of biogas production from co-digestion of pig waste and grass clippings. Proceedings of world congress on Engineering 2016 vol 2 wce, London, U.K



Heavy metal ion detection using Immobilized ALP enzyme

K.Valarmathy*, Kala Sai Sarwani, H. Geethabhai, Eric Joseph

Department of Biotechnology, The Oxford College of Engineering, Bommanhalli, Bangalore-560068
mathy.valar@gmail.com

Abstract: Environment pollution by toxic heavy metals (HM) presents a real life threat for human health. Accumulation of heavy metals like Cadmium, Mercury, Cobalt and Copper in water causes toxic actions if the tolerance level is exceeded. Alkaline Phosphatase (ALP) activity was used for estimation of heavy metal ions in drinking water. It was based on inhibition of Alkaline Phosphatase enzyme activity exerted by metal ions. Kinetics of ALP was performed and maximum activity was found to be at using 2U/ml concentration of enzyme and hence was chosen for further studies. ALP immobilization was carried out by sol-gel method and sodium alginate method on two different surfaces: glass and stainless steel. Inhibition characteristics of ALP were tested using different concentrations of individual heavy metals ranging from 10mM to 10^{-5} mM and also using combination of heavy metals of concentration 10^{-4} mM. The reaction showed uncompetitive inhibition. Amongst the four heavy metals used, the amount of inhibition was found to be more in mercury compared to other metals.

Index Terms— Alkaline Phosphatase, Sol-Gel, Inhibition, metal ions

1. INTRODUCTION

The accumulation of toxic substances in the environment continuously increases due to diverse pollutants from the industries. Heavy metals in drinking water pose a serious threat to human health if the respective tolerance level is exceeded. Populations are exposed to heavy metals primarily through water consumption, but few heavy metals can accumulate in the human body (e.g., in lipids and gastrointestinal system) and may induce cancer and other risks. Hence, fast and accurate detection of metal ions has become a critical issue. Due to the high toxicity caused by the heavy metal ions there is an obvious need to determine them rapidly at trace levels. The present investigation aims determining heavy metal ions based on the inhibition studies of ALP on different metals.

2. MATERIALS AND METHODS

2.1 ENZYME KINETIC STUDIES

2.1.1 PNP STANDARD CURVE:

Enzyme kinetics was studied by plotting the pNP Standard Curve and carrying out the Enzyme Activity Assay by using 0.05M p-nitro phenyl phosphate (pNPP) as the substrate. The release of p-nitrophenol (pNP) in the reaction mixture (2.5ml) was continuously measured at 405nm spectrophotometrically (Thermo-Fischer), over the linear period. Different concentrations of standard pNP ranging from 0 μ g to 50 μ g were taken in a series volume of different test tubes. 1ml of distilled water is added to the test tubes. 2ml of 0.1M Sodium Hydroxide was added to make up the final reaction mixture to 4ml. Absorbance readings were taken at 405nm.

2.1.2 INHIBITION STUDIES OF FREE ALP WITH DIFFERENT HEAVY METAL IONS:

The effect of Hg²⁺, Cu²⁺, Co²⁺ and Mn²⁺ on ALP activity was studied. Various concentrations of the chosen heavy metals were added to the 0.1M Sodium Carbonate-Bicarbonate buffer followed by the addition of 0.1ml

enzyme. 1ml of 0.05M p-NPP substrate was then added to study the inhibition of the enzyme activity. 1ml of 0.2M NaOH was added to the final reaction mixture and the absorbance was measured at 405 nm spectrophotometrically.

2.2 IMMOBILIZATION OF ENZYME

2.2.1 SOL GEL METHOD

The stock gel solution for immobilization was prepared by adding 570 μ l of methanol 50 μ l of TEOS and 10 μ l of 3.8% CTAB (Cetyl Tri methyl Ammonium Bromide) solution in a small test tube at room temperature The solution was vigorously mixed. It was then cooled to 4 $^{\circ}$ C immediately after mixing. The enzyme stock solution was prepared by dissolving a known quantity of ALP in 50ml 0.02M phosphate buffer (pH- 7.0).The enzyme solution was cooled at 4 $^{\circ}$ C.

2.2.2 SODIUM ALGINATE METHOD (SA):

The sodium alginate method was performed by adding 0.6gms of Sodium alginate to 20ml of distilled water(solution 1) and 50 μ l of ALP (2U/ml) (solution 2). The Solution 1 and 2 were mixed and stirred for 30 minutes covering the electrode.

2.3 ACTIVITY OF IMMOBILIZED ENZYME ON DIFFERENT SURFACES

Immobilization was performed on two different types of surfaces (Glass and Stainless Steel) and by two different methods (Sol Gel and Sodium Alginate). 1ml of pNPP substrate was added to 0.4ml sodium carbonate-bicarbonate buffer .The enzyme immobilized glass beads, stainless steel fork prangs and stainless steel plates were added and incubated at 37 $^{\circ}$ C for 15minutes. glass beads, stainless steel fork prangs and stainless steel plates were removed. 1ml NaOH was then added and absorbance was measured at 405nm. Enzyme was not immobilized on the glass surface using the Sol Gel method as it specifically requires a conducting medium

2.4 pNPP SUBSTRATE KINETICS

The primary function of the inhibitor is to reduce the rate of reaction. Hence the need to study the rate of the reaction is highly necessary to study the properties of inhibition.

2.4.1 pNP ASSAY

Various volumes of standard pNP (0, 0.2, 0.4, 0.6, 0.8, 1.0 ml) were taken in a series of test tubes. The Volume was made upto 1ml using distilled water. 2ml of 0.1M NaOH was then added to all the test tubes and absorbance was measured at 405nm

2.4.2 pNPP ASSAY

1ml of different concentrations of pNPP was added to 0.4ml buffer followed by the addition of 0.1ml enzyme. It was then incubated at 37 $^{\circ}$ C for 5minutes. 1ml of 0.2M NaOH was then added to the test tubes and the absorbance was measured at 405nm.

2.4.3 MM PLOT FOR pNPP SUBSTRATE

The Michaelis-Menton plot was plotted for the substrate to find the rate of the reaction. It is a plot with concentration on x-axis and activity on y-axis. The formula used to calculate the activity is:-

Activity = (concentration of pNP x dilution factor) in μ mol/min
(mol. wt of pNP x Vol. of enzyme x Incubation time)

2.4.3 LB PLOT OF pNPP

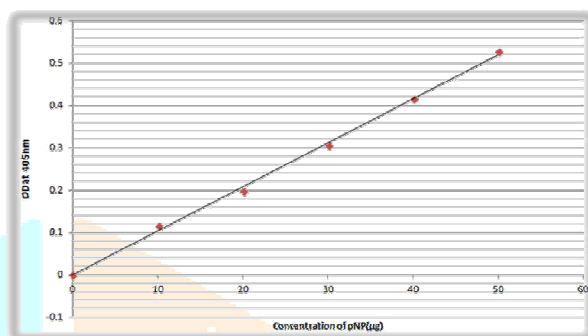
The Lineweaver-Burk plot is widely used to determine important terms in enzyme kinetics, such as K_m and V_{max} . The y-intercept of such a graph is equivalent to the inverse of V_{max} . The x-intercept of the graph represents $-1/K_m$. It also gives a quick, visual impression of the different forms of enzyme inhibition. The LB plot was plotted for the substrate to use as a reference to fine the type of inhibition exhibited by the heavy

metals.

3. RESULTS AND DISCUSSION

3.1 STANDARDIZATION OF pNP

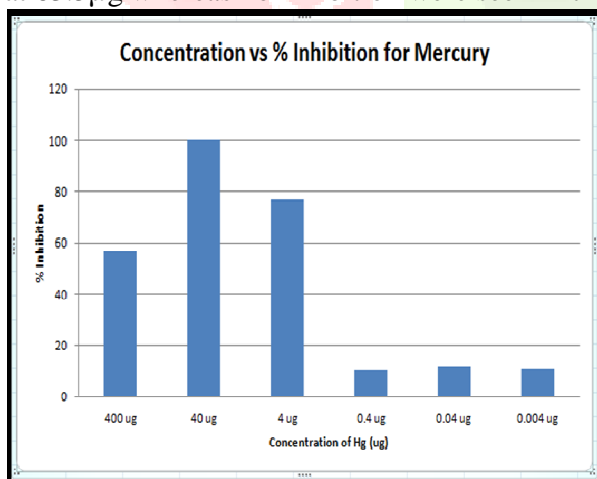
A graph was plotted with concentration of pNP taken on the x-axis and absorbance on y-axis. From the results it was observed that there was a linear increase in the absorbance level against increasing concentrations of pNP



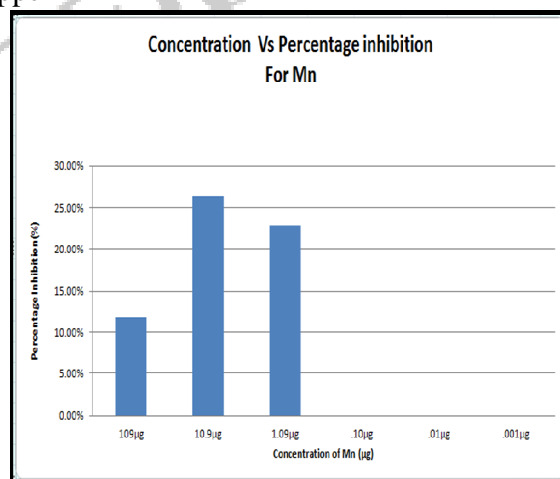
Graph 1: Standard Curve for pNP

3.2 INHIBITION STUDIES OF THE FREE ENZYME ALP

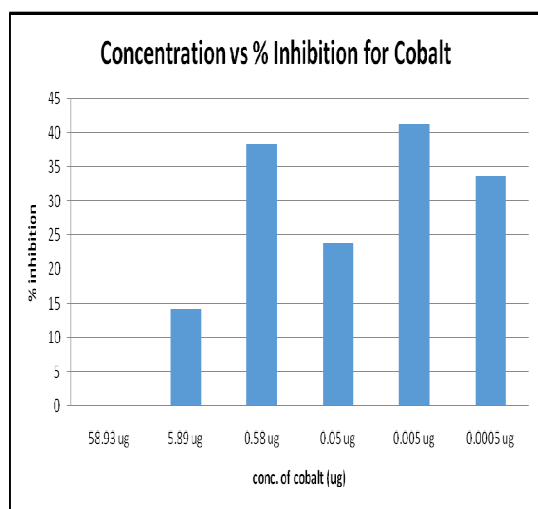
The compounds HgCl_2 , MnSO_4 , CoSO_4 and CuSO_4 were used as inhibitors and the percentage inhibition exerted by the respective individual heavy metals i.e. Hg^{2+} , Mn^{2+} , Co^{2+} and Cu^{2+} is given below. The percentage inhibition was calculated for different concentrations of Mercury, Manganese, cobalt and copper.. It was found that maximum inhibition was exhibited by $40\mu\text{g}$ of Mercury whereas minimum inhibition was shown by $0.4\mu\text{g}$ of Mercury and maximum inhibition was exhibited by $10.9\mu\text{g}$ of Manganese whereas no inhibition was seen after concentrations of $0.10\mu\text{g}$. It was found that maximum inhibition was exhibited by $0.005\mu\text{g}$ of Cobalt whereas no inhibition was seen in $58.93\mu\text{g}$ of Cobalt and it was found that high inhibitions were seen in $6.35\mu\text{g}$ and $0.06\mu\text{g}$ concentrations of Copper, lesser inhibition at $63.5\mu\text{g}$ whereas no inhibition were seen in the by $0.4\mu\text{g}$ of Copper



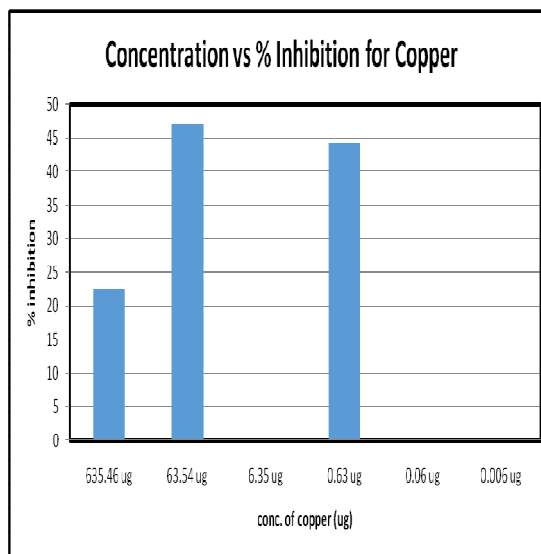
Graph 2: Concentration of Mercury vs. Percentage Inhibition



Graph 3: Concentration of Manganese vs. Percentage Inhibition



Graph 4: Concentration of Cobalt vs. Percentage Inhibition



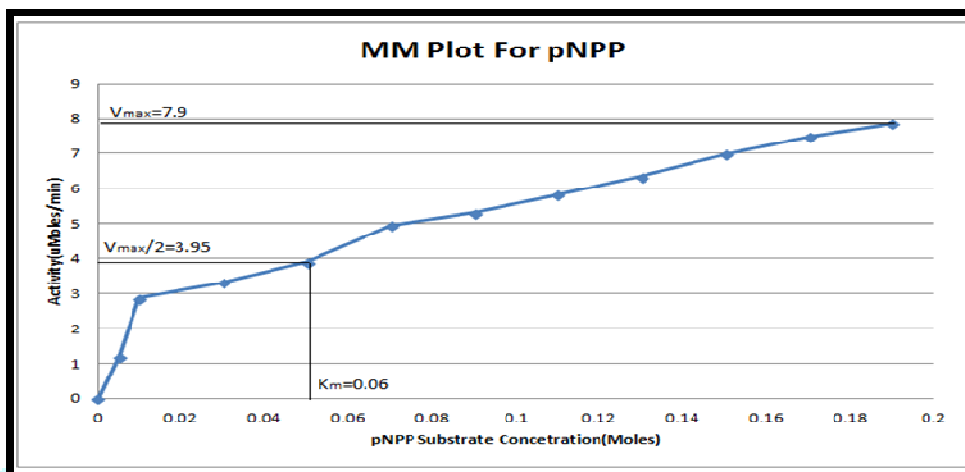
Graph 5: Concentration of Copper vs. Percentage Inhibition

3.3 RESULTS OF ACTIVITY OF IMMOBILIZED ENZYME ON DIFFERENT SURFACES

Immobilization was performed on two different types of surfaces (Glass and Stainless Steel) and by two different methods (Sol Gel and Sodium Alginate). The test was performed to find the activity of the immobilized enzyme on the glass beads. The sample (S) which had the enzyme immobilized glass beads showed negligible activity while the left over Sodium Alginate Extract (E) of the glass beads comparatively showed some activity. This showed that the enzyme had not been immobilized on to the glass surface using this method. The ALP immobilized prongs were tested for enzyme activity for a period of one week. The Immobilized enzyme showed high activity on the 1st day, which steadily decreased on the 2nd day and was almost negligible on the 7th day. This concluded that the enzyme showed stability for 1 week when it was immobilized with Sodium Alginate. For the Sol Gel Immobilized Surface, activity was found to be maximum on the 1st day which decreased over the 2nd and the 7th day. Moreover the activity for Stainless Steel Fork Prongs using Sodium Alginate Method had considerable good activity on day 2 whereas for the Sol Gel Immobilized prongs lost a greater amount of activity on the day 2 itself. Here the Sodium Alginate Immobilized Surface was tested for enzyme activity. This experiment showed considerably good activity on the 1st day which was rapidly lost on the 2nd. The results did not require us to proceed with testing the activity further ahead. The sol gel immobilized enzyme surface was then tested for enzyme activity. For this type of immobilization, the activity had reduced drastically from the 1st day to the 2nd. Moreover the activity for Stainless Steel Plates using Sol Gel method seemed to exhibit higher activity than that of the Sodium Alginate Method. The inhibition characteristics for four different metals i.e. Mercury, manganese, cobalt, copper were tested. All the metals were found to produce 100% inhibition.

3.4 MM PLOT FOR pNPP SUBSTRATE

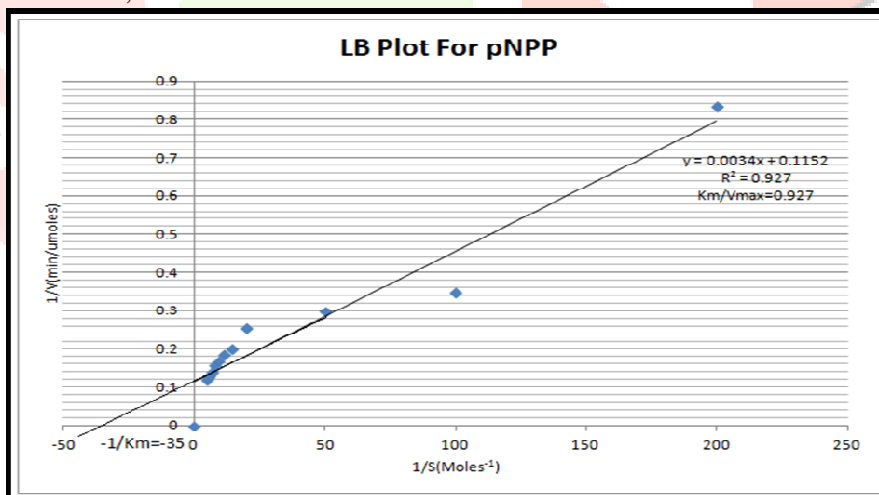
In the Michaelis-Menton curve obtained, it was seen that the rate of the reaction was found to increase with increasing concentrations of the substrate. This would tell us about the amount of the product pNP formed from the substrate pNPP. From the graph the V_{max} was found to be 7.9 and the K_m value was found to be 0.06



Graph 7: MM plot for substrate

3.5 LB PLOT OF PNPP

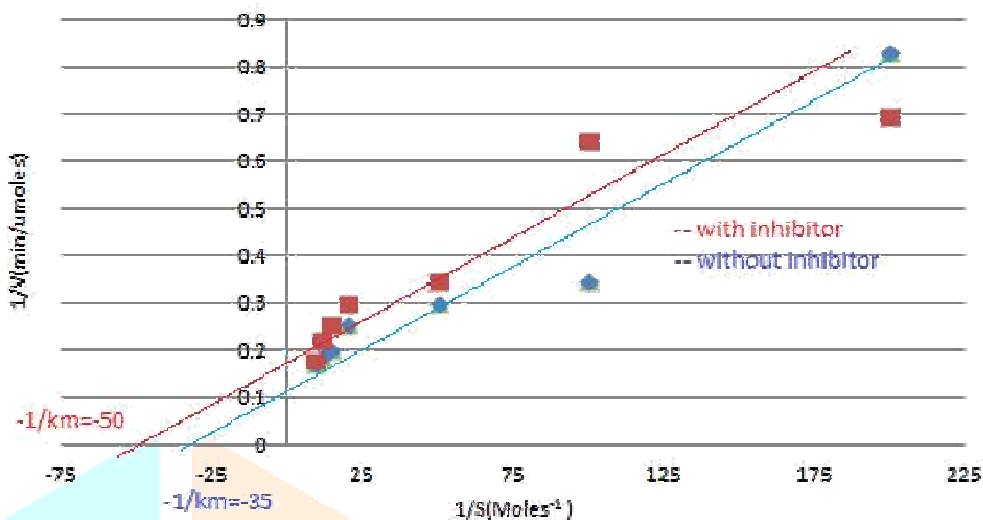
From the resulting LB plot, the substrate was used as a reference to find the type of inhibition exhibited by the heavy metals. From this, the K_m was found to be 0.028 and V_{max} was found to be 0.0302.



Graph 8: LB plot of pNPP

3.6 TYPE OF INHIBITION

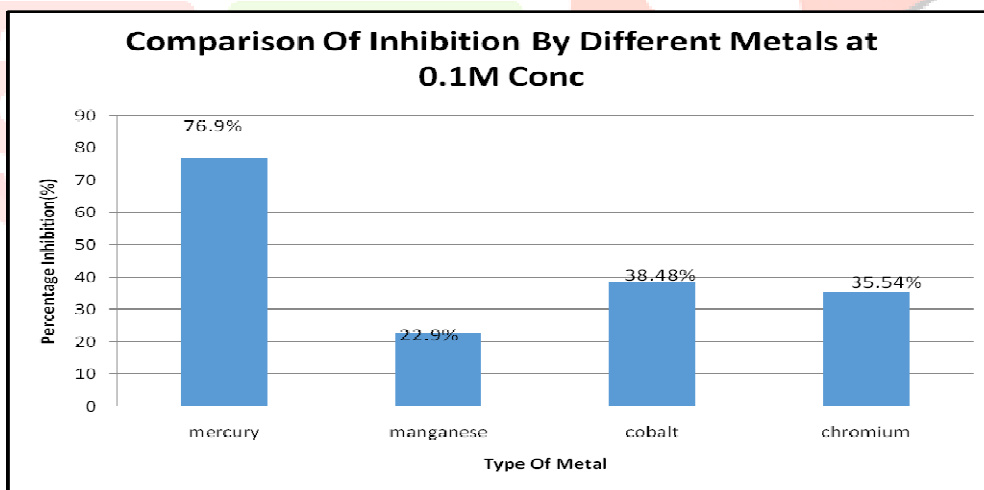
The Lineweaver-burk plot was plotted for the substrate with and without the inhibitor and the inhibition was found to be of uncompetitive type. Uncompetitive inhibition implies that the inhibitor can bind only to the substrate-enzyme complex. This was concluded due to the parallel slopes obtained for the respective curves.



Graph 9: LB plot with inhibitor

3.7 COMPARISON OF INHIBITION BY DIFFERENT METALS AT 0.1 M CONCENTRATIONS

The results obtained were plotted on a graph. It was found that Mercury exhibited maximum inhibition of 76.9% while Manganese seemed to show the least inhibition of 22.9%.



Graph 10: Comparison of Inhibition by Different Metals

4. CONCLUSION

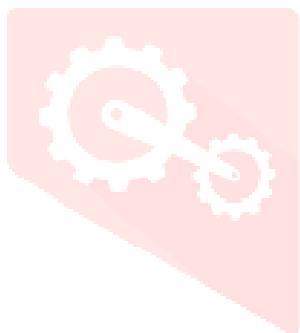
The present study concluded that maximum activity for Alkaline Phosphatase enzyme was exhibited at 2U/ml concentration. Hence, this concentration was chosen for further work. On comparing the immobilization by the two techniques used, we observed that Sodium Alginate immobilized surface retained higher activity compared to Sol gel immobilized surface. By studying the effect of various

heavy metals on the free and immobilized enzyme, it was found that Mercury exhibited maximum inhibition on the activity of the enzyme Alkaline Phosphatase and Manganese was found to have the least inhibition. The heavy metals Copper and Cobalt showed unstable inhibition readings due to the inherent color exhibited by them which caused hindrance in Absorbance readings. The concentration range of heavy metals that can be detected by using this sensor is 10-4mM to 10mM .A Line weaver – Burk plot was plotted for the pNPP substrate with and without the inhibitor. The graph obtained showed that the inhibition was of uncompetitive type. This implies that the enzyme inhibitor can bind only to the complex formed between the enzyme and the substrate. This could imply that the binding site for the inhibitor is accessible only after the enzyme has bound to its substrate.

5. REFERENCES

1. R. Ilangoan, D. Daniel, A. Krastanov, C. Zachariah & R. Elizabeth (2006) Enzyme based Biosensor for Heavy Metal Ions Determination, *Biotechnology & Biotechnological Equipment*, 20:1, 184-189.
2. Maitha M. Alnuaimi, Ibtisam A Saeed and S. Salman Ashraf (2012) Effect of various heavy metals on the enzymatic activity of E.coli ALP, *International Journal of Biotechnology and Biochemistry*, Vol 8, 47-59.
3. Lata Sheo Bachan Upadhyay and Nishant Verma (2015) ALP inhibition based conductometric biosensor for phosphate estimation in biological fluids., *Elsevier*, Vol 68, 611-616.
4. Abollino, O., Aceto, M., Malandrino, M., Mentasti, E., Sarzanini, C., Barberis, R., (2002). Distribution and mobility of metals in contaminated sites. Chemometric investigation of pollutant profiles. *Environ. Pollut.* 119: 177-193.
5. Alpat, S., Alpat, S.K., Adirci, B.H.C., Yas, a, I. and Telefoncu, A. (2008) A novel microbial biosensor based on *Circinella* sp. modified carbon paste electrode and its voltammetric application. *Sens. Actuators B* 134(1): 175–181.
6. Alpat, S.K., Alpat, S., Kutlu, B., Zbayrak, O.O. and B'uy'ukis, ik, H.B. (2007) Development of biosorption-based algal biosensor for Cu(II) using *Tetraselmis chuii*. *Sens. Actuators B* 128(1): 273–278.
7. Amine A., Mohammadi H., Bourais I. and Palleschi G. (2006) Enzyme inhibition-based biosensors for food safety and environmental monitoring. *Biosens. Bioelectron.* 21: 1405–1423.
8. Amine A., Mohammadi H., Bourais I. and Palleschi G. (2006) Enzyme inhibition-based biosensors for food safety and environmental monitoring. *Biosens. Bioelectron.* 21: 1405–1423.
9. Anh, T.M., Dzyadevych, S.V., Prieur, N. (2006) Detection of toxic compounds in real water samples using a conductometric tyrosinase biosensor. *Materials Science and Engineering C* 26(2-3): 453–456
10. Appenroth, K.J. (2010) Definition of “Heavy Metals” and their role in biological systems, Sherameti, I. and Varma, A. (eds.), *Soil Heavy Metals*, *Soil Biology*. 19: 19-29. DOI 10.1007/978-3-642-02436-8_2, © Springer-Verlag Berlin Heidelberg 2010
11. Babkina, S.S. and Ulakhovich, N.A. (2004) Amperometric biosensor based on denature DNA for the study of heavy metals complexing with DNA and their determination in biological, water and food samples. *Bioelectrochem.* 63(1-2): 261–265.
12. Bagal-Kestwal, D., Karve, M. S., Kakade, B. and Pillai, V. K. (2008) Invertase inhibition based electrochemical sensor for the detection of heavy metal ions in aqueous system: application of ultra-microelectrode to enhance sucrose biosensor's sensitivity. *Biosens. Bioelectron.* 24(4): 657– 664.

13. Barcelo, J., Poschenrieder, C. (2004) Structural and ultrastructural changes in heavy metal exposed plants. In: Prasad MNV (ed) Heavy metal stress in plants, 3rd edn. Springer, Berlin, 223–248
14. Barrocas, P.R.G., Landing, W.M. and Hudson, J.M. (2010) Assessment of mercury(II) bioavailability using a bioluminescent bacterial biosensor: practical and theoretical challenges. *J. Environ. Sc.* 22(8): 1137– 1143.
15. Belkin, S., (2003) Microbial whole-cell sensing systems of environmental pollutants. *Curr. Opin. Microbiol.* 6: 206-212
16. Bentley A., Atkinson A., Jezek J. and Rawson D. M. (2001) Whole cell biosensor electrochemical and optical approaches to ecotoxicity testing. *Toxicol. Vitro* 15: 469-475.
17. Berezhtskyy, A.L., Sosovska, O.F., Durrieu, C., Chovelon, J., Dzyadevych, S.V., Tran- Minh, C. (2008) Alkaline phosphatase conductometric biosensor for heavy-metal ions determination. *ITBM-RBM* 29(2–3): 136–140.
18. Biran, R., Babai, L., Klimentiy, J., Rishpon and Ron, E.Z. (2000) Online and in situ monitoring of environmental pollutants: electrochemical biosensing of cadmium. *Environ Microbiol.* 2: 285-290
19. Blake, D.A., Jones, R.M., Blake, R.C. 2nd, Pavlov, A.R., Darwish, I.A., Yu, H. (2001)
20. Antibody-based sensors for heavy metal ions. *Biosens. Bioelectron.* 16(9–12): 799–809.
21. Bontidean, A., Mortari, S. and Leth N.L. (2004) Biosensors for detection of mercury in contaminated soils, *Environ. Poll.* 131(2): 255–262.
22. Bontidean, C., Berggren, G., Johansson, E., Csoregi, B., Mattiasson, J.R., Lloyd, K.J., Jakeman and Brown, N.L. (1998) Detection of Heavy Metal Ions at Femtomolar Levels
23. Using Protein-Based Biosensors. *Anal. Chem.* 70: 4162-4169.
24. Bontidean, I. (2002) Design, development and applications of highly sensitive protein based capacitive biosensors. Lund University Dissertation Abstracts.
25. Bontidean, I., Ahlqvist, J. and Mulchandani, A. (2003) Novel synthetic phytochelatin based capacitive biosensor for heavy metal ion detection. *Biosens. Bioelectron.* 18(5-6): 547– 553



SCREENING OF POTENTIAL PHYTOCHEMICALS FOR WOUND HEALING

¹Dr. B.K. Manjunatha*, ²Tanusree Chaudhuri, ³B.S. Rithu, ⁴K Soundarya Vadhulas, ⁵Harish.M

¹ Professor and Head of Department, ² Assistant professor, ^{3,4,5} Student
Department of Biotechnology,
The Oxford College of Engineering, Bengaluru, Karnataka-
560068, India.

Abstract: Traditional therapies, including the use of dietary components for wound healing and skin regeneration, are very common in Asian countries such as China and India. The increasing evidence of health-protective benefits of phytochemicals, components derived from plants is generating a lot of interest, warranting further scientific evaluation and mechanistic studies. Among different plants showing positive activity towards wound healing, *Capparis spinosa*-*C. spinosa* has many active constituents such as flavonoids such kaempferol and quercetin. Nature fruits of *C. spinosa* have glucose as 1-H Indole-3-acetonitrile etc, whereas *C. zeylanica* has reported to have fatty acids such as E-octodec-7enyonic acid isolated from chloroform extract of the roots. Extracts of *C. decidua* stems and flowers showed insecticidal and oviposition inhibitory activities against *Bruchus chinensis*. The phytochemical from these plant extracts were found to possess significant wound healing promoting activity. In the present study, we have identified 12 potent active constituents viz., Capparis spine, Glucocapparin, kaempferol, kaempferol-7-rhamnoside, Polyprenols, Proline betaine, Quercetin, Quercetin-3-rutinoside, Rhamnetin, Rutin, Saccharose, Sinigrin for wound healing promoting ability. These active constituents were subjected for docking study using a well established target GSK 3 Beta responsible for wound healing process in human. Our results, indicated that Capparis spine, Glucocapparin, kaempferol, Polyprenols, Quercetin, Quercetin-3-rutinoside, Rhamnetin have a potent wound healing property among other compounds. In vivo/ in vitro studies to validate the present finding and to understand the exact mechanism and potential targets of these phytochemicals are under process.

Keywords: Wound healing, Ethanol leaf extract, *C. decidua*, *C. spinosa* and *C. Zeylanica*, Antimicrobial activity, Docking.

I. INTRODUCTION

Wound infection has become a major medical distress in recent years. Wound is defined simply as the disruption of the cellular and anatomic continuity of a tissue. Wound may be originated by physical, chemical, thermal, microbial or immunological insult to the tissue. Wound healing is a structured biological process that restores tissue continuity after injury and is a combination of physical, chemical and cellular events that recreate the wounded tissue or replace it with collagen. Wound healing can be divided into three stages, including inflammation, proliferation and re-modelling and maturation phases which includes the interaction of various cells, cytokines and growth factors. The normal healing starts immediately after the injury. When blood spills at the site of injury, the blood platelets interact with collagen and other components of the extracellular matrix. This stimulates the release of clotting factors as well as essential growth factors and cytokines such as platelet-derived growth factor (PDGF) and transforming growth factor beta (TGF- β). The inflammatory phase begins after the migration of neutrophils to the wound site to clean the tissue. The fibroblasts migrate into the tissue to unfold into the proliferative phase and deposit new extracellular matrix. This new collagen matrix gets cross linked and organized.

Capparis is one of the important genus of the family Capparidaceae. Leaves of *Capparis decidua* are used as plaster for boils and swellings, to relieve tooth ache, as antidote to poison, stem bark as laxative, anthelmintic, in treating cough, asthma and inflammation, fruits in cardiac troubles, root and root bark in fever and rheumatism (Chopra, et al., 1956), fruits are known as appetizer, stem bark is used in the treatment of cardiac diseases, whole plant is used in debility, joint pains, pyorrhoea, rheumatism, skin disorders (Keshava Murthy, 1994), fruits and shoots are reported for hypolipidaemic (Purohit and Vyas, 2005), antistress and antidiabetic (Yadav, et al., 1997), anti-inflammatory activity. Leaves of *C. spinosa* are used as poultice in gout, in nervous disorders, stem bark is used in treating paralysis, rheumatism, tooth ache and tuberculosis (Keshava Murthy, 1994), root bark as tonic, diuretic, expectorant, anthelmintic, analgesic, in rheumatism, paralysis, enlarged spleen and tubercular glands (Chopra, et al., 1956), antihepatitis, anti-inflammatory, antifungal, antidiabetic, in treating chondrocytes (Panico, et al., 2005), as hypolipidaemic (Eddouks, et al., 2005), as antiallergic and antihistaminic (Trombetta, et al., 2005), as antioxidant (Bonina, et al., 2002; Germano, et al.,

2002). The plant contains glucoside, triglucoside, rutin, pentosans, ronic acid, pectic acid and saponin (Chopra, et al., 1956), glucosinolates, fatty acid, sterol and tocopherol (Matthaus and Ozcan, 2005). Leaves of *C. zeylanica* is used in treating cholera, fruits in treating blisters and boils, roots in treating coryza, elephantiasis, hemiplegia, neuralgia, oedema, piles, pneumonia, rheumatism, snakebite, ulcer and vomiting (Keshava Murthy, 1994), as sedative, in treating cholera and stomachic, the plant contains an alkaloid, phytosterols, water soluble acids (Chopra, et al., 1956) and E-octadec-7-en-5-ynoic acid. The tribal groups of Davanagere district, Karnataka state, India use leaves of above mentioned plants in healing septic wound (Fresh leaves were ground with lime juice and mixed with one teaspoon full of honey, a thick paste so obtained is applied to septic wounds) (Manjunatha, 2002).

Critical review of the literature revealed that the wound healing potency of these plants has not been subjected to clinical evaluation. In the present study, we have identified 12 potent active constituents viz., Capparispinine, Glucocapparin, kaempferol, kaempferol-7-rhamnoside, Polyphenols, Proline betaine, Quercetin, Quercetin-3-rutinoside, Rhamnetin, Rutin, Saccharose, Sinigrin for wound healing promoting ability. These active constituents were subjected for docking study using a well established target GSK 3 Beta responsible for wound healing process in human. Our results, indicated that Capparispinine, Glucocapparin, kaempferol, Polyphenols, Quercetin, Quercetin-3-rutinoside, Rhamnetin have a potent wound healing property among other compounds. In vivo/ in vitro studies to validate the present finding and to understand the exact mechanism and potential targets of these phytochemicals are under process.

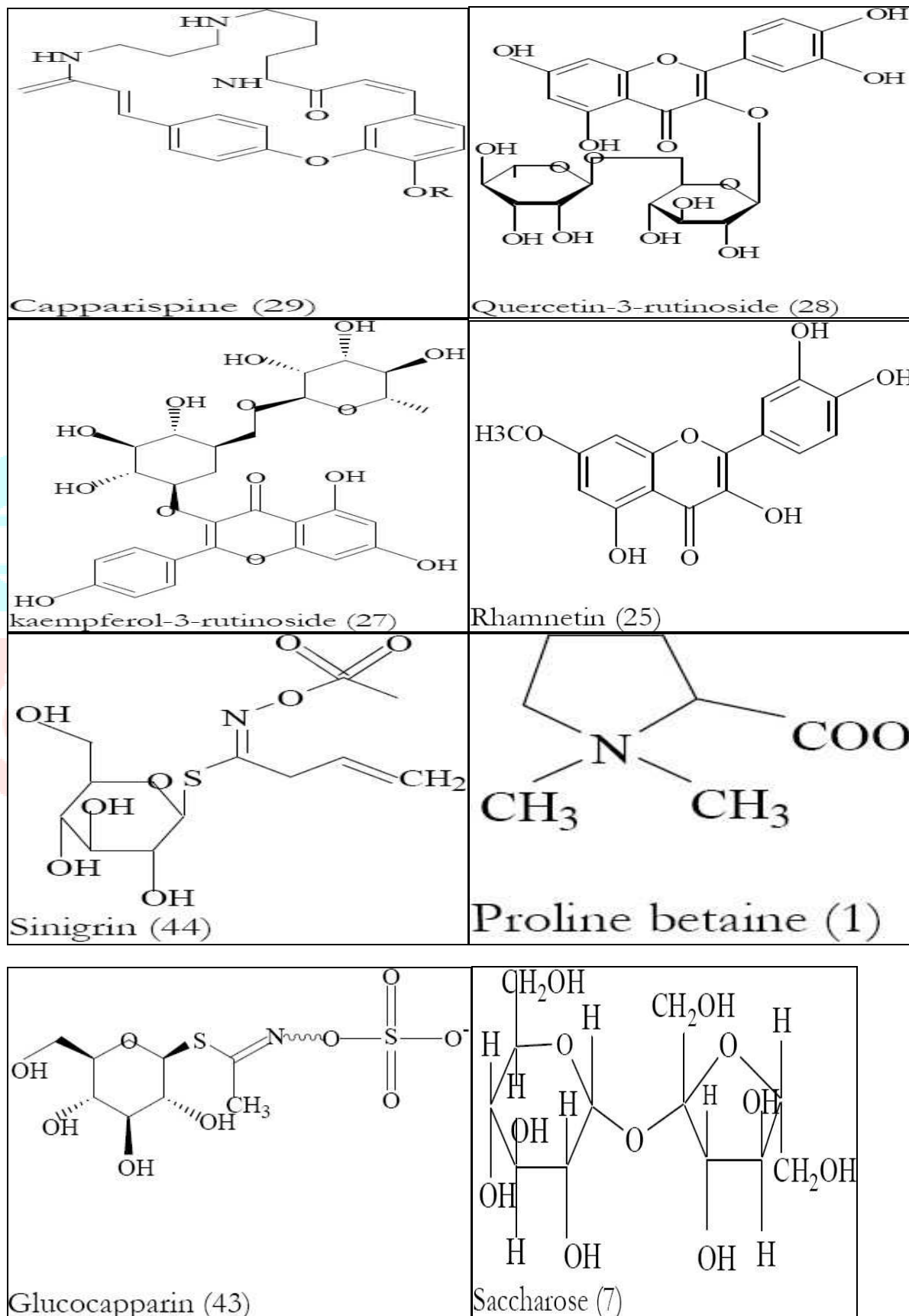
II. MATERIALS AND METHODS

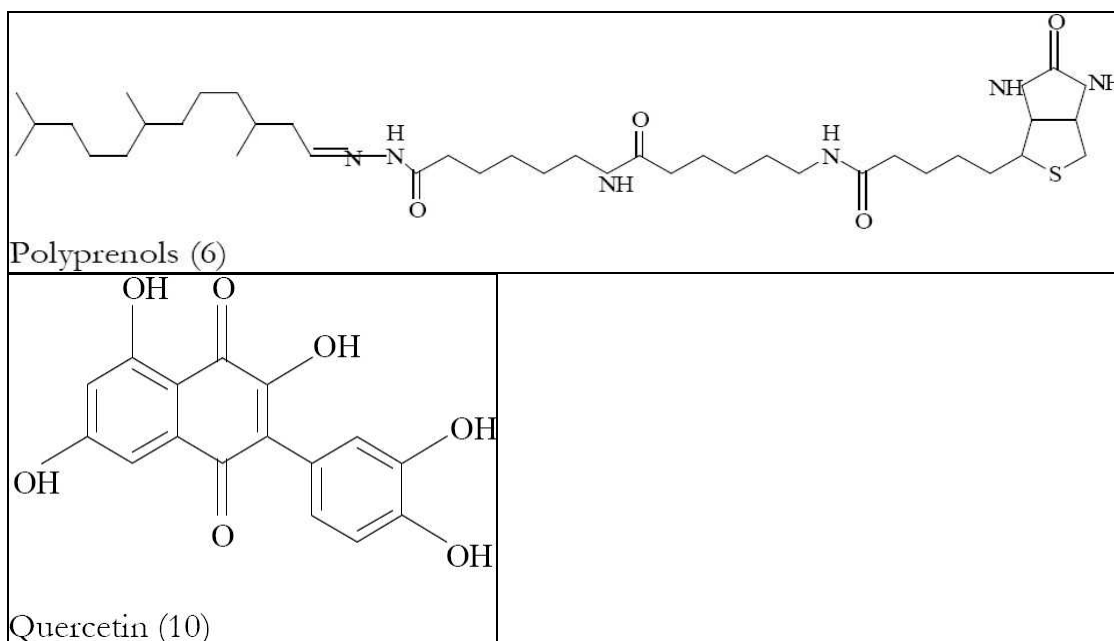
- 1. Target Identification:** Glycogen synthase kinase-3 (GSK-3) is a widely expressed and highly conserved serine/threonine protein kinase encoded by 2 genes, GSK3A and GSK3B. Both Gsk3b-CKO mice and fibroblasts showed elevated expression and production of endothelin-1 (ET-1) compared with control mice and cells. Antagonizing ET-1 reversed the phenotype of Gsk3b-CKO fibroblasts and mice. Thus, GSK-3beta appears to control the progression of wound healing and fibrosis by modulating ET-1 levels. These results suggest that targeting the GSK-3beta pathway or ET-1 may be of benefit in controlling tissue repair and fibrogenic responses in vivo. So, we performed Automated docking was used to determine the orientation of inhibitors bound in the active site of GSK3-b. The protein structure file 1Q5K was taken from PDB (www.rcsb.org/pdb) was edited by removing the hetero atoms, adding C terminal oxygen (Binkowski et al., 2003).
- 2. Ligand Identification:** 12 ligands namely Capparispinine, Glucocapparin, kaempferol, kaempferol-7-rhamnoside, Polyphenols, Proline betaine, Quercetin, Quercetin-3-rutinoside, Rhamnetin, Rutin, Saccharose, Sinigrin was identified through literature, which have potential wound healing activity belonging to *Capparis spp.* All ligands were searched for the three dimensional structure in the pubchem database, and nonpolar hydrogen atoms were merged in the corresponding three dimensional structure.
- 3. Docking:**
 - 1. Target preparation:** The following steps were followed to prepare the protein file: First the water molecules were removed from protein. Next, we need to add hydrogen because X-ray crystallography usually does not locate hydrogen; hence most PDB files do not include them. Later pdbqt file of protein was generated.
 - 2. Ligand preparation:** to generate the ligand pdbqt file, the following steps were followed. In Autodock Tools, torsion tree and no of torsions were selected. And finally it was saved Save as .pdbqt
 - 3. Autodock vina working protocol:** Docking studies were carried out using AUTODOCK software. AUTODOCK Vina is a suite of automated docking tools. Autodock Vina was performed in the cmd command terminal using the following command.
“C:\Program Files (x86)\The Scripps Research Institute\Vina\vina.exe” -- config conf.txt
-- log log.txt.
- 4. Visualization of docking results:** PyMOL and DISCOVERY STUDIO are the software used for visualization of interactions between targets and ligands. These help in finding in different types of interactions between our ligand and the target molecule.

III. RESULTS AND DISCUSSION:

- 12 ligands namely Capparispinine, Glucocapparin, kaempferol, kaempferol-7-rhamnoside, Polyphenols, Proline betaine, Quercetin, Quercetin-3-rutinoside, Rhamnetin, Rutin, Saccharose, and Sinigrin was identified through

literature, which have potential wound healing activity belonging to *Capparis spp.* The structure of all the 12 ligands are as follows:





The protein structure file 1Q5K was taken from PDB (www.rcsb.org/pdb) was edited by removing the hetero atoms, adding C terminal oxygen is being given as follows:

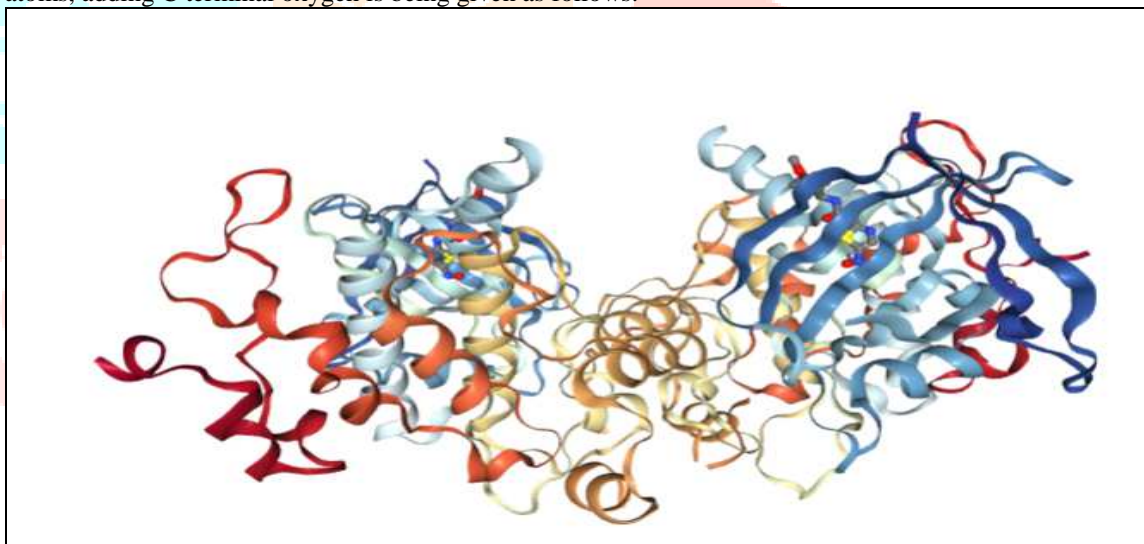


Figure1: Structure of 1Q5K protein

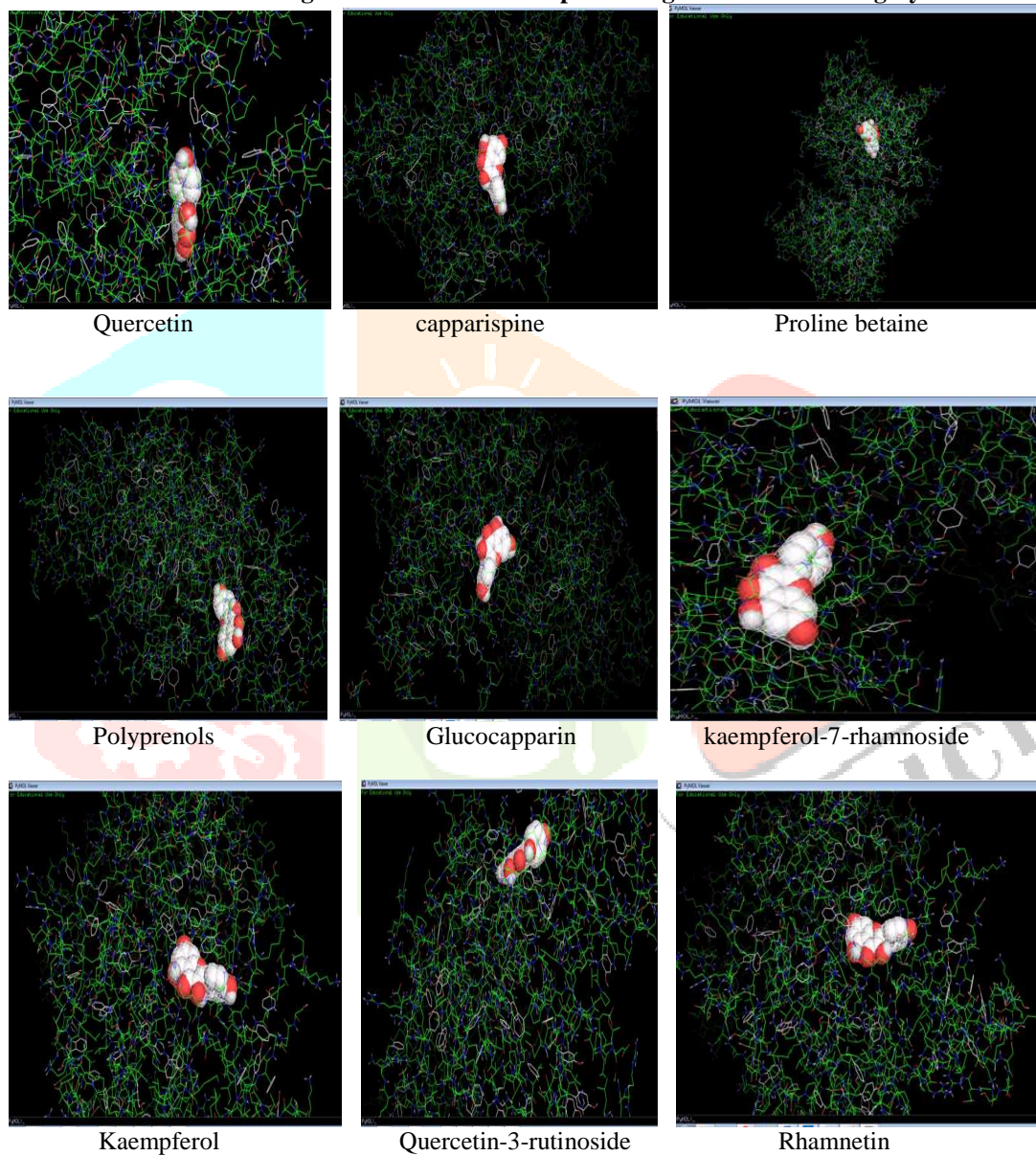
Using Autodock Vina software, docking is done and the results are obtained in the form of dlq files. These files are converted to PDBQT files and then into PDB file. Binding energy score and corresponding PDB structure is obtained for the runs. The run giving the highest negative score for estimated binding energy in kcal/mol is considered for complex file formation.

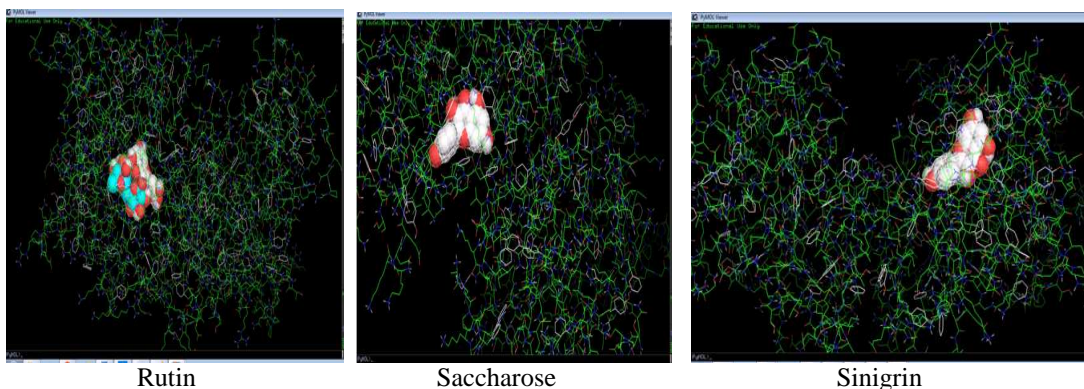
Table-1
Affinity values after Docking studies.

| Sl no. | Ligand Compounds | Affinity values |
|--------|-------------------------|-----------------|
| 1 | Capparispine | -8.4 |
| 2 | Glucocapparin | -8.4 |
| 3 | kaempferol | -8.4 |
| 4 | kaempferol-7-rhamnoside | -7.4 |
| 5 | Polyrenols | -8.4 |

| | | |
|----|------------------------|------|
| 6 | Proline betaine | -8.1 |
| 7 | Quercetin | -8.4 |
| 8 | Quercetin-3-rutinoside | -8.4 |
| 9 | Rhamnetin | -8.4 |
| 10 | Rutin | -9.1 |
| 11 | Saccharose | -8.4 |
| 12 | Sinigrin | -8.5 |

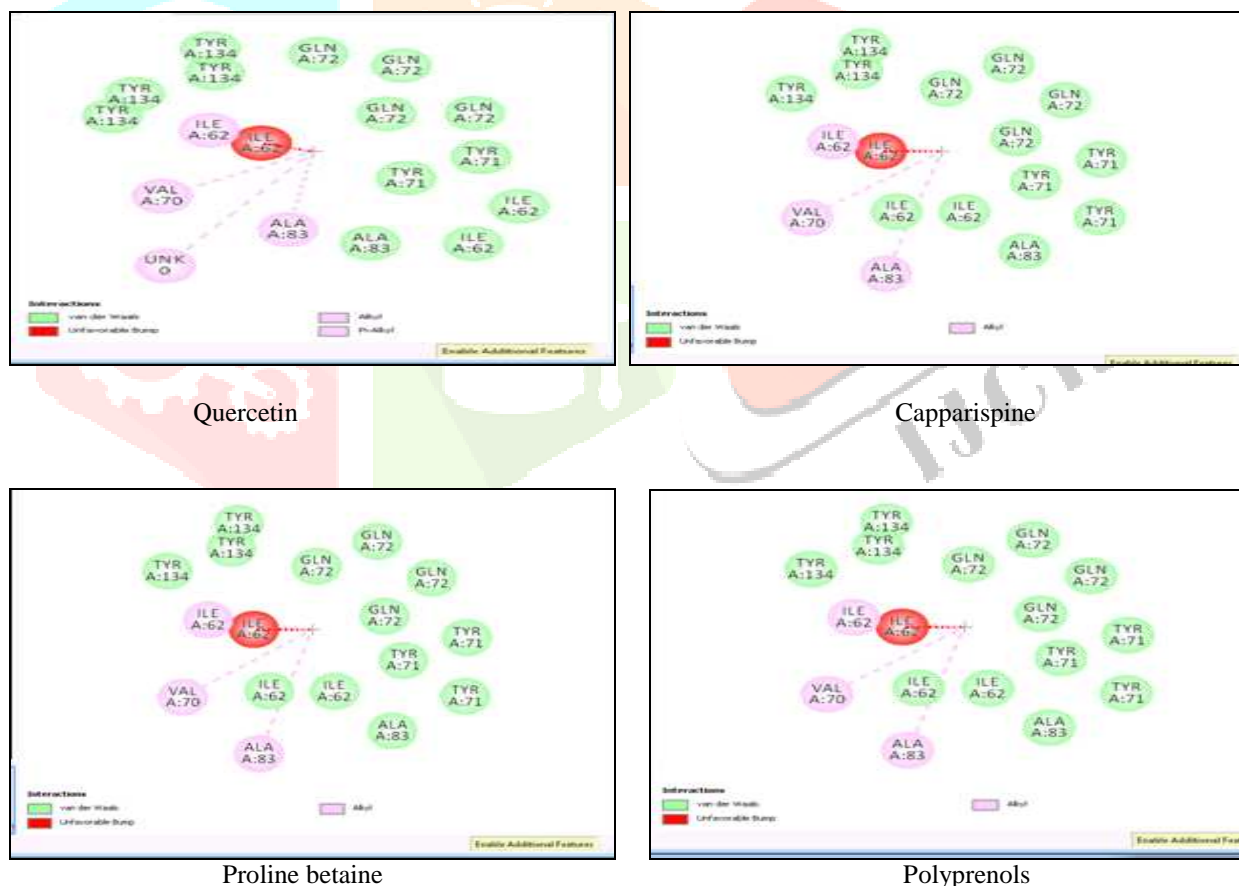
Figure 2: Visualization of protein-ligand structure using Pymol.





From the docked complex, pharmacophore is being identified and analyzed through protein ligand 2-D interaction. It is being observed that the Tyr and Gln are the most two important amino acids present in the active site of the target protein, making the favourable interaction with the ligand molecule.

Figure3: Protein ligand 2-D interaction of Pharmacophore



| | |
|---------------------------|--------------------|
| Van der walls interaction | Val, Tyr, Gln, Ile |
| Alkyl, pi-alkyl | Val, Ile and ala |

IV. DISCUSSION

In the present investigation preliminary phytochemical analysis revealed the presence of glycosides, triterpenoids, flavonoids, alkaloids, saponins, sterols and tannins. These phytoconstituents are known to inhibit lipid peroxidation and increases the viability of collagen fibrils by increasing the strength of collagen fibers, by increasing the circulation, by preventing the cell damage and by promoting the DNA synthesis (Geite, et al., 2002). Thus wound healing potency of *C. decidua*, *C. spinosa* and *C. zeylanica* may be attributed to the antibacterial and antioxidant property of the phytoconstituents present in them which may be either due to their individual or additive effect which help the process of wound healing. Among the ligands studied for wound healing Capparispine, Glucocapparin, kaempferol, Polyphenols, Quercetin, Quercetin-3-rutinoside, Rhamnetin showed very high potential towards wound healing.

V. ACKNOWLEDGEMENTS

The authors is very grateful to Girimaji N. Raj Gopal, S.V.Thimmaiah and Prof. Darmanada Rao National Educational Society, Shimoga.

VI. REFERENCES

- Ageel, A.M., Parmar, N.S., Mossa, J.S., Al-Yahya, M.A., Al-Said, M.S. and Tariq, M., *Agents Actions*, 1986, 17(3-4), 383.
- Azad, S. 2002. Essentials of surgery. PARAS Medical Publishers, Hyderabad, India.
- Bonina, F., Puglia, C., Ventura, D., Aquino, R., Tortora, S., Sacchi, A., Saija, A., Tomaino, A., Pellegrino, M.L. and de Caprariis, P. 2002. *In vitro* antioxidant and *in vivo* photoprotective effects of a lyophilized extract of *Capparis spinosa* L. buds. *J. Cosmet. Sci.* 53(6), 321-335.
- Calis, I., Kuruuzum-Uz, A., Lorenzetto, P.A. and Ruedi, P., *Phytochem.*, 2002, 59(4), 451.
- Chopra, R.N., Nayar, S.L. and Chopra, I.C. 1956. Glossary of Indian Medicinal Plants. C.S.I.R. Publications, New Delhi.
- Ehrlich, H.P. and Hunt, T.K. 1968. Effect of cortisone and vitamin A on wound healing. *Ann. Surg.* 167, 324.
- Germano, M.P., De Pasquale, R., De Angelo, V., Catania, S., Silvari, V. and Costa, C. 2002. Evaluation of extracts and isolated fraction from *Capparis spinosa* L. buds as an antioxidant source. *J. Agric. Food Chem.* 50(5), 1168-1171.
- Getie, M., Gebre Mariam, T., Reitz, R. and Neubert, R.H. 2002. Evaluation of the release profiles of flavonoids from topical formulations of the crude extract of the leaves of *Dodonea viscosa* (Sapindaceae). *Pharmazie.* 57, 320-322.
- Haque, M.E., Haque, M., Rahman, M.M., Rahman, M.M., Khondkar, P., Wahed, M.I., Mossadik, M.A., Gray, A.I. and Sarker, S.D., *Fitoter.*, 2004, 75(2), 130.
- Keshavamurthy, K.R. 1994. Medicinal plants of Karnataka. Karnataka Forest Department (ed.), Bangalore, India.
- Kokate, C.K., Purohith, A.P. and Gokhale, S.B. 1990. Pharmacognosy. Nirali Prakashan, Pune.
- Lee, K.H. 1968. Studies on mechanism of action of salicylates, retardation of wound healing by aspirin. *J. Pharm. Sci.* 57(6), 1042-1043.
- Manjunatha, B.K. 2002. Floristic composition of davanagere district, Karnataka, India. Ph. D. Thesis, Kuvempu University, Shankaraghatta, Karnataka, India.
- Matthaus, B. and Ozcan, M. 2005. Glucosinolates and fatty acid, sterol and tocopherol composition of seed oils from *Capparis spinosa* Var. *spinosa* and *Capparis ovata* Desf. Var. *canescens* (Coss.) Heywood. *J. Agric. Food Chem.* 53 (18) 7136-7141.
- Morton, J.P. and Malone, M.H. 1972. Evaluation of vulnerary activity by an open wound procedure in rats. *Arch. Int. Pharmacodyn.* 196(6), 117-136.
- Panico, A.M., Cardile, V., Garufi, F., Puglia, C., Bonina, F. and Ronsisvalle, G. 2005. Protective effect of *Capparis spinosa* on chondrocytes. *Life Sci.* 77 (20) 2479-2488.
- Patil, M.B., Jalalpure, S.S. and Nagoor, V.S. 2004. Wound healing activity of the roots of *Eclipta alba* Linn. *Indian Drugs.* 41(1), 40-45.
- Purohit, A. and Vyas, K.B. 2005. Hypolipidaemic efficacy of *Capparis decidua* fruit and shoot extracts in cholesterol fed rabbits. *Indian J. Exp. Biol.* 43 (10) 863-866.
- Trombetta, D., Occhiuto, F., Perri, D., Puglia, C., Santagati, N.A., De Pasquale, A., Saija, A. and Bonina, F. 2005. Antiallergic and antihistaminic effect of two extracts of *Capparis spinosa* L. flowering buds. *Phytother Res.* 19 (1): 29-33.

20. Woessner, J.F. 1963. The determination of hydroxyproline in tissue and protein samples containing small proportions of the iminoacid. *Archiv. Biochem.* 93, 440-447.
21. Yadav, P., Sarkar, S. and Bhatnagar, D., *Pharmacol. Research*, 1997, 36(3), 221.



Screening Of Antibacterial And Antioxidant Activities Of *Streptomyces* Species Isolated From Western Ghats Region Of Karnataka

Almas Fathima, Daaniyah Belgami, S S Naziya Saba, Smriti Aurora, B K Manjunatha and Divakara R
Department of Biotechnology, The Oxford College of Engineering, Bommanahalli, Bengaluru-560068

ABSTRACT

Soil *Actinomycetes*' secondary metabolites possess wide range of biologically active compounds and are the potential source of novel bioactive metabolites. Currently *Actinomycetes* emerged as an important source for bioactive natural products with chemical diversity. In this study, *Actinomycetes* strain was isolated from the Western Ghats region of Karnataka and characterized by the 16S rRNA gene sequence. The strain was identified as *Streptomyces* species. The strain was characterized for antioxidant and antibacterial activity. The isolated strain exhibited broad spectrum of antibacterial activity against Gram positive bacteria (*S. aureus* and *B. subtilis*) and Gram negative bacteria (*P. aeruginosa* and *E. coli*). The ethyl acetate extract showed 86.6 % and 98 % of 2, 2-diphenyl-1-picrylhydrazyl (DPPH) and 2, 2'-azinobis-(3-ethylbenzothiazoline-6-sulfonic acid) radical scavenging assay at 11 mg/ml and 8.25 mg/ml respectively. However, purification and further characterization of bioactive metabolites from *Streptomyces* species is required for their optimum utilization towards antibacterial and antioxidant purposes.

INTRODUCTION

Actinomycetes are a group of prokaryotic organisms belonging to subdivision of the Gram-positive bacteria phylum. Most of them are grouped under subclass Actinobacteridae, order Actinomycetales. The members of this order are characterized by the high G+C content which accounts about >55 mol% in their DNA (Stackebrandt *et al*, 1997). These are one of the richest source of important natural products especially antibiotics. So far, approximately 10,000 antibiotics were reported, and almost half of them are produced by soil actinomycetes *Streptomyces* (Lazzarini *et al*, 2000). Bioactive metabolites produced from *Streptomyces* have high commercial value and important applications in human as well as livestock medicine and in agriculture (Wathe *et al*, 2001). The biological active compounds produced by actinomycetes are being used as antibiotics, immunosuppressant, extracellular hydrolytic enzymes, plant growth promoters, lytic enzymes, herbicides, insecticides, antitumor agents and siderophores. Approximately World's 80% antibiotics are obtained by actinomycetes, majorly from genus *Streptomyces* and *Micromonospora* (Pandey *et al*, 2004).

Chemotherapy using antimicrobial agents has been a leading cause for the rise of average life expectancy in the past Century. However, infectious agents that have become resistant to antibiotic drug therapy are an increasing public health problem. Currently, about 70% of the bacteria which cause infections to humans in hospitals are resistant to at least one of the drugs most commonly used for treatment of infection caused by them. Certain organisms are resistant to all approved antibiotics and infections caused by these organisms can only be treated with experimental and potentially toxic drugs. The increase in antibiotic resistance of bacterial will cause community acquired infections and also causes morbidity (Bisht *et al*, 2009). Development of antibiotic resistance in bacteria, as well as economic incentives has resulted in identification new antibiotic strains of actinomycetes in order to maintain a pool of effective drugs at all times (Stephen & Kennedy, 2011).

Free radicals and oxidants play a dual role as both toxic and beneficial compounds, since they can be either harmful or helpful to the body. It has been implicated in the development of many human diseases. A few of them include arthritis, inflammatory diseases, kidney diseases, cataracts, inflammatory bowel disease, colitis, lung dysfunction, pancreatitis, drug reactions, skin lesions and aging (Lakhtakia *et al*, 2011). They are produced either from normal cell metabolism *in situ* or from external sources (like pollution, cigarette smoke, radiation and medication). When an overload of free radicals cannot gradually be destroyed, their accumulation in the body generates a phenomenon called oxidative stress. This process plays a major part in the development of several chronic and degenerative illnesses (Pham-Huy *et al*, 2008).

Moreover, it has been shown that antioxidants and free radical scavengers are crucial in the prevention of pathologies, in which reactive oxygen species (ROS) or free radicals are implicated (Rathna Kala and Chandrika, 1993). Synthetic antioxidants have been used in stabilization of foods (Hajji *et al*, 2010). But their use is being restricted nowadays because of their toxic and carcinogenic effects (Kekuda *et al*, 2010). Thus, interest in finding natural antioxidants, without any undesirable effects has increased greatly (Rechner *et al*, 2002). Oxidative stress is ultimately involved in endothelial dysfunction, a condition which is evident in adults suffering from various cardiovascular diseases including thalassemia (Shinar and Rachmilewitz, 1990; Hebbel, 1990; Grinberg *et al*, 1995). Antioxidant and other supportive therapies protect red blood cells against oxidant damage (Filburn, 2007; Kukongviriyapan *et al*, 2008). It is well known that the generation of free radicals happens because of microbial infection which leads to DNA damage (Maeda and Akaike, 1998). In the present study, we point out biological activities of secondary metabolites produced by actinomycetes in effort to combat infectious diseases.

MATERIALS AND METHODS

Soil sampling and pretreatment: Soil samples were collected from forest areas of Western Ghat region of Karnataka and Kerala. Each collection will be made from 10-15 cm depth of the soil. These were air-dried for 1 week, crushed and sieved. The sieved soils were then used for actinomycetes isolation.

Isolation of Actinomycetes: Each sample were air-dried at room temperature (about 25 ± 2 °C) for 5 to 7 days and then ground in a mortar and used for further study. Dilution technique was used to isolate actinomycetes from the soil samples. Soil samples were serially diluted with sterile 0.9% (w/v) saline solution to give final concentrations of 10^{-2} and 10^{-3} . Using a sterile glass rod, the soil suspensions were spread onto sterile Glycerol Asparagine Agar (GAA). All plates were incubated at 28 °C for 7 days.

Characterization of actinomycetes: The isolated actinomycetes were characterized by morphological and biochemical methods. Morphological characterization was done by macroscopic and microscopic methods. Microscopic characterization was carried out by cover slip culture method (Kawato and Sinobu, 1979) by observing mycelium structure, color and arrangement of conidiospore and arthospore on the mycelium through the oil immersion (100X). The observed morphological characters were compared with Bergey's manual of determinative bacteriology and the isolate was characterized.

Screening for antimicrobial activity: Antimicrobial activities of isolates were tested preliminarily by cross streak method on Nutrient Agar plates (Egorov, 1985). Actinomycetes isolates were streaked across diameter on nutrient agar plates. After incubation at 28 °C for 6 days, 24 hrs cultures of test organisms were streaked perpendicular to the central strip of actinomycetes culture. All plates were again incubated at 37 °C for 24 hrs and zone of inhibition was measured.

Extraction of antimicrobial compounds: The antibacterial compounds were isolated from the actinomycetes isolates by following Westley *et al*, 1979 and Liu *et al*, 1986 method with slight modifications. The selected antagonistic actinomycete isolates were inoculated into Yeast Extract Malt Extract (YEME) broth, and incubated at 28 °C in a shaker (200-250 rpm) for seven days. After incubation the broths were filtered through Whatman No.1 filter paper. To the culture filtrate, equal volume ethyl acetate was added and shaken vigorously for 1 hr for the extraction of antimicrobial compound. The ethyl acetate extract was evaporated to dryness in rotary flash evaporator. The extracts were tested for their antimicrobial activity by well diffusion method (Sen *et al*, 1995) against the test pathogens. The antimicrobial efficacy was assessed by measuring the zone of inhibition after 24 hrs of incubation.

DETERMINATION OF ANTIOXIDANT ACTIVITY:

DPPH scavenging activity: DPPH scavenging activity of the EA extract was determined by the method of Manjunatha *et al*, 2013 with slight modifications. 100 µM methanol DPPH solutions were mixed with different concentrations of EA extract. Ascorbic acid (standard) was used as positive control. The tubes were incubated at room temperature in dark for 30 min and the optical density was measured at 517 nm. The absorbance of the control, DPPH• alone (containing no sample), was also noted (Khalaf NA, 2008). The percentage of radical scavenging activity of the extract against the stable DPPH• was calculated using following equation:

$$\% \text{ DPPH}\cdot \text{ Scavenging activity} = [A_{\text{control}} - A_{\text{sample}}] / A_{\text{control}} \times 100$$

ABTS scavenging activity: To generate ABTS radical cation, 50ml of 2mM ABTS and 0.3mL of 17mM Potassium persulfate were mixed together and incubated in the dark for 12-16 h to develop Prussian blue colored ABTS•+ solution which has an absorption maxima at 734nm [Re *et al.*, 1999]. To determine scavenging activity of extracts of different concentrations was added to 1.6ml of ABTS•+ solution. The absorbance was measured at 734nm after 20 minutes at room temperature. All readings were performed in triplicates and the free radical scavenging activity was calculated from equation:

$$\% \text{ ABTS Scavenging activity} = [A_{\text{control}} - A_{\text{sample}}] / A_{\text{control}} \times 100$$

Molecular characterization of actinomycetes strain by 16S rDNA sequence: The actinomycetes strain was grown at 30 °C for 5 days in shake flasks, containing 100 ml of ISP 2 medium (4 g/l yeast extract, 10 g/l malt extract and 4 g/l glucose). Mycelium was obtained by centrifugation and washed twice with bi-distilled water. Approximately, 200 mg of mycelium were used for genomic DNA extraction as follows: the sample was dispersed in 800 µl of the lysis solution (100mM Tris-HCl, pH 7.4, 20mM EDTA; 250mM NaCl; 2% SDS; 1 mg/ml; lysozyme; 100 µl H₂O), added with 5 µl of RNase (50 mg/ml) and incubated at 37 °C for 60 min. Then 10 µl of proteinase K solution (20 mg/ml) were added, and the lysis solution was reincubated at 65 °C for 30 min. The lysate was extracted two times with an equal volume of phenol, centrifuged and then re-extracted with chloroform (v/v) to remove residual phenol. DNA was precipitated by adding NaCl (at a final concentration of 150 mM) and 2 volumes of 95% cool ethanol. After centrifugation, the DNA was cleaned with 50 µl of ethanol 70%, centrifuged, and then re-suspended in 50 µl of TE buffer (10mM Tris-HCl, pH 7.4; 1mM EDTA, pH 8.0). The DNA purity and quantity were checked by spectrophotometer at 260 and 280 nm.

PCR amplification of the 16S rDNA of actinomycetes strain was performed using two primers: 27f (50-AGAGTTTGATCCTGGCTCAG-30) and 1492r (50-GGTTACCTTGTTACGACTT-30). The 16S rDNA was amplified by PCR using Promega kit. The final volume of reaction mixture of 50 µl contained 1X PCR buffer (10mM Tris-HCl, 50mM KCl, pH 9.0 at 25 °C), 1.5mM MgCl₂, 200 mM of each dNTP, 1mM of each primer, 1.25 U of Taq DNA polymerase and 500ng of template DNA. The amplification was performed according to the following profile: an initial denaturation step at 98 °C for 3 min, after which Taq DNA polymerase was added, followed by 30 amplification cycles of 94 °C for 1 min, 52 °C for 1 min and 72 °C for 2 min, and a final extension step of 72 °C for 10 min. The PCR product was detected by agarose gel electrophoresis and was visualized by UV fluorescence after ethidium bromide staining.

The PCR products obtained were submitted to Genome Express for sequence determination. The same primers as above and an automated sequencer were used for this purpose. The sequence determined was compared for similarity level with the reference species of bacteria contained in genomic database banks, using the NCBI Blast available at the ncbi.nlm.nih.gov Web site.

RESULTS

Cultural characteristics and Microscopic study:

The actinomycetes isolate was named as SBR1 (1). The colony characteristics of the isolate were studied on the GAA, Inorganic salt-starch agar (ISSA) and Oat Meal Agar (OMA) media. The growth was good on GAA and ISSA whereas moderate growth was observed on OMA. The color of substrate and aerial mycelium varied in different media. The organism produced colonies of 3 mm diameter, white colony with secondary black metabolites, blue pigmentation, greys at centre and hard on GAA with inhibition of neighbored colony, on oat meal agar it produced colony with poor growth, 3 mm diameter, cream colored spores with entire and umbonate margin, on ISSA colonies were light cream colored entire, elevated margin, good growth, outer periphery shows ring of spores. The organism was gram positive and positive for starch hydrolysis, casein hydrolysis and lecithinase and lipase production, negative for gelatine hydrolysis, citrate utilization. Based on morphological biochemical and on characterization of the organism it was shown to be *Streptomyces* sp.

Table 1: Cultural characteristics of SBR 1(1)

| Media | Growth | Substrate mycelium | Aerial mycelium | Diffusile pigment |
|-------|----------|--------------------|-----------------|-------------------|
| GAA | Good | Grey | White | Blue |
| OMA | Moderate | Grey | Cream | --- |
| ISSA | Good | Grey | White | --- |

Preliminary antibacterial activity and MIC: A total of 7 isolates were recovered from the soil samples. All the isolates were subjected for cross streak method in order to assess antagonistic property against gram negative and gram positive bacteria. Presence of clear zone or reduced growth of test bacteria near the growth of actinomycetes was considered as positive for antagonistic activity. All the isolates were potent enough to inhibit at least one of the test bacteria. SBR 1(1) showed prominent inhibition of test bacteria in cross streak technique, so it was selected for further study.

The antibacterial efficacy of the ethyl acetate extract of SBR 1(1) is studied using 3 Gram positive and 2 Gram negative bacteria. It was observed that extract was having broad spectrum antibacterial activity inhibiting both Gram positive and Gram negative bacteria. The study of MIC has shown that MIC of ethyl acetate extract was <25 µg for Gram positive bacteria (*B. subtilis* and *S. aureus*) and 75 µg for Gram negative bacteria (*E. coli*) (Table 2 & 3; Figure 1).

Table 2: Antibacterial activity of ethyl acetate extract of isolate SBR 1(1)

| Test Bacteria | Zone of inhibition in cm | | |
|--------------------|--------------------------|-------------------------------|------|
| | SBR 1(1) | Standard (Streptomycin 10 µg) | DMSO |
| <i>B. cereus</i> | 2.6 | 2.0 | 0.0 |
| <i>E. coli</i> | 2.0 | 1.1 | 0.0 |
| <i>B. subtilis</i> | 2.7 | 1.9 | 0.0 |
| <i>S. aureus</i> | 2.5 | 2.4 | 0.0 |
| <i>P. putida</i> | 1.0 | 1.3 | 0.0 |

Table 3: Minimum Inhibitory Concentration (MIC) of ethyl acetate extract of isolate RHC-1

| Test bacteria | MIC for ethyl acetate extract of isolate SBR 1(1) Zone of Inhibition in cm | | | | |
|--------------------|--|-------|-------|-------|--------|
| | Standard 10 µg | 25 µg | 50 µg | 75 µg | 100 µg |
| <i>E. coli</i> | 2.5 | - | - | 1.1 | 1.3 |
| <i>B. subtilis</i> | 1.2 | 1.5 | 1.7 | 1.8 | 1.9 |
| <i>S. aureus</i> | 1.8 | 1.2 | 1.4 | 1.5 | 1.7 |



Figure 1: MIC for ethyl acetate extract of RHC-1

Screening of antioxidant activity:

DPPH Radical Scavenging Assay: Study of DPPH scavenging ability of the extract showed that ethyl acetate extract has free radical scavenging ability but the activity of extract is less when compared with the ascorbic acid standard. DPPH scavenging studies have revealed that the extract possesses 86.6% scavenging ability at a concentration of 11 mg/ml and the DPPH free radical scavenging ability of the extract was dose dependent (Figure. 2).

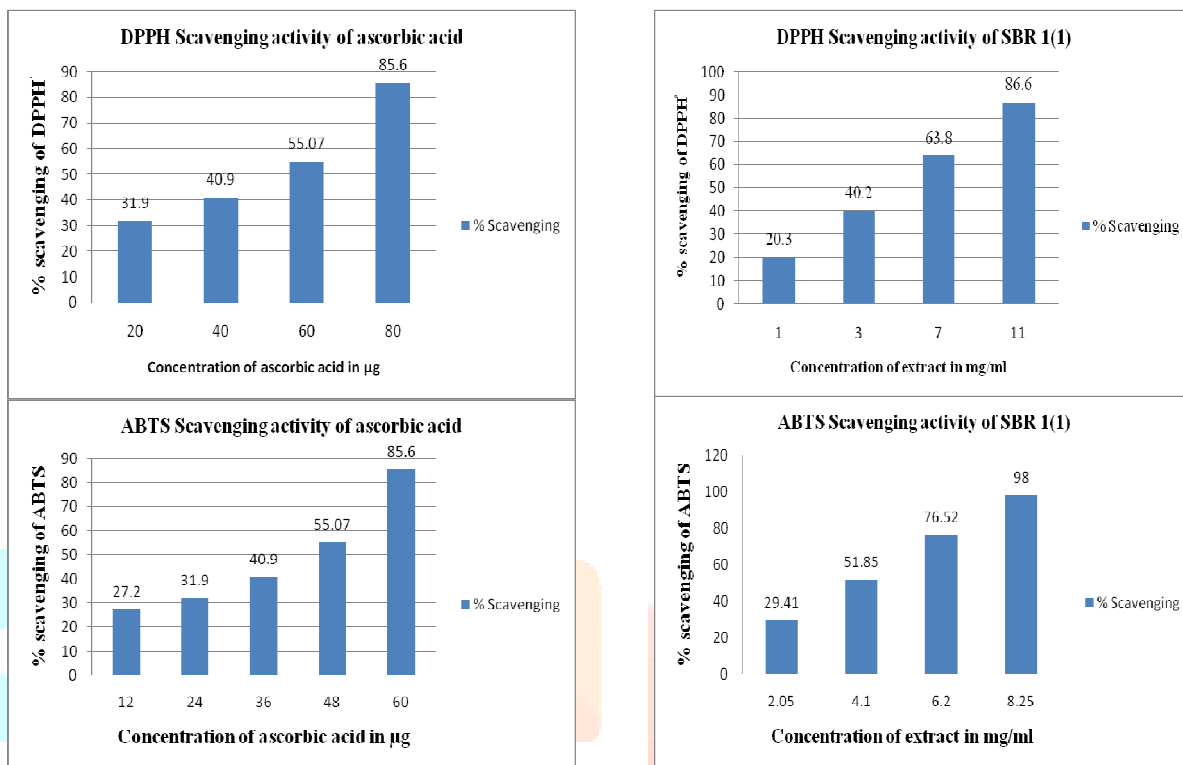


Figure 2: Antioxidant activity of ethyl acetate extract of SBR 1(1)

Assay of ABTS scavenging activity: ABTS scavenging studies have revealed that the ethyl acetate extract of SBR 1(1) is capable of scavenging the ABTS radical efficiently. But ability of the extract is less when compared with ascorbic acid standard. The ethyl acetate extract had 98% scavenging activity at a concentration of 8.25 mg/ml. Even ABTS free radical scavenging ability of the extract is also dose dependent (Figure 2).

Molecular characterization by 16S rDNA sequencing: Through 16S rDNA sequence analysis, an amplified fragment of 747 bp was obtained and compared with sequences of the reference species of bacteria contained in genomic database banks. The similarity level ranged from 96.3% to 97.8% with Streptomyces species 13636G having the closest match. The phylogenetic tree obtained by applying the neighbor joining method is illustrated in Fig. 8. The sequence results for SBR 1(1) as follows:

```
GGCGTTTTTTCGCTCTCAGCGTCAGTAATGGCCCAGAGATCCGCCTTCGC
CACCGGTGTTCTCCTGATATCTGCGCATTTACCGCTACACCAGGAATT
CCGATCTCCCTACCACACTCTAGCTAGCCCGTATCGAATGCAGACCCGG
GGTTAAGCCCCGGGCTTTCACATCCGACGTGACAAGCCGCCTACGAGCTC
TTTACGCCAATAAATTCCGGACAACGCTTGCGCCCTACGTATTACCGCGG
CTGCTGGCACGTAGTTAGCCGGCGCTTCTTCTGCAGGTACCGTCACTTGC
GCTTCTCCCTGCTGAAAGAGGTTTACAACCCGAAGGCCGTCATCCCTCA
CGCGCGTCGTCATCAGGCTTTCGCCCATTTGTGCAATATTCCCACTG
CTGCCCTCCGTAGGATGCTGGGCCGTGTCTCAGTCCCAGTGTGGCCGGTC
GCCCTCTCAGGCCGGCTACCCGTCGCTCGCCTTGGTAGGCCATTACCCAC
CAACAAGCTGATAGGCCGCGGGCTCATCCTTACCCGCCGAGCTTTCAAC
CCCGTCCCATGCGGAACAGAGTATTATCCGGTATTAGACCCCGTTTCCAG
GGCTTGTCCAGAGTGAAGGGCAGATTGCCACGTGTTACTACCCGTTT
GCCACTAATCCACCACCGAAGCGGCTTCATCGTTTCCACTTGCATGTGTTA
AGCACGCCGCCAGCGTTCGTCTGAGCTGTTTTAAAACTTAAAAAC.FASTA
```

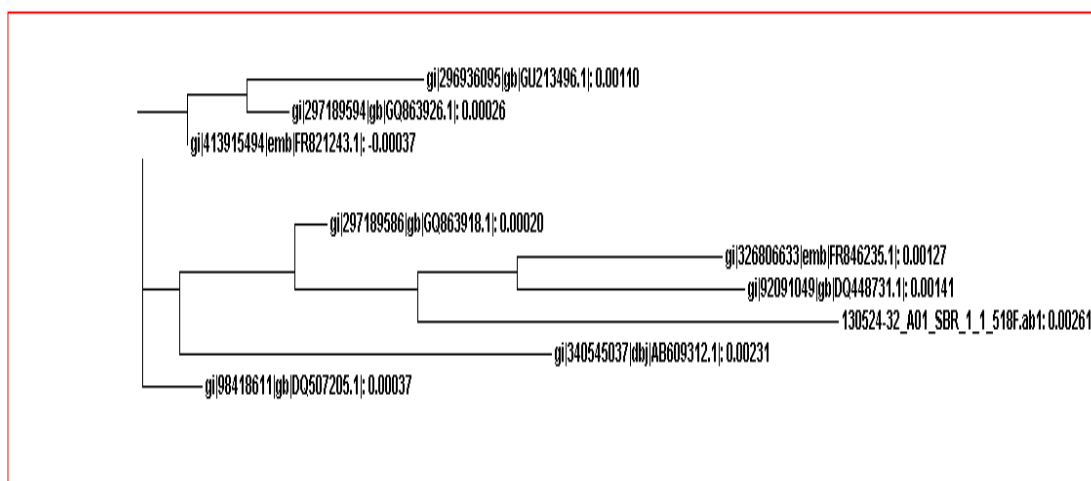


Figure 3:

Phylogram based on 16S rDNA sequences showing the relations between strain SBR 1(1) and type species of the genus *Streptomyces*

DISCUSSION

Western Ghats of India are the less explored regions for actinomycetes diversity and this study has shown that Western Ghats contain diverse species producing the antibiotic. The plant root primarily determines the nature and abundance of the rhizosphere soil microflora, when conditions affect root growth or metabolism, it will be reflected in quantitative and qualitative changes in microbial populations of rhizosphere. Conversely, microbial communities can affect rooting patterns, stimulate and promote plant root growth (e.g., release of hormones, neutralizing toxic substances, etc.), and influence the supply of available nutrients for plant uptake. Microbial turnover of rhizo-deposits plays an important role in carbon flow through soils [Rathna Kala and Chandrika, 1993; Rechner et al, 2002; Behal, 2003; Kekuda et al., 2010]. Actinomycetes are an important class of bacteria and constitute one of the important groups of the rhizosphere microflora. Members of *Streptomyces* are most abundant in soil and accounts for about 90% of actinomycetes isolated from soil [Shinar and Rachmilewitz, 1990; Rathna Kala and Chandrika, 1993; Khamna et al., 2009;]. In the present study, we have recovered 07 actinomycetes isolates from a rhizosphere soil collected at Western Ghats of Karnataka. All the isolates were subjected to primary screening for antibacterial activity by cross streak method. This dual culture method is widely used to screen the ability of actinomycetes strains to produce antimicrobial metabolites [Shinar and Rachmilewitz, 1990, Hebbel et al., 1990; Kekuda et al., 2012]. Out of 07 isolates, all the 7 isolates have shown inhibition of all test bacteria. We have selected a potent isolate SBR 1(1) which inhibited both gram positive and Gram negative bacteria. The characterization of SBR 1(1) revealed that the isolate is a *Streptomyces* species. The life cycle of *Streptomyces* provides 3 distinct features for microscopic characterization namely vegetative mycelium, aerial mycelium bearing chains of spores and the characteristic arrangement of spores and the spore ornamentation. The latter two features produce most diagnostic information [Kukongviriyapan et al., 2008, Filburn et al., 2007]. Details on cultural and microscopic characteristics together with biochemical properties assisted the researchers to classify actinomycetes as members of the genus *Streptomyces*. Many studies have been carried out where the actinomycetes isolates were identified as species of *Streptomyces* based these properties or characteristics (Ceylan et al, 2008; Pham-Huy et al, 2008; Grinberg, 1995; Maeda and Akaike, 1998; Jeffrey et al, 2007; Sahin and Ugur, 2003). In the present study, the cultural and microscopic characteristics of the isolate SBR1(1) were consistent with its classification as a member of the genus *Streptomyces*.

The members of *Streptomyces* can be distinguished from other sporing actinomycetes based on morphology and hence morphology plays an important role in the Antimicrobial agents play an indispensable role in decreasing morbidity and mortality associated with infectious diseases caused by bacteria, fungi, viruses and parasites. However, selective pressure exerted by the use of antimicrobial drug became the major driving force behind the emergence and spread of drug-resistance pathogens. In addition, resistance has been developed in pathogens after discovery of major class of antimicrobial drugs, varying in time from as short as 1 year in case of penicillin to >10 years in case of Vancomycin (Jeffrey et al, 2007). This alarming situation necessitated search of new bioactive compounds capable of acting against pathogens in particular drug resistant pathogens. It is well known that microorganisms, in particular bacteria and fungi are an unexhaustible source of natural compounds having several therapeutic applications. In the present study, it was found that both Gram positive bacteria and Gram negative bacteria were susceptible to high extent (Singh et al, 2006; Pandey et al, 2004).

Free radicals are chemical species containing one or more unpaired electrons that make them highly unstable and cause damage to other molecules by extracting electrons from them in order to attain stability. In recent years much attention has been devoted to natural antioxidant and their association with health benefits (Ali et al, 2008).

DPPH is a stable, organic and nitrogen centered free radical, it has absorption maximum band around 515-528 nm (517 nm) in alcoholic solution. It accepts an electron or hydrogen atom and becomes a stable diamagnetic molecule. Though a number of *in vitro* assays have been developed to evaluate radical scavenging activity of compounds, the model of scavenging of the stable DPPH radical is one of the widely used protocols. The effect of antioxidants on scavenging DPPH radical is due to their hydrogen donating ability. In this assay, the antioxidants reduce the purple colored DPPH radical to a yellow colored compound diphenylpicrylhydrazine, and the extent of reaction will depend on the hydrogen donating ability of the antioxidants. In the

present study, a decrease in the absorption of DPPH solution in the presence of various concentrations of ethyl acetate extract was measured at 517 nm. It was observed that the radical scavenging activities of extract and ascorbic acid increased on increasing concentration. The scavenging effect of ethyl acetate extract was much lesser when compared with ascorbic acid. Although the scavenging abilities of extract was lesser, it was evident that the extracts showed hydrogen donating ability and therefore the extract could serve as free radical scavengers, acting possibly as primary antioxidants (Ali *et al*, 2008).

The ABTS radical cation decolorization assay is one of the methods for the screening of the antioxidant activity (Re *et al*, 1999). Therefore, the ABTS radical scavenging activity of the ethyl acetate extract was determined. The results indicated that the ethyl acetate extract showed a lesser tendency to decay ABTS radicals at low concentrations of reaction than at high concentrations (Fig. 6). The extract scavenged ABTS radicals in a concentration-dependent manner. The ABTS antioxidant assay, also known as the Trolox equivalent anti-oxidant capacity (TEAC) assay, assesses the total radical scavenging capacity of the plant extracts. This is determined through the ability of these extracts to scavenge the long-lived specific ABTS radical cation chromophore in relation to that of Trolox, the water-soluble analogue of vitamin E [Zhong *et al.*, 2011].

The antioxidant activities of recognized antioxidants have been attributed to various mechanisms, including the prevention of chain initiation, binding of transition metal ion catalysts, decomposition of peroxides, prevention of hydrogen abstraction, and radical scavenging [Diplock, 1997].

According to the results of the DPPH radical-scavenging assay and ABTS radical-scavenging assay, it was found that the isolate SBR 1(1) had antioxidant abilities.

CONCLUSION:

In this study, the results have suggested that actinomycetes isolate RHC-1 has closely related with *Streptomyces* spp. 13636G, having the capability to show antimicrobial and antioxidant activity and the present study highlights the necessity of further researches towards the goal of searching for novel bioactive compounds from less explored regions like Western Ghats.

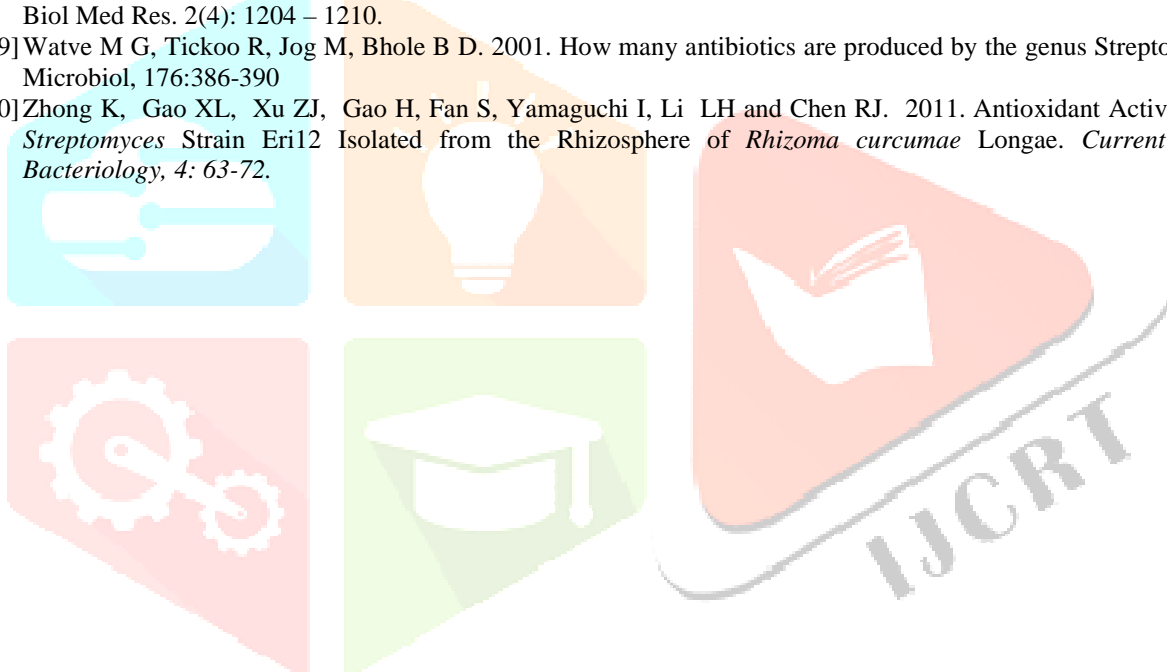
Acknowledgement:

We express our deep gratitude to Founder Chairman Sri. NarasaRaju, President Sri. Ramesh Raju, Principal Dr. R. V. Praveen Gowda and Head, Dept. of Biotechnology Dr. Manjunath B K, The Oxford College of Engineering, Bangalore, for providing facilities to conduct work and kind support and encouragement.

REFERENCES:

- [1] Amit Pandey, Imran Ali, Kailash Singh Butola, TanushriChatterji, Vidyottma Singh. 2004. Isolation and characterisation of actinomycetes from soil and evaluation of antibacterial activities of actinomycetes against pathogens. *ActaBiol Med Exper*, 15:113-115
- [2] Behal V. 2003. Alternative sources of biologically active substances. *Folia Microbiol (Praha)*; 48:563-71.
- [3] Bisht R, Katiy ARA, Singh R, Mittal P. 2009. Antibiotic Resistance –A Global Issue of Concern. *Asian Journal of Pharmaceutical and Clinical Research*. 2 (2); 34-39.
- [4] Ceylan O, Okmen G and Ugur A.2008.Isolation of soil *Streptomyces* as source antibiotics active against antibiotic-resistant bacteria.*EurAsian Journal of BioSciences*.2, 73-82.
- [5] Diplock, AT. 1997. Will the 'good fairies' please prove to us that vitamin E lessens human degenerative disease. *Free Rad.Res*.27 (5),511-532.
- [6] Filburn CR, Kettenacker R, Griffin DW. 2007. Bioavailability of a silybin-phosphatidylcholine complex in dogs. *J Vet PharmacolTher*; 30:132-8.
- [7] Grinberg LN, Rachmilewitz EA, Kitrossky N, Chevion M. 1995. Hydroxyl radical generation in β -thalassemia red blood cells. *Free Rad Biol Med*; 18:611-5.
- [8] Hajji M, Jarraya R, Lassoued I, Masmoudi O, Damak M, Nasri M. 2010. GC/MS and LC/MS analysis, and antioxidant and antimicrobial activities of various solvent extracts from *Mirabilis jalapa* tubers. *Process Biochem*; 45:1486-93.
- [9] Hebbel RP, Leung A, Mohandas N.1990. Oxidation-induced changes in microheologic properties of the red cell membrane. *Blood*; 76:1015-20.
- [10]Jeffrey L.S.H., A.M. Sahilah, R. Son and S. Tosiah. 2007. Isolation and screening of actinomycetes from Malaysian soil for their enzymatic and antimicrobial activities. *J. Trop. Agric. and Fd. Sc*. 35(1): 159– 164.
- [11]Kekuda PTR, Shobha KS, Onkarappa R, Gautham SA, Raghavendra HL. 2012. Screening biological activities of a *Streptomyces* species isolated from soil of Agumbe, Karnataka, India, *International Journal of Drug Development and Research*, 4(3), 104-114.
- [12]Kekuda PTR, Shobha KS, Onkarappa R. 2010. Studies on antioxidant and anthelmintic activity of two *Streptomyces* species isolated from Western Ghat soil of Agumbe, Karnataka, *Journal of Pharmacy Research*, 3(1), 26-29.
- [13]Khamna S, Yokota A, Lumyong S. 2009. Actinomycetes isolated from medicinal plant rhizosphere soils: diversity and screening of antifungal compounds, indole-3-acetic acid and siderophore production, *World Journal of Microbiology and Biotechnology*, 25(4), 649-655.
- [14]Kukongviriyapan V, Somparn N, Senggunprai L, Prawan A, Kukongviriyapan U, Jetsrisuparb A. 2008. Endothelial Dysfunction and Oxidant Status in Pediatric Patients with Hemoglobin E-beta Thalassemia. *PediatrCardiol*; 29:130-5.
- [15]Lakhtakia R, Ramji MT, Lavanya K, Rajesh K, Jayakumar K, Sneha C, Narayan A, Ramya B, Ramana G, Chari PVB, Chaitanya KV.2011. The role of antioxidants in human health maintenance: Small molecules with infinite functions. *IJPSR*; 2:1395-402.
- [16]Lazzarini A, Cavaletti L, Toppo G and Marinelli F. 2000. Rare genera of actinomycetes as potential producers of new antibiotics.*Antonie van Leeuwenhoek* 78:399–405

- [17] Maeda H, Akaike T. 1998. Nitric oxide and oxygen radicals in infection, inflammation, and cancer. *Biochemistry (Moscow)*; 63:854-65.
- [18] Manjunatha BK, Syed Murthuza, Divakara R, Archana M, Sarvani RJ, Verghees S, Paul K. 2013. Antioxidant and anti-inflammatory potency of *Mesua ferrea* L. *Indian Journal of Applied Research*. 3(8); 55-59.
- [19] Pandey, B. Ghimire, P. Agrawal, V.P. 2004. Studies on antibacterial activity of Actinomycetes isolated from the Khumbu region of Nepal. *J Biol.Sci.*, 23:44-53.
- [20] Pham-Huy LA, He H, Pham-Huyc C. 2008. Free radicals, antioxidants in disease and health. *Int J Biomed Sci*; 4:89-96.
- [21] Rathna Kala R, Chandrika V. 1993. Effect of different media for isolation, growth and maintenance of actinomycetes from mangrove sediments. *Indian J Mar Sci*; 22:297-9.
- [22] Re R, Pellegrini N, Proteggente A, Pannala A, Yang M, Rice-Evans C. 1999. Antioxidant activity applying an improved ABTS radical cation decolorization assay. *Free Radical Biol. Medicine*. 26(9):1231-1237.
- [23] Rechner AR, Kuhnle G, Bremmer P, Hubbard GP, Moore KP, Rice-Evans CA. 2002. The metabolic fate of dietary polyphenols in humans. *Free Radic Biol Med*; 33:220-35.
- [24] Sahin N, Ugur A. 2003. Investigation of the antimicrobial activity of some *Streptomyces* isolates, *Turkish Journal of Biology*, 27, 79-84.
- [25] Shinar E, Rachmilewitz EA. 1990. Oxidative denaturation of red blood cells in thalassemia. *Semin Hematol*; 27:70-82.
- [26] Singh, S.L., Baruha, I and Bora, T.C. 2006. Actinomycetes of loktak habitat isolation and screening of antimicrobial activity. *Biotech*. 5 (2): 217-221.
- [27] Stackebrandt E, Rainey F A and Ward-Rainey N L. 1997 Proposal for a new hierarchic classification system, Actinobacteria classis Nov. *Int. J. Syst. Bacteriol*, 47:479-491.
- [28] Stephen T Odonkor & Kennedy K Addo. 2011. Bacteria Resistance to Antibiotics: Recent Trends and Challenges. *Int J Biol Med Res*. 2(4): 1204 – 1210.
- [29] Watve M G, Tickoo R, Jog M, Bhole B D. 2001. How many antibiotics are produced by the genus *Streptomyces*? *Arch. Microbiol*, 176:386-390
- [30] Zhong K, Gao XL, Xu ZJ, Gao H, Fan S, Yamaguchi I, Li LH and Chen RJ. 2011. Antioxidant Activity of a Novel *Streptomyces* Strain Eri12 Isolated from the Rhizosphere of *Rhizoma curcuma* Longae. *Current Research in Bacteriology*, 4: 63-72.



Construction of Cancer Diseasome through Graph Theoretical Approach

Chetan H, Shujaat Afzal, Tanusree Chaudhuri, B. K. Manjunath

Student, Student, Asst. Professor, Head of the Department

Department of Biotechnology, The Oxford College Of Engineering, Bangalore, India

Abstract

Diseasome is a collection of networks that relates human diseases with the disease causing human genes. A network of disorders and disease genes linked by known disorder–gene associations offers a platform to explore in a single graph-theoretic framework all known phenotype and disease gene associations, indicating the common genetic origin of many diseases. The Online Mendelian Inheritance in Man (OMIM) is used as the data source for disease-gene relations in Diseasome. Mouse is the primary model organism to study mammalian genetics. The genome of mouse is incisively and specifically modified and controlled to study the mutations in the human genome, to discover the molecular mechanisms of various complex human diseases such as cancers, diabetes, hereditary and neurological disorders. Researchers have already identified that, essential human genes are likely to encode hub proteins and are expressed widely in most tissues, suggesting that disease genes also would play a central role in the human interactome. In our present study we have constructed and classified the human diseasome network for cancer for the better understanding of disease gene association in different types of cancer. This project aims to map the human cancer disease network onto the mouse genotype/phenotype data pertaining to different types of cancer, by generating multi-partite networks of human cancer vs – human/mouse genes – phenotypic abnormalities observed in targeted knock-out-mouse models in cancer. The resulting networks will enrich the effort to curate specific symptoms and effects of different types of cancer to improve medical diagnosis.

Key words: Cancer, Human, Mouse, OMIM, Disease, Diseasome

I. Introduction:

Diseasome is a compilation of networks between human diseases with the genes causing disease (Goh et al., 2007). It is a network based study that relates human genetic disorders with the corresponding genes (Martignoni M et al., 2006). Genes associated with similar disorders show both higher likelihood of physical interactions between their products and higher expression profiling similarity for their transcripts, supporting the existence of distinct disease-specific functional modules (Hulbert AJ 2008). The Online Mendelian Inheritance in Man (OMIM) is used as the data source for disease-gene relations in Diseasome (Joanna S. Amberger et al., 2004). Mouse is the primary model organism to study mammalian genetics. The Genetic resemblance between mouse and human organisms is the reason behind using mouse as a model organism to study human diseases (McKusick, V.A., 1998). More than 90% of the mouse and human genomes can be divided into related conserved syntenic regions, which show the gene order in the genomes (Robert L. Perlman., 2016). The Diseasome mapping consists of multiple networks namely: the human disease network (HDN), the disease genes network (DGN) and the bi-partite human disease and gene network. In the study of, Goh et al. It was proposed that the disorders can be associated with each other using the shared disease-causing genes. The main list of Diseasome contained 1,284 disorders and 1,777 disease genes and all diseases are categorized based on 22 distinct disease classes (Olson H et al., 2000). Diseasome particularly focuses on the molecular relationships between genetic variation and phenotypic information, and it is a seminal work in terms of discovering the mechanisms of complex diseases. It is important here to note that, revealing complex disease mechanisms is one of the most crucial problems in biomedical research, currently (Botstein and Risch, 2003, Kann, 2009). It had already been stated in the literature that many human diseases occur due to the factors related to genetic variations (Hirschhorn and Daly, 2005). Up to date, various databases are constructed for annotating the relations between genes and diseases of human such as OMIM (Hamosh et al., 2005), CTDTM (Davis et al., 2010) and NHGRI-EBI GWAS catalog (Welter et al., 2013). Due to the nature of database curation process the associations are not complete, so the integration of multiple existing resources usually leads to more comprehensive view of the current biomedical knowledge.

Cancer, is one of leading cause of death worldwide. There are several analysis that have been performed, which enables the better understanding towards cancer proteomics by deciphering genetic and epigenetic data for gene regulatory networks analysis. These data has uncovered very important protein-protein interaction (PPI) pairs which are integrative part of the cancer network.

In our present study we have created a diseasome network for different types of cancer, which will eventually help us to better understand the cancer processes to identify biomarkers and therapeutic targets, and predict the prognosis of cancer in acute cancer patients.

II. Materials and methods:

2.1 DATA DOWNLOAD AND PROCESSING :

Curated morbid map file was being downloaded from Online Mendelian Inheritance in man (OMIM). Morbid Map (MM) of the OMIM is one of the most comprehensive and highly curated disorder gene association database. The OMIM MM shows the cytogenetic map location of disease genes in OMIM. The link www.omim.org is being opened up, wherein download tab in menu is selected and registration for download is done.

Two different datasets about human and mouse organisms were extracted. Dataset 1 contains the Human disease – human gene relation information and downloaded from Disasome resource and the Dataset 2 contains Mouse affected system (phenotype) – mouse gene information derived from MGI and Human data were downloaded from OMIM. Mouse genes attribute was chosen as a foreign key, to relate these two sets.

2.2 DATASET DOWNLOAD FROM DISEASOME & DATA PROCESSING:

Disasome dataset was created from curated OMIM data, that has been used as the source to constitute Dataset 1. It includes disease ID, disease name, disorder class, size (s) that show the number of associated genes, degree (k) shows number of disorder classes it connects to, class degree (K) is the number of distinct disorder classes it connects to and genes written as comma delimited at the last column.

The curated table contains the Disease ID, Disorder name, Human Gene Symbols, OMIM ID, Chromosome Position of the related gene and Disorder Class information. Disorder names were aligned in an alphabetical order and distinct consecutive numbers are given in ascending order starting from 1. These numbers are called as Disease ID and assigned for analysis in Gephi. Disorder names are distinctly ordered with their related human genes and in accordance OMIM IDs are retrieved. If a disorder has more than one genes related to it, these genes are separated with comma.

Mouse orthologues of human genes were converted and extracted with the online converter tool called as HCOP: Orthologue Predictions Search.

2.3 DATASET DOWNLOAD FROM MGI & DATA PROCESSING:

Mouse affected systems information (i.e. phenotypes) was collected from the MGI database. Collected mouse orthologue genes with HCOP were imported to the MGI batch summary tool for creating Dataset 2.

Only the targeted null/knock-out mouse genes were taken into consideration during the generation of Dataset 2.

The dataset 2 includes affected system information with unique “Mammalian phenotype ID” of all recorded mouse genes with marker symbols in that database. It also provides unique MGI IDs for these genes, allele type and allele attribute information.

2.4 Collection of Cancer data: Curated Morbid map from dataset 1 was searched rigorously for different types of cancer information. A total set of 74 different types of cancer with the involvement of 202 gene was identified. Dataset 2 was constructed for this set following the process in 2.3.

2.5 INTEGRATION OF DATA & GENERATING THE NETWORKS.

The data integration was based on connecting human diseases and mouse affected systems (i.e. phenotypes) by using mouse/human orthologous genes. We have followed the genes as nodes strategy to generate the networks.

Human diseases are indirectly connected to the mouse phenotypes (i.e. affected systems) while using mouse/human orthologous genes as the mediator. Relations in-between genes-diseases-phenotypes. Human diseases are indirectly connected to the mouse phenotypes (i.e. affected systems) while using mouse/human orthologous genes as the mediator.

III Result and Discussion:

3.1 Creation of Dataset 1:

Dataset 1 was created with required disease name corresponding disease ID, human genes, OMIM ID, Chromosome Position of the related gene and Disorder Class information. Disorder names were aligned in an alphabetical order and distinct consecutive numbers are given in ascending order starting from 1. These numbers are called as Disease ID and assigned for analysis in Gephi. The Figure 3.1 shows a screenshot the curated dataset1

| Disease ID | Disorder name | Gene symbols | OMIM ID | Chromosome | Class |
|------------|--|---|---------|---------------|-------------------|
| 427 | Diabetes mellitus, type 1, 125853 (3) | AKT2 | 184731 | 19q13.1-q13.2 | Endocrine |
| 427 | Diabetes mellitus, type 1, susceptibility to, 125853 (3) | IFF1 | 600733 | 13q12.1 | Endocrine |
| 918 | Lung cancer, 211980 (3) | KRAS2, RASK2 | 190070 | 12p12.1 | Cancer |
| 918 | Lung cancer, 211980 (3) | PPP2R1B | 603113 | 11q22-q24 | Cancer |
| 918 | Lung cancer, 211980 (3) | SLC22A1L, BWSCR1A, IMPT1 | 602631 | 11p15.5 | Cancer |
| 918 | Lung cancer, somatic, 211980 (3) | MAP3K8, COT, EST, TPL2 | 191195 | 10p11.2 | Cancer |
| 1324 | Rheumatoid arthritis, progression of, 180300 (3) | IL10, CSF | 124092 | 1q31-q32 | Connective tissue |
| 1324 | Rheumatoid arthritis, susceptibility to, 180300 (3) | MHC2TA, C2TA | 600005 | 16p13 | Connective tissue |
| 1324 | Rheumatoid arthritis, susceptibility to, 180300 (3) | NFKB1L1 | 601022 | 6p21.3 | Connective tissue |
| 1324 | Rheumatoid arthritis, susceptibility to, 180300 (3) | PADI4, PADI5, PAD | 605347 | 1p36 | Connective tissue |
| 1324 | Rheumatoid arthritis, susceptibility to, 180300 (3) | PTPN8, PEP, PTPN22, LYP | 600716 | 1p13 | Connective tissue |
| 1324 | Rheumatoid arthritis, susceptibility to, 180300 (3) | RUNX1, CBF4A, ANK1 | 151385 | 21q22.3 | Connective tissue |
| 1324 | Rheumatoid arthritis, susceptibility to, 180300 (3) | SLC22A4, OCTN1 | 604190 | 5q31 | Connective tissue |
| 1324 | Rheumatoid arthritis, systemic juvenile, susceptibility to, 180300 (3) | MF | 153620 | 22q11.2 | Connective tissue |
| 1304 | Rapid progression to AIDS from HIV1 infection (3) | CX3CR1, GFR13, V28 | 601470 | 3pter-q21 | Immunological |
| 1305 | Rapp-Hodgkin syndrome, 129400 (3) | TP73L, TP63, KET, EEC3, SHFM4, LMS, RHS | 603273 | 3q27 | multiple |
| 70 | AIDS, delayed/rapid progression to (3) | KIR3DL1, NKAT3, NKB1, AMB11, KIR3DS1 | 604946 | 19q13.4 | Immunological |
| 70 | AIDS, rapid progression to, 609423 (3) | IFNG | 147570 | 12q14 | Immunological |
| 70 | AIDS, resistance to (3) | CXCL12, SDF1 | 600835 | 10q11.1 | Immunological |
| 1043 | Mycobacterium tuberculosis, susceptibility to infection by (3) | NRAMP1, NRAMP | 600266 | 2q35 | Immunological |
| 1400 | Sjogren-Larsson syndrome, 270200 (3) | ALDH3A2, ALDH10, SLS, FALDH | 609523 | 17p11.2 | Metabolic |
| 1454 | Stroke, susceptibility to, 1, 606799 (3) | PDE4D, DPDE3, STRK1 | 600129 | 5q12 | Cardiovascular |
| 1454 | Stroke, susceptibility to, 601367 (3) | ALOX5AP, FLAP | 603700 | 13q12 | Cardiovascular |
| 1533 | Tuberculosis, susceptibility to (3) | IFNGR1 | 107470 | 6q23-q24 | Respiratory |

FIGURE 3.1: Sample Dataset 1

For our present study, we have identified 74 different types of cancer, with 202 human genes with their OMIM Id, chromosome location.

| | A | B | C | D | E | F |
|-----|---|--------------------------------|------------|---------------|------------|-------|
| | DISEASE ID | DISEASE NAME | HUMAN GENE | OMIM ID | CHROMOSOME | CLASS |
| 207 | Bladder cancer, 109800 (3) | FGFR3, ACH | 134934 | 4p16.3 | Cancer | |
| 207 | Bladder cancer, 109800 (3) | KRAS2, RASK2 | 190070 | 12p12.1 | Cancer | |
| 207 | Bladder cancer, 109800 (3) | RB1 | 180200 | 13q14.1-q14.2 | Cancer | |
| 207 | Bladder cancer, somatic, 109800 (3) | HRAS | 190020 | 11p15.5 | Cancer | |
| 228 | Breast and colorectal cancer, susceptibility to (3) | CHEK2, RAD53, CHK2, CDS1, LFS2 | 604373 | 22q12.1 | Cancer | |
| 228 | Breast cancer, 114480 (3) | PK3CA | 171834 | 3q26.3 | Cancer | |
| 228 | Breast cancer, 114480 (3) | PPM1D, WIP1 | 605100 | 17q22-q23 | Cancer | |
| 228 | Breast cancer, 114480 (3) | SLC22A1L, BWSCR1A, IMPT1 | 602631 | 11p15.5 | Cancer | |
| 228 | Breast cancer, 114480 (3) | TP53, P53, LFS1 | 191170 | 17p13.1 | Cancer | |
| 228 | Breast cancer-1 (3) | BRCA1, PSCP | 113705 | 17q21 | Cancer | |
| 228 | Breast cancer 2, early onset (3) | BRCA2, FANCD1 | 600185 | 13q12.3 | Cancer | |
| 228 | Breast cancer (3) | TSG101 | 601387 | 11p15.2-p15.1 | Cancer | |
| 228 | Breast cancer, early-onset, 114480 (3) | BRIP1, BACH1, FANCI | 605882 | 17q22 | Cancer | |
| 228 | Breast cancer, invasive intraductal (3) | RAD54L, HR54, HRAD54 | 603615 | 1p32 | Cancer | |

Figure 3.2: Dataset 1 for cancer diseases

3.2 Creation of Dataset 2:

Dataset 2 consists of phenotype terms with their MP ID's and targeted knock-out mouse orthologues of human genes. Human gene column again was added for the ease of understanding. This dataset is based on mouse data. Mouse affected systems information (i.e. phenotypes) was collected from the MGI database. An example dataset 2 is described in figure 3.3

| MP ID | AFFECTED SYSTEM (PHENOTYPE) | MOUSE GENE | HUMAN GENE | DISEASE ID | HUMAN DISEASE | DISORDER CLASS |
|---------------|--|------------|------------|------------|----------------------------|-------------------|
| 1 MP:0002078 | abnormal glucose homeostasis | Akt2 | AKT2 | 427 | Diabetes mellitus, type II | Endocrine |
| 2 MP:0014169 | decreased brown adipose tissue mass | Akt2 | AKT2 | 427 | Diabetes mellitus, type II | Endocrine |
| 4 MP:0009356 | decreased liver triglyceride level | Akt2 | AKT2 | 427 | Diabetes mellitus, type II | Endocrine |
| 5 MP:0030022 | decreased muscle cell glucose uptake | Akt2 | AKT2 | 427 | Diabetes mellitus, type II | Endocrine |
| 6 MP:0014146 | decreased white adipose tissue mass | Akt2 | AKT2 | 427 | Diabetes mellitus, type II | Endocrine |
| 7 MP:0005378 | growth/size/body region phenotype | Akt2 | AKT2 | 427 | Diabetes mellitus, type II | Endocrine |
| 8 MP:0000316 | cellular necrosis | Kras2 | KRAS2 | 918 | Lung cancer | Cancer |
| 9 MP:0010856 | dilated respiratory conducting tubes | Kras2 | KRAS2 | 918 | Lung cancer | Cancer |
| 10 MP:0005379 | endocrine/exocrine gland phenotype | Kras2 | KRAS2 | 918 | Lung cancer | Cancer |
| 11 MP:0010771 | integument phenotype | Kras2 | KRAS2 | 918 | Lung cancer | Cancer |
| 12 MP:0010768 | mortality/aging | Kras2 | KRAS2 | 918 | Lung cancer | Cancer |
| 13 MP:0002006 | neoplasm | Kras2 | KRAS2 | 918 | Lung cancer | Cancer |
| 14 MP:0001954 | respiratory distress | Kras2 | KRAS2 | 918 | Lung cancer | Cancer |
| 15 MP:0010768 | mortality/aging | Kras2 | KRAS2 | 918 | Lung cancer | Cancer |
| 16 MP:0005387 | immune system phenotype | Pad | PAD | 1324 | Rheumatoid arthritis | Connective tissue |
| 17 MP:0004924 | abnormal behavior | Pad | PAD | 1324 | Rheumatoid arthritis | Connective tissue |
| 18 MP:0003935 | abnormal craniofacial development | Tp73l | TP73L | 1305 | Rapp-Hodgkin syndrome | multiple |
| 19 MP:0000428 | abnormal craniofacial morphology | Tp73l | TP73L | 1305 | Rapp-Hodgkin syndrome | multiple |
| 20 MP:0001672 | abnormal embryo development | Tp73l | TP73L | 1305 | Rapp-Hodgkin syndrome | multiple |
| 21 MP:0010942 | abnormal respiratory epithelium morphology | Tp73l | TP73L | 1305 | Rapp-Hodgkin syndrome | multiple |
| 22 MP:0000549 | absent limbs | Tp73l | TP73L | 1305 | Rapp-Hodgkin syndrome | multiple |
| 23 MP:0005380 | embryo phenotype | Tp73l | TP73L | 1305 | Rapp-Hodgkin syndrome | multiple |
| 24 MP:0010771 | integument phenotype | Tp73l | TP73L | 1305 | Rapp-Hodgkin syndrome | multiple |
| 25 MP:0010768 | mortality/aging | Tp73l | TP73L | 1305 | Rapp-Hodgkin syndrome | multiple |

Figure 3.3: Sample dataset for dataset 2

For this project 1567 mouse affected systems information (i.e. phenotypes) was collected from MGI report along with their MP ID's. These mouse affected systems were aligned to their corresponding human orthologs and dataset 3 was created for the construction of cancer Diseases. Figure 3.4 shows the glimpse of cancer diseases.

| MOUSE GENE | HUMAN GENE | MP ID | phenotype |
|------------|------------|------------|--|
| Mdm2 | MDM2 | MP:0005384 | cellular phenotype |
| Mdm2 | MDM2 | MP:0006043 | decreased apoptosis |
| Mdm2 | MDM2 | MP:0001262 | decreased body weight |
| Mdm2 | MDM2 | MP:0000333 | decreased bone marrow cell number |
| Mdm2 | MDM2 | MP:0001698 | decreased embryo size |
| Mdm2 | MDM2 | MP:0002875 | decreased erythrocyte cell number |
| Mdm2 | MDM2 | MP:0005378 | growth/size/body region phenotype |
| Egfr | EGFR | MP:0002161 | abnormal fertility/fecundity |
| Egfr | EGFR | MP:0000763 | abnormal filiform papillae morphology |
| Egfr | EGFR | MP:0006257 | abnormal fungiform papillae morphology |
| Egfr | EGFR | MP:0008325 | abnormal gonadotroph morphology |
| Braf | BRAF | MP:0002182 | abnormal astrocyte morphology |
| Braf | BRAF | MP:0000297 | abnormal atrioventricular cushion morphology |
| Braf | BRAF | MP:0010029 | abnormal basicranium morphology |
| Braf | BRAF | MP:0001614 | abnormal blood vessel morphology |
| Braf | BRAF | MP:0001777 | abnormal body temperature homeostasis |
| Braf | BRAF | MP:0004259 | small placenta |
| Braf | BRAF | MP:0001209 | spontaneous skin ulceration |
| Braf | BRAF | MP:0005426 | tachypnea |
| ErbB2 | ERBB2 | MP:0000920 | abnormal myelination |
| ErbB2 | ERBB2 | MP:0003871 | abnormal myelin sheath morphology |

Figure 3.4 : dataset 2 for Cancer

3.4 Construction of Dataset 3:

Dataset 1 and Dataset 2 were merged by integrating the human and mouse data tables to create Dataset 3. A link was established between human and mouse data using the targeted knock-out mouse orthologues of human genes. A sample dataset 3 is shown in figure 3.5.

| MP ID | AFFECTED SYSTEM (PHENOTYPE) | MOUSE GENE | HUMAN GENE | DISEASE ID | HUMAN DISEASE | DISORDER CLASS |
|------------|--|------------|------------|------------|----------------------------|-------------------|
| MP:0002078 | abnormal glucose homeostasis | Akt2 | AKT2 | 427 | Diabetes mellitus, type II | Endocrine |
| MP:0014169 | decreased brown adipose tissue mass | Akt2 | AKT2 | 427 | Diabetes mellitus, type II | Endocrine |
| MP:0009356 | decreased liver triglyceride level | Akt2 | AKT2 | 427 | Diabetes mellitus, type II | Endocrine |
| MP:0030022 | decreased muscle cell glucose uptake | Akt2 | AKT2 | 427 | Diabetes mellitus, type II | Endocrine |
| MP:0014146 | decreased white adipose tissue mass | Akt2 | AKT2 | 427 | Diabetes mellitus, type II | Endocrine |
| MP:0005378 | growth/size/body region phenotype | Akt2 | AKT2 | 427 | Diabetes mellitus, type II | Endocrine |
| MP:0000316 | cellular necrosis | Kras2 | KRAS2 | 918 | Lung cancer | Cancer |
| MP:0010856 | dilated respiratory conducting tubes | Kras2 | KRAS2 | 918 | Lung cancer | Cancer |
| MP:0005379 | endocrine/exocrine gland phenotype | Kras2 | KRAS2 | 918 | Lung cancer | Cancer |
| MP:0010771 | integument phenotype | Kras2 | KRAS2 | 918 | Lung cancer | Cancer |
| MP:0010768 | mortality/aging | Kras2 | KRAS2 | 918 | Lung cancer | Cancer |
| MP:0002006 | neoplasm | Kras2 | KRAS2 | 918 | Lung cancer | Cancer |
| MP:0001954 | respiratory distress | Kras2 | KRAS2 | 918 | Lung cancer | Cancer |
| MP:0010768 | mortality/aging | Kras2 | KRAS2 | 918 | Lung cancer | Cancer |
| MP:0005387 | immune system phenotype | Pad | PAD | 1324 | Rheumatoid arthritis | Connective tissue |
| MP:0004924 | abnormal behavior | Pad | PAD | 1324 | Rheumatoid arthritis | Connective tissue |
| MP:0003935 | abnormal craniofacial development | Tp73l | TP73L | 1305 | Rapp-Hodgkin syndrome | multiple |
| MP:0000428 | abnormal craniofacial morphology | Tp73l | TP73L | 1305 | Rapp-Hodgkin syndrome | multiple |
| MP:0001672 | abnormal embryo development | Tp73l | TP73L | 1305 | Rapp-Hodgkin syndrome | multiple |
| MP:0010942 | abnormal respiratory epithelium morphology | Tp73l | TP73L | 1305 | Rapp-Hodgkin syndrome | multiple |
| MP:0000549 | absent limbs | Tp73l | TP73L | 1305 | Rapp-Hodgkin syndrome | multiple |
| MP:0005380 | embryo phenotype | Tp73l | TP73L | 1305 | Rapp-Hodgkin syndrome | multiple |
| MP:0010771 | integument phenotype | Tp73l | TP73L | 1305 | Rapp-Hodgkin syndrome | multiple |
| MP:0010768 | mortality/aging | Tp73l | TP73L | 1305 | Rapp-Hodgkin syndrome | multiple |

Figure 3.5: Sample Dataset 3

Again, we have created a dataset 3 for the construction of cancer diseaseome with name of different types of cancer, disease ID(3 is specified for cancer), phenotype, mouse and human gene, MP ID's . Figure 3.6 shows the cancer diseaseome

| MP ID | MOUSE GENE | HUMAN GENE | HUMAN DISEASE | phenotype | CLASS |
|------------|------------|------------|---|---|--------|
| MP:0005384 | Mdm2 | MDM2 | Accelerated tumor formation, susceptibility to (3) | cellular phenotype | CANCER |
| MP:0006043 | Mdm2 | MDM2 | Accelerated tumor formation, susceptibility to (3) | decreased apoptosis | CANCER |
| MP:0001262 | Mdm2 | MDM2 | Accelerated tumor formation, susceptibility to (3) | decreased body weight | CANCER |
| MP:0000333 | Mdm2 | MDM2 | Accelerated tumor formation, susceptibility to (3) | decreased bone marrow cell number | CANCER |
| MP:0001698 | Mdm2 | MDM2 | Accelerated tumor formation, susceptibility to (3) | decreased embryo size | CANCER |
| MP:0002875 | Mdm2 | MDM2 | Accelerated tumor formation, susceptibility to (3) | decreased erythrocyte cell number | CANCER |
| MP:0005378 | Mdm2 | MDM2 | Accelerated tumor formation, susceptibility to (3) | growth/size/body region phenotype | CANCER |
| MP:0002161 | Egfr | EGFR | Adenocarcinoma of lung, response to tyrosine kinase inhib | abnormal fertility/fecundity | CANCER |
| MP:0000763 | Egfr | EGFR | Adenocarcinoma of lung, response to tyrosine kinase inhib | abnormal filiform papillae morphology | CANCER |
| MP:0006257 | Egfr | EGFR | Adenocarcinoma of lung, response to tyrosine kinase inhib | abnormal fungiform papillae morphology | CANCER |
| MP:0008325 | Egfr | EGFR | Adenocarcinoma of lung, response to tyrosine kinase inhib | abnormal gonadotroph morphology | CANCER |
| MP:0002182 | Braf | BRAF | Adenocarcinoma of lung, somatic, 211980 (3) | abnormal astrocyte morphology | CANCER |
| MP:0000297 | Braf | BRAF | Adenocarcinoma of lung, somatic, 211980 (3) | abnormal atrioventricular cushion morphol | CANCER |
| MP:0010029 | Braf | BRAF | Adenocarcinoma of lung, somatic, 211980 (3) | abnormal basicranium morphology | CANCER |
| MP:0001614 | Braf | BRAF | Adenocarcinoma of lung, somatic, 211980 (3) | abnormal blood vessel morphology | CANCER |
| MP:0001777 | Braf | BRAF | Adenocarcinoma of lung, somatic, 211980 (3) | abnormal body temperature homeostasis | CANCER |
| MP:0004259 | Braf | BRAF | Adenocarcinoma of lung, somatic, 211980 (3) | small placenta | CANCER |
| MP:0001209 | Braf | BRAF | Adenocarcinoma of lung, somatic, 211980 (3) | spontaneous skin ulceration | CANCER |
| MP:0005426 | Braf | BRAF | Adenocarcinoma of lung, somatic, 211980 (3) | tachypnea | CANCER |
| MP:0000920 | ErbB2 | ERBB2 | Adenocarcinoma of lung, somatic, 211980 (3) | abnormal myelination | CANCER |
| MP:0003871 | ErbB2 | ERBB2 | Adenocarcinoma of lung, somatic, 211980 (3) | abnormal myelin sheath morphology | CANCER |

Figure 3.6: Cancer Dataset 3

3.5 Clustering and analysis of the network:

The network visualisation was done in gephi tool. The disease names were taken as nodes and the edges was for assigned for the phenotypes. The network for different types of cancer was created, which has been shown in figure 3.7. In this figure the genes partening to different types of cancer is used as the nodes, and phenotypes for cancer is being used as the edges. After analysis of the network it is being observed a very high modularity in cancer phenotypes. Specially the genes, that are present at the core of the network shows similar kind of phenotypes rather than the nodes present on the surface of the network.

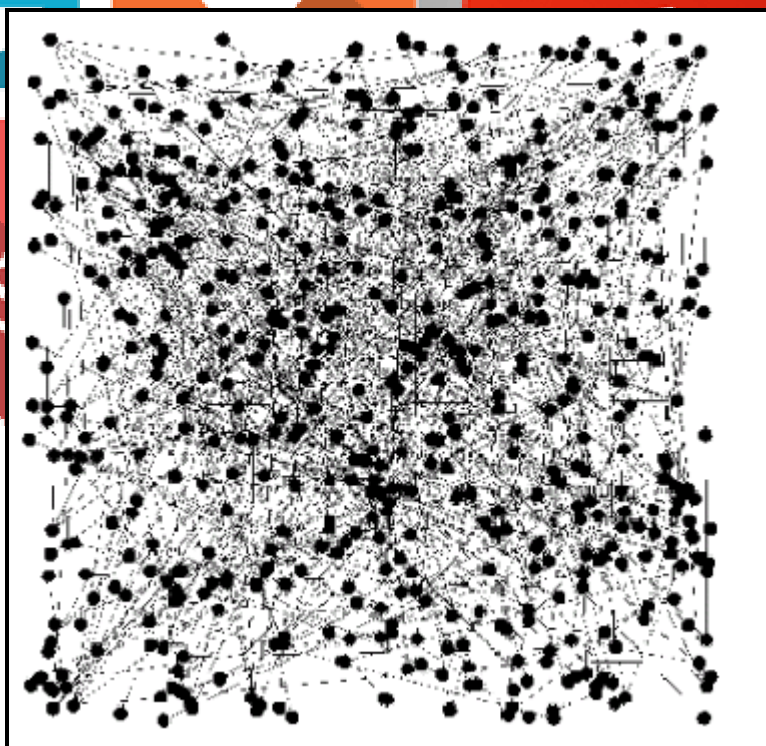


Figure 3.7 Cancer Diseaseome.

So, to analyze the genes present in the network, we have reconstructed the network only with the genes as nodes without edges. This time we have used a unique color code for the genes. The color code is shown in figure 3.8(a). The network is reconstructed using the color code in 3.8(b). In this new network it is being observed that KRAS2 is the gene that shows majority of the phenotypes in cancer (Fig 3.8 a)

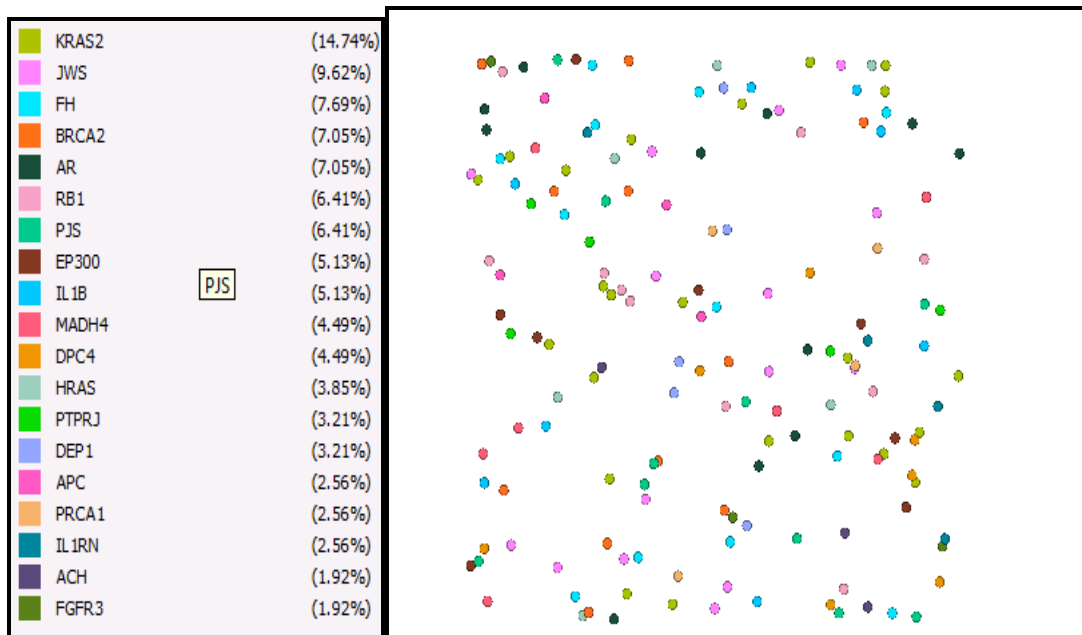


Figure 3.8: a) colour codes of genes. b) network constructed according to the colour code.

So, to analyze, the core part of the network more intensely as well as the phenotypes associated with it, we decided to break the main network into different modules. Figure 3.9 shows the modularity in the cancer network. After analysis of the modularity in the cancer network, it has been found that there are 813 different modules that are present and the most dominant phenotypes in cancer are nervous system phenotype modularity 34, abnormal dermis papillary layer morphology modularity 27, abnormal embryo development modularity 21 etc.

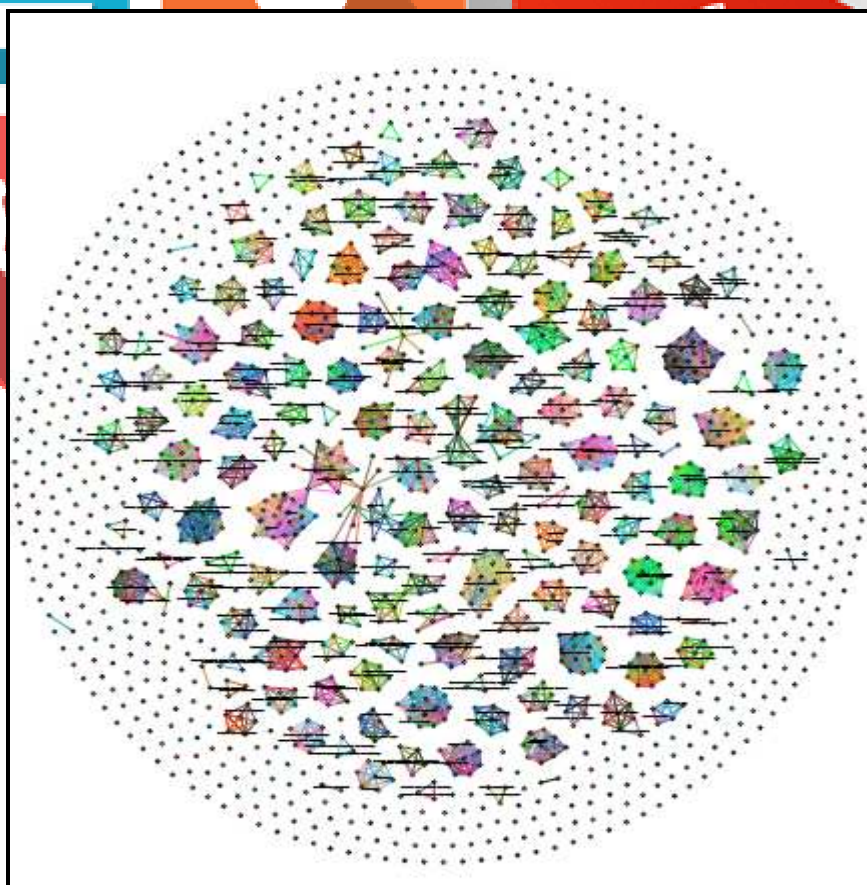


Fig 3.9: Modularity in cancer network.

so, to make our conclusion more apprehensive, we have given detailed diagram of some of the modularity in the following figure 3.10.

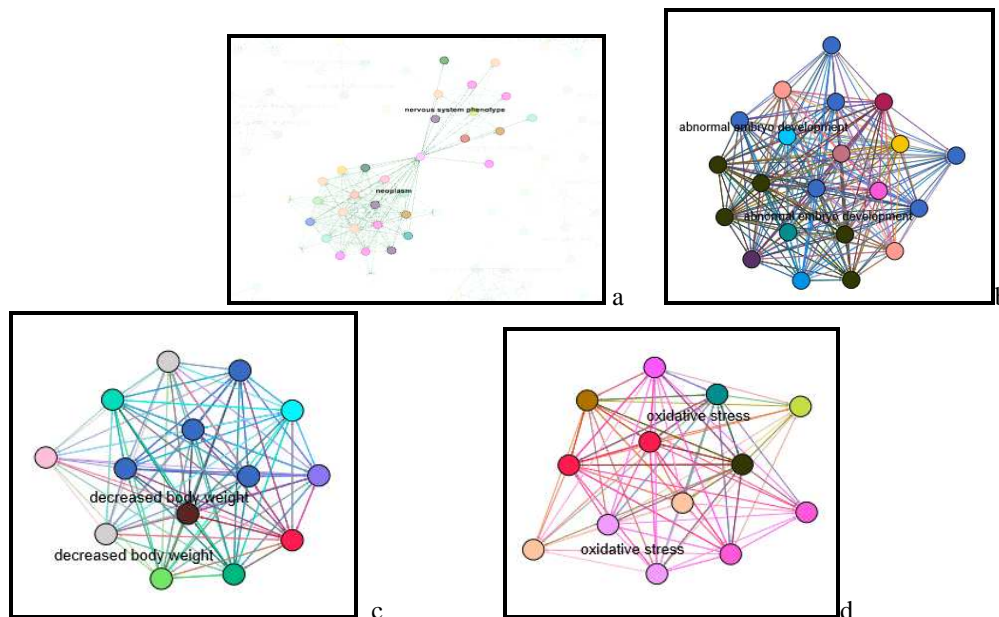


Figure 3.10: a) Cluster of neoplasm and nervous system phenotype b) Cluster of abnormal embryo development c) Cluster of decreased body weight d) Cluster of oxidative stress.

In our present study , we have even listed out the major phenotypes that occur during different types across different stages of cancer. Table 3.1 shows a detailed list of mostly occur phenotypes in cancer.

| phenotype | modularity_class | No of Occurance |
|---|------------------|-----------------|
| nervous system phenotype | 119 | 34 |
| abnormal dermis papillary layer morphology | 298 | 27 |
| abnormal embryo development | 771 | 21 |
| ventricular septal defect | 328 | 16 |
| decreased incidence of tumors by chemical induction | 108 | 16 |
| enlarged thymus | 62 | 16 |
| increased tumor incidence | 565 | 15 |
| decreased embryo size | 291 | 15 |
| premature death | 302 | 14 |
| decreased body weight | 35 | 13 |
| prenatal lethality, incomplete penetrance | 741 | 13 |
| no abnormal phenotype detected | 562 | 13 |
| abnormal thyroid-stimulating hormone level | 307 | 13 |
| abnormal bone marrow cell morphology/development | 339 | 12 |
| increased apoptosis | 146 | 12 |
| increased thyrotroph cell number | 83 | 12 |
| respiratory distress | 512 | 11 |
| abnormal cell physiology | 340 | 11 |
| cardiovascular system phenotype | 332 | 11 |
| abnormal hematopoietic system morphology/development | 299 | 11 |
| increased or absent threshold for auditory brainstem response | 281 | 11 |
| abnormal long bone diaphysis morphology | 173 | 10 |
| decreased cardiac muscle contractility | 153 | 10 |
| abnormal coat appearance | 121 | 10 |
| abnormal myocardium layer morphology | 9 | 10 |

Table 3.1: The common phenotypes of all cancer.

In our present study, we have created diseaseome for all types of cancer in human. From the diseaseome, we have identified the major phenotypes that occur from different types to different stages of cancer. This analysis of diseaseome has been carried out using knockout mouse model will help in characterization of different types of cancer. This study will have a significant impact on the development of methodological approaches toward precise identification of pathological cells and would allow for more effective detection of cancer-related changes.

IV Reference:

1. KWANG-IL GOH, MICHAEL E. CUSICK, DAVID VALLE, BARTON CHILDS, MARC VIDAL, AND ALBERT-LÁSZLÓ BARABÁSI, 2007. **THE HUMAN DISEASE NETWORK**
2. McKusick, V.A. (1998) Mendelian Inheritance in Man. A Catalog of Human Genes and Genetic Disorders, 12th edn. Johns Hopkins University Press, Baltimore, MD.
3. Ada Hamosh*, Alan F. Scott, Joanna S. Amberger, Carol A. Bocchini and Victor A. McKusick, 2004 Online Mendelian Inheritance in Man (OMIM), a knowledgebase of human genes and genetic disorders.
4. Olson H, Betton G, Robinson D et al., 2000 Concordance of the toxicity of pharmaceuticals in humans and in animals.; 32:56–67.
5. Martignoni M, Groothuis GM, de Kanter R. 2006 Species differences between mouse, rat, dog, monkey and human CYP-mediated drug metabolism, inhibition and induction. *Expert Opin Drug Metab Toxicol* ;2:875–94.
6. Suarez RK, Darveau CA. 2005 Multi-level regulation and metabolic scaling. *J Exp Biol*;208:1627–34.
7. Hulbert AJ 2008. The links between membrane composition, metabolic rate and lifespan. *Comp Biochem Physiol A Mol Integr Physiol* ;150:196–203.
8. Berry RJ, Bronson FH 1992. Life history and bioeconomy of the house mouse. *Biol Rev Camb Philos Soc* ;67:519–50.
9. Phelan JP, Rose MR. 2005 Why dietary restriction substantially increases longevity in animal models but won't in humans. *Age Res Rev* ;4:339–50.
10. Nguyen TL, Vieira-Silva S, Liston A et al. 2015 How informative is the mouse for human gut microbiota research? *Dis Model Mech* ;8:1–16.
11. Mestas J, Hughes CC. 2004 Of mice and not men: differences between mouse and human immunology. *J Immunol* ;172:2731–8.
12. Nachman MW, Searle JB. 1995 Why is the house mouse karyotype so variable? *Trends Ecol Evol* ;10:397–402.
13. Austad SN. 2002 A mouse's tale. *Nat Hist* ;111:64–70.
14. Paigen K. 2003 One hundred years of mouse genetics: an intellectual history the classical period (1902–1980). *Genetics* 2003;163:1–7.

Acknowledgement:

We sincerely thank the management of The Oxford College of Engineering and VGST for providing the opportunity to work.

The logo for the International Journal of Creative Research Thoughts (IJCRT) is a large, stylized graphic. It features a central white shape resembling a book or a flame, set against a red background. This is surrounded by various colored geometric shapes: a blue square, a green triangle, and a grey triangle. The letters 'IJCRT' are written in a bold, black, sans-serif font across the bottom right of the graphic.

IJCRT

ISOLATION, CHARACTERIZATION AND BIOLOGICAL ACTIVITY OF FLAX LECTIN

¹Dr Suma TK, ²Vasudha TK, ²Raghavi G, ²Rajalakshmi V, ²Nisha S, ²Priyadarshini M, ²B Preethi, ²M Vaishali Krishna and ³Dr BK Manjunath

¹Asst Professor, ²Student, ³Professor and Head
Department of Biotechnology
The Oxford College of Engineering, Bangalore, India
For correspondence – tksuma@gmail.com

Abstract: Lectins are a class of non-covalent carbohydrate-binding proteins of non-immune origins; possessing at least one non-catalytic domain, they can reversibly recognize and bind to monosaccharides or oligosaccharides. Legume lectins have been demonstrated to possess antifungal and antiproliferative potency on tumor cells. Seed lectin from *Linum usitatissimum* (flax) was extracted and partially purified by acetone precipitation followed by DEAE-cellulose ion exchange chromatography and Sephadex G-100 gel filtration chromatography. Carbohydrate binding specificity of lectin was determined by the hemagglutination method and found to be specifically binding to N-acetyl galactosamine. Purified lectin was characterized for their biological activity like antiproliferative, antioxidant, anti-inflammatory and antimicrobial activity using *in vitro* assays and found to possess significant biological activities.

(Index terms : flax, lectin, hemagglutination, carbohydrate binding, anti-oxidant)

I. INTRODUCTION

Lectins are proteins/glycoproteins which bind reversibly to carbohydrates. Lectins with specific carbohydrate specificity have been isolated from distinct sources such as viruses, bacteria, fungi, algae, animals, and plants [Sharon and Lis2004]; they show specificity to distinct carbohydrates, such as mannose, sialic acid, fucose, N-acetylglucosamine, galactose/N-acetylgalactosamine, complex glycans, and glycoproteins [Wu A. M *et al* 2009].

Recent studies have demonstrated the potential of lectins from different origin and carbohydrate specificities as antifungal and antiparasitic agents [Hamed *et al* 2017]. Plant lectins investigated for antifungal potential, mainly against phytopathogenic species, have most reported antifungal effects binding to hyphae, causing inhibition of growth and prevention of spore germination.

Lectins from several origins exert cytotoxic effects such as inhibition of proliferation and activation of cell death pathways, on different types of cancer cells. In addition, many anticancer lectins usually possess low cytotoxicity to nontransformed cells. This fact is probably associated with the distinct expression of glycans on surface of cancer and normal cells, allowing lectins specifically to recognize malignant cells [Przybyłomet al 2002, Varki *et al* 2009]. Since lectins have the property to bind carbohydrates their ability to antagonize, *in vivo*, neutrophil migration induced by inflammatory stimuli is well established (Alencar NM *et al* 2004). There is also data to suggest that some lectins down-regulate telomerase activity and hence inhibit angiogenesis (Sharon and Lis, 2004). A natural outcome of these studies has been the application of several lectins as therapeutic agents which favorably bind to cancer cell membranes or their receptors, thereby triggering cancer cell agglutination which translates into cytotoxicity, apoptosis, and inhibition of tumour growth (Sharon and Lis, 2004).

With the background of a wide variety of lectins isolated from diverse sources and studied for multiple biological activities, the current project was formulated to identify potential novel sources of lectins with useful properties. Flax seed or *Linum usitatissimum* is important in the nutraceutical market, as an alternate source of fish oil being naturally high in polyunsaturated fatty acids (PUFA). Intake of flaxseed in daily diet may reduce the risk of cardiovascular diseases such as coronary heart disease and stroke. There is also evidence that flax has anticancer effects in breast, prostate and colon cancers. Information on lectins isolated from flax seeds and their properties is very little. The focus of the present study was to isolate, purify and characterize lectin from the seeds of *Linum usitatissimum*(flax) and analyze *in vitro* antioxidant, anti-inflammatory and antiproliferative activities.

II. MATERIALS AND METHODS

a) Materials

Human blood of groups A, B and O were collected from healthy persons. Animal blood was collected from nearby veterinary hospitals. Flax (*Linum usitatissimum*) seeds were obtained from local markets.

b) Extraction of lectin

Dry seeds were first powdered in a blender. Seed powders were then weighed and extracted using cold extraction buffer, 1X PBS overnight at 4°C. The extract was then centrifuged for 15 minutes at 10,000 rpm at 4°C and clear supernatant was collected. Protein was estimated by Bradford method using BSA as a standard protein (Bradford 1976).

c) Hemagglutination activity of lectins

Seed extracts were assayed for the presence of lectin with whole blood of different blood types (Jawade AA et al 2016). 10µl of whole blood was used as negative control. 10µl of human blood types A, B, AB and O are taken on a clean and dry slide. The whole blood was mixed with 20µl of seed extract and hemagglutination observed.

In order to confirm that hemagglutination is due to lectin interacting with RBC cell surface carbohydrates, agglutination test of lectin was done by using 2% suspension of erythrocytes (Deshpande&Patil 2003). 50µl of 2% RBC suspension was mixed with 20µl of seed extract and hemagglutination observed.

Hemagglutination assay was also performed in 96 well plates (John Shi et al., 2007). 50µl of PBS and 10µl each of whole blood of human blood types A, B, AB and O was added to wells. 20µl of sample was then added to the wells. 50µl of PBS and 10µl of whole blood of any blood type served as negative control. Hemagglutination was observed after one hour.

d) Carbohydrate inhibition assay

Agglutination inhibition assay was done by testing the ability of different carbohydrates like disaccharides, pentoses, hexoses, oligosaccharides to inhibit the agglutination (Kurokawa et al. 1976). To confirm sugar specificity of extracted lectins, 100 µl of 500 mM sugar solutions were incubated with 100 µl lectin for 30 minutes at room temperature. 20µl of incubated mixture was mixed with 50µl of 2% RBC suspension. Hemagglutination or its absence was observed under a transilluminator.

e) Purification of lectin

Crude lectin extract was fractionated using ammonium sulfate salt (0 - 75%) (Devi et al., 2014). The salt precipitate was allowed to stand overnight in the cold for complete precipitation. After centrifugation, pellets were suspended in minimal volume of 1X PBS buffer and extensively dialysed against the extraction buffer for 24 hr in the cold for complete salt removal. Alternatively, crude extracts were treated with ice-cold acetone at 4°C and allowed for complete precipitation overnight. The precipitate was then centrifuged, air dried and dissolved in PBS. Protein concentration and hemagglutination activity were determined for the precipitates.

f) Chromatographic separation of lectin (Devi et al., 2014)

Acetone-precipitated flax seed extract was fractionated on a Sephadex G-100 gel filtration column equilibrated with 1X PBS, pH 7.4. Fractions were collected at a flow rate of 0.5ml/min and the protein was monitored by measuring absorbance at 280nm. Hemagglutination activities of the fractions were then assayed. The fractions containing hemagglutinating activities were pooled and again loaded on to a DEAE-cellulose ion exchange column pre-equilibrated with 1X PBS, pH 7.4. Fractions of 1 ml volume each were collected at a flow rate of 1 ml/min. The bound proteins were eluted with 1M KCl in 1X PBS, pH 7.4. All fractions were measured for absorbance at 280nm as well as for hemagglutination activity.

g) SDS-PAGE

Polyacrylamide gel electrophoresis of lectin samples was performed by the method of Laemmli (1970) with 15% polyacrylamide gel in the presence of sodium dodecyl sulfate (SDS) and 2-mercaptoethanol (SDS-PAGE). After electrophoresis the gel was stained with 0.2% Coomassie brilliant blue (R250) (Bluh et al 1987) and then destained.

h) pH and temperature stability studies

The effect of pH on activity of lectin was studied using different buffers in the pH range of 4-9 by the method described earlier (Devi et al., 2014). The thermal behavior of the partially purified lectin was also evaluated by incubating the lectin sample at temperatures of 17°C–77°C for 15min.

i) Antioxidant activity of lectin

Antioxidant activity of lectin was assessed by DPPH (1,1-diphenyl-2-picrylhydrazyl) radical scavenging assay (Janardhan et al 2014) and ABTS (2, 2'-azinobis, 3-ethylbenzothiazoline-6-sulfonic acid di-ammonium salt) radical scavenging assay (Lee et al 2014). Standard used in assay was ascorbic acid.

j) Anti-inflammatory activity of lectin

To assess the anti-inflammatory activity of flax lectin, proteinase inhibition assay was performed according to the modified method of Oyedepo et al 1995 and Sakat et al 2010 and inhibition of albumin denaturation technique according to Mizushima et al 1968 and Sakat et al 2010 with minor modifications. The percentage inhibition of proteinase inhibitory and protein denaturation activity was calculated.

k) Anti-proliferative activity of lectins

MCF-7 and HEPG2 cell line were cultured in DMEM and EMEM medium respectively supplemented with 10% inactivated Fetal Bovine Serum (FBS), penicillin (100 IU/ml), streptomycin (100 µg/ml) in a humidified atmosphere of 5% CO₂ at 37°C until confluent. The cells were dissociated with TPVG solution (0.2 % trypsin, 0.02 % EDTA, 0.05 % glucose in PBS). The viability of the cells is checked and centrifuged. Further, 50,000 cells / well of MCF-7 and HEPG2 were seeded in a 96 well plate and incubated for 24 hrs at 37°C, 5 % CO₂ incubator. The monolayer cell

culture was trypsinized and the cell count was adjusted to 1.0×10^5 cells/ml using respective media containing 10% FBS. To each well of the 96 well microtiter plate, 100 μ l of the diluted cell suspension (50,000cells/well) was added. After 24 h, when a partial monolayer was formed, 100 μ l of different concentrations of test samples were added and plates incubated at 37°C for 24hrs in 5% CO₂ atmosphere. Later, test solutions in the wells were discarded and 100 μ l of MTT (5 mg/10 ml of MTT in PBS) was added to each well and incubated for 4 h at 37°C. The supernatant was removed and 100 μ l of DMSO was added and the plates were gently shaken to solubilize the formed formazan. The absorbance was measured using a microplate reader at a wavelength of 590 nm. The percentage growth inhibition was calculated using the following formula and concentration of test drug needed to inhibit cell growth by 50% (IC₅₀) values is generated from the dose-response curves for each cell line. % Inhibition = $100 - (\text{OD of sample}/\text{OD of Control}) \times 100$.

III. RESULTS AND DISCUSSION

Lectins were extracted from flax seeds into PBS and precipitated using salt or acetone. All extracts were tested for hemagglutination with human and animal blood. Table 1 shows hemagglutination of human blood types and animal blood by flax seed extracts. It showed hemagglutination reaction with only human blood group A (and AB) indicating its specificity to N-Acetylgalactosamine (Fig. 1).

Table 1 : Agglutination study of *Linum usitatissimum* seed lectin with human and animal erythrocytes

| Erythrocytes | Agglutination |
|--------------|---------------|
| Human 'O' | - |
| Human 'A' | +++ |
| Human 'AB' | +++ |
| Human 'B' | - |
| Rabbit | - |
| Sheep | - |
| Hen | - |

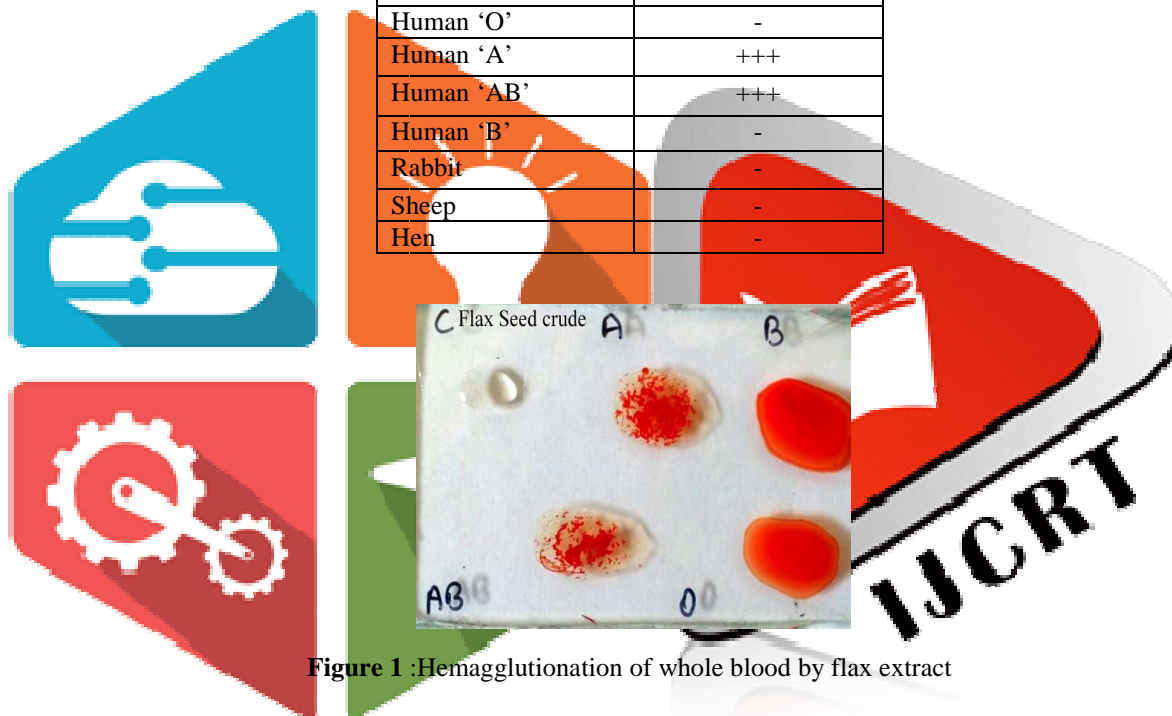


Figure 1 : Hemagglutination of whole blood by flax extract

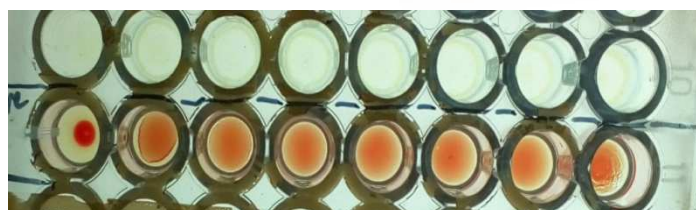


Figure 2: Hemagglutination assay in 96 well plate

Hemagglutination assay was also performed by using human erythrocyte suspension in microtitre plates. Formation of red button of RBCs at the bottom of the well indicated absence of hemagglutination. (Fig. 2).

In order to determine the absolute specificity of flax lectins towards various carbohydrates, carbohydrate inhibition assay was carried out. Table 2 shows the inhibition of lectin by different carbohydrates. Flax lectin was inhibited by N- Acetyl galactosamine (GalNac) alone and no other carbohydrate indicating the absolute specificity of this lectin for GalNac.

Table 2: Inhibition of lectin by different carbohydrates

| Carbohydrates | Agglutination |
|---------------|---------------|
|---------------|---------------|

| | |
|------------------------|-----|
| Glucose | +++ |
| Galactose | +++ |
| Mannose | +++ |
| Lactose | +++ |
| Fucose | +++ |
| N-acetyl galactosamine | - |

- = inhibits lectin
+ = does not inhibit lectin

Flax lectin was purified from the acetone precipitated extract using Sephadex G-100 gel filtration column equilibrated with 1X PBS buffer, pH 7.4. Fig. 3 gives the purification profile of flax lectin by gel filtration chromatography. Hemagglutination activity was detected in the initial fractions (maximum in fraction 3) denoting the high molecular weight of the purified lectin. None of the later eluting protein peaks showed any trace of hemagglutination activity. Although gel filtration chromatography is commonly employed for lectin separations (Zhang et al 2014), such purification of *Linum usitatissimum* lectin using Sephadex G-100 has not been reported earlier.

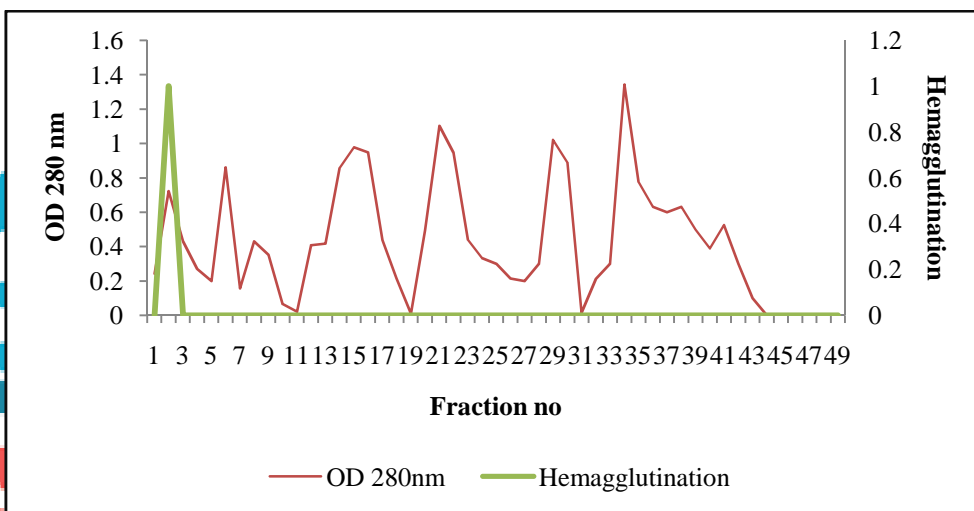


Figure 3: Sephadex G-100 gel filtration purification profile of flax lectin

Flax lectins were further purified on DEAE cellulose ion exchange column. The fractions were assayed for protein by measuring their absorbance at 280nm as well as for the hemagglutination activity. Among the fractions collected, activity was recovered in the unbound fractions and no activity was seen in bound (Fig. 4), indicating its anionic nature.

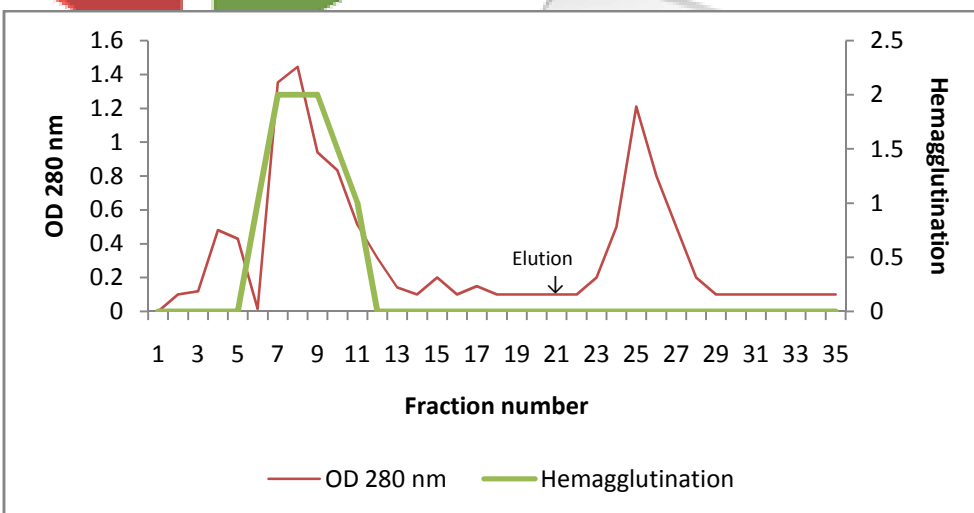


Figure 4: DEAE-cellulose ion exchange purification profile of flax lectin

SDS-PAGE analysis of lectin at each stage of purification was done to determine purity as well as molecular weight. Fig. 5 shows the gel profile of crude and partially purified flax lectin preparation on a 15% SDS-PAGE gel. In comparison with crude extract

and salt and acetone precipitates, different types of protein bands were seen in unbound and gel filtration fraction signifying a level of purification. The presence of protein bands in between that of BSA and lysozyme molecular markers shows that the molecular weight of the lectin or its subunits is between 14.3 kDa (lysozyme) and 66.5 kDa (Bovine serum albumin). This profile of unbound and gel filtration fractions was associated with hemagglutination activity while bound had no hemagglutination activity.

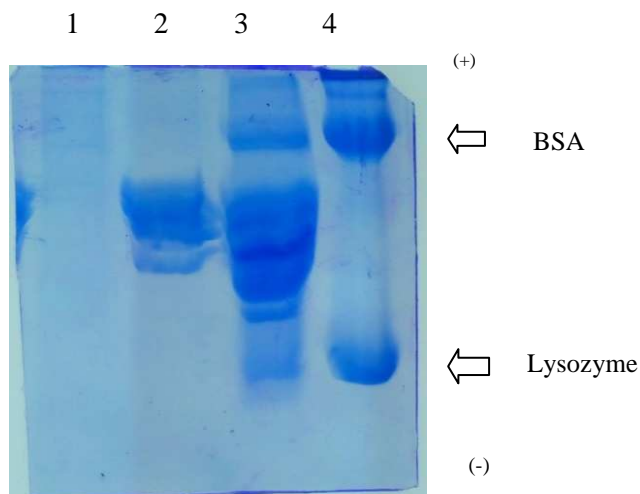


Figure 5: SDS-PAGE profile of flax crude and partially purified samples. 15% polyacrylamide gel was run with following samples and stained with Coomassie Brilliant Blue for visualization. From left to right: Lane 1: Gel-filtration pooled fraction, Lane 2: Flax ion-exchange unbound fraction, Lane 3: acetone precipitate, Lane 4: BSA + Lysozyme molecular marker.

The antioxidant activity of lectins has been well-established (Sadananda *et al.*, 2014). Anti-oxidant assays of DPPH and ABTS were performed for lectin extracts. The percentage scavenging activity of flax lectin was tested against that of ascorbic acid which is known to have potent antioxidant activity (Fig. 6 and 7). The IC₅₀ value for flax lectin was found to be 3.008 mg/ml. The IC₅₀ value for ascorbic acid at same concentration as lectin was found to be 3.018mg/ml.

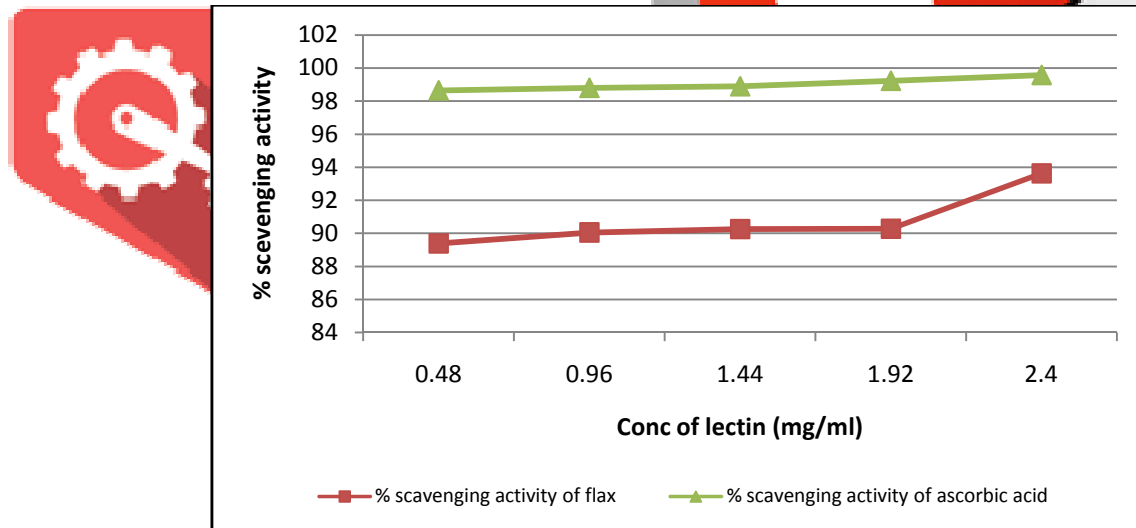


Figure 6: Antioxidant activity of flax lectin by DPPH assay. The reduction capability of DPPH radical was determined by the decrease in its absorbance at 517nm which is induced by different antioxidants.

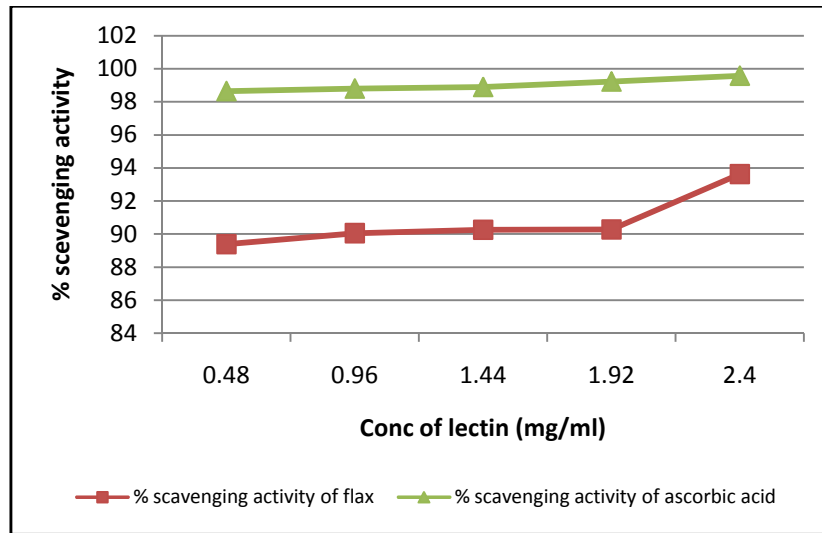


Figure 7: Antioxidant activity of flax lectin by ABTS assay. The decrease in absorbance due to scavenging of the proton radicals is monitored spectrophotometrically at 734nm

Lectins have been shown to have anti-inflammatory activity (Janaina K.L. Campos *et al.*, 2016). Proteinase inhibition assay and albumin denaturation assays were performed to demonstrate anti-inflammatory activity. Fig. 8 shows the anti-inflammatory activity of flax lectin. Flax lectin exhibited significant antiproteinase activity at different concentrations and showed 100% inhibition at 3.2mg/ml of lectin.

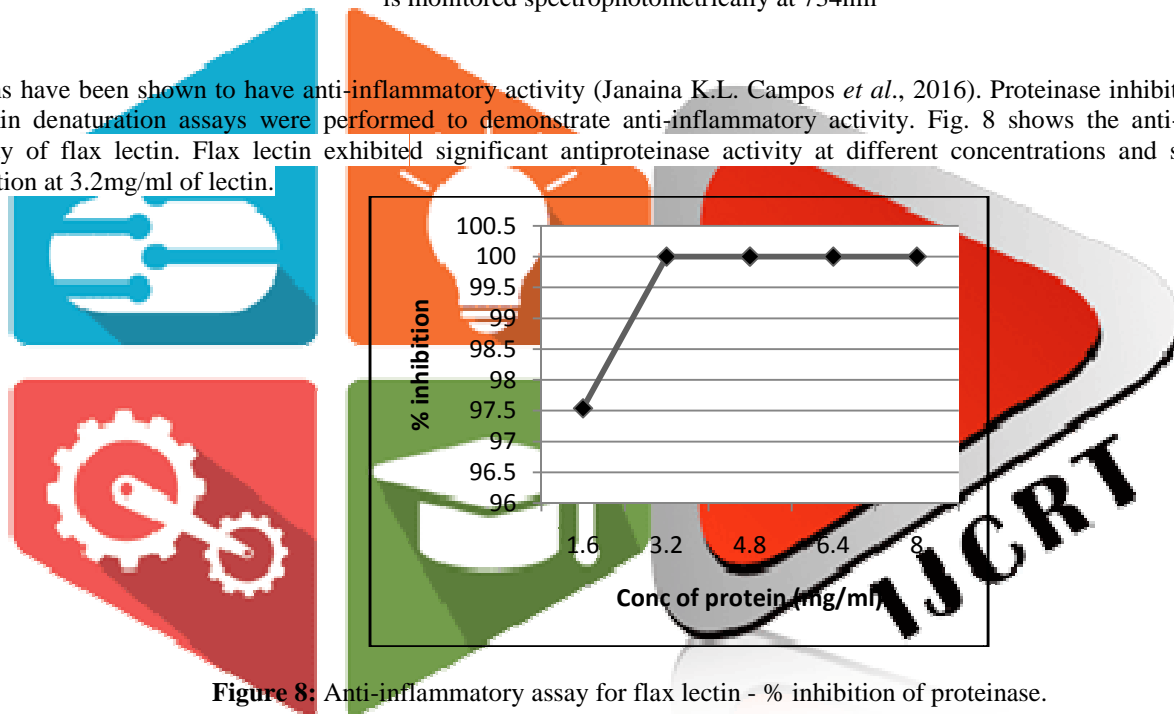


Figure 8: Anti-inflammatory assay for flax lectin - % inhibition of proteinase.

As part of the investigation on the mechanism of the anti-inflammation activity, ability of lectin to inhibit protein denaturation was studied (Fig. 9). It was effective in inhibiting heat induced albumin denaturation. Inhibition of 100% was observed at 8 mg/ml for flax lectin.

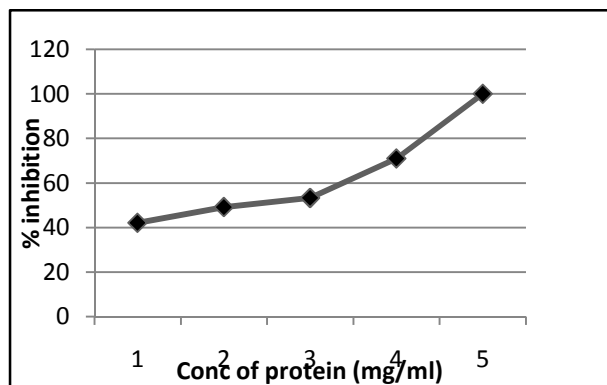


Figure 9: Anti-inflammatory assay for flax lectin - % inhibition of protein denaturation.

Flax lectins were tested for their pH stability by incubating the lectins in buffers of different pH. The lectins showed remarkable pH stability in the range 4-9 which was confirmed by hemagglutination of the lectins after incubation. When tested at a range of temperatures between 17-100°C, flax and lectins showed decreased activity beyond 57°C.

To evaluate the cytotoxic effect of flax lectin against cancer cells, human breast carcinoma cells (MCF-7) were incubated with different dosages of flax lectin samples. After 24 hours of incubation, cell viability was determined by MTT assay. Flax lectin extract was found to induce cell toxicity in a concentration dependant manner (Table 4). Dose response curves between the range 10µg/ml to 320µg/ml express decreased number of viable cells with increase in the concentration of compound. Results indicate that the cytotoxic effect steadily strengthens with increase in concentration.

Table 4: Cytotoxicity assays using flax lectin

| MCF-7 | | | |
|----------------------------|-------------|-------------|--------------|
| Sample | Conc. µg/ml | OD at 590nm | % inhibition |
| <i>Linum usitatissimum</i> | 10 | 0.911 | 4.27 |
| | 20 | 0.875 | 7.95 |
| | 40 | 0.833 | 12.47 |
| | 80 | 0.811 | 14.78 |
| | 160 | 0.766 | 19.50 |
| | 320 | 0.721 | 24.19 |

IV. CONCLUSION

Very little information is currently available on flax seed lectins. In one study, hemagglutination activity and carbohydrate specificity of lectin seedlings revealed their role in plant adaptation to abiotic stresses (Levchuket *et al* 2013). A similar study on amaranth-like lectin genes in flax induced by defence hormones has also been reported (Kashfia Faruque *et al* 2015).

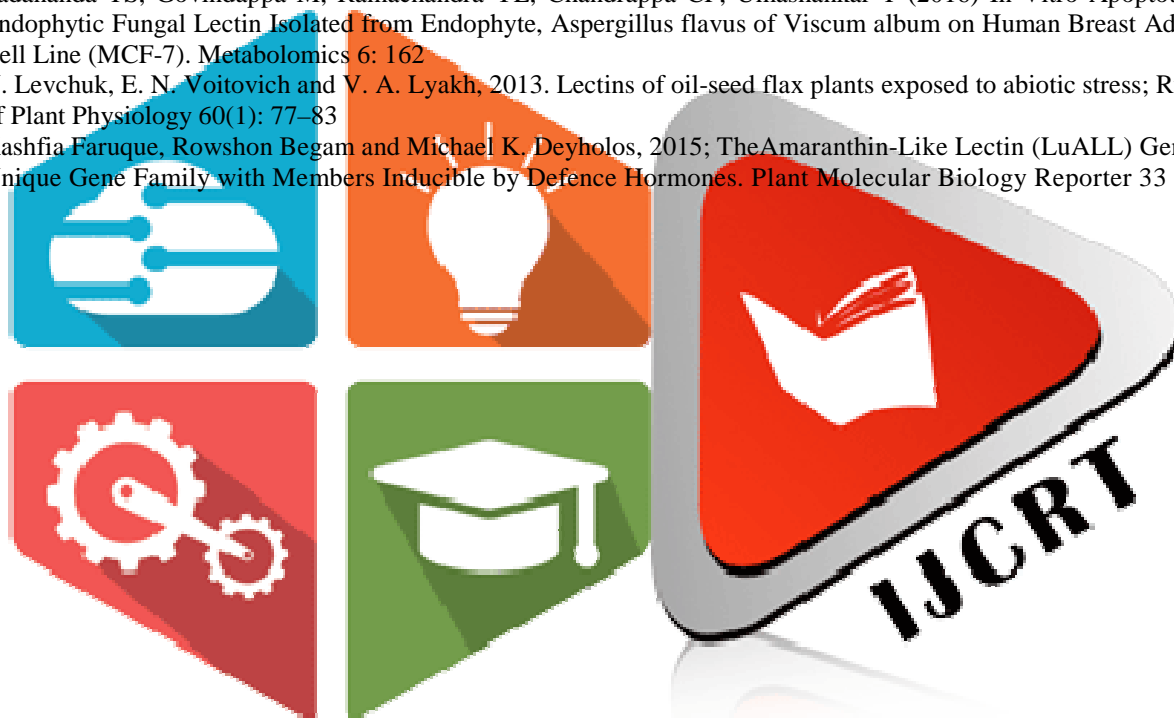
The current report sheds light on the hemagglutination activity, carbohydrate specificity, purification strategies and biological activity of flax seed lectins. *Linum usitatissimum* (Flax) lectin extracts were found to be specific to N-Acetylgalactosamine. Purification was achieved by concurrent use of gel filtration and ion exchange chromatography and it was found to be a high molecular weight cationic protein. Purified lectin was shown to possess anti-oxidant, anti-inflammatory and anti-proliferative properties and remarkable pH and temperature stability. These results support the general finding of lectins to be biologically active in different ways. Further work is warranted to establish possible utilization of flax lectin for specific applications.

Acknowledgment

V. References

- Nathan, Sharon and Halina Lis, 2004; History of lectins: from hemagglutinins to biological recognition molecules; *Glycobiology* 14 (11): 53R-62R
- Wu AM, Lisowska E, Duk M and Yang Z, 2009; Lectins as tools in glycoconjugate research; *Glycoconj* 26(8):899-913.
- Hamed El-SE, Ibrahim El-AMM, Mounir SM (2017) Antimicrobial Activities of Lectins Extracted from Some Cultivars of *Phaseolus vulgaris* Seeds. *J MicrobBiochemTechnol* 9:109-116
- Przybylo M, Hoja-Lukowicz D, Litynska A and Laidler P. 2002; Different glycosylation of cadherins from human bladder non-malignant and cancer cell lines. *Cancer Cell Int.* 18;2:6.
- Varki A, Varki NM and Borsig L, 2009; Molecular basis of metastasis (correspondence). *N. Engl. J. Med.* 360: 1678-1680
- Nylane M.N. Alencar, Ana M.S. Assreuy, David N. Criddle, Emmanuel P. Souza, Pedro M.G. Soares, AlexandreHavt, Karoline S. Aragao, Daniel P. Bezerra, Ronaldo A. Ribeiro, Benildo S. Cavada, 2004. VataireaMacrocarpaLectin Induces Paw Edema With Leukocyte Infiltration. *Protein & Peptide Letters* 11(2), 195-200
- Bradford, Marion (1976). "A Rapid and Sensitive Method for the Quantification of Microgram Quantities of Protein Utilizing the Principle of Protein-Dye Binding" (PDF). *Analytical Biochemistry*. 72: 248–254.
- Jawade AA, Pingle SK, Tumane RG, Sharma AS, Ramteke AS & Jain RK (2016) Isolation and characterization of lectin from the leaves of *Euphorbia tithymaloides* (L.). *Tropical Plant Research* 3(3): 634– 641)
- Deshpande&Patil 2003
- John Shi, Sophia Jun Xue, Yukio Kakuda, Sanjallic, and Daniel Kim; 2007; Isolation and characterization of lectins from kidney beans (*Phaseolus vulgaris*); *Process Biochemistry* 42: 1436–1442.
- Kurokawa T, Tsuda M and Sugino Y, 1976. Purification and characterization of a lectin from *Wistaria floribunda* seeds. *J Biol Chem.* 251(18):5686-93
- B. Gayatri Devi and K.P.J HemaLatha. 2014; Isolation, Partial Purification and Characterization of Alkaline Serine Protease from seeds of *CucumisMelo* Var. *International Journal of Research in Engineering and Technology.* 3:6

13. Helmut Blum, HildburgBeier and Hans J. Gross; 1987; Improved silver staining of plant proteins, RNA and DNA in polyacrylamide gels; *Electrophoresis* 8(2): 93-99
14. Janardhan A, Kumar AP, Viswanath B, Saigopal DV and Narasimha G. 2014. Production of bioactive compounds by actinomycetes and their antioxidant properties. *Biotechnol Res Int.* 2014:217030.
15. Lee DR, Lee SK, Choi BK, Cheng J, Lee YS, Yang SH and Suh JW, 2014. Antioxidant activity and free radical scavenging activities of *Streptomyces* sp. strain MJM 10778. *Asian Pac J Trop Med.* 7(12):962-7
16. O.O. Oyedapo & A. J. Famurewa, 1995. Antiprotease and Membrane Stabilizing Activities of Extracts of *FagaraZanthoxyloides*, *OlaxSubscorpioides* and *TetrapleuraTetraptera*. *International Journal of Pharmacognosy* 33(1), 65-69
17. Sakat S, Juvekar AR, Gambhire MN. 2010 In vitro antioxidant and anti-inflammatory activity of methanol extract of *Oxalis corniculata* Linn. *International Journal of Pharma and Pharmacological Sciences*; 2(1):146-155
18. Mizushima Y and Kobayashi M. 1968 Interaction of anti-inflammatory drugs with serum proteins, especially with some biologically active proteins. *J of Pharma Pharmacol*; 20:169- 173.
19. T. S. Sadananda, M. Govindappa and Y. L. Ramachandra, 2014; In vitro Antioxidant Activity Of Lectin from Different Endophytic Fungi of *Viscum album* L; *British Journal of Pharmaceutical e research* 4(5): 01-15.
20. Janaína K.L. Campos, Chrisjacele S.F. Araújo, Tiago F.S. Araújo, Andréa F.S. Santos, José A. Teixeira, Vera L.M. Lima, Luana C.B.B. Coelho, 2016; Antiinflammatory and antinociceptive activities of *Bauhinia monandra* leaf lectin. *Biochimie* 01: 62–68.
21. Weiwei Zhang, Guoting Tian, Xueran Geng, Yongchang Zhao, Tzi Bun Ng, Liyan Zhao and Hexiang Wang. 2014. Isolation and Characterization of a Novel Lectin from the Edible Mushroom *Stropharia rugosoannulata*. *Molecules* 19, 19880-19891
22. Sadananda TS, Govindappa M, Ramachandra YL, Chandrappa CP, Umashankar T (2016) In Vitro Apoptotic Activity of Endophytic Fungal Lectin Isolated from Endophyte, *Aspergillus flavus* of *Viscum album* on Human Breast Adenocarcinoma Cell Line (MCF-7). *Metabolomics* 6: 162
23. N. Levchuk, E. N. Voitovich and V. A. Lyakh, 2013. Lectins of oil-seed flax plants exposed to abiotic stress; *Russian Journal of Plant Physiology* 60(1): 77–83
24. Kashfia Faruque, Rowshon Begam and Michael K. Deyholos, 2015; TheAmaranthin-Like Lectin (LuALL) Genes of Flax: a Unique Gene Family with Members Inducible by Defence Hormones. *Plant Molecular Biology Reporter* 33 (3), 731–741.



SIGNIFICANCE ANALYSIS OF TARGET PROFILE IN TUBERCULOSIS USING GENE INTERACTIONS AND INSILICO DOCKING APPROACH TO FIND POTENTIAL LIGANDS

Dr. Manjunath, Shambhu M.G Apeksha, Chandana N, Lakshmi S, Mounika S.

Department of Biotechnology, The Oxford College of Engineering, Bengaluru-560068

*correspondence should be addressed to Mr Shambhu M G : shambhumg13@gmail.com

Abstract: Tuberculosis is a common and deadly infectious disease caused by *Mycobacteria*. WHO estimates that one third of global population is infected with *Mycobacterium tuberculosis*. Tuberculosis is a Multidrug resistant since there are a lot of mutations occur in genes. Our study focused on uncharacterized mutated tuberculosis target identification by using Systems Biology Approach, which is used to find the better drug targets. From the advance search by using UniProt we observed seven receptors are the significant targets 2CCA, 1P44, 3VZ1, 3IFZ, 1KOR, 2EYQ. Tuberculosis target candidates are screened and validated by docking studies using Auto dock Software. Analysis has revealed that among 14 ligands it has been observed that Josamycine and Rifapentine showed a better interaction score (-10.3 kcal/mol and -12.7 kcal/mol) and could be potential ligands. These potential ligands have also shown better ADMET properties in *Insilico* studies by using ADMET SAR software.

1. INTRODUCTION

Tuberculosis (TB) is caused by *Mycobacterium tuberculosis*. TB is an infectious disease that usually affects the lungs. Some strains of the TB bacteria developed resistance to the standard drugs through genetic changes [2]. TB affects 24% of world's total population. According to WHO its world's top infectious disease, about 5000 people deaths occurs everyday. *Mycobacterium tuberculosis* (MTB) is a rod shaped bacteria that can thrive only human beings [3]. TB is often called Multidrug resistance (MDR). The TB bacteria has natural defences against some drugs, and can acquire drug resistance through genetic mutations. The bacteria does not have the ability to transfer genes for resistance between organisms through plasmids some mechanisms of drug resistance include: **Cell wall:** The cell wall of *M. tuberculosis* (TB) contains complex lipid molecules which act as a barrier to stop drugs from entering the cell [9]. **Drug modifying & inactivating enzymes:** The TB genome codes for enzymes (proteins) that inactivate drug molecules. These enzymes usually phosphorylate, acetylate, or adenylate drug compounds. **Drug efflux systems:** The TB cell contains molecular systems that actively pump drug molecules out of the cell. **Mutations:** Spontaneous mutations in the TB genome can alter proteins which are the target of drugs [6], making the bacteria drug resistant. In the present study, Initially the receptors are obtained from the target pathogen database 30 receptors were obtained from the literature survey. Among the 30 receptors, 7 potential genes were obtained by string software. Validation was performed using Rampage software. Homology model was performed for all seven receptors. Among the seven receptors, only two receptors model was not found. These two receptors model was built using Swiss model and validated using Rampage and ERATT tool. Fourteen potential ligands were obtained from drug bank. These ligands satisfied and passed Lipinski's rule which were performed to obtain better drug candidates. Interaction studies between the receptors and ligands were observed by docking studies by using Autodockvina software. It was observed that among the 14 ligands, two ligands showed good interaction studies they are Rifapentine and Josamycin. *Insilico* ADMET properties predictions was performed using ADMET SAR SOFTWARE.

2. MATERIALS AND METHODS

2.1 IDENTIFICATION AND PREPARATION OF TARGET PROTEIN

Target identification is the process of identifying the direct molecular target for example protein or nucleic acid of a small molecule. In clinical pharmacology, target identification is aimed at finding the efficacy target of a drug/pharmaceutical. Target proteins are functional biomolecules that are addressed and controlled by biologically active compounds [1]. Target proteins control the action and the kinetic behaviour of drugs within the organism. Initially by using database Target pathogen and literature review 4000 genes was obtained which occurred in Tuberculosis [1]. These 4000 genes was further analyzed and screened by using the string software. By using string software on the basis of protein-protein interaction 30 potential genes were screened based on their functions and characteristics using UniProt advance filters.

2.2 GENES NETWORK STUDIES

Using string database these 30 genes were screened based on their functions and characteristics using UniProt advance filters .Seven significant genes involved in tuberculosis were shortlisted among 30 targets. All the 7 targets were further studied based on structural information[15]. Among these seven targets we observed that 2 targets did not have the structure which was further modelled using Swiss model.

2.3 HOMOLOGY MODELLING

The Homology Modelling server template library ExpDB is extracted from the PDB. To select templates for a given protein, the sequences of the template structure library are searched. If these templates cover distinct regions of the target sequence, the modeling process will be split into separate independent batches. Homology modelling was used for the construction of atomic resolution model of the target protein. Swiss model was used to obtain 3d protein structure models for the genes which we have selected for finding the better drug candidate. The template protein of gabD1 is 3VZL and of mfd is 2EYQ. For two protein the model was built based on template as the structure was not available and this was done using Swiss model.

2.4 VALIDATION

The Ramachandran plot has been the mainstay of protein structure validation for many years. Its detailed structure has been continually analysed and refined as more and more experimentally determined models of protein 3D structures have become available, particularly at high and ultra-high resolution. These plots are typically split in forbidden and allowed regions. Around 40% of all the amino acids in a structure are contained in just the 2% of the Ramachandran plot the so called "allowed areas". Rampage revealed the information of the dihedral angles of residues with respect to protein structures. Ramachandran plot was analysed for the 2 protein models by giving the pdb format. Validation was done using the ERRAT tool and this tool analyzes the statistics of non-bonded interactions between different atom types and plots the value of the error function versus position of a 9-residue sliding window, calculated by a comparison with statistics from highly refined structures. We uploaded the pdb file of modeled protein and we obtained a graph which specifies the error % and the warning %. These graphs were used for the validation process.

2.5 SCREENING OF LIGANDS

The ligands were collected from the DRUGBANK and advance search. The ligands were screened based on the Lipinski's rule which states that poor adsorption is anticipated, if the molecular weight is greater than 500 LogP is greater than 5 and hydrogen bond acceptors is greater the all the ligands should satisfies Lipinski's rule and also indicates good drug candidates. In our study 14 potential ligands were screened[17].

2.6 DOCKING

AutoDockVina, a new program for molecular docking and virtual screening, is presented. AutoDockVina significantly improves the accuracy of the binding mode predictions, than the Autodock 4. Six targets were docked with the selected 14 ligands. The best interaction is taken based on the score given by autodockvina. The general functional form of the conformation-dependent part of the scoring function AutoDockVina (referred to as Vina here) is designed to work with is [7],

$$c = \sum_{i < j} f_{t_i t_j}(r_{ij}),$$

Where the summation is over all of the pairs of atoms that can move relative to each other, normally excluding 1–4 interactions, *i.e.* atoms separated by 3 consecutive covalent bonds. Here, each atom i is assigned a type t_i , and a symmetric set of interaction functions $f_{t_i t_j}$ of the interatomic distance r_{ij} should be defined.

$$c = c_{\text{inter}} + c_{\text{intra}}$$

This value can be seen as a sum of intermolecular and intramolecular contributions [7]. The optimization algorithm, described in the following section, attempts to find the global minimum of c and other low-scoring conformations, which it then ranks.

2.7 ADMET (Absorption, Distribution, Metabolism, Excretion, and toxicity) Test

ADMET stands for Adsorption, Distribution, Metabolism, Excretion, Toxicity. To select drug-like molecule, ADMET SAR software was used to screen the selected five molecules based on filters namely Lipinski's rule [16], Quantitative Estimate of Drug likeness. The selected compounds in SDF format was given to the ADMET software interface and proceeded to calculate the properties.

3. RESULTS AND DISCUSSIONS

3.1 IDENTIFICATION OF TARGET PROTEIN

After the characterization of genes we obtained 1373 unknown genes. Analysis of genes was carried out based on their functional characteristics. Among the 30 targets, 7 targets have to be further analyzed through network analysis. The mapping of genes was carried out using UniProt ID mapping. The several specific genes were obtained as such when provided with identifiers from UniProtKB AC/ID to PDB.

3.2 Gene interaction network analysis

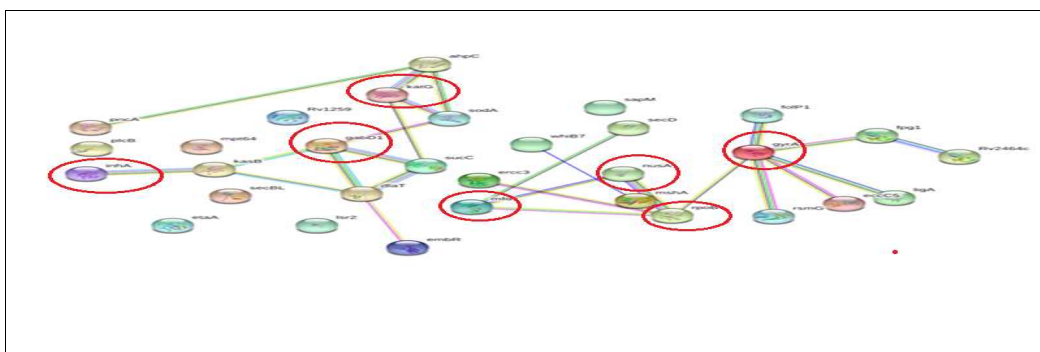
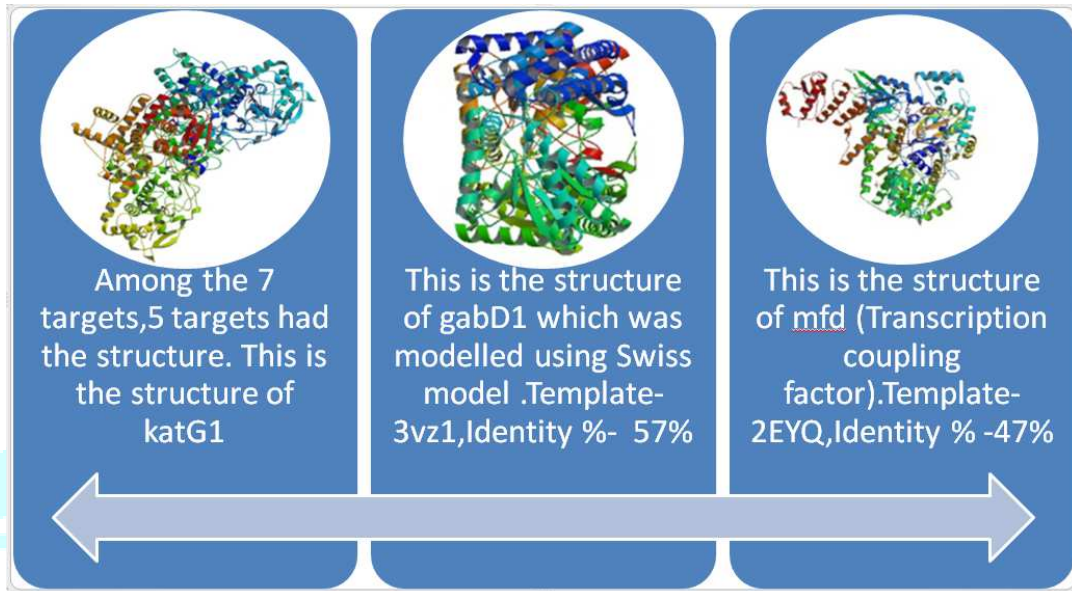


Fig 2: protein-protein interactions where done using the string database and 7 targets were found to have better interactions and those genes were inhA, katG, r

The 30 Target protein which were obtained from the advance search n the characterized genes, these were given to string software and using the string software we found out the gene-gene interactions and among the 30 genes we found that 7 genes had the better drug interactions and based on these interactions the 7 genes were shortlisted and those are the inhA,katG,rpoB,gabD1,mfd,gyrA,nusA. Among these 7 genes 5[22] had the structures and 2 did not have the structures which were modelled using the homology modeling.

3.2 HOMOMOLOGY MODELLING



In the homology modelling we used the swiss model software and the 2 genes which did not have the structure was built a model and the template was found for the these genes and we obtained the structure.

3.3 VALIDATION

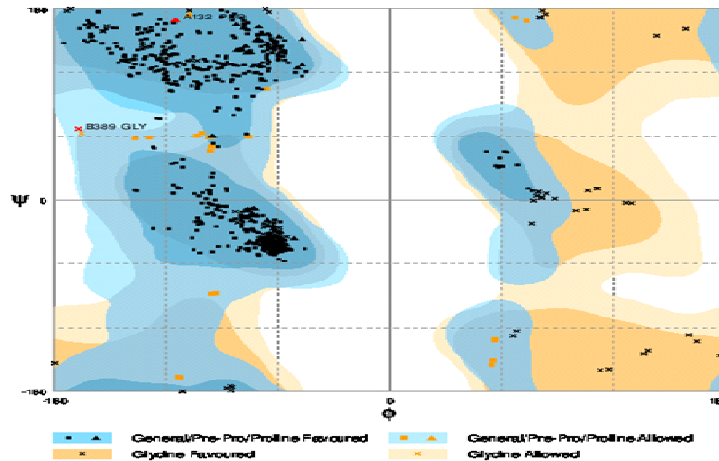


FIGURE 8:
 Number of residues in favoured region (~98.0% expected) : 881 (97.5%)
 Number of residues in allowed region (~2.0% expected) : 21 (2.3%)

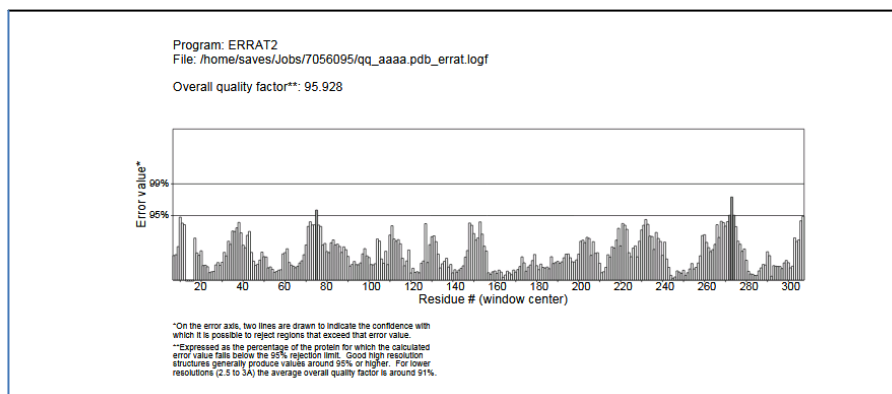


Fig 7 : Validation of molecules using ERRAT tool

3. 4 DOCKING

Autodockvina was performed to predict the bound conformation the binding affinity[23].The grid maps will be automatically formed by the software.The configuration values will be saved in a text file called conf.The PDBQT file of target and the ligand was obtained.

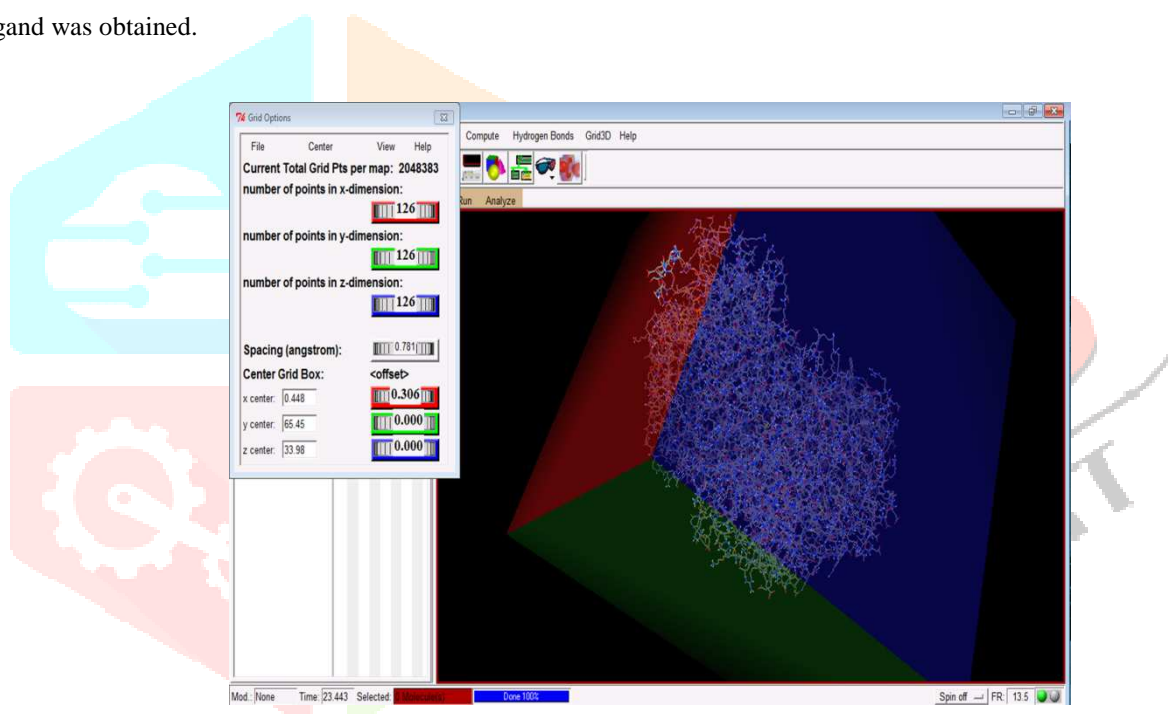


Fig8:Grid box formed by the Autodock for 1KOR.

Similarly the grid box and the configuration was done for other genes.14 ligands were taken for docking purpose, where Josamycine and Rifapentine showed the better result compared to other ligands.

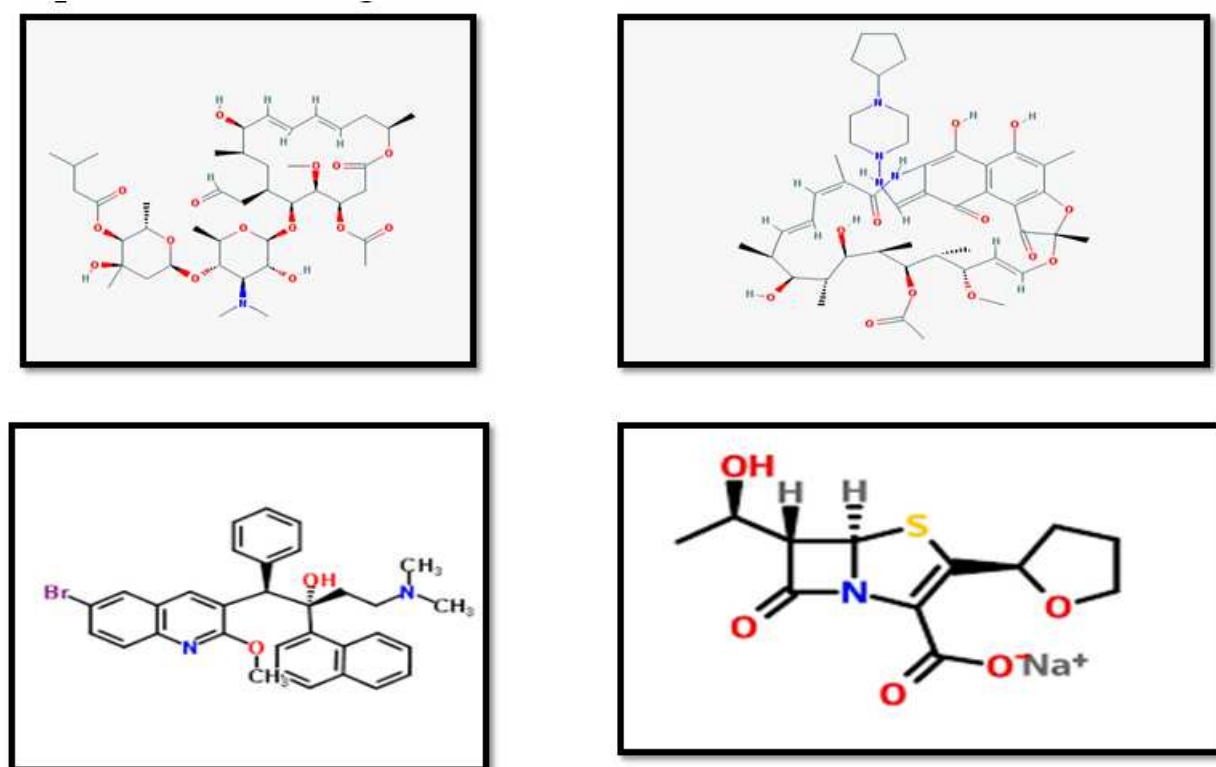


Fig9 : Ligands structure a.Josamycin, b.Rifampentine, c.Bedaquiline, d.Faropenem

Further the command prompt was used to run the program, where the conffile ,gene and ligand pdbqt file was saved in one folder.Further the docking analysis is performed based on the binding energy value and the interaction was analysed using pymol software.

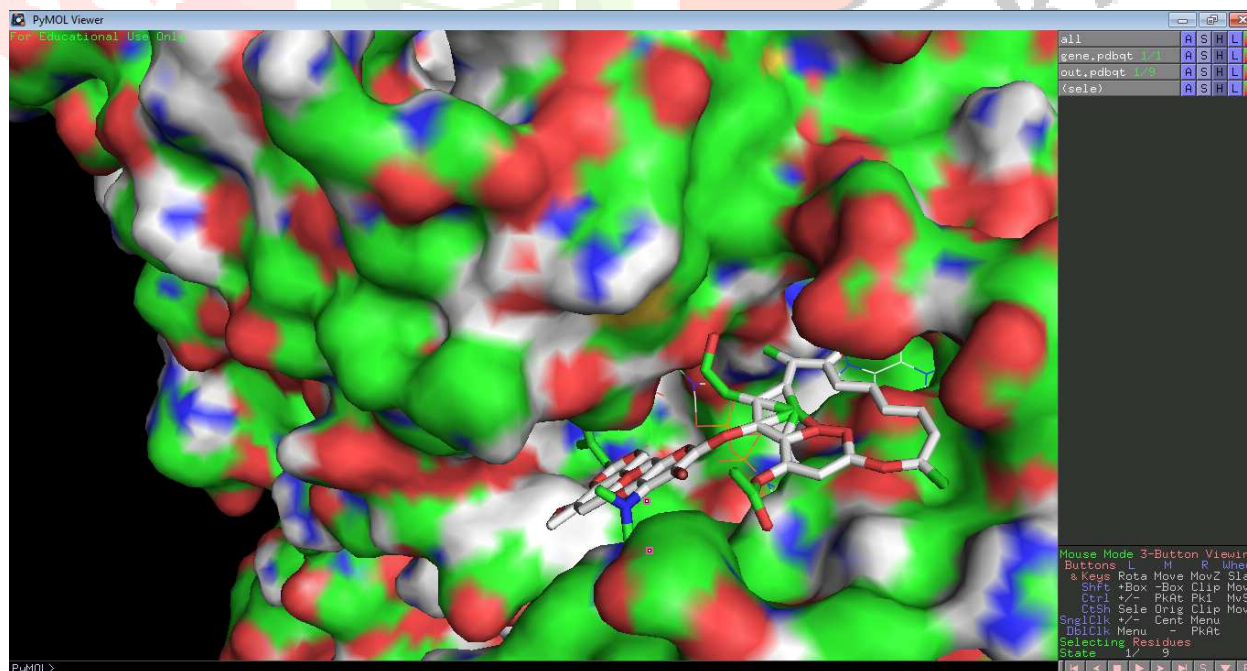


Fig10: Docking result of Josamycin which is docked with the 1KOR

Rifapentine was shown the better result for the gene 2CCA.

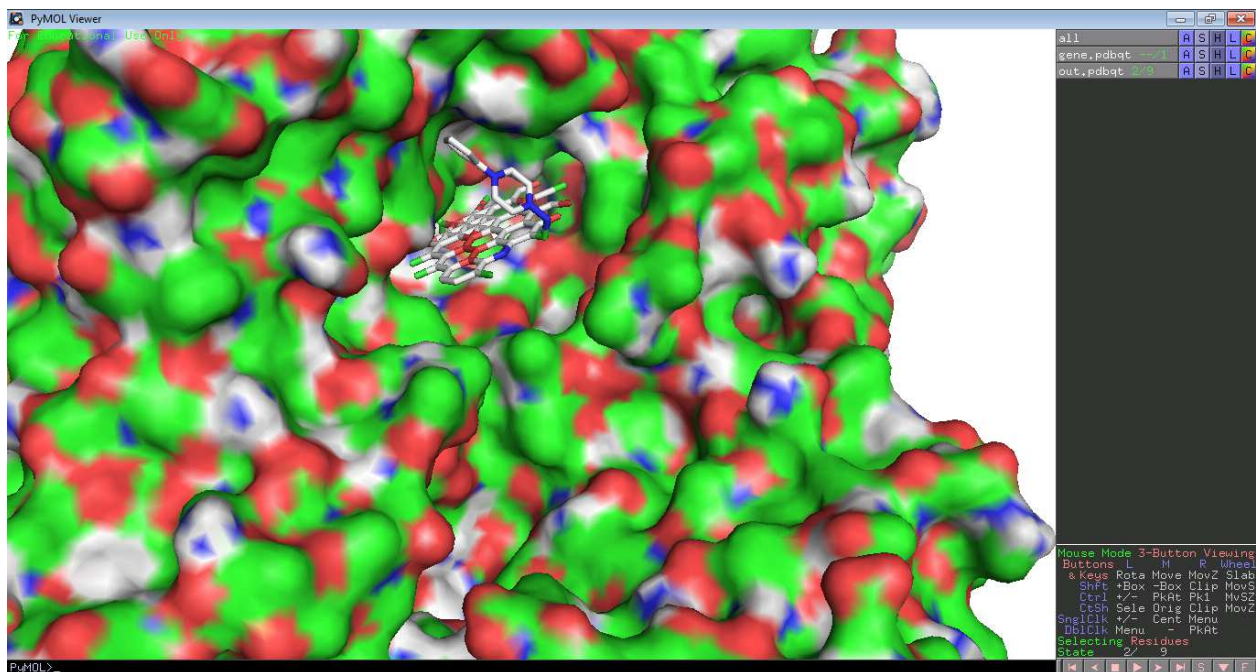


Fig15: 2CCA was docked with the ligand Rifapentine.

Docking was performed between the 6 genes and the listed ligands using the autodockvina. The software will predict the proper binding site. Further the analysis of the result was done based on the values.

| 1 | LIGANDS | 2CCA | 1P44 | 3VZ1 | 3IFZ | 1KOR | 2EYQ |
|----|------------------------------------|-------|-------|-------|-------|-------|-------|
| 2 | 5 Amino-1,3,4,thiadiazole -2 thiol | -4.6 | -3.7 | -4.4 | -3.7 | -4 | -4.1 |
| 3 | Bedaquiline | -9.8 | -8.2 | -8.2 | -9.9 | -9.3 | -8.7 |
| 4 | Delamanid | -8 | -9 | -9.7 | -9.5 | -8 | -9.2 |
| 5 | Faropenem | -8.1 | -6.6 | -6.1 | -6.3 | -7.1 | -7 |
| 6 | Isoniazid | -5.8 | -4.7 | -4.9 | -4.3 | -4.7 | -4.7 |
| 7 | Josamycin | -9.2 | -9 | -9.1 | -9.3 | -10.3 | -10.1 |
| 8 | KanamycinA | -8.1 | -9.2 | -7.4 | -7.5 | -8.2 | -9.1 |
| 9 | Levofloxacin | -7.4 | -8.9 | -6.8 | -7.1 | -7.3 | -7.7 |
| 10 | Pretomanid | -7.2 | -7.8 | -7.4 | -7.3 | -7.9 | -8.2 |
| 11 | Protionamide | -5.2 | -7 | -5.2 | -5 | -5.3 | -5.2 |
| 12 | Pyrazinamide | -5.1 | -4.8 | -5.3 | -4.2 | -4.8 | -4.6 |
| 13 | Rifapentine | -12.7 | -10.9 | -11.8 | -12.4 | -11.8 | -13.1 |
| 14 | SQ-109 | -5 | -5.1 | -6.2 | -5.1 | -6.7 | -6.8 |
| 15 | Terizidone | -7.2 | -7 | -6.6 | -6.4 | -8 | -6.7 |



3.5 ADMET PROPERTIES

| SL.NO | LIGAND NAME | PROPERTY | MODEL | RESULT | PROBABLIITY |
|-------|-------------|--------------|-----------------------------|-----------------|-------------|
| 1 | REFAPENTINE | ABSORPTION | Blood-Brain Barrier | BBB- | 0.9659 |
| | | | Human Intestinal Absorption | HIA+ | 0.66848 |
| | | DISTRIBUTION | Subcellular localisation | Mitochondria | 0.5477 |
| | | METABOLISM | CYP450IA2 Inhibitor | Non-Inhibitor | 0.8865 |
| | | TOXICITY | Carcinogens | Non-carcinogens | 0.8147 |
| 2 | JOSAMYCINE | ABSORPTION | Blood-Brain Barrier | BBB- | 0.9659 |
| | | | Human Intestinal Absorption | HIA+ | 0.5235 |
| | | DISTRIBUTION | Subcellular localisation | Mitochondria | 0.5110 |
| | | METABOLISM | CYP450IA2 Inhibitor | Non-Inhibitor | 0.9070 |
| | | TOXICITY | Carcinogens | Non-carcinogens | 0.9287 |

ADMET properties of Rifapentine and Josamycine.

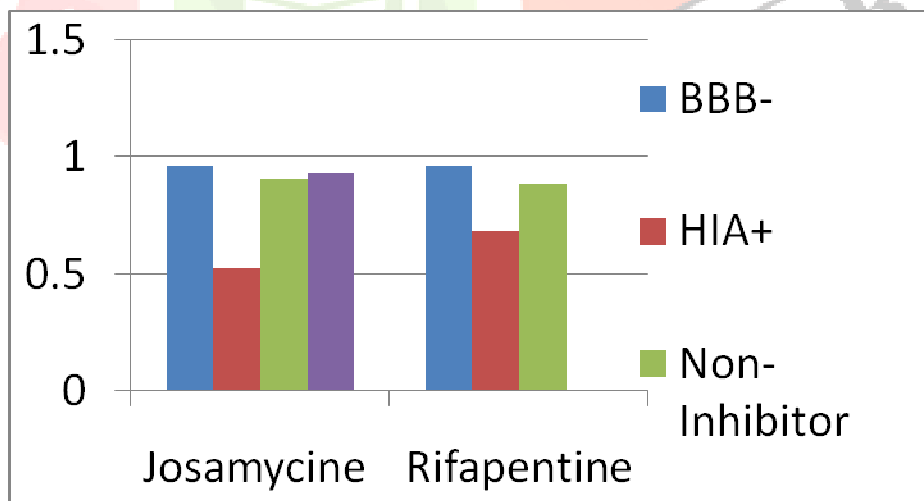


Fig16 : Result of ADMET properties.

4. CONCLUSION

Tuberculosis (TB) is caused by *Mycobacterium tuberculosis*. TB is an infectious disease that usually affects the lungs. Some strains of the TB bacteria developed resistance to the standard drugs through genetic changes and *Mycobacterium tuberculosis* (MTB) is a rod shaped bacteria that can thrive only human beings .TB is often called Multidrug resistance(MDR) or Multi drug resistance is antimicrobial resistance shown by a species of microorganisms to multiple anti-microbial drugs .MDR is most threatening to public health. MDR bacteria that is resist multiple antibiotics

A dataset of genes was reviewed using the TARGET PATHOGEN database where the characterization of the genes were carried out such that separate the characterized genes and uncharacterized genes and we concentrated on the un characterized genes for our project and among the 4000 genes we obtained 1373 characterized gens and 2627 of characterized genes.

These genes were further shortlisted to 30 genes based on their functional characteristics which were suitable for the *Mycobacterium tuberculosis*. Further to know the gene-gene interactions of these 30 genes, these genes were submitted to gene interaction analysis.

In the gene network analysis we used the STRING software to find out the gene-gene interaction where we submitted 30 genes to STRING and gene network was formed from which 6 genes were shortlisted because they had better drug interactions.

Modelling of the protein was carried out using SWISS MODEL .Among the seven genes which had better interactions, two genes did not have the structure so they were modelled using the SWISS MODEL and the template was obtained for these 2 targets.

Validation of these structures obtained from SWISS MODEL was carried out using RAMPAGE and ERRAT tool was also used for the validation of the structures.RAMPAGE showed the allowed regions and favourable regions based on which the modelled structures were validated and in ERAT tool the percentage of error and the warning percentage were given and 99% of the residues were below the threshold and 1% of which were above the threshold. Thus the modelled structures were validated.

Further the docking studies were carried out using AUTODOCK VINA software and the docking results showed that two ligands had better interaction score and those were REFAPENTINE (-13.1 kcal/mol) and JOSAMYCINE (- 10.1 kcal/mol). ADMET properties were studied using ADMET SAR software and these two ligands also showed better properties compared to other ligands and these ligands are non-carcinogenic and non-toxic.

Hence we conclude that based on the docking studies and ADMET properties ,two ligands REFAPENTINE (-13.1 kcal/mol) and JOSAMYCINE (- 10.1 kcal/mol) have shown better interactions and these can be the potential drug molecules for Tuberculosis.

ACKNOWLEDGEMENT

The Authors would like to thank CCMC-VGST (under KFIST Level 1) Govt of Karnataka , Department of Biotechnology and the management TOCE Bengaluru for the support and Infrastructure provided and for their undiminished encouragement and valuable inputs for the project.

5.REFERENCE

1. Sosa EJ, Burguener G, Lanzarotti E Target-Pathogen: a structural bioinformatic approach to prioritize drug targets in pathogens , journal nucleic acids research. published in 2018.
2. Nisha T,nair,Shefin Nisthar identification of novel drug candidate against Mycobacterium Tuberculosis Inh A protein through computer aided drug discovery, journal, Indian journal of pharmaceutical education and research. published in 2016.
3. V.R.Bollela, E.I.Nambuurete, Detection of kat G and inh A mutations to guide isoniazid and ethionamid use of drug resistant tuberculosis and journal is HHS PUBLIC ACCESS published in 2016.
4. Marva Seifert, Donald Catanzaro, Genetic mutations associated with isoniazid resistance in mycobacterium tuberculosis and the journal is PLOS ONE published in 2015.
5. Danil V Zimenkov, Olga V Antonova, Detection of second line drug resistance in mycobacterium tuberculosis using oligonucleotides microarrays and journal is BMC INFECTIOUS DISEASES and it is published in 2013.
6. Wanil Kang, Yu Pang, Current status of new tuberculosis vaccine in children and the journal is HUMAN VACCINE IMMUNOTHERAPEUTICS and it is published in 2016.
7. Marva V.J, Autodock Vina:Improving the speed and accuracy of docking with scoring function and journal is HHS PUBLIC ACCESS published in 2011.
8. Charles C Wang, System approach to tuberculosis vaccine development and journal is RESPIROLOGY published in 2013.
9. Asad Amir, Khyti Rana, M TB H37 RV , In silico drug targets, Identification by metabolic pathway analysis and the journal is INTERNATIONAL JOURNAL OF EVOLUTIONARY BIOLOGY published in 2014.
10. Mustafa AS, In silico analysis and experimental variation of M TB specific protein and peptides M TB for immunological diagnosis and vaccine development, journal MEDICAL PRINCIPLE AND PRACTICE published in 2013.
11. Beban Kai Sheng Chung, Thomas dick, In silico analysis for discovery of tuberculosis drug targets, journal ANTIMICROBIAL CHEMOTHERAPY published in 2013.
12. Edivi W Tiwemera, Natural history of tuberculosis duration and fatality of untreated pulmonary TB in HIV negative patients, journal PLOS ONE published in 2011.
13. Molebogeng X Rangaka, Controlling the seed beads of TB, Diagnosis and tereatment of TB infection, journal HSS PUBLIC ACCESS published in 2015.
14. Ragini Singh, Basanhi Ramachandran, In silico based high throughput screening for discovery of novel combinations of TB treatment, journal ANTIMICROBIAL AGENTS AND CHEMOTHERAPY published in 2015.

15. Dipendra Gurnung, String software,intelligent predictive string search algorithm, journal SCIENCE DIRECT published in 2016.
16. V.C Sheng, Comprehensive source and free tool for assessment of chemical ADMET properties, journal CHEMICAL INFORMATION AND MODELLING published in 2012.
17. David S Wishart, Comprehensive resource for in silico drug discovery and exploration, journal NUCLEIC ACID RESEARCH published in 2006.



Pharmacognosy

Journal of Pharmacognosy and Phytochemistry

Printed Journal Indexed Journal Refereed Journal Peer Reviewed Journal

Search



Menu



Journal of Pharmacognosy and Phytochemistry

Vol. 8, Issue 3 (2019)

Morphological characterization of *Pyricularia oryzae* causing blast disease in rice (*Oryza sativa* L.) from different zones of Karnataka

Author(s):

B Manjunatha and M Krishnappa

Abstract:

Study was conducted to describe the cultural and morphological characteristics such as colour and texture of the leaf blast pathogen *Pyricularia oryzae* on different solid media viz., Host extract agar, Oat meal agar, Potato dextrose agar and Richard's agar medium. Among all the solid media the highest mean mycelial growth (diameter) of the fungus *Pyricularia oryzae* was recorded on Host extract agar (40.80mm) followed by Oat meal agar (38.33 mm) and least mean mycelial growth of the *P. oryzae* on Rechar's agar (28.4 mm). The highest mean dry mycelial weight(mg) Rechar's agar(300.65mg) followed by Oat meal agar (234.67 mg) and least mean mycelial weight was recorded in Potato Dextrose agar (96.31 mg). In general, among all solid media the Host extract agar media is more appropriate for cultural and morphological study of rice blast fungus *P. oryzae*.

Pages: 3749-3753 | 211 Views 48 Downloads

[Download \(619KB\)](#)**How to cite this article:**

B Manjunatha and M Krishnappa. Morphological characterization of *Pyricularia oryzae* causing blast disease in rice (*Oryza sativa* L.) from different zones of Karnataka. J Pharmacogn Phytochem 2019;8(3):3749-3753.

[Subscribe Print Journal](#)

UPCOMING CONFERENCE

UPCOMING CONFERENCES

JOURNAL CODE(S)

E-ISSN: 2278-4136

P-ISSN: 2349-8234

CODEN Code: JPPOHO

Abbr: J Pharmacogn Phytochem

See discussions, stats, and author profiles for this publication at: <https://www.researchgate.net/publication/326000500>

Stability Analysis for Yield and Yield Attributing Traits in Rice (*Oryza sativa* L.)

Article in *International Journal of Current Microbiology and Applied Sciences* · June 2018

DOI: 10.20546/ijcmas.2018.706.194

CITATIONS

2

READS

105

3 authors, including:



B. Manjunatha

University of Agricultural & Horticultural

9 PUBLICATIONS 8 CITATIONS

[SEE PROFILE](#)



Dr Niranjana Kumara

The Trans-disciplinary University

23 PUBLICATIONS 27 CITATIONS

[SEE PROFILE](#)

Some of the authors of this publication are also working on these related projects:



AICRP on Rice [View project](#)

Original Research Article

<https://doi.org/10.20546/ijcmas.2018.706.194>

Stability Analysis for Yield and Yield Attributing Traits in Rice (*Oryza sativa* L.)

B. Manjunatha*, C. Malleshappa and B. Niranjana Kumara

Department of Genetics and Plant Breeding, Agricultural and Horticultural Research Station,
Kathalagere- 577219 (Karnataka), India
(University of Agricultural and Horticultural Sciences,
Shivamogga-577204, Karnataka, India)

*Corresponding author

ABSTRACT

Keywords

Stability, Linear,
Genotype x
Environment,
Variance

Article Info

Accepted:
17 May 2018
Available Online:
10 June 2018

The present investigation was carried out during *kharif* 2016 at the Agricultural and Horticultural Research Station, Kathalagere and other five locations under University of Agricultural and Horticultural Sciences, Shivamogga, Karnataka, to know the stability of the Twenty three advanced genotypes including three checks of paddy. Highly significant differences among genotypes were observed for all the characters except number of tillers, panicles fertility percent. The variance due to Genotype x Environment found significant for the characters like days to maturity, Plant height, Panicle length (cm) and number of spikelets per plant. Environment (linear) interaction component was significant for all the traits. The variance due to pooled deviation (non- linear) was highly significant for all the characters except for harvest index which reflect considerable genetic diversity in the material. Out of 23 genotypes studied six entries viz., JT-2-16-1, JT-2-22-5, JA-4-3, JT-2-15-1, JB-1-20-2 and JK-1-7-5 were consistent and high yielding compared to local checks, from the present study genotype JA-6-2 was found to be a stable across the environments.

Introduction

Rice (*Oryza sativa* L.), belongs to the family Graminae, recognized as “Millennium Crop” expected to contribute towards food security in the world, as it is one of the staple cereal crops of the world and a primary source of food for more than half the world’s population. With an alarming increase in the population throughout the world, the demand for rice will continue to increase in near future. Therefore, rice breeders across the world aim at increasing the grain yield of rice

(Song *et al.*, 2007). Worldwide, rice is cultivated in an area of about 161.4 million hectares, production of about 506.3 million tonnes and productivity of 3.14 tonnes per hectare. In India area under rice cultivation is 44.11 million hectare and production of about 105.48 million tonnes with 2.39 tonnes per hectare productivity. In Karnataka, it is grown in an area of 13.26 lakh hectares with production of 3541 thousand tons and productivity of 2.67 tonnes per ha (Annon, 2016). Yield is a complex quantitative character and is greatly influenced by

environmental fluctuations; hence, the selection for superior genotypes based on yield *per se* at a single location in a year may not be very effective (Shrestha *et al.*, 2012). The assessment of stability of a genotype under different environments is useful for recommending cultivars for known conditions of cultivation. The stability of varieties over wide range of environments with high yield potential is desirable. It has always been emphasized by breeders as base before releasing an ideal variety for commercial cultivation (Singh and Shukla, 2001). For a genotype to be commercially successful, it must perform well across the range of environment likely to be encountered in a target region over the entire array of years in which the genotype could be in use. Beyond seasonal and location differences, however, cultivation conditions within season do transit from one condition to the other, as dictated by variability in moisture and other environmental indices.

The presence of G x E interaction is naturally makes it difficult to fully realise the potential of a genotype for a region in which weather varies from year to year. When the G x E interaction is significant, the plant and environmental factors that play a major role in causing differential performance, and their significance in determining desirable breeding strategies, must be carefully considered (Kang and Martin, 1987 and Yan and Hunt, 2000). Understanding the genotype x environment interaction has long been a key issue for plant breeders and geneticists. In crop performance, the observed phenotype is a function of genotype (G), environment (E) and genotype × environment interaction (GEI). GEI is said to occur when different cultivars or genotypes respond differently to diverse environments. Researchers agree that GEI is important only when it is significant and causes considerable changes in genotype ranks in different environments. If this interaction is more, then

the stable performance of the variety is less and vice versa. Hence, testing of newly developed genotypes for their stable performance is vital across the different environments.

Materials and Methods

The experimental material for the contemporary study comprises of twenty advanced breeding lines of F₆ generation (Table 1.) with three checks Jyothi, KHP-2 and Tunga collected from Department of Genetics and Plant breeding, College of Agriculture Shivamogga. The research was carried out during *kharif* 2016. The experiment was laid out in Randomized Complete Block Design (RCBD) with two replications in puddle field at all locations (Table 2). Five plants in all the advanced breeding lines were selected at random from each replication for recording of observations on metric characters of these advanced breeding lines were used for recording all the below cited characters. The average of observations recorded on these five plants was considered for statistical analysis. Similarly plant morphological characters of each genotype were recorded by selecting single or group of plants depending on all characters at different stages of crop growth. Days to fifty per cent flowering, Days to maturity, Plant height (cm), Panicle length (cm), Number of tillers, Number of productive tillers per plant, Number of spikelets per plant, Number of grains per panicle, Panicle fertility (per cent), Test weight (g), Grain yield (kg/ha), Straw yield (kg/ha) and Harvest Index (%). To analyze the data over six environments the stability model proposed by Eberhart and Russel (1966) have proposed a dynamic approach for studying and interaction phenotypic stability from regression analysis. It enables selection of genotypes that may reasonably show stable performance over a range of environment was adopted.

Results and Discussion

In the present study stability parameters such as mean (μ), regression coefficient (bi) and deviation from regression (S^2_{di}), as suggested by Eberhart and Russel (1966) were considered to explain and discuss the stability of different advanced breeding lines for various characters under consideration. From the pooled analysis of variance, it was evident that the significant mean squares due to environment (linear) for grain yield revealed differential response of the genotypes and environment, mean square for pooled deviation were significant for all most all the characters studied (Table 3). The results supported with the reports of Vanave *et al.*, 2014.

Table 4 shows that the advanced breeding lines JB-1-22-2 and JA-4-3 had less mean value for days to fifty per cent flowering than the population mean had regression coefficient unity and least deviation from regression, indicating that with respect to days to fifty per cent flowering, these advanced breeding lines show stable performance across the environments.

So, by using these advanced breeding lines in breeding programme can develop medium duration or short duration cultivars. JK-1-11-8, JA-4-2, JB-1-22-2, JA-6-3, JA-6-4 and JA-6-2 are identified as stable lines for specific locations these results were in associated with Basavaraj (1994) and Subramanya (1996). In other hand Koli *et al.*, (2015) reported that days to fifty per cent flowering is a stable character across the environment. The advanced breeding line JB-1-20-2 had less mean value for days to maturity than population mean, also had regression coefficient value is around unity and less deviation from regression. So, it is indicated that this advanced breeding line had stable performance across the environments and less

sensitive to environment it can adapt to the diverse environments. These findings are agreement with those of Sawant *et al.*, (2006) and Praveen *et al.*, (2013). JA-4-2 and JA-6-2, JA-4-3, JA-6-2, JA-4-2, JA-6-2 and JA-4-2 identified as stable lines for specific locations. The advanced breeding line JT-2-16-1 had more mean value for plant height than the population mean also had regression coefficient value is around unity and less deviation from regression. Significant regression co-efficient was observed for JT15-3 and JK2 15-2 indicate that they were highly sensitive to environmental changes and rest of the advanced breeding lines had average stability. Basavaraj (1994) also identified advanced breeding lines with average responsiveness and also advanced breeding lines with higher environmental sensitivity.

Subramanya (1996) noted unpredictability of the genotypes for this trait. Similar results were also reported by Koli *et al.*, (2015). JT-2-16-1, JT-2-16-1, JT-2-22-5, JT-2-16-1, JT-2-22-5 and JT-2-16-1 are identified as stable lines for specific locations. The advanced breeding line JK-1-12-1 had more mean value than the population mean and also had regression coefficient value is around unity and less deviation from regression.

Similar results were reported Mahapatra and Sujathadas (1999). JT-2-16-1, JT-2-16-1, JB-1-11-7, JA-6-4, JA-6-2 and JA-6-4 identified as stable lines for specific locations. High mean values than the population mean, regression coefficient around unity and least deviation from regression were recorded for number of tillers per plant in the advanced breeding lines JB-1-11-7 and JA-6-3 indicating that their stability over wide range of environments. These findings are agreement with those of Umadevi *et al.*, (2008). JA-6-2, JK-1-7-5, JT-2-15-1, JT-2-16-1, JK-1-13-2 and JT-2-16-1 are identified as stable lines for specific locations.

Table.1 List of advanced breeding lines (F₆) used under present investigation including checks

| Cross combinations | Code | Advanced breeding lines | Grain shape | Grain color |
|--------------------|------|-------------------------|----------------|-------------|
| JYOTI x BILIYA | G1 | JB-1-11-7 | Medium slender | Light red |
| | G2 | JB-1-20-2 | Medium slender | Light red |
| | G3 | JB-1-22-1 | Medium slender | Light red |
| | G4 | JB-1-22-2 | Medium slender | Light red |
| | G5 | JB-1-22-3 | Medium slender | Light red |
| JYOTI x KESARI | G6 | JK-1-7-5 | Medium bold | Dark red |
| | G7 | JK-1-11-8 | Medium bold | Light red |
| | G8 | JK-1-12-1 | Medium bold | Light red |
| | G9 | JK-1-13-1 | Medium bold | Light red |
| | G10 | JK2-2-1-8-1 | Medium bold | Light red |
| | G11 | JK2-1-12-1 | Medium bold | Light red |
| JYOTI x AKKALU | G12 | JA-4-1 | Medium slender | Light red |
| | G13 | JA-4-2 | Medium slender | Light red |
| | G14 | JA-4-3 | Medium slender | Light red |
| | G15 | JA-6-2 | Medium slender | Light red |
| | G16 | JA-6-3 | Medium slender | Light red |
| | G17 | JA-6-4 | Medium slender | Light red |
| JYOTI x TUNGA | G18 | JT-2-15-1 | Medium slender | Light red |
| | G19 | JT-2-16-1 | Medium slender | Light red |
| | G20 | JT-2-22-5 | Medium slender | white |
| JYOTHI | G21 | | Bold | Red |
| KHP-2 | G22 | | Slender | Red |
| TUNGA | G23 | | Bold | white |

Table.2 Location of experiments conducted to evaluate rice genotypes for stability analysis

| SL. NO. | Particulars | Environments | | | | | |
|---------|---------------------|-------------------|------------------|-----------------|-----------------|-----------------|-----------------|
| 1 | Locations | AHRS, Kattalagere | UAHS, Shivamogga | AHRS, Honnavile | ZAHRS, Mudigere | AHRS, Bhavikere | AHRS, Ponnampet |
| 2 | Latitude | 16°12' N | 13.054° N, | 13.9299° N, | 13°8'3"N | 12.50° N, | 12.14907°N |
| 3 | Longitude | 74°54' E | 75.03930° E | 75.5681° E | 75°38'30" E | 77.35° E | 75.94052 °E |
| 4 | Elevation | 598 meters | 569 meters | 570 meters | 915 meters | 566.7met | 851 meters |
| 5 | Average temperature | 25.5 °C | 24.8 °C | 24.6 °C | 23.2 °C | 36 °C | 22.6 °C |
| 6 | Average rainfall | 567 mm | 909 mm | 863 mm | 610 mm | 1104.2 mm | 2173 mm |

Table.3 Pooled ANOVA values for thirteen quantitative traits over six environments

| Source of Variations | DF | X1 | X2 | X3 | X4 | X5 | X6 | X7 |
|----------------------|-----|-----------|----------|-----------|----------|----------|---------|-----------|
| Rep within Evn. | 6 | 0.82 | 13.52 | 4.62 | 0.53 | 1.67 | 0.51 | 57.53 |
| Varieties | 22 | 168.92** | 868.42** | 512.17** | 2.48** | 4.67* | 5.29** | 522.81** |
| Env.+(Var.x Env.) | 115 | 51.62** | 8.71 | 74.93** | 1.66** | 4.42* | 1.71 | 184.72 |
| Environments | 5 | 868.06** | 15.24 | 1293.62** | 25.77** | 35.45** | 8.56** | 845.53** |
| Var.x Env. | 110 | 14.51 | 8.41 | 19.53 | 0.57 | 3.01 | 1.40 | 154.68 |
| Environments(Lin.) | 1 | 4340.31** | 76.20 | 6468.11** | 128.86** | 177.27** | 42.81** | 4227.68** |
| Var.x Env.(Lin.) | 22 | 18.42 | 4012 | 3.40 | 0.72 | 3.46 | 1.24 | 152.29 |
| Pooled Deviation | 92 | 12.94 | 9.07 | 22.54** | 0.50** | 2.77** | 1.38** | 148.53** |
| Pooled error | 132 | 0.66 | 3.39 | 8.69 | 0.23 | 0.96 | 0.87 | 65.71 |
| Total | 137 | 70.45 | 146.77 | 145.14 | 1.79 | 4.46 | 2.29 | 23.01 |

| Source of Variations | DF | X8 | X9 | X10 | X11 | X12 | X13 |
|----------------------|-----|-----------|----------|---------|--------------|--------------|---------|
| Rep within Evn. | 6 | 60.46 | 1.15 | 0.33 | 57622.57 | 139889.49 | 1.05 |
| Varieties | 22 | 563.92** | 11.93* | 10.48** | 3332866.56** | 2807513.59* | 42.77** |
| Env.+(Var.x Env.) | 115 | 157.35 | 7.37 | 1.92 | 296132.08* | 479592.10 | 4.89 |
| Environments | 5 | 694.63** | 23.30** | 4.67* | 1437879.31** | 1873335.65** | 3.32 |
| Var.x Env. | 110 | 132.93 | 6.65 | 1.79 | 244234.48 | 416240.12 | 4.96 |
| Environments(Lin.) | 1 | 3473.16** | 116.52** | 23.49** | 7189396.54** | 9366678.25** | 16.61 |
| Var.x Env.(Lin.) | 22 | 106.99 | 7.82 | 2.55* | 435198.69** | 631680.12* | 4.66 |
| Pooled Deviation | 92 | 133.35** | 6.08** | 1.53** | 18750.23* | 346624.47** | 4.82** |
| Pooled error | 132 | 66.17 | 0.50 | 0.26 | 124084.59 | 187533.05 | 2.39 |
| Total | 137 | 222.64 | 8.11 | 3.29 | 783782.87 | 853418.90 | 10.97 |

* & ** Significant at 5% and 1% respectively

Where,

| | | | |
|--------------------------|---------------------------------|---------------------------|-----------------------|
| X1 Days to 50% flowering | X5 Number of Tillers per plant | X9 Panicles fertility (%) | X13 Harvest index (%) |
| X2 Days to maturity | X6 Number of Productive tillers | X10 Test weight | |
| X3 Plant Height | X7 No. Of spikelets tillers | X11 Grain Yield (kg/ha) | |
| X4 Panicle Length | X8 No. Of grains per panicle | X12 Straw yield | |

Table.4 Mean and stability parameters in 23 advanced genotypes of Rice

| Sl. No. | Advanced breeding lines | Days to fifty per cent flowering | | | Days to maturity | | | Plant height (cm) | | | Panicle length (cm) | | | Number of tillers per plant | | | Number of productive tillers per plant | | | Number of spikelets per panicle | | |
|---------|-------------------------|----------------------------------|-------------------|-------|------------------|-------------------|--------|-------------------|-------------------|------|---------------------|-------------------|-------|-----------------------------|-------------------|-------|--|-------------------|-------|---------------------------------|-------------------|---------|
| | | Mean | S ² di | Bi | Mean | S ² di | bi | Mean | S ² di | bi | Mean | S ² di | bi | Mean | S ² di | bi | Mean | S ² di | bi | Mean | S ² di | bi |
| 1 | JB-1-11-7 | 96.83 | 1.61* | 1.14 | 125.58 | -1.74 | 0.31 | 67.08 | 19.20* | 0.77 | 19.28 | 0.24 | 0.15* | 19.21 | -0.62 | 0.91 | 19.21 | -0.62 | 0.91 | 161.92 | 864.08** | -0.90 |
| 2 | JB-1-20-2 | 97.33 | 10.99** | 1.14 | 128.33 | 2.73 | 0.96 | 77.66 | 12.65* | 1.00 | 19.58 | -0.08 | 0.83 | 18.67 | -0.61 | 1.20 | 18.67 | -0.61 | 1.20 | 169.58 | 17.25 | 0.80 |
| 3 | JB-1-22-1 | 96.83 | 27.02** | 1.07 | 127.08 | 4.84 | 0.78 | 82.44 | 6.05 | 1.06 | 19.59 | -0.18 | 1.06 | 18.24 | -0.16 | 2.17 | 18.24 | -0.16 | 2.17 | 162.25 | -31.93 | 0.86 |
| 4 | JB-1-22-2 | 93.92 | 41.45** | 1.00 | 125.92 | -1.53 | -0.87 | 82.67 | 2.45 | 0.90 | 19.38 | -0.20 | 0.79 | 18.08 | -0.21 | 1.79 | 18.08 | -0.21 | 1.79 | 163.17 | -38.36 | 0.55 |
| 5 | JB-1-22-3 | 96.25 | 8.15** | 1.14 | 126.75 | 8.60* | 3.19 | 83.91 | 0.91 | 1.06 | 20.32 | 0.65** | 1.03 | 18.78 | 1.22 | 0.99 | 18.78 | 1.22 | 0.99 | 174.67 | 45.20 | 1.15 |
| 6 | JK-1-7-5 | 95.50 | 0.65 | 1.40* | 126.92 | 14.01** | 2.15 | 80.89 | -3.71 | 1.15 | 19.37 | 0.14 | 1.01 | 19.33 | -0.79 | 1.54* | 19.33 | -0.79 | 1.54* | 163.50 | -37.32 | 1.17 |
| 7 | JK-1-11-8 | 94.75 | 13.74** | 1.37 | 125.92 | 0.80 | 1.75 | 81.68 | -4.17 | 1.11 | 19.00 | -0.02 | 0.87 | 18.73 | -0.17 | 1.55 | 18.73 | -0.17 | 1.55 | 171.00 | 94.29* | -0.35 |
| 8 | JK-1-12-1 | 95.00 | 7.75** | 1.30 | 126.67 | 3.18 | 1.48 | 81.29 | 3.51 | 1.04 | 19.72 | -0.10 | 0.98 | 18.98 | -0.51 | 0.93 | 18.98 | -0.51 | 0.93 | 165.50 | -20.01 | 1.77 |
| 9 | JK-1-13-1 | 96.67 | 11.30** | 1.28 | 127.67 | 7.61* | 2.58 | 79.91 | 4.02 | 0.98 | 19.37 | 0.20 | 1.26 | 19.13 | 1.66* | 1.79 | 19.13 | 1.66* | 1.79 | 170.33 | 112.46* | 1.05 |
| 10 | JK2-2-1-8-1 | 97.58 | 16.72** | 0.87 | 124.25 | 5.13 | 1.69 | 81.11 | 1.25 | 0.99 | 20.03 | -0.09 | 1.03 | 18.72 | -0.35 | 1.88 | 18.72 | -0.35 | 1.88 | 153.08 | 75.66 | 2.07 |
| 11 | JK2-1-12-1 | 98.58 | -0.47 | 0.94 | 126.33 | 14.17** | 3.10 | 78.59 | -3.55 | 1.17 | 19.62 | 0.68** | 0.63 | 20.00 | 0.04 | -0.70 | 20.00 | 0.04 | -0.70 | 154.67 | 58.46 | 1.19 |
| 12 | JA-4-1 | 99.83 | 7.46** | 0.81 | 120.42 | 0.73 | 1.50 | 84.12 | 5.95 | 0.86 | 19.95 | 0.02 | 1.05 | 18.95 | -0.23 | 1.31 | 18.95 | -0.23 | 1.31 | 159.67 | 13.48 | 0.20 |
| 13 | JA-4-2 | 93.25 | 22.77** | 1.33 | 118.42 | 2.52 | 0.49 | 81.18 | -5.31 | 0.90 | 20.12 | 0.66** | 1.46 | 19.88 | 0.09 | 0.70 | 19.88 | 0.09 | 0.70 | 162.92 | -6.79 | 1.73 |
| 14 | JA-4-3 | 95.67 | 9.55** | 1.00 | 118.75 | -0.08 | 1.08 | 80.87 | -2.02 | 0.94 | 19.70 | -0.17 | 1.36* | 19.58 | 1.50* | 0.55 | 19.58 | 1.50* | 0.55 | 162.83 | 17.08 | 2.16 |
| 15 | JA-6-2 | 92.58 | 4.91** | 0.47* | 118.58 | -2.68 | -0.89* | 82.58 | 0.08 | 0.84 | 20.45 | 0.74** | 0.61 | 21.10 | 1.99* | -1.03 | 21.10 | 1.99* | -1.03 | 178.33 | 28.69 | 0.89 |
| 16 | JA-6-3 | 95.17 | 7.29** | 0.68 | 119.17 | -2.11 | 0.53 | 80.38 | -5.70 | 1.01 | 19.34 | 0.50* | 0.99 | 19.40 | 0.61 | 0.64 | 19.40 | 0.61 | 0.64 | 163.50 | 271.68** | 0.67 |
| 17 | JA-6-4 | 96.92 | 19.00** | 0.05* | 120.17 | -2.56 | 0.72 | 82.15 | -0.27 | 1.01 | 20.59 | 0.62** | 1.62 | 18.84 | 0.04 | 2.05 | 18.84 | 0.04 | 2.05 | 165.08 | -13.86 | 1.48 |
| 18 | JT-2-15-1 | 102.75 | 11.46** | 1.22 | 149.67 | 14.60** | 0.18 | 100.85 | 36.12** | 1.08 | 20.16 | -0.08 | 1.06 | 19.88 | 3.63** | 1.42 | 19.88 | 3.63** | 1.42 | 162.58 | -30.54 | 0.12 |
| 19 | JT-2-16-1 | 100.92 | 9.70** | 0.84 | 149.08 | 22.75** | -0.64 | 107.89 | 71.88** | 0.95 | 20.69 | 1.75** | 1.85 | 19.23 | 1.06 | 0.15 | 19.23 | 1.06 | 0.15 | 155.67 | -52.95 | -0.26** |
| 20 | JT-2-22-5 | 98.83 | 6.71** | 0.87 | 149.67 | 18.33** | 0.23 | 102.12 | 102.80** | 1.07 | 19.77 | -0.05 | 0.96 | 20.31 | 3.21** | 0.26 | 20.31 | 3.21** | 0.26 | 166.58 | 302.55** | 1.26 |
| 21 | Jyothi | 96.83 | 8.63** | 1.21 | 132.17 | -3.16 | 0.19 | 78.16 | 19.08* | 0.94 | 17.62 | 0.33 | 0.97 | 16.50 | 0.86 | 0.78 | 16.50 | 0.86 | 0.78 | 135.67 | 103.70* | 2.98 |
| 22 | KHP-2 | 109.92 | 9.67** | 0.81 | 153.25 | 3.17 | 1.33 | 82.84 | 35.39** | 1.22 | 19.14 | 0.26 | 0.52 | 17.58 | 0.56 | 0.53 | 17.58 | 0.56 | 0.53 | 148.00 | 39.32 | 2.05 |
| 23 | Tunga | 116.00 | 26.21** | 1.06 | 155.67 | 11.29** | 1.14 | 98.78 | 26.14** | 0.97 | | | | 18.35 | -0.75 | 1.62 | 18.35 | -0.75 | 1.62 | 149.17 | 100.86* | 0.38 |
| | Mean | 98.17 | | | 130.28 | | | 84.31 | | | 19.66 | | | 19.04 | | | 19.04 | | | 161.72 | | |

Continued...

| Sl. No. | Advanced breeding lines | Number of grains per panicle | | | Panicle fertility (per cent) | | | Test weight (g) | | | Grain yield (kg/ha) | | | Straw yield (kg/ha) | | | Harvest index | | |
|---------|-------------------------|------------------------------|-------------------|---------|------------------------------|-------------------|--------|-----------------|-------------------|---------|---------------------|-------------------|---------|---------------------|-------------------|--------|---------------|-------------------|--------|
| | | Mean | S ² di | Bi | Mean | S ² di | bi | Mean | S ² di | bi | Mean | S ² di | bi | Mean | S ² di | bi | Mean | S ² di | bi |
| 1 | JB-1-11-7 | 144.83 | 455.18** | -0.60 | 89.90 | 9.23** | 2.87 | 30.74 | 0.29 | -0.05 | 6026.63 | -92232.61 | 0.83 | 7942.50 | 128655.11 | 2.46 | 43.24 | 0.82 | 2.50 |
| 2 | JB-1-20-2 | 153.95 | 46.69 | 0.38 | 90.78 | 8.69** | 1.42 | 30.06 | 5.85** | -0.28 | 6466.69 | 277102.89* | 0.44 | 8093.33 | 117713.20 | 1.96 | 44.44 | 10.26** | 3.89 |
| 3 | JB-1-22-1 | 145.16 | -42.84 | 0.65 | 89.51 | 12.11** | 0.29 | 31.52 | 0.62* | -0.55 | 6490.38 | -102165.83 | 0.30* | 8119.17 | 40851.44 | 1.31 | 44.48 | 1.34 | 0.14 |
| 4 | JB-1-22-2 | 147.37 | 1.08 | 0.10 | 90.27 | 6.78** | -0.29 | 29.61 | 0.80** | -0.15 | 6530.04 | 175040.21* | 0.22 | 8337.50 | 39571.17 | 1.97 | 43.95 | 8.49** | 4.90 |
| 5 | JB-1-22-3 | 156.19 | 124.66* | 1.36 | 89.28 | 10.81** | 0.50 | 29.81 | -0.08 | 2.64* | 6459.36 | 303364.99** | -0.43 | 8346.67 | 35105.38 | -0.06 | 43.60 | 2.95 | 5.66 |
| 6 | JK-1-7-5 | 147.33 | -31.59 | 0.87 | 90.13 | 6.05** | 2.15 | 29.62 | 0.20 | 2.66 | 6875.67 | 176756.09* | -0.43 | 8728.33 | -41520.19 | 0.57 | 44.04 | 1.63 | 1.98 |
| 7 | JK-1-11-8 | 152.93 | 240.29** | 0.09 | 89.24 | 9.04** | 1.56 | 29.75 | -0.11 | 1.68 | 6397.34 | -12557.51 | 1.24 | 8105.83 | 361806.04* | 2.23 | 44.24 | 1.83 | 2.38 |
| 8 | JK-1-12-1 | 144.50 | -54.80 | 1.35 | 87.41 | 6.65** | -0.99 | 30.64 | 0.04 | 1.35 | 6575.67 | 95776.87 | 1.26 | 8006.67 | 3470.32 | 0.70 | 45.11 | 1.76 | -0.25 |
| 9 | JK-1-13-1 | 155.08 | 80.27 | 0.96 | 91.02 | 0.07 | -0.48* | 29.69 | 0.16 | 2.68 | 6549.13 | 244994.25* | 1.54 | 8340.83 | -4518.89 | 0.70 | 43.90 | 0.95 | -0.81 |
| 10 | JK2-2-1-8-1 | 138.13 | 82.61 | 1.96 | 90.21 | 5.04** | 2.56 | 30.11 | 1.62** | 2.80 | 6352.49 | -26221.86 | 1.29 | 8435.00 | 135465.77 | -0.78 | 42.90 | 3.88* | 2.21 |
| 11 | JK2-1-12-1 | 140.82 | 10.61 | 1.02 | 91.10 | 3.63** | 1.93 | 29.88 | 0.26 | 0.24 | 6177.71 | 54428.55 | 0.61 | 7824.17 | -11295.77 | 0.23 | 44.09 | -0.49 | 1.27 |
| 12 | JA-4-1 | 145.70 | -6.66 | -0.02 | 91.23 | 1.23* | 0.87 | 28.42 | 0.05 | -1.32* | 6634.93 | -11067.75 | 0.46 | 8472.50 | -34684.04 | -0.12 | 43.91 | 1.10 | 0.85 |
| 13 | JA-4-2 | 146.95 | -32.34 | 2.22 | 90.11 | 1.77** | 1.46 | 30.27 | 2.23** | 1.42 | 6584.93 | -45167.91 | 0.63 | 8474.17 | -106266.60 | -0.35* | 43.73 | 0.51 | 2.29 |
| 14 | JA-4-3 | 148.17 | 19.85 | 2.21 | 90.94 | 0.46 | 1.76 | 30.93 | 1.24** | 0.79 | 6696.80 | 66107.04 | 0.21 | 8395.83 | -152853.91 | 0.34 | 44.36 | -0.30 | 1.81 |
| 15 | JA-6-2 | 167.83 | -4.39 | 1.12 | 94.12 | -0.18 | -0.09* | 30.76 | 0.05 | 0.08 | 6865.83 | -344.27 | 0.94 | 8599.17 | -143760.05 | 0.30 | 44.38 | -0.87 | 2.26 |
| 16 | JA-6-3 | 146.17 | 163.47** | 0.95 | 89.50 | 6.30** | 2.62 | 29.89 | 1.68** | 2.39 | 6477.90 | -69897.93 | 1.36 | 8460.00 | 276175.59* | 0.90 | 43.44 | 1.17 | 0.51 |
| 17 | JA-6-4 | 149.10 | -0.05 | 2.10 | 90.19 | 3.84** | 1.56 | 30.40 | 2.07** | 2.27 | 6456.39 | -2367.73 | 2.27 | 8963.33 | 9808.13 | 1.67 | 41.83 | 2.12 | 1.06 |
| 18 | JT-2-15-1 | 146.47 | 5.54 | 0.78 | 90.01 | 4.54** | 2.05 | 30.09 | 0.31 | 1.02 | 7059.60 | 242504.26* | 3.78 | 9891.67 | 848675.82** | 3.98 | 41.51 | 3.65* | 1.14 |
| 19 | JT-2-16-1 | 142.33 | -63.61 | -0.29** | 91.43 | 2.28** | -0.76 | 29.32 | 1.48** | -0.55 | 6827.72 | 248044.72* | 3.41 | 9737.50 | 547211.51** | 2.87 | 41.19 | 1.24 | 0.13 |
| 20 | JT-2-22-5 | 152.17 | 341.57** | 1.45 | 91.25 | 9.03** | 2.16 | 30.51 | 3.02** | -0.25 | 7177.53 | 110844.45 | 2.81 | 10135.83 | 651461.76** | 2.56 | 41.46 | 0.43 | -1.15 |
| 21 | Jyothi | 118.42 | 181.04** | 2.39 | 87.22 | 4.80** | 0.95 | 25.09 | -0.07 | -1.97** | 4093.06 | 52475.53 | 0.91 | 6994.17 | 50195.35 | 0.08 | 36.90 | 11.32** | 0.34 |
| 22 | KHP-2 | 132.73 | -49.05 | 1.55 | 89.94 | 12.96** | -1.42 | 27.37 | 6.20** | 1.56 | 4881.40 | -81675.58 | 0.53 | 8443.33 | 471340.13** | -0.06 | 36.72 | 2.48 | 4.27 |
| 23 | Tunga | 132.10 | 83.43 | 0.41 | 88.53 | 2.60** | 0.33 | 29.93 | 1.22** | 4.56* | 4788.67 | -68369.08 | -1.15** | 8680.83 | 484138.77** | -0.44 | 35.57 | 0.83 | -5.83* |
| | Mean | 145.84 | | | 90.14 | | | 29.76 | | | 6323.73 | | | 8501.23 | | | 42.69 | | |

The three advanced breeding lines JB-1-11-7 and JA-4-2 had more mean value for number of productive tillers per plant than population mean, also had regression coefficient value is around unity and very less deviation from regression. So, it is indicated that the genotype had stable performance across the environments. These findings are agreement with those of Vishnuvardhan *et al.*, (2015). JA-6-2 and JT-2-22-5, JA-6-2 and JT-2-22-5, JT-2-15-1, JB-1-22-3 and JK-1-7-5, JK2-1-12-1 and JK2-1-12-1 are identified as stable lines. The advanced breeding line JA-6-2 had more mean value for test weight than population mean also had regression coefficient value is around unity and less deviation from regression. So, it is indicated that this advanced breeding line had stable performance across the environments and less sensitive to environment it can adapt to the diverse environments. JA-6-4, JA-6-4, JA-4-2, JA-4-2, JB-1-20-2 and JA-4-2 are identified as stable lines for specific locations. This is on par with results of Deshpande *et al.*, (2003), Arumugam *et al.*, (2007), Panwar *et al.*, (2008), Ramya and Senthilkumar (2008) and Krishnappa *et al.*, (2009). Among twenty advanced breeding lines including checks line JA-6-2 had more mean value than population mean also had regression coefficient value is around unity and less deviation from regression. Therefore, it is indicated that this advanced breeding line had stable performance across the environments and it can adapt to the diverse environments. Hence, it can be used as stable line adopted across the environments and could be released for large scale trials. JT-2-16-1, JT-2-22-5, JA-4-3, JT-2-15-1, JB-1-20-2 and JK-1-7-5 are identified as suitable lines for specific locations. These results are also reported by Mall *et al.*, (2013). The advanced breeding line JK-1-7-5 had more mean value for straw yield per hectare than population mean also had regression coefficient value is around unity and less deviation from regression. So,

it is indicated that the advanced breeding line had stable performance across the environments and less sensitive to environment it can adapt to the diverse environments. JT-2-22-5, JT-2-15-1, Tunga, JT-2-15-1, JT-2-15-1 and JT-2-22-5 are identified as stable lines for specific locations. These findings are in conformity with Patil *et al.*, (2013). High mean value than the population mean, regression coefficient around unity and least deviation from regression were recorded for harvest index in the advanced breeding line JA-4-1 indicating that their stability over wide range of environment. JK2-2-1-8-1, JK-1-12-1, JA-6-3, JB-1-22-2, JA-4-1 and JB-1-20-2 are identified as stable lines for specific locations. (Gourishankar *et al.*, (2008), Ramya and Senthilkumar (2008) and Krishnappa *et al.*, (2009)).

Different measures of stability have been used by various workers earlier, Finlay and Wilkinson (1963) considered linear regression slopes as a measure of stability. Eberhart and Russel (1966) emphasized the need of considering both linear and nonlinear component of Genotype x Environment interaction in judging the stability of genotypes. Later Breese (1969); Samuel *et al.*, (1970); Paroda and Hayes (1971) and Jatasra and Paroda (1978) emphasized that the linear regression could simply be regarded as a measure of response of a particular genotype whereas deviation around the regression line was the most suitable measure of stability. In the present study the stability was assessed by the parameters suggested by Eberhart and Russel (1966).

The term stable genotype has been used for the average performance in all environments. Hence, such a stable variety has a high mean, unit regression and a minimum deviation from regression. From the present study it is concluded that genotypes JA-6-2 was found

to be a stable across the environments and this genotype can also be used as a donor parent for generating new breeding material for development of variety with good stability for irrigated conditions. However, this needs to be verified by testing the breeding lines over the season and over the locations for one more year under rain fed condition.

References

- Amrithadevarathinam, A., 1987, Stability analysis of some released varieties and local cultivars in dry and semidry condition. *Madras Agric. J.*, 24 (10-11): 434-439.
- Anonymus, 2016, FAO data, <http://faostat.fao.org/>.
- Arumugam, M., M. P. Rajenna and B. Vidyachandra., 2007, Stability of rice genotypes for yield and yield components over extended dates of sowing under Cauvery command area in Karnataka. *Oryza.*, 44:104-107.
- Basavaraj, D.M., 1994, Stability analysis of promising genotypes of low land rice of hill zone of Karnataka. *M.Sc (Agri) Thesis* submitted to Univ. Agric. Sci., Bangalore. 58-75.
- Deshpande, V. N., Dalvi, V. V., Awadoot, G. S., and Desai, S. B. 2003, Stability analysis in hybrid rice. *J. Maharashtra Agri Univ.*, 28 (1): 87-88.
- Eberhart, S.A., and Russell, W.A. 1966, Stability parameters for comparing varieties. *Crop Sci.*, 6 (1): 36-40.
- Ganesh, S. K., and Soundarapandian, G., 1987, Association studies for stability parameters in short duration varieties of rice (*Oryza sativa* L.). *Madras Agric.J.*, 74: 208-212.
- Gourishankar, V., Ansari, N. A., and Ilyas A., 2008, Stability analysis using thermo-sensitive genic male sterility (TGMS) system in rice (*Oryza sativa* L.). *Res. on Crops*, 9 (1): 141-146.
- Kang, M.S., & Martin, F. A. 1987, A review of important aspect of genotype-environmental interactions and practical suggestions for sugarcane breeders. *J. of American Soci.of Sugarcane Techn.*, 7: 36-38.
- Karnataka. *Crop Res.*, 38:141-143.
- Koli, N. R., Bagri, R.K., Kumhar, B. L., Chandra, P., Mahawar, R. K. and Punia, S. S., 2015, Assessment of stability performance in scented rice genotypes under transplanted condition of south-eastern plain zone of Rajasthan. *Electronic J. Plant Breed*, 6 (4): 992-995.
- Krishnaappa, M. R., Chandrappa, H. M. and Shadakshari. H. G., 2009, Stability analysis of medium duration hill zone rice genotypes of Karnataka. *Crop Res.*, 38:141-143.
- Mahapatra, K.C. and Sujathadas, 1999, Stability of yield in relation to component traits in rice. *Oryza*, 36: 301-305.
- Mall, A. K., Swain, P., Singh, O. N. and Baig, M. J., 2013, Use of Genotype x Environment Interactions and Drought Susceptibility Index for Identification of Drought Tolerant Genotypes at Vegetative Stage in Upland Rice. *Indian J. Dryland Agric. Res Development*, 27: 73-78.
- Maurya, D.M. and Singh, D.P., 1977, Adaptability in rice. *Indian J. Genet.*, 37:403-410.
- Panwar, L. L., Joshi, V. N. and Ali, M., 2008, Genotype x environment interaction in scented rice. *Int J. Rice.*, 45 (2):103-109.
- Patil, A. B., Desai, R. T., Patil, S. A., chougule, Girish. R. and Shinde, D. A., 2013, Stability Analysis for Grain Yield and Its Component Traits in Rice (*Oryza sativa* L.). *Trends in Biosciences.*, 6 (3):281-287.

- Praveen, S., Anil, P., and Rajesh, K., 2013, Stability study in aromatic rice (*Oryza sativa* L.). *Crop Res.*, 45 (1-3):59-65.
- Ramya, K. and Senthilkumar, N., 2008, Genotype x environment interaction for yield and its component traits in rice (*Oryza sativa* L.). *Crop Improvement.*, 35 (1): 11-15).
- Sawant, D. S., Kunkerkar, R. L., Shetye, V. N. and Shirdhankar, M. M., 2005, Stability assessment in late duration rice hybrids. In National seminar on “*Rice and Rice Based Systems for Sustainable Productivity, Extended summaries.*”, ICAR Research Complex for Goa”, 18-19th October. 75- 76.
- Shrestha SP, Asch F, Dusserre J, Ramanantsoanirine A, Brueck H, 2012, Climate effects on yield components as affected by genotypic responses to variable environmental conditions in upland rice systems at different altitudes. *Field Crops Res*, 134:216-228.
- Singh, S. P., and Shukla, S., 2001, Stability parameters for opium and seed yield in opium poppy (*Papaver somniferum* L.). *Indian J. Agril. Sci.*, 71:313-315.
- Song, X.J., Huang, W., Shim, Z. M. and Lin, H. 2007, A QTL for rice grain width and weight encodes a previously unknown RING- type E3 Ubiquitin ligase. *Nat Genet.* 3(9): 623–630.
- Subramanya, H., 1996, *Stability analysis in rice (Oryza sativa L.) hybrids.* *M.Sc (Agri) Thesis* submitted to Univ. Agric. Sci., Bangalore. 48-103.
- Umadevi, M., Veerabadhiran, P. and Manonmani, S., 2008, Stability Analysis for Grain Yield and its Component Traits in Rice (*Oryza sativa* L.). *J. Rice Res.*, 3 (1): 10-12.
- Vanave, P. B., Apte, U. B., Kadam, S. R. and Thaware, B. L., 2014, Stability analysis for straw and grain yield in rice (*Oryza sativa* L.). *Electronic J. Plant Breed.*, 5: 442-444.
- Vishnuvardhan, B. R., Payasi, K., Devendra and Anwar, Y., 2015, Stability analysis for yield and its components in promising rice hybrids. *Int Quarterly J. Envir sci.*, 9 (1-2): 311-321.
- Yan W., Hunt, L. A., Sheng, Q., & Szlavnic, Z. (2000). Cultivar evaluation and mega environment investigation based on the GGE biplot. *Crop Sci.*, 40(3):597–605.

How to cite this article:

Manjunatha B., C. Malleshappa and Niranjana Kumara B. 2018. Stability Analysis for Yield and Yield Attributing Traits in Rice (*Oryza sativa* L.). *Int.J.Curr.Microbiol.App.Sci.* 7(06): 1629-1638. doi: <https://doi.org/10.20546/ijcmas.2018.706.194>

See discussions, stats, and author profiles for this publication at: <https://www.researchgate.net/publication/329058866>

Performance Evaluation of Maize Hybrids (Zea mays L.)

Article in International Journal of Current Microbiology and Applied Sciences · November 2018

DOI: 10.20546/ijcmas.2018.711.139

CITATIONS

2

READS

927

3 authors, including:



B. Manjunatha

University of Agricultural & Horticultural

9 PUBLICATIONS 8 CITATIONS

SEE PROFILE



Dr Niranjana Kumara

The Trans-disciplinary University

23 PUBLICATIONS 27 CITATIONS

SEE PROFILE

Some of the authors of this publication are also working on these related projects:



AICRP on Rice [View project](#)

Original Research Article

<https://doi.org/10.20546/ijcmas.2018.711.139>

Performance Evaluation of Maize Hybrids (*Zea mays* L.)

B. Manjunatha*, B. Niranjana Kumara and G.B. Jagadeesh

Agricultural and Horticultural Research Station, Kathalagere, University of Agricultural and Horticultural Sciences, Shivamogga, Karnataka, India

*Corresponding author

ABSTRACT

Keywords

Heritability, Hybrids,
Genetic advance,
Correlation, PCV, GCV

Article Info

Accepted:

10 October 2018

Available Online:

10 November 2018

The study was conducted to evaluate the performance of 100 maize hybrids and to assess the association between yield and yield component traits of maize hybrids. The Experiment was carried out in randomized complete block designs (RCBD) with three replications in 2017 main cropping season. The analysis of variance revealed significant differences between hybrids for all measured parameters. The highest and lowest grain yield were recorded for VH132059 (11.11ton/ha) and VH141651 (6.06 ton/ha) respectively. Among the Hybrids VH15471 and VH15884 were early maturing varieties, while VH11153 and VH112944 are late maturing hybrids. Higher phenotypic coefficient of variation (PCV) and Genotypic coefficient of variation (GCV) were recorded for the traits plant aspect, ear aspect, number of cobs per plant and grain yield. High heritability and high genetic advance were recorded for plant height, number of grain per row and cob length VH132059 and VH11128 are good performed hybrids.

Introduction

Maize (*Zea mays* L.) is the third most important cereal crop after wheat and rice. Improving maize production is considered to be one of the most important strategies for food security in the developing countries (Iqbal *et al.*, 2001). Maize grain today is recognized worldwide as a strategic food and feed crop that provides an enormous amount of protein and energy for humans and livestock (FAOSTAT, 2008).

Maize production in the area suffers much from low fertility, low management, lack of improved varieties, and very severe infections of foliar diseases like turcicum leaf blight,

high infestations of striga and stalk borers (Assefa, 1998). As a result, evaluating the performance of hybrid maize genotypes in specific agro ecology on different traits is very crucial. Maize improvement in India started an century ago and several promising hybrids and composite varieties were introduced and evaluated at different locations (Benti *et al.*, 1997).

However, the changing environmental conditions affect the performance of maize genotypes which requires a breeding program that needs to take into account the consequences of environment and genotype interaction in the selection and release of improved varieties. Hence, the overall

objectives of this study were to evaluate the performance of the tested hybrid maize and to identify superior maize germplasms for better productivity to maize growers.

Materials and Methods

The experiment was laid out in a randomized complete block design (RCBD) with three replications composed of 100 hybrids (Table 1) conducted under rain fed condition during 2016 in *kharif* season at Agricultural and Horticultural Research Station, Kathalagere, Davangere district under University of Agricultural and Horticultural Sciences, Shivamogga, Karnataka.

Each plot comprised of 5.1m long with the spacing of 0.60m between rows and 0.30m between plants. Two seeds were planted per hill and later thinned out to one healthy plant. The recommended fertilizer dose (urea@150 kg/ha and DAP@150 kg/ha) was used. DAP fertilizer was applied once at planting while urea was applied twice equally at planting and at knee height stage of the crop. All other management practices were uniformly applied to all experimental plots as per package of practice.

Data were recorded on plot and plant basis for the following characteristics; days to 50% anthesis, days to 50% silk emergence, days to maturity, grain yield, plant height, ear height and number of cobs/plant.

Analysis of variance (ANOVA) was done by using INDOSTAT software. The phenotypic and genotypic coefficients of variation were estimated according to the method suggested by Burton and De Vane (1953).

Broad sense heritability (h^2) expressed as the percentage of the ratio of the genotypic variance to the phenotypic variance as described by Allard (1960).

Results and Discussion

Analysis of variance

The results of analysis of variance (ANOVA) of the quantitative traits of the tested genotypes are presented in (Table 2). The analysis of variance result showed that there were considerable amount of variation between the tested hybrids. Results showed highly significant variation ($p < 0.01$) for days to 50% anthesis, days to 50% silking, days to 50% maturity, plant height, plant aspect, cob weight, cob length and number of grains per row and significant variation ($p < 0.05$) for ear height, ear aspect, number of cobs per plant, grain yield. This result is in agreement with the findings of Soza *et al.*, (1996); Sallah *et al.*, (2001); Ram Reddy *et al.*, (2013). Maximum grain yield (11.11 ton/ha) was observed for VH132059 whereas the minimum grain yield (6.06 ton/ha) was recorded for VH141651 (Table 2).

Phenotypic and genotypic variation

The phenotypic variance was separated into genotypic and environmental variances to estimate the contribution of each to the total variation. The minimum (0.2) and maximum (50.9) percentages of phenotypic coefficient of variation (PCV) were observed for plant height and number of diseased cobs, respectively.

The PCV values for number of diseased cobs and ear height were high. It indicates on these traits the phenotypic difference between the tasted genotypes is high. PCV values for number of cobs per plant, cob weight and number of grains per row, stand count at harvest and cob length were medium. It indicates the phenotypic difference between the tested maize genotypes with the above traits is moderate (Bello *et al.*, 2012; Golam *et al.*, 2014). Days to maturing, plant height,

days to anthesis, days to silking and grain yield had low PCV values (Ram Reddy *et al.*, 2012). Low PCV observed for days to maturing, plant height, days to anthesis and days to silking. Genotypic coefficient of variation measures the genetic variability with in a character. The extent of the environmental influence on any character is indicated by the magnitude of the differences between the genotypic and phenotypic coefficients of variation. Large differences reflect high environmental influence, while small differences reveal that the influence of environment on the genetic variance is low (Manjunatha *et al.*, 2018). The small difference between PCV and GCV of these traits indicated the possibility of genetic improvement of the traits. Genotypic coefficients of variability (GCV) values were low for days to maturing, days to anthesis and days to silking. Medium GCV was observed for plant height, ear height, number of cobs per plant, number of grain per row, cob weight (Golam *et al.*, 2014).

Higher PCV and GCV were recorded for the traits number of cobs per plant, grain yield and number of diseased cobs. It shows that the selection can be effective for these traits and also indicated the existence of substantial variability, ensuring ample scope for their improvement through selection. From this result by selecting the genotype with higher number of cobs per plant, better grain yield and less number of diseased cobs can improve the grain yield of maize.

The difference between PCV with the corresponding GCV values was relatively higher for plant height, ear aspect and grain yield, indicating the higher influence of the environment on the traits. However, this difference was comparatively low for days to anthesis, days to silking, days to maturing, number of grain per row, stand count at harvest and cob length. The small difference

indicating that there is a minimal influence of environment on the expression of these traits. In addition, it indicates the presence of sufficient genetic variability for observed traits may facilitate the selection process. Therefore, selection based on phenotypic performance of the traits would be effective to bring considerable improvement in these traits.

Heritability and genetic advance

Heritability is the proportion of genetic variance and phenotypic variance. It is a major parameter for the selection of superior population improvement method. Knowledge about heritability of quantitative traits of a crop plant is of extreme interest to plant breeders. The heritability estimates detected for the characters studied ranged between 39.7% for number of cobs per plant to 98.9% for date of anthesis. High levels of heritability were estimated for days to anthesis, days to silking, days to maturing, plant height, number of grains per row, stand count at harvest and cob length (Beyene, 2005); Muhammad (2009) for days to anthesis and number of grains per row Sarlangue *et al.*, (2007).

High heritability of the above traits indicated that influence of environment on these characters is negligible or low. Therefore, selection can be effective on the basis of phenotypic expression of these traits in the individual plant by implementing simple selection methods. Medium heritability was recorded for ear height, number of cob per plant, cob weight, grain yield. The moderate levels of heritability indicated that this trait was moderately influenced by environmental factors (Lorenzana and Bernardo, 2008). Genetic advance under selection (GA) refers to the improvement of traits in genotypic value for the new population compared with the base population less than one cycle of population at a given intensity (Singh, 2001).

Table.1 List of hybrids

| | | | | | |
|----|----------|----------|-----|------------|---------------------|
| 1 | VH131306 | VH131306 | 51 | VH112744 | VH112744 |
| 2 | VH133273 | VH133273 | 52 | VH141640 | VH141640 |
| 3 | VH141552 | VH141552 | 53 | VH121082 | VH121082 |
| 4 | VH125 | VH125 | 54 | VH11128 | VH11128 |
| 5 | VH11431 | VH11431 | 55 | ZH112035 | ZH112035 |
| 6 | VH11301 | VH11301 | 56 | VH123389 | VH123389 |
| 7 | VH11441 | VH11441 | 57 | VH141651 | VH141651 |
| 8 | VH113012 | VH113012 | 58 | VH123061 | VH123061 |
| 9 | VH13296 | VH13296 | 59 | VH12328 | VH12328 |
| 10 | VH13305 | VH13305 | 60 | VH13554 | VH13554 |
| 11 | VH13306 | VH13306 | 61 | VH141682 | VH141682 |
| 12 | VH13700 | VH13700 | 62 | VH15911 | VH15911 |
| 13 | VH13729 | VH13729 | 63 | ZH115995 | ZH115995 |
| 14 | VH13740 | VH13740 | 64 | KH141554 | KH141554 |
| 15 | VH112888 | VH112888 | 65 | VH16161 | VH16161 |
| 16 | VH11131 | VH11131 | 66 | VH122850 | VH122850 |
| 17 | VH11153 | VH11153 | 67 | VH131199 | VH131199 |
| 18 | VH112944 | VH112944 | 68 | VH123031 | VH123031 |
| 19 | VH11134 | VH11134 | 69 | VH11812 | VH11812 |
| 20 | VH13917 | VH13917 | 70 | VH131376 | VH131376 |
| 21 | VH1640 | VH1640 | 71 | VH133765 | VH133765 |
| 22 | VH132079 | VH132079 | 72 | VH153409 | NK30 |
| 23 | VH132059 | VH132059 | 73 | VH153410 | Swarna |
| 24 | VH151139 | VH151139 | 74 | VH153411 | Mukta |
| 25 | VH132169 | VH132169 | 75 | VP15297 | African tall |
| 26 | VH16100 | VH16100 | 76 | TA5024 | TA5024 |
| 27 | VH123015 | VH123015 | 77 | TA5104 | TA5104 |
| 28 | VH1230 | VH1230 | 78 | TA5114 | TA5114 |
| 29 | VH161055 | VH161055 | 79 | TA5144 | TA5144 |
| 30 | VH15471 | VH15471 | 80 | TA5084 | TA5084 |
| 31 | VH15496 | VH15496 | 81 | VH112651 | NK6240 |
| 32 | VH132461 | VH132461 | 82 | VH112649 | 900MGold |
| 33 | VH1652 | VH1652 | 83 | VH131025 | DKC8101 |
| 34 | VH15884 | VH15884 | 84 | VH112667 | 30V92 |
| 35 | VH1660 | VH1660 | 85 | VH153412 | D2244 |
| 36 | VH15537 | VH15537 | 86 | VH112655 | HTMH5101 |
| 37 | VH141618 | VH141618 | 87 | VH131019 | P3396 |
| 38 | VH112972 | VH112972 | 88 | 31Y45 | 31Y45 |
| 39 | VH11150 | VH11150 | 89 | VH151758 | Pratap QPM Hybrid-1 |
| 40 | VH11138 | VH11138 | 90 | AH1223 | 9108 |
| 41 | VH1253 | VH1253 | 91 | DHM121 | DHM121 |
| 42 | VH12264 | VH12264 | 92 | WIN Orange | WIN Orange |
| 43 | VH11130 | VH11130 | 93 | Hema | Hema |
| 44 | VH112906 | VH112906 | 94 | VH171212 | Ravi-81 |
| 45 | VH113027 | VH113027 | 95 | VP1760 | Pant Sankar Makka-3 |
| 46 | VH12241 | VH12241 | 96 | VH171213 | P3502 |
| 47 | VH151280 | VH151280 | 97 | VH171214 | HTMH5106 |
| 48 | VH131026 | VH131026 | 98 | VH171215 | DKC9144 |
| 49 | VH141229 | VH141229 | 99 | VH171254 | Shaktiman-4 |
| 50 | VH112740 | VH112740 | 100 | VH151757 | Shaktiman-5 |

Table.2 Estimates of range, mean and genetic parameters on the tested maize hybrids

| | Grain yield | Days to Anthesis | Days to Silking | Plant height | Ear height | Ear position | Lodging root | Cobs/plant |
|---------------------|-------------|------------------|-----------------|--------------|------------|--------------|--------------|------------|
| Mean | 8.17 | 51.3 | 54.9 | 260.8 | 107.4 | 0.42 | 2.9 | 1.10 |
| Min | 3.74 | 45.1 | 49.4 | 196.6 | 77.3 | 0.32 | -1.4 | 0.65 |
| Max | 12.14 | 56.7 | 59.7 | 294.2 | 136.6 | 0.52 | 70.8 | 1.63 |
| Lower Limit | 0.00 | 50.0 | 50.0 | 30.0 | 30.0 | 0.10 | 0.0 | 0.00 |
| Upper Limit | 15.00 | 110.0 | 110.0 | 250.0 | 200.0 | 0.70 | 101.0 | 3.00 |
| Phenotypic Variance | 1.76 | 10.3 | 9.2 | 324.5 | 140.4 | 0.00 | 73.9 | 0.02 |
| Error Variance | 0.62 | 3.7 | 3.2 | 138.4 | 79.4 | 0.00 | 17.5 | 0.01 |
| Genotypic Variance | 1.14 | 6.5 | 6.0 | 186.1 | 61.0 | 0.00 | 56.4 | 0.01 |
| Heritability | 0.65 | 0.6 | 0.7 | 0.6 | 0.4 | 0.15 | 0.8 | 0.66 |

The genetic advance as percent of mean (GA%) was high for plant height, ear height, plant aspect, ear aspect, cob weight, number of grains per row, stand count at harvest, grain yield, number of diseased cob and cob length (Emmanuel, 2013). Genetic advance as percent of mean was moderate for days to 50% anthesis, days to 50% silking and number of cobs per plant. Genetic advance as percent of mean was low for days to 50% maturity (Badu *et al.*, 2012).

In view of the fact that, high heritability does not always indicate a high genetic gain, heritability should be used together with genetic advance in predicting the ultimate effect for selecting superior varieties. In this study, high heritability and high genetic advance were recorded for plant height number of grains per row, stand count at harvest and cob length which could be considered as essential traits for maize improvement by selection (Bello *et al.*, 2012).

The study showed variation for almost all the traits studied among the tested hybrids, which is an indication of the presence of sufficient variability and can be exploited through selection. The significant difference in grain yield and other agronomic traits among various hybrids were probably due to diverse back

ground from which the hybrids were developed. VH132059 and VH11128 were shown higher grain yield compared to others. Consequently, these hybrids can be a preferable choice for further crop improvement. The higher grain yield of the above genotypes could be correlated to the higher number of grain per row and cob weight. Among the tested hybrids VH15471 and VH15884 are early maturing, while VH11153 and VH112944 are late maturing varieties.

Acknowledgement

The authors are highly acknowledged to CIMMYT, Global maize programme, Hyderabad for providing materials for testing in our station.

References

- Allard RW (1960). Principles of Plant Breeding. John Willy and Sons Inc., USA.
- Annapura D, Khan HA, Mohammad S (1998). Genotypic phenotypic Correlations and path coefficient analysis between seed yield and other associated characters in tall genotypes of maize. Crop Research 16: 205-9.
- Assefa T (1998). Survey of maize diseases in western and north- western Ethiopia. In

- the sixth Eastern and Southern Africa Regional Maize Conference, CIMMYT. Addis Ababa, Ethiopia. pp. 121-124.
- Badu AB, Fakorede MAB, Menkir A, Sanogo D. Editors (2012). Conduct and management of maize field trials. IITA, Ibadan, Nigeria. 59 pp.
- Bello OB, Ige SA, Azeez MA, Afolabi MS, Abdulmalik SY, Mahamood J (2012). Heritability and Genetic Advance for Grain Yield and its Component Characters in Maize (*Zea mays* L.). *IJPR*, 2(5): 138-145.
- Benti, T, K Mulata, W Olde L, W Olku M, Tulu L (1997). Reflections on the successful achievements of hybrid maize breeding program in Ethiopia. In: Ransom (ed.). Maize Productivity gains through research and technology dissemination. Fifth Eastern and Southern Africa Regional Maize Conference Arusha Tanzania. CIMMYT, Addis Ababa, Ethiopia.
- Beyene YA (2005). Phenotypic diversity of morphological and agronomical traits in traditional Ethiopian highland maize accessions. *South African J. Plant and Soil*. 22:100-105.
- Burton GW, De vane EH (1953). Estimating heritability in Tall Fescue (*Festuca arundinacea*) from replicated clonal material. *Agronomy Journal*. 45: 481-487.
- Daniel T (2014). Evaluation of Improved Maize Genotypes for Grain Yield and Yield Components in Chilga District, North Western Ethiopia. *IJSR*: 2319-7064.
- Gardeah Vah E (2013). Evaluation of maize top cross hybrids for grain yield and associated traits: 82.
- FAOSTAT, (2008). Monitoring and Assessment of Greenhouse Gas Emissions and Mitigation Potential in Agriculture (MAGHG)
- GolamMd A, Umakanta SM, Bhagya RB (2014). Genetic variability of yield and its contributing characters on CIMMYT maize in breders under drought stress. *Bangladesh J. Agril. Res.* 39(3): 419-426.
- Iqbal, M., M. Saleem and O. Rashid (2001). Inter-racial heterosis in maize hybrids. *Pak. J. Sci. Indus. Res.*, 44: 239-243.
- Johnson HW, Robinson HF, Comstock RE (1955). Estimates of genetic and environmental variability in soybeans. *Agronomy Journal*, 47: 314-318.
- Lorenzana RE, Bernardo R (2008). Genetic correlation between corn performance in organic and conventional production systems. *Crop Sci.* 48: 903-910.
- Manivannan NA (1998). Character association and components analysis in maize. *Madras Journal of Agriculture* 85:293-294.
- Manjunatha B and Niranjana Kumara B (2018), Variability Studies in Advanced Genotypes of Rice (*Oryza sativa* L.), *Trends in Biosciences* 10(41), 8707-8708.
- Muhammad I (2009). Genetic analysis of maturity and yield attributes in subtropical maize. Department of plant breeding and genetics faculty of crop production sciences agricultural university, Peshawar Pakistan. 112 – 113.
- Ram Reddy, Farzana Jabeen, Sudarshan MR, Seshagiri Rao A (2012). Studies on genetic variability, heritability, correlation and path Analysis in maize (*Zea mays* L.) Over locations. *IJABPT*, 4: 0976- 4550.

How to cite this article:

Manjunatha, B., B. Niranjana Kumara and Jagadeesh, G.B. 2018. Performance Evaluation of Maize Hybrids (*Zea mays* L.). *Int.J.Curr.Microbiol.App.Sci*. 7(11): 1198-1203.
doi: <https://doi.org/10.20546/ijcmas.2018.711.139>

**Cookies on
CAB Direct**

Like most websites we use cookies. This is to ensure that we give you the best experience possible.

Continuing to use www.cabdirect.org means you agree to our use of cookies. If you would like to, you can learn more about the cookies we use.

Close

Find out more (<http://www.cabi.org/cookie-information/>)[Home \(/cabdirect\)](#)[Other CABI sites ▼](#)[About \(/cabdirect/about\)](#)[Help](#)[Mobile](#)[Instant Access \(/cabdirect/instant-access\)](#)[Login](#)

(/cabdirect)

CAB DirectSearch: [Keyword](#) [Advanced](#) [Browse all content](#) [Thesaurus](#) [\[?\] \(http://www.cabi.org/cabthesaurus/\)](http://www.cabi.org/cabthesaurus/)[clear search \(/cabdirect/search/?search-directive=clear-search\)](#)

Enter keyword search

[Search](#)[Search \(/cabdirect/search/\)](#)

Actions



Tools



Genetic variability, path analysis, character association for yield and its attributing traits in F₂ population of cross BPT-5204 × IET-21214 in rice (*Oryza sativa* L.).

Author(s) : [Pradeep, P. \(/cabdirect/search/?q=au%3a%22Pradeep%2c+P.%22\)](#); [Malleshappa, C. \(/cabdirect/search/?q=au%3a%22Malleshappa%2c+C.%22\)](#); [Manjunatha, B. \(/cabdirect/search/?q=au%3a%22Manjunatha%2c+B.%22\)](#); [Kumara, B. N. \(/cabdirect/search/?q=au%3a%22Kumara%2c+B.+N.%22\)](#); [Harish, D. \(/cabdirect/search/?q=au%3a%22Harish%2c+D.%22\)](#)

Author Affiliation : Department of Genetics and Plant Breeding College of Agriculture, University of Agricultural and Horticultural Sciences, Shivamogga, India.

Author Email : manjugpb@gmail.com (<mailto:manjugpb@gmail.com>)

Journal article : [Environment and Ecology \(/cabdirect/search/?q=do%3a%22Environment+and+Ecology%22\)](#), 2018 Vol.36 No.2 pp.437-442 ref.11

Abstract : The present investigation in rice (*Oryza sativa* L.) was undertaken during *kharif*, 2015 to study variability parameters, character association and path analysis and identification of transgressive segregants in respect of grain yield and its component traits in F₂ population of BPT5204 × IET21214 crosses. The distribution pattern of F₂ populations indicated large number of genes with dominance based complementary interaction in the inheritance of total tillers per plant, number of panicles per plant, number of grains per panicle, grain yield per plant and L:B ratio in both crosses but duplicate type of interaction was noticed for days to 50% flowering, panicle length, number of spikelets per panicle, spikelets fertility, test weight, grain length and grain breadth, panicle length and harvest index in BPT5204 × IET21214. GCV and PCV values were relatively higher with high heritability coupled with high genetic advance for total tillers per plant, productive tillers per plant and grains per panicle and grain yield per plant in both the crosses indicating additive gene action in their genetic control. Grain yield per plant was exhibited significant positive correlation with plant height, total tillers per plant, number of panicles per plant, panicle length, number of spikelets per panicle, number of grains per plant and spikelets. Path analysis in F₂ generation of indicated the positive direct effect of total tillers per plant, number of panicles per plant, grains per panicle and panicle length and harvest index on grain yield.

ISSN : [0970-0420 \(/cabdirect/search/?q=sn%3a%220970-0420%22\)](#)

URL : <http://www.environmentandecology.com/> (<http://www.environmentandecology.com/>)

Record Number : 20183128922

Publisher : [MKK Publication \(/cabdirect/search/?q=pb%3a%22MKK+Publication%22\)](#)

Location of publication : [Kolkata \(/cabdirect/search/?q=lp%3a%22Kolkata%22\)](#)

Country of publication : [India \(/cabdirect/search/?q=cp%3a%22India%22\)](#)

Language of text : [English \(/cabdirect/search/?q=la%3a%22English%22\)](#)

Indexing terms for this abstract:

Organism descriptor(s) : *Oryza sativa*

Explore similar records

[Genetic variability, correlation and path... \(/cabdirect/abstract/20183035357\)](#)

[Correlation and path coefficient analysis of... \(/cabdirect/abstract/20173014882\)](#)

[Correlation and path analysis in Vandana ×... \(/cabdirect/abstract/20093238917\)](#)

[Selection indices for identification of... \(/cabdirect/abstract/20203173938\)](#)

[Evaluation of nature and magnitude of gene... \(/cabdirect/abstract/20173244177\)](#)

[Study of combining ability using CMS line in... \(/cabdirect/abstract/20183199593\)](#)

[Show all similar records \(/cabdirect/search/?q=similar:20183128922\)](#)

Search or refine using Index terms :



Show indexing terms:

Organism Descriptors : (1)**Descriptors** : (15)**Identifiers** : (5)**Broad Terms** : (14)**Geographic Location** : (2)

Other sources of full text :



View PDF

[Download full issue](#)

Beni-Suef University Journal of Basic and Applied Sciences

Volume 7, Issue 4, December 2018, Pages 719-723

Full Length Article

In vitro and *in vivo* evaluation of anti-inflammatory potency of *Mesua ferrea*, *Saraca asoca*, *Viscum album* & *Anthocephalus cadamba* in murine macrophages raw 264.7 cell lines and Wistar albino rats

Syed Murthuza, B.K. Manjunatha

[Show more](#) [Outline](#) | [Share](#) [Cite](#) <https://doi.org/10.1016/j.bjbas.2018.10.001>[Get rights and content](#)Under a Creative Commons [license](#)[open access](#)

Highlights

- Present paper reports antiinflammatory efficacy of *Mesua ferrea*, *Viscum album*, *Saraca asoca* and *Anthocephalus cadamba* using *In vitro* and *in vivo* methods. For *in vitro* LPS-activated murine macrophage RAW 264.7 cell lines were used, Carrageenan-induced paw edema model in Wistar albino rats models was used for *In vivo* study.
- Results of the study provide scientific validation for ethnomedicinal claims of the selected plants.
- Further studies on bioactive compound isolation and its pharmacological profiling is in progress.

Abstract

The present study reports the *in-vitro* and *in-vivo* anti-inflammatory potency of *Mesua ferrea*, *Saraca asoca*, *Viscum album* and *Anthocephalus cadamba*, potent medicinal plants of Western Ghats of Karnataka India. Lipopolysaccharide (LPS)-activated murine macrophage RAW 264.7 cell line was used in *in-vitro* assay. Pretreatment with methanolic extracts at non toxic concentrations abridged the LPS-induced protein levels. Among the four plants tested, methanolic extract of *Viscum album* (70.20 ± 1.094) and *Mesua ferrea* (68.29 ± 2.862) showed potent anti-inflammatory activity at 100 μg concentration with an IC_{50} value of 57.23 ± 1.922 and 63.36 ± 3.791 $\mu\text{g}/\text{ml}$. *In vivo* anti-inflammatory activity was evaluated using carrageenan-induced paw edema in Wistar albino rats, *Viscum album* (0.6167 ± 0.01667) and *Mesua ferrea* (0.6833 ± 0.01667) showed potent anti-inflammatory activity (at 100 mg/kg.bw). The obtained results indicate the potency of active constituents of *Mesua ferrea* and *Viscum album* in the development of effective anti-inflammatory drugs.

[Previous](#)[Next](#)

Analysis and Design of Blast Resistant Structures

Sharlin Sheeba

PG Student, Department of Civil Engineering
The Oxford College of Engineering,
Bangalore, Karnataka, India

B. K. Raghu Prasad

Professor, Department of Civil Engineering
The Oxford college of Engineering,
Bangalore, Karnataka, India

Abstract: To design structures to resist blast is becoming important these days. Although designing structures to blast is well understood to obtain the effect of attenuation through soil on buried structures using the certain existing software is to be explored, therefore a point worth highlighting in this paper is a novel technique of an imaginary boundary is created on which the overpressure from the explosive is determined based on distance and yield of the explosive. The pressure on the imaginary boundary is thus applied which furthers transferred to the building model through the soil which is modeled in SAFE SOFTWARE. The pressure which reaches the model would have been subjected to the soil properties like attenuation. The above novel technique is developed in order to obtain the effect of soil on buried structures.

Keyword: Attenuation

I. INTRODUCTION

Blast resistant materials or Blast resistance design might be a costly affair. Its knowledge is far beyond the reach of common people.

But, the common people are not far from the reach of blast attacks.

To help common people and our armed forces too to survive these kinds of blast. We have tried to find an affordable and accessible solution.

Buildings get displaced enormously during blasts, due to which lives are lost.

So considering this aspects of Blast, after doing lot of research and experiments

We have developed a solution.

We found out that instead of Blast resistant Structures or design, we can minimize the response and effects due to blast by the way we construct it.

We have made an attempt to find out the responses of the structures situated above ground level and also structures situated below ground level using ETABS and SAFE software.

II. ABOUT : SAFE

This paper describes blast response analysis results of a single storey (RCC and STEEL) using ETABS above ground level and is compared the analysis result with those from a SAFE below ground level.

We have used SAFE mainly for soil modeling.

III. LITERATURE REVIEW

Sourish Mukherjee et.al (2017)¹

The main aim of this paper is to study the review paper and its work on the effect of the blast loading on the structures that has previously done and is continuing till now. For designing the blast resistant structures would be uneconomic. It describes information about explosion.

Gautam.C,pathak. R (2013)²

They designed and developed a shock blast resistance structures capable of withstanding dynamic loading of 12psi and a static pressure of 1.5m earth cover due to blast.and evaluated it experimentally.

Abhroop goswami, alaukk Singh satadru Das abhikary(2017)³

In this journal experiment had proved that ultra-high performance Fiber concrete is effective in resisting blast load.

Sajal Verma, mainak choudhury purnachandra Saha (2015)⁴

In this paper they made an attempt to review the different methods which are been applied to various type of structures like concrete, steel and masonry. In this paper they discussed FRP retrofit technique to protect the blast made of steel structures with dampers due to which no cracks are visible and there is no damage occurred in any of the walls and steel structures as the internal energy is dissipated by the dampers.

IV. OBJECTIVE:

The main aim of this work is to find out the responses of the structure situated below and above the Ground level. Thus analyzing which structure is more blast resistant.

V. METHODOLOGY

Two similar models of plan dimensions 5m*4m*3m are considered. The thickness of wall and slab are 200mm and 150 mm respectively. The plan of structure situated above ground level is as shown in figure 1. To this structure an over pressure is applied to the side of the model and also a soil pressure is applied to the model and is analyzed. The plan of a structure situated below ground level is as shown in figure 2. To this structure an over pressure is applied

considering an imaginary line away from the model and a soil pressure is applied around it and is analyzed. Thus analyzing which structure is more blast resistant. The calculations are based on **IS: 4991-1968** which is the criteria for blast resistant design of structures for explosions above ground. Basically the manual calculation is done using code **IS: 4991-1968** keeping the same blast load and varying the standoff distance the overpressure is calculated and then the manually calculated overpressure is applied to the models. The analysis is carried out using ETABS (2016) and SAFE

VI. MODELING AND ANALYSIS

A single storey building of plan dimension 5*4*3m the size of beam 200*300 and size of column 300*300 for concrete structures are used for modeling. For steel structures ISWB is used for column and ISLB is used for beams. In the above structures the models are made using ETABS and below structures are made using SAFE software's.

The analysis was carried out for the model as described as follows.

Model 1: Reinforced structure situated above ground level

Model 2: Reinforced structure situated below ground level

Model 3: Steel structure situated above ground level

Model 4: Steel structure situated below ground level

Different Models:

MODEL1.1- Blast load of 200kg yield at 20m standoff distance

MODEL1.2- Blast load of 200kg yield at 40m standoff distance

MODEL1.3- Blast load of 300kg yield at 20m standoff distance

MODEL 1.4- Blast load of 300kg yield at 40m standoff distance

MANUAL CALCULATION

200kg yield used from 20m standoff distance.

$x = \text{actual distance}/w^{1/3}$

$x = 20/(0.2)^{1/3}$

$x = 34.199\text{m}$

From IS 4991-1968

$P_{so} = 1.12006\text{kg/cm}^2$

$P_{ro} = 3.17\text{kg/cm}^2$

$q_o = 0.388\text{kg/cm}^2$

Scaled time to and t_d

$t_o = 25.65*(0.2)^{1/3} = 15.002$

$t_d = 16.9614*(0.2)^{1/3} = 9.919$

$M = 1.396$

$a = 344\text{m/s}$ $u = 480.224 = 0.48\text{m/millisecond}$

Pressure on building

$H = 3\text{m}$ $L = 4\text{m}$ $B = 5\text{m}$

$S = H$ or $B/2$ whichever is less

$t_c = 3S/u = 3*2.5/0.4802 = 15.6184\text{millisecond}$

$t_t = L/u = 4/0.4802 = 8.329\text{millisecond}$

$t_r = 4s/u = 4*2.5/0.4802\text{millisecond}$

$t_r > t_d$ no pressure on back face and is zero

For roof and sides $c_d = -0.4$

$P_{so} + c_d q_o = 1.120 + (0.4)*0.388 = 0.964\text{kg/cm}^2$

Conversion from kg/cm^2 to kN/m^2

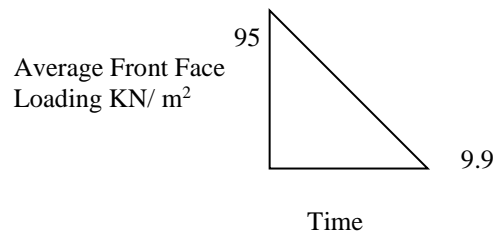
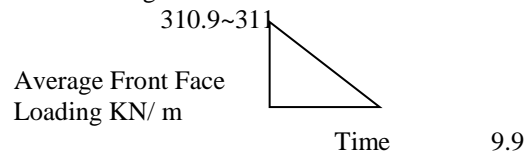
$P_{so} + c_d q_o = 94.56\text{kN/m}^2$

$3.17\text{kg/cm}^2 = 3.17*9.81\text{ N/cm}^2$

$= (31.09\text{N}) / (10^{-4}\text{m}^2)$

$= 310.9\text{kN/m}^2$

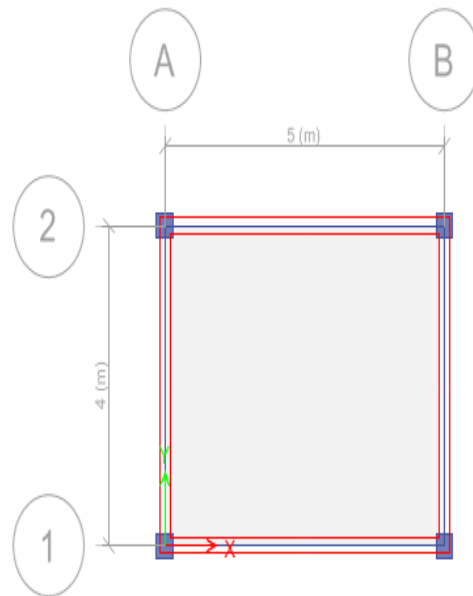
Pressure diagram

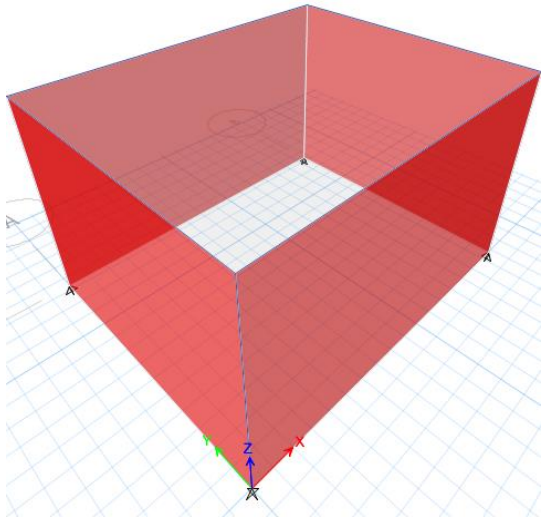


P_{so} = Peak side-on overpressure

P_{ro} = Peak reflected overpressure

M = Mach number for incident shock front





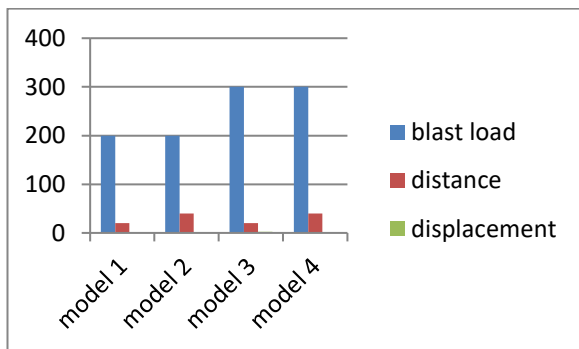
3-D view of a structure above ground level

VII. ANALYSIS AND RESULTS:

The overpressure is applied to the models and is analyzed. The analysis results are tabulated below

Response values for concrete above ground level

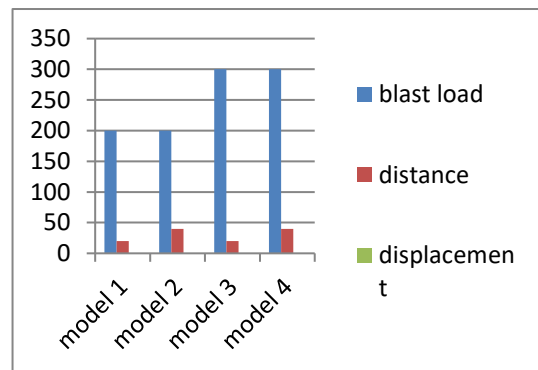
| Blast load(Kg) | stand off distance(m) | Over pressure (kN/m ²) | displacement (mm) | Moment (kN-m) | Max stress | Shear force (kN) |
|----------------|-----------------------|------------------------------------|-------------------|---------------|------------|------------------|
| 200 | 20 | 311 | 0.0629 | 0.0635 | -0.08 | -0.0262 |
| 200 | 40 | 72 | 0.01421 | -0.0094 | 0.0255 | 0.0044 |
| 300 | 20 | 419 | 0.0827 | -0.0547 | -0.15 | -0.0254 |
| 300 | 40 | 91.88 | 0.018135 | 0.012 | -0.022 | -0.0056 |



| | Blast load | distance | displacement |
|---------|------------|----------|--------------|
| Model 1 | 200 | 20 | 0.0629 |
| Model 2 | 200 | 40 | 0.01421 |
| Model 3 | 300 | 20 | 0.0827 |
| Model 4 | 300 | 40 | 0.018135 |

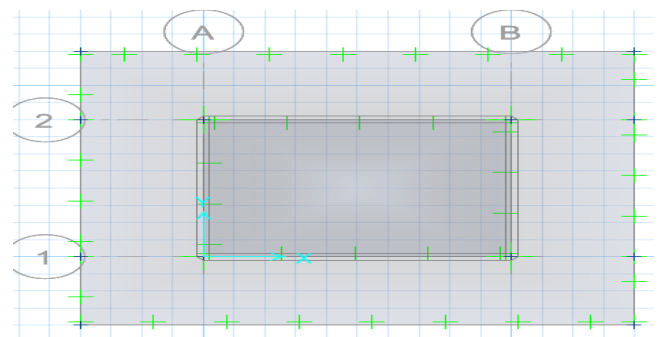
Response values for steel above ground level

| Blast load(Kg) | stand off distance(m) | Over pressure (kN/m ²) | displacement (mm) | Max stress | Moment (kN-m) | Shear force (kN) |
|----------------|-----------------------|------------------------------------|-------------------|------------|---------------|------------------|
| 200 | 20 | 311 | 0.0075 | -0.24 | 0.0914 | -0.0516 |
| 200 | 40 | 72 | 0.00174 | -0.028 | -0.0212 | -0.0119 |
| 300 | 20 | 419 | 0.0101 | -0.48 | 0.1231 | -0.0695 |
| 300 | 40 | 91.88 | 0.00222 | -0.068 | -0.027 | -0.0152 |



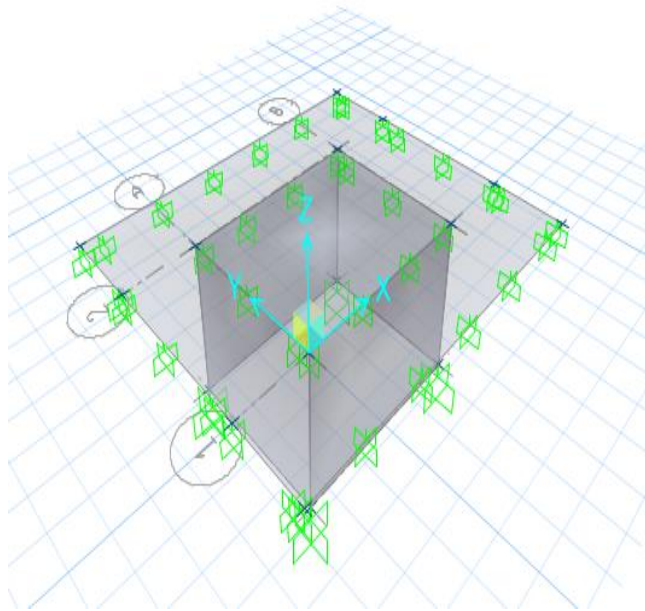
| | Blast load | distance | displacement |
|---------|------------|----------|--------------|
| Model 1 | 200 | 20 | 0.0075 |
| Model 2 | 200 | 40 | 0.00174 |
| Model 3 | 300 | 20 | 0.0101 |
| Model 4 | 300 | 40 | 0.00222 |

Response values for structures below ground level



Plan of a structure above ground level

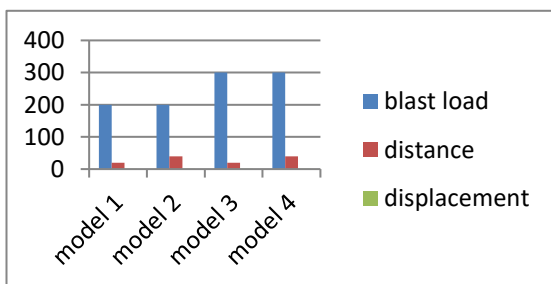
Here we considered imaginary line away from structure; soil pressure is applied around it and An overpressure is applied to the side of a structure



3-D view of a structure below ground level

Response value of concrete below ground level

| Blast load(Kg) | standoff distance(m) | Over pressure (kN/m ²) | Nodal displacement (mm) | Max stress | moment | Shear force |
|----------------|----------------------|------------------------------------|-------------------------|------------|---------|-------------|
| 200 | 20 | 311 | 0.0093 | 107.54 | 740.36 | 199.80 |
| 200 | 40 | 72 | 0.0045 | 11.905 | 23.5649 | -82.817 |
| 300 | 20 | 419 | 0.0088 | 72.168 | 57.1206 | -566.02 |
| 300 | 40 | 91.88 | 0.0087 | 15.312 | 30.1223 | -108.24 |

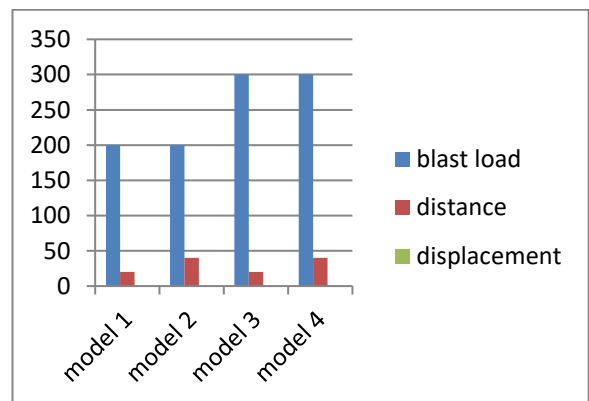


| | Blast load | distance | displacement |
|---------|------------|----------|--------------|
| Model 1 | 200 | 20 | 0.0093 |
| Model 2 | 200 | 40 | 0.0045 |
| Model 3 | 300 | 20 | 0.0088 |
| Model 4 | 300 | 40 | 0.0087 |

Response value of steel below ground level

| Blast load(Kg) | standoff distance(m) | Over pressure (kN/m ²) | Nodal displacement (mm) | Max stress | moment | Shear force |
|----------------|----------------------|------------------------------------|-------------------------|------------|--------|-------------|
| 200 | 20 | 311 | 0.01085 | 62.25 | 113.81 | -333.65 |
| 200 | 40 | 72 | 0.014732 | 14.43 | 26.94 | -77.316 |
| 300 | 20 | 419 | 0.01102 | 86.16 | 153.34 | -456.56 |
| 300 | 40 | 91.88 | 0.014736 | 18.0167 | 34.24 | -95.31 |

| | Blast load | distance | displacement |
|---------|------------|----------|--------------|
| Model 1 | 200 | 20 | 0.01085 |
| Model 2 | 200 | 40 | 0.014732 |
| Model 3 | 300 | 20 | 0.01102 |
| Model 4 | 300 | 40 | 0.014736 |



VIII. CONCLUSIONS

1. Although, effect of blast loads on structures above ground is well understood, the effect of buried structures is not so well understood because to model and soil which attenuates the blast effect is very complex.
2. Very important structures like government offices, historical structures and malls should be analyzed and designed to withstand blast load.
3. With the advent of the modern software such as SAFE which can model soil effectively it has been possible to set the effect of attenuation through soil.
4. But even modeling using SAFE is not very straightforward, a new technique of creating an imaginary boundary on which the overpressure are obtained .then the effect of attenuation of the blast effect from the imaginary boundary onwards towards the building is obtained.
5. In the present work, using SAFE the soil has been modeled and the effect of a attenuation has been obtained.
6. It is found that the effect of the blast loads on buried structures is significantly less compared to that on above structures.

IX. ACKNOWLEDGMENT

I would like to thank Professor B.K. RAGHUPRASAD and also our principal R V PRAVEENA GOWDA who gave me a chance for doing this innovative technique on ANALYSIS AND DESIGN OF BLAST RESISTANT STRUCTURES .At last I would like to thank my loved parents and friends.

X. REFERENCES

- [1] Sourish Mukherjee et.al review paper on blast loading and blast resistant structures,(IJCIET) Volume8, issue8, August 2017.
- [2] Gautam. C andpathak. R defence science journal volume 47, no.2. (2013).
- [3] abhroop goswami, alaukk Singh satadru Das adhikary,blast resistant of ultra high performance of concrete structures, IJETAE, volume 7,(2017).
- [4] sajal Verma, mainak choudhury, purnachandra Saha, blast resistant design of structures, IJRET, volume 4, special issue 13, Dec 2015

Response of RCC Asymmetric Building Subjected to Earthquake Ground Motions

Davda Karan Kishorbhai
Dept. of Civil Engg.

The Oxford College of Engineering
Bangalore, Karnataka, India

Prof. B.K. Raghu Prasad
Dept. of Civil Engg.

The Oxford College of Engineering
Bangalore, Karnataka, India

Prof. Amarnath K
Dept. of Civil Engg.

The Oxford College of Engineering
Bangalore, Karnataka, India

Abstract: The post-earthquake analysis of a structure has always revealed that most of the time the structure was unable to perform well due to the structure irregularities present in it either plan or elevation or in both. Nowadays because of the architectural constraints, or due to urbanization, there is less space available for construction due to which symmetric structure is nearly impossible. A regular structure is one which has a continuous load path and irregular structure is one which has a discontinuity in geometry (setback), mass or load resisting element. Though many researchers were conducted till date but the structural irregularity study as per latest revision IS 1893:2016 was limited and hence it was taken. In the present study, a G+12 existing RCC building asymmetric in the plan is taken to assess the effect irregularities present in it as defined by seismic code IS 1893:2002 and IS 1893:2016 with the help of ETABS (2017) software. Assessment is carried out using Time history method (EL-CENTRO & BHUJ). Several models are prepared in ETABS includes a soft story, str. with basement, etc. The measured response includes story displacement, base shear, etc. The aim of this study is to make a designer aware of the effects of irregularities mainly soft story and also a structure with torsion irregularity and to make the structure good enough to withstand the possible lateral load.

Keywords—Structural irregularity; soft story; torsion irregularity; time-history;

I. INTRODUCTION

Field investigations of a post-earthquake disaster have always found that asymmetric structure or irregular structures suffer more damage than the regular one. Nowadays due to the increase in urbanization there is less space available for parking or for the usage of the space the ground floors are generally kept open due to which their arises discontinuity in the load path and thus structure becomes asymmetric and vulnerable to more damage during earthquake, thus a detailed study regarding behavior of structure during earthquake is always required.

An irregular structure is one in which the load path is not continuous due to improper mass or stiffness distribution. Structural irregularities are of two types:

- 1) Plan irregularity- re-entrant corners, diaphragm discontinuity, and non-uniform distribution of the lateral force resisting system.
- 2) Vertical irregularity- stiffness irregularity in elevation, very long projection and mass irregularity.

Previously many researchers have studied the structural irregularities. B.K. Raghu Prasad and Jagadish K S (1989)¹

have found out the effect of eccentricity in plan and the increase in the torsion response on a single story building when it is subjected to strong earthquake motion (EL-Centro). They observed that eccentricity up to $0.05b$ (' b ' is the plan dimension) can significantly increase the ductility demand on the columns.

B.K. Raghu Prasad et al. (2007)² have presented an analytical method of quantification and location of seismic damage, through system identification methods. A G+3 structure was taken and the response of weak or soft first story was compared with the normal structure using a non-linear dynamic analysis program (IDARC). Multi-resolution analysis using wavelets was also done for damage identification of soft-story columns.

S. Vardharajan et al. (2013)³ have studied different criteria of irregularities defined by different codes (IS 1893:2002, EC8:2004, etc.) and found the limitation of types of irregularities prescribed by the standard codes. Regarding the vertical irregularity, they have found that strength irregularity had more impact than mass irregularity on seismic response and during analysis, a dynamic analysis method was found to be more accurate than modal pushover analysis even after the improvement.

B.K. Raghu Prasad et al. (2016)⁴ have studied the response of buildings symmetric and asymmetric in the plan. In the study, a single story structure was taken in which columns were modeled as fixed as well as with spring supports. A G+11 structure was taken to study the response of the structure. In both cases, it was found that the asymmetric structure was subjected to more lateral force and was subjected to torsion because of the eccentricity between the center of mass and center of rigidity.

Hemanth Kumar et al. (2018)⁵ have studied the response of G+14 RCC asymmetric building using time history method and modal pushover method by considering three models of the structure i.e. bare frame, with infill and soft story and concluded that soft-story buildings are more vulnerable to damage.

II. OBJECTIVES

The objective of this work is to analyze a G+12 RCC existing building asymmetric in plan and to know its responses for EL-CENTRO (MAY, 1940) time history and BHUJ (JAN, 2001) time history. Though many researchers were conducted till date but the structural irregularity study as per latest revision IS 1893:2016 was limited, hence it was taken and will help make the designer aware about the effects of irregularity in structures.

III. METHOD OF ANALYSIS

A) Equivalent Static Method

For a symmetric building up to a certain height defined by IS codes and a structure situated in the less seismic prone region this method can be adopted and this method requires less computational efforts. By this method, design base shear is computed for the whole building and it is then distributed along with the height of the building. The lateral forces obtained are distributed to the individual lateral resisting element. This method is less accurate because it does not consider the dynamic effect.

B) Response Spectrum Method

It is linear dynamic analysis; Response spectrum is a set of ordinates that describes max response (acceleration, velocity, displacement) of a set of SDOF systems subjected to ground motion. These max values are plotted against the undamped natural periods for various damping values.

C) Time History Analysis

Time History Method is the most accurate method among all and is also used for both elastic and inelastic analysis. This method requires the ground acceleration data of the previous earthquakes. It is a step by step analysis of the dynamic response of the structure to a specified loading which varies with time

IV. MODELING AND ANALYSIS

A G+12 RCC existing structure asymmetric in plan situated in seismic zone III having soil condition medium. The building consists of two groups of a column of 200mm x 700mm, 200mm x 600mm and beams of different size 200mm x 450mm, 200mm x 800mm and slab thickness of 125mm. The building is analyzed for its irregularities defined as per IS 1893 (Part 1): 2002 & 2016 in a structure modeling software ETABS 2017 with response reduction factor-3 and for 5% damping. The plan and elevation are described in fig.1 and fig.2 respectively. The base dimension in X-direction is 36.5m and in Y-direction is 17.34m. The structure has two parts which can be seen in plan and among which the second part is at 13° to X-axis because of the site configuration.

The analysis was carried out on a four structure models described as follows:

Model 1: A model of the building with a floor height of 3m was used as a reference model to compare the results for the irregularities.

Model 2: The building is divided into two parts by providing a separation joint between two wings. In software a gap element is provided between the two wings thus the software understands the structure as a single structure.

Model 3: A ground soft story model was created to know the behavior of the building for the stiffness irregularity, in which ground story height was kept as 4m and was kept open as such buildings are nowadays created and used for the parking place due to lack of space available for it.

Model 4: A fourth model was created by adding a basement to the building which is the next common thing to open story used for the parking, storage, etc.

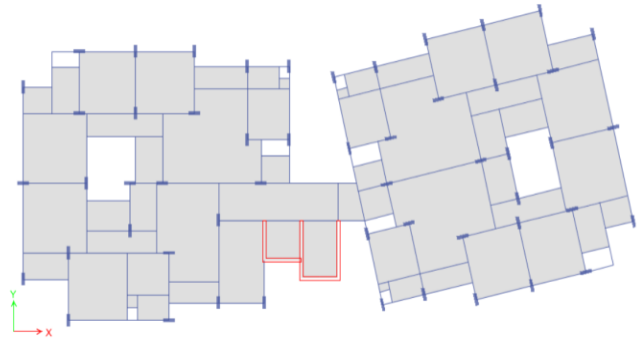


Figure 1: Plan

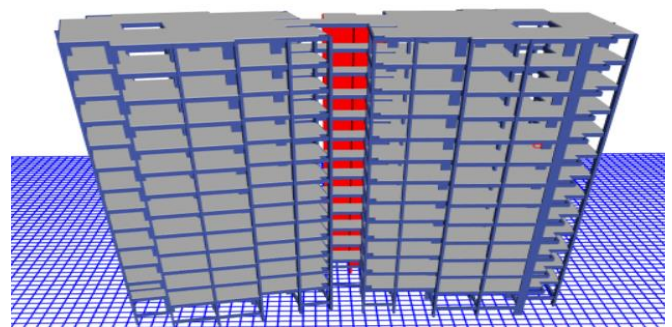


Figure 2: Elevation

The analysis of the building is carried out using time history method. The accelerogram of previous earthquakes i.e. El-Centro (1940), USA and Bhuj (2001), India were applied to the building.

The details of El-Centro (1940) earthquake are as follows:

- 1) Magnitude- 6.9
- 2) Duration- 54 s
- 3) Peak ground acceleration- 0.347g at 2.41 s.

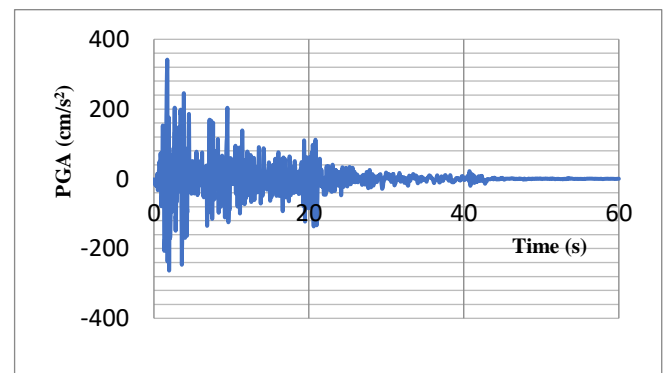


Figure 3: Time-History of El-Centro (May, 1940)

The details of Bhuj (2001) earthquake are as follows:

- 1) Magnitude- 7
- 2) Duration- 135 s but considered up-to 60 s as PGA was achieved
- 3) Peak ground acceleration- 0.105g at 46.94 s.

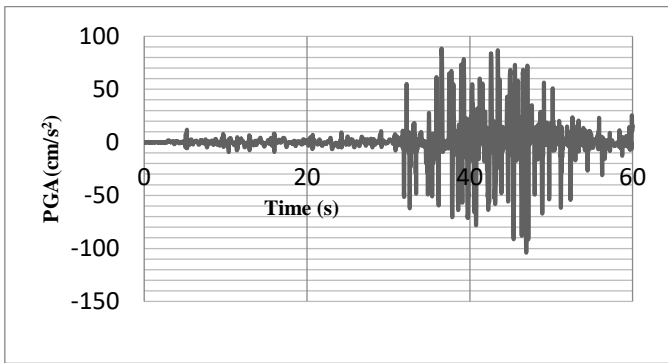


Figure 4: Time-History of Bhuj (Jan, 2001)

V. RESULTS AND DISCUSSION

The above RCC building is analyzed using the static and dynamic method and results are as follows:

A) Base Shear comparison

The Fig.5-Fig.8 shows the base shear in the principal X direction and Y direction for IS 1893:2002 and 2016 and it was seen that base shear in model 1 is high compared to all in each case. The base shear in response spectrum analysis obtained was less compared to base shear from the equivalent static method (EQ/RS).

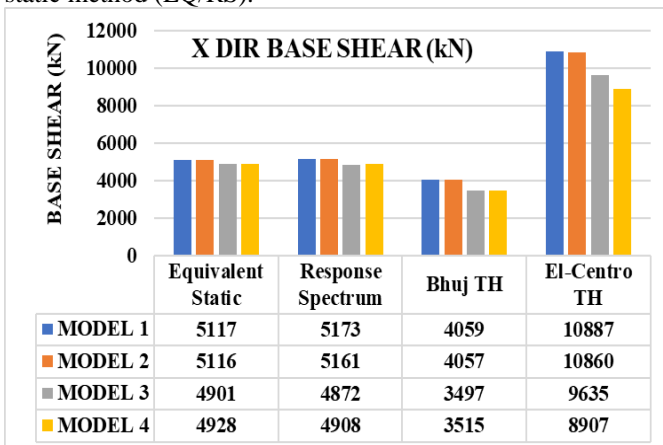


Figure 5: Base Shear (kN) in X-dir.(IS 1893:2002)

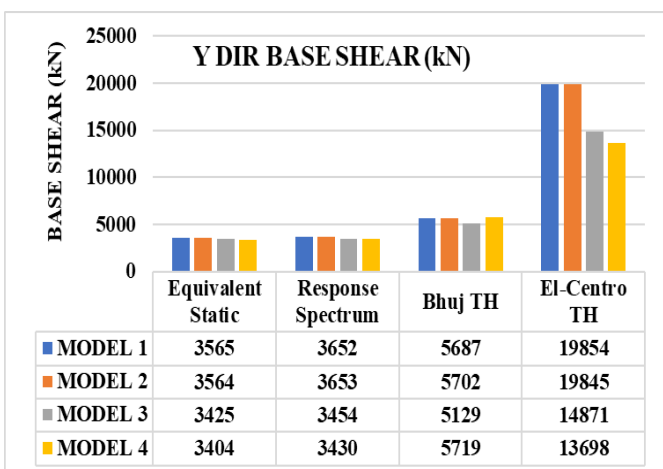


Figure 6: Base Shear (kN) in Y-dir.(IS 1893:2002)

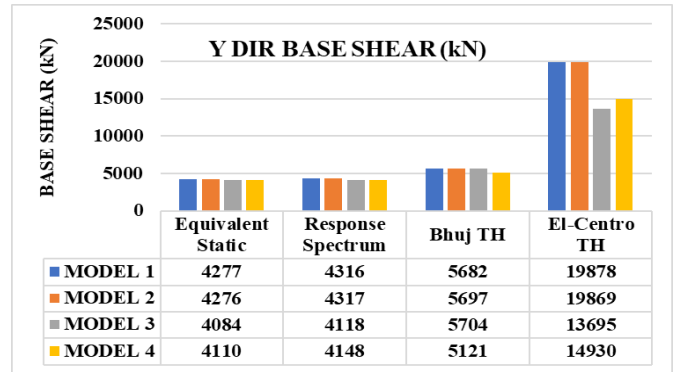


Figure 7: Base Shear (kN) in X-dir.(IS 1893:2016)

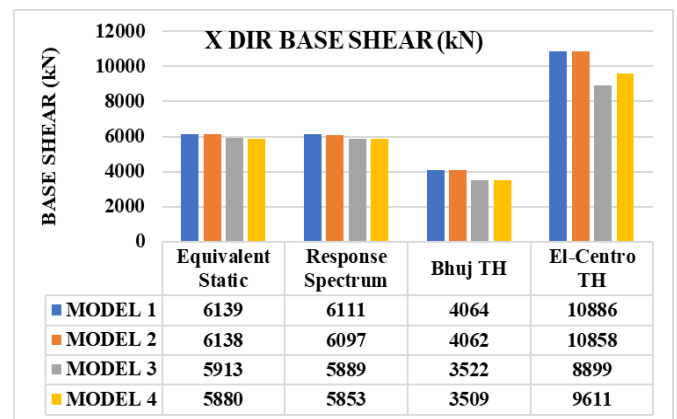


Figure 8 Base Shear (kN) in X-dir.(IS 1893:2016)

B) Maximum Top Story Displacement

IS 456 and IS 1893 have specified limit for lateral sway of any structure which should not exceed (height/250). Maximum Permissible Lateral Sway in different models as per IS 1893:2002 & 2016 shown in table 1

Table 1: Max. Allowable Sway

| Model | Lateral Sway (mm) |
|---------|-------------------|
| MODEL 1 | 163 |
| MODEL 2 | 163 |
| MODEL 3 | 168 |
| MODEL 4 | 179 |

The graphs (Fig.9 & Fig.12) showing the displacement values shows that model 1 has very less lateral sway and is also in the limiting range specified by the standards.

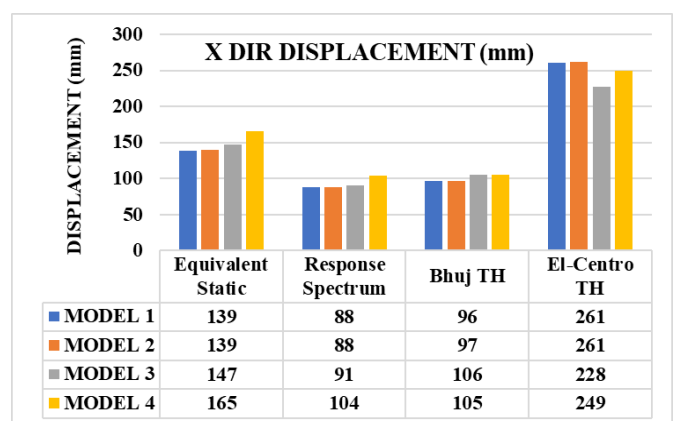


Figure 9: Max Story Displacement X-dir. (IS 1893:2002)

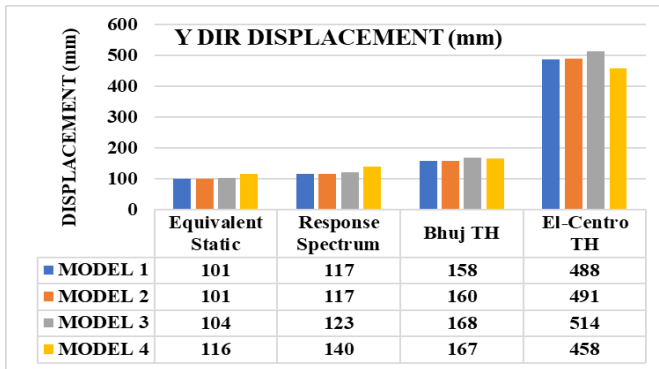


Figure 10: Max Story Displacement Y-dir. (IS 1893:2002)

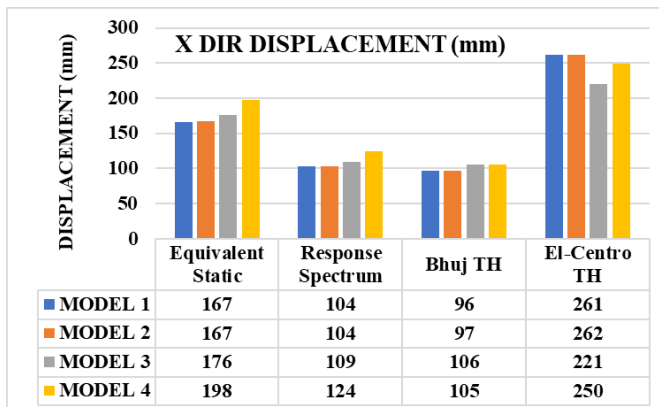


Figure 11: Max Story Displacement X-dir. (IS 1893:2016)

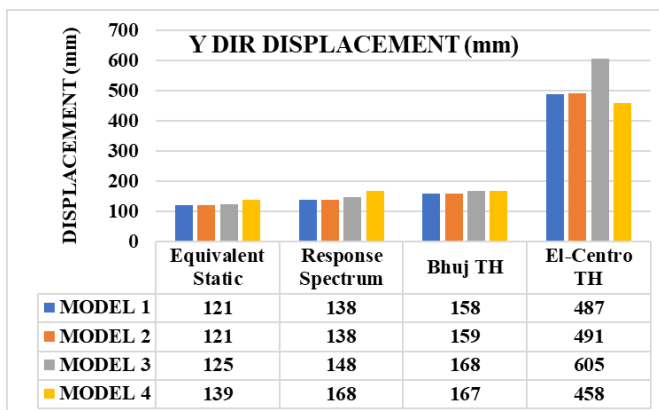


Figure 12: Max Story Displacement Y-dir. (IS 1893:2016)

Torsion irregularity is one of the most important factors which can cause severe damage to the structure. The irregularity depends on a number of factors such as plan geometry, the arrangement of structural elements and their dimensions and also on the story numbers. This ratio governs the multi-directional response of the structure and also recognizes the ability of elements resisting lateral forces.

Torsion irregularity to be considered to exist when the maximum story drift, computed with design eccentricity, at one end of the structure transverse to an axis is more than 1.2 times the average of the story drifts at the two ends of the structure. The limiting ratio ($\Delta_{max} / \Delta_{avg}$) ≤ 1.2 defined as per IS 1893:2002 is 1.2, and ($\Delta_{max} / \Delta_{min}$) as per IS 1893:2016 in the range of 1.5-2.0 and if the ratio exceeds 2.0, the building configuration to be revised. When the building is subjected to a torsion irregularity, it is affected by differential deformation in plan and will affect the seismic performance of the structure and thus the design of resisting elements should be formulated in such a way that it reduces the torsional effects.

Tables 2 and 3 show the torsion irregularity ratios ($\Delta_{max} / \Delta_{avg}$) and ($\Delta_{max} / \Delta_{min}$) as defined by IS 1893:2002 and 2016 respectively of different models for the response spectrum analysis of the building under lateral load and was seen that all models have torsion irregularity because of plan deformation in geometry.

C) Torsional irregularity

Table 2: Torsion irregularity ratio ($\Delta_{max} / \Delta_{avg}$) of different models in X-dir. And Y-dir. as per IS (1893:2002)

| DIR → STORY | MODEL 1 | | MODEL 2 | | MODEL 3 | | MODEL 4 | |
|----------------|---------|------|---------|------|---------|------|---------|------|
| | X | Y | X | Y | X | Y | X | Y |
| 12 | 1.12 | 1.26 | 1.12 | 1.26 | 1.12 | 1.27 | 1.12 | 1.27 |
| 11 | 1.12 | 1.27 | 1.12 | 1.27 | 1.12 | 1.28 | 1.12 | 1.28 |
| 10 | 1.12 | 1.28 | 1.11 | 1.28 | 1.11 | 1.29 | 1.11 | 1.29 |
| 9 | 1.11 | 1.29 | 1.11 | 1.29 | 1.11 | 1.30 | 1.11 | 1.30 |
| 8 | 1.11 | 1.30 | 1.11 | 1.30 | 1.10 | 1.31 | 1.10 | 1.30 |
| 7 | 1.10 | 1.31 | 1.10 | 1.31 | 1.10 | 1.31 | 1.10 | 1.31 |
| 6 | 1.10 | 1.32 | 1.10 | 1.32 | 1.10 | 1.33 | 1.10 | 1.32 |
| 5 | 1.09 | 1.33 | 1.09 | 1.33 | 1.11 | 1.34 | 1.11 | 1.33 |
| 4 | 1.10 | 1.34 | 1.10 | 1.35 | 1.12 | 1.35 | 1.12 | 1.35 |
| 3 | 1.10 | 1.36 | 1.10 | 1.36 | 1.13 | 1.38 | 1.13 | 1.37 |
| 2 | 1.10 | 1.39 | 1.10 | 1.39 | 1.13 | 1.40 | 1.14 | 1.39 |
| 1 | 1.10 | 1.42 | 1.10 | 1.42 | 1.13 | 1.44 | 1.14 | 1.42 |
| 0 | 1.09 | 1.46 | 1.09 | 1.46 | 1.12 | 1.49 | 1.15 | 1.46 |
| BASEMENT | | | | | | | 1.14 | 1.52 |

Table 3: Torsion irregularity ratio ($\Delta_{max} / \Delta_{min}$) of different models in X-dir. And Y-dir. (IS 1893:2016)

| DIR → STORY | MODEL 1 | | MODEL 2 | | MODEL 3 | | MODEL 4 | |
|----------------|---------|------|---------|------|---------|------|---------|------|
| | X | Y | X | Y | X | Y | X | Y |
| 12 | 1.27 | 1.71 | 1.27 | 1.71 | 1.27 | 1.73 | 1.27 | 1.73 |
| 11 | 1.27 | 1.74 | 1.27 | 1.75 | 1.26 | 1.77 | 1.27 | 1.77 |
| 10 | 1.26 | 1.78 | 1.26 | 1.79 | 1.25 | 1.80 | 1.26 | 1.80 |
| 9 | 1.25 | 1.82 | 1.25 | 1.82 | 1.24 | 1.84 | 1.24 | 1.84 |
| 8 | 1.24 | 1.85 | 1.23 | 1.85 | 1.23 | 1.88 | 1.23 | 1.87 |
| 7 | 1.22 | 1.89 | 1.22 | 1.89 | 1.22 | 1.92 | 1.22 | 1.90 |
| 6 | 1.21 | 1.93 | 1.21 | 1.93 | 1.22 | 1.96 | 1.22 | 1.95 |
| 5 | 1.21 | 1.98 | 1.21 | 1.99 | 1.25 | 2.02 | 1.25 | 2.00 |
| 4 | 1.22 | 2.05 | 1.22 | 2.05 | 1.27 | 2.09 | 1.27 | 2.06 |
| 3 | 1.22 | 2.14 | 1.23 | 2.14 | 1.28 | 2.20 | 1.30 | 2.15 |
| 2 | 1.22 | 2.27 | 1.23 | 2.27 | 1.30 | 2.35 | 1.32 | 2.27 |
| 1 | 1.21 | 2.45 | 1.21 | 2.45 | 1.29 | 2.59 | 1.34 | 2.45 |
| 0 | 1.19 | 2.67 | 1.19 | 2.67 | 1.27 | 2.92 | 1.34 | 2.73 |
| BASEMENT | | | | | | | 1.33 | 3.19 |

D) Stiffness Irregularity (Soft Story)

A soft story is one which has more openings such as in one or more floor there are more windows or large openings for doors, which may result in a decrease in stiffness of the floor. A typical soft story building is defined as a building with three or more stories in which ground level is kept open for parking or for the stores having large openings for doors or windows or the structure which is designed for less strength on the upper story also known as upper soft story, such structures performance is less during an earthquake and is seen in the past earthquakes that most of the building got damage at soft story termed as soft story failure.

A soft story is one whose stiffness is less than 70% of the story above or 80% of the average of above three stories defined as per code.

Tables 4 shows the value of stiffness of the different models. It was found that in soft story model 3, the stiffness of the ground floor is less than 70% of the first floor and model is irregular in stiffness.

| STORY | MODEL1 kN/m | MODEL 2 kN/m | MODEL 3 kN/m | MODEL 4 kN/m |
|----------|----------------|-----------------|-----------------|-----------------|
| 12 | 167130 | 166442 | 151719 | 143535 |
| 11 | 306186 | 304859 | 286778 | 272273 |
| 10 | 382326 | 380600 | 366030 | 349450 |
| 9 | 407757 | 405985 | 394484 | 379005 |
| 8 | 427820 | 425985 | 415674 | 399925 |
| 7 | 448249 | 446352 | 435340 | 417518 |
| 6 | 474653 | 472690 | 458822 | 436519 |
| 5 | 512410 | 510390 | 491891 | 461770 |
| 4 | 563914 | 561852 | 539512 | 498178 |
| 3 | 626907 | 624883 | 604567 | 550011 |
| 2 | 708355 | 705745 | 659653 | 615853 |
| 1 | 828136 | 825353 | 712676 | 653751 |
| 0 | 1065720 | 1062753 | 519295 | 562048 |
| Basement | | | | 658200 |

Table 4 Stiffness of the building (IS 1893:2016)

VI. CONCLUSIONS

In this study, the existing structure of G+12 RCC was assessed for irregularities defined as per IS 1893:2002 and IS 1893:2016. The analysis for the lateral load is carried out using time history of past earthquake i.e. EL-CENTRO (May

1940) and BHUJ (Jan 2001) on four different models and the following conclusions are summarized:

- From the analysis, it was found that base shear in model 1 is the largest.
- The lateral sway was more than the allowable limit in all the models.
- All the models undergo torsion irregularity.
- The structure configuration for model 2, model 3 and model 4 need to be revised as torsion irregularity ratio exceeds 2.0 as per latest revision of the seismic code
- The soft story model 3 has stiffness irregularity which may result in soft story failure.
- To make the structure less un-symmetric a separation joint should be provided somewhere in between.
- Irregularity in the structure either in mass or stiffness will increase the forces to be resisted by the structural elements which will affect the overall cost of the structure.
- When the results were compared from both the codes it is seen that the latest edition of the code is stringent towards the structural irregularity.

REFERENCES

- [1] B K Raghu Prasad and Jagadish K S, "Inelastic torsional response of a single story framed structure", Journal of engineering mechanics, ASCE, vol.115, number 08, pp 1782-1797, August 1989.
- [2] B.K Raghu Prasad, N. Lakshmanan, K. Muthumani, N. Gopalakrishnan and R. Sreekala. Seismic damage estimation through measurable dynamic characteristics, Computers, and Concrete, Vol. 4, No. 3 (2007) 167-186.
- [3] S.Vardharajan, V.K.Sehgal and Babita Saini (2013). Review of structural irregularities, Journal of Structural Engineering, Vol.39, NO.5, pp 538-563.
- [4] B.K. Raghuprasad, Vinay S, Amarnath K (2016). Seismic analysis of buildings symmetric and asymmetric in the plan, SSRG-IJCE- Vol.3, Issue 5- May-2016 (ISSN: 2348-8352).
- [5] Hemant Kumar M, H Eramma, Madhukaran (2018). Seismic evaluation of symmetric and asymmetric buildings by pushover and time history method, IRJET, Vol.5, e-ISSN: 2395-0056.
- [6] Gunay Ozmen, Konuralp Girgin, Yavuz Durgun (2014). Torsional irregularity in structures, International Journal of Advanced Structural Engineering, DOI 10.1007/s 40091-014-0070-5.

- [7] Neha P. Modakwar, Sangitta S. Meshram, Dinesh W. Gawatre (2014). Seismic Analysis of Structures with Irregularities, IOSR-JMCE, e-ISSN: 2278-1684, p-ISSN: 2320-334X, pp 63-66.
- [8] IS 1893:2002 (Part 1)
- [9] IS 1893:2016 (Part 1)
- [10] Pankaj Agarwal and Manish Shrikande. Earthquake Resistant Design OF Structures, Sixteenth printing, PHI publications-India.
- [11] Anil K. Chopra. Dynamics of Structure, Fourth Edition.

CASE HARDENING EFFECTS ON MECHANICAL PROPERTIES IN GRAPHITE REINFORCED AL6061 MMCS

¹H. S. Siddesha, ²Raju B.R., ³R.Sivasubramaniam

¹Associate Professor, ²Professor, ³Associate Professor

¹Department of Mechanical Engineering

¹ ACS College of Engineering, Bangalore, Karnataka, India

Abstract: In recent times the application of Aluminium based composites are increasing in various industries, owing to their improved mechanical properties. These materials are of much interest to the researchers from past four decades. In this paper it is aimed to present the experimental results of the studies conducted regarding effect of a case hardening process like Nitriding on mechanical properties of Al6061 – Graphite composites. The composites are prepared using the liquid metallurgy technique, in which graphite particulates were dispersed in the base matrix in steps of 0, 3 and 5 wt. %. The experimental results showed that, after Nitriding of the Graphite reinforced Al6061 metal matrix composite material, the values of the mechanical properties like Brinell's hardness, Tensile strength, Young's modulus and % elongation compared to those values without Nitriding were found to be improved.

IndexTerms - Al6061, graphite, case hardening, nitriding, composites, mechanical properties

I. INTRODUCTION

Metal matrix composites (MMC) are of wide interest owing to their high strength, fracture toughness and stiffness. The light metals such as Al and its alloys form superior composites suitable for elevated temperature applications when reinforced with ceramic particulates [1]. It was found that the matrix hardness has a strong influence on the dry sliding wear behaviour of Al₂O₃ particulate Al6061 MMC [2]. In the investigation on the tribological behavior on Al6061 reinforced with Al₂O₃ particles it was concluded that a characteristic physical mechanism exists during the wear process [3]. When a sufficiently high load is applied on the contact, the matrix phase is plastically deformed, and the strain is partially transferred to the particulates, which are brittle with small failure strains. It was clearly demonstrated that the effects of applied load and temperature on the dry sliding wear behavior of Al6061 alloy matrix composites reinforced with SiC whiskers or SiC particulates and concluded that, the wear rate decreased as the applied load is increased [4]. At higher normal loads (60N), severe wear and silicon carbide particles (SiC) cracking and seizure of the composite was observed in pin-on-disc test during dry sliding wear of Al2219 alloy MMCs [5]. MMCs having SiC of 3.5, 10 and 20 μm size with 15 vol. %, produced by P/M route displayed good wear resistance with increasing particle size in sliding wear [6]. Sliding distance has the highest effect on the dry sliding wear of MMCs compared to load and sliding speed [7]. Addition of 20% reinforcements increases the wear resistance of the composites, but beyond that no improvement was observed [8]. In the investigation of wear behaviour of Al6061 alloy filled with short fiber (Saffil) it was concluded that Saffil reinforcement are significant in improving wear resistance of the composites [9]. Self-lubricating graphite was incorporated in Al6061 alloy to prepare composites [10]. The above literature reveals that the nitriding effects on mechanical behavior of the composites are not discussed, further very little information is available with MMCs of Al6061 reinforced with graphite particulates. Hence the present paper describes the mechanical behavior of nitrided and graphite filled Al6061 metal matrix composites.

II. EXPERIMENTAL DETAILS AND MATERIALS USED

The following section highlights the material, its properties and methods of composite preparation and testing. The matrix material for the present study is Al6061. The reinforcing material selected was graphite. Table 1 gives the chemical composition Al6061 and table 2 gives the physical and mechanical properties of Al6061 and graphite.

TABLE 1. CHEMICAL COMPOSITION OF AL6061 BY WT%

| Si | Fe | Cu | Mn | Mg | Cr | Zn | Ti | Al |
|------|------|------|------|------|------|------|------|-----|
| 0.62 | 0.23 | 0.22 | 0.03 | 0.84 | 0.22 | 0.10 | 0.01 | Bal |

TABLE 2. PHYSICAL & MECHANICAL PROPERTIES OF AL6061 AND GRAPHITE

| Material | Elastic Modulus(GPa) | Density (g/cc) | Hardness (HB500) | Tensile Strength(MPa) |
|----------|----------------------|----------------|------------------|-----------------------|
| Al6061 | 70-80 | 2.7 | 30 | 115 |
| Graphite | 8-15 | 2.09 | 1.7* | 20 – 200** |

*Mohs scale; ** Compressive Strength (MPa)

III. PREPARATION OF COMPOSITES

The liquid metallurgy route (stir casting technique) has been adopted to prepare the cast composites as described below. Preheated graphite powder of laboratory grade purity was introduced into the vortex of the molten alloy after effective degassing. Mechanical stirring of the molten alloy for duration of 10 min was achieved by using ceramic-coated steel impeller. A speed of 400 rpm was maintained. A pouring temperature of 730⁰C was adopted and the molten composite was poured into cast iron moulds. The extent of incorporation of graphite in the matrix alloy was varied from 0, 3 and 5 wt%. Thus composites containing particles 0, 3 and 5 wt% were obtained in the form of cylinders of diameter 22mm and length 210mm

IV. CASE HARDENING BY NITRIDING OF COMPOSITES

Among various case hardening processes, Nitriding is selected in the present research. The nitriding process is primarily used to increase the hardness, corrosion resistance and wear resistance etc, of the components/parts used in the various industrial applications. There are various methods for nitriding. For this experimentation Gas Nitriding was used. Because of the absence of a quenching requirement with attendant volume changes, and the comparatively low temperatures employed in this process, gas nitriding produces less distortion and deformation than either carburizing or conventional hardening. Some growth occurs as a result of nitriding but volumetric changes are relatively small. The cast composites were heated to a temperature of 500⁰C in a gas tight furnace and then ammonia gas was introduced into the furnace chamber. This process of nitriding was carried out, in the presence of the nitrogen that is evolved from the decomposition of the ammonia gas, for a period of 24 hrs maintaining the temperature of 500⁰C.

V. TESTING OF COMPOSITES

The cast composites were machined and the specimens for the measurement of hardness, as well as for mechanical behavior were prepared as per ASTM standards. Brinell's hardness tester was used to measure the Hardness of the composites before and after nitriding. The mechanical properties were evaluated before and after nitriding using Akash make computerized universal testing machine of 40-ton capacity.

VI. RESULTS AND DISCUSSIONS

The test results of Al6061 and its composites containing graphite at various weight percentages, without and with nitriding, are presented in these sections.

Effect of nitriding on the mechanical properties

The effect of nitriding on mechanical properties such as hardness, tensile strength property, % elongation, Young's modulus, compressive strength property test results of Al6061 and Al6061 composites containing graphite at various weight percentages are presented in these sections.

a. Hardness

The change in the hardness of composites with varying content of graphite reinforcement, without and with nitriding is shown in Fig. 1. The figure represents the variation in hardness evaluated at a load of 500kg with increasing percentage of graphite in Al6061 with and without nitriding. It is observed that the hardness of Al6061 composites decreases with increased content of the graphite reinforcement.

There is a good reason for this phenomenon, though, since graphite, being a soft dispersoid, does not contribute positively to the hardness of the composite. K.H.W Seah et al., [11] have reported a reduction in hardness from 107 BHN to 77 BHN (about 28% differences) on addition of similar weight percentages of graphite to ZA-27 (Zinc Aluminium) alloy. Such a monotonic decrease in the hardness of the composite as graphite content is increased poses a limit to how much graphite may be added to enhance its other mechanical properties, since hardness is directly related to wear resistance. Consequently, a compromise is necessary when deciding how much graphite should be added to enhance the ductility, UTS, compressive strength, and Young's modulus of the composite without sacrificing too much of its hardness, especially in components like engine bearings, pistons,

piston rings and cylinder liners, in which wear resistance is of paramount importance [12]. Further the hardness values of the composites were found to be increased after nitriding compared to those values before nitriding. This is clearly depicted in the Fig.1.

b. Tensile properties

From the study of Fig. 2 it can be seen that the tensile strength increases with increasing percentage of graphite. From the figure, it can be observed that the tensile strength of the composites is higher than that of the matrix alloy. Further, from the graph, the trends of the tensile strength can be found to be increased with increase in graphite content in the composites. This increase in tensile strength may be due to the graphite

particulates acting as barriers to dislocations in the microstructure [13]. One great advantage of this dispersion-strengthening effect is that it is retained even at elevated temperatures and for extended time periods because the particles are unreactive with the matrix phase [14]. Also the tensile strength of the composites was found to be increased after nitriding compared to that before nitriding. This is clearly seen in the Fig. 2.

c. % Elongation

From the study of Fig. 3 it can be seen that the % elongation increases with increasing percentage of graphite. From the figure, it can be observed that the % elongation of the composites is higher than that of the matrix alloy. Further, from the graph, the trends of the % elongation can be found to be increased with increase in graphite content in the composites. This considerable increase in ductility is due to the graphite additions, being an effective solid lubricant [15-19], eases the movement of grains along the slip planes. The effect of graphite is expected to be mechanical in nature since the particles are un-reactive with the matrix phase [14]. It was also observed that the % elongation of the composites is increased after nitriding. This is clearly illustrated in the Fig. 3.

d. Young's Modulus

From the study of Fig. 4 it can be seen that the Young's modulus increases with increasing percentage of graphite. From the figure, it can be observed that the Young's modulus of the composites is higher than that of the matrix alloy. Further, from the graph, the trends of the Young's modulus can be found to be increased with increase in graphite content in the composites. Similar results have been obtained in aluminium matrix composites where the Young's modulus has been reported to increase with increase in the content of the reinforcing material, regardless of the type of

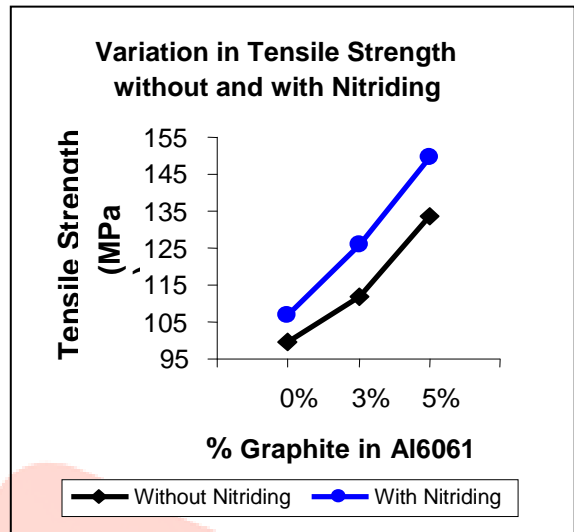


Figure 2. Variation in tensile strength of Al6061 with increasing wt% of Graphite (Without and with nitriding)

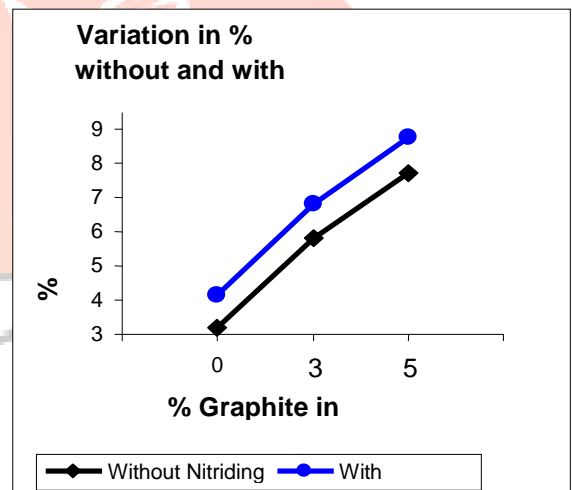


Figure 3. Variation in % Elongation of Al6061 with increasing wt% of Graphite (Without and with

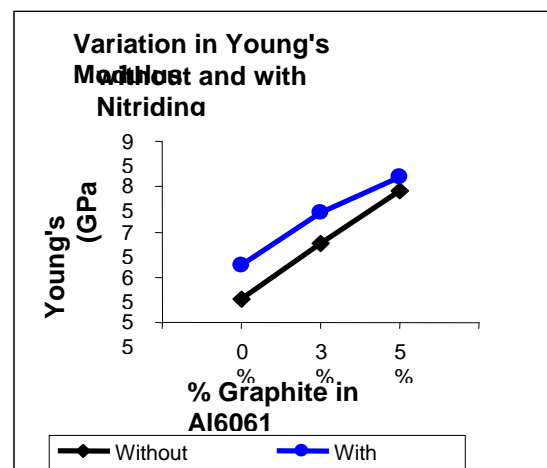


Figure 4. Variation in Young's modulus of Al6061 with increasing wt% of Graphite (Without and with nitriding)

reinforcement used [20]. The values of the Young's modulus of the composite were found to be enhanced after nitriding. This is clearly seen in the Fig. 4.

e. Compressive properties

From the study of Fig. 5 it can be seen that the compressive strength increases with increasing percentage of graphite. From the figure, it can be observed that the compressive strength of the composites is higher than that of the matrix alloy. Further, from the graph, the trends of the compressive strength can be found to be increased with increase in graphite content in the composites. Also the compressive strength values of the composites were found to be improved after nitriding compared to those values before nitriding. This is clearly depicted in the Fig. 5.

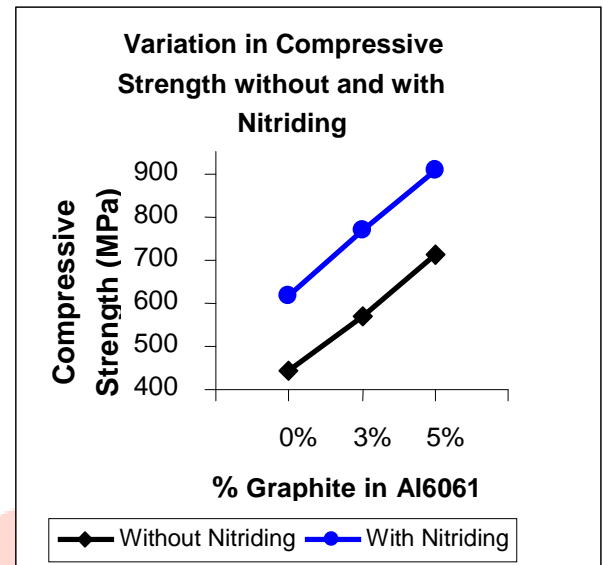


Figure 5. Variation in Compressive strength of Al6061 with increasing wt% of Graphite (Without and with nitriding)

VII. CONCLUSION

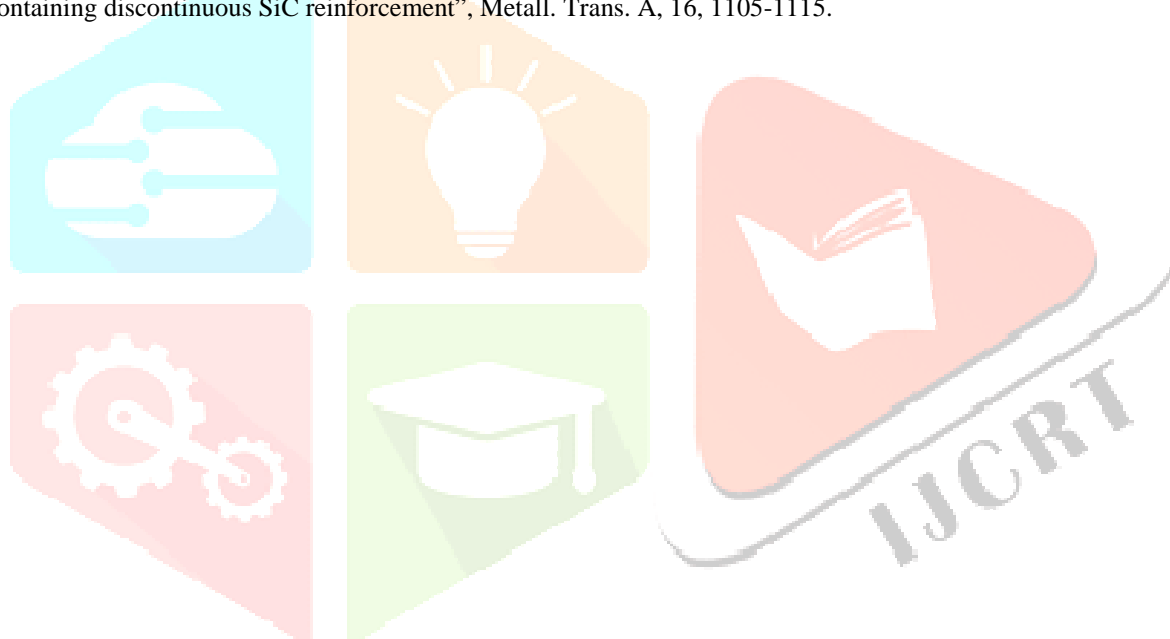
The significant conclusions of the studies carried out on Case Hardening of Al6061 - Graphite composites are as follows.

1. Cast Al6061 – Graphite composites were prepared successfully using liquid metallurgy techniques.
2. The properties of the cast Al6061-graphite composites are significantly changed by varying the amount of graphite therein. It was found that increasing the graphite content within the matrix material resulted in significant improvement in ductility, tensile strength, compressive strength and Young's modulus, but a decrease in the hardness.
3. The mechanical properties like hardness, tensile strength, % elongation, Young's modulus and compressive strength of the composites were found enhanced with the nitriding heat treatment process.

REFERENCES

- [1] ASM, (2001), Handbook of Composites, Volume 21.
- [2] Straffellini, G., Bonollo, F., Tiziani, A., (1997), "Influence of matrix hardness on the sliding behavior of 20 vol% Al_2O_3 -particulate reinforced 6061 Al MMC", *Wear* 211, 192-197.
- [3] Martin, A., Rodriguez, J. Llorca, J., (1999), "Temperature effects on the wear behavior of particulate reinforced Al-based composites", *Wear*, 225-229, 615-620.
- [4] Szu Ying Yu, Hitoshi Ishii, Keiichiro Tohgo, Young Tae Cho, Dongfeng Diao, (1997), "Temperature dependence of sliding wear behavior in SiC whisker or SiC particulate reinforced 6061 aluminum alloy composite", *Wear*, 213, 21-28.
- [5] Basavarajappa, S., Chandramohan, G., Subramanian, R., Chandrasekar, (2006), "Dry sliding wear behaviour of Al2219/SiC MMC", *Materials Science-Poland*, 24(2/1), 357-366.
- [6] Liang, Y. N., Ma, Z. Y., Li, S. Z., Li, S. and Bi, J., (1995), "Effect of particle size on wear behavior of SiC particulate-reinforced aluminum alloy composites", *Journal of Materials Science Letters*, 14, 114-116.
- [7] Basavarajappa S. and Chandramohan G., (2005), "Wear studies on metal matrix composites-Taguchi approach", *Journal of Mat Sci and Tech*, 21(6), 845-850.
- [8] Lee, C. S., Kim, Y. H. and Han, K. S., (1992), "Wear Behaviour of Aluminium Matrix Composite Materials", *Journal of Materials Science*, 27, 793-800.
- [9] How, H.C., Baker, T.N., (1997), "Dry sliding wear behaviour of Saffil-reinforced AA6061 composites", *Wear*, 210, 263-272.
- [10] Jen Fin Lin, Ming Guu Shih, Yih Wei Chen, (1996), "The tribological performance of 6061 aluminum alloy / graphite composite materials in oil lubricants with EP additives", *Wear*, 198, 58-70.

- [11] K.H.W Seah ., S.C.Sharma., B.M.Girish, (1995), “Mechanical properties of cast ZA-27/graphite particulate composites” , Materials and Design, 16, 271- 275.
- [12] A. Ramesha, J. N. Prakash, A. S. Shiva Shankare Gowda and Sonnappa Appaiah, (2009), Journal of Minerals & Materials Characterization & Engg”, Vol. 8, No.2, pp 93-106.
- [13] Dieter, G. E. (1988), “Mechanical Metallurgy”, McGrawHill, New York, pp. 212-19.
- [14] Callister, W. D. Jr, (1991), “Materials Science and Engineering: An Introduction, 2nd edition, John Wiley, New York, pp. 536.
- [15] Rohatgi, P. K., Ray, S. and Lin, Y., (1992), “Tribological properties of metal matrix graphite particle composites”, International Materials Review, 37, No.3, 129.
- [16] Biswas, S., Santharam, A., Rao, N.A.P, Narayanaswamy, K ., Rohatgi, P. and Biswas, S. K. (1980), Tribology Internationa, 8, 171.
- [17] Pai, B. C., Pillai, R.M. and Sathyanarayana, K. G, (1994), “Prospects for graphite aluminium composites in engineering industries”, Indian Journal of Engineering and Materials Science, 1, October, 279.
- [18] Krishnan, B.P., Raman, N., Narayanaswamy, K and Rohtagi, P.K., (1980) Wear, 60, 1.
- [19] Bragg, W. L. Introduction to Crystal Analysis, Bell and Son, London, 1928, p. 64.
- [20] McDanel, D. L., (1985), “Analysis of stress-strain, fracture and ductility behaviour of aluminium matrix composites containing discontinuous SiC reinforcement”, Metall. Trans. A, 16, 1105-1115.



Investigation on Mechanical and Tribological Characterization of Nano Particulate Filled Fiber Reinforced Hybrid Composites for Automobile Applications

¹Dr. Raju B.R., ²Shreyas Shenoy, ³Somanna K K, ⁴Supreeth Shetty, ⁵Vasuki K

¹Professor & Head, ^{2,3,4,5}Students

^{1,2,3,4,5}Department of Automobile Engineering,

^{1,2,3,4,5}The Oxford College Of Engineering, Bengaluru, India

Abstract: In this study the abrasive wear behaviour and mechanical behaviour of glass fibre reinforced epoxy (G-E), Nano Silicon dioxide filled with G-E (SiO₂-G-E) and Nano Aluminium oxide filled with G-E (Al₂O₃-G-E) composites have been carried out by using a rubber wheel abrasion test (RWAT), Pin-on-disc test, along with Tensile strength test, Impact strength test and hardness test. Samples of G-E with 0%, 5%, 10% and 15wt% content of SiO₂ and Al₂O₃ were tested under different loads and abrading distances. Also, conventional weighing of specimen, determination of wear volume of the specimen, specific wear rate of the specimen, and examination of the worn surface morphological features by scanning electron microscopy (SEM) were done. The results showed varied responses under different abrading distance because of the inclusion of different wt% of SiO₂ and Al₂O₃ filler loading. Further, the test results show that glass fabric reinforcement obviously improves the strength of epoxy and glass fabric- Al₂O₃ exhibits a synergistic effect on the wear resistance and reinforcing epoxy simultaneously. Further, it was also noticed that G-E composite wear is reduced to a greater extent by addition of the Nano fillers of SiO₂ and further more by Al₂O₃, selected mechanical properties such as hardness, tensile strength, and elongation at fracture were analysed for investigating wear property correlations.

Index Terms – Glass fabric reinforced epoxy composite, SiO₂ filler, Al₂O₃ filler, Abrasive wear, wear mechanisms.

I. INTRODUCTION

Glass fiber reinforced polymer matrix composites have been extensively used in various fields such as aerospace industries, automobiles, marine, and defence industries [1]. Their main advantages are good corrosion resistance, lightweight, dielectric characteristic, and better damping characteristics than metals. Fabric reinforced and particulate filled polymer composites have become attractive because of their wide spread applications and low cost. A possibility that the incorporation of both particles and fibers in polymer could provide a synergism in terms of improved properties and performance has not been adequately explored so far. However, some recent reports suggest that by incorporating filler particles into the matrix of fiber reinforced composites, synergistic effects may be achieved in the form of higher modulus and reduced material cost, yet accompanied with decreased strength and impact toughness [2].

One part of composite material for engineering applications may be represented by a thermosetting polymer matrix, e.g. an epoxy resin, which already covers alone some of the demanded properties. Diglycidyl of bisphenol A (DGEBA) type epoxy resin being the most widely matrix for innumerable applications, owing to its well-balanced chemical, adhesive, thermal and processing characteristics. However, the high coefficient of linear expansion, low thermal conductivity and limited mechanical properties of epoxies limit their use in mechanical and tribological applications. Recently many attempts were made to develop epoxy resin composites modified by fibers and fillers to improve the mechanical and tribological performance of the epoxy matrix [3-5]. Bahadur and Zheng [6], in their studies on short glass fiber (SGF) reinforced polyester by varying SGF up to 60 wt% described the effect of glass fiber on mechanical properties of the composites. Epoxy resins are superior to polyesters in resisting moisture and other environmental influences and offer lower shrinkage and better mechanical properties. However, the structural application of epoxy resin and its composites is usually limited owing to the relatively poor thermal stabilities and load carrying capacity. In order to enhance the wear resistance and thermal stability, many research studies have been carried out. One of these is the fiber reinforcement into the epoxy matrix. Different synthetic fibers and hard ceramic or metal particles have been tried as fillers in the epoxy matrix [7-9]. Kim et al. [10] reported that the damage could occur during the fabrication process, storage, service, transport, and maintenance. They are susceptible to mechanical damage when they are subjected to effects of tension, compression, and flexure, which can lead to interlayer delamination. The increase of external load favors the propagation of delamination through the interlayer leading to the catastrophic failure of the component. Another work reported by Unal and Mimaroglu [11] evaluated mechanical properties of Nylon-6 by incorporating one or a combination of more than one filler by varying the weight percent. They observed that the tensile strength and modulus of elasticity of Nylon-6 composites increased with increase in filler weight percent. Osmani [12] evaluated the mechanical properties of alumina filled glass-epoxy (G-E)

composites and reported that tensile and shear strengths decreased with increase in alumina content and flexural strength and modulus increased. Suresha et al. [13] studied the mechanical and sliding wear behavior of SiC filled G-E composites and concluded that the SiC filler addition improved the mechanical as well as wear resistance of G-E composites. Wetzel et al. [14] evaluated the mechanical and tribological properties of epoxy filled with nano- Al_2O_3 and micro CaSiO_3 hybrid composites. They concluded that incorporation of micro-and nano-scale particles improved the mechanical as well as tribological properties.

Among the wear types, the abrasive wear situation encountered in industries connected with power, automobile, pumps handling industrial fluids, and earth moving equipment has been received increasing attention. Glass/carbon fibers are the best known and most widely used reinforcing fibers in advanced polymeric composites. Reports related to application of polymer matrix composites on mechanical and tribological components such as gears, cams, wheels, and impellers are cited in literature. The importance of the tribological properties convinced various researchers to study the wear behavior and to improve the wear resistance of polymers and fiber-reinforced polymeric composites. Chand et al. [15] reported the three-body abrasive wear behavior of short glass fiber reinforced polyester composite. Chand and Gautam [16] reported the influence of load on the abrasion of fly ash, glass fiber- reinforced composites. Suresha et al. [17-19] investigated the abrasive wear behavior of epoxy/vinyl ester filled with or without particulate filler and glass/carbon fabrics. An investigation on the wear behavior of the composite materials with epoxy matrix filled with hard powders was reported by Visconti et al. [20]. Studies were also made on the effect of various fillers on the abrasive wear behavior of polymeric materials [21] and polymer composites [22-24].

A survey of the literature indicates that the effect of fiber/filler on the abrasion of polymer/composites is a complex and unpredictable phenomenon [25]. This is because physical effects such as fiber fragmentation, debonding, pullout, etc., affect the behavior of composite material subject to the abrasive wear process. It is also difficult to predict their relative contribution because various other mechanisms and influencing factors are involved (ploughing, cutting and cracking of the matrix). Although, a good amount of work has been reported on mechanical and three-body wear behavior of polymer matrix composites as discussed earlier in this section, no literature could be cited on the mechanical and abrasive wear aspect of G-E filled with Al_2O_3 particles. For sliding elements under tribological loading, however, the industrial acceptability of polymers is often limited by their thermal behaviors. The degradation of their mechanical properties at elevated temperature restricts the possibility to apply of these materials at high sliding speed and loading conditions. That is why high temperature resistant polymers are generally preferred for such tribological applications. Therefore an attempt has, therefore, been made to study the three-body abrasive wear behavior of G-E composite filled with different proportions of very fine Al_2O_3 particles (particle size $\leq 5 \mu\text{m}$) under two different loads and for different abrading distances (250-1000 m). The abrasive wear behavior has been quantified in terms of wear volume and specific wear rate. The different wear mechanisms under different abrasive wear conditions have also been reported.

II. EXPERIMENTAL DETAILS

A. Materials and preparation method

The matrix material selected is an epoxy resin and woven glass plain weave fabrics made of glass fibers are used as the reinforcing material in all composites. Woven glass plain weave fabrics made of 360 g/meter square containing glass fibers of diameter of about $12 \mu\text{m}$ is employed. The epoxy resin (LAPOX L-12) is mixed with the hardener (K-6, supplied by ATUL India Ltd., Gujarat, India) in the ratio 100: 12 by weight. The average particle size of Silica and Alumina particles are in Nano meter. As regards to the processing, on a Teflon sheet, E-glass woven fabric are placed over which the epoxy matrix system consisting of epoxy and hardener was smeared. Dry hand lay-up technique is employed to fabricate the composites as represented in fig 1. The stacking procedure consists of placing the fabric one above the other with the resin mix well spread between the fabrics.

A porous Teflon film is used multiple times to complete the stack. To ensure uniform thickness of the sample, a 3 mm spacer is used. The mould plates are coated with release agent in order to aid the ease of separation on curing. The sheets of fiberglass are placed over the mold and rolled down into the mold using steel rollers. The material must be securely attached to the mold; air must not be trapped in between the fiberglass and the mold. Additional resin is applied and additional sheets of fiberglass. Rollers are used to make sure the resin is between all the layers, the glass is wetted throughout the entire thickness of the laminate, and any air pockets are removed. The work must be done quickly enough to complete the job before the resin starts to cure. Laminates are left to cure under standard atmospheric conditions. The cast of each composite after 12 h of impregnation and dried for 2 h at 80°C followed by compression moulding at a temperature of 100°C & pressure of 7.35 MPa. The slabs so prepared measured 250 mm x 250 mm x 3 mm by size. To prepare different wt. % of Silica and Alumina filled G-E composites, besides the epoxy hardener mixture, additional wt. % of Silica and Alumina particles were included to form the resin mix.

The details of the composites (including wt% of the constituents) prepared are shown in Table 1. The mechanical and abrasion test samples were prepared according to ASTM standards from the cured slabs filled with Silicon dioxide filled G-E (SiO_2 -G-E) and Aluminium oxide G-E (Al_2O_3 -G-E) using abrasive cut-off machine.

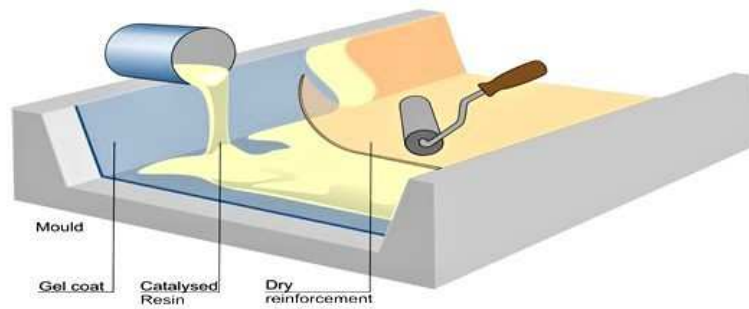


Fig 1: Hand lay-up technique.

Table 1: Composite Prepared For Present Work

| Composites | Compositions |
|------------|--|
| C1 | Glass Fiber (55wt %) + Epoxy (45wt %) |
| C2 | Glass Fiber (55wt %) + Epoxy (40wt %) + Nano Silicon dioxide (5 wt %) |
| C3 | Glass Fiber (55wt %) + Epoxy (35wt %) + Nano Silicon dioxide (10wt %) |
| C4 | Glass Fiber (55wt %) + Epoxy (30wt %) + Nano Silicon dioxide (15wt %) |
| C5 | Glass Fiber (55wt %) + Epoxy (40wt %) + Nano Aluminum oxide (5 wt %) |
| C6 | Glass Fiber (55wt %) + Epoxy (35wt %) + Nano Aluminum oxide (10wt %) |
| C7 | Glass Fiber (55wt %) + Epoxy (30wt %) + Nano Aluminum oxide (15wt %) |

B. Characterization

Density of the composites was determined by using a high precision electronic balance (Mettler Toledo, Model AX 205) using Archimedes principle. Hardness (Shore-D) of the samples was measured as per ASTM D2240, by using a Hiroshima make hardness tester (Durometer). Three readings at different locations were noted and average value is reported. Tensile properties were measured using a computerized Universal testing machine in accordance with the ASTM D-3039 procedure at a cross head speed of 1 mm/min and a gauge length of 70 mm. The tensile strength and modulus were determined from the stress-strain curves. Two samples were tested in each set and the average value was reported. The tensile tests were carried out on a fully automated Kalpak Universal testing machine connected to a computer with DAPMAT software.

The three-body abrasive wear tests (Rubber Wheel Abrasive Test) were conducted using a dry sand/rubber wheel abrasion tester as per ASTM G-65. The details of the samples preparation and wear testing procedure have been described elsewhere [17].

The experiments were carried out at three different abrading distances (150, 300 and 450 m) under constant load (30 N). Densities of the composites were determined using a high precision weighing balance by using Archimedes' principle. The wear was measured by the loss in weight, which was then converted into wear volume using the measured density data. After the wear test, the sample was again cleaned. The specific wear rate (K_s) was calculated from the equation:

$$\text{Specific wear rate} = (\text{Wear volume}) / (\text{Load} \times \text{Abrading distance}) \text{ in } \text{m}^3/\text{Nm}$$

III. RESULTS AND DISCUSSION

3.1 Effect of Filler Loading on Hardness

By using Duro-hardness tester, the Shore-D hardness of the composites is measured; the values recorded are given in Table 2. The hardness of G-E composite increased with increase of SiO₂ and Al₂O₃ filler loading. From Table 2, we can see that the SiO₂ and Al₂O₃ filler greatly increased the hardness of G-E, which can be attributed to the higher hardness and more uniform dispersion of SiO₂ and Al₂O₃ filler. The higher hardness is exhibited by the 15 wt% Al₂O₃ filled G-E compared to other Nanocomposites. The table shows that for a 15 wt% increase in Al₂O₃ content there is 12% increase in hardness. The increase in Al₂O₃ content results in an increase in brittleness of the composite. Hence this results in an increase in hardness value of the composite. Particulate filled G-E composites with sufficient surface hardness is resistant to in-service scratches that can compromise the fatigue strength and lead to premature failure. Therefore, under an indentation loading, particles would undergo elastic rather than plastic deformation, as compared to unfilled G-E composites.

Table 2: Hardness of the materials

| Materials | G+E | G+E+5%SiO ₂ | G+E+10%SiO ₂ | G+E+15%SiO ₂ | G+E+5%Al ₂ O ₃ | G+E+10%Al ₂ O ₃ | G+E+15%Al ₂ O ₃ |
|-----------|-----|------------------------|-------------------------|-------------------------|--------------------------------------|---------------------------------------|---------------------------------------|
| Hardness | 63 | 65 | 70 | 74 | 66 | 72 | 75 |

3.2 Abrasive Wear Volume and Specific Wear Rate

A. Three Body Abrasion Test:

Dry sand rubber wheel abrasion test is one of the most widely used abrasion testing method. The abrasive, for example dry sand, is fed between the specimen and the rotating rubber wheel. Other abrasives can be used depending on the application such as, industrial equipment for grinding grain, paints, plastics, coatings, slurry abrasion, construction and automobile equipment. The test specimen is fitted as shown in Fig 2

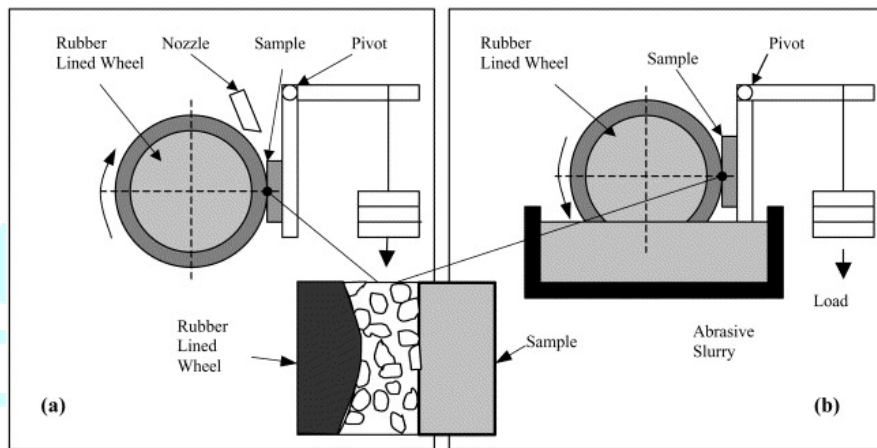


Fig 2: Schematic Representation of Rubber Wheel Abrasion Test

The specimen gets hit by the rotating rubber wheel and sand. The sand is sandwiched between the specimen and the rubber wheel. The frictional force due to the load and the speed along with the distance of abrasion will affect the wear of the specimen. We can observe that the wear is high for the G-E specimen compared to that of the SiO₂ material filled specimen, and SiO₂ wear is greater compared to that of Al₂O₃.

Figure 3a (SiO₂ filler specimen) and 3b(Al₂O₃ filler specimen) show the wear volume loss with load for different abrading distances. It is evident from these figures that irrespective of the type of samples used, there is a linear trend of wear volume loss. The Al₂O₃ filled G- E composite exhibited considerably lower wear volume loss than that of SiO₂ and G-E composite. This is attributed to the glass fiber reinforcement in epoxy decrease the abrasive wear resistance due to debonding and tearing at the glass/matrix interface.

Figure 4a and b shown as histograms for specific wear rate of the specimens, the comparative abrasive wear performance of G-E, SiO₂ and Al₂O₃-G-E composites at 150m, 300m and 450m distance respectively. The specific wear rate data reveals that initially the specific wear rate tends to decrease with increasing abrading distance and further it strongly depends on the applied load for both samples. Also observed is the earlier noted fact that G-E composite exhibits the highest specific wear rate. We can observe that for Al₂O₃-G-E system, the specific wear rate is on the lower side.

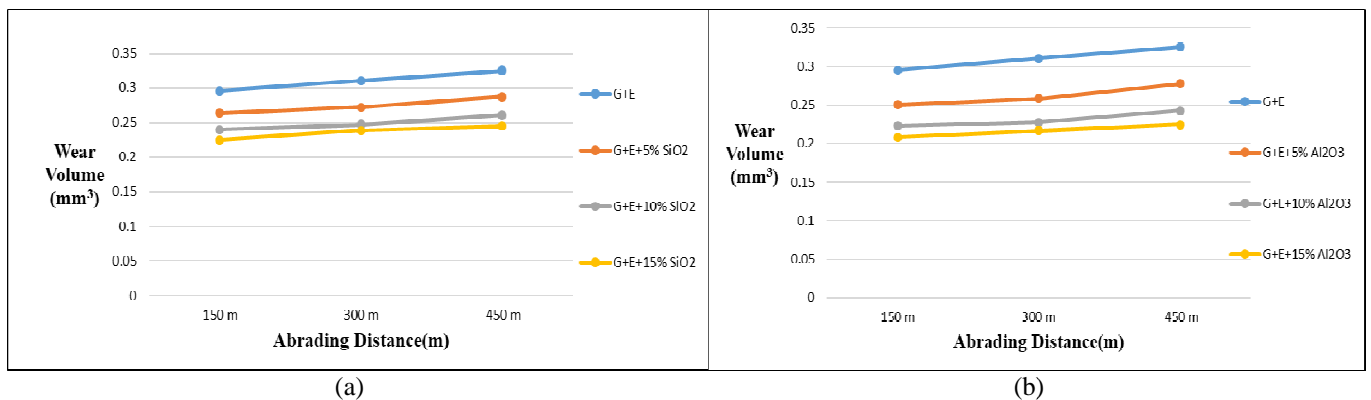


Fig 3: Wear Volume Loss of Unfilled, SiO₂ & Al₂O₃ Filled G-E Composites

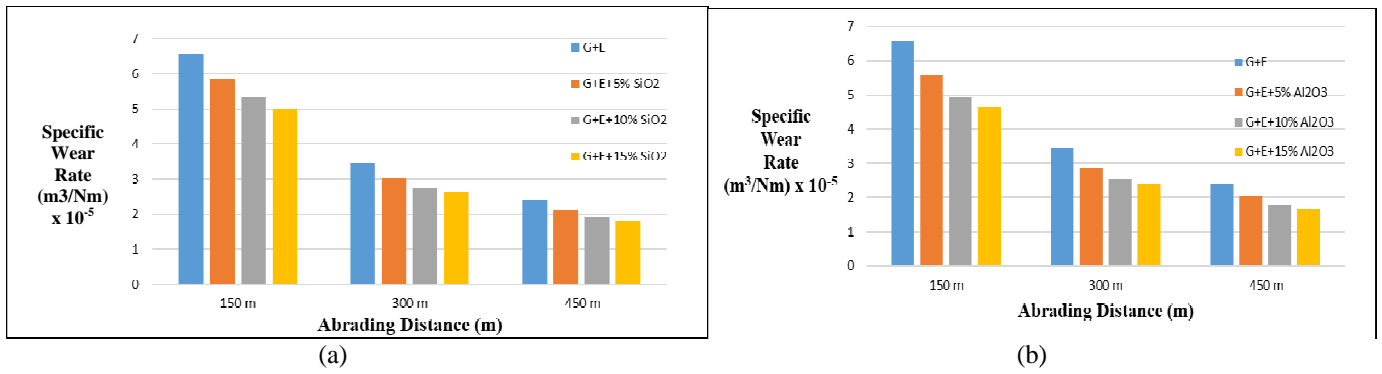


Fig 4: Specific Wear Rate of Unfilled, SiO2 and Al2O3 Filled G-E Composites

B. Two Body Abrasion Test

The standard equipment used to determine the wear resistance of surfaces is the pin on disc tester. The pin on disc machine is versatile unit designed to evaluate the wear and friction characteristics on a variety of materials exposed to sliding contacts in dry or lubricated environments. The sliding friction test occurs between stationary pin stylus and a rotating disk. Normal load, rotational speed, and wear track diameter can be varied. Electronic sensors monitor wear and the tangential force of friction as a function of load, speed, lubrication, or environmental condition.

The specimen was tested for constant abrading distance and varying loads i.e. for 20N and 30N loads. Here also we can see the effect of fillers acting on the wear of the materials. From Figure 5 (a), (b) i.e. wear volume vs load and Figure 6 (c), (d) i.e. specific wear rate vs load, we can conclude that for constant sliding distance under various loads the wear volume and specific wear rate of Nano Aluminum oxide filled glass epoxy composites are lower compared to glass epoxy with and without Nano Silicon dioxide. Therefore, the addition of fillers plays an important role in decreasing the wear of the composites.

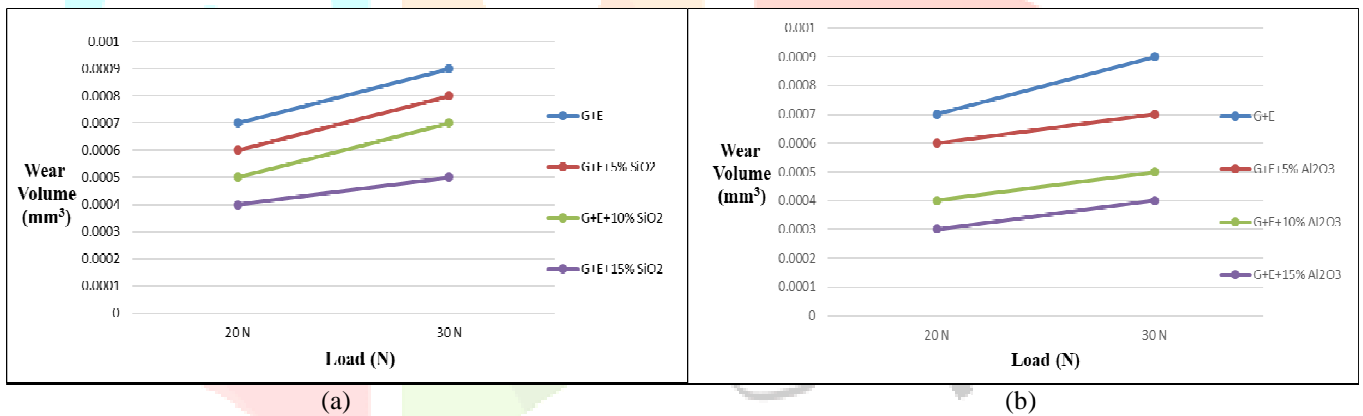


Fig 5: Wear Volume Loss of Unfilled, SiO2 & Al2O3 Filled G-E Composites

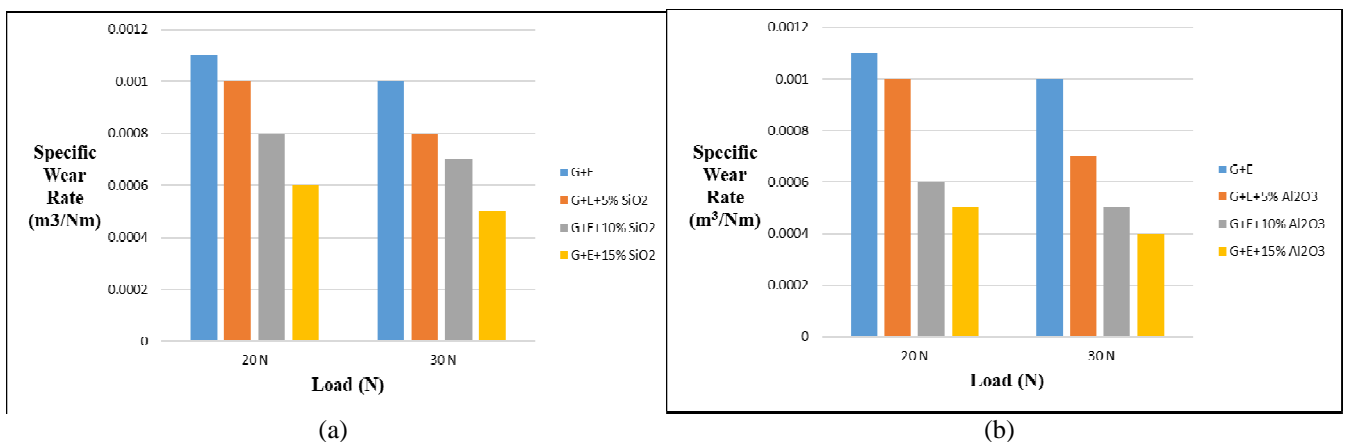


Fig 6: Specific Wear Rate of Unfilled, SiO2 and Al2O3 Filled G-E Composites

3.3 Worn surface analysis

Worn surfaces of the materials were examined by SEM to find out the wear mechanisms. Abrasive wear occurs by three different wear mechanisms, i.e. micro ploughing, micro cutting and micro cracking. SEM photographs of abraded surfaces are given below in Figure 7

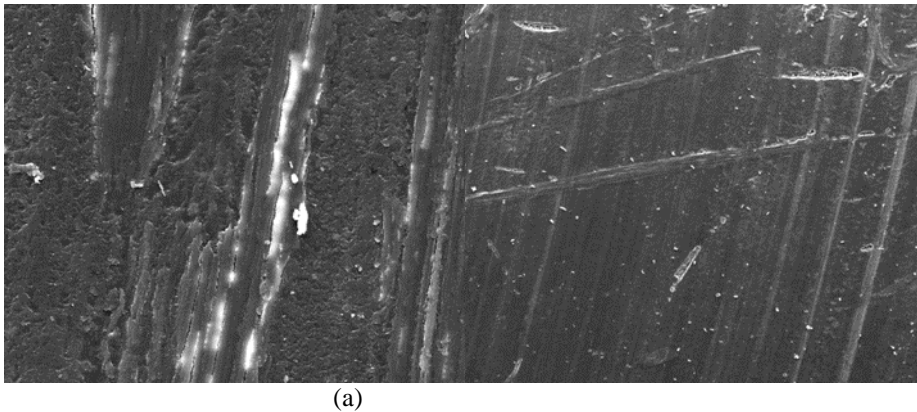


Fig 7: (a) and (b) Wear Mechanism Under Two body abrasion test(Pin on Disc Test)

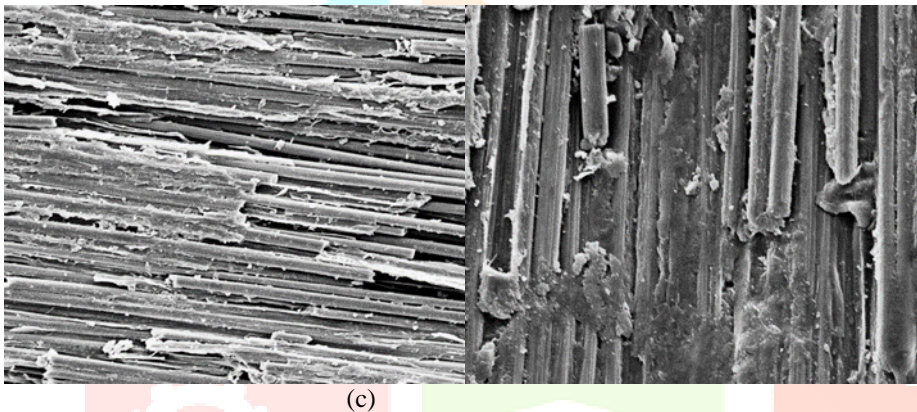


Fig 7: (c) and (d) Wear Mechanism Under Rubber Wheel Abrasion Test

IV. CONCLUSION

The experimental investigations of tribological properties of Silicon dioxide (SiO_2) filled and Aluminum oxide (Al_2O_3) filled glass epoxy composites leads to the following conclusions.

1. This work shows that successful fabrication of a Glass fiber reinforced epoxy composites filled with Silicon carbide and Silicon dioxide is possible by simple hand lay-up technique.
2. It is noticed that there is a significant improvement in the tribological properties like Wear with addition of Silicon dioxide and Aluminum oxide fillers in the glass epoxy composites.
3. The wear volume of unfilled glass epoxy blend as compared to that of Silicon dioxide and Aluminium oxide filled glass epoxy blend is high.
4. The specific wear rate is also low for the Silicon dioxide and Aluminium oxide filled glass epoxy when compared to the unfilled glass epoxy composites.
5. SEM studies of worn surfaces support the involved mechanisms and indicate damage to the matrix and filler as well as debonding of matrix and fillers of Aluminium Oxide and Silicon Dioxide filled glass epoxy composites.

V. REFERENCES

1. Kuljanin, J., Vuckovic, M., Comor, M.I., Bibic, N., Djokovic, V., Nedeljkovic, J.M., Influence of CdS-filler on the thermal properties of polystyrene, *European Polymer Journal*, 2002, 38(8), pp 1659–1662 .
2. Weidenfeller, B., Hofer, M., Schilling, F., Thermal conductivity, thermal diffusivity, and specific heat capacity of particle filled polypropylene, *Composites Part A: Applied Science and Manufacturing*, 2004, 35 (4), pp 423–429.
3. Ferreira, J.M., Pires, J.T.B., Costa, J.D., Zhang, Z.Y., Errajha ,O.A., and Richardson, M., Fatigue Damage Analysis of Aluminized Glass Fiber Composites, *Materials Science and Engineering A*, 2005, 407, pp 1–6

4. Amuzu, J.K.A., Briscoe, B.J. and Tabor, D., Polymers as Bearing and Lubricants; Aspects and Fundamental Research: Advances in Tribology, 1978, pp 59-62.
5. Kaushal, S., and Kishore, Analysis of Deformation Behaviour and Fracture Features in Glass-epoxy Composites Toughened by Rubber and Carbon Additions, Journal of Materials Science Letters, 1992, 11, pp 86–88.
6. Bahadur, S., and Zheng, Y., Mechanical and Tribological Behaviour of Polyester Reinforced with Short Glass Fibers, Wear, 1990, 137, pp 251-266.
7. Zhang, Y., Pickels, C.A., and Cameron, J., The Production and Mechanical Properties of Silicon Carbide and Alumina Whisker-Reinforced Epoxy Composites, Journal of Reinforced Plastics and Composites, 1992, 11, pp 1176–1186.
8. Cao, Y., and Cameron, J., Flexural and Shear Properties of Silica Particle Modified Glass Fiber Reinforced Epoxy Composite, Journal of Reinforced Plastics and Composites, 2006, 25, pp 347–359.
9. Srivastava, V.K., Pathak, J.P., and Tahzibi, K., Wear and Friction Characteristics of Mica-filled Fiber Reinforced Epoxy Resin Composites, Wear, 1992, 152, pp 343–350.
10. D-H kim Composite structures for civil and architectural engineering.
11. Unal, H., and Mimargolu, A., Influence of filler addition on the mechanical properties of nylon-6 polymer, Journal of Reinforced Plastics and Composites, 2004, 23, pp 5461-69.
12. Osmani, Mechanical Properties of Glass-Fiber Reinforced Epoxy Composites Filled with Al₂O₃ Particles. Journal of Reinforced Plastics and Composites, 28, 2861-2867 (2009).
13. Suresha, B., Siddharamaiah, Kishore, Seetharamu, S., Sampathkumaran, P., Investigations on the influence of graphite filler on dry sliding wear and abrasive wear behaviour of carbon fabric reinforced epoxy composites, Wear, 2009, pp 267
14. Wetzel, B., Hauptert, F., Zhang, M.Q., Epoxy nanocomposites with high mechanical and tribological performance, Composite Science and Technology, 2003, 63, pp 2055-2067.
15. Chand, N., Naik, A.M, and Neogi, S., Three-Body Abrasive Wear of Short Glass Fiber Polyester Composite, Wear, 2000, 242(1-2), pp 38-46.
16. Chand N., and Gautam, K.K.S., Influence of Load on Abrasion of Fly Ash-glass Fiber reinforced Composites, Journal of Materials Science Letters, 1994, 13(4), pp 227-300.
17. Suresha, B., Chandramohan, G., Siddaramaiah, Sampathkumaran, P., and Seetharamu, S., Three-Body Abrasive Wear Behavior of Carbon and Glass Fiber Reinforced Epoxy Composites, Mater. Sci. Eng. A, 2007, 443(1-2), pp 285-292.
18. Suresha, B., and Chandramohan, G., Three-Body Abrasive Wear Behavior of Particulate- Filled Glass-Vinyl Ester Composites, J. Mater. Process. Tech., 2008, 200(1), pp 306-311.
19. Suresha, B., Chandramohan, G., Kishore, Sampathkumaran, P., and Seetharamu, S., Mechanical and Three-Body Abrasive Wear Behavior of SiC Filled Glass-Epoxy Composites, Polym. Compos., 2008, 29(9), pp 1020-1025 .
20. Visconti, I.C., Langella, A., and Durante, M., The Wear Behaviour of Composite Materials with Epoxy Matrix Filled with Hard Powder, Applied Composite Materials, 2001, 8(3), pp 179-189.
21. Vaziri, M., Spurr, R.T., and Stott, F.H., An Investigation of the Wear of Polymeric Materials, Wear, 1988, 122(3), pp 329-342.
22. Vishwanath, B., Verma A.P., and Rao, C.V.S.K., Wear Study of Glass Woven Roving Composite, Wear, 1989, 131(2), pp 197-205.
23. Suresha, B., Chandramohan, G., Siddaramaiah and Jayaraju, T., Three-body Abrasive Wear Behavior of E-glass Fabric Reinforced/Graphite-filled Epoxy Composites, Polymer Composites, 2008, 29(6), pp 631-637.
24. Suresha, B., Chandramohan, G. and Mohanram, P.V., Role of fillers on three-body abrasive wear behavior of glass fabric reinforced epoxy composites, Polymer Composites, 2009, Vol. 30(8), pp. 1106-1113.
25. Bartenov, G.M., and Lavrentov, V.V., Lee L.H., and Ludema, K.C., Friction and Wear of Polymers, Tribology Series 6, Elsevier, Amsterdam, 1981.
26. Jayshree Bijwe, John Rajesh, J., Jeyakumar, A., Gosh A., and Tewari, U.S., Tribology International, 2000, 33, 6971.

A simple Approach on Premises Deployment Model Techniques Provider with Encrypt Transfers Technology

Dharamvir¹ Dr. M S Shashidhara²

¹Asst. Professor, ² Professor & Head, Department of MCA

^{1,2} The Oxford College of Engineering, Bommanahalli Hosur Road Bangalore-68

Abstract : Proactive consideration of all the related organization regarding numerous foundations in the reference to various worldwide customer applications will give all the related arrangements required in a uniquely sorted out changes and classes. The principle objective is to guarantee that all the related block attempts as for the segment of capacity can be improved and checked. The application recognition with all related system impact independent of the area and reconciliation worry as various customers will utilize diverse system procedure and framework mixes. The application will give the intelligent teach of the efficiency tuning that is required for appropriate recognizable proof and Solutions arrangements for various mechanical articles. The application will be founded on multi ability part administration as the weighted can be more as for various customers.

Keywords: *Analysis, Monitoring, Capacity enhancement, Server setup, Security, proclamation Information tunneling, Reports, categorization*

1. INTRODUCTION

PROJECT DESCRIPTION

The application interface design is to provide multiple facilities to the uses of different companies and prospective to help manage all the related application development, collaboration, data management, security, version design, scalability etc. The application design will help the users to manage all the company related work management with all related and required tools as the application will incorporate different application solutions for the working. Application also integrates and provides a subjective working where all methods for the custom design of the resources will be provided to the users so that requirements can be structured for the working based on the platform as a service interface. The application provides all the related integration that is required for the working as the application can be designed and can be used on the same platform with different authentication and the relative configuration required for multi user working. All the related assets with respect to the development will be provided to the users for the design and development with relation to the customized working.

Application incorporates multiple data pages design that will help to design different required designs for example multiple reports section, chart system, form designs, calendar systems, schedule managements etc. can be designed. The application provides a detailed table system management there all the related data tables will be managed with respect to multi customized options provided for example integrated download set of data, auto numbering and

reset, find, new entries etc. The design system provided will help the companies to establish the related modeling structure required.

The application also takes in consideration the related authentication options provided which will help the uses to integrate different methodology with respect to the user authentication as the applications designed can be used for the commercial where multiple users are required to be integrated and validated. The application also provide multiple design styles that will help for the fast design and implementation as the needed style is pre built and is provided to the users.

The application supports multiple users working with the help of the control and granted rights and process design options. The applications will structure all the related users with different permission. The application helps to design all different environment application design and integration with the help of the connection provided where all the factors are integrated. The application is provided for the referral working where the company can have multiple options of usage and its meaning according to the requirements. These aspects are divided into 2 modules, they are

The Basic Classifications

The application will help the partners to have a chance to upgrade the separate application improvement with every one of the prospects required in an all-out based consideration where the application will give the related check to more reasonable advancement.

The application will give dashboard where all the separate insights about the related framework instruments are given to the clients to better understanding and review

The application will give every one of the alternate routes required that can be utilized as a specific from the dashboard itself

The application will approached the Associates for multi alternative where coordinate combination should be possible with the forthcoming application furnished with the related new advancement

That plan configurations will be shown with the ordering subtle elements on the dashboard

The relationship of the improvement that will be given to the clients would have different area based where it will naturally diverted as the new application outline advancement will be given to the application

The incorporation of the affiliation will contain the plans of the accompanying

Pages with the reports reconciliation, distinctive exclusively based shape definition will be given particular concerned and tablet must be incorporated for the simplicity of the work

Numerous perspectives definition support will be given

Auto expansion as for the immediate coding of that will be given; the application will support various coding sorts that can be incorporated

Various formats in combination will be given to the client so they can utilize the layouts for the general convenience of the application movement execution

Component and standards coordinated outcome based interface must be given to the clients so that the clients can characterize all the related components that are required to be delineated on pages with all the general and field choices that must be incorporated with a few guidelines

Localizing

The application will give Authenticator where all the diverse organizing of the Associates can be furnished with different level validation base and the standards that must be characterized can be contribution by the preeminent client

The application will likewise give the immediate import and fare of the source based information that can be straightforwardly incorporated with the assistance of the application interface

Numerous fare choices will be given regard to the customization and all the detail forthcoming of the substance will be appeared

Application even give the point by point configuration arrange where the outline sheet can be tweaked by necessity with all the sort names graphic essential educational and so on can be characterized for the plan planned

Application will support the direct CSS coding concerning the different plan organize in connection to the style generalizing

The application will support the considerations of numerous configuration data regarding give the adaptability in the work use in administration

Application charge supplier limiting choice where the applications can be set up on the confining mode for more secure and protection required which will give characterized working arrangement. The configuration wizard window will be accommodated the progression incorporations and administration

Advantages

- The different upgrades and changes that are required can be designed and operated properly and easily
- The application design is geographically designed so that all different companies with respect to different domain working can be integrated
- The application helps to control the workflow and the related application integration at one place
- Application is very cost effective as it is chargeable according to the usage in based on service working
- All the related design style and templates are provided to the users
- With the help of the application platform the design of the applications will be mark on the custom basis where the exact requirements will be full filled with respect to the working

2. LITERATURE SURVEY

Disseminated registering is a standout amongst the most sizzling topics in IT as it on an exceptionally fundamental level changes the ways associations and associations are managing their figuring needs (Han, 2010). Circulated processing is truly enlisting as a Service Oriented Architecture. Consequently, it gains the qualities and inadequacies of this perspective. The service mechanism perspective is about moving a long way from the thing change prologue to a presentation which is revolved around organization movement. Advantage service mechanism offers many purposes of enthusiasm for associations.

Meanwhile, there are numerous troubles in its use and organization. Remembering the true objective to fulfill a compelling service mechanism use numerous segments must be seen as like honest to goodness business and IT game plan, service mechanism execution issues and possible impacts of service mechanism on an affiliation. In light of the above, Cloud Computing offers numerous inclinations to affiliations and organizations yet it in like manner has issues that must be taken into concern. Circulated figuring relies on upon the points of interest that the budgetary parts of economies of scale offer. Regardless, meanwhile it encounters the disservices that overconcentration of benefits and power can make.

Advantage service mechanism is a game plan of gauges and theories for arranging and making programming as interoperable organizations. This kind of programming building gets from the organization arranged perspective. Advantage acquaintance is an arrangement perspective with collect PC programming as organizations. Like other layout perfect models (e.g. address presentation), advantage acquaintance gives a speaking to path with management motorize business reason as scattered structures (Erl, 2012). Arsanjani et al (2004) portray service mechanism as the compositional style that support roughly coupled organizations to enable business versatility in a bury operable, advancement doubter way.

Advantage service mechanism includes a composite game plan of business-balanced organizations that support a versatile and effectively re-configurable end-to-end business frames affirmation using interface-based organization depictions. Advantage service mechanism perspective can be enlarged and associated on the level of a business affiliation and structure. So to speak, associations can use service mechanism to change their model and approach customers by offering organizations instead of things.

Advantage service mechanism has a movement of purposes of enthusiasm of over the conventional thing based arrangement of activity and approach. Accenture (2012) sees the going with three which are a) deftness b) cost diminish c) Return of Investment (ROI) bolster. Preparation suggests that service mechanism engages relationship to respond quickly to new business goals, make specific new limits and utilize existing organizations for veritable responsiveness. Incurred significant damage diminish implies the reuse of existing assets, extending viability and lessening application headway costs.

2. EXISTING SYSTEM

Adding compliance customization in respect to the working identities is not possible and even for the required identity support multiple utility configured and purchased. Some of the main points of the existing system

- Compatibility with respect to different environments is a concern
- Restriction based on the customization
- Central work stage for selection and customization is not supported
- Implementation and connections are not supported
- Custom setup is not provided
- Structuring with respect to tables and pages are not supported
- Pre-built support with respect to multiple designs are not provided
- Multi user support is not provided

3. PROPOSED SYSTEM

Proposed system design is to provide all the related management concerns for a procedure incorporated working style. Application provides the enhanced collaborative design Wizard format working. Some of the main points of proposed system

- Application can be used on a service places whenever required
- Multiple connection status are provided
- Step work for proper understanding will be provided
- Different functionalities will be integrated
- Multiple security provisions are provided
- Multiple working securities is provided to the users
- Structuring and designing can be operated properly
- Multiple utilities are provided for the use

4. System Transmission Identification

The application requires the preparing framework that will be characterized by the client as required as for various instruments that must be considered for the organization working. Event give various alternatives where the plan can be utilized that will be given to the clients so that the working can be passed in without the learning of Technical observations the working can be enhanced and overseen. Application gives all the related association so that is required so that after the improvement of the application that application can be utilized as a part of the earth where is really required and intended for.

Application will give all the related security setup status required for the working and combination of the application. Different Security System are given so that all the related confirmations and extremely patient can be overseen legitimately. The application will give the plan point of view where the clients can structure of the related outlines concerning the pages and as for the working. The application will help the utilizations to play out all the related outline organizes that are required to be incorporated into the specific plan application required for the working of the coveted action.

Legitimate data ought to be accumulated as for the advancement and identified with that data the proficient client to know something about the application configuration can chip away at the application to give all the related orders and as indicated by the variables chose to working will be overseen. The application is exceptionally adaptable and working and all the related work can be organized as indicated by the procedure configuration require and the application will handle every one of the information as indicated by the working style chose. Different work arrangements and alternatives can be coordinated with the assistance of all the related plan highlights gave to the clients.

Application gives a custom database framework where all the related information this will be composed and upgraded. Application chips away at the administration framework so that at whatever point the organizations oblige something to be outlined and created on a quick however this application can be utilized as a part of an extremely easy to utilize development strategies provided.

Scope and objective

- To provide all the related process design required
- To provide all the related instrumental application from one place
- To provide all the related service integration
- Provide all the related application versioning in security prospective
- Provide all the related storage and scalability for the working

5. Nonfunctional requirements

Reliable

Application is designed to handle any situation with respect to the information management and working. All the related working for the work situation will be handled by the application properly

Availability

Application is available on the cloud working platform, related working will be based on the service as required by the company they have to provide account integration that will be integrated by the valid authentication, and the meantime for working has been calculated to 15 second

Security

Security perspective has to be taken as the application requires to be designed for different work usage and all the related integrated application should support the related features of the security. The application will be integrated with instructions for the design.

Legal

Application will have the legal documents that are required to be discussed by the user and has to be implemented with respect to the copyrights of the design and other working requirements

Maintain

Application is maintained by the hosting company where all the related upgrade send update system for including more resources and the support management will be provided. For the organizational working that mistake I will be having the rights for update

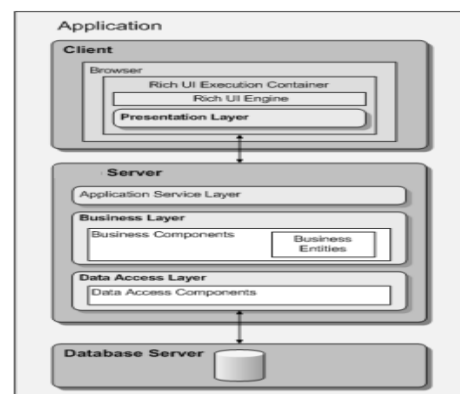


Fig 1 Architecture diagram

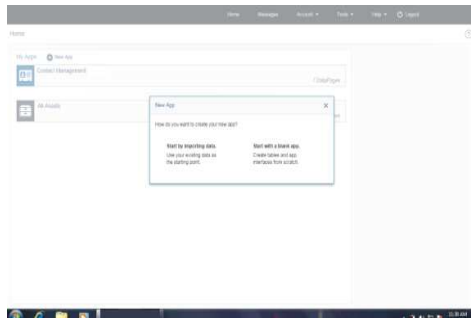


Fig 2: Options for new application

The developer can select the application of which type if the developer wants to import prebuilt software otherwise the developer can create their own specific requirement applications name has generated. This application can also import the Data, Application, and object. The developer can select the form type on basis of application. It consists of Submission form, Single update record, Password recovery.

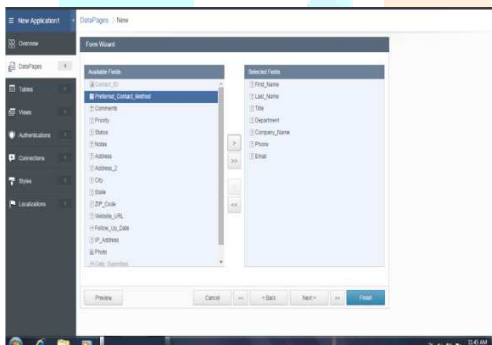


Fig 3: System Design

The form shows the fields then design the page using the field option.

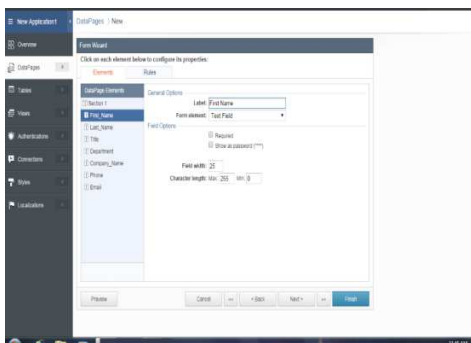


Fig 4: Manage configuration

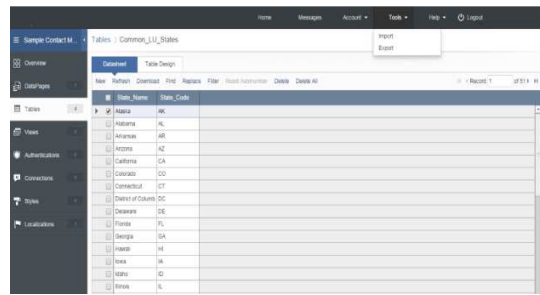


Fig 5: Check tools option

6. Conclusion and Future Enhancement

We can describe our application platform as a interface where all needed infrastructural association and development will be supported, the application provides all the related configuration that is required for transfer and usage of the designed tools with the help of the related components provided to the users. The application will help the guided development that is very much important for the non-technical peoples to associate with our application transform. Application in corporate all the needed perspective of the development as the company will define the tools and the development process accordingly.

7. Reference

- [1] S.G. Lee, Y. Mao, A.M. Gokhale, J. Harris, M.F. Horstemeyer (2009), Application of encrypt transform technology of cracked constituent particles/inclusions in wrought aluminum alloys, Elsevier, Materials Characterization, 60(9), pp.964-970.
- [2] D. Deb, S. Hariharan, U.M. Rao, Chang-Ha Ryu (2008), Automatic detection and analysis of discontinuity geometry of rock mass from digital images, Elsevier, Computers & Geosciences, 34(2), pp.115-126.
- [3] Zhanfeng Shen, Jiancheng Luo, Chenghu Zhou, Guangyu Huang, Weifeng Ma, Dongping Ming (2005), System design and implementation of digital-image processing using computational grids, Elsevier, Computers & Geosciences, 31(5), pp. 619-630.
- [4] D.W.Moolman, C. Aldrich, J.S.J. Van Deventer, and W.W. Stange (1994), Digital Image Processing as a tool for online monitoring of froth in flotation plants, Elsevier, Minerals Engineering, 7(9), pp. 1149-1164.
- [5] S.Vandenberg and C. F. Osborne(1992), Digital image processing techniques, fractal dimensionality and scale-space applied to surface roughness, Elsevier, Wear, 159(1), pp.17-30.

Conference Paper

An Empirical study on Ticket Classification using Machine learning in Osticket System"; Published in IJCRT-ISSN(2320-2882) UGC approved Open Access Journal & 5.97 impact factor volume 6 Issue 1 January 2018; &p_id=IJCRT1705154

January 2018

Conference: An Empirical study on Ticket Classification using Machine learning in Osticket System · At: http://www.ijcrt.org/viewfull.php?&p_id=IJCRT1705154

Authors:



Dr. M. S Shashidhara The Oxford Educational Institutions

Request full-text

Download citation

Copy link



To read the full-text of this research, you can request a copy directly from the author.

Abstract

In today's world, everyone is trying to get support online. An issue raised by the end user need to be addressed by the Support team. Support team has to play a key role in verifying issue and classifying the issue to get support from other teams. Classification needs to be done properly to provide improved end user satisfaction. In many organizations, ticket classification still done manually, which is time consuming and requires human effort. There may be human errors, which leads to wrong classification. Manual classification also increases the response time, which results in decrease end user satisfaction. There are automatic multiple choice phone support systems which provide the user to choose the related categories, but these systems are not much useful because users have never used the system before, usually have no idea about the which option to choose from the menu. In web-based support system, End users do not want to fill long forms, which are needed to identify the issue. In this study, Support team needs classification of the ticket in ticketing tool automatically is proposed. In this system, we have used bag of word approach and machine learning techniques. This method helps the support person to classify the ticket and transfer to the relevant team. It reduces manual efforts and human errors. It helps to improve the end-user satisfaction, also helps in improving the SLA. Index Terms - Tracking System, Automatic Assignment, Ticket Classification, Machine Learning

Discover the world's research

- 20+ million members
- 135+ million publications
- 700k+ projects [Join for free](#)

No full-text available

To read the full-

Conference Paper

Study On Eye Troubles Using Palm Print And Image Processing Technique

May 2016

Conference: International Journal of Recent Trends in Engineering & Research-IJRTER

Authors:



Dr. M. S Shashidhara
The Oxford Educational Institutions

Request full-text

Download citation

Copy link



To read the full-text of this research, you can request a copy directly from the author.

Abstract

- Palm and Finger Print Identification is widely used in all sectors for identification and recognition. Most of the governments have collected all finger prints and palm prints of all Individuals which are used for various purposes. Palm print is also used as security tool in some of the organizations. Palm print not only used for identification it also reveals information about diseases and health condition of the human body. Doctors also use patients palm and to get assistance in diagnosing diseases. Medical Palmistry is scientific study human palm. Digital Image processing techniques are used in medical field for diagnosing diseases and also store data for future reference. In this paper we propose to study the palm imprints which affect human eye leading to eye deficiencies like short site and long sites. In current Digital world Childern get affected by watching TV, Tablets, Mobile, and Video Gaming. With such background we carried out study on eye troubles by reading palm imprints using image processing techniques. Key Words: Palm, Digital Image Processing, Sobel, Eye Trouble

Discover the world's research

- 20+ million members
- 135+ million publications
- 700k+ projects [Join for free](#)

No full-text available



To read the full-text of this research, you can request a copy directly from the author.

Request full-text PDF

A Simple Approach on Web Based Classification of Face Recognition Based on Individual Data using Internet on Things and its Applications

Dharamvir ¹ , Dr. Poornima Nataraja ²

¹Associate Professor, Department of MCA, The Oxford College of Engineering , Bangalore -560068

²Professor & Head Department of MCA, Dayanand Sagar College of Engineering , Bangalore -560078

Abstract: This proposed research is a new methodology of recognizing face using Individual Eigen Subspaces and it's implemented in the field of Image Processing for Personnel verification or recognition using basic components and Data Applications of Internet on Things and its Applications. A major objective of this proposed work is to develop a tool for face recognition, which can help in quicker and effective analysis of a face from the face set, thus reducing false acceptance rate and false rejection rate. Face recognition has been widely explored in the past years. A lot of techniques have been applied in various applications. Robustness and reliability have become more and more important for these applications especially in security systems. In this proposed research , a variety of approaches for face recognition are reviewed first using Internet on Things with Data Classification methods . These approaches are classified according to three basic tasks: face representation, face detection, and face identification. An implementation of the appearance-based face recognition method, the eigenface recognition approach, is reported. This method utilizes the idea of the principal component analysis and decomposes face

images into a small set of characteristic feature images called eigenfaces. This proposed work is intended to develop, multiple face Eigen subspaces. With each one is corresponding to one known subject privately, rather than all individuals sharing one universal subspace as in the traditional eigenface method.

Keywords : *Face Recognition ,Image Processing , IoT Applications*

1. Introduction

The proposed method also makes use of Fuzzy Logic rules along with necessary image processing procedure. Fuzzy logic serves as a front part of the face recognition especially defined for skin area detection within the image frame. The experiments strongly supports the proposed area in which an effective performance over the traditional "eigenface" has been observed when tested on the same face base. Most of the previous work dealt with an single pose of an individual. Some common techniques included single template matching and eigenfaces. These systems were not real-

time and not rotation invariant. Eigenfaces described in represented face images in low dimensional feature space using PCA. Initially face recognition systems focused only on single expression images. However during the previous research on face recognition system dealt with the recognition of many different views of a single image and still the recognition of the person when his expression varies is a great problem, the face recognition system is facing. Mostly in the previous researches, they use traditional eigen value method which makes the recognition very difficult as only a single image is formed from the calculated eigen values of a set of images. Moreover there are no implemented methods to identify the face from a real time image in the preprocessing stage when eigen face algorithm is used as the feature extraction method. The performance of the face recognition system significantly drops when there are a large number of poses. When illumination variation is also present the task of face recognition becomes even more difficult. Another main drawback is that it is extremely difficult to recognize the facial areas from a real time image.

The Proposed method will be trained to identify the individuals face with different expressions. The system identifies the person's image, no matter how the expression of the face is. Individual eigenface method is to be used rather than traditional eigenvalue method. So the drawback in the traditional eigen face method is overcome by using single eigenvalue method.

Here the calculation of eigenvalue for all the images in the database will be done and these eigen values are compared individually with the query images eigenvalue using Euclidean distance and the results are given. Hence the performance of the system greatly increases when the identification is done with a large number of expressions.

When a real time image is given as input, fuzzy logic is used for the identification of the facial areas from the image. This is done using the fuzzy inference system (FIS). The fuzzy logic rules are implemented in the FIS and the face areas are cropped from them. The eigen values are then calculated for these face areas and is recognized normally.

2. Literature Review

This is deals with literature survey on image processing recognition methods, has been studied for more than two decades. This survey has been conducted in order to establish a roadmap that is to forecast the future developments of image processing technology.[1]

In this proposed research , a novel method is proposed for discovering fuzzy rules and to detect faces under lighting and angle constraint. The thesis is organized into nine chapters. The first chapter is introductory in nature and the subsequent chapters discuss the proposed techniques in detail. The list o each chapter is provided here under.[2]

This part of System deals with data acquisition for face recognition. The training sets of images are acquired first. Ten

different face images are taken for every individual. By using Internet of Things and Data Applications can be compiles and works.[3]

It describes about the fuzzy logic rules which are implemented through the fuzzy inference system (FIS) in MATLAB. The process of fuzzy inference involves all of the pieces that are described in the previous sections: Membership Functions, Logical Operations, and If-Then Rules. [5]

In mathematical terms, this is equivalent to finding the principal components of the distribution of faces, or the eigenvectors of the covariance matrix of the set of face images, treating an image as a point (or vector) in a very high dimensional space. The eigenvectors are ordered, each one accounting for a different amount of the variation among the face images.

These eigenvectors can be thought of as a set of features, which together characterize the variation among face images. Each image contributes some amount to each eigenvector, so that each eigenvector formed from an ensemble of face images appears as a sort of ghostly face image, referred to as an *eigenface*. Each eigenface deviates from uniform gray where some facial feature differs among the set of training faces collectively, they map of the variations between faces.

3. Objective of Proposed Research

The face images captured has to converted into gray scale format for the easy accessing of the image in the calculation of

Eigen values. The size of the images is also converted to a standard format before accessing them for the feature extraction. The images are resized to 92×112 matrix size and all images of any format like JPEG, BMP, and PGM are converted into PGM format.

Each individual face image can be represented exactly in terms of a linear combination of the eigenfaces. Each face can also be approximated using only the “best” eigenfaces those that have the largest eigenvalues, and which therefore account for the most variation within the set of face images. The best M eigenfaces span an M -dimensional subspace face space of the space of all possible images. Because eigenfaces will be an orthonormal vector set, the projection of a face image into face space is analogous to the well-known Fourier transform. In the FT, an image or signal is projected onto an orthonormal basis set of sinusoids at varying frequencies and phase. Each location of the transformed signal represents the projection onto a particular sinusoid. The original signal or image can be reconstructed exactly by a linear combination of the basis set of signals, weighted by the corresponding component of the transformed signal. If the components of the transform are modified, the reconstruction will be approximate and will correspond to linearly filtering the original signal.

4. Study Area and Methodology

In the proposed research work the images must be first added to a text file for easy retrieval and processing. So a database

text file is created and all the images are stored in it. Now, every image is taken from the database and the mean value is calculated from the image matrix.

Our system will be trained to identify the individuals face with different expressions. The system identifies the person's image, no matter how the expression of the face is. We use individual eigenface method rather than traditional eigenvalue method. So the drawback in the traditional Eigen face method is overcome by using single eigenvalue method.

Here we calculate the eigenvalue for all the images in the database and these Eigen values are compared individually with the query images eigenvalue using Euclidean distance and the results are given. Hence the performance of the system greatly increases when the identification is done with a large number of expressions.

When a real time image is given as input, we use fuzzy logic for the identification of the facial areas from the image. This is done using the fuzzy inference system (FIS). The fuzzy logic rules are implemented in the FIS and the face areas are cropped from them. The Eigen values are then calculated for these face areas and are recognized normally.

5. Expected Outcomes

Design is essentially the bridge between requirement specification and final solution for satisfying requirements. System has to be designed in various aspects such as the

input, output. There may be many correct possible designs. The goal of the design process is not simply to produce a design for the system. Instead the goal is to find the best possible design within the limitations imposed by the requirements and the physical and social environment in which the system will operate.

Modularization is breaking the project into different smaller units. Modularization helps in debugging of modules involved in the project and also helps in reuse of code. This helps in faster development, implementation and maintenance of software.

The training sets of images are acquired first. Ten different face images with different face expressions of the same person are taken for every individual. Five individuals' images with ten different expressions for each individual are taken with a total of 50 images. These face images are in RGB format with a matrix size of 256×256 . The image has to be converted into gray scale format for the easy accessing of the image in the calculation of Eigen values. The size of the images is also converted to a standard format before accessing them for the feature extraction. The images are resized to 92×112 matrix size and all images of any format like JPEG, BMP, PGM are converted into PGM format with a file extension of *.pgm. The images are given a filename and file type for accessing them in Eigen value calculation. This happens in the first module. The working of subsequent modules is explained below.

The images must be first added to a text file for easy retrieval and processing. So a database text file is created and all the images are stored in it. Now, every image is taken from the database and the mean value is calculated from the image matrix. The difference between the image matrix and the mean value is calculated and the covariance of the matrix is evaluated by squaring this difference value. Then the Eigen value is calculated for the image from the obtained covariance value. The result will be obtained as two matrices. The second matrix is taken and the diagonal values are sorted and stored in a array. This vector stored in the array is the value taken for further processing. This generally consists of 92 values as the images taken for processing are 92×112 format .In the same way, the Eigen value is calculated for every image in the database.

5. References

- [1] Anagnostopoulos C, Vergados D., Loumos V., Kayafas E.,” A Probabilistic Neural Network for Human Face Identification based on Fuzzy Logic Chromatic Rules”,Vol.22 No.1,2017.
- [2] C. P. Papageorgiou, M. Oren ,and T. Poggio,A general framework for object detection, Proceedings of international Conference on Computer Vision (2017) 555{562}
- [3] Costen N, Craw I, Robertson G, Akamatsu S (2015). "Automatic Face Recognition: What Representation?", 4th European Conference on Computer Proceedings, Springer-Verlag, Berlin, Germany, pp. 504-513
- [4] Olivier de Vel and Stefan Aeberhard “Line-Based Face Recognition under Varying Pose”

IEEE TRANSACTIONS ON PATTERN ANALYSIS AND MACHINE INTELLIGENCE, Vol. 21, No. 10, OCTOBER 2014

- [5] Reisfeld D, Yeshurun Y (2013).”Preprocessing of Face Images: Detection of Features and Pose Normalization”, Computer Vision and Image Understanding.
- [6] Soirovich, Kerby: *Low-dimensional procedure for the characterization of human faces*. Opt. Soc. Am. A, 87
- [7] Yang ,M.H and Ahuja.N.,”Detecting Human Faces in Color Images”,Proceedings of IEEE International conference on Image processing, Vlo.1,pp128-30

DOI: 10.1007/s10989-018-9734-5 • Corpus ID: 49667396

Share This Paper    

In Silico Identification of Piperazine Linked Thiohydantoin Derivatives as Novel Androgen Antagonist in Prostate Cancer Treatment

Shipra Bhati, V. Kaushik, Joginder Singh • Published 2018 • Chemistry • International Journal of Peptide Research and Therapeutics

Prostate cancer is the most prevalent deadly cancer in men worldwide. Androgen receptors are widely recognized for their prognostic and predictive roles in prostate cancer. The current study deals with the pharmacological analysis and preclinical trials of newly designed piperazine linked thiohydantoin derivatives incorporating various five or six-membered heterocyclic moieties using in silico techniques as androgen antagonist. The designed ligands were subjected to molecular properties... [Expand](#)

6 Citations

Background Citations 1
Methods Citations 1

[View All](#)

[View on Springer](#)

 Save

 Alert

 Feed

[Abstract](#)

[Figures and Tables](#)

[6 Citations](#)

[56 References](#)

[Related Papers](#)

Figures and Tables from this paper

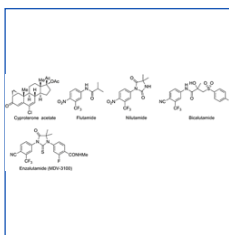


Figure 1

| Sl. No. | Compound | LogP | TPSA | QED | TPSA | QED | TPSA | QED |
|---------|----------|-------|-------|-----|--------|-----|------|-----|
| 1 | 1 | -0.25 | 85.86 | 25 | 360.43 | 9 | 1 | 3 |
| 2 | 2 | 0.16 | 82.36 | 25 | 367.43 | 9 | 0 | 3 |
| 3 | 3 | 0.32 | 89.23 | 25 | 363.50 | 8 | 0 | 3 |
| 4 | 4 | 0.12 | 74.12 | 25 | 366.45 | 9 | 0 | 3 |
| 5 | 5 | -1.32 | 95.23 | 25 | 366.42 | 10 | 0 | 3 |
| 6 | 6 | -0.03 | 82.12 | 25 | 368.68 | 9 | 0 | 3 |
| 7 | 7 | 1.28 | 89.93 | 25 | 365.57 | 8 | 0 | 3 |
| 8 | 8 | -0.02 | 87.96 | 25 | 367.64 | 10 | 1 | 3 |
| 9 | 9 | -1.08 | 96.94 | 25 | 366.42 | 11 | 0 | 3 |
| 10 | 10 | -1.01 | 87.96 | 25 | 367.64 | 10 | 0 | 3 |
| 11 | 11 | 0.09 | 82.14 | 26 | 375.46 | 9 | 0 | 3 |
| 12 | 12 | 0.09 | 77.96 | 26 | 376.58 | 10 | 0 | 3 |
| 13 | 13 | 0.06 | 86.96 | 26 | 376.03 | 8 | 0 | 3 |
| 14 | 14 | 0.24 | 89.09 | 27 | 382.47 | 9 | 1 | 3 |
| 15 | 15 | -0.01 | 89.09 | 27 | 383.58 | 10 | 0 | 3 |
| 16 | 16 | -0.01 | 76.14 | 31 | 383.88 | 8 | 1 | 3 |

Table 1

| Sl. No. | Compound | LogP | TPSA | QED | TPSA | QED | TPSA | QED |
|---------|----------|-------|-------|-----|--------|-----|------|-----|
| 17 | 17 | 0.16 | 82.36 | 25 | 367.43 | 9 | 0 | 3 |
| 18 | 18 | 0.32 | 89.23 | 25 | 363.50 | 8 | 0 | 3 |
| 19 | 19 | 0.12 | 74.12 | 25 | 366.45 | 9 | 0 | 3 |
| 20 | 20 | -1.32 | 95.23 | 25 | 366.42 | 10 | 0 | 3 |
| 21 | 21 | 0.03 | 82.12 | 25 | 368.68 | 9 | 0 | 3 |
| 22 | 22 | 1.28 | 89.93 | 25 | 365.57 | 8 | 0 | 3 |
| 23 | 23 | -0.02 | 87.96 | 25 | 367.64 | 10 | 1 | 3 |
| 24 | 24 | -1.08 | 96.94 | 25 | 366.42 | 11 | 0 | 3 |
| 25 | 25 | -1.01 | 87.96 | 25 | 367.64 | 10 | 0 | 3 |
| 26 | 26 | 0.09 | 82.14 | 26 | 375.46 | 9 | 0 | 3 |
| 27 | 27 | 0.09 | 77.96 | 26 | 376.58 | 10 | 0 | 3 |
| 28 | 28 | 0.06 | 86.96 | 26 | 376.03 | 8 | 0 | 3 |
| 29 | 29 | 0.24 | 89.09 | 27 | 382.47 | 9 | 1 | 3 |
| 30 | 30 | -0.01 | 89.09 | 27 | 383.58 | 10 | 0 | 3 |
| 31 | 31 | -0.01 | 76.14 | 31 | 383.88 | 8 | 1 | 3 |

Table 1

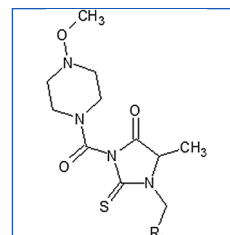


Figure 2

| Sl. No. | Compound | LogP | TPSA | QED | TPSA | QED | TPSA | QED |
|---------|----------|-------|-------|-----|--------|-----|------|-----|
| 1 | 1 | -0.25 | 85.86 | 25 | 360.43 | 9 | 1 | 3 |
| 2 | 2 | 0.16 | 82.36 | 25 | 367.43 | 9 | 0 | 3 |
| 3 | 3 | 0.32 | 89.23 | 25 | 363.50 | 8 | 0 | 3 |
| 4 | 4 | 0.12 | 74.12 | 25 | 366.45 | 9 | 0 | 3 |
| 5 | 5 | -1.32 | 95.23 | 25 | 366.42 | 10 | 0 | 3 |
| 6 | 6 | -0.03 | 82.12 | 25 | 368.68 | 9 | 0 | 3 |
| 7 | 7 | 1.28 | 89.93 | 25 | 365.57 | 8 | 0 | 3 |
| 8 | 8 | -0.02 | 87.96 | 25 | 367.64 | 10 | 1 | 3 |
| 9 | 9 | -1.08 | 96.94 | 25 | 366.42 | 11 | 0 | 3 |
| 10 | 10 | -1.01 | 87.96 | 25 | 367.64 | 10 | 0 | 3 |
| 11 | 11 | 0.09 | 82.14 | 26 | 375.46 | 9 | 0 | 3 |
| 12 | 12 | 0.09 | 77.96 | 26 | 376.58 | 10 | 0 | 3 |
| 13 | 13 | 0.06 | 86.96 | 26 | 376.03 | 8 | 0 | 3 |
| 14 | 14 | 0.24 | 89.09 | 27 | 382.47 | 9 | 1 | 3 |
| 15 | 15 | -0.01 | 89.09 | 27 | 383.58 | 10 | 0 | 3 |
| 16 | 16 | -0.01 | 76.14 | 31 | 383.88 | 8 | 1 | 3 |

Table 2

[View All 16 Figures & Tables](#)

6 Citations

Exploration and evaluation of bioactive phytochemicals against BRCA proteins by in silico approach.

H. Prabhavathi, K. R. Dasegowda, K. H. Renukananda, K. Lingaraju, H. R. Naika • Biology, Medicine • Journal of biomolecular structure & dynamics • 2020

NOTICE: Ukraine: Read IOP Publishing's statement.

PAPER • OPEN ACCESS

An extension of golden section algorithm for n-variable functions with MATLAB code

G Sandhya Rani¹, Sarada Jayan¹ and K V Nagaraja¹

Published under licence by IOP Publishing Ltd

IOP Conference Series: Materials Science and Engineering, Volume 577, International Conference on Advances in Materials and Manufacturing Applications (IConAMMA-2018) 16–18 August 2018, Bengaluru, India

Citation G Sandhya Rani *et al* 2019 *IOP Conf. Ser.: Mater. Sci. Eng.* **577** 012175

sandhya.reddyj@gmail.com

j_sarada@blr.amrita.edu

kv_nagaraja@blr.amrita.edu

¹ Department of Mathematics, Amrita School of Engineering, Bengaluru, Amrita Vishwa Vidyapeetham, India

<https://doi.org/10.1088/1757-899X/577/1/012175>

[Sign up for new issue notifications](#)

[Create citation alert](#)

Abstract

PDF

Golden section search method is one of the fastest direct search algorithms to solve single variable optimization problems, in which the search space is reduced from $[a, b]$ to $[0,1]$. This paper describes an extended golden section search method in order to find the minimum of an n-variable function by transforming its n-dimensional cubic search space to the zero-one n-dimensional cube. The paper also provides a MATLAB code for two-dimensional and three-dimensional golden section search algorithms for a zero-one n-dimensional cube. Numerical results for some benchmark functions up to five dimensions and a comparison of the proposed algorithm with the Nelder Mead Simplex Algorithm is also provided.

Help

This site uses cookies. By continuing to use this site you agree to our use of cookies. To find out more, see our Privacy and Cookies policy.





Journal of Emerging Technologies and Innovative Research

(An International Scholarly Open Access Journal, Peer-reviewed, Refereed Journal)

Impact factor 7.95 Calculate by Google Scholar and Semantic Scholar | AI-Powered Research Tool, Multidisciplinary, Monthly, Multilanguage Journal

UGC Approved Journal no 63975

ISSN: 2349-5162 | ESTD Year : 2014

Call for Paper

Volume 9 | Issue 6 | June-2022

JETIR **E**XPLORE- Search Thousands of research papers

[Home](#)[Editorial / RMS](#)[Call For Paper](#)[Research Areas](#)[For Author](#)[Current Issue](#)[Archives](#)[NEW FAQs](#)[Contact Us](#)

Published in:

Volume 6 Issue 5
May-2019
eISSN: 2349-5162

UGC and ISSN approved
7.95 impact factor UGC
Approved Journal no
63975

7.95 impact factor calculated
by Google scholar

Unique Identifier

Send message...

Published Paper ID:
JETIR1905G44

Registration ID:
210879

Number

295-305

Post-Publication

Download
eCertificate,
Confirmation Letter
editor board member
JETIR front page
Journal Back Page
UGC Approval 14 June W.e.f
of CARE List UGC Approved
Journal no 63975

Share This Article

Important Links:

[Current Issue](#)
[Archive](#)
[Call for Paper](#)
[Submit Manuscript online](#)

Jetir RMS

Title

CONVEXITY FOR THE PROPORTION OF ONE MEAN WITH RESPECT TO ANOTHER PROPORTION OF MEAN

Authors

SREENIVASA REDDY PERLA
S PADMANABHAN

Abstract

Convexity/Concavity nature proportion of contrast of means are for the most part dis-cussed. In any case, in this paper relative investigation of Convexity/Concavity between proportion of distinction of means are found and these outcomes are deciphered in Vander Monde determinants.

Key Words

CONVEXITY FOR THE PROPORTION OF ONE MEAN WITH RESPECT TO ANOTHER PROPORTION OF MEAN

Cite This Article

"CONVEXITY FOR THE PROPORTION OF ONE MEAN WITH RESPECT TO ANOTHER PROPORTION OF MEAN", International Journal of Emerging Technologies and Innovative Research (www.jetir.org), ISSN:2349-5162, Vol.6, Issue 5, page no.295-305, May-2019, Available :<http://www.jetir.org/papers/JETIR1905G44.pdf>

ISSN

2349-5162 | Impact Factor 7.95 Calculate by Google Scholar

An International Scholarly Open Access Journal, Peer-Reviewed, Refereed Journal Impact Factor 7.95 Calculate by Google Scholar and Semantic Scholar | AI-Powered Research Tool, Multidisciplinary, Monthly, Multilanguage Journal Indexing in All Major Database & Metadata, Citation Generator

Cite This Article

"CONVEXITY FOR THE PROPORTION OF ONE MEAN WITH RESPECT TO ANOTHER PROPORTION OF MEAN", International Journal of Emerging Technologies and Innovative Research (www.jetir.org | UGC and issn Approved), ISSN:2349-5162, Vol.6, Issue 5, page no. pp295-305, May-2019, Available at : <http://www.jetir.org/papers/JETIR1905G44.pdf>

Publication Details

Published Paper ID: JETIR1905G44

Registration ID: 210879

Published In: Volume 6 | Issue 5 | Year May-2019

DOI (Digital Object Identifier):

Download PDF



Downloads

0002681

Print This Page



Impact Factor:

7.95 WhatsApp
Contact
Click Here

[Impact Factor
Calculation click here](#)

Current Call For Paper

Volume 9 | Issue 6
June-2022

[Call for Paper](#)
Click Here For More
Info [Contact Us](#)
Click Here

Important L

[Current Issue](#)
[Archive](#)
[Call for Paper](#)
[Submit Manuscript online](#)

Jetir RMS

ON SCHUR M- POWER CONVEXITY FOR PROPORTION OF DISTINCTION OF SOME SPECIAL MEANS IN TWO VARIABLES

SREENIVASA REDDY PERLA AND S PADMANABHAN

Abstract. In this paper, we discuss the Schur m-power convexity on $(0, \infty) \times (0, \infty)$. For proportion of distinction of some special means in two variables, such as arithmetic, geometric, harmonic, root-square means and the like, and obtain some inequalities related to proportion of distinction of means.

1. MEAN OF ORDER t

Let us consider the following well known *mean of order t* :

$$(1.1) \quad B_t(a, b) = \begin{cases} \left(\frac{a^t + b^t}{2} \right)^{1/t}, & t \neq 0 \\ \sqrt{ab}, & t = 0 \\ \max \{a, b\}, & t = \infty \\ \min \{a, b\}, & t = -\infty \end{cases}$$

for all $a, b, t \in \mathbb{R}$, $a, b > 0$.

In particular, we have

$$B_{-1}(a, b) = H(a, b) = \frac{2ab}{a+b}$$

$$B_0(a, b) = G(a, b) = \sqrt{ab}$$

$$B_{1/2}(a, b) = N_1(a, b) = \left(\frac{\sqrt{a} + \sqrt{b}}{2} \right)^2$$

$$B_1(a, b) = A(a, b) = \frac{a+b}{2}$$

$$B_2(a, b) = S(a, b) = \sqrt{\frac{a^2 + b^2}{2}}$$

The means, $H(a, b)$, $G(a, b)$, $A(a, b)$ and $S(a, b)$ are known in the literature as *harmonic*, *geometric*, *arithmetic* and *root-square means* respectively. For simplicity we can call the measure, $N_1(a, b)$ as *square-root mean*. It is well know that [1] the *mean of order s* given in (1.1) is monotonically increasing in s , then we can write

$$(1.2) \quad H(a, b) \leq G(a, b) \leq N_1(a, b) \leq A(a, b) \leq S(a, b)$$

Dragomir and Pearce [3] (page 242) proved the following inequality:

$$(1.3) \quad \frac{a^r + b^r}{2} \leq \frac{b^{r+1} - a^{r+1}}{(r+1)(b-a)} \leq \left(\frac{a+b}{2}\right)^r$$

Let us consider two parameter

$$\frac{a^r + b^r}{2} \leq \frac{\frac{b^{r+1} - a^{r+1}}{(r+1)(b-a)}}{\frac{b^{s+1} - a^{s+1}}{(s+1)(b-a)}} \leq \left(\frac{a+b}{2}\right)^r$$

$$(1.4) \quad \frac{a^r + b^r}{2} \leq \frac{(s+1)(b^{r+1} - a^{r+1})}{(r+1)(b^{s+1} - a^{s+1})} \leq \left(\frac{a+b}{2}\right)^r$$

For all $a, b > 0, a \neq b, r \in (0,1),$ and $s \in (0,1).$ in particular take $r = \frac{1}{2}$ we get

$$\frac{\sqrt{a} + \sqrt{b}}{2} \leq \frac{2(s+1)(b^{3/2} - a^{3/2})}{3(b^{s+1} - a^{s+1})} \leq \left(\frac{a+b}{2}\right)^{1/2}$$

Multiply by $\frac{\sqrt{a} + \sqrt{b}}{2}$

$$\left(\frac{\sqrt{a} + \sqrt{b}}{2}\right)^2 \leq \frac{(s+1)(b^{\frac{3}{2}} - a^{\frac{3}{2}})(\sqrt{a} + \sqrt{b})}{3(b^{s+1} - a^{s+1})} \leq \left(\frac{a+b}{2}\right)^{1/2} \frac{\sqrt{a} + \sqrt{b}}{2}$$

$$(1.5) \quad \left(\frac{\sqrt{a} + \sqrt{b}}{2}\right)^2 \leq \frac{(s+1)(b-a)(a+b+\sqrt{ab})}{3(b^{s+1} - a^{s+1})} \leq \left(\frac{a+b}{2}\right)^{1/2} \frac{\sqrt{a} + \sqrt{b}}{2}$$

$$(1.6) \quad \left(\frac{\sqrt{a} + \sqrt{b}}{2}\right)^2 \leq \frac{\text{If } s=0}{3} \frac{(a+b+\sqrt{ab})}{3} \leq \left(\frac{a+b}{2}\right)^{1/2} \frac{\sqrt{a} + \sqrt{b}}{2}$$

$$\text{i.e.,} \quad N_1(a,b) \leq H_e(a,b) \leq N_2(a,b)$$

If $s=1/2$ from (1.5)

$$(1.7) \quad \left(\frac{\sqrt{a} + \sqrt{b}}{2}\right)^2 \leq \frac{(b-a)}{2(\sqrt{b} - \sqrt{a})} \leq \left(\frac{a+b}{2}\right)^{1/2} \frac{\sqrt{a} + \sqrt{b}}{2}$$

$$\left(\frac{\sqrt{a} + \sqrt{b}}{2}\right)^2 \leq \frac{\sqrt{a} + \sqrt{b}}{2} \leq \left(\frac{a+b}{2}\right)^{1/2} \frac{\sqrt{a} + \sqrt{b}}{2}$$

If $s=1$ from (1.5)

$$\left(\frac{\sqrt{a} + \sqrt{b}}{2}\right)^2 \leq \frac{2(b-a)(a+b+\sqrt{ab})}{3(b^2 - a^2)} \leq \left(\frac{a+b}{2}\right)^{1/2} \frac{\sqrt{a} + \sqrt{b}}{2}$$

$$\left(\frac{\sqrt{a} + \sqrt{b}}{2}\right)^2 \leq \frac{2(a+b+\sqrt{ab})}{3(a+b)} \leq \left(\frac{a+b}{2}\right)^{1/2} \frac{\sqrt{a} + \sqrt{b}}{2}$$

On the other side we can easily check that

$$\left(\frac{a+b}{2}\right)^{1/2} \frac{\sqrt{a} + \sqrt{b}}{2} \leq \frac{a+b}{2}$$

$$\left(\frac{\sqrt{a} + \sqrt{b}}{2}\right)^2 \leq \frac{N_3}{A} \leq \left(\frac{a+b}{2}\right)^{1/2} \frac{\sqrt{a} + \sqrt{b}}{2}$$

Here $N_1 = \left(\frac{\sqrt{a} + \sqrt{b}}{2}\right)^2$, $N_2 = \left(\frac{a+b}{2}\right)^{1/2} \frac{\sqrt{a} + \sqrt{b}}{2}$, $N_3 = \frac{a+b+\sqrt{ab}}{3}$, and $N_4 = \frac{N_3}{A}$

Finally the expressions (1.5), (1.6) lead us to the following inequalities [7]

$$H(a,b) \leq G(a,b) \leq N_1(a,b) \leq H_e(a,b) \leq N_2(a,b) \leq A(a,b) \leq S(a,b)$$

Let us consider the following distinction of means was studied in [17].

$$(1.8) \quad M_{SA}(a,b) = S(a,b) - A(a,b)$$

$$(1.9) \quad M_{SN_2}(a,b) = S(a,b) - N_2(a,b)$$

$$(1.10) \quad M_{SH_e}(a,b) = S(a,b) - H_e(a,b)$$

$$(1.11) \quad M_{SN_1}(a,b) = S(a,b) - N_1(a,b)$$

$$(1.12) \quad M_{SG}(a,b) = S(a,b) - G(a,b)$$

$$(1.13) \quad M_{SH}(a,b) = S(a,b) - H(a,b)$$

$$(1.14) \quad M_{AN_2}(a,b) = A(a,b) - N_2(a,b)$$

$$(1.15) \quad M_{AG}(a,b) = A(a,b) - G(a,b)$$

$$(1.16) \quad M_{AH}(a,b) = A(a,b) - H(a,b)$$

$$(1.17) \quad M_{N_2N_1}(a,b) = A(a,b) - N_2(a,b)$$

$$(1.18) \quad M_{N_2G}(a,b) = N_2(a,b) - G(a,b)$$

Clearly the above distinction of means are nonnegative and convex in $\mathfrak{R}^2_+ = (0, \infty) \times (0, \infty)$.

In this paper, we defined new distinction of means and by using these we define some special means, then we discussed "Schur m - power convexities for special means".

2.Special Means

From the distinction of means defined in the equations 1.8 to 1.18, we define the following difference between the means

$$(2.1) \quad M_{SN_2}(a,b) - M_{SA}(a,b) = A - N_2$$

$$(2.2) \quad M_{SH_e}(a,b) - M_{SN_2}(a,b) = N_2 - H_e$$

$$(2.3) \quad M_{SH_e}(a,b) - M_{SA}(a,b) = A - H_e$$

$$(2.4) \quad M_{SN_1}(a,b) - M_{SH_e}(a,b) = H_e - N_1$$

$$(2.5) \quad M_{SN_1}(a,b) - M_{SN_2}(a,b) = N_2 - N_1$$

$$(2.6) \quad M_{N_1H}(a,b) - M_{GH}(a,b) = N_1 - G$$

$$(2.7) \quad M_{SH}(a,b) - M_{SG}(a,b) = G - H$$

Clearly, the above difference of the means are convex for all positive real value of 't'.

Now, by using the (2.1) to (2.7) difference of means, we establish the special means as follows:

$$(2.8) \quad \frac{M_{SN_2} - M_{SA}}{M_{SH_e} - M_{SN_2}} = \frac{A - N_2}{N_2 - H_e}$$

$$(2.9) \quad \frac{M_{SN_1} - M_{SH_e}}{M_{NH} - M_{GH}} = \frac{H_e - N_1}{N_1 - G}$$

Lemma 2.1. In [14] J.Rooin and M Hassni , introduced the homogeneous functions, the function

$$(2.10) \quad f(x) = \frac{a^x - b^x}{c^x - d^x} \text{ and } g(x) = \frac{a^x - b^x}{c^x - d^x} . \text{ For } a > b \geq c > d > 0 \text{ where } x \in (-\infty, \infty) \text{ is}$$

- (i) Convex, if $ad - bc > 0$
- (ii) Concave, if $ad - bc < 0$ and
- (iii) Equality holds, if $ad - bc = 0$

3. Preliminaries

We begin with recalling some basic concepts and notations in the theory of majorization. For more details, we refer the reader to [1,2].

Definition 3.1 . Let $x = (x_1, x_2, x_3, \dots, x_n)$ and $y = (y_1, y_2, y_3, \dots, y_n) \in R^n$

- i) x is said to be majorized by y (in symbols $x < y$), $\sum_{i=1}^k x_{[i]} \leq \sum_{i=1}^k y_{[i]}$ for $k=1, 2, 3, \dots, n-1$ and $\sum_{i=1}^n x_i = \sum_{i=1}^n y_i$ where $x_{[1]} \geq \dots \geq x_{[n]}$ and $y_{[1]} \geq \dots \geq y_{[n]}$ are rearrangement of x and y in a descending order.
- ii) $\Omega \subset R^n$ is called a convex set, if $(\alpha x_1 + \beta y_1, \alpha x_2 + \beta y_2, \dots, \alpha x_n + \beta y_n) \in \Omega$, for any x and $y \in \Omega$, where α and $\beta \in [0,1]$ with $\alpha + \beta = 1$
- iii) Let $\Omega \subset R^n$, the function $\varphi : \Omega \rightarrow R^n$ is said to be schur convex function on Ω if $x < y$ on Ω implies $\varphi(x) \leq \varphi(y)$. φ is said to be a Schur concave function on Ω , if and only if $-\varphi$ is Schur convex function.

Definition 3.2 . Let $x = (x_1, x_2, x_3, \dots, x_n)$ and $y = (y_1, y_2, y_3, \dots, y_n) \in R_+^n$.

$\Omega \subset R^n$ is called geometrically convex set, if $(x_1^\alpha y_1^\beta, x_2^\alpha y_2^\beta, \dots, x_n^\alpha y_n^\beta) \in \Omega$, for any x and $y \in \Omega$, where $\alpha, \beta \in [0,1]$ with $\alpha + \beta = 1$.

A generalization of Schur convex functions was introduced by Yang [14], as follows

Definition 3.3. Let $f : R_{++} \rightarrow R$ be defined by

$$f(x) = \begin{cases} \frac{x^m - 1}{m}, & m \neq 0 \\ \ln x, & m = 0 \end{cases}$$

Lemma 2.4. Let $\varphi : \Omega \rightarrow R_+$ be continuous on Ω and differentiable on Ω^0 . Then φ is Schur m -power convex on function $x = (x_1, x_2, x_3, \dots, x_n) \in \Omega^0$ if and only if φ is symmetric on Ω and

$$\frac{x_1^m - x_2^m}{m} \left[x_1^{m-1} \frac{\partial \varphi(x)}{\partial x_1} - x_2^{m-1} \frac{\partial \varphi(x)}{\partial x_2} \right] \geq 0 \text{ if } m \neq 0$$

and

$$(\log x_1 - \log x_2) \left[x_1^m \frac{\partial \varphi(x)}{\partial x_1} - x_2^m \frac{\partial \varphi(x)}{\partial x_2} \right] \geq 0 \text{ if } m = 0$$

4. Main Results

In this paper, we discuss the Schur m -power Convexity of the distinguishes special means, in the following theorems.

Theorem 4.1. For $m \neq 0$, the proportion of distinction of means $\frac{M_{SN_2} - M_{SA}}{M_{SH_e} - M_{SN_2}}$ is Schur m -power convex function in R_+^2 .

Proof. Let

$$f(a, b) = \frac{M_{SN_2} - M_{SA}}{M_{SH_e} - M_{SN_2}} = \frac{A - N_2}{N_2 - H_e}$$

By Lemma 2.1

$$f(a, b) = \frac{AH_e - N_2^2}{24}$$

$$f(a, b) = \frac{a^2 + b^2 + 2ab - 2a\sqrt{ab} - 2b\sqrt{ab}}{24}$$

by finding the partial derivatives of $f(a, b)$ and simple manipulation gives we have

$$\frac{\partial f}{\partial a} = \frac{2a + 2b - 3\sqrt{ab} - b \left(\frac{\sqrt{b}}{\sqrt{a}} \right)}{24}$$

$$\frac{\partial f}{\partial b} = \frac{2b + 2a - 3\sqrt{ab} - a\left(\frac{\sqrt{a}}{\sqrt{b}}\right)}{24}$$

By m -power Schur convexity,

$$\begin{aligned} \Delta &= \frac{a^m - b^m}{m} \left[a^{1-m} \frac{\partial f}{\partial a} - ab^{1-m} \frac{\partial f}{\partial b} \right] \\ &= \frac{a^m - b^m}{24m} \left[(2a + 2b - 3\sqrt{ab})(a^{1-m} - b^{1-m}) - \frac{ab\sqrt{b}}{a^m\sqrt{a}} + \frac{ab\sqrt{a}}{b^m\sqrt{b}} \right] \\ &= \frac{a^m - b^m}{24ma^m b^m} \left[(2a + 2b - 3\sqrt{ab})(ab^m - ba^m) - \sqrt{ab}(b^{m+1} - a^{m+1}) \right] \\ &= \frac{a^m - b^m}{24ma^m b^m} \left[(2a + 2b - 3\sqrt{ab})(ab^m - ba^m) - \sqrt{ab}(b^{m+1} - a^{m+1}) \right] \\ &= \frac{a^m - b^m}{24ma^m b^m} \left[(2a + 2b - 3\sqrt{ab})(ab^m - ba^m) + \sqrt{ab}(a^{m+1} - b^{m+1}) \right] \end{aligned}$$

Thus $\Delta \geq 0$. From Lemma 3.2, it follows that the proportion of distinction of mean is Schur 'm'-power convex functions in R_{++}^n .

Theorem 4.2. For $m \neq 0$, the proportion of distinction of means $\frac{M_{SH_e} - M_{SA}}{M_{SN_1} - M_{SH_e}}$ is Schur m-power

convex function in R_+^2 .

Proof. Let $f(a, b) = \frac{M_{SH_e} - M_{SA}}{M_{SN_1} - M_{SH_e}} = \frac{A - H_e}{H_e - N_1}$

By Lemma 3.2

$$f(a, b) = AN_1 - H_e^2$$

$$f(a, b) = \frac{a^2 + b^2 + 6ab - 2a\sqrt{ab} + 2b\sqrt{ab}}{72}$$

by finding the partial derivatives of $f(a, b)$ and simple manipulation gives we have

$$\frac{\partial f}{\partial a} = \frac{2a - 6b + 3\sqrt{ab} + b\left(\frac{\sqrt{b}}{\sqrt{a}}\right)}{72}$$

$$\frac{\partial f}{\partial b} = \frac{2b - 6a + 3\sqrt{ab} + a\left(\frac{\sqrt{a}}{\sqrt{b}}\right)}{72}$$

By m -power Schur convexity,

$$\begin{aligned} \Delta &= \left(\frac{a^m - b^m}{m}\right) \left[a^{1-m} \frac{\partial f}{\partial a} - ab^{1-m} \frac{\partial f}{\partial b} \right] \\ &= \left(\frac{a^m - b^m}{72m}\right) \left[(3\sqrt{ab})(a^{1-m} - b^{1-m}) + a(2a^{1-m} + 6b^{1-m}) - b(6a^{1-m} + 2b^{1-m}) + \frac{ab\sqrt{b}}{a^m\sqrt{a}} - \frac{ab\sqrt{a}}{b^m\sqrt{b}} \right] \\ &= \left(\frac{a^m - b^m}{72m}\right) \left[\frac{1}{a^m} (2a^2 + \sqrt{ab}(3a+b) - 6ab) + \frac{1}{b^m} (2b^2 - \sqrt{ab}(3b+a) + 6ab) \right] \\ &= \left(\frac{a^m - b^m}{72ma^m b^m}\right) \left[b^m (2a^2 + \sqrt{ab}(3a+b)) + a^m (2b^2 - \sqrt{ab}(3b+a)) + 6ab(a^m - b^m) \right] \geq 0 \end{aligned}$$

Thus $\Delta \geq 0$. From Lemma 3.2, it follows that the proportion of distinction of mean is Schur ' m '-power convex functions for $x \in R_{++}^n$.

5. Conclusion

In this paper, we distinguished special means and discussed about the Schur properties of Schur ' m '-power convexities on the proportion of distinction of special means.

References

- [1] B. Y. Wang, Foundations of majorization inequalities (Chinese), Beijing Normal University Press, Bei-jing, China, 1990.
- [2] A. W. Marshall, I. Olkin, and B. C. Arnold, Inequalities: Theory of Majorization and its Applications, 2nd Ed., Springer Verlag, New York-Dordrecht-Heidelberg-London, 2011; Available online at <http://dx.doi.org/10.1007/978-0-387-68276-1>.
- [3] F. QI, Integral representations and properties of Sterling numbers of the first kind, J. Number Theory 133 (2013), no. 7, 23072319; Available online at <http://dx.doi.org/10.1016/j.jnt>.
- [4] H.-N. Shi, J. Zhang, and D.-M. Li, Schur-geometric convexity for differences of means, Appl. Math. E-Notes 10 (2010), 275284.
- [5] I. J. Taneja, Nested inequalities among divergence measures, Appl. Math. Inf. Sci. 7 (2013), No.1 4972; Available online at <http://dx.doi.org/10.12785/amis/070106>.
- [6] I. J. Taneja, On a difference of Jensen inequality and its applications to mean divergence measures, RGMIA Res. Rep. Coll. 7 (2004), no. 4, Art. 16; Available online at <http://rgmia.org/v7n4.php>.
- [7] I.J.Taneja, Refinement of inequalities among means, J. Comb. Inf. Syst. Sci. 31 (2006), no. 1-4, 343364.

- [8] I.J.Taneja, Sequence of inequalities among differences of Gini means and divergence measures, *J. Appl. Math. Statist. Inform.* 8 (2012), no. 2, 4965; Available online at <http://dx.doi.org/10.2478/v10294-012-0014-2>.
- [9] I.J.Taneja, Seven means, generalized triangular discrimination, and generating divergence measures, *Information* (2013) no. 4, 198239; Available online at <http://dx.doi.org/10.3390/info4020198>.
- [10] B.-Y.Wang, *Foundations of Majorization Inequalities*, Beijing Normal Univ. Press, Beijing, China, 1990. (Chinese)
- [11] Y. Wu and F. QI, Schur-harmonic convexity for differences of some means, *Analysis (Munich)* 32 (2012), no. 4, 263270; Available online at <http://dx.doi.org/10.1524/anly.2012.1171>.
- [12] Y. Wu, F. QI, and H.-N. Shi, Schur-harmonic convexity for differences of some special means in two variables, *J. Math. Inequal.* 8, 2 (2014), 321330; Available online at <http://dx.doi.org/10.7153/jmi-08-23>.
- [13] W.-F. Xia and Y.-M. Chu, Schur-convexity for a class of symmetric functions and its applications *J. Inequal. Appl.* 2009 (2009), Article ID 493759, 15 pages; Available online at <http://dx.doi.org/10.1155/2009/493759>.
- [14] Z.-H. Yang, Schur power convexity of Stolarsky means, *Publ. Math. Debrecen* 80 (2012), no. 12, 4366; Available online at <http://dx.doi.org/10.5486/PMD.2012.4812>.
- [15] E.F. Beckenbach and R. Bellman, *Inequalities*, Springer-Verlag, New York, 1971.
- [16] S.S.Dragomir and C.E.M. Pearce, *Selected Topics on Hermite-Hadamard Inequalities and Applications*, Research Report Collection, Monograph, 2002,
- [17] I.J.Taneja, Refinement of inequalities among means, *Journal of Combinatorics, Information and System Sciences*, 31(2006), 343-364.

(sreenivasa Reddy Perla) Department of Mathematics, The Oxford College Of ENGG
E-mail address: srireddy_sri@yahoo.co.in

(S Padmanabhan) Department of Mathematics, R N S I T, Uttarahalli-Kengeri Road, Bangalore - 560 098, India



CHILDREN'S EDUCATION SOCIETY (Regd.)
THE OXFORD COLLEGE OF ENGINEERING

(Recognised by the Govt. of Karnataka, Affiliated to Visvesvaraya Technological University, Belagavi.

Approved by A.I.C.T.E. New Delhi.

Recognised by UGC Under Section 2(f)

Bommanahalli, Hosur Road, Bangalore - 560 068.

Ph: 080-61754601/602, Fax: 080 - 25730551

E-mail: engprincipal@theoxford.edu Web: www.theoxfordengg.org

| Sl.NO | Title of paper | Name of the author/s | Department of the teacher | Name of journal | Year of publication | ISSN number | Link to website of the Journal | Link to article/paper/abstract of the article | Is it listed in UGC Care list/Scopus/Web of Science/other, mention |
|-------|--|--|---------------------------|-----------------------------|---------------------|-------------|---|---|--|
| 1 | Clustering with Modified Mutation Strategy in Differential Evolution | Seema Patil and Anandhi Rajamani Jayadharmarajan | CSE | Pertanika J. Sci. & Technol | 2020 | 0128-7680 | http://www.pertanika.upm.edu.my/resources/files/Pertanika%20PAPER%20S/JST%20Vol.%2028%20(1)%20Jan.%202020/08%20JST-1709-2019.pdf | http://www.pertanika.upm.edu.my/resources/files/Pertanika%20PAPER%20S/JST%20Vol.%2028%20(1)%20Jan.%202020/08%20JST-1709-2019.pdf | UGC |
| 2 | A REAL TIME HAND GESTURERE COGNITION AND HUMANCOM | J. Jesy Janet Kumari | CSE | JETIR | 2019 | 2349-5162 | https://www.jetir.org/papers/JETIRCD06052.pdf | https://www.jetir.org/papers/JETIRCD06052.pdf | Google Scholar |



CHILDREN'S EDUCATION SOCIETY (Regd.)
THE OXFORD COLLEGE OF ENGINEERING

(Recognised by the Govt. of Karnataka, Affiliated to Visvesvaraya Technological University, Belagavi.

Approved by A.I.C.T.E. New Delhi.

Recognised by UGC Under Section 2(f)

Bommanahalli, Hosur Road, Bangalore - 560 068.

Ph: 080-61754601/602, Fax: 080 - 25730551

E-mail: engprincipal@theoxford.edu Web: www.theoxfordengg.org

| | | | | | | | | | |
|---|---|--------------------------------------|-----|--------------------------------------|------|-----------|---|---|----------------|
| | PUTER INTERACTION SYSTEM USING OPENCV | | | | | | | | |
| 3 | PREDICTIVE MODEL DEVELOPMENT FOR LULC DATA USING ADAPTIVE MLP NEURAL NETWORK ARCHITECTURE | Shobha T | CSE | IJSIA | 2020 | | http://article.nadiapub.com/IJSIA/vol115_no1/2.html | http://article.nadiapub.com/IJSIA/vol15_no1/2.html | Google Scholar |
| 4 | Rate adaptation performance and quality analysis of adaptive HTTP streaming methods | Selvaraj Kesavan & E. Saravana Kumar | CSE | Selvaraj Kesavan & E. Saravana Kumar | 2020 | 2511-2104 | https://link.springer.com/article/10.1007/s41870-019-00350-6 | https://www.springer.com/journal/41870 | Google Scholar |



**CHILDREN'S EDUCATION SOCIETY (Regd.)
THE OXFORD COLLEGE OF ENGINEERING**

(Recognised by the Govt. of Karnataka, Affiliated to Visvesvaraya Technological University, Belagavi.

Approved by A.I.C.T.E. New Delhi.

Recognised by UGC Under Section 2(f)

Bommanahalli, Hosur Road, Bangalore - 560 068.

Ph: 080-61754601/602, Fax: 080 - 25730551

E-mail: engprincipal@theoxford.edu Web: www.theoxfordengg.org

| | | | | | | | | | |
|---|---|-----------------------------|-----|---|------|-----------|---|---|------------|
| 5 | Diversity based self-adaptive clusters using PSO clustering for crime data | Seema Patil & R. J. Anandhi | CSE | International Journal of Information Technology | 2019 | 2511-2112 | https://www.springer.com/journal/41870 | https://doi.org/10.1007/s41870-019-00311-z | UGC/Scopus |
| 6 | Adaptive strategy operators-based GA for rule discovery | T. Shobha, R. J. Anandhi | CSE | International Journal of Information Technology | 2019 | 2511-2112 | https://www.springer.com/journal/41870 | https://doi.org/10.1007/s41870-019-00303-z | UGC/Scopus |
| 7 | Extreme Precipitation Events in Chennai Metro City Using Data Mining | R.Senthil Kumar | CSE | International Journal of Innovative Technology and Exploring Engineering (IJITEE) | 2019 | 2278-3075 | https://www.ijitee.org/ | https://www.ijitee.org/wp-content/uploads/papers/v8i11/I99780881019.pdf | Scopus |
| 8 | An investigation on adaptive HTTP media streaming Quality-of-Experience (QoE) and agility using | Dr. E. Saravana Kumar | CSE | International Journal of Computers and Applications | 2019 | 1925-7074 | https://www.tandfonline.com/action/journalInformation?journalCode=tjca20 | https://doi.org/10.1080/1206212X.2019.1575034 | Scopus |



CHILDREN'S EDUCATION SOCIETY (Regd.)
THE OXFORD COLLEGE OF ENGINEERING

(Recognised by the Govt. of Karnataka, Affiliated to Visvesvaraya Technological University, Belagavi.

Approved by A.I.C.T.E. New Delhi.

Recognised by UGC Under Section 2(f)

Bommanahalli, Hosur Road, Bangalore - 560 068.

Ph: 080-61754601/602, Fax: 080 - 25730551

E-mail: engprincipal@theoxford.edu Web: www.theoxfordengg.org

| | | | | | | | | | |
|----|---|-------------|-----|--------|------|----------------------|---|---|----------------|
| | cloud media services | | | | | | | | |
| 9 | An automated serving robot based on artificial intelligence | S Preethi | ISE | IJRCCE | 2020 | 2320-9801, 2320-9798 | https://www.ijrce.com/ | http://ijrce.com/admin/main/storage/app/pdf/4f7R1oyUawy6UIGefLcmGbbdhe5gTC3rUVFnqq5J.pdf | Google Scholar |
| 10 | Personal Assistant Robot System Using Node MCU | Borra Ramya | ISE | IJRCCE | 2020 | 2320-9801, 2320-9798 | https://www.ijrce.com/ | http://ijrce.com/admin/main/storage/app/pdf/EQGzDOFKG3dwrW6WMOLeTNPfnGFf7FP5EwFRvGxh.pd8f | Google Scholar |
| 11 | Voice Control Chatbot for Ticket Booking Using NLP | Nipam Rawal | ISE | IJRCCE | 2020 | 2320-9801, 2320-9798 | https://www.ijrce.com/ | http://ijrce.com/admin/main/storage/app/pdf/C0PEnjqcAs269pN1eD2TKAGwmbOjiMCnlw45ffjZ.pdf | Google Scholar |



CHILDREN'S EDUCATION SOCIETY (Regd.)
THE OXFORD COLLEGE OF ENGINEERING

(Recognised by the Govt. of Karnataka, Affiliated to Visvesvaraya Technological University, Belagavi.

Approved by A.I.C.T.E. New Delhi.

Recognised by UGC Under Section 2(f)

Bommanahalli, Hosur Road, Bangalore - 560 068.

Ph: 080-61754601/602, Fax: 080 - 25730551

E-mail: engprincipal@theoxford.edu Web: www.theoxfordengg.org

| | | | | | | | | | |
|----|--|-----------------------|-----|--------|------|----------------------|---|---|----------------|
| 12 | A Novel Approach for User-Cloud Interaction using RAAC | Shwetha Balaji | ISE | IJIRCE | 2020 | 2320-9801, 2320-9798 | https://www.ijrce.com/ | http://ijrce.com/admin/main/storage/app/pdf/nYQCdwXwl32wbCiP3MxB51S01RRcmrXZdF9nzP2r.pdf | Google Scholar |
| 13 | Secured and Cardless ATM using Iris | C R Sai Ruchitha Babu | ISE | IJIRCE | 2020 | 2320-9801, 2320-9798 | https://www.ijrce.com/ | http://ijrce.com/admin/main/storage/app/pdf/c7OKLbugcaJvV66ReogA6R39hUi2QlqDpTN1eveB.pdf | Google Scholar |
| 14 | Smart Irrigation System with Safety and Security using Alarm Systems | S Kavitha | ISE | IJIRCE | 2020 | 2320-9801, 2320-9798 | https://www.ijrce.com/ | http://ijrce.com/admin/main/storage/app/pdf/jVg3IzlWG26GoWKWMAjpYze5ApgDwQnI9hNxEf1Q.pdf | Google Scholar |
| 15 | Automated Smart Sericulture System Based | Monica K V | ISE | IJIRCE | 2020 | 2320-9801, 2320-9798 | https://www.ijrce.com/ | http://ijrce.com/admin/main/storage/app/pdf/pGPZ | Google Scholar |



CHILDREN'S EDUCATION SOCIETY (Regd.)
THE OXFORD COLLEGE OF ENGINEERING

(Recognised by the Govt. of Karnataka, Affiliated to Visvesvaraya Technological University, Belagavi.

Approved by A.I.C.T.E. New Delhi.

Recognised by UGC Under Section 2(f)

Bommanahalli, Hosur Road, Bangalore - 560 068.

Ph: 080-61754601/602, Fax: 080 - 25730551

E-mail: engprincipal@theoxford.edu Web: www.theoxfordengg.org

| | | | | | | | | | |
|----|---|-------------------|-----|--------|------|----------------------|---|---|----------------|
| | on Image Processing Technique | | | | | | | MplZ2IV6Cgipm0U9KhnrTxh4o07jt3LPyggF.pdf | |
| 16 | GloveBlu: Many-to-Many Communication among Disabled Users | Rachana | ISE | IJRCCE | 2020 | 2320-9801, 2320-9798 | https://www.ijrcc.com/ | http://ijrcc.com/admin/main/storage/app/pdf/FCYNQCRZV6IP29C2QtRG1BqreQAv9Nzsnk62HLNx.pdf | Google Scholar |
| 17 | 3-D Hologram Using Hand Gestures | Ameerunisa Daniya | ISE | IJRCCE | 2020 | 2320-9801, 2320-9798 | https://www.ijrcc.com/ | http://ijrcc.com/admin/main/storage/app/pdf/VamaIX1a3khNLoLVp4NmgIJTZNI8FgeVAmSJcP5z.pdf | Google Scholar |
| 18 | An Automated Cooking Robot Using Embedded C | Prakruthi K.S | ISE | IJRCCE | 2020 | 2320-9801, 2320-9798 | https://www.ijrcc.com/ | http://ijrcc.com/admin/main/storage/app/pdf/0n8ZIYdgMUjkjYXBzh8BVQHj | Google Scholar |



CHILDREN'S EDUCATION SOCIETY (Regd.)
THE OXFORD COLLEGE OF ENGINEERING

(Recognised by the Govt. of Karnataka, Affiliated to Visvesvaraya Technological University, Belagavi.

Approved by A.I.C.T.E. New Delhi.

Recognised by UGC Under Section 2(f)

Bommanahalli, Hosur Road, Bangalore - 560 068.

Ph: 080-61754601/602, Fax: 080 - 25730551

E-mail: engprincipal@theoxford.edu Web: www.theoxfordengg.org

| | | | | | | | | | |
|----|--|----------------|-----|----------|------|----------------------|---|---|----------------|
| | | | | | | | | 19TMpZ9kdwZzoKsZYm.pdf | |
| 19 | Hand Gesture Technology Using Image Processing | Faisal Shariff | ISE | IJIRCCCE | 2020 | 2320-9801, 2320-9798 | https://www.ijrccce.com/ | http://ijrccce.com/admin/main/storage/app/pdf/KXIYDESUnUIHG5MAFD7oAQSW9NzVYRFjWfkBCUOk.pdf | Google Scholar |
| 20 | USB to USB Data Transfer using Raspberry Pi | Rachana R | ISE | IJIRCCCE | 2020 | 2320-9801, 2320-9798 | https://www.ijrccce.com/ | http://ijrccce.com/admin/main/storage/app/pdf/pjltADrYLLT0V6QpYqFicBfWPfVjPsHeNwQpgR11.pdf | Google Scholar |
| 21 | Virtual Technology for Library Using VR Box | Ramya S | ISE | IJIRCCCE | 2020 | 2320-9801, 2320-9798 | https://www.ijrccce.com/ | http://ijrccce.com/admin/main/storage/app/pdf/3uUHC TC5cILwdglBTsOOr0FZddbMpTSae | Google Scholar |



CHILDREN'S EDUCATION SOCIETY (Regd.)
THE OXFORD COLLEGE OF ENGINEERING

(Recognised by the Govt. of Karnataka, Affiliated to Visvesvaraya Technological University, Belagavi.

Approved by A.I.C.T.E. New Delhi.

Recognised by UGC Under Section 2(f)

Bommanahalli, Hosur Road, Bangalore - 560 068.

Ph: 080-61754601/602, Fax: 080 - 25730551

E-mail: engprincipal@theoxford.edu Web: www.theoxfordengg.org

| | | | | | | | | | |
|----|--|--------------|-----|--------|------|----------------------|---|---|----------------|
| | | | | | | | | DBn51HQ.pdf | |
| 22 | Automated Beach Security System using Autopilot Drone | Arpitha P | ISE | IJRCCE | 2020 | 2320-9801, 2320-9798 | https://www.ijrce.com/ | http://ijrce.com/admin/main/storage/app/pdf/hyLIPV9btcSraD8nC aGU7meDHwN6nzNU4N ODnhbJ.pdf | Google Scholar |
| 23 | Eye Tracking Password Using Blinking Verification System | Sristi V | ISE | IJRCCE | 2020 | 2320-9801, 2320-9798 | https://www.ijrce.com/ | http://ijrce.com/admin/main/storage/app/pdf/AUAeoUy4KssWB6t1DjJ3JTyUzEfe3MDPmlIsDwbH.pdf | Google Scholar |
| 24 | Suspicious Human Activity Detection Using Image Processing | Harshith T R | ISE | IJRCCE | 2020 | 2320-9801, 2320-9798 | https://www.ijrce.com/ | http://ijrce.com/admin/main/storage/app/pdf/jqV9Z5AQnRfPyRcK5VlfVsxxciTUpuxAZpc2QfIC.pdf | Google Scholar |



CHILDREN'S EDUCATION SOCIETY (Regd.)
THE OXFORD COLLEGE OF ENGINEERING

(Recognised by the Govt. of Karnataka, Affiliated to Visvesvaraya Technological University, Belagavi.

Approved by A.I.C.T.E. New Delhi.

Recognised by UGC Under Section 2(f)

Bommanahalli, Hosur Road, Bangalore - 560 068.

Ph: 080-61754601/602, Fax: 080 - 25730551

E-mail: engprincipal@theoxford.edu Web: www.theoxfordengg.org

| | | | | | | | | | |
|----|---|-----------------|-----|---------|------|----------------------|---|---|----------------|
| 25 | A Secured Data sharing among Vehicles to Keep Track of Road Conditions | Rahul Chatterje | ISE | IJIRCCE | 2020 | 2320-9801, 2320-9798 | https://www.ijrce.com/ | http://ijrce.com/admin/main/storage/app/pdf/BtpCW rPpI5PFFEna ACAoZpW6 Rojq4NBchm mEhIvj.pdf | Google Scholar |
| 26 | Encasement for Walking Assistance using Robotic Technology Aishwarya M | Aishwarya M | ISE | IJIRCCE | 2020 | 2320-9801, 2320-9798 | https://www.ijrce.com/ | http://ijrce.com/admin/main/storage/app/pdf/vTgWs AoNvBV4Jp TqFGtvKCO Uc7Dty7LD4 QTbKkxw.pdf | Google Scholar |
| 27 | Medical Mirror Using Face Recognition | Abhishek M | ISE | IJIRCCE | 2020 | 2320-9801, 2320-9798 | https://www.ijrce.com/ | http://ijrce.com/admin/main/storage/app/pdf/xBkV4 AkFGeO4G Kq4j9X2JWp mfFlFRDog NcrJLWSF.pdf | Google Scholar |



CHILDREN'S EDUCATION SOCIETY (Regd.)
THE OXFORD COLLEGE OF ENGINEERING

(Recognised by the Govt. of Karnataka, Affiliated to Visvesvaraya Technological University, Belagavi.

Approved by A.I.C.T.E. New Delhi.

Recognised by UGC Under Section 2(f)

Bommanahalli, Hosur Road, Bangalore - 560 068.

Ph: 080-61754601/602, Fax: 080 - 25730551

E-mail: engprincipal@theoxford.edu Web: www.theoxfordengg.org

| | | | | | | | | | |
|----|---|--|-----|---|------|----------------------|---|---|----------------|
| 28 | Blockchain Based Video Surveillance System | Ritesh S | ISE | IJIRCCE | 2020 | 2320-9801, 2320-9798 | https://www.ijrce.com/ | http://ijrce.com/admin/main/storage/app/pdf/EtSQYc3h0A5PvuAc4G9tUNwXpzHgI16Q0WGoK2Uj.pdf | Google Scholar |
| 29 | Design of ultra-high sensitive biosensor to detect E. Coli in water | Sandip Kumar Roy, Preeta Sharan | ECE | International Journal of Information Technology | 2019 | 2511-2112 | https://www.springer.com/journal/41870 | https://doi.org/10.1007/s41870-019-00327-5 | UGC/Scopus |
| 30 | A Traffic Delay and Bandwidth Based Multipath Scheduling Approach for Optimal Routing in Underwater Optical Network | R. Bhargava Rama Gowd, S. Thenappan & M. N. GiriPrasad | ECE | Wireless Personal Communications | 2019 | 1572-834X | https://www.springer.com/journal/11277 | https://doi.org/10.1007/s11277-019-06632-3 | UGC/Scopus |



CHILDREN'S EDUCATION SOCIETY (Regd.)
THE OXFORD COLLEGE OF ENGINEERING

(Recognised by the Govt. of Karnataka, Affiliated to Visvesvaraya Technological University, Belagavi.

Approved by A.I.C.T.E. New Delhi.

Recognised by UGC Under Section 2(f)

Bommanahalli, Hosur Road, Bangalore - 560 068.

Ph: 080-61754601/602, Fax: 080 - 25730551

E-mail: engprincipal@theoxford.edu Web: www.theoxfordengg.org

| | | | | | | | | | |
|----|---|---------------------|-----|--|------|-----------|---|---|----------------|
| 31 | Effect of Chanting, Recitation of Mantras, Slokas, Duas, Music on Plants and Trees using EMF Radiations: A Sudy | Dr. Thenappan S | ECE | TEST | 2020 | 0193-4120 | http://www.testmagzine.biz/index.php/testmagzine | http://testmagzine.biz/index.php/testmagzine/article/view/9212/7041 | Scopus |
| 32 | Parameter Analysis of CMOS Amplifier Topologies for Biosensors | Mrs.Jyoti M R, | ECE | International Journal of Advanced Science and Technology | 2020 | 2005-4238 | http://oaji.net/journal-detail.html?number=3107 | http://sersc.org/journals/index.php/IJAST/article/view/24865 | Google Scholar |
| 33 | Design of a Low Latency and High Throughput Packet Classification Module on FPGA Platform | Anita P, Manju Devi | ECE | IJITEE | 2020 | 2278-3075 | https://www.ijitee.org/ | http://www.ijitee.org/wp-content/uploads/papers/v9i6/F4195049620.pdf | Google Scholar |



CHILDREN'S EDUCATION SOCIETY (Regd.)
THE OXFORD COLLEGE OF ENGINEERING

(Recognised by the Govt. of Karnataka, Affiliated to Visvesvaraya Technological University, Belagavi.

Approved by A.I.C.T.E. New Delhi.

Recognised by UGC Under Section 2(f)

Bommanahalli, Hosur Road, Bangalore - 560 068.

Ph: 080-61754601/602, Fax: 080 - 25730551

E-mail: engprincipal@theoxford.edu Web: www.theoxfordengg.org

| | | | | | | | | | |
|----|--|---------------------|-----|-------|------|----------------------|---|--|----------------|
| 34 | Design and Development of Mach Zehnder Interferometer based Optical Sensors to Detection of Arsenic compound in Drinking Water | Shaikh Afzal Nehal | ECE | IJET | 2020 | 2227-524X | https://www.sciencepubco.com/index.php/IJET | https://www.sciencepubco.com/index.php/IJET | Google Scholar |
| 35 | Power Analysis of Photonic Sensor for Detection of E-coli in Water | Afzal Shaikh | ECE | IEEE | 2020 | | https://ieeexplore.ieee.org/Xplore/home.jsp | https://doi.org/10.1109/WRAP47485.2019.9013691 https://ieeexplore.ieee.org/document/9013691 | IEEE Xplore |
| 36 | Smart E – Cane for the Visually Challenged and Blind using ML Concepts | Adam Filbert Ashwal | ECE | IRJET | 2020 | 2395-0056, 2395-0072 | https://www.irjet.net/ | https://www.irjet.net/archives/V7/i3/IRJET-V7I3735.pdf | Google Scholar |



CHILDREN'S EDUCATION SOCIETY (Regd.)
THE OXFORD COLLEGE OF ENGINEERING

(Recognised by the Govt. of Karnataka, Affiliated to Visvesvaraya Technological University, Belagavi.

Approved by A.I.C.T.E. New Delhi.

Recognised by UGC Under Section 2(f)

Bommanahalli, Hosur Road, Bangalore - 560 068.

Ph: 080-61754601/602, Fax: 080 - 25730551

E-mail: engprincipal@theoxford.edu Web: www.theoxfordengg.org

| | | | | | | | | | |
|----|---|--------------------------------|-----|--|------|-----------|---|---|----------------|
| 37 | A Novel Low Power 8-Bit Binary Weighted Charge Steering DAC with Integrated Power Supply using CMOS | Bharathesh Patel N, Manju Devi | ECE | IJEAT | 2020 | 2249-8958 | https://www.ijeat.org/download/volume-9-issue-4/ | https://www.ijeat.org/wp-content/uploads/papers/v9i4/D6666049420.pdf | Scopus |
| 38 | The Tiled Cache Implementation for High Performance Processor | Suma Sannamani | ECE | International Journal of Advanced Science and Technology | 2020 | 7430-7438 | http://oaji.net/journal-detail.html?number=3107 | http://sersc.org/journals/index.php/IJAST/article/view/18237 | Google Scholar |
| 39 | Turbo Decoder for LTE High Speed band Efficient Architecture | Rashmi R, Manju Devi | ECE | IJFGCN | 2020 | 2233-7857 | http://sersc.org/journals/index.php/IJFGCN/issue/archive | http://sersc.org/journals/index.php/IJFGCN/article/view/6687 | Google Scholar |
| 40 | Voice Assisted Smart E-Cane for the Visually Challenged using Machine Learning | Adam Filbert Ashwal | ECE | IJRASET | 2020 | 2321-9653 | https://www.ijraset.com/archive-detail.php?AID=107 | http://doi.org/10.22214/ijraset.2020.6316 | Google Scholar |



CHILDREN'S EDUCATION SOCIETY (Regd.)
THE OXFORD COLLEGE OF ENGINEERING

(Recognised by the Govt. of Karnataka, Affiliated to Visvesvaraya Technological University, Belagavi.

Approved by A.I.C.T.E. New Delhi.

Recognised by UGC Under Section 2(f)

Bommanahalli, Hosur Road, Bangalore - 560 068.

Ph: 080-61754601/602, Fax: 080 - 25730551

E-mail: engprincipal@theoxford.edu Web: www.theoxfordengg.org

| | | | | | | | | | |
|----|--|---|----|---|------|-------------|---|---|----------------|
| 41 | Dry Sliding Wear Behavior of B4C Particulates Reinforced Al7020 Alloy Composites | Raviprakash M | ME | International Journal of Applied Engineering Research | 2019 | 0973-4562 | http://www.ripublication.com/ | https://www.ripublication.com/ijaer19/ijaerv14n2_14.pdf | Google Scholar |
| 42 | Influence of Nickel Coated B4C particulates Addition on the Mechanical Characterization of Al7020 Alloy Composites | Raviprakash M1* , R Saravanan2 | ME | International Journal of Computational Engineering Research | 2019 | 2250 – 3005 | http://www.ijceronline.com/ | http://www.ijceronline.com/papers/Vol9_issue5/B09051218.pdf | Google Scholar |
| 43 | Microstructure , Hardness and Tensile Behavior of Micro B4C Reinforced Al7020 Alloy Composites | Raviprakash M R Saravanan, Madeva Nagaral | ME | Advanced Materials Manufacturing & Characterization | 2019 | 2347-1891 | http://www.ijammc-griet.com/ | http://www.ijammc-griet.com/attach/1506612609_8.pdf | Google Scholar |



CHILDREN'S EDUCATION SOCIETY (Regd.)
THE OXFORD COLLEGE OF ENGINEERING

(Recognised by the Govt. of Karnataka, Affiliated to Visvesvaraya Technological University, Belagavi.

Approved by A.I.C.T.E. New Delhi.

Recognised by UGC Under Section 2(f)

Bommanahalli, Hosur Road, Bangalore - 560 068.

Ph: 080-61754601/602, Fax: 080 - 25730551

E-mail: engprincipal@theoxford.edu Web: www.theoxfordengg.org

| | | | | | | | | | |
|----|--|---|--------------|---|------|----------------------|---|---|----------------|
| 44 | Characterization and Tensile Fractography of Nano ZrO ₂ Reinforced Copper-Zinc Alloy Composites | Prasad H Nayak | ME | Frattura ed integrità strutturale | 2019 | 1971-8993 | https://doi.org/10.3221/IGF-ESIS.48.35 | https://www.fracturae.com/index.php/fis/article/view/2261 | Scopus |
| 45 | FPGA BASED DIGITAL LOGIC ANALYZER FOR DIGITAL AUTOMATIC TEST EQUIPMENT | Manjula C and Jayadevappa D | Mechatronics | International Journal of Future Generation Communication and Networking | 2020 | 2321-2234 | http://sersc.org/journals/index.php/IJFGCN/article/view/4837 | http://sersc.org/journals/index.php/IJFGCN/article/view/4837 | Google Scholar |
| 46 | Estimation of genetic diversity for yield and yield attributing traits in rice (Oryza sativa L.) | Manjunatha B, Nagaraja Kusagur and Niranjana kumara B | BioTech | Journal of Pharmacognosy and Phytochemistry | 2020 | 2278-4136, 2349-8234 | https://www.phytojournal.com/ | https://www.phytojournal.com/archives/2020/vol9issue4/PartAD/9-4-269-108.pdf | Google Scholar |



CHILDREN'S EDUCATION SOCIETY (Regd.)
THE OXFORD COLLEGE OF ENGINEERING

(Recognised by the Govt. of Karnataka, Affiliated to Visvesvaraya Technological University, Belagavi.

Approved by A.I.C.T.E. New Delhi.

Recognised by UGC Under Section 2(f)

Bommanahalli, Hosur Road, Bangalore - 560 068.

Ph: 080-61754601/602, Fax: 080 - 25730551

E-mail: engprincipal@theoxford.edu Web: www.theoxfordengg.org

| | | | | | | | | | |
|----|---|--|---------|--|------|-------------------------|---|---|----------------|
| 47 | Variability, Heritability and Genetic Advance Studies in Advanced Genotypes of Rice (<i>Oryza sativa</i> L.) | R Manjunatha , Dr Niramjama Kumara | BioTech | IJCMAS | 2020 | 2319-7692, 2319-7706 | https://www.ijcmas.com/ | https://doi.org/10.20546/ijcmas.2020.908.191 | Google Scholar |
| 48 | ASIC Implementation of Random Perturbation Algorithm for Neural Network Application | Dharamvir , Arul Kumar V | MCA | TEST Engineering | 2020 | 0193-4120 | http://www.testmagzine.biz/index.php/testmagzine/article/view/7871 | http://www.testmagzine.biz/index.php/testmagzine/article/view/7871 | Google Scholar |
| 49 | Recommendation based on guided analytics for Product prediction in retail space | J C Achutha | MCA | International Journal of Combined Research & Development (IJCRD) | 2020 | 2321-225X | http://www.ijcrd.com/files/Vol_8_issue_5/2503.pdf | http://www.ijcrd.com/files/Vol_8_issue_5/2503.pdf | Google Scholar |



CHILDREN'S EDUCATION SOCIETY (Regd.)
THE OXFORD COLLEGE OF ENGINEERING

(Recognised by the Govt. of Karnataka, Affiliated to Visvesvaraya Technological University, Belagavi.

Approved by A.I.C.T.E. New Delhi.

Recognised by UGC Under Section 2(f)

Bommanahalli, Hosur Road, Bangalore - 560 068.

Ph: 080-61754601/602, Fax: 080 - 25730551

E-mail: engprincipal@theoxford.edu Web: www.theoxfordengg.org

| | | | | | | | | | |
|----|--|---|-------------|--|------|----------------|---|---|----------------|
| 50 | Data Normalization Techniques on Intrusion Detection for Dataset Applications | Dharamvir, Arul Kumar V | MCA | International Journal of Advanced Science and Technology | 2020 | 2321-2234 | http://sersc.org/journals/index.php/IJAST/article/view/25793 | http://sersc.org/journals/index.php/IJAST/article/view/25793 | Google Scholar |
| 51 | A Study and Application Development for POMP Decorum and its Transformation System | Dr M S Shahsidhara | MCA | International Journal of Combined Research & Development (IJCRD) | 2020 | ISSN:2321-225X | http://www.ijcrd.com/files/Vol_8_issue_5/2501.pdf | http://www.ijcrd.com/files/Vol_8_issue_5/2501.pdf | Google Scholar |
| 52 | An extension of golden section algorithm for n-variable functions with MATLAB code | G Sandhya Rani, Sarada Jayan and K V Nagaraja | Mathematics | IOP Conf. Ser.: Mater. Sci. Eng. | 2019 | -- | https://iopscience.iop.org/ | https://iopscience.iop.org/article/10.1088/1757-899X/577/1/012175 | Scopus |
| 53 | On Schur M-Power Convexity For Proportion Of Distinction Of | Sreenivasa reddy Perla and S Padmanabhan | Mathematics | JETIR | 2019 | 2349-5162 | http://www.jetir.org/ | https://www.researchgate.net/publication/333917262_CONVEXIT | UGC |



CHILDREN'S EDUCATION SOCIETY (Regd.)
THE OXFORD COLLEGE OF ENGINEERING
 (Recognised by the Govt. of Karnataka, Affiliated to Visvesvaraya Technological University, Belagavi.

Approved by A.I.C.T.E. New Delhi.

Recognised by UGC Under Section 2(f)

Bommanahalli, Hosur Road, Bangalore - 560 068.

Ph: 080-61754601/602, Fax: 080 - 25730551

E-mail: engprincipal@theoxford.edu Web: www.theoxfordengg.org

| | | | | | | | | | |
|----|---|--|--------|---------------------------------------|------------|--------------------|---|---|----------------|
| | Some Special Means In Two Variables | | | | | | | Y_OF_ONE_MEAN_WITH_RESPECT_TO_ANOTHER_MEAN | |
| 54 | 'A study on Compartmental models, Epidemiological Characteristics and Stability Analysis of pandemic COVID-19' in INDIA | Dr. Sreenivasa Reddy P. | MAT HS | GIS Science Journal, Volume7, Issue 6 | June 2020. | pp. 8224-8235. | https://www.researchgate.net/publication/342657308_A_study_on_Compartmental_models_Epidemiological_Characteristics_and_Stability_Analysis_of_pandemic_COVID-19_in_INDIA | https://www.researchgate.net/publication/342657308_A_study_on_Compartmental_models_Epidemiological_Characteristics_and_Stability_Analysis_of_pandemic_COVID-19_in_INDIA | Google Scholar |
| 55 | Degree domination Number of a graph | Dr. Mallikarjun K. and Moumita Kali Chatterjee | MAT HS | GIS SCIENCE JOURNAL | Jun-20 | ISSN NO: 1869-9391 | https://drive.google.com/file/d/1M_-dFhazMQ7sM55WY2cv0J11PvQFW4hF/view?usp=sharing | https://drive.google.com/file/d/1M_-dFhazMQ7sM55WY2cv0J11PvQFW4hF/view?usp=sharing | Google Scholar |



CHILDREN'S EDUCATION SOCIETY (Regd.)
THE OXFORD COLLEGE OF ENGINEERING

(Recognised by the Govt. of Karnataka, Affiliated to Visvesvaraya Technological University, Belagavi.

Approved by A.I.C.T.E. New Delhi.

Recognised by UGC Under Section 2(f)

Bommanahalli, Hosur Road, Bangalore - 560 068.

Ph: 080-61754601/602, Fax: 080 - 25730551

E-mail: engprincipal@theoxford.edu Web: www.theoxfordengg.org

| | | | | | | | | | |
|----|--|--|--------|--|-------------|-----------------|---|---|----------------|
| 56 | Vertex Polynomial of Middle Line and Total Graphs of some standard Graphs, | Dr. Mallikarjun K. and Sridhara K. R. | MAT HS | International Journal of Management and Humanities | April 2020. | ISSN:2394-0913, | https://www.ijmh.org/wp-content/uploads/papers/v4i8/H0794044820.pdf | https://www.ijmh.org/wp-content/uploads/papers/v4i8/H0794044820.pdf | Google Scholar |
| 57 | on Schur Geometric Convexity of Related Function for Holders Inequality with Application | Dr. Sreenivasa Reddy P., | MAT HS | EJPAM. | 2020 | pp. 8224-8235. | https://www.ejpm.com/index.php/ejpm/article/view/3741 | https://www.ejpm.com/index.php/ejpm/article/view/3741 | Google Scholar |
| 58 | on Schur Harmonic Convexity of Related Function for Holders Inequality with Application | Dr. Sreenivasa Reddy P., | MAT HS | International Journal of Advanced Science and Technology Vol. 29, No. 7, (2020), | 2020 | pp. 8224-8235. | http://sersc.org/journals/index.php/IJAST/article/view/24646 | http://sersc.org/journals/index.php/IJAST/article/view/24646 | Google Scholar |
| 59 | Transitive Domination Polynomial of a Graphs, | Dr. Mallikarjun K. and Sridhara K. R., | MAT HS | (UGC Care Journal | 2020 | ISSN: 2394-3114 | https://papers.ssrn.com/sol3/papers.cfm?abstract_id=3667497#:~:text=The%20transitive | https://papers.ssrn.com/sol3/papers.cfm?abstract_id=3667497#:~:text=The%20transitive | Google Scholar |



CHILDREN'S EDUCATION SOCIETY (Regd.)
THE OXFORD COLLEGE OF ENGINEERING

(Recognised by the Govt. of Karnataka, Affiliated to Visvesvaraya Technological University, Belagavi.

Approved by A.I.C.T.E. New Delhi.

Recognised by UGC Under Section 2(f)

Bommanahalli, Hosur Road, Bangalore - 560 068.

Ph: 080-61754601/602, Fax: 080 - 25730551

E-mail: engprincipal@theoxford.edu Web: www.theoxfordengg.org

| | | | | | | | | | |
|--|--|--|--|--|--|--|---|---|--|
| | | | | | | | %20domination% 20polynomial%2 0of,dominating% 20sets%20of%20 cardinality%20j. | ext=The%20t ransitive%20 domination% 20polynomial %20of,domin ating%20sets %20of%20ca rdinality%20j . | |
|--|--|--|--|--|--|--|---|---|--|

Original Research | Published: 25 April 2019

Diversity based self-adaptive clusters using PSO clustering for crime data

[Seema Patil](#)  & [R. J. Anandhi](#)

International Journal of Information Technology **12**, 319–327 (2020)

81 Accesses | **1** Citations | [Metrics](#)

Abstract

Diversity is the key parameter which plays the important role in defining the exploration capability of natural computing algorithms. Poor convergence is guaranteed, once diversity has lost prematurely. It is also true that there are number of sensitive parameters available with all paradigms of natural computing, whose optimal values drives the quality of solution. In this proposed work, diversity based self-adaption has been applied to particle swarm optimization to obtain better clusters. This diversity has been achieved with parameters like inertia weight, social and cognition constant. The proposed work has been applied over numeric benchmark and cluster data set to validate. Also new algorithm has been applied on crime datasets of Karnataka and Bengaluru to determine similar and different crime characteristics.

Original Research | Published: 06 April 2019

Adaptive strategy operators based GA for rule discovery

[T. Shobha](#)  & [R. J. Anandhi](#)

International Journal of Information Technology **12**, 1365–1375 (2020)

30 Accesses | [Metrics](#)

Abstract

A new variant of genetic algorithm, which provides equal opportunity for all parent solution to produce the offspring solution, has been applied in discovery of classification rules from continuous datasets. The main objective of proposed algorithm is used to discover classification rule with three measures like accuracy, coverage (completeness) and comprehensibility, using which easily understandable, accurate and comprehensible rules can be generated. A new process has been defined to simplify the generated rules by reducing the features dimension, according to their role in the success of discovering rules. Adaptive approach for crossover and mutation operations has been applied to handle the exploration and exploitation in dynamic manner. Algorithm has been tested on UCI benchmark dataset. The results show the better classification accuracy and optimal selection of features. It is also observed that, proposed

Extreme Precipitation Events in Chennai Metro City Using Data Mining

R.Senthil Kumar, C.Ramesh

Abstract: A information mining approach is displayed and connected to examine the climatic reasons for outrageous climatic occasions. Our methodology involves two primary strides of information extraction connected progressively, so as to decrease the trouble of the first informational index. The objective is to recognize an a lot littler subset of climatic factors that may in any case have the option to portray or even anticipate the outrageous occasions. The initial step applies a class correlation strategy. The subsequent advance comprises of a choice tree learning calculation utilized as a prescient model to outline set of measurably most huge atmosphere factors recognized in the past advance to classes of precipitation quality. The procedure is utilized to the investigation the climatic reasons for two outrageous occasions happened in India the most recent decade: the Chennai 2015 extraordinary precipitation disaster and the Tamilnadu(except Chennai) inadequacy of 2016. In the two cases, our outcomes are in great concurrence with investigations distributed in the writing.

Keywords : Extreme event, Drought, Intense rainfall, KDD (Knowledge Discovery in Databases), Data mining, Classification, Decision tree.

I. INTRODUCTION

Tamil Nadu, located in southeast peninsular India, receives the major part of its annual rainfall during the northeast monsoon season (the three-month period from October to December). Coastal Tamil Nadu (including Chennai, Cuddalore, Nagapattinam, Ramanathapuram and Kanyakumari) receives about 60% of its annual rainfall and interior Tamil Nadu receives about 40-50% of annual rainfall during northeast monsoon. In comparison with Indian summer monsoon, the Northeast monsoon is characterized by limited aerial extent and average lesser rainfall amount[1-3]. During northeast monsoon season, Tamil Nadu generally receives rainfall due to the formation of tough of low, cyclonic circulation, easterly waves, low pressure area in the Coastal, depression and cyclonic storm over Bay of Bengal, because, the northeast monsoon season is the major rainy season in the Tamilnadu state. The vicissitudes of the rainfall of Tamil Nadu state has led to considerable and widespread interest among the public, farmers as well as in government circles in recent years, in view of the frequent failure of northeast monsoon rainfall over Tamil Nadu. There are several papers and documents to explain the relation between OLR and Northeast monsoon rainfall. The inter-annual variation of the outgoing long-wave radiation

for the summer monsoon period showing a close association with the large-scale monsoon rainfall over India has been mentioned by Prasad and Verma (Prasad and Verma, 1985)[4-6]. They have concluded that the satellite-derived outgoing long-wave radiation can be used to monitor more comprehensively, the large-scale monsoon circulation and its year-to year variability, in view of its spatial coverage over oceanic areas. Prasad and Bansod have found the relationship between averaged OLR for west central India and the Indian summer monsoon rainfall to be stable (Prasad and Bansod, 1964). The inter-annual variability of Indian summer monsoon rainfall and Northeast monsoon rainfall is determined by external forcing and nonlinear internal dynamics. Surface air temperature is one of the factors that influence monsoon variability. The distribution of surface air temperature over land and sea determines the locations of heat source and sink which in turn affect circulation patterns through thermal and latent heat energy exchange between atmospheres and the surface beneath. A number of studies addressed the relationship between Indian summer monsoon and land and sea surface temperatures (Sikka, 1980; Verma. et al, 1985)[7].

Many studies (Rajeevan.et al, 1998; Pai, 2003) examined the global land surface air temperature anomaly patterns in association with inter annual variability of Indian summer monsoon rainfall[8]. Balachandran et al (2006) suggested that, in the correlation coefficient patterns, the positive correlation coefficient regions indicate that when the surface air temperature over these areas are Southeast India, especially Tamil Nadu and Puducherry experienced unprecedented rainfall activity during November and early December 2015 leading to devastating flood over Tamil Nadu[9]. Chennai was worst affected during the end of November and early part of December. The extremely heavy rainfall over north coastal Tamil Nadu including Chennai occurred in three different spells, viz., 8-9 Nov, 16-17 November and 30 Nov.-1- Dec., 2015. Details of the synoptic situations for these three spells are presented. It was mainly due to a Deep depression over southwest Bay of Bengal, well marked low pressure area over southwest bay of Bengal and a trough of low with embedded cyclonic circulation extending up to middle troposphere level respectively. The performance of the IMD GFS and WRF model for these three extreme spells are evaluated and presented[10-13].

S
Revised Manuscript Received on September 03, 2019

* Correspondence Author

R.Senthil Kumar*, Research Scholar, Department of Computer Science and Engineering, Satyabama University, Chennai.

Dr.C.Ramesh, Research Supervisor, Satyabama University,Chennai.

Extreme Precipitation Events in Chennai Metro City Using Data Mining

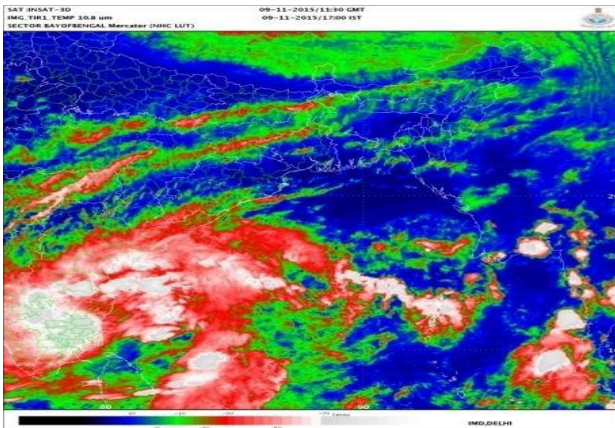


Fig.1a INSAT-3D satellite imagery of DD (08-10 Nov 2015) based on 09th/1130 UTC, Doppler Weather Radar, Chennai imagery based on 09th/1400 UTC

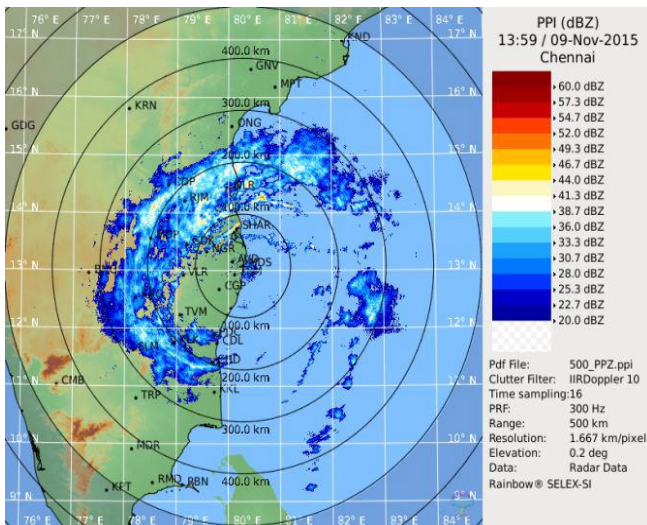


Figure 1-b- Spatial distribution of 24-hr heavy rainfall occurrences as on 0300 UTC of 08-11 November 2015).

Data mining – a step in the more general process of knowledge discovery in databases (KDD) – attempts to uncover hidden patterns in large data sets. Its main goal is to extract information from a data set and transform it into an understandable structure for further use, in order to facilitate a better interpretation of existing data [8]. These patterns can be seen as a kind of summary of the input data and may be used in further analysis. Data mining may, for instance, identify multiple clusters or subsets in the data, which can then be used to obtain more accurate prediction results by a decision support system. For more several decades, climatologists have been using data mining techniques in an assortment of studies. For a review see [9] and references therein. However, within the particular context of extreme rainfall-associated events, data mining technologies were applied in a relatively small number of studies[10,11]. Here it is present an innovative data mining approach to investigate the climatic causes of extreme events such as the Chennai of 2015 tragedy, and the Chennai of 2016 droughts. Our approach comprises two main steps of knowledge extraction, applied successively in order to reduce the complexity of the original dataset, and identify a much smaller subset of climatic variables that may explain the event being studied. In the first step, it is follow along the lines of [14], and apply

a class comparison technique commonly used as a tool to analyze large data sets of genome-wide studies. This step results in a series of-spatial fields that identify which climatic variables behave differently across pre-defined classes of rainfall intensity. More generally, it permits to identify coherent spatial patterns that might indicate the existence of plausible links between different climate subsystems. The second step consists of a decision tree (DT) learning algorithm used as a predictive model to map the set of statistically most significant climate variables identified in the previous step to classes of rainfall intensity. A decision tree is a flowchart-like structure in which internal nodes represent tests on attributes, each branch represents the outcome of a test, and each leaf node represents a class label. A path from the root to a given leaf represents a set of classification rules [15]. In the present context, the final result identifies a small subset of climatological variables that may explain or even forecast the extreme event in study. The remainder of this paper is organized as follows. Section 2 presents the methodology and data sets used in this investigation. Section 3 presents our results, while in Section 4 conclusions and discuss some further developments.

II. METHODOLOGY

The data mining approach here employed comprises two main steps of knowledge extraction: 1)Class-Comparison, and 2)Decision Trees. These methods are applied successively to reduce the difficulty of the original dataset (obtained from Chennai Meteorological Department: <http://www.imdchennai.gov.in/>) and recognize a much smaller subset of climatic variables that may explain the event being studied.

A.. Class-Comparison

Class comparison methods are used for comparing two or more pre-defined classes in a data set. Here, it is apply the class-comparison to time series of climatic grid box values or indices, but not to the entire fields. The objective is to determine which variables in our data set behave differently across pre-defined classes of rainfall strength (“high”, “neutral”, and “low”, for example). The “no-difference” case corresponds to a null hypothesis. The classes are defined in such a way so as to captured in the correct class the main episodes of drought or extreme rainfall that occurred during the period being evaluated. There are several methods for checking whether differences in variable values are statistically significant[16]. The F-test is a generalization of the well-known t-test, which measures the distance between two samples in units of standard deviation. Large absolute values of the F-statistic suggest that the observed differences among classes are not due to chance, and that the null hypothesis can therefore be rejected. Supposing there are J1 data points of class 1 and J2 data points of class 2, the t-test score is computed as:

$$t = \frac{\bar{x}_1 - \bar{x}_2}{\sqrt{s_p^2 \left(\frac{1}{J_1} + \frac{1}{J_2} \right)}} \quad (1)$$

where,

$$s_p^2 = \frac{(J_1 - 1)s_1^2 + (J_2 - 1)s_2^2}{J_1 + J_2 - 2}, \quad (2)$$

and for $i=1,2$,

$$s_i^2 = \frac{1}{J_i - 1} \sum_{j=1}^{J_i} (x_{ij} - \bar{x}_i)^2, \quad (3)$$

where \bar{x}_1 = mean of samples class 1,
 \bar{x}_2 = mean of samples class 2.

For more than two classes, an F-statistic shall be computed. In this case, the alternative to the null hypothesis is that at least one of the classes has a distribution that is different from the others. The t-test and F-test scores may be converted into probabilities, known as p-value. A p-value is the probability that one would observe under the null hypothesis a t-statistic (or F-statistic) as large as or larger than the one computed from the data. Both the t-test and F-test assume that the means are normally distributed, which may not hold, particularly when the number of data points is small. In this case, one could use the non-parametric counterparts of these tests, such as the Wilcoxon test, the Kruskal-Wallis, or a permutation method. The probability of observing an F-statistic as large as or larger than the one computed from the data is called a “p-value”. It is a measure of statistical significance in the sense that one expects to observe, under the null hypothesis, p-values less than 0.01 only 1% of the time. Permutations methods, which do not rely on data normality assumptions, are commonly used for computing p-values [17]. For this, after calculating t-test scores for each variable, the class labels of the J_1 and J_2 are randomly permuted, so that a random J_2 of the samples are temporarily labeled as class 1, and the remaining J_2 samples are labeled as class 2. Using these temporarily labels, a new t-test score is calculated, say t^* . The labels are then reshuffle many times again, with a t^* being computed at each permutation. The p-value from the permutation t-test is given by:

p-value from the permutation t-test is given by:

$$p\text{-value} = \frac{1 + \# \text{ of random permutation where } |t| \geq |t^*|}{1 + \# \text{ of random permutation}} \quad (4)$$

B. Decision Tree

Usually, DT learners use the divide-and-conquer strategy to construct a suitable tree from a training set. For this, the problem is successively divided into smaller sub-problems until each subgroup addresses only one class, or until one of the classes shows a clear majority not justifying further divisions. Most algorithms attempt to build the smallest trees without loss of predictive power. To this end, the J4.8

Table 1: Data set used in this study

algorithm relies on a partition heuristic that maximizes the “information gain ratio”, the amount of information generated by testing a specific attribute. This approach permits to identify the attributes with the greatest discrimination power among classes, and select those that will generate a tree that is both simple and efficient.

The information gain is measured in terms Shannon’s entropy reduction. Given a set A with two classes P and N, the information content (in bits) of a message that identifies the class of a case in A is then

$$I(p, n) = -\frac{p}{p+n} \log_2 \left(\frac{p}{p+n} \right) - \frac{n}{p+n} \log_2 \left(\frac{n}{p+n} \right), \quad (1)$$

where p is the total number of objects belonging to class P, and n is total number of the objects into the classes N. If A is partitioned into subsets A_1, A_2, \dots, A_v by a given test T, the information gained is given by

$$G(A; T) = I(A) - \sum_{i=1}^v \frac{p_i + n_i}{p+n} I(A_i), \quad (2)$$

where A_i has p_i objects from the class P, and n_i from the class N. The algorithm chooses the test T that maximizes the information gain ratio $G(A;T)/P(A;T)$, with

$$P(A; T) = -\sum_{i=1}^v \frac{p_i + n_i}{p+n} \log_2 \left(\frac{p_i + n_i}{p+n} \right), \quad (3)$$

being the information gain from the partition itself. The process is repeated recursively to obtain the other nodes, structuring the decision tree with the rest of the subsets.

III. RESULTS

The climatic causes of the Chennai 2016 tragedy and the Tamilnadu droughts of 2005 and 2010 are investigated. The entire data sets used in the analysis can be freely downloaded from the Web (obtained from Chennai Meteorological Department: <http://www.imdchennai.gov.in/>). Surface- and pressure-level atmospheric fields have a spatial resolution of 2.5o x 2.5o and were extracted from NCEP/NCAR Reanalyzes. Sea Surface Temperatures (SSTs) on a 2o x 2o grid were obtained from the NOAA Optimum Interpolation SST Analysis, version 2 [20]. The objective of this study is to determine which variables in our dataset behave differently across pre-defined classes of precipitation intensity. The “no-difference” case corresponds to the null hypothesis for the applications considered here.

A. Extreme Rainfall over Chennai of Tamilnadu

The data set used in this study comprises 3.781 time series (Table 1). Gridded data cover a region delimited by latitudes 20oS and 50oS, and longitudes 30oW and 60oW. Since the episode of extreme rainfall in Chennai was an event of short duration, pentad-averaged anomalies were used in the analysis.



Extreme Precipitation Events in Chennai Metro City Using Data Mining

| Variable | Units | Observations | No. of Time Series |
|--------------------------|-------|---|--------------------|
| Sea Surface Temperature | oC | Surface | 147 |
| Sea Level Pressure - SLP | Pa | 1000 hPa | 170 |
| Air Temperature | oC | Surface | 170 |
| Specific Humidity | g/kg | At 850 and 1000hPa | 331 |
| Omega | Pa/s | At 100,200,300,400,500,600,700,850, and hPa | 1478 |
| Geopotential Height | m | At 1000hPa | 174 |
| Zonal Wind | m/s | At 200,500,850 hPa | 512 |
| Meridional Wind | m/s | at 200,500,850 hPa | 516 |
| Cloud Cover | % | Surface | 174 |

A. Class-Comparison

The goal is to identify variables that might correlate with observed differences among classes of rainfall in the region of Chennai (red colored dots in Figs.3 to 5), one of the most affect areas by the 2015 disaster. To this end, we analyzed 12 years (January 1994 up to December 2016) of pentad averages, comprising 3,781 environmental variables. Precipitation data in the region of Chennai (Fig.2) is an average of five measurement stations of Chennai Meteorological Department. For classification purposes, the pentads of this time series were divided in three classes of precipitation intensity: “strong”, “moderate”, and “light” rainfall. The standard t-test (eq.1) was applied, as recommended for applications with two classes: “strong”

(precipitation greater than 8), and “moderate” (precipitation between 0 and 8). Results for the most significant variables identified by this procedure are presented in Figs.3 to 5. These results represent p-value fields, where coherent spatial patterns of low p-values indicate the existence of a possible links between omega and zonal/meridional wind anomalies, at different levels, and the precipitation intensity in the region of Chennai (Fig.2). The red isolines in Fig. 3 and 4 correspond to omega anomalies averaged over the period November 22 up to 26, 2015, the period of most intense precipitation in and around Chennai (delimited by the red bars in Fig.1). The wind fields in Fig.4 are also anomalies averaged over the same period.

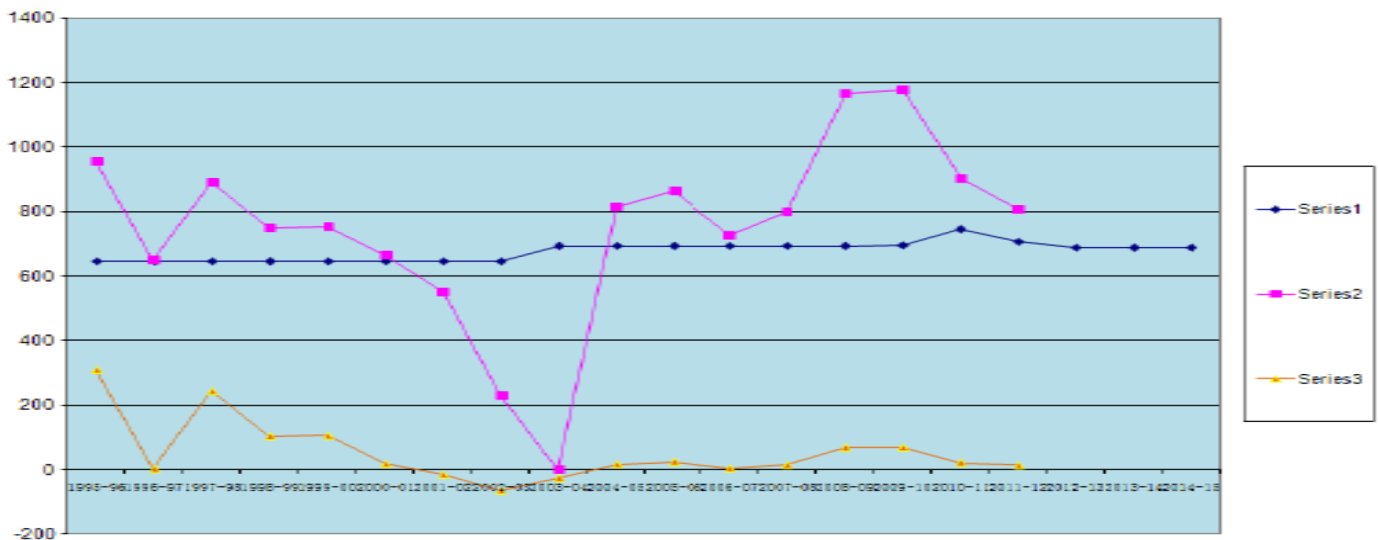
Table 2: Time Series Data Of Rainfall By Seasons (Last 20 Years)-2015-2016

| S.NO | Year | Hot Weather or Normal Season | | South West Normal Monsoon | | North East Normal Monsoon | | Winter Normal Season | | Total Normal | | Deviation fPercentage |
|------|---------|------------------------------|--------|---------------------------|--------|---------------------------|--------|----------------------|--------|--------------|--------|-----------------------|
| | | Actual | Actual | Actual | Actual | Actual | Actual | Actual | Actual | Actual | | |
| | | Normal | Actual | Normal | Actual | Normal | Actual | Normal | Actual | Normal | Actual | |
| 1. | 1994-95 | 135.1 | 164.4 | 158.2 | 754.3 | 328.2 | 567.6 | 25.6 | 0.1 | 647.2 | 956.3 | +309.1 |
| 2. | 1995-96 | 135.1 | 177.3 | 158.2 | 579.9 | 328.2 | 194.1 | 25.6 | 0.5 | 647.2 | 956.3 | +309.1 |
| 3. | 1996-97 | 135.1 | 126.6 | 158.2 | 181.4 | 328.2 | 340.5 | 25.6 | 1.2 | 647.2 | 649.7 | +2.5 |
| 4. | 1997-98 | 135.1 | 75.0 | 158.2 | 167.7 | 328.2 | 571.9 | 25.6 | 0.6 | 647.2 | 890.2 | +243.0 |
| 5. | 1998-99 | 135.1 | 69.8 | 158.2 | 229.7 | 328.2 | 434.8 | 25.6 | 16.0 | 647.2 | 750.3 | +103.1 |
| 6. | 1999-00 | 135.1 | 92.3 | 158.2 | 87.1 | 328.2 | 504.7 | 25.6 | 68.7 | 647.2 | 752.6 | +105.4 |
| 7. | 2000-01 | 135.1 | 141.9 | 158.2 | 339.0 | 328.2 | 179.8 | 25.6 | 5.0 | 647.2 | 665.7 | +18.5 |
| 8. | 2001-02 | 135.1 | 66.20 | 158.3 | 152.4 | 328.2 | 327.0 | 25.6 | 6.1 | 647.2 | 551.8 | -14.74 |
| 9. | 2002-03 | 135.1 | 69.6 | 158.3 | 78.6 | 328.2 | 62.8 | 25.6 | 17.6 | 647.2 | 228.6 | -64.67 |
| 10 | 2003-04 | 148.4 | 202 | 192.9 | 90.1 | 327 | 205.4 | 26.1 | 16.7 | 694.4 | 514.2 | -180.2 |

| | | | | | | | | | | | | |
|----|---------|-------|-------|-------|-------|-------|-------|------|------|-------|--------|-------|
| 11 | 2004-05 | 148.4 | 294.7 | 192.9 | 233.3 | 327.0 | 260.2 | 26.1 | 26.6 | 694.4 | 814.8 | 17.3 |
| 12 | 2005-06 | 148.4 | 162.1 | 192.9 | 177.6 | 327.0 | 505.7 | 26.1 | 17.7 | 694.4 | 863.1 | 24.3 |
| 13 | 2006-07 | 148.4 | 128.4 | 192.9 | 141.5 | 327.0 | 444.3 | 26.1 | 11.1 | 694.4 | 725.3 | 4.4 |
| 14 | 2007-08 | 148.4 | 190.8 | 192.9 | 204.3 | 327.0 | 378.0 | 26.1 | 25.0 | 694.4 | 798.1 | 14.9 |
| 15 | 2008-09 | 148.4 | 157.3 | 192.9 | 695 | 327.0 | 312.2 | 26.1 | 1.3 | 694.4 | 1165.8 | 67.89 |
| 16 | 2009-10 | 150.2 | 101.5 | 192.9 | 765.4 | 327 | 306.1 | 26.1 | 4.8 | 696.2 | 1177.8 | 69.2 |
| 17 | 2010-11 | 150.3 | 194.6 | 233.1 | 188.0 | 341.9 | 437.0 | 20.3 | 82.9 | 745.6 | 902.5 | 21.0 |
| 18 | 2011-12 | 168.0 | 140.4 | 189.8 | 252.9 | 328.9 | 410.7 | 20.3 | 2.6 | 707.0 | 806.6 | 14.1 |
| 19 | 2012-13 | 150.3 | 121.2 | 189.8 | 162.4 | 320.9 | 278.5 | 20.3 | 57.8 | 689.3 | 619.9 | -11.2 |
| 20 | 2013-14 | 150.3 | 141 | 189.8 | 596.7 | 328.9 | 257.9 | 20.3 | 5.1 | 689.3 | 1000.7 | 45.2 |
| 21 | 2014-15 | 150.3 | 342.3 | 189.8 | 764.2 | 328.9 | 311.6 | 20.3 | 0 | 689.3 | 1418.1 | 105.7 |
| 22 | 2015-16 | 150.3 | 118 | 189.8 | 309.4 | 328.9 | 341.1 | 20.3 | 23 | 689.3 | 791.5 | 15 |

Source: Directorate of Economics and Statistics, Chennai. mm and Extremely Heavy: ≥ 244.5 mm; Spatial distribution: Isolated (ISOL): 1-25% of stations reporting rainfall.

Actual and Normal Rainfall for the year 1995-96 to 2014-15



Extreme Precipitation Events in Chennai Metro City Using Data Mining

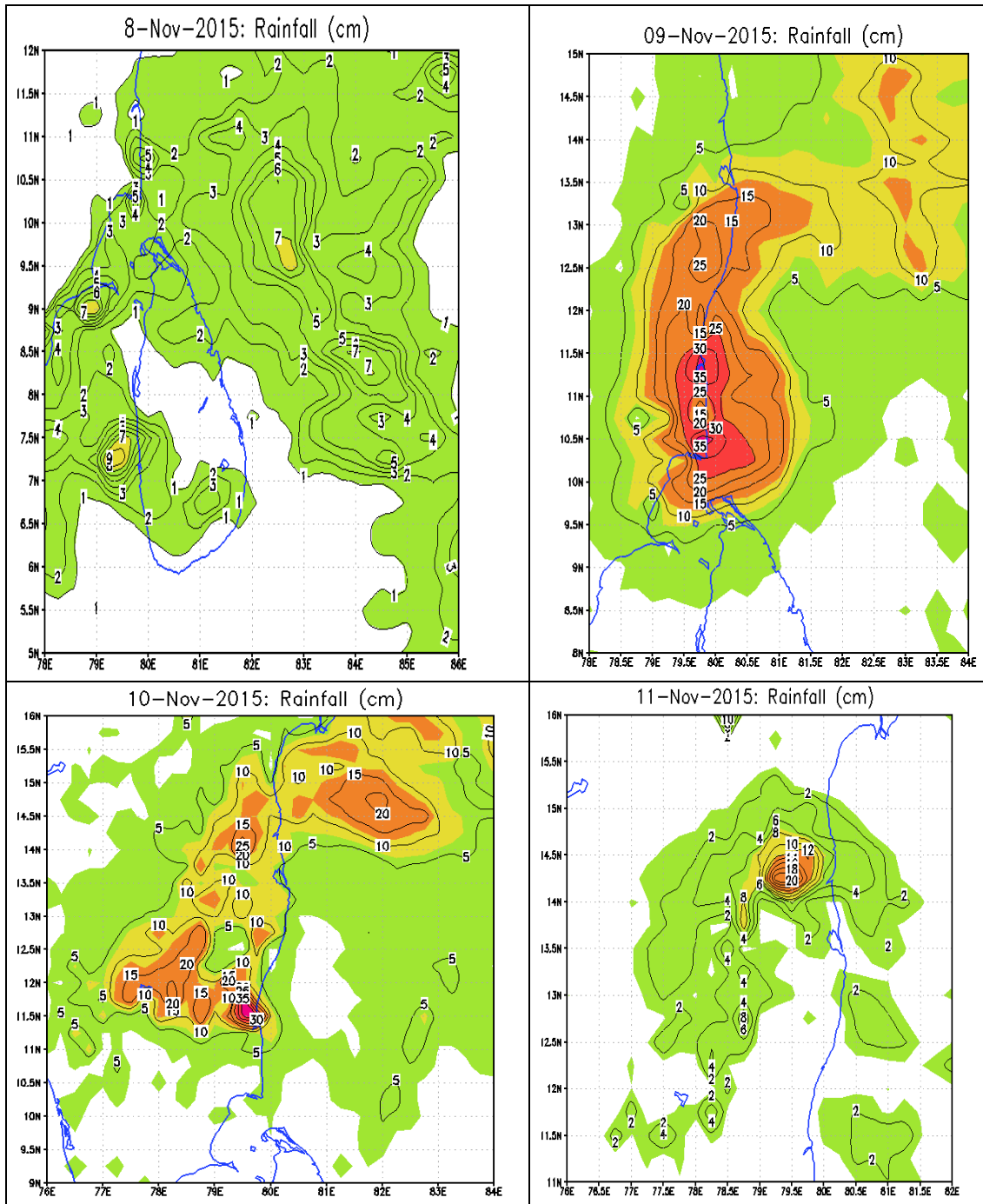


Fig.2c Rainfall realised in association with Deep Depression (08-10 Nov 2015) (based on IMD-NCMRWF GPM gauge merged rainfall data)

Well marked Low pressure area over South West Bay of Bengal (12-18 November 2015) Associated with this system, rainfall activity occurred over coastal Tamil Nadu during 12-18 November. Heavy to extremely heavy rainfall occurred along the entire north Tamil Nadu coastal belt during the

24-hr ending 0300 UTC of 16th and isolated heavy to very heavy rainfall on the other days. Spatial distribution of 24-hr heavy rainfall occurrences as on 0300 UTC of 13-19 November 2015) is depicted in Fig.2b.

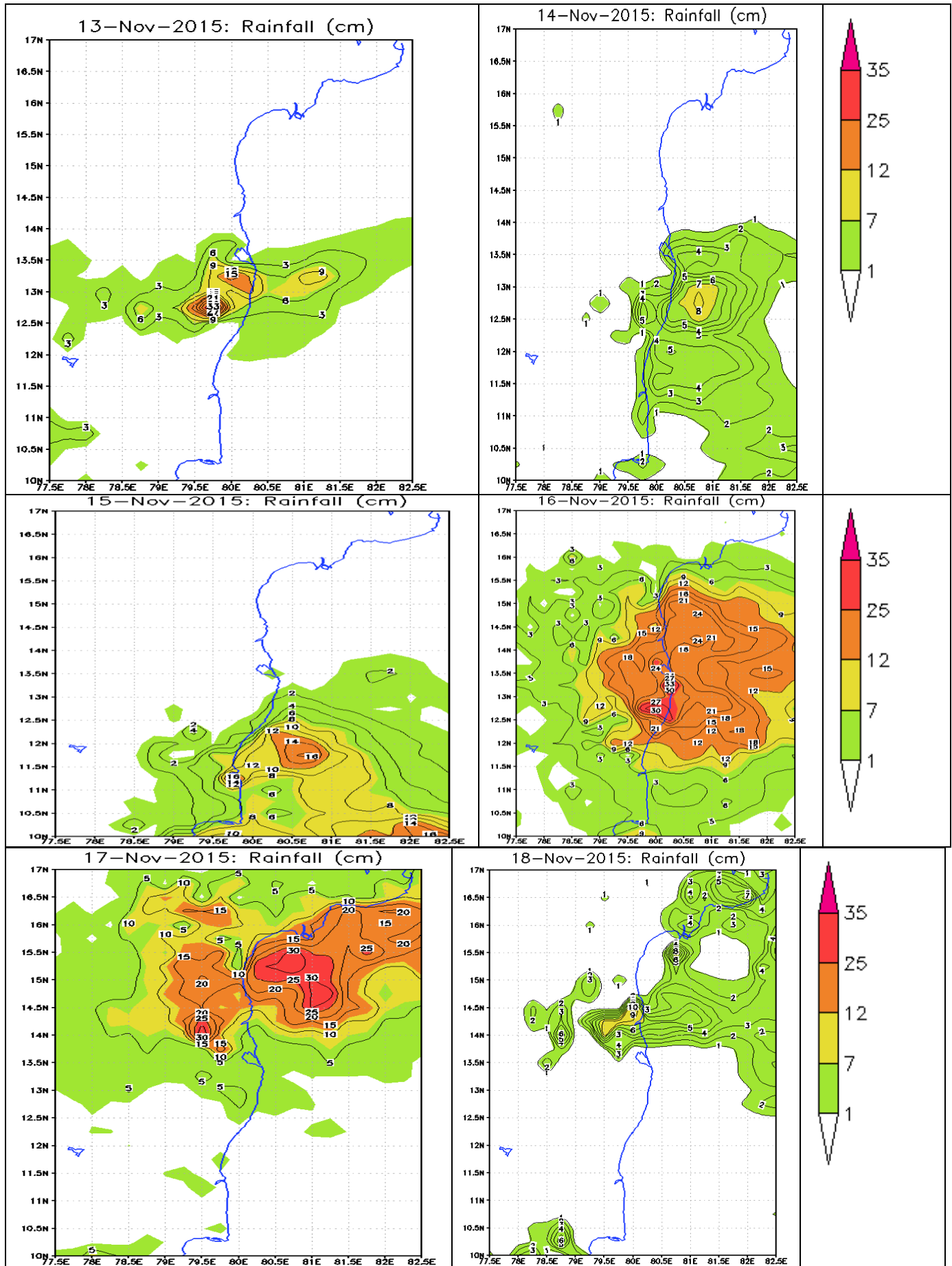


Fig.2b 24-hr accumulated rainfall as on 0300 UTC of 13-18 November 2015 in association with well marked low of 12-18 Nov 2015 (based on IMDNCRWF GPM gauge merged rainfall data)



Regions with darker shades indicate the grid parameters with lower p-values. A p-value <0.01 , for example, indicates probability lower than 1% of being a false positive. Figures 3 and 4 show a dense dark area of low p-values for omega at different levels, which extends from the Chennai city of Tamilnadu state. During the extreme rainfall episode, it is also observe (see the isolines) that omega values are negative over the continent (upward vertical motion) and positive over the ocean (downward vertical movement). It is well known that upward vertical motion over the continent can result in rainfall. This rainfall is fed by moisture transported from the ocean to the continent by easterly winds that predominated in the area in late November (see Fig. 4). According to the location of a blocking anticyclone on the Bay of Bengal Ocean (with winds that rotate in anti-clockwise on the Southern Hemisphere) determined the occurrence of easterly winds on large part of the South Region coast, resulting in a large scale moisture transport from the ocean to the continent.

B.. Decision Tree

The decision tree with the J4.8 algorithm was created with confidence factor used for pruning (0.25), and number of instances per leaf(8). Several tests were performed: with fixed number of attributes (meteorological variable for different coordinates are considered different attribute) with smallest p-values. The best result was obtained with the 5 different climatological variables, considering 10 different

coordinates for each variable, with smallest p-values (total 50 attributes). To this goal, the precipitation time series were divided over the area of Chennai(red dot) in two classes: “light” (values below the median), and “strong” (values above the median), corresponding to episodes of low and high rainfall, respectively. The training set comprised data from 2000 up to 2016. The years of 1999, 2007, 2008, 2009, and 2010 were used to evaluate the tree performance. Figure 1shows two rainfall intense episodes: July 1999, and November 2008. The event at July 1999 was less intense than November 2008.

The resulting tree, displayed in Fig.5, has 7 leafs (4 “strong” and 3 “light”) and 6 decision nodes. The variable with the highest information gain is omega at 500 hPa, and at coordinates 50oW and 25oS. As expected, these coordinates are as near to the disaster zone as the limited spatial resolution of the gridded data permits. Note that all but one decision nodes are also associated with omega, at different pressure levels but always in the vicinity of the affected area. These results highlight the key role played in the episode of extreme rainfall in Chennai 2015 by the vertical transport of the moisture, brought from the ocean by sustained easterly winds. As a predictor, the tree was able to forecast 100% of the cases of extreme rainfall during the evaluation years (1995, 2007-2016), including the episode occurred in November 2015.

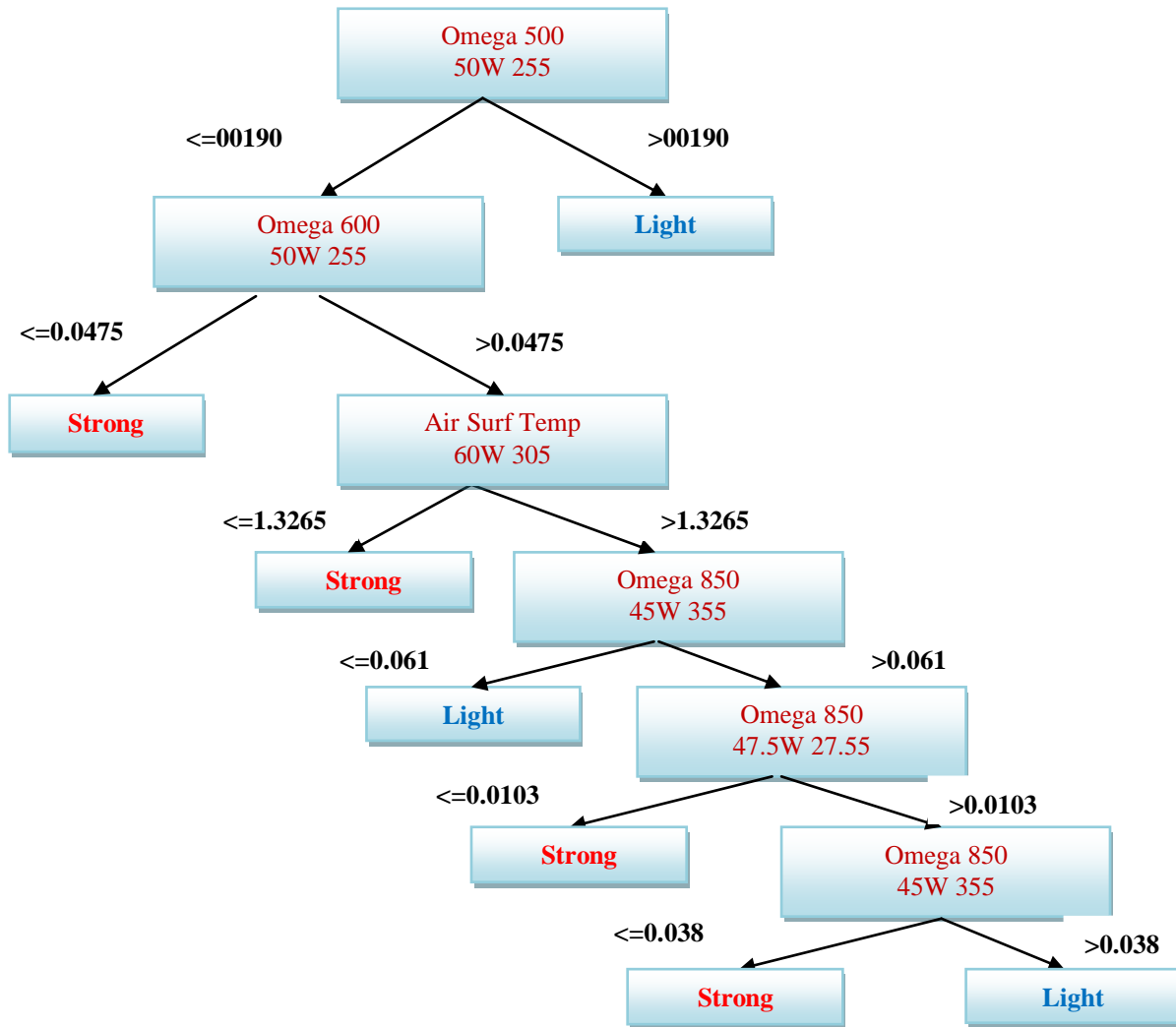


Figure 5. Decision tree generated: training set from 2000 up to 2016; test set:1999, 2007-2016

C. Tamilnadu Droughts

This analysis has used climatological data covering the period from January 1995 up to December 2016. Monthly anomalies were computed relative to the mean values over the period. The entire data set used in this illustrative study comprises 2.455 time series.

D. Class-Comparison

Class-classification was based on a time series of monthly accumulated precipitation anomalies, averaged over the area delimited by latitudes 4oS and 8oS and longitudes 68oW and 72oW. This time series was used as proxy of drought in our analysis. This region, located in the east costal area was strongly affected by the droughts of 2005 and 2010. In this time series, the range of anomalies was split into 3 sub-classes: “dry”, “neutral” and “wet”. To this end, the interval is divided between the highest and the lowest precipitation anomaly into three parts, assigning the upper and lower 37% bins to the “wet” and “dry” classes, respectively, and the remaining 26% to the “neutral” class. The results represents class comparison between "dry" and "neutral" classes.

IV. CONCLUSION

In this work our technique was used to generate decision trees and rules for classifying weather parameters such as maximum temperature, minimum temperature, rainfall, evaporation and wind speed in terms of the month and year. The data used was for Tamilnadu metropolis obtained from the meteorological station between 2009 and 2016. The results show how these parameters have influenced the weather observed in these months over the study period. Given enough data the observed trend over time could be studied and important deviations which show changes in climatic patterns identified. This work is important to climatic change studies because the variation in weather conditions in term of temperature, rainfall and wind speed can be studied using these data mining techniques.

REFERENCES

1. Ruivo H. M.; Sampaio G.; Ramos F. M; Knowledge extraction from large climatological data sets using a genome-wide analysis approach: application to the 2005 and 2010 Amazon droughts; Climatic Change; pages 1-15 (2014).

Extreme Precipitation Events in Chennai Metro City Using Data Mining

2. Rokach, L., Maimon, O.: Data Mining with Decision Trees: Theory and Applications. World Scientific Publishing. Vol. 270, (2007).
3. Simon, R. M. et al.: Design and analysis of DNA microarray investigations Springer Vol 209, (2003).
4. Hardin J, Mitani A, Hicks L, VanKoten B., A robust measure of correlation between two genes on a microarray. BMC Bioinformatics 8:220. (2007).
5. Witten, I. H., Frank, E. S.: Data mining: Practical machine learning tools and techniques with java implementation Morgan Kaufmann Publishers. (2000).
6. Hunt, E.B. Concept learning: An information processing problem. New York: Wiley (1962).
7. Quinlan, J. R.: C4.5: programs for machine learning. Morgan Kaufmann Publishers. (1993).
8. Kalnay, E., Kanamitsu, M., Kistler, R., Collins, W., Deaven, D. et al.: The NCEP/NCAR 40-Year Reanalyses Project. Bull Amer Meteor Soc Vol 77, pages 437-471. (1996).
9. Reynolds, R.W., Rayner, N.A., Smith, T.M., Stokes, D.C., Wang, W.: An improved in situ and satellite SST analysis for climate Journal Of Climate Vol 15, pages 1609-1625. (2002).
10. NOAA - Earth System Research Laboratory: Multivariate ENSO index (MEI), U.S. Department of Commerce, National Oceanic and Atmospheric Administration, <http://www.cdc.noaa.gov/people/klaus.wolter/MEI/>, Accessed 19 Jul. 2010 (2007).
11. Huffman GJ, Bolvin DT (2011) TRMM and Other Data Precipitation Data Set Documentation. Laboratory for Atmospheres, NASA Goddard Space Flight Center and Science Systems and Applications Inc. [ftp://meso.gsfc.nasa.gov/pub/trmmdocs/3B42\\$_3B43\\$_sd oc.pdf](ftp://meso.gsfc.nasa.gov/pub/trmmdocs/3B42$_3B43$_sd oc.pdf). Accessed 30 Jun 2011.
12. Lewis SL, Brando PM, Phillips OL, van der Heijden GMF, Nepstad D: The 2010 Amazon Drought. Science 331:554--554. doi: 10.1126/science.1200807. (2011).
13. Sistema Nacional de Informações sobre Recursos Hídricos (SNIRH) – Agência Nacional de Águas (ANA) - Available in: <http://ana.gov.br/portalsnirh/>. Accessed March 2010.
14. Chao WC: Multiple quasi equilibria of the ITCZ and the origin of monsoon onset. Journal of the atmospheric sciences, 57(5), 641-652.(2000).
15. Cook B, Zeng N, Yoon and J-H: Climatic and ecological future of the Amazon: likelihood and causes of change. Earth Syst. Dynam. Discuss. (2010).
16. Marengo JA, Tomasella J, Alves LM, Soares WR, Rodriguez DA: The drought of 2010 in the context of historical droughts in the Amazon region. Geophys Res Lett 38 L12703, doi:10.1029/2011GL047436.(2011).
17. Marengo JA, Nobre CA, Tomasella J, Cardoso MF, Oyama MC: Hydro-climatic and ecological behaviour of the drought of Amazonia in 2005. Philos Trans R Soc B 363:1773--1778. (2008).
18. R.Senthil Kumar, Dr. C.Ramesh, " Analysis of Extreme Rainfall Events in Chennai Using a Novel Data Mining Approach", Sylwan Journals, 163(7), Pp.14-29.



Home ▶ All Journals ▶ International Journal of Computers and Applications ▶ List of Issues
▶ Volume 43, Issue 5 ▶ An investigation on adaptive HTTP media ...



International Journal of Computers and Applications >

Volume 43, 2021 - Issue 5

1217

Views

0

CrossRef citations to date

Altmetric

Sustainable Computing for Intelligent Systems

An investigation on adaptive HTTP media streaming Quality-of-Experience (QoE) and agility using cloud media services

Selvaraj Kesavan , E. Saravana Kumar , Abhishek Kumar  & K. Vengatesan 

Pages 431-444 | Received 15 Nov 2018, Accepted 23 Jan 2019, Published online: 06 Feb 2019

 Download citation

 <https://doi.org/10.1080/1206212X.2019.1575034>



ABSTRACT

Web services is software entity allows machine to machine communication, operates as standalone unit and interoperability over network using standard web technologies such as Hypertext transfer protocol (HTTP) and eXtensible markup language (XML). With the rapid growth of cloud platform, infrastructure and emergence of multiple Digital transformation technologies, more and more conventional applications are transformed into web-based services. Service-based approach creates tremendous impact on multimedia content storage, retrieval, delivery and communication. With cloud infrastructure and service, get economically viable, real time, high resolution multimedia content on-the-go anywhere and everywhere using adaptive http streaming approach. This paper presents convergence of adaptive http streaming from conventional infrastructure to cloud enabled model and presents the advancement and architecture of

Clustering with modified mutation strategy in Differential Evolution

Seema Patil*, R. J Anandhi**

* Department of Computer Science & Engineering, The Oxford College of Engineering

** Department of Information Science & Engineering, New Horizon College of Engineering

Abstract- In this paper, a clustering approach based on modified mutation strategy in the Differential Evolution has been proposed. The objectives of modification are to achieve high rate of convergence and to obtain better cluster efficiency. The proposed form of modification has been applied on probabilistic environment to define the differential vector through randomly selected members and the best solution has been obtained. Over number of benchmark dataset, clustering efficiency have been estimated and compared with Conventional Differential Evolution as well as Particle Swarm Optimization. The proposed solution has delivered the superior and consistent performance over the considered benchmark.

Index Terms- Clustering, Convergence, Differential evolution, Mutation, Particle swarm optimization

I. INTRODUCTION

The tremendous growth of data-based knowledge in scientific studies has presented lot of challenges before the researchers to extract useful information from them using traditional data base techniques. Hence effective mining methods are essential to discover the implicit knowledge from huge data warehouses. Data based knowledge offer numerous opportunities in various practical applications like bioinformatics, engineering, biology, healthcare, medicine, prediction analysis, forecasting the crime and various computing techniques.

To perform this, knowledge extraction is done with the help of data mining techniques such as classification and clustering. The important task of combining various population or data points into clusters is clustering which performs similarity of points. It is one of iterative process of discovery of knowledge which involves major trial and failure. The clustering process does not require any kind of feedback to perform similarity of data points, it is self-organized [1]. Clustering defines a new swarm intelligence (SI) for partitioning any datasets into an optimal number of groups through one run of optimization. SI is an innovative distributed intelligent paradigm for solving optimization problems that originally took its inspiration from the biological examples by swarming, flocking and herding phenomena in vertebrates.

Data clustering is a popular approach of automatically finding classes, concepts, or groups of patterns. Particle Swarm Optimization (PSO) incorporates swarming behaviors observed in flocks of birds, schools of fish, or swarms of bees, and even human social behavior, from which the idea is emerged. Data clustering using PSO can be used to find the centroids of a user specified number of clusters. For automatic clustering of large unlabeled data sets, Differential Evolution (DE) is used. [2]

This work proposed the method for clustering, based on differential evolution. Even though DE is very efficient, but sometimes it suffers from the issue of slow convergence and difficulties in achieving the global solution. To overcome these, balance between exploration and exploitation has been maintained by adding the two modules in the conventional DE. To increase the level of exploitation, under the probabilistic mode, selection between best and randomly selected member takes place. The Differential vector made by best solution, deliver the fast change in the solution and results in faster convergence. The

multi-culture approach helps in exploration of new and efficient solution. Gathering and selection of solution from different environments will maintain the diversity in the population.

II. RELATED WORK

The author Gupta [3] et al., has proposed a new efficient clustering approach which was applied on k harmonic means (KHM) by using PSO. The local optimum problem of KHM was overcome by PSO. Also, fuzzy logic was used to control the various parameters of PSO. The author Pranav [4] et al., has achieved the global optima on clustering by making use of two validation indices criteria. These indices were simple and robust against other outliers and shown best clustering which has lower computation cost and parallel execution and faster convergence. The author Wang [5] et al., combines PSO and DE approach by taking velocity update of PSO and mutation parameter of DE to generate the new population. The DE re-mutation, crossover and selection are performed throughout the optimization process to get the good results. This approach gives the best result compared to inertia weight PSO and comprehensive learning PSO and basic DE. The author Zhu et al., [6] has discussed complications associated with K-means clustering algorithm and centroid all rank distance concept has been presented. To overcome the difficulties associated with density and delta-distance clustering (DDC) when data derived from the two indicators are large, an efficient and intelligent DDC algorithm has been discussed by author Liu et al [7]. A robust recommendation algorithm based on kernel principal component analysis and fuzzy c-means clustering has been presented by author Huawei et al., [8]. The author has presented a variation of differential evolution (DE) algorithm to solve an automatic clustering problem [9]. The author [10] describes the new improved approach of PSO by improving the diversity mechanism and mutation operator to employ new neighborhood search strategy. These new approaches were tested on well-defined benchmark data sets. Based on matrix partitioning a hierarchical clustering algorithm has been presented in [11].

III. PROPOSED WORK

A. Modified Mutated DE (MMDE)

To increase the convergence speed of DE, a new approach in mutation operation has been presented. It has two possibilities of differential change under the probabilistic environment. In the first case, differential change is defined through best member and random selected member while in second case three random members are selected to define the differential change. A threshold value is defined to determine the selection of differential change type. Best member based differential change generate the faster change, while the random member-based selection tries to prevent from suboptimal convergence. The pseudo code for applied mutation strategy has been shown below.

- Define the Threshold value (Thr)
- $r = U [0, 1]$; a random number generated through uniform distribution in range of [0 1];
- *if* $r < Thr$
 - Select two members' $m1$ & $m2$ randomly from population
 - Select best member BM from population
 - Mutation vector defined as: $Mv = m1 + mf * [BM - m2]$;
- Else*
 - Select three members $m1$, $m2$ & $m3$ randomly from population
 - Mutation vector defined as: $Mv = m1 + mf * [m2 - m3]$
- *End*

B. Multi-domain-based DE

A multi-culture concept called “Multi-culture modified mutation Differential Evolution” has been developed to evolve the individual population independently and later exploit to form a better community to search the solution space efficiently. This approach is inspired very much by present human society, where at fundamental level two things happen (i) the independent existence of a number of separate population, and they get their progress under the same environment up to a certain period of time. (ii) with respect to objectives, a number of individuals are selected from the different population and form a new population to achieve the objectives. Rather than working under monoculture formed by one population as in conventional PSO, multiculture environment has been proposed, where a number of different environments created by a different set of population independently. Each population has evolved socially, independently to generate the multiculture and later among all, best individuals are selected to finish the task. This is a dual stage process where first stage finds some potential solution discovered from different regions of solution space, and later in the second phase, each individual contributes more efficiently to find a global solution. Even with the small size of the population, the proposed method has achieved better quality solution with the very high value of consistency.

In the working principle of MMDE, population (POP) are the initial random population, which is evolved by the DE process individually and independently for a fewer number of iterations and creates the multi-culture new population (NPOP). Even though the process of creating the NPOP is same for all POP, because of difference in leadership and different community surrounding, each NPOP has different characteristics. Through the fitness-based selection process, among all members from all NPOP, better members are selected to form a new population (SPOP), which has the same size as initial POP. In SPOP, there are a number of good candidates, which are different and have higher fitness value, hence the high level of diversity exists. Finally, over SPOP, MMDE has been applied till terminating criteria has not meet, to obtain the Final Population (FPOP).

IV. EXPERIMENTAL RESULTS AND ANALYSIS

For the data set namely “Wine data”, “Iris”, and “Glass” data set which are available in UCI repository[12] have been considered to analyze the work. In the first part, only the MMDE has been applied and performances have been obtained for 5 independent trials. Comparison has been made with conventional DE(CDE) and dynamic weighted PSO(DYPSO). For all the cases, the size of population has been considered as 100, mutation rate and crossover rate as 0.4 and 0.5. The allowed number of iterations were 600. The performances have been represented in terms of correctly placed data samples in the clusters, number of data samples placed wrongly, cluster efficiency and total intra cluster distance value. In second part, multidomain based experiment has been included with MMDE and performances have been estimated over “Glass” data set. Experimental process has been developed in the MATLAB environment.

A. Dataset: Wine Data

There are total 178 set of data carrying 3 clusters. Each data contains 13 attributes.

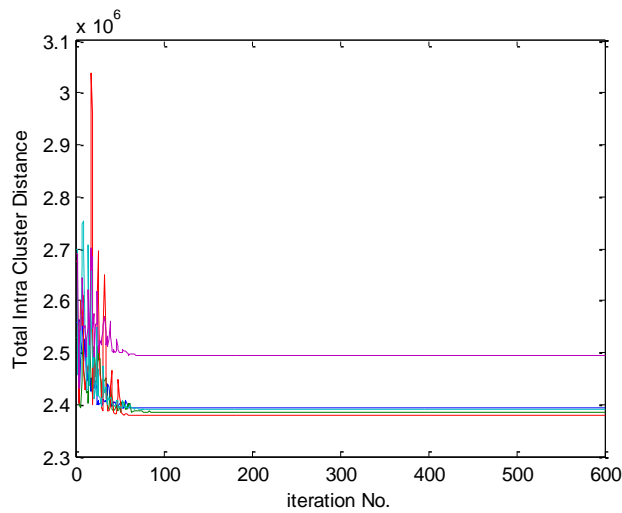


Fig.1 DYP SO based convergence in 5 trials for wine data set

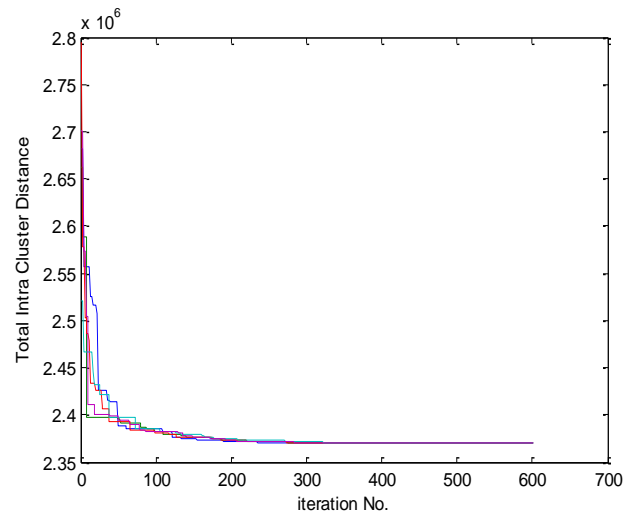


Fig.2 CDE based convergence in 5 trials for wine data set

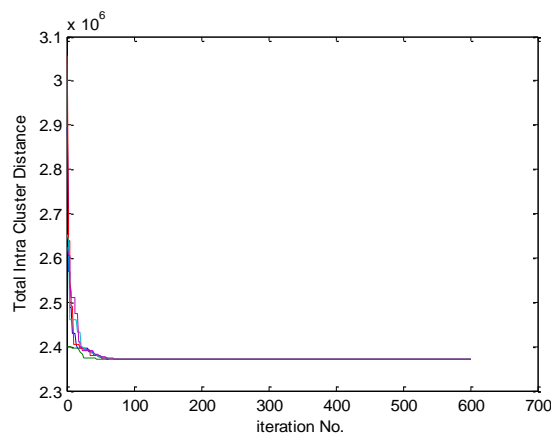


Fig.3: MMDE based convergence in 5 trials for wine data set

Table1: Mean Performance over 5 trials by different algorithm over wine data set

| | Correctly clustered data samples | Wrongly clustered data samples | Clustered efficiency | Total Intra Cluster Distance value $1.0e+006$ * |
|-------|----------------------------------|--------------------------------|----------------------|---|
| DWPSO | 125 | 53 | 70.22 | 2.4088e+006 |
| CDV | 125 | 53 | 70.22 | 2.3707e+006 |
| MMDV | 125 | 53 | 70.22 | 2.3707e+006 |

Table 2: Centroid position for winedata

| | | | | | | | | | | | | | |
|-----------|--------|--------|--------|--------|--------|--------|--------|--------|--------|--------|--------|--------|--------|
| C1 | 3.0351 | 3.0067 | 3.0065 | 3.0541 | 3.2816 | 3.0057 | 3.0043 | 3.0108 | 3.0041 | 3.0154 | 3.0024 | 3.0067 | 4.9797 |
| C2 | 3.0375 | 3.0051 | 3.0065 | 3.0462 | 3.2867 | 3.0078 | 3.0081 | 3.0008 | 3.0051 | 3.0154 | 3.0029 | 3.0084 | 6.2486 |
| C3 | 3.0339 | 3.0067 | 3.0062 | 3.0565 | 3.2508 | 3.0057 | 3.0048 | 3.0010 | 3.0040 | 3.0111 | 3.0024 | 3.0067 | 4.2455 |

The performances obtained under 5 independent trials by different algorithms have been shown in Table1. It can be observed that all the three algorithms have nearly the same performances, while there is little more distance measure appeared for the DYPSO. The obtained centroid value by MMDE for 1st trail have been shown in Table2. The convergence characteristics for DYPSO, CDE and MMDE have been shown in Fig.1 to Fig.3. To get the relative convergence speed, Fig.4 has plotted the mean convergence characteristics. Proposed MMDE has shown the fastest rate of convergence while DYPSO was the poorest.

B Dataset: IRIS Data

Contain total 150 data set and each data has 4 attributes. Three different global clusters exist in dataset. The convergence performances of DYPSO, CDE and MMDE have been shown in Fig. 5 to Fig.7, while the statistical performances have been shown in Table 3 to Table 5. It can be observed that MMDE has shown very consistent performance in all trials and in Fig.8 comparative convergence has been shown. The obtained best value of centroid has been shown in Table 6.

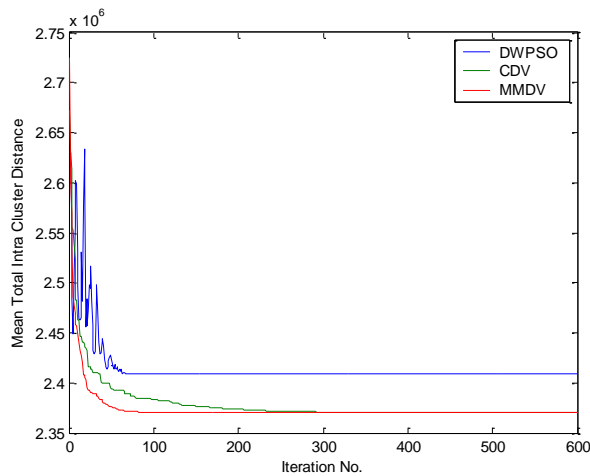


Fig.4: Mean convergence comparison for Iris data set

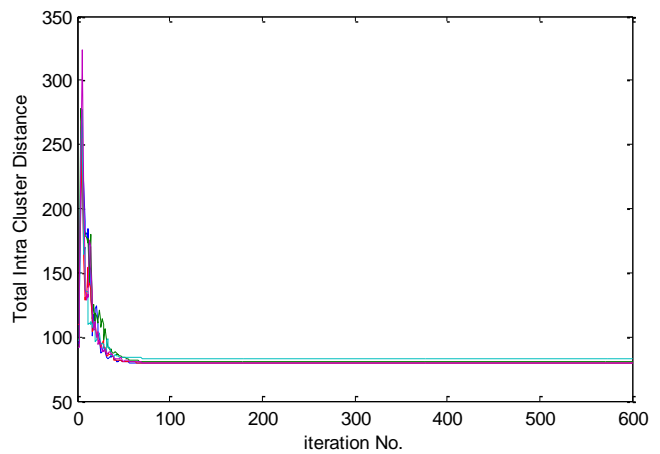


Fig.5: DYPSO based convergence in 5 trials for Iris data set

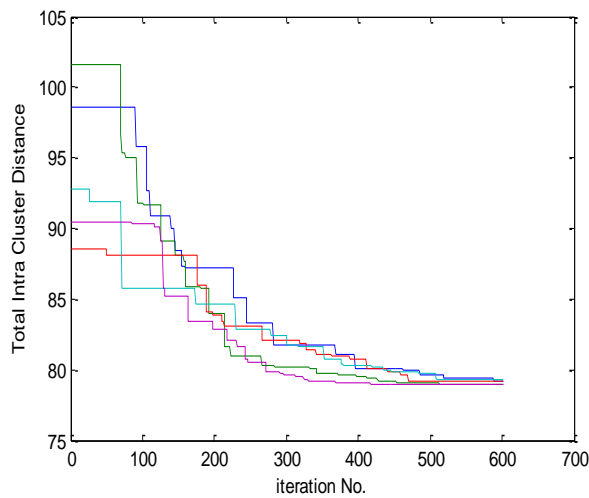


Fig.6: CDE based convergence in 5 trials for Iris data set

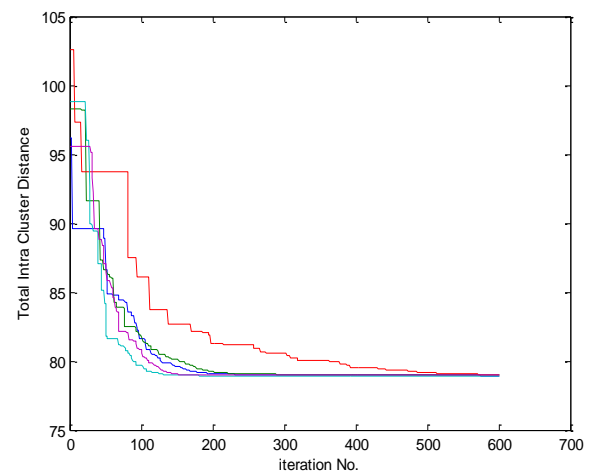


Fig.7: MMDE based convergence in 5 trials for Iris data set

Table 3: DYPSO performance over Iris data

| Trial No. IRIS(PSO) | Correctly clustered data samples | Wrongly clustered data samples | Clustered efficiency | Total Intra Cluster Distance value |
|---------------------|----------------------------------|--------------------------------|----------------------|------------------------------------|
| 1 | 134 | 16 | 89.33 | 79.3157 |
| 2 | 134 | 16 | 89.33 | 80.2949 |
| 3 | 133 | 17 | 88.67 | 79.4755 |
| 4 | 136 | 14 | 90.67 | 83.2333 |
| 5 | 133 | 17 | 88.67 | 79.7068 |
| Mean | 134 | 16 | 89.33 | 80.4052 |

Table 4: CDE performance over Iris data

| Trial No. IRIS(CDV) | Correctly clustered data samples | Wrongly clustered data samples | Clustered efficiency | Total Intra Cluster Distance value |
|---------------------|----------------------------------|--------------------------------|----------------------|------------------------------------|
| 1 | 134 | 16 | 89.33 | 79.2028 |
| 2 | 134 | 16 | 89.33 | 78.9563 |
| 3 | 133 | 17 | 88.67 | 79.1462 |
| 4 | 134 | 16 | 89.33 | 79.2389 |
| 5 | 134 | 16 | 89.33 | 78.9430 |
| Mean | 133.8 | 16.2 | 89.2 | 79.0974 |

Table 5: MMDE performance over Iris data

| Trial No. IRIS(MMDV) | Correctly clustered data samples | Wrongly clustered data samples | Clustered efficiency | Total Intra Cluster Distance value |
|-------------------------|----------------------------------|--------------------------------|----------------------|------------------------------------|
| 1 | 134 | 16 | 89.33 | 78.9471 |
| 2 | 134 | 16 | 89.33 | 78.9631 |
| 3 | 134 | 16 | 89.33 | 79.0133 |
| 4 | 134 | 16 | 89.33 | 78.9454 |
| 5 | 134 | 16 | 89.33 | 78.9494 |
| Mean | 134 | 16 | 89.33 | 78.9637 |

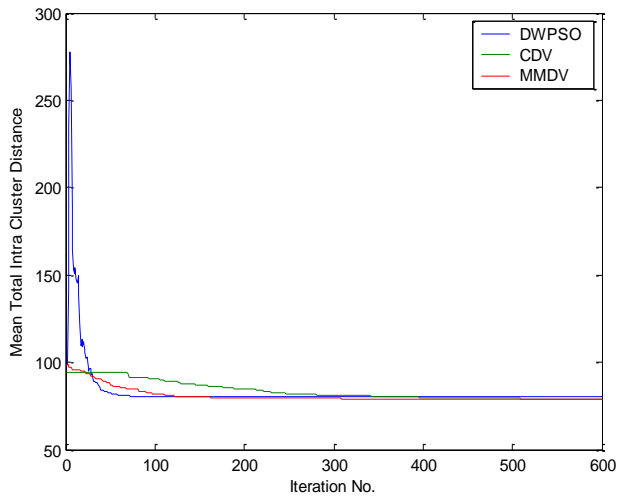


Fig.8: Mean convergence comparison for Iris data set

| Centroids of IRIS Dataset | | | | |
|---------------------------|--------|--------|--------|--------|
| C1 | 5.8863 | 2.7456 | 4.3731 | 1.4115 |
| C2 | 5.0173 | 3.4385 | 1.4452 | 0.2704 |
| C3 | 6.8326 | 3.1128 | 5.7640 | 2.0469 |

Table 6: Centroids value for Iris data set

C. Dataset: Glass Data

This data set contains total 214 data set. Each data set carried 10 attributes and 6 clusters exists.

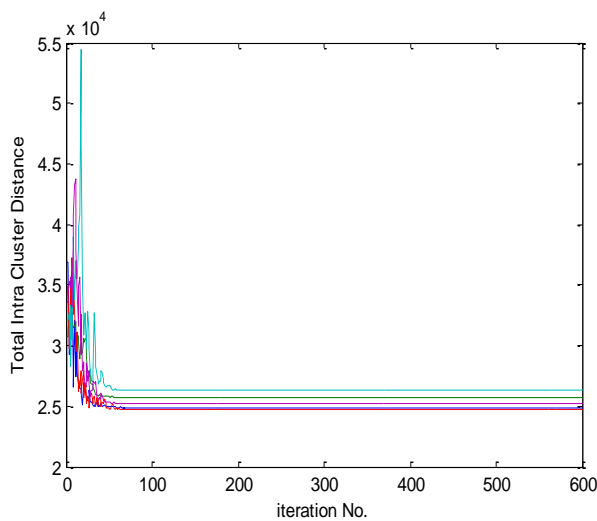


Fig.9: DYPPO based convergence in 5 trials for Glass data set

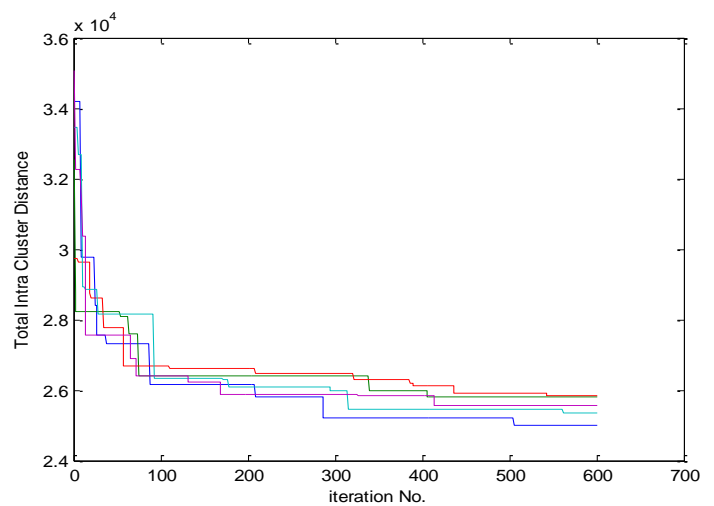


Fig.10: CDE based convergence in 5 trials for Glass data set

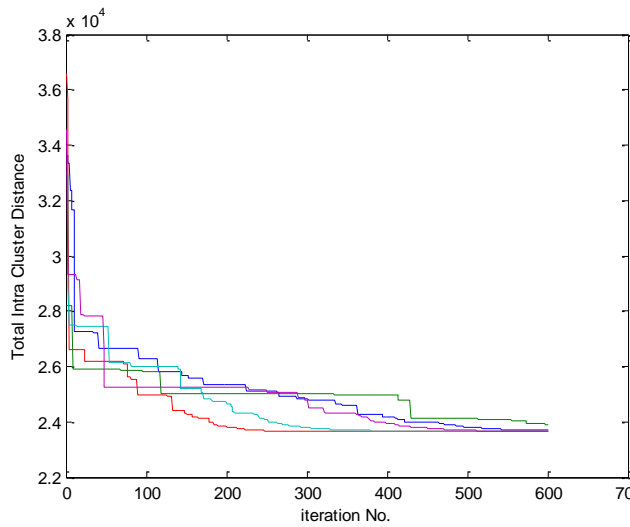


Fig.11: MMDE based convergence in 5 trials for Glass data set

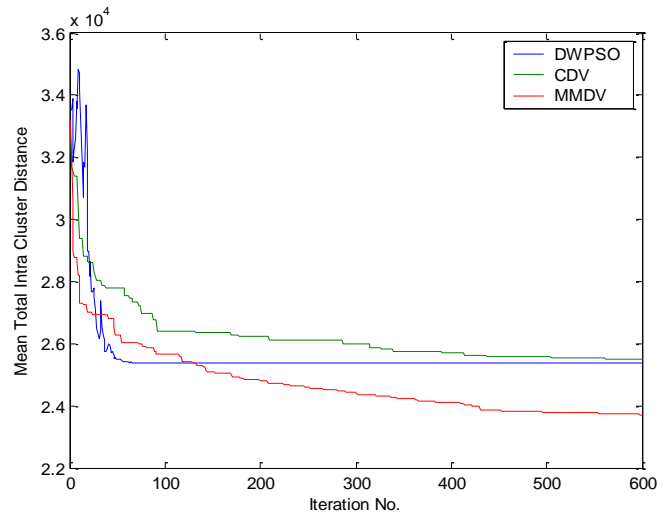


Fig.12: Mean convergence comparison for Glass data set

Table 7: DYPSO performance over Glass data

| Trial No. Glass (PSO) | Correctly clustered data samples | Wrongly clustered data samples | Clustered efficiency | Total Intra Cluster Distance value |
|-----------------------|----------------------------------|--------------------------------|----------------------|------------------------------------|
| 1 | 183 | 31 | 85.51 | 2.4897 e+004 |
| 2 | 189 | 25 | 88.32 | 2.5737 e+004 |
| 3 | 178 | 36 | 83.18 | 2.4721 e+004 |
| 4 | 184 | 30 | 85.98 | 2.6271 e+004 |
| 5 | 188 | 26 | 87.85 | 2.5209 e+004 |
| Mean | 184.4 | 29.6 | 86.17 | 2.5367e+004 |

Table 8: CDE performance over Glass data

| Trial No. Glass (CDE) | Correctly clustered data samples | Wrongly clustered data samples | Clustered efficiency | Total Intra Cluster Distance value |
|-----------------------|----------------------------------|--------------------------------|----------------------|------------------------------------|
| 1 | 183 | 31 | 85.51 | 2.4990 e+004 |
| 2 | 189 | 25 | 88.32 | 2.5797 e+004 |
| 3 | 178 | 36 | 83.18 | 2.5850e+004 |
| 4 | 184 | 30 | 85.98 | 2.5368 e+004 |
| 5 | 188 | 26 | 87.85 | 2.5546 e+004 |
| Mean | 184.4000 | 29.6000 | 86.17 | 2.5510e+004 |

Table9: MMDE performance over Glass data

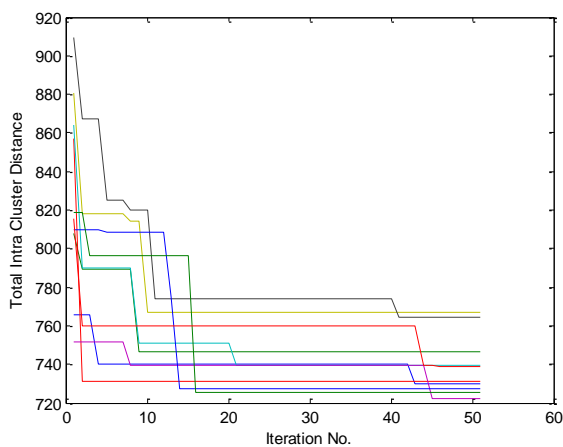
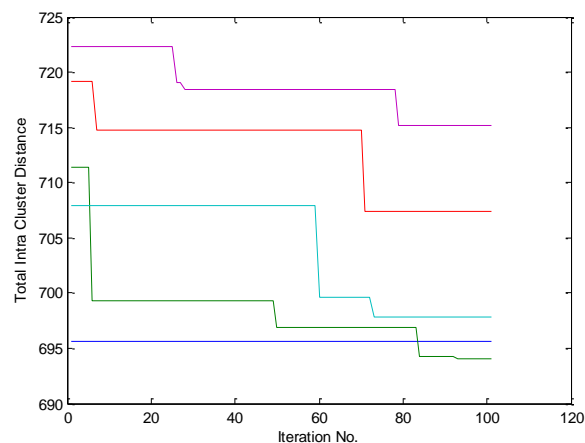
| Trial No. Glass (MMDE) | Correctly clustered data samples | Wrongly clustered data samples | Clustered efficiency | Total Intra Cluster Distance value |
|------------------------------|--|--------------------------------------|-------------------------|--|
| 1 | 187 | 27 | 87.38 | 2.4990 e+004 |
| 2 | 187 | 27 | 87.38 | 2.5797 e+004 |
| 3 | 187 | 27 | 87.38 | 2.5850 e+004 |
| 4 | 189 | 25 | 88.32 | 2.5368 e+004 |
| 5 | 184 | 30 | 85.98 | 2.5546 e+004 |
| Mean | 186.8 | 27.2 | 87.29 | 2.5510e+004 |

Table10: Centroids value for Glass data set

| | | | | | | | | | | |
|-----------|----------|--------|---------|--------|--------|---------|--------|---------|---------|---------|
| C1 | 166.0782 | 2.4471 | 13.7061 | 3.5266 | 2.2563 | 73.3031 | 2.4611 | 10.7421 | -0.1976 | 0.5747 |
| C2 | 198.4844 | 2.5638 | 16.2827 | 3.2212 | 2.7751 | 73.5565 | 1.7972 | 9.9803 | 1.6024 | -0.1853 |
| C3 | 54.2369 | 2.1344 | 14.2542 | 4.4666 | 1.9043 | 72.6730 | 1.0457 | 9.7003 | 1.4352 | 0.2335 |
| C4 | 18.5031 | 2.1863 | 13.2582 | 4.4278 | 1.5191 | 74.4194 | 1.3567 | 10.2181 | 0.4565 | 10.1096 |
| C5 | 129.9205 | 0.8875 | 13.9521 | 4.3390 | 2.7228 | 75.5818 | 0.9168 | 8.7067 | 1.4468 | 1.4522 |
| C6 | 91.0957 | 2.8459 | 14.1901 | 3.6017 | 2.9122 | 72.2789 | 0.9257 | 10.0617 | 0.7071 | 1.1787 |

For the Glass data set the obtained convergence characteristics have been shown in Fig.9 to Fig.11. Comparative mean convergence has been shown in Fig.12. It can be observed that, in spite of more number of clusters, superior convergence has appeared. The obtained statistical performance has been shown in Table7 to Table9. For MMDE, maximum cluster efficiency has been obtained. The obtained best centroid value has also been shown in Table10.

D. Multidomain based MMDE


Fig.13 Convergence characteristics in 1st Stage for multidomain MMDE

Fig.14 Convergence characteristics in 2nd stage for multidomain MMDE

Convergence characteristics over Glass data set for multidomain MMDE has been shown in Fig.13, for the 1st stage and in Fig.14 for the 2nd stage. The obtained performances have been shown in Table11. It can be observed that maximum efficiency 87.48% has been obtained. The corresponding centroid value has also been shown in Table 12.

Table11: Multidomain MMDE performance over Glass data

| Trial No. (MMDE) GLASS | Correctly clustered data samples | Wrongly clustered data samples | Clustered efficiency | Total Intra Cluster Distance value |
|---------------------------------------|---|---|---------------------------------|---|
| 1 | 188 | 26 | 87.85 | 695.5811 |
| 2 | 188 | 26 | 87.85 | 694.0454 |
| 3 | 189 | 25 | 88.32 | 707.4350 |
| 4 | 190 | 24 | 88.79 | 697.8723 |
| 5 | 181 | 33 | 84.58 | 715.1624 |
| Mean (Std.Dev) | 187.2 (3.5637) | 26.8 (3.5637) | 87.48 (0.1252) | 702.0192 (9.042) |

Table12: Centroid values by Multidomain MMDE

| | | | | | | | | | | |
|-----------|----------|--------|---------|--------|--------|---------|--------|--------|--------|--------|
| C1 | 16.0000 | 1.5165 | 13.4754 | 3.3530 | 2.4072 | 74.6342 | 0.0100 | 8.7993 | 0.0894 | 0.2050 |
| C2 | 201.3622 | 1.5122 | 14.7074 | 0.1029 | 1.2528 | 72.3216 | 0.1859 | 8.6580 | 1.3473 | 0.0031 |
| C3 | 165.4855 | 1.5189 | 12.7370 | 2.3479 | 2.1774 | 71.8032 | 0.7419 | 7.7070 | 0.2396 | 0.0068 |
| C4 | 48.0214 | 1.5246 | 11.9324 | 4.4900 | 1.1781 | 72.9279 | 0.7290 | 9.8281 | 0.0987 | 0.0876 |
| C5 | 88.8809 | 1.5116 | 13.4721 | 3.3903 | 1.0875 | 72.9210 | 0.3255 | 7.9812 | 0.0100 | 0.1157 |
| C6 | 127.1936 | 1.5134 | 13.9751 | 3.8544 | 1.4775 | 73.6876 | 0.2323 | 9.0625 | 0.0100 | 0.1454 |

E. Comparative study of MMDE with K-Means

Comparative performance between Multi-Domain MMDE and K-Means over all the three different data sets have been shown in Table13-15. For each data set 5 independent trials have been applied. It can be observed with outcomes that the problems with K-Means algorithm are twofold. First it may not deliver the optimal performances, second, there is high level of variations in the performances over trails which is really a serious issue from the practical point of view. This happens because of sensitivity of K-Means algorithm towards initialization. Whereas the proposed method Multi-domain MMDE has delivered not only better performance because of exploration but also variation level is very less.

Table 13: Comparative Performance of MMDE and K-means for Wine Data

| WineData | Multi-Domain MMDE Samples | | K-Means K means Samples | |
|-------------------|--------------------------------------|------------------------------|------------------------------------|------------------------------|
| Trial | Correctly clustered | Wrongly Clustered | Correctly clustered | Wrongly Clustered |
| 1 | 125 | 53 | 125 | 53 |
| 2 | 125 | 53 | 120 | 58 |
| 3 | 125 | 53 | 120 | 58 |
| 4 | 125 | 53 | 120 | 58 |
| 5 | 125 | 53 | 120 | 58 |
| Mean | 125 | 53 | 123.75 | 54.28 |
| Efficiency | 70.22 | | 67.98 | |

Table 14: Comparative Performance of MMDE and K-means for Iris Data

| Iris Data | Multi-Domain | | K-Means | |
|-------------------|----------------------------|--------------------------|----------------------------|--------------------------|
| Trial | MMDE Samples | | K means Samples | |
| | Correctly clustered | Wrongly Clustered | Correctly clustered | Wrongly Clustered |
| 1 | 135 | 15 | 134 | 16 |
| 2 | 134 | 16 | 134 | 16 |
| 3 | 137 | 13 | 100 | 50 |
| 4 | 133 | 17 | 134 | 16 |
| 5 | 134 | 16 | 100 | 50 |
| Mean | 134.6 | 15.4 | 120.4 | 29.6 |
| Efficiency | 89.73 | | 80.27 | |

Table 15: Comparative Performance of MMDE and K-means for Glass Data

| Glass Data | Multi-Domain | | K-Means | |
|-------------------|----------------------------|--------------------------|----------------------------|--------------------------|
| Trial | MMDE Samples | | K means Samples | |
| | Correctly clustered | Wrongly Clustered | Correctly clustered | Wrongly Clustered |
| 1 | 188 | 26 | 187 | 27 |
| 2 | 188 | 26 | 187 | 27 |
| 3 | 189 | 25 | 187 | 27 |
| 4 | 190 | 24 | 187 | 26 |
| 5 | 191 | 33 | 187 | 27 |
| Mean | 187.2 | 26.8 | 187 | 26.8 |
| Efficiency | 87.48 | | 87.38 | |

V. CONCLUSION

In this paper, a modified mutation strategy for differential evolution has been proposed to facilitate the clustering requirement of data. This modification increases the convergence rate and deliver the cluster efficiency up to the mark. To increase the level of exploration, two stage based a multimodal structure has also been proposed. With this structure, the bias variation sensitivity of cluster activity decreased. Number of benchmarks have been tested which had the number of clusters from 2 to 6 to ensure the generalize capability. Proposed solution has outperformed the conventional form of DE as well as dynamic weighted form of PSO. Proposed work has been evaluated only using datasets of UCI Repository, further it can be applied on application oriented dataset to evaluate performance.

ACKNOWLEDGMENT

I would like to offer my special thanks to Dr. R J Anandhi, Professor and Head, Department of Information Science and Engineering, New Horizon College of Engineering, Bengaluru, my research supervisor, for her patient guidance, enthusiastic encouragement and useful critiques of this research work. I would also like to thank Dr. R V Praveena Gowda, Principal, The Oxford College of Engineering, Bengaluru, for his advice and assistance in keeping my progress on schedule. Finally, I wish to thank my husband and parents for their support and encouragement throughout my research work.

REFERENCES

- [1] “Nuria Gómez Blas, Octavio López Tolic, “Clustering using Particle Swarm Optimization”, *International Journal Information Theories and Applications*. 23, pp24-33, 2016
- [2] Swagatam Das, Ajith Abraham, “Automatic Clustering Using an Improved Differential Evolution Algorithm”, *IEEE Transactions on Systems, Man, And Cybernetics—Part A: Systems And Humans*, Vol. 38, NÓ. 1, pp 218-237, JANUARY 2008
- [3] Yogesh Gupta, Ashish Saini, “A new swarm-based efficient data clustering approach using KHM and fuzzy-logic”, *Soft Computing*, Springer, pp 145-162, 2019.
- [4] Pranav Nerurkar, Aruna Pavate, Mansi Shah and Samuel Jacob, “Performance of Internal Cluster Validations Measures for Evolutionary Clustering”, *Computing, Communication and Signal Processing*, Springer pp 305-312 2019
- [5] H. Wang, L. L. Zuo, J. Liu, W. J. Yi, B. Niu1, “Ensemble particle swarm optimization and differential evolution with alternative mutation method”, *Natural Computing*, Springer Nature pp 1-14,2018
- [6] Yehang Zhu, Mingjie Zhang, Feng Shi, “Application of Algorithm CARDBK in Document Clustering”, *Wuhan University Journal of Natural Sciences*, December 2018, Volume 23, Issue 6, pp 514–524
- [7] Xuejuan Liu, Jiabin Yuan, Hanchi Zhao, “Efficient and Intelligent Density and Delta-Distance Clustering Algorithm”, *Arabian Journal for Science and Engineering*, December 2018, Volume 43, Issue 12, pp 7177–7187
- [8] Huawei Yi “Robust Recommendation Algorithm Based on Kernel Principal Component Analysis and Fuzzy C-means Clustering”, *Wuhan University Journal of Natural Sciences*, April 2018, Volume 23, Issue 2, pp 111–119.
- [9] Kuo, R.J. & Zulvia, F.E. “An improved differential evolution with cluster decomposition algorithm for automatic clustering”, *Soft Computing*, Springer, pp 1–17, 2018.
- [10] Dang Cong Trana, c., Zhijian Wua and Changshou Dengb, “An improved approach of particle swarm optimization and application in data clustering”, *Intelligent Data Analysis* 2015 pp 1049–1070
- [11] Hewijin Christine Jiau, “MPM: a hierarchical clustering algorithm using matrix partitioning method for non-numeric data”, *Journal of Intelligent Information Systems*, May 2006, Volume 26, Issue 3, pp 303–306.
- [12] <https://archive.ics.uci.edu/ml/index.php>

A REAL TIME HAND GESTURE RECOGNITION AND HUMAN COMPUTER INTERACTION SYSTEM USING OPENCV

¹J. Jesy Janet Kumari, ²Hirpara Divyang, ³Jaykumar Savani, ⁴Ajay Mourya, ⁵Heena Kouser,

¹Assistant Professor, Department Of Computer Science And Engineering, ^{2,3,4,5}BE Students, Department Of Computer Science And Engineering, The Oxford College Of Engineering, Bommanahalli, Hosur Road Bangalore-560068

Abstract: The Project is on Real time Human Computer Interaction System based on hand gesture. The System created with 3 part : Gesture detection, Gesture recognition and Human computer interaction and it realizes the robust control of keyboard events with higher accuracy of gesture recognition. To recognize gestures and make it attainable to identify relatively complex gestures using camera. The developed system is highly extendable and can be used in human-robotics or other human-machine interaction scenarios with more complex command formats rather than just mouse and keyboard events. In the proposed system, the model is trained with a custom dataset and perform specific events specifically keyboard events to control the system. Once the model is trained, it can be easily integrated into an application with a graphical interface. The system can be implemented in various applications depending on the use case, for example a physically impaired person would be able to control device just with simple gestures, there can be a video player controlled by simple hand gestures or a person could give a presentation without the hassle of going near a system by just using simple hand gestures.

Index terms: Python, OpenCV, Hand Gesture, Haar Cascade, XML, Keyboard, PyautoGUI, Convex Hull Algorithm, Human Computer Interaction

I. INTRODUCTION

Human-computer system is communication between human and computer. Trend of human-computer interaction is becoming more interested day by day and is forward operation humanity and easy. Computer vision technology is interaction between human and machines. The important input device like mouse and keyboard used to interact with computer.

By using hand gesture user can pass on more information in short period of time. Human-computer Interaction system has great application by using elaborating interface between user and computer. The main aim of proposed system is to identify the specific gesture and we can use it to express the information or can control any device or robot. Static affectation of hand is defined as posture.

There are two techniques which are used to interpret gestures for human computer interaction.

(i) Data Gloves technique:

In this technique hardware part like sensors and gloves are used to detect the gestures. In this human had to wear the gloves, helmet and other apparatuses. That equipment Transfer finger flexing into electrical signals for determining the hand gesture.



Fig 1.1: Data gloves based Hand Gesture Recognition

(ii) Computer Vision technique:

Computer vision technique is nature, easy and cheap in cost comparing. This technique extract the feature from the video frame. Web camera in laptop is taking the frame continuously and program extract the feature from the frame, process on the frame as required.

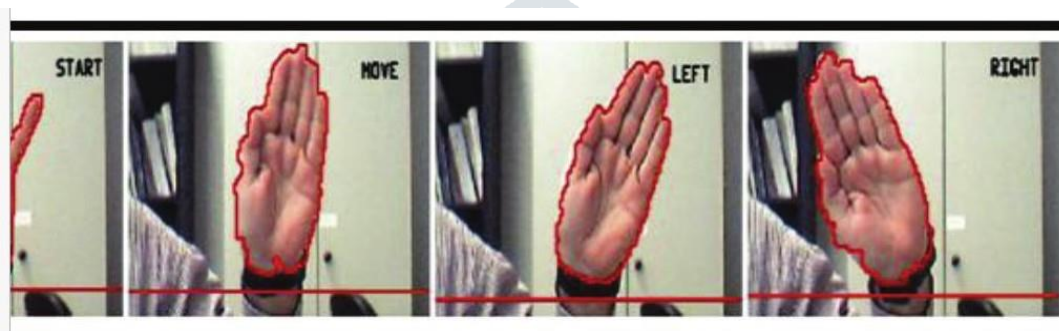


Fig 1.2: Hand Pose taken by camera

II: LITERATURE SURVEY

In vision based approach, there are many method used in hand detection, gesture training, background subtraction and fingertip detection.

A number of recognition techniques are available. Researchers worked on various aspects like skin color or background subtraction for hand segmentation. Some worked on plain, uniform background[1][4] whereas some worked on complex background[6]. Usually a static background where no other object is moving is used. Segmentation on such static background is comparatively simpler than on dynamic background. Hand localization is much easier on uniform background.

One approach is image segmentation which uses HSV color space model rather than RGB color space to determine the color of human skin. This algorithm gives better result for background separation and region boundary but it can't detect the object of skin color with similar color background [3]. Another approach is learning based gesture recognition in Adaptive Boosting algorithm that can integrate the information of same category of objects. It trains the network by combining all weak classifiers into one strong classifier.

Another technique is based on convex hulls. Palm Detection have many algorithm. In this section some of existing algorithms will be discussed which are used in our proposed technique. Jarvis's March or Gift wrapping Algorithm, Divide and Conquer algorithm, Graham's Scan Algorithm, Quick hull algorithm and Chan's algorithm. Graham Scan computes the convex hull of any given set of points. To implement the system for hand tracking and simple gesture recognition in real time, there is no need to touch or carry a peripheral device by user. By comparative analysis, we can conclude that only one detection technique not enough because different kind of methods can deal with different problem during detection & recognition. There are various available machine learning algorithms that are AdaBoost, support vector machine technique, hidden markov model, & principle component analysis for training classifiers [2]. There may also have different convex hull and contour detection of boundary of hand region.

Using this method, we implemented system for hand detection and haar classifier algorithm to train the classifier. Here we tend to additionally use HSV color model for background subtraction & noise removal, convex hull algorithm for drawing contour around palm and fingertip detection.

There are multiple softwares for image processing application but among them OpenCV (Open Source for Computer Vision) software is very popular for Real time image processing applications such as object detection & gesture recognition. The major advantage is that one will simply integrate the code with hardware. We implement the projected system on OpenCV library supported UNIX operating system setting.

III: METHODOLOGY

In this System, we start taking the input from web camera. Based on the input system will detect the gesture and do the further process on the frame as required and remove the noise also eliminate the background from the image and recognize the gesture.

The simple Haar-like features are used in the Viola and Jones algorithm. The integral image at the location of pixel $[x, y]$ contains the sum of the pixel intensity values located directly above the pixel location $[x,y]$ and at the left side of this pixel. So $AI[x,y]$ is the original image and $AI[x,y]$ is the integral image that is calculated by below equation 1:

$$AI[x,y] = IA[x',y']$$

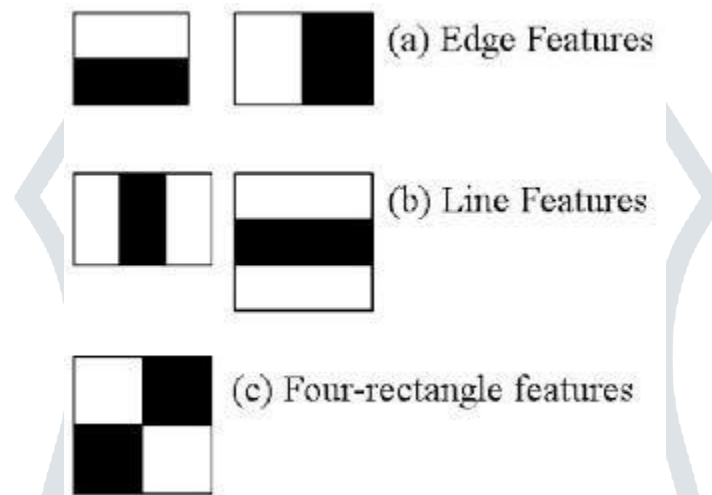


Fig 3.1: Common haar like features for integral images[5]

Not one Haar-like feature can identify the object with high accuracy. However, it is not complex to find one Haar-like feature-based classifier that has good accuracy than the random guessing.

In convex Hull algorithmic rule start is segmentation of the hand image that contains the hand to be placed. In order to create this method it's potential to use shapes, however they'll be modified greatly in interval that hand moves naturally.

So, we tend to choose skin-color to induce characteristic of hand. The skin-color could be a distinctive cue of hands and it's invariant to scale and rotation.

In the next step we tend to use the estimated hand state to extract many hand options to outline as settled method of finger recognition. After the hand is segmented from the background, a counter is extracted. The counter vector contains the series of coordinates of edges of hand. Then the process of counter vector provides the placement of the fingertip.

Calculate the points with min and max of x and y coordinates in Convex Hull and join these points. There also are other points for that find convex defects i.e. between each arm of hull. We have used opencv library for this project is called open computer vision (openCV).

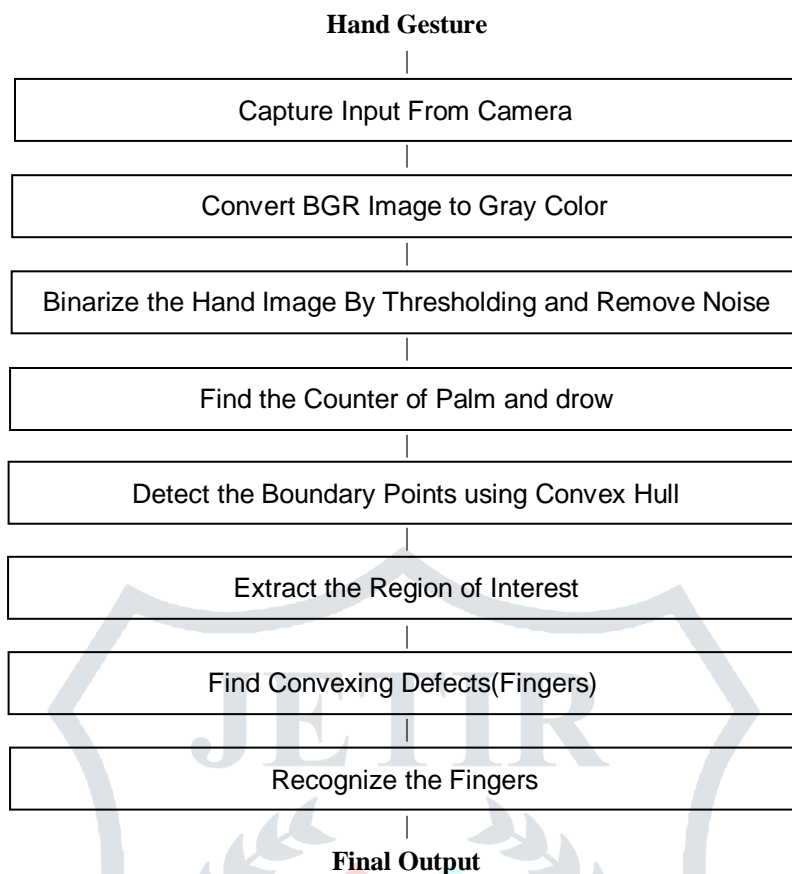


Fig 3.2: Flow of Methodology for finger counter

IV: SOFTWARE IMPLEMENTATION

Human Computer Interaction, robotics, biometrics, image processing and other area where openCV library can be used. Visualization is most important and that include implementation of Haar Classifier detection and training. Two set of images are required to train the haar classifier. One set which refers positive image which will be our model object for gesture recognition and another set image refers negative image which does not contains an interested objects. It is also important that they should be different in background and lighting.

In our trained model, 4 hand postures are tested the "palm" posture, "fist" posture, "OK" posture, "point" posture against negative postures. Low cost Web camera of laptop is used for the video input. Camera Provides video capture with max resolution of 640*480. Gaussian blur is applied in implementation for smothering the image. we collected positive image in range of 400 to 500 with different scales for each posture and 500 random images for negative samples. after all positive images and negative image samples are ready, it is generated in xml file which will latter used in system for detection and recognition of gesture.

V: RESULT AND CONCLUSION

First, We try palm detection based on our trained xml file in openCV. Then capturing live streaming of camera the initialization has been done. Four gesture such as palm, fist, okey and point by green rectangle which is trained by integral images. Second step is extracting image gesture which is compared with stored positive-negative integral image dataset and perform finger tip tracking by contour detection. which is compared with stored positive-negative integral image dataset and perform finger tip tracking by contour detection. With help of 2.40 GHz intel® coreTM processor Linux based opencv image processing software & jupyter notebook and sublime text editor is used to analyze a 640 x 480 image size, a frame rate of 30 frame/second has achieved.

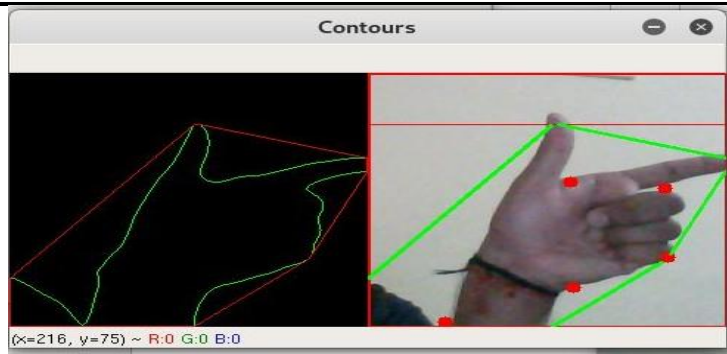


Fig 5.1: Pointdetection

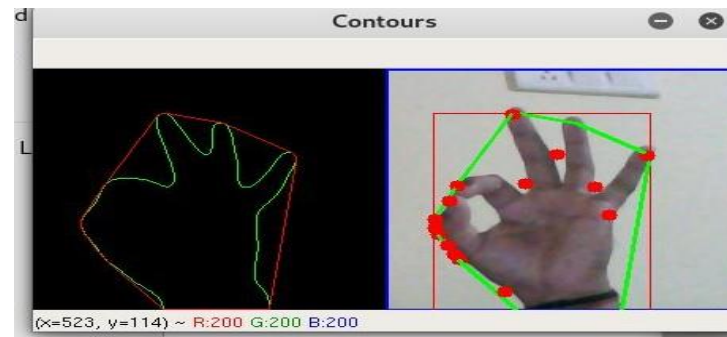


Fig 5.2: okeydetection

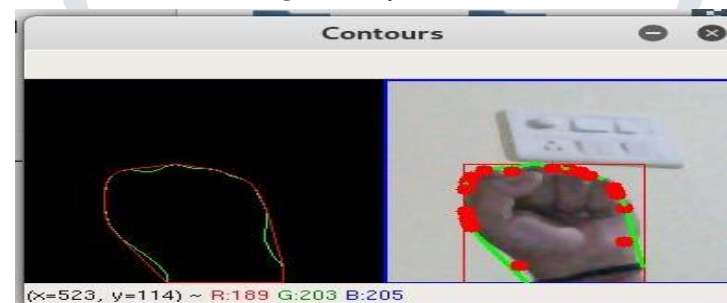


Fig 5.3: fist detection

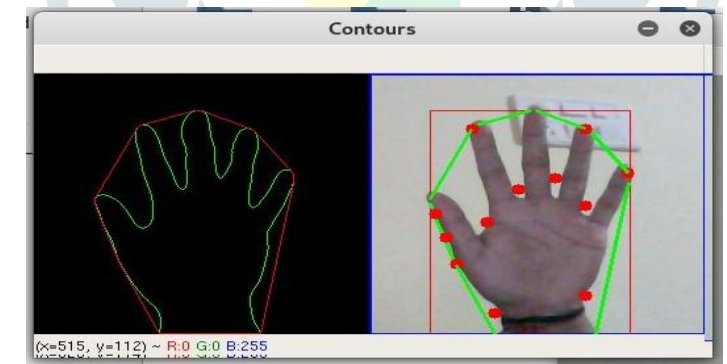


Fig 5.4: Palm detection

Fig. 5.1, 5.2, 5.3, 5.4 shows the detection of Point, Okey, Fist, Palm respectively by using python programming language. all above figure shows various finger gestures detected by proposed algorithm and also contain segmented image and Identified gestures.

The aim of project is to develop a real time hand Gesture recognition system. It is shown that contour is very important feature and can be used to discriminate two different gesture.

Reference

- [1] M.Ali Qureshi, Abdul Aziz, Muhammad Ammar Saeed, Muhammad Hayat, Jam Shahid Rasool, "Implementation of an Efficient Algorithm for Human Hand Gesture Identification," Electronics Communications and Photonics Conference (SIECPC), Saudi International,2011.
- [2] : Ruchi Manish Gurav, "Real time finger tracking and contour detection for gesture recognition using OpenCV", IEEE 2015
- [3] Qing Chen Nicolas, D. Georganas, and Emil M. Petriu "Hand Gesture Recognition Using Haar-Like Features And A Stochastic Context-Free Grammar" IEEE ,Vol. 57, No. 8, August2008
- [4] Asanterabi Malima, Erol Ozgur and Mujdat Cetin, "A Fast Algorithm for Vision-Based Hand Gesture Recognition for Robot Control," IEEE Conference on Signal Processing and Communications Applications, 2006,pp1-4.
- [5] Nasser H. Dardas And Nicolas D. Georganas "Real-Time Hand Gesture Detection And Recognition Using Bag-Of-Features And Support Vector Machine Techniques", IEEE Vol. 60, No. 11, November2011
- [6] Means Xingyan Li, "Gesture Recognition Based on Fuzzy C- Clustering Algorithm," TechnicalReport,2005.



NADIA

Advancement Through Research

- [Home](#)
- [Contents](#)

[IJSIA Articles](#)

[PREDICTIVE MODEL DEVELOPMENT FOR LULC DATA USING ADAPTIVE MLP NEURAL NETWORK ARCHITECTURE](#)

[31 Mar 2021 | [vol. 15](#) | [no. 1](#) | pp. 11-22]

[About Authors:](#)

Shobha T1* and R J Anandhi2

-1Research Scholar, Department of CSE, The Oxford College of Engineering, Bengaluru, Affiliated to Visvesvaraya Technological University, Belagavi, Karnataka, India

-2Professor and Head, Department of ISE, New Horizon College of Engineering, Bengaluru, Affiliated to Visvesvaraya Technological University, Belagavi, Karnataka, India

[Abstract:](#)

Land Use and Land Cover (LULC) data from remote sensing imagery have given various dimensions of benefits in different applications. Proposed work has applied a next-level approach to extract the pattern of change in the objects of LULC with time. The LULC mapped data has been applied to develop the predictive model for the LULC objects. The adaptive form of multilayer perceptron (MLP) architecture has been applied to make predictor efficient. The different regions of Karnataka state have been considered for analyzing the experimental results. The proposed model has shown a high level of prediction accuracy and can be considered as a support system for remote sensing-based applications for LULC.

[Keywords:](#)

Adaptive Architecture, Land Cover Land Use, Neural Network, Predicting Model

About IJCA

IJSIA aims to facilitate and support research related to security and its applications. Our Journal provides a chance for academic and industry professionals to discuss recent progress in the area of security and its applications.

Original Research | [Published: 06 August 2019](#)

Rate adaptation performance and quality analysis of adaptive HTTP streaming methods

[Selvaraj Kesavan](#)  & [E. Saravana Kumar](#)

International Journal of Information Technology **12**, 453–465 (2020)

173 Accesses | [Metrics](#)

Abstract

Media streaming is the key innovation in technology era brings high quality on-demand and live media content to the consumer on-the-go anywhere, any time. Achieving best quality-of-service and quality-of-experience (QoE) are major concerns in the current circumstances due to increasing network usage and user demand to high quality media content. Conventional streaming approaches face numerous challenges in delivering media content to the users without degradation of quality. An adaptive HTTP streaming is emerging content delivery approach which provides real time content delivery without compromising quality and ensuring superlative QoE. The dynamic and robust bit rate selection based on the network and client key performance indices helps to achieve best class of service to the consumer. As many standards and processes emerge in the field of Adaptive HTTP



An Automated Serving Robot Based On Artificial Intelligence

S Preethi¹, Rabya Suroor², Sahana L³, Sangeetha U Hottigoudra⁴, Amaresha⁵

Final year B.E Students (UG), Department of Information Science & Engineering, The Oxford College of Engineering,
Bangalore, India^{1,2,3,4}

Assistant Professor, Department of Information Science & Engineering, The Oxford College of Engineering,
Bangalore, India⁵

ABSTRACT: As the technology is growing and it is been applied in all the fields and is being used in every aspect of life. As our life becomes busy due to work, we prefer to eat outside in some good restaurant to enjoy the food and to spend quality of time. Along with the good food a good environment is also required as the people demand. A modern restaurant can be equipped with robots or up to date new technologies. In our proposed project work, we are going to design a restaurant that can be controlled and services can be provided automatically using the modern technologies. In today's world the use of robot is going on increasing. Robots are able to carry out every work more effectively and efficiently than a man can do. Hence one of such application of robot could be SERVING ROBOT. There are many areas of research that could be done for a serving robot. We have used image processing to detect the old customer to recognize them automatically. Customers can access the menu sitting at the table itself and can place the order and the food is being served by the robot. In this paper we have try to demonstrate a prototype of Autonomous Serving Robot which will serve the food to the customer. The implementation is done with available resources to reduce the cost of project.

KEYWORDS: Support vector machine, Face recognition, Automatic Food Delivery, Internet of things, Cooking status, Android application.

I. INTRODUCTION

Robot being a great advancement in the field of technology can serve well as a waiter at restaurants and hotels. With their time efficient and dedicated task performance robot can be a perfect solution in catering work. The traditional way of serving comprises of a human waiter, who goes around the customer asking for the order. The main drawback of traditional human waiter is that it is very time consuming and employing a human can cost more as he need to be paid for his service, also when they get sick the work suffers for the owner.

In this paper we have proposed a robotic foodway track which work on the technique of following an assigned coordinated path which is based on 2 dimensional axis that is x and y axis. The robotic tray carry the meal to the tables with their assigned area over a 2 dimensional path separated with x and y coordinate and stop at the point at which table is placed.

An RF module used at the counter section of the restaurant help to guide the robot to the table number at which the meal should be delivered act as an remote control of the waiter robot.

In today's restaurant Digital multi-touch menu cards and other forms of digital facility are replacing old fashioned services like-waiters can take order from customer and serve them. Intelligent Restaurant system delivers almost infinite flexibility in promoting meal and snack options. Intelligent Restaurant system uses technologies innovatively in a modern restaurant such as multi-touch LCD with Arduino mega, RF module, database & line following Robot to enhance quality of services and to enrich customer's dining experience.

The whole system makes use of RF technology. Robot automatically checks the status of the person. It reaches the correct destination and person passes his order to robot. The robot sends the order by wireless technology (RF technology) to counter where a receiver is placed, this receiver receives the signal from the robot (through RF technology) and the person at the counter checks the order, prepare it and put it on the robot and robot again provides proper service to respective person automatically. The robot can take the order from multiple people by reaching near their tables on their call.



The robot can serve to a customer as well as take order from another customer at the same time.

II. PROPOSED SYSTEM

In today’s restaurant Digital multi-touch menu cards and other forms of digital facility are replacing old fashioned services like-waiters can take order from customer and serve them. Intelligent Restaurant system delivers almost infinite flexibility in promoting meal and snack options. Intelligent Restaurant system uses technologies innovatively in a modern restaurant such as multi-touch Tab, Robotic module, database & line following Robot to enhance quality of services and to enrich customer’s dining experience. A line following robot is designed using sensor operated motors to keep track the line path predetermined for meal serving. Online payment with auto generated bill. In this paper we have made a robot which provides proper service to customer in restaurant. Customers can select the food items from the menu display on the table and place the order. The person at the counter checks the order, prepare it and put it on the robot and robot deliver the food to the respective table. Real time face tracking refers to the task of locating human faces in a video stream and tracking the detected or recognized faces.

Advantages:

- Cost Efficient
- Error free
- Attract customers
- Gain in business

III. METHODOLOGY

◆ MENU MANAGEMENT SYSTEM

The menu management will be authorized by the authorized person from restaurant.

In this they can manage their menu and can hide/delete/add the required item and with pictures of food.

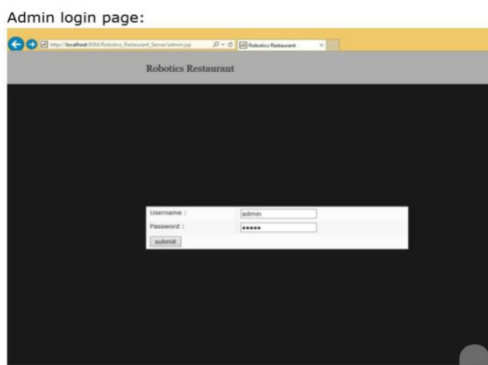


Fig 1: Schematic Design of Admin Login page



Fig 2: Schematic Design of select Menu page

◆ WEB ORDERING SYSTEM

Customers can place their order via their smart phone or smart tap. Customers can select the food items from the menu display on the table and place the order. Customer can order the desired dishes and view them in the cart. After clicking on the button of “order now”, it directly flashes on the screen of kitchen side. Then Kitchen’s employee will update the food prepare status, after that customer can check the food prepare status.



Fig 3.Android design page



◆ ORDER RETRIEVAL SYSTEM

In this system, restaurant employee will keep track on each and every order receive/serve.

Total amount:



Fig 4. Order Retrieval Page

◆ DELIVER FOOD

The person at the counter checks the order, prepare it and put it on the robot and robot deliver the food to the respective table. Robot will serve the food original position to customer’s position.

Update status page:

Total amount:



Fig 5. Deliver Food Page

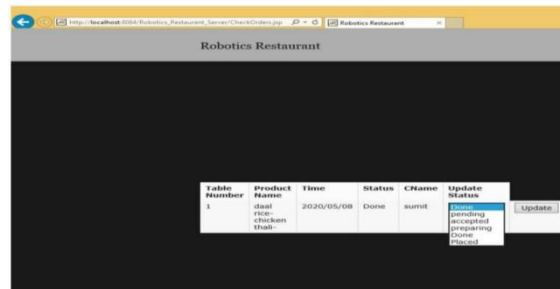


Fig 6. Update Status Page

FACE RECOGNITION

Real time face tracking refers to the task of locating human faces in a video stream and tracking the detected or recognized faces. After recognized robot can tell to customer like how are you Mr. aa, welcome to our restaurant.

ALGORITHM DESCRIPTION

Face recognition: Real time face tracking refers to the task of locating human faces in a video stream and tracking the detected or recognized faces. After recognized robot can tell to customer like how are you Mr. aa, welcome to our restaurant.

We are using Linear Support Vector Machine (LSVM) in this project. Linear Support Vector Machine (LSVM) are used to train. Certain steps are to be followed in HOG (Histogram of Oriented Gradients). They are:

Extracting HOG descriptors from the positive samples of trained images.

Extracting HOG descriptors from the negative samples that don't contain any objects.

Training LSVM on the samples.

Computing HOG descriptors and applying classifiers on samples which are called as hard negative mining.

Collecting the false negative samples which are found from the hard negative mining stage and sort them.

Testing with dataset.

Finally face recognition is done by using Euclidean distance method.



V. SYSTEM DESIGN AND MODULE DESCRIPTION

◆ INTRODUCTION

A good system design is to organise the program modules in such a way that are easy to develop and change. Structured design techniques help developers to deal with the size and complexity of programs. Analysts create instructions for the developers about how code should be written and how pieces of code should fit together to form a program.

◆ SYSTEM ARCHITECTURE

The architecture of a system describes its major components, their relationships (structures), and how they interact with each other. Software architecture and design includes several contributory factors such as Business strategy, quality attributes, human dynamics, design, and IT environment. We can segregate Software Architecture and Design into two distinct phases: Software Architecture and Software Design. In Architecture, nonfunctional decisions are cast and separated by the functional requirements. In Design, functional requirements are accomplished.

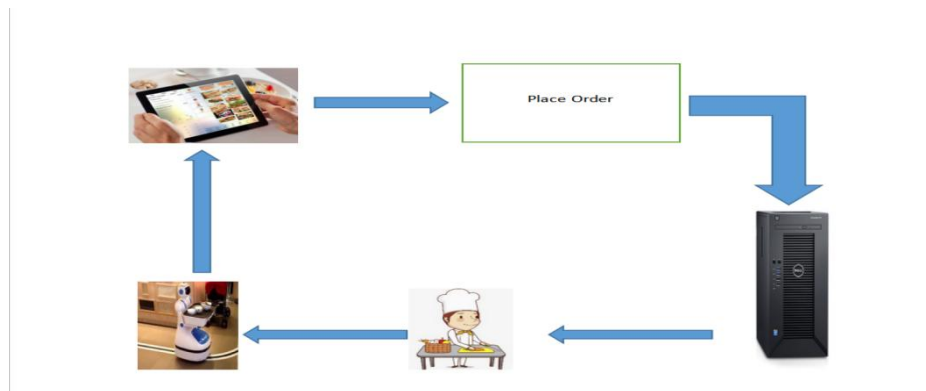


FIG 7. SYSTEM ARCHITECTURE

The Step by step process of the system:

1. Admin can add the menu items and details are saved in the server
2. Customer can check the menu items using the mobile app
3. Customer selects the items and add into the cart
4. Customer can make payment using the mobile app
5. Once order is placed, cook can view the order details and update the status of the cooking process
6. Customer can view the status of the items ordered
7. Once food is prepared, cook updates the status and server sends the instruction to the robot
8. Robot once receives the instruction , moves to the cook to collect
9. Cook places the food items on the tray of the robot and sets the table number
10. Robot than moves to the table to deliver the food
11. Robot once moves to the table trigger the camera and captures the photo
12. The photo is sent to the server for processing
13. Server applies the face recognition algorithm to check the old customer. If old customer is recognized, sends the information to the robot and robot interact with the customer
14. If it's a new customer, server saves the face images in the server.
15. Robot and customer can interact to discuss about the food

VI. DESIGN CONSIDERATION

◆ REQUIREMENT SPECIFICATION

A software requirements specification (SRS) is a document that captures complete description about how the system is expected to perform. It is usually signed off at the end of requirements engineering phase. Framework Requirement Specification (SRS) is a focal report, which outlines the foundation of the item headway handle. It records the



necessities of a structure and in addition has a delineation of its noteworthy highlight. A SRS is basically an affiliation's seeing (in making) of a customer or potential client's edge work necessities and conditions at a particular point in time (for the most part) before any veritable design or change work. It's a two-way insurance approach that ensures that both the client and the affiliation understand exchange's necessities from that perspective at a given point in time.

◆ SOFTWARE DESCRIPTION

ANDROID DESCRIPTION

Android applications are written in the Java programming language. The Android SDK tools compile the code along with any data and resource files into an Android package, an archive file with an .apk suffix. All the code in a single .apk file is considered to be one application and is the file that Android-powered devices use to install the application. Once installed on a device, each Android application lives in its own security sandbox. The Android operating system, is a multi-user Linux system in which each application is a different user.

ARDUINO IDE

The Arduino Integrated Development Environment (IDE) is a cross-platform application (for Windows, macOS, Linux) that is written in the programming language Java. It is used to write and upload programs to Arduino compatible boards, but also, with the help of 3rd party cores, other vendor development boards.

The source code for the IDE is released under the GNU General Public License, version 2.

The Arduino IDE supports the languages C and C++ using special rules of code structuring. The Arduino IDE supplies a software library from the Wiring project, which provides many common input and output procedures.

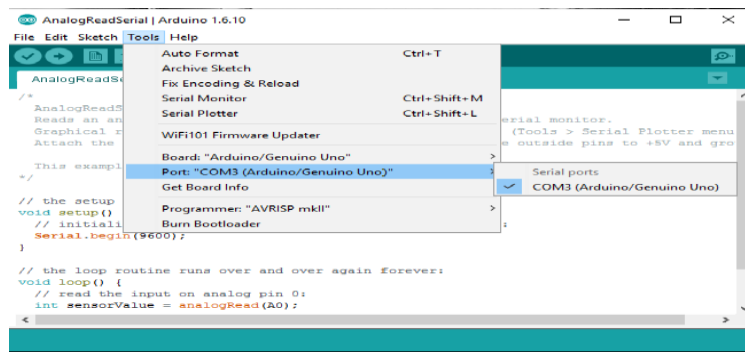


Fig 8. Arduino IDE

NET BEANS IDE

NetBeans IDE is the official IDE for Java 8. With its editors, code analyzers, and converters, you can quickly and smoothly upgrade your applications to use new Java 8 language constructs, such as lambdas, functional operations, and method references. NetBeans IDE provides different views of your data, from multiple project windows to helpful tools for setting up your applications and managing them efficiently, letting you drill down into your data quickly and easily, while giving you versioning tools via Subversion, Mercurial, and Get integration out of the box. When new developers join your project, they can understand the structure of your application because your code is well-organized.

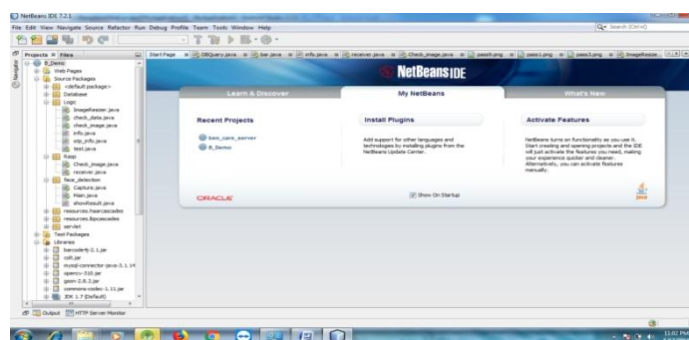


Fig 9. Snap Shot of Net Beans



MySQL

MySQL ("My Sequel") is (as of 2008) the world's most widely used open source relational database management system (RDBMS) that runs as a server providing multi-user access to a number of databases. The SQL phrase stands for Structured Query Language.

MySQL is a popular choice of database for use in web applications, and is a central component of the widely used LAMP open source web application software stack (and other 'AMP' stacks). LAMP is an acronym for "Linux, Apache, MySQL, Perl/PHP/Python." Free-software-open source projects that require a full-featured database management system often use MySQL.

NAVICAT PREMIUM

Navicat Premium is a multi-connections database administration tool allowing you to connect to MySQL, MariaDB, SQL Server, and SQLite, Oracle and PostgreSQL databases simultaneously within a single application, making database administration to multiple kinds of database so easy.

Navicat Premium combines the functions of other Navicat members and supports most of the features in MySQL, MariaDB, SQL Server, SQLite, Oracle and PostgreSQL including Stored Procedure, Event, Trigger, Function, View, etc.

Navicat Premium enables you to easily and quickly transfer data across various database systems, or to a plain text file with the designated SQL format and encoding.

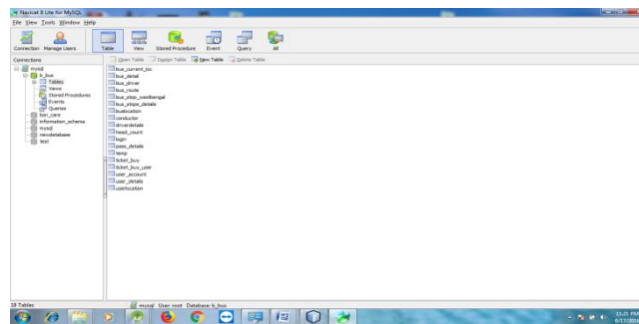


Fig 10. Navicat Lite for MySQL

IV. RESULTS ANALYSIS

The Result of this project is to develop a small scale robot, called the Serving Robot, which can help in the progress in the field of the robotic assistance technologies. A robot that functions as a personal assistant should be able to help in different environments, whether it would be a research lab, a hospital, or even at home. The basic objective of the Serving Robot is to serve the customer effectively. It takes their orders and takes care of transporting food/refreshment to them.

We have used image processing to detect the old customer to recognize them automatically. Customers can access the menu sitting at the table itself and can place the order and the food is being served by the robot. In this paper we have tried to demonstrate a prototype of Autonomous Serving Robot which will enhance the dining experience for the customers. The implementation is done with available resources to reduce the cost of project.

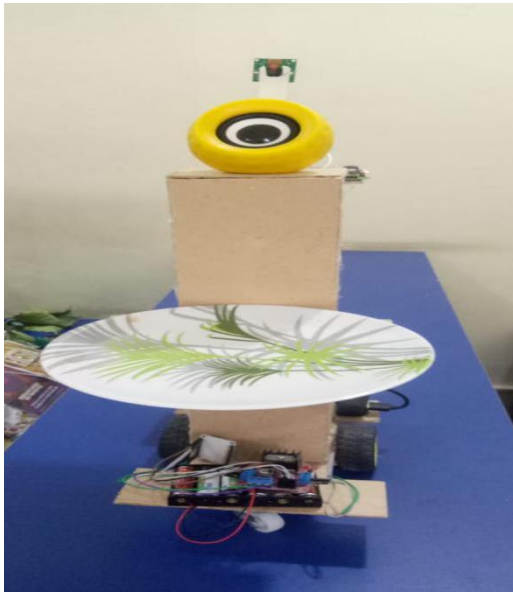


Fig .11(a) Final prototype

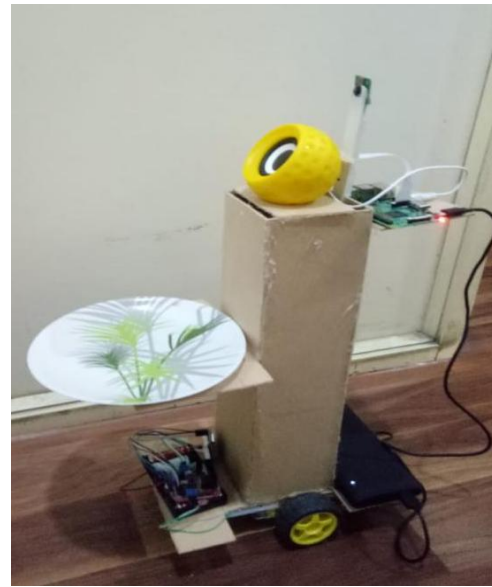


Fig .12(b) Final prototype

V. FUTURE SCOPE OF THIS STUDY

- Cost Efficient
- Error free
- Attract customers
- Gain in business
- The purpose of this project was to create a robotic waiter that would assist restaurant staffs in delivering food.
- Manpower is still an issue in the industry with workers being inefficient and having no-shows.
- They would still need to be trained and paid.
- Reduces customer waiting time.
- One time investment in the system.
- Work can be faster and may reduce the cost of labouring.
- As customers place their own orders, waiter's staff numbers can be reduced.
- Applications are performed with precision and high repeatability

VI. CONCLUSION

As we see the robots are increasingly becoming the part of everyday life; the use of Serving Robot can be extend to various functional purposes.

This system allows customers to order food by android app which is wirelessly connected to the kitchen side.

A line following robot is used to carry meal from counter to customer.

Based on our experiences and literature, the restaurant service process will mainly include human service also in the future.

The robotic restaurant system has to fulfill both the needs of the customer and the restaurant's personnel and it has to provide added value to the restaurant's business.

The introduced robotic restaurant system Smart menu creates a new way of working because the extensions of the digital menu offer features that help the waiting staff to communicate better with the kitchen.

REFERENCES

- [1] P. Lessel, M. Böhmer, A. Kröner and A. Krüger, "User requirements and design guidelines for digital restaurant menus," Proceedings of the 7th Nordic Conference on Human-Computer Interaction: Making Sense Through Design , pp. 524-533
- [2] S. Pieskä, M. Luimula, J. Jauhiainen and V. Spitz, "Social Service Robots in Wellness and Restaurant Applications.," Journal of Communication and Computer, Vol 10, No. 1, 2013, pp. 116-123



- [3] T.-H. Tan and C.-S. Chang, "Development and evaluation of an RFID- based e-restaurant system for customer-centric service," *Expert Systems with Applications* 37 (2010), pp. 6482–6492
- [4] P. Baranyi and A. Csapo, "Definition and synergies of cognitive infocommunications," *Acta Polytechnica Hungarica* 2012; 9(1), pp. 67– 83, 2012.
- [5] G. Sallai, "The Cradle of the Cognitive Infocommunications," *Acta Polytechnica Hungarica* Vol. 9, No. 1, pp. 171-181, 2012.
- [6] E.W.T. Ngai, F.F.C. Suk and S.Y.Y. Lo, "Development of an RFID- based sushi management system: The case of a conveyor-belt sushi restaurant," *Int. J. Production Economics* 112 (2008), pp. 630–645
- [7] Y. Qing-xiao, Y. Can, F. Zhuang and Z. Yan-zheng, "Research of the Localization of Restaurant Service Robot," *International Journal of Advanced Robotic Systems*, Vol. 7, No. 3 (2010), pp. 227-238
- [8] E-TableTM, The unique restaurant interactive ordering system Available at: <http://www.e-table-interactive.com/>, Accessed 3.10.2013



Personal Assistant Robot System Using Node MCU

Borra Ramya¹, Deeksha N², Dhannarapu Guna³, Divya M⁴, Channappa Gowda⁵

Final year B.E Students (UG), Department of Information Science & Engineering, The Oxford College of Engineering, Bangalore, India^{1,2,3,4}

Assistant Professor, Department of Information Science & Engineering, The Oxford College of Engineering, Bangalore, India⁵

ABSTRACT: In our case robot is mainly designed for this group of people as its main purpose is to offer assistance to an elderly or disabled person. The main objective of the project is to create a robot that can provide useful services, but that also exhibits personality and character. The robot will be designed for ease of interaction without requiring any training or expertise, and to serve the patient with water, food & tablet. Interactions between the end users and robot are done by using the natural English language which is taken as a command by the robot.

KEYWORDS: Robotic Nurse, Helping paralyzed people, Updating family about medicines, Serving water, food and medicines to paralyzed people.

I. INTRODUCTION

We live in a world in which technology embraces us, makes our lives easier and more enjoyable. Technology is growing at an unexpectedly fast pace with the unveiling of the family friendly robots that play the role of a personal assistant at home.

Man has already started interacting with computers and smartphones. It is anticipated that social robots shall replace these computers and smartphones in the near future. This work is delving into the design of one such social robot, which supports the above proposition.

Although we all benefit from this emerging technology, certain groups of people need more help and support than others: elderly or disable people. For them technology means a way of having an almost normal life. So we focused our attention on an age old concept: the smart house, more precisely a personal assistant robot that is a part of the smart house paradigm. This robot is mainly designed for this group of people as its main purpose is to offer assistance to an elderly or disabled person.

II. RELATED WORK

In [1] Hospital nurse regularly bring her instrument to the patient using cart. They need to push or pull the cart to the patient bed and bring it back many times in a day. This can be tiresome for nurses because they need to treat many patients in the hospital. This research is mainly to solve this problem by constructing a mobile robot for nurses that is able to follow and carry the medical equipment and at the same time perform obstacle avoidance. In [2] Here, the authors present the ACCOMPANY project, a pan-European project which focuses on home companion technologies. The projects aims to progress beyond the state of the art in multiple areas such as empathic and social human robot interaction, robot learning and memory visualisation, monitoring persons and chores at home, and technological integration of these multiple approaches on an existing robotic platform, Care-O-BotR 3, and in the context of a smart-home environment utilising a multitude of sensor arrays. In [3] A major contribution and novelty of this project is the development of a human-robot interaction system and the new DTW algorithm capable of measuring the quality of imitation interaction between a humanoid robot and a human subject. This system enables consistent objective measurement of the imitation behavior that can be used to glean information about the ASD condition. In [4] Here, firstly the authors have presented user-centred design and aimed to evaluate the first system prototype after the requirements set by the preliminary focus groups and pilot experiments. To this end, they recruited elderly participants and asked them to realistically experiment some of the services in our test sites, because older people generally have difficulties to make the imaginative leap to seeing fictional demonstrations as representing an actual application. Secondly, study was focused on the evaluation of the MMUI only. In [5] Care-O-bot 4 is a general purpose service robot that is apt to adapt to different environments, situations and requirements. Its design blends in every configuration with the situation and it is able to create a positive emotional bond on all three levels (visceral, behavioral, and



reflective) providing the necessary social cues. As with its predecessors, the Care-O-bot 4 may be deployed in different environments from a home setting to a medical assistant and assumes different roles, where it is perceived as social actor. In [6] All trials were carried out in private homes of single-living senior adults. Each trial with one user lasted three weeks. In total, the robot was deployed for 371 days. Assessment by means of qualitative interviews and questionnaires took place at four stages of each trial: pre-trial, mid-term, end of trial, and post-trial (i.e. one week after the trial had ended). Results of the qualitative interviews as well as perceived safety measured by the Falls Efficacy Scale (FES) are reported here. Quantitative data were analyzed using SPSS by means of descriptive statistics and nonparametric methods (Friedman ranking-test). In [7] This paper presents the proposed experimental layout of the preliminary test to observe the initial response and behavior of ASD children when they are exposed to a humanoid robot NAO. The HRI procedure involves the robot executing basic, simple modules of interaction. The adaptation of real ASD characteristics in the proposed architecture can be applied to develop new therapy procedures applying close human-robot integration to cater various individual characteristics of autistic children. In [8] The paper discusses a novel human-robot communication system for people with disability using electromyography (EMG, signals via a Personal Digital Assistant (PDA). The system contains six primary components: the EMG signal processing, the Morse code command generate, the command decomposition, the robot task manager, the status User Interfaces (UIs), the event-triggered adaptation, and the database. In [9] Here, the authors has presented a service oriented architecture based application which is fully expandable without modifying the existing modules. This approach of creating plug-and-play based modules which could be added upon like present day android marketplace could only help the cause for making this application feature-rich. Also, by specifying the priorities of these modules or behaviors, they could help the robot be more intelligent through the use of the reactive architecture. In [10] The authors had developed a kind of personal assistant robot platform especially for students and employee to help to manage their learning, life and work better, in the fields of curriculum management, diary management, financing management and chatting system. They adopted the structured design method of MVC framework and the optimized algorithm. We created a dependable and convenient system that can effectively identify the information from a database and timely deal with it.

III. PROPOSED SYSTEM

We have proposed a robotic personal assistant for elderly person which can take care of the elderly. Robotic personal assistant can sense the person and help them with the essentials. The receptionist is fitted with a medicine chamber where it can keep the medicine. The robotic personal assistant can interact with the patients. The personal assistant serves the patient with water and also serve them with their medicines (tablets). The user gets notification about the medicine to be taken in their android application.

IV. METHODOLOGY

This stage is the underlying stage in moving from issue to the course of action space. Accordingly, starting with what is obliged; diagram takes us to work towards how to full fill those requirements. System plot portrays all the critical data structure, record course of action, yield and genuine modules in the structure and their Specification is picked. This assumes an essential part on the grounds that as it will give the last yield on which it was being working. In our work we use four modules, these modules are listed below.

Initial setup: We are using Arduino uno microcontroller which is connected Bluetooth module. Here we made personal robot nurse. We made robot nurse by using DC motor, Wheel based car that will serve the medicine to patient. Another technology we are using android application to interact between patient and nurse. To active the robot nurse we used chargeable battery.

Water check: Robot will check water inside the water-tank. We have made the water-tank for one Liter. When water will be empty inside water-tank then robot nurse will give alert for empty water.

Process instruction: Robot will feed the patient when the patient is at meal time. After that When it comes time to feed, the robot will feed medicine to patient and water. When medicine time will come then robot nurse will give alert automatically.

Interaction patient to robot: Patient can use android app to interact with robot nurse. Patient can start the app for help from robot nurse. If the patient needs some water, robot nurse can serve the water. When patient will say something like "I need some water" then this speech will be convert speech to text using NLP algorithm and robot will get the instruction.

V. SYSTEM ARCHITECTURE

The architectural configuration procedure is concerned with building up a fundamental basic system for a framework. It includes recognizing the real parts of the framework and interchanges between these segments. The beginning configuration procedure of recognizing these subsystems and building up a structure for subsystem control and correspondence is called construction modeling outline and the yield of this outline procedure is a portrayal of the product structural planning. The proposed architecture for this system is given below. It shows the way this system is designed and brief working of the system.

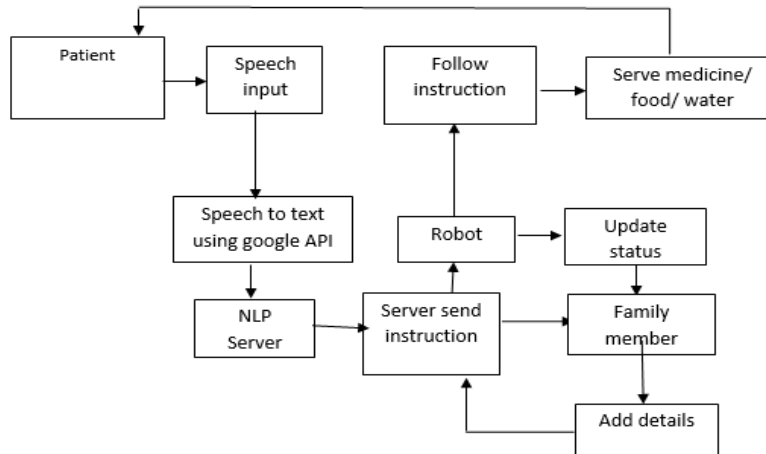


Fig 1. System Architecture of the model

The Step by step process of the system;

1. When the patient requests something to the robot, the message from the patient is received by the Mic which will be with the patient and that speech message is converted into the text message using the Speech to text Google API and that sentence is inputted to the NLP server.
2. NLP server detects the kind of request, it may be for the food or water. And it informs the family member about the request.
3. Robot receives the particular information about the food or water and moves near the patient and serves accordingly.
4. If the food or medicines or water is not available when requested, robot checks it and the server sends a message to the android app handled by the patient's caretaker or family member.
5. When the family member again fills the details in the server then the database will get updated.
6. The medicines will be served to the patient automatically according to the time set in the server.

V. DESIGN CONSIDERATIONS

Software Requirements

1. Operating system : Windows 7/8
2. JDK 1.8
3. Android SDK
4. IDE: NetBeans, arduino
5. Data Base: MYSQL
6. Server: Apache Tomcat Server 7.0
7. Programming Language : Java, C



Some snapshots of our android app are:

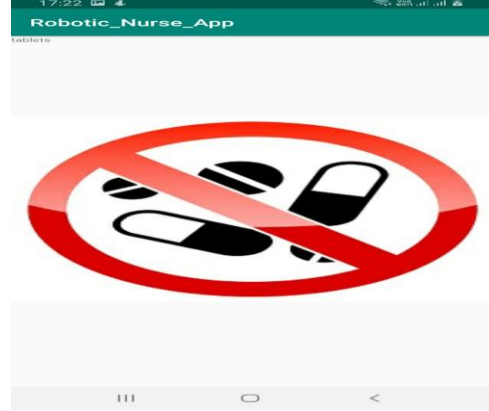
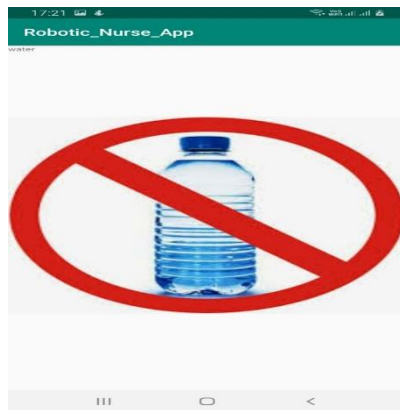


Fig 2 Android Application UI

Fig 3. Water Alert in the Android App

Fig 4. Medicines Alert in the Android App

Some snapshots of our Web Application are:

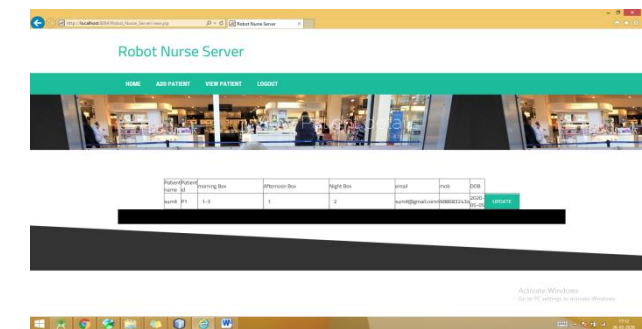
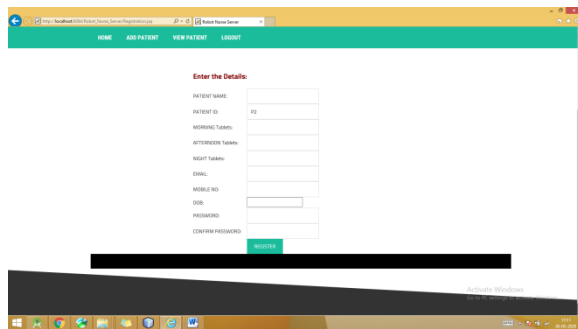
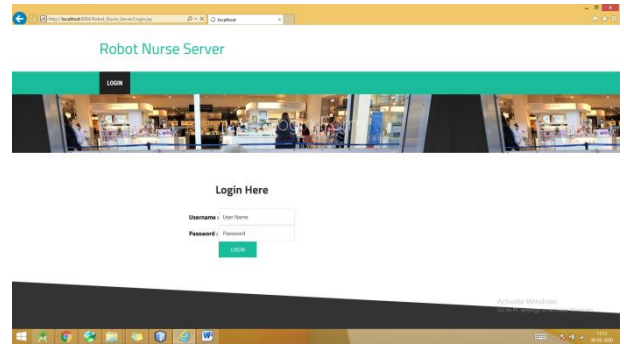
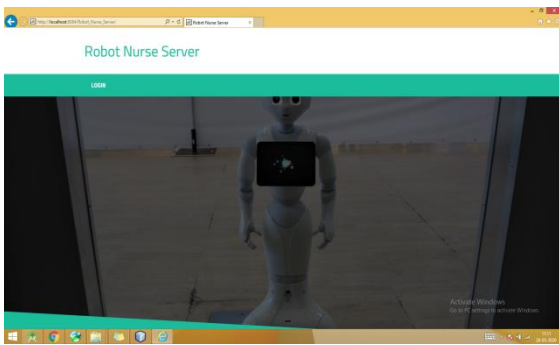


Fig 6. Service Pages in the Website for the care taker to add details about the medicines and the time

Hardware Requirements

Processor : Any Processor above 500 MHz, RAM : 4 GB, Hard Disk : 80 GB, Android Phone, Arduino Uno, Water pump, DC Motor, Relay, Power Supply, Servo motor, NodeMCU.

Power Supply: Control supply is a reference to a wellspring of electrical compel. A contraption or system that provisions electrical or diverse sorts of essentialness to a yield load or assembling of weights is known as constrain supply unit or PSU. The term is most generally associated with electrical essentialness supplies, less much of the time to mechanical ones, and once in a while to others. This power supply segment is required to change over AC flag to DC flag furthermore to decrease the plenitude of the flag. The available voltage motion from the mains is 230V/50Hz which is an AC voltage, yet the required is DC voltage (no repeat) with the sufficiency of +5V and +12V for various applications.

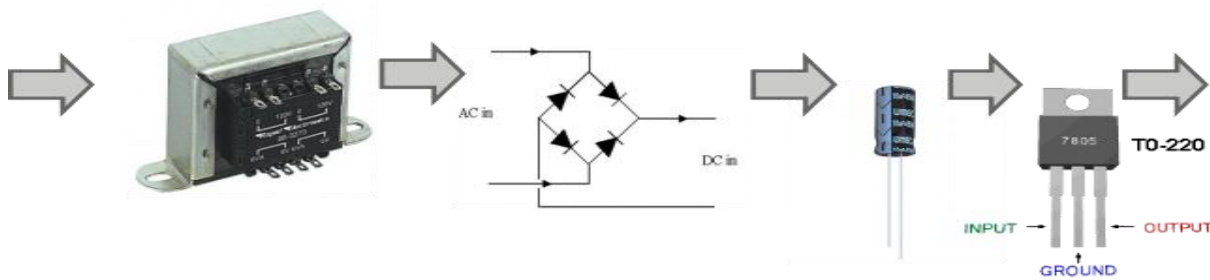


Fig 7. Power Supply and transistors

DC Motor: The DC Motor or Direct Current Motor to give it its full title, is the most commonly used actuator for producing continuous movement and whose speed of rotation can easily be controlled, making them ideal for use in applications where speed control, servo type control, and/or positioning is required. A DC motor consists of two parts, a “Stator” which is the stationary part and a “Rotor” which is the rotating part. The result is that there are basically three types of DC Motor available.

Servo Motor: A servo motor is an electrical device which can push or rotate an object with great precision. If you want to rotate an object at some specific angles or distance, then you use a servo motor. It is just made up of a simple motor which runs through servo mechanism. If a motor is used is DC powered then it is called a DC servo motor, and if it is AC powered then it is called an AC servo motor. We can get a very high torque servo motor in a small and light weight package. Due to these features they are being used in many applications like toy car, RC helicopters and planes, Robotics, Machine etc.



Fig 8. Servo Motor



Fig 9. DC Motor

Arduino Concepts: An Arduino is an open-source microcontroller development board. In plain English, you can use the Arduino to read sensors and control things like motors and lights. This allows you to upload programs to this board which can then interact with things in the real world. With this, you can make devices which respond and react to the world at large. An Arduino board is a one type of microcontroller based kit. The first Arduino technology was developed in the year 2005 by David Cuartielles and Massimo Banzì. The designers thought to provide an easy and low cost board for students, hobbyists and professionals to build devices. An Arduino board can be purchased from the seller or directly we can make it at home using various basic components. The best examples of Arduino for beginners and hobbyists include motor detectors and thermostats, and simple robots. In the year 2011, Adafruit Industries expected that over 3 lakhs Arduino boards had been produced. But, 7 lakhs boards were in user’s hands in the year 2013. Arduino technology is used in many operating devices like communication or controlling.

The pin configuration of the Arduino Uno board is shown in the above. It consists of 14 digital i/o pins. Wherein 6 pins are used as pulse width modulation o/p and 6 analog i/p, a USB connection, a power jack, a 16MHz crystal oscillator, a reset button and an ICSP header. An Arduino board can be powered either from the personal computer through a USB or external source like a battery or an adaptor. This board can operate with an external supply of 7-12V by giving voltage reference through the IOREF pin or through the pin VIN.



Fig 10. Arduino UNO

VI. RESULTS

The result of this project mainly focuses on the robot helping the disabled or paralyzed person with their medicines on time and when they are thirsty, when they are hungry. And here the device comes to the patient from its resting place with 5 cm and 1 degree precision using AMCL. And also it pumps the required amount of water and when the patients says stop the robot stops and goes back to its position again. And whenever the tablets or water or medicine are over in the containers then the robot detects it and sends a message from the server to the android app which is handled by the patients care taker. When the water quantity is below 250 ml only the robot sends the alert to the caretaker about water level.

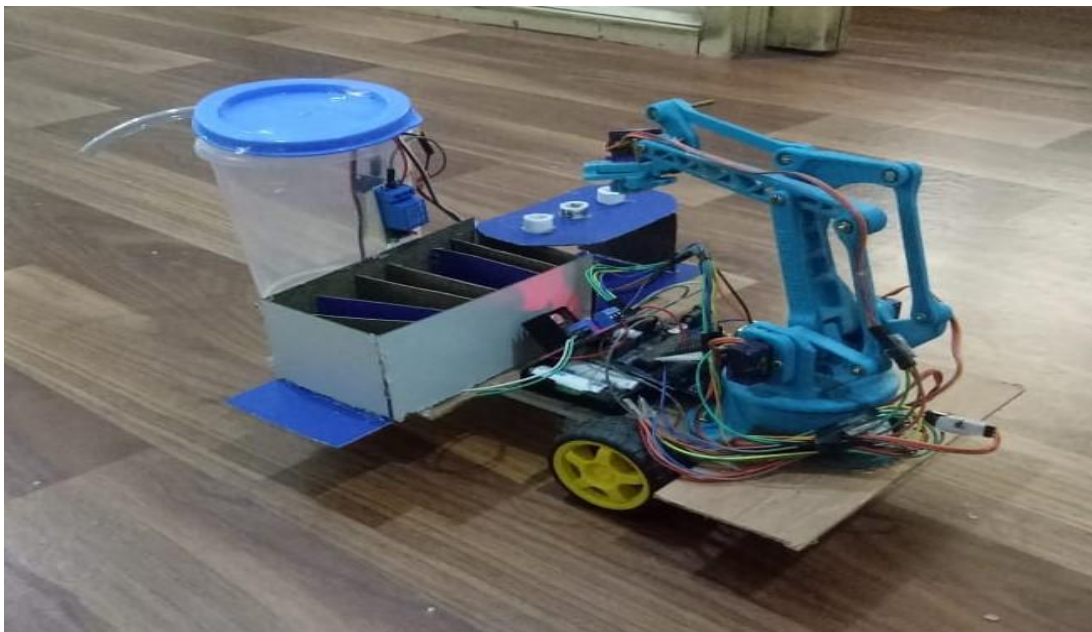


Fig 11. Final Model of the Personal Assistant Robot System using Node MCU

VII. CONCLUSION AND FUTURE WORK

The Health IoT thus helps the hospital / home authorities to have continuous monitoring on the patients as well as it reminds the patient to have the medicines in time. With the increase in the use of family friendly robots this voice based personal assistant robot finds useful applications in modern homes. The robot presented in this paper creates an interactive environment for the user and assists him virtually. This justifies its cause of a personal assistance. A sample instance of the interaction environment of the system. We will be using raspberry pi camera in future enhancement. This camera will capture images of patient and find the particular patient from database, after that process will be starting.



REFERENCES

1. Bukhari Ilias, R. Nagarajan, M. Murugappan, Khaled Helmy, Awang Sabri Awang Omar and Muhammad Asyraf Abdul Rahman, 'Hospital nurse following robot: hardware development and sensor integration' [Online] Available: https://www.researchgate.net/publication/264836811_Hospital_nurse_following_robot_Hardware_dvelopment_and_sensor_integration
2. Farshid Amirabdollahian, Rieks op den Akker, Sandra Bedaf, Richard Bormann, Heather Drape Year-2013 IEEE, 'Acceptable robotics companions for Ageing Years - Multidimensional Aspects of Human-System Interactions', Available : https://www.researchgate.net/publication/265551588_Assistive_technology_design_and_development_for_acceptable_robotics_companions_for_ageing_years
3. Nicoleta Bugnariu, Carolyn Garver, Carolyn Young & Dan Popa, Year- 2013 IEEE, ' Human-robot interaction as a tool to evaluate and quantify motor imitation behavior in children with Autism Spectrum Disorders', Available : <https://ieeexplore.ieee.org/document/6662088>
4. Alessandro Di Nuovo, Frank Broz, Ning Wang, Tony Belpaeme, Angelo Cangelosi, Year- 2017, ' The multi-modal interface of Robot-Era multi-robot services tailored for the elderly', Available: <https://link.springer.com/article/10.1007/s11370-017-0237-6>
5. AlGabri Ralf Kittmann, Tim Fröhlich, Johannes Schäfer, Ulrich Reiser2, Florian Weißhardt, Andreas Haug, Year- 2015, ' Let me Introduce Myself: I am Care-O-bot 4, a Gentleman Robot', Available: <https://dl.gi.de/handle/20.500.12116/7892>
6. Jürgen Pripfl, Tobias Körtner, Daliah Batko-Klein, Denise Hebesberger, Markus Weninger, Christoph Gisinger., Year-2016 IEEE, ' Results of a Real World Trial with a Mobile Social Service Robot for Older Adults', Available: <https://ieeexplore.ieee.org/document/7451824>
7. Shilpa jain and Syamimi Shamsuddin, Hanafiah Yussof, Luthffi Ismail, Fazah Akhtar Hanapiah, Salina Mohamed, Hanizah Ali Piah, Year-2012 IEEE, 'Initial Response of Autistic Children in Human-Robot Interaction Therapy with Humanoid Robot NAO', Available: <https://ieeexplore.ieee.org/document/6194716>
8. Nobuo Ezaki, Phongchai Nilas, Year- IEEE 2006, 'A PDA-based human-robot interaction for disabled persons using electromyography', Available: <https://ieeexplore.ieee.org/document/4054526>
9. Soumyarka Mondal and G. C. Nandi, Year- 2017 IEEE, 'Personal Robot: Towards developing a complete Humanoid Robot Assistant using the Internet of Things' , Available: <https://ieeexplore.ieee.org/abstract/document/8397453>
10. Yu Zhang, Yishen Hu, Panpan Zhang & Wenxie Zhang, Year- 2014 IEEE, 'Design of Personal Assistant Robot with Interactive Interface of Learning and Working', Available: <https://ieeexplore.ieee.org/document/7280961>



Voice Control Chatbot for Ticket Booking Using NLP

Nipam Rawal¹, Sandip Das², Soumya Dhoundiyal³, Tapaswini Swain⁴, Mr. Channappa Gowda DV⁵

Assistant Professor, Department of Information Science & Engineering, The Oxford College of Engineering,
Bangalore, India⁵

Final year B.E Students (UG), Department of Information Science & Engineering, The Oxford College of Engineering,
Bangalore, India^{1,2,3,4}

ABSTRACT: This report presents a VOICE CONTROL CHATBOT FOR TICKET BOOKING to provide a much easier way of booking tickets since this system is capable of accepting voice as an input along with the text. The chatbot application developed using various programming languages with user interface to send input and receive response contains certain boundaries and limitations. This paper proposes a chatbot application for assisting the information regarding the colleges with the use of artificial intelligence. This system has been embedded artificial intelligence to help the user to resolve the questions by providing a human way interaction to identify the sentences and making a decision itself as response to answer a question overcoming the use of programming languages. The technology at the core of the rise of the chatbot is natural language processing (“NLP”). Recent advances in machine learning have greatly improved the accuracy and effectiveness of natural language processing, making chatbots a viable option for many organizations. This improvement in NLP is firing a great deal of additional research which should lead to continued improvement in the effectiveness of chatbots in the years to come. Most commercial chatbots are dependent on platforms created by the technology giants for their natural language processing. These include Amazon Lex, Microsoft Cognitive Services, Google Cloud Natural Language API, Facebook Deep Text, and IBM Watson. Platforms where chatbots are deployed include Facebook Messenger, Skype, and Slack, among many others.

I. INTRODUCTION

A chatbot is a program that communicates with you. It is a layer on top of, or a gateway to, a service. Sometimes it is powered by machine learning (the chatbot gets smarter the more you interact with it). Or, more commonly, it is driven using intelligent rules (i.e. if the person says this, respond with that). The services a chatbot can deliver are diverse. Important life-saving health messages, to check the weather forecast or to purchase a new pair of shoes, and anything else in between. The term chatbot is synonymous with text conversation but is growing quickly through voice communication. The chatbot can talk to you through different channels; such as Facebook Messenger, Siri, WeChat, Telegram, SMS, Slack, Skype and many others. Consumers spend lots of time using messaging applications (more than they spend on social media). Therefore, messaging applications are currently the most popular way companies deliver chatbot experiences to consumers. A bot is a software application that performs automated task and chatbots come under the category of bots that live in various chat platforms. A chatbot can converse with humans so the idea of conversation is primary to a chatbot. Chatbots run on platforms such as Facebook Messenger, Slack, Telegram, Skype, SMS and even on websites. Each platform has its own salient features which determine the possible ways in which the chatbot can interact with the user, however, the actual behavior of the chatbot is determined by the bot itself.

II. METHODOLOGY

With the prevalence of Chatbot Technology and its public APIs curated by several largest IT companies like Google, IBM, Microsoft and Amazon, developers should now find it much easier to make one. Here we introduce some of the well-established Bot framework and their public APIs. As already mentioned, the present system is a user-friendly interface that aims at cutting down the inconvenience and hassle caused during the tedious process of booking tickets. Chatbot becomes more natural interaction than graphic base interface so will be broadly used in humanizing computer interaction to human. Chatbot can give 24 hours service which can become an advantage besides using a human personal assistant.



Additionally, it also supports a smooth ticket booking for people who are differently abled people. Communication has been the essence of life from the beginning of times. Thus, with the evolution of technology, the mode and style of communication has also evolved. In the early days, conversations were restricted to verbal and textual interaction between humans. These interactions are usually guided by emotions, context, and awareness. A bot is a form of virtual assistant that acts as an intelligent intermediary between people, digital systems, and Internet-enabled things. Bots are intelligent with machine learning, natural language processing, and other forms of advanced.

III. DIALOGFLOW

Dialogflow is a natural language understanding platform used to design and integrate a conversational user interface into mobile apps, web applications, devices, bots, interactive voice response systems, and so on. Dialogflow is a Google-owned developer of human-computer interaction technologies based on natural language conversations. It is a natural language processing (NLP) platform that can be used to build conversational applications and experiences for a company's customers in various languages and on multiple platforms. The Google-powered product enables developers to create text-based and voice conversation interfaces for responding to customer queries in different languages.

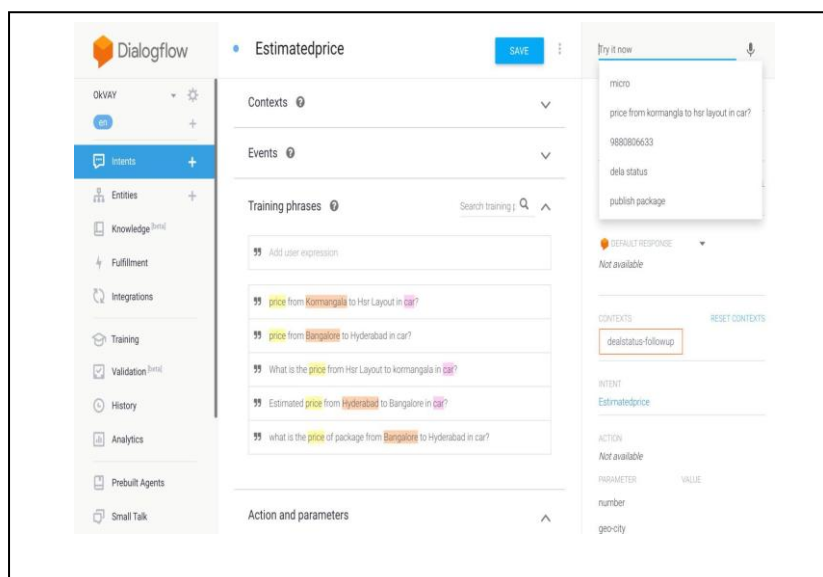


Fig 1: Overview of Dialogflow

Our proposal considers two main phases:

- (i) **Knowledge modelling** - This phase determines how knowledge is represented and stored in the knowledge base.
- (ii) **Conversation flow** - Both the lexicon used by the tutor and the order in which ideas are presented should be defined in this phase.

- **PHASE I: KNOWLEDGE MODELING, EXTRACTION AND STORING:**

The sets of queries and responses are to be defined first, and there are several ways to perform that task. To deal with knowledge extraction and representation, for example, of the form <input, response>, which are constructed by ranking the replies of a web forum thread as either 'fascinating', 'acceptable' or 'unsuitable', on the other hand, focus on automatic emotion detection of news headlines to give meaning to the input using self-organizing maps. Both ideas revolve around a medium-sized knowledge base, with a couple of concepts and queries.

The tutor language may be either casual and relaxed, or a bit more abstract and rigorous depending on the context. For example, in the field of mathematics—using abstract constructs and precise notations—the input from an expert is advised, since technology alone does not guarantee that students learn mathematics better than using only a regular textbook. Moreover, problem situations can be represented in several ways, even in natural language.



The use of an appropriate lexicon is important for students to incite them to translate everyday situations to mathematical models. Although many data structures exist to store the knowledge base, most chat-bot conversation structures are based on trees. Each node in the tree represents a unique response, from a simple greeting to detailed information about previous queries. It is also important to note that in order for the conversation service to determine which response the user is looking for, the similarity between the user input and all known queries must be calculated. This process is usually done by machine learning algorithms using similarity measures between sentences in which each word or character may represent a single dimension, and its accuracy is refined by providing thousands of correctly labelled examples of user inputs.

Therefore, it is advised to group knowledge units by similarity of the user input that will trigger them, rather than clustering by topic.

For instance, grouping the examples provided by intent, one can see that all three queries using the function tell time have a similar input:

- What's the time now?
- What time is it here?
- What is the time in New Zealand?

The tell time function input is somewhat different from that of the show function, in which the phrase Show me is predominant. Creating branches according to intents therefore reduces the complexity of the search.

● **PHASE II: CONVERSATION FLOW**

Once knowledge is separated into small atomic units, designing how to present them is the next step. An efficient way to do that is the creation of a glossary and a naming convention to keep track of the available queries and manage their trigger order. For instance, for the creation of the intelligent tutor for the introductory mathematics course, each knowledge unit in the tree was given a unique ID. The ID was generated automatically from abbreviation of the names of the intents and the entities, with a hyphen separating the intent from the entities, and the entities separated by a plus sign: def-N was used to represent the definition of the natural numbers, corresponding to the question 'What is a natural number?' or 'What is the definition of natural numbers?'. Some conversation frameworks allow entities to be grouped into categories, as it is the case of IBM Watson.

Entities are then combined with intents to formulate a unique set of conditions that are needed to trigger their response, which were written by the expert considering the pedagogical aspect of the language employed in the answer. In this way, instructors can easily work along knowledge engineers to effectively model the queries and generate the knowledge base.

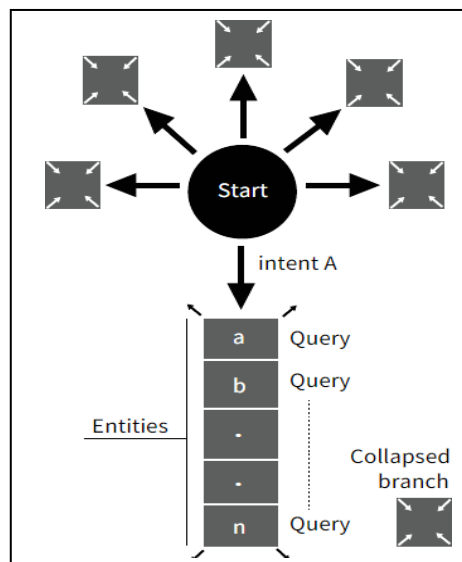


Fig 2: An abstract representation of the knowledge base built by grouping queries by intent

IV. SYSTEM DESIGN

The structural setup methodology is worried with working up a fundamental essential framework for a system. It incorporates perceiving the genuine parts of the structure and exchanges between these fragments. The starting design technique of perceiving these subsystems and working up a structure for subsystem control and correspondence is



called development demonstrating plot and the yield of this framework method is a depiction of the item basic arranging. The proposed design for this framework is given beneath. It demonstrates the way this framework is outlined and brief working of the framework.

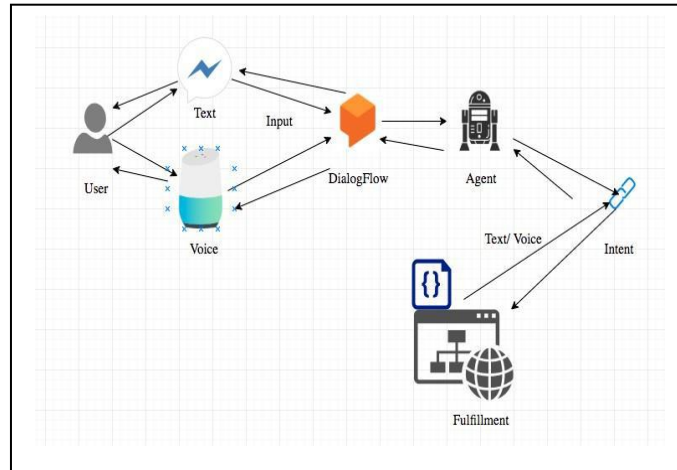


Fig 3: System Design Architecture

V. RESULT

The voice booking chatbot is able to perform operations of booking a flight by using voice and text as inputs. At this stage, the system is only equipped to make bookings for flights and not any other mode of transportation. The current system has only been trained on a very small database. The person looking to book tickets will have to stick by the parameters that are included in the system and only then will it be possible for the system to make the required booking.

FINAL PROTOTYPE



Fig 4: Login Page

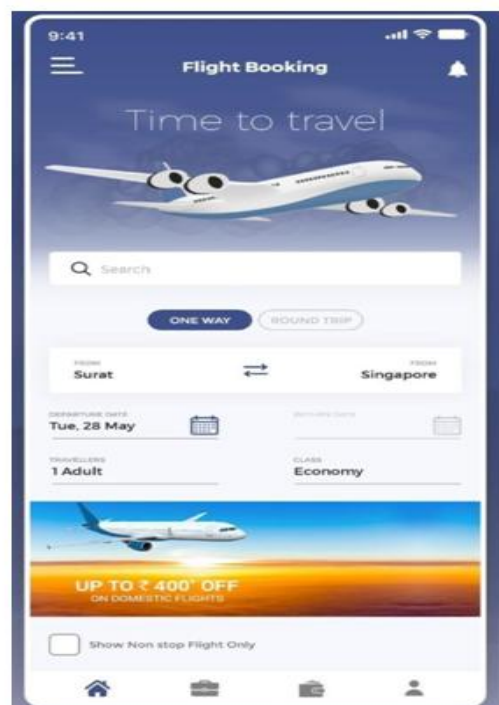


Fig 5: Flights Selection Portal

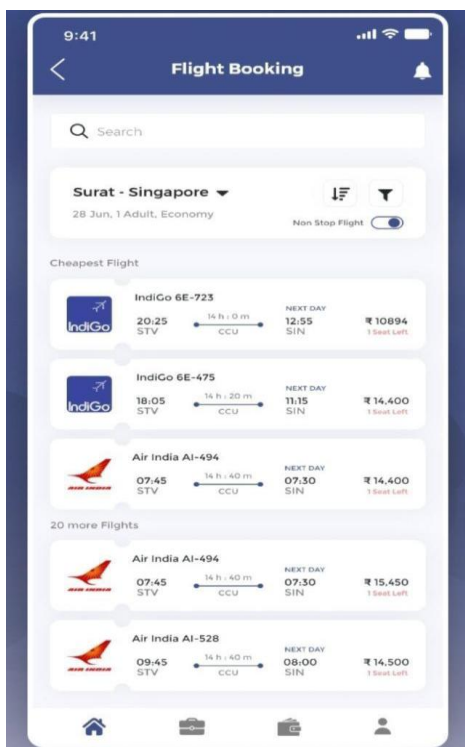


Fig 6: Booking Page

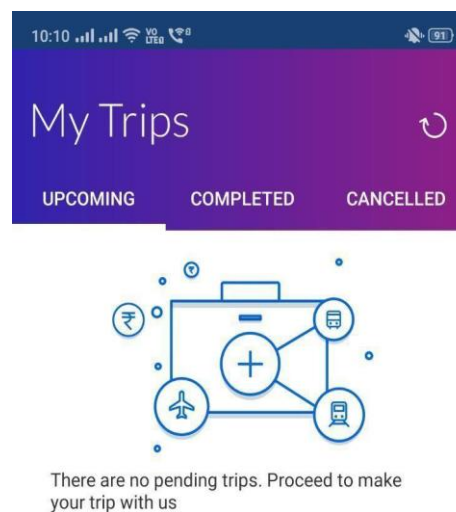


Fig 7: Booking Details

IV. CONCLUSION

Voice is a more natural way of functioning for humans than texting. It is informal, intuitive and immediate. This shift provides a natural and seamless flow to processes and therefore it proves to be the most desirable and convenient. The novelty lies in the way chatbot intelligence can cover and overcome out of topic and also mistyping situation that commonly occurs. Also, in the future chat history can be considered as chat experience so the behavior of the user can be analyzed.

The proposed chatbot has functionalities of ticket booking along with different filters that a user is free to apply catering to the need of a wide range of user and specifically taking care that it makes the process of ticket booking a hassle-free affair for the differently abled. There is a wide range of chatbot building platforms that are available for various enterprises, such as e-commerce, retail, banking, travel and so on. Chatbots can reach out to large audience on apps and be more effective than humans.

They may develop into capable info-gathering tool in the near future. The development costs of chatbots are getting cheaper. More and more industries wish to tap into the potential of the same and deliver enhanced customer experience. We expected certain industries easily adopting chatbots but a few have shown resistance. Inarguably the development world is working on top priority to remove the barriers to major mainstream augmented by efficient and quick chatbots. After becoming one of the trendiest words of the past year, chatbots are predicted to disrupt the travel industry and set a new standard in the online booking arena.

V. FUTUREWORK

The project aims at bringing the new technology for smart life. A chatbot is a program that communicates with you. It is a layer on top of, or a gateway to, a service. Sometimes it is powered by machine learning (the chatbot gets smarter the more you interact with it). Or, more commonly, it is driven using intelligent rules (i.e. if the person says this, respond with that). The services a chatbot can deliver are diverse. Important life-saving health messages, to check the weather forecast or to purchase a new pair of shoes, and anything else in between.



From the result testing, Chatbots with AI are dramatically changing businesses. There is a wide range of chatbot building platforms that are available for various enterprises, such as e-commerce, retail, banking, travel and so on. Chatbots can reach out to large audience on apps and be more effective than humans. They may develop into capable info-gathering tool in the near future. The development costs of chatbots are getting cheaper. More and more industries wish to tap into the potential of the same and deliver enhanced customer experience. We expected certain industries easily adopting chatbots but a few have shown resistance. Inarguably the development world is working on top priority to remove the barriers to major mainstream adoption and we will soon be witnessing employees being augmented by efficient and quick chatbots.

REFERENCES

1. Mohammed Javed, P. Nagabhushan, B.B. Chaudhari, "A Direct Approach for Word and Character Segmentation in Run-Length Compressed Documents with an Application to Word Spotting", 13th International Conference on Document Analysis and Recognition, 2015.
2. Naeun Lee, Kirak Kim, Taeseon Yoon, "Implementation of Robot Journalism by Programming Custombot using Tokenization and Custom Tagging", 2017.
3. Bo Chen, Donghong Ji, "Chinese Semantic Parsing based on Dependency Graph and Feature Structure", International Conference on Electronic and Mechanical Engineering and Information Technology, 2011.
4. Zhenghua Li, Min Zhang, Wanxiang Che, Ting Liu, and Wenliang Chen, "Joint Optimization for Chinese POS Tagging and Dependency Parsing", IEEE/ACM transactions on audio, speech, and language processing, Vol. 22, No. 1, January 2014.
5. Naganna Chetty, Kunwar Singh Vaisla, Nagamma Patil, "An improved Method for Disease Prediction using Fuzzy Approach", 2nd International Conference on Advances in Computing and Communication Engineering, 2015.
6. Bhavika R. Ranoliya, Nidhi Raghuwanshi, Sanjay Singh, "Chatbot for University FAQs". [14] Ming-Hsiang Su, Chung-Hsien Wu, Kun-Yi Huang, Qian-Bei Hong, Hsin-Min Wang, "A Chatbot Using LSTM-based MultiLayerEmbedding for Elderly Care".



A Novel Approach for User-Cloud Interaction using RAAC

Shwetha Balaji¹, Sriraksha², Vaishnavi M³, Wasim Akram⁴, Mrs. Geetha Rani⁵

Final year B.E Students (UG), Department of Information Science & Engineering, The Oxford College of Engineering, Bangalore, India^{1,2,3,4}

Assistant Professor, Department of Information Science & Engineering, The Oxford College of Engineering, Bangalore, India⁵

ABSTRACT: Data access and security control is the challenging issue faced with regards to public cloud systems. Ciphertext-Policy Based Encryption (CP-ABE) has been adopted in order to provide flexibility, fine-grained and secure data access control with secure access to various cloud servers. In the existing CP-ABE schemes, the single attribute authority must execute the time-consuming user legitimacy verification and secret key distribution, and hence it results in a single-point performance bottleneck when a CP-ABE scheme is adopted in a large-scale cloud storage system. Although multiauthority access control schemes have been proposed, these schemes still cannot overcome the drawbacks of single-point bottleneck and low efficiency, due to the fact that each of the authorities still independently manages a disjoint attribute set. RAAC removes the problem of single-point performance bottleneck and provides a more efficient access control scheme with an auditing mechanism. It employs multiple attribute authorities to share the load of user legitimacy verification. Meanwhile, RAAC consists of a CA (Central Authority) to generate secret keys for legitimacy verified users. Unlike other multiauthority access control schemes, each of the authorities programmed in by RAAC manages one whole attribute set individually. RAAC enhanced security by including an auditing mechanism to detect which AA (Attribute Authority) has incorrectly or maliciously performed the legitimacy verification procedure. The goal of this project is to guarantee the security requirements needed for accessing data stored remotely as well as improving the user-system interaction performance by making use of key generation techniques.

KEYWORDS: Cloud storage, Access control, Auditing, CPABE

I. INTRODUCTION

To address the issue of data access control in cloud storage, there have been quite a few schemes proposed, among which Ciphertext-Policy Attribute-Based Encryption (CP-ABE) is regarded as one of the most promising techniques. A salient feature of CP-ABE is that it grants data owners direct control power based on access policies, to provide flexible, fine grained and secure access control for cloud storage systems. In CP-ABE schemes, the access control is achieved by using cryptography, where an owner's data is encrypted with an access structure over attributes, and a user's secret key is labelled with his/her own attributes. Only if the attributes associated with the user's secret key satisfy the access structure, can the user decrypt the corresponding ciphertext to obtain the plaintext. RAAC not only employs a single CA but multiple RAs as well and thus proposes a robust and auditable access control scheme (named RAAC) for public cloud storage to promote the performance while keeping the flexibility and fine granularity features of the existing CP-ABE schemes. CA generates the secret key for the user on the basis of the received intermediate key, with no need of any more verification. In this way, multiple AAs can work in parallel to share the load of the time-consuming legitimacy verification and standby for each other so as to remove the single-point bottleneck on performance. With the help of intermediate keys, CA is able to not only generate secret keys for legitimacy verified users more efficiently but also trace an AA's mistake or malicious behaviour to enhance the security. The main contributions of this work can be summarized as follows: 1) To address the single-point performance bottleneck of key distribution existed in the existing schemes, a robust and efficient heterogeneous framework with single CA (Central Authority) and multiple AAs (Attribute Authorities) for public cloud storage is implemented. 2) It includes an auditing mechanism that helps the system trace an AA's misbehaviour on user's legitimacy verification.



II. LITERATURE REVIEW

In cloud computing, searchable encryption scheme over outsourced data is a hot research field. However, most existing works on encrypted search over outsourced cloud data follow the model of “one size fits all” and ignore personalized search intention.[1]

With the increasing adoption of cloud computing, a growing number of users outsource their datasets into cloud. The datasets usually are encrypted before outsourcing to preserve the privacy.[2]

With the popularity of group data sharing in public cloud computing, the privacy and security of group sharing data have become two major issues. The cloud provider cannot be treated as a trusted third party.[3]

A novel Multi-message Ciphertext Policy Attribute-Based Encryption (MCP-ABE) technique is presented, and employs the MCP-ABE. The scheme is efficient and flexible.[4]

The recent adoption and diffusion of the data sharing paradigm in distributed systems such as online social networks or cloud computing, there have been increasing demands and concerns for distributed data security. Ciphertext policy attribute-based encryption (CP-ABE) is becoming a promising cryptographic solution to this issue.[5]

III. PROBLEM STATEMENT

The main problem with the existing system is the presence of only one authority which is in charge of all the attributes in single authority schemes, offline/crash of this authority makes all secret key requests unavailable during that period. The similar problem exists in multi-authority schemes, since each of multiple authorities manages a disjoint attribute set. The inefficiency of the authority’s service results in single-point performance bottleneck, which will cause system congestion such that users often cannot obtain their secret keys quickly, and have to wait in the system queue. On the other hand, if there is only one authority that issues secret keys for some particular attributes, single-point performance bottleneck problem arises affecting the efficiency of secret key generation service and immensely degrades the utility of the existing schemes to conduct access control in large cloud storage systems.

IV. EXISTING SYSTEM

To address the issue of data access control in cloud storage, there have been quite a few schemes proposed, among which Ciphertext-Policy Attribute-Based Encryption (CP-ABE) is regarded as one of the most promising techniques. A salient feature of CP-ABE is that it grants data owners direct control power based on access policies, to provide flexible, fine grained and secure access control for cloud storage systems. In CP-ABE schemes, the access control is achieved by using cryptography, where an owner’s data is encrypted with an access structure over attributes, and a user’s secret key is labelled with his/her own attributes.

V. PROPOSED SYSTEM

Inspired by the heterogeneous architecture with single CA and multiple RAs, we propose a robust and auditable access control scheme (named RAAC) for public cloud storage to promote the performance while keeping the flexibility and fine granularity features of the existing CP-ABE schemes. In this scheme, the procedure of user legitimacy verification from the secret key generation, and assign these two sub-procedures to two different kinds of authorities was separated. There are multiple authorities (named attribute authorities, AAs), each of which is in charge of the whole attribute set and can conduct user legitimacy verification independently. Meanwhile, there is only one global trusted authority (referred as Central Authority, CA) in charge of secret key generation and distribution. Before performing a secret key generation and distribution process, one of the AAs is selected to verify the legitimacy of the user’s attributes and then it generates an intermediate key to send to CA. CA generates the secret key for the user on the basis of the received intermediate key, with no need of any more verification. In this way, multiple AAs can work in parallel to share the load of the time-consuming legitimacy verification and standby for each other so as to remove the single-point bottleneck on performance. Meanwhile, the selected AA doesn’t take the responsibility of generating final secret keys to users. Instead, it generates intermediate keys that associate with users’ attributes and implicitly associate with its own identity, and sends them to CA. With the help of intermediate keys, CA is able to not only generate secret keys for



legitimacy verified users more efficiently but also trace an AA’s mistake or malicious behaviour to enhance the security.

A.SYSTEM ARCHITECTURE

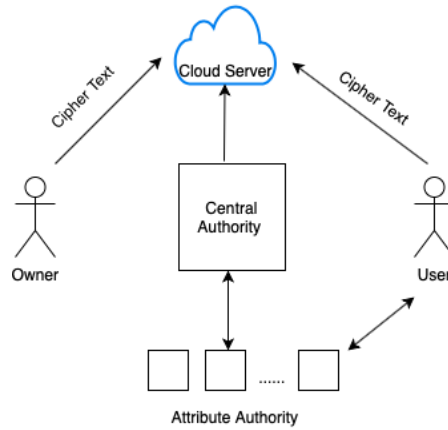


Fig 1: System Architecture

1. **Data Owner/User:** Data owner can upload files to the cloud and possesses the authority to decide who can access the files uploaded by him. Whereas the user can only view/download the files.
2. **Attribute Authorities:** Does all the user legitimacy verification and generates the intermediate key for the user.
3. **Central Authority:** Central Authority is the administrator of the entire system. For a key request from a user, CA is responsible for generating secret keys for the user on the basis of the received intermediate key associated with the user’s legitimate attributes verified by an AA. Once the user is authenticated, he shall be given access to the files.
4. **Cloud Server:** Cloud Server provides a public platform for owners to store and share their encrypted data. The cloud server doesn’t conduct data access control for owners. The encrypted data stored in the cloud server can be downloaded freely by any user.

B.WORKING

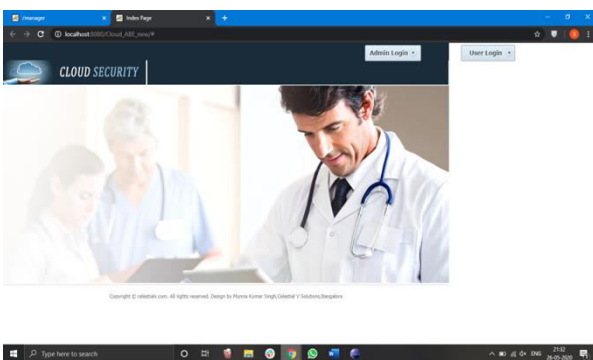


Figure 2: Home page

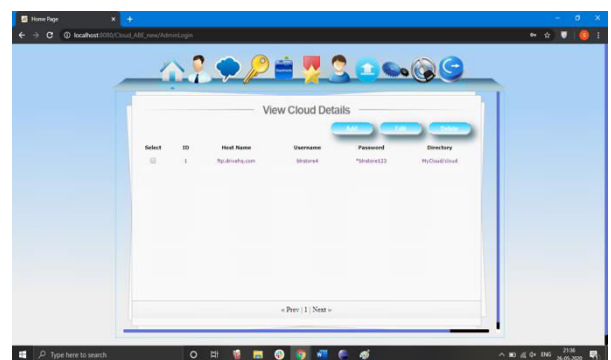


Figure 3: Cloud Details

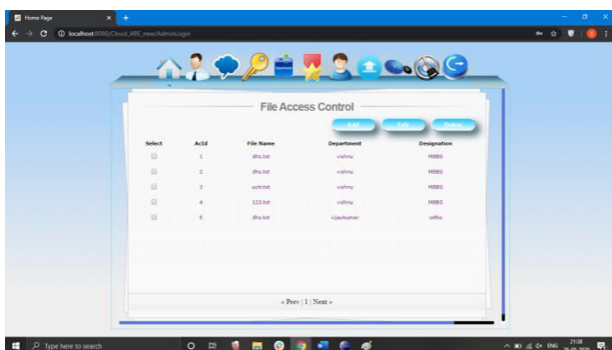


Figure 4: File access control



Figure 5: User Profile

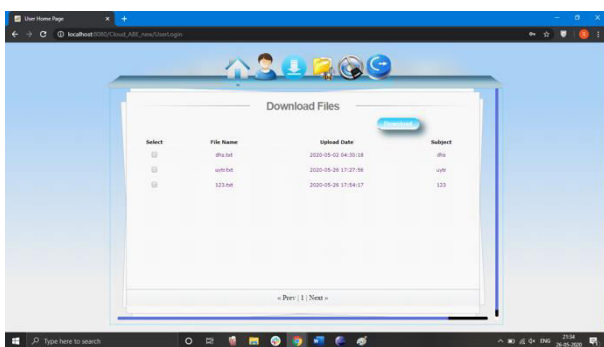


Figure 6: Files in cloud

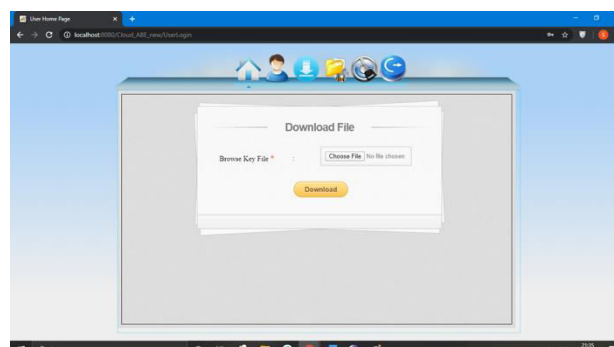


Figure 7: Downloading Files

The following is the implementation of the system based on the images shown in the above figure. The figures above shows the working of the project. The Home page contains the link to both Admin and user panel where they can log in to their respective accounts. The admin, after logging into his account, can upload new files to the cloud. The admin can also view the list of users requesting access to his files. He can grant access permissions to any of the new users. The Admin also has the power to modify the access given to any existing user for any of his files in the cloud. The user after being authenticated should upload the private key he possesses in order to view or download the file.

VI. RESULTS

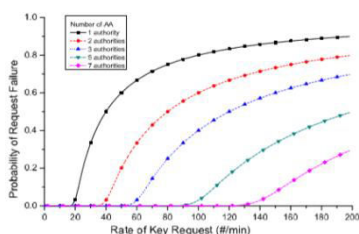


Figure 8

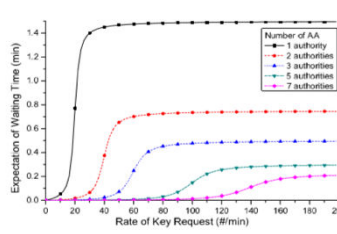


Figure 9

When multi AAs is filled with N users, it means that K users are waiting in the queue and all AAs are occupied, the newly arriving users are rejected. We analyse the probability of failure to show how to lower this failure rate with more AAs. Based on the emulation of the scheme, the average time of generating a secret key for an attribute is about 35ms. Furthermore, we assume that users possess 10 attributes on average and the verification takes tenfold amount of time of that of the key generation. The performance analysis in terms of the average failure rate and the average waiting time is



shown in below graphs. The first graph shows the failure rate versus the arrival rate and the number of AAs. The second graph shows that the average waiting time increases rapidly with the increase of arrival rate when the arrival rates are low.

VII. CONCLUSION AND FUTURE WORK

The goal of this research is to eliminate the single-point performance bottleneck of the existing CP-ABE schemes proposed. By effectively reformulating CP-ABE cryptographic technique along with RAAC to provide a fine-grained, robust and efficient access control with one CA/multi-AAs for public cloud storage. RAAC employs multiple AAs to share the load of the time-consuming legitimacy verification and standby for serving new arrivals of user's requests. It was also confirmed that the auditing method to trace an attribute authority's potential misbehaviour would be included, along with a detailed security and performance analysis to verify that RAAC is secure and efficiency is confirmed. The security analysis shows that RAAC could effectively resist to individual and colluded malicious users, as well as the honest-but-curious cloud servers. The security analysis shows that RAAC could effectively resist to individual and colluded malicious users, as well as the honest-but-curious cloud servers. Besides, with the proposed auditing & tracing scheme, no AA could deny its misbehaved key distribution. Further performance analysis based on queuing theory showed the superiority of RAAC over the traditional CP-ABE based access control schemes for public cloud storage.

REFERENCES

- [1] Z. Fu, K. Ren, J. Shu, X. Sun, and F. Huang, "Enabling personalized search over encrypted outsourced data with efficiency improvement," *IEEE Transactions on Parallel & Distributed Systems*, vol. 27, no. 9, pp. 2546–2559, 2016.
- [2] Z. Fu, X. Sun, S. Ji, and G. Xie, "Towards efficient content-aware search over encrypted outsourced data in cloud," in *Proceedings of 2016 IEEE Conference on Computer Communications (INFOCOM 2016)*. IEEE, 2016, pp. 1–9.
- [3] K. Xue and P. Hong, "A dynamic secure group sharing framework in public cloud computing," *IEEE Transactions on Cloud Computing*, vol. 2, no. 4, pp. 459–470, 2014.
- [4] Y. Wu, Z. Wei, and H. Deng, "Attribute-based access to scalable media in cloud-assisted content sharing," *IEEE Transactions on Multimedia*, vol. 15, no. 4, pp. 778–788, 2013.
- [5] J. Hur, "Improving security and efficiency in attribute-based data sharing," *IEEE Transactions on Knowledge and Data Engineering*, vol. 25, no. 10, pp. 2271–2282, 2013.



Secured and Cardless ATM using Iris

C R Sai Ruchitha Babu¹, Divyashree C², Kanchana³, Likhitha P⁴, Indu K S⁵

Final year B.E Students(UG) , Department of Information Science & Engineering, The Oxford College of Engineering,
Bangalore, India^{1,2,3,4}

Assistant Professor Department of Information Science & Engineering, The Oxford College of Engineering,
Bangalore, India⁵

ABSTRACT: A biometric framework gives automatic identity proof of an individual based on unique characteristics or features of the individual. As demands on secure identification are hiking and as the human iris gives a pattern that is phenomenal for identification, the utilization of inexpensive equipment could help iris recognition turn into another standard in security framework. Iris recognition is viewed as the most reliable and precise biometric identification framework available. The principal point of this project is to study the unique pattern of the iris in the eye.

KEYWORDS: Iris Scanner; Arduino based micro-controller; recognition of iris ; matching the templates ; withdrawal of money through iris scanning.

I. INTRODUCTION

As demands on secure identification are hiking and as the human iris gives a pattern that is phenomenal for identification, the utilization of inexpensive equipment could help iris recognition turn into another standard in security framework. Iris recognition is viewed as the most reliable and precise biometric identification framework available. A test situation depending upon the open source code can be built to measure the performance of iris recognition techniques, image quality, and acceptance rate. In this project, the image quality of images as data from a database acquired from a standard camera is surveyed, the most imperative issue areas recognized, and the overall general recognition performance measured. The purpose of this project will be to implement an iris recognition and identification system which can authenticate the claimed performance of the methodology. The main objective of the proposed application is to identify an individual with high efficiency and accuracy by analyzing the random patterns visible within the iris of an eye.

II. PROBLEM STATEMENT

Conventionally passwords, secret codes and PINs are used for identification which can be easily stolen, observed or forgotten. In pattern recognition problems, the key issue is the relation between inter-class and intra-class variability: objects can be reliably classified only if the variability among different instances of a given class is less than the variability between different classes. For example in face recognition, difficulties arise from the fact that the face is a changeable social organ displaying a variety of expressions, as well as being an active 3D object whose image varies with viewing angle, pose, illumination, accoutrements, and age. So as an alternative we propose to use biometrics (iris recognition) system to identify an individual.

III. PROPOSED SYSTEM

In the proposed system image processing technique is used to extract the unique iris patterns from a digitized image of the eye, and encode it into a biometric template, which can be stored in a database. The biometric template contains objective mathematical representations of unique information stored in the iris, and allows the comparison to be made between the templates. When subject wishes to be identified by iris recognition system, their eyes are first photographed, and then template is created for their iris region. This template is then compared with the other templates stored in the database until a either a matching template is found and the subject is identified, or a no match is found and the subject is unidentified.

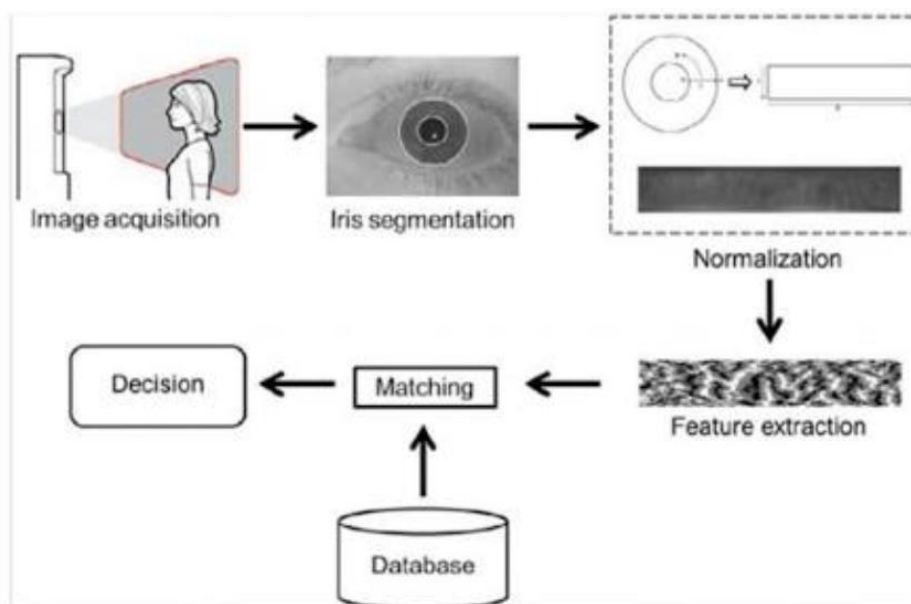


FIG 1 SYSTEM ARCHITECTURE

The step by step process is given below.

1. Firstly, Admin of the bank account use the desktop based application which is developed using java swings. Once the admin's login credentials are verified by the server, he can add the customer and scan the iris of the customer. These details are stored in the server. Admin can add the amount to customer's account. Whenever the customer goes to the ATM machine, his iris will be scanned using the iris scanner to get a better image clarity.
2. In the second step, image processing will be done to enhance the image. Here, grayscale is used for image processing. Grayscale is preferred over the colored ones to simplify the mathematics. During preprocessing RGB image is converted into grayscale. As computer can understand only grayscale images so it is preferred over the colored ones. Grayscale images are stored as an 8-bit integers in the form of 0's and 1's.
3. Next, segmentation will be carried out. It is the process of partitioning the image into multiple segments so that the representation of the image will be more easier and meaningful to analyze. Image segmentation is basically performed to locate the Iris object in image. Two methods to perform the segmentations are

iCanny edge Detection

Here edge() function is used. Edge function will take an image as input. General form is
 Output= EDGE(Input,'canny', THRESH)
 Edge function will return a array with the values 1's and 0's.

ii Hough Transform:

This method is used to find the circles in the image. Equation of the circle is:

$$r^2=(x-a)^2+(y-b)^2 \quad r \text{ is the radius of the circle. } (a,b)= \text{ center co-ordinates of the circle.}$$

Here we need to detect two circles, outer circle of pupil and outer circle of iris. For every value of pixel (x,y) and r we have to plot circle in 3D axis so that we get many cone shaped circles. After this we should find the point with the maximum number of intersections. This point gives the (a,b,r) value. From that we can detect the two circles which represents the iris

4. Once the iris is segmented, next stage is to transform the iris region so that it has fixed dimensions in order to allow the comparisons. Normalization process involves unwrapping the iris and converting it on to its polar equivalent. This process is done using Daughman's Rubbersheet model.
5. Next is the feature extraction. It is the process of reducing the raw data into more informative data. In order to recognize the individuals accurately, the most discriminating features that present in the region must be extracted. The iris contains unique features such as, stripes, freckles, rings and zigzag collarette. Feature extraction is done using Fast wavelet Transform algorithm.
6. Next step is to classify the iris. It is done with the help of various features calculated in the previous step. For this we will use support vector machine algorithm. Classification can either supervised or unsupervised, but we are using supervised classifications. SVMs are based on the idea of finding a hyperplane that best divides a



datasets into two classes. On x-axis we take the extracted features and on y-axis we take each customer's name and plot the graph.

- Final step is analyse the result. Once the iris is being scanned and detected, the linked account number is checked. Based on that account number account information is being sent to the ATM machine display. The display is connected to raspberry pi and touch screen option. It displays features like balance check, cash withdrawal, transfer amount. Based on the requested amount the controller sends the requests and cash will be dispensed.

IV. SOFTWARE & HARDWARE

A. Software

ARDUINO IDE

The **Arduino** Integrated Development Environment (**IDE**) is a cross-platform application (for Windows, macOS, Linux) that is written in the programming language Java. It is used to write and upload programs to Arduino compatible boards, but also, with the help of 3rd party cores, other vendor development boards.

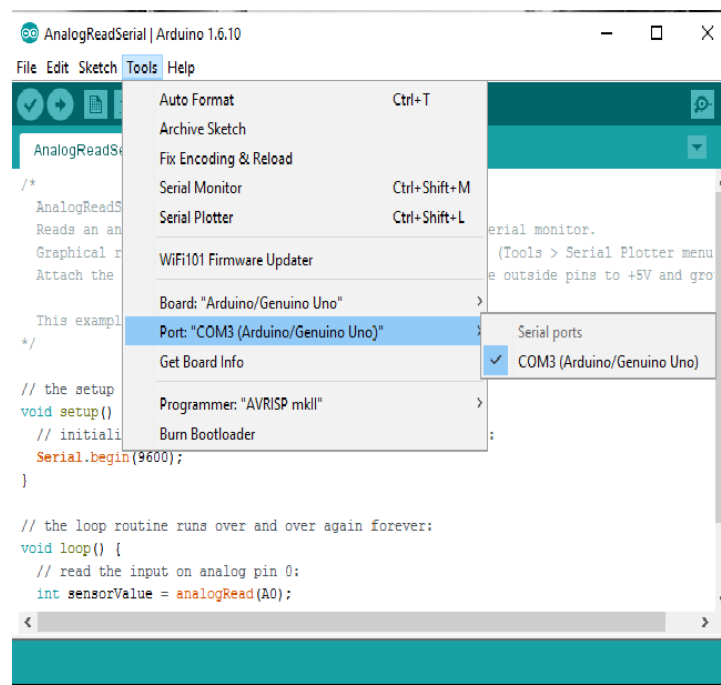


Fig 2 Arduino IDE

NET BEANS IDE

NetBeans IDE is the official IDE for Java 8. With its editors, code analyzers, and converters, you can quickly and smoothly upgrade your applications to use new Java 8 language constructs, such as lambdas, functional operations, and method references. Batch analyzers and converters are provided to search through multiple applications at the same time, matching patterns for conversion to new Java 8 language constructs. With its constantly improving Java Editor, many rich features and an extensive range of tools, templates and samples, NetBeans IDE sets the standard for developing with cutting edge technologies out of the box. An IDE is much more than a text editor. The NetBeans Editor Indent lines, matches words and brackets, and highlight source code syntactically and semantically. It also provides code templates, coding tips, and refactoring tools.

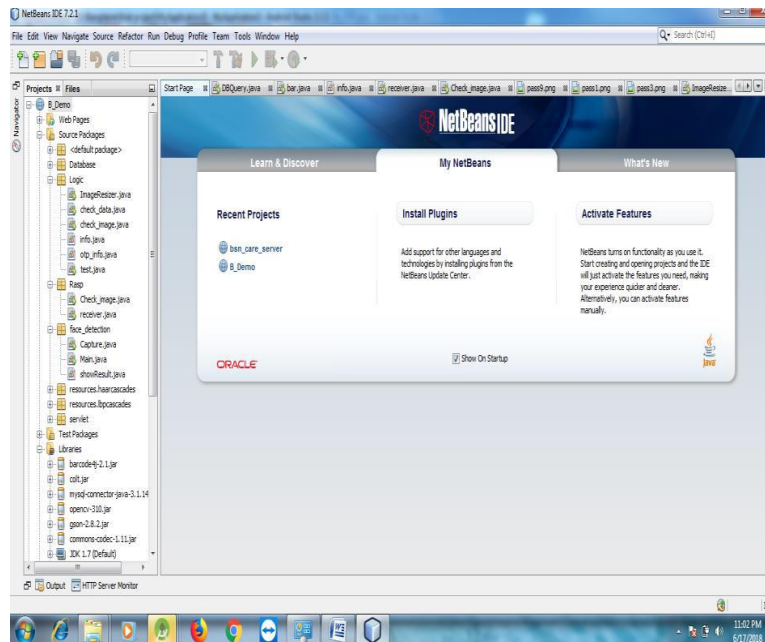


Fig 3 Net Beans IDE

MySQL

MySQL ("My Sequel") is (as of 2008) the world's most widely used open source relational database management system (RDBMS) that runs as a server providing multi-user access to a number of databases. The SQL phrase stands for Structured Query Language.

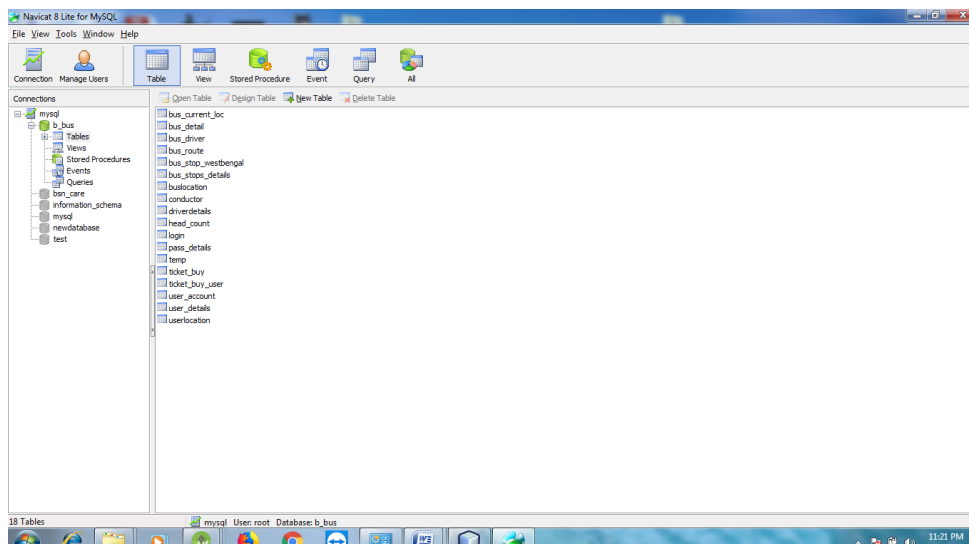


Fig 4 MySQL

B.Hardware

ARDUINO

An Arduino is an open-source microcontroller development board. In plain English, you can use the Arduino to read sensors and control things like motors and lights. This allows you to upload programs to this board which can then interact with things in the real world. With this, you can make devices which respond and react to the world at large.



Fig 5 Arduino

RASPBERRY PI

The Raspberry Pi device looks like a motherboard, with the mounted chips and ports exposed (something you'd expect to see only if you opened up your computer and looked at its internal boards), but it has all the components you need to connect input, output, and storage devices and start computing. You'll encounter two models of the device: **Model A** and **Model B**. The only real differences are the addition of Ethernet and an extra USB port on the more expensive Model B.

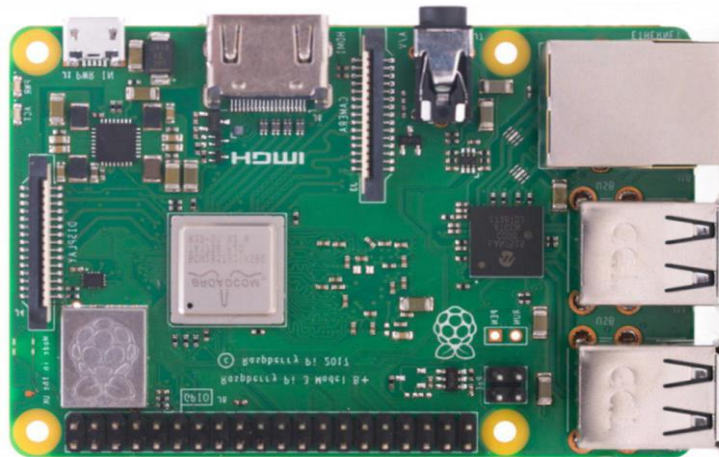


Fig 6 Raspberry Pi

IRIS SCANNER



Fig 7 Iris Scanner

V. RESULTS

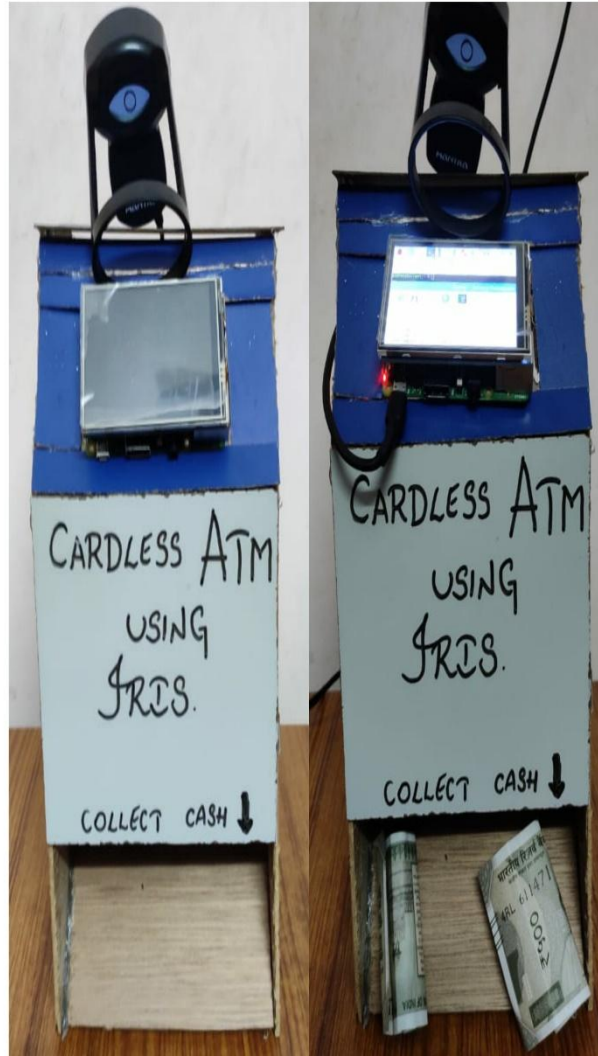


Fig 8 Cardless ATM Machine model

VI. CONCLUSION

The use of iris recognition system has been seen in various areas of life such as airport, crime detection, business application, various research firm and industries, experts anticipate the growth of iris recognition system. The study showed that the use of iris recognition system is expanding worldwide as the public has been oriented about the necessity of iris recognition system. For instance, iris recognition system is used in banks where it is incorporated into the Automated Teller Machines (ATMs).

REFERENCES

- [1] Automated Teller Machine - ATM," <http://www.investopedia.com/terms/a/atm.asp>"
- [2] Anil K. Jain, Patrick Flynn and Arun A. Ross, Handbook of Biometrics. Michigan State University, USA, University of Notre Dame, USA and West Virginia University, USA.
- [3] Personal Finance Tips, "<http://www.thinkpesos.com/8-different-types-ofatm-fraud-everyone-should-be-aware-of/>"



- [4] Ofir Pele and Michael Werman, "The Quadratic-Chi Histogram Distance Family, " 11th European Conference on Computer Vision, Heraklion, Crete, Greece, September 2010, Proceedings, Part II, pp 749-762
- [5] Akio Ogihara, Hiroyuki Matsumura and Akira Shiozaki, "Biometric Verification Using Keystroke Motion and Key Press Timing for ATM User Authentication," International Symposium on Intelligent Signal Processing and Communication Systems (ISPACS2006) Yonago Convention Center, Tottori, Japan, 2006.
- [6] Mr Abhijeet S. Kale and Prof.Sunpreet Kaur Nanda, "Design of Highly Secured Automatic Teller Machine System by Using Aadhaar Card and Fingerprint," www.ijesi.org Volume 3, Issue 5, pp.22-26, May 2014 [International Journal of Engineering Science Invention ISSN (Online), p. 2319 – 6734, ISSN (Print): 2319 – 6726]
- [7] Mr. Mahesh A. Patil, Mr. Sachin P.Wanere, Mr. RupeshP.Maighane and Mr. AashayR.Tiwari, "ATM Transaction Using Biometric Fingerprint Technology," International Journal of Electronics, Communication & Soft Computing Science and Engineering Volume 2, Issue 6, pp. 22-27
- [8] Bin Li, Kuan-Quan Wang and D. Zhang, "On-line Signature Verification for E-Finance and E-Commerce Security System," Machine Learning and Cybernetics, 2003 International Conference on 5-5 Nov. 2003, pp. 3002-3007.



Smart Irrigation System with Safety and Security using Alarm Systems

S Kavitha¹, Sathya V², Srilekha B C³, Manisha N⁴, Mrs. Indu K S⁵

Final year B.E Students(UG), Department of Information Science & Engineering, The Oxford College of Engineering, Bangalore, India^{1,2,3,4}

Assistant Professor Department of Information Science & Engineering, The Oxford College of Engineering, Bangalore, India⁵

ABSTRACT : The Smart Irrigation System is an IOT based device which is capable of automating the irrigation process by analyzing the moisture of soil and the climate condition. It provides water supply at the right time, in right quantity and at the right place in field which place a vital role in plants growth. Water management remotely is also a challenging task, especially the management becomes more difficult during the storage of water, which may otherwise damage the crop. The system has a distributed wireless network of soil moisture and temperature sensors place in the root zone of the plants. Soil parameters like soil moisture, pH, humidity are measured and the pressure sensor and sensed values are displayed in LCD. By using sensors like moisture, rain, etc. Water supply for irrigation can be managed easily by analyzing the condition of soil and climate. Soil moistures sensors smartly measure the moisture and based on that data, field is get irrigated automatically with less human interventions. The IR sensor senses the animals nearing the fields and produces the huge alarm sounds. The intruder detection system is done with the help of PIR sensor where the birds are repelled from entering into the fields. The GSM module has been used to establish a communication link between the farmer and the field. The current field status will be intimated to the farmer via SMS. The farmer can access the server about the field condition anytime, anywhere thereby reducing the man power and time.

KEYWORDS: Microcontroller, Sensors, Intruder Detection System, IOT, Monitoring and Controlling System

I.INTRODUCTION

India is basically an agricultural country, and all its resources depend on the agricultural output. Even in the modern span of industrialization, agriculture is the key area that decides the economy growth of the country. Agriculture also accounts for 8.56% of the country's total exports.

Irrigation is the science of planning and designing an efficient, low cost, economic irrigation system designed in such a way to fit natural conditions. By the construction of proper distribution system and providing of adequate water supply will increase the yield of crops. Rising population, there is a need for increase at the cultural production. In order to support greater production in farms, the requirement of the amount of fresh water used in irrigation also raises. Currently, agriculture accounts 83% of the total water consumption in India. Unplanned use of water inadvertently results in wastage of water.

In the internet era, where information place a key role in people's lives, agriculture is rapidly becoming a very data intensive industry where farmers need to collect and evaluate a huge amount of information from a diverse number of devices in order to become more efficient in production and communicating appropriate information. With the advent of open source Arduino boards along with cheap moisture sensors, it is viable to create devices that can monitor the soil moisture content and accordingly irrigating the feels or the landscape as and when needed. The propose system makes use of microcontroller LPC2148 on Arduino platform and IOT which enable farmers to remotely monitor the status of sprinklers installed on the farm by knowing the sensor values there by, making the farmers work much easier as they can concentrate on other farm activities.

II.LITERATURE REVIEW

In order to effectively reduce the impact of inadequate water resources on China's economy, from modern agricultural cultivation and management perspective, according to the basic principles of Internet, with wireless sensor technology, this article proposes precision agriculture irrigation systems based on the Internet of things (IOT) technology, and



focuses on the hardware architecture, network architecture and software process control of the precision irrigation system. [1]

The paper discusses about wireless technology using various sensors for precision agriculture has become a popular research with the greenhouse effect. Ethernet network, RF module and ZigBee wireless network are used to transmit data in Remote Monitoring System. This paper gives a review of remote control and monitoring systems based on existing technologies and a ZigBee. [2]

The project aims at making agriculture smart using automation and IOT technologies. The features of this project includes smart GPS based remote controlled robot to perform tasks like weeding, spraying, moisture sensing, bird and animal scaring, etc.. Secondly, it includes smart irrigation with smart control and intelligent decision making based on the accurate real time field data. Thirdly, it includes smart warehouse management and theft detection in the warehouse. Controlling of all these operations will be through any remote smart device or computer connected to internet and the operations will be performed by interfacing sensors, wi-fi or ZigBee modules, camera and actuators with microcontrollers. [3]

They explained that agriculture is the broadest economy sector and plays an important role in the overall economic development of a nation. In this paper, they have proposed a novel methodology for smart farming by linking a smart sensing system and smart irrigator system through wireless communication technology. Our system focuses on the measurement of physical parameters such as soil moisture content, nutrition content, and pH of the soil that plays a vital role in farming activities. Based on the essential physical and chemical parameters of the soil is measured, the required quantity of green manure, compost, and water is splashed on the crops using a smart irrigator, which is mounted on a movable overhead crane system. The detailed modelling and the control strategies of a smart irrigator and smart farming system are demonstrated. [4]

Indian farmers face a multitude of problems. Some of the issues faced, such as irregular monsoons and insufficient rainfall, are not in the realm of problems that can be addressed of technology, as of now. But, there are numerous problems that can indeed be solved with proper advice to farmers, at the right time. They can be made to acquire essential farming skills such as how to maximize yield by growing compatible crops, along with main ones, various crop rotation strategies depending on the location, soil. [5]

III.SYSTEM ARCHITECTURE

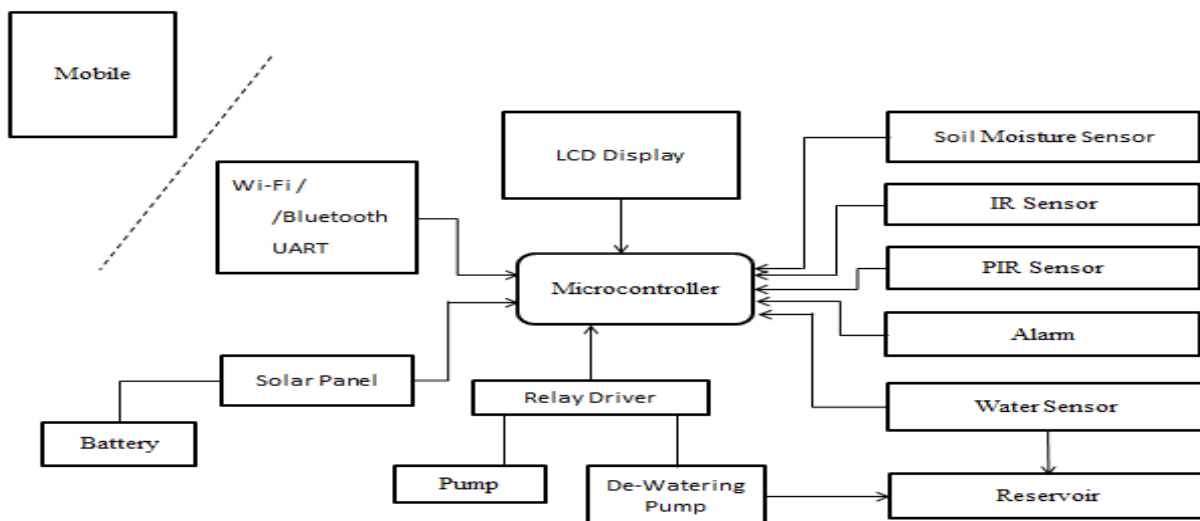


Figure 3.1: System Architecture

MICROCONTROLLER:

A LPC2148 Microcontroller is a small computer on a single metal-oxide-semiconductor integrated circuit chip.

SOLAR PANEL:

It works in dual mode. Firstly, it absorbs the light rays emitted from the sun and converts it to the electrical energy. Secondly, it works by absorbing the light rays from the rays emitting equipment and stores it in the battery.



SOIL MOISTURE SENSOR:

It measures the volumetric water content in soil.

IR SENSOR:

It is an electronic device, that emits in order to sense some aspects of the surroundings.

WATER SENSOR:

It is a device used in the detection of the water level for various applications.

RELAY DRIVER:

It is an electro-magnetic switch that helps switching between pump and de-pump.

LCD Display:

LCD uses a liquid crystal to produce a visible image.

Data flow diagrams:

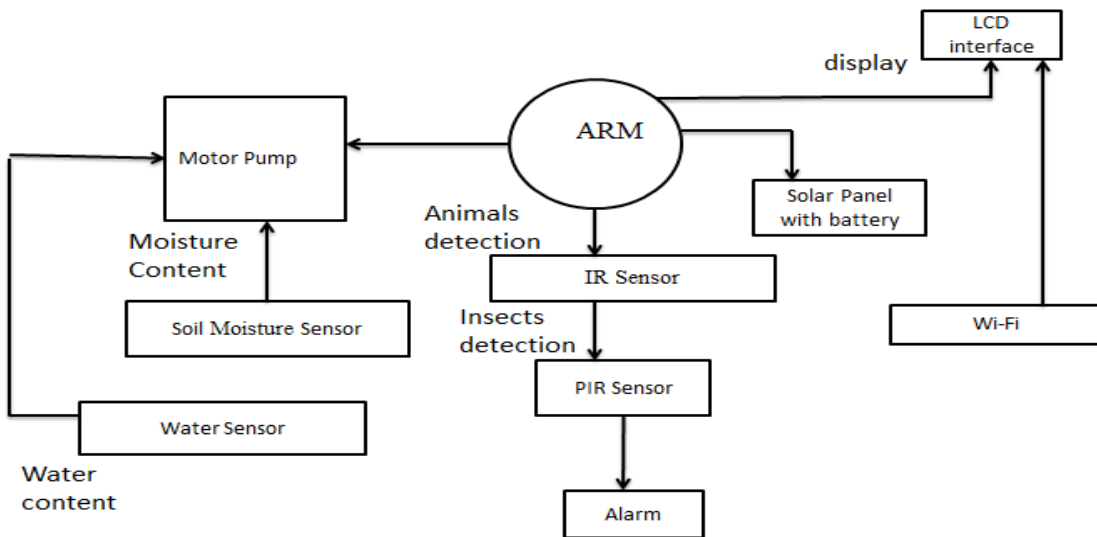


Figure 3.2: Data Flow Diagram

Data Flow:

The DFD is clear graphical formalism that can be used to address a structure the extent that the data to the system, diverse get ready did on this data and the yield data made by the structure. From the soil moisture sensor, the moisture content data is been observed and motor gets ON or OFF accordingly. Likely, water content data is been observed with the help of water sensor. If incase excess water is found it is stored in the reservoir for future purposes. The motion of animals and/or insects that are nearing the field will be detected by the IR sensor and PIR sensor respectively. The notifications will be intimated to the user via wi-fi.

IV.MODULE SETS

Soil Moisture Module

Soil moisture sensors measure the volumetric water content in soil. Since the direct gravimetric measurement of free soil moisture requires removing, drying and weighing of a sample, soil moisture sensors measure the volumetric water content indirectly by using some other property of the soil, such as electrical resistance, dielectric constant, or interaction with neutrons, as a proxy for the moisture content. The relation between the measured property and soil moisture must be calibrated and may vary depending on environmental factors such as soil type, temperature, or electric conductivity. The threshold water content is defined for different crops. So based on water content and threshold value the plants are irrigated. The plants are watered using automatic motor, which works based on the output of soil moisture sensors.

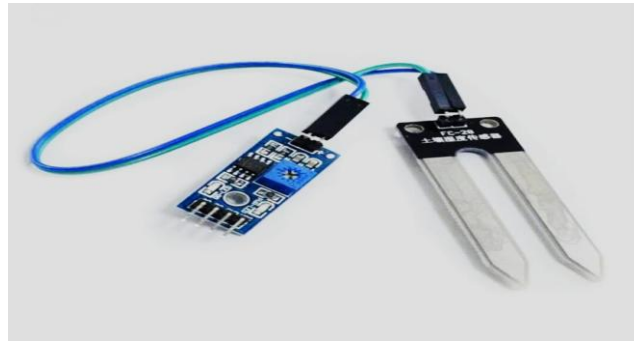


Figure 4.1: Soil Moisture Sensor

IR Sensor Module

An infrared sensor is an electronic device, that emits in order to sense some aspects of the surroundings. It can measure the heat of an object as well as detects the motion. These types of sensors measure only infrared radiation, rather than emitting it. The emitter is simply an IR LED and the detector is simply an IR photodiode that is sensitive to IR light of the same wavelength as that emitted by the IR LED. The intruder deduction system is done with the help of PIR sensor where the birds, insects are repelled from entering into the field. An IR sensors senses movements in the land and detects physical intruders such as animals etc. An intrusion in farmland is notified to the user. An alarm system is activated and produce huge sound as the physical intrusion is detected.

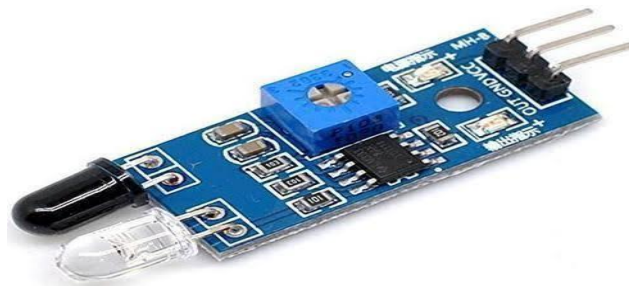


Figure 4.2: IR Sensor

Water Sensor Module

A water sensor is a device used in the detection of the water level for various applications. Water level senses are used to detect the level of substances that can flow. Level measurements can be done inside containers or it can be the level of a river or lake. Such measurements can be used to determine the amount of materials within a closed container or the flow of water in open channels. Water sensor brick is designed for water detection, which can be widely used in sensing the rainfall. During heavy rains, the excess water from the field is de pumped into the reservoir. This information is notified to the user.



Figure 4.3: Water Sensor



V.IMPLEMENTATION

SOIL MOISTURE MODULE

Function Name: #define WATER (IOPIN0 & (1<<23))

Input: Moisture content of land.

Output: Should ON the motor if less water content.

```

if(!(WATER))      //Motor Off
{
IOCLR1=m1p;      // p1 24,25      are motor pins
IOCLR1=m1n;
water();
LcdCmd(0x01); // Shift cursor position to left
LcdCmd(0x80); // Sets cursor to line 1 of display
LcdWriteText("MOTOROFF");
gsmSend();str_serial_0("MOTOROFF\n");
delayseconds(1);
gsmSend(); //notifies user
str_serial_0("SOIL MOISTURE DETECTED,MOTOR OFF\r\n");
delayseconds(2);
}

```

The above code explains when there is no water needed for the farm land and calls the function water() hence it displays in the LCD as “MOTOR OFF”, and also it calls predefined function gsmSend () and sends notification as “SOIL MOISTURE DETECTED, MOTOR OFF”

```

void water() //Water detected in soil moisture
{
LcdCmd(0x01); // Shift cursor position to left LcdCmd(0x80); //Sets
cursor to line 1 of display LcdWriteText("WATER DETECTED");
delayseconds(1);
LcdCmd(0x01);
}

```

The above snippet function tells water is present and sends notification as “WATER IS DETECTED”.

```

if(WATER) // Motor On
IOCLR1=m1p; // p1 24,25 are motor pins
IOCLR1=m1n;
delayseconds(2);
LcdCmd(0x01); // Shift cursor position to left LcdCmd(0x80); // Sets cursor
to line 1 of display LcdWriteText("MOTOR ON");
gsmSend(); //notifies user
str_serial_0("SOIL MOISTURE NOT DETECTED,MOTOR ON\n");
delayseconds(2);
}

```

The above snippet tells there is no moisture content in the farm land and hence water is needed for crops and sends notification as “SOIL MOISTURE NOT DETECTED, ON THE MOTOR”.



WATER LEVEL MODULE

Function Name: #define RAIN (IOPIN0 & (1<<20))

Input: Level of water

Output: Pump to the reservoir

```

if(RAIN) //Water is de-pumped
{
  IOCLR0=(1<<12);
  IOCLR0=(1<<13);
  LcdCmd(0x01); // Shift cursor position to left LcdCmd(0x80); // Sets cursor
  to line 1 of display LcdWriteText("RAIN MOTOR OFF");
  gsmSend();
  str_serial_0("WATER IS DEPUMPED\n");
  delayseconds(2);
}

```

This function explains that there is no excess water in the land and sends notification as “RAIN MOTOR OFF” and also notifies user as Water is de-pumped.

```

if(!(RAIN)) //Rain water depumping to reservoir
{
  IOSET0=(1<<12);
  IOCLR0=(1<<13);
  LcdCmd(0x01); // Shift cursor position to left LcdCmd(0x80); // Sets cursor
  to line 1 of display LcdWriteText("RAIN MOTOR On");
  gsmSend();
  str_serial_0("RAIN DETECTED DEPUMPING TO RESIVOIR\n");
  delayseconds(2);
}

```

This above snippet explains there is excess of water in land and that water is transferred into reservoir so it gives message as Rain Motor ON. And sends notification to user as “RAIN DETECTED DEPUMPING TO RESERVIOR”.

IR MODULE

Function Name: #define IR (IOPIN0 & (1<<18))

Input: Physical intruders

Output: Buzzer ON

```

if(IR) // Object Detection
{
  LcdCmd(0x01); //Shift cursor position to left
  LcdCmd(0x80);
  LcdWriteText("OBJECT DETECTED");
  delayseconds(1);
  IOSET0=(1<<16); //LEDOuput
  IOSET0=(1<<15);
  delayseconds(2); IOCLR0=(1<<16);
  IOCLR0=(1<<15);
  //BuzzergsmSend();
  str_serial_0("OBJECT DETECTED\n");
  delayseconds(2);
}

```

This function explains whether any intrusion present in the farm land. If any obstacles in the farm land then IR sensor detects and sends the message as “OBJECT DETECTED”.



V.EXPERIMENTAL RESULTS

User Application



Figure 6.1: Output of Soil Moisture



Figure 6.2:Output of Soil Moisture



Figure 6.3: Output of Water Level Module



Figure 6.4: Output of IR Module



Figure 6.5: Solar Panel



LCD

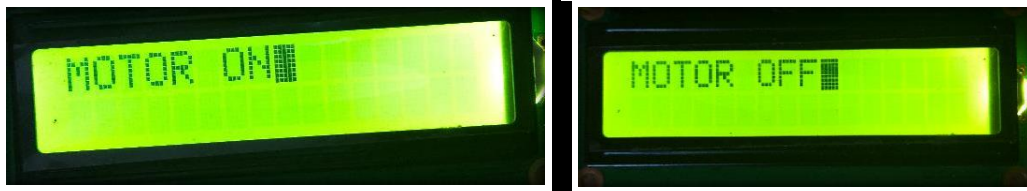


Figure 6.6: Output on LCD

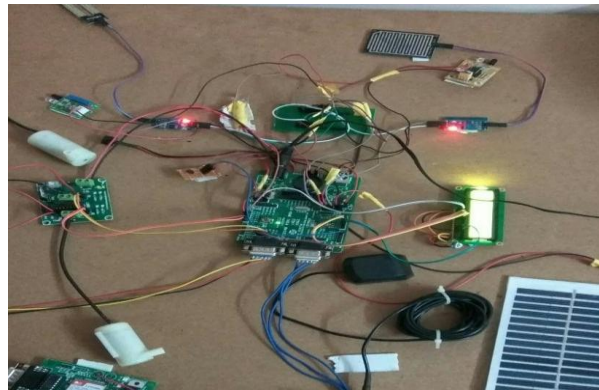


Figure 6.7: Hardware Kit

VI.CONCLUSION

In this system, it provides all kind of help that a farmer needs to know about the crops, start to end process is included in the proposed application where farmers can easily get the information about soil condition, temperature condition and also about solar panel as well as motor. The application proposes new techniques of securing and maintaining the farmland in a better way. It also has cattle tracking where we can track the cattle beyond certain distance. The farmers will get notification about the farm land. There is also a reservoir that is used when there is a heavy rain, excess of water gets stored in that reservoir and used in the future. Farmers can ON and OFF the motor through his android application handheld device. It cures all issues of existing system as it reaches everyone and can be accessible by every farmer.

REFERENCES

- [1] Sanbo Li, "Application of the internet of things technology in precision agriculture irrigation systems," International Conference on Computer Science and Service System, 2012.
- [2] Prof C. H. Chavan, Mr. P. V. Karande, "Wireless Monitoring of Soil Moisture, Temperature and Humidity Using Zigbee in Agriculture", International Journal of Engineering Trends and Technology (IJETT), Volume 11 Number 10- May 2014.
- [3] Prof Nikesh Gondchawar ,Prof.Dr.R.S.Kawitkar, "IoT based Smart Agriculture", International Journal of Advanced Research in Computer and Communication Engineering, Vol. 5, Issue 6, June 2016.
- [4] Chetan Dwarkani M, Ganesh Ram R, Jagannathan S, R. Priyatharshini, " smart Farming system Using sensors for Agricultural Task Automation" , IEEE International Conference on Technological Innovations in ICT for Agriculture and Rural Development (TIAR), 2015.
- [5] N. Shashwathi, Priyam Borkotoky, Suhas K, "Smart Farmig :A Step Towards TechnoSavvy Agriculture", International Journal of Computer Applications (0975-8887) Volume 57-No.18, November 2012.
- [6] Helikson,H.J et al, Pumping water for irrigation using solar energy,University of Florida, USA, 2007.
- [7] Trakia Journal of Sciences, Vol. 3, No. 7, pp 7-11, 2015 http://www.abayaran.com/pdf/technical_papers/pumps/SOLAR%20POWERED%20WATER%20PUM%20PING%20SYSTEMS.pdf
- [8] "SunPower e20 Module". Retrieved 7 April 2014 http://www.wikipedia.com/solar_panel.html.
- [9] Uni-solar, solar energy produces catalogue and brochures, USA, 2001.
- [10] Energy efficient wireless sensor network used for farmland soil moisture monitoring by Zhang Ruirui,Chen Liping,Guo Jianhua,Meng Zhijun,Xu Gang,Beijing Research Centre of Intelligent Equipment for Agriculture , Beijing China.
- [11] Bogart, Theodore F, "Electronic Devices and Circuits"Fourth Edition Prentice Hall, 1997.
- [12] Cirronet, ZMN2405/HP ZigbeeTM Module Developer"s Kit User Manual, Rev A 2015.



Automated Smart Sericulture System Based on Image Processing Technique

Monica K V¹, Monisha R Shetty², Nandini R³, Neethu K⁴, Ms.Jeevitha⁵

Final year B.E Students (UG), Department of Information Science & Engineering, The Oxford College of Engineering, Bangalore, India^{1,2,3,4}

Assistant Professor, Department of Information Science & Engineering, The Oxford College of Engineering, Bangalore, India⁵

ABSTRACT: Sericulture is a art of rearing silk worms for silk production. India is the second largest producer of silk in the world. Sericulture is the root of social, economical ,cultural and political progress of India. Temperature and humidity plays an important role in the development of healthy silkworms in every states, especially during the development of larva. Disinfection is one of the critical parameters to be considered for healthy and successful silk worm rearing.

KEYWORDS: Automated smart sericulture system, Silkworm rearing , temperature, Humidity, disinfection reduced human intervention.

I.INTRODUCTION

The Internet of Things(IoT) is a recent paradigm that has made a variety of each and every things/objects to sense, actuate and communicate through internet by recognizing itself with a unique addressing scheme and interacting wirelessly with each other to create a smart implementation.

Silkworms are stenophagous insects that are fed solely with mulberry leaves and/or silkworm chow.In the adult phase of the lifecycle, the silkworm moths do not eat or drink.There are 4 different stages namely egg, larva, pupa and moth.Sericulture activities are broadly classified into two:the agro-based sector and the industrial sector.The agro-based part involves two distinct phases of activities that is, mulberry cultivation and silkworm rearing. Silkworm rearing is differentiated into two stages:young age rearing from first and second instar.The intermediate stage will be 3rd instar and the rearing will be 4th and 5th instars which comes under late age rearing.The sensor network utilized in our smart sericulture system comprises of smart sensor nodes interfaced with temperature and humidity sensors to collect real time accurate readings inside the system. The autocontrolled actuators namely exhaust fan,heater and sprinkler maintains the temperature and humidity of the system within the threshold levels.Image processing technologies is utilized to capture the pictures of sericulture process and to analyze the status of sericulture process.Image processing is a method mainly to convert an image into digital form and to perform some operations on it, in order to get an enhanced image or to extract some useful information from it.Here the raw data from serial camera is collected and it will undergo various phases of processing.The 3 general phases that all types of data have to undergo while using digital technique are pre-processing, enhancement and display, information extraction.

II.PROBLEM STATEMENT

The existing systems use the controllers like microcontroller and PIC controller which maintains the parameters like temperature and humidity only.Hence without proper management of other parameters the existing systems are not very efficient in producing silk in healthier manner.

III.PROPOSEDSYSTEM

The sensor network utilized in our smart sericulture system comprises of smart sensor nodes interfaced with temperature and humidity sensors to collect real time accurate readings inside the system. The auto controlled actuators namely, exhaust fan, heater and sprayer maintain the temperature and humidity of the system within the threshold levels. Both the temperature and humidity sensors provide and analog output. We have used three relay circuits, for the three actuation systems the switching operation enabling the actuator to operate for desired time. The sensors collect real time data are connected to the raspberrypi.



IV. METHODOLOGY

This stage is the underlying stage in moving from issue to the course of action space. Accordingly, starting with what is obliged; diagram takes us to work towards how to full fill those requirements. System plot portrays all the critical data structure, record course of action, yield and genuine modules in the structure and their Specification is picked. This assumes an essential part on the grounds that as it will give the last yield on which it was being working. In our work we use following modules, these modules are listed below.

Controlling water pump

The greenhouse model is equipped with soil moisture sensor and a water pump. Based on the captured soil moisture level by the soil moisture sensor, it passes the data to raspberry pi and if the moisture level is below threshold value the water pump is triggered high so that it can supply water to the soil. The water pump is connected with the relay so that the raspberry pi can provide instructions to the water pump that needs to be switched on/off. The water pump is fitted inside a water tank filled with water.

Controlling window

The greenhouse has window inside it. The window is fitted with Servo Motor so that when the window is need to be open, the Servo Motors get the instruction to rotate in particular angle and when it has to be closed, the servo motor rotates in anti-clockwise direction. The humidity sensor is connected with the raspberry pi. When the humidity level reaches the threshold value the microcontroller triggers the servo motor to rotate so that the window opens up and when the humidity level goes down to normal level the servo motor rotates in anti-clockwise direction to close the window.

Controlling upper lid and fan

The upper lid of the greenhouse is fitted with the servo motors and it can be open or closed based on the requirement. Controlling the upper lid is based on the in house temperature the temperature sensor is fitted with the raspberry board and the LDR sensor is also connected with the raspberry pi board as well. The LDR sensor detects the amount of light and the temperature sensor senses the in house temperature. When the temperature reaches its threshold level, the microcontroller checks the input from the LDR sensors and if there is enough light then the upper lid of the greenhouse opens up. To open up, the servo motor rotates in clockwise direction and based on the delay the servo motor is stopped. If there is no enough light present inside the greenhouse we consider it as a night time and the fan is triggered on so that it can maintain the temperature. The servo motor as well as the fan operates with Ac current so both the devices are connected with a relay.

Controlling exhaust fan

The greenhouse is fitted with an mq9 sensor that can sense the carbon monoxide level. Inside the Greenhouse sensor is connected with the raspberry pi. The sensor operates at 5V, if the gas level reaches the threshold level, it triggers the exhaust fan so that the unwanted gas can go out of the greenhouse. The exhaust fan operates at Ac current circuit so it is connected with relay.

Accessing data

Raspberry pi can send the data to the tomcat server. User can check the details using his/her android based app.

V. SYSTEM ARCHITECTURE

The architectural configuration procedure is concerned with building up a fundamental basic system for a framework. It includes recognizing the real parts of the framework and interchanges between these segments. The beginning configuration procedure of recognizing these subsystems and building up a structure for subsystem control and correspondence is called construction modeling outline and the yield of this outline procedure is a portrayal of the product structural planning. The proposed architecture for this system is given below. It shows the way this system is designed and brief working of the system.

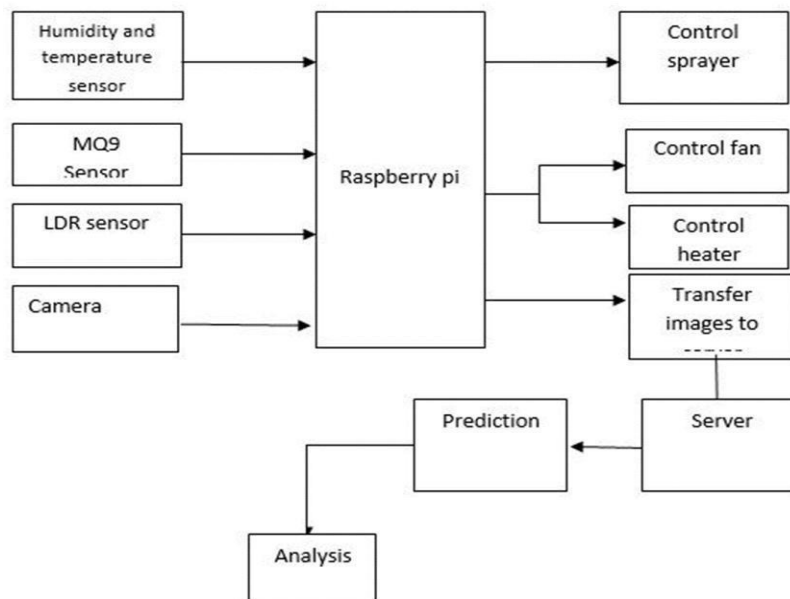


Fig 1: System Architecture

The Step by step process of the system;

1. Humidity and temperature sensor, MQ9 sensor, LDR sensor and camera are connected to raspberry piboard.
2. Humidity and temperature sensor captures temperature and humidity level in the greenhouse model, MQ9 sensor captures the amount of carbon monoxide level, LDR sensor captures the amount of light inside the model and camera captures the videos and pictures of silkworm and all these data are sent to raspberry pi and is stored on a server to take necessary action based on obtained data.
3. When the moisture level captured by soil moisture sensor present in the model is below a threshold value, the data is passed to the raspberry pi which triggers the water pump to spray water using a control sprayer.
4. When the amount of carbon monoxide level increases a threshold value then the exhaust fan is triggered on so that it can maintain the inhouse temperature.
5. When the temperature and humidity reaches a threshold value the controlling lid and window is triggered to open up to maintain the parameters in a normal level.
6. The images and videos captured by raspberry pi camera are sent to the server for comparing and then predicting if it's a healthier or unhealthier silkworm.

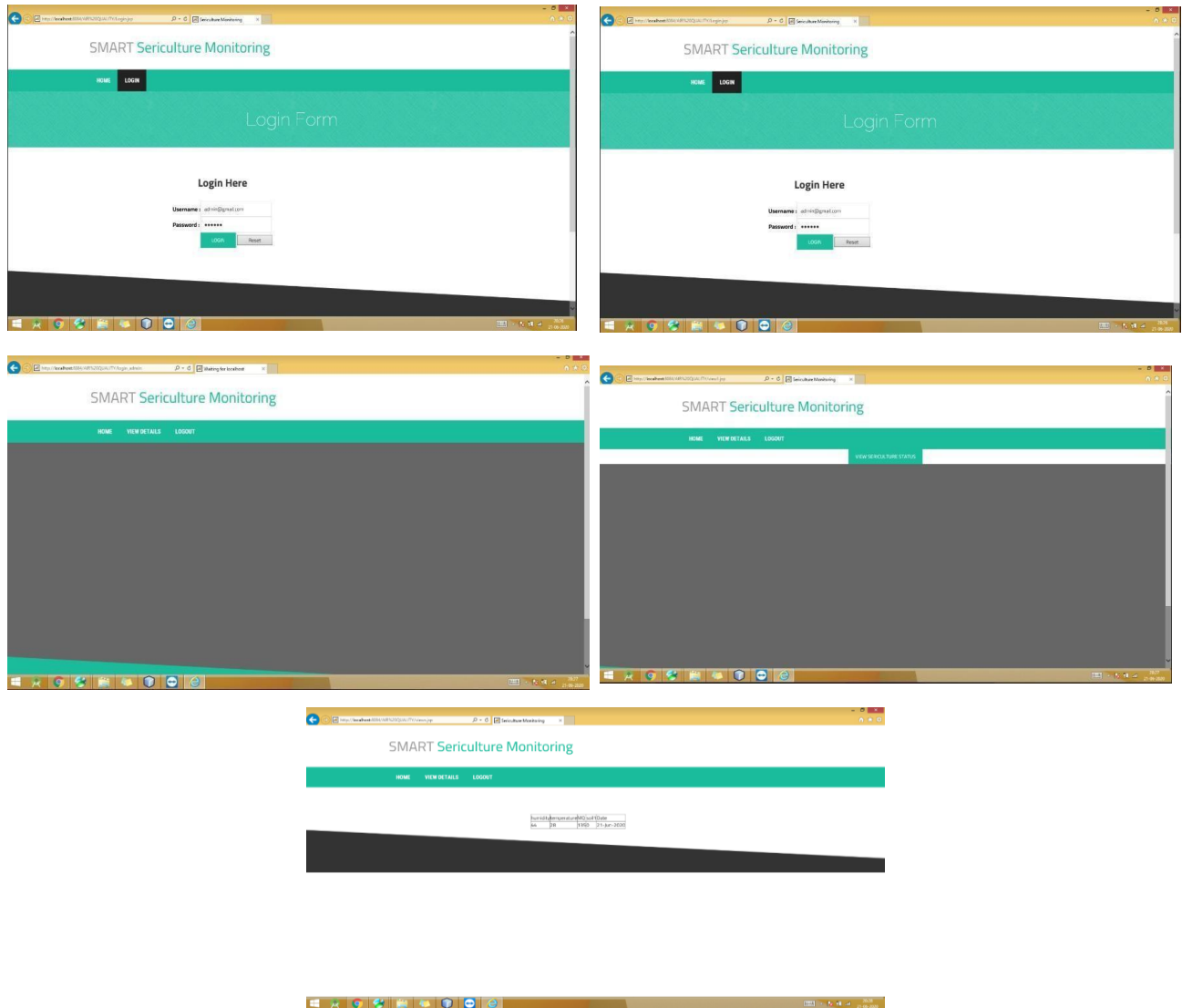
VI. DESIGN CONSIDERATIONS

Software Requirements

1. Operating system : Windows 7/8
2. JDK 1.8
3. Android SDK
4. IDE: NetBeans, Arduino, python 3.7
5. Data Base: MYSQL
6. Server: Apache Tomcat Server 7.0
7. Programming Language : Java, C



Some snapshots of our Web Application are:



Power Supply: Control supply is a reference to a wellspring of electrical compel. A contraption or system that provisions electrical or diverse sorts of essentialness to a yield load or assembling of weights is known as constrain supply unit or PSU. The term is most generally associated with electrical essentialness supplies, less much of the time to mechanical ones, and once in a while to others. This power supply segment is required to change over AC flag to DC flag furthermore to decrease the plenitude of the flag. The available voltage motion from the mains is 230V/50Hz which is an AC voltage, yet the required is DC voltage (no repeat) with the sufficiency of +5V and +12V for various applications.

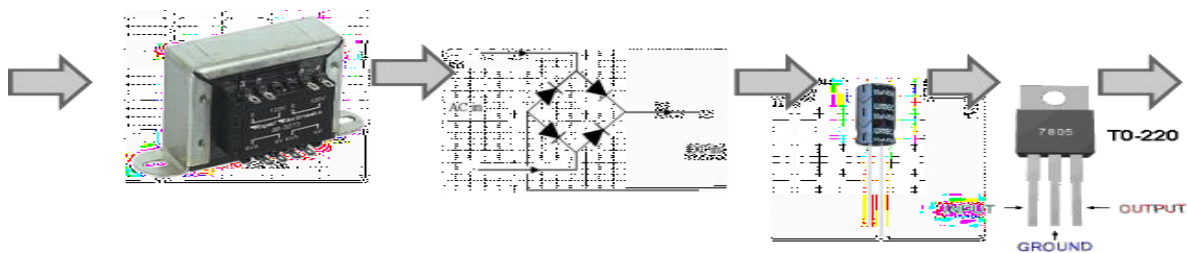


Fig 2: Power Supply



DHT 11 : This DHT11 Temperature and Humidity Sensor features a calibrated digital signal output with the temperature and humidity sensor capability. It is integrated with a high-performance 8-bit microcontroller. Its technology ensures the high reliability and excellent long-term stability. This sensor includes a resistive element and a sensor for wet NTC temperature measuring devices. It has excellent quality, fast response, anti-interference ability and high performance.

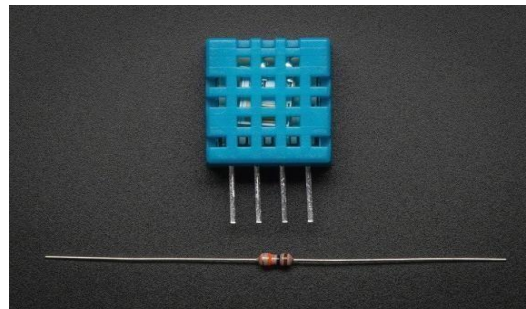


Fig 3: DHT 11

Servo Motor : A **servo motor** is an electrical device which can push or rotate an object with great precision. If you want to rotate an object at some specific angles or distance, then you use servo motor. It is just made up of simple motor which run through **servo mechanism**. If motor used is DC powered then it is called DC servo motor, and if it is AC powered motor then it is called AC servo motor. We can get a very high torque servo motor in a small and light weight packages. Due to these features they are being used in many applications like toy car, RC helicopters and planes, Robotics, Machines etc.



Fig 4: Servo Motor

Arduino Concepts : An Arduino is an open-source microcontroller development board. In plain English, you can use the Arduino to read sensors and control things like motors and lights. This allows you to upload programs to this board which can then interact with things in the real world. With this, you can make devices which respond and react to the world at large. An Arduino board is a one type of microcontroller based kit.

The pin configuration of the Arduino Uno board is shown in the below. It consists of 14- digital i/o pins. Wherein 6 pins are used as pulse width modulation o/p/s and 6 analog i/p/s, a USB connection, a power jack, a 16MHz crystal oscillator, a reset button, and an ICSP header. Arduino board can be powered either from the personal computer through a USB or external source like a battery or an adaptor. This board can operate with an external supply of 7- 12V by giving voltage reference through the IOREf pin or through the pinVin..



Fig 5: Arduino



Raspberry pi : The Raspberry Pi device looks like a motherboard, with the mounted chips and ports exposed (something you'd expect to see only if you opened up your computer and looked at its internal boards), but it has all the components you need to connect input, output, and storage devices and start computing.



Fig 6: Raspberry Pi

LDR sensor : A **Light Dependent Resistor** (LDR) or a photo resistor is a device whose resistivity is a function of the incident electromagnetic radiation. Hence, they are light sensitive devices. They are also called as photo conductors, photo conductive cells or simply photocells. They are made up of semiconductor materials having high resistance. There are many different symbols used to indicate a **LDR**, one of the most commonly used symbol is shown in the figure below. The arrow indicates light falling on it.

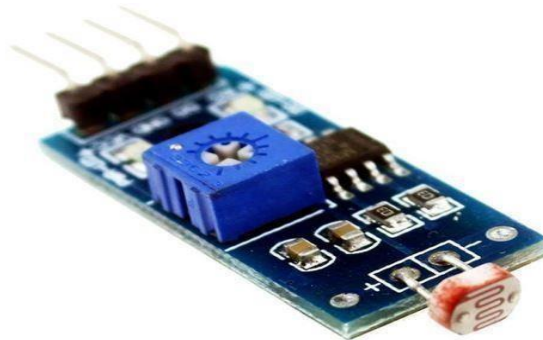


Fig 7: LDR Sensor

Exhaust Fan : Main features are:

1. Starts or stops at 5V and is connected to a controller port and supports PWM speed control of fan with program.
2. Power supply voltage input range : 3-6VDC
3. With LED indicator , it will light up after being switched on.
4. Material :FR-4
5. Easy operation, it can give rise to your interest in electronic circuits and enlighten your creative thinking.



Fig 8: Exhaust Fan



VI. RESULT

The result of this project mainly focuses on the effective rearing of silkworm in a healthier manner so that finally the outcome is a good quality of silk produced. Since the svm algorithm is used, the images captured by raspberry pi camera is in rgb form which is preprocessed to convert into grayscale that is computer understandable format and then it is segmented to locate the silkworm for feature extraction and then finally is classified by comparing it with the trained dataset stored in the server as healthier or unhealthier silkworm. This project also has reduced the continuous human intervention which is otherwise required, because here all environmental parameters are properly managed and maintained. This leads to a production of better quality of silk.

Final Prototype:



Fig 9: Final prototype

VII. CONCLUSION

IoT is widely used in connecting devices and used to gather information. The system is designed to remotely monitor the greenhouse parameters such as soil moisture, temperature, and light, this information can be collected by the farmers with the help of cloud account and internet connection. There is also controlling action taken automatically that is greenhouse windows/ doors roll on/off based on the soil moisture levels. Thus, the system will help the farmers to avoid physical visit to the field, and increase the yield with the maintenance of precise parameters such as soil moisture, temperature, and light in the greenhouse with the help of IoT. Future work is to automatically supply medicines to diseased silkworms.

REFERENCES

1. Karuna Chandraul, Archana Singh, "An agriculture application research on cloud computing", International Journal of Current Engineering and Technology, volume 3, No.5, pp. 2084-2087, October 2010.
2. Ronald Haley, Riley Wortman, Yiannis Ampatzidis, Matthew Whiting, "An Integrated cloud-based platform for labor monitoring and data analysis in precision agriculture", IEEE 14th International Conference on Information Reuse and Integration, pp. 349-356, August 2013.
3. Mistsuyoshi Hori, Eiji Kawashima, Tomihiro Yamazaki, "Application of cloud Computing to agriculture and prospects in other fields", FUJITSU Sci. Tech. J., volume 46, No. 4, October 2010.
4. B. K. Jha, S. K. Jha, R. Mukharjee, D. Basak, "Development of guided SMS solution in local language for Demand-driven Access of agriculture information", 7th International Conference on Communication Systems and Networks (COMSNETS), pp. 1-5, January 2015.
5. D. D. Chaudhary, S. P. Nayse, L. M. Waghmare, "Application of wireless sensor network for greenhouse parameter control in precision agriculture", International Journal of Wireless and Mobile Networks (IJWMN), volume 3, No.1, 2011.47
6. O. T. Denmead and R. H. Shaw, "Availability of soil water to plants as affected by soil moisture content and meteorological conditions", Agronomy journal, 1962.
7. Ahmad Nizar Harun, Mohamed Rawidean Mohd Kassim, Ibrahim Mat, Siti Sarah Ramli, "Precision Irrigation using Wireless Sensor Network", International Conference on Smart Sensors and Application (ICSSA), 2015.



GloveBlu: Many-to-Many Communication among Disabled Users

Rachana¹, Sneha K², Soundarya SBV³, Thanuja K⁴, Kalaiselvi⁵

Final year B.E Students (UG), Department of Information Science & Engineering, The Oxford College of Engineering, Bangalore, India^{1,2,3,4}

Assistant Professor, Department of Information Science & Engineering, The Oxford College of Engineering, Bangalore, India⁵

ABSTRACT: Communication is also one of the activities which are considered as crucial issues at the basis of daily activities of deaf-blind people and of people with disabilities in general, since they are essential in order to have a social life. Today, the perspectives are changed with the introduction of assistive technologies, that are products, devices or systems, which allow to overcome existing digital barriers. This is the context where the GloveBlu project was born. GloveBlu is a low-cost solution supporting users to autonomously communicate with the rest of the world, letting them directly interact with other persons, without the need of an assistant or of an interpreter. The aim is to enable many-to-many communication between many users exploiting the potentiality of tuple centers as coordination media.

KEYWORDS: wearable devices, many-to-many communication, deaf-blind users, people with disability, accessibility.

I. INTRODUCTION

Communication has a key role in our daily life and in particular in daily activities of people with disabilities, since it represents a means of inclusion and of integration in the society and a way to enhance their independence. It takes on further importance in severe disability cases like deaf blindness that is the combination of blindness and deafness. Communication is of crucial importance for deaf-blind people, but it is also very complex, because communicating does not just mean talking, but also getting in touch with other people, breaking the barriers of isolation. Usually, in order to communicate and to interact with the others, several deaf-blind people need the constant presence of a caregiver, who acts as an interpreter with the rest of the world. Communication is also one of the activities which are considered as crucial issues at the basis of daily activities of deaf-blind people and of people with disabilities in general, since they are essential in order to have a social life.

II. LITERATURE REVIEW

Title: Expectations for User Experience in Haptic Communication with Mobile Devices

Author: Jani Heikkinen, Thomas Olsson & Kaisa Väänänen-Vainio-Mattila

- The main contribution of the study is the new knowledge about the expectations and user experience of potential users of haptic communication systems. The authors gained insight into the expectations towards the holistic user experience with haptic systems with mobile devices.

Title: DroidGlove: An Android-Based Application for Wrist Rehabilitation

Author: Silvia Mirri, Catia Prandi, Paola Salomoni & Lorenzo Monti

- This illustrates an original application we have created that combines serious gaming, healthcare, and smart phones to create a digital tool for wrist rehabilitation, namely Droid- Glove.

A Multimedia Broker to Support Accessible and Mobile Learning Through Learning Objects Adaptation

Author: Paola Salomoni, Silvia Mirri, Stefano Ferretti, Marco Rocchetti

-This described LOT (Learning Object Transcoder), an automatic system for the production of accessible and portable learning materials. The system offers a brokering service to transcode digital video lectures based on specific student and device profiles.

Personalizing Pedestrian Accessible Way-finding with mPASS

Author: Silvia Mirri, Catia Prandi, Paola Salomoni



-This introduced mPASS, a system with the goal of equipping citizen with personalized pedestrian paths and a mapping of urban accessibility. mPASS collects data from many sources to improve the accessibility of urban environments, meeting special needs of citizen with disabilities and elderly people.

III. SYSTEM ARCHITECTURE

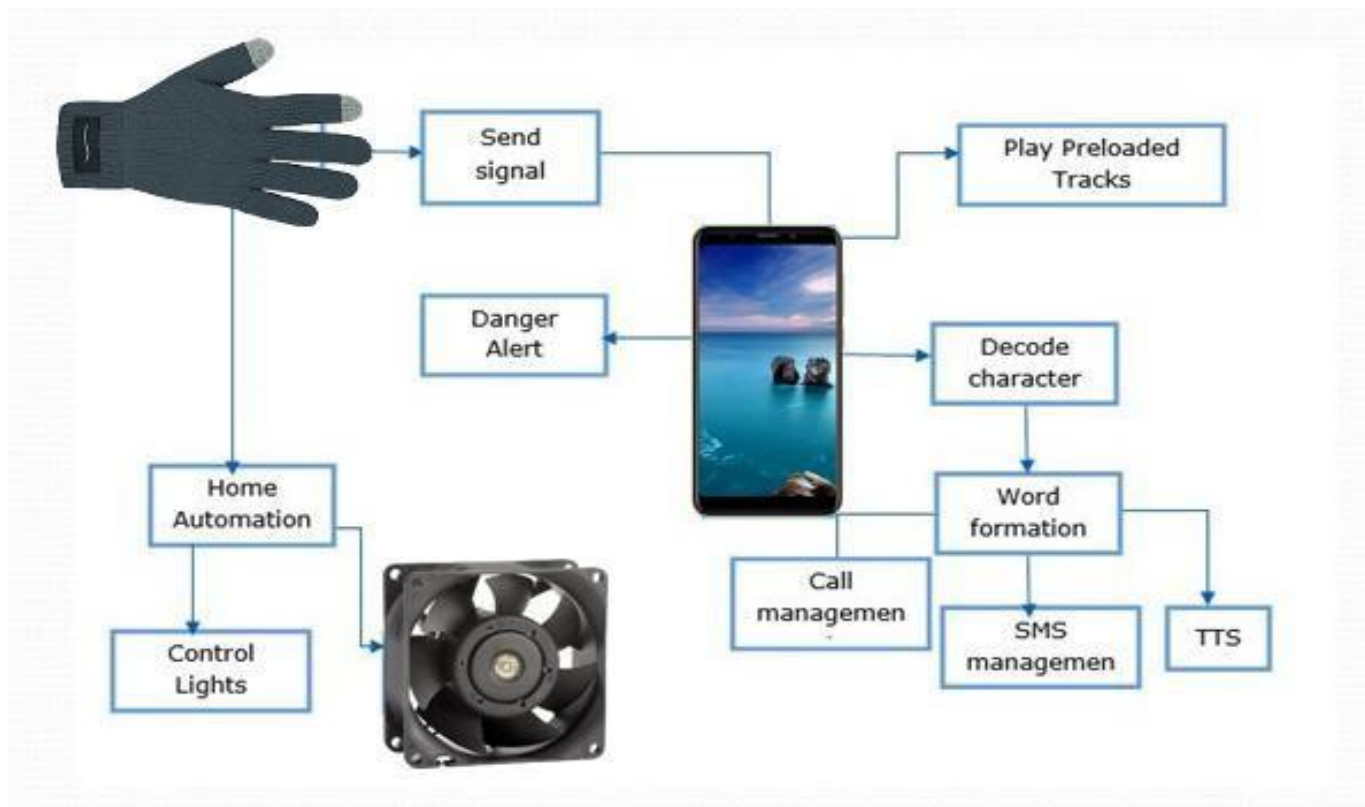


Figure:3.1

The architecture shown in 3.1 has glove which is fitted with multiple buttons that perform various operations. The glove is fitted with a battery for the power supply. The android phone has an application which is used to display the characters pressed on the glove and also show the operations performed. The phone is connected to the glove via Bluetooth. The functions performed from the android phone are shown in the architecture in 3.1. Node MCU is used for home automation such as controlling lights, fans etc. It is connected to glove via Wi-Fi module.

IV. MODULE SETS

Interaction: Using the proposed glove the deaf and dumb people can interact with others. The glove comes with several buttons. With the help of the buttons they can type whatever they want to speak. Once a button is pressed, the respective character is transferred to the android app via Bluetooth. The android app forms the words and that results into sentence. We have used google TTS API to read out the sentence. In the reverse way when a user says something, the app listens to it and converts the speech into text and display.

Home Automation: We have connected the lights and fans with the Arduino Uno microcontroller using H-Bridge. The Arduino Uno is connected with the Bluetooth HC-05. When the user wants to control the home appliances using the glove, they can use dedicated buttons to control the home appliances. So, this glove can be used by the disable people too. When there is a smoke or fire at home the kit sends a signal to the glove. The glove is fitted with a buzzer. Once receives the signal, the buzzer sets the alarm.

Call and SMS: Using the same proposed glove, blind user can send SMS or make calls. When a user wants a SMS to someone, they can use the dedicated buttons to type the sentence and special buttons to type the numbers. The details



are sent to the android app and SMS is sent from the android phone. In the same way user can type the number and press on the call button to make calls using the android phone.

Safe Button: The safety button is a special button fitted with the glove. When the user feels like danger, he/she can press the button and signal is sent to the android app. The app after that send an alert to the family members with the current location of the user.

V. IMPLEMENTATION



Fig 5.1 Glove Fitted with Buttons and Arduino

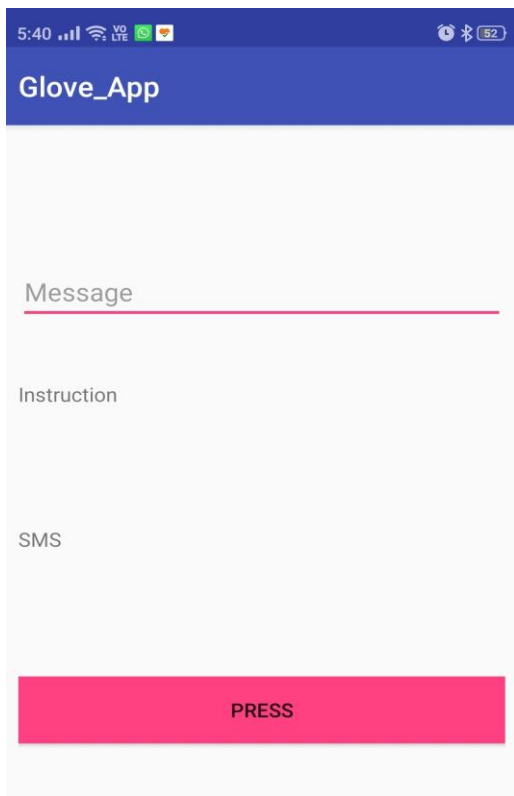


Fig 5.2 The Android App

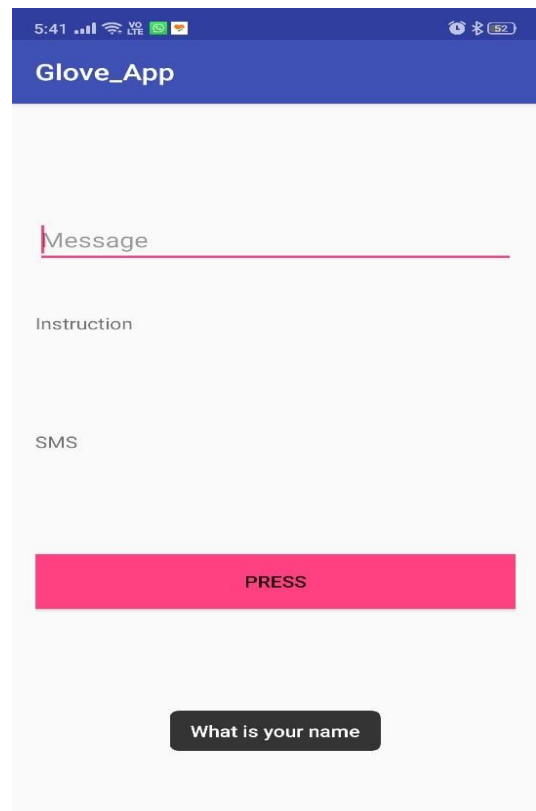


Fig 5.3 Read out Predefined Message

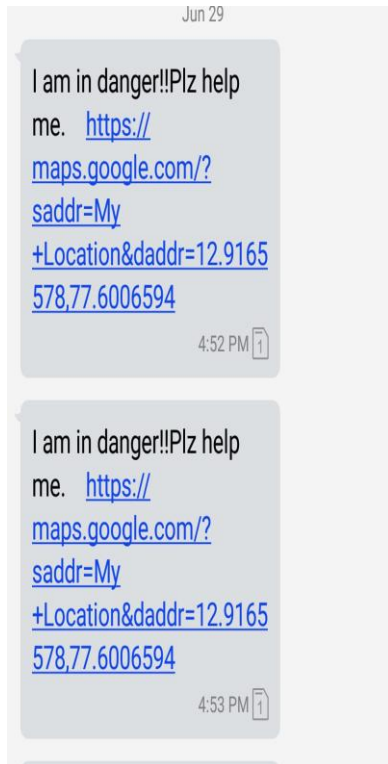


Fig 5.4 Danger Alert send to Registered phone number

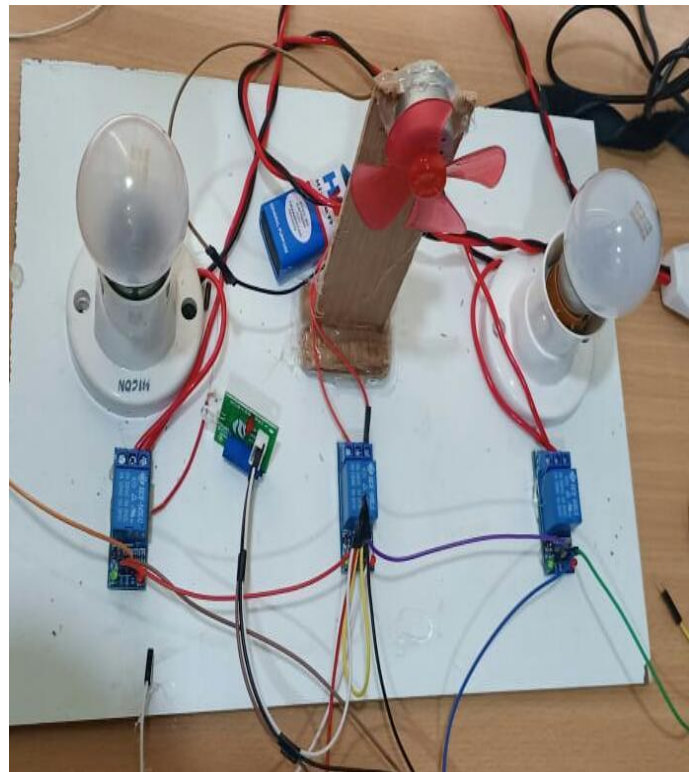


Fig 5.5 Home Automation Setup

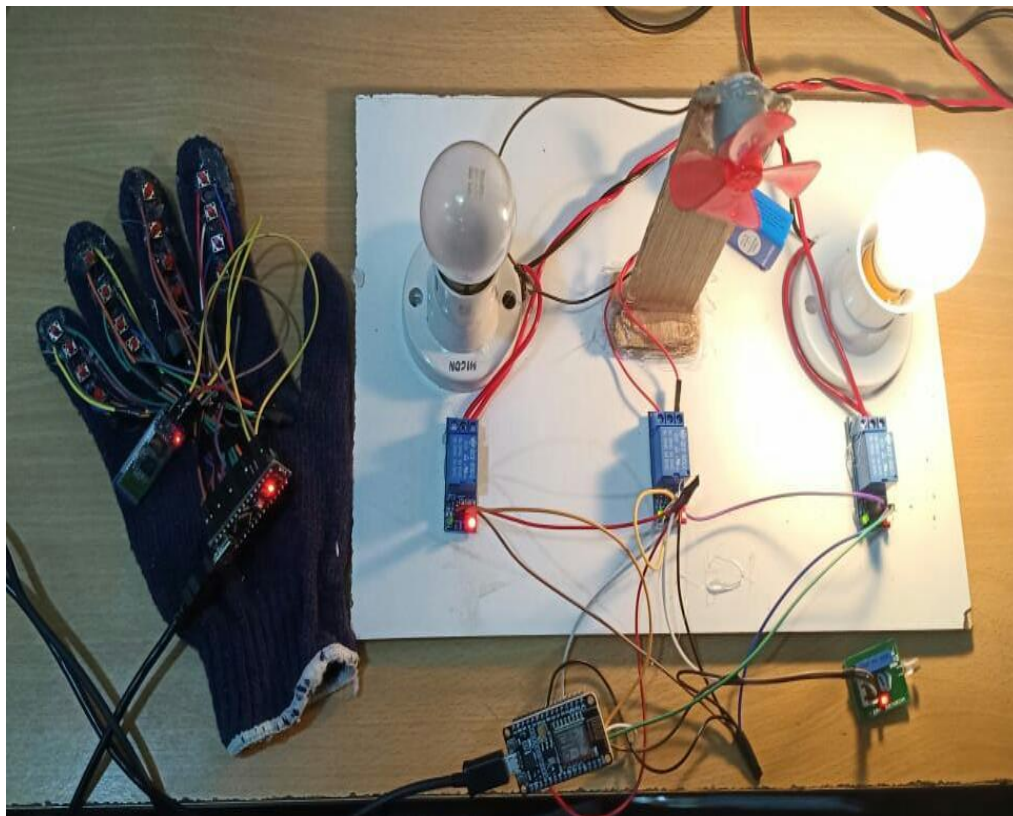


Fig 5.6 Overall Project Setup



VI. EXPERIMENTAL RESULTS

Assistive technologies supporting people with disabilities can be a strategic tool to enhance their inclusion, integration, and independence, in particular for persons with disabilities that involve more senses, such as deaf-blindness, which is the combination of blindness and deafness. Deaf-blind users can communicate by mainly exploiting the sense of touch. Focusing on this kind of communication, we have designed and developed Glove-pi, a low-cost wearable device, based on a glove equipped with mobile devices via Bluetooth. All the systems, services, devices and appliances that are used by disabled people to help in their daily lives, make their activities easier. GloveBlu is an open source assistive system, developed employing low costs hardware components. In particular, the system architecture is composed by three main components: (i) a glove; (ii) an Arduino Uno; (iii) a button. Moreover, an android app has been developed to communicate with the user and display and listen the phases created by the deaf-blind user, using the glove. Using the glove user can send the alert message.

| | |
|-----------------|--|
| S2 # Test Case | UTC- 2 |
| Name of Test | Working of several buttons. |
| Expected Result | With the help of the buttons the user can type whatever they want to speak. According to the respective buttons the characters are transferred to the android app via Bluetooth. |
| Actual output | Same as expected. |
| Remarks | Successful |

Fig 6.1 Testcases for working of several buttons

| | |
|-----------------|--|
| S3 # Test Case | UTC- 3 |
| Name of Test | Call/SMS management. |
| Expected Result | Some specified buttons are used to type the sentence to send the message and special buttons to type the numbers and make the calls. |
| Actual output | Same as expected. |
| Remarks | Successful |

Fig 6.2 Testcases for call and SMS of the glove

VII. CONCLUSION AND FUTURE WORK

In this project we presented Glove Blu, an open source assistive system developed employing low costs hardware components. In particular, the system architecture is composed by three main components: (i) a glove; (ii) an Arduino Uno; (iii) a button. Moreover, an android app has been developed to communicate with the user and display and listen the phases created by the deaf-blind user, using the glove. Using the glove user can send the alert message.

As a future work, it will be interesting to investigate the two-way communication of data not only from glove to the mobile app, but also from the mobile app to the glove.

REFERENCES

- [1] J. Medina, Brain Rules: 12 Principles for Surviving and Thriving at Work, Home, and School (Large Print 16pt). ReadHowYouWant. com, 2011.



- [2] J. Delwiche, "The impact of perceptual interactions on perceived flavor," *Food Quality and preference*, vol. 15, no. 2, pp. 137–146, 2004.
- [3] S. Mirri, C. Prandi, M. Roccetti, and P. Salomoni, "Food and gastronomic heritage: Telling a story of eyes and hands," in *Computers and Communication (ISCC), 2016 IEEE Symposium on*. IEEE, 2016, pp. 6–9.
- [4] S. Mirri, P. Salomoni, A. Pizzinelli, M. Roccetti, and C. E. Palazzi, "" di piazza in piazza": Reimagining cultural specific interactions for people entered exhibitions," in *2016 International Conference on Computing, Networking and Communications (ICNC)*. IEEE, 2016, pp. 1–5.
- [5] J. F. Delwiche, "You eat with your eyes first," *Physiology & behaviour*. Vol 107, no. 4, pp. 502– 504, 2012.
- [6] C. Spence, K. Okajima, A. D. Cheok, O. Petit, and C. Michel, "Eating with our eyes: from visual hunger to digital satiation," *Brain and cognition*, 2015.
- [7] S. Ferretti, S. Mirri, C. Prandi, and P. Salomoni, "Automatic web content personalization through reinforcement learning," *Journal of Systems and Software*, 2016.
- [8] "User centred and context dependent personalization through experiential transcoding," in *2014 IEEE 11th Consumer Communications and Networking Conference (CCNC)*. IEEE, 2014, pp. 486–491.
- [9] S. Mirri, C. Prandi, and P. Salomoni, "A context-aware system for personalized and accessible pedestrian paths," in *High Performance Computing & Simulation (HPCS), 2014 International Conference on*. IEEE, 2014, pp. 833–840.
- [10] P. Salomoni, C. Prandi, M. Roccetti, V. Nisi, and N. J. Nunes, "Crowdsourcing urban accessibility: Some preliminary experiences with results," in *Proceedings of the 11th Biannual Conference on Italian SIGCHI Chapter*. ACM, 2015, pp. 130–133.
- [11] M. Roccetti, S. Ferretti, C. E. Palazzi, P. Salomoni, and M. Furini, "Riding the web evolution: from egoism to altruism," in *2008 5th IEEE Consumer Communications and Networking Conference*. IEEE, 2008, pp. 1123–1127.



3-D Hologram Using Hand Gestures

¹Ameerunisa Daniya, ²Ameema Azhar, ³Ameera Shafi, ⁴Aakanksha Singh,

⁵Dr. R. Kanagavalli

^{1,2,3,4}Final year B.E Students(UG) , Department of Information Science & Engineering, The Oxford College of Engineering, Bangalore, India.

⁵Professor & Head, Department of Information Science & Engineering, The Oxford College of Engineering, Bangalore, India.

ABSTRACT: Holography is the next stage of photography and conventional film and its three-dimensionality creates completely new possibilities for use, such as for product presentation. A 3D hologram displays products, objects, and animated sequences three-dimensionally and enables seemingly real objects or animations to appear to float completely freely in space. Unlike a conventional film on a standard screen, a 3D hologram is visible from all sides, which means the observer can walk around the hologram, enabling an absolutely realistic-looking image to form. Hologram makers, render 3D projections whether it's inside a glass tube or suspended in thin air. 3D multi-dimensional images enable users to interact with content in a totally unique way from a 360-degree seeing point. The way to the operation of holographic projectors is the 3D image. A holographic projector utilizes part illuminations reflected together from multiple viewing angles of the subject in a combined form to reproduce a picture of the subject in a 3D state.

KEYWORDS: Zooming K-Time algorithm, Image processing, Arduino UNO, Raspberry Pi, Flex sensor, Hand gestures, Holographic effects.

I. INTRODUCTION

A hologram is a physical recording of an interference pattern which uses diffraction to reproduce a three-dimensional light field, resulting in an image which retains the depth, parallax, and other properties of the original scene. A hologram is a photographic recording of a light field, rather than an image formed by a lens. A 3D hologram is a 3D projection that exists freely in space and is visible to everyone without the need for 3D glasses. Holography is the next stage of photography and conventional film and its three-dimensionality creates completely new possibilities for use, such as for product presentation. A 3D hologram displays products, objects, and animated sequences three-dimensionally and enables seemingly real objects or animations to appear to float completely freely in space. Unlike a conventional film on a standard screen, a 3D hologram is visible from all sides, which means the observer can walk around the hologram, enabling an absolutely realistic-looking image to form. 3D hologram object is a record pattern of the light method. Digital holography was invented in 1900. The improvement of computer science led to delivering the recording. Nowadays, holography has a broad range of applications various sciences. Display paradigm for unrestricted viewing of real-world objects that employs all real 3D principles. A holographic projector utilizes part illuminations reflected together from multiple viewing angles of the subject in a combined form to reproduce a picture of the subject in a 3D state. The main objective of our project is to develop a fully functional 3D video capture. Our project allows the user to change the image using hand gestures without the help of any device.

II. PROBLEM STATEMENT

Many problems can be faced when using the traditional methods of viewing the pictures or any conventional films. Some of them can be accommodation-vergence rivalry that arises when a viewer's eyes converge or diverge in response to disparity between the left and right images, giving the illusion that part of the scene is coming in front of or behind the screen, but all the time the eyes must focus exactly on the screen. The other problem can be no motion parallax that arises when users move their heads slightly in 3D cinema, the objects do not move as they should if it was a 3D scene, this can give rise to visual discomfort. Everyone in the cinema sees the same perspective decided by cinematographer, changing seat does not give a new perspective of the 3D scene, as in the case in live theatre. Holography could be used to overcome some of these problems. The existing system discuss the creation of a three dimensional (3D) effect for an image by rotating the two dimensional (2D) one on a computer screen in order to add the required sense of image depth depending on image processing techniques. In the traditional system while



explaining something we use board or projector. Traditional system requires more time to demonstrate and need to draw image for different orientation

III. PROPOSED SYSTEM

In the proposed model we have created a 3D holographic box which will be used to display the image. The hologram box is made up of a wood. The top frame is simply a rectangle with a lip on the inside of the frame for the edges of the monitor to sit on. The bottom frame is similar to the top frame except for the inner lip. The top and bottom frame hold together the acrylic frustum within it. The frustum is three pieces of acrylic sheet brought together to form a three-sided pyramid with a 45 degree slope. The acrylic sheets used in developing frustum must be of exact dimensions. The dimensions are highly dependent on the size of the monitor used. The base and back of the hologram box is covered with PVC sheets or any similar material that serve the 3D holographic effects by blocking off the light and creating a dark background for the hologram. For the hand gestures we are using one wrist band which consist of an Arduino Nano, ADXL and a Bluetooth module HC05. For image modification such as zoom in or zoom out we make use of a flex sensor. Image is displayed in the holographic box along with the information provided to it. The proposed system uses a Raspberry Pi controller based system to achieve holographic projections. The power supply unit is designed such that it is connected to both the Raspberry Pi board and the Gesture Interface board simultaneously, both circuits are provided with different voltage and power requirements. The power supply unit consists of a bridge rectifier, capacitive filters and voltage regulators (LM7805).

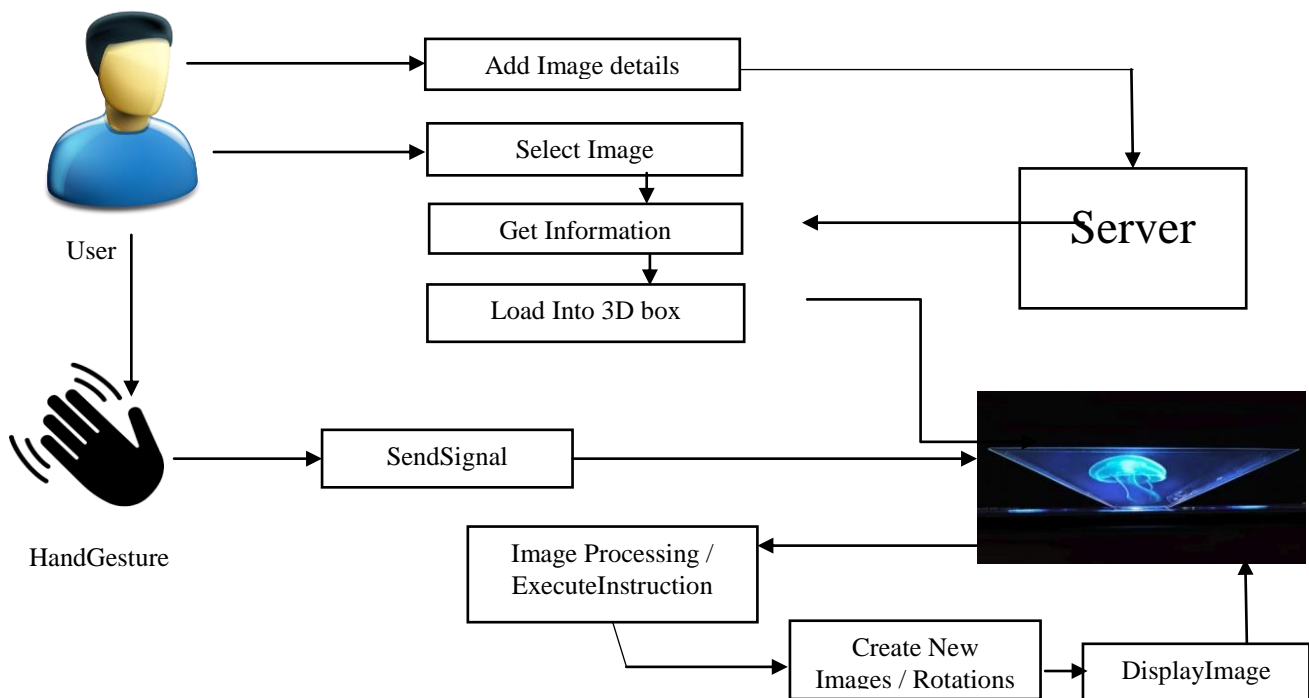


Fig 1: Working of the System

The step by step process how the images are displayed in hologram box is given

1. First the images and videos which needs to be displayed are stored in the web app along with its information. The application can be used in any smartphones.
2. The app is connected to the monitor of the hologram box using a Bluetooth. The images selected by the user is transferred through the Bluetooth to be displayed in the box.
3. There is a Raspberry Pi placed on the monitor. Once the Raspberry Pi receives the instructions from the android based mobile app, those instructions are applied on the selected images and displayed in the hologram box.
4. The user can change the images using hand gestures without the help of the mobile app. One wrist band is used for the hand gestures which consist of an Arduino Nano, ADXL and a Bluetooth module HC05. The ADXL detects the hand movement based on x, y, z axes and passes the data to the Arduino and the Arduino transmit the instruction to the raspberry pi. For zoom in and zoom out we will use flex sensor.



5. Based on the instructions given by the user the images are modified using the python program in the raspberry and is displayed in the hologram box.
6. When the zoom in and zoom out instruction is given the image processing algorithm is applied to zoom in and zoom out the images

IV. IMPLEMENTATION

A. Implementation

An android based mobile application is developed, to store the images along with its information that is needed to be displayed in the hologram box.

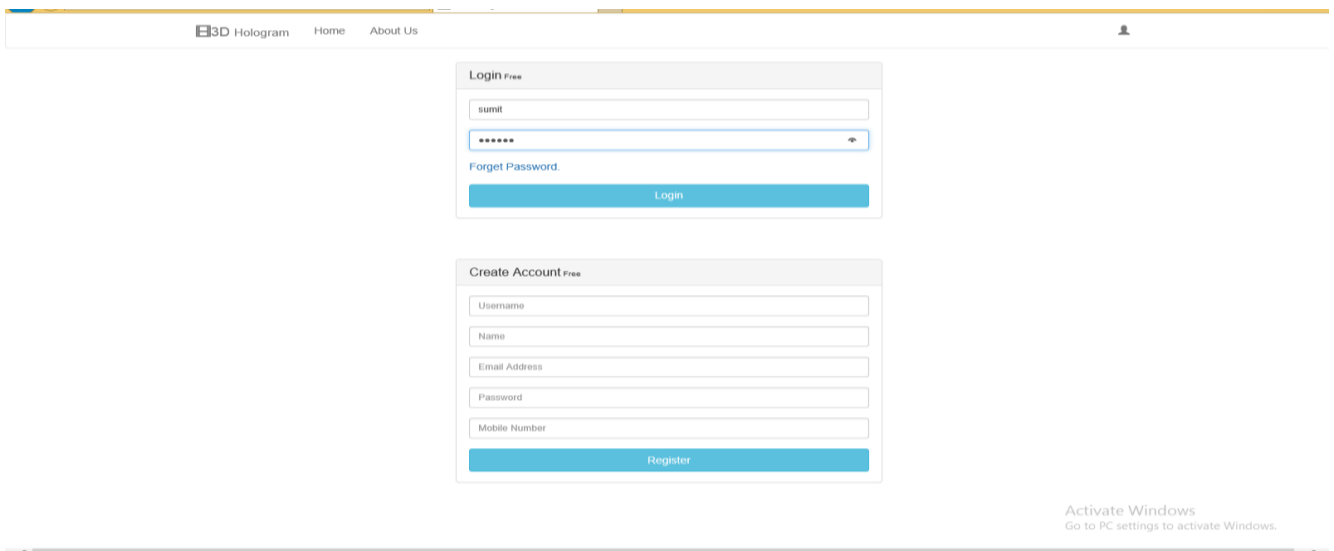


Fig 2: Login Page of the app

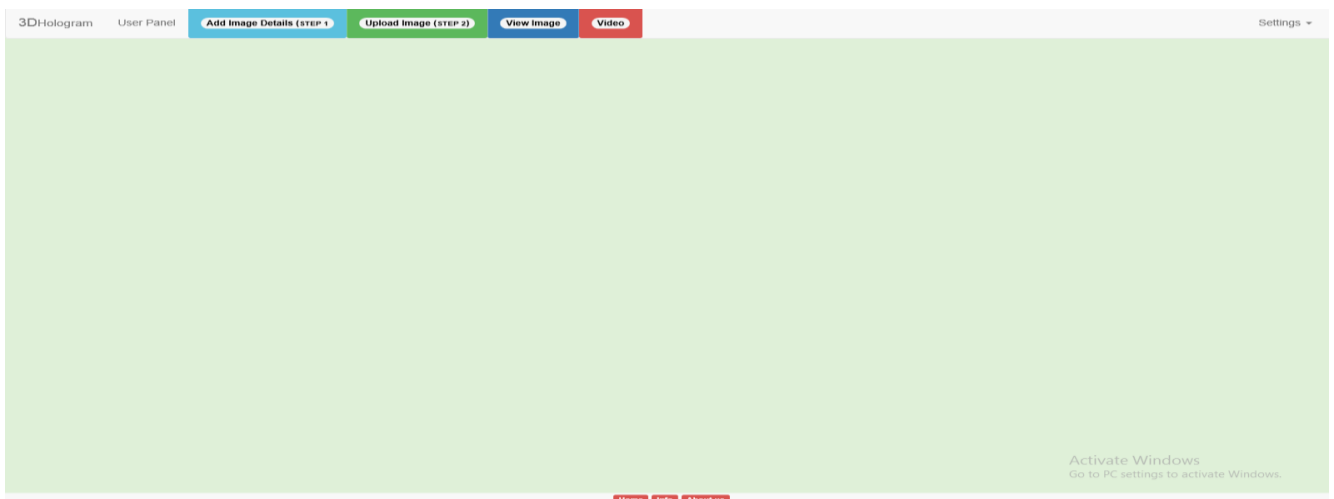


Fig 3: Home page of the user



The image shows two web forms stacked vertically. The top form is titled 'Adding New Image' and contains the following fields: 'Image Name' (text input), 'Description' (text input), 'Image View' (dropdown menu with 'Top View' selected), and 'Image Category' (dropdown menu with 'Science' selected). A blue button labeled 'Add Image' is at the bottom. The bottom form is titled 'Adding New Video' and contains the following fields: 'Video Name' (text input), 'Description' (text input), 'Video View' (dropdown menu with 'Top View' selected), and 'Video Category' (dropdown menu with 'Science' selected). A blue button labeled 'Add Video' is at the bottom.

Fig 4: Adding image and video details

The image shows two web forms. The left form is titled 'Set Image' and contains a 'Select Image' dropdown menu and a button labeled 'Click Me To Upload Image'. A blue button labeled 'Set Image' is at the bottom. The right form is titled 'Adding New Video' and contains the same fields as in Fig 4: 'Video Name' (text input), 'Description' (text input), 'Video View' (dropdown menu with 'Top View' selected), and 'Video Category' (dropdown menu with 'Science' selected). A blue button labeled 'Add Video' is at the bottom.

Fig 5: Adding images and videos

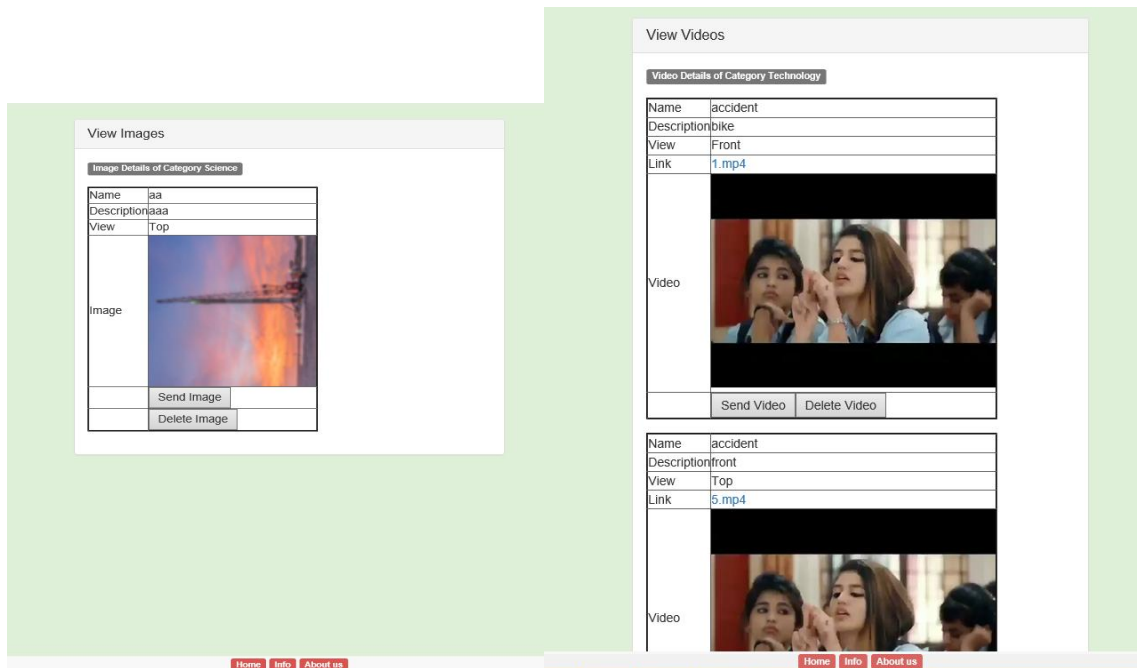


Fig 6: View images and videos

B. Software

For software purpose, we used 4 different software for different purpose in our project.

1. NetBeans 8.2
2. Jdk8
3. Python 3.7
4. Mysql5.1

V. HARDWARE

A.1. Hologram Box

The hologram Box is made up of wood as its base and top frame. The top frame holds the monitor within its inner lip. The top and bottom frames are held together by wooden pillars. The frustum is made of acrylic sheets, they are made in the shape of a pyramid with 45 degree. The image is seen within the frustum.

B.1. Arduino UNO

Arduino Uno is used to control the relay signal which will direct the signal based on their given code, the signals given by flex sensor are controlled and work accordingly.

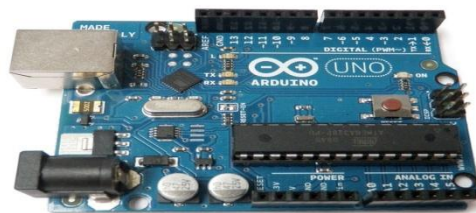


Fig 7: Arduino UNO

B.2. Raspberry pi

The Raspberry Pi device looks like a motherboard, with the mounted chips and ports exposed (something you'd expect to see only if you opened up your computer and looked at its internal boards), but it has all the components you need to connect input, output, and storage devices and start computing. There are two models of the device: **Model A** and **Model B**. The only real differences are the addition of Ethernet and an extra USB port on the more expensive Model B.



Fig 8: Raspberry Pi

B.3. Glove for hand gesture

The wrist band consists of an Arduino nano, ADXL and a Bluetooth module HC05. The ADXL detects the hand movement based on x, y, z axes and passes the data to the Arduino and the Arduino transmit the instruction to the raspberry pi. Based on the instruction, the python program in the raspberry, receives the instruction and applies on the image. For zoom in and zoom out we will use flex sensor. A Bluetooth is also connected to it.

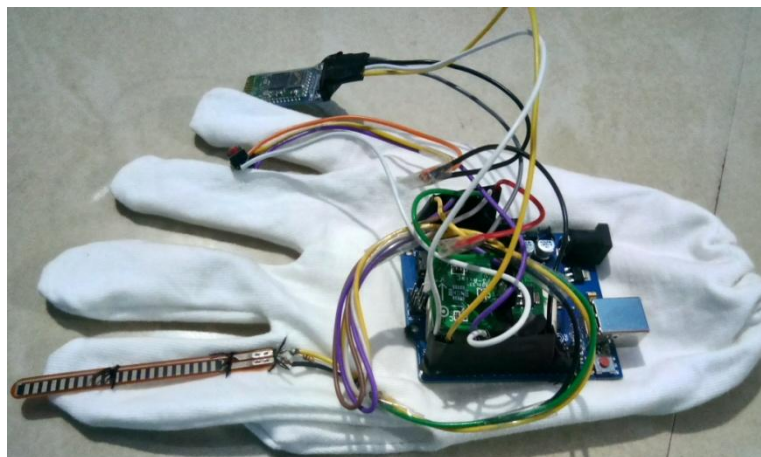


Fig 9: Glove for Hand Gesture

C.1. Power Supply

The power supply unit is designed such that it is connected to both the Raspberry Pi board and the Gesture Interface board simultaneously, both circuits are provided with different voltage and power requirements. The power supply unit consists of a bridge rectifier, capacitive filters and voltage regulators (LM7805).



VI. RESULT ANALYSIS

The result of the project mainly focuses on two part. The hardware result which will focus on how the device is running displaying the images and videos selected, if the goal is being achieved properly. And the software result which will focus on storing the images and videos required to be displayed along with its information to be displayed in the hologram box.



Fig 10: Hologram box

The app consist of different views of a single image i.e. top view, bottom view, right view, left view and each of the view has its own information to be displayed in the hologram box. When an image is selected to be displayed, same image is same from all four directions for the user.

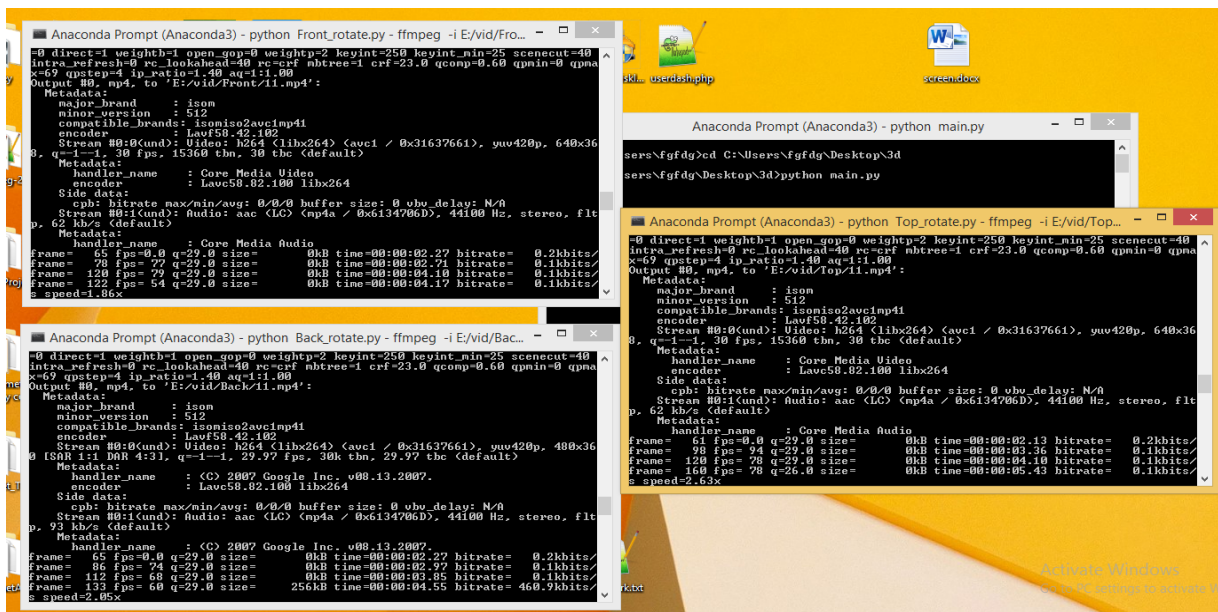


Fig 11: Command prompt to run the code for changing the view



VII. CONCLUSION

A digital display system is simulated to be capable of displaying 3-D images having all the relevant information and visual properties of the scenes to be viewed. The simulated model is a fast simple display technique without need to install optical system or even real objects. The created 3D images are viewed with depth impression and are scaled to a desired size. It is also possible to combine the constructed images with some graphical effects to be more enjoyable. This 3-D hologram is constructed in such a way that it is user friendly as well as can be used in almost every domain in order to deliver ideas in a creative way. The use of hand gestures will make it easy for the user to have control on the 3-D hologram as well as the image that is being represented inside it. Thus it plays an important role in digitizing most of the domains with latest technologies being inculcated in it.

VIII. FUTURE SCOPE OF THE STUDY

The future of holographic technology is said to be a game changer, set to revolutionize industries beyond the conventional standards we live in today. 3D holographic projection technology clearly has a big future ahead. As this audio visual display continues to get high profile credibility, we are likely to see more companies advertising their products or marketing their business in this way. Whether it be large scale, big budget product launches or smaller retail POS systems, they are likely to become a common feature in the advertising world. The images that were being viewed in 2-D perspective can now be viewed from all sides and also in a 3-D manner with the help of the 3-D hologram. Along with the features of a 3-D hologram, it also enables the users to use hand gestures in order to have full control of the image inside the holographic box. In the near future, the 3-D hologram box will be very essential in digital education, as it will allow the users to teach in a visually appealing way and also act as an amazing device for modern education. Along with being beneficial in the field of education, it also plays an important role in the medical and health care domain by providing a 3-D view of any scan report. The entire project is not only sustainable but very essential in mostly all of the domains which require a device to convey their ideas in a very creative way. The future integration of hologram technology in different sectors is thought to revolutionize certain industries like space research, medical research, information storage, architecture, non-photorealism and even entertainment. Holograms have the potential to dramatically improve training, design, and visualization in many business settings and production facilities, being able to look at, zoom in and manipulate 3D versions of in-progress designs.

REFERENCES

- [1] <http://holocenter.org/what-is-holography/?gclid=CNaPzYbYnNICFUQfaAodoBsD7g>
- [2] S. Amabdiyil, D. Sekhar and V. P. M. Pillai, "One step 3D hologram master origination for security applications," 2015 Workshop on Recent Advances in Photonics (WRAP), Bangalore, 2015, pp. 1-3, doi: 10.1109/WRAP.2015.7805981.
- [3] NurulMaziah, MohdBarkhaya, Noor Dayana Abd Halim, "A review of application of 3d hologram in education: A meta-analysis", IEEE 8th International Conference on Engineering Education (ICEED), 2016.
- [4] Wen Chen, "Three Dimensional optical correlation based on binary computer-generated hologram", IEEE 27th International Symposium on Industrial Electronics (ISIE), 2018.
- [5] P.A. Cheremkhin, E.A. Kurbatova, "Optical dynamic reconstruction of quantized digital and computer-generated holograms", International Conference Laser Optics (ICLO), 2018, doi: 10.1109/LO.2018.8435412.
- [6] Takashi Kakue, Takashi Nishitsuji, Tetsuya Kawashima, Tomoyoshi Shimobaba, Tomoyoshi Ito, "Aerial projection of 3d images reconstructed from computer generated image holograms", 14th Workshop on Information Optics (WIO), 2015.
- [7] ThibaultLeportier, Min-Chul Park, Taegeun Kim, Jung-Young Son, "Generation of binary hologram preserving the 3d information", 13th Workshop on Information Optics (WIO), 2014, doi: 10.1109/WIO.2014.6933301.
- [8] ThibaultLeportier, Min-Chul Park, Kwang-hoon Lee, "Binary hologram generation of real objects by combination of color and depth map", 15th Workshop on Information Optics (WIO), 2016, doi: 10.1109/WIO.2016.7745578.
- [9] Mohammedhusen H Manekiya, Arulmozhivarman.P, "3D volume reconstruction using hologram", International Conference on Communication and Signal Processing (ICCS), 2016, doi: 10.1109/ICCS.2016.7754423.
- [10] TharoeunThap, Hee-won Chung, Yunyoung Nam, Jinseok Lee, "Simplified 3d hologram heart activity monitoring using a smartphone", 9th International Conference on Innovative Mobile and Internet Services in Ubiquitous Computing, 2015, doi:10.1109/IMIS.2015.87.



An Automated Cooking Robot Using Embedded C

Prakruthi K.S¹, Raksha S²., Saroja N Patgar³, Sindhu M.S⁴, Dr. R. Kanagavalli.⁵

Final year B.E Students (UG), Department of Information Science & Engineering, The Oxford College of Engineering,
Bangalore, India^{1,2,3,4}

Assistant Professor and HOD, Department of Information Science & Engineering, The Oxford College of Engineering,
Bangalore, India⁵

ABSTRACT: Electric household appliances are now an indispensable component of our life. Microwave ovens cook our meals, dishwashers clean the dishes and laundry machines wash and dry our clothes. However, most of these machines operate in a closed environment (box) and it significantly limits what they can do. We foresee that next generation electric household appliances (systems) should execute more advanced tasks in an open environment that is shared with users. We are developing a cooking system as an initial example of such household systems. Cooking in a closed environment consumes too much space for typical home kitchens. We therefore, designed a system that works in an open environment. When using the system, the user puts pre-processed cooking ingredients on the table and has small robots execute the cooking tasks using a pot on an induction heating (IH) cooker. When not using the system, the user can cook on the same table using the same cooker. Consideration to human factors is critically important for the successful deployment of such open household systems. They must be safe and able to adapt to dynamic changes of the environment because they share the space with the user. They also must provide an appropriate user interface for controlling complicated real-world tasks. We address these issues in the design of our cooking system.

KEYWORDS: Cooking robot, Internet of things, Android application, automation, intelligent systems, robotics, cooking systems, Arduino.

I. INTRODUCTION

We propose a cooking system that operates in an open environment. The system cooks a meal by pouring various ingredients into a boiling pot on an induction heating cooker and adjusts the heating strength according to the user's instructions. We then describe how the system incorporates robotic- and human-specific elements in a shared workspace so as to achieve a cooperative rudimentary cooking capability. First, we use small mobile robots instead of built-in arms to save space, improve flexibility and increase safety. Second, we use detachable visual markers to allow the user to easily configure the real-world environment. Third, we provide a graphical user interface to display detailed cooking instructions to the user. We hope insights obtained in this experiment will be useful for the design of other household systems in the future.

The Kitchen is an essential part of human life. Cooking food is considered as special skill. Cooking food in present day busy life is a tedious work. For a busy life schedule, solutions such as restaurants, packaged food, ready to eat food came into existence. These solutions turned out to high profit and medium scale industries. The quality of food and adulteration became major factors in restaurants, addition of chemicals for long lasting food in packaged and ready to eat food products may affect the health of human-life. And the taste in these foods are depended on the chief chef of the particular industry. In this paper, authors describes a mechanism to overcome the above-mentioned problem with a solution of an autonomous cooking system which cooks the desired dishes in the home kitchen which can be controlled from android application.

Present day kitchen automation system includes features like smart notifications, scheduled notifications, smart displays, prediction of dishes from the ingredients available [1]. But most of these methods are software oriented. Most of the commercially available devices, which is used to cook are specific to one dish and are costly for use in home and medium scale applications. The mechanism discussed in this paper integrates device that is capable of cooking multiple recipes and can be cooked on a single pan using up to nine or more ingredients with churning, cooking, frying mechanisms and smart weigh scale.



II. PROPOSED SYSTEM

We are creating a special table and placed it higher than the pot so that the robots can easily pour ingredients and seasonings. We also created special plates so that the robots can handle them and the user can place a visual marker on it. Inside the IH cooker we implanted a micro controller circuit and Bluetooth communication module for controlling the temperature level remotely. We carefully designed the environment so that the user can also cook without using the system. The user can use the table as a working space and put ingredients on the same plates. We are developing three types of customized small IoT robots, one for transporting the ingredients on plates, one for transporting seasonings in bottles, and one for stirring the pot. The first robot grabs a plate using a single arm, moves to the pot, and tilts the plate to drop the ingredients into the pot. The second robot grabs a bottle by using a hand with two fingers, moves to the pot, and shakes the bottle to sprinkle the seasoning into the pot. The stirring robot stirs the pot at appropriate times. Before cooking begins, the user needs to select and attach a cooking utensil to the robot. We are developing a cooking system as an initial example of such household systems. Cooking in a closed environment consumes too much space for typical home kitchens. When not using the system, the user can cook on the same table using the same cooker. This robot can cook egg, boil, rice, coffee, tea and vegetables item etc.

Advantages:

- It works really well
- It looks fantastic
- Helpful for elder people
- They make it easier/help people who are stressed

III. METHODOLOGY

In our work we use four modules, these modules are listed below.

➤ Chopping Vegetables:

Vegetable cutting dicing is a daily domestic task which takes up a lot of time and effort. So here we propose a motorized vegetable cutting machine that does this in a fully automatic manner. The vegetable cutter machine consists of a narrow feeder which is attached to a motorized blade cutter arrangement. The blade is contained in a circular transparent vessel to collect cut vegetables. The system consists of a narrow feed pipe used to insert vegetables. This feed pipe is fabricated to the cutting blade area. As soon as the vegetable is pushed through it rotating blade which is connected to a powerful motor through a custom designed coupling is continuously rotating as per the speed we set for it. The motor mount is fabricated with the lower collector vessel which is used to collect the diced vegetable pieces.

➤ Process Request:

The users can select the cook/chef as per their interest. The cook might specialize in preparing Indian or maybe something else. Under this section, the users can send the request to the desired cook as per their preferences.

➤ Cook Process:

When Robot Cook gets instruction from the user then Robot cook will be working automatically. Like lemon-rice -It takes around 20 minutes for the meal to be cooked and the entire procedure is completely unaided. The recipes can be pre-programmed into the bot and after loading the required ingredients; the bot functions independently.



➤ **Android Application:**

In this paper, the cooking robot is connected with the android app through the low power hc05 (Bluetooth) technology based on the technology of the internet of things. User are able to use android app to give the instructions to the Arduino microcontroller.

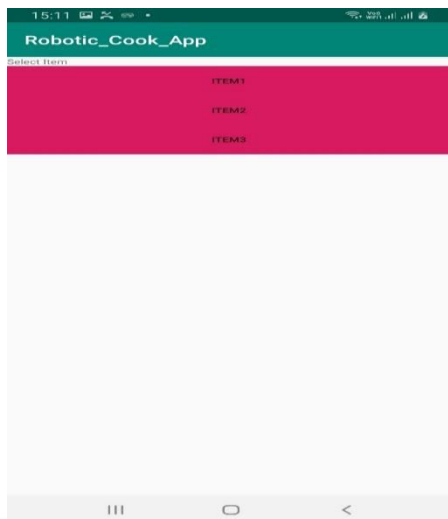


Fig1 application pg1

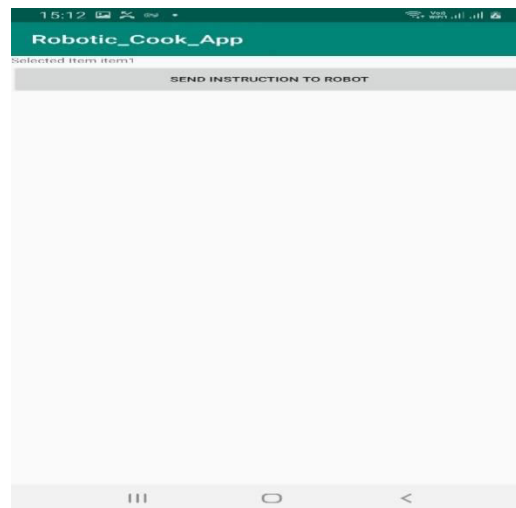


Fig 2 application pg2

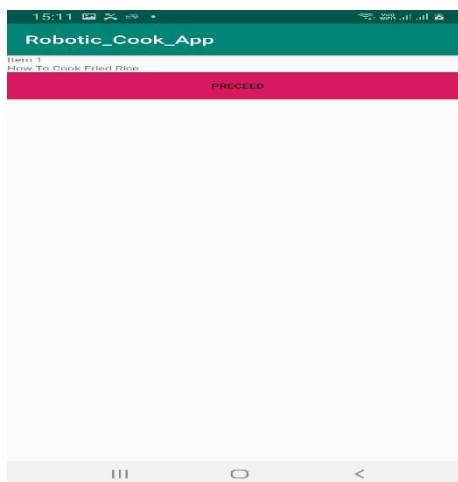


Fig 3 application pg 3

SYSTEM DESIGN AND MODULE DESCRIPTION

◆ **INTRODUCTION**

A good system design is to organise the program modules in such a way that are easy to develop and change. Structured design techniques help developers to deal with the size and complexity of programs. Analysts create instructions for the developers about how code should be written and how pieces of code should fit together to form a program.

◆ **SYSTEM ARCHITECTURE**

The architecture of a system describes its major components, their relationships (structures), and how they interact with each other. Software architecture and design includes several contributory factors such as Business strategy, quality attributes, human dynamics, design, and IT environment. We can segregate Software Architecture and Design into two distinct phases: Software Architecture and Software Design. In Architecture, non-functional decisions are cast and separated by the functional requirements. In Design, functional requirements are accomplished.

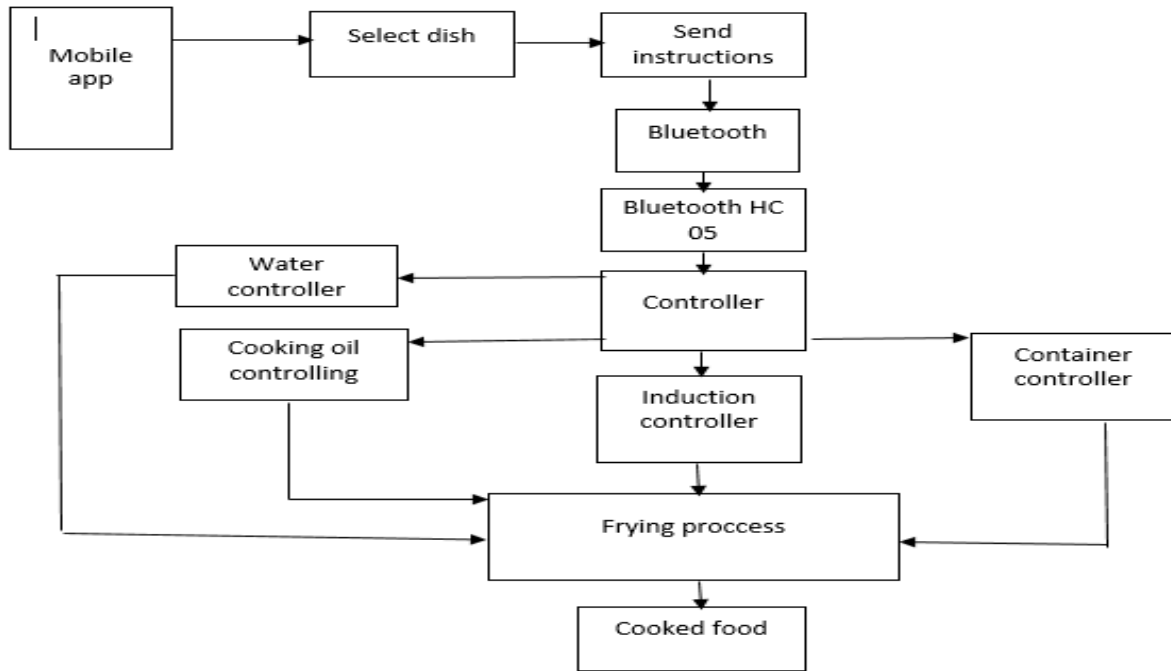


FIG 4. SYSTEM ARCHITECTURE

IV. DESIGN CONSIDERATION

◆ REQUIREMENT SPECIFICATION

A software requirements specification (SRS) is a document that captures complete description about how the system is expected to perform. It is usually signed off at the end of requirements engineering phase. Framework Requirement Specification (SRS) is a focal report, which outlines the foundation of the item headway handle. It records the necessities of a structure and in addition has a delineation of its noteworthy highlight. A SRS is basically an affiliation's seeing (in making) of a customer or potential client's edge work necessities and conditions at a particular point in time (for the most part) before any veritable design or change work. It's a two-way insurance approach that ensures that both the client and the affiliation understand exchange's necessities from that perspective at a given point in time.

◆ SOFTWARE REQUIREMENT

ANDROID DESCRIPTION

Android applications are written in the Java programming language. The Android SDK tools compile the code along with any data and resource files into an Android package, an archive file with an .apk suffix. All the code in a single .apk file is considered to be one application and is the file that Android-powered devices use to install the application. Once installed on a device, each Android application lives in its own security sandbox. The Android operating system, is a multi-user Linux system in which each application is a different user.

ARDUINO IDE

The Arduino Integrated Development Environment (IDE) is a cross-platform application (for Windows, macOS, Linux) that is written in the programming language Java. It is used to write and upload programs to Arduino compatible boards, but also, with the help of 3rd party cores, other vendor development boards.

The source code for the IDE is released under the GNU General Public License, version 2.

The Arduino IDE supports the languages C and C++ using special rules of code structuring. The Arduino IDE supplies a software library from the Wiring project, which provides many common input and output procedures.

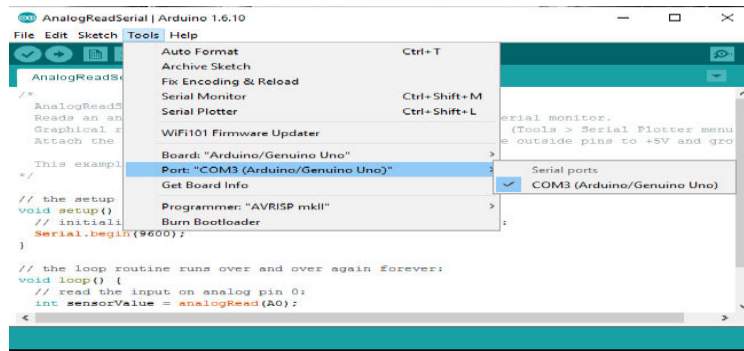


Fig 5.Arduino ide

BLUETOOTH HC05

HC05 module has an internal 3.3v regulator and that is why you can connect it to 5v voltage. But we strongly recommend 3.3V voltage, since the logic of HC05 serial communication pins is 3.3V. Supplying 5V to the module can cause damage to the module. In order to prevent the module from damages and make it work properly, you should use a resistance division circuit (5v to 3.3v) between Arduino TX pin and module RX pin.

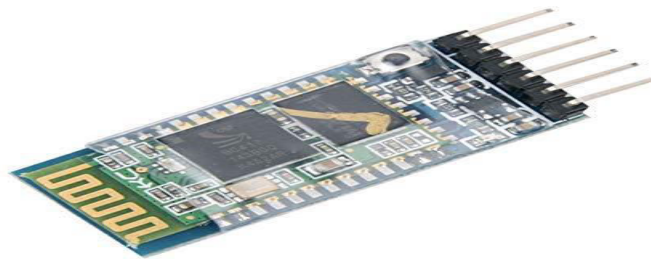


Fig 6. Bluetooth hc 05

ANDROID APPLICATION

Android applications are written in the Java programming language. The Android SDK tools compile the code along with any data and resource files into an Android package, an archive file with an .apk suffix. All the code in a single .apk file is considered to be one application and is the file that Android-powered devices use to install the application. Once installed on a device, each Android application lives in its own security sandbox: The Android operating system, is a multi-user Linux system in which each application is a different user. By default, the system assigns each application a unique user ID (the ID issued only by the system and is unknown to the application). The system sets permissions for all the files in an application so that only the user ID assigned to that application can access them. Each process has its own virtual machine (VM), so an application's code runs in isolation from other applications. By default, every application runs in its own Linux process. Android starts the process when any of the application's components need to be executed, then shuts down the process when it's no longer needed or when the system must recover memory for other applications.

V. RESULTS ANALYSIS

We proposed a cooking system in a shared cooking environment with the user, called Cooky. User can send the instruction to Arduino (smart robotic cooking frame). Smart robotic cooking frame can receive the instruction from mobile app. This robot can cook rice, coffee, tea and vegetables item etc. The user gives cooking instructions to the system such as timing for the ingredients adding, stirring a pot, and controlling an electric cooker. Also, we developed small robots for the actual cooking tasks. The robots perform their tasks according to the user's instructions. We tested the system and confirmed that it successfully cooked a meal with given instructions.



Fig .11(a)Final prototype

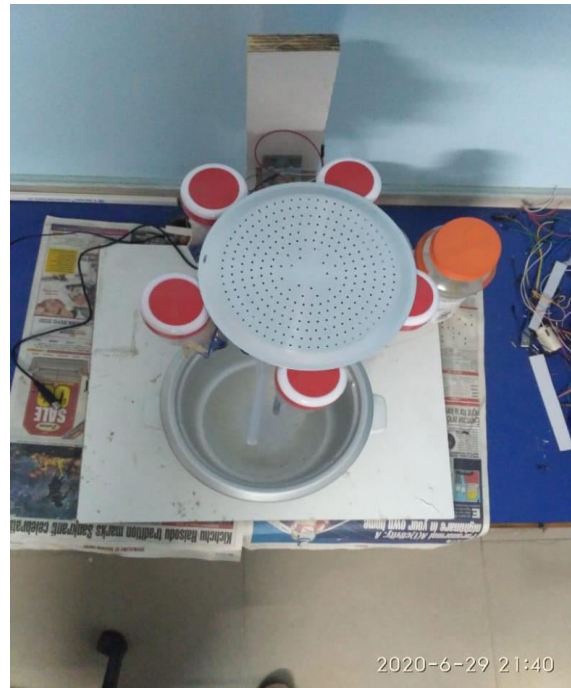


Fig .12(b) Final prototype

VI. FUTURE SCOPE OF THIS STUDY

- To reduce the man power
- Make cooking process automated.
- To maintain the test food quality
- Robotic cook for disable person, elder people, fast-food restaurant who doesn't know how to cook
- They make it easier/help people who are stressed
- Vegetable cutting dicing is a daily domestic task which takes up a lot of time and effort. So here we propose a motorized vegetable cutting machine that does this in a fully automatic manner.
- The users can select the cook/chef as per their interest. The cook might specialize in preparing Indian or maybe something else.
- smart robotic cook is able to manage automatically

VII. CONCLUSION

We proposed a cooking system in a shared cooking environment with the user, called Cooky. The system uses recipes, which include cooking instructions and visual markers; for simple cooking tasks. The user gives cooking instructions to the system such as timing for the ingredients adding, stirring a pot, and controlling an electric cooker. Also, we developed small robots for the actual cooking tasks. The robots perform their tasks according to the user's instructions. We tested the system and confirmed that it successfully cooked a meal with given instructions. The design result is including system design machines, physical machines design, also interface designed that will be embedded in the machine. Later, if this system implemented successfully, this machine will be very helpful in terms of shortening the cooking process. This machine is expected can work automatically so that users do not need to wait from start to finish in cooking process.



REFERENCES

1. Forlizzi, J. How robotic products become social products: an ethnographic study of cleaning in the home. In Proc. HRI2007. ACM (2007), 129-136.
2. Guo, C. and Sharlin, E. Exploring the use of tangible user interfaces for human-robot interaction: a comparative study. In Proc. CHI 2008. ACM (2008), 121-130.
3. Hamada, R., Okabe, J., Ide, I., Satoh, S., Sakai, S., and Tanaka, H. Cooking navi: assistant for daily cooking in kitchen. In Proc. MULTIMEDIA 2005. ACM (2005), 371-374.
4. Kato, F., Shiina, M., Tokizaki, T., Mitake, H., Aoki, T., and Hasegawa, S. Culinary art designer. In Proc. ACE 2008, vol. 352. ACM (2008), 398-398.
5. Kemp, C. C., Anderson, C. D., Nguyen, H., Trevor, A. J., and Xu, Z. A point-and-click interface for the real world: laser designation of objects for mobile manipulation. In Proc. HRI 2008, (2008), 241-248.
6. Nakauchi, Y., Fukuda, T., Noguchi, K., and Matsubara, T. Time Sequence Data Mining for Cooking Support Robot. In Proc. CIRA 2005, No.We-B3-4, 2005
7. Okada, K., Ogura, T., Haneda, A., Fujimoto, J., Gravot, F., and Inaba, M. Humanoid motion generation system on HRP2-JSK for daily life environment. In Proc. ICMA 2005, IEEE (2005), Vol. 4, 29, 1772-1777.
8. Sakamoto, D., Honda, K., Inami, M. and Igarashi, T. Sketch and run: a stroke-based interface for home robots. In Proc. CHI 2009, ACM (2009), 197-200



Hand Gesture Technology Using Image Processing

Faisal Shariff¹, Lohith Kumar², Mahalakshmi M³, Mohd Rehan⁴, Karthik Raj SL⁵

Final year B.E Students(UG) ,Department of Information Science & Engineering, The Oxford College of Engineering, Bangalore,India^{1,2,3,4}

Assistant Professor, Department of Information Science & Engineering, The Oxford College of Engineering, Bangalore,India⁵

ABSTRACT: The project consists of a system used for human-computer interaction (HCI) using simple hand gestures. The system has 3 phases: hand gesture detection, gesture recognition, and command execution. The system allows for better and simplified HCI than that compared to a traditional mouse and keyboard control. The algorithms used are for higher accuracy and faster gesture recognition. This project provides a cost effective and simple interaction than the current 3D based technologies. The gestures can be extended for other purposes which can be further programmed in the computer. During the HCI stage, we develop a simple strategy to avoid the false recognition caused by noises - mostly transient, false gestures, and thus to improve the reliability of interaction. The developed system is highly extendable and can be used in human-robotic or other human-machine interaction scenarios with more complex command formats rather than just mouse and keyboard events.

KEYWORDS: Gesture recognition, human-computer interaction, mouse keyboard control.

I. INTRODUCTION

In this modern era computers are being used by a large number of people and its demand is still growing. In accordance with the Moore's Law, it is being expected that the technology will advance at a very high rate and computers will be in reach of common people. With the advancement in ubiquitous computing the emphasis on use of natural user interface is required. Today mouse, keyboards and pens are not enough for interaction with machines. Gestures are being used in HCI since many years. Earlier, hardware based gesture recognition was more prevalent. User had to wear gloves, helmet and other heavy apparatus. Sensor, actuator and accelerometer were used for gesture recognition. But the whole process was difficult in real time environment.

Recent trend is to use Computer Vision techniques for gesture recognition. Principal component analysis is being used for hand gesture recognition. However, this made the whole system slower and required more memory. For head gesture recognition, Hidden Markov model is being used. But this requires training of head gestures. Many multimodal HCI based system are also being developed, most of them uses a combination of hand and facial expression or hand and speech recognition or facial expression and speech recognition. Very little work in the area of multimodal HCI using hand and head is being done.

The objective of our work is to develop a vision-based multimodal human computer interaction method where hand and head can be simultaneously used to control any computer application. Shape recognition algorithm is being used for hand gesture recognition. Hand contour is being made and the number of defects, orientation and direction of movement of hand is being observed. For head gesture recognition optical flow is being used to observe the direction of movement of head. Thereafter, finite state automata are being used for head gesture recognition.

II. LITERATURE REVIEW

Title: Review on Image Segmentation Based on Colour Space and Its Hybrid [2016]

Author: Maheswari . S

- They proposed an efficient method for capturing images using RGB-HSV hybrid combination rather than RGB or HSV, which provides better information even in poor background with improved color preservation. The RGB colour space is not trust worthy or accurate for computer vision applications. It is hence not suitable for an application like human hand tracking and gesturing.



Title: Hand Gesture Recognition Based on Hog Feature Extraction and K-NN Classification [2017]

Author: Tejashree P. Salunke

- The author proposes a static hand gesture recognition in real-time that facilitates effective and effortless human-computer interaction. This system does not make use of traditional methods for hand gesture recognition such as by using hand-gloves, markers, rings, pens or any other devices.

The image captured from the input data is then processed and then histogram of oriented gradients features is extracted from it. The processed image is then compared with the database of gesture images.

III. PROBLEM STATEMENT

The main problem in the existing system is that user need to be in front of the laptop to use it. If they are busy with some other work and need to any application in the laptop, they need to go in front of the laptop and perform the operation. This causes reduction in user control especially in a productivity and fast environment. There is a need for faster input to a computer and which can be performed from a distance or even remotely. Also there is a need to check if the operation specified by the user is executed and the user can visually verify the output.

IV. EXISTING SYSTEM

The various HCI Interfaces that are being used since earlier times having some demerits. They block the improvement of computer dependent devices or systems. It is now a general tendency to lessen human efforts and overcome the usual, traditionally being used computer dependent devices. There are various technologies which uses different sensors and hardware to control computers. Instrumented data glove approach involves the use of sensor devices to recognize the hand gestures Sixth Sense Technology is a wearable gestural interface. Coloured Markers approaches are gloves that are worn by the human hand.

V. PROPOSED SYSTEM

The proposed system is used to control the mouse cursor and implement its function using a real-time camera. We implemented mouse movement, selection of the icons and its functions like right, left, double click and scrolling. This system is based on image comparison and motion detection technology to do mouse pointer movements and selection of icon. The proposed system is a real time video processing that is based on a real time application system. This can replace one of the traditionally used input device i.e. mouse so that simply by using the hand gestures the user will be able to interact naturally with their computer. The goal is two-fold. First, gesture recognition can complement other forms of human computer interaction (keyboard and mouse), but provides such control at a distance without touch. Second, it can be used as a convenient computer interface to the millions of people who are unable to adequately use typical computer interaction techniques. The system uses a standard windows PC and an inexpensive commercially available USB camera. This arrangement does not require any connection to the user.

A. SYSTEM ARCHITECTURE

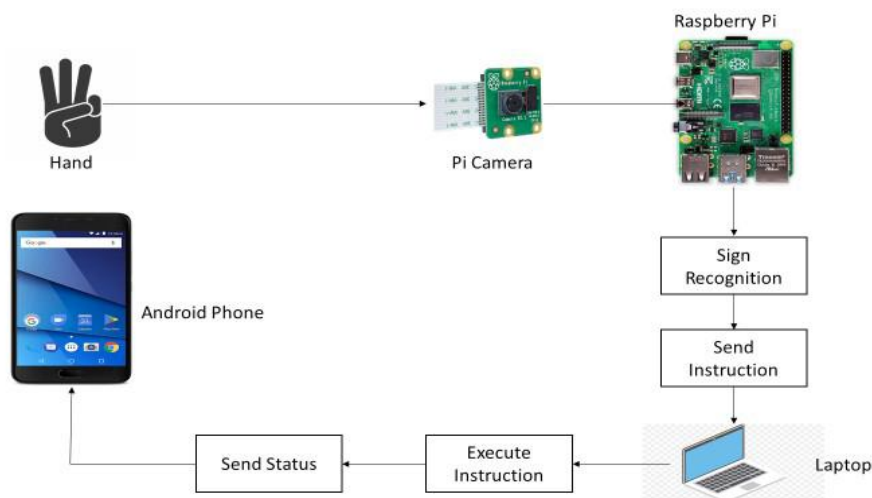


Fig1: System Architecture

The system consists of 5 parts. The hand is used for input to the system in the form of gesture commands. The pi camera is connected to the Raspberry Pi which collects the input and relays it to the Raspberry Pi setup. This is placed in a remote location and can be operated wirelessly. The Pi module processes the image in 5 steps: Input image from webcam, preprocessing and segmentation, feature extraction, classification, and Result analysis. It completes and converts the image in the readable format.

The laptop obtains the processed image and compares it with its trained and tested data samples. On match of the image it executes the operation related to the image and shows the output on the screen. The user if present in a remote location and wish to operate the system can view the output using an android app for verification. After execution of the command the live screenshot is forwarded to the laptop.

B. WORKING

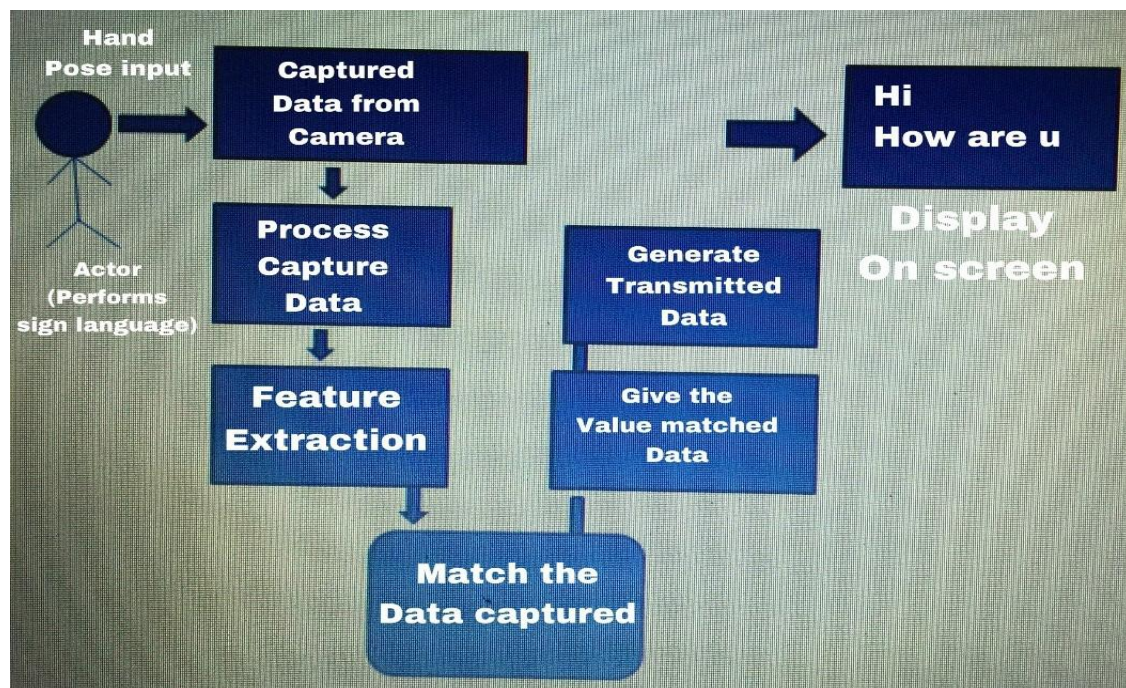


Fig2 : Steps Needed to Process the Gesture Input of the User

The following shows the step by step implementation of the system. These are based on the images shown in the above figure.

The steps start from capturing data from camera, processing data, feature extraction, match captured data, give values of matched data, generate transmitted data and show the output. This is summarized in the following steps:

- 1) The Pi camera is connected to the Raspberry pi.
- 2) The Raspberry pi is connected to a power supply, the Raspberry module then executes the Gesture recognition software.
- 3) The camera setup is positioned and connected to the Apache Tomcat server. The Server-Client Transmit software is run, this creates a connection between the laptop and the Raspberry module so that the module can transmit the final images to the laptop.
- 4) The laptop is also connected to the Tomcat server. The laptop runs a Client-Server receivesoftware which is used to receive the images from the raspberri pi.
- 5) This is hence used to establish a gateway where both the Raspberry pi module and the laptop are connected to the same network ensuring that the images only get transmitted to the laptop.
- 6) The laptop executes the train and test python program. This converts the images into gesture based commands which is already loaded into the laptop.
- 7) These gestures can be to open the browser, execute a script, play a media file or other server based commands.



- 8) The user's hand shows the gestures to the camera, this can be simple commands which is already trained by the system and fed as training data. The hand image is captured and the image is processed.
- 9) The laptop executes the instruction and shows the requested command output.
- 10) The user also receives an acknowledgement via the mobile Android app.

There are two options:

- If the user wishes to see the final output screenshot, this is useful when operation is simple.
- If the user wants to see a process running, then by selecting the View Live can see the operation being streamed to the app from the laptop or computer.

VI.HARDWARE REQUIREMENTS

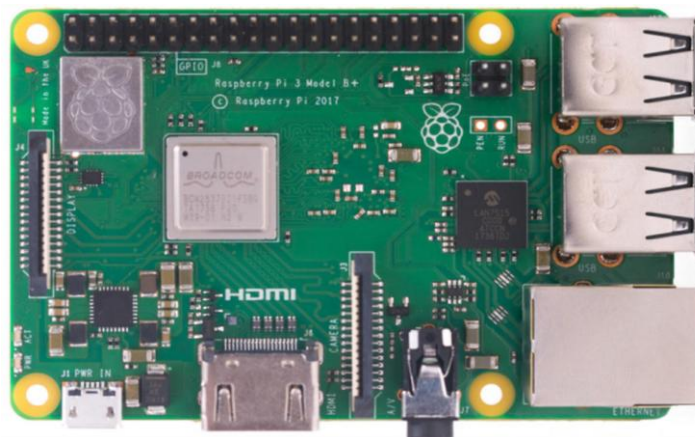


Fig 3 : Raspberry pi

The Raspberry Pi device looks like a motherboard, with the mounted chips and ports exposed, but it has all the components you need to connect input, output, and storage devices and start computing. It is a capable device that enables computing, and used to learn how to program in languages like Scratch and Python.

Here are the various components on the Raspberry Pi board:

- **ARM CPU/GPU** -- This is a Broadcom BCM2835 System on a Chip (SoC) that's made up of an ARM central processing unit (CPU) and a Videocore 4 graphics processing unit (GPU). The CPU handles all the computations that make a computer work (taking input, doing calculations and producing output), and the GPU handles graphics output.
- **GPIO** -- These are exposed general-purpose input/output connection points that will allow the real hardware hobbyists the opportunity to tinker.
- **RCA** -- An RCA jack allows connection of analog TVs and other similar output devices.
- **Audio out** -- This is a standard 3.55-millimeter jack for connection of audio output devices such as headphones or speakers. There is no audio in.
- **LEDs** -- Light-emitting diodes, for all of your indicator light needs.
- **USB** -- This is a common connection port for peripheral devices of all types (including your mouse and keyboard). Model A has one, and Model B has two. You can use a USB hub to expand the number of ports or plug your mouse into your keyboard if it has its own USB port.
- **HDMI** -- This connector allows you to hook up a high-definition television or other compatible device using an HDMI cable.
- **Power** -- This is a 5v Micro USB power connector into which you can plug your compatible power supply.
- **SD cardslot** -- This is a full-sized SD card slot. An SD card with an operating system (OS) installed is required for booting the device. They are available for purchase from the manufacturers, but you can also download an OS and save it to the card yourself if you have a Linux machine and the wherewithal.
- **Ethernet** -- This connector allows for wired network access and is only available on the Model B.



Fig 4 : Pi Camera

Pi Camera

Pi Camera Module. The Pi camera module is a portable light weight camera that supports RaspberryPi. It communicates with Pi using the MIPI camera serial interface protocol. It is normally used in image processing, machine learning or in surveillance projects.

1. ANDROID APP:

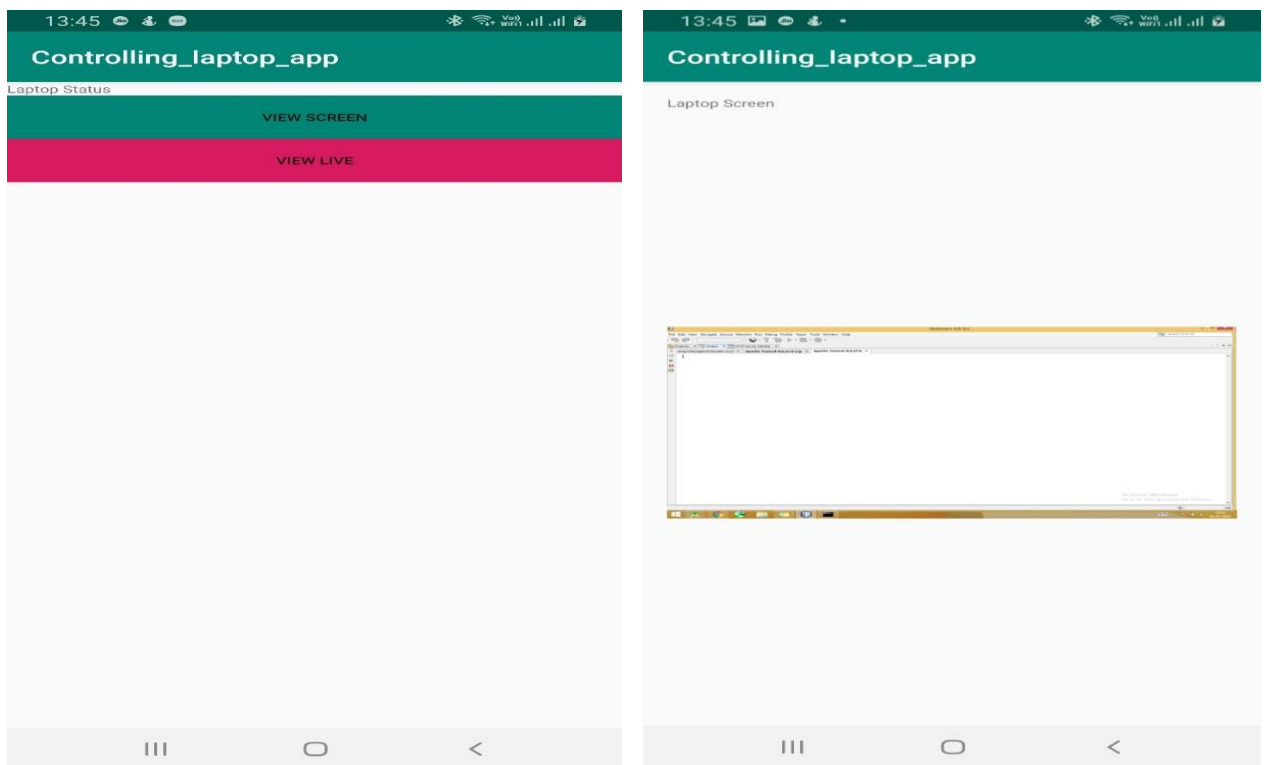


Fig 5 : Android App to display the output acknowledgement

In the figure, the Android App is used to collect the output from the laptop and display it to the user. The first image shows the menu to View the screen and View Live. The second image shows the streaming video of the operation.

VII.RESULT AND IMPLEMENTATION

In this modern world, where technology is at the peak, there are many facilities available for offering input to any applications running on the computer systems, some of the inputs can be offered using physical touch and some of



them without using physical touch (like speech, hand gestures, head gestures etc.). Using hand gestures many users can handle applications from distance without even touching it.

But there are many applications which cannot be controlled using hand gestures as an input. This technique can be very helpful for physically challenged people because they can define the gesture according to their need. The present system which we have implemented although seems to be user friendly as compared to modern device or command based system but it is less robust in detection and recognition as we have seen in the previous step.

We need to improve our system and try to build more robust algorithm for both recognition and detection even in the cluttered background and a normal lighting condition. We also need to extend the system for some more class of gestures as we have implemented it for only 6 classes. However, we can use this system to control applications like power point presentation, games, media player, windows picture manager etc.

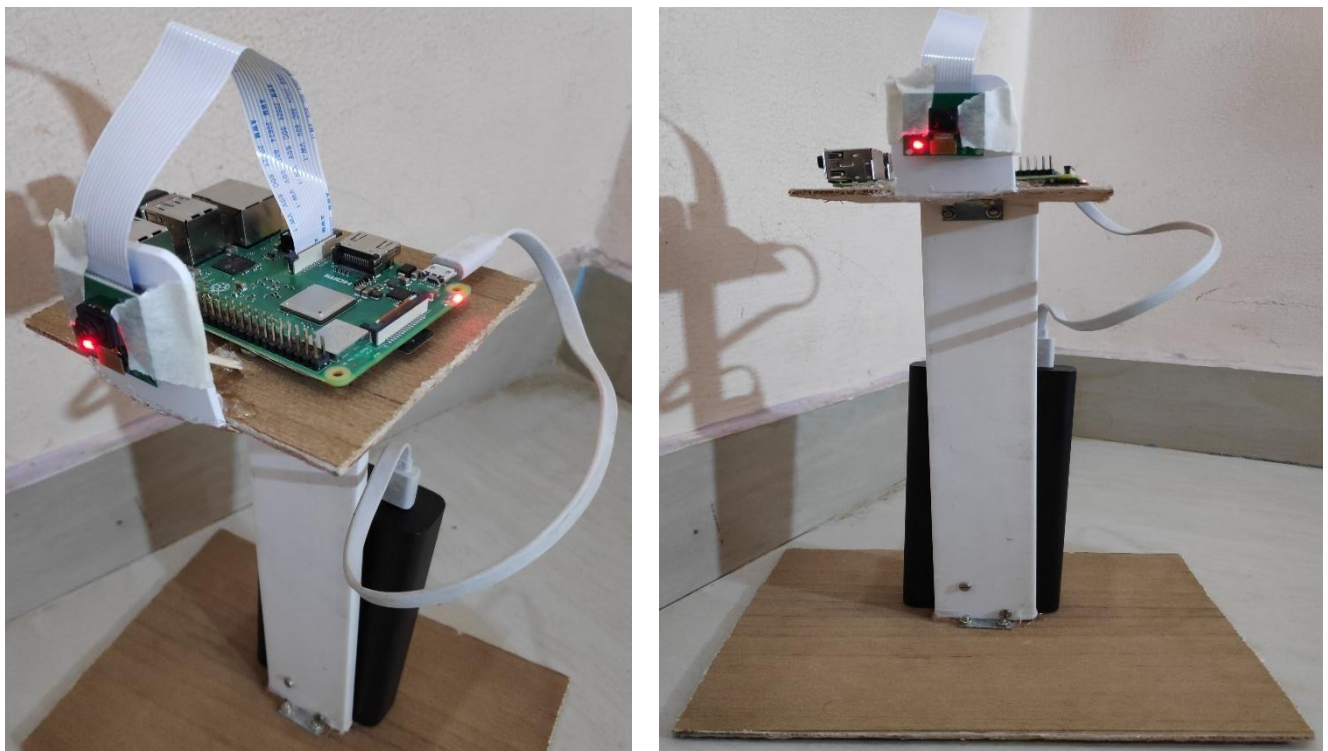


Fig 6 : Shows the setup of the Raspberry image capturing setup

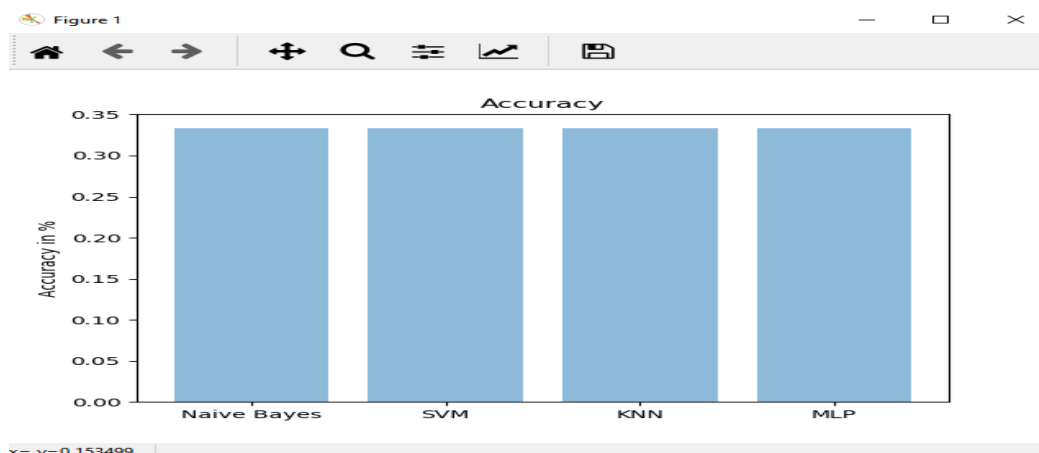


Fig 7 : Shows the accuracy score of training



Fig 8 : Shows the score performed by each Algorithm

VIII.CONCLUSION AND FUTURE WORK

We were able to create a hand gesture recognition system that did not utilize any markers, hence making it more user friendly and low cost. In this gesture recognition system, we have aimed to provide gestures, covering almost all aspects of HCI such as system functionalities, launching of applications and opening some popular websites.

In future we would like to improve the accuracy further and add more gestures to implement more functions. Finally, we target to extend our domain Hand Gesture Technology Using Image Processing scenarios and apply our tracking mechanism into a variety of hardware including digital TV and mobile devices. We also aim to extend this mechanism to a range of users including disabled users.

REFERENCES

- [1] S. S. Rautaray and A. Agrawal, "Interaction with virtual gamethrough hand gesture recognition."2011 International Conferenceon Multimedia, Signal Processing and CommunicationTechnologies(IMPACT), 2011, pp. 244–247.
- [2] D. Avola, M. Spezialetti, and G. Placidi, "Design of an efficientframework for fast prototyping of customized human–computerinterfaces and virtual environments for rehabilitation,"ComputerMethods and Programs in Biomedicine, vol. 110, no. 3,pp. 490 – 502, 2013.
- [3] G. Placidi, D. Avola, D. Iacoviello, and L. Cinque, "Overall design and implementation of the virtual glove," Computers inBiology and Medicine, vol. 43, no. 11, pp. 1927–1940, 2013.
- [4] W. Lu, Z. Tong, and J. Chu, "Dynamic hand gesture recognitionwith leap motion controller," IEEE Signal Processing Letters,vol. 23, no. 9, pp. 1188–1192, 2016.
- [5] G. Marin, F. Dominio, and P. Zanuttigh, "Hand gesture recognitionwith jointly calibrated leap motion and depth sensor,"Multimedia Tools Appl., vol. 75, no. 22, pp. 14 991–15 015, 2016.



USB to USB Data Transfer using Raspberry Pi

Rachana R¹, Rashmi Srikanth Shanbhag², Shilpa J³, Spoorthi P⁴, Kokila P⁵

Final year B.E Students (UG), Department of Information Science & Engineering, The Oxford College of Engineering,
Bangalore, India^{1,2,3,4}

Assistant Professor, Department of Information Science & Engineering, The Oxford College of Engineering,
Bangalore, India⁵

ABSTRACT: The purpose of the proposed system is to describe the efficient data transfer between pen drives without the support of PC. Now day's portability is most important. Utilizing the system one can not only transfer the data but also transfer the particular file which is to be sent by using LCD display. Currently to transfer data between two USB device we use PC or laptop, but it is not always possible to carry such a large device only for the data transfer. So to overcome the problem a system is designed, which is more compact. In the proposed system, transfer of data between two USB devices is done without using any computers or laptops. As shown in the block, whenever two pen drives are inserted into the USB port of Raspberry Pi, as done by giving the command to the processor, the processor indicates that the pen drive is inserted successfully till the user can not send any command to processor, the operation will not be initiated. After sending the particular command to processor, the processor will start fetching the data from source pen drive into buffer and the ARM processor wait for the signal from destination pen drive. When the processors receives the signal from destination pen drive, the data transfer operation will start. Only the ARM processor should get the external hard key input signal from the user. Once the user press the hard key the ARM processor get the information to transfer the data between two pen drive. While transferring the data the LED blinking rate will be increased when data transfer is completed then LED will stop blinking. The total operation is performed on the Raspberry Pi board by using a "Raspbian" operating system.

KEYWORDS: USB to USB, Without PC, Raspbian OS.

I. INTRODUCTION

Today the need for the portable devices is well known to us. One can easily find the USB and its applications everywhere around us. The applications of the USB are computer peripherals such as keyboard, pointing devices, digital cameras, printers, portable media players, disk drives and network adapter, both to communicate and to supply electric power. It has become common place on other devices, such as smart phones, PDAs and video game consoles. USB has effectively replaced a variety of earlier interfaces, such as serial and parallel ports, as well as separate power chargers for portable devices. But the main disadvantage of USB devices is that it requires the use of PC for their operation. Carrying a PC just for the sake of data transfer is not affordable these days in the age when people want all devices to be handy. Moreover, transferring data via a computer involves a lot of power to be wasted. Also, the threat of viruses and malware has made the life of computer users more complicated. These viruses get activated as soon as the device is plugged into the system and get copied along with other data from one device into another. So a solution is provided by means of implementation of a small device that carries out the required task. The small footprint and ease of portability makes it a choice for the data transfer. This device will help the user to select a particular data file from the mass storage device connected to one of the ports and transfers it to the other mass storage device using some controls like list, copy provided on the front panel.

The main objective is to design and implement a cost friendly device to effectively transfer data without using pc, from one pen drive to another pen drive. It is a portable device which ensures data transfer securely. Aims at evaluating feasibility and performance. The system is designed in such a way that it assures no loss of data, is simple and easy to adapt.

Problem Statement- Nowadays the transfer of data between two PC's can be done with either net access or LAN network, but transfer of data between PC's is not secured. For transferring data between pen drives in general we require PC's. Disadvantage of an existing system – we can transfer the data from one place to another place by using net access, but if we transfer the data between PC's the data is not secured and also it requires two PC's to communicate. Moreover, transferring data via a computer involves a lot of power to be wasted, since the computer has to be entirely before it can transfer data. Also, the threat of virus and malware has made the life of computer users more



complicated. These viruses get activated as soon as the device is plugged into system and get copied along with other data from one ash device into another.

Proposed System- this project here can provide a valuable solution to all the problems faced by a person in the existing system. The aim of the project is to build a small and handy device to transfer data from one USB device to another.

This system pen drive to pen drive data transfer without PC is done by using raspberry pi. The pen drives are connected to USB module through USB hub, the communication between two pen drives is done by using raspberry pi.

The purpose of this paper is to describe the efficient data transfer between pen drives without the support of PC. The probability of the device is achieved using a small credit-card sized, yet a powerful computer, Raspberry Pi. Raspberry Pi is responsible for the execution of the main software and display of the render images on the screen. This paper includes literature review and commentary on this topic that has been addressed by professionals, researchers and practitioners. Effective data transfer between the drives without PC achieved with a good speed estimate is valuable. The value in addressing this topic is to examine the notion of efficient transfer of data without PC and its suggested uses in various fields to ensure accurate performance, portability and usability.

II.PROBLEM STATEMENT

Nowadays the transfer of data between two PC's can be done with either net access or LAN network, but transfer of data between PC's is not secured. For transferring data between pen drives in general we require PC's .Disadvantage of an existing system – we can transfer the data from one place to another place by using net access, but if we transfer the data between PC's the data is not secured and also it requires two PC's to communicate. Moreover, transferring data via a computer involves a lot of power to be wasted, since the computer has to be entirely before it can transfer data. Also, the threat of virus and malware has made the life of computer users more complicated. These viruses get activated as soon as the device is plugged into system and get copied along with other data from one ash device into another.

III.PROPOSED SYSTEM

This project here can provide a valuable solution to all the problems faced by a person in the existing system. The aim of the project is to build a small and handy device to transfer data from one USB device to another. This system pen drive to pen drive data transfer without PC is done by using raspberry pi.The pen drives are connected to USB module through USB hub, the communication between two pen drives is done by using raspberry pi.

IV.METHODOLOGY

Transfer of data through USB in today's scenario is the very easy task. But the problem is that to transfer the data to a personal computer or laptop is not easy if you don't have one or the only intention is transfer data.

So to overcome this problem we implement device using the following :-

1. Initial Setup:

In this system, the user inputs two pen drive i.e., source pen drive and destination pen drive. Selects the desired file or folder to be transferred, which will be displayed on the screen. The progress of the data transfer destination pen drive. Selects the desired file or folder to be transferred, which will be displayed on the screen. The progress of the data transfer will be displayed on the screen so that the user might take further actions based on it.

2. Detection of Pendrive:

The Raspberry pi has the two USB port and it has the central host controller. The host controller manages attachment and removal of USB devices Manage data flow between host and devices Provide and manage power to attached devices monitor activity on the bus. The 2.0 USB connector are connected to the ARM processor this two USB port are used to connect the other device such as keyboard, mouse, and external hubs. For communication it's most important to connect the two pen drives into the USB ports of controller. When it connects to the system first it does the job of initialization and then we provide the option such as copy, paste, cut etc. by using switches for dealing with the data.

3. Display of Data:

The touch screen is used which is of 10" tablet with high quality IPS screen, a great 1280×800 resolution, capacitive multi-point touch screen and uses Raspberry Pi as a heart. The contents of the mass storage device are displayed on the touch screen. This helps the user to view and select the files or folders of interest from the USB device. Also the options like select, copy for data transfer are put on to the touch screen. It displays the start and finish of the data transfer.

4. User Interface:

This module obtains the user input and displays the user requested information through a touch screen. It has three major blocks, the touch screen Controller, Navigation and Screen Display Formatter. The touch screen is used to select



the file and displays the path or Long File Name (LFN) format of a file or directory. The inputs from the touch panel are used to execute the operation to be performed. All the content on touch panel are displays the information of the USB drive.

5. Data Transfer:

Universal Serial Bus (USB) is a master- slave device which is made up of many slaves and a single master. The slaves are called the peripherals and the master is the host. Only the host has the ability to begin data transfer. The slaves cannot initiate data transfer. They only respond to the master’s instructions. A USB device can have 32 connections- two of which are reserved for giving Ack. So a total of 30 are present for normal use for the data transfer in bidirectional manner.

V.SYSTEM ARCHITECTURE

A good system design is to organize the program modules in such a way that are easy to develop and change. Structured design techniques help developers to deal with the size and complexity of programs. Analysts create instructions for the developers about how code should be written and how pieces of code should fit together to form a program.

Several structural design considerations should be taken into account for economical and efficient welding. Many of these apply to other joining methods, and all apply to both subassemblies and the complete structure. The architectural design of a system emphasizes the design of the system architecture that describes the structure, behaviour and more views of that system and analysis.

The architecture of a system describes its major components, their relationships (structures), and how they interact with each other. Software architecture and design includes several contributory factors such as Business strategy, quality attributes, human dynamics, design, and IT environment. We can segregate Software Architecture and Design into two distinct phases: Software Architecture and Software Design. In Architecture, non-functional decisions are cast and separated by the functional requirements. In Design, functional requirements are accomplished.

VI.BLOCK DIAGRAM AND ITS COMPONENTS

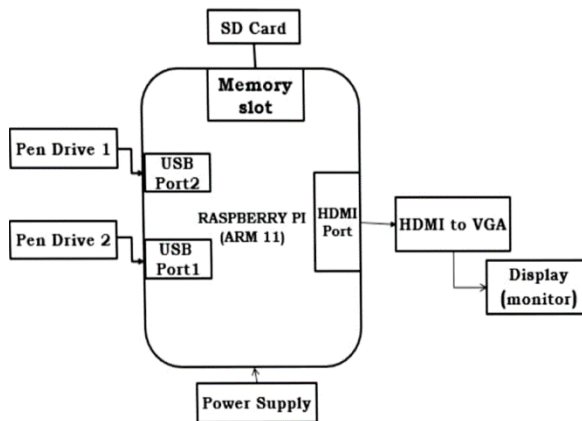


Fig. 1 Block diagram

A block diagram is a graphical representation of a system – it provides a functional view of a system. Block diagrams give us a better understanding of a system’s functions and help create interconnections within it. Block diagrams derive their name from the rectangular elements found in this type of diagram. They are used to describe hardware and software systems as well as to represent processes. Block diagrams are described and defined according to their function and structure as well as their relationship with other blocks.

Block diagram can represent Source, destination, storage and flow of data using the following set of components:-

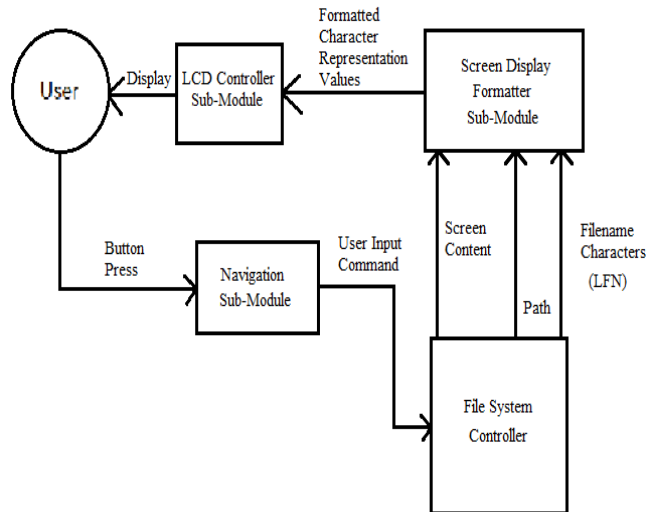


Fig. 2 User Interface Controller Module Block Diagram

1. User Interface Controller Module: This module obtains the user input and displays the user requested information through a touch screen. It consists of three sub modules namely the touch screen Controller, Navigation and Screen Display Formatter. The touch screen is used to select the file and displays the path or Long File Name (LFN) format of a file or directory. The inputs from the touch screen are converted to their corresponding command codes and are forwarded to the File System Controller module for execution. All information to be displayed is received from the File System Controller module.

A. Touch screen Controller: The touch screen controller is used to interface the touch screen to the main hardware system. It has two USB ports and ARM7 controller which consists of driver files for the touch screen.

B. Navigation: The Navigation sub module is the input handling hardware of the system. It sends corresponding signal for each touch pressed to the microcontroller that controls the touch screen so that it could update the screen and/or send commands to the File System Controller module for processing.

C. Screen Display formatter: The Screen Display formatter is the software part of the User Interface module. It arranges and orders the contents of the touch screen. It formats the screen to display the appropriate option menus, folder contents, path names, content type (folder or file).It receives the names of the files and folders to be displayed from the File System.

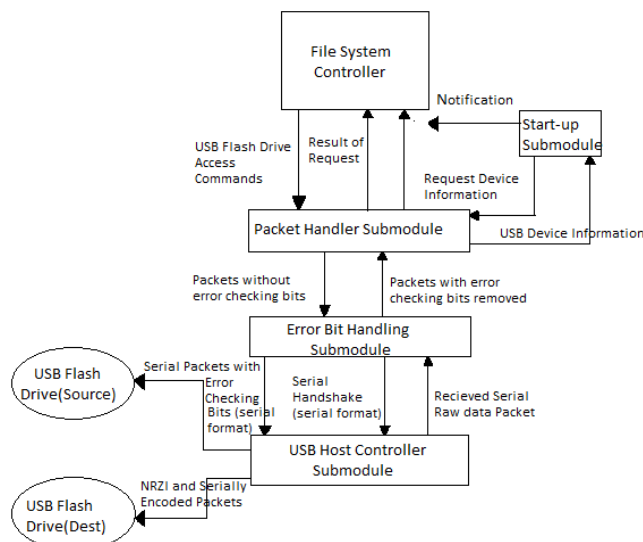


Fig. 3 USB Host Controller Module Block Diagram

2. USB Host Controller Module: The USB Host Controller sub module is the main hardware used by both the USB Controller Module and the File System Controller Module. It interfaces the USB flash drives and converts raw data and



information to their proper NRZI encoding as specified by the USB technical specifications. Furthermore, the sub module is capable of encoding or decoding the incoming NRZI data from the USB flash drives and forwards it to their respective sub modules for further processing. The system uses the Raspberry pi, a programmable microcontroller and USB multi-role embedded host /peripheral controller, which has its own Basic Input/output system and framework program. Most of the software sub modules make use of the available framework where the functions are already abstracted and simply need to be enabled and customized depending on the application.

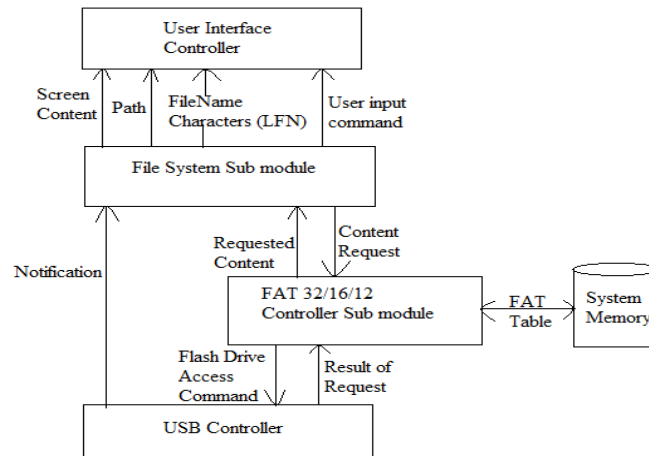


Fig. 4 File System Controller Module Block Diagram

3. File System Controller Module: The File System Controller is responsible for all file management processes and FAT file system access for the system. It mediates between the display/user interface and USB communications module. A large percentage of the systems software is found in this module, contains most of the systems core functions. The major commands handled by the sub module include the navigation touch screen and the different functions like copy, delete, browsing through files/folders and the back command.

VII.IMPEMENTATION

The data transfer is having four types:

- Interrupt transfers:** For the devices needing quick but guaranteed response. For the files up to 20 KB this type of data transfer will take place (e.g. small text file).
- Isochronous transfers:** For some fixed data rate but data loss may take place. For the files between 20 KB and 1024 KB this type of data transfer will take place
- Control transfers:** used for simple status check.
- Bulk transfers:** uses available bandwidth with no fixed data rate. For the files more than 1024 KB this type of data transfer will take place (e.g. file transfer).

6. Implementation Algorithm:

The Implementation Algorithm is as follows

- 1) Select the suitable development board.
- 2) Check whether the OS is ported or not
- 3) Connect the USB device to check functionality
- 4) Inter face the touch screen and keypad as a User interfaces.
- 5) Check the communication between the USB device and the board.
- 6) Explore the device content son touch screen.
- 7) Select a particular file, and by using the option COPY, copy that file to destination device Move Button on touch screen.
- 8) The selected file is then copied into destination USB device that is connected in one of the two USB ports.
- 9) If another copy operation is to be performed, then go to step 7.
- 10) Terminate the process.

VIII.RESULT

The project undertaken satisfies the needs of the current generation that requires portable means of carrying data transfers. The important thing is data transfer is done without the involvement of PC. It also provides much security as



Linux is a much secured Operating System. It has been developed by integrating features of all the hardware component & software used, using advanced raspberry pi board & with the help of growing technology the project has been successfully implemented. The advantage of this device is that it is battery operated, so there is no need of connecting power supply & data transfer can be take place at any time.

IX.CONCLUSION AND FUTURE WORK

Transferring the data through USB in today's scenario is the most common task. But the problem is that for transferring the data to a personal computer or laptop is difficult if you don't have any of them. Therefore, we came up with an easy and affordable device which can transfer the data between two USB data drives without the help of PC or laptops. For future work Keypad and graphical LCD could be replaced by touch screens which could make human work easier by drag and drop method. And it can It can be implemented with photocopier machine.

REFERENCES

- [1] Rohan Kulashresta, Rajeev Ranjan, Shreyas Barati , Rakesh M, Vibha T G. Wireless Data Transfer Of USB Devices Using Wifi Technology: International Journal of Advanced Scientific Research and Management, Vol. 2 Issue 7, July 2017.
- [2] VanaparthiUpendhar, Anand Babu. Device - to - Device communication (Pen drive) without PC: UpendharVanaparthi, Babu Anand, International Journal of Advance Research, Ideas and Innovations in Technology.
- [3] PushpakDhangar, Sonam Kanade, Aishwarya kute, Kavita Labhade. Implementation Paper On Data Transmission And Reception Using Raspberry Pi: International Journal of Scientific Research Engineering & Technology (IJSRET), ISSN 2278 – 0882 Volume 5, Issue 6, June 2016.
- [4] Rupali C. Bachalkar, Shrutika D. Durge, Purvaja V. Pote, Sapana V. Ajmire, Prof. Reetesh V. Golhar. Data Transfer between Two Pendrives without PC: International Journal of Advanced Research in Computer Science and Software Engineering, Volume 5, Issue 1, January 2015.
- [5] Singh Harpreet , Kaur Kamaldeep. Flash Drive Communication Using Embedded System: International Journal Of Engineering And Computer Science ISSN:2319-7242 Volume 3 Issue 2 February,2014 Page No. 3947-3950.
- [6] Tushar Sawant, Bhagya Parekh, Naineel Shah. Computer Independent USB to USB Data Transfer Bridge: 2013 Sixth International Conference on Emerging Trends in Engineering and Technology.
- [7] Ms. Disha Juriasinghani, Mr. Tanay Krishna Dev / International Journal of Engineering Research and Applications (IJERA) ISSN: 2248-9622 www.ijera.com Vol. 2, Issue 1,Jan-Feb 2012, pp.798-800.
- [8] Prof. Rakesh R. Yadav, Prof. Monali Patil, Prof. Vijay Gupta. USB to USB Data Transfer without Pc: International Journal for Research in Applied Science & Engineering Technology (IJRASET) ISSN: 2321-9653; IC Value: 45.98; SJ Impact Factor: 6.887 Volume 5 Issue IX, September2017- Available at www.ijraset.com.



Virtual Technology for Library Using VR Box

Ramya S¹, Gnanalaxmi S², Sargam P³, Smitha T C⁴, Madhusmitha,⁵

Final year B.E Students(UG), Department of Information Science & Engineering, The Oxford College of Engineering,
Bangalore, India^{1,2,3,4}

Assistant Professor, Department of Information Science & Engineering, The Oxford College of Engineering,
Bangalore, India⁵

ABSTRACT: This paper describes the design and the development of hardware and software of a portable Virtual Reality Headset. The portability of the device is achieved using an Android smart phone. It is responsible for the execution of the main software and display of the rendered images on the screen. The Inertial Measurement Unit (IMU) present in the device tracks the user's head movements and communicates with Android smart phone. This technology focuses on developing a dedicated hardware platform for the Virtual Reality purposes. Throughout the design phase of the project, cost was kept minimal without compromising on the performance of the system.

KEY WORDS: VR, Virtual Reality, 3D, Online Book Reading, VR Library.

I. INTRODUCTION

VR library is a new type of library based on the new technology of digital, network-based, intelligent and the new concepts of management, which has gradually become the future library model. Generally, VR library has three characteristics: interconnectivity, efficiency, convenience, which is the product of the information age along with the technology of cloud computing, big data, Social Local Mobile (SoLoMo), wearable technology and virtual reality. In recent years, with the development of information technology, virtual reality (VR) technology has been applied in the military, entertainment, education, business and other fields. VR technology was proposed by Jaron Lanier, the founder of the VPL Company in United States in the 1980s, also known as virtual technology or artificial illusion. VR technology aims to improve the experience of human computer interaction by comprehensive computer graphics, artificial interaction, sensor and artificial intelligence technology. The users interact with the virtual world in a natural way in 3D virtual environment to achieve real visual, tactile, auditory and factory experience. We intend to use the VR technology to develop a virtual library system. The system realize the virtual library scene construction, virtual roaming and scene interaction and book retrieving by connected with the library management system to realize book location require and other functions.

II. PROBLEM STATEMENT

In designing any kind of learning environment, there are a number of issues one has to consider. In designing a learning environment based on new and relatively unexplored tools, such as virtual reality (VR), these issues become even more complex. These systems require a processor with a good computational power and a Graphic Processing Unit (GPU). Due to the above-mentioned constraints, the user cannot move around wearing the headset.

III. PROPOSED SYSTEM

We propose a virtual reality system in which the user will be having immersive experience for exercising in 3D world. Live streaming of the video could be done with the help of Android smart phone. The device will capture the images or videos from camera and place these images or videos in background to render in real-time. This will enable superimposing the real and virtual world images, thereby giving an entirely new viewing experience. This system creates a visual sensation to the user in the form of virtual or mixed reality. The rendered images are updated on the screen of the Head Mounted Display (HMD) according to the movement of the user. The architectural configuration procedure is concerned with building up a fundamental basic system for a framework. It includes recognizing the real parts of the framework and interchanges between these segments. The beginning configuration procedure of recognizing these subsystems and building up a structure for subsystem control and correspondence is called



construction modeling outline and the yield of this outline procedure is a portrayal of the product structural planning. The proposed architecture for this system is given below. It shows the way this system is designed and brief working of the system.

The step by step process how the Virtual box works is given

1. First the images and videos which need to be displayed are stored in the web app along with its information. The application can be used in any smartphones.
2. The app is connected to the monitor of the virtual box using a Bluetooth. The book selected by the user is transferred through the Bluetooth to be displayed in the virtual box.
3. There is a Android smart phone placed on the monitor. Once the Android smart phone receives the instructions from the android based mobile app, those instructions are applied on the selected book and displayed in the virtual box.
4. The user can change the book using hand gestures without the help of the mobile app.
5. Based on the instructions given by the user the contents of books are modified using the python program in the Android smart phone and is displayed in the virtual box.
6. When the change button is pressed through hand gesture the instruction is given to the virtual box and the respective books are displayed.
7. The client side shows the user the respective scene roaming and the respective book the user clicks is displayed.
8. The server side stores the data about the user, model, scene and book details which acts as a database

IV. IMPLEMENTATION, HARDWARE AND SOFTWARE

A. Implementation

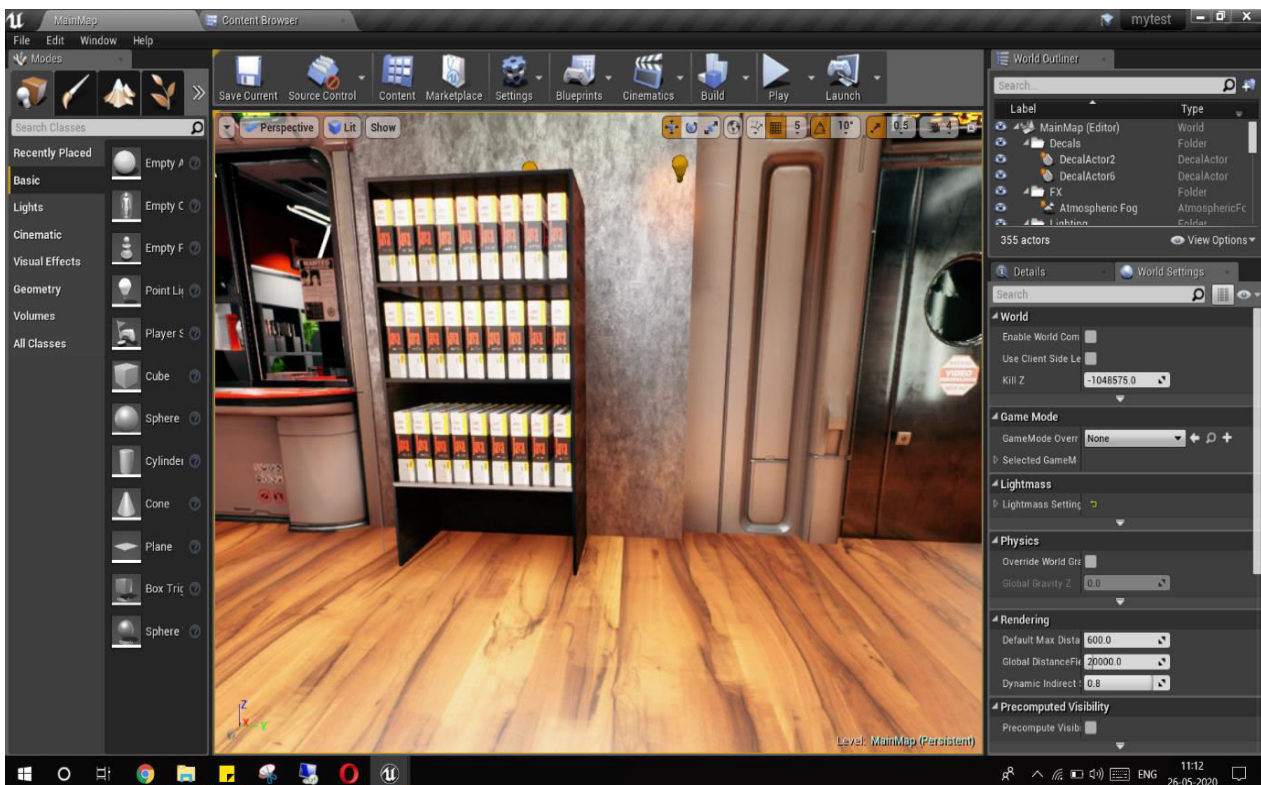


Fig: Library Design Page

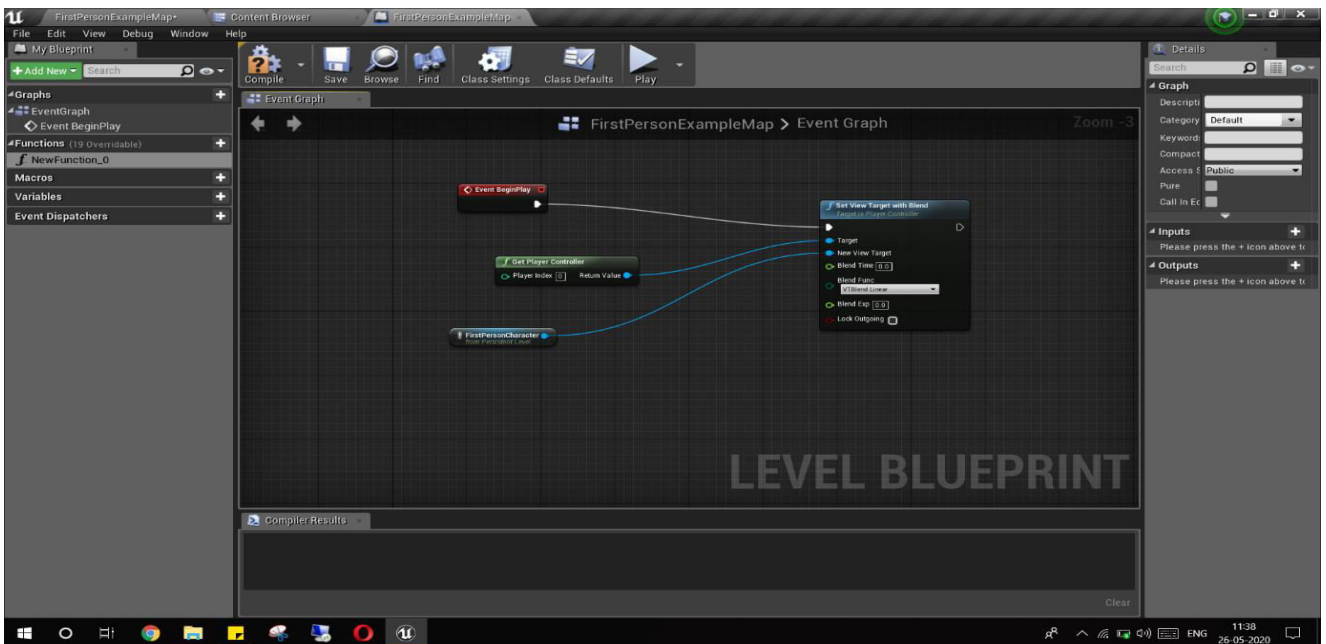


Fig: Blueprint Design Page

Home Page:

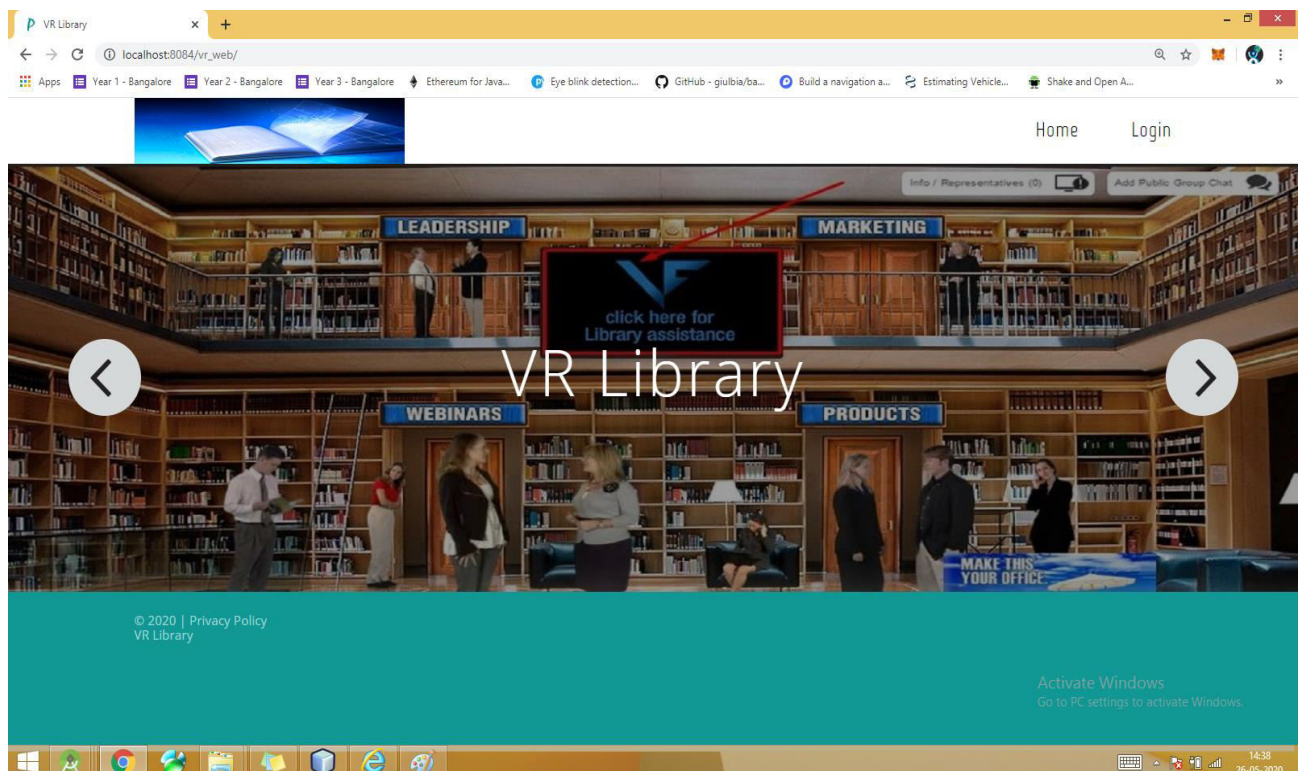


Fig: Home Page



Login page:

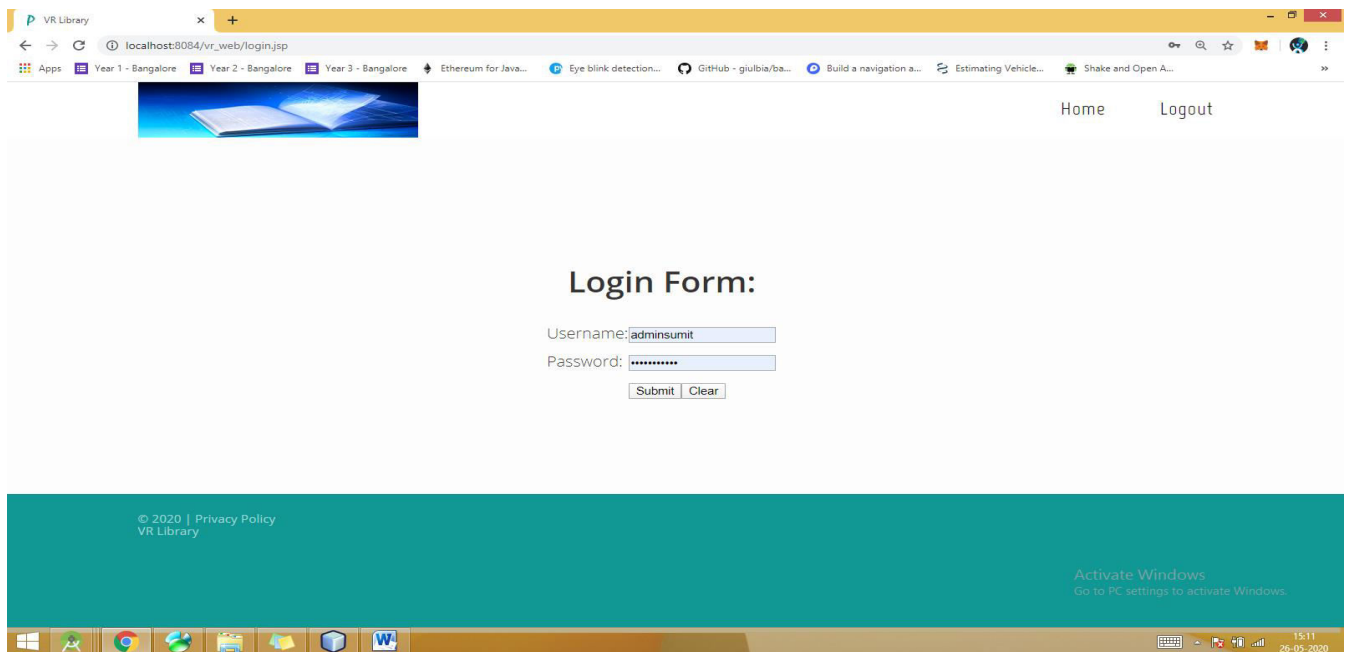


Fig: Login page

Admin Home Page:

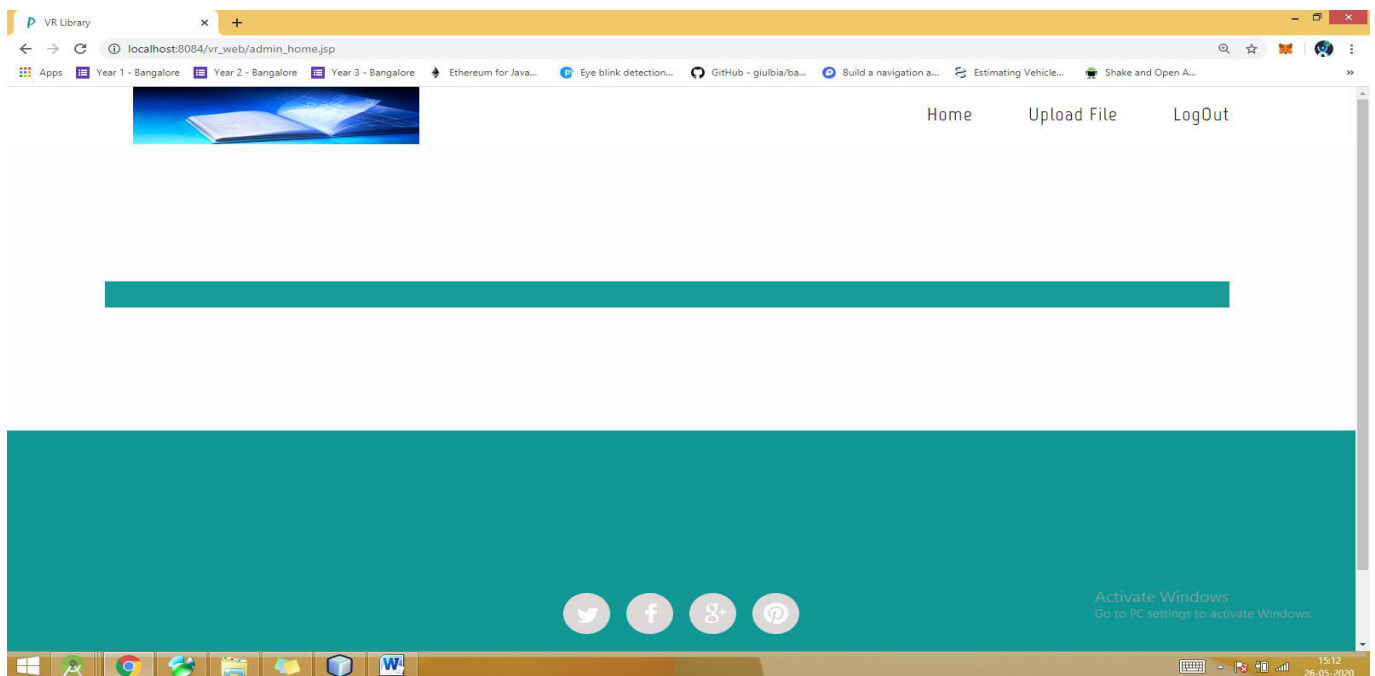


Fig: Admin Home Page



Upload E-Book Page:

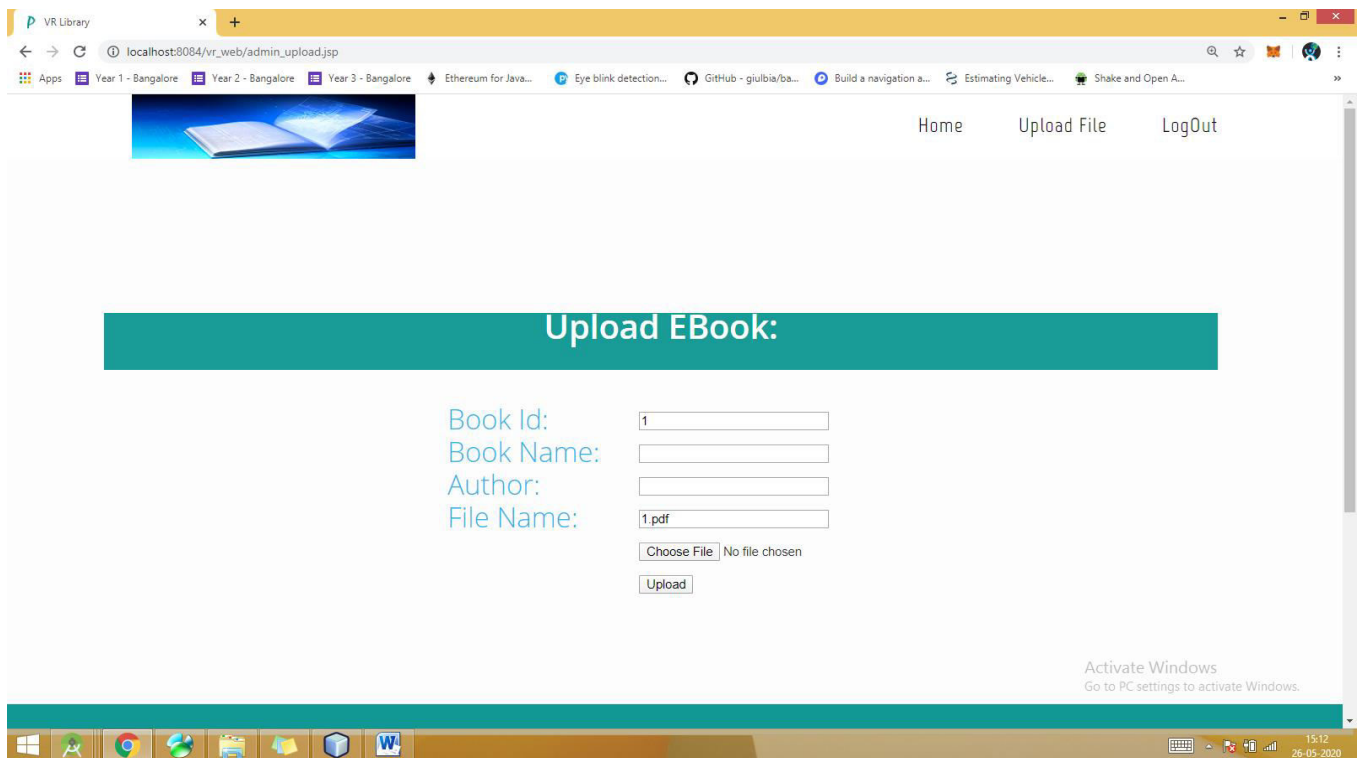


Fig: Upload E-Book

B. Hardware requirements

- System : Intel i5 3 GHZ
- Memory : 8GB.
- Hard Disk : 250 GB SSD
- GPU : NvidiaGforce GTX1050Ti
- Arduino, Node MCU
- ADXL
- Android Phone
- Power supply

C. Software requirements

- Operating System : Windows 10.
- Language : Java, Python, C
- Tool : Unreal Engine 4, Netbeans IDE

V. RESULT ANALYSIS

The result of the project mainly focuses on providing the user with virtual experience of the library. The hardware result which will focus on how the device is running displaying the book selected, if the goal is being achieved properly. And the software result which will focus on storing the books and graphical view of library required to be displayed along with its information to be displayed in the VR box.



Fig: VR BOX

VI. CONCLUSION

The key motivation for developing this product was to design and develop a dedicated hardware and software for VR purposes to make portability possible. Available devices use either the phone's processor and display or Personal Computers' hardware. The next version of the device will be developed with better display to address the problem of aliasing. Even the casing design for the device will be optimized for shape and mass. We also plan to incorporate cameras in the device to make AR possible. The device will capture the images from camera and place these images in background to render in real-time. This will enable superimposing the real and virtual world images, thereby giving an entirely new viewing experience.

REFERENCES

- [1] K. S. Hale and K. M. Stanney, Handbook on Virtual Environments, 2nd edition, CRC Press, 2015.
- [2] Steaven M. Lavelle, Virtual Reality URL: <http://msl.cs.uiuc.edu/vr/>, 2015.
- [3] <https://www.oculus.com/en-us/>, 2015.
- [4] <http://www.htcvive.com/us/>, 2015.
- [5] <https://www.playstation.com/enin/explore/ps4/features/playstation-vr/>, 2015.
- [6] <https://www.visusvr.com/>, 2015.
- [7] William R. Bussone, Linear and Angular Head Accelerations in Daily Life, URL : <http://scholar.lib.vt.edu/theses/available/etd-08182005-222028/unrestricted/thesis.pdf>, 2005.
- [8] InvenSense, "MPU-6000 and MPU-6050 Product Specification Revision 3.4", URL : http://store.invensense.com/datasheets/invensense/MPU6050_DataSheet_V3%204.pdf, 2013.
- [9] Arduino, "Arduino Uno", URL: <https://www.arduino.cc/en/Main/ArduinoBoardUno>, 2015.



Automated Beach Security System using Autopilot Drone

¹Arpitha P, ²Hemalatha R, ³Hindu Priya C, ⁴Kavitha C, ⁵Ms.P Kokila,

^{1,2,3,4}Final year B.E Students (UG), Department of Information Science & Engineering, The Oxford College of Engineering, Bangalore, Karnataka, India

⁵Assistant Professor, Department of Information Science & Engineering, The Oxford College of Engineering, Bangalore, Karnataka, India

ABSTRACT: Beach is the most attractive holiday spot to visit, over 35% of people in the India visit beach every year and witnessing 9% of drowning accidents per annum. The life-guards saves the drowning victim when the lifeguard spots the victim and reaches out there which takes a mean time of 240 minutes. This paper presents the design of the lifesaving system using the autopilot drone which delivers life-rings to victim; thus, the victim survives long enough until the lifeguard reaches them. The proposed system focuses on identifying the RIP Current and the drowning victim using Machine learning classification algorithms and trigger an action like Broadcasting the emergency situation to Life guard and dropping a life ring using drone. Thus, The Automated beach security system using autopilot drones results in a reduction in mean time to reach a victim and increasing the probability of a successful rescue from 93.2% to 99.6%.

KEYWORDS: video processing, autopilot drone, drowning, machine learning algorithms.

I. INTRODUCTION

Drones are an emerging technology as such there is a lot of research on potential applications. With the amount of weight, a drone can carry and with the speed a drone can travel, they seem ideal for emergency and fast responder work and hence drones were chosen to the rescue of drowning victims in hopes of saving lives.

Machine Learning has been great advancement in the field of technology, Machine learning is the brain where all the learning takes place. The way the machine learns is similar to the human being. Humans learn from experience. The more we know, the more easily we can predict. Machines are trained the same. To make an accurate prediction, the machine sees an example. When we give the machine a similar example, it can figure out the outcome. The core objective of Machine Learning here is to find the people who are swimming in RIP Currents and classify whether the person is drowning or not using the classification algorithms. This makes 24/7 observance on the beach through a fixed camera and if a drowning victim is detected it triggers the live location of the victim to drone. The paper enhances in automating the beach security process using the advanced technologies which are mentioned above such that it is more efficient than the existing manual beach security process.

II. LITERATURE SURVEY

The research was done on various aspects to find the existing system and drone laws in India and found few papers related and accepted universally, few of them are listed below

Design of the Life-Ring Drone Delivery System for RIP Current Rescue

Authors: Gang Xiang, Andrew Hardy, Mohammed Rajesh And Lahari Venuthurupalli.

The manually operated drone delivers the life ring to the drowning victim, System dynamics, UAV, stochastic simulation etc. were the methodologies

Drone laws in India with new updates in 2019 According to the Ministry of Civil Aviation, Govt. of India flying a drone is legal in India, the drone then according to the Drone Laws in India you must have to register your drone with the respective authority like [Digital Sky](#).

An Automatic Video-based Drowning Detection System for Swimming Pools Using Active Contours

Authors: Nasrin Salehi and Maryam Keyvanara and Seyed Amirhassan Monadjemmi.

In this paper, a real time drowning detection method based on HSV color space analysis is presented which uses prior



knowledge of the video sequences to set the best values for the color channels, HSV Color Space Analysis, Contour Detection were the methodologies.

Oceanography is an Earth science covering a range of topics, including ocean currents, waves, plate tectonics and the sea floor. Nearshore research comprises one area of oceanographic research, understanding this is very important as the RIP currents are the major cause for drowning.

III. PROBLEM STATEMENT

The existing systems use the manually operated lifebuoy ring delivery drone system when a drowning victim is found by the life guard. Hence without proper management by life guard or other parameters the existing systems is not very efficient to save the lives.

IV. PROPOSED SYSTEM

The live video streaming is done to detect the drowning victim, if found the latitude and longitude points of the location of victim is updated to the drone, thus the drone flies to the location and drops the lifebuoy ring. Thus the entire existing system is automated.

V. METHODOLOGY

Prototype methodology is selected to implement the system and all the activities done for each and every stage is discussed below.

5.1 Planning

A feasibility study was conducted mainly under three categories. They are time, cost and scope. Even though this is a research project, it needed to complete within a very limited time period. Is it possible? Then check whether the project was able to complete with the limited budget which the project team had. The technologies, hardware and software components which are needed to implement the system were new to the research team. Therefore, check whether project team has interest and ability to adapt or learn new frameworks or other new technologies. After conducting these feasibility study project team identified this project was enough feasible to start implementing in the planning phase.

5.2 Requirement gathering & analysis

The requirement gathering was done using primary data and secondary data. As primary data interviews were conducted with the Disaster Recovery Center. The results of interviews were, current methods are the life guard or other person finding the drowning victim and rescuing him, whereas if no person is there at that time it may cost the loss of a life. Therefore, proper method like object detection through video streaming is done to find the drowning victim and then drone which is very small compared to other delivery methods is most suitable way to deliver goods in order to rescue human's life was the final conclusion of the interviews. As the secondary data project team went through several research papers. In this, research team researched for existing similar systems and analyzed their functionalities, to better understand the methodologies used. Information regarding object detection and autopilot techniques of the drone were analyzed using existing research as well.

5.3 Designing

The object detection structure, Convolutional Neural Network (CNN) algorithm is used as to detect the drowning victim and reports the location of the victim. The research was done in finding the best machine learning algorithm among various other, CNN algorithm stood best among it by providing more accuracy.

The drone structure, collision detection algorithm, obstacle avoidance algorithm, autopilot system and interfaces are designed as main component of the system in this phase. Hardware parts needed to implement the drone structure was contained several varieties and it is very difficult to find the best ones with the limited budget. Therefore, first small designing plan was made for the behavior of the flight controller, Power supply module, GPS Mast and how they were placed in the drone frame in more organizing way.

Figure 1 is illustrated the Architecture diagram. It is explained about main relationships between the user and other system components. The camera is connected to the personal computer (PC) and performs live video processing, if the drowning victim is detected the location is updates to the drone flight controller through the PC, the operator is used to maintain the PC functions as well as the transmitter.

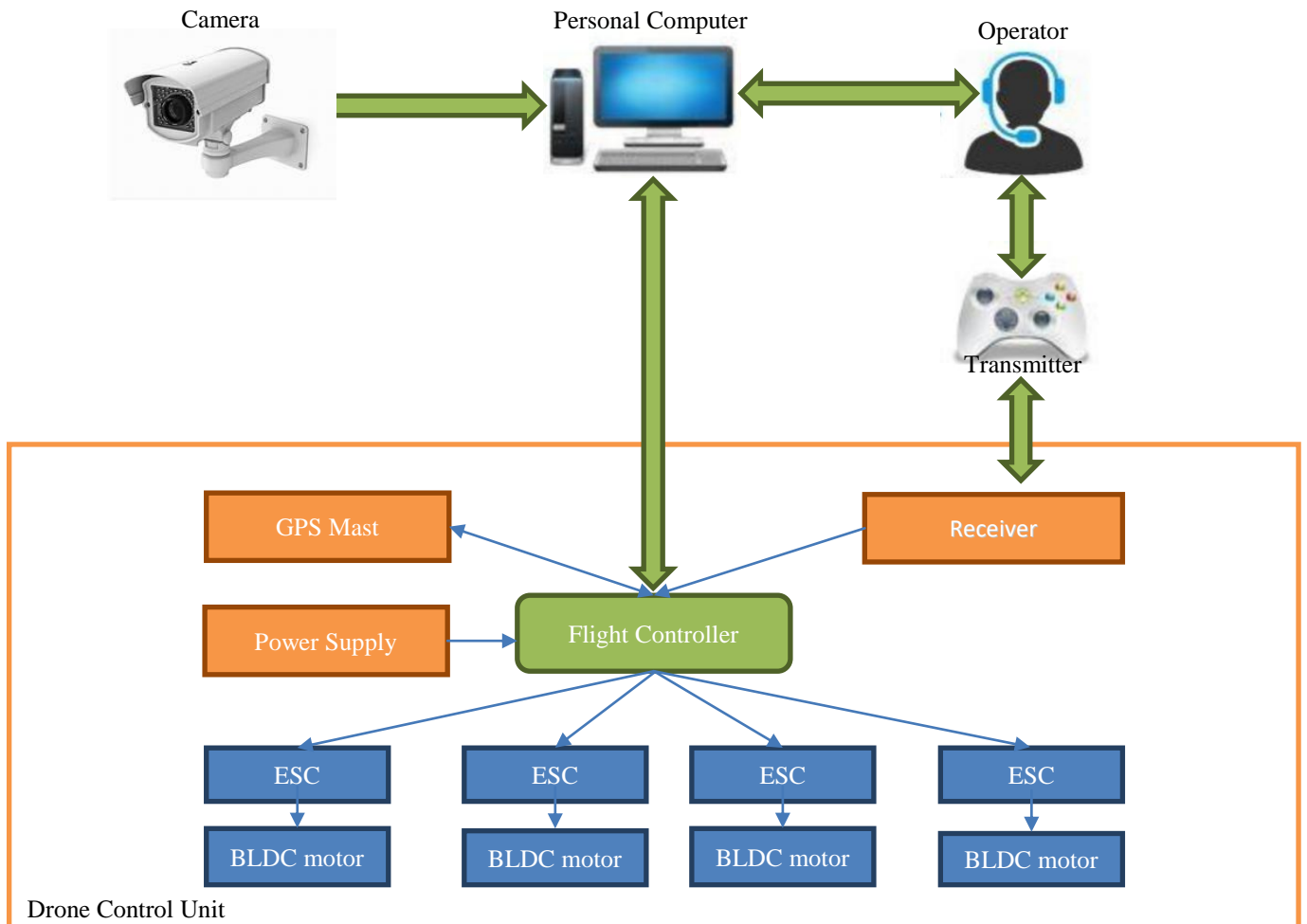


Figure 1: Architecture Diagram

4.4 Implementation

As a first step for this phase drone was implemented by combining all the hardware parts as shown in figure 2. The System is developed as separate units for the purpose of developing the code. The requirements are met by developing the system separately as smaller units and integrating to form one full system. The python language was used to code for CNN algorithm, the train and test data was sorted in 7:3 ratio for training and testing respectively. The drone was incorporated with ArduPilot flight controller and certain settings for uploading the location and other was made. Figure 2 is the prototype of the drone.

4.5 Testing

All testing was done in the “prototype level”. The two main testing methodologies used were Black-Box testing and White Box testing. Black box testing was done to ensure all the functionality of the system is working as specified. Structure of the functionalities is checked using white box testing.



Figure 2: Drone prototype

VI. RESULT

The “Automated beach security system using autopilot drone” System has two subsystems and the result of both are shown below, the system was trained to detect three activities like Normal, Drowning and Swimming and the output of that activity detection is shown in Figure 3 Figure 4 and Figure 6 respectively. The ArduPilot software used to set the GPS Co-ordinates is shown in the Figure 5, thus the flight path is set. Now the drone is set for its flight to the victim and drop the lifebuoy ring.



Figure 3: Activity Drowning detected



Figure 4: Activity Normal detected

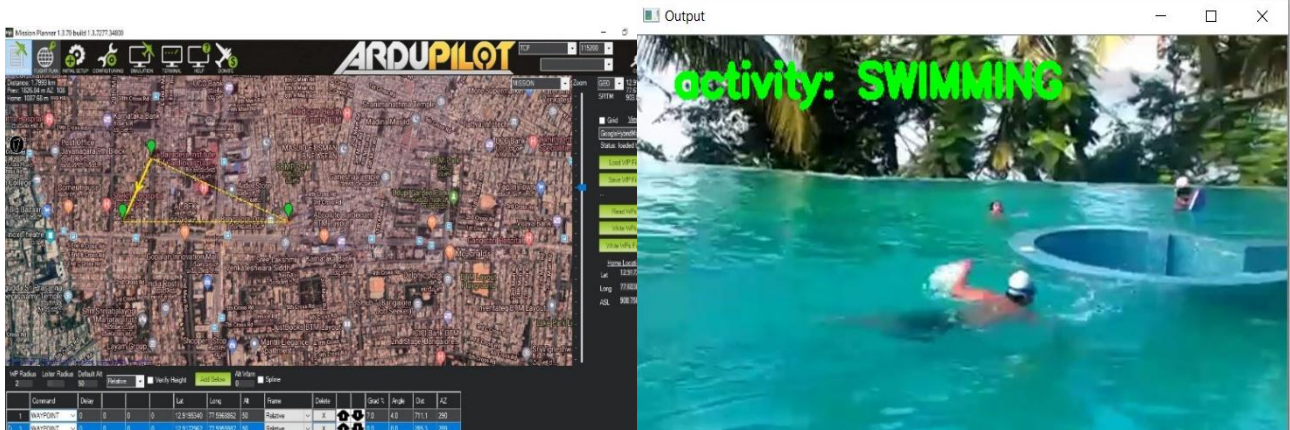


Figure 5: Drone GPS Co-ordinates fix

Figure 6: Activity Swimming detected

VII. CONCLUSION

The system is developed to save life of drowning victim, it increases the victim survival time during the rip current rescue process. This is an autonomous drone delivery system which can easily reach to any area without any trouble and through video processing the drowning victim can be detected easily.

With all these functionalities, this system has some limitations as well. This system is completely depending on power supply. If it is not supplied, system can stop the operation. This system is not capable of travelling to long distance because of the less battery power, less motor speeds and other hardware component capacity issues in the drone. When situation like bad weather condition is occurred, this system cannot handle itself because of the less battery capacity, insufficient esc power thus not capable enough to give 100 percent accurate result.

REFERENCES

- [1] Design of the Life-Ring Drone Delivery System for RIP Current Rescue (2016) by Gang Xiang, Andrew Hardy, Mohammed Rajesh And Lahari Venuthurupalli for System dynamics, UAV, stochastic simulation.
- [2] GPS Tracking System Coupled With Image Processing in Traffic Signals to Enhance Life Security (2013) by Manoj Prabhakar K And Manoj Kumar S for Image processing, Ambulance GPS tracking system, pattern recognition, shortest path algorithm.
- [3] Implementation of Real-time Image and Video Processing, and AR on Mobile Devices (2015) by Dr. Hamid Mehrvar and Farzin Farhadi-Niaki for Real time image processing, face detection, viola-Jonas algorithm, augmented reality.
- [4] Accident Detection System using Image Processing and MDR (2007) by Yong-Kul Ki† for Image processing.
- [5] IMAGE PROCESSING APPLICATIONS IN LIFE SAVER DRONES (2018) S K Shankar, Balasubramani.S, Joyce John, GokulaKrishnan.V (2018) for BPM, face detection using deep learning.
- [6] An Automatic Video-based Drowning Detection System for Swimming Pools Using Active Contours (2016) by Nasrin Salehi and Maryam Keyvanara and Seyed Amirhassan Monadjemmi for Drowning detection, color space analysis, real time image detection.
- [7] Drone Delivery System for Flooded Area (2017) by T. L. H. Gammedda, W. V. Dilushika and W. C. I. D. Silva for Video streaming, obstacle collision detection.



Eye Tracking Password Using Blinking Verification System

Sristi V¹, Sushmitha Katherine J², Tejasvi M G³, Tinki Rani⁴, Ms. Sandhya Rani⁵

Final year B.E Students (UG), Department of Information Science & Engineering, The Oxford College of Engineering,
Bangalore, India^{1,2,3,4}

Assistant Professor, Department of Information Science & Engineering, The Oxford College of Engineering,
Bangalore, India⁵

ABSTRACT: Personal identification numbers are widely used for user authentication and security. Password authentication using PINs requires users to physically input the PIN, which could be vulnerable to password cracking via shoulder surfing or thermal tracking. PIN authentication with hands-off gaze-based PIN entry techniques, on the other hand, leaves no physical footprints behind and therefore offers a more secure password entry option. Gaze based authentication refers to finding the eye location across sequential image frames, and tracking the center of the eye over time. This paper presents a real-time application for gaze-based PIN entry, and eye detection and tracking for PIN identification using a smart camera.

KEYWORDS: Pins, Smart camera, Real-time systems, Authentication, Gaze tracking, Password

I. INTRODUCTION

The use of Personal Identification numbers (PINs) is a common user authentication method for many applications, such as money management in automatic teller machines (ATMs), approving electronic transactions, unlocking personal devices, and opening doors.

Flawless identity authentication remains a challenge even when PIN authentication is used, such as in financial systems and gate access control. According to the European ATM Security, fraud attacks on ATMs increased by 26% in 2016 compared to that of 2015. The fact that an authorized user must enter the code in open or public places make PIN entry vulnerable to password attacks, such as shoulder surfing and thermal tracking.

The purpose of this work is to enter and identify gaze-based PINs using a smart camera through real-time eye detection and tracking. NIVisionBuilder and LabVIEW are used for eye tracking and for recording eye center location on board the camera real-time.

The smart camera allows on-board data processing and collection. Non-contact PIN based authentication adds a layer of security to physical PIN entries and are expected to reduce the vulnerability of the authentication process.

II. LITERATURE REVIEW

The current state of functioning systems in offline mode

- With the project of digitalization of academic and administrative affairs in UP, the phase of complete computerized services has begun. The results obtained from this work are tested and successfully implemented in the Electronic Student Management System (ESMS) also developed from UP. The aim of this paper is to provide new results for data synchronization in different platforms through Web services, which allow software applications to run or to be executed online and offline as well.

Implementation of the proposed solution for ESMS in offline mode

- Files will be transferred as data and not as files, but the central server will return the file format. To provide both modes of operation, ESMS has built a system which enables the data synchronization between faculties that are working offline with the primary system, in the main data base, so that the data could still be synchronous and up to date with the work done in all the different units. For this purpose, it has been provided the data synchronization, for the units working in "Offline" mode, with the primary system and the network infrastructure that will support the



implementation of such technology serving the UP and its data synchronization in both “Offline” and “Online” mode and vice versa.

III. PROBLEM STATEMENT

The main problem in the existing system is that it is not very secure. Passwords typed on a keypad are easy to hack, which poses a major question on its security. Another problem that exists in the existing system is accuracy. Most of the existing systems are sensor based that makes them inaccurate. Also, not to mention the inconvenience that comes with some head-controlled systems where physical movement is required.

IV. EXISTING SYSTEM

Systems that have been used for a long time now have some demerits. They have undoubtedly served their purpose but there are instances that make us question the security and accuracy of these systems. As we all know, keypad-based systems are easy to hack, voice-controlled systems are user specific and most systems are sensor dependent which make them mostly inaccurate. It is now a general tendency to make systems more convenient for the users. Hence, the attempt to upgrade from the inconvenience of using head-controlled systems where physical movements are required.

V. PROPOSED SYSTEM

The proposed system is an eye recognition-controlled locker. Eye tracking technology, which is based on an eye tracker that measures the movement and positions of the eye. A mounted camera will recognize the eye and lock and unlock the locker. NI Smart Cameras are industrial, high-quality image sensors combined with powerful processors to create rugged, all-in-one solutions for machine vision applications. The first part is the head mounted camera that will track the camera wearer’s eye using Arduino. The microprocessor will take a USB output from the camera and convert the signal into signals that will be sent to the locker. The final part of the project is the motor drivers to interface with the locker itself.

A. SYSTEM ARCHITECTURE

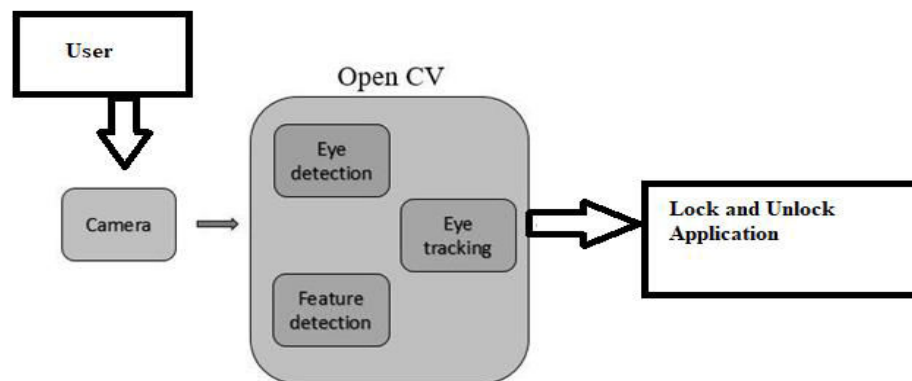


Fig 1: System Architecture



The system consists of 4 parts. The user looks into the camera and the user's face is captured by the camera. The image is then processed using the Haar Cascade and the Facial Landmark algorithm to calculate the structure of the face and to detect the eyes on it. Then the pupil is detected.

After which the process of feature extraction takes place. Once that is done, the data is trained and tested based on the prior data stored.

B. WORKING

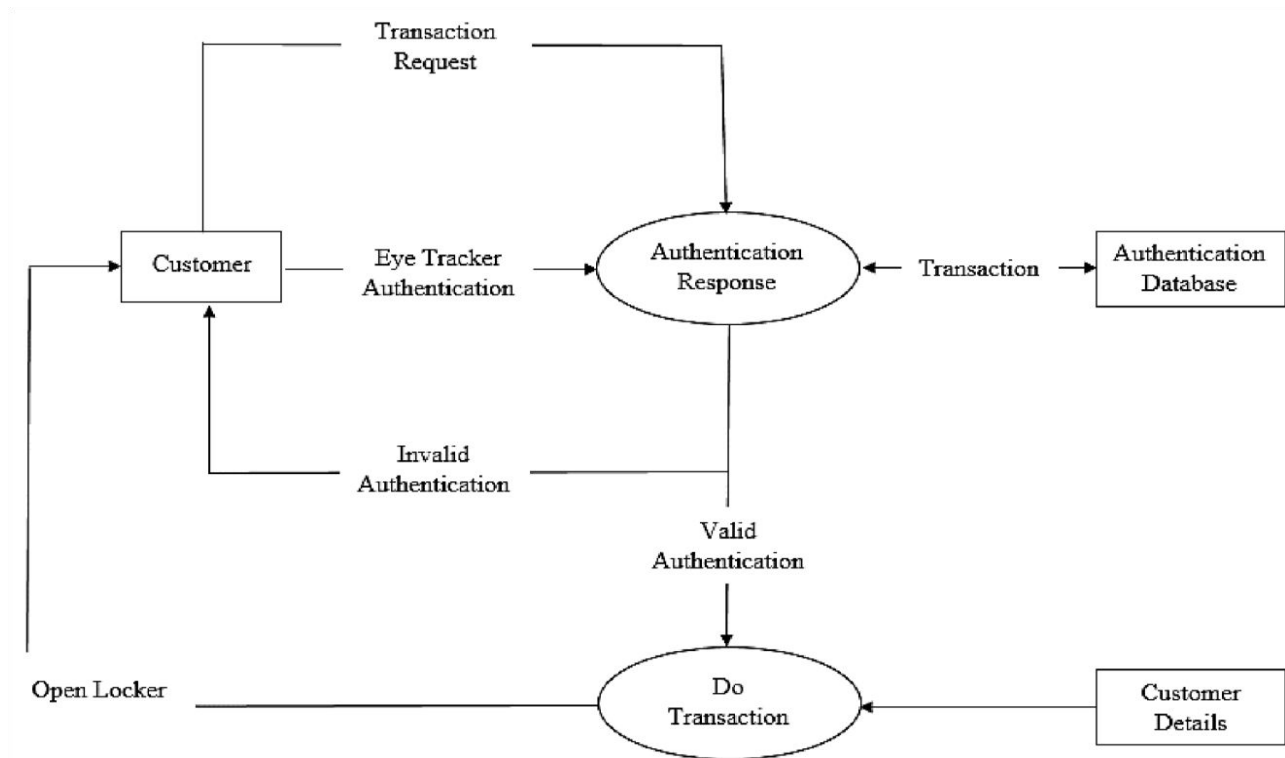


Fig 2: Shows the working of the system

The following shows the working of the system.

The steps start from capturing the image from the camera, then processing the image, detecting the face, detecting the eye, extracting features and testing and training. This is summarized in the following steps:

- i. The user/customer requests a transaction by looking into the camera.
- ii. The camera captures the face of the user by the process of image acquisition.
- iii. The image is then processed by using the Haar Cascade and the Facial Landmark algorithm to calculate the structure of the face and to detect eyes on it.
- iv. The complete eye data is captured based on the pupil detected.
- v. After which, the features are extracted from the face and eye detection process.
- vi. The system then checks if the user is an authorized user or not by checking the authentication database.
- vii. If the authentication is valid, then the transaction is done and the locker is opened.
- viii. In case of invalid authentication, the control is directed back to the user.



VI. HARDWARE REQUIREMENTS



Fig 3: Arduino

The Arduino hardware and software were designed for creating interactive objects or environments. Arduino can interact with buttons, LEDs, motors, speakers, GPS units, cameras, the internet, and even your smart-phone or your TV, thus making it very flexible. Both the Arduino hardware and software are easy to learn.

- **Processor**—x86 compatible processor with 1.7GHz Clock Sleep
- **Microcontroller**-- Arduino
- **RAM**—512MB or greater
- **Monitor**—VGA/SVGA, WEB CAM
- **Keyboard**—104 keys standard
- **Mouse**—2/3 button. Optical/Mechanical

VII. IMPLEMENTATION

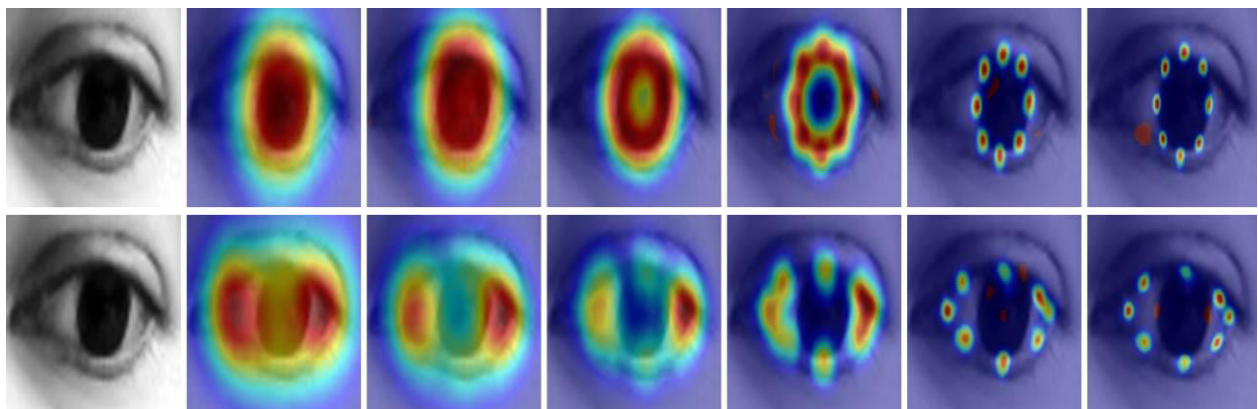


Fig 4: Eye landmarking for recognizing layers

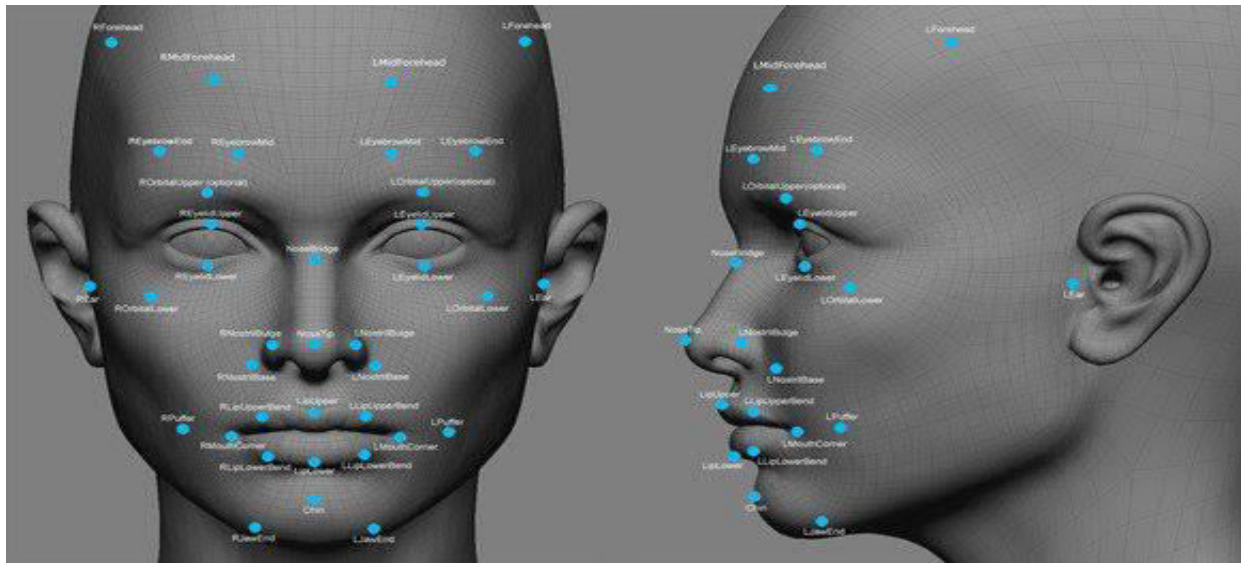


Fig 5: Face and eye detection



Fig 6:Pupil detection

VIII. RESULT

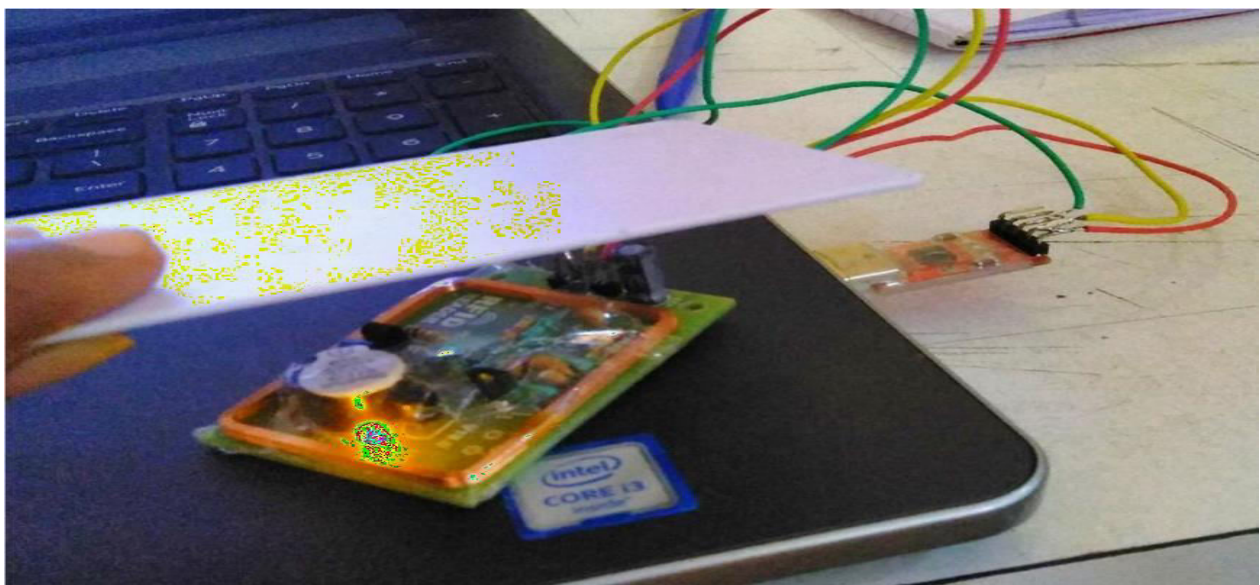


Fig 7: RFID card reading and relay operation



Today, we have various security systems such keypad-based systems, voice-controlled systems, head-controlled systems and so on. But the Eye Tracker Password system truly stands out as they are much more secure and accurate compared to the traditional security systems and not to mention the convenience of a completely hands-off gaze-based system.

This system can especially be useful to the physically challenged as now, they can have access to security systems without having to manually type out a password or make any physical movements.

The Eye Tracker Password system in addition to being secure and accurate also consumes less power. The project is fairly easy to implement and uses commonly available components, which made it quite cost effective. This system can be used schools, banks, or just about anywhere where security is a want or need.

```
--
Scanned the ID
$000133433
Welcome Rajesh
Generating the OTP
['1', '5', '7', '2']
['1', '5', '7', '2']
Enter the above generated password
```

Fig 8: OTP generation after eye scanning

IX. CONCLUSION AND FUTURE WORK

A smart camera-based eye tracking system has been incorporated as a new application for gaze-based PIN identification. The system has been successfully tested with numbers and can be extended to character and digit combination password entry. It mainly protects the user password from various attacks like shoulder surfing and thermal tracking.

Future work includes incorporating the PIN identification algorithm to the real time framework for all in one password identification system. In addition, gaze-based password entry can be extended to mobile devices and other camera-based systems.

REFERENCES

1. R. Revathy and R. Bama, "Advanced Safe PIN-Entry Against Human Shoulder-Surfing," IOSR Journal of Computer Engineering, vol 17, issue 4, ver. II, pp. 9-15, July-Aug. 2015. (Available: <http://www.iosrjournals.org/iosr-jce/papers/Vol17-issue4/Version2/B017420915.pdf>)
2. J. Weaver, K. Mock and B. Hoanca, "Gaze-Based Password Authentication through Automatic Clustering of Gaze Points," Proc. 2011 IEEE Conf. on Systems, Man and Cybernetics, Oct. 2011. (DOI: 10.1109/ICSMC.2011.6084072)
3. "ATM Fraud, ATM Black Box Attacks Spread Across Europe", European ATM Security Team (E.A.S.T.), online, posted 11 April 2017. (Available: <https://www.european-atm-security.eu/tag/atmfraud/>)
4. K. Mowery, S. Meiklejohn and S. Savage, "Heat of the Moment: Characterizing the Efficacy of Thermal Camera-Based Attacks," WOOT '11, pp. 1-8, August 2011. (Available: <https://cseweb.ucsd.edu/~kmowery/papers/thermal.pdf>)
5. M. Mehrübeoglu, H. T. Bui and L. McLauchlan, "Real-time iris tracking with a smart camera," Proc. SPIE 7871, 787104, 2011. (DOI:10.1117/12.872668)
6. M. Mehrübeoglu, L. M. Pham, H. T. Le, M. Ramchander, and D. Ryu, "Real-time eye tracking using a smart camera," Proc. 2011 IEEE Applied Imagery Pattern Recognition Workshop (AIPR '11), pp. 1-7, 2011. (DOI: 10.1109/AIPR.2011.6176373)
7. M. Mehrübeoglu, E. Ortlieb, L. McLauchlan, L. M. Pham, "Capturing reading patterns through a real-time smart camera iris tracking system," Proc. SPIE, vol. 8437, id. 843705, 2012. (DOI: 10.1117/12.922875)
8. Smart Cameras for Embedded Machine Vision, (product information) National Instruments (Available: http://www.ni.com/pdf/products/us/cat_ni_1742.pdf)



Suspicious Human Activity Detection Using Image Processing

Harshith T R¹, Gurushekara K², Kumar Shivam³, S Vidhya⁴

Final year B.E Students (UG), Department of Information Science & Engineering, The Oxford College of Engineering, Bangalore, India^{1,2,3}

Assistant Professor Department of Information Science & Engineering, The Oxford College of Engineering, Bangalore, India⁴

ABSTRACT: In today's insecure world the video surveillance plays an important role for the security of the indoor as well as outdoor places. The components of video surveillance system such as behavior recognition, understanding and classifying the activity as normal or suspicious can be used for real time applications. In this paper the hierarchical approach is used to detect the different suspicious activities such as loitering, fainting, unauthorized entry etc. This approach is based on the motion features between the different objects. First of all, the different suspicious activities are defined using semantic approach. Then the object detection is done using background subtraction. The detected objects are then classified as living (human) or nonliving (bag). These objects are required to be tracked which is done using correlation technique. Finally using the motion features & temporal information the events are classified as normal or suspicious. As the semantic based approach is used computational complexity is less and the efficiency of the approach is more.

KEYWORDS: Video Surveillance, Suspicious activity, Object detection.

I. INTRODUCTION

Computer vision is mainly used to study how to interpret, reconstruct and understand 3D scenes from its 2D images in terms of the properties of the structures present in the scene. Computer vision mainly includes methods for acquiring, analyzing, processing and understanding digital images. Video processing is a prominent research area in the field of computer vision. The detection and tracking of moving objects and activity recognition of these objects in video surveillance is one of the important tasks.

Human detection and tracking are a major component in many of the intelligent video management and monitoring applications in recent times. This finds application in surveillance video analysis for security, sports video analysis, detection of abnormal activities, patient monitoring, traffic monitoring and many more. Human activity recognition is mainly used for human-to-human interaction as it provides information about a person's identity, their personality and many more. As a result, it has many applications in video surveillance systems, human-computer interaction and robotics for characterization of human behavior all these require multiple activity recognition systems.

The two main approaches of detecting and tracking humans are frame difference method and background modelling method. Frame difference method is most suitable for no change in background and when there is a relatively static situation. Background modelling method is based on the Gaussian mixture model (GMM), Graph cut method. GMM and Graph cut methods are more complex and a larger amount of calculation is involved. The activity recognition approaches can be termed as local or global approaches. Local approach of video analysis mainly uses local interest points wherein each interest point contains a local descriptor which describes the characteristics of a point. By the analysis of these descriptors motion analysis is done. Scale Invariant Feature Transform (SIFT) and Space Time Interest Points (STIP) are some of the most commonly used local descriptors for videos. Global approach mainly uses the overall movement characteristics of the video. Most of the methods make use of optical flow to represent motion in a frame of video.

The classifier used for human activity recognition is mainly categorized into three basic types. Conditional Random Field (CRF), Hidden Markov Model (HMM) and Support vector machine (SVM). Where the CRF and HMM belong to the state model method, wherein due to the continuous change in activity sequence, activity recognition can be manipulated by modelling. Whereas, SVM uses nonlinear classification function which is established by known



samples to classify activities and hence overcomes the difficulties of parameter estimation in state model method. There is no need for considering the probability distribution. Hence it has its own wide variety of applications.

II. PROBLEM STATEMENT

The need for automated surveillance systems have become urgent as reliance on the human factor gives inaccurate results in the recognition of suspicious activities. Public places like subway stations, airports, and government buildings require detection of abnormal and suspicious activities to prevent crime before an occurrence such as automatic reporting of a person with Suspicious activity at the airport and to overcome crime. In this video surveillance moving object detection and recognition is the important research area of computer vision. Detection and recognition of moving is not an easy task as continuous deformation of objects takes place during movement. Any moving object has several attributes in temporal and spatial spaces. In spatial space objects vary in size whereas in temporal space it varies in moving speed.

III. PROPOSED SYSTEM

The proposed system is to automatically detect and estimate the 2D pose of humans in images recorded under uncontrolled environments. This project emphasis on detecting suspicious activities in public places like subway stations, airports, and government buildings require detection of abnormal and suspicious activities to prevent crime before an occurrence. In this video surveillance moving object detection and recognition is the important research area of computer vision. Detection and recognition of moving is not an easy task as continuous deformation of objects takes place during movement. Any moving object has several attributes in temporal and spatial spaces. In spatial space objects vary in size whereas in temporal space it varies in moving speed. This work mainly focuses on multiple human detection and activity recognition. Multiple human video datasets are considered and in order to detect and track multiple humans. Background subtraction technique is used for detecting moving multiple humans. Histogram of Oriented Gradient feature descriptor is used to extract features. For human activity recognition Support Vector Machine classifier is used.

Advantages:

- No need of human intervention as automatic Functioning performs the proper operation without any supervision.
- Complete automated operation.
- One-time installation.
- Low maintenance cost

IV. METHODOLOGY

1. Input Data:

The input for the system is video stream. As the system is to be implemented to detect the suspicious activity its input is to be taken from the CCTV.

2. Background Image Acquisition:

The background image is dynamically updated so that any new object entered the scene can be captured.

3. Image Pre-Processing:

The changing light conditions, movement of reference background cause some noise introduced in the image.

4. Object detection:

The foreground image is obtained by the subtraction of the input image from the background image. From this foreground image the required object is detected.

5. Object Tracking:

The detected object is tracked in the scene so that we can determine if any new object is entered in the scene or if any object left the scene i.e. the person walk off the scene.

V. SYSTEM ARCHITECTURE

The architecture of a system describes its major components, their relationships (structures), and how they interact with each other. Software architecture and design includes several contributory factors such as Business strategy, quality attributes, human dynamics, design, and IT environment. We can segregate Software Architecture and Design into two distinct phases: Software Architecture and Software Design. In Architecture, non-functional decisions are cast and separated by the functional requirements. In Design, functional requirements are accomplished.



BLOCK DIAGRAM AND ITS COMPONENTS

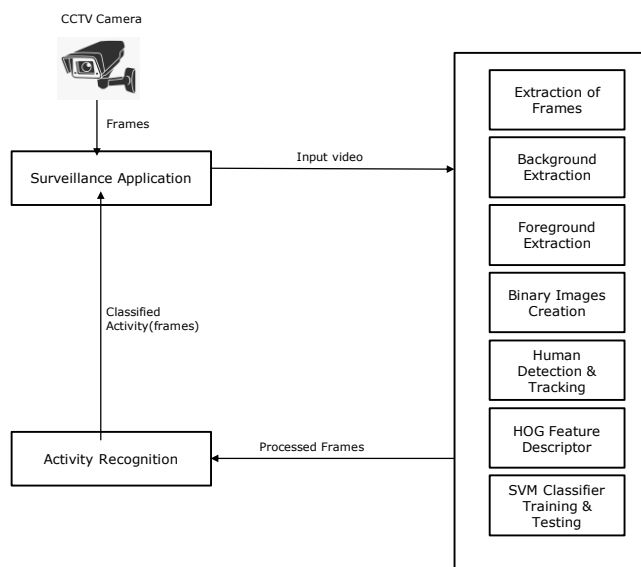


Fig. 1 Block diagram of approach used in the proposed system

A block diagram is a graphical representation of a system – it provides a functional view of a system. Block diagrams give us a better understanding of a system’s functions and help create interconnections within it. Block diagrams derive their name from the rectangular elements found in this type of diagram. They are used to describe hardware and software systems as well as to represent processes. Block diagrams are described and defined according to their function and structure as well as their relationship with other blocks.

Extraction of frames is necessary as videos cannot be processed directly. Later, background subtraction technique is used to find the moving humans. In this technique a background image is considered, where each frame is subtracted by background image to obtain foreground images which show the moving human location. Convert the obtained foreground RGB image to grayscale images. Onto this result 2-D median filtering is used to remove noise components present in the video.

Once noise removal is done the grey scale images will be converted to binary images of 0s and 1s, where binary 1 is used for representing human region which is filled with white color and apart from moving human region binary 0 is used which represents absence of humans. Hence, binary image creation is useful for extracting any moving humans and objects in a video sequence. Followed by which dilation process is carried out which is typically applied on binary images obtained.

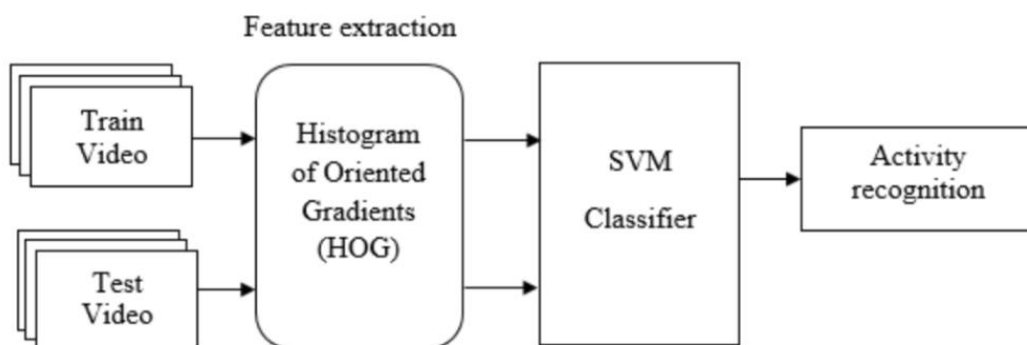


Fig. 2 Framework of Suspicious Activity Recognition

Figure 2 shows Human activity recognition in which HOG feature descriptor and SVM classifier along with train and test video dataset.

Once after detecting each individual human the next stage is recognizing their activities. After detecting the moving humans in a video, it is also necessary to determine the number of humans present later which activity recognition is



carried out. HAR consists of two phases: training and testing.

The flow chart of training and testing phase is as shown Figure 4.3.3. In the training phase the video dataset will be loaded first, then frames extraction is carried out. Training folder is created which contains the frames belonging to particular activities. Useful features are extracted for each activity being performed. HOG feature extraction technique is used for extraction of features. SVM classifier is used to train this extracted feature and it saves this trained SVM model which will be further used for testing. In the testing phase, the testing video is loaded and frames extraction, background subtraction, binary image creation and HOG feature extraction steps will be done on the loaded test video. The obtained result will be inputted to the earlier trained SVM classifier, depending upon the feature match SVM classifier will recognize the particular activities performed.

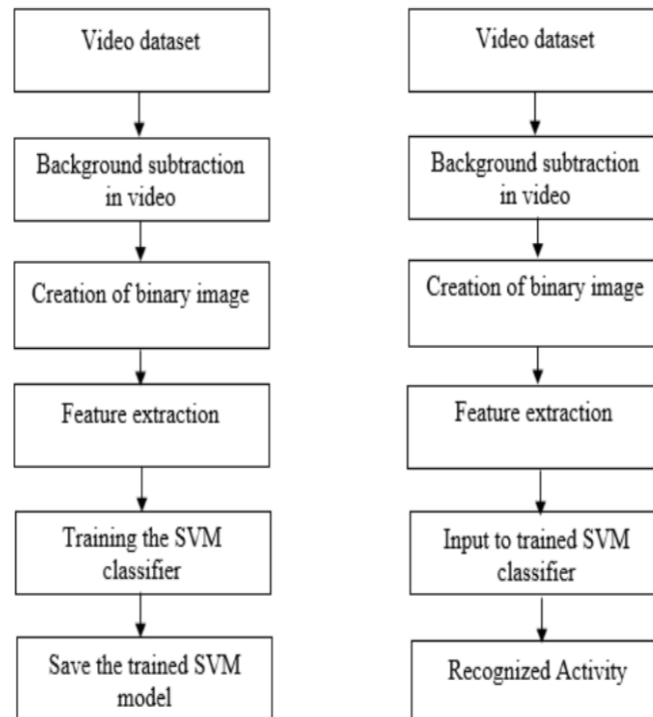


Fig. 3 Flow Chart of Training and Testing Phase

VI. IMPEMENTATION

Object Detection:

The template matching is used for object detection. In this method the cross correlation between a template image & the new image is performed.

Object Tracking:

For tracking the objects detected in the scene we use the correlation-based tracking method. In this method a small tracking window is centered on the object in the first frame.

Object Features Extraction:

Once the object in the frame to be tracked is fixed then its features are required to be extracted.

Defining the Suspicious Activities:

There are lots of activities which come under suspicious activity. But for the project work we have selected the following activities-

- Abandoned luggage
- Unauthorized Access
- Stabbing
- Shooting
- Fighting



VII. RESULT

The suspicious activity detection in the video data is a challenging task. It has a number of difficulties such as complexity of scene, illumination of light, camera angle etc. Also, the definition of the suspect activity is scene/place dependant. Another problem is that the standard and challenging data sets are not easily available for testing.



Fig. 4 Detected the suspicious objects in frame

VIII. CONCLUSION AND FUTURE WORK

The system was tested on the video recorded from a CCTV that captured scenes where a group of volunteers were exhibiting suspicious actions. The system has been tested on different real scenarios offering promising results.

The future work of this paper will include the detection of suspicious objects such as unmovable bags to make the system more effective. Reducing the computational time is also an important factor that can be improved.

Abandoned object detection and theft detection Majority of the works have been done for the abandoned object detection from surveillance videos captured by static cameras. Few works detected the static human as an abandoned object. To resolve such problems, human detection methods should be very effective and the system should check the presence of the owner in the scene, if the owner is invisible in the scene for a long duration then alarm should be raised. To resolve the problem of theft or object removal, the face of the person who is picking up the static object, should match with the owner otherwise an alarm must be raised to alert the security. Future work may also resolve the low contrast situation i.e. similar color problems such as black bag and black background which lead to miss detections. Future improvements may be integration of intensity and depth cues in the form of 3D aggregation of evidence and occlusion analysis in detail. Spatial-temporal features can be extended to 3-dimensional space for the improvement of abandoned object detection methods for various complex environments. Thresholding based future works can improve the performance of the surveillance system by using adaptive or hysteresis thresholding approaches. Few works have been also proposed for abandoned object detection from the multiple views captured by multiple cameras. To incorporate these multiple views to infer the information about abandoned objects can also be improved. There is a large scope to detect abandoned objects from videos captured by moving cameras.

Falling detection Most of the works have been done for fall detection of single people in indoor videos based on human shape analysis, posture estimation analysis and motion-based analysis. Future works can include the integration of multiple elderly monitoring which is able to monitor more than one person in the indoor scene. Many older people go for morning walks every day in public areas such as parks; to monitor these elder people, a future work can include one or more than one human fall detection from outdoor surveillance videos.

Accidents, illegal parking, and rule breaking traffic detection Several researchers have presented accidents detection, illegal parking detection and illegal U-turn detections from static video surveillance. These systems become incapable to detect these abnormal activities in more crowded traffic on roads. Future works should be based on unsupervised learning of transportation systems because no standard dataset is available for the training.

Violence detection Several research works have been done for the prevention of violence activities such as vandalism, fighting, shooting, punching, and hitting. To detect such violence activities, a single view static video camera has been used but sometimes this system fails in occlusion handling. Therefore, a multi-view system has been proposed by few researchers to resolve this problem but it requires important cooperation between all views at the low-level steps for abnormal activity detection. Future work may be an automatic surveillance system for moving videos. Improvements are required in accuracy, false alarm reduction, and frame rate to develop an intelligent surveillance system for the road traffic monitoring.

Fire detection Future work can include more improvement in accuracy, frame rate, false alarms reduction and also it



can be improved to detect far distant small fire covered by dense smoke.

REFERENCES

- [1] Hanan Samir, "Suspicious Human Activity Recognition using Statistical Features." *2018 13th International Conference on Computer Engineering and Systems (ICCES)* (2018): 589-594.
- [2] Mohannad Elhamod and Martin D. Levine, "Automated Real-Time Detection of Potentially Suspicious Behavior in Public Transport Areas", *IEEE Transactions on Intelligent Transportation Systems*, vol. 14, no. 2, June 2013.
- [3] Sandesh Patil and Kiran Talele, "Suspicious Movement Detection and Tracking based on Color Histogram", *2015 International Conference on Communication Information & Computing Technology (ICCICT)*, Jan. 16–17
- [4] P. Birch, W. Hassan, N. Bangalore, R. Young and C. Chatwin, "Stationary traffic monitor", *Proc. 4th Internat. Conf. on Imaging for Crime Detection and Prevention (ICDP-11)*, pp. 1-6, 2011.
- [5] Y. Tian, R. Feris, H. Liu, A. Humpapur and M.-T. Sun, "Robust detection of abandoned and removed objects in complex surveillance videos", *Proc. IEEE*, 2010.
- [6] F. Porikli, Y. Ivanov and T. Haga, "Robust abandoned object detection using dual foregrounds", *EURASIP Journal on Advances in Signal Processing* 2008, 2008.
- [7] James Ferryman et al., "Robust abandoned object detection integrating wide area visual surveillance and social context" in *Pattern Recognition Letters*, Elsevier, vol. 34, pp. 789-798, 2013.
- [8] Mohannad Elhamod and Martin D. Levine, "Real-Time Semantics-Based Detection of Suspicious Activities in Public Spaces", *Proc. 9th Conf. CRV*, 2012.
- [9] Achkar F, Amer A (2007) Hysteresis-based selective gaussian mixture models for real-time background maintenance. *SPIE Vis Commun Image Process* 6508: J1–J11.
- [10] Adam A, Rivlin E, Shimshoni I, Reinitz D (2008) Robust real-time unusual event detection using multiple fixed-location monitors. *IEEE Trans Pattern Anal Mach Intell* 30(3):555–560



A Secured Data sharing among Vehicles to Keep Track of Road Conditions

Rahul Chatterje¹, Ramya R², Venkatesh M³, Vinod kumar⁴, Mrs. Visalini S⁵

Final year B.E Students(UG) , Department of Information Science & Engineering, The Oxford College of Engineering,
Bangalore, India^{1,2,3,4}

Assistant Professor, Department of Information Science & Engineering, The Oxford College of Engineering,
Bangalore, India⁵

ABSTRACT: The main objective is to improve the travel efficiency and safety of transportation system and it represents the design of a road side authority, such that it needs to monitor real-time road conditions with the help of a cloud server so that it could make sound responses to emergency cases timely. Vehicles on site are able to report the information to a cloud server engaged by the authority when they detect some bad road conditions, for example some geologic hazard or accidents. The main goal is to provide authorized reporting of the vehicles. A vehicle can collect the real time road condition information and encrypt it with the root authority's public key, its secret key and the token issued by the administrative RU and the cloud server is engaged to perform much of the monitoring work. The entities in RCoM system such as sub-authorities, vehicles and roadside units are recognized with their identities.

KEYWORDS: Data privacy, vehicular ad hoc network, cloud computing, authentication.

I. INTRODUCTION

In real world application scenario, the road side authority may need to monitor real time road conditions so that it could respond quickly in emergency cases. Each vehicle with an embedded on-board unit is able to collect and communicate the current road/traffic information with the help of distributed road side unit. When T (toe) or more road condition reports for the same location are received, where T denotes the threshold in the monitoring system, the root authority considers it as an emergency case and then makes response. Mainly, the vehicles have to be authorized by some roadside unit. To guarantee the privacy against the cloud server, the road condition information should be reported in cipher text format. The cloud server and authority should be able to validate the report source. So in this way, every nearby recipient vehicle would be able to get better awareness of driving environment and change driving plan if needed. However this approach requires root authority to equip with powerful computing and storage resources, which would bring unaffordable costs to RA.

II. LITERATURE REVIEW

Title: Efficient Hierarchical Identity-Based Signature with Batch Verification for Automatic Dependent Surveillance-Broadcast System

Author: Debiao He, Neeraj Kumar, Kim-Kwang Raymond Choo, and Wei Wu

- They proposed an efficient TLHIBS scheme and show it is provably secure and can meet summarized security requirements.

Title: How to Protect ADS-B: Confidentiality Framework and Efficient Realization Based on Staged Identity-Based Encryption

Author: JoonsangBaek, EmanHableel, Young-Ji Byon, Duncan S. Wong, Kitae Jang, and Hwasoo Yeo

- The author proposes a modified version which they call a "Staged Identity-Based Encryption (SIBE)" scheme, to address the aforementioned challenges of providing ADS-B with confidentiality



SYSTEM ARCHITECTURE

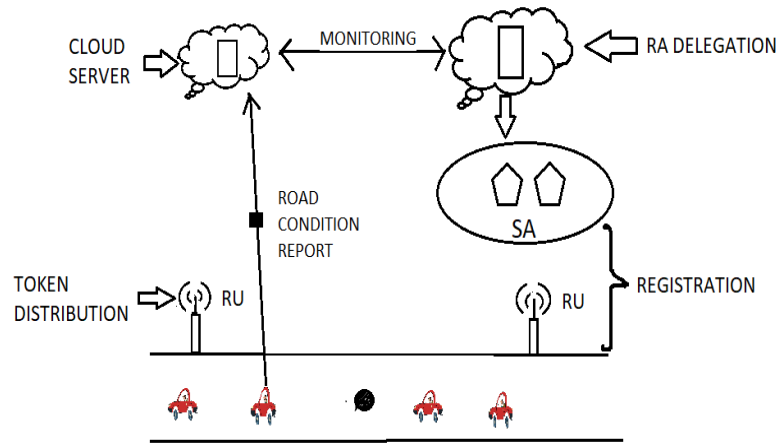


Figure:3.1

The system architecture consists of five types of entities, that is, a root authority (RA), many sub-authorities (SAs), many roadside units (RUs), a cloud server, and many vehicles. As in VANET, RA, SAs and RUs are the trusted participants. In real-world applications, RA can be the Department of Transportation. The goal of RA is to monitor the real-time road conditions with the help of a cloud server, so that it could make timely response to emergency cases. The cloud server is maintained by some cloud service provider (CSP), which has significant computing and storage resources, and provides on-the-move access to outsourced data (i.e., road condition information) to end users. In RCoM, the cloud server is a curious entity, which is engaged by RA to maintain and process all road information collected by vehicles.

III. MODULE SETS

Setup(1^k)->(par, msk): On input 1^k where k is a security parameter, the RCoM system setup algorithm, which is run by the root authority RA, generates the public parameter par for the system and a master secret key msk for itself. **SAdlg(par, msk; SA_i)** ->ssk_i: On input the public parameter par, the master secret key msk and the identity of some sub-authority SA_i, the delegation algorithm, which is run by RA, generates a secret key ssk_i for SA_i. Sub-authority SA_i should be able to validate ssk_i before accepting it as secret key. **VHreg(par, SA_i, ssk_i, V_j)** ->vsk_j: On input the public parameter par, the identity SA_i and secret key ssk_i of some sub-authority, and the identity of some vehicle V_j, the vehicle registration algorithm, which is run by SA_i, generates a secret key vsk_j for V_j. Vehicle V_j should be able to validate vsk_j before accepting it as secret key. **RUreg(par, SA_i, ssk_i, RU_l)** ->rsk_l: On input the public parameter par, the identity SA_i and secret key ssk_i of some sub-authority, and the identity of some roadside unit RU_l, the roadside unit registration algorithm, which is run by SA_i, generates a secret key rsk_l for RU_l. Roadside unit RU_l should be able to validate rsk_l before accepting it as secret key. **TKdis(par, (SA_i, V_j, vsk_j), (SA_l, RU_l, rsk_l))** ->T₁ / L: On input the public parameter par, the token distribution protocol, which is jointly run by vehicle V_j and roadside unit RU_l with (SA_i, vsk_j) and (SA_l, rsk_l), respectively, outputs an authentication tuple T₁ including a token theta₍₁₎ if both sides are honest, or L otherwise. Here, SA_i and SA_l denote the administrative sub-authorities of V_j and RU_l, respectively. **RCrep(par, vsk_j, T₁, RU_l, I)** -> (U, W): On input the public parameter par, the secret key vsk_j of vehicle V_j, an authentication tuple T₁, a roadside unit identity RU_l and some road condition information I, the road condition report algorithm, which is run by vehicle V_j, outputs a ciphertext U and a tuple W. **CLpro(par, U, W)** ->{0, 1}: On input the public parameter par and a pair of (U, W), the cloud processing algorithm, which is run by the cloud server, outputs “1” if the pair (U, W) can be inserted into some group; otherwise it outputs “0”. **RApro(par, msk, U, W)** -> (RU_l, I): On input the public parameter par, the master secret key msk and a pair of (U, W), the RA processing algorithm, which is run by the root authority, outputs a decrypted pair of (RU_l, I).



IV. IMPLEMENTATION

Step 1:

The screenshot shows a login page with the following elements: a title "Login Page", a "Username" input field, a "Password" input field, a red "SUBMIT" button, and a link "Not registered yet? Register HERE" below the button.

Login from app

Step 2:

The screenshot shows a registration page with the following elements: a title "Registration Page", "Name", "Email Address", "Mobile", and "Password" input fields, a "Gender" section with radio buttons for "Male" and "Female", a "Confirm Password" input field, and a red "SUBMIT" button.

Registration



Step 3:



User homepage and updating GPS location

Step 4:



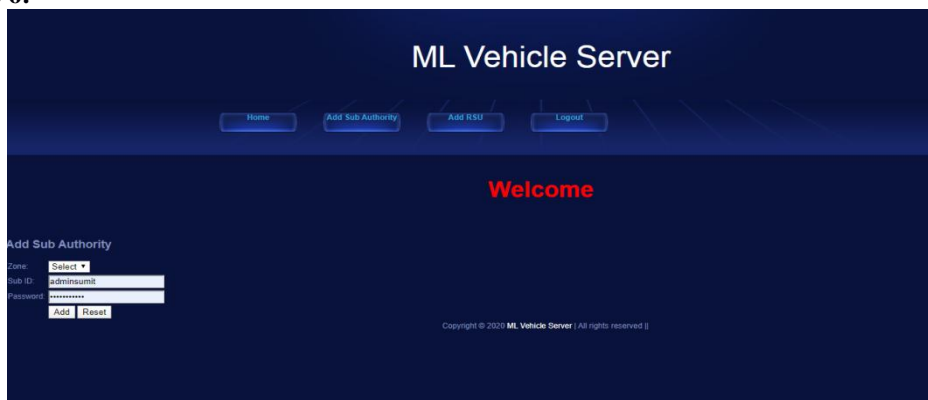
GPS tracker

Step 5:



Authority home

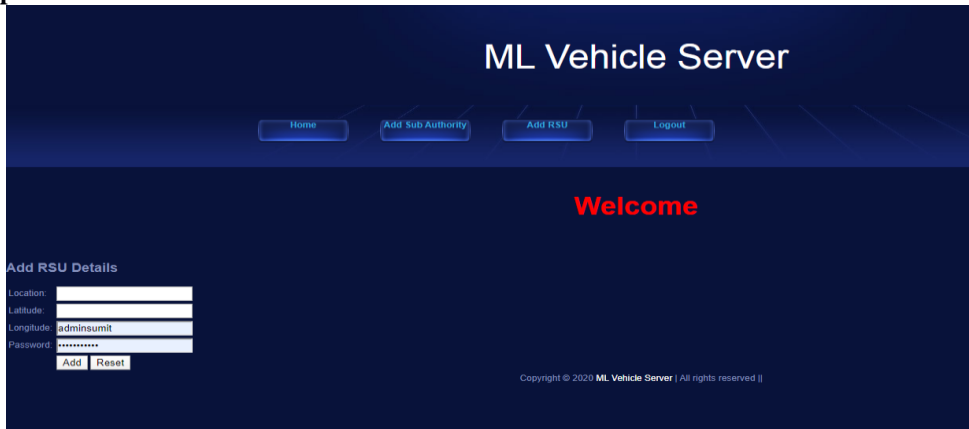
Step 6:



Add Sub-authority



Step 7:



Add RSU

V. EXPERIMENTAL RESULTS

The performance of the Setup, SAdlg, VHreg and RUreg algorithms are shown in Figure 1. The evaluation shows that the Setup algorithm can be completed in less than 20 msec, which is mainly determined by two exponentiations in G. For a delegation, RA can generate a secret key sski for some sub-authority SA_i in roughly 7 msec, whereas SA_i is able to validate sski with less than 8 msec. These two procedures are presented by DelGen and DelVrf in the figure. The vehicle registration enjoys the comparable performance of the roadside unit registration, that is, the secret keys vskj and rskl can be generated by sub-authorities in roughly the same time, and the verification at respective sides of vehicle and roadside unit also takes the similar time. Figure 2 plots the performance of the token distribution TKdis protocol, and the RCrep and RApr algorithms. The experiment results are shown in Figure 3, which demonstrate that the performance linearly determined by the number of equivalence classes at the cloud server side. It is easy to see that the average execution time of comparing with a single equivalence class is roughly 4 msec.

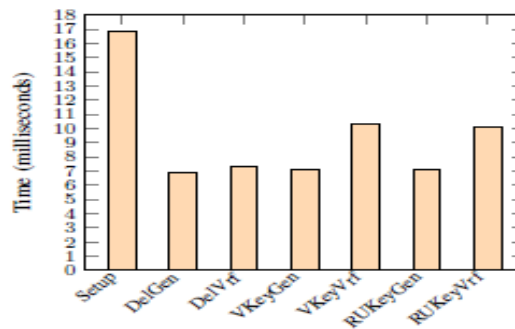


Fig.1. Performance evaluation of the Setup, SAdlg, VHreg and RUreg algorithms.

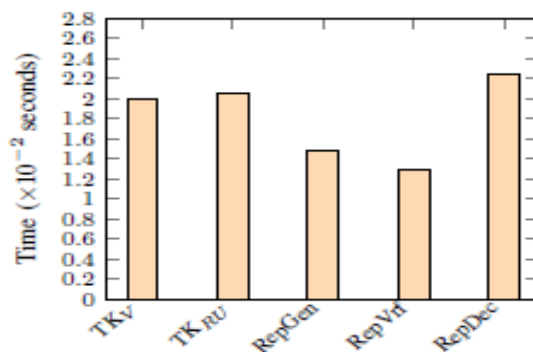


Fig.2 Performance evaluation of the TKdis protocol, and the RCrep and RApr algorithms.

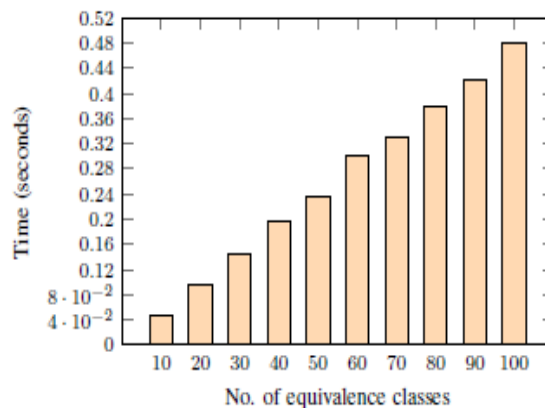


Fig. 3. : Performance evaluation of the CLpro algorithm.

VI. CONCLUSION AND FUTURE WORK

In this article, we considered the problem of a secured data sharing among vehicles to keep track of road condition. There are two levels of authorities such that the root authority delegates sub authorities to perform registration for vehicles and RUs. RA monitors real-time road conditions through a third party intermediary, that is, vehicles report the detected road conditions to the cloud server for verification and processing, in this way, only the valid information sent from legitimate vehicles will be picked out for RA to make response. To protect the privacy against the cloud server, the road condition report should be uploaded in cipher text format, which brings another challenge for the cloud server to distinguish the same road condition for the same place from lots of reports. In response to these functionalities and security and privacy requirements, we presented an efficient scheme and compared it with related techniques. Through extensive theoretical and experimental analyses, we demonstrate that the proposed RCoM scheme is practical in application settings and we can increase the performance of privacy requirements.

REFERENCES

- [1] Q. Wu, J. Domingo-Ferrer, and U. Gonzalez-Nicolas, "Balanced trustworthiness, safety, and privacy in vehicle-to-vehicle communications," *IEEE Transactions on Vehicular Technology*, vol. 59, no. 2, pp. 559–573, Feb 2010.
- [2] M. Armbrust, A. Fox, R. Griffith, A. D. Joseph, R. Katz, A. Konwinski, G. Lee, D. Patterson, A. Rabkin, I. Stoica, and M. Zaharia, "A view of cloud computing," *Commun. ACM*, vol. 53, no. 4, pp. 50–58, Apr. 2010.
- [3] G. Yang, C. H. Tan, Q. Huang, and D. S. Wong, "Probabilistic public key encryption with equality test," in *Topics in Cryptology - CT-RSA 2010: The Cryptographers' Track at the RSA Conference 2010, San Francisco, CA, USA, March 1-5, 2010. Proceedings*, J. Pieprzyk, Ed. Berlin, Heidelberg: Springer Berlin Heidelberg, 2010, pp. 119–131.
- [4] L. Chen, S. L. Ng, and G. Wang, "Threshold anonymous announcement in vanets," *IEEE Journal on Selected Areas in Communications*, vol. 29, no. 3, pp. 605–615, March 2011.
- [5] D. Song, E. Shi, I. Fischer, and U. Shankar, "Cloud data protection for the masses," *IEEE Computer*, vol. 45, no. 1, pp. 39–45, Jan 2012.



Encasement for Walking Assistance using Robotic Technology

¹Aishwarya M, ²Akanksha P, ³Akahaya Kumari S, ⁴Krithika P, ⁵Mrs. Visalini S

Final year B.E Students (UG), Department of Information Science & Engineering, The Oxford College of Engineering, Bangalore, India^{1,2,3,4}

Assistant Professor, Department of Information Science & Engineering, The Oxford College of Engineering, Bangalore, India⁵

ABSTRACT: Our project represents the design of an exoskeleton robotic technology to assist the paralyzed people to move on their own, by supporting them physically and move their leg independently like a human leg. The working prototype has been designed of two features, one is support and the second one is motion with the help of Arduino based micro-controller support. In support part the robot is holding the whole physique of the paralyzed person and keep the person stand with support. The motion part is taking decision whether to sit down, stand up and walk based on the manual switch that will give command to the microcontroller which assess the command, and move the exoskeleton based on it. The prototype is developed with the intention to help the paralyzed people for helping them walk and remove them from the entitlement of disability.

KEYWORDS: Exoskeleton robotic technology; Arduino based micro-controller; Assess the command ; move the exoskeleton ; entitlement of disability.

I. INTRODUCTION

There are many people with disabilities in today's country's population. Our project is mainly dedicated to them who are paralyzed and can't move their lower body part. Patient of this kind of disease usually uses wheelchair or someone else's help to move or do any kind of mobility-based work. By introducing this device to them they can sit, stand and walk.

This will help them stand up while keeping balance and support their whole body. The revolution of robotic exoskeleton started at the last half of the 20th century. People who could not walk or move started to embrace robotics. In 1965, General Electric (in the US) was in progress with the Hardiman, a large full-body exoskeleton intended to enhance the user's strength to assist in lifting heavy objects. At the end of 1960s and at the start of 1970s, the first gait assistance exoskeletons were developed at the Mihajlo Pupin Institute Serbia and University of Wisconsin-Madison in the US, respectively. The exoskeleton project was recently modified by many other companies such as ReWalk, Ekso GT and Phoenix Medical.

These projects are state of the art which possess more advance technology with better and faster control system for the patient to use. They are primarily made for the rehabilitation of the paralyzed people but can also be used for their day to day like necessities with convenient advance programs and features. And while they are state of the art, they come at prices far beyond reach for normal or poor people to afford. And this is where the assistive exoskeleton shine giving the basic movement at much lower price.

II. PROBLEM STATEMENT

Exoskeletons are dressed external and support the body movement like a power suit. Exoskeletons were developed to support disabled or handicapped people during their rehabilitation process and to support the everyday life, for example, of paralyzed patients. The motivation to use Exoskeletons in industry to assist and help workers to achieve daily tasks, is based on these two different approaches. Exoskeletons will be able to assist disabled workers at work and therefore give them the ability to reintegrate. As a result a reduction of lost work days can be expected.

III. PROPOSED SYSTEM

In the proposed system we developed a metallic exoskeleton which mostly consists of several metallic frame and some electrical parts to run the device in an automated way. The metallic bar holds the overall structure of the exoskeleton. The robust element will support the overall structure of the exoskeleton and give it, its base to work on the whole

exoskeleton. A Relay module is an electrically worked switch of mains voltage. It implies that it can be turned on or off, releasing the current through or not.

The relay module will take command from the Arduino and give signal to the actuators of respective relay part to control their movement. The Arduino Uno control the relay signal which will direct the signal based on their given code, and according to those signals, the actuator will move accordingly moving the exoskeleton. We are using 2 8400 mAh LiPo Battery to ensure the functionality of the actuator and other electronics peripherals with it. This will let the device sustain for a minimum 5 hours of functionality.

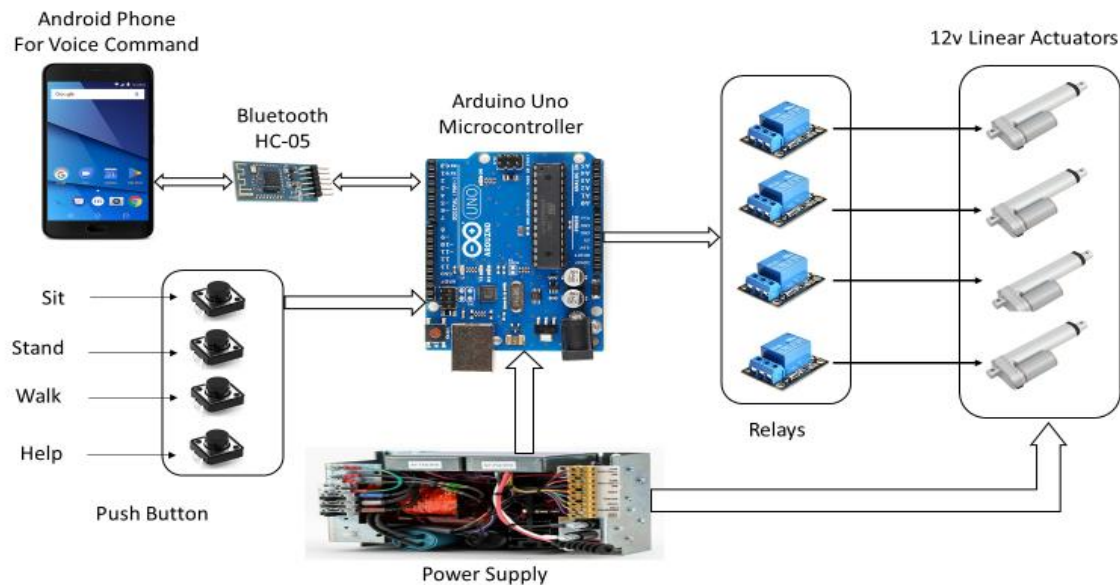


Fig 1: Working Method of the System

The step by step process of the device running with a command signal is given below.

1. Firstly, when the switching command is pressed, the relay sends signal to the microcontroller. There are 8 relay which gives different set of signals to the microcontroller based on the movement to be made.
2. The device when given the walk signal starts moving forward.
3. First, the left leg is lifted up and moved forward when relay 1 and 2 are high. The leg will start coming down to the ground when relay 3 and 4 are on. Half cycle complete.
4. Next, the right leg is lifted up and moved forward when relay 5 and 6 are high. The leg will start coming down to the ground when relay 7 and 8 are on. In this way, full cycle of 1 step is complete. After pressing the switch of the walk button, the whole function will start with a delay of 1 second, and will fully complete the full cycle within a time of 18 second.
5. By the combination of the movement of the left leg and the right leg using 8 relay signal, it can be seen that the exoskeleton achieved its goal by moving a paralyzed patient based on the command given to them.
6. During the movement of standing and sitting up, all the relay works together at the same time. The function of the stand and sit is reciprocal to one another. While the device is in stand position, when pressing the stand button, the device will not do anything. But if the sit button is pressed, all the relay will signal all the 4 actuator at both the leg to go down at the same time.

IV. SIMULATION & SOFTWARE

A. Simulation

To avoid theoretical error and unexpected circumstances in this project, some simulation of the designed circuit and hardware are done before implementing the physical parts. By this way, better understanding of the work by the system is achieved and the validity of the project is ensured.

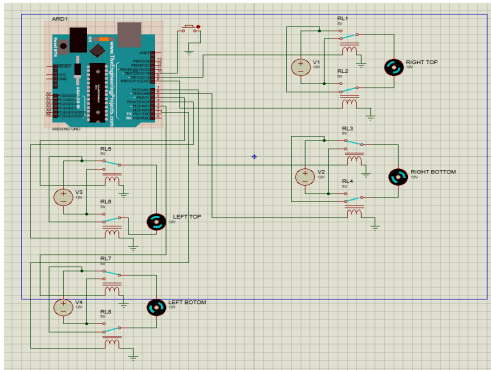


Fig 2: Schematic Design of the Arduino and Relay Module.

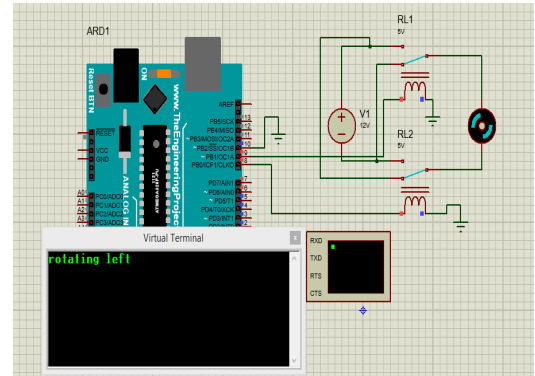


Fig. 3: Relay signal for motor to turn left.

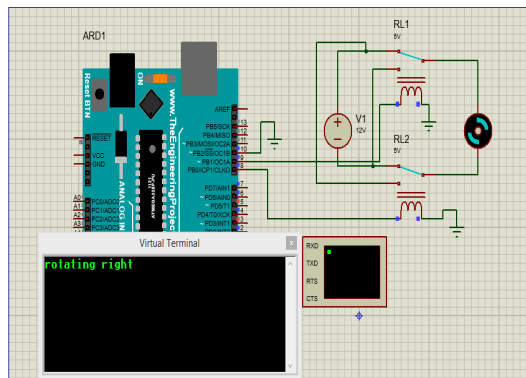


Fig. 4: Relay Signal for motor to turn right

In the above picture 8-relay module is connected to the Arduino Uno. The 8-relay signal worked when the command of the relay was transferred to the microcontroller where the code was set of 8 different relay signals. The code was completed and executed in the Arduino software and the circuit design was accomplished in the Proteus 8 Professional Software. The function that were executed by the code of the 8 relays in the Arduino software is given below. In the figure 3, the relay signal has been given for the motor to turn left representing the pull of the actuator. In the figure 4, the opposite can be seen.

B. Software

For software purpose, we used 3 different software for different purpose in our project.

1. Solidworks computer aided design software
2. Arduino IDE for Arduino programming
3. Arduino Embedded C.
4. Android Program



Solid Works Modelling



Fig. 5: Solid works modeling back movement



Fig. 6: Solid works modeling forward movement

The main design of the exoskeleton was done by using Solidworks, which is a computer-aided design and computer-aided engineering computer program. By using this software, a virtual product was made to understand the functionality and the sustainability of the project device. In figure 5, we can see the actuator moving down moving the leg frame towards the ground. In figure 6, the actuator fully lifts the leg up to move the leg forward.

Android App

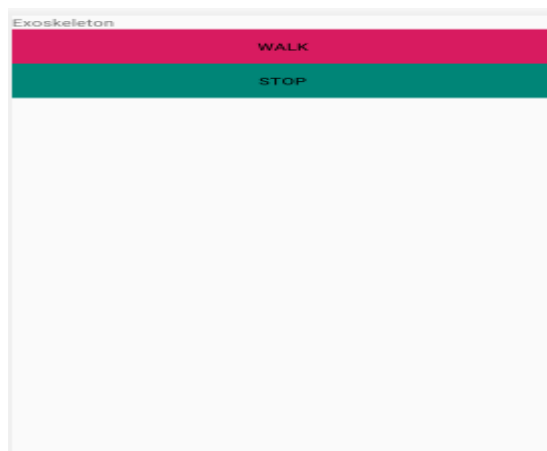


Fig. 7: Android App to control device

In figure 7, the Android app is been created which has two button, one to Walk and another to Stop where the paralysed person can access the exoskeleton model through phone by using this app.

V. HARDWARE

The Assistive Exoskeleton is a metallic exoskeleton which mostly consists of several metallic frame and some electrical parts to run the device in an automated way.

A.1 Metallic Frame

Made of Steel, this metallic bar holds the overall structure of the exoskeleton. Compare to carbon fiber they maybe heavier, but the robust element will support the overall structure of the exoskeleton and give it, its base to work on the whole exoskeleton and help keep the integrity of the device in the long run. Also, it is very much cheaper than carbon fiber and available in the local market since low cost is one of the novelty of this project.



A.2 Actuators

4 Linear actuator
Brand: Louie
Model: XTL100
Stroke: 100mm or 4inch
Push Load: 1000N
Voltage: 12V DC
Speed: 12mm/s

In this project, 2 of them are used, 1 on the upper thigh, and 1 on the back calf of the leg. These actuators will be used to control the overall movement of the exoskeleton by moving them according to the command they are given in a synchronized motion.



Fig. 8: Linear Actuator

B.1 Relay Module as MotorDriver

A Relay module is an electrically worked switch of mains voltage. It implies that it can be turned on or off, releasing the current through or not. The relay module will take command from the Arduino and give signal to the actuators of respective relay part to control their movement.

B.2 Arduino UNO

Arduino Uno is used to control the relay signal which will direct the signal based on their given code, and according to those signals, the actuator will move accordingly moving the exoskeleton [8].

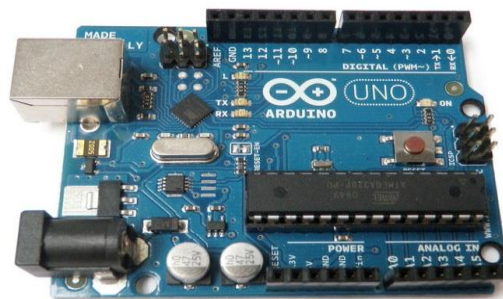


Fig.9. Arduino UNO



C.1 Power Supply

Control supply is a reference to a wellspring of electrical compel. A contraption or system that provisions electrical or diverse sorts of essentialness to a yield load or assembling of weights is known as constrain supply unit or PSU. The term is most generally associated with electrical essentialness supplies, less much of the time to mechanical ones, and once in a while to others

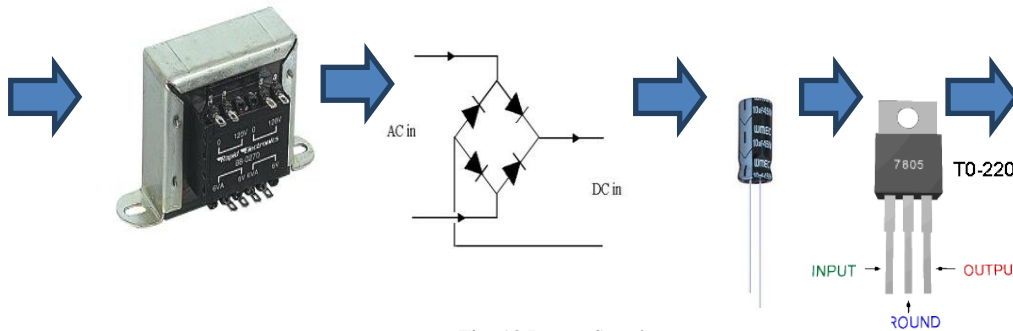


Fig .10 Power Supply

VI. RESULTS ANALYSIS

The result of the project mainly focuses on two part. The hardware result which will focus on how the device is running with a patient, if the goal is being achieved properly. And the software result which will focus on the simulation of the electrical part of the device if the different control signals are properly delivered with each command.

It is to be mentioned again the design of the whole frame with the accurate placement position of the actuators will allow the movement of the frame in the desired position which has been already simulated in the Solidworks software. While the device can fully support the patient physically, the stability of the patient is maintained using two elbow crutch which are to be held at both hand of the patient to keep the balance of the device and the body of the patient.

Also, the device is made mimicking the movement of the simulation, so the patient should be able to walk or stand still comfortably both when the switch is turned on or off respectively

The step by step process of the device running with a command signal is given below

1. Firstly, when the switching command is pressed, the relay sends signal to the microcontroller. There are 8 relay which gives different set of signal to the microcontroller based on the movement to be made.

2. The device when given the walk signal starts moving forward.

3. First, the left leg is lifted up and moved forward when relay 1 and 2 are high. The leg will start coming down to the ground when relay 3 and 4 are on. Half cycle complete.

4. Next, the right leg is lifted up and moved forward when relay 5 and 6 are high. The leg will start coming down to the ground when relay 7 and 8 are on. In this way, full cycle of 1 step is complete. After pressing the switch of the walk button, the whole function will start with a delay of 1 second, and will fully complete the full cycle within a time of 18 second.

5. By the combination of the movement of the left leg and the right leg using 8 relay signal, it can be seen that the exoskeleton achieved its goal by moving a paralyzed patient based on the command given to them.

6. During the movement of standing and sitting up, all the relay works together at the same time. The function of the stand and sit is reciprocal to one another. While the device is in stand position, when pressing the stand button, the device will not do anything. But if the sit button is pressed, all the relay will signal all the 4 actuator at both the leg to go down at the same time. The device is designed in a way that the frame will take into position of sitting just by the movement of the actuator. The whole process will take 8sec.



Fig .11 Lower Limb Exoskeleton with Linear Actuator

VII. FUTURE SCOPE OF THIS STUDY

The assistive exoskeleton that was developed in this project can be used in other purpose like robotics research, medical research etc. The sustainability of the project is directly proportional to the importance of the project. The importance of the project is determined by the usage of the project. In India, hundreds and thousands of people are paralyzed in some way or another. Most of them are poor.

The Assistive Exoskeleton is targeted specifically for this kind of people. With high demand, this project under proper observation can flourish on a large scale and mass manufacture of the device can be started with proper sponsor. After further development of the project in future, the device can be exported on global scale to different other countries of the world. There are many points and spaces for future development which will improve the usability of the device and make it more user friendly.

Differential Gear will be used instead of actuator which will give us faster operation and better mobility. IOT (Internet of things) technology can be used to monitor the patients' health status and also keep it informed to the family member and the physician of the patient. Wireless input system for information gathering and command system can be added which will let the exoskeleton to be controlled in a wireless manner. Furthermore, it can mainly target to control the system by simply thinking or by using brain wave. This can open up vast scope of study for this project

VIII. CONCLUSION

The Assistive Exoskeleton will be extremely useful for the physically paralyzed individuals in terms of movement. Paralyzed individuals will be able to move from one place to another independently. The Exoskeleton will act as a base of more improved design from generation to generation of development in the upcoming future as more research will be done towards it. The developed prototype gives us better result at moving a paralyzed person from one position to another, thus giving us an accurate estimate of the real deal to come. This project can change the world of paralyzed



people who are poor and cannot afford to spend millions of moneys to walk and can take us to the betterment of mankind.

REFERENCES

- [1] Shuaib, M. (n.d.). List of Contributors in the Preparation of the Monograph, BANGLADESH BUREAU OF STATISTICS (BBS), 2015, p.1-91.
- [2] Amputee-coalition.org, 2018. [Online]. Available: <https://www.amputee-coalition.org/resources/a-brief-history-of-prosthetics/>. [Accessed: 13- Dec-2018].
- [3] Esquenazi A, Talaty M, Packel A, Saulino M., "The ReWalk powered exoskeleton to restore ambulatory function to individuals with thoracic-level motor-complete spinal cord injury", Am J Phys Med Rehabil.2012;91:911–21.
- [4] Ekso exoskeleton for rehabilitation in people with neurological weakness or paralysis | Guidance and guidelines | NICE", Nice.org.uk, 2018. [Online]. Available: <https://www.nice.org.uk/advice/mib93>. [Accessed: 13- Dec-2018].
- [5] "A new budget exoskeleton could help paraplegics walk at a drastically lower price." [Online]. Available:<https://www.extremetech.com/extreme/222396-a-new-budget-exoskeleton-could-help-paraplegics-walk-at-a-dramatically-lower-price.html>. [Accessed8-Aug-2018].
- [6] "About Actuators." [Online]. Available:[www.thomasnet.com.html](http://www.thomasnet.com/html). [Accessed8-Aug-2018].
- [7] "Guide for Relay Module with Arduino." [Online]. Available: <https://randomnerdtutorials.com/guide-for-relay-module-with-arduino.html>. [Accessed 8-Aug-2018].
- [8] "What is an Arduino?" [Online]. Available: <https://learn.sparkfun.com/tutorials/what-is-an-arduino.html>. [Accessed 8-Aug-2018].
- [9] Bruno Scrosati, K. M. Abraham, Walter A. van Schalkwijk, Jusef Hassoun (ed), Lithium Batteries: Advanced Technologies and Applications, John Wiley & Sons, 2013 ISBN 1118615395,page44
- [10] "Decorative Trim" [Online]. Available: http://www.kroh-wagner.com/decorative_trim.html [Accessed 8- Aug-2018].



Medical Mirror Using Face Recognition

Abhishek M¹, Manish kumar², Madan R³, Mr. Yadhu Krishna M. R⁴

Final year B.E Students (UG), Department of Information Science & Engineering, The Oxford College of Engineering,
Bangalore, India ^{1,2,3}

Assistant Professor, Department of Information Science & Engineering, The Oxford College of Engineering,
Bangalore, India ⁴

ABSTRACT: We propose a video surveillance system based on blockchain system. The proposed system consists of a blockchain network with trusted internal managers. The metadata of the video is recorded on the distributed ledger of the blockchain, thereby blocking the possibility of forgery of the data. The proposed architecture encrypts and stores the video, creates a license within the blockchain, and exports the video. Since the decryption key for the video is managed by the private DB of the blockchain, it is not leaked by the internal manager unauthorizedly. In addition, the internal administrator can manage and export videos safely by exporting the license generated in the blockchain to the DRM-applied video player.

KEYWORDS: Smart Mirror, Medical Data, Database.

I. INTRODUCTION

Internet of Things (IoT) is a term used to describe “technologies, systems, and design principles associated with the emerging wave of Internet-connected things that are based on the physical environment”. It refers to a network of uniquely identifiable things (objects) and their virtual representations in an Internet-like structure, which are able to collect and exchange data and are remotely controlled across existing network infrastructure. It comprises of major components including sensing function, heterogeneous access, information processing, security, privacy, and applications and services. According to the International Telecommunication Union (2013), the term Internet of Things (IoT) is defined as a global structure for society that enables Internet service to connect to physical matter based on information and communication technologies available. IoT is also seen in a broader perspective and nonetheless brings quite a huge implication of technology on society. Along with the development of technology, various information can be found easily and the emergence of the concept of Smart Mirror Smart Education has become increasingly widespread. The Smart Mirror system which is based on the concept of Internet of Things (IoT) is developed specifically to allow users to manage and control education levels through voice recognition. In this case, it has been identified as the main problem faced by most people. There are just too many things to be done at one time and at certain point, users are not able to multitask such daunting chores. For example, when a to-do-list with a number of studies has been recorded on a paper, but the paper is lost because it is misplaced. Another example is when users are too busy managing their daily activities until some trivial-yet-critical things have happened, which can eventually lead to energy wastage.

II. PROBLEM STATEMENT

In the existing system managing education related things were done by the people themselves which led them to face many problems and it has been identified as the main problem faced by most people.

There are just too many things to be done at one time and at certain point, users are not able to multitask such daunting chores. There are plethoras of Smart Mirrors in existence by now. Mostly, developed to display time, date, and weather-related information. But you will hardly find all these features in a single Smart Mirror. Especially in India, this concept has not made strides yet. Also, human detection system is not implemented into Smart Mirrors on a large scale. By implementing human detection module, one can get instant control along with that can save electricity.

III. PROPOSED SYSTEM

In the proposed system, we develop an android application. This android application is connected to the smart mirror through Wi-Fi. When the user opens the presentation in his/her android mobile it automatically gets projected in the smart mirror. While connecting the device with the smart mirror its going to display the information to the smart screen so it enables the user to smartly handle and organize the various study levels in an efficient manner.



IV. METHODOLOGY

In our work we used some modules, these modules/methodology are listed below.

Initial setup:

In this system, admin can add patient detail and medical report. Admin can update medical reports. Admin is able to add patient picture for face detection and recognition. Admin can check all record and patient detail from web application.

Voice Control: To interact with the mirror it uses microphones. Microphone is using to power the voice recognition capabilities. The first microphone is a simple one connected Through a USB sound card and Raspberry Pi

Motion Sensing: Using a PIR sensor for your Raspberry Pi you can have your display turn on only when there is someone in the room. PIR sensor will detect the human.

Facial Recognition: In this project, we are using machine learning algorithm SVM for recognizing the patient. Camera placed behind the mirror is used to recognize the user standing in front of the mirror. By recognizing the person, the mirror knows how to interact or behave next.

Medicine box: after recognized, if medicine is needed then medicine box will be open for particular patient.

V. SYSTEM ARCHITECTURE

The architecture of a system describes its major components, their relationships (structures), and how they interact with each other. Software architecture and design includes several contributory factors such as Business strategy, quality attributes, human dynamics, design, and IT environment. We can segregate Software Architecture and Design into two distinct phases: Software Architecture and Software Design. In Architecture, nonfunctional decisions are cast and separated by the functional requirements. In Design, functional requirements are accomplished

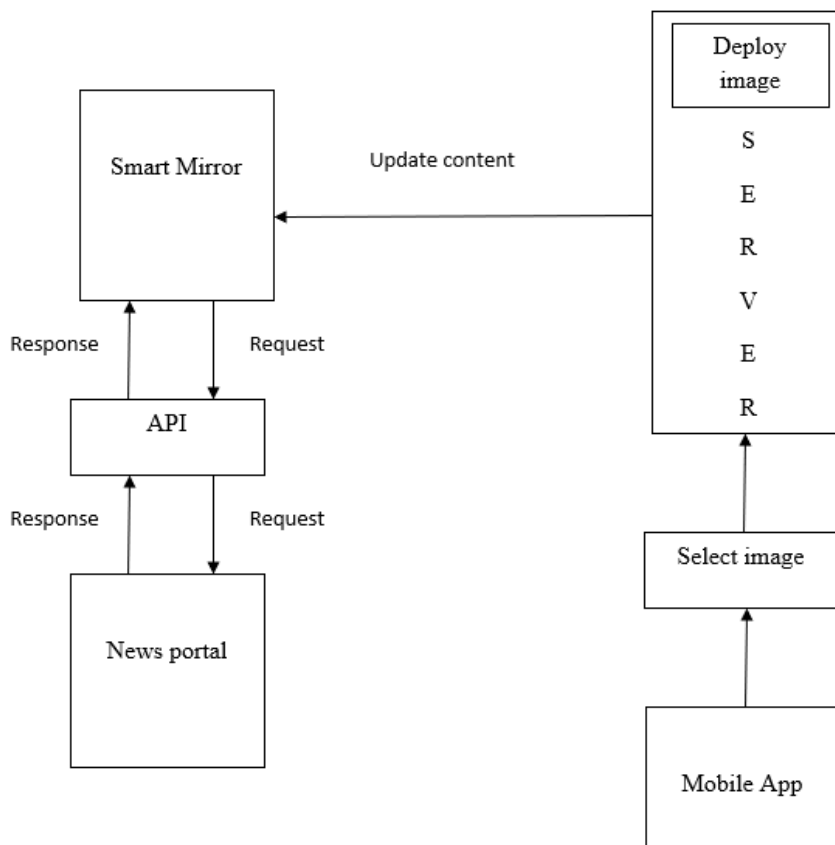


Fig 1: System Architecture



VI. IMPLEMENTATION

Prototype of the Project:

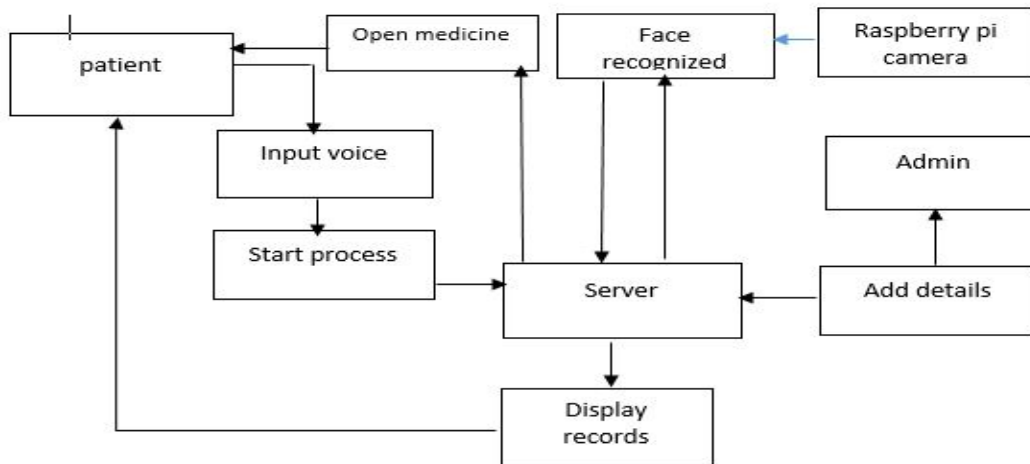


Fig 2: Implementation of the overall System

Methodology

1. Registration
2. Update details
3. Face Recognition
4. Display Information

Registration

Admin first login into the portal to add the patient details. Admin can add the patient details along with the face image. All these details are saved in the application server. The patient details are sent from web browser to the application server using HTTP protocol. The students details are saved in the my sql database. The captured customer face images are trained in the server using Linear Support Vector Machine (LSVM) and the trained model will be updated. Admin can add the patient details and provides the login credential.

Update details

Admin can login into the portal and add or update patients report details. The patient details are stored in the mysql database.

Face Recognition

HOG image descriptors and Linear Support Vector Machine (LSVM) are used to train. Certain steps are to be followed in HOG. They are:

- Extracting HOG descriptors from the positive samples of trained images.
- Extracting HOG descriptors from the negative samples that don't contain any objects.
- Training LSVM on the samples.
- Testing with dataset.
- Finally face recognition is done by using Euclidean distance method.

Server fetch the corresponding patient id and send back to the controller.

Display Information

As soon as server recognizes the patient, it fetches the patient information from database and send to the raspberry pi connected to the smart mirror. On receiving the information, raspberry pi displays the information on the smart mirror



and welcomes the patient using text to speech API. The smart mirror is fitted with a microphone. If any patient wants to check his/her report or any other information can input the speech input. Raspberry Pi process the speech and converts into text using google TTS API. Based on the query raspberry pi send request to the server and get the data from the server and displays on the screen.

Medicine Box

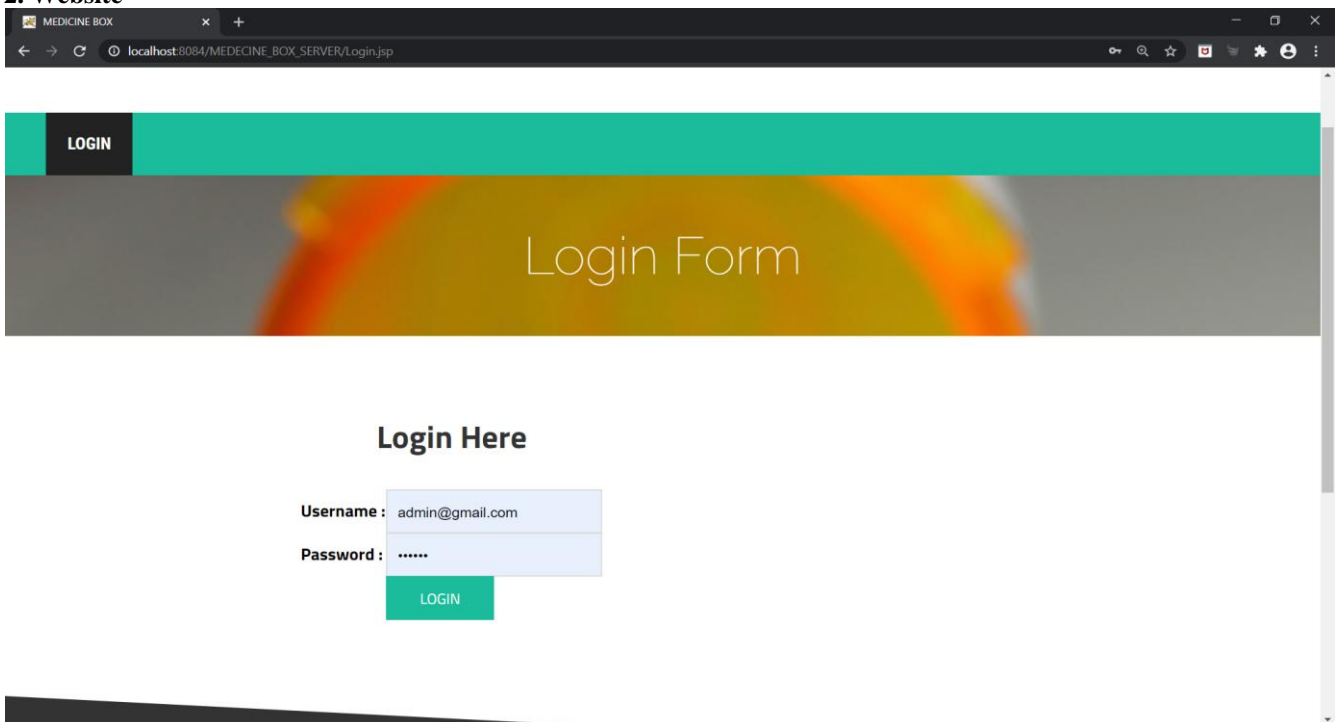
The Medicine Box is made of server motor which is controlled by the code to rotate at certain degrees. It includes 4 slots for the medicine and based upon the patients data the medicine box rotates and provides the particular medicine .It also has an IR sensor attached which detects the motion and updates the details if the patient has taken the particular medicine or not

Pictures

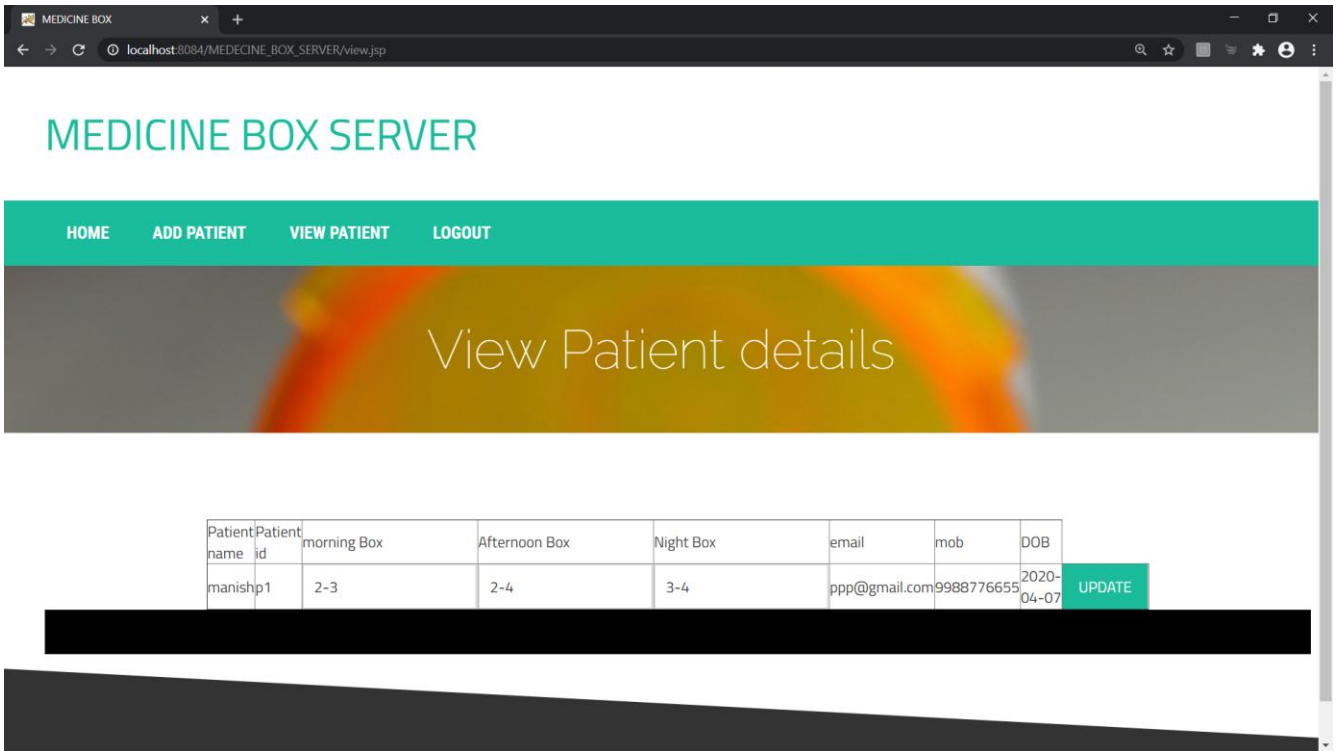
1.Project



2. Website

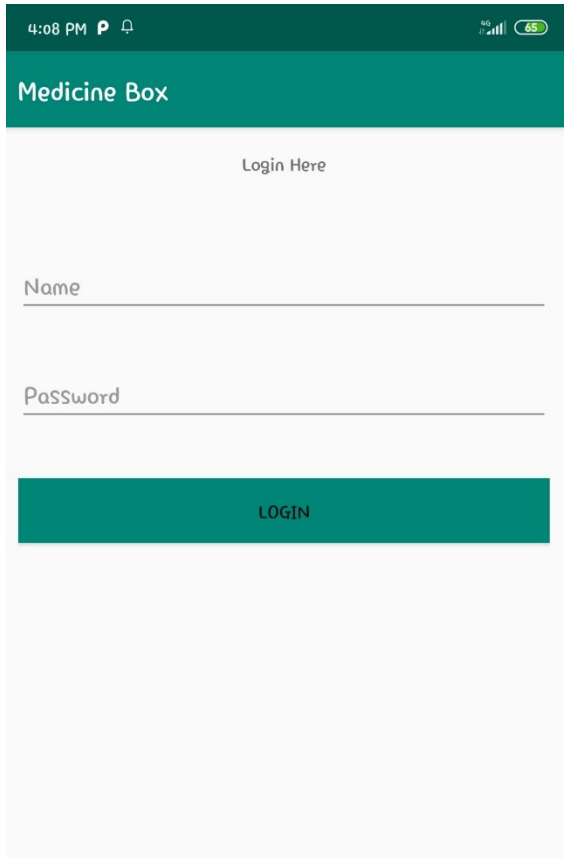


Login page

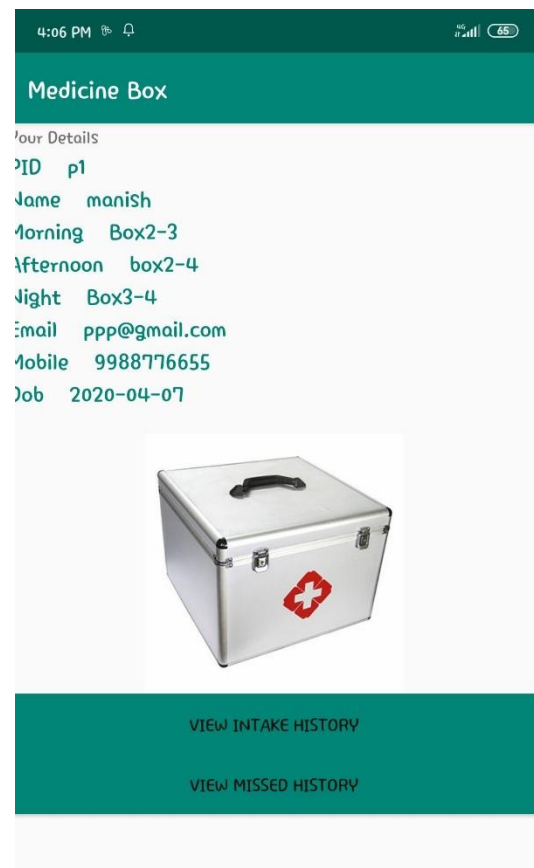


Patient details

3. Android App



App login



Patient details



VII. RESULT

The Users who want to access the videos which are uploaded into the blockchain can register themselves in the “BLOCKCHAIN VSS” website. They are provided with all the options to change their password or their credentials in case they want to edit. The users need to verify themselves by providing the portal with their registered email and phone number, a code will be sent to both, by entering both the codes in the portal a user gets verified. After his/her verification the user can download the desired videos which are present in the blockchain network in a read only format i.e, he/she can only view the videos and cannot make any changes to it.

VIII. CONCLUSION AND FUTURE WORK

As a conclusion, the application is the new technology for smart life. From the result testing, most of the function of the application are functioning well and there still need some improvement to the development of the newest functionality on smart mirror.

We have designed futuristic smart mirror that provides natural interaction between patients and the ambient medical services. The mirror display is provided by a flat led display monitor which display all the necessary information which are useful for the patient.

The mirror also provides a picture-in-picture sub-display to facilitate the display of services such as reports, prescriptions and other important patient details.

Future scope: in our future work we will investigate how the surrounding context of the patient and the environment can be utilized in order to provide optimal service experiences in the home environment.

The system can be made much more useful to the patients by adding more functionality like integrating speech processing, medicine disposal etc

REFERENCES

- [1] Holler J., Tsiatsis V., Mulligan C., Avesand S., Karnouskos S., Boyle D. M2M to IoT—the vision: from M2M to IoT From Machine-to-Machine to the Internet of Things: Introduction to a New Age of Intelligence 2014 1st chapter 2, section 2.2 Oxford, UK Academic Press 1418 Google Scholar
- [2] Chen M., Wan J., Li F. Machine-to-machine communications: architectures, standards and applications KSII Transactions on Internet and Information Systems 2012 6248049710.3837/tiis.2012.02.0022-s2.0- 84861022395 Google Scholar CrossRef
- [3] Internet of Things Global Standards Initiative 2015 Geneva, Switzerland ITU: Committed to connecting the world
- [4] Williams J. Internet of Things: Science Fiction or Business Fact? Harvard Business Review Analytic Services Report, December 2014
- [5] International Telecommunication Union (2013). Harnessing the Internet of Things for Global Development. <https://www.itu.int/en/action/broadband/Documents/Harnessing-IoT-Global-Development.pdf>
- [6] Centers for Medicare & Medicaid Services (CMS) Office of Information Service (2008). Selecting A Development Approach. Retrieved on October 27, 2016 from www.cms.gov/Research-Statistics-Data-and-Systems/CMSInformation-Technology/XLC/Downloads/SelectingDevelopmentApproach.pdf
- [7] Ian Sommerville (2007). Software Engineering. 8th ed. United States: Pearson Education, Inc.
- [8] R. A. Carter, A. I. Anton, A. Dagnino and L. Williams, "Evolving beyond requirements creep: a risk-based evolutionary prototyping model," *Proceedings Fifth IEEE International Symposium on Requirements Engineering*, Toronto, Ont., 2001, pp. 94-101.
- [9] Kasim, S., Hafit, H., Yee, N. P., Hashim, R., Ruslai, H., Jahidin, K., & Arshad, M. S. (2016, November). CMIS: Crime Map Information System for Safety Environment. In IOP Conference Series: Materials Science and Engineering (Vol. 160, No. 1, p. 012096). IOP Publishing.
- [10] Kasim, S., Hafit, H., Leong, T. H., Hashim, R., Ruslai, H., Jahidin, K., & Arshad, M. S. (2016, November). SRC: Smart Reminder Clock. In IOP Conference Series: Materials Science and Engineering (Vol. 160, No. 1, p. 012101). IOP Publishing.
- [11] Kasim, S., Hafit, H., Juin, K. P., Afif, Z. A., Hashim, R., Ruslai, H., ... & Arshad, M. S. (2016, November). BBIS: Beacon Bus Information System. In IOP Conference Series: Materials Science and Engineering (Vol. 160, No. 1, p. 012097). IOP Publishing.
- [12] Kasim, S., Xia, L. Y., Wahid, N., Fudzee, M. F. M., Mahdin, H., Ramli, A. A., ... & Salamat, M. A. (2016, August). Indoor Navigation Using A* Algorithm. In International Conference on Soft Computing and Data Mining (pp. 598-607). Springer, Cham.



- [13] Kasim, S., Azahar, U. A., Samsudin, N. A., Fudzee, M. F. M., Mahdin, H., Ramli, A. A., & Suparjoh, S. (2016, August). E-Code Checker Application. In International Conference on Soft Computing and Data Mining (pp. 570-578). Springer, Cham.
- [14] Mahdin, H., Senan, N., Kasim, S., Ibrahim, N., & Abdullah, N. A. (2014). Teaching computer programming to IPAD generation.



Blockchain Based Video Surveillance System

Ritesh S¹, Syed Hussain², Sujith Chandrashekar Sarang³, Mr. Yadhu Krishna M. R⁴

Final year B.E Students (UG), Department of Information Science & Engineering, The Oxford College of Engineering,
Bangalore, India^{1,2,3}

Assistant Professor, Department of Information Science & Engineering, The Oxford College of Engineering,
Bangalore, India⁴

ABSTRACT: We propose a video surveillance system based on blockchain system. The proposed system consists of a blockchain network with trusted internal managers. The metadata of the video is recorded on the distributed ledger of the blockchain, thereby blocking the possibility of forgery of the data. The proposed architecture encrypts and stores the video, creates a license within the blockchain, and exports the video. Since the decryption key for the video is managed by the private DB of the blockchain, it is not leaked by the internal manager unauthorizedly. In addition, the internal administrator can manage and export videos safely by exporting the license generated in the blockchain to the DRM-applied video player.

KEYWORDS: Video Surveillance, Blockchain, Database.

I. INTRODUCTION

Video surveillance is a vital tool for protecting people and property around the clock. The increasing availability and, thus, lower cost of higher-quality cameras makes improving the effectiveness of video more affordable. However, a new issue now holds back users increased storage requirements. In a normal retail environment, it is common for video storage costs to exceed 50% of the entire surveillance system cost. There is also a problem of the Security provided to such videos stored which includes the leaks from the unauthorized users and the internal administrators. Video surveillance involves the act of observing a scene or scenes and looking for specific behaviors that are improper or that may indicate the emergence or existence of improper behavior. Common uses of video surveillance include observing the public at the entry to sports events, public transportation (train platforms, airports, etc.), and around the perimeter of secure facilities, especially those that are directly bounded by community spaces. The video surveillance process includes the identification of areas of concern and the identification of specific cameras or groups of cameras that may be able to view those areas. If it is possible to identify schedules when security trends have occurred or may be likely to occur, that is also helpful to the process. Then, by viewing the selected images at appropriate times, it is possible to determine if improper activity is occurring. A blockchain is a distributed ledger that is completely open to any and everyone on the network. Once an information is stored on a blockchain, it is extremely difficult to change or alter it. Each transaction on a blockchain is secured with a digital signature that proves its authenticity.

II. PROBLEM STATEMENT

The video surveillance system monitors video output from IP cameras and stores video information. It consists of a camera, a transmission device, a storage device, and a playback device. In recent decades, video surveillance systems have become increasingly large-scale to be managed with the rapid dissemination of CCTV (closed circuit television) for the purpose of crime prevention and facility management. The videos stored in the video surveillance system must be managed safely, but the videos are leaked out to unauthorized persons or viewed, resulting in the infringement of personal information. To solve this problem, a system has been developed that applies access control to video surveillance system, but there is still insufficient research to prevent unauthorized leakage by internal administrator

III. PROPOSED SYSTEM

The Proposed System consists of the Blockchain based Video surveillance and the usage of blockchain technology. Blockchain is a distributed database that stores data records that continue to grow, controlled by multiple entities. Blockchain (distributed ledger) is a trustworthy service system to a group of nodes or non-trusting parties, generally blockchain acts as a reliable and reliable third party to keep things together, mediate exchanges, and provide secure computing machines.



IV. METHODOLOGY

This stage is the underlying stage in moving from issue to the course of action space. Accordingly, starting with what is obliged; diagram takes us to work towards how to full fill those requirements. System plot portrays all the critical data structure, record course of action, yield and genuine modules in the structure and their Specification is picked. This assumes an essential part on the grounds that as it will give the last yield on which it was being working. In our work we use following modules, these modules are listed below:

- **Users Profile Operations**

Here, the end users can perform various operations on their profiles. Firstly, the users can register a new account and thus getting an access to the portal. And then the users can login to their accounts using the registered email ID and password to access various other divisions in the portal. The users can then choose to update their profile by providing the new values to the fields they have provided during the registration phase, or the user can wish to change their password by providing their old password and new password. The user can also opt to delete their accounts in case they wish to no longer access our portal. The user can also logout from the portal to make sure the session created for them during login is terminated.

- **Blockchain implementation**

Here, we implement the core Distributed Ledger network (Blockchain Architecture). We also create an interface to the users where they can setup the blockchain node by entering its IP address. Users can add as many nodes as they want. More the nodes, better the security.

- **Surveillance Application**

Here, we implement the application which communicates with CCTV/ Web Camera to capture the video frames. This can be set-up by the users by providing the IP address of the node where CCTV is pushing the video streams.

- **Blockchain Service Implementation**

Here, we provide couple of services w.r.t blockchain. The first service is called 'Video Write' service which will be used by the surveillance application to write the videos to blockchain network. The second service is called 'Video Read' service which allows the authorized users to download the video frames from the blockchain network.

- **Surveillance data Access implementation**

Here, we implement the Authorization mechanism to the Blockchain data. The authorized users can then read the video frames from Blockchain network using the previous module.

➤ SYSTEM ARCHITECTURE

The architectural configuration procedure is concerned with building up a fundamental basic system for a framework. It includes recognizing the real parts of the framework and interchanges between these segments. The beginning configuration procedure of recognizing these subsystems and building up a structure for subsystem control and correspondence is called construction modeling outline and the yield of this outline procedure is a portrayal of the product structural planning. The proposed architecture for this system is given below. It shows the way this system is designed and brief working of the system.

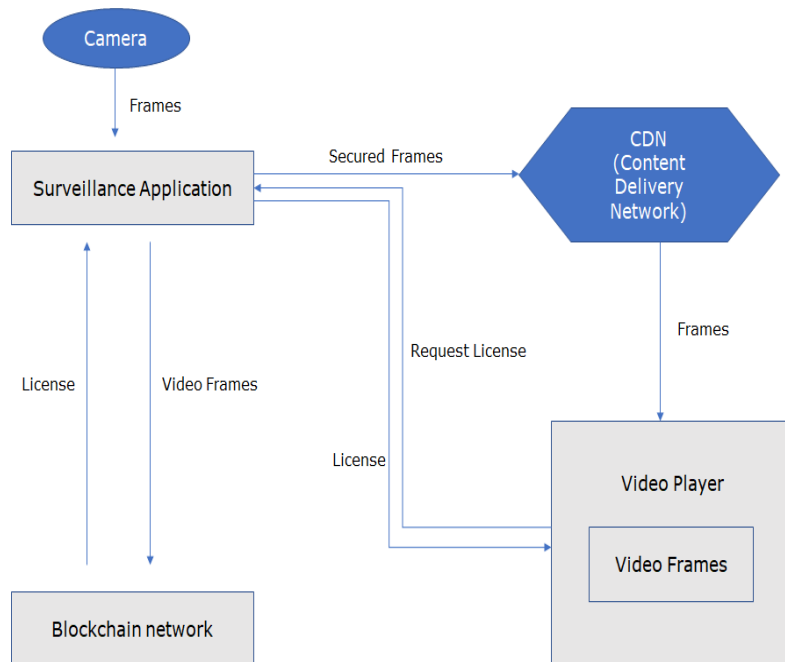


Fig 1: System Architecture

➤ **IMPEMENTATION**

Prototype of the Project:

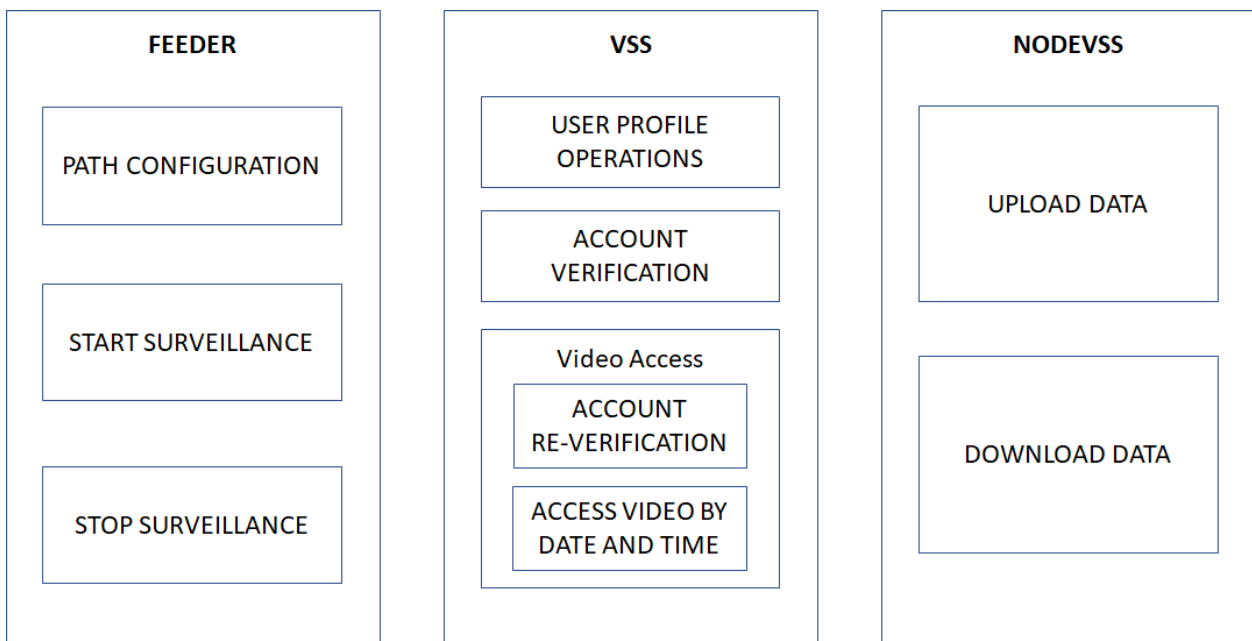


Fig 2: Implementation of the overall System



Feeder Application:

Feeder application is developed using Java-EE framework. This application is installed at the physical premises where the surveillance camera has to be installed (Ex: Shopping malls, Hospitals, Colleges, Offices, Shops, etc). Since this application is installed at a particular premises, only the admin/owner of the premises will have an access to this application. The Feeder application will provide the following three operations to the admin:

- **Path Configuration:** This is the configuration admin has to do before performing the surveillance operation. Here the admin will have select/specify the path where the surveillance video frames will be temporarily stored before they picked up by the bridge which uploads to the blockchain network
- **Start Surveillance:** The admin can start the surveillance operation. The video camera starts collecting the frames and dump them into the path configured above which will eventually be picked up by the bridge and pushed to the blockchain network
- **Stop Surveillance:** The admin can stop the surveillance operation.

Blockchain Node:

This Module implements the Blockchain Node. A node is the one which will have the entire blockchain data stored in it. The node will get the blockchain data when the Feeder components' bridge picks up all the frames from the configured path and constructs the blockchain out of it and then eventually uploads it to the Blockchain Node. There would be multiple blockchain nodes. More the number of nodes, stronger the security of the blockchain data. The blockchain Node application provides the two operations. Upload data and Download data to push and get the blockchain data correspondingly

VSS Application

This application provides the following four operations to the end users

- **User Profile Operations:** This module implements the basic user profile operations on the prototype application. The user profile operations include creating a new account, logging in to the existing account, logging out, editing the profile, changing the password, and deleting the profile if not needed anymore. This application is also deployed on the cloud server so that this can be accessed by anyone across the globe using the IP address of this cloud server. The implementation is done using the J2EE architecture and for the database needs we have used SQLITE3.
- **User Profile Verification:** Here, the user will have to verify their email ID and the mobile number specified during the registration operation. The system will generate an OTP separately for email and mobile and sends it to the user. The user will then have to provide the OTP in order to verify his/her profile. Without the profile verification, the system doesn't allow the user to download the video footage from the blockchain network.
- **Profile re-verification:** Here, the user will have to prove his/her identity again in order to verify that his/her session is not hacked by someone else. This re-verification is done in the same way as the profile operation. i.e, through sending an OTP to user's mobile number and email ID.
- **Video Retrieval:** Once the profile re-verification is done, the user will then get to select the date and time of the video at which he/she wants to retrieve for performing the monitoring operation. And then the system downloads the video from that date and time and provides the same to the user.



V. RESULT

The Users who want to access the videos which are uploaded into the blockchain can register themselves in the “BLOCKCHAIN VSS” website. They are provided with all the options to change their password or their credentials in case they want to edit. The users need to verify themselves by providing the portal with their registered email and phone number, a code will be sent to both, by entering both the codes in the portal a user gets verified. After his/her verification the user can download the desired videos which are present in the blockchain network in a read only format i.e., he/she can only view the videos and cannot make any changes to it.

Snapshots from the website:

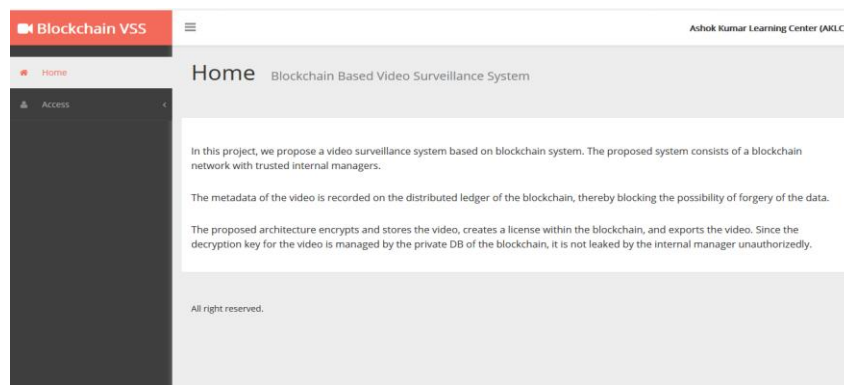


Fig 3: Index Page

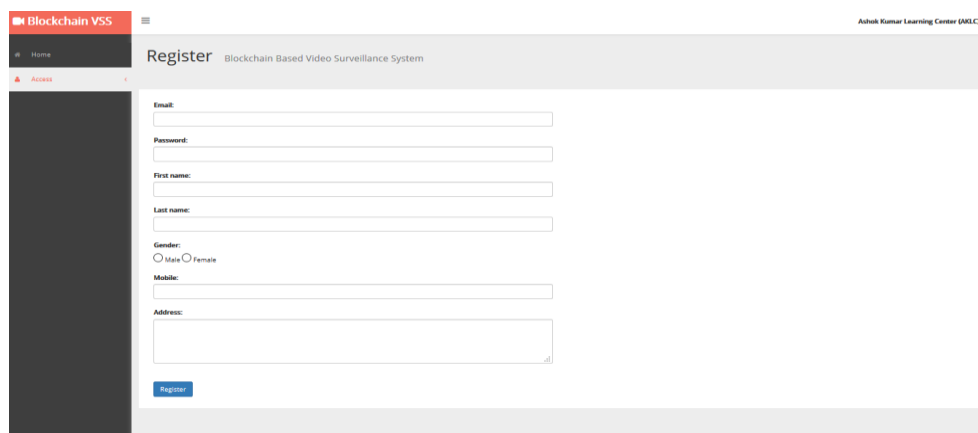


Fig 4: Register page

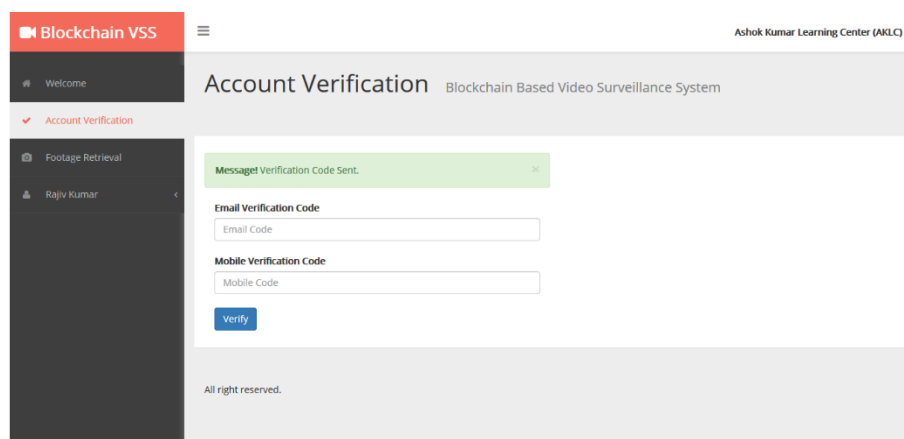


Fig 5: Account Verification page

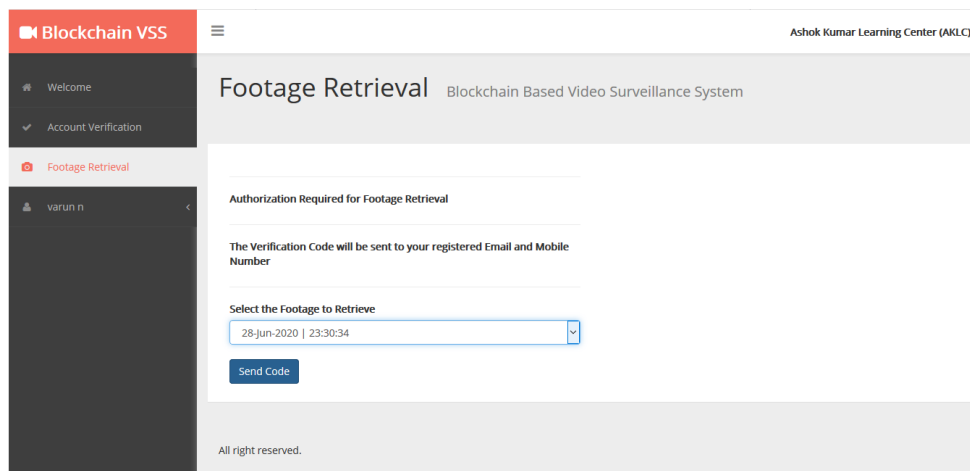


Fig 6: Footage Retrieval Page

VI. CONCLUSION AND FUTURE WORK

In this project, we propose a video surveillance system based on blockchain. Videos recorded from IP cameras are encrypted and stored in IPFS through a private blockchain network composed of trusted administrators. The decryption key for the video is not stored in the block but stored in the DB of the specific node having the collection authentication authority so that the internal manager cannot confirm the decryption key. Also, when a person who wants to view a video receives approval from the blockchain network or an internal manager monitors video on the screen, the internal manager executes a verification algorithm for exporting the video. In the verification algorithm, the code is sent to users email and mobile. In the proposed blockchain structure, the video surveillance system can securely manage videos from external persons and internal administrators. Also, it is possible to manage the objective record whether the video export is well managed.

In Future, we aim at extending the solution across multiple nodes and scaling it to a large cluster of videos using Big data computing environment.

REFERENCES

- [1] Holler J., Tsiatsis V., Mulligan C., Avesand S., Karnouskos S., Boyle D. M2M to IoT—the vision: from M2M to IoT From Machine-to-Machine to the Internet of Things: Introduction to a New Age of Intelligence 2014 1st chapter 2, section 2.2 Oxford, UK Academic Press 1418 Google Scholar.
- [2] Chen M., Wan J., Li F. Machine-to-machine communications: architectures, standards and applications KSII Transactions on Internet and Information Systems 2012 6(2):480-497 10.3837/tiis.2012.02.0022-s2.0-84861022395 Google Scholar CrossRef.
- [3] Internet of Things Global Standards Initiative 2015 Geneva, Switzerland ITU: Committed to connecting the world.
- [4] Williams J. Internet of Things: Science Fiction or Business Fact? Harvard Business Review Analytic Services Report, December 2014.
- [5] International Telecommunication Union (2013). Harnessing the Internet of Things for Global Development. <https://www.itu.int/en/action/broadband/Documents/Harnessing-IoT-Global-Development.pdf>.
- [6] Centers for Medicare & Medicaid Services (CMS) Office of Information Service (2008). Selecting A Development Approach. Retrieved on October 27, 2016 from www.cms.gov/Research-Statistics-Data-and-Systems/CMSInformation-Technology/XLC/Downloads/SelectingDevelopmentApproach.pdf.
- [7] Ian Sommerville (2007). Software Engineering. 8th ed. United States: Pearson Education, Inc
- [8] R. A. Carter, A. I. Anton, A. Dagnino and L. Williams, "Evolving beyond requirements creep: a risk-based evolutionary prototyping model," *Proceedings Fifth IEEE International Symposium on Requirements Engineering*, Toronto, Ont., 2001, pp. 94-101.
- [9] Kasim, S., Hafit, H., Yee, N. P., Hashim, R., Ruslai, H., Jahidin, K., & Arshad, M. S. (2016, November). CMIS: Crime Map Information System for Safety Environment. In *IOP Conference Series: Materials Science and Engineering* (Vol. 160, No. 1, p. 012096). IOP Publishing.



- [10] Kasim, S., Hafit, H., Leong, T. H., Hashim, R., Ruslai, H., Jahidin, K., & Arshad, M. S. (2016, November). SRC: Smart Reminder Clock. In IOP Conference Series: Materials Science and Engineering (Vol.160, No. 1, p. 012101). IOP Publishing.
- [11] Kasim, S., Hafit, H., Jain, K. P., Afif, Z. A., Hashim, R., Ruslai, H., ... & Arshad, M. S. (2016, November). BBIS: Beacon Bus.Information System. In IOP Conference Series: Materials Science and Engineering (Vol. 160, No. 1, p. 012097). IOP Publishing.
- [12] Kasim, S., Xia, L. Y., Wahid, N., Fudzee, M. F. M., Mahdin, H., Ramli, A. A., ... & Salamat, M. A. (2016, August). Indoor Navigation Using A* Algorithm. In International Conference on Soft Computing and Data Mining (pp. 598-607). Springer, Cham.

Original Research | Published: 12 July 2019

Design of ultra-high sensitive biosensor to detect *E. Coli* in water

[Sandip Kumar Roy](#)  & [Preeta Sharan](#)

International Journal of Information Technology **12**, 775–780 (2020)

62 Accesses | 2 Citations | [Metrics](#)

Abstract

Escherichia coli (abbreviated as *E. coli*) are bacteria found in water, in food. The present work focuses applications of surface plasmon resonance (SPR) based biosensors to detect *E. coli*. SPR is a label-free technology that is used to detect biological samples. The SPR based biosensor design consists of optical wave guide with different structures of metal–dielectric interfaces and effort has been done to optimize design parameters for improved sensitivity. Metal-dielectric structures considered are Au–Si, Ag–Si, Au–GaAs and Ag–GaAs. Obtained simulation results indicates that the performance of the proposed sensor can be enhanced by varying the thickness and material of metal–dielectric interfaces. The device sensitivity obtained 1071.42 nm/RIU by considering metal-dielectric interface of Gold (thickness 0.074 μm) and Gallium Arsenide (thickness 0.22 μm). This result is significantly higher than sensitivity value

[Download PDF](#)

Published: 30 July 2019

A Traffic Delay and Bandwidth Based Multipath Scheduling Approach for Optimal Routing in Underwater Optical Network

[R. Bhargava Rama Gowd](#) , [S. Thenappan](#) & [M. N. GiriPrasad](#)

Wireless Personal Communications **116**, 1009–1023 (2021)

117 Accesses | **1** Citations | [Metrics](#)

Abstract

Optical networks are future networks that will support the vast bandwidth demand for communication in diverse domain and service applications scale to worldwide through underwater fiber optical for the demand of broadband Internet-traffic. The distribution of this network has grown to its extent, which can be utilized to get benefited through efficient multipath routing dynamically across multiple fiber-optic links to meet the bandwidth requirements, network load balancing and resource optimization. The increase in invariable traffic rate in communication make it very challenging to manage and provide the QoS. In this paper, we aim to present a solution on the efficiency of multipath routing based on the comprehensive bandwidth remaining and the variable traffic delay

Effect of Chanting, Recitation of Mantras, Slokas, Duas, Music on Plants and Trees using EMF Radiations: A Study

¹Dr. Thenappan S, *Professor, Dept. of ECE, KNSIT, Bengaluru*

²Dr. Sridhar N, *Asst. Professor, Dept. of ECE, CMRIT, Bengaluru*

³Bhargava Ramagoud, *Asst. Professor, Dept. of ECE, TOCE, Bengaluru*

⁴S.Senthil Kumar, *Assoc. Professor, Dept. of ECE, GRTIET, Tiruttani*

⁵Dr. Anantha Padmanabhan, *Professor & HOD, Dept. of ECE, GCEM, Bengaluru*

¹honey.souri@gmail.com, ²sridhar.n@cmrit.ac.in, ³rbg4u84@gmail.com, ⁴senthil.swamyg@gmail.com, ⁵ananthu.padmanabhan@gmail.com

Article Info

Volume 83

Page Number: 11481 - 11484

Publication Issue:

May-June 2020

Abstract:

The psychological stress is less in plants and trees and also the stillness, reactivity when exhibited in the electromagnetic field emanations are advantageous when compared to animals [8]. Study is going on in the field of vegetation regarding the effect of plants and trees when exposed to electromagnetic field emanations. From the seeds to fruits the effect of growing plants are carried out by scientists in different parts of the world. Inside a TEM (Transverse Electromagnetic Cell), seeds were exposed for various periods, and then they will let to germinate at different frequencies [3].

In this review paper mantras, slokas, duas and music replaces different EMF radiations of electromagnetic spectrum. This audio as input to the antennas emits electromagnetic radiation in the range of 20Hz to 20KHz. Seeds, plants and trees are exposed to different audio EMF emanations and the growth of plants, trees and their yields are observed. In Rigveda so many mantras are available for growing plants and trees. The antenna used here may be isotropic or directional according to the requirement. Before experimentation this audio should be simulated by using an antenna to find different antenna parameters.

Article History

Article Received: 19 November 2019

Revised: 27 January 2020

Accepted: 24 February 2020

Publication: 19 May 2020

Keywords: EMF radiation, Slokas, Mantras, Duas, Music, Seeds, Plants, Trees, Antenna.

I. INTRODUCTION

The growth of plants, trees and fertility of the soil can be improved by EMF radiations. Small amplitude of high frequency electromagnetic field (HF-EMF) will be perceived by plants for the developmental scheme by molecular responses [4]. Electromagnetic radiations (EMR) has many advantages in the agricultural sector. For rice plant the utility of EMR, will increase the growth of plants

[2].

Specific Absorption Rate (SAR) of plants can be determined by different methods, for different plants. This review paper can be considered at three levels.

- i) Pre-treatment of seeding
- ii) Seed germinations
- iii) Plant growth and development.

A brief introduction of these is given in the

methodology of the paper.

Plants are grown in different environment, three hours, plants are exhibited to EMF at the cut stage some plants are exhibited to type-1 exposure and type-2 exposure, for 40 days, 60 days, and 80 days. Type-2 exposure will have an amplitude of 200 vm^{-1} , 30 minutes, 900 MHz EMF signal [5]. When seeds are exposed to static magnetic field, then increase in the speed of germination was noticed. Also plants with larger longitude and weight were observed. The trees which are nearer to antenna have grown quickly in a forest, some trees will have positive effect, and some trees will not have any effect of these electromagnetic field radiations [10].

II. LITERATURE REVIEW

The biological exposure of plants to HF-EMF emanations and their responses at the molecular and whole plant level, educe changes in plants metabolism. At the sub cellular level reactions takes place, involving modification of enzymatic molecular events. Many experiments were conducted on plants by HF-EMF radiations, compare to humans and animals, plants are excellent models [4].

Plant growth, seed germination, yield quantity and water have been affected by magnetic field (MF). The quantity and quality of seed germination can be increased by magnetic fields. In the past 20 years development in enzyme activity, germination, water uptake in seeds were determined. Wastes of any kind will not be developed and harmful radiations will not be evolved [1].

Microbiological activity in the soil and quality and quantity of crop can be enhanced by electromagnetic stimulation. Frequency of the range between 10MHz and 1 KHz are used to develop the plant growth by using electromagnetic pulses. The structural change of water in the cells in plants which are very much useful for plant growth, this process can be done by EMF emissions on plants [7].

An increase in plant growth was absorbed when

plant seeds were exposed to EMF radiations at 900 MHz. The Chlorophyll ratio zeamays plantlets were increased in long duration [9].

Zeamays seeds were exhibited to 1GHz frequency inside a TEM cell for different exhibiting periods, then decrease in photo-assimilation of pigments and nucleic acid contents were observed [6].

III. METHODOLOGY

Audio EMF emissions can be used for the seeds and growth of plants, to get more yield in terms of quality and quantity (which has to be studied). First and foremost is to do the simulation. The SAR level of different types of plants are established. The input to the antenna is an audio which may be a mantra, sloka, dua and music. Here the SAR level and other parameters like power density, distance with which the electromagnetic wave travels without distortion etc. are to be determined. These parameters of the antenna should be as per the EMF standards for plants.

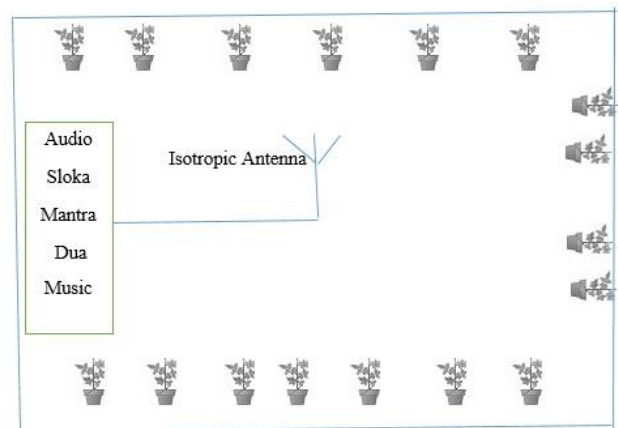


Fig.1. Practical Antenna set up Indoor

From Vedas, there are so many mantras like Gayathri mantra to chant and recite to grow plants. In Rigveda, there are so many mantras which are familiar for plants growth. In this review paper, instead of EMF radiations due to the wireless communication we are taking mantras and slokas from vedas and these as the input to the antenna produces electromagnetic wave emanations, these radiations are utilized for seeds and growth of plants.

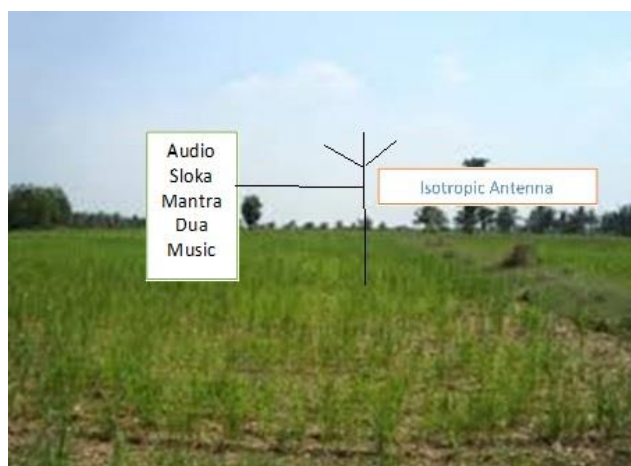


Fig.2. Practical Antenna set up Outdoor

In Fig.1 and Fig.2 plant growth in the indoor and outdoor environment is shown by using an antenna. If the EMF emanations are distorted, then modulation may be carried out to travel longer distance without distortion. In this case the antenna length will be greater and lengthier. So modulation may be carried out to decrease the antenna height. But for experimentation purpose, without modulation may also be carried and growth of the plants may be observed.

IV. CONCLUSIONS & FUTURE SCOPE

EMF radiations from these mantras, slokas, duas and music are emanated towards the plants by using a directive antenna or isotropic antenna. The experimentation is carried out in indoor and outdoor in both these cases, a detailed study has to be conducted with

- a) Recitation of mantras, slokas, duas and music in audio form on plants and trees.
- b) EMF radiations of mantras, slokas, duas and music on plant and trees.
- c) Without a & b.

All these three should be compared in terms of quality, quantity etc by doing respective tests in agricultural research centres.

In the case of EMF radiations of the audio signal, the

audio frequency range is of 20Hz to 20 KHz, so the antenna length will also be increased, in this case the antenna of smaller size is chosen and we need to study the antenna parameters by simulation and experimental basis. If this is not satisfied then we have to modulate the audio signal and plants and trees are exposed or exhibited to the EMF radiations of the modulated audio signals. In this case also a detailed study has to be conducted in to two ways,

- a) With modulation, with minimum size of antenna and
- b) With modulation and with antenna design

Safeguarding the plants, trees and the mother earth is protecting our human community. So by using these audio signals EMF emanations, it can be studied, and try to achieve positive results through positive vibrations.

If the proposed technique gives positive results then we can try the following techniques also. Bihar, Uttar Pradesh and Rajasthan are the states in India, in these states young children were dead with unknown cause. We feel each disease will be having a negative energy and frequency. In future this may be jammed by having powerful mantras, duas and music in the form of electromagnetic wave emanations. For this deeper study in our scriptures should be carried out. For rainfall, these electromagnetic wave radiations from varuna mantras in atherva veda can be tried in the sky.

Further the need for pesticides and fertilizers plays an important role in growing plants and trees, by utilizing these audio EMF emanations, it can be studied that whether the use of pesticides and fertilizers can be avoided or not. Also by using these audio EMF emanations fertility of the soil can be tested.

REFERENCES

1. Neo E. Nyakane, E. D. Markus and M. M. Sedibe, "The Effects of Magnetic Fields on Plants Growth: A Comprehensive Review",

- International Journal of Food Engineering
Vol. 5, No. 1, March 2019.
2. S. Batool, A. Bibi, F. Frezza and F. Mangini, "Benefits and hazards of electromagnetic waves, telecommunication, physical and biomedical: a review", *European Review for Medical and Pharmacological Sciences*, vol.23, pp.3121-3128, 2019.
 3. Mihaela Răcuciu, Cora Iftode, and Simona Miclăuș, "Ultrahigh frequency-low power electromagnetic field impact on physiological parameters of two types of cereals", *Romanian Reports in Physics* 69, 712 2017.
 4. Alain Vian, Eric Davies, Michel Gendraud, and Pierre Bonnet, "Plant Responses to High Frequency Electromagnetic Fields", *BioMed Research International*, Hindawi Publishing Corporation, vol.2016.
 5. Alexandre Grémiaux, Sébastien Girard, Vincent Guérina, Jérémy Lothier, Frantisek Baluska, Eric Davies, Pierre Bonnet and Alain Viana, "Low-amplitude, high-frequency electromagnetic field exposure causes delayed and reduced growth in Rosa hybrid", *Journal of Plant Physiology*, vol.190, pp.44-53, 2016.
 6. Mihaela Răcuciu, Cora Iftode, and Simona Miclăuș, "Inhibitory Effects of low Thermal Radiofrequency Radiation on Physiological Parameters of Zea Mays Seedlings Growth", *Article in Romanian Journal of Physics* · January 2015.
 7. D. Dicu, and P. Pîrșan, "The Effect of Electromagnetic Waves on Zea Mays Plants Germination", *Research Journal of Agricultural Science*, vol.46 no.4, 2014.
 8. Alain Vian, Catherine Faure, Sébastien Girard, Eric Davies, Francis Hallé, Pierre Bonnet, Gérard Ledoigt, Françoise and Paladian, "Plants respond to GSM-Like radiation", *Article in Plant signaling and behavior*, vol.2:6, pp.522-524, December 2007.
 9. Mihaela Răcuciu and Simona Miclăuș, "Low-level 900 MHz Electromagnetic field Influence on Vegetal Tissue", *Romanian J.Biophys.*, vol. 17, no. 3, pp.149–156, Bucharest, 2007.
 10. Alfonso Balmori Martínez, "The Effects of Microwaves on the Trees and other Plants", December 2003.
 11. Majeed, A.S. Eco-friendly design of flow injection system for the determination of bismarck brown R dye (2018) *International Journal of Pharmaceutical Research*, 10 (3), pp. 399-408.
 12. IBRAHIM R. "Workstation Cluster's Hadoop Distributed File System Simulation and Modeling." *International Journal of Communication and Computer Technologies* 8 (2020), 1-4. doi:10.31838/ijccts/08.01.01

Parameter Analysis of CMOS Amplifier Topologies for Biosensors.

¹Mrs.Jyoti M R,² Dr.Manju Devi

CMR Institute of Technology, Bengaluru,² TOCE,Bengaluru
¹jyoti.r@cmrit.ac.in VTU Scholar, ²manju3devi@gmail.com

Abstract

In this paper we designed amplifiers with different topologies for different application including biosensors. Parameters of all topologies are simulated and compared. We designed two stage, folded cascade with low power as these two designs are used in many applications. The circuits are designed and simulated in VLSI CAD Cadence 180nm technology. Folded cascade amplifiers are used in design of Trans impedance amplifier which is first stage of biosensor interface, which measures low redox current generated by sensor. Parameter analyzed in this work are transconductance, power, area and gain. Results shows folded cascade gain 77.97Db and power 0.925 mW since folded cascade amplifier is mainly considered one of important amplifier in Trance Impedance Amplifier (TIA) for analog front end design.

Keywords: *folded cascode, gain, area, power, Transimpedance amplifier, VLSI CAD.*

1. Introduction

Bio-potential signals are important to physicians for diagnosing medical conditions in patients. These signals are very weak in the presence of stronger common mode signals. Extracting such signal is challenging task. To perform such ask high gain low noise stable amplifier will be used. The ability of an amplifier to amplify required differential Signals by rejecting unwanted common mode signals is known as common mode rejection ratio (CMRR). An op-amp has several parameters based on the applications each of the parameter has its own significance. Among them a high voltage gain of greater than 80dB and high CMRR of greater than 90dB is preferred for Bio-medical application. These amplifiers found in many biomedical applications such amplifiers are called bio amplifiers. A high gain, high CMRR operational amplifier is a fundamental requirement for Bio-medical applications in the Analog front end circuits since bio signals have low amplitude and frequency [1].

First stage of any bio amplifier is signal conditioning block which is used to acquire redox current from electrochemical reaction of sensor. This block plays very important part in sensor. For signal conditioning circuits different techniques are used to convert redox current to different process parameters. Many article shows redox current is converted into voltage, frequency, impedance etc. dependence on the application where it used redox current is converted. The challenge is there is this design of converter for the design of front end converter circuit different amplifier topologies are used.

In this paper we discussed different amplifier topologies for analog front end for signal condition circuits. We start from basic differential amplifier two stage operational amplifier, and different cascade amplifiers with gain boosting techniques[1].Any signal condition circuit needs it front part must differential stage so it required to analyse each amplifier with all constrains like area, power, trans conductance ,current and voltage capabilities.For any VLSI analog circuit differential amplifier is the most important block. A differential amplifier circuit amplifies the difference of any two input signals and rejects any two common signals [2]. Infinite CMRR, infinite gain, bandwidth, high input impedance low output admittance are important features of any differential amplifier.

These are widely used due to less distortion in the output and are widely used in linear amplification circuits. These amplifiers can be single ended and double ended outputs. Because of its high immunity to noise and linearity fully differential amplifiers are preferred in bio application but designer has to compromise with large area. In this paper we showed how differential amplifiers behaves with different amplitude signals over band of frequencies. For the amplification of bio signals single stage is not enough to achieve high gain, for this constraint two stage operational amplifier, cascade with miller compensation are considered for better performance of amplifier [3]. Mainly folded cascade amplifier is used in the design of Transimpedance amplifier.

Transimpedance amplifiers are used in a variety of applications, and cover an extremely broad range of specifications. Common applications include detecting signal from photodiodes in high-speed optical communication, and detecting current from accelerometers in micro electromechanical systems applications. A transimpedance amplifier can be thought of simply as a current to voltage converter, which linearly converts a current input to a corresponding voltage output. The input/output relationship can be described using Ohm's law, and the overall transimpedance gain is measured in Volts/Amperes, or simply in Ohms [4]. This folded-cascode architecture achieves wide dynamic range and bandwidth at the cost of high power (nearly double) and area consumption. Since for biomedical application amplifier with high bandwidth are not required. Amplifier with less than 20 KHz is enough to use for bio amplifier. But in this paper amplifier parameters are analyzed up to MHz range of frequencies.

2. Amplifier Design Steps

The specification for two stage operational amplifier is shown in the following table 1.

Table 1: Specification of two stage OP-AMP

| Parameter | Value |
|--------------------------|---------------------------------|
| Slew Rate | $\geq 10 \text{ V}/\mu\text{s}$ |
| P_{diss} | $\leq 3 \text{ mW}$ |
| C_L | 5 pf |
| Small signal gain, A_v | $\geq 6000 \text{ V/V}$ |
| GB | $\geq 5 \text{ MHz}$ |
| $ICMR_{\text{min}}$ | -0.6V |
| $ICMR_{\text{max}}$ | 1.6V |
| Vout Range | $\pm 2 \text{ V}$ |

The following table 2 shows 180nm technology parameters for design of transistors.

Table 2-180nm technology parameters.

| Parameter | Value |
|-------------------------|------------------------------|
| $V_{DD} = -V_{SS}$ | 1.8 V |
| $\lambda_n = \lambda_p$ | 0.1 V^{-1} |
| V_{TN} | 0.43 V |
| V_{TP} | -0.38 V |
| $\mu_n C_{ox}$ | $300 \mu\text{A}/\text{V}^2$ |
| $\mu_p C_{ox}$ | $100 \mu\text{A}/\text{V}^2$ |

For the amplifier design following python program is considered.

```

Uncox=float(input("enter the value of process parameter"))
vtn =float(input("enter the value of threshold voltages for nmos and pmos transistor"))
vtp= float(input("enter the value of threshold voltages for nmos and pmos transistor"))
print("enter all specification of your design")
print("enter ICMR+,ICMR- for the amplifier")
icmr+ -=float(input())
icmr-=float(input())
print("Enter small signal gain of an amplifier")
gain=float(input())
Printf("enter load capacitor value")
CL=int(input())
Print("enter slew rate")
SR=float(input())
Print("enter gain bandwidth product")
    
```

$$\text{Slew Rate} = \frac{I_{SS}}{C_L} \tag{1}$$

$$I_{SS} = 100 \mu A \tag{2}$$

Assume Bias currents in output cascode We need to assume bias currents in the output cascode higher than the tail current. Hence it is required to assume.

$$I_{SS} = 1.2 \times 100 \mu A = 120 \mu A \tag{3}$$

ISS is assumed 125 uA

$$V_{DS5}(sat) = V_{DS7}(sat) = \frac{V_{DD} - V_{out}(max)}{2} \tag{4}$$

$$S_4 = S_5 = S_{14} = \frac{8 \times I_5}{\mu_{pcox} \times V_{SD5}^2} \tag{5}$$

$$S_6 = S_7 = S_{13} = \frac{8 \times I_7}{\mu_{pcox} \times V_{SD7}^2} \tag{6}$$

$$S_8 = S_9 = \frac{2 \times I_9}{\mu_{pcox} \times V_{SD9}^2} \tag{7}$$

$$S_{10} = S_{11} = \frac{8 \times I_{11}}{K_P' V_{SD11}^2} \tag{8}$$

$$S_1 = S_2 = \frac{GB^2 \times C_L^2}{\mu_{ncox} \times I_3} \tag{9}$$

$$S_3 = \frac{2 \times I_{SS}}{\mu_{ncox} \times \left[V_{in}(min) - V_{SS} - \sqrt{\frac{I_3}{\mu_{ncox} \times S_1}} - V_{thM1} \right]^2} \tag{10}$$

$$S_{12} = \frac{I_{12}}{I_3} \times S_3 \tag{11}$$

To calculate the gain of the amplifier

$$A_V = \frac{(2 + K)}{2 \times (1 + K)} \times g_m \times R_1 \tag{12}$$

Where S_1 to S_{14} are saturation voltages of transistor M_1 to M_{14} . With values of W/L of all transistors now we need to find g_m and g_{ds} of all the transistors,

$$g_m = \sqrt{2 \times K_p' \times S_4 \times I_{SS}} \quad (13)$$

$$R_9 = g_{m_9} \times \frac{1}{g_{ds9}} \times \frac{1}{g_{ds11}} \quad (14)$$

$$R_{11} = R_9 \parallel (g_{m_9}) \times (r_{ds7}) \times (r_{ds1} \parallel r_{ds4}) \quad (15)$$

$$A_V = \frac{(2 + K)}{2 \times (1 + K)} \times g_m \times R_1 \quad (16)$$

Where K is

$$K = \frac{R_9 (g_{ds2} + g_{ds4})}{g_{m7} r_{ds7}} \quad (17)$$

$$P_{diss} = (V_{DD} - V_{SS})(I_3 + I_{12} + I_{10} + I_{11}) \quad (18)$$

Where K is

$$K = \frac{R_9 (g_{ds2} + g_{ds4})}{g_{m7} r_{ds7}} \quad (19)$$

$$P_{diss} = (V_{DD} - V_{SS})(I_3 + I_{12} + I_{10} + I_{11}) \quad (20)$$

Using all these formula and mapped in python to get theoretical values. Similar way theoretically all parameter are calculated for two-stage operational amplifier, folded cascade and folded cascade with Wilson mirror circuit also.

The following table 3 shows aspect ratios of all transistors after running python program. The schematic considered for two stage operational amplifier (OP-AMP) is shown below figure 1.

The circuit in figure 1 is a two stage operational amplifier for which the first stage is a differential circuit and the latter is a common source circuit. The idea being having two stage amplifiers is to increase the gain and to have high swing in the output voltage. The circuit above satisfies both the properties hence is used for performance analysis in the project. In this circuit, transistors M_1 to M_6 form differential stage whereas M_7 and M_8 form a common source arrangement. The gain of the amplifier is given by gain of each amplifier and is given as

$$A_V = A_1 + A_2$$

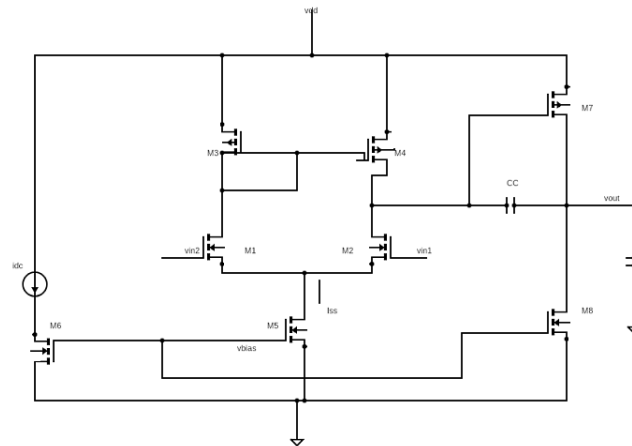


Fig1. Two stage OP-AMP circuit diagram with miller compensation schematic.

Figure 3 shows the folded cascade op-amp. In this circuit the circuit includes the cascading in its output stage with the differential stage and a biasing circuit which is used to increase the gain of the op-amp and “to achieve good input common mode range, folded cascade op-amp offers self-compensation and good input common mode range . Since, to achieve high gain and good input common mode range differential amplifier is not enough to provide a single ended output with the single stage. Hence to achieve that the designers have moved on to more than one stage amplifiers to get the better stability along with the high gain including the compensation circuits. Folded cascade does not require perfect balance of currents in the differential amplifier because excess dc current can flow into or out of the current mirror The Bias currents I_3 , I_4 and I_5 should be designed in such a way that the DC current in the cascade mirror never goes to zero. This might cause the delay in the circuit because of the parasitic capacitances. Hence to avoid this I_4 and I_5 should be kept between the values of I_3 and $2I_3$. Now, speaking about the gain of the op-amp, the gain includes parasitic resistances forming self-compensation in the circuit, and is given by R_1 , R_2 ; which are resistances connected to the drain of M_{13} and M_8 respectively and R_A and R_B are the resistances looking into the sources of transistors M_6 and M_7 respectively.

Table3-Aspect ratio of all transistors

| Parameters used for the design | Value ($\mu\text{m}/\mu\text{m}$) |
|--------------------------------|-------------------------------------|
| $(W/L)_{1,2}$ | 1 |
| $(W/L)_{3,4}$ | 80 |
| $(W/L)_5$ | 5 |
| $(W/L)_6$ | 23 |
| $(W/L)_7$ | 126 |
| $(W/L)_8$ | 4 |

The amplifier which is designed specifically to amplify the difference in the input signal and to give high performance is called as differential amplifier. As we know, differential amplifier has two modes of operation: differential mode and common mode. And the best suitable in most designs is the differential mode. “Differential amplifiers are compatible with matching properties of IC technology” where two transistors which form the differential counterpart of a transistor to divide the current into two branches equally called as tail current and transistor pairs forming a current mirror load to give a single ended output with a high voltage gain[3].

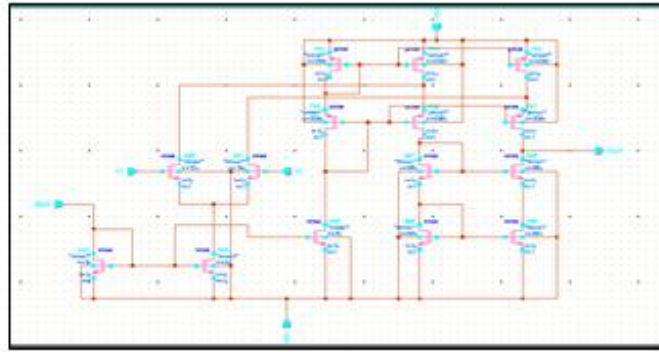


Fig 2. Folded cascode amplifier schematic with designed aspect ratio

3. Comparison of Performance Parameters of Amplifiers

The following results are monitored for all differential amplifiers.

a) Comparison of Power

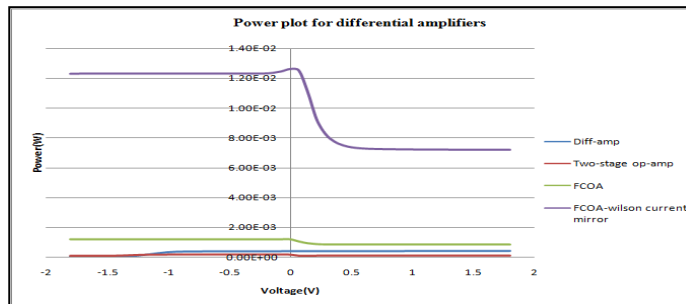


Figure 3: Power Plot for differential amplifiers

b) Comparison of current

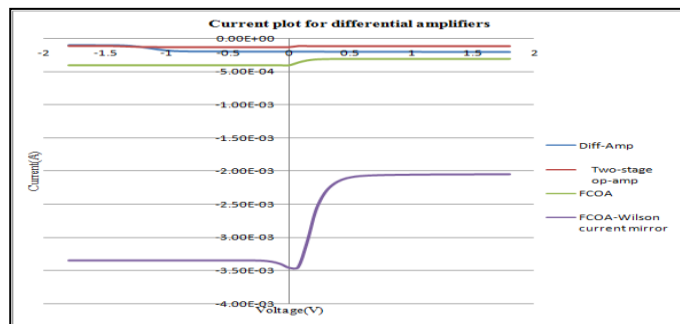


Figure 4: Current Plot for differential amplifiers

From figure 3 and 4 it can be seen that power dissipation and current is more in case of folded cascode op-amp. And it is less in case of two-stage op-amp, later it is less for differential amplifier. Even if power dissipation is more in folded cascode op-amp it provides comparatively higher gain among all other op-amp designs. This comparison of gain is as shown in figure 6.

c) **Comparison of Area**

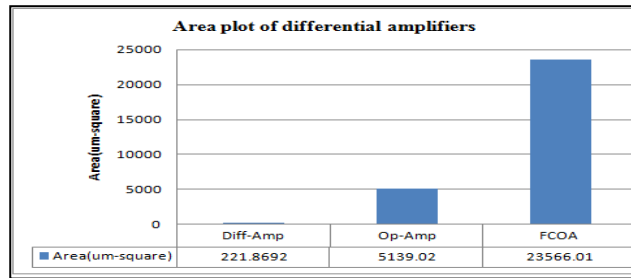


Figure 5. Area Plot for amplifiers

Figure 6. it is shown that the gain of FCOA is higher than other op-amps and two-stage op-amp and FCOA with Wilson current mirror provides almost the same gain hence can be used in high gain applications.

d) **Comparison of Gain**

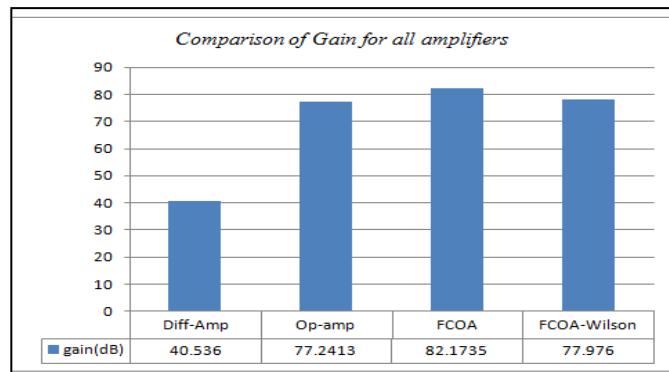


Figure6: Gain Plot for amplifiers

includes more number of transistors in covers more area compared to other amplifiers. Since area is more cost will be more for FCOA but it provides high gain hence trade-off between area and gain can be acceptable.

e) **Comparison of trans conductance**

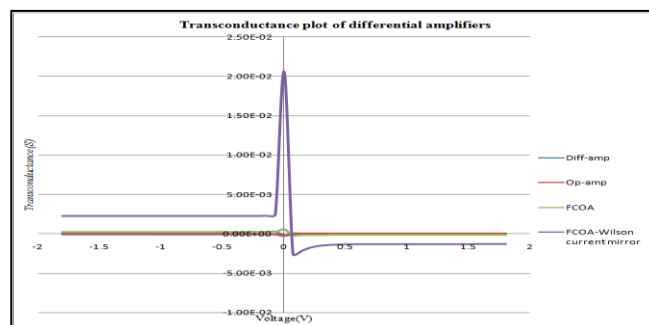


Figure 7: trans conductance Plot for amplifiers

Figure 7 gives comparison of Trans conductance possessed by all amplifiers. FCOA with Wilson current mirror gives higher Trans conductance value compared to rest other amplifiers and is a reason for decrease in the gain value than the folded cascode op-amp.

And also Figure 6 provides the gain- bandwidth comparison of all differential amplifiers. Gain-bandwidth is high in case of the differential amplifier and less for two-stage op-amp but provides less gain than the multi-stage amplifiers. Hence it is preferable to use high gain amplifiers and with low bandwidth. Since this characteristics of amplifiers is required for bio signals like ECG, EEG and neuro signal which have less amplitude and low bandwidth, Amplification bio signal using single stage amplifiers is not enough with respect to specification gain multistage amplifiers are preferred.

f) **Comparison of Gain-Bandwidth**

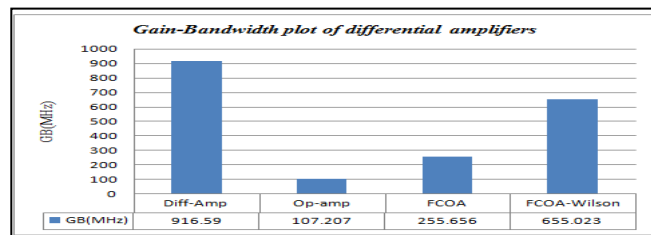


Figure 8: Gain-Bandwidth Plot for amplifiers

Figure 8 provides the gain- bandwidth comparison of all differential amplifiers. Gain-bandwidth is high in case of the differential amplifier and less for two-stage op-amp but provides less gain than the multi-stage amplifiers. Hence it is preferable to use high gain amplifiers and with low bandwidth.

Figure 9 provides the stability plot for all the amplifiers, which means it gives the plot for power where it becomes stable for the small change in the voltage value. And the respective stability attained by the all amplifiers is as shown in the figure 9.1.and 9.2. Table 4 gives the comparison of obtained gain, power and gain-bandwidth for all differential amplifiers designed for 180 nm technology. The results in the table are without extraction of the rc-parameters in the layout simulation.

g) **dP/dV plot of all differential amplifier**

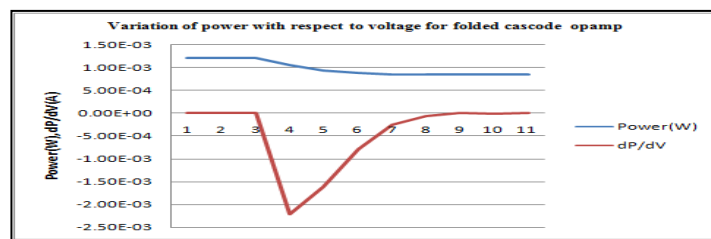


Figure 9.1: variation of power with respect voltage for folded cascode OP-AMP

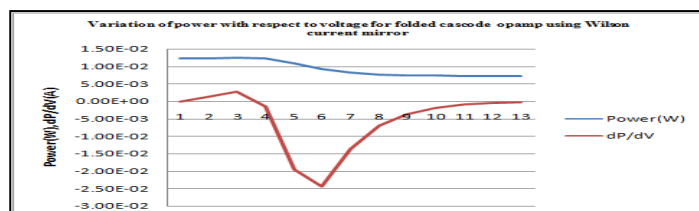


Figure 9.2: variation of power with respect voltage for folded cascode with Wilson current mirror OP AMP

Table 4: Comparison of parameters for differential amplifiers

| Parameters | Diff-Amp | Two-stage op-amp | Folded cascode op-amp | Folded cascode op-amp-Wilson current mirror |
|----------------------|----------|------------------|-----------------------|---|
| Gain (dB) | 40.536 | 77.2413 | 82.1735 | 77.976 |
| Power (mW) | 0.445 | 0.121 | 0.933 | 0.925 |
| Gain-Bandwidth (MHz) | 916.59 | 107.207 | 255.656 | 655.025 |

4. Conclusion

The design and experimental results of folded cascode operational transconductance Amplifier, differential amplifier and two stage op-amp parameters are compared in terms of gain, power and area. Results has been presented, based on 0.18um CMOS process, The amplifiers shows good performances with gain varies from 40dB to 80 dB approximately from 1Hz to 100KHz and average power of 0.445mW to 0.925mW for all three topologies at a power supply of 1.8 V.

REFERENCES

- [1]. Design and Performance Analysis of Differential Amplifier for Various Applications Journal of Computational and Theoretical Nanoscience Vol. 15, 3501–3508, 2018 M. R. Jyoti1 *, H. Chetan1, and Manjudevi2.
- [2]Low Leakage and High CMRR CMOS Differential Amplifier for Bio-medical Application. Prateek Jain, Amit Mahesh Joshi. 2017.
- [3]. Design of Miller Compensated Two Stage Operational Amplifier for Data Converter Applications. Prema Kumar. G, Shravan Kudikala. 2015.
- [4] CMOS Transimpedance Amplifier for Biosensor Signal Acquisition Mark M. R. Ibrahim and Peter M. Levine.
- [5] Analysis of Simple Half-Shared Transimpedance Amplifier for Pico ampere Biosensor Measurements Geoffrey Mulberry, Kevin A. White, Brian N. Kim IEEE transactions on biomedical circuits and systems, vol. 13, no. 2, April 2019.
- [6]. Design of 1V, 0.18 um Folded Cascode Operational Amplifier for Switch Capacitor Sigma Delta Modulator. Ratnaprabha W. JAsutkar, P.R. BAjaj, A.Y.Deshmukh. 2013.
- [7] A Low Power 100MΩ CMOS Front-End Trans-impedance Amplifier for Biosensing Applications Jiaping Hu, Yong-Bin Kim, Joseph Ayers IEEE 2010.
- [8]. Design and Analysis of Two Stage Miller Compensated Op-Amp Suitable for ADC Applications. D.S.Shylu, D. Jackuline Moni, Banazir Kooran. 2014.
- [9]. Allen, P.E. Analog Integrated Circuits and Systems. 2000.
- [10]. Razavi, Behzad. “Design of Analog CMOS Integrated Circuits”, McGrawHill,2002.

Design of a Low Latency and High Throughput Packet Classification Module on FPGA Platform

Anita P, Manju Devi

Abstract: The Packet classification method plays a significant role in most of the Network systems. These systems categories the incoming packets in various flows and takes suitable action based on the requirements. If the size of the network is vast and complexity will arise to perform the different operations, which affects the network performance and other constraints also. So there is the demand for high-speed packet classifiers to reduce the network complexity and improve the network performance. In this article, The Bit vector Packet classifier (BV-PC) Module is designed to improve the network system performance and overcome the existing limitation of Packet classification approaches on FPGA. The BV-PC Module contains Packet generation Unit (PGU) to receive the valid incoming packets, Memory Unit (MU) to store valid packets, Header Extractor Unit (HEU) extracts the IP Header address information from the Valid packets, The BV-Based Source and Destination Address (BV-SA, BV-DA) unit receives the IP packet header Information and Process with BV based rule set and aggregates the BV-SA and BV-DA outputs, Priority Encoder encodes the Highest priority BV Rule for the generation of Classified output. The BV-PC utilizes <2% Chip area (slices), works at 509.38MHz, and consumed Less 0.103 W of total Power on Artix-7 FPGA. The BV-PC operates with a latency of 5 clock cycles and works at 815.03Mpps throughput. The BV-PC is compared with existing approaches and provides Better improvements in Hardware constraints.

Keywords: Bit vector (BV), Packet classifier, Ruleset, FPGA, Throughput, Packet generation Unit, Source Address, Destination Address, Latency.

I. INTRODUCTION

The demand for Network constraints like Security, Traffic analysis, Load Balancing, and Quality of Service (QoS) is increasing exponentially by increasing the Network System speed. To link up these, the Packet classification approach is necessary and much needed. The packet classification is the Process of matching the packet header fields with a suitable rule set. In general, there are 5 different classification fields used in Process, Namely, Source and Destination Address (SA and DA), Source and Destination Port (SP and DP), and Protocol. The different approaches use only 5- fields or 15 fields for classification to match the rule set [1-4]. The challenges of Packet classification are Classification Speed, Scalability, Modularity, Power consumption, fast updation,

implementation flexibility, and Storage Space. Many approaches are available to design the Packet classification, which includes clustering-based, Tree-based, Tuple space-based, geometrical approaches, and Bit Vector-based approaches. Similarly, many Hardware-based Packet classification approaches are available, which includes, Ternary Content Addressable Memory (TCAM) based, RAM based, FPGA based, and Multi-core Processor approaches [5-8]. The packet classification is used many applications to improve network security [9] and Network-on-Chip (NoC) [10] Performance on FPGA Chip.

In this article, The Bit vector Packet classifier (BV-PC) is designed and implemented on Artix-7 FPGA, Which provides low latency and High throughput performance on FPGA, which also consumes less amount memory and supports more massive Rule sets. Section 1.1 provides the background of the current research works of different packet classifiers, followed by findings. The proposed Bit vector Packet classifier (BV-PC) hardware architecture and its sub modules are discussed in section 2. Section 3 elaborates on the results and discussion by concerning the hardware constraints of BV-PC and comparison of the BV-PC with existing approaches with improvements. The overall work with improvements and future scope is highlighted in Section 4

A. The Background

This section describes the existing approaches of different Packet classifier approaches and applications. Li et al. [11] discuss the high-speed classification using the Binary tree approach, which provides quick rule updation and better memory performance. The binary tree approach has binary tree searching Nodes with rule set followed by Linear matching for rules. The binary tree searching module contains mainly leaf node with rule's base address followed by a middle node with child node address and also has Main root node contains first level, second-level, and third-level nodes with rule address. The linear searching Module contains storage rules with the upper boundary and lower memory field address. This linear search engine compares the lower and upper boundary values to provide the output matching results. Ganegedara et al. [12] explain the high-performance packet classification module with scalable and modular architectures. The modular BV for high-speed PC on FPGA also introduces the Stride BV architectures, which improves the optimization goal in Modular BV and provides the scalability features, which is quite better than Conventional approaches. The range search module in incorporated in Modular BV to eliminates the rule set enlargement. The modular BV supports 100Gbps speed and supports broad rule set up to 28K on on-chip Memory.

Revised Manuscript Received on March 30, 2020.

* Correspondence Author

Anita P*, Research scholar, Department of Electronics & Communication Engineering, TOCE, Bengaluru, India. Email: anitasp2002@gmail.com

Dr. Manju Devi, Professor & Head, Department of Electronics & Communication Engineering, TOCE, Bengaluru, India

Yun Qu et al. [13] discuss the dynamically Updatable PC engine, which provides high performance and high Throughput on FPGA. The 2-dimensional array of modular Processing Elements (PEs) are used, which provides exact memory allocation and prefix match effectively. The Dynamic updateable PC also supports optimization features like striding, power-gating, dual-port Memory, and clustering. The Modular PE's are self-reconfigurable, which updates the ruleset dynamically. The dynamically Updatable PC engine sustains 650Mpps Throughput on FPGA and better than the Existing TCAM approach.

Qu et al. [14] explain the many field PC on FPGA, Graphical Processing Unit (GPU), and General propose Processor (GPP) with multi-core support. The Many filed PC is optimized using Module PE and is designed and concatenated using systolic array and also divides the generic ranges into multiple parts. The multi filed PC works at 500Mpps, 14.7 Mpps, and 30.5 Mpps throughput for FPGA, GPP, and GPU platforms. The multi filed PC works also support 1.5K Rule sets, 32Krule sets, 32K rule sets for FPGA, GPP, and GPU platforms. Zhou et al. [15] discuss the large scale PC on the FPGA Platform, which uses a decomposition approach, which has searching and merging phases. The searching phases use BV algorithms or Rule Identifier Set (RIDS), and the merge phase provides the intermediate results, both the results concatenated each other for the generation of final results. The Large scale PC works at 147 Mpps and supports 256k Rules on the FPGA platform. Chang et al. [16] describe the Range Enhanced PC on FPGA, which is a hybrid combination of Stride BV features and a sub-range comparison method. The Range Search PC uses 12 tuple header fields to support multi-field PC and also used to store pre-computed values in Memory. The field lengths are defined as per open flow 1.0 in Range Search PC. The Range Search PC contains Range BV Encoding (RBVE) method has lower and Upper Boundary, which is split into Strides to improve the optimization in PC. Khan et al. [17] present high-performance Module design for PC, which contains essential XNOR gate operation for matching input packets against Rule sets and generates the BV of same size and AND'ing all the bits in BV to generates the final Matched Results. The design supports 4bits per Rules with low latency. Yu et al./ [18] present the static-RAM (SRAM) based PC works in one memory access, also exhibit the behavior of pseudo-TCAM. The SRAM-based PC provides header fields that are encoded using the Prefix Inclusion Coding (PIC) technique. The bit selection method is used to map the encoded rules with SRAM –based Match units. The SRAM-based PC works at 426 Mpps and supports 10K to 100K Rules. The existing Packet classification approaches have many limitations and challenges to address, which includes multiple fields matched against the large rule sets and the drastic increment in network traffic data rate, which causes complexity and performance metrics in PC. There is a need for PC which maintain high performance, high Throughput, and Low latency for Networks.

II. PACKET CLASSIFICATION ARCHITECTURE

The Packet classification plays a vital role in many network systems like the Intrusion detection system, Routing systems, Firewalls, Traffic control systems, and many. These network

systems need data packets that are divided based on the various design flows to address the different application requirements. This functionality much suited and provided by the Packet classifier (PC), which is defined by a set of rules. This section contains the methodology used in the research for BV-Packet classification, and detailed architecture is discussed in detail.

a. Research Methodology: The proposed methodology of the Packet classification is represented in Figure 1. The Proposed BV-Packet Classifier Module contains Packet Generation Unit (PGU), Memory Unit (MU), Header Extractor Unit (HEU), Packet classification module using Bit Vector (BV), Packet Aggregator and Priority Encoder. The Packet generation Unit (PGU) mainly used to receive valid Incoming from any external sources or by the user. It receives only valid and proper data packets for Futureclassification. The Memory Unit is used to store the incoming packets based on write enable signal. The Header extractor unit (HEU) is a central part of the packet classification process. The HEU generates different header addresses, which includes TCP header, IP header, and Ethernet header along with primary 32-bit packet data for future usage in packet classification.

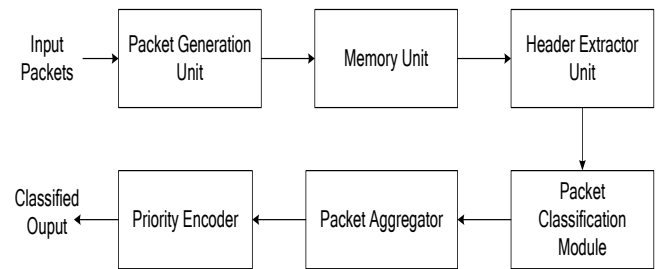


Figure 1 Methodology used in BV- Packet Classifier Module

The Packet Classification Module is designed Using the Bit Vector (BV) approach. The HEU provides the Internet protocol (IP) address used as Packet header information in the BV method. The BV source and destination address modules are matched with the corresponding memory location, which is set by rules. The BV Source and Destination address output information is aggregated using Packet Aggregator. The priority encoder encodes the highest priority rule that matches the incoming packet for the generation of the classified packet. The detailed internal Architecture of BV-PC is explained in the below section.

b. Bit Vector Packet Classifier (BV-PC) Design: The Bit Vector Packet Classifier (BV-PC) design is used to receive the incoming packet and Process with BV and generates the classified output. The detailed internal architecture of Bit Vector Packet Classifier (BV-PC) design is represented in figure 2.

Packet Generation Unit (PGU): The packet generation Unit mainly used to receives valid Incoming from any external sources or by a user. It receives only valid and proper data packets for Future communications. In this design, 76-bytes are receiving for the formation of 608-bit Valid Packets. The design incorporates the Main control signals like sop (Start of the packet) to initiates the PGU process, the valid signal indicates receives only valid packets, eop (End of the packet) indicates the last packet of the PGU.

These control signals are analyzing and validating the incoming Packets for the formation PGU. The PGU receives 76-bytes of incoming packets and generates the 608-bit outgoing packets. The 7-bit Packet counter is used to count the number of packets until it reaches 76. The Error output signal will be activated if the control signals and the error signal violates the conditions.

Memory Unit (MU):The Memory Unit is used to store the Incoming generated packets based on write enable signal. The MU receives 608-bits of packets, and once write enable signal is activated. The MU has 16-memory locations, and each memory location can hold 608-bit packets. Based on the user address, stored packets can read and send to the next Process. When the write enables is low, memory location will be read and stores the results in 608-bit Memory out.

Header Extractor Unit (HEU):The Header Extractor Unit is a central part of the packet classification process. The HEU is working based on Internet Version protocol 4 (IPv4). It generates different header address which includes TCP header, IP header, and Ethernet header along with primary 32-bit packet data for future communication in packet classification. The Header extractor unit extracts the different header addresses like 208-bits Ethernet header, 160-bits for IP header, and 160-bits TCP header. These TCP header, IP header, and Ethernet headers are acts as a source and destination address in detailed packet classification process like Bit vector (BV) and other processes. Out of 160-bit IP header values, The BV Process uses the first 32-bits [31:0] for a Destination address (DA) and next 32-bit [63:32] for Source Address (SA).

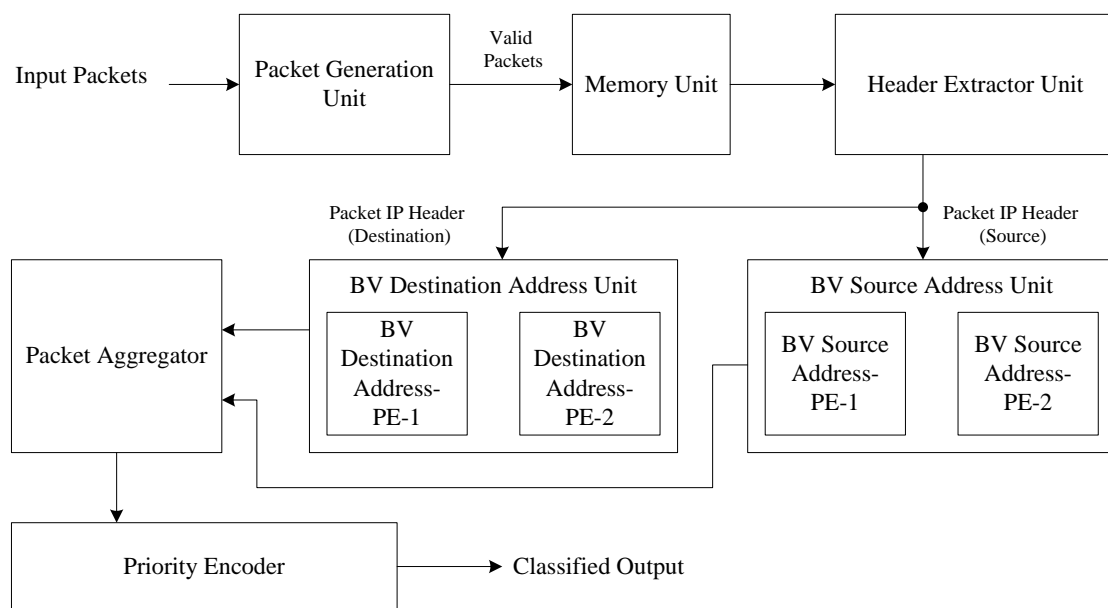


Figure 2 Internal Architecture of BV- Packet Classifier

Bit Vector Architecture:

The Bit Vector (BV) process is also considered as Field-Split BV (FSBV) method [13], and its associates split each field into several sub-fields. The Ruleset is mapped onto each sub-field based on {0, 1, *} ternary string. The Memory operations (Lookup table) is performed in all the sub-fields in a pipelined manner. BV of corresponding bits defines the temporary results of each processing element (PE). The Final Results are obtained by merging all the extracted BV bits using logical AND operations on FPGA. BV architecture is represented in figure 3.

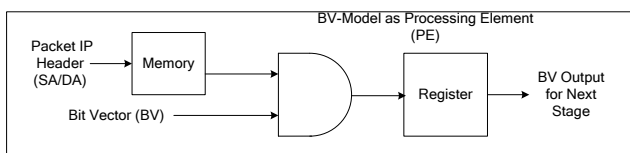


Figure 3 Bit Vector Architecture

The HEU generates the Packet IP address, which is divided into 32-bit Source and Destination IP address. Each Source and destination IP Address acts as packet header address to BV-SA and BV-DA process. Each BV-SA and BV-DA unit contains Two Processing elements, which perform the BV process. The Packet IP Header of SA PE-1, acts as header address in Memory, and finds the corresponding field Value and Perform Logical AND operation with User BV data and results are stored in temporary Register. The

Register Output is input to the next BV-SA of PE-2 and perform the same BV process and generates the Final Results of BV-SA output. A similar process is applied for BV-SA of PE-1 and PE-2 and generates the BV-DA Output. The Memory Unit contains 16 locations, and each location has 32-bit information.

Packet Aggregator: The Aggregator is used to Perform Logical AND operation of BV-SA output and BV-DA output and generates 32-bit Aggregator Output, which is input to priority encoder.

Priority Encoder: The encoder extracts the highest priority rule that should match with an incoming packet. The 32-bit encoder input performs bit-wise rule checking with the highest priority for the generation of classified output.

The example of the BV process is illustrated in figure 4. The BV process is applied to match the 4-bit header address field, which is against with rule of 4-bits width. The input header field is either SA or DA address is set to 1100. The 3 rulesets are defined with corresponding field (F) values. Splitting the 4-bit field into 1-bits, to get Bit vectors of each sub-fields: F [3], F [2], F[1], and F[0]. The subfield F[0] and others are either '0' or '1' field value. For bit 3 or (F [3]) of the ruleset is "101". Based on field values, The Ruleset generates BV values. So The R1 has 1111, R2 has 0100, and R3 has 1111. The extracted BV values R1, R2, and R3, are performed logical AND (&) operation. The matched results are obtained by using R1& R2& R3. So for this example, the Matched Results is 101.

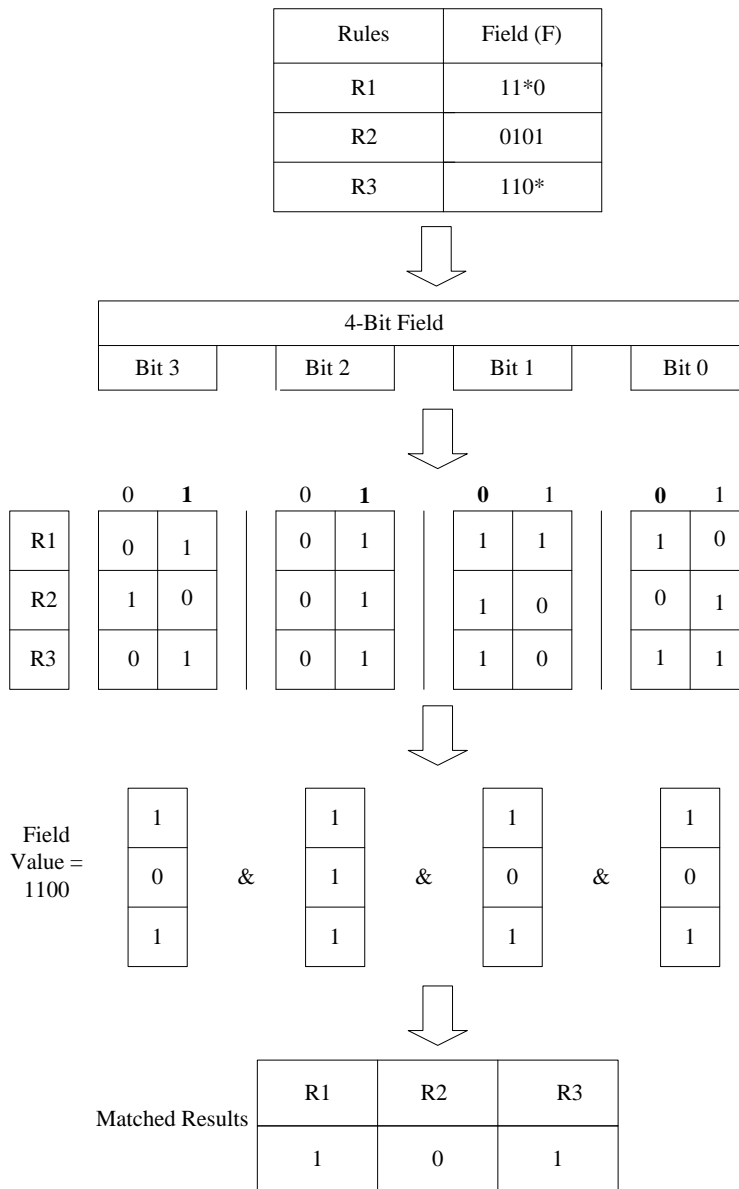


Figure 4 Example of BV Process

III. RESULTS AND ANALYSIS

An efficient Bit-Vector Packet Classifier (BV-PC) module is designed and implemented on Artix-7 FPGA. The BV-PC module is simulated on the Modelsim simulator and used for the calculation of latency. The Synthesized results are generated on the Xilinx14.7 ISE environment. The resource constraints like Chip area, Frequency, power, latency, and

Throughput are tabulated in table 1 for the BV-PC module. The BV-PC utilizes the 3636 Slice registers, 2641 LUT's, and 2453 LUT-FF pairs. The BV-PC is operating at 509.398 MHZ on Artix-7 FPGA with a minimum period of 1.963ns and a combinational delay of 1.061ns. The present Classifier consumes a total power of 0.103W with the inclusion of static power 0.082W and Dynamic power of 0.021W.

Table 1 Resource Utilization of BV-packet Classifier on Artix-7

| Resources | BV_Packet Classifier |
|--------------------------|----------------------|
| Area Utilization | |
| Slice Registers | 3636 |
| Slice LUT's | 2641 |
| LUT-FF pairs | 2453 |
| Timing Analysis | |
| Minimum Period (ns) | 1.963 |
| Max. Frequency (MHz) | 509.398 |
| Combinational Delay (ns) | 1.061 |

| Power Utilization | |
|------------------------|-------|
| Dynamic Power (W) | 0.021 |
| Total Power (W) | 0.103 |
| Latency and Throughput | |
| Latency (Clock cycles) | 5 |
| Throughput (Gbps) | 61.94 |

The BV-PC module receives 76 bytes of input packets for classifying the packet at high speed based on the BV algorithm and Ruleset. The BV-PC module is simulated on ModelSim Simulator for latency calculation, and the Classifier takes 5 clock cycles (50ns) to complete the classification for 76 bytes of packets. The Throughput is calculated using ((Number of bits * Frequency)/latency). The 76 bytes packets contain 608-bits, and the maximum operating Frequency of BV-PC is 509.398 MHz with a

latency of 5 clock cycles. So BV-PC is working with a throughput (speed) of 61.94Gbps. The Throughput is also represented in terms of Millions Packet per second (MPPS), so the BV-PC works at 815.03 MPPS.

The BV-PC module consists of sub-modules of the Packet generation Unit (PGU), Memory unit (MU), Header Extraction Unit (HEU), BV-Source address, and destination Address Unit, and finally Priority Encoder. The Area utilization and operating Frequency of submodules in the BV-PC module is tabulated in table 2.

Table 2 BV-PC sub-modules Area utilization and operating Frequency

| BV-PC Sub Modules | Slice Registers | Slice LUT's | Max. Frequency (MHz) |
|------------------------|-----------------|-------------|----------------------|
| Packet Generation Unit | 1237 | 28 | 584.62 |
| Memory Unit | 608 | 610 | 870.09 |
| Header Extractor Unit | 1744 | 2281 | 1023.227 |
| Bit Vector SA | 14 | 46 | NA |
| Bit Vector DA | 15 | 46 | NA |
| Priority Encoder | 1 | 31 | NA |

The PGU, MU, and HEU consume more slices registers and LUTs. The PGU, MU, and HEU operate Frequency of 584.62MHz, 870.09MHz, and of 1023.22MHz, respectively. The HEU is used for the extraction of Internet protocol (IP) and TCP header address information. The HEU boosts the BV-PC performance and reduces the complexity by providing headers information. Each BV-Source Address (SA) and Destination Address (DA) contains two processing Elements (PEs). Each PE is designed using Packet header and BV inputs.

classifiers like Decision Tree [20], Large Scale [21], Ultra scale [22], and HiCuts [23] are implemented on different FPGA devices. The Performance metrics like Chip area, Frequency, and Throughput (Speed) are analyzed with Proposed BV-PC. The proposed efficient high throughput Bit Vector-Based Packet classifier (BV-PC) is designed using the Bit Vector approach with pipelined architecture. The BV-PC is implemented on Low-cost Artix-7 FPGA. The BV-PC utilizes only 3636 slices, operated at Frequency of 509.398 MHz on Artix-7 with a high throughput of 815.03 Mpps, and it supports more massive rule sets

The performance comparison of BV-PC with other existing Packet classifier is tabulated in table 3. The existing Packet

Table 3 Performance Comparison of Classifiers on Different FPGA's platform

| Packet Classifier Approach | FPGA Device | Slices | LUT's | FF's | Block RAMs | Frequency (MHz) | Speed (Mpps) |
|----------------------------|-------------|--------|-------|------|------------|-----------------|--------------|
| Decision Tree PC [20] | Spartan 3E | NA | 6442 | 5336 | 22 | 100 | NA |
| Large Scale PC [21] | Virtex-5 | 10307 | NA | NA | 407 | 125.4 | 250 |
| Ultra-scale PC [22] | Stratix-III | 40 070 | NA | NA | NA | 219 | 433 |
| HiCuts [23] | Stratix-IV | 15936 | NA | NA | NA | 150 | 100 |
| Proposed BV-PC | Artix-7 | 3636 | 2641 | 2453 | 1 | 509.39 | 815.03 |

The Decision Tree Packet classifier [20] uses 8-parallel instances of 4-stages with pipelined architecture for packet classification, which utilizes 6442 LUT's, 5336 Flip-flops (FFs) and Block RAM of 22. The Decision Tree PC works at 100 MHz using Spartan -3E FPGA Board. The Large Packet wire-speed (LPWS) classifier [21] is designed using decision Tree-based, Multi-field, 2dual pipelined architecture. The Large Packet wire-speed classifier is implemented on Virtex-5 FPGA. The LPWSclassifier utilizes 10307 Slices, operated at 125.4 MHz on Virtex-5 with a throughput of 250

Mpps, and it supports 12 pipeline stage rules. The Ultra-scale Packet classifier [22] is designed using Cutting Scheme with the Decision Tree algorithm. The Ultra-scale Packet classifier is implemented on Stratix-IV and Cyclone III FPGA's. The Ultra-scale Packet classifier utilizes 40070 Logical elements (Slices), a peak power of 9.03W, operated at 219 MHz on Stratix-IV with a throughput of 433Mpps and it supports large rule sets. The HiCuts Based Packet classifier [23] is designed with high degree

pipelined and parallel architecture using decision Tree and rule memory approach. The HiCuts Based Packet classifier is implemented on Stratix-IV FPGA. The HiCuts Based Packet classifier utilizes 15936 Logical elements (Slices); operated at 150 MHz on Stratix-IV with a throughput of 100Mpps and it supports 500 rule sets. The proposed BV-PC provides better resource utilization and Throughput than existing Packet classifier approaches.

IV. CONCLUSION AND FUTURE WORK

The High-performance Bit Vector Packet classifier is designed and implemented on Artix-7 FPGA. The BV-PC works at Low latency and high Throughput on FPGA. The BV-PC is used to receive the Incoming packets and Process through the BV module and generates the classified output. This BV-PC is used in Most of the Network modules for Packet classification and also improves the system performance. The BV –PC main contains PGU, Memory Unit, HEU, BV-SA, and DA Unit and Packet aggregator, also Priority encoder. The BV-PC results are analyzed and discussed using hardware constraints like Chip area, Frequency, and Power. The BV-PC Utilizes < 2% slices resources and works at 509.39 MHz and also consumed 0.103W of total power on Artix-7 FPGA. The BV-PC is simulated on Modelsim Simulator for Latency calculation, and BV-PC uses 5 clock cycles for 76 Bytes packets process. The BV-PC works at 815.03Mpps Throughput Supports a more extensive rule set and utilizes less amount of Memory on FPGA. The BV-PC is compared with existing Packet classification approaches by concerning performance parameters with improvements. In the future, The BV-PC is optimized using striding, clustering, and other approaches with the help of a Modified BV approach to improving the Network performance further.

REFERENCES

1. Kumar, V. Anand Prem, Vidya Thiyagarajan, and N. Ramasubramanian. "A Survey of Packet Classification Tools and Techniques." In 2015 International Conference on Computing Communication Control and Automation, pp. 103-107. IEEE, 2015.
2. Nagpal, Bharti, Nanhay Singh, Naresh Chauhan, and Radhika Murari. "A survey and taxonomy of various packet classification algorithms." In 2015 international conference on advances in computer engineering and applications, pp. 8-13. IEEE, 2015.
3. Srinivasan, T., N. Dhanasekar, M. Nivedita, R. Dhivyakrishnan, and A. A. Azeezunnisa. "Scalable and parallel aggregated bit vector packet classification using the prefix computation model." In International Symposium on Parallel Computing in Electrical Engineering (PARELEC'06), pp. 139-144. IEEE, 2006.
4. Choorat, Thapana, and Akharin Khunkitti. "A packet classification algorithm." In 2010 The 2nd International Conference on Computer and Automation Engineering (ICCAE), vol. 1, pp. 145-148. IEEE, 2010.
5. Song, Haoyu, and John W. Lockwood. "Efficient packet classification for network intrusion detection using FPGA." In Proceedings of the 2005 ACM/SIGDA 13th international symposium on Field-programmable gate arrays, pp. 238-245. 2005.
6. Taylor, David E., and Jonathan S. Turner. "Scalable packet classification using distributed cross producing of field labels." In Proceedings IEEE 24th Annual Joint Conference of the IEEE Computer and Communications Societies. vol. 1, pp. 269-280. IEEE, 2005.
7. Linan, Chen, Lin Zhaowen, Ma Yan, Huang Xiaohong, and Li Chunqiang. "Multidimensional packet classification with improved cutting." In 2014 4th IEEE International Conference on Network Infrastructure and Digital Content, pp. 409-413. IEEE, 2014.
8. Li, Wei, and Xiufen Yu. "An online flow-level packet classification method on multi-core network processor." In 2015 11th International

- Conference on Computational Intelligence and Security (CIS), pp. 407-411. IEEE, 2015.
9. Pak, Wooguil, and Young-June Choi. "High performance and high scalable packet classification algorithm for network security systems." IEEE Transactions on Dependable and Secure Computing 14, no. 1 (2015): 37-49.
10. Guruprasad, S. P., and B. S. Chandrasekar. "An Efficient Bridge Architecture for NoC Based Systems on FPGA Platform." In International Conference on Intelligent and Interactive Systems and Applications, pp. 377-383. Springer, Cham, 2019.
11. Li, Jingjiao, Yong Chen, Cholman Ho, and Zhenlin Lu. "Binary-tree-based high speed packet classification system on FPGA." In The International Conference on Information Networking 2013 (ICOIN), pp. 517-522. IEEE, 2013.
12. Ganegedara, Thilan, Weirong Jiang, and Viktor K. Prasanna. "A scalable and modular architecture for high-performance packet classification." IEEE Transactions on Parallel and Distributed Systems 25, no. 5 (2013): 1135-1144.
13. Qu, Yun R., and Viktor K. Prasanna. "High-performance and dynamically updatable packet classification engine on FPGA." IEEE Transactions on Parallel and Distributed Systems 27, no. 1 (2015): 197-209.
14. Qu, Yun R., Hao H. Zhang, Shijie Zhou, and Viktor K. Prasanna. "Optimizing many-field packet classification on FPGA, multi-core general purpose processor, and GPU." In 2015 ACM/IEEE Symposium on Architectures for Networking and Communications Systems (ANCS), pp. 87-98. IEEE, 2015.
15. Zhou, Shijie, Yun R. Qu, and Viktor K. Prasanna. "Large-scale packet classification on FPGA." In 2015 IEEE 26th International Conference on Application-specific Systems, Architectures and Processors (ASAP), pp. 226-233. IEEE, 2015.
16. Chang, Yeim-Kuan, and Chun-Sheng Hsueh. "Range-enhanced packet classification design on FPGA." IEEE Transactions on Emerging Topics in Computing 4, no. 2 (2015): 214-224.
17. Khan, Ausaf Umar, Yogesh Suryawanshi, Manish Chawhan, and Sandeep Kakde. "Design and implementation of high performance architecture for packet classification." In 2015 International Conference on Advances in Computer Engineering and Applications, pp. 598-602. IEEE, 2015.
18. Yu, Weiwen, Srinivas Sivakumar, and Derek Pao. "Pseudo-TCAM: SRAM-based architecture for packet classification in one memory access." IEEE Networking Letters 1, no. 2 (2019): 89-92.
19. Huang, Jiamin, Yueming Lu, and Kun Guo. "A Hybrid Packet Classification Algorithm Based on Hash Table and Geometric Space Partition." In 2019 IEEE Fourth International Conference on Data Science in Cyberspace (DSC), pp. 587-592. IEEE, 2019.
20. Saqib, Fareena, Aindrik Dutta, Jim Fussquellie, Philip Ortiz, and Marios S. Pattichis. "Pipelined decision tree classification accelerator implementation in FPGA (DT-CAIF)." IEEE Transactions on Computers 64, no. 1 (2013): 280-285.
21. Jiang, Weirong, and Viktor K. Prasanna. "Large-scale wire-speed packet classification on FPGAs." In Proceedings of the ACM/SIGDA international symposium on Field programmable gate arrays, pp. 219-228. 2009.
22. Kennedy, Alan, and Xiaojun Wang. "Ultra-high throughput low-power packet classification." IEEE Transactions on Very Large Scale Integration (VLSI) Systems 22, no. 2 (2013): 286-299.
23. Tao, Zhang, Wang Yonggang, Zhang Lijun, and Yang Yang. "High throughput architecture for packet classification using FPGA." In Proceedings of the 5th ACM/IEEE Symposium on Architectures for Networking and Communications Systems, pp. 62-63. 2009.

AUTHORS PROFILE



Anita P is a research scholar in the department of ECE at The Oxford College of Engineering Bangalore. She had worked as assistant professor at CMRIT, Bangalore. She obtained her B.E (ECE) degree in 2002 from (GVIT) Bangalore University, M.Tech degree in VLSI Design and Embedded system from CMRIT. She has almost nine years of academic teaching experience and worked for both NBA and NAAC. She has almost 4 publications in international journals. Her areas of interest are VLSI design, Analog and Digital Electronics.



Dr. Manju Devi is working as Professor and head in the department of ECE at The Oxford College of Engineering Bangalore. She has worked as Vice-Principal and professor at BTLIT, Bangalore. She obtained her B.E (ECE) degree in 1996 from Anna University, M.Tech degree in Applied Electronics from BMSCE, and Ph.D from Visvesvaraya Technological University (VTU), Karnataka. She has almost twenty two years of academic teaching experience and worked for both NBA and NAAC. She has almost 75 publications in international conference and journals. She is guiding eight students from Visvesvaraya Technological University (VTU), Karnataka. Her areas of interest are VLSI design, Analog and Mixed mode VLSI design and Digital Electronics.



Design and Development of Mach Zehnder Interferometer based Optical Sensors to Detection of Arsenic compound in Drinking Water

Shaikh Afzal Nehal¹, Anindita Mukherjee² and Dr. Manju Devi³

¹Research Scholar, VTU-RRC, Belagavi, Karnataka, India

²M.Tech(VLSI and Embedded System), CMR Institute of Technology, BANGALORE, KARNATAKA, INDIA
aninditamukherjee84@gmail.com

³Prof. & HOD, Dept. of ECE, The Oxford College of Engineering, Bangalore, Karnataka, India
manju3devi@gmail.com

Abstract

Water, the inevitable need of any individual, must be monitored. Detection of the arsenic chemical present in water leads to contagious diseases. The legacy makes people difficult to survive. The consequences are cancer, other diseases. Employing photonic crystal waveguide with the rally round of mach Zehnder interferometer, it is feasible to correctly compute arsenic compound level in water. MZI sensor has many compensation, diminutive, least use of instrumentation, and ready to be used with CMOS technology. Follows in the paper, arsenic compound level of wavelength range of 1530–1565 nm is analyzed and detected. Experiential program from the band arrangement that for minute change in refractive index is accounted, subsequently logical shift in the frequency and amplitude will be evident enlarging mach Zehnder interferometer will behave as a sensor. Thus projected alternate included optical Mach Zehnder Interferometer (MZI), composed of graded index channel waveguide that can be frequently used as chemical and biological sensor in this manuscript. This dissertation describes how the MZI operates two arms predominantly to conquer the industrial challenges. Manuscript represents test data, graph and results that exemplify the performance of whole system.

Keywords: Nanocavity-Coupled Waveguide; Hexagonal Sensor Meep; Mach Zehnder Interferometer Using Beam Prop.

1. Introduction

Arsenic is a natural compound and present in water. This element found all over the environment. As a consequence, millions of people are in problem for long-time because of arsenic poisoning from the water they drink [1]. For longer period obsessive of arsenic that can effect skin and lung cancers, as well as cancers of the urinary tract, kidney, and liver; Reproductive system and growth in child health can be effected. [2,3].

The main aim of this paper is to propose an evolution of a system that can be used at the establishment of scientist to continuously observe qualitative water parameters. In different laboratory tests, Simple and low-cost colorimetric kits are used to test arsenic testing range from drinking water. So these kind of tests in laboratory has lots of disadvantages such as lack of accuracy, superior limit of detection and used toxic chemicals as test reagents [4]. We have been inspired by these clear advantages and proposed a optimum device which is an opto-photonics devices, that uses MZI for the detection of arsenic. Mach Zehnder Interferometer offered with good sensitivity with two arms of one is for sensitive and other arm for reference. The reference arm is comprising of a strip wave guide. We have exploited and came close to included optics for designing of the 2 dimensional photonic crystal based sensor for treating agents causing physical problem which is the source of water. Because of arsenic that present in water which causes many health issues in human body that can be detected using a

combination of the clinical depiction. Many complex laboratory methods [10-12] is used to quantify accurate measurement of arsenic level in water. The occurrence of broadcasting of light within the Photonic crystal is explained and examined that has been quantified for the accurate measurement of arsenic compound level. These exclusive procedure present good sensitivity and accuracy, but needed particular laboratories, proper training and more time to perform the experiment. So these experiments are not accessible for monitor the arsenic levels on routine basis in field. So the enlargement of biosensors and chemical sensors for the recognition of arsenic compound in water that is an attractive alternative method to colorimetric detection. We have presented in this manuscript, that to design a lab-on-chip photonic crystal sensor using MZI sensor which is very simple to design and can be scalable yet reconfigurable. This lab on chip sensor can be able to identify inorganic compound arsenic in water. The proposed sensor can provide accurate spectral signatures for different compound of arsenic like indium arsenide, gallium arsenide, cadmium telluride, selenium etc that presence in water. This conventional hexagonal ring structure may be suitable for, Mach-Zehnder interferometer (MZI) based sensors that is easy to construct and fabricate.

We demonstrated photonic wave guide that based on defect process and controls the current of beam of glow inside the photonic crystal [10]. Photonic band structure can be referred as optical insulator where transmission of light beam wave travels and that can be prohibited because of presence of band structure photonic

crystal. So the property of band gap can be altered by creating defect engineering. Defects can be classified into dot defect or row defect. The circulation of beam of light in photonic crystal is explained by the master equation (Eq1). The main equation is observed by solving Maxwell's electromagnetic equations

$$\nabla \times \left(\frac{1}{\epsilon} \nabla \times H \right) = \left(\frac{\omega}{c} \right)^2 \times H \quad (1)$$

The glow beam is divided into two arm with one light path containing to be tested sample with hexagonal sensor and the other arm performing as a reference in a conventional MZI sensor configuration. Fig(1). SiO₂ substrate [5-6] is present in MZI which is consisting of particular mode channel wave guide and made by photolithography process and come together with the ion exchange. The active arm of Sensors is made-up of using a silicon waveguide core layer over a SiO₂ masked oxide layer. the increased wave length of MZI and hexagonal ring resonator offer sensitivity. The design of sensor is characterized by using TE polarization from light source with the wave length of $\lambda=1550$ nm into the sensor and measuring the waveguide output light to notice the analytic value. The interference of light beam is travelling through two arms of MZI result in intensity modulation at the output of the waveguide. The relationship between oscillating output is expressed by between input light intensity and output light intensity and that can be denoted by the equation of

$$\frac{I_{out}}{I_{in}} \propto 1 + V \cos(\Delta\phi + \Delta\phi_0) \quad (2)$$

Where $\Delta\phi_0$ is the initial phase change of normalized of two arm. After applying RI value of analyte $\Delta\phi$ is the changed of two arms.

Hexagonal ring resonators mechanisms have been included on the chip.

$$\phi = \left(\frac{2\pi L}{\lambda} \right) N_{eff} \quad (3)$$

From equation 2 phase ϕ which depends on its effective refractive index value for a given wave length λ of the active arm of MZI sensor. Arm length is denoted by L. This kind of design and can be integrated with optical technique.

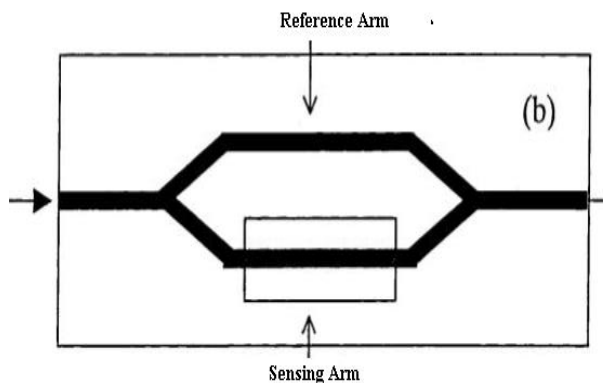


Fig-1: Schematic diagram Of MZI

In this paper, theoretical and tentative investigation of quality factor based on dissimilar value of refractive index of a photonic crystal (PhC) resonators are planned with the help of MEEP simulations, the change in refractive index, quality factor is observed. The use of biosensor for detection of bimolecular or chemical molecules has been observed quick growth since last two decades. Addition of sensor with microelectronics and wireless communication provides high sensitivity and that allow the real

time monitoring. The various technique is used by biosensor to detection of various analyte and that bio sensing technique is used for their simplicity in fabrication, small footprint, low cost and real time detection and high sensitivity. A light beam is divided through MZI device into two identical arms, sensor and reference arm by means of Y junction. Light beam will travel through distance of arms length L, by means another, by means another Y junction. In the sensor arm, the specific area is etched, now electromagnetic waves interact with specified analyte. This kind of interaction causes change in effective refractive index of the sensor arm which will cause another parameter that is phase change between the light beam travelling through both the arms. Because of difference in effective refractive indices of the sensor and reference arm and on the interaction length of sensor area that produces phase difference.

2. Theory

Photonic crystals (PCs) comprising of a intermittent arrangement of regularly formed materials having different dielectric constants in a substrate [7]. Photonic crystals are divided into three types based on their structure as follows

- i) 1-dimensional (1D) structures
- ii) 2-dimensional (2D) structures and
- iii) 3-dimensional (3D) structures.

There is insufficient band gap in 1-Dimensional photonic crystal structures and to make 3D structures is very difficult because of their small lattice size [8]. 2D structures are easy to create compared to 3D structure, because 2D structures are having complete band gap. By Solving the Maxwell equations, we can explain the propagation of light within the photonic crystals.

Photonic crystals have many applications in various fields like optical field. Photonic crystals are having many applications since they offer a common proposal to fabricate a huge number of optical components on an array configuration.

The working principle of both resonator and interferometer based on the changes of the effective refractive index (N_{eff}) of the waveguide mode due to changes in the ambient refractive index via the passing field interaction.

$$\Delta N_{eff} = \frac{\partial n_{eff}}{\partial n_{ambient}} \quad (3)$$

$$S = \frac{2\pi L}{\lambda} \frac{\partial N_{eff}}{\partial n_c} \quad (4)$$

From equation (4) sensitivity can be calculated by using N_{eff} value from the practical graph which is shown in the graph 4. The coupling of the complete sensor is done with the help of two structure explained below:

A. HEXAGONAL RESONATOR:

Light beam can be passed into a hexagonal waveguide with circumference L using MZI. Silicon waveguide based hexagonal structure can be integrated with MZI optical wave guide by using mode conversion process.

B. Mach-Zehnder Interferometer (MZI) :

MZI device has been constructed using silicon-on-insulator (SOI) [10-12]. MZI is constructed using a strip waveguide and slot wave guide. MZI sensor uses slot waveguide instead of conventional sensor of a sensing path to achieved a high sensitivity. Strip wave guide is considered as reference arm and slot wave guide is considered as sensing arm. Mode converter converts strip wave guide into slot waveguide through sensing arm. The visibility factor depended on splitting ratios of the input and output Y junction and on the differential propagation loss of the strip waveguide and slot wave guide of the 2 (two) arms[9].

3. Sensor Design

MEEP simulation tool is applied to design and formed bio and chemical sensor. This kind of sensor is based on two dimensional square lattice photonic crystal structure with row defect. A two dimensional photonic crystal is periodic along two if its axes and homogeneous along the third axis [4]. We have designed a hexagonal resonator structure that is sensitive, we proposed two structures one is hexagonal structure and MZI sensor based on different RI value e.g. chemical RI value.

Design specification:

1. Configuration used- Rods in air.
2. Diameter of the Silicon rods used is = 20 nm.
3. The dielectric constant of the defect rods used is 12
4. Tallness of rods used is = infinity.
5. Beam resource used is: Gaussian Pulse.
6. Lattice constant of the crystal structure used and is denoted by, 'a'= 1 nm

Proposed Structure

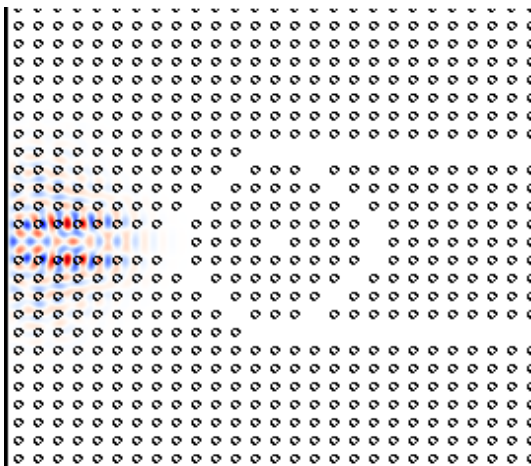


Fig-2: Hexagonal structure (Rods In Air)

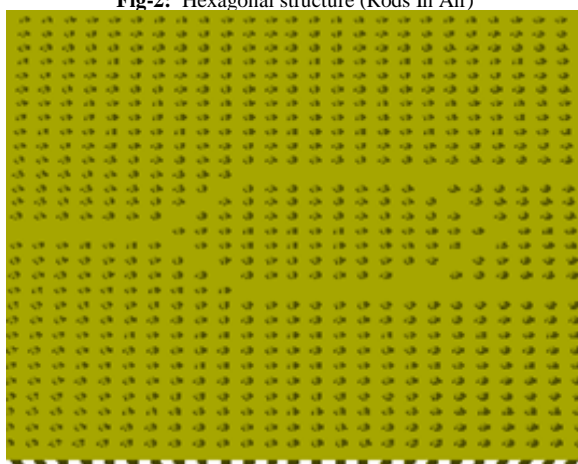


Fig-3: Structure of photonic Wave guide

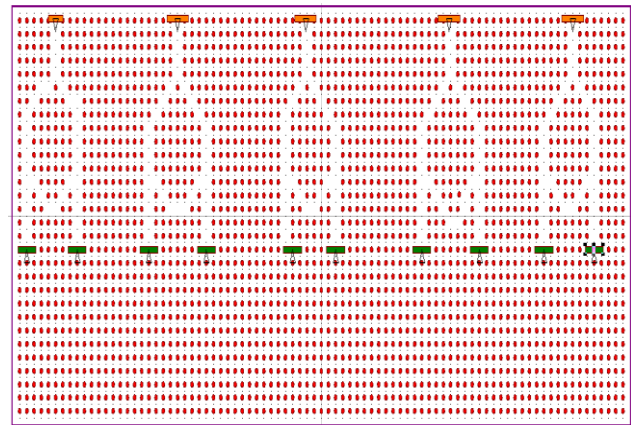


Fig-4: Array structure of wave guide

We have made array structure of photonic crystal sensor of hexagonal resonator to determine the arsenic compound in water. This array structure can be used for mass volume capacity construction to determine the large amount of arsenic compound.

Design description for MZI:

Table-1 Shows the specification of MZI Construction

| | |
|------------------------|-------------|
| Simulation Tool | Beam Prop |
| Excitation Wave Length | 1.55um |
| Index Of Background | 1.46 |
| Width Of Component | 5 |
| Dimension | 3-Dimension |
| Index Difference | 1.98 |

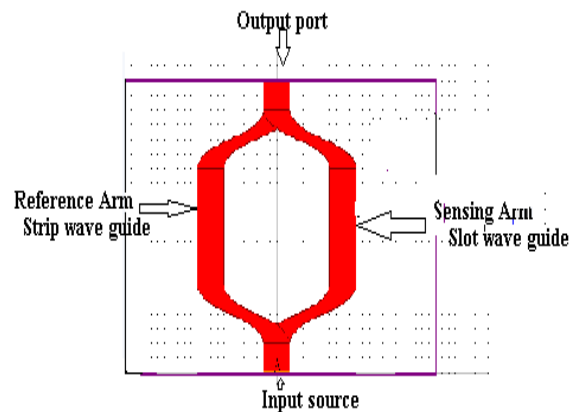


Fig -5: Structure of MZI and Structure of Strip Waveguide

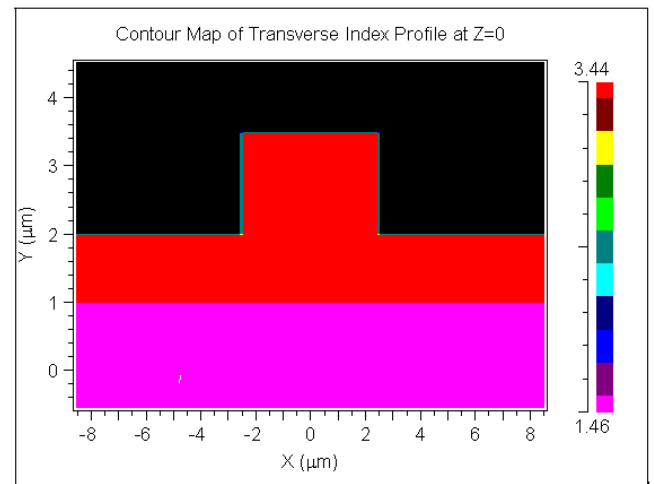


Fig 6: Strip Waveguide

From Fig.6 we can observe the structure of strip wave guide which is the part of reference arm of MZI. Fig. 4 shows that Material has taken for MZI construction that is SOI(silicon on insulator).To conclude (from the above figure 6) its inferred that 1.46 value indicate silicon di oxide material and 3.44 value indicate si material which is used for MZI construction. The sensor MZI is designed and is done using Beam-prop technology, we carefully look after the manufactured acceptance of the MZI, especially with respect to the difference of the waveguide size and length and observed fabrication errors. Fabrication error variation in terms of width of waveguide causes a change in designed value. The material has taken as SOI for MZI configuration. MZI is about 7 nm, which for the two-channel MZI in Fig. 5.

4. Simulation Results

Table-2 Comparison of water and other arsenic compound and observe quality factor

| Name Of Arsenic Compound | Amplitude (V) | Frequency (Thz) | Quality Factor |
|--------------------------|---------------|-----------------|----------------|
| Water | 0.03 | 0.8449 | 19998 |
| Indium Arsenide | 0.031 | 0.861 | |
| Gallium Arsenide | 0.0249 | 0.854 | |

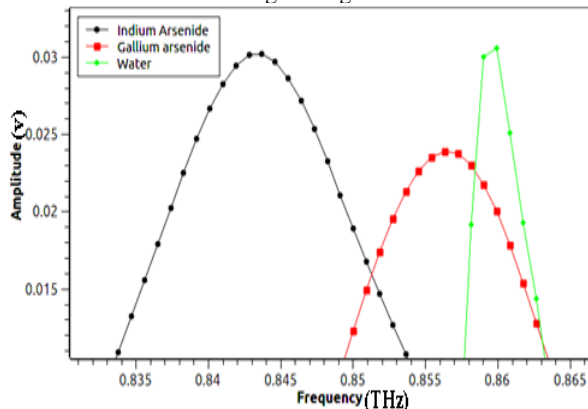
Table-3 Comparison of water and other arsenic compound and observe quality factor

| Name Of Arsenic Compound | Amplitude (V) | Frequency (Thz) | Quality Factor |
|--------------------------|---------------|-----------------|----------------|
| Water | 0.008 | 0.8179 | 19998 |
| Cadmium Sul-fide | 0.000608 | 0.861 | |
| Zinc Sulfide | 0.0104 | 0.81509 | |

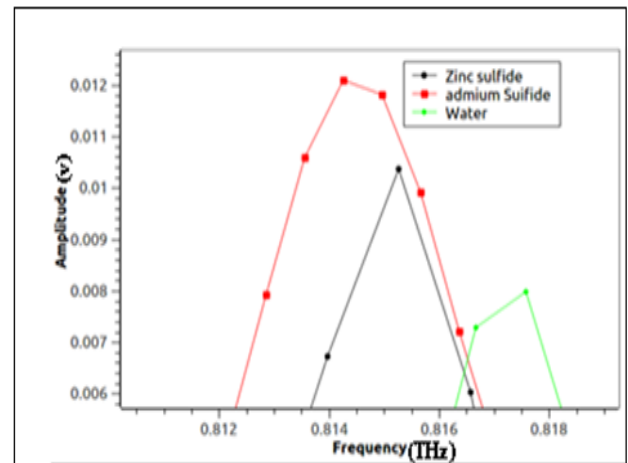
Table-4 Comparison of water and other arsenic compound and observe quality factor

| Name Of Arsenic Compound | Amplitude (V) | Frequency (Thz) | Quality Factor |
|--------------------------|---------------|-----------------|----------------|
| Water | 0.12390 | 0.823 | 19998 |
| Cadmium Tel-luride | 0.031 | 0.8231 | |
| Selenium | 0.00066 | 0.8209 | |

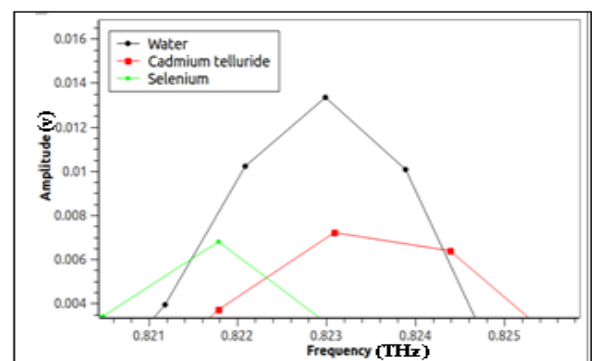
There is a variations in the resonant frequencies of arsenic present in water are obtained by using MEEP simulation tool and are shown in Table 2,3,4 and observed quality factor. Quality factor is observed by means of propagation of light through wave guide . we have to make sure that all the way through wave guide during propagation there will be very less loss or less scattering .So that we can demonstrate a strong wave guide .



Graph-1: Observe the peak amplitude of normal water and other peak amplitude of arsenic present in waetr with different R.I value of Arsenic



Graph-2: Observe the peak amplitude of normal water and other peak amplitude of arsenic present in waetr with different R.I value of Arsenic



Graph-3: Observe the peak amplitude of normal water and other peak amplitude of arsenic present in waetr with different R.I value of Arsenic

Graphs are presented here to show about arsenic present in water with different peak amplitude. For a particular frequency changes we have observed maximum peak value of amplitude for arsenic compound and water . Different arsenic compound has been observed which is present in the water with the help of their respective RI value . Silicon based material is used to fabricate high sensitive MZI sensor. RI value of si and sio2 is 3.45 and 1.44 has taken .

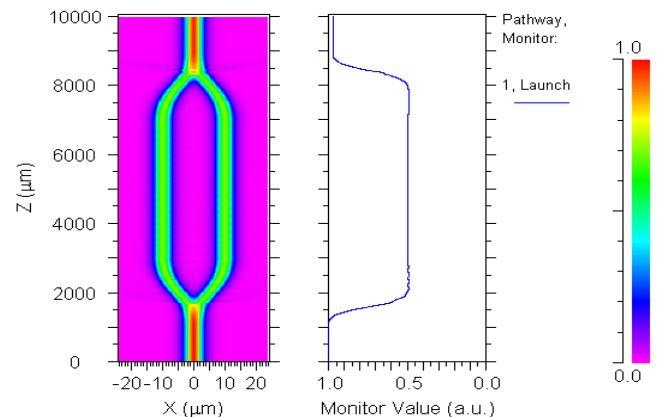
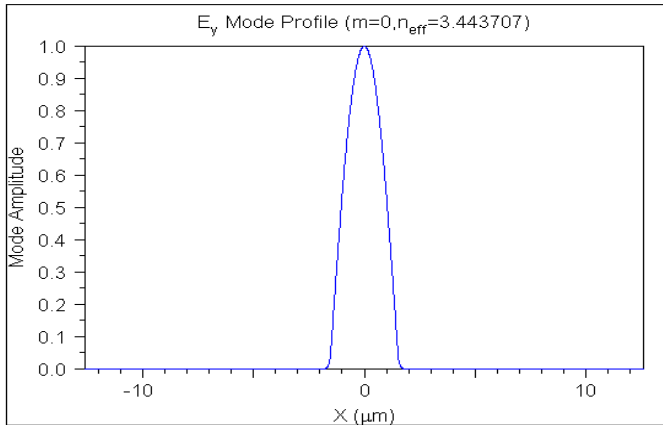


Fig-7: Light Propagation through MZI and observe the output power without

sensing layer



Graph-4: Observe the Neff value for MZI calculation of Sensitivity

MZI waveguide sensor was experimented which can determine existence of arsenic compound in water. In this paper we have considered fundamental mode. Determination of arsenic compound in water is inevitable for the detection and identification of transferable or inborn diseases. By using equation 4 and from graph [4] Sensitivity of a common MZI for length of 7 nm of the channel length was accounted to be 78.5. So to achieve high sensitivity of MZI construction SOI material is used.

5. Conclusion

The design and optimization of a highly sensitive MZI of a waveguide biosensor is presented in this paper. MZI Biosensors comprises of slot wave guide and strip wave guide. This provides high sensitivity and high optical intensity region of MZI. The slot wave guide is integrated with sensing arm of MZI. From fig 7 we can conclude that this is normalized output power without sensing the arm with analyte. But after interact with sensor that is resonator, there will be change in propagation of light beam. This waveguide based MZI sensor has ability to perform in the platform for highly sensitive analytical device by combining the MZI's unique characteristic and photonic devices which are easier and simple to design. Design of a sensor should be cost effective, small and possible to fabricate lab on chip. Both the proposed sensor are highly sensitive and with the help of both the sensor minute change can be detected when input refractive index of arsenic that is present in water is applied to the input terminal of sensor. Designed a photonic crystal sensor is part of sensing module but we have to monitor to represent a complete sensor that is complete lab on chip sensor that can be possible to implement by using MZI sensor.

References

- [1] Ahuja, Satinder.; "The Problem of Arsenic contamination of groundwater." Arsenic Contamination of Ground water: Mechanism, Analysis, and Remediation (2008).
- [2] R G Heidman, P.V. Lambeck.; "Remote opto with extreme sensitivity: Design, fabrication and performance of pigtailed integrated optical phase modulated Mach Zehnder Interferrometer system", sense actuat. B 61(1999)100-127
- [3] Sarkar, I. Jamal, S.K. Mitra.; "Analysis, Design, and Fabrication of optical wave guide for Mach Zehnder Interferrometer". Opt. Commun, 311, (338-345) 2013
- [4] Marazulela, M Moreno Bondi. Fibre optic.; "Biosensor overview. Anal. Bioanal. Chem". 372(5-6)
- [5] S. Chandran, R. K. Gupta, and B. K. Das.; "Dispersion-free SOI interleaver for DWDM application, Journal lightwave technology", vol. 30 no. 1, pp. 140-146, 2012

- [6] X. Fan, I. M. White, S. I. Shopova, H. Zhu, J. D. Suter, and Y. Sun.; "Sensitive optical biosensors for unlabeled targets: A review," Anal. Chim. Acta 620, 8-26 (2008).
- [7] K. Zinoviev, L.G. Carrascosa, J. Sanchen del Rio, B. Sepulveda, C. Dominenguiz, L.M. Lekhuga, "In Advances in optical technology, 2008, Silicon Photonic Biosensor for lab on chip application", 2008
- [8] Frazao, O.; Silva, S.F.O.; Viegas, J.; Baptista, J.M. Santos, J.L.; Kobelke, J.; Schuster, K.; "All fibre Mach Zehnder Interferrometer based on suspended twin-core fibre". IEEE Photon. Technol. Lett. 22, 1300-1302, 2010.
- [9] Zhu, J.J.; Zhag, A.P.; Xia, T.H.; He, S.; Xue, W. "Fibre optic High-temperature sensor based on thin-core fibre modal interferometer" IEEE Sens. J., 10, 1415-1418, 2010
- [10] D. a. Marry-Arrijoja, P. Likam W. Sa, J.J. Sanchez-Mondragon, R. j Selvas Agular, and I. Torres -Gomez.; "A reconfigurable multi-mode interference splitter for sensing application," meas Sci. Technol vol. 18, no. 10, pp. 3241-3246, Oct.
- [11] S.K. Raghawanish, V. Kumar, D. Chack, and Kumar.; "Propagation study of Y-junction optical splitter using BPM,"

Power Analysis of Photonic Sensor for Detection of E-coli in Water

Afzal Shaikh⁽¹⁾, Preeta Sharan⁽²⁾, Manju Devi⁽³⁾

(1) Research Scholar, The Oxford College of Engineering, Bangalore, Karnataka, India

(2) Professor, The Oxford College of Engineering, Bangalore, Karnataka, India

(3) Professor & Head of ECE, The Oxford College of Engineering, Bangalore, Karnataka, India
afzal.aiktc@gmail.com¹, sharanpreeta@gmail.com², manju3devi@gmail.com³

Abstract— An optical photonic crystal sensor design is proposed, which contains Silicon (Si) circular rods, made in a square lattice structure. The input point has a light source of wavelength 1.55 μ m and has two output point to observe the output. The paper proposed different Photonic Crystal structure and power analysis for the same. The calculation for change in Refractive index value and power - wavelength shift for various analyte (bacteria in water, is analyzed, and plotted. The procedure repeated for proposed different structures. The scope of applications of the splitter is becoming broader day by day owing to fast progress in complementary technologies such as nanophotonics and integrated photonic sensing. Using a new design of 2D slab, we have achieved 84.4% power output from a 1 \times 2 power splitter.

Keywords— Nanocavity-coupled waveguide; MEEP; Photonic crystal;

I. INTRODUCTION

The power splitter is a critical component in a silicon chip. The prominent applications of silicon chips include photonic computing, long haul fiber communication, and bio-photonic sensing. Photonic Crystals (PC) are dielectric formation with periodical spatial rotations of the refractive index on the order of the wavelength of the light [1, 2]. Photonic bandgap can be realized and artificially introduce defects to control the light emanation and transmission and the trapping of the photons. The photonic bandgap (PBG) formation due to periodicity and the electromagnetic waves propagation gets forbidden for all wave vectors inside this bandgap. Therefore, the detection of the unwanted and harmful content which is present in water is a crucial issue in decimating its adverse impact on public health and hygiene. So the determination of Escherichia coli (E-coli) and observation of the power for a different structure is essential. In the paper, we have used RI value of analyte, the harmful content present in water. Power splitting technique is performed using 2D and 2D slab PC line defect waveguides by investigating different structure for 1 \times 2. For power splitter experiment, the required components are input and output waveguide channels which act like branches of the splitter. The intersect point from where the branches are coming out is called a junction [2]. From the intersection of power division, one input and two output branches form 120° waveguide bend with each other [3]. Further, the two output branches make an extra 60° bend with the input branch. To perform the function for the power splitter, the transmission of light power should be maximum without suffering any reflection. The efficient and well-executed design of waveguide bends is essential to achieve the above objectives.

II. THEORY

Organization of the periodic structure is Photonic crystal and it is comprising of different dielectric constants in a substrate [4]. Depending on the geometry of the structure, photonic are offering three kinds of architecture such as one-dimensional (1D), two dimensional (2D), and three dimensional (3D) arrangements. With the help of Maxwell equations, the propagating light within the PC is manipulated. Photonic crystal platform is employed to fabricate a large number of optical components on a single chip. The frequency of the light is not allowed to pass within the PBG range. The photons are entirely forbidden within PBG if a particular defect is introduced in the PCs structure. In various applications, these PC bandgap structures are utilized [5-7]. Figure 1 shows the structure of the splitter consisting of two parts, the input port and two output ports. The power is given to the input port, which is divided equally into two output ports without any reflection and radiation loss.

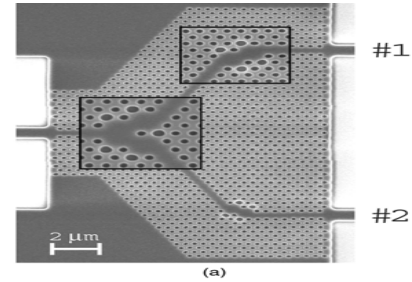


Fig. 1. Y-junction power splitter based on Photonic Crystal.

The Finite Difference Time Domain (FDTD) method is used as a numerical analysis technique to solve the differential equations [8].

$$\nabla \times E^{\vec{r}} = -\partial B^{\vec{r}} / \partial t \quad \nabla \times H^{\vec{r}} = J + \partial D^{\vec{r}} / \partial t \quad (1)$$

The Gaussian pulse is used as a source for this power splitter experiment. The frequency response over a wide range of this system is possible to obtain. The 2D MEEP method is applied to perform the simulation and the propagation of the electromagnetic waves can be obtained within the waveguides.

III. SENSOR DESIGN

The sensor is designed using Rods in Air configuration in both OptiFDTD and MEEP software. The sensor design checked for various analyte by changing their R.I. values. Here we are analyzing the propagation of the TE polarized light in the designed sensor. We are observing the variation in the light property after passing through the various refractive index of the analyte. Here the relationship between the output

power and the wavelength shows the changes recorded for different refractive index by the designed sensor.

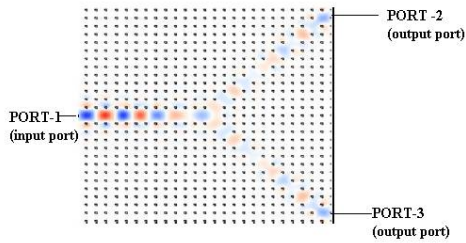


Fig. 2. Proposed Structure Design 1 in MEEP.

Figure 2 is called Y structure, Figure 3 is called as PI structure and Figure 4 is called as Cantilever structure. Light propagation is observed from the PBG structure. Port 1 is acting as input and Port 2 and Port 3 as output.

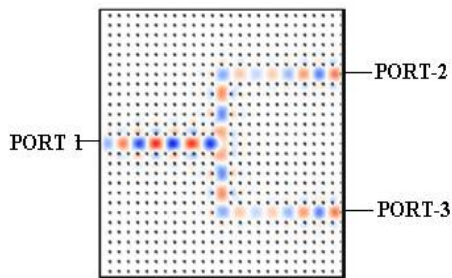


Fig. 3. Proposed Structure Design 2 in MEEP..

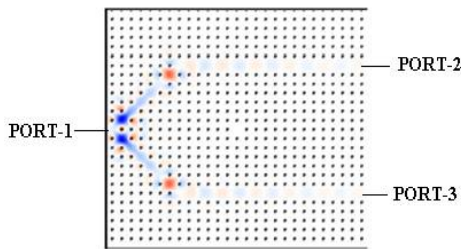


Fig. 4. Proposed Structure Design 3 in MEEP.

TABLE I. DESIGN PARAMETER FOR SENSOR

| Sr. No. | Description |
|---------|-----------------------------------|
| 1. | Configuration is rods in air |
| 2. | Lattice constant "a"=1 |
| 3. | Structure is square lattice |
| 4. | The radius of rods "R"=0.21um |
| 5. | 0.65um is the height OF RODS |
| 6. | 12 is dielectric constant of rods |
| 7. | Light source:gaussian source |

IV. SIMULATION RESULTS

A. Design 1: Y Structure

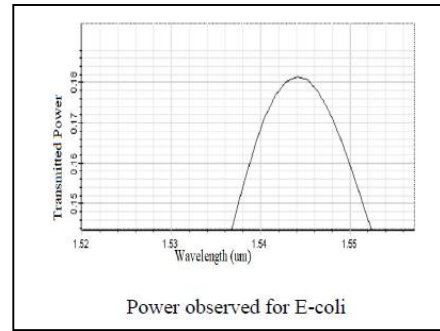


Fig. 5. Graph for Transmitted Power vs Wavelength for Structure 1 in OptiFDTD

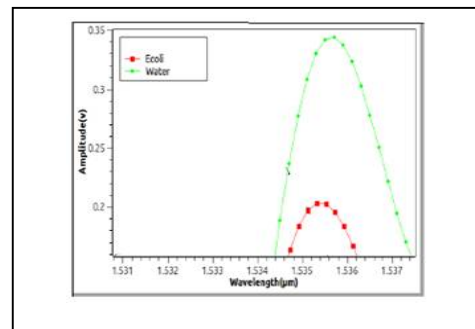


Fig. 6. Graph for Amplitude vs Wavelength for Structure 1

B. Design 2: PI Structure

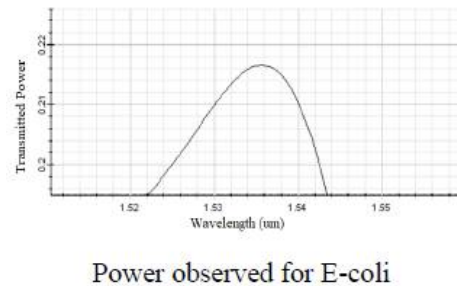


Fig. 7. Graph for Transmitted Power vs Wavelength for Structure 2 in OptiFDTD

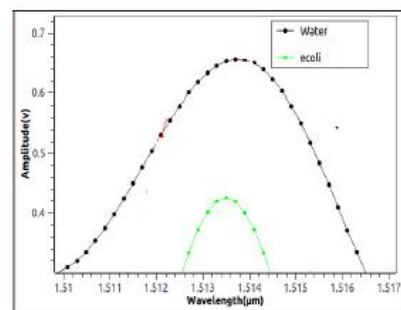
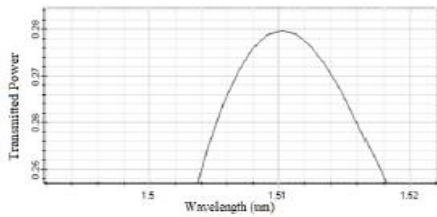


Fig. 8. Graph for Amplitude vs Wavelength for Structure 1

C. Design 3: Cantilever Structure



Power observed for E-coli

Fig. 9. Graph for Transmitted Power vs Wavelength for Structure 2 in OptiFDTD

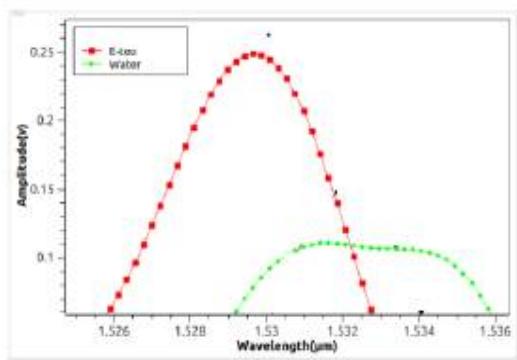


Fig. 10. Graph for Amplitude vs Wavelength for Structure 1

TABLE II. TRANSMITTED POWER OBSERVED

| Name of Structure | Name of Analyte | Transmitted Power |
|----------------------|-----------------|-------------------|
| Y Structure | E-coli | 18% |
| PI Structure | | 29% |
| Cantilever Structure | | 28% |

TABLE III. DETECTION OF E-COLI IN WATER AND OBSERVED QUALITY FACTOR

| Name of Structure | Name of Analyte | Amplitude | Quality Factor |
|----------------------|-----------------|-----------|----------------|
| Y Structure | Water | 0.34 | 5282 |
| | E-coli | 0.2 | |
| PI Structure | Water | 0.66 | 21508 |
| | E-coli | 0.42 | |
| Cantilever Structure | Water | 0.11 | 25954 |
| | E-coli | 0.25 | |

From Table II, we can come up to the culmination that power is considered more for PI and cantilever structure and Table III, we can conclude that cantilever structure provided more quality factor compared to the other structure hence

propagation loss though the cantilever structure is less. Hence PI and Cantilever structure will be considered to design and put on for fabrication as good PBG structure for different application like biomedical, networking

V. CONCLUSION

The power splitter is a promising topic of research in photonics. The development of complementary technologies such as nano-photonics, spectroscopy, and optical coherence tomography (OCT) accelerates the research in power splitter. We briefed the different architectures of the power splitter. We have observed the power division method using different technology. Further, the realization of the power using analyte, which is present in water for the proposed structure. Ecoli that is very harmful to human beings is detected through three different PBG structures. Also came to the ending decision that Y and PI structures are preferable for fabrication to discover any analyte. Also, the current developments and applications of power splitter are explained. Finally, the potential of the splitter in future such as in Smartphone, biomedical device, and networking device can be used.

References

- [1] Varsha Sharma , Vijay Laxmi Kalyani, “ Design Four Channel Nano cavities coupled Photonic Crystal Based Bio-sensor for detection of Bacteria” International Conference on Computing and Communication Technologies for Smart Nation (IC3TSN), IEEE, pp. 84-88, 2017.
- [2] Praveen Kumar Kerimani, Fleming Dackson Gudagunti, Preeta Sharan, Srinivas Talabuttata, “Photonic Crystal Based Nano Scaled Sensor for the Ahents causing Typhoid in water”, IEEE ICCSP Conference, pp. 1171-1175, 2015.
- [3] Preeta Sharan, Pooja Deshmukh, Sandipn Kumar Roy, “Mapping of Aqua Constituents Using Photonic Crystal” IEEE R10-HTC 2013, pp. 320-325.
- [4] Varsha Sharma, Vijay Laxmi Kalyani, Shivam Upadhaya, “Photonic Crystal Based BIO sensor Detection in Cancer cell Using FDTD Method”, 8th ICCCNT 2017, Conference Paper, July 2017, IEEE – 40222, ResearchGate.
- [5] Joyti, Vinita, “ Design and analysis of PCF of Silica and Gallium Phosphide using OPTI FDTD”, Imperial Journal of Interdisciplinary Research (IJIR) Vol-2, Issue-11, 2016, pp. 740-742
- [6] Ashutosh Kumar Dikshit, M Bhargav, Yeswanth Kumar, Usha Rani, Subhashish Tiwari, Bipin k Singh, “Tunability of Resonator Based Photonic Crystal. Switch By Elliptical Rods”, WRAP2015, pp. 1-4, 2015.
- [7] Poonam Sharma, Preeta Sharan, “Design of Photonic Crystal based Biosensor for Detection of Glucose Concentration in Urine”, IEEE SENSORS JOURNAL, VOL. 15, NO. 2, FEBRUARY, 2015, pp. 1035-1042.
- [8] Fleming Dackson, Gudagunti, Preeta Sharan, Srinivas Talabattula, Nainitej V, “Early Stage Detection of Breast Cancer Using Hybrid Photonic Crystal Ring Resonator,” 2014 IEEE International Conference on Advanced Communication Control and Computing Technologies (ICACCCT), pp. 1542-1545.

Smart E – Cane for the Visually Challenged and Blind using ML Concepts

Adam Filbert Ashwal¹, Kimberly Claudia Dsouza², Meghana S³, Muhammad Hashim Iqbal Husain⁴, Dr. Manju Devi⁵

^{1,2,3,4}Student, Dept. of ECE, The Oxford College of Engineering, Bangalore, Karnataka, India

⁵Professor and HOD, Dept. of ECE, The Oxford College of Engineering, Bangalore, Karnataka, India

Abstract - Eyes are the organs through which one can recognize and identify the surroundings with. Sadly, there are people deprived of their sight. Sometimes, they can be effortlessly confused or obtain inadequate data because of which they can't complete their proposed work. This paper plans to show light on a proposed smart stick and wearable band which can offer help to the visually impaired in their movement by giving precise area subtleties and cause them to feel free. The Smart E-Cane will involve the essential and modern sensors for obstruction discovery and area-based input. The Smart E-Cane will also be able to detect a rise in surface level as the blind person is walking using machine learning and report back what kind of a raised surface is in front of him. This would be very useful when the person encounters an obstacle that is detected as a raised surface or object but doesn't specify whether it is stairs, or an inclination, or a misplaced rock. This Smart E-Cane gives assurance of independency along with security when it comes to walking without assistance from another person.

Key Words: E-Cane, Blind Stick, Machine Learning, GPS, IoT, Voice Assistance, Object Detection

1. INTRODUCTION

Visual impairment or vision loss is a decreased ability to see to an extent that causes problems not fixable by typical means. The term blindness is for complete or nearly complete vision deficit.[1] The World Health Organization (WHO) gauges that 80% of visual debilitation is either preventable or reparable with treatment. Starting at 2015, 246 million had low vision and 39 million were visually impaired. [2] Hence there is a compelling need to find better and much advanced solutions to assist the less fortunate individuals who are deprived of their vision.

In the past, and recent years, there have been many advancements towards designing tools through smart phones, wearables, smart sticks, etc. With each new product being designed and developed, there are new features or upgrades being made that aid the visually challenged in a much better way. This paper, along with proposing a system, will also provide a review of the existing applications and models, to give a wider perception of what is in store and what can be, for better awareness and implementation.

2. LITERATURE SURVEY

A paper based on the recognition/identification of images in real-time. They identify, arrange and gauge the rough position utilizing raspberry pi as the processor that interfaces with the camera to catch the general condition. The capacity to make sense of specific obstructions, examined later, that are a crucial for the visually challenged person to be warned about was lacking in this paper.

Another paper we came across uses a voice play back framework through a mobile android application. Whatever the gadget detects and senses, it provides a criticism through the android application dependent on Natural Language Processing (NLP).

The concept of utilizing real time video processing is likewise applied. The video is processed through Google's Cloud Video Intelligence API, for better navigational guidelines. It is a rather cost-effective method for providing constant recordings.

An improvement of the smart walking stick, a device which is considered to be a robot cane, screens occasions and recognizes impediments just when placed on a level surface. The alarm is activated when the visually challenged person seems to lose balance and is detected to be falling down.

3. PROPOSED SYSTEM

3.1 Existing Systems

There are several existing frameworks that were designed in such a way that they stood out when it came to assisting the blind in moving from one place to another. Not merely do these systems help in travelling but additionally in distinguishing proof of objects that we use in daily life. They likewise provide the facility of voice to text conversion and vice versa to allow for a better interaction with the device. A few of them are briefly described below:

One application that allows for ease of wandering about is Google Maps. There is an element that furnishes individuals with the capacity to get progressively particularized voice direction and new types of verbal declarations for on foot trips. Google Maps proactively announces the correct route, the distance until the next turn and the direction one is walking in. As the individual approaches large intersections, a heads-up notification is received to cross with added

caution. Also, if they accidentally depart from their route, they get a spoken notification that they're being re-routed.[3]

A company which helps in assisting the blind using the most advanced technologies is an organization called Be My Eyes.[4] The manner in which this application works is sighted volunteers offer their vision to solve tasks to assist the blind and low-vision people. There are numerous ways a visually impaired can look for help through this platform. It helps them identify packages, identify colour, food, reading recipes, setting up gadgets, navigating, coordinating an outfit, getting support with Gmail, troubleshooting Skype, etc.

eSight, another product to assist the visually challenged, is advanced electronic glasses.[5] It uses a cutting-edge camera, smart algorithms and high-resolution screens, to create a crystal clear, real-time image of what is in front. It utilizes innovation to help distinguish faces, continue with normal work or secure positions, feel sure about new conditions. It is a lightweight gadget that gives ongoing input of the environment around the individual.

3.2 Methodology

The proposed framework includes various sensors and specialized ideas that help in making this framework a superior model. The use of machine learning concepts is an added advantage as the gadget will have the option to not just perceive and synchronize information of the environment yet in addition learn and store that information for future use. The project theoretical implementation is divided into obstacle detection and emergency notification. The machine learning concepts will be executed in the impediment identification part of the framework. Navigation in this proposed system will be based on google directions API. Different sensors are likewise included to upgrade the nature of the framework and provide better feedback and feeling of independence.

3.3 Obstacle Detection

The different segments that ought to be utilized for obstacle detection incorporate ultrasonic and infrared sensors to ascertain and gauge the separation among objects and the individual, and a magnetometer to recognize change in surface level, however not in the conventional ways. The integration of the information gathered from the sensors alongside the magnetometer information will be utilized in this prototype.

First is the utilization of the magnetometer to prepare the model to comprehend the normal inclination the stick will be positioned in. In this approach, model will initially be prepared to distinguish surface level. The information will be handled so as to recognize the items, for example, stairs, inclinations or pits, and so forth. There will be a scope of qualities that will be expressed as expected surface level.

After that will be a set of recorded values that will be founded on different surface level inclinations. Those values will be stored on cloud and integrated with the values recorded from the ultrasonic and IR sensors.

At that point there is the information gathered from the ultrasonic/IR sensors. Here, as the inclination of the magnetometer changes, the ultrasonic and IR sensors will likewise distinguish the estimation of the obstacles before the individual. Assume there is an inclination, the information from the three sensors set before the stick will rise linearly. Presently assume there are staircases before the stick, the sensors will distinguish the adjustment in a step rise. Hence the data is captured for many other obstacles and the machine forms an understanding of the correlation between the data. This will be done via the supervised learning.

The magnetometer will only be used as a reference. Later an addition of a camera which will be integrated along with raspberry pi will be present, to help in obstacle identification. This information will be contrasted and the information obtained from the cloud so as to make the framework increasingly dependable.

3.4 SOS Wearable Band

To help in emergency situations, we have proposed a wearable band that will have two buttons. One that will locate the position of the stick in case the visually challenged person is unable to figure out where he kept the stick. Another button that will send the person's location via IoT on the off chance that he is lost. It will likewise provide a voice feedback, expressing where precisely the individual is and will request for the destination to be entered and provide an audio feedback to direct him/her back home. It will likewise send the present location by means of IoT to the individual's emergency contacts in case they don't have a sense of security going back alone.

4. REPRESENTATION OF PROPOSED SYSTEM

The below framework depicted in figure 1 gives a comprehension of the connection of the various components in the framework. The primary processors will be the arduino, raspberry pi and Node MCU. The arduino will be utilized to interface the sensors while the node mcu will be used to implement the Smart Band and finally the Raspberry pi module will be utilised to implement the machine learning part of our framework.

The ultrasonic sensors will be used for obstacle detection and the feedback will be provided via a vibrator whose intensity will increase as the stick gets closer to the obstacle.

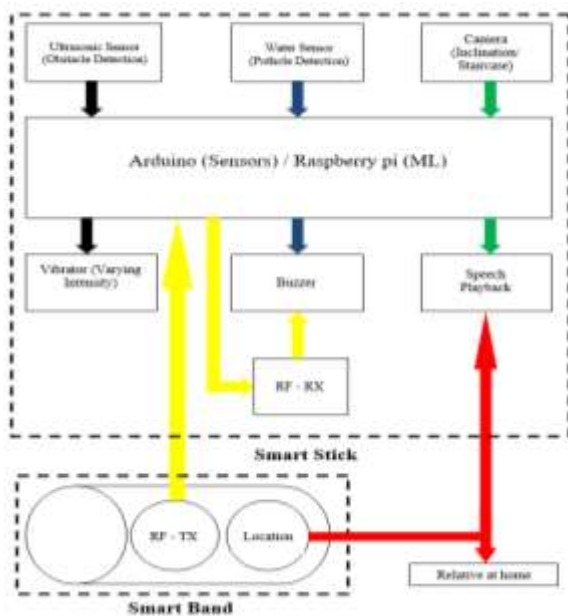


Figure 1

The water sensor will be used to detect wet areas, potholes containing water etc. and the feedback will be provided by a buzzer. This concludes the Smart Cane part.

The smart stick is combined with a smart band for added features such as safety and location tracking. It consists of two buttons. The first button is connected to an RF Transmitter, and the RF Receiver is mounted on to the smart stick. This feature would help the user to locate the smart stick in the near vicinity and the feedback is provided using the same Buzzer.

The second button is used by the user if they are in a situation where they find themselves lost. Here when the second button is pressed, it would send the location about the user to the concerned people at home as well as provide the location feedback to the user via speech playback.

Finally, one of the most important features of our project is to detect any raised surface level such as a staircase, ramp, inclined plane using Anomaly Detection which is one of the Machine Learning concepts.

One way to implement the feature is that there would be a device such as a Magnetometer which would be used to provide a range of reference values. While the camera continuously monitors to detect any raised surface level such as a staircase, ramp, inclined plane etc., if it does encounter any such surface it must send the data and the difference value has to be calculated. By having numerous data, using the concept of machine learning it should provide the user with a cautionary message via speech playback of the type of surface it may encounter before the user even steps on it.

Here the reference data provided by the Magnetometer is used against the sudden change in data provided by the

camera. The difference value or the change in value when compared to the reference value is treated as an Anomaly and thus the concept of Anomaly detection is used. Along with this the machine learns from various data in order to give more accurate results, thus the machine learning part is also incorporated onto the stick.

5. CONCLUSIONS

The Smart E-Cane along with the Smart Band will provide the visually challenged with much of the important features than a modern-day blind stick.

The location tracking feature along with the detection of any raised surface level by machine learning will not only provide accurate results with huge number of data learnt but also allow a wide range of opportunities for future scope.

REFERENCES

- [1] Maberley DA, Hollands H, Chuo J, Tam G, Konkal J, Roesch M, et al. (March 2006). "The prevalence of low vision and blindness in Canada". *Eye*. 20 (3): 341-6. doi:10.1038/sj.eye.6701879. PMID 15905873.
- [2] "Visual impairment and blindness Fact Sheet N°282". August 2014. Archived from the original on 12 May 2015. Retrieved 23 May 2015.
- [3] Wakana Sugiyama, "Voice guidance in Maps, built for people with impaired vision", Published Oct 10, 2019. Retrieved 13 March 2020. URL: <https://www.blog.google/products/maps/better-maps-for-people-with-vision-impairments/>
- [4] Will Butler, "100 Ways to Use Be My Eyes", Published January 28, 2020. Retrieved 13 March 2020. URL: <https://www.bemyeyes.com/blog/100-ways-to-use-be-my-eyes>
- [5] eSight, "eSight", Retrieved 13 March 2020. URL: <https://www.esighteyewear.eu/>
- [6] P. Rohit, M. S. Vinay Prasad, S. J. Ranganatha Gowda, D. R. Krishna Raju and I. Quadri, "Image Recognition based SMART AID FOR VISUALLY CHALLENGED PEOPLE," 2019 International Conference on Communication and Electronics Systems (ICCES), Coimbatore, India, 2019, pp. 1058-1063.
- [7] D. Bharatia, P. Ambawane and P. Rane, "Smart Electronic Stick for Visually Impaired using Android Application and Google's Cloud Vision," 2019 Global Conference for Advancement in Technology (GCAT), BANGALURU, India, 2019, pp. 1-6.
- [8] P. Ambawane, D. Bharatia and P. Rane, "Smart e-stick for Visually Impaired using Video Intelligence API," 2019 IEEE Bombay Section Signature Conference (IBSSC), Mumbai, India, 2019, pp. 1-6.
- [9] S. Srinivasan and M. Rajesh, "Smart Walking Stick," 2019 3rd International Conference on Trends in Electronics and Informatics (ICOEI), Tirunelveli, India, 2019, pp. 576-579.
- [10] M. P. Menikdiwela, K. M. I. S. Dharmasena and A. M. H. S. Abeykoon, "Haptic based walking stick for visually impaired people," 2013 International conference on Circuits, Controls and Communications (CCUBE), Bengaluru, 2013, pp. 1-6.

- [11] S. Mohapatra, S. Rout, V. Tripathi, T. Saxena and Y. Karuna, "Smart Walking Stick for Blind Integrated with SOS Navigation System," 2018 2nd International Conference on Trends in Electronics and Informatics (ICOEI), Tirunelveli, 2018, pp. 441-447.
- [12] S. Gupta, I. Sharma, A. Tiwari and G. Chitranshi, "Advanced guide cane for the visually impaired people," 2015 1st International Conference on Next Generation Computing Technologies (NGCT), Dehradun, 2015, pp. 452-455.
- [13] S. Innet and N. Ritnoom, "An application of infrared sensors for electronic white stick," 2008 International Symposium on Intelligent Signal Processing and Communications Systems, Bangkok, 2009, pp. 1-4.
- [14] A. Krishnan, G. Deepakraj, N. Nishanth and K. M. Anandkumar, "Autonomous walking stick for the blind using echolocation and image processing," 2016 2nd International Conference on Contemporary Computing and Informatics (IC3I), Noida, 2016, pp. 13-16.
- [15] Nada, Ayat & Mashali, Samia & Fakhr, Mahmoud & Seddik, Ahmed. (2015). Effective Fast Response Smart Stick for Blind People. 10.15224/978-1-63248-043-9-29.
- [16] Dimitra P. Marini. March 2018, BSc Thesis, National and Kapodistrian University Of Athens School Of Science Department Of Informatics And Telecommunication, "Electronic Smart Canes for Visually Impaired People", S.N.: 1115201100044.
- [17] K. B. Swain, R. K. Patnaik, S. Pal, R. Rajeswari, A. Mishra and C. Dash, "Arduino based automated STICK GUIDE for a visually impaired person," 2017 IEEE International Conference on Smart Technologies and Management for Computing, Communication, Controls, Energy and Materials (ICSTM), Chennai, 2017, pp. 407-410.
- [18] A. R. García, R. Fonseca and A. Durán, "Electronic long cane for locomotion improving on visual impaired people. A case study," 2011 Pan American Health Care Exchanges, Rio de Janeiro, 2011, pp. 58-61.

A Novel Low Power 8-Bit Binary Weighted Charge Steering DAC with Integrated Power Supply using CMOS

Bharathesh Patel N, Manju Devi

Abstract: the design and implementation of binary weighted charge steering DAC architectures is discussed in this paper. Charge steering DAC were designed and successfully implemented in CMOS 90nm and 180nm technology. For bigger planning contrasts there is an exchange off between powerful number of bits, and equipment cost and basic way. Taking everything into account, an 8 piece two fold weighted accuse directing DAC of coordinated force supply was effectively planned in 90 and 180nm CMOS innovation utilizing Cadence apparatuses. As indicated by the reproduction results, the proposed DAC is exceptionally straight with the most pessimistic scenario DNL of 0.99LSB and INL of 0.008LSB, and furthermore has low force utilization esteem 96.36mW.

Keywords: DAC, CMOS, DNL, INL.

I. INTRODUCTION

In the vast majority of the electronic frameworks the information and yield signals are simple in nature. Subsequently there are simple preparing gadgets like speakers as information and yield gadgets. Anyway Most of the changes to be completed on the info flags before getting the yields are done in advanced space. Along these lines, there is a need to change over the simple information Signals into computerized signals at the info end, and in the wake of preparing them in the advanced area; they must be changed over go into simple signals in the majority of the applications. The circuits That convert simple signs to computerized signals are known as A/D Converters and the circuits That convert advanced signs to simple signs are called D/A Converters (DACs) The penetration of electronics into areas like computers, communications, instrumentation and embedded systems such as mobile phones, camcorders, HDTVs has given rise to the need for DACs with stringent requirements. The requirements span over features like high Accuracy, linearity, reliability, high speed, low power and so on. There are various approaches adopted to achieve specific characteristics as given below:

- Speed: - Higher speed is generally achieved by the use of current steering DAC architecture.
- Accuracy: - Accuracy can be improved by adopting the segmentation approach in the design of current source array architecture where the ratio of transistor widths is not too high in each segment.

•Power: - Use of low current value for LSB reduces the power consumption in the DAC. Also, power consumption can be reduced by lowering the supply voltage provided to the DAC. The current-controlling DAC as an appropriate contender for fast and high-goals correspondence applications. This design needn't bother with any yield cradle. It will anyway get touchy to limited yield impedance. Further, the current-directing DAC can be actualized with MOS-just parts and still arrive at rather high exactness. Resistor-string or R–2R stepping stools are likewise quick, yet they require high-precision on-chip resistors. Rather, we centre on the unadulterated current-controlling renditions where various weighted current sources are utilized to frame the transformation work

This paper manages this sort of a video DAC that devours less force and least zone while giving a full scale current yield. In these sorts of DAC's, static and dynamic exhibitions are significant. Along these lines, many blended sign IC configuration engineers have directed research on progress of CMOS ebb and flow mode DAC. Static mistakes are brought about by jumble of transistors inside cells and dynamic blunders are created by synchronization of computerized input voltages. These blunders limit the general execution of DAC. Right now configuration considers the exchange off between execution, goals and zone. The proposed circuit depends on the notable portioned engineering; comprising of current directing structures, for example, parallel weighted and thermometer coded.

II. CHARGE STEERING DAC

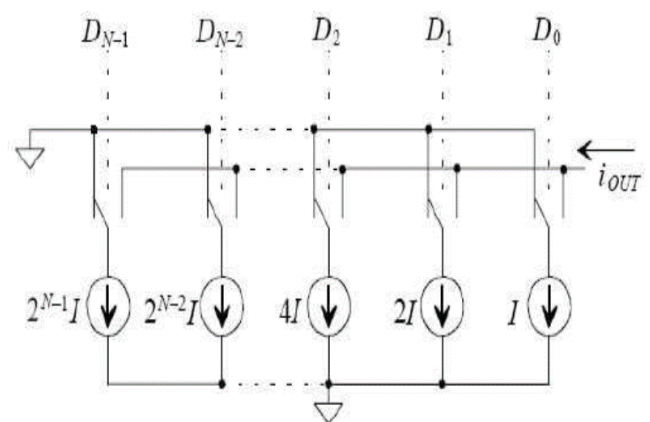


Fig. 1. N-bit charge-steering DAC

Revised Manuscript Received on March 17, 2020.

Bharathesh patel N, Assistant Professor, GSSSIETW, Mysore, Department Electrical & Electronics.

Dr.Manju Devi, Professor, TOCE, Bangalore

This architecture consists of weighted currents produced by current mirrors, switches to steer the current and an added. The reference elements are current sources and sum elements are only wire connections. The switches are normally MOS transistors. The switches are controlled by the input bits. In the figure, binary-weighted current sources are produced by the use of current mirrors. This means that every element is weighted with $2^1, 2^2, 2^3, \dots, 2^N$ where N is the number of bits. The output current is given by

In Figure 1, an N -bit current-steering DAC is shown. The current-steering DAC in the figure is binary-weighted, as can be seen from the weighting of the current sources. The switches are controlled by the input word. Depending on the input word, the current source is switched to the load or to the ground which improves the speed of the DAC. The advantage of current steering architecture is the ease of implementing the elements on the chip. The current sources are current mirrors implemented using FETs. The weightage in the current values can be obtained by simply varying the widths of the transistors. All the switches can also be realized by using FETs. Thus, all the elements in current steering DAC can be realized using MOSFETs. The power efficiency is also very high since most of the power is dissipated in the small load resistor at the output. This architecture is thus suitable for high speed design and cost-effective to implement.

The major difficulty is to realize current sources with ideal characteristics because of device mismatches, and to avoid the switching related glitches suitable for high speed design and cost-effective to implement. The major difficulty is to realize current sources with ideal characteristics because of device mismatches, and to avoid the switching related glitches.

III. PROPOSED CHARGE STEERING DAC ARCHITECTURE

A. 8-bit Charge Steering DAC

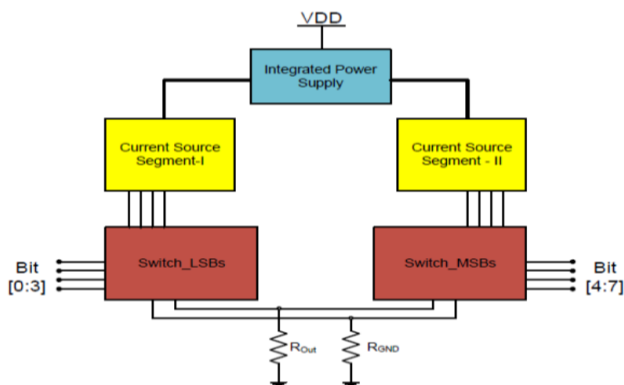


Fig. 2. 8 Bit Charge- Steering Architecture

The block diagram of the DAC with integrated power supply is shown in Figure 2, It consists of a highly stabilized power supply, a power supply-DAC interface i.e. source follower, one 4-bit DAC corresponding to LSBs (segment-I) and another 4-bit DAC corresponding to MSBs (segment-II). With a view to reduce the total number of transistors, a segmentation approach consisting of two current source segments has been adopted for implementing the current sources. Contingent on the information computerized word, separate current sources from both the portions are exchanged into the yield load. At the point when the changed flows from

these two DACs are included, one gets the yield relative to the info advanced word.

B. Current Source

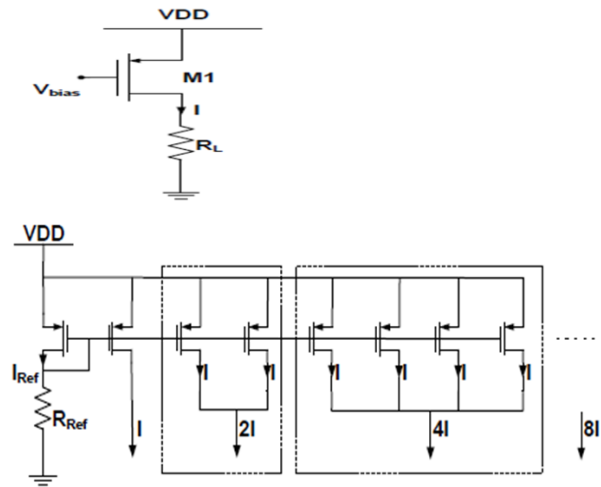


Fig.3. Current source and Current Sources with Parallel Transistors Connection

A present source is one of the most significant components of the present directing DAC. It creates the necessary current to be given at the yield of the DAC. In view of the info word, the flows produced by number of current sources are appropriately exchanged and added at the yield hub. The present source can be acknowledged either by utilizing NMOS or PMOS transistors. The simplest current source which corresponds to a LSB current source as shown in Figure 3 is realized by a single transistor, biased with a fixed voltage to provide constant current value. The other current sources are simply realized by using the required number of transistors in parallel. For example, a current source which supplies 8 times the current through the LSB source has 8 transistors in parallel. The current sources with transistors connected in parallel are shown in Figure 3.

C. DAC Current Source Segments

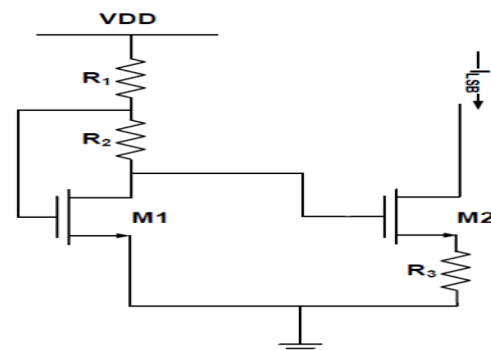


Fig. 4. Current Peaking Source

The stable current source of $2\mu A$ has been generated using peaking current source as shown in Fig. 4.4. Peaking current source enables realization of small currents with reasonably. Small resistor values. It has been to get an output current of $2\mu A$ with transistor sizes of $W = 1.6\mu A$ and $L = 0.18\mu A$, and resistor values $R1 = 500 \Omega$, $R2 = 2 k \Omega$ and $R3 = 4.2 k \Omega$. The supply voltage used is 1.8 V. This current source has itself been simulated and checked for the stability of the current with respect to supply.

On the same lines, the source current of $32\mu A$ is generated. These two current sources are mirrored into segments -I and segments -II respectively to generate various current sources for different outputs of DAC. The stable VDD has been generated using a highly stabilized voltage reference.

D. Current Switches

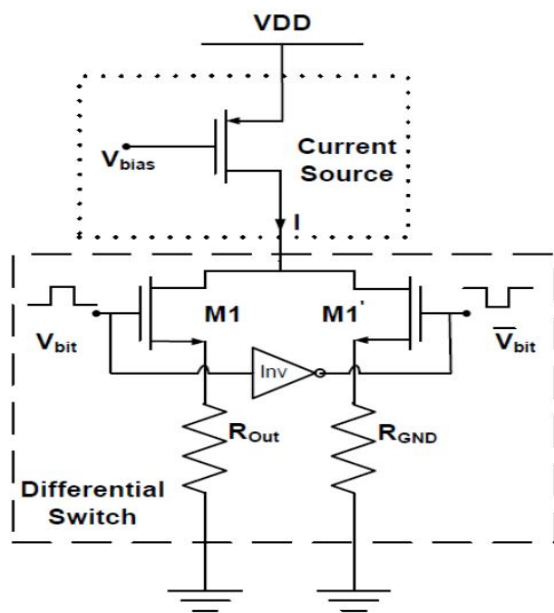


Fig. 5. A Differential Switch

A current source is supposed to supply current irrespective of the load connected. If the current is to flow into the load, the current source should be connected to the load. When it is not connected to the load, there is a need for diverting this current to some other sink. In our case when the source current is not flowing in the load, it is diverted to ground, thus ensuring that the current flowing through the source is always maintained. The circuit diagram indicating the current steering or switching mechanism is given in Figure 5. From the figure, it may be seen that there are 2 switches used, one 'M1' for connecting the current source to the load and the other 'M1'' to ground.

The switches are operated by the corresponding bit in the input digital word and its complement. If the bit is high '1', switch M1 is on and switch M1' receives the complement of the bit, namely '0' and it is put off.

E. CMOS Inverter

As the inverter that has been used to obtain the complement of the bit is CMOS inverter as shown in Fig. 4.6. It is the usual CMOS inverter with PMOS as load and NMOS as active device. The inverter itself has some amount of delay while propagating the signal from its input to the output and this delay should be as small as possible to improve the speed of the DAC without degrading its accuracy. It has been found

that the width of the inverter transistor is dependent on the width of the transistors in differential switch. As the width of the switched transistor is increased at higher currents, the inverter transistor width is also increased to minimize the propagation delay of the inverter. The widths of switches and inverter transistors for 8 input bits are given in Table 4.1. This arrangement also ensured that glitches due to delay between input bit signal and its inverted signal, are reduced. In this 8-bit DAC, 8 CMOS inverters are used. Since input bit voltage, when high is 1.8 volts, the VDD of every inverter is also 1.8 volts. The width of the PMOS transistor has been taken as 2.5 times the width of NMOS transistor. The minimum width of the NMOS transistor in inverter is $3 \mu m$ and the propagation delay of each inverter.

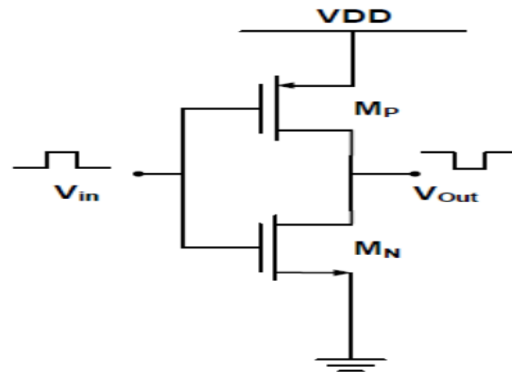


Fig. 6: CMOS inverter

F. Op-amp

Operational amplifier (op-amp) is a fundamental building block in analog integrated circuit design. Op-amp is one of the cores of a whole reference generator circuit. The op-amp gives the output to the reference generator circuit. Therefore it is important that the op-amp circuit functions well.

Figure 7 shows the circuit diagram of op-amp. The Op-amp used in this circuit is a differential amplifier. In this op-amp, input offset voltage and DC gain can be varied by changing the values of the parameters in the design. The function of the Op-amp is to set the same voltage at the gates of the two PMOS devices connected to the bipolar devices.

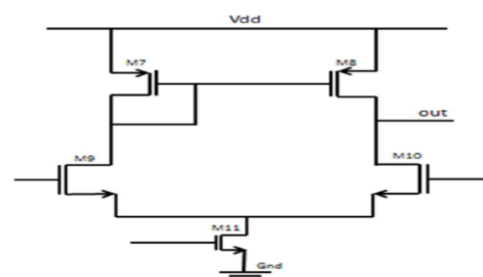


Fig. 7: Op-amp Circuit.

The two PMOS devices connected to the bipolar operate in principle as a current mirror to the output node of the PTAT circuit. So, the value that appears at the PMOS devices is reflected at the output node.

G. Reference Generator

The proposed reference voltage delivers a temperature autonomous current which when goes through a resistor gives a temperature free voltage. Since, the controlled amount for the circuit is current, any reference voltage under 1.2V can without much of a stretch be created. In addition, the stockpile voltage confinement looked in the ordinary voltage-mode circuit is evacuated in the new current-mode design. The subtleties of the design are talked about there.

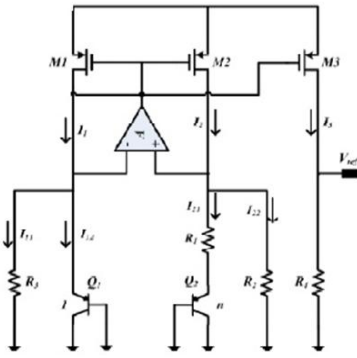


Fig. 8: Reference Generator circuit

H. Reference Generator with regulated output.

Low voltage activity and low force utilization are significant plan factors for versatile electronic gadgets. Procedure innovations are creating and the line widths are decreasing, likewise the most extreme passable force supply voltage will downsize

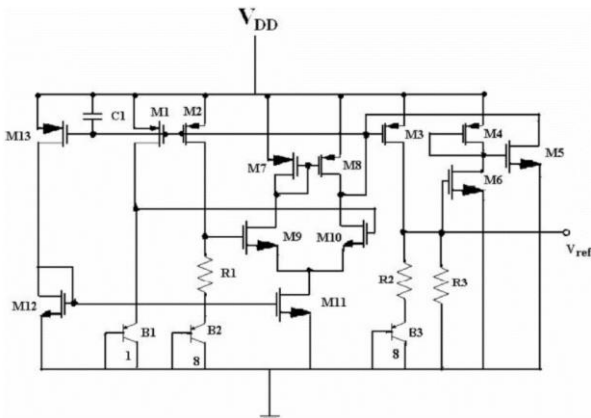


Fig. 9: Reference Generator with regulated circuit

The figure 9: above shows a reference generator circuit that has been chosen to be used as the right architecture for the designing a reference generator circuit of the from the text book “Behzad Razavi”. Some parameters are included in the circuit such as a resistors and CMOS transistor to obtain the desired result. Once the circuits has been designed separately, the three parts of the circuits are joined together to form a reference generator circuit. Then once again a thorough design is done according to the desired design. The desired current flow and node voltages are check to match required expected result. Simulations are done to check on the voltage reference when the temperature and supply voltage is varied.

IV. PROPOSED BINARY WEIGHTED CHARGE STEERING DAC WITH INTEGRATED POWER SUPPLY

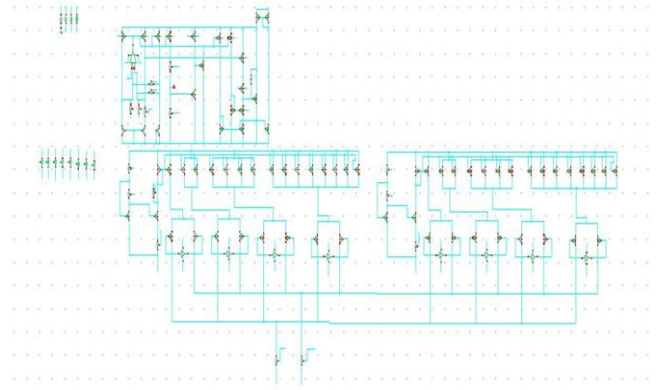


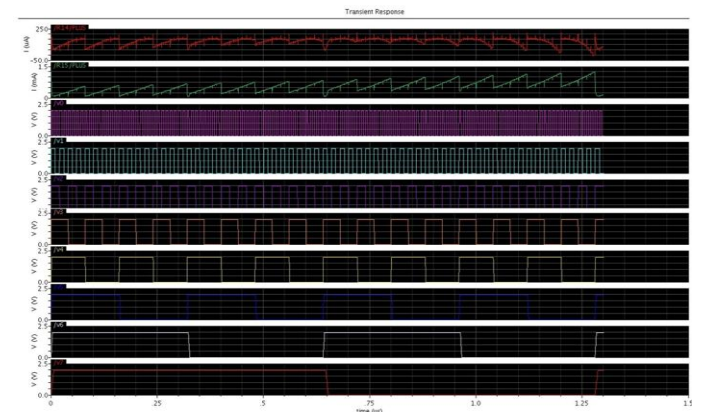
Fig. 10: Binary weighted charge steering DAC with integrated Power supply

Figure 10: shows Proposed Binary weighted current steering DAC with integrated power supply which contains reference generator circuit, current source and current switches.

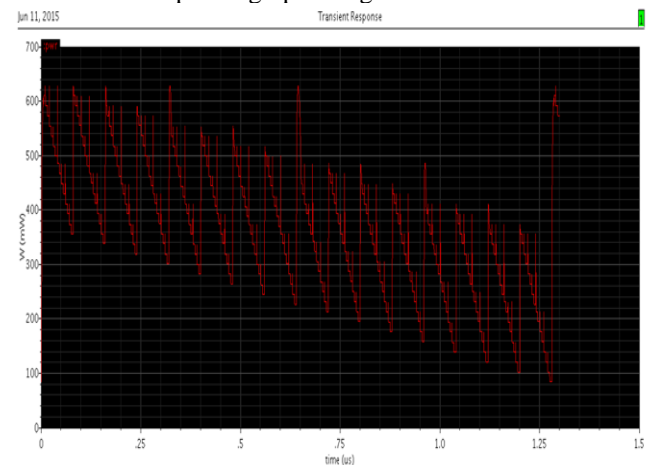
V. SIMULATION RESULTS AND DISCUSSION

A. Simulation

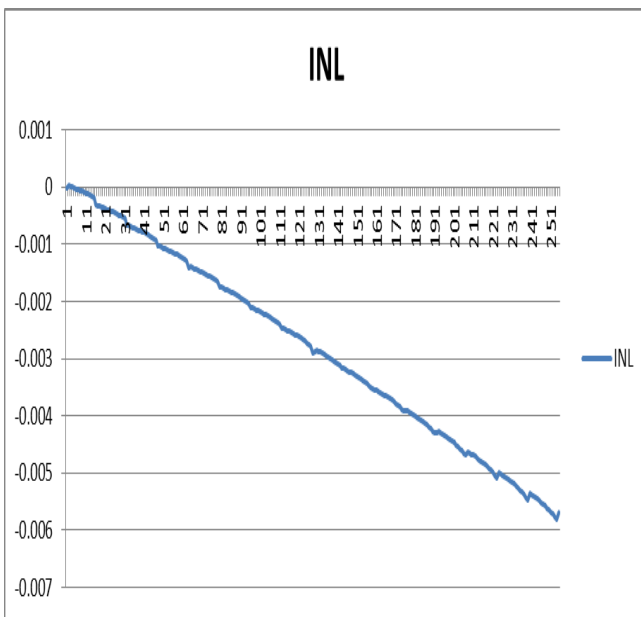
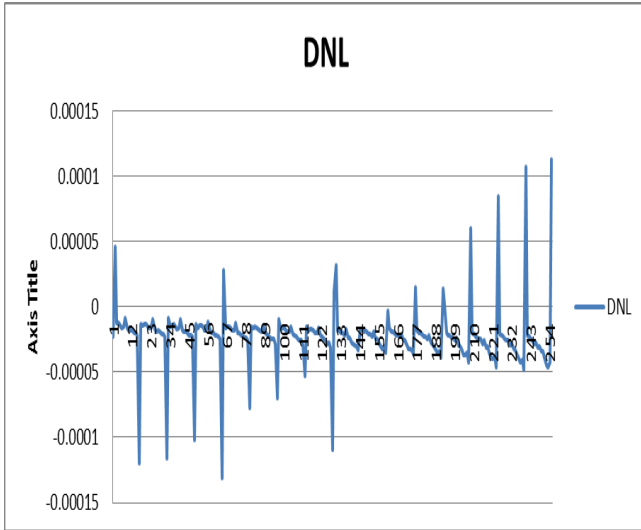
1. 8-bit current steering DAC output using 90nm CMOS



2. Power Dissipation graph using 90nm CMOS



3. Analysis of INL and DNL using EXCEL work Sheet analysis



VI. LAYOUT IMPLEMENTATION

Timing is significant, so directing for the comparator and multiplexer ought to be same, comparator is a simple square, regular centroid is utilized for coordinating information transistors and entomb digitisation for current mirrors. Operation amp and inverter is an advanced square, so there isn't a lot of requirements for it. All resistors are made into serpentine structure to diminish the territory. Top level steering is troublesome, so metal 4 is utilized.

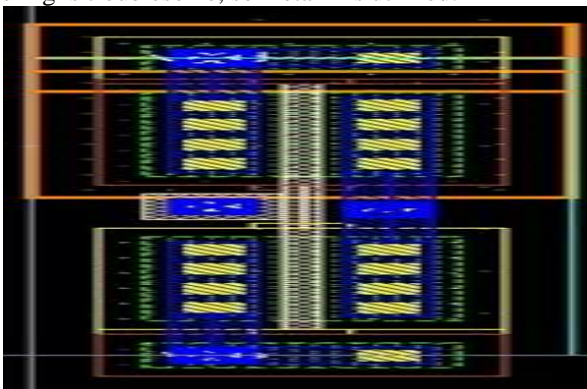


Fig. 11. Inverter Layout

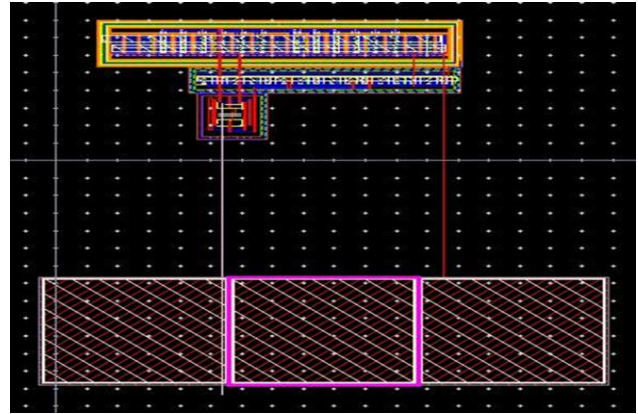


Fig. 12. Op-Amp Layout

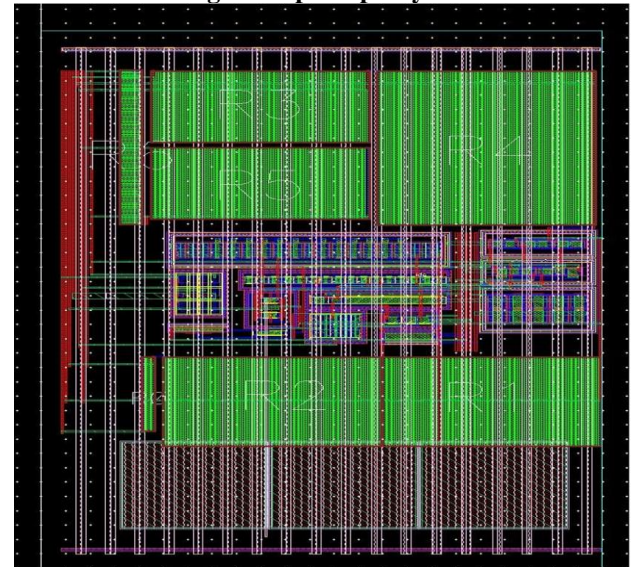


Fig. 13. Integrated power supply Layout

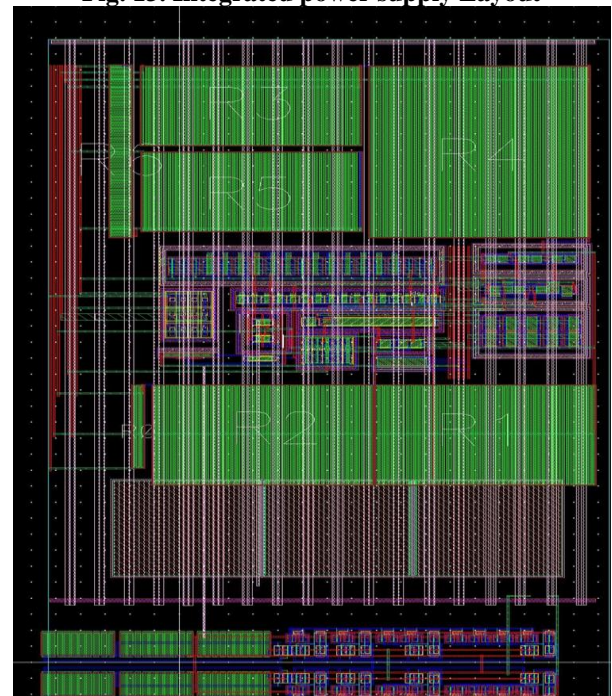


Fig. 13. Top Level Layout

VII. COMPARISON OF TECHNOLOGY, PERFORMANCE AND TRANSISTOR COUNT

Table No I: Comparison of the performance

| | Proposed DAC | [1] | [2] | [3] |
|-------------------|---------------------|---------------------|--------------------|---------------------|
| Architecture | Charge steering | Charge steering | Charge steering | Charge steering |
| Resolution | 8bit | 12 | 8 | 8 |
| Power supply | 1.8v | 5v | 5v | 1.8 |
| Technology | 90nm | 350nm | 500nm | 90nm |
| Power consumption | 96.36mW | 144.9mW | 320mW | 800mW |
| DNL | 0.99LSB | 0.4LSB | 0.3LSB | 0.23LSB |
| INL | .008LSB | 0.47LSB | 0.6LSB | 0.3LSB |
| SNR | 49.92db | 74db | 49.92db | 49.92db |
| Input frequency | 100MHZ | 10GHZ | 800MHZ | 500MHZ |
| Area | 0.23mm ² | 1.37mm ² | 3.2mm ² | 1.37mm ² |

Table No II: Transistor counts in the proposed design

| Functional Module | No. of Transistors |
|---------------------------|--------------------|
| 1.Integrated power supply | 25 |
| 2. current source | 36 |
| 3. current switch | 32 |
| Total No. of transistors | 93 |

Table No III: DAC performance summary

| Parameter | Specification |
|-------------------|---------------------|
| Architecture | Charge steering |
| Resolution | 8bit |
| Power supply | 1.8V |
| Technology | 90nm |
| Power Dissipation | 96.36mW |
| DNL | 0.99LSB |
| INL | 0.008LSB |
| output frequency | 41.41MHZ |
| Input frequency | 100MGHZ |
| SNR | 49.92dB |
| Area | 0.23mm ² |

Table No IV: Technology Comparison

| Technology | 90nm | 180nm |
|--------------|-----------------|-----------------|
| Architecture | Charge-steering | Charge-steering |
| Resolution | 8-bit | 8-bit |

| Power supply | 1.8v | 5v |
|-------------------|----------|----------|
| Power Dissipation | 96.36mW | 260.80mW |
| DNL | 0.99LSB | 0.16LSB |
| INL | 0.008LSB | 3.6LSB |
| Output frequency | 41.41MHZ | 838.MHZ |
| SNR | 49.92db | 49.92db |
| Input frequency | 100MHZ | 29.3GHZ |

VIII. CONCLUSION

The plan and usage of parallel weighted current directing DAC designs is talked about right now. Current guiding DAC were structured and effectively executed in CMOS 90nm and 180nm innovation. For bigger planning contrasts there is an exchange off between successful number of bits, and equipment cost and basic way. Taking everything into account, a 8 piece twofold weighted current guiding DAC with incorporated force supply was effectively structured in 90and 180nm CMOS innovation utilizing Cadence apparatuses. As indicated by the reproduction results, the proposed DAC is profoundly direct with the most pessimistic scenario DNL of 0.99LSB and INL of 0.008LSB, and furthermore has low force utilization esteem 96.36mW.

The presentation, innovation rundown demonstrated segment VI, Based on the reproduction results current controlling DAC structures improve the exhibition regarding rate and force utilization. In addition, it is additionally accepted that, the proposed DAC engineering is alluring for architects from plan intricacy perspective. The format photograph of the total converter is appeared in Layout Section. Correlation result appeared in Table No 3 and Table No 4. The physical design of the coordinated force supply, operation amp, complete current controlling DAC as appeared in area VII has been drawn utilizing CADENCE VIRTUSO LAYOUT EDITOR.

FUTURE ENHANCEMENT

As a future work, the presentation of the proposed paired weighted current controlling DAC structure will be contrasted with elective kinds of current directing DAC execution. What's more, further upgrades are arranged in the Dual incline DAC engineering.

In future can even structure and look at these plans in all conceivable Nano-meter advancements like 32nm, 22nm, 14nm, 12nm, etc

REFERENCES

1. Anshul Agarwal "Design of Low Power 8-Bit Digital-to-Analog Converter with Good Voltage"-Stability in the proceedings of IEEE Asia Symposium on Quality Electronic Design (ASQED 2009), Kuala Lumpur, Malaysia, 15-16 July 2009"
2. KS.GOPakumar, P Cyril Prasanna Raj, S.L Pinjare 3 "Design and Implementation of High Speed, Low Power to-bit DAC for Video Application
3. Dominik Przyborowski and Marek Idzik4 "A 10-bit Low-Power Small-Area High-Swing CMOS DAC.
4. Piyush K. Mathurkar1 and Madan B. Mali 5 CMOS 8-BIT BINARY TYPE CURRENT-STEERING DAC.
5. JurgenDeveugele, Member, IEEE, and Michiel S. J. Steyaert, Fellow, IEEE A 10-bit 250-MS/s Binary-WeightedCurrent-Steering DAC.
6. Amit S Durgannavar, Rohit D Patil1, Vardhaman K Desai, Chethan Kuma M DESIGN AND IMPLEMENTATION OF HIGH RESOLUTION DIGITAL TO ANALOG.
7. D. Johns, and K. Martin, \Analog integrated circuit design," John Wiley & Sons, 1997, ISBN: 0-471-14448-7.
8. J. Baker, H. Li, and D. Boyce, \CMOS - circuit design, layout, and simulation," IEEE Press, 1998, ISBN 0-7803-3416-7.
9. J. Deveugele, and M.S.J. Steyaert, \A 10-bit 250-MS/s binary-weighted current-steering DAC," Solid-State Circuits, IEEE Journal of, vol. 41, no. 2, pp. 320-329, Feb. 2006.
10. D.A. Mercer, Low-Power Approaches to High-Speed Current-Steering Digital-to-Analog Converters in 0.18- μ m CMOS," Solid-State Circuits, IEEE Journal of, vol. 42, no. 8, pp.1688-1698, Aug. 2007.
11. R. J. van de Plassche, \Integrated Analog-to-Digital and Digital-to-Analog Converters," Kluwer Academic Publishers, Boston, MA, USA, 1994, ISBN 0-7923-9436-4.
12. B. Razavi, \Design of analog CMOS integrated circuits," McGraw-Hill Higher Education, 2001, ISBN 0-07-2388032-2.
13. Chi-Hung Lin and, Klaas Bult, \A 10-b 500-MSample/s CMOS DAC in 0.6 μ m²," IEEE JOURNAL OF SOLID-STATE CIRCUITS, vol. 33, no. 12, Dec. 1998.
14. Chueh-Hao Yu, Ching-Hsuan Hsieh, Tim-Kuei Shia and, Wen-Tzao Chen, \A 90nm 10- bit 1GS/s current-steering DAC with 1-V supply voltage," VLSI Design, Automation and Test, 2008. VLSI-DAT 2008. IEEE International Symposium on, pp.255-258, 23-25 April 2008
15. Takeshi Uedo, Takafumi Yamaji, and Tetsuro Itakura, \A 1.2-V 12-bit 200MSample/s current-steering D/A Converter in 90-nm CMOS," IEEE Custom Integrated Circuits Conference (CICC), pp. 26-4-1 - 26-4-4, 2005.

AUTHORS PROFILE



Bharathesh patel N, BE Electrical and Electronics, M.tech in VLSI & embedded systems, pursuing Ph.D in VLSI Design, Published two research papers, working as assistant professor in GSSSIETW, Mysore in department electrical & electronics.



Dr. Manju Devi, BE in Electronics and communication, M.Tech in VLSI Design, Ph.D in VLSI Design, 30 publications in research work, 20 years' experience, Head and professor in TOCE, Bangalore

The Tiled Cache Implementation for High Performance Processor

**Suma Sannamani¹, Dr. Manjudevi², Suganya S³*

Visvesvaraya Technological University, Belagavi, India

Oxford College of Engineering, Bangalore, India,

CMR Institute of Technology, Bangalore, India,

sumabs2014@gmail.com, manju3devi@gmail.com, suganya.senthil2005@gmail.com

Abstract

Embedded Processors demand cache hierarchies which can satisfy needs of industries, improvisation in performance and reduction in power requirement. Here, work involves introducing tiled cache implementation for high performance processor. Tiled Cache memory implementation involves basic operation Search, Transport and Replacement. From VLSI implementation tiles incur minimal latency and area. Tile cache implementation involves search, transport and replacement operations. Tile cache improve the performance in multi core processor. We use Xilinx simulation tool to model tile architecture for cache.

Keywords: Cache memory, Multi-core processor, Latency

Introduction

As technology scales latency, area are the basic requirements for performance of processors. In order to reduce the costs embedded systems integrated SOCs. Tile based Cache has recently emerged as architecture of choice for many core processor. It has multiple tiles connected over network. Initially cache were designed to have uniform search for the data. Alternative is to divide large cache into multiple banks. System designs uses Chip multiprocessors as a dominant model[1]. Most of the microprocessors includes multiple cores which shares cache in between them. Number of cores varies from 2 to 8. As there is scale of integration, around 64 processor cores are placed on to chip. Maintaining the homogeneous access time, these multi-core systems uses shared caches. Soc's shows CPU follow high performance.

Cache memory first become noticeable in 1968 to improve performance developed by IBM system/360 Model 85 computer, which were designed to reduce latency gap between the CPU and main memory that helped to increase performance of system. Gigantic chip-vendors initiated the use of cache memory in processors[5][6]. With cache memory ,system consume more energy and system more unpredictable[7][8][9]. Multi-core evolved the modern computing. In multi-core

embedded systems, the cache memory hierarchy and applications effects the performance and energy consumptions significantly. There is decrease in performance, if there is more cache miss or if required energy is more. Different architectures are available to reduce cache miss frequency. Recent research show that by executing multiple instructions per cycle multi-core design improves performance [10][11][12], which is called parallel processing. Memory optimization is important for performance as we use more number of cores.

2. Tile Organization

Tile is the on-chip interconnect. Implementation of tiled cache involves basic operation search, transport and replacement. There is a availability of various mapping techniques .Here we are using direct mapping. Search network responsible to send miss request to cache tile. When a cache tile receives a search request and assumes if cache tile experience miss-data is not found, then it replacement network works. Or if the cache tile found data to be searched-hit, it transport data to processor. Search network may send a new request in every cycle to transport network. Replacement involves reading data from memory and placing into cache. Replacement is based on LRU policy. It takes three consecutive cycle. One cycle is to receive block. Second cycle is to find the target location in cache. During this cycle if the target location has valid data, it is removed. During third cycle, write block to target way.

Mapping Techniques: There are availability of different technique.1)Direct Mapping

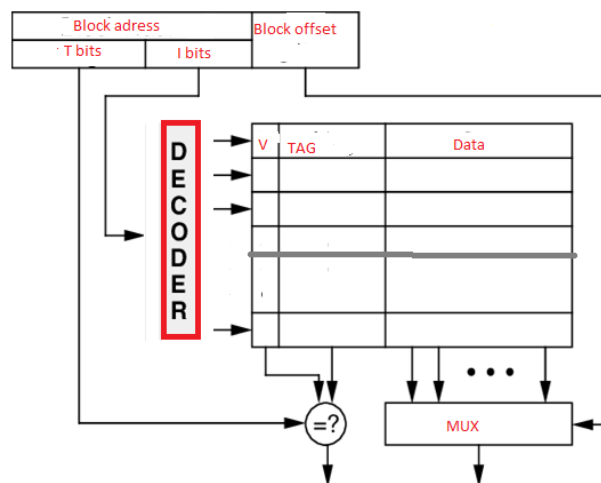


Figure 1. Address Decoding

In a direct-mapping technique, the entire cache is arranged into several sets, each

set includes one cache line . Memory block is mapped to single cache line depending on its address. The cache will have n rows and 1 column.

1) Write data block to cache: Bits obtained from **the** address of memory determine the set are called I bits. Data block of memory is placed onto recognized set. T bits are placed to tag field. If cache has previous data, new data placed in and previous data is removed.2)Processor to read word from the cache: I bits determine the set. The T bits of the memory block address are compared with the T bits of set in cache memory .

Cache hit: T address bits of memory block and the tag address bits of cache memory are same, which is called as cache hit has occurred.

Cache miss: T address bits of memory block and the tag address bits of cache memory , doesn't match, which called as cache miss has occurred. Hence, memory block is derived from main memory.

Advantages of using Direct mapping technique: Direct placement of memory block helps to reduce the power requirement. It reduces unnecessary search through all cache lines. Hence data placement and replacement become simple.

It is cost effective. as hardware required is of low cost because only one tag address bit are verified at a time.

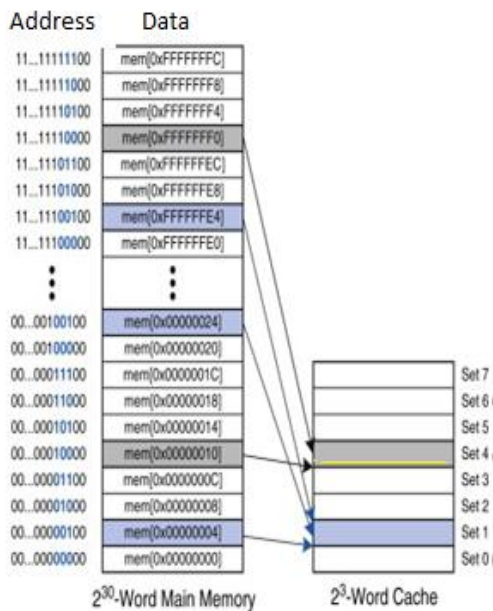


Figure 2.Example of main memory mapping

Disadvantage of Direct mapping: Number hits are less, as there availability of one

cache line in each set. There is need to associate a new memory every time to same set. which also results clash in miss data. In direct mapping cache memory has one block per set, so it has equal number of sets and blocks. Consider main memory partitioned into d -word blocks. Data block 0 of main memory maps to set 0 of cache, Data block 1 of main memory maps to set 1 of cache, continued till $d-1$ block of main memory maps to Set $d-1$ of cache.

This data mapping technique is discussed with example as shown in Figure(2) for a direct mapping technique. Cache has total 8 sets, where one data word block fits to one set. Least significant bits of the main memory address are always zero. Considering logarithm base of 8 bits, which is equal to 3. These 3 bits decides, to which set memory address maps. Hence, locations with address 4, 16, 36 locations maps to set 0 of cache memory

3. MULTICORE PROCESSOR

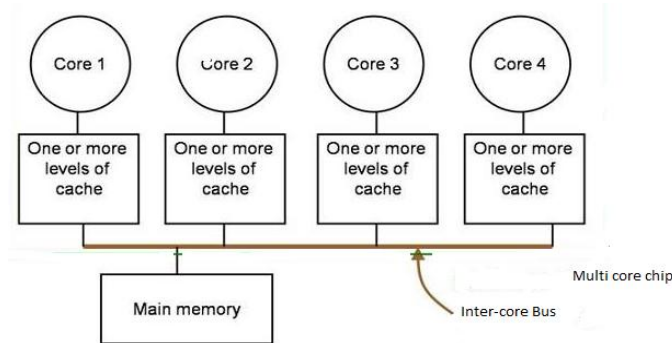


Figure 3. Shared cache

Multi core processors have become necessary in our real life in devices like smart phones, tablet etc. More processors require large cache to increase speed by supporting the concurrent applications. A multi-core processor is a single calculating unit, which has many processing elements, those units can read and execute program instructions. Software and its implementation decides the performance progress while using multi-core processors. [13] describes performance improvement by decreasing delay in multi-core system. Also involves design for the system-wide shared last-level caches placed between the memory and the node private cache memories.

Cache memory is included in almost every PC built. The cache memory appeared first time in IBM System in 1968. Usually, multi-core processors have dedicated lower level cache memory and shared upper level cache memory, where upper level cache resides on the motherboard. Along with that upper level cache is also seen on the microprocessor itself. In some computers there is connection of microprocessor and the upper level cache with a backside bus to improve the performance. Multi-core

processors are used by manufacturers in embedded systems to reduce power and to increase processing speed.

Hardware-software methodology is used to make coherency with shared memory in heterogeneous multiprocessors[14]. This paper Disadvantage of using more hardware to gain low miss rate. There by increasing performance. By reducing miss rate latency required is reduced. This approach removes the burden of software synchronization and hence embedded system designer can clear understand about shared data. This methodology is neither applicable for dedicated CL2 architecture nor suitable for calculation of power requirement.

In [15][16], Two ways, which helps handle Forecast problem due to cache in real-time systems . Cache data is locked, thereby it is possible to predict time required to access main memory and cache-related preemption delay . Still more work to be done to see the applicability of static cache locking techniques on various level-2 cache schemes and the impact of these approaches on delay and power requirement .

4.PROCESS FLOW

Here, we are investigating tiled cache area requirement and latency.

To write the data to memory, we access the RAM with data and address where we want to write. To search the data, we have to address cache. If necessary data is not found in cache, then it accesses the RAM by copying data from there.

Here each individual block is represented as module in verilog As cache is not an independent part of fast memory, and for its proper operation it needs to take data from another memory RAM. To get results with cache we have to simulate whole RAM module which includes cache as well, but actual execution of work involves cache simulation. Here we are considering Ram is of 32-bit wide and it has 4k size. Tiled cache has 64 locations. Here we are XILINX ISE software tool to simulate the module

5.RESULTS

In this paper, we worked to find the effect of tiled cache on performance of shared cache between multi-core system. We use latency to express performance .We developed RAM of size 4k.which is the part of tile. Main component is cache memory, which has 64 locations.

Here mode 1 is used to write data addressed location in memory, where as mode 0 to fetch the required data by processor. Latency obtained from XILINX simulation software tool .Maximum output time after clock is 0.723ns. Here we have shown

provided for this work.

REFERENCES

- [1] P. Frost Gorder, “Multicore processors for science and engineering,” *Computing in Science & Engineering*, March-April 2007.
- [2] T. R. Halfhill, “The rise of licensable SMP,” *Microprocessor Rep.*, vol.24, no. 2, pp. 11–18, 2010.
- [3] “PowerPC Processor (476FP) Embedded Core Product Brief,” LSI Corp., 2010 [Online]. Available: <http://www.lsi.com/Distribution-System/AssetDocument/PPC476FP-PB-v7.pdf>
- [4] “MIPS32 1004K Coherent Processing System (CPS),” MIPS Technol., 2010 [Online]. Available: http://www.mips.com/media/files/MIPS32_1004K_410.pdf
- [5] cache-SmartComputing2008.
<http://www.smartcomputing.com/editorial/dictionary/detail.asp?guid=&searchtype=&DicID=16600&RefType=Encyclopedia>
- [6] L.Schoeb,G.Darnell,"Large Processor L2 cache sizes in dell Power edge servers",Dell,1999
- [7] D.Lenoski,J.Laudon,M.S.Lam,et al.,"The Stanford Dash Multiprocessor".IEEE,1992.
- [8] R.Wilhem,J.Engblom,S.Rhesing,D.Whalley," The determination of worst executiontimes",ARTIST,2003.
- [9] R.Wilhelm,L.Thiele,"Timing Predictability-a must for avionics system",ARTIST,2006.
- [10] R.M. Ramanathan, “Intel Multi-Core Processors:Making the Move to Quad-Core and Beyond”, WhitePaper, 2006.
- [11] V. Romanchenko, “Quad-Core Opteron: architectureand roadmaps”, Digital-Daily.com, 2006.
- [12] V. Romanchenko, “Evaluation of the multi-core processor architecture Intel core: Conroe, Kentsfield...”, Digital-Daily.com, 2006.
- [13] Preethi P Damodaran,Stefan Wallentowitz, Andreas Herkersdorf ,“Distributed Cooperative Shared Last-Level Caching in Tiled Multiprocessor System on Chip”, Technische Universität at München, Germany.
- [14] T. Suh, D. Kim, H.-H.S. Lee, “Cache Coherence Support for Non-Shared Bus Architecture on Heterogeneous MPSOCs”, *Proceedings of the 42nd annual conference on Design automation (CA-2005)*, 2005, pp. 553-558.
- [15] I. Puaut, D. Decotigny, “Low-Complexity Algorithmsfor Static Cache Locking in Multitasking Hard Real-Time Systems”, *IEEE*, 2002.
- [16] I. Puaut, “Cache Analysis Vs Static Cache Lockingfor Schedulability Analysis in Multitasking Real-TimeSystems”, 2006.

<http://citeseer.ist.psu.edu/534615.html>

***Suma Sannamani**

Suma Sannamani graduated from visvesvaraya Technological University with her Bachelor's degree and Master's degree. She had been with Electronics and Communication Engineering Department at CMR Institute of Technology since 2014 - 2017.

At present she is a Researcher Scholar at visvesvaraya Technological University, Belagavi, Karnataka, India. She has published her research papers and also presented papers in National Conferences. Her current research interest includes Cache memory, Multi core processors, dealy problems.



Dr,Manju Devi

Dr,Manju Devi is working as Professor and head in the department of ECE at The Oxford College of Engineering Bangalore. She has worked as Vice-Principal and professor at BTLIT, Bangalore. She obtained her B.E (ECE) degree in 1996 from Anna University, M.Tech degree in Applied Electronics from BMSCE, and Ph,D from Visvesvaraya Technological University (VTU), Karnataka. She has almost twenty two years of academic teaching experience and worked for both NBA and NAAC. She has almost 75 publications in international conference and journals. She is guiding eight students from Visvesvaraya Technological University (VTU), Karnataka. Her areas of interest are VLSI design, Analog and Mixed mode VLSI design and Digital Electronics.



Suganya.S

Suganya.S graduated from Anna University with her Bachelor's degree and Master's degree. She has been with Electronics and Communication Engineering Department at CMR Institute of Technology since 2006, where she is currently an Associate Professor and a Researcher.

She has published her research papers in standard International Journals, IEEE explorer and also presented more than 15 papers in National and International Conferences. Her current research interest includes LTE Unlicensed, Resource allocation problems and Heterogeneous networks



Turbo Decoder for LTE High Speed band Efficient Architecture

Rashmi R*, Manju Devi**

**Asst Professor, Department of Electronics and Communication Engineering,
Vemana Institute of Technology, affiliated to Visvesvaraya Technological University,
Belagavi, Karnataka, India*

*** Professor, H o D, Department of Electronics and commutation Engineering,
The Oxford College of engineering, affiliated to Visvesvaraya Technological University,
Belagavi, Karnataka, India*

Abstract

The evolution of wireless communications for the next generation is well beyond 3 Gbps of wireless communication standards. Hence, reliable data communication is possible because of Wireless communication system. Turbo codes that is used by the Channel decoder delivers good bit rate performance and also performs error-correction, making the code widely acceptable by numerous wireless communication standard. Wireless communication that is 3G and 4G includes turbo codes within it for accurate error correction. The turbo decoder is restricted by the inherent iterative process to compile the data at a higher rate. Bit error rate (BER) is calculated depending on the size of the frame and the interleaver type that is required in the implementation of encoder and decoder. A coding loss of around 0.2 dB is exhibited by the decoder while comparing BER performance with simulated BER values. High decoding latency is the major flaw of Turbo coding implementation. The three major obstacles faced in turbo coding architecture are: The forward recursions or recursions occurring backward in maximum a posteriori (MAP) decoder, the repetitive nature of the decoding algorithm and interleaver or de-interleaver units between the MAP decoders. The above-mentioned obstacles are of utmost importance when we integrate the codes written using turbo coding in a communication standard of throughput which is high like LTE. To predict latency reduction and parallelization methods in the implementation of hardware components of Turbo decoder, we fulfill the data rates mentioned above. A serial data dependency imposed is the problem of decoding a received signal. The severe bottleneck is created conventional turbo decoder by the limited processing throughput of the.

Keywords-wireless communication; 5G communication; FEC - Forward Error Correcting channel Coding; Turbo Codes; LTE - Long Term Evolution; Cellular Technology

I. THE NEED FOR TURBO CODES

The easy accessibility of unwired technology has altered the way the world communicates today. Technologies like cellular and others makes it possible for individuals to be connected to others around the globe from anywhere, at any time. Every wireless network requires transmission of information quickly and timely, at a high rate accurately. To ensure that there is optimal accuracy or for recovering the unaltered signal at the receiver's end, there has been implementation of forward error correction. There are various categories of techniques for error correction that can be used like convolution method of coding. However, this method does not succeed in maintaining the signal's lower bound values to the noise ratio with the increase in code length. To overcome this, turbo coding which is a latter version of coding, was introduced which helps in achieving performance levels which is closer to theoretical bounds compared to the conventional coding systems.

One of the most proficient type of Forward Error-Correcting channel type of coding is Turbo coding. With the rise in systems of communication done digitally, there is a need for rectification of errors. This issue arises because of the non-idealistic nature of realistic channels for communication, often with disturbance caused due to noise. To reimburse for the errors that get produced by this noise, there is a requirement for error correction. An effective solution is forward error channel coding. The reason turbo code is widely accepted in wireless network of communication that are wireless in nature is the power over other correction codes. The turbo encoder and decoder are a recent progress done in the area of forward error correction (FEC) codes that is useful in the achievement of Shannon-limit performance. This encoder and decoder fulfill the requirement of high throughput in Wimax/LTE network by providing a relatively good performance. The key feature of these turbo codes is decoding algorithms which improves BER performance of wireless networks. To achieve optimized performance, we then will have to find the best option of turbo codes.

There is no need for a back-channel hence avoiding retransmission of data which can be an advantage of forward error correction. Hence where retransmitting can be relatively impossible to be done or costly, FEC is applied. The coding scheme for Long Term Evolution (LTE) Turbo coding. Some of the characteristic features of turbo codes are its repetitive decoding mechanism, reoccurring systematic encoders and also the use of interleavers. This paper presents the structure of turbo encoder and decoder and its respective operations. The above-mentioned operations are further defined by various techniques. An integral part of wireless communication system is a channel decoder which is responsible for communication of data that is reliable in nature. A decoder for channel employing turbo codes for correction of errors produces bit-error-rate performance that can be excellent which makes various wireless communication standards accept this code [1]. Peak data-rates of standards of 3G and 4G communication wireless in nature which include turbo codes for the correction of errors are shown in Fig. 1

These components must be created which in turn must incorporate the criteria that can be applicable.

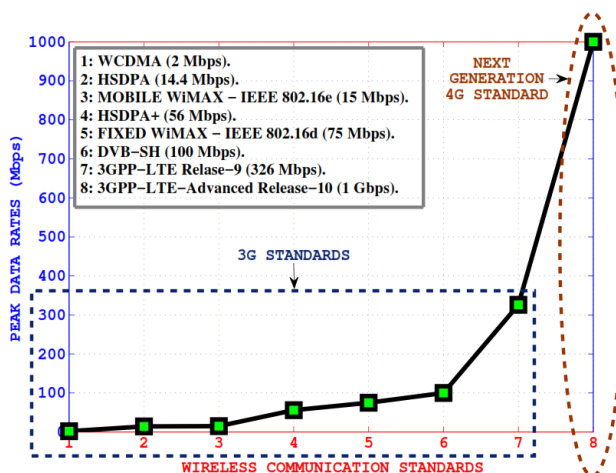


Fig 1: Ever increasing peak data rates of various wireless communication standards which include turbo code as their error.

II. RELATED WORKS

Lekha S. Yeldi, Jagdish D. Kene et al [1], proposed the key features of turbo coding method are the algorithms for decoding which improve the wireless network’s BER performance. To have an optimized performance, the paper attempts to find the best possible option that exists of turbo code. The simulation results that are produced that of the BER performance of that of log map and of max-log

Map show that these maps of log functions scans be implemented much easily thereby giving a bit error rate which has low SNR, desired in nature. This also reduces additional complexity by performing with lesser number of states. The paper also shows the results produced in Log-Map which has different quantized levels and values of that of forward, backward and branch metric. Log MAP best suits the decoding algorithm with low bit error rate in comparison to max-log map and MAP.

Prabhavathi D Bahirgonde, S K Dixit et al [2], presented that the extremely challenging task is to reduce the complexity produced in computation of Turbo decoding implementation in 3GPP-LTE that is wireless communication standard. The difficulty in execution of a turbo encoder is much lesser than the complexity in that of turbo decoder. This difficulty of Turbo decoder depends on decoding algorithm. The performance degrades with less complexity in decoding. The number of iterations also influences Turbo decoder performance during decoding. Different types of iterative Turbo decoding algorithm are described in this paper. Discussion is done about the factor of correction and how it changes when in different algorithms. Different Turbo decoding algorithms go through BER. MATLAB simulation is used to show how the number of iterations has an effect on Max-Log-MAP decoding. A good method of testing the performance of coding using Turbo code is BER analysis. The number of parameters can be used to test the performance over using hardware of Turbo decoder, the BER analysis becomes difficult to carry. A simulation tool used for performing BER analysis is MATLAB. BER analysis can also be used for algorithms for decoding, the number of interactions and the frame size is carried out in this paper.

Yogesh Beeharry, Tulsi Pawanfowdur, Krishnaraj M. S. Soyjaudah et al [3], proposed that between two concatenated decoders, Turbo codes affect a mechanism for message passing which is iterative. Code Division and Long-Term Evolution for Multiple Access 2000 are some of the communication standards in which there is their widespread adoption due to their astounding performance. When there is usage of Sign Difference Ratio, it has been observed that as there is increase in E_b/N_0 , the decoding methods' complexity decreases strikingly. Moreover, assessment of Bit Error Rate performance of these methods was also compared for multiple schemes of modulation. These results show that performance differs when varying methods are applied in the waterfall and in the error-floor regions with multiple schemes of variation. Moreover, it is also seen that the Method 2 needs less overall computation steps when compared to those in Methods 1 and 3 in the computational complexity analysis. When considering Binary LTE Turbo codes with BPSK, Binary LTE Turbo with Q-PSK and Binary LTE Turbo of 16-QAM, three varying methods of decoding have been shown. These methods have performance which is similar in general E_b/N_0 range, with BPSK modulation. With QPSK modulation, it is seen that these methods have extremely similar performance over E_b/N_0 range. Gaining 0.1dB avg. when considering the range $E_b/N_0 > 2.4$ dB, the method 2 and method 3 perform better than method 1, with 16-QAM.

Zhongfeng Wang, Zhipei Chi, Keshab K. Parhi et al [4], presented that the decoding done by turbo decoder have throughput which is low and large decoding inactivity due to decoding iteratively. Decoding schemes that are high speed in nature must be used to increase this low throughput and to reduce the value of latency. Comparison on the number of units of computation, the general inactivity in decoding and storage requirement is also mentioned in this paper for different decoding schemes which have different parallelism levels. For the implementation of very high level parallelism, an attractive solution are Hybrid parallel decoding schemes. While some overhead must be paid when it comes to power and area, Turbo decoders which employ these decoding schemes are presumed to gain multiple times the value of throughput of a serial decoding decoder. Simulation results have shown that performance degradations do not occur when considering decoding schemes that are parallel and area-efficient.

Rahul Shrestha, Roy P. Paily et al [5], focused their work on the design aspect concerning the VLSI of maximum *a posteriori* (MAP) probability decoders that are high-speed in nature which are also are intrinsic building-blocks of parallel turbo decoders. For the computation of backward state metrics, the paper has presented a non-grouped backward recursion technique for the algorithm used in MAP decoders which is logarithmic-Bahl–Cocke–Jelinek–Raviv (LBCJR). To achieve higher clock frequency, based on this technique, MAP decoder can be extensively pipelined and retimed which is unlike such conventional decoder architectures. Additionally, in the state metric normalization technique, there has been reduction critical with 8 and 64 parallel MAP decoders in 90nm CMOS technology, which is employed in designing an add-compare-select-unit (ACSU). An achievement of maximum throughput of the rate 439 Mbps with 0.11 nJ/bit/iteration energy-efficiency was received in an 8-parallel turbo-decoder with VLSI implementation. Similarly, maximum throughput of 3.3 Gbps was achieved in 64 parallel turbo-decoder which has an energy-efficiency of 0.079 nJ/bit/iteration. 3GPP-LTE's peak data-rates and that of LTE-Advanced standards have been met by these high-throughput decoders.

Ardimas Andi Purwita, Arnaud Setio, Trio Adiono et al [6], presented that coding using Turbo code is able to closely reach Shannon limits' channel capacity which is also a high-performance channel coding. A new architecture of encoder based on Turbo coding which is based on 3GPP standard is also mentioned in the paper. By the implementation of dual RAM in internal interleaver, with an optimized parallel architecture that has 8-level, this architecture is developed. To simulate the system and to profile the system, the paper also uses MATLAB software which ensures functionality of the algorithm being proposed and even the architecture. To increase hardware implementation performances of system, compare the performance between un-optimized, un-parallelized, and an optimized encoder of turbo coding which is 8 level. Parallel processing architecture is employed in the algorithm defined to improve inactivity of the clock and to reduce the encoders' size. In order to reduce clock latency, double RAM has also been implemented in internal interleaver of the type turbo coding. When compared to conventional architecture with size smaller than 50%, this proposed architecture increases the efficiency of the encoder by increasing its' speed by 16 times.

Liang Li, Robert G. Maunder, Bashir M. Al-Hashimi, Lajos Hanzo et al [7], recently they have considered turbo codes for the application of wireless communication that can be restrained by energy, as turbo codes help in low energy consumption when it comes to transmission. Here, the usage of magnitude which is a few gates lesser than the architectures of latest LUT-Log-BCJR, which further facilitates a reduction in the consumption of energy by 71%, 71% lower of 0.4 nJ/bit/iteration in this architecture is demonstrated.

Cristian Anghel, Constantin Paleologu et al [8], presents that advantage was taken of the quadratic permutation polynomial (QPP) interleaver proprieties and also when a few of the characteristics of FPGA block memory were considered, a simplified parallel decoding architecture are proposed in this paper. When high decoding latency is introduced by the serial decoding, it should be especially used for large data blocks. N , that is the parallelization factor is usually in the powers of two, 8 is the maximum considered value. The serial decoding latency is N times greater than the received parallel decoding latency. Only one interleaver is used with the cost of very low latency added to proposed parallel architecture, independent of N 's value. The serial wise implemented turbo decoder architecture was implemented and developed in a methodical manner, which especially is done from the view of the interleave or the deinterleaver. To make sure the interleaver process works effectively when implemented other than in the process of a decoder especially, the interleaver memory ILM was introduced. The data fed as input together with ILM was typed, whereas the block predecessor to the current block was still decoding. Using this method, the architecture shifted to parallel wise by the use of concatenated values only when in similar memory locations.

Lohith Kumar H G, Manjunatha K N, Suma M S, C K Raju, Prof. Cyril Prasanna Raj P. et al [9], presented in the paper for a turbo decoder that is 3GPP advanced by the use of an interleaver convolutional in nature, proposed to design and to develop VLSI architecture that is efficient in nature. This advanced Turbo code needs implementation of turbo decoder to produce high throughput. The main obstacle to the decoder implementation is an interleaver and the introduction of latency which arises due to the collisions that occur during memory access. This paper also places a proposition of a Soft Input Soft Output (SISO) turbo decoder which has low complexity for the architecture of memory which thereby enables the decoding to achieve least latency. Trade-offs that occur in design in terms of throughput efficiency and area are then explored to find the architecture optimal in nature. Simulink is used to model the proposed Turbo decoder; and to estimate the performances various test cases are used. The Bit Error Rate (BER) and Turbo decoder and channel specifications are analysed for the rate of 3 samples which is 0.000254 which is of the order of (10^{-3}) .

Guohui Wang, Aida Vosoughi, HaoShen, Joseph R. Cavallaro, and Yuanbin Guo et al [10], present that there is a need for parallel architecture to produce a high throughput using a decoder; this can be implemented to meet the requirements of the data rate of the communication systems that are wireless in nature. However, the major challenge that causes the desired interleaver designs' throughput to become unachievable is due to conflict in memory. Furthermore, the hardware for generation of parallel interleaving address becomes difficult to execute because of the increasing complexity of the interleaver algorithm. An interleaver architecture that is parallel in nature and can generate multiple addresses of interleaving is proposed in this paper. A scheduling scheme is proposed which has better and efficient buffer structures that can be used to get rid of contention of memory. The produced results show that with new scheduling scheme, proposed architecture can reduce complexity in hardware and usage of memory significantly. Great flexibility along with scalability can be shown in proposed architecture.

Samir Jasim Mohammed, Ansam Abbas Obaid et al [11], proposed that after many decoder types have been introduced which include multiple parameters, with work design and implementation of turbo code, obtain the Ber for each of the cases, and comparing the results. To study each of the parameters' effect on the turbo codes' performance, multiple parameters have been described that give the desired result of these codes. The UMTS interleaver and the BPSK modulation are assumed for the proposed system. After that, changing many parameters, many types of decoders were done from this work and the results conclude that BER decrease for the same and the performance improves when the number of iteration increased the. The increase in length of code and number of frames improves the performance, different code length applied (256,512,1024 and 4096) and number of frame (512 and 1024) were performed and comparison was done between the results obtained for each case. The results of the SOVA and MAX-Log-MAP is in comparison worse than other types of decoding techniques applied (SOVA, Log-MAP and MAX-Log-MAP) by using log-MAP technique when applied for the same conditions of the system (512 b/f, 1024 f, 4 iterations and), also the gain is obtained about in log-MAP compare with SOVA and in log-MAP comparison with MAX-Log-MAP. To increase the rate of the system, puncturing technique was used, but the BER degrades by increasing the rate. Also the generator polynomial of the system was changed and compared with the standard generator polynomial, where two addition generators polynomials are used, finally two types of channel used in this simulation obtained results for each case and comparison as done when using AWGN channel the performance is best than the fading channel.

Christoph Studer, Christian Benkeser et al [12], proposed the use of turbo decoding for 3GPP LTE standard for communication that occurs in wireless way is a challenging task when considering consumption of power and complexity in computation of the related cellular devices. The implementation aspect of the turbo decoders occurring parallelly that cross 326.4 Mb/s LTE peak data-

rate using various Soft Input Soft Output decoders that work parallelly are also researched in this paper. When a more realistic 100 Mb/s LTE milestone is considered that is required by the industry today, the decoder implementing turbo code only consumes 69 mW. On analysing the throughput/area trade-offs that are usually associated with the parallelly implemented turbo decoders, it is noticed that in the combination of radix-4 and instances of eight M-BCJR are needed to reach maximum data rate of 0.13 μm in LTE in CMOS technology. There was achievement of parallel access and access of interleaving to memory spaces with high throughput by developing master-slave Batchner network. Optimizing the radix-4 M-BCJR unit has caused to reach a performance higher and lesser area of architecture of turbo decoder ; including the setting record in the throughput achieved which are both ultralow-power and cost effective in implementation.

Prabhavati D. Bahirgonde, Shantanu K. Dixit et al [14], implemented trellis of 8 state which is of the form of radix-2 and the radix-4 form. When considering a system that is practical, the foremost MAP algorithm is much more difficult to implement. To calculate LLR values, all the branch metrics required are stored in a RAM. There is implementation of the Max function to increase the performance with the correction factor. The algorithm defined when implemented is similar to the max. function. While there is increase in the need for various rates of data and services that come with system of communication re-configurability becomes necessary. Constant Log-MAP algorithm is proposed to use the MAP algorithm in the domain of log, and this produces result that are extremely similar to those produced by max Log-MAP algorithm.

Shivshankar Mishra et al [15] presents a paper that implements Turbo encoding algorithm, where two parallel concatenated RSC codes are used to design 1/3 rate encoder. MAX-LOG-MAP algorithm is used for decoding along with Turbo, results of simulation were obtained as expected at the side of the receiver. The paper also analyzes and simulates the mentioned algorithm and the observation was made with the increase in number of iterations, the BER gets better. This performance of BER depends on even the type of interleaver and the size of the frame that has been used for implementing decoder and encoder.

Cristin Anghel et al [16] proposed with the use of decoding architecture that is parallel in nature, the main methods used for sorting is turbo codes that are used in LTE systems. Mostly, the number of required interleavers is represented by the parallelization factor N. The paper proposes an architecture of a decoder which has a single Quadratic Permutation Polynomial (QPP) interleaver. On same memory location, every interleaved address is then placed as a result of the properties of algebraic QPP interleaver. But there must be sorting to be performed before the correct should be sent to each of the decoder unit. Comparison is done for all the methods of sorting to find the one that suits implementation of Field Programmable Gate Array (FPGA) mostly.

III. OBJECTIVES OF THE RESEARCH WORK

A. Need for the Research Problem

A major drawback of implementation of turbo code is its high inactivity in the decoding. There are three important issues which are presented in architectures of turbo codes : the recursions that take place both in forward and backward direction in the maximum a posteriori (MAP) decoders in this repetitive process, the repeating nature of the algorithm for decoding, and the interleaver and the deinterleaver units that are present between the MAP decoders. When there is integration of turbo in the codes of high throughput standard of communication like LTE, these above mentioned challenged become important. To fulfill the rate of data that is mentioned, there must be foretelling of parallelization and reduction in inactivity techniques in turbo decoders' implementation of hardware. A serial data dependency is imposed to overcome the problem of decoding received signal; a severe

bottleneck is imposed by limiting the throughput of procession of the standard implementation of the turbo decoder upon the general throughput of the schemes of communication in real-time.

- Decoding algorithm
- Signal to noise ratio (E_b/N_0)
- BER
- Frame size
- Puncture/un-puncture
- Maximum iterations
- Number of errors in the frame that need to be terminated

B. Primary Objective

The primary objectives of this proposed research work are to develop efficient Turbo Decoder Architecture when considering the throughput of processing, the inactivity of processing, the energy consumed by each frame and normalized core area. Another objective is for reviewing literature on Turbo Decoder Architecture in LTE communication based on BER. This objective also focuses on validation of effective Turbo Decoder Architecture when considering processing of the throughput, the latency's processing, consumption of energy in every area along with normalized core region. This primary objective includes evaluation of efficiency of Turbo Decoder Architecture when considering the throughput processed, procession of latency, energy taken by the individual frames with the normalized care but definitely not limited to these above-mentioned objectives.

IV. RESEARCH CONDUCTED

This section discusses about the work carried out till date. The entire work is classified into Preliminary Review, Research methodology, and Possible Outcomes.

A. Preliminary Review

The preliminary research phase is the phase where the motive was to investigate the existing issues that are associated with turbo decoder's performance analysis and to propose areas in which the execution of the turbo decoder may be further upgraded by in turn improving BER performance of wireless networks, by ensuring balance in the network and for obtaining better performance for turbo decoders.

The study outcome of the preliminary phase of research performed is published in a review paper titled "*Evolution of Wireless Communication Along with Encoders*". In "International Journal of Innovative technology and Exploring Engineering (IJITEE)", the paper is published.

B. Research Methodology

The methodologies adopted by the proposed system are as listed below:

- Conduction of literature surveys on different Architectures of Decoders implemented using Turbo Coding in LTE Communication (as per BER) and then will be carried out from IEEE papers, white papers and journals.
- Development of efficient architecture of turbo decoder for wireless LTE communication standards must also be carried out.
- Literature survey on LTE Communication and challenges that can be faced in LTE Communication (asper BER) must be carried out from different IEEE papers, white papers and journals.
- Validation of efficient Turbo Decoder Architecture when considering processing latency, processing throughput, energy consumption for each frame and area of the core that is normalized will be carried out.

- Evaluating and optimization the Turbo Decoder Architecture when considering to process the throughput, the latency, and the consumption of energy by each and normalized core area must also be carried out.

C. Possible Outcomes

In all wireless telecommunications systems, the channel coding procedure which is also known as Forward Error Coding (FEC), is used in such a way to identify and also correct any potential errors which may occur during radio transmission the constituent encoder and the interleaver are the main components of a turbo code. Turbo codes are used in Long Term Evolution (LTE) systems and Universal Mobile Telecommunications Systems (UMTS), respectively. Parallel decoding architectures are considered to solve this problem.

We propose an architecture that are decoding in nature with just a single Quadratic Permutation Polynomial (QPP) interleaver. On the same memory location, every address interleaved are placed as a result of algebraic properties of QPP interleaver, but this needs the data to be sorted before the correct data is sent to each unit of decoder. Comparison of these methods of sorting are performed to find the most fitting for Field Programmable Gate Array (FPGA) implementation. The method of sorting selected is even-odd merge sorting method, and the results that are found are in terms of resources occupied and maximum speed.

The performance measured based on the Bit-error-rate (BER) of the decoder implemented has shown coding loss of approximately 0.2 dB when compared with the simulated BER values.

V. FURTHER RESEARCH

With the discussion and researched carried out, it is seen that the proposed study has helped in accomplishing the first objective of the study designing of low BER turbo decoder. Hence, the next phase that must be accomplished will be focusing on achieving the remaining objective of the study, which also includes focusing on three different challenges that become very important to focus on when integration of codes produced by turbo coding must be performed in standards of communication that has high throughput such as LTE. To fulfil the data rates that are mentioned, one must foretell parallelization and methods for reducing the latency in the implementation of hardware/e of turbo decoders.

A. Implementation Techniques

The proposed solution must perform implementation on MATLAB for software side and CMOS VLSI architecture will be used for hardware side. The proposed communication system must follow the following block diagram which includes stages such as Formatting Digitization, Source Coding, Channel Coding, Multiplexing, Modulation and Access techniques. The data transmission and receiving order is represented with the help of arrows.

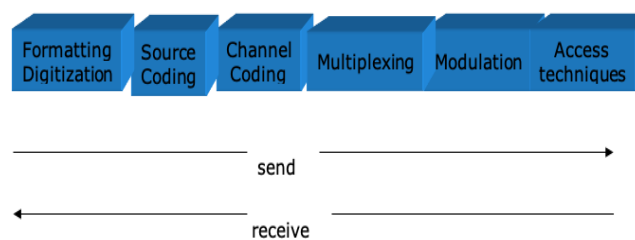


Fig 2: Communication System

The proposed channel encoder performs encoding using an input sequence of k bits and encoding to produce an output sequence of n bits with a code rate k/n and the redundancy factor of $(n-k)$. The diagram of the encoder block of the channel is represented below

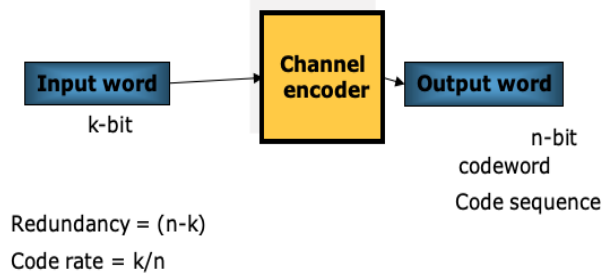


Fig 3: The channel encoders' block diagram

The encoding performed by the channel encoder faces challenges in the form of

1. The performance of error vs. Bandwidth with High redundancy consumption bandwidth
2. Power vs. Bandwidth that has Reduction in E_b/N_0
3. The data rate vs. Bandwidth in a Higher Rate

In the architecture represented below, the inputs pass through the Recursive Systematic module which then generates systematic code word. This is again passed through an Interleaver module and then Recursive Systematic module for further systematic code word.

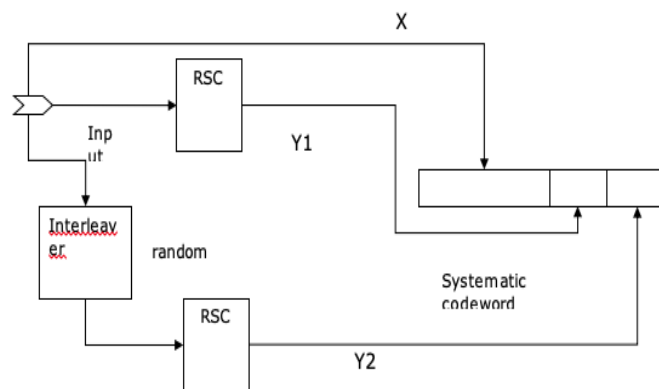


Fig 4: Coding Architecture

To develop the system model of iterative turbo code decoder, attesting frames are generated which are an integer to a vector of binary bits. At the receiver's end, serial to parallel de-multiplex has been designed. to encode the frames, recursive Systematic Convolutional encoder has been developed which uses turbo encoding process. To complete the decoding process, the encoded data is converted from vector of bits to integer, and set up trellis for the encoded data. For the simulation of the turbo encoding and turbo decoding system, assuming a uniform distribution, the information bits are randomly generated. There is generation of a random interleaver for bits of each frame. The code performance is calculated from the average performance among all interleavers.

VI. RESULTS

The performance of turbo decoder has been realized on developed communication model with AWGN channel. Number of iterations has been tried on developed communication model. Plotted result has been shown in in Fig 5. Fig 5 shows the bit error rate gradually reduces with increase of signal to noise ratio. Number of iteration affects the bit error rate as shown in fig 5.

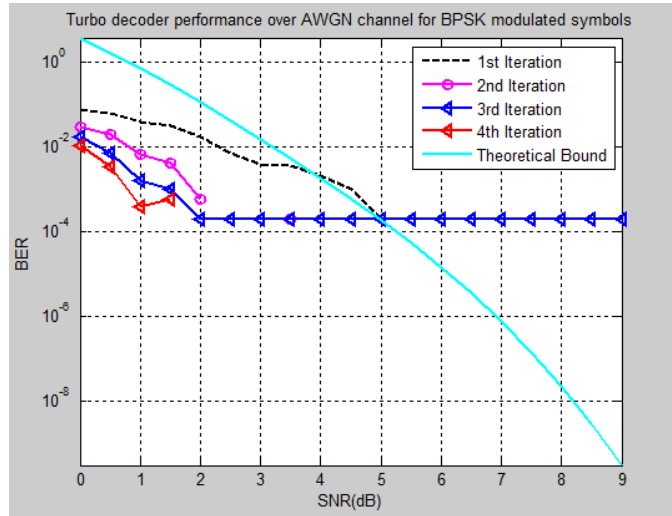


Fig 5 : Turbo decoder performance for BPSK modulated system over AWGN channel.

Developed communication model of turbo decoder is verified with different AWGN channels and different iterations. Result has been plotted and shown in Fig 6. In Fig 6 bit error rate behaviour are almost same in different AWGN channels, The SNR value increases when compared to the initial channel.

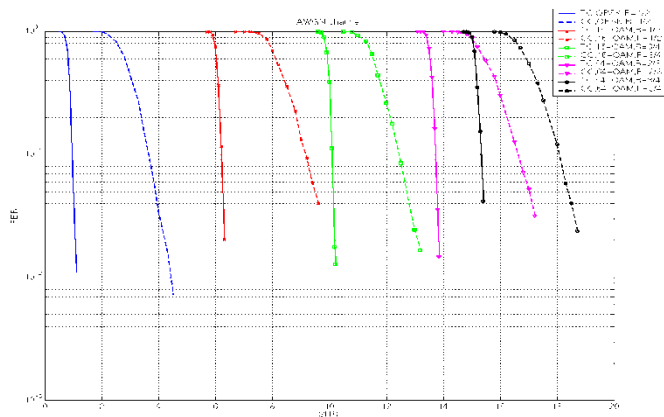


Fig 6 : Comparison between SNR(x-axis) and BER(y-axis) in AWGN channel

The number of iterations can be then adjusted to achieve better performance and complexity trade – off. The coding system comparison graph of BER (bit error rate) and SNR(signal to noise ratio) obtained from the coding architecture is shown below.

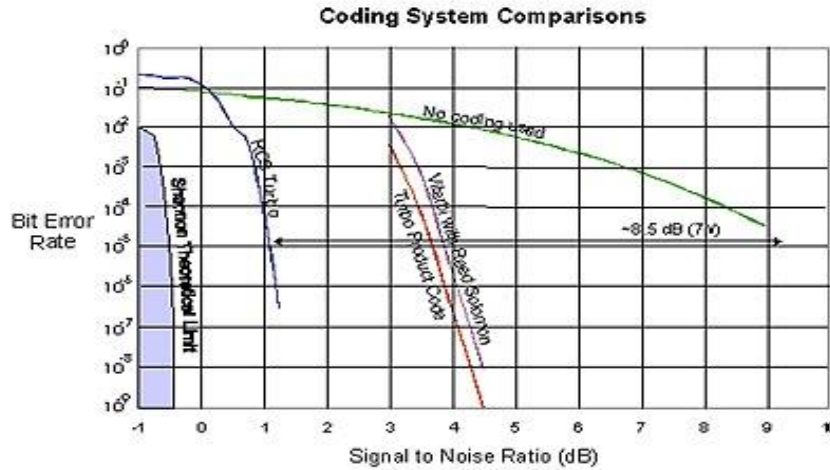


Fig 7 : Comparison of the SNR and BER of Coding system

CONCLUSION

Cellular and other technology makes it possible for people to be connected to the rest of the world from anywhere, anytime. All these wireless networks demand for high rate of transmission quickly, timely and accurately. For providing the good accuracy or to recover the original signal at the receiver end, forward error correction codes have been implemented. There are several types of error correcting techniques used like convolution coding, but it fails to maintain the lower values of signal to noise ratio as the length of code increases. So a new version of coding called turbo coding was introduced that can achieve a level of performance that comes closer to theoretical bounds than more conventional coding systems. The inherent iterative process of decoding restricts turbo decoder to process data at higher data-rate. BER performance also depends on frame size and interleaver type used for implementation of encoder and decoder. Bit-error-rate (BER) performance of the implemented decoder has shown a coding loss of approximately 0.2 dB in comparison with the simulated BER values. We have investigated the techniques of message ling and state metric normalization, which improve the BER performance and prevent potential overflow, respectively. Furthermore, a bypass mechanism is proposed for allowing a hard-wired interleaver to support the decoding of frames having different lengths and interleaver patterns. In order to fulfil the data rates mentioned above, The performance of turbo decoder has been realized on developed communication model with AWGN channel and The problem of decoding in received signal has been realized.for further hardware implementation of turbo decoder for LTE standard communication with efficient hardware architecture.

REFERENCES

- [1] Rashmi R and Manju Devi , "Evolution of Wireless Communication along with Encoders" International Journal of Innovative Technology and Exploring Engineering (IJITEE), Volume 9, Issue 1, November 2019,Page No 2589-2593.
- [2] Lekha S and Jagdish D. kene, "Review on Role of Turbo Encoder and Decoder in LTE Network" International Journal of Science, Engineering and Technology Research (IJSETR), Volume 5, Issue 1, January 2016.
- [3] Prabhavati D. Bahirgonde and S. K. Dixit, "BER Analysis of Turbo Decoding Algorithms" Foundation of Computer Science FCS, New York, USA Volume 4– No.3. 26-29, 2016.

- [4] Yogesh BEEHARRY, Krishnaraj M. S. SOYJAUDAH and Tulsı Pawan FOWDUR, "Performance of Bit-Level Decoding Algorithms for Binary LTE Turbo Codes with Early Stopping" Yogesh BEEHARRY et al. / IU-JEEE Vol. 17(2), 3399-3415, 2017.
- [5] Zhongfeng Wang, Zhipei Chi and Keshab K. Parhi, "Area-Efficient High-Speed Decoding Schemes for Turbo Decoders" IEEE transactions on very large scale integraton(VLSI systems, VOL. 10, NO. 6. 902-912, 2002.
- [6] Rahul Shrestha and Roy P. Paily, "High-Throughput Turbo Decoder with Parallel Architecture for LTE Wireless Communication Standards" IEEE transactions on circuits and systems-1: REGULAR PAPERS. 1-12, 2017.
- [7] Ardimas Andi Purwita, Arnaud Setio and Trio Adiono, "Optimized 8-Level Turbo Encoder Algorithm and VLSI Architecture for LTE" I2011 International Conference on Electrical Engineering and Informatics. 17-19, 2011.
- [8] Liang Li, Robert G. Maunder, Bashir M. Al-Hashimi and Lajos Hanzo, "A Low-Complexity Turbo Decoder Architecture for Energy-Efficient Wireless Sensor Networks" 1-9.
- [9] Cristian Anghel and Constantin Paleologu, "Simplified Parallel Architecture for LTE-A Turbo Decoder Implemented on FPGA" Advances in Circuits, Systems, Signal Processing and Telecommunications. 102-111, 2009.
- [10] Lohith Kumar H G, Manjunatha K N, Suma M S, C K Raju and Prof.Cyril Prasanna Raj P, "Design and Performance analysis of a 3GPP LTE/LTE-Advance turbo decoder using software reference models" International Journal of Scientific & Engineering Research Volume 2, 1-4, July-2011.
- [11] Guohui Wang, Aida Vosoughi, Hao Shen, Joseph R. Cavallaro, and Yuanbin Guo, "Parallel Interleaver Architecture with New Scheduling Scheme for High Throughput Configurable Turbo Decoder".
- [12] Samir Jasim Mohammed and Ansam Abbas Obaid, " Design and Implementation Different Types of Turbo Decoder with Various Parameters ", International Journal of Computer Applications (0975-8887), Volume 166 –NO 11, May 2017.
- [13] Christoph Studer, Christian Benkeser, Sandro Belfanti and Qiuting Huang Fellow” Design and Implementation of a Parallel Turbo-Decoder ASIC for 3GPP-LTE" ITO APPEAR IN IEEE JOURNAL OF SOLID-STATE CIRCUITS, 1-9, 2011.
- [14] Prabhavati D. Bahirgonde, Shantanu K. Dixit, " Low Complexity Modified Constant Log- Map Algorithm for Radix-4 Turbo Decoder" 2015 International Conference on Pervasive Computing (ICPC)
- [15] Shivshankar Mishra and Harshit Shukla and Suneel Madhekar,” Implementation of Turbo Decoder Using MAX-LOG-MAP Algorithm in VHDL " IEEE INDICON 2015 1570169743.
- [16] Cristian Anghel and Cristian Stanciu and Constantin Paleologu, " Sorting Methods Used in Parallel Turbo Decoding for LTE Systems ".
- [17] C. Berrou, A. Glavieux, and P. Thitimajshima, "Near Shannon Limit Error-Correcting Coding and Decoding: Turbo-Codes," in Proc. 1993 *International Conference on Communications* (ICC '93), Geneva, Switzerland May 1993, pp. 1064–1070.
- [18] Claude Berrou, Alain Glavieux and Punya Thitimajshima "Near shannon limit error – correcting Coding and decoding turbo-codes" IEEE Transactions on Communications, 44:1261 – 1271, Oct.1996.
- [19] Third Generation Partnership Project, "3GPP home page" www.3gpp.org.
- [20] Vogt.J and Finger.A, "Improving the max-log-MAP turboDecoder," Electron. Lett., vol. 36, no.23, pp.1937 1939, Nov 2000.

- [21] K. Loo, T. Alukaidey, and S. Jimaa, "High performance parallelised 3GPP turbo decoder," in *IEEE Personal Mobile Communications Conference*, April 2003, pp. 337- 342.
- [22] A.J. Viterbi. An intuitive justification and a simplified implementation of the MAP decoder for convolutional codes. *IEEE J.Sel. Areas Commun.*, vol.16:pp.260–264, Feb.1998.
- [23] R. Dobkin, M.Peleg, and R.Ginosar. Parallel interleaver design and vlsi architecture for low-latency map turbo decoders. *IEEE Trans.VLSI Syst.*, 13(4):427–438,200.



IJRASET

International Journal For Research in
Applied Science and Engineering Technology



INTERNATIONAL JOURNAL FOR RESEARCH

IN APPLIED SCIENCE & ENGINEERING TECHNOLOGY

Volume: 8 Issue: VI Month of publication: June 2020

DOI: <http://doi.org/10.22214/ijraset.2020.6316>

www.ijraset.com

Call:  08813907089

E-mail ID: ijraset@gmail.com

Voice Assisted Smart E-Cane for the Visually Challenged using Machine Learning

Adam Filbert Ashwal¹, Kimberly Claudia Dsouza², Meghana S³, Muhammad Hashim Iqbal Husain⁴, Manju Devi⁵

^{1, 2, 3, 4}Dept of Electronics and Communication Engineering, The Oxford College of Engineering, Bangalore, India

⁵Head of Department, ECE, The Oxford College of Engineering, Bangalore, India

Abstract: *This prototype device focuses on aiding the visually challenged in terms of movement. The device includes a Smart E-Cane implemented using Raspberry Pi and sensors for obstacle, water detection and vibration, buzzer as feedback respectively. The device also includes a Smart Band implemented using Node MCU which provides safety and security features such as sending the location to the user's relatives at home and locating the Smart E-Cane within the user's vicinity. The prototype is trained to detect staircase in real-time using YOLOv3, deep learning concept and report back to the user via speech playback. This Smart E-Cane promises independency along with security in terms of walking without assistance.*

Keywords: *Blind Stick, Staircase Detection, Raspberry Pi, Node MCU, IoT, YOLOv3, Deep Learning.*

I. INTRODUCTION

There are many people who suffer from visual impairment and need to go through expensive treatments or mental and physical challenges to cope with their disability. This was the ideology behind our project. The prototype consists of a Smart E – Cane and a Smart Band. The Smart E – Cane is to assist the visually challenged while the Smart Band provides safety and security features to the user.

The Smart E – Cane is implemented using Raspberry Pi microprocessor and incorporates with various sensors and feedback mechanisms that will aid the user for navigation and alerting purposes. While the most important is the detection of raised surface level such as a staircase using Raspberry Pi and Pi Camera.

The prototype also focuses on providing accurate location information when needed to the user's contacts. It includes a wearable Smart Band for emergencies. The Smart Band is implemented using NodeMCU. The framework detects an ascent in surface level such as a staircase as the individual is walking, using deep learning and reports back what sort of raised surface is ahead. This Smart E – Cane not only provides independency but security too in terms of walking without any sort of assistance.

II. LITERATURE SURVEY

After referring many papers, we found umpteen devices that aid the visually challenged and blind to go about their daily life. Few of the implementations that stood out were:

“Real Time Object Detection Using YOLOv3” by Omkar Masarekar, Omkar Jadhav, Prateek Kulkarni, Shubham Patil. They have created a model to distinguish only three objects which can be scaled additionally to detect manifold quantity of objects. In this, they had used the Bounding box method for localization of the objects to overcome the drawbacks of the sliding window method. [1]

“Smart Stick for Blind using Machine Learning” by Mohamedarif Regade, S Bibi Ayesha Khazi, Sushmita Sunkad, Mrityunjay C.K, Sharda K.S. A wall-following platform is overlaid so the user will walk straight in a passage in an inhouse environment. Head level obstacle recognition can also be carried out.

Programmable wheels to be inured to steer the stick off from the obstructions. [3] “Electronic Smart Canes for Visually Impaired People” by Dimitra P. Marini in her B.Sc Thesis book, mentioned that this project includes capturing the background via a camera and estimating the background details to form required path to be taken for the blind person. This path is then provided to the user through auditory response. [4] “Smart Walking Stick for Blind integrated with SOS Navigation System” by Saurav Mohapatra, Subham Rout, Varun Tripathi, Tanish Saxena, Yepuganti Karuna. It is a device that integrated a blind stick with Smart navigation system for emergency situations. It assists in identifying obstacles through live streaming system and directs the users next move based on the obstacle in front of them. [5]

III. TOOLS AND TECHNOLOGIES

A. Hardware Tools Used in Smart E-Cane

The different hardware tools that are used in the Smart E-Cane are as follows:

- 1) *Raspberry Pi*: The Raspberry Pi microprocessor is like a credit card size computer capable of controlling the various I/O devices connected to it. The main processor which is used to control the various hardware components used in the Smart E – Cane is the Raspberry Pi 3 model B microprocessor. The Raspberry Pi 3 is interfaced with ultrasonic sensor (HC-SR04), moisture sensor and moisture meter (YL-69 & YL-38), Raspberry Pi camera (rev 1.3, 5MP), motor driver board (L293D-R1), 2.4 GHz RF receiver, vibrator motor and magnetic buzzer.
- 2) *Ultrasonic Sensor*: An ultrasonic sensor is a device which is used in measuring distance or sensing objects. When triggered, the ultrasonic transmitter transmits 8 ultrasonic pulses which travel in air and the echo pin is kept at a high logic state. When the transmitted waves are reflected by an object, they are reflected back towards the sensor and are received by the ultrasonic receiver. At this instant the echo pin is brought back to the low logic state. The amount of time during which the echo pin stays high is measured by the microprocessor as it gives the time taken for the ultrasonic waves to return back to the sensor. Using this value, the distance of the obstacle can be measured using the simple speed-distance formula. We have used HC-SR04 ultrasonic sensor to detect obstacle on the path.
- 3) *Moisture Sensor and Moisture Meter*: The presence of wet surface is detected by using a moisture sensor along with a moisture meter. We have used a combination of YL-69 moisture sensor and YL-38 moisture meter to detect wet surfaces such as water puddles. The moisture sensor acts as a variable resistor whose resistance varies inversely according to the water content in water puddle. The YL-38 moisture meter which is attached to the moisture sensor produces a voltage (analog) which is equivalent to the resistance value. The LM393 comparator chip which is incorporated in the moisture meter is used to digitize the analog voltage signal.
- 4) *Raspberry Pi Camera*: The Raspberry Pi camera is a portable light weight camera module which is compatible with the different Raspberry Pi microprocessor models. It communicates with the Raspberry Pi processor using the MIPI camera serial interface protocol. We have used Raspberry Pi rev 1.3 5MP camera as the input device to record the images of the environment so that these recorded images can be processed to detect the presence of staircase in the environment.

B. Hardware Tools Used in Smart Band

The different hardware tools that are used in the Smart Band are as follows:

- 1) *Node MCU*: Node MCU is the pairing of firmware and hardware based around the ESP8266-12E module which is a low cost Wifi enabled microchip with a full TCP/IP stack and microcontroller capabilities. Node MCU is the main microcontroller which is used to control the various hardware components used in the Smart Band. Node MCU is interfaced with GPS module (SKG13BL), 2.4GHZ RF transmitter and the two 4-pin push buttons.
- 2) *GPS Receiver Module*: GPS (Global Positioning System) is a satellite-based system that sends a signal to the GPS receiver. This signal contains information such as exact time of signal transmission, orbital position of the satellite, etc. The GPS receiver uses the received information signals to calculate its distance from the GPS satellites. This is done by measuring the time required for the signals to travel from GPS satellites to the GPS receiver and then multiplying the measured time with speed of light. The GPS receiver requires signals from at least 4 GPS satellites to calculate its location accurately. We have incorporated GPS receiver module (SKG13BL) in our Smart Band to help the visually impaired user to determine and send the location details to user's relative's mobile in the case of emergency.
- 3) *RF Transmitter and Receiver Modules*: RF modules (transmitter and receiver) are small size electronic devices that are used to aid in wireless communication between an embedded system and another device. This communication is accomplished by using radio frequency signals. Communication over radio frequency is advantageous as it doesn't require a line of sight connection between the transmitter and receiver and the range of RF communication is very high when compared to IR communication. We have used 2.4 GHz RF transmitter and receiver modules in order to establish wireless communication between the Smart E – Cane and the Smart Band.

C. Software Tools

The major software tools which were used to program the different sensors, output devices, microprocessor and microcontroller used in our entire project are as follows:

- 1) *Anaconda*: Anaconda is an open source distribution of the Python and R programming languages for scientific computing that aims to simplify package management and deployment. It includes a desktop graphical user interface called Anaconda Navigator. Package management in Anaconda is done by using conda which is an open source, cross-platform package manager and environment management system that installs, runs, and updates various packages and their dependencies. We have used conda package manager to install various libraries and their dependencies which were needed in implementing staircase detection.
- 2) *Blynk App*: Blynk is an IoT (Internet of Things) platform which enables users to control hardware components such as different sensors remotely, display sensor data, store the sensor data and visualize it using android devices. We have used this app to display the location details of the user in the user's relative's mobile.
- 3) *VOTT*: VOTT (Visual Object Tagging Tool) aids user to label different objects in different images. These labelled images can be then used to train object detector models. We have used VOTT to annotate staircases in different images (250 images).
- 4) *VNC Viewer*: VNC (Virtual Network Computing) is a graphical desktop sharing system that uses the RFB (Remote Frame Buffer) protocol to remotely control another computer by transmitting the keyboard and mouse events from one computer to another and relaying the graphical screen updates back in the other direction over a common network. We need a VNC server application for the computer which we want to control and a VNC viewer application for the computer we want to control from. We have used VNC viewer to control Raspberry Pi 3 Model B microprocessor remotely.

D. Software Libraries

- 1) *Keras*: Keras is an open source neural network library written in Python. It is capable of running on top of TensorFlow, Microsoft Cognitive Toolkit, R, Theano, or PlaidML libraries. Keras library contains numerous implementations of commonly used neural network building blocks such as layers, objectives, activation functions and optimizers. It also contains a host of tools to make working with image and text data easier to simplify the coding necessary for writing deep neural network code [22].
- 2) *OpenCV*: OpenCV (Open Source Computer Vision Library) is an open source computer vision and machine learning software library [23]. This library includes a set of both classic and state-of-the-art computer vision and machine learning algorithms which are used in real time image and video processing.
- 3) *TensorFlow*: TensorFlow is an end-to-end open source platform for machine learning [24]. This library uses data flow graphs to build models and also allows developers to create large-scale neural networks with many layers. TensorFlow library is mainly used for classification, perception, understanding, discovering, prediction and creation. It provides a variety of toolkits that allow users to construct models at their preferred level of abstraction. The library is written using python programming language and is built to run on multiple CPUs or GPUs.
- 4) *YOLOv3*: You Only Look Once (YOLO) is a state-of-the-art, real-time object detection system. It applies a single neural network to the full image. This network divides the image into regions and predicts bounding boxes and probabilities for each region. These bounding boxes are weighted by the predicted probabilities [16]. YOLOv3 is an updated version of YOLO that includes additional features such as multi-scale predictions and a better backbone classifier. YOLOv3 predicts an object likelihood score for each bounding box using logistic regression. Each box predicts the classes the bounding box may contain using multi label classification [25]. One of the salient features of YOLOv3 is that it makes detections at three different scales [27]. YOLOv3 is a very strong detector that excels at producing decent boxes for objects [25].
- 5) *gTTS API*: gTTS (Google Text-to-Speech), a Python library and CLI tool to interface with Google Translator's text-to-speech API [26]. There are several APIs available to convert text to speech in python. One of such APIs is the Google Text to Speech API commonly known as the gTTS API. gTTS is a very easy to use tool which converts the text entered, into audio which can be saved as a mp3 file. It features flexible pre-processing and tokenizing. The speech can be delivered in any one of the two available audio speeds, fast or slow.

IV. DESIGN AND IMPLEMENTATION

A. Design

The prototype model consists of a Smart E-Cane and a Smart Band as in figure 1. The Smart E-Cane's main processor is the Raspberry Pi and consists of Ultrasonic sensor, Moisture sensor, Raspberry Pi Camera, Vibrator Motor, Magnetic Buzzer, RF Receiver module and a Motor Driver. The ultrasonic sensor and moisture sensor implement the obstacle detection and wetness detection respectively.

The feedback for obstacle detection is provided via a vibrator motor and feedback for wetness detection is provided via a magnetic buzzer. The Smart Band main controller is the Node MCU and consists of a GPS module, two push buttons and a RF Transmitter module. The Smart Band provides safety and security features to the user. The two push buttons are utilised to provide these features. Finally, the most important feature of our prototype model is the detection of staircase using Deep Learning. Here we use YOLOv3 for staircase detection while the core libraries include Keras, TensorFlow and for image processing, OpenCV is used.

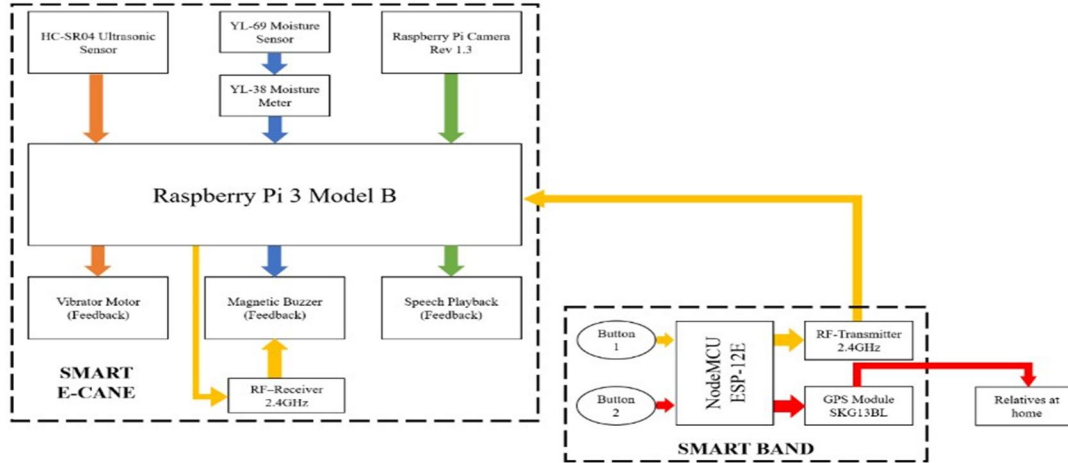


Fig. 1: Generalized Block diagram of Voice Assisted Smart E – Cane for the Visually Challenged Using Machine Learning

B. Implementation

1) *Hardware:* The Smart E – Cane which contains the ultrasonic sensor, moisture sensor, RF receiver module, the Pi camera and the Raspberry Pi microprocessor (shown in figure 2) is the main processing unit of this project. When the device is connected to the power source, the sensors are all active and provide constant feedback.

TABLE I. Hardware Components List

| | |
|---------------------------------------|------------------------------|
| Raspberry Pi 3 Model B Microprocessor | Node MCU ESP-12E |
| HC-SR04 Ultrasonic Sensor | YL-69 Moisture Sensor |
| YL-38 Moisture Meter | Magnetic Buzzer |
| Vibrator Motor | 4 Pin Push Button |
| Raspberry Pi Camera Rev 1.3 | GPS Module SKG13BL |
| 9V Power Supply | Radio Frequency TX/RX 2.4GHz |
| L293D R1 Motor Driver | |

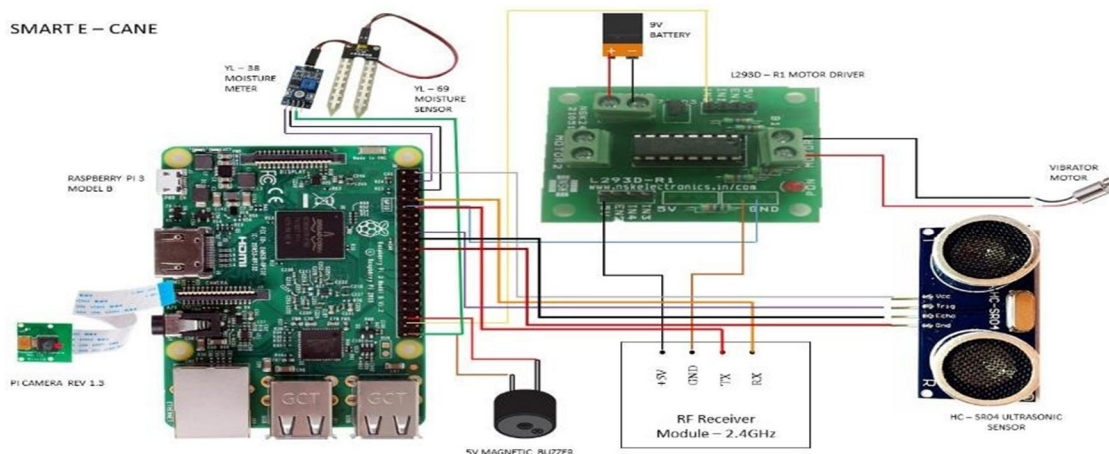


Fig. 2: Smart E – Cane pin diagram

The ultrasonic sensor uninterruptedly measures the distance to sense if there are any obstacles present in front of the user. To measure the distance the sound has travelled in air we use the formula: $\text{Distance} = (\text{Time} \times \text{Speed of Sound in Air}) / 2$. The "2" represents the sound travelling back and forth. To read the distance as centimetres we use the formula: $\text{Centimetres} = ((\text{Microseconds} / 2) / 29)$. Here, we take into consideration the temperature while calculating the speed of sound in air. On detecting an object within the range of 100cms, the vibrator motor is turned on and alerts the user. If the user approaches the object closer than 50cms, the intensity of vibrations increases. The moisture sensor also continuously provides feedback if in contact with water. The feedback is given via the buzzer to differentiate between obstacles.

The reason we use these two different feedback mechanisms by two different sensors is because, the probability of obstacles being detected is more compared to wet areas, hence to avoid causing disturbances to surrounding people the feedback from ultrasonic sensor (obstacle detection) is provided by vibrations by the vibrator motor as it is sound-free (sound of vibrations compared to that of the magnetic buzzer is assumed to be negligible). Moreover, the possibility of confusion is much greater when the sensors are connected to the same feedback device.

The raised surface detection is implemented using the Raspberry Pi microprocessor on the Smart E – Cane. The Raspberry Pi microprocessor receives data from the image captured by the Pi camera. Deep learning is a subset of machine learning that uses multi-layered neural network to progressively extract higher level features from the raw input data. Since this is a prototype model, only staircase detection has been trained into the machine by data sets and the deep learning mechanism is used on various staircase. The flowchart for the staircase detection is explained in the figure 3. A threshold value of 0.25 is set, so that images detected as staircases below 25% confidence value are discarded. The feedback from this process is provided via speech playback using a speaker or earphones.

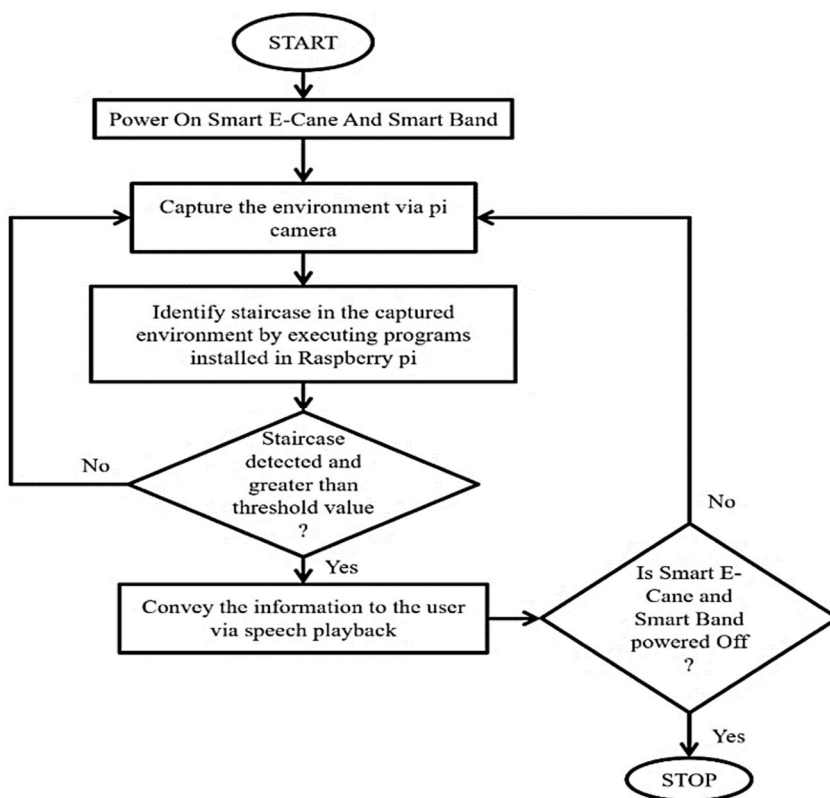


Fig. 3: Staircase Detection Using Deep Learning Flowchart

Once the code is dumped onto the processor and a power supply is provided, the Smart Band which contains the NodeMCU, the GPS module, RF transmitter module and the push buttons (as shown in figure 4) is turned on. The code contains the BlynkSimpleEsp8266 header file which was included to provide access to the Blynk app. Another library called TinyGPS is included for parsing NMEA data streams provided by GPS modules. This library provides compact and easy-to-use methods for extracting position, date, time, altitude, speed, and course from consumer GPS devices.

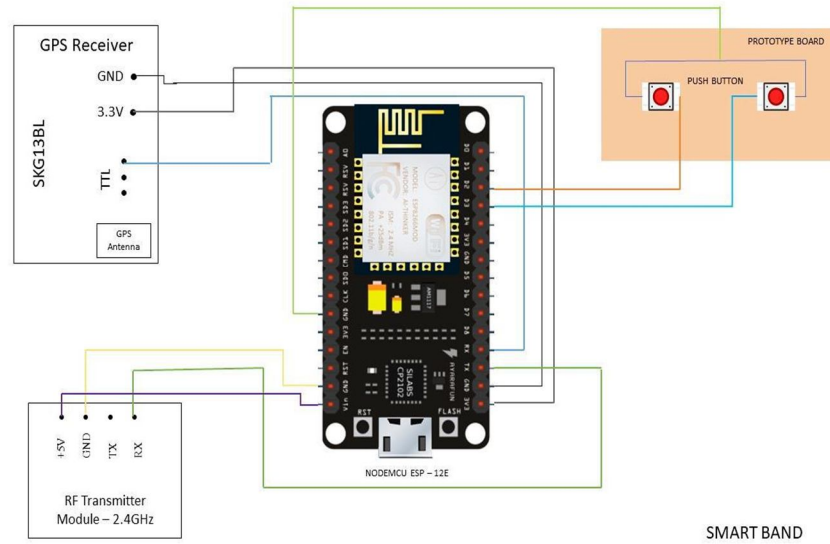


Fig. 4: Smart Band pin diagram

As seen, there are two push buttons. One works as an SOS button and the other is used to locate the Smart E – Cane. When the user presses Button 2 (the SOS button), the GPS module collects the location information and send it to Blynk (latitude first, then longitude), along with a “HELP!!!” message indicating the user is in some kind of situation that needs the attention of his contacts. The emergency contacts will be able to view his location on a map. When Button 1 is LOW, the RF transmitter sends a signal to the RF receiver on the Smart E – Cane, which activates the buzzer.

2) *Software:* The software part of our project is based on image processing using deep learning and machine learning algorithms. We use yolov3 which is a quick, real time, image processing tool.

TABLE II
Software Components List

| Python 3 | OpenCV |
|-----------------|-------------|
| TensorFlow | YOLOv3 |
| Blynk | Vott |
| Keras | Arduino IDE |
| VNC Viewer | Anaconda |
| Raspberry Pi OS | gTTS API |

a) *Step 1: Image Annotation*

For detecting staircases in pictures, it needs to be fed with labelled training data. For accurate results, we labelled about 250 objects. Labelling is done using Microsoft’s Visual Object Tagging Tool (VoTT). Once the images are classified and the coordinates are established, and we export it as csv file shown in figure 5.

```
"image", "xmin", "ymin", "xmax", "ymax", "label"
"9k_%20(1).jpg", 79.57432922407541, 3.0179032258064513, 215.0891950688905, 143.72129032258064, "Staircase"
"9k_%20(2).jpg", 59.43710609243698, 6.045714285714285, 174.3266619147659, 126.4342857142857, "Staircase"
"2Q_%20(1).jpg", 26.52356780275562, 15.133688842482101, 106.929659173314, 87.18022822195704, "Staircase"
"2Q_%20(2).jpg", 86.63551136363635, 2.3005714285714283, 196.61732954545454, 124.23085714285713, "Staircase"
"2Q_%.jpg", 3.4578606592465753, 0.8868571428571429, 106.12652504280823, 103.31885714285714, "Staircase"
"9k_%20(4).jpg", 95.65192168237853, 29.751827267303103, 150.57868020304568, 79.45349791169451, "Staircase"
"9k_%20(5).jpg", 135.09789702683102, 4.32421875, 265.69253081943435, 130.57421875, "Staircase"
"9k_%20(3).jpg", 65.82857142857142, 48.857142857142854, 177.17142857142855, 152.74285714285713, "Staircase"
"9k_%20(6).jpg", 145.25868486352357, 54.57142857142857, 212.95099255583125, 129.22514285714286, "Staircase"
"9k_%20(7).jpg", 80.65844815083393, 39.45290322580645, 179.5300942712111, 137.41790322580647, "Staircase"
"9k_%20(7).jpg", 148.09064539521393, 0, 248.48005801305294, 100.78306451612903, "Staircase"
"9k_%.jpg", 25.509090909090908, 0, 185.95369318181815, 161.66742857142853, "Staircase"
"Z%20(2).jpg", 187.30964467005077, 0, 268.67295141406817, 69.77331606217615, "Staircase"
"Z%20(3).jpg", 13.483670295489889, 0, 247.25349922239502, 170.41142857142862, "Staircase"
"Z%20(4).jpg", 79.95935828877006, 58.28, 184.91764705882355, 171.61599999999999, "Staircase"
"Z%20(1).jpg", 46.416052756654, 3.7645714285714282, 142.6137713878327, 100.17942857142856, "Staircase"
"Z.jpg", 117.18662827557058, 22.057142857142857, 235.000660397295, 127.49028571428573, "Staircase"
"Z.jpg", 5.55011094674562, 84.25828571428572, 103.50784551986476, 179.54514285714288, "Staircase"
"images%20(1).jpg", 8.831926323867997, 9.252571428571429, 194.93323100537222, 168.64914285714286, "Staircase"
"images%20(10).jpg", 55.808, 23.296, 118.52799999999999, 82.176, "Staircase"
```

Fig. 5: Annotations_export.csv

In the final step, we convert the VoTT csv format to the YOLOv3 format by, running the conversion script within the Image_Annotation folder:

```
>>> python Convert_to_YOLO_format.py
/home/ubuntu/TrainYourOwnYOLO/Data/Source_Images/Training_Images/vott-csv-export/9k_%20(1).jpg 80,3,215,144,0
/home/ubuntu/TrainYourOwnYOLO/Data/Source_Images/Training_Images/vott-csv-export/9k_%20(2).jpg 59,6,174,126,0
/home/ubuntu/TrainYourOwnYOLO/Data/Source_Images/Training_Images/vott-csv-export/2Q_%20(1).jpg 27,15,107,87,0
/home/ubuntu/TrainYourOwnYOLO/Data/Source_Images/Training_Images/vott-csv-export/2Q_%20(2).jpg 87,2,197,124,0
/home/ubuntu/TrainYourOwnYOLO/Data/Source_Images/Training_Images/vott-csv-export/2Q_%20(3).jpg 3,1,106,103,0
/home/ubuntu/TrainYourOwnYOLO/Data/Source_Images/Training_Images/vott-csv-export/9k_%20(4).jpg 96,30,151,79,0
/home/ubuntu/TrainYourOwnYOLO/Data/Source_Images/Training_Images/vott-csv-export/9k_%20(5).jpg 135,4,266,131,0
/home/ubuntu/TrainYourOwnYOLO/Data/Source_Images/Training_Images/vott-csv-export/9k_%20(3).jpg 66,49,177,153,0
/home/ubuntu/TrainYourOwnYOLO/Data/Source_Images/Training_Images/vott-csv-export/9k_%20(6).jpg 145,55,213,129,0
/home/ubuntu/TrainYourOwnYOLO/Data/Source_Images/Training_Images/vott-csv-export/9k_%20(7).jpg 81,39,180,137,0 148,0,248,101,0
/home/ubuntu/TrainYourOwnYOLO/Data/Source_Images/Training_Images/vott-csv-export/9k_%20(1).jpg 46,4,143,100,0
/home/ubuntu/TrainYourOwnYOLO/Data/Source_Images/Training_Images/vott-csv-export/2%20(2).jpg 187,0,269,70,0
/home/ubuntu/TrainYourOwnYOLO/Data/Source_Images/Training_Images/vott-csv-export/2%20(3).jpg 13,0,247,170,0
/home/ubuntu/TrainYourOwnYOLO/Data/Source_Images/Training_Images/vott-csv-export/2%20(4).jpg 80,58,185,172,0
/home/ubuntu/TrainYourOwnYOLO/Data/Source_Images/Training_Images/vott-csv-export/9k_%20(7).jpg 46,4,143,100,0
/home/ubuntu/TrainYourOwnYOLO/Data/Source_Images/Training_Images/vott-csv-export/Z.jpg 117,22,235,127,0 6,84,104,100,0
/home/ubuntu/TrainYourOwnYOLO/Data/Source_Images/Training_Images/vott-csv-export/images%20(1).jpg 9,9,195,169,0
/home/ubuntu/TrainYourOwnYOLO/Data/Source_Images/Training_Images/vott-csv-export/images%20(10).jpg 56,23,119,82,0
/home/ubuntu/TrainYourOwnYOLO/Data/Source_Images/Training_Images/vott-csv-export/images%20(100).jpg 109,86,154,124,0
```

Fig. 6: data_train.txt

This script generates two output txt files: data_train.txt and data_classes.txt. The data_train file is shown in figure 6 and the data_classes.txt contains the class of the recognizable images which, in our project, is the staircase.

b) Step 2: Training

By means of the training images and the annotation file data_train.txt which we have created in the earlier step we now train our YOLOv3 detector. Before this we download the pre-trained YOLOv3 weights and convert them to keras format. These weights are pre-trained under ImageNet 1000 dataset and thus work quite well for object detection that are very similar to the images and objects in the ImageNet 1000 dataset. The final weights are saved in Model_weights.

c) Step 3: Inference

In this step, we test our detector on staircase images located in Test_Images. The outputs are saved and stored into the Test_Image_Detection_Results. The outputs include the original images with bounding boxes and confidence scores as well as a file called Detection_Results.csv containing the image file paths and the bounding box coordinates.

C. Sequence Flow

When the device is ON, the Raspberry Pi runs the scheduled processes. Once the Ultrasonic sensor detects the object that is in its range, it activates the vibrator through the Raspberry Pi. A similar process takes place when the moisture sensor comes in contact with water; it activates the buzzer through the processor. When the Pi camera captures an image, it stores the image. Based on the parameters and trained model sets, the image is processed by yolov3 and if the staircase is detected, it sends the feedback to the processor which then activates a voice message stating the obstacle that is detected.

When the Button 1 on the Smart Band is pressed, it activates the buzzer through Radio frequency transmission. When the Button 2 on the Smart Band is pressed, it initiates the GPS module to send location via IoT back to the NodeMCU which then sends that location with an alert message to the application of the contacts having the Blynk application.

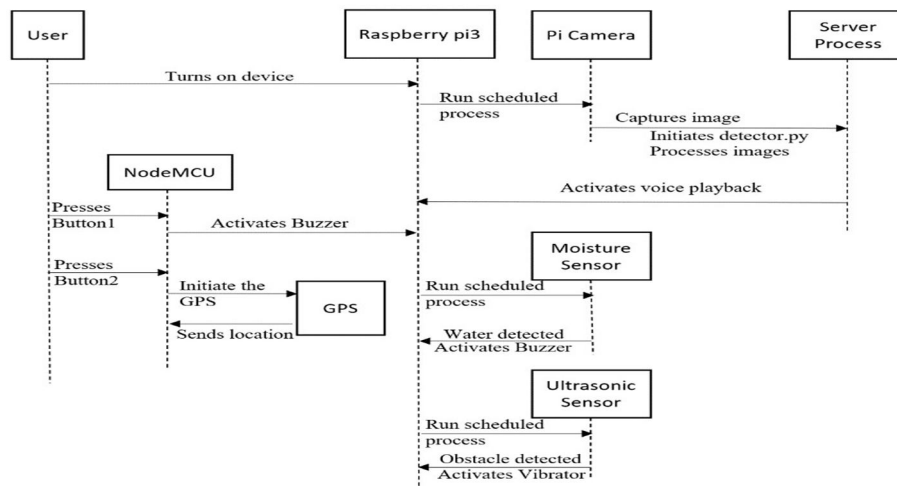


Fig. 7: Sequence Flow of Raspberry Pi and NodeMCU

V. RESULTS

The Smart E – Cane and Smart Band devices are powered on when a power source of 9V or more is provided to them. In order to initiate the working of Smart E – Cane and to view the output from various sensors along with the status of output devices they are connected to, we execute the run command in the terminal window of Raspberry Pi.

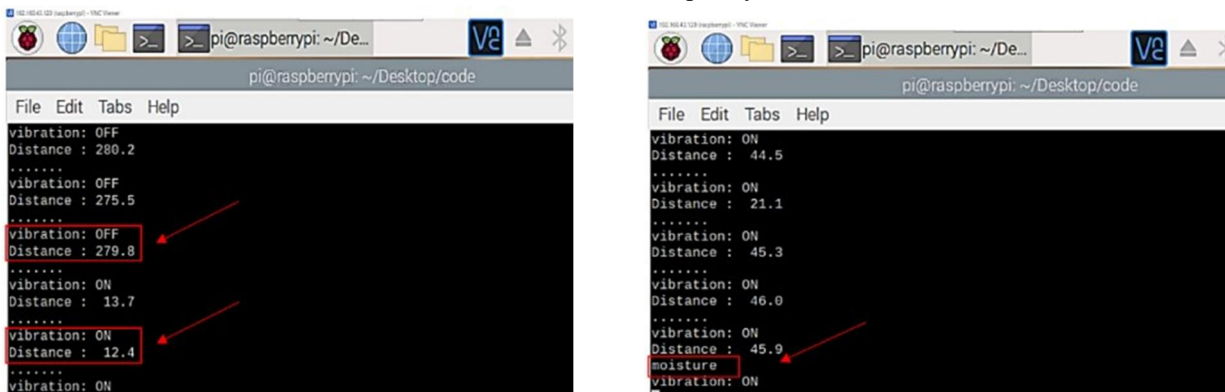


Fig. 8: (Left) Output of Ultrasonic sensor showing distance from object with vibrator status. (Right) Output on command prompt showing water detected by moisture sensor

When Button 1 on the Smart Band is pressed to locate the Smart E – Cane, the receiver on the Smart E – Cane receives the signal from the transmitter on the Smart Band and activates the buzzer on the Smart E – Cane. This is depicted in figure 9.

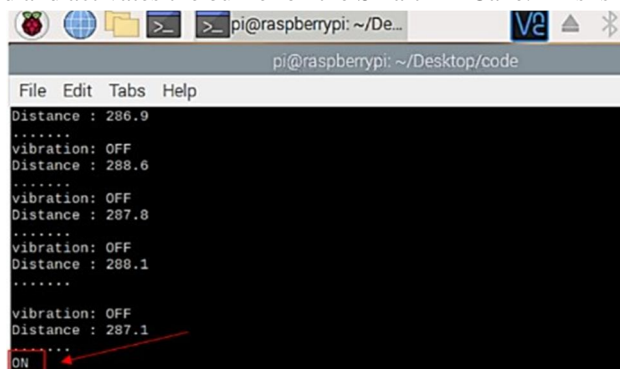


Fig. 9: Button 1 on Smart Band pressed, activating buzzer on Smart E – Cane

When the Button 2 on the Smart Band is pressed, the GPS module obtains and sends the location to the NodeMCU which then sends it to the Blynk app, which alerts the respective contact of the user. When the button isn't pressed, the status is left blank as shown in figure 10.

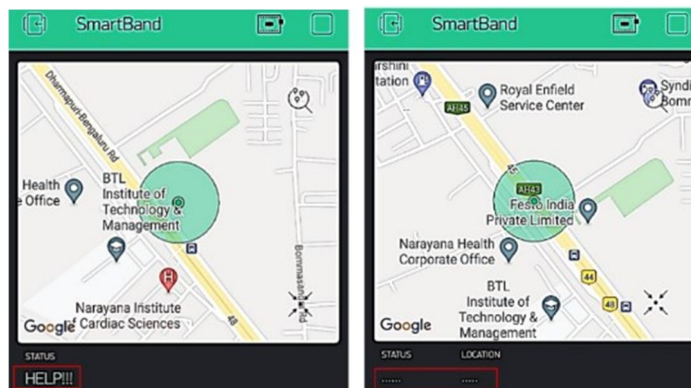


Fig. 10: (Left) Location of user with alert notification on Blynk app of the emergency contact. (Right) Location of the user with blank status on Blynk app

When the user comes in front of an obstacle such as the staircase, the processor detects it and produces an output as shown in figure 11. A voice message alerts the user if the staircase is detected. We have used YOLOv3 object detection algorithm in our project to detect staircase. YOLOv3 produces a confidence score beside the object class when detecting an image. The score is a number between 0 and 1 that indicates confidence that the object was genuinely detected [24]. The closer the number is to 1, the more confident the model is. In our staircase detector model, we have defined cut-off threshold level as 0.25. In that case, we would ignore the remaining objects because those confidence scores are below 0.25.

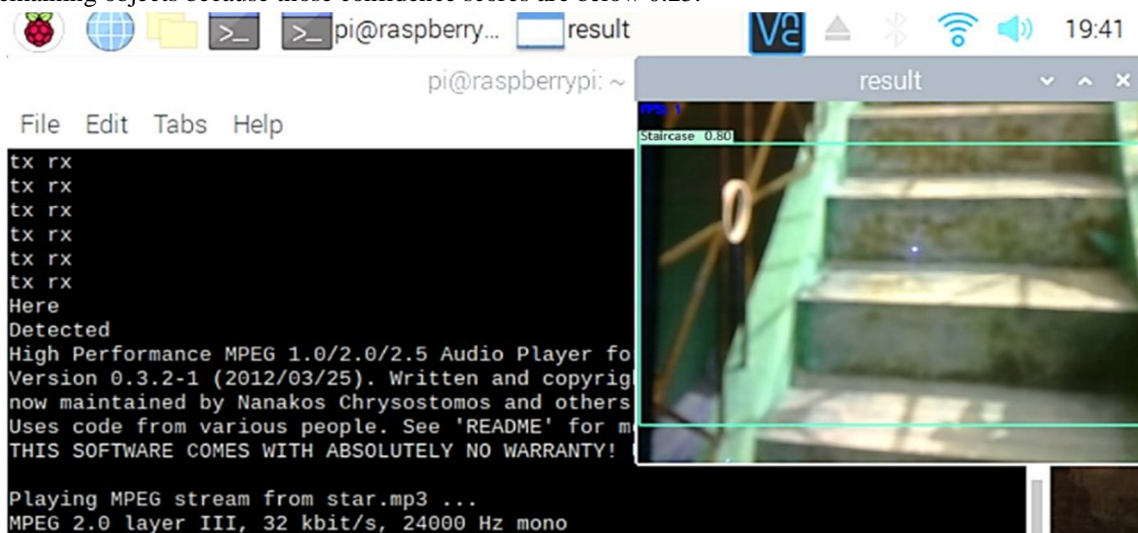


Fig. 11: Staircase detection with a confidence score of 0.80 or 80%.

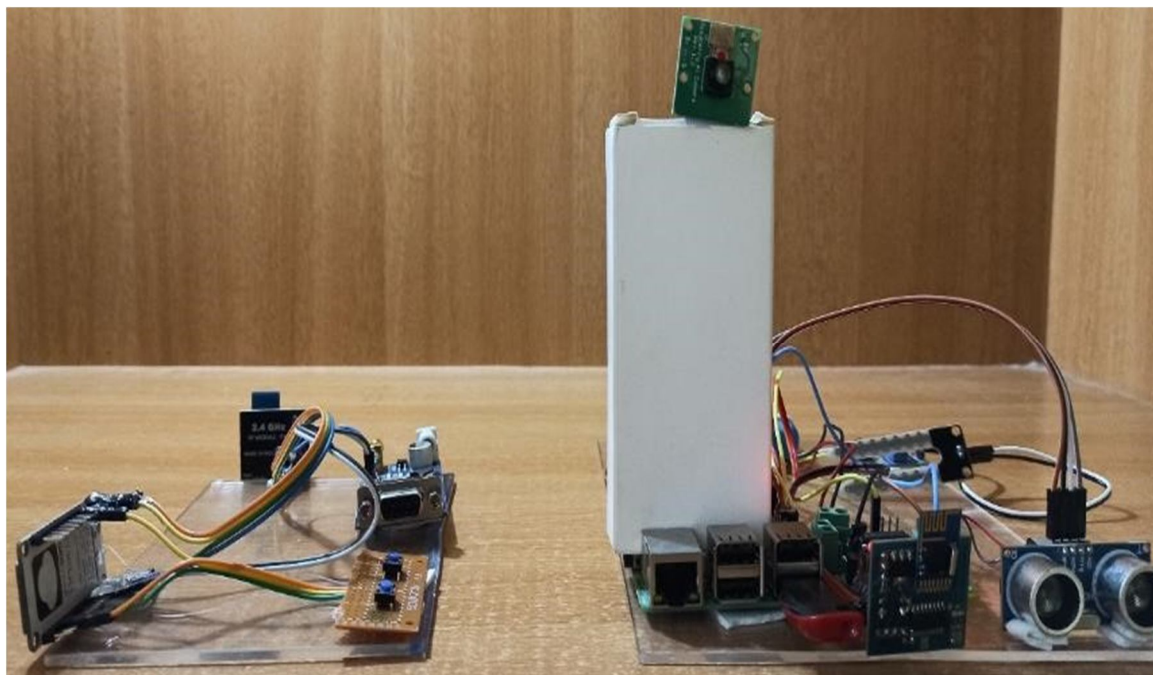


Fig. 12: Prototype model of Voice Assisted Smart E-Cane for the Visually Challenged Using Machine Learning

VI. CONCLUSIONS

Voice Assisted Smart E-Cane for the Visually Challenged Using Machine Learning, this prototype model is a great electronic aid for the visually challenged and the blind. It not only alerts the user if the obstacle is detected but also provides security for the user. The Smart E-Cane with Raspberry Pi microprocessor detects the obstacles using ultrasonic sensors and alerts the user by vibrator motor. Intensity of the vibrations depends on how far the obstacle is located, if the obstacle is far the intensity is low otherwise the intensity is high.

The Smart E-Cane detects the water in the surrounding using moisture sensor and alerts the user by buzzer sound. Most important feature is the detection of staircase and it is done using Deep Learning and Neural Network concepts, where it uses YOLOv3 the latest, popular object detection algorithm. If the staircase is detected the voice playback saying “STAIRCASE FOUND” is played.

VII. FUTURE SCOPE

Our prototype model can further be powered by solar cells instead of Li-ion battery as they have to be replaced often. Can establish wireless communication between the components to achieve the compactness of the system. As the prototype model only detects staircase, further it can be trained to detect other elevated surfaces like ladder, an inclined plane, ramp etc. To increase the processing speed and to reduce the delay occurred, one can go with GPU (Graphical Processing Unit) or high-speed processors. Moreover, earphones can be made use for the better clarity of the voice playback and to speak to the concerned person at any location.

REFERENCES

- [1] Omkar Masurekar, Omkar Jadhav, Prateek Kulkarni, Shubham Patil, “Real Time Object Detection Using YOLOv3”, 2020, International Research Journal of Engineering and Technology (IRJET) e-ISSN: 2395-0056. Volume: 07 Issue: 03, Mar 2020.
- [2] Habib, A., Islam, M.M., Kabir, M.N., Mredul, M.B., Hasan, M. (2019). “Staircase detection to guide visually impaired people: A hybrid approach”, *Revue d'Intelligence Artificielle*, Vol. 33, No. 5, pp. 327-334. Accessible at: <https://doi.org/10.18280/ria.33050>.
- [3] Mohamedarif Regade, S Bibi Ayesha Khazi, Sushmita Sunkad, Mrityunjay C.K, Sharda K.S, “Smart Stick for Blind using Machine Learning”, 2019, International Journal of Innovative Science and Research Technology ISSN No: 2456-2165, Volume 4, Issue 5. May 2019.
- [4] Dimitra P. Marini, BSc THESIS: “Electronic Smart Canes for Visually Impaired People”, 2018, National and kapodistrian university of athens school of science department of informatics and telecommunication. Athens.
- [5] Saurav Mohapatra, Subham Rout, Varun Tripathi, Tanish Saxena, Yepuganti Karuna, “Smart Walking Stick for Blind integrated with SOS Navigation System”, 2018, Proceedings of the 2nd International Conference on Trends in Electronics and Informatics (ICOEI 2018) IEEE Conference Record: # 42666, IEEE Xplore ISBN:978-1-5386-3570-4.
- [6] Kunja Bihari Swain, Rakesh Kumar Patnaik, Suchandra Pal, Raja Rajeswari, Aparna Mishra and Charusmita Dash, “Arduino based Automatic Stick Guide for a Visually Impaired Person”, 2017, IEEE International conference on smart technologies and management for computing, communication, controls, energy and materials (ICSTM) 4 August 2017, Veltch Dr. RR & Dr. SR university, Chennai, TN, India.
- [7] Akhilesh Krishnan, Deepakraj G, Nishanth N, Dr.K.M.Anandkumar, “Autonomous Walking Stick For The Blind Using Echolocation And Image Processing”, 2016, 2nd International Conference on Contemporary Computing and Informatics.
- [8] S. Murali, R. Shrivatsan, V. Sreenivas, S. Vijjappu, S. J. Gladwin and R. Rajavel, “Smart walking cane for the visually challenged”, 2016 IEEE Region 10 Humanitarian Technology Conference (R10-HTC), Agra, 2016, pp. 1-4, doi: 10.1109/R10-HTC.2016.7906791.
- [9] Alejandro R. Garcia Ramirez, Renato Fonseca Livramento da Silva, Milton Jose Cinelli, Alejandro Durán Carrillo de Albornoz, “Evaluation of Electronic Haptic Device for Blind and Visually Impaired People: A Case Study”, 2015, *Journal of Medical and Biological Engineering* 2015, 32(6): 423-428.
- [10] Mohammad Hazzaz Mahmud, Rana Saha, Sayemul Islam, “Smart walking stick - an electronic approach to assist visually disabled persons”, 2013, International Journal of Scientific & Engineering Research, Volume 4, Issue 10, ISSN 2229-5518, October 2013.
- [11] S.Koley and R. Mishra, “Voice Operated Outdoor Navigation System for Visually Impaired Persons”, 2012, International journal of engineering trends and technology, Vol.3 Issue 2.
- [12] Farnel, Newark, element14, “Raspberry Pi 3 Model B”, URL: <https://us04web.zoom.us/j/71160940605?pwd=ZEZUeTFNcG1naHA3ZjRvWmlEV3dGdG09>, Retrieved on 04/05/2020.
- [13] Components 101, “Pi Camera Module – 5MP”, URL: <https://components101.com/misc/Pi-camera-module>, Published on 09/12/2018, Retrieved on 04/05/2020.
- [14] Proto Supplies, “ESP8266 NodeMCU V1.0 ESP-12E Wi-Fi Module”, URL: <https://protosupplies.com/product/esp8266-nodemcu-v1-0-esp-12e-wifi-module/>, Retrieved on 06/05/2020.
- [15] Amy Unruh, “What is the TensorFlow machine intelligence platform?”, OpenSource, 09 Nov 2017. Available at: <https://opensource.com/article/17/11/intro-tensorflow>. Accessed on 06/05/2020.
- [16] Redmon, Joseph and Farhadi, Ali, “YOLOv3: An Incremental Improvement”, *yolov3*, arXiv, 2018. URL: <https://pjreddie.com/darknet/yolo/>. Accessed on 06/05/2020.
- [17] Lucy, “How does VNC technology work?”, RealVNC, August 23, 2019. Available at: <https://help.realvnc.com/hc/en-us/articles/360002320638-How-does-VNC-technology-work->, Accessed on 07/05/2020.
- [18] Tegan, “Understanding VNC Server Modes”, RealVNC, August 15, 2019. Available at: <https://help.realvnc.com/hc/en-us/articles/360002253238-Understanding-VNC-Server-Modes>, Accessed on 12/05/2020.
- [19] diycode, “VoTT”, diycode, Available at: <https://www.diycode.cc/projects/Microsoft/VoTT>, Accessed on 20/05/2020.
- [20] tutorialspoint, “Python 3 Tutorial”, tutorialspoint, Available at: <https://www.tutorialspoint.com/python3/index.htm>, Accessed on: 22/05/2020.
- [21] Raspberry Pi foundation, “Raspberry Pi OS”, Raspberry Pi organisation, Available at: <https://www.raspberrypi.org/documentation/raspbian/>, Accessed on 01/06/2020.
- [22] Wikipedia, “Keras”, Wikipedia, the free encyclopedia, Accessible by URL: <https://en.wikipedia.org/wiki/Keras#:~:text=Keras%20is%20an%20open%2Dsource,friendly%2C%20modular%2C%20and%20extensible>, Accessed on 08/06/2020.
- [23] OpenCV Team, “About OpenCV”, OpenCV, Accessible at URL: <https://opencv.org/about/>, Accessed at 08/06/2020.



- [24] TensorFlow, “*Object Detection*”, For Mobile and IoT, TensorFlow, 04/06/2020. Available at: https://www.tensorflow.org/lite/models/object_detection/overview, Accessed on: 08/06/2020.
- [25] Joseph Redmon, Ali Farhadi, “*YOLOv3: An Incremental Improvement*”, University of Washington, Accessible at: <https://pjreddie.com/media/files/papers/YOLOv3.pdf>
- [26] Pierre Nicolas Durette, “*gTTS*”, Built with Sphinx using a theme provided by Read the Docs, Accessible at: <https://gtts.readthedocs.io/en/latest/>. Accessed on 22/06/2020.
- [27] Ayoosh Kathuria, “*What’s new in YOLO v3?*”, Towards Data Science, A Medium publication sharing concepts, ideas, and codes. Available at: <https://towardsdatascience.com/yolo-v3-object-detection-53fb7d3bfe6b>, Accessed on 22/06/2020.



10.22214/IJRASET



45.98



IMPACT FACTOR:
7.129



IMPACT FACTOR:
7.429



INTERNATIONAL JOURNAL FOR RESEARCH

IN APPLIED SCIENCE & ENGINEERING TECHNOLOGY

Call : 08813907089  (24*7 Support on Whatsapp)



Corpus ID: 221081556

Share This Paper

Dry Sliding Wear Behavior of B4C Particulates Reinforced Al7020 Alloy Composites

[R. Prakash](#), [R. Saravanan](#) · Published 2019

The work is carried out to investigate the dry sliding wear behavior of B4C reinforced Al7020 alloy metal matrix composites. In the present work Al7020 alloy was taken as the base matrix and B4C particulates as reinforcement material to prepare metal matrix composites by stir casting method. For metal matrix composites the reinforcement material was varied from 0 to 4 wt. % in steps of 2 wt. %. The wear resistance of metal matrix composites was studied by performing dry sliding wear test using a pin on disc apparatus. The experiments were conducted at a constant sliding speed of 300rpm and sliding distance of 4000m over a varying load of 1, 2 and 3Kg. Similarly, experiments were conducted at a constant load of 3Kg and sliding distance of 4000m over a varying sliding speed of 200, 300 and 400rpm. The results showed that the wear resistance of Al7020-2% B4C and 4% B4C composites were better than the unreinforced alloy. The wear in terms of height loss found to increase with the load and sliding speed. To study the dominant sliding wear mechanism for various test conditions, the worn surfaces were analyzed using scanning electron microscopy. [Collapse](#)

[PDF](#) [ripublication.com](#)

Save

Alert

Feed

[Abstract](#)

[Figures](#)

By clicking accept or continuing to use the site, you agree to the terms outlined in our [Privacy Policy](#), [Terms of Service](#), and [Dataset License](#)

ACCEPT & CONTINUE

Influence of Nickel Coated B₄C particulates Addition on the Mechanical Characterization of Al7020 Alloy Composites

Raviprakash M^{1*}, R Saravanan²

¹Research Scholar, Department of Mechanical Engineering, UVCE, Bangalore-560001, Karnataka, India

²Assistant Professor, Department of Mechanical Engineering, UVCE, Bangalore-560001, Karnataka, India

*Corresponding Author : Raviprakash M

ABSTRACT: In the present work investigations have been made on effect of nickel coated B₄C particulates addition on the tensile behavior of Al7020 alloy. Nickel coating on the B₄C particles was done by using electroless coating method. Composites were prepared by using liquid melt method, 6 and 8 wt.% of B₄C particulates were used to fabricate the Al7020 alloy composites. Samples were tested for microstructural characterization by using scanning electron microscope and X-Ray diffraction. Mechanical behaviors like hardness, ultimate tensile strength, yield strength and percentage elongation were evaluated as per ASTM standards. Scanning electron micro photographs revealed the uniform distribution of nickel coated B₄C particulates in the Al7020 alloy and confirmed XRD patterns. Further, hardness and tensile properties of base matrix Al7020 alloy was enhanced with the addition of B₄C particulates and ductility was slightly reduced. Fractography study was conducted on the tensile fractured specimens.

Keywords: Al7020 Alloy, Nickel Coated B₄C particulates, Microstructure, Hardness, Tensile Strength, Fractography

Date of Submission: 07-05-2019

Date of acceptance: 24-05-2019

I. INTRODUCTION

Aluminum matrix composites are under consideration in aerospace, automotive and military industries, because of their low weight, high strength and excellent abrasion resistance [1]. Stir casting is a preferred method for fabrication of aluminum matrix composites due to its low cost, simplicity, flexibility and capability of mass production. However, this method has always been accompanied by the formation of lots of structural defects in composite materials. Poor wettability and nonuniform distribution of reinforcing particles, segregation and agglomeration of the reinforcement particles in the matrix, weak matrix-reinforcement interface and presence of porosity and destructive phases are some important structural defects of stir casted composites [2].

Poor wettability of reinforcements in the melt means that the molten matrix cannot wet the surface of reinforcement particles. Therefore, when the reinforcement particles are added into the molten matrix, they float on the melt surface [3, 4]. Poor wettability of reinforcing particles in the molten metal could be a cause of oxide films on the melt surface or presence of a gas layer on the ceramic particles surface. More importantly, very large specific surface area and increased surface energy during combining two different phases lead to reducing the wettability of ceramic particles within the molten matrix [5].

Various techniques are used for increasing the wettability of reinforcing ceramic particles in molten metal. Modification of surface oxide layer on the molten metal by addition of some alloying elements such as magnesium and calcium and heat-treating the particles for desorption of gases adsorbed on the particles are appropriate techniques for improving the reinforcement's wettability [6]. Metal coating of the reinforcement particles is known as the most favorite techniques for improving the ceramic particulates wettability through modification of surface tension. A considerable focus of studies on fabrication of metal matrix composites using coated reinforcing particles were carried out in recent years. In this study, nickel coating of B₄C reinforcement particles is considered for successful fabrication of aluminum matrix composites, free of any structural defects.

Coatings enhance the mechanical and tribological properties of the base material. Electroless Ni coating is one of the popular techniques used in scientific as well as in industrial domains [7, 8]. Recently the electroless coatings have gained wide popularity in automobile, chemical, mechanical, and aerospace industries due to its ability to produce hard, wear resistant, friction resistant, and corrosion resistant surface. Completely new material concepts are successfully used, especially for coatings, to implement key optimizations of properties often with reduced material consumption, with low technical effort, and at low process costs. The electroless

deposition of metallic nickel from aqueous solution in the presence of hypophosphite was first noted as a chemical accident by Wurtz in 1844 (Mallory and Hajdu 1990). Electroless plating is an autocatalytic process, where the substrate develops a potential when it is dipped in electroless solution called electroless bath, which contains a source of metallic ions, reducing agent, complexing agent, stabilizer, additives, and wetting agents etc.

The present study is to synthesize Al7020-B₄C particulate MMC using stir casting method, by taking uncoated and nickel coated B₄C particulates as the reinforcement material. In order to improve wettability and distribution of reinforcing particles a novel two stage mixing combined with preheating of the reinforcing particles is being adopted and the as cast Al7020 and 6 and 8wt. % of B₄C particulates of the prepared composites were subjected to metallographic studies, hardness and tensile behavior as per ASTM standards.

II. EXPERIMENTAL DETAILS

Materials Used

In the present study Al7020 is used as the matrix material, most of the applications in areas such as aerospace, automobile, marine make use of 7xxx series, aluminium zinc series alloys. Al7020 normally has 5% zinc. The theoretical density of Al7020 is taken as 2.84 g/cm³.

Table 1: Chemical composition of Al7020 Alloy

| Element | Si | Cu | Mg | Mn | Fe | Zn | Cr | Al |
|---------|------|-----|-----|------|------|-----|------|---------|
| Wt. (%) | 0.35 | 0.2 | 1.2 | 0.50 | 0.40 | 5.0 | 0.30 | Balance |

In the present work, micro B₄C particulates are used as the reinforcement materials, 80 to 90 micron particulates were used procured from Speedfam Ltd., Chennai. The density of boron carbide is lesser than the matrix material, which is 2.52 g/cm³.

III. METHODOLOGY

In the present study B₄C particulates were used as the reinforcement particles. These B₄C particles were coated by nickel by using the electroless coating process to enhance the wettability between the matrix and the reinforcement. The fabrication of Al7020-B₄C composites were carried out by liquid metallurgy route via stir casting technique. Calculated amount of the Al7020 alloy ingots are charged into the furnace for melting. The melting point of aluminium alloy is 660 °C. The melt superheated to a temperature of 730°C. The temperature was recorded using achrome-alumel thermocouple. The molten metal is then degassed using solid hexachloroethane (C₂Cl₆) for 3 min. A stainless-steel impeller coated with zirconium is used to stir the molten metal to create a vortex. The stirrer will be rotated at a speed of 300rpm and the depth of immersion of the impeller was 60 percent of the height of the molten metal from the surface of the melt. Further, the nickel coated B₄C particulates were preheated in a furnace upto 500 °C will be introduced into the vortex. Stirring is continued until interface interactions between the reinforcement particulates and the matrix promotes wetting. Then, Al7020- 6wt. % B₄C mixture was poured into permanent cast iron mold having dimensions 120mm length and 15mm diameter. Similarly, composites are prepared for 8weight percentage of nickel coated B₄C particles reinforced composites.

Evaluation of Properties

The castings thus obtained were cut to appropriate size of 15 mm diameter and 5 mm thickness which is then subjected to different levels of polishing to get required sample piece for microstructure study. Initially, the sliced samples were polished with emery paper upto 1000grit size followed by polishing with Al₂O₃ suspension on apolishing disc using velvet cloth. This was followed by polishing with 0.3 microns diamond paste. The polished surface of the samples etched with Keller's reagent and finally subjected to microstructure study under the scanning electron microscope.

Hardness test was conducted by using Brinell hardness testing machine as per ASTM E10 standard. The tensile study was carried out on the cut specimens as per ASTM E8 [9] standards using Electronic Universal Testing machine at room temperature to study properties like tensile strength, yield stress and percentage of elongation.

IV. RESULTS AND DISCUSSION

Microstructural Study

Figure 1a and b-c shows the SEM micrographs of as cast alloy Al7020 and the composites of 6 and 8 wt. % of nickel coated B₄C reinforced with Al7020 alloy composites. These two examined samples were chosen from the middle segment from the cylindrical specimens. The microstructure of as cast Al7020 alloy comprises of fine grains of aluminium solid solution with an enough dispersion of inter-metallic precipitates.

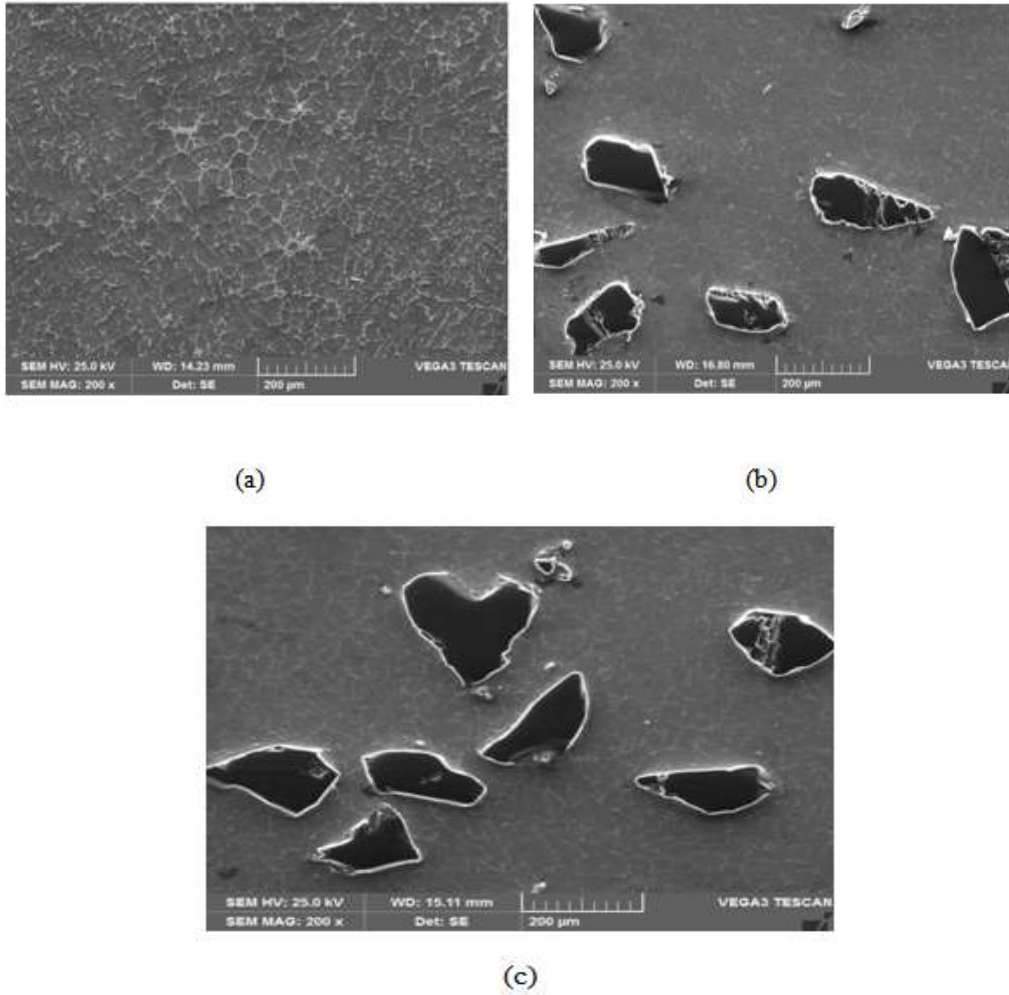


Fig. 1 Scanning electron micrographs of (a) as cast Al7020 alloy (b) Al7020-6 wt. % Nickel coated B₄C (c) Al7020-8 wt.% Nickel coated B₄C particles reinforced composites

The strong interfacial bonding between the Al7020 alloy and B₄C particulates obtained due to the addition of nickel coated B₄C particles. Fig. 1b-c represents the SEM micrographs of 6 and 8 wt. % nickel coated B₄C particulates reinforced composites. From the micrographs, it is revealed that the composites are free from pores and other surface damages. Nickel coated particles are uniformly distributed all over the Al7020 alloy matrix. This is mainly due to the enhanced wettability of the B₄C particulates due to the nickel coating.

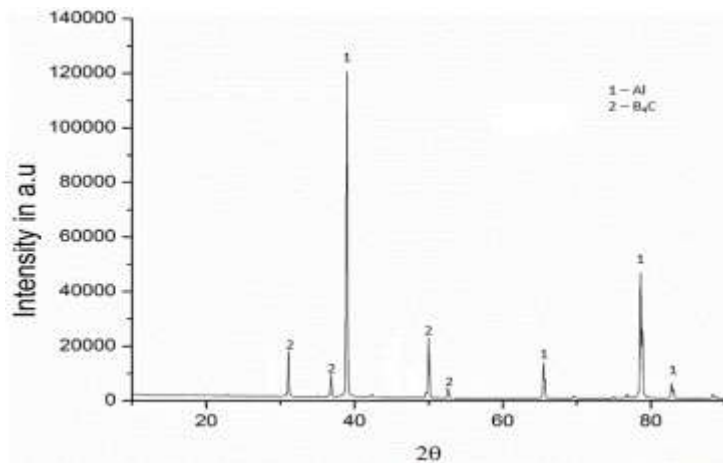


Fig.2: X-ray diffraction pattern of Al7020-8 wt.% of Nickel coated B₄C particles reinforced composites

Fig. 2 shows the X-ray diffraction (XRD) pattern taken for Al7020 alloy with 8 wt.% of B₄C particulates reinforced composites. It can be observed that peak height increases and then decreases on 2-theta scale indicating the presence of different phases of material. In fig. 2 it is visible that X-ray intensities of peak are higher at 38°, 65°, 78° & 83° indicating the presence of aluminium phase. Similarly, B₄C particulates phases are identified at 31°, 37°, 50° and 53°.

Hardness Measurements

From the fig.3, it is observed that there is an increase in the hardness of Al7020 with addition of 6 and 8wt % of nickel coated B₄C particulates addition. The graph shows the variation of hardness of Al7020 alloy with B₄C reinforcement particulate. It can be concluded that the addition of wt. % of B₄C particulate results in increasing the hardness. The hardness of a soft material such as Aluminum matrix is increased when it is reinforced with a hard particulate i.e., B₄C [10, 11].

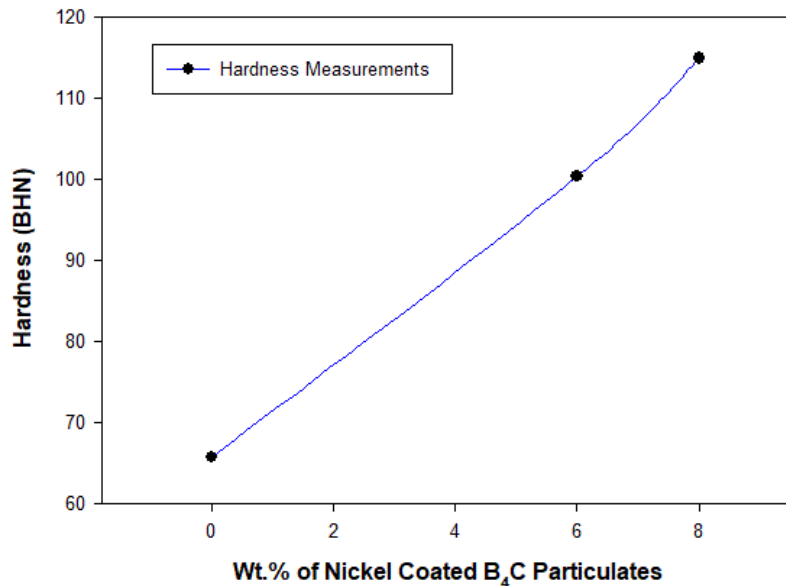
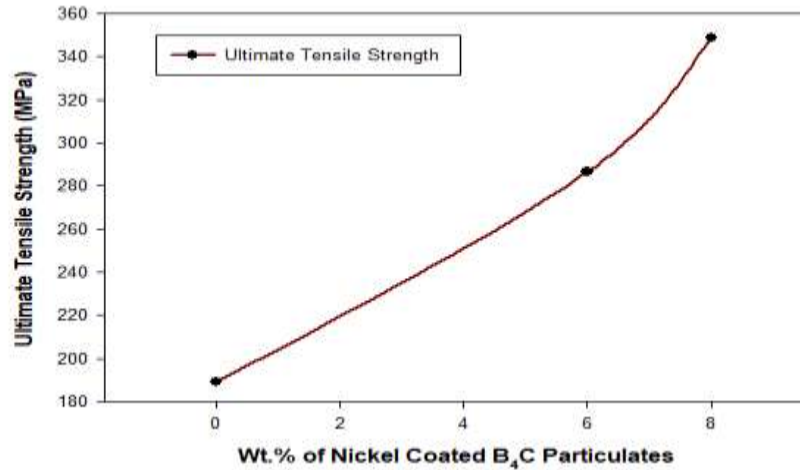


Fig. 3: Hardness measurements of Al7020-6 and 8 wt.% of Nickel coated B₄C composites

Ultimate Tensile Strength

Fig.4 shows the variation of ultimate tensile strength (UTS) of base alloy, when reinforced with 6 and 8 wt. % of nickel coated B₄C particulates. The ultimate tensile strength of Al7020- B₄C composite material increases as compared to the cast base Al7020 alloy. The microstructure and properties of hard ceramic B₄C particulates control the deformation of the composites. Due to the strong interface bonding, load from the matrix transfers to the reinforcement resulting in increased ultimate tensile strength. This increase in ultimate tensile strength mainly is due to presence of B₄C particles which are acting as barrier to dislocations in the microstructure [12]. The improvement in ultimate tensile strength may also be due to alloy strengthening of the matrix, followed with a reduction in grain size of the composites, and the formation of a high dislocation density in the Al7020 alloy matrix due to the difference in the thermal expansion between the metal matrix and the B₄C reinforcement. Further, the enhanced strength is mainly due to the addition of nickel coated B₄C particulates, which created the strong interfacial bonding between the Al7020 alloy and the 90 micron size nickel coated B₄C particles.

Fig. 4: Showing the ultimate tensile strength of Al7020 alloy-6 and 8 wt.% of nickel coated B₄C composites



Yield Strength

Fig.5 shows variation of yield strength (YS) of Al7020 alloy matrix with 6 and 8 wt. % of micro B_4C particulate reinforced composite. By adding 6 and 8 wt. % of nickel coated B_4C particulates yield strength of the Al alloy increased from 162.80 MPa to 241.7MPa and 291.25 MPa respectively. This increase in yield strength is in agreement with the results obtained by several researchers, who have reported that the strength of the particle reinforced composites is highly dependent on the volume fraction of the reinforcement. The increase in YS of the composite is obviously due to presence of hard nickel coated B_4C particles which impart strength to the soft aluminum matrix resulting in greater resistance of the composite against the applied tensile load [13]. In the case of particle reinforced composites, the dispersed hard particles in the matrix create restriction to the plastic flow, thereby providing enhanced strength to the composite [14].

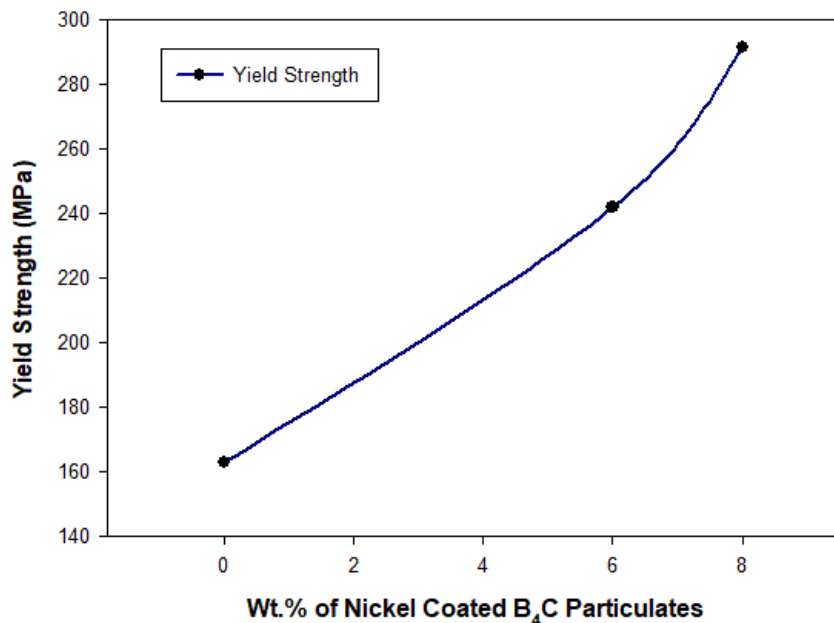


Fig. 5: Showing the yield strength of Al7020 alloy-6 and 8 wt.% of nickel coated B_4C composites

Percentage Elongation

Fig. 6 demonstrating the impact of micro B_4C content on the elongation (ductility) of the composites. It can be seen from the chart that the flexibility of the composites diminish essentially with the 6 and 8 wt. % B_4C fortified composites. This diminishing in rate prolongation in correlation with the base amalgam is a most usually happening detriment in particulate fortified metal lattice composites [15]. The lessened pliability in composites can be ascribed to the nearness of B_4C particulates which may get broke and have sharp corners that make the composites inclined to restricted split start and proliferation [16].

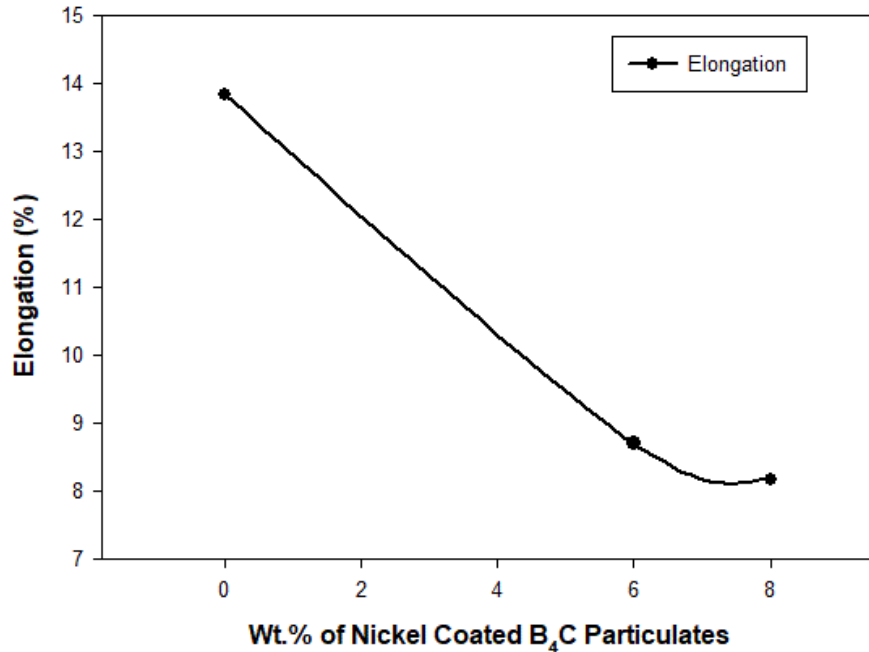


Fig. 6 Showing the percentage elongation of Al7020 alloy-6 and 8 wt.% nickel coated B₄C particulates reinforced composites

Fracture Studies

Fracture mechanisms of as cast alloy and composite samples after tensile testing were studied by using SEM images of fracture surfaces (figure 7a-c). The as cast Al7020 alloy fracture mode is a ductile fracture mode as shown in figure 7-a, which has large number of dimple shaped structures, no crack can be seen.

Figure 7b and 7c shows that 6 and 8 wt. % B₄C reinforced MMCs fracture structures have less ductile failure. During tensile test it is accepted that particle cracking along with matrix material fracture, de-bonding between the alumina particles and Al matrix alloy interface are some of the reasons for failure MMCs. Small voids observed in the case of 8 wt. % B₄C composites, fractured surfaces showed local stresses at the interfaces is more and so crack at reinforcement particles mechanism is observed.

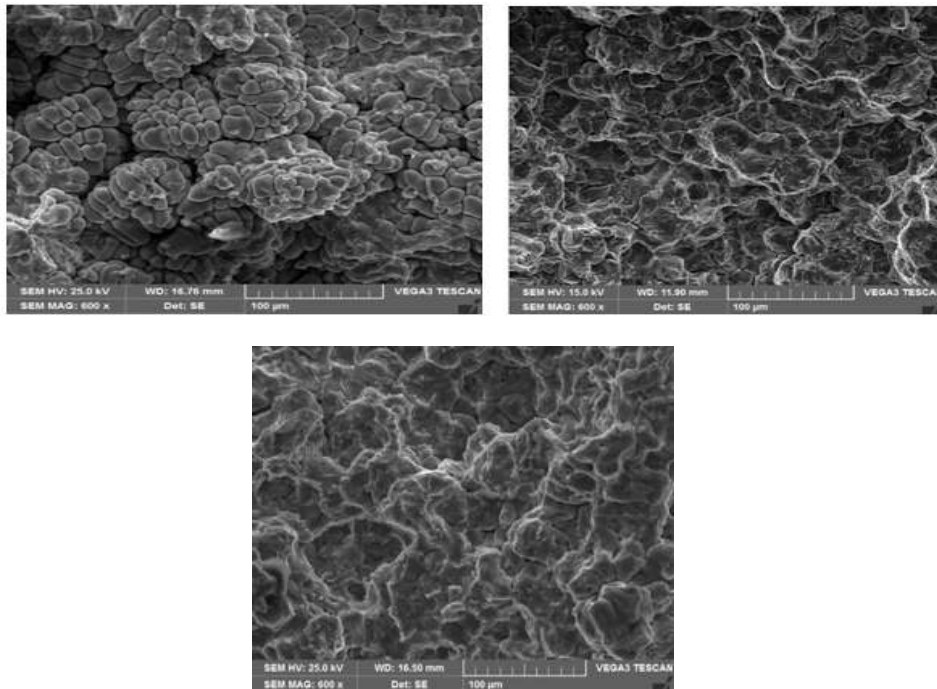


Fig. 7:Showing the SEM micrographs of tensile fractured surfaces of (a) as cast Al7020 alloy (b) Al7020-6 wt.% of Nickel coated B₄C (c) Al7020-8 wt.% of Nickel coated B₄C particulates reinforced composites

V. CONCLUSIONS

In this research, Al7020 alloy with 6 and 8 weight % of nickel coated B₄C particles reinforced composites have been fabricated by stir casting method. The microstructure, ultimate tensile strength, yield strength, percentage elongation and fractography of prepared samples are studied. The matrix is almost pore free and uniform distribution of micro particles, which is evident from SEM microphotographs. The XRD analysis confirms the presence of B₄C particles in the Al alloy matrix. The hardness and tensile properties of Al7020-6 and 8 wt. % nickel coated B₄C composites are superior to those of unreinforced material. There was slight decrease in the ductility of the composites as compared to the base Al7020 alloy matrix. The fracture surface of the composite material consists of voids which formed by the strain localization. These voids were then coalesced during tensile loading, resulting in the formation of dimple appearance at the fracture surface.

REFERENCES

- [1]. N. G. Siddesh Kumar, G. S. Shivashankar, S. Basavarajappa, R. Suresh, "Some studies on mechanical and machining characteristics of Al2219/n-B₄C/MoS₂ nano hybrid metal matrix composites", *Measurement*, 107, 2017, pp. 1-11.
- [2]. Sathyashankara Sharma, AchutaKini, Gowri Shankar, T. C. Rakesh, H. Raja, "Tensile fractography of artificially aged Al6061-B₄C composites", *Journal of Mechanical Engineering and Sciences*, 12, 3, 2018, pp. 3866-3875.
- [3]. Bao Sarina, Tang Kia, K. Anne, Thorvald Engh, Merete Tangstad, "Wetting of pure aluminium on graphite, SiC and Al₂O₃ in aluminium filtration", *Transactions of Nonferrous Metals Society of China*, 22, 2012, pp. 1930-1938.
- [4]. A. Amouri, Sh. Kazemi, A. Momeni, M. Kazazi, "Microstructure and mechanical properties of Al/nano-micro SiC composites produced by stir casting technique", *Materials Science and Engineering A*, 674, 2016, pp. 569-578.
- [5]. B. F. Schultz, J. B. Ferguson, P. K. Rohatgi, "Microstructure and hardness of Al₂O₃ nanoparticle reinforced Al-Mg composites fabricated by reactive wetting and stir mixing", *Materials Science and Engineering A*, 530, 2011, pp. 87-97.
- [6]. H. Zhang, K. T. Ramesh, E.S.C. Chin, "Effects of interfacial bonding on the rate dependent response of metal matrix composites", *Acta Materialia*, 53, 2005, pp. 4687-4700.
- [7]. M. L. Ted Guo, Chi. Y. A. Tsao, "Tribological behavior of aluminiumSiC-nickel coated graphite hybrid composites", *Materials Science and Engineering A*, 333, 2002, pp. 134-145.
- [8]. Suhas, Jaimon Quadras, N. L. Vaishak, "Evaluation and characterization of tensile properties of short coated carbon fiber reinforced aluminium 7075 alloy metal matrix composites via liquid stir casting method", *Material Science Research India*, 13, 2, 2016, pp. 66-73.
- [9]. H. Zhang, M. W. Chen, K. T. Ramesh, J. Ye, J. M. Schoenung, E. S.C. Chin, "Tensile behavior and dynamic failure of aluminium 6092-B₄C composites", *Materials Science and Engineering A*, 433, 2006, pp. 70-82.
- [10]. Amir Pakdel, Agnieszka Witecka, Gauthier Rydzek, Dayangku Noorfazidah Awang Shri, Valeria Nicolosi, "A comprehensive analysis of extrusion behavior, microstructural evolution and mechanical properties of 6063 Al-B₄C composites produced by semisolid stir casting", *Materials Science and Engineering Materials A*, 2018.
- [11]. Dinesh Patidar, R. S. Rana, "Effect of B₄C reinforcement on the various properties of aluminium matrix composites: a survey paper", *Materials Today Proceedings*, 4, 2017, pp. 2981-2988.
- [12]. K. T. Akhil, Jerry Verghese, Arun Raphel, Frenosh Francis, "To study the cooling rate and influence of boron carbide on mechanical properties of aluminium LM13 matrix B₄C reinforced composites", *Materials Today Proceedings*, 4, 2017, pp. 7202-7207.
- [13]. Keshav Singh, R. S. Rana, Anjaney Pandey, "Fabrication and mechanical properties characterization of aluminium alloy LM24-B₄C composites", *Materials Today Proceedings*, 4, 2017, pp. 701-708.
- [14]. Madeva Nagal, Shivananda Kalgudi, Virupaxi Auradi, Shivaputrapa Kori, "Mechanical characterization of ceramic nano B₄C-Al2618 alloy composites synthesized by semi solid processing", *Transactions of the Indian Ceramic Society*, Vol.77, No.3, pp. 1-4, 2018.
- [15]. T H Manjunatha, Y Basavaraj, Madeva Nagal, V Venkataramana, "Investigations on mechanical behavior of Al7075-nano B₄C composites", *IOP Conf. Series: Materials Science and Engineering*, 376, 012091, 2018.
- [16]. Pankaj R Jadhav, B R Sridhar, Madeva Nagal, Jayasheel Harti, "Evaluation of mechanical properties of B₄C and graphite particulates reinforced A356 alloy hybrid composites", *Materials Today Proceedings*, 4, 9, pp. 9972-9976, 2017.

Raviprakash M" Influence of Nickel Coated B₄C particulates Addition on the Mechanical Characterization of Al7020 Alloy Composites" *International Journal of Computational Engineering Research (IJCER)*, vol. 09, no. 5, 2019, pp 12-18



Advanced Materials Manufacturing & Characterization

journal home page: www.ijammc-griet.com



Microstructure, Hardness and Tensile Behavior of Micro B₄C Reinforced Al7020 Alloy Composites

Raviprakash M^{1*}, R Saravanan², Madeva Nagara³

¹Research Scholar, Department of Mechanical Engineering, UVCE, Bangalore-560001, Karnataka, India

²Assistant Professor, Department of Mechanical Engineering, UVCE, Bangalore-560001, Karnataka, India

³Design Engineer, Aircraft Research and Design Centre, Hindustan Aeronautics Limited, Bangalore-560037, Karnataka, India

Abstract

Micro particulates reinforced metal matrix composites are well suited for large number of automotive and marine applications. In the current study, an investigation made on fabrication of B₄C reinforced Al7020 alloy composites and evaluation of properties. Al7020- B₄C composites were synthesized by melt stirring process. The weight percentage of B₄C particulates were varied in steps of 2 and 4 %. Microstructural characterization was carried out by using scanning electron microscope and energy dispersive spectroscope. Prepared composites were evaluated for hardness and tensile strength as per ASTM standards. Scanning electron micro photographs revealed the distribution of B₄C particulates in the Al matrix and were confirmed by EDX analysis. B₄C particulates reinforced composites were shown more enhanced properties as compared to A7020 alloy.

Keywords: Al7020 Alloy, B₄C particulates, Microstructure, Hardness, Tensile Strength

1. Introduction

Aluminium matrix composites AMCs have evolved as a potential materials to alternate conventional monolithic aluminium alloys in many applications owing to its high specific strength and stiffness, low density, low thermal expansion coefficient and high wear resistance [1]. AMCs are used in

numerous industries that are not limited to aerospace, automotive, defense, naval and electronic packaging.

For structural applications, the strength of aluminium is enhanced by alloying or reinforcing with ceramic particles. However, the strength obtained by alloying is limited to lower temperatures whereas the dispersion of inert hard particles helps in getting high strength not only at low temperature but also retaining it at high temperature. Several aluminium matrix composites have been developed for a wide range of applications with reinforcements of SiC, TiC, Al₂O₃ and B₄C [2]. Amongst these reinforcements, boron carbide is the lightest (density 2.52 g/cc) and the hardest material. B₄C is known to be neutron absorber and so the Al-B₄C composite is used as a nuclear fuel storage material. Also, due to its light weight and high wear resistance, this composite finds application as armour plates [3].

An important issue in the production of metal matrix composites is the chemical compatibility between the matrix and the reinforcement, particularly when using liquid metal processes [4, 5]. Casting of MMCs is an attractive processing method since it is relatively inexpensive and offers a wide selection of materials and processing conditions. But poor wetting

- Corresponding author Raviprakash M E-mail address: madev.nagaral@gmail.com
- Doi: <http://dx.doi.org/10.11127/ijammc2017.10.08> Copyright@GRIET Publications. All rights reserved.

between Al and B₄C below 1100°C means that it is difficult to produce Al-B₄C composites by mixing particles into the liquid phase. In order to enhance the wettability of ceramics and improve their incorporation behavior into Al melts, particles often heat treated or coated.

Therefore, K₂TiF₆ flux is used in order to increase the wetting between Al and B₄C and facilitate the incorporation of B₄C particles into molten aluminium. To avoid insufficient reaction phase at the interface and to lower the processing cost, no additional processes except the traditional casting methods were used in this study.

In this study, an attempt has been made to prepare Al7020 alloy composites by adding 2 & 4 wt. % of B₄C particulates into matrix by using a novel two stage reinforcement addition method. Further, the prepared Al7020 – B₄C composites were studied for hardness and tensile behavior.

EXPERIMENTAL DETAILS

Materials Used

Metal matrix composites containing 2 and 4 weight rates of B₄C particles were created by liquid metallurgy course. For the generation of MMCs, an Al7020 alloy was utilized as the framework material while B₄C were utilized as the fortifications. The theoretical density of grid material Al7020 amalgam is 2.80g/cm³ and support particulates B₄C is 2.52g/cm³. The chemical substance of Al7020 composite utilized as a part of the work is given in the table 1.

Table.1 Shows the chemical composition of the Al7020 alloy used in the present study.

| Elements | Si | Fe | Cu | Mn | Mg | Cr | Zn | Al |
|------------|------|-----|-----|-----|-----|-----|-----|---------|
| Percentage | 0.35 | 0.4 | 0.2 | 0.5 | 1.2 | 0.3 | 5.0 | Balance |

Preparation of Composites

The B₄C particle reinforced Al7020 alloy metal matrix composites have been produced by using a vortex method. Initially calculated amount of Al7020 alloy was charged into SiC crucible and superheated to a temperature 730°C in an electrical resistance furnace. The furnace temperature was controlled to an accuracy of ±10 degree Celsius using a digital temperature controller. Once the required temperature is achieved, degassing is carried out using solid hexachloroethane (C₂Cl₆) to expel all the absorbed gases. The melt was agitated with the help of a zirconia coated mechanical stirrer to form a fine vortex. A spindle speed of 300 rpm and stirring time 3-5 min. were adopted. The B₄C particulates were preheated to a temperature of 500 degree Celsius in a pre-heater to increase the wettability. The pre-heated B₄C particles introduced into melt in steps of two at constant feed rate of 1.2-1.4 g/sec. After holding the melt for a period of 5 min., the melt was poured from 710 degree Celsius into a preheated cast iron mould having dimensions of 120mm length x 15mm diameter.

Testing

Metallographic test specimens of 5mm thickness were prepared by cutting the as cast and B₄C strengthened Al7020 combination composites. Test samples were polished according to the standard metallographic methodology and etched with Keller's reagent. The microstructure was viewed utilizing scanning electron microscope instrument.

The tensile properties of the example were measured by utilizing a universal testing machine at room temperature in light of ASTM E 8 standard. Hardness of as cast Al7020-B₄C amalgam composites were directed to know the impact of small scale B₄C particles in the network material ASTM E 10 standard. The cleaned examples were tried for their hardness, utilizing Brinell hardness testing machine having ball indenter for 250 kg stack and abide time of 30 sec.,

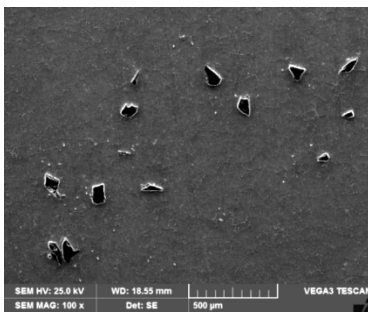
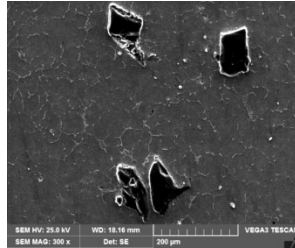
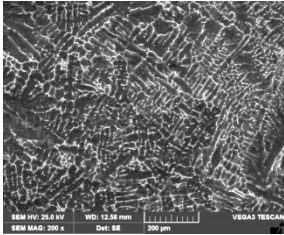
three arrangements of readings were taken at better places of the example and a normal esteem was utilized for figuring.

RESULTS AND DISCUSSION

Microstructural Studies

(a)

(b)



(c)

Fig. 1. a-c Showing the scanning electron microphotographs of (a) as cast Al7020 alloy (b) with 2 wt.% of B₄C & (c) with 4 wt.% of B₄C

Figure 1 (a-c) shows the SEM microphotographs of Al7020 alloy as cast and Al7020 with 2 and 4 wt. % of B₄C particulate composites. This reveals the uniform distribution of B₄C particles and very low agglomeration and segregation of particles, and porosity.

Fig. 1 b-c clearly show and even distribution of B₄C particles in the Al7020 alloy matrix. In other words,

no clustering of B₄C particle is evident. There is no evidence of casting defects such as porosity, shrinkages, slag inclusion and cracks which is indicative of sound castings. In this, wetting effect between particles and molten Al7020 alloy matrix also retards the movement of the B₄C particles, thus, the particles can remain suspended for a long time in the melt leading to uniform distribution.

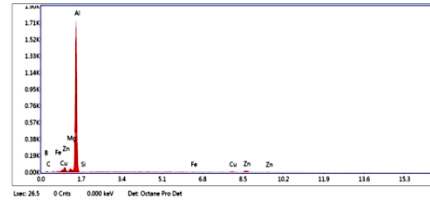
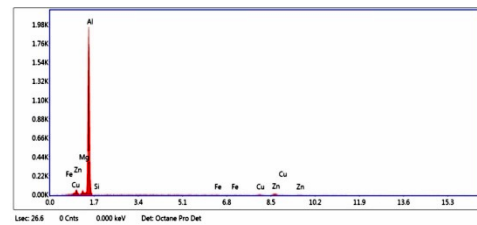


Fig. 2 EDS spectrum of (a) as cast Al7020 alloy (b) Al7020-4% B₄C composites



In order to confirm the presence of B₄C energy dispersive spectroscopy analysis was carried out at the edge of the B₄C particle and Al alloy matrix. The EDS spectrum reveals the presence of Al, Zn, Cu, Mg, B and C in the interface reaction layer (fig. 2-b).

Hardness Measurements

Hardness is a property of a material that indicates the ability of the material to resist local plastic deformation. Fig. 3 shows the influence of the micro B₄C particle contents on the hardness of the Al7020 alloy. The hardness values are positively correlated with the weight percentage of micro particles, because particles strengthened the matrix. Furthermore, the results show that B₄C reinforced MMCs harder than Al7020 alloy due

to Hall-Petch and Orowan strengthening mechanisms as well as the good interface between the reinforcement and matrix [6]. Al7020-4 wt.% B₄C composites shows more hardness, the increase in hardness of these composites as the B₄C fraction increases can be attributed to the dispersion strengthening effect [7]. By adding 4 wt. % B₄C particulates into the Al7020 alloy, the hardness increased of Al7020 alloy increased to 85 BHN from 63 BHN.

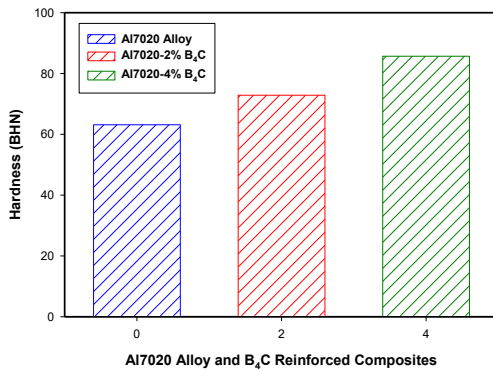


Fig. 3 Shows the hardness of Al7020 alloy and B₄C reinforced composites

Tensile Behavior

Fig. 4 and 5 shows the ultimate and yield strength of aluminium matrix composites (AMCs) reinforced with 2 and 4% micro B₄C particles. The ultimate tensile and yield strength of the composite increases as the content of reinforcement increases to 4%. The increase in tensile strength of AMCs containing B₄C is mainly due to the load bearing effect and mismatch of the strengthening mechanism. The difference between the co-efficient of thermal expansion of B₄C ($5 \times 10^{-6}/^{\circ}\text{C}$) and the aluminium matrix ($25 \times 10^{-6}/^{\circ}\text{C}$) results in a high dislocation density and thermally induced residual stresses [8-10]. These induced dislocations and thermal stresses act as a barrier to the dislocation movement. Hence, the strength of the AMCs containing micro sized B₄C increases.

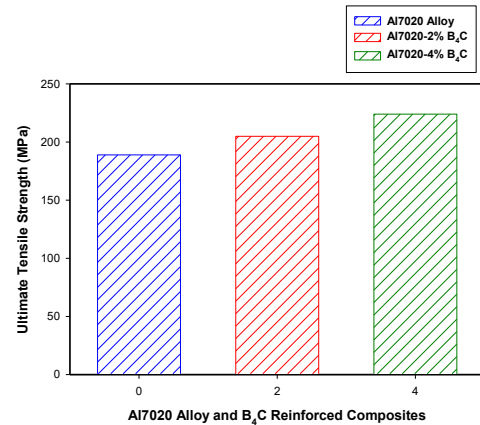


Fig. 4 Shows the ultimate tensile strength of Al7020 alloy and B₄C reinforced composites

The increase in the ultimate tensile strength and yield strength upon the addition of B₄C particles is 18.5% and 17.7% respectively. This is mainly due to Hall-Petch strengthening mechanism, which results from grain size refinement, the load bearing effect, and the Orowan and mismatch strengthening mechanisms [11, 12].

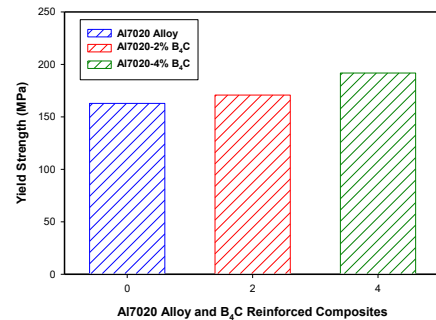


Fig. 5 Shows the yield strength of Al7020 alloy and B₄C reinforced composites

CONCLUSIONS

The present work entitled, "Microstructure, hardness and tensile behavior of micro B₄C reinforced Al7020 alloy composites" has led to the following conclusions:

- The liquid metallurgy technique was successfully adopted in the preparation of

Al7020 alloy reinforced with 2 and 4wt. % B₄C particulates.

- The micro structural studies from scanning micro photographs revealed the uniform distribution of the B₄C particulates in the Al7020 alloy matrix.
- The Energy Dispersive (EDS) analysis revealed the presence of B₄C particles in Al7020 alloy composites.
- Hardness of the Al7020-B₄C composite was found to be more than base Al matrix.
- The ultimate tensile strength of the composites was found to be higher than that of base matrix. The improvements in UTS by adding 4 wt. % of B₄C was increased by 18.5 %.
- The yield strength of the composites found to be higher than that of base matrix. The yield strength of base matrix Al7020 is increased from 162.8 MPa to 191.7 MPa after addition of 4 wt. % of B₄C particulates.

REFERENCES

1. M. Kok, Production and mechanical properties of Al₂O₃ particle reinforced 2024 aluminium alloy composites. *Journal of Materials Processing Technology*, 161, 381-387, 2005.
2. Madeva Nagaral, Pavan R, Shilpa P S and V Auradi, Tensile behavior of B₄C particulate reinforced Al2024 alloy metal matrix composites. *FME Transactions*, 45, 93-96, 2017.
3. Madeva Nagaral, V Auradi, S A Kori, Reddappa H N, Jayachandran and Veena Shivaprasad, Studies on 3 and 9 wt. % B₄C particulates reinforced Al7025 alloy composites. *AIP Conference Proceedings*, 1859, 020019, 2017.
4. K. H. W. Seah, S. C. Sharma, B. M. Girish, Effect of artificial aging on the hardness of cast ZA-27/Graphite particulate composites. *Materials and Design* Vol. 16, No. 6, 337, 1995.
5. S. A. Sajjadi, H. R. Ezatpour, M. Torabi, "Comparison of microstructure and mechanical properties of A356 aluminium alloy-Al₂O₃ composites fabricated by stir and compo casting processes", *Materials and Design*, 34, 2012, pp. 106-111.
6. Ranjith Bauri, M. K. Surappa, "Processing and properties of Al-Li-SiCp composites", *Science and Technology of Advanced Materials*, 8, 2007, pp. 494-502.
7. G. B. Veeresh Kumar, C.S.P. Rao, N. Selvaraj, "Studies on mechanical and dry sliding wear of Al6061-SiC composites", *Composites Part B*, 43, 2012, pp. 1185-1191.
8. J. Hashim, L. Looney, M. S. J. Hashmi, "Particles distribution in cast metal matrix composites part-I", *Journal of Materials Processing Technology*, 123, 2002, pp. 251-257.
9. R. K Everest, R. J. Arsenault, "Metal Matrix Composites: Processing and Interfaces", 1991.
10. B. Vijaya Ramnath, C. Elanchezian, M. Jaivignesh, S. Rajesh, C. Parswajinan, "Evaluation of mechanical properties of aluminium alloy -alumina-boron carbide metal matrix composites", *Materials and Design*, 58, 2014, pp. 332-338.
11. Nagaral M, Attar S, Reddappa H N, Auradi V, Sureshkumar S, Raghu S, Mechanical behavior of Al7025-B₄C particulates reinforced composites. *Journal of Applied Mechanical Engineering*, 4-6, 2015.
12. S A Sajjadi, H R Ezatpour, M Torabi, Comparison of microstructure and mechanical properties of A356 aluminium alloy-Al₂O₃ composites fabricated by stir and compo-casting process. *Materials and Design*, 34, 106-111, 2012.

Home (<https://www.fracturae.com/index.php/fis/index>)
/ Archives (<https://www.fracturae.com/index.php/fis/issue/archive>)
/ Vol. 13 No. 48 (2019): April 2019 (<https://www.fracturae.com/index.php/fis/issue/view/301>) / Articles

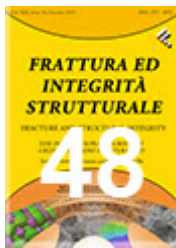
🐦 Follow on Twitter (<https://twitter.com/IGFfrattura>)

f Like on Facebook (<https://www.facebook.com/FISJournal/>)

📡 Follow on RSS

📄 Follow on Telegram (<https://t.me/joinchat/UBFJlmlawcVOCFUh>)

Characterization and Tensile Fractography of Nano ZrO₂ Reinforced Copper-Zinc Alloy Composites



(<https://www.fracturae.com/index.php/fis/issue/view/301>)

PDF (<https://www.fracturae.com/index.php/fis/article/view/2261/2415>)

Visual Abstract (<https://www.fracturae.com/index.php/fis/article/view/2261/2416>)

Published Mar 2, 2019

DOI <https://doi.org/10.3221/IGF-ESIS.48.35> (<https://doi.org/10.3221/IGF-ESIS.48.35>)

Madeva Nagara

Hindustan Aeronautics Limited Bangalore

Prasad H. Nayak

VTU RRC, Belgaum, Dept. of Mechanical Engineering, Oxford College of Engineering, Bangalore, Karnataka, India

H. K. Srinivas

Dept. of Mechanical Engineering, SJBIT, Bangalore, Karnataka, India

V. Auradi

Dept. of Mechanical Engineering, SIT, Tumkur, Karnataka, India

Abstract

Nano particulates fortified metal lattice composites are finding extensive variety of utilizations in car and sports hardware fabricating businesses. In the present investigation, an endeavor has been made to create copper-zinc-nano ZrO₂ particulates strengthened composites by utilizing fluid liquefy technique. 4, 8 and 12 wt. % of nano ZrO₂ particulates were added to the Cu-Zn base grid. Microstructural studies were finished by utilizing SEM and EDS examination. Mechanical behavior of Cu-Zn-4, 8, 12 wt. % of nano ZrO₂ composites were assessed according to ASTM benchmarks. Checking electron micrographs uncovered the uniform dispersion of nano ZrO₂ particulates in the copper zinc composite network. EDS examination affirmed the nearness of Zr and O components in nano ZrO₂ strengthened composites. Further, it was noticed that hardness, UTS, yield quality of Cu-Zn composite expanded with the expansion of 4, 8 and 12 wt. % of nano



E-ISSN: 2278-4136

P-ISSN: 2349-8234

www.phytojournal.com

JPP 2020; 9(4): 3078-3080

Received: 10-05-2020

Accepted: 12-06-2020

Manjunatha BAgricultural and Horticultural
Research Station, Kattalagere,
Karnataka, India**Nagaraja Kusagur**Agricultural and Horticultural
Research Station, Kathalagere,
Karnataka, India**Niranjana kumara B**Agricultural and Horticultural
Research Station, Kathalagere,
Karnataka, India

Estimation of genetic diversity for yield and yield attributing traits in rice (*Oryza sativa* L.)

Manjunatha B, Nagaraja Kusagur and Niranjana kumara B

Abstract

The present investigation was carried out in Agricultural and Horticultural Research Station, Kattalagere. The nature and magnitude of genetic divergence were estimated in 23 rice genotypes in six environments using Mahalanobis D² – statistics by considering 13 quantitative characters. D² analysis revealed considerable amount of diversity in the material. The genotypes were grouped into six clusters. Cluster I constituted maximum number of genotypes (16). The genotypes falling in cluster II had the maximum divergence. The inter cluster distance was maximum between cluster I and IV (10.34) followed by cluster III and V (9.82), suggesting that the genotypes constituted in these clusters may be used as parents for future breeding programme. Traits like; days to maturity, plant height(cm), Number of grains per panicle, Test weight (g), Harvest Index (%), Days to 50% flowering, Panicle length (cm) were the major contributors to genetic divergence.

Keywords: Estimation of genetic attributing traits in rice horticultural *Oryza sativa* L

Introduction

Rice (*Oryza sativa* L.), belongs to the family Graminae, recognized as “millennium crop” expected to contribute towards food security in the world, as it is one of the staple cereal crops of the world and a primary source of food for more than half the world’s population. With an alarming increase in the population throughout the world, the demand for rice will continue to increase in near future. Therefore, rice breeders across the world aim at increasing the grain yield of rice (Song *et al.*, 2007). Genetic diversity is pre-requisite for any crop improvement programme, as it helps in the development of superior recombinants (Manonmani and Fazlullah Khan, 2003) [3]. Genetic divergence among the genotypes plays an important role in selection of parents having wider variability for different characters (Nayak *et al.* 2004) [4]. Genetic divergence is the total number of genetic characteristics in the genetic makeup of a species. It serves as a way for populations to adapt to changing environments. Information on the nature and degree of genetic divergence would help the plant breeder in choosing the right parents for breeding program. The D² technique based on multivariate analysis developed by Mahalanobis (1936) [2] had been found to be a potent tool in quantifying the degree of divergence in germplasm.

Material and methods: The present investigation was carried out in Agricultural and Horticultural Research Station, Kathalagere. The experiment was laid out in Randomized Complete Block Design (RCBD) with two replications in puddle field at all locations. Seeds of rice genotypes were sown on 22nd of June 2018 at Kattalagere in raised beds of one sq m each. Twenty days old seedlings were transplanted to the main field at the rate of one seedling per hill by following Randomized Complete Block Design. The recommended packages of practice were followed to get a normal healthy crop. List of advanced breeding lines (F6) used under present investigation including checks (Table 1). Genetic diversity was assessed using Mahalanobis’ (1936) [2] D² statistics using WINDOSTAT software.

Results and discussion: The amount of diversity available in the crop decides the success of any crop improvement programme with manifold objectives. Assemblage and assessment of divergence in the germplasm is essential to know the spectrum of diversity. Improvement in grain yield is normally attained through involvement of the genetically diverse parents in breeding programmes. For identifying such diverse parents for crossing, by means of Mahalanobis’s D² statistics has been used in several crops. It is a powerful tool used to quantify the genetic divergence between the genotypes and to relate clustering pattern with the geographical origin. The present study was focused to assess the genetic diversity in twenty

Corresponding Author:**Manjunatha B**Agricultural and Horticultural
Research Station, Kathalagere,
Karnataka, India

three rice advanced breeding lines using Mahalanobis' D2 statistics. Of the several methods available, Mahalanobis' generalized distance estimated by D2 statistic (Rao, 1952) [5] is a unique tool for discriminating populations considering a set of parameters together rather than inferring from indices based upon morphological similarities, eco- geographical diversity and phylogenetic relationship. So as to enumerate the diversity in twenty advanced breeding lines of rice, thirteen quantitative characters were studied and their fitness was assessed using the concept of Mahalanobis' generalized distance (D2). Genetic diversity analysis assists in studying nature of diversity among the advanced breeding lines. With the purpose of finding the genetically diverse genotypes for their uses in recombination breeding programme, Mahalanobis' generalized (D²) analysis was carried out with thirteen characters studied. Advanced breeding lines distributed into five clusters. This cluster pattern showed that cluster I consists of maximum of sixteen number of advanced breeding lines, cluster II consists of three, cluster IV consists two and remaining two clusters are solitary. The distribution pattern of rice advanced breeding lines into five clusters is shown in Table 2. Intra and inter relation of clusters judged by average D2 values. The maximum intra cluster distance noticed in cluster IV (1.58). Diversity among the clusters was in the range of 1.47 to 10.34. Cluster I and cluster IV showed maximum inter cluster distance (10.34) followed by the cluster III and cluster IV (9.82). The lowest inter cluster distance was observed between cluster I and cluster III (1.47). The average D² values of intra and inter clusters distances are mentioned in Table 2. The cluster means regarding thirteen characters across the five clusters are mentioned in Table 3. The advanced breeding lines with respect to days to fifty per cent flowering belongs to cluster IV showed highest mean value of (104.63), while cluster III showed the least mean value days to fifty per cent flowering (85.75). The advanced breeding lines belong to cluster III showed the least mean value days to maturity (125.00). While cluster IV showed highest mean value for days to days to maturity (131.63). With respect to plant height, advanced breeding lines belongs

to cluster I showed highest mean value of (86.06 cm), while cluster II showed the least mean value of plant height (76.72 cm) Table 4. Across the thirteen characters with the five clusters, the cluster II with total score of 36 secured first rank followed by cluster III and cluster V with 38 score secured second rank. Cluster IV with two advanced breeding lines is the most divergent group with a maximum intra-cluster distance (1.58) and these results are on par with the results of Tuhina *et al.* (2012) [7] as they obtained five clusters for forty three upland rice accessions and they had noted the highest number of advanced breeding lines (14) in cluster I and lowest in cluster II, III and IV (01). The clustering pattern of the genotypes revealed that the clustering did not follow any particular patterning clustering with respect to the origin (Ushakumari and Rangaswamy, 1997). It is desirable to select advanced breeding lines from these clusters showing high inter cluster distance and also with high grain yield as parents in recombination breeding programme for obtaining wide variability and desirable segregants. Sixteen advanced breeding lines were present in cluster I. likewise in cluster II, two in cluster IV and one genotype each were present in III and V clusters. These results are in conformity with the observations made by Sohrabi *et al.* (2012) [6].

Proportion of contribution of each character to total D2 statistics showed significant differences and they are mentioned in Table 2. The selection and choice of parents mainly depends upon contribution of characters towards divergence (Nayak *et al.*, 2004) [4]. The most important character contributing to the divergence among the thirteen quantitative characters studied was days to maturity which is more responsible for increasing grain yield. This was followed by plant height (cm), number of grains per panicle, test weight, harvest index, days to fifty per cent flowering, panicle length (cm), number of tillers per plant, number of spikelets per panicle, panicle fertility (%), straw yield (kg/ha), grain yield (kg/ha), days to maturity and number productive of tillers per plant. These observations are in accordance with the findings of Banumathy *et al.* (2010) [1].

Table 1: List of advanced breeding lines (F6) used under present investigation including checks.

| Cross combinations | Code | Advanced breeding lines | Grain shape | Grain color |
|--------------------|------|-------------------------|----------------|-------------|
| Jyoti X Biliya | G1 | JB-1-11-7 | Medium slender | Light red |
| | G2 | JB-1-20-2 | Medium slender | Light red |
| | G3 | JB-1-22-1 | Medium slender | Light red |
| | G4 | JB-1-22-2 | Medium slender | Light red |
| | G5 | JB-1-22-3 | Medium slender | Light red |
| Jyoti X Kesari | G6 | JK-1-7-5 | Medium bold | Dark red |
| | G7 | JK-1-11-8 | Medium bold | Light red |
| | G8 | JK-1-12-1 | Medium bold | Light red |
| | G9 | JK-1-13-1 | Medium bold | Light red |
| | G10 | JK2-2-1-8-1 | Medium bold | Light red |
| | G11 | JK2-1-12-1 | Medium bold | Light red |
| Jyoti X Akkalu | G12 | JA-4-1 | Medium slender | Light red |
| | G13 | JA-4-2 | Medium slender | Light red |
| | G14 | JA-4-3 | Medium slender | Light red |
| | G15 | JA-6-2 | Medium slender | Light red |
| | G16 | JA-6-3 | Medium slender | Light red |
| | G17 | JA-6-4 | Medium slender | Light red |
| Jyoti X Tunga | G18 | JT-2-15-1 | Medium slender | Light red |
| | G19 | JT-2-16-1 | Medium slender | Light red |
| | G20 | JT-2-22-5 | Medium slender | white |
| Jyothi | G21 | | Bold | Red |
| KHP-2 | G22 | | slender | Red |
| Tunga | G23 | | Bold | white |

Table 2: Per cent contribution of character towards divergence of twenty advanced breeding lines of rice.

| S. No. | Characters | Contribution (%) |
|--------|--|------------------|
| 1. | Days to maturity | 54.1 |
| 2. | Plant height (cm) | 9.88 |
| 3. | Number of grains per panicle | 5.14 |
| 4. | Test weight (g) | 5.14 |
| 5. | Harvest Index (%) | 4.74 |
| 6. | Days to 50% flowering | 4.35 |
| 7. | Panicle length (cm) | 4.35 |
| 8. | Number of tillers per plant | 3.16 |
| 9. | Number of spikelets per panicle | 2.37 |
| 10. | Panicle fertility (%) | 2.2 |
| 11. | Straw yield (kg/ha) | 1.8 |
| 12. | Grain yield (kg/ha) | 1.58 |
| 13. | Number of productive tillers per plant | 1.19 |

Table 3: Distribution of twenty advanced breeding lines of rice into different clusters.

| Clusters | Number of advanced breeding lines | Advanced breeding lines |
|----------|-----------------------------------|---|
| I | 16 | JB-1-20-2, JB-1-22-1, JB-1-22-2, JB-1-22-3, JK-1-7-5, JK-1-11-8, JK-1-12-1, JK-1-13-1, JK2-2-1-8-1, JK2-1-12-1, JA-4-1, JA-4-2, JA-4-3, JA-6-2, JA-6-3, JA-6-4. |
| II | 3 | JT-2-15-1, JT-2-16-1, JT-2-22-5. |
| III | 1 | JB-1-11-7. |
| IV | 2 | KHP-2, Tunga. |
| V | 1 | Jyothi |

Table 4: Average intra and inter cluster distance values of twenty advanced breeding lines of rice

| Cluster | I | II | III | IV | V |
|---------|------|------|------|-------|------|
| I | 0.65 | 6.34 | 1.47 | 10.34 | 4.84 |
| II | | 0.33 | 7.86 | 3.56 | 8.12 |
| III | | | 0.00 | 9.82 | 5.37 |
| IV | | | | 1.58 | 7.44 |
| V | | | | | 0.00 |

References

- Banumathy S, Manimaran R, Sheeba A, Manivannan N, Ramya B, Kumar D. Genetic diversity analysis of rice germplasm lines for yield attributing traits. *Electron. J. Plant. Breed.* 2010; 1(4):500-504.
- Mahalanobis PC. A statistical study at Chinese head measurement. *J Asiatic society Bengal.* 1936; 25:301-77.
- Manomani S, Fazlullah khan AK. Analysis of genetic diversity for selection of parents in rice. *Oryza.* 2003; 40:54-56.
- Nayak AR, Chaudhury D, Reddy JN. Genetic divergence in scented rice. *Oryza.* 2004; 41(384):79-82.
- Rao CR. *Advance statistical methods in biometric research.* John Wiley and Sons Inc., New York, 1952.
- Sohrabi MY, Rafii, Latif MA. Genetic Diversity of Upland Rice Germplasm in Malaysia Based on Quantitative Traits. *Scientific World J.* 2012; 15:416-491.
- Tuhina K, Mohamed H, Mohd RY, Wong MY, Faezah M Sallish, Jannatul F. Genetic Variation, Heritability, and Diversity Analysis of Upland Rice (*Oryza sativa L.*) Genotypes Based on Quantitative Traits. *BioMed Res. Int.* 2012; 7(2):1-7.
- Usha Kumary RU, Rangasamy P. Studies on genetic diversity in International early rice genotypes. *Ann. of Agric Res.* 1997; 18(1):29-33.

See discussions, stats, and author profiles for this publication at: <https://www.researchgate.net/publication/343935616>

Variability, Heritability and Genetic Advance Studies in Advanced Genotypes of Rice (*Oryza sativa* L.)

Article in *International Journal of Current Microbiology and Applied Sciences* · June 2020

DOI: 10.20546/ijcmas.2020.908.191

CITATIONS

0

READS

24

3 authors, including:



B. Manjunatha

University of Agricultural & Horticultural

9 PUBLICATIONS 8 CITATIONS

[SEE PROFILE](#)



Dr Niranjana Kumara

The Trans-disciplinary University

23 PUBLICATIONS 27 CITATIONS

[SEE PROFILE](#)

Some of the authors of this publication are also working on these related projects:



AICRP on Rice [View project](#)

Original Research Article

<https://doi.org/10.20546/ijcmas.2020.908.191>

Variability, Heritability and Genetic Advance Studies in Advanced Genotypes of Rice (*Oryza sativa* L.)

B. Manjunatha, Nagaraja Kusagur and B. Niranjanja Kumara

Agricultural and Horticultural Research Station, Kathalagere, University of Agricultural and Horticultural Sciences, Shivamogga, Karnataka, India

*Corresponding author

ABSTRACT

Keywords

Heritability, Rice, Variability

Article Info

Accepted:

18 July 2020

Available Online:

10 August 2020

The experiment was composed of thirty five advanced rice genotypes with two replications in Randomized Complete Block Design conducted in Agricultural and Horticultural Research Station, Kathalagere, University of Agricultural and Horticultural Sciences, Shivamogga in *kharif* 2018. The traits panicles per square metre and yield kg/ha had higher GCV and PCV as well as high genetic variability and phenotypic variability. Yield kg/ha had high heritability coupled with GCV and PCV.

Introduction

Rice (*Oryza sativa* L.) is regarded as one of the major cereal crops with high agronomic and nutritional importance. It is a major source of human food for more than half of the world's population (1). Rice is one of the food crops for which complete genome sequence is available. Therefore, it is an ideal model plant for study of grass genetics due to its relatively small genome size of 430 Mb compared to other plants (2). Rice is a self-pollinated cereal crop belonging to the family Gramineae (synonym-Poaceae) under the order Cyperales and class Monocotyledon having chromosome number $2n=24$ (1). The

genus *Oryza* includes a total of 25 recognized species out of which 23 are wild species and two, *Oryza sativa* and *Oryza glaberrima* are cultivated (2). It can survive as a perennial crop and can produce a ratoon crop for up to 30 years but cultivated as annual crop and grown in tropical and temperate countries over a wide range of soil and climatic condition. Rice and agriculture are still fundamental to the economic development of most of the Asian countries. In much of Asia, rice plays a central role in politics, society and culture, directly or indirectly employs more people than any other sector. A healthy rice industry, especially in Asia's poorer countries, is crucial to the livelihoods of rice

producers and consumers alike. Farmers need to achieve good yields without harming the environment so that they can make a good living while providing the rice-eating people with a high-quality, affordable staple. Underpinning this, a strong rice research sector can help to reduce costs, improve production and ensure environmental sustainability. Indeed, rice research has been a key to productivity and livelihood.

Rice is the second largest produce cereal in the world in 158.3million hectare area with annual production of about 685.24 millionmetric tons (3) and also the staple food for over one third of the world's population (4) and more than 90% to 95% of rice is produced and consumed is Asia (5). Rice (*Oryza sativa* L.) is the staple food in india and grown in a wide range of environments ranging from the upland areas like Chittagong Hill Tracts, Sylhet and Garo Hills, with little moisture, to situations where the water is 3-4 meter deep(6).

Yield enhancement is the major breeding objective in rice breeding programmes and knowledge on the nature and magnitude of the genetic variation governing the inheritance of quantitative characters like yield and its components is essential for effective genetic improvement. A critical analysis of the genetic variability parameters, namely, Genotypic Coefficient of Variability (GCV), Phenotypic Coefficient of Variability (PCV), heritability and genetic advance for different traits of economic importance is a major pre-requisite for any plant breeder to work with crop improvement programs. The present investigation was under taken in this context to elucidate information on variability, heritability, genetic advance, character associations and path of effect in promising rice genotypes. A good knowledge of genetic resources might also help in identifying desirable genotypes for future hybridization program.

Materials and Methods

The experiment was carried out during *khariif*, 2018 at Agricultural and Horticultural Research station, kathalagere under University of Agricultural and Horticultural Sciences, Shivamogga, Karnataka. The material comprised of thirty five advanced rice genotypes own in a randomized complete block design with two replications with spacing of 20 X 15 cm. Data were recorded on five randomly selected plants in each entry in each replications for the traits days to 50% flowering, Plant height (cm), Productive tillers/m² and Yield kg/ha. The data subjected to INDOSTAT software to estimate Genetic coefficient of variation (%), phenotypic coefficient of variation (%), Heritability (%) (Broad sense), Genetic Advance and Genetic Advance as percent of mean. The estimates for variability treated as per the categorization proposed by Siva Subramanian and Madhavamenon (4), heritability and genetic advance as percent of mean estimates according to criteria proposed by Johnson *et al.*, (2).

Results and Discussion

In the present study analysis of variance revealed the existence of significant differences among genotypes for all traits studied. The mean, variability estimates *i.e.*, Genetic coefficient of variation (%), phenotypic coefficient of variation (%), Heritability (%) (Broad sense), Genetic Advance as percent of mean are presented in table 1. All traits under studied have higher phenotypic coefficient of variation than genotypic coefficient of variation. The magnitude of phenotypic coefficient of variation and genotypic coefficient of variation was moderate to high for the traits panicles per square metre and yield (3, 5). The high PCV observed for yield per hectare (5).

Table.1 Variability, heritability and genetic advance for quantitative traits in rice

| Character | Mean | Genetic coefficient of variation (%) | Phenotypic coefficient of variation (%) | Heritability (%) | Genetic advance (%) | Genetic advance as percent mean |
|---------------------------------|------|--------------------------------------|---|------------------|---------------------|---------------------------------|
| Days to fifty percent flowering | 117 | 9.90 | 11.04 | 0.98 | 25.88 | 21.46 |
| Plant height(cm) | 76 | 17.78 | 17.40 | 0.93 | 23.18 | 33.44 |
| Panicles per m ² | 389 | 22.05 | 20.65 | 0.80 | 155.00 | 34.66 |
| Yield kg/ha | 3558 | 30.6 | 30.36 | 0.95 | 2258.00 | 53.54 |

The high GCV obtained for number of panicles per square metre indicating the improvement is possible through selection. Genotypic coefficient of variation measures the extent of genetic variability percent for a trait but does not assess the amount of genetic variation which is heritable. Heritability estimates were high for all the characters.

The heritability estimates along with genetic advance can be useful to predict effect of selection in selection programmes. The traits like days to fifty percent flowering, yield (7) and plant height exhibited high magnitude of genetic advance as percent of mean.

The traits plant height, days to fifty percent flowering, panicles per square metre and yield have high heritability along with genetic advance as percent of mean indicate that these characters attributable to additive gene effects which are fixable revealing that improvement in these characters would be possible through direct selection.

References

1. Genetic variability and association analysis in rice. *International Journal of Applied*

Biology and Pharmaceutical Technology. 5(2): 63-65.

- Johnson, H.W. Robinson, H.F. and Costock, R.E., Estimates of genetic and environmental variability in Soyabean. *Agronomy Journal*, 47(7): 314-318 (1955)
- Roy, B. Hossain, M. and Hossain, F., Genetic variability in yield components of rice (*Oryza sativa* L.). *Environment and Ecology*. 19(1): 186-189 (2001).
- Siva Subramanian, S. and madhavamenon, P., Combining ability in rice. *Madras Agricultural Journal*. 60: 419-421 (1973)
- ThirumalaRao, V. Chandra Mohan, Y. Bhadru, D. Bharathi, D. and Venkanna,. V. (2014).
- Venkanna, V., Lingaiah, N., Raju, Ch and Rao, V.T., Genetic studies for quality traits of F₁ population of rice (*Oryzasativa* L.). *International Journal of Applied Biology and PharmaceuticalTechnology*. 5(2): 125-127 (2014)
- Vaithiyalingan, M. and Nadarajan, N., Genetic variability, heritability and genetic advance in F population of inter sub-specific crosses of rice. *Crop Research*. 31(3): 476-477 (2006).

How to cite this article:

Manjunatha, B., Nagaraja Kusagur and Niranjana Kumara, B. 2020. Variability, Heritability and Genetic Advance Studies in Advanced Genotypes of Rice (*Oryza sativa* L.). *Int.J.Curr.Microbiol.App.Sci*. 9(08): 1668-1670. doi: <https://doi.org/10.20546/ijcmas.2020.908.191>

ASIC Implementation of Random Perturbation Algorithm for Neural Network Application

Dharamvir¹, Arul Kumar V²

¹Research Scholar, ²Asst. Professor

^{1,2}School of CSA, REVA University, Bengaluru, India

Article Info

Volume 83

Page Number: 3474-3476

Publication Issue:

May-June 2020

Article History

Article Received: 19 August 2019

Revised: 27 November 2019

Accepted: 29 January 2019

Publication: 12 May 2020

Abstract

An Analog VLSI Implementation of an on-chip learning neural network is described in this paper. The network considered comprises an analog feed forward network with digital weights and update circuitry. The chip consists of a comparator, incrementer and decremter circuit to update the weights. The training algorithm used is Random Perturbation Algorithm. From experimental results it is seen that the weights are updated as per the algorithm. Intense simulations were carried out in HSPICE simulation tool using 0.18 μ m technology to verify its functioning.

Keywords : Neural Networks, Perturbation Algorithms, Incrementer, Data Connectivity, Image Transformations

1. Introduction

One of the major impediments to implement an artificial neural network is the complexity of the hardware required to implement the training algorithm.[1,2]. A VLSI neural network can be applied in many situations requiring fast, low power operations [3].

Artificial Neural Networks require to be trained to solve any problem. The training can be either offline or online. The offline training involves using the weights generated by simulation. The weights are represented using fixed number of bits for hardware implementation. This results in quantization error. On chip learning can adjust the weights to obtain the desired functionality and reduce the quantization error.

The back propagation method as well as Random Perturbation has been used in hardware implementation for training the network. The back propagation method involves implementation of circuits to estimate mean square error and derivatives of the error function[4]. This results in a complex circuit. A simple method of implementing training by Random Perturbation has been reported by Kush et al. The neural network is implemented as mixed signal circuits using multiplying DAC. The analog circuit is used to implement the weight perturbation method. Here we report an alternative method to perturb the weight using partly digital implementation based on

incrementer and decremter circuits. The weights are stored as charge on capacitors. This requires frequent refreshing as capacitors loose their charge over time. The weights are updated bit by bit and are stored in the memory. Thus the network needs to be trained only once or only when a new number needs to be solved. The second section gives the basic algorithm of Random Perturbation. Third section looks into the hardware implementation of the training algorithm. The fourth section analysis the test results obtained and the finally the conclusion is provided in the 5th section.

2. Random Perturbation Algorithm

The artificial neural network consists of a processor, control circuit, a training algorithm and a memory to store the weights as shown in figure 1.

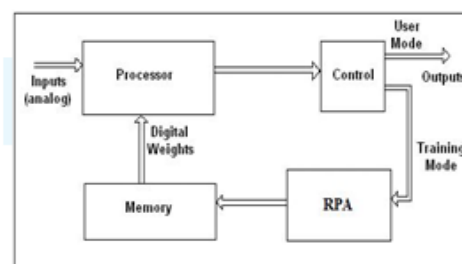


Figure 1: Neural Network Block Diagram

The processor consists of an analog multiplier and a summer. There are different architectures of analog neural network reported earlier in literature [5,6,7]. The control circuit decides whether neural network will be operated in user mode or training mode. Once training mode is selected the training algorithm is executed and finally the updated weights are stored in memory.

The neural network is trained here by using the Random Perturbation Algorithm also called as parallel weight update rule[8]. The algorithm begins with the generation of random weights and then adjusts the weights during every iteration. The following is an outline of the algorithm [1]

```

Initialize Weights;
Get the error; While (error > error goal);
Perturb Weights;
Get New Error;
If (New Error < Error), Weights=New Weights; Error = New Error; Else Restore Old Weights; End End
    
```

The flow of the algorithm has been implemented using the flow chart shown in figure 2.

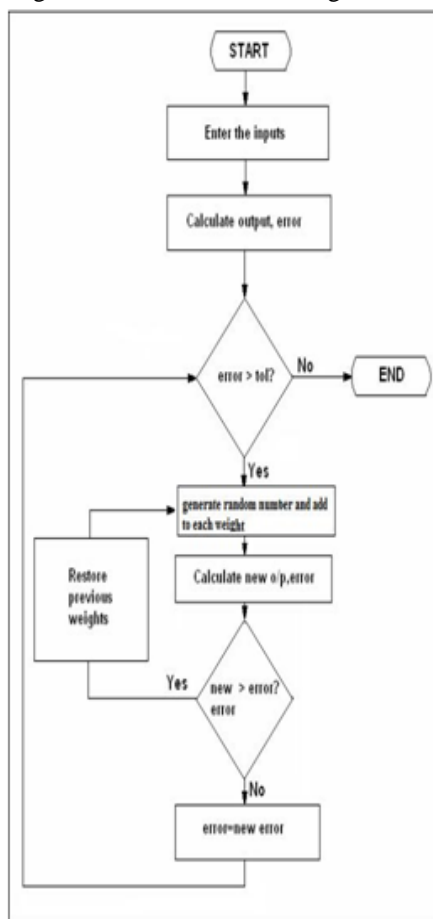


Figure 2: Flowchart of RPA

Hardware implementation

The hardware implementation of the algorithm includes an operational amplifier, and an incrementer and decrementer circuits as shown in figure 3.

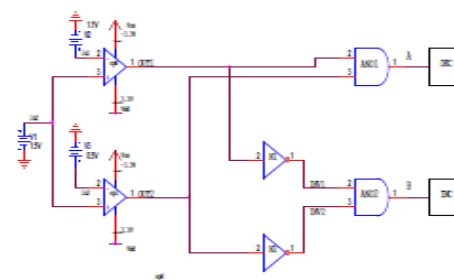


Figure 3: Hardware implementation of RPA

Op Amp as a Comparator

The circuit diagram of the two stage Op Amp is shown in figure 4.

The two stage Op Amp is used as a comparator. The first Op Amp is used to compare the input voltage V1 with the target plus tolerance voltage V2. The output OUT1 of this Op Amp is high if the V1 is greater than the V2. Else it is low.

The second Op Amp is used to compare the input Voltage V1 with the target minus tolerance Voltage V3. The output OUT2 of this Op Amp is high if the V1 is greater than the V3. Else it is low. The operational amplifier is designed to meet low power dissipation requirements of analog circuits [9].

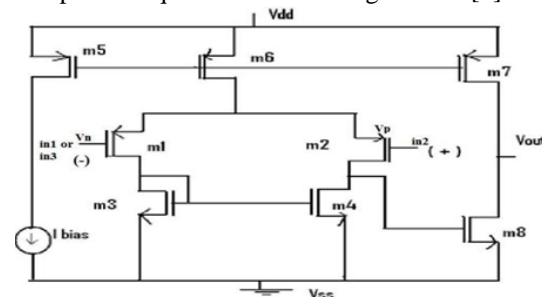


Figure 4:Two Stage Op Amp

Decrementer Circuit (DEC)

The gate level description of a one bit incrementer is shown in figure 5.

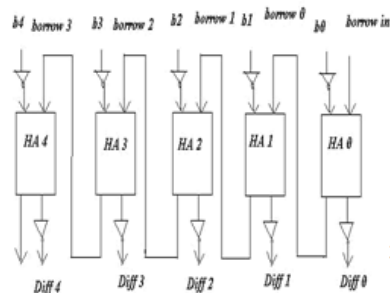


Figure 5: One bit Decrementer Circuit

The decrementer circuit has been implemented to carry out two's complement subtraction. The circuit decrements the LSB bit of the weight one bit every iteration if the input is higher than the target plus

tolerance voltage. If the input voltage V1 is greater than target plus tolerance voltage V2 then it V1 is also greater than target minus tolerance VoltageV3. Thus if OUT1 and OUT2 are both high then the decremter is executed and the weight is decremented by one bit.

Incrementer Circuit (INC)

The gate level description of a one bit Incrementer is shown in figure 6.

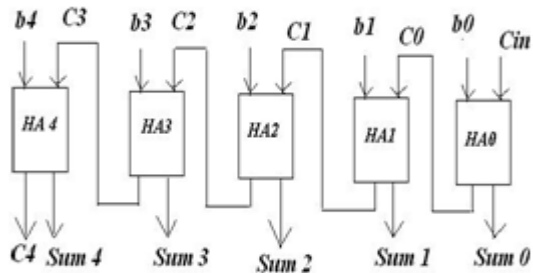


Figure 6: One bit Incrementer Circuit

The circuit increments the LSB bit of the weight one bit every iteration if the input is lesser than the target plus tolerance voltage. It is obvious that if the input voltage V1 is lesser than target minus tolerance voltage V3 then V1 is also lesser than target plus tolerance VoltageV2. Thus if OUT1 and Out2 are both low then incrementer is executed and the weight is incremented by one bit.

The incrementer and decremter circuit consist of a series of Half Adders (HA) arranged in a carry ripple fashion. In this work the Random Perturbation Algorithm is implemented to update 5 bit weight [5,6,7 Hence five Half Adders are used in the incrementer and decremter circuits.

3. Test Results

Intense simulations were carried out in HSPICE simulation tool using 0.18µm technology to verify the functioning of the hardware mentioned in section 3 of this paper. For various combinations of the input voltage, the various outputs have been recorded as shown in table 1.

Table 1: Output details at each stage of RPA

| V1 | V2 | V3 | OUT1 | OUT2 | A | B |
|-----|-----|-----|-------|-------|-----|-----|
| 1.5 | 1.1 | 0.5 | 3.3 | 3.3 | 3.3 | 0 |
| 1.1 | 1.1 | 0.5 | -0.23 | 3.3 | 0 | 0 |
| 0.5 | 1.1 | 0.5 | -3.3 | -0.55 | 0 | 0 |
| 0.4 | 1.1 | 0.5 | -3.3 | -3.3 | 0 | 3.3 |

Hardware Implementation

As explained in section 3, the weights have to be updated if the new error is greater than old error. Here the weight is decremented if the above mentioned case is true as is seen in table 1 where when V1 is

greater than V2, V1 is also greater than V3 and so OUT1 is and OUT2 are high indicated by 3.3V (logic 1) and hence A is high and B is low triggering the decremter circuit to decrement the weight. Also the weights are updated if the input voltage V1 is lesser than target minus tolerance Voltage V3 and hence V1 is also lesser than V2, in which case the weight is incremented by one as is obvious from the table1, when V1 0.4V and V2 is 1.1V and V3 is 0.5V, OUT1 and OUT2 both are low (-3.3V Logic 0) and B is high and A is low. This triggers the incrementer circuit and the weight is incremented by one bit. If the input voltage is anywhere in between the target minus tolerance Voltage and target plus tolerance Voltage, the outputs A and B both are zero and neither the incrementer nor the decremter are executed. Thus the old weights are retained as per the Random Perturbation Algorithm.

4. Conclusion

A VLSI implementation of an on Chip training algorithm for artificial neural network is demonstrated in this paper. The Random Perturbation Algorithm is implemented using Op Amp as a comparator and the decremter and incrementer to decrease and increase the weights respectively. The simulation results show that the training circuit follows the algorithm to a large extent. The can be extended to update the weights constantly and on the fly.

References

- [1] Vincent F. Koosh, Rodney Goodman, "VLSI Neural Network with Digital Weights and Analog Multipliers", 0-7803-6685-9/01/IEEE, 2018
- [2] Paul W. Hollis, John J.Paulos," A Neural Network Learning Algorithm Taiolored for VLSI Implementation", IEEE Transactions on Neural Networks, Vol 5, September 2014
- [3] R.Coggins, M.Jabri, B.Flower and S.Pickard, "A Hybrid Analog and digital VLSI Neural Network for Intracardiac Morphology Classification", IEEE J. of Solid -Sate Circuits, vol.30, no.5, pp.542-550, May 2017.
- [4] Perry D Moerland, Emile Fiester, " Neural Network adaptations to hardware implementations", in Handbook of Neural System Data Classification with Computation, 10P Publishing and oxford university press, 2018, 97/1, pp E1.2:1
- [5] Sujith Sudarshan, Santosh K and S.L.Pinjare, "MDAC Synapse – Neuron for Analog Neural Networks", National Conference on convergence ofsignal processing, communication and VLSI Design, NCSCV10-13, 186, 2019.

Recommendation based on guided analytics for Product prediction in retail space

J C Achutha

Assistant Professor

Department of Master Of Computer Applications
The Oxford College of engineering Bangalore

Abstract— Production and Data Reliability based on Cyber-attacks are becoming an increasing threat to people and daily businesses regularly. Attackers have also been evolving their strategies and methods with time. Every attack carried out has the potential to exploit the system on a large scale. Various Artificial Intelligence (AI) algorithms are used to defend such vulnerabilities. This paper analyzes a novel attack and extracts attackers' intrusion scenarios. Evolutionary Computation Techniques have been remarkably used in the field of cybersecurity. This paper particularly discusses the Distributed Denial Of Service (DDoS) attack. The effect of this attack ranges from a disturbance of an elementary service to causing major threats to critical services. In recent times these attacks have become more intricate and carry a significant threat. Therefore, there is a necessity for an intelligent Intrusion Detection System (IDS) to recognize attacks. In this study, work is carried on the latest dataset called Modern DDoS. This paper comprises of comparing the results of six established classification techniques: Random Forest, Naive Bayes, Stochastic Gradient Descent, Decision Trees, Logistic Regression, and K-Nearest Neighbour (KNN) with the proposed Genetic Programming model. The results show that the proposed Genetic Programming model has better accuracy when compared to various existing methods.

Keywords—Intrusion Detection System (IDS), Distributed Denial of Service (DDoS), Modern DDoS dataset, Evolutionary Computation (EC), Genetic programming (GP), Principal Component Analysis (PCA).

I. INTRODUCTION

Cybersecurity is becoming a regular struggle for organization asset's and businesses. The effort to hinder the integrity, confidentiality, or availability of system is called intrusions. [3] "Intrusion Detection is the process of investigating and monitoring the events occurring in the network or computer system which are violations or impeding threats of computer security policies" [5]. An Intrusion detection system (IDS) is an application that defends your network from suspicious activities, threats, and vulnerabilities when detected [7]. However, IDS faces several issues such as unbalanced data distributions, large traffic volumes, continuously changing environments and the need to recognize normal and abnormal behavior [14].

A Cyber attack is a deliberate attempt that targets one or more computers against multiple computers or networks. The Cyber Attacks such as Denial-of-service (DoS) and Distributed Denial-of-service (DDoS), Man-in-the-Middle (MitM) attack,

Phishing, and Spear-Phishing attacks, Cross-site Scripting (XSS) attack, Malware attack, etc have attracted the attention of researchers over the years [16]. The primary focus of this study is particularly restricted to DDoS attacks which will be extended to various attacks in future and thus coming up with a model capable of detecting attacks of various kinds and providing an immediate remedy of the attack in case attack happens. A DDoS attack is a pernicious attack on network wherein the targeted system (a server or website or any other network resources) gets affected by causing the denial of services to the user of the targeted system (or resources)

[23]. Hackers make use of botnets to flood an IP address with thousands of messages and connection requests thereby denying services to legitimate users.

Advances in Machine Learning (ML) and Deep Learning (DL) [24], [25] have a profound impact on science and technology. These technologies have many recent successes in the field of Cyber-security. The study focuses on the usage of ML and Evolutionary Computation (EC) algorithms specifically Genetic Programming to investigate the IDS building process more effectively than the existing methods [26]. "Genetic programming (GP) is an evolutionary approach towards computing that focuses on optimal classification. GP is a meta-heuristic approach that is capable of using complex pattern representations such as trees" [27]. This paper demonstrates a comprehensive analysis of detecting DDoS attacks using various classification models as well as the proposed method using genetic programming. Within this evaluation, six ML models namely Random Forest, Naive Bayes, Stochastic Gradient Descent, Decision Trees, Logistic Regression, K-Nearest Neighbour (KNN), [28] and genetic programming model are explored for detecting DDoS attacks and their performances are evaluated based on experiments on Modern DDoS dataset.

The rest of the paper is organized as follows: Section II encapsulates the available literature. Section III sums up the genetic programming fundamentals and explanation. In section IV, the proposed method is reported in detail. Section V furnishes the experiments and results. Section VI bestows conclusions and future scope of the work.

Data Normalization Techniques on Intrusion Detection for Dataset Applications

^[1] Dharamvir, ^[2] Arul Kumar V

^[1] Research Scholar, School of CSA, REVA University, Bangalore, India.

^[2] Asst. Professor, School of CSA, REVA University, Bangalore, India.

^[1] dhiruniit@gmail.com

Abstract

Intrusion Detection System (IDS) is an important security tool for safeguarding the network from both internal and external threats. Conventional IDSs employ signature-based methods or anomaly-based methods which rely on dataset for training and testing the system. KDD CUP 99 is one such widely used dataset. Artificial Neural Networks (ANN), Machine learning, Data mining, Evolutionary computing, Statistical methods, Computational Intelligence, etc., algorithms make use of this KDD CUP 99 dataset for testing. The dataset consists of symbolic, binary, numeric, and continuous features scattered in different range of values. In statistical methods such as Euclidean distance, the larger value dominates the distance measurement. In clustering algorithms, the larger values shift the cluster center. Such disadvantages could be overcome by ensuring uniformity to the dataset while retaining the exactness of the features mapped which could be achieved by a process known as Normalization. Data normalization is a data preprocessing stage which maps data from different ranges on to a common scale. In this paper, a detailed analysis of the existing various data normalization techniques that can be applied on KDD CUP 99 dataset is presented along with the illustration. From the analysis, it was found that different normalization techniques are suitable for different subsets of KDD CUP 99 dataset. The problem under investigation is to prove that the new dataset generated on application of various normalization techniques exhibits the same characteristics as that of the original KDD CUP 99 dataset. Also, the effect of data normalization techniques, viz., of Min-max, Z-Score, Log, and Sigmoid on the neural Network algorithm in terms of detection rate and false alarms were compared and it was experimentally found that the log and sigmoid data normalization techniques result in better detection rate.

Keywords - IDS, Data Normalization, KDD CUP 99

1. Introduction

Intrusion is an act by which a person enters another person's/organization's computer network without rights or permission. Over a decade, intrusion detection system (IDS) has got considerable importance in the field of network security. One important attribute to the growth of IDS is the paradigm shift of the mentality of attackers from script kiddies to sophisticated spy network agents who are politically and monetarily motivated. This has led to strengthen the security premises of network using firewall, IDS [1], Intrusion Prevention System (IPS), etc. IDS can be broadly classified into two methods, viz., signature-based or misuse detection and anomaly-based detection. In misuse detection techniques, signature or pattern of previously seen attack is calculated and configured in to the IDS which in turn alerts the administrator in case of similar attacks. On the other hand, anomaly detection techniques [2], calculate the normalcy of network behavior/activity and fix the activity as an attack on finding any deviating activity from the normal behavior. Misuse detection has high detection rate where as anomaly detection aids in detecting zero day attacks which are never seen before. Anomaly detection and misuse detection are orthogonal to each other.

1.1 KDD CUP 1999 dataset

KDD CUP 99 dataset is the most popular IDS dataset [3]. It consists of a large labeled training data and testing data. Testing data consists of attacks which are not present in the training dataset. The algorithms developed for anomaly detection systems can be tested using this dataset [9]. The dataset contains the four different types of attack data, viz., DoS, Probe, Remote-to-Local (R2L), and User-to-Superuser (U2R) attacks. The dataset is a U*A matrix where U is the set of data instances and A,

A Study and Application Development for POMP Decorum and its Transformation System

¹Ushasree R , ²Dr M S Shashidhara,

¹Assistant Professor, ²Professor & Head
Dept of MCA, The Oxford College of Engineering
¹ushasree19832000@gmail.com

Abstract: POMP is an App for decorum (events and functions) organizing an android application project that provide the basic functionality of a decorum organizer. The application will grant only existed users to log in, and new customers are permitted to register in the application. It is proposed to be an Android application. The plan provides the majority of the essential functions necessary for an occasion. It allows the user to select from a list of occasions and foyers list for every category of occasion. Once the user choose the occasion type, for example, Marriage, Birthday, Conference, Product launch, etc. The application grant the users to select the date and time of the hall or foyer if any additional requirements needed can be placed in front of the admin view. Since the app contains a list of the hall so the user can select the foyer according to his/her preferences, every information is stored in the record, and the customer can check out their bookings in the booking section. The user data is then transferred to the admin of the application, and if any unavailability of date is occurred will notified to the user immediately. And user data stored in the database. Along with that, a gallery provided to the user or customers to have a view over the halls or foyer for every particular event.

Keywords: *Foyer, Booking, Firebase, Possessor, Occasion*

1. INTRODUCTION: It is an android application which mainly

focuses on decorum (events and functions). It is a known fact that everyone needs to celebrate an occasion grandly, so we come up with an idea to ease the needs of the customer or end-user who are in search for a foyer or function hall. The fact of today's world is smart phones, and android apps, everything from small to more significant works are carried out through apps in smart phones. Back in the old days, when a person wants to search for a foyer for any occasion, the end-user has to take a physical tour i.e., the customer has to move around several places to fix a lobby, which is time-consuming and stressful. This app mainly focuses on customer needs people who are looking foyer or hall for occasions like marriage, birthday, conference meetings, etc. We bring all kinds of lobbies required for different events into a single app. This app contains all the information about the foyer and details about the owner who owns and what are the services provided by the particular foyer.

Unlike another database system, here we used a powerful and firmly secured server database which is provided by the Google

FPGA BASED DIGITAL LOGIC ANALYZER FOR DIGITAL AUTOMATIC TEST EQUIPMENT

¹Manjula C and ²Jayadevappa D

¹Oxford College of Engineering, Bengaluru, VTU, India

²JSS Academy of Technical Education, Bengaluru, VTU, India

Abstract

Simulation is necessary to identify the defects in most of the digital circuits before the final unit is formed. The process of simulation generally caters for displaying logic analysis. Usually, discrete logic circuits which are complex in nature are verified by input simulation and testing of outputs by boundary scan methods. Logic analysers used for such purposes may uncover hardware defects that are not found in simulation. This work covers design and simulation of Digital logic analyser and its sub modules Dual Port Random Access Memory (DPRAM), Parallel to serial converter (PTSC), Multi Standard Baud Rate Generator and Universal Asynchronous Receiver Transmitter (UART). Simulation is done using Xilinx ISE 14.5v EDA tool and FPGA implementation is carried out on Xilinx Spartan3 FPGA board.

Keywords: Digital Pattern Generator, Digital Logic Analyser, Dual port RAM, Baud Rate Generator, UART.

1. Introduction

Multiple analysis of signals from various digital circuits and systems can be analysed using an electronic instrument called logic analyser. These instruments converts the captured information to protocol decodes, timing diagrams machine traces and assembly language. When the users required to have relationships between many signals in digital systems [1], [2], there are advanced capabilities of triggering features in logic analysers. The overall ATE (Automatic Testing Equipment) system consists of Digital Pattern Generator (DPG), Digital Logic Analyser (DLA), Controller to configure DPG and DLA as per CUT (Circuit under Test). Whenever CUT is changed, controller will configure DPG and DLA accordingly to make ATE effective). Figure 1 shows the design of proposed Digital Test Pattern Generator (DTPG) implemented on Xilinx Spartan FPGA.

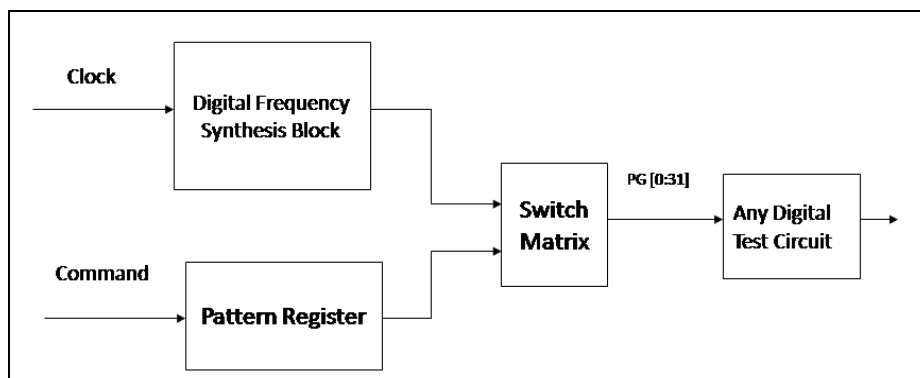


Figure 1. Digital Pattern Generator.

The design and simulation results of all individual sub modules; Digital Frequency Synthesizer, Pattern Generator, Switch Matrix and DUT of the FPGA based DTPG was published in IEEE Digital Library Journal.

When the system is under test, the logic analyser can be triggered to capture the data in a larger scale from the digital systems to analyse the complicated sequences of data. At the time when the logic analyser was put into use, it was a tradition to attach several hundred clips to a digital system. Later, due to the applications of specialized connectors, the development of probes of logic analysers have resulted to a common footprint that support multiple vendors, which enhanced added freedom to consumers. The connector less technology was demonstrated in 2002 and which was recognized by various vendors specifically with trade names such as Soft Touch, D-Max and Compression Probing [3]. Later they became very popular also. These provided a strong, durable and reliable electrical and mechanical connection between the circuit board and probes with less than 0.5 to 0.7 pF loading per signal. Once the information is captured, logic analysers can present it in so many ways starting from simple like displaying waveforms or listing of states etc., to complex way i.e. displaying traffic of decoded Ethernet protocol. Similarly, some of the logic analysers can also work in a compare mode. In this case, captured data will be compared with previously loaded data set. This is helpful for the testing of empirical data for long time. Recent developed logic analysers can even adjusted to set to email a copy of the test information to the in charge on a successful trigger [4], [5].

2. Related Work

In 1960's integrated circuits and digital computing process started and at the same time, a new and complex issues have begun to file up because of inability of oscilloscopes for handling troubles. Early solutions made an attempt to combine hardware from multiple oscilloscopes into single unit, but a lack of definite data interpretation, screen clutter and the constraints of probes made this solution applicable for only marginal usage.

In 1973, the HP 5000A logic analyser was introduced, this was published in Hewlett Packard newsletter. Probably this was the first instrument commercially available namely Logic Analyser. However, the HP 5000A was limited to only two channels and information was usually presented by means of 32 LEDs with two rows. The HP 1601L was the first truly parallel instrument which has 12 channel. This was a plug-in for the HP 180 series oscilloscope mainframes and used the oscilloscope screen to present 16 rows of 12 bit words as 1s and 0s.

At present, there are 3 varieties of logic analysers are available in the market. The first one is the modular logic analyser which consist of either a chassis or mainframe and logic analyser modules [6]. In this case, the mainframe or chassis has display, controls, computer control and also multiple slots where the actual data capturing hardware is installed. In the modules, each have a specific number of channels and multiple modules may be combined to get a very high channel count. This type of logic analysers are generally very expensive. The cost justification for higher performance logic analysers depends on the ability to combine multiple modules to yield for the higher channel count. The user often must provide their own host PC or purchase an embedded controller compatible with the system for the very high end modular logic analysers [7], [8].

Portable LAs, are also called as standalone logic analysers [9], [10]. These analysers combines everything into a single unit, with options installed at the factory. But, portable logic analysers have lower performance as compared to their modular counterparts, they are often applied for general purpose debugging by cost conscious users.

In case of PC based logic analysers, the hardware connects to a computer through a USB or Ethernet connection and transmits the signals which are captured to the software on the computer. These devices are generally much smaller and cost effective because they make use of existing keyboard, display and CPU of personal computers.

3. Proposed Approach

The figure 2 shows the design of proposed Digital Logic Analyser (DLA) to be implemented on FPGA. The design consists of following blocks; Dual port RAM with simultaneous READ and

WRITE, Parallel to serial converter, UART, MAX232 level converter and RS232 cable. The design consideration of DLAL is as follows.

- The width of the FIFO DPRAM is fully programmable and is dependent on processor data bus.
- If there is a difference between the width of FIFO and processor data memory latency will be more
- In DPRAM, there is a separate port for data read & write with the condition with the condition first read and then write
- RS232 has a fixed frequency i.e., around 5KHz
- If processor speed is in KHz then DPRAM can be replaced by a single row shift register of data bus width.
- If processor is 10MHZ (data writing speed), data reading speed is 10KHZ, then data reading is slower by 10^3 compared to writing speed. Hence 10^3 rows of DPRAM is required for data missing.

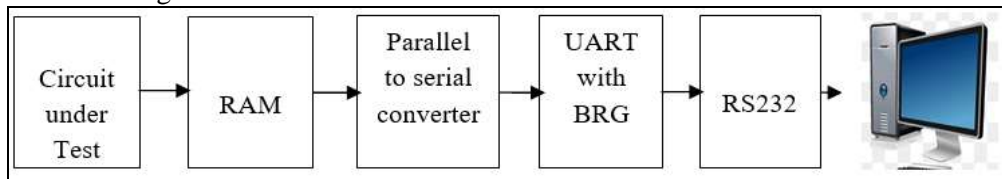


Figure 2. Proposed block diagram of Digital Logic Analyser.

4. Design and Simulation Results of DLA

4.1 DPRAM

Figure 4 (a) shows the RTL schematic of DPRAM (16x8) with 16 locations of each 8 bits, 2 separate ports, 2 address buses and 2 clocks for reading and writing data into the memory. This will perform read and write memory operations from the single RAM, with a condition that reading and writing operations will happen from different memory locations. There is a minimum prescribed data settling time (latency) of 3 write clocks time, before reading data from various locations of the RAM. The input and output pins/buses and their respective functionalities are as follows.

- data_in[7:0] – 8 bit input data bus or input data port to write data into the memory location as per corresponding write address.
- data_out[7:0] - 8 bit input data bus or input data port to read data into the memory location as per corresponding read address.
- read_addr[3:0] - 4 bit read address bus that specifies the memory location, from where the data is read
- write_addr[3:0] - 4 bit write address bus that specifies the memory location, from where the data is written
- clk_read - clock frequency at which data will be read from the memory
- clk_write - clock frequency at which data will be written into the memory
- rd_en- read enable signal to activate memory read operation
- wr_en–write enable signal to activate memory write operation



Figure 4. (a) RTL schematic of DPRAM and (b) Simulation waveform of DPRAM.

This latency time between successive write and read operation can be noted only in post layout timing simulation and not indicated in behavioural simulation. The simulation waveform of DPRAM is illustrated in figure 4(b). As can be seen from the simulation waveforms,

- Write clock is running at 200MHz frequency or $t=10ns$.
- Read clock is running at 100MHz frequency or $t=20ns$.
- Write enable and read enable signal are held high from 0 to 400ns, all through the simulation snapshot window.
- Write clock frequency is more than read clock frequency.
- Between 0 to 150ns, 4 bit Write address is incremented in DPRAM and the write address is varied from 0 to 14, for each of the 14 clock pulses.
- During the same duration of 0 to 150ns, 8 bit-14 different data are written into respective data locations of DPRAM as per the addresses.
- Between 0 to 300ns, 4 bit read address is incremented in DPRAM and read address varied from 0 to 14, for each of the 14 clock pulses.
- During the same duration of 0 to 300ns, 8 bit-14 different data are read from respective data locations of DPRAM as per the addresses.
- DPRAM is having Dual ports and facilitate simultaneous read and write from different data locations and different read and write clock rates.
- Hence, the DPRAM successively designed, coded in Verilog and simulated in Xilinx ISE simulator is working and the functionality is fully verified.

4.2 Parallel to Serial Converter

In figure 5, the digital design of parallel to serial converter is described. This design contains 4 D-type flip-flops connected in cascade (output of each flip-flop is connected to input of next flip-flop via mux). Mux provides for serial or parallel loading of input data to each of the flip-flops. For serial input data loading, the select line of the mux [cntl =0], then, at the next active clock edge $d[2]=q3=d3$ i.e., d3 data is loaded to d2 and with next successive clock pulses, d3 will move from q3 to q2 to q1 and finally to q0, the last flip-flop in the 4 flip-flop cascade.

- If cntl=1, mux data [md] inputs - md2, md1 and md0 will be applied directly to flip-flop inputs d2, d1 and d0 respectively and hence this method of data loading to a converter is called Parallel data loading. During the next immediate active clock edge, $q3=d3$, $q2=d2=md2$, $q1=d1=md1$ and $q0=d0=md0$.
- If the data output is read out from the 4 flip-flop outputs [q3, q2, q1 and q0] during this immediate active clock edge, we get parallel data output.
- If the data is parallel loaded and parallelly read out, then such a system is called parallel in and parallel out converter (PIPO).
- If the data is loaded parallelly with cntl=1 and data is read out from q0, after every active edge of 4 clock cycles, such a system is called Parallel to Serial converter.

Hence using the above circuit, we can realize SISO, PISO, SIPO and PIPO. But in the proposed research experiment requirement will be to implement parallel to serial converter only.

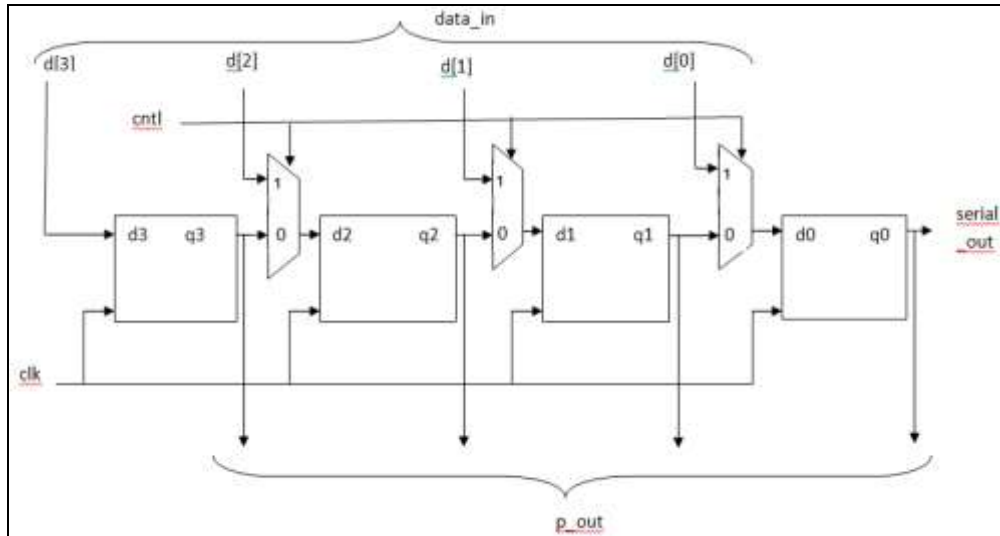


Figure 5. Digital circuit diagram of Parallel to Serial converter.

If the data is loaded parallelly with cntl=1 and data is read out from q0, after every active edge of 4 clock cycles, such a system is called Parallel to Serial converter. Hence using the above circuit, we can realize SISO, PISO, SIPO and PIPO.

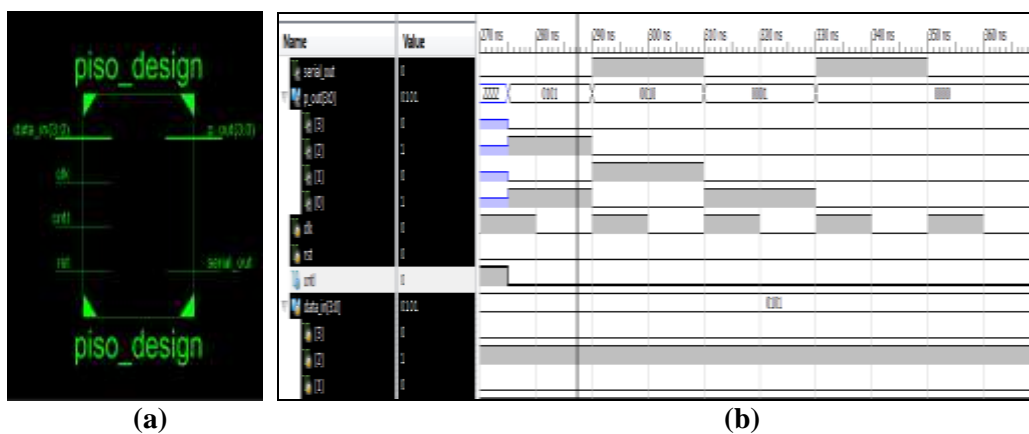


Figure 6. (a) RTL schematic of Parallel to serial converter and (b) Simulation result of Parallel to Serial Converter.

But our research experiment requirement will be to implement Parallel to Serial converter only. The figure 6(a) shows the RTL schematic of PISO after synthesis using Xilinx ISE tool. As can be seen,

- Data_in[3:0] is 4 bit data input to the PISO
- P_out[3:0] is 4 bit parallel output
- Serial_out is 1 bit serial output of PISO
- Cntl is 1 bit input signal to control the mux. [If cntl =0, serial in & if cntl=1, parallel input]
- Reset signal=1 will clear all 4 flip flops & Reset signal=0 will allow PISO to function normally.

The table1 shows data transition happening through all 4 flip-flops with respective parallel inputs is applied at various clock edges and the corresponding serial outputs, at various values of cntl signals and corresponding clock transitions.

Table 1. Truth table for all 4 flip-flops.

| Clk | Cntl | Data in | D ₃ | D ₂ | D ₁ | D ₀ | Serial Out |
|-----|------|---------|----------------|----------------|----------------|----------------|------------|
| 1 | 1 | 0101 | 0 | 0 | 0 | 1 | - |
| 2 | 0 | | 0 | 0 | 1 | 0 | 1 |
| 3 | 0 | | 0 | 0 | 0 | 1 | 0 |
| 4 | 0 | | 0 | 0 | 0 | 0 | 1 |
| 5 | 0 | | 0 | 0 | 0 | 0 | 0 |
| 6 | 1 | 1111 | 1 | 1 | 1 | 1 | - |
| 7 | 0 | | 0 | 1 | 1 | 1 | 1 |
| 8 | 0 | | 0 | 0 | 1 | 1 | 1 |
| 9 | 0 | | 0 | 0 | 0 | 1 | 1 |
| 10 | 0 | | 0 | 0 | 0 | 0 | 1 |

The following aspects can be observed from the simulation waveform.

- 500MHZ frequency Clock is applied to the PISO converter
- Reset is held low all through the simulation.
- From 270ns to 400ns, parallel input data_in[3:0] is held at 0101.
- Cntl is held high initially between 270 to 280ns and parallel data output pout [3:0] is tristated.
- From 280ns to 400ns, Cntl =0, to facilitate serial loading of data to the cascade of 4 flip-flops in the PISO converter
- At 280ns, parallel data input data_in[3:0]=0101, pout[3:0]= 0101 and serial_out=0.
- At the clock edge of 290ns, parallel data input applied at 270ns will get shifted right once or by 1 bit and hence pout= 0010 and serial_out=1.
- At the clock edge of 310ns, parallel data input applied at 290ns will get shifted right once or by 1 bit and hence pout= 0010 and serial_out=0.
- At the clock edge of 330ns, parallel data input applied at 310ns will get shifted right once or by 1 bit and hence pout= 0010 and serial_out=1.
- And the similar chain of events repeats. Thereby converting 4 bit parallel data input applied into 4 bit serial data output.
- The total number of clock pulses required to convert parallel input data into serial output data= the number of bits of parallel data.
- Hence PISO functionality is verified.

4.3 Standard Baud Rate Generator for FPGA

The multiple standard baud rate generator (BRG) for the FPGA board having 10 MHz as master clock is used in the design of DLA. The table 2 indicates multiple standard baud Rates and strategy to derive the multiple specific baud clocks from master clock on the FPGA board of 10MHz.

For instance, to transmit data from UART at 1200bps, a baud rate clock of 600Hz has to be derived from the master clock of 10MHz. This is achieved by dividing master clock of 10MHz by a factor of 16666 and thereby the duration between pulses of 1.66ms is achieved. Likewise, all other standard baud rates can be achieved by using suitable dividing factor, to thereby achieve respective baud rates and pulse duration.

Table 2. Multiple Standard Baud Rates and Clock for FPGA.

| Standard Baud Rate in bps | Master clock to be divided a factor | Specific Baud clock in HZ | Duration b/w pulses |
|---------------------------|-------------------------------------|---------------------------|---------------------|
| 1200 | 16666 | 600 | 1.66 ms |
| 2400 | 8333 | 1200 | 0.833ms |
| 4800 | 4167 | 2400 | 0.416 ms |

| | | | |
|---------------|------|-------|----------------|
| 9600 | 2083 | 4800 | 208.35 μ s |
| 19200 | 1041 | 9600 | 104.14 μ s |
| 38400 | 520 | 19200 | 52.0 μ s |
| 57600 | 260 | 38400 | 26.05 μ s |
| 115200 | 174 | 57600 | 17.45 ms |

The figure 7 shows multiple BRG clock design wherein master clock is divided by suitable division factor to achieve required baud clock.

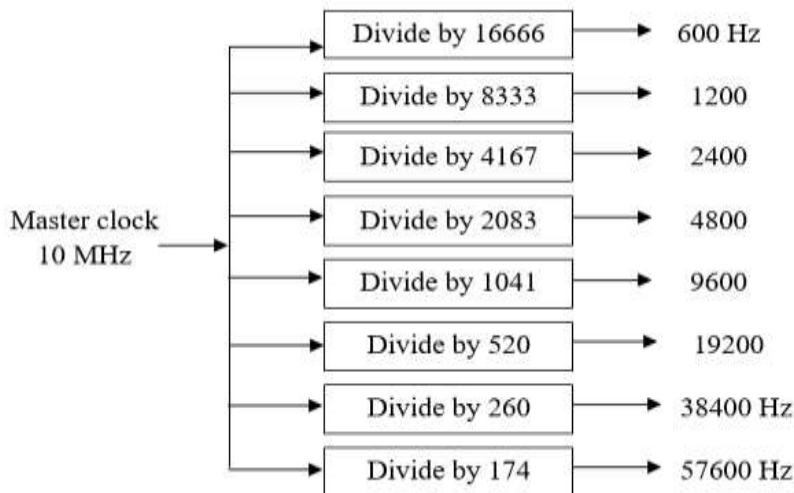


Figure 7. Baud Rate Generator (BRG) clock Design.

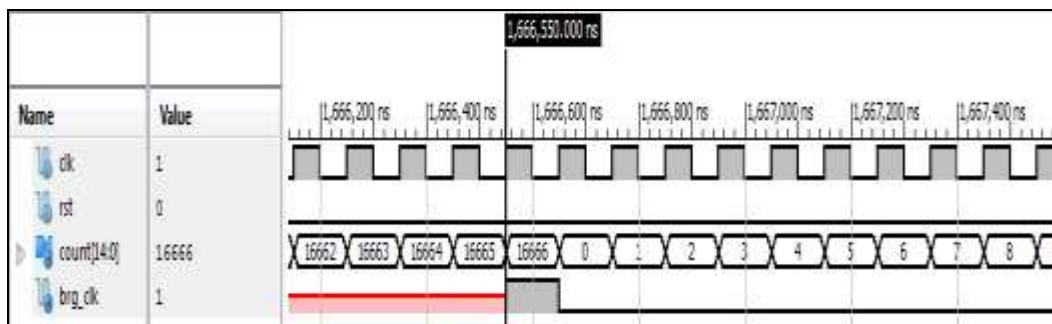
4.3.1 Simulations results for different Baud rate and Baud rate clock

A. Baud rate 1200 bps and baud rate clock 600 Hz

The simulation of Baud rate generator (1200 bps) of baud clock 600 is shown in figure 8. The following are the simulation results implications.

- Master Clock frequency is 10 MHz=20Mbps.
- BRG to be generated at 1200bps [frequency=600Hz], hence the clock has to be divided by a factor of 16666.
- Using multiple clock dividers, the master clock is divided by 16, again divided by 10 three times.
- Alternative method a 16666 counter's terminal counter signal will provide the required 9600bps or 4800Hz more accurately.

As can be seen from the simulation waveforms, Baud rate pulses or frequency are generated after every 16666 clock pulses and are indicated by B_clk dotted signals.



- Using multiple clock dividers, the master clock is divided by 4, again divided by 10 three times.
- Alternative method a 4167 counter's terminal counter signal will provide the required 4800bps or 2400Hz more accurately.

As can be seen from the simulation waveforms, Baud rate pulses or frequency are generated after every 4167 clock pulses and are indicated by B_clk dotted signals.

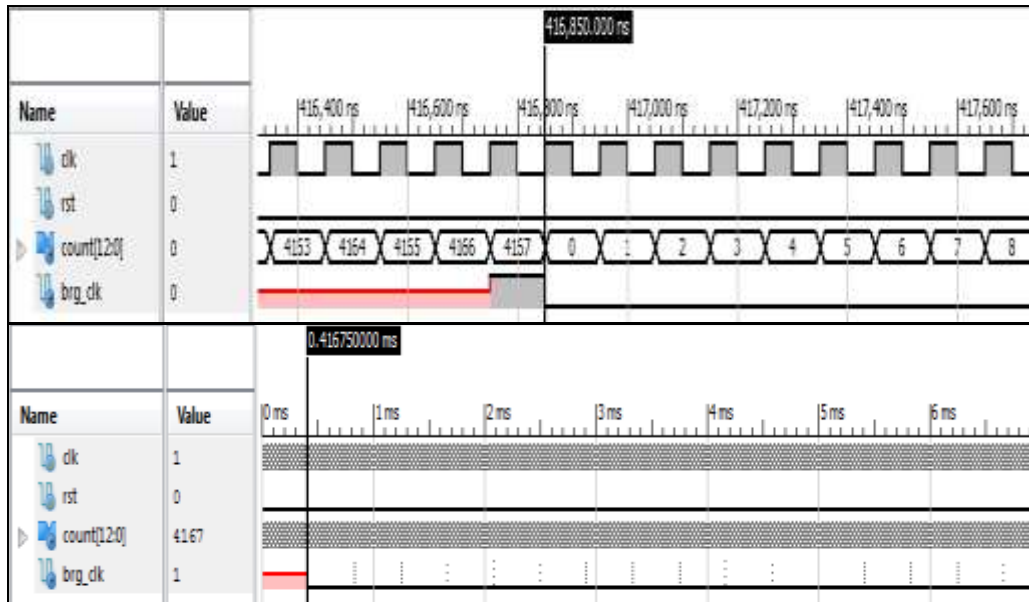
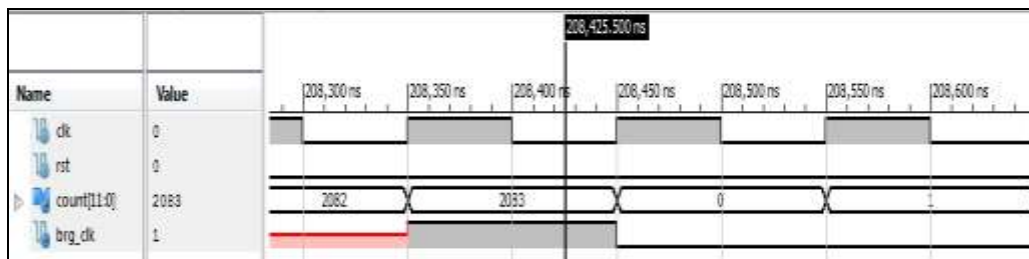


Figure 10. Simulation of Baud rate generator of Baud clock 4800.

D. Baud rate 9600 bps and baud rate clock 4800 Hz

- Master Clock frequency is 10 MHz=20Mbps.
- BRG to be generated at 9600bps [frequency=4800Hz], hence the clock has to be divided by a factor of 2083 [approximately 2000].
- Using multiple clock dividers, the master clock is divided by 2, again divided by 10 three times.
- Alternative method a 2083 counter's terminal counter signal will provide the required 9600bps or 4800Hz more accurately.

As can be seen from the simulation waveforms, Baud rate pulses or frequency are generated after every 2083 clock pulses and are indicated by B_clk dotted signals.



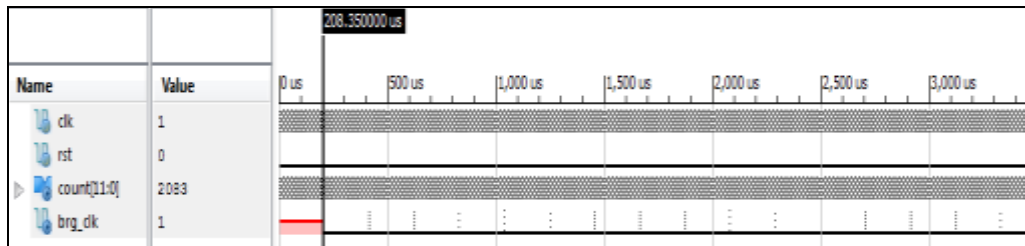


Figure 11. Simulation of Baud rate generator of Baud clock 4800.

E. Baud rate 19200 bps and baud rate clock 9600 Hz

- Master Clock frequency is 10 MHz=20Mbps.
- BRG to be generated at 19200bps [frequency=9600Hz], hence the clock has to be divided by a factor of 1041.
- Using multiple clock dividers, the master clock is divided by 10 three times.
- Alternative method a 1041 counter's terminal counter signal will provide the required 19200bps or 9600Hz more accurately.

As can be seen from the simulation waveforms, Baud rate pulses or frequency are generated after every 1041 clock pulses and are indicated by B_clk dotted signals.

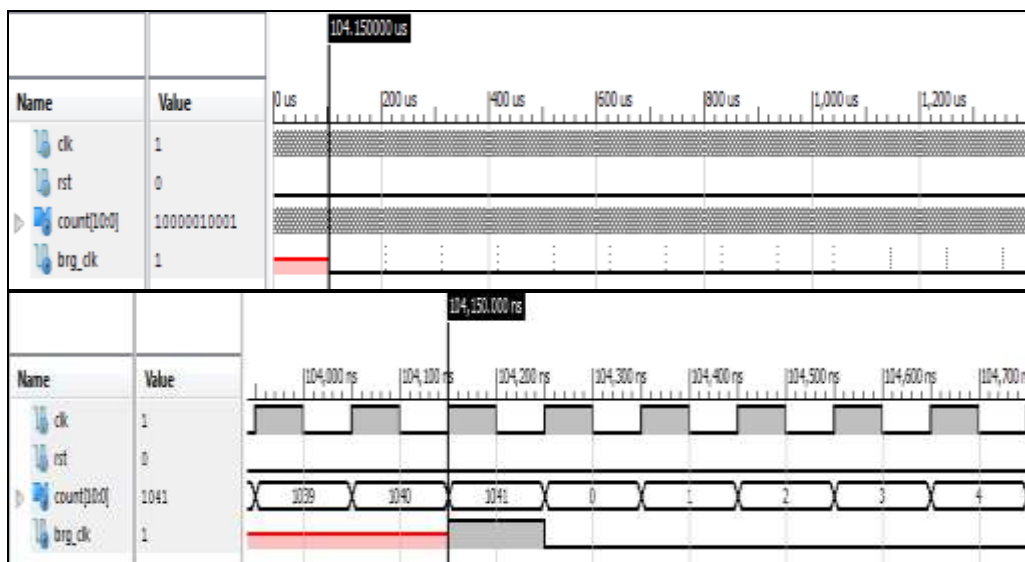


Figure 12. Simulation of Baud rate generator of Baud clock 9600.

F. Baud rate 38400 bps and baud rate clock 19200 Hz

- Master Clock frequency is 10 MHz=20Mbps.
- BRG to be generated at 38400bps [frequency=19200Hz], hence the clock has to be divided by a factor of 520.
- Using multiple clock dividers, the master clock is divided by 5, again divided by 10 two times.
- Alternative method a 520 counter's terminal counter signal will provide the required 38400bps or 19200Hz more accurately.

As can be seen from the simulation waveforms, Baud rate pulses or frequency are generated after every 520 clock pulses and are indicated by B_clk dotted signals.

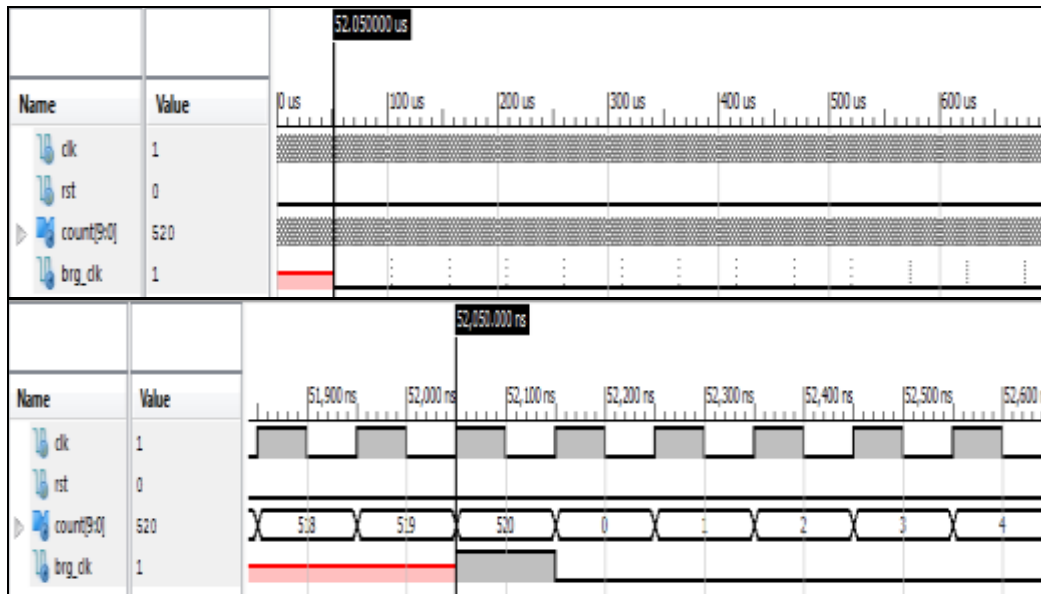


Figure 13. Simulation of Baud rate generator of Baud clock 19200.

G. Baud rate 57600 bps and baud rate clock 38400 Hz

- Master Clock frequency is 10 MHz=20Mbps.
- BRG to be generated at 57600bps [frequency=38400Hz], hence the clock has to be divided by a factor of 260.
- Using multiple clock dividers, the master clock is divided by 2, divided by 13 and again divide by 10.
- Alternative method a 260 counter's terminal counter signal will provide the required 57600bps or 38400Hz more accurately.

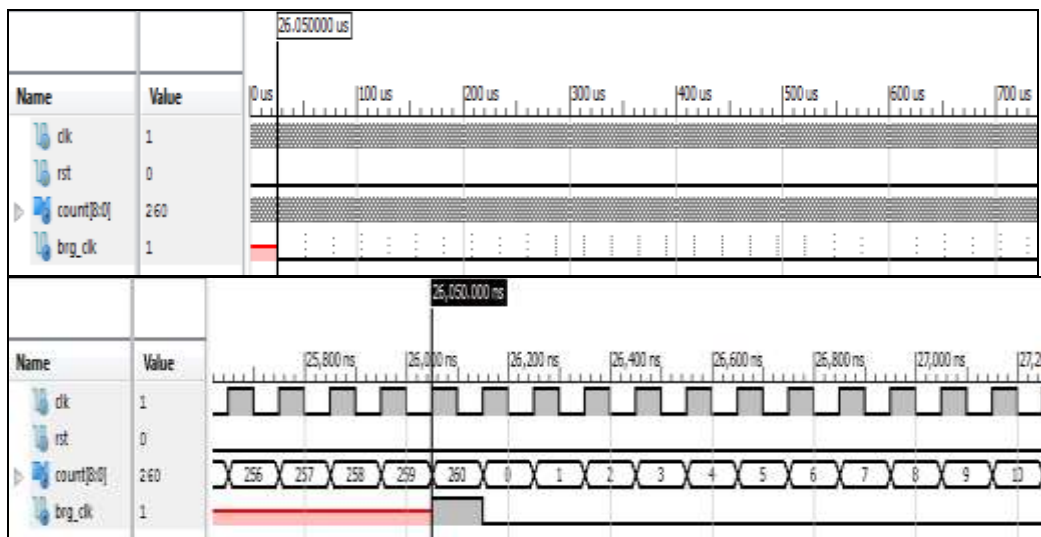


Figure 14. Simulation of Baud rate generator of frequency 38400.

As can be seen from the simulation waveforms, Baud rate pulses or frequency are generated after every 260 clock pulses and are indicated by B_clk dotted signals.

H. Baud rate 115200 bps and baud rate clock 57600 Hz

- Master Clock frequency is 10 MHz=20Mbps.

- BRG to be generated at 115200bps [frequency=4800Hz], hence the clock has to be divided by a factor of 174.
- Using multiple clock dividers, the master clock is divided by 13, again divided by 13.
- Alternative method a 174 counter's terminal counter signal will provide the required 115200bps or 57600Hz more accurately.

As can be seen from the simulation waveforms, Baud rate pulses or frequency are generated after every 174 clock pulses and are indicated by B_clk dotted signals.

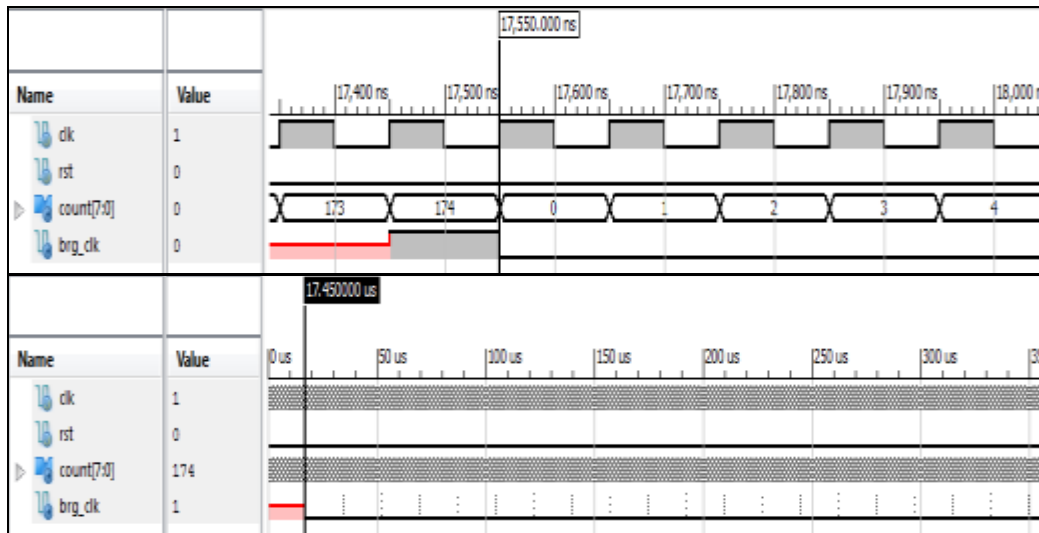


Figure 15. Simulation of Baud rate generator of Baud clock 57600.

4.4 UART Design

The top level block diagram of UART is depicted in figure 16. It consists of digital modules, Parallel to serial converter, Multiple Baud Rate Generator which provides Universal data rates [1200, 2400, 4800, 9600, 19200, 38400, 57600 and 115200]. In UART, the transmission Buffer Register [TBR] sends transmission data serially at desired baud rates and the Baud Rate select Mux is used to select required Baud clock for data transmission based on specified Baud rate.

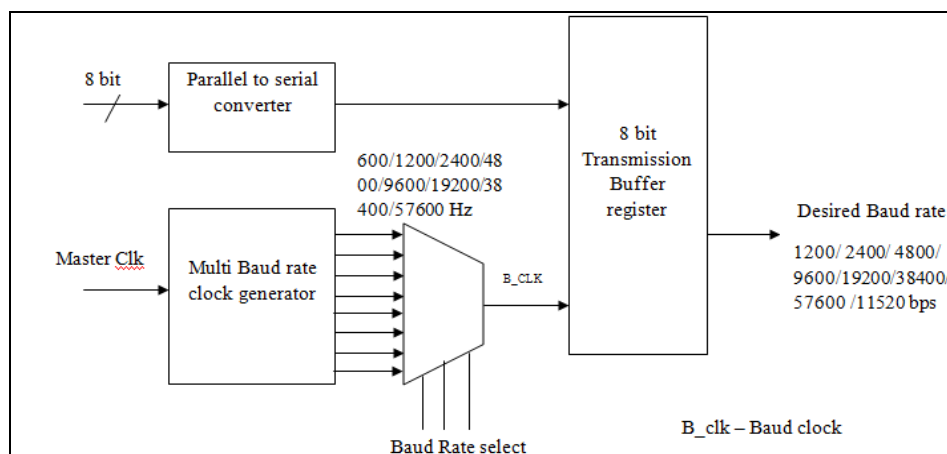


Figure 16. Block diagram of UART.

5. Conclusion

In this paper, novel and innovative design was undertaken to implement all the sub modules of a Digital Logic Analyzer. Multi Baud rate generator is a specialized module that would make this DLA acquire data from low or high frequency DUT channels and enable high speed data acquisition and display. Till date, several products are available in the market with varied specifications and functionalities with respect to Digital Logic Analyzers. But no research has been undertaken to design and develop a Digital ATE on FPGA. Hence this research experiment is very unique and important as compared to the existing systems.

References

- [1] Amit Dhir, “Programmable logic solutions enabling digital consumer technology”, the digital consumer technology handbook, chapter 19, (2004), pp. 516-537.
- [2] S.Adilakshmi, K.Rajasekhar and T.B.K.Manoj kumar, “Integrating Logic Analyzer Functionality into VHDL designs”, International Journal of Computer Science and Information Technologies, vol. 3, no. 1, (2012), pp. 3107-3111.
- [3] D Nanda Kishore and S K Ghoshal, “Design and implementation of a PC-based FPGA Tester”, IETE Technical Review, vol.12, (2015), pp. 119-132.
- [4] Sonam M. Tiple, Swetansha C, Aishwarya S, V. P. Mulik, A. P. Yadav , “Arm Based Logic Analyzer”, International Journal of Advanced Research in Computer Science and Software Engineering, vol. 5, Issue 3, (2015).
- [5] Chaitanya Kilaru, J K R Sastry and K RajaSekhara Rao, “Testing distributed embedded systems through logic analyzer”, International Journal of Engineering and Technology, 7 (2.7), (2018), pp. 297-302.
- [6] Ranjan Kumar Sen, Ajit Pal and A. K. Choudhury, “A Programmable Logic State Analyser”, IETE Journal of Research, vol. issue 7, (2015), pp. 434-439.
- [7] Sheng-Luen Chung , Cheng-Wei Chu , Yu Fu and , Embedded control system design and practice”, Journal of the Chinese Institute of Engineers, vol. 30, issue 6, (2011), pp. 1103-1107.
- [8] W F Clocksin, “Logic Programming and Digital Circuit Analysis”, Journal of Logic Programming, (1987), pp. 59-82.
- [9] Fei Tao, Y. Tang, X. Zou, Q. Qi, “A field programmable gate array implemented fibre channel switch for big data communication towards smart manufacturing”, Robot. Comput.-Integr. Manuf. vol.57, (2019), pp. 166–181.
- [10] J. Li, X. Dai, Z. Meng, “Automatic reconfiguration of petri net controllers for reconfigurable manufacturing systems with an improved net rewriting system-based approach”, IEEE Trans. Autom. Sci. Eng. vol. 6, (2009), pp. 156–167.

PAPER • OPEN ACCESS

An extension of golden section algorithm for n-variable functions with MATLAB code


G Sandhya Rani¹, Sarada Jayan¹ and K V Nagaraja¹

Published under licence by IOP Publishing Ltd

IOP Conference Series: Materials Science and Engineering, Volume 577, International Conference on Advances in Materials and Manufacturing Applications (IConAMMA-2018) 16–18 August 2018, Bengaluru, India

Citation G Sandhya Rani *et al* 2019 *IOP Conf. Ser.: Mater. Sci. Eng.* **577** 012175sandhya.reddyj@gmail.comj_sarada@blr.amrita.edukv_nagaraja@blr.amrita.edu¹ Department of Mathematics, Amrita School of Engineering, Bengaluru, Amrita Vishwa Vidyapeetham, India<https://doi.org/10.1088/1757-899X/577/1/012175>

Buy this article in print

 Journal RSS

Sign up for new issue notifications

Create citation alert

Abstract

Golden section search method is one of the fastest direct search algorithms to solve single variable optimization problems, in which the search space is reduced from $[a, b]$ to $[0,1]$. This paper describes an extended golden section search method in order to find the minimum of an n-variable function by transforming its n-dimensional cubic search space to the zero-one n-dimensional cube. The paper also provides a MATLAB code for two-dimensional and three-dimensional golden section search algorithms for a zero-one n-dimensional cube. Numerical results for some benchmark functions up to five dimensions and a comparison of the proposed algorithm with the Nelder Mead Simplex Algorithm is also provided.

PDF

Help

This site uses cookies. By continuing to use this site you agree to our use of cookies. To find out more, see our [Privacy and Cookies policy](#).



Article

CONVEXITY OF ONE MEAN WITH RESPECT TO ANOTHER MEAN

August 2016

Authors:



K.M. Nagaraja
JSS Academy of Technical Education Bangalore



P S K Reddy



Sridevi K.
Rashtreeya Vidyalaya College of Engineering

[Request full-text](#)

[Download citation](#)

P S K Reddy

This person is not on ResearchGate, or hasn't claimed this research yet.

To read the full-text of this research, you can request a copy directly from the authors.

[Citations \(2\)](#)

[References \(14\)](#)

Discover the world's research

- 20+ million members
- 135+ million publications
- 700k+ research projects

[Join for free](#)

No full-text available



To read the full-text of this research, you can request a copy directly from the authors.

[Request full-text PDF](#)

[Citations \(2\)](#)

[References \(14\)](#)

Convexities of Stolarsky's Mean With Respect to Well Known Greek Means

[Article](#) [Full-text available](#)

Apr 2018

K.M. Nagaraja · P.Siva Kota Reddy · Sampath kumar. R

[View](#) [Show abstract](#)

Convexities of Stolarsky's Mean With Respect to Well Known Greek Means

[Article](#) [Full-text available](#)

Apr 2018

Sampath kumar. R · K.M. Nagaraja

[View](#) [Show abstract](#)

See discussions, stats, and author profiles for this publication at: <https://www.researchgate.net/publication/342657308>

A study on Compartmental models, Epidemiological Characteristics and Stability Analysis of pandemic COVID-19 in INDIA

Article · July 2020

CITATIONS

0

READS

114

1 author:



Umesha Veerakyathaiah

Dayananda Sagar Institutions

6 PUBLICATIONS 6 CITATIONS

SEE PROFILE

A study on Compartmental models, Epidemiological Characteristics and Stability Analysis of pandemic COVID-19 in INDIA

S Padmanabhan¹, Umesh V², Anand K S³, Baskar P⁴, Sreenivasa Reddy Perla⁵,
Narasimhan G¹, Sampathkumar R¹

¹Department of Mathematics, RNS Institute of Technology, Bangalore, India

²Department of Mathematics, Dayananda Sagar College of Engineering, Bangalore, India

³Department of Mathematics, APS College of Engineering, Bangalore, India

⁴Department of Mathematics, New Horizon College of Engineering, Bangalore, India

⁵Department of Mathematics, The Oxford College of Engineering, Bangalore, India

Abstract: In this paper, we attempted to describe the outbreak of Severe Acute Respiratory Syndrome (SARS) Coronavirus 2 (COVID-19) via various compartmental models. We first simulate the COVID-19 situation in India. Dynamics of the models are presented. The basic reproduction number R_0 is determined for real data and finally reviewed the comprehensive stability analysis. The data used from health care agencies, the Government Organizations and the Planning Commission www.worldometers.info/coronavirus, www.covid19india.org/ and www.mygov.in/covid-19 to make suitable arrangements to fight the pandemic.

Keywords: Novel Coronavirus, compartmental models, reproduction number, epidemiological parameters, stability analysis.

1. Introduction

The novel coronavirus disease (COVID-19) was first confirmed in the Chinese city of Wuhan, late December, 2019. The rapidity of its spread in many countries around the globe made the World Health Organization (WHO) declare it as a global pandemic and public health emergency, raising concerns that if countries with robust healthcare systems to detect and control disease outbreak are having challenges managing the disease, countries with weak healthcare system need to put adequate measures in place to contain the spread [1]. The coronavirus disease (COVID-19) caused by the Severe Acute Respiratory Syndrome Coronavirus-2 (SARS-CoV-2) presents clinical features which are similar to the diseases caused by other coronaviruses, Severe Acute Respiratory Syndrome (SARS) and Middle East Respiratory Syndrome such as lower respiratory illness with fever, dry cough, myalgia, shortness of breath etc. The Coronavirus disease is “novel” in the sense that, it is a new strain of zoonotic origin which has not been previously discovered to affect humans. Historically, the COVID-19 pandemic is a major human coronavirus epidemic in the last two decades aside SARS [2] and MERS [3, 4] respectively. The incubation period of COVID-19 is between 2-14 days with symptoms averagely between 5-7 days. Its basic reproduction number is averaged 2.2 [5] and even more ranging from 1.4 – 6.5 in [6].

The COVID-19 outbreak is currently on-going and the number of infections has been fast growing since the onset of the epidemic. As on June 18, 2020, 17:07 GMT, the virus had affected 213 countries and territories globally with 8,512,149 confirmed cases, of which

453,425 have passed away, 4,455,403 recovered, 3,548,708 (98%) are in Mild condition and 54,613 (2%) cases are in critical condition (worldometers.info).

The first case of the COVID-19 pandemic in India was reported on 30 January 2020, originating from China. As on 18th June 2020, the Ministry of Health and Family Welfare have confirmed a total of 377,122 cases, 200,358 recoveries and 12,501 deaths in the country. India currently has the Fourth largest number of confirmed cases in world with number of cases breaching the 400,000 mark on 18th June 2020. The highest single day surge in new cases was 12,881 cases were reported recorded on 17th June 2020. India's case fatality rate is relatively lower at 3.09%, against the global 6.63% as of 18th June 2020. Five cities account for around half of all reported cases in the country – Mumbai, Delhi, Ahmedabad, Chennai and Pune. As of 18th June 2020, only a region, Lakshadweep has not reported a case.

Due to lack of appropriate vaccination and its highly contagious nature, there is still a possibility that the outbreak could become more intense and cause high mortality around the world. There is no doubt that the pandemic has profound effects on world economy and our private and professional sectors. To avoid the risk of worst condition of this pandemic outbreak, the central government and local governments of all the infected countries had tightened preventive measures and large-scale movement of population is strictly prohibited. As the outbreak grows to a greater extent, severally infected areas are imposing a more massive quarantine.

Recent analysis by the World Health Organisation (WHO) suggests that out of total infected cases, 80% of infected patients are asymptomatic or at an initial stage, 15% are severely infected, suffering from dyspnoea and 5% are requiring ventilation as they are at critical stage. Mainly two types of human to human virus transmission are reported, symptomatic, pre-symptomatic transmission. Symptomatic transmission occurs while exposed individuals come in contact with the infected respiratory droplets spread through coughing or sneezing by symptomatic individuals.

The incubation period for COVID-19 is on usual 5-6 days, and can be extend up to 14 days, which makes it hard to find and quarantine infected individuals before symptoms onset. The duration of this pre-symptomatic period which is more hazardous, since some infected persons can be contagious in this duration and they can infect others unknowingly.

The outbreak has been declared an epidemic in more than a dozen states and union territories, where provisions of the Epidemic Diseases Act, 1897 have been invoked, and educational institutions and many commercial establishments have been shut down. India has suspended all tourist visas, as a majority of the confirmed cases were linked to other countries.

Mathematical formulation of disease models is very effective to understand epidemiological prototypes of diseases, as well as it helps us to take necessary measures of public health intrusions by controlling the spread of the diseases. In this paper, we briefly discussed about the basic terminologies, epidemiological characteristics, various compartmental SIR/SIRS, SEIR/SEIRS, SEQIR and SEQIDR models to study the transmission of the COVID-19 infection in India. Its basic reproduction number is calculated using real data and reviewed the comprehensive stability analysis.

2. Basic Terminologies

Pathogen: a bacterium, virus, or other microorganism that can cause disease.

Susceptible: A person who is not infected but is at a risk of catching infection.

Exposed: A person who has contracted the infection but does not have visible symptoms.

Infectious: A person who has the disease with symptoms and is capable of passing infection to others.

Recovered/Removed: After treatment, the symptoms are gone and the person is no more infectious.

Incubation period: It is the duration between exposure to the infection and having first apparent symptom of the disease.

Endemic: A disease is said to be endemic if it is regularly found in a population or a particular area.

Epidemic: A disease is said to be in epidemic stage if the number of cases substantially increases within a short duration in a given population.

Pandemic: A disease is said to be pandemic if it is prevalent in the entire country or the world.

Isolation: Infected people are isolated from contact with other people. Only sanitary professionals are in contact with them. However, contamination of those professionals also occurs. Isolated patients receive an adequate medical treatment that reduces the COVID-19 fatality rate.

Quarantine: Movement of people in the area of origin of an infected person is restricted and controlled (e.g. quick sanitary check-points at the airports) to avoid that possible infected people spread the disease.

Tracing: The objective of tracing is to identify potential infectious contacts which may have infected a person or spread COVID-19 to other people. Increase the number of tests in order to increase the percentage of detected infected people.

Interquartile range (IQR): It is a measure of variability, based on dividing a data set into quartiles. Quartiles divide a rank-ordered data set into four equal parts. The values that divide each part are called the first, second, and third quartiles; and they are denoted by Q_1 , Q_2 , and Q_3 , respectively.

- Q_1 is the "middle" value in the first half of the rank-ordered data set.
- Q_2 is the median value in the set.
- Q_3 is the "middle" value in the second half of the rank-ordered data set.

In order to find the difference between the upper and lower quartile, you'll need to subtract the 25th percentile from the 75th percentile. The formula is written as: $IQR = Q_3 - Q_1$.

Basic reproduction number: The average number of secondary cases generated by a single case in an entirely susceptible population is called a basic reproduction number and is denoted by R_0 . For a pathogen with direct person-to-person transmission.

i.e., $R_0 = \text{Rate of transmission} \times \text{Infectious period} \times \text{Population size}$

Mortality rate or death rate: It is a measure of the number of deaths in a particular population, scaled to the size of that population, per unit of time.

3. Epidemiological parameters

In the early days of the pandemic, limited data availability led the first generation epidemiological models to predict that hundreds of millions would be infected with the virus, and millions of lives lost. Fortunately, the reality so far has turned out to be very different. However, the situation is still worrisome. From 657 cases on March 25, India has more than 285,000 cases today. Even more troubling are those active cases continued to grow, despite a significant slowdown since the national lockdown.

To understand the future trajectory of the pandemic and to frame appropriate policy responses, we need granular data based on contact tracing at the level of a city or district to provide information on three important epidemiological parameters.

1. Incubation period, which is the interval between infection and symptoms. The distribution of this parameter helps the government and experts understand the nature, extent and possible future scenarios of the outbreak. It also informs in the evaluation of the disease-control strategy.
2. The serial interval, which is the time between the onset of the illness in the primary case (infector) and illness onset in the secondary case (infectee). If the estimated average of the serial interval is shorter than the estimated average incubation period, then pre-symptomatic transmission is more likely to happen than symptomatic transmission. Research from Japan has indicated that the median serial interval for Covid-19 is 4.1 days, which is less than the mean incubation period of approximately five days. The public policy implication of this is that containment via case isolation might be a challenging task. Containment would, therefore, require to be guided by an aggressive testing and rapid contact tracing strategy.
3. The basic reproduction ratio (also popularly known as R_0), which is the average number of secondary cases per primary case. There has been a great deal of focus on this parameter, because if the R_0 is greater than one, then the probability that there will be an outbreak is extremely high.

The importance of the parameter R_0 , one has to exercise great caution in interpreting and estimating it. Most models that estimate this parameter assume that all individuals have a homogenous transmission and constant recovery rate. Therefore, a population-based R_0 is estimated with the implication that if this is greater than one, then outbreaks from a single infected person is highly likely to happen. However, research based on the previous Severe Acute Respiratory Syndrome (SARS) epidemic in 2003 has shown that there is a great deal of variability in individual infectiousness. The variability of R_0 plays an important role in the dynamics of an outbreak. Models that account for individual variability show that even if the population-based R_0 is greater than one, an outbreak could still be a low-probability event.

In the Indian context, this might explain why Mumbai is experiencing an explosive outbreak, while many other large, highly-dense cities with significant populations dwelling in slums, are not experiencing such an outbreak.

Crude mortality rate (CMR) is not really applicable during an ongoing epidemic. And to reach herd immunity for COVID-19 and effectively end the epidemic, approximately two thirds (67%) of the population would need to be infected.

The patients affected in India had a median age of 36 years with IQR of 25-54 years. Largest percentage of affected patients was in the age group of 20-39 years. There were 66.34% male patients and 33.66% female patients. The median age for affected males was 35 years (IQR 25-50) and for females was 40 years (IQR 24.5-59). Both in male patients and female patients the largest number of affected patients was in the 20-39 years age group accounting for 54.38% of males and 41.01% of females. This was followed by the age group 40-59 years accounting for 25.91% of males and 26.62% of females. According to the data, 16 patients out of 413 had died accounting for 3.8 % cases, with 68.75% of all the deaths among 60-79 years, accounting for 11 deaths. The median age of deceased patients was 65 years with IQR 59.25-69. The mortality rate in male patients was 4.38% and for female patients was 2.88%. For recovered patients, most were in the 20-39 age group followed by the 40-59 years age group. Median 36 years with IQR 21.75-56.25.

4. Model formulation

Disease models play an important role in understanding and managing the transmission dynamics of various pathogens. We can use them to describe the spatial and temporal patterns of disease prevalence, as well as to explore or better understand the factors that influence infection incidence. Modelling is a key step in understanding what treatments and interventions can be most effective, how cost-effective these approaches may be, and what specific factors need to be considered when trying to eradicate disease. Mathematicians, data scientists and statisticians have proposed various models called compartmental models to decipher and predict the behaviour of the epidemic in various environments in the early 20th century; these models stratify a population into groups, generally based on their risk or infection status. Underlying these models is a system of differential equations that track the number of people in each category over time.

4.1. Formulation of SIR/SIRS models

In SIR models, individuals in the recovered state gain total immunity to the pathogen whereas in SIRS models, that immunity wanes over time and individuals can become reinfected.

The SIR/SIRS diagram below shows how individuals move through each compartment in the model. The dashed line shows how the SIR model becomes an SIRS (Susceptible - Infectious - Recovered - Susceptible) model, where recovery does not confer lifelong immunity, and individuals may become susceptible again.

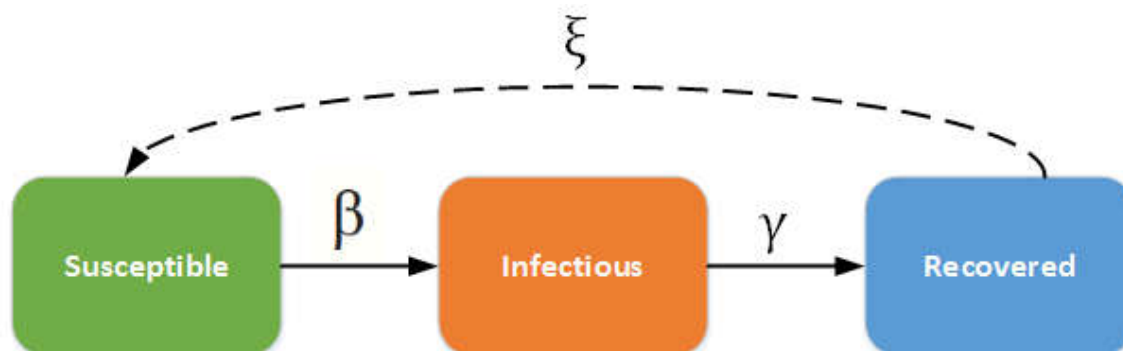


Figure 1: SIR/SIRS Model

The infectious rate β , controls the rate of spread which represents the probability of transmitting disease between a susceptible and an infectious individual. Recovery rate, $\gamma = 1/D$, is determined by the average duration, D , of infection. For the SIRS model, ξ is the rate which recovered individuals return to the susceptible state due to loss of immunity.

4.1.1 SIR - Model

A starting point for the use of mathematical models to study the spread of epidemics was the SIR (Susceptible-Infected-Recovered) model developed in 1927 by Mc Kendrick and Kermack [1]. The model studied a population in which an epidemic could develop and divided the population into three groups:

- $S(t)$: the number of susceptibles
- $I(t)$: the number of infectives
- $R(t)$: the number recovered (recovered, died, or naturally immune to the disease)

The population is considered closed for any time, that is to say, neither births nor migrations are taken into account, in such a way that

$$N = S(t) + I(t) + R(t)$$

where N is the total population of India (N is itself a variable, but treated as a constant in this model consistent with the fact that the course of this epidemic is short compared with the lifetime of an individual).

The flow of transitions from one group to another follows the scheme below:

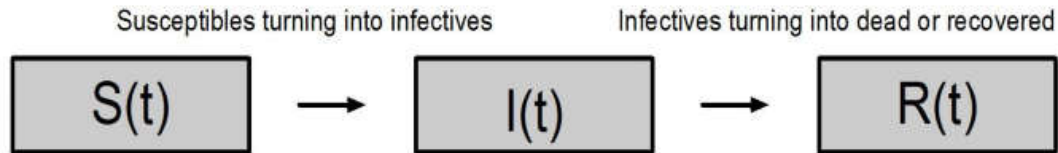


Figure 2: SIR Model

From what is known about corona viruses (COVID-19), it is evident that the per capita rate of increase in the number of infectives is directly proportional to the number of susceptible in the vicinity of an infective and hence, the total intake in the first compartment looks like (βSI) , where β signifies the rate of transmission indicated by the average number of people who will catch the virus from one infected person.

Recovery rate: It takes on the average about 14 days to recover. Then $(1/14)^{\text{th}}$ of the infected population will recover per day.

i.e., $\frac{dR}{dt} = \left(\frac{1}{14}\right)I = \gamma I$, where γ is the recovery rate constant.

Transmission rate: First let us consider a single susceptible person on a single day and let I number of sick people in the population on that day. We expect only a couple of persons will be in the same place with average susceptible. So the fraction of contacts is $p = 2/I$

The 2 contacts themselves can be expressed as

$$2 = (2/I)I = pI \text{ contacts per day per susceptible.}$$

Number of daily contacts the whole susceptible population is pIS . Not all contacts lead to new infections; only a certain fraction q does, we can expect $pqSI$ new infections per day. This becomes βSI , if we define β , for convenience, to be the product pq . Every time a person becomes sick the number of susceptible persons decreases by one. So the rate of change of the susceptible population is the negative of the transmission rate. i.e., $\frac{dS}{dt} = -\beta SI$

Infection rate: The rate of change of the infected population is affected by the transmission rate as well as the recovery rate. i.e., $\frac{dI}{dt} = \beta SI - \gamma I$

In the deterministic form, the SIR model without vital dynamics (birth and death can be ignored) can be written as the following ordinary differential equation (ODE):

$$\begin{aligned} \frac{dS}{dt} &= -\beta SI \\ \frac{dI}{dt} &= \beta SI - \gamma I \\ \frac{dR}{dt} &= \gamma I \end{aligned} \quad (1)$$

where γ is the rate at which infectives recover or die; and clearly, these individuals can no longer remain infective. In a closed population with no vital dynamics, an epidemic will eventually die out due to an insufficient number of susceptible individuals to sustain the disease. Infected individuals who are added later will not start another epidemic due to the lifelong immunity of the existing population. Looking at the statistics worldwide (<https://www.who.int/>) the value of β is somewhere between 1.4 and 2.5. For the sake of visualization let us take the total world population to be 100 and a single infective to begin with. A plot code in Mathematica for $\beta = 2$ (which is much lower than the actual β for many countries at present) gives a striking sketch (Figure 3).

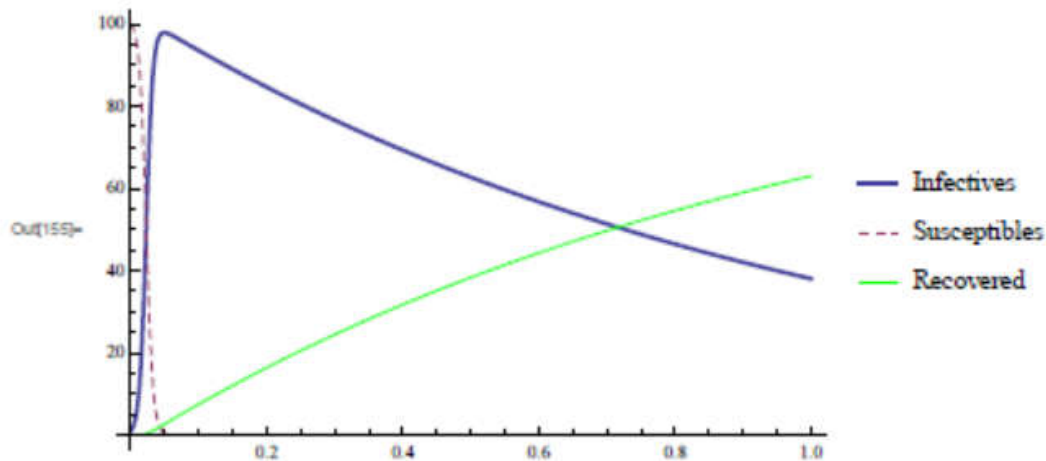


Figure 3: SIR outbreak

Starting with just a single infective, the infection peaks up to almost the total population size before starting to fall down. The situation in India is summarized in the following website <https://www.mohfw.gov.in/>.

At present, community transmission has not been validated and the β value is significantly less than 1 in India. The infection will still continue growing initially before attaining a peak lower than the total susceptible population this time, as indicated by Figure 4.

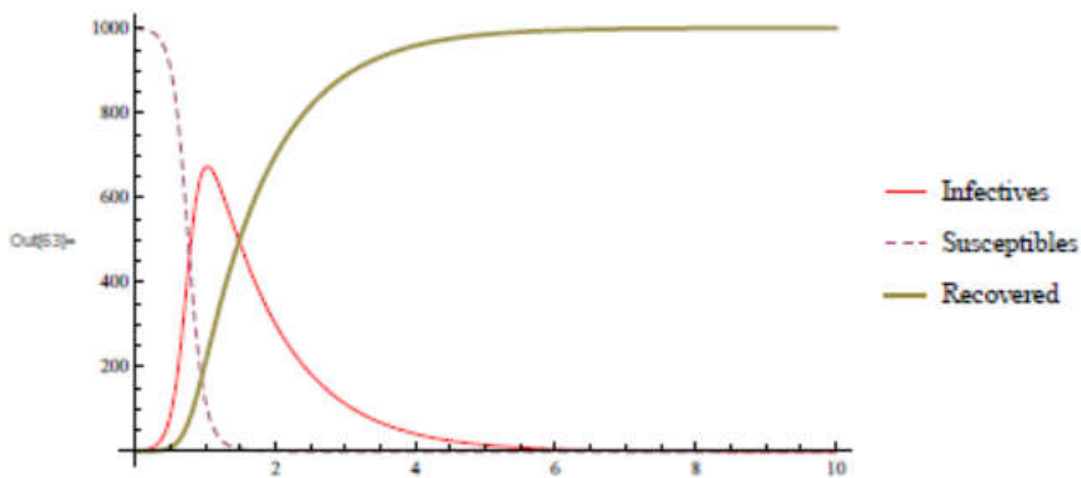


Figure 4: SIR

To contain the transmission of this virus, it is extremely important to contain the value of β . This β value is supposedly dependent on many factors that involve both natural (temperature, humidity) and non-natural factors or personal provisioning measures such as physical distancing, infectives wearing masks, good hygiene practices such as washing hands with soap for 20 seconds, and so on.

If β is greater than 1, then the disease will grow exponentially after a critical stage and becomes an epidemic. The average number of secondary cases generated by a single case in an entirely susceptible population is called a basic reproduction number and is denoted by R_0 . The R_0 for measles is around 12, the R_0 for COVID19 is around 2.6, and for seasonal flu it is around 1.3. Figure 5 shows how the number of new cases (per transmission) for seasonal flu is negligible as compared to COVID19.

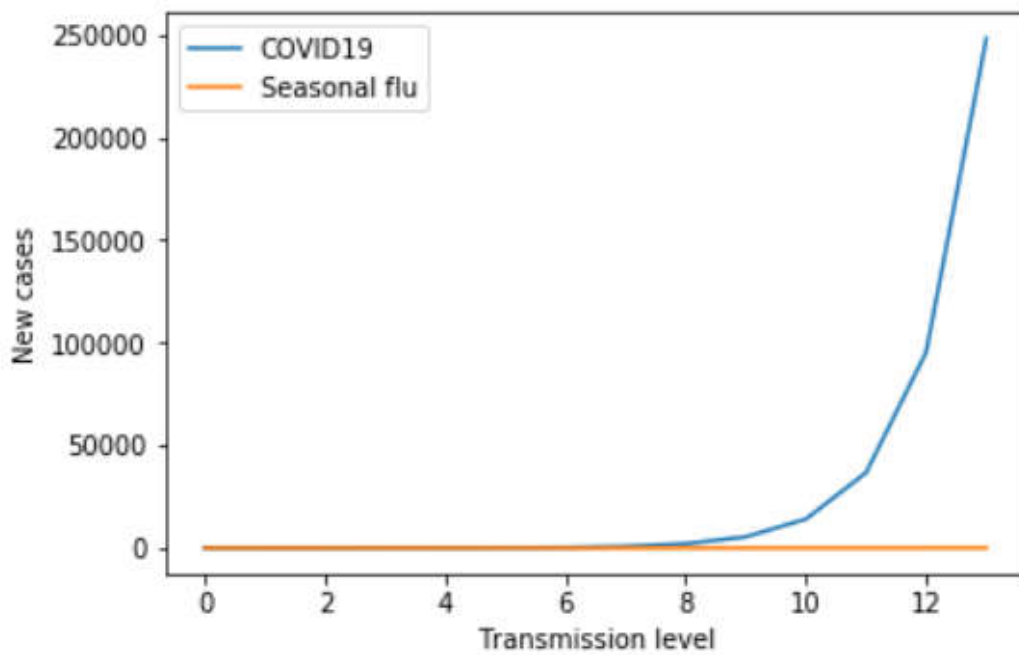


Figure 5: Seasonal flu Vs COVID19

SIR with vital dynamics

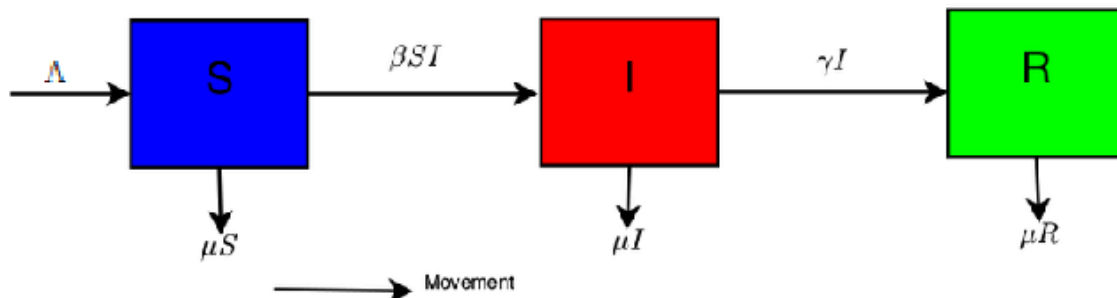


Figure 6: SIR with vital dynamics

However in a population with vital dynamics, new births can provide more susceptible individuals to the population, sustaining an epidemic or allowing new introductions to spread throughout the population. In a realistic population like this, disease dynamics will reach a

steady state. This is the case when diseases are endemic to a region. Let ν and μ represent the birth and death rates, respectively, for the model. To maintain a constant population, assume that $\nu = \mu$. In steady state $\frac{dI}{dt} = 0$. The ODE then becomes:

$$\begin{aligned}\frac{dS}{dt} &= \Lambda - \beta SI - \mu S \\ \frac{dI}{dt} &= \beta SI - \gamma I - \mu I \\ \frac{dR}{dt} &= \gamma I - \mu R\end{aligned}\quad (2)$$

where the parameter Λ represents the population influx i.e., $\Lambda = \nu N$.

4.1.2 SIRS – Model

The SIRS model is used to allow recovered individuals to return to a susceptible state.

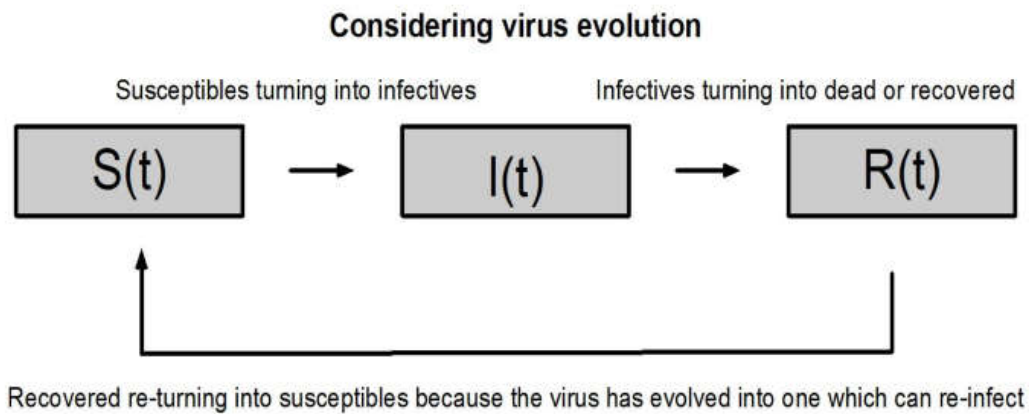


Figure 7: SIRS model

SIRS without vital dynamics

If there is sufficient influx to the susceptible population, at equilibrium the dynamics will be in an endemic state with damped oscillation. The ODE then becomes:

$$\begin{aligned}\frac{dS}{dt} &= -\beta SI + \xi R \\ \frac{dI}{dt} &= \beta SI - \gamma I \\ \frac{dR}{dt} &= \gamma I - \xi R\end{aligned}\quad (3)$$

SIRS with vital dynamics

We can also add vital dynamics to an SIRS model, where ν and μ represent the birth and death rates, respectively. To maintain a constant population, assume that $\nu = \mu$. In steady state $\frac{dI}{dt} = 0$. The ODE then becomes:

$$\begin{aligned}\frac{dS}{dt} &= \Lambda - \beta SI + \xi R - \mu S \\ \frac{dI}{dt} &= \beta SI - \gamma I - \mu I \\ \frac{dR}{dt} &= \gamma I - \xi R - \mu R\end{aligned}\quad (4)$$

where the parameter Λ represents the population influx i.e., $\Lambda = \nu N$.

The graph below show damped oscillation due to people losing immunity and becoming susceptible again.

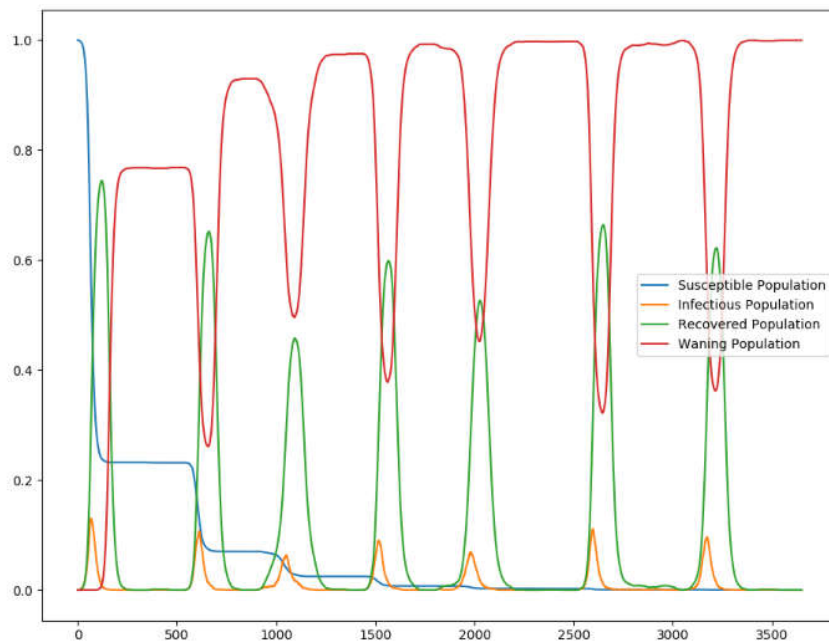


Figure 8: SIRS damped oscillation

For a pathogen with direct person-to-person transmission. Control policies optimally reduce transmission so that $R_0 < 1$, since at that level epidemic cannot sustain itself. Hence control policies need to eliminate a fraction of transmission. i.e., 33% for $R_0 = 1.5$ or 50% of $R_0 = 2$. This can be achieved by

- Reducing contact (quarantine, increasing social distances)
- Reducing susceptibility (Vaccination)
- Reducing infectiousness (treatment)

We do care about R_0 so much, because

- R_0 is threshold parameter, which determines whether disease will persist in the population or not?
- R_0 determines the initial rate of increase of an epidemic.
- R_0 determines the control effort required to achieve eradication.

However, the exponential growth process can only continue

- 1) If there are sufficiently many susceptible individuals available. Once a larger fraction of the population has gone through the infection and has become immune, the probability of an infected person transmitting the infection decreases. But as shown in the previous figures, in every transmission from person to person, the numbers

increase exponentially, and we would not have enough hospitals beds, medical staff and equipment to treat all infected individuals if exponentially increasing number of people have to be admitted in hospitals every day! We cannot risk such a situation because any healthcare system (of even the richest and most developed country) will breakdown and we would have unnecessary deaths. As humans, we have the knowledge to overcome such situations. We have the knowledge of science, and we should use this to avoid unnecessary deaths. This is where the second option becomes important to practice, that is

- 2) Physical distancing to ensure we do not spread (or receive) the virus to (or from) other people. This way, the virus surviving within the bodies of already infected individuals can no longer survive by jumping to other persons. The viruses would stop surviving in the infected persons' bodies after its 14-day incubation period in that host. This way, we can reduce the number of deaths, and also reduce the number of infected by blocking the virus from spreading.

Though the transmission rate is very low in India now, the number of infectives is bound to increase with time. The only way to get the graph of infectives as a decreasing function of time as per this model is that the interaction term βSI in the equation (1) tends to zero. That can only happen when infectives are totally isolated from the susceptible population. The variables will keep on changing with each passing day as the virus has just reached stage 2 of its disease cycle where there are no mass casualties and things are under control.

3.2. Formulation of SEIR/SEIRS models

In this category of models, individuals experience a long incubation duration (the “exposed” category), such that the individual is *infected* but not yet *infectious*. Many diseases have a latent phase during which the individual is infected but not yet infectious. This delay between the acquisition of infection and the infectious state can be incorporated within the SIR model by adding a latent/exposed population, E, and letting infected (but not yet infectious) individuals move from S to E and from E to I. The SEIR/SEIRS diagram below shows how individuals move through each compartment in the model. The dashed line shows how the SEIR model becomes an SEIRS (Susceptible – Exposed – Infectious – Recovered – Susceptible) model, where recovered people may become susceptible again (recovery does not confer lifelong immunity).

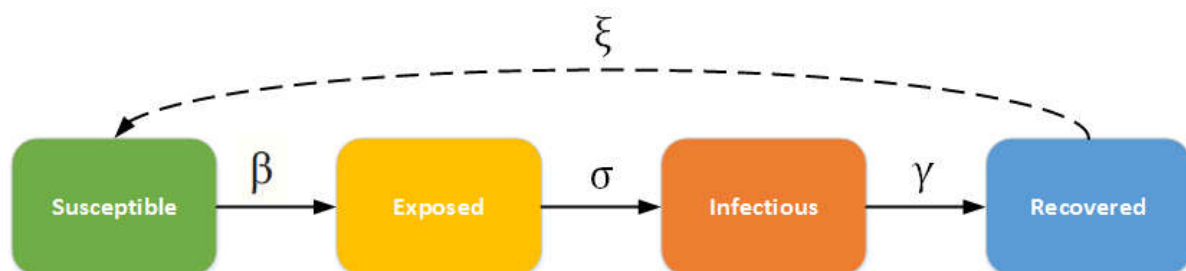


Figure 9: SEIR/SEIRS models

The infectious rate β , controls the rate of spread which represents the probability of transmitting disease between a susceptible and an infectious individual. The incubation rate σ , is the rate of latent individuals becoming infectious (average duration of incubation is $1/\sigma$). Recovery rate, $\gamma = 1/D$, is determined by the average duration, D , of infection. For the SEIRS

model, ξ is the rate which recovered individuals return to the susceptible statue due to loss of immunity.

4.2.1 SEIR - Model

This model studied a population in which an epidemic COVID-19 could develop and divided the population into four compartments:

- $S(t)$: the number of susceptible
- $E(t)$: the number of exposed
- $I(t)$: the number of infectives
- $R(t)$: the number recovered (recovered, died, or naturally immune to the disease)

The population is considered closed for any time, that is to say, neither births nor migrations

are taken into account, in such a way that $N = S(t) + E(t) + I(t) + R(t)$

where N is the total population of India (N is itself a variable, but treated as a constant in this model consistent with the fact that the course of this epidemic is short compared with the lifetime of an individual).

The flow of transitions from one group to another follows the scheme below:

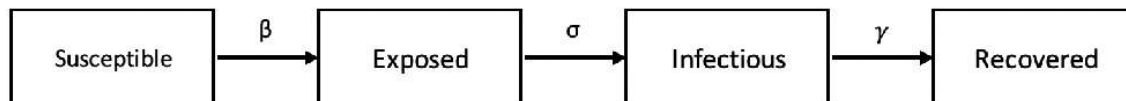


Figure 10: SEIR model

In a closed population with no births or deaths, the SEIR model becomes:

$$\begin{aligned}
 \frac{dS}{dt} &= -\beta SI \\
 \frac{dE}{dt} &= \beta SI - \sigma E \\
 \frac{dI}{dt} &= \sigma E - \gamma I \\
 \frac{dR}{dt} &= \gamma I
 \end{aligned}
 \tag{5}$$

Since the latency delays the start of the individual's infectious period, the secondary spread from an infected individual will occur at a later time compared with an SIR model, which has no latency. Therefore, including a longer latency period will result in slower initial growth of the outbreak. However, since the model does not include mortality, the basic reproductive number, $R_0 = \beta/\gamma$, does not change. The complete course of outbreak is observed. After the initial fast growth, the epidemic depletes the susceptible population. Eventually the virus cannot find enough new susceptible people and dies out. Introducing the incubation period does not change the cumulative number of infected individuals.

The following graph shows typical SEIR outbreaks, one with an incubation period of 8 days and one with an incubation period of 2 days. Notice how the outbreak depletes the susceptible population more quickly when the incubation period is shorter but that the cumulative infections remain the same.

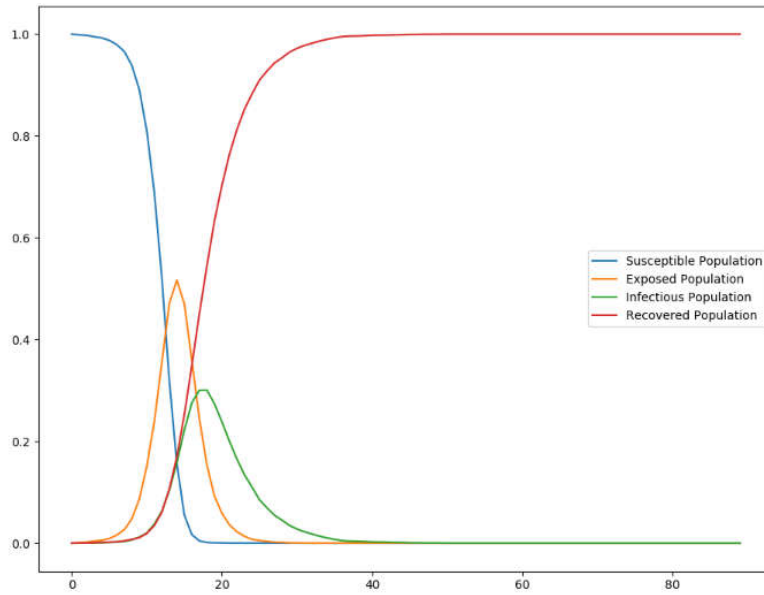


Figure 11: SEIR epidemic course for 8-day incubation period

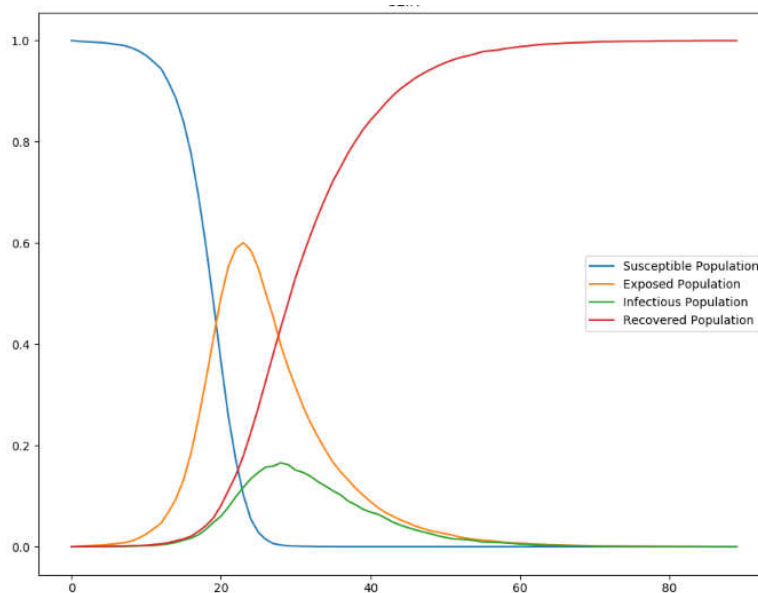


Figure 12: SEIR epidemic course for 2-day incubation period

SEIR with vital dynamics

The flow of transitions from one group to another with accounting new births and deaths follows the scheme below:

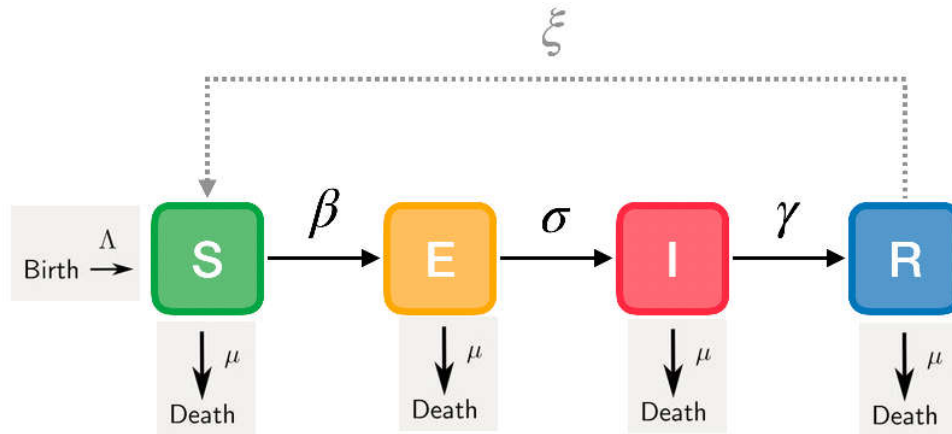


Figure 13: SEIR model with vital dynamics

As with the SIR model, enabling vital dynamics (births and deaths) can sustain an epidemic or allow new introductions to spread because new births provide more susceptible individuals. In a realistic population like this, disease dynamics will reach a steady state, where υ and μ represent the birth and death rates, respectively, and are assumed to be equal to maintain a constant population, the ODE then becomes:

$$\begin{aligned}
 \frac{dS}{dt} &= \Lambda - \beta SI - \mu S \\
 \frac{dE}{dt} &= \beta SI - \sigma E - \mu E \\
 \frac{dI}{dt} &= \sigma E - \gamma I - \mu I \\
 \frac{dR}{dt} &= \gamma I - \mu R
 \end{aligned}
 \tag{6}$$

The following graph shows periodic reintroductions of an SEIR outbreak in a population with vital dynamics.

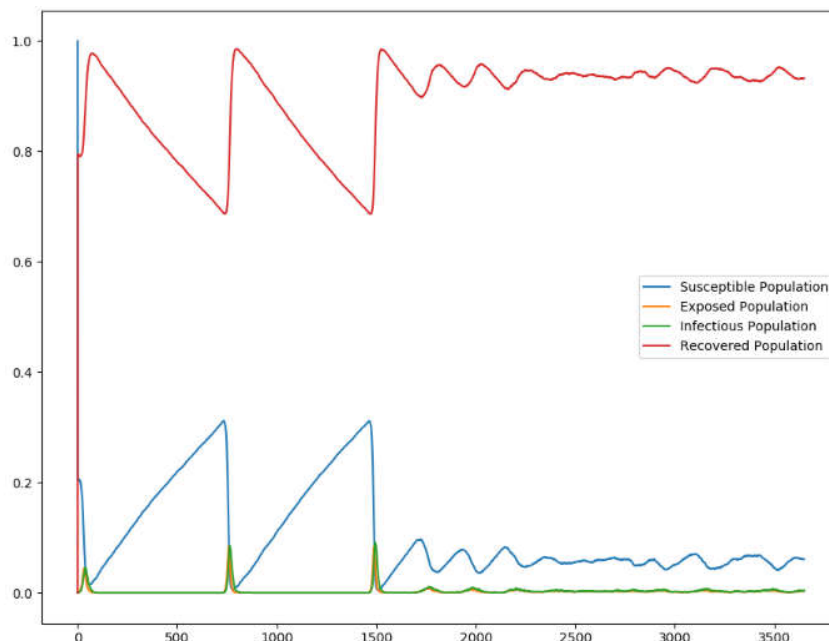


Figure 14: SEIR outbreak

4.2.2 SEIRS – Model

The SEIR model assumes people carry lifelong immunity to a disease upon recovery, but for many diseases the immunity after infection wanes over time. In this case, the SEIRS model is used to allow recovered individuals to return to a susceptible state. Specifically, ξ is the rate which recovered individuals return to the susceptible state due to loss of immunity. If there is sufficient influx to the susceptible population, at equilibrium the dynamics will be in an endemic state with damped oscillation. The SEIRS ODE is:

$$\begin{aligned} \frac{dS}{dt} &= -\beta SI + \xi R \\ \frac{dE}{dt} &= \beta SI - \sigma E \\ \frac{dI}{dt} &= \sigma E - \gamma I \\ \frac{dR}{dt} &= \gamma I - \xi R \end{aligned} \tag{7}$$

SEIRS with vital dynamics

We can also add vital dynamics to an SEIRS model, where υ and μ again represent the birth and death rates, respectively. To maintain a constant population, assume that $\upsilon = \mu$. In the steady state $\frac{dI}{dt} = 0$. The ODE then becomes:

$$\begin{aligned} \frac{dS}{dt} &= \Lambda - \beta SI + \xi R - \mu S \\ \frac{dE}{dt} &= \beta SI - \sigma E - \mu E \\ \frac{dI}{dt} &= \sigma E - \gamma I - \mu I \\ \frac{dR}{dt} &= \gamma I - \xi R - \mu R \end{aligned} \tag{8}$$

The following graph shows the complete trajectory of a fatal SEIRS outbreak: the disease endemicity due to vital process and waning immunity and the effect of vaccination campaigns that eradicate the outbreak after day 500.

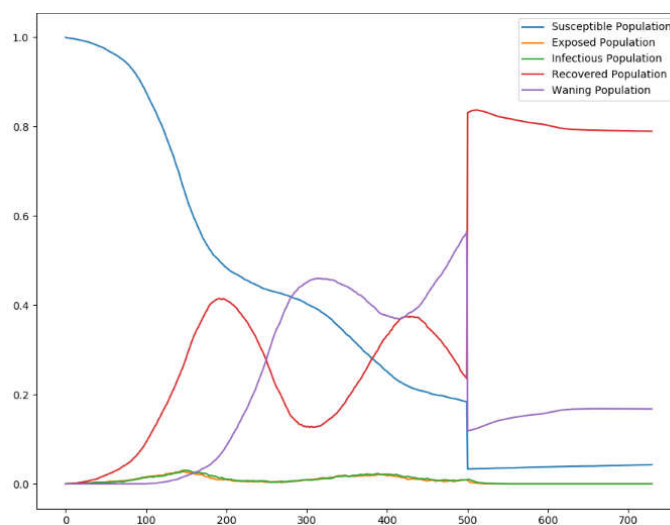


Figure 15: SEIRS outbreak

4.3. Improved SEIR - Model

A mathematical improved SEIR (Susceptible-Exposed-Infected-Recovered) model developed by Chayu Yang and Jin Wang [2] to investigate the current outbreak of the corona virus disease 2019 (COVID-19) in Wuhan, China. This model describes the multiple transmission pathways in the infection dynamics, and emphasizes the role of the environmental reservoir in the transmission and spread of this disease. This model also employs non-constant transmission rates which change with the epidemiological status and environmental conditions and which reflect the impact of the on-going disease control measures. They conducted a detailed analysis of this model, and demonstrate its application using publicly reported data. Among other findings, their analytical and numerical results indicate that the corona virus infection would remain endemic, which necessitates long-term disease prevention and intervention programs.

This model studied a population in which an epidemic could develop and divided the population into four compartments:

- $S(t)$: the number of susceptible
- $E(t)$: the number of exposed
- $I(t)$: the number of infectives
- $R(t)$: the number recovered (recovered, died, or naturally immune to the disease)

Individuals in the infected class have fully developed disease symptoms and can infect other people. Individuals in the exposed class are in the incubation period; they do not show symptoms but are still capable of infecting others. Thus, another interpretation of the E and I compartments in their model is that they contain asymptomatic infected and symptomatic infected individuals, respectively.

The differential equations system [SEIR-Model] that captures the problem is given by:

$$\begin{aligned}
 \frac{dS}{dt} &= \Lambda - \beta_1 ES - \beta_2 SI - \beta_3 SV - \mu S, \\
 \frac{dE}{dt} &= \beta_1 ES + \beta_2 SI + \beta_3 SV - (\alpha + \mu) E, \\
 \frac{dI}{dt} &= \alpha E - (w + \gamma + \mu) I, \\
 \frac{dR}{dt} &= \gamma I - \mu R, \\
 \frac{dV}{dt} &= \xi_1 E + \xi_2 I - \sigma V,
 \end{aligned} \tag{9}$$

where V is the concentration of the corona virus in the environmental reservoir. The parameter Λ represents the population influx, μ is the natural death rate of human hosts, α is the incubation period between the infection and the onset of symptoms, w is the disease-induced death rate, γ is the rate of recovery from infection, ξ_1 and ξ_2 are the respective rates of the exposed and infected individuals contributing the corona virus to the environmental reservoir, and σ is the removal rate of the virus from the environment. The functions β_1 and β_2 represent the direct, human-to-human transmission rates between the exposed and susceptible individuals, and between the infected and susceptible individuals, respectively, and the function β_3 represents the indirect, environment-to human transmission rate. They assumed that β_1 , β_2 and β_3 are all non-increasing functions, given that higher values of E , I and V would motivate stronger control measures that could reduce the transmission rates.

The above system (9) has a unique Disease-Free Equilibrium (DFE) at

$$X_0 = (S_0, E_0, I_0, R_0, V_0) = \left(\frac{\Lambda}{\mu}, 0, 0, 0, 0 \right)$$

The infection components in this model are E , I and V . The new infection matrix F and the transition matrix V are given by

$$F = \begin{bmatrix} \beta_1(0)S_0 & \beta_2(0)S_0 & \beta_3(0)S_0 \\ 0 & 0 & 0 \\ 0 & 0 & 0 \end{bmatrix} \text{ and } V = \begin{bmatrix} \alpha + \mu & 0 & 0 \\ -\alpha & w + \gamma + \mu & 0 \\ -\xi_1 & -\xi_2 & \sigma \end{bmatrix},$$

The basic reproduction number of model (9) is then defined as the spectral radius of the next generation matrix FV^{-1} [3]; i.e.,

$$R_0 = \rho(FV^{-1}) = \frac{\beta_1(0)S_0}{\alpha + \mu} + \frac{\alpha\beta_2(0)S_0}{(w + \gamma + \mu)(\alpha + \mu)} + \frac{((w + \gamma + \mu)\xi_1 + \alpha\xi_2)\beta_3(0)S_0}{\sigma(w + \gamma + \mu)(\alpha + \mu)}$$

i.e., $R_0 = R_1 + R_2 + R_3$

which provides a quantification of the disease risk. The first two parts R_1 and R_2 measure the contributions from the human-to-human transmission routes (exposed-to-susceptible and infected-to susceptible, respectively), and the third part R_3 represents the contribution from the environment-to human transmission route. These three transmission modes collectively shape the overall infection risk for the COVID-19 outbreak.

4.4. Formulation of SEQIR model

After the outbreak of the COVID-19 epidemic, the government has taken many effective measures to combat the epidemic, such as inspection detention, isolation treatment, isolation of cities, and stopping traffic on main roads. However, the traditional SEIR model cannot fully describe the impact of these measures on different populations [4-7]. Depending on the recent situation, Indian Government has taken some strategies to stop spreading COVID-19 virus. This section presents a SEQIR model of COVID-19 based on the current situation of the disease in Indian environment. We espouse an alternate that reproduces several key epidemiological properties of COVID-19 virus. The present model structure of COVID-19 describes the dynamics of five sub-populations of Indians such as

- $S(t)$ People who may be infected by the virus
- $E(t)$ Infected with the virus but without the typical symptoms of infection
- $Q(t)$ Diagnosed and quarantined
- $I(t)$ Infected with the virus and highly infectious but not quarantined
- $R(t)$ People who are cured after infection

We assume total population size of India is $N(t)$ and $N(t) = S(t) + E(t) + Q(t) + I(t) + R(t)$.

In this model, quarantine refers to the separation of infected individuals from the common Indian population when the populace is infected but not infectious. By Infected Indian population, we guess that the Indian individual who have confirmed infected by the COVID-19 virus. Again by population in secured zone, we presume those Indian individuals who have not affected by corona virus disease. To make this SEQIR model more realistic, D. Palin and et al, in [22] several demographic effects by assuming a proportional natural death rate $d_1 > 0$ in each of the five Indian sub-populations. Furthermore, we incorporate a net inflow of susceptible Indian individuals into the county (India) at a rate $\Lambda (> 0)$ per unit time. Λ comprises of new birth of Indian child, immigration and emigration from and in India. The flow diagram of the COVID-19 infection model in present situation of India is depicted through Figure 16.

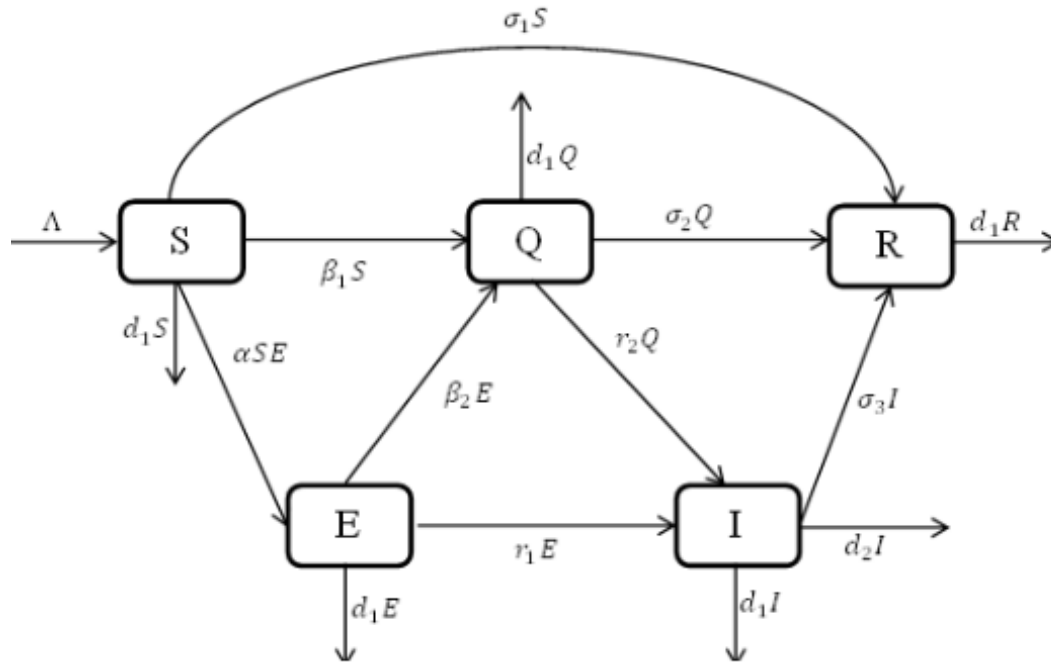


Figure 16: SEQIR model

Explanation of parameters exploited in SEQIR model structure is as follows:

| Parameters | Meaning |
|------------|---|
| Λ | The recruitment rate at which new individuals enter in the Indian population |
| α | The transmission rate from susceptible population to infected but not detected by testing population |
| β_1 | The transmission coefficient from susceptible population to quarantine population |
| β_2 | The transmission coefficient from infected but not detected by testing population to quarantine population |
| σ_1 | The transmission rate from susceptible population to secured zone population |
| σ_2 | The transmission coefficient from infected but not detected by testing population to secured zone population |
| σ_3 | The transmission rate from quarantine population to secured zone population |
| r_1 | The transmission rate from infected but not detected by testing population to infected population for treatment |
| r_2 | The transmission rate from quarantine population to infected population for treatment |
| d_1 | Natural death rate of all five sub-populations |
| d_2 | Death rate of Infected population due to Covid-19 infection |

In the deterministic form, the SIR model can be written as the following ordinary differential equation (ODE):

$$\begin{aligned}\frac{dS}{dt} &= \Lambda - \alpha SE - \beta_1 S - \sigma_1 S - d_1 S \\ \frac{dE}{dt} &= \alpha SE - r_1 E - \beta_2 E - d_1 E \\ \frac{dQ}{dt} &= \beta_1 S + \beta_2 E - r_2 Q - \sigma_2 Q - d_1 Q \\ \frac{dI}{dt} &= r_1 E + r_2 Q - \sigma_3 I - d_1 I - d_2 I \\ \frac{dR}{dt} &= \sigma_1 S + \sigma_2 Q + \sigma_3 I - d_1 R\end{aligned}\quad (10)$$

with initial densities:

$$S(0) > 0, E(0) \geq 0, I(0) \geq 0, Q(0) \geq 0, R(0) > 0.$$

The above SEQIR model formulation (10) can be rewritten as

$$\begin{aligned}\frac{dS}{dt} &= \Lambda - \alpha SE - AS \\ \frac{dE}{dt} &= \alpha SE - BE \\ \frac{dQ}{dt} &= \beta_1 S + \beta_2 E - CQ \\ \frac{dI}{dt} &= r_1 E + r_2 Q - DI \\ \frac{dR}{dt} &= \sigma_1 S + \sigma_2 Q + \sigma_3 I - d_1 R\end{aligned}\quad (11)$$

where $A = \beta_1 + \sigma_1 + d_1$, $B = r_1 + \beta_2 + d_1$, $C = r_2 + \sigma_2 + d_1$ and $D = \sigma_3 + d_1 + d_2$.

The above system (11) has a unique Disease-Free Equilibrium (DFE) at

$$E_0 = (S_0, E_0, Q_0, I_0, R_0, V_0) = \left(\frac{\Lambda}{A}, 0, 0, 0, 0, 0 \right)$$

The infection components in this model are E , I and V . The new infection matrix F and the transition matrix V are given by

$$F = \begin{bmatrix} \frac{\alpha\Lambda}{A} & 0 & 0 \\ 0 & 0 & 0 \\ 0 & 0 & 0 \end{bmatrix} \quad \text{and} \quad V = \begin{bmatrix} B & 0 & 0 \\ -\beta_2 & C & 0 \\ -r_1 & -r_2 & D \end{bmatrix},$$

The basic reproduction number R_0 of the model (11) is then defined as the spectral radius of the next generation matrix FV^{-1} [3]; i.e.,

$$R_0 = \rho(FV^{-1}) = \frac{\alpha\Lambda}{AB} = \frac{\alpha\Lambda}{(\beta_1 + \sigma_1 + d_1)(r_1 + \beta_2 + d_1)} > 0$$

It is notable that $\frac{\Lambda}{A}$ represents the number of susceptible individual at the DFE. Based on the each of the parameters of R_0 a sensitivity analysis is performed to check the sensitivity of the basic reproduction number. The value of R_0 will be enhanced if the value of α is raised. On the contrary, the value of the R_0 will be as well reduced in the same proportion if the value of α diminished. Again it is also noticed that the parameters β_1 , σ_1 , d_1 , r_1 and β_2 are related to R_0 inversely. Therefore, for any increasing value of any of this mentioned parameters will definitely reduce the value of R_0 . Therefore, the sensitive analysis of the basic reproduction number emphasized that prevention is better than treatment.

4.5. Formulation of SEQIDR model

After the outbreak of the COVID-19 epidemic, the government has taken many effective measures to combat the epidemic, such as inspection detention, isolation treatment, isolation of cities, and stopping traffic on main roads. However, the traditional SEIR model cannot fully describe the impact of these measures on different populations [4-7]. Based on the analysis of the actual situation and existing data, divided the population into different warehouses and established a more effective model for the dynamic spread of infectious diseases. According to the actual situation of the epidemic, Yichi Li and et al in [21], established a SEQIDR model by dividing the population into 6 different categories to comply with the current spread of COVID-19.

- $S(t)$ People who may be infected by the virus
- $E(t)$ Infected with the virus but without the typical symptoms of infection
- $Q(t)$ Diagnosed and quarantined
- $I(t)$ Infected with the virus and highly infectious but not quarantined
- $D(t)$ Suspected cases of infection or potential victims
- $R(t)$ People who are cured after infection

Since the incubation period of the COVID-19 is as long as 2 to 14 days, there are already infected but undetected people (E) in the natural environment of the susceptible population (S), when the first case is identified. Some people who have been infected need to go through a certain incubation period before suspected symptoms can be detected (Q). Chest CT imaging was used to observe whether there were glassy shadows in the lungs to determine whether the diagnosis was confirmed (D). Another part of the population has been infected and has been sick, because not isolated, is highly infectious in the population. After a period of quarantine treatment, these two groups of people will be discharged from hospital (R), or face death due to basic diseases. The diagnosed patients will become healed after a certain period of isolation and treatment.

To build a dynamic discrete model for a certain period of time for COVID-19, the authors ignored the impact of factors such as population birth rate and natural mortality and also assumed that the latent population of COVID-19 and the infected but not yet isolated population have the same range of activities and capabilities, that is, for COVID-19, the population $E(t)$ and the crowd $I(t)$ have the same contact rate.

The flow of transitions from one group to another follows the scheme below:

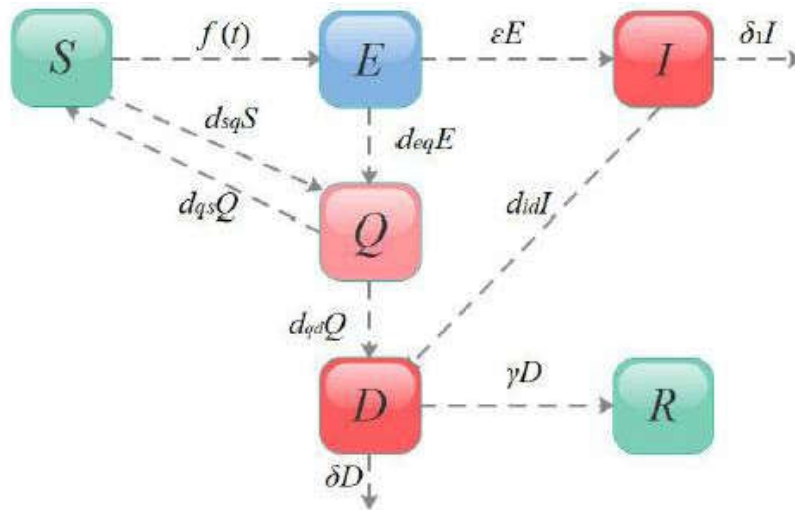


Figure 17: SEQDIR model

Explanation of parameters exploited in SEQDIR model structure is as follows:

| Parameters | Meaning |
|------------|---|
| $f(t)$ | The incidence rate of the susceptible population $S(t)$, which to some extent can reflect the infection degree of COVID-19 in the susceptible population. |
| ϵ | The proportion of latent persons who were converted to free infection |
| d_{sq} | The rate at which suspected patients are converted into quarantine |
| d_{qd} | The rate at which suspected patients are converted into confirmed cases represents a measure of quarantine intensity due to the constant changes in medical procedures. |
| d_{id} | The rate at which some highly infectious people in the free environment will be transferred to confirmed cases. |
| d_{qs} | The rate at which susceptible population has also been converted to suspected cases. |
| d_{eq} | The susceptible population in the free environment will become latent after being infected by COVID-19 and gradually develop after the incubation period |
| δ | The fatality rate of new pneumonia, reflecting the lethal intensity of COVID-19. |
| γ | The cure rate that is diagnosed by the proportion of people who are cured per day to those, which reflects the local level of care and, to another extent, the difficulty of the condition. |

In the deterministic form, the SEDQIR model can be written as the following ordinary differential equation (ODE):

$$\begin{aligned}
\frac{dS}{dt} &= d_{qs}Q(t) - f(t) - d_{sq}S(t), \\
\frac{dE}{dt} &= f(t) - \varepsilon E(t) - d_{eq}E(t), \\
\frac{dD}{dt} &= d_{qd}Q(t) + d_{id}I(t) - (\gamma + \delta)D(t), \\
\frac{dQ}{dt} &= d_{eq}E(t) + d_{sq}S(t) - d_{qs}Q(t) - d_{qd}Q(t), \\
\frac{dI}{dt} &= \varepsilon E(t) - d_{id}I(t) - \delta I(t), \\
\frac{dR}{dt} &= \gamma D(t).
\end{aligned} \tag{12}$$

In order to study the deeper COVID-19 transmission rule, they performed a detailed analysis of some parameters to transform the degree of infection into a form more conducive to data expression [8]. Adopt the degree of infection of COVID-19 in susceptible populations $f(t)$, the mathematical expression is as follows:

$$f(t) = (\beta_1 CE + \beta_2 CI) \frac{S}{S + E + I + R} = \frac{\beta_1 CS}{S + E + I + R} (kE + I), \text{ where } k = \frac{\beta_1}{\beta_2}.$$

$$\text{i.e., } f(t) = \beta(kE + I),$$

Among them, they referred to the infection rate coefficients of latent and freely infected people in susceptible populations as β_1 and β_2 . At this stage, the epidemic caused by COVID-19 may still be in the early stages of spreading among the population.

The infection rate $\beta(t)$ can be estimated and fitted based on the existing data, and k value reflects the infectivity of the latent person relative to the infected person. Furthermore, according to the definition of incidence, the rate of infection can be expressed by the number of people diagnosed over a period of time [9]. If the number of people diagnosed on day t is F , the infection rate can be expressed as

$$\beta(t) = \frac{F(t + d_1 + d_2)}{\sum_{j=0}^{d_2-1} F(t + j) + k \sum_{j=d_2}^{d_1+d_2-1} F(t + j)}$$

Among them, d_1 is the average incubation period of COVID-19, and d_2 is the time during which the incubator is isolated after the incubation period. Based on the available data, the infectious rate was calculated numerically.

5. Stability analysis

By constructing a suitable Lyapunov function, the authors in [21], proved the following stability theorems

Theorem 1. The following statements hold for the model (8).

- (1) If $R_0 \leq 1$, the DFE of system (8) is globally asymptotically stable in Ω .
- (2) If $R_0 > 1$, the DFE of system (8) is unstable and there exists a unique endemic equilibrium. Moreover, the disease is uniformly persistent in the interior of Ω , denoted by $\dot{\Omega}$; namely, $\liminf_{t \rightarrow \infty} (E(t), I(t), V(t)) > (\varepsilon, \varepsilon, \varepsilon)$ for some $\varepsilon > 0$.

Theorem 2. Assume that β_1, β_2 and β_3 are non-decreasing functions of variables E, I and V , respectively. If $R_0 > 1$, then the unique endemic equilibrium X^* of system (8) is globally asymptotically stable in $\dot{\Omega}$.

Also, by constructing a suitable Jacobian matrix of the system (11), the authors in [21] proved the following stability nature of the Diseases Free Equilibrium (DFE) $E_0 = \left(\frac{\Lambda}{A}, 0, 0, 0, 0 \right)$

Theorem 3. The SEQIR model structure (11) at DFE at $E_0 = \left(\frac{\Lambda}{A}, 0, 0, 0, 0 \right)$ is locally asymptotically stable under the condition $R_0 < 1$ and unstable if $R_0 > 1$.

Theorem 4. The SEQIR model structure (11) at DFE at $E_0 = \left(\frac{\Lambda}{A}, 0, 0, 0, 0 \right)$ is globally asymptotically stable under the condition $R_0 < 1$ and unstable if $R_0 > 1$.

Theorem 5. The DFE E_0 of the system (12) is locally asymptotically stable if $R_0 < 1$.

6. Conclusion:

In this paper, we have briefly discussed various epidemic models of COVID-19 disease which is transferred from human to human. So far the daily confirmed COVID-19 cases are increasing day by day worldwide. Therefore, prediction about infected individual is very much important for health concern arrangement of the citizens. It is also important to control spread rate of the COVID-19 virus with restricted supply. Our mathematical study is based on COVID-19 virus spread in India. We tried to fit various compartmental model systems to COVID-19 disease in India as per as data are available. The basic reproduction number R_0 is determined and reviewed the comprehensive stability analysis.

Therefore, analyzing all results of various models and observing the situation of different countries, we may conclude that India may be in a big trouble in very near future due to COVID-19 virus. To avoid this big trouble, Indian Government should take stricter measures other than quarantine, lock down etc. So far the Indian Government are continuously changing its policy to protect India from COVID-19 virus. Recently, all districts of India are classified by Indian Government into three zones namely Red zones (hotspots), Orange zones (non hotspots) and Green zones (save zones). Preliminarily 170 districts of India are hotspots zones, where rapid testing facility is available for the public. As the time progress more strategies are applied by the Government of India as well as all state Governments to stop the spread of COVID-19 virus in India. Therefore, we may assume that if the Indian Government take proper step time to time then the infected number of population will be differ from our predicted number as time progress, and India will recover from this virus in recent future. Lastly, we say that public of India should help the Indian Government to fight against this dangerous COVID-19 as per the compartmental models.

Given the current development of COVID-19, it is widely speculated that this disease would persist in the human world and become endemic. Our mathematical analysis and

numerical simulation results support this speculation. The findings in this study imply that we should be prepared to fight the coronavirus infection for a much longer term than that of the current epidemic wave, in order to reduce the endemic burden and potentially eradicate the disease eventually. Among other intervention strategies, new vaccines for the novel coronavirus, which are currently in research and development, could play an important role in achieving that goal. Scientists need to gear up for the task and come forward to do collaborative research work to understand the spread, containment and eventualities of the pandemic outbreak. For this, interdisciplinary teams must work together to come out with some concrete strategy. Research teams have to develop vaccines for which funding, infrastructure, and adequate facilities are required. So, Covid-19 is a reminder that science cannot take a back seat and health care, education and research should always hold a top priority. Faith in science and scientists, and optimism is important at this juncture so that India comes out as a winner in the battle.

Acknowledgments

Authors would like to thank the anonymous referees for their valuable comments and careful reading to the improvement of the manuscript.

References

- [1] Kermack WO and Mc Kendrick AG “Contributions to the Mathematical Theory of Epidemics”, proceedings of the Royal Society A 115 (1927), 700-721.
- [2] Chayu Yang and Jin Wang “A mathematical model for the novel coronavirus epidemic in Wuhan, China” *Mathematical Biosciences and Engineering*, 17(3): 2708–2724.
- [3] P. V. D. Driessche, J. Watmough, Reproduction numbers and sub-threshold endemic equilibria for compartmental models of disease transmission, *Math. Biosci.*, 180 (2002), 29–48.
- [4] Hansun S. A New Approach of Brown’s Double Exponential Smoothing Method in Time Series Analysis. *Balkan J Electric Comput Engineering*.2016;4(2):75-8.
- [5] Chadsuthi S, Modchang C, Lenbury Y, Iamsirithaworn S, Triampo W. Modeling seasonal leptospirosis transmission and its association with rainfall and temperature in Thailand using time-series and ARIMAX analyses. *Asian Pac J Trop Med*. 2012;5(7):539-46.
- [6] Ming W, Huang J, Zhang CJP. Breaking down of healthcare system: Mathematical modeling for controlling the novel coronavirus (COVID-19) outbreak in Wuhan, China. *bioRxiv*. 2020.
- [7] Chowell G, Castillo-Chavez C, Fenimore PW, Kribs-Zaleta CM, ArriolaL, Hyman JM. Model parameters and outbreak control for SARS. *Emerg Infect Dis*. 2004;10(7):1258.
- [8] Luo H, Ye F, Sun T, Yue L, Peng S, Chen J, et al. In vitro biochemical and thermodynamic characterization of nucleocapsid protein of SARS. *Biophysical chemistry*. 2004;112(1):15-25.
- [9] Dye C, Gay N. Modeling the SARS epidemic. *Science*. 2003; 300 (5627):18845.
- [10] Chen T, Ka-Kit Leung R, Liu R, Chen F, Zhang X, Zhao J, et al. Risk of imported Ebola virus disease in China. *Travel Med Infect Dis*. 2014;12:650–8.
- [11] Yi B, Chen Y, Ma X, Rui J, Cui JA, Wang H, et al. Incidence dynamics and investigation of key interventions in a dengue outbreak in Ningbo City, China. *PLoS Negl Trop Dis*. 2019;13: e0007659
- [12] Chen T, Leung RK, Zhou Z, Liu R, Zhang X, Zhang L. Investigation of key interventions for shigellosis outbreak control in China. *PLoS One*. 2014;9: e95006.
- [13] Zhang S, Hu Q, Deng Z, Hu S, Liu F, Yu S, et al. Transmissibility of acute haemorrhagic conjunctivitis in small-scale outbreaks in Hunan Province, China. *Sci Rep*. 2020;10:119.

- [14] Chen S, Yang D, Liu R, Zhao J, Yang K, Chen T. Estimating the transmissibility of hand, foot, and mouth disease by a dynamic model. *Public Health*. 2019;174:42–8.
- [15] Cui J-A, Zhao S, Guo S, Bai Y, Wang X, Chen T. Global dynamics of an epidemiological model with acute and chronic HCV infections. *Appl Math Lett*. 2020;103:106203.
- [16] Russell T.W., Hellewell J., Abbott S., Golding N., Gibbs H., Jarvis C.I., et al. Using a delay-adjusted case fatality ratio to estimate under-reporting. Report from the Centre for Mathematical Modelling of Infectious Diseases. https://cmmid.github.io/topics/covid19/severity/global_cfr_estimates.html; 2020a.
- [17] Ivorra B., Ramos A.M., Ngom D. Be-CoDiS: A mathematical model to predict the risk of human diseases spread between countries. Validation and application to the 2014 Ebola Virus Disease epidemic. *Bulletin of Mathematical Biology*. 2015;77(9):1668–1704. doi: 10.1007/s11538-015-0100-x. [PubMed] [CrossRef] [Google Scholar]
- [18] Ferrández M.R., Ivorra B., Ortigosa P.M., Ramos A.M., Redondo J.L. Application of the Be-CoDis model to the 2018-19 Ebola Virus Disease outbreak in the Democratic Republic of Congo. *ResearchGate Preprint*. 2019;23 July 2019:1–17. doi: 10.13140/RG.2.2.13267.63521/2. [CrossRef] [Google Scholar]
- [19] Ferrández M.R., Ivorra B., Redondo J.L., Ramos A.M., Ortigosa P.M. A multi-objective approach to estimate parameters of compartmental epidemiological models. Application to Ebola Virus Disease epidemics. *researchgatenet*. 2020:1–49. doi: 10.13140/RG.2.2.25778.56006. [CrossRef] [Google Scholar].
- [20] B. Ivorra, M.R. Ferrández, M. Vela-Pérez, and A.M. Ramos, Mathematical modeling of the spread of the coronavirus disease 2019 (COVID-19) taking into account the undetected infections. The case of China *Commun Nonlinear Sci Numer Simul*. 2020 Apr 30 : 105303 doi: 10.1016/j.cnsns.2020.105303
- [21] Yichi Li and et al, Mathematical Modeling and Epidemic Prediction of COVID-19 and Its Significance to Epidemic Prevention and Control Measures, *Annals of Infectious Disease and Epidemiology*, Volume 5, Issue 1, Mar, 2020.
- [22] D. Pal and et al, Mathematical Analysis of a COVID-19 Epidemic Model by using Data Driven Epidemiological Parameters of Diseases Spread in India, *medRxiv preprint* doi: <https://doi.org/10.1101/2020.04.25.20079111>, April 29, 2020.
- [23] https://www.worldometers.info/coronavirus/?utm_campaign=homeAdvegas1?
- [24] <https://www.covid19india.org/>
- [25] [Ministry Of Health & Family Welfare](#)

Appendix – 1

State wise COVID - 19 Cases in India as on 18th June 2020

(Sourced from state health ministry's: <https://covidindia.org/>)

| State | Confirmed Cases | Recoveries | Deaths |
|-----------------------------|-----------------|------------|--------|
| Andaman and Nicobar Islands | 45 | 35 | 0 |
| Andhra Pradesh | 7496 | 3772 | 92 |
| Arunachal Pradesh | 103 | 7 | 0 |
| Assam | 4861 | 2848 | 9 |
| Bihar | 7040 | 4961 | 44 |
| Chandigarh | 373 | 306 | 6 |

| State | Confirmed Cases | Recoveries | Deaths |
|-----------------------------------|-----------------|---------------|--------------|
| Chhattisgarh | 1946 | 1202 | 10 |
| Dadar & Nagar Haveli; Daman & Diu | 57 | 12 | 0 |
| Delhi | 47102 | 17457 | 1904 |
| Goa | 705 | 109 | 0 |
| Gujarat | 25601 | 17819 | 1591 |
| Haryana | 9218 | 4556 | 134 |
| Himachal Pradesh | 595 | 373 | 8 |
| Jammu and Kashmir | 5555 | 3144 | 71 |
| Jharkhand | 1919 | 1198 | 11 |
| Karnataka | 7944 | 4983 | 114 |
| Kerala | 2794 | 1413 | 21 |
| Ladakh | 687 | 95 | 1 |
| Lakshadweep | 0 | 0 | 0 |
| Madhya Pradesh | 11426 | 8632 | 486 |
| Maharashtra | 120504 | 60838 | 5751 |
| Manipur | 606 | 199 | 0 |
| Meghalaya | 44 | 30 | 1 |
| Mizoram | 130 | 1 | 0 |
| Nagaland | 193 | 103 | 0 |
| Odisha | 4512 | 3144 | 14 |
| Puducherry | 271 | 109 | 7 |
| Punjab | 3615 | 2570 | 83 |
| Rajasthan | 13857 | 10742 | 330 |
| Sikkim | 70 | 5 | 0 |
| Tamil Nadu | 52334 | 28641 | 625 |
| Telangana | 5675 | 3071 | 192 |
| Tripura | 1146 | 614 | 1 |
| Unassigned | 8703 | 0 | 0 |
| Uttar Pradesh | 14598 | 8904 | 435 |
| Uttarakhand | 2103 | 1386 | 26 |
| West Bengal | 12735 | 7001 | 518 |
| Total | 376563 | 200280 | 12485 |

Appendix - 2

Current Rules and Guidelines

The Ministry of Health and Family Welfare has issued SOP's on prevention of COVID-19 at different places. The general guidelines are

- Pregnant women, persons above 65 years of age, children below the age of 10 years, and persons with comorbidities are advised to stay at home.
- Everyone should maintain a distance minimum of 6 feet in public places.
- Use of face covers/masks to be mandatory.
- Spitting should be strictly prohibited.
- Use of the Aarogya Setu App shall be advised.
- Cover your mouth and nose while sneezing or coughing with a tissue/handkerchief/flexed elbow and dispose of the used tissues properly.
- Practice frequent hand washing with soap (for at least 40-60 seconds) even when hands are not visibly dirty. Use of alcohol-based hand sanitizers (for at least 20 seconds) can be made wherever feasible.

The ministry also issued specific guidelines to be followed at different places to contain COVID. Click on links below to view them.

- Religious places
- Restaurants
- Offices
- Shopping malls
- Hospitality units

Prevention of COVID-19

The announcement of Unlock-1 led to opening up of many places; and the government has advised to follow all the necessary precautions.

The following are basic hygiene practices that are recommended in different work, travel and household settings to prevent the spread of COVID-19.

- Teach your house help about COVID 19: What the virus is, how it spreads and the precaution to be taken.
- S/he should sanitise properly before entering the house. Keep soap and water or an alcohol-based sanitizer (with at least 70% alcohol) handy at the entrance.
- S/he should wear face mask at all times.
- Ask him/her to wash their hand / sanitise every time you send them out for essential items.
- When they are sent to buy essential items they should wear proper masks, plastic washable slippers, and a sanitizer (to use in case if she/he touches anything suspicious in the market/shop).
- Instruct the house help to maintain a safe physical distance of 6 feet from others.

- Try to keep away the material from your body when carrying from market. It is better to have a plastic basket/bucket with you when going to the market. Put the material in bucket and carry it to your home.
- Tender exact money for the products purchased so that one can avoid getting the change back from the shopkeeper.
- If you have a full-time house help, ask him/her to wash her/his hand thoroughly and frequently with soap and running water throughout the day.
- Maintain physical distancing (6 feet) with domestic help. Don't stay close to him/her at the time for giving instructions.
- If s/he shows any symptom(s) of COVID-19, s/he should be asked to isolate/home quarantine.
- If s/he shows any symptom of COVID-19, s/he should be taken for testing and medical check-up immediately. Provide him/her with necessary support for getting medical help immediately.

Advisory on Social Distancing

Social distancing is a non-pharmaceutical infection prevention and control intervention implemented to avoid/decrease contact between those who are infected with a disease causing pathogen and those who are not, so as to stop or slow down the rate and extent of disease transmission in a community.

In addition to the social distance, get to know about a few other things such as covering mouth while sneezing, washing hands regularly for 20 seconds, etc which will help to slow down the transmission.

DEGREE DOMINATION NUMBER OF A GRAPH

Mallikarjun Basanna Kattimani¹, Moumita Kali Chatterjee²
 Department of Mathematics,
 The Oxford College of Engineering, Bangalore-560 068, India.

Abstract

Let $G = (V, E)$ be a graph. A set $D \subseteq V(G)$ is a dominating set of G if every vertex not in D is adjacent to at least one vertex in D . The domination number $\gamma(G)$ is the minimum cardinality of a dominating set. The degree of a vertex v_i , where $i = 1, 2, 3, \dots, n$ of a graph G is denoted by d_i or $\deg(v_i)$ is the number of edges incident with v_i . We define, a set $D_k \subseteq V(G)$, where $k = 1, 2, 3, \dots, n$ is a dominating set and $u_i \in D_k$, where $i = 1, 2, 3, \dots, n$ then $\deg(D_k) = \left\{ \sum_i^n \deg(u_i) \right\} = x$ is the degree of a dominating set D_k . A set $D_i \subseteq V(G)$ is a *degree dominating set* of a graph G if $\deg(D_i) = x$ is minimum. The *degree domination number* $\gamma^*(G)$ is the minimum cardinality of a degree dominating set and an upper degree domination number $\Gamma^*(G)$ is the maximum cardinality of a degree dominating set of G .

Introduction

The graphs considered here are simple, finite, undirected, connected, without loops or multiple edges or isolated vertices. For undefined terms or notations in this paper may be found in Harary [2].

Let $G = (V, E)$ be a graph. A set $D \subseteq V(G)$ is a dominating set of G if every vertex not in D is adjacent to at least one vertex in D . The domination number $\gamma(G)$ is the minimum cardinality of a dominating set.

The degree of a vertex v_i , where $i = 1, 2, 3, \dots, n$ of a graph G is denoted by d_i or $\deg(v_i)$ is the number of edges incident with v_i .

We define, a set $D_k \subseteq V(G)$, where $k = 1, 2, 3, \dots, n$ is a dominating set and $u_i \in D_k$, where $i = 1, 2, 3, \dots, n$ then $\deg(D_k) = \left\{ \sum_i^n \deg(u_i) \right\} = x$ is the degree of a dominating set D_k . A set $D_i \subseteq V(G)$ is a *degree dominating set* of a graph G if $\deg(D_i) = \delta$ is minimum. The *degree domination number* $\gamma^*(G)$ is the minimum cardinality of a degree dominating set and an *upper degree domination number* $\Gamma^*(G)$ is the maximum cardinality of a degree dominating set of G .

In this paper, we initiate a study of this new parameter. The *degree domination number* $\gamma^*(G)$ reduces the congestion in traffic network and is having more application in electricity transmission network, and distribution, in telecommunication system, in water supply channels, in railway network, in circuit design and in the Management information System. Etc.

Results:

We list the exact values for some standard graphs.

Proposition 1.

- (i) For any complete graph K_p , $p \geq 2$ vertices, $\gamma^*(K_p) = 1$, $\delta = p - 1$
- (ii) For any cycle C_p , $p \geq 3$ vertices, $\gamma^*(C_p) = \left\lceil \frac{p}{3} \right\rceil$, $\delta = \left\lceil \frac{p}{3} \right\rceil \times 2$
- (iii) For any path P_p , $p \geq 2$ vertices, $\gamma^*(P_p) = \left\lceil \frac{p}{3} \right\rceil$, $\delta = \left\lceil \frac{2p}{3} \right\rceil$
- (iv) For any wheel W_p , $p \geq 4$ vertices, $\gamma^*(W_p) = 1$, $\delta = p - 1$
- (v) For any star $K_{1,n}$, $n \geq 2$ vertices, $\gamma^*(K_{1,n}) = 1$, $\delta = p - 1$
- (vi) For any star $K_{m,n}$, $m \geq 2$, $n \geq 2$ vertices, $\gamma^*(K_{m,n}) = 2$, $m \leq n$, $\delta = m + n$

Theorem 1. For any graph G , $\gamma(G) \leq \gamma^*(G)$, equality hold for K_p , W_p , $K_{1,n}$, $K_{m,n}$... (1)

Proof. This follows from the fact that every degree dominating set is dominating set, (1) holds.

Theorem 2. For any graph G , $p \geq 2$ vertices, $\gamma^*(G) = p - \gamma(G)$

Proof. Let $G = (V, E)$ be a graph, consider the following two cases.

Case1. Suppose G be a complete graph K_p , every pair of its p vertices adjacent.

We know that $\gamma(K_p) = 1$ and

By theorem 1 a) we have $\gamma^*(K_p) = 1$

Thus, $\gamma^*(K_p) \leq p - \gamma(K_p)$

$$1 \leq p - 1$$

$$2 \leq p$$

....(2)

Case 2. Suppose G be path

We know that $\gamma(P_p) = \left\lfloor \frac{p+2}{3} \right\rfloor$ and

By theorem 1 c) we have $\gamma^*(P_p) = \left\lfloor \frac{p}{3} \right\rfloor$

Thus, $\gamma^*(P_p) \leq p - \gamma(P_p)$

$$\left\lfloor \frac{p}{3} \right\rfloor \leq p - \left\lfloor \frac{p+2}{3} \right\rfloor$$

$$\left\lfloor \frac{p}{3} \right\rfloor \leq \left\lfloor \frac{3p - p - 2}{3} \right\rfloor$$

$$p \leq 2p - p$$

$$2 \leq 2p - p$$

$$2 \leq p.$$

...(3)

From (2) and (3) given results holds true for any graph.

Proposition 2. Let T be a tree with $c(T) \leq 4$ cut-vertices, then $\gamma^*(T) = |e|$, where e is the number of pendent vertices.

Proposition 3. If T is a tree, $|c(T)| = 1$, where $c(T)$ is the number of cut vertex of T , then $\gamma^*(T) = 1$.

Proposition 4 If T is a tree, $|c(T)| = 2$, where $c(T)$ is the number of cut vertex of T e be the number of end vertex, then $\gamma^*(T) = |e|$.

Proposition 5 If T is a tree with $|c(T)| = 3$, where $c(T)$ is number of cut vertex of T , then

$$\gamma^*(T) = \left\lfloor \frac{p-2}{2} \right\rfloor.$$

Theorem 3. For any graph G , $\gamma^*(G) \leq \left\lfloor \frac{P}{2} \right\rfloor$, $\delta \leq p$

Proof. Let us assume that $\gamma^*(G) > \left\lfloor \frac{P}{2} \right\rfloor$

$$\Rightarrow 2\gamma^*(G) > P$$

There exists, $\gamma^*(G) = 1 \Rightarrow 2 > p$ which is contradiction by theorem (3). Hence our assumption is wrong.

Thus, $\gamma^*(G) \leq P$ The converse is obvious.

Theorem 4. For any tree T , $\gamma^*(T) \leq c(T)$, where $c(T)$ is number of the cut vertex and p is the number of pendent vertex in T .

Proof. Consider a tree T with $p \geq 3$ vertices, obviously contains cut vertices and end vertices.

Consider the following two cases:

Case 1. Suppose a tree T , $p = 3$ vertices, is a path P_3 by Proposition 1 (iii) $\gamma^*(T) = 1$, thus $\gamma^*(T) = c(T)$

Case 2. Suppose a tree T , $p > 3$ vertices, which is having more than one cut vertex and more than one end vertex, definitely $\{c(T)\}$ and $\{p\}$ are dominating set called a set A and B respectively. Then $\deg(A) < \deg(B)$, since each bridge is contributing two degree to the cut vertices.

Thus $\deg(A) < \deg(B)$. Hence $\gamma^*(T) < |c(T)|$.

REFERENCES:

- [1] Cockayne E.J., Hartnell B.L. and Hedetniemi S.T. Well domination in graphs, Ars. Combinatorics 387-395 (1987).
- [2] F. Harary, Graph theory, Addison Wesley, Reading Mass (1969).
- [3] Haynes T.W, Hedetniemi S.T. and Slater P J. Fundamentals of domination in graphs. Marcel Dekker Inc. New York. (1998).
- [4] Kulli V.R. and Kattimani M B. Accurate domination in graphs. In V.R. Kulli, ed., Advances in Domination Theory I, Vishwa International Publications, Gulbarga, India 1-8 (2012).
- [5] Kulli V.R. and Kattimani M B. A note on maximal domination number of a graph, Graph Theory Notes of New York, New York Academy of Sciences 39, 35-36, (2000).

Vertex Polynomial of Middle, Line and Total Graphs of some standard Graphs



Mallikarjun Basanna Kattimani, Sridhara K.R.

Abstract: In this article, we have obtained vertex polynomial of Middle, Line and Total graphs of some standard graphs namely complete graph, star, path, cycle and wheel graph.

Keywords: Vertex polynomial, Middle graph, Line Graph, Total Graph

1. INTRODUCTION

In this paper, we have considered only finite graphs which are non-trivial, undirected, having no self-loops and having no parallel edges. Two edges of a graph are adjacent if they have a common vertex. If a vertex v is an end vertex of an edge e , then edge e is incident on vertex v . Vertices and edges are called elements of a graph and are neighbors if they are either incident or adjacent. $K_{1,n}$ represents a star. A wheel graph W_n and is defined as $W_n = K_1 + C_{n-1}$. A graph G is k -regular if each vertex has degree k . If $x = uv$ is an edge of a graph G , and w is not a vertex of G , then x is said to be subdivided if it is replaced by the edges uw and vw . For terminologies and notations, we refer [1]. The vertex polynomial of the graph G [2] is defined as $V(G; x) = \sum_{k=0}^{\Delta(G)} v_k x^k$, where $\Delta(G) = \max \{d(v) : v \in V(G)\}$ and v_k is the number of vertices of degree k . The roots of a vertex polynomial are called vertex polynomial roots.

2. MIDDLE GRAPH, LINE GRAPH, TOTAL GRAPH AND VERTEX POLYNOMIAL WITH AN EXAMPLE.

In this part, we list the definitions of Middle graph, Line graph and Total graph of a graph with an example. Also we show their vertex polynomials.

Let G be a graph with $|V| = m$ and $|E| = n$. Its line graph $L(G)$ contains vertices which are edges of G and edges in $L(G)$ are drawn between vertices if they have common vertex in G . Middle graph $M(G)$ has vertex set containing all vertices and all edges of G and edges of $M(G)$ between new vertices are drawn only when the edges corresponding in G are adjacent. Total graph $T(G)$ has vertex set containing all vertices of G and all edges of G and two vertices of total graph are adjacent if they happen to be neighbors in G . The following figures show a graph, its line graph, middle graph and total graph with their vertex polynomials.



Figure 1– Graph G .

In this graph, we find 1, 2 and 1 vertices of degrees 1, 2 and 3 respectively. Thus $V(G; x) = x + 2x^2 + x^3$. Now we consider its line graph as in Figure 2.

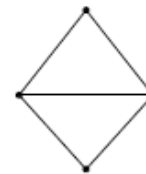


Figure 2– $L(G)$

We note that $L(G)$ has four vertices of which two are of degree 2 and remaining two are of degree 3. Thus $V(L(G); x) = 2x^2 + 2x^3$

Now, we consider middle graph $M(G)$ as shown in Figure 3.

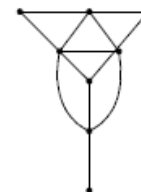


Figure 3– $M(G)$

The middle graph has one vertex of degree 1, two vertices of degree 2, one vertex of degree 3, two vertices of degree 4 and two vertices of degree 5. Thus $V(M(G); x) = x + 2x^2 + x^3 + 2x^4 + 2x^5$. Now we consider total graph $T(G)$ as shown in Figure 4.

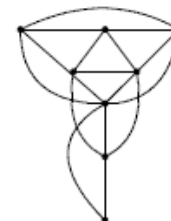


Figure 4– $T(G)$

Revised Manuscript Received on April 03, 2020.

* Correspondence Author

Mallikarjun Basanna Kattimani, Department of Mathematics, The Oxford College of Engineering, Bangalore, India, mathshodxford@gmail.com

Sridhara K.R.*, Department of Mathematics, A.P.S. College of Engineering, Bangalore, India, sridharwi@gmail.com

© The Authors. Published by Blue Eyes Intelligence Engineering and Sciences Publication (BEIESP). This is an open access article under the CC BY-NC-ND license (<http://creativecommons.org/licenses/by-nc-nd/4.0/>)

Vertex Polynomial of Middle, Line and Total Graphs of some standard Graphs

$T(G)$, the total graph has 1, 4, 2 and 1 vertices of degrees 2, 4, 5 and 6 respectively.

$$\text{Thus } V(T(G); x) = x^2 + 4x^4 + 2x^5 + x^6$$

III. MAIN RESULTS

Theorem 3.1: If $M(K_n)$ is middle graph of K_n , then

$$V(M(K_n); x) = nx^{n-1} + \frac{n(n-1)}{2}x^{2n-2}$$

Proof: We note that K_n has n vertices, whereas its middle graph $M(K_n)$ has $\frac{n^2+n}{2}$ vertices by definition of middle graph. We can partition vertex set of $M(K_n)$ into two disjoint subsets V_1 and V_2 as follows:

V_1 : Vertex set with $|V_1| = n$, degree being $(n-1)$ for each vertex and

V_2 : Vertex set with $|V_2| = \frac{n^2-n}{2}$, degree being $(2n-2)$ for each vertex.

$$\text{Hence } V(M(K_n); x) = nx^{n-1} + \frac{n(n-1)}{2}x^{2n-2}$$

Theorem 3.2: If $M(K_{1,n})$ is middle graph of $K_{1,n}$, then

$$V(M(K_{1,n}); x) = nx^{n+1} + x^n + nx \text{ for } n \geq 2$$

Proof: We note that $K_{1,n}$ has $(n+1)$ vertices, whereas its middle graph $M(K_{1,n})$ has $(2n+1)$ vertices by definition of middle graph. We can partition the vertex set of $M(K_{1,n})$ into disjoint subsets V_1, V_2 and V_3 as follows:

V_1 : Vertex set containing 1 vertex of degree n ,

V_2 : Vertex set with $|V_2| = n$, each vertex being pendant and

V_3 : Vertex set $|V_3| = n$, degree being $(n+1)$ for each vertex.

$$\text{Thus } V(M(K_{1,n}); x) = nx^{n+1} + x^n + nx$$

Theorem 3.3: If $M(P_n)$ is the middle graph of P_n , then

$$V(M(P_n); x) = 2x + (n-2)x^2 + (n-1)x^3, n \geq 3$$

Proof: We note, by definition of middle graph that, $M(P_n)$ contains $(2n-1)$ vertices. We can partition the vertex set of $M(P_n)$ into three disjoint subsets V_1, V_2 and V_3 as follows:

V_1 : Vertex set containing 2 vertices, each of degree 1,

V_2 : Vertex set with $|V_2| = n-2$, degree being 2 for each vertex and

V_3 : Vertex set with $|V_3| = n-1$, degree being 3 for each vertex.

$$\text{Thus } V(M(P_n); x) = 2x + (n-2)x^2 + (n-1)x^3$$

Theorem 3.4: If $M(C_n)$ is the middle graph of C_n , then

$$V(M(C_n); x) = nx^2 + nx^4$$

Proof: We note, by definition of middle graph that, $M(C_n)$ contains $2n$ vertices. We can partition the vertex set of $M(C_n)$ into V_1 and V_2 as follows:

V_1 : Vertex set containing n vertices of C_n , each of degree 2 and

V_2 : Vertex set containing n new vertices obtained by definition of middle graph, each of degree 4.

$$\text{Thus } V(M(C_n); x) = nx^2 + nx^4$$

Corollary 3.5: The vertex polynomial roots of $M(C_n)$ are 0, 0 and $\pm i$

Proof: In view of Theorem 3.4, vertex polynomial roots of $M(C_n)$ can be obtained by taking

$$nx^2 + nx^4 = 0 \Rightarrow x = 0, 0 \text{ and } \pm i$$

Theorem 3.6: If $M(W_n)$ is the middle graph of W_n , then

$$V(M(W_n); x) = (n-1)x^{n+2} + x^{n-1} + (n-1)x^6 + (n-1)x^3, \text{ for } n \geq 5$$

Proof: We note, by definition of middle graph that, $M(W_n)$ contains $(3n-2)$ vertices. We can partition vertex set of $M(W_n)$ into four disjoint subsets V_1, V_2, V_3 and V_4 as follows:

V_1 : Vertex set containing a single vertex of degree $(n-1)$,

V_2 : Vertex set with $|V_2| = n-1$, degree being 3 for each vertex,

V_3 : Vertex set $|V_3| = n-1$, degree being 6 for each vertex, and

V_4 : Vertex set $|V_4| = n-1$, degree being $n+2$ for each vertex.

$$\text{Thus } V(M(W_n); x) = (n-1)x^{n+2} + x^{n-1} + (n-1)x^6 + (n-1)x^3$$

Theorem 3.7: If $L(K_n)$ is the line graph of K_n , then

$$V(L(K_n); x) = \frac{n(n-1)}{2}x^n$$

Proof: Using definition of line graph, we easily understand that $L(K_n)$ is a $n-2$ regular graph with $\frac{n(n-1)}{2}$ vertices and every vertex will be of degree $n-2$.

$$\text{Thus } V(L(K_n); x) = \frac{n(n-1)}{2}x^{n-2}$$

Theorem 3.8: If $L(K_{1,n})$ is the line graph of $K_{1,n}$, then

$$V(L(K_{1,n}); x) = nx^{n-1}$$

Proof: By definition of line graph, of a graph, we easily understand that $L(K_{1,n})$ is a complete graph K_n and therefore every vertex will be of degree $(n-1)$.



Thus $V(L(K_{1,n}; x)) = nx^{n-1}$.

Theorem 3.9: If $L(P_n)$ is the line graph of P_n , then $V(L(P_n); x) = 2x + (n - 3)x^2, n \geq 3$

Proof: By definition of line graph, we easily understand that $L(P_n)$ is a path graph P_{n-1} .

Thus $V(L(P_n); x) = V(P_{n-1}; x)$.

It is easy to note that path graph P_{n-1} will have 2 pendant vertices and remaining $(n - 3)$ internal vertices will be of degree 2.

Thus $V(L(P_n); x) = 2x + (n - 3)x^2$.

Theorem 3.10: If $L(C_n)$ is the line graph of C_n , then is $V(L(C_n); x) = nx^2$.

Proof: By definition of line graph, we easily understand that $L(C_n) = C_n$ itself. As degree of every vertex of C_n is 2 and as it has n vertices, we find $V(L(C_n); x) = nx^2$.

Corollary 3.11: The vertex polynomial root of $L(C_n)$ is 0 with multiplicity 2.

Proof: In view of Theorem 3.10, vertex polynomial roots of $L(C_n)$ can be obtained by taking

$$nx^2 = 0 \Rightarrow x = 0, 0 \text{ as } n \neq 0$$

Theorem 3.12: If $L(W_n)$ is the line graph of W_n , then $V(L(W_n); x) = (n - 1)x^4 + (n - 1)x^n, n \geq 4$

Proof: We know, a wheel graph W_n will have n vertices and $(2n - 2)$ edges. The vertex set of $L(W_n)$ will have $(2n - 2)$ vertices and we can partition the vertex set into two disjoint subsets V_1 and V_2 as follows:

V_1 : Vertex set with $|V_1| = n - 1$, degree being 4 for each vertex

V_2 : Vertex set with $|V_2| = n - 1$, degree being n for each vertex

Thus $V(L(W_n); x) = (n - 1)x^4 + (n - 1)x^n$

Theorem 3.13: If $T(K_n)$ is the total graph of K_n , then

$$V(T(K_n); x) = \frac{n(n + 1)}{2} x^{2n-2}$$

Proof: We note that K_n will have n vertices and $\frac{n(n-1)}{2}$ edges. By definition of total graph of a graph, we note that, total graph $T(K_n)$ will have $n + \frac{n(n-1)}{2} = \frac{n(n+1)}{2}$ vertices and each vertex will be of degree $(2n - 2)$.

Thus

$$V(T(K_n); x) = \frac{n(n + 1)}{2} x^{2n-2}$$

Theorem 3.14: If $T(K_{1,n})$ is the total graph of $K_{1,n}$, then

$$V(T(K_{1,n}); x) = nx^2 + nx^{n+1} + x^{2n}$$

Proof: We know a star graph $K_{1,n}$ will have $n + 1$ vertices and n edges. We note that total graph $T(K_{1,n})$ of star graph $K_{1,n}$ will have $(2n + 1)$ by the way in which total graph is defined and we can partition this the vertex set into 3 disjoint subsets V_1, V_2 and V_3 as follows:

V_1 : Vertex set containing a single vertex of degree $2n$,

V_2 : Vertex set with $|V_2| = n - 1$, degree being 2 for each vertex and

V_3 : Vertex set $|V_3| = n$, degree being 2 for each vertex.

Thus $V(T(K_{1,n}); x) = nx^2 + nx^{n+1} + x^{2n}$

Theorem 3.15: If $T(P_n)$ is the total graph of $T(P_n)$, then

$$V(T(P_n); x) = 2x^2 + 2x^3 + (2n - 5)x^4, n \geq 3$$

Proof: We know, a path graph P_n will have n vertices and $(n - 1)$ edges. By definition of total graph, we note $T(P_n)$ will have $(2n - 1)$ vertices and we can partition this vertex set into 3 disjoint subsets V_1, V_2 and V_3 as follows:

V_1 : Vertex set containing 2 vertices, each of degree 2,

V_2 : Vertex set containing 2 vertices, each of degree 3 and

V_3 : Vertex set containing $(2n - 5)$ vertices, each of degree 4.

Thus $V(T(P_n); x) = 2x^2 + 2x^3 + (2n - 5)x^4$

Theorem 3.16: If $T(C_n)$ is the total graph of C_n , then

$$V(T(C_n); x) = 2nx^4$$

Proof: We know, a cycle graph C_n has n vertices. By definition of total graph of a graph, we note that, $T(C_n)$ of C_n is a 4-regular graph with $2n$ vertices and each vertex will be of degree 4. Thus $V(T(C_n); x) = 2nx^4$.

Corollary 3.17: The vertex polynomial root of $T(C_n)$ is 0 with multiplicity 4.

Proof: In view of Theorem 3.16, result is obvious.

Theorem 3.18: If $T(W_n)$ is the total graph of W_n , then

$$V(T(W_n); x) = (2n - 2)x^6 + (n - 1)x^{n+2} + x^{2n-2}, \text{ for } n \geq 5$$

Proof: We know a wheel graph W_n has n vertices and $2n - 2$ edges. By definition of total graph, we note that $T(W_n)$ of W_n will have $(3n - 2)$ vertices and we can partition this vertex set into three disjoint subsets V_1, V_2 and V_3 as follows:

V_1 : Vertex set containing $(2n - 2)$ vertices, each of degree 6,



Vertex Polynomial of Middle, Line and Total Graphs of some standard Graphs

V_2 : Vertex set containing a single vertex of degree $(2n - 2)$ and

V_3 : Vertex set containing $(n - 1)$ vertices, each of degree $(n + 2)$.

Thus $V(T(W_n; x)) = (2n - 2)x^6 + (n - 1)x^{n+2} + x^{2n-2}$

IV.CONCLUSION

Vertex polynomial is one of the possible ways in which we can represent a graph algebraically. We can compare this polynomials with other polynomials associated with graph also.

REFERENCES

1. F.Haray, Graph Theory, Addison-Wesley, Reading- Mass (1969).
2. J.Devaraj and E.Sukumaran, On Vertex Polynomial, International J. of Math. Sci. & Engg. Appls. (IJMSEA), Vol. 6 No. I (January, 2012), pp. 371-380.
3. A.M.Anto and P.Paul Hawkins, Vertex Polynomial of Graphs with New Results, Global Journal of Pure and Applied Mathematics, Volume 15, Number 4 (2019), pp. 469-475.
4. Mallikarjun Basanna Kattimani and Sridhara K.R., Transitive domination polynomial in graphs, Studies in Indian Place Names (UGC Care Journal), ISSN: 2394-3114, Vol-40-Issue-70-March 2020, pp. 440-447.

AUTHORS' PROFILE



Dr.Mallikarjun Basanna Kattimani , He is working as Professor and Head, Department of Mathematics & Dean of Examinations at The Oxford College of Engineering, Bangalore. His current area of research interest is Graph Theory. He has successfully guided one student for Ph.D. and presently guiding 6 students for Ph.D. He has introduced many domination parameters in Graph Theory and has published 12 research papers in national and international journals. In addition, he has 7 extended research articles to his credit. He has around 28 years of rich teaching experience.



Sridhara K.R., He is working as Assistant Professor and Head, Department of Mathematics, A.P.S. College of Engineering, Bangalore. His research area of interest is Graph Theory. He has around 21 years of teaching experience.



[Home](#) / [Archives](#) /

[Vol. 13 No. 5 \(2020\): Special Issue Dedicated to Professor Hari M. Srivastava on the Occasion of his 80th Birthday](#) /
[Special Issue Dedicated to Professor Hari M. Srivastava on the Occasion of his 80th Birthday](#)

Schur Geometric Convexity of Related Function for Holders Inequality with Application

Sreenivasa Reddy Perla

<https://orcid.org/0000-0001-7112-0278>

S. Padmanabhan

RNS Institute of Technology, VTU

V. Loksha

VSK UNIVERSITY

DOI: <https://doi.org/10.29020/nybg.ejpam.v13i5.3741>

Keywords: Holders Inequality, majorization inequality, schur geometric convex, schur geometric concave

Keywords: Holders Inequality, majorization inequality, schur geometric convex, schur geometric concave

Abstract

In this paper, we investigated the Schur geometric convexity of related function for Holders Inequality by using majorization inequality theory and some applications are established.

Author Biographies

Sreenivasa Reddy Perla

S. Padmanabhan, RNS Institute of Technology, VTU

 PDF

How to Cite

Perla, S. R., Padmanabhan, S., & Loksha, V. (2020). Schur Geometric Convexity of Related Function for Holders Inequality with Application. *European Journal of Pure and Applied Mathematics*, 13(5), 1199–1211. <https://doi.org/10.29020/nybg.ejpam.v13i5.3741>

International Journal of Advanced Science and Technology

[Home](#)[Editorial Board](#)[Journal Topics](#)[Archives](#)[About the Journal](#)[Submissions](#)[Privacy Statement](#)[Contact](#)[Home](#) / [Archives](#) / [Vol. 29 No. 7 \(2020\)](#) / [Articles](#)

Schur Harmonic Convexity of Related Function for Holders Inequality with Application

Sreenivasa Reddy Perla , S. Padmanabhan

Abstract

In this paper, make use of majorization inequality theory investigated the Schur harmonically convex regarding related function of Holders Inequality, giving a complete essential condition of Schur harmonically convex function to Holders Inequality and some applications are established.

[PDF](#)

How to Cite

Sreenivasa Reddy Perla , S. Padmanabhan. (2020). Schur Harmonic Convexity of Related Function for Holders Inequality with Application. *International Journal of Advanced Science and Technology*, 29(7), 8224-8235. Retrieved from <http://serisc.org/journals/index.php/IJAST/article/view/24646>

[More Citation Formats](#)

Issue

[Vol. 29 No. 7 \(2020\)](#)

Section

[Articles](#)



(https://www.ssrn.com/)

Product
&
Services

Subscribe

Submit
a
paper

Browse

Rankings

Contact



(https://papers.ssrn.com/sol3/ShoppingCa



Download This Paper (Delivery.cfm/SSRN_ID3667497_code3253098.pdf?abstractid=3667497&mirid=1)

Open PDF in Browser (Delivery.cfm/SSRN_ID3667497_code3253098.pdf?abstractid=3667497&mirid=1&type=2)

★ Add Paper to My Library

Share:

Transitive Domination Polynomial of Graphs

Institute of Scholars (InSc), 2020

7 Pages

Posted: 18 Sep 2020

Mallikarjun Basanna Kattimani (https://papers.ssrn.com/sol3/cf_dev/AbsByAuth.cfm?per_id=4314501)

The Oxford College of Engineering

Sridhara K R (https://papers.ssrn.com/sol3/cf_dev/AbsByAuth.cfm?per_id=4314502)

A.P.S. College of Engineering

Date Written: August 5, 2020

Abstract

Let $G=(V,E)$ be a connected simple graph with n vertices. A set of vertices D is called a Transitive Dominating set if every vertex in $V-D$ is adjacent to at least one of the vertices in D through a path of length at most two [4]. Transitive domination number, denoted by $\gamma_{\text{trd}}(G)$ is the minimum of the cardinalities of all possible transitive dominating sets of the graph. In this paper, we introduce a new domination polynomial called Transitive Domination Polynomial of a graph. The transitive domination polynomial of a graph G with n vertices is denoted by $D_{\text{trd}}(G,x)$ and is defined as:

$D_{\text{trd}}(G,x) = \sum_{j=\gamma_{\text{trd}}(G)}^n [d_{\text{trd}}(G,j)] x^j$, where $d_{\text{trd}}(G,j)$ represents the number of transitive dominating sets of cardinality j . The roots of transitive domination polynomial are called transitive dominating roots. In this paper, we have obtained transitive domination polynomials of some standard graphs. Also transitive dominating roots of some graphs are obtained.

Keywords: Domination, Transitive Domination, Transitive Domination Polynomial, Transitive Domination Roots

[Suggested Citation](#) >

[Show Contact Information](#) >



Download This Paper (Delivery.cfm/SSRN_ID3667497_code3253098.pdf?abstractid=3667497&mirid=1)

Open PDF in Browser (Delivery.cfm/SSRN_ID3667497_code3253098.pdf?abstractid=3667497&mirid=1&type=2)

7 References

1. F Haray
Graph Theory
Posted: 1969
2. J L Arocha, B Llano
Mean value for the matching and dominating polynomial
Discuss.Math.Graph Theory, volume 20, issue 1, p. 57 - 69
Posted: 2000
Crossref (https://doi.org/10.7151/dmgt.1106)
3. S Alikhani, Y H Peng
Introduction to domination polynomial of a graph
Ars Combinatoria, volume 114, p. 257 - 266
Posted: 2014

TRANSITIVE DOMINATION NUMBER OF A GRAPH

Mallikarjun B. Kattimani and **Selastina Mary A** Department of Mathematics The Oxford College of Engineering :: mallikarjunbk64@gmail.com

Abstract

A Subset D of $V(G)$ of a graph G is said to be a transitive dominating set if every vertex not in D is adjacent to at least one vertex in D through a path of length at most two. The minimum cardinality of the transitive dominating set of G is called the transitive domination number $\gamma_{tr}(G)$ of G . Similarly; we define upper transitive domination number $\Gamma_{tr}(G)$ of G as the maximum number of vertices in a transitive dominating set. In this paper, bounds for $\gamma_{tr}(G)$ and its exact values for some standard graphs are found and also relations between $\gamma_{tr}(G)$ with known parameters are established.

Introduction

In this paper, a graphs considered here will be finite, undirected, without isolated vertices and contain no loops or multiple edges, any undefined terms or notations in this paper may be found in Harary [3].

A set of D vertices of a graph G is a dominating set, if every vertex not in D is adjacent to at least one vertex in D . The minimum cardinality of a dominating set is called domination number of a graph G and is denoted by $\gamma(G)$.

We introduce a new parameter called a transitive dominating set of a graph is which is well defined and some results obtained on this parameter.

A subset D of $V(G)$ of a graph G is said to be transitive dominating set if every vertex not in D is adjacent to at least one vertex in D through a path of length at most two. The minimum cardinality of the transitive dominating set of G is called the transitive domination number of a graph G and which is denoted by $\gamma_{tr}(G)$.

For any real number x , $\lceil x \rceil$ denote the least integer not less than x and $\lfloor x \rfloor$ denote the greatest integer not greater than x .

Results

We list the exact values of $\gamma_{tr}(G)$ for some standard graphs.

Proposition 1:

1. For any path P_p , with $P \geq 2$ vertices, $\gamma_{tr}(P_p) = \lceil \frac{p}{5} \rceil$
2. For any cycle C_p , $\gamma_{tr}(C_p) = \lceil \frac{p}{5} \rceil$, $P \geq 3$.
3. For complete graph K_p , $\gamma_{tr}(K_p) = 1, P \geq 2$.
4. For complete bipartite graph $K_{m,n}$,



CHILDREN'S EDUCATION SOCIETY (Regd.)
THE OXFORD COLLEGE OF ENGINEERING
 (Recognised by the Govt. of Karnataka, Affiliated to Visvesvaraya Technological University, Belagavi.

Approved by A.I.C.T.E. New Delhi.

Recognised by UGC Under Section 2(f)

Bommanahalli, Hosur Road, Bangalore - 560 068.

Ph: 080-61754601/602, Fax: 080 - 25730551

E-mail: engprincipal@theoxford.edu Web: www.theoxfordengg.org

| Sl.No | Title of paper | Name of the author/s | Department of the teacher | Name of journal | Year of publication | ISSN number | Link to website of the Journal | Link to article/paper/abstract of the article | Is it listed in UGC Care list/Scopus/ Web of Science/other , mention |
|-------|--|-----------------------|---------------------------|--|---------------------|-------------|---|---|--|
| 1 | DCUIS: An Exhaustive Algorithm for Pre Processing of Web Log File | Sowmya H.K | CSE | International Journal of Engineering Trends and Technology | 2020 | 2231-5381 | https://ijettjournal.org/ | http://www.internationaljournals.org/uploads/specialissuepdf/ICT-2020/2020/OTHERS/P127.pdf | Scopus |
| 2 | Robust Classifier Design with Ensemble Neural Network using Differential Evolution | Shobha T | CSE | International Journal of Engineering Trends and Technology | 2020 | 2231-5381 | https://ijettjournal.org/ | http://www.internationaljournals.org/uploads/specialissuepdf/ICT-2020/2020/OTHERS/P127.pdf | Scopus |
| 3 | An Approach for Remove Missing Values in Numerical and Categorical Values Using Two Way Table Marginal Joint Probability | Dr. E. Saravana Kumar | CSE | International Journal of Advanced Science and Technology | 2020 | 2005-4238 | http://sersc.org/journals/index.php/IJAST/article/view/11383 | https://www.emerald.com/insight/content/doi/10.1108/IJIUS-10-2020-0060/full/html#:~:text=The%20smart%20city%20utilizes%20hybrid,et%20al.%2C%202020).&text=A%20Web%20camera%20with%20street,be%20implemente | Scopus |



CHILDREN'S EDUCATION SOCIETY (Regd.)
THE OXFORD COLLEGE OF ENGINEERING

(Recognised by the Govt. of Karnataka, Affiliated to Visvesvaraya Technological University, Belagavi.

Approved by A.I.C.T.E. New Delhi.

Recognised by UGC Under Section 2(f)

Bommanahalli, Hosur Road, Bangalore - 560 068.

Ph: 080-61754601/602, Fax: 080 - 25730551

E-mail: engprincipal@theoxford.edu Web: www.theoxfordengg.org

| | | | | | | | | | |
|---|---|--|-----|---|------|---------|---|---|--------|
| | | | | | | | | d%20in%20Bhopal%20city. | |
| 4 | An improved watermarking algorithm for robustness and imperceptibility of data protection in the perception layer of internet of things | Moham mad Kamrul Hasan , Samar Kamil , Muhammad Shafiq , Yuvaraj S , E. Saravana Kumar , Rajiv | CSE | Pattern Recognition Letter | 2021 | 1678655 | https://www.sciencedirect.com/journal/pattern-recognition-letters | https://www.sciencedirect.com/science/article/pii/S0167865521003901 | Scopus |
| 5 | Artificial intelligence and machine learning approaches to COVID-19 outbreak: A survey | Sowmya, H. K.; Jesy Janet Kumari, J.; Naidu, R. Ch A.; Vengatesan, K. | CSE | Turkish Journal of Physiotherapy and Rehabilitation | 2021 | 1783454 | https://pesquisa.bvsalud.org/global-literature-on-novel-coronavirus-2019-ncov/resource/pt/covidwho-1250726 | https://pesquisa.bvsalud.org/global-literature-on-novel-coronavirus-2019-ncov/resource/pt/covidwho-1250726 | Scopus |



CHILDREN'S EDUCATION SOCIETY (Regd.)
THE OXFORD COLLEGE OF ENGINEERING

(Recognised by the Govt. of Karnataka, Affiliated to Visvesvaraya Technological University, Belagavi.

Approved by A.I.C.T.E. New Delhi.

Recognised by UGC Under Section 2(f)

Bommanahalli, Hosur Road, Bangalore - 560 068.

Ph: 080-61754601/602, Fax: 080 - 25730551

E-mail: engprincipal@theoxford.edu Web: www.theoxfordengg.org

| | | | | | | | | | |
|---|---|--|-----|--|------|------------|---|---|--------|
| 6 | Comprehensive Analysis of Cloud based Databases | E. Saravana Kumar, R Ch A Naidu | CSE | IOP Conference Series: Materials Science and Engineering | 2021 | 1757-899X | https://www.researchgate.net/publication/350903294_Comprehensive_Analysis_of_Cloud_based_Databases | https://www.researchgate.net/publication/350903294_Comprehensive_Analysis_of_Cloud_based_Databases | Scopus |
| 7 | Internet of things (IoT)-based unmanned intelligent street light using renewable energy | E. Saravana Kumar | CSE | International Journal of Intelligent Unmanned Systems | 2021 | 2049-6427 | https://www.emerald.com/insight/2049-6427.htm | https://www.emerald.com/insight/2049-6427.htm | Scopus |
| 8 | PULMONOLOGICAL DISORDERS CAUSED DUE TO COVID-19 PANDEMIC | Shobha, T.; Patil, S.; Naidu, R. C. H. A.; Saravana Kumar, E.; Vengatesan, K.. | CSE | Turkish Journal of Physiotherapy Rehabilitation | 2021 | 1300-0101. | https://pesquisa.bvsalud.org/global-literature-on-novel-coronavirus-2019-ncov/resource/pt/covidwho-1362972 | https://pesquisa.bvsalud.org/global-literature-on-novel-coronavirus-2019-ncov/resource/pt/covidwho-1362972 | Scopus |
| 9 | Review on side-effects of COVID-19 in the growth of | Shobha, T.; Patil, S.; Naidu, | CSE | Turkish Journal of Physiotherapy and | 2021 | 1300-0101. | https://pesquisa.bvsalud.org/global-literature-on-novel- | https://pesquisa.bvsalud.org/global-literature-on-novel-coronavirus-2019- | Scopus |



CHILDREN'S EDUCATION SOCIETY (Regd.)
THE OXFORD COLLEGE OF ENGINEERING

(Recognised by the Govt. of Karnataka, Affiliated to Visvesvaraya Technological University, Belagavi.

Approved by A.I.C.T.E. New Delhi.

Recognised by UGC Under Section 2(f)

Bommanahalli, Hosur Road, Bangalore - 560 068.

Ph: 080-61754601/602, Fax: 080 - 25730551

E-mail: engprincipal@theoxford.edu Web: www.theoxfordengg.org

| | | | | | | | | | |
|----|--|---|-----|---|------|-----------------|---|---|------------|
| | neurologic diseases | R. C. H. A.; Saravana Kumar, E.; Vengatesan, K.. | | Rehabilitation | | | coronavirus-2019-ncov/resource/pt/covidwho-1218842 | ncov/resource/pt/covidwho-1218842 | |
| 10 | Gradient flow-based deep residual networks for enhancing visibility of scenery images degraded by foggy weather conditions | Dr. R Kanagavalli | ISE | Journal of Ambient Intelligence and Humanized Computing | 2020 | ISSN: 1868-5137 | https://www.springer.com/journal/12652 | https://link.springer.com/article/10.1007%2Fs12652-020-02225-2 | UGC/Scopus |
| 11 | Highly sensitive photonic crystal based biosensor for Bacillus cereus | S. S. Ajey,H. R. Bhanumathi, P. C. Srikanth, Preeta Sharan2 | ECE | International Journal of Information Technology | 2020 | 2511-2112 | https://www.springer.com/journal/41870 | https://doi.org/10.1007/s41870-020-00507-8 | UGC/Scopus |



CHILDREN'S EDUCATION SOCIETY (Regd.)
THE OXFORD COLLEGE OF ENGINEERING
 (Recognised by the Govt. of Karnataka, Affiliated to Visvesvaraya Technological University, Belagavi.

Approved by A.I.C.T.E. New Delhi.

Recognised by UGC Under Section 2(f)

Bommanahalli, Hosur Road, Bangalore - 560 068.

Ph: 080-61754601/602, Fax: 080 - 25730551

E-mail: engprincipal@theoxford.edu Web: www.theoxfordengg.org

| | | | | | | | | | |
|----|---|--|-----|---|------|-----------|---|---|----------|
| 12 | Integrated MOEMS based cantilever sensor for early detection of cancer | Mr Anup, Dr Preeta Sharan, Maneesh Srivastava | ECE | Optik | 2020 | 0030-4026 | https://www.journals.elsevier.com/optik | https://doi.org/10.1016/j.ijleo.2020.165321 | SCI |
| 13 | Novel automated framework for water impurity detection | Afzal sheikh, Preeta Sharan, Manju Devi | ECE | International Journal of Information Technology | 2021 | 2511-2112 | https://link.springer.com/article/10.1007/s41870-020-00601-x#citeas | https://dx.doi.org/10.1007/s41870-020-00601-x | Scopus |
| 14 | Characterization of hydroacoustic optical fibre Bragg grating pressure sensor using different materials | Hareesh Kumar, Preeta Sharan, Sreerangaraju, M Narasimhaiiah | ECE | Results in Optics | 2021 | 2666-9501 | https://www.sciencedirect.com/science/article/pii/S2666950120300377#:~:text=The%20sensitivity%20of%20FBG%20sensor,are%20titanium%2C%20gold%20and%20polyamide. | https://doi.org/10.1016/j.rio.2020.100037 | Elsevier |
| 15 | Computational analysis of core cavity | Sundaresan, Vishalatchi | ECE | Indian Journal of Engineering | 2021 | 0971-4588 | http://nopr.niscair.res.in/handle/123456789/57649 | http://nopr.niscair.res.in/handle/123456789/57649 | SCIE |



CHILDREN'S EDUCATION SOCIETY (Regd.)
THE OXFORD COLLEGE OF ENGINEERING
 (Recognised by the Govt. of Karnataka, Affiliated to Visvesvaraya Technological University, Belagavi.

Approved by A.I.C.T.E. New Delhi.

Recognised by UGC Under Section 2(f)

Bommanahalli, Hosur Road, Bangalore - 560 068.

Ph: 080-61754601/602, Fax: 080 - 25730551

E-mail: engprincipal@theoxford.edu Web: www.theoxfordengg.org

| | | | | | | | | | |
|----|--|---|-----|---|------|-------------------|---|---|----------------|
| | Mach-Zehnder interferometer based optical sensor for various types of virus | Saravana ; Ramrao, Nagaraj ; Sharan, Preeta ; Murugan , Kalpana | | and Materials Sciences | | | | | |
| 16 | Detection of oral cancerous cells using highly sensitive one-dimensional distributed Bragg's Reflector Fabry Perot Microcavity | Ranjit Gowda, Sara, Preeta Sharan | ECE | Optil | 2021 | 0030-4026 | https://doi.org/10.1016/j.ijleo.2021.167599 | https://www.sciencedirect.com/science/article/abs/pii/S0030402621012080?via%3Dihub | SCI |
| 17 | Real Time Email Alert For Visitor Monitoring System For Surveillance Applications | Sunitha L., Dr. Harish H. M., Dr. Yedukon dalu U. | ECE | International Journal of Future Generation Communication and Networking | 2021 | 2233-7857 | http://sersc.org/journals/index.php/IJFGCN/index | http://sersc.org/journals/index.php/IJFGCN/article/view/36130 | Google Scholar |
| | Analysis and Design of an Optical Biosensor | Somwya Padukone | ECE | Innovative Design, Analysis | 2021 | 978-981-13-2697-4 | https://link.springer.com/book/10.1 | https://link.springer.com/book/10.1007/978-981-13-2697-4 | Scopus |



CHILDREN'S EDUCATION SOCIETY (Regd.)
THE OXFORD COLLEGE OF ENGINEERING
 (Recognised by the Govt. of Karnataka, Affiliated to Visvesvaraya Technological University, Belagavi.

Approved by A.I.C.T.E. New Delhi.

Recognised by UGC Under Section 2(f)

Bommanahalli, Hosur Road, Bangalore - 560 068.

Ph: 080-61754601/602, Fax: 080 - 25730551

E-mail: engprincipal@theoxford.edu Web: www.theoxfordengg.org

| | | | | | | | | | |
|----|--|---|-----|---|------|-----------|---|---|----------------|
| | Using Mathematical Modeling | | | and Development Practices in Aerospace and Automotive Engineering | | | 007/978-981-13-2697-4 | | |
| 18 | Cascade H Bridge Multilevel Inverter with Pwm for Lower Thd, Emi & Rfi Reduction | Jayakumar N, Dr.B. Devi, Vighneshwari Monalisa Mohanty | EEE | Annals of the Romanian Society for cell biology | 2021 | 1583-6258 | https://www.annalsofscb.ro/index.php/journal/article/view/6013 | https://www.annalsofscb.ro/index.php/journal/article/view/6013 | Google Scholar |
| 19 | Fault Tolerant Discrete Control Technique for PV Fed Stepper Motor Drive | Viji Ka, K Chitrab, Raicel Ruby Mc, Sandhya Raid, and Someswari T | EEE | Turkish Journal of Computer and Mathematics Education | 2021 | 1583-6258 | https://turcomat.org/index.php/turkbiltmat/article/view/2982 | https://doi.org/10.17762/turcomat.v12i9.2982 | Google Scholar |



CHILDREN'S EDUCATION SOCIETY (Regd.)
THE OXFORD COLLEGE OF ENGINEERING

(Recognised by the Govt. of Karnataka, Affiliated to Visvesvaraya Technological University, Belagavi.

Approved by A.I.C.T.E. New Delhi.

Recognised by UGC Under Section 2(f)

Bommanahalli, Hosur Road, Bangalore - 560 068.

Ph: 080-61754601/602, Fax: 080 - 25730551

E-mail: engprincipal@theoxford.edu Web: www.theoxfordengg.org

| | | | | | | | | | |
|----|---|--|----|---|------|-----------|---|---|------------|
| 20 | Design and analysis of moems based displacement sensor for detection of muscle activity in human body | Preeta Sharan,K . V. Sandhya, Rakesh Barya, Mohit Bansal, Anup M. Upadhya ya | ME | International Journal of Information Technology | 2020 | 2511-2112 | https://www.springer.com/journal/41870 | https://doi.org/10.1007/s41870-020-00533-6 | UGC/Scopus |
| 21 | Performance analysis of optomechanical-based microcantilever sensor with various geometrical shapes | Mr. Anup M Upadhya ya, Preeta Sharan, Maneesh Srivastava | ME | Microwave and Optcal Technology letter | 2020 | 1098-2760 | https://onlinelibrary.wiley.com/journal/10982760 | https://onlinelibrary.wiley.com/doi/abs/10.1002/mop.32652 | SCI |
| 22 | Hot corrosion behavior of plasma-sprayed NiCrAlY/TiO ₂ and NiCrAlY/Cr ₂ O ₃ /YSZ cermets | Dr Madhu Sudan Reddy G | ME | Surface and Interface | 2020 | 2468-0230 | https://www.journals.elsevier.com/surfaces-and-interfaces | https://www.sciencedirect.com/science/article/pii/S2468023020308026#:~:text=The%20NiCrAlY%2B%20Cr2O,coatings%20to%20high%2Dtemperature%20corrosion. | SCI |



CHILDREN'S EDUCATION SOCIETY (Regd.)
THE OXFORD COLLEGE OF ENGINEERING

(Recognised by the Govt. of Karnataka, Affiliated to Visvesvaraya Technological University, Belagavi.

Approved by A.I.C.T.E. New Delhi.

Recognised by UGC Under Section 2(f)

Bommanahalli, Hosur Road, Bangalore - 560 068.

Ph: 080-61754601/602, Fax: 080 - 25730551

E-mail: engprincipal@theoxford.edu Web: www.theoxfordengg.org

| | | | | | | | | | |
|----|--|--|------|------------------------------|------|-----------|---|---|--------|
| | coatings on alloy steel | | | | | | | | |
| 23 | Investigation & characterization of plasma sprayed cermet coatings on special steel alloy for gas turbine applications | Dr Madhusudana Reddy G | ME | Material Today Proceeding | 2021 | 2214-7853 | https://www.journals.elsevier.com/materials-today-proceedings | https://www.sciencedirect.com/science/article/pii/S2214785321011548 | Scopus |
| 24 | Estimation of mechanical parameters for orthodontic retraction loops using finite element analysis | Raviprakash M. , Prasad H. Nayak Rahul D | Mech | Materials Today: Proceedings | 2021 | | https://www.sciencedirect.com/journal/materials-today-proceedings | https://doi.org/10.1016/j.matpr.2020.11.066 | Scopus |
| 25 | Estimation of stress and deformation on steel coil holder fixtures using finite element analysis | Raviprakash M. , Prasad H. Nayak Rahul D | Mech | Materials Today: Proceedings | 2021 | | https://www.sciencedirect.com/journal/materials-today-proceedings | https://doi.org/10.1016/j.matpr.2020.11.052 | Scopus |



CHILDREN'S EDUCATION SOCIETY (Regd.)
THE OXFORD COLLEGE OF ENGINEERING

(Recognised by the Govt. of Karnataka, Affiliated to Visvesvaraya Technological University, Belagavi.

Approved by A.I.C.T.E. New Delhi.

Recognised by UGC Under Section 2(f)

Bommanahalli, Hosur Road, Bangalore - 560 068.

Ph: 080-61754601/602, Fax: 080 - 25730551

E-mail: engprincipal@theoxford.edu Web: www.theoxfordengg.org

| | | | | | | | | |
|----|--|---|------|---|------|---|---|--------|
| 26 | Silicon nanostructure-based photonic MEMS sensor for bio-sensing application | Anup M. Upadhyaya, Maneesh C. Srivastava, Preeti Sharan, Sandip Kumar Roy | Mech | Society of Photo-Optical Instrumentation Engineers (SPIE) | 2021 | https://www.spiedigitallibrary.org/journals/journal-of-nanophotonics/ | https://doi.org/10.1117/1.JNP.15.026001 | SCI |
| 27 | Investigation & characterization of plasma sprayed cermet coatings on special steel alloy for gas turbine applications | Madhu Sudana Reddy | Mech | Materials Today: Proceedings | 2021 | https://www.sciencedirect.com/journal/materials-today-proceedings | https://doi.org/10.1016/j.matpr.2021.02.092 | Scopus |
| 28 | Hot corrosion behavior of plasma-sprayed NiCrAlY/TiO and NiCrAlY/Cr O /YSZ cermets coatings on alloy steel | Madhu Sudana Reddy | Mech | Surfaces and Interfaces | 2021 | https://www.sciencedirect.com/journal/surfaces-and-interfaces | https://doi.org/10.1016/j.surfin.2020.100810 | SCI |



CHILDREN'S EDUCATION SOCIETY (Regd.)
THE OXFORD COLLEGE OF ENGINEERING

(Recognised by the Govt. of Karnataka, Affiliated to Visvesvaraya Technological University, Belagavi.

Approved by A.I.C.T.E. New Delhi.

Recognised by UGC Under Section 2(f)

Bommanahalli, Hosur Road, Bangalore - 560 068.

Ph: 080-61754601/602, Fax: 080 - 25730551

E-mail: engprincipal@theoxford.edu Web: www.theoxfordengg.org

| | | | | | | | | | |
|----|---|---|------------|--|------|--------------|---|---|--------|
| 29 | Microstructure and Wear Behavior of Al2218-B4C Nano Composites | Vidyadhar Poojar | Mech | Pal Arch journal of archaeology | 2021 | 1567-214X | https://www.archives.palarch.nl/index.php/jae/index | https://archives.palarch.nl/index.php/jae/article/view/3717 | Scopus |
| 30 | Mechanical Behavior and Fractography of Al2218-Nano B4C Metal Composites | Vidyadhar Poojar | Mech | International Journal of Engineering and Advanced Technology | 2021 | 2249 – 8958` | https://www.ijeat.org/ | https://www.ijeat.org/wp-content/uploads/papers/v9i4/D7816049420.pdf | Scopus |
| 31 | Investigations on microstructure and tensile properties of as-cast ZA-27 metal matrix composite reinforced with zircon sand | G.R. Gurunagendra a,† , B.R. Raju b , Vijayakumar Pujara , D.G. Amitha , H.G. Hanumantharajuc , Santosh Angad | Automobile | Materials Today: Proceedings | 2021 | 22147853 | https://www.sciencedirect.com/science/article/pii/S2214785321009937 | https://www.sciencedirect.com/journal/materials-today-proceedings | Scopus |



CHILDREN'S EDUCATION SOCIETY (Regd.)
THE OXFORD COLLEGE OF ENGINEERING

(Recognised by the Govt. of Karnataka, Affiliated to Visvesvaraya Technological University, Belagavi.

Approved by A.I.C.T.E. New Delhi.

Recognised by UGC Under Section 2(f)

Bommanahalli, Hosur Road, Bangalore - 560 068.

Ph: 080-61754601/602, Fax: 080 - 25730551

E-mail: engprincipal@theoxford.edu Web: www.theoxfordengg.org

| | | | | | | | | | |
|----|--|---|------------|--|------|----------|---|---|--------|
| 32 | Mechanical, wear and corrosion properties of micro particulates reinforced ZA-27 hybrid MMC by stir casting: A review | G.R. Gurunagendra a,†, B.R. Raju b, Vijayakumar Pujar, D.G. Amitha, Poornachandra, H.S. Siddesh | Automobile | Materials Today: Proceedings | 2021 | 22147853 | https://www.sciencedirect.com/journal/materials-today-proceedings | https://www.sciencedirect.com/science/article/pii/S2214785321009895 | Scopus |
| 33 | Microstructure, Dislocation Density and Thermal Expansion Behavior Using Thermo Elastic Models of Zircon Sand Reinforced as Cast ZA-27 Composite | G. R. Gurunagendra1*, V. Bharat1, B. R. Raju2, D. G. Amith1, Vijayakumar Pujar1, | Automobile | Journal of Minerals and Materials Characterization and Engineering | 2021 | 22147853 | https://www.scirp.org/journal/journalarticles.aspx?journalid=1753 | https://www.scirp.org/ | Scopus |



CHILDREN'S EDUCATION SOCIETY (Regd.)
THE OXFORD COLLEGE OF ENGINEERING

(Recognised by the Govt. of Karnataka, Affiliated to Visvesvaraya Technological University, Belagavi.

Approved by A.I.C.T.E. New Delhi.

Recognised by UGC Under Section 2(f)

Bommanahalli, Hosur Road, Bangalore - 560 068.

Ph: 080-61754601/602, Fax: 080 - 25730551

E-mail: engprincipal@theoxford.edu Web: www.theoxfordengg.org

| | | | | | | | | | |
|----|---|--|-----|--|------|------------|---|---|----------------|
| | | C. Ravi Keerthi | | | | | | | |
| 34 | Towards a Competency Framework for Business School Faculty Members | A. Sahana, Dr. Vijila K, Dr. K Tharaka Rami Reddy | MBA | Alochana Chakra Journal | 2020 | 2231-3990 | http://www.alochanachakra.in/ | http://www.alochanachakra.in/gallery/372-acj-june-2133.pdf | UGC |
| 35 | The role of training and work environment on retention and job satisfaction as a mediator at start-ups, bangalore | Padmaja P, Balakote shwari, Richa Tiwari, R V Dhanalakshmi | MBA | INTERNATIONAL JOURNAL OF MANAGEMENT | 2020 | 0976-6502 | http://www.iaeme.com/Ijm/index.asp | 10.34218/IJM.11.9.2020.112 | Scopus |
| 36 | Image Scheduling using Cloud Energy Data Computational Techniques | Dharamvir, Dr. Hemanth K S | MCA | Turkish Journal of Computer Mathematics and Applications | 2021 | 1300-0101. | https://turcomat.org/index.php/turkbilmat/article/view/6641 | https://turcomat.org/index.php/turkbilmat/article/view/6641 | Google Scholar |



CHILDREN'S EDUCATION SOCIETY (Regd.)
THE OXFORD COLLEGE OF ENGINEERING
 (Recognised by the Govt. of Karnataka, Affiliated to Visvesvaraya Technological University, Belagavi.

Approved by A.I.C.T.E. New Delhi.

Recognised by UGC Under Section 2(f)

Bommanahalli, Hosur Road, Bangalore - 560 068.

Ph: 080-61754601/602, Fax: 080 - 25730551

E-mail: engprincipal@theoxford.edu Web: www.theoxfordengg.org

| | | | | | | | | | |
|----|---|----------------------------|-----|--|------|-----------|---|---|----------------|
| 37 | Data Normalization Techniques on Intrusion Detection for Dataset Applications | Dharamvir, Arul Kumar V | MCA | International Journal of Advanced Science and Technology | 2020 | 2207-6360 | http://sersc.org/journals/index.php/ijast | http://sersc.org/journals/index.php/IJAST/article/view/25793 | Scopus |
| 38 | Prospective Analysis with Expansion Monitoring System and Its Applications | Dharamveer, M S Shashidara | MCA | Kala Sarovar | 2021 | 0975-4520 | https://scholar.google.com/citations?user=QmsEk74AAAAJ&hl=en | https://scholar.google.com/citations?user=QmsEk74AAAAJ&hl=en | Google Scholar |
| 39 | Exploring Service Oriented Routing Protocol Network Architecture for Multicast Functionality in Internet of Things and its Applications | Dharamveer, M S Shashidara | MCA | Design Engineering | 2021 | 0975-4520 | https://scholar.google.com/citations?user=QmsEk74AAAAJ&hl=en | https://scholar.google.com/citations?user=QmsEk74AAAAJ&hl=en | Google Scholar |
| 40 | Framework for Improving Telecom Services by Standardization of Virtual Network | Chennappa, M S Shashidara | MCA | Design Engineering | 2021 | 0975-4520 | https://scholar.google.com/citations?user=QmsEk74AAAAJ&hl=en | https://scholar.google.com/citations?user=QmsEk74AAAAJ&hl=en | Google Scholar |



CHILDREN'S EDUCATION SOCIETY (Regd.)
THE OXFORD COLLEGE OF ENGINEERING

(Recognised by the Govt. of Karnataka, Affiliated to Visvesvaraya Technological University, Belagavi.

Approved by A.I.C.T.E. New Delhi.

Recognised by UGC Under Section 2(f)

Bommanahalli, Hosur Road, Bangalore - 560 068.

Ph: 080-61754601/602, Fax: 080 - 25730551

E-mail: engprincipal@theoxford.edu Web: www.theoxfordengg.org

| | | | | | | | | | |
|----|---|--|-------------|--|------|-----------|---|---|----------------|
| | Function on Boarding | | | | | | | | |
| 41 | An Approach to Electro Photonic Image classification in Thyroid Patents using BBNN Method | Indrakumar S , M S Shashidara | MCA | Design Engineering | 2021 | 0975-4520 | https://scholar.google.co.in/citations?user=gYdxjCMAAAJ&hl=en | https://scholar.google.co.in/citations?user=gYdxjCMAAAJ&hl=en | Goolge Scholar |
| 42 | Review Dimension reduction techniques for transformational image processing | Dharamveer, Hemant | MCA | Design Engineering | 2021 | 0975-4520 | https://scholar.google.co.in/citations?user=gYdxjCMAAAJ&hl=en | https://scholar.google.co.in/citations?user=gYdxjCMAAAJ&hl=en | Goolge Scholar |
| 43 | Transitive Domination number of a Graph | Dr.Mallikarjun K. and Selastina Mary A, | Mathematics | Journal of The Maharaja Sayajirao university Of Baroda | 2020 | 0025-0422 | https://www.ssrn.com/index.cfm/en/ | https://papers.ssrn.com/sol3/papers.cfm?abstract_id=3667497#:~:text=A%20set%20of%20vertices%20D,dominating%20sets%20of%20the%20graph. | UGC |
| 44 | Schur Geometric Convexity of Related Function for Holders | Sreenivasa reddy Perla and S | Mathematics | European Journal of Pure and Applied | 2020 | 1307-5543 | https://www.ejpm.com/index.php/ejpm | https://www.ejpm.com/index.php/ejpm/article/view/3741 | Scopus |



CHILDREN'S EDUCATION SOCIETY (Regd.)
THE OXFORD COLLEGE OF ENGINEERING

(Recognised by the Govt. of Karnataka, Affiliated to Visvesvaraya Technological University, Belagavi.

Approved by A.I.C.T.E. New Delhi.

Recognised by UGC Under Section 2(f)

Bommanahalli, Hosur Road, Bangalore - 560 068.

Ph: 080-61754601/602, Fax: 080 - 25730551

E-mail: engprincipal@theoxford.edu Web: www.theoxfordengg.org

| | | | | | | | | | |
|----|---|--|-------------|--|------|--------------------|---|---|----------------|
| | Inequality with Application | Padmanabhan | | Mathematics | | | | | |
| 45 | Schur Harmonic Convexity of Related Function for Holders Inequality with Application -. | Sreenivasa reddy Perla and S Padmanabhan | Mathematics | International Journal of Advanced Science and Technology | 2020 | 2207-6360 | http://sersec.org/journals/index.php/IJAST/index | http://sersec.org/journals/index.php/IJAST/article/view/24646 | Scopus |
| 46 | Vertex Polynomial of Middle Line and Total Graphs of some standard Graphs, | Dr. Mallikarjun K. and Sridhara K. R | Mathematics | International Journal of Management and Humanities | 2020 | 2394-0913 | https://www.ijmh.org/ | https://www.ijmh.org/wp-content/uploads/papers/v4i8/H0794044820.pdf | UGC |
| 47 | Anti-domination Number of a Graph | Mallikarjun B Kattimani | MATHS | Journal of Multidisciplinary Research & | 2021 | 44 ISSN: 2360-821X | https://www.ajmrd.com/wp-content/uploads/2021/07/G374044.pdf | https://www.ajmrd.com/wp-content/uploads/2021/07/G374044.pdf | Google Scholar |
| 48 | Maximal Transitive Domination Number of a Graph, | Mallikarjun B. Kattimani and Smita K Phadmis | MATHS | Journal of the Maharaja Sayajirao University of Baroda, | 2021 | ISSN: 0025-0422 | https://scholar.google.co.in/citations?user=C3gumn4AAAJ&hl=en | https://scholar.google.co.in/citations?user=C3gumn4AAAJ&hl=en | Google Scholar |

DCUIS: An Exhaustive Algorithm for Pre-Processing of Web Log File

Sowmya H.K., Dr. R.J. Anandhi

**Department of Computer Science and Engineering, #Department of Information Science and Engineering*

**The Oxford College of Engineering, Affiliated to VTU, Bangalore, India*

#New Horizon College of Engineering, Affiliated to VTU, Bangalore, India

hk.sowmyakiran@gmail.com, rjanandhi@hotmail.com

Abstract— The recent growth of Internet and World Wide Web lead to exponential development of Internet usage for various purposes such as online shopping, social media, education etc. Every hit to the web site is recorded in log file which includes user request, IP address, date and time of page demanded etc. This information can be utilized to derive favorable perceptions. Web Usage Mining is one such approach, which is applied to log file to automatically discover user navigational pattern. This research work, presented a novel algorithm termed DCUIS: Data Cleaning, User Identification and Sessionization. It is an exhaustive algorithm which considers all stages of pre-processing phase. The proposed algorithm has taken raw log file as input, and performed cleaning operation to obtain data of superior quality. This data is used in the next step of algorithm to uniquely identify users and which in succession assists to find user sessions.

Keywords— Web Usage Mining, User Identification, Sessionization, Pre-processing, log file

I. INTRODUCTION

World-wide usage of internet for retrieving facts and details produces large volume of data daily. This overflowing data cannot be applied for analysis straightly. Thus Web Mining came into picture, which is the exercising of techniques available in data mining area to explore patterns from the data present on the internet. It is used to generate impressive outcomes on investigation which may possibly support the enterprise in captivating additional customers. Web mining can be classified into Web Content, Web Usage and Web Structure mining. Web Content mining implies, drawing out knowledge from web page which includes text, images, videos etc. Web Structure Mining finds knowledge from hyper link structure. Whereas Web Usage Mining discovers access pattern of user from web logs.

Web Usage mining is determining and analyzing visitors' navigational patterns by realizing different data mining strategies on log files of server or proxy, client. These navigational patterns are well realized in diversified policies such as website restructuring, web page recommendation and web content personalization, and improvisation of server activities. The process of Web usage mining can be divided into three major phases: Data pre-processing,

Pattern Discovery and Pattern analysis. Data pre-processing phase is a intricate job and spends longer time in web usage mining process due to the large volume of log data and its unstructured nature. It includes sub tasks such as data cleaning, user and session identification. This phase takes log file as input and identifies visitors of the web site and produces sessions which can then be used for pattern extraction and evaluation.

The entire paper is divided in to 4 sections. First section describes literature survey of existing approaches for pre-processing. Second section presents problem formulation of various stages of pre-processing. Third section explains various phases of Web Usage Mining and proposed novel exhaustive algorithm. Fourth section implements a new algorithm and compares it with existing algorithm which shows that our proposed algorithm produces better result.

II. LITERATURE SURVEY

P. Sukumar et.al [4] proposed De-Spidering heuristic algorithms was used to remove web robots. This algorithm used for data cleaning isolated the entries with file extension .css, .gif, .jpeg etc. It retained only the entries with status code in the range [200-299]. Additionally, the appeal initiated by web Crawlers, Robot or Spider is detached.

Sudheer Reddy et. al. [7], proposed preprocessing methods used to remove irrelevant entries with file extension .gif, .jpeg, .css and error codes. They gave algorithm for user identification, which determines new user by checking IP address. In case IP address is identical at that point, it compares with web browser and Operating System.

Patel et.al. [3], gave an algorithm for data cleaning which removed entries having extension .js, .css, .gif, .png, .jpg, .svg and error status codes. They also gave visitor identification algorithm which is developed on IP address and user agent to uniquely determine user. Session identification algorithm identifies user session based upon IP address and threshold time of 30 minutes.

Srivatsava et. al. [5], presented algorithm that considered unsuccessful inquiry, appeals of multimedia and other irrelevant files, and HTTP mechanism except GET comprising demands. This also removes failed status codes and links for pdf and

image files. This algorithm eliminate records of URL ending like jpg, gif and css file.

Michal Munk et.al. [2], presented an approach to pre-process educational data and identified phases which are needed in case of pre-processing for increased usage of understanding analytics methods. Outcome of their experiment revealed that session identification algorithm with reference length had a notable influence on grade of extricated series conventions. Path completion technique had remarkable effect on quantity of extracted sequence rules.

Mary et.al. [8], proposed a method to enhance the performance of session identification to find accurate user navigational behavior. To identify a new session, it has considered set of pages that are shared between different sessions of same user. Suppose shared pattern does not exists, at that point ,such session of same user will be rejected. This improves quality of session.

Mitali Srivastava et.al. [1], developed a new algorithm for user identification based on MapReduce method. They identified user by IP address and user agent information. The proposed algorithm is free to address machine recognition and expandability affairs. Author have not considered details of referrer and site layout for identifying visitors.

III. PROBLEM FORMULATION

Each time user demands for a web page from a web site, an access is documented against a web server log file. Server log file exists in different formats like IIS standard/Extended, NCSA Common/Combined, and Netscape Flexible etc. NCSA extended common log format is most popular log format. Data cleaning, User identification and Session identification problem formation for ECLF format is in this manner.

Consider $IP=\{ip_1,ip_2,\dots,ip_n\}$ is set of each respective IP addresses of n users, who browsed website. $WR=\{wr_1,wr_2,\dots,wr_n\}$ denotes the web resources of website, $UA=\{ua_1,ua_2,\dots,ua_n\}$ represents user agents of visitor of the web and $EL=\{el_1,el_2,\dots,el_n\}$ is a set of external links. Now log record in ECLF possibly specified as $LE=\langle ip_i;t;m;v;sc;bt;[Ref_i];[ua_i];[cookies] \rangle$, where $ip_i \in IP$, $wr_i \in WR$, $Ref_i \in RUEL$, $ua_i \in UA$, t denotes timestamp, m represents access method, sc represents status code and bt depicts amount of bytes moved. Ref_i and ua_i are attributes. Web server log file comprises $WL= \{wl_1,wl_2,\dots,wl_n\}$. So data cleaning issue perhaps depicted in this manner: Taking into account a web server log file WL, remove all irrelevant entries and prepared log file can be represented as $CL= \{cl_1, cl_2,\dots,cl_n\}$, which contains only relevant entries and $cl_i=\langle ip_i;wr_i;[Ref_i];[ua_i] \rangle$. Suppose $U=\{u_1,u_2,\dots,u_n\}$ is a group of users who browsed website. A user's visit can be defined as $v_i=\langle u_i,E_i \rangle$, where $E_i=\langle (t_1,wr_1,[Ref_1]);(t_2,wr_2,[Ref_2]);\dots (t_n,wr_n,[Ref_n]) \rangle$; $t_{i+1}>t_i$. Now user

identification problem can be defined as follows: From the cleaned log file CL, identify set of visitors $V=\{v_1,v_2,\dots,v_n\}$. Enter V inside user activity file. Further, session identification question possibly specified in this fashion: From the user activity file, identify set of sessions $S=\{(v_1=\langle s_1,s_2,\dots,s_k \rangle);(v_2=\langle s_1,s_2,\dots,s_k \rangle);\dots(v_n=\langle s_1,s_2,\dots,s_k \rangle)\}$, where $\langle s_1,s_2,\dots,s_k \rangle$ represents k different session of the visitor. Write this into user session activity file.

IV. PROPOSED METHODOLOGY

Web Usage Mining deals with approaches that may potentially speculate the user attitude when they are communicating with the WWW. Web usage mining uncover browsing patterns of visitor and attempt to discover the appropriate information from web log file.

The entire Web usage mining system can be splitted into three vital stages as shown in Figure 1. The pre-processing stage, the log file having click stream data is prepared to remove very noisy and ambiguous bunch of user activities during their visit to the site.

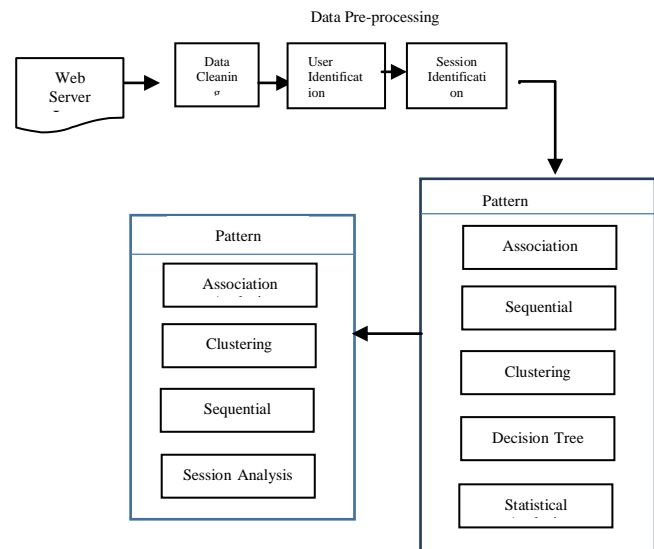


Fig. 1. Phases of Web Usage Mining Process

Data pre-processing is the basic step in data preparation step. Its objective is to reformat the web log file to identify users and user sessions. Web server makes an entry in the log file for each user hit to request resource from the website. Log data can be saved as Common Log Format (CLF) or Extended Log Format (ECLF). These files have fields such as User's IP address, User Identification, Authentication, Access date and time, Request method, Status code, Number of bytes transmitted, Referrer and User agent Field.

3. Extract IP address, User agent and Referrer field of the entry
4. For each entry do the following
5. If (Two successive IP addresses are identical)
6. Then
7. Check web browser and OS
8. If (Two successive entries IP address and User Agent are identical)
9. Then
10. Examine Referrer field
11. If(Web page can be accessed with Referrer link)
12. Same User
13. Else
14. New User, UID++
15. For new User create next Session,
16. Inside User Session
17. If (referrer ==NULL)
18. If(Time of current request – time of previous request)<Page Stay Time Threshold
19. Then
20. Same Session
21. Else if((Time of current request – time of first request)<Session Time Threshold
22. Then
23. Same Session
24. Else
25. New Session
26. Else
27. If referrer page is same as previous request
28. Then
29. Same Session
30. Else if(Time of current request – time of previous request)<Page Stay Time Threshold
31. Then
32. Same Session
33. Else if (Time of current request – time of first request)<Session time Threshold
34. Then
35. Same Session
36. Else
37. New Session

Above DCUIS algorithm provides complete solution to pre-processing of web log file by performing complete steps of pre-processing starting from data cleaning to session identification. It commences from data cleaning, then performs user identification by verifying IP address and user agent. Identified user details are stored in a file. Soon afterward sessions are spotted by matching up the duration of current request and previous request with threshold time. Output of algorithm is a set of user sessions which are stored in session file.

V. RESULTS AND DISCUSSION

The exhaustive DCUIS algorithm has implemented in java Eclipse Platform and experiments run on a laptop machine equipped with Intel I3 processor and 8GB memory.

Input applied to algorithm is taken from the link <http://www.almhuetten-raith.at/apache-log/access.log> which contains 9874 records. It holds browsing history of web user from 12th December 2015 to 21st December 2015. Algorithm is implemented in Java Eclipse platform using Java programming language. Results of data cleaning is stored in a separate file which is used as input for user identification process. The outcome of user identification is saved in user activity file. Further, this file is used as input for session identification, which produces set of user sessions, which are then saved in user session file.

When the user appeals for web page, if it succeeds then status code entered in web log file is in the range 200-299. Other kind of codes represent, unsuccessful request. Details of status codes present in raw log file is shown in the Table I.

TABLE I. SUMMARY OF STATUS CODES

| Status Code | Number of Records in web log file | Percentage |
|-------------|-----------------------------------|------------|
| 200 | 9180 | 92.97 |
| 300 | 450 | 4.55 |
| 400 | 229 | 2.319 |

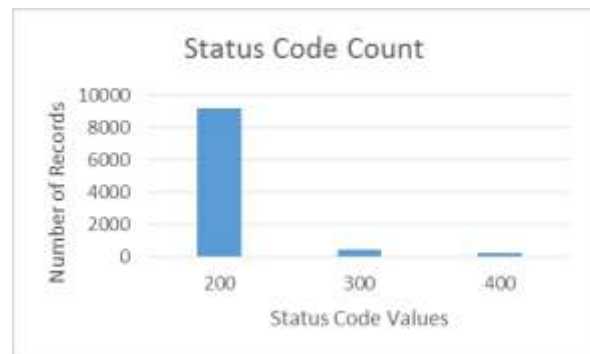


Fig. 3. Status Codes of Web Log File

The Raw web log file contains, enclosed image files, audio and multimedia files, which are not preferred and has to be cleaned. Our algorithm has cleaned the various types of irrelevant files as shown in the Table II.

TABLE II. SUMMARY OF FILE TYPES

| File Type | Number of Records | Percentage |
|------------|-------------------|------------|
| Script | 330 | 3.34 |
| Multimedia | 79 | 7.73 |
| Image | 764 | 0.80 |

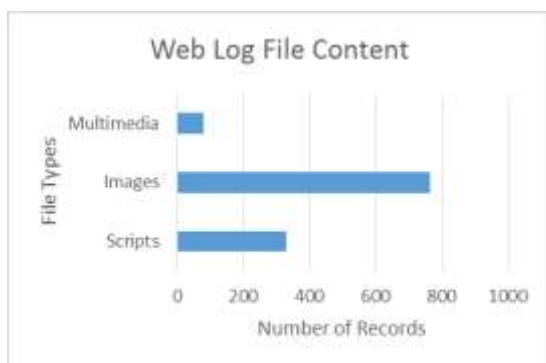


Fig. 4. Various File Types in Web Log File



Fig. 5. Sessions Identified for Various Threshold Values

Proposed data cleaning algorithm performs elimination of all unwanted records and retains, only valid records for further action. Table III shows result of the experiment after data cleaning operation.

TABLE III. RESULT OF DATA CLEANING PROCESS

| Days | Size of Raw log file(KB) | Number of Raw Log Record | Number of valid records | % of valid Record |
|------------------------------------|--------------------------|--------------------------|-------------------------|-------------------|
| 10 Days (12/12/2015 to 21/12/2015) | 1870 | 9874 | 5104 | 52% |

After accomplishing data cleaning operation, users are identified by our algorithm. Details about user identification is given in Table IV.

TABLE IV. RESULT AFTER IDENTIFYING UNIQUE USERS

| Days | Number of records in a web log file | Number of User sessions |
|------------------------------------|-------------------------------------|-------------------------|
| 10 Days (12/12/2015 to 21/12/2015) | 9874 | 1264 |

Sessions are identified for the unique users based on session threshold time and page stay time. Table V depicts the number of user sessions for various values of threshold time.

TABLE V. RESULT AFTER IDENTIFYING USER SESSIONS

| Session Threshold Time (minutes) | Page Stay Threshold Time(minutes) | Original Records | Number of Sessions Identified |
|----------------------------------|-----------------------------------|------------------|-------------------------------|
| 15 | 5 | 9874 | 3019 |
| 20 | 7 | 9874 | 3017 |
| 25 | 9 | 9874 | 3015 |

VI. CONCLUSION

Preprocessing of web log file is a major and complex task in web usage mining process which needs significant algorithms to perform data cleaning, identification of user and session. Several authors have proposed various algorithms for the different phases of preprocessing, but a complete algorithm for entire process is not available. So a new algorithm named DCUIS (Data cleaning, User Identification and Sessionization) is proposed for entire preprocessing phase. Hypothetical and experimental analysis have shown productiveness and relevance of empirical rooted preprocessing methods and algorithm policies. It shows that proposed novel algorithm is more efficient one which can be evolved as tool to administer exhaustive formula for preprocessing stage. The outcome of proposed algorithm can be used as input for subsequent phases of web usage mining.

Acknowledgment

I would like to thank to Dr. R J Anandhi, Professor and Head, Department of Information Science and Engineering, New Horizon College of Engineering, Bengaluru, my research supervisor, for her valuable guidance and encouragement towards this research work. I would like to express my special thanks of gratitude to Dr. A S Arvind, Principal, The Oxford College of Engineering, Affiliated to VTU, Bengaluru, for his advice and assistance that helped me during this research work. I would also like to thank Visvesvaraya Technological University for supporting me to do research work. Finally, a special thanks to my family for their support throughout my research work.

References

- [1] Mitali Srivastava, Rakhi Garg, and P K Mishra, "A Map Reduced-Based User Identification Algorithm for Web Usage Mining", International Journal of Information Technology and Web Engineering. Volume 13, Issue 3, April – June 2018.
- [2] Michal Munk, Martin Drlik, Benko and Reichel, "Quantitative and Qualitative Evaluation of Sequence Patterns Found by Application of Different Educational Data Preprocessing Techniques", IEEE Access 5, 8989-9004, 2017.

- [3] Patel, Parikh, "Preprocessing on Web Server Log Data for Web Usage Pattern Discovery", International Journal of Computer Applications, Volume 165, May 2017
- [4] Sukumar, Robert, Yuvraj, "Review on Modern Data Preprocessing Techniques in Web Usage Mining", International Conference on Computational System and Information Systems for Sustainable Solutions, 2016.
- [5] Mitali Srivastava, Rakhi Garg, and P K Mishra, "Analysis of Data Extraction and Data Cleaning in Web Usage Mining", ICARCSET '15, March 06 - 07, 2015, Unnao, India.
- [6] Anupama and Gowda, "Clustering Of Web User Sessions to Maintain Occurrence of Sequence in Navigation Pattern", Second International Symposium on Computer Vision and the Internet, vol. 58, pp. 558–564, 2015.
- [7] K. Sudheer Reddy, G. Partha Saradhi Varma, and M. Kantha Reddy, "An Effective Preprocessing Method for Web Usage Mining" International Journal of Computer Theory and Engineering, Vol. 6, No. 5, October 2014.
- [8] Mary, Baburaj, "Performance Enhancement in Session Identification", International Conference on Control, Instrumentation, Communicational and Computational Technology (ICCICCT), 2014.
- [9] Ramya and Kavitha, "An Efficient Preprocessing Methodology for Discovering Patterns and Clustering of Web Users using a Dynamic ART1 Neural Network", Fifth International Conference on Information Processing, pp. 1–6, 2011.
- [10] <http://www.almhuette-raith.at/apache-log/access.log>
- [11] CU, O., and P. Bhargavi. "Analysis of Web Server log by web usage mining for extracting users patterns." International Journal of Computer Science Engineering and Information Technology Research (IJCEITR) 3.2 (2013): 123-136.
- [12] DA, Adeniyi. "Design and Realization of On-Line, Real Time Web Usage Data Mining and Recommendation System Using Bayesian Classification Method." International Journal of Computer Science Engineering and Information Technology Research (IJCEITR) 6.3 (2016): 19-38.
- [13] DHARMARAJAN, K., and K. ABIRAMI. "DATA PREPROCESSING ALGORITHMIC APPROACH TO IDENTIFYING USER PATTERN BEHAVIOR FROM WEB SERVER LOG FILE." International Journal of Mechanical and Production Engineering Research and Development (JMPERD) 8, Special Issue 3 (2018): 1434-1446
- [14] SOLANKI, NIDHI, and AMAN DUREJA. "COMPUTING FOR INNOVATION IN TECHNOLOGY." International Journal of Industrial Engineering & Technology (IJET) 3.2 (2013): 87-94
- [15] LATHA, N. PUSHPA, KV N. BHANU PRAKASH, and K. VENKATESWARA REDDY. "HYBRID METHODOLOGY TO ANALYZE WEB USER BEHAVIOR IN WEB MINING AND FUZZY NETWORKS." International Journal of Computer Science and Engineering (IJCE) 3.3 (2014): 157-166
- [16] KUMAR, T. VIJAYA, and HS GURUPRASAD. "Clustering of web usage data using fuzzy tolerance rough set similarity and table filling algorithm." International Journal of Computer Science Engineering and Information Technology Research (IJCEITR) 3.2 (2013): 143-152.

Robust Classifier Design with Ensemble Neural Network using Differential Evolution

Shobha T¹ and Dr. R J Anandhi²

¹Research Scholar, Department of CSE, The Oxford College of Engineering, Bengaluru
Visvesvaraya Technological University, Belagavi, Karnataka, India

²Professor and Head, Department of ISE, New Horizon College of Engineering, Bengaluru
Visvesvaraya Technological University, Belagavi, Karnataka, India

Abstract — An ensemble neural network using Differential Evolution (DEENN) for the classification has been designed and implemented in this work. The ensemble structure with two levels of classifier has been proposed and designed. Four multilayer perceptron classifiers of the first level have been trained with same sized data with overlapping and learnt through gradient descent algorithm. Second level single-layer neural network fuses the output of first level classifiers and the final output has been derived using differential evolution (DE). To demonstrate the performance of proposed work, the decision integrating methods, majority voting method and mean decision value method has also been implemented, tested and compared. Results show that the proposed method is highly efficient and resistant to trial variation.

Keywords — Classification, Differential Evolution, Ensemble Neural Network, Feed forward Architecture

I. INTRODUCTION

Machine learning refers to a data analysis method that can automatically build an analytical model without explicit programming. Classification is one of the important mechanism available in machine learning. It is a supervised learning method that gains knowledge from the given data and uses this learning to predict the labels of new data. There are various classification algorithms in machine learning such as support vector machine, nearest neighbour, swarm intelligence, neural network, decision tree, evolutionary algorithm etc.

Artificial Neural Networks (ANN) are considered as one of the very powerful classifiers [6]. ANN is a biological neural networks based computational model for information processing. The main drawback of the single classifier is not having generalized knowledge of classification. And also

single classifiers fail to provide satisfactory results when dealing with the data with more category and noise [5]. To overcome the problems of single classifiers, one common solution is to use an ensemble of classifiers, which combines the decisions of multiple classifiers to obtain a better and efficient result. Ensemble neural network (ENN) originated from Hansen and Salamon's work [3], showed that the generalization ability of an NN system can be significantly improved through ensembling several NNs. Hence, ENN has been extensively studied by many researchers [1-12], due to its remarkable improvement in the aspect of the generalization ability. It has already been applied to diversified areas such as protein modification detection[2], syntax analysis of natural language [4], metabolomics studies[1], time series prediction [7], human pose estimation[8], blur image identification [9], protein-protein interactions [10] etc.

Structure formation and identifying the importance of each classifier are the very important factors of ensemble network that effects its generalization capability. The generalization ability of ENN can be enhanced, by improving the generalization ability of individual NN as well as an increase in diversity between individual NN [4]. For aggregating the decisions of individual NN, general approaches used are majority voting [3,4,9], simple averaging[5,10] and weighted averaging[6]. There are many other approaches for aggregating the decisions such as entropy [11], Akaike information criterion [12], type 2 fuzzy system [7], genetic algorithm [13] etc. The proposed method in this paper uses differential evolution (DE) based aggregation of decisions, which is not been found in any other similar work.

In this proposed work, the two-level classifier has been designed using feed-forward NN (FF-NN) at the first level and using differential evolution, an ensemble of NN architecture has been developed. Gradient descent learning method is used to train each of the FF-NN. Some overlapping training data has been used to introduce diversity for each individual classifier. A single layer feed-forward architecture has been used in the second-level classifier, whose weights have been evolved using DE.

To understand the quality involved with the developed algorithm, the algorithm has to be evaluated over the complex and standard dataset. With this respect, the NN benchmark problem XOR is considered because of its nonlinear classification characteristics. To analyze the capability of the proposed work, the proposed differential evolution based learning method was evaluated on benchmark XOR classification problem. Further, to define classification over other data sets, ensemble network with DE has been developed.

II. PROPOSED METHODOLOGY

It is well known that all-natural computing paradigms have some kind of variability in their outcomes with the repetition of the process. The minimum value of variability is always desired characteristics of any classifier. To minimize the variability, the ensemble of different classifiers (which may differ in their structure and/or in their knowledge) is one of the best possible approaches, which has been considered in this work. The issue that occurs in optimal ensemble architecture design is assigning the weightage to individual classifier outcome, which provides the challenge. In this work, the difference in the knowledge of the classifier has been considered by providing the different set of training data set to same sized architecture. To ensemble the classifier, rather than assigning linear weighted or efficiency-based weightage, a single layer feed-forward neural network architecture has been considered which decides the weightage of the individual classifier through the differential evolution based learning process. Such a process considers the individual outcomes of each classifier for final weightage value.

The detailed structure of the development of first stage classifiers is as shown in Figure 1. For each classifier, a partial overlapping training data have been given along with their corresponding targets.

The learning of optimal weights to minimize the error has been given through the gradient descent based algorithms. Such a process provides some kind of similarity as well as diversity in their solution development knowledge.

In the second stage, a neural network ensemble has been provided to integrate the classifier as shown in Figure 2. Each classifier outcomes become the input to this neural network ensemble which try to deliver the corresponding target outcome by weight upgradation through the differential evolution. The use of differential evolution provides the facility to explore the weight domain in an optimal manner. The weight exploration process through differential evolution has been shown in Figure 3, where the first dimension of the solution is decided through the available number of the classifier. Hence a parent solution in DE will have the same size length as the number of classifiers. It is necessary that there should be relative weightage of each classifier outcome, hence the weight of each classifier will have the value in the range of [0,1]. So, in each iteration weight values have been normalized using Equation (1).

$$x_n = \frac{x - x_{mn}}{x_{mx} - x_{mn}} \quad (1)$$

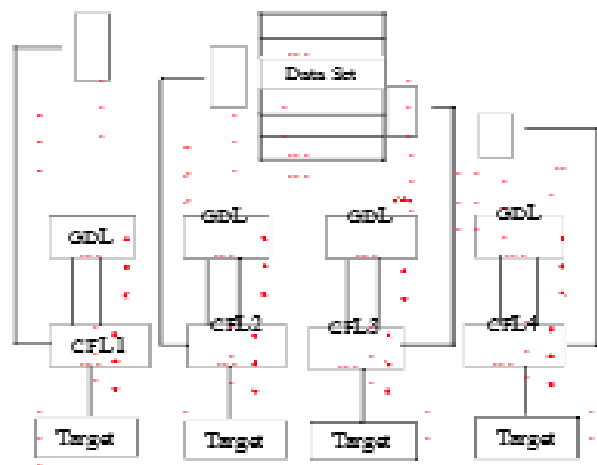


Figure 1: Architecture of training phase of first stage Neural Network

A. Differential Evolution

Differential evolution is a population-based meta-heuristic algorithm. It is a member of evolutionary computation with a high level of exploration that leads to delivering the global solution. As in the case of Genetic algorithm, there are three main operators which help to create the next generation

III. DATASETS USED IN THE EXPERIMENT

A. Exclusive OR(XOR) dataset

A well-known classic problem XOR in Artificial Neural Network research has been considered for performance evaluation of the proposed ENN with Differential Evolution. The important feature of XOR data is that it is not linearly separable. The XOR dataset that is used for training is shown in Table 1. A feedforward NN architecture with size [2 3 1] has been considered.

TABLE 1: XOR DATASET

| Input 1 | Input 2 | Target |
|---------|---------|--------|
| 0 | 0 | 0 |
| 0 | 1 | 1 |
| 1 | 0 | 1 |
| 1 | 1 | 0 |

B. Heart Disease dataset

We have also used a publicly available benchmark data, “Heart Disease” dataset from the UCI repository [14]. This database contains 303 datasets with 76 attributes, but the only subset of 13 of them from processed Cleveland database has been considered. Dataset has two classes, that refers to whether the heart disease is present or not in the patient. A feedforward NN architecture with size [13 6 1] has been considered.

IV. RESULTS AND DISCUSSION

A. Experimental Results with XOR dataset

The learning of neural weights using DE has been confirmed with the benchmark XOR classification problem. The success over this problem provides the guarantee of nonlinear classification capability of the classifier. The XOR problem has been considered as a benchmark because of its high non-linear separable characteristics. In this work, a feed-forward neural network architecture having a size of [2 3 1] has been considered where each active nodes has the nonlinear activation function as a sigmoid function. The learning iterations has been terminated based on self-terminating criteria when the mean square error becomes less than 0.007. The population size of 100 has been considered for the DE. This is basically a 9-dimensional problem where each weight represents a component. The explored weight for the hidden

layer and output layer by the DE has been shown in Table 2 and Table 3. Figure 4 shows the convergence characteristics for the best member in each generation and the population mean. A very close progress in the convergence path can be observed which indicates that complete population converge to the global solution. The obtained final classified outcome for the different classes has been shown in Table 4. From Table 4, it can be observed that the difference between the target and delivered output is very small. Such kind of performance of learning ensures that DE can be very effective optimizer for the neural weights.

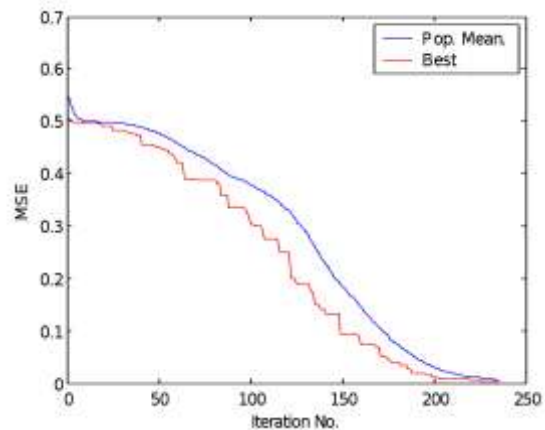


Figure 4: Learning error convergence characteristics for Ensemble Neural Network with Differential Evolution

TABLE 2: HIDDEN LAYER WEIGHTS OBTAINED AFTER COMPLETION OF LEARNING USING DEENN

| Input node | Hidden node1 | Hidden node2 | Hidden node3 |
|------------|--------------|--------------|--------------|
| 1 | -4.3461 | 6.1494 | 12.0642 |
| 2 | 15.4913 | 9.5075 | -5.7447 |

TABLE 3: OUTPUT LAYER WEIGHTS OBTAINED AFTER COMPLETION OF LEARNING USING DEENN

| Hidden node | Output node |
|-------------|-------------|
| 1 | -17.5399 |
| 2 | 22.6341 |
| 3 | -16.2271 |

TABLE 4: FINAL OBTAINED OUTPUT BY DEENN

| Input Data | | Target | DEENN Output |
|------------|---|--------|--------------|
| 0 | 0 | 0 | 0.0038 |
| 0 | 1 | 1 | 0.9936 |
| 1 | 0 | 1 | 0.9978 |
| 1 | 1 | 0 | 0.0000 |

A. Experimental Results with Heart Disease dataset

To check the practical applicability of the proposed method, it has been applied over the heart disease data available in the UCI repository. Dataset has 13 attributes and 303 data samples. Here we have considered the four different classifiers, each classifier has training data of 100 data samples while remaining data samples have been used for test cases. For the 1st classifier, data samples from 1-100 have been used for training data, while for 2nd classifier it is 51-150, for 3rd classifier, it is 101-200 and for 4th classifier has training data from 151-250. Such distribution ensures the similarity because of overlapping while diversity because of the inclusion of other datasets. The parameter of gradient learning, learning rate and momentum constant have been considered as 0.2 and 0.1. A low value of learning rate ensures the exploration of local space much better. The number of iterations for each classifier was 2000. In Figure 5, the convergence characteristics for all the four classifiers have been shown. The classifier performances over training and test data along with final mean square error have been shown in Table 5. The outcome efficiency for each classifier over the training data is appreciating and is around [98.6%, 98.4%, 81.2% and 79%]. While performances were disappointed over test data and are [77%, 76.6%, 81.2% and 79%] for the individual classifier in sequence from 1st to 4th. Such performances are the cause of worry particularly for critical applications like health care.

The possibilities of ensembles have been defined previously through the voting system or average tendency. In voting system, decision is counted and the majority decision is the final outcome. Such a process has the limitation of complete ignorance of classifier decision which was not part of majority decision. In the averaging decision process, the outcome value of individual classifier has been considered and the final outcome value is estimated by averaging and later a threshold value is applied to decide the final decision. This process has the advantage of using each classifier outcomes and it is

also observed that the averaging based performances are superior in comparison to the voting-based decision.

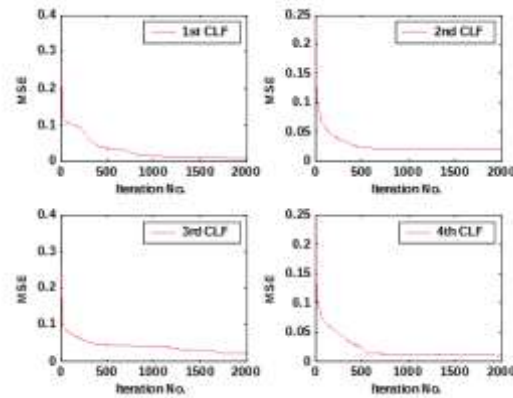


Figure 5. Error Convergence of Individual classifier

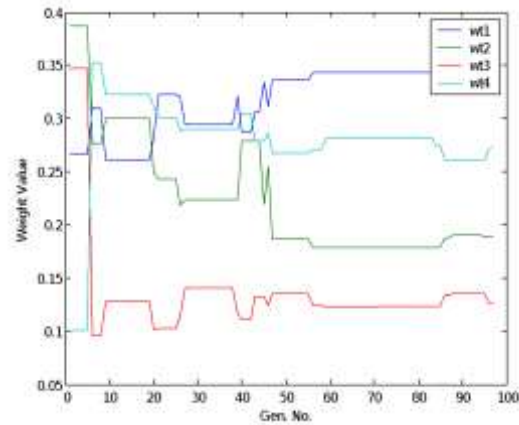


Figure 6. Weight evolution for ensemble by Differential Evolution

But the problem of averaging approach is that each classifier decision is given equal importance, which suppresses the cause of nullification i.e., means a better decision value is suppressed by inferior decision. The proposed DE based ensemble approach has been applied over 5 independent trials and their performance over training and test data along with obtained weightage for individual classifier has been shown in Table 6. The path of weights convergence for individual classifiers have shown in Figure 6 while Figure 7 represents the learning convergence of the proposed ensemble approach.

TABLE 5: EACH CLASSIFIER MEAN SQUARE ERROR / TRAINING/ TESTDATA PERFORMANCE

| Trail No. | CLF-1 | | | CLF-2 | | | CLF-3 | | | CLF-4 | | |
|--------------------------|----------------|-----|----------------|----------------|----------------|------|----------------|----------------|------|----------------|----------------|------|
| | MSE | Tr. | Test | MSE | Tr. | Test | MSE | Tr. | Test | MSE | Tr. | Test |
| 1 | 0.107 | 100 | 80 | 0.198 | 99 | 77 | 0.325 | 98 | 82 | 0.0106 | 98 | 82 |
| 2 | 0.0108 | 99 | 79 | 0.0105 | 98 | 77 | 0.0157 | 97 | 77 | 0.0105 | 98 | 80 |
| 3 | 0.0122 | 99 | 78 | 0.0205 | 99 | 78 | 0.0312 | 98 | 85 | 0.0016 | 99 | 79 |
| 4 | 0.0306 | 98 | 74 | 0.0204 | 99 | 78 | 0.0315 | 98 | 83 | 0.0103 | 100 | 80 |
| 5 | 0.0117 | 100 | 77 | 0.0105 | 98 | 78 | 0.0313 | 98 | 84 | 0.0106 | 100 | 80 |
| Mean (Tr. / Test) | 99.2000 | | 77.6000 | 98.6000 | 77.6000 | | 97.8000 | 82.2000 | | 99.0000 | 80.2000 | |

TABLE 6: PERFORMANCE OF DIFFERENT TYPES OF ENSEMBLE NEURAL NETWORK FOR HEART DISEASE DATASET

| Trial No. | MJVT Efficiency% | MNDS Efficiency% | DEENN | | | | | Efficiency % |
|-----------|------------------|------------------|----------|----------|----------|----------|-------|--------------|
| | | | CLF-1 WT | CLF-2 WT | CLF-3 WT | CLF-4 WT | | |
| 1 | 88.5183 | 88.8890 | 0.3535 | 0.1892 | 0.1267 | 0.2745 | 92.01 | |
| 2 | 87.4075 | 90.1 | 0.2524 | 0.3338 | 0.1977 | 0.3379 | 92.02 | |
| 3 | 90.1 | 90.7409 | 0.3948 | 0.1858 | 0.2796 | 0.1001 | 93.01 | |
| 4 | 88.8890 | 89.6298 | 0.1407 | 0.4415 | 0.2580 | 0.2869 | 92.02 | |
| 5 | 88.6847 | 89.7255 | 0.2439 | 0.3350 | 0.1730 | 0.3449 | 92.03 | |

And also efficiency obtained for ensemble neural network with majority voting (MJVT) and mean value integration method (MNDS), over 5 independent trials have been shown in Table 6.

The proposed method (DEENN), has achieved high efficiency of 92%, along with consistent performance over 5 trials.

In the heart disease dataset, 13 attributes define a very complex co-relationship in the decision landscape, which makes the classification with high efficiency, very difficult. But with the proposed system, it can be observed that the outcome even over

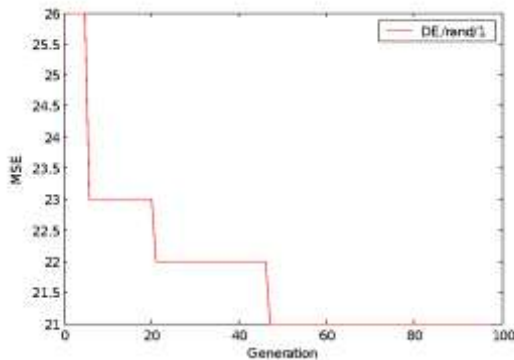


Figure 7. Learning error minimization by Differential Evolution for ensemble

such a complex landscape is very appreciable and also practically acceptable.

Table 7 illustrates the comparison of performances of all the three types of ensemble neural network classifiers (DEENN, MJVT, MNDS) and individual classifiers (CLF1-CLF4). Figure 8, shows the graph of performance comparison with respect to classification efficiency. It can also be observed that ensemble structures are more beneficial when compared to any individual classifier.

Each of the individual classifier performances was also evaluated in terms of sensitivity and specificity to know their predictable capabilities. Sensitivity and specificity performances of different classifier structures have been shown in Table 8. It can be observed that all the individual neural network classifier (CLF 1-CLF 4) have relatively the same performance.

From Table 8, it is clear that ensemble neural network has shown better specificity and sensitivity on the given dataset in comparison with individual NN classifiers (CLF 1-CLF 4), MJVT and MNDS.

TABLE 7: PERFORMANCE COMPARISON OF ALL THE CLASSIFIERS

| CLF -1 | CLF -2 | CLF -3 | CLF -4 | MJV T | MN DS | DEE NN |
|--------|--------|--------|--------|--------|--------|--------|
| 77.000 | 76.600 | 81.200 | 79.000 | 88.699 | 89.796 | 92.200 |

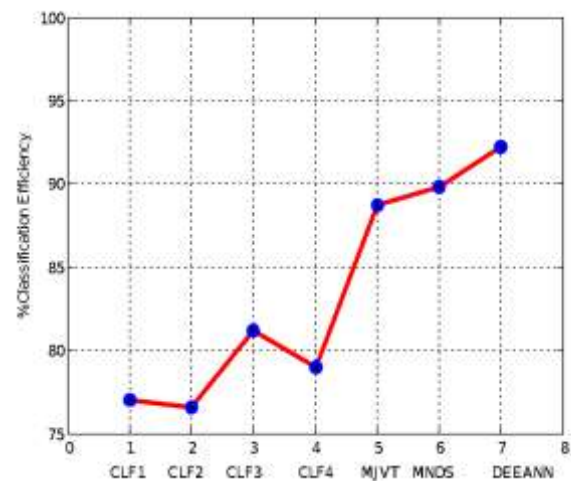


Figure 8. Performance comparison of different classifiers

TABLE 8: DIFFERENT CLASSIFIER STRUCTURES SENSITIVITY AND SPECIFICITY PERFORMANCES

| Classifier | Sensitivity(%) | Specificity(%) |
|------------|----------------|----------------|
| CLF-1 | 85.84 | 83.35 |
| CLF-2 | 84.18 | 86.01 |
| CLF-3 | 82.51 | 92.68 |
| CLF-4 | 82.51 | 90.01 |
| MJVT | 78.35 | 97.35 |
| MNDS | 84.19 | 94.02 |
| DEENN | 90.02 | 93.35 |

V. CONCLUSION

This proposed work shows the efficiency of ensemble neural network in the classification area. Experimental results prove that ensemble classifier is always better than any single classifier. Evolutionary process-based ensemble structure has achieved outstanding efficiency and high-level consistency. When compared to the conventional form of ensemble methods, the proposed method is computationally efficient and also has achieved improvement in quality. Evaluation of proposed work has been done only on single UCI dataset. Further, the algorithm can be enhanced and tested on more application-specific datasets.

ACKNOWLEDGEMENT

We gratefully thank the UCI Machine Learning Repository [<http://archive.ics.uci.edu/ml>] for providing datasets. We also thank the Visvesvaraya Technological University, Jnana Sangama, Belagavi for giving an opportunity and support for this research work.

REFERENCES

- [1] (Asakura, T., Date, Y., & Kikuchi, J. (2018). Application of ensemble deep neural network to metabolomics studies. *Analytica Chimica Acta*, 1037, 230-236. doi:10.1016/j.aca.2018.02.045
- [2] Bao, W., Yang, B., Li, D., Li, Z., Zhou, Y., & Bao, R. (2019). CMSENN: Computational Modification Sites with Ensemble Neural Network. *Chemometrics and Intelligent Laboratory Systems*, 185, 65-72. doi:10.1016/j.chemolab.2018.12.009
- [3] Hansen, L.K., & Salamon, P. (1990). Neural Network Ensembles. *IEEE Transactions on Pattern Analysis and Machine Intelligence*, 12(10), 993-1001. doi:10.1109/34.58871
- [4] Kim, K., Jin, Y., Na, S.-H., & Kim, Y.-K. (2017). Center-shared sliding ensemble of neural networks for syntax analysis of natural language. *Expert Systems with Applications*, 83(C), 215-225. doi:10.1016/j.eswa.2017.04.048
- [5] Li, H., Wang, X., & Ding, S. (2016). Research of multi-sided multi-granular neural network ensemble optimization method. *Neurocomputing*, 197(C), 78-85. doi:10.1016/j.neucom.2016.02.013
- [6] Manjón, J. V., Coupé, P., Raniga, P., Xia, Y., Desmond, P., Fripp, J., & Salvado, O. (2018). MRI white matter lesion segmentation using an ensemble of neural networks and overcomplete patch-based voting. *Computerized Medical Imaging and Graphics*, 69, 43-51. doi:10.1016/j.compmedimag.2018.05.001
- [7] Pulido, M., Melin, P., & Castillo, O. (2014). Particle swarm optimization of ensemble neural networks with fuzzy aggregation for time series prediction of the Mexican Stock Exchange. *Information Sciences*, 280, 188-204. doi:10.1016/j.ins.2014.05.006
- [8] Ukita, N., Kawana, Y., Huang, J.-B., & Yang, M.-H. (2018). Ensemble convolutional neural networks for pose estimation. *Computer Vision and Image Understanding*, 169, 62-74. doi:10.1016/j.cviu.2017.12.005
- [9] Wang, R., Li, W., & Zhang, L. (2018). Blur image identification with ensemble convolution neural networks. *Signal Processing*, 155, 73-82. doi:10.1016/j.sigpro.2018.09.027
- [10] Zhang, L., Yu, G., Xia, D., & Wang, J. (2018). Protein-protein interactions prediction based on ensemble deep neural networks. *Neurocomputing*, 324, 10-19. doi:10.1016/j.neucom.2018.02.097
- [11] Zhao, Z., & Zhang, Y. (2011). Design of ensemble neural network using entropy theory. *Advances in Engineering Software*, 42(10), 838-845. doi:10.1016/j.advengsoft.2011.05.027
- [12] Zhao, Z., Zhang, Y., & Liao, H. (2008). Design of ensemble neural network using the Akaike information criterion. *Engineering Applications of Artificial Intelligence*, 21(8), 1182-1188. doi:10.1016/j.engappai.2008.02.007
- [13] Zhou, Z.-H., Wu, J., & Tang, W. (2002). Ensembling neural networks: Many could be better than all. *Artificial Intelligence*, 137(1-2), 239-263. doi:10.1016/s0004-3702(02)00190-x
- [14] Dua, D. and Graff, C. (2019). UCI Machine Learning Repository [<http://archive.ics.uci.edu/ml>]. Irvine, CA: University of California, School of Information and Computer Science..

International Journal of Advanced Science and Technology

[Home](#) [Editorial Board](#) [Journal Topics](#) [Archives](#) [About the Journal](#) [Submissions](#)[Privacy Statement](#) [Contact](#) [Home](#) / [Archives](#) / [Vol. 29 No. 05 \(2020\): Vol. 29 No. 05 \(2020\)](#) / [Articles](#)

An Approach for Remove Missing Values in Numerical and Categorical Values Using Two Way Table Marginal Joint Probability

Vengatesank, E Saravana Kumar, S. Yuvaraj, Punjabi Shivkumar Tanesh, Abhishek Kumar

Abstract

Data analytics is a wide area which helps to extract the essential information from a huge volume of data. Data gathered from different sources are not in the same format, hence it is very difficult for pre-processing such data. Each and every data set has different categories of data types such as numerical or categorical data types. In this proposed work, we will discuss about identifying the missing values from the dataset using statistical techniques such as two-way table joint probability, two-way table marginal probabilities and two-way table conditional probability. The work also focuses on how to extract the essential features from the data set. Different visualization methods are used to easily understand the data set and feature prediction.

Keywords: Data Analytics, Missing values, Joint Probability, Visualization.

[PDF](#)

How to Cite

Vengatesank, E Saravana Kumar, S. Yuvaraj, Punjabi Shivkumar Tanesh, Abhishek Kumar. (2020). An Approach for Remove Missing Values in Numerical and Categorical Values Using Two Way Table Marginal Joint Probability.



Pattern Recognition Letters

Volume 152, December 2021, Pages 283-294

An improved watermarking algorithm for robustness and imperceptibility of data protection in the perception layer of internet of things

Mohammad Kamrul Hasan ^a, Samar Kamil ^b, Muhammad Shafiq ^c✉, Yuvaraj S ^d, E. Saravana Kumar ^e, Rajiv Vincent ^f, Nazmus Shaker Nafi ^g

Show more 

 Share  Cite

<https://doi.org/10.1016/j.patrec.2021.10.032>

[Get rights and content](#)

Abstract

Emergence of Internet of Things (IoT) and modern digital applications such as digital financial services and deliveries make it easy to reproduce and re-distribute digital contents thus give room to so many copyright violations of illegal use of contents that need to be resolved. Researcher have been presenting the watermarking algorithms to prevent these illicit activities to a document before distribution. However, several issues have been identified for the digital transactions in the IoT. Thus, this research proposes a new text document image watermarking algorithm which emphasizes on two most important measures, visual quality, and robustness. To boost these measures, third least significant bit has been used for insertion. In addition, to further strengthen the technique, the Pascal Triangle is applied to determine the best position for embedding. Experimental results on the standard dataset have revealed that the proposed watermarking has achieved very encouraging results with PSNR and NCC averaged 54.95db and 0.98, respectively.

Introduction

The digital watermarking technique overcomes many challenges copyright violations, including illegal duplication or redistribution of digital content of IoT (Hasan et al. [1]). There

Artificial intelligence and machine learning approaches to COVID-19 outbreak: A survey

Sowmya, H. K.; Jesy Janet Kumari, J.; Naidu, R. Ch A.; Vengatesan, K.

Turkish Journal of Physiotherapy and Rehabilitation ; 32(3):690-697, 2021.

Artigo em Inglês | EMBASE | ID: covidwho-1250726

ABSTRACT

Corona viruses are group of viruses which may cause illness in both animals and humans. A person can easily get COVID-19 from the other people who have the virus. It is a serious disease, which disseminates through tiny water droplets from the nose or mouth, which are thrown out when a COVID-19 infected person coughs, sneezes, or speaks. This disease was first discovered in China and has since spread throughout the world at breakneck speed. At this pandemic time, the entire world should take an adequate and efficient step to analyze the disease and get rid of the effects of this epidemic. The applications of Machine Learning (ML) and Artificial Intelligence (AI) techniques play an important role to detect and predict potential effect of this virus in future by gathering and examining most recent and past data. Furthermore, it can be used in realizing and recommending the enhancement of a vaccine for COVID-19. This paper focuses on reviewing the role of AI and ML approaches used for examining, analyzing, predicting, contact tracking of existing patients and potential patients.

PAPER • OPEN ACCESS

Comprehensive Analysis of Cloud based Databases

To cite this article: E. Saravana Kumar *et al* 2021 *IOP Conf. Ser.: Mater. Sci. Eng.* **1131** 012021

View the [article online](#) for updates and enhancements.



240th ECS Meeting ORLANDO, FL

Orange County Convention Center **Oct 10-14, 2021**

Abstract submission deadline extended: April 23rd

SUBMIT NOW

Comprehensive Analysis of Cloud based Databases

¹Dr. E. Saravana Kumar, ²Dr. Selvaraj Kesavan, ³Dr. R. Ch. A Naidu,

⁴Dr. Senthil Kumar R, ⁵Latha

¹Associate Professor,

²Advisor Solution Architect in DXC Technology, India,

³Professor & H.O.D ,

⁴Associate Professor,

⁵Assistant Professor

^{1, 3,4,5} Dept. of CSE, The Oxford College of Engineering,
Bommanahalli, Bangalore-560068

saraninfo@gmail.com, selvarajkesavan@gmail.com,

chanr789@gmail.com, senkr.raj@gmail.com,

latha.shreeram@gmail.com

Abstract

With standard change in the computing architecture and distributed, wide range processing approach leverage the large data to be analyzed and extract the content. The recent advancement in Web technology enables the user to produce process and ingest content of any structure. Cloud computing helps to provide computing infrastructure, centralized storage and seamless services for organizations and users. In a digital world, data is core aspect of the economy, become part of government, enterprise, social sectors and every individual in a day to day life. Data analysis is gathering of strength in both research and production communities. There are many social networking sites, web, enterprise and IoT data require being stored in secured, centralized data store. It also demands data to be stored without any predefined schema and able to retrieve in near real time. When demand goes up application needs to be scaled to sustain for the demand. Similarly, data store should support scalability to support applications demand. Cloud providers and third-party organization offers numerous data storage, database options. This article highlights various available data storage options, suitability and limitations.

Keywords: Open-Source Database, Cloud storage, Data Storage

1. Introduction

Data science becoming the integral part of every business and individual life. Organizations are spending huge amount in data science to keep up the heat in today's competition and improve their business outcome. It helps to derive business insights, key metrics and predictive analysis from the data captured. Data science and its relevant fields are highly valuable; it helps management teams to make strategic business decisions. Many companies around the world are exploring the data science and trying to build the data science platforms.



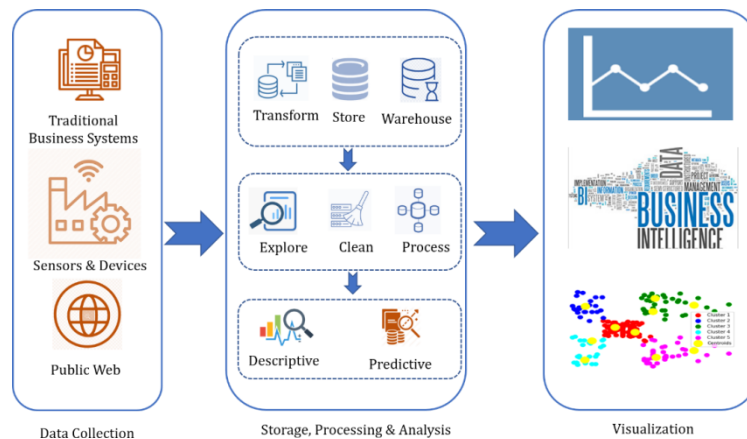


Figure 1. Data science pipeline

With the invent of Web technologies, data with volume, velocity and variety coming from major sources such as Internet of things/sensors, web & social network and traditional business systems. The data source may be structured varieties or unstructured varieties or combinations of both. Data science uses the numerous approaches to clean, explore, transform the data before applying techniques like machine learning deep learning data visualization text analytics to analyze the data. It is tightly integrated with artificial intelligence to make reality of decision-making robots. The Fig.1 shows the architecture of data science Pipeline with detailed manner.

Data science extracts knowledge and provides insights of various form of data for business process efficiency data is important and key part of cloud computing. Data captured from many industry verticals/users such as business & commerce, Entertainment, Science, social network, medical, manufacturing etc.. Data in raw or extracted format brings lot of value to organizations and individual. It helps to expedite the business decisions and improve quality of life. The evolving technologies help to capture Terabytes of data, store in large repositories, and analyze the data with complex data analysis approach using distributed/parallel processing. Data store to Data warehousing helps to store, process, analyze commutative and historical data from single or multiple data sources. Data analysis tools, algorithms and framework helps to derive descriptive and predictive analytics from data and aids to quick decision. The critical aspect of the pipeline is to collect and store the data from diverse sources which produce different data formats.

The data captured from various sources includes structured, single dimension, multidimensional, tabular, spreadsheet, time series, documents formats. The storage mechanism is simultaneously evolving to address the need and support for multiple applications and data formats. The selection of data base is depending on multiple factors such as

- Requirement of Relational between elements
- Amount of data to store
- Real Time Streaming of Data
- Scalability, reliability and availability requirement
- Multi-tenancy
- Cost

Structured Query Language (SQL) is mainly designed for the data requires relational with elements. It deals structured data with defined attributes. The scalability of SQL recognized by Web2.0 companies with large, increasing data and framework needs Facebook, Amazon and Google etc. Because of its sheer size and lack of structure, traditional relational database management system (RDBMS) unable to handle very large big data. These kinds of very large data require a flexible non-relational model that supports fast access to data for processing.

Relational databases are predefined, expensive to scale, and have high storage costs. They are also transactional, consistent, and use mature SQL and a relational mindset. There is no SQL database that can meet this need. On the other hand, non-relational (NoSQL) databases are flexible, scalable, and resilient. They feature commodity storage, are not transaction-oriented, and are eventually consistent. Non-relational databases are also programmable with SQL-like and use a new mindset. No-SQL databases are playing vital role in recent applications in multiple fields. It provides free flow operations without any bottleneck in the performance and use a different types of data models, which includes text document, graphical models, dictionary and columns, helps unique way to query the data. Horizontal scaling and flexible data model definitions. Distributed and developed for very large-scale forms of data storage and enormous parallel processing data across a different number of servers and achieve speed at scale, overcoming RDBMS limitations and inefficiencies. With built-in high-resiliency architecture, it helps to store dynamic schema, semi-structured data for low-latency applications and update, retrieval in real time. This increasing interest among NoSQL and DBMS's evolved with a focus on improved performance and consistence with reliability. The major No-SQL data bases are Mongo DB(Document), Redis (Key-value),Amazon Redshift (Columnar), Cassandra (Columnar), HBase (Columnar),Dynamo DB(Document DB-stores JSON/XML) and GraphDB .

The major contributions of the proposed paper covers three main points.

- Provides list of various available data storage options, highlights the criteria to choose appropriate database, cache and limitations.
- Elaborately discuss the No-SQL architecture, retrieval mechanism and Caching strategy
- Detailed comparison of various No-SQL storage options with key metrics

Apart from the main points the remaining the paper is organized in other section. Section 2 presents the various related research work in the area of data base and data storage mechanisms and options. The evolution of database paradigm and classifications are discussed in Section 3. The various aspects of No-SQL Database Storage architecture, retrieval mechanism and selection strategy are captured in Section 4. In section 5, the comparison of key No-SQL databases with key metrics are discussed in detail. Finally, section 6 concludes the paper.

2. Related work

Database helps applications to store, update and retrieve information. SQL and No-SQL databases are widely used by the organizations for storing data collected from various sources. Cloud and IoT evolving exponentially, it is critical to have appropriate databases for store, retrieve, and process data on real time. Sensors/Things connected to server via network and deliver connected industry solutions for efficient control and improved human experience. Billions of connected devices are an indicator of IoT and transmits data in high velocity, variety and volume. The real value of IoT is on data which helps business insight and enable data-driven economy.

Database management systems (DBMS) and databases are critical to everyday business and work

[1]. Relational Database Management Systems (RDBMS) is old, pioneer system used many years [2]. The need of new databases is inevitable to develop and use new generation digital applications such as social networking, business visualizations, web 3.0 and connected sensors/devices [3]. Authors [4] performs independent investigation on the NoSQL and SQL performance of databases based on dictionary of key-value stores. The various operations such as comparing reading, writing, deleting and instance operations on key-value stores of SQL and NoSQL. Apart from that, authors investigated the operation of iteration across all the keys. A framework of abstract key-value pair [5] designed implemented and tested using the above basic operations. A detailed comprehensive survey [6] of various approaches and deployment mechanisms of data-intensive areas in the cloud gains major attention in both research and industry. An analysis of different design decisions of every approach and its fitness to support various areas of applications and different end-users. Different views of some of the open issues and future questions related to scalability of large scale database in economical processing on the cloud is addressed. Bartholomew [7] explains the differences of SQL and NoSQL databases and its history. The authors [8] compared functional and non-functional features of graph database; dictionary based key value stores, column store database and documents. In each category, authors selected one database on document store (MongoDB), column database (Cassandra) stores, key value stores and graph based databases (Redis and Neo4j)

A qualitative research [9] has been conducted on SQL and No-SQL data base and detailed, intensive analysis and comparison performed. The NoSQL and SQL performance compared experimented and analyzed by the authors [10]. IoT and IIoT are one of the major sources in providing data. The authors [11] have analyzed and performed comparisons of SQL, NoSQL in the context of Internet of Things. Authors [12] performed analysis on the effectiveness problem of data format for the purpose of storing and processing in RDBMS technology. SQL and NoSQL databases have been compared [13] to use for an small IoT application of water sprinkler system and analyses the merits, fitness, performance of NoSQL and SQL under different scenarios.

Even though, the various research papers discuss the functionalities and applications of different databases, it does not provide complete view and comparison of multiple databases and applications with various metrics. However, it is important to have all-in-oneview of different databases along with features, architecture, flexibility, limitations and applications. This paper gives comprehensive view of data storage in the market, selection strategy and comparison which helps for developers, organizations to understand the functionalities and choose right data base for their need.

2.1 Evolution of Database and classification

Information Systems and data bases are the two components concurrently existing in the computer science technology. Appropriate data base management system required for storing and retrieval of data in a meaningful manner. RDBMS databases applies the ACID model in transactions management strong atomicity, consistency with Isolation and Durability property. Unfortunately the transaction properties cannot be applied on NOSQL databases because the priorities are different. The NOSQL applies the BASE model which ensures the Basic Availability of the database, Soft state of the model and the Eventual consistency of the database. Over the years, many researchers have conducted various researches in the mentioned field to justify BASE in NOSQL and ACID properties of RDBMS database.

Various structures were applied and improved to enhance the read operation searching techniques. Big companies developed Proprietary NoSQL to focus on their needs. Google developed BigTable and Amazon developed DynamoDB. The successful outcome of these proprietary softwares started the open source community to develop such a software, Hbase, MongoDB, Cassandra, DynamoDB, Hypertable, and Redis are the popular NoSQL database developed by these communities.

2.2 Data quality and governance

2.2.1 Data store

Persistently store and manage repository of data, files, organized and unorganized data. It includes file system, SQL, No-SQL databases etc. Quick access of data on very large number of nodes allowed in non relational database management systems like distributed DBMS. Distributed DBMS has very good access performance and rich query abilities which are limited key-value semantic in other databases. These limitations are noted in Bigtable , Azure and Dynamo models performs comparatively better in peer-to-peer network.

2.2.2 Data Lake

Data lake is a repository to hold large amount of structured, unstructured data accumulated from various sources at any scale. It is act as a raw repository which holds data in original format as it received from the sources. It stores all data types whether structured or unstructured. Storing data in data lake is comparatively cheap .It is suitable for Machine Learning, Predictive analytics, data discovery and profiling

Ex: Amazon S3, Amazon Glacier

2.2.3 Data Warehouse

A data warehouse is a database optimized to store data which are formatted / processed to give shape to the data. The data structure, schema are defined in advance in order to optimize read / write operations. The data helps to derive insights, analytics which helps organization to take management decisions. Storing data in data warehouse is comparatively costlier than Data Lake. It is suitable for Batch reporting, BI and visualizations

Ex: Amazon Redshift

2.2.4 Database

Technology stores data in an organized manner using Data base management system. It is classified as SQL and No- SQL Databases. Entire row is stored Row-oriented databases in a physical block. Secondary indexes used to achieve the high performance in read operations. Instead of packing the whole rows into a block each column organized into set of physical blocks in Column-oriented databases. Better performance achieved in master/slave architecture type with an overhead that single point of failure presented in master node. Every node is identical in peer-to-peer cluster and same responsibilities assigned to each node. Every node achieves fault tolerance with overhead of consistency maintenance is high.

RDBMS, usually executes query language (SQL), is combination interrelated tables. The tables contains rows and columns. The schema represents the relationships among tables and column represents the attribute. These RDBMS databases are highly consistent by design. RDBMS queries are used in banking applications for online transactions. Cloud providers which are popular are IBM DB2 , SQL Server , MySQL and Oracle. MySQL platform is open source cloud platform.

Table model is not used in non-relational databases which is called NoSQL because it stores the content as a document regardless of any structure. Unstructured data is well-suited in non-relational databases technology like image and video contents of social media.

2.2.5 SQL Databases

SQL data bases have predefined schema. Database stores data in table row format in the databases

such as MS SQL Server Oracle DB Server open source MySQL, PostgreSQL and SQL databases. Traditionally data warehouse was used in these systems in which online transactional processing (OLTP) implemented better than for analytical purposes.

In a SQL database, all of the columns are read by query for all of the rows to satisfy the query condition. It creates a bottleneck in the performance especially analysis related use cases. But in relational database systems it is well suited for transaction processing across many tables. The multiple tables joined using complex join operations.

2.2.6 No-SQL Databases

A different scalable paradigm instead of relational databases are No-SQL data base. The cloud computing currently uses scalable applications but the challenge of scalable database is storing models. NoSQL data base based on cloud can be considered as an alternative. No fixed scheme is required for distributed data bases which used No-Sql. It is well suitable for unstructured data which need to fit into schema based database or the design changes frequently. Different data model varieties utilized such as key- value based data model, columnar data model, graphs and document model

The familiar, widely used No-SQL DB are

- Document -Mongo DB,
- Columnar - Amazon Redshift, Cassandra, HBase, Dynamo DB
- Key-Value – Redis, Riak, Dynamo DB, Berkeley DB
- Graph - Neo4J

2.2.7 Key - Value -Redis, riak

Implementation of NOSQL database is based on Key-value based databases, which are simple. It uses hash method of dictionary. By using hash it matches the key to the values. A hash table will be implemented to separately store the unique keys with pointers refers to the corresponding values. Scalar data types can be used for values, for example integer and complex structures. BLOB, List structure and JSON are the complex structures. In NoSQL databases design and implementation can be performed using key value stores. The API such as get, put, delete can be used by clients for reading, writing using NoSQL. These operations are uses primary key concept. It enable scalability and high performance can be achieved.

2.2.8 Document based – Mongo DB, CouchDB

Mongo DB, CouchDB database systems are not relied on schemas which is storing the document. Each record in document databases is an associated data which treats the document as semi-structured data.

A database object encapsulate everything related to document database. It gives less dependency and more agility. The encapsulated and encoded database objects are provided in some formats like JSON an XML. JSON provided object notation of java script.

The JSON, BSON and XML formats uses stored data structure. It uses Key-Value pair in document store and each key has a corresponding value provides the data structure. This is called as *document*. An object containing metadata value with array, string, binary and date. It gives a method to index and apply query based on features in document

2.2.9 Graph based- Neo4j, GraphDB

Graph based databases are entirely different when compared with NOSQL database. Graph based databases that rely on graph structure. In graph structure nodes and edges are connected with others through structure relations like tree. Property Graphs contains *nodes* . The *relationships* among the nodes represented in property graphs. Properties are the attributes which can be store nodes along with relationships. Nodes represented as entities of graph, Node metadata tagged with *labels* used to represent the contexts. Direction provided by relationships which can be bi- directional. The connections are named among two nodes. More than one relationship can be specified between two different nodes and each relationship with a direction, type, start and an end node.

2.2.10 Columnar – Casandra, H-Base

Data stored n Column databases, is cells of columns. These are grouped into families of column. Multidimensional nested sorted map of maps format used in these databases. data identified in the innermost map contains a timestamp. A cell is used to store the data This will be mapped to column and mapped with column family. A Collection of column families found using a row key. The row key on sets of columns implemented for read and write operations. It will be stored as a continuous entry in the storage which is improving the performance.

2.3 Choosing Appropriate Database

| Scenario | Database Type |
|---|------------------------------|
| Session Storage, user preference, shopping cart data | Key value |
| Blogging, web Analytics, real time analytics, ecommerce applications | Document Database |
| Content management, IoT,log analysis | Columnar DB |
| Spatial Data ,Social network, transport, routing Applications | Graph DB |
| - Distribute Static and media contents Low cost ,highly durable - Data store for computation and large-scale analytics | Object Storage |
| Structured data with Query | Relational DB |
| Meta data store | Key value and Caching |
| Uninterrupted Key-Value | Object and key value storage |

2.3.1 No-SQL Database Storage and retrieval mechanism

The storage and retrieval of No-SQL contains strong consistency. All clients performs two-phase commit protocol on updating the dataset which uses XA transactions, ACID properties. It provides high availability: The availability of requested data to all the clients found at least one copy of the data, even if some of the machines in a cluster is down, Partition-tolerance: the total system keeps its characteristic even when being deployed on different servers, transparent to the client. Flexible schema supported in NoSQL databases which enables developers to quickly adopt the databases. The schema supports structured and unstructured data enables efficient processing which supports high performance in executing queries in the vary large scale environment.

2.3.2 Master less Ring Architecture

Identical role played by all the nodes in master less ring architecture; Without the master node concept all the other nodes are communicating with each other nodes through scalable and

distributed protocol called as "gossip." across datacenters architecture based on a peer-to-peer ring can be deployed which can be done by Cassandra.

The Cassandra performs logical division of racks and the required switches inside the cluster, this installation determines the best node to be stored and rack for replicas of the node

Mongos query routers are used to build the hierarchal architecture MongoDB. The architecture contains one or more routers and one or more shards used to run the mongod. The replica node built the mongodb and it sets consist of a primary node and secondary nodes.

A master-less peer-to-peer architecture architecture along with many data centers is supported by Riak Commercial version architecture. One datacenter acts primary and many different data centers supports with primary node which will be synchronized.

A peer-to-peer architecture Couchbase, consists of cluster manager, index, query in each and every node. The multiple datacenter in Couchbase support, updation flowing from one datacenter to other datacenters. These flowing can be done bilaterally where conflicts can be resolved by each cluster which is the owner of certain set of partitions.

2.3.3 Peer To Peer Architecture Systems

The upshot of the discussion is that the client-server model generates a service hot-spot at the server and increasingly hot network utilization the closer one gets to the server. Traffic that is diffuse toward the client is concentrated near the serve. The system is represented in fig.2

Distributing the service helps. But, as long as clients out number servers, there is a natural imbalance. The solution to this imbalance is a peer to peer architecture where services are provided (hopefully, but not likely) in proportion to their use.

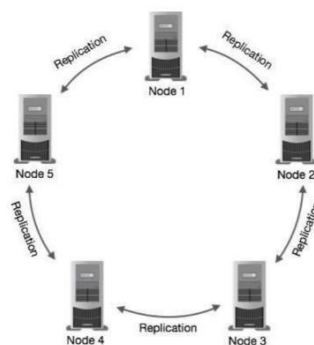


Figure 2: Peer-to-Peer System

3. Challenges of Peer-to-Peer systems

The peer-to-peer architecture systems present several challenges:

- Describing and searching for content
- Naming
- Finding objects and directory services
- Stability of the peers
- Trust of the peers

It becomes difficult to search for object in peer-to-peer systems because high-level searches don't

localize well. For this type of thing, we really do want a distributed map-reduce or other parallel search or large, in memory monolithic database, or both. We don't want to have to ask a large number of distant peers and then need to coordinate the results.

Once can identify each object we want, we need to find it. One option is a fully distributed directory service, another is a directory service distributed among select peers, and a third is a distributed hash. Stability of peers is obviously an issue. Some peers will be well resourced and stable, others will be thin and brittle. The stability of the system depends upon having enough stable resources to mitigate the impact of a smaller quantity of brittle resources. One common solution here is to appoint willing, richer, more stable, longer-serving peers as "super peers" and giving them more responsibility, perhaps incentivizing them by proving more or better service (or just by the good feeling from being a good citizen).

Trust is the nearly impossible part. Insert the whole discussion about public key infrastructure here. It is really challenging to trust the identity of hosts. With luck, we can get a hash of what we want from enough sources trusted enough to trust the answer -- and then we can check that what we get matches the hash. Thus, the most brittle part of this is really trusting the search results and/or human-name to hash-name mapping.

3.1 Distributed Hashing: Consistent Hashing and Chords

Another idea for a peer to peer system is to implement a huge distributed hash table. The problem with traditional hash tables, though, is that they don't handle growth well. The hash function produces a large number, which is then taken modulus the table size. As a result, the table size can't change without needing to rehash the entire table -- otherwise the keys can't be found.

A hash value which is independent of the hash table size is used by a hashing scheme in distributed hashing. Keys can be found from the result even if the table size changes. This is not supported of a distributed hash table, The keys found even the nodes enter the system.

Chord protocol is a technique for doing this hashing. A logical ring used to view the world in this protocol. For the selected m , number of bit key, the bit contains the logical positions 0 to 2^m-1 . Think of them as hours on a clock. Some of these positions have actual nodes assigned to them, others do not. Every node "need" the successor only like the token ring, but the topology is known for the entire ring which will be used to handle failures.

For more than one key each and every node is responsible because there are only fewer nodes than actual addresses which is hours on the clock. Mapping is performed on keys to actual nodes by identifying the keys to the "closest" node which can be equal or greater than in number.

a brute force searching technique is use to find a key of the circle, but instead each node keeps a "finger" which points to the next node, 2, or 4 or 8 nodes away, etc. In other words, every node points to nodes exponential manner farther and farther away. These pointers are stored in a table such that the i^{th} entry of the table contains a pointer to a node that is 2^i away from it, e.g. at position node number + 2^i . The keys, if suppose any node is not present at the exact location then the next passing greater node will be used. This modified arrangement enables the possibility of search for a bucket with the time complexity $O(\log n)$. The time complexity found with each step, which either find the right node, or performs cutting the search space into half.

In order for a node to join, it simply is added to an unrepresented position (hour on the clock) within the hash table. It gets its portion of the keys from its successor, and then goes live. Similarly, disappearing from the hash simply involves spilling ones keys to one's successor.

3.2 Schema less Architecture

NoSQL DB provides Schema less architecture which helps to create schema on-the-fly and it does not need any predefined schema.

| Database | Architecture | When to Use |
|-----------|--------------|--|
| Cassandra | peer-to-peer | SQL-style data types Steep learning curve when switching from SQL |
| MangoDB | master-slave | Lots of highly unstructured data Loosely coupled objectives |

3.3 Caching Design Patterns and Strategy

- Consistent Caching (Sharding)
 - Issue with Modulo (CRC32) ,keys mapped to new node when scaled
 - Consistent hashing – Ring methodology
 - Client libraries
- Lazy population (updated cache when app reads , cache miss lead to direct query)
- Write on through
 - Cache upgraded to real time when database updated
 - Cache miss avoided
 - Minimize app fetch delay
 - Cache always up-to date
 - Filled unnecessary objects
 - Lot of cache churn due to repeated update
 - No strategy to repopulate cache node when it fails
- Expiration Date
 - TTL to cache keys
 - Short TTL for rapid changing data types (news, leaderboards etc)
 - **Russian doll caching** – nested records with own cache keys , delete only cache keys which needs to be updated (suspect that it will affected by database update)
- Thundering Herd (Dog piling)
 - Cache miss , millions of user hit the DB in parallel increases DB throttling
 - Setting TTL to popular data will impact DB performance (if data not updated but TTL expire will trigger millions to request to be routed to DB)
 - When new cache node added , many requests routed to DB
 - Run script to populate cache before app make requests
 - For new node , run script to populate data in new cache node
 - Prewarming node (incase regular addition/deletion of cache node?)
- Cache everything
 - Heavily hit queries and expensive calculations
 - Caching data is stale data (no longer fresh and not appropriate in some scenarios)

3.3.1 Comparison

- HBase (ordered keys, semi-structured data), Cassandra, BigTable,
- CouchDB (name or value in text)
- Sherpa or PNuts (JSON, unordered keys)
- MongoDB (based on JSON)

| Name of the tools | Cassandra Database model | GraphDB | MongoDB | Neo4j | Redis |
|--|--|---|--|--|---|
| Descriptions of the comparative model | Supports wide-column store based on ideas of BigTable and DynamoDB | The graphs uses Enterprise RDF and with reasoning, external index cluster and synchronization support | One of the most popular document stores | The tools supports Open source graph database | In-memory data structure store, used as database, cache and message broker |
| Supported programming languages | Java, JSS,PHP, Python,Ruby,Scala,.Net | C#,C++,Clojure, Erlang,Go,Haskell,Java, JSS,PHP,Python, Ruby,Scala | Java, JSS,PHP,Python,Ruby,Scala,.Net, coldFusion | Java, JSS,PHP,Python,Ruby,Scala,.Net,Go, Groovy | Java, JSS,PHP,Python, Ruby,Scala, .Net, Crystal |
| The scripting of server-side | no | Java Server Plugin | JavaScript | yes | Lua |
| Partitioning techniques | Sharding supported | none | Sharding supported | none | Sharding supported |
| Replication techniques | Supports selectable replication factor | Supports Master- master replication | Supports Master-slave replication | Causal Clustering using Raft protocol | Multi-master replication, Master-slave replication |
| Consistency concepts of the models | Supports Immediate Consistency, Eventual Consistency | Supports Immediate Consistency, Eventual consistency | Supports Immediate Consistency Eventual Consistency, | Eventual and Causal Consistency configurable in Causal Cluster setup Immediate Consistency in stand-alone mode | Strong eventual consistency with CRDT |

| | | | | | |
|--|--|---------------------------------|--|---|---|
| Transacti on technique s | Not support ed | ACID Properties supported | ACID Transactions on Multi- document with snapshot isolation | ACID Prop erties supp orted | Atomic execution of commands blocks and scripts and Optimisti c locking, |
| User concepts supported in models | Per object the access rights for users can be defined | Supported | Allows the access rights for users and roles | Supports standards wth Users, roles and permission s. Pluggable authentic ation (Active Directory , Kerberos , LDAP) | Supports password- based access control |

4. Factors impacts database Performance

4.1 Merits

- The databases support elastic scalability which is designed for low-cost commodity hard wares.
- Massive volumes of Big Data Applications can be handled by NoSQL
- Economy: NoSQL databases installation is cheap in commodity hardware even with data volumes and transaction increase. But installation of RDBMS is expensive storage in proprietary servers. Processing and storage is less cost.
- Dynamic schemas: No schema design required for NoSQL databases. In RDBMS, a schema has to be defined first, it makes more difficult because the schema has to be changed every time when the requirements are changed. It ensures that data quality control should be performed on the application. NoSQL has no schema, of the data must be organized properly.
- Auto-sharding: In RDBMS scalability supported vertically, which makes a lot of databases spread among many servers and takes the disk space from multiple servers needed t work. Auto sharding is normally supported in NoSQL databases. Naturally NoSQL automatically spread the data across multiple arbitrary servers. These servers does not required even the application used composition of server pool
- Replication: Automatic database replication is supported in most of the NoSQL databases. This replication used to maintain availability of data all the time. Event maintenance or event of outages maintained using replication. Fully self-healing supported by most of the sophisticated NoSQL which provides automated failover and data recovery. Replication provides the ability to distribution of database across many geographic regions to avoid the regional failures and supports localization.
- Integrated caching: Integrated caching is supported in most of the NoSQL technologies, the frequently-used data kept in the system memory for storing and removing.

4.2 Limitations of Cloud Database

- Multiple-Data has no relationships among all the data.
- Multi-operation Transactions: Failure to save any one of key among many keys and if any transactions aborted then implementing roll back operation is very difficult
- Query Data by 'value': It support the searching by keys, which is based on information found in the 'value' of the key.
- Operation by groups: Simultaneously several keys cannot run as operations are grouped to one key at a time

5. Conclusion

If the application consists of a small amount of traffic Cloud Datastore will work well and performs better. if database is scaled up to very large number of requests then performance decreases. No wasted capacity will be made for the request given. It is expensive than using data store and required to know the capacity in advance. These will be charged for the additional capacity. Amazon announced auto scaling will be supported in cloud database in near future. Getting the provisioned capacity will help to write the own scripts to handle the scalability issue. Depending on the more capacity requirement it is provisioned, then start to deplete accumulated credits. If credits depleted, then the request will be throttled or failed some time. Depending on the options, the scalability available databases is alluring. The tradeoffs and selecting the right pricing model suitable for the application, enable to free the user from constraints of RDBMS.

References:

1. K. L. Berg, T. Seymour and R. Goel, "History of databases," *International Journal of Management & Information Systems*, vol. 17, no. 1, pp. 29-35, 2013.
2. U. Bhat and S. Jadhav, "Moving Towards Non-Relational Databases," *International Journal of Computer Application*, vol. 1, no. 13, pp. 40-46, 2010.
3. R. P. Padhy, M. R. Patra and S. C. Satapathy, "RDBMS to NoSQL: Reviewing Some Next-Generation," *International Journal of Advanced Engineering Science and Technologies*, vol. 11, no. 1, pp. 15-30, 2011
4. Y. Li and S. Manoharan, "A performance comparison of SQL and NoSQL databases," *2013 IEEE Pacific Rim Conference on Communications, Computers and Signal Processing (PACRIM)*, Victoria, BC, 2013, pp. 15-19.
5. J. C. Anderson, J. Lehnardt, and N. Slater, *CouchDB: The Definitive Guide*. O'Reilly Media, January 2010.
6. S. Sakr, A. Liu, D. Batista, and M. Alomari, "A survey of large scale data management approaches in cloud environments," *Communications Surveys Tutorials, IEEE*, Vol. 13, no. 3, pp. 311-336, 2011.
7. Mahrishi M., Shrotriya A., Sharma D (2012). "Globally Recorded binary encoded Domain Compression algorithm in Column Oriented Databases" in *Global Journal of Computer Science and Technology*, [S.l.], ISSN 0975-4172.
8. A. Gupta, S. Tyagi, N. Panwar, S. Sachdeva and U. Saxena, "NoSQL databases: Critical analysis and comparison," *2017 International Conference on Computing and Communication Technologies for Smart Nation (IC3TSN)*, Gurgaon, 2017, pp. 293-299, doi: 10.1109/IC3TSN.2017.8284494.
9. K. Sahatqija, J. Ajdari, X. Zenuni, B. Raufi and F. Ismaili, "Comparison between relational and NOSQL databases," *2018 41st International Convention on Information and Communication Technology, Electronics and Microelectronics (MIPRO)*, Opatija, 2018, pp. 0216-0221, doi: 10.23919/MIPRO.2018.8400041.
10. Kumar, A., Vengatesan, K., Vincent, R., Rajesh, M., Singhal, A. : A novel Arp approach for cloud resource management; *International Journal of Recent Technology and Engineering (IJRTE)* at Volume-7 Issue-6, March 2019
11. K. Fraczek and M. Plechawska-Wojcik, "Comparative Analysis of Relational and Non-relational

- Databases in the Context of Performance in Web Applications", *Proceedings 13th International Conference Beyond Databases Architectures and Structures (BDAS 2017)*, pp. 153-164, May 30 - June 2, 2017.
12. F. Haleemunnisa and W. Kumud, "Comparison of SQL NoSQL and NewSQL Databases for Internet of Things", *IEEE Bombay Section Symposium*, pp. 1-6, Dec. 2016.
 13. K.B. Kumar, SrivydiaSundhara and S. Mohanavalli, "A performance comparison of document oriented NoSQL databases", *Computer Communication and Signal Processing (ICCCSP) 2017 International Conference on*, 2017.

[Skip to main content](#) [Journals](#) / [International Journal of Intelligent Unmanned Systems](#) / [Volume 10 Issue 1](#)
Internet of things (IoT)-based unmanned intelligent street light using renewable energy

Access and authentication: Please [visit our page](#).

Close ✕

Enter your search terms here



Advanced search

Internet of things (IoT)-based unmanned intelligent street light using renewable energy

[Dinesh Kumar Anguraj, S. Balasubramanian, E. Saravana Kumar, J. Vakula Rani, M. Ashwin](#)

[International Journal of Intelligent Unmanned Systems](#)

DOWNLOADS



ISSN: 2049-6427

Article publication date: 12 January 2021

Standard

Issue publication date: 7 January 2022

Serial

Number.)

Abstract

Purpose

The purpose of the research is to concentrate on the most important smart metropolitan applications which are smart living, smart security and smart maintainable. In that, Power management and security is a most important problem in the current metropolitan situation.

Design/methodology/approach

A smart metropolitan area utilizes recent innovative technologies to improve its living, security and maintainable. The aim of this study is to recognize and resolve the difficulties in metropolitan area applications.

Findings

The main aim of this study is to reduce the metropolitan foremost energy consumption, to recharge the electric vehicles and to increase the lifetime of smart street lights.

Originality/value

The hybrid renewable energy street light applies smart resolutions to substructure and facilities in rural and metropolitan areas to create them well. This study will be applying smart metropolitan solar and wind turbine street light using renewable energy for existing areas. In future, the smart street light work will be implemented everywhere else.

Keywords

Wi-Fi

LED lights

Micro-wind turbine

Internet of things (IoT)

Citation

Related articles

[Investigating the information security management role in smart city organisations](#)

Mohamad Amin Hasbini et al., World Journal of Entrepreneurship, Management and Sustainable Development, 2018

[Security architectures for network clients](#)

Victoria Skoularidou et al., Information Management & Computer Security, 2003

[Systematic literature review on the security challenges of blockchain in IoT-based smart cities](#)

Zhihao Yu et al., Kybernetes, 2021

[Drones role in the city - municipal drone best practices](#)

South African Health Review, 2017

[Drones role in the city - municipal drone best practices](#)

SABI Magazine, 2017

[Overall Survival With Palbociclib And Fulvestrant in Women With HR+/HER2- ABC: Updated Exploratory Analyses of PALOMA-3, a Double-Blind, Phase 3 Randomized Study | Clinical Cancer Research | American Association for Cancer Research](#)

Brought to you by Pfizer Medical Affairs

PULMONOLOGICAL DISORDERS CAUSED DUE TO COVID-19 PANDEMIC

Patil, S.; Shobha, T.; Naidu, R. C. A.; Kumar, E. S.; Vengatesan, K.

Turkish Journal of Physiotherapy Rehabilitation-Turk Fizyoterapi Ve Rehabilitasyon Dergisi ; 32(2):1589-1594, 2021.

Artigo em Inglês | Web of Science | ID: covidwho-1362972

ABSTRACT

This paper talks about the new corona virus disease (COVID - 19). The corona virus is highly communicable, which makes it even more dangerous to the mankind. It spreads through water, touch and even when you come in contact with an infected person. Until now, only 30% of the virus has been studied, studies about the virus are yet being done by the scientists of every country in the world. The indications of the virus are very likely to those of common cold and pneumonia, which is why most of the time people neglect it and the virus continues to spread across. The virus has caused more than 5lakh deaths, 10.1 million cases and around 5.1 million people have been recovered. Scientists and doctors claim that it would take around 6 - 7 months to find an antivirus medicine for the disease. This paper has described about the virus, its causes, prevention and other related diseases this virus can spread. Abstract goes here.

Review on side-effects of COVID-19 in the growth of neurologic diseases

Shobha, T.; Patil, S.; Naidu, R. C. H. A.; Saravana Kumar, E.; Vengatesan, K.

Turkish Journal of Physiotherapy and Rehabilitation ; 32(2):1595-1598, 2021.

Artigo em Inglês | Scopus | ID: covidwho-1218842

ABSTRACT

Recent studies on risk factors and characteristics of the corona virus disease 2019 epidemic, have set up evidences that suggests persons afflicted by corona virus may suffer from neurological deficiency. Severely affected patients suffer from acute respiratory dysfunction, high levels of cytokines, immune response and neuroinflammation. These factors are the main causes for neurodegeneration that plays a vital role in Alzheimer Disease (AD). It is also said that the aged people are further vulnerable to AD after corona virus disease 2019 infection. This review gives the insight about risk factors of severely infected and elderly patients of COVID-19 developing cognitive decline, and gradually to AD, after recovering from SARS-CoV-2 infection. The main intention behind this review is to provide the base on future studies and investigations on corona virus and its effects on the neuro system. And also, to provide the awareness among the caretakers of corona virus infected persons with AD. © 2021 Turkish Physiotherapy Association. All rights reserved.

[Download PDF](#)Original Research | [Published: 30 June 2020](#)

Gradient flow-based deep residual networks for enhancing visibility of scenery images degraded by foggy weather conditions


[R. Suganya](#)  & [R. Kanagavalli](#)[Journal of Ambient Intelligence and Humanized Computing](#).**12**, 1503–1516 (2021)**88** Accesses | [Metrics](#)

Abstract

In the recent years, the vehicles are incorporated with camera-based modern driver support systems for facilitating the drivers to confirm their safety under different conditions of driving. However, lower contrast and faded scene visibility is considered as the main issue faced by the driver assistance system while driving in foggy weather conditions. At this juncture, deep neural network methods are considered to be potent in solving the limitations of manually designing haze-related features. In this paper, gradient flow-based deep residual network is utilized for improving the scenery images which are degraded through foggy weather conditions. This proposed scheme uses an undetermined complex function for mathematically modeling the fog in an image, which can be subsequently approximated by

Original Research | Published: 30 August 2020

Highly sensitive photonic crystal based biosensor for *Bacillus cereus*

[S. S. Ajey](#) , [H. R. Bhanumathi](#), [P. C. Srikanth](#) & [Preeta Sharan](#)

International Journal of Information Technology **12**, 1393–1402 (2020)

73 Accesses | [Metrics](#)

Abstract

The *Bacillus cereus* or *B. cereus* group comprises genetically closely related species with variable toxigenic characteristics. Most human food poisoning is caused by *B. cereus*. *B. cereus* is associated with nosocomial and opportunistic infections, particularly in immunocompromised patients. The motivation for this work was to provide an alternate method of detection of *B. cereus* on the fly. The purpose of the current study is to establish an innovative method to detect *B. cereus*. The proposed technique relies on a change in refractive index (RI) between normal and *B. cereus* infected blood. This involves the spectral analysis of the sample and uses the unique RI of the bacteria as a spectral signature for detection. The design incorporates an optical biosensor based on the photonic crystal (PC). Here we have considered two configurations—concentric and the side by side hexagonal ring resonators for PC based biosensor



Download PDF

[Download full issue](#)

Optik

Volume 227, February 2021, 165321

Original research article

Integrated MOEMS based cantilever sensor for early detection of cancer

Anup M. Upadhyaya ^a, Maneesh C. Srivastava ^a, Preeta Sharan ^b[Show more](#) [Outline](#) | [Share](#) [Cite](#)<https://doi.org/10.1016/j.ijleo.2020.165321>[Get rights and content](#)

Highlights

- Design of Photonic Resonator Based Integrated Microcantilever Sensor.
- Design of different shape of microcantilever.
- Optomechanical analysis of sensing device for cancer application.
- Investigation of sensor device performance, sensitivity, Q factor.

Abstract

In this paper, we present a novel microcantilever sensor for early detection of cancer in human body using an integrated optical micro ring resonator. Effect of geometrical modification of microcantilever on sensitivity and quality factor of proposed sensor is investigated. Regular rectangular and triangular profile are the two types of microcantilever considered during the analysis. The concept of integration of triangular and regular rectangular microcantilever profile with six hexagonal ring with hexagonal lattice configuration is novel work considered here. Finite element method simulation were carried out to obtain the surface stress of microcantilever and finite difference time domain method are used to obtain the transmission characteristics of photonic resonator structure. Range of pressure exerted on microcantilever due to binding of carcino embryonic antigen molecules on surface microcantilever is calculated as 0–2 MPa for specific number of molecules. High resolution with high quality factor 11,458 and pressure sensitivity of 60 nm/MPa is obtained for triangular microcantilever profile. Regular rectangular microcantilever has shown sensitivity of 0.01 nm/MPa and maximum quality factor of 3805. Both the sensor configuration has shown transmission efficiency above 90%. Thus a novel photonic resonator based microcantilever sensor configurations shows a promising linear characteristic as MOEMS sensor.

[Previous](#)[Next](#)

Keywords

Photonics; Microcantilever; Cancer; Ring resonator; Rectangular microcantilever; Triangular microcantilever; Carcino embryonic antigen (CEA)

Original Article | Published: 13 February 2021

A novel automated framework for water impurity detection

[Afzal Shaikh](#) , [Preeti Sharan](#), [P. C. Srikanth](#) & [Manju Devi](#)

International Journal of Information Technology **13**, 785–792 (2021)

31 Accesses | [Metrics](#)

Abstract

Proposed work involves the development of algorithm and computer simulation of a Hexagonal Ring Structure-based photonic sensor for the detection of harmful water impurities. An optical sensor ring structure is used to detect impurities such as Lead, DDT, Chlorine, PCB, Arsenic, Mercury, Fluoride, Aluminum. A comparison between two types of sensing structures is investigated for different water impurities. It is observed that the designed optical sensor is giving more amplitude variation for e. g 1.7 for lead impurities as compared to MZI based optical sensor with an output value of 0.4 and gives fast appropriate output. A sensitivity of 350 nm/RIU and Q factor of 3453 is obtained for the designed sensing sensor. The result has shown a feasible fabrication possibility in the future for sensing applications. Work carried having tremendous

Home 2 More ▾



Article Full-text available

Characterization of Hydroacoustic Optical Fibre Bragg Grating Pressure Sensor Using Different Materials

December 2020

DOI: [10.1016/j.rio.2020.100037](https://doi.org/10.1016/j.rio.2020.100037)

License · [CC BY-NC-ND 4.0](#)

Hareesh Kumar · M.N Sreerangaraju · Dr preeta Sharan

Research Interest ⓘ

Citations

Recommendations

Reads ⓘ

[See details](#)

1.7

0

0 new 0

7 new 47

Download Share ▾ More ▾

Overview Stats Comments Citations References (23) ⋮

Abstract and figures

The Exploration of the ocean with sound waves submarines, object tracking, bed deposits, and ocean communications requires a high sensitive hydroacoustic pressure sensor. Design of highly sensitive hydroacoustic challenges and needs of the present scenario. Proposed work involves the design and development of fiber Bragg grating hydroacoustic pressure sensors for underwater communication. Here side hole package is designed and analyzed in Ansys Multiphysics. Three different coating material is such as the layer of titanium, polyamide, and gold is coated on core fiber of fiber Bragg grating sensor and specific mechanical properties of the layer have been assigned. Centre wavelength and sensitivity of the designed FBG sensor is investigated by applying pressure in the range of 100 MPa to 900 MPa. From the results it is also observed that even for small pressure value sensitivity obtained was considerably high, thus satisfying the requirement of hydroacoustic pressure sensor to detect the low-pressure acoustic signals. The high sensitivity of 4590 nm/RIU obtained for the coating material of polyamide. The result obtained has shown feasibility for the fabrication of FBG for different applications such as underwater acoustic, ocean communication.



Indian Journal of Engineering and Materials Sciences (IJEMS)

[OP-HOME](#) [IJEMS-HOME](#) [ABOUT](#) [LOG IN](#) [REGISTER](#)
[SEARCH](#) [CURRENT](#) [ARCHIVES](#) [ANNOUNCEMENTS](#)
[NISCAIR](#) [NOPR](#)

14-Sep-2021
13:09:45 IST

[Journal Help](#)

Home > Vol 28, No 2 (2021) > **SSundaresan**

USER

Username

Password

Remember me

NOTIFICATIONS

- [View](#)
- [Subscribe / Unsubscribe](#)

JOURNAL
CONTENT

Search

All

Browse

- [By Issue](#)
- [By Author](#)
- [By Title](#)
- [Other Journals](#)

FONT SIZE

INFORMATION

- [For Readers](#)
- [For Authors](#)
- [For Librarians](#)

Computational analysis of core cavity Mach-Zehnder interferometer based optical sensor for various types of virus

SSundaresan, Vishalatchi Saravana; Ramrao, Nagaraj ; Sharan, Preeta ; Murugan, Kalpana

Abstract

In this effort, the demonstration has been done for designing the new optical sensor for the detection of various viruses. In this design, we have revealed about Photonic crystal based CCMZIs (Core Cavity Mach-Zehnder interferometers) structures namely CCMZI_1, CCMZI_2, CCMZI_3, and CCMZI_4. These structural designs are commonly referred here as CCMZI_X cavity sensors where X denotes the gradual decrement of scattering rods present in the cavity sensors. By selecting four types of viruses we are interested to detect these viruses in bio-sample using the device, CCMZI_X based sensor for light wave propagation. It has been found that, while removing the number of rods in the structure distinct transmission patterns are obtained. By the consideration of the sensitivity part, further simulation has been done by using the signature of the viruses. The analysis of virus existence is simulated in the FDTD tool. The optimization has been done to provide the higher amplitude spectrum with the range up to 0.8712 and the sensitivity can be calculated in the range of 200-250 μ m which are obtained by comparing the structures having corresponding analytes.

Keyword(s)

Photonic crystal, FDTD, Mach-Zehnder, virus analysis, Optical sensor, HIV

Full Text: [PDF](#) (downloaded 119 times)

Refbacs

There are currently no refbacs.

This abstract viewed **99** times



View PDF

[Download full issue](#)

Optik

Volume 244, October 2021, 167599

Original research article

Detection of oral cancerous cells using highly sensitive one-dimensional distributed Bragg's Reflector Fabry Perot Microcavity

Ranjith B. Gowda ^a , K. Saara ^a , Preeta Sharan ^b [Show more](#) [Outline](#) | [Share](#) [Cite](#) <https://doi.org/10.1016/j.ijleo.2021.167599>[Get rights and content](#)

Abstract

In the proposed work, a multi-layered Distributed Bragg's Reflector (DBR) Fabry Perot Microcavity resonator is proposed theoretically to sense bio-analyte. One dimensional Photonic-Crystal (PhC) sensor is designed and analysed to sense the presence of oral cancerous cells in the analyte. The Characteristic Matrix Method (CMM) is used to design, model and analyse the proposed sensor. A multi-layer structure with a central defect having 3 pairs of high and low refractive index layers on either side of the defect is analysed for its sensing performance. The incident light having wavelength in the range of mid-infrared frequency is used at input source, which enhances the sensor sensitivity. Five normal (INOK) cells and oral cancerous (YD-10B) cells are considered for the analysis of sensor performance. The effect of variation in the geometrical length of central defect layer and the number DBR layers on resonant wavelength, sensitivity, and Q factor is performed. A highest sensitivity of 3630 nm/RIU with a Q-factor of 11,323 and a very minimum resolution of 9.5×10^{-5} RIU is obtained. The sensor proposed in this work is suitable for label-free, easy fabrication, cost-effective, and highly sensitive sensor designs for biomedical applications.

[< Previous](#)[Next >](#)

Keywords

Photonic crystal; Distributed Bragg's Reflector; Fabry Perot Micro-cavity; Bio-sensor; Oral cancerous cells; Characteristic Matrix Method

1. Introduction

Cancer is one of the major diseases that cause more death across the world than coronary heart disease and other major diseases. It is expected to have more than 20 million cases by 2025, particularly in countries with low and middle income [1]. GLOBOCAN 2018 database contains the estimates of all cancer mortality rates for the year 2018 [2]. Global Cancer Observatory (GCO) of WHO updates, day to day and future possible mortality burden across the globe. Pathologists and medical practitioners are facing difficulty in the detection and identification of various cancer cells in their early stages. Cancer cells identification based on microscopic imaging methods varies from person to person based on their experience, detailed observation, and accurate predictions [3]. There exists various analytical and experimental studies, methods for the early detection of cancerous cells [4], [5], [6], [7]. Cancer cells detection in the early stage may save the life of a person by undergoing various tests & observations. There exist various techniques for the detection and identification of these malignant cells based on their biophysical properties [8], [9], [10] like chemical, bio-mechanical,

Real Time Email Alert For Visitor Monitoring System For Surveillance Applications

Sunitha L

Dept. of E&CE

The Oxford College of Engineering ,
Bangalore, Karnataka, India

sunirjbhairava@gmail.com

Dr. Harish H M

Dept. of E&CE

Government College of Engineering
Haveri, Karnataka, India

hmharish@gmail.com

Dr. Yedukondalu U

Dept. of E&CE

SVEC, Tadepalligudem
Andhra Pradesh, India

drykudara@gmail.com

Abstract

The design and implementation of the Visitor Monitoring and Email Alert System (VMES) for Surveillance Applications is the focus of this paper. This framework is primarily focused on achieving a cost-effective VMES in public locations such as railway stations, bus stations, government offices, schools, universities, and other similar locations, with the aim of improving current visitor tracking in log book registers through security personnel and information management practices. In a variety of commercial and non-commercial contexts, people are observed and visitors are welcomed. The number of people entering or leaving stores, the occupancy of office buildings, and the passenger count of commuter trains all provide valuable data to shop keepers and advertisers, police officers, and train operators. In particular, VMES eliminates the need for security personnel to manually record visitor details during visitor registration by using a log book register. The VMES allows for the retrieval of visitor information from the device, which is then used to verify their identification as they reach campus premises. According to this report, the percentage of improvement achieved by using VMES is 30 to 60% higher than that achieved by manual recording, while the percentage of improvement achieved by using VMES for a current visitor scheme is 80 to 90%. This study's additional analysis includes the use of email alert authentication methods such as images and video clips to replace the existing manual recording process with a faster reading speed, as well as a notification mechanism to notify the visitor's arrival to the visiting person.

Keywords: Raspberry Pi, Monitoring, Visitor, Pi Camera, Sensor

1. Introduction

Visitor Monitoring and email alert system, typically refer as a structure to keep tracking visitor's activities in organization or public building. It can provide necessary output and information to the users and record the incoming visitors within the shortest time and also keeps the count of the visitors. Nevertheless, VMES also capable to make more efficient way of monitoring process and provide an authentic and integrated data of the visitors. [1] Generally, there are many government buildings or public premises are still using the conventional paper log or guest book to record the access of the visitors. This manual method consumes longer time when the number of visitors is exceeded the limit. Meanwhile, an increasing number of visitors indicates that the security issues should be concern in the government buildings or public premises. [2] This is mainly because the operators are lack of time to verify the identification of each visitor when they are tons of guest entering the building. [3] Moreover, paper log is inadequate to offer greater

traceability in which cannot be archived or efficiently retrieved after several years. [4] Due to above circumstances, VMES contribute a good solution to solve the problems exist in the conventional method. To enter the building is an easy way and to identify and record the visitor's information. [5] This authentication system also helps the security officer to determine whether the visitors are giving the right to enter the building. [6] In this paper, an automated VMES is designed and developed to assure the simplification of process before entering the premises.

4. Literature Survey

4.1 A People Counting Technology

People counting are a widely studied and commercially exploited subject. This section briefly reviews the typical technologies used for people counting. *B Video Cameras* In the authors describe an approach to people counting (and localization) using multiple video cameras. The focus lies on extracting the size and moving patterns of individuals passing. By means of motion histograms based on frame-differenced images, the histograms classify detected movements. Probabilistic correlation is applied to determine a people count. The results of multiple cameras are joined in order to form a movement vector for each individual recognized. In contrast, proposes a solution based on a single ceiling-mounted camera, which identifies people by background extraction of the camera image. A non-background “blob” is recognized, and its size is estimated and compared to previously established bounds of people's pixel dimensions. A people count is derived from the results of this analysis. The system reaches a claimed accuracy of 98.5%. The major disadvantage of a camera-based system is that it requires an ambient light source and relatively powerful computer resources to perform image processing.

4.2 Ultrasonic Sensors

The authors of introduce a system employing ultrasonic sensors. Per each observed area a three-node sensor cluster is established, whereby each sensor node mounts an ultrasonic sensor. Multiple clusters are joined to cover a wider area. Nodes in each cluster communicate sensor readings by an RF link to the cluster's coordinator node. The latter contributes its own sensor measurements. By means of a distributed algorithm, nodes decide on whether to count a detected person. The sensor nodes require clock synchronization at the millisecond level in order to correlate the data exchanged. Despite the availability of clock synchronization protocols this imposes a disadvantage to this approach. The system achieves an overall counting accuracy of 90% using a probabilistic estimate of the total count, despite individual clusters achieving only around 50-70% accuracy.

4.3 Infrared Sensor

IR arrays combine a matrix of IR sensors to form array detectors. As the name suggests the sensor signals are provided as a matrix, where each element of the matrix corresponds to one IR sensor. Pattern recognition algorithms are able to detect people moving across the sensor's view at a claimed accuracy of 95%. This holds true even if two pedestrian's paths cross, or people walk in parallel. IR arrays provide a cost-effective solution and also operate without any ambient light source. IR arrays are widely used in commercial systems.

4.4 Infrared Motion Sensors

In people counting system based on PIR motion detectors, for each passage monitored, three PIR sensors are installed at a distance of 0.8m. The sensors are connected to a coordinator by a wireless RF link. Sensors detect motion events and send these data to the coordinator. The coordinator infers a people count from correlating the number, phase and time difference of peaks found in the signal. The system achieves a rate of 100% to detect the direction of movement, and accurately detects 89% of the number of people passing. PIR sensors provide an alternative to IR sensor arrays, however the cost and effort of employing multiple sensor nodes for each entry/exit point is a cost-side disadvantage. The goal of this thesis is to develop a system based on just one PIR sensor and one sensor node per each observed entry/exit point. Sensor Fusion Results of a building occupancy estimation system applying different types of sensors is found in [6]. The system consists of camera, CO₂ and PIR sensors. It uses a Hidden Markovian Model (HMM) based on an Extended Kalman Filter (EKF) in order to derive building occupancy. The approach integrates historical data and current sensor readings to estimate the true state of the system, adjusting for sensor noise (false observations) and stochastic processes, e.g. uncertain people movement patterns.

4.5 Open CV Simple Motion Detection

This project is a program use OpenCV to detect motion and save pictures. Publish by Cédric Verstraeten on website: www.cedricve.me on February 5th, 2013. This program introduction an algorithm use OpenCV to compare different between two images. The algorithm is supposed have 2 images, the images are a taken with some delay c between them. If we compare every pixel of the 2 images and they're all the same, we could say the 2 images are same. But if they don't, we could say there something happen during the delay time c . Maybe someone place an object in front of the camera or passing.

4.6 Motion Detection and Object Tracking in Image Sequences

Artificial intelligence is an important topic of the current computer science research. In order to be able to act intelligently a machine should be aware of its environment. The visual information is essential for humans. Therefore, among many different possible sensors, the cameras seem very important. Automatically analyzing images and image sequences is the area of research usually called 'computer vision'. This thesis is related to the broad subject of automatic extraction and analysis of useful information about the world from image sequences. The focus in this thesis is on a number of basic operations that are important for many computer vision tasks. These basic steps are analyzed and improvements are proposed.

4.7 Motion Detection and Object Tracking in Image Sequences

It had introduction algorithm of how to detect motion using image. The algorithm is a static camera observing a spot is a common case of a monitor system [12, 30, 8,23]. Detecting invade objects is a necessary step in analyzing the spot. A usually applicable hypothesis is that the images of the spot without the invade objects exhibit some regular behavior that can be well depict by a statistical model. If we have a statistical model of the spot, an invade object can be

detected by spotting the parts of the image that don't fit the model. This process is usually known as "background subtraction".

Usually a simple bottom-up way is applied and the spot model has a probability density function for each pixel divided. A pixel from a new image is considered to be a background pixel if its new value is well depicted by its density function. For example for a static spot the simplest model could be just an image of the spot without the invade objects. The next step would be, for example, to forecast appropriate values for the change of the pixel intensity levels from the image since the change can vary from pixel to pixel. However, pixel values often have complex layout and more elaborate models are needed. In this project, consider two popular models: the parametric Gaussian mixture and the non-parametric k nearest neighbors (k-NN) estimate. The spot could change from time to time (suddenly or slow illumination changes, static objects deleted etc.). The model should be frequently updated to incarnate the most current situation. The main problem for the background subtraction algorithms is how to automatically and efficiently update the model. This project analyzes the results from the literature and extracts some basic principles. Based on the extracted principles we recommend, analyze and compare two efficient algorithms for the two models: Gaussian mixture and k-NN estimate. The Gaussian mixture density function is a popular flexible probabilistic model. A Gaussian mixture having a fixed number of components is constantly updated using a set of heuristic equations. Based on the results from the previous chapter of this thesis and some additional approximations we propose a set of theoretically supported but still very simple equations for updating the parameters of the Gaussian mixture. The important improvement compared to the previous approaches is that at almost no additional cost also the number of components of the mixture is constantly adapted for each pixel. By choosing the number of components for each pixel in an on-line procedure, the algorithm can automatically fully adapt to the scene. We propose an efficient algorithm based on the more appropriate nonparametric k-NN based model. The both algorithms have similar parameters with a clear meaning and that are easy to set. This project also suggests some typical values for the parameters that work for most of the situations. Finally, we analyze and compare the two proposed algorithms.

5. Design Methodology

5.1 System Architecture

Before starting to develop and design the VMES, it is necessary to identify the system requirement for the items that used in this project. The system requirement of the VMES is the configuration, functional and data requirement as well as the quality constraint of the processor. The objective of system requirement is to ensure the VMES is running smoothly and efficiently so that it could make the monitoring process faster and easier.

In this paper, to count the number of people entering from the door, Raspberry Pi board has been used which is a SBC, on which we interfaced a Picamera. Picamera is used for capturing the images of the people. The Raspberry Pi board is connected to the monitor (Display) through HDMI port, for getting the results. The monitor shows the number of people captured by Picamera. The number of face detected is displayed on the counter. OpenCV is a library which is used for interfacing the camera to the board.

In this, a Pi camera is used to capture the images of visitors, when a sensor detects a movement of a persons. A DC motor is used as a gate. Whenever anyone wants to enter in the place then he/she needs to push the button. After pushing the button, Raspberry Pi sends command to Pi Camera to click the picture and save it. After it, the gate is opened for a while and then gets closed again. The buzzer is used to generate sound when sensor senses the movement of persons and LED is ON, and system is ready for operation.

Here the images of visitors are saved in Raspberry Pi with the name which itself contains the time and date of entry. Means there is no need to save date and time separately at some other place as we have assigned the time and date as the name of the captured image.

Requirements and specifications.

Components required

- Raspberry Pi
- Pi camera
- PIR Sensor
- 16x2 LCD
- DC Motor
- Buzzer
- LED
- Power supply

Description:

a Raspberry Pi Board :The Raspberry Pi Camera Board figure 1 is a custom designed add-on module for Raspberry Pi hardware. It attaches to Raspberry Pi hardware through a custom CSI interface. The sensor has 5 megapixel native resolutions in still capture mode. In video mode it supports capture resolutions up to 1080p at 30 frames per second. The camera module is light weight and small making it an ideal choice for mobile projects.

In this example figure 2 you will learn how to create a camera board object to connect to the Raspberry Pi Camera Board, capture images from the camera and process them in Python programming. Raspberry Pi Model B has 512Mb RAM, 2 USB ports and an Ethernet port. It has a Broadcom BCM2835 system on a chip which includes an ARM1176JZF-S 700 MHz processor, Video Core IV GPU, and an SD card. It has a fast 3D core accessed using the supplied OpenGL ES2.0 and OpenVG libraries. This board is the central module of the whole embedded image capturing and processing system as given in figure 3.1. Its main parts include: main processing chip, memory, power supply HDMI Out, Ethernet port, USB ports and abundant global interfaces.

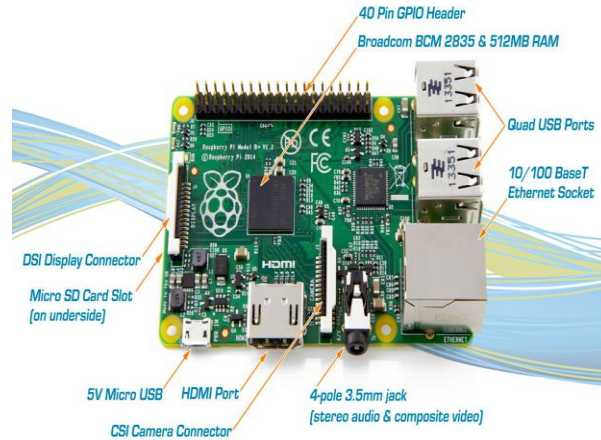


Figure 1: Raspberry Pi Module

The Raspberry Pi 2 delivers 6 times the processing capacity of previous models. This second generation Raspberry Pi has an upgraded Broadcom BCM2836 processor, which is a powerful ARM Cortex-A7 based quad-core processor that runs at 900MHz. The board also features an increase in memory capacity to 1Gbyte.

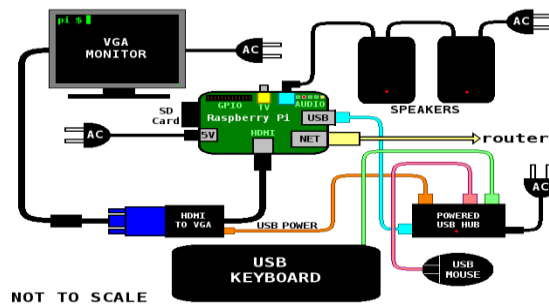


Figure 2: Circuit diagram of camera interfacing with Raspberry pi.

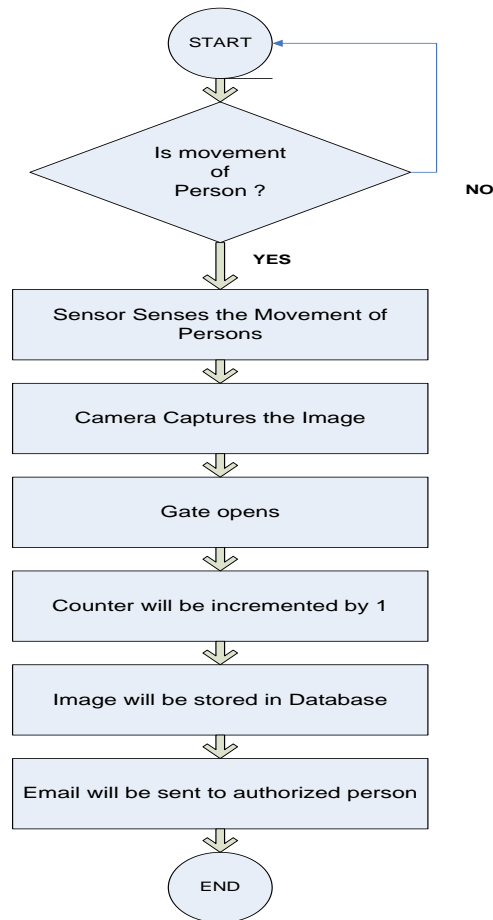


Figure 3: Flow Chart

6. Implementation Diagram

This time we are here with our next interesting part which is Visitors Monitoring System with Image capture functionality. Here we are interfacing Pi camera with Raspberry Pi to capture the image of every visitor which has entered through the Gate or door. In this paper, whenever any person is arrived at the Gate, PIR sensor sense the movement of the visitors, automatically opens the Gate, and at the same time, his/her image will be captured and saved in the system with the date and time of the entry. An Email alert will be sent to authorize person/s email ID which is registered with this system. This can be very useful for security and surveillance purpose which is presented in figure 4.

This system is very useful in offices or factories where visitor entry record is maintained for visitors and attendance record is maintained for employees. This Monitoring system will digitize and automate the whole visitor entries and attendances, and there will be no need to maintain them manually. This system automatically works for very visitor.

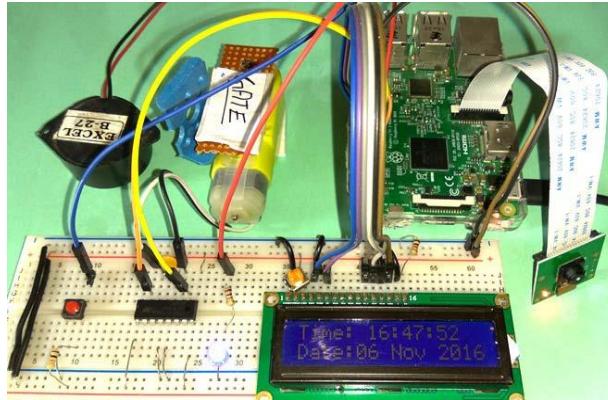


Figure 4: System Setup with Hardware

Working Explanation

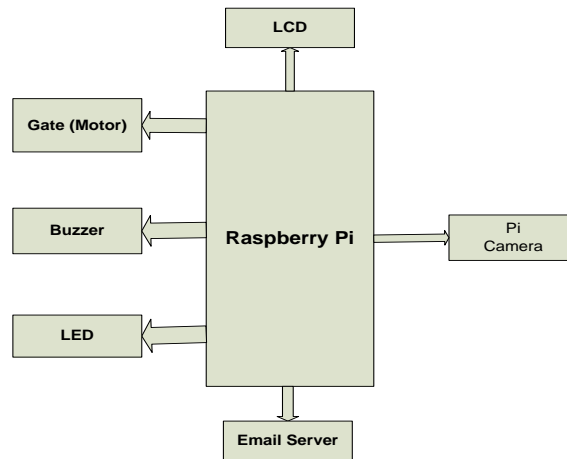


Figure 5: Block diagram of the proposed system

Here the pictures of visitors are saved in Raspberry Pi with the name which itself contains the time and date of entry. Means there is no need to save date and time separately at some other place as we have assigned the time and date as the name of the captured picture.

Circuit Explanation

Circuit of this Raspberry Pi Visitor monitoring System is very simple. Here a Liquid Crystal Display (LCD) is used for displaying Time/Date of visitor entry and some other messages. LCD is connected to Raspberry Pi in 4-bit mode. Pins of LCD namely RS, EN, D4, D5, D6, and D7 are connected to Raspberry Pi GPIO pin number 18, 23, 24, 16, 20 and 21. Pi camera module in figure 7 is connected at camera slot of the Raspberry Pi. A buzzer is connected to GPIO pin 26 of Raspberry Pi for indication purpose. LED is connected to GPIO pin 5 through a 1k resistor and a PIR sensor is connected to GPIO pin 19 with respect to ground, to trigger the camera and open the Gate. DC motor (as Gate) is connected with Raspberry Pi GPIO pin 17 and 27 through Motor Driver IC (L293D). Rest of connections is shown in circuit diagram.

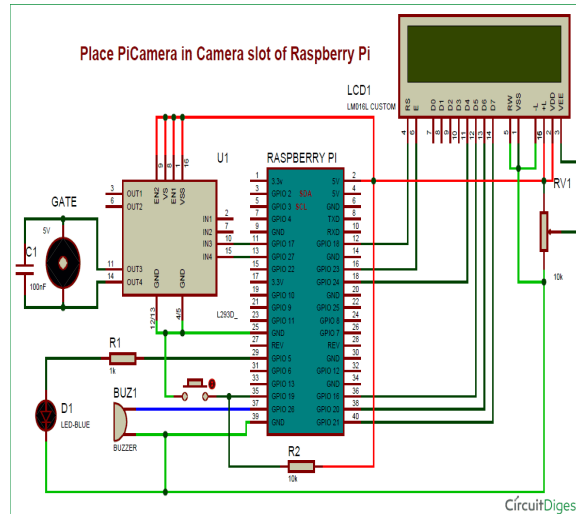


Figure 6: Circuit Connections

To connect the Pi Camera, insert the Ribbon cable of Pi Camera into camera slot, slightly pull up the tabs of the connector at RPi board and insert the Ribbon cable into the slot, then gently push down the tabs again to fix the ribbon cable.

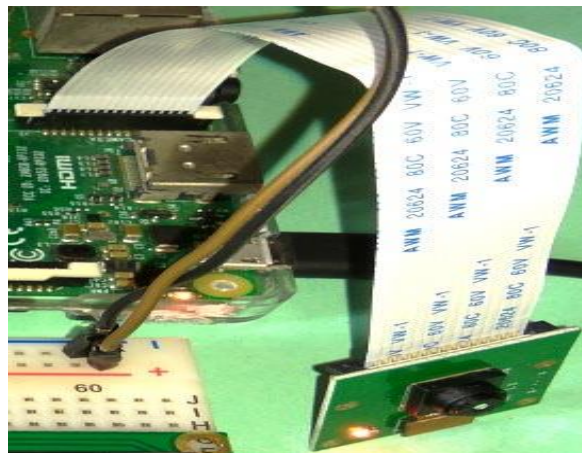


Figure 7: Pi Camera Module

7. Results

While designing PCB for relay circuitry, LED and relay were not working simultaneously. Relays are used as a switch, which is used to reset and give pulse for counter. So the LED was removed and circuitry containing relays, connectors, resistors, transistors, diodes was designed. Counter was added so that number of face detected could be visible in numbers. Regarding program some algorithms were added, for proper face detection

Work Flow in Snaps

Step 1

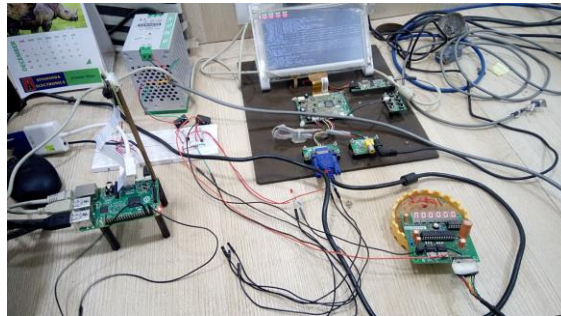


Figure 8: Initialization of Raspberry Pi and Counter

In this paper counter circuitry has been used for counting the images figure 8 detected by the Picamera and also shows the count of stored images.

The counter can count upto range 000000 to 999999.

Step 2 (Option 1: Capture image from camera and sending email)

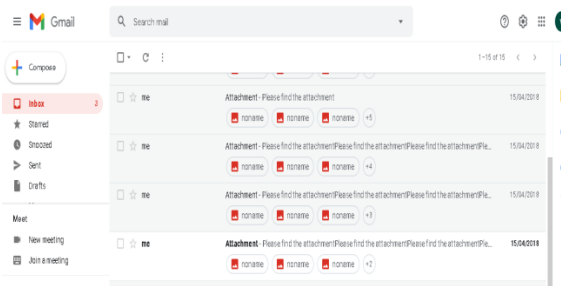


Figure 9: Capture and sending image through email to authorized persons

Conclusion

This current paper is focused with an objective of design and development a VMES that is affordable for the government buildings or public premises. The proposed VMES has a lower average cost than other current VMS on the market in this project. According to the findings of the study, the proposed VMES will reduce the time it takes to track visitors to government buildings or public places. Furthermore, since the VMES could produce an aggregate report immediately, it massively decreased the security officer's workload. In reality, despite being over budget for the project and approaching the submission deadline, there is more that can be improved. The lack of authentication tools to authenticate the visitor's identity in the VMES built in this project. This can allow a visitor with criminal intent to steal information from others to gain access to government buildings or public areas. As a result, a biometric fingerprint device may be used to improve the reliability of the visitor monitoring system. As soon as a guest approaches the entrance, an email message will be sent. Furthermore, facial recognition should be used on this guest tracking device because it has a higher degree of security than other biometric methods. To do this, a higher-quality camera could be used to capture more pixels of the visitor's face image. Moreover, the processing speed can be increased to speed up the

monitoring process. For a faster reading rate, the time it takes to retrieve information may be reduced from 30 seconds to less than a minute. Last but not least, this project has the potential to improve in a variety of areas since it can still be updated and modified to meet the needs of the users. As a result, it is clear that there are many ways to improve this project on a daily basis that are not limited to a single aspect.

References

- [1] K. Terada, D. Yoshida, S. Oe, and J. Yamaguchi, A method of counting the passing people by using the stereo images, International conference on image processing, 0-7803-5467-2, 1999
- [2] Haritaoglu and M. Flickner, Detection and tracking of shopping groups in stores, Proceedings of the 2001 IEEE Computer Society Conference on Computer Vision and Pattern Recognition , 0-7695- 1272-0,2001.
- [3] Gary Conrad and Richard Johnson baugh, A real-time people counter, Proceedings of the 1994 ACM symposium on Applied computing, 0-89791-647-6, 1994[ROS94] : M. Rossi and A. Bozzoli, Tracking and Counting Moving People, IEEE Proc. of Int. Conf. Image Processing, , 1994.
- [4]. Roy Ellwood. (2011). Build A Home Webserver
- [5]. Price, Peter.(2011). "Can a £15 computer solve the programming gap?". BBC Click.
- [6]. Moorhead, Joanna.(2012). "Raspberry Pi device will reboot computing in schools". The Guardian (London).
- [7]. Gary Bradski. (2008). Learning OpenCV: Computer Vision with the OpenCV Library. ISBN-13:978-059616130
- [8]. Daniel LellisBaggio. (2012). Mastering OpenCV with Practical Computer Vision Projects. ISBN-13: 978-184517829
- [9] Carlo Tomasi Takeo Kanad Detection and Tracking of Point Feature Technical Report CMU-CS-91-1350
- [10] Nicolai Petkov· Easwar Subramanian Motion detection, noise reduction, texture suppression, and contour enhancement by spatiotemporal Gabor filters with surround inhibition Publishedonline:25October2007
- [11]Motion_Detection_Programming_Guide_V1.1 GM8126
- [12] Price, Peter "Can a £15 computer solve the programming gap?". BBC Click. 2 July 2011.
- [13] "David Braben on Raspberry Pi". Edge. 25 November 2011. 8 December 2011.
- [14] Moorhead, Joanna "Raspberry Pi device will 'reboot computing in schools'". The Guardian (London). 20 January 2012.
- [15] "What is web server?". Web developers notes. 23 November 2013.
- [16] "Distributed Application Architecture". Sun Microsystem.16 July 200951.
- [17] "Interview with Eben Upton – Raspberry Pi Founder". International Business Times. 19 March 2012.
- [18] "Linux news showing the first release of Debian Squeeze for Raspberry running on QEMU". Linuxnewshare.com. 16 July 20012
- [19] "Raspberry Pi maker says code for ARM chip is now open source". ArsTechnica. 3 November 2012.
- [20] Shead, Sam. "Raspberry Pi delivery delays leave buyers hungry (and angry)". ZDNet. 18 October 2012.
- [21] Vallance, Chris. "Raspberry Pi bids for success with classroom coders". BBC News. 29 February 2012.
- [22] Steve Silva(2008). Web Server Administration.ISBN-13: 978-1423903239
- [23] Alan Winston(2002). OpenVMS with Apache, WASD, and OSU: The Nonstop Webserver (HP Technologies). ISBN-13: 978-1555582647

Home 15 More ▾




Chapter

Analysis and Design of an Optical Biosensor Using Mathematical Modeling

January 2021

DOI: [10.1007/978-981-15-6619-6_53](https://doi.org/10.1007/978-981-15-6619-6_53)

In book: Innovative Design, Analysis and Development Practices in Aerospace and Automotive Engineering

G. Sowmya Padukone · H. Uma Devi ·  Shivaputra Valsange · Meenakshi L. Rathod

Research Interest 

Citations

Recommendations

Reads 

[See details](#)

 0.3

0

0 new 0

1 new 7

Request full-text

Share ▾

More ▾

Overview

Stats

Comments

Citations

References (9)



Abstract

Photonics is a branch of science which deals with creation, perception, and arrangement of light in a suitable form. The waves are electromagnetic waves (EM waves) where electric and magnetic waves are perpendicular to each other. These sensors are used to detect diseases like cancer, forensic analysis, pattern, parental recognition, pattern recognition, etc. But, photonic biosensors are first designed so as to get the optical-designed simulation pattern using MEEP and opti-FDTD algorithms. The patterns are nothing but light wave patterns. These patterns are analogous to electromagnetic waves. These waves are linked mathematically by using different laws and equations. The study of mathematical model for generation of images and simulation is done mainly in this paper. Mathematical modeling of any sensor is an excellent approach to design and model it.

 Public Full-texts



Home (<https://www.annalsofrscb.ro/index.php/journal/index>)

/ Archives (<https://www.annalsofrscb.ro/index.php/journal/issue/archive>)

/ Vol. 25 No. 6 (2021) (<https://www.annalsofrscb.ro/index.php/journal/issue/view/30>)

/ Articles

Cascade H Bridge Multilevel Inverter with Pwm for Lower Thd, Emi & Rfi Reduction

PDF (<https://www.annalsofrscb.ro/index.php/journal/article/view/6013/4594>)

Jayakumar N, Dr.B. Devi Vighneshwari, Monalisa Mohanty, Subash Ranjan Kabat, Bibhu Prasad Ganthia, Nisha C Rani , L Vadivel Kannan

Abstract

Solar inverter has entered the market, where it is a combination of multilevel, a multi monitoring transformer, and with a solar charger. Although most are single-level inverters, others are multi ported. This is the primary benefit of multilevel inverters as opposed to single level ones: minimum harmonic distortion, lower EMI/RFI the Multilevel inverters can be set to run on any voltage between 115 and 230VAC. Sinusoidal and trapezoidal implementations of active control have different waveforms, which can be implemented with different multi-stage inverters. by adding PWM power, we can optimize the benefit of the inverters. The most straightforward way to simulate multivalent DC sources with modulations is to intersect the modulating signal with a triangular-shaped carrier waveform. in this article, we are creating a microcontroller based Solar Multivel Pulse Width Modulator utilizing cascade H bridge topology. We are also implementing MPT to enhance our overall performance. We will use the capacity of the full duration of the day to capture the greatest amount of sunshine during the day.

How to Cite

L Vadivel Kannan, J. N. D. D. V. M. M. S. R. K. B. P. G. N. C. R. , . (2021). Cascade H Bridge Multilevel Inverter with Pwm for Lower Thd, Emi & Rfi Reduction. *Annals of the Romanian Society for Cell Biology*, 25(6), 2972–2977. Retrieved from <https://www.annalsofrscb.ro/index.php/journal/article/view/6013>

More Citation Formats ▾

Issue

Fault Tolerant Discrete Control Technique for PV Fed Stepper Motor Drive

[PDF \(https://turcomat.org/index.php/turkbilmat/article/view/2982/2555\)](https://turcomat.org/index.php/turkbilmat/article/view/2982/2555)

DOI: <https://doi.org/10.17762/turcomat.v12i9.2982> (<https://doi.org/10.17762/turcomat.v12i9.2982>)

Viji K , et. al.

Abstract

This paper deals with the fault tolerant discrete control technique for the Photo Voltaic (PV) fed 3-phase stepper motor (SM). The operation of stepper motor is complex under high speed applications due to difficulty in locating the step-angle and there is a chance of missing the step-angle. A robust discrete sliding mode control (DSMC) algorithm is developed to overcome this problem along with the fault tolerant topology. The drive is powered by PV array and using perturb and observe (P&O) algorithm maximum power is retrieved from the source. The closed loop control of this drive is implemented using MATLAB/SIMULINK simulation software and the speed control of stepper motor is achieved by introducing stepped reference signal. The fault tolerance is verified by introducing open circuit (OC) and short circuit (SC) faults in the driver circuit and the speed response of the same is plotted. The robustness of the discrete controller is proved by introducing changes in the irradiance of PV array, changes in reference speed and faults in the driver circuit. The overall system is cheap, compact, robust and reliable under all test conditions and suitable for very low and very high speed applications.

Issue

[Vol. 12 No. 9 \(2021\) \(https://turcomat.org/index.php/turkbilmat/issue/view/43\)](https://turcomat.org/index.php/turkbilmat/issue/view/43)

Section

Articles

[Login \(https://turcomat.org/index.php/turkbilmat/login\)](https://turcomat.org/index.php/turkbilmat/login)

[Submit Articles \(https://turcomat.org/index.php/turkbilmat/about/sut\)](https://turcomat.org/index.php/turkbilmat/about/sut)

[Download Paper Template \(/download/paper_template.docx\)](/download/paper_template.docx)

[Home \(https://turcomat.org/index.php/turkbilmat\)](https://turcomat.org/index.php/turkbilmat)


[Aims and Scope \(https://turcomat.org/index.php/turkbilmat/aims_and_scope\)](https://turcomat.org/index.php/turkbilmat/aims_and_scope)

[Author Guidelines \(https://turcomat.org/index.php/turkbilmat/author_guidelines\)](https://turcomat.org/index.php/turkbilmat/author_guidelines)

[Ethical Principles and Publication Policy \(https://turcomat.org/index.php/turkbilmat/ethics_and_policies\)](https://turcomat.org/index.php/turkbilmat/ethics_and_policies)

Original Research | Published: 11 October 2020

Design and analysis of moems based displacement sensor for detection of muscle activity in human body

[Preeti Sharan](#) , [K. V. Sandhya](#), [Rakesh Barya](#), [Mohit Bansal](#) & [Anup M. Upadhyaya](#)

International Journal of Information Technology **13**, 397–402 (2021)

48 Accesses | [Metrics](#)

Abstract

Proposed work consist of simple and micro size optical MEMS based displacement sensor for detection of muscle movement in human body. Optical MEMS based structure, analyzed with rods-in air and hole-in slab configuration of photonic crystal. Remarkable shift in wavelength is observed in RIA configuration with high quality factor of 3245 compare to holes in slab in the photonic sensing structure with Q factor 1456. Optical sensitivity of device with rods in air configuration is 350 nm/RIU is obtained and from the result, the distinctly visible shift in wavelength is found to be optimum for fabrication of projected device. Proposed work is applicable for the muscle movement of human body during medical diagnosis and for daily life activities.

Performance analysis of optomechanical-based microcantilever sensor with various geometrical shapes

Anup M. Upadhyaya ✉ Maneesh C. Srivastava Preeta Sharan

First published: 22 September 2020

<https://doi.org/10.1002/mop.32652>

Abstract

This paper presents a performance analysis of different microcantilever shapes integrated with the optical MEMS system in different fluid mediums. Microcantilevers such as rectangular, trapezoidal, and triangle profile are coupled with optical sensing layers. Here, the concept of integration of optical sensing layer with different shapes of microcantilever is novel. The cantilever is designed and developed in CAD tools. Numerical analysis of different shapes of microcantilever was carried out with the help of Ansys Workbench. Optimal design of the regular microcantilever is considered during the analysis. The pressure is applied to the free end of the cantilever in the range of 100 to 250 kPa. The complete photonic sensing layer is analyzed with the help of a finite difference time domain (FDTD) tool called MIT Electromagnetic Equation Propagation (MEEP). The transmission spectrum is obtained for each microcantilever model. The pressure-induced refractive index is calculated for the equivalent maximum stress generated. The result shows that a remarkable Q factor was obtained for rectangular, trapezoidal, and triangular profile microcantilevers with an optical system. Triangular and rectangular profiles have shown remarkable contribution over quality factor for air mediums such as 10 120, 1300, respectively. High pressure sensitivity of 1.92 nm/kPa was obtained for rectangular microcantilever in air. Least sensitivity of 0.16 nm/kPa was obtained for triangle microcantilever in the water medium. The proposed work successfully distinguishes various shapes of microcantilever in terms of sensitivity and Q factor. It is having tremendous application in sensing biofluids and in device miniaturization.

Supporting Information



| Filename | Description |
|----------|-------------|
| | |



Download PDF

[Download full issue](#)

Surfaces and Interfaces

Volume 22, February 2021, 100810

Hot corrosion behavior of plasma-sprayed NiCrAlY/TiO₂ and NiCrAlY/Cr₂O₃/YSZ cermets coatings on alloy steel

MadhuSudana Reddy ^a, C Durga Prasad ^b , Pradeep Patil ^c, M.R. Ramesh ^d, Nageswara Rao ^e[Show more](#) [Outline](#) | [Share](#)  [Cite](#) <https://doi.org/10.1016/j.surfin.2020.100810>[Get rights and content](#)

Abstract

The objective of the Present research work is to evaluate the hot corrosion resistance of plasma-sprayed 70% NiCrAlY+ 30% TiO₂ and 70% NiCrAlY+ 25% Cr₂O₃+5% YSZ coatings on MDN 420 alloy. Hot corrosion tests are carried out under molten salt environment of Na₂SO₄+60 % V₂O₅ salt mixture at 700°C for 50 cycles. Each cycle consisting of 1 hour heating in a silicon carbide tubular furnace followed by 20 min of cooling. The thermogravimetric technique was used to determine the kinetics of corrosion. The scanning electron microscopy (SEM), energy dispersive analysis (EDAX), electron probe microanalyser (EPMA) and X-ray diffracton (XRD) techniques were used to evaluate the characterization of coatings with regard to coating bondstrength, thickness, microhardness and porosity. The parabolic rate constants of coated steels are lower when compared to the uncoated substrate. The NiCrAlY+ Cr₂O₃+YSZ coating is found to be more protective when compared to NiCrAlY+ TiO₂ coating. The oxides of Al₂O₃, NiCr₂O₄, and Cr₂O₃ are formed on the outermost layer of the coatings which gives the resistance the coatings to high-temperature corrosion.

[Previous](#)[Next](#)

Keywords

Plasma spray; NiCrAlY/TiO₂; NiCrAlY/Cr₂O₃/YSZ; Hot Corrosion; MDN-420 alloy

1. Introduction

Power stations are one of the significant or major sectors where severe problems are encountered, like erosion and corrosion [1]. During the operation of the gas turbines, the blades and vanes are subjected to greater mechanical and thermal load. In addition to these, they are exposed to high-temperature corrosion and erosion [2], [3], [4], [5]. The high strength alloys alone are sufficient only to meet high-temperature requirements but not sufficient to overcome the corrosion, oxidation, and wear problems. Hence coating gives the way of enlarging the curb of usage of the materials at the superior end of their standard capacity by permitting the substrate mechanical properties, which is to be conserved while guarding them beside the corrosion or erosion [6], [7], [8]. Different varieties of coatings are available, out of which, nickel-based coatings show excellent corrosion, oxidation & wear-resistant properties and are widely used or suitable for high-temperature environments [9], [10], [11]. Plasma spraying is one of creating novel techniques for prospering the coatings on the alloys and metals [12], [13], [14], [15]. It has been declared as one of the best coating technology, which is popular and successfully used all over in the industrial applications [16] with despicable cost in thermal, biomedical & electrical fields where the high-temperature corrosion and erosion variables are induced [17], [18], [19]. Present coatings used in gas turbines are thermal barrier coatings (TBC), which are bi-material coatings consisting of a thermally insulating ceramic topcoat, usually yttria or



Get Access

Materials Today: Proceedings

Available online 26 February 2021

In Press, Corrected Proof

Investigation & characterization of plasma sprayed cermet coatings on special steel alloy for gas turbine applications

Madhu Sudana Reddy ^a, Pradeep P. Patil ^b, M. Muniraju ^b, K. Gagan Shetty ^c, T. Nageswara Rao ^b

Show more

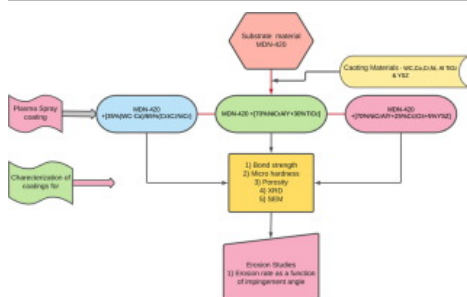
Outline | Share | Cite

<https://doi.org/10.1016/j.matpr.2021.02.092>[Get rights and content](#)

Abstract

The gas turbines are the components which are commonly affected by severe high-temperature erosion wear due to impingement of solid particles entrained in the stream of fluid. The present investigation focuses on the applicability of plasma sprayed coatings for turbines by improving the erosion resistance of the base material. The present work includes high-temperature solid particle erosion behaviour of [35%(WC-Co)/65%(Cr₃C₂NiCr), [70%NiCrAlY + 30%TiO₂] & [70%NiCrAlY + 25%Cr₂O₃ + 5%YSZ] coatings deposited by atmospheric plasma spray (APS) process. All the coating materials are considered by weight (%). The effect of impact angle on erosion performance of uncoated and coated specimens were comparatively studied by using the air-jet erosion tester (ASTM G76-13). The eroded surface morphology was analysed by using a porosity tests, microhardness values, scanning electron microscopy & X-ray diffraction analysis. All Coatings exhibits the ductile erosive mechanism at the temperature of 700 °C with severe plastic deformation. The NiCrAlY + TiO₂ coating is more protective than the other two coatings in high temperature and erosion environments due to its higher ductility, homogenous microstructure, and lesser porosity of the coatings. However, uncoated MDN 420 steel exhibits lesser wear loss when compared to the coated substrates. This may be due to the alumina particles' embedment onto the coated surface, which might present a shielding effect against further material loss to occur.

Graphical abstract

[Download : Download high-res image \(83KB\)](#)[Download : Download full-size image](#)

Keywords

Plasma spray coatings; Solid particle erosion; Special steel alloy; X-ray diffraction (XRD); Scanning electron microscope (SEM)

 [Get Access](#)

Oxford College of Engineering does not subscribe to this content.



Materials Today: Proceedings

Volume 42, Part 2, 2021, Pages 686-692

Estimation of mechanical parameters for orthodontic retraction loops using finite element analysis

Raviprakash M. ^a, Ananda G.K. ^b, Prasad H. Nayak ^a, Rahul D. ^a[Show more](#) [Outline](#) | [Share](#) [Cite](#)<https://doi.org/10.1016/j.matpr.2020.11.066>[Get rights and content](#)

Abstract

Forces and moments are the main parameters deciding the safety of many of the engineering as well as biomaterials. Since every material has certain yield or ultimate strength, it is always desirable to work in the safe limits to maintain the integrity of the systems. In the present analysis, five standard loops used in the orthodontic applications (T-Loop, Vertical Loop, Opus70, Mushroom and Helix) were analysed using finite element analysis for a fixed horizontal length of 14mm and a vertical height of 10mm. Analysis is carried out using 3D beam elements with an element size of 0.25 mm as the accuracy of finite elements are mainly based on element size. For all the analysis, the load deflection rate, vertical force generation and moment values are recorded with carried out in the nonlinear domain to capture the results better. The results shows that minimum force and moment development when the loop is positioned at centre. It is positioned near any bracket, maximum forces and moments are create near the activation bracket. Higher the elastic modulus, the wire is inducing higher moments and forces which are key to the stability of the orthodontic structure. Finite element analysis is effectively used to estimate the load deflection rate, force and moment generation based on different types of loops, positions and materials.

[Previous](#)[Next](#)

Keywords

Domain; Forces; Helix loop; Load deflection; Reaction forces; Reverse loop

[Special issue articles](#)[Recommended articles](#)[Citing articles \(0\)](#)

© 2020 Elsevier Ltd. All rights reserved. Selection and peer-review under responsibility of the scientific committee of the Second International Conference on Recent Advances in Materials and Manufacturing 2020.



About ScienceDirect

Remote access

[Get Access](#)

Materials Today: Proceedings

Volume 42, Part 2, 2021, Pages 660-670

Estimation of stress and deformation on steel coil holder fixtures using finite element analysis

Raviprakash M. ^a, Ananda G.K. ^b, Prasad H. Nayak ^a, Rahul D. ^a[Show more](#) [Outline](#) | [Share](#) [Cite](#)<https://doi.org/10.1016/j.matpr.2020.11.052>[Get rights and content](#)

Abstract

For engineering components, fixtures are essential elements for holding proper design and provide safety of the work-space. Any failure results are occurs in chain type hindrance of manufacturing process and system delivery causes delay in production time. In this present works, a steel coil holder has been selected for alignment of fixtures with coil capacity of 40tons. The components are shell slide, support channel, connecting plate, channel connector, pipe elements, and final assembly of top cylinder. Finite element analysis (FEA) was chosen to optimization of design factors and material of the plate SAILMA550 with allowable stress (250 MPa). A physical parameters are load-withstands and deformation of the plate were examined. Results show that optimization of initial stress has found 1443.5 MPa and final stress component falls to 253.85 MPa. The higher load deflection of initial design was obtained 4.8489 mm and lower deflection of the plate is reached to 4.5833 mm. However, the initial setting results shows heavy stress on the components (shell slide, support channel & pipe element) it leads more sufficient allowable stress performed on steel coil holder within their limits.

[Previous](#)[Next](#)

Keywords

Connecting plate; Deformation; Pipe element; Shell slide; Steel coil holder; Support channel

[Special issue articles](#)[Recommended articles](#)[Citing articles \(0\)](#)

© 2020 Elsevier Ltd. All rights reserved. Selection and peer-review under responsibility of the scientific committee of the Second International Conference on Recent Advances in Materials and Manufacturing 2020.

[About ScienceDirect](#)[Remote access](#)[Shopping cart](#)

RELX™

26 April 2021

Select Language ▼

[Translator Disclaimer](#)

Silicon nanostructure-based photonic MEMS sensor for biosensing application

[Anup M. Upadhyaya \(/profile/Anup.M-Upadhyaya-4326477\)](#), [Maneesh C. Srivastava](#), [Preeti Sharan \(/profile/Preeti.Sharan-8844\)](#), [Sandip Kumar Roy](#)

[Author Affiliations + \(\)](#)

J. of Nanophotonics, 15(2) ([/journals/journal-of-nanophotonics/volume-15/issue-2](#)), 026001 (2021).
<https://doi.org/10.1117/1.JNP.15.026001> (<https://doi.org/10.1117/1.JNP.15.026001>)

ARTICLE

FIGURES &
TABLES

REFERENCES

CITED BY

Abstract

We explored the design of an optical pressure sensor. The objective is to create a photonic microelectromechanical system-based cantilever sensor design to detect prostate-specific antigen, a protein biomarker associated with prostate cancer. Sensor's performance for the early detection of cancerous cells is dependent on sensitivity. The designed sensor consists of a hexagonal ring integrated with microcantilevers. Two types of microcantilever such as rectangular profile and V profile with integrated photonic sensing layer are investigated for sensitivity, quality factor, and resonant wavelength. The analysis shows that a geometrical modification of microcantilever has a significant effect on sensitivity enhancement. The finite difference time domain tool is used for designing photonic ring resonator patches. Numerical analysis of microcantilever is considered to investigate surface stress behavior. The cantilever deformation due to applied pressure resulted in a change in the index of refraction. Results show that the sensitivity of 55 nm / MPa for a triangular-shaped microcantilever obtained is higher compared to the rectangular-shaped microcantilever with a sensitivity of 0.19 nm / MPa. The designed structures have significantly higher sensitivities than the previously published sensitivity of 3.27 nm / MPa at wavelength 1550 nm. The maximum quality factor obtained for the rectangular shape is 2852 and 77,510 for the triangular shape. Triangular-shaped microcantilever can minimize winding inflexibility or stiffness. This capability of the triangular-shaped microcantilever enhances feasibility in making the final packaging and future fabrication.

© 2021 Society of Photo-Optical Instrumentation Engineers (SPIE) 1934-2608/2021/\$28.00 © 2021 SPIE

Citation [Download Citation ▼](#)

[Anup M. Upadhyaya \(/profile/Anup.M-Upadhyaya-4326477\)](#), [Maneesh C. Srivastava](#), [Preeti Sharan \(/profile/Preeti.Sharan-8844\)](#), and [Sandip Kumar Roy](#). "Silicon nanostructure-based photonic MEMS sensor for biosensing application," *Journal of Nanophotonics* 15(2), 026001 (26 April 2021).
<https://doi.org/10.1117/1.JNP.15.026001> (<https://doi.org/10.1117/1.JNP.15.026001>)

Received: 6 January 2021; Accepted: 31 March 2021; Published: 26 April 2021

JOURNAL ARTICLE
11 PAGES

DOWNLOAD PAPER

SAVE TO MY LIBRARY

SHARE

GET CITATION

[Subscribe to Digital Library \(/subscribe-page\)](#)

[Receive Erratum Email Alert \(\)](#)

ACCESS THE FULL ARTICLE

PERSONAL SIGN IN

Full access may be available with your subscription

Email or Username

[Forgot your username? \(https://spie.org/account/forgotusername?redir=https%3a%2f%2fwww.spiedigitallibrary.org%2fjournals%2fjournal-of-nanophotonics%2fvolume-15%2fissue-2%2f026001%2fSilicon-nanostructure-based-photonic-MEMS-sensor-for-biosensing-application%2f10.1117%2f1.JNP.15.026001.short%3fSSO%3d1\)](#)

PURCHASE THIS CONTENT

[INTERESTED IN A FREE CORPORATE TRIAL? \(/institutionaltrial\)](#)


SUBSCRIBE TO DIGITAL LIBRARY

50 downloads per 1-year subscription

Password

[Forgot your password?](https://spie.org/account/forgotpassword?redirect=https%3a%2f%2fwww.spiedigitallibrary.org%2fjournals%2fjournal-of-nanophotonics%2fvolume-15%2fissue-2%2f026001%2fSilicon-nanostructure-based-photonic-MEMS-sensor-for-biosensing-application%2f10.1117%2f1.JNP.15.026001.short%3fSSO%3d1) (<https://spie.org/account/forgotpassword?redirect=https%3a%2f%2fwww.spiedigitallibrary.org%2fjournals%2fjournal-of-nanophotonics%2fvolume-15%2fissue-2%2f026001%2fSilicon-nanostructure-based-photonic-MEMS-sensor-for-biosensing-application%2f10.1117%2f1.JNP.15.026001.short%3fSSO%3d1>)

 Show

Keep me signed in 

SIGN IN

Members: \$195
Non-members: \$335

ADD TO CART
(/shoppingcart?
fuseaction=cartadditem&productid=DLX&qty=50)

25 downloads per 1 - year subscription

Members: \$145
Non-members: \$250

ADD TO CART
(/shoppingcart?
fuseaction=cartadditem&productid=DLX&qty=25)

PURCHASE SINGLE ARTICLE

Includes PDF, HTML & Video, when available

Members: \$24.00
Non-members: \$28.00

ADD TO CART
(/shoppingcart?
urlId=10.1117%2f1.JNP.15.026001)

No SPIE account? [Create an account](https://spie.org/account/create/accountinfo)
(<https://spie.org/account/create/accountinfo>)

Institutional Access:

[Sign in with your institutional credentials](https://spie.org/account/institutionalsignin?redirect=https%3a%2f%2fwww.spiedigitallibrary.org%2fjournals%2fjournal-of-nanophotonics%2fvolume-15%2fissue-2%2f026001%2fSilicon-nanostructure-based-photonic-MEMS-sensor-for-biosensing-application%2f10.1117%2f1.JNP.15.026001.short%3fSSO%3d1)
(<https://spie.org/account/institutionalsignin?redirect=https%3a%2f%2fwww.spiedigitallibrary.org%2fjournals%2fjournal-of-nanophotonics%2fvolume-15%2fissue-2%2f026001%2fSilicon-nanostructure-based-photonic-MEMS-sensor-for-biosensing-application%2f10.1117%2f1.JNP.15.026001.short%3fSSO%3d1>)



Oxford College of Engineering does not subscribe to this content.



Materials Today: Proceedings

Available online 26 February 2021

In Press, Corrected Proof

Investigation & characterization of plasma sprayed cermet coatings on special steel alloy for gas turbine applications

Madhu Sudana Reddy ^a, Pradeep P. Patil ^b, M. Muniraju ^b, K. Gagan Shetty ^c, T. Nageswara Rao ^b

Show more

Outline | Share | Cite

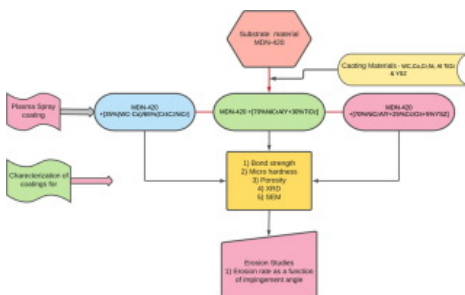
<https://doi.org/10.1016/j.matpr.2021.02.092>

Get rights and content

Abstract

The gas turbines are the components which are commonly affected by severe high-temperature erosion wear due to impingement of solid particles entrained in the stream of fluid. The present investigation focuses on the applicability of plasma sprayed coatings for turbines by improving the erosion resistance of the base material. The present work includes high-temperature solid particle erosion behaviour of [35%(WC-Co)/65%(Cr₃C₂NiCr), [70%NiCrAlY + 30%TiO₂] & [70%NiCrAlY + 25%Cr₂O₃ + 5%YSZ] coatings deposited by atmospheric plasma spray (APS) process. All the coating materials are considered by weight (%). The effect of impact angle on erosion performance of uncoated and coated specimens were comparatively studied by using the air-jet erosion tester (ASTM G76-13). The eroded surface morphology was analysed by using a porosity tests, microhardness values, scanning electron microscopy & X-ray diffraction analysis. All Coatings exhibits the ductile erosive mechanism at the temperature of 700 °C with severe plastic deformation. The NiCrAlY + TiO₂ coating is more protective than the other two coatings in high temperature and erosion environments due to its higher ductility, homogenous microstructure, and lesser porosity of the coatings. However, uncoated MDN 420 steel exhibits lesser wear loss when compared to the coated substrates. This may be due to the alumina particles' embedment onto the coated surface, which might present a shielding effect against further material loss to occur.

Graphical abstract



Download : Download high-res image (83KB)

Download : Download full-size image

Keywords

Plasma spray coatings; Solid particle erosion; Special steel alloy; X-ray diffraction (XRD); Scanning electron microscope (SEM)



View PDF

[Download full issue](#)

Surfaces and Interfaces
Volume 22, February 2021, 100810

Hot corrosion behavior of plasma-sprayed NiCrAlY/TiO₂ and NiCrAlY/Cr₂O₃/YSZ cermets coatings on alloy steel

MadhuSudana Reddy ^a, C Durga Prasad ^b, Pradeep Patil ^c, M.R. Ramesh ^d, Nageswara Rao ^e

[Show more](#)

Outline | Share Cite

<https://doi.org/10.1016/j.surfin.2020.100810>

[Get rights and content](#)

Abstract

The objective of the Present research work is to evaluate the hot corrosion resistance of plasma-sprayed 70% NiCrAlY+ 30% TiO₂ and 70% NiCrAlY+ 25% Cr₂O₃+5% YSZ coatings on MDN 420 alloy. Hot corrosion tests are carried out under molten salt environment of Na₂SO₄+60 % V₂O₅ salt mixture at 700°C for 50 cycles. Each cycle consisting of 1 hour heating in a silicon carbide tubular furnace followed by 20 min of cooling. The thermogravimetric technique was used to determine the kinetics of corrosion. The scanning electron microscopy (SEM), energy dispersive analysis (EDAX), electron probe microanalyser (EPMA) and X-ray diffracton (XRD) techniques were used to evaluate the characterization of coatings with regard to coating bondstrength, thickness, microhardness and porosity. The parabolic rate constants of coated steels are lower when compared to the uncoated substrate. The NiCrAlY+ Cr₂O₃+YSZ coating is found to be more protective when compared to NiCrAlY+ TiO₂ coating. The oxides of Al₂O₃, NiCr₂O₄, and Cr₂O₃ are formed on the outermost layer of the coatings which gives the resistance the coatings to high-temperature corrosion.

[Previous](#)

[Next](#)

Keywords

Plasma spray; NiCrAlY/TiO₂; NiCrAlY/Cr₂O₃/YSZ; Hot Corrosion; MDN-420 alloy

1. Introduction

Power stations are one of the significant or major sectors where severe problems are encountered, like erosion and corrosion [1]. During the operation of the gas turbines, the blades and vanes are subjected to greater mechanical and thermal load. In addition to these, they are exposed to high-temperature corrosion and erosion [2], [3], [4], [5]. The high strength alloys alone are sufficient only to meet high-temperature requirements but not sufficient to overcome the corrosion, oxidation, and wear problems. Hence coating gives the way of enlarging the curb of usage of the materials at the superior end of their standard capacity by permitting the substrate mechanical properties, which is to be conserved while guarding them beside the corrosion or erosion [6], [7], [8]. Different varieties of coatings are available, out of which, nickel-based coatings show excellent corrosion, oxidation & wear-resistant properties and are widely used or suitable for high-temperature environments [9], [10], [11]. Plasma spraying is one of creating novel techniques for prospering the coatings on the alloys and metals [12], [13], [14], [15]. It has been declared as one of the best coating technology, which is popular and successfully used all over in the industrial applications [16] with despicable cost in thermal, biomedical & electrical fields where the high-temperature corrosion and erosion variables are induced [17], [18], [19]. Present coatings used in gas turbines are thermal barrier coatings (TBC), which are bi-material coatings consisting of a thermally insulating ceramic topcoat, usually yttria or magnesia stabilized zirconia [16], which are deposited on top of a metallic bond coat. Due to the inherent brittleness of ceramics, failure of a thermal barrier system often occurs by debonding along the interface between the bond coating and its thermal grown protective oxide (TGO) layer. The failure of thermal barrier system can also occur by the result of decohesion of ceramic layer [15].

PalArch's Journal of Archaeology of Egypt / Egyptology

Microstructure and Wear Behavior of Al2218-B₄C Nano Composites

¹Vidyadhar Pujar, ²Srinivas H K, ³Sahadeva G N, ⁴Mamunuri Sailender, ⁵Madeva Nagara

¹Research Scholar, Department of Mechanical Engineering, Don Bosco Institute of Technology, Bangalore, Karnataka, India & Assistant Professor, Department of Mechanical Engineering, Oxford College of Engineering, Bangalore, Karnataka

²Professor, Department of Mechanical Engineering, SJBIT, Bangalore, Karnataka

³Professor, Department of Mechanical Engineering, EPCET, Bangalore, Karnataka

⁴Manager, ARDC, Hindustan Aeronautics Limited, Bangalore, Karnataka

⁵Deputy Manager, ARDC, Hindustan Aeronautics Limited, Bangalore, Karnataka

Email: v8123340411@gmail.com

Vidyadhar Pujar, Srinivas H K, Sahadeva G N, Mamunuri Sailender, Madeva Nagara: Microstructure and Wear Behavior of Al2218-B₄C Nano Composites -- Palarch's Journal Of Archaeology Of Egypt/Egyptology 17(9). ISSN 1567-214x

Keywords: Al2218 Alloy, Nano B₄C particles, Stir Casting, Microstructure, Wear, Worn Surface

ABSTRACT

The effect of nano B₄C particle addition on the wear behaviour of Al2218 alloy composites has been investigated. Al2218 combination with 2 to 8 wt. % of nano B₄C composites were manufactured by stir technique. Microstructural study was completed by utilizing SEM and EDS. A pin-on-disc machine was used to evaluate the wear loss of examples, in which a set EN32 steel plate was used as the counter face. Wear tests were went with on Al2218 compound with nano B₄C particles strengthened composites at different loads of 9.8 N, 19.6 N, 29.4 N and 39.2 N with steady sliding rate of 2.8 m/sec and 2000 m sliding separation. Also, Wear tests were went with on Al2218 amalgam with nano B₄C particles strengthened composites at different paces of 1.4 m/sec, 1.8 m/sec, 2.3 m/sec and 2.8 m/sec with consistent load of 39.2 N and 2000 m sliding separation. The wear opposition of Al2218 compound improved with the gathering of B₄C particulates. Further, worn surface morphology and wear debris of prepared composites were studied to know the different wear phenomena.

1. Introduction

The normal name being composite material or basically a composite is mix of at least two materials with non-indistinguishable physical or substance properties, when intermixed delivers completely extraordinary item with unique attributes when contrasted and the individual material trademark. The mixing of the material is normally done at a perceptible level. These materials

are intermixed in such a proportion that its specific properties get improved. The proportions of two materials are advanced dependent on their applications. The subsequent composite material has an equilibrium of its properties that is greatly improved to any of the constituent materials [1, 2]. These composites are utilized for their extemporized mechanical properties, yet in addition for warm, electrical and ecological applications. These materials are commonly favoured for various applications like cements, strengthened plastics, for example, fiber fortified polymers, metal composites, clay composites. Artistic lattice composites and metal grid composites are commonly utilized for structures, extensions and structures, for example, boat shelter, pool boards, race vehicle bodies, baths, stockpiling tanks and likewise progressed materials in shuttle's and airplanes building which are sought after [3, 4].

The metal matrix composite (MMC) is the one in which metals are matrix phase & the reinforcing phase may be a metal other than base metal/matrix metal or another material like organic compound or a ceramic. The reinforcing material may be in the form of particles or whiskers or fibers and the properties of the MMC's can be varied with variation of size of reinforcing material [5]. Though MMC's are not widely used as the PMC's, but the properties like stiffness, high strength & fracture toughness are creating the trend towards MMC's. The MMC's can withstand high temperature, corrosive environment better than that of the composites made of PMC's. Most metals and alloys can be used as matrices which require reinforcement materials that are to be stable at high temperatures and are to be non-reactive too. It has to be kept in mind that if MMC's have to offer good strength then the reinforcing material used should have high modulus & high tensile strength.

In the current work an exertion has been made to know the impact of nano B₄C support expansion on the wear conduct of Al2218 aluminum composite. Al2218 composite with 2 to 8 wt. % of nano composites were created. Further, these readied tests were assessed for dry sliding wear conduct at different loads and sliding rates according to ASTM G99 norms.

2. Experimental Details

Materials

In the present study Al2218 is used as the matrix material, most of the applications in areas such as aerospace, automobile, marine make use of 2xxx series, aluminium-copper alloys. Al2218 normally has 4.5% of copper and 1.8% of magnesium. The theoretical density of Al2218 alloy is taken as 2.80 g/cm³.

Table 1: Chemical composition of Al2218 Alloy

| Element | Si | Cu | Mg | Mn | Fe | Zn | Ni | Al |
|---------|------|-----|-----|------|-----|------|-----|---------|
| Wt. (%) | 0.90 | 4.5 | 1.8 | 0.20 | 1.0 | 0.25 | 1.5 | Balance |

In the present work, nano B₄C particulates are used as the fortification materials, 500 nm particulates were used, which were obtained from Reinste

Nano Ventures Ltd., Delhi. The density of B₄C is smaller than the matrix material, which is 2.52 g/cm³.

Methodology

The manufacture of Al2218-B₄C composites were completed by liquid metallurgy through stir cast method. Determined measure of the Al2218 compound ingots were kept into the heater for liquefying. The melting temperature of aluminum composite is 660°C. The Al2218 alloy melt was superheated to 750°C temperature. The temperature of the melt was recorded utilizing a chrome-alumel thermocouple. The molten metal is then degassed utilizing solid hexachloroethane (C₂Cl₆) for 3 min [6]. A hardened steel impeller covered with zirconium is utilized to mix the liquid metal to make a vortex. The stirrer will be turned at a speed of 300rpm and the profundity of drenching of the impeller was 60 percent of the height of the liquid metal from the outside of the liquefy. Further, the B₄C particulates were preheated in a heater upto 400°C will be brought into the vortex. Stirring was proceeded until interface connections between the fortification particulates and the Al matrix advances wetting. At that point, Al2218-2 wt. % nano B₄C melt was poured into the cast iron mold having measurements of 120mm length and 15mm width. Additionally, composites were set up for 4, 6 and 8 weight level of nano B₄C particles in the similar method.

Evaluation of Properties

The castings in this way got were sliced to a size of 15 mm diameter across and 5 mm thickness which is then exposed to various dimensions of cleaning to get required example piece for microstructure studies. At first, the cut examples were cleaned with emery paper up to 1000grit size pursued by cleaning with Al₂O₃ suspension on a cleaning disc utilizing velvet material. The cleaned surface of the examples etched with Keller's reagent lastly exposed to microstructure in an electron microscope.

The wear conduct of Al2218 compound and B₄C fortified composites were done by utilizing wear machine. The preliminaries were gone with according to ASTM G-99 wear testing standard [7] on 8 mm in measurement and 30 mm length roundabout example. The wear misfortune was determined in the wake of leading the dry sliding wear tests at 9.8 N to 39.2 N differing loads at 2.826 m/sec sliding velocity for 2000 m sliding separation in 90 mm distance across wear track. Likewise, one more arrangement of dry sliding wear conduct of Al2218 combination composites were dissected at different sliding velocities of 1.4 m/sec to 2.826 m/sec at 39.2 N load and 2000 m sliding separation. The wear misfortune was noted regarding stature misfortune and introduced in the work.

At the time of conducting wear tests utilizing wear machine, wear trash were gathered and these debris were read for the different wear instruments utilizing SEM micrographs. Further, worn surface morphology likewise done utilizing examining electron micrographs to know the different wear conduct associated

with the Al2218 amalgam and Al2218 composite with 2 to 8 wt. % of nano B₄C composites.

3. Results And Discussion

Microstructural Study

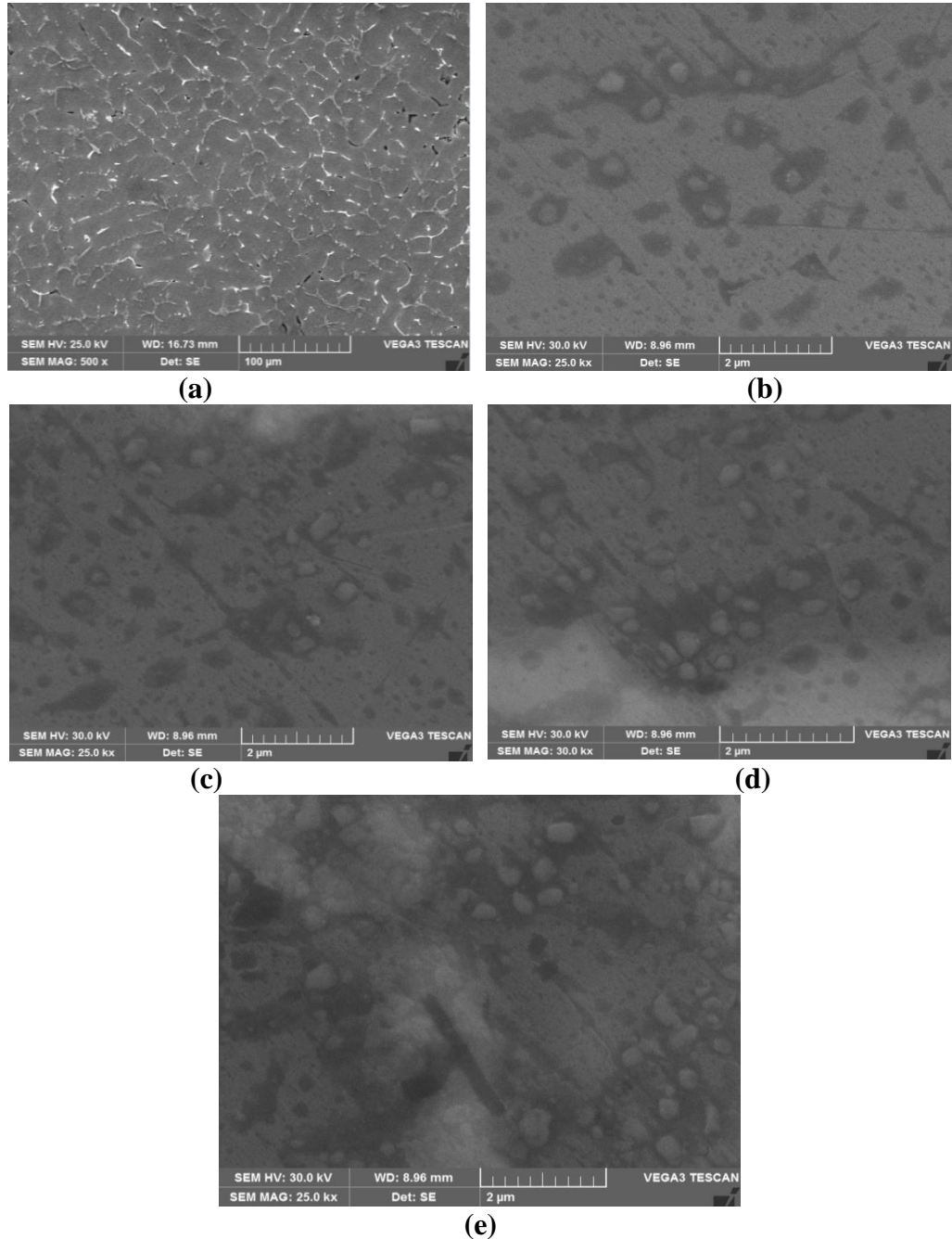
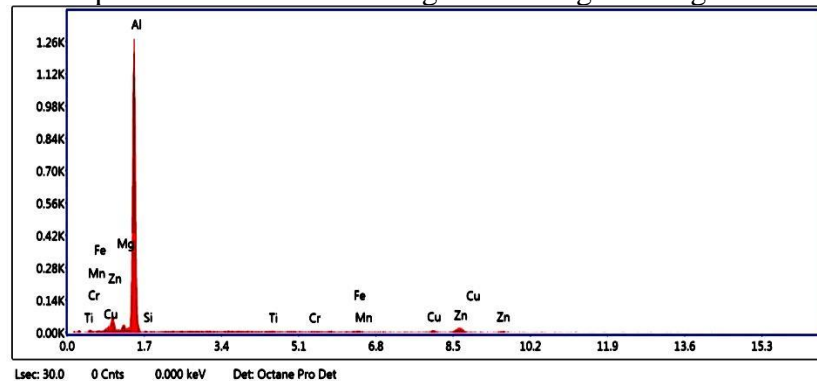


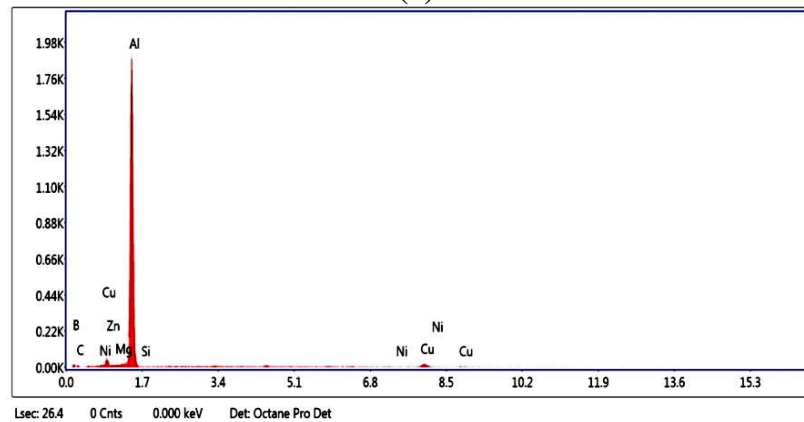
Figure 2: SEM of (a) as cast Al2218 alloy (b) Al2218-2 wt. % B₄C (c) Al2218-4 wt. % B₄C (d) Al2218-6 wt. % B₄C and (e) Al2218-8 wt. % B₄C composites

Figure 1a-e shows the SEM micrographs of as cast alloy Al2218 and the composites of 2 to 8 wt. % of nano B₄C reinforced with Al2218 alloy composites. The microstructure of as cast Al2218 alloy comprises of fine grains of aluminium solid solution with an enough dispersion of inter-metallic precipitates.

It also exhibits the incredible bonding between the matrix system and the nano particles so uniform homogenous dissemination of nano evaluated B₄C particulates with no agglomeration and clustering in the composites. This is basically a direct result of the suitable mixing action achieved all through the extension of the fortress by two stages. The nano particles wherever all through the grain furthest reaches of the cross section hinder the grain improvement and contradict the partition advancement of grains during stacking.



(a)



(b)

Figure 2: EDS images of (a) as cast Al2218 alloy (b) Al2218-8 wt. % B₄C composites

Figure 2 (a-b) represents the EDS spectrum of as cast Al2218 alloy and Al2218 alloy with 8 wt. % of nano B₄C reinforced composites. As cast Al2218 alloy EDS spectrum is showing the major elements like Al, Cu, Si, Mg, Mn and Fe in the Al2218 alloy matrix. Further, Al2218 with 8 wt. % of B₄C composites EDS spectrum is indicating boron (B) and carbon (C) elements in the prepared composites and confirms the presence of B₄C reinforcement in the Al2218 alloy composites.

Wear Properties

The wear misfortune was determined in the wake of directing the dry sliding wear tests at 9.8 N to 39.2 N differing loads at 2.826 m/sec sliding pace for 2000 m sliding distance in 90 mm width wear track. Likewise, one more arrangement of dry sliding wear conduct of Al2218 combination composites were investigated at different sliding paces of 1.4 m/sec to 2.826 m/sec at 39.2 N load and 2000 m sliding separation. The wear misfortune was noted regarding height loss and introduced in the work.

Effect of Load on Wear Rate

Fig. 3 is indicating the correlation of wear conduct Al2218 amalgam and Al2218 composite with 2 to 8 wt. % of nano B₄C composites at different loads of 9.8 N to 39.2 N fluctuating loads at 2.826 m/sec sliding rate for 2000 m sliding separation in 90 mm wear track. From the diagram it is obvious that as the load increment from 9.8 N to 39.2 N, there is an increment in wear misfortune in Al2218 combination and Al2218-B₄C particles fortified composites. The load influenced the wear conduct of both as cast and B₄C strengthened examples. The expanded wear misfortune as load increments from 9.8 N to 39.2 N is chiefly because of the improved contact territory between the example and the steel plate. This expanded region of contact during wear test creates more warmth, which causes the delamination in the compound and composites [8].

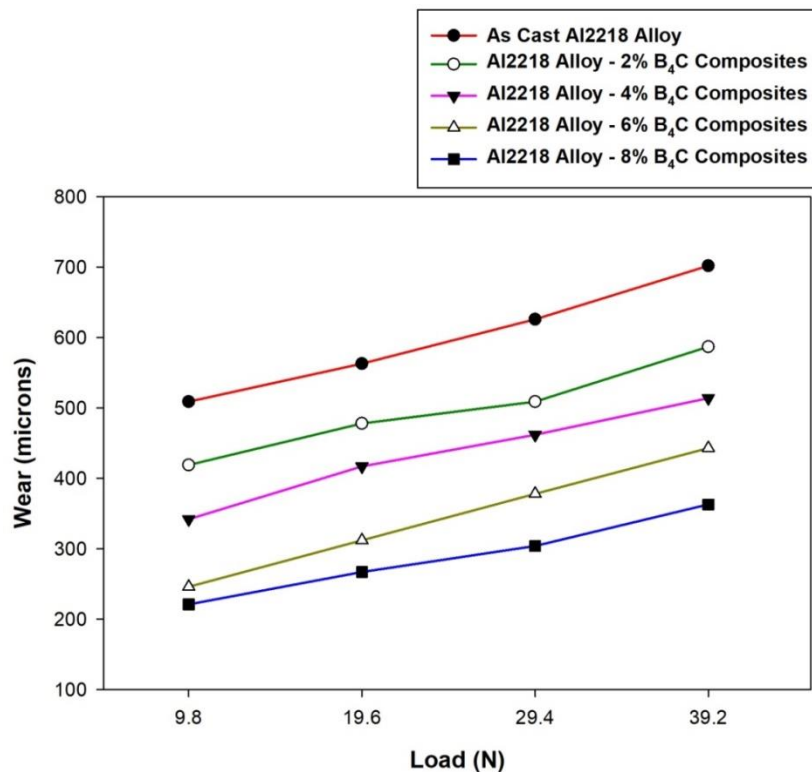


Figure 3 Wear loss of Al2218 alloy with nano B₄C reinforced composites at varying loads and constant velocity

Effect of Sliding Speed on Wear Rate

Fig. 4 shows the wear misfortune with the variety of speed for a several samples with varying content of B₄C. The test is directed with differing speed of 1.4 m/sec, 1.8 m/sec, 2.3 m/sec and 2.8 m/sec by holding load of 39.2 N. From the Fig. 4, it is presumed that wear misfortune increments with the speeding up. For base Al2218 amalgam the impact of sliding velocity is more when contrasted with B₄C fortified nano composites.

From the graph 4 as the speed increases from 1.4 m/sec to 2.8 m/sec, there is an increase in wear of Al2218 alloy and Al2218 alloy with 2 to 8 wt. % of nano B₄C reinforced composites. Further, from the plot it is evident that the nano B₄C particles reinforced composites shown more wear resistance as compared to Al2218 alloy. The addition of nano B₄C particles improves the hardness of Al2218 alloy with strong bonding between the matrix and reinforcement. This enhanced bonding helps in improving wear resistance of Al2218 alloy by acting these particles as barrier for the deformation during wear process [9].

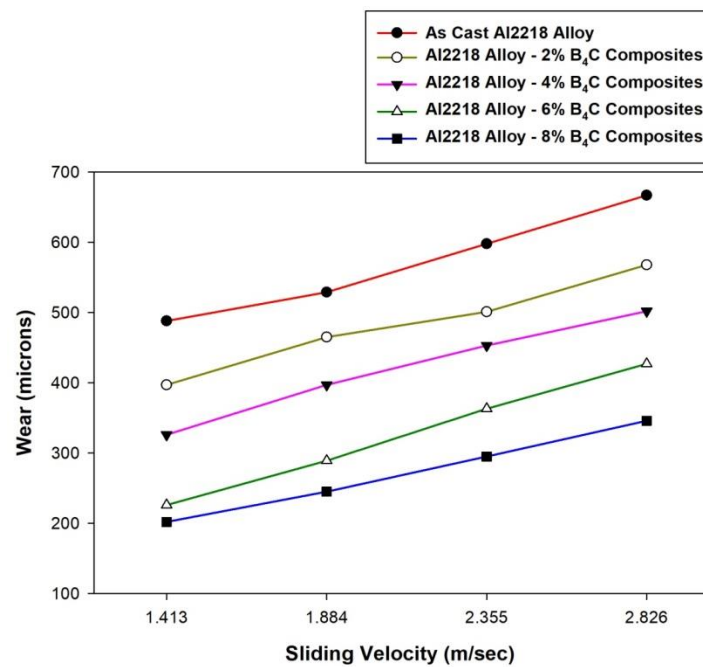


Figure 4 Wear loss of Al2218 alloy with nano B₄C reinforced composites at varying speeds and constant load

Worn Surface morphology and Wear Debris

It's significant to study the worn-out surface morphology of Al2218 alloy and its nano composites as it shows the type of wear the materials with different composition have undergone. During sliding the Al2218 matrix is softer than the rubbing disk material and hence shows viscous flow in Al2218 matrix, which is in the form of pin causing plastic deformation of the specimen surface, resulting in very high material loss. The worn surface of Al2218 alloy shows presence of grooves, micro-pits and fractured oxide layer as shown in Fig. 5 (a), which would have caused the increase of wear loss. Whereas 8 wt. %

of B₄C particles in Al2218 alloy composites restrict the viscous flow of the matrix as shown in Fig .5 (b), it is observed that the grooves or erosion have reduced with increase in B₄C particles means there is more and more resistance to wear loss [10]. Meanwhile, the stress seems to be transferred on B₄C particles and strain concentration occurs around these B₄C particles and worn surface area shows less and less cracks and grooves with increasing B₄C particles.

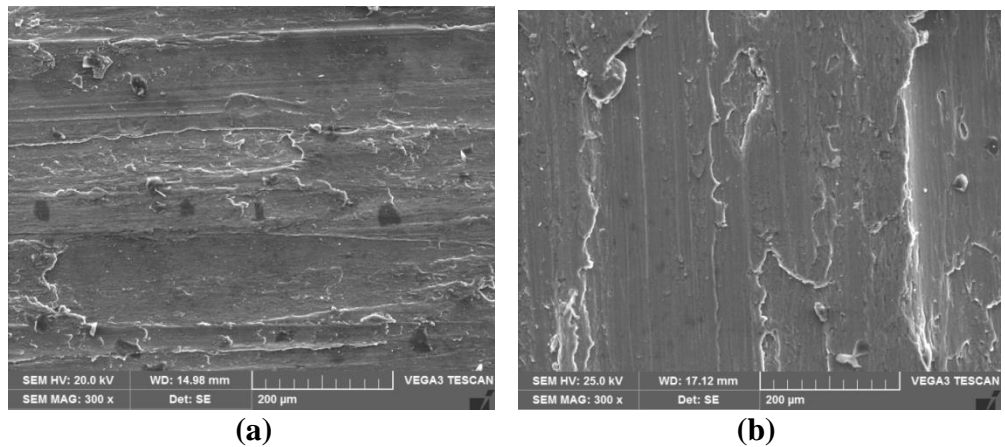


Figure 5 Worn surfaces SEM micrographs of (a) Al2218 Alloy (b) Al2218 – 8 wt. % B₄C composites

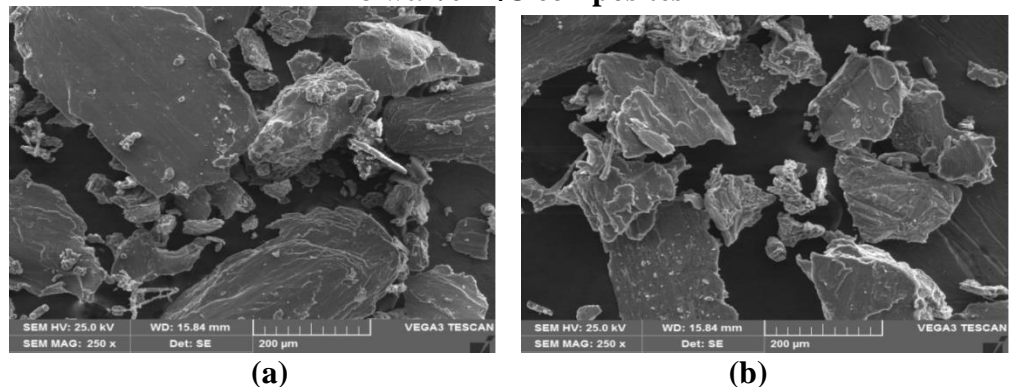


Figure 6 Wear debris SEM micrographs of (a) Al2218 Alloy (b) Al2218 – 8 wt. % B₄C composites

The byproducts obtained in the form of particles after wear test are called wear debris. During the course of rubbing action always the softer material wears out. In wear debris analysis the worn-out particles are observed in SEM to understand type of wear the material has undergone. The various images obtained from SEM are shown in above Fig. 6 (a-b).

Fig. 6 (a) shows image of debris resulted from wear of Al2218 aluminium alloy. The size of the debris due to wear mechanism shows the extent of wear, Al2218 alloy has under gone. The long layers formed from wear surface were not able to withstand the high load and hence the layers were pulled and thrown away in the form of thin plate, these thin long mechanical layers resulted due to the ductility of test sample. Fig. 6 (b) shows wear debris of

Al2218-8 wt. % of B₄C composites, the debris can be seen in the form of fragments which are crushed between test piece & rotating disc. The wear debris of B₄C based composites exhibits less wear with small particles like fragments pulled out from the pin.

4. Conclusions

Al2218 alloy with nano B₄C composites have been manufactured by stir casting technique by taking 2 to 8 wt. % of B₄C particles. The microstructure and wear practices of Al2218 compound nano composites were analyzed. SEM microphotographs uncovered the even circulation of B₄C particles in the Al2218 compound. Further, nano support particles were eminent by the EDS examination. The impact of load and the sliding velocity was seen on the Al2218 amalgam and its B₄C particles fortified composites. As the load and speed improved, there was enhanced wear loss of Al2218 amalgam and nano composites. The improved wear opposition was seen on account of Al2218 amalgam with 8 wt. % of nano B₄C composites.

References

- Mohammed Imran, A. R. Anwar Khan, JMRT, 8 (3), 2019, pp. 3347-3356.
R. Devanathan, J. Ravikumar, Materials Today Proceedings, 22, 2020, pp. 3136-3144.
V. Bharath, V. Auradi, Madeva Nagaral, Satish Babu Bopanna, JurnalTribologi, 25, 2020, pp. 29-44.
Nosaidusuyi, John I. Olayinka, JMRT, 8 (3), 2019, pp. 3338-3346.
V. Bharath, V. Auradi, Madeva Nagaral, Satish Babu Bopanna, Journal of Bio and Tribo Corrosion, 6, 45, 2020.
Madeva Nagaral, V Auradi, SAKori, Vijayakumar Hiremath, JMES, 13, 1, 2019, pp. 4623-4635.
Zhang Mei Juan, Transactions of Nonferrous Metals Society of China, 20, 2010, pp. 471-475.
C. S. Ramesh, R. Keshavmurthy, B. H. Channabasappa, S. Pramod, Materials and Design, 30, 2009, pp. 3713-3722.
Madeva Nagaral, Applied Mechanics and Materials, Vol. 592-594, 2014, pp.170-174.
C. Mallikarjuna, Materials and Design, 32, 2011, pp. 3554-3559.

Mechanical Behavior and Fractography of Al2218-Nano B₄C Metal Composites

Vidyadhar Pujar, Srinivas H K, Madeva Nagaral, V Auradi

Abstract : In the present examination, the mechanical properties of Al2218-nano B₄C composites displayed. The composites containing 4 to 8 wt. % of nano boron carbide in ventures of 4 wt.% were readied utilizing liquid metallurgy method through stir casting. For every composite, fortification particles were preheated to a temperature of 400°C and afterward added in ventures of two into the vortex of liquid Al2218 compound to improve the wettability and dispersion. Microstructural examination was carried out by SEM and elemental investigation was finished by EDS. XRD Analysis used to recognize the B₄C phases in the Al grid. Density, tensile, compression and hardness tests were done to distinguish various properties of composites. The aftereffects of this investigation uncovered that as the weight % level of nano B₄C particles were expanded, there was noteworthy increment in hardness, UTS, yield and compression strength of Al2218 amalgam composites. Further, there was slight drop in the density and malleability of the Al2218 amalgam composites when contrasted with the base. Tensile fractured surfaces analysis was conducted by using SEM.

Keywords: Al2218 Alloy, Nano B₄C particles, Stir Casting, Microstructure, Mechanical Behaviour, Fractography

I. INTRODUCTION

Aluminum compound nano-composites are valuable in the aviation, car, marine, and auxiliary applications. The nano-composites have superior properties by using diverse ceramic powders, for example, boron carbide, zirconia, aluminum oxide and silicon carbide are added to the lightweight aluminum composite to improve the mechanical properties. Aluminum matrix composites (AMCs) are broadly utilized in aerospace, autos, and marine field because of the great quality, light weight and ease. Mechanical and wear conduct can be seen in brakes, gears, valves, cams, cylinder liners, grasps and different applications including sliding contact or moving contact [1]. AMCs are one of the propelled building materials that have been created for weight basic applications in the aviation, and more as of late in the automotive enterprises because of their astounding properties of high specific quality and better wear obstruction [2]

Hard earthenware particulates, for example, zirconia, alumina (Al₂O₃) and silicon carbide (SiC) [3], have been brought into aluminum-based framework to build the quality,

Revised Manuscript Received on April 25, 2020.

* Correspondence Author

Vidyadhar Pujar*, Research Scholar, Don Bosco Institute of Technology, Bangalore and Assistant Professor, Dept., of Mechanical Engineering, The Oxford College of Engineering, Bangalore, India. Email: prasadnayak990@gmail.com

Srinivas H K, Professor, Department of Mechanical Engineering, SJBIT Bangalore, India. Email: khsri2006@gmail.com

Madeva Nagaral, Deputy Manager, Aircraft Research and Design Centre, HAL, Bangalore, India. Email: madev.nagaral@gmail.com

V. Auradi, Associate Professor, Department of Mechanical Engineering, Siddaganga Institute of Technology, Tumkur, India. Email: vsauradi@gmail.com

stiffness, wear opposition, erosion obstruction, weariness obstruction and high temperature resistance. Among these fortifications, B₄C is artificially perfect with aluminum (Al) and structures an enough bond with the grid [4]. Wear rate of aluminum lattice composites fortified with B₄C and SiC particles created through a similar course (weight less infiltration strategy) were dissected; the wear rate and contact coefficient of Al– B₄C was observed to be lower than those of Al– SiC under similar conditions.

The point of the present examination is to assess the microstructure and mechanical conduct of Al2218 compound strengthened with nano B₄C particles. The stir technique is picked for the processing of AMCs. The impact of nano B₄C expansion on the hardness, tensile and compression strength of composite is researched. The microstructures of the example are considered utilizing SEM for the particle circulation and fractography examination.

II. EXPERIMENTAL STUDY

A. Materials

In the present study Al2218 is used as the matrix material, most of the applications in areas such as aerospace, automobile, marine make use of 2xxx series, aluminium-copper alloys. Al2218 normally has 4.5% of copper and 1.8% of magnesium. The theoretical density of Al2218 alloy is taken as 2.80 g/cm³.

Table1-I: The chemical composition of Cu-Zn alloy

| Elements | Content wt. % |
|----------|---------------|
| Si | 0.90 |
| Cu | 4.50 |
| Mg | 1.80 |
| Mn | 0.20 |
| Fe | 1.00 |
| Zn | 0.25 |
| Ni | 1.5 |
| Al | Bal |

In the present work, nano B₄C particulates are used as the fortification materials, 500 nm particulates were used, which were obtained from Reinste Nano Ventures Ltd., Delhi. The density of B₄C is smaller than the matrix material, which is 2.52 g/cm³.

B. Methodology

The manufacture of Al2218-B₄C composites were completed by liquid metallurgy through stir cast method. Determined measure of the Al2218 compound ingots were kept into the heater for liquefying.

Mechanical Behavior and Fractography of Al2218-Nano B₄C Metal Composites

The melting temperature of aluminum composite is 660°C. The Al2218 alloy melt was superheated to 750°C temperature. The temperature of the melt was recorded utilizing a chrome-alumel thermocouple. The liquid metal is then degassed utilizing solid hexachloroethane (C₂Cl₆) for 3 min [5]. A hardened steel impeller covered with zirconium is utilized to mix the liquid metal to make a vortex. The stirrer will be turned at a speed of 300rpm and the profundity of drenching of the impeller was 60 percent of the height of the liquid metal from the outside of the liquefy. Further, the B₄C particulates were preheated in a heater upto 400°C will be brought into the vortex. Stirring was proceeded until interface connections between the fortification particulates and the Al matrix advances wetting. At that point, Al2218-4 wt. % nano B₄C melt was poured into the cast iron mold having measurements of 120mm length and 15mm width. Additionally, composites were set up for 8 weight level of nano B₄C particles in the similar method.

C. Methodology

The castings in this way got were sliced to a size of 15 mm diameter across and 5 mm thickness which is then exposed to various dimensions of cleaning to get required example piece for microstructure studies. At first, the cut examples were cleaned with emery paper up to 1000grit size pursued by cleaning with Al₂O₃ suspension on a cleaning disc utilizing velvet material. The cleaned surface of the examples etched with Keller's reagent lastly exposed to microstructure in an electron microscope.

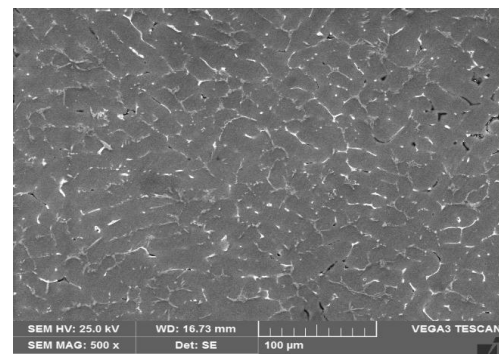
Hardness tests were performed on the cleaned surface of the examples utilizing Brinell hardness testing machine having a indenter of 5 mm diameter and 250 kg load for a stay time of 30 seconds, five arrangement of readings were taken at better places of the cleaned surface of the example and test was performed according to ASTM E10 [9]. The tensile and compression test was done on the cut examples according to ASTM E8 and E9 [10] standards utilizing universal testing machine at room temperature to ponder properties like UTS, yield strength, % of elongation and compression quality.

III. RESULTS AND DISCUSSION

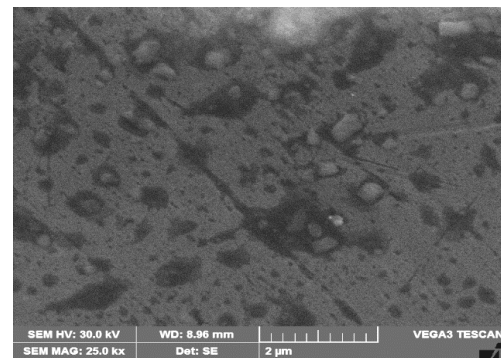
A. Microstructural Analysis

Figure 1a-c shows the SEM micrographs of as cast alloy Al2218 and the composites of 4 and 8 wt. % of nano B₄C reinforced with Al2218 alloy composites. The microstructure of as cast Al2218 alloy comprises of fine grains of aluminium solid solution with an enough dispersion of inter-metallic precipitates.

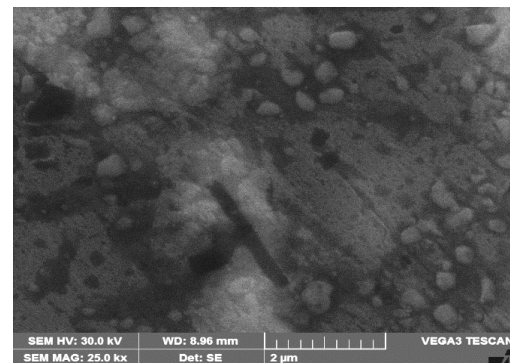
It also exhibits the incredible bonding between the matrix system and the nano particles so uniform homogenous dissemination of nano evaluated B₄C particulates with no agglomeration and clustering in the composites. This is basically a direct result of the suitable mixing action achieved all through the extension of the fortress by two stages. The nano particles wherever all through the grain furthest reaches of the cross section hinder the grain improvement and contradict the partition advancement of grains during stacking.



(a)



(b)



(c)

Fig. 1 SEM of (a) as cast Al2218 alloy (b) -4 wt. % B₄C (c) Al2218-8 wt.% B₄C composites

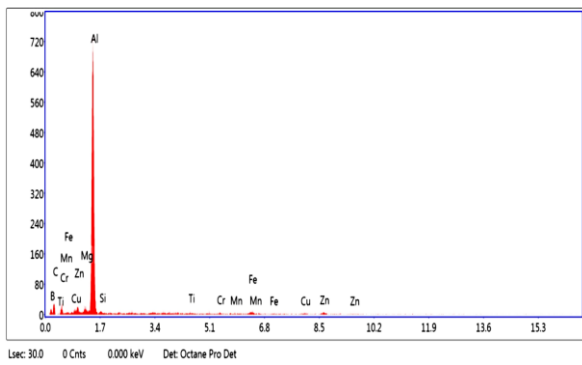


Fig. 2 Showing the EDS of Al2218-8 wt. % B₄C composites

From the figure 2 it is evident that nano B₄C particles are presented in the Al2218 alloy matrix in the form of B and C elements along with Al and Cu.

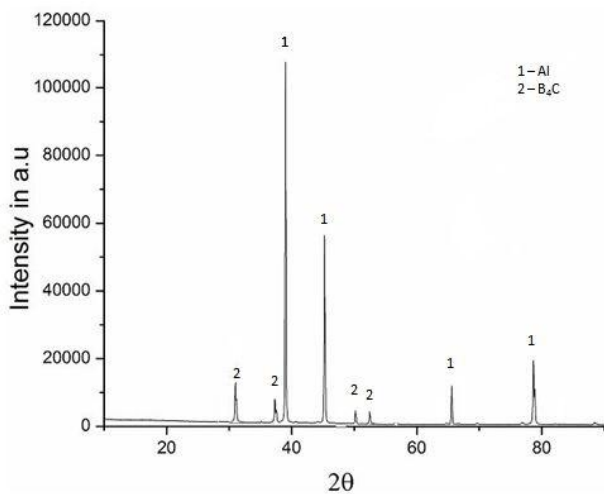


Fig. 3 XRD pattern of Al2218- 8 wt. % of nano B₄C composite

Figure 3 shows XRD pattern taken for Al2218- 8 wt.% B₄C nano composites to verify its quality and standard XRD pattern. It can be detected that peak height surges and then declines on 2-theta scale representing the occurrence of diverse phases of material. In fig. 3 it is visible that X-ray intensities of peak are higher at 38°, 45°, 65° & 78° demonstrating the occurrence of aluminium stage. Similarly, in fig. 3 it is observed the peaks for altered segments of boron carbide at 32°, 37°, 50° and 53°.

B. Density Measurements

Above figure 4 compares the theoretical & experimental densities of as cast Al2218 alloy, Al2218 – 4 and 8 wt. % B₄C composites. Aluminium alloy Al2218 has density of 2.8 g/cc, boron carbide has density of 2.52 g/cc. When aluminium alloy Al2218 is reinforced with 4 and 8 wt. % B₄C, the complete density of compound becomes less as B₄C density is lesser than Al2218 alloy. Further, it can be witnessed that experimental densities are slighter than the theoretical densities. Figure 5 demonstrates the variety in hardness with the expansion of 4 and 8 wt. % of nano B₄C particulates to the Al2218 composite. The hardness of a material is a mechanical parameter demonstrating the capacity of opposing nearby plastic twisting. The hardness of Al-B₄C composite is found to increment with the expansion of 4 and 8 wt. % nano B₄C

particulates. This expansion is seen from 63.13 BHN to 96.7 BHN for Al composites. This can be attributed essentially to the closeness of harder carbide particles in the cross section, and moreover the higher limitation to the restricted framework disfigurement amid space because of the nearness of harder stage. Furthermore, B₄C, as like different fortresses strengthens the framework by creation of high-density disengagements in the midst of cooling to room temperature due to the qualification of coefficients of thermal extension improvements between the B₄C and network Al2218 compound. Confound strains created between the support and the lattice deters the development of separations, bringing about progress of the hardness of the composites.

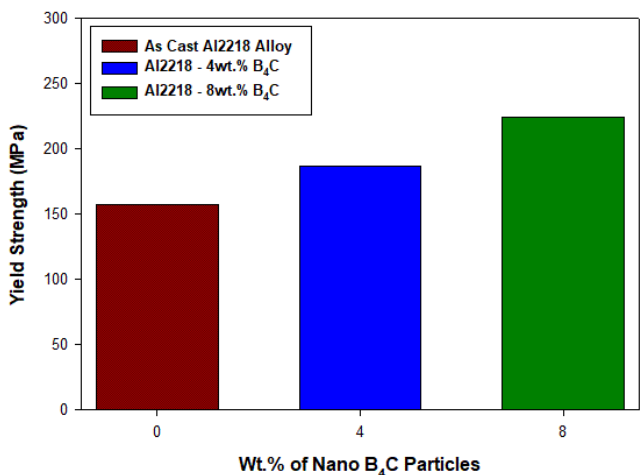
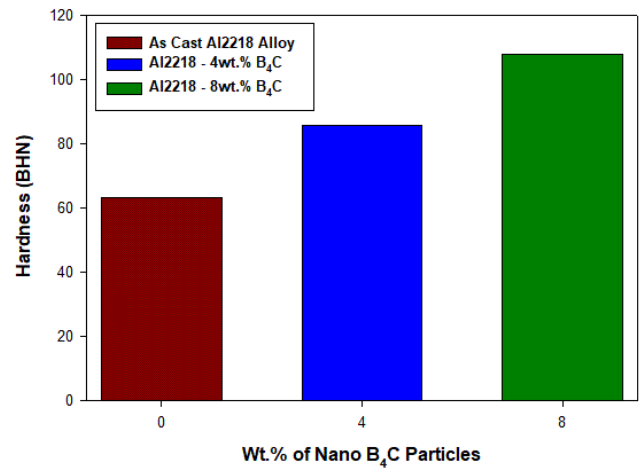


Fig. 5 showing the hardness of Al2218 alloy-4 and 8 wt. % B₄C nano composites

C. Ultimate Tensile and Yield Strength

The plot of ultimate strength (UTS) with 4 and 8 wt. % of nano B₄C dispersoid in metal grid composite has been presented in figure 6. The conscious estimations of UTS were plotted as a segment of weight rate of nano boron carbide particles. There has been a difference in 64 MPa in UTS regard when appeared differently in relation to base Al2218 compound when contrasted with 8 wt.% of nano B₄C strengthened composites.

The development in quality is credited on account of genuine contact between the matrix structure and nano materials. Better the grain gauge better is the hardness and nature



Mechanical Behavior and Fractography of Al2218-Nano B₄C Metal Composites

of composites provoking to upgrade the wear opposition additionally. The improvement in UTS is credited to the closeness of hard nano B₄C particulates, which presents quality to the structure amalgam, along these lines giving improved unbending nature [6]. The extension of these particles may have offered climb to immense waiting compressive nervousness made in the midst of solidifying due to differentiate in coefficient of advancement between adaptable lattice and particles.

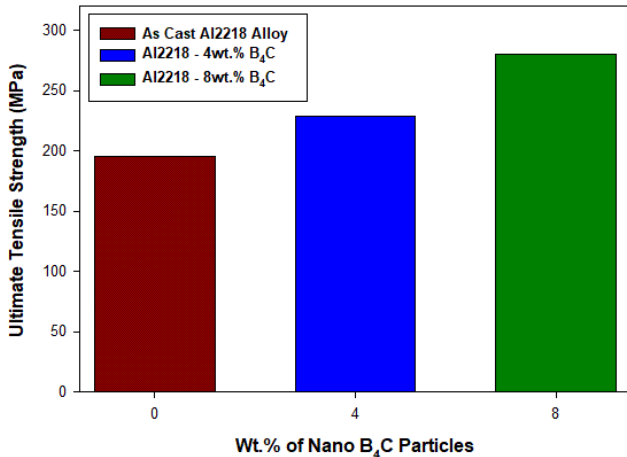


Fig. 6 Showing the ultimate tensile strength of Al2218 alloy-4 and 8 wt.% B₄C nano composites

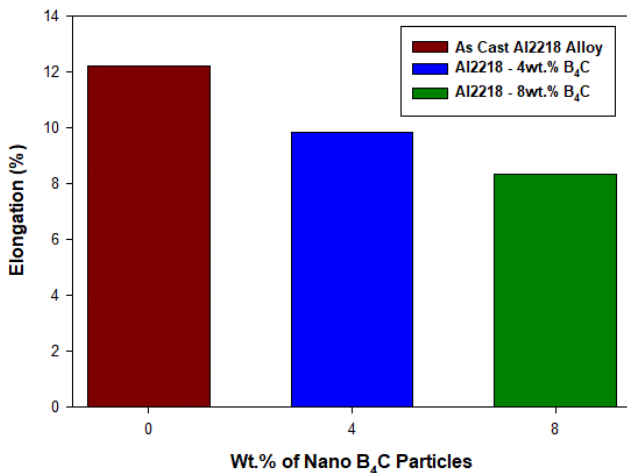


Fig. 7 Showing the yield strength of Al2218 alloy-4 and 8 wt.% B₄C nano composites

Figure 7 indicates variety of yield quality (YS) of Al2218 compound grid with 4 and 8 wt. % of nano B₄C particulate fortified composite. It tends to be seen that by including 4 and 8 wt. % of B₄C particulates yield quality of the Al amalgam expanded from 157.10 MPa to 165.30 MPa, and 211.12 MPa separately. The development in YS of the composite is plainly a result of proximity of hard B₄C particles which concede quality to the aluminum arrange achieving progressively conspicuous opposition of the composite against the associated load. Because of particles fortified composites, the dispersed hard particles in the matrix make impediment to the plastic stream, along these lines giving redesigned quality to the composite.

D. Percentage Elongation

Figure 8 showing the effect of nano B₄C content on the elongation (malleability) of the composites. It tends to be seen from the diagram that the adaptability of the composites

decreases basically with the 4 and 8 wt. % B₄C sustained composites. This reducing in rate prolongation in connection with the base amalgam is a most often happening method in particulate invigorated metal cross section composites.

Fig. 8 showing the percentage elongation of Al2218 alloy-4 and 8 wt. % B₄C nano composites

E. Compression Strength

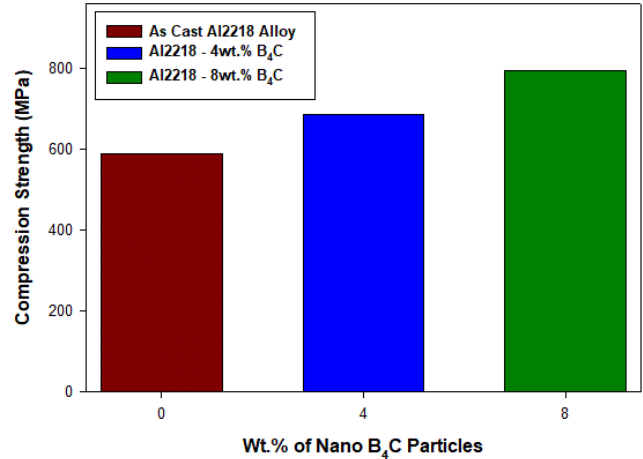
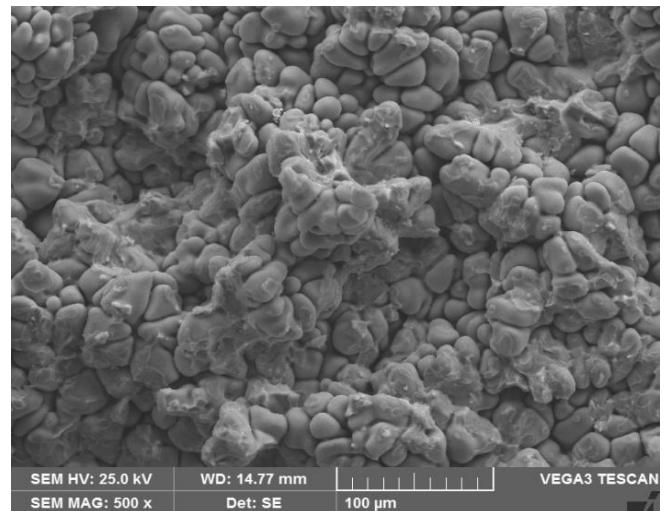


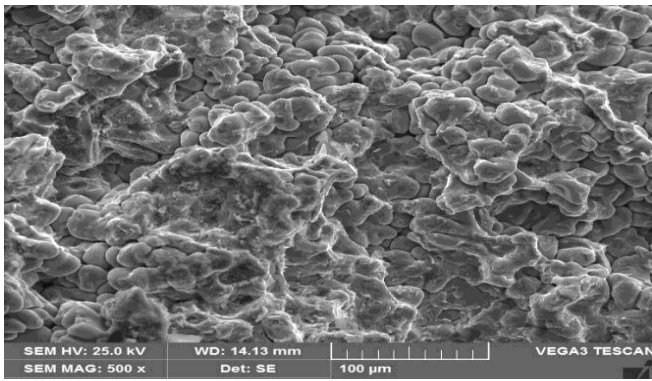
Fig. 9 Showing the compression of Al2218 alloy-4 and 8 wt.% B₄C nano composites

Figure 9 shows variation of compression strength (YS) of Al2218 alloy matrix with 4 and 8 wt. % of nano B₄C reinforced composite. By adding 4 and 8 wt. % of B₄C particulates compression strength of the Al alloy increased from 587.4 MPa to 684.97 MPa and 793.77 MPa respectively. This increase in compression strength is primarily due to the presence of hard ceramic particles in the Al2218 alloy matrix.

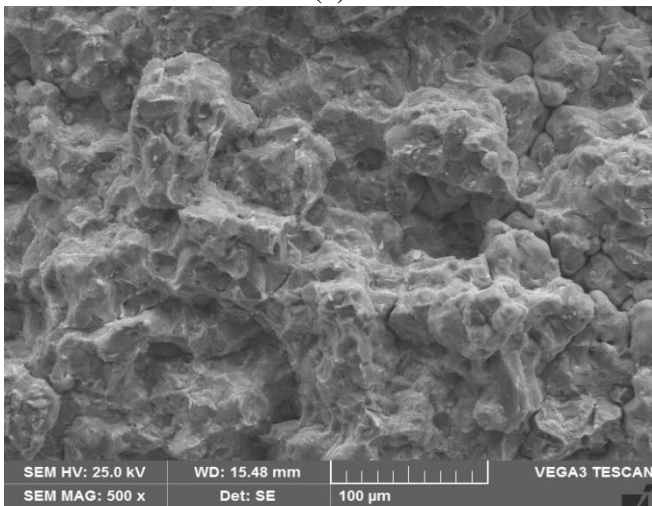
F. Fracture Studies



(a)



(b)



(c)

Fig. 10 Showing the tensile fractured specimens of (a) Al2218 alloy (b) Al2218-4 wt.% B₄C (c) Al2218-8 wt. %

B₄C nano composites Tensile fracture of as cast compound and composite examples after tensile testing were examined by utilizing SEM pictures of crack surfaces (figure 10 a-c).

Figure 10b and 10c demonstrates that 4 and 8 wt. % B₄C strengthened MMCs fracture surfaces respectively. The brittle fracture has been observed in the case of B₄C reinforced composites. The surface indicates the particle full out during the tensile loading.

IV. CONCLUSIONS

In this exploration, Al2218-B₄C nano composites have been manufactured by stir casting technique by taking 4 and 8 wt. % of secondary particles. The microstructure, hardness, UTS, yield quality, rate prolongation, compression quality and fractography of arranged examples are examined.

The framework or composite is free from pores and uniform dispersion of nano particles, which is apparent from SEM microphotographs. The EDS and XRD examination affirm the nearness of B₄C particles in the Al2218 matrix. The mechanical properties of Al2218-4 and 8 wt. % nano B₄C composites are improved as compared to Al matrix material. The tensile fractured surfaces of the composite material indicate ductile and brittle fracture in Al matrix and its composites respectively.

REFERENCES

1. Xian Zhu et al., Journal of Alloys and Compounds. 2016; 674:145-152.
2. Prasad H Nayak et al., Frattura ed Integrita Strutturale, 48, 2019, 370-376.
3. Meijuan Li, Materials Science & Engineering A, 2016; 256:241-248.
4. Shashidhar S, et al., Materials Today Proceedings, 5, pp. 25158-25164, 2018.
5. Chandrashekar G L, et al., AIP Conference Proceedings, 2039, 020017, 2018.
6. Madeva Nagaral, et al., Transactions of the Indian Ceramic Society, Vol.77, No.3, pp. 1-4, 2018.

AUTHORS PROFILE



Mr. Vidyadhar Pujar has received the B.E degree in Mechanical Engineering from Bellary Institute of Technology and Management, Bellary and obtained M.Tech degree in Design Engineering from Dayanandsagar College of Engineering, Bangalore. Currently working has Assistant Professor Department of Mechanical Engineering, The Oxford College of Engineering, Bangalore, Karnataka, India. He

made significant contributions are made in the fields of metal matrix composites.



Dr. H.K. Srinivas received his B.E. from Mysore University, M.Tech. and PhD from VTU Belagavi, Karnataka State, where he is currently Professor of Mechanical Engineering in SJB Institute of Technology, Bangalore. He has attended more than five international conferences and 15 national conferences. He has published ten research articles in reputed international journals.



Mr. Madeva Nagaral is working as a Deputy Manager in Configuration and Mass Properties Group, Aircraft Research and Design Centre (ARDC), Hindustan Aeronautics Limited (HAL, Bangalore since Jan 2012. He has done his BE and M.Tech from Basaveshwar Engineering College, Bagalkot. Presently he is pursuing his Ph.D in Siddaganga Institute of Technology, Tumkur.

Previously, he worked as an Assistant Professor in the Department of Mechanical Engineering, MVJ College of Engineering, Bangalore, for the period of three years (2009-2011). Also, has worked as an Engineer in Bharat Electronics Limited, for the period of one year. Since 2012, his 102 research papers have been published in National and International Journals and he has presented more than 100 research papers in national and international conferences organized at various engineering colleges all over the country. His research papers are having more than 280 Google Scholar Citations. He guided more than 48 UG and 32 PG projects. 26 international journal papers were reviewed, as a reviewer. 21 guest talks were delivered as a key note resource speaker in various engineering colleges of India. He has chaired as a Guest and Session Judge for National and International Conferences held at various Engineering Colleges.



Dr. Virupaxi Auradi did his M. Tech degree in Materials and Metallurgical Engineering from KREC, Surathkal in the year 2002 and Ph. D. in Mechanical Engineering from Visvesvaraya Technological University, Belgaum in the year 2007. Currently, he is working as Associate Professor in the Department of Mechanical Engineering of Siddaganga Institute of

Technology, Tumkur. From July 2002 to February 2007, he worked as Research Associate under the projects sponsored by Ministry of Defense, DRDO, New Delhi, India. He made significant contributions are made in the fields of Grain refinement and modification of Al and its Alloys, Metal Matrix Composites (MMCs), In situ Composites, Tribology, Synthesis of Al Alloys for Aerospace Applications. He has undertaken R&D projects from agencies like AR&DB and AICTE New Delhi.



Contents lists available at ScienceDirect

Materials Today: Proceedings

journal homepage: www.elsevier.com/locate/matpr

Investigations on microstructure and tensile properties of as-cast ZA-27 metal matrix composite reinforced with zircon sand

G.R. Gurunagendra ^{a,*}, B.R. Raju ^b, Vijayakumar Pujar ^a, D.G. Amith ^a, H.G. Hanumantharaju ^c, Santosh Angadi ^a

^a Department of Mechanical Engineering, Global Academy of Technology, VTU, Bangalore 560098, India

^b Department of Automobile Engineering, The Oxford College of Engineering, VTU, Bangalore 560068, India

^c Department of Mechanical Engineering, UVCE, Bangalore 560001, India

ARTICLE INFO

Article history:

Received 18 December 2020

Received in revised form 11 January 2021

Accepted 27 January 2021

Available online xxxxx

Keywords:

Density

Porosity

Dislocation density

Tensile strength

as- cast ZA-27

Micro-structure

ABSTRACT

Zinc-Aluminum alloys are employed as a bearing material in various machinery. In the present work zircon sand microparticles of size, 100 μm are dispersed in ZA-27 alloy with weight fractions of 1.5 wt%, 3.0 wt%, 4.5 wt%, and 6.0 wt% to synthesize ZA-27 metal matrix composites by stir casting. Microstructure studies using, SEM/EDAX conducted to determine the morphology of the particles and the ZA-27 composites. Physical properties like density and porosity of the zircon sand microparticle reinforced ZA-27 are evaluated and their effect on strength and ductility of the composites are evaluated using the tensile test. Dispersion of zircon sand is seen in the SEM micrographs and EDAX confirms the same. The results obtained revealed an increase in tensile strength and yield strength at 3.0 wt%, 4.5 wt and 6.0 wt% at the cost of a reduction in percentage elongation when compared to ZA-27 alloy. The tensile behavior of ZA-27 composites is found to be affected by the dispersion of reinforcement in the matrix arising due to dislocation density.

© 2021 Elsevier Ltd. All rights reserved.

Selection and peer-review under responsibility of the scientific committee of the 3rd International Conference on Materials, Manufacturing and Modelling.

1. Introduction

Researchers worldwide now paying attention and interest in developing Metal-Matrix Composites (MMC) due to their unique physical/mechanical properties and performance. MMC exhibits elevated temperature strength, high thermal conductivity, specific strength, and low coefficient of thermal expansion (CTE), wear strength, and good damping characteristics. MMC comprises of metal or alloy as matrix and ceramic fillers as reinforcements in various shapes and sizes [1,2]. The zinc family of alloys such as ZA-8, ZA-12, and ZA-27 had exhibited exceptional mechanical and tribological properties giving competition to cast-iron and bronze as a traditional bearing material. ZA-27 is a less dense and low melting alloy among the ZA family and possesses good strength, ease of casting, and machinability. One of the shortcomings of this ZA alloy is the instability of dimension at a temperature of more than 100 °C. Performing thermal treatment and inclusion of ceramic particles to the alloy will improve the properties of

the ZA-27 alloy but with reduced machinability, with the addition of solid lubricants machinability and wear characteristics are enhanced [3–5]. Apart from synthetic ceramic particles such as alumina, boron carbide, silicon carbide garnet, graphite, agricultural by-products, and Industrial waste are nowadays explored as reinforcement agents in fabricating both ZA-27 MMC and ZA-27 hybrid MMC [5–9]. ZA-27 alloy research reports containing more than one reinforcement for the manufacture of composites such as a synthetic ceramic filler and dry lubricant like graphite are fabricated to counter the problems of ease of machining [10,11]. Recent researchers are also carrying out studies on introducing nanofillers to the ZA-27 alloy using different composite preparation techniques namely, stir casting, double stir casting, squeeze casting, powder metallurgy and ultrasonic agitation to obtain sound casting and better properties [1,10]. There are very few research articles on the characterization of ZA-27 MMC reinforced with zircon sand microparticles. Especially, beyond the micro-mechanical behavior of such composites exceeding 5.0 wt% [6]. The coefficient of thermal expansion (CTE) plays a key role in the performance of ZA-27 composites as bearing material and needs to be evaluated and understood. However, the challenges in

* Corresponding author.

E-mail address: gurunagendra.gn@gmail.com (G.R. Gurunagendra).

obtaining composites include low ductility, poor particle–matrix bonding, particle cracking, particle pull out agglomeration are some of the difficulties in the preparation of composites [3,12].

In the present work, ZA-27 MMC is fabricated by a stir casting route that is widely adopted in preparing ZA-27 composites owing to its ease of mass manufacturing, simplicity, and low cost. There is also ample scope to investigate the behavior of microparticle zircon sand containing ZA-27 as main reinforcement and organic or solid lubricant as secondary reinforcement.

2. Experimental procedure

2.1. Matrix

ZA-27 alloy containing a high percentage of aluminium content is used as a matrix alloy in the present work. This alloy is a promising material for bush and bearing applications. The chemical composition of the matrix alloy is shown in (Table 1).

2.2. Reinforcement

Zircon sand ($ZrSiO_4$) of particle size 100mesh is used in this work as a key reinforcement in the ZA-27 matrix. Zircon sand's chemical composition is 65 percent zircon oxide and hafnium and 24 percent silica with traces of Alumina, oxides of iron, and Titanium [13] (Fig. 6).

2.3. Preparation of composite by stir casting

The stir casting process is known to be inexpensive and suitable for a large volume of production compared to other manufacturing techniques, produced composite. In preparing 2000 g of ZA-27 alloy, 1.5 wt%, 3 wt%, 4.5 wt% and 6 wt. % percent of Zircon sand was calculated. Zircon sand particles were preheated to about 200 °C to remove any moisture. In the graphite crucible, ZA-27 alloy ingots are placed and superheated to a melting temperature of 550 °C, and stirring was performed after the temperature was reduced to 450 °C (semi solid-state) for homogenization. The reinforcement particles are now fed slowly around 20 g/min and continuously stirred at a rate of 350 rpm for 3 min to get vortex to achieve proper particle distribution., 10 g of borax powder is added to improve wettability, before which the melt is degassed using hex chloroethylene tablets to minimize void and eradicates the formation of air bubbles. The ZA-27 composite is poured at 500 °C onto the preheated cast iron die [14] for achieving solidification of the casting (Fig. 1).

2.4. Density and void fraction

Density has a profound impact in many engineering applications where low weight is desirable. The relative proportion of both the matrix and the reinforcements affects the value of density obtained. Density difference of experimental and theoretical value exists due to the inclusion of voids during castings. Mechanical and endurance strength of composites have a direct bearing on the presence of voids in the composites.

Rule of mixtures is used to compute theoretical density,

$$\rho_{\text{theoretical}} = \frac{100}{\sum_{i=1}^n \frac{x_i}{p_i}} \quad (1)$$

Table 1
Composition of ZA-27 alloy.

| Al | Mg | Cu | Fe | silicon | Zinc |
|--------|-------|-------|-------|---------|-----------|
| 25.60% | 0.07% | 2.10% | 0.04% | 0.001 | Remainder |

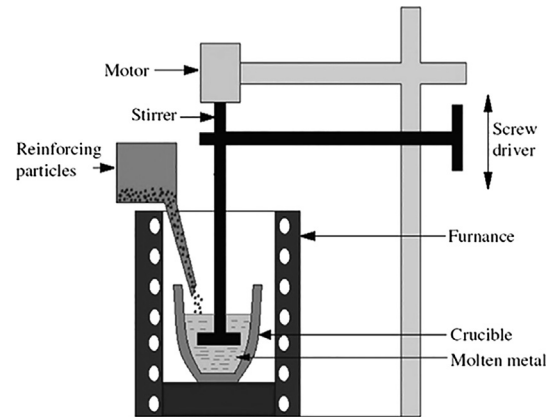


Fig. 1. Diagram of stir casting set up.

Experimental density is determined by measuring the known volume of water displaced by the base alloy and composite specimens using the Archimedes principle.

Density (ρ) is the ratio of the mass of the composite samples to the volume of water displaced

$$\% \text{Porosity} = \frac{\rho_{th} - \rho_{exp}}{\rho_{th}} \times 100 \quad (2)$$

2.5. X-Ray diffraction

X-ray diffraction works on the principle of Bragg's law. Various phases present in the composite samples are determined by XRD studies.

2.6. Microstructure studies

Scanning electron microscopy studies are performed on composite samples prepared as per the metallographic procedure. Electron backscattered diffraction (EBSD) arrangement attached to the spectroscopy detector is used to observe the morphology of the different composition of composites as well as elemental composition.

2.7. Hardness test

Hardness is the resistance to indentation by the material. The hardness of a material is the property that makes it withstand deformation, scratching, abrasion. Brinell hardness number (BHN) of the samples of the ZA-27 composites is measured for a dwell time of 15 s using indentation of a 10 mm ball indenter under a load of 500kgf. An average value was calculated and tabulated for the readings obtained during the experiments.

2.8. Tensile strength

Tensile testing is a destructive test procedure that provides knowledge about the material's tensile strength, yield strength, and ductility. The force needed to crack a composite is determined and also the degree to which the specimen elongates to that breaking point.

Tensile strength is evaluated as per ASTM E8 standard on a computerized universal testing machine by applying a uniaxial tensile load on a cylindrical dog bone specimen as shown in Fig. 2. Three specimens were tested, and the average reading of the strength was obtained.

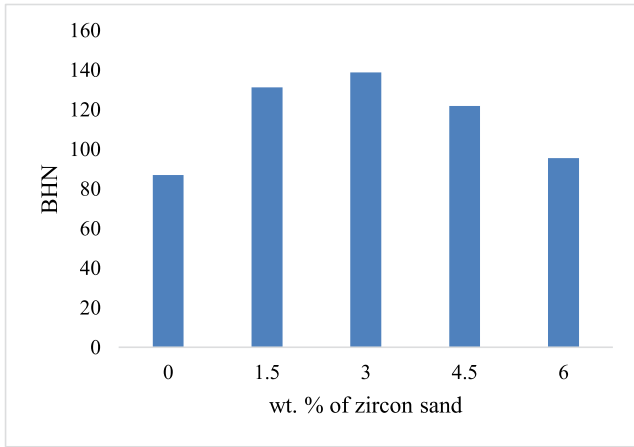


Fig. 5. Variation of Hardness with the composition of reinforcement.

zirconium, silicon, and oxides at the interface due to reaction as shown in Figs. 8 and 9.

3.5. Tensile test

Fig. 10(a). shows the Tensile strength (TS) values with zircon sand addition to ZA-27 matrix whereas Fig. 10(b) shows Yield strength (YS) values with increase in weight percentage of zircon sand and Fig. 11 reveals Percentage Elongation values of the ZA-27/zircon sand composites. with the increase in zircon sand content the tensile strength and yield strength increase for 3 wt%, 4.5 wt%, and 6.0 wt% composition but at 1.5 wt% because of the poor particle–matrix interface. Porosity and particle cracking seen from Fig. 7(a) in 1.5 wt% zircon sand reinforcement depicts a low value of strength compared to 3 wt%, 4.5 wt%, and 6.0 wt% zircon sand. It is confirmed from the work done by several researchers that the ductility of composites is reduced with an increase in reinforcement content. The reduction in percentage elongation shown in Fig. 11 may be ascribed to the zircon sand particles increasing the localized stress concentration. The strength obtained for a given matrix material depends largely on the particle–matrix wetting of the liquid metal and reinforcement, which needs a tight bond for efficient load transfer [16].

3.6. Strength and dislocation density of the composites

Dislocation density is the average dislocation length of thickness of the crystal. macroscopic deformation is influenced by the microscopic dislocation motion. The influence on strength and

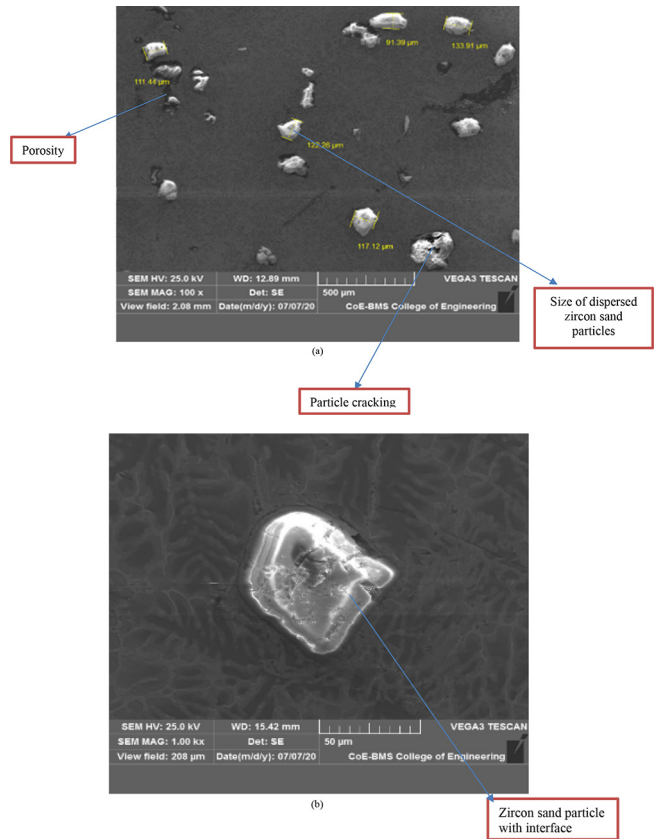


Fig. 7. SEM of (a) dispersion of zircon sand microparticles of 1.5 wt% in ZA-27 alloy and (b) interface at 3 wt% zircon sand.

hardness of ceramic particles present in the ductile alloy matrix was previously studied by theories such as quenching reinforcement, Orowan reinforcement, work hardening, grain reinforcement / Hall Petch strengthening [17].

Coefficient of thermal expansion (CTE) mismatch at the interface due to work hardening gives rise to dislocations produced during composite cooling whose movements are arrested. This is due to the high interface dislocation density increasing the strength of the composites [17].

4. Conclusion

ZA-27 composites with 1.5 wt%, 3.0 wt%, 4.5 wt% and 6.0 wt% zircon sand are fabricated by stir casting and the microstructure

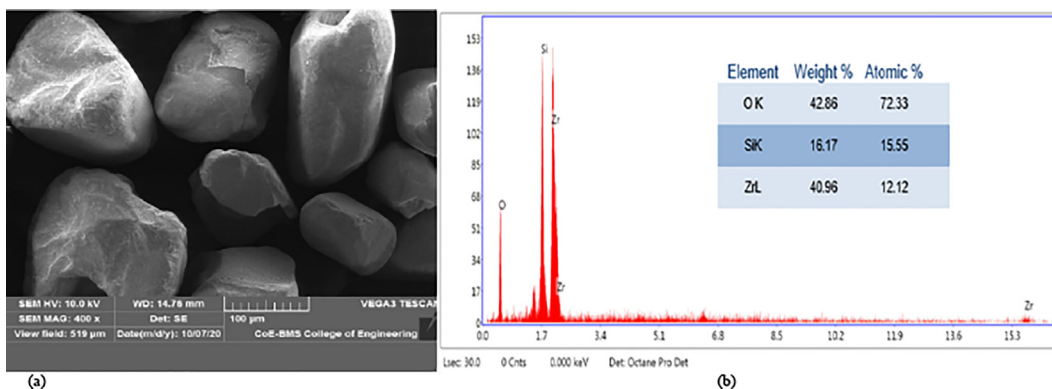


Fig. 6. SEM of (a) Zircon sand microparticles. (b) EDAX of Zircon sand.

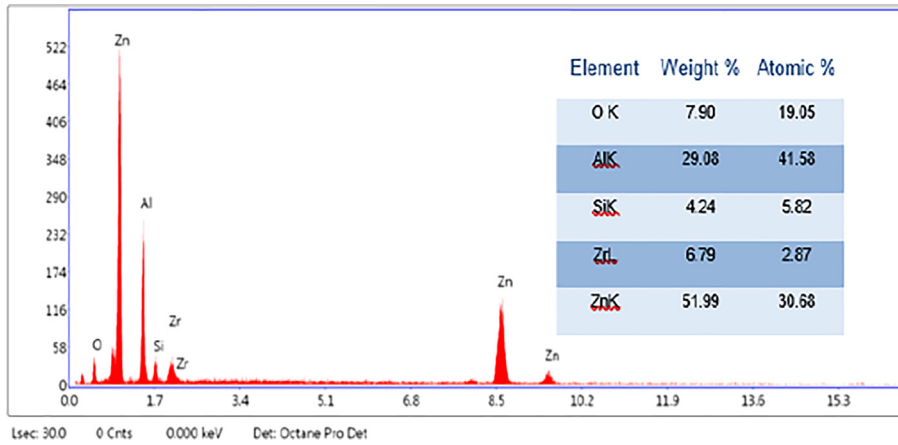


Fig. 8. EDAX results from 3 wt% Zircon reinforced ZA-27 composites.

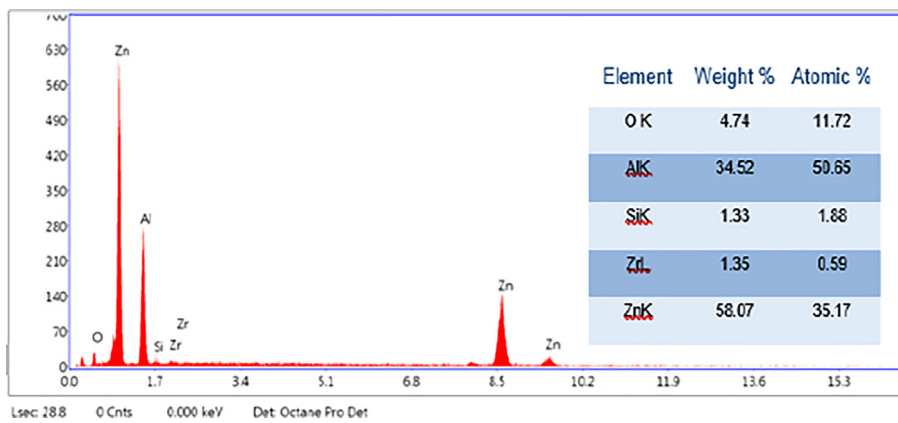


Fig. 9. EDAX results from 6 wt% Zircon reinforced ZA-27 composites.

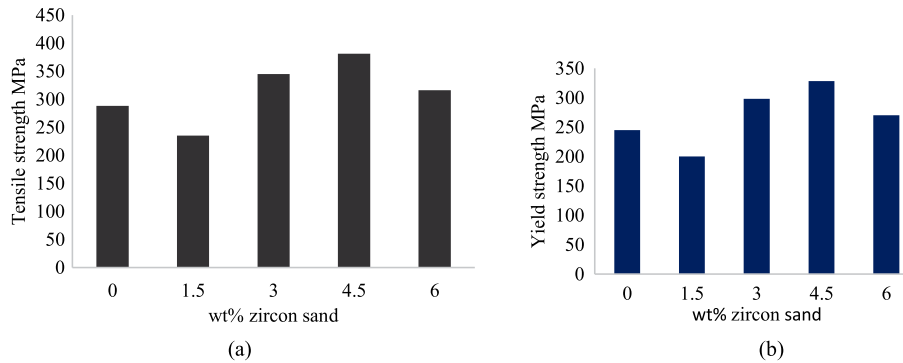


Fig. 10. (a). Effect of zircon sand weight fraction on tensile strength (b). Effect of zircon sand weight fraction on tensile strength.

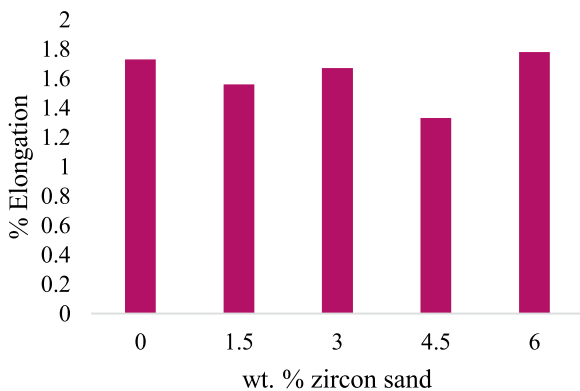


Fig. 11. Percentage elongation with the increase in weight percentage of zircon sand.

reveals the distribution of zircon sand particles. Experimental density is less for composites which is desirable for weight-sensitive applications. The porosity increases with an increase in zircon sand content and is maximum for 3 wt% zircon sand. SEM pictures graphs indicate the distribution of particles and the interface of matrix and particles. EDAX confirms the elements found in the composites. Tensile strength and yield strength are found to increase at 3.0 wt%, 4.5 wt% but reveal a slight drop in value at 6.0 wt% zircon sand. Tensile strength increases by 32% for 4.5 wt % zircon sand. The ductility is low for 4.5 wt% reinforcement but improves at 6.0 wt% zircon sand of course with slightly better strength that is desirable in engineering applications. The dislocation density of the composites is calculated and shows an upward trend with an increase in zircon sand particles but at 6.0 wt% its

value drops and correlates with the tensile strength of the 6.0 wt% ZA-27 composites.

CRedit authorship contribution statement

G.R. Gurunagendra: Writing original draft, Conceptualization, Data curation, Investigation, Methodology. **B.R. Raju:** Review & Editing. **Vijayakumar Pujar:** Validation. **D.G. Amith:** Validation. **H.G. Hanumantharaju:** Validation. **Santosh Angadi:** Review & Editing.

Declaration of Competing Interest

The authors declare that they have no known competing financial interests or personal relationships that could have appeared to influence the work reported in this paper.

References

- [1] B.O. Fatile, B.O. Adewuyi, H.T. Owoyemi, Synthesis and characterization of ZA-27 alloy matrix composites reinforced with zinc oxide nanoparticles, *Eng. Sci. Technol. Int. J.* 20 (3) (2017) 1147–1154, <https://doi.org/10.1016/j.jestch.2017.01.001>.
- [2] M.O. Bodunrin, K.K. Alaneme, L.H. Chown, Aluminium matrix hybrid composites: A review of reinforcement philosophies; mechanical, corrosion and tribological characteristics, *J. Mater. Res. Technol.* 4 (2015) 434–445, <https://doi.org/10.1016/j.jmrt.2015.05.003>.
- [3] M. Babić, R. Ninković, S. Mitrović, I. Bobić, Influence of heat treatment on tribological behavior of Zn-Al alloys, *Tribol. Ind.* 29 (2007) 23–31.
- [4] T.S. Kiran, M. Prasanna Kumar, S. Basavarajappa, B.M. Viswanatha, Dry sliding wear behavior of heat treated hybrid metal matrix composite using Taguchi techniques, *Mater. Des.* 63 (2014) 294–304, <https://doi.org/10.1016/j.matdes.2014.06.007>.
- [5] T.S. Kiran, M. Prasanna Kumar, S. Basavarajappa, B.M. Vishwanatha, Mechanical properties of as-cast ZA-27/Gr/SiCp hybrid composite for the application of journal bearing, *J. Eng. Sci. Technol.* 8 (2013) 557–565.
- [6] S. Gangwar, V. Payak, V.K. Pathak, A. Jamwal, P. Gupta, Characterization of mechanical and tribological properties of graphite and alumina reinforced zinc alloy (ZA-27) hybrid metal matrix composites, *J. Compos. Mater.* 54 (30) (2020) 4889–4901, <https://doi.org/10.1177/0021998320938442>.
- [7] K.K. Alaneme, B.O. Fatile, J.O. Borode, Mechanical and corrosion behaviour of Zn-27Al based composites reinforced with groundnut shell ash and silicon carbide, *Tribol. Ind.* 36 (2014) 195–203.
- [8] K.K. Alaneme, M.O. Bodunrin, A.A. Awe, Microstructure, mechanical and fracture properties of groundnut shell ash and silicon carbide dispersion strengthened aluminium matrix composites, *J. King Saud Univ. - Eng. Sci.* 30 (2018) 96–103, <https://doi.org/10.1016/j.jksues.2016.01.001>.
- [9] S.S. Owoeye, D.O. Folorunso, B. Oji, S.G. Borisade, Zinc-aluminum (ZA-27)-based metal matrix composites: a review article of synthesis, reinforcement, microstructural, mechanical, and corrosion characteristics, *Int. J. Adv. Manuf. Technol.* 100 (2019) 373–380, <https://doi.org/10.1007/s00170-018-2760-9>.
- [10] N. Shiva Kumar, Mechanical and wear behavior of ZA-27/SiC/Gr hybrid metal matrix composites, *Mater. Today Proc.* 5 (9) (2018) 19969–19975, <https://doi.org/10.1016/j.matpr.2018.06.363>.
- [11] T.R. Hemanth Kumar, R.P. Swamy, T.K. Chandrashekar, An experimental investigation on wear test parameters of metal matrix composites using Taguchi technique, *Indian J. Eng. Mater. Sci.* 20 (2013) 329–333.
- [12] D.S. Prasad, C. Shoba, N. Ramanaiah, Investigations on mechanical properties of aluminum hybrid composites, *J. Mater. Res. Technol.* 3 (1) (2014) 79–85, <https://doi.org/10.1016/j.jmrt.2013.11.002>.
- [13] V. Ramesha, T.B. Prasad, V. Nayak, V.L. Neelakantha, A study on mechanical properties of Al-17Si metal matrix composites, *IOP Conf. Ser. Mater. Sci. Eng.* 376 (2018), <https://doi.org/10.1088/1757-899X/376/1/012100>.
- [14] S.C. Sharma, B.M. Girish, D.R. Somashekar, R. Kamath, B.M. Satish, Mechanical properties and fractography of zircon-particle-reinforced ZA-27 alloy composite materials, *Compos. Sci. Technol.* 59 (12) (1999) 1805–1812, [https://doi.org/10.1016/S0266-3538\(99\)00040-8](https://doi.org/10.1016/S0266-3538(99)00040-8).
- [15] S. Agrahari, I. Panda, F.M. Patel, M. Gupta, C.P. Mohanty, Effect of cooling rate on microstructures and mechanical property of Al 1230 alloy in a sand casting process, *Mater. Today Proc.* 26 (2019) 1771–1775, <https://doi.org/10.1016/j.matpr.2020.02.372>.
- [16] S. Madhusudan, M.M.M. Sarcar, N.B.R.M. Rao, Mechanical properties of Aluminum-Copper(p) composite metallic materials, *J. Appl. Res. Technol.* 14 (5) (2016) 293–299, <https://doi.org/10.1016/j.jart.2016.05.009>.
- [17] W.S. Miller, F.J. Humphreys, Strengthening mechanisms in particulate metal matrix composites, *Scr. Metall. Mater.* 25 (1) (1991) 33–38.



Contents lists available at ScienceDirect

Materials Today: Proceedings

journal homepage: www.elsevier.com/locate/matpr

Mechanical, wear and corrosion properties of micro particulates reinforced ZA-27 hybrid MMC by stir casting: A review

G.R. Gurunagendra ^{a,*}, B.R. Raju ^b, Vijayakumar Pujar ^a, D.G. Amith ^a, Poornachandra ^a, H.S. Siddesha ^c

^a Department of Mechanical Engineering, Global Academy of Technology, VTU Bangalore, 560098 India

^b Department of Automobile Engineering, The Oxford College of Engineering, VTU Bangalore, 560068 India

^c Department of Mechanical Engineering, ACS College of Engineering, VTU Bangalore 560074 India

ARTICLE INFO

Article history:

Received 17 December 2020

Received in revised form 28 December 2020

Accepted 27 January 2021

Available online xxx

Keywords:

Microstructure

Tensile strength

Density

Ductility

ABSTRACT

During the last few years, ZA-27 alloys are commercially used as a bearing material due to their excellent tribological properties. This alloy also possesses advantages like good mechanical properties, low energy consumption, and ease of machining. It is found that ZA-27 alloys lose their dimensional stability above 100 °C during its usage. This has inspired many researchers in recent years to explore the possibility of reinforcing ZA-27 alloy with synthetic ceramic reinforcement like SiC, Alumina, boron carbide Agricultural and industrial wastes along with solid lubricant such as graphite for tribological applications. This article reviews the microstructure, physical, mechanical, wear, and corrosion properties of ZA-27 hybrid MMC reinforced with microparticles like SiC, and Alumina, Rice husk ash, Groundnut ash, Quarry dust, and Bamboo leaf ash fabricated by stir casting technique. This paper summarizes the work done by several researchers in optimizing the stirring parameters for better distribution of microparticle reinforcements and mechanical, corrosion and wear behavior of the hybrid ZA-27 composites.

© 2021 Elsevier Ltd. All rights reserved.

Selection and peer-review under responsibility of the scientific committee of the 3rd International Conference on Materials, Manufacturing and Modelling.

1. Introduction

In recent times, there is a huge demand for stronger, light, and low-cost engineering materials. Components in service are required to be made of materials that are required to possess niche properties that are difficult to obtain using conventional metals and alloys. Metal matrix composites are found to possess such unique properties for various industrial applications. Some of these properties include load-bearing ability, Low values of coefficient of thermal expansion, fatigue resistance, wear strength and good damping. To improve the properties of MMC compared to monolithic metals/alloys, the matrix made of monolithic metal or alloy is embedded with hard particles. Matrix materials based on aluminum, magnesium, titanium, copper, and zinc are also used in a variety of applications.

Studies on zinc-based alloys have been performed over the last few decades and have shown excellent tribo-mechanical properties, apart from the low melting point, good casting ability, and machinability. In contrast, to cast iron, bronze, and plastics, several

studies have shown that the Zinc-Aluminum family of alloys such as ZA-12 and ZA-27 possess greater strength as components having relative motion like bearings working at moderate temperature. The limitations of ZA alloy are that it exhibits dimensional instability at a temperature greater than 100 °C, despite good tribo-mechanical characteristics. This limitation can be overcome by heat treatment techniques and the addition of ceramic particles to the alloy at the cost of a decrease in machinability, which can be minimized by adding dry lubricants [1,2].

In preparing this review article it is found that researchers are motivated to improve the strength of ZA alloys by adding reinforcement particles and whiskers like synthetic ceramics such as Alumina, silicon carbide, Garnet, Glass, boron carbide, Graphite, and Agricultural/Industrial Waste. Also, some researchers had tried to combine synthetic ceramic particles and industrial waste/Agricultural waste to develop a new class of materials called hybrid composites to achieve improved mechanical, wear, and thermal characteristics. Hybrid composites such as ceramic fillers and solid lubricants are also tried to reduce the effects of ceramic fillers on ease of machining [3,4]. To obtain casting with enhanced properties researchers are recently adding fillers of nano size to the cast ZA27 alloy and synthesize the MMC using various metallurgi-

* Corresponding author.

E-mail address: gurunagendra.gn@gmail.com (G.R. Gurunagendra).

cal processes such as stir casting, double stir casting, squeeze casting, powder metallurgy, and also ultrasonic-assisted stir casting [4].

Hybrid MMCs are promising materials consisting of two or more reinforcing agents tailored for highly demanding applications. Hybrid MMCs fabricated using stir casting route is a good prospect for low cost and mass production of castings.

This paper aims to review the studies carried out on the different combinations of reinforcing microparticles used in the production of hybrid ZA-27 MMC by stir casting method and their behavior which paves the way for developing low-cost and sustainable hybrid ZA-27 MMC for various engineering applications.

1.1. Processing of ZA-27 hybrid MMC by stir casting and characterization:

Fig. 1 outline the fabrication of ZA-27 hybrid MMC by stir casting and characterization techniques. Due to its ease, large quantity of castings made the Stir casting technique is the less expensive process for manufacturing ZA27 hybrid MMC. Although there have been widely documented concerns about the homogeneous distribution of reinforcing particles, formation of pores, wettability clustering and the development of undesirable secondary phases, methods for containing these problems have been well reported. By optimizing mixing parameters such as stirring speed, time of stirring, pouring temperature [5] segregation of reinforcement particles and cluster formation can be avoided.

Grain refiners, degassers, covering flux and wetting agents like borax and magnesium are used to obtain quality ZA-27 composites.

Once the casting is obtained the ZA-27 composite samples are subjected to various characterization techniques. To begin with, Microstructure evaluation using Scanning electron microscopy (SEM) which gives the information about interface/bonding between particles and matrix and reinforcement particles distribution in the ZA-27 alloy. A strong interface is essential for distribution of the load in matrix and reinforcement resulting in enhancement of strength required for structural applications. Energy dispersive spectroscopy (EDAX) gives the chemical constituents of the composites. Physical properties like density and void fraction helps in identifying the quality of composites produced for structural and machine members. A very important requirement for a bush and bearing applications are high strength, low coefficient of thermal expansion (CTE), thermal conductivity, wear resistance and corrosion strength that needs to be evaluated and optimized [6,7].

1.2. Materials

In the present review ZA-27 is used as a matrix material. ZA-27 is the lightest alloy in the family of zinc alloy Table 1. It is widely used as bearing material in high load and low-speed applications in

Table 1
The chemical compositions of ZA-27 alloy.

| | | | | | |
|--------|-------|-------|-------|---------|-----------|
| Al | Mg | Cu | Fe | Silicon | Zinc |
| 25.60% | 0.07% | 2.10% | 0.04% | 0.001 | Remainder |

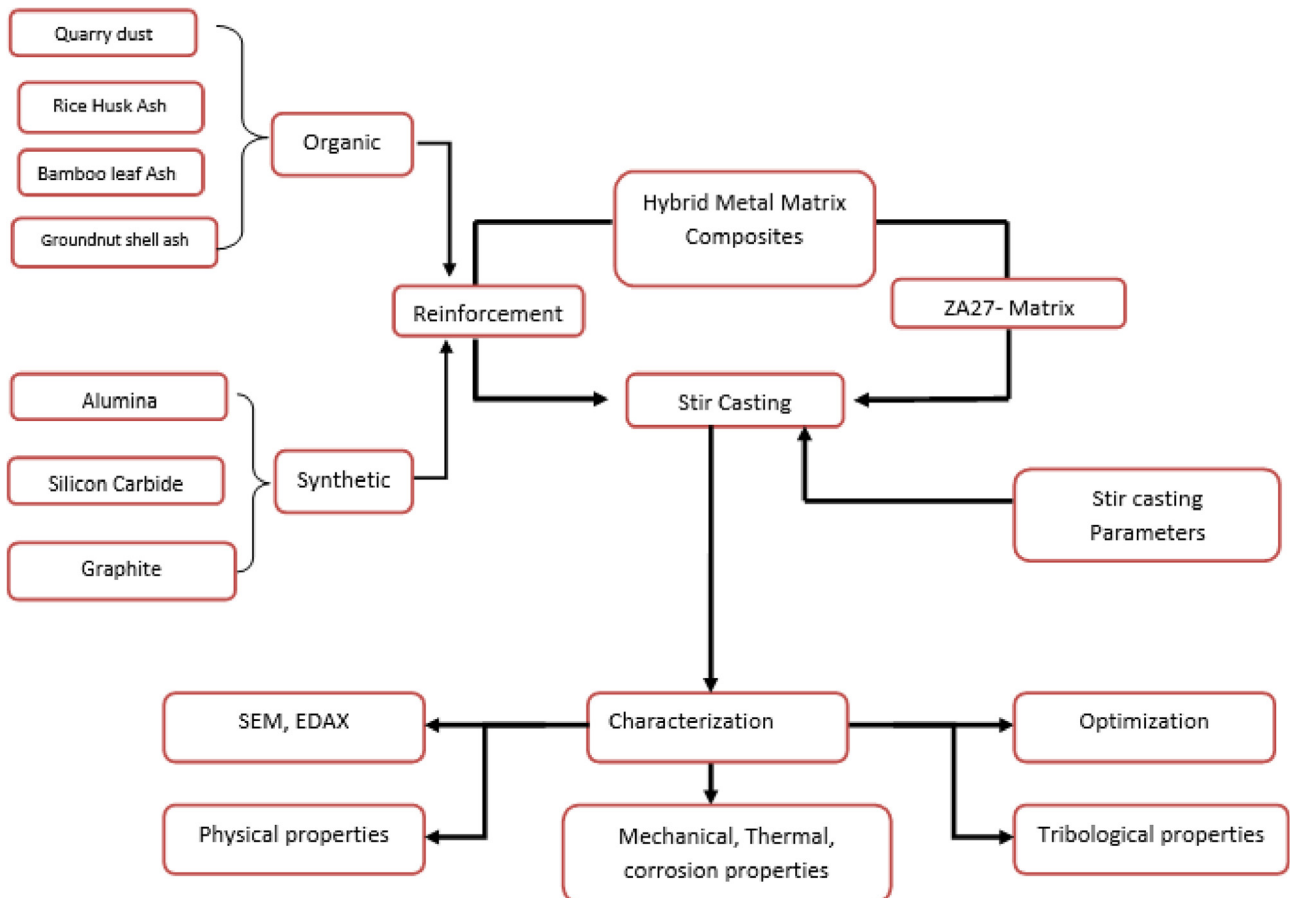


Fig. 1. Flow chart of fabrication and characterization of ZA 27 hybrid MMC by stir casting.

the areas of agriculture machinery, construction machinery, machine tools and wear parts.

1.3. Reinforcement materials:

The reinforcement materials are generally stronger, discontinuous, and harder than matrix materials. Several researchers have used varieties of synthetic ceramic filler materials like Silicon carbide, Alumina, ZrO_2 , garnet, TiC, TiB_2 . In recent years for structural and tribological applications researchers are adding more than one reinforcement material along with addition of dry lubricants for nullifying the effects of hard fillers during machining and for improved tribological properties. In recent times researchers are also adding Agri waste like bamboo leaf ash (BFA), Rice Husk ash (RHA) Ground nutshell ash (GSA) and industrial wastes like fly ash and Quarry dust. These are also called green hybrid composites due to the recycling of by-products of Agri and industrial wastes.

Alumina ($\rho = 3.96 \text{ g/cc}$) and silicon carbide ($\rho = 3.18 \text{ g/cc}$) are synthetic ceramic particles used as reinforcement due to better interfacial bond between matrix and reinforcement resulting in increased strength of the ZA-27 composites. Alumina is a hard and possess high thermal conductivity find its use as insulator. whereas silicon carbide which is expensive and limited in terms of availability is the most widely used reinforcement in weight sensitive and electronic packaging industries [8]. Both these particles enhance wear resistance required in Journal bearing applications. In addition to silicon carbide and alumina. Graphite is added as secondary reinforcement to optimize the wear properties in hybrid ZA-27 MMC as it is a very good solid lubricant also augment machinability of the hybrid composites [9].

Rice husk ash (RHA), Bamboo leaf ash (BLA), Ground nutshell ash (GSA) obtained by burning of dry husk, bamboo leaf and ground nut an agricultural by-product used as organic reinforcement materials in ZA-27 composites. They are of low cost and abundantly available in developing countries reducing the dependence on exorbitant synthetic ceramic particles. The density of RHA ($\rho = 0.31 \text{ g/cc}$), BLA ($\rho = 0.36 \text{ g/cc}$) and GSA ($\rho = 1.54 \text{ g/cc}$) are low when compared to synthetic ceramic fillers. These Agri waste contain oxides of aluminium, iron, and silicon suitable for replacing synthetic ceramic fillers with a good cost advantage. GSA contain low silica content compared to RHA and BLA but with high alumina content also density resulting in less dense composites for weight sensitive applications [10].

Quarry dust ($\rho = 1.9 \text{ g/cc}$) obtained by crushing rock is an industrial waste and found to be a substitute for synthetic ceramic like silicon carbide when added to ZA-27 alloy matrix helps in achieving specific strength with improved tribological properties suitable for journal bearing applications [11]. It consists of oxides of silicon, aluminium and iron and purchased at low cost when compared to silicon carbide. The use of quarry dust as reinforcement reduces the problem of disposal thereby reducing environmental pollution.

2. Literature review

The literature review is carried out under the following categories

1. Hybrid ZA-27 MMC containing two synthetic ceramic particles.
2. Hybrid ZA-27 MMC containing synthetic ceramic particles and Agricultural wastes in different proportions.
3. Hybrid ZA-27 MMC containing synthetic ceramic particles and industrial wastes in different proportions.

2.1. Hybrid ZA27 MMC containing synthetic ceramic particles

There are a lot of research articles published on ZA-27 MMC reinforced with various synthetic ceramic particles like SiC_p , Alumina, garnet, ZrO_2 , boron carbide, graphite, MoS_2 , etc. But there are very few articles published containing two synthetic ceramic particulates in ZA-27 alloy they are silicon carbide with alumina, silicon carbide with graphite, and Alumina with graphite are most studied.

Kiran [12] has discussed the influence of silicon carbide with graphite addition on ZA-27 alloy for journal bearing with the increase in silicon carbide content from 0 to 9 wt% and keeping graphite with 3 wt% constant. Tensile strength was found to increase due to the dislocation density of reinforcement in the matrix whereas ductility dropped marginally as shown in Fig. 2. The addition of graphite in ZA27 matrix along with silicon carbide resulted in low coefficient of friction.

Kiran [9] has conducted wear test under dry sliding conditions on ZA-27 hybrid metal matrix composite reinforced with 9 wt% silicon carbide and graphite 3 wt% by stir casting. It is found that Thermal treatment of the traditional ZA alloys enhance the dimensional stability and ductility of the dimensions. Most of the heat treatments lead to a decrease in hardness and tensile strength, at the same time achieve enhanced tribological characteristics, despite decreased hardness. In regulating the structural, mechanical, and tribological properties of ZA alloys, the temperature and period for homogenization and ageing play the dominant role. For all applied loads, the heat-treated alloy samples exhibited increased tribological performance (reduced friction coefficient and wear rate) over the cast ones. Despite decreased hardness, the enhanced tribological performance of the heat-treated alloys could be attributed to finer and more uniform distributed micro constituents and decreased cracking propensity [13].

The castings were subjected to thermal processing (T6 heat treatment) to reduce residual stresses and the authors have also optimized the wear test results using Taguchi techniques. L_{27} orthogonal array with three factors of load, sliding distance and three levels of load (15 N, 45 N, 75 N), Sliding distance (1000 m, 3000 m, 5000 m) and sliding speed (0.63 m/s, 1.88 m/s, 3.14 m/s) ANOVA was performed to understand the interactions of various factors. The hybrid composites exhibited mild wear where as ZA27 alloy exhibited severe wear as per the SEM studies of worn surfaces as shown in Fig. 3. Graphite as secondary reinforcement along with SiC_p improved the wear strength forming a protective layer for wear loss.

Shravan Kumar Yadav [14] conducted experiments to determine hardness, impact strength and tensile strength of ZA-27 alloy containing Alumina and graphite as reinforcement particles. The alumina weight percent was varied from 0 to 3 wt% keeping graphite content as 3 wt% constant. Hardness value is found to be high for 3 wt% Alumina but decreased with the addition of graphite. Tensile strength and impact strength increased with increase in Alumina content.

Ajith G Joshi [15] studied the tribological properties of ZA-27 reinforced with Alumina and Graphite. The composite was prepared by stir casting route. Microstructure details revealed good bonding with ZA27 matrix and particle despite the high residual strength developed due to coefficient of thermal expansion mismatch between matrix and reinforcement particles and a uniform distribution is noticed. The highest wear resistance was observed for hybrid MMC with 9 wt% Al_2O_3 and 3% graphite. At high loads of 50 N severe form of wear was observed. Increasing the sliding distance also resulted in wear loss. worn surface SEM revealed a

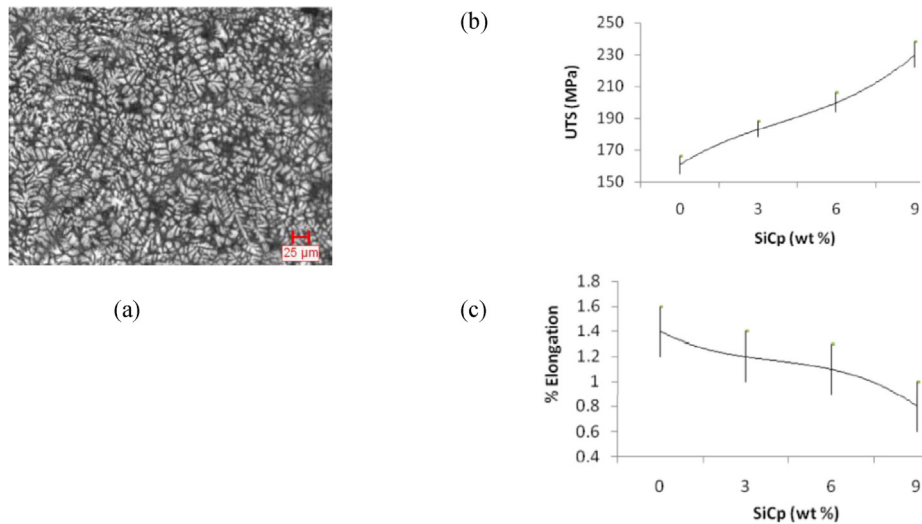


Fig. 2. (a) Microstructure of ZA27 MMC containing SiC and graphite. (b) Variation of strength with SiC content (c) Percentage of elongation with increase in SiC content [12].

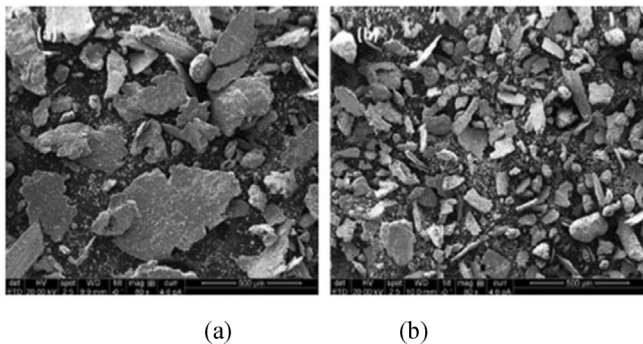


Fig. 3. (a) Worn out particles of ZA27 alloy (b) Worn out particles of hybrid composite [9].

tribo-film layer due to the presence of solid lubricant graphite. Whereas at a higher percentage of reinforcement Alumina (9 wt %) clustered with graphite particles and caused pullout of alumina particles by ploughing mechanism and there was an abrasive (3-body) wear observed instead of adhesive (dry sliding) wear mechanism.

Swati Gangwar [16] In this work ZA-27 alloy (99% parts) is mixed with same size graphite particles (30 μm) and alumina (30 μm) in the preparation of hybrid MMC to obtain better bonding at the interface.

ZA-27 alloy reinforced with graphite alumina hybrid MMC were fabricated using stir casting method. From phase diagram melting range of ZA-27 lies between 350 °C–450 °C. Since solidification occurs during pending eventually resulting in casting defects, the temperature of melting is increased to 540 °C. Preheated alumina and graphite are mixed with continuous stirring at 400 rpm for 30 min and poured into a hardened steel die and then samples are quenched water. Rockwell hardness number, compression strength, and impact strength increased with an increase in graphite and alumina weight percentage. Density values of the composites showed differences in experimental and theoretical one due to the pores resulting in lower fatigue strength and water penetration. 10.5 wt% of hybrid reinforcement in the matrix alloy shows high porosity. At higher graphite presence hardness reduces. The compressive strength increased with increase in wt. % of reinforcement particles. But at a high rate of reinforcement, the compression test revealed reduction strength due to the

agglomeration effect presence of a huge amount of graphite presence in the composite. Sliding wear studies of composites is conducted using a Pin-on-disc machine for four loads of 10 N to 40 N in steps of 10 N for different sliding speeds of (1.309, 2.618, 3.927, and 5.236 m/s) with constant 1000 m of sliding distance. The wear rate of ZA-27/Alumina/Graphite MMC reduced with an increase in reinforcement content because of presence of alumina and graphite micro particulates as dry lubricant further reduce the wear rate of composites. Alumina and graphite will impart strength and lubricating qualities in the composites since the Alumina has the same HCP crystal structure as boron nitride a good solid lubricant [17].

Although many research articles and review papers exist on microstructure, tensile, wear, and corrosion behavior of ZA27 composites with single synthetic ceramic particles as reinforcement. There is a scope to explore the effect of two or more synthetic ceramic fillers of a different type, size, and shape on distribution, tensile, wear, and corrosion characteristics of ZA27 hybrid MMCs.

2.2. Hybrid ZA27 MMC with synthetic ceramic particles and agricultural wastes in different proportions

Due to the high cost of synthetic ceramic materials and lack of availability, a combination of agricultural waste and conventional ceramic fillers can be used in the production of Hybrid ZA-27 MMC. Agri waste offers the advantages of ease of availability, low cost, sustainability, and eco-friendly. In countries like India and other developing countries which are the agrarian economy, Agri waste/by-products are generated in large amount and can be used as reinforcement in making new composites. This paper gives an overview of some of the Agri waste used in the preparation of hybrid ZA-27 MMC like Bamboo leaf ash (BLA), rice husk ash (RHA), and Ground nutshell ash (GSA) in mix ratio with conventional ceramic particles.

Kenneth Kanayo Alaneme [5] investigated the rice husk ash (RHA), silicon carbide, and graphite particles reinforced ZA-27 aluminum alloy reinforced with fabricated by liquid metallurgy route. The microstructure and mechanical properties of RHA (Rice husk ash) an Agri waste during rice production of particle size (50 μm), SiC (30 μm) and graphite (30 μm) is determined with weights of reinforcement in the ratio of 7 wt% and 10 wt% with (RHA; SiC; graphite) in the composites. With an increase in rice husk ash, hardness is found to decrease even though RHA contains

traces of oxides like silica, ferric oxides, magnesium oxides whose hardness is less than the silicon carbide. Both the 7 wt% and 10 wt% reinforced composites showed decreased hardness values with an increase in the weight percent of RHA but with reduced SiC_p weight percent in the reinforcement phase of the composites. The strength for 7 wt% and 10 wt% reinforced composites reduced with an increase in the weight ratio of RHA and SiC_p in the composites. With 40 wt% of Rice husk ash, reduction of 8.5% in tensile strength was found.

K.K. Alaneme [18] investigated the mechanical and corrosion behavior of hybrid Zn-Al composites containing 7 wt% and 10 wt% of Ground nutshell ash (GSA) and SiC varied weight ratios (GSA: SiC). It is found that the hardness of hybrid composites and ultimate tensile strength reduced with an increasing weight percent of GSA. Even though the elongation percentage decreased somewhat with the GSA content increasing, the trend was not as consistent as that of hardness and tensile strength. With an increase in the GSA in the composites, the fracture strength of the hybrid composites improved.

Kenneth Kanayo alaneme [19] investigated the strength and corrosion properties of ZA-27 alloy reinforced with Bamboo leaf ash (BLA) and SiC . The tensile strength, percentage elongation and corrosion performance of composites based on Zn-27Al alloy reinforced with 7wt. % and 10wt. % percent Bamboo leaf ash (BLA) and SiC in different weight ratios (BLA: SiC) was investigated. mechanical strength has improved although a slight decrease in ductility was found as the BLA contains silicon oxides as a major element that is softer than silicon carbide particles. It is found that the presence of BLA and SiC as reinforcement in Zn-27Al composites showed good corrosion resistance in acidic environments when compared with the use of synthetic ceramic fillers SiC reinforced Zn-27Al composite.

2.3. Hybrid ZA27 MMC containing synthetic ceramic particles and industrial wastes in different proportions

Industrial wastes/by-products are generated during various processing activities like red mud in aluminium refineries, quarry dust in rock crushing plant, fly ash in thermal power generation to name a few. These wastes contain various oxides that help make hard, wear-resistant, and strong composites. There are a lot of research articles on incorporating these industrial wastes as primary reinforcement in synthesizing composites for understanding the mechanical, tribological, thermal, and corrosion properties.

Davies Oladayo Folorunso [20] investigated the effect of industrial waste i.e., quarry dust (QD) and SiC particles with 8 wt% and 10 wt% of QD: SiC_p in the ZA27 hybrid MMC. The hybrid composites is synthesized by stir casting. Metallographic studies revealed the distribution of quarry dust and SiC particles in the dendritic ZA27 matrix. Void fraction was low in the produced composites samples paving the way for improved strength in the composites. The fracture toughness values of the composites increased with the increase in QD and SiC particles which is a good sign for the composites applied in shock load applications. The wear properties of hybrid composites containing 50% and 75% quarry dust for both 8 wt% and 10 wt% was encouraging.

3. Industrial applications of ZA-27 hybrid metal matrix composites

Zinc Aluminum alloy itself has proved to be commercially successful due to its superior and low cost antifriction alloy compared to traditional bronze alloys like leaded bronze and phosphor bronze and also cast iron. ZA-27 composites are developed to over-

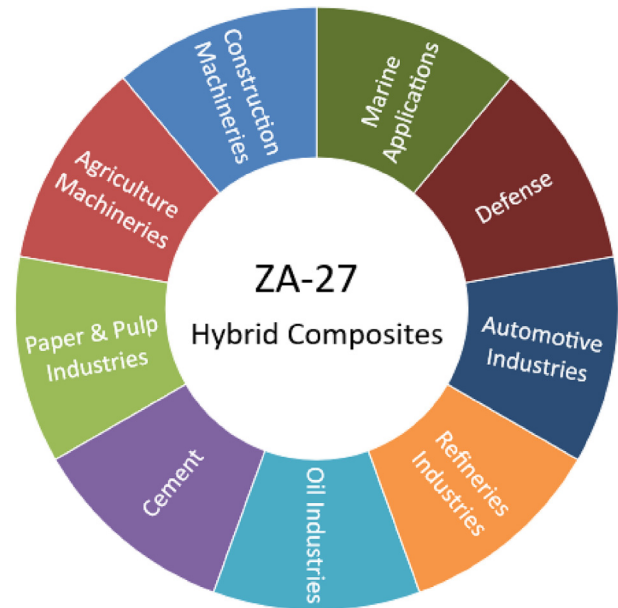


Fig. 4. Industrial applications of ZA27 hybrid composites.

come the shortcomings of deterioration of strength and ductility above 100 °C.

Composites of ZA-27 are potential candidate for industrial applications especially as bush and bearing elements, wear plates for high load and low speed conditions in construction machineries, Agriculture machineries, paper and pulp industries, cement, oil industries, refineries, automotive, defense and marine engineering due to its excellent structural, tribological and corrosion properties as illustrated in Fig. 4.

4. Conclusion

This paper has tried to discuss in detail the different reinforcements like conventional/synthetic micro-ceramic fillers and Agri and industrial waste by-products in fabricating ZA-27 hybrid composites by conventional stir casting route only. Stir casting is the easy way of fabricating ZA-27 composites due to its advantages of simplicity, and economical manufacturing. It is found that ceramic particles are extensively used as reinforcement and use of fibers are not attempted much due to their interfacial strength and distribution of particles are better in the composite, mechanical strength are seen to improve with the increase in reinforcement, but percentage elongation is found to decrease. Fracture toughness value decreased with increasing reinforcement content for hybrid ZA-27 MMC. Wear and corrosion studies carried by few authors are revealing encouraging results in terms of improvement in wear strength and reduced corrosion rate in these composites. There is still enormous scope for further exploring the material of ZA-27 by reinforcing with different oxides, carbides of various sizes and shapes with different Agri wastes and industrial waste both as primary and secondary reinforcement for synthesizing ZA-27 hybrid MMC and conduct test to evaluate the material for mechanical corrosion and wear characteristics.

The above review reveals that there is scope for exploring the properties of hybrid metal matrix composites for various Engineering applications. Even though there are very few papers on ZA-27 hybrid MMC processed by stir casting route. There is scope to research ZA-27 alloy by including solid lubricants along with ceramic particles as reinforcement. There are researchers evincing interest in adding Agri waste like Rice husk ash (RHA), bamboo leaf

ash (BLA), Groundnut shell ash (GSA), and industrial wastes like quarry dust particles (QD) as reinforcement replacing synthetic oxides and carbides widely researched by various authors. This paper does not review the research articles on alternate fabrication routes of making the ZA-27 hybrid composites like powder metallurgy, squeeze casting, spray forming, Rheo-casting, electromagnetic stir casting, etc.

The mechanical wear and corrosion properties of ZA- 27 hybrid MMC obtained by the above literature review is encouraging in applying these materials in highly demanding applications at an affordable cost. The review also highlights the ample scope for using recycled waste as reinforcement particles in varied weight percentages thereby reducing the problem of disposal of industrial waste and improving sustainability.

CRediT authorship contribution statement

G.R. Gurunagendra: Conceptualization, Data curation, Investigation, Methodology, Writing - original draft. **B.R. Raju:** Writing - review & editing, Supervision. **Vijayakumar Pujar:** Writing - review & editing. **D.G. Amith:** Writing - review & editing. **Poornachandra:** Writing - review & editing. **H.S. Siddesha:** Writing - review & editing, Supervision.

Declaration of Competing Interest

The authors declare that they have no known competing financial interests or personal relationships that could have appeared to influence the work reported in this paper.

References

- [1] M. Babić, R. Ninković, Zn-Al alloys as tribomaterials, *Tribol. Ind.* 26 (2004) 3–7.
- [2] M. Babić, R. Ninković, S. Mitrović, I. Bobić, Influence of heat treatment on tribological behavior of Zn-Al alloys, *Tribol. Ind.* 29 (2007) 23–31.
- [3] N. Shiva Kumar, Mechanical and wear behavior of ZA-27/SiC/Gr hybrid metal matrix composites, *Mater. Today Proc.* 5 (9) (2018) 19969–19975, <https://doi.org/10.1016/j.matpr.2018.06.363>.
- [4] B.O. Fatile, B.O. Adewuyi, H.T. Owoyemi, Synthesis and characterization of ZA-27 alloy matrix composites reinforced with zinc oxide nanoparticles, *Eng. Sci. Technol. Int. J.* 20 (3) (2017) 1147–1154, <https://doi.org/10.1016/j.jestch.2017.01.001>.
- [5] K.K. Alaneme, O.J. Ajayi, Microstructure and mechanical behavior of stir-cast Zn-27Al based composites reinforced with rice husk ash, silicon carbide, and graphite, *J. King Saud Univ. - Eng. Sci.* 29 (2) (2017) 172–177, <https://doi.org/10.1016/j.jksues.2015.06.004>.
- [6] J. Hashim, L. Looney, M.S.J. Hashmi, Particle distribution in cast metal matrix composites - Part II, *J. Mater. Process. Technol.* 123 (2) (2002) 258–263, [https://doi.org/10.1016/S0924-0136\(02\)00099-7](https://doi.org/10.1016/S0924-0136(02)00099-7).
- [7] D. Miracle, Metal matrix composites - From science to technological significance, *Compos. Sci. Technol.* 65 (15-16) (2005) 2526–2540, <https://doi.org/10.1016/j.compscitech.2005.05.027>.
- [8] A. Ramanathan, P.K. Krishnan, R. Muraliraja, A review on the production of metal matrix composites through stir casting - Furnace design, properties, challenges, and research opportunities, *J. Manuf. Process.* 42 (2019) 213–245, <https://doi.org/10.1016/j.jmapro.2019.04.017>.
- [9] T.S. Kiran, M. Prasanna Kumar, S. Basavarajappa, B.M. Viswanatha, Dry sliding wear behavior of heat treated hybrid metal matrix composite using Taguchi techniques, *Mater. Des.* 63 (2014) 294–304, <https://doi.org/10.1016/j.matdes.2014.06.007>.
- [10] K.K. Alaneme, M.O. Bodunrin, A.A. Awe, Microstructure, mechanical and fracture properties of groundnut shell ash and silicon carbide dispersion strengthened aluminium matrix composites, *J. King Saud Univ. - Eng. Sci.* 30 (1) (2018) 96–103, <https://doi.org/10.1016/j.jksues.2016.01.001>.
- [11] K.K. Alaneme, B.J. Bamike, Characterization of mechanical and wear properties of aluminium based composites reinforced with quarry dust and silicon carbide, *Ain Shams Eng. J.* 9 (4) (2018) 2815–2821, <https://doi.org/10.1016/j.asej.2017.10.009>.
- [12] T.S. Kiran, M. Prasanna Kumar, S. Basavarajappa, B.M. Vishwanatha, Mechanical properties of as-cast ZA-27/Gr/SiCp hybrid composite for the application of journal bearing, *J. Eng. Sci. Technol.* 8 (2013) 557–565.
- [13] M. Babic, S. Mitrovic, B. Jeremic, The influence of heat treatment on the sliding wear behavior of a ZA-27 alloy, *Tribol. Int.* 43 (1-2) (2010) 16–21, <https://doi.org/10.1016/j.triboint.2009.04.016>.
- [14] S.K. Yadav, G. Karuna Kumar, R. Vijaya Prakash, Preparation and characterization of ZA27-alumina-graphite reinforced hybrid composites, *Mater. Today Proc.* 18 (2019) 57–65, <https://doi.org/10.1016/j.matpr.2019.06.277>.
- [15] A.G. Joshi, R.S. Desai, M. Prashanth, S. Sandeep, Study on Tribological Behavior of ZA-27/Al₂O₃/Gr MMC, *Int. J. Emerg. Technol.* 7 (2016) 117–122, <https://doi.org/10.1016/j.jksues.2015.06.004>.
- [16] S. Gangwar, V. Payak, V.K. Pathak, A. Jamwal, P. Gupta, Characterization of mechanical and tribological properties of graphite and alumina reinforced zinc alloy (ZA-27) hybrid metal matrix composites, *J. Compos. Mater.* 54 (30) (2020) 4889–4901, <https://doi.org/10.1177/0021998320938442>.
- [17] M.O. Bodunrin, K.K. Alaneme, L.H. Chown, Aluminium matrix hybrid composites: A review of reinforcement philosophies; Mechanical, corrosion and tribological characteristics, *J. Mater. Res. Technol.* 4 (4) (2015) 434–445, <https://doi.org/10.1016/j.jmrt.2015.05.003>.
- [18] K.K. Alaneme, S.I. Adama, S.R. Oke, Mechanical properties and corrosion behaviour of Zn-27Al based composites reinforced with silicon carbide and bamboo leaf ash, *Leonardo Electron. J. Pract. Technol.* 13 (2014) 58–71.
- [19] K.K. Alaneme, B.O. Fatile, J.O. Borode, Mechanical and corrosion behaviour of Zn-27Al based composites reinforced with groundnut shell ash and silicon carbide, *Tribol. Ind.* 36 (2014) 195–203.
- [20] D.O. Folorunso, S.S. Owoeye, Influence of quarry dust-silicon carbide weight percentage on the mechanical properties and tribological behavior of stir cast ZA-27 alloy based hybrid composites, *J. King Saud Univ. - Eng. Sci.* 31 (3) (2019) 280–285, <https://doi.org/10.1016/j.jksues.2017.07.003>.

Microstructure, Dislocation Density and Thermal Expansion Behavior Using Thermo Elastic Models of Zircon Sand Reinforced as Cast ZA-27 Composites

G. R. Gurunagendra^{1*}, V. Bharat¹, B. R. Raju², D. G. Amith¹, Vijayakumar Pujar¹, C. Ravi Keerthi¹

¹Global Academy of Technology, Bangalore, India

²The Oxford College of Engineering, Bangalore, India

Email: *gurunagendra.gn@gmail.com

How to cite this paper: Gurunagendra, G.R., Bharat, V., Raju, B.R., Amith, D.G., Pujar, V. and Keerthi, C.R. (2021) Microstructure, Dislocation Density and Thermal Expansion Behavior Using Thermo Elastic Models of Zircon Sand Reinforced as Cast ZA-27 Composites. *Journal of Minerals and Materials Characterization and Engineering*, 9, 100-115.

<https://doi.org/10.4236/jmmce.2021.91008>

Received: November 23, 2020

Accepted: January 26, 2021

Published: January 29, 2021

Copyright © 2021 by author(s) and Scientific Research Publishing Inc.

This work is licensed under the Creative Commons Attribution International License (CC BY 4.0).

<http://creativecommons.org/licenses/by/4.0/>



Open Access

Abstract

In the present work stir casting route is used to fabricate the ZA27 Metal matrix composites containing 3 wt%, 6 wt%, 9 wt%, and 12 wt%. Zircon sand particulates of size 100 mesh. Microstructure studies using Optical Microscopy, SEM-EDAX are carried out to ascertain the distribution and morphology of particulates in the composites. Effect of zircon sand as reinforcement on bulk density, porosity, of the fabricated composites is studied. SEM studies are carried out to understand the behavior of as-cast ZA27 alloy reinforced with zircon sand. The dislocation density of the fabricated composite affects the strength of the composites and depends on the strain due to thermal mismatch and is found to increase with increase in weight% of zircon sand. However, it does not consider casting defects of voids/clustering observed in micrographs of the fabricated composite. Porosity in composites does not have influence on Coefficient of thermal expansion (CTE) of the ZA27 composites studied using thermoelastic models like Kerner and turner model and rule of mixtures of composite.

Keywords

Density, Porosity, Dislocation Density, Thermoelastic Models, Rule of Mixtures

1. Introduction

Over the years, Metal matrix composites are playing a significant role in aerospace, automotive, space engineering and other industrial applications due to

their superior mechanical, tribological and thermal properties.

Matrix is made of monolithic Metal or alloy and embedded with hard particulates to augment the properties of MMC compared to the monolithic metals/alloys. Aluminum, Magnesium, titanium, copper and Zinc based alloys are widely employed as matrix materials in various applications.

Over the past few decades research on zinc-based alloys are being carried out and found to exhibit excellent tribo-mechanical properties apart from low melting point, good cast ability and machinability. Several research have proved the Zinc-Aluminum family of alloys like ZA12 and ZA27 are possessing better strength when compared to cast-iron, bronze and plastics as tribo-elements for operating at moderate temperature condition. In spite of good tribo-mechanical properties The ZA alloy exhibits dimensional instability at temperature greater than 100°C. With heat treatment techniques of cast alloy and addition of high melting point ceramic particles to the alloy the properties of the alloy can be improved at the expense of reduction in machinability which can be reduced by addition of dry lubricants [1] [2].

Nowadays researchers are inspired to reinforce these alloys with reinforcement particles and whiskers like Al₂O₃, Sic, Garnet, glass, Tic, graphite, Agri and industrial waste etc. to achieve better mechanical, wear and thermal characteristics. There are research reports of ZA27 alloy containing more than one reinforcement to produce hybrid composites like a ceramic filler and a solid lubricant like graphite to offset the negative effects of ceramic fillers on machinability [3] [4]. Also in recent times, researchers are adding nanofillers in recent times to the as-cast ZA27 alloy and fabricating the MMC using different metallurgical processes like, stir casting, double stir casting, squeeze casting, powder metallurgy and also ultrasonic-assisted stir casting for obtaining better casting and improved properties [3] [5]. There is not much work carried out on characterization of zircon sand reinforced with ZA27 alloy especially beyond 5% weight fraction also micro-mechanical behavior of such composites [6]. Coefficient of thermal expansion (CTE) plays an important role in ZA27 materials used as tribo-elements and needs to be estimated for better performance of the elements. Thermoelastic models are used to predict the CTE of the ZA27/zircon sand composites [7]. Effects of presence of voids on dislocation density of composites and cracking/agglomeration of zircon particles in ZA27 matrix with increased weight fraction on CTE of composites and their effects on strength is addressed [8]. preparation of composites by various routes and its processing, matrix-reinforcement bonding and characterization poses significant challenge in the end use of composites, also decrease in ductility, poor matrix-reinforcement interface, particle cracking, debonding/pull out of particles and agglomeration of particulates are some of the challenges in preparation of composites. composites are subjected to age hardening to obtain better strength and improved ductility as well as tribological properties [2] [9].

Stir casting is widely adopted route in preparing these composites due to their advantages like bulk manufacturing, ease of fabrication and economy. Also,

there is enough scope to investigate and understand the behavior of ZA-27 containing microparticulate zircon sand as primary reinforcement and hybrid composites with dry lubricants as secondary reinforcement.

2. Experimental Procedure (Figure 1 and Table 1)

In this work Zircon sand ($ZrSiO_4$) of particle size 100 mesh is used as a primary reinforcement in the matrix of ZA-27. Chemical composition of Zircon sand is Zircon oxide and hafnium of 65% and silica of 24% with traces of Al_2O_3 , TiO_2 and Fe_2O_3 [10]. The thermal coefficients of zircon sand is low compared to other oxides of ceramics improving the interface strength, also the density of zircon sand ($\rho = 4.56$ g/cc) is in close proximity with the density of ZA-27 ($\rho = 4.5$ g/cc) alloy which reduces the problems of gravity segregation due to large density difference between matrix phase and dispersed phase (Figure 2 and Table 2).



Figure 1. (a) Zircon sand particles (b) ZA-27 ingot.

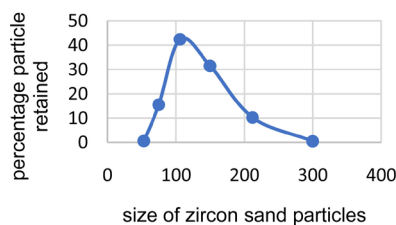


Figure 2. Particle size by sieve analysis.

Table 1. The chemical compositions of ZA-27 alloy.

| Al | Mg | Cu | Fe | silicon | Zinc |
|--------|-------|-------|-------|---------|-----------|
| 25.60% | 0.07% | 2.10% | 0.04% | 0.001 | Remainder |

Table 2. Properties of zircon sand.

| | |
|--|------------|
| Melting point ($^{\circ}C$) | 2500 |
| Hardness (Mohs) | 7.5 |
| Density (g/cc) | 4.5 |
| linear coefficient of expansion (10^{-6} K) | 4.5 |
| crystal structure | Tetragonal |

Preparation of ZA27 MMC by Stir Casting

Composite was fabricated by stir casting method regarded as the most economical and suitable for mass production compared to other techniques of fabrication. The setup is as shown in **Figure 3**. To begin with the weight of reinforcements for 3 wt%, 6 wt%, 9 wt% and 12 wt% Zircon sand to prepare 2000 g of ZA-27 alloy was calculated. Zircon sand particles were preheated to around 200°C in an oven to remove presence of moisture in it ZA27 alloy ingots were placed in the graphite crucible and super-heated to a melting temperature and stirring was done for homogenizing temperature later the temperature was reduced to 450°C (semi solid state) Now, the reinforcement particles are fed at a rate of 20 g/min and the mixture with continued heating is stirred at a speed of 350 rpm to create vortex for 5 minutes for better distribution of particles. 10 g of Magnesium rod was added to improve wettability and the melt is degassed using C₂Cl₆ (hex chloroethylene tablets) in order to eliminate porosity and remove air presence in the mixture. The composite was poured at 500°C into the preheated cast iron die for better solidification [6].

3. Results and Discussion

Theoretical density and experimental density of the base alloy and composite with different weight percentage of composite is evaluated. There will be difference in the values of densities due to the voids and pores generated during casting. Due to the presence of voids mechanical properties will get reduced so it is obvious to determine the density and porosity of the composites for ascertaining the quality of composites produced. Theoretical density is calculated using the rule of mixture,

$$\rho_{\text{theoretical}} = \frac{100}{\sum_{i=1}^n \frac{x_i}{\rho_i}} \quad (1)$$

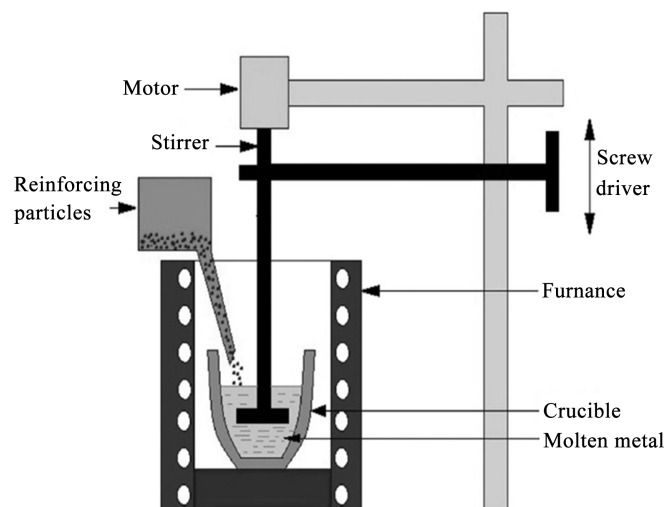


Figure 3. Diagram of stir casting set up.

Experimental density is determined using the Archimedes principle by measuring the known volume of water displaced by the base alloy and composite specimens. The mass of the specimen is measured using a weighing balance (make: shimadzu-Electronic balance) of readability of 0.0001 grams.

ρ = mass of the specimen/volume of water displaced

$$\% \text{Porosity} = \frac{\rho_{th} - \rho_{exp}}{\rho_{th}} \times 100 \quad (2)$$

From the values of density of base alloy and composite it is observed that density decreases with increase in reinforcement as shown in **Figure 4**. Porosity of the composite was found to increase with the reinforcement content (**Figure 5**). The increase in porosity is attributed to gas entrapment during mixing, shrinkage, and presence of air bubbles in the composite slurry.

3.1. Hardness Test (Figure 6)

Hardness is the ability of the material for indentation. Rockwell Hardness number of the bulk specimen of the base alloy and composites is measured using indentation of 1/16' ball indenter under a load of 100 Kgf for dwell time of 15 seconds. An average of values of readings obtained during the tests were taken and tabulated. The hardness was found to increase with increase in weight (%) of zircon sand particles.

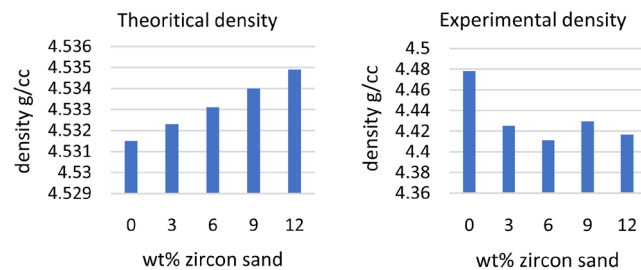


Figure 4. Variation of measure density with composition of reinforcement.

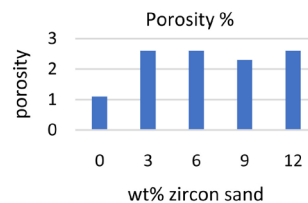


Figure 5. Porosity with increase in weight percentage of zircon sand.

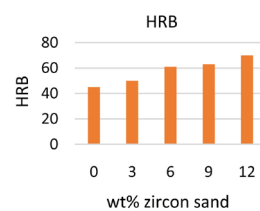


Figure 6. Brinell Hardness for the ZA-27 composite.

The ZA27 alloy is strengthened due to solid solution strengthening, while the ZA27 composite is dispersion strengthened due to presence of zircon sand particulates in the zinc aluminum matrix. The hardness testing is compressive in nature and the area under the indentation is work hardened, resulting in enhanced values.

3.2. Microstructure Studies

When the Zinc alloy is solidified it results information of various phases like, $\alpha + L$, β , $\alpha + \beta$ and $\alpha + \eta$ as shown in **Figure 7** The microstructure in **Figure 2(a)** of ZA-27 alloy reveals the Aluminum rich matrix (α FCC) and dendrite Zinc phase (η HCP), CuZnO_4 at 382°C and $\text{Al}_4\text{Cu}_3\text{Zn}$ at 275°C [11] (**Figure 7**, **Figure 8** and **Figure 9**).

The wavelength of X-rays is in the range of 0.01nm to 10nm that can penetrate through the crystal structure to reveal the properties of material while exiting out of it. XRD is used to characterize different types of materials. Interplanar spacing (d) = Order of Reflection (n) \times Wavelength (λ) / $2 \times \sin\theta$ using Braggs law.

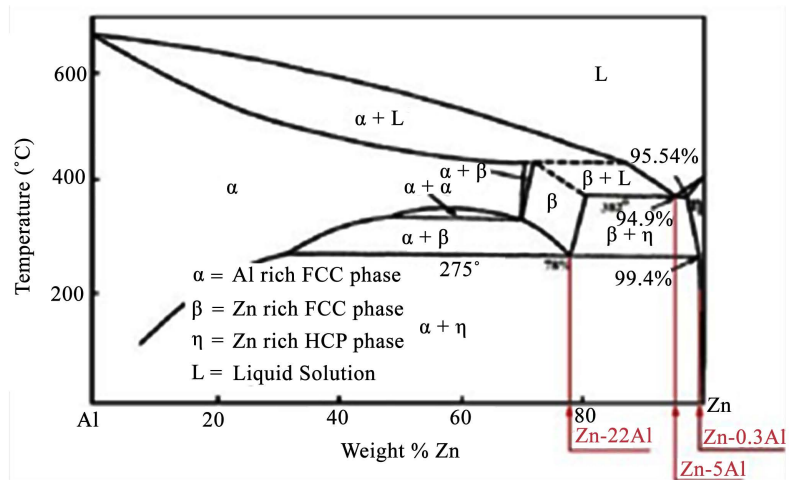


Figure 7. Phase diagram, of ZA-27 alloy.

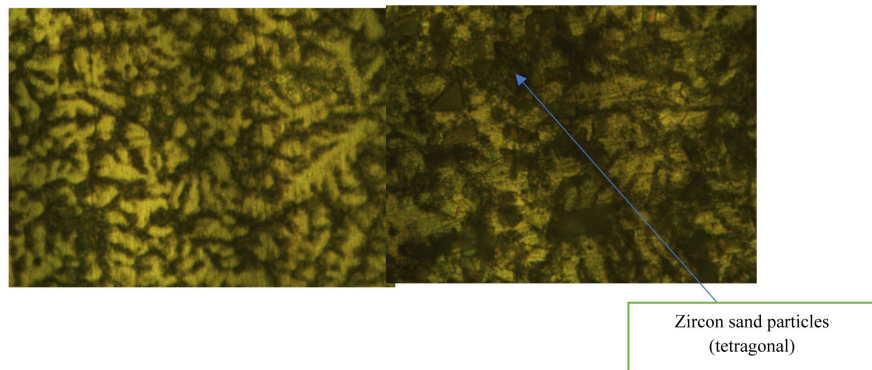


Figure 8. Optical microscope pictures of zircon sand reinforced ZA-27 (100 \times Magnification).

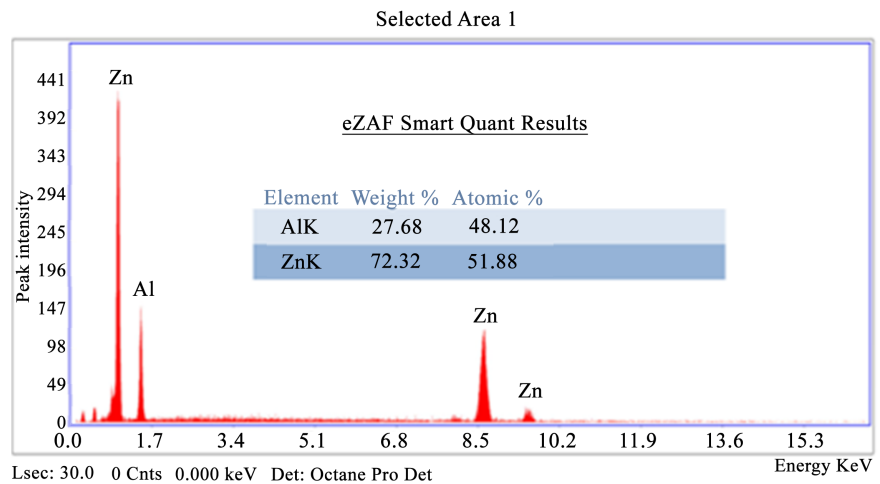


Figure 9. EDAX of ZA-27.

3.3. SEM/EDAX Studies

To study the morphology of the different composition of composites SEM (Make: TESCAN VEGA3) was used with EBSD arrangement attached with EDS detector. The micrographs reveal the presence of distribution of zircon particles and their distribution. The average size of the zircon sand particles is found to be 100 - 150 microns distributed in the matrix of ZA27 alloy and confirms the sieve analysis shown in **Figure 2**. The EDS detector confirms the existence of zinc, aluminum, zircon, and silicon along with the oxides due to chemical reactions at the interface.

Principle of Bragg's law is the basis for X-Ray diffraction. XRD is conducted to identify different phases present in the ZA27 composite samples using PAN-Analytical-Xpert³ powder XRD fitted with Ni filter operated at 30 mA and 40 kV generator settings using Cu- α radiation with a wavelength of 1.5418 Å. The diffraction angle (2θ) range is varied from 20° to 90°.

XRD of the zircon sand and composites confirmed the presence of elements like zircon, silicon, and oxygen in the reinforcement as shown in **Figure 10**. XRD of ZA-27 composites containing 3% and 12% zircon sand reveals the presence of zirconium silicate and their compounds. The compounds are found at the interface of matrix and particles due to chemical reaction of Zinc aluminum with zircon sand (**Figure 11**, **Figure 12** and **Figure 14**).

The presence of voids will bring down the strength of the composite developed. With increase in zircon sand reinforcement content there occurs agglomeration of particles because of which voids get accumulated during deformation. The agglomeration of particulates is undesirable in fabrication of metal matrix composites due to which strength of the fabricated composites certainly reduces. The strength is also obtained by good wetting of the zircon sand and ZA27 alloy, resulting in strong interface for efficient load transfer [12].

The bonding strength at the interface will affect the mechanical and physical properties like coefficient of thermal expansion, thermal conductivity, and

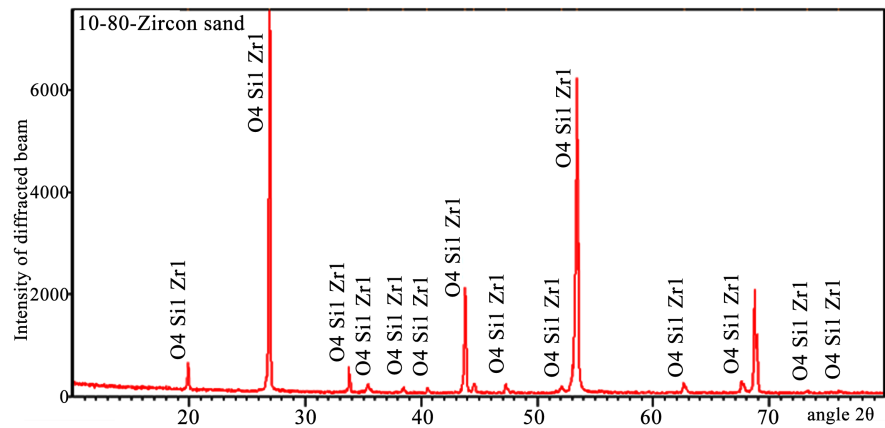


Figure 10. XRD of Zircon sand particles.

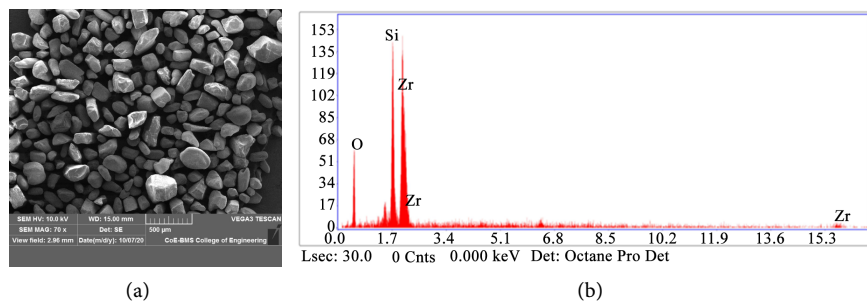


Figure 11. (a) SEM of Zircon sand particles (b) EDAX of Zircon sand particles.

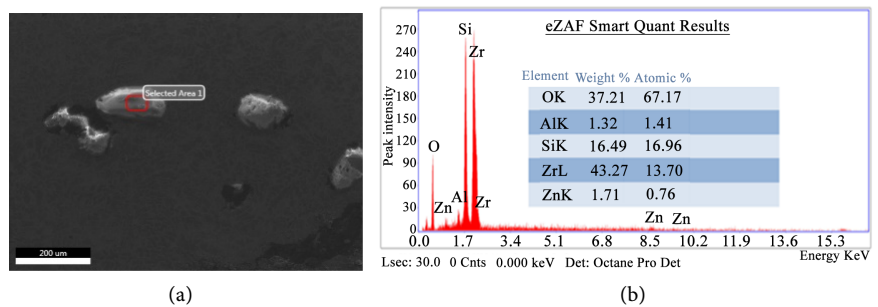
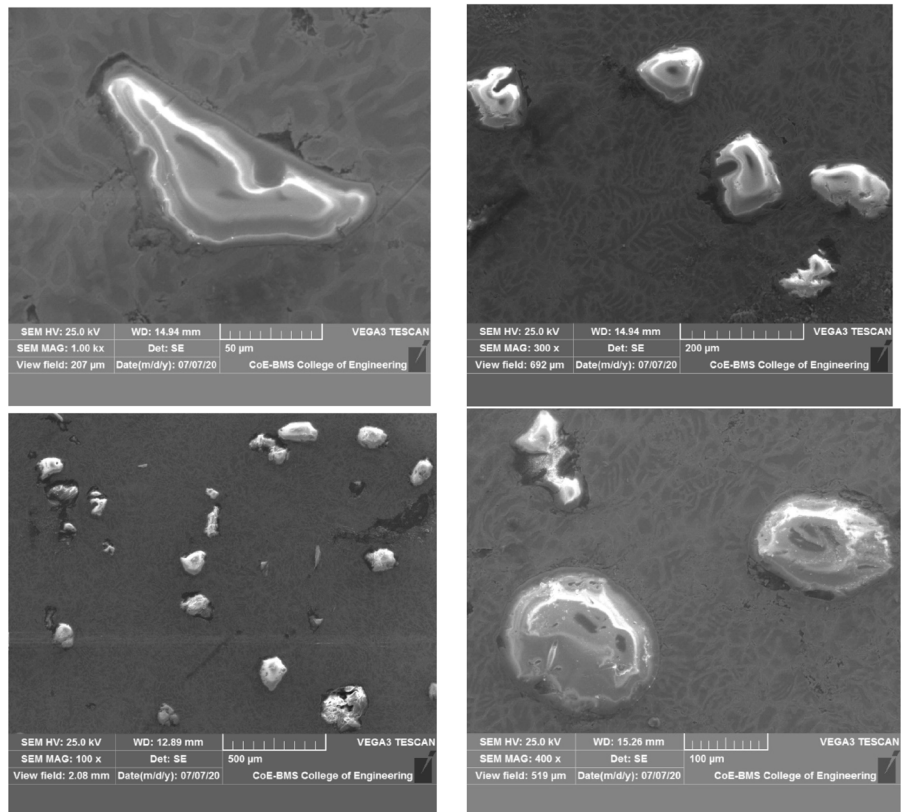


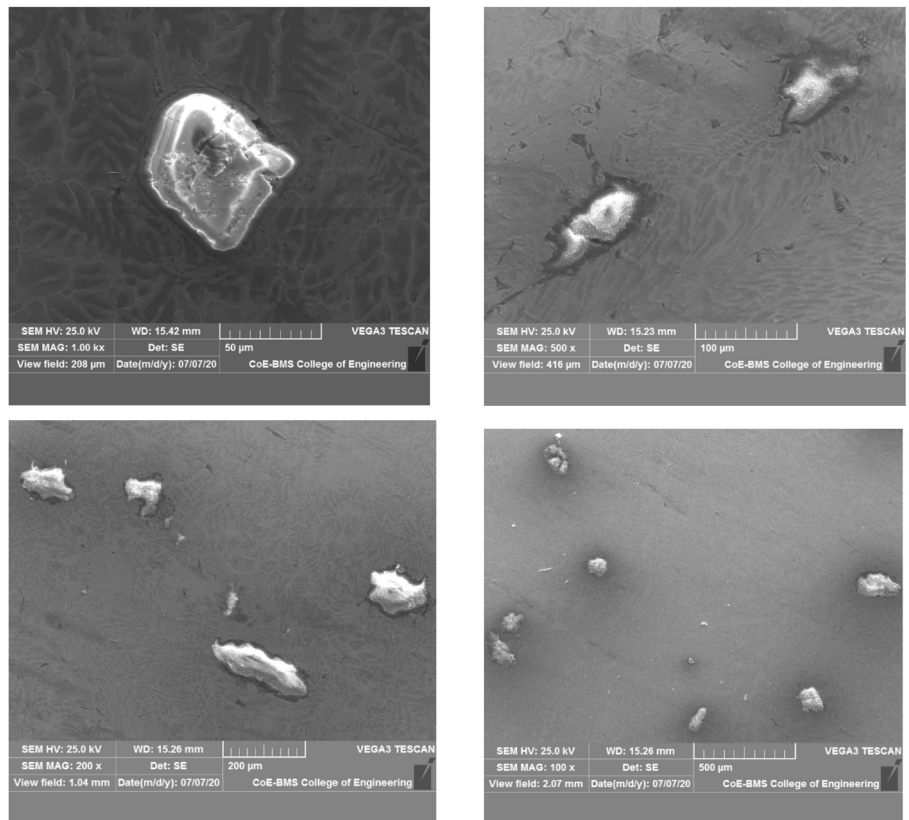
Figure 12. (a) SEM for ZA-27 composite containing zircon sand (b) EDAX for ZA-27 composite containing zircon sand.

damping. Coefficient of thermal expansion is a major criterion for the ZA27 composites with good dimensional stability. To obtain better interface characteristics there are process variables that need to be controlled such as processing technique, pouring temperature, stirring time, stirring speed etc. as well as reinforcement content and chemical properties of matrix and reinforcement [13].

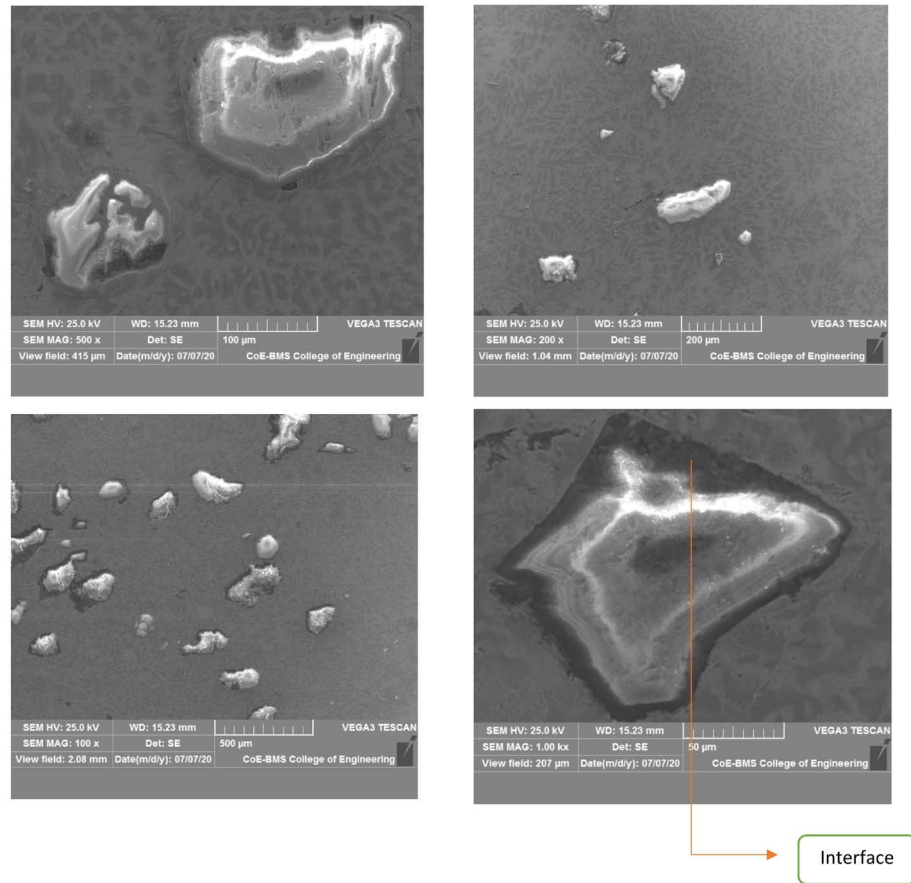
It follows from SEM pictures in **Figure 13** that the multiple microcracks observed in the regions of particle agglomeration will result in reduction in ductile region of the composite. The addition of the hard zircon particles as reinforcement in the ductile soft ZA-27 alloy matrix results in resistance to deformation. Subsequently, causing triaxial stress state ZA27 matrix results in the formation of voids and growth in the matrix and also debonding at the interface of the particle



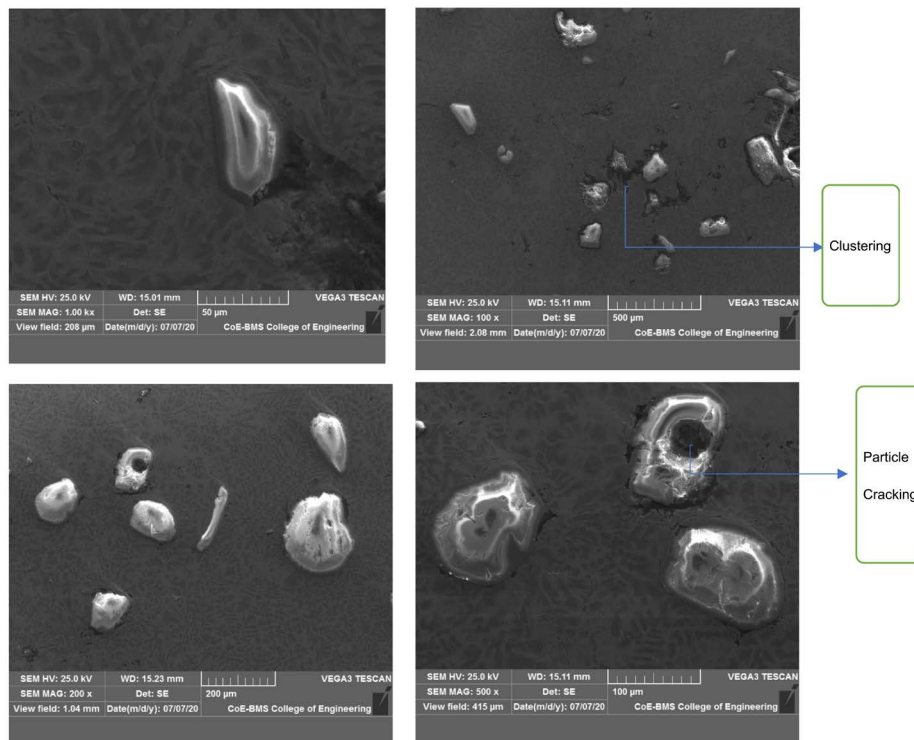
(a)



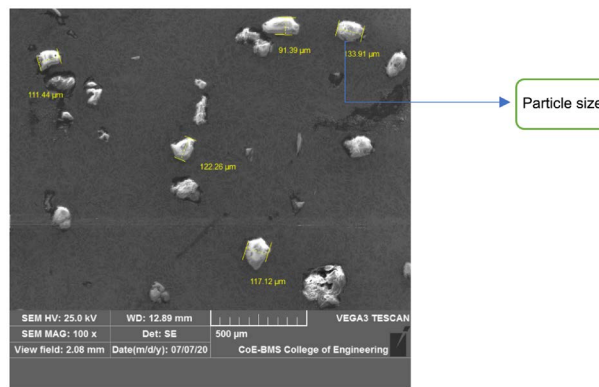
(b)



(c)



(d)



(e)

Figure 13. (a) SEM images of ZA27 composites of magnification 100×, 200×, 300×, 1000× for 3 wt%; (b) SEM images of ZA27 composites of magnification 100×, 200×, 300×, 1000× for 6 wt%; (c) SEM images of ZA27 composites of magnification 100×, 200×, 300×, 1000× for 9 wt%; (d) SEM images of ZA27 composites of magnification 100×, 200×, 300×, 1000× for 12 wt%; (e) Size of the particles distributed in ZA-27 alloy (Magnification: 100×).

and the matrix [12] Shrinkage cavities are seen in the micrographs due to porosity linking to reduction in strength of the composite. Hence, distribution of the particles is an important factor governing the behaviour of the composites. It is very essential to control particle clustering and voids to in the microstructure of the composite [6] (Figure 14).

Apart from the above challenges in processing of composites by liquid metallurgy route it is necessary to understand strong chemical bond that exists between reinforcement and matrix. It is very important to know the various advantages and limitations of fabrication techniques like liquid metallurgy, powder metallurgy, spray deposition or in-situ route of preparation of composites. Also, due consideration to be given to the disparity in the physical properties of Zircon sand as reinforcement and ZA27 matrix in order to obtain a satisfactory interface between the reinforcement and matrix [14]. Large differences in the coefficients of thermal expansion in the reinforcement and matrix lead to the formation of residual stresses in the composite during the fabrication process.

3.4. Dislocation Density of the Composite Due to Difference in CTE

Dislocation density is total length of dislocation to volume of the crystal. It is well known that microscopic movement of dislocation will be having significant effect on the macroscopic deformation of materials. Effect of ceramic particles present in ductile alloy matrix on strength and hardness has been studied earlier [15] by theories like, quench strengthening, Orowan strengthening, work hardening, grain strengthening/Hall Petch mechanism of the composites. During solidification and cooling of composite to room temperature if the particle-reinforcement interface bonding is good then tensile and compressive stresses is developed in ZA27 alloy and zircon sand particles, respectively. Because of large difference of coefficient of thermal expansion (CTE) and temperature

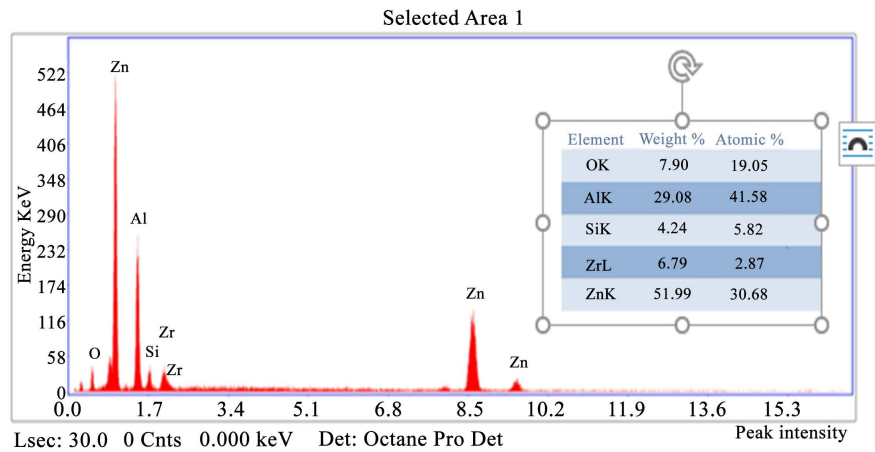


Figure 14. EDAX conforming the presence of reinforcement.

difference (ΔT) due to cooling of composites, plastic deformation of ZA27 alloy matrix is likely to occur in order to accommodate elastic residual stress that forms in matrix, CTE mismatch will be large at interface due to work hardening setting up dislocations formed during cooling of composite whose movements are arrested at particle and matrix interface and exhibits large hardness which decreases with increasing distance from interface. This is due to high density of dislocation at the interface and can be predicted using the model of [15] The dislocation density of particulate composite at the interface is given by Equation (3) where $b = 0.26$ nm burgers vector for zinc alloy [15] $d =$ particle size.

$$\rho = \frac{12\Delta C\Delta T V_p}{bd(1-V_p)} \quad (3)$$

Thermal mismatch strain,

$$\Delta C = \alpha_m - \alpha_p \quad (4)$$

$\Delta T =$ Temperature difference during cooling of casting from solidus temperature.

It is understood that coefficient of thermal expansion of the composites depends on several material parameters like the composition, the microstructure of the matrix, the reinforcement volume fraction and distribution as well as residual stresses formed due to the CTE mismatch, porosity, volume fraction, and the interface strength [16].

Thermo-elastic models like Kerner and Turner have been used to understand the behavior of thermal expansion of composites. It is important to note that these models can predict the CTE relying on the reinforcement content and elastic nature of the matrix [16] [17], however, they do not take into account the case of plasticity of the matrix nor the voids formed in the composites [18].

By Rule of mixture CTE (α) of composites are calculated using,

$$\alpha_c = \alpha_p V_p + \alpha_m V_m \quad (5)$$

Based on Turner model,

$$\alpha_c = \frac{\alpha_m K_m V_m + \alpha_p K_p V_p}{K_m V_m + K_p V_p} \quad (6)$$

Based on Kerner's model.

$$\alpha_c = \alpha_m V_m + \alpha_p V_p + V_m V_p (\alpha_p - \alpha_m) \times \frac{K_p - K_m}{V_m K_m + V_p K_p + \frac{3K_m K_p}{4G_m}} \quad (7)$$

where, α , E , G , K , V are CTE, Young's modulus, Shear modulus, bulk modulus, and volume fraction, respectively. Subscripts m , p , c indicates matrix, particles, and composites.

The Bulk modulus of the material is calculated using,

$$K = \frac{E}{3 \left(3 - \frac{E}{G} \right)} \quad (8)$$

It is important to understand the mechanism of the reduction in CTE values in the ZA27 composites due to presence of voids. From **Table 3** it is found the CTE and elastic modulus of the reinforcement are lower and higher than those of matrix resin, respectively. When this composite is subjected to temperature rise, Thermal mismatch strain, $\Delta C = \alpha_m - \alpha_p$ is induced. This mismatch strain initiates the formation of compressive and tensile stress in the matrix and reinforcement (**Table 4** and **Table 5**, **Figure 15** and **Figure 16**).

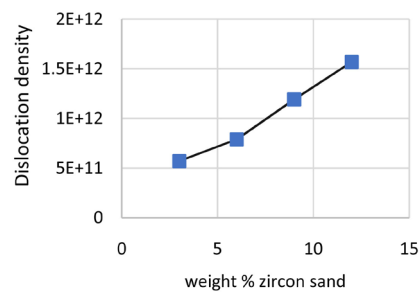


Figure 15. Variation of dislocation density vs weight percent of zircon sand.

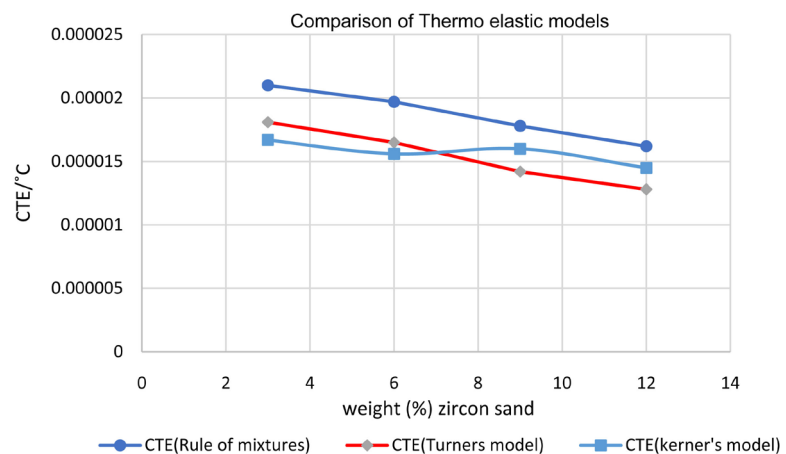


Figure 16. CTE comparison of composite using by thermoelastic models.

Table 3. Elastic constants and CTE of ZA27 and zircon sand.

| Material | <i>E</i> GPa | <i>G</i> Gpa | <i>K</i> Gpa | CTE/ ^o C |
|-------------|--------------|--------------|--------------|----------------------|
| ZA27 | 77 | 31 | 49.7 | 26×10^{-6} |
| Zircon sand | 97.1 | 36.5 | 95.27 | 4.5×10^{-6} |

Table 4. Results of dislocation density.

| Slmo. | Sample | Weight (%) zircon sand | Dislocation density (ρ) |
|-------|--------|------------------------|--------------------------------|
| 1 | A | 0 | - |
| 2 | B | 3 | 5.69×10^{11} |
| 3 | C | 6 | 7.89×10^{11} |
| 4 | D | 9 | 1.19×10^{12} |
| 5 | E | 12 | 1.57×10^{12} |

Table 5. Comparison of CTE values using thermo elastic models.

| Sl No | Sample | Weight (%) zircon sand | CTE (Rule of mixtures) | CTE (Turners model) | CTE (Kerner's model) |
|-------|--------|------------------------|------------------------|-----------------------|-----------------------|
| 1 | A | 0 | - | - | - |
| 2 | B | 3 | 2.10×10^{-5} | 1.81×10^{-5} | 1.67×10^{-5} |
| 3 | C | 6 | 1.97×10^{-5} | 1.65×10^{-5} | 1.56×10^{-5} |
| 4 | D | 9 | 1.78×10^{-5} | 1.42×10^{-5} | 1.60×10^{-5} |
| 5 | E | 12 | 1.62×10^{-5} | 1.28×10^{-5} | 1.45×10^{-5} |

If micro voids are dispersed in the matrix, they are subjected to the compressive stresses, resulting in the shrinkage of the void volume. Hence, the overall CTE of the ZA27 composite is reduced and shape of the voids results CTE reduction. The reduction of CTE values of the composite is also due to low volume fraction of the matrix and existence of voids in the composite. Hence, the ZA27 matrix, with large CTE value is reduced with increase of volume fraction of voids, affecting the overall CTE value of ZA27 composites [7] [8] [16].

If the interface between zircon sand and matrix of ZA27 is good, then a significant amount of the reduction of CTE value of the composite occurs. However, it is more likely that these high thermal stress values induce fracture at the interface. So the compressive thermal stress, which is the main driving force of the composite CTE reduction due to voids, is relaxed in this respect so that the effect of voids on CTE values are reduced [13].

4. Conclusions

The experimental density is reduced with increase in weight fraction of zircon sand and the bulk hardness of the ZA27/zircon composite prepared by stir casting route is found the increase with increase in zircon sand reinforcement. The Optical microscopy studies of the ZA27/zircon composites and microstructure

obtained from SEM/EDAX and XRD studies indicate the presence and distribution of zircon sand particles and intermetallic compounds in the ZA27 matrix along with agglomeration.

The SEM pictures also show the presence of voids and particle clustering in the matrix. The role of particle-matrix interface as revealed from the microstructure of the composite is studied to understand the thermal expansion behavior of composites. Strengthening of composites due to mechanism of dislocation density is obtained analytically.

From the analytical results obtained by the rule of mixtures it is found that the value of CTE decreases with the increase in zircon sand reinforcement. The values are closely predicted by thermoelastic energy principles like Turners and Kerner's model using Equation (6) and Equation (7) in comparison to rule of mixtures Equation (5). The reason for decrease in CTE values is due to the presence of voids and agglomeration during the fabrication of the ZA27 MMC.

The dislocation density is found to increase with the increase in reinforcement content and depicts the inverse relation with CTE values. Thermoelastic models reveal that Zircon sand particles as reinforcement is affecting the augmentation of strength of the composites due to increase in dislocation density arising out of large difference in CTE values during solidification of the composites. But it does not consider casting defects like voids or poor interface between ZA27matrix and Zircon sand particulates.

Acknowledgements

All acknowledgments (if any) should be included at the very end of the paper before the references and may include supporting grants, presentations, and so forth.


Conflicts of Interest

The authors declare no conflicts of interest regarding the publication of this paper.


References

- [1] Babić, M. and Ninković, R. (2004) Zn-Al Alloys as Tribomaterials. *Tribology in Industry*, **26**, 3-7.
- [2] Babić, M., Ninković, R., Mitrović, S., *et al.* (2007) Influence of Heat Treatment on Tribological Behavior of Zn-Al Alloys. *Tribology in Industry*, **29**, 23-31.
- [3] Shiva Kumar, N. (2018) Mechanical and Wear Behavior of ZA-27/Sic/Gr Hybrid Metal Matrix Composites. *Materials Today Proceedings*, **5**, 19969-19975. <https://doi.org/10.1016/j.matpr.2018.06.363>
- [4] Hemanth Kumar, T.R., Swamy, R.P. and Chandrashekar, T.K. (2013) An Experimental Investigation on Wear Test Parameters of Metal Matrix Composites Using Taguchi Technique. *Indian Journal of Engineering and Materials Sciences*, **20**, 329-333.
- [5] Fatile, B.O., Adewuyi, B.O. and Owoyemi, H.T. (2017) Synthesis and Characteriza-

- tion of ZA-27 Alloy Matrix Composites Reinforced with Zinc Oxide Nanoparticles. *Engineering Science and Technology*, **20**, 1147-1154. <https://doi.org/10.1016/j.jestch.2017.01.001>
- [6] Sharma, S.C., Girish, B.M., Somashekar, D.R., *et al.* (1999) Mechanical Properties and Fractography of Zircon-Particle-Reinforced ZA-27 Alloy Composite Materials. *Composites Science and Technology*, **59**, 1805-1812. [https://doi.org/10.1016/S0266-3538\(99\)00040-8](https://doi.org/10.1016/S0266-3538(99)00040-8)
- [7] Panwar, R.S. and Pandey, O.P. (2013) Study of Wear Behavior of Zircon Sand-Reinforced LM13 Alloy Composites at Elevated Temperatures. *Journal of Materials Engineering and Performance*, **22**, 1765-1775. <https://doi.org/10.1007/s11665-012-0383-0>
- [8] Shoba, C., Ramanaiah, N. and Rao, D.N. (2014) Ageing Behavior of Aluminum Hybrid Metal Matrix Composites. *Materials Science. An Indian Journal*, **3**, 79-85.
- [9] Prasad, D.S., Shoba, C. and Ramanaiah, N. (2014) Investigations on Mechanical Properties of Aluminum Hybrid Composites. *Journal of Materials Research and Technology*, **3**, 79-85. <https://doi.org/10.1016/j.jmrt.2013.11.002>
- [10] Ramesha, V., Prasad, T.B., Nayak, V. And Neelakantha, V.L. (2018) A Study on Mechanical Properties of Al-17Si Metal Matrix Composites. *IOP Conference Series: Materials Science and Engineering*, **376**, 012100. <https://doi.org/10.1088/1757-899X/376/1/012100>
- [11] Gurunagendra, G., Ravishankar, T.N., Ravikeerthi and Raju, B.R. (2019) Dry Sliding Wear Studies of Zinc Aluminium Alloy Containing Micro and Nano Solid Lubricants. *International Journal of Engineering Research and Advanced Technology*, **5**, 7-13. <https://doi.org/10.31695/IJERAT.2019.3457>
- [12] Madhusudan, S., Sarcar, M.M.M. and Rao, N.B.R.M. (2016) Mechanical Properties of Aluminum-Copper(p) Composite Metallic Materials. *Journal of Applied Research and Technology*, **14**, 293-299. <https://doi.org/10.1016/j.jart.2016.05.009>
- [13] Mitra, R. and Mahajan, Y.R. (1995) Interfaces in Discontinuously Reinforced Metal Matrix Composites: An Overview. *Bulletin of Materials Science*, **18**, 405-434. <https://doi.org/10.1007/BF02749771>
- [14] Chappell, P.J.C. (1990) Reinforcement-Matrix Interface Effects in Metal Matrix Composites. MRL Technical Note, MRL-TN-562.
- [15] Miller, W.S. and Humphreys, F.J. (1991) Strengthening Mechanisms in Particulate Metal Matrix Composites. *Scripta Metallurgica et Materialia*, **25**, 33-38. [https://doi.org/10.1016/0956-716X\(91\)90349-6](https://doi.org/10.1016/0956-716X(91)90349-6)
- [16] Hatta, H., Takei, T. and Taya, M. (2000) Effects of Dispersed Microvoids on Thermal Expansion Behavior of Composite Materials. *Materials Science and Engineering: A*, **285**, 99-110. [https://doi.org/10.1016/S0921-5093\(00\)00721-8](https://doi.org/10.1016/S0921-5093(00)00721-8)
- [17] Bharat, V., Prasad, B.D. and Venkateswarlu, K. (2017) Effect of Beryllium Aluminum Cyclosilicate on Thermal Expansion Behavior of Al-Based Composites. *Journal of Minerals and Materials Characterization and Engineering*, **5**, 140-152. <https://doi.org/10.4236/jmmce.2017.53012>
- [18] Nam, T.H., Requena, G. and Degischer, P. (2008) Thermal Expansion Behaviour of Aluminum Matrix Composites with Densely Packed SiC Particles. *Composites Part A: Applied Science and Manufacturing*, **39**, 856-865. <https://doi.org/10.1016/j.compositesa.2008.01.011>

 Download This Paper (Delivery.cfm/SSRN_ID3773954_code4560868.pdf?abstractid=3773954&mirid=1)

Open PDF in Browser (Delivery.cfm/SSRN_ID3773954_code4560868.pdf?abstractid=3773954&mirid=1&type=2)

 Add Paper to My Library
Share:    

Towards a Competency Framework for Business School Faculty Members a. Sahana#1, Dr. Vijila K*2, Dr. K Tharaka Rami Reddy*3

Alochana Chakra Journal (UGC Care Group-1)

11 Pages

Posted: 18 Feb 2021

Dr. K. Tharaka Rami Reddy (https://papers.ssrn.com/sol3/cf_dev/AbsByAuth.cfm?per_id=4560868)

The Oxford College of Business Management Bangalore


Date Written: June 27, 2020

Abstract

entTertiary Education System in India has the largest number of Higher Education Institutions in the world (33,723) and the second highest student enrolment in the world (26.7 Million). Since independence the number of Universities in India has increased from 20 Universities in 1947 to 819 Universities in 2017. Apart from these Universities, autonomous institutes like 23 IITs, 31 NITs, 23 IIITs, 20 IIMs and 43 other Institutes of National importance have also been established. In a 30 year period from the year 1950 to1980 the average growth rate of management institutes is 4 per annum. While in a 7 year time frame from 2000 to 2007, 1528 new management institutes have been opened, that is an average of 218 institutions per year. From the year 2007 to 2011, 1300 new management institutes have been added with an average growth rate of 325 colleges per year. According to EY Analysis, it is expected to increase to 42 million in the coming years. However, today management education has crossed its pre-set boundaries and new technologies are acting as catalysts for change and educational mergers are creating large, ingenious competitors. Employability skills and survival skills of the students play an important role in effectively managing complex work situations that are science and technology driven, along with progression in work-life practices. Common challenges faced by Indian Business Schools include rapid increase in competition, decrease in funding from government sources, greater government scrutiny, inability in delivering corporate consultancy assignments, retention of quality faculty members who are the right blend of academics, research and consulting, managing student placement opportunities. There is a need for Business Schools to reposition themselves to manage the present wave of change in the business because management education has entered an era of receptive transition driven by technology. Therefore, faculty needs to analyze and upgrade their skills and abilities to be able to provide MBA students with the necessary skills and talents to help them accept the challenges and compete in the global scenario. To be a successful performer at the job, the faculty has to be competent in the domains of curriculum and pedagogy; research and consultancy; administration and governance; and knowledge dissemination. There is a need to recognize the competencies of Business School faculty in the domain of knowledge, skills, and abilities. This study attempts to explore the competencies of Business School faculty in the realm of knowledge, skills, and abilities. For the study the roles and responsibilities for HEIs by AICTE and the API developed by UGC has been used as the standard for developing the framework.er Abstract Body]

Keywords: Business School, Skills, abilities


JEL Classification: MBA

[Suggested Citation >](#)
[Show Contact Information >](#)
 Download This Paper (Delivery.cfm/SSRN_ID3773954_code4560868.pdf?abstractid=3773954&mirid=1)

Open PDF in Browser (Delivery.cfm/SSRN_ID3773954_code4560868.pdf?abstractid=3773954&mirid=1&type=2)

48 References

1. A A Adediwura, B Tayo
Perception of teachers' Knowledge Attitude and Teaching Skills as predictor of Academic performance in Nigerian Secondary schools
Educational Research and Review, volume 2, issue 7, p. 165 - 171
Posted: 2007

 Download This Paper (Delivery.cfm/SSRN_ID3712067_code2083654.pdf?abstractid=3712067&mirid=1)

Open PDF in Browser (Delivery.cfm/SSRN_ID3712067_code2083654.pdf?abstractid=3712067&mirid=1&type=2)

☆ Add Paper to My Library

Share:    

The Role of Training and Work Environment on Retention and Job Satisfaction as a Mediator at Startups, Bangalore

International Journal of Management, 11(9), 2020, pp. 1181-1191

11 Pages

Posted: 9 Dec 2020

Padmaja P (https://papers.ssrn.com/sol3/cf_dev/AbsByAuth.cfm?per_id=4427622)

Assistant Professor, Department of MBA, The Oxford College of Engineering, Bangalore

Dr. Bala Koteswari (https://papers.ssrn.com/sol3/cf_dev/AbsByAuth.cfm?per_id=4427626)

Dean Academics Sanskriti Group Of Institutions, Puttaparthi, Andhra Pradesh, India

Dr.R.V Dhanalakshmi (https://papers.ssrn.com/sol3/cf_dev/AbsByAuth.cfm?per_id=4427633)

Professor & HOD, Department of MBA, The Oxford College of Engineering, Bangalore

Richa Tiwari (https://papers.ssrn.com/sol3/cf_dev/AbsByAuth.cfm?per_id=4427637)

Assistant Professor, NITTE School of Management, Bangalore

Date Written: October 15, 2020

Abstract

Purpose: Employee Retention is a buzz topic in today's Knowledge based era, Very few empirical studies were carried out in the rapid-growing Startup sector and this present study address the gap in the literature. The Comprehensive literature reviews reported that Job Satisfaction is an important contributor of retention. Work environment and training are the topmost pertinent factors in raising the level of job Satisfaction towards organization. This paper investigates the impact of the above factors over Job satisfaction and explores the effects of Job satisfaction on retention and verifies the mediating effect of Job satisfaction on the relationship between proposed antecedents and employee retention.

Design/methodology: A Structured Questionnaire framed, consisting of elements acquired from earlier literatures were used to collect the data. A Simple random sampling technique employed in selecting the sample size. Questionnaire has been circulated to various employees working in Startups located at Bangalore in India, 270 responses have been recorded and used for the analysis.

Findings: Findings disclose that Job satisfaction influences retention and among the above factors work environment has significant relation with retention. In addition, Job satisfaction acts as a mediator between the proposed factors and outcome variable. However, mediation analysis indicated that training did not have any direct effect on retention.

Research limitations: This present study was carried out at startups in Bangalore. Sample size is not very large, since startups are having less manpower very difficult to increase sample size.


Practical implications: This paper suggests few recommendations to the Startups in employee retention as it is very essential to sustain. If Startups provide healthy work environment and effective training in order to increase Job satisfaction and leads to increase the level of retention in the organization.

Originality/value: This research paper highlights the significant factors that contribute to employee retention in startups

Keywords: Work Environment, Training, Job Satisfaction, Employee Retention

[Suggested Citation](#) >

[Show Contact Information](#) >

 Download This Paper (Delivery.cfm/SSRN_ID3712067_code2083654.pdf?abstractid=3712067&mirid=1)

Open PDF in Browser (Delivery.cfm/SSRN_ID3712067_code2083654.pdf?abstractid=3712067&mirid=1&type=2)

30 References

1. M Wells, L &thelen

What does your workplace say about you? The Influence of personality status and workplace on personalization

Journal of Environmental and Behaviour Sciences, volume 34, issue 3, p. 300 - 321

Posted: 2002

2. C K Okioga

The Contribution of a Developed Reward System on Employee Retention: A Case of Kisii Bottlers Limited: Kenya

European Journal of Business and Management, volume 4, issue 16, p. 9 - 21

Posted: 2012

3. K Al-Jarradi

An Investigation into the Effectiveness of the Reward System in the Government Sector in the Sultanate of Oman and the Potential for Introducing a Total Reward Strategy

Posted: 2011

4. Worldatwork

Total Reward Model, A framework for Strategies to attract, motivate and retain employees

Load more

Do you have a job opening that you would like to promote on SSRN?

Place job opening (<https://www.ssrn.com/index.cfm/en/Announcements-Jobs/>)

Paper statistics

DOWNLOADS 50

ABSTRACT VIEWS 148

30 References

PlumX Metrics



https://plu.mx/ssrn/a/?ssrn_id=3712067
Related eJournals

Organizations & Markets: Policies & Processes eJournal (https://papers.ssrn.com/sol3/ELJOUR_Results.cfm?form_name=journalBrowse&journal_id=2543961)

Follow ⓘ

Labor: Personnel Economics eJournal (https://papers.ssrn.com/sol3/ELJOUR_Results.cfm?form_name=journalBrowse&journal_id=1480989)

Follow ⓘ

View more >

Feedback ↻

Submit a Paper > (<https://hq.ssrn.com/submissions/CreateNewAbstract.cfm>)

SSRN Quick Links



SSRN Rankings



About SSRN



f (<https://www.facebook.com/SSRNcommunity/>)

in ([https://www.linkedin.com/company/493409?](https://www.linkedin.com/company/493409?trk=tyah&trkInfo=clickedVertical%3Acompany%2CentityType%3AentityHistoryName%2CclickedEntityId%3Acompany_493409)

[trk=tyah&trkInfo=clickedVertical%3Acompany%2CentityType%3AentityHistoryName%2CclickedEntityId%3Acompany_493409](https://www.linkedin.com/company/493409?trk=tyah&trkInfo=clickedVertical%3Acompany%2CentityType%3AentityHistoryName%2CclickedEntityId%3Acompany_493409)

t (<https://twitter.com/SSRN>)

(<https://www.elsevier.com/>)

Copyright (<https://www.ssrn.com/index.cfm/en/dmca-notice-policy/>)

Terms and Conditions (<https://www.ssrn.com/index.cfm/en/terms-of-use/>)

Privacy Policy (<https://www.elsevier.com/legal/privacy-policy>)

We use cookies to help provide and enhance our service and tailor content.



To learn more, visit [Cookie Settings](#).

(<http://www.relx.com/>)

(<https://papers.ssrn.com/sol3/updateInformationLog.cfm?process=true>)

International Journal of Advanced Science and Technology

[Home](#) [Editorial Board](#) [Journal Topics](#) [Archives](#) [About the Journal](#) [Submissions](#)
[Privacy Statement](#) [Contact](#)

[Home](#) / [Archives](#) / [Vol. 29 No. 7s \(2020\): Vol 29 No. 7s \(Special Issue\)](#) / [Articles](#)

Data Normalization Techniques on Intrusion Detection for Dataset Applications

Dharamvir, Arul Kumar V

Abstract

Intrusion Detection System (IDS) is an important security tool for safeguarding the network from both internal and external threats. Conventional IDSs employ signature-based methods or anomaly-based methods which rely on dataset for training and testing the system. KDD CUP 99 is one such widely used dataset. Artificial Neural Networks (ANN), Machine learning, Data mining, Evolutionary computing, Statistical methods, Computational Intelligence, etc., algorithms make use of this KDD CUP 99 dataset for testing. The dataset consists of symbolic, binary, numeric, and continuous features scattered in different range of values. In statistical methods such as Euclidean distance, the larger value dominates the distance measurement. In clustering algorithms, the larger values shift the cluster center. Such disadvantages could be overcome by ensuring uniformity to the dataset while retaining the exactness of the features mapped which could be achieved by a process known as Normalization. Data normalization is a data preprocessing stage which maps data from different ranges on to a common scale. In this paper, a detailed analysis of the existing various data normalization techniques that can be applied on KDD CUP 99 dataset is presented along with the illustration. From the analysis, it was found that different normalization techniques are suitable for different subsets of KDD CUP 99 dataset. The problem under investigation is to prove that the new dataset generated on application of various normalization techniques exhibits the same characteristics as that of the original KDD CUP 99 dataset. Also, the effect of data normalization techniques, viz., of Min-max, Z-Score, Log, and Sigmoid on the neural Network algorithm in terms of

Image Scheduling using Cloud Energy Data Computational Techniques

Dharamvir ¹, Dr. Hemanth K S ²

¹ Research Scholar Department of CSA, REVA UNIVERSITY, Bengaluru, India

² Associate Professor Department of CSA, REVA UNIVERSITY, Bengaluru, India

Article History: Received: 11 January 2021; Revised: 12 February 2021; Accepted: 27 March 2021; Published online: 10 May 2021

Abstract: In proposed research Paper we are classifying the process of data intensive business and image scheduling through data computational techniques. The process of Image scheduling computing are having an advantage of tracking data from all available image using data computational specification. In such a domain, computing, data stockpiling and image transformation changes into a utility. It is a sensible form of computing which allow image data for optimal cost of processing operations as in task distribution specification. Since, the classification of present industry are increasing the efficiency of computing was not the aim; instead the goal was to facilitate faster computing by packing more power of computational hardware in form of distributed computing, grids architecture, parallel computing and cloud image transformation . Thereby, the power consumption of such high performance computing architectures lead to increase of power usages and heat which is accompanied by equal amount of energy. Similarly we are going to develop Image scheduling data transformation to achieve required goals

Keywords : Energy efficiency , Cloud Data Server , Parallel Computing , Computational Data System

1. Introduction

As a fact, the cooling frameworks often require more energy usage than that required for the IT data centre (S. Zhang et al. 2013). In IT server farms, to guarantee such elevated level of regular power consumption, readily available is stockpiling, power dissemination along with cooling units. In this way, the utilization of energy is unaccountable to give a quantifiable values corresponding to the workload to process. To gauge this waste of energy, the Green Grid Consortium formed two types of metrics to be deployed i.e, the Power Usage Effectiveness (PUE) and the Data Center Infrastructure Efficiency (DCIE) Together PUE and DCIE represent the level of energy consumed by the IT server farms with respect to the aggregate power utilized by it. As of now, almost 40% of the aggregate electrical energy is aggressively utilized by the IT server farms .Different computational frameworks adding to the energy utilizations of servers are cooling and power circulation frameworks which in turn average around 50% and 25% of aggregate energy utilization.The previous technique, ordinarily alluded to as Dynamic Power Management (DPM) which brings about the vast amount of the external investment or funds because the normal workload usually remains beneath 40% in cloud computing server farms . The second option relates to the Dynamic Voltage and Frequency Scaling (DVFS) technique to facilitate lower power usage by coordinating the comparing attributes of the given workload. Here, we present a learning based method for an energy aware cloud computing framework which streamlines the utilization of power at the cloud server farm while dynamically adjusting the computational workload. A successful dissemination of system activity enhances Quality of Service (QoS) by lessening processing delay. The system is tested and simulated on GreenCloud simulator to give best performance as per need of system .

In particular, the principle commitments of our work are the accompanying: Devise of a scheduler that improves energy proficiency along with load adjusting of system activity in cloud computing server farms. Devise of a conventional model is based on Q-Learning based scheduler for the scheduling and dissemination of processing load on a cloud server farm workload on continuous basis. The procedure of deploying scientific workflow load in the simulation is exponentially conveyed to imitate reasonable scheduling of the clients as in actual workflow setting as shown in Figure 5.1. The presented scheduler uses Q-learning based approach to manage resource allocation based on best configuration for minimal cost. Here, the computational job is divided into several IP bundles and sent over the IT cloud server farm and there it got rearranged based on the configuration set by the scheduler to accommodate three IP parcels having 1500 bytes. When the process reach at the server, the execution of computational job begins. Upon execution, the process returns the results to the end client, which is sent over the server farm and through the central switches. The way of executing job in each section relates itself to the wide-range attributes which dictate the association between the availability of server farm and the end client. To and fro of information is carried out through Transmission Control Protocol (TCP) and is used to dictate sending rate in order to match transmission capacity (stream control) and resolve any clog or connection related information. The underlying conflict among various information streams in the given cloud topology is multiplexed to focus in similar fashion as with rack-switch or a total switch as shown in Figure 2.

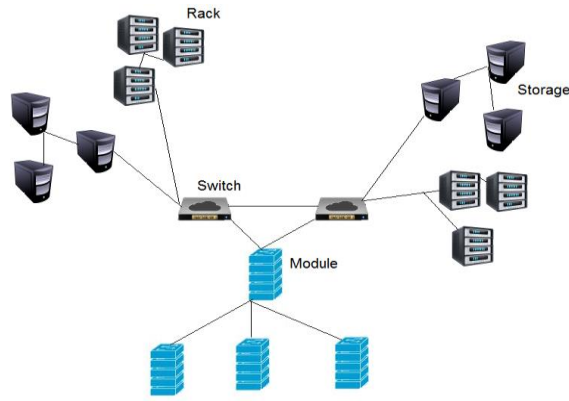


Figure 1: Cloud Architecture Module distribution

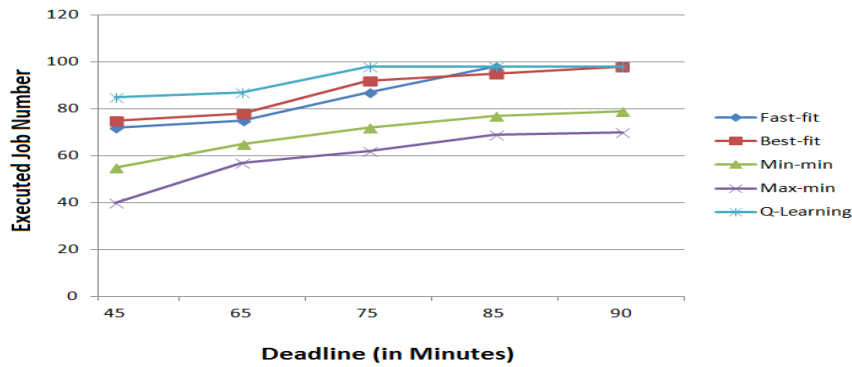


Figure 2: Comparison of the performance data Analysis methods

The energy consumption analysis of the cloud server image transformation with different activities is defined by a comparison of data transformation with different methods and their equivalent values. To use the maximum and minimum scheduler activities to perform image transformations we can transmit the data segments and its co-components. The cloud server farm in the simulation initially used full capacity because no power management was enabled. Using the proposed algorithm for scheduling and power management has resulted in a 78 percent reduction in overall power consumption for the system and its Learning-based schedulers. The Learning based scheduler significantly facilitates a reduction of roughly 37 percent when image administration is activated in switches. It's not common practice to use a scheduler to manage power in switches.

Server farm switches, in general, operate in unison, particularly in the centre and complete systems, to provide a reliable communication network.

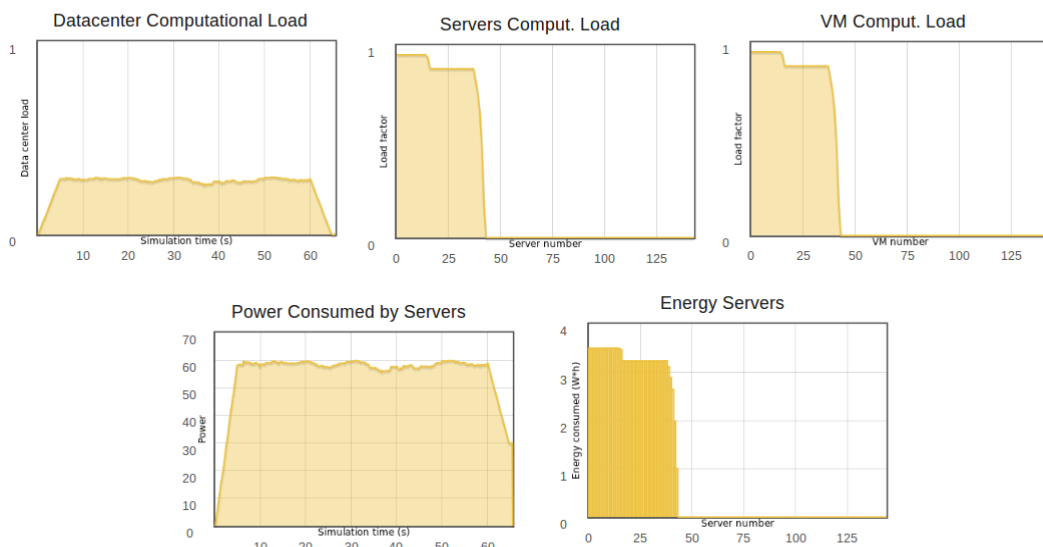


Figure 3: System performance energy saving by the presented algorithm

Figures 2 and 3 shows the data classification system that is used to generate energy-aware scheduling. As seen in Figure 2, various measurements are used to distinguish between the earliest execution before the deadline and the computing work performed on the server. The cost of operation, the time taken by the device minute task is effectively coordinated out of the server farm. Despite what one would anticipate, the proposed strategy limits the postponement of individual jobs with extended deadlines to a minimum of 40-50 milliseconds, which is significantly less than the spread deferral of a device filled with transmission queues.

2. Task Allocation using GPU Image Scheduling

Modern multi-core graphics processors Tesla are having highly parallel, fully programmable architectures with up to 230 processor cores and 1 TFLOP peak performance. Since GPUs are difficult to programme, their current applications are usually limited to physics simulation and scientific computing. The GPU's powerful architecture is restricted to its full-fledged use in much other fields. In reality; the best sorting method for GPUs is currently the subject of heated debate. Recent research has been conducted in this area, and as a result, the comparison-based Thrust Merge method has emerged. Later, its sort method emerged, which outperformed the previous sorting method. It does, however, have one drawback.

In this paper, we examine a different sorting method for GPUs that overcomes the drawbacks of sorting methods by operating even with dynamic data flow. It also performs well when it comes to sorting and has a higher memory quality.

Let the state of a task can be explained by two parametric sets i.e., states corresponding to set of each tasks and actions a -1 or +1 required to reduce the overall ranking within the sets of tasks T.

For proper VM-PM process functioning, the overheads incurred during communication along with the job scheduling time need to be reduced. Hence, the transformation of tasks can be achieved using algorithm below:

Algorithm: Reinforced Learning based Spatial Sorting Algorithm

Input: An array.

Output: Structure of Sorted Array of tasks.

Step 1. Divide the array into m array

Step 2. Perform Sub Sort

Step 3. Perform Local Sort

Step 4. Perform sorting of all samples

Step 5. Perform Data Relocation:

Step 6. Rep steps 1-5

End

The first step in the algorithm is to split the array n/m . Which are having items each where n/m is the shared memory. The second step is performing the Sub sort. In this step, Sort is performed on distribution of occupied image memory as a cache unit with master Node with system data transformation.

The Initialization steps are as follows:

By using the same history sets for different steps to update history for reinforced learning for the state and activities associated with each mission. The local sort is performed as the third step:

Multiple stacks are chosen, and a p Insertion sort is performed in parallel with the total number of P samples by subdividing the task yields the centroid (C) of the linked dimension (CC). The data relocation is the fifth phase. All P sorted positions of the changed array consisting of Cut sub sort are swapped here. The sixth step is to repeat the previous five steps until all subsorts have been divided into local sort and the sample size has been met.

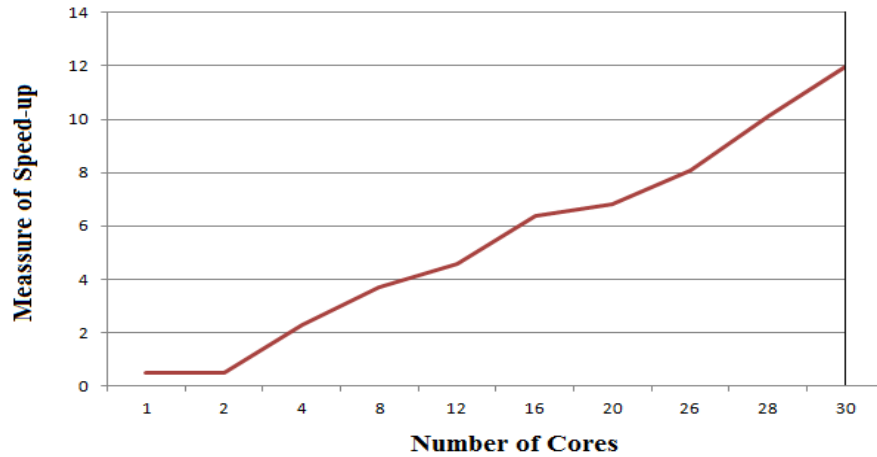


Figure 4: GPU Measurement statuses

The memory mapping is decreased which leads to the allocation of assigned data jobs by rank prioritization. The assigned data source are having 64 bit image transform data identification with minimal data occurred during Grade-I GPU processors. The simulator result of GPU measurement assign multiform data transformation using numbers of cores and its measurement Speed.

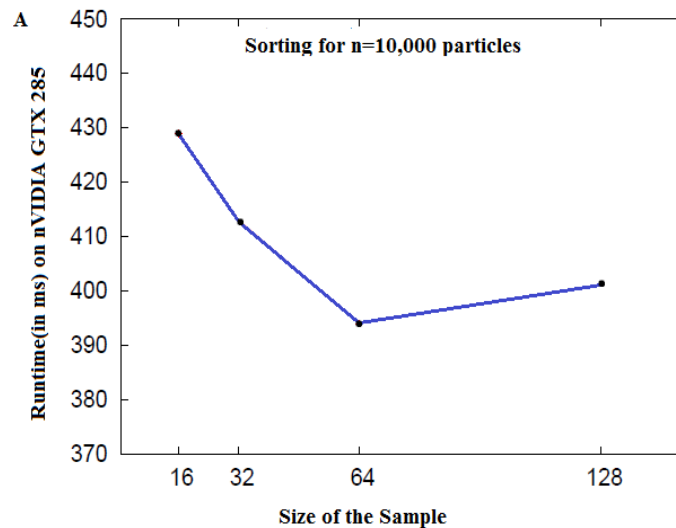


Figure 5: Runtime Algorithm with System Applications .

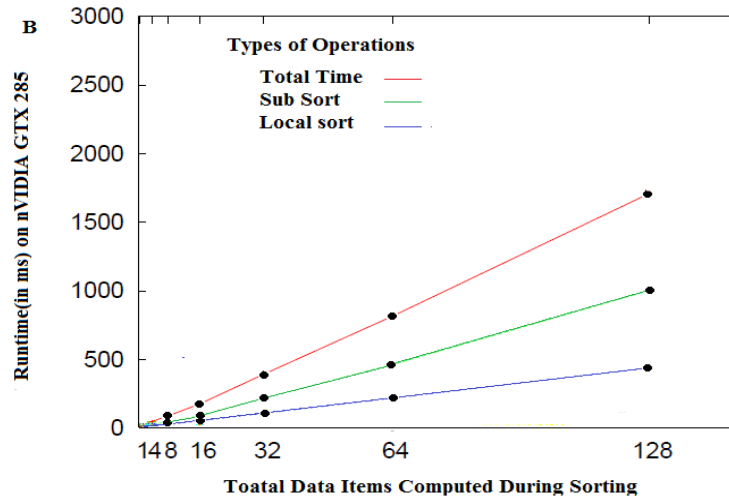


Figure 6: Performance of spatial sorting for three types of operations

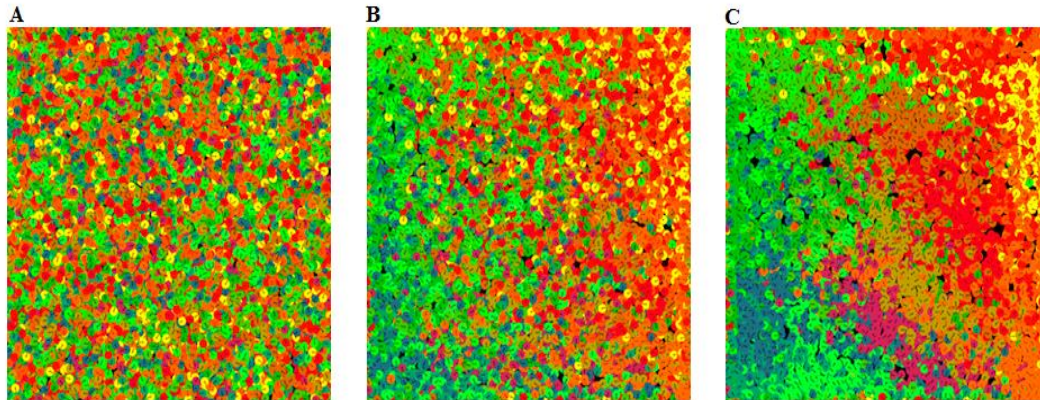


Figure 7: Performance of Visualization

3. Data Transformation and its Applications

Data transformation with visualized effects is having classification ranking to adopt multiple visualization method with minimum efficiency control system. For such linked microprocessors, there is no pre-existing infrastructure. It can be determined by the network to be enforced. End nodes have no limits in MPI networking. Multi-memory hops may be present in node-to-node routes.

There are some points related to cloud computing MPI networking, such as a) Nodes act as processors to forward packets for each other, and b) Node mobility can cause routes to change. Routes are modified based on networking mobility. c) This is a very useful strategy for MPI routing. On the current architecture, a simulation was run to run a costly workload. This job generates a large number of pipelining threads, each of which performs a specific task for the slaves.

When we raise the number of worker threads from 1-6, we see a drastic change in computation and execution time (as shown in Figure7).

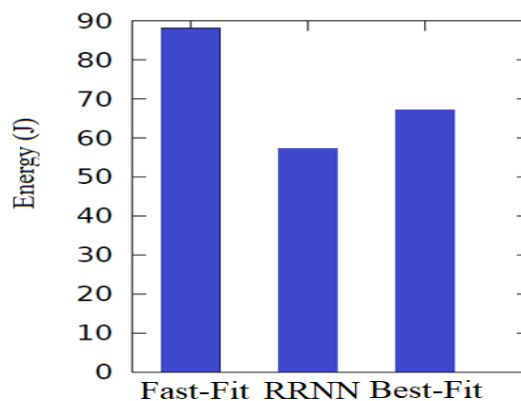


Figure 8: Comparison plot while using different method

The micro benchmarking operations, on the other hand, are carried out using three different protocols. The energy consumption plot in Figure 7 shows that the threading mechanism achieves optimal threading for efficient computation in Bluetooth data stream parallelization. In addition, the performance of the RRNN allowed parallelization shows that it is best suited for cloud infrastructure. The higher consumption of the other process results in significant overheads in workload data streams. Since it necessitates data transformation in order to resolve compatibility issues. For each of the four setups: A total of 100 free instances were generated, each recreating the system's output for 1000 seconds. A single M2M class is considered for each machine event, involving 100 M2M devices. The objective and the actual QoS output are indistinguishable if enough M2M bandwidth is considered. The following is noted in each of the four set-up results. The relative contrast of the two algorithms is shown in Figure 8.



Figure 9: Comparison of the performance of hierarchy based models

4. Conclusion

The main goal of this method is to provide a complete Image transformation which will enable to design more new schemes in order to evaluate and improve the transformational workload traffic behavior and distribution on network topologies defined by the user. The presented approach enables generation of procedurally generated hub-spoke topologies for routing mechanism and performs better when put in comparison with other methods such as Locality, Waxman, Barabasi-Albert and hierarchical models. It also takes in consideration of mobility patterns as per the model layout of random walk model in an unidentified networked topology. Hence, we have developed a learning based pipelining in image structural strategy for efficiently employing the resources offered by multi-core architectures embedded system in parallel with the networked devices in the localized area using a custom modelled learning protocol for pipelining and communication between running cores for assigning computing jobs in parallel. However, this idea has been novel in this field of research which restricts the heavy citations of preliminary approach for Image scheduling transformational activity .

References

1. Abhinandan. S, Prasad and Shrisha Rao A., Mechanism Design Approach to Resource Procurement in Cloud Computing IEEE Transactions on Computers (1),(2018) 17-30.
2. Abishi Chowdhury and PriyankaTripathi Enhancing Cloud Computing reliability Using Efficient Scheduling by Providing Reliability as a Service International Conference on Parallel, Distributed and Grid Computing (2019)
3. Zaharia M, Borthakur D, Sen Sarma J, Elmeleegy K, Shenker S, and Stoica I, Delay Scheduling: A Simple Technique for Achieving Locality and Fairness in Cluster Scheduling, Proc. European Conf. Computer Systems (EuroSys '10), (2010)
4. Bila N, Lara E D, Joshi K, Lagar-Cavilla H A, Hiltunen M, and Satyanarayanan M, Jettison: Efficient Idle Desktop Consolidation with Partial VM Migration, Proc. ACM European Conf. Computer Systems (EuroSys '18), (2018).
5. Jinzhao Liu, Yaoxue Zhang, Yuezhi Zhou, Member, IEEE, Di Zhang, and HaoLiu., Aggressive Resource Provisioning for Ensuring QoS in Virtualized Environments" IEEE Transactions On Cloud Computing, 1 (1), 2019)
6. James M. Kaplan, William Forrest, and Noah Kindle. Revolutionizing DataCenter Energy Efficiency. Technical report, McKinsey & Company, July 2018.
7. Scaling up energy efficiency a cross the data center industry: evaluating key drivers and barriers, nrdc, august 2014. <http://www.nrdc.org/energy/files/data-center-efficiency-assessment-IP.pdf>.
8. Erica Naone. Conjuring clouds. Technology Review, 112(4):54{56, 2019}

Data Normalization Techniques on Intrusion Detection for Dataset Applications

[¹] Dharamvir, [²] Arul Kumar V

[¹] *Research Scholar, School of CSA, REVA University, Bangalore, India.*

[²] *Asst. Professor, School of CSA, REVA University, Bangalore, India.*

[¹] *dhiruniit@gmail.com*

Abstract

Intrusion Detection System (IDS) is an important security tool for safeguarding the network from both internal and external threats. Conventional IDSs employ signature-based methods or anomaly-based methods which rely on dataset for training and testing the system. KDD CUP 99 is one such widely used dataset. Artificial Neural Networks (ANN), Machine learning, Data mining, Evolutionary computing, Statistical methods, Computational Intelligence, etc., algorithms make use of this KDD CUP 99 dataset for testing. The dataset consists of symbolic, binary, numeric, and continuous features scattered in different range of values. In statistical methods such as Euclidean distance, the larger value dominates the distance measurement. In clustering algorithms, the larger values shift the cluster center. Such disadvantages could be overcome by ensuring uniformity to the dataset while retaining the exactness of the features mapped which could be achieved by a process known as Normalization. Data normalization is a data preprocessing stage which maps data from different ranges on to a common scale. In this paper, a detailed analysis of the existing various data normalization techniques that can be applied on KDD CUP 99 dataset is presented along with the illustration. From the analysis, it was found that different normalization techniques are suitable for different subsets of KDD CUP 99 dataset. The problem under investigation is to prove that the new dataset generated on application of various normalization techniques exhibits the same characteristics as that of the original KDD CUP 99 dataset. Also, the effect of data normalization techniques, viz., of Min-max, Z-Score, Log, and Sigmoid on the neural Network algorithm in terms of detection rate and false alarms were compared and it was experimentally found that the log and sigmoid data normalization techniques result in better detection rate.

Keywords - IDS, Data Normalization, KDD CUP 99

1. Introduction

Intrusion is an act by which a person enters another person's/organization's computer network without rights or permission. Over a decade, intrusion detection system (IDS) has got considerable importance in the field of network security. One important attribute to the growth of IDS is the paradigm shift of the mentality of attackers from script kiddies to sophisticated spy network agents who are politically and monetarily motivated. This has led to strengthen the security premises of network using firewall, IDS [1], Intrusion Prevention System (IPS), etc. IDS can be broadly classified into two methods, viz., signature-based or misuse detection and anomaly-based detection. In misuse detection techniques, signature or pattern of previously seen attack is calculated and configured in to the IDS which in turn alerts the administrator in case of similar attacks. On the other hand, anomaly detection techniques [2], calculate the normalcy of network behavior/activity and fix the activity as an attack on finding any deviating activity from the normal behavior. Misuse detection has high detection rate where as anomaly detection aides in detecting zero day attacks which are never seen before. Anomaly detection and misuse detection are orthogonal to each other.

1.1 KDD CUP 1999 dataset

KDD CUP 99 dataset is the most popular IDS dataset [3]. It consists of a large labeled training data and testing data. Testing data consists of attacks which are not present in the training dataset. The algorithms developed for anomaly detection systems can be tested using this dataset [9]. The dataset contains the four different types of attack data, viz., DoS, Probe, Remote-to-Local (R2L), and User-to-Superuser (U2R) attacks. The dataset is a $U \times A$ matrix where U is the set of data instances and A ,

the set of features. There are 41 features which are extracted from network packets and classified into four different categories. In this, the first 9 features 1-9 are extracted from the header of network packets. Features 10-22 represent the content area/payload portion of network packets. The next two categories are time window (2 seconds) based features (23-31) and connection-window (100 connections) based features (32-41). The dataset contains 4 lakhs training instances and 2 lakhs testing instances. The training dataset contains 24 different attack vectors and the testing dataset contains 14 extra attack vectors.

2. Data Normalization

Data preprocessing is an important step in knowledge discovery process. It is considered as the fundamental block of data mining. Feature Extraction, Transformation, and Loading (ETL) are the three steps performed before loading the dataset to the learning algorithm. Data normalization technique, a sub division of data analysis, is a process where the attribute data or features are scaled so as to fall within a specific range such as -1.0 to 1.0, or 0.0 to 1.0, has the following advantages:

- enables data mining algorithms to be applied easily
- improves the effectiveness and the performance of mining algorithms
- makes data suitable for a specific analysis to be performed
- improves the normality of the variables/features
- reduces Type I (overestimation/false positives) and Type II (underestimation/false negatives) errors

In many practical applications, the dataset has features which lie in different range of values. Features are not uniform throughout the dataset. It contains both nominal [7] and numeric features with different range values. This results in the feature having larger values dominating the cost function than the features with smaller values, leading to the deterioration in the performance of the algorithm. Therefore the dataset could not be used in non-parametric models, where data does not belong to any particular distribution, such as neural networks, support vector machines, classification algorithms, clustering algorithms, etc., without data

Normalization

The study on intrusion detection is widely spread on the application of Artificial Neural Networks (ANN), data mining algorithms, statistical methods, etc. In statistical methods, Euclidean distance method has been used for grouping the inputs into clusters. In Euclidean distance calculation, the squared distance between two data instances are calculated, on non normalized data instances. A large deviation between instances which are statistically in the same category could be observed. This large deviation, in terms of distance, is due to the large range feature in the data set. Therefore, in order to minimize the large deviation, large range values of the instances must be normalized necessitating the need for normalization techniques.

In neural network algorithms, the need for data normalization arises because the output is normally represented by -1, 0, and 1. So the input to the neural network should be in the range of [-1, 1] or [0, 1]. Hence, data normalization is a prerequisite for neural network algorithms.

Data Normalization [8] is a technique by which data values in different ranges are mapped on to a common scale, preferably in the range [0-1]. The process of normalization [4] should maintain two main properties, viz., robustness and efficiency [6]. Robustness is the property of ensuring that the outliers, data instances which behave in an unexpected way or have abnormal properties, not affect the normalization process. Efficiency of normalization determines the quality by which the exact nature/property of features are retained and not lost in the new range.

Figure 1 shows the taxonomy of data normalization techniques. The data normalization schemes are classified into two schemes, viz., Feature-based schemes and Input vector-based schemes [5].

In feature-based schemes, the normalization is done feature wise. This helps to map each feature value in the dataset to the corresponding value in the new range. Feature-based schemes are further

divided into two methods, viz., linear methods and non-linear methods. The distribution of data around the mean

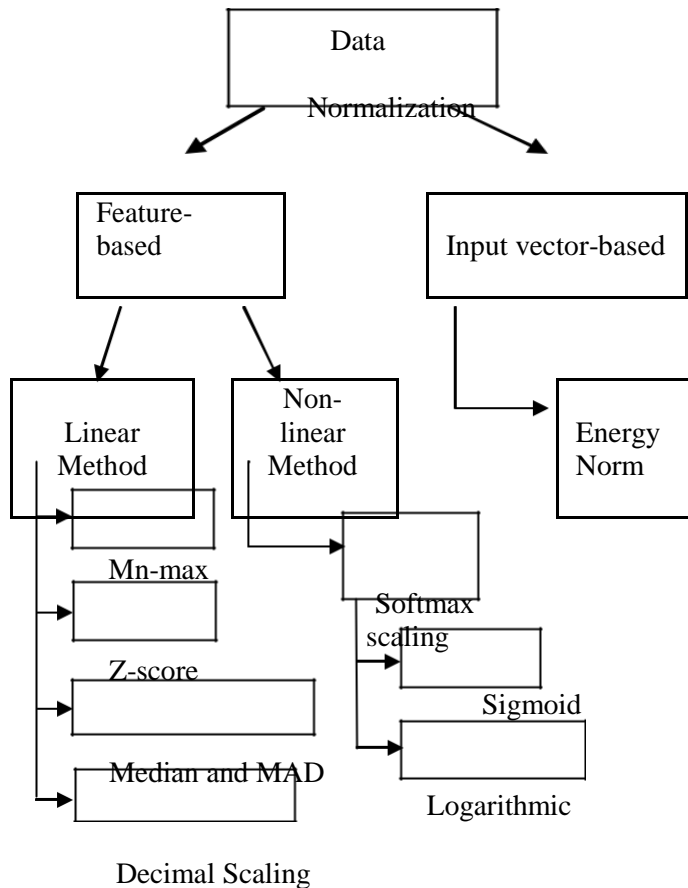


Figure 1. Taxonomy of Data Normalization Techniques

differentiates between the two methods.

2.1 Linear Methods

Linear methods are those where the data lie equally distributed around the mean. The following are the linear method feature-based data normalization schemes:

- Min-max normalization
- Z-score normalization
- Median and MAD normalization
- Decimal scaling normalization
-

A. Min-max Normalization

Min-max Normalization performs a linear interpolation using (1). The underlying distribution of the corresponding feature with the new range of values is sustained.

$$x' = \frac{x - \min f}{\max f - \min f} (n_{\max} - n_{\min}) + n_{\min}$$

- x - Feature value to be normalized
- x' - Normalized feature value of x.
- minf - Actual minimum value for feature f^c in the given dataset
- maxf - Actual maximum value for feature f^c in the given dataset
- n_minf - Lower value in the new range
- n_maxf - Upper value in the new range

B. Z-score Normalization

Z-score normalization is the most commonly used method in normalization. The values are mapped using (2) and (3) to a scale where the mean, the local estimator, is zero and the standard deviation, the scatter estimator, is one. It obeys the standard normal distribution principle. An important aspect of Z-score normalization is the ability to reduce the effect of outliers in the dataset.

$$x' = \frac{x - \mu}{\sigma} \quad (2)$$

$$\text{Mean, } \mu = \frac{1}{N} \sum_{i=1}^N x_i \quad \text{S.D. } \sigma = \sqrt{\frac{1}{N-1} \sum_{i=1}^N (x_i - \mu)^2} \quad (3)$$

- x - Feature value to be normalized
-
- x' - Normalized feature value of x.
-
- μ - Mean value for feature f^c
-
- σ - Standard Deviation (S.D.) for feature f^c
-
- N - Number of data instances

C. Median and Median Absolute Deviation (MAD)

Median and Median Absolute Deviation is a rehashed form of Z-score normalization done using (4). MAD is suitable if the feature values are continuous in the given range.

$$x' = \frac{x - \text{median}}{\text{MAD}} \quad \text{where, } \text{MAD} = \text{median}(|x_i - \text{median}|) \quad (4)$$

D. Decimal Scaling Normalization

Decimal Scaling Normalization transforms the data into [0, 1] range by moving the decimal point of values of the attribute, using (5). The capability of this normalization lies in the mapping of very large values in the range [0, 10000] to the range [0, 1].

$$x' = \frac{x}{10^s} \text{ where, } s = \log_{10}(\max_f) \quad (5)$$

x - Feature value to be normalized
 x' - Normalized feature value of x .

2.2 Non-linear Methods

In non-linear methods the data are not evenly distributed around the mean and the deviations are very large. In such cases, transformations are based upon non-linear functions such as sigmoid or logarithmic to map the data within the specified interval of [0, 1]. Such transformations are known as Softmax scaling. The functions sigmoid and logarithmic are known as squashing function which is used to limit the data in the range of [0, 1].

A. Logarithmic Normalization

In many cases the values of features are exponentially distributed. The logarithmic process of normalization using (6) enables to get more resolution to the lower feature values. If

TABLE I. KDD CUP 99 FEATURES

| Sl. No | Features | Type | Range |
|--------|--------------------|------------|------------|
| 1 | Duration | Discrete | 0-100000 |
| 2 | Protocol_type | Symbolic | NA |
| 3 | Service | Symbolic | NA |
| 4 | Flag | Symbolic | NA |
| 5 | Src_bytes | Discrete | 0-10000000 |
| 6 | Dst_bytes | Discrete | 0-10000000 |
| 7 | Land | Binary | 0/1 |
| 8 | Wrong_fragments | Discrete | 0-25 |
| 9 | Urgent | Discrete | 0-30 |
| 10 | Hot | Discrete | 0-35 |
| 11 | Num_failed_logins | Discrete | 0-35 |
| 12 | Logged_in | Binary | 0/1 |
| 13 | Num_compromised | Discrete | 0-1000 |
| 14 | Root_shell | Binary | 0/1 |
| 15 | Su_attempted | Binary | 0/1 |
| 16 | Num_root | Discrete | 0-1000 |
| 17 | Num_file_creations | Discrete | 0-28 |
| 18 | Num_shells | Discrete | 0-40 |
| 19 | Num_access_files | Discrete | 0-60 |
| 20 | Num_outbound_cmds | Discrete | 0-60 |
| 21 | Is_host_login | Binary | 0/1 |
| 22 | Is_guest_login | Binary | 0/1 |
| 23 | Count | Discrete | 0-1000 |
| 24 | Srv_count | Discrete | 0-1000 |
| 25 | Error_rate | Continuous | 0-1 |

| | | | |
|----|-----------------------------|------------|-------|
| 26 | Srv_serroro_rate | Continuous | 0-1 |
| 27 | Rerror_rate | Continuous | 0-1 |
| 28 | Srv_error_rate | Continuous | 0-1 |
| 29 | Same_srv_rate | Continuous | 0-1 |
| 30 | Diff_srv_rate | Continuous | 0-1 |
| 31 | Srv_diff_host_rate | Continuous | 0-1 |
| 32 | Dst_host_count | Discrete | 0-255 |
| 33 | Dst_host_srv_count | Discrete | 0-255 |
| 34 | Dst_host_same_srv_rate | Continuous | 0-1 |
| 35 | Dst_host_diff_srv_rate | Continuous | 0-1 |
| 36 | Dst_host_same_src_port_rate | Continuous | 0-1 |
| 37 | Dst_host_srv_diff_host_rate | Continuous | 0-1 |
| 38 | Dst_host_serror_rate | Continuous | 0-1 |
| 39 | Dst_host_srv_serror_rate | Continuous | 0-1 |
| 40 | Dst_host_rerror_rate | Continuous | 0-1 |
| 41 | Dst_host_srv_rerror_rate | Continuous | 0-1 |

the minimum values are known a priori, it might be a good idea to use it as in (6) for initialization during the normalization.

$$x' = \log(x - m + 1) \text{ where } m = \min(x_i) \quad (6)$$

x - Feature value to be normalized

B. Sigmoid/Logistic Normalization

Sigmoid normalization as shown in (7) not only normalizes the current dataset values in the range [0, 1] but also ensures

Table II. Subset-1: Attribute Values For Decimal Scaling Norm

Decimal Scaling

| <i>Features</i> | <i>Value of 's'</i> | <i>x'</i> |
|-----------------|---------------------|-----------|
| 1 | 4.766 | 0.087 |
| 5 | 6.710 | 1.000 |
| 6 | 6.712 | 0.000 |
| 13 | 2.946 | 0.000 |
| 16 | 2.997 | 0.000 |
| 23 | 2.708 | 0.002 |
| 24 | 2.708 | 0.002 |
| 32 | 2.407 | 0.000 |
| 33 | 2.407 | 0.000 |

Table III. Subset-2: Attribute Values For Z-Score Norm

Z-Score

| <i>Features</i> | <i>Mean</i> | <i>Standard Deviation</i> | <i>x'</i> |
|-----------------|-------------|---------------------------|-----------|
| 8 | 0.035 | 0.782 | 0.044 |
| 9 | 0.000 | 0.006 | 0.000 |
| 10 | 0.000 | 0.006 | 0.000 |
| 11 | 0.000 | 0.016 | 0.000 |
| 17 | 0.001 | 0.096 | 0.028 |
| 18 | 0.001 | 0.096 | 0.028 |
| 19 | 0.001 | 0.036 | 0.028 |
| 20 | 0.001 | 0.036 | 0.028 |

that any larger data value than the present set maps to [0, 1]. The transformation is more-or-less linear in the middle range around mean value, and has a smooth nonlinearity at the end which ensures that all values are within the range. Values away from the mean are squashed exponentially.

$$x' = \frac{1 - e^{-y}}{r} \quad \text{where, } y = \frac{x - \mu}{\sigma} \quad (7)$$

and r is a user defined value .

C. Input vector-based: Energy Normalization

Energy normalization is an input-vector based normalization scheme where normalization is performed on each data instance independently using (8).

$$x_i' = \frac{x_i}{M_n(x)} \quad \text{where, } M_n(x) = \left(\sum_{i=1}^n |x_i|^n \right)^{\frac{1}{n}} \quad (8)$$

- x_i - Each feature in a data instance
- x_i' - Normalized data instance
- $M_n(x)$ - Minkowski norm, $n=1, 2$
-
- N - Number of features

It is based on Minkowski Norm. In (8), if the value of $n=1$, then it is L1 or Taxicab norm. If $n=2$, then it is L2 or Euclidean norm.

3. Normalization On Kdd Cup 99 Dataset

Table I shows the feature type and the range of values the features possess in the KDD CUP 99 dataset. This facilitates to choose the appropriate data normalization technique for a particular feature. From the Table I it can be noticed that 3 features are symbolic and 6 features take binary values (either 0 or 1). Out of the 32 features which are numeric, 15 features are continuous in the desired range of [0-1]. So the process of data normalization should be applied on the remaining 17 features, which are discrete, whose value lie in different ranges of the order of [0-1000] and [1-10000000]. These features if not normalized will not give good support to the modeling algorithms. One of the

4. Comparison Of Distribution

This section compares the distribution of the KDD CUP 99 dataset before and after normalization. SOM toolbox, a software library for MATLAB, is used to perform the data normalization techniques on the KDD CUP 99 training dataset. The dataset consists of 4,94,021 data instances. X-axis represents the data instances and Y-axis represents the feature values in Figures 2 to 5.

4.1 Feature-6 of KDD CUP dataset

Feature 6, `dst_bytes` in KDD CUP 99, denotes the number of bytes transferred from destination address-port pair to source address-port pair. Figure 2 shows the plot of the distribution for feature 6, `dst_bytes`, and its feature values. The resultant distribution of `dst_bytes` on application of Min-max, Z-score, and Decimal scaling normalization techniques are plotted in Figures 3, 4, and 5 respectively.

It can be seen from Figure 3 that the application of Min-max data normalization technique on feature 6 maps the data instances into the range $[-1,0]$ without disturbing the underlying data distribution. The range from -1 to 0 could be mapped into 0 to 1 by taking the modulus values.

Figure 4 shows the distribution of Z-Score normalization on Feature 6. It can be seen from Figure 4 that the range is still high from -20 to 160.

Figure 5 shows the distribution of Decimal scaling normalization on Feature 6.

Therefore it could be concluded that both Min-max and Decimal scaling normalization techniques preserve the distribution. Further it indicates that either Min-max or Decimal scaling normalization technique is suitable as the range is 0 to 1 in both cases.

5. Experiment And Results

Under Matlab 7.6, Network Pattern Recognition Tool, `npr tool`, was used to conduct the experiments. KDD CUP 99 training dataset was used. The dataset was split in the ratio 0.70, 0.15, and 0.15 for training, validation, and testing purposes. The parameters chosen to conduct the experiment, common for all the four data normalization methods, are as follows:

- Training function: Scaled conjugate gradient, `trainscg`

Error function: Mean Squared Error, `mse`

Validation: 6 rounds

The experiment was conducted as shown in Figure 8. The measured performance metrics, viz., detection rate, sensitivity, specificity, and error are tabulated in Table IV.

| | |
|------------------|--|
| Detection rate : | It is the combined ratio of true positives and true negatives to the total number of instances |
| Sensitivity : | Proportion of actual positives which are correctly classified |
| Specificity : | Proportion of actual negatives which are correctly classified |
| Error : | Low error attained during training iteration |
| Epochs : | Number of iterations performed |
| Time : | Time taken, in minutes, to complete the training process |

From the Table IV it can be inferred that non-linear methods such as log and sigmoid normalization are the best normalization methods for KDD CUP99 Intrusion Detection dataset, which result in a detection rate of 99.9%.

TABLE IV. COMPARISON OF NORMALIZATION TECHNIQUES

| Norm Method | Detection Rate | Sensitivity | Specificity | Error | Epoch | Time |
|-------------|----------------|-------------|-------------|---------|-------|------|
| Min-max | 99.8 | 99.6 | 99.9 | 0.00017 | 181 | 25 |
| Z-Score | 99.6 | 99.3 | 99.7 | 0.00280 | 295 | 90 |
| Log | 99.9 | 99.9 | 99.9 | 0.00039 | 200 | 29 |
| Sigmoid | 99.9 | 99.8 | 99.9 | 0.00051 | 170 | 28 |

6. Summary

In this paper a detailed survey on the various data normalization schemes that can be applied on KDD CUP 99 dataset where the features lie in different range of values is presented. This non uniformity in data which when used in pattern recognition algorithms leads to biased output depending only on a subset of the feature space. These data normalization techniques even out the dataset and ensure a fair representation of all features with the actuality preserved. The application of Min-max, Z-Score, and Decimal Scaling techniques on the KDD CUP 99 dataset has been illustrated. The results are seen to be in the desired range. Further, it has also been shown that the resultant dataset on application of normalization techniques retains the original property as that of the original dataset. Moreover, it is seen that non-linear methods such as log and sigmoid data normalization techniques result in better detection rate.

References

- [1] Animesh Patcha and Jung-Min Park, —An Overview of Anomaly Detection Techniques: Existing Solutions and Latest Technological Trends, Computer Networks Vol. No. 51, 2017, pp. 3448-3470.
- [3] KDD CUP 1999. Available on: <http://kdd.ics.uci.edu/databases/kddcup99/kddcup99.html>.
- [4] S. Theodoridis and K. Koutroubas, Pattern Recognition, Second Edition, Elsevier Academic Press, 2018
- [5] Kevin L. Priddy, Paul E. Keller, —Artificial Neural Networks: An Introduction, First Edition, SPIE – The International Society for Optical Engineering, 2019.
- [6] J. Song, H. Takakura, Y. Okabe, and Y. Kwon, —A Robust Feature Normalization Scheme and an Optimized Clustering Method for Anomaly-Based Intrusion Detection System, In Proceedings of the 12th International Conference on Database Systems for Advanced Applications, 2017, pp. 140-151.
- [7] Mei-Ling Shyu, Kanoksri Sarinnapakorn, Indika Kuruppu-Appuhamilage, Shu-Ching Chen, LiWu Chang, and Thomas Goldring, —Handling Nominal Features in Anomaly Intrusion Detection Problems, In Proceedings of the 15th International Workshop on Research Issues in Data Engineering: Stream Data Mining and Applications, 2015, pp. 55-62.

- [8]Long-zheng Cai, Jian Chen, Yun Ke, Tao Chen, and Zhi-gang Li, —A new data normalization method for unsupervised anomaly detectionl, Journal of Zhejiang University SCIENCE-C (Computers and Electronics), Vol. No. 11, 2018, pp. 778-784.
- [9]Manbod Tavallae, Ebrahim Bagheri, Wei, Lu, and Ali A. Ghorbani, —A detailed Analysis of the KDD CUP 99 Datasetl, In Proceedings of the IEEE Symposium on Computational Intelligence in Security and Defense Applications (CISDA), 2019, pp. 1-6.

Prospective Analysis with Expansion Monitoring System and Its Applications

Dharamvir¹, Arul Kumar V²
¹ Research Scholar ² Asst. Professor
School of CSA, REVA University
Bangalore, India
dhiruniit@gmail.com¹

Abstract— Application is deliberate and intent to bring out, clarify, examine or analyze the essentials, and overseeing the parts of budgetary requirements of complex association. The monetary status, processing, execution and any changes made in budgetary value position of a given ventures being explained, given clarity and identified with a money related association stand. Explanations increasing their productivity, extensive variety of clients for financial opinion on settling down. All the complicated related queries of budgetary information can be caught at a single hub which is clubbed together under single software. Includes assets list and claims in balance sheets, trial balances, income related multi product and client based reports, tax management and cash flow reports. The software is provided with a customized opinion for each and every individual client who is using, as a impact on or for style of working. Automated and complication related financial calculations can be obtained and maintained. The desire, needful, an exposure to automate the bank feeds and account statements management and tracking, the error detection is made simpler and easier. Here live updating shown and managed, the payment integration with security encryptions is managed.

Keywords— Databases, User interface, System Reports, Analysis, and Dashboard.

I. INTRODUCTION

Businesses are often found large and small, hence requirement to keep accurate records of their finances regularly made easy and must [1],[2] to avoid such confliction around. In some situation, a part is forked, but the thing is most detailed about records and specific records of financial analysis that are fine good practices. [3] it might be impossible to completely eradicate error made by humans and bugs in any endeavor, [4] but financial analysis software can simplify aspects of keeping records, invoicing, reporting, billing. [3]-[5] “Manage all your finances from one place in a centralized way and Organizes your business with application and get the financial information you need to retrieve is accessed faster”.

A **financial forecasting** is a money related statements that is been estimated, for the future financial outcomes for the betterment of a a company or for money based markets. historical based internal financial analysis and data related to sales, including to external markets for a financial forecast, based on historic data, an economist's decisions to predict the estimates to the company that, whats going to happen in terms of finance for a given duration



Fig. 1 Financial planning Process.

The desire, needful, an exposure to automate the bank feeds and account statements management and tracking, the error detection is made simpler and easier. Here live updation shown and managed, the payment integration with security encryptions is managed. In the process of Business Management process and Notation, which offers for a new template of the Requirement Selection Process Management to assist the companies. Its being understood and known that the employees are structured and branched at different position with different wages allowances allotted so the software is so automated in such situation a report as to be generated exactly correct and exact wages by calculating the work done, even the time based calculation is possible, automated tax and provident fund calculations are done, not only calculations but helps to fix liabilities with detailed

reportings, also helps to get loans from the financial institutions as it requires complete report and detailed information about the company's activities includes profit ,loss, investment and expenses. The data security is taken with great concern to protect by using encryption algorithm, the data is transferred encrypted also data auto synchronization on few related platform is taken care.

The advent and main motto of business world is to eradicate the doing of manual reentering of data related accessing by the users, lessened the need for custom interfaces between systems,because the dashboard made it simple to understand, simple way of cross departmental transaction processing, the full touch of business cycle processes has enabled real-time information analysis and reporting easier

The process covers:

- a. Related user can check the reports in different format of budgetary information details.
- b. Transfer and integration of banking system
- c. Live updates will be managed.
- d. Time based wages calculation.

II. LITERATURE SURVEY

In the year 1994 two person named Jog and Srivastava took a study that seems the financial status by using decision-making model, few of the abroad companies like the Canadian companies, the usual techniques they made in used to do decisions on money budget, financing.

The funding opportunity are nearly related to investment results decision and the cost effective method they used are as simple as they do, the methods used are internal rate of return and the netvalue.

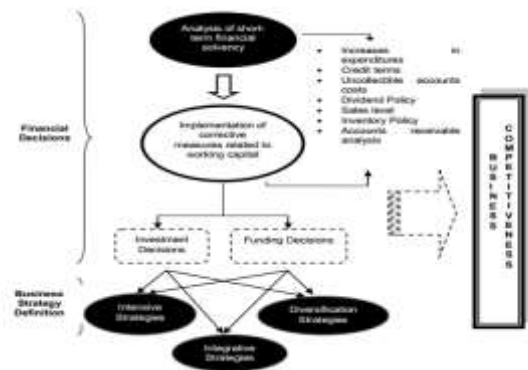


Fig. 2 decision model

In decision making model the analysis of shorterm financial solvency which gives chance to check increased expenditure is there ,to check the credit terms,sales levels and dividend policy are made.after being analysed,the implementation which is being related to money workings.later on implementing can be done based on two decisions are made one is investment decisions and second one is funding decisions also they follow few strategies such as intense strategies, integrated strategies and diversified strategies.

III Existing System:

The traditional ways to manage various activities of finance is the existing or current scenario followed in the existing system. As the current scenario makes use of the traditional process to manage financial activities, the automation and synchronization off the data related to business falls lack in the management of the system.

- Lack of automate in synchronization
- Lack of graphical and visual output.
- Use of multi-application or tools.
- Unaffordable and Expensive in nature.
- Human power required to do manual entries to manage the financial analysis system .
- Lack of Security concerns, unauthentication.
- Insufficient knowledge to define the structure.
- Complication in integrating banking system.

IV Implementation and Result Analysis

The proposed system is essential to provide centralized place for all activities related to business

that can be managed and organized. Proper data resource of business related planning can be managed, also the applications are provided with graphical reporting facility system. Few considerations are taken as main points are as follows.

- Centralized work platform and cloud support,
- Automation of synchronization mechanism
- Multi teen collaborative work and Centralized workspace
- Graphical Reporting system generated for analysis and static reasons.
- Bank Integration with banking system that is bank reconciliation.
- Use of encryption for secure data transfer, data sharing and data management
- Scheduled process to enhance the invoicing
- Customized design approach for uniqueness.
- Structured management of the functionalities as needed

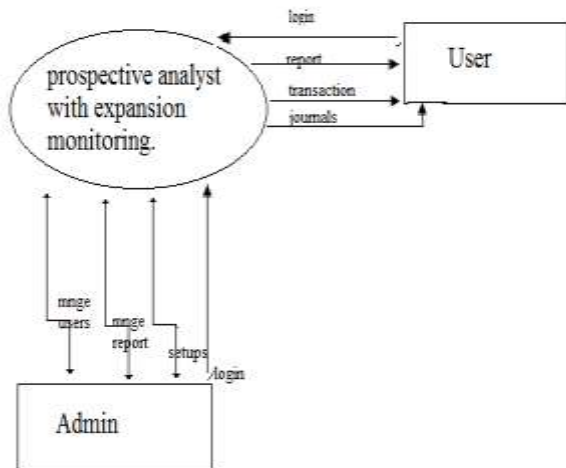


Fig. 3 context diagram of the system

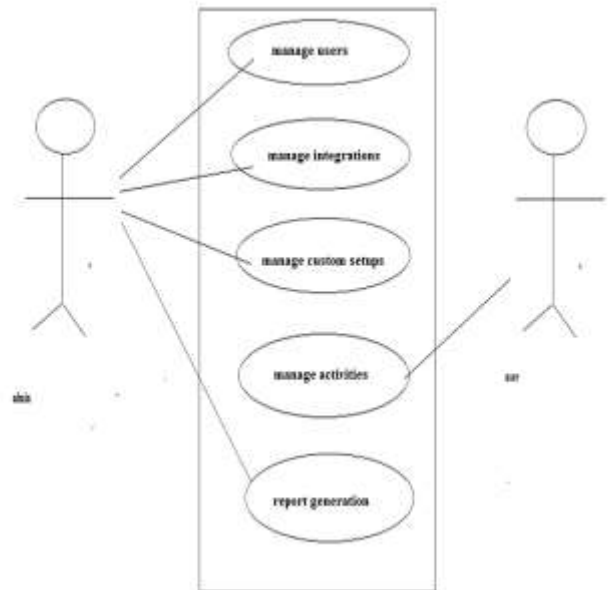


Fig. 4 Interaction of admin and user

1. MODULES
a) Budgetary

In this module, all the complicated budgetary information is managed and clubbed at the one place by the software, related people can check the reports in the proper way. All the entities related can be checked in different format. The main reports it After implementing the proposed system the results obtained are as follows: helps to check are balance sheet, trial sheet, tax management report, cash flow detailed report, profit and loss account.

b) Automated rule

In this module, the automated rule based invoicing, analyzed. Based on the analyzed results bills are generated. Automated financial calculation, template option are provided to save the template.

c) Wages calculation

In this module, the employees are structured in different formats management is also very complicated to manage so in the software we can easily calculate wages and automate the management. time based calculation, time frame based, always encrypted data transfer, device data integrated for the auto calculations, form based self service and data management, benefit calculation.

d) Transfer and integration

In this module, all the need for tracking for the budgetary information can be tracked with full clarity software will help to automate the bank feeds and statements management and track ,the error detection is easy, encrypted transfers and information gathering will be done by using the encryption ,direct connect will be managed with the banking platforms.

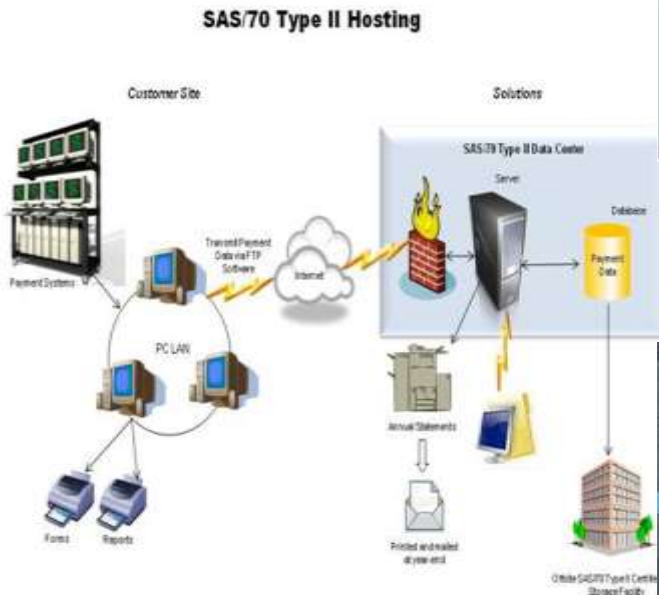


Fig.5: Block diagram for Proposed System

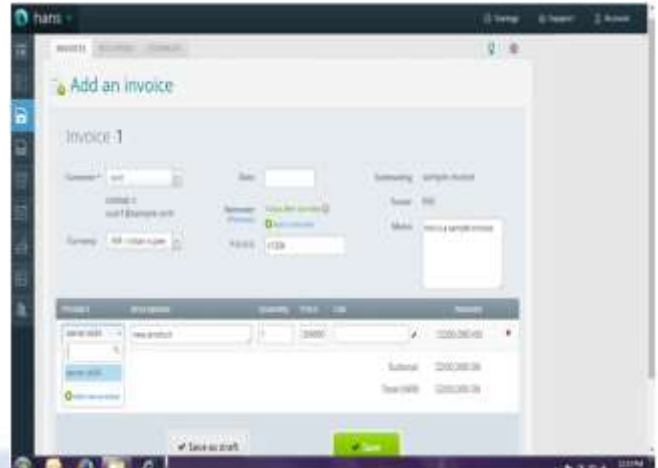


Fig .7: invoice management
Billing is made eaiier



Fig.8: Account management and Billing Report

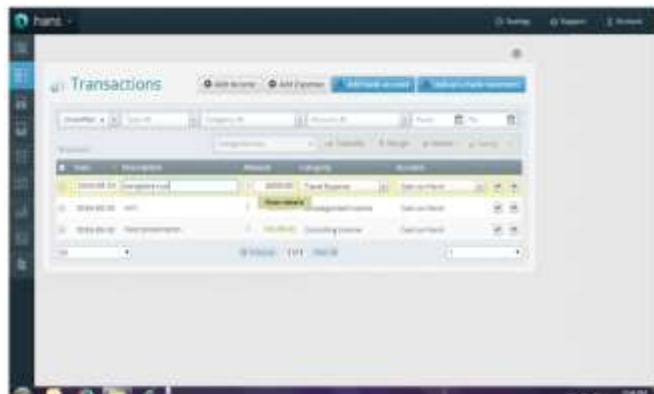


Fig. 6: Managing Transaction

Managing any number of transaction under single hub.

VII CONCLUSION

This paper proposes Our application helps in managing overall invoicing, accounts, payrolls and reporting for easy managing, synchronizing, and tracking and analyzing business activities. Application benefits realized included for worked area that is a Increased discount as each time the account is earned or received. There is reduction of costs of cost rates . As reports are generated at timely bases so there is Improvement in working capital ie money. Reports are collected for Improved accounting practices. Everything is done computerized way they cannot be any loss of document. Development of relationships between the stakeholders. Development can be seen at internal controls.

Automated year end reporting is also being generated, few reports are archived such as pay slips and annual reports which may be needed in later enhancement. the application

helps us to incorporate,orit gets integrated with timesheet systems ,the information about how long hours worked, Application generates the following general-purpose, external, financial statements:

1. The outcomes of the operations workings or the earnings are meant to be shown under income statement.
2. The position of financial reviews and statements are clearly specified in balance sheet.
3. The benefits and loss are shown in the statement of cash flow which is being given very clearly

VIII. Future Enhancement

With the fast technique used and advancement in technology for this logic environment world it is being waste of time to say what is going to happen in the real world of business how its going to work with improvement and there will be expansion in the coming years. From the working of current project , plan of advancement is done for enhancing future enhancement. We can do the implement for practicing mode so that the upcoming new technique for unknown users can have a some idea of management what it is meant to be developed, user gets a clear picture to understand.

Can do the inclusion of more features of data regression and modelling techniques in the application so that the analytics part is more flexible. We can do the inclusion of tax calculating part for future enhancement..

IX. REFERENCES

1. Deren LI and Shuliang WANG, -Concepts, principles and applications of spatial data mining and knowledge discovery,in ISSTM 2005, August, 27-29, 2015, Beijing, China.
2. W. Wang, J. Yang, and R. Muntz. -STING: A statistical information grid approach to spatial data mining in International Conference on Very Large Data Bases, Athens, Greece, Morgan Kaufman, San Mateo, CA, pp. 186-195,2018
3. M. S. Chen, J. Han, P. S. Yu. -Data mining, an overview from database perspective, *IEEE Transactions on Knowledge and data Engineering*, 2018.
4. U. Fayyad, G. P.-Shapiro, and P. Smyth. -From data mining to knowledge discovery in databases, *AI magazine*, Vol. 17 No. 3, pp. 37-54, fall 2017.
5. U. Fayyad, G.P.Shapiro, P.Smyth, and R.uthurusamy, editors. *Advances in Knowledge Discovery and Data Mining*. AAAI /MIT Press, Menlo Park, CA, 2015.

Exploring Service Oriented Routing Protocol Network Architecture for Multicast Functionality in Internet of Things and its Applications

Dharamvir^{1,a}, Dr. M S Shashidhara^{2,b}

¹Department of MCA, The Oxford College of Engineering ,
Bengaluru, India -560068

²Department of MCA, The Oxford College of Engineering ,
Bengaluru, India -560068

Corresponding author: ^adhiruniit@gmail.com

^bmsshashidhara@gmail.com

Abstract -Emerging demands of applications and capabilities of network technologies are often conflicting and contradicting. The diversity of applications on Internet requires flexible and customizable network technologies. Changing protocol of TCP/IP stack is a complex task because of its implicit dependencies between layers and tight coupling. Demand of flexible Internet architecture is arising to see that protocols can be easily added and removed from a pool of protocols without disturbing rest of the services. Service Oriented Network Architecture (SONATE) provides flexible Internet architecture in which protocol selection and composition is based on the application and network constraints. In this paper the author proposed an agent based multicast infrastructure for SONATE which is being explored as one of the possible Architecture Framework for Future Internet.

Keywords—Internet Architecture, SOA, Future Internet, Multicast, SONATE.

INTRODUCTION

In the early 1980's with the objective of computers connectivity in network TCP/IP protocol suite was developed. Still today, the same Internet technology protocol is being in use by Internet community. Looking at future demands of applications and network technologies many workaround have been introduced from time to time like cross-layer composition, multiple protocol layer switching at layer 2.5, transport layer switching at layer 4.5. Many types of end-to-end model are already introduced such as Middle Boxes, Firewalls and Network Address Translator (NAT) etc., [4]. Because of these developments in Internet resulted in increased complexity and hard to modify anything in the current system of TCP/IP protocol suit. The following main reasons to identify for this identifications , such as:

- i. Adhere to the strict layering policy of current TCP/IP protocol suit which prevented from cross layer communication and resulted in hard coupling between layers.
- ii. One Protocol header is placed inside the header of another protocol that led to sequential processing of protocols which is principle of layered structure.

Selection of Protocol is hard coded in the application, that is application will select the protocol with different data.

it should be used for completion of the task. Because of this type of dependency the developer has to know the architecture of a system well in advance on which the application is intended to be run during the development phase of the application [2].

Future Internet architecture must be flexible enough to support variant types of network devices and applications from user perspective. Thus can increase by changing or adding new

A Framework for Improving Telecom-Services by Standardization of Virtual Network Function on Boarding

Chengappa MR¹, Dr. M S Shashidhara MS²

¹Research Scholar, ²Professor & Head Department of Computer Applications

The Oxford College of Engineering

Bangalore, India

chengappa.mr@gmail.com¹, msshashidhara@gmail.com²

Abstract— Driven by a grievous push from Communication Service Providers and with the advent of 5G, Network Function Virtualization is maturing towards reality from being a mere buzz word. Communication Service Providers (CSPs) are racing towards adoption via Proof-of-Concepts (POCs) and trials. On the one side, significant investment is being made for defining and implementing the Network Function Virtualization (NFV) platform, Virtual Network Function (VNF) vendors are making severe investments to virtualize network functions which will be deployed on the NFV platform and on the other side CSPs and VNF vendor are finding it difficult on how to define the requirements in a standard manner. The framework proposed and described here is on VNF onboarding, deployment, reporting, and publishing system – a means to industrialize the process end-to-end. The solution will produce repeatable artifacts which can be used to redeploy the VNFs and will help reduce the Total cost of ownership (TCO) as well as time-to-value of the VNFs and the network services that are composed within VNFs.

Keywords -NFV, CSP, on-boarding, VNF, NFV-I.

I. INTRODUCTION

Telecom operators are adopting NFV and are looking for means to accelerate deployment of virtual network functions independent of the underlying hardware, thereby reducing the capex and opex involved in the maintenance and implementation of network services [1]. Network Function Virtualization Infrastructure provides the foundation for the deployment of Virtualized Network Functions. With VNF services being the end product of a successful NFV deployment, in the absence of a common standard for defining and deploying a VNF, Communication Service Providers are faced with challenges concerning their implementation. The solution proposed and described here averts these challenges and provides a means to rapidly define VNF deployment requirements, generate reusable, error-free deployment templates in multiple formats and hence assist a Telco attain the objective of time to value through the adoption of NFV. Deployment of VNF is achieved using orchestration templates, which contains information on resource requirements. As the first step to VNF deployment, there should be a means to define the resource requirements of the VNF. This includes standard resource requirements, and specific

An Approach to Electro Photonic Image classification in Thyroid Patents using BBNN Method

Indrakumar S S Prof. M S Shashidhara

Research Scholar , Dept. of Computer Applications,
VTU , The Oxford College of Engineering, elgaum, Bangalore-560068,India

indra181@gmail.com commsshshidhara@gmail.com

Abstract: Human body suffers from many ailments and diseases, identifying them is critical to treat the disease. Diagnosis of disease is done in many ways, Electro Photonic images help in diagnosing disease. Electro photonic imaging is capable of measuring the energy fields. We can measure energy fields of water, crystals, plants and humans. A specialized camera used to capture these images also referred to as EPI camera. This paper gives insight into the classification of Thyroid Electro Photonic Images using Backpropagation Algorithm. Different ANN methods can be used to for detecting diseases, images were processed using Backpropagation Algorithm used to detect and classify Thyroid patients.

Keywords: *kirlian photography, Medical diagnosis, Energy, Aura, Chakras, Thyroid*

1. Introduction

According to modern science human organism made of molecules, these molecules need energy which is provided in the form of food, light and water the overall energy in the body creates an energy field we are leaning to measure this energy fields using Kirlian cameras.

Diagnosis of disease is done in many ways methods, also using some devices. Electro photonic images can be used to for measuring out the energy levels of the body. Diseases can be identified using these images. Images collected from Non Thyroid and Thyroid. These images are classified using backpropagation Neural Network method as Non Thyroid and Thyroid.

Review of Dimensionality Reduction Techniques for Transformational Image Signals

Dharamvir¹, Hemanth K. S.²

¹Research Scholar ²Associate Professor

School of CSA, REVA University
Bangalore, India

dhirunii@gmail.com¹ hemanth.ks@reva.edu²

Abstract— In recent years, graphs have become a primary method of representation of large data sets generated through ubiquitous sensing devices and there is a need for dimensionality reduction techniques to perform processing, analysis and storing of these large data sets in the graph setting effectively. However finding suitable dimensionality algorithms, for a particular application has become cumbersome and even more difficult for real-time applications concerned. So in this paper, we have attempted to review dimensionality techniques proposed for processing, analyzing the large data sets in the graph setting. We have kept our review based on the computational complexity of dimensionality reduction techniques.

Keywords— Dimensionality Reduction, Graph Signal Processing, Graph Laplacian.

I. INTRODUCTION

Graphs have emerged as a fundamental way of representing data used in many scientific and engineering fields such as bio-molecular research, social networks, energy, transportation, sensor, neural network, commerce, and security. The complexity of networks and interaction between the components in these networks shows that the data do not only reside irregularly, it also has complex structures. This complex structure and irregularity of the data domain, does not give much freedom to us to use the standard signal processing tools for processing, analyzing and storing of the data.

Graphs have the ability to capture the structure and interaction among the components of these complex and irregular data domain. The data on these graphs collectively called a graph signal and can be visualized as samples taken at each vertex [1]. An example of a graph signal has been illustrated in figure 1. Graph Signal Processing (GSP) has become a new research domain that extends the techniques used in the current digital signal processing for signals defined on the nodes of the graph [1],[2].

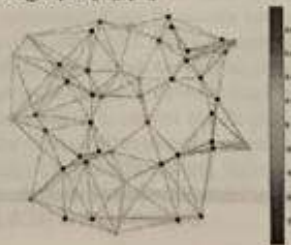


Fig 1: Network of 50 sensors as nodes and their sample values represented using color-coding.

[15007]

[Download This Paper \(Delivery.cfm/SSRN_ID3667497_code3253098.pdf?abstractid=3667497&mirid=1\)](#)[Open PDF in Browser \(Delivery.cfm/SSRN_ID3667497_code3253098.pdf?abstractid=3667497&mirid=1&type=2\)](#)[★ Add Paper to My Library](#)Share: [f](#) [t](#) [✉](#) [🔗](#)

Transitive Domination Polynomial of Graphs

Institute of Scholars (InSc), 2020

7 Pages

Posted: 18 Sep 2020

Mallikarjun Basanna Kattimani (https://papers.ssrn.com/sol3/cf_dev/AbsByAuth.cfm?per_id=4314501)

The Oxford College of Engineering

Sridhara K R (https://papers.ssrn.com/sol3/cf_dev/AbsByAuth.cfm?per_id=4314502)

A.P.S. College of Engineering

Date Written: August 5, 2020

Abstract

Let $G=(V,E)$ be a connected simple graph with n vertices. A set of vertices D is called a Transitive Dominating set if every vertex in $V-D$ is adjacent to at least one of the vertices in D through a path of length at most two [4]. Transitive domination number, denoted by $\gamma_{trd}(G)$ is the minimum of the cardinalities of all possible transitive dominating sets of the graph. In this paper, we introduce a new domination polynomial called Transitive Domination Polynomial of a graph. The transitive domination polynomial of a graph G with n vertices is denoted by $D_{trd}(G,x)$ and is defined as:

$D_{trd}(G,x) = \sum_{j=\gamma_{trd}(G)}^n [d_{trd}(G,j)] x^j$, where $d_{trd}(G,j)$ represents the number of transitive dominating sets of cardinality j . The roots of transitive domination polynomial are called transitive dominating roots. In this paper, we have obtained transitive domination polynomials of some standard graphs. Also transitive dominating roots of some graphs are obtained.

Keywords: Domination, Transitive Domination, Transitive Domination Polynomial, Transitive Domination Roots[Suggested Citation >](#)[Show Contact Information >](#)[Download This Paper \(Delivery.cfm/SSRN_ID3667497_code3253098.pdf?abstractid=3667497&mirid=1\)](#)[Open PDF in Browser \(Delivery.cfm/SSRN_ID3667497_code3253098.pdf?abstractid=3667497&mirid=1&type=2\)](#)

7 References

1. F Haray
Graph Theory
Posted: 1969
2. J L Arocha, B Llano
Mean value for the matching and dominating polynomial
Discuss.Math.Graph Theory, volume 20, issue 1, p. 57 - 69
Posted: 2000
Crossref (<https://doi.org/10.7151/dmgt.1106>)
3. S Alikhani, Y H Peng
Introduction to domination polynomial of a graph
Ars Combinatoria, volume 114, p. 257 - 266
Posted: 2014



European Journal of Pure and Applied Mathematics

[Home \(https://www.ejpam.com/index.php/ejpam/index\)](https://www.ejpam.com/index.php/ejpam/index) > [Vol 13, No 5 \(2020\)](#)
(<https://www.ejpam.com/index.php/ejpam/issue/view/61>) > [Perla](#)
(<https://www.ejpam.com/index.php/ejpam/article/view/3741/0>)

Schur Geometric Convexity of Related Function for Holders Inequality with Application

Sreenivasa Reddy Perla, S. Padmanabhan, V. Loksha

Abstract

In this paper, we investigated the Schur geometric convexity of related function for Holders Inequality by using majorization inequality theory and some applications are established.

Keywords

Holders Inequality, majorization inequality, schur geometric convex, schur geometric concave

Full Text:

[PDF](#)
(<https://www.ejpam.com/index.php/ejpam/article/view/3741/962>)

DOI: <https://doi.org/10.29020/nybg.ejpam.v13i5.3741>
(<https://doi.org/10.29020/nybg.ejpam.v13i5.3741>)

Tweet

(<http://www.addthis.com/bookmark.php>)

Article Tools



[Print this article](#)
([javascript:openRTWir](#))

[Indexing metadata](#)
([javascript:openRTWir](#))

[How to cite item](#)
([javascript:openRTWir](#))

[Finding References](#)
([javascript:openRTWir](#))

Email this article

(Login required)

Email the author

(Login required)

User

Username

Password

Remember me

OUR AFFILIATED JOURNALS

» [Journal of Algebraic Statistics](#)
(<https://jalgstat.com>)

» [European Journal of](#)

International Journal of Advanced Science and Technology

- Home
- Editorial Board
- Journal Topics
- Archives
- About the Journal
- Submissions
- Privacy Statement
- Contact

[Home](#) / [Archives](#) / [Vol. 29 No. 7 \(2020\)](#) / [Articles](#)

Schur Harmonic Convexity of Related Function for Holders Inequality with Application

Sreenivasa Reddy Perla , S. Padmanabhan

Abstract

In this paper, make use of majorization inequality theory investigated the Schur harmonically convex regarding related function of Holders Inequality, giving a complete essential condition of Schur harmonically convex function to Holders Inequality and some applications are established.



How to Cite

Sreenivasa Reddy Perla , S. Padmanabhan. (2020). Schur Harmonic Convexity of Related Function for Holders Inequality with Application. *International Journal of Advanced Science and Technology*, 29(7), 8224-8235. Retrieved from <http://sersc.org/journals/index.php/IJAST/article/view/24646>

Issue

[Vol. 29 No. 7 \(2020\)](#)

Section

Articles

Vertex Polynomial of Middle, Line and Total Graphs of some standard Graphs

Mallikarjun Basanna Kattimani, Sridhara K.R.

Abstract: In this article, we have obtained vertex polynomial of Middle, Line and Total graphs of some standard graphs namely complete graph, star, path, cycle and wheel graph.

Keywords: Vertex polynomial, Middle graph, Line Graph, Total Graph

I. INTRODUCTION

In this paper, we have considered only finite graphs which are non-trivial, undirected, having no self-loops and having no parallel edges. Two edges of a graph are adjacent if they have a common vertex. If a vertex v is an end vertex of an edge e , then edge e is incident on vertex v . Vertices and edges are called elements of a graph and are neighbors if they are either incident or adjacent. $K_{1,n}$ represents a star. A wheel graph W_n and is defined as $W_n = K_1 + C_{n-1}$. A graph G is k -regular if each vertex has degree k . If $x = uv$ is an edge of a graph G , and w is not a vertex of G , then x is said to be subdivided if it is replaced by the edges uw and vw . For terminologies and notations, we refer [1]. The vertex polynomial of the graph G [2] is defined as $V(G; x) = \sum_{k=0}^{\Delta(G)} v_k x^k$, where $\Delta(G) = \max\{d(v) : v \in V(G)\}$ and v_k is the number of vertices of degree k . The roots of a vertex polynomial are called vertex polynomial roots.

II. MIDDLE GRAPH, LINE GRAPH, TOTAL GRAPH AND VERTEX POLYNOMIAL WITH AN EXAMPLE.

In this part, we list the definitions of Middle graph, Line graph and Total graph of a graph with an example. Also we show their vertex polynomials.

Let G be a graph with $|V| = m$ and $|E| = n$. Its line graph $L(G)$ contains vertices which are edges of G and edges in $L(G)$ are drawn between vertices if they have common vertex in G . Middle graph $M(G)$ has vertex set containing all vertices and all edges of G and edges of $M(G)$ between new vertices are drawn only when the edges corresponding in G are adjacent. Total graph $T(G)$ has vertex set containing all vertices of G and all edges of G and two vertices of total graph are adjacent if they happen to be neighbors in G . The following figures show a graph, its line graph, middle graph and total graph with their vertex polynomials.



Figure 1– Graph G .

In this graph, we find 1, 2 and 1 vertices of degrees 1, 2 and 3 respectively. Thus $V(G; x) = x + 2x^2 + x^3$. Now we consider its line graph as in Figure 2.

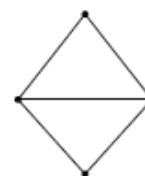


Figure 2– $L(G)$

We note that $L(G)$ has four vertices of which two are of degree 2 and remaining two are of degree 3. Thus $V(L(G); x) = 2x^2 + 2x^3$

Now, we consider middle graph $M(G)$ as shown in Figure 3.

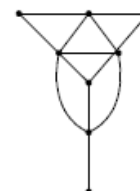


Figure 3– $M(G)$

The middle graph has one vertex of degree 1, two vertices of degree 2, one vertex of degree 3, two vertices of degree 4 and two vertices of degree 5. Thus $V(M(G); x) = x + 2x^2 + x^3 + 2x^4 + 2x^5$. Now we consider total graph $T(G)$ as shown in Figure 4.

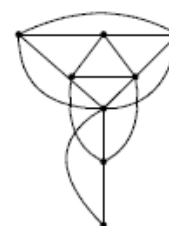


Figure 4– $T(G)$

Revised Manuscript Received on April 03, 2020.

* Corresponding Author

Mallikarjun Basanna Kattimani, Department of Mathematics, The Oxford College of Engineering, Bangalore, India, mathshodoxford@gmail.com

Sridhara K.R.* , Department of Mathematics, A.P.S. College of Engineering, Bangalore, India, sridharwi@gmail.com

Vertex Polynomial of Middle, Line and Total Graphs of some standard Graphs

$T(G)$, the total graph has 1, 4, 2 and 1 vertices of degrees 2, 4, 5 and 6 respectively.

$$\text{Thus } V(T(G); x) = x^2 + 4x^4 + 2x^5 + x^6$$

III. MAIN RESULTS

Theorem 3.1: If $M(K_n)$ is middle graph of K_n , then

$$V(M(K_n); x) = nx^{n-1} + \frac{n(n-1)}{2}x^{2n-2}$$

Proof: We note that K_n has n vertices, whereas its middle graph $M(K_n)$ has $\frac{n^2+n}{2}$ vertices by definition of middle graph. We can partition vertex set of $M(K_n)$ into two disjoint subsets V_1 and V_2 as follows:

V_1 : Vertex set with $|V_1| = n$, degree being $(n-1)$ for each vertex and

V_2 : Vertex set with $|V_2| = \frac{n^2-n}{2}$, degree being $(2n-2)$ for each vertex.

$$\text{Hence } V(M(K_n); x) = nx^{n-1} + \frac{n(n-1)}{2}x^{2n-2}$$

Theorem 3.2: If $M(K_{1,n})$ is middle graph of $K_{1,n}$, then

$$V(M(K_{1,n}); x) = nx^{n+1} + x^n + nx \text{ for } n \geq 2$$

Proof: We note that $K_{1,n}$ has $(n+1)$ vertices, whereas its middle graph $M(K_{1,n})$ has $(2n+1)$ vertices by definition of middle graph. We can partition the vertex set of $M(K_{1,n})$ into disjoint subsets V_1, V_2 and V_3 as follows:

V_1 : Vertex set containing 1 vertex of degree n ,

V_2 : Vertex set with $|V_2| = n$, each vertex being pendant and

V_3 : Vertex set $|V_3| = n$, degree being $(n+1)$ for each vertex.

$$\text{Thus } V(M(K_{1,n}); x) = nx^{n+1} + x^n + nx$$

Theorem 3.3: If $M(P_n)$ is the middle graph of P_n , then

$$V(M(P_n); x) = 2x + (n-2)x^2 + (n-1)x^3, n \geq 3$$

Proof: We note, by definition of middle graph that, $M(P_n)$ contains $(2n-1)$ vertices. We can partition the vertex set of $M(P_n)$ into three disjoint subsets V_1, V_2 and V_3 as follows:

V_1 : Vertex set containing 2 vertices, each of degree 1,

V_2 : Vertex set with $|V_2| = n-2$, degree being 2 for each vertex and

V_3 : Vertex set with $|V_3| = n-1$, degree being 3 for each vertex.

$$\text{Thus } V(M(P_n); x) = 2x + (n-2)x^2 + (n-1)x^3$$

Theorem 3.4: If $M(C_n)$ is the middle graph of C_n , then

$$V(M(C_n); x) = nx^2 + nx^4$$

Proof: We note, by definition of middle graph that, $M(C_n)$ contains $2n$ vertices. We can partition the vertex set of $M(C_n)$ into V_1 and V_2 as follows:

V_1 : Vertex set containing n vertices of C_n , each of degree 2 and

V_2 : Vertex set containing n new vertices obtained by definition of middle graph, each of degree 4.

$$\text{Thus } V(M(C_n); x) = nx^2 + nx^4$$

Corollary 3.5: The vertex polynomial roots of $M(C_n)$ are 0, 0 and $\pm i$

Proof: In view of Theorem 3.4, vertex polynomial roots of $M(C_n)$ can be obtained by taking

$$nx^2 + nx^4 = 0 \Rightarrow x = 0, 0 \text{ and } \pm i$$

Theorem 3.6: If $M(W_n)$ is the middle graph of W_n , then

$$V(M(W_n); x) = (n-1)x^{n+2} + x^{n-1} + (n-1)x^6 + (n-1)x^3, \text{ for } n \geq 5$$

Proof: We note, by definition of middle graph that, $M(W_n)$ contains $(3n-2)$ vertices. We can partition vertex set of $M(W_n)$ into four disjoint subsets V_1, V_2, V_3 and V_4 as follows:

V_1 : Vertex set containing a single vertex of degree $(n-1)$,

V_2 : Vertex set with $|V_2| = n-1$, degree being 3 for each vertex,

V_3 : Vertex set $|V_3| = n-1$, degree being 6 for each vertex, and

V_4 : Vertex set $|V_4| = n-1$, degree being $n+2$ for each vertex.

$$\text{Thus } V(M(W_n); x) = (n-1)x^{n+2} + x^{n-1} + (n-1)x^6 + (n-1)x^3$$

Theorem 3.7: If $L(K_n)$ is the line graph of K_n , then

$$V(L(K_n); x) = \frac{n(n-1)}{2}x^n$$

Proof: Using definition of line graph, we easily understand that $L(K_n)$ is a n -regular graph with $\frac{n^2-n}{2}$ vertices and every vertex will be of degree n .

$$\text{Thus } V(L(K_n); x) = \frac{n(n-1)}{2}x^n.$$

Theorem 3. 8: If $L(K_{1,n})$ is the line graph of $K_{1,n}$, then

$$V(L(K_{1,n}); x) = nx^{n-1}$$

Proof: By definition of line graph, of a graph, we easily understand that $L(K_{1,n})$ is a complete graph K_n and therefore every vertex will be of degree $(n-1)$.



Thus $V(L(K_{1,n}; x)) = nx^{n-1}$.

Theorem 3.9: If $L(P_n)$ is the line graph of P_n , then $V(L(P_n); x) = 2x + (n-3)x^2, n \geq 3$

Proof: By definition of line graph, we easily understand that $L(P_n)$ is a path graph P_{n-1} .

Thus $V(L(P_n); x) = V(P_{n-1}; x)$.

It is easy to note that path graph P_{n-1} will have 2 pendant vertices and remaining $(n-3)$ internal vertices will be of degree 2.

Thus $V(L(P_n); x) = 2x + (n-3)x^2$.

Theorem 3.10: If $L(C_n)$ is the line graph of C_n , then is $V(L(C_n); x) = nx^2$.

Proof: By definition of line graph, we easily understand that $L(C_n) = C_n$ itself. As degree of every vertex of C_n is 2 and as it has n vertices, we find $V(L(C_n); x) = nx^2$.

Corollary 3.11: The vertex polynomial root of $L(C_n)$ is 0 with multiplicity 2.

Proof: In view of Theorem 3.10, vertex polynomial roots of $L(C_n)$ can be obtained by taking

$$nx^2 = 0 \Rightarrow x = 0, 0 \text{ as } n \neq 0$$

Theorem 3.12: If $L(W_n)$ is the line graph of W_n , then $V(L(W_n); x) = (n-1)x^4 + (n-1)x^n, n \geq 4$

Proof: We know, a wheel graph W_n will have n vertices and $(2n-2)$ edges. The vertex set of $L(W_n)$ will have $(2n-2)$ vertices and we can partition the vertex set into two disjoint subsets V_1 and V_2 as follows:

V_1 : Vertex set with $|V_1| = n-1$, degree being 4 for each vertex

V_2 : Vertex set with $|V_2| = n-1$, degree being n for each vertex

Thus $V(L(W_n); x) = (n-1)x^4 + (n-1)x^n$

Theorem 3.13: If $T(K_n)$ is the total graph of K_n , then

$$V(T(K_n); x) = \frac{n(n+1)}{2} x^{2n-2}$$

Proof: We note that K_n will have n vertices and $\frac{n(n-1)}{2}$ edges. By definition of total graph of a graph, we note that, total graph $T(K_n)$ will have $n + \frac{n(n-1)}{2} = \frac{n(n+1)}{2}$ vertices and each vertex will be of degree $(2n-2)$.

Thus

$$V(T(K_n); x) = \frac{n(n+1)}{2} x^{2n-2}$$

Theorem 3.14: If $T(K_{1,n})$ is the total graph of $K_{1,n}$, then

$$V(T(K_{1,n}); x) = nx^2 + nx^{n+1} + x^{2n}$$

Proof: We know a star graph $K_{1,n}$ will have $n+1$ vertices and n edges. We note that total graph $T(K_{1,n})$ of star graph $K_{1,n}$ will have $(2n+1)$ by the way in which total graph is defined and we can partition this the vertex set into 3 disjoint subsets V_1, V_2 and V_3 as follows:

V_1 : Vertex set containing a single vertex of degree $2n$,

V_2 : Vertex set with $|V_2| = n-1$, degree being 2 for each vertex and

V_3 : Vertex set $|V_3| = n$, degree being 2 for each vertex.

Thus $V(T(K_{1,n}); x) = nx^2 + nx^{n+1} + x^{2n}$

Theorem 3.15: If $T(P_n)$ is the total graph of $T(P_n)$, then

$$V(T(P_n); x) = 2x^2 + 2x^3 + (2n-5)x^4, n \geq 3$$

Proof: We know, a path graph P_n will have n vertices and $(n-1)$ edges. By definition of total graph, we note $T(P_n)$ will have $(2n-1)$ vertices and we can partition this vertex set into 3 disjoint subsets V_1, V_2 and V_3 as follows:

V_1 : Vertex set containing 2 vertices, each of degree 2,

V_2 : Vertex set containing 2 vertices, each of degree 3 and

V_3 : Vertex set containing $(2n-5)$ vertices, each of degree 4.

Thus $V(T(P_n); x) = 2x^2 + 2x^3 + (2n-5)x^4$

Theorem 3.16: If $T(C_n)$ is the total graph of C_n , then

$$V(T(C_n); x) = 2nx^4$$

Proof: We know, a cycle graph C_n has n vertices. By definition of total graph of a graph, we note that, $T(C_n)$ of C_n is a 4-regular graph with $2n$ vertices and each vertex will be of degree 4. Thus $V(T(C_n); x) = 2nx^4$.

Corollary 3.17: The vertex polynomial root of $T(C_n)$ is 0 with multiplicity 4.

Proof: In view of Theorem 3.16, result is obvious.

Theorem 3.18: If $T(W_n)$ is the total graph of W_n , then

$$V(T(W_n); x) = (2n-2)x^6 + (n-1)x^{n+2} + x^{2n-2}, \text{ for } n \geq 5$$

Proof: We know a wheel graph W_n has n vertices and $2n-2$ edges. By definition of total graph, we note that $T(W_n)$ of W_n will have $(3n-2)$ vertices and we can partition this vertex set into three disjoint subsets V_1, V_2 and V_3 as follows:

V_1 : Vertex set containing $(2n-2)$ vertices, each of degree 6,

Vertex Polynomial of Middle, Line and Total Graphs of some standard Graphs

V_2 : Vertex set containing a single vertex of degree $(2n - 2)$
and

V_3 : Vertex set containing $(n - 1)$ vertices, each of degree $(n + 2)$.

Thus $V(T(W_n; x)) = (2n - 2)x^6 + (n - 1)x^{n+2} + x^{2n-2}$

IV. CONCLUSION

Vertex polynomial is one of the possible ways in which we can represent a graph algebraically. We can compare this polynomials with other polynomials associated with graph also.

REFERENCES

1. F.Haray, Graph Theory, Addison-Wesley, Reading- Mass (1969).
2. J.Devaraj and E.Sukumaran, On Vertex Polynomial, International J. of Math. Sci. & Engg. Appls. (IJMSEA), Vol. 6 No. I (January, 2012), pp. 371-380.
3. A.M.Anto and P.Paul Hawkins, Vertex Polynomial of Graphs with New Results, Global Journal of Pure and Applied Mathematics, Volume 15, Number 4 (2019), pp. 469-475.
4. Mallikarjun Basanna Kattimani and Sridhara K.R., Transitive domination polynomial in graphs, Studies in Indian Place Names (UGC Care Journal), ISSN: 2394-3114, Vol-40-Issue-70-March 2020, pp. 440-447.

AUTHORS' PROFILE



Dr. Mallikarjun Basanna Kattimani

He is working as Professor and Head, Department of Mathematics & Dean of Examinations at The Oxford College of Engineering, Bangalore. His current area of research interest is Graph Theory. He has successfully guided one student for Ph.D. and presently guiding 6 students for Ph.D. He has introduced many domination parameters in Graph Theory and has published 12 research papers in national and international journals. In addition, he

has 7 extended research articles to his credit. He has around 28 years of rich teaching experience.



Sridhara K.R.

He is working as Assistant Professor and Head, Department of Mathematics, A.P.S. College of Engineering, Bangalore. His research area of interest is Graph Theory. He has around 21 years of teaching experience.

